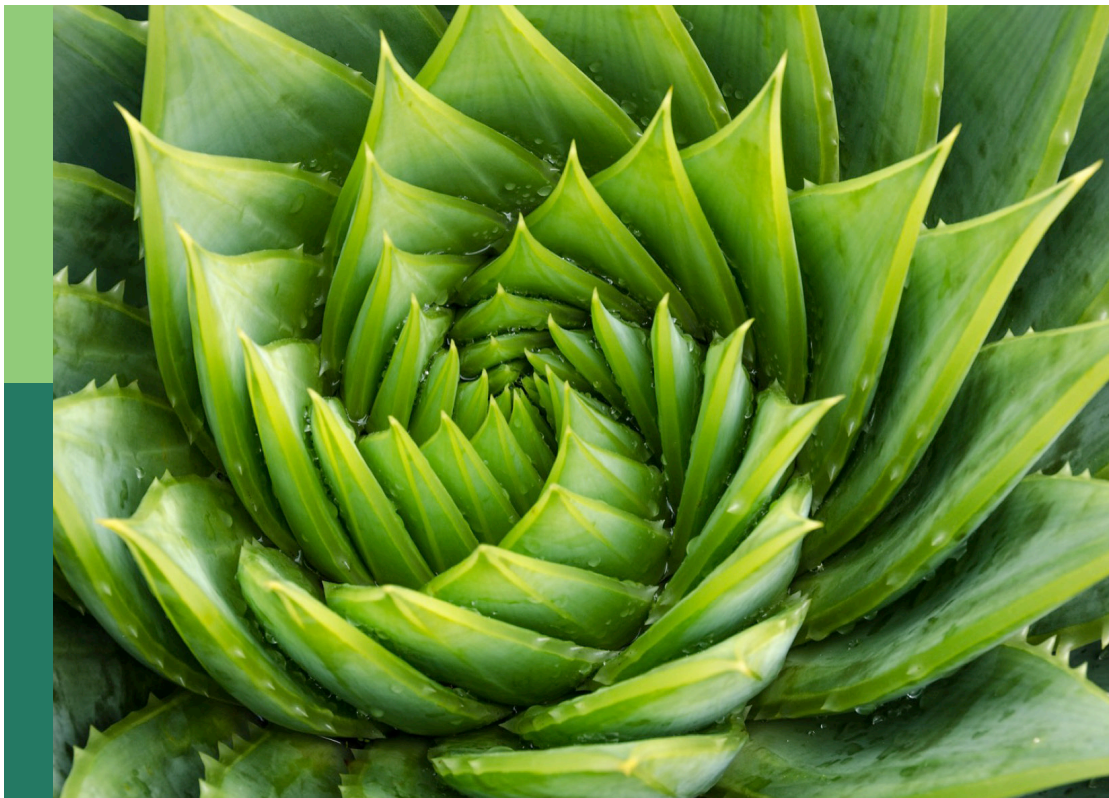
frontiers | Research Topics

Mechanisms of abiotic stress responses and tolerance in plants: Physiological, biochemical and molecular interventions, volume II

Edited by
Shabir Hussain Wani, Guo-Liang Jiang, Mohammad Anwar Hossain, David John Burritt, Hatem Rouached and Fulai Liu

Published in
Frontiers in Plant Science



FRONTIERS EBOOK COPYRIGHT STATEMENT

The copyright in the text of individual articles in this ebook is the property of their respective authors or their respective institutions or funders. The copyright in graphics and images within each article may be subject to copyright of other parties. In both cases this is subject to a license granted to Frontiers.

The compilation of articles constituting this ebook is the property of Frontiers.

Each article within this ebook, and the ebook itself, are published under the most recent version of the Creative Commons CC-BY licence. The version current at the date of publication of this ebook is CC-BY 4.0. If the CC-BY licence is updated, the licence granted by Frontiers is automatically updated to the new version.

When exercising any right under the CC-BY licence, Frontiers must be attributed as the original publisher of the article or ebook, as applicable.

Authors have the responsibility of ensuring that any graphics or other materials which are the property of others may be included in the CC-BY licence, but this should be checked before relying on the CC-BY licence to reproduce those materials. Any copyright notices relating to those materials must be complied with.

Copyright and source acknowledgement notices may not be removed and must be displayed in any copy, derivative work or partial copy which includes the elements in question.

All copyright, and all rights therein, are protected by national and international copyright laws. The above represents a summary only. For further information please read Frontiers' Conditions for Website Use and Copyright Statement, and the applicable CC-BY licence.

ISSN 1664-8714
ISBN 978-2-8325-3575-2
DOI 10.3389/978-2-8325-3575-2

About Frontiers

Frontiers is more than just an open access publisher of scholarly articles: it is a pioneering approach to the world of academia, radically improving the way scholarly research is managed. The grand vision of Frontiers is a world where all people have an equal opportunity to seek, share and generate knowledge. Frontiers provides immediate and permanent online open access to all its publications, but this alone is not enough to realize our grand goals.

Frontiers journal series

The Frontiers journal series is a multi-tier and interdisciplinary set of open-access, online journals, promising a paradigm shift from the current review, selection and dissemination processes in academic publishing. All Frontiers journals are driven by researchers for researchers; therefore, they constitute a service to the scholarly community. At the same time, the *Frontiers journal series* operates on a revolutionary invention, the tiered publishing system, initially addressing specific communities of scholars, and gradually climbing up to broader public understanding, thus serving the interests of the lay society, too.

Dedication to quality

Each Frontiers article is a landmark of the highest quality, thanks to genuinely collaborative interactions between authors and review editors, who include some of the world's best academicians. Research must be certified by peers before entering a stream of knowledge that may eventually reach the public - and shape society; therefore, Frontiers only applies the most rigorous and unbiased reviews. Frontiers revolutionizes research publishing by freely delivering the most outstanding research, evaluated with no bias from both the academic and social point of view. By applying the most advanced information technologies, Frontiers is catapulting scholarly publishing into a new generation.

What are Frontiers Research Topics?

Frontiers Research Topics are very popular trademarks of the *Frontiers journals series*: they are collections of at least ten articles, all centered on a particular subject. With their unique mix of varied contributions from Original Research to Review Articles, Frontiers Research Topics unify the most influential researchers, the latest key findings and historical advances in a hot research area.

Find out more on how to host your own Frontiers Research Topic or contribute to one as an author by contacting the Frontiers editorial office: frontiersin.org/about/contact

Mechanisms of abiotic stress responses and tolerance in plants: Physiological, biochemical and molecular interventions, volume II

Topic editors

Shabir Hussain Wani — Sher-e-Kashmir University of Agricultural Sciences and Technology, India

Guo-Liang Jiang — Virginia State University, United States

Mohammad Anwar Hossain — Bangladesh Agricultural University, Bangladesh

David John Burritt — University of Otago, New Zealand

Hatem Rouached — Institut National de recherche pour l'agriculture, l'alimentation et l'environnement (INRAE), France

Fulai Liu — University of Copenhagen, Denmark

Citation

Wani, S. H., Jiang, G.-L., Hossain, M. A., Burritt, D. J., Rouached, H., Liu, F., eds. (2023). *Mechanisms of abiotic stress responses and tolerance in plants: Physiological, biochemical and molecular interventions, volume II*. Lausanne: Frontiers Media SA. doi: 10.3389/978-2-8325-3575-2

Table of contents

08 Editorial: Mechanisms of abiotic stress responses and tolerance in plants: physiological, biochemical and molecular interventions, volume II
Shabir Hussain Wani

14 Alpha Tocopherol-Induced Modulations in the Morphophysiological Attributes of Okra Under Saline Conditions
Maria Naqve, Xiukang Wang, Muhammad Shahbaz, Athar Mahmood, Safura Bibi and Sajid Fiaz

26 Advances in "Omics" Approaches for Improving Toxic Metals/Metalloids Tolerance in Plants
Ali Raza, Javaria Tabassum, Zainab Zahid, Sidra Charagh, Shanza Bashir, Rutwik Barmukh, Rao Sohail Ahmad Khan, Fernando Barbosa Jr., Chong Zhang, Hua Chen, Weijian Zhuang and Rajeev K. Varshney

54 Phytohormones Trigger Drought Tolerance in Crop Plants: Outlook and Future Perspectives
Shehzad Iqbal, Xiukang Wang, Iqra Mubeen, Muhammad Kamran, Iqra Kanwal, Gonzalo A. Díaz, Aqleem Abbas, Aasma Parveen, Muhammad Nauman Atiq, Huda Alshaya, Tarek K. Zin El-Abedin and Shah Fahad

68 Preharvest UV-C Hormesis Induces Key Genes Associated With Homeostasis, Growth and Defense in Lettuce Inoculated With *Xanthomonas campestris* pv. *vitians*
Amadou Sidibé, Marie Thérèse Charles, Jean-François Lucier, Yanqun Xu and Carole Beaulieu

86 Genome-Wide Identification and Expression Profiling of DUF221 Gene Family Provides New Insights Into Abiotic Stress Responses in Potato
Madiha Zaynab, Jiaofeng Peng, Yasir Sharif, Mohammed Albaqami, Rashid Al-Yahyai, Mahpara Fatima, Muhammad Azhar Nadeem, Khalid Ali Khan, Saqer S. Alotaibi, Ibrahim A. Alaraidh, Hassan O. Shaikhaldein and Shuangfei Li

100 Transgenic *Medicago truncatula* Plants That Accumulate Proline Display Enhanced Tolerance to Cadmium Stress
Vanesa S. García de la Torre, Teodoro Coba de la Peña, M. Mercedes Lucas and José J. Pueyo

112 Exogenous Application of Salicylic Acid and Hydrogen Peroxide Ameliorate Cadmium Stress in Milk Thistle by Enhancing Morpho-Physiological Attributes Grown at Two Different Altitudes
Mereen Nizar, Kanval Shaukat, Noreen Zahra, Muhammad Bilal Hafeez, Ali Raza, Abdul Samad, Qasim Ali, Manzer H. Siddiqui and Hayssam M. Ali

130 Genome-Wide Identification and Expression Profiling of Germin-Like Proteins Reveal Their Role in Regulating Abiotic Stress Response in Potato
Madiha Zaynab, Jiaofeng Peng, Yasir Sharif, Mahpara Fatima, Mohammed Albaqami, Rashid Al-Yahyai, Khalid Ali Khan, Saqer S. Alotaibi, Ibrahim A. Alaraidh, Hassan O. Shaikhaldein and Shuangfei Li

149 Corrigendum: Genome-Wide Identification and Expression Profiling of Germin-Like Proteins Reveal Their Role in Regulating Abiotic Stress Response in Potato
Madiha Zaynab, Jiaofeng Peng, Yasir Sharif, Mahpara Fatima, Mohammed Albaqami, Rashid Al-Yahyai, Khalid Ali Khan, Saqer S. Alotaibi, Ibrahim A. Alaraidh, Hassan O. Shaikhaldein and Shuangfei Li

151 Zinc Oxide Nanoparticles Interplay With Physiological and Biochemical Attributes in Terminal Heat Stress Alleviation in Mungbean (*Vigna radiata* L.)
Hafiz Abdul Kareem, Muhammad Farrukh Saleem, Sana Saleem, Shabir A. Rather, Shabir Hussain Wani, Manzer H. Siddiqui, Saud Alamri, Ritesh Kumar, Nikhil B. Gaikwad, Zhipeng Guo, Junpeng Niu and Quanzhen Wang

166 The Combined Inoculation of *Curvularia lunata* AR11 and Biochar Stimulates Synthetic Silicon and Potassium Phosphate Use Efficiency, and Mitigates Salt and Drought Stresses in Rice
Arjun Adhikari, Muhammad Aaqil Khan, Muhammad Imran, Ko-Eun Lee, Sang-Mo Kang, Jin Y. Shin, Gil-Jae Joo, Murtaza Khan, Byung-Wook Yun and In-Jung Lee

180 Calcium Nanoparticles Impregnated With Benzenedicarboxylic Acid: A New Approach to Alleviate Combined Stress of DDT and Cadmium in *Brassica alboglabra* by Modulating Bioacummulation, Antioxidative Machinery and Osmoregulators
Samavia Mubeen, Iqra Shahzadi, Waheed Akram, Wajid Saeed, Nasim Ahmad Yasin, Aqeel Ahmad, Anis Ali Shah, Manzer H. Siddiqui and Saud Alamri

195 Mechanistic Insights Into Trehalose-Mediated Cold Stress Tolerance in Rapeseed (*Brassica napus* L.) Seedlings
Ali Raza, Wei Su, Ziqi Jia, Dan Luo, Yi Zhang, Ang Gao, Muhammad Azhar Hussain, Sundas Saher Mehmood, Yong Cheng, Yan Lv and Xiling Zou

209 Multidimensional Role of Silicon to Activate Resilient Plant Growth and to Mitigate Abiotic Stress
Rakeeb Ahmad Mir, Basharat Ahmad Bhat, Henan Yousuf, Sheikh Tajamul Islam, Ali Raza, Masood Ahmad Rizvi, Sidra Charagh, Mohammed Albaqami, Parvaze A. Sofi and Sajad Majeed Zargar

235 Effects on Photosynthetic Response and Biomass Productivity of *Acacia longifolia* ssp. *longifolia* Under Elevated CO_2 and Water-Limited Regimes
Muhammad Mansoor Javaid, Xiukang Wang, Singarayer K. Florentine, Muhammad Ashraf, Athar Mahmood, Feng-Min Li and Sajid Fiaz

249 The Multifaceted Roles of MYC2 in Plants: Toward Transcriptional Reprogramming and Stress Tolerance by Jasmonate Signaling
Cheng Song, Yunpeng Cao, Jun Dai, Guohui Li, Muhammad Aamir Manzoor, Cunwu Chen and Hui Deng

263 Genome-Wide Identification and Expression Profiling of *KCS* Gene Family in Passion Fruit (*Passiflora edulis*) Under *Fusarium kyushuense* and Drought Stress Conditions
Hafiz Muhammad Rizwan, Fang Shaozhong, Xiaoting Li, Muhammad Bilal Arshad, Ahmed Fathy Yousef, Yang Chenglong, Meng Shi, Mohammed Y. M. Jaber, Muhammad Anwar, Shuai-Ya Hu, Qiang Yang, Kaiwei Sun, Mohamed A. A. Ahmed, Zheng Min, Ralf Oelmüller, Lin Zhimin and Faxing Chen

296 Exogenous Methyl Jasmonate Application Improved Physio-Biochemical Attributes, Yield, Quality, and Cadmium Tolerance in Fragrant Rice
Adam Sheka Kanu, Umair Ashraf, Lamin R. Mansaray, Farhat Abbas, Sajid Fiaz, Sikandar Amanullah, Christen Shaka Charley and Xiangru Tang

308 Melatonin Rescues Photosynthesis and Triggers Antioxidant Defense Response in *Cucumis sativus* Plants Challenged by Low Temperature and High Humidity
Bakht Amin, Muhammad Jawaad Atif, Huanwen Meng, Muhammad Ali, Shuju Li, Hesham F. Alharby, Ali Majrashi, Khalid Rehman Hakeem and Zhihui Cheng

323 Effects of Fallow Management Practices on Soil Water, Crop Yield and Water Use Efficiency in Winter Wheat Monoculture System: A Meta-Analysis
Muhammad Adil, Shaohong Zhang, Jun Wang, Adnan Noor Shah, Mohsin Tanveer and Sajid Fiaz

336 Melatonin-Mediated Abiotic Stress Tolerance in Plants
Wen Zeng, Salma Mostafa, Zhaogeng Lu and Biao Jin

357 Silicon Supplementation Modulates Physiochemical Characteristics to Balance and Ameliorate Salinity Stress in Mung Bean
Musa Al Murad and Sowbiya Muneer

376 Expression of Potato *StDRO1* in Arabidopsis Alters Root Architecture and Drought Tolerance
Chao Sun, Wenjun Liang, Kan Yan, Derong Xu, Tianyuan Qin, Sajid Fiaz, Philip Kear, Zhenzhen Bi, Yuhui Liu, Zhen Liu, Junlian Zhang and Jiangping Bai

386 Research Progress in the Field of Microbial Mitigation of Drought Stress in Plants
Shifa Shaffique, Muhamad Aaqil Khan, Muhamad Imran, Sang-Mo Kang, Yong-Sung Park, Shabir Hussain Wani and In-Jung Lee

403 Leaf Functional Traits of Invasive Grasses Conferring High-Cadmium Adaptation Over Natives
Muhammad Ilyas, Sakhawat Shah, Ya-Wen Lai, Jan Sher, Tao Bai, Fawad Zaman, Farkhanda Bibi, Monika Koul, Shabir Hussain Wani, Ali Majrashi, Hesham F. Alharby, Khalid Rehman Hakeem, Yong-Jian Wang and Shabir A. Rather

422 Integration of Metabolomics and Transcriptomics for Investigating the Tolerance of Foxtail Millet (*Setaria italica*) to Atrazine Stress
Lifang Sun, Libin Liu, Yuting Wang, Yanfei Feng, Wei Yang, Di Wang, Shuren Gao, Xingfen Miao and Wentao Sun

436 NAC Transcription Factor *TwNAC01* Positively Regulates Drought Stress Responses in Arabidopsis and Triticale
Meng Wang, Li-Tong Ren, Xiao-Yong Wei, Yue-Ming Ling, Hai-Tao Gu, Shan-Shan Wang, Xue-Feng Ma and Guang-Chao Kong

452 Comprehensive Genome-Wide Identification and Expression Profiling of *Eceriferum* (*CER*) Gene Family in Passion Fruit (*Passiflora edulis*) Under *Fusarium kyushuense* and Drought Stress Conditions
Hafiz Muhammad Rizwan, Abdul Waheed, Songfeng Ma, Jiankun Li, Muhammad Bilal Arshad, Muhammad Irshad, Binqi Li, Xuelian Yang, Ahmad Ali, Mohamed A. A. Ahmed, Nusrat Shaheen, Sandra S. Scholz, Ralf Oelmüller, Zhimin Lin and Faxing Chen

482 Salicylic Acid Priming Regulates Stomatal Conductance, Trichome Density and Improves Cadmium Stress Tolerance in *Mentha arvensis* L.
Abbu Zaid, Firoz Mohammad and Kadambot H. M. Siddique

497 *Bacillus thuringiensis* PM25 ameliorates oxidative damage of salinity stress in maize *via* regulating growth, leaf pigments, antioxidant defense system, and stress responsive gene expression
Baber Ali, Aqsa Hafeez, Saliha Ahmad, Muhammad Ammar Javed, Sumaira, Muhammad Siddique Afridi, Turki M. Dawoud, Khalid S. Almaary, Crina Carmen Muresan, Romina Alina Marc, Dalal Hussien M. Alkhalifah and Samy Selim

520 Isolation and characterization of peroxidase P7-like gene and Rab-GDI like gene from potential medicinal plants: A step toward understanding cell defense signaling
Raheela Jabeen, Atia Iqbal, Farah Deeba, Faisal Zulfiqar, Ghulam Mustafa, Haq Nawaz, Ume Habiba, Muhammad Nafees, Abbu Zaid and Kadambot H. M. Siddique

531 New opportunities in plant microbiome engineering for increasing agricultural sustainability under stressful conditions
Muhammad Siddique Afridi, Muhammad Ammar Javed, Sher Ali, Flavio Henrique Vasconcelos De Medeiros, Baber Ali, Abdul Salam, Sumaira, Romina Alina Marc, Dalal Hussien M. Alkhalifah, Samy Selim and Gustavo Santoyo

553 Proteomic analysis response of rice (*Oryza sativa*) leaves to ultraviolet-B radiation stress
Saroj Kumar Sah, Salah Jumaa, Jiaxu Li and K. Raja Reddy

569 Recent advancement in OMICS approaches to enhance abiotic stress tolerance in legumes
Amjad Ali, Muhammad Tanveer Altaf, Muhammad Azhar Nadeem, Tolga Karaköy, Adnan Noor Shah, Hajra Azeem, Faheem Shehzad Baloch, Nurettin Baran, Tajamul Hussain, Saowapa Duangpan, Muhammad Aasim, Kyung-Hwan Boo, Nader R. Abdelsalam, Mohamed E. Hasan and Yong Suk Chung

594 Enhancing *Rubisco* gene expression and metabolites accumulation for better plant growth in *Ficus deltoidea* under drought stress using hydrogen peroxide
Mohammad Moneruzzaman Khandaker, Rosnah Jamaludin, Ali Majrashi, Zalilawati Mat Rashid, Sarker Mohammad Rezaul Karim, Hatim M. Al-Yasi, Noor Afiza Badaluddin, Mekhled Mutiran Alenazi and Khamsah Suryati Mohd

617 Indole pyruvate decarboxylase gene regulates the auxin synthesis pathway in rice by interacting with the indole-3-acetic acid–amido synthetase gene, promoting root hair development under cadmium stress
Gulmeena Shah, Sajid Fiaz, Kotb A. Attia, Naeem Khan, Muhammad Jamil, Adeel Abbas, Seung Hwan Yang and Tu Jumin

frontiers | Frontiers in Plant Science

TYPE Editorial
PUBLISHED 13 September 2023
DOI 10.3389/fpls.2023.1272255

Check for updates

OPEN ACCESS

EDITED AND REVIEWED BY
Boon Chin Tan,
University of Malaya, Malaysia

*CORRESPONDENCE
Shabir Hussain Wani
shabirhussainwani@gmail.com
shabirhwani@skuastkashmir.ac.in

RECEIVED 03 August 2023
ACCEPTED 31 August 2023
PUBLISHED 13 September 2023

CITATION
Wani SH (2023) Editorial: Mechanisms of abiotic stress responses and tolerance in plants: physiological, biochemical and molecular interventions, volume II. *Front. Plant Sci.* 14:1272255. doi: 10.3389/fpls.2023.1272255

COPYRIGHT
© 2023 Wani. This is an open-access article distributed under the terms of the Creative Commons Attribution License (CC BY). The use, distribution or reproduction in other forums is permitted, provided the original author(s) and the copyright owner(s) are credited and that the original publication in this journal is cited, in accordance with accepted academic practice. No use, distribution or reproduction is permitted which does not comply with these terms.

Editorial: Mechanisms of abiotic stress responses and tolerance in plants: physiological, biochemical and molecular interventions, volume II

Shabir Hussain Wani*

Mountain Research Centre for Field Crops, Khudwani, Sher-e-Kashmir University of Agricultural Sciences and Technology, Srinagar, Jammu and Kashmir, India

KEYWORDS

abiotic stress, molecular mechanism, drought, phytohormomes, salinity, transcription factors

Editorial on the Research Topic

Mechanisms of abiotic stress responses and tolerance in plants: physiological, biochemical and molecular interventions, volume II

Amid climate change, abiotic stresses such as extreme temperatures, drought, salinity, and heavy metal toxicity significantly impact plant growth and productivity, leading to impaired morphological development and negative effects on plant health (Hasanuzzaman and Fujita, 2022; Bhardwaj et al., 2023). These stresses cause morphological changes in plants, such as reduced shoot and root growth, poor anther dehiscence, loss of pollen viability, increased flower drop, decreased flower fertilization, seed shrinking, and shortened grain filling periods. In addition, leaf senescence, chlorosis, necrosis, burning, and abscission further contribute to the detrimental impacts on plant growth. (Saxena et al., 2019; Dumanović et al., 2021; Hasanuzzaman and Fujita, 2022; More et al., 2023). To counteract these detrimental effects, plants employ various adaptation and tolerance mechanisms. Recent studies have focused on unraveling the mechanisms underlying plant responses to abiotic stress. Physiological interventions, such as stomatal regulation mediated by the abscisic acid (ABA) signaling pathway, ion homeostasis, and osmotic adjustment, are crucial for plant adaptation to drought and salt stress (Kuromori et al., 2022; Li et al., 2020). Additionally, the involvement of reactive oxygen species (ROS)-scavenging enzymes and antioxidant systems in mitigating heat-induced oxidative damage and promoting thermotolerance has been elucidated (Dumanović et al., 2021; Mittler et al., 2022). The crosstalk between hormonal signaling pathways and the regulation of antioxidant defence systems, ion homeostasis, and osmotic adjustment have been highlighted (Ramegowda et al., 2020; Singhal et al., 2021). Genome-wide transcriptomic studies have provided valuable insights into stress-responsive genes including transcription factors, microRNAs, and stress-responsive proteins (Liu et al., 2022). The successful application of CRISPR-Cas9 technology has been observed in developing abiotic stress-resilient crops, facilitated by bioinformatics tools for designing suitable CRISPR/Cas9

vectors (Zafar et al., 2020; Wang et al., 2022). Understanding the mechanisms underlying abiotic stresses is crucial for the development of strategies that enhance plant stress tolerance and ensure sustainable agriculture. By uncovering the roles of physiological, biochemical, and molecular interventions, researchers aim to promote the resilience of crops to abiotic stresses, thus safeguarding global food security in the face of abrupt global climate change.

In this Research Topic, 35 articles have been put together, which comprise of original research as well as review articles, to obtain the crux of the variety of intrusions made by global researchers through application of advances in physiological, biochemical and molecular interventions to better understand the mechanisms underlying abiotic stress responses and tolerance in plants.

To advance a context on the theme and to lay a sturdy footing for the Research Topic, nine review articles have been published. One, entitled *"The multifaceted roles of MYC2 in plants: Toward transcriptional reprogramming and stress tolerance by Jasmonate signaling*" by Song et al., details recent investigations in several facets of *MYC2*-mediated JA signaling and their role in plant growth and stress response. Melatonin controls plant stress responses by unswervingly impeding the deposition of reactive oxygen and nitrogen species, and by circuitously affecting stress response pathways. Therefore, a review on "*Melatonin-mediated abiotic stress tolerance in plants*" by Zeng et al. was also included in this Research Topic. In this review, a recent update on melatonin biosynthesis, metabolism, and antioxidation was highlighted, and further emphasis was given to melatonin-mediated tolerance to abiotic stresses including drought, waterlogging, salt, heat, cold, heavy metal toxicity, and light-induced stresses. It was also proven that melatonin acts as a signaling molecule, regulating the expression of genes involved in stress responses, antioxidant production, and phytohormone pathways, such as ABA, ET, and JA. In a recent study by Amin et al., the exogenous application of melatonin resulted in improved low temperature and high humidity stress tolerance in cucumber. It also resulted in an upsurge in the transcript levels of genes encoding antioxidant enzymes under stress conditions. Another review entitled "*Phytohormones trigger drought tolerance in crop plants: Outlook and future perspectives*" by Iqbal et al. emphasized the role of phytohormones in drought tolerance via regulation of morphological, physiological, biochemical, and molecular processes. The morphological and physiological processes encompass vagaries in the composition of leaves, root growth, and stomatal control. The biochemical method consists of altering the levels of phytohormones. Molecular progressions comprise phytohormone-mediated signals, leading to the stimulation of many transcription factors that ground the expression of genes essential for plant endurance under abiotic stresses, particularly drought stress. Improving the water use efficiency (WUE) in winter wheat using agronomic practices has been proposed by Adil et al., which is described in a systematic review entitled "*Effects of fallow management practices on soil water, crop yield and water use efficiency in winter wheat monoculture system: A meta-analysis*". In this review, the authors conclude that no tillage in combination with straw mulching significantly increased WUE and wheat yield under erratic climatic conditions.

Further, another review entitled "*Recent advancement in OMICS approaches to enhance abiotic stress tolerance in legumes"* by Ali et al. described the role played by genomics, transcriptomics, metabolomics, and proteomics for elucidating the complex abiotic stress mechanisms in legumes. The authors also gave an idea about the application of genome editing and genomic selection for abiotic stress mitigation in legumes and concluded that there is a need to change the narrative regarding orphan crops for legumes, as nowadays most legumes have been studied deeply and are at par with cereal crops in terms of genomics resources available in databases. Another review entitled "*Advances in "Omics" approaches for improving toxic metals/metalloids tolerance in plants"* by Raza et al. focused on the current novelties in "omics" that possibly accelerate the progress of toxic metals/metalloids tolerant plants.

One imperative area in the field of abiotic stress mitigation is engineering of the plant microbe interaction; therefore, a review entitled *"New opportunities in plant microbiome engineering for increasing agricultural sustainability under stressful conditions"* by Afridi et al. was also included. This review resolved various facts, for instance, the effect of secondary metabolites of microorganisms on beneficial microbes of the plant microbiome, variation of constant environmental condition and their influence on the host and its allied microbial communities, and the amalgamation of agronomic practices with synthetic biology and their adjustment and suitability to each other. There is enough evidence that microbes play a role in plant drought tolerance, which obliged us to include another review entitled *"Research progress in the field of microbial mitigation of drought stress in plants"* by Shaffique et al., in which stress was waylaid upon instigation of drought tolerance arbitrated by plant inoculation with fungi, bacteria, viruses, and quite a few bacterial elements. It was concluded that microbial connotations play a probable role in facilitating plant protection responses to drought, which is a vital aspect for agricultural production systems that are affected by climatic aberrations.

Silicon amends biotic and abiotic stress situations in plants by regulating the physiological, biochemical, and molecular responses. Therefore, another review on the *"Multidimensional role of silicon to activate resilient plant growth and to mitigate abiotic stress*" by Mir et al. was included in this Research Topic. All of these reviews helped to further sharpen the concepts and processes related to advancements in the field of abiotic stress, such as drought and toxic metalloid stress mitigation using state of the art biochemical, physiological, and molecular approaches in various crop plants.

Salinity is one of the most damaging abiotic stresses affecting 7% of land area and 33% of irrigated lands worldwide. Extricating the specific functions of various stress-related genes, including those responsible for salinity stress in plants, is still a challenge in many crops, and such gene products have been categorized as hypothetical domains of unknown function, or *DUFs*. These are characterized in the *Pfam* database and named using the prefix *DUF* followed by a number, for example, *DUF1* and *DUF2*. These proteins are extensively distributed in different plants and restrain at least one extremely conserved domain of *DUF* (Bateman et al., 2010). Zaynab et al. reported that genome-wide identification and expression profiling of the *DUF221* gene family offers innovative

understandings into abiotic stress, including salt stress responses in potato. The authors also concluded that *StDDP7* exhibited high transcript abundance against salt stress in potatoes. Germin-like proteins (*GLPs*) are persistent proteins considered to be water-soluble glycoproteins, and may be involved in different abiotic and biotic stresses (He et al., 2021). To decipher the possible involvement of *GLPs* in potato, a comprehensive genome-wide analysis was executed in the potato genome by Zaynab et al., which led to identification of 70 *GLPs*. Gene structure, synteny, phylogenetic motifs, promotor, and miRNA analyses were carried out to further elucidate the mechanisms involved. Further, the *StGLP5* gene exhibited the highest expression in response to salt stress. Plant growth-promoting rhizobacteria (PGPR) are the most auspicious advantageous microorganisms that can be used to progress plant responses against biotic and abiotic stresses, including salinity stress. Ali et al. demonstrated that *Bacillus thuringiensis* PM25 ameliorates oxidative damage caused by salinity stress in maize by regulating growth, leaf pigments, the antioxidant defence system, and stress responsive gene expression. This study also revealed that *B. thuringiensis PM25* plays an imperative role in reducing salinity stress by regulating antioxidant defence and abiotic stress-related genes.

To counter the deleterious effects of salinity stress, plants adopt physio-biochemical and molecular signaling defensive mechanistic cascades to prevail over salinity stress; however, unrelenting vulnerability can overcome the defence system, causing cell death and the breakdown of crucial gadgets. Taming plant vigour and defence responses can thus escalate plant stress tolerance and productivity. On the other hand, the apparently vital element silicon (Si)—the second-most widely available element in the Earth's crust—is employed by plants and applied exogenously to fight salinity stress and progress plant growth by augmenting physiological, metabolomic, and molecular responses (Khan et al., 2019). To support the above fact, Murad and Muneer studied the beneficial effect of silicon supplementation, which resulted in increased growth in mungbean and alleviated salinity stress as evidenced by the results of their physio-chemical experiments. Similarly, in another study by Adhikari et al., silicon applied in combination with biochar, K_2HPO_4, and rhizospheric fungus *Curvularia lunata* isolate (AR11) significantly improved the salt and drought stress tolerance in rice. Such studies help to lower fertilizer use, production costs, and environmental pollution, minimize food toxicity, and foster sustainable agriculture.

A foliar spray of antioxidants is a cost effective and realistic tactic to fight the various deleterious effects of salinity stress in agricultural crops. Naqve et al. demonstrated that foliar application of α-tocopherol reduced salinity-induced impairment in okra by enhancing growth, photosynthetic pigments, and leaf gas exchange traits, and by conceivably shielding chloroplasts as a result of its antioxidant potential. Foliar application of H_2O_2 led to an increase in plant growth of *Ficus deltoidea* under drought stress via accumulation of metabolites and Rubisco gene expression (Khandaker et al.). The authors further demonstrated that application of H_2O_2 resulted in elevated photosynthesis, stomatal conductance, chlorophyll fluorescence, carotene, total phenols, total flavonoids, sugar content, and antioxidant activities under drought stress conditions. Defensin genes are included in a plant's defence system and are triggered when plants are subjected to biotic or abiotic stress. They play a key role in regulating several signaling pathways responsible for many plant defence systems. Jabeen et al. reported the isolation and characterization of the *peroxidase P7-like* and *Rab-GDI* like genes, which are novel defensin genes from particular medicinally important plants, to explore their signaling mechanisms and defence-associated roles for breeding.

Heavy metal (HM)-arbitrated poisonous effects on plants have received substantial attention worldwide as they unswervingly lurk in the food supply chain. Plants growing in Cd-polluted soils constitute cadmium's main entry into the food chain, presenting a serious threat to animal and human health (Peralta-Videa et al., 2009). A study on the extrinsic application of salicylic acid and hydrogen peroxide to ameliorate cadmium stress in milk thistle was carried out by Nizar et al., which revealed that the toxic effects of heavy metal (Cd^{2+}) impeded the morphological and physiological traits of milk thistle. However, priming and foliar treatment of plant-signaling molecules with SA and H_2O_2 exhibited a constructive influence on decreasing the toxic effect of Cd^{2+}. The secondary metabolites displayed enhanced tolerance to the Cd^{2+} concentration. Their work suggests mining of the genes responsible for amending the heavy metal toxicity in medicinal plants of economic importance grown at varied altitudes, for which very few studies have been conducted. Another article by Kanu et al. described the detrimental effects of Cd stress on fragrant rice cultivar; exogenous application of methyl jasmonate resulted in improved antioxidant activity and chlorophyll content and reduced oxidative damage under Cd stress conditions. According to Zaid et al., the application of plant growth regulators such as salicylic acid helps to lower Cd uptake, mitigates Cd toxicity, and improves the yield and quality traits, thus serving as a remunerative, concrete, and viable tactic for crop plants in general and for medicinal and aromatic plants in particular. A similar study by Ilyas et al. showed that *Pennisetum purpureum* and *Paspalum dilatatum* are bio-accumulators of cadmium and can be suggested for plantation in Cd-contaminated soils. Further, probable incursion by alien plants in contaminated soil environments takes place within the introduced array. Therefore, non-invasive alien plants and native plants should be endorsed to enable land phytoremediation in contaminated environments. Another study tackling the detrimental effects of the combined stress of Cd and dichlorodiphenyltrichloroethane (DDT) was conducted by Mubeen et al., in which a novel approach using calcium nanoparticles impregnated with benzenedicarboxylic acid was used to alleviate the combined stress of DDT and cadmium in Kale. The growth and physiological characteristics of Kale were efficaciously enhanced by Ca- and Bd-dependent Bd_{Ca} under several stress conditions caused by Cd and DDT pollution. By reducing the biosynthesis of ROS, improving the antioxidative machinery, and modulating the synthesis of osmoregulators, the externally applied Bd_{Ca} augmented plant resistance to the combined abiotic stressors. In addition, Bd_{Ca} repressed the accumulation of DDT in plant tissues and reduced its translocation factor. Consequently, innovative treatment with Bd_{Ca} is suggested for mitigating manifold stresses to ensure a viable crop production system. Compatible solute accumulation, such as proline, in plants in response to abiotic

stress is a well-known phenomenon. To check the preventive property of accumulated proline against Cd stress, a study was conducted by Garcia de la Torre et al. on transgenic and wild type *Medicago trunculata* plants. The results reported in this study were in line with the earlier proven fact that the expression of *VaPC5S* and the ensuing high proline accumulation resulted in alleviated Cd stress in *M. truncatula* transgenic plants. Conversely, this upsurge in tolerance is not exclusively due to proline build-up, but to a proline-induced upregulation of many vital genes associated with proline uptake, phyto-chelatins biogenesis, antioxidant machinery, and *NADPH*-recycling in the transgenic plants, which turn out to be well-armoured to tackle the Cd stress. Similarly, Shah et al. reported that *Indole pyruvate decarboxylase gene (IDPC)* regulates the auxin synthesis pathway in rice by interacting with the in*dole-3-acetic acid–amido synthetase* gene, promoting root hair development under cadmium stress. *IPDC* transgenic lines exhibited a 40% surge in lateral roots. The results showed an increase in root hairs (RHs) and lateral root density, as well as changes in auxin levels and the expression of the *YUCCA* gene.

A considerable increase in the atmospheric CO_2 level has occurred since the industrial revolution, and it is anticipated that it will reach 700 ppm by the year 2050 (IPCC, 2018). This upsurge in atmospheric CO_2 will result in global warming (Mikhaylov et al., 2020), eventually leading to water stress, a major limiting factor of crop productivity. However, increased CO_2 (eCO_2) is thought to hasten the photosynthetic rate and hinder photorespiration (Li et al., 2019). This fact was supported by results from Javaid et al., wherein the authors studied the photosynthetic response and biomass productivity in *A. longifolia* under elevated CO_2 and water limited conditions. eCO_2 enhanced the photosynthetic activity, water use efficiency, and general growth-related traits of *A. longifolia ssp. longifolia* under both well-watered and water limited conditions.

The spatial architecture of a root system has a key influence on plant growth and development, which includes the firmness of the soil, uptake of water and essential nutrients, and interrelation with beneficial soil microorganisms. Root system architecture is quantified by numerous parameters. Another vital architectural factor is the alignment of root growth (Waite et al., 2020). Therefore, interest has grown among scientists working on plant stress biology. As a consequence, the gene *DEEPER ROOTING 1* (*DRO1*) was first mined in rice from a quantitative trait locus associated with root orientation and overall root system depth (Uga et al., 2013). Recently, ABA inducible *DRO1* was found to improve the adaptation to water stress in maize (Feng et al., 2022). Sun et al. studied the expression of Potato *StDRO1* in *Arabidopsis* in terms of DRO1 function for the control of root architecture and drought tolerance. The ectopic expression of *StDRO1* in *Arabidopsis* generated a substantial upsurge in biochemical parameters (e.g., *SOD*, *POD*, and *CAT*) and proline content under drought stress conditions, which showed that *StDRO1* is likely a major player for potato drought stress tolerance. The above, and similar related studies published in the literature support the hypothesis of improving root architecture for abiotic stress tolerance in plants. In a recent study on passion fruit by Rizwan et al., important transcription factors (TFs) such as *ERF*, *AP2*, *MYB*, and *bZIP* were predicted and envisaged in a TF regulatory network with *PeCER* genes. Gene ontology (GO) and Kyoto encyclopaedia of genes and genomes (KEGG) annotation analyses showed that *PeCER* genes were particularly associated with fatty acid, cutin, wax biosynthesis, plant-pathogen interactions, and stress response pathways. It has been shown in several studies that drought tolerance is regulated by many genes, including TFs, that permit plants to endure adverse conditions. These remain likely genomic candidates for extensive application in crop breeding. These TFs consist of vital molecular switches managing the control of plant developmental processes in response to an array of stresses (Joshi et al., 2016). Wang et al. reported that *NAC* Transcription Factor *TwNAC01* positively regulates drought stress responses in *Arabidopsis* and *Triticale*. Overexpression of the transcription factor gene *TwNAC01* in *A. thaliana* improved the drought tolerance of *A. thaliana* by boosting the water holding tendency of the leaves, lowering cellular membrane injury, reducing the production of ROS in the leaves, and promoting root elongation. Plant growth and development is impaired due to growing abiotic and biotic stresses. To counter these stress conditions, the majority of the plants are shielded with a hydrophobic protective layer generally known as cuticle wax, which is the primary blockade between the environment and plants (Trivedi et al., 2019). Cuticle wax comprises very-long-chain fatty acids (*VLCFAs*) and their cognates. β-Ketoacyl-CoA synthase (*KCS*) is a crucial enzyme in the development of *VLCFAs* and offers a precursor for the synthesis of cuticle wax. Rizwan et al. reported the identification of 32 *KCS* genes in the passion fruit genome, and phylogenetically grouped them as *KCS1*-like, *FAE1*-like, *FDH*-like, and *CER6*-like. Moreover, 31 *PeKCS* genes were positioned on seven chromosomes, while one *PeKCS* was localized to the unassembled genomic scaffold. Cis-element analysis allows understanding of the likely role of *PeKCS* genes in phytohormones and stress responses.

In another interesting measure to tackle abiotic stress such as heat stress, Kareem et al. demonstrated that zinc oxide nanoparticles interact with physiological and biochemical traits in terminal heat stress mitigation in mungbean (*Vigna radiata* L.). Nanotechnology is transforming global agriculture, particularly zinc oxide nanoparticles (nano-ZnO), which have garnered substantial research interest due to their unique properties and countless practical applications against abiotic stresses. Thus, the foliar application of nano-ZnO can be recommended as a robust way to shield crops from heat stress-mediated impairment, with low chances of nanoparticle release to the environment.

Sunlight releases extensive radiation such as visible light, ultraviolet (UV), and infrared radiation that are finally received by the surface of the earth (Kumar et al., 2016). Among these different types of radiation, UV rays affect the development of plants during their life cycle. UV-B radiation strength is largely affected by the depth of the stratospheric ozone layer and is particularly damaging to plants (Sztatelman et al., 2015). Sah et al. reported the proteomic responses of rice (*Oryza sativa*) leaves to UV-B radiation stress. Protein expression under various levels of UV-B was observed in rice cultivars, and it differed among the two rice varieties under study. The differentially expressed proteins reported in the above study are related to plant growth

and development, cell defence and redox homeostasis, metabolism, cell wall architecture, photosynthesis, signal transduction, stress response, and ABA signaling. In another study, Sidibe et al. concluded that transcriptome analysis of lettuce in response to UV-C alone or together with Xcv revealed that the differentially expressed genes (*DEGs*) are linked to homeostasis, growth, and defence. To wrap up, UV-C hormesis applied in the present study is a potent eustress that does not hinder the capability of treated plants to restart normal growth or to guard themselves against possible stressors.

The detrimental effect of the herbicide atrazine in the form of its persistence for a long duration in soil has been reported. Sun et al. integrated metabolomics and transcriptomics for investigating the tolerance of Foxtail millet (*Setaria italica*) to atrazine stress. The results indicated that 2,208 *DEGs* and 192 differentially expressed metabolites (*DEMs*) were recognized in atrazine-treated GA2. A bioinformatics analysis of *DEGs* and *DEMs* revealed that several biosynthetic metabolism pathways were suggested to be augmented in GA2, such as glutathione metabolism, amino acid biosynthesis, and phenylpropanoid biosynthesis. In this study, an atrazine-resistant millet variety was investigated, which resulted in the generation of valuable data that may help refine our understanding of the multifaceted molecular apparatus underlying the response to atrazine stress in millet.

Contemporary studies including full genome sequencing, mutational transgenic plant analyses, and genome editing have facilitated a profound perception of the multifaceted transcriptional machinery that operates under cold stress in plants. Variations in gene expression in response to cold stress are followed by upsurges in the levels of numerous metabolites with defending effects to counter the detrimental effects of cold stress (Sanghera et al., 2011; Islam et al., 2023). Among the various gene types whose role in cold stress has been elucidated, compatible solutes, including trehalose, may play a major protective role. In a recent study, Raza et al. demonstrated that the exogenous application of trehalose augmented the osmoprotectants soluble sugar (*SS*), soluble protein (*SP*), and proline (Pro), as well as the activities of antioxidant enzymes such as catalase (*CAT*), peroxidase (*POD*), superoxide dismutase (*SOD*), and ascorbate peroxidase (*APX*) under cold stress conditions. Therefore, trehalose controls the antioxidant and osmotic balance and also plays an active role in metabolism and the signaling network to improve the cold stress tolerance in crops such as rapeseed.

In conclusion, abiotic stresses still pose a great threat to sustainable agriculture nowadays and in the near future, and with the advent of erratic weather conditions and extreme temperatures as a consequence of climate change, these abiotic stresses will become more lethal for crop growth and productivity. Adequate research has been conducted to unravel the physiological, biochemical, and molecular mechanisms underlying abiotic stress tolerance in crop plants. More focused research needs to be carried out to better comprehend plant responses to abiotic stresses. This is conceivable with the dawn of emerging scientific inventions in the field of plant biology, such as genome editing and the advancement in artificial intelligence, which aid the food requirements of the ever-increasing human population.

Author contributions

SW: Writing – original draft, Writing – review & editing.

Acknowledgments

Reviewers have painstakingly reviewed all the papers to make this Research Topic a success. Efforts by authors, reviewers, co-editors, and editorial staff of the journal are highly acknowledged.

Conflict of interest

The author declares that the research was conducted in the absence of any commercial or financial relationships that could be construed as a potential conflict of interest.

Publisher's note

All claims expressed in this article are solely those of the authors and do not necessarily represent those of their affiliated organizations, or those of the publisher, the editors and the reviewers. Any product that may be evaluated in this article, or claim that may be made by its manufacturer, is not guaranteed or endorsed by the publisher.

References

Bateman, A., Coggill, P., and Finn, R. D. (2010). DUFs: families in search of function. *Acta Crystallogr. Sect. F Struct. Biol. Cryst. Commun.* 66, 1148–1152. doi: 10.1107/S1744309110001685

Bhardwaj, R., Lone, J. K., Pandey, R., Mondal, N., Dhandapani, R., Meena, S. K., et al. (2023). Insights into morphological and physio-biochemical adaptive responses in mungbean (Vigna radiata L.) under heat stress. *Front. Genet.* 14, 1206451. doi: 10.3389/fgene.2023.1206451

Dumanović, J., Nepovimova, E., Natić, M., Kuča, K., and Jaćević, V. (2021). The significance of reactive oxygen species and antioxidant defense system in plants: A concise overview. *Front. Plant Sci.* 11, 552969. doi: 10.3389/fpls.2020.552969

Feng, X., Jia, L., Cai, Y., Guan, H., Zheng, D., Zhang, W., et al. (2022). ABA-inducible DEEPER ROOTING 1 improves adaptation of maize to water deficiency. *Plant Biotechnol. J.* 20 (11), 2077–2088. doi: 10.1111/pbi.13889

Hasanuzzaman, M., and Fujita, M. (2022). Plant responses and tolerance to salt stress: Physiological and molecular interventions. *Int. J. Mol. Sci.* 23 (9), 4810. doi: 10.3390/ijms23094810

He, Z. D., Tao, M. L., Leung, D. W. M., Yan, X. Y., Chen, L., Peng, X. X., et al. (2021). The rice germin-like protein OsGLP1 participates in acclimation to UV-B radiation. *Plant Physiol.* 186 (2), 1254–1268. doi: 10.1093/plphys/kiab125

IPCC. (2018). *IPCC Special Report on Global Warming of 1.5°C. United Nations Intergovernmental Panel on Climate Change.* (Switzerland: IPCC).

Islam, F., Khan, M. S. S., Ahmed, S., Abdullah, M., Hannan, F., and Chen, J. (2023). *OsLPXC* negatively regulates tolerance to cold stress via modulating oxidative stress, antioxidant defence and JA accumulation in rice. *Free Radical Biol. Med.* 199, 2–16. doi: 10.1016/j.freeradbiomed.2023.02.008

Joshi, R., Wani, S. H., Singh, B., Bohra, A., Dar, Z. A., Lone, A. A., et al. (2016). Transcription factors and plants response to drought stress: current understanding and future directions. *Front. Plant Sci.* 7, 1029. doi: 10.3389/fpls.2016.01029

Khan, A., Khan, A. L., Muneer, S., Kim, Y.-H., Al-Rawahi, A., and Al-Harrasi, A. (2019). Silicon and salinity: crosstalk in crop-mediated stress tolerance mechanisms. *Front. Plant Sci.* 10, 1429. doi: 10.3389/fpls.2019.01429

Kumar, J., Babele, P. K., Singh, D., and Kumar, A. (2016). UV-B radiation stress causes alterations in whole cell protein profile and expression of certain genes in the rice phyllospheric bacterium enterobacter cloacae. *Front. Microbiol.* 7, 1440. doi: 10.3389/fmicb.2016.01440

Kuromori, T., Fujita, M., Takahashi, F., Yamaguchi-Shinozaki, K., and Shinozaki, K. (2022). Inter-tissue and inter-organ signaling in drought stress response and phenotyping of drought tolerance. *Plant J.* 109 (2), 342–358. doi: 10.1111/tpj.15619

Li, D., Zhang, X., Li, L., Aghdam, M. S., Wei, X., Liu, J., et al. (2019). Elevated CO2 delayed the chlorophyll degradation and anthocyanin accumulation in postharvest strawberry fruit. *Food Chem.* 285, 163–170. doi: 10.1016/j.foodchem.2019.01.150

Li, S., Li, X., Wei, Z., and Liu, F. (2020). ABA-mediated modulation of elevated CO2 on stomatal response to drought. *Curr. Opin. Plant Biol.* 56, 174–180. doi: 10.1016/j.pbi.2019.12.002

Liu, P., Zhu, Y., Liu, H., Liang, Z., Zhang, M., Zou, C., et al. (2022). A combination of a genome-wide association study and a transcriptome analysis reveals circRNAs as new regulators involved in the response to salt stress in maize. *Int. J. Mol. Sci.* 23 (17), 9755. doi: 10.3390/ijms23179755

Mikhaylov, A., Moiseev, N., Aleshin, K., and Burkhardt, T. (2020). Global climate change and greenhouse effect. *Entrepreneurship Sustain. Issues* 7 (4), 2897. doi: 10.9770/jesi.2020.7.4(21)

Mittler, R., Zandalinas, S. I., Fichman, Y., and Van Breusegem, F. (2022). Reactive oxygen species signalling in plant stress responses. *Nat. Rev. Mol. Cell Biol.* 23 (10), 663–679. doi: 10.1038/s41580-022-00499-2

More, S. J., Bardhan, K., Ravi, V., Pasala, R., Chaturvedi, A. K., Lal, M. K., et al. (2023). Morphophysiological responses and tolerance mechanisms in cassava (Manihot esculenta Crantz) under drought stress. *J. Soil Sci. Plant Nutr.* 23 (1), 71–91. doi: 10.1007/s42729-023-01127-4

Peralta-Videa, J. R., Lopez, M. L., Narayan, M., Saupe, G., and Gardea-Torresdey, J. (2009). The biochemistry of environmental heavy metal uptake by plants: implications for the food chain. *Int. J. Biochem. Cell Biol.* 41 (8-9), 1665–1677. doi: 10.1016/j.biocel.2009.03.005

Ramegowda, V., Da Costa, M. V. J., Harihar, S., Karaba, N. N., and Sreeman, S. M. (2020). "Abiotic and biotic stress interactions in plants: a cross-tolerance perspective," in *Priming-mediated stress and cross-stress tolerance in crop plants* (United States: Academic Press), 267–302.

Sanghera, G. S., Wani, S. H., Hussain, W., and Singh, N. B. (2011). Engineering cold stress tolerance in crop plants. *Curr. Genomics* 12 (1), 30. doi: 10.2174/138920211794520178

Saxena, R., Kumar, M., and Tomar, R. S. (2019). Plant responses and resilience towards drought and salinity stress. *Plant Arch.* 19 (Suppl 2), 50–58.

Singhal, R. K., Jatav, H. S., Aftab, T., Pandey, S., Mishra, U. N., Chauhan, J., et al. (2021). Roles of nitric oxide in conferring multiple abiotic stress tolerance in plants and crosstalk with other plant growth regulators. *J. Plant Growth Regul.* 40, 2303–2328. doi: 10.1007/s00344-021-10446-8

Sztatelman, O., Grzyb, J., Gabryś, H., and Banaś, A. K. (2015). The effect of UV-B on Arabidopsis leaves depends on light conditions after treatment. *BMC Plant Biol.* 15, 281. doi: 10.1186/s12870-015-0667-2

Trivedi, P., Nguyen, N., Hykkerud, A. L., Häggman, H., Martinussen, I., Jaakola, L., et al. (2019). Developmental and environmental regulation of cuticular wax biosynthesis in fleshy fruits. *Front. Plant Sci.* 10, 431. doi: 10.3389/fpls.2019.00431

Uga, Y., Sugimoto, K., Ogawa, S., Rane, J., Ishitani, M., and Hara, N. (2013). Control of root system architecture by DEEPER ROOTING 1 increases rice yield under drought conditions. *Nat. Genet.* 45, 1097–1102. doi: 10.1038/ng.2725

Waite, J. M., Collum, T. D., and Dardick, C. (2020). *AtDRO1* is nuclear localized in root tips under native conditions and impacts auxin localization. *Plant Mol. Biol.* 103, 197–210. doi: 10.1007/s11103-020-00984-2

Wang, Y., Zafar, N., Ali, Q., Manghwar, H., Wang, G., Yu, L., et al. (2022). CRISPR/Cas genome editing technologies for plant improvement against biotic and abiotic stresses: advances, limitations, and future perspectives. *Cells* 11 (23), 3928. doi: 10.3390/cells11233928

Zafar, S. A., Zaidi, S. S. E. A., Gaba, Y., Singla-Pareek, S. L., Dhankher, O. P., Li, X., et al. (2020). Engineering abiotic stress tolerance via CRISPR/Cas-mediated genome editing. *J. Exp. Bot.* 71 (2), 470–479. doi: 10.1093/jxb/erz476

frontiers in Plant Science

ORIGINAL RESEARCH
published: 21 December 2021
doi: 10.3389/fpls.2021.800251

Alpha Tocopherol-Induced Modulations in the Morphophysiological Attributes of Okra Under Saline Conditions

Maria Naqve[1], Xiukang Wang[2], Muhammad Shahbaz[1], Athar Mahmood[3]*, Safura Bibi[1] and Sajid Fiaz[4]*

[1] Department of Botany, University of Agriculture, Faisalabad, Pakistan, [2] College of Life Sciences, Yan'an University, Yan'an, China, [3] Department of Agronomy, University of Agriculture, Faisalabad, Pakistan, [4] Department of Plant Breeding and Genetics, The University of Haripur, Haripur, Pakistan

OPEN ACCESS

Edited by:
Shabir Hussain Wani, Sher-e-Kashmir University of Agricultural Sciences and Technology, India

Reviewed by:
Mehmet Zahit Yeken, Abant Izzet Baysal University, Turkey
Renata Gamrat, West Pomeranian University of Technology, Poland

****Correspondence:***
Xiukang Wang
wangxiukang@yau.edu.cn
Athar Mahmood
athar.mahmood@uaf.edu.pk

Specialty section:
This article was submitted to Plant Breeding, a section of the journal Frontiers in Plant Science

Received: *22 October 2021*
Accepted: *16 November 2021*
Published: *21 December 2021*

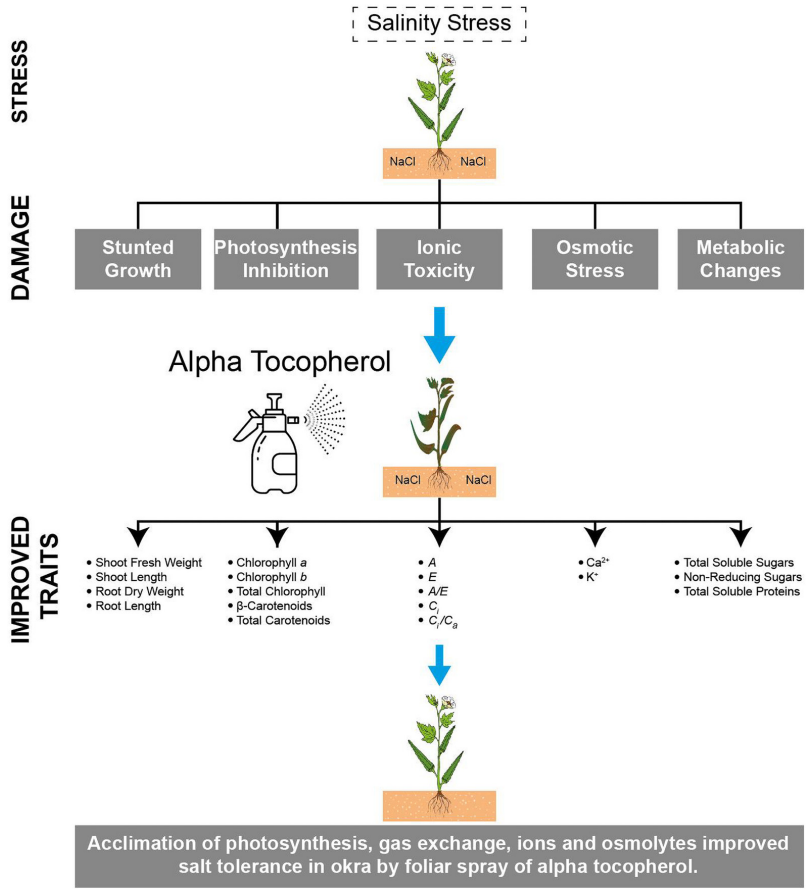
Citation:
Naqve M, Wang X, Shahbaz M, Mahmood A, Bibi S and Fiaz S (2021) Alpha Tocopherol-Induced Modulations in the Morphophysiological Attributes of Okra Under Saline Conditions. Front. Plant Sci. 12:800251. doi: 10.3389/fpls.2021.800251

Foliar spray of antioxidants is a pragmatic approach to combat various effects of salinity stress in agricultural crops. A pot trial was conducted to examine the effect of exogenously applied α-tocopherol (α-Toc) as foliar spray to induce morpho-physiological modulations in two varieties (Noori and Sabzpari) of okra grown under salt stress conditions (0 mM and 100 mM NaCl). After 36 days of salinity treatments, four levels (0, 100, 200 and 300 mg L^{-1}) of α-tocopherol were sprayed. Salt stress significantly reduced root and shoot fresh and dry biomass, photosynthesis rate (*A*), transpiration rate (*E*), water use efficiency (*A*/*E*), stomatal conductance, internal CO_2 concentration (C_i)and C_i/C_a), and photosynthetic pigments. Foliar spray of α-tocopherol proved effective in improving the growth of okra by significantly enhancing root dry weight, root length, shoot fresh weight, shoot length, Chl. *a*, Chl. *b*, Total chl., β-Car., Total Car., *A, E, A/E,* C_i, and C_i/C_a, leaf and root Ca^{2+} and K^+ ion content, total soluble sugars, non-reducing sugars and total soluble protein content by significantly reducing root Na^+ ion content. The Okra variety Noori performed better than Sabzpari in the examined attributes, and 300 mg L^{-1} application of α-tocopherol was more pronounced in improving the growth of okra by alleviating salinity effects. Therefore, the use of α-tocopherol (300 mg L^{-1}) as a foliar spray is recommended to improve okra production in saline soils.

Keywords: alpha tocopherol, salinity, okra, biomass, photosynthetic attributes

INTRODUCTION

Okra [*Abelmoschus esculentus* (L.) Moench] is the most popular mallow crop, and its capsules and leaves are mainly consumed as vegetables, capsules are rich source of vitamin A, B6, C and K (Aboyeji et al., 2021). potassium, calcium, carbohydrates, unsaturated fatty acids such as linolenic acid, oleic acid and minerals along with enormous amounts of mucilage with medicinal properties (Naqve et al., 2018; Schafleitner et al., 2021). Salt stress significantly reduced K^+ and Ca^{2+} ions and yield and increased H_2O_2, malondialdehyde (MDA), Na^+, glycine betaine (GB), total free proline,



GRAPHICAL ABSTRACT | Salinity stress mitigation by the application of alpha tocopherol in okra.

total phenolics, and the activities of catalase (CAT), guaiacol peroxidase (GPX), and protease in Noori (salt tolerant) and Sabzpari (salt sensitive) (Naqve et al., 2018).

Okra is classified as a moderately sensitive crop to salinity stress by the Food and Agriculture Organization (FAO), and it is susceptible to salinity stress in areas where summers are dry (Elshaikh et al., 2018). Based on germination, growth and yield characteristics, salinity tolerant (8 dSm^{-1}) varieties of okra (OH-713, OH-139, OH-138, OH-2324 and OH-001) has been reported whereas the sensitive genotypes include Kiran, Okra-1548, Ikra-3, Sabzpari, Okra-7100, Sitara-9101, and Okra-7080 (sensitive 4 dSm^{-1}). However, increasing salinity stress decreases the per hectare productivity of okra (Mushtaq et al., 2020). Among abiotic stresses, salinity is a major threat to crop productivity (Ahmad et al., 2019). Cultivated land in Asia is expected to be affected by 50% by soil salinization by the year 2050 (Khan et al., 2019). Soil salinity (2 to 3 dSm^{-1}) aggravates the fertility of soil and drastically decreases crop yield (Shilev, 2020). Among all other soluble salts causing adverse effects on plants, NaCl is most dominant, and a high concentration of NaCl hampers various plant processes, including seed germination, root growth, nutrient uptake, and photosynthesis (Naveed et al., 2020). Reduced root and shoot growth are primary symptoms of salinity effects (Liu et al., 2020). Salinity affects plant growth and yield by reducing the photosynthesis rate, biomass, and water use efficiency (Moles et al., 2019). Increased levels of saline stress decrease stomatal conductance, photosynthesis, and chlorophyll content in the leaves of plants (Sun et al., 2018).

Due to reduced plant height and the number of leaves and root and shoot biomass under saline conditions, plant growth is severely affected (Naqve and Shahbaz, 2019). Reduced uptake of CO_2 is associated with increased salinity, which alters stomatal functions, photosynthesis, and transpiration (Hussain et al., 2018). Salt stress alters the ionic status of plants, which aggravates enzymatic activities, cellular turgor, and protein biogenesis by shunting osmotic stress (Chokshi et al., 2017). Oxidative stress is also a major threat to crop production under saline regimes due to the overproduction of reactive oxygen species (ROS) (Mehla et al., 2017). To resist salinity, plants adapt various responses at the molecular level by the upregulation of plant hormones, organic osmotica and antioxidants (Soni et al., 2017). Primarily, plants cope with salinity-induced oxidative bursts by up-regulating defensive antioxidants, including catalase, peroxidases, ascorbic acid, flavonoids, phenolics and α-tocopherol (Hasanuzzaman et al., 2020). Maintaining optimal ROS concentrations by ROS

quenchers regulates various processes essential for the growth and development of plants (Mittler, 2017). Thus, exogenous application of these compounds can be helpful for plants to resist salinity, which can be a potentially simple, economical, and culturally feasible approach compared with introgression and genetic engineering (Sadiq et al., 2019). Foliar spraying of α-tocopherol is one such approach to improve plant growth under salinity stress (Surówka et al., 2020). Tocopherols are members of the vitamin E family and consist of alpha, beta, gamma, and delta forms (Shahidi and De Camargo, 2016). Alpha tocopherol is more active than all other categories of vitamin E, as it protects photosystem II and lipid membranes in chloroplasts from salinity-induced damage (Sadiq et al., 2019; Surówka et al., 2020). α-tocopherol also protects chloroplasts by quenching ROS, thus improving photosynthetic efficiency in plants (Hasanuzzaman et al., 2020). Moreover, it also protects plants by quenching free radical species produced under salinity stress by enhancing the production of other antioxidants (Semida et al., 2014), thus improving the growth and yield of plants (Surówka et al., 2020)The agricultural economy of Pakistan is important for the food of 207 million people, which is threatened by salinity. The total area of Pakistan is 79.6 mha, of which 22 mha is cultivated land and 6.28 mha is affected by salt (GOP, 2020). Salinity has serious socioeconomic issues in the agricultural communities of the country. Selection and breeding for improved tolerance against salinity in different vegetables and crops is considered a high priority due to economic benefits and is the best alternative for the farming community. Okra is a commonly consumed vegetable in Pakistan, but its per ha productivity is being reduced due to the increasing land salinity problem in Pakistan. Hence, it is urgent to introduce cost-effective strategies for farmers, such as foliar spraying of compounds that are naturally produced by plants such as α-tocopherol, to combat salinity problems. These strategies can be more effective than the application of synthetic fertilizers that are organic in nature. Such compounds as α-tocopherol are beneficial for plants and humans as well. Therefore, the present study aimed to investigate the effect of foliar spray application of α-Toc on the morpho-physiological attributes of okra under salt stress.

MATERIALS AND METHODS

To evaluate whether foliar spray of α-tocopherol could alleviate salinity-induced negative effects on okra, the current experiment was laid out in the research area of the Old Botanical Garden, University of Agriculture Faisalabad, Pakistan. Okra varieties (Sabzpari and Noori) differing in salinity tolerance were selected, and seeds of selected varieties were obtained from the Ayub Agricultural Research Institute (AARI), Faisalabad, Pakistan.

The experiment was conducted twice in plastic pots (24 cm wide and 30 cm deep), each containing 10 kg well-washed dry sand. In each pot, six plants were maintained after thinning, and the experiment was carried out with four replicates under a completely randomized design (CRD). After sowing full strength (2 L per pot), Hoagland's nutrient solution was supplied weekly. During the experiment, salinity stress was maintained by NaCl levels (0 mM and 100 mM) in full-strength Hoagland's nutrient solution after 21 days of germination. Concentration of NaCl was maintained in aliquot parts of 50 mM to prevent osmotic shock. Thus, salinity level was maintained in two phases. In first phase 50 mM NaCl level was maintained and after 2 days of this level, the required level of 100 mM was maintained. Foliar fertigation of α-tocopherol concentrations [0 (distilled water), 100, 200 and 300 mg L^{-1}] was performed on 36-day-old plants. Each pot was supplied with a 25 mL solution of each concentration of α-tocopherol just before sunset for maximum absorption and to avoid sunburn of leaves. For enhancement at absorption, Tween 20 (0.1%) was used as the surfactant. After 3 weeks of foliar spray from each replicate, two plants were uprooted carefully and washed, and data were recorded.

Photosynthetic Pigments

The protocol described by Arnon (1949) was followed to measure the concentrations of various photosynthetic pigments. Fresh leaves (0.5 g) were extracted in 80% acetone (10 ml). Chlorophyll was extracted by thoroughly grinding it in a mortar pesto. The absorbance of photosynthetic pigments was read at OD 663, OD 645, OD 505, OD 453, and OD 470 nm by using a spectrophotometer (IRMECO-U2020) and, calculations were made by using following formulae

$$\text{Chl. } a \text{ (mg ml}^{-1}) = [12.7\ (\text{OD } 663) - 2.69(\text{OD}645)] \times [V/(1000 \times W)]$$

$$\text{Chl. } b \text{ (mg ml}^{-1}) = [22.9\ (\text{OD } 645) - 4.68(\text{OD}663)] \times [V/(1000 \times W)]$$

$$\text{Carotenoids (g ml}^{-1}) = [\text{A}^{\text{car}}/\text{Em}100\%] \times 100$$

$$\text{A}^{\text{car}} = [(\text{OD } 480) + 0.114(\text{OD } 663) - 0.638(\text{OD}645)]$$

Where,

V is the volume of the sample.

W is the weight of fresh tissue taken for extraction.

Em100% = 2500.

Growth Attributes

After calculating fresh masses of roots and shoots, the same plant was oven-dried using an electric oven at 70°C for 48 h, and their dry masses were calculated using a digital electronic balance.

Leaf Gas Exchange Characteristics

For the assessment of leaf gaseous exchange traits, an LCA-4 portable infrared gas analyzer (IRGA) was used with specifications of ambient pressure (P), 98.5 kPa, gas flow rate, (U) 252 μmol S^{-1}, ambient CO_2 concentration 350 μmol mol^{-1}, water vapor pressure, 6.0–9.0 mbar, temperature, 28–32°C, relative humidity, 41.1% and air flow/unit leaf area (Us) 22.05 mol m^{-2} S^{-1}. Data were recorded during 9: 00 A.M. to 12: 00 P.M. under suitable weather conditions.

Nutrients Analysis for Leaf and Root

Dried leaf and root tissues were used separately for the analysis of nutrients (Na, K and Ca) by following the acid digestion protocol as proposed by Wolf (1982).

Acid Digestion Method

Leaf- and root-dried material (0.1 g) was digested in 2.5 ml of conc. H_2SO_4 overnight at room temperature in digestion flasks. To it was then added one mL of 35% H_2O_2 and the flask was heated at 350°C until the production of fumes. The heating process continued for approximately 30 min, then 1 mL of 35% H_2O_2 was again added while the heating process continued. This process was repeated until the mixture became colorless, and it was then diluted with distilled water up to 50 mL and filtered. The filtrate was used for the determination of mineral ions by using a flame photometer.

Total Soluble Proteins

Fresh plant leaves (0.5 g) were crushed with 10 ml (50 mM) potassium phosphate buffer with pH 7.0 in a chilled environment, and the extract (5 μL) was then homogenized with 1 ml of Bradford dye and 0.1 N HCl. The optical density was read at 595 nm by following the protocol of Bradford (1976).

Sugars Content

The procedure of Dubois et al. (1951) was followed to estimate the total soluble sugar content. The reaction mixture was prepared by adding (0.5mL) sample, 5% phenol solution (0.25 mL) and 96% sulfuric acid (1.25 mL), and the absorbance was measured at 490 nm by using an IRMECO-U2020 spectrophotometer.

For the determination of reducing sugars, reaction solution was set in test tubes by adding sample, H_2O and DNS reagent. Absorbance was noted at 540 nm using an IRMECO-U2020 spectrophotometer by following (Miller et al., 1973). In this way, the non-reducing sugars were determined by the difference in reducing and total soluble sugars.

Statistical Analysis

Collected data were investigated for analysis of variance of data for all the recorded traits by following Snedecor and Cochran (1980), and the means were compared using least significant difference (LSD) at a probability level of 5% by using COSTAT software.

RESULTS

Growth Attributes

The root fresh weight (RFW) of okra varieties was significantly decreased by salinity stress in the present study. The data showed that Noori exhibited considerably higher RFW than Sabzpari. Foliar spray of α-tocopherol did not significantly affect this attribute under the control and stress treatments (**Table 1** and **Figure 1A**).

The current study revealed that salt stress induced a significant reduction in the RDW of both okra varieties. Noori was superior in RDW than that of Sabzpari. Sprays of α-tocopherol markedly enhanced the RDW of salt-stressed and non-stressed plants. Furthermore, a higher concentration (300 mg L^{-1}) of α-tocopherol increased the RDW of both varieties (**Table 1** and **Figure 1B**).

A significant reduction was observed in the root length (RL) of both tested varieties of okra. However, Noori produced more RL than Sabzpari. Foliar supplementation with α-tocopherol significantly improved the RL of okra. Additionally, foliage spray of α-tocopherol (200 mg L^{-1} and 300 mg L^{-1}) improved RL under salinity. Overall, a 300 mg L^{-1} concentration of α-tocopherol showed a pronounced effect in increasing the RL of okra varieties under stressed and non-stressed conditions (**Table 1** and **Figure 1C**).

The data revealed that saline (NaCl) stress significantly reduced the shoot fresh weight (SFW) of the tested okra varieties. However, Noori was superior to Sabzpari with respect to SFW. Foliar fertigation of α-tocopherol significantly increased the SFW of both varieties. However, among the effects of various levels of α-tocopherol under salt stress conditions, 300 mg L^{-1} was more effective in enhancing shoot growth than the other levels (**Table 1** and **Figure 2A**).

Salt stress significantly reduced the shoot dry weight of both tested varieties, and this reduction was more pronounced in Sabzpari than in Noori. Surprisingly, foliar application of α-tocopherol did not affect the shoot dry weight (SDW) of either tested variety under either salinity treatment. However, 200 and 300 mg L^{-1} levels of α-tocopherol spray showed little improvement in the SDW of stressed and non-stressed plants (**Table 1** and **Figure 2B**).

A reduction in shoot length (SL) of both tested varieties was observed under salinity stress (100 mM NaCl). However, foliar spraying with higher levels of α-tocopherol (300 mg L^{-1}) caused a significant increase in the SL of the tested varieties under stressed and non-stressed conditions. This increase in SL was more pronounced in Noori than in Sabzpari (**Table 1** and **Figure 2C**).

Photosynthetic Pigments

Root medium salinity stress remarkably suppressed chlorophyll *a*, *b* and β-carotene contents. The response of both okra varieties was also significant in terms of these traits. Moreover, varying concentrations of α-tocopherol applied as foliar spray markedly boosted the level of these pigments in both varieties. While 300 mg L^{-1} improved pigment concentrations under stressed and non-stressed plants of both okra varieties, Noori showed relatively higher accumulation of these pigments than Sabzpari under saline and non-saline conditions. Significant interactions of NaCl levels, α-tocopherol application, and the tested varieties were observed in terms of chlorophyll *a* and *b* content. The Okra variety Noori reached higher concentrations of both pigments at a 300 mg L^{-1} spray of α-tocopherol under salinity, whereas the minimum concentration of these pigments was recorded in Sabzpari (**Table 1** and **Figures 3A,B**, **4C**).

A significant effect of salinity was observed on the chlorophyll *a*/*b* ratio (Chl. *a*/*b*). Both okra varieties showed comparable values of Chl. *a*/*b*. The data of the present study revealed that

TABLE 1 | Analysis of variance (mean squares) for growth traits and photosynthetic attributes of okra plants treated with α-tocopherol as foliar spray under saline and non-saline conditions.

Source	df	RFW	RDW	RL	SFW	SDW	SL	Chl. *A*	Chl. *B*	Chl. *a/b*	Total Chl.	β-Car.	Total Car.
V	1	0.81*	0.01***	4.05ns	20.47**	0.66**	503.44***	15131.8***	360.63***	0.001ns	21780.12***	2.45*	0.86ns
S	1	4.0***	0.10***	103.78***	152.76***	1.17***	1018.40***	19117.6***	1633.23***	34.252***	29555.42***	2.79*	252.55***
α-Toc	3	0.25ns	0.003*	36.83***	16.43***	0.17 ns	72.54**	9276.5***	225.12***	0.404ns	5308.77***	2.37**	16.10**
V x S	1	0.02ns	0.001ns	6.06ns	1.17ns	0.03 ns	2.28ns	289.1ns	0.18 ns	0.019ns	5305***	1.01ns	8.55ns
V x α-Toc	3	0.03ns	2.72 ns	0.33ns	0.67ns	0.02 ns	8.98ns	114.5ns	22.53**	2.096ns	769.03*	1.69*	14.65**
S x α-Toc	3	0.02ns	5.72 ns	2.35ns	1.51ns	0.02 ns	13.88ns	326.9ns	3.32ns	3.123*	194.70ns	1.50*	4.88ns
V x S x α-Toc	3	0.04ns	5.66 ns	1.39ns	1.84ns	0.01 ns	7.01ns	1063.7*	37.95***	3.563*	661.16*	1.33ns	12.20*
Error	48	0.13	8.02	4.05ns	1.84	0.08	15.19	292.50	5.23	1.050	264.06	422.67	0.002
V (LSD 0.05%)		0.18	0.014	1.00	0.68	0.14	1.95	8.59	1.15	0.51	6.90	0.36	0.89
S (LSD 0.05%)		0.18	0.014	1.00	0.68	0.14	1.95	8.59	1.15	0.51	6.90	0.36	0.89
α-Toc (LSD 0.05%)		0.25	0.02	1.42	0.96	0.20	2.77	12.15	1.62	0.72	9.76	0.5	1.26

**, **, and ***Significant at 0.05, 0.01 and 0.001 levels, respectively; ns, non-significant; V, Varieties; S, Salinity; α-toc, Alpha tocopherol; RFW, Root Fresh Weight; RDW, Root Dry Weight; SFW, Shoot Fresh Weight; SDW, Shoot Dry Weight; SL, Shoot Length; Chl. a, Chlorophyll a; Chl.b, Chlorophyll b; Chl. a/b, Chlorophyll a/b; Total Chl., Total Chlorophyll; β-Car., Beta Carotenoids; Total Car., Total Carotenoids.*

exogenously applied α-tocopherol did not show any change in this ratio. A significant interactive effect was recorded between NaCl stress and foliar application of α-tocopherol. At the 100 mg L^{-1} level of α-tocopherol, okra variety Noori performed better in terms of Chl. *a*/*b* (**Table 1** and **Figure 3C**).

Total chlorophyll (Total Chl.) content was significantly decreased under salt (NaCl) stress. A significant impact of

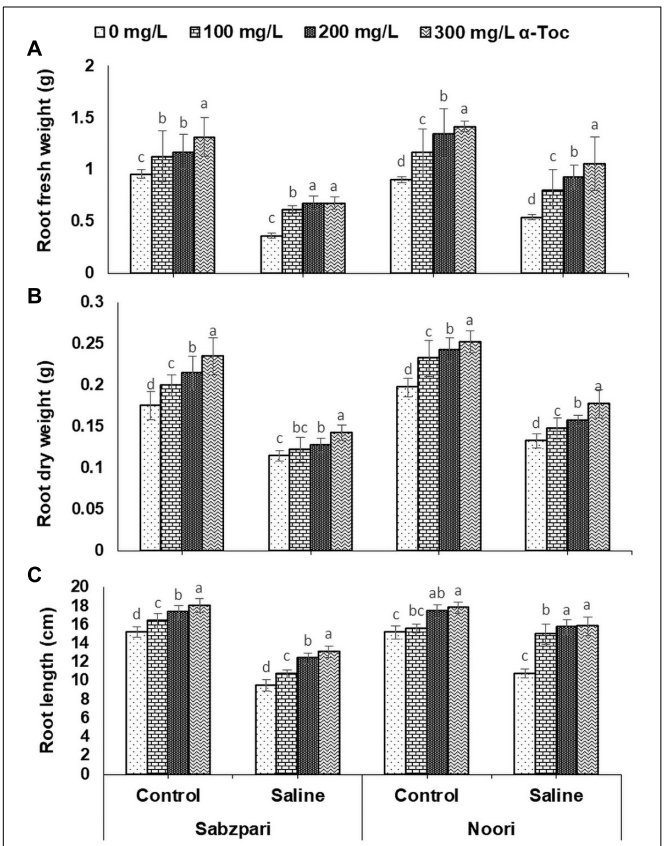


FIGURE 1 | Root fresh weight **(A)**, Root dry weight **(B)**, Root length **(C)** of okra varieties sprayed with different levels of α-tocopherol under saline conditions. Values represent means ± S.D. Significant differences among row spacing were measured by the least significant difference (LSD) at $p > 0.05$ and indicated by different letters.

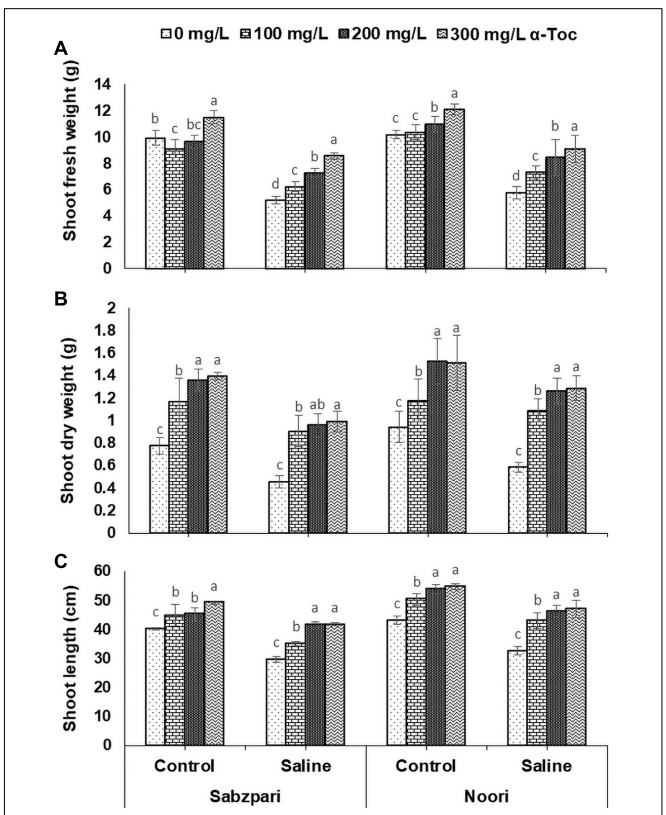


FIGURE 2 | Shoot fresh weight **(A)**, Shoot dry weight **(B)** and Shoot length **(C)** of okra varieties sprayed with different levels of α-tocopherol under saline conditions. Values represent means ± S.D. Significant differences among row spacing were measured by the least significant difference (LSD) at $p > 0.05$ and indicated by different letters.

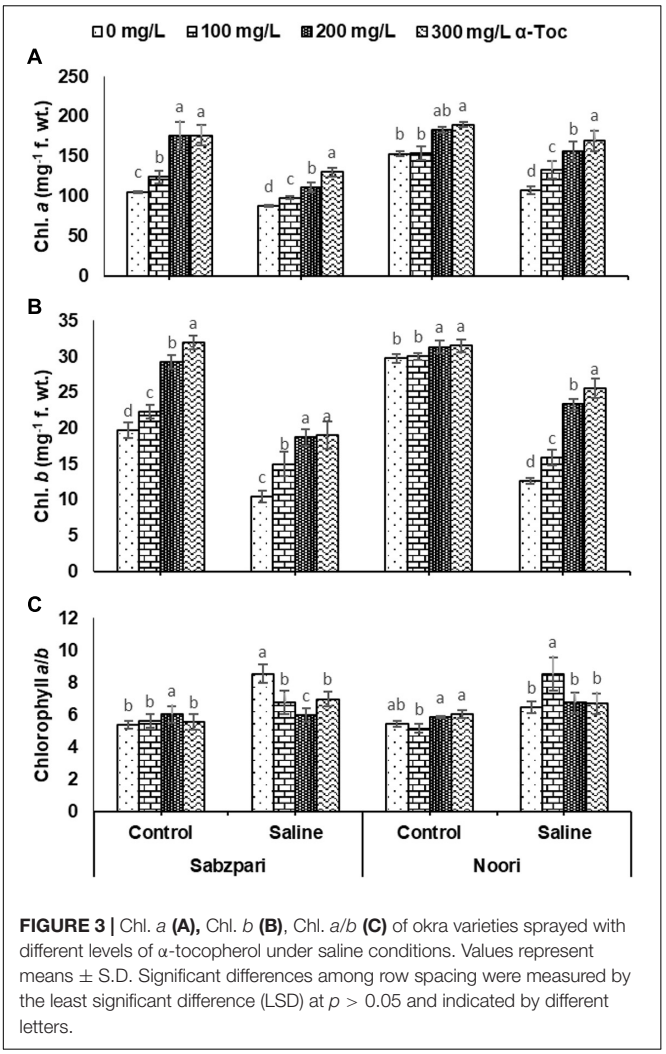


FIGURE 3 | Chl. *a* **(A),** Chl. *b* **(B)**, Chl. *a*/*b* **(C)** of okra varieties sprayed with different levels of α-tocopherol under saline conditions. Values represent means ± S.D. Significant differences among row spacing were measured by the least significant difference (LSD) at $p > 0.05$ and indicated by different letters.

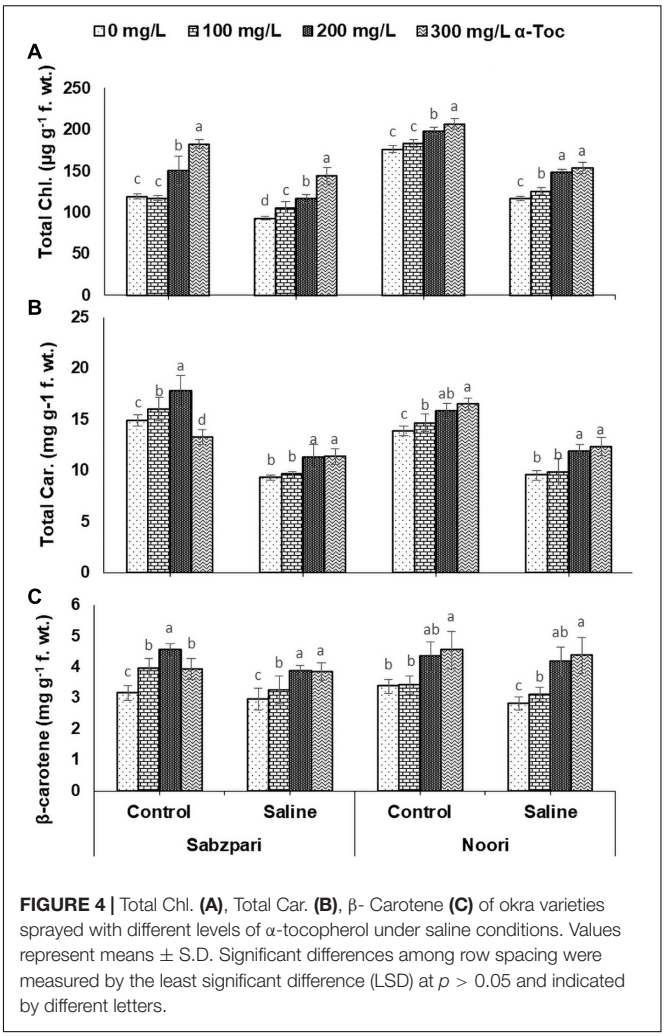


FIGURE 4 | Total Chl. **(A)**, Total Car. **(B)**, β- Carotene **(C)** of okra varieties sprayed with different levels of α-tocopherol under saline conditions. Values represent means ± S.D. Significant differences among row spacing were measured by the least significant difference (LSD) at $p > 0.05$ and indicated by different letters.

α-tocopherol (300 mg L^{-1}) application was noticed regarding total chlorophyll under stressed and non-stressed conditions. A significant interactive effect of variety and α-tocopherol was noticed with respect to the total chlorophyll content. Noori showed the highest total chlorophyll content at a higher level of α-tocopherol (300 mg L^{-1}) (**Table 1** and **Figure 4A**).

In the current study, a significant reduction was observed in total carotenoids (Total Car.) content in both varieties under salt stress than in non-stressed plants. However, foliar application of varying levels of α-tocopherol enhanced the total carotenoid content of both varieties under saline- and salinity-free treatments. The variety Noori performed better with respect to total carotenoids content than Sabzpari at 300 mg L^{-1} foliar spray of α-tocopherol under 100 mM NaCl stress (**Table 1** and **Figure 4B**).

Gas Exchange Characteristics

Salt stress (100 mM NaCl) significantly reduced photosynthetic traits. However, significant improvement was observed in transpiration rate (*E*), photosynthesis rate (*A*) and water use efficiency (*A*/*E*) after foliar spray of α-tocopherol (300 mg L^{-1}) under saline and controlled conditions. Noori was superior to Sabzpari in these attributes. A significant interaction was observed among the tested varieties and treatments regarding *A*, and the highest *A* level was determined in the variety Noori combined with 300 mg L^{-1} α-tocopherol under 100 mM NaCl (**Table 2** and **Figures 5A–C**).

A significant reduction was observed in the stomatal conductance (g_s) of the tested okra plants under the saline regime. The Okra variety Noori showed higher stomatal conductance (g_s) than Sabzpari under saline conditions. In contrast, a similar performance of both varieties was observed regarding stomatal conductance under non-stressed conditions. Exogenous application of α-tocopherol (300 mg L^{-1}) as foliar spray had a remarkable effect on stomatal conductance (g_s) in both varieties (**Table 2** and **Figure 6A**).

The substomatal internal CO_2 concentration (C_i) significantly decreased in both okra varieties under salinity. Both tested varieties exhibited similar performance toward substomatal internal CO_2 concentrations. Moreover, foliar application of α-tocopherol significantly improved the C_i of the tested varieties under salt stress. A higher level (300 mg L^{-1}) of foliar

TABLE 2 | Analysis of variance (mean squares) for leaf gas exchange attributes of okra plants treated with α-tocopherol as foliar spray under saline and non-saline conditions.

Source	df	*A*	*E*	*A/E*	g_s	C_i	C_i/C_a
V	1	5.02ns	0.23ns	0.16ns	976.56ns	1881.39*	0.025***
S	1	285.94***	3.97**	27.29***	27639.06 ***	9225.60***	0.002ns
α-Toc	3	16.61*	2.06**	0.64*	1926.56 ***	6984.22***	0.078***
V x S	1	1.65ns	0.85ns	0.22ns	976.56ns	6756.84***	0.024**
V x α-Toc	3	29.14**	0.64ns	0.97**	64.06ns	861.60ns	0.005ns
S x α-Toc	3	19.86*	0.05ns	0.26ns	68.22ns	6573.09***	0.188 ***
V x S x α-Toc	3	16.82*	0.34ns	0.30ns	305.72ns	603.31ns	0.024 ***
Error	48	4.73	0.34	0.21	264.06	422.67	0.002
V (LSD 0.05%)		1.09	0.29	0.23	8.16	10.33	0.02
S (LSD 0.05%)		1.09	0.29	0.23	8.16	10.33	0.02
α-Toc (LSD 0.05%)		1.54	0.41	0.32	11.55	14.61	0.03

**, **, and ***Significant at 0.05, 0.01, and 0.001 levels, respectively; ns, non-significant; V, Varieties; S, Salinity; α-toc, Alpha tocopherol: Photosynthetic rate (A), Transpiration rate (E), Water use efficiency (A/E), Stomatal conductance (g_s), Internal CO_2 concentration (C_i), Ratio of internal and ambient CO_2 concentration (C_i/C_a).*

α-tocopherol application clearly improved the C_i of both varieties under stressed conditions (**Table 2** and **Figure 6B**).

Similarly, a significant effect on the ratio of internal and ambient CO_2 C_i/C_a of both varieties was also observed. Foliar fertigation of tested plants with α-tocopherol markedly improved the C_i/C_a concentration in both okra varieties (**Figure 6C**). Overall, (200 and 300 mg L^{-1}) spray of α-tocopherol proved better in enhancing C_i/C_a in both varieties under saline regime. The interactive effects of the Noori variety with foliar α-tocopherol (200 mg $L^{-}1$) spray under 100 mM NaCl stress exhibited a higher combined effect than the other treatments (**Table 2** and **Figure 6B**).

Ionic Content

The application of salt remarkably decreased leaf Ca^{2+} and K^+ contents in both okra varieties. Tested okra varieties (Noori and Sabzpari) had no significant impact on leaf Ca^{2+} content, while in terms of leaf K^+ content, both varieties differed significantly, as Noori accumulated more K^+ than Sabzpari. The α-tocopherol spray significantly enhanced the leaf Ca^{2+} and K^+ contents of both varieties of okra under saline and non-saline regimes (**Table 3** and **Figures 7A,B**).

The saline regimen markedly enhanced the concentration of leaf Na^+ ions. However, the trend of Na^+ ion accumulation in the leaves of both okra varieties (Noori and Sabzpari) differed non-significantly. Moreover, the response of both okra varieties was also non-significant for the foliar spray of α-tocopherol in decreasing Na^+ ion concentration (**Table 3** and **Figure 7C**).

Both okra varieties showed non-significant differences in terms of root ion content, i.e., Ca^{2+}, K^+, and Na^+. The addition of salt stress non-significantly reduced the root Ca^{2+} content in Sabzpari, while an increase was observed in Noori. Salt stress markedly decreased the K^+ ion content in the roots of both tested varieties of okra. Root medium salt stress significantly enhanced the root Na^+ ion concentration in both tested varieties. Sprays of α-tocopherol did not significantly affect the concentrations of root Ca^{2+} and K^+. Foliar application of α-tocopherol at 300 mg L^{-1} significantly reduced the inhibitory effect of Na^+ ion concentration in both okra varieties under saline stress (**Table 3** and **Figures 8A–C**).

Soluble Sugars and Protein Content

Salt stress increased the concentration of total soluble sugars and reducing and non-reducing sugars in both varieties of okra. Both varieties (Noori and Sabzpari) differed non-significantly in terms of total soluble sugars and non-reducing sugars. However, reducing sugar content showed a significant difference in the performance of both okra varieties, as Noori was superior in the accumulation of reducing sugars than Sabzpari under salt and non-salt conditions. A prominent increase was observed in the concentration of total soluble sugars and non-reducing sugars in both varieties of okra due to α-tocopherol spray. However, the effect of exogenously applied α-tocopherol as foliar spray on okra plants was non-significant in enhancing the reducing sugar content (**Table 3** and **Figures 9A–C**).

Both okra varieties showed significant differences in terms of total soluble protein content. Noori was superior to Sabzpari in this attribute. Total soluble protein content was markedly enhanced under saline stress. The effect of foliar-applied α-tocopherol on enhancing the total soluble protein content was not remarkable, whereas a significant interaction was observed among the varieties, NaCl treatment and foliar spray of α-tocopherol (**Table 3** and **Figure 10**).

DISCUSSION

Plant growth is an important criterion to evaluate salinity tolerance in plants, as higher accumulation of NaCl in plant tissues adversely affects plant growth (Kachout et al., 2016). In the current study, suppression of growth in terms of root and shoot fresh and dry weights and their lengths was observed for okra plants under salinity stress. Reduced growth is directly linked with reduced photosynthetic activity and stunted growth of vegetative plant parts under saline regimes. Decreased growth is linked to blocked activity of photosynthesis

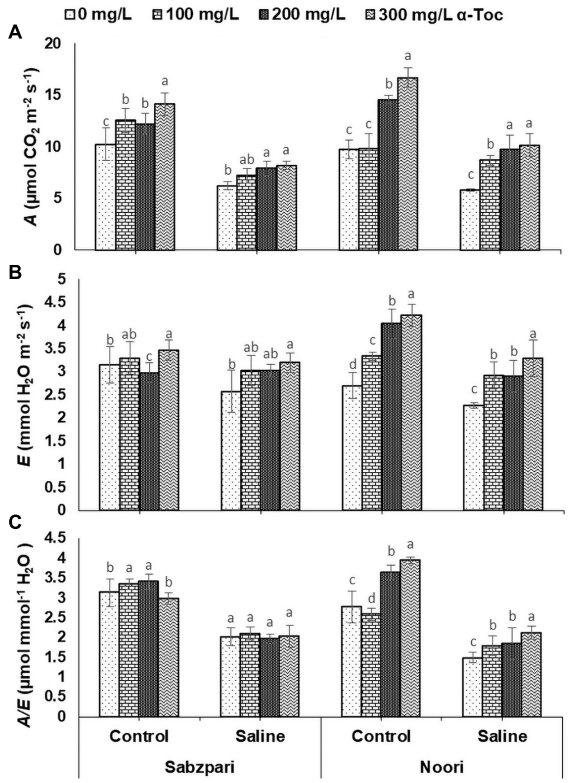


FIGURE 5 | Photosynthetic rate *A* **(A)**, Transpiration rate *E* **(B)**, Water use efficiency *A*/*E* **(C)**, of okra varieties sprayed with different levels of α-tocopherol under saline conditions. Values represent means ± S.D. Significant differences among row spacing were measured by the least significant difference (LSD) at $p > 0.05$ and indicated by different letters.

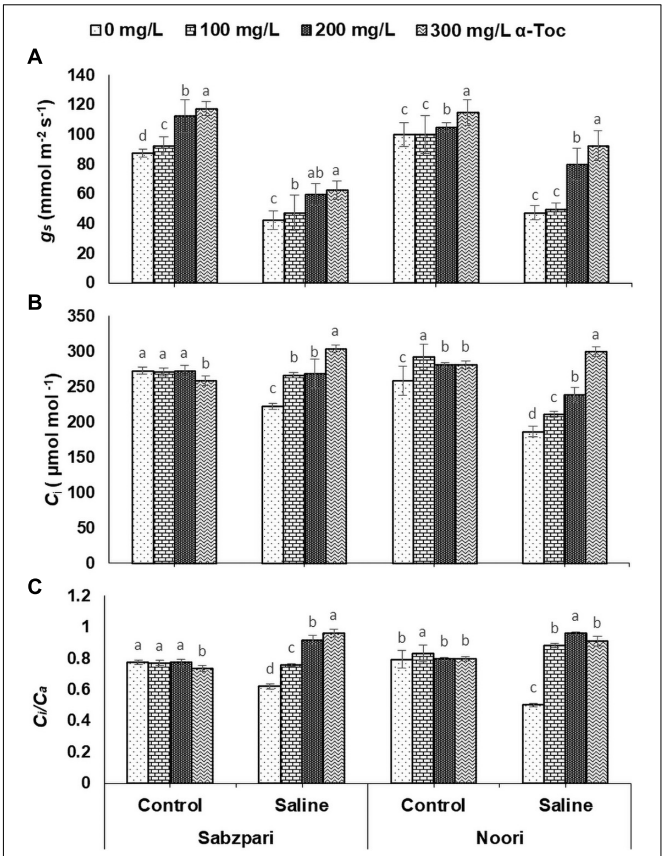


FIGURE 6 | Stomatal conductance g_s **(A)**, Internal CO_2 concentration C_i **(B)** C_i/C_a **(C)** of okra varieties sprayed with different levels of α-tocopherol under saline conditions. Values represent means ± S.D. Significant differences among row spacing were measured by the least significant difference (LSD) at $p > 0.05$ and indicated by different letters.

and inhibited uptake of essential ions (Farooq et al., 2017). However, foliar fertigation of α-tocopherol alleviated the adverse effects of salinity by improving these growth attributes. This shows that α-tocopherol stimulates various signaling factors involved in growth stimulation. Improved photosynthesis is also linked with upregulation of α-tocopherol, which is linked with enhanced growth (Orabi and Abdelhamid, 2016). Abiotic factors, including salinity, reduce the photosynthetic rate. Elevated levels

TABLE 3 | Analysis of variance (mean squares) for leaf gas exchange attributes of okra plants treated with α-tocopherol as foliar spray under saline and non-saline conditions.

Source	df	Total soluble proteins	Reducing sugars	Non-reducing sugars	Total soluble sugars	Leaf Ca^{2+}	Leaf K^+	Leaf Na^+	Root Ca^{2+}	Root K^+	Root Na^+
V	1	28532.84***	22.65***	15.59ns	10.95ns	0.47ns	26.26**	3.28ns	1.56ns	0.66ns	4.25ns
S	1	8883.06***	5.51*	113.63***	61.02***	17.53***	19.14**	14.53 ***	1ns	98.75 ***	38.28 ***
α-Toc	3	607.43ns	2.53ns	129.17***	90.82***	4.48***	11.54**	0.58ns	1.38ns	2.72ns	10.50 ***
V x S	1	70.84ns	18.36***	121.27***	55.90**	13.59***	9.76ns	0.19ns	4.51 *	3.28ns	21.97 ***
V x α-Toc	3	48183.32***	0.30ns	20.74**	11.88ns	0.53ns	3.08 ns	0.23ns	0.82ns	1.04ns	11.47 ***
S x α-Toc	3	18282.91***	6.08**	94.19***	52.95***	2.82**	3.35 ns	0.50ns	1.01ns	3.03ns	8.62 **
V x S x α-Toc	3	7053.95***	0.50ns	38.03***	35.97***	1.13ns	1.02 ns	3.72 *	0.04ns	2.31ns	7.46 **
Error	48	404.83	1.13	4.44	4.55	0.62	2.42	0.91	1.05	2.00	1.56
V (LSD 0.05%)		10.11	0.53	1.05	1.07	0.39	0.78	0.48	0.51	0.71	0.62
S (LSD 0.05%)		10.11	0.53	1.05	1.07	0.39	0.78	0.48	0.51	0.71	0.62
α-Toc (LSD 0.05%)		14.3	0.75	1.49	1.51	0.56	1.10	0.67	0.73	1.00	0.88

**, **, and ***Significant at 0.05, 0.01 and 0.001 levels, respectively; ns, non-significant; V, Varieties; S, Salinity; α-toc, Alpha tocopherol.*

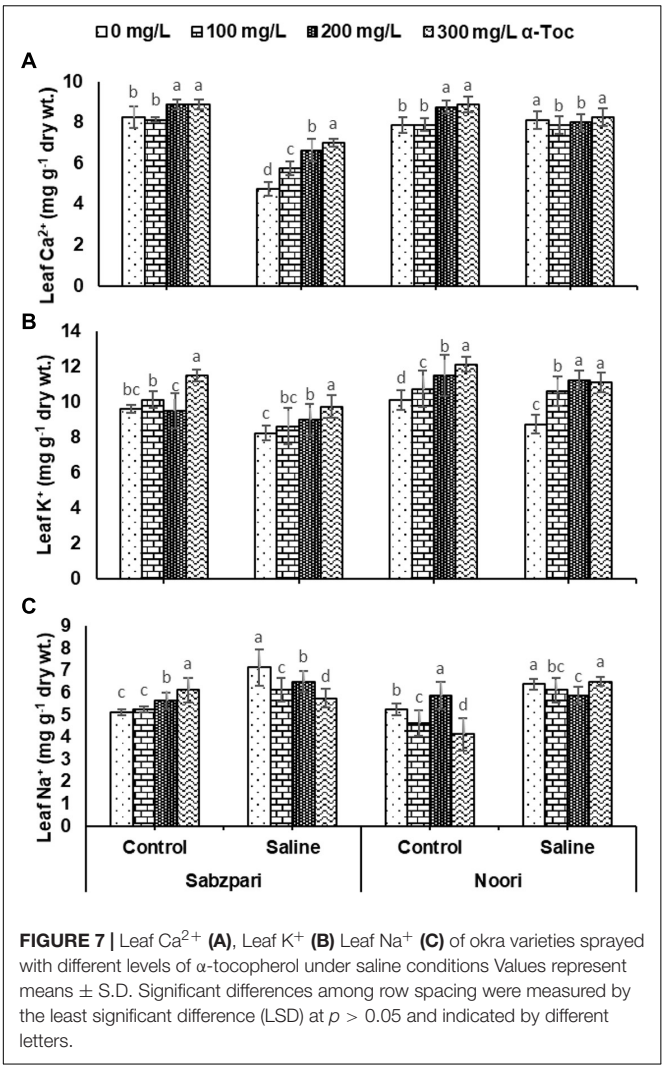


FIGURE 7 | Leaf Ca^{2+} **(A)**, Leaf K^{+} **(B)** Leaf Na^{+} **(C)** of okra varieties sprayed with different levels of α-tocopherol under saline conditions Values represent means ± S.D. Significant differences among row spacing were measured by the least significant difference (LSD) at $p > 0.05$ and indicated by different letters.

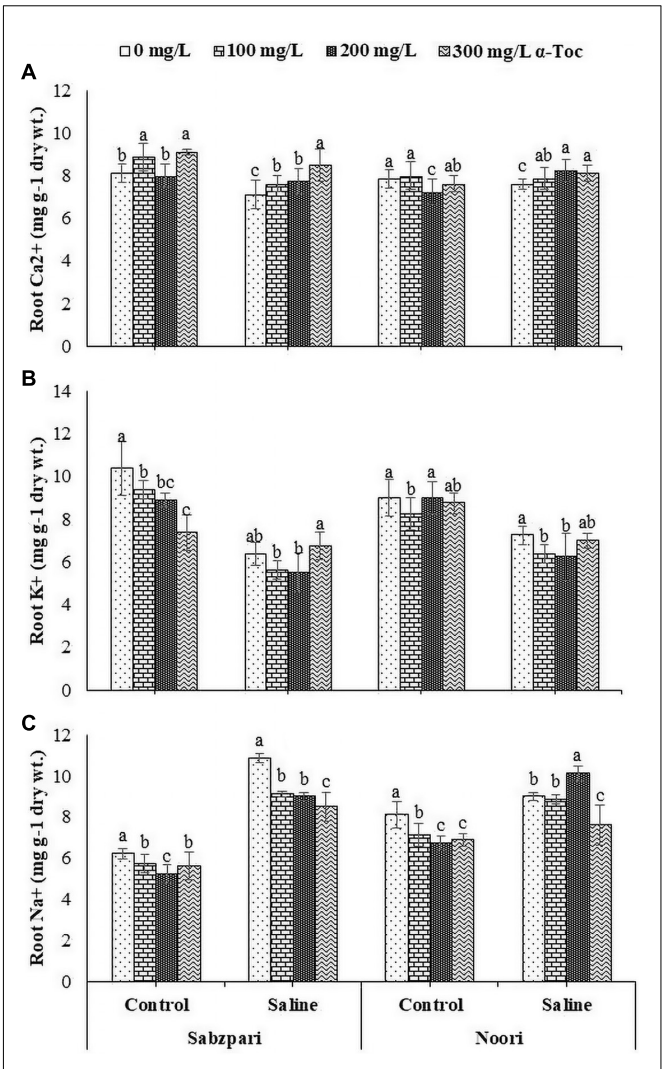


FIGURE 8 | Root Ca^{2+} **(A)**, Root K^{+} **(B)** Root Na^{+} **(C)** of okra varieties sprayed with different levels of α-tocopherol under saline conditions. Values represent means ± S.D. Significant differences among row spacing were measured by the least significant difference (LSD) at $p > 0.05$ and indicated by different letters.

of NaCl also hamper stomatal function, uptake of CO_2 and ultimately photosynthesis (Hnilickova et al., 2021). In the present study, a reduction in photosynthetic pigments was markedly observed under salinity stress in the tested okra varieties. Salinization disturbs the biosynthesis of photosynthetic pigments by disorganizing the structure of chlorophyll (Kumar et al., 2013). The process of photosynthesis comprises various components, and damage by salinity stress at any stage may reduce the plant's overall photosynthetic rate. However, different levels of α-tocopherol applied as foliar spray significantly altered the content of photosynthetic pigments, including chlorophyll *a* and *b,* β-carotenes, total carotenoids and total chlorophyll of okra, under salinity stress. α-Tocopherol protects chloroplast structure from salinity-induced photoinhibition (Sh, 2014), as the effects of salinity on photosynthesis may involve inhibition of electron transport and inactivation of photosystem II (PSII) reaction centers (Mehta et al., 2010). α-Tocopherol also enhances the production of chlorophyll pigments by acting as an antioxidant and combating salinity-induced oxidative bursts as α-tocopherol is synthesized in plastids (Surówka et al., 2020).

Photosynthetic absorption of solar energy and CO_2 fixation are directly linked with fluctuations in CO_2 assimilation (Joshi et al., 2018). The rate of photosynthesis can be affected by environmental factors at all levels, and many researchers have reported a reduction in the rate of photosynthesis due to salinity. Stomatal regulation is extremely sensitive to salinity stress, which results in a reduced photosynthetic rate, transpiration rate, chlorophyll content and stomatal conductivity (Tang et al., 2020). In the present study, salinity stress markedly reduced gas exchange characteristics (*A, E, A/E, gs,* C_i and C_i/C_a) in the tested okra varieties. Reduced stomatal conductance is linked with reduced intercellular CO_2, which decreases the activity of several enzymes, including RUBISCO. However, gas exchange characteristics (*A, E, A/E, gs,* C_i, and C_i/C_a) were improved due to foliar spray of α-tocopherol under salinity stress in okra plants

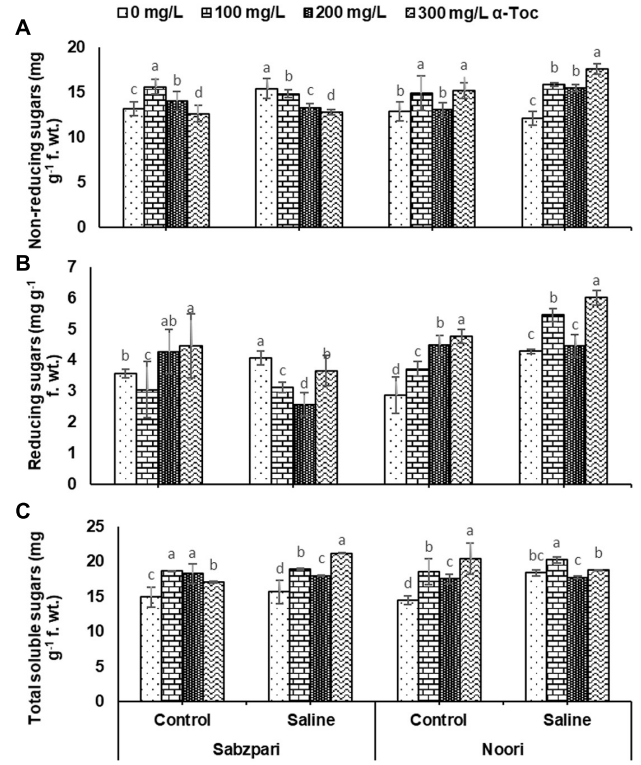


FIGURE 9 | Non-reducing sugars **(A)**, Reducing sugars **(B)**, Total soluble sugars **(C)** of okra varieties sprayed with different levels of α-tocopherol under saline conditions. Values represent means ± S.D. Significant differences among row spacing were measured by the least significant difference (LSD) at $p > 0.05$ and indicated by different letters.

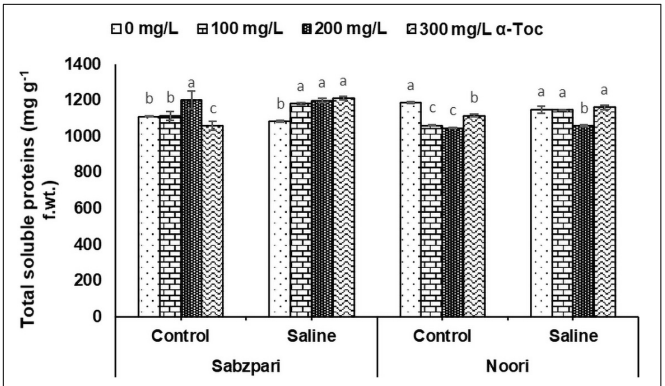


FIGURE 10 | Total soluble proteins of okra varieties sprayed with different levels of α-tocopherol under saline conditions. Values represent means ± S.D. Significant differences among row spacing were measured by the least significant difference (LSD) at $p > 0.05$ and indicated by different letters.

in the current study. This augmentation in the conductance efficiency of okra plants by exogenous supply of α-tocopherol is due to its antioxidative property. As an antioxidant, it protects photosystems and plastid membranes from lipid peroxidation by scavenging salinity-induced oxidative bursts (Fritsche et al., 2017). All these findings recommend the salinity mitigation role of α-tocopherol as a shielding agent by protecting chlorophyll pigments from photoinhibition. Agricultural crops suffer severe nutritional disorders due to competition among Na^+, Ca^{2+}, and K^+ ions (Singh et al., 2021). In this study, higher concentrations of Na^+ were observed in the leaf and root tissues of okra plants under saline regimes. Enhanced Na^+ concentrations disturb photosynthesis, plant metabolism, and enzymatic activities and thus affect overall crop productivity (Ashraf and Harris, 2013). Reduced uptake of Ca^{2+} is correlated with an enhanced concentration of Na^+. Foliar spray of α-tocopherol proved effective in minimizing the toxic concentrations of Na^+ ions in root and leaf tissues of okra plants, suggesting the role of α-tocopherol in osmotolerance by lowering Na^+ levels in plants (Sadak and Dawood, 2014). Foliar spray of alpha tocopherol enhanced the concentration of K^+ and Ca^{2+} ion contents in root and leaf of okra plants in the present study although, root medium applied salt stress decreased the concentration of these ions in root and leaf tissues of okra plants. High salt (NaCl) concentrations in soil and groundwater affect the ability of plants to take up K^+ and adversely affect enzymatic activities, cellular turgor and protein biosynthesis (Ahmed et al., 2021). Calcium plays a vital role in plants by providing structural stability and as a signaling molecule, but high concentrations of toxic salts reduce the uptake of Ca^{2+}. α-Tocopherol supplementation helps lower Na^+ ion content and enhances the uptake of K^+ under abiotic stress and non-stressed conditions (Ahmed et al., 2021). Total soluble proteins function as compatible solutes and are upregulated during abiotic stress conditions (Singh and Husen, 2019). In the current study, salt stress conditions enhanced the total soluble proteins in okra. On the other hand, foliar application of α-tocopherol induced a non-significant rise in soluble protein content. Alpha tocopherol is involved in the biosynthesis of proteins. A positive correlation also exists between exogenous application of α-tocopherol and protein biosynthesis (Sadak and Abdelhamid, 2015). It is hypothesized that enhanced levels of total soluble proteins enhance SOD activities in plants and minimize adverse effects of ROS generated under salinity stress.

The accumulation of carbohydrates (such as sugars) under stress conditions is one of most important plant response mechanisms to attain stress tolerance by osmoprotection, osmoregulation, carbon storage, and working against ROS. Total soluble sugars and reducing sugars were remarkably enhanced in the tested okra varieties under salinity. A significant increase was observed in total soluble sugars and non-reducing sugars due to α-tocopherol spray. Salinity tolerance may have been achieved due to the accumulation of carbohydrates as a protection mechanism (Sadiq et al., 2017). The accumulation of sugars due to abiotic stresses is thought to be a symbol of membrane damage due to stress-induced ROS (Islam et al., 2016). Alpha tocopherol helps quench ROS and is also responsible for the higher buildup of carbohydrates in plants (Sadak et al., 2015) under salinity stress conditions, the accumulation of sugars helps plants adjust osmotically. Plants have been attributed to adaptation by an increase in carbohydrate levels in response to stresses. In addition to osmoregulators, soluble sugars may act as osmoprotectants for proteins under stressed conditions.

CONCLUSION

Foliar application of α-tocopherol proved effective in alleviating salinity-induced damage in okra by enhancing growth, photosynthetic pigments, and leaf gas exchange attributes, possibly by protecting chloroplasts due to its antioxidant potential. Among the tested okra varieties, Noori showed enhanced tolerance against salinity, and 300 mg L^{-1} α-tocopherol was more effective. Thus, this study points to the use of the okra variety Noori to be grown in saline soils with foliar spray of α-tocopherol (300 mg L^{-1}) to increase okra production under field conditions. Exogenous application of α-tocopherol is also recommended to apply on other crops to alleviate salinity induced damages. Other modes of exogenous application of α-tocopherol e.g., seed priming can also be tested to cope with salinity stress in other crops.

DATA AVAILABILITY STATEMENT

The original contributions presented in the study are included in the article/supplementary material, further inquiries can be directed to the corresponding author/s.

AUTHOR CONTRIBUTIONS

MN and MS conceived the idea. XW and AM provided the technical expertise to strengthen the basic idea. SF and SB helped in the collection of data and its analysis. AM helped in the proofreading and discussion of the manuscript. All authors have read the first draft, helped in revision and approved the article.

FUNDING

The publication of the present work is supported by the Natural Science Basic Research Program of Shaanxi Province (Grant No. 2018JQ5218) and the National Natural Science Foundation of China (51809224), Top Young Talents of Shaanxi Special Support Program.

ACKNOWLEDGMENTS

The authors would like to thank the UAF (University of Agriculture Faisalabad) for providing the Infrastructure and Facilities to carry out this study.

REFERENCES

Aboyeji, C. M., Dahunsi, S. O., Olaniyan, D. O., Dunsin, O., Adekiya, A. O., and Adeniyi, O. (2021). Performance and quality attributes of okra (*Abelmoschus esculentus* (L.) Moench) fruits grown under soil applied Zn-fertilizer, green biomass and poultry manure. *Sci. Rep.* 11:8291. doi: 10.1038/s41598-021-87663-4

Ahmad, P., Ahanger, M. A., Alam, P., Alyemeni, M. N., Wijaya, L., Ali, S., et al. (2019). Silicon (Si) supplementation alleviates NaCl toxicity in mung bean [*Vigna radiata* (L.) Wilczek] through the modifications of physio-biochemical attributes and key antioxidant enzymes. *J. Plant Growth Regulat.* 38, 70–82. doi: 10.1007/s00344-018-9810-2

Ahmed, K. B. M., Singh, S., Sadiq, Y., Khan, M. M. A., Uddin, M., Naeem, M., et al. (2021). Photosynthetic and cellular responses in plants under saline conditions. *Front. Plant Soil Interact.* 2021:293–365. doi: 10.1016/B978-0-323-90943-3.00007-9

Arnon, D. I. (1949). Copper enzymes in isolated chloroplasts. Polyphenoloxidase in Beta vulgaris. *Plant Physiol.* 24:1. doi: 10.1104/pp.24.1.1

Ashraf, M., and Harris, P. J. C. (2013). Photosynthesis under stressful environments: an overview. *Photosynthetica* 51, 163–190. doi: 10.1007/s11099-013-0021-6

Bradford, M. M. (1976). A rapid and sensitive method for the quantitation of microgram quantities of protein utilizing the principle of protein-dye binding. *Analyt. Biochem.* 72, 248–254. doi: 10.1016/0003-2697(76)90527-3

Chokshi, K., Pancha, I., Ghosh, A., and Mishra, S. (2017). Salinity induced oxidative stress alters the physiological responses and improves the biofuel potential of green microalgae Acutodesmus dimorphus. *Bioresour. Technol.* 244, 1376–1383. doi: 10.1016/j.biortech.2017.05.003

Dubois, M., Gilles, K., Hamilton, J., Rebers, P., and Smith, F. (1951). A colorimetric method for the determination of sugars. *Nature* 168, 167–167.

Elshaikh, N. A., Zhipeng, L., Dongli, S., and Timm, L. C. (2018). Increasing the okra salt threshold value with biochar amendments. *J. Plant Interact.* 13, 51–63. doi: 10.1080/17429145.2017.1418914

Farooq, M., Hussain, M., Nawaz, A., Lee, D. J., Alghamdi, S. S., and Siddique, K. H. (2017). Seed priming improves chilling tolerance in chickpea by modulating germination metabolism, trehalose accumulation and carbon assimilation. *Plant Physiol. Biochem.* 111, 274–283. doi: 10.1016/j.plaphy.2016.12.012

Fritsche, S., Wang, X., and Jung, C. (2017). Recent advances in our understanding of tocopherol biosynthesis in plants: an overview of key genes, functions, and breeding of vitamin E improved crops. *Antioxidants* 6:99. doi: 10.3390/antiox6040099

GOP (2020). *Economic survey of Pakistan, Economic Advisor's Wing, Ministry of Finance*. Government of Pakistan.

Hasanuzzaman, M., Bhuyan, M., Zulfiqar, F., Raza, A., Mohsin, S. M., Mahmud, J. A., et al. (2020). Reactive oxygen species and antioxidant defense in plants under abiotic stress: Revisiting the crucial role of a universal defense regulator. *Antioxidants* 9:681. doi: 10.3390/antiox9080681

Hnilickova, H., Kraus, K., Vachova, P., and Hnilicka, F. (2021). Salinity Stress Affects Photosynthesis, Malondialdehyde Formation, and Proline Content in Portulaca oleracea L. *Plants* 10:845. doi: 10.3390/plants10050845

Hussain, H. A., Hussain, S., Khaliq, A., Ashraf, U., Anjum, S. A., Men, S., et al. (2018). Chilling and drought stresses in crop plants: implications, cross talk, and potential management opportunities. *Front. Plant Sci.* 9:393. doi: 10.3389/fpls.2018.00393

Islam, F., Ali, B., Wang, J., Farooq, M. A., Gill, R. A., Ali, S., et al. (2016). Combined herbicide and saline stress differentially modulates hormonal regulation and antioxidant defense system in Oryza sativa cultivars. *Plant Physiol. Biochem.* 107, 82–95. doi: 10.1016/j.plaphy.2016.05.027

Joshi, R., Sahoo, K. K., Tripathi, A. K., Kumar, R., Gupta, B. K., Pareek, A., et al. (2018). Knockdown of an inflorescence meristem-specific cytokinin oxidase–OsCKX2 in rice reduces yield penalty under salinity stress condition. *Plant Cell Environ.* 41, 936–946. doi: 10.1111/pce.12947

Kachout, S., Ennajah, A., Mechergui, R., Ben Mansoura, A., Ouerghi, Z., and Bouraoui, N. (2016). Effect of seed weight and salinity on the germination of garden orache (Atriplex hortensis L.). *Acad. J. Agricult. Res.* 4, 404–410.

Khan, A., Khan, A. L., Muneer, S., Kim, Y.-H., Al-Rawahi, A., and Al-Harrasi, A. (2019). Silicon and salinity: crosstalk in crop-mediated stress tolerance mechanisms. *Front. Plant Sci.* 10:1429. doi: 10.3389/fpls.2019.01429

Kumar, S., Singh, R., and Nayyar, H. (2013). α-Tocopherol application modulates the response of wheat (Triticum aestivum L.) seedlings to elevated temperatures by mitigation of stress injury and enhancement of antioxidants. *J. Plant Growth Regulat.* 32, 307–314. doi: 10.1007/s00344-012-9299-z

Liu, C., Zhao, X., Yan, J., Yuan, Z., and Gu, M. (2020). Effects of salt stress on growth, photosynthesis, and mineral nutrients of 18 pomegranate (Punica granatum) cultivars. *Agronomy* 10:27. doi: 10.3390/agronomy10010027

Mehla, N., Sindhi, V., Josula, D., Bisht, P., and Wani, S. H. (2017). An introduction to antioxidants and their roles in plant stress tolerance. *React. Oxyg. Spec. Antioxid. Syst. Plants* 2017, 1–23. doi: 10.1007/978-981-10-5254-5_1

Mehta, P., Jajoo, A., Mathur, S., and Bharti, S. (2010). Chlorophyll a fluorescence study revealing effects of high salt stress on Photosystem II in wheat leaves. *Plant Physiol. Biochem.* 48, 16–20. doi: 10.1016/j.plaphy.2009.10.006

Miller, T., Arison, B., and Albers-Schonberg, G. (1973). Isolation of a cyclitol antibiotic: 2, 3, 4, 5-tetrahydroxycyclohexanemethanol. *Biotechnol. Bioengine.* 15, 1075–1080. doi: 10.1002/bit.260150606

Mittler, R. (2017). ROS are good. *Trends Plant Sci.* 22, 11–19. doi: 10.1016/j.tplants.2016.08.002

Moles, T. M., de Brito Francisco, R., Mariotti, L., Pompeiano, A., Lupini, A., Incrocci, L., et al. (2019). Salinity in autumn-winter season and fruit quality of tomato landraces. *Front. Plant Sci.* 10:1078. doi: 10.3389/fpls.2019.01078

Mushtaq, Z., Faizan, S., and Gulzar, B. (2020). Salt stress, its impacts on plants and the strategies plants are employing against it: a review. *J. Appl. Biol. Biotechnol.* 8, 81–91. doi: 10.7324/JABB.2020.80315

Naqve, M., and Shahbaz, M. (2019). "Enhancing Morpho-Physiological Responses And Yield Potential In Okra," in *Crop Production Technologies for Sustainable Use and Conservation*, ed. A. E. L. Moench (Folrida, FL: Apple Academic Press), 103–320. doi: 10.1201/9780429469763-13

Naqve, M., Shahbaz, M., Wakeel, A., and Waraich, E. A. (2018). Seed priming with alpha tocopherol improves morpho-physiological attributes of okra under saline conditions. *Int. J. Agricult. Biol.* 20, 2647–2654. doi: 10.17957/IJAB/15.0805

Naveed, M., Sajid, H., Mustafa, A., Niamat, B., Ahmad, Z., Yaseen, M., et al. (2020). Alleviation of salinity-induced oxidative stress, improvement in growth, physiology and mineral nutrition of canola (Brassica napus L.) through calcium-fortified composted animal manure. *Sustainability* 12:846. doi: 10.3390/su12030846

Orabi, S. A., and Abdelhamid, M. T. (2016). Protective role of α-tocopherol on two Vicia faba cultivars against seawater-induced lipid peroxidation by enhancing capacity of anti-oxidative system. *J. Saudi Soc. Agricult. Sci.* 15, 145–154. doi: 10.1016/j.jssas.2014.09.001

Sadak, M. S., and Abdelhamid, M. T. (2015). Influence of amino acids mixture application on some biochemical aspects, antioxidant enzymes and endogenous polyamines of Vicia faba plant grown under seawater salinity stress. *Gesunde Pflanzen* 67, 119–129. doi: 10.1007/s10343-015-0344-2

Sadak, M. S., and Dawood, M. G. (2014). Role of ascorbic acid and tocopherol in alleviating salinity stress on flax plant (*Linum usitatissimum* L.). *J. Stress Physiol. Biochem.* 10, 93–111.

Sadak, S. H. M., Abdelhamid, M. T., and Schmidhalter, U. (2015). Effect of foliar application of aminoacids on plant yield and some physiological parameters in bean plants irrigated with seawater. *Acta Biol. Colomb.* 20, 141–152. doi: 10.15446/abc.v20n1.42865

Sadiq, M., Akram, N. A., and Ashraf, M. (2017). Foliar applications of alpha-tocopherol improves the composition of fresh pods of *Vigna radiata* subjected to water deficiency. *Turk. J. Bot.* 41, 244–252. doi: 10.3906/bot-1610-24

Sadiq, M., Akram, N. A., Ashraf, M., Al-Qurainy, F., and Ahmad, P. (2019). Alpha-tocopherol-induced regulation of growth and metabolism in plants under non-stress and stress conditions. *J. Plant Growth Regulat.* 38, 1325–1340. doi: 10.1007/s00344-019-09936-7

Schafleitner, R., Lin, C. Y., Lin, Y. P., Wu, T. H., Hung, C. H., Phooi, C. I., et al. (2021). The World Vegetable Center Okra (Abelmoschus esculentus) Core Collection as a Source for Flooding Stress Tolerance Traits for Breeding. *Agriculture* 11:165. doi: 10.3390/agriculture11020165

Semida, W., Taha, R., Abdelhamid, M., and Rady, M. (2014). Foliar-applied α-tocopherol enhances salt-tolerance in Vicia faba L. plants grown under saline conditions. *South Afr. J. Bot.* 95, 24–31. doi: 10.1016/j.sajb.2014.08.005

Sh, S. M. (2014). Role of ascorbic acid and α tocopherol in alleviating salinity stress on flax plant (Linum usitatissimum L.). *J. Stress Physiol. Biochem.* 10, 93–111.

Shahidi, F., and De Camargo, A. C. (2016). Tocopherols and tocotrienols in common and emerging dietary sources: Occurrence, applications, and health benefits. *Int. J. Mol. Sci.* 17:1745. doi: 10.3390/ijms17101745

Shilev, S. (2020). Plant-growth-promoting bacteria mitigating soil salinity stress in plants. *Appl. Sci.* 10:7326. doi: 10.3390/app10207326

Singh, S., and Husen, A. (2019). Role of nanomaterials in the mitigation of abiotic stress in plants. *Nanomater. Plant Potent.* 2019, 441–471.

Singh, U. B., Malviya, D., Singh, S., Singh, P., Ghatak, A., Imran, M., et al. (2021). Salt-Tolerant Compatible Microbial Inoculants Modulate Physio-Biochemical Responses Enhance Plant Growth, Zn Biofortification and Yield of Wheat Grown in Saline-Sodic Soil. *Int. J. Environ. Res. Public Health* 18:9936. doi: 10.3390/ijerph18189936

Snedecor, G. W., and Cochran, G. W. (1980). *Statistical Methods*, 7th Edn. Ames, IA: Lowa State University Press.

Soni, R., Kumar, A., Kanwar, S. S., and Pabbi, S. (2017). Efficacy of liquid formulation of versatile rhizobacteria isolated from soils of the North-Western Himalayas on Solanum lycopersicum. *Ind. J. Tradit. Knowl.* 16, 660–668.

Sun, Y., Niu, G., Masabni, J. G., and Ganjegunte, G. (2018). Relative salt tolerance of 22 pomegranate (Punica granatum) cultivars. *HortScience* 53, 1513–1519. doi: 10.21273/HORTSCI13362-18

Surówka, E., Potocka, I., Dziurka, M., Wróbel-Marek, J., Kurczyńska, E., Żur, I., et al. (2020). Tocopherols mutual balance is a key player for maintaining Arabidopsis thaliana growth under salt stress. *Plant Physiol. Biochem.* 156, 369–383. doi: 10.1016/j.plaphy.2020.09.008

Tang, N., Zhang, B., Chen, Q., Yang, P., Wang, L., and Qian, B. (2020). Effect of salt stress on photosynthetic and antioxidant characteristics in purslane (Portulaca oleracea). *Int. J. Agricult. Biol.* 24, 1309–1314. doi: 10.17957/IJAB/15.1564

Wolf, B. (1982). A comprehensive system of leaf analyses and its use for diagnosing crop nutrient status. *Commun. Soil Sci. Plant Anal.* 13, 1035–1059. doi: 10.1080/00103628209367332

Conflict of Interest: The authors declare that the research was conducted in the absence of any commercial or financial relationships that could be construed as a potential conflict of interest.

Publisher's Note: All claims expressed in this article are solely those of the authors and do not necessarily represent those of their affiliated organizations, or those of the publisher, the editors and the reviewers. Any product that may be evaluated in this article, or claim that may be made by its manufacturer, is not guaranteed or endorsed by the publisher.

Copyright © 2021 Naqve, Wang, Shahbaz, Mahmood, Bibi and Fiaz. This is an open-access article distributed under the terms of the Creative Commons Attribution License (CC BY). The use, distribution or reproduction in other forums is permitted, provided the original author(s) and the copyright owner(s) are credited and that the original publication in this journal is cited, in accordance with accepted academic practice. No use, distribution or reproduction is permitted which does not comply with these terms.

frontiers in Plant Science

REVIEW
published: 04 January 2022
doi: 10.3389/fpls.2021.794373

Advances in "Omics" Approaches for Improving Toxic Metals/Metalloids Tolerance in Plants

Ali Raza[1†], Javaria Tabassum[2], Zainab Zahid[3], Sidra Charagh[2†], Shanza Bashir[3], Rutwik Barmukh[4], Rao Sohail Ahmad Khan[5], Fernando Barbosa Jr.[6], Chong Zhang[1], Hua Chen[1], Weijian Zhuang[1] and Rajeev K. Varshney[1,4,7]**

[1] Key Laboratory of Ministry of Education for Genetics, Breeding and Multiple Utilization of Crops, Center of Legume Crop Genetics and Systems Biology/College of Agriculture, Oil Crops Research Institute, Fujian Agriculture and Forestry University (FAFU), Fuzhou, China, [2] State Key Laboratory of Rice Biology, China National Rice Research Institute, Chinese Academy of Agricultural Sciences (CAAS), Hangzhou, China, [3] School of Civil and Environmental Engineering (SCEE), Institute of Environmental Sciences and Engineering (IESE), National University of Sciences and Technology (NUST), Islamabad, Pakistan, [4] Center of Excellence in Genomics & Systems Biology, International Crops Research Institute for the Semi-Arid Tropics (ICRISAT), Hyderabad, India, [5] Centre of Agricultural Biochemistry and Biotechnology (CABB), University of Agriculture, Faisalabad, Pakistan, [6] Department of Clinical Analysis, Toxicology and Food Sciences, University of Sao Paulo, Ribeirão Preto, Brazil, [7] State Agricultural Biotechnology Centre, Centre for Crop and Food Innovation, Food Futures Institute, Murdoch University, Murdoch, WA, Australia

OPEN ACCESS

Edited by:
Shabir Hussain Wani, Sher-e-Kashmir University of Agricultural Sciences and Technology, India

Reviewed by:
Suprasanna Penna, Bhabha Atomic Research Centre (BARC), India
Timothy O. Jobe, University of Cologne, Germany

***Correspondence:**
Weijian Zhuang
weijianz@fafu.edu.cn
Rajeev K. Varshney
R.K.Varshney@cgiar.org;
rajeev.varshney@murdoch.edu.au

†ORCID:
Ali Raza
orcid.org/0000-0002-5120-2791
Sidra Charagh
orcid.org/0000-0002-8077-7324

Specialty section:
This article was submitted to Plant Breeding, a section of the journal Frontiers in Plant Science

Received: *13 October 2021*
Accepted: *22 November 2021*
Published: *04 January 2022*

Citation:
Raza A, Tabassum J, Zahid Z, Charagh S, Bashir S, Barmukh R, Khan RSA, Barbosa F Jr, Zhang C, Chen H, Zhuang W and Varshney RK (2022) Advances in "Omics" Approaches for Improving Toxic Metals/Metalloids Tolerance in Plants. Front. Plant Sci. 12:794373. doi: 10.3389/fpls.2021.794373

Food safety has emerged as a high-urgency matter for sustainable agricultural production. Toxic metal contamination of soil and water significantly affects agricultural productivity, which is further aggravated by extreme anthropogenic activities and modern agricultural practices, leaving food safety and human health at risk. In addition to reducing crop production, increased metals/metalloids toxicity also disturbs plants' demand and supply equilibrium. Counterbalancing toxic metals/metalloids toxicity demands a better understanding of the complex mechanisms at physiological, biochemical, molecular, cellular, and plant level that may result in increased crop productivity. Consequently, plants have established different internal defense mechanisms to cope with the adverse effects of toxic metals/metalloids. Nevertheless, these internal defense mechanisms are not adequate to overwhelm the metals/metalloids toxicity. Plants produce several secondary messengers to trigger cell signaling, activating the numerous transcriptional responses correlated with plant defense. Therefore, the recent advances in omics approaches such as genomics, transcriptomics, proteomics, metabolomics, ionomics, miRNAomics, and phenomics have enabled the characterization of molecular regulators associated with toxic metal tolerance, which can be deployed for developing toxic metal tolerant plants. This review highlights various response strategies adopted by plants to tolerate toxic metals/metalloids toxicity, including physiological, biochemical, and molecular responses. A seven-(omics)-based design is summarized with scientific clues to reveal the stress-responsive genes, proteins, metabolites, miRNAs, trace elements,

stress-inducible phenotypes, and metabolic pathways that could potentially help plants to cope up with metals/metalloids toxicity in the face of fluctuating environmental conditions. Finally, some bottlenecks and future directions have also been highlighted, which could enable sustainable agricultural production.

Keywords: abiotic stress, CRISPR/Cas system, genomics, metabolomics, proteomics, speed breeding, miRNAomics

INTRODUCTION

Over the last few decades, intensive anthropogenic activities and modern farming practices have led to the contamination of ecosystems by toxic metals/metalloids (Rai et al., 2019), an alarming global concern. Toxic metals/metalloids are ubiquitous in the earth's crust and possess multiple benefits but can be harmful to the ecosystem when present in excess amounts (Gashi et al., 2020). Abiotic stresses (e.g., toxic metals/metalloids contamination, drought, salinity, etc.) are amongst some important factors affecting the growth and productivity of crop plants, resulting in up to 70% yield losses (Rai et al., 2019; Raza et al., 2020, 2021a; Roorkiwal et al., 2020; Varshney et al., 2021c). Climate changes give rise to several environmental stresses, including toxic metals/metalloids. Consequently, climate change significantly impacts the toxic metals/metalloids pollutions based on bioavailability, fate, and toxicity (Wijngaard et al., 2017; Wu et al., 2017; Oyewo et al., 2020). Among various environmental stresses, drought stress may cause an upsurge in eutrophication and toxic metals/metalloids meditations. Whereas the flooding stress may cause more toxic metals/metalloids meditations owing to desorption or re-suspension signifying that climate change determined impacts on toxic metals/metalloids transport is a composite and dynamic environmental problem, demanding a systematic understanding of toxic metals/metalloids accessibility, transport, and uptake pathways (Wijngaard et al., 2017; Wu et al., 2017; Oyewo et al., 2020).

Plants require mineral nutrients for proper growth and development. For instance, they need macro-nutrients and micro-nutrients to carry out primary functions like metabolism, photosynthesis, synthesis of enzymes, DNA and pigments, chlorophyll (Chl) functioning, nitrogen (N) fixation, etc. (Malar et al., 2016; Patel et al., 2020; Salim and Raza, 2020). Among these nutrients, some metals/metalloids such as copper (Cu), zinc (Zn), nickel (Ni), iron (Fe), selenium (Se), etc. are required in trace amounts (Karthika et al., 2018; Hasanuzzaman et al., 2020a), and can be toxic when taken up in excess by the plants (Pandey et al., 2019; Hasanuzzaman et al., 2020a). Besides, other non-essential metals/metalloid elements, like arsenic (As), cadmium (Cd), lead (Pb), mercury (Hg), are toxic to plant even at low amounts (Asati et al., 2016; Mawia et al., 2020; Raza et al., 2021a). The toxicity of non-essential toxic metals/metalloids in plants can lead to severe damages, including reduced or inhibited growth, low biomass and reduced production, chlorosis, water and nutrient imbalance, denaturation of essential enzymes and proteins, production of reactive oxygen species (ROS), disturbed electron transport chain, lipid peroxidation, and at times ultimately plant death (Rucińska-Sobkowiak, 2016; Venkatachalam et al., 2017; Jalmi et al., 2018; Tiwari and Lata, 2018; Gashi et al., 2020; Salehi et al., 2021). As a mechanism of toxicity, some non-essential toxic metals/metalloids tend to replace the essential ones in enzymes and pigments, thus disrupting their functioning (Sarwar et al., 2017; Erickson et al., 2019). Thus, plants need these metals/metalloids at a low amount to perform their metabolic activities.

Various biotechnological techniques are being implied to get an insight and in-depth understanding of the mechanisms and pathways involved in plant responses and tolerance toward toxic metals/metalloids toxicity. "Omics" approaches such as genomics (genes and complete DNA), transcriptomics (coding RNA and its types), proteomics (proteins), metabolomics (profiling of metabolites), ionomics (micro and macro ions profiling), miRNAomics (non-coding RNA), and phenomics (plant phenotype) are being widely implied for this purpose (Jamla et al., 2021a; Khan et al., 2021; Raza et al., 2021a). Molecular regulators (genes, RNA, metabolites, and proteins) and their related activities like replication, translation, post-translation, transcription, etc., play a pivotal role in the performance and maintenance of critical plant functions. Since they also determine plant responses to toxic metals/metalloids stress, the understanding of regulatory principles at the genetic level is necessary. Genomics and transcriptomics approaches hold the potential to provide insights into such complex and intricate processes during plant development (Pirzadah et al., 2019). Proteomics offers insights into the stress-inducible proteins and their involvement in mitigation against toxic metals/metalloids toxicity (Wen et al., 2019). It also provides cues into protein profiles from the cellular to organ level and offers insights into protein behavior under stress conditions (Wen et al., 2019). Metabolomics enables an understanding of the differentially regulated metabolites and complex metabolic activities occurring within the plant under diverse conditions (Razzaq et al., 2019; Raza, 2020). Furthermore, ionomics provides insights into the nutrient and trace element composition of the plant, as well as activities and mechanisms involved in uptake, storage, assimilation, and the plants' responses to toxic metals (Stich et al., 2020). MicroRNAs (miRNAs), a group of single-stranded, non-coding micro RNAs, have been shown to regulate gene expression at a post-transcriptional level. Plants respond to stress (including toxic metals/metalloids) by triggering the miRNAs that work by cleaving or neutralizing the transcribed mRNA according to the plant needs under stressed conditions (Dubey et al., 2021; Jamla et al., 2021b).

In this review, we start by discussing the physiological, biochemical, and molecular responses of the plants toward toxic

metals/metalloids toxicity. We then describe recent innovations in "omics" approaches such as genomics, transcriptomics, proteomics, metabolomics, ionomics, miRNAomics, and phenomics that could empower the development of toxic metals/metalloids tolerant plants. Further, we summarize some important online databases/tools for the integration of omics data. Additionally, an overview of some plant-based remediation approaches has also been discussed. We aim to offer a comprehensive overview of intricate plant responses to toxic metal stress and highlight the potential of omics approaches for developing toxic metals/metalloids tolerant plants in future.

PLANT RESPONSES TO TOXIC METALS/METALLOIDS TOXICITY

Since plants constitute the primary level of the food chain, harmful metals/metalloids may enter the food chain through plants, thereby posing a threat of exposure to animals and especially humans, and may cause several physiological, morphological, and metabolic disorders and abnormalities (Rai et al., 2019). Increased metals/metalloids toxicity has resulted in reduced crop and food production by disturbing the demand and supply equilibrium, demanding an urgent need to develop strategies for combating the situation and enhancing plant tolerance toward toxic metals/metalloids (Rai et al., 2019; Gashi et al., 2020).

Plants being sessile organisms, have no escape when it comes to unfavorable environmental conditions. Several physiological, biochemical, and molecular responses are generated in the plant due to toxic metals/metalloids toxicity, as these toxicants interfere with several natural processes (**Figure 1**; Raza et al., 2021a). The interference of toxic metals/metalloids with plant processes takes place mainly through: (i) competition at the root absorption surface level with the essential metal ions for uptake; (ii) displacement of ions from specific binding sites and essential biomolecules; (iii) displacement of a critical functional group from proteins (e.g., sulfhydryl group, -SH), denaturing them and making them inactive; and (iv) the formation of ROS which interacts with and deteriorates biomolecules and disrupts the metabolic activities (Ghori et al., 2019; Mishra S. et al., 2019).

The early responses of the plant to toxic metals/metalloids stress are easier to study, whereas signal transduction at later stages of exposure is difficult to detect (Jalmi et al., 2018). Detection of stress triggers plants' defense mechanisms through various pathways (Raza et al., 2021a). For instance, root endings detect the presence of metals and send signals from the roots throughout the plant cells and into different cell organelles (Dalvi and Bhalerao, 2013). Plants first attempt to prevent the entry of metal ions into the body by immobilizing ions with the help of their mycorrhizal associations and converting them to complexes of organic acids, amino acids, etc., secreted from the root endings (Dalvi and Bhalerao, 2013; Jalmi et al., 2018). Toxic metals/metalloids that enter the plant body may get accumulated within vacuoles and/or get bound to the cell wall and proteins, thereby causing a further modification of physiological, biochemical, and molecular activities when transported to different plant parts (**Figure 1**; Jalmi et al., 2018).

Physiological Responses

Toxic metals/metalloids toxicity induces and alters many physiological responses in plants. One of the most observed plant responses is the reduction or inhibition of plant growth and development (Rucińska-Sobkowiak, 2016; Ghori et al., 2019; Raza et al., 2020, 2021a). For instance, Zn, Cd, Cu, Hg, As, Ni, chromium (Cr), and many other prominent metal toxicants have been reported to retard plant growth, seed germination and cause other morphological modifications (Ghori et al., 2019). Moreover, Pb has been reported to reduce growth in alfalfa (Hattab et al., 2016) and *Acalypha indica* (Venkatachalam et al., 2017). Increasing concentrations of Hg from 5 to 80 $\mu g\ mL^{-1}$ decreased roots, shoots, and leaves content in *Jatropha curcas* (Marrugo-Negrete et al., 2016). Nickel has been reported to reduce seed germination in sunflower due to lower α-amylase and protease activities (Ashraf et al., 2011). Furthermore, adverse effects on leaf area due to Cd contamination were observed in tomato (Rehman et al., 2011), and production of chlorosis by Cd was reported in *Phaseolus vulgaris* (Bahmani et al., 2012). An account of the effect on pollen germination has been found in *Pisum sativum* by Cd and Cu toxicity (Sabrine et al., 2010).

Since roots represent the first plant parts to encounter toxic metals/metalloids stress in the soil, a decrease in root growth, root hair surface, and enhanced root dieback has been observed (Rucińska-Sobkowiak, 2016). Root cells tend to harden their cell walls and inhibit growth by avoiding the entrance of Cu ions in *Festuca arundinacea* and *Lolium perenne* (Zhao et al., 2010). Root cells further stimulated the entered metals/metalloids ions into the vacuole to prevent their interference with the organelle functions. For instance, Eleftheriou et al. (2015) reported Cr sequestration in the cell wall and vacuole in *Arabidopsis thaliana*. The plasma membranes in cells work in a highly controlled fashion, preventing unwanted materials from entering the organelles and mediating the harmful effects of various stresses. Despite this, Cd has been reported to disrupt the structure and functionality of the plasma membrane (Janicka-Russak et al., 2012). Such effects can further produce many undesirable outcomes, such as disruption of water and nutrient supply.

Although few metals/metalloids such as Zn, Fe, Cu, cobalt (Co), molybdenum (Mo), and manganese (Mn) are considered as essential elements for photosynthesis (Schmidt et al., 2020), their increased concentration has been shown to alter photosynthetic activities in plants (Chandra and Kang, 2016). Some metals/metalloids (e.g., Fe) act as necessary co-factors for various enzymes involved in the photosynthetic process (Balk and Schaedler, 2014); however, they tend to retard normal activities when present at higher concentrations (Asati et al., 2016). For instance, Pb and Cd were found to inhibit photosynthetic pigments in *Davidia involucrate* (Yang Y. et al., 2020). Toxic metals/metalloids toxicity also affects the overall photosynthetic apparatus and the rate of photosynthesis, causing a reduction in Chl content and mesophyll thickness (Pereira et al., 2016; Schmidt et al., 2020). In wheat, Cr has been reported to

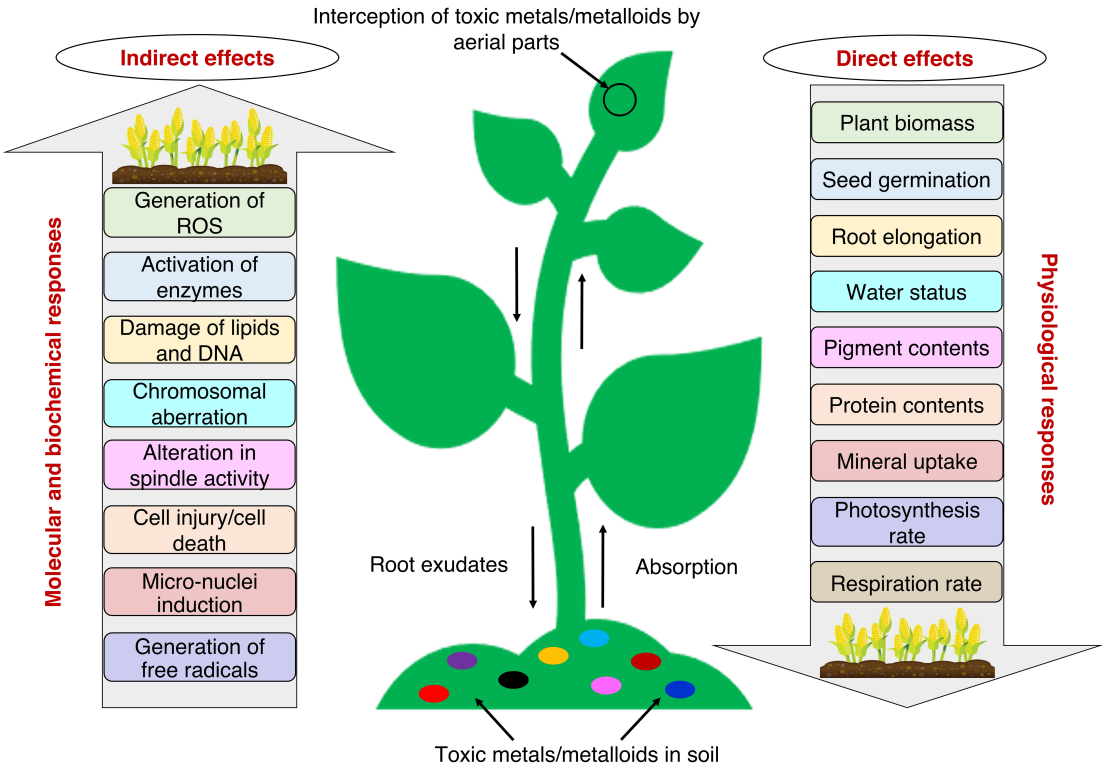


FIGURE 1 | Plant responses to toxic metals/metalloids toxicity with possible direct and indirect effects on crop productivity. Plants interact with toxic metals/metalloids via above-ground and/or below-ground parts. The toxic effects of several toxic metals/metalloids decrease the physiological responses and increase the molecular and biochemical responses.

reduce the electron transport chain rate and negatively affect light-harvesting complex of photosystem II (PSII) by reducing the number of active reaction sites (Mathur et al., 2016).

Toxic metals/metalloids toxicity tends to affect the nutrient uptake, water uptake, and their translocation and assimilation in plants. Several alterations in plant functions, including dehydration due to inhibition of water translocation (Hussain et al., 2013), reduced transpiration, and altered stomatal activity, have also been observed (Wani et al., 2018). Decreased transpiration was observed for poplar hybrid in response to Cd, Cu, Cr, and Zn exposure (Chandra and Kang, 2016). In contrast, reduced stomatal activity was observed in *Pistacia vera* due to Zn toxicity (Tavallali, 2017). Moreover, xylem and phloem functionality were affected due to toxic metals/metalloids contamination, e.g., reduction in root xylem area was observed in *Salix caprea* in response to Zn and Cd exposure (Vaculík et al., 2012). Toxic ions have been found to compete with essential ions for translocation throughout the plant (Rucińska-Sobkowiak, 2016). For example, Cd was identified to compete with essential ions such as Fe, Mg, and calcium (Ca), among others (Raza et al., 2020).

Biochemical Responses

Toxic metals/metalloids usually trigger biochemical responses by displacing/replacing essential ions or blocking functional groups. They compete with crucial nutrients at bindings sites of enzymes, rendering them denatured and inhibiting their activity (Ghori et al., 2019). For instance, the biochemical response of Cr on mung bean seeds showed a significant decline in protein, Chl, and starch content under 50% metal contaminated soil (Rath et al., 2019). Similarly, Se-stressed rice plants were found to promote Chl and protein degradation in response to metal accumulation. Alteration in these biochemical processes caused significant physiological toxicity symptoms in plants (Gouveia et al., 2020). Different ornamental plant species grown under urban Pb-contaminated soil showed a decline in their net photosynthetic rate and root activity due to stress responses. In contrast, the levels of soluble sugars, leaf proline content, and membrane stability index, altogether maintain osmotic adjustment, form metal-proline complexes and identify the extent of membrane damage, respectively, were found to increase significantly (Song et al., 2020b). The biochemical responses of kenaf (*Hibiscus cannabinus* L.) revealed Cu-induced damage in root and shoot tissues as observed through excess production of malondialdehyde (MDA), hydrogen peroxide (H_2O_2), and electrolyte leakage. Its negative impacts on the plant were mediated through antioxidative enzyme activities, which increase with enhancing metal concentration (Saleem et al., 2020).

The assessment of cowpea subjected to Fe toxicity showed an increase in the MDA content (Ifie et al., 2020). Another study on halophytic phytoremediator of Cu, *Sesuvium portulacastrum*, also reported similar findings where plants were affected

by the toxic effects of Cu at higher concentrations. The MDA production was mediated through an active antioxidant mechanism in plants to counteract the damage caused by ROS production (Lokhande et al., 2020). The antioxidants work by searching, neutralizing, and removing the reactive species (Hasanuzzaman et al., 2020b). An assessment of biochemical responses in alfalfa plants showed high peroxidase (POD) and glutathione *S*-transferase (GST) activity upon its exposure to Ni. The data on antioxidant enzymes was also in corroboration with the expression transcripts of the *Prx1C* gene, showing elevated biochemical activity in plants as a function of plant defense (Helaoui et al., 2020).

Furthermore, carbon dioxide (CO_2) fixation and assimilation activities are also greatly affected by metal toxicity. For instance, inhibition of CO_2 assimilation was reported in wheat by excessive concentrations of Cd and Zn (Paunov et al., 2018). Rubisco activity was observed to be reduced due to toxic metals/metalloids stress, as they react with the thiol group of the enzyme and render denaturing it (Son et al., 2014). Nitrogen metabolism is a crucial mechanism in plant growth and development that suffers from metal stress. For example, Cr lowered nitrate and ammonia assimilation enzymes in *Cyamopsis tetragonoloba* by enhancing their destruction through protease increase (Sangwan et al., 2014).

Molecular Responses

As a defense mechanism to toxic metals/metalloids stimuli, root growth is reduced and inhibited by terminating the mitotic activity (Campos et al., 2018). Pavlova (2017) detected a decrease in meristem mitosis in *Plantago lanceolate* due to Ni toxicity, inhibiting root elongation. Similarly, Cr has also been described to inhibit mitotic cell division by delaying and extending the cell cycle in rice (Sundaramoorthy et al., 2010). ROS production in response to toxic metals/metalloids stress can cause damage to cellular membranes, nucleic acids, lipids, and proteins (Hasanuzzaman et al., 2020b). For example, Cu and Zn caused severe damage to cellular structures in the Populus species (Benyó et al., 2016). Plants also produce various metal binding structures, chelating agents or ligands as a defense or detoxification mechanism, such as organic acids, amino acids, phytochelatins (PCs), and metallothionein (MT), among others (Raza et al., 2020, 2021a).

Although plants have different mechanisms to prevent metal ions from reaching the nucleus, the entry of metals/metalloids causes cross-linking of DNA and proteins, DNA mutation (deletion, addition, modification), alter the base structure of the DNA, or cause DNA strands to break (Emamverdian et al., 2015). They further disrupt lipids, damage Chl, disturb cell homeostasis, and also interfere with the electron transport chain and energy production and assimilation through ATP molecules, leading to programmed cell death (Parmar et al., 2013).

Exposure to Cd was found to display an enhanced expression of *Chit5* (one of the chitinase encoding genes) in roots by 7. 3-, 3. 9-, and 3.7-fold, compared with its expression in shoots in *Amaranth. cruentus*, *A. hypochondriacus* × *A. hybridus*, and *A. hypochondriacus* × *A. hybridus*, respectively (Lancíková et al., 2020). Alfalfa plant experienced a 25- and 29-fold increase in detoxifying enzyme superoxide dismutase (SOD) transcripts in response to bulk Cu and nano Cu, respectively (Cota-Ruiz et al., 2020). Research has established melatonin expression to help alleviate Cd stress in radish plants (Xu L. et al., 2020). Gao et al. (2020) demonstrated *PtrMTP* (*Populus trichocarpa* metal tolerance proteins) gene to play a significant role in inducing tolerance toward metal contamination in roots, stems, and leaves of *Populus trichocarpa* through homeostasis and detoxification mechanisms.

MicroRNAs have been reported to play a significant role in plant response and tolerance to toxic metals/metalloids stress by regulating chelation, antioxidant response, auxin signaling, and cytokinin signaling, among others (Ding et al., 2020). For instance, Casarrubia et al. (2020) reported microRNA to play a significant role in combination with the mycorrhizal association for regulating the response of *Vaccinium myrtillus* against Cd contamination. MicroRNA expression in terms of biosynthesis/biogenesis of various secondary metabolites has been found to play a major role in enhancing Al and Cd tolerance in transgenic tobacco (Cedillo-Jimenez et al., 2020). Notably, the expression of different microRNAs, including miR156, miR162, miR164, miR166, miR172, miR398, and miR408, were found to regulate the expression of their respective target genes in *Carthamus tinctorius* as a result of Cd exposure (Kouhi et al., 2020).

SEVEN-(OMICS)-BASED APPROACHES TO IMPROVE TOXIC METALS/METALLOIDS TOLERANCE IN PLANTS

Plant responses to toxic metals/metalloids toxicity rely on the regulation of molecular factors. Therefore, an integrated omics approach has been extensively used to comprehend the plant's biological interactions and molecular mechanisms against toxic metals/metalloids toxicity. Regardless of the incredible advancements in genomics, it is essential to evaluate other omics tools for wide-ranging knowledge at the molecular level (**Figure 2**). Scientific investigations and existing information derived by omics tools target signaling pathways, key molecular regulators, and integrated mechanisms to enhance tolerance toward toxic metals/metalloids toxicity for crop improvement.

Genomics

Genomics includes characterization, data sequencing, structural organization, genetic alignments, interactions, and functions of a whole organism (plant) (Gilliham et al., 2017). Genomics is interrelated to the terms like transcriptomics, metabolomics, transgenomics, epigenomics, and phenomics. These approaches, associated with high throughput (HTP) technologies, have made significant advancements in plant genomics research and have enabled the improvement of multiple important crop plants (Varshney et al., 2020, 2021a). Genomics can help to identify genes, enzymes, or other molecular factors involved in stimulating toxic metals/metalloids stress. Genomics-based

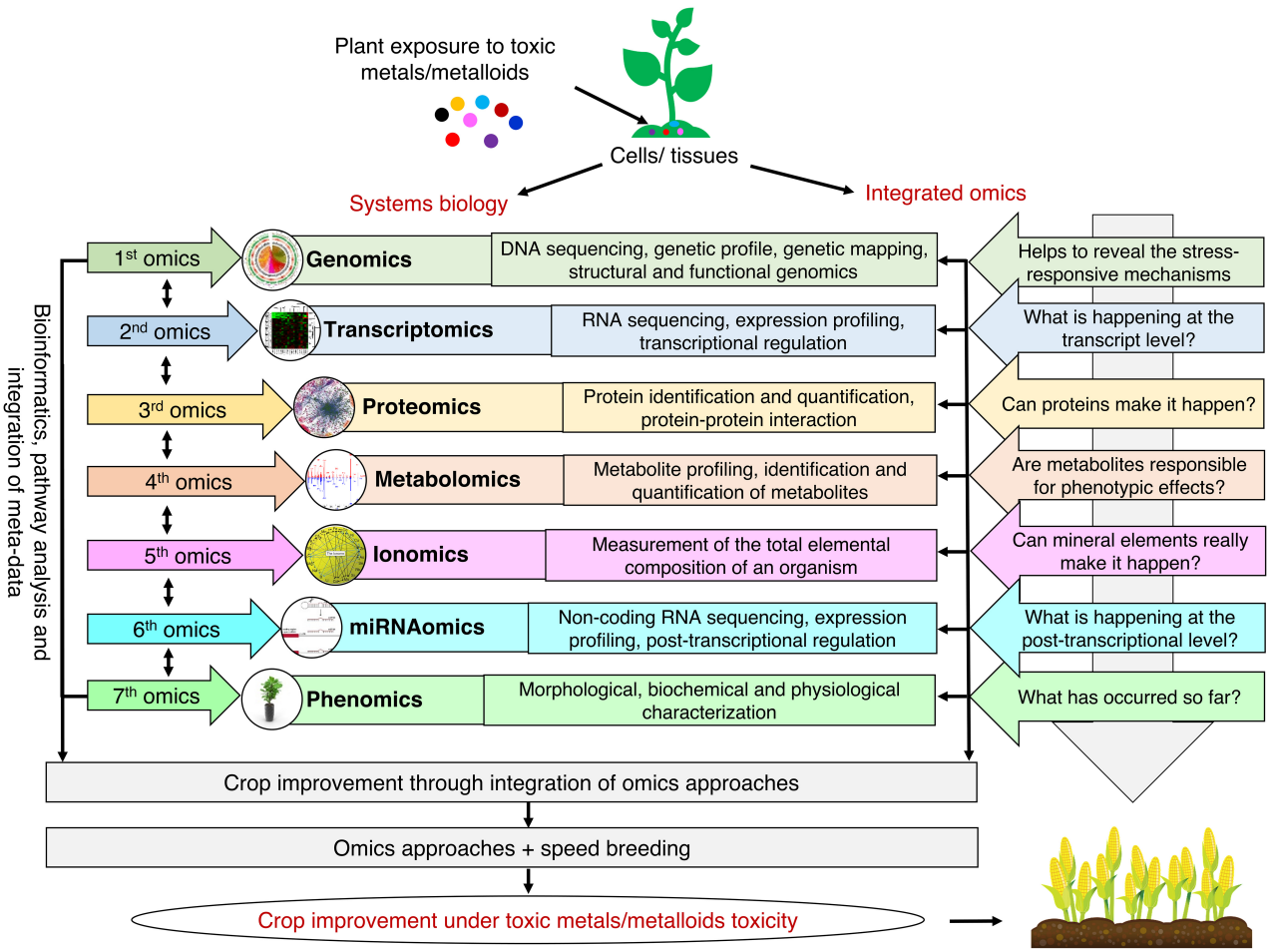


FIGURE 2 | Integrated omics approach for developing toxic metals/metalloids tolerant plants. The use of multi-omics approach can help to reveal stress-responsive mechanisms at the genomic level, understand what is happening at the transcript and proteome level, provide clues about the interaction of metabolites with the phenotype, understand the role of different mineral elements, and unravel phenotypic changes in plants in response to toxic metals/metalloids toxicity. Integrating state-of-the-art omics approaches with speed breeding will help to meet the challenge of feeding a burgeoning human population.

findings and online genomic data sets provide a way forward to open new windows for multi-omics technologies and genome editing tools.

Quantitative Trait Locus Mapping

Various trait mapping methods, such as quantitative trait locus (QTL) mapping, QTL-sequencing (QTL-seq), and RNA-sequencing (RNA-seq), have been established to switch the fine-mapping course as it can distinguish candidate genes within major QTLs quickly. For example, the genetic architecture and regulation of Cd tolerance in barley plants identified two QTLs, one minor-effect and other major-effect QTL, with a phenotypic variance of 47.24 and 38.59%, respectively, associated with Cd tolerance. This analysis also identified 16 candidate genes linked with Cd tolerance (Derakhshani et al., 2020). Marker-trait association study was conducted for As related traits using 704 SNPs. About 9 QTLs were identified with a phenotypic variance ranged from 8.6 to 12.6%, out of which six QTLs (*qAsS2, qAsS5.1, qAsS5.2, qAsS6, qAsS9.1,* and *qAsS9.2*) for As content in shoots were mapped on chromosome 2, 5, 6, and 9, two QTLs in roots (*qAsR8.1* and *qAsR8.2*) on chromosome 8 and one QTL (*qRChlo1*) for relative Chl content was mapped on chromosome 1. Using these QTL intervals, 25 associated candidate genes were identified, showing transcription regulation for As toxicity-related traits (Murugaiyan et al., 2019). A total of four QTLs (*qAsTSL8, qAsTSL12, qAsTRL8,* and *qAsTRSB8*) for As phytotoxicity tolerance were found on chromosomes 8 and 12 using a composite interval mapping approach. A significantly effective QTL for As phytotoxicity tolerance in root contributing 24.9% phenotypic discrepancies was found on chromosome 8 with apparent pleiotropic effect on root-shoot biomass and shoot length (Syed et al., 2016).

QTL mapping in bread wheat for Al stress response revealed 79 QTLs, out of which 22 were putative, showing a range of phenotypic variance from 4.38 to 12.24%. Identified stable QTLs related to days to heading and grain yield were co-located with those of Al concentration with zero × additive environment interaction (Farokhzadeh et al., 2020b). Two

bi-parental populations were used for QTL identification against Al toxicity in rice accessions. Fourty eight regions with a phenotypic variation of 57% were identified for Al tolerance, out of which four were co-localized with previously reported QTLs and three new regions (*ART1*, *STAR2*, *Nrat1*) on chromosome 1, 9, and 12 found inducing Al sensitive rice mutants. The study revealed that mapping with *Indica/Japonica* background identified QTLs where *indica* parent enhanced Al tolerance in *Japonica* background (Famoso et al., 2011). In another QTL map-based study of rice against Al resistance, a QTL named *Alt12.1*, was identified for Al resistance and ultimately considered *ART1* as a primary candidate gene for this QTL region. The presence of the *ART1* allele in different parental backgrounds has reportedly affected the expression of many genes in rice against Al tolerance (Arbelaez et al., 2017). A recent study in tomato identified 103 QTLs, out of which six QTLs were for fruit and leaf Fe contents while eight QTLs were for yield Fe content (FeUEc). Also, two relevant candidate genes encoding for specific proteins of tomato xylem sap were identified under Fe deficiency, thus affecting fruit yield and quality traits (Asins et al., 2020). Eight QTLs were detected for Al resistance in common bean (*Phaseolus vulgaris*) with a phenotypic variation of 7.6–14.7%. QTLs found were related to traits such as root length (RL), root dry weight (RDW), and shoot dry weight (SDW). This study identified the resistant Al activated transporter candidate gene (Phvul.007G025900) underlying the target QTL (Njobvu et al., 2020). QTL mapping for toxic metals/metalloids stress tolerance in rice identified one QTL related to Cu and Hg, three QTLs for As, and two QTLs for Fe and Zn contents. Candidate genes underlying the target QTLs for Zn (*LOC_Os01g14440, LOC_Os01g18584, LOC_Os01g20160*) and Fe (*LOC_Os04g34600*) were predicted to improve Zn and Fe stress tolerance in rice (Zhu et al., 2020). A total of 40 QTLs for Al stress tolerance were mapped on the A genome in wheat using composite interval mapping (CIM) and mixed composite interval mapping (MCIM) algorithms, which showed significant QTL × environment interactions (Farokhzadeh et al., 2020c). Another study in wheat revealed 58 QTLs associated with Al stress tolerance affecting spikelet-related traits (Farokhzadeh et al., 2020a). A further list of QTLs mapped for toxic metals/metalloids tolerance in different plant species is provided in **Table 1**.

Genome-Wide Association Study

Genome-wide association study (GWAS) is a method utilized in genetics to relate definite genetic variations with certain traits in different individuals. It overcomes many constraints of traditional trait mapping (QTL) by offering advanced resolution, often to the gene level, and using trials from formerly examined populations in which frequently occurring genetic variations can be coupled with a phenotypic difference. For example, a GWA study for low Cd accumulation in rice identified *OsABCB24* gene underlying a novel QTL (*qCd1-3*) (Pan et al., 2020). A recent GWA study in wheat identified five loci (*qSCd−1A*, *qSCd−1D*, *qZn−2B1*, *qZn−2B2*, and *qFe−6D)* associated with Cd stress tolerance (Safdar et al., 2020a). Analysis of a large collection of rapeseed accessions identified four QTLs and underlying candidate genes, including *GSTUs, BCATs, UBP13, TBR,* and *HIPP01,* responsible for Pb tolerance (Zhang et al., 2020a). GWAS investigation on rice grains for Fe and Zn traces have identified novel marker-trait associations with a phenotypic variation of 2.1–53%, which could be helpful to identify candidate genes for improving Fe and Zn tolerance (Bollinedi et al., 2020). Rice crop has also been studied for Fe toxicity using a GWAS approach, and three linkage disequilibrium (LD) blocks

TABLE 1 | Summary of QTL/gene mapping for toxic metals/metalloids tolerance in different plant species.

Metals/metalloids	Plant species	QTLs/genes mapped	Number of lines/accessions used	Chromosome	Key observations	References
Cadmium	*Hordeum vulgare*	One minor and one major	87 DH lines	2H, 6H	One major-effect and one minor-effect QTL along with 16 candidate genes for Cd tolerance were detected.	Derakhshani et al., 2020
Aluminum	*Triticum aestivum*	79	RIL population (167 lines)	1, 4	79 QTLs were identified, some of which were stable and were associated with grain yield traits.	Farokhzadeh et al., 2020b
Aluminum	*Phaseolus vulgaris*	8	RIL population (150 lines)	Pv02, Pv04, Pv06, Pv07, Pv09, Pv1	Eight QTLs identified for Al resistance with a phenotypic variation of 7.6–14.7%. QTLs found were related to root length, root dry weight, and root fresh weight.	Njobvu et al., 2020
Aluminum	*Triticum aestivum*	40	RIL population (167 lines)	1A, 1B, 1D-a, 2A-b, 2A-d, 2B, 2D, 4A, 4B, 6A-a, 6B, 7A, and 7D	Nine out of 40 QTLs were putative detected by CIM method. 20 additive and six pairs of epistatic stable QTLs identified by MCIM method.	Farokhzadeh et al., 2020c
Iron	*Solanum lycopersicum*	14	RIL population (121 lines)	9, 12	Six QTLs identified for fruit and leaf Zn content, while eight QTLs identified for FeUEc. Two putative candidate genes were identified under Fe deficiency.	Asins et al., 2020
Iron, zinc, copper, mercury, and arsenic	*Oryza sativa*	9	RIL population (120 lines)	1, 2	One QTL related to Cu, Hg; three QTLs for As; two QTLs for Fe and Zn contents were identified against metal ion stress.	Zhu et al., 2020

DH, double haploid; RIL, recombinant inbred line; QTL, quantitative trait locus; CIM, composite interval mapping; MCIM, mixed composite interval mapping.

were found to mainly contribute to Fe omission. These LD blocks were detected on chromosomes 1, 2, 3, 4, and 7 for vegetative and generative stages, facilitating tolerance against Fe toxicity (Utami et al., 2020). Integration of approaches like genome-wide association, genome-wide epistasis (GWE), and gene expression proved to be an effective strategy for identifying novel QTLs related to Fe tolerance (69 genomic regions) across 19 chromosomes (Assefa et al., 2020). GWA study in barley for potassium (K) tolerance identified three primary QTLs responsible for K translocation and also identified some candidate genes for improving potassium-use efficiency (Ye et al., 2020).

Furthermore, a GWA study in bread wheat identified 534 significant MTAs for K-related traits, which included 11 stable loci and 16 M-QTLs. This study also identified potential candidate genes involved in critical pathways associated with stress tolerance, nutrient uptake, and sugar metabolism, which possessed the potential to develop K stress tolerant wheat cultivars (Safdar et al., 2020b). Zhao Z. et al. (2018) performed a GWA study and found six SNPs associated with four non-redundant QTLs significantly related to As accumulation. The loci, localized from 25.71 to 25.77 Mb on chromosome 1, co-localized with already reported QTLs (*CAsA1/CAsS1*), and just one candidate gene *GRMZM2G130987* was discovered. The identified gene encodes a protein with P-P-bond hydrolysis-driven protein transmembrane transporter activity and contributes to As ion transport. Other SNPs located on chromosome 2 were found within the *BAsA2/XAsA2* QTL. Five candidate genes are present in this QTL, and the *GRMZM2G125495* candidate gene encodes a protein with extracellular glutamate-gated ion channel activity. This study provides a solid reason to further study the gene's function in As accumulation (Zhao Z. et al., 2018). Liu X. et al. (2019) performed a GWA study against toxic metals in rice grain and found 22, 17, and 21 QTLs for grain associated with As, Cd, and Pb toxicity, respectively. The authors examined the candidate gene in *qGAS1*, a QTL for grain arsenic, with the best *P*-value found for the whole population. Toxin extrusion and transport protein of the multidrug might be the candidate gene for this QTL (Liu X. et al., 2019). Examples of GWA studies conducted in different crop plants for identifying toxic metals/metalloids tolerance loci have been described in **Table 2**.

CRISPR/Cas9 System

Clustered regularly interspaced short palindromic repeats (CRISPR)/CRISPR-associated protein 9 (Cas9) system is a valuable editing tool with high efficiency, specificity, and possessing a wide range of applications (Zafar et al., 2020). Targeted knock-in/out, deletion, insertion, and substitution mutations generated by CRISPR/Cas9 system have explored regulatory functions of genes and their impact on other biochemical processes and have helped to improve many crops by increasing their scavenging capacity under toxic metals/metalloids toxicity (**Table 3**).

Knock-out of *OsNRAMP1* gene responsible for the uptake of metals like Cd, Fe, As, and Mn, significantly reduced the uptake of Cd and Mg and their storage in rice shoots and grains (Chang et al., 2020). Furthermore, *OsIRO3* gene knock-out using the CRISPR/Cas9 approach highlighted the function of this gene in the regulation of Fe homeostasis. *OsIRO3* gene mutants accumulated ROS, and their growth and development were affected under Fe deficiency (Wang et al., 2020c). Single, double, and triple mutants developed against Cd toxicity in tomato by CRISPR/Cas9 system were found to protect chloroplasts by mutating members of class II glutaredoxin (GRXs) from Cd toxicity (Kakeshpour, 2020). Knock-out mutant lines generated by CRISPR/Cas9 system in rice targeting *OsZIP9* gene against Zn toxicity showed a substantial reduction in growth, which revealed Zn as an essential element for growth (Yang M. et al., 2020). In *Arabidopsis, OZS3* gene knock-out reduced the growth of roots and elusive development of plants, further damaged embryos, and caused early flowering (Weber et al., 2020). Cd accumulation was studied in rice by knocking out a segment of the *OsABCG3* gene via CRISPR/Cas9 technology. Knock-out mutants accumulated Cd in roots cells and routed Cd contents out of the cell sap to detoxify its effect, thus generating tolerance against Cd (Fu et al., 2019). In *Arabidopsis*, the variant *GSNOR* has been observed to generate tolerance and promote root growth against Fe toxicity. The mutant lines produced using the CRISPR/Cas9 vector were also found to be highly sensitive toward high Fe content, which affected the whole seedlings and produced leaves that were smaller than the wild type (Li et al., 2019). Loss of *AtPDF2.6* gene has been reported to reduce tolerance against Cd along with its significant accumulation in root cells when exposed to Cd stress (Luo et al., 2019). Genome editing using the CRISPR/Cas system has a promising future for sustainable agricultural production to feed the world's growing population. In the near future, more genome editing works need to be performed under the toxicity of different metals/metalloids like As, Pb, Hg, Ni, Cr, etc., in different crop plants to explore the stress resistance mechanisms.

Transcriptomics

The term transcriptomics refers to a set of techniques that are used to study the RNA transcripts in an organism. Several transcriptomic techniques are widely used to measure the abundance of the transcripts of interest (Lowe et al., 2017; Mehmood et al., 2021; Raza et al., 2021c). Studies have shown that stress-induced changes in gene expression may lead to the synthesis of novel proteins, stress mediating metabolic compounds, or encode transcription factors (TFs), which help to regulate the stress-responsive genes (**Table 4**).

Transcriptomic techniques represent an effective method to enhance toxic metals/metalloids tolerance in plants by better understanding signaling mechanisms and gene ontology (GO). The transcriptomic profile screening of two contrasting varieties of rice (Fe susceptible "Hatcha" and Fe tolerant "Lachit") revealed 22 out of 35 metal homeostasis genes in the tolerant variety. Furthermore, leaf transcriptome showed a more pronounced response in Hatcha, leading to a high degree of differential gene regulation (Kar et al., 2020). High and low grain Zn and Fe containing wheat genotypes revealed enrichment of GO terms such as Zn and Fe binding, Chl synthesis, ATP-synthase coupled transport, and oxidoreductase activity (Mishra V. K. et al., 2019).

TABLE 2 | Summary of key GWA studies for toxic metals/metalloids toxicity in different crop plants.

Metals/ metalloids	Plant species	Platform	No. of QTLs	No. of lines/ accessions used	Chromosome	SNPs	Key observations	References
Cadmium	*Brassica napus*	Illumina Brassica SNP60 Bead chip	25	419	A3, A5, A9, C3, C5, C8	98	QTLs identified for root, shoot, and for Cd translocation. Homologs of key *Arabidopsis* genes identified that can be further used for Cd tolerance in other plants.	Chen et al., 2018
Cadmium	*Oryza sativa*	SLAF-seq, Illumina-HiSeq 2500	35	338	1, 2, 3, 4, 5, 6, 7, 8, 9, 11, 12	203	Identified 35 significant QTLs for low Cd accumulation, including a novel QTL, *qCd1-3.* Differential expression of *OsABCB24*, a candidate gene underlying *qCd1-3.*	Pan et al., 2020
Cadmium, iron, and zinc	*Triticum aestivum*	Illumina iSelect 90K	5	120	1A, 1D, 2B, 6D	179	Five novel loci detected to be associated with Cd toxicity.	Safdar et al., 2020a
Copper	*Triticum aestivum*	Wheat 660K SNP assay	4	243	1D, 6A, 6B, 7D	489	Four significant QTLs with a phenotypic variation of 4.71–8.66% regulating GCC in wheat were observed.	Zhao et al., 2020
Lead	*Brassica napus*	60 K Brassica Infinium SNP array	4	472	A9, C3, C4	9	Identified four QTLs and nine candidate genes associated with Pb tolerance.	Zhang et al., 2020a
Iron and zinc	*Oryza sativa*	50 K SNP chip	29	192	1, 2, 3, 4, 6, 7, 8, 9, 10	31,132	Total of 29 marker-trait associations (MTAs) were identified, showing a phenotypic variation of up to 53% for traits controlling Fe and Zn contents.	Bollinedi et al., 2020
Iron	*Oryza sativa*	384 SNP chip	8	288	1, 2, 3, 4, 7	384	Three LD blocks containing QTLs for Fe toxicity tolerance were found that can be used for rice breeding programs for specific land types.	Utami et al., 2020
Iron	*Glycine max*	Illumina Infinium SoySNP50K BeadChip	69	460	3, 5, 16	36,000	Integration of approaches like genome-wide association (GWA), genome-wide epistasis (GWE), and gene expression enabled identification of novel Fe tolerance QTLs, with a significant QTL found on chromosome Gm03.	Assefa et al., 2020
Potassium	*Hordeum vulgare*	Diversity Array Technology (DArT)	3	179	1H, 6H	13,634	Identified three significant QTLs associated with K uptake and translocation.	Ye et al., 2020
Potassium	*Triticum aestivum*	90 K Infinium SNP array	11	150	1A, 1B, 1D, 2A, 3A, 3B-I, 3B-II, 4A-I, 4A-II, 4B, 5B-I, 5B-II, 6A, 6B, 7A, and 7B	20,853	Total of 534 significant MTAs were identified for potassium related traits, which included 11 stable loci and 16 M-QTLs. Identified potential candidate genes involved in crucial pathways related to stress tolerance, nutrient uptake, and sugar metabolism.	Safdar et al., 2020b
Aluminum and iron	*Oryza sativa*	44 K SNP array	6	373	1, 2, 9, 12	36,901	Identified forty eight regions associated with Al tolerance. Six Al tolerant QTL were detected for root growth, out of which three (*ART1*, *STAR2*, *Nrat1*) were used to induce Al sensitive rice mutant. Promoted the selectively introgressing alleles for trait enhancement	Famoso et al., 2011

The molecular insights into transcriptome expression profiling of chickpea under toxic metals/metalloids [As(III), Cr(III), and Cd(II)] showed induction of crucial metabolic pathways under stressed conditions. Moreover, nine genes that played a major role in regulating these metabolic pathways were found to be differentially expressed in response to stress conditions (Yadav et al., 2019). Recently, Di et al. (2021) studied the stress-responsive genes of upland rice exposed to As(III) and As(V). Under metals toxicity, many genes were down-regulated compared to those that were up-regulated. Arsenic treatment resulted in unique transcriptome profiles changes, and a novel set of typical response genes were found. The antioxidant enzyme activities were consistent with the antioxidant enzyme-related genes expression, and several transports and defense

TABLE 3 | Summary of genome editing studies for toxic metals/metalloids tolerance in different plant species.

Metals/ metalloids	Plant species	Gene target	Modification	Key observations	References
Iron	*Arabidopsis thaliana*	*GSNOR*	Knock-out	Mutants were found to be sensitive to high Fe toxicity, showing this gene to generate tolerance in roots against Fe stress.	Li et al., 2019
Cadmium	*Oryza sativa*	*OsABCG36*	Knock-out	Targeted gene could transport Cd out of the cell to detoxify its effect. Mutants were tolerant to Cd accumulation in roots, but not in shoots.	Fu et al., 2019
Cadmium	*Arabidopsis thaliana*	*AtPDF2.6*	Knock-out	Loss of *AtPDF2.6* gene reduced tolerance against Cd and was significantly accumulated when exposed to Cd stress. Mainly expressed in root tissues.	Luo et al., 2019
Cadmium and manganese	*Oryza sativa*	*OsNRAMP1*	Knock-out	Reduced uptake and transportation of Mg, Fe, Cd, and As.	Chang et al., 2020
Cadmium	*Solanum lycopersicum*	*class II glutaredoxin*	Knock-out	Knockout mutation on members of class II glutaredoxin (GRXs) against Cd toxicity protected chloroplasts of cells.	Kakeshpour, 2020
Zinc and copper	*Oryza sativa*	*OsZIP9*	Knock-out	Higher concentration of Zn improved the growth of plants.	Yang M. et al., 2020
Iron and zinc	*Oryza sativa*	*OsIRO3*	Knock-out	Accumulation of ROS. Maintenance of Fe homeostasis by tolerating Fe deficiency or toxicity.	Wang et al., 2020c
Zinc	*Arabidopsis thaliana*	*OZS3*	Knock-out	Complete loss of the *OZS3* gene resulted in reduced growth, early flowering and long petioles.	Weber et al., 2020

enzyme-related pathways were identified (Di et al., 2021). Shukla T. et al. (2018) studied the response of *Arabidopsis* accessions under As(V) toxicity. Differential transcriptome modulation was found in sensitive "Slavi-1" and tolerant "Col-0" accessions. The results showed that As-induced genes are linked with stress response and detoxification pathways (Shukla T. et al., 2018).

According to Komarkova et al. (2020), Cd resulted in alteration of poplar's gene transcripts, which not only regulated the plant defense mechanism through differential gene expression but also led to the production of phytohormones. Additionally, long-term exposure to stress was found to reduce the Cd toxicity in plants (Komarkova et al., 2020). Another transcriptomic study carried out on Chinese flowering cabbage (*Brassica parachinensis*) showed that Cd toxicity was mediated through some important tolerance-inducing genes, including *HMA3, HMA4,* and *Nramp1* (Wang et al., 2017). Furthermore, the genetic insights in two contrasting wheat genotypes (low Cd accumulating L17 and high Cd accumulating H17) revealed 1,269 genes to be differentially expressed. These genes showed heme-binding as the most active GO network, followed by metal binding. In contrast, phenylpropanoid biosynthesis and glutathione metabolism were found to be the major pathways active under Cd stress (Zhou et al., 2019). The analysis of the transcriptional data set of *Verbena bonariensis* under Cd stress revealed ROS scavenging system, photosynthesis, transpiration mechanism, chelating reaction, and production of secondary metabolites associated with DEGs as analyzed through GO and KEGG pathways (Wang et al., 2019).

The transcriptional analysis of the creeping bentgrass identified four transcription factors (bZIP, WRKY, MYB, and ERF) linked with Cd stress (Yuan et al., 2018). In a Cd-hyperaccumulator, *Siegesbeckia orientalis*, the comparative transcriptome analysis of roots with and without Cd treatment revealed a high number of DEGs, indicating the involvement of multiple biological pathways to cope up with Cd stress at the molecular level (Xu X. et al., 2020). Among such functional pathways, the ubiquitin-proteasome system (UPS) in plants has been reported to act through sequential actions of a cascade of enzymes. A comparative transcriptional study on a Cd hyperaccumulator *Viola baoshanensis* and its non-tolerant counterpart *Viola inconspicua* showed overexpression of genes involved in the UPS pathway under Cd exposure in *V. baoshanensis,* thereby supporting the hypothesis that high transcript levels of the genes involved in the UPS pathway can enhance tolerance to Cd toxicity (Shu et al., 2019).

Another study on the transcriptomic response of alfalfa plants, while assessing its phytoremediation potential for Ni, showed high expression of peroxiredoxin-1C, glutathione-S-transferase (GST), and phytochelatins (PCs). These genes were linked to an antioxidative response, prevention of cell damage, and Ni detoxification through its binding with PCs forming Ni-PC complexes, respectively (Helaoui et al., 2020). Kök et al. (2020) evaluated B accumulator *Puccinellia distans* for Se tolerance. Here, RNA-seq data showed induction of Se assimilation and stress response genes under stress conditions, which in turn altered the expression of gene transcripts involved in developmental (2.2%), transcriptional and translational (7.3%) processes, biotic (2.2%), and abiotic (17.7%) stress responses in *P. distans.* It further restricted the movement of Se by trapping it in the cell wall through the up-regulation of lignin production-related transcripts (Kök et al., 2020). Transcriptomic analysis of the Co stress response in *Salix babylonica* showed 2,002 DEGs, out of which 1,165 were identified in root and 837 in shoots. In addition, 107 transcription factors were identified from the DEGs, and most of them were reported to belong to the NAC and ERC families (Wang et al., 2020f). Another technique, translating ribosome affinity purification (TRAP) has been used to study transcriptional program in *Arabidopsis* against Fe stress. Using this technique, the excess Fe was sensed in *opt3* leaves. This study highlighted the first tissue, vasculature, in comparison with roots and leaves to respond against Fe deprivation and supply, thus maintaining Fe homeostasis through xylem and phloem. Moreover, a total of 1,143 DEGs were identified with more than

TABLE 4 | Summary of key transcriptomics, proteomics, metabolomics, and ionomics studies under toxic metals/metalloids toxicity in different plant species.

Transcriptomics

Plant species	Stress conditions	Target tissues	Approach	Functional annotation methods	Key observations	References
Phytolacca americana	50 mg kg^{-1} $CdCl_2$; 15 days	Roots, leaves, and stem	RNA-Seq	NR, SWISS-PROT, GO, KEGG	1,515 differentially expressed genes (DEGs) were identified. 12 DEGs validated using qRT-PCR. Genes related to toxic metal tolerance identified including nicotianamine synthases (8), ABC transporter (3), expansins (11), metallothionein (3), ZRT/IRT protein (4), and aquaporins (4)	Chen et al., 2017
Brassica juncea	25 μM $CdSO_4$; 24 h	Roots	Microarray	Gene chip Arabidopsis ATH1 genome array	38 DEGs identified, and six DEGs validated by qRT-PCR. The DEGs were mainly involved in Cd metabolism.	Dalyan et al., 2017
Oryza sativa	100 μML^{-1} $AlCl_3$; 24 h	Root tips	RNA-seq	KEGG, WEGO 2.0	14,550 DEGs identified, of which most were related to Al tolerance. Total of 92 genes were reported to be linked with different pathways that mediated Al-induced inhibition in plants.	Zhang et al., 2019c
Verbena bonariensis	100 mg kg^{-1} $CdCl_2$; 20 days	Root	RNA-seq	GO and KEGG	23,424 DEGs identified. 10 DEGs validated by qRT-PCR. DEGs encoding lignin synthase, chalcone synthase, and anthocyanidin synthase identified under Cd stress.	Wang et al., 2019
Triticum aestivum	100 μM $CdCl_2$; 24 h	Roots	RNA-seq	GO-GO network and pathway network analysis	1,269 and 399 DEGs identified in low and high Cd accumulation genotypes. Six genes validated using qRT-PCR. DEGs related to Cd uptake and transport include antioxidant defense, ATP binding, plant hormone signal transduction, and phenylpropanoid biosynthesis.	Zhou et al., 2019
Vicia faba	5, 10, 15, 20, 25 μM U; 72 h	Roots	RNA-seq	NR, KOG, GO, Swiss-Prot, eggNOG, KEGG, Pfam	4,974 DEGs identified. The uranium induction significantly up- and down-regulated 1,654 and 3,320 genes, respectively, involved in the regulation of cell metabolism and other processes, and processing of environmental and genetic information.	Lai et al., 2020
Fagopyrum tataricum	2,000, 10,000 bmgkg^{-1} $Pb(NO_3)_2$; 72 h	Leaves	RNA-seq	GO, KEGG	12,595 DEGs identified. Majority of DEGs were associated with phenylpropanoid synthesis pathway and up-regulated the expression of MAPKs and GSH metabolic genes along with the regulation of plant protecting metabolites and hormones.	Wang et al., 2020d
Medicago sativa	50, 150, 250, 500 mg kg^{-1} $NiCl_2$; 60 days	Roots and shoots	RNA-seq	Fern Base, NCBI	Highly expressed prx1C, GST, and PC genes in roots and shoots actively mediated the negative impact of Ni on plant growth.	Helaoui et al., 2020
Oryza sativa	15 mM $FeSO_4$; 2 days	Roots and leaves	RNA-seq	Top GO, Ensembl Plants, TAIR	1,147 and 1,038 DEGs identified under control and Fe treatment. The Fe stress affected "Hacha" genotype more abundantly by causing alterations in roots' gene expression pattern. Total of 1,248 and 1,161 DEGs were less abundant in "Lachit" roots under control and Fe stress conditions.	Kar et al., 2020
Dendrobium officinale	2, 5, 9, 14 mg L^{-1} $CdSO_4$; 30 days	Roots	RNA-seq	GO and KEGG	2,469 DEGs identified. DEGs helped identify complex metabolic pathways and regulated the transcription factors involved in regulating Cd stress.	Jiang et al., 2020

Proteomics

Plant species	Stress conditions	Target tissue	Extraction protocol	Analytical approach	Key observations	References
Artemisia annua	100 μM As + 100 μM Se; 3 days	Roots, shoots	TCA	2D- PAGE, MALDI-TOF-MS	20 differentially abundant proteins (DAPs) identified. The DAPs were involved in energy metabolism, secondary metabolism, photosynthesis, transcriptional regulators, transport proteins, and lipid metabolism.	Kumari and Pandey-Rai, 2018
Capsicum annuum	0 or 100 ppm Na_2SeO_4; 24 h	Shoots	EDTA	LC-MS/MS	4,693 DAPs identified. Identified DAPs were associated with protein processing, post-translational modification, chaperones, protein turnover, and metabolic process.	Zhang et al., 2019a

(Continued)

TABLE 4 | (Contiuned)

Proteomics

Plant species	Stress conditions	Target tissue	Extraction protocol	Analytical approach	Key observations	References
Eucalyptus camaldulensis	30, 50, 100 μM, $CuSO_4 \cdot 5H_2O$; 6 weeks	Leaves, roots	TCA/acetone	MS	26 DAPs were identified. 11 DEPs were up-regulated, and 15 DAPs were down-regulated. Identified DEPs were involved in antioxidant enzymes, photosynthesis, metabolism, transcription, and translation.	Alotaibi et al., 2019
Arachis hypogaea	2 μM $CdCl_2$; 7 days	Roots	TCA/Acetone	LC-ESI-MS/MS, RT-PCR	30 DAPs were found to be linked with heavy metal transport, while 86 DAPs were found to be associated with cell wall modification.	Yu R. et al., 2019
Stylosanthes guianensis	5 or 400 μM $MnSO_4$; 10 days	Shoots, roots	Tris-HCl	LC-MS/MS	356 DAPs identified. 172 DAPs were strongly induced, while 96 DAPs were completely suppressed. Identified DAPs were involved in carbon fixation, defense response, signaling, metabolism, photosynthesis, and cell wall modulation.	Liu P. et al., 2019
Oryza sativa	25 μM AsIII, $NaAsO_2$ + 25 μM SeIV, Na_2SeO; 15 days	Roots, shoots	Acetone	MALDI-TOF/TOF, qRT-PCR	Significantly enhanced expression of 14,303 proteins for As + Se exposure, compared to As alone. In As stress, Se application effectively mitigated As toxicity, improving plant growth via regulation of 14-3-3 proteins. FBPase, AtpB, GLN1, and GLN2 proteins were found to be involved in defense, photosynthesis, and energy metabolism upon Se exposure.	Chauhan et al., 2020
Setaria italica	120 g hm^{-2} Na_2SeO_3; 72 h	Grains	HEPES-based buffer	LC-MS/MS	123 DAPs identified. The DAPs were mainly involved in amino acid and carbohydrate metabolism.	Liang et al., 2020
Nicotiana tabacum	5.36 mg kg^{-1} Zn^{+2}; 10 days	Leaves	TCA/Acetone	LC-MS/MS	Zn stress resulted in the down-regulation of 8 proteins. Chl synthesis was not inhibited significantly, and only a few proteins involved in the electron transport chain showed down-regulation. Zn-stress did not significantly inhibit photosynthetic function in tobacco leaves.	Zhang et al., 2020b
Allium cepa	5–15 μM $Pb(NO_3)_2$; 6, 12, and 24 h	Roots	Tris-HCl	2-DE, AutoFlex TOF/TOF II-MS	17 DAPs identified. Lowered expression of *Anx D1*, *SHMTI*, and *COMT2* resulted in decreased defensive response, respiration, and the response of other functions, respectively. Improved expression of *NDPK*, *PR1*, and *CHI1* resulted in increased transcription, translation, and better pathogen invasion, respectively.	Lyu et al., 2020
Cichorium intybus	100, 200, and 300 μM Pb; 46 days	Leaves	Tris-HCl	SDS-PAGE	81 DAPs identified. Total of 16 proteins were up-regulated and 13 were down-regulated. Identified proteins were associated with plant-stress response and adaptation toward metal toxicity.	Malik and Pirzadah, 2020

Metabolomics

Plant species	Stress conditions	Target tissue	Analytical platform	Data analysis	Key observations	References
Cucumis sativus	10, 100, and 500 mg L^{-1} CuSO4; 7 days	Leaves	GC-TOF-MS, LC-MS/MS	PLS-DA	Total of 149 primary and 79 secondary metabolites were quantified. 1.4–2.4-folds of intermediates involved in TCA were found to be down-regulated upsetting carbohydrate metabolism.	Zhao L. et al., 2018
Glycine max	0.1–100 mg L^{-1} Mo; 48 h	Leaves, roots	UPLC, LC-MS	PCA, OPLS-DA, KEGG	Identified 42 and 19 significantly different metabolites (SDMs) in roots and leaves, respectively. Organic acids, gluconic acid, D-glucarate, and citric acid were amplified by 107. 63-, 4.42- and 2.87-folds after Mo exposure. Organic compounds such as 2-oxoarginine, L-nicotine, gluconic acid, D-glucarate, and citric acid played a significant role in chelating Mo and decreasing its toxicity.	Xu et al., 2018
Oryza sativa	400 ppm $FeSO_4.7H_2O$; 10 days	Roots, shoots	GC-MS	PCA, PLS-DA	Levels of elaidic acid increased, while linoleic- and linolenic acid decreased. In shoot and root, alteration of the fatty acid composition suggested metabolites alteration.	Turhadi et al., 2019

(Continued)

TABLE 4 | (Contiuned)

Metabolomics

Plant species	Stress conditions	Target tissue	Analytical platform	Data analysis	Key observations	References
Glycine max	25 μM Fe (III)−EDTA; 10 days	Roots, leaves	GC-MS	OPLS-DA	N assimilation was inhibited, which reduced proteins in roots and nodules. Sugars increased or maintained at a constant level in different tissues under Fe deficiency, which probably relates to oxidative stress, cell wall damage, and feedback regulation. Increased levels of ascorbate, nicotinate, raffinose, galactinol, and proline in different tissues possibly helped resist the oxidative stress induced by Fe deficiency.	Chu et al., 2019
Helianthus annuus	1, 5, and 25 mg L^{-1} Cr(VI); 7 days	Roots	capHPLC-ESI-QTOF-MS	PLS	70% of metabolites involved in LA metabolic pathway are affected by Cr(VI) stress. Detection of four EKODE isomers not included in LA metabolism and found only in the exposed roots. Oxidation of LA to HpODE isomers upon incubation with Cr(VI).	Ibarra et al., 2019
Brassica napus	100 μM $CdCl_2.2.5H_2O$; 8 days	Leaves	UPLC/MS	PCA, PLS-DA, KEGG	644 SDMs found in sensitive genotype ZD622, and 487 SDMs in tolerant genotype CB671. Most SDMs were involved in Cd-mediated stress tolerance pathways.	Mwamba et al., 2020
Elodea nuttallii	280 μg L^{-1} Cd as $Cd(NO_3)_2$; 24 h	Shoots	GC-MS, LC analysis	PCA, MetaboAnalyst KEGG	Cd stress caused significant variations in aminoacyl-tRNA biosynthesis and branched-chain amino acid pathways. In the shoot, Cd induces a concentration of 11 amino acids, 2 sugars, adonitol, and pipecolic acid in the cytosol, and Cd induces a concentration of glycine, ammonium, hydroxy.	Cosio and Renault, 2020
Cucumis melo L.	300 μmol L^{-1} $CuSO_4$; 3 days	Roots	UPLC/MS	KEGG	70 DEGs identified; 42-downregulated and 28-upregulated. 318 SDMs identified, 150-downregulated and 168-upregulated. Identified SDMs and DEGs were involved in JA biosynthesis; comprising lipoxygenase related genes, and lecithin and linoleic acid metabolites.	Hu et al., 2020
Cucumis sativus L.	3 μM Se (Na_2SeO_3)–50 μM Cd ($CdCl_2$); 7 days	Leaves, roots	GC-MS	OPLS-DA, PCA, HCA, KEGG	Intermediates of TCA, glycolysis, and some amino acids were upregulated. Differentially regulated metabolites have a significant role in developing Se-mediated Cd tolerance.	Sun et al., 2020
Vicia faba	25 μM U [$UO_2(NO_3)_2{\cdot}6H_2O$, 238U]; 72 h	Roots	GC-MS	KEGG	53 SDMs identified to be related to carbohydrate metabolism; including 12-downregulated and 13-upregulated metabolites. U led to the imbalance of the expression of related metabolites in the energy metabolism pathway of plant cells.	Zhang et al., 2020d
Ipomoea batatas L.	1.68–5.16 mg kg^{-1} U, 0.78–2.02 mg kg^{-1} Cd; 150 days	Roots	UPLC-MS	PCA, OPLS-DA, KEGG	634 SDMs identified in U + Cd; including 428 up-regulated and 214 down-regulated metabolites. Induced expression of plant hormones and cyclic nucleotides in cells. Regulated primary and secondary root-metabolism to induce U and Cd toxicity resistance.	Zhang-Xuan et al., 2020

Ionomics

Plant species	Approach	Element	Tissue	Key observations	References
Zea mays	ICP−OES	Cd, Mo, Ca, Cu, Fe, K, Mg, Mn, P, S, and Zn	Shoot	Significant genotypic variation found among all minerals. *ZmHMA2/3* and *ZmMOT1* were found to be responsible for Cd and Mo contents in shoot.	Stich et al., 2020
Brassica napus	ICP−OES	B, Ca, Cu, Fe, K, Mg, Mn, Na, P, S, and Zn	Shoot and root	Total of 133 and 123 QTLs identified for the shoot and root ionome under OP and LP. Six QTL clusters were identified to be influencing mineral elements.	Wang et al., 2020e
Oryza sativa	Ex-3600 ED-XRF spectrometer	F, Co, Si, Ca, K, S, Zn, Cu, Ni, Fe, Mn, V, and Se	Seedling	Reduced fluoride toxicity and stimulated plant growth.	Banerjee et al., 2020
Solanum tuberosum	ICP-AES	Co, Zn, Cd, and Pb	Tubers	Reduced contamination of heavy metals in potato tubers	Muntean et al., 2019
Oryza sativa	ICP-MS	As, B, Ca, Cd, Cu, K, Mg, Mn, Mo, Na, Ni, P, Zn, and Ti	Straw and grain	Identified 70 novel ionomic QTLs and *OsMOT1* as a causative gene underlying a QTL controlling Mo tolerance.	Wang et al., 2020a

2-fold change, including 539 DEGs in roots and 604 DEGs in leaves, thus an up-regulation of iron deficiency responsive genes (Khan et al., 2018).

Laf vasculature from *Arabidopsis* leaves have also been used to execute single-cell RNA analysis and identified 19 clusters of all cell types, including mesophyll, guard cells, vascular cells, hydathodes, and some metabolic pathways to recognize their roles. The results identified potential roles of these clusters in sugar transport, amino acid transport, hormone biosynthesis, and defense-related responses (Kim et al., 2021). Single-cell transcriptome analysis has not been studied so far. Yet, there is a dire need to implement single-cell transcriptome analysis against the toxic metals/metalloids toxicity and may provide key resources and molecular insights to develop new strategies regulating the flux of ions, signals, and metabolites. Taken together, the analysis of transcriptomics data obtained through various studies suggests that it not only brings useful insights to functional genomics but also has a great potential to support molecular breeding, genetic engineering, phytoremediation, and metal complexation pathways. Meanwhile, there is a need to make smart use of comprehensive tools to integrate transcriptomics with other omics data and get useful insights into unidentified linkages. Summary of some experiments performed using transcriptomic approaches under toxic metals/metalloids toxicity is discussed in **Table 4**.

Proteomics

Proteomics comprehensively covers the encoded proteins in living organisms at a particular instance and plays a vital role in understanding all cellular routes at the molecular level (Mehmood et al., 2021). Recently, proteomics has appeared as a vital tool to convey data on the survival of plants and adaptation toward toxic metals/metalloids toxicity in several plants (**Table 4**). From a methodological viewpoint, proteomics technology has progressed quite fast from the first generation (i.e., two-dimensional electrophoresis-mass spectrometry (2DE-MS); to second-generation (i.e., isobaric/isotopic tagging); to third-generation (i.e., shotgun and gel/label-free approaches); and lastly to fourth generation (i.e., mass western, targeted, SRM/MRM approaches) (Jorrin-Novo et al., 2019). Innovative proteomic systems provide a comprehensive understanding of metal-responsive proteins for plant stress tolerance (**Table 4**).

For instance, plant vascular systems like xylem sap transport minerals, water, and toxic metals (Cd) from roots to shoots. Proteomic variations in xylem sap significantly detoxify Cd in plants (Luo and Zhang, 2019). *Brassica* seedlings were treated with Cd (0 and 10 μM) for 3 days, and the collected xylem sap was subjected to lyophilization. Notably, 672 proteins from the xylem sap of Cd-treated rapeseed plants were identified through proteomic analysis (LC-MS/MS, shotgun). Most affected metabolic pathways between these proteins were found to be linked with stress/oxidoreductases, protein/lipid metabolism, and cell wall modification. Protein-like defensins, *BnPDFL,* found in xylem sap behaved as a Cd-chelating agent, confirming its positive role in regulating Cd tolerance (Luo and Zhang, 2019). In another study, the iTRAQ approach illustrated dynamic changes in root proteome in maize seedlings (Wen et al., 2019). Plant's roots were exposed to 200 mg L^{-1} $CdCl_2$, and both root and shoot growth were found to be severely inhibited in the first 72 h. The different numbers of differentially abundant proteins (DAPs; 733, 307, 499, and 576) were isolated after 12, 24, 48, and 72 h, respectively. These DAPs displayed numerous functions like energy and carbohydrate metabolism, ribosomal synthesis, cellular metabolism, ROS homeostasis, and cell wall organization. Amongst these GSTs, *GRMZM2G308687* showed extra abundance after 12, 48, and 48 h Cd-treatment. GST protein was found to be mainly tangled in PCs generation for Cd tolerance (Wen et al., 2019). Label-free proteomic analysis of Cd treated *Iris lactea* revealed 163 and 196 DAPs expressed in shoots and roots, respectively. Bioinformatic studies revealed that these DAPs, which are responsive to Cd, were majorly involved in redox reactions, signal transduction, ion transport, and other biochemical mechanisms. They were not only involved in lignin and amino acid biosynthesis pathways but also assisted GSH and glycerolipid metabolism. From *I. lactea*, a mannose-specific lectin (Cd-induced) was found to increase Cd-sensitivity and enhance Cd-accumulation in yeast (Liu et al., 2020).

Chauhan et al. (2020) performed a transcriptomic and proteomic analysis in rice to explore the molecular cross-talk involving Se-mediated tolerance of As-toxicity. Se supplementation restored the structural deformities caused by As, which comprised the cell wall and membrane disintegration. As-transporter gene expression viz., *ABCG5, NIP1;1, NIP2;1, TIP2;2, NRAMP1, NRAMP5*, and sulfate transporters *SULTR3;1, SULTR3;6* were found to be high in As + Se treated plants when compared to As alone. This not only resulted in low As concentration but also reduced the toxicity. During As + Se exposure, the GST, GRX, and PRX up-regulation also confirmed that elevation of As resulted in oxidative stress (Chauhan et al., 2020). Proteomic analysis (LC-MS/MS) of Se-treated pepper seedlings revealed up-regulation of 172 proteins, while 28 proteins were found to be down-regulated. Identified DAPs were mainly associated with metabolic processes, protein turnover, protein processing, post-translational modifications, and chaperones. Furthermore, various heat shock proteins (HSPs) were also identified as DAPs, which helped to cope with metal toxicity (Zhang et al., 2019a). Zeng et al. (2019) performed quantitative proteomics (iTRAQ) to study differential protein expression in Se-enriched and non-Se-enriched rice seedlings. Overall, 3235 proteins were detected, of which 3,161 proteins were quantified from 401 DAPs. Interestingly, 77 targeted significant DAPs were screened further and classified into 10 sets comprising of actin, synthetases, hydrolases, tubulin, ligases, lyases, isomerases, heat shock proteins, oxidoreductases, and transferases. These findings indicated that active oxygen metabolism, anti-stress, anti-oxidation, amino acid, and carbohydrate metabolism of Se-enriched rice seedlings was higher as compared to non-Se-enriched plants (Zeng et al., 2019).

In another study, proteomic analysis of Cu-treated young seedlings of *Eucalyptus camaldulensis* revealed 26 targets taking part in protein expression. Elevated Cu levels up-regulated the expression of 11 proteins and down-regulated

expression of 15 proteins. Identified proteins were associated with antioxidant enzymes, photosynthesis, metabolism, transcription, and translation (Alotaibi et al., 2019). Furthermore, Ceballos-Laita et al. (2018) used two different proteomic approaches, i.e., shotgun and 2-DE, to study the effects of Mn toxicity on tomato root proteome. The shotgun approach identified 367 reliable proteins, while 2-DE yielded 340 consistent spots. A total of 54 proteins were detected using a 2-DE approach, which was found to be altered in relative abundance, while shotgun found variations in 118 proteins. Only 7% of DAPs were found to be common in both methods. The most affected metabolic pathways were signaling, protein metabolism, and oxidoreductases. Further findings suggested that Mn-toxicity mediated protein-turnover impaired the roots for energy production, leading to changes in oxidative phosphorylation, glycolysis, TCA, and pyruvate metabolism. Root proteome indicated a slowdown of metabolic activities, including call wall integrity, protein turnover, and energy production (Ceballos-Laita et al., 2018). Nevertheless, Mn interaction with Cd and attenuation of the toxic effects on plants are also found to play a major role in photosynthesis. Oliveira et al. (2020) studied the mechanisms of Mn-response in Cd toxicity mitigation in young plants of cacao by analyzing the alterations in DAPs and exclusive proteins (EP). Few significant proteins were produced in the presence of Cd while repressed in the presence of Cd + Mn, and vice versa. These findings suggested that Mn mitigated the adverse effects of Cd on cacao plants (Oliveira et al., 2020).

Two *Brassica napus* cultivars, ZS758 and ZD622, were treated with high As concentrations, and their response to As toxicity has been studied through iTRAQ-based proteomics analysis. The chlorophyll fluorescence attributes revealed that As pressure significantly lowered the photochemical efficiency of photosystem I and photosystem II and closed stomata detected under scanning electron microscopy. Metabolic pathways, followed by ribosome and secondary metabolites biosynthesis, were the dominant functional annotation among the differentially expressed proteins. Many genes involved in stress defense and primary metabolism were As-responsive DAPs (Farooq et al., 2021). Alka et al. (2021) performed histological and proteome analysis and found that *Microbacterium foliorum* lowered the As toxicity in *Melastoma malabathricum*. 2D gel electrophoresis and transmission electron microscopy were used to conduct the histological and proteome analysis. When As-treated cells were compared to untreated cells, considerable changes were discovered. Compared to control, root cells ultra-structure showed intact cell wall, cytoplasm, and vacuole under As + bacteria. To further understand the As + bacteria, proteome profiling of root cells was analyzed. It has been found that proteins involved in photosynthesis, defense, signaling, and protein biogenesis were higher in As + bacteria than As alone (Alka et al., 2021).

Metabolomics

Metabolomics is considered as an emerging field that broadly detects and quantifies all exogenous and endogenous molecules of low molecular weight (<1 kDa), including metabolites present in living organisms (Razzaq et al., 2019; Raza, 2020). Multiple analytical techniques have been developed to understand plant metabolic responses like inductively joined MS, liquid, and gas chromatography-MS (LC-MS, GC-MS), and nuclear magnetic resonance spectroscopy (NMR) (Razzaq et al., 2019; Raza, 2020). **Table 4** shows some examples of metabolomics studies under toxic metals/metalloids toxicity in different plants.

Xie et al. (2019) performed LC-MS/MS and HPLC analysis for metabolites and thiol compounds in *Amaranthus hypochondriacus* under Cd stress. *A. hypochondriacus* leaves accumulated Cd levels 40 times more than the control plant and also enhanced the PCs contents. Out of 12,084 metabolites identified, 41 were found to be significantly different metabolites (SDMs) among two groups and known to take part in seven different metabolic pathways. Among them, 12 SDMs related to PCs were associated with three different pathways, namely Arg and Pro metabolism, Val, Leu and Ile biosynthesis, and Ala, Asp, and Glu metabolism (Xie et al., 2019). An HPLC coupled with MS-based metabolome profiles of rice was analyzed in response to Cd and Cu toxicity. A total of 112 metabolites were identified, of which 97 metabolites were subsequently confirmed under Cd toxicity. Importantly, the secondary metabolism, amino acid metabolism-like purine, carbon, and glycerolipid metabolism pathways were found to be greatly affected. Furthermore, reduction in plant growth, photosynthetic capacity, and induction of defense systems to protect cell damage have also been observed (Navarro-Reig et al., 2017). In yet another study, GC-TOF-MS and LC-MS/MS-based metabolome profiling were performed to study the effect of Cu stress on cucumber plants (Zhao L. et al., 2018). Metabolomics helped in the identification of 149 primary and 79 secondary metabolites. Down-regulation of TCA intermediates (up to 1.4–2.4-fold) was observed, indicating disturbed carbohydrate metabolism. Excess Cu affected the aldarate and ascorbate metabolism and shikimate phenylpropanoid biosynthesis (Zhao L. et al., 2018). In soil, excess Se may appear destructive to plants. Zhang et al. (2019b) carried out an untargeted metabolome analysis of Se-treated and control celery seedlings and identified 24 sulfur and seleno-compound metabolic unigenes to be differentially expressed. Moreover, 1,774 metabolites and 237 SDMs were found through UHPLC-MS/MS. Results revealed that identified metabolites could be associated with significant biological pathways regulating Se tolerance (Zhang et al., 2019b). Furthermore, an untargeted metabolomics method was used to study the effects of 5 days application of 100 μmol L^{-1} selenate on broccoli sprouts metabolome. Multivariate statistical analysis displayed that tyrosine, D-erythronolactone, serine, and melezitose were up-regulated, while citric acid, D-glyceric acid, and succinic acid were down-regulated after selenate application. Selenate application also affected the metabolism of GSH, β-alanine, and plant-metabolite biosynthesis associated with glucosinolate precursors (Tian et al., 2018).

The metabolomic responses of tea plants toward Zn stress showed that Zn excess or deficiency differentially affected the metabolic pathways in tea leaves (Zhang et al., 2017). Zn-deficiency influenced carbohydrates metabolism, whereas Zn-excess affected the metabolism of flavonoids. Furthermore, it was observed that both Zn-excess and Zn-deficiency led

to lowered nicotinamide concentrations, which accelerated NAD^+ breakdown and resulted in low energy metabolism (Zhang et al., 2017). Furthermore, UHPLC/Q-TOF based metabolic investigation was conducted to study the effects of 100 mM NaCl and 100 mM $ZnSO_4$ on lettuce root metabolic profiling (Rouphael et al., 2016). Most of the compounds identified in $ZnSO_4$/NaCl environments were lipids, carbohydrates, glucosinolate, phenolics, or hormones. Results showed that osmotic stress and redox-imbalance have an essential role in defining lettuce root metabolic response; while polyamines and polyamine conjugates were found to be elicited as a precise reaction to $ZnSO_4$ (Rouphael et al., 2016). *Qualea grandiflora* plants were grown in Murashige and Skoog (MS) medium with or without Al supplementation for 120 days. Metabolite profiling of *Qualea grandiflora* plants was performed through GC-MS under Al stress. *Q. grandiflora* plants with starved Al showed shorter roots and shoots, chlorotic leaves, and low biomass. Al was found to be critical for lignin synthesis, cell wall, processing of genetic information, and organic acid metabolism. Furthermore, Al was predicted to help plants uptake phosphorous (Cury et al., 2020).

Cosio and Renault (2020) studied physiology and shoot metabolomic profiles of *Elodea nuttallii* exposed to methyl-Hg (30 ng L^{-1}), inorganic Hg (70 ng L^{-1}), and Cd (280 μg L^{-1}) for 24 h. KEGG pathway analysis revealed that MeHg exposure resulted in numerous biochemical changes like aminoacyl-tRNA biosynthesis, serine, glycine, threonine, proline, arginine, and nitrogen metabolism. In contrast, Cd-stress resulted in important alterations in aminoacyl-tRNA biosynthesis and branched-chain amino acid pathways. Data supported the argument that MeHg impacts N homeostasis, Cd caused an osmotic stress-like pattern, and inorganic Hg had less impact on both features (Cosio and Renault, 2020). In a different study, Pb-treated vetiver plants grown in a hydroponic setup were used for LC/MS/MS-based metabolome analysis of shoot, and root tissues. Multivariate metabolite analysis displayed tremendous induction of vital metabolic pathways like amino acid metabolism, sugar metabolism, enhanced osmoprotectants production like polyols and betaine, and metal chelating organic acids (Pidatala et al., 2016). For Pb remediation, vetiver grass is considered a superior choice due to its Pb-hyperaccumulation ability. Pidatala et al. (2018) performed comparative metabolic profiling of maize and vetiver under Pb-stress conditions. Vetiver plants displayed a massive increase of metabolites under Pb-stress, including coenzymes, amino acids, and organic acids; whereas, maize displayed a modest increase in the same metabolites with no significant effect on other metabolites (Pidatala et al., 2018). Furthermore, Zhang et al. (2019d) performed metabolic profiling of *Malus halliana* leaves under Fe-deficiency through GC/MS and identified a total of 18, 39, and 17 metabolites in three pairs L12h vs. L0h, L3d vs. L0h, and L3d vs. L12h, respectively. The findings showed that trehalose and sucrose are the most abundant metabolites in glucose metabolism and have a role in balancing photosynthetic activity in *M. halliana* leaves with the utilization of photo-assimilate. Overall, identified metabolites were found to play a major role in the positive regulation of Fe-deficiency response (Zhang et al., 2019d).

Das et al. (2021) investigated the differential expression of two *Andrographis paniculata* genotypes under As stress. The As distribution was found to be higher in roots than in other tissues with TF <1. APMS (wild collection) was more tolerant and accumulated less As than APwC (mass selection line). HPLC was used to quantify the metabolites in sample extract, and metabolites detection was performed at 223 nm by photodiode array detector (PDA). Arsenic enhanced flavonoids production like 5,7,2′,3′-tetramethoxyflavone in *A. paniculata*. The main secondary metabolites, oxidative enzymes, and nutrient uptake showed a significant difference in the detoxification process under As stress. The improved *Ap2* expression proposed its involvement in metabolic flux channeling toward the ent-LRDs biosynthesis under As stress (Das et al., 2021). NMR-based metabolomics approach provides a quick snapshot of metabolites without prior knowledge of organisms. Thus, Arora et al. (2018) validated the applicability of NMR-based metabolomics using freshwater microalga *Scenedesmus* sp. Using NMR spectroscopy, the authors identified and quantified around 45 metabolites, comprising organic acids, sugars, amino acids, nucleotides, phosphagens, and osmolytes. These findings revealed that microalga tolerated the As toxicity by accumulating these diverse metabolites (Arora et al., 2018).

Ionomics

Plants require minerals in appropriate amounts to perform their functions properly. Ionome or ionomics are the mineral elements needed in trace amounts for plant growth, development, and removal of toxic metals/metalloids (Stich et al., 2020). Nitrogen is an essential plant nutrient and forms an integral part of nucleic acids, proteins, vitamins, and hormones. It reduces toxic metals/metalloids toxicity by synthesizing Chl, N-containing antioxidants, and metabolites (Lin T. et al., 2011). Punshon et al. (2013) used the ionomic approach of multi-element imaging synchrotron X-ray fluorescence microscopy (SXRF) with *A. thaliana* for studying the phenotype, gene identification, and screening. Su et al. (2017) performed Fourier transform infrared spectrometry (FTIR) analysis to examine the subcellular distribution, accumulation, alteration in metabolic activity, and physiology of *S. polyrhiza* under Cd stress (5, 10 μM for 4 days). In another study, ICP-MS ionomic approach was applied to sunflower growth under Cd stress (50, 350, and 750 mg as $CdCl_2$). Increased doses of Cd caused necrosis and chlorosis and led to disproportion in Cu/Zn homeostasis (Júnior et al., 2014). Some recent examples of ionomics studies under toxic metals/metalloids toxicity are provided in **Table 4**.

Zhu et al. (2010) reported 16 mM N fertilizer $(NH_4)_2SO_4$ to reduce the Cd toxicity in Sedum. In *S. nigrum,* the fertilizers, $(NH_4)_2SO_4$ and CH_4N_2O application increased plant biomass by up to 2.0 and 2.1-folds, respectively, as compared to control under Cd stress (2 mg kg^{-1}) (Yang et al., 2019). Mg, which is an essential component of Chl, reduced Cd toxicity by enhancing the activity of antioxidant enzymes (Chou et al., 2011). In Japanese mustard spinach, Cd stress and accumulation caused by a dose of 0.25 μM was reduced by up to 40% after the application of 10 mM Mg (Kashem and Kawai, 2007). Calcium not only regulates the metabolic activity of plants but also reduces the

toxicity caused by toxic metals/metalloids. For instance, 30 mM Ca reduced Cd quantity from 46.7 to 17.4 μg in *A. thaliana* (Suzuki, 2005). Feng et al. (2017) performed inductively coupled plasma-MS (ICP-MS) determination of Cd/As to demonstrate a distinct transport of elements to 14 parts of 21 different brown rice genotypes. Interestingly, sixteen other elements were also determined in roots, and associated with the highest Cd accumulation fraction and increased glycolytic activity. Cu, Zn, Mg, and Co distribution was found to be associated with Cd concentration in roots and nodes. Ionomic profile indicated that all elements are correlated with different plant parts, and distribution occurs through them, while node1 had the highest accumulation rate of Cd (Feng et al., 2017).

The ionome of maize shoot has been studied under the Fe regime using recombinant inbred line population, and significant genotypic variance among 12 mineral elements was identified using inductively coupled plasma optical emission spectrometry (ICP−OES) (Stich et al., 2020). Besides, *ZmHMA2/3* and *ZmMOT1* were also proposed to cause genetic variation of Cd and Mo contents in maize shoots. Another ionome study targeting shoots and roots of *Brassica* species identified a total of 133 and 123 QTLs under optimal and low P (OP/LP) conditions (Wang et al., 2020e). These QTL clusters are predicted to reveal the uptake and transport mechanisms of mineral elements. Ionome study in rice seedlings, when mediated by nano-Si-priming (SiNP), generated fluoride tolerance by reducing fluoride uptake and bioaccumulation. This improved photosynthetic activity and uptake of mineral nutrients by lowering oxidative damage, thus ensuring a safe rice cultivation method (Banerjee et al., 2020). During 3 consecutive years, a decreasing trend of low contamination of toxic metals/metalloids was observed in an ionome study of potato tubers (Muntean et al., 2019). A study on rice grain and straw identified 70 novel ionomic QTLs for 15 nutrient elements. The study identified a molybdate transporter gene *OsMOT1;1* underlying *qMo8* QTL controlling Mo concentration in both grain and straw tissues (Wang et al., 2020a). Ionomic variations of rice had also been compared to *Arabidopsis* against sodium, molybdenum, and nitrogen using genome-wide association studies from 529 accessions. This comprehensive study with 6.4 million SNPs identified 72 loci for ionomic variation and further identified candidate genes, sodium transporter gene *Os-HKT1, Os-MOLYBDATE TRANSPORTER,* and thus grain number, plant height, and heading date thus featured the molecular mechanism controlling rice ionome (Yang et al., 2018). Mišúthová et al. (2021) studied the growth and developments of maize plants in response to silicon (Si) and As metalloids. The experimental findings revealed increased As (75 and 150 μM) concentration reduced the biomass and root length, and 2.5 μM Si supplementation to the medium did not affect root growth. Further, Si application did not affect the uptake of micro-and macro-elements into the roots (Ni, Ca, Zn, P, Cu, Mo, and K). While, Si significantly reduced the presence of hydrogen peroxide and superoxide in roots suffering from As toxicity and increased root antioxidant enzymes (Mišúthová et al., 2021). In another study, Xiao et al. (2021) investigated the transcriptomic variations and ionomic profiles to understand the molecular mechanism of alleviating the As(III) stress. Under As(III) stressed and control conditions, a total of 29 elements were found through inductively coupled plasma mass spectrometry (ICP-MS) in the rice roots and shoots. Strong connections were observed between transcriptome and ionome in the rice shoots. Overall, 3,812 DEGs were discovered in the As(III)-applied shoots than control shoots, and these DEGs were mainly associated with transmembrane transport and ion binding. The rice plants preferred to translocate more nutrients to cope with arsenic toxicity (Xiao et al., 2021).

miRNAomics

miRNAs are tiny non-coding RNA species and key post-transcriptional regulators. They have also emerged as an important technique like other omics approaches to develop toxic metals/metalloids tolerant plants (Dubey et al., 2021; Jamla et al., 2021b). Some successful studies have been completed to identify metals/metalloids responsive miRNAs. For instance, miRNA against Cd toxicity have been reported in many crop plants, including wheat (Qiu et al., 2016), rice (Huang et al., 2009), maize (Gao et al., 2019), barley (Yu J. et al., 2019) and rapeseed (Jian et al., 2018). These successful studies depicted miRNAs regulating toxic metal uptake and transport, inducing oxidative stress and antioxidative defense, thus maintaining homeostasis. The exploration of miRNAs in plants, along with other omics approaches and computational tools, may act as potential targets for improving plants to confer toxic metals/metalloids tolerance (Dubey et al., 2021). Some recent reports of miRNAs against toxic metals/metalloids stress and their impact on plants are mentioned below.

The role of *miR156j* from *miR156* family was observed in rice for physiological growth stages against As toxicity. Expression analysis revealed the functional role of *Osa-miR156j* at various developmental stages and plant tissues under As(V) exposure. Further, stress-responsive *cis*-acting regulatory elements confirmed its involvement during stress conditions. The results altogether showed the obvious role of *miR156j* in metabolic activities under As toxicity and can be used to develop As stress-tolerant varieties (Pandey et al., 2020). The genome-wide identification analysis in *Brassica juncea* identified some novel miRNAs, including 11 miRNAs and 56 transcripts against Cd stress response, using transcriptomic and sRNA sequencing technology. This study found *bra-miR172b-3p* regulating *ATCCS* playing a significant role against Cd stress and highlighted the regulatory relationship between miRNAs and transcripts, thus providing insights into molecular mechanisms in response to Cd stress in plants (Liu et al., 2021). A library of more than 2,000 artificial microRNAs (amiRNAs) has been developed in *Arabidopsis* to overcome the limitation for dissecting As responsive mechanisms. The research identified six transformant lines in response to As(V) and Cd exposure. However, further characterization of miRNA line closely related to homologous CBF and ERF transcriptional factor genes revealed *ERF34* and *ERF35* as important resistant TFs against Cd stress. The CBF1, CBF2, and CBF3 TFs were mediating negative regulation under As exposure and can be further used in the future to identify Cd and As induced transcriptional control networks (Xie et al., 2021).

Another miRNA named *miR1511* for the *MIR1511* gene responded against Al toxicity in common bean and then targeted against *ALS3* (*Aluminum Sensitive Protein 3*) gene. Both the genes opposed each other for sensitive genotypes as decreased expression of *miR1511* showed increased *ALS3* transcript level under Al toxicity and vice versa, thus revealing the prominent role of *miR1511* for inducing resistance against Al stress in plants (Ángel et al., 2021). Overexpression of *miR156* had significantly reduced the endogenous ROS in *Arabidopsis* and enhanced tolerance against Cd stress by reducing the effect of Cd-related transporters (Zhang et al., 2020c). In *Miscanthus sinensis*, high-throughput miRNA sequencing for Cr toxicity identified a total of 104 conserved miRNAs and 158 non-conserved miRNAs, out of which 45 differentially expressed miRNAs were linked with roots while 13 differentially expressed miRNAs were linked with leaves under Cr stress. GO, and KEGG analysis identified *miR167a, novel-miR15,* and *novel-miR22* as potential candidates that were involved in Cr transportation and chelation. Moreover, *miR156a, miR164, miR396d,* and novel *miR155* were involved in physiological and biochemical metabolisms and detoxifying the toxic effect of Cr in plants (Nie et al., 2021). Overall, these studies showed that miRNA significantly regulates genes expression and plays a key role in mitigating the adverse effect of toxic metals/metalloids. Thus, miRNAomics should be more exploited in identifying tiny key players (miRNAs) in regulating the stress-responsive mechanisms against a variety of toxic metals in different crop plants.

Phenomics

A phenome is a set of all biological, physical, and biochemical processes expressed by an organism in the form of phenotypes (qualitative and quantitative features) in a specific living condition. Plant phenomics depicts the phenotypic and genotypic expression within a particular living condition (Pratap et al., 2019). The phenotype of a plant may have a diverse manifestation within the same genotype due to different environmental conditions, i.e., abiotic stresses. The plant phenotype can be identified by using accomplishments made via genomic innovations and bioinformatics with the application of analytical techniques/phenomics technologies determining the relationship between plant genotype and environmental stress (Walter et al., 2015). The significance of phenomics is highly appreciable in the post-genomic era and is noticeable after using approaches like genomic selection, marker-assisted selection, GWAS, and QTL mapping, which are highly dependent on HTP for crop improvement. HTP technologies collect large data samples with automated digital analysis, interpret and process the data accurately with adequate statistical processing (Awada et al., 2018). The use of recent approaches for genetic dissection, knowledge of plant structure, and investigation of all functional processes enable the identification of plant phenotypic expression (Pratap et al., 2019). Some reported and widely used tools for phenotyping plants are provided in **Supplementary Table 1**. The integration of phenomics with other omics approaches forms the basis of crop breeding to identify plants with the best acceptable phenotype. It is the most promising approach for achieving sustainability in agriculture by understanding the plant's response to multiple stresses, including toxic metals/metalloids toxicity.

Recently, root system architecture (RSA) traits have been studied in soybean using the phenome approach to identify genetic diversity since it is difficult to analyze RSA traits manually for a large number of accessions (Falk et al., 2020). Genotype and phenotype-based clusters of accessions showed similarity, in which genotype-based clusters depicted co-relation by geographical origins. This analysis provides opportunities for the breeding of root traits using beneficial functional genetic diversity that can be used in the future for crop improvements (Falk et al., 2020). In *A. thaliana*, a dataset of stress-responsive signals has been developed under a wide range of biotic and abiotic stresses, including Al and Fe toxicity, temperature, light, osmotic, and oxidative stresses. This research highlighted several shared and unshared biological processes, molecular functions, metabolic pathways, and phenomic characteristics that may help develop improved varieties using genome editing techniques (Naika et al., 2013). Since minimal applications of phenomics are reported against toxic metals/metalloids toxicity in plants, there is a margin to fulfill this gap by utilizing the phenomics approach to develop tolerant varieties by breeding crop plants against metals/metalloids toxicity.

ONLINE DATABASES/TOOLS FOR EFFECTIVE INTEGRATION OF OMICS DATA

The diversity and large volumes of omics data present a need for various tools required for data analysis. Several omics platforms have been developed to meet the needs and to integrate better the generated multi-omics data (Hernández-de-Diego et al., 2018). These tools are useful to decipher plant responses and behavior through results from the varying levels of molecular information. A few selected databases and tools/software for effective integration of the multi-omics data are discussed in this section. Some other examples, along with their functionality, have been provided in **Supplementary Table 2**.

One of the web databases, the Plant Omics Data Centre (PODC), allows gene mining by acquiring publicly available transcriptomics data obtained through RNA-sequencing of different model and crop plants. It also comprehensively integrates the gene expression networks and provides some essential features on inter species diversity by comparing gene expression networks, manual addition of information on published genes, and functional gene annotation through text mining (Shenton et al., 2019). Another web database, CATchUP, deals with the Spatio-temporal gene expression, i.e., genes expressed under specific conditions, by identification of the maximum expression difference of the transcripts. Owing to its unique data mining properties under particular treatment/conditions, it is mainly useful to find tissue-specific genes expressed at a certain developmental stage (Shenton et al., 2019). The National Genomics Data Centre (NGDC) processes a wide range of genomics-related data available through

a family of database resources. This suite of databases has allowed data integration and curation, which can be accessed in either of three categories of resources, namely meta and sequenced data, standardized information, and processed data. Some prominent databases maintained by NGDC include manually curated Genome-Wide Variant-Trait Association (GWAS) Atlas, Genome Warehouse (GWH), Genome Variation Map (GVM), Plant Editosome Database (PED), and The Methylation Bank/MethBank (National Genomics Data Center Members and Partners, 2020).

Studies have shown that different tools and techniques involving joint visualization of the multi-omics data provide molecular context and a better understanding of the molecular interconnections (Hernández-de-Diego et al., 2018). One of the metabolic pathway-based data visualization tools, KaPPa-View, allows the integration of transcript and metabolite data into pathway maps (Hernández-de-Diego et al., 2018) and hence helps to find a correlation with the biological knowledge. Similarly, a protein classification and annotation framework, MapMan4, supports multiple omics platforms, including transcriptomics, proteomics, and metabolomics (Schwacke et al., 2019). Another web-based tool, PaintOmics3, lays a framework for interactive exploration of multi-omics data via the KEGG pathway diagram and has enabled researchers to understand different levels of regulation in a biological system (Hernández-de-Diego et al., 2018). MetaBridge is a database that uses data from KEGG and MetaCyc metabolic pathway databases. It is useful for data integration and gene mapping for specific metabolites (Blimkie et al., 2020). The Miodin (MultI-Omics Data INtegration) R package allows users to integrate the omics data in a streamlined workflow-based syntax either based on vertical (across experiments on the same samples) or horizontal (across studies on the same variables) integration of samples. It supports the multi-omics modalities and enables workflows to import efficiently, process, and analyze the multi-omics data (Ulfenborg, 2019).

Besides the fact that these tools and databases have proved useful for researchers, the fast-evolving multi-omics platforms have resulted in the lack of uniformity among the available tools. This necessitates committed efforts for quality assessment and validation from scientific communities across the world.

AN OVERVIEW OF PLANT-BASED REMEDIATION APPROACHES FOR TOXIC METALS/METALLOIDS

Rapid industrialization has resulted in a large number of toxic metals/metalloids pollutants into the soil, water, and air, which then enter crops directly or indirectly through various pathways, posing significant health and wildlife risks (Rai et al., 2019; Raza et al., 2020, 2021a). Nevertheless, different plant-based remediation techniques have been developed to solve these issues, and some of the major techniques have been briefly discussed in the subsequent sections.

Bioremediation

Bioremediation, particularly biochar amended phytoremediation, is one of the most promising remediation strategies that is widely used to remediate toxic metals/metalloids in the soil (Shukla A. et al., 2018; Wang et al., 2021). Biochar has many significant properties that make it a good remediation material for contaminated soils, including a large internal surface area, negative charge, and resistance to degradation. It is also the most important bioremediation strategy since it not only serves to remediate soil pollution and improve soil quality but is also a cost-effective product that decreases the global environmental challenge of solid waste management (Shukla A. et al., 2018; Wang et al., 2021). A recent study shows that the addition of 10% of biochar generated from rice straw to Cu-contaminated soil reduced Cu availability by 96% (Rehman et al., 2019). Furthermore, biochar made from rice husk pyrolysis was found to be a useful agricultural by-product and an excellent immobilizer of metals contaminants such as Zn, Pb, and Cd (Dhiman et al., 2021). Sulfur-modified rice husk biochar advanced its sulfur content and was utilized as a "green bioremediation approach" to stabilize Hg-polluted soil (O'Connor et al., 2018). Metal pollutants are taken in and concentrated by hyperaccumulators and organic soil remedies, resulting in their precipitation within the root's innards (Huang et al., 2018). *Cassia alata*, a promising photo stabilizer with biochar aid to improve soil pH, nitrogen content, and total carbon, reduces Pb and Cu metal contamination in mine tailings and also leads to increased plant shoot and root biomass (Huang et al., 2018).

Phytostabilization

Phytostabilization is the process in which plant species with high metal tolerance are used to immobilize toxic metals/metalloids below ground and reduce their bioavailability, thus preventing metals from migrating into the environment and reducing the probability of metals/metalloids entering the food chain (Raza et al., 2020; Yan et al., 2020). In this approach, toxic metals/metalloids are physically and chemically immobilized in the rhizosphere through sorption on roots of plants, fixation with soil amendments, complexation, precipitation, or reduction in metals valence (Mthembu et al., 2020). Phytostabilization requires the identification of appropriate plant species with high resistance to toxic metals/metalloids (Yan et al., 2020). Because of their better tolerance to toxic metals/metalloids, territorial expansion, and evapotranspiration, some plant species, particularly crop grasses and willows (*Salix* spp.), are effective for phytostabilization (Sylvain et al., 2016). Plants such as *Festuca* spp. and *Agrostis* spp. are commonly used to phytostabilize Pb, Zn, and Cu contaminants in soil (Galende et al., 2014). Lands with increased metals/metalloids contamination or physical disturbances lack natural flora; hence, phytostabilization techniques can be used to rebuild a vegetative cover. Wind erosion of surface soils and leaching to groundwater is reduced when metal-tolerant plants are planted in such areas (Mthembu et al., 2020).

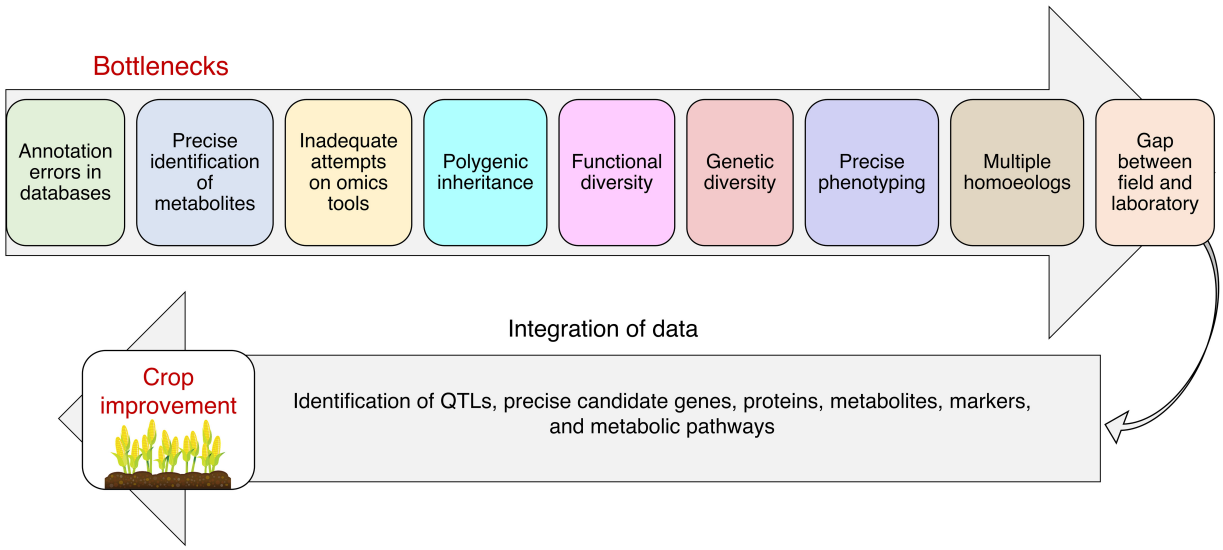


FIGURE 3 | Persisting bottlenecks in the exploitation of omics approaches (Raza et al., 2021b). Although an outstanding revolution has been accomplished in the biotechnological era, many queries and bottlenecks presently limit the utilization of omics approaches for stress tolerance research in several plant species. The amendment of these bottlenecks using molecular tools will help us to exploit the innovative manifesto in developing toxic metals/metalloids tolerant plants.

Phytoextraction

Phytoextraction is the process of absorbing, transporting, and accumulating toxic metals/metalloids in the biomass of harvestable plant parts using specialized and highly adapted hyperaccumulators (Diarra et al., 2021). The electrochemical characteristics of the metals being extracted, as well as their absorption, transport, and accumulation in the plants, all influence the efficiency of the phytoextraction process (Saini and Dhania, 2020). The most important factor determining the viability and success of phytoextraction is plant selection criteria; therefore, hyperaccumulators with exceptional tolerance and bioaccumulation of a broad range of toxic metals/metalloids are preferred (Diarra et al., 2021). Over 500 plant species from 45 different families, including Lamiaceae, Caryophyllaceae, Poaceae, Asteraceae, Fabaceae, and Brassicaceae, have been identified as hyperaccumulators so far. Brassicaceae is the most common family among those identified (Gul et al., 2021). In a recent study, the flowering plant *Lantana camara* L. exhibited all of the desired criteria of a hyperaccumulator plant, including a translocation factor (TF) >1 and Cd content in aerial portions of >100 mg kg^{-1}. As a result, it was proposed as a Cd hyperaccumulator (Liu S. et al., 2019). *Artemisia vulgaris* was recently identified as a promising plant for metal phytoremediation, with TF > 11 for As, Cd, Cu, Cr, Ni, and Pb, while *Silene vulgaris* had a TF greater than 1 for Cd (Antoniadis et al., 2020).

CONCLUSION AND FUTURE PROSPECTS

Climate change and agricultural production are highly correlated, as climate change is the leading cause of several environmental stresses, including toxic metals/metalloids toxicity in the soil and environment. Increasing metals/metalloids toxicity poses a severe threat to agricultural production by hampering plant growth and yield. The toxic effects of these toxic metals/metalloids also significantly affect the plant's physiological, biochemical, and molecular mechanisms, which are vital for healthy plant growth and improved yield. Several plant-based remediation approaches have also been successfully used to remediate the toxicity of the toxic metals/metalloids in the soil and environment. Under metals/metalloids toxicity, plants adjust themselves by modifying genes, proteins, and metabolites expression levels to cope with unfavorable conditions. Thus, a comprehensive understanding of the biological processes is required to cope with toxic metals/metalloids toxicity in the emerging technological era. During the last few years, significant progress has been made in utilizing state-of-the-art "omics" approaches to develop climate-smart plants. Interestingly, genome-wide omics analysis holds the potential to identify stress-related genes, metabolites, proteins, minor and major elements, miRNAs, stress regulators, and metabolic pathways precisely associated with plant phenotype under stressful environments.

Nevertheless, some persisting bottlenecks in exploiting omics approaches demand urgent attention (**Figure 3**; Raza et al., 2021b,d). Polygenic inheritance and genetic diversity are significant bottlenecks among the existing ones. Therefore, releasing these bottlenecks using molecular tools will help us to feat the new strategy to develop stress resistance plants; and consecutively will guarantee global food safety. For instance, recent developments in high-throughput technologies enable the analysis of global genetic diversity. Genomic selection and haplotype-based breeding are expected to lessen the genetic diversity of a breeding plan in the long term. Consequently, sustaining genetic diversity in breeding programs will be

essential for maintaining genetic gains from breeding revolutions (Varshney et al., 2021a,b,c). Therefore, integrating ideal selection contributions with these methodologies may help preserve genetic diversity while enhancing genetic gains. Furthermore, effective crop breeding programs with an improved genetic base will speed up fast-forward breeding, proposed by Varshney et al. (2021b). Briefly, genomics-assisted breeding, including haplotype-GWAS, haplotype-assisted breeding, and haplotype-assisted genomic selection, will effectively utilize superior haplotypes to accelerate future breeding advancement (Bhat et al., 2021). Moreover, modern machine learning tools and artificial intelligence methodologies systematically incorporate the overflow of data rolling through multi-omics approaches (van Dijk et al., 2020; Jung et al., 2021). Hence, system-level knowledge will help clarify functional diversity and regulatory networks underlying intricate phenotypes of agricultural value.

Genome editing by CRISPR/Cas systems and genetic engineering of stress-associated genes could be essential prospects for improving stress tolerance. Likewise, the engineering of metabolic pathways could also provide new avenues for the development of climate-resilient plants. Recently, speed breeding has emerged as the most powerful and time-saving tool to shorten the breeding cycle and enhance genetic gains in plants. Therefore, omics approaches could be galvanized by utilizing speed breeding to facilitate plant breeders to keep pace with increasing environmental fluctuations and burgeoning human population.

AUTHOR CONTRIBUTIONS

AR conceived the idea and prepared the figures. AR, JT, ZZ, SC, SB, RB, CZ, and HC contributed in writing. AR, JT, ZZ, and SC designed the tables. AR, RB, FBJ, RSAK, RKV, and WZ reviewed and edited the manuscript. All authors have read and approved the final version of the manuscript.

FUNDING

This work was supported by grants from the National Science Foundation (NSF) of China (U1705233 to WZ) and the Fujian Agriculture and Forestry University, Fuzhou, China. Further, RKV is thankful to Bill & Melinda Gates Foundation, USA, and Australia-India Strategic Research Fund from the Department of Biotechnology, Government of India, for supporting this work in part.

ACKNOWLEDGMENTS

AR would like to thank the Fujian Agriculture and Forestry University (FAFU) and the Fujian Provincial Government for providing Post-doc Research Fellowship. We are grateful to many scientists and colleagues for scientific discussions, which enabled the development of this up-to-date comprehensive review. We apologize to colleagues whose relevant work could not be cited due to space limitations.

SUPPLEMENTARY MATERIAL

The Supplementary Material for this article can be found online at: https://www.frontiersin.org/articles/10.3389/fpls.2021.794373/full#supplementary-material

REFERENCES

Alka, S., Shahir, S., Ibrahim, N., Rahmad, N., Haliba, N., and Abd Manan, F. (2021). Histological and proteome analyses of *Microbacterium foliorum*-mediated decrease in arsenic toxicity in *Melastoma malabathricum*. *3 Biotech* 11, 1–17. doi: 10.1007/s13205-021-02864-y

Alotaibi, M. O., Mohammed, A. E., Almutairi, T. A., and Elobeid, M. M. (2019). Morpho-physiological and proteomic analyses of *Eucalyptus camaldulensis* as a bioremediator in copper-polluted soil in Saudi Arabia. *Plants* 8:43. doi: 10.3390/plants8020043

Ángel, M. R. J., Ariani, A., Leija, A., Elizondo, A., Fuentes, S. I., Ramirez, M., et al. (2021). *Phaseolus vulgaris* MIR1511 genotypic variations differentially regulate plant tolerance to aluminum toxicity. *Plant J.* 105, 1521–1533. doi: 10.1111/tpj.15129

Antoniadis, V., Shaheen, S. M., Stark, H. J., Wennrich, R., Levizou, E., Merbach, I., et al. (2020). Phytoremediation potential of twelve wild plant species for toxic elements in a contaminated soil. *Environ. Int.* 146:106233. doi: 10.1016/j.envint.2020.106233

Arbelaez, J. D., Maron, L. G., Jobe, T. O., Piñeros, M. A., Famoso, A. N., Rebelo, A. R., et al. (2017). ALUMINUM RESISTANCE TRANSCRIPTION FACTOR 1 (ART1) contributes to natural variation in aluminum resistance in diverse genetic backgrounds of rice (*O. sativa*). *Plant Direct.* 1:4. doi: 10.1002/pld3.14

Arora, N., Dubey, D., Sharma, M., Patel, A., Guleria, A., Pruthi, P. A., et al. (2018). NMR-based metabolomic approach to elucidate the differential cellular responses during mitigation of arsenic (III, V) in a green microalga. *ACS Omega* 3, 11847–11856. doi: 10.1021/acsomega.8b01692

Asaari, M. S. M., Mertens, S., Dhondt, S., Inzé, D., Wuyts, N., and Scheunders, P. (2019). Analysis of hyperspectral images for detection of drought stress and recovery in maize plants in a high-throughput phenotyping platform. *Comput. Electron. Agric.* 162, 749–758.

Asati, A., Pichhode, M., and Nikhil, K. (2016). Effect of heavy metals on plants: an overview. *Int. J. Appl. Innov. Eng. Manag.* 5, 56–66.

Ashraf, M. Y., Sadiq, R., Hussain, M., Ashraf, M., and Ahmad, M. S. A. (2011). Toxic effect of nickel (Ni) on growth and metabolism in germinating seeds of sunflower (*Helianthus annuus* L.). *Biol. Trace Element Res.* 143, 1695–1703. doi: 10.1007/s12011-011-8955-7

Asins, M., Raga, M., Torrent, D., Roca, D., and Carbonell, E. (2020). QTL and candidate gene analyses of rootstock-mediated tomato fruit yield and quality traits under low iron stress. *Euphytica* 216, 1–19. doi: 10.9734/cjast/2019/v38i630452

Assefa, T., Zhang, J., Chowda-Reddy, R., Lauter, A. N. M., Singh, A., O'Rourke, J. A., et al. (2020). Deconstructing the genetic architecture of iron deficiency chlorosis in soybean using genome-wide approaches. *BMC Plant Biol.* 20:42. doi: 10.1186/s12870-020-2237-5

Awada, L., Phillips, P. W., and Smyth, S. J. (2018). The adoption of automated phenotyping by plant breeders. *Euphytica* 214:148.

Bahmani, R., Bihamta, M., Habibi, D., Forozesh, P., and Ahmadvand, S. (2012). Effect of cadmium chloride on growth parameters of different bean genotypes (*Phaseolus vulgaris* L.). *ARPN J. Agric. Biol. Sci.* 7, 35–40.

Balk, J., and Schaedler, T. A. (2014). Iron cofactor assembly in plants. *Ann. Rev. Plant Biol.* 65, 125–153. doi: 10.1146/annurev-arplant-050213-035759

Banerjee, A., Singh, A., Sudarshan, M., and Roychoudhury, A. (2020). Silicon nanoparticle-pulsing mitigates fluoride stress in rice by fine-tuning the

ionomic and metabolomic balance and refining agronomic traits. *Chemosphere* 262:127826. doi: 10.1016/j.chemosphere.2020.127826

Benyó, D., Horváth, E., Németh, E., Leviczky, T., Takács, K., Lehotai, N., et al. (2016). Physiological and molecular responses to heavy metal stresses suggest different detoxification mechanism of *Populus deltoides* and *P. x canadensis*. *J. Plant Physiol.* 201, 62–70. doi: 10.1016/j.jplph.2016.05.025

Bhat, J. A., Yu, D., Bohra, A., Ganie, S. A., and Varsheny, R. K. (2021). Features and applications of haplotypes in crop breeding. *Commun. Biol.* 4:1266. doi: 10.1038/s42003-021-02782-y

Blimkie, T., Lee, A. H. Y., and Hancock, R. E. (2020). MetaBridge: an integrative multi-omics tool for metabolite-enzyme mapping. *Curr. Protoc. Bioinform.* 70:e98. doi: 10.1002/cpbi.98

Bollinedi, H., Yadav, A. K., Vinod, K., Krishnan, S. G., Bhowmick, P. K., Nagarajan, M., et al. (2020). Genome-wide association study reveals novel marker-trait associations (MTAs) governing the localization of Fe and Zn in the rice grain. *Front. Genet.* 11:213. doi: 10.3389/fgene.2020.00213

Borjigin, C., Schilling, R. K., Bose, J., Hrmova, M., Qiu, J., Wege, S., et al. (2020). A single nucleotide substitution in TaHKT1; 5-D controls shoot Na+ accumulation in bread wheat. *bioRxiv* [Preprint]. doi: 10.1101/2020.01.21.909887

Campos, N. V., Arcanjo-Silva, S., Freitas-Silva, L., de Araújo, T. O., Souza-Fernandes, D. P., and Azevedo, A. A. (2018). Arsenic hyperaccumulation in *Pityrogramma calomelanos* L.(Link): adaptive traits to deal with high metalloid concentrations. *Environ. Sci. Pollut. Res.* 25, 10720–10729. doi: 10.1007/s11356-017-1085-9

Canzler, S., Schor, J., Busch, W., Schubert, K., Rolle-Kampczyk, U. E., Seitz, H., et al. (2020). Prospects and challenges of multi-omics data integration in toxicology. *Arch. Toxicol.* 94, 371–388. doi: 10.1007/s00204-020-02656-y

Carroll, A. A., Clarke, J., Fahlgren, N., Gehan, M. A., Lawrence-Dill, C. J., and Lorence, A. (2019). NAPPN: who we are, where we are going, and why you should join us! *Plant Phenome J.* 2, 1–4.

Casarrubia, S., Martino, E., Daghino, S., Kohler, A., Morin, E., Khouja, H.-R., et al. (2020). Modulation of plant and fungal gene expression upon cd exposure and symbiosis in ericoid mycorrhizal *Vaccinium myrtillus*. *Front. Microbiol.* 11:341. doi: 10.3389/fmicb.2020.00341

Caspi, R., Billington, R., Ferrer, L., Foerster, H., Fulcher, C. A., Keseler, I. M., et al. (2016). The MetaCyc database of metabolic pathways and enzymes and the BioCyc collection of pathway/genome databases. *Nucleic Acids Res.* 44, D471–D480.

Ceballos-Laita, L., Gutierrez-Carbonell, E., Imai, H., Abadía, A., Uemura, M., Abadía, J., et al. (2018). Effects of manganese toxicity on the protein profile of tomato (*Solanum lycopersicum*) roots as revealed by two complementary proteomic approaches, two-dimensional electrophoresis and shotgun analysis. *J. Proteom.* 185, 51–63. doi: 10.1016/j.jprot.2018.06.016

Cedillo-Jimenez, C. A., García-Ortega, L. F., Martínez-Reséndiz, M., Arné-Robles, D., Cruz-Hernandez, A., and Guevara-Gonzalez, R. G. (2020). Response of transgenic tobacco overexpressing the CchGLP gene to cadmium and aluminium: phenotypic and microRNAs expression changes. *Physiol. Mol. Biol. Plant* 26, 3–13. doi: 10.1007/s12298-019-00716-x

Chandra, R., and Kang, H. (2016). Mixed heavy metal stress on photosynthesis, transpiration rate, and chlorophyll content in poplar hybrids. *Forest Sci. Technol.* 12, 55–61. doi: 10.1080/21580103.2015.1044024

Chang, J. D., Huang, S., Yamaji, N., Zhang, W., Ma, J. F., and Zhao, F. J. (2020). OsNRAMP1 transporter contributes to cadmium and manganese uptake in rice. *Plant Cell Environ.* 43, 2476–2491. doi: 10.1111/pce.13843

Chauhan, R., Awasthi, S., Indoliya, Y., Chauhan, A. S., Mishra, S., Agrawal, L., et al. (2020). Transcriptome and proteome analyses reveal selenium mediated amelioration of arsenic toxicity in rice (*Oryza sativa* L.). *J. Hazard. Mater.* 390:122122. doi: 10.1016/j.jhazmat.2020.122122

Chen, L., Wan, H., Qian, J., Guo, J., Sun, C., Wen, J., et al. (2018). Genome-wide association study of cadmium accumulation at the seedling stage in rapeseed (*Brassica napus* L.). *Front. Plant Sci.* 9:375. doi: 10.3389/fpls.2018.00375

Chen, Y., Zhi, J., Zhang, H., Li, J., Zhao, Q., and Xu, J. (2017). Transcriptome analysis of *Phytolacca americana* L. in response to cadmium stress. *PLoS One* 12:e0184681. doi: 10.1371/journal.pone.0184681

Chong, J., Soufan, O., Li, C., Caraus, I., Li, S., Bourque, G., et al. (2018). MetaboAnalyst 4.0: towards more transparent and integrative metabolomics analysis. *Nucleic Acids Res.* 46, W486–W494. doi: 10.1093/nar/gky310

Chou, T.-S., Chao, Y.-Y., Huang, W.-D., Hong, C.-Y., and Kao, C. H. (2011). Effect of magnesium deficiency on antioxidant status and cadmium toxicity in rice seedlings. *J. Plant Physiol.* 168, 1021–1030. doi: 10.1016/j.jplph.2010.12.004

Chu, Q., Sha, Z., Maruyama, H., Yang, L., Pan, G., Xue, L., et al. (2019). Metabolic reprogramming in nodules, roots, and leaves of symbiotic soybean in response to iron deficiency. *Plant Cell Environ.* 42, 3027–3043. doi: 10.1111/pce.13608

Colmer, J., O'Neill, C. M., Wells, R., Bostrom, A., Reynolds, D., Websdale, D., et al. (2020). SeedGerm: a cost-effective phenotyping platform for automated seed imaging and machine-learning based phenotypic analysis of crop seed germination. *New Phytol.* 228, 778–793. doi: 10.1111/nph.16736

Cosio, C., and Renault, D. (2020). Effects of cadmium, inorganic mercury and methyl-mercury on the physiology and metabolomic profiles of shoots of the macrophyte *Elodea nuttallii*. *Environ. Pollut.* 257:113557. doi: 10.1016/j.envpol.2019.113557

Cota-Ruiz, K., Ye, Y., Valdes, C., Deng, C., Wang, Y., Hernández-Viezcas, J. A., et al. (2020). Copper nanowires as nanofertilizers for alfalfa plants: understanding nano-bio systems interactions from microbial genomics, plant molecular responses and spectroscopic studies. *Sci. Total Environ.* 742:140572. doi: 10.1016/j.scitotenv.2020.140572

Cury, N. F., Silva, R. C., Andre, M. S., Fontes, W., Ricart, C. A., Castro, M. S., et al. (2020). Root proteome and metabolome reveal a high nutritional dependency of aluminium in *Qualea grandiflora* Mart. (Vochysiaceae). *Plant Soil* 446, 125–143.

Dalvi, A. A., and Bhalerao, S. A. (2013). Response of plants towards heavy metal toxicity: an overview of avoidance, tolerance and uptake mechanism. *Ann. Plant Sci.* 2, 362–368.

Dalyan, E., Yüzbaşıoğlu, E., Keskin, B. C., Yıldızhan, Y., Memon, A., Ünal, M., et al. (2017). The identification of genes associated with Pb and Cd response mechanism in *Brassica juncea* L. by using *Arabidopsis* expression array. *Environ. Exp. Bot.* 139, 105–115. doi: 10.1016/j.envexpbot.2017.05.001

Das, P., Khare, P., Singh, R. P., Yadav, V., Tripathi, P., Kumar, A., et al. (2021). Arsenic-induced differential expression of oxidative stress and secondary metabolite content in two genotypes of *Andrographis paniculata*. *J. Hazard. Mater.* 406:124302. doi: 10.1016/j.jhazmat.2020.124302

de Alvarenga Mudadu, M., and Zerlotini, A. (2020). Machado: open source genomics data integration framework. *bioRxiv* [Preprint]. doi: 10.1101/2020.05.08.084731

Derakhshani, B., Jafary, H., Maleki Zanjani, B., Hasanpur, K., Mishina, K., Tanaka, T., et al. (2020). Combined QTL mapping and RNA-Seq profiling reveals candidate genes associated with cadmium tolerance in barley. *PLoS One* 15:e0230820. doi: 10.1371/journal.pone.0230820

Dhiman, S., Ibrahim, M., Devi, K., Sharma, N., Kapoor, N., Kaur, R., et al. (2021). "Biochar assisted remediation of toxic metals and metalloids." in *Handbook of Assisted and Amendment: Enhanced Sustainable Remediation Technology*, ed. M. N. V. Prasad (Hoboken, NJ: Wiley-Blackwell), 131–162. doi: 10.1002/9781119670391.ch7

Di, X., Zheng, F., Norton, G. J., Beesley, L., Zhang, Z., Lin, H., et al. (2021). Physiological responses and transcriptome analyses of upland rice following exposure to arsenite and arsenate. *Environ. Exp. Bot.* 183:104366. doi: 10.1016/j.envexpbot.2020.104366

Diarra, I., Kotra, K. K., and Prasad, S. (2021). Assessment of biodegradable chelating agents in the phytoextraction of heavy metals from multi–metal contaminated soil. *Chemosphere* 273:128483. doi: 10.1016/j.chemosphere.2020.128483

Ding, Y., Ding, L., Xia, Y., Wang, F., and Zhu, C. (2020). Emerging roles of microRNAs in plant heavy metal tolerance and homeostasis. *J. Agric. Food Chem.* 68, 1958–1965. doi: 10.1021/acs.jafc.9b07468

Dubey, S., Shri, M., and Chakrabarty, D. (2021). MicroRNA mediated regulation of gene expression in response to heavy metals in plants. *J. Plant Biochem. Biotechnol.* [Epub ahead of print]. doi: 10.1007/s13562-021-00718-5

Eleftheriou, E. P., Adamakis, I.-D. S., Panteris, E., and Fatsiou, M. (2015). Chromium-induced ultrastructural changes and oxidative stress in roots of *Arabidopsis thaliana*. *Int. J. Mol. Sci.* 16, 15852–15871. doi: 10.3390/ijms160715852

Emamverdian, A., Ding, Y., Mokhberdoran, F., and Xie, Y. (2015). Heavy metal stress and some mechanisms of plant defense response. *Sci. World J.* 2015, 756120. doi: 10.1155/2015/756120

Erickson, T. B., Brooks, J., Nilles, E. J., Pham, P. N., and Vinck, P. (2019). Environmental health effects attributed to toxic and infectious agents following

hurricanes, cyclones, flash floods and major hydrometeorological events. *J. Toxicol. Environ. Health, Part B* 22, 157–171. doi: 10.1080/10937404.2019.1654422

Falk, K. G., Jubery, T. Z., O'Rourke, J. A., Singh, A., Sarkar, S., Ganapathysubramanian, B., et al. (2020). Soybean root system architecture trait study through genotypic, phenotypic, and shape-based clusters. *Plant Phenomics* 2020:1925495. doi: 10.34133/2020/1925495

Famoso, A. N., Zhao, K., Clark, R. T., Tung, C. W., Wright, M. H., Bustamante, C., et al. (2011). Genetic architecture of aluminum tolerance in rice (*Oryza sativa*) determined through genome-wide association analysis and QTL mapping. *PLoS Genet.* 7:e1002221. doi: 10.1371/journal.pgen.1002221

Farokhzadeh, S., Fakheri, B. A., Nezhad, N. M., Tahmasebi, S., Mirsoleimani, A., and Heidari, B. (2020b). Mapping QTLs associated with grain yield and yield-related traits under aluminum stress in bread wheat. *Crop Past. Sci.* 71, 429–444.

Farokhzadeh, S., Fakheri, B. A., Nezhad, N. M., Tahmasebi, S., Mirsoleimani, A., and McIntyre, C. L. (2020c). Genetic control of some plant growth characteristics of bread wheat (*Triticum aestivum* L.) under aluminum stress. *Genes Genomics* 42, 245–261. doi: 10.1007/s13258-019-00895-7

Farokhzadeh, S., Fakheri, B. A., Nezhad, N. M., Tahmasebi, S., and Mirsoleimani, A. (2020a). Genetic dissection of spike-related traits in wheat (*Triticum aestivum* L.) under aluminum stress. *Genet. Resour. Crop Evol.* 67, 1221–1243. doi: 10.1007/s10722-020-00907-6

Farooq, M. A., Hong, Z., Islam, F., Noor, Y., Hannan, F., Zhang, Y., et al. (2021). Comprehensive proteomic analysis of arsenic induced toxicity reveals the mechanism of multilevel coordination of efficient defense and energy metabolism in two *Brassica napus* cultivars. *Ecotoxicol. Environ. Saf.* 208:111744. doi: 10.1016/j.ecoenv.2020.111744

Feng, X., Han, L., Chao, D., Liu, Y., Zhang, Y., Wang, R., et al. (2017). Ionomic and transcriptomic analysis provides new insight into the distribution and transport of cadmium and arsenic in rice. *J. Hazard. Mater.* 331, 246–256. doi: 10.1016/j.jhazmat.2017.02.041

Fu, S., Lu, Y., Zhang, X., Yang, G., Chao, D., Wang, Z., et al. (2019). The ABC transporter ABCG36 is required for cadmium tolerance in rice. *J. Exp. Bot.* 70, 5909–5918. doi: 10.1093/jxb/erz335

Galende, M. A., Becerril, J. M., Barrutia, O., Artetxe, U., Garbisu, C., and Hernández, A. (2014). Field assessment of the effectiveness of organic amendments for aided phytostabilization of a Pb-Zn contaminated mine soil. *J. Geochem. Explor.* 145, 181–189. doi: 10.1016/j.scitotenv.2016.04.080

Gao, J., Luo, M., Peng, H., Chen, F., and Li, W. (2019). Characterization of cadmium-responsive MicroRNAs and their target genes in maize (*Zea mays*) roots. *BMC Mol. Biol.* 20:14. doi: 10.1186/s12867-019-0131-1

Gao, Y., Yang, F., Liu, J., Xie, W., Zhang, L., Chen, Z., et al. (2020). Genome-wide identification of metal tolerance protein genes in *Populus trichocarpa* and their roles in response to various heavy metal stresses. *Int. J. Mol. Sci.* 21:1680. doi: 10.3390/ijms21051680

Gashi, B., Osmani, M., Aliu, S., Zogaj, M., and Kastrati, F. (2020). Risk assessment of heavy metal toxicity by sensitive biomarker δ-aminolevulinic acid dehydratase (ALA-D) for onion plants cultivated in polluted areas in Kosovo. *J. Environ. Sci. Health B* 55, 462–469. doi: 10.1080/03601234.2020.1721229

Ghori, N.-H., Ghori, T., Hayat, M., Imadi, S., Gul, A., Altay, V., et al. (2019). Heavy metal stress and responses in plants. *Int. J. Environ. Sci. Technol.* 16, 1807–1828.

Ghosh, S., Datta, A., Tan, K., and Choi, H. (2019). SLIDE–a web-based tool for interactive visualization of large-scale–omics data. *Bioinformatics* 35, 346–348. doi: 10.1093/bioinformatics/bty534

Gilliham, M., Able, J. A., and Roy, S. J. (2017). Translating knowledge about abiotic stress tolerance to breeding programmes. *Plant J.* 90, 898–917. doi: 10.1111/tpj.13456

Gouveia, G. C. C., Galindo, F. S., Lanza, M. G. D. B., da Rocha Silva, A. C., de Brito Mateus, M. P., da Silva, M. S., et al. (2020). Selenium toxicity stress-induced phenotypical, biochemical and physiological responses in rice plants: characterization of symptoms and plant metabolic adjustment. *Ecotoxicol. Environ. Saf.* 202:110916. doi: 10.1016/j.ecoenv.2020.110916

Gui, S., Yang, L., Li, J., Luo, J., Xu, X., Yuan, J., et al. (2020). ZEAMAP, a comprehensive database adapted to the maize multi-omics era. *iScience* 23:101241. doi: 10.1016/j.isci.2020.101241

Gul, I., Manzoor, M., Hashim, N., Shah, G. M., Waani, S. P. T., Shahid, M., et al. (2021). Challenges in microbially and chelate-assisted phytoextraction of cadmium and lead–A review. *Environ. Pollut.* 287:117667. doi: 10.1016/j.envpol.2021.117667

Hasanuzzaman, M., Bhuyan, M. B., Raza, A., Hawrylak-Nowak, B., Matraszek-Gawron, R., Al Mahmud, J., et al. (2020a). Selenium in plants: boon or bane? *Environ. Exp. Bot.* 178:104170. doi: 10.1016/j.envexpbot.2020.104170

Hasanuzzaman, M., Bhuyan, M., Zulfiqar, F., Raza, A., Mohsin, S. M., Mahmud, J. A., et al. (2020b). Reactive oxygen species and antioxidant defense in plants under abiotic stress: revisiting the crucial role of a universal defense regulator. *Antioxidants* 9:681. doi: 10.3390/antiox9080681

Hattab, S., Hattab, S., Flores-Casseres, M. L., Boussetta, H., Doumas, P., Hernandez, L. E., et al. (2016). Characterisation of lead-induced stress molecular biomarkers in *Medicago sativa* plants. *Environ. Exp. Bot.* 123, 1–12.

Helaoui, S., Boughattas, I., Hattab, S., Mkhinini, M., Alphonse, V., Livet, A., et al. (2020). Physiological, biochemical and transcriptomic responses of *Medicago sativa* to nickel exposure. *Chemosphere* 249:126121. doi: 10.1016/j.chemosphere.2020.126121

Hernández-de-Diego, R., Tarazona, S., Martínez-Mira, C., Balzano-Nogueira, L., Furió-Tarí, P., Pappas, G. J. Jr., et al. (2018). PaintOmics 3: a web resource for the pathway analysis and visualization of multi-omics data. *Nucleic Acids Res.* 46, W503–W509. doi: 10.1093/nar/gky466

Hu, Z., Fu, Q., Zheng, J., Zhang, A., and Wang, H. (2020). Transcriptomic and metabolomic analyses reveal that melatonin promotes melon root development under copper stress by inhibiting jasmonic acid biosynthesis. *Hortic. Res.* 7, 1–15. doi: 10.1038/s41438-020-0293-5

Huang, L., Li, Y., Zhao, M., Chao, Y., Qiu, R., Yang, Y., et al. (2018). Potential of *Cassia alata* L. coupled with biochar for heavy metal stabilization in multi-metal mine tailings. *Int. J. Environ. Res. Public Health* 15:494. doi: 10.3390/ijerph15030494

Huang, S. Q., Peng, J., Qiu, C. X., and Yang, Z. M. (2009). Heavy metal-regulated new microRNAs from rice. *J. Inor. Biochem.* 103, 282–287. doi: 10.1016/j.jinorgbio.2008.10.019

Hussain, M. B., Ali, S., Azam, A., Hina, S., Farooq, M. A., Ali, B., et al. (2013). Morphological, physiological and biochemical responses of plants to nickel stress: a review. *Afr. J. Agric. Res.* 8, 1596–1602.

Ibarra, A. A. G., Wrobel, K., Barrientos, E. Y., Escobosa, A. R. C., Corona, J. F. G., Donis, I. E., et al. (2019). Impact of Cr (VI) on the oxidation of polyunsaturated fatty acids in *Helianthus annuus* roots studied by metabolomic tools. *Chemosphere* 220, 442–451. doi: 10.1016/j.chemosphere.2018.12.145

Ifie, J., Ifie-Etumah, S., and Ikhajiagbe, B. (2020). Physiological and biochemical responses of selected cowpea (*Vigna unguiculata* (L.) Walp.) accessions to iron toxicity. *Acta Agric. Slovenica* 115, 25–38.

Jalmi, S. K., Bhagat, P. K., Verma, D., Noryang, S., Tayyeba, S., Singh, K., et al. (2018). Traversing the links between heavy metal stress and plant signaling. *Front. Plant Sci.* 9:12. doi: 10.3389/fpls.2018.00012

Jamla, M., Khare, T., Joshi, S., Patil, S., Penna, S., and Kumar, V. (2021a). Omics approaches for understanding heavy metal responses and tolerance in plants. *Curr. Plant Biol.* 27:100213. doi: 10.1016/j.cpb.2021.100213

Jamla, M., Patil, S., Joshi, S., Khare, T., and Kumar, V. (2021b). MicroRNAs and their exploration for developing heavy metal-tolerant plants. *J. Plant Growth Regul.* [Epub ahead of print]. doi: 10.1007/s00344-021-10476-2

Jang, Y., Yu, N., Seo, J., Kim, S., and Lee, S. (2016). MONGKIE: an integrated tool for network analysis and visualization for multi-omics data. *Biol. Direct* 11, 1–9. doi: 10.1186/s13062-016-0112-y

Janicka-Russak, M., Kabała, K., and Burzyński, M. (2012). Different effect of cadmium and copper on H+-ATPase activity in plasma membrane vesicles from *Cucumis sativus* roots. *J. Exp. Bot.* 63, 4133–4142. doi: 10.1093/jxb/ers097

Jian, H., Yang, B., Zhang, A., Ma, J., Ding, Y., Chen, Z., et al. (2018). Genome-wide identification of microRNAs in response to cadmium stress in oilseed rape (*Brassica napus* L.) using high-throughput sequencing. *Int. J. Mol. Sci.* 19:1431. doi: 10.3390/ijms19051431

Jiang, W., Wu, Z., Wang, T., Mantri, N., Huang, H., Li, H., et al. (2020). Physiological and transcriptomic analyses of cadmium stress response in *Dendrobium officinale* seedling. *Plant Physiol. Biochem.* 148, 152–165. doi: 10.1016/j.plaphy.2020.01.010

Jorrin-Novo, J. V., Komatsu, S., Sanchez-Lucas, R., and de Francisco, L. E. R. (2019). Gel electrophoresis-based plant proteomics: past, present, and future. Happy 10th anniversary Journal of Proteomics! *J. Proteom.* 198, 1–10. doi: 10.1016/j.jprot.2018.08.016

Jung, J., Maeda, M., Chang, A., Bhandari, M., Ashapure, A., and Landivar-Bowles, J. (2021). The potential of remote sensing and artificial intelligence as tools to improve the resilience of agriculture production systems. *Curr. Opin. Biotechnol.* 70, 15–22. doi: 10.1016/j.copbio.2020.09.003

Júnior, C. A. L., Mazzafera, P., and Arruda, M. A. Z. (2014). A comparative ionomic approach focusing on cadmium effects in sunflowers (*Helianthus annuus* L.). *Environ. Exp. Bot.* 107, 180–186. doi: 10.1016/j.envexpbot.2014.06.002

Kakeshpour, T. (2020). *Tomato Class II Glutaredoxin Mutants Generated Via Multiplex CRISPR/Cas9 Genome Editing Technology are Susceptible to Multiple Abiotic Stresses*. Doctoral dissertation. Manhattan, KS: Kansas State University.

Kanehisa, M., Sato, Y., Furumichi, M., Morishima, K., and Tanabe, M. (2019). New approach for understanding genome variations in KEGG. *Nucleic Acids Res.* 47, D590–D595. doi: 10.1093/nar/gky962

Kar, S., Mai, H.-J., Khalouf, H., Abdallah, H. B., Flachbart, S., Fink-Straube, C., et al. (2020). Transcriptomic expression patterns of two contrasting lowland rice varieties reveal high iron stress tolerance. *bioRxiv* [Preprint]. doi: 10.1101/2020.05.01.070516

Karthika, K., Rashmi, I., and Parvathi, M. (2018). "Biological functions, uptake and transport of essential nutrients in relation to plant growth," in *Plant Nutrients and Abiotic Stress Tolerance*, eds M. Hasanuzzaman, M. Fujita, H. Oku, K. Nahar, and B. Hawrylak-Nowak (Berlin: Springer), 1–49. doi: 10.1007/978-981-10-9044-8_1

Kashem, M. A., and Kawai, S. (2007). Alleviation of cadmium phytotoxicity by magnesium in Japanese mustard spinach. *Soil Sci. Plant Nutr.* 53, 246–251. doi: 10.1111/j.1747-0765.2007.00129.x

Khan, M. A., Castro-Guerrero, N. A., McInturf, S. A., Nguyen, N. T., Dame, A. N., Wang, J., et al. (2018). Changes in iron availability in *Arabidopsis* are rapidly sensed in the leaf vasculature and impaired sensing leads to opposite transcriptional programs in leaves and roots. *Plant Cell Environ.* 41, 2263–2276. doi: 10.1111/pce.13192

Khan, M. I. R., Chopra, P., Chhillar, H., Ahanger, M. A., Hussain, S. J., and Maheshwari, C. (2021). Regulatory hubs and strategies for improving heavy metal tolerance in plants: chemical messengers, omics and genetic engineering. *Plant Physiol. Biochem.* 164, 260–278. doi: 10.1016/j.plaphy.2021.05.006

Kim, J. Y., Symeonidi, E., Pang, T. Y., Denyer, T., Weidauer, D., Bezrutczyk, M., et al. (2021). Distinct identities of leaf phloem cells revealed by single cell transcriptomics. *Plant Cell* 33, 511–530. doi: 10.1093/plcell/koaa060

Kök, A. B., Mungan, M. D., Doğanlar, S., and Frary, A. (2020). Transcriptomic analysis of selenium accumulation in *Puccinellia distans* (Jacq.) Parl., a boron hyperaccumulator. *Chemosphere* 245:125665. doi: 10.1016/j.chemosphere.2019.125665

Komarkova, M., Chromy, J., Pokorna, E., Soudek, P., and Machova, P. (2020). Physiological and transcriptomic response of grey Poplar (*Populus* × *Canescens* Aiton Sm.) to cadmium stress. *Plants* 9:1485. doi: 10.3390/plants9111485

Kouhi, F., Sorkheh, K., and Ercisli, S. (2020). MicroRNA expression patterns unveil differential expression of conserved miRNAs and target genes against abiotic stress in safflower. *PLoS One* 15:e0228850. doi: 10.1371/journal.pone.0228850

Kumari, A., and Pandey-Rai, S. (2018). Enhanced arsenic tolerance and secondary metabolism by modulation of gene expression and proteome profile in *Artemisia annua* L. after application of exogenous salicylic acid. *Plant Physiol. Biochem.* 132, 590–602. doi: 10.1016/j.plaphy.2018.10.010

Lai, J.-L., Liu, Z.-W., and Luo, X.-G. (2020). A metabolomic, transcriptomic profiling, and mineral nutrient metabolism study of the phytotoxicity mechanism of uranium. *J. Hazard. Mater.* 386:121437. doi: 10.1016/j.jhazmat.2019.121437

Lancíková, V., Tomka, M., Žiarovská, J., Gažo, J., and Hricová, A. (2020). Morphological responses and gene expression of grain Amaranth (*Amaranthus* spp.) growing under Cd. *Plants* 9:572. doi: 10.3390/plants9050572

Li, B., Sun, L., Huang, J., Göschl, C., Shi, W., Chory, J., et al. (2019). GSNOR provides plant tolerance to iron toxicity via preventing iron-dependent nitrosative and oxidative cytotoxicity. *Nat. Commun.* 10, 1–13. doi: 10.1038/s41467-019-11892-5

Liang, K., Liang, S., and Zhu, H. (2020). Comparative proteomics analysis of the effect of selenium treatment on the quality of foxtail millet. *Lebensm. Wiss. Technol.* 131:109691.

Lin, K., Kools, H., de Groot, P. J., Gavai, A. K., Basnet, R. K., Cheng, F., et al. (2011). MADMAX–Management and analysis database for multiple˜ omics experiments. *J. Integr. Bioinfor.* 8, 59–74.

Lin, T., Zhu, X., Zhang, F., and Wan, X. (2011). The detoxification effect of nitrogen on cadmium stress in *Populus yunnanensis*. *Bot. Res. J.* 4, 13–19.

Liu, H., Wang, F., Xiao, Y., Tian, Z., Wen, W., Zhang, X., et al. (2016). MODEM: multi-omics data envelopment and mining in maize. *Database* 2016:baw117. doi: 10.1093/database/baw117

Liu, L., Yin, H., Liu, Y., Shen, L., Yang, X., Zhang, D., et al. (2021). Analysis of cadmium-stress-induced microRNAs and their targets reveals bra-miR172b-3p as a potential Cd2+-specific resistance factor in *Brassica juncea*. *Processes* 9:1099. doi: 10.3390/pr9071099

Liu, P., Huang, R., Hu, X., Jia, Y., Li, J., Luo, J., et al. (2019). Physiological responses and proteomic changes reveal insights into Stylosanthes response to manganese toxicity. *BMC Plant Biol.* 19:212. doi: 10.1186/s12870-019-1822-y

Liu, Q., Zhang, Y., Wang, Y., Wang, W., Gu, C., Huang, S., et al. (2020). Quantitative proteomic analysis reveals complex regulatory and metabolic response of *Iris lactea* Pall. var. chinensis to cadmium toxicity. *J. Hazard. Mater.* 400:123165. doi: 10.1016/j.jhazmat.2020.123165

Liu, S., Ali, S., Yang, R., Tao, J., and Ren, B. (2019). A newly discovered Cd-hyperaccumulator *Lantana camara* L. *J. Hazard Mater.* 371, 233–242. doi: 10.1016/j.jhazmat.2019.03.016

Liu, X., Chen, S., Chen, M., Zheng, G., Peng, Y., Shi, X., et al. (2019). Association study reveals genetic loci responsible for arsenic, cadmium and lead accumulation in rice grain in contaminated farmlands. *Front. Plant Sci.* 10:61. doi: 10.3389/fpls.2019.00061

Lokhande, V. H., Patade, V. Y., Srivastava, S., Suprasanna, P., Shrivastava, M., and Awasthi, G. (2020). Copper accumulation and biochemical responses of *Sesuvium portulacastrum* (L.). *Mater. Today Proc.* 31, 679–684. doi: 10.1016/j.matpr.2020.07.117

Lowe, R., Shirley, N., Bleackley, M., Dolan, S., and Shafee, T. (2017). Transcriptomics technologies. *PLoS Comput. Biol.* 13:e1005457. doi: 10.1371/journal.pcbi.1005457

Luo, J.-S., Gu, T., Yang, Y., and Zhang, Z. (2019). A non-secreted plant defensin AtPDF2.6 conferred cadmium tolerance via its chelation in *Arabidopsis*. *Plant Mol. Biol.* 100, 561–569. doi: 10.1007/s11103-019-00878-y

Luo, J.-S., and Zhang, Z. (2019). Proteomic changes in the xylem sap of *Brassica napus* under cadmium stress and functional validation. *BMC Plant Biol.* 19:280. doi: 10.1186/s12870-019-1895-7

Luo, W., Pant, G., Bhavnasi, Y. K., Blanchard, S. G. Jr., and Brouwer, C. (2017). Pathview Web: user friendly pathway visualization and data integration. *Nucleic Acids Res.* 45, W501–W508. doi: 10.1093/nar/gkx372

Lyu, G., Li, D., Li, S., Ning, C., and Qin, R. (2020). Genotoxic effects and proteomic analysis on *Allium cepa* var. agrogarum L. root cells under Pb stress. *Ecotoxicology* 29, 959–972. doi: 10.1007/s10646-020-02236-x

Malar, S., Vikram, S. S., Favas, P. J., and Perumal, V. (2016). Lead heavy metal toxicity induced changes on growth and antioxidative enzymes level in water hyacinths [*Eichhornia crassipes* (Mart.)]. *Bot. Stud.* 55, 1–11. doi: 10.1186/s40529-014-0054-6

Malik, B., and Pirzadah, T. B. (2020). Lead induced changes in biomarkers and proteome map of Chicory (*Cichorium intybus* L.). *Curr. Bot.* 11, 111–116.

Marrugo-Negrete, J., Durango-Hernández, J., Pinedo-Hernández, J., Enamorado-Montes, G., and Díez, S. (2016). Mercury uptake and effects on growth in *Jatropha curcas*. *J. Environ. Sci.* 48, 120–125. doi: 10.1016/j.jes.2015.10.036

Mathur, S., Kalaji, H., and Jajoo, A. (2016). Investigation of deleterious effects of chromium phytotoxicity and photosynthesis in wheat plant. *Photosynthetica* 54, 185–192.

Mawia, A. M., Hui, S., Zhou, L., Li, H., Tabassum, J., Lai, C., et al. (2020). Inorganic arsenic toxicity and alleviation strategies in rice. *J. Hazard. Mater.* 408:124751. doi: 10.1016/j.jhazmat.2020.124751

Mehmood, S. S., Lu, G., Luo, D., Hussain, M. A., Raza, A., Zafar, Z., et al. (2021). Integrated analysis of transcriptomics and proteomics provides insights into the molecular regulation of cold response in *Brassica napus*. *Environ. Exp. Bot.* 187:104480.

Mishra, S., Bharagava, R. N., More, N., Yadav, A., Zainith, S., Mani, S., et al. (2019). "Heavy metal contamination: an alarming threat to environment and human health," in *Environmental Biotechnology: For Sustainable Future*, eds R. C. Sobti, N. K. Arora, and R. Kothari (Cham: Springer), 103–125.

Mishra, V. K., Gupta, S., Chand, R., Yadav, P. S., Singh, S. K., Joshi, A. K., et al. (2019). Comparative transcriptomic profiling of High-and Low-grain Zinc and

Iron containing Indian wheat genotypes. *Curr. Plant Biol.* 18:100105. doi: 10.1016/j.cpb.2019.100105

Mišúthová, A., Slováková, Ľ, Kollárová, K., and Vaculík, M. (2021). Effect of silicon on root growth, ionomics and antioxidant performance of maize roots exposed to As toxicity. *Plant Physiol. Biochem.* 168, 155–166. doi: 10.1016/j.plaphy.2021.10.012

Montague, E., Stanberry, L., Higdon, R., Janko, I., Lee, E., Anderson, N., et al. (2014). MOPED 2.5—an integrated multi-omics resource: multi-omics profiling expression database now includes transcriptomics data. *Omics J. Integr. Biol.* 18, 335–343. doi: 10.1089/omi.2014.0061

Mthembu, M. S., Odinga, C. A., Bux, F., and Swalaha, F. M. (2020). "Constructed wetlands: an eco-sustainable phytotechnology for degradation and detoxification of industrial wastewaters," in *Bioremediation of Industrial Waste for Environmental Safety*, eds G. Saxena and R. N. Bharagava (Singapore: Springer), 291–312.

Muntean, E., Muntean, N., Duda, M., and Michalski, R. (2019). Heavy metals' uptake from soil in potato tubers: an ionomic approach. *ProEnvironment* 12, 159–162.

Murugaiyan, V., Ali, J., Mahender, A., Aslam, U. M., Jewel, Z. A., Pang, Y., et al. (2019). Mapping of genomic regions associated with arsenic toxicity stress in a backcross breeding populations of rice (*Oryza sativa* L.). *Rice* 12:61. doi: 10.1186/s12284-019-0321-y

Mwamba, T., Islam, F., Ali, B., Lwalaba, J., Gill, R., Zhang, F., et al. (2020). Comparative metabolomic responses of low-and high-cadmium accumulating genotypes reveal the cadmium adaptive mechanism in *Brassica napus*. *Chemosphere* 250:126308. doi: 10.1016/j.chemosphere.2020.126308

Nagel, K. A., Lenz, H., Kastenholz, B., Gilmer, F., Averesch, A., Putz, A., et al. (2020). The platform GrowScreen-Agar enables identification of phenotypic diversity in root and shoot growth traits of agar grown plants. *Plant Methods* 16, 1–17. doi: 10.1186/s13007-020-00631-3

Naika, M., Shameer, K., and Sowdhamini, R. (2013). Comparative analyses of stress-responsive genes in *Arabidopsis thaliana*: insight from genomic data mining, functional enrichment, pathway analysis and phenomics. *Mol. BioSyst.* 9, 1888–1908. doi: 10.1039/c3mb70072k

National Genomics Data Center Members and Partners (2020). Database resources of the National Genomics Data Center in 2020. *Nucleic Acids Res.* 48, D24–D33. doi: 10.1093/nar/gkz913

Navarro-Reig, M., Jaumot, J., Piña, B., Moyano, E., Galceran, M. T., and Tauler, R. (2017). Metabolomic analysis of the effects of cadmium and copper treatment in *Oryza sativa* L. using untargeted liquid chromatography coupled to high resolution mass spectrometry and all-ion fragmentation. *Metallomics* 9, 660–675. doi: 10.1039/c6mt00279j

Nie, G., Liao, Z., Zhong, M., Zhou, J., Cai, J., Liu, A., et al. (2021). MicroRNA-mediated responses to chromium stress provides insight toward to tolerance characteristics of *Miscanthus sinensis*. *Front. Plant Sci.* 12:666117. doi: 10.3389/fpls.2021.666117

Njobvu, J., Hamabwe, S. M., Munyinda, K., Kelly, J. D., and Kamfwa, K. (2020). Quantitative trait loci mapping of resistance to aluminum toxicity in common bean. *Crop Sci.* 60, 1294–1302. doi: 10.1007/s00122-009-1051-0

O'Connor, D., Peng, T., Li, G., Wang, S., Duan, L., Mulder, J., et al. (2018). Sulfur-modified rice husk biochar: a green method for the remediation of mercury contaminated soil. *Sci. Total Environ.* 621, 819–826. doi: 10.1016/j.scitotenv.2017.11.213

Oliveira, B. R. M., de Almeida, A.-A. F., Pirovani, C. P., Barroso, J. P., Neto, C. H. C., Santos, N. A., et al. (2020). Mitigation of Cd toxicity by Mn in young plants of cacao, evaluated by the proteomic profiles of leaves and roots. *Ecotoxicology* 29, 340–358. doi: 10.1007/s10646-020-02178-4

Oyewo, O. A., Adeniyi, A., Bopape, M. F., and Onyango, M. S. (2020). "Heavy metal mobility in surface water and soil, climate change, and soil interactions," in *Climate Change and Soil Interactions*, eds M. N. V. Prasad and M. Pietrzykowski (Amsterdam: Elsevier), 51–88. doi: 10.1016/b978-0-12-818032-7.00004-7

Pan, X., Li, Y., Liu, W., Liu, S., Min, J., Xiong, H., et al. (2020). QTL mapping and candidate gene analysis of cadmium accumulation in polished rice by genome-wide association study. *Sci. Rep.* 10:11791. doi: 10.1038/s41598-020-68742-4

Pandey, A. K., Gautam, A., and Dubey, R. S. (2019). Transport and detoxification of metalloids in plants in relation to plant-metalloid tolerance. *Plant Gene* 17:100171. doi: 10.1007/s11356-020-10293-2

Pandey, A. K., Gedda, M. R., and Verma, A. K. (2020). Effect of arsenic stress on expression pattern of a rice specific miR156j at various developmental stages and their allied co-expression target networks. *Front. Plant Sci.* 11:752. doi: 10.3389/fpls.2020.00752

Papoutsoglou, E. A., Faria, D., Arend, D., Arnaud, E., Athanasiadis, I. N., Chaves, I., et al. (2020). Enabling reusability of plant phenomic datasets with MIAPPE 1.1. *New Phytol.* 227, 260–273. doi: 10.1111/nph.16544

Parmar, P., Dave, B., Sudhir, A., Panchal, K., and Subramanian, R. (2013). Physiological, biochemical and molecular response of plants against heavy metals stress. *Int. J. Curr. Res.* 5, 80–89.

Patel, M., Rangani, J., Kumari, A., and Parida, A. K. (2020). Mineral nutrient homeostasis, photosynthetic performance, and modulations of antioxidative defense components in two contrasting genotypes of *Arachis hypogaea* L. (peanut) for mitigation of nitrogen and/or phosphorus starvation. *J. Biotechnol.* 323, 136–158.

Paunov, M., Koleva, L., Vassilev, A., Vangronsveld, J., and Goltsev, V. (2018). Effects of different metals on photosynthesis: cadmium and zinc affect chlorophyll fluorescence in durum wheat. *Int. J. Mol. Sci.* 19:787. doi: 10.3390/ijms19030787

Pavlova, D. (2017). Nickel effect on root-meristem cell division in *Plantago lanceolata* (Plantaginaceae) seedlings. *Aust. J. Bot.* 65, 446–452. doi: 10.1071/bt17054

Pereira, M. P., de Almeida Rodrigues, L. C., Corrêa, F. F., de Castro, E. M., Ribeiro, V. E., and Pereira, F. J. (2016). Cadmium tolerance in *Schinus molle* trees is modulated by enhanced leaf anatomy and photosynthesis. *Trees* 30, 807–814. doi: 10.1007/s00468-015-1322-0

Pidatala, V. R., Li, K., Sarkar, D., Ramakrishna, W., and Datta, R. (2016). Identification of biochemical pathways associated with lead tolerance and detoxification in *Chrysopogon zizanioides* L. Nash (Vetiver) by metabolic profiling. *Environ. Sci. Technol.* 50, 2530–2537. doi: 10.1021/acs.est.5b04725

Pidatala, V. R., Li, K., Sarkar, D., Wusirika, R., and Datta, R. (2018). Comparative metabolic profiling of vetiver (*Chrysopogon zizanioides*) and maize (*Zea mays*) under lead stress. *Chemosphere* 193, 903–911. doi: 10.1016/j.chemosphere.2017.11.087

Pinu, F. R., Beale, D. J., Paten, A. M., Kouremenos, K., Swarup, S., Schirra, H. J., et al. (2019). Systems biology and multi-omics integration: viewpoints from the metabolomics research community. *Metabolites* 9:76. doi: 10.3390/metabo9040076

Pirzadah, T. B., Malik, B., and Hakeem, K. R. (2019). "Integration of "Omic" approaches to unravel the heavy metal tolerance in plants," in *Essentials of Bioinformatics*, ed. J. Xiong (Berlin: Springer), 79–92. doi: 10.1007/978-3-030-19318-8_4

Pratap, A., Gupta, S., Nair, R. M., Gupta, S., Schafleitner, R., Basu, P., et al. (2019). Using plant phenomics to exploit the gains of genomics. *Agronomy* 9:126. doi: 10.3389/fpls.2021.626565

Punshon, T., Ricachenevsky, F. K., Hindt, M. N., Socha, A. L., and Zuber, H. (2013). Methodological approaches for using synchrotron X-ray fluorescence (SXRF) imaging as a tool in ionomics: examples from *Arabidopsis thaliana*. *Metallomics* 5, 1133–1145. doi: 10.1039/c3mt00120b

Qiu, Z., Hai, B., Guo, J., Li, Y., and Zhang, L. (2016). Characterization of wheat miRNAs and their target genes responsive to cadmium stress. *Plant Physiol. Biochem.* 101, 60–67. doi: 10.1016/j.plaphy.2016.01.020

Rai, P. K., Lee, S. S., Zhang, M., Tsang, Y. F., and Kim, K.-H. (2019). Heavy metals in food crops: health risks, fate, mechanisms, and management. *Environ. Int.* 125, 365–385. doi: 10.1016/j.envint.2019.01.067

Rath, B. P., Hota, S., Subhadarshini, S., Dash, D., and Das, P. K. (2019). Consequence of chromium-tainted soil on physical and biochemical responses of *Vigna radiata* L. *J. Appl. Biol. Biotechnol.* 7, 35–41.

Raza, A. (2020). Metabolomics: a systems biology approach for enhancing heat stress tolerance in plants. *Plant Cell Rep.* [Epub ahead of print]. doi: 10.1007/s00299-020-02635-8

Raza, A., Habib, M., Charagh, S., and Kakavand, S. N. (2021a). "Genetic engineering of plants to tolerate toxic metals and metalloids," in *Handbook of Bioremediation*, eds M. Hasanuzzaman and M. N. V. Prasad (Cambridge, MA: Academic Press), 411–436. doi: 10.1016/b978-0-12-819382-2.00026-0

Raza, A., Habib, M., Kakavand, S. N., Zahid, Z., Zahra, N., Sharif, R., et al. (2020). Phytoremediation of cadmium: physiological, biochemical, and molecular mechanisms. *Biology* 9:177. doi: 10.3390/biology9070177

Raza, A., Razzaq, A., Mehmood, S. S., Hussain, M. A., Wei, S., He, H., et al. (2021b). Omics: the way forward to enhance abiotic stress tolerance in *Brassica napus* L. *GM Crops Food* 12, 251–281. doi: 10.1080/21645698.2020.1859898

Raza, A., Su, W., Hussain, M. A., Mehmood, S. S., Zhang, X., Cheng, Y., et al. (2021c). Integrated analysis of metabolome and transcriptome reveals insights for cold tolerance in rapeseed (*Brassica napus* L.). *Front. Plant Sci.* 12:721681. doi: 10.3389/fpls.2021.721681

Raza, A., Tabassum, J., Kudapa, H., and Varshney, R. K. (2021d). Can omics deliver temperature resilient ready-to-grow crops? *Crit. Rev. Biotechnol.* 7, 1–24. doi: 10.1080/07388551.2021.1898332

Razzaq, A., Sadia, B., Raza, A., Khalid Hameed, M., and Saleem, F. (2019). Metabolomics: a way forward for crop improvement. *Metabolites* 9:303. doi: 10.3390/metabo9120303

Rehman, F., Khan, F., Varshney, D., Naushin, F., and Rastogi, J. (2011). Effect of cadmium on the growth of tomato. *Biol. Med.* 3, 187–190.

Rehman, M., Liu, L., Bashir, S., Saleem, M. H., Chen, C., Peng, D., et al. (2019). Influence of rice straw biochar on growth, antioxidant capacity and copper uptake in ramie (*Boehmeria nivea* L.) grown as forage in aged copper-contaminated soil. *Plant Physiol. Biochem.* 138, 121–129. doi: 10.1016/j.plaphy.2019.02.021

Rohart, F., Gautier, B., Singh, A., and Lê Cao, K.-A. (2017). mixOmics: an R package for 'omics feature selection and multiple data integration. *PLoS Comput. Biol.* 13:e1005752. doi: 10.1371/journal.pcbi.1005752

Roorkiwal, M., Bharadwaj, C., Barmukh, R., Dixit, G. P., Thudi, M., Gaur, P. M., et al. (2020). Integrating genomics for chickpea improvement: achievements and opportunities. *Theor. Appl. Genet.* 133, 1703–1720. doi: 10.1007/s00122-020-03584-2

Rouphael, Y., Colla, G., Bernardo, L., Kane, D., Trevisan, M., and Lucini, L. (2016). Zinc excess triggered polyamines accumulation in lettuce root metabolome, as compared to osmotic stress under high salinity. *Front. Plant Sci.* 7:842. doi: 10.3389/fpls.2016.00842

Rucińska-Sobkowiak, R. (2016). Water relations in plants subjected to heavy metal stresses. *Acta Physiol. Plant* 38:257.

Sabrine, H., Afif, H., Mohamed, B., Hamadi, B., and Maria, H. (2010). Effects of cadmium and copper on pollen germination and fruit set in pea (*Pisum sativum* L.). *Sci. Hortic.* 125, 551–555. doi: 10.1016/j.scienta.2010.05.031

Safdar, L. B., Almas, F., Sarfraz, S., Ejaz, M., Ali, Z., Mahmood, Z., et al. (2020a). Genomewide association study identifies five new cadmium uptake loci in wheat. *Plant Genome* 13:e20030. doi: 10.1002/tpg2.20030

Safdar, L. B., Andleeb, T., Latif, S., Umer, M. J., Tang, M., Li, X., et al. (2020b). Genome-wide association study and QTL meta-analysis identified novel genomic loci controlling potassium use efficiency and agronomic traits in bread wheat. *Front. Plant Sci.* 11:70. doi: 10.3389/fpls.2020.00070

Saini, S., and Dhania, G. (2020). "Cadmium as an environmental pollutant: ecotoxicological effects, health hazards, and bioremediation approaches for its detoxification from contaminated sites," in *Bioremediation of Industrial Waste for Environmental Safety*, eds R. N. Bharagava and G. Saxena (Singapore: Springer), 357–387.

Sakurai, N., Ara, T., Ogata, Y., Sano, R., Ohno, T., Sugiyama, K., et al. (2011). KaPPA-View4: a metabolic pathway database for representation and analysis of correlation networks of gene co-expression and metabolite co-accumulation and omics data. *Nucleic Acids Res.* 39, D677–D684. doi: 10.1093/nar/gkq989

Saleem, M. H., Fahad, S., Rehman, M., Saud, S., Jamal, Y., Khan, S., et al. (2020). Morpho-physiological traits, biochemical response and phytoextraction potential of short-term copper stress on kenaf (*Hibiscus cannabinus* L.) seedlings. *PeerJ* 8:e8321. doi: 10.7717/peerj.8321

Salehi, H., Chehregani Rad, A., Raza, A., and Chen, J. T. (2021). Foliar application of CeO2 nanoparticles alters generative components fitness and seed productivity in bean crop (*Phaseolus vulgaris* L.). *Nanomaterials* 11:862. doi: 10.3390/nano11040862

Salim, N., and Raza, A. (2020). Nutrient use efficiency (NUE) for sustainable wheat production: a review. *J. Plant Nutr.* 43, 297–315. doi: 10.1080/01904167.2019.1676907

Sangwan, P., Kumar, V., and Joshi, U. (2014). Effect of chromium (VI) toxicity on enzymes of nitrogen metabolism in clusterbean (*Cyamopsis tetragonoloba* L.). *Enzyme Res.* 2014:784036. doi: 10.1155/2014/784036

Sarwar, N., Imran, M., Shaheen, M. R., Ishaque, W., Kamran, M. A., Matloob, A., et al. (2017). Phytoremediation strategies for soils contaminated with heavy metals: modifications and future perspectives. *Chemosphere* 171, 710–721. doi: 10.1016/j.chemosphere.2016.12.116

Schmidt, S. B., Eisenhut, M., and Schneider, A. (2020). Chloroplast transition metal regulation for efficient photosynthesis. *Trends Plant Sci.* 25, 817–828. doi: 10.1016/j.tplants.2020.03.003

Schwacke, R., Ponce-Soto, G. Y., Krause, K., Bolger, A. M., Arsova, B., Hallab, A., et al. (2019). MapMan4: a refined protein classification and annotation framework applicable to multi-omics data analysis. *Mol. Plant.* 12, 879–892. doi: 10.1016/j.molp.2019.01.003

Shenton, M., Kudo, T., Kobayashi, M., Nakamura, Y., Ohyanagi, H., and Yano, K. (2019). "Plant omics data center and CATchUP: web databases for effective gene mining utilizing public RNA-Seq-based transcriptome data," in *The Model Legume Medicago Truncatula*, ed. F. J. de Bruijn (Hoboken, NJ: Wiley), 1137–1146.

Shu, H., Zhang, J., Liu, F., Bian, C., Liang, J., Liang, J., et al. (2019). Comparative transcriptomic studies on a cadmium hyperaccumulator *Viola baoshanensis* and its non-tolerant counterpart *V. inconspicua*. *Int. J. Mol. Sci.* 20:1906. doi: 10.3390/ijms20081906

Shukla, A., Srivastava, S., and D'Souza, S. F. (2018). An integrative approach toward biosensing and bioremediation of metals and metalloids. *Inter. J. Environ. Sci. Technol.* 15, 2701–2712.

Shukla, T., Khare, R., Kumar, S., Lakhwani, D., Sharma, D., Asif, M. H., et al. (2018). Differential transcriptome modulation leads to variation in arsenic stress response in *Arabidopsis thaliana* accessions. *J. Hazard Mat.* 351, 1–10. doi: 10.1016/j.jhazmat.2018.02.031

Son, J. A., Narayanankutty, D. P., and Roh, K. S. (2014). Influence of exogenous application of glutathione on rubisco and rubisco activase in heavy metal-stressed tobacco plant grown in vitro. *Saudi J. Biol. Sci.* 21, 89–97. doi: 10.1016/j.sjbs.2013.06.002

Song, X., Nie, F., Chen, W., Ma, X., Gong, K., Yang, Q., et al. (2020a). Coriander genomics database: a genomic, transcriptomic, and metabolic database for coriander. *Hortic. Res.* 7, 1–10.

Song, X., Zhang, C., Chen, W., Zhu, Y., and Wang, Y. (2020b). Growth responses and physiological and biochemical changes in five ornamental plants grown in urban lead-contaminated soils. *Plant Environ. Int.* 1, 29–47. doi: 10.1002/pei3.10013

Stich, B., Benke, A., Schmidt, M., Urbany, C., Shi, R., and von Wirén, N. (2020). The maize shoot ionome: its interaction partners, predictive power, and genetic determinants. *Plant Cell Environ.* 43, 2095–2111. doi: 10.1111/pce.13823

Su, C., Jiang, Y., Li, F., Yang, Y., Lu, Q., Zhang, T., et al. (2017). Investigation of subcellular distribution, physiological, and biochemical changes in *Spirodela polyrhiza* as a function of cadmium exposure. *Environ. Exp. Bot.* 142, 24–33.

Sun, H., Wang, X., Li, H., Bi, J., Yu, J., Liu, X., et al. (2020). Selenium modulates cadmium-induced ultrastructural and metabolic changes in cucumber seedlings. *RSC Adv.* 10, 17892–17905. doi: 10.1039/d0ra02866e

Sundaramoorthy, P., Chidambaram, A., Ganesh, K. S., Unnikannan, P., and Baskaran, L. (2010). Chromium stress in paddy:(i) nutrient status of paddy under chromium stress;(ii) phytoremediation of chromium by aquatic and terrestrial weeds. *Comptes Rendus Biol.* 333, 597–607. doi: 10.1016/j.crvi.2010.03.002

Suzuki, N. (2005). Alleviation by calcium of cadmium-induced root growth inhibition in *Arabidopsis* seedlings. *Plant Biotechnol.* 22, 19–25.

Syed, M. A., Iftekharuddaula, K., Mian, M. K., Rasul, M. G., Rahmam, G. M., Panaullah, G. M., et al. (2016). Main effect QTLs associated with arsenic phyto-toxicity tolerance at seedling stage in rice (*Oryza sativa* L.). *Euphytica* 209, 805–814. doi: 10.1007/s10681-016-1683-5

Sylvain, B., Mikael, M. H., Florie, M., Emmanuel, J., Marilyne, S., Sylvain, B., et al. (2016). Phytostabilization of As, Sb and Pb by two willow species (*S. viminalis* and *S. purpurea*) on former mine technosols. *Catena* 136, 44–52. doi: 10.1016/j.catena.2015.07.008

Tavallali, V. (2017). Interactive effects of zinc and boron on growth, photosynthesis, and water relations in pistachio. *J. Plant Nutr.* 40, 1588–1603. doi: 10.1080/01904167.2016.1270308

Tian, M., Xu, X., Liu, F., Fan, X., and Pan, S. (2018). Untargeted metabolomics reveals predominant alterations in primary metabolites of broccoli sprouts in response to pre-harvest selenium treatment. *Food Res. Int.* 111, 205–211. doi: 10.1016/j.foodres.2018.04.020

Tiwari, S., and Lata, C. (2018). Heavy metal stress, signaling, and tolerance due to plant-associated microbes: an overview. *Front. Plant Sci.* 9:452. doi: 10.3389/fpls.2018.00452

Turhadi, T., Hamim, H., Ghulamahdi, M., and Miftahudin, M. (2019). Iron toxicity-induced physiological and metabolite profile variations among tolerant and sensitive rice varieties. *Plant Signal. Behav.* 14:1682829. doi: 10.1080/15592324.2019.1682829

Ulfenborg, B. (2019). Vertical and horizontal integration of multi-omics data with miodin. *BMC Bioinform.* 20:649. doi: 10.1186/s12859-019-3224-4

Utami, D. W., Rosdianti, I., Chrisnawati, L., Subardi, S., Nurani, S., and Suwarno, S. (2020). Identification of iron tolerant candidate loci in rice determined through genome-wide association study. *Indonesian J. Agric. Sci.* 21, 17–29. doi: 10.1186/s12864-017-4221-5

Vaculík, M., Konlechner, C., Langer, I., Adlassnig, W., Puschenreiter, M., Lux, A., et al. (2012). Root anatomy and element distribution vary between two *Salix caprea* isolates with different Cd accumulation capacities. *Environ. Pollut.* 163, 117–126. doi: 10.1016/j.envpol.2011.12.031

van Dijk, A. D. J., Kootstra, G., Kruijer, W., and de Ridder, D. (2020). Machine learning in plant science and plant breeding. *Iscience* 24:101890. doi: 10.1016/j.isci.2020.101890

Varshney, R. K., Bohra, A., Yu, J., Graner, A., Zhang, Q., and Sorrells, M. E. (2021c). Designing future crops: genomics-assisted breeding comes of age. *Trends Plant Sci.* 26, 631–649. doi: 10.1016/j.tplants.2021.03.010

Varshney, R. K., Bohra, A., Roorkiwal, M., Barmukh, R., Cowling, W. A., Chitikineni, A., et al. (2021b). Fast-forward breeding for a food-secure world. *Trends Genet.* 37, 1124–1136. doi: 10.1016/j.tig.2021.08.002

Varshney, R. K., Barmukh, R., Roorkiwal, M., Qi, Y., Kholova, J., Tuberosa, R., et al. (2021a). Breeding custom-designed crops for improved drought adaptation. *Adv. Genet.* 2:e202100017.

Varshney, R. K., Sinha, P., Singh, V. K., Kumar, A., Zhang, Q., and Bennetzen, J. L. (2020). 5Gs for crop improvement. *Curr. Opin. Plant Biol.* 56, 190–196. doi: 10.1016/j.pbi.2019.12.004

Venkatachalam, P., Jayalakshmi, N., Geetha, N., Sahi, S. V., Sharma, N. C., Rene, E. R., et al. (2017). Accumulation efficiency, genotoxicity and antioxidant defense mechanisms in medicinal plant *Acalypha indica* L. under lead stress. *Chemosphere* 171, 544–553. doi: 10.1016/j.chemosphere.2016.12.092

Walter, A., Liebisch, F., and Hund, A. (2015). Plant phenotyping: from bean weighing to image analysis. *Plant Methods* 11, 1–11. doi: 10.1186/s13007-015-0056-8

Wang, C., Tang, Z., Zhuang, J.-Y., Tang, Z., Huang, X.-Y., and Zhao, F.-J. (2020a). Genetic mapping of ionomic quantitative trait loci in rice grain and straw reveals OsMOT1; 1 as the putative causal gene for a molybdenum QTL qMo8. *Mol. Genet. Genomics* 295, 391–407. doi: 10.1007/s00438-019-01632-1

Wang, D., Fan, W., Guo, X., Wu, K., Zhou, S., Chen, Z., et al. (2020b). MaGenDB: a functional genomics hub for *Malvaceae* plants. *Nucleic Acids Res.* 48, D1076–D1084. doi: 10.1093/nar/gkz953

Wang, F., Itai, R. N., Nozoye, T., Kobayashi, T., Nishizawa, N. K., and Nakanishi, H. (2020c). The bHLH protein OsIRO3 is critical for plant survival and iron (Fe) homeostasis in rice (*Oryza sativa* L.) under Fe-deficient conditions. *Soil Sci. Plant Nutr.* 66, 579–592.

Wang, J., Li, H., Zou, D., Zhao, J., Fan, L., and Wu, T. (2017). Transcriptome profile analysis of cadmium tolerance in Chinese flowering cabbage. *Hortic. Environ. Biotechnol.* 58, 56–65. doi: 10.1007/s13580-017-0075-7

Wang, L., Rinklebe, J., Tack, F. M., and Hou, D. (2021). A review of green remediation strategies for heavy metal contaminated soil. *Soil Use Manag.* 37, 936–963.

Wang, L., Zheng, B., Yuan, Y., Xu, Q., and Chen, P. (2020d). Transcriptome profiling of *Fagopyrum tataricum* leaves in response to lead stress. *BMC Plant Biol.* 20:54. doi: 10.1186/s12870-020-2265-1

Wang, M.-Q., Bai, Z.-Y., Xiao, Y.-F., Li, Y., Liu, Q.-L., Zhang, L., et al. (2019). Transcriptomic analysis of *Verbena bonariensis* roots in response to cadmium stress. *BMC Genomics* 20:877. doi: 10.1186/s12864-019-6152-9

Wang, W., Ding, G., White, P. J., Wang, M., Zou, J., Xu, F., et al. (2020e). Genetic dissection of the shoot and root ionomes of *Brassica napus* grown with contrasting phosphate supplies. *Ann. Bot.* 126, 119–140. doi: 10.1093/aob/mcaa055

Wang, X., Zhang, J., He, S., Gao, Y., Ma, X., Gao, Y., et al. (2018). HMOD: an omics database for herbal medicine plants. *Mol. Plant* 11, 757–759. doi: 10.1016/j.molp.2018.03.002

Wang, Y.-M., Yang, Q., Xu, H., Liu, Y.-J., and Yang, H.-L. (2020f). Physiological and transcriptomic analysis provide novel insight into cobalt stress responses in willow. *Sci. Rep.* 10, 1–12. doi: 10.1038/s41598-020-59177-y

Wani, W., Masoodi, K. Z., Zaid, A., Wani, S. H., Shah, F., Meena, V. S., et al. (2018). Engineering plants for heavy metal stress tolerance. *Rend. Lincei Sci. Fis. Nat.* 29, 709–723.

Weber, M., Beyene, B., Nagler, N., Herfert, J., Schempp, S., Klecker, M., et al. (2020). A mutation in the essential and widely conserved DAMAGED DNA BINDING1-Cullin4 ASSOCIATED FACTOR gene OZS3 causes hypersensitivity to zinc excess, cold and UV stress in *Arabidopsis thaliana*. *Plant J.* 103, 995–1009. doi: 10.1111/tpj.14779

Wen, R., Ya, L., Zhou, M.-Y., Zi, S., Wang, T.-Y., Zhao, J.-R., et al. (2019). Dynamic changes of root proteome reveal diverse responsive proteins in maize subjected to cadmium stress. *J. Integr. Agric.* 18, 2193–2204.

Wijngaard, R. R., van der Perk, M., van der Grift, B., de Nijs, T. C., and Bierkens, M. F. (2017). The impact of climate change on metal transport in a lowland catchment. *Water Air Soil Pollut.* 228:107. doi: 10.1007/s11270-017-3261-4

Wu, Q., Qi, J., and Xia, X. (2017). Long-term variations in sediment heavy metals of a reservoir with changing trophic states: implications for the impact of climate change. *Sci. Total Environ.* 609, 242–250. doi: 10.1016/j.scitotenv.2017.04.041

Xiao, W., Liu, P., Wang, K., Yang, Z., and Wang, L. (2021). Relationship between ionomics and transcriptomics of rice plant in response to arsenite stress. *Environ. Exp. Bot.* 189:104565.

Xie, M., Chen, W., Lai, X., Dai, H., Sun, H., Zhou, X., et al. (2019). Metabolic responses and their correlations with phytochelatins in *Amaranthus hypochondriacus* under cadmium stress. *Environ. Pollut.* 252, 1791–1800. doi: 10.1016/j.envpol.2019.06.103

Xie, Q., Yu, Q., Jobe, T. O., Pham, A., Ge, C., Guo, Q., et al. (2021). An amiRNA screen uncovers redundant CBF and ERF34/35 transcription factors that differentially regulate arsenite and cadmium responses. *Plant Cell Environ.* 44, 1692–1706. doi: 10.1111/pce.14023

Xu, L., Zhang, F., Tang, M., Wang, Y., Dong, J., Ying, J., et al. (2020). Melatonin confers cadmium tolerance by modulating critical heavy metal chelators and transporters in radish plants. *J. Pineal Res.* 69:e12659. doi: 10.1111/jpi.12659

Xu, S., Hu, C., Hussain, S., Tan, Q., Wu, S., and Sun, X. (2018). Metabolomics analysis reveals potential mechanisms of tolerance to excess molybdenum in soybean seedlings. *Ecotoxicol. Environ. Saf.* 164, 589–596. doi: 10.1016/j.ecoenv.2018.08.062

Xu, X., Zhang, S., Cheng, Z., Li, T., Jia, Y., Wang, G., et al. (2020). Transcriptome analysis revealed cadmium accumulation mechanisms in hyperaccumulator *Siegesbeckia orientalis* L. *Environ. Sci. Pollut. Res.* 27, 18853–18865. doi: 10.1007/s11356-020-08387-y

Yadav, B. S., Singh, S., Srivastava, S., Singh, N. K., and Mani, A. (2019). Whole transcriptome expression profiling and biological network analysis of chickpea during heavy metal stress. *J. Plant Biochem. Biotechnol.* 28, 345–352. doi: 10.1007/s13562-019-00486-3

Yan, A., Wang, Y., Tan, S. N., Mohd Yusof, M. L., Ghosh, S., and Chen, Z. (2020). Phytoremediation: a promising approach for revegetation of heavy metal-polluted land. *Front. Plant Sci.* 11:359. doi: 10.3389/fpls.2020.00359

Yang, M., Li, Y., Liu, Z., Tian, J., Liang, L., Qiu, Y., et al. (2020). A high activity zinc transporter OsZIP9 mediates zinc uptake in rice. *Plant J.* 103, 1695–1709. doi: 10.1111/tpj.14855

Yang, M., Lu, K., Zhao, F. J., Xie, W., Ramakrishna, P., Wang, G., et al. (2018). Genome-wide association studies reveal the genetic basis of ionomic variation in rice. *Plant Cell* 30, 2720–2740. doi: 10.1105/tpc.18.00375

Yang, W., Dai, H., Dou, X., Zhang, Q., and Wei, S. (2019). Effect and mechanism of commonly used four nitrogen fertilizers and three organic fertilizers on *Solanum nigrum* L. hyperaccumulating Cd. *Environ. Sci. Pollut. Res.* 26, 12940–12947. doi: 10.1007/s11356-019-04848-1

Yang, Y., Zhang, L., Huang, X., Zhou, Y., Quan, Q., Li, Y., et al. (2020). Response of photosynthesis to different concentrations of heavy metals in *Davidia involucrata*. *PLoS One* 15:e0228563. doi: 10.1371/journal.pone.0228563

Ye, Z., Zeng, J., Ye, L., Long, L., and Zhang, G. (2020). Genome-wide association analysis of potassium uptake and translocation rates under low K stress in Tibetan wild barley. *Euphytica* 216:35.

Yu, R., Jiang, Q., Xv, C., Li, L., Bu, S., and Shi, G. (2019). Comparative proteomics analysis of peanut roots reveals differential mechanisms of cadmium detoxification and translocation between two cultivars differing in

cadmium accumulation. *BMC Plant Biol.* 19:137. doi: 10.1186/s12870-019-1739-5

Yu, J., Wu, L., Fu, L., Shen, Q., Kuang, L., Wu, D., et al. (2019). Genotypic difference of cadmium tolerance and the associated microRNAs in wild and cultivated barley. *Plant Growth Regul.* 87, 389–401. doi: 10.1007/s10725-019-00479-1

Yuan, J., Bai, Y., Chao, Y., Sun, X., He, C., Liang, X., et al. (2018). Genome-wide analysis reveals four key transcription factors associated with cadmium stress in creeping bentgrass (*Agrostis stolonifera* L.). *PeerJ* 6:e5191. doi: 10.7717/peerj.5191

Zafar, S. A., Zaidi, S., Gaba, Y., Singla-Pareek, S. L., Dhankher, O. P., Li, X., et al. (2020). Engineering abiotic stress tolerance via CRISPR/Cas-mediated genome editing. *J. Exp. Bot.* 71, 470–479. doi: 10.1093/jxb/erz476

Zeng, R., Farooq, M. U., Wang, L., Su, Y., Zheng, T., Ye, X., et al. (2019). Study on differential protein expression in natural selenium-enriched and non-selenium-enriched rice based on iTRAQ quantitative proteomics. *Biomolecules* 9:130. doi: 10.3390/biom9040130

Zhang, C., Xu, B., Geng, W., Shen, Y., Xuan, D., Lai, Q., et al. (2019a). Comparative proteomic analysis of pepper (*Capsicum annuum* L.) seedlings under selenium stress. *PeerJ* 7:e8020. doi: 10.7717/peerj.8020

Zhang, C., Xu, B., Zhao, C.-R., Sun, J., Lai, Q., and Yu, C. (2019b). Comparative de novo transcriptomics and untargeted metabolomic analyses elucidate complicated mechanisms regulating celery (*Apium graveolens* L.) responses to selenium stimuli. *PLoS One* 14:e0226752. doi: 10.1371/journal.pone.0226752

Zhang, P., Zhong, K., Zhong, Z., and Tong, H. (2019c). Mining candidate gene for rice aluminum tolerance through genome wide association study and transcriptomic analysis. *BMC Plant Biol.* 19:490. doi: 10.1186/s12870-019-2036-z

Zhang, X.-Y., Jia, X.-M., Zhang, R., Zhu, Z.-L., Liu, B., Gao, L.-Y., et al. (2019d). Metabolic analysis in Malus halliana leaves in response to iron deficiency. *Sci. Hortic.* 258:108792.

Zhang, F., Xiao, X., Xu, K., Cheng, X., Xie, T., Hu, J., et al. (2020a). Genome-wide association study (GWAS) reveals genetic loci of lead (Pb) tolerance during seedling establishment in rapeseed (*Brassica napus* L.). *BMC Genomics* 21:139. doi: 10.1186/s12864-020-6558-4

Zhang, H., Xu, Z., Guo, K., Huo, Y., He, G., Sun, H., et al. (2020b). Toxic effects of heavy metal Cd and Zn on chlorophyll, carotenoid metabolism and photosynthetic function in tobacco leaves revealed by physiological and proteomics analysis. *Ecotoxicol. Environ. Saf.* 202:110856. doi: 10.1016/j.ecoenv.2020.110856

Zhang, L., Ding, H., Jiang, H., Wang, H., Chen, K., Duan, J., et al. (2020c). Regulation of cadmium tolerance and accumulation by miR156 in *Arabidopsis*. *Chemosphere* 242:125168. doi: 10.1016/j.chemosphere.2019.125168

Zhang, Y., Lai, J.-L., Ji, X.-H., and Luo, X.-G. (2020d). Unraveling response mechanism of photosynthetic metabolism and respiratory metabolism to uranium-exposure in *Vicia faba*. *J. Hazard. Mater.* 398:122997. doi: 10.1016/j.jhazmat.2020.122997

Zhang, Y., Wang, Y., Ding, Z., Wang, H., Song, L., Jia, S., et al. (2017). Zinc stress affects ionome and metabolome in tea plants. *Plant Physiol. Biochem.* 111, 318–328. doi: 10.1016/j.plaphy.2016.12.014

Zhang-Xuan, D., Xiao-Hui, J., and Xue-Gang, L. (2020). Absorption and Interaction mechanisms of uranium & cadmium in purple sweet potato (*Ipomoea batatas* L.). *J. Hazard. Mater.* 400:123264. doi: 10.1016/j.jhazmat.2020.123264

Zhao, L., Pan, Y., Dong, Z., Zheng, Y., Liu, J., Geng, J., et al. (2020). Investigation and genome-wide association study of grain copper content in Chinese common wheat. *J. Cereal Sci.* 95:102991.

Zhao, S., Liu, Q., Qi, Y., and Duo, L. (2010). Responses of root growth and protective enzymes to copper stress in turfgrass. *Acta Biol. Cracoviensia Series Bot.* 52, 7–11.

Zhao, Z., Zhang, H., Fu, Z., Chen, H., Lin, Y., Yan, P., et al. (2018). Genetic-based dissection of arsenic accumulation in maize using a genome-wide association analysis method. *Plant Biotechnol. J.* 16, 1085–1093. doi: 10.1111/pbi.12853

Zhao, L., Huang, Y., Paglia, K., Vaniya, A., Wancewicz, B., and Keller, A. A. (2018). Metabolomics reveals the molecular mechanisms of copper induced cucumber leaf (*Cucumis sativus*) senescence. *Environ. Sci. Technol.* 52, 7092–7100. doi: 10.1021/acs.est.8b00742

Zhou, M., Zheng, S., Liu, R., Lu, J., Lu, L., Zhang, C., et al. (2019). Comparative analysis of root transcriptome profiles between low-and high-cadmium-accumulating genotypes of wheat in response to cadmium stress. *Funct. Integr. Genomics* 19, 281–294. doi: 10.1007/s10142-018-0646-4

Zhu, E., Liu, D., Li, J., Li, T., Yang, X., He, Z., et al. (2010). Effect of nitrogen fertilizer on growth and cadmium accumulation in *Sedum alfredii* Hance. *J. Plant Nutr.* 34, 115–126.

Zhu, H., Wang, S., Zhang, Y., Lin, H., Lu, M., Wu, X., et al. (2020). QTL excavation and analysis of candidate genes in contents of As, Cu, Fe, Hg and Zn in rice grain. *Sci. Sin. Vitae* 50, 623–632. doi: 10.1360/ssv-2020-0052

Conflict of Interest: The authors declare that the research was conducted in the absence of any commercial or financial relationships that could be construed as a potential conflict of interest.

Publisher's Note: All claims expressed in this article are solely those of the authors and do not necessarily represent those of their affiliated organizations, or those of the publisher, the editors and the reviewers. Any product that may be evaluated in this article, or claim that may be made by its manufacturer, is not guaranteed or endorsed by the publisher.

Copyright © 2022 Raza, Tabassum, Zahid, Charagh, Bashir, Barmukh, Khan, Barbosa, Zhang, Chen, Zhuang and Varshney. This is an open-access article distributed under the terms of the Creative Commons Attribution License (CC BY). The use, distribution or reproduction in other forums is permitted, provided the original author(s) and the copyright owner(s) are credited and that the original publication in this journal is cited, in accordance with accepted academic practice. No use, distribution or reproduction is permitted which does not comply with these terms.

frontiers in Plant Science

REVIEW
published: 13 January 2022
doi: 10.3389/fpls.2021.799318

Phytohormones Trigger Drought Tolerance in Crop Plants: Outlook and Future Perspectives

Shehzad Iqbal[1†], Xiukang Wang[2†], Iqra Mubeen[3†], Muhammad Kamran[4*], Iqra Kanwal[5], Gonzalo A. Díaz[1*], Aqleem Abbas[6], Aasma Parveen[7], Muhammad Nauman Atiq[6], Huda Alshaya[8], Tarek K. Zin El-Abedin[9] and Shah Fahad[10,11*]*

[1] Faculty of Agriculture Sciences, Universidad De Talca, Talca, Chile, [2] Shaanxi Key Laboratory of Chinese Jujube, College of Life Sciences, Yan'an University, Yan'an, China, [3] Key Lab of Integrated Crop Disease and Pest Management of Shandong Province, College of Plant Health and Medicine, Qingdao Agricultural University, Qingdao, China, [4] School of Agriculture, Food, and Wine, The University of Adelaide, Adelaide, SA, Australia, [5] Department of Plant Pathology, University of Agriculture, Faisalabad, Pakistan, [6] College of Plant Science and Technology, Huazhong Agricultural University, Wuhan, China, [7] Department of Soil Science, Faculty of Agriculture and Environmental Sciences, The Islamia University of Bahawalpur, Bahawalpur, Pakistan, [8] Cell and Molecular Biology, University of Arkansas, Fayetteville, NC, United States, [9] Department of Agriculture and Biosystems Engineering, Faculty of Agriculture (El-Shatby), Alexandria University, Alexandria, Egypt, [10] Hainan Key Laboratory for Sustainable Utilization of Tropical Bioresource, College of Tropical Crops, Hainan University, Haikou, China, [11] Department of Agronomy, The University of Haripur, Haripur, Pakistan

OPEN ACCESS

Edited by:
Shabir Hussain Wani, Sher-e-Kashmir University of Agricultural Sciences and Technology, India

Reviewed by:
Amjad Iqbal, Abdul Wali Khan University Mardan, Pakistan
Veysel Turan, Bingöl University, Turkey

***Correspondence:**
Xiukang Wang
wangxiukang@yau.edu.cn
Muhammad Kamran
kamiagrarian763@gmail.com
Gonzalo A. Díaz
g.diaz@utalca.cl
Shah Fahad
shah_fahad80@yahoo.com

[†] These authors have contributed equally to this work

Specialty section:
This article was submitted to Plant Biotechnology, a section of the journal Frontiers in Plant Science

Received: *29 October 2021*
Accepted: *27 December 2021*
Published: *13 January 2022*

Citation:
Iqbal S, Wang X, Mubeen I, Kamran M, Kanwal I, Díaz GA, Abbas A, Parveen A, Atiq MN, Alshaya H, Zin El-Abedin TK and Fahad S (2022) Phytohormones Trigger Drought Tolerance in Crop Plants: Outlook and Future Perspectives. Front. Plant Sci. 12:799318. doi: 10.3389/fpls.2021.799318

In the past and present, human activities have been involved in triggering global warming, causing drought stresses that affect animals and plants. Plants are more defenseless against drought stress; and therefore, plant development and productive output are decreased. To decrease the effect of drought stress on plants, it is crucial to establish a plant feedback mechanism of resistance to drought. The drought reflex mechanisms include the physical stature physiology and biochemical, cellular, and molecular-based processes. Briefly, improving the root system, leaf structure, osmotic-balance, comparative water contents and stomatal adjustment are considered as most prominent features against drought resistance in crop plants. In addition, the signal transduction pathway and reactive clearance of oxygen are crucial mechanisms for coping with drought stress via calcium and phytohormones such as abscisic acid, salicylic acid, jasmonic acid, auxin, gibberellin, ethylene, brassinosteroids and peptide molecules. Furthermore, microorganisms, such as fungal and bacterial organisms, play a vital role in increasing resistance against drought stress in plants. The number of characteristic loci, transgenic methods and the application of exogenous substances [nitric oxide, ($C_{28}H_{48}O_6$) 24-epibrassinolide, proline, and glycine betaine] are also equally important for enhancing the drought resistance of plants. In a nutshell, the current review will mainly focus on the role of phytohormones and related mechanisms involved in drought tolerance in various crop plants.

Keywords: phytohormones, drought stress, microorganisms, tolerance mechanisms, genes

INTRODUCTION

Plants are influenced by both biotic and abiotic factors, and in response to these factors, numerous internal changes occur in plants. These biotic and abiotic factors influence plant growth and development along with productivity. Biotic factors are interactions of organisms with plants that have both positive and negative effects. Positive effects may have a beneficial influence on plant

growth. Negative effects may include allelopathy, herbivory influence, or pathogen infection in plants (Ciura and Kruk, 2018). Plant defense systems with various chemical compounds help to resist those negative effects (Li et al., 2019; Riaz et al., 2021), as described briefly in **Figure 1**. Plant cell walls are proteins (antimicrobial) and secondary metabolites reservoirs with a highly weighted molecular layer of polysaccharides that resist pathogen physical penetration and growth.

Notably, the innate immune defense system of plants limits pathogen expansion through PTI (pattern-triggered immunity), PRRs (pattern recognition receptors), and ETI (effector-triggered immunity). ETI forms lesions on plant surfaces that restrict the further movement of pathogens from the infection site (Nishiyama et al., 2013). These defense systems activate a league of defense responses against pathogens in plant infection sites (Teixeira et al., 2019). In response to biotic and abiotic factors, plants have growth regulatory hormones that play a crucial function (Ciura and Kruk, 2018; Ali et al., 2021a). Plant growth hormones, primarily known as phytohormones, are organic, natural and small lipophilic compounds. Phytohormones play a significant role in response to different biotic and abiotic stresses along with the coordination and regulation among most developmental and growth functions in plants (Jiang and Asami, 2018). Also, they regulate cellular processes and respond very effectively to external stimuli and changing environmental conditions, even at very low concentrations (Nowicka et al., 2018).

Phytohormones with low molecular weights are more frequently adopted defense mechanisms of plants to receive external stimuli precisely against biotic stresses (Cao et al., 2011; Parveen et al., 2020). Based on phytohormone physiological functions and chemical structures, there were only a few regulatory hormones, namely jasmonic acid (JA), salicylic acid (SA), ethylene (ET), auxins (IAA), gibberellins (GAs), abscisic acid (ABA), and cytokinins (CKs), which have been more often studied by plant biologists (Dubois et al., 2018). However, presently, brassinosteroids (BRs), jasmonic acid-based compounds, cytokinins based compounds (zeatin), salicylic acid-based compounds, strigolactones, and peptides are also being investigated as plant hormones (Hu et al., 2020). Based on the chemical structures of some specific groups, phytohormones are further subdivided (Péret et al., 2013) and are responsible for the formation of roots and tropism and elongation. Seed and bud dormancy occurs by inhibiting phytohormones that resist abiotic stresses, and growth becomes active after the environment becomes favorable for growth (Liu J. et al., 2019). Various derivatives of all phytohormones are present, such as transport, activated or inactivated storage forms, degradation metabolites and, most importantly, sugar or amino acid conjugates. The biological effects of many plant growth hormones are the result of the combined induction of more than one hormone. Free hormones show similar biological activity to these derivatives; therefore, a precise concentration is required for maximum effect estimations (Zhao et al., 2019), and the estimation of the effect is shown in **Figure 2**. Many techniques have been used for phytohormone separation to study their effects more deeply. First, thin layer chromatography techniques (Stec et al., 2016) and high-performance liquid chromatography techniques are most commonly used for plant growth hormone separation (Floková et al., 2014). GC-MS-based methods are used to profile and study phytohormone profiles in citrus species, particularly in *Citrus sinensis* L., to recognize the responses to biological and environmental stresses. Specific ionic monitoring (SIM) methods were used to evaluate the description of phytohormones. Two derivation reagents, N-Methyl-N-(trimethylsilyl) trifluoroacetamide (MSTFA) and methyl chloroformate (MCF), and one extraction solvent mixture were used. This method showed recovery with a high extraction percentage and reproducibility with a low limit of quantification and detection. With this method, they detected thirteen (13) phytohormones, such as auxins, salicylic acids, gibberellin, jasmonic acid, and abscisic acid, that belong to different groups. Jasmonic acid and auxins were only present in the vegetation of plants, abscisic acid was in the leaves and roots and salicylic acid, cytokinins and gibberellins were found in all plants. Phytohormones are present at extremely low concentrations in plants, making their analysis more difficult. Salicylic acid (SA) is the most abundant phytohormone present in various tissues, mostly ranging from 59 to 70% of growth hormones. ABA phytohormone was the highest among SA groups, and GA7 was the most abundant among all GA groups and was made from GA12 in the 3β-hydroxy gibberellic acid pathway (Farrow and Facchini, 2014).

Drought being one of the abiotic stresses, is the most compelling ecological issue that significantly damages plant photosynthesis, development and growth (Rizwan et al., 2015; Fahad et al., 2017). Perennial fruit trees and crops demand well-drained soils for healthy growth and development and to obtain the maximum level of productivity. Even for a short time, poor drainage can markedly affect the productivity of perennial fruit trees for extended durations (Fahad et al., 2017; Fuller and Stevens, 2019). Moreover, drought stress causes an imbalance in carbon metabolism, which is the primary source of carbohydrates, leading to partial stomatal closure at carboxylation sites with less carbon dioxide availability (Hu et al., 2019). In addition, drought stress also causes the shoot respiration level to increase to sustain metabolic activity. Then, a decrease in the carbohydrate reserves occurs in the storage organs of citrus plants (Fahad et al., 2017).

Moderate drought stress leads to increased leaf soluble carbohydrate concentrations, a reduction in starch concentrations and a low photosynthesis rate in leaves. Plants may use stored carbohydrates because changes in carbon availability are observed under low photosynthesis rates. To meet the plant metabolic demand, these plants stored reservoirs to overcome stressful drought conditions (Fahad et al., 2017; Liu Y. N. et al., 2019). However, severe drought stress reduces starch and soluble fraction levels (Rizwan et al., 2015; Fahad et al., 2017). Plants exposed to saline environments experience a decline in plant growth because of the effect of specific ions on metabolism and antagonistic environmental connections. Various technologies have been used to exploit citrus plant growth under drought stress. Attempts are being made through conventional breeding methods to improve plants tolerance to

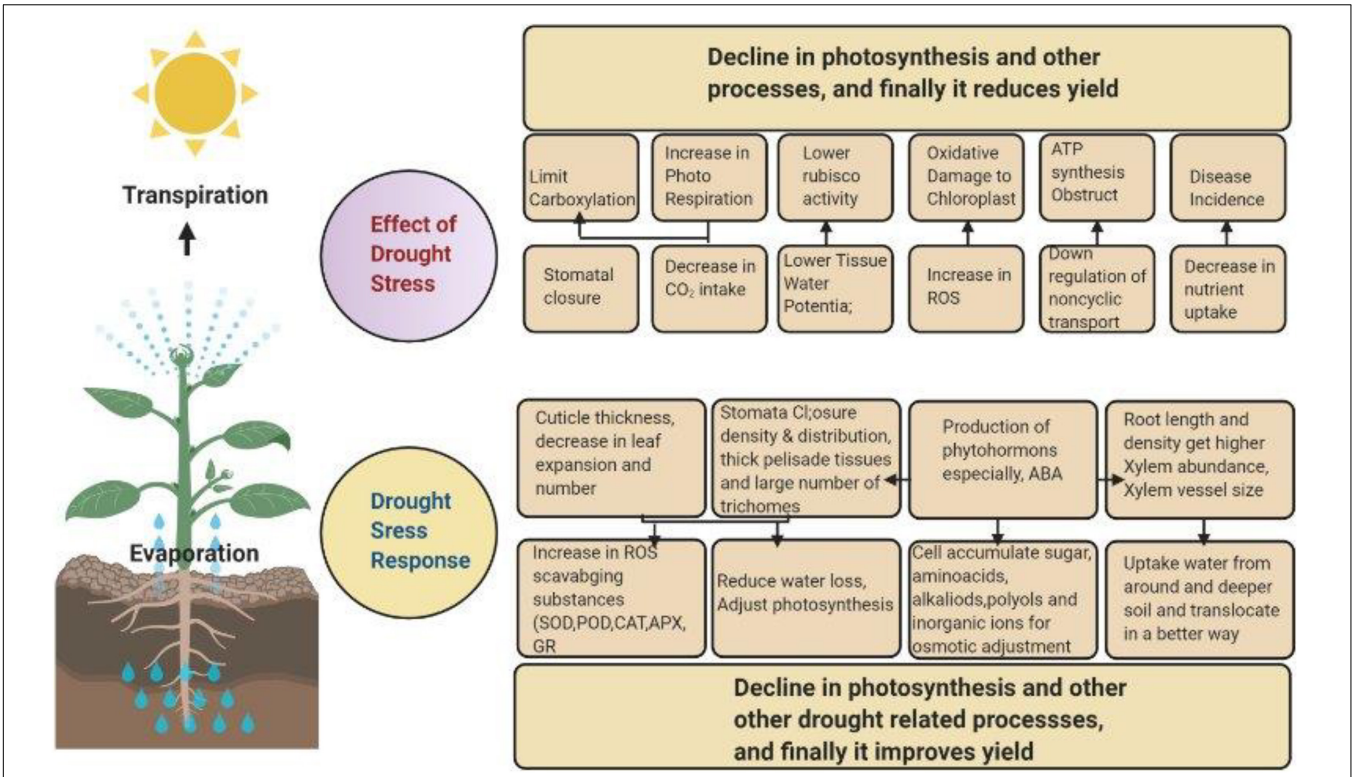


FIGURE 1 | Crop response, from physiological and morphological perspectives to drought stress. Drought stress affects the normal functioning of plants by lowering the rate of photosynthesis. To overcome this issue, plants increase the production of hormones and photosynthesis-related components as a defense mechanism.

drought stress, and these methods are laborious and based on the prevailing genetic changeability. Recently various drought resistance genes were overexpressed in plants, and plants become tolerant to drought stress. In most cases, a higher yield was recorded in the transgenic plants than the wild type plants. Some of the drought-tolerant plants have been listed in **Table 1**.

In response to abiotic stresses, i.e., drought and salinity, plants have developed various physiology, phenology, morphology, and biochemical-based mechanisms to sustain their cellular osmotic potential (Fahad et al., 2015, 2017, 2018, 2020, 2021a,b,c,d,e,f; Kamran et al., 2019; Ali et al., 2021a). Various studies on these mechanisms are ongoing due to the involvement of multiple phytohormones acting as sole mediators for avoidance, tolerance, and the adverse effect of water stress. Plant hormones vitally regulate the development and growth of plants along with drought stress reflexes throughout the lifespans of plants (Sah et al., 2016; Ullah et al., 2017). In response to drought stress, plants produce phytohormones that transduce the pathway to regulate its impact (Fahad et al., 2017; Hamayun et al., 2018). Also, phytohormones activate different developmental and physiological processes, such as negative phototropism in roots, osmotic balance, and closing stomata (Lim et al., 2015; Zahid et al., 2016).

Exogenous applications of plant growth regulators are also employed to overcome these stressed conditions (Kamran et al., 2021). As mentioned, phytohormones were applied to improve drought tolerance in plants (see **Table 2**) and increase growth, development, and productivity. Phytohormones play important roles in modifying the plant reflex to strains at very low concentrations, and their chemical messenger properties are produced in one part of the plant and transferred to entire parts of plants. Phytohormones are natural products synthesized chemically as plant growth regulators (Sah et al., 2016).

PLANT HORMONES IMPROVE DROUGHT RESISTANCE IN PLANTS

Auxins

Auxin is an important phytohormone. Auxins are involved in cell division, cell elongation and the differentiation of cellular tissues, embryogenesis, root formation, apical dominance, phyllotaxis, and tropic responses. Auxin genes are important biotechnological targets for modifying plant size and shape and improving plant yield. Therefore, they play a vital role in cell and growth development (Asgher et al., 2015). Auxins also play a dynamic role in mediating and improving plant tolerance to non-infectious stresses, such as deficiency conditions, as represented by many research reports (Kazan, 2013). Indole-3-acetic acid was one of the first hormones recognized in this group and is most commonly found among the auxins (Hamayun et al., 2021c). Indole 3-acetic acid is produced from tryptophan and is chemically similar to it. Alterations in gene expression patterns

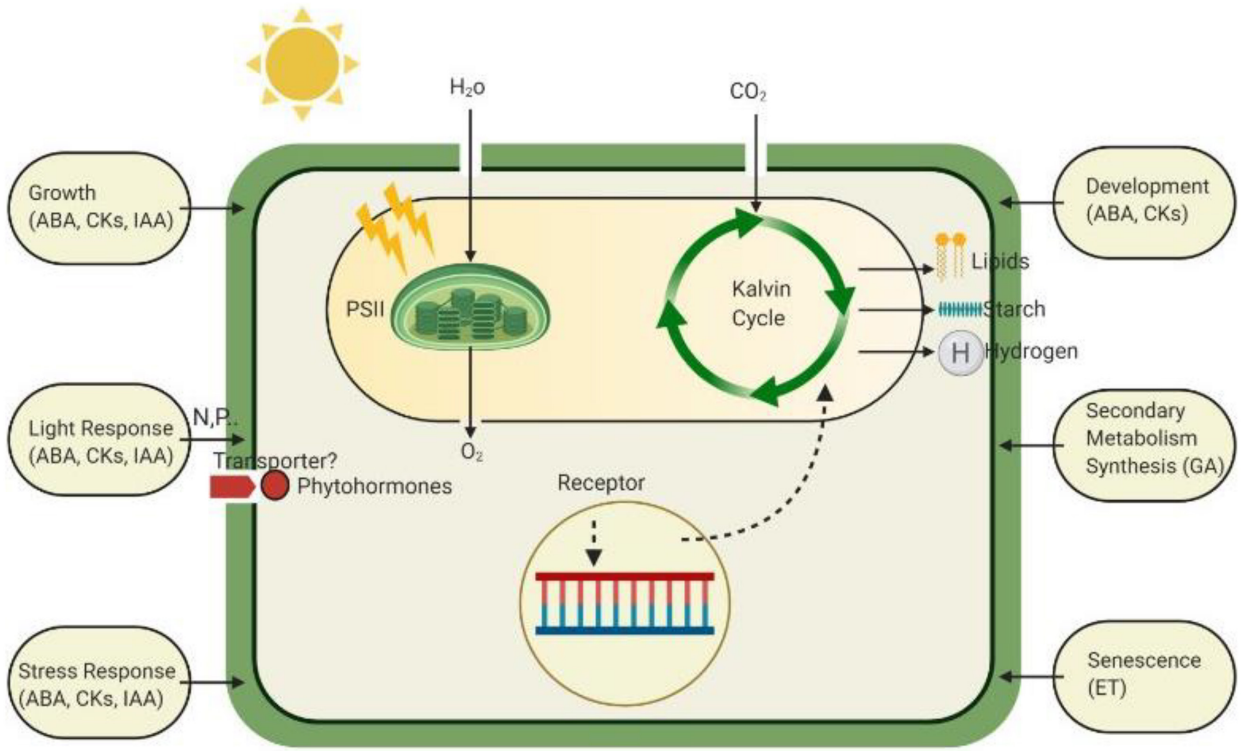


FIGURE 2 | The role of various phytohormones in plants to defend against different stressed conditions by increasing or decreasing their levels. Unstable levels of these hormones work within the defense mechanism of plants to ensure healthy normal growth.

were used to control auxin-mediated growth and development. When plants are exposed to drought and other stress conditions, varied modulations in the synthesis, metabolism, transport, and activity of auxins take place, as depicted in various reports (Ljung, 2013). A decline in the IAA level under stress conditions can increase the ABA level in plants to induce growth modulation by auxins. Jung et al. (2015) mentioned that among auxin-coding genes recognized in rice plants, some genes were activated by drought stress. Previous studies also reported the overexpression of YUC6 in poplar and potato, resulting in auxin-enhanced drought tolerance and phenotypes (Ke et al., 2015). Auxins also promote root branching and have a potential role in drought tolerance mechanisms in tobacco seedlings (Verma et al., 2016; Wang et al., 2018). Auxin response factors (ARFs) bind directly to the promoters of auxin-responsive genes, allowing them to be activated or repressed transcriptionally and enhance stress tolerance in tomatoes (Bouzroud et al., 2018). In addition, these ARFs regulate genes *(WRKY108715*, *MYB14*, *DREB4,* and *bZIP 107*) involved in drought stress response and enhanced tolerance in clovers (Zhang et al., 2020).

The role of auxin in drought stress has been explored via TLD1/OsGH3.13 which encodes indole-3-acetic acid (IAA)-amido synthase; it then enhanced the expression of late embryogenesis abundant (LEA) genes, which then increase the resistance in plants against drought stress. In addition, genes Aux/IAA genes were identified in rice and most of these genes were expressed under drought stress. In a study, YUC6 was overexpressed in potato and poplar which showed auxin-overproduction phenotypes and enhanced drought tolerance (Colebrook et al., 2014b). Auxin also enhanced drought resistance by interacting with other phytohormones. For example, auxin regulates various members of the ACS (1-aminocyclopropane-1-carboxylate synthase) gene family, which is a rate-limiting enzyme in ethylene biosynthesis. This interaction enhances resistance in plants against drought stress (Colebrook et al., 2014b).

Cytokinin

Cytokinins were discovered in 1950, and they are the most important phytohormones that stimulate cell division and induce variations. The first natural cytokinin was *trans*-zeatin, which was isolated from maize (Miller, 1961). These compounds are adenine byproducts derived from isoprene or an aromatic side chain at the *N6* position of purine. Folke Skoog and his assistants isolated kinetin (the cytokinesis-promoting factor) from autoclaved herring sperm DNA (Miller, 1961). These hormones are essential for the growth of plant regulation and acclimation to drought stress (Li et al., 2016). Cytokinins have both negative and positive impacts on drought stress (Ha et al., 2012; Li et al., 2016).

The enhancement or reduction of the cytokinin level depends on the period and severity of the drought stress (Zwack and Rashotte, 2015). The beneficial aspects are enhanced intolerance against drought stress. CKs are also

TABLE 1 | Transgenic crops under drought stress experienced altered yields through the phytohormone signaling pathway.

Gene(s)	Expressing plant	Signaling pathway	Stress type	Environmental condition(s)	Effect on yield (increase (%)	References
AtYUCCA6	*Solanum tuberosum*	Auxin	Drought	Greenhouse	Data not shown	Im Kim et al., 2013
LOS5ABA3	*Glycine max*	ABA	Drought	Growth chamber and field	21%	Li et al., 2013
AtEDT1/HDG11	*Oryza sativa*	ABA	Drought	Greenhouse and field	16%	Yu et al., 2013
AtGAMT1	*Solanum lycopersicum*	GAs	Drought	Greenhouse	Data not shown	Nir et al., 2014
AtEDT1/HDG11	*Gossipium hirsutum*	ABA	Drought and salinity	Laboratory, greenhouse and field	43%	Yu et al., 2016
GhABF2	*Gossipium hirsutum*	ABA	Drought and salinity	Laboratory, greenhouse, and field	46%	Liang et al., 2016
JIOsPR10	*Oryza sativa*	JA	Drought, salt and *Magnaporthe oryzae*	Greenhouse	No change	Wu et al., 2016
GA2ox	*Oryza sativa*	GAs	Drought and disease	Greenhouse and field	10–30%	Lo et al., 2017
OsERF109	*Oryza sativa*	JA and ABA	Drought	Greenhouse	30–45%	Yu et al., 2016

TABLE 2 | Phytohormones functions to prevent plants from drought stress.

Functions	Hormones	References
Involved in cell division, cell elongation, apical dominance, phyllotaxis and tropic responses	Auxin	Im Kim et al., 2013
Root branching	Auxin	Im Kim et al., 2013
Growth of plant parts and the flowering stage	Cytokinins	Liang et al., 2016
Development of female gametes and embryos	Cytokinins	Wu et al., 2016
Photomorphogenesis and leaf senescence	Cytokinins	Ha et al., 2012
Cell elongation and increasing the cell division	Gibberellins	Colebrook et al., 2014a
Enhance the vegetative and reproductive stages of plants	Gibberellins	Li et al., 2012a
Stomatal closure, gene upregulation and compatible osmolyte synthesis	Abscisic acid (ABA)	Shi et al., 2018
Photosynthetic activity, stomatal regulation, root growth, and germination	Abscisic acid (ABA)	Seo and Koshiba, 2011
Defense responses	Salicylic acid (SA)	Miura et al., 2013
Progressive responses against elevated temperature stress	Salicylic acid (SA)	Munne-Bosch and Penuelas, 2003
Stomatal closure	Salicylic acid (SA)	Dempsey et al., 2011a
Drought tolerance by lessening transpiration, squeezing the aperture of the stomata, and thinning the cuticle	Ethylene	Zandalinas et al., 2016
Appraisal of growth, drought tolerance, and yields	Brassinosteroids	Li et al., 2012b
Stomatal closing	Jasmonic Acid (JA)	De Ollas et al., 2013
Increase the antioxidant activity of plants under drought	Jasmonic Acid (JA)	Dong and Hwang, 2014
Root growth, pollen tube growth, stomatal development	Peptides	Shi et al., 2018

reported to stimulate transgene expression in transgenic plants, i.e., isopentenyl transferase gene expression. The transgenic plants indicated significant drought tolerance through delayed senescence by restricting drought-induced leaf senescence. The negative effects of CK accumulation on drought tolerance have also been reported along with the positive effects of CK accumulation. CK oxidase/dehydrogenase (CKX) catalyzes CK and is involved in the overexpression and breakdown of CKX in *Arabidopsis*, which results in a decrease in endogenous CK contents (Werner et al., 2010; Hamayun et al., 2021b). Therefore, *CKX1, CKX2, CKX3, and CKX4* were overexpressed independently in *Arabidopsis*, resulting in transgenic lines with reduced CK levels and subsequently greater drought tolerance.

Cytokinins are helpful in plant tissue culture techniques and support the thoughtful study of plant biological processes, such as the growth of plant parts and the flowering stage. These compounds are responsible for stimulating different processes during the growth and development of female gametes and embryos of a plant. Notably, cytokinins also participate in seed germination, vascular development, photomorphogenesis, shoot apical meristem development, floral development, and leaf senescence. It also helps plants to induce adaptive responses to drought and adverse ecological conditions (Mao et al., 2020). Moreover, different hormones and macronutrients control the transcription of cytokinin biosynthetic genes. In *Arabidopsis*, cytokinins stimulate cell division by antagonizing auxin. Auxin promotes the expression of *AtIPT5* and *AtIPT7*, whereas cytokinins suppress the expression of *AtIPT1*, *AtIPT3*, *AtIPT5*, and *AtIPT7* in the shoot meristem (Ismail H. M. et al., 2020).

All the genes related to cytokinin in *Arabidopsis* were overexpressed individually, and transgenic lines of *Arabidopsis* with decreased levels of cytokinin gradually improved tolerance to drought conditions (Nishiyama et al., 2011). The current need is to elucidate the signaling and role of cytokinins under drought conditions.

Gibberellins

Gibberellins are tetracyclic diterpenoids of carboxylic acids. The primary purpose of GAs in plants is as growth hormones and

to provide resistance against drought stress and other abiotic stresses. GAs continues their functions in plants throughout the plant life cycle. The primary purpose of gibberellins is to enhance the development of plant tissues by cell elongation and increasing the cell division process enhances the immature and adult stages of plant growth. It also helps to enhance the vegetative and reproductive stages of plants (Colebrook et al., 2014b; Kang et al., 2019).

SIDREB (drought-responsive element-binding protein) increases drought tolerance in tomatoes by decreasing the expression of gibberellin biosynthesis genes (Colebrook et al., 2014a). Drought tolerance is said to be enhanced if the GA level is reduced in plants. Transgenic tomatoes are produced by the overexpression of the *AtGAMT1* (*Arabidopsis thaliana* GA Methyl Transferase-1) gene. *AtGAMT1* encodes an enzyme that causes a breakdown in the methylation of active GA to make inactive GA methyl esters. The transgenic tomato indicated a reduction in gibberellins by enhanced drought tolerance. An increased water level in leaves was observed in transgenic tomatoes under drought stress because of transpiration in plants (Nir et al., 2014). The ectopic expression of GA2ox (GA 2-oxidase) increased drought tolerance. This protein also helps to enhance resistance in rice plants (Lo et al., 2017). The *DELLAs* proteins are the primary stimulators of GA responses in drought conditions faced by plants. The functions of this group of nuclear regulators are to suppress gibberellin stimulation in plants. Gibberellins binding to the receptor GID1 (GA in-sensitive dwarf 1) lead to the degradation of *DELLAs* by the 26S proteasome and the stimulation of gibberellin responses (Li et al., 2012c).

Drought tolerance in plants is appreciably enhanced by gibberellins, as reported in many studies (Li et al., 2012a; Colebrook et al., 2014a). Tomatoes make the transgene by overexpressing the gene (methyltransferase 1). *GAMT1* encodes an enzyme catalyzing active gibberellin methylation to form inactivated GA methyltransferase in *Arabidopsis* spp. The resulting tomato plant expressed a typical GA-deficient phenotype, which showed drought tolerance. A high-water content was prominent in transgene tomato plants because of decreased transpiration (Ullah et al., 2018). By contrast, applying hormones resulted in the reappearance of normal growth, and plants became prone to drought again (Nir et al., 2014). In addition, the external expression of GA oxidase enzyme (GA 2-oxidase) improved drought and disease hindrance in rice plants (Lo et al., 2017). *SIDREB* (drought-reflexing binding protein) also improved drought tolerance in tomatoes by suppressing the genes involved in GA biosynthesis (Li et al., 2012a). DELLAs protein factors also primarily regulate response to GA, and this group of nuclear regulators especially act to suppress the GA response. GA binding to the insensitive dwarf1 receptor of GA will result in *DELLA* degradation, similar to 26S proteasome and GA response stimulation (Li et al., 2013).

Abscisic Acid

Abscisic acid is an important signaling phytohormone under drought stress (De Ollas et al., 2013). Abscisic acid plays a significant role in regulating stomatal closure, gene upregulation and compatible osmolyte synthesis. 9-Neoxanthin cis-epoxicarotenoid dioxygenase (NCED) is used in abscisic acid synthesis and is considered a bottleneck, covering 9-neoxanthins to xanthins. This enzyme is used in the upregulation of an increased level of abscisic acid. Abscisic acid is cleaved into 8′-OH-ABA, and this process is catalyzed by an ABA 8′-hydroxylase (CYP707A) enzyme. This reaction is used to inactivate abscisic acid. ABA 8′-hydroxylase compounds are spontaneously converted into dehydrophaseic acid (DPA) and phaseic acid (PA), the primary degradation products. Another path that is used to inactivate abscisic acid pools is through conjugation to hexoses catalyzed by the ABA O-glycosyl transferase enzyme. This process yielded the ABA-glycosyl ester (ABAGE) compound (Dong and Hwang, 2014). After the cleavage of the ABA glycosyl ester (ABAGE) compound by an ABA glycosyl ester β-glycosidase (BG18) enzyme, active abscisic acid is released. Both species have increased levels of phasic acid (PA) and dehydrophaseic acid (DPA) under drought stress, but Cleopatra exhibited a more increased level of ABA-glycosyl ester (ABAGE).

Abscisic acid signaling pathways have vital role in the expression of drought stress-responsive genes because various stress situations can occur in plants. Abscisic acid receptors are very important in the transduction of signals. In the subcellular state, many receptors are recognized. Under normal conditions, ABA is expressed at low concentrations in plants (Parveen et al., 2021). SnRK2 activity in protein kinases is inhibited by the phosphatase PP_2C, leading to dephosphorylation. As plants develop ABA concentrations, they start to bind with PYRs, PYLs, and RCARs, which bind to deactivate PP_2C phosphatase activity (Danquah et al., 2014). These PYRs and PYLs are essential receptors for the abscisic acid response encoded by different genes, such as 11 genes in rice and 14 genes in *Arabidopsis* encoding these receptors (Klingler et al., 2010). The autoactivation of $SnRK_2$ (protein kinases that enhance the abscisic acid response) occurs when the protein is dissociated from phosphatase PP_2Cs (Hrabak et al., 2003; Ullah et al., 2017), and the rest of the SnRKs are involved in the abscisic acid response (SnRK2.2, SnRK2.3, and SnRK2.6) (Feng et al., 2014). In *Arabidopsis*, only the A clade participates in the signaling of abscisic acid out of seventy-six PP_2Cs. Additionally, the ABA signaling pathway is also dependent on branches of various transcription factors, such as MYC, NAC and MYBs. The responsive elements of abscisic acid also play a role in ABA signaling (De Ollas and Dodd, 2016). CDPKs (CDPKs) also proved very important in the pathway related to signaling. Calcium-dependent protein kinases also participate in ABA signaling, and 34 CDPKs have been reported in *Arabidopsis*, along with 29 in rice, 20 in wheat and 35 in maize. Two CDPKs, CPK4, and CPK11, have been reported to be involved in the regulation of ABA signaling in *Arabidopsis*. $SnRK_2$ activation triggers the phosphorylation of down–target genes, resulting in the induction of molecular and physiological responses to ABA triggering, such as photosynthetic activity, stomatal regulation, root growth, and germination (Altaf et al., 2020). Abscisic acid also regulates many other genes related to drought stress to develop drought

tolerance in plants. The abscisic acid-induced pathway is shown in **Figure 3**.

Salicylic Acid

The salicylic acid (SA) hormone is associated with drought tolerance and signaling in plants (Miura and Tada, 2014). In response to drought stress, SA biosynthesis takes place via both the isochorismate pathway and the phenylpropanoid pathway. Both pathways require the chemical chorismate generated from the shikimate pathway (**Figure 4A**). However, the isochorismate pathway is known to be the major pathway in most plants (De Ollas et al., 2013). The phenylpropanoid pathway for SA biosynthesis begins with phenylalanine (Phe) being converted to trans-cinnamic acid (t-CA) by phenylalanine ammonia lyase (PAL). It is then transformed into benzoic acid (BA). Researchers have yet to discover the enzyme that converts t-CA to benzoic acid. After that, the enzyme benzoic acid 2-hydroxylase catalyzes the hydroxylation reaction that yields SA from BA (BA2H) (**Figure 4A**). The isochorismate pathway requires enzyme ICS1 (isochorismate synthase 1) that converts chorismate to isochorismate, and isochorismate is then converted to SA by isochorismate pyruvate lyase (IPL) (Danquah et al., 2014). Salicylic acid also plays a significant role in defense responses against drought stress, as shown in **Figure 4B**. NPR1 (non-expresser of pathogenesis-related genes 1) is a master regulator of defensive signals mediated by SA. SA binds to NPR1 and NPR1 homologs directly, perhaps regulating NPR1 activity and stability. Increased cellular SA levels cause a redox shift in the cytoplasm, causing NPR1 to transition from oligomer to monomer forms (**Figure 4B**). The active monomers then go to the nucleus, where SA binds to NPR3 and NPR4 to block their transcriptional repression activity. NPR1 interacts with TGAs (TGACG-binding factors), activating defense responses against drought stress. However, in cells with low SA levels, NPR1 forms oligomers and persists in the cytosol, while NPR3 and NPR4 bind residual NPR1 in the nucleus to block NPR1 function (**Figure 4B**; Dempsey et al., 2011b). Salicylic acid accumulation in plants improves responses to various abiotic stress conditions, such as drought

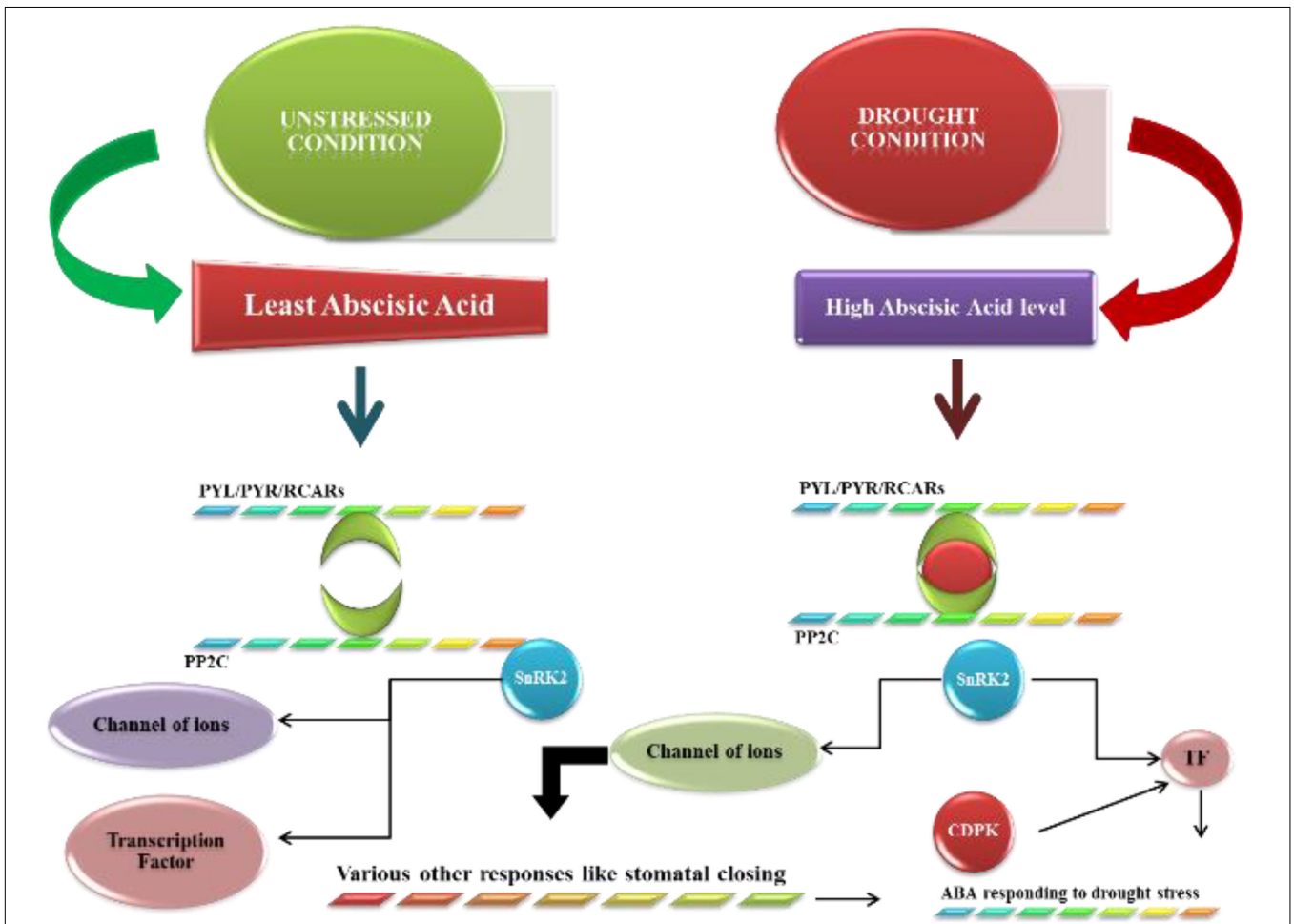


FIGURE 3 | ABA's fundamental signaling mechanism during stressful situations. The ABA levels are lower under ideal circumstances, and the function of SnRK2 protein kinase is blocked by PP2C phosphatases. The cellular ABA level rises during high-pressure situations, and ABA then attaches to PYR/PYL/RCARs, which connect to and deactivate PP2Cs in response. If they are detached from PP2C, then SnRK2s are automatically activated. Switched on SnRK2s phosphorylate the following targets and provoke molecular and physiological reactions through ABA.

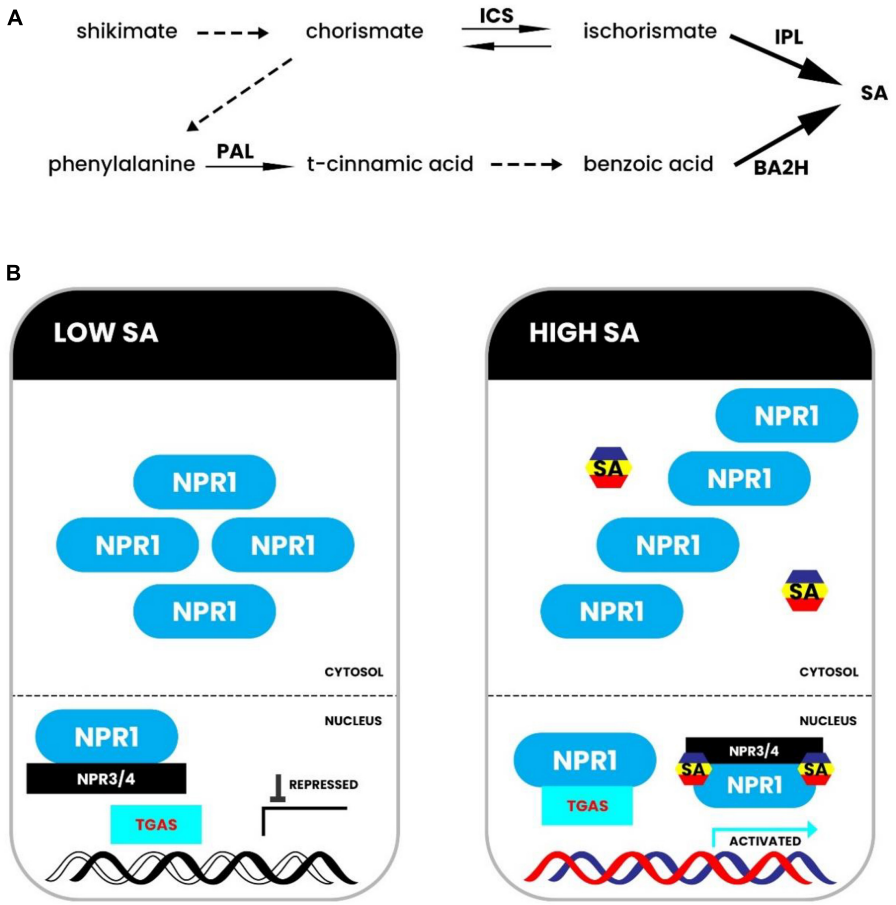


FIGURE 4 | Biosynthesis and signaling of salicylic acid. **(A)** In *Arabidopsis,* a model for salicylic acid (SA) production has been proposed. Genetic investigations showed the isochorismate pathway in the upper panel. Biochemical research showed the phenylpropanoid pathway in the lower panel. **(B)** NPR1 forms an oligomer in the cytosol in cells with low SA levels, and NPR3 and NPR4 bind leftover NPR1 in the nucleus to block NPR1 activity. NPR1 becomes monomeric and reaches the nucleus in cells with high SA levels, where SA binds to NPR3 and NPR4 to disrupt their transcriptional repression action. NPR1 interacts with TGAs in SA-responsive promoters, causing defensive responses to be activated. BA2H stands for benzoic acid 2-hydroxylase; ICS stands for isochorismate synthase; IPL stands for isochorismate pyruvate lyase; NPR stands for non-expresser of pathogenesis-related genes; PAL stands for phenylalanine ammonia lyase; SA stands for salicylic acid; TGA stands for TGACG-binding factor. Adapted from Li et al. (2019).

and salinity (Miura and Tada, 2014), antioxidant activity and photosynthetic machinery protection, which prevents electron leakage (Ismail I. et al., 2020; Malik et al., 2021). Previous studies showed that drought increased endogenous levels of abscisic acid (ABA) and jasmonic acid (JA) in *Brassica napus*, resulting in a rise in ABA/SA and (ABA + JA)/SA (Lee et al., 2019). The increase of ROS and proline, as well as a loss of reducing potential [NAD(P)H/NAD(P) + and GSH/GSSG], paralleled the changes in endogenous hormonal balance. Drought-induced O_2 buildup was scavenged by SA pretreatment (Lee et al., 2019). Moreover, drought increased ROS generation and, as a result, lipid peroxidation, which is a specific indicator of oxidative damage. On the other hand, Exogenous SA application substantially reduced oxidative damage in rice seedlings in hydroponic and soil systems by upregulating antioxidant enzymes (Ali et al., 2021b). Furthermore, drought stress lowered photosynthetic pigment concentration, gas exchange parameters, proline, soluble sugars, total phenolic, flavonoids, growth, and biomass output. On the other hand, SA promoted *Portulaca oleracea* growth and biomass production by improving photosynthetic pigments, gas exchanges, suitable solutes, and secondary metabolites (Hamayun et al., 2021a). In *Impatiens walleriana*, dehydration increased the quantity of electrolyte leakage (EL), malondialdehyde (MDA), peroxidase (POD), and ascorbate peroxidase (APX) activities, along with proline content. P5CR (gene for 1-pyrroline-5-carboxylate reductase) has a similar expression pattern to P5CS, with minor changes in intensity. Through improved antioxidant activity and water balance, SA lowered the amount of EL and MDA in the plant (Safari et al., 2021). When compared to non-SA pretreated *Brassica rapa*, SA pretreatment dramatically boosted proline concentration via upregulating the expression of genes expressing pyrroline-5-carboxylate synthase (P5CSA and P5CSB) and down-regulating the expression of the gene encoding proline dehydrogenase (PDH). In another case, the Carrizo citrus plant variety showed greater tolerance to drought and heat stress in combination. Drought stress increased salicylic

acid levels in the leaves of certain citrus species, such as Carrizo and Cleopatra. Chlorophyll fluorescence, gas exchange parameters and malondialdehyde (MDA) accumulation indicate that Cleopatra mandarin is susceptible to drought and heat stress (Hamayun et al., 2018). Phenotypic traits of citrus plants occur in response to a combination of drought and heat stress. Whole sprouts (%) of Cleopatra and Carrizo seedlings were exposed to drought and heat stress (40°C) in combination for 10 days. For each genotype, asterisks denote statistical significance concerning the initial values at $P \leq 0.05$ (Hamayun et al., 2021a).

The salicylic acid levels also increased in plants under drought stress, which may be five times that of the normal level recorded in evergreen shrubby plants in *Phillyrea augustifolia* (Munné-Bosch and Peñuelas, 2003; Hamayun et al., 2021c). The enhanced drought tolerance and disorder resistance found in mutants of *Arabidopsis* spp. such as adr_1, acd_6, myb_{96-1}, and cpr_5 are due to the presence of salicylic acid (Seo and Koshiba, 2011; Miura et al., 2013). In *Arabidopsis*, stomatal closing was also observed due to salicylic acid accumulation under stressed conditions because the SA-regulated induction of *PR* gene expression led to drought tolerance by shutting the stomatal openings (Liu et al., 2013; Miura et al., 2013), and stomatal closure occurred through the accumulation of SA under the influence of SIZI in *Arabidopsis*, significantly increasing the drought tolerance.

In another study, the exogenous application of SA positively regulated *ICS1* gene (isochorismate synthase) and enhanced drought tolerance in *Arabidopsis*. Furthermore, it revealed that SA activated *WRKYs* and *TGAs* genes, which then enhanced the plant immune system against drought stress (Klingler et al., 2010).

Jasmonic Acid

Drought tolerance in plants is induced by closing stomata, shifting reactive oxygen species, and deep root growth in the case of jasmonic acid. Studies have revealed that JAs participate in stomatal closing regulation as a result of drought stress (Riemann et al., 2015). A case study revealed that treating *Arabidopsis* with 12-OPDA led to stomatal shutting. It is also involved in indirectly decreasing stomatal gaps, favoring drought tolerance. Drought also prevents the alteration of OPDAs to jasmonic acid; in this case, OPDA coupled with ABA or individually leads to the closing of stomata (Savchenko et al., 2014; Kazan, 2015). High ROS foraging was found (Fang et al., 2016) in transgenic plants overexpressing VaNAC26, which showed relatively more drought tolerance. JA-related genes were highly regulated in overexpressed lines under drought and ordinary conditions. The external application of JA led to a perfect reflex by plants to drought stress. External JA application was also shown to enhance the activity of antioxidants under drought stress (Shan et al., 2015). Another case revealed that JA was found to be an enhancer of different enzymes in young wheat, such as ascorbate peroxidases (APX) and ascorbate reductases monodehydroascorbate reductase and glutathione reductase, under stress conditions (Shan et al., 2015). JA also plays a significant role in water conductivity from soil under restricted moisture conditions (De Ollas et al., 2013; Sánchez-Romera et al., 2014) found that the transient presence of jasmonic acid in roots is required under drought stress to increase the abscisic acid levels. However, the function of JA still must be clarified under drought stress to obtain highly tolerant plants. The exogenous application of JA increased the antioxidant activity of plants under drought conditions, as shown in **Figure 5**. The proteins JAI3/JAZ bind to various transcription factors, including MYC2, and limit their activity under normal conditions. However, during drought stress, the degradation of JAZ proteins occurs, resulting in active transcription factors that upregulate genes of JA, which enhances tolerance in plants against drought stress (De Ollas and Dodd, 2016). Moreover, JA signaling pathways interact with ABA signaling pathways, suggesting their role in response to drought stress. It has been recently revealed that JA enhanced the hydraulic conductivity of plant roots under drought stress by interacting with calcium and ABA-dependent and independent signaling pathways (De Ollas and Dodd, 2016).

Brassinosteroids

Brassinosteroids play a role in stress responses along with roles in plant growth and nourishment. These stresses include drought, cold, hypersalinity, metallic heaviness, raised temperature, and infectious agents (Chen et al., 2017). It was previously mentioned that in *Arabidopsis*, wheat, and *Brassica* spp., brassinosteroids played a positive role in response to drought stress (Divi et al., 2010). *Arabidopsis* biosynthetic gene (DWF_4) overexpression resulted in the appraisal of growth, drought tolerance, and yields (Sahni et al., 2016). By contrast, there was a negative response from the brassinosteroids. Additionally, mutants of Brs showed functional loss, but increased drought tolerance (Northey et al., 2016; Ye et al., 2017), and knocking out BR_1 by miRNA technique led to more drought tolerance in *Brachypodium distachyon* (Feng et al., 2015). These phytohormones play a crucial role in drought stress tolerance. They act synergistically in response to drought stress.

Recently, various WRKY transcription factors have been discovered in *Arabidopsis thaliana* and these transcription factors are reported to be involved in plant growth and response to drought stress. To regulate plant growth, BRs extensively interact with these transcription factors and GA in response to drought stress (Clarke et al., 2004; Xue et al., 2013; Sánchez-Romera et al., 2014; Sánchez-Martín et al., 2015).

Ethylene

Ethylene was found to be actively involved in enhancing drought tolerance in plants. In a study on cotton, ethylene-responsive genes or binding protein elements such as AP_2, EREBPs, and $APETELA_2$ were identified in response to heat and drought stress (Liu and Zhang, 2017). One analysis revealed that members of ERFs (responsive factors of ethylene), $GmERF_3$ isolated from *Glycine max,* whose expression was induced by drought stress, ABA, SA, JA, and ET. $GmERF_3$ in overexpressing tobacco plants exhibited more tolerance to drought stress because of the high contents of proline and solubilized sugar compared to wild plants. Transgenic plants showed increased resistance to *Ralstonia solancearum, Alternaria alternata*, and tobacco mosaic virus due to the high expression of pathogenesis-related protein-coding genes (Hamayun et al., 2019). The overexpression

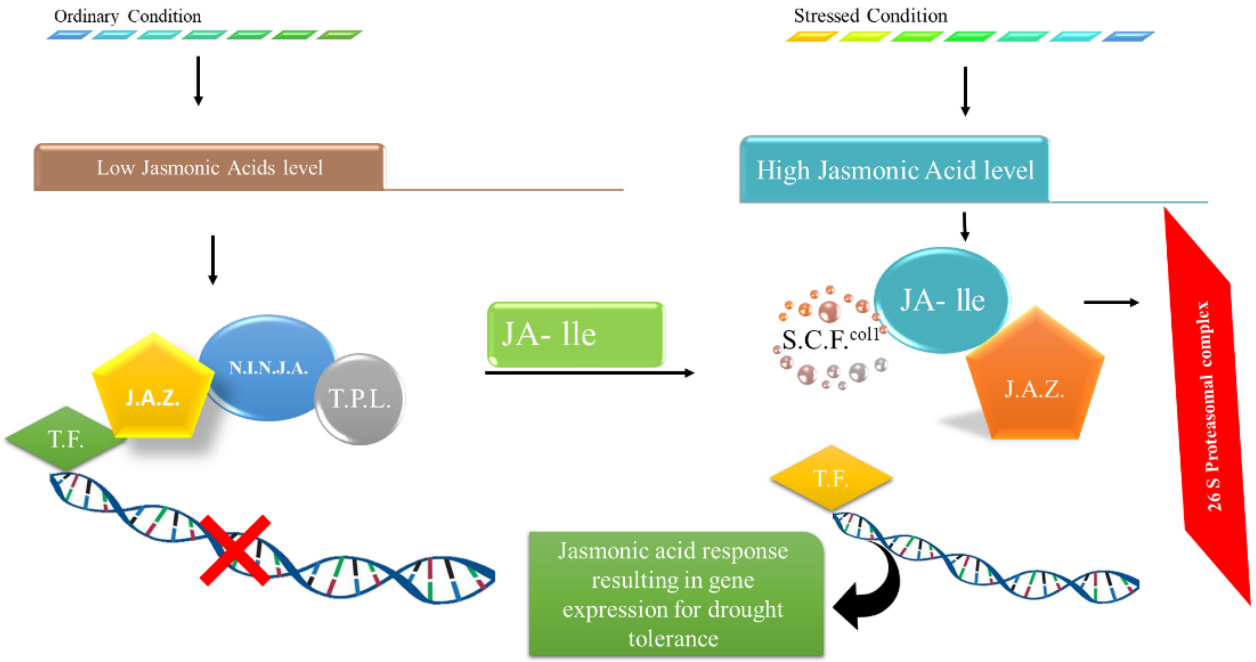


FIGURE 5 | Changes in JA signals under stressful situations. JAI3/JAZ proteins attach to different transcription components and restrict their function along with reduced levels of JA under ideal circumstances. The JA concentrations are high and deteriorate JAZ proteins under stressful situations, leading to the activation of transcriptional components that upregulate genes associated with stress responses.

of the ERF gene (*ERF019*) in *Arabidopsis* delayed aging and flowering time. Transgenes also exhibit drought tolerance by lessening transpiration, squeezing the aperture of the stomata, and thinning the cuticle (Scarpeci et al., 2017). In signal transduction, ETR_1 codes for receptors of ET but negatively regulates the response; other receptors of this family always close down the signaling, whether ethylene is present or not (Shi et al., 2016) of the other members of the family include ERS_1, ETR_2, EIN_4, and ERS_2. CTR_1 regulates ET signaling. In *Arabidopsis*, CTR_1 is involved in ET signaling, while in tomato 3, CTR_1 is involved in ET signaling. There is no evidence of a decrease in the stream substrate of CTR_1. When the receptor finds ethylene, it shuts off the activity of ethylene, thus leading to a reflex action for tolerance to drought conditions.

Peptides

Recently several secreted peptides were found to mediate the cellular development in plants. However, it was unclear whether these peptides mediate long-distance signaling in response to drought stress. Among the peptides, CLAVATA3 (CLV3) is a well-characterized plant peptide involved in shoot apical meristem formation. In land plants, phytohormone abscisic acid plays a significant role in the regulation of stomatal movement to prevent water loss. However, no mobile signaling molecules have yet been discovered that can enhance the abscisic acid accumulation in leaves (Nir et al., 2014). Recently, CLE25 peptide was found to transmit water-deficiency signals through vascular tissues in Arabidopsis and affects abscisic acid biosynthesis and stomatal control of transpiration. The gene related to these peptides was expressed in the vascular tissues and enhanced root response to drought stress. These peptides move from the roots to the leaves and induce stomatal closure by modulating abscisic acid accumulation, enhancing resistance to drought stress. Recently, another peptide gene in rice, OsDSSR1, was discovered, which was expressed mainly in the root, stem, node, leaf, and panicle, and this expression was induced by drought stress. The peptide is localized in the nucleus and cytoplasm and exhibited enhanced drought stress tolerance and decreased ABA sensitivity compared to the wild type (Yu et al., 2016). Other peptides such as phytosulfokine (PSK), a growth related to cell proliferation; rapid alkalinization factor (RALF), which regulates root growth; LUREs, which guides pollen tube growth; STOMAGEN, which is related to stomatal development; and casparian strip integrity factor (CIF), which is associated with the formation of the casparian strip diffusion barrier; Another peptide, AtPep3 which plays an important role in the drought and salinity stresses were also recently discovered (Nir et al., 2014; Liang et al., 2016; Yu et al., 2016).

CONCLUSION AND FUTURE PERSPECTIVES

An ever-growing population and diminishing natural resources have made it difficult for farmers to produce enough food to meet their needs. Drought is a major constraint on crop productivity worldwide and is expected to worsen in the near future. Besides, droughts are becoming more

common, severe, and widespread due to climate change. Hence, scientists are attempting to develop drought-tolerant crops and understand different drought tolerance mechanisms. This review's underlying theme is that plants typically respond to drought stress by adjusting the levels of phytohormones, such as abscisic acid, jasmonic acid, auxin, ethylene, and gibberellin, cytokinin, brassinosteroids, and small peptide molecules. These phytohormones trigger tolerance to drought stress via regulation of various morphological, physiological, biochemical and molecular processes. The morphological and physiological processes involve changes in the composition of the leaves, root growth and stomatal control. The biochemical process includes adjusting the levels of phytohormones. Molecular processes include phytohormone-mediated signals, leading to the activation of various transcription factors that causes the expression of genes required for plant survival in drought stress (Saleem et al., 2020).

However, due to the high level of complexity, most of the mechanisms by which phytohormones trigger drought tolerance in crops are poorly understood and requires further study. Besides, scientists could not comprehend the crosstalk among the phytohormones against drought stress. Since crosstalk is so intricate, the underlying mechanisms are also unknown and need further investigation. Recently scientists are attempting to understand the mechanisms of drought tolerance in plants through the exogenous application of phytohormones. In addition, drought stress in plants is alleviated by applying plant microbiomes. These plant microbiomes induce drought stress-responsive genes and play a crucial role in the acquisition of drought tolerance (Ismail A. H. et al., 2020). In the future, newly developed large-scale OMIC methods and high-throughput bioinformatic analysis will be used to seek a better understanding of the mechanisms by which phytohormones trigger drought tolerance in crops, which will ultimately lead to the development of drought-resistant crop plants with significant agronomic features.

AUTHOR CONTRIBUTIONS

SI, XW, IM, and MK wrote the manuscript. SI, MK, and XW designed the study idea and applied the mode. GD, AP, SF, HA, TZ, and AA collected and arranged the whole database. AA, IK, MK, and MNA analyzed and discussed the contents of the manuscript. SF, MK, IK, and SI critically revised the manuscript. All authors contributed to the article and approved the submitted version.

FUNDING

This research was funded by the National Natural Science Foundation (51809224). The APC was funded by the National Natural Science Foundation (51809224).

REFERENCES

Ali, M., Afzal, S., Parveen, A., Kamran, M., Javed, M. R., Abbasi, G. H., et al. (2021a). Silicon mediated improvement in the growth and ion homeostasis by decreasing Na+ uptake in maize (*Zea mays* L.) cultivars exposed to salinity stress. *Plant Physiol. Biochem.* 158, 208–218. doi: 10.1016/j.plaphy.2020.10.040

Ali, M., Kamran, M., Abbasi, G. H., Saleem, M. H., Ahmad, S., Parveen, A., et al. (2021b). Melatonin-induced salinity tolerance by ameliorating osmotic and oxidative stress in the seedlings of two tomato (*Solanum lycopersicum* L.) cultivars. *J. Plant Growth Regulat.* 40, 2236–2248.

Altaf, M. A., Shahid, R., Ren, M. X., Mora-Poblete, F., Arnao, M. B., Naz, S., et al. (2020). Phytomelatonin: an overview of the importance and mediating functions of melatonin against environmental stresses. *Physiol. Plant.* 172, 820–846. doi: 10.1111/ppl.13262

Asgher, M., Khan, M. I., Anjum, N. A., and Khan, N. A. (2015). Minimising toxicity of cadmium in plants–role of plant growth regulators. *Protoplasma* 252, 399–413. doi: 10.1007/s00709-014-0710-4

Bouzroud, S., Gouiaa, S., Hu, N., Bernadac, A., Mila, I., Bendaou, N., et al. (2018). Auxin response factors (ARFs) are potential mediators of auxin action in tomato response to biotic and abiotic stress (*Solanum lycopersicum*). *PLoS One* 13:e0193517. doi: 10.1371/journal.pone.0193517

Cao, F. Y., Yoshioka, K., and Desveaux, D. (2011). The roles of ABA in plant-pathogen interactions. *J. Plant Res.* 124, 489–499. doi: 10.1007/s10265-011-0409-y

Chen, J., Nolan, T. M., Ye, H., Zhang, M., Tong, H., Xin, P., et al. (2017). Arabidopsis WRKY46, WRKY54, and WRKY70 Transcription Factors Are Involved in Brassinosteroid-Regulated Plant Growth and Drought Responses. *Plant Cell* 29, 1425–1439. doi: 10.1105/tpc.17.00364

Ciura, J., and Kruk, J. (2018). Phytohormones as targets for improving plant productivity and stress tolerance. *J. Plant Physiol.* 229, 32–40. doi: 10.1016/j.jplph.2018.06.013

Clarke, S. M., Mur, L. A., Wood, J. E., and Scott, I. M. (2004). Salicylic acid dependent signaling promotes basal thermotolerance but is not essential for acquired thermotolerance in Arabidopsis thaliana. *Plant J.* 38, 432–447. doi: 10.1111/j.1365-313X.2004.02054.x

Colebrook, E. H., Thomas, S. G., Phillips, A. L., and Hedden, P. (2014b). The role of gibberellin signalling in plant responses to abiotic stress. *J. Exp. Biol.* 217, 67–75. doi: 10.1242/jeb.089938

Colebrook, E. H., Thomas, S. G., Phillips, A. L., and Hedden, P. (2014a). The role of gibberellin signalling in plant responses to abiotic stress. *J. Exp. Biol.* 217, 67–75.

Danquah, A., De Zelicourt, A., Colcombet, J., and Hirt, H. (2014). The role of ABA and MAPK signaling pathways in plant abiotic stress responses. *Biotechnol. Adv.* 32, 40–52. doi: 10.1016/j.biotechadv.2013.09.006

De Ollas, C., and Dodd, I. C. (2016). Physiological impacts of ABA-JA interactions under water-limitation. *Plant Mol. Biol.* 91, 641–650. doi: 10.1007/s11103-016-0503-6

De Ollas, C., Hernando, B., Arbona, V., and Gómez-Cadenas, A. (2013). Jasmonic acid transient accumulation is needed for abscisic acid increase in citrus roots under drought stress conditions. *Physiol. Plant* 147, 296–306. doi: 10.1111/j.1399-3054.2012.01659.x

Dempsey, D. A., Vlot, A. C., Wildermuth, M. C., and Klessig, D. F. (2011b). Salicylic Acid biosynthesis and metabolism. *Arabidopsis Book* 9:e0156.

Dempsey, D., Vlot, A., Wildermuth, M., and Klessig, D. (2011a). *The Arabidopsis Book*. Rockville MD: The American Society of Plant Biologists, e0156.

Divi, U. K., Rahman, T., and Krishna, P. (2010). Brassinosteroid-mediated stress tolerance in Arabidopsis shows interactions with abscisic acid, ethylene and salicylic acid pathways. *BMC Plant Biol.* 10:151. doi: 10.1186/1471-2229-10-151

Dong, T., and Hwang, I. (2014). Contribution of ABA UDP-glucosyltransferases in coordination of ABA biosynthesis and catabolism for ABA homeostasis. *Plant Signal Behav.* 9:e28888. doi: 10.4161/psb.28888

Dubois, M., Van Den Broeck, L., and Inzé, D. (2018). The Pivotal Role of Ethylene in Plant Growth. *Trends Plant Sci.* 23, 311–323. doi: 10.1016/j.tplants.2018.01.003

Fahad, S., Bajwa, A. A., Nazir, U., Anjum, S. A., Farooq, A., Zohaib, A., et al. (2017). Crop production under drought and heat stress: Plant responses and Management Options. *Front. Plant Sci.* 8:1147. doi: 10.3389/fpls.2017.01147

Fahad, S., Muhammad, Z. I., Abdul, K., Ihsanullah, D., Saud, S., Saleh, A., et al. (2018). Consequences of high temperature under changing climate optima for rice pollen characteristics-concepts and perspectives. *Archives Agron. Soil Sci.* 2018:1443213. doi: 10.1080/03650340.2018.1443213

Fahad, S., Nie, L., Chen, Y., Wu, C., Xiong, D., Saud, S., et al. (2015). Crop plant hormones and environmental stress. *Sustain Agric. Rev.* 15, 371–400.

Fahad, S., Hasanuzzaman, M., Alam, M., Ullah, H., Saeed, M., Ali, K. I., et al. (eds) (2020). *Environment, Climate, Plant and Vegetation Growth*. New York, NY: Springer Nature, doi: 10.1007/978-3-030-49732-3

Fahad, S., Sönmez, O., Saud, S., Wang, D., Wu, C., Adnan, M., et al. (eds) (2021a). *Plant growth regulators for climate-smart agriculture, First edition. ed, Footprints of climate variability on plant diversity*. Boca Raton, FL: CRC Press.

Fahad, S., Sonmez, O., Saud, S., Wang, D., Wu, C., Adnan, M., et al. (eds) (2021b). *Climate change and plants: biodiversity, growth and interactions, First edition. ed, Footprints of climate variability on plant diversity*. Boca Raton, FL: CRC Press.

Fahad, S., Sonmez, O., Saud, S., Wang, D., Wu, C., Adnan, M., et al. (eds) (2021c). *Developing climate resilient crops: improving global food security and safety, First edition. ed, Footprints of climate variability on plant diversity*. Boca Raton, FL: CRC Press.

Fahad, S., Sönmez, O., Turan, V., Adnan, M., Saud, S., Wu, C., et al. (eds) (2021d). *Sustainable soil and land management and climate change, First edition. ed, Footprints of climate variability on plant diversity*. Boca Raton, FL: CRC Press.

Fahad, S., Sönmez, O., Saud, S., Wang, D., Wu, C., Adnan, M., et al. (eds) (2021e). *Engineering Tolerance in Crop Plants Against Abiotic Stress, First edition. ed, Footprints of climate variability on plant diversity*. Boca Raton, FL: CRC Press.

Fahad, S., Saud, S., Yajun, C., Chao, W., and Depeng, W. (eds) (2021f). *Abiotic stress in plants*. London: IntechOpen United Kingdom, doi: 10.5772/intechopen.91549

Fang, L., Su, L., Sun, X., Li, X., Sun, M., Karungo, S. K., et al. (2016). Expression of Vitis amurensis NAC26 in Arabidopsis enhances drought tolerance by modulating jasmonic acid synthesis. *J. Exp. Bot.* 67, 2829–2845. doi: 10.1093/jxb/erw122

Farrow, S. C., and Facchini, P. J. (2014). Functional diversity of 2-oxoglutarate/Fe(II)-dependent dioxygenases in plant metabolism. *Front. Plant Sci.* 5:524. doi: 10.3389/fpls.2014.00524

Feng, C. Z., Chen, Y., Wang, C., Kong, Y. H., Wu, W. H., and Chen, Y. F. (2014). Arabidopsis RAV1 transcription factor, phosphorylated by SnRK2 kinases, regulates the expression of ABI3, ABI4, and ABI5 during seed germination and early seedling development. *Plant J.* 80, 654–668. doi: 10.1111/tpj.12670

Feng, Y., Yin, Y., and Fei, S. (2015). Down-regulation of BdBRI1, a putative brassinosteroid receptor gene produces a dwarf phenotype with enhanced drought tolerance in Brachypodium distachyon. *Plant Sci.* 234, 163–173. doi: 10.1016/j.plantsci.2015.02.015

Floková, K., Tarkowská, D., Miersch, O., Strnad, M., Wasternack, C., and Novák, O. (2014). UHPLC-MS/MS based target profiling of stress-induced phytohormones. *Phytochemistry* 105, 147–157. doi: 10.1016/j.phytochem.2014.05.015

Fuller, D. Q., and Stevens, C. J. (2019). Between domestication and civilization: the role of agriculture and arboriculture in the emergence of the first urban societies. *Veg. Hist. Archaeobot.* 28, 263–282. doi: 10.1007/s00334-019-00727-4

Ha, S., Vankova, R., Yamaguchi-Shinozaki, K., Shinozaki, K., and Tran, L.-S. P. (2012). Cytokinins: metabolism and function in plant adaptation to environmental stresses. *Trends Plant Sci.* 17, 172–179. doi: 10.1016/j.tplants.2011.12.005

Hamayun, M., Hussain, A., Iqbal, A., Khan, S. A., and Lee, I.-J. (2018). Endophytic fungus *Aspergillus japonicus* mediates host plant growth under normal and heat stress conditions. *BioMed Res. Internat.* 2018:2018. doi: 10.1155/2018/7696831

Hamayun, M., Hussain, A., Afzal Khan, S., Iqbal, A., and Lee, I.-J. (2019). *Aspergillus flavus* promoted the growth of soybean and sunflower seedlings at elevated temperature. *BioMed. Res. Internat.* 1:2019. doi: 10.1155/2019/1295457

Hamayun, M., Hussain, A., Iqbal, A., Khan, S. A., Khan, M. A., and Lee, I.-J. (2021c). An Endophytic Fungus *Gliocladium cibotii* Regulates Metabolic and Antioxidant System of Glycine max and *Helianthus annuus* under Heat Stress. *Polish J. Env. Stud.* 2021:30.

Hamayun, M., Hussain, A., Iqbal, A., Khan, S. A., Gul, S., Khan, H., et al. (2021b). *Penicillium Glabrum* Acted as a Heat Stress Relieving Endophyte in Soybean and Sunflower. *Polish J. Env. Stud.* 2021:30.

Hamayun, M., Hussain, A., Iqbal, A., Khan, S. A., Ahmad, A., Gul, S., et al. (2021a). *Aspergillus foetidus* regulated the biochemical characteristics of soybean and sunflower under heat stress condition: role in sustainability. *Sustainability* 13:7159.

Hrabak, E. M., Chan, C. W., Gribskov, M., Harper, J. F., Choi, J. H., Halford, N., et al. (2003). The Arabidopsis CDPK-SnRK superfamily of protein kinases. *Plant Physiol.* 132, 666–680. doi: 10.1104/pp.102.011999

Hu, L., Wang, J., Yang, C., Islam, F., Bouwmeester, H. J., Muños, S., et al. (2020). The Effect of Virulence and Resistance Mechanisms on the Interactions between Parasitic Plants and Their Hosts. *Int. J. Mol. Sci.* 2020:21. doi: 10.3390/ijms21239013

Hu, W., Ren, T., Meng, F., Cong, R., Li, X., White, P. J., et al. (2019). Leaf photosynthetic capacity is regulated by the interaction of nitrogen and potassium through coordination of CO(2) diffusion and carboxylation. *Physiol. Plant* 167, 418–432. doi: 10.1111/ppl.12919

Im Kim, J., Baek, D., Park, H. C., Chun, H. J., Oh, D.-H., Lee, M. K., et al. (2013). Overexpression of Arabidopsis YUCCA6 in potato results in high-auxin developmental phenotypes and enhanced resistance to water deficit. *Molecular plant* 6, 337–349. doi: 10.1093/mp/sss100

Ismail, I., Hamayun, M., Hussain, A., Iqbal, A., Khan, S. A., and Lee, I.-J. (2020). *Aspergillus niger* boosted heat stress tolerance in sunflower and soybean via regulating their metabolic and antioxidant system. *J. Plant Interact.* 15, 223–232.

Ismail, A. H., Mehmood, A., Qadir, M., Husna, A. I., Hamayun, M., and Khan, N. (2020). Thermal stress alleviating potential of endophytic fungus *rhizopus oryzae* inoculated to sunflower (*Helianthus annuus* L.) and soybean (*Glycine max* L.). *Pak. J. Bot.* 52, 1857–1865.

Ismail, H. M., Anwar, H., Sumera, A. K., Amjad, I., and In-Jung, L. (2020). An endophytic fungus *Aspergillus violaceofuscus* can be used as heat stress adaptive tool for *Glycine max* L. and *Helianthus annuus*. *L. J. Appl. Bot. Food Q.* 93:112.

Jiang, K., and Asami, T. (2018). Chemical regulators of plant hormones and their applications in basic research and agriculture. *Biosci. Biotechnol. Biochem.* 82, 1265–1300. doi: 10.1080/09168451.2018.1462693

Jung, H., Lee, D.-K., Do Choi, Y., and Kim, J.-K. (2015). OsIAA6, a member of the rice Aux/IAA gene family, is involved in drought tolerance and tiller outgrowth. *Plant Sci.* 236, 304–312. doi: 10.1016/j.plantsci.2015.04.018

Kamran, M., Danish, M., Saleem, M. H., Malik, Z., Parveen, A., Abbasi, G. H., et al. (2021). Application of abscisic acid and 6-benzylaminopurine modulated morpho-physiological and antioxidative defense responses of tomato (*Solanum lycopersicum* L.) by minimizing cobalt uptake. *Chemosphere* 263:128169. doi: 10.1016/j.chemosphere.2020.128169

Kamran, M., Malik, Z., Parveen, A., Zong, Y., Abbasi, G. H., Rafiq, M. T., et al. (2019). Biochar alleviates Cd phytotoxicity by minimizing bioavailability and oxidative stress in pak choi (*Brassica chinensis* L.) cultivated in Cd-polluted soil. *J. Env. Manag.* 250:109500. doi: 10.1016/j.jenvman.2019.109500

Kang, S.-M., Hamayun, M., Khan, M. A., Iqbal, A., and Lee, I.-J. (2019). *Bacillus subtilis* JW1 enhances plant growth and nutrient uptake of Chinese cabbage through gibberellins secretion. *J. Appl. Bot. Food Qual.* 92, 172–178.

Kazan, K. (2013). Auxin and the integration of environmental signals into plant root development. *Ann. Bot.* 112, 1655–1665. doi: 10.1093/aob/mct229

Kazan, K. (2015). Diverse roles of jasmonates and ethylene in abiotic stress tolerance. *Trends Plant Sci.* 20, 219–229. doi: 10.1016/j.tplants.2015.02.001

Ke, M., Zheng, Y., and Zhu, Z. (2015). Rethinking the origin of auxin biosynthesis in plants. *Front. Plant Sci.* 6:1093. doi: 10.3389/fpls.2015.01093

Klingler, J. P., Batelli, G., and Zhu, J.-K. (2010). ABA receptors: the START of a new paradigm in phytohormone signalling. *J. Exp. Bot.* 61, 3199–3210. doi: 10.1093/jxb/erq151

Lee, B.-R., Zhang, Q., Park, S.-H., Islam, M. T., and Kim, T.-H. (2019). Salicylic acid improves drought-stress tolerance by regulating the redox status and proline metabolism in *Brassica rapa*. *Horticult. Env. Biotechnol.* 60, 31–40.

Li, N., Han, X., Feng, D., Yuan, D., and Huang, L. J. (2019). Signaling Crosstalk between Salicylic Acid and Ethylene/Jasmonate in Plant Defense: Do We Understand What They Are Whispering? *Int. J. Mol. Sci.* 2019:20. doi: 10.3390/ijms20030671

Li, Q. F., Wang, C., Jiang, L., Li, S., Sun, S. S., and He, J. X. (2012c). An interaction between BZR1 and DELLAs mediates direct signaling crosstalk between brassinosteroids and gibberellins in Arabidopsis. *Sci Signal* 5:ra72. doi: 10.1126/scisignal.2002908

Li, J., Sima, W., Ouyang, B., Wang, T., Ziaf, K., Luo, Z., et al. (2012a). Tomato SlDREB gene restricts leaf expansion and internode elongation by downregulating key genes for gibberellin biosynthesis. *J. Exp. Bot.* 63, 6407–6420. doi: 10.1093/jxb/ers295

Li, Q.-F., Wang, C., Jiang, L., Li, S., Sun, S. S., and He, J.-X. (2012b). An interaction between BZR1 and DELLAs mediates direct signaling crosstalk between brassinosteroids and gibberellins in Arabidopsis. *Sci. Signal.* 5, ra72–ra72.

Li, W., Herrera-Estrella, L., and Tran, L. P. (2016). The Yin-Yang of Cytokinin Homeostasis and Drought Acclimation/Adaptation. *Trends Plant Sci.* 21, 548–550. doi: 10.1016/j.tplants.2016.05.006

Li, Y., Zhang, J., Zhang, J., Hao, L., Hua, J., Duan, L., et al. (2013). Expression of an A rabidopsis molybdenum cofactor sulphurase gene in soybean enhances drought tolerance and increases yield under field conditions. *Plant Biotechnol. J.* 11, 747–758. doi: 10.1111/pbi.12066

Liang, C., Meng, Z., Meng, Z., Malik, W., Yan, R., Lwin, K. M., et al. (2016). GhABF2, a bZIP transcription factor, confers drought and salinity tolerance in cotton *(Gossypium hirsutum* L.). *Sci. Rep.* 6, 1–14. doi: 10.1038/srep35040

Lim, C. W., Baek, W., Jung, J., Kim, J.-H., and Lee, S. C. (2015). Function of ABA in stomatal defense against biotic and drought stresses. *Internat. J. Mole. Sci.* 16, 15251–15270. doi: 10.3390/ijms160715251

Liu, C., and Zhang, T. (2017). Expansion and stress responses of the AP2/EREBP superfamily in cotton. *BMC Genom.* 18:118. doi: 10.1186/s12864-017-3517-9

Liu, J., Feng, K., Hou, X., Li, H., Wang, G., Xu, Z., et al. (2019). Transcriptome profiling reveals the association of multiple genes and pathways contributing to hormonal control in celery leaves. *Acta Biochim. Biophys. Sin.* 51, 524–534. doi: 10.1093/abbs/gmz034

Liu, P., Xu, Z. S., Pan-Pan, L., Hu, D., Chen, M., Li, L. C., et al. (2013). A wheat PI4K gene whose product possesses threonine autophophorylation activity confers tolerance to drought and salt in Arabidopsis. *J. Exp. Bot.* 64, 2915–2927. doi: 10.1093/jxb/ert133

Liu, Y. N., Xi, M., Zhang, X. L., Yu, Z. D., and Kong, F. L. (2019). [Carbon storage distribution characteristics of wetlands in China and its influencing factors.]. *Ying Yong Sheng Tai Xue Bao* 30, 2481–2489. doi: 10.13287/j.1001-9332.201907.036

Ljung, K. (2013). Auxin metabolism and homeostasis during plant development. *Development* 140, 943–950. doi: 10.1242/dev.086363

Lo, S. F., Ho, T. D., Liu, Y. L., Jiang, M. J., Hsieh, K. T., Chen, K. T., et al. (2017). Ectopic expression of specific GA2 oxidase mutants promotes yield and stress tolerance in rice. *Plant Biotechnol. J.* 15, 850–864. doi: 10.1111/pbi.12681

Malik, Z., Afzal, S., Dawood, M., Abbasi, G. H., Khan, M. I., Kamran, M., et al. (2021). Exogenous melatonin mitigates chromium toxicity in maize seedlings by modulating antioxidant system and suppresses chromium uptake and oxidative stress. *Environ. Geochem Health* 2021, 1–19. doi: 10.1007/s10653-021-00908-z

Mao, C., He, J., Liu, L., Deng, Q., Yao, X., Liu, C., et al. (2020). OsNAC2 integrates auxin and cytokinin pathways to modulate rice root development. *Plant Biotechnol. J.* 18, 429–442. doi: 10.1111/pbi.13209

Miller, C. O. (1961). A kinetin-like compound in maize. *Proc. Natl. Acad. Sci. U S A* 47, 170–174. doi: 10.1073/pnas.47.2.170

Miura, K., Okamoto, H., Okuma, E., Shiba, H., Kamada, H., Hasegawa, P. M., et al. (2013). SIZ1 deficiency causes reduced stomatal aperture and enhanced drought tolerance via controlling salicylic acid-induced accumulation of reactive oxygen species in Arabidopsis. *Plant J.* 73, 91–104. doi: 10.1111/tpj.12014

Miura, K., and Tada, Y. (2014). Regulation of water, salinity, and cold stress responses by salicylic acid. *Front. Plant Sci.* 5:4. doi: 10.3389/fpls.2014.00004

Munne-Bosch, S., and Penuelas, J. (2003). Photo-and antioxidative protection, and a role for salicylic acid during drought and recovery in field-grown Phillyrea angustifolia plants. *Planta* 217, 758–766. doi: 10.1007/s00425-003-1037-0

Munné-Bosch, S., and Peñuelas, J. (2003). Photo- and antioxidative protection, and a role for salicylic acid during drought and recovery in field-grown Phillyrea angustifolia plants. *Planta* 217, 758–766.

Nir, I., Moshelion, M., and Weiss, D. (2014). The Arabidopsis gibberellin methyl transferase 1 suppresses gibberellin activity, reduces whole-plant transpiration and promotes drought tolerance in transgenic tomato. *Plant Cell Environ.* 37, 113–123. doi: 10.1111/pce.12135

Nishiyama, R., Watanabe, Y., Fujita, Y., Le, D. T., Kojima, M., Werner, T., et al. (2011). Analysis of cytokinin mutants and regulation of cytokinin metabolic genes reveals important regulatory roles of cytokinins in drought, salt and abscisic acid responses, and abscisic acid biosynthesis. *Plant Cell* 23, 2169–2183. doi: 10.1105/tpc.111.087395

Nishiyama, R., Watanabe, Y., Leyva-Gonzalez, M. A., Van Ha, C., Fujita, Y., Tanaka, M., et al. (2013). Arabidopsis AHP2, AHP3, and AHP5 histidine phosphotransfer proteins function as redundant negative regulators of drought stress response. *PNAS* 110, 4840–4845. doi: 10.1073/pnas.1302265110

Northey, J. G., Liang, S., Jamshed, M., Deb, S., Foo, E., Reid, J. B., et al. (2016). Farnesylation mediates brassinosteroid biosynthesis to regulate abscisic acid responses. *Nat. Plants* 2:16114. doi: 10.1038/nplants.2016.114

Nowicka, B., Ciura, J., Szymańska, R., and Kruk, J. (2018). Improving photosynthesis, plant productivity and abiotic stress tolerance - current trends and future perspectives. *J. Plant Physiol.* 231, 415–433. doi: 10.1016/j.jplph.2018.10.022

Parveen, A., Ahmar, S., Kamran, M., Malik, Z., Ali, A., Riaz, M., et al. (2021). Abscisic acid signaling reduced transpiration flow, regulated Na+ ion homeostasis and antioxidant enzyme activities to induce salinity tolerance in wheat (*Triticum aestivum* L.) seedlings. *Env. Technol. Innov.* 24:101808.

Parveen, A., Saleem, M. H., Kamran, M., Haider, M. Z., Chen, J.-T., Malik, Z., et al. (2020). Effect of citric acid on growth, ecophysiology, chloroplast ultrastructure, and phytoremediation potential of jute (*Corchorus capsularis* L.) seedlings exposed to copper stress. *Biomolecules* 10:592. doi: 10.3390/biom10040592

Péret, B., Middleton, A. M., French, A. P., Larrieu, A., Bishopp, A., Njo, M., et al. (2013). Sequential induction of auxin efflux and influx carriers regulates lateral root emergence. *Mol. Syst. Biol.* 9:699. doi: 10.1038/msb.2013.43

Riaz, M., Kamran, M., Fang, Y., Wang, Q., Cao, H., Yang, G., et al. (2021). Arbuscular mycorrhizal fungi-induced mitigation of heavy metal phytotoxicity in metal contaminated soils: a critical review. *J. Hazard. Material.* 402:123919. doi: 10.1016/j.jhazmat.2020.123919

Riemann, M., Dhakarey, R., Hazman, M., Miro, B., Kohli, A., and Nick, P. (2015). Exploring Jasmonates in the Hormonal Network of Drought and Salinity Responses. *Front. Plant Sci.* 6:1077. doi: 10.3389/fpls.2015.01077

Rizwan, M., Ali, S., Ibrahim, M., Farid, M., Adrees, M., Bharwana, S. A., et al. (2015). Mechanisms of silicon-mediated alleviation of drought and salt stress in plants: a review. *Environ. Sci. Pollut. Res. Int.* 22, 15416–15431. doi: 10.1007/s11356-015-5305-x

Safari, M., Mousavi-Fard, S., Nejad, A. R., Sorkheh, K., and Sofo, A. (2021). Exogenous salicylic acid positively affects morpho-physiological and molecular responses of Impatiens walleriana plants grown under drought stress. *Internat. J. Env. Sci. Technol.* 2021, 1–16.

Sah, S. K., Reddy, K. R., and Li, J. (2016). Abscisic Acid and Abiotic Stress Tolerance in Crop Plants. *Front. Plant Sci.* 7:571. doi: 10.3389/fpls.2016.00571

Sahni, S., Prasad, B. D., Liu, Q., Grbic, V., Sharpe, A., Singh, S. P., et al. (2016). Overexpression of the brassinosteroid biosynthetic gene DWF4 in Brassica napus simultaneously increases seed yield and stress tolerance. *Sci. Rep.* 6:28298. doi: 10.1038/srep28298

Saleem, M. H., Ali, S., Kamran, M., Iqbal, N., Azeem, M., Tariq Javed, M., et al. (2020). Ethylenediaminetetraacetic acid (EDTA) mitigates the toxic effect of excessive copper concentrations on growth, gaseous exchange and chloroplast ultrastructure of *Corchorus capsularis* L. and Improves copper accumulation capabilities. *Plants* 9:756. doi: 10.3390/plants9060756

Sánchez-Martín, J., Heald, J., Kingston-Smith, A., Winters, A., Rubiales, D., Sanz, M., et al. (2015). A metabolomic study in oats (Avena sativa) highlights a drought tolerance mechanism based upon salicylate signalling pathways and the modulation of carbon, antioxidant and photo-oxidative metabolism. *Plant Cell Environ.* 38, 1434–1452. doi: 10.1111/pce.12501

Sánchez-Romera, B., Ruiz-Lozano, J. M., Li, G., Luu, D. T., Martínez-Ballesta Mdel, C., Carvajal, M., et al. (2014). Enhancement of root hydraulic conductivity by methyl jasmonate and the role of calcium and abscisic acid in this process. *Plant Cell Environ.* 37, 995–1008. doi: 10.1111/pce.12214

Savchenko, T., Kolla, V. A., Wang, C. Q., Nasafi, Z., Hicks, D. R., Phadungchob, B., et al. (2014). Functional convergence of oxylipin and abscisic acid pathways controls stomatal closure in response to drought. *Plant Physiol.* 164, 1151–1160. doi: 10.1104/pp.113.234310

Scarpeci, T. E., Frea, V. S., Zanor, M. I., and Valle, E. M. (2017). Overexpression of AtERF019 delays plant growth and senescence, and improves drought tolerance in Arabidopsis. *J. Exp. Bot.* 68, 673–685. doi: 10.1093/jxb/erw429

Seo, M., and Koshiba, T. (2011). Transport of ABA from the site of biosynthesis to the site of action. *J. Plant Res.* 124, 501–507. doi: 10.1007/s10265-011-0411-4

Shan, C., Zhou, Y., and Liu, M. (2015). Nitric oxide participates in the regulation of the ascorbate-glutathione cycle by exogenous jasmonic acid in the leaves of wheat seedlings under drought stress. *Protoplasma* 252, 1397–1405. doi: 10.1007/s00709-015-0756-y

Shi, J., Drummond, B. J., Wang, H., Archibald, R. L., and Habben, J. E. (2016). Maize and Arabidopsis ARGOS Proteins Interact with Ethylene Receptor Signaling Complex, Supporting a Regulatory Role for ARGOS in Ethylene Signal Transduction. *Plant Physiol.* 171, 2783–2797. doi: 10.1104/pp.16.00347

Shi, S., Li, S., Asim, M., Mao, J., Xu, D., Ullah, Z., et al. (2018). The Arabidopsis Calcium-Dependent Protein Kinases (CDPKs) and Their Roles in Plant Growth Regulation and Abiotic Stress Responses. *Int. J. Mol. Sci.* 2018:19. doi: 10.3390/ijms19071900

Stec, N., Banasiak, J., and Jasiñski, M. (2016). Abscisic acid - an overlooked player in plant-microbe symbioses formation? *Acta Biochim. Pol.* 63, 53–58. doi: 10.18388/abp.2015_1210

Teixeira, P. J. P., Colaianni, N. R., Fitzpatrick, C. R., and Dangl, J. L. (2019). Beyond pathogens: microbiota interactions with the plant immune system. *Curr. Opin. Microbiol.* 49, 7–17. doi: 10.1016/j.mib.2019.08.003

Ullah, A., Manghwar, H., Shaban, M., Khan, A. H., Akbar, A., Ali, U., et al. (2018). Phytohormones enhanced drought tolerance in plants: a coping strategy. *Environ. Sci. Pollut. Res. Int.* 25, 33103–33118. doi: 10.1007/s11356-018-3364-5

Ullah, A., Sun, H., Yang, X., and Zhang, X. (2017). Drought coping strategies in cotton: increased crop per drop. *Plant Biotechnol. J.* 15, 271–284. doi: 10.1111/pbi.12688

Verma, V., Ravindran, P., and Kumar, P. P. (2016). Plant hormone-mediated regulation of stress responses. *BMC Plant Biol.* 16, 1–10. doi: 10.1186/s12870-016-0771-y

Wang, C., Zhao, Y., Gu, P., Zou, F., Meng, L., Song, W., et al. (2018). Auxin is involved in lateral root formation induced by drought stress in tobacco seedlings. *J. Plant Growth Regulat.* 37, 539–549. doi: 10.1111/ppl.12444

Werner, T., Nehnevajova, E., Köllmer, I., Novák, O., Strnad, M., Krämer, U., et al. (2010). Root-specific reduction of cytokinin causes enhanced root growth, drought tolerance, and leaf mineral enrichment in Arabidopsis and tobacco. *Plant Cell* 22, 3905–3920. doi: 10.1105/tpc.109.072694

Wu, J., Kim, S. G., Kang, K. Y., Kim, J.-G., Park, S.-R., Gupta, R., et al. (2016). Overexpression of a pathogenesis-related protein 10 enhances biotic and abiotic stress tolerance in rice. *Plant Pathol. J.* 32:552.

Xue, L. J., Guo, W., Yuan, Y., Anino, E. O., Nyamdari, B., Wilson, M. C., et al. (2013). Constitutively elevated salicylic acid levels alter photosynthesis and oxidative state but not growth in transgenic populus. *Plant Cell* 25, 2714–2730. doi: 10.1105/tpc.113.112839

Ye, H., Liu, S., Tang, B., Chen, J., Xie, Z., Nolan, T. M., et al. (2017). RD26 mediates crosstalk between drought and brassinosteroid signalling pathways. *Nat. Commun.* 8:14573. doi: 10.1038/ncomms14573

Yu, L., Chen, X., Wang, Z., Wang, S., Wang, Y., Zhu, Q., et al. (2013). Arabidopsis enhanced drought tolerance1/HOMEODOMAIN GLABROUS11 confers drought tolerance in transgenic rice without yield penalty. *Plant Physiol.* 162, 1378–1391. doi: 10.1104/pp.113.217596

Yu, L. H., Wu, S. J., Peng, Y. S., Liu, R. N., Chen, X., Zhao, P., et al. (2016). Arabidopsis EDT 1/HDG 11 improves drought and salt tolerance in cotton and poplar and increases cotton yield in the field. *Plant Biotechnol. J.* 14, 72–84. doi: 10.1111/pbi.12358

Zahid, K. R., Ali, F., Shah, F., Younas, M., Shah, T., Shahwar, D., et al. (2016). Response and tolerance mechanism of cotton Gossypium hirsutum L. to elevated temperature stress: a review. *Front. Plant Sci.* 7:937. doi: 10.3389/fpls.2016.00937

Zandalinas, S. I., Rivero, R. M., Martínez, V., Gómez-Cadenas, A., and Arbona, V. (2016). Tolerance of citrus plants to the combination of high temperatures and drought is associated to the increase in transpiration modulated by a reduction in abscisic acid levels. *BMC Plant Biol.* 16, 1–16. doi: 10.1186/s12870-016-0791-7

Zhang, Y., Li, Y., Hassan, M. J., Li, Z., and Peng, Y. (2020). Indole-3-acetic acid improves drought tolerance of white clover via activating auxin, abscisic acid and jasmonic acid related genes and inhibiting senescence genes. *BMC Plant Biol.* 20, 1–12. doi: 10.1186/s12870-020-02354-y

Zhao, J., Yu, N., Ju, M., Fan, B., Zhang, Y., Zhu, E., et al. (2019). ABC transporter OsABCG18 controls the shootward transport of cytokinins and grain yield in rice. *J. Exp. Bot.* 70, 6277–6291. doi: 10.1093/jxb/erz382

Zwack, P. J., and Rashotte, A. M. (2015). Interactions between cytokinin signalling and abiotic stress responses. *J. Exp. Bot.* 66, 4863–4871. doi: 10.1093/jxb/erv172

Conflict of Interest: The authors declare that the research was conducted in the absence of any commercial or financial relationships that could be construed as a potential conflict of interest.

Publisher's Note: All claims expressed in this article are solely those of the authors and do not necessarily represent those of their affiliated organizations, or those of the publisher, the editors and the reviewers. Any product that may be evaluated in this article, or claim that may be made by its manufacturer, is not guaranteed or endorsed by the publisher.

Copyright © 2022 Iqbal, Wang, Mubeen, Kamran, Kanwal, Díaz, Abbas, Parveen, Atiq, Alshaya, Zin El-Abedin and Fahad. This is an open-access article distributed under the terms of the Creative Commons Attribution License (CC BY). The use, distribution or reproduction in other forums is permitted, provided the original author(s) and the copyright owner(s) are credited and that the original publication in this journal is cited, in accordance with accepted academic practice. No use, distribution or reproduction is permitted which does not comply with these terms.

frontiers in Plant Science

ORIGINAL RESEARCH
published: 17 January 2022
doi: 10.3389/fpls.2021.793989

Preharvest UV-C Hormesis Induces Key Genes Associated With Homeostasis, Growth and Defense in Lettuce Inoculated With *Xanthomonas campestris* pv. *vitians*

Amadou Sidibé[1,2], Marie Thérèse Charles[1,2], Jean-François Lucier[1], Yanqun Xu[3] and Carole Beaulieu[1]*

[1] Department of Biology, Université de Sherbrooke, Sherbrooke, QC, Canada, [2] Saint-Jean-sur-Richelieu Research and Development Centre, Agriculture and Agri-Food Canada, Saint-Jean-sur-Richelieu, QC, Canada, [3] College of Biosystems Engineering and Food Science, Zhejiang Key Laboratory for Agri-Food Processing, Zhejiang University, Hangzhou, China

OPEN ACCESS

Edited by:
Shabir Hussain Wani, Sher-e-Kashmir University of Agricultural Sciences and Technology of Kashmir, India

Reviewed by:
Silvia Proietti, Tuscia University, Italy
Alessio Aprile, University of Salento, Italy

***Correspondence:**
Marie Thérèse Charles
marietherese.charles@agr.gc.ca

Specialty section:
This article was submitted to Plant Biotechnology, a section of the journal Frontiers in Plant Science

Received: *12 October 2021*
Accepted: *22 December 2021*
Published: *17 January 2022*

Citation:
Sidibé A, Charles MT, Lucier J-F, Xu Y and Beaulieu C (2022) Preharvest UV-C Hormesis Induces Key Genes Associated With Homeostasis, Growth and Defense in Lettuce Inoculated With Xanthomonas campestris pv. vitians. Front. Plant Sci. 12:793989. doi: 10.3389/fpls.2021.793989

Preharvest application of hormetic doses of ultraviolet-C (UV-C) generates beneficial effects in plants. In this study, within 1 week, four UV-C treatments of 0.4 kJ/m2 were applied to 3-week-old lettuce seedlings. The leaves were inoculated with a virulent strain of *Xanthomonas campestris* pv. *vitians* (*Xcv*) 48 h after the last UV-C application. The extent of the disease was tracked over time and a transcriptomic analysis was performed on lettuce leaf samples. Samples of lettuce leaves, from both control and treated groups, were taken at two different times corresponding to T2, 48 h after the last UV-C treatment and T3, 24 h after inoculation (i.e., 72 h after the last UV-C treatment). A significant decrease in disease severity between the UV-C treated lettuce and the control was observed on days 4, 8, and 14 after pathogen inoculation. Data from the transcriptomic study revealed, that in response to the effect of UV-C alone and/or UV-C + Xcv, a total of 3828 genes were differentially regulated with fold change ($|\log2\text{-FC}| > 1.5$ and false discovery rate (FDR) < 0.05. Among these, of the 2270 genes of known function 1556 were upregulated and 714 were downregulated. A total of 10 candidate genes were verified by qPCR and were generally consistent with the transcriptomic results. The differentially expressed genes observed in lettuce under the conditions of the present study were associated with 14 different biological processes in the plant. These genes are involved in a series of metabolic pathways associated with the ability of lettuce treated with hormetic doses of UV-C to resume normal growth and to defend themselves against potential stressors. The results indicate that the hormetic dose of UV-C applied preharvest on lettuce in this study, can be considered as an eustress that does not interfere with the ability of the treated plants to carry on a set of key physiological processes namely: homeostasis, growth and defense.

Keywords: bacterial disease, cell homeostasis, defense mechanisms, eustress, leaf spot disease, lettuce, physiological processes, plant growth

INTRODUCTION

Plants live in a complex and constantly changing environment, where they continuously interact with biotic and abiotic factors (Foyer et al., 2016). These factors can be the cause of severe economic losses in edible plants such as lettuce, one of the most widely consumed leafy vegetables in the world (Moraes et al., 2018). The susceptibility of lettuce to certain diseases such as bacterial leaf spot (BLS), caused by *Xanthomonas campestris* pv. *vitians* (*Xcv*) can result in 100% yield losses (Lu and Raid, 2013). The bacterium can remain viable for months in buried plant debris or in surface irrigation water (Fayette et al., 2018) and penetrates leaves through stomata or wounds, resulting in bacterial clusters in the substomatal chamber (Bull et al., 2007). Typical symptoms of BLS begin as dark, oily looking spots and then cluster into large necrotic patches in warm, moist conditions (Bull et al., 2007) making the lettuce heads unsaleable. Confine Extra (mono and di-potassium salts of phosphorous acid) is the only chemical pesticide registered for the control of BLS in 2017 (Health Canada, 2019). To obtain the expected biological response, pesticides are used excessively and repeatedly, resulting in enormous costs and posing a serious threat to the environment and human health (Konatu and Jardim, 2018). Therefore, new and effective biological approaches to improve the control of BLS are urgently needed.

Recent scientific literature indicates increased interest in the use of biotic or abiotic agents as eustressors to improve plants' functional quality and protect them against harmful levels of stressors. A biotic or abiotic eustressor is defined as a factor of biological, chemical or physical origin that can impact the physiological status of the plants in a beneficial way (Vázquez-Hernández et al., 2019). Very little is known about the cellular and molecular responses of plants to combined stimulation by a biotic disease-causing agent and an abiotic eustressor.

In response to biotic stresses, plants have developed a series of molecular pathways to adapt using proteins involved in cellular mechanisms as key players in the maintenance of cell homeostasis. Through regulation of physiological parameters, proteins participate directly in the response to biotic stresses giving rise to new plant phenotypes with peculiar characteristics (Feussner and Polle, 2015). The sequential effect of a certain combination of abiotic and biotic stresses may have a positive or negative impact on the plant's response in terms of pathogen resistance and tolerance to abiotic stresses (Zhang and Sonnewald, 2017), depending on the level applied. For example, the effect of drought stress on tomato plant growth has led to increased resistance to *Botrytis cinerea* and *Oidium neolycopersici* (Achuo et al., 2006).

Research has shown that following applications of abiotic stresses such as heat stress, plants activate several molecular cascades involving kinases that regulate genes, transcription factors (TFs), microRNAs, reactive oxygen species (ROS) and Hsps (Muthusamy et al., 2017). Abiotic stresses result in the activation of numerous ion channels, signaling pathways of different hormonal cascades (ethylene, salicylic acid, abscisic acid, jasmonic acid) to overcome the adverse effects caused by the stress situation (Murcia et al., 2017). A recent study showed that proteometabolomic and physiological changes in algae due to ultraviolet-C (UV-C) doses of radiation are characterized by an increase in redox homeostasis, ROS production, protein damage and repair, avoidance elements, photosynthetic electron flux, carbon fixation, and C/N metabolism (Colina et al., 2020).

A complete understanding of metabolic and signaling pathways and their interactions during stress response is critical to enabling the development of stress-tolerant plants. The use of data from transcriptomics studies can provide comprehensive information on the interactions that occur in response to a specific stress (Bagati et al., 2018) such as UV-C. While in strawberries, studies have shown that treatment with UV-C has a significant impact on gene expression and leads to the overexpression of a set of genes required for effective defense in plant-pathogen interaction (Xu et al., 2019), the impact of UV-C on gene expression in lettuce is unknown.

Numerous studies have shown the beneficial effects of postharvest UV-C hormesis in several plant species (for a review, see Duarte-Sierra et al., 2019). When applied at the preharvest stage, the beneficial effects of UV-C hormesis have been shown in strawberry (Janisiewicz et al., 2016a,b; Xie et al., 2016; Xu et al., 2019), tomato (Valencia et al., 2017), and lettuce (Vàsquez et al., 2017; Sidibé et al., 2021). Among the beneficial effects of UV-C on lettuce, Sidibé et al. (2021) showed an increase in dry matter and resistance against *Xcv* with no negative impact on yield. The work of Sidibé et al. (2021) suggests that the lettuce plant is able to integrate the negative effects of UV-C-induced oxidative stress signals, return to a state of homeostasis and pursue normal growth while mounting an effective defense fight against BLS. Based on these premises, using transcriptomics in the present study, we propose a hypothetical model describing the regulatory mechanisms that may underlie the beneficial effects induced by preharvest hormetic doses of UV-C radiation on lettuce.

MATERIALS AND METHODS

Plant Material and Inoculation

The lettuce cultivar 'Parris Island Cos', which is known to be susceptible to the pathogen *Xanthomonas campestris* pv. *vitians*-B07-007 (*Xcv*) (Nicolas et al., 2018), was used in this study. Seeding was carried out in a 98-well tray in a germinator for 2 weeks, and seedlings were then transferred to growth chambers as described by Sidibé et al. (2021). The plants were watered daily, alternating between water and a nutrient solution containing 200 ppm nitrogen, 71 ppm potassium and 200 ppm phosphorus. Inoculation was done with a virulent *Xcv* strain B07-007 isolated from lettuce fields in Montérégie (QC, Canada).

The inoculation conditions were described by Nicolas et al. (2018). Briefly, *Xcv* B07-007 was recovered in sterile distilled water after 48 h culture on YDC agar medium at a final concentration of 10^8 colony forming units (CFU) per mL and then sprayed up to runoff on the adaxial and abaxial surfaces of the leaves of 18 lettuce plants, 9 control, and 9 UV-C treated (**Supplementary Figure 1**) using a manual sprayer.

Ultraviolet-C Treatments

Ultraviolet-C treatments began 3 weeks after sowing, corresponding to the transplanting stage of lettuce in the field as described by Sidibé et al. (2021). The growth chambers (Conviron, PGV40, MB, Canada) were modified with a set of three UV-C lamps (254 nm, 160 W, Clean Light Inc., Vineland Station, ON, Canada). The lamps were placed at 80 cm over the tops of the plants. During treatment, the intensity of the lamps was 1.1 mW/cm^2 measured with a radiometer (ML1400A, Miltec UV, Stevensville, MD, United States) equipped with a SEL240 # 6090 sensor (ML1400A, Miltec UV). The time required to administer the treatment dose of 0.4 kJ/m^2 was 1 min. Four UV-C doses of 0.4 kJ/m^2 (**Supplementary Figure 1**) at intervals of 48 h between the first three doses and 72 h for the last dose was applied (Nicolas et al., 2020). In total, lettuce plants in the treated group received 1.6 kJ/m^2 over a 1-week period. Forty-eight hours after the last UV-C treatment, lettuce was inoculated with *Xcv* B07-007 as described above and in **Supplementary Figure 1**.

Evaluation of the Effect of Ultraviolet-C Treatments on Bacterial Leaf Spot Symptom Expression

The method of Nicolas et al. (2018) was used to assess BLS symptom development. The severity of the disease is the proportion of the foliar surface with symptoms of disease (Nicolas et al., 2018). The area under the disease progress curve (AUDPC) was calculated using equation (1) for trapezoidal integration of disease incidence as described by Shaner and Finney (1977).

$$AUDPC = \sum_{i=1}^{n} \left(\frac{Y_{i+n1} + Y_i}{2} \right) (X_{i+1} + X_i) \quad (1)$$

where Y is the disease severity (per unit) at the *i*th observation, X*i* is the time (days) at the *i*th observation, and n is the total number of observations.

This experiment was repeated three times.

RNA Extraction, Transcriptomic and qPCR Analysis

A transcriptomic study was carried on lettuces in three independent completely randomized experiments (E1, E2, E3), each designed with three replicates of three experimental units (**Supplementary Table 1** and **Supplementary Figure 1**). Fully extended lettuce leaves without the main vein from each replicate were sampled at two different times, T2 and T3 (**Supplementary Figure 1**). For each experiment, a total of 54 plants were randomly selected after transplantation and acclimatization. At this time, the plants were separated into two groups: 27 plants received the UV-C treatment and 27 plants served as control. In each group (UV-treated and control), 48 h after the last UV treatment (T2), nine plants (3 rep × 3EU) were randomly sampled as UV-48 h and C-48 h. Also at T2 inoculation was performed on nine plants from each group but there was no sampling. Later, at 24 h post-inoculation (T3), nine plants from each inoculated group were sampled to provide UVi-24 h and Ci-24 h. At the same time (T3) as an un-inoculated reference set, the nine remaining plants from each group were sampled to provide UV-72 h and C-72 h. Once the leaf samples were severed from the plants, they were immediately flash-frozen in liquid nitrogen and stored at −80°C until RNA extraction.

The total RNA of the leaves (0.1 g) was extracted using a Qiagen total RNA isolation system (RNeasy Plant Mini Kit, 74904, Qiagen, Valencia, CA, United States) according to the manufacturer's protocol. Any contaminating genomic DNA that may have been extracted along with the total RNA was removed using the RNase free DNase kit according to the instructions provided by the manufacturer (Qiagen, Germantown, United States). The verification of RNA sample purity was performed by the Bioanalyzer Agilent 2100 system using the Nano 6000 Assay RNA kit (Bioanalyzer 2100, CA, United States). This system provides the quantity and size of the RNA strands and the evaluation of the purity of the RNA samples. The RNA integrity number (RIN) minimum accepted was 5 and the mean RIN of the samples obtained was 8.

The transcriptomic analysis was performed by Genome Quebec (Canada). The cDNA libraries were built up from RNA samples by paired-end (PE) points sequencing following the Illumina Next-Generation Sequencing (NGS) protocol. The sequencing of the PE (2 × 100 bp) was performed on the Illumina HiSeq 2000 platform at a rate of 200 million sequences per line with an error rate < 0.1% (Illumina, San Diego, CA, United States). The RNA-seq library reads were trimmed using Trimmomatic 0.36 and aligned on lettuce reference genome Lsat_Salinas_v7 (GCF_002870075.1) using the STAR aligner v2.5.3a[1].

The expression profile of 10 randomly selected lettuce genes from RNA-seq data was validated using qPCR. List of primers used in this study is presented in **Supplementary Table 2**. For each gene, three biological replicates with two technical replicates were used. The EXP45 gene was chosen as reference genes (Borowski et al., 2014). Prior to -qPCR, cDNA biosynthesis was performed from 5 μg of each RNA sample using the Maxima Mix reverse transcription kit (Thermo Scientific) according to the manufacturer's instructions.

qPCR reactions were performed in a final volume of 20 μl and contained 10 μl of the ROX qPCR Master Mix from Thermo Fisher Scientific, 0.5 μM of each primer, and 2 μl of cDNA, equivalent to 20 ng of total RNA. PCR thermocycling conditions were set at 95°C for 3 min, 35 cycles at 95°C for 5 s, 60°C for 30 s, in a QuantStudioTM 3. Specificity of amplification as well as the absence of primer dimers was confirmed by melting curve analysis at the end of each reaction.

To correct for technical variations in reverse transcription and qPCR reactions as well as expression data for biological variations, these were normalized to the geometric mean of the EXP45 reference gene. The fold change (±SD) is expressed as treatment versus control is calculated by the 2-ΔΔCt method (Livak and Schmittgen, 2001).

[1]https://bitbucket.org/mugqic/genpipes/src/master/

Statistical Analysis

The experiment consisted of three independent repeats in a completely randomized design with three replicates of three experimental units, an experimental unit being 1 lettuce plant in a pot. For each experiment, the lettuce seedlings were randomly assigned to two separate groups 3 weeks after sowing. One group received the UV-C treatment according to the different modalities described above (see section "Ultraviolet-C Treatments"). Another group received no treatment and served as the control group. Symptoms of BLS data were subjected to a multi-factor analysis of variance (ANOVA) with interactions on R (v3.6.2), and Python was used to create the time-based disease assessment curve. The statistical procedures for the ANOVA and the time-based disease assessment curve can be found at https://bitbucket.org/asidibe2011/bls_data_analysis and https://bitbucket.org/asidibe2011/python_curve, respectively. RNA-Seq differential transcript expression levels were computed using Cufflinks v2.2.1, and differential relative gene expression analyses were computed using DESEQ and EDGER from the Bioconductor Rtools suite v3.5.0. Heatmaps were generated with R (v3.6.2) using the "pheatmap" package to show the relative expression of genes in the different samples. The procedures are available at https://bitbucket.org/asidibe2011/heatmaps/src/66fad937f2b5?at=master. Transcripts indicating a fold change $\geq$ 1.5 with FDR $<$ 0.05 were confirmed to be differentially expressed. It should also be noted that the selection of the genes presented in the results is based on their function as described in the literature (**Supplementary Table 3**).

RESULTS

Increased Resistance in Ultraviolet-C-Treated Lettuce to *Xanthomonas campestris* pv. *vitians*

Significant differences were observed between UV-C treated lettuce and controls in terms of *Xcv* symptom expression on days 4, 8, and 14 after inoculation (**Figure 1**). On day 4, UV-C treated lettuce leaves showed very few apparent symptoms, resulting in an AUDPC value close to 0, while on the leaves of the control lettuce, some dark and oily spots were observed, resulting in an AUDPC value of around 80. From day 8 on, the symptoms appearing on the lettuces were small necrotic spots, evolving to larger spots by day 14. This evolution was weak in UV-C treated lettuces compared to controls. As a result, AUDPC was significantly smaller in the treated group, with UV-C treatment resulting in a 62, 52, and 30% reduction in symptoms at 4, 8, and 14 days after *Xcv* inoculation, respectively, indicating an increase in AUDPC over time. However, this increase was significantly higher in control lettuces.

Differential Relative Expression of the RNA Sequences

RNA sequencing of the 54 samples from three biological replicas yielded a total gross readings of around 3 billion 94 million. Net readings of 3 billion 29 million, or around 97.88% of gross readings, were associated with the reference genome of

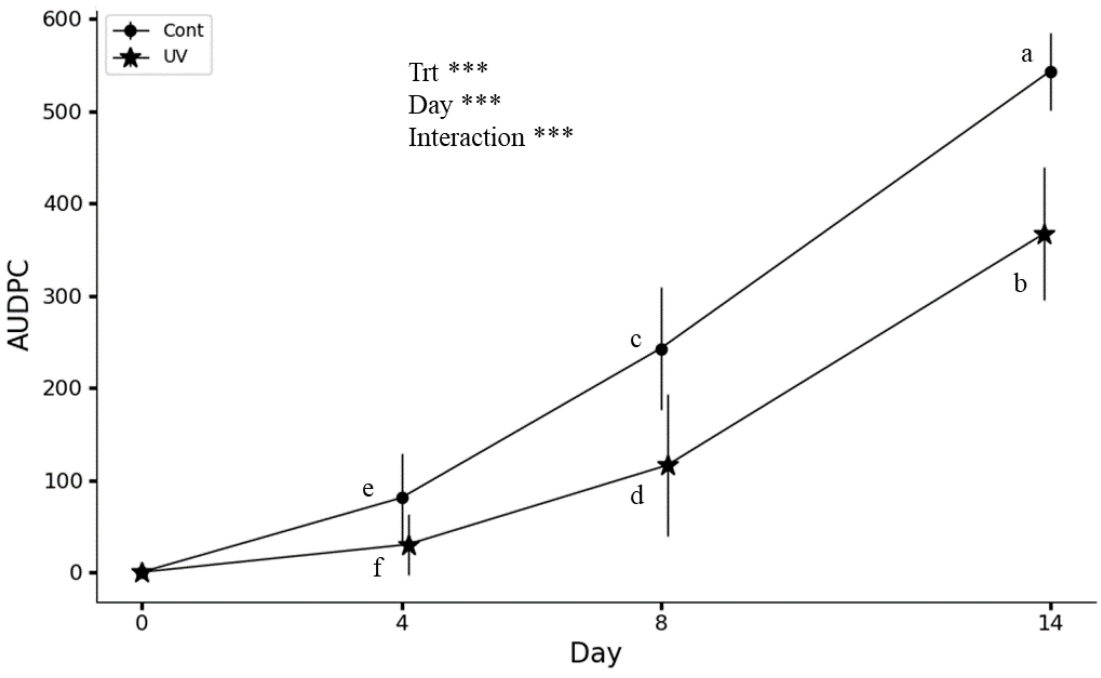


FIGURE 1 | Effect of UV-C treatments on AUDPC (area under the disease progress curve). Treatments (Trt): Cont (control), UV (1.6 kJ/m^2). Two-way ANOVA indicates a significant effect of treatments, assessment days (0, 4, 8, and 14) for BLS (bacterial leaf spot) and their interaction. AUDPC means are statistically different at $P < 0.05$ according to the Duncan's multiple range test, $n = 9$, $^{***}P < 0.001$. Different letters indicate a significant difference between treatments at the same day or on different days (4, 8, and 14). The vertical bars show the standard deviation.

Lactuca sativa L. (**Supplementary Table 4**). A total of 46,150 transcripts were identified. In UV-C treated lettuces, UV-48 h and UV-72 h and their controls C-48 h and C-72 h, respectively, 31538, 31371, 31370, and 31000 transcripts were detected, while in inoculated UV-C treated lettuces and the corresponding inoculated controls, 30930 and 31231 transcripts were detected, respectively (**Supplementary Figure 2**). The number of differentially expressed genes were 265, 2329, 2683, 2399, and 2653 in UV-48 h, UV-72 h, C-72 h, Ci-24 h and UVi-24 h respectively (**Table 1** and **Supplementary Figure 3**).

Overall Functions of Genes Affected by Preharvest Ultraviolet-C and *Xcv*

By comparing the identified transcripts of the samples from the different groups of lettuce with the C-48 h, 3828 differentially expressed transcripts with |log2-FC| > 1.5 and false discovery rate (FDR) < 0.05 were detected. The functions of 59% of these transcripts (2270) have been defined (**Supplementary Table 5**). Among these 2270 genes, some were unique to the different treatments: 44 genes belonged to UV-48 h, 257 genes to UV-72 h, 422 genes to C-72 h, 107 genes to Ci-24 h, and 238 genes to UVi-24 h. These differentially expressed genes are associated with 14 biological functions including stress and antioxidant response (**Table 2** and **Figure 2**); cell homeostasis and cell cycle (**Table 3**); metal transport (**Figure 2**); cell morphology and plant growth (**Table 4**); primary metabolism (**Figure 3** and **Supplementary Table 4**); cell wall (**Table 5**); defense mechanisms (**Figure 4**); chloroplasts, phytohormones and other phenylpropanoids (**Table 6**). These differentially expressed genes can therefore explain the modification of the lettuce transcriptome following the effect of UV-C treatments followed by *Xcv* inoculation at three levels: homeostasis state, resumption of normal growth and activation of defense mechanisms.

Genes Linked to Homeostasis State

Table 2 and **Figure 2** show that the combined effect of UV-C and inoculation resulted in the relative overexpression of 13 genes, including those of the WRKY TFs, while the single effect of UV-C 72 h after treatment resulted in the relative overexpression of four genes and the downregulation of a single gene. At the level of genes associated with WRKY TFs and upregulated, there was only one gene (40915) induced by UV-C and two genes (25732 and 23563) induced by the combined effect of UV-C and inoculation. In addition, the combined effect of UV-C and inoculation resulted in positive regulation of the genes 22470, 44623, 31324, and 1939 associated with homogentisate phytyltransferase (HPT), peroxidase N1-like, probable carboxylesterase and epidermis-specific secreted glycoprotein (EP1), respectively.

A total of six genes (19989, 27642, 39875, 4352, 11830, 33035) linked to cell homeostasis calcium-binding protein PBP1-like, calcium-binding protein CML38-like, inorganic phosphate transporter 1-4-like, AAA-ATPase At5g57480-like, protein early flowering 3 and calcium-dependent protein kinase 7-like were differentially expressed (**Table 3**). The differential expression of these genes is due to the combined effect of UV-C and *Xcv*, with the exception of the genes encoding calcium-binding protein PBP1-like, calcium-binding protein CML38-like, inorganic phosphate transporter 1-4-like, which are due respectively to the effect of UV-C 48 h and 72 h after the last treatment. All these genes were upregulated with the exception of gene 19989 encoding a calcium-binding protein PBP1-like.

The gene 27642 linked to the calcium binding protein CML38-like (calmodulin-like proteins) and the gene 33035 linked to the calcium-dependent protein kinase 7-like were positively regulated in samples UV-72h and UVi-24h, respectively. In the UV-48h samples, gene 38678, associated with the U-box domain-containing protein 1-like, was observed to be downregulated. In

TABLE 1 | Overall number of unique genes per sample.

Samples[1]	Number of genes	Number of genes specific to the sample
UV-48 h	265	44 (20-up, 24-down regulated)
C-72 h	2683	422 (161-up, 261-down regulated)
UV-72 h	2329	257 (117-up, 140-down regulated)
Ci-24 h	2399	107 (107-up regulated)
UVi-24 h	2653	238 (238-up regulated)
Unique genes	3828	

[1]Sample genes result from their comparison with the C-48 h sample as control. C-48 h, control corresponding to treated 48 h after UV. UV-48 h, UV after 48 h treatment; C-72 h, control corresponding to treated 72 h after UV; UV-72 h, UV after 72 h treatment; Ci-24 h: Control 24 h after inoculation; UVi-24 h, UV 24 h after inoculation. The genes were filtered out with a threshold |log2-FC| > 1.5 and FDR < 0.05.

TABLE 2 | Relative expression of stress and antioxidant response genes.

Samples	Gene ID	Log2-FC	Protein name
C-48 h*UV-72 h	7750	1.735	Probable serine/threonine-protein kinase PBL22
	25745	1.582	Probable protein phosphatase 2C 39
	40915	1.531	Probable WRKY transcription factor 40
	44001	1.525	BURP domain protein USPL1
	33752	−1.709	Peptidyl-prolyl cis-trans isomerase-like
C-48 h*UVi-24 h	22470	2.475	Homogentisate phytyltransferase 1, chloroplastic-like
	31324	2.24	Probable carboxylesterase 18
	45305	2.129	CBL-interacting serine/threonine-protein kinase 7-like
	25732	1.994	Probable WRKY transcription factor 70
	33507	1.789	Protein ABHD18
	25564	1.788	Sulfate transporter 1.3
	44623	1.706	Peroxidase N1-like
	1939	1.659	Epidermis-specific secreted glycoprotein EP1-like
	4132	1.624	Monothiol glutaredoxin-S2-like
	17850	1.614	Calmodulin-binding transcription activator 3-like
	36553	1.61	Heme oxygenase 1, chloroplastic-like
	23563	1.523	Probable WRKY transcription factor 31
	8354	1.505	Receptor-like cytoplasmic kinase 176

The genes were filtered out with a threshold |log2-FC| > 1.5 and FDR < 0.05. C-48 h, control corresponding to treated 48 h after UV. UV-48 h, UV after 48 h treatment; UV-72 h, UV after 72 h treatment; UVi-24 h, UV 24 h after inoculation.

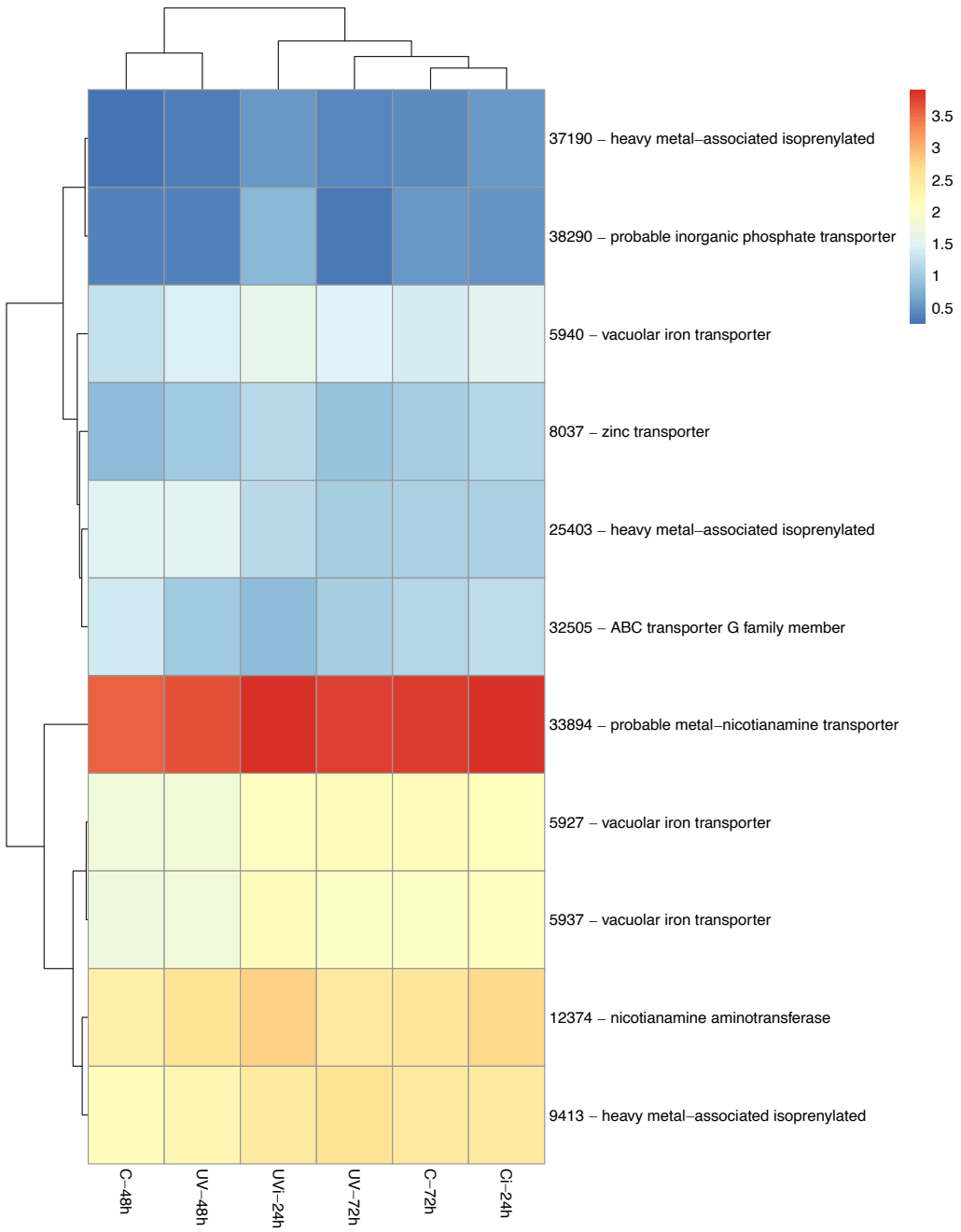


FIGURE 2 | Genes related to metal transport differentially expressed in response to UV and *Xcv* inoculation. Test of hierarchical DEG (HCA) groupings. The colors reflect the level of relative gene expression. The columns and rows represent the samples and ID_genes associated with the name/function of the corresponding proteins that were grouped according to their relative expression profile, respectively. C-48 h, control corresponding to treated 48 h after UV; UV-48 h, UV after 48 h treatment; C-72 h, control corresponding to treated 72 h after UV; UV-72 h, UV after 72 h treatment; Ci-24 h, control 24 h after inoculation; UVi-24h, UV 24 h after inoculation. The genes were filtered out with a threshold $|\log2\text{-FC}| > 1.5$ and FDR < 0.05.

the UV-72h samples, the genes (14274, 7029) linked to cyclin D5-3-like and 19-like protein containing the U-box domain were downregulated and upregulated, respectively.

A treatment-dependent regulation of three heavy-metal-binding protein biosynthesis genes (25403, 37190, and 9413) was observed (**Figure 2**). Genes 25403 and 9413 are respectively downexpressed and overexpressed in response to UV-72h, while lettuce in response to UVi-24 h resulted in positive regulation of gene 37190. In addition, UVi-24 h caused the relative overexpression of three genes (5927, 5937, and 5940) linked to the vacuolar iron transporter1 (VIT1) and one gene (12374) linked to nicotianamine aminotransferase A-like (NA).

TABLE 3 | Relative expression of cell homeostasis and cell cycle arrest genes.

Processes	Samples	Gene ID	Log2-FC	Protein name
Homeostasis	C-48 h*UV-48 h	19989	−1.957	Calcium-binding protein PBP1-like
	C-48 h*UV-72 h	27642	1.761	Calcium-binding protein CML38-like
	C-48 h*UVi-24 h	39875	1.838	Inorganic phosphate transporter 1–4-like
		4352	1.776	AAA-ATPase At5g57480-like
		11830	1.604	Protein EARLY FLOWERING 3
		33035	1.557	Calcium-dependent protein kinase 7-like
Cell cycle arrest	C-48 h*UV-48 h	38678	−1.506	U-box domain-containing protein 1-like
	C-48 h*UV-72 h	7029	1.502	U-box domain-containing protein 19-like
		14274	−1.717	Cyclin-D5-3-like
	C-48 h*UVi-24 h	9509	1.624	Cyclin-dependent kinase inhibitor 3-like
		44951	1.606	U-box domain-containing protein 13-like
		26329	1.539	U-box domain-containing protein 29-like

The genes were filtered out with a threshold |log2-FC| > 1.5 and FDR < 0.05. C4–8 h, control corresponding to treated 48 h after UV. UV-48 h, UV after 48 h treatment; UV-72 h, UV after 72 h treatment; UVi-24 h, UV 24 h after inoculation.

Genes Linked to Resumption of Normal Growth

Among the genes involved in cell morphology, five were differentially expressed (**Table 4**) in UVi-24 h samples, one gene, 35244, which is associated with the cell number regulator 7-like (CNR), is overexpressed. In samples UV-48 h and UV-72 h, a positive regulation is observed with gene 38675, associated with zinc finger protein, Constans-like 10-like, and gene 45199, associated with zinc finger protein ZAT12-like, respectively.

Table 4 also indicates the upregulation of four genes (18254, 20982, 32107, and 32104) associated with ATL (RING-H2 finger protein) and of gene 35967 linked to BRI1-EMS suppressor1/brassinazole-resistant1 (BES1/BZR1) homolog protein 4-like in response to the effect of UV-C and *Xcv* (**Table 2**). The effect of UV-C alone 72 h after treatment resulted in the upregulation of gene 25468 linked to phosphoprotein ECPP44-like.

Concerning photosynthesis, gene 7707 associated with ruBisco (ribulose-1,5-bisphosphate carboxylase/oxygenase) was positively regulated following UV-C 48 and 72 h after the last treatment and also in response to the combined effect of UV-C and *Xcv* with respective FDR of 0.006, 1.4E-13, 7.2E-14 and log2-FC of 1.42, 2.84, and 2.96. Similarly, gene 35073 linked to bisphosphoglycerate was overexpressed by the combined effect of UV-C and *Xcv*, with a FDR of 1.5E-14 and log2-FC of 0.7.

TABLE 4 | Relative expression of cell morphology and growth genes.

Processes	Samples	Gene ID	Log2-FC	Protein name
Morphology	C-48 h*UV-48 h	38675	2.246	Zinc finger protein CONSTANS
	C-48 h*UV-72 h	45199	2.025	Zinc finger protein ZAT12
		20999	−1.552	Very-long-chain enoyl-CoA reductase
		41210	−1.636	Zinc finger MYM-type protein 1
	C-48 h*UVi-24 h	35244	1.593	Cell number regulator 7
Growth	C-48 h*UV-72 h	29487	2.222	Protein DOG1
		44813	1.725	Splicing factor U2af small subunit B
		32006	1.66	NAC domain-containing protein
		23793	1.62	Scarecrow-like protein 15
		25468	1.615	Phosphoprotein ECPP44
		37511	1.584	Scarecrow-like protein 8
		45340	−1.775	Ribonuclease H2 subunit B
		43958	−4.114	Protein JINGUBANG
	C-48 h*UV-i24 h	20982	2.775	RING-H2 finger protein ATL70
		40351	2.107	Inositol 2-dehydrogenase 2
		6073	2.049	Serine/threonine-protein kinase
		32107	1.788	RING-H2 finger protein
		9835	1.736	Serine/threonine-protein kinase
		2883	1.707	Upstream activation factor
		19997	1.698	Nuclear transcription factor Y
		32907	1.691	LanC-like protein GCL1
		29278	1.686	Probable mediator of RNA
		20239	1.624	Serine/threonine-protein kinase
		16308	1.602	Nucleolar GTP-binding protein
		15163	1.578	Protein DOG1
		25756	1.572	Protein cup-shaped cotyledon
		26522	1.56	NAC transcription factor
		33732	1.552	Myb-related protein 308
		18254	1.55	RING-H2 finger protein ATL54
		35967	1.538	BES1/BZR1 homolog protein
		32104	1.523	RING-H2 finger protein ATL78

The genes were filtered out with a threshold |log2-FC| > 1.5 and FDR < 0.05. C-48 h, control corresponding to treated 48 h after UV; UV-48 h, UV after 48 h treatment; UV-72 h, UV after 72 h treatment; UVi-24 h, UV 24 h after inoculation.

The heatmap presented in **Figure 3** show the relative expression of the genes mainly involved in primary metabolism. They include a group of five highly induced genes (38054, 1879, 33672, 28184, and 23004) encoding delta (12) fatty acid

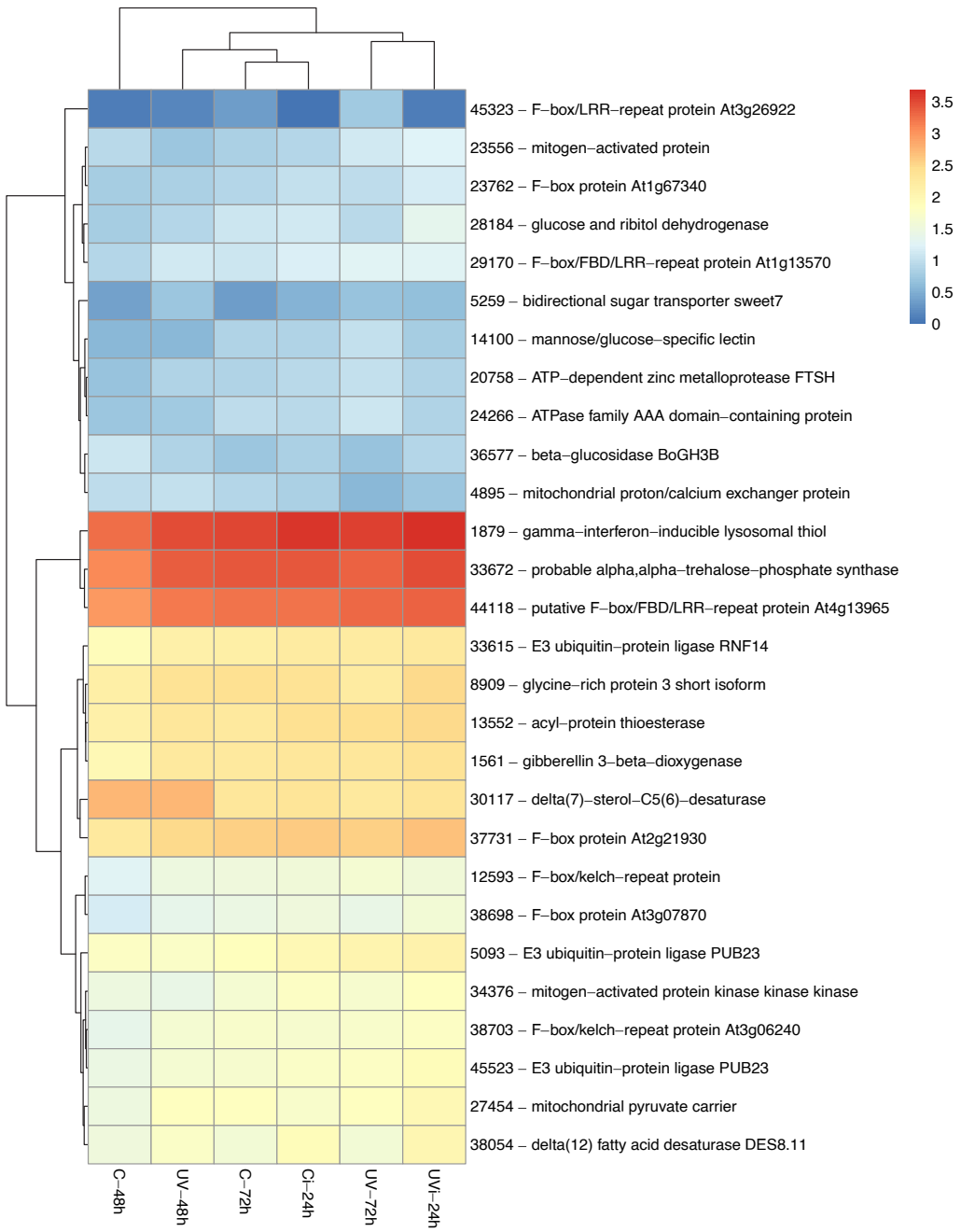


FIGURE 3 | Primary metabolism-related genes differentially expressed in response to the influence of UV and *Xcv* inoculation. Test of hierarchical DEG (HCA) groupings. The colors reflect the level of relative gene expression. The columns and rows represent the samples and ID_genes associated with the name/function of the corresponding protein that were grouped according to their relative expression profile, respectively. C-48 h, control corresponding to treated 48 h after UV; UV-48 h, UV after 48 h treatment; C-72 h, control corresponding to treated 72 h after UV; UV-72 h, UV after 72 h treatment; Ci-24 h, control 24 h after inoculation; UVi-24 h, UV 24 h after inoculation. The genes were filtered out with a threshold $|\log2\text{-FC}| > 1.5$ and FDR < 0.05.

desaturase (DES8.11), gamma-interferon-inducible lysosomal thiol reductase, probable alpha alpha-trehalose phosphate synthase (TPS10) and glucose ribitol dehydrogenase-like. There were also two groups of moderately expressed genes linked to the F-box family. Of the F-box family, the gene associated with the repeat protein F-box/LRR At3g26922 is strongly overexpressed in response to UV-C, 72 h after the last treatment, with a fold change > 3 (**Supplementary Table 5**).

Several genes in **Figure 3** and **Table 3** are involved in protein ubiquitination. These are the genes associated with E3 ubiquitin-protein ligase PUB23-like (gene 45523), E3 ubiquitin-protein ligase PUB23-like (gene 5093), and E3 ubiquitin-protein

TABLE 5 | Relative expression of cell wall genes.

Samples	Gene ID	Log2-FC	Protein name
C-48 h*UV-72 h	4681	1.704	WAT1-related protein At2g39510-like
	23001	–1.518	Expansin-A15-like
	5596	–1.524	UPF0481 protein At3g47200-like
	23655	–1.57	Putative receptor-like protein kinase At5g39000
	39520	–1.618	G2/mitotic-specific cyclin C13-1-like
	32919	–1.746	Classical arabinogalactan protein 2-like
	17410	–1.919	Extensin-3-like
C-48 h*UVi-24 h	14233	3.193	Putative receptor protein kinase ZmPK1
	6251	2.61	Extensin-2-like
	5010	2.189	Probable receptor-like protein kinase At5g38990
	23417	2.186	Berberine bridge enzyme-like 8
	27222	2.095	Clavaminate synthase-like protein At3g21360
	33528	1.748	UPF0481 protein At3g47200-like
	15855	1.663	Probable serine/threonine-protein kinase PIX13
	8086	1.662	Extensin-1
	38017	1.641	Heparanase-like protein 1
	11861	1.613	Probable receptor-like protein kinase At5g20050
	37407	1.608	Formin-like protein 4
	35108	1.583	Protein LURP-one-related 10-like

The genes were filtered out with a threshold |log2-FC| > 1.5 and FDR < 0.05. C-48h, control corresponding to treated 48 h after UV; UV-48 h, UV after 48 h treatment; UV-72h, UV after 72 h treatment; UVi-24 h, UV 24 h after inoculation.

ligase RNF14-like (gene 33615), with respective fold changes of 1.863, 1.539, and 1.503 (**Figure 3** and **Supplementary Table 5**). In the treated and inoculated lettuce, three upregulated genes (9509, 44951, and 26329) were differentially expressed: cyclin-dependent kinase inhibitor 3-like, U-box domain-containing protein 13-like and U-box domain-containing protein 29-like. Two protein-associated genes (20758 and 24266) of the protease subfamily, namely the ATP-dependent zinc metalloprotease FtsH 6, located in the chloroplast, and At1g05910-like, a member of the ATPase family AAA (ATPase Associated with various cellular Activities), were positively regulated, with a respective fold change of 1.6 and 1.5 (**Figure 3** and **Supplementary Table 5**) in response to the UV-C effect 72 h after treatment.

Our results indicate a positive upregulation of two genes (34376 and 23556) linked to mitogen-activated protein kinase 18-like, one gene (27454) related to mitochondrial pyruvate carrier (**Figure 3** and **Supplementary Table 5**), and one gene (41814) linked to protein glutamine dumper 2-like (**Figure 4**) following the combined effect of UV-C and the pathogen *Xcv*.

In UV-72h samples, a single gene 4681 linked to WAT1-related protein At2g39510-like was overexpressed. However, in response to the combined effect of UV-C and inoculation, all 12 genes observed in **Table 5** (14233, 6251, 5010, 23417, 27222, 33528, 15855, 8086, 38017, 11861, 37407, and 35108) were positively regulated and were associated with 12 different cell wall-related proteins. Among the proteins positively regulated in response to the combined effect of UV-C and inoculation are two clavaminate synthase-like proteins (**Tables 2**, **3**). The combined effect of UV-C and inoculation also resulted in the relative overexpression of five genes (**Figure 4** and **Tables 4**, **5**) coding for proteins related to the maintenance of the cell wall: BES1/BZR1 homolog protein, leucine-rich repeat extensin protein (LRX), leucine-rich repeat receptor protein kinase and two extensin proteins.

Genes Linked to Activation of Defense Mechanisms

Our results (**Figure 4**) show a relative overexpression of five genes (11156, 3972, 11409, 34826, and 22073) linked to the receptor-like kinase (RLK) family protein biosynthesis and one ankyrin repeat-containing protein ITN1-like following the combined effect of UV-C and *Xcv* inoculation. The coding sequence of gene 28479, a precursor of the CRK proteins, was positively regulated in response to the combined effect of UV-C and inoculation.

As indicated in **Figure 4**, positive regulation was observed in response to the effect of UV-C and inoculation of three *AZI1* genes (29649, 29650, and 29654), gene 10636, which is associated with the biosynthesis of Bcl-2-associated athanogene (BAG) family, and gene 36183, which is associated with the biosynthesis of PR-1 (Pathogenesis Related) proteins. The pEARLI1-like lipid transfer protein 1 biosynthesis genes are known as AZI1.

The effect of UV-C alone 72 h after the last treatment resulted in downregulation of gene 31015 involved in the biosynthesis of receptor-like proteins (RLPs) and gene 30766 associated with L-type lectin receptor kinase (LECRKs). However, the combined effect of UV-C and inoculation resulted in the positive regulation of five RLP genes (11411, 40213, 23652, 44570, and 21772), one LECRKs gene (30760), and one wall-associated receptor kinase-like 2 (WAK) protein biosynthesis gene (34502) (**Figure 2**).

The data from **Figure 4** show relative overexpression in response to UVi-24h of 9 genes (6901, 38608, 28479, 34172, 37962, 8404, 20089, 17391, and 41842). Gene 20089 is a presumed homologue of the mildew resistance protein R1A-10, and genes 17391 and 41842 are associated with the biosynthesis of proteins of the leucine-rich repeated extensin (LRX) family. With respect to the cell wall, the effect of UVi-24 h resulted in the relative overexpression of two genes (9999 and 9998) associated with the inhibition of pectin methylesterase proteins (PME) and three genes (43380, 9999, and 9998) linked to the biosynthesis of cell wall proteins (CWPs) and pectin. Gene 33943, a precursor of β-1,3:1,4-Glucan, and gene 25131, associated with glycan metabolism, are highly overexpressed as a result of UV-C and inoculation.

Figure 4 also shows positive regulation of four other disease resistance genes. The relative overexpression of genes 16977, 16993, and 27132, which are related to disease resistance proteins RML1A-like, RML1B-like and RGA3, is due to the combined effect of UV-C and inoculation with *Xcv*. The upregulation of gene 5918 associated with disease resistance is due solely to the effect of UV-C 72 h after the last treatment. Genes

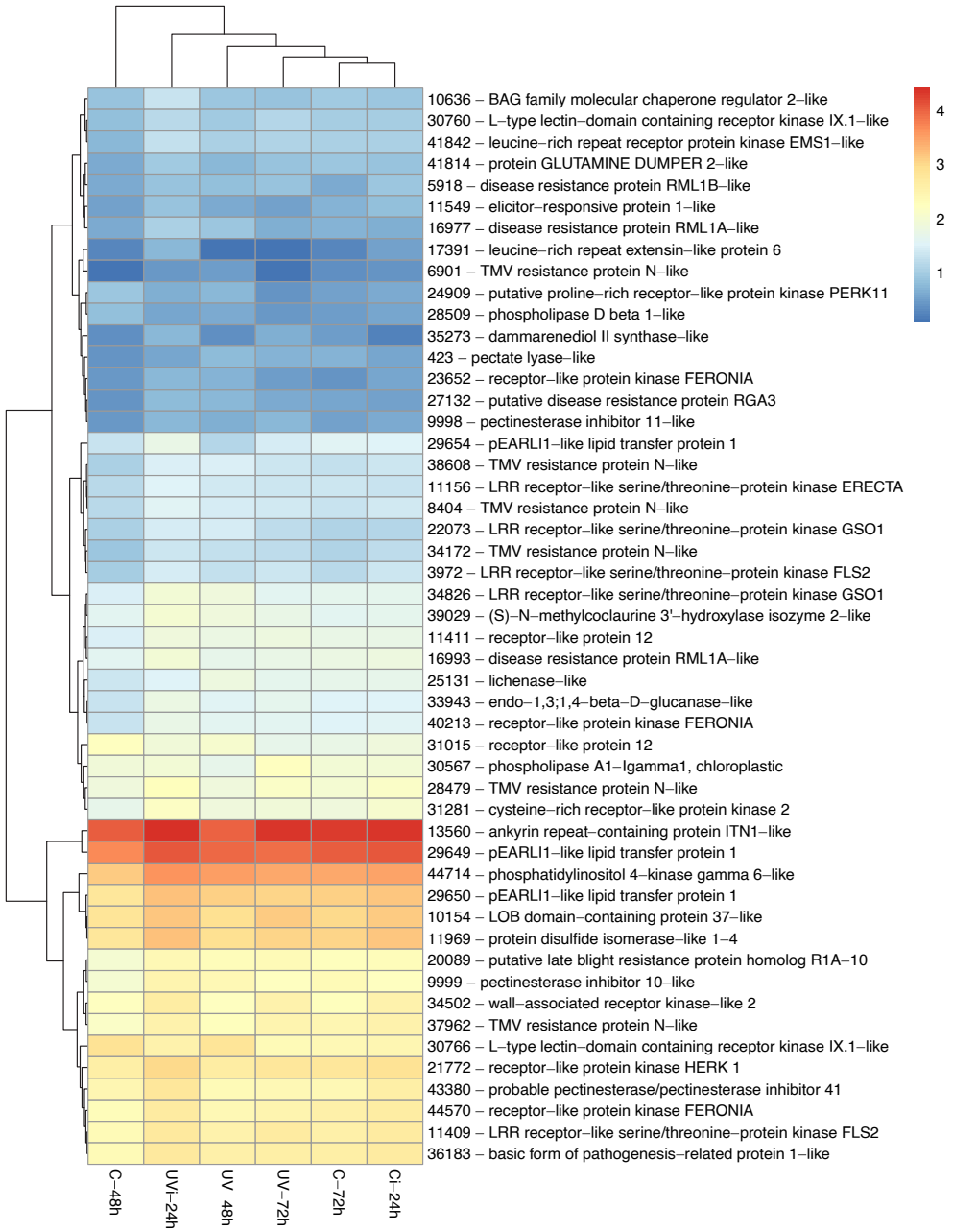


FIGURE 4 | Genes related to defense mechanisms differentially expressed in response to UV and *Xcv* inoculation. Test of hierarchical DEG (HCA) groupings. The colors reflect the level of relative gene expression. The columns and rows represent the samples and ID_genes associated with the name/function of the corresponding protein that were grouped according to their relative expression profile, respectively. C-48 h, control corresponding to treated 48 h after UV; UV-48 h, UV after 48 h treatment; C-72 h, control corresponding to treated 72 h after UV; UV-72 h, UV after 72 h treatment; Ci-24 h, control 24 h after inoculation; UVi-24 h, UV 24 h after inoculation. The genes were filtered out with a threshold $|\log2\text{-FC}| > 1.5$ and FDR < 0.05.

24266 and 20758, linked to the AAA ATPase family (**Figure 3**) overexpressed in response to the effect of UV-C, are also involved in plant defense.

The results presented in **Table 6** indicate that two genes (21432 and 22355) associated with cytochrome P450 were downexpressed in UV-72h. However, the combined effect of UV-C and inoculation with *Xcv* resulted in a positive regulation of two other genes (10522 and 24501) linked to cytochrome P450 and two genes (40902 and 27222) linked to clavaminate synthase-like protein.

Our study showed 10 differentially expressed hormone-related genes (**Tables 4**, **6**). The effect of UV light 72 h after the last treatment resulted in relative overexpression of gene 1159, which is associated with the ethylene-responsive transcription factor

TABLE 6 | Relative expression of phytohormones, chloroplast, and phenylpropanoids biosynthesis genes.

Processes	Samples	Gene ID	Log2-FC	Protein name
Phytohormones	C-48 h*UV-72 h	1159	2.076	Ethylene-responsive transcription factor
		27723	1.761	Geraniol 8-hydroxylase
		16982	–1.792	Glutamate receptor 3.6
	C-48 h*UVi-24 h	23265	1.8	Ethylene-responsive transcription factor
		24354	1.771	Glutamate receptor 2.8
		45812	1.748	Auxin-responsive protein
		34865	1.636	Glutamate receptor 1.3
		16974	1.61	Glutamate receptor 3.6
		17418	1.573	Ethylene-responsive transcription
		2086	1.546	Glutamate receptor 1.2
Chloroplast	C-48 h*UV-72 h	22355	–1.518	Cytochrome P450 89A2
		21432	–1.706	Cytochrome P450 71A4
	C-48 h*UVi-24 h	24501	1.89	Cytochrome P450 94B3
		10522	1.739	Cytochrome P450 71A6
		40902	1.72	Clavaminate synthase-like protein
Other phenylpropanoids	C-48 h*UV-72 h	29845	2.179	β-galactosidase 15
		11168	1.589	*S*-norcoclaurine synthase 2
		23316	1.531	β-amyrin 28-oxidase
		14651	1.503	Serine carboxypeptidase
		46017	–1.529	Palmitoyl-acyl carrier protein
		36801	–2.339	Hydroxycinnamoyltransferase
		46011	–2.698	Palmitoyl-acyl carrier protein
	C-48 h*UVi-24 h	13938	1.967	Vinorine synthase
		768	1.899	Vitellogenin-2
		38075	1.778	Isoflavone 2′-hydroxylase
		36806	1.593	Putrescine hydroxycinnamoyltransferase
		6395	1.52	Protein SRC2

The genes were filtered out with a threshold |log2-FC| > 1.5 and FDR < 0.05. C-48 h, control corresponding to treated 48 h after UV; UV-48 h, UV after 48 h treatment; UV-72 h, UV after 72 h treatment; UVi-24 h, UV 24 h after inoculation.

ERF017-like. In addition, the combined effect of UV-C and inoculation resulted in the relative overexpression of two genes (23265 and 17418) involved in the biosynthesis of ERF family proteins and of four genes (24354, 34865, 16974, 2086) associated with the glutamate receptor GLRs.

Table 6 shows the relative overexpression of five genes (29845, 11168, 23316, 14651, and 27723) in UV-72h samples. These genes are related to biosynthesis of several enzymes, namely, β-galactosidase 15-like, *S*-norcoclaurine synthase 2-like, β-amyrin 28-oxidase-like, serine carboxypeptidase-like and geraniol 8-hydroxylase-like (G8H).

Table 6 show that the combined effect of UV-C and inoculation with *Xcv* resulted in the positive regulation of six genes (13938, 768, 38075, 36806, 6395, and 39029) associated with the biosynthesis of vinorin synthase-like, vitellogenin-2-like, isoflavone 2′-hydroxylase-like, putrescine hydroxycinnamoyltransferase 1-like (PHT), protein SRC2-like, and (*S*)-*N*-methylcoclaurine 3′-hydroxylase isozyme (CYP80B1). Two other genes (16310 and 25705) linked to shikimate *O*-hydroxycinnamoyltransferase-like (CST) and caffeoylshikimate esterase-like (CSE), with respectively FDR of 2.5E-9, 7.2E-47 and log2-FC of 1.719, 5.196, were overexpressed in response to UV-C treatment and *Xcv*.

Comparison of RNA-seq Analysis to qPCR

Real-time quantitative polymerase chain reaction (qPCR) was performed on ten selected genes that were induced by the different treatments in our experimental conditions. Among these ten genes, *ATL5* and *ERF* are associated with defense mechanisms, *BGAL15*, *DES8.11,* and *FBXL22* are involved in plant growth recovery, *FtsH*, *GLR1.2*, *MAPKK18*, *MAPKK19*, and *WAK2* play a role in the return of homeostasis state following UV effects. All treatments were included in this validation, and all ten genes showed consistent trend of fold change expression between RNA-seq and qPCR (**Figure 5**).

Although the trend is similar for all tested genes (overexpression) for both PCR and RNSeq data, discrepancy in the amplitude of FCs can be observed for several genes. This is illustrated for example for ALT54 at UV-72 h (qPCR < RNA-seq), ERF017 at UV-48 h (qPCR > RNA-seq), ERF017 at UVi-24 h (qPCR > RNA-seq) and WAK2 at UV-72 h (qPCR > RNA-seq). At this point, we can only postulate that these apparent discrepancies are related to differences between the two techniques and handling error bias.

DISCUSSION

This work confirms that a UV-C treatment of 1.6 kJ/m^2 applied as described by Nicolas et al. (2020) falls within the hormetic dose range conferring a protective effect on lettuce against BLS. This is consistent with previous studies that have reported the efficacy of hermetic treatment of UV-C radiation in reducing the symptoms observed in a variety of plant-pathogen interactions (Janisiewicz et al., 2016a,b; Xu et al., 2019; Aarrouf and Urban, 2020; Nicolas et al., 2020; Vàsquez et al., 2020). **Figure 6**, which served as a framework for the discussion below, was developed using original data from the present study and available data from the literature. This figure shows that the early responses of lettuce treated with UV-C followed by *Xcv* inoculation led to a change in the transcriptome, which likely translated into a return to homeostasis, resumption of normal growth and the activation of defense mechanisms.

Return to Homeostasis

The change in lettuce transcriptome demonstrated a return to the homeostasis state revealed by the relative overexpression of several genes. These genes act directly or indirectly on the

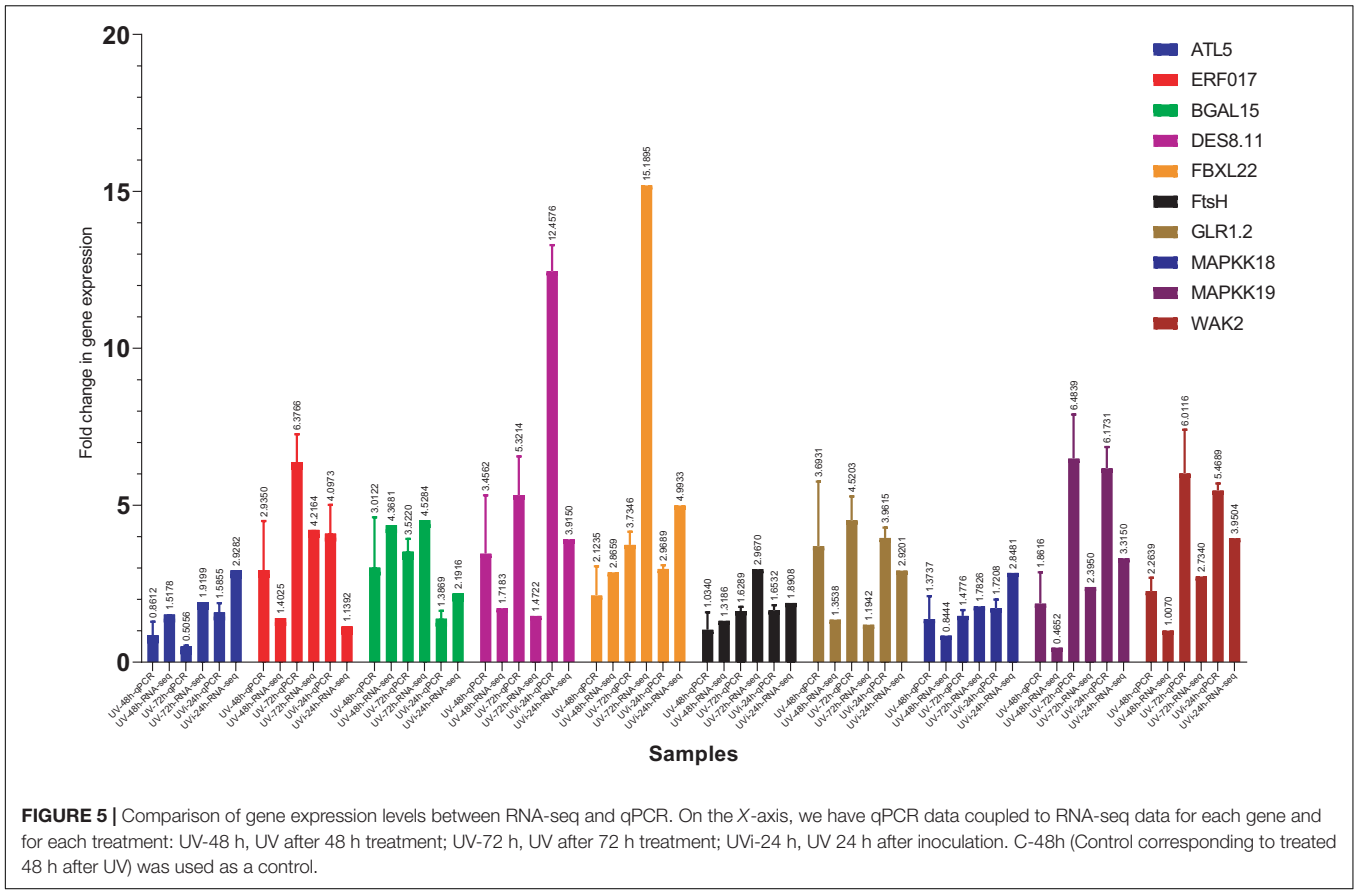


FIGURE 5 | Comparison of gene expression levels between RNA-seq and qPCR. On the *X*-axis, we have qPCR data coupled to RNA-seq data for each gene and for each treatment: UV-48 h, UV after 48 h treatment; UV-72 h, UV after 72 h treatment; UVi-24 h, UV 24 h after inoculation. C-48h (Control corresponding to treated 48 h after UV) was used as a control.

production or removal of ROS to ensure the return and/or maintenance of homeostasis (Mittler et al., 2004).

Among those genes, the relative overexpression of *SRC2* genes and protein kinase biosynthesis genes (*MAPKK18/19*, *CPK7*, *WAK2*) was found. The *SRC2* genes induce the expression of NADPH oxidases, which are homologous proteins to respiratory burst oxidase homologs (RBOHs) (Kawarazaki et al., 2013). The latter are enzymes that contribute to the generation of ROS in response to hormonal and environmental signals (Suzuki et al., 2011). The *SRC2* genes encoding SRC2 proteins are involved in the activation of Ca^{2+} influx-dependent ROS generation in *Arabidopsis thaliana* (Kawarazaki et al., 2013). The relative overexpression of *SRC2* genes therefore suggests (**Figure 6**) ROS production. This would be in agreement with the work of Xu et al. (2014, 2019), who showed induction of ROS production in response to UV-C and bacterial flagellin, respectively.

In plants, RBOHs have an N-terminal cytosolic extension consisting of two Ca^{2+}-binding EF-hand motifs and phosphorylation target sites that are important for their activity (Drerup et al., 2013). Considering the relative overexpression of SRC2, CML38 (calmodulin-like proteins), an increase in Ca^{2+} concentration can be presumed. Ca^{2+} is known to be essential to many plants cellular processes, including regulation of cellular ROS levels (Hu et al., 2018), division, differentiation, and programmed cell death (López-Fernández and Maldonado, 2015).

In contrast to SRC2, protein kinases negatively regulate RBOHD-dependent ROS production by, for instance, limiting the phosphorylation cascades that drive ROS production in response to stress (Escudero et al., 2019). Studies have shown that plants possess a comprehensive antioxidant system, consisting of enzymatic and non-enzymatic antioxidants, that can scavenge ROS (Baxter et al., 2014). Following the effect of UV-C treatment alone or in combination with *Xcv* inoculation, the relative overexpression of genes associated with the production of enzymatic antioxidants, such as SOD, CAT, and peroxidases (POD), and non-enzymatic antioxidants, such as tocopherols was found (Savidge et al., 2002). Tocopherols limit the oxidation of lipids to protect the thylakoid membrane from photo-oxidation. They also have antioxidant properties against oxidative damage caused by ROS. Our results also indicate an upregulation of metals such as Fe and Zn. Metal ions are cofactors of ROS detoxification enzymes (Ravet and Pilon, 2013). FtsH, an ATP-dependent metalloprotease with zinc as a cofactor, has been found to play a role in thylakoid membrane biogenesis, quality control in photosystem II repair, and the assembly of several protein complexes in photosynthetic electron transport pathways in *A. thaliana* (Kato and Sakamoto, 2018).

Our results indicate the relative overexpression of *PUB*, *WRKY*, and *EP1* genes with UV-C treatments alone or in combination with *Xcv* inoculation. *PUB* genes in several plant species are involved in the regulation of intracellular trafficking

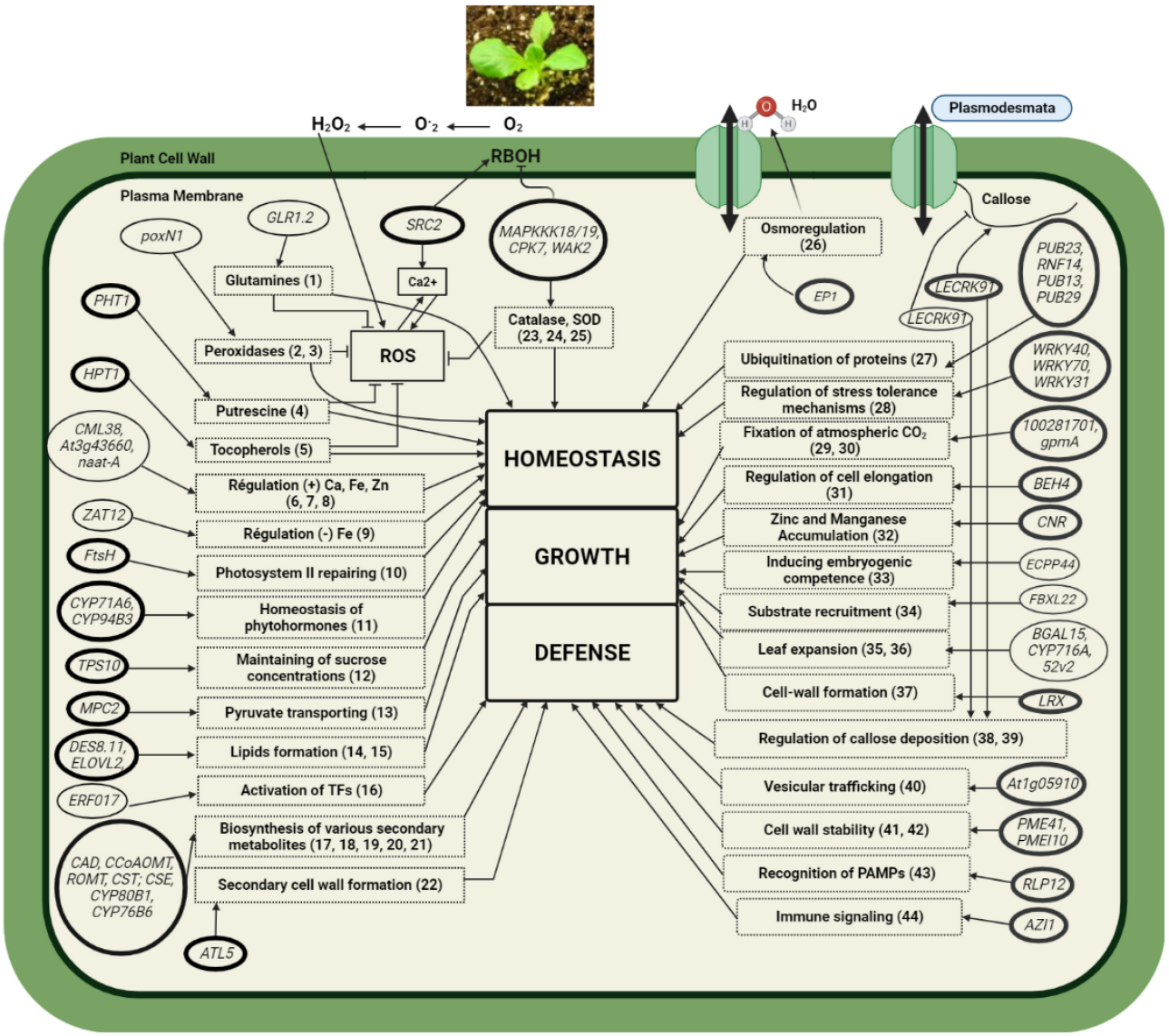


FIGURE 6 | Representative model of the regulation mechanisms induced in lettuce by the preharvest application of hormetic doses of UV-C and inoculation with the pathogen *Xcv*. Thick-bordered rectangular boxes: Physiological (or biological) processes; dashed rectangular boxes: Function or molecules associated with genes as reported in the literature. Thin-bordered ellipses: genes affected by UV-C alone; thick-bordered ellipses: genes affected by UV-C + *Xcv* infection. The pointed arrows indicate activation reactions and the blunt arrows indicate inhibition reactions. The numbers in brackets in the rectangular boxes represent the reference source(s). (1) Cheng et al. (2018); (2) Kim et al. (2007); (3) Wang et al. (2016); (4) Pushpa et al. (2014); (5) Savidge et al. (2002); (6) Lokdarshi et al. (2016); (7) Gollhofer et al. (2014); (8) Cassin et al. (2009); (9) Le et al. (2016); (10) Kato and Sakamoto (2018); (11) Yan et al. (2016); (12) Lunn et al. (2014); (13) Shen et al. (2017); (14) Doan et al. (2009); (15) Nayeri and Yarizade (2014); (16) Dey and Vlot (2015); (17) Zhang and Liu (2015); (18) Ma et al. (2005); (19) Ziegler and Facchini (2008); (20) Sung et al. (2011); (21) Höfer et al. (2013); (22) Noda et al. (2013); (23) Zhou et al. (2014); (24) Bundó and Coca (2017); (25) Li et al. (2020); (26) van Engelen et al. (1993); (27) Kimura and Tanaka (2010); (28) Ashrafi-Dehkordi et al. (2018); (29) Hauser et al. (2015); (30) Li et al. (2018); (31) Chaiwanon et al. (2016); (32) Qiao et al. (2019); (33) Tan and Kamada (2000); (34) Skaar et al. (2013); (35) Ban et al. (2020); (36) Han et al. (2013); (37) Zhao et al. (2018); (38) Lannoo and Van Damme (2014); (39) De Storme and Geelen (2014); (40) Zhu et al. (2016); (41) Lionetti et al. (2017); (42) Niu and Wang (2020); (43) Jamieson et al. (2018); (44) Dutton et al. (2019).

and ROS production (Tian et al., 2015) and in cell homeostasis (Kimura and Tanaka, 2010; Proietti et al., 2014). Genes associated with the hypothetical WRKY transcription factors participate in plant response to biotic (Scarpeci et al., 2013) and abiotic stresses (Scarpeci et al., 2013; Buti et al., 2019), by enabling dynamic cellular homeostatic reprogramming (Phukan et al., 2016). Studies have hypothesized that *EP1* genes may be involved in the regulation of water flow through the cell wall (van Engelen et al., 1993).

Resumption of Normal Growth

In addition to the return and/or maintenance of homeostasis, the effect of UV-C treatments alone or in combination with *Xcv* inoculation was followed by a resumption of normal growth likely

corresponding to an increase in photosynthetic activity. This increase in photosynthetic activity could generate an increase in dry matter synthesis (Farahbakhsh et al., 2017). Our recent work has also indicated an increase in dry matter in lettuce following preharvest treatments with hormetic doses of UV-C (Sidibé et al., 2021). In the present study, the effect of UV-C treatments alone or in combination with *Xcv* resulted in the relative overexpression of 13 genes directly or indirectly associated with the resumption of normal growth. Four of these genes (*ECPP44*, *BGAL15*, *FBXL22*, *CYP716A52v2*) were induced in response to the effect of UV-C alone. During somatic embryogenesis in plants, the phosphoprotein ECPP44 induces embryogenic competence in plants (Tan and Kamada, 2000). The induction of ECPP44 in response to the single effect of UV-C is therefore consistent with the overexpression of genes associated with embryogenic processes in cassava in response to drought (Wu et al., 2018). The β-galactosidases, such as BGAL15, are involved in polysaccharide metabolism (Ban et al., 2020) and in the separation of cellulose microfibrils during wall extension and remodeling (Sampedro et al., 2012). The released galactose fragments can serve as energy sources and substrates, which would explain the observed relative overexpression of the *FBXL22* gene. *FBXL22* is associated with F-box family proteins and is known to be involved in substrate recruitment (Skaar et al., 2013), plant growth, signal transduction (Huo et al., 2014), and disease tolerance (Kumar et al., 2020). The *CYP716A52v2* gene encodes the β-amyrin 28-oxidase enzyme, which catalyzes the triterpene hydroxylation responsible for the biosynthesis of oleic-type saponins (Han et al., 2013). Studies have shown that saponins and their biosynthetic intermediates are involved in plant growth and development (Moses et al., 2014) by stimulating chlorophyll biosynthesis, as observed in radish and pea (Boiteau and Ratsimamanga, 1956).

Seven genes (*DES8.11*, *TPS10*, *BEH4*, *MPC2*, *CNR,* and *LRX*) were induced in response to the joint effect of UV-C and *Xcv*. These seven genes code for proteins known to be involved in plant growth and development. The *DES8.11* gene is associated with fatty acid desaturase proteins, which at the plasma membrane site produce unsaturated fatty acids by introducing double bonds into fatty acid hydrocarbon chains (Nayeri and Yarizade, 2014). *DES8.11* gene induction is in agreement with the work of Gierz et al. (2017), who showed overexpression of fatty acid-encoding genes in algae (*Symbiodinium* sp.) in response to heat stress.

The *TPS* genes encode for a trehalose-6-phosphate synthase, which is a key enzyme for trehalose biosynthesis in yeast (Yeo et al., 2000). In beans (*Phaseolus vulgaris*), induction of trehalose-6-phosphate synthase biosynthesis has been shown to increase yield and improve drought tolerance (Suárez et al., 2008). BEH4 proteins of the BES1/BZR1 BES1 family integrate a variety of plant signaling pathways (Yin et al., 2005), such as brassinosteroid (BR) signaling. BRs are phytohormones involved in the regulation of cell elongation and lateral organ development (Chaiwanon et al., 2016). Pyruvate, as the end product of glycolysis, is derived from sources in the cell cytoplasm, and much of the pyruvate is transported into mitochondria by MPC2 proteins for oxidative metabolism of the Krebs cycle (Shen et al., 2017). Studies have shown that the *CNR* gene, which is relatively overexpressed in rice, has increased tolerance to otherwise toxic levels of Zn and Mn (Qiao et al., 2019). Mn has been shown to be an essential micronutrient for all stages of plant development, including as a catalytic center for photosystem II (Yang et al., 2007). The *LRX* gene is responsible for maintaining cell wall integrity through cross-linking with other cell wall components, such as pectin (Zhao et al., 2018). Overexpression of these genes (*TPS10*, *BEH4*, *MPC2*, *CNR,* and *LRX*) associated with cell tissue expansion is consistent with the increase in dry matter observed in lettuce following preharvest UV-C applications (Sidibé et al., 2021).

Activation of Defense Mechanisms

The model in **Figure 6** proposes an activation of defense mechanisms in lettuce via the relative overexpression of 15 genes following the effect of UV-C alone or in combination with *Xcv*. The effect of UV-C treatments alone resulted in the induction of the *ERF017* gene and the inhibition of the *LECRK91* gene. Genes associated with the structural reinforcement of the cell wall (*LECRK91*, *RLP12*, *ATL5*, *PMEI10*, *PME41*, *AZI1*, *At1g05910*, *CYP80B1*, *CYP76B6*, *PAL*, *CST,* and *CSE*) were induced by the effect of UV-C and *Xcv*. The induction of these genes suggests a "priming effect" of UV-C treatments in lettuce against the pathogen.

The inhibition of the *LECRK91* gene in response to the single effect of UV-C and its activation following the combined effect of UV-C and *Xcv* observed in the present study is not surprising. In *A. thaliana*, inhibition of *LECRK* gene expression has been established under various oxidative stresses (UV-B, drought, heat) (Mondal and Das, 2020). Conversely, overexpression of *LECRK* family genes was observed in response to infection by bacterial pathogens (Balagué et al., 2017). Receptor-like proteins (RLPs) often associate with receptor-like kinases (RLKs) and are involved in the development of immunity and growth (Jamieson et al., 2018). RLK proteins (Quezada et al., 2019) and Bcl-2-associated athanogenes (BAGs) (Williams et al., 2010) have been shown to cause cell death associated with a hypersensitivity reaction. For their part, the lectin receptor kinase (LECRK) and L-type lectin domain proteins (LLP) proteins (Hofberger et al., 2015) are pathogen recognition receptors (PRRs) involved in the recognition of carbohydrate structures of microbial organisms (Lannoo and Van Damme, 2014). The *ERF* gene induces the Ethylene-Responsive Factor (ERF) family of proteins, which in turn induce physiological responses to stress in plants (Dey and Vlot, 2015). Secondary wall biosynthesis in plants is induced by the *ATL5* gene (Noda et al., 2013). Also, it should be noted that the RING domain of ATL proteins is essential for E3 ubiquitin ligase (PUB) function in response to pathogen invasion (Deng et al., 2017). Therefore, it would be logical to assume that some complementarity between ATL and PUB proteins enabled the control of BLS observed in the present study.

Pectin methylesterase proteins can contribute to the generation of pectic fragments, some of which are reported to induce plant defense mechanisms (Wormit and Usadel, 2018). As PME activity is modulated by pectin methylesterase inhibitors (PMEI) (Wormit and Usadel, 2018), it is therefore appropriate to speculate that in this study, in conjunction with the relative

overexpression of PME, the increased activity of PMEI10 contributes to protecting the lettuce cell wall from degradation by *Xcv*-secreted pectinases. It is well known that *Xcv* pectinases are important factors of virulence (Kazemi-Pour et al., 2004).

AZI1 genes inducing pEARLI1-like lipid transfer protein biosynthesis link to glycerol-3-phosphate accumulation required for systemic acquired resistance conferred by azelaic acid (Yu et al., 2013). In rice plants, the AAA ATPase family protein-associated gene *At1g05910* is involved with the *PUB* genes in the induction of multivesicular body (MVB) trafficking of the plant defense system (Zhu et al., 2016). This result therefore suggests a complex feedback regulatory loop between AZI1, AAA ATPases, PUB, and glycerol-3-phosphate proteins.

In *A. thaliana*, the Geraniol 8-hydroxylase (G8H) (CYP76B6) biosynthetic gene have been shown to be involved in the flavonoid (Sung et al., 2011), alkaloid, and monoterpenoid biosynthetic pathway (Höfer et al., 2013). The precursors of G8H enzymes are derived from the deamination of L-phenylalanine (Baucher et al., 1998) which is catalyzed by PAL, the main entry point in the biosynthetic pathway of phenylpropanoids, including flavonoids, which play a role in pathogen defense and UV protection (Buer et al., 2010). Other enzymes, such as Caffeoyl shikimate esterase (CSE) and Shikimate *O*-hydroxycinnamoyltransferase-like (CST), which are involved in the lignin biosynthetic pathway (Vanholme et al., 2013), are relatively overexpressed in response to the effect of UV-C and *Xcv*. In addition to the overexpression of the latter two genes (*CSE* and *CST*), the overexpression of *ATL5* and *LECRK91* genes suggests that the protection of UV-C-treated lettuce would be partly due to the reinforcement of structural barriers. This UV-C effect was previously observed in tomato treated at the postharvest stage (Charles et al., 2008).

CONCLUSION

The control of BLS following the application of the total UV-C treatment of 1.6 kJ/m^2 observed in this study can be explained by a change in several physiological processes in lettuce. Transcriptome analysis of lettuce in response to UV-C alone or in combination with *Xcv* showed that the differentially expressed genes are associated with homeostasis, growth and defense. These results allow us to conclude that UV-C hormesis applied under the conditions described in the present study is an effective eustress that does not interfere with the ability of treated plants to resume normal growth or to defend themselves against potential stressors.

DATA AVAILABILITY STATEMENT

The original contributions presented in the study are publicly available in NCBI under accession number SUB10516369.

AUTHOR CONTRIBUTIONS

AS, MTC, and CB conceived and designed the study. AS performed the experiments. AS, MTC, J-FL, and YX analyzed the data. AS, MTC, and CB wrote the manuscript with valuable contributions from J-FL and YX. All authors read and approved the final manuscript.

FUNDING

This work was financially supported by Agriculture and Agri-Food Canada (Grant # J-001300) and the AgroPhytoSciences program at Centre SÈVE, Sherbrooke University.

ACKNOWLEDGMENTS

The authors would like to thank Karine Fréchette and Bertrand Riendeau for maintenance of lettuce plants; Daniel Rolland, Dominique Roussel, Pierre-Yves Véronneau, Marie Ciotola, and Mélanie Cadieux for their assistance in monitoring the experiments; Benjamin Mimee, Etienne Lord, Martin Laforest, and Joel Lafond-Lapalme for their assistance in bioinformatics; as well as Sylvain Lerat and Mamadou Lamine Fall for critical review of the manuscript.

SUPPLEMENTARY MATERIAL

The Supplementary Material for this article can be found online at: https://www.frontiersin.org/articles/10.3389/fpls.2021.793989/full#supplementary-material

REFERENCES

Aarrouf, J., and Urban, L. (2020). Flashes of UV-C light: an innovative method for stimulating plant defences. *PLoS One* 15:e0235918. doi: 10.1371/journal.pone.0235918

Achuo, E. A., Prinsen, E., and Höfte, M. (2006). Influence of drought, salt stress and abscisic acid on the resistance of tomato to *Botrytis cinerea* and *Oidium neolycopersici*. *Plant Pathol.* 55, 178–186. doi: 10.1111/j.1365-3059.2006.01340.x

Ashrafi-Dehkordi, E., Alemzadeh, A., Tanaka, N., and Razi, H. (2018). Meta-analysis of transcriptomic responses to biotic and abiotic stress in tomato. *PeerJ* 6:e4631. doi: 10.7717/peerj.4631

Bagati, S., Mahajan, R., Nazir, M., Dar, A. A., and Zargar, S. M. (2018). "'Omics': a gateway towards abiotic stress tolerance," in *Abiotic Stress-Mediated Sensing and Signaling in Plants: An Omics Perspective*, eds S. Zargar and M. Zargar (Singapore: Springer), 1–45. doi: 10.1007/978-981-10-7479-0_1

Balagué, C., Gouget, A., Bouchez, O., Souriac, C., Haget, N., Boutet-Mercey, S., et al. (2017). The *Arabidopsis thaliana* lectin receptor kinase LecRK-I. 9 is required for full resistance to *Pseudomonas syringae* and affects jasmonate signalling. *Mol. Plant Pathol.* 18, 937–948. doi: 10.1111/mpp.12457

Ban, Q., Jiao, J., He, Y., Jin, M., and Rao, J. (2020). Ectopic expression of the persimmon β-galactosidase gene DkGAL2 promotes leaf growth, delays dark-induced senescence and enhances tolerance to abiotic stress in *Arabidopsis*. *Sci. Hortic.* 265:109232. doi: 10.1016/j.scienta.2020.109232

Baucher, M., Monties, B., Montagu, M. V., and Boerjan, W. (1998). Biosynthesis and genetic engineering of lignin. *Crit. Rev. Plant Sci.* 17, 125–197. doi: 10.1080/07352689891304203

Baxter, A., Mittler, R., and Suzuki, N. (2014). ROS as key players in plant stress signalling. *J. Exp. Bot.* 65, 1229–1240. doi: 10.1093/jxb/ert375

Boiteau, P., and Ratsimamanga, A. R. (1956). Asiaticoside extracted from *Centella asiatica* and its therapeutic uses in cicatrization of experimental and refractory wounds (leprosy, cutaneous tuberculosis and lupus). *Therapie* 11, 125–149.

Borowski, J. M., Galli, V., da Silva Messias, R., Perin, E. C., Buss, J. H., e Silva, S. D. D. A., et al. (2014). Selection of candidate reference genes for real-time PCR studies in lettuce under abiotic stresses. *Planta* 239, 1187–1200. doi: 10.1007/s00425-014-2041-2

Buer, C. S., Imin, N., and Djordjevic, M. A. (2010). Flavonoids: new roles for old molecules. *J. Integr. Plant Biol.* 52, 98–111. doi: 10.1111/j.1744-7909.2010.00905.x

Bull, C. T., Goldman, P. H., Hayes, R., Madden, L. V., Koike, S. T., and Ryder, E. (2007). Genetic diversity of lettuce for resistance to bacterial leaf spot caused by *Xanthomonas campestris* pv. *vitians*. *Plant Health Prog.* 10, 1094–2007. doi: 10.1094/PHP-2007-0917-02-RS

Bundó, M., and Coca, M. (2017). Calcium-dependent protein kinase OsCPK10 mediates both drought tolerance and blast disease resistance in rice plants. *J. Exp. Bot.* 68, 2963–2975. doi: 10.1093/jxb/erx145

Buti, M., Baldoni, E., Formentin, E., Milc, J., Frugis, G., Lo Schiavo, F., et al. (2019). A meta-analysis of comparative transcriptomic data reveals a set of key genes involved in the tolerance to abiotic stresses in rice. *Int. J. Mol. Sci.* 20:5662. doi: 10.3390/ijms20225662

Cassin, G., Mari, S., Curie, C., Briat, J. F., and Czernic, P. (2009). Increased sensitivity to iron deficiency in *Arabidopsis thaliana* overaccumulating nicotianamine. *J. Exp. Bot.* 60, 1249–1259. doi: 10.1093/jxb/erp007

Chaiwanon, J., Wang, W., Zhu, J. Y., Oh, E., and Wang, Z. Y. (2016). Information integration and communication in plant growth regulation. *Cell* 164, 1257–1268. doi: 10.1016/j.cell.2016.01.044

Charles, M. T., Goulet, A., and Arul, J. (2008). Physiological basis of UV-C induced resistance to *Botrytis cinerea* in tomato fruit: IV. Biochemical modification of structural barriers. *Postharvest Biol. Technol.* 47, 41–53. doi: 10.1016/j.postharvbio.2007.05.019

Cheng, Y., Zhang, X., Sun, T., Tian, Q., and Zhang, W. H. (2018). Glutamate receptor homolog3.4 is involved in regulation of seed germination under salt stress in *Arabidopsis*. *Plant Cell Physiol.* 59, 978–988. doi: 10.1093/pcp/pcy034

Colina, F., Carbó, M., Meijón, M., Cañal, M. J., and Valledor, L. (2020). Low UV-C stress modulates *Chlamydomonas reinhardtii* biomass composition and oxidative stress response through proteomic and metabolomic changes involving novel signalers and effectors. *Biotechnol. Biofuels* 13:110. doi: 10.1186/s13068-020-01750-8

De Storme, N., and Geelen, D. (2014). Callose homeostasis at plasmodesmata: molecular regulators and developmental relevance. *Front. Plant Sci.* 5:138. doi: 10.3389/fpls.2014.00138

Deng, F., Guo, T., Lefebvre, M., Scaglione, S., Antico, C. J., Jing, T., et al. (2017). Expression and regulation of ATL9, an E3 ubiquitin ligase involved in plant defense. *PLoS One* 12:e0188458. doi: 10.1371/journal.pone.0188458

Dey, S., and Vlot, A. C. (2015). Ethylene responsive factors in the orchestration of stress responses in monocotyledonous plants. *Front. Plant Sci.* 6:640. doi: 10.3389/fpls.2015.00640

Doan, T. T., Carlsson, A. S., Hamberg, M., Bülow, L., Stymne, S., and Olsson, P. (2009). Functional expression of five *Arabidopsis* fatty acyl-CoA reductase genes in *Escherichia coli*. *J. Plant Physiol.* 166, 787–796. doi: 10.1016/j.jplph.2008.10.003

Drerup, M. M., Schlücking, K., Hashimoto, K., Manishankar, P., Steinhorst, L., Kuchitsu, K., et al. (2013). The calcineurin B-like calcium sensors CBL1 and CBL9 together with their interacting protein kinase CIPK26 regulate the *Arabidopsis* NADPH oxidase RBOHF. *Mol. Plant* 6, 559–569. doi: 10.1093/mp/sst009

Duarte-Sierra, A., Charles, M. T., and Arul, J. (2019). "UV-C hormesis: a means of controlling diseases and delaying senescence in fresh fruits and vegetables during storage," in *Postharvest Pathology of Fresh Horticultural Produce*, 1st Edn. eds L. Palou and J. Smilanick (Boca Raton, FL: CRC Press), 539–594.

Dutton, C., Hõrak, H., Hepworth, C., Mitchell, A., Ton, J., Hunt, L., et al. (2019). Bacterial infection systemically suppresses stomatal density. *Plant Cell Environ.* 42, 2411–2421. doi: 10.1111/pce.13570

Escudero, V., Torres, M. Á, Delgado, M., Sopeña-Torres, S., Swami, S., Morales, J., et al. (2019). Mitogen-activated protein kinase phosphatase 1 (MKP1) negatively regulates the production of reactive oxygen species during *Arabidopsis* immune responses. *Mol. Plant Microbe Interact.* 32, 464–478. doi: 10.1094/MPMI-08-18-0217-FI

Farahbakhsh, H., Pasandi Pour, A., and Reiahi, N. (2017). Physiological response of henna (*Lawsonia inermise* L.) to salicylic acid and salinity. *Plant Prod. Sci.* 20, 237–247. doi: 10.1080/1343943X.2017.1299581

Fayette, J., Jones, J. B., Pernezny, K., Roberts, P. D., and Raid, R. (2018). Survival of *Xanthomonas campestris* pv. *vitians* on lettuce in crop debris, irrigation water, and weeds in south Florida. *Eur. J. Plant Pathol.* 151, 341–353. doi: 10.1007/s10658-017-1377-4

Feussner, I., and Polle, A. (2015). What the transcriptome does not tell—proteomics and metabolomics are closer to the plants' patho-phenotype. *Curr. Opin. Plant Biol.* 26, 26–31. doi: 10.1016/j.pbi.2015.05.023

Foyer, C. H., Rasool, B., Davey, J. W., and Hancock, R. D. (2016). Cross-tolerance to biotic and abiotic stresses in plants: a focus on resistance to aphid infestation. *J. Exp. Bot.* 67, 2025–2037. doi: 10.1093/jxb/erw079

Gierz, S. L., Forêt, S., and Leggat, W. (2017). Transcriptomic analysis of thermally stressed *Symbiodinium* reveals differential expression of stress and metabolism genes. *Front. Plant Sci.* 8:271. doi: 10.3389/fpls.2017.00271

Gollhofer, J., Timofeev, R., Lan, P., Schmidt, W., and Buckhout, T. J. (2014). Vacuolar-iron-transporter1-like proteins mediate iron homeostasis in *Arabidopsis*. *PLoS One* 9:e110468. doi: 10.1371/journal.pone.0110468

Han, J. Y., Kim, M. J., Ban, Y. W., Hwang, H. S., and Choi, Y. E. (2013). The involvement of β-amyrin 28-oxidase (CYP716A52v2) in oleanane-type ginsenoside biosynthesis in *Panax ginseng*. *Plant Cell Physiol.* 54, 2034–2046. doi: 10.1093/pcp/pct141

Hauser, T., Popilka, L., Hartl, F. U., and Hayer-Hartl, M. (2015). Role of auxiliary proteins in Rubisco biogenesis and function. *Nat. Plants* 1, 1–11 doi: 10.1038/nplants.2015.65

Health Canada (2019). *Search Product Label, Pest Management Regulatory Agency*. Available online at: http://pr-rp.hc-sc.gc.ca/ls-re/index-eng.php (accessed November 1, 2020).

Hofberger, J. A., Nsibo, D. L., Govers, F., Bouwmeester, K., and Schranz, M. E. (2015). A complex interplay of tandem-and whole-genome duplication drives expansion of the L-type lectin receptor kinase gene family in the *Brassicaceae*. *Genome Biol. Evol.* 7, 720–734. doi: 10.1093/gbe/evv020

Höfer, R., Dong, L., André, F., Ginglinger, J. F., Lugan, R., Gavira, C., et al. (2013). Geraniol hydroxylase and hydroxygeraniol oxidase activities of the CYP76 family of cytochrome P450 enzymes and potential for engineering the early steps of the (seco) iridoid pathway. *Metab. Eng.* 20, 221–232. doi: 10.1016/j.ymben.2013.08.001

Hu, W., Yan, Y., Tie, W., Ding, Z., Wu, C., Ding, X., et al. (2018). Genome-wide analyses of calcium sensors reveal their involvement in drought stress response and storage roots deterioration after harvest in cassava. *Genes* 9:221. doi: 10.3390/genes9040221

Huo, D., Zheng, W., Li, P., Xu, Z., Zhou, Y., Chen, M., et al. (2014). Identification, classification, and drought response of F-box gene family in foxtail millet. *Acta Agron. Sin.* 40, 1585–1594. doi: 10.3724/SP.J.1006.2014.01585

Jamieson, P. A., Shan, L., and He, P. (2018). Plant cell surface molecular cypher: receptor-like proteins and their roles in immunity and development. *Plant Sci.* 274, 242–251. doi: 10.1016/j.plantsci.2018.05.030

Janisiewicz, W. J., Takeda, F., Glenn, D. M., Camp, M. J., and Jurick, W. M. (2016a). Dark period following UV-C treatment enhances killing of *Botrytis cinerea* conidia and controls gray mold of strawberries. *J. Phytopathol.* 106, 386–394. doi: 10.1094/PHYTO-09-15-0240-R

Janisiewicz, W. J., Takeda, F., Nichols, B., Glenn, D. M., Jurick, W. M. II, and Camp, M. J. (2016b). Use of low-dose UV-C irradiation to control powdery mildew caused by *Podosphaera aphanis* on strawberry plants. *Can. J. Plant Pathol.* 38, 430–439. doi: 10.1080/07060661.2016.1263807

Kato, Y., and Sakamoto, W. (2018). FtsH protease in the thylakoid membrane: physiological functions and the regulation of protease activity. *Front. Plant Sci.* 9:855. doi: 10.3389/fpls.2018.00855

Kawarazaki, T., Kimura, S., Iizuka, A., Hanamata, S., Nibori, H., Michikawa, et al. (2013). A low temperature-inducible protein AtSRC2 enhances the ROS-producing activity of NADPH oxidase AtRbohF. *Biochim. Biophys. Acta* 1833, 2775–2780. doi: 10.1016/j.bbamcr.2013.06.024

Kazemi-Pour, N., Condemine, G., and Hugouvieux-Cotte-Pattat, N. (2004). The secretome of the plant pathogenic bacterium *Erwinia chrysanthemi*. *Proteomics* 4, 3177–3186. doi: 10.1002/pmic.200300814

Kim, Y. H., Lim, S., Han, S. H., Lee, J. C., Song, W. K., Bang, J. W., et al. (2007). Differential expression of 10 sweetpotato peroxidases in response to sulfur dioxide, ozone, and ultraviolet radiation. *Plant Physiol. Biochem.* 45, 908–914. doi: 10.1016/j.plaphy.2007.07.019

Kimura, Y., and Tanaka, K. (2010). Regulatory mechanisms involved in the control of ubiquitin homeostasis. *J. Biochem.* 147, 793–798. doi: 10.1093/jb/mvq044

Konatu, F. R. B., and Jardim, I. C. S. F. (2018). Development and validation of an analytical method for multiresidue determination of pesticides in lettuce using QuEChERS–UHPLC–MS/MS. *J. Sep. Sci.* 41, 1726–1733. doi: 10.1002/jssc.201701038

Kumar, D., Kumar, A., Chhokar, V., Gangwar, O. P., Bhardwaj, S. C., Sivasamy, M., et al. (2020). Genome-wide association studies in diverse spring wheat panel for stripe, stem and leaf rust resistance. *Front. Plant Sci.* 11:748. doi: 10.3389/fpls.2020.00748

Lannoo, N., and Van Damme, E. J. (2014). Lectin domains at the frontiers of plant defense. *Front. Plant Sci.* 5:397. doi: 10.3389/fpls.2014.00397

Le, C. T. T., Brumbarova, T., Ivanov, R., Stoof, C., Weber, E., Mohrbacher, J., et al. (2016). Zinc finger of *Arabidopsis thaliana*12 (ZAT12) interacts with FER-like iron deficiency-induced transcription factor (FIT) linking iron deficiency and oxidative stress responses. *J. Plant Physiol.* 170, 540–557. doi: 10.1104/pp.15.01589

Li, Q., Hu, A., Qi, J., Dou, W., Qin, X., Zou, X., et al. (2020). CsWAKL08, a pathogen-induced wall-associated RLK in sweet orange, confers resistance to citrus bacterial canker via ROS control and JA signaling. *Hortic. Res.* 7:42. doi: 10.1038/s41438-020-0263-y

Li, Y., Chang, D., Yang, H., Wang, J., and Shi, H. (2018). Metabolome and molecular basis for carbohydrate increase and nitrate reduction in burley tobacco seedlings by glycerol through upregulating carbon and nitrogen metabolism. *Sci. Rep.* 8:13300. doi: 10.1038/s41598-018-31432-3

Lionetti, V., Fabri, E., De Caroli, M., Hansen, A. R., Willats, W. G., Piro, G., et al. (2017). Three pectin methylesterase inhibitors protect cell wall integrity for *Arabidopsis* immunity to *Botrytis*. *Plant Physiol.* 173, 1844–1863. doi: 10.1104/pp.16.01185

Livak, K. J., and Schmittgen, T. D. (2001). Analysis of relative gene expression data using real-time quantitative PCR and the 2– ΔΔCT method. *Methods* 25, 402–408.

Lokdarshi, A., Conner, W. C., McClintock, C., Li, T., and Roberts, D. M. (2016). Arabidopsis CML38, a calcium sensor that localizes to ribonucleoprotein complexes under hypoxia stress. *J. Plant Physiol.* 170, 1046–1059. doi: 10.1104/pp.15.01407

López-Fernández, M. P., and Maldonado, S. (2015). Programmed cell death in seeds of angiosperms. *J. Integr. Plant Biol.* 57, 996–1002. doi: 10.1111/jipb.12367

Lu, H., and Raid, R. (2013). A novel screening method for evaluation of lettuce germplasm for bacterial leaf spot resistance. *Hortscience* 48, 171–174. doi: 10.21273/HORTSCI.48.2.171

Lunn, J. E., Delorge, I., Figueroa, C. M., Van Dijck, P., and Stitt, M. (2014). Trehalose metabolism in plants. *Plant J.* 79, 544–567. doi: 10.1111/tpj.12509

Ma, X., Koepke, J., Panjikar, S., Fritzsch, G., and Stöckigt, J. (2005). Crystal structure of vinorine synthase, the first representative of the BAHD superfamily. *J. Biol. Chem.* 280, 13576–13583. doi: 10.1074/jbc.M414508200

Mittler, R., Vanderauwera, S., Gollery, M., and Van Breusegem, F. (2004). Reactive oxygen gene network of plants. *Trends Plant Sci.* 9, 490–498. doi: 10.1016/j.tplants.2004.08.009

Mondal, R., and Das, P. (2020). Data-mining bioinformatics: suggesting *Arabidopsis thaliana* L-type lectin receptor kinase IX. 2 (LecRK-IX. 2) modulate metabolites and abiotic stress responses. *Plant Signal. Behav.* 15:1818031. doi: 10.1080/15592324.2020.1818031

Moraes, R. M., Carvalho, M., Nery, F. C., Filho, P. R. S., Nogueira, M. L., and Barbosa, S. (2018). Effects of hydrogen peroxide on initial growth and enzymatic antioxidant system of *Lactuca sativa* L (Asteraceae). *Pak. J. Bot.* 50, 1769–1774.

Moses, T., Papadopoulou, K. K., and Osbourn, A. (2014). Metabolic and functional diversity of saponins, biosynthetic intermediates and semi-synthetic derivatives. *Crit. Rev. Biochem. Mol.* 49, 439–462. doi: 10.3109/10409238.2014.953628

Murcia, G., Fontana, A., Pontin, M., Baraldi, R., Bertazza, G., and Piccoli, P. N. (2017). ABA and GA3 regulate the synthesis of primary and secondary metabolites related to alleviation from biotic and abiotic stresses in grapevine. *Phytochemistry* 135, 34–52. doi: 10.1016/j.phytochem.2016.12.007

Muthusamy, S. K., Dalal, M., Chinnusamy, V., and Bansal, K. C. (2017). Genome-wide identification and analysis of biotic and abiotic stress regulation of small heat shock protein (HSP20) family genes in bread wheat. *J. Plant Physiol.* 211, 100–113. doi: 10.1016/j.jplph.2017.01.004

Nayeri, F. D., and Yarizade, K. (2014). Bioinformatics study of delta-12 fatty acid desaturase 2 (FAD2) gene in oilseeds. *Mol. Biol. Rep.* 41, 5077–5087. doi: 10.1007/s11033-014-3373-5

Nicolas, O., Charles, M. T., Chabot, D., Aarrouf, J., Jenni, S., Toussaint, V., et al. (2020). Preliminary evaluation of the impact of preharvest UV-C on lettuce: potential for the control of *Xanthomonas campestris*. *Acta Hortic.* 1271, 387–394. doi: 10.17660/ActaHortic.2020.1271.53

Nicolas, O., Charles, M. T., Jenni, S., Toussaint, V., and Beaulieu, C. (2018). Relationships between *Xanthomonas campestris* pv. *vitians* population sizes, stomatal density and lettuce resistance to bacterial leaf spot. *Can. J. Plant. Pathol.* 40, 399–407. doi: 10.1080/07060661.2018.1495269

Niu, L., and Wang, W. (2020). Defensive forwards: stress-responsive proteins in cell walls of crop plants. *bioRxiv* [Preprint]. doi: 10.1101/2020.02.15.950535v1

Noda, S., Takahashi, Y., Tsurumaki, Y., Yamamura, M., Nishikubo, N., Yamaguchi, M., et al. (2013). ATL54, a RING-H2 domain protein selected by a gene co-expression network analysis, is associated with secondary cell wall formation in *Arabidopsis*. *Plant Biotechnol. J.* 30, 169–177. doi: 10.5511/plantbiotechnology.13.0304a

Phukan, U. J., Jeena, G. S., and Shukla, R. K. (2016). WRKY transcription factors: molecular regulation and stress responses in plants. *Front. Plant Sci.* 7:760. doi: 10.3389/fpls.2016.00760

Proietti, S., Giangrande, C., Amoresano, A., Pucci, P., Molinaro, A., Bertini, L., et al. (2014). *Xanthomonas campestris* lipooligosaccharides trigger innate immunity and oxidative burst in *Arabidopsis*. *Plant Physiol. Biochem.* 85, 51–62. doi: 10.1016/j.plaphy.2014.10.011

Pushpa, D., Yogendra, K. N., Gunnaiah, R., Kushalappa, A. C., and Murphy, A. (2014). Identification of late blight resistance-related metabolites and genes in potato through nontargeted metabolomics. *Plant Mol. Biol. Rep.* 32, 584–595. doi: 10.1007/s11105-013-0665-1

Qiao, K., Wang, F., Liang, S., Wang, H., Hu, Z., and Chai, T. (2019). New biofortification tool: wheat TaCNR5 enhances zinc and manganese tolerance and increases zinc and manganese accumulation in rice grains. *J. Agric. Food Chem.* 67, 9877–9884. doi: 10.1021/acs.jafc.9b04210

Quezada, E. H., García, G. X., Arthikala, M. K., Melappa, G., Lara, M., and Nanjareddy, K. (2019). Cysteine-rich receptor-like kinase gene family identification in the *Phaseolus* genome and comparative analysis of their expression profiles specific to mycorrhizal and rhizobial symbiosis. *Genes* 10:59. doi: 10.3390/genes10010059

Ravet, K., and Pilon, M. (2013). Copper and iron homeostasis in plants: the challenges of oxidative stress. *Antioxid. Redox Signal.* 19, 919–932. doi: 10.1089/ars.2012.5084

Sampedro, J., Gianzo, C., Iglesias, N., Guitián, E., Revilla, G., and Zarra, I. (2012). AtBGAL10 is the main xyloglucan β-galactosidase in *Arabidopsis*, and its absence results in unusual xyloglucan subunits and growth defects. *Plant Physiol.* 158, 1146–1157. doi: 10.1104/pp.111.192195

Savidge, B., Weiss, J. D., Wong, Y. H. H., Lassner, M. W., Mitsky, T. A., Shewmaker, C. K., et al. (2002). Isolation and characterization of homogentisate phytyltransferase genes from *Synechocystis* sp. PCC 6803 and *Arabidopsis*. *J. Plant Physiol.* 129, 321–332. doi: 10.1104/pp.010747

Scarpeci, T. E., Zanor, M. I., Mueller-Roeber, B., and Valle, E. M. (2013). Overexpression of AtWRKY30 enhances abiotic stress tolerance during early growth stages in *Arabidopsis thaliana*. *Plant Mol. Biol.* 83, 265–277. doi: 10.1007/s11103-013-0090-8

Shaner, G., and Finney, R. E. (1977). The effect of nitrogen fertilization on the expression of slow-mildewing resistance in knox wheat. *J. Phytopathol.* 67, 1051–1056.

Shen, J. L., Li, C. L., Wang, M., He, L. L., Lin, M. Y., Chen, D. H., et al. (2017). Mitochondrial pyruvate carrier 1 mediates abscisic acid-regulated stomatal closure and the drought response by affecting cellular pyruvate content in *Arabidopsis thaliana*. *BMC Plant Biol.* 17:217. doi: 10.1186/s12870-017-1175-3

Sidibé, A., Charles, M. T., Nicolas, O., and Beaulieu, C. (2021). Preharvest UV-C affects lettuce resistance to *Xanthomonas campestris* pv. *vitians* and quality. *Sci. Hortic.* 285:110094. doi: 10.1016/j.scienta.2021.110094

Skaar, J. R., Pagan, J. K., and Pagano, M. (2013). Mechanisms and function of substrate recruitment by F-box proteins. *Nat. Rev. Mol. Cell Biol.* 14, 369–381. doi: 10.1038/nrm3582

Suárez, R., Wong, A., Ramírez, M., Barraza, A., Orozco, M. D. C., Cevallos, M. A., et al. (2008). Improvement of drought tolerance and grain yield in common bean by overexpressing trehalose-6-phosphate synthase in rhizobia. *Mol. Plant Microbe Interact.* 21, 958–966. doi: 10.1094/MPMI-21-7-0958

Sung, P. H., Huang, F. C., Do, Y. Y., and Huang, P. L. (2011). Functional expression of geraniol 10-hydroxylase reveals its dual function in the biosynthesis of terpenoid and phenylpropanoid. *J. Agric. Food Chem.* 59, 4637–4643. doi: 10.1021/jf200259n

Suzuki, N., Miller, G., Morales, J., Shulaev, V., Torres, M. A., and Mittler, R. (2011). Respiratory burst oxidases: the engines of ROS signaling. *Curr. Opin. Plant Biol.* 14, 691–699. doi: 10.1016/j.pbi.2011.07.014

Tan, S. K., and Kamada, H. (2000). Initial identification of a phosphoprotein that appears to be involved in the induction of somatic embryogenesis in carrot. *Plant Cell Rep.* 19, 739–747. doi: 10.1007/s002999900186

Tian, M., Lou, L., Liu, L., Yu, F., Zhao, Q., Zhang, H., et al. (2015). The RING finger E3 ligase STRF1 is involved in membrane trafficking and modulates salt-stress response in *Arabidopsis thaliana*. *Plant J.* 82, 81–92. doi: 10.1111/tpj.12797

Valencia, M. A., Hoyos, L. F. P., Ramírez, J. H., Sánchez, D. A. C., Gómez, J. A., and Quijano, J. C. (2017). Using UV-C radiation and image analysis for fungus control in tomato plants. *Opt. Pura Apl.* 50, 369–378.

van Engelen, F. A., Hartog, M. V., Thomas, T. L., Taylor, B., Sturm, A., van Kammen, A., et al. (1993). The carrot secreted glycoprotein gene EP1 is expressed in the epidermis and has sequence homology to *Brassica* S-locus glycoproteins. *Plant J.* 4, 855–862. doi: 10.1046/j.1365-313X.1993.04050855.x

Vanholme, R., Cesarino, I., Rataj, K., Xiao, Y., Sundin, L., Goeminne, et al. (2013). Caffeoyl shikimate esterase (CSE) is an enzyme in the lignin biosynthetic pathway in *Arabidopsis*. *Science* 341, 1103–1106. doi: 10.1126/science.1241602

Vàsquez, H., Ouhibi, C., Forges, M., Lizzi, Y., Urban, L., and Aarrouf, J. (2020). Hormetic doses of UV-C light decrease the susceptibility of tomato plants to *Botrytis cinerea* infection. *J. Phytopathol.* 168, 524–532. doi: 10.1111/jph.12930

Vàsquez, H., Ouhibi, C., Lizzi, Y., Azzouz, N., Forges, M., Bardin, M., et al. (2017). Pre-harvest hormetic doses of UV-C radiation can decrease susceptibility of lettuce leaves (*Lactuca sativa* L.) to *Botrytis cinerea* L. *Sci. Hortic.* 222, 32–39. doi: 10.1016/j.scienta.2017.04.017

Vázquez-Hernández, M. C., Parola-Contreras, I., Montoya-Gómez, L. M., Torres-Pacheco, I., Schwarz, D., and Guevara-González, R. G. (2019). Eustressors: chemical and physical stress factors used to enhance vegetables production. *Sci. Hortic.* 250, 223–229. doi: 10.1016/j.scienta.2019.02.053

Wang, X. Y., Li, D. Z., Li, Q., Ma, Y. Q., Yao, J. W., Huang, X., et al. (2016). Metabolomic analysis reveals the relationship between AZI1 and sugar signaling in systemic acquired resistance of *Arabidopsis*. *Plant Physiol. Biochem.* 107, 273–287. doi: 10.1016/j.plaphy.2016.06.016

Williams, B., Kabbage, M., Britt, R., and Dickman, M. B. (2010). AtBAG7, an *Arabidopsis* Bcl-2–associated athanogene, resides in the endoplasmic reticulum and is involved in the unfolded protein response. *Proc. Natl. Acad. Sci. U.S.A.* 107, 6088–6093. doi: 10.1073/pnas.0912670107

Wormit, A., and Usadel, B. (2018). The multifaceted role of pectin methylesterase inhibitors (PMEIs). *Int. J. Mol. Sci.* 19:2878. doi: 10.3390/ijms19102878

Wu, C., Hu, W., Yan, Y., Tie, W., Ding, Z., Guo, J., et al. (2018). The late embryogenesis abundant protein family in cassava (*Manihot esculenta* Crantz): genome-wide characterization and expression during abiotic stress. *Molecules* 23:1196. doi: 10.3390/molecules23051196

Xie, Z., Fan, J., Charles, M. T., Charlebois, D., Khanizadeh, S., Rolland, D., et al. (2016). Preharvest ultraviolet-C irradiation: influence on physicochemical parameters associated with strawberry fruit quality. *Plant Physiol. Biochem.* 108, 337–343. doi: 10.1016/j.plaphy.2016.07.026

Xu, J., Xie, J., Yan, C., Zou, X., Ren, D., and Zhang, S. (2014). A chemical genetic approach demonstrates that MPK 3/MPK 6 activation and NADPH oxidase-mediated oxidative burst are two independent signaling events in plant immunity. *Plant J.* 77, 222–234. doi: 10.1111/tpj.12382

Xu, Y., Charles, M. T., Luo, Z., Mimee, B., Veronneau, P. Y., Rolland, D., et al. (2019). Ultraviolet-C priming of strawberry leaves against subsequent *Mycosphaerella fragariae* infection involves the action of reactive oxygen species, plant hormones, and terpenes. *Plant Cell Environ.* 42, 815–831. doi: 10.1111/pce.13491

Yan, Q., Cui, X., Lin, S., Gan, S., Xing, H., and Dou, D. (2016). GmCYP82A3, a soybean cytochrome P450 family gene involved in the jasmonic acid and ethylene signaling pathway, enhances plant resistance to biotic and abiotic stresses. *PLoS One* 11:e0162253. doi: 10.1371/journal.pone.0162253

Yang, Z. B., You, J. F., and Yang, Z. M. (2007). Manganese uptake and transportation as well as antioxidant response to excess manganese in plants. *J. Plant Physiol. Mol. Biol.* 33, 480–488.

Yeo, E. T., Kwon, H. B., Han, S. E., Lee, J. T., Ryu, J. C., and Byu, M. O. (2000). Genetic engineering of drought resistant potato plants by introduction of the trehalose-6-phosphate synthase (TPS1) gene from *Saccharomyces cerevisiae*. *Mol. Cells* 10, 263–268.

Yin, Y., Vafeados, D., Tao, Y., Yoshida, S., Asami, T., and Chory, J. (2005). A new class of transcription factors mediates brassinosteroid-regulated gene expression in *Arabidopsis*. *Cell* 120, 249–259. doi: 10.1016/j.cell.2004.11.044

Yu, K., Soares, J. M., Mandal, M. K., Wang, C., Chanda, B., Gifford, A. N., et al. (2013). A feedback regulatory loop between G3P and lipid transfer proteins DIR1 and AZI1 mediates azelaic-acid-induced systemic immunity. *Cell Rep.* 3, 1266–1278. doi: 10.1016/j.celrep.2013.03.030

Zhang, X., and Liu, C. J. (2015). Multifaceted regulations of gateway enzyme phenylalanine ammonia-lyase in the biosynthesis of phenylpropanoids. *Mol. Plant* 8, 17–27. doi: 10.1016/j.molp.2014.11.001

Zhang, H., and Sonnewald, U. (2017). Differences and commonalities of plant responses to single and combined stresses. *Plant J.* 90, 839–855. doi: 10.1111/tpj.13557

Zhao, C., Zayed, O., Yu, Z., Jiang, W., Zhu, P., Hsu, et al. (2018). Leucine-rich repeat extesin proteins regulate plant salt tolerance in *Arabidopsis*. *Proc. Natl. Acad. Sci. U.S.A.* 115, 13123–13128. doi: 10.1073/pnas.1816991115

Zhou, J., Xia, X. J., Zhou, Y. H., Shi, K., Chen, Z., and Yu, J. Q. (2014). RBOH1-dependent H2O2 production and subsequent activation of MPK1/2 play an important role in acclimation-induced cross-tolerance in tomato. *J. Exp. Bot.* 65, 595–607. doi: 10.1093/jxb/ert404

Zhu, X., Yin, J., Liang, S., Liang, R., Zhou, X., Chen, Z., et al. (2016). The multivesicular bodies (MVBs)-localized AAA ATPase LRD6-6 inhibits immunity and cell death likely through regulating MVBs-mediated vesicular trafficking in rice. *PLoS Genet.* 12:e1006311. doi: 10.1371/journal.pgen.1006311

Ziegler, J., and Facchini, P. J. (2008). Alkaloid biosynthesis: metabolism and trafficking. *Annu. Rev. Plant Biol.* 59, 735–769. doi: 10.1146/annurev.arplant.59.032607.092730

Conflict of Interest: The authors declare that the research was conducted in the absence of any commercial or financial relationships that could be construed as a potential conflict of interest.

Publisher's Note: All claims expressed in this article are solely those of the authors and do not necessarily represent those of their affiliated organizations, or those of the publisher, the editors and the reviewers. Any product that may be evaluated in this article, or claim that may be made by its manufacturer, is not guaranteed or endorsed by the publisher.

Copyright © 2022 Sidibé, Charles, Lucier, Xu and Beaulieu. This is an open-access article distributed under the terms of the Creative Commons Attribution License (CC BY). The use, distribution or reproduction in other forums is permitted, provided the original author(s) and the copyright owner(s) are credited and that the original publication in this journal is cited, in accordance with accepted academic practice. No use, distribution or reproduction is permitted which does not comply with these terms.

frontiers in Plant Science

ORIGINAL RESEARCH
published: 20 January 2022
doi: 10.3389/fpls.2021.804600

Genome-Wide Identification and Expression Profiling of DUF221 Gene Family Provides New Insights Into Abiotic Stress Responses in Potato

*Madiha Zaynab[1†], Jiaofeng Peng[2†], Yasir Sharif[3], Mohammed Albaqami[4], Rashid Al-Yahyai[5], Mahpara Fatima[6], Muhammad Azhar Nadeem[7], Khalid Ali Khan[8,9,10], Saqer S. Alotaibi[11], Ibrahim A. Alaraidh[12], Hassan O. Shaikhaldein[12] and Shuangfei Li[1]**

[1] Shenzhen Key Laboratory of Marine Bioresource and Eco-Environmental Sciences, College of Life Sciences and Oceanography, Shenzhen University, Shenzhen, China, [2] Instrument Analysis Center, Shenzhen University, Shenzhen, China, [3] College of Plant Protection, Fujian Agriculture and Forestry University, Fuzhou, China, [4] Department of Biology, Faculty of Applied Science, Umm Al-Qura University, Makkah, Saudi Arabia, [5] Department of Plant Sciences, College of Agricultural and Marine Sciences, Sultan Qaboos University, Muscat, Oman, [6] College of Agriculture, Fujian Agriculture and Forestry University, Fuzhou, China, [7] Faculty of Agricultural Sciences and Technologies, Sivas University of Science and Technology, Sivas, Turkey, [8] Research Center for Advanced Materials Science (RCAMS), King Khalid University, Abha, Saudi Arabia, [9] Unit of Bee Research and Honey Production, Faculty of Science, King Khalid University, Abha, Saudi Arabia, [10] Faculty of Science, King Khalid University, Abha, Saudi Arabia, [11] Department of Biotechnology, College of Science, Taif University, Taif, Saudi Arabia, [12] Botany & Microbiology Department, Science College, King Saud University, Riyadh, Saudi Arabia

OPEN ACCESS

Edited by:
Shabir Hussain Wani, Sher-e-Kashmir University of Agricultural Sciences and Technology, India

Reviewed by:
Shoaib Ur Rehman, Muhammad Nawaz Shareef University of Agriculture, Pakistan
Sajid Fiaz, The University of Haripur, Pakistan

***Correspondence:**
Shuangfei Li
sfli@szu.edu.cn

[†]These authors share first authorship

Specialty section:
This article was submitted to Plant Biotechnology, a section of the journal Frontiers in Plant Science

Received: *29 October 2021*
Accepted: *07 December 2021*
Published: *20 January 2022*

Citation:
Zaynab M, Peng J, Sharif Y, Albaqami M, Al-Yahyai R, Fatima M, Nadeem MA, Khan KA, Alotaibi SS, Alaraidh IA, Shaikhaldein HO and Li S (2022) Genome-Wide Identification and Expression Profiling of DUF221 Gene Family Provides New Insights Into Abiotic Stress Responses in Potato. Front. Plant Sci. 12:804600. doi: 10.3389/fpls.2021.804600

The domain of the unknown function 221 proteins regulate several processes in plants, including development, growth, hormone transduction mechanism, and abiotic stress response. Therefore, a comprehensive analysis of the potato genome was conducted to identify the deafness-dystonia peptide (DDP) proteins' role in potatoes. In the present study, we performed a genome-wide analysis of the potato domain of the unknown function 221 (DUF221) genes, including phylogenetic inferences, chromosomal locations, gene duplications, gene structures, and expression analysis. In our results, we identified 10 *DDP* genes in the potato genome. The phylogenetic analysis results indicated that *StDDPs* genes were distributed in all four clades, and clade IV was the largest clade. The gene duplication under selection pressure analysis indicated various positive and purifying selections in *StDDP* genes. The putative stu-miRNAs from different families targeting *StDDPs* were also predicted in the present study. Promoter regions of *StDDP* genes contain different *cis*-acting components involved in multiple stress responses, such as phytohormones and abiotic stress-responsive factors. The analysis of the tissue-specific expression profiling indicated the *StDDPs* gene expression in stem, root, and leaf tissues. We subsequently observed that *StDDP4*, *StDDP5*, *and StDDP8* showed higher expressions in roots, stems, and leaves. *StDDP5* exhibited high expression against heat stress response, and *StDDP7* showed high transcript abundance against salt stress in potatoes. Under abscisic acid (ABA) and indole acetic acid (IAA) treatments, seven *StDDP* genes' expressions indicated that ABA and IAA

performed important roles in immunity response. The expression profiling and real-time qPCR of stems, roots, and leaves revealed *StDDPs'* significant role in growth and development. These expression results of *DDPs* are primary functional analysis and present basic information for other economically important crops.

Keywords: gene family, miRNA, expression, duplication, phylogeny

INTRODUCTION

Almost 70% of annual potential crop yield losses are due to variations in the environment (Leng et al., 2021). Abiotic factors are the major limiting stress factors that affect plants during their vegetative and reproductive growth, resulting in abrupt economic and agricultural losses worldwide (Sade et al., 2018; Hafeez et al., 2021; Li et al., 2021). Salt and drought stress factors are the chief abiotic stress factors affecting geographical plant distribution, threatening food security, and limiting crop production (Muhammad Ahmad et al., 2021). Generally, plants lack a structure that works directly with environmental impacts, but they can respond to climate change (Mahalingam and Fedoroff, 2003; Huang et al., 2021; Raza et al., 2021c). Plants exhibit extensive defense responses at molecular and cellular levels to oppose the cell damage caused by stress factors (Kim et al., 2014; Raza et al., 2021b).

Plant biologists have always been attracted to gene families' structure, function, and evolutionary model. The interaction and adaptation between the environment and plants are well studied based on the information of these gene families (Zhao et al., 2021). Among them, the domain of unknown function (DUF) proteins are extensively distributed in different plants and restrain at least one extremely conserved domain of DUF (Bateman et al., 2010). Many studies on DUF genes have revealed the importance of DUFs in plants in various functions, one of which is abiotic stress tolerance (Zhang et al., 2021). However, there have been reports of other DUF gene families in many plants. These include the DUF221, DUF810, DUF866, DUF936, and DUF1618 gene families in rice and the DUF581 and DUF724 gene families in Arabidopsis (Zhao et al., 2021). Furthermore, DUF proteins act as integral membrane proteins and are associated with other membrane proteins (Rai et al., 2012). Resistance to DUF-mediated strains has been studied in various plants, while a comprehensive study of the DUF family gene remains to be conducted in other plants. Additionally, in transgenic *Oryza sativa* (rice) and *Arabidopsis thaliana*, *OsSGL* presents significant drought stress tolerance, whereas other diverse stress-responsive genes have been altered significantly in transgenic rice. Xin et al. (2007) reported that in *A. thaliana,* the *AT3g55990* (*ESK1* gene) is associated with the DUF283 family gene, considered a novel negative cold acclimation gene regulator. The *AtCSC1* gene in Arabidopsis (Hou et al., 2014) and its homologous gene in rice are known *OsCA1*, responsible for osmotic regulation (Yuan et al., 2014), *ERD4* is known as a dehydration-responsive gene in *Brassica juncea* (Rai et al., 2012), whereas *DUF27* and *DUF538* have chlorophyll-binding capabilities (Gholizadeh, 2016). Moreover, the superfamily of *DUF283* is important for siRNA processing (in gene silencing) in Arabidopsis (Qin et al., 2010). Another study in *A. thaliana* illustrated the reduced effect of ABA mediation (drought stress gene) after inhibiting the gene expression of both *ATRDUF2* (RING-DUF1117 E3 ubiquitin ligases) (Kim et al., 2012). From rice, two genes (*DUF1644* and *OsSIDP366*) positively regulate the drought and salt stresses by overexpressing *OsSIDP366* in transgenic rice, which enhances tolerance against drought and salinity factors (Guo et al., 2016). In *O. sativa*, other DUF family genes have been related to abiotic stress factors, including *OsDUF810.7* (Li et al., 2018), *DUF1644* (*SIDP361*) (Li et al., 2016), and *DUF966* (*OsDSR2*) (Luo et al., 2014). Three family members of deafness-dystonia peptides (DDPs) in *Medicago truncatula* reported dehydration (*MtST2* and *MtST3*) and modulation through nutritional status (*MtST1*) during development (Albornos et al., 2017).

Potato is an important food source and cash crop worldwide (Zaynab et al., 2021c). In 2018, about 368,168,914 tons of potatoes were harvested globally from 17,578,672 ha of land, and over one billion people consume them. Among the potato-producing countries, China holds the first position, producing about 90,321,442 tons of potatoes from 4,813,542 ha of land in 2018 (Rashid et al., 2021). Though, like other plants, potato yield is also at risk to abiotic and biotic stress factors (Zaynab et al., 2021f). The objective of the present research was to characterize the *DDP* genes family across the potato genomes. Thus, based on the putative role of *DDPs* against abiotic stress, we carried out a comprehensive analysis of *DDP* genes in the potato genome against abiotic stress. To date, *DDP* genes expression analysis against abiotic has not been reported in potatoes. We examine the expression profiling of *StDDPs* under phytohormones, salt, and heat stress. These data may potentially explain the validated functional foundation of potato *DUF221* genes and their functions according to growth and development in potatoes under unfavorable/stressful conditions.

MATERIALS AND METHODS

Identification and Phylogenetic Analysis of the StDDP Genes

The Arabidopsis *DDPs* sequences were attained from the TIAR[1] and used as the query to search the potato *DDP* genes from the Phytozome site[2]. A local BLASTP similarity search was carried out to find the *DDPs* in the *S. tuberosum* genome.

[1]http://www.arabidopsis.org/

[2]https://phytozome.jgi.doe.gov/

The collected gene sequences were subjected to PfamScan and Batch CDD-NCBI search to validate the presence of the Pfam domain (PF14703). The data redundancy was removed, and the identified genes were analyzed for further study. The protein physiochemical properties, including isoelectric point (PI), and molecular weight (MW), were forecasted by Expasy[3] server.

A phylogenetic tree was constructed to observe evolutionary relationships among *A. thaliana*, *Solanum tuberosum*, and *Solanum lycoperiscum* by MEGA 7 software. The entire protein sequences were arranged by using MUSCLE through 16 iterations. Then, the protein sequence alignment was used to make the phylogenetic tree through the Neighbor-Joining method through 1,000 bootstrap values.

Chromosomal Location, Synteny, and Selection Pressure Analysis

The information about *StDDPs* was retrieved from the Potato Genome Sequencing Consortium (PGSC). The TBtools software[4] was used to map the chromosomal positions of *StDDPs*. The comparative synteny analysis was executed to visualize the genome conservation through the Circoletto Tool (tools.bat.infspire.org/circoletto/). Further, the duplicated genes' coding sequences were arranged by the Muscle program in MEGA 7. The synonymous and non synonymous substitution rates (Ka = No. of nonsynonymous substitution/nonsynonymous site; Ks = No. of synonymous substitution/synonymous site) were calculated by KaKs_ Calculator 2.0 software tool through the exchange rate ($r = 2.6 \times 10^{-9}$; Li et al., 2019).

Gene Structure and Conserved Motif Analysis

For the gene structure analysis, we used Gene Structure Display Server, and DDP proteins' conserved motifs were determined by MEME tool[5] through the following parameters: optimum width ranges: 6–200; no. of motifs: 20. TB tools software[4] was used to figure out the distribution of motifs.

Cis-Elements Analysis miRNAs Prediction and Orthologous Genes Identification

To analyze the *cis*-regulatory elements of potato *DDP* genes, the promoter sequences (2,000 bp upstream of the ATG initiation codon) were taken from the *S. tuberosum* genome database in a generic file format. The promoter sequences were scanned with the PlantCARE database[6]. The coding sequence of *StDDPs* was used to identify potential miRNAs targeting the *StDDPs* using the psRNATarget database[7] with default parameters. The orthologous DDPs proteins in *A. thaliana*, *S. tuberosum*, and *S. lycoperiscum* were identified using orthovenn2 https://orthovenn2.bioinfotoolkits.net/home. Protein sequences of three species were used for analysis. Each species was individually assessed with each other for the identification of orthologous gene clusters.

Expression Analysis of StDDP Genes

For the *StDDP* genes expression analysis, fragments per kilobase million (FPKM) values in root, stem, and leaf tissues were used. The data was collected and assembled with enormously expressed tissues, including leaves, stems, and roots. The FPKM values were used to illustrate the heat map by using TBtools. The $\log_2$ normalized values were used to construct the heat maps (Zaynab et al., 2021a).

Plant Sampling and Material Collection

Potato tubers were obtained from the NARC (National Agricultural Research Center), Islamabad, Pakistan, and planted in the glasshouse under controlled conditions at National Institute for Genomics and Advanced Biotechnology (NIGAB) NARC, Islamabad, Pakistan. Later, 25 days after germination, the roots, stems, and leaves were

[3]https://web.expasy.org/protparam/

[4]https://github.com/CJ-Chen/TBtools

[5]http://meme-suite.org/

[6]http://bioinformatics.psb.ugent.be/webtools/plantcare/html/

[7]http://plantgrn.noble.org/psRNATarget/

TABLE 1 | List of identified putative *StDDPs* and their features.

Gene ID	Genomic	CDS	Location	Star-end	No. of amino acids	Molecular weight	PI
StDDP1	7254	2106	ST4.03ch04	66454282..66461536	701	79,307.25	9.5
StDDP2	9609	2655	ST4.03ch12	56091976..56101585	884	99,784.46	9.35
StDDP3	7570	2304	ST4.03ch02	17639083..17646653	767	87,867.64	9.24
StDDP4	6811	1245	ST4.03ch02	36697175..36703986	414	47,703.76	9.4
StDDP5	8295	2151	ST4.03ch02	45947456..45955751	716	81,093.79	8.95
StDDP6	7418	2256	ST4.03ch09	46690336..46697754	751	85,855.55	9.11
StDDP7	8795	2679	ST4.03ch08	48862785..48871580	892	102,546.31	8.86
StDDP8	6811	300	ST4.03ch02	36697175..36703986	99	11,371.45	9.74
StDDP9	5772	1137	ST4.03ch08	29755774..29761546	378	42,947.2	9.29
StDDP10	7418	972	ST4.03ch09	46690336..46697754	323	37,409.37	9.12

CDS, coding sequence; pI, isoelectric point.

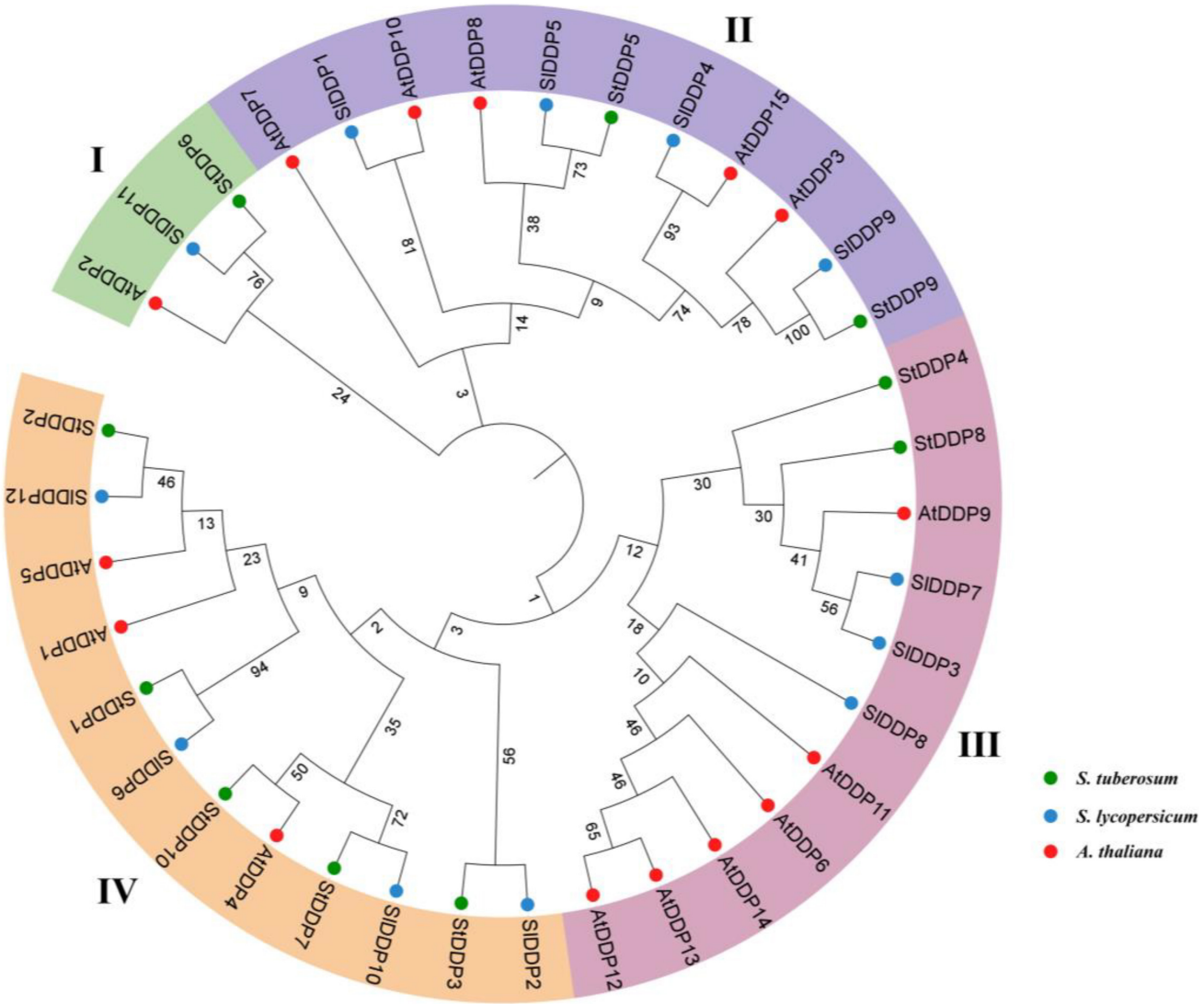


FIGURE 1 | Phylogenetic tree of deafness-dystonia peptide (DDP) proteins from *Arabidopsis, Solanum lycoperiscum*, and *Solanum tuberosum*. The colored arcs indicate different groups. The stars' colors, represent proteins of *Arabidopsis S. lycoperiscum*, and *S. tuberosum*.

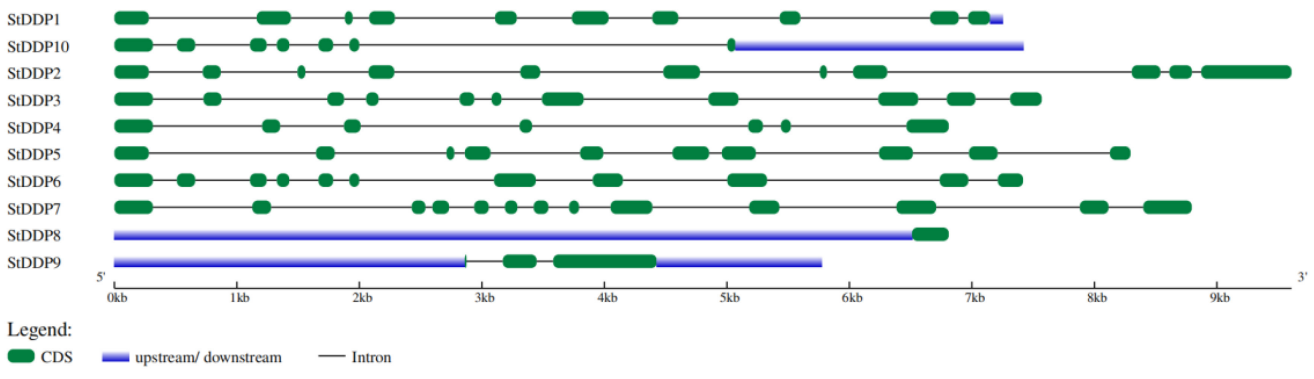


FIGURE 2 | Distribution of exons, introns, and UTR (untranslated regions) in *StDDP* gene sequences.

collected in replicates and for RNA extraction stored in liquid nitrogen.

RNA Extraction and RT-qPCR Analysis

The total RNA from roots, stems, and leaves was extracted by a quick isolation Ribonucleic acid (RNA) Kit (Huayueyang, Beijing, China) following the manufacture's protocol. The quality of RNA was assessed through gel electrophoresis using 1% agarose gel. The first cDNA strand was prepared from 0.5 μg RNA. The qRT-PCR was executed in BioRad CFX96 RT-PCR Detection System instrument (BioRad Laboratories) with a 20 μL reaction mixture through SYBR® Green RT-PCR Master (TOYOBO QPK-210, Shanghai, China) using gene-specific primers. The thermocycler was set according to the given protocol: denaturation at 95°C for 15 s, annealing occurs at 55°C for 15 s, and extension takes to play at 72°C for 15 s.

Target gene amplification was monitored with SYBR Green fluorescence in each cycle. In addition, the qRT-PCR amplification specificity was routinely checked with the melting curve. The data were observed through the $2^{-\Delta\Delta Ct}$ method (Zaynab et al., 2018), while results were represented through relative gene expression level (Zaynab et al., 2021d). Through this analysis report, elongation factor 1 elongation factor 1 - α was considered housekeeping gene. In the whole experimental observation, four technical replicates were conducted (Zaynab et al., 2021b). The sequences of all primers used are mentioned in **Supplementary Table 1**.

RESULTS

Identification and Phylogenetic Analysis of StDDP Genes

The results showed that 10 *DDP* genes were found after genome-wide identification in the potato genome. Similar genes with diverse transcripts were not considered in this study. Although all the identified genes contain conserved *DDP* domains with Pfam ID (PF14703). The details of 10 *DDPs*, including their molecular weight (MW), chromosome number, isoelectric point (PI), and protein length, are shown in **Table 1**. Moreover, the protein lengths ranged from 99 to 892 amino acids (aa), the PI was 8.86–9.74, and the MW was from 11.371 to 10.2546 kDa. The evolutionary relationship of *DDPs* was observed through a phylogenetic tree by MEGA7.0 software using the Neighbor-joining method with 1,000 bootstrap values. The phylogenetic tree was classified into four clades. The results of the phylogenetic

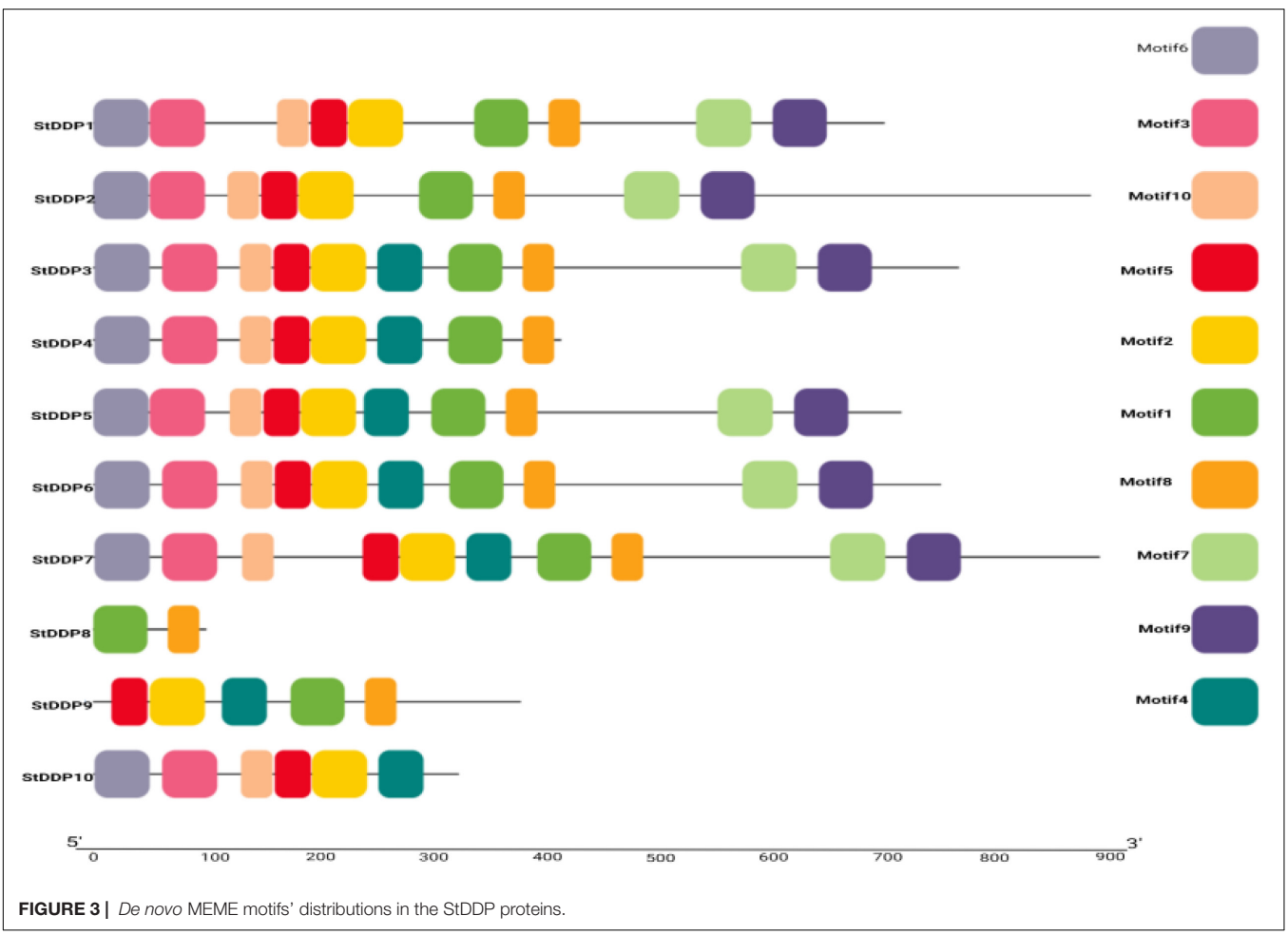


FIGURE 3 | *De novo* MEME motifs' distributions in the StDDP proteins.

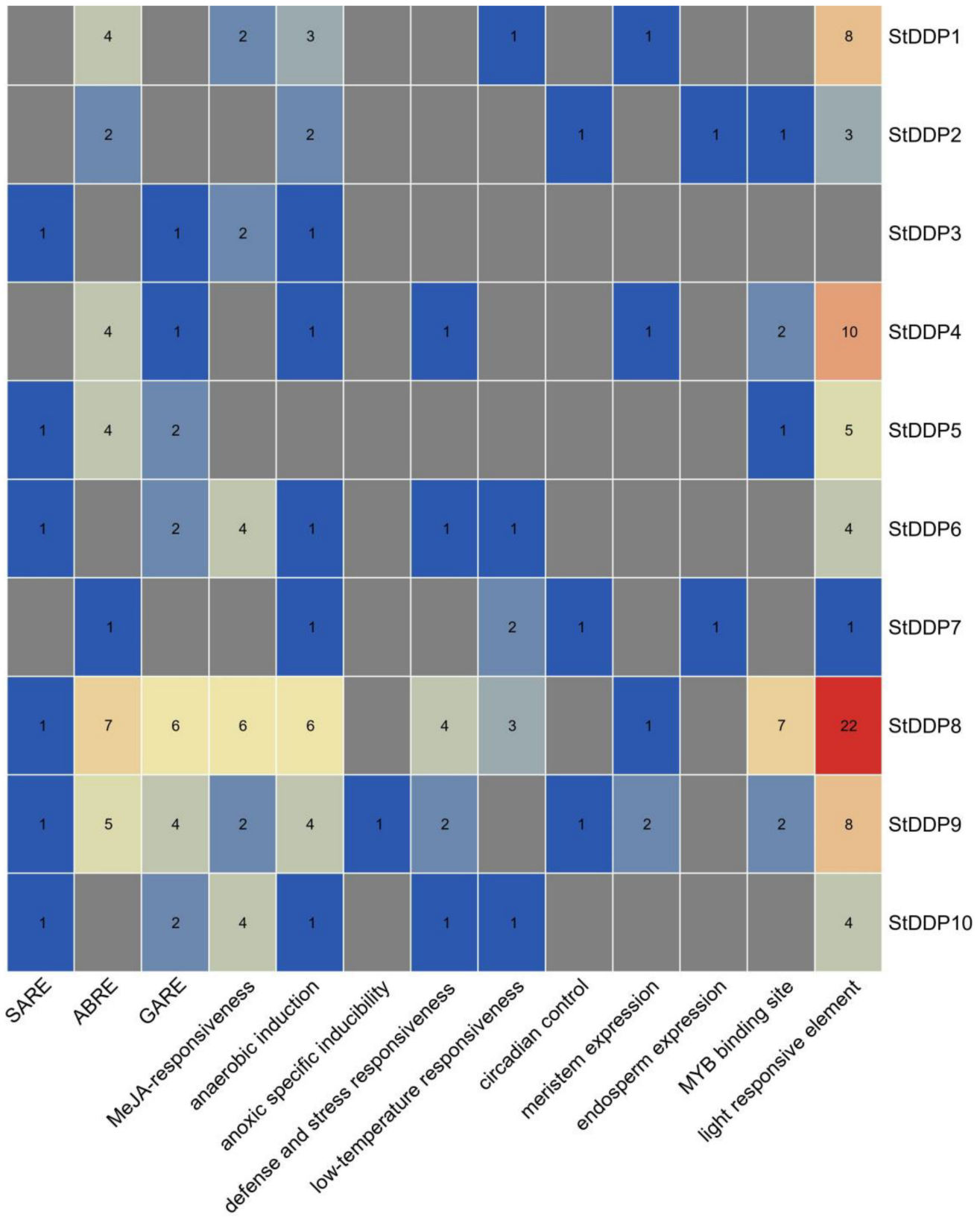


FIGURE 4 | Predicted *cis*-acting elements in *StDDP* promoters. Promoter sequences (2,000 bp) of ten *StDDP* genes were analyzed by PlantCARE.

TABLE 2 | Gene duplication and selection pressure of *StDDPs*.

Seq_1	Seq_2	Ka	Ks	Ka_Ks	Time (MYA)
StDDP1	*StDDP2*	0.215171807	0.614484198	0.350166542	118.1700381
StDDP6	*StDDP10*	0.02600552	0.037007255	0.702714102	7.116779808

Ka, no. of nonsynonymous substitutions per nonsynonymous site; Ks, no. of synonymous substitutions per synonymous site; MYA, million years ago.

analysis indicated that *StDDPs* genes were distributed in all four clades and clade IV was the largest clade (**Figure 1**).

Gene Structure and Conserved Motif Analysis

The genomic DNA and coding DNA sequences were used for exon-intron structure analysis in *S. tuborosum*. The number, length, and distribution of introns-exons were not the same among all genes. For instance, *StDDP2* was the most extended, whereas *StDDP9* was the smallest gene. The number of *StDDP* exons ranged from 1 to 13. In our results, *StDDP8* has only one exon, whereas *StDDP7* has a maximum of 13 exons. However, some genes, such as *StDDP2*, *StDDP3*, and *StDDP6* have a similar number of exons. In addition, *StDDP1* and *StDDP5* have an equal number of exons but with different sequence lengths (**Figure 2**).

The architecture of StDDP proteins was also investigated using DDP amino acids sequences. The MEME motif analysis identified several common and unique motifs in *StDDPs*. Commonly shared motifs tended to cluster in the same groups, indicating similar functions. The first motifs were observed in all *StDDPs*, except *StDDP10*, whereas the second motif was observed in most of the proteins except *StDDP8*. Motif 3 was absent in *StDDP8*.

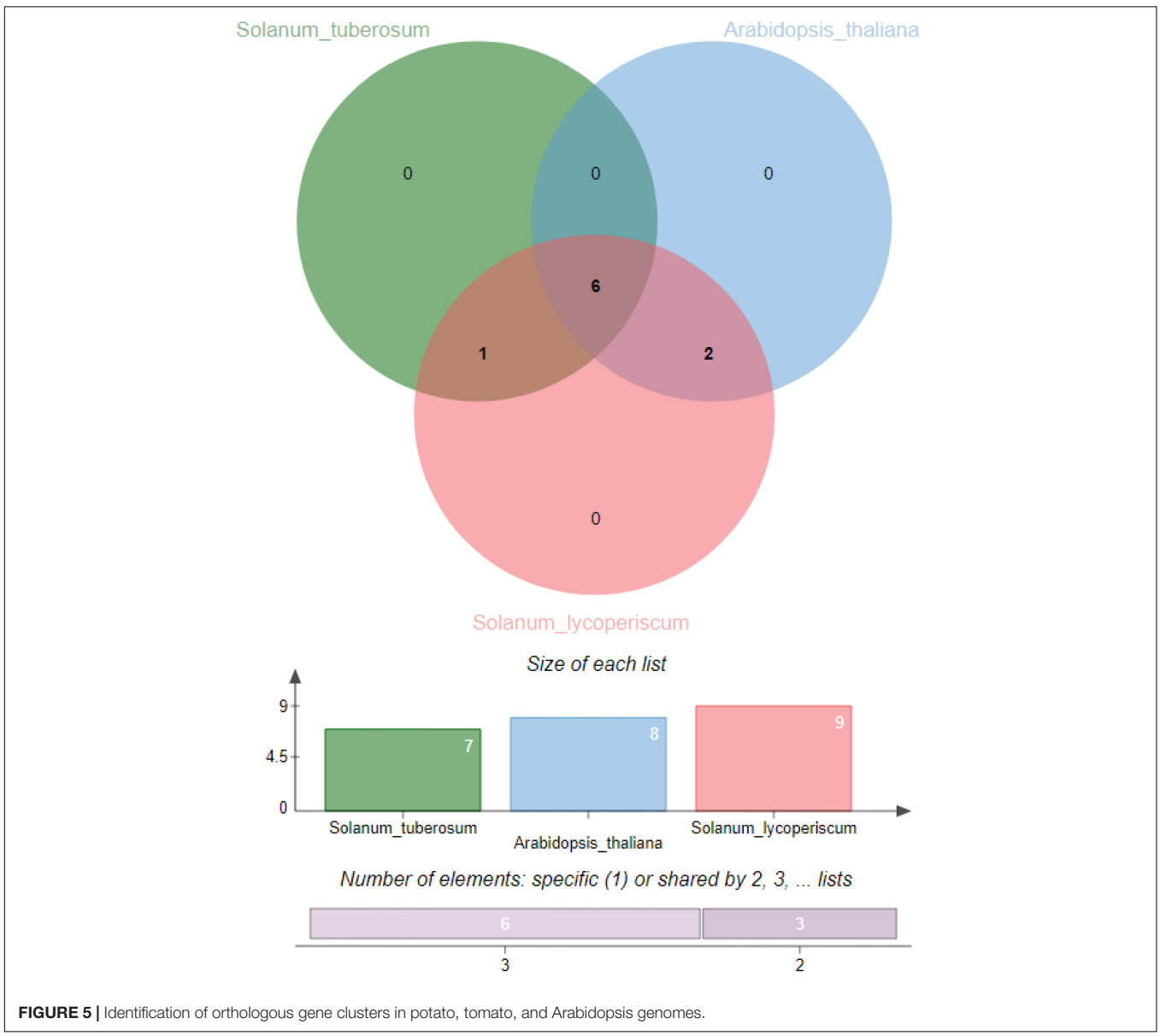


FIGURE 5 | Identification of orthologous gene clusters in potato, tomato, and Arabidopsis genomes.

In summary, some motifs were family-specific, group-specific, clade, and taxa-specific. The length of motifs also varied; for example, the first and ninth motifs had 49 amino acids, the second, third, sixth, and seventh motifs had 50 amino acids and the eighth, tenth, and fifth motifs had 29 amino acids (**Figure 3**).

Chromosomal Distribution and Cis Element Analysis

The numbers of *StDDP* genes were present unequally on chromosomes. The maximum number of *DDP* genes was observed on chromosome # 2 (four genes). A total of two *DDP* genes were present on chromosomes # 8 and 9. Only one gene was present on chromosomes # 4 and 10 (**Table 1**). The results of the *cis*-element analysis indicated that generally, the *cis*-acting elements were from growth and development, phytohormones, and stress-responsive classes. Light and MYB binding were the most enriched elements. Furthermore, anaerobic induction, stress-responsive components, and defense were also enriched in their promoters among stress-responsive components. The MeJRE and ABA response elements were enriched in phytohormones

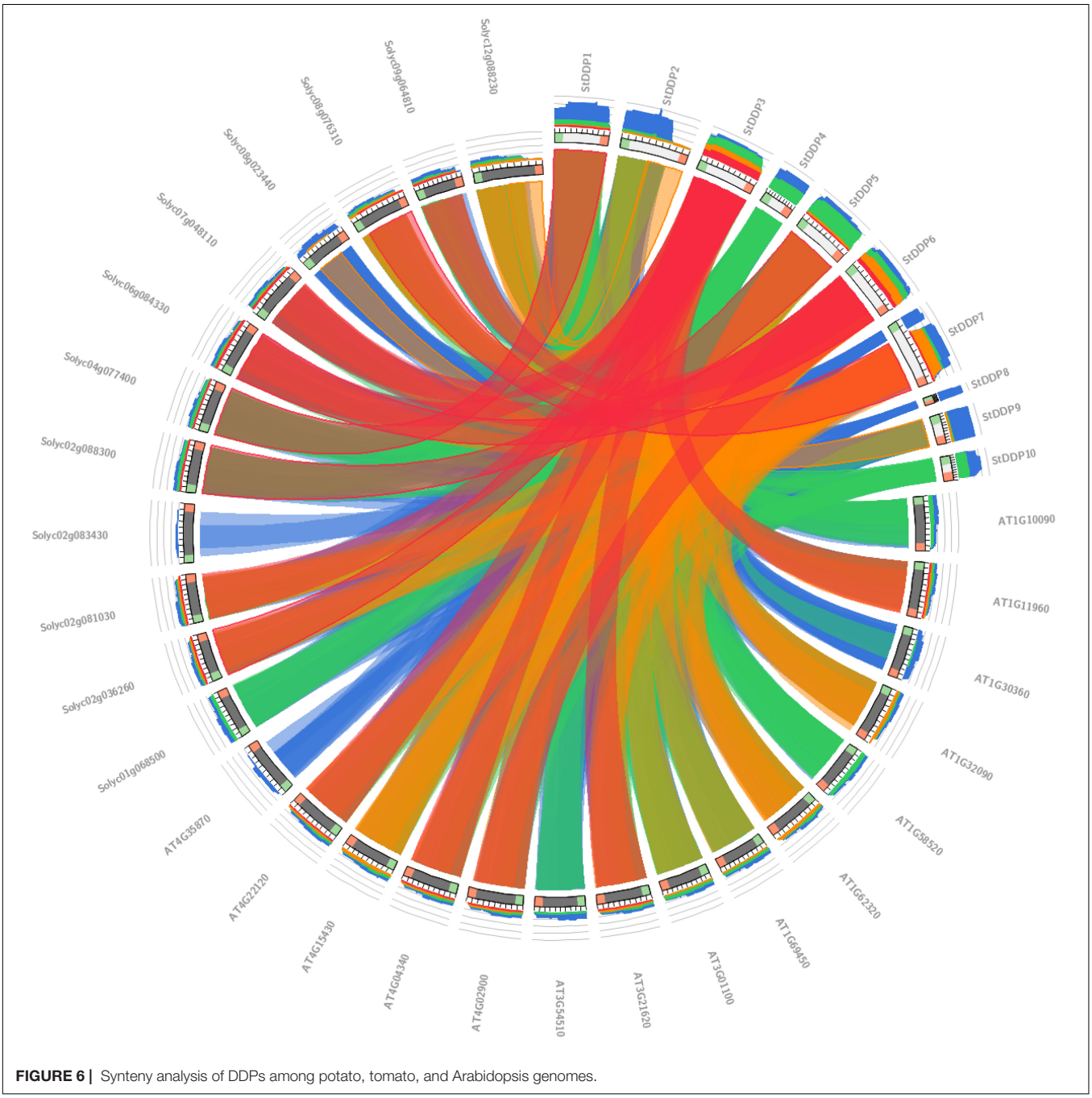


FIGURE 6 | Synteny analysis of DDPs among potato, tomato, and Arabidopsis genomes.

responsive elements. Consequently, it was observed that various *cis*-regulatory elements carried out *DDP* gene expression (**Figure 4**).

Genes Duplications and Identification of Orthologous Gene Clusters

The rate of molecular evolution was measured for entire duplicated gene pairs with estimating the rate of Ka/Ks. The value of Ka/Ks > 1 was a positive selection factor, whereas the Ks/Ks < 1 were indicated as a purifying selection factor. Ka/Ks = 1 was indicated a neutral selection amongst the duplicated genes. Our results illustrated that the majority of the *DDP* duplicated genes tolerated the pressure of purifying selection during the duplication process, implying that the role of the *DDP* duplicated genes may not alter comprehensively in successive evolutionary processes. The time deviation among duplicated gene pairs was also approximated. The cosmic majority of *DDP* genes illustrated the Ks > 0.52 value, although the resulting time deviation may be greater than 100 MYA (millions of years ago). Surprisingly, in the present study, the *Ks* value for the duplicated gene (*StDDP1/StDDP2*) was 0.614, while the deviation time was 118.17 MYA (**Table 2**).

The corresponding evaluation was carried out to determine orthologous clusters of DDPs in potato, tomato, and Arabidopsis genomes. This will aid in analyzing processes related to polyploidization throughout the evolutionary period of the DDP gene family in the genome of *S. tuberosum*. Spotted orthologous gene clusters and their imbricated regions of *S. tuberosum* are depicted in **Figure 5**. The highest number of in-paralogous genes was noted in *S. lycopersicum*. Seven in-paralogous genes were identified in *S. tuberosum*, and eight in-paralogous genes were identified in *A. thaliana*.

Comparative Synteny and miRNA Analysis

The synteny analysis in *A. thaliana*, *S. lycopersicum*, and *S. tuberosum* illustrated the significant relationship between gene evolution, duplication, triplication, expression, and function. The *Solyc12g088230* gene sequence showed synteny in tomatoes with the *StDDP2* gene sequence of potato. Likewise, the potato gene *StDDP2* showed synteny with tomato *Solyc02g036260*. Potato *StDDP2* presented synteny with tomato *Solyc08g076310* (**Figure 6**).

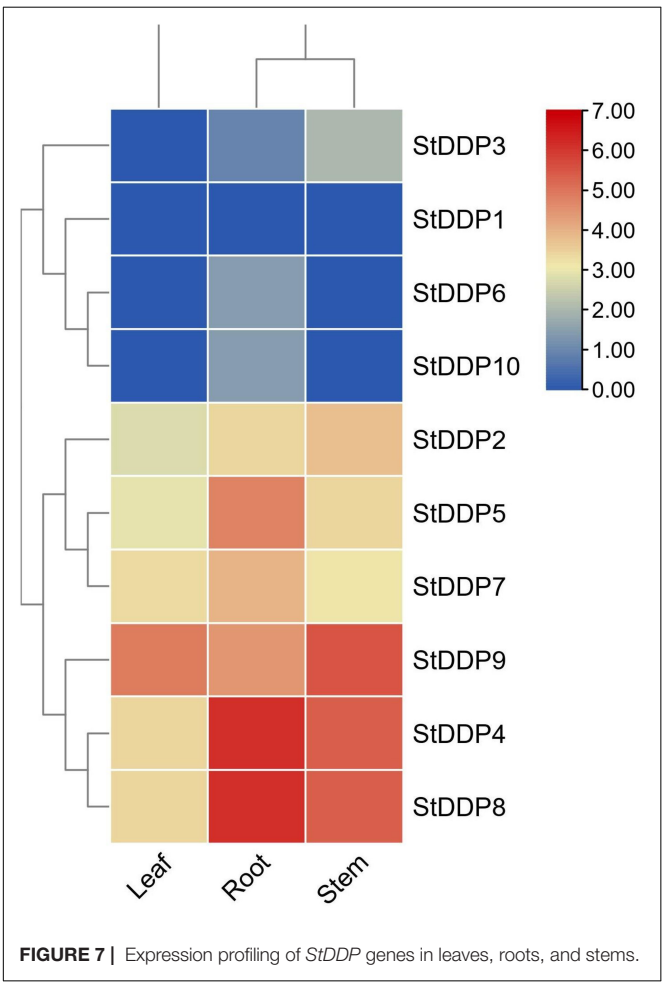


FIGURE 7 | Expression profiling of *StDDP* genes in leaves, roots, and stems.

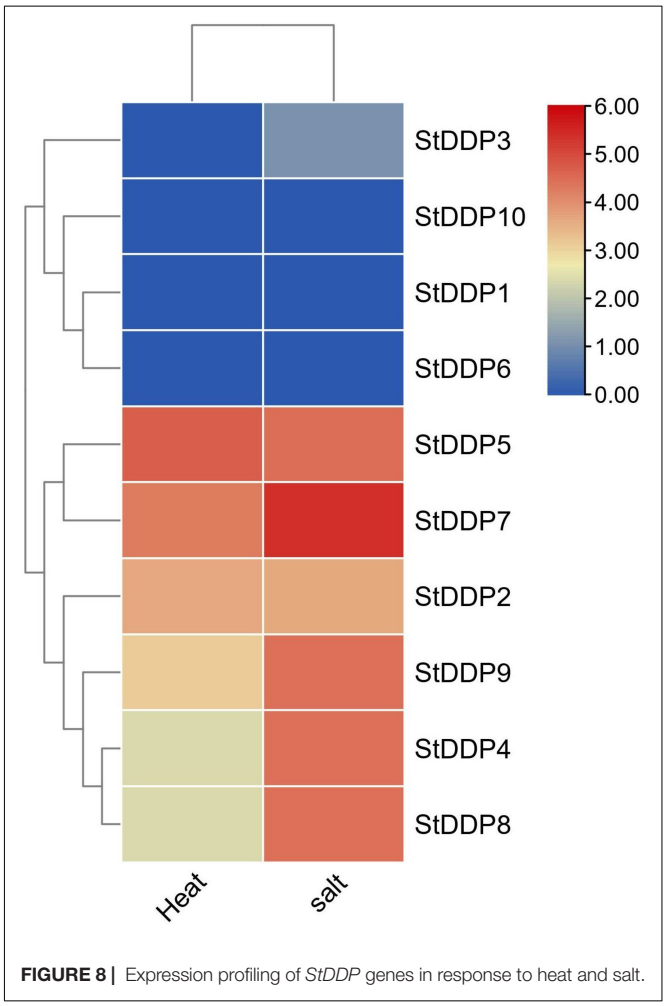


FIGURE 8 | Expression profiling of *StDDP* genes in response to heat and salt.

In the previous few years, various studies have revealed miRNA-mediated regulation escorts stress responses in plants. The comprehensive information of entire miRNA targeted sites/genes is shown in **Supplementary Table 2**. These results illustrated that 10 members of the stu-miR395 targeted *StDDP4*. Three members of miR319-3p, stu-miR319a-3p, and stu-miR319b targeted two genes (*StDDP1* and *StDDP5)*. The stu-miR172a-5p targeted *StDDP7*, stu-miR172b-5p targeted *StDDP2* and stu-miR172d-3p targeted *StDDP1*. Furthermore, stu-miR8033-3p targeted *StDDP6. StDDP5, StDDP4, StDDP2,* and *StDDP1* genes were estimated to be targeted with more miRNAs. These results revealed that miRNAs have significant biological functions in the genome of the potato.

Tissue-Specific Expression Profiling

The expression profiling suggests that most *DDP* genes represented comparatively higher transcriptional abundance in roots than in stems and leaves. Though, some detected genes do not illustrate any expression, while others show a tissue-specific expression. Such as, *StDDP8* was expressed in leaf, root, and stem tissues. In our results, the *StDDP8* gene had high transcript abundance in the roots, and the *StDDP9* gene was highly expressed in stems and leaves (**Figure 7**).

Expression Patterns of StDDP Genes in Response to Heat and Salt Stress

Based on the transcription levels of *StDDPs* in potatoes under heat stress, we inferred that *StDDPs* might take part against potato heat stress. Six *StDDP* genes were expressed against heat treatment, although the transcription levels of *StDDP2*, *StDDP5*, and *StDDP7* are remarkably enhanced in potatoes after heat treatment (**Figure 8**). However, the expression level of *StDDP5* was observed to be higher than those of *StDDP2* and *StDDP7*. The expression of *StDDP4* was lower compared with those of other genes. A total of 7 *DDP* genes were upregulated against salt treatment, although the transcription levels of *StDDP5*, *StDDP7*, and *StDDP9* were remarkably enhanced in potatoes after salt treatment (**Figure 8**). The expression level of *StDDP7* was observed to be higher than those of StDDP5 and *StDDP9* in potatoes in response to salt treatment.

Expression Patterns of StDDP Genes in Response to Phytohormones

Indole acetic acid (IAA) and abscisic acid (ABA) were selected to identify the *DDP* genes' transcriptional responses toward hormones treatments. Leaf tissues were treated with ABA, and the expression pattern of all 10 genes was observed. A total of seven *DDP* genes showed expression against ABA treatment, and *StDDP9* showed higher expression compared to other *StDDPs*. Similarly, a total of seven *DDP* genes showed expression against IAA in treated leaves, and *StDDP7* showed higher expression compared to other *StDDPs* (**Figure 9**). These results indicated a strong correlation between gene clusters or their expression in IAA and ABA treatments.

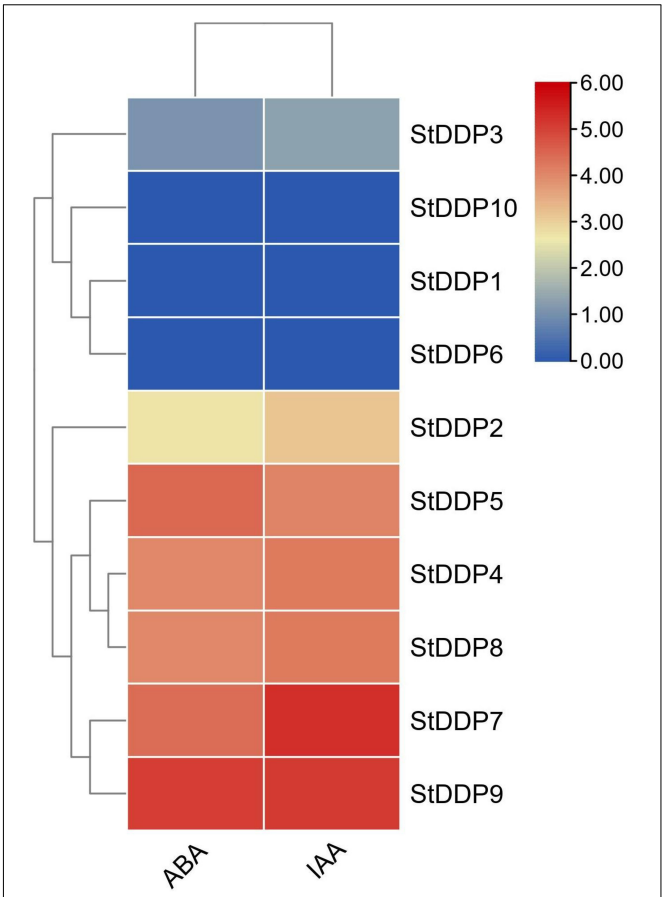


FIGURE 9 | Expression profiling of *StDDP* genes in response to ABA and IAA.

RT-qPCR Analysis

The RT-qPCR analysis also reported the expressions of the *StDDP2*, *StDDP5*, *StDDP7*, *StDDP8*, and *StDDP9* genes in leaves, roots, and stems. The comparative expression analysis pattern illustrated that *StDDP5*, *StDDP7*, and *StDDP8* have higher expressions in roots. Furthermore, *StDDP2* and *StDDP9* showed higher expression in stems than in roots and leaves. These results validate the RNA-Sequencing results. The higher expression in the roots demonstrates their strong association with the soil and environment (**Figure 10**).

DISCUSSION

Most plants bear destruction from biotic and abiotic stress agents (Zaynab et al., 2020), which influence their productivity and survival rate throughout their life cycle (Zaynab et al., 2018). *DDPs* are implicated in several regulatory processes, including development, growth, biotic and abiotic stresses (Zaynab et al., 2021e). Plants have evolved tolerance systems to change their cellular biochemistry and physiology during stress by changing gene expression (Zaynab et al., 2017). One of the domains known as DUF221 is considered a more conserved membrane-associated protein and acts to stimulate calcium osmoregulation

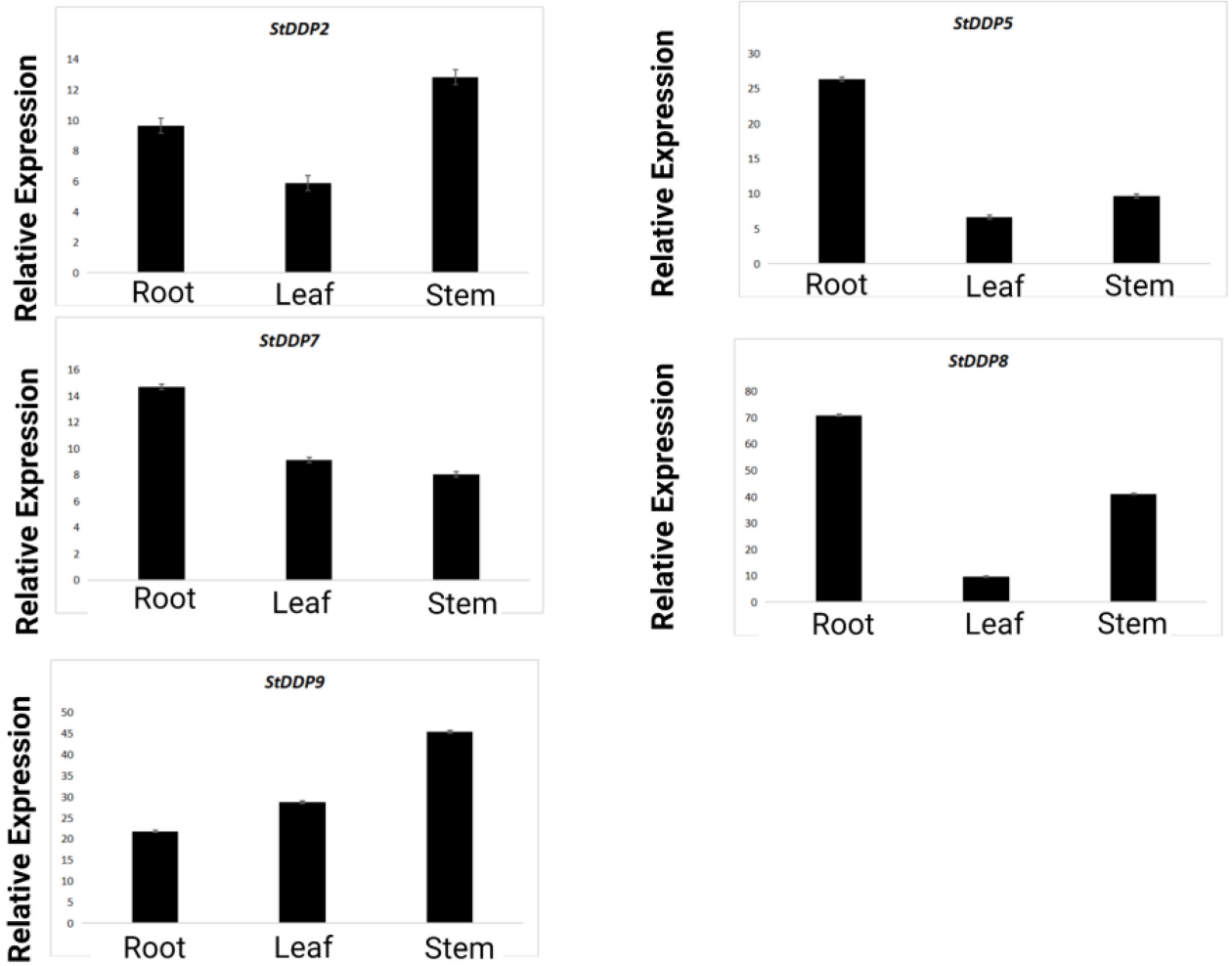


FIGURE 10 | Real-time relative expressions of *StDDPs* in leaves, roots, and stems.

through the cellular membrane (Hou et al., 2014). Thus far, the status of *DUF221* genes has been primarily unexplored. In this analysis, the DDP genes were observed in, salt, heat, and phytohormones stress, in keeping with previous identification in maize (Ding et al., 2019), rice (Li et al., 2015), and Arabidopsis (Yuan et al., 2014).

The structural identification of *StDDPs* is supportive during functional analysis.

All obtained *StDDP* genes were categorized into four phylogenetic groups. Similar phylogenetic grouping was also observed in other plant species. The comparative analysis of phylogeny illustrated that the organizations of *A. thaliana*, *S. lycopersicum*, and *S. tuberosum* proteins were relatively similar with each other in four clades, representing that all *StDDP* genes in representing groups may originate from a common ancestor. Previous studies have also reported the classification of *DDPs* into four clades in Arabidopsis (Yuan et al., 2014) and rice (Yuan et al., 2014; Li et al., 2015), and rice (Li et al., 2015).

Furthermore, evolutionary evidence found that exon-intron alignment affects gene family evolution (Moore and Purugganan, 2005). This is related to prior Scientific researches that several genes are subject to be kept in plants that could not have introns/short introns during the evolutionary process (Flagel and Wendel, 2009). In plants, gene expression levels are low with few and no introns (Mattick and Gagen, 2001). Moreover, a conserved gene configuration can allow a fast expression response toward an exogenous and endogenous gene stimulus (Jeffares et al., 2008). The structure analysis of the gene reported that the *StDDP* gene sequences illustrated a similarity in exon-intron number with analogous functional characters due to the origination of duplication course in evolutionary processes (Waqas et al., 2019). Some important factors, including gene distribution, genome size, and duplications, are involved in the genetic diversity of plants. However, the duplication factor of genetics has been extensively studied throughout the gene families' expression origins, complexity, and evolutionary novelty. We also identified several duplication events in *StDDPs*, which played an important role in *StDDP* amplification. Gene duplication is an important event in expansion, diversification, and neofunctionalization

(Lavin et al., 2005); correspondingly, the distribution and mapping of *StDDP* genes at the chromosomal level will support potato breeders in producing desired traits. *Cis*-element studies may illustrate an important foundation for functional analysis of the *StDDP* genes (Wen et al., 2021). Moreover, we also identified that all *StDDP* promoters hold multiple stress-responsive *cis*-elements, such as the low-temperature responsive elements, ABRE, the MeJA responsive elements, and the SA responsive elements (Raza et al., 2021a). These *Cis*-elements perform an essential function in stress response through stress-responsive gene regulation (Wu et al., 2014). Therefore, in *StDDP*s, these vital *Cis*-acting points propose their response to various environmental stress factors.

Over the past few years, through genome-wide examination, abundant miRNAs have been recognized in the potato to employ in different environmental factors. In addition obtained results reported that the DDPs in potatoes were targeted through miR172, miR8033, and miR319 members. These findings revealed that a particular gene may be regulated through multiple miRNAs. Some studies have reported the relationship between the *ZmDDP* (Ding et al., 2019) and *AtDDP* proteins (Zhao et al., 2015). The dynamic phytohormones and abiotic responsive expression patterns of *StDDP* genes are still ambiguous. The analysis of the expression pattern of *StDDP* genes supported us to understand their potential functions and propose a systematic base for future analysis. Therefore, *StDDPs*' expression profiling and its validation are useful for deeper consideration of the potato genome. A current analysis presented a high transcript abundance of *DDPs* in plant roots; this finding was also established in a previous analysis (Yang et al., 2020) and helped in our results, in which *StDDP4*, *StDDP5,* and *StDDP8* showed high expression in roots.

The results of RT-qPCR indicated that *StDDP7* and *StDDP8* were particularly upregulated in roots. This suggests that potato *StDDP* genes play a vital function in development, growth and, diverse stress responses. So far, an increasing number of studies have illustrated the importance of *StDDPs* against various stresses (Zhao et al., 2021). Furthermore, in potatoes, *StDDP2*, *StDDP5*, and *StDDP7* were upregulated against heat stress. Though, the hormones can affect the physiological and biochemical reactions in plants during multiple signal transduction processes (Fatima et al., 2021). Moreover, IAA and ABA are important hormones in plant immunity. Numerous analyses have reported that *DDP*s are concerned with stress response and are involved in hormonal and developmental signaling (Waseem et al., 2021). To evaluate whether the *StDDPs* in potatoes were expressed by hormonal signaling, the potato leaves were treated with IAA and ABA, and gene expression was examined. After the ABA and IAA treatments, seven genes were influenced, indicating that various members of *StDDPs* played several roles in ABA- and IAA-induced immune response. During the ABA and IAA treatments, the upregulation of seven StDDP genes identified that ABA and IAA played important roles in the immune system, in accordance with previous studies. results (Waseem et al., 2021). The expression of genes and their clusters highlighted a strong correlation between gene groups and their analysis in various tissues during various stresses. This co-occurrence and co-expression illustrate their putative character related to plant adaptation under varied environmental stresses.

CONCLUSION

Overall, a total of 10 *StDDP* genes were identified in *S. tuberosum*. The relative evolutionary analysis illustrated the existence of four main groups in the *DDP* gene family. Furthermore, the conserved structural and functional motifs were identified in *StDDPs*, through a slight change between groups and members. The high expression of *StDDPs* in roots demonstrated their significant role in plant–soil associations. The existing consequences present a profound understanding of main potato development and growth challenges under different stresses. In potatoes, *StDDP5* represented higher expression analysis in response to heat stress. During ABA and IAA treatments, the seven *StDDP* gene expressions demonstrated that ABA and IAA played essential roles in defense. Furthermore, the *StDDP9* gene showed higher expression against ABA treatment, and the *StDDP7* gene showed higher expression against IAA treatment.

DATA AVAILABILITY STATEMENT

The datasets presented in this study can be found in online repositories. The names of the repository/repositories and accession number(s) can be found in the article/ **Supplementary Material**.

AUTHOR CONTRIBUTIONS

MZ, YS, and RA-Y performed the experiments and wrote the manuscript. HS, IA, MN, KK, and SA revised the manuscript. SL revised and supervised the manuscript. All authors contributed to the article and approved the submitted version.

FUNDING

This work was supported by the Shenzhen Special Project for Sustainable Development (KCXFZ20201221173211033). The authors appreciate the support of the Research Center for Advanced Materials Science (RCAMS) at King Khalid University Abha, Saudi Arabia through a grant KKU/RCAMS/G002-21. Taif University Researchers Supporting Project number (TURSP-2020/38), Taif University, Taif, Saudi Arabia. This project was also supported by the King Saud University, Deanship of Scientific Research, College of Science Research.

SUPPLEMENTARY MATERIAL

The Supplementary Material for this article can be found online at: https://www.frontiersin.org/articles/10.3389/fpls.2021.804600/full#supplementary-material

REFERENCES

Albornos, L., Martín, I., Labrador, E., and Dopico, B. (2017). Three members of Medicago truncatula ST family are ubiquitous during development and modulated by nutritional status (MtST1) and dehydration (MtST2 and MtST3). *BMC Plant Biol.* 17:117. doi: 10.1186/s12870-017-1061-z

Bateman, A., Coggill, P., and Finn, R. D. (2010). DUFs: families in search of function. *Acta Crystallogr. Sect. F Struct. Biol. Cryst. Commun.* 66, 1148–1152. doi: 10.1107/S1744309110001685

Ding, S., Feng, X., Du, H., and Wang, H. (2019). Genome-wide analysis of maize OSCA family members and their involvement in drought stress. *PeerJ* 7:e6765. doi: 10.7717/peerj.6765

Fatima, M., Ma, X., Zhou, P., Zaynab, M., and Ming, R. (2021). Auxin regulated metabolic changes underlying sepal retention and development after pollination in spinach. *BMC Plant Biol.* 21:166. doi: 10.1186/s12870-021-02944-4

Flagel, L. E., and Wendel, J. F. (2009). Gene duplication and evolutionary novelty in plants. *New Phytol.* 183, 557–564. doi: 10.1111/j.1469-8137.2009.02923.x

Gholizadeh, A. (2016). DUF538 protein superfamily is predicted to be chlorophyll hydrolyzing enzymes in plants. *Physiol. Mol. Biol. Plants* 22, 77–85. doi: 10.1007/s12298-015-0331-1

Guo, C., Luo, C., Guo, L., Li, M., Guo, X., Zhang, Y., et al. (2016). OsSIDP366, a DUF1644 gene, positively regulates responses to drought and salt stresses in rice. *J. Integr. Plant Biol.* 58, 492–502. doi: 10.1111/jipb.12376

Hafeez, M. B., Zahra, N., Zahra, K., Raza, A., Khan, A., Shaukat, K., et al. (2021). Brassinosteroids: molecular and physiological responses in plant growth and abiotic stresses. *Plant Stress* 2, 100029.

Hou, C., Tian, W., Kleist, T., He, K., Garcia, V., Bai, F., et al. (2014). DUF221 proteins are a family of osmosensitive calcium-permeable cation channels conserved across eukaryotes. *Cell Res.* 24, 632–635. doi: 10.1038/cr.2014.14

Huang, F., Abbas, F., Fiaz, S., Imran, M., Yanguo, K., Hassan, W., et al. (2021). Comprehensive characterization of guanosine monophosphate synthetase in *Nicotiana tabacum*. *Mol. Biol. Rep.* 1–8. doi: 10.1007/s11033-021-06718-x

Jeffares, D. C., Penkett, C. J., and Bahler, J. (2008). Rapidly regulated genes are intron poor. *Trends Genet.* 24, 375–378. doi: 10.1016/j.tig.2008.05.006

Kim, S. J., Ryu, M. Y., and Kim, W. T. (2012). Suppression of Arabidopsis RING-DUF1117 E3 ubiquitin ligases, AtRDUF1 and AtRDUF2, reduces tolerance to ABA-mediated drought stress. *Biochem. Biophys. Res. Commun.* 420, 141–147. doi: 10.1016/j.bbrc.2012.02.131

Kim, Y., Tsuda, K., Igarashi, D., Hillmer, R. A., Sakakibara, H., Myers, C. L., et al. (2014). Mechanisms underlying robustness and tunability in a plant immune signaling network. *Cell Host Microbe* 15, 84–94.

Lavin, M., Herendeen, P. S., and Wojciechowski, M. F. (2005). Evolutionary rates analysis of leguminosae implicates a rapid diversification of lineages during the tertiary. *Syst. Biol.* 54, 575–594. doi: 10.1080/10635150590947131

Leng, Z.-X., Liu, Y., Chen, Z.-Y., Guo, J., Chen, J., Zhou, Y.-B., et al. (2021). Genome-wide analysis of the DUF4228 family in soybean and functional identification of GmDUF4228–70 in response to drought and salt stresses. *Front. Plant Sci.* 12:628299. doi: 10.3389/fpls.2021.628299

Li, G., Hou, M., Liu, Y., Pei, Y., Ye, M., Zhou, Y., et al. (2019). Genome-wide identification, characterization and expression analysis of the non-specific lipid transfer proteins in potato. *BMC Genomics* 20:375. doi: 10.1186/s12864-019-5698-x

Li, L.-H., Lv, M.-M., Li, X., Ye, T.-Z., He, X., Rong, S.-H., et al. (2018). The rice OsDUF810 family: OsDUF810.7 may be involved in the tolerance to salt and drought. *Mol. Biol.* 52, 489–496. doi: 10.1134/S002689331804012X

Li, M., Guo, L., Guo, C., Wang, L., and Chen, L. (2016). Over-expression of a DUF1644 protein gene, SIDP361, enhances tolerance to salt stress in transgenic rice. *J. Plant Biol.* 59, 62–73. doi: 10.1007/s12374-016-0180-7

Li, W., Huai, X., Li, P., Raza, A., Mubarik, M. S., Habib, M., et al. (2021). Genome-wide characterization of glutathione peroxidase (GPX) gene family in rapeseed (*Brassica napus* L.) revealed their role in multiple abiotic stress response and hormone signaling. *Antioxidants* 10, 1481. doi: 10.3390/antiox10091481

Li, Y., Yuan, F., Wen, Z., Li, Yihao, Wang, F., et al. (2015). Genome-wide survey and expression analysis of the OSCA gene family in rice. *BMC Plant Biol.* 15:261. doi: 10.1186/s12870-015-0653-8

Luo, C., Guo, C., Wang, W., Wang, L., and Chen, L. (2014). Overexpression of a new stress-repressive gene OsDSR2 encoding a protein with a DUF966 domain increases salt and simulated drought stress sensitivities and reduces ABA sensitivity in rice. *Plant Cell Rep.* 33, 323–336. doi: 10.1007/s00299-013-1532-0

Mahalingam, R., and Fedoroff, N. (2003). Stress response, cell death and signalling: the many faces of reactive oxygen species. *Physiol. Plant.* 119, 56–68. doi: 10.1034/j.1399-3054.2003.00156.x

Mattick, J. S., and Gagen, M. J. (2001). The evolution of controlled multitasked gene networks: the role of introns and other noncoding RNAs in the development of complex organisms. *Mol. Biol. Evol.* 18, 1611–1630. doi: 10.1093/oxfordjournals.molbev.a003951

Moore, R. C., and Purugganan, M. D. (2005). The evolutionary dynamics of plant duplicate genes. *Curr. Opin. Plant Biol.* 8, 122–128. doi: 10.1016/j.pbi.2004.12.001

Muhammad Ahmad, H., Wang, X., Fiaz, S., Rahman, M. U., Azhar Nadeem, M., Aslam Khan, S., et al. (2021). Comprehensive genomics and expression analysis of eceriferum (CER) genes in sunflower (*Helianthus annuus*). *Saudi J. Biol. Sci.* 28, 6884–6896. doi: 10.1016/j.sjbs.2021.07.077

Qin, H., Chen, F., Huan, X., Machida, S., Song, J., and Yuan, Y. A. (2010). Structure of the Arabidopsis thaliana DCL4 DUF283 domain reveals a noncanonical double-stranded RNA-binding fold for protein–protein interaction. *RNA* 16, 474–481. doi: 10.1261/rna.1965310

Rai, A., Suprasanna, P., D'Souza, S. F., and Kumar, V. (2012). Membrane topology and predicted rna-binding function of the 'early responsive to dehydration (ERD4)' plant protein. *PLoS One* 7:e32658. doi: 10.1371/journal.pone.0032658

Rashid, M.-O., Li, J.-H., Liu, Q., Wang, Y., and Han, C.-G. (2021). Molecular detection and identification of eight potato viruses in Gansu province of China. *Curr. Plant Biol.* 25, 100184. doi: 10.1016/j.cpb.2020.100184

Raza, A., Tabassum, J., Kudapa, H., and Varshney, R. K. (2021c). Can omics deliver temperature resilient ready-to-grow crops? *Crit. Rev. Biotechnol.* 41, 1209–1232.

Raza, A., Su, W., Hussain, M. A., Mehmood, S. S., Zhang, X., Cheng, Y., et al. (2021b). Integrated analysis of metabolome and transcriptome reveals insights for cold tolerance in rapeseed (*Brassica napus* L.). *Front. Plant Sci.* 12:721681. doi: 10.3389/fpls.2021.721681

Raza, A., Su, W., Gao, A., Mehmood, S. S., Hussain, M. A., Nie, W., et al. (2021a). Catalase (CAT) gene family in rapeseed (*Brassica napus* L.): genome-wide analysis, identification, and expression pattern in response to multiple hormones and abiotic stress conditions. *Int. J. Mol. Sci.* 22:4281.

Sade, N., del Mar Rubio-Wilhelmi, M., Umnajkitikorn, K., and Blumwald, E. (2018). Stress-induced senescence and plant tolerance to abiotic stress. *J. Exp. Bot.* 69, 845–853. doi: 10.1093/jxb/erx235

Waqas, M., Azhar, M. T., Rana, I. A., Azeem, F., Ali, M. A., Nawaz, M. A., et al. (2019). Genome-wide identification and expression analyses of WRKY transcription factor family members from chickpea (*Cicer arietinum* L.) reveal their role in abiotic stress-responses. *Genes Genomics* 41, 467–481. doi: 10.1007/s13258-018-00780-9

Waseem, M., Aslam, M. M., and Shaheen, I. (2021). The DUF221 domain-containing (DDP) genes identification and expression analysis in tomato under abiotic and phytohormone stress. *GM Crops Food* 1–14. doi: 10.1080/21645698.2021.1962207

Wen, Y., Raza, A., Chu, W., Zou, X., Cheng, H., Hu, Q., et al. (2021). Comprehensive in silico characterization and expression profiling of TCP gene family in rapeseed. *Front. Genet.* 12:794297. doi: 10.3389/fgene2021.794297

Wu, J., Wang, J., Pan, C., Guan, X., Wang, Y., Liu, S., et al. (2014). Genome-wide identification of MAPKK and MAPKKK gene families in tomato and transcriptional profiling analysis during development and stress response. *PLoS One* 9:e103032. doi: 10.1371/journal.pone.0103032

Xin, Z., Mandaokar, A., Chen, J., Last, R. L., and Browse, J. (2007). *Arabidopsis* ESK1 encodes a novel regulator of freezing tolerance. *Plant J.* 49, 786–799. doi: 10.1111/j.1365-313X.2006.02994.x

Yang, Q., Niu, X., Tian, X., Zhang, X., Cong, J., Wang, R., et al. (2020). Comprehensive genomic analysis of the DUF4228 gene family in land plants and expression profiling of ATDUF4228 under abiotic stresses. *BMC Genomics* 21:12. doi: 10.1186/s12864-019-6389-3

Yuan, F., Yang, H., Xue, Y., Kong, D., Ye, R., Li, C., et al. (2014). OSCA1 mediates osmotic-stress-evoked Ca2+ increases vital for osmosensing in *Arabidopsis*. *Nature* 514, 367–371. doi: 10.1038/nature13593

Zaynab, M., Hussain, A., Sharif, Y., Fatima, M., Sajid, M., Rehman, N., et al. (2021c). Mitogen-activated protein kinase expression profiling revealed its role in regulating stress responses in potato (*Solanum tuberosum*). *Plants* 10, 1371. doi: 10.3390/plants10071371

Zaynab, M., Wang, Z., Hussain, A., Bahadar, K., Sajid, M., Sharif, Y., et al. (2021f). ATP-binding cassette transporters expression profiling revealed its role in the development and regulating stress response in *Solanum tuberosum*. *Mol. Biol. Rep.* 1–14.

Zaynab, M., Chen, H., Chen, Y., Ouyang, L., Yang, X., Hu, Z., et al. (2021a). Signs of biofilm formation in the genome of *Labrenzia* sp. PO1. *Saudi J. Biol. Sci.* 28, 1900–1912. doi: 10.1016/j.sjbs.2020.12.041

Zaynab, M., Pan, D., Fatima, M., Sharif, Y., Chen, S., and Chen, W. (2021d). Proteomics analysis of Cyclobalanopsis gilva provides new insights of low seed germination. *Biochimie* 180, 68–78. doi: 10.1016/j.biochi.2020.10.008

Zaynab, M., Chen, H., Chen, Y., Ouyang, L., Yang, X., Xu, W., et al. (2021b). Transcriptome analysis revealed transporter proteins role in the growth of *Labrenzia* sp. PO1 and SY1. *J. King Saud Univ. Sci.* 33:101433. doi: 10.1016/j.jksus.2021.101433

Zaynab, M., Sharif, Y., Abbas, S., Afzal, M. Z., Qasim, M., Khalofah, A., et al. (2021e). Saponin toxicity as key player in plant defense against pathogens. *Toxicon* 193, 21–27. doi: 10.1016/j.toxicon.2021.01.009

Zaynab, M., Fatima, M., Abbas, S., Sharif, Y., Umair, M., Zafar, M. H., et al. (2018). Role of secondary metabolites in plant defense against pathogens. *Microb. Pathog.* 124, 198–202. doi: 10.1016/j.micpath.2018.08.034

Zaynab, M., Kanwal, S., Furqan, M., Islam, W., Noman, A., Ali, G. M., et al. (2017). Proteomic approach to address low seed germination in *Cyclobalnopsis gilva*. *Biotechnol. Lett.* 39, 1441–1451. doi: 10.1007/s10529-017-2393-3

Zaynab, M., Sharif, Y., Fatima, M., Afzal, M. Z., Aslam, M. M., Raza, M. F., et al. (2020). CRISPR/Cas9 to generate plant immunity against pathogen. *Microb. Pathog.* 141:103996. doi: 10.1016/j.micpath.2020.103996

Zhang, L., Hou, D., Li, C., Li, X., Fan, J., Dong, Y., et al. (2021). Molecular characterization and function analysis of the rice OsDUF1664 family. *Biotechnol. Biotechnol. Equip.* 35, 53–60. doi: 10.1080/13102818.2020.1853606

Zhao, J., Wang, P., Gao, W., Long, Y., Wang, Y., Geng, S., et al. (2021). Genome-wide identification of the DUF668 gene family in cotton and expression profiling analysis of GhDUF668 in *Gossypium hirsutum* under adverse stress. *BMC Genomics* 22:395. doi: 10.1186/s12864-021-07716-w

Zhao, X., Xu, M., Wei, R., and Liu, Y. (2015). Expression of OsCAS (calcium-sensing receptor) in an *Arabidopsis* mutant increases drought tolerance. *PLoS One* 10:e0131272. doi: 10.1371/journal.pone.0131272

Conflict of Interest: The authors declare that the research was conducted in the absence of any commercial or financial relationships that could be construed as a potential conflict of interest.

Publisher's Note: All claims expressed in this article are solely those of the authors and do not necessarily represent those of their affiliated organizations, or those of the publisher, the editors and the reviewers. Any product that may be evaluated in this article, or claim that may be made by its manufacturer, is not guaranteed or endorsed by the publisher.

Copyright © 2022 Zaynab, Peng, Sharif, Albaqami, Al-Yahyai, Fatima, Nadeem, Khan, Alotaibi, Alaraidh, Shaikhaldein and Li. This is an open-access article distributed under the terms of the Creative Commons Attribution License (CC BY). The use, distribution or reproduction in other forums is permitted, provided the original author(s) and the copyright owner(s) are credited and that the original publication in this journal is cited, in accordance with accepted academic practice. No use, distribution or reproduction is permitted which does not comply with these terms.

frontiers in Plant Science

ORIGINAL RESEARCH
published: 26 January 2022
doi: 10.3389/fpls.2022.829069

Transgenic *Medicago truncatula* Plants That Accumulate Proline Display Enhanced Tolerance to Cadmium Stress

Vanesa S. García de la Torre[1], Teodoro Coba de la Peña[2†], M. Mercedes Lucas[1*†] and José J. Pueyo[1*†]*

[1] Instituto de Ciencias Agrarias, Consejo Superior de Investigaciones Cientiíficas (ICA-CSIC), Madrid, Spain, [2] Centro de Estudios Avanzados en Zonas Áridas (CEAZA), La Serena, Chile

OPEN ACCESS

Edited by:
Mohammad Anwar Hossain, Bangladesh Agricultural University, Bangladesh

Reviewed by:
Habib Khoudi, Centre of Biotechnology of Sfax, Tunisia
M. Nasir Khan, University of Tabuk, Saudi Arabia

***Correspondence:**
Teodoro Coba de la Peña
teodoro.cobadelapena@ceaza.cl
M. Mercedes Lucas
mlucas@ica.csic.es
José J. Pueyo
jj.pueyo@csic.es

[†] These authors have contributed equally to this work and share senior authorship

Specialty section:
This article was submitted to Plant Biotechnology, a section of the journal Frontiers in Plant Science

Received: *04 December 2021*
Accepted: *03 January 2022*
Published: *26 January 2022*

Citation:
García de la Torre VS, Coba de la Peña T, Lucas MM and Pueyo JJ (2022) Transgenic Medicago truncatula Plants That Accumulate Proline Display Enhanced Tolerance to Cadmium Stress. Front. Plant Sci. 13:829069. doi: 10.3389/fpls.2022.829069

Cadmium (Cd) accumulation in agricultural soils constitutes a serious problem for crop yields and food safety. It is known that proline (Pro) can rapidly accumulate in plant tissues in response to abiotic stress. To analyze the potential protective effect of Pro accumulation against Cd toxicity, we compared the response to Cd stress of wild-type (WT) *Medicago truncatula* and a transgenic line that we had previously obtained and characterized (p18), which expressed the Δ^1-*pyrroline-5-carboxylate synthetase* gene from *Vigna aconitifolia* (*VaP5CS*), and accumulated high Pro levels. Cadmium significantly reduced germination of WT seeds compared to p18 seeds, and seedling relative root growth, a valid indicator of metal tolerance, was significantly higher for p18 than WT seedlings. We analyzed the relative expression of genes related to Pro metabolism, phytochelatin biosynthesis. antioxidant machinery, and NADPH recycling, which are relevant mechanisms in the response to Cd stress. They presented differential expression in the seedlings of both genotypes both under control conditions and under Cd stress, suggesting that the Cd response mechanisms might be constitutively activated in the transgenic line. Pro accumulation promoted higher survival, enhanced growth performance, and minor nutrient imbalance in transgenic p18 plants compared to WT plants. These facts, together with the recorded gluthatione levels, lipid peroxidation and antioxidant enzyme activities strongly suggested that *VaP5CS* expression and Pro accumulation conferred enhanced Cd tolerance to *M. truncatula* p18 plants, which was likely mediated by changes in Pro metabolism, increased phytochelatin biosynthesis and a more efficient antioxidant response. Moreover, p18 roots accumulated significantly higher Cd amounts than WT roots, while Cd translocation to the aerial part was similar to WT plants, thus suggesting that high Pro levels increased not only Cd tolerance, but also Cd phytostabilization by rhizosequestration.

Keywords: Δ^1-pyrroline-5-carboxylate synthetase, P5CS, proline, *Medicago truncatula*, cadmium, phytochelatin biosynthesis, antioxidant response

INTRODUCTION

The occurrence of polluted soils with trace metal elements, also known as heavy metals (Pourret et al., 2020), is an increasing agricultural problem due to industry-derived metal contamination and to the use of soil amendments and agrochemicals. Cadmium (Cd) presents a high mobility and bioavailability and it is extremely toxic for all living organisms (Clemens et al., 2013). Plants growing in Cd-polluted soils constitute its main entry into the food chain, and present a serious threat for animal and human health (Peralta-Videa et al., 2009). Therefore, the identification of Cd-tolerant cultivars that do not translocate the metal to the edible parts of the plant becomes a priority in global food security.

Multiple studies in different plant species report that Cd is highly phytotoxic and can cause germination inhibition, nutritional imbalance, growth reduction and plant death, among other detrimental effects (Sanità di Toppi and Gabbrielli, 1999; Benavides et al., 2005; Seneviratne et al., 2019; El Rasafi et al., 2020; García de la Torre et al., 2021). Cd contributes to the generation of reactive oxygen species (ROS) (Sharma and Dietz, 2009; Romero-Puertas et al., 2019), which are considered the main source of the damage to plant tissues (Cuypers et al., 2010). Enzymatic and non-enzymatic antioxidant defense systems participate in ROS scavenging. The primary defense against ROS includes the superoxide dismutase (SOD) enzymes that catalyze the dismutation of O_2^- (superoxide) to O_2 and H_2O_2. Then, catalases and peroxidases can detoxify H_2O_2. Levels of the antioxidant metabolites ascorbate, glutathione, NADPH and the enzymes of the ascorbate-glutathione cycle are also of pivotal importance to maintain the redox state of the cell. NAPDH is considered a limiting metabolite in the plant antioxidant capacity because many ROS-detoxifying reactions are NADPH-dependent (Foyer and Noctor, 2011). This enzyme cofactor and reducing agent can be produced in different pathways, including enzymatic reactions catalyzed by isocitrate dehydrogenase (ICDH), glucose 6-phosphate dehydrogenase (G6PDH) or 6-phosphogluconate dehydrogenase (6PGDH), which are induced in response to oxidative stress caused by different factors, including Cd stress (Marino et al., 2007, 2013; Pérez-Chaca et al., 2014). The Cd-induced gene expression of these enzymes might be key for Cd tolerance in some *M. truncatula* cultivars (García de la Torre et al., 2021). Another plant response to Cd stress is the synthesis of phytochelatins (PCs) by phytochelatin-synthases (PCS), using glutathione as a substrate. It has been suggested that PCs are important for Cd chelation, detoxification and tolerance (Schat et al., 2002; Sobrino-Plata et al., 2009; Ahmad et al., 2019).

Proline (Pro) is a compatible solute accumulated under several environmental stresses in plants, such as osmotic stress and metal-induced stress, and increased levels of this amino acid have been shown to correlate with enhanced stress tolerance in several plants (Sharma and Dietz, 2006; Hayat et al., 2012; Hossain et al., 2015). The role of Pro in drought and salt stress tolerance has been widely discussed (Hayat et al., 2012; El Moukhtari et al., 2020); however, not so much is known about the contribution of Pro to Cd tolerance in plants. Pro functions as a mediator in osmotic adjustment (Ben Ahmed et al., 2011), and contributes to the protection of membranes, enzymes and proteins under various stresses (Hayat et al., 2012; Singh et al., 2015). Furthermore, Pro contributes to maintain redox homeostasis by scavenging free radicals and ROS (Sharma and Dietz, 2006; Hoque et al., 2008; Aggarwal et al., 2011). Oxidation of Pro by proline dehydrogenase (ProDH) and proline-5-carboxylate dehydrogenase (P5CDH) enhances the reducing potential of mitochondria during stress (Szabados and Savouré, 2010). Pro can also act as a metabolic signal that controls cellular homeostasis in response to changing environmental conditions (see review by Alvarez et al., 2021).

In plants, Pro is synthesized from glutamic acid (Glu) or from ornithine (Orn), depending on the availability of the substrates. Under stress conditions, Pro was proposed to be synthesized through the Glu pathway, which involves Δ^1-pyrroline-5-carboxylate reductase (P5CR) and Δ^1-pyrroline-5-carboxylate synthetase (P5CS) activities (Delauney and Verma, 1993; Mansour and Ali, 2017; Funck et al., 2020). The Orn pathway, which involves ornithine δ-aminotransferase (OAT) and P5CR, has been described as an alternative pathway that is considered non-essential for Pro biosynthesis (Funck et al., 2008), although it seems to be the predominant pathway in legumes (Abdelgawad et al., 2015). It has been reported that transgenic plants overexpressing Pro biosynthetic pathway genes display osmotic and oxidative stress tolerance (see review by Kumar et al., 2015).

Legume crops are capable to grow in nutrient-poor soils as they do not depend on nitrogen fertilization (Coba de la Peña and Pueyo, 2012). The model plant *Medicago truncatula* is related to alfalfa (*M. sativa*), it constitutes a source for genetic improvement and an optimal model to elucidate metal tolerance mechanisms. This forage legume presents a high biomass production and good soil coverage. *M. truncatula* cultivars with enhanced Cd tolerance and metal accumulation restricted to roots have the potential to be used as a forage crop in mildly Cd-contaminated soils (García de la Torre et al., 2021).

In a previous work, we generated a *M. truncatula* transgenic line, namely p18, that expressed the *Δ¹-pyrroline-5-carboxylate synthetase* gene from *Vigna aconitifolia* (*VaP5CS*), accumulated high Pro levels and displayed enhanced tolerance to osmotic stress (Verdoy et al., 2006). The aim of the present work was to elucidate the role of Pro in Cd tolerance in this transgenic line. We evaluated Cd tolerance and determined the expression profiles of relevant genes involved in Pro metabolism, PC biosynthesis, antioxidant machinery and NADPH recycling in wild type (WT) and transgenic (p18) *M. truncatula* plants at the seedling stage. We also comparatively assessed Cd effect on germination, survival, metal accumulation and nutritional status at longer exposure times. Some markers related to Cd-induced antioxidant defenses were also analyzed. Our results indicated that the expression of *VaP5CS,* and the consequent Pro accumulation, remarkably enhanced the capacity of *M. truncatula* transgenic plants to cope with Cd stress.

MATERIALS AND METHODS

Plant Material and Germination Assay

Seeds of wild-type *Medicago truncatula* Gaertn. R-108-1 (c3) and transgenic p18 *M. truncatula*, expressing the *Vigna aconitifolia* Δ^1*-pyrroline-5-carboxylate synthetase* gene (*VaP5CS*) (Verdoy et al., 2006), were scarified, sterilized with 10% bleach for 15 min, rinsed (4 × 20 min) and imbibed in sterile water at 4°C. For the germination assay in the presence of Cd, WT and transgenic p18 *M. truncatula* seeds were transferred to Petri dishes containing 1% agar supplemented with 0, 0.5, 1.0, or 1.5 mM $CdCl_2$ (25/19°C, 16/8 h). Germination percentage was evaluated after 7 days in darkness. Three biological replicates, each containing 12 seeds per genotype and treatment, were assayed.

Cadmium Stress at the Seedling Stage

For this and all subsequent experiments, scarified, sterilized and imbibed seeds (as described above) were germinated on 1% agar Petri dishes (25/19°C, 16/8 h) for 48 h in darkness. Seedlings were acclimatized to the different growth systems with Hoagland solution (pH 5.4) prior to Cd treatment. All experiments were performed at 180 μmol photon m^{-2} s^{-1} light intensity and 25/19°C, 16/8 h photoperiod.

Germinated WT and transgenic p18 *M. truncatula* seedlings were transferred to a glass box hydroponic culture system (García de la Torre et al., 2013, 2021) for 24 h before Cd treatment was applied, and seedlings were subsequently exposed to 0 or 10 μM $CdCl_2$ for 48 h. Seedling relative root growth (RRG), which is a proven indicator of metal tolerance (Sledge et al., 2005; García de la Torre et al., 2013, 2021) was determined. The $CdCl_2$ concentration and time of exposure were determined in a previous study as optimal to identify Cd-sensitive and Cd-tolerant cultivars (García de la Torre et al., 2021). Two biological replicates, each containing 10 seedlings per genotype and treatment (control or Cd), were performed.

Gene Expression Profiles

Germinated WT and transgenic p18 *M. truncatula* seedlings were acclimatized for 72 h in a glass box hydroponic culture and then exposed to Cd stress. Seedlings were exposed to 0 or 50 μM $CdCl_2$ for 12 h. Roots and shoots were separately frozen in liquid nitrogen and stored at −80°C until use for RNA isolation and RT-qPCR analysis. Four biological replicates, each containing 10 seedlings per genotype and treatment, were assayed. Total RNA was isolated using the TRIZol (Invitrogen) reagent and treated with RNase-free DNase I (Thermo Scientific). Determination of RNA concentration and integrity, and reverse transcription were performed as detailed by García de la Torre et al. (2021). qPCR analyses were performed with a 7300 Real-Time PCR Sequence Detection System (PE Applied Biosystems), as described (García de la Torre et al., 2021). Fold-changes ≥ 2 were considered as significant. Specific primers were designed using the Primer3 software[1] (**Supplementary Table 1**). *MtACTIN11* was used as a housekeeping gene (García de la Torre et al., 2021). Four biological replicates, each containing 10 seedlings per cultivar and treatment, were analyzed.

[1]http://bioinfo.ut.ee/primer3-0.4.0/

Plant Growth and Survival Assays

Scarified, sterilized, imbibed WT and transgenic p18 *M. truncatula* seeds were germinated on 1% agar in Petri dishes (25/19°C) for 48 h in the dark. Germinated seedlings were acclimatized for 7 days in pots containing vermiculite (350 mL) and then watered with Hoagland nutrient solution (pH 5.4) containing 0, 0.1, 0.2, 0.4, 0.6 or 1.0 mM $CdCl_2$ every 48 h. Plants were grown at 180 μmol photon m^{-2} s^{-1} light intensity, 25/19°C and 16/8 h photoperiod. After 32 days, the survival percentage was evaluated. Plants growing at 0 and 100 μM $CdCl_2$ were selected for further analyses. 100 μM $CdCl_2$ was chosen as a concentration that had an effect on plant growth, yet did not result in plant death, so that the differential response of WT and p18 plants could be analyzed. Shoots and roots of sixteen plants were independently frozen in liquid nitrogen and stored at –80°C for quantification of Pro and glutathione, lipid peroxidation, and SOD and CAT activities. Ten plants were used to analyze shoot and root weights, root length, number of leaves and chlorophyll content. Relative parameters (RX) were calculated as: $RX = (\Delta\text{Parameter } X_{Cd}/\Delta\text{Parameter } X_{Control}) \times 100$. The same plants were used for determination of Cd and nutrients contents.

Cadmium and Nutrient Contents

At harvest, after 32-day treatment, plant tissues were washed with 10 mM Na_2EDTA and then rinsed with distilled water. Shoots and roots were stove-dried at 60°C. Pools of two to three plants per genotype and treatment were digested with nitric-perchloric acid (7:3). Elemental analyses were performed using an ICP-OES (Perkin Elmer Optima 4300 DV). Three to five replicates (pools) per genotype and treatment were analyzed.

Determination of Free Proline, Glutathione, Lipid Peroxidation and Antioxidant Enzyme Activities

Shoots and roots of WT and transgenic p18 *M. truncatula* plants were ground in liquid nitrogen and homogenized in 5% (w/v) sulfosalicylic acid (0.2 g FW mL^{-1}). Homogenates were centrifuged (15,000 *g*, 5 min, 4°C), and the supernatant was used for free Pro determination as previously described (Bates et al., 1973). The reaction mixture included the supernatant, acid ninhydrin and glacial acetic acid (1:1:1). The acid ninhydrin solution was prepared in the dark by mixing 30 mL glacial acetic acid, 20 mL 6 M phosphoric acid and 1.25 g ninhydrin. The reaction mixture was boiled for 1 h and the reaction was stopped on ice. Proline-ninhydrin chromophore complex was extracted using 0.6 mL toluene. Absorbance of the organic phase was determined at 520 nm. Content of Pro was determined with a calibration curve performed with L-proline. Four biological replicates per genotype and treatment were analyzed.

Total glutathione (GSH + GSSG) and reduced glutathione (GSH) were determined as we previously described (García de la Torre et al., 2021) in roots and shoots of WT and transgenic *M. truncatula* p18 plants grown at 0 or 100 μM

$CdCl_2$ for 32 days. Four biological replicates per genotype and treatment were analyzed.

Malondialdehyde (MDA) determination was carried out using the thiobarbituric acid method (Singh et al., 2007). Plant tissue was ground in liquid nitrogen and homogenized in 0.1% TCA solution and MDA was determined as described by Redondo et al. (2009). Four biological replicates per genotype and treatment were analyzed.

The enzyme activities were assayed in roots and shoots of WT and transgenic p18 *M. truncatula* plants grown in the presence of 0 or 100 μM $CdCl_2$ for 32 days. Plant tissue was ground in liquid nitrogen and homogenized (García de la Torre et al., 2021). SOD and CAT activities were determined as described (Redondo et al., 2009). Total protein content in the homogenates was quantified in 1:5 dilutions at 595 nm with the Bradford protein assay (BioRad) using BSA as a standard. The enzymatic activities were calculated in units per mg of protein. One unit of SOD is the amount of enzyme that will inhibit the rate of reduction of cytochrome c by 50% in a coupled system, using xanthine and xanthine oxidase at pH 7.8 at 25°C. One catalase unit will decompose 1.0 μmole of H_2O_2 per minute at pH 7.0 at 25°C. Four biological replicates per genotype and treatment were analyzed.

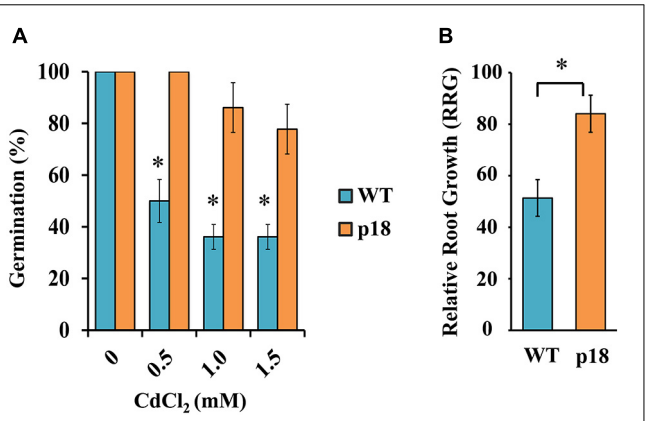


FIGURE 1 | Effects of cadmium on germination and seedling relative root growth of *M. truncatula* WT and p18 lines. **(A)** Germination percentage of *M. truncatula* WT and transgenic p18 seeds at different $CdCl_2$ concentrations for 7 days. * Indicates significant differences between control and Cd treatment (Chi-squared (χ^2), $p < 0.05$, $n = 3$ replicates per treatment, each containing 12 seeds). **(B)** Relative root growth (RRG) of *M. truncatula* WT and transgenic p18 seedlings in the presence of Cd (40 μM $CdCl_2$, 48 h). * Indicates significant differences between genotypes, one-way ANOVA, $p < 0.05$, $n = 10$. Bars indicate standard deviation.

Statistical Analyses

The IBM SPSS Statistics 20 software (SPSS Inc., Chicago, IL, United States) was used. Root length and the relative growth parameters were analyzed by ANOVA ($p < 0.05$). Cadmium and nutrient contents were analyzed by ANOVA ($p < 0.05$, Tukey HSD). The germination and survival percentages were analyzed by Pearson's Chi-squared test (χ^2) ($p < 0.05$). The glutathione and Pro contents, SOD and CAT activities and lipid peroxidation were analyzed by ANOVA ($p < 0.05$) and the Tukey HSD test was used for pair-wise comparisons.

RESULTS

Expression of *VaP5CS* in *M. truncatula* Reduces the Negative Effects of Cadmium Stress on Germination and on Root Growth at the Seedling Stage

As a first approach to determine whether Pro accumulation had an effect on *M. truncatula* tolerance to Cd, we compared the effect of Cd on seed germination. WT and p18 seeds were germinated in the presence of increasing $CdCl_2$ concentrations. Cadmium induced a strong and significant decrease in the germination percentage of WT seeds at all tested Cd concentrations. A slight decrease could be observed in p18 seed germination, but Cd had a much lesser effect (**Figure 1A**).

To examine how Pro accumulation influenced Cd tolerance, we compared the relative root growth (RRG) of *M. truncatula* p18 and WT seedlings growing in a miniaturized hydroponic system. RRG at the seedling stage is considered a valid indicator of metal tolerance in plants (Sledge et al., 2005; García de la Torre et al., 2013, 2021). These conditions were previously described as adequate to identify Cd-sensitive and Cd-tolerant cultivars (García de la Torre et al., 2021). Upon Cd treatment, both genotypes displayed a significant decrease in root growth compared to control conditions (**Figure 1B**). However, whereas Cd affected more severely WT seedlings (RRG ≈ 50%), p18 seedlings root growth was reduced by about 17% in the presence of Cd. These results suggested that *VaP5CS* expression and the consequent Pro accumulation led to increased tolerance to Cd stress in p18 plantlets.

Pro Metabolism, Phytochelatin Biosynthesis, and Antioxidant Response Related Genes Display Different Relative Expression in p18 and Wild-Type Seedlings

The expression of *VaP5CS* and the consequent Pro accumulation, influenced the transcriptional response of several important genes related to Pro metabolism, phytochelatin (PC) biosynthesis, antioxidant machinery and NADPH biosynthesis both in the absence and the presence of Cd (**Figure 2**). In the absence of Cd, most tested genes showed significantly higher expression in p18 than in WT roots. *MtOAT* showed significantly lower expression in p18 than in WT roots, *MtProDH* expression decreased in p18 roots, although non-significantly, and *MtCuZnSODs* expression did not show any significant differences (**Figure 2A**). On the contrary, most genes showed a lower expression in p18 than in WT shoots. A significant downregulation was observed for most genes involved in biosynthesis, transport and degradation of Pro (*MtPC5CS1*, *MtPC5CS2*, *MtP5CR*, *MtP5CDH* and *MtProT*), for *MthGSHS*, *MtPCS* involved in PC biosynthesis, and for antioxidant response related *MtFeSOD* and *MtCAT*. Only *MtCuZnSODa* showed

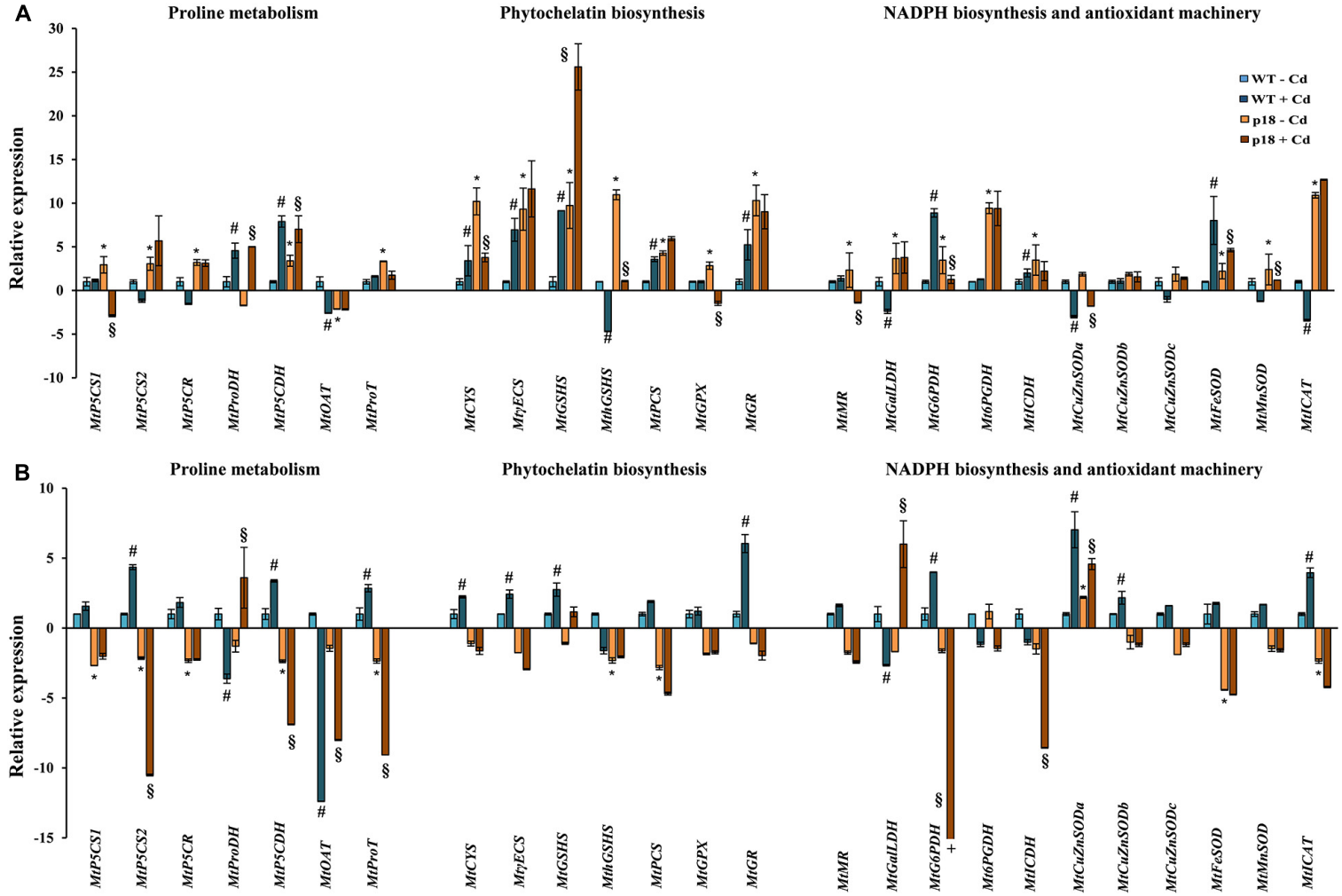


FIGURE 2 | Transcript accumulation of genes involved in Pro metabolism, PC biosynthesis, antioxidant machinery and NADPH biosynthesis in *M. truncatula* WT and transgenic p18 seedlings roots **(A)** and shoots **(B)** grown in the absence or presence of 50 μM $CdCl_2$ for 12 h. Data are mean of four biological replicates (10 seedlings per replicate). * Indicates significant differences (fold change ≥ 2) between untreated WT and p18 seedlings; #, significant differences between untreated and Cd-treated WT seedlings; §, significant differences between untreated and Cd-treated p18 seedlings; + , the actual value is –37.8. Abbreviations: *MtP5CS1*: *M. truncatula* Δ^1-pyrroline-5-carboxylate synthetase 1; *MtP5CS2*: Δ^1-pyrroline-5-carboxylate synthetase 2; *MtP5CR*: pyrroline-5-carboxylate reductase; *MtP5CDH*: Δ^1-pyrroline-5-carboxylate dehydrogenase; *MtProDH*: proline dehydrogenase; *MtOAT*: ornithine δ-aminotransferase; *MtProT*: proline transporter; *MtCYS*: cysteine synthase; *MtECS*: γ-glutamylcysteine synthetase; *MtGSHS*: glutathione synthetase; *MthGSHS*: homoglutathione synthetase; *MtPCS*: phytochelatin synthase; *MtGPX*: glutathione peroxidase; *MtGR*: glutathione reductase; *MtMR*: monodehydroascorbate reductase; *MtGalLDH*: galactono-1, 4-lactone dehydrogenase; *MtG6PDH*: glucose-6-phosphate dehydrogenase; *Mt6PGDH*: 6-phosphogluconate dehydrogenase; *MtICDH*: isocitrate dehydrogenase; *MtCuZnSODa*, *MtCuZnSODb*, *MtCuZnSODc*: cooper/zinc superoxide dismutases; *MtFeSOD: ferric SOD; MtMnSOD*: manganese SOD; *MtCAT*: catalase.

significantly higher expression in p18 than in WT shoots. Most genes involved in glutathione, ascorbate and NADPH biosynthesis showed no significant changes in expression between p18 and WT shoots (**Figure 2B**).

In WT roots, Cd stress caused an upregulation of *MtProDH*, *MtP5CDH*, of most of the genes involved in GSH and PCs biosynthesis, and several genes involved in NADPH biosynthesis and antioxidant response (*MtG6PDH*, *MtICDH* and *MtFeSOD*). *MtOAT*, *MthGSHS, MtGalLDH*, *MtCuZnSODa* and *MtCAT* showed lower expression in WT roots under Cd stress (**Figure 2A**). In WT shoots, most genes were upregulated upon Cd exposure, and this upregulation was significant for *MtP5CS2*, *MtP5CDH*, *MtProT*, *MtCYS*, *MtECS*, *MtGSHS*, *MtGR*, *MtG6PDH*, *MtCuZnSODa* and *MtCuZnSODb*, and *MtCAT*. Only a few genes (*MtProDH, MtOAT* and *MtGalLDH*) were significantly downregulated upon Cd exposure in WT shoots (**Figure 2B**). On the other hand, only a few genes (*MtProDH*, *MtP5CDH, MtGSHS* and *MtFeSOD*) were significantly upregulated in p18 roots upon Cd stress in comparison with untreated p18 roots, whereas a significant downregulation was observed for *MtP5CS1*, *MtCYS*, *MthGSHS, MtGPX, MtMR*, *MtG6PDH*, *MtCuZnSODa* and *MtMnSOD* expression in Cd-treated p18 roots (**Figure 2A**). Cd stress led to significantly increased expression of *MtProDH, MtGalLDH* and *MtCuZnSODa* in p18 shoots, and to significantly reduced expression of several genes related to Pro metabolism (*MtP5CS2*, *MtP5CDH*, *MtOAT*, *MtProT*), and NADPH biosynthesis (*MtG6PDH* and *MtICDH*). Genes related to the biosynthesis of glutathione and PC were not affected upon Cd exposure in p18 shoots (**Figure 2B**).

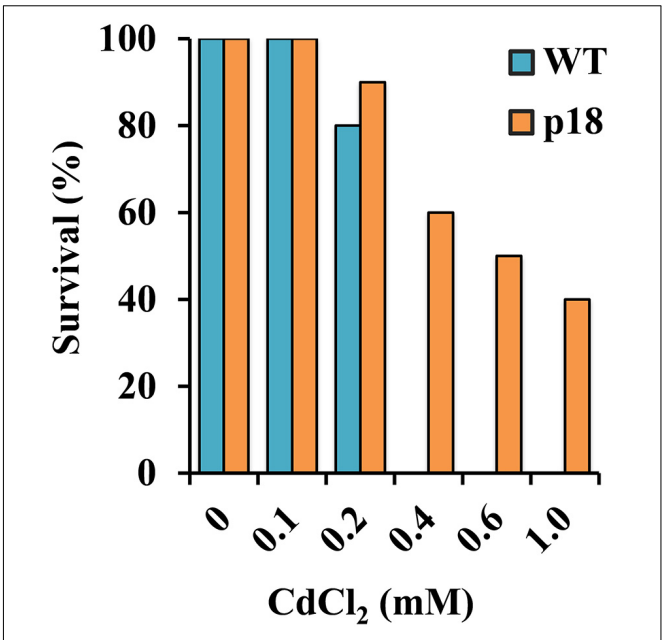


FIGURE 3 | Survival percentage of WT and p18 plants upon exposure to different $CdCl_2$ concentrations ($n = 30$). The germination percentages were analyzed by Pearson's Chi-squared test ($\chi 2$) ($p < 0.05$).

Proline Accumulation Enhances Cadmium Tolerance in Transgenic *M. truncatula* p18 Plants, and Affects the Nutritional Status of Cd-Stressed Plants

Plants of both genotypes grown in vermiculite were watered with nutrient solution containing different $CdCl_2$ concentrations for 32 days. Survival was negatively affected in both genotypes at concentrations of $CdCl_2$ higher than 100 μM. WT plants did not survive exposure to 400 μM $CdCl_2$ or to higher concentrations. The transgenic line was affected, but displayed notable survival percentages when exposed to 400 μM $CdCl_2$ and higher concentrations up to 1 mM $CdCl_2$ (**Figure 3**). To further characterize the role of Pro accumulation in the *M. truncatula* transgenic line Cd tolerance, and to determine the differences between WT and p18 plants after a longer exposure to Cd, we selected plants subsets grown in the absence of Cd or in the presence of 100 μM $CdCl_2$, a concentration that did not affect survival of WT or p18 plants. Pro content, growth parameters, Cd accumulation and nutrients contents were measured in roots and shoots. The content of Pro was significantly higher in p18 compared to WT plants, both in roots and shoots in the absence or presence of Cd (**Figure 4A**), due to expression of *VaP5CS* gene. However, Cd induced a significant increase in Pro accumulation in shoots of WT plants only (**Figure 4A**). Differences in plant growth between WT and transgenic p18 plants were observed after Cd stress (**Figure 4B**). Relative growth parameters calculated as percentages of the values recorded for plants grown in the absence of Cd were significantly higher for p18 than for WT plants subjected to Cd stress, including the relative number of leaves (RNL), relative root fresh weight (RRFW), relative root dry weight (RRDW), relative shoot fresh weight (RSFW), relative shoot dry weight (RSDW) and relative chlorophyll content (RCC). The difference was not significant for relative root growth (RRG) (**Figure 4C**).

Regarding metal accumulation and translocation to the aerial part, Cd accumulated mainly in roots and relatively small amounts were translocated to the aerial part of the plants (**Table 1**). Transgenic p18 plants accumulated a significantly higher content of Cd in roots (about 1.5-fold). In shoots, differences in Cd content, while still significant, were much smaller. In consequence, the translocation factor was significantly higher in WT plants (**Table 1**).

The content of macro and micronutrients did not show striking differences between WT and p18 plants grown under control conditions for 32 days (**Table 2**). In roots, only S content was significantly lower in p18 than in WT plants, and Zn and Cu contents were significantly higher in p18 compared to WT roots. In shoots, p18 plants showed significantly lower contents of K and P than WT plants; while Ca, Na and Zn contents were significantly higher in p18 than in WT shoots.

In WT roots, the Cd treatment promoted a significant increase of the contents of K, Ca, Na, Zn and Cu, and a significant decrease in Mg, P, S and Fe contents. The effect of Cd on p18 roots was similar to that observed in WT roots, with the exceptions of P (that was not significantly affected by the Cd treatment) and

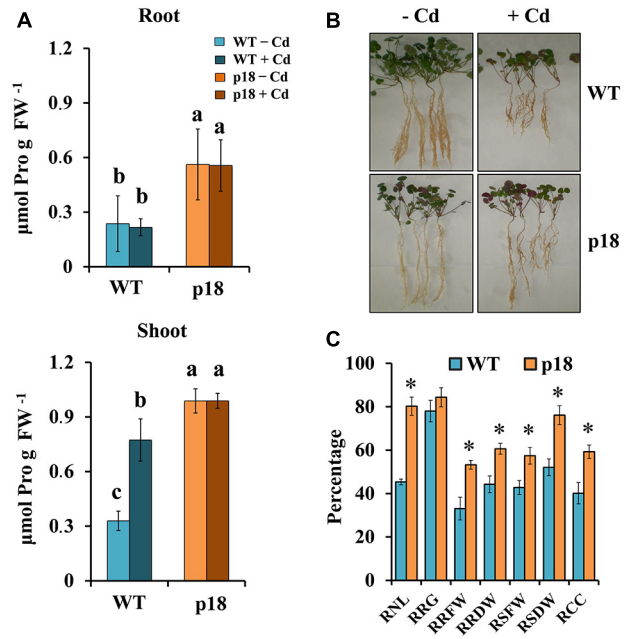


FIGURE 4 | Effects of cadmium treatment on *M. truncatula* WT and transgenic p18 plants after 32 days of growth in pots in the presence of 0 or 100 µM $CdCl_2$. **(A)** Pro content in roots (upper panel) and shoots (lower panel). Different letters denote significant differences between lines and treatments in roots or shoots, Tukey HSD, $p < 0.05$, $n = 4$. **(B)** Representative image of *M. truncatula* WT and p18 plants grown for 32 days in the absence or presence of 100 µM $CdCl_2$. **(C)** Relative growth parameters of Cd-treated *M. truncatula* WT and p18 plants calculated as percentages of the values recorded for plants grown in the absence of Cd. Bars indicate standard error. * Indicates significant differences between genotypes (ANOVA, $p < 0.05$, $n = 10$). RNL, relative number of leaves; RRG, relative root growth; RRFW, relative root fresh weight; RRDW, relative root dry weight; RSFW, relative shoot fresh weight; RSDW, relative shoot dry weight; RCC, relative chlorophyll content.

TABLE 1 | Cadmium content in roots and shoots of WT and transgenic p18 *M. truncatula* plants.

	[Cd] mg/kg		Translocation factor%
	Root	Shoot	
WT	893.56 ± 295.28 b	62.03 ± 8.84 b	7.94 ± 3.60 a
p18	1327.51 ± 153.19 a	70.13 ± 3.60 a	5.37 ± 0.88 b

Plants were grown in pots containing vermiculite with 0 or 100 µM $CdCl_2$ for 32 days.
Means ± SD are shown.
Different letters denote significant differences between WT and p18 plants (Tukey HSD, $p < 0.05$, $n = 3–5$).

Mn (that displayed a significant decrease upon Cd treatment); Mn content was significantly lower than in treated p18 than in treated WT roots. Zn and Cu contents were significantly higher in p18 than in WT roots, both in the absence and in the presence of Cd.

In WT shoots, Cd treatment induced a significant increase in the contents of Na and Mg, and a significant decrease in the contents of K, P, Zn and Cu. In Cd-treated p18 shoots, a significant increase in Na content was observed, but no significant changes were observed in the contents of Mg. Na levels remained significantly higher than those observed for Cd-treated WT shoots, and the opposite was observed for Mg levels. Significant decreases in the amounts of Ca, S and Zn were observed in p18 shoots exposed to Cd; Ca levels remained at similar levels than those observed in WT shoots upon Cd treatment, and S levels were significantly lower than those observed in Cd-treated WT shoots. The contents of K, P and Cu were not affected by the Cd treatment in p18 shoots, but Cu levels were significantly higher than those in Cd-treated WT shoots.

TABLE 2 | Macro and micronutrients contents in roots and shoots of WT and transgenic p18 *M. truncatula* plants.

		Root		Shoot	
	$CdCl_2$ (µM)	WT	p18	WT	p18
		Macronutrients (mg kg^{-1})			
K	0	46,500	49,442	62,701 a	53,112 b
	100	58,797 *	55,182 *	51,769 *	51,908
Ca	0	1,293	1,384	3,634 b	4,267 a
	100	1,771 *	1,675 *	3,430	3,177 *
Na	0	2,230	2,235	858 b	1,028 a
	100	3,147 *	2,956 *	1,292 *b	1,775 *a
Mg	0	10,069	10,458	11,246	12,214
	100	9,729 *	8,113 *	13,276 *a	11,418 b
P	0	1,210	1,077	2,128 a	1,953 b
	100	741 *b	1,233 a	1,898 *	1,870
S	0	5,781 a	2,610 b	4,240	4,423
	100	1,796 *	857 *	4,436 a	2,198 *b
		Micronutrients (mg kg^{-1})			
Fe	0	943	1,104	70	90
	100	445 *	696 *	73	75
Mn	0	183	233	37	40
	100	162 a	88 *b	47	39
Zn	0	20 b	33 a	11 b	16 a
	100	26 *b	35 *a	5 *	7 *
Cu	0	31 b	56 a	16	17
	100	63 *b	87 *a	12 *b	19 a

Plants were grown in pots containing vermiculite with 0 or 100 µM $CdCl_2$ for 32 days.
An asterisk indicates significant differences between treatments; different lowercase letters indicate significant differences between WT and p18 plants (ANOVA, $p < 0.05$, $n = 3–5$).

Wild-Type and Transgenic p18 *M. truncatula* Plants Display Differential Antioxidant Responses to Cadmium Stress

To investigate whether the antioxidant defense was affected in the transgenic plants, we analyzed roots and shoots of WT and p18 plants grown for 32 days in presence of 0 or 100 µM $CdCl_2$. The contents of oxidized (GSSG) and reduced glutathione (GSH), and the GSH/GSSG ratio, lipid peroxidation, and the SOD and CAT enzyme activities were determined.

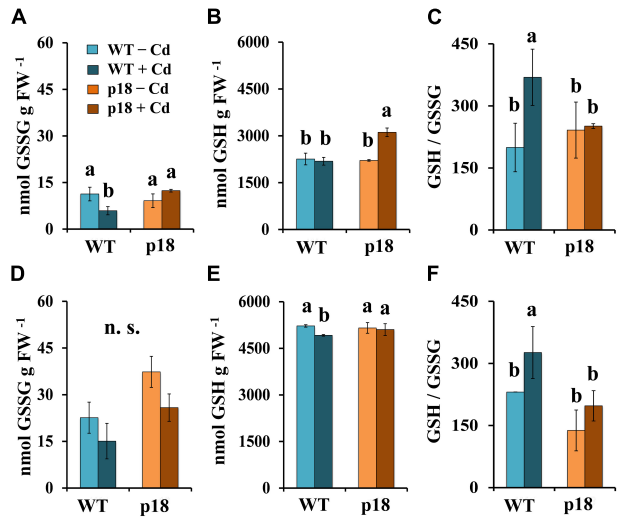


FIGURE 5 | Cadmium effect on the levels of oxidized gluthathione (GSSG), reduced glutathione (GSH) and GSH/GSSG ratio in *M. truncatula* WT and transgenic p18 roots **(A–C)** and shoots **(D–F)**. Plants were grown in pots with 0 or 100 μM $CdCl_2$ for 32 days. Bars indicate standard deviation. Different letters denote significant differences, Tukey HSD, $p < 0.05$, $n = 4$; n.s. not significant.

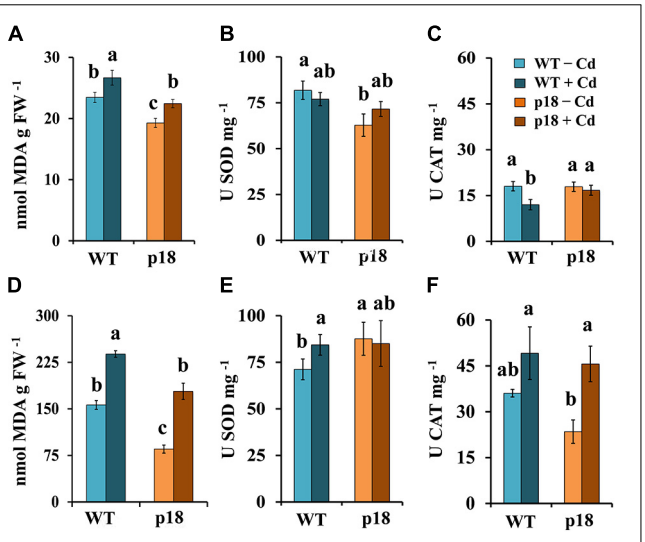


FIGURE 6 | Lipid peroxidation (MDA), superoxide dismutase and catalase activities in *M. truncatula* WT and p18 roots **(A–C)** and shoots **(D–F)**. Plants were grown in pots with 0 or 100 μM $CdCl_2$ for 32 days. Bars indicate standard deviation. Different letters denote significant differences, Tukey HSD, $p < 0.05$, $n = 4$.

No significant differences in GSSG or GSH contents were observed when comparing WT and p18 plants in absence of Cd, neither in roots nor in shoots. A significant decrease in GSSG levels was observed in WT roots upon Cd exposure (**Figure 5A**), and a significant increase in GSH levels was observed in roots of Cd-treated transgenic p18 plants (**Figure 5B**). In shoots, GSSG levels were not significantly affected by the Cd treatment in either genotype (**Figure 5D**). A small, yet significant decrease in GSH levels was observed in Cd-treated WT shoots, whilst no significant changes were observed in p18 shoots (**Figure 5E**). Significant increases of the GSH/GSSG ratio were observed in WT roots (**Figure 5C**) and shoots (**Figure 5F**) upon Cd exposure, while no significant differences for this parameter were observed between control and Cd-treated p18 plants (**Figures 5C,F**).

The oxidative damage was estimated by measuring lipid peroxidation (as MDA content). In the absence of Cd, MDA levels in roots and shoots of p18 plants were significantly lower than those in roots and shoots of WT plants (**Figures 6A,D**). Cadmium exposure promoted a significant increase of MDA levels in roots and shoots of both genotypes; however, MDA levels in Cd-treated p18 roots and shoots remained significantly lower than those in Cd-treated WT roots and shoots, respectively (**Figures 6A,D**). SOD and CAT enzymatic activities were determined. In the absence of Cd, SOD activity levels were significantly higher in WT roots compared with those in p18 roots (**Figure 6B**), and the opposite was observed in shoots (**Figure 6E**). Upon Cd treatment, SOD activity was significantly induced in WT shoots, reaching to similar values to those observed in p18, which were not significantly affected by Cd (**Figure 6E**). Catalase activity was similar in WT and p18 roots (**Figure 6C**) in the absence of Cd, and it was higher, although non-significantly in WT than in p18 shoots (**Figure 6F**). Exposure to Cd induced a significant decrease of catalase activity in WT roots (**Figure 6C**), and an increase in both WT and p18 shoots that was statistically significant for p18 (**Figure 6F**).

DISCUSSION

Plants accumulate Pro under a variety of abiotic stresses including salinity, drought and heavy metal-induced stress (Sharma and Dietz, 2006; Hayat et al., 2012). This amino acid functions in plants as a signaling molecule (Singh et al., 2017), as a mediator in osmotic adjustment (Ben Ahmed et al., 2011), a stabilizer of sub-cellular structures (Singh et al., 2015), and as a ROS scavenger (Aggarwal et al., 2011). However, little is known about the role of Pro in plants under Cd stress.

To obtain a deeper insight into the role of Pro in Cd tolerance in *M. truncatula*, we used a transgenic line, p18, that expresses the Δ^1-pyrroline-5-carboxylate synthetase gene from *Vigna aconitifolia* (*VaP5CS*) and accumulates high Pro levels (Verdoy et al., 2006). In our previous work we used two different transgenic lines, p2 and p18, which behaved in an identical manner, only p2 showed relatively higher *VaP5CS* transcript and Pro accumulation than p18. However, p2 germination was extremely poor and we decided to use only p18 in the present study. We evaluated Cd tolerance, expression profiles of relevant genes involved in Pro biosynthesis and response to Cd stress, as well as growth performance, Cd accumulation, and nutritional status in WT *M. truncatula* plants and in the transgenic line.

Expression of the *VaP5CS* transgene in wheat (Sawahel and Hassan, 2002), tobacco (Razavizadeh and Ehsanpour, 2009), chickpea (Ghanti et al., 2011), sugarcane (Guerzoni et al., 2014),

rice (Kumar et al., 2010) and pigeon pea (Surekha et al., 2014) has been proven to promote high levels of Pro accumulation and, to different extents, better plant performance under salt stress. Expression of *VaP5CS* has been reported to increase Cd stress tolerance in the green algae *Chlamydomonas reinhardtii* (Siripornadulsil et al., 2002). To our knowledge, the effect on Cd tolerance of *VaP5CS* (or any other *P5CS* homolog) expression, and the consequent Pro accumulation, has not been reported in higher plants to date. In the present work, we show that expression of *VaP5CS* leads to Pro accumulation and increased tolerance to Cd stress in *M. truncatula*.

Compared with other developmental stages, germination is very sensitive to Cd stress (Rahoui et al., 2008; Seneviratne et al., 2019; El Rasafi et al., 2020). Our results indicated that the expression of *VaP5CS* allowed elevated germination in the presence of Cd concentrations that significantly decreased germination of *M. truncatula* WT seeds. Seedling relative root growth (RRG) is considered as a valid indicator of metal tolerance (Sledge et al., 2005; García de la Torre et al., 2013, 2021; Rahoui et al., 2014). The RRG assay showed that *M. truncatula* transgenic line p18 displayed significantly higher tolerance to Cd stress than WT *M. truncatula* at the seedling stage.

In general, Pro accumulation upon stress involves the Glu pathway by increased expression and/or activity of P5CS (Delauney et al., 1993; Zhen and Ma, 2009; Lei et al., 2016; Mansour and Ali, 2017; Funck et al., 2020). *MtOAT* expression was significantly decreased in shoots and roots of WT seedlings exposed to Cd, while *MtP5CS2* expression was significantly induced in shoots of WT seedlings exposed to Cd, suggesting that the Glu pathway might be the main source of Pro accumulation upon Cd stress in *M. truncatula* at the seedling stage. Nevertheless, the Orn pathway seems to play a role in Pro accumulation in adult *M. truncatula* plants under salt stress (Verdoy et al., 2006). In the absence of Cd, the roots of p18 transgenic plantlets displayed higher expression of most genes related to Pro biosynthesis and transport *(MtP5CS1*, *MtP5CS2*, *MtP5CR,* and *MtProT*), in comparison with WT plantlets.

In addition to scavenge, stabilize and detoxify ROS, Pro accumulation might lead to an activation of the antioxidant machinery and the biosynthesis of phytochelatins (PCs) (Siripornadulsil et al., 2002; Sharma and Dietz, 2006; Szabados and Savouré, 2010; Hayat et al., 2012; Ahmad et al., 2019). The plant antioxidant machinery plays a fundamental role in Cd tolerance (Terrón-Camero et al., 2020). To maintain redox homeostasis, SOD and CAT are the first enzymes to face ROS accumulation. In addition, GSH has a dual role as an antioxidant molecule and as a substrate for phytochelatin biosynthesis (Noctor et al., 2012; Sobrino-Plata et al., 2014). NAPDH-recycling enzymes play an important role in Pro biosynthesis. In plants, NADPH is key in the antioxidant defense response (Foyer and Noctor, 2011) and Cd tolerance appears to be dependent on NADPH levels in some species (León et al., 2002; Pérez-Chaca et al., 2014). Genes codifying for NAPDH-recycling enzymes have been proposed to be key in the strategy to cope Cd stress in a Cd-tolerant *M. truncatula* cultivar (García de la Torre et al., 2021). Our results showed that, in the absence of Cd, the expression of *VaP5CS* promoted enhanced expression of most tested genes related to the antioxidant machinery, PC biosynthesis and NADPH-recycling in p18 transgenic roots compared to WT roots, suggesting that p18 plants possess a constitutive capacity to better counteract Cd toxicity. In transgenic shoots, though, most genes showed lower expression than in WT shoots. Upon Cd treatment, most genes showed enhanced expression in both WT roots and shoots, while only a few genes were upregulated in the transgenic plants, suggesting that the Cd treatment was stressful for WT plants and induced a transcriptomic response, while p18 plants were less affected. Increased glutathione reductase (*GR*) expression is considered as a marker of Cd stress in plants (Romero-Puertas et al., 2007; DalCorso et al., 2008; Chou et al., 2012). Interestingly, *MtGR* expression was higher in transgenic roots than in WT roots in the absence of Cd. This elevated *MtGR* expression cannot be ascribed to stress, and it is most likely a result of Pro accumulation. When Cd treatment was applied, WT plants displayed a significant increase in *MtGR* expression, indicating a response to Cd stress, while such increase was not observed in p18 roots or shoots, suggesting that the transgenic line was less stressed by the Cd treatment.

We analyzed WT and p18 plants grown in the absence or presence of Cd for 32 days. As expected, Pro content was significantly higher in roots and shoots of the transgenic line than in WT plants. Cd treatment did not induce changes in Pro contents except for a significant increase in WT shoots, which nevertheless, remained lower than that in p18 shoots. Our results on Cd contents suggest that, due to Pro accumulation, certain mechanisms are likely triggered in p18 plants that induce Cd accumulation, mainly in roots. The enhanced expression of phytochelatin synthase (*PCS*) in p18 roots could contribute to increased Cd chelation by phytochelatins and subsequent Cd storage in the vacuole (El Rasafi et al., 2020). Other genes and proteins, such as metal transporters, phytochelatin transporters and metallothioneins might also be involved (Ismael et al., 2019), but were not the object of the present study. It has been proposed that Pro may form non-toxic complexes with Cd (Rehman et al., 2017; El Rasafi et al., 2020). It is well known that Cd causes plant nutritional imbalance by impairing the uptake and transport of several nutrients (Ismael et al., 2019; Qin et al., 2020). The decreases in Fe and Mn contents in roots under Cd stress might suggest that Fe and/or Mn transporters could be involved in Cd uptake by *M. truncatula* roots (Vert et al., 2002; Sasaki et al., 2012). Phosphorus (P) and Mg are essential elements for photosynthesis. The contents of these two elements were not impaired in the shoots of p18 plants upon Cd stress, in agreement with the higher chlorophyll content in p18 plants compared to WT plants after Cd treatment.

In plants, glutathione plays a key role as an antioxidant, chelator and a signaling molecule (Jozefczak et al., 2012). Cadmium promoted an increase of the GSH/GSSG ratio in roots and shoots of WT plants, while the transgenic p18 plants remained unaltered. This result might appear unexpected, as it would suggest a better redox balance. However, an increase of GSH might be needed to activate PC biosynthesis, which is in good agreement with the increased expression of *MtGR, MtCYS, MtγECS, MtGSHS* and *MtPCS* observed in WT seedling roots

upon Cd treatment. The expression of these genes is basally higher in p18, and their expression changes are not so marked after Cd exposure.

Cadmium stress induces oxidative damage that leads to lipid peroxidation in different plant species, including *M. truncatula* (Sobrino-Plata et al., 2009; Rahoui et al., 2017; García de la Torre et al., 2021). Lipid peroxidation, SOD and CAT activities were measured in shoots and roots of WT and p18 plants. Lipid peroxidation was significantly higher after Cd stress in both genotypes. Pro accumulation seemed to have a positive effect as lipid peroxidation remained always lower in p18 than in WT plants. Moreover, MDA content observed in both organs of p18 plants subjected to Cd stress were similar to those observed in unstressed WT plants. SOD activity was slightly, but significantly lower in p18 than in WT roots in the absence of Cd, and the opposite was observed in shoots. This higher basal SOD activity in p18 shoots might provide an intrinsic advantage, as Cd promoted a significant increase of SOD activity in WT shoots reaching to levels measured in non-stressed p18 shoots. Two of the SOD genes analyzed (*MtFeSOD, MtMnSOD*) showed higher expression in p18 than in WT roots. Only *MtCuZnSODa* displayed significantly higher expression in p18 than in WT shoots, while *MtFeSOD* showed a significantly lower expression. In presence of Cd, catalase activity decreased in WT roots and increased in WT shoots, in agreement with the changes in expression observed for *MtCAT*. While catalase activity was significantly higher in p18 roots than in WT roots upon Cd exposure, CAT activities did not seem to correspond to the variations in *MtCAT* (*MTR_3g115370*) expression. Catalase activity increased in the shoots of both genotypes in the presence of Cd, most probably as a response to ROS produced by the impaired photosynthetic activity (Foyer et al., 1994; Mittler, 2002), but again the activity values did not reflect the changes in *MtCAT* expression. These differences might be due to the presence of at least another *CAT* gene in the *M. truncatula* genome (*MTR_1386s0010*), which we were not able to amplify and might display different expression patterns.

The results presented here support the hypothesis that the expression of *VaPC5S* and the consequent high Pro accumulation contribute to alleviate Cd stress in *M. truncatula* transgenic p18 line. However, this increase in tolerance is not due exclusively to Pro accumulation, but to a Pro-induced upregulation of several important genes related to Pro metabolism, PC biosynthesis, antioxidant machinery, and NADPH-recycling in the transgenic line, which in this way becomes constitutively better equipped to cope with Cd stress. Moreover, the increased accumulation of Cd in p18 roots compared to WT roots, with only a slightly higher Cd levels in p18 than in WT shoots suggest that Pro accumulation also appears to increase the plant phytostabilization capacity through rhizosequestration.

DATA AVAILABILITY STATEMENT

The raw data supporting the conclusions of this article will be made available by the authors, without undue reservation.

AUTHOR CONTRIBUTIONS

VSGT, TCP, JJP, and MML designed the project and conceived the experiments. VSGT performed the experiments. TCP contributed to the experimental part. JJP, MML, and TCP supervised the experiments and corrected and wrote the final version. VSGT wrote the first draft. All authors approved the content of the manuscript.

FUNDING

This work was supported by Comunidad de Madrid (grant S2009/AMB-151 to MML, and a contract to TCP), MINECO (grant AGL2013-40758-R to JJP and MML), AEI/FEDER-UE (grant AGL2017- 88381-R to JJP and MML), and Fundación Areces (grant to JJP). VSGT was the recipient of an FPU fellowship from the Spanish Ministry of Education. We acknowledge support of 25% of the publication fee by the CSIC Open Access Publication Support Initiative through its Unit of Information Resources for Research (URICI).

SUPPLEMENTARY MATERIAL

The Supplementary Material for this article can be found online at: https://www.frontiersin.org/articles/10.3389/fpls.2022.829069/full#supplementary-material

REFERENCES

Abdelgawad, H., De Vos, D., Zinta, G., Domagalska, M. A., Beemster, G. T. S., and Asard, H. (2015). Grassland species differentially regulate proline concentrations under future climate conditions: an integrated biochemical and modelling approach. *New Phytol.* 208, 354–369. doi: 10.1111/nph.13481

Aggarwal, M., Sharma, S., Kaur, N., Pathania, D., Bhandhari, K., Kaushal, N., et al. (2011). Exogenous proline application reduces phytotoxic effects of selenium by minimising oxidative stress and improves growth in bean (*Phaseolus vulgaris* L.) seedlings. *Biol. Trace Elem. Res.* 140, 354–367. doi: 10.1007/s12011-010-8699-9

Ahmad, J., Ali, A. A., Baig, M. A., Iqbal, M., Hag, I., and Qureshi, M. I. (2019). "Role of phytochelatins in cadmium stress tolerance in plants," in *Cadmium Toxicity and Tolerance in Plants: From Physiology to Remediation*, eds M. Hasanuzzaman, M. N. V. Prasad, and M. Fujita (Cambridge, MA: Academic Press), 185–212. doi: 10.1016/C2017-0-02050-5.99

Alvarez, M. E., Savouré, A., and Szabados, L. (2021). Proline metabolism as regulatory hub. *Trends Plant Sci.* 27, 39–55. doi: 10.1016/j.tplants.2021.07.009

Bates, L. S., Waldren, R. P., and Teare, I. D. (1973). Rapid determination of free proline for water-stress studies. *Plant Soil* 207, 205–207. doi: 10.1007/BF00018060

Ben Ahmed, C., Magdich, S., Ben Rouina, B., Sensoy, S., Boukhris, M., and Ben Abdullah, F. (2011). Exogenous proline effects on water relations and ions contents in leaves and roots of young olive. *Amino Acids* 40, 565–573. doi: 10.1007/s00726-010-0677-1

Benavides, M., Gallego, S. M., and Tormaro, M. (2005). Cadmium toxicity in plants. *Braz. J. Plant Physiol.* 17, 21–34. doi: 10.1590/S1677-04202005000100003

Chou, T. S., Chao, Y. Y., and Kao, C. H. (2012). Involvement of hydrogen peroxide in heat shock- and cadmium-induced expression of ascorbate peroxidase and glutathione reductase in leaves of rice seedlings. *J. Plant Physiol.* 169, 478–486. doi: 10.1016/j.jplph.2011.11.012

Clemens, S., Aarts, M. G. M., Thomine, S., and Verbruggen, N. (2013). Plant science: the key to preventing slow cadmium poisoning. *Trends Plant Sci.* 18, 92–99. doi: 10.1016/j.tplants.2012.08.003

Coba de la Peña, T., and Pueyo, J. J. (2012). Legumes in the reclamation of marginal soils, from cultivar and inoculant selection to transgenic approaches. *Agron. Sustain. Dev.* 32, 65–91. doi: 10.1007/s13593-011-0024-2

Cuypers, A., Plusquin, M., Remans, T., Jozefczak, M., Keunen, E., Gielen, H., et al. (2010). Cadmium stress: an oxidative challenge. *Biometals* 23, 927–940. doi: 10.1007/s10534-010-9329-x

DalCorso, G., Farinati, S., Maistri, S., and Furini, A. (2008). How plants cope with cadmium: staking all on metabolism and gene expression. *J. Integr. Plant Biol.* 50, 1268–1280. doi: 10.1111/j.1744-7909.2008.00737.x

Delauney, A., and Verma, S. (1993). Proline biosynthesis and osmoregulation in plants. *Plant J.* 4, 215–223. doi: 10.1046/j.1365-313X.1993.04020215.x

Delauney, A. J., Hu, C. A., Kishor, P. B. K., and Verma, D. P. S. (1993). Cloning of ornithine delta- aminotransferase cDNA from *Vigna aconitifolia* by trans-complementation in *Escherichia coli* and regulation of proline biosynthesis. *J. Biol. Chem.* 268, 18673–18678. doi: 10.1016/S0021-9258(17)46682-8

El Moukhtari, A., Cabassa-Hourton, C., Farissi, M., and Savouré, A. (2020). How does proline treatment promote salt stress tolerance during crop plant development? *Front. Plant Sci.* 11:1127. doi: 10.3389/fpls.2020.01127

El Rasafi, T., Oukarroum, A., Haddioui, A., Song, H., Kwon, E. E., Bolan, N., et al. (2020). Cadmium stress in plants: a critical review of the effects, mechanisms, and tolerance strategies. *Crit. Rev. Environ. Sci. Technol.* doi: 10.1080/10643389.2020.1835435

Foyer, C., Lelandais, M., and Kunert, K. (1994). Photooxidative stress in plants. *Physiol. Plant.* 92, 696–717. doi: 10.1111/j.1399-3054.1994.tb03042.x

Foyer, C. H., and Noctor, G. (2011). Ascorbate and glutathione: the heart of the redox Hub. *Plant Physiol.* 155, 2–18. doi: 10.1104/pp.110.167569

Funck, D., Baumgarten, L., Stift, M., von Wirén, N., and Schönemann, L. (2020). Differential contribution of P5CS isoforms to stress tolerance in *Arabidopsis*. *Front. Plant Sci.* 11:565134. doi: 10.3389/fpls.2020.565134

Funck, D., Stadelhofer, B., and Koch, W. (2008). Ornithine-δ-aminotransferase is essential for arginine catabolism but not for proline biosynthesis. *BMC Plant Biol.* 8:40. doi: 10.1186/1471-2229-8-40

García de la Torre, V. S., Coba de la Peña, T., Lucas, M. M., and Pueyo, J. J. (2013). Rapid screening of *Medicago truncatula* germplasm for mercury tolerance at the seedling stage. *Environ. Exp. Bot.* 91, 90–96. doi: 10.1016/j.envexpbot.2013.03.004

García de la Torre, V. S., Coba de la Peña, T., Pueyo, J. J., and Lucas, M. M. (2021). Cadmium-tolerant and -sensitive cultivars identified by screening of *Medicago truncatula* germplasm display contrasting responses to cadmium stress. *Front. Plant Sci.* 12:595001. doi: 10.3389/fpls.2021.595001

Ghanti, S. K. K., Sujata, K. G., Kumar, B. M. V., Karba, N. N., Reddy, K. J., Rao, K. J., et al. (2011). Heterologous expression of *P5CS* gene in chickpea enhances salt tolerance without affecting yield. *Biol. Plant.* 55:634. doi: 10.1007/s10535-011-0161-0

Guerzoni, J. T. S., Belintani, N. G., Moreira, R. M. P., Hoshino, A. A., Domingues, D. S., Filho, J. C. B., et al. (2014). Stress-induced Δ^1-pyrroline-5-carboxylate synthetase (*P5CS*) gene confers tolerance to salt stress in transgenic sugarcane. *Acta Physiol. Plant.* 36, 2309–2319. doi: 10.1007/s11738-014-1579-8

Hayat, S., Hayat, Q., Alyemeni, M. N., Wani, A. S., Pichtel, J., and Ahmad, A. (2012). Role of proline under changing environments: a review. *Plant Signal. Behav.* 7, 1456–1466. doi: 10.4161/psb.21949

Hoque, M. A., Banu, M. N. A., Nakamura, Y., Shimoishi, Y., and Murata, Y. (2008). Proline and glycinebetaine enhance antioxidant defense and methylglyoxal detoxification systems and reduce NaCl-induced damage in cultured tobacco cells. *J. Plant Physiol.* 165, 813–824. doi: 10.1016/j.jplph.2007.07.013

Hossain, M. A., Burritt, D. J., and Fujita, M. (2015). "Proline and glycine betaine modulate cadmium-induced oxidative stress tolerance in plants," in *Plant Environment Interaction: Responses and Approaches to Mitigate Stress*, eds M. M. Azooz and A. A. Parvaiz (Chichester: John Wiley & Sons), 97–123. doi: 10.1002/9781119081005.ch6

Ismael, M. A., Elyamine, A. M., Moussa, M. G., Cai, M., Zhao, X., and Hu, C. (2019). Cadmium in plants: uptake, toxicity, and its interactions with selenium fertilizers. *Metallomics* 11, 255–277. doi: 10.1039/c8mt00247a

Jozefczak, M., Remans, T., Vangronsveld, J., and Cuypers, A. (2012). Glutathione is a key player in metal-induced oxidative stress defenses. *Int. J. Mol. Sci.* 13, 3145–3175. doi: 10.3390/ijms13033145

Kumar, V., Shriram, V., Hossain, M. A., and Kishor, P. K. (2015). "Engineering proline metabolism for enhanced plant salt stress tolerance," in *Managing Salt Tolerance in Plants: Molecular and Genomic Perspectives*, eds S. H. Wani and M. A. Hussain (Oakville, ON: Apple Academic Press), 349–368. doi: 10.1201/b19246-20

Kumar, V., Shriram, V., Kishor, P. B. K., Jawali, N., and Shitole, M. G. (2010). Enhanced proline accumulation and salt stress tolerance of transgenic indica rice by over-expressing P5CSF129A gene. *Plant Biotechnol. Rep.* 4, 37–48. doi: 10.1007/s11816-009-0118-3

Lei, P., Xu, Z., Liang, J., Luo, X., Zhang, Y., Feng, X., et al. (2016). Poly(γ-glutamic acid) enhanced tolerance to salt stress by promoting proline accumulation in *Brassica napus* L. *Plant Growth Regul.* 78, 233–241. doi: 10.1007/s10725-015-0088-0

León, A., Palma, J., Corpas, F., Gomez, M., Romero-Puertas, M., Chatterjee, D., et al. (2002). Antioxidative enzymes in cultivars of pepper plants with different sensitivity to cadmium. *Plant Physiol. Biochem.* 40, 813–820. doi: 10.1016/S0981-9428(02)01444-4

Mansour, M. M. F., and Ali, E. F. (2017). Evaluation of proline functions in saline conditions. *Phytochemistry* 140, 52–68. doi: 10.1016/j.phytochem.2017.04.016

Marino, D., Damiani, I., Gucciardo, S., Mijangos, I., Pauly, N., and Puppo, A. (2013). Inhibition of nitrogen fixation in symbiotic *Medicago truncatula* upon Cd exposure is a local process involving leghaemoglobin. *J. Exp. Bot.* 64, 5651–5660. doi: 10.1093/jxb/ert334

Marino, D., González, E. M., Frendo, P., Puppo, A., and Arrese-Igor, C. (2007). NADPH recycling systems in oxidative stressed pea nodules: a key role for the $NADP^+$ -dependent isocitrate dehydrogenase. *Planta* 225, 413–421. doi: 10.1007/s00425-006-0354-5

Mittler, R. (2002). Oxidative stress, antioxidants and stress tolerance. *Trends Plant Sci.* 7, 405–410. doi: 10.1016/s1360-1385(02)02312-9

Noctor, G., Mhamdi, A., Chaouch, S., Han, Y., Neukermans, J., Marquez-Garcia, B., et al. (2012). Glutathione in plants: an integrated overview. *Plant Cell Environ.* 35, 454–484. doi: 10.1111/j.1365-3040.2011.02400.x

Peralta-Videa, J. R., Lopez, M. L., Narayan, M., Saupe, G., and Gardea-Torresdey, J. (2009). The biochemistry of environmental heavy metal uptake by plants: implications for the food chain. *Int. J. Biochem. Cell Biol.* 41, 1665–1677. doi: 10.1016/j.biocel.2009.03.005

Pérez-Chaca, M. V., Rodríguez-Serrano, M., Molina, A. S., Pedranzani, H. E., Zirulnik, F., Sandalio, L. M., et al. (2014). Cadmium induces two waves of reactive oxygen species in *Glycine max* (L.) roots. *Plant Cell Environ.* 37, 1672–1687. doi: 10.1111/pce.12280

Pourret, O., Bollinger, J. C., and van Hullebusch, E. D. (2020). On the difficulties of being rigorous in environmental geochemistry studies: some recommendations for designing an impactful paper. *Environ. Sci. Pollut. Res.* 27, 1267–1275. doi: 10.1007/s11356-019-06835-y

Qin, S., Liu, H., Nie, Z., Rengel, Z., Gao, W., Li, C., et al. (2020). Toxicity of cadmium and its competition with mineral nutrients for uptake by plants: a review. *Pedosphere* 30, 168–180. doi: 10.1016/S1002-0160(20)60002-9

Rahoui, S., Ben, C., Chaoui, A., Martinez, Y., Yamchi, A., Rickauer, M., et al. (2014). Oxidative injury and antioxidant genes regulation in cadmium-exposed radicles of six contrasted *Medicago truncatula* genotypes. *Environ. Sci. Pollut. Res. Int.* 21, 8070–8083. doi: 10.1007/s11356-014-2718-x

Rahoui, S., Chaoui, A., and El Ferjani, E. (2008). Differential sensitivity to cadmium in germinating seeds of three cultivars of faba bean (*Vicia faba* L.). *Acta Physiol. Plant.* 30, 451–456. doi: 10.1007/s11738-008-0142-x

Rahoui, S., Martinez, Y., Sakouhi, L., Ben, C., Rickauer, M., El Ferjani, E., et al. (2017). Cadmium-induced changes in antioxidative systems and differentiation in roots of contrasted *Medicago truncatula* lines. *Protoplasma* 254, 473–489. doi: 10.1007/s00709-016-0968-9

Razavizadeh, R., and Ehsanpour, A. A. (2009). Effects of salt stress on proline content, expression of delta-1-pyrroline-5-carboxylate synthetase, and activities of catalase and ascorbate peroxidase in transgenic tobacco plants. *Biol. Lett.* 46, 63–75. doi: 10.2478/v10120-009-0002-4

Rehman, M. Z. U., Rizwan, M., Ali, S., Ok, Y. S., Ishaque, W., Saifullah, et al. (2017). Remediation of heavy metal contaminated soils by using *Solanum nigrum*: a review. *Ecotoxicol. Environ. Saf.* 143, 236–248. doi: 10.1016/j.ecoenv.2017.05.038

Redondo, F. J., Coba de la Peña, T., Morcillo, C. N., Lucas, M. M., and Pueyo, J. J. (2009). Overexpression of flavodoxin in bacteroids induces changes in antioxidant metabolism leading to delayed senescence and starch accumulation in alfalfa root nodules. *Plant Physiol.* 149, 1166–1178. doi: 10.1104/pp.108.129601

Romero-Puertas, M. C., Corpas, F. J., Rodríguez-Serrano, M., Gómez, M., del Río, L., and Sandalio, L. M. (2007). Differential expression and regulation of antioxidative enzymes by cadmium in pea plants. *J. Plant Physiol.* 164, 1346–1357. doi: 10.1016/j.jplph.2006.06.018

Romero-Puertas, M. C., Terrón-Camero, L. C., Peláez-Vico, M. A., Olmedilla, A., and Sandalio, L. M. (2019). Reactive oxygen and nitrogen species as key indicators of plant responses to Cd stress. *Environ. Exp. Bot.* 161, 107–119. doi: 10.1016/j.envexpbot.2018.10.012

Sanità di Toppi, L., and Gabbrielli, R. (1999). Response to cadmium in higher plants. *Environ. Exp. Bot.* 41, 105–130. doi: 10.1016/S0098-8472(98)00058-6

Sasaki, A., Yamaji, N., Yokosho, K., and Ma, J. F. (2012). Nramp5 is a major transporter responsible for manganese and cadmium uptake in rice. *Plant Cell* 24, 2155–2167. doi: 10.1105/tpc.112.096925

Sawahel, W. A., and Hassan, A. H. (2002). Generation of transgenic wheat plants producing high levels of the osmoprotectant proline. *Biotechnol. Lett.* 24, 721–725. doi: 10.1023/A:1015294319114

Schat, H., Llugany, M., Vooijs, R., Hartley-Whitaker, J., and Bleeker, P. M. (2002). The role of phytochelatins in constitutive and adaptive heavy metal tolerances in hyperaccumulator and non-hyperaccumulator metallophytes. *J. Exp. Bot.* 53, 2381–2392. doi: 10.1093/jxb/erf107

Seneviratne, M., Rajakanura, N., Rizwan, M., Madawala, H. M. S. P., Ok, Y. S., and Vithanage, M. (2019). Heavy metal-induced oxidative stress on seed germination and seedling development: a critical review. *Environ. Geochem. Health* 41, 1813–1831. doi: 10.1007/s10653-017-0005-8

Sharma, S. S., and Dietz, K. J. (2006). The significance of amino acids and amino acid-derived molecules in plant responses and adaptation to heavy metal stress. *J. Exp. Bot.* 57, 711–726. doi: 10.1093/jxb/erj073

Sharma, S. S., and Dietz, K.-J. (2009). The relationship between metal toxicity and cellular redox imbalance. *Trends Plant Sci.* 14, 43–50. doi: 10.1016/j.tplants.2008.10.007

Singh, A., Sharma, M. K., and Sengar, R. S. (2017). Osmolytes: proline metabolism in plants as sensors of abiotic stress. *J. Appl. Nat. Sci.* 9, 2079–2092. doi: 10.31018/jans.v9i4.1492

Singh, M., Singh, D., and Rai, M. (2007). Assessment of growth, physiological and biochemical parameters and activities of antioxidative enzymes in salinity tolerant and sensitive Basmati rice varieties. *J. Agron. Crop Sci.* 193, 398–412. doi: 10.1111/j.1439-037X.2007.00267.x

Singh, S., Parihar, P., Singh, R., Singh, V. P., and Prasad, S. M. (2015). Heavy metal tolerance in plants: role of transcriptomics, proteomics, metabolomics and ionomics. *Front. Plant Sci.* 6:1143. doi: 10.3389/fpls.2015.01143

Siripornadulsil, S., Traina, S., Verma, P. S., and Sayre, R. T. (2002). Molecular mechanisms of proline-mediated tolerance to toxic heavy metals in transgenic microalgae. *Plant Cell* 14, 2837–2847. doi: 10.1105/tpc.004853

Sledge, M. K., Pechter, P., and Payton, M. E. (2005). Aluminum tolerance in *Medicago truncatula* germplasm. *Crop Sci.* 45, 2001–2004. doi: 10.2135/cropsci2004.0673

Sobrino-Plata, J., Meyssen, D., Cuypers, A., Escobar, C., and Hernández, L. E. (2014). Glutathione is a key antioxidant metabolite to cope with mercury and cadmium stress. *Plant Soil* 377, 369–381. doi: 10.1007/s11104-013-2006-4

Sobrino-Plata, J., Ortega-Villasante, C., Flores-Cáceres, M. L., Escobar, C., Del Campo, F. F., and Hernández, L. E. (2009). Differential alterations of antioxidant defenses as bioindicators of mercury and cadmium toxicity in alfalfa. *Chemosphere* 77, 946–954. doi: 10.1016/j.chemosphere.2009.08.007

Surekha, C., Kumari, K. N., Aruna, L. V., Suneetha, G., Arundhati, A., and Kavi Kishor, P. B. (2014). Expression of the *Vigna aconitifolia P5CSF129A* gene in transgenic pigeonpea enhances proline accumulation and salt tolerance. *Plant Cell Tissue Organ. Cult.* 116, 27–36. doi: 10.1007/s11240-013-0378-z

Szabados, L., and Savouré, A. (2010). Proline: a multifunctional amino acid. *Trends Plant Sci.* 15, 89–97. doi: 10.1016/j.tplants.2009.11.009

Terrón-Camero, L. C., del Val, C., Sandalio, L. M., and Romero-Puertas, M. C. (2020). Low endogenous NO levels in roots and antioxidant systems are determinants for the resistance of *Arabidopsis* seedlings grown in Cd. *Environ. Pollut.* 256, 113411. doi: 10.1016/j.envpol.2019.113411

Verdoy, D., Coba de la Peña, T., Redondo, F. J., Lucas, M. M., and Pueyo, J. J. (2006). Transgenic *Medicago truncatula* plants that accumulate proline display nitrogen-fixing activity with enhanced tolerance to osmotic stress. *Plant Cell Environ.* 29, 1913–1923. doi: 10.1111/j.1365-3040.2006.01567.x

Vert, G., Grotz, N., Dédaldéchamp, F., Gaymard, F., Guerinot, M. L., Briat, J.-F., et al. (2002). IRT1, an *Arabidopsis* transporter essential for iron uptake from the soil and for plant growth. *Plant Cell* 14, 1223–1233. doi: 10.1105/tpc.001388

Zhen, W. B., and Ma, Q. H. (2009). Proline metabolism in response to salt stress in common reed [*Phragmites australis* (Cav.) Trin. ex Steud]. *Bot. Mar.* 52, 341–347. doi: 10.1515/BOT.2009.007

Conflict of Interest: The authors declare that the research was conducted in the absence of any commercial or financial relationships that could be construed as a potential conflict of interest.

Publisher's Note: All claims expressed in this article are solely those of the authors and do not necessarily represent those of their affiliated organizations, or those of the publisher, the editors and the reviewers. Any product that may be evaluated in this article, or claim that may be made by its manufacturer, is not guaranteed or endorsed by the publisher.

Copyright © 2022 García de la Torre, Coba de la Peña, Lucas and Pueyo. This is an open-access article distributed under the terms of the Creative Commons Attribution License (CC BY). The use, distribution or reproduction in other forums is permitted, provided the original author(s) and the copyright owner(s) are credited and that the original publication in this journal is cited, in accordance with accepted academic practice. No use, distribution or reproduction is permitted which does not comply with these terms.

frontiers in Plant Science

ORIGINAL RESEARCH
published: 27 January 2022
doi: 10.3389/fpls.2021.809183

Exogenous Application of Salicylic Acid and Hydrogen Peroxide Ameliorate Cadmium Stress in Milk Thistle by Enhancing Morpho-Physiological Attributes Grown at Two Different Altitudes

Mereen Nizar[1], Kanval Shaukat[1,2], Noreen Zahra[2], Muhammad Bilal Hafeez[3], Ali Raza[4]*, Abdul Samad[1], Qasim Ali[5], Manzer H. Siddiqui[6] and Hayssam M. Ali[6]*

[1] Department of Botany, University of Balochistan, Quetta, Pakistan, [2] Department of Botany, University of Agriculture, Faisalabad, Pakistan, [3] Department of Agronomy, University of Agriculture, Faisalabad, Pakistan, [4] Key Laboratory of Ministry of Education for Genetics, Breeding and Multiple Utilization of Crops, Center of Legume Crop Genetics and Systems Biology/College of Agriculture, Oil Crops Research Institute, Fujian Agriculture and Forestry University (FAFU), Fuzhou, China, [5] Institute of Food and Agriculture Sciences, University of Florida, Gainesville, FL, United States, [6] Department of Botany and Microbiology, College of Science, King Saud University, Riyadh, Saudi Arabia

OPEN ACCESS

Edited by:
Mohammad Anwar Hossain, Bangladesh Agricultural University, Bangladesh

Reviewed by:
Mohammad Irfan, Cornell University, United States
Sadettin Çelik, Bingöl University, Turkey

***Correspondence:**
Kanval Shaukat
kanval_shaukat777@yahoo.com
Ali Raza
alirazamughal143@gmail.com

Specialty section:
This article was submitted to Plant Breeding, a section of the journal Frontiers in Plant Science

Received: *04 November 2021*
Accepted: *08 December 2021*
Published: *27 January 2022*

Citation:
Nizar M, Shaukat K, Zahra N, Hafeez MB, Raza A, Samad A, Ali Q, Siddiqui MH and Ali HM (2022) Exogenous Application of Salicylic Acid and Hydrogen Peroxide Ameliorate Cadmium Stress in Milk Thistle by Enhancing Morpho-Physiological Attributes Grown at Two Different Altitudes. Front. Plant Sci. 12:809183. doi: 10.3389/fpls.2021.809183

Cadmium (Cd^{+2}) is a potential and widespread toxic environmental pollutant, mainly derived from a rapid industrial process that has inhibitory effects on growth, physiological, and biochemical attributes of various plant species, including medicinal plants such as *Silybum marianum* L. Gaertn commonly known as milk thistle. Plant signaling molecules, when applied exogenously, help to enhance/activate endogenous biosynthesis of potentially important signaling molecules and antioxidants that boost tolerance against various abiotic stresses, e.g., heavy metal stress. The present study documented the protective role of salicylic acid (SA;0.25 μM) and hydrogen peroxide (H_2O_2; 10 μM) priming, foliar spray, and combinational treatments in reducing Cd^{+2} toxicity (500 μM) in milk thistle grown at two diverse ecological zones of Balochistan Province of Pakistan i.e., Quetta (Qta) and Turbat (Tbt). The morpho-physiological and biochemical attributes of milk thistle were significantly affected by Cd^{+2} toxicity; however, priming and foliar spray of SA and H_2O_2 significantly improved the growth attributes (root/shoot length, leaf area, and root/shoot fresh and dry weight), photosynthetic pigments (Chl *a*, *b*, and carotenoids) and secondary metabolites (Anthocyanin, Soluble phenolics, and Tannins) at both altitudes by suppressing the negative impact of Cd^{+2}. However, the oxidative damage parameters, i.e., MDA and H_2O_2, decreased astonishingly under the treatment of signaling molecules, thereby protecting membrane integrity under Cd^{+2} stress. The morphological variations were profound at the low altitude (Tbt) as compared to the high altitude (Qta). Interestingly,

the physiological and biochemical attributes at both altitudes improved under SA and H_2O_2 treatments, thus hampered the toxic effect of Cd^{+2}. These signaling compounds enhanced tolerance of plants under heavy metal stress conditions with the consideration of altitudinal, and ambient temperature variations remain to be the key concerns.

Keywords: cadmium stress, oxidative damage, chlorophyll, milk thistle, high altitude

INTRODUCTION

Milk thistle (*Silybum marianum* L. Gaertn) is a medicinal weed belonging to the Asteraceae family. It grows well at an altitude of 1,800–2,400 m a.s.l in sandy or rocky soil. The optimum temperature for germination of milk thistle seeds ranges between 28 and 29°C. The density of plants reaches up to 4.5 plant/m^2 (Karkanis et al., 2011; Heidari et al., 2014). Medicinal plants are of very high significance because they provide the community with health care and prevention from diseases. A rapid increase in the population and pharmaceutical industry needs medicinally important plants with active ingredients to enhance and promote their cultivation and production (Valková et al., 2021; Zahra et al., 2021c). Compounds of pharmaceutical properties are derived from milk thistle fruits, i.e., achenes. Seed and dry pericarp accumulate a large flavonolignans group called silymarin, being the precursor taxifolin (Bijak, 2017).

The environmental contamination to heavy metals and other pollutants hailing from the **eighteenth** century (Andrade et al., 2014) in which cadmium (Cd^{+2}) is the most toxic heavy metal for the living biota (Raza et al., 2020). Heavy metals toxicity has been widely recognized (Raza et al., 2021a, 2022; Salehi et al., 2021; Zahra et al., 2021a). Cd^{+2} is a non-degradable trace metal contaminant, ranked seventh among the top recognized pollutants in the environment. When Cd^{+2} enters the cells of plants, it interferes and disrupts the metabolic process because of an interaction with some organic compounds within organelles of cells and the cytosol (Ali et al., 2013; Mwamba et al., 2020; Raza et al., 2020). Furthermore, it may interact with proteins and lipids that result in affecting the enzyme and fluidity of the membrane by causing oxidative damage that initiates free radical formation (Yu et al., 2018; Mwamba et al., 2020; Raza et al., 2021b, 2022). It binds to sulfhydryl groups in proteins that also replace the important metal ions metalloproteins (Raza et al., 2021c). The mountainous areas plants, in contrast to land plants, display changes in physiognomy, anatomy, and physiology. Plant characteristics can be divided into two groups with the elevation changes. The variations of recorded data confirmed the higher antioxidant activity of plant extracts, which were derived from low to high altitude (Spitaler et al., 2008).

Salicylic acid is widely used to promote the plants' growth and their development under varying favorable and unfavorable conditions of the ambient environment. SA has a crucial role in mediating the responses to the toxicity of heavy metals. Recently, it has been reported that SA ameliorates Cd^{+2} stress by improving germination and protecting membrane (Lu et al., 2018; Majumdar et al., 2020). Hydrogen peroxide (H_2O_2) is recognized as one of the main chemicals, having the properties of inducing tolerance under biotic and abiotic stress (Dikilitas et al., 2020). H_2O_2 as a signaling molecule also plays a key role within plants and acts as a messenger molecule involved in signaling, which triggers stress tolerance against different stresses of abiotic conditions. Growing milk thistle across the altitudinal gradient for exploring the tolerance potential under Cd^{+2} toxicity is a pragmatic approach to exploring the mechanisms for its tolerance and survival in diverse environmental regimes. Recently, variation in morpho-physiological attributes has been reported with different milk thistle ecotypes grown at a single ecological zone under different stresses (Zahra et al., 2021b,d). However, the information about Cd^{+2} tolerance of milk thistle under priming and foliar of H_2O_2 and SA, grown at the diverse ecological zones, is still lacking. The data on morpho-physiological attributes of milk thistle grew at varying altitudes under Cd^{+2} stress are not reported from Balochistan, Pakistan. In the present study, an effort has been made to explore the tolerance potential of milk thistle to Cd^{+2} stress under priming and foliar treatments of H_2O_2 and SA grown at the Quetta and Turbat area of Balochistan, Pakistan.

MATERIALS AND METHODS

Experimental Detail

A study was planned to explore/evaluate the role of H_2O_2 and SA in alleviating cadmium toxicity in milk thistle that was grown across the altitudinal gradient, i.e., at Quetta (1,679 m) and Turbat (129 m). Both areas have diverse environmental regimes with varying maximum and minimum temperatures around the year (**Figure 1**). A Randomized Complete Block Design (RCBD) experiment was designed in which the field was divided into two major plots: control and cadmium (500 μM). Each plot further contained ten treatments with three replicates. The experimental plot was 57 × 12 feet (each plot, i.e., control and cadmium) at both experimental sites. Here, control treatment means no foliar and no priming treatment in both cadmium treated and untreated plants/control plants). Prior to the sowing of seeds, the soil of both experimental sites was analyzed for its physio-chemical properties (**Table 1**). Seeds were sown at 1-inch depth, row to row, and plant-to-plant distance was 1 ft.

Priming and Foliar Spray

Seeds of milk thistle were collected from Balochistan Agriculture Research and Development Centre (BARDC), Quetta for experiment. The seeds of milk thistle were primed in concentrations of 0.25 μM salicylic acid (SA), 10-μM hydrogen peroxide (H_2O_2), and with distilled water (H_2O) for 8 h, and

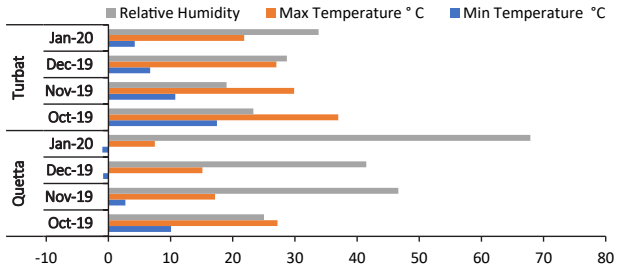


FIGURE 1 | Average monthly maximum, minimum temperature, and relative humidity during the experiment period October 2019–January 2020.

then seeds were sown in the field. After 15 days of germination, Cd^{+2} was applied at both altitude fields with a concentration of 500 μM. These concentrations were selected based on our preliminary trial (data not shown); thus, one suitable level was selected for the present study. In the field of cadmium, a black sheet was placed at 5-foot depth in order to avoid its leaching. After 15 days of cadmium treatment, plants were foliarly treated using the same level of SA, H_2O_2 treatment as used for priming (P). Moreover, after 15 days of foliar spray (FS), the milk thistle plants were harvested from both experimental sites, and data were recorded for various morpho-physiological attributes.

Determination of Growth Attributes

Root and shoot length (cm), number of leaves, leaf area (cm^2), root and shoot fresh (g), along with dry weight (g), were determined. Three plant samples were randomly collected for measuring root and shoot length by using a scale, and the number of total leaves/per plant was counted. Plants were harvested carefully. Before harvest, the field was fully watered to make safe and easy removal of roots from soil without any mechanical damage. The area of the leaf was calculated by following an equation developed by Cain and Castro (1959) by using the given formula, A 1/4.75 × L × W. The L described the length of the leaf, while W showed the width of the leaf, and 0.75 was being utilized for the correction factor that was used for conservation of the leaf length and width rectangular product into the area of the leaf. Lastly, three roots and shoots were separately weighted to determine the fresh weight (FW) and placed in an oven (65–75°C, 72 h) to obtain dry weight (DW).

Physiological Analysis

Photosynthetic Pigment Analysis

Leaf samples (0.1 g) were extracted with acetone (80%). The absorbance was recorded at 663 nm, 645 nm and 480 nm against 80% acetone (Arnon, 1949; Kirk and Allen, 1965). Chlorophyll *a*, *b*, and carotenoids contents were measured using the following formulas:

$$\text{Chlorophyll } a \text{ (mg/g fresh wt.)} = (1.27\,(OD663) - 2.69\,(OD645) \times V/1000 \times W$$

$$\text{Chlorophyll } b \text{ (mg/g fresh wt.)} = (22.9\,(OD645) - 4.68\,(OD663) \times V/1000 \times W$$

$$\text{Carotenoids (mg/g fresh wt.)} = (OD480 + 0.114\,(OD663) - 0.638\,(OD645)/2500) \times 1000$$

Determination of Anthocyanins

For anthocyanins contents determination, 0.1 g of plant sample was taken and extracted in 1–2-ml acidified methanol. The samples were placed in a water bath at 50°C for 1 h. The absorbance was measured at 535 nm by an spectrophotometer using acidified methanol as blank (Strack and Wray, 1989).

Soluble Phenolic

Soluble phenolic was determined by taking 0.1 g of a plant sample by grinding in 1–2 ml of 80% acetone. In the test tube, 1 ml of distilled water was added in 100 μL of the sample, followed by the addition of 0.5 ml folin phenol reagent, and then 2.5 ml of 20% Na_2CO_3 (sodium carbonate) was added. The absorbance at 745 nm was measured using 80% acetone as blank (Julkunen-Tiitto, 1985).

Tannins

A sample (root and shoot) was taken and added 2 ml of diethyl ether and left overnight, and then decanted the solution, and 1 ml of 70% acetone was added and kept overnight. From each sample, 50 μL of the extract was taken in each test tube, and the volume was made up to 1 ml with distilled water. After dilution, 0.5 ml of folin phenol reagent was added vortexed, and then added 2.5 ml of 20% Na_2CO_3 solution mixed very well and kept for 40 min at

TABLE 1 | Physio-chemical analysis of the soil of experimental sites.

Region	Exchangeable potassium	Available phosphorus	Total nitrogen	Cadmium	Organic matter	pH	Electrical conductivity
	(mg/kg)	(mg/kg)	(mg/kg)	(mg/kg)	%		(dS/m)
Quetta	241	4.9	0.275	0.36	0.502	8.05	1.52
Turbat	197	4.1	0.165	0.31	0.195	7.84	9.08
References	Bremner and Mulvaney, 1982	Olsen et al., 1954	Richards, 1954	Lindsay and Norvell, 1978	Walkley and Black, 1934	McLean, 1983	Rhoades, 1982

room temperature. The absorbance was recorded at 725 nm using 70% acetone as a blank.

Hydrogen Peroxide (H_2O_2)

Fresh plant samples (0.1 g) were grinded in 2 ml of 0.1% (w/v) trichloroacetic acid (TCA) under pre-chilled conditions by crushing the tissues (placed on ice bath). The homogenized material was then centrifuged at 12,000 rpm for 15 min. The supernatant (0.5 ml) was mixed with 0.5 ml of a potassium phosphate buffer (pH 7.0), and 1 ml of potassium iodide solution, thoroughly mixed, and absorbance was recorded at 390 nm. Distilled water was used as a blank (Velikova et al., 2000).

Malondialdehyde

Malondialdehyde (MDA) was determined by the method developed by Heath and Packer (1968). A plant sample (0.1 g) of plant fresh material was grinded in 1 ml of (1% w/v) TCA and centrifuged at 12,000 rpm for 15 min. About 1 ml of supernatant was taken and mixed with 1 ml of 0.5% thiobarbituric acid in 20% TCA [0.5% in 20% (w/v) TCA] and kept in a water bath preheated at 95°C for 50 min. The sample extract was cooled in an ice bath. Absorbance was measured at 532 nm and 600 nm. For comparison, 1% TCA was used as a blank. MDA contents were calculated using their absorption coefficient of 155,000 nmol/mol as:

$$\mathrm{MDA[nmolml^{-1}} = (\mathrm{A532} - \mathrm{A600})/155,000]10^6$$

Statistical Analysis

The recorded data from each parameter were analyzed statistically using "STATISTIX 8.1." The graphs and mean standard deviation were calculated using MS. EXCEL.

RESULTS

Morphological Parameters

Root Length

Results were obtained for the root length of milk thistle grown at two different altitudes (Qta and Tbt), under Cd^{+2}, toxicity (500 μM) showed statistically significant results (**Figure 2B**) ($p < 0.05$). Results revealed that treatment of SA priming + foliar spray (P + FS) under control at high-altitude Qta was best, while the treatment of salicylic acid FS under control was the least effective. However, the priming and foliar spray helped to reduce the impact of Cd^{+2} toxicity in milk thistle grown at Qta and Tbt (**Figure 2B**).

The trend of root length at Qta was SA P + FS control > H_2O priming control > H_2O_2 P + FS control > H_2O_2 P + FS control > H_2O P + FS Cd^{+2} > H_2O_2 priming control > H_2O_2 spray control > H_2O_2 P + FS Cd^{+2} > H_2O_2 spray Cd^{+2} > Control of Control > SA P + FS Cd^{+2} > SA spray Cd^{+2} > Control Cd^{+2} > H_2O spray control > SA priming control > H_2O spray Cd^{+2} > SA priming Cd^{+2} > H_2O P + FS Cd^{+2} > SA spray control.

Considering Tbt, the trend observed for root length was as follows: H_2O_2 spray control > SA P + FS control > SA spray control > H_2O priming control > H_2O P + FS control > H_2O priming Cd^{+2} > H_2O_2 P + FS Cd^{+2} > H_2O_2 spray control > SA priming Cd^{+2} > SA priming control > H_2O_2 priming control > H_2O P + FS Cd^{+2} > SA P + FS Cd^{+2} > H_2O_2P + FS Cd^{+2} > H_2O_2 priming Cd^{+2} > H_2O_2 spray Cd^{+2} > SA spray Cd^{+2} > Control of Control > H_2O spray Cd^{+2} > control Cd^{+2} (Control; no foliar no priming treatment in both cadmium-treated and -untreated plants/control plants).

In a nutshell, the root length of milk thistle at both altitudes affected under Cd^{+2} toxicity; however, the priming and foliar application of Hydrogen peroxide (H_2O_2) and salicylic acid (SA) helped significantly to reduce the impacts of Cd^{+2} toxicity in milk thistle (**Figure 2B**).

Shoot Length

Data recorded for shoot length of milk thistle grown at two different altitudes (Qta and Tbt) under Cd^{+2} toxicity (500 μM) reported statistically significant results ($p < 0.05$) in which H_2O_2 P + FS treatment at high-altitude Qta under control conditions produced plants with greater shoot length while minimum shoot length was observed in SA P + FS of Qta under Cd^{+2} stress. Milk thistle at low altitude (Tbt) had healthy plants as compared to Qta, which demonstrated that the temperature of Tbt supported enhancing the growth of plants' ambient conditions (**Figure 2A**).

The order of improvement at Qta was observed as H_2O_2 P + FS control > SA P + FS control > Control of Control > H_2O_2 priming control > H_2O P + FS control > control Cd^{+2} > H_2O priming control > H_2O_2 priming Cd^{+2} > SA priming control > H_2O P + FS Cd^{+2} H_2O_2 P + FS Cd^{+2} > SA spray Cd^{+2} > SA priming Cd^{+2} > H_2O priming Cd^{+2} > H_2O spray Cd^{+2} > SA spray control > SA P + FS Cd^{+2}.

However, the order for growth in Tbt was H_2O_2 P + FS control > SA spray control > H_2O P + FS control > H_2O priming control > SA P + FS control > Control of Control > SA priming control > H_2O_2 spray control > H_2O spray control > H_2O_2 priming control > H_2O_2 priming Cd^{+2} > H_2O spray Cd^{+2} > control Cd^{+2} > H_2O priming Cd^{+2} > SA priming Cd^{+2} > SA P + FSCd^{+2} > H_2O P + FS Cd^{+2} > SA spray Cd^{+2} > H_2O_2 Cd^{+2} > H_2O_2 P + FS Cd^{+2}.

Overall, it has been observed that the priming and foliar spray with SA and H_2O_2 decreased the toxic effects of Cd^{+2} in milk thistle. However, in control conditions, both plant signaling molecules helped to significantly enhance the shoot length (**Figure 2A**).

Number of Leaves

Results obtained for the number of leaves of milk thistle plants grown at both the altitudes of Qta along with Tbt under the concentration of 500-μM Cd^{+2} stress displayed highly significant ($p < 0.05$) data (**Figure 3D**). Data for leaves count from respective treatment revealed that the highest number of leaves was recorded from H_2O P + FS under control conditions at low-altitude Tbt, while the less number of leaves counted from SA spray under control of Qta (**Figure 3D**).

In Qta, the order was observed as SA P + FS control > H_2O_2 P + FS control > H_2O priming control > H_2O P + FS control > Control of Control > SA priming control > SA spray Cd^{+2} > H_2O_2 spray control > H_2O_2 priming control > H_2O_2 spray Cd^{+2} > SA P + FS Cd^{+2} > H_2O_2 priming Cd^{+2} > H_2O

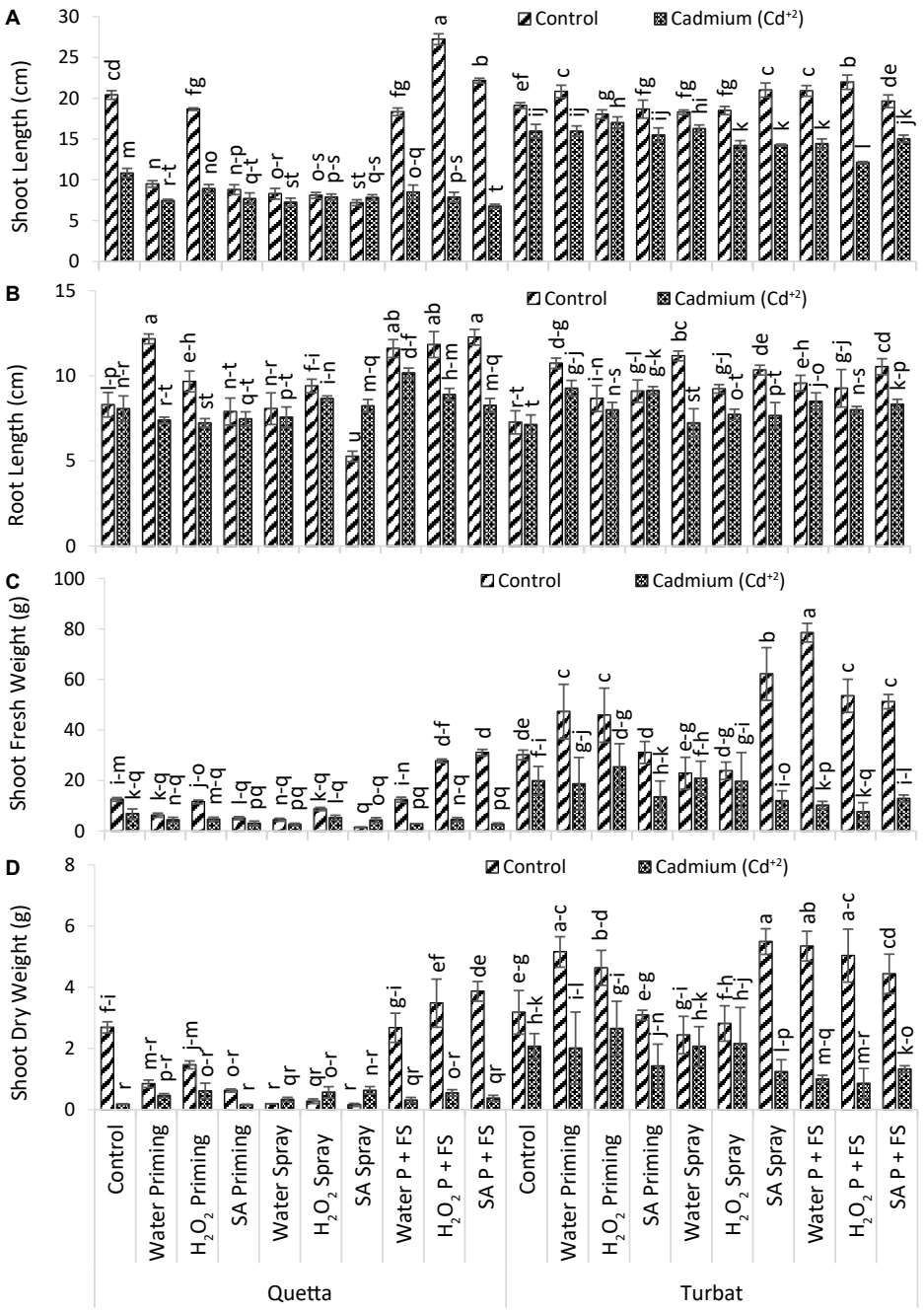


FIGURE 2 | Growth parameters; shoot length **(A)**, root length **(B)**, shoot fresh weight **(C)**, shoot dry weight **(D)** of milk thistle as affected by SA and H_2O_2 treatment grown at Quetta and Turbat under cadmium stress. The same letters on graphs represent statistically similar effect ($p < 0.05$).

spray Cd^{+2} > H_2O_2 P + FS Cd^{+2} > control Cd^{+2} > H_2O spray control > H_2O P + FS Cd^{+2} > SA priming Cd^{+2} > H_2O priming Cd^{+2} > SA spray control.

While the order of treatments at Tbt was denoted as H_2O P + FS control > H_2O priming control > H_2O_2 P + FS control > SA P + FS control > SA spray control > H_2O_2 priming control > H_2O_2 spray control > H_2O spray control > H_2O_2 spray Cd^{+2} > Control of Control > SA priming control > control Cd^{+2} > H_2O_2 priming Cd^{+2} > H_2O priming Cd^{+2} > SA spray Cd^{+2} > H_2O spray Cd^{+2} > SA P + FS Cd^{+2} > H_2O P + FS Cd^{+2} > SA priming Cd^{+2} > H_2O_2 P + FS Cd^{+2}.

Considering the total number of leaves among the treatments of both altitudes, it has been observed that, under control conditions, milk thistle was reported to have flourished well as compared to Cd^{+2} stress, while H_2O_2 and SA

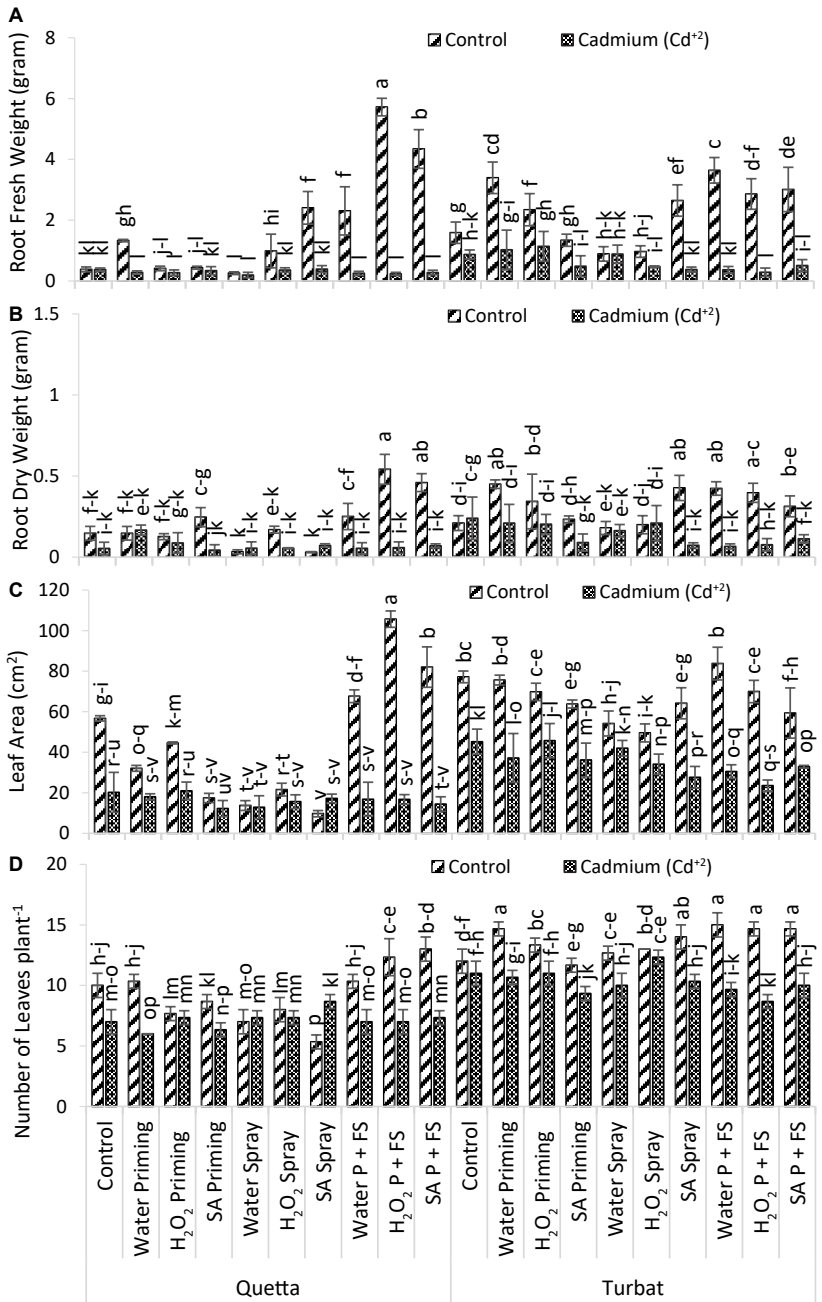


FIGURE 3 | Growth parameters; root fresh weight **(A)**, root dry weight **(B)**, leaf area **(C)**, no of leaves plant^{-1} **(D)** of milk thistle as affected by SA and H_2O_2 treatment grown at Quetta and Turbat under cadmium stress. The same letters on graphs represent statistically similar effect ($p < 0.05$).

priming with foliar spray decreased the impact of Cd^{+2} toxicity (**Figure 3D**).

Leaf Area

Data recorded for leaf area of milk thistle grew at two different altitudes (Qta and Tbt) under 500-μM Cd^{+2} concentration reported significant ($p < 0.05$) results statistically (**Figure 3C**). Results for the leaf area revealed that the greater leaf area was recorded from H_2O_2 P + FS of control at high-altitude Qta, while the lowest was observed for SA spray of control under same-altitude Qta (**Figure 3C**).

The order of leaf area improvement at Qta was observed as H_2O_2 P + FS > SA P + FS > H_2O P + FS > Control of Control > H_2O_2 priming control > H_2O_2 spray control > H_2O_2 priming Cd^{+2} > Control Cd^{+2} > H_2O priming Cd^{+2} > SA priming control > SA spray Cd^{+2} > H_2O P + FS Cd^{+2} > H_2O_2 P + FS Cd^{+2} > H_2O_2 spray Cd^{+2} > SA P + FS

Cd^{+2} > H_2O spray control > H_2O spray Cd^{+2} > SA priming Cd^{+2} > SA spray control.

While order of improvement at Tbt was much better as compared to Qta that is as follows: H_2O P + FS control > Control of Control > H_2O priming control > H_2O_2 P + FS control > H_2O_2 priming control > SA spray control > SA priming control > SA P + FS control > H_2O spray control > SA spray control > H_2O_2 priming Cd^{+2} > Control Cd^{+2} > H_2O spray Cd^{+2} > H_2O priming Cd^{+2} > SA priming Cd^{+2} > H_2O_2 spray Cd^{+2} > SA P + FS Cd^{+2} > H_2O P + FS Cd^{+2} > SA spray Cd^{+2} > H_2O_2 P + FS Cd^{+2}.

Considering the leaf area of both altitudinal fields, results favor a considerable enhancement of the leaf area at Tbt under control as compared to Qta plants. It is also recorded that H_2O_2 and SA priming + foliar spray hampered the impact of Cd^{+2} toxicity much better at low-altitudinal field Tbt as compared to Qta (**Figure 3C**).

Root Fresh Weight

Data obtained for root fresh weight of milk thistle comprising at both altitudinal fields, i.e., Qta and Tbt under Cd^{+2} stress reported significant results statistically ($p < 0.05$) described in **Figure 3A**. Results indicated that maximum root fresh weight was observed in H_2O_2 P + FS treatment under control at high-altitude Qta. However, the minimum weight was recorded from H_2O spray under Cd^{+2} stress at the same altitude (**Figure 3A**).

The order of improvement of Qta was observed as H_2O_2 P + FS control > SA P + FS control > SA spray control > H_2O P + FS control > H_2O priming control > H_2O_2 spray control > SA priming control > H_2O_2 priming control > SA spray Cd^{+2} > Control of Control > Control Cd^{+2} > SA priming Cd^{+2} > H_2O_2 spray Cd^{+2} > H_2O priming Cd^{+2} > SA P + FS Cd^{+2} > H_2O_2 priming Cd^{+2} > H_2O_2 spray Cd^{+2} > H_2O P + FS Cd^{+2} > H_2O_2 P + FS Cd^{+2} > H_2O spray Cd^{+2}.

While, under low-altitude Tbt, the order of treatment was H_2O P + FS control > H_2O priming control > SA P + FS control > H_2O_2 P + FS control > SA spray control > H_2O_2 priming control > Control of Control > SA priming control > H_2O_2 priming Cd^{+2} > H_2O priming Cd^{+2} > H_2O_2 spray control > H_2O spray control > H_2O_2 spray Cd^{+2} > Control Cd^{+2} > SA P + FS Cd^{+2} > SA priming Cd^{+2} > H_2O_2 spray Cd^{+2} > SA spray Cd^{+2} > H_2OP + FS Cd^{+2} > H_2O_2 P + FS Cd^{+2}.

Concludingly, data revealed that, under Qta control, there was the maximum fresh weight of the root in contrast with Tbt control. However, considering Cd^{+2}, the root fresh weight of Tbt resulted in having much improvement as compared to Cd^{+2} at Qta (**Figure 3A**). Overall results indicate a minimum root fresh weight, among which H_2O_2 and SA were quite effective in enhancing the root fresh weight of milk thistle to a very significant extent at both the altitudes (**Figure 3A**).

Shoot Fresh Weight

Data recorded for shoot fresh weight of milk thistle grown at two different altitudes (Qta and Tbt) statistically reported significant ($p < 0.05$) results (**Figure 2C**). Results revealed that H_2O P + FS under control of area Tbt showed greater shoot fresh weight, while the lower shoot fresh weight was observed in SA spray under control at Qta (**Figure 2C**).

The order of shoot fresh weight at Qta was recorded as SA P + FS control > H_2O_2 P + FS control > Control of Control > H_2O P + FS control > H_2O_2 priming control > H_2O_2 spray control > Control Cd^{+2} > H_2O priming control > H_2O_2 spray Cd^{+2} > SA priming control > H_2O_2 priming Cd^{+2} > H_2O_2 P + FS Cd^{+2} > H_2O priming Cd^{+2} > H_2O spray control > SA spray Cd^{+2} > SA priming Cd^{+2} > H_2O P + FS Cd^{+2} > SA P + FS Cd^{+2} > H_2O spray Cd^{+2} > SA spray control.

While, at low-altitude Tbt, the order of improvement reported was H_2O P + FS control > SA spray control > H_2O_2 P + FS control > SA P + FS control > H_2O priming control > H_2O_2 priming control > SA priming control > Control of Control > H_2O_2 priming Cd^{+2} > H_2O_2 spray control > H_2O spray control > H_2O spray Cd^{+2} > Control Cd^{+2} > H_2O_2 spray Cd^{+2} > H_2O priming Cd^{+2} > SA priming Cd^{+2} > SA P + FS Cd^{+2} > SA spray Cd^{+2} > H_2O P + FS Cd^{+2} > H_2O_2 P + FS Cd^{+2}.

In a nutshell, the observed data for shoot fresh weight revealed that the low-altitudinal field Tbt reported highly significant variations under control and Cd^{+2} toxicity in contrast with Qta. On the other hand, the application of SA along with H_2O_2 helped to suppress Cd^{+2} stress and enhance shoot fresh weight of milk thistle grown at Tbt, which describes a very healthy and effective growth of milk thistle at low altitude (**Figure 2C**).

Root Dry Weight

Results obtained for root dry weight of milk thistle grown at two varying altitudes (Qta and Tbt) under Cd^{+2} toxicity reported statistically significant results ($p < 0.05$) by revealing that the highest value for root dry weight was observed in H_2O_2 P + FS under control at Qta, while the minimum root dry weight was obtained from SA spray in control at Qta (**Figure 3B**).

At Qta, the order of treatment was H_2O_2 P + FS control > SA P + FS control > H_2O P + FS control > SA priming control > H_2O_2 spray control > H_2O priming Cd^{+2} > H_2O priming control > Control of Control > H_2O_2 priming control > H_2O_2 priming Cd^{+2} > SA spray Cd^{+2} > SA P + FS Cd^{+2} > H_2O_2 P + FS Cd^{+2} > H_2O spray Cd^{+2} > H_2O_2 spray Cd^{+2} > H_2O P + FS Cd^{+2} > Control Cd^{+2} > SA priming Cd^{+2} > H_2O spray control > SA spray control.

While, at Tbt, the trend observed for root dry weight was as follows: H_2O priming control > SA spray control > H_2O P + FS control > H_2O_2 P + FS control > H_2O_2 priming control > SA P + FS control > Control Cd^{+2} > SA priming control > H_2O priming Cd^{+2} > H_2O_2 spray Cd^{+2} > Control of Control > H_2O_2 priming Cd^{+2} > H_2O_2 spray control > H_2O spray Cd^{+2} > SA P + FS Cd^{+2} > SA priming Cd^{+2} > H_2O_2 P + FS Cd^{+2} > SA spray Cd^{+2} > H_2O P + FS Cd^{+2}.

Concludingly, the statistical analysis for root dry weight revealed that milk thistle showed a significant variation in root dry weight at both altitudes. However, under control, SA and H_2O_2 proved to be effective, moreover it also reduced the impacts of Cd^{+2} toxicity (**Figure 3B**).

Shoot Dry Weight

Data obtained for shoot dry weight of milk thistle grown at two different altitudes, i.e., Qta and Tbt, revealed statistically significant ($p < 0.05$) differences under Cd^{+2} toxicity (**Figure 2D**). Data revealed that, under Cd^{+2} stress, SA and H_2O_2 supplementations were effective in increasing shoot dry weights. Maximum weight was recorded in SA spray under control at Tbt, while the least was observed in SA spray under control of Qta, which illustrates that the supplementation with signaling molecules at Tbt performed better (**Figure 2D**).

However, the order of improvement recorded at Qta was SA P + FS control > H_2O_2 P + FS control > Control of Control > H_2O P + FS control > H_2O_2 priming control > H_2O priming control > SA spray Cd^{+2} > SA priming Cd^{+2} > H_2O_2 priming Cd^{+2} > H_2O_2 spray Cd^{+2} > H_2O_2 P + FS Cd^{+2} > H_2O priming Cd^{+2} > SA P + FS Cd^{+2} > H_2O spray Cd^{+2} > H_2O P + FS Cd^{+2} > H_2O_2 spray Cd^{+2} > H_2O spray Cd^{+2} > Control Cd^{+2} > SA priming Cd^{+2} > SA spray Cd^{+2}.

While, at low-altitude Tbt, the order was SA spray control > H_2O P + FS control > H_2O priming control > H_2O_2 P + FS control > H_2O_2 priming control > SA P + FS control > Control of Control > SA priming control > H_2O_2 Spray control > H_2O_2 priming Cd^{+2} > H_2O spray control > H_2O_2 spray Cd^{+2} > Control Cd^{+2} > H_2O spray Cd^{+2} > H_2O priming Cd^{+2} > SA priming Cd^{+2} > SA P + FS Cd^{+2} > SA spray Cd^{+2} > H_2OP + FS Cd^{+2} > H_2O_2 P + FS Cd^{+2}.

Considering the overall improvement of milk thistle shoot dry weight, it can be observed that respective treatments at Tbt showed highly significant results reducing toxicity of Cd^{+2}. While, at Qta, the SDW reduced to a greater extent both under control and Cd^{+2} conditions. The fluctuating temperature may have a profound effect on the growth of the milk thistle; therefore, a varying trend can be recorded in shoot dry weight (**Figure 2D**).

Photosynthetic Pigments

Chlorophyll *a*

Results obtained for chlorophyll *a* of milk thistle grown at two varying altitudes (Qta and Tbt) under Cd^{+2} stress of 500-μM concentration revealed statistically non-significant results ($p > 0.05$) (**Figure 4A**). The data further revealed that the maximum Chl *a* content was observed in H_2O_2 P + FS under control at Qta, while the minimum Chl *a* content was recorded in the control field at Tbt (**Figure 4A**).

However, the trend observed in Qta was H_2O_2 P + FS control > SA P + FS control > SA spray Cd^{+2} > H_2O priming Cd^{+2} > H_2O_2 priming control > H_2O P + FS control > H_2O spray Cd^{+2} > SA priming control > H_2O_2 priming Cd^{+2} > SA priming Cd^{+2} > H_2O_2 spray control > SA spray control > Control of Control > SA P + FS Cd^{+2} > H_2O spray Cd^{+2} > H_2O_2 P + FS Cd^{+2} > H_2O_2 spray Cd^{+2} > Control Cd^{+2} > H_2O priming control.

While the order of improvement at Tbt was observed as H_2O_2 spray control > H_2O spray control > H_2O_2 P + FS control > H_2O_2 priming control > SA P + FS control > SA priming control > SA P + FS Cd^{+2} > SA priming Cd^{+2} > H_2O priming Cd^{+2} > H_2O P + FS control > H_2O spray Cd^{+2} > H_2O_2 spray Cd^{+2} > H_2O_2 P + FS Cd^{+2} > H_2O P + FS Cd^{+2} > control Cd^{+2} > SA spray Cd^{+2} > SA spray control > H_2O_2 priming Cd^{+2} > H_2O_2 priming Cd^{+2} > H_2O priming control > Control of Control.

Statistical data revealed a slight increase in chlorophyll *a* at both altitudes due to the priming and foliar spray of plant-signaling molecules, i.e., H_2O_2 and SA becoming highly helpful in reducing Cd^{+2} toxicity, thereby proving the role of signaling molecules in enhancing the content of photosynthetic pigments (**Figure 4A**).

Chlorophyll *b*

Data recorded for chlorophyll *b* of milk thistle grown at two different altitudes, i.e., Qta and Tbt, under toxicity of heavy metal (Cd^{+2}) of 500-μM concentration showed statistically non-significant ($p > 0.05$) results (**Figure 4B**), in which data depict that SA P + FS under control of Qta was the best treatment, while H_2O priming under Cd^{+2} stress at low-altitude Tbt proved to be the least non-significant treatment for chlorophyll *b* content (**Figure 4B**).

At high altitude (Qta), the trend recorded for Chl *b* was H_2O_2 P + FS control > H_2O spray control > Control Cd^{+2} > SA priming Cd^{+2} > H_2O_2 spray Cd^{+2} > H_2O spray Cd^{+2} > SA priming control > H_2O priming control > SA P + FS Cd^{+2} > SA spray Cd^{+2} > H_2O_2 priming Cd^{+2} > H_2O priming Cd^{+2} > H_2O P + FS Cd^{+2} > Control of Control > SA P + FS control > SA spray control > H_2O_2 priming control > H_2O_2 spray control > H_2O P + FS control > H_2O_2 P + FS Cd^{+2}.

However, at low altitude (Tbt), the trend was observed as SA P + FS control > SA priming control > Control of Control > H_2O_2 priming control > H_2O_2 P + FS control > H_2O_2 spray control > H_2O spray control > SA priming Cd^{+2} > H_2O_2 priming Cd^{+2} > H_2O P + FS control > Control Cd^{+2} > SA P + FS Cd^{+2} > SA spray control > H_2O_2 spray Cd^{+2} > H_2O_2 P + FS Cd^{+2} > H_2O priming Cd^{+2} > H_2O spray Cd^{+2} > H_2O P + FS Cd^{+2} > SA spray Cd^{+2} > H_2O priming Cd^{+2}.

Overall data statistically revealed that values for chlorophyll *b* were not significant ($p > 0.05$); therefore, it was established that, under control, the respective treatments at both the altitude (Qta and Tbt) were at their best, but the priming and foliar application of SA and H_2O_2 enhanced chlorophyll *b* content in milk thistle (**Figure 4B**).

Carotenoids

Results obtained for carotenoids of milk thistle, which was grown at two different altitudes (Qta and Tbt) under heavy metal stress of Cd^{+2}, reported statistically non-significant results ($p > 0.05$). Data further revealed that the best treatment was SA priming under Cd^{+2} stress at Tbt, while the least carotenoids contents were observed in the SA priming treatment of control of Qta (**Figure 4C**).

The order of improvement at Qta was observed as SA spray control > H_2O_2 P + FS control > SA P + FS control > Control Cd^{+2} > H_2O_2 spray Cd^{+2} > SA spray Cd^{+2} > H_2O spray

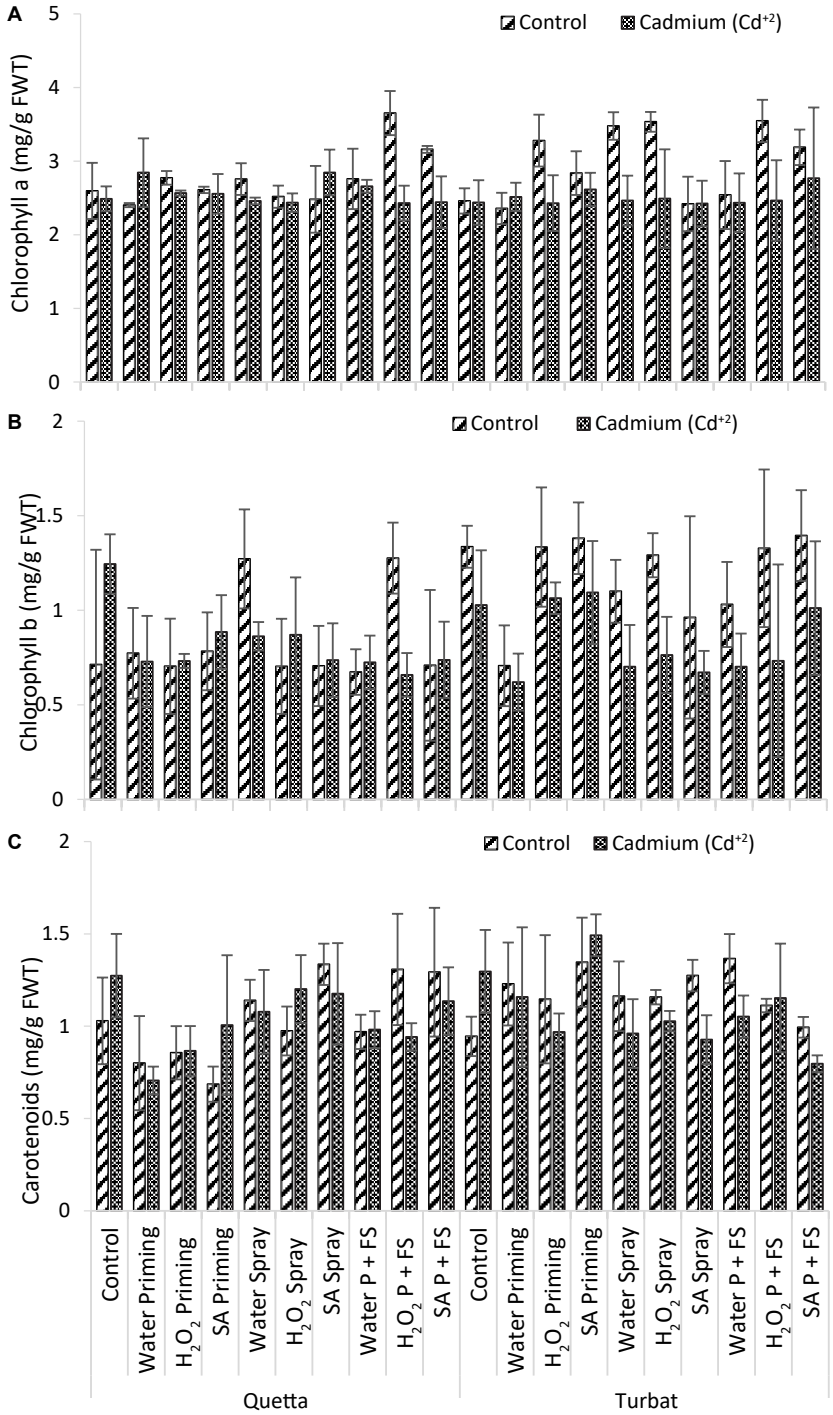


FIGURE 4 | Photosynthetic pigments; Chlorophyll *a* **(A)**, Chlorophyll *b* **(B)**, carotenoids **(C)** of milk thistle as affected by SA and H_2O_2 treatment grown at Quetta and Turbat under cadmium stress.

control > SA P + FS Cd^{+2} > H_2O spray Cd^{+2} > Control of Control > SA priming Cd^{+2} > H_2O P + FS Cd^{+2} > H_2O_2 spray control > H_2O P + FS control > H_2O_2 P + FS Cd^{+2} > H_2O_2 priming Cd^{+2} > H_2O_2 priming control > H_2O priming control > SA priming control.

While the order at Tbt was recorded as follows: SA priming Cd^{+2} > H_2O P + FS control > SA priming control > Control Cd^{+2} > SA spray control > H_2O priming control > H_2O spray control > H_2O priming Cd^{+2} > H_2O_2 spray control > H_2O_2 P + FS Cd^{+2} > H_2O_2 priming control > H_2O_2 P + FS

control > H_2O P + FS Cd^{+2} > H_2O_2 spray Cd^{+2} > SA P + FS control > H_2O_2 priming Cd^{+2} > H_2O spray Cd^{+2} > Control of Control > SA spray Cd^{+2} > SA P + FS Cd^{+2}.

Overall data for carotenoids contents revealed that the application of SA both under control and Cd^{+2} conditions of priming and foliar spray highly improved the carotenoids contents at both varying altitudes, i.e., Qta and Tbt. However, under heavy metal concentration (Cd^{+2}), the treatments showed a remarkable increase in carotenoids contents, which proves it plays a defensive role in alleviating Cd^{+2} toxicity in milk thistle (**Figure 4C**).

In a nutshell, considering results, it is proved that the presence of SA and H_2O_2 in leaves of milk thistle is highly helpful for accumulation and reduction of the toxic effects of Cd^{+2} (**Figures 4A–C**).

Oxidative Damage/Stress Measurement

Hydrogen Peroxide (H_2O_2) Content

Data recorded for H_2O_2 of milk thistle both (roots and shoots) under a concentration of 500-μM Cd^{+2} toxicity grown at two different altitudes (Qta and Tbt) in which the root showed statistically significant ($p < 0.05$) and shoot non-significant ($p > 0.05$) results (**Figures 5A,B**). Data for root H_2O_2 content revealed that highest concentration was observed in Qta and SA P + FS treatment under Cd^{+2} toxicity while the lowest content of H_2O_2 in root was observed in Control of Control of the same altitude.

The order of improvement in hydrogen peroxide (H_2O_2) content of root at high-altitude Qta was recorded as follows: SA P + FS Cd^{+2} > H_2O_2 priming Cd^{+2} > H_2O_2 P + FS Cd^{+2} > SA spray Cd^{+2} > H_2O_2 spray Cd^{+2} > SA P + FS control > SA priming Cd^{+2} > H_2O_2 P + FS control > H_2O_2 priming control > Control Cd^{+2} > H_2O P + FS Cd^{+2} > H_2O_2 spray control > H_2O_2 spray Cd^{+2} > SA spray control > H_2O P + FS control > SA priming control > H_2O spray control > H_2O priming Cd^{+2} > H_2O priming control > Control of Control.

While, at low-altitude Tbt, the order of changes reported to be in the following sequence: H_2O_2 spray Cd^{+2} > SA P + FS Cd^{+2} > H_2O P + FS Cd^{+2} > H_2O_2 P + FS Cd^{+2} > SA P + FS control > H_2O_2 priming Cd^{+2} > SA priming Cd^{+2} > H_2O_2 P + FS control > SA spray Cd^{+2} > Control of Cd^{+2} > H_2O priming Cd^{+2} > H_2O_2 spray control > H_2O spray Cd^{+2} > Control of Control > H_2O P + FS control > SA priming control > H_2O_2 priming control > SA spray control > H_2O spray control > H_2O priming control.

Furthermore, results obtained for shoot H_2O_2 content revealed that maximum hydrogen peroxide content was observed in H_2O P + FS under Cd^{+2} stress at Qta, while minimum content of H_2O_2 was observed in SA priming under control at Tbt (**Figure 5A**).

The order of shoot H_2O_2 content at Qta was recorded as H_2O P + FS Cd^{+2} > H_2O spray Cd^{+2} > H_2O_2 priming Cd^{+2} > SA spray Cd^{+2} > SA P + FS control > SA priming Cd^{+2} > H_2O_2 spray Cd^{+2} > H_2O_2 priming control > SA priming control > H_2O priming control > H_2O_2 P + FS Cd^{+2} > Control of Control > H_2O_2 P + FS control > H_2O priming Cd^{+2} > H_2O P + FS control > Control Cd^{+2} > H_2O spray control > SA P + FS Cd^{+2} > H_2O_2 spray control > SA spray control.

In contrast, the order of improvement at the low-altitude Tbt was recorded as follows: H_2O_2 P + FS Cd^{+2} > H_2O P + FS Cd^{+2} > H_2O P + FS control > H_2O spray Cd^{+2} > H_2O_2 P + FS control > Control Cd^{+2} > SA P + FS control > H_2O priming Cd^{+2} > H_2O_2 spray Cd^{+2} > H_2O spray control > SA spray Cd^{+2} > SA P + FS Cd^{+2} > H_2O_2 spray control > H_2O priming control > SA priming Cd^{+2} > H_2O_2 priming control > H_2O_2 priming Cd^{+2} > Control of Control > SA spray control > SA priming control.

Considering H_2O_2 content in the root of milk thistle, it was observed that the priming and foliar spray of signaling molecules, i.e., H_2O_2 and SA, were most effective in lowering hydrogen peroxide content in roots under Cd^{+2} toxicity. Similar findings were observed for shoots as well, proving the beneficial role of exogenous supplementation of SA and H_2O_2 in alleviating heavy metal toxicity (Cd^{+2}). However, the interactions and trends toward hampering oxidative damage by SA and H_2O_2 in alleviating Cd^{+2} toxicity vary in roots and shoots (**Figures 5A,B**).

Malondialdehyde

Results obtained for MDA content of roots and shoots of milk thistle under heavy metal toxicity Cd^{+2} (500 μM) at two different altitudes, i.e., Qta and Tbt showed a significant ($p < 0.05$) difference (**Figures 5C,D**). Data for root MDA content revealed that the maximum MDA content was observed in H_2O_2 P + FS under control at Tbt, while the least was observed at Qta under Cd^{+2} toxicity, i.e., H_2O_2 P + FS.

However, the trend in root MDA content at Qta was observed as H_2O_2 priming Cd^{+2} > H_2O_2 P + FS control > SA priming Cd^{+2} > H_2O spray control > H_2O_2 spray control > SA spray control > H_2O spray Cd^{+2} > SA P + FS control > H_2O_2 spray Cd^{+2} > Control Cd^{+2} > H_2O P + FS control > Control of Control > H_2O priming Cd^{+2} > H_2O_2 priming control > H_2O priming control > SA priming control > SA spray Cd^{+2} > H_2O P + FS Cd^{+2} > H_2O_2 P + FS Cd^{+2}.

While, at low altitude (Tbt), the order was recorded as H_2O_2 P + FS control > SA priming Cd^{+2} > H_2O_2 P + FS Cd^{+2} > H_2O priming Cd^{+2} > H_2O_2 P + FS Cd^{+2} > SA P + FS Cd^{+2} > SA spray Cd^{+2} > H_2O_2 spray Cd^{+2} > SA P + FS control > Control Cd^{+2} > H_2O spray Cd^{+2} > H_2O P + FS Cd^{+2} > H_2O P + FS control > Control of Control > H_2O spray control > H_2O_2 spray control > H_2O priming control > SA priming control > SA spray control > H_2O_2 priming control.

Furthermore, data for MDA content in the shoot of milk thistle also revealed significant data ($p < 0.05$) in which the maximum MDA content was reported in control under Cd^{+2} stress at Tbt; however, the H_2O P + FS under Cd^{+2} stress at Qta was reported to have a minimum content of MDA (**Figure 5C**).

The order of changes in MDA content in the shoot at Qta was observed as H_2O_2 priming Cd^{+2} > H_2O priming Cd^{+2} > Control Cd^{+2} > SA priming Cd^{+2} > H_2O spray Cd^{+2} > SA priming control > SA P + FS control > SA P + FS Cd^{+2} > SA spray Cd^{+2} > H_2O_2 P + FS Cd^{+2} > H_2O priming control > H_2O P + FS control > H_2O_2 priming

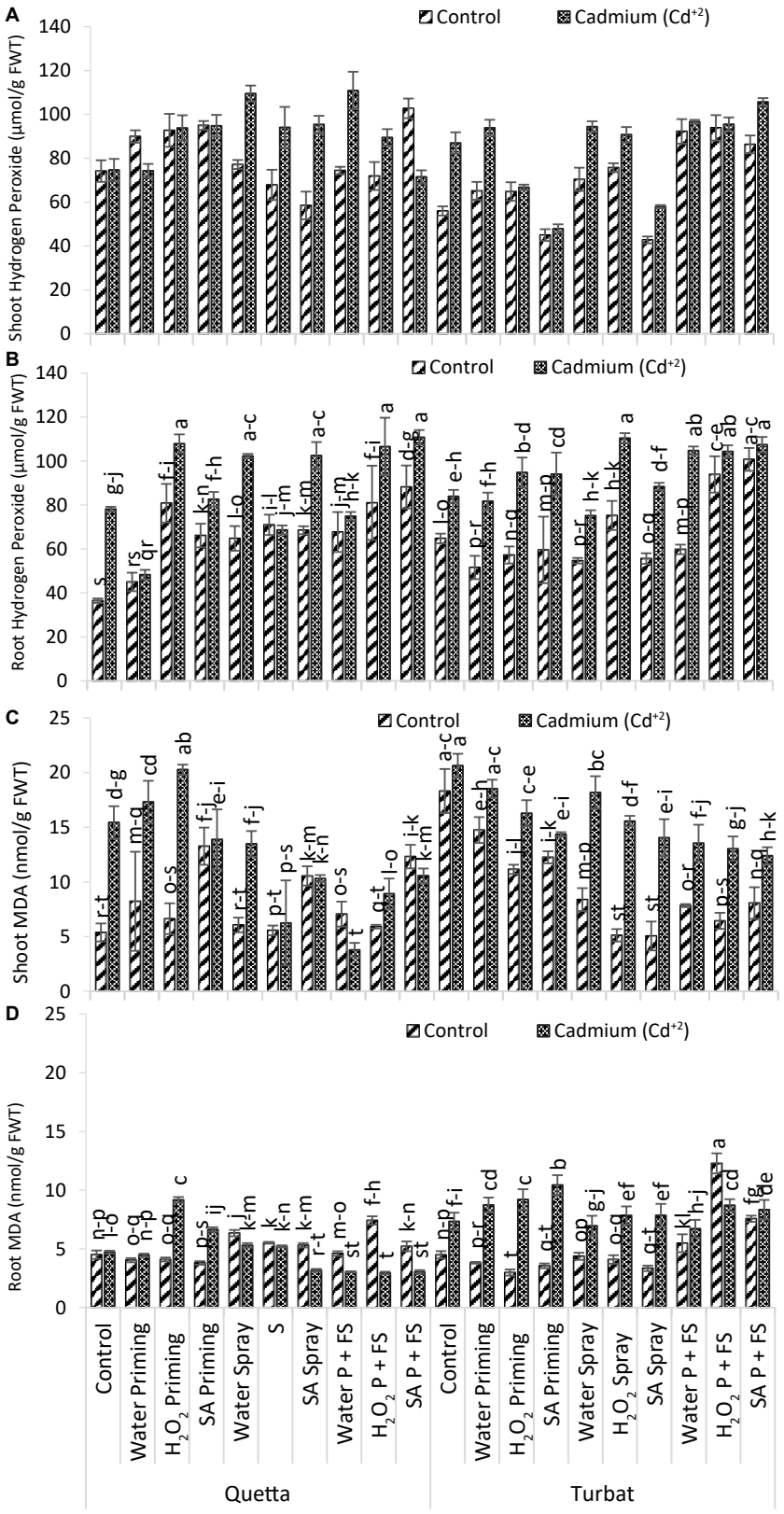


FIGURE 5 | Oxidative damage parameters; shoot H_2O_2 **(A)**, root H_2O_2 **(B)**, shoot MDA **(C)**, root MDA **(D)** of milk thistle as affected by SA and H_2O_2 treatment grown at Quetta and Turbat under cadmium stress. The same letters on graphs represent statistically similar effects ($p < 0.05$).

control > H_2O_2 spray Cd^{+2} > H_2O spray control > H_2O_2 P + FS control > H_2O_2 spray control > Control of Control > H_2O P + FS Cd^{+2}.

While the trend at Tbt was recorded as follows: Control Cd^{+2} > H_2O priming Cd^{+2} > Control of Control > H_2O spray Cd^{+2} > H_2O_2 priming Cd^{+2} > H_2O_2 spray Cd^{+2} > H_2O priming control > SA priming Cd^{+2} > SA spray Cd^{+2} > H_2O P + FS Cd^{+2} > H_2O_2 P + FS Cd^{+2} > SA P + FS Cd^{+2} > SA priming control > H_2O_2 priming control > H_2O spray control > SA P + FS control > H_2O P + FS control > H_2O_2 P + FS control > H_2O_2 spray control > SA spray control.

Overall data of MDA content in milk thistle revealed that maximum MDA content in milk thistle had been reported in shoots both in control and Cd^{+2} conditions; in contrast, MDA content in root was reported very low. In root, the interactions of SA and H_2O_2 with Cd^{+2} were reported to be different. There is a significant difference in both altitudes along with the stress, i.e., Control and Cd^{+2}. Considering the Cd^{+2} toxicity, it is considered that the plant-signaling molecules (i.e., SA and H_2O_2) reported a synergistic effect of these molecules in relation to accumulation and uptake of Cd^{+2} toxicity in the roots and shoots, thus enhancing the role of signaling molecules and suppressing the heavy metal toxicity (**Figures 5C,D**).

Secondary Metabolites

Anthocyanin Content

Results obtained for anthocyanin content (roots and shoots) manifested significant differences in milk thistle grown at two different altitudinal fields, i.e., Qta and Tbt under heavy metal toxicity (500 μM). Data further revealed that, in the roots, the maximum anthocyanin content was determined in H_2O P + FS under Cd^{+2} stress at low-altitude Tbt, while the minimum anthocyanins in roots were observed in H_2O priming under Cd^{+2} toxicity at the same altitude, showing statistically non-significant ($p > 0.05$) results (**Figure 6B**).

However, the trend for root anthocyanin at Qta was observed as SA P + FS Cd^{+2} > SA P + FS control > H_2O_2 priming Cd^{+2} > SA priming Cd^{+2} > H_2O_2 P + FS Cd^{+2} > H_2O priming Cd^{+2} > H_2O priming control > SA spray Cd^{+2} > H_2O_2 spray Cd^{+2} > H_2O P + FS control > H_2O_2 P + FS control > H_2O_2 priming control > H_2O spray control > control Cd^{+2} > SA spray control > H_2O P + FS Cd^{+2} > H_2O spray control > SA priming control > Control of Control > H_2O spray Cd^{+2}.

While the order of improvement at Tbt was H_2O P + FS Cd^{+2} > SA P + FS Cd^{+2} > H_2O spray Cd^{+2} > SA P + FS control > SA spray Cd^{+2} > H_2O_2 P + FS Cd^{+2} > H_2O_2 priming Cd^{+2} > Control Cd^{+2} > H_2O P + FS control > H_2O_2 spray Cd^{+2} > H_2O spray Cd^{+2} > H_2O_2 P + FS control > H_2O_2 priming control > SA priming Cd^{+2} > H_2O_2 spray control > Control of Control > SA spray control > SA priming control > H_2O priming control > H_2O priming Cd^{+2}.

Moreover, anthocyanin content in the shoot was the highest in H_2O_2 spray under heavy metal toxicity (Cd^{+2}) at Tbt; in contrast, SA P + FS under control remained the lowest treatment observed at Qta. The results for shoot anthocyanin content statistically showed significant ($p < 0.05$) data in milk thistle (**Figure 6A**).

On the other hand, the order of changes in attribute of anthocyanin contents in the shoot at Qta was recorded as SA P + FS Cd^{+2} > H_2O spray Cd^{+2} > H_2O P + FS Cd^{+2} > H_2O_2 spray Cd^{+2} > SA spray Cd^{+2} > H_2O priming Cd^{+2} > SA priming Cd^{+2} > H_2O_2 priming control > H_2O priming control > H_2O_2 P + FS Cd^{+2} > Control of Control > Control Cd^{+2} > H_2O_2 P + FS control > H_2O_2 spray control > SA spray control > H_2O_2 priming Cd^{+2} > H_2O P + FS control > SA priming control > H_2O_2 spray control > SA P + FS control.

At Tbt, the order of improvement was observed as follows: H_2O_2 spray Cd^{+2} > H_2O_2 priming Cd^{+2} > H_2O P + FS Cd^{+2} > SA spray Cd^{+2} > SA priming Cd^{+2} > SA P + FS Cd^{+2} > H_2O priming Cd^{+2} > Control Cd^{+2} > H_2O_2 P + FS Cd^{+2} > H_2O_2 priming control > Control of Control > H_2O spray Cd^{+2} > H_2O_2 P + FS control > H_2O priming control > H_2O spray control > H_2O P + FS control > H_2O_2 spray control > SA spray control > SA priming control > SA P + FS control.

Considering anthocyanin (i.e., roots and shoots) content at two different altitudes (i.e., Qta and Tbt), it was established that there was a significant difference with the prescribed altitudes. Overall results indicate that anthocyanin content in both roots and shoots showed a small degree of differentiation statistically at Qta and Tbt under heavy metal toxicity (Cd^{+2}). Thus, it proved that, along with altitudinal variations, the application of SA and H_2O_2 proved to be the best by reducing the toxic effect and stress of Cd^{+2}. As compared to roots, there was a maximum increase in shoot anthocyanin content (**Figures 6A,B**).

Soluble Phenolics Content

Statistical analysis for roots and shoots of soluble phenolics in milk thistle grown at high (Qta) and low (Tbt) altitudes showed statistically significant ($p < 0.05$) results under application of heavy metal Cd^{+2} (500 μM). Considering root soluble phenolics content, it has been observed that the best and effective treatment was SA spray under control at Tbt; however, the less effective treatment was recorded H_2O spray under Cd^{+2} stress at the same altitude (**Figures 6C,D**).

The order of improvement in root phenolics contents in Qta was SA spray control > H_2O_2 priming control > H_2O spray control > H_2O_2 P + FS control > SA priming Cd^{+2} > SA P + FS Cd^{+2} > H_2O spray Cd^{+2} > H_2O_2 spray Cd^{+2} > H_2O P + FS Cd^{+2} > SA spray Cd^{+2} > Control Cd^{+2} > Control of Control > SA P + FS control > H_2O priming Cd^{+2} > H_2O_2 spray control > H_2O_2 P + FS Cd^{+2} > H_2O priming control > H_2O P + FS control > H_2O_2 priming Cd^{+2} > SA priming control.

While the order of changes at Tbt was SA spray control > H_2O_2 priming Cd^{+2} > H_2O spray control > SA priming Cd^{+2} > Control of Control > H_2O_2 P + FS control > SA spray Cd^{+2} > Control Cd^{+2} > H_2O P + FS Cd^{+2} > H_2O_2 spray control > H_2O_2 P + FS Cd^{+2} > H_2O_2 spray Cd^{+2} > SA P + FS control > H_2O_2 priming control > SA P + FS Cd^{+2} > SA priming control > H_2O P + FS control > H_2O priming control > H_2O priming Cd^{+2} > H_2O spray Cd^{+2}.

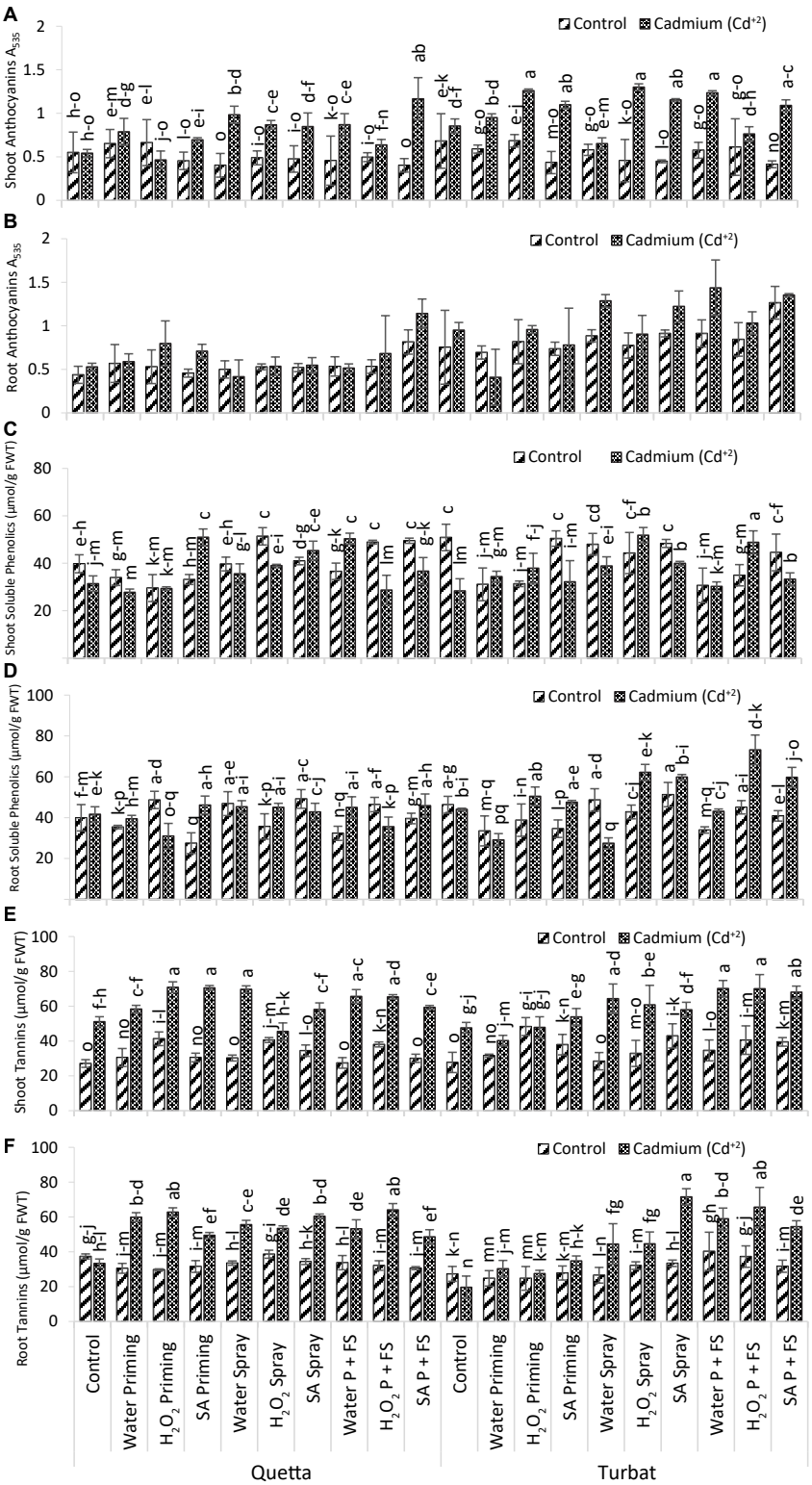


FIGURE 6 | Secondary metabolites; shoot anthocyanin **(A)**, root anthocyanin **(B)**, shoot soluble phenolics **(C)**, root soluble phenolics **(D)** shoot tannins **(E)** root tannins **(F)** of milk thistle as affected by SA and H_2O_2 treatment grown at Quetta and Turbat under cadmium stress. The same letters on graphs represent a statistically similar effect ($p < 0.05$).

On the other hand, Soluble phenolics in shoots reported maximum content in H_2O_2 P + FS under heavy metal (Cd^{+2}) toxicity at Tbt, while the minimum phenolics content was reported in H_2O priming under Cd^{+2} toxicity at Qta (**Figure 6C**).

The order for shoot phenolics content at Qta was observed as follows: H_2O_2 spray control > SA priming Cd^{+2} > H_2O P + FS Cd^{+2} > SA P + FS control > H_2O_2 P + FS control > SA spray Cd^{+2} > SA spray control > Control of Control > H_2O spray control > H_2O_2 spray Cd^{+2} > SA P + FS Cd^{+2} > H_2O P + FS control > H_2O spray Cd^{+2} > H_2O priming control > SA priming control > Control Cd^{+2} > H_2O_2 priming control > H_2O_2 priming Cd^{+2} > H_2O_2 P + FS Cd^{+2} > H_2O priming Cd^{+2}.

However, at Tbt, the order of improvement was recorded as H_2O P + FS Cd^{+2} > H_2O_2 spray Cd^{+2} > SA spray Cd^{+2} > SA P + FS Cd^{+2} > Control of Control > SA priming control > SA spray control > H_2O spray control > SA spray Cd^{+2} > SA P + FS control > H_2O_2 spray control > H_2O spray Cd^{+2} > H_2O_2 priming Cd^{+2} > H_2O_2 P + FS control > H_2O priming Cd^{+2} > SA priming Cd^{+2} > H_2O_2 priming control > H_2O priming control > H_2O priming control > H_2O P + FS Cd^{+2} > Control Cd^{+2}.

Considering the overall observed results of soluble phenolics contents in both roots and shoots, it has been observed that the maximum phenolic content was observed in shoots as compared to the roots. Data pertaining to this attribute revealed that foliar spray and priming with plant signaling molecules (SA and H_2O_2) played a significant role in reducing the Cd^{+2} toxicity and enhanced the phenolics content in both roots and shoots. Supplementation with SA and H_2O_2 had a stronger effect on the attribute of milk thistle under Cd^{+2} stress as compared to control plants (**Figures 6C,D**).

Tannins Content

Results obtained for Tannins content in both roots and shoots showed statistically significant results ($p < 0.05$) in milk thistle grown at two different altitudinal fields (i.e., Qta and Tbt) under Cd^{+2} toxicity (500 μM). Data revealed that, in the roots, the highest content of tannins was recorded in SA spray under Cd^{+2} stress at Tbt, while the lowest tannins content was observed in control treatment of Cd^{+2} at the same altitude (Tbt) (**Figures 6E,F**).

However, the trend for root tannins contents in Qta was observed as H_2O_2 P + FS Cd^{+2} > H_2O_2 priming Cd^{+2} > H_2O_2 priming Cd^{+2} > SA spray Cd^{+2} > H_2O priming Cd^{+2} > H_2O spray Cd^{+2} > H_2O_2 spray Cd^{+2} > H_2O P + FS Cd^{+2} > SA priming Cd^{+2} > SA P + FS Cd^{+2} > H_2O_2 spray control > Control of Control > SA spray control > H_2O P + FS control > H_2O spray control > Control Cd^{+2} > H_2O_2 P + FS control > SA priming control > SA P + FS control > H_2O priming control > H_2O_2 priming control.

Considering Tannin content in roots of milk thistle grown at Tbt, following order of improvement was observed: SA spray Cd^{+2} > H_2O_2 P + FS Cd^{+2} > H_2O P + FS Cd^{+2} > SA P + FS Cd^{+2} > H_2O_2 spray Cd^{+2} > H_2O spray Cd^{+2} > H_2O P + FS control > H_2O_2 P + FS control > SA priming Cd^{+2} > SA spray control > H_2O_2 spray control > SA P + FS control > H_2O priming Cd^{+2} > SA priming control > H_2O_2 priming Cd^{+2} > Control of Control > H_2O spray control > H_2O priming control > H_2O_2 priming control > Control Cd^{+2}.

Moreover, data recorded for shoot tannins in milk thistle also showed significant variations ($p < 0.05$) under Cd^{+2} toxicity at both altitudes (Qta and Tbt). Furthermore, the obtained results revealed that the maximum tannin contents in shoot were found in H_2O_2 priming under Cd^{+2} toxicity at Qta, while the minimum shoot tannins were observed in control at the same altitude (**Figure 6E**).

The order of improvement in shoot tannins at Qta was observed as H_2O_2 priming Cd^{+2} > SA priming Cd^{+2} > H_2O spray Cd^{+2} > H_2O P + FS Cd^{+2} > H_2O_2 P + FS Cd^{+2} > SA P + FS Cd^{+2} > H_2O priming Cd^{+2} > SA spray Cd^{+2} > Control Cd^{+2} > H_2O_2 spray Cd^{+2} > H_2O_2 priming control > H_2O_2 spray control > H_2O_2 P + FS control > SA spray control > SA priming control > H_2O priming control > H_2O spray control > SA P + FS control > H_2O P + FS control > Control of control.

While the trend for Tbt was recorded as follows: H_2O P + FS Cd^{+2} > H_2O_2 P + FS Cd^{+2} > SA P + FS Cd^{+2} > H_2O spray Cd^{+2} > H_2O_2 spray Cd^{+2} > SA spray Cd^{+2} > SA priming Cd^{+2} > H_2O_2 priming control > H_2O_2 priming Cd^{+2} > Control Cd^{+2} > SA spray control > H_2O_2 P + FS control > H_2O priming Cd^{+2} > SA P + FS control > SA priming control > H_2O P + FS control > H_2O_2 spray control > H_2O priming control > H_2O spray control > Control of Control. In a nutshell, the data statistically revealed significant results by applying plant-signaling molecules in alleviating Cd^{+2} toxicity in milk thistle grown under two varying altitudes, i.e., Qta and Tbt. Compared to control field plants at both altitudes, the Cd^{+2} stress plants showed significantly enhanced tannin content in milk thistle, thus indicating the activation of the defensive mechanism by the synthesis of secondary metabolites (**Figures 6E,F**).

Correlations With Shoot and Root Dry Weights

Drawing correlations of various morpho-physiological attributes with shoot and root dry weights (**Table 2**) revealed that shoot length positively significantly correlated with the dry weights even under Cd^{+2} stress; however, root length showed a negative non-significant correlation under stress. Considering milk thistle leaf area's correlation with shoot dry weights revealed that, in Qta, under unstressed conditions, the leaf area positively correlated, while, in Tbt, under cadmium stress, the leaf area positively correlated with the SDW. Photosynthetic pigments, i.e., chlorophyll *a*, *b*, and carotenoids showed non-significant correlations except for Chl *a* at Qta in control milk thistle plants that showed significant positive correlations. Secondary metabolites showed non-significant correlations with the shoot and root dry weights under both control and Cd^{+2} stress except for shoot soluble phenolics and root tannin showing significant negative correlation under control conditions and Cd^{+2} stressed plants, respectively, of the Tbt area.

TABLE 2 | Correlation of changes in various morpho-physiological attributes of milk thistle with shoot and root dry weights grown at Quetta and Turbat under cadmium stress (n = 10).

Parameter	Stress	Area	
		Quetta	Turbat
Root length	Control	0.681*	0.157^{ns}
	Cd^{+2}	-0.380^{ns}	-0.050^{ns}
Shoot length	Control	0.943**	0.774**
	Cd^{+2}	-0.254^{ns}	0.760*
Leaf area	Control	0.957**	0.588^{ns}
	Cd^{+2}	0.351^{ns}	0.881**
Root fresh weight	Control	0.824**	0.921**
	Cd^{+2}	-0.09^{ns}	0.781**
Shoot fresh weight	Control	0.909**	0.911**
	Cd^{+2}	0.076^{ns}	0.993**
Chlorophyll *a*	Control	0.717*	-0.411^{ns}
	Cd^{+2}	0.303^{ns}	-0.156^{ns}
Shoot soluble phenolics	Control	0.322s	−0.649*
	Cd^{+2}	-0.323^{ns}	-0.325^{ns}
Root tannins	Control	-0.296^{ns}	0.379^{ns}
	Cd^{+2}	0.374^{ns}	−0.750**
Shoot MDA	Control	-0.024^{ns}	-0.193^{ns}
	Cd^{+2}	-0.037^{ns}	0.758*

*Significant at: *$p < 0.05$; **$p < 0.01$, and $^{ns}p > 0.05$.*

DISCUSSION

The results of this study on milk thistle illustrate the significant role of plant-signaling molecules SA and H_2O_2 in alleviating Cd^{+2} toxicity at two varying altitudes of Balochistan (Qta and Tbt), Pakistan. However, the priming and foliar spray of SA and H_2O_2 enhanced the germination, morpho-physiological effectiveness at both altitudes, thus thereby ameliorating the toxic effect of Cd^{+2} in milk thistle. Cd^{+2} is widely recognized as a toxic heavy metal in soil by destabilizing the integrity of membrane and status of nutrients; that inhibits biosynthesis of chlorophyll that resulted in the reduction in plant growth and development (Lu et al., 2018; Majumdar et al., 2020). Considering the growth attributes of the present study, it was observed that roots, shoot length, and weights decreased under Cd^{+2} toxicity; however, the supplementation of SA and H_2O_2 helps the milk thistle plants to alleviate the toxic impacts in single or combinational treatments at both experimental sites. Khatamipour et al. (2011) reported the various Cd^{+2} concentrations significantly reduce root length in milk thistle. The decline in root length was more pronounced because of the Cd^{+2} treatment as compared to shoot length. The toxicity of Cd^{+2} was previously reported in different plant species and groups (Kaur et al., 2017; Lu et al., 2018; Kaya et al., 2019; Majumdar et al., 2020). The attributes for growth in *Brassica juncea,* such as shoot/root length, dry and fresh weight, along with the leaf area, decreased by the application of Cd^{+2} (Faraz et al., 2020). However, the findings of Migahid et al.'s (2019) research suggested that priming of seeds with H_2O_2 increased the leaf area, dry weight of roots and shoots, and root and shoot fresh weight of milk thistle (Gaertn) in comparison with control (Wahid et al., 2007). Furthermore, in the present study, it has been reported that Cd^{+2} toxicity decreased the leaf area at high altitude (Qta), but by the priming and foliar application of plant-signaling molecules (i.e., SA and H_2O_2), the morphological parameters (i.e., root/shoot length, the number of leaves, shoot and root fresh weight) increased and also alleviated the toxic effects of heavy metal cadmium (**Figures 2A–C**, **3A,D**).

The application of Cd^{+2} concentration reduces the rate of photosynthesis by targeting various electron transport chain components in carboxylation reactions along with PSII (Shah et al., 2020). Study, conducted by Guo et al. (2019) also reported a decrease in contents of chlorophyll and fluorescence under Cd^{+2} toxicity. In this study, milk thistle plants treated with priming and foliar spray of SA and H_2O_2 have a propounding effect on alleviating the toxicity of Cd^{+2} on the photosynthetic pigments (**Figures 4A–C**). The carotenoid contents in plants were reduced because of high cadmium Cd^{+2} (Cai et al., 2011), while our findings showed non-significant ($p > 0.05$) results under both control and Cd^{+2} conditions. Carotenoid contents are enhanced due to plant-signaling molecules (SA and H_2O_2) at high- (Qta) and low-altitude Tbt (**Figure 4C**). Carotenoids are the potent antioxidants that serve as reactive oxygen species (ROS) against disruption of photo-oxidative in photosystems (Zahra et al., 2021d), thus suggesting the putative role of SA and H_2O_2 in improving plant defense mechanisms.

MDA is considered the main product for peroxidation of the lipid membrane. Contents of MDA reflect the damage to structures of cell membranes (Parida and Jha, 2010). While, under Cd^{+2} toxicity, high-level MDA accumulation is reported to enhance O_2^- and H_2O_2 (Wang et al., 2013a; Xu et al., 2014). Furthermore, Krantev et al. (2008) reported that seeds of maize were presoaked with 500 mM SA before applying the Cd^{+2} has a protective effect by diminishing MDA accumulation, which is involved in the protection against oxidative damage. Wang et al. (2013a,b) and Bai et al. (2015) also reported pretreatment of SA under cadmium stress-reduced MDA contents. In the present study, it has been reported that MDA content enhanced in roots of milk thistle under Cd^{+2} stress (**Figure 5D**). Popova et al. (2008) reported that Cd^{+2} was accumulated in roots of the plants because it is the basic organ that was exposed to heavy metals in soil and translocated to shoots as well. Cd^{+2} stress was reported to cause lipid peroxidation in roots of pea seedlings with increasing levels of H_2O_2 (Podazza et al., 2012). The outcome of the report was further shown in the study of El Dakak and Hassan (2020) that H_2O_2 was not significantly accumulated ($p > 0.05$); hence, our findings support the same findings that H_2O_2 content in shoots showed non-significant results in milk thistle under Cd^{+2} stress (**Figure 5A**). Song et al. (2014) reported enhancing activities of antioxidative enzymes (i.e., SOD and POD) along with some other enzymatic antioxidants such as CAT and APX decreased by the exposure of Cd^{+2} toxicity. Liu et al. (2010) reported that Cd^{+2}-generated oxidative damage interacts with antioxidant defense system. While the increasing activity of SOD and POD

indicated detoxifying of ROS (Ferreira et al., 2002; Krantev et al., 2008). Furthermore, POD activated by Cd^{+2} at a minimum level is responsible for the removal of H_2O_2, which insignificantly ($p > 0.05$) increased.

Plant secondary metabolites play a key role in defense against environmental stresses (Yang et al., 2018). A slow process was observed due to secondary metabolites accumulation during the stress conditions in lemongrass, which reported greater accumulation in soluble phenolics, flavonoids, and anthocyanin, while the accumulation of tannins content was minimum both in the shoots and roots (Shaukat et al., 2020) after exposure to different altitudes. Basically, tannins are of two types (i.e., condensed and hydrolysable). The condensed tannins are physiologically less significant due to being much complex, not soluble, but hydrolysable tannins played a significant role in growth attributes along with development under adverse conditions (Tiku, 2020). Such compounds, apart from tannin, are mainly found in the soluble phase, which increases in the concentration of secondary metabolites under adverse environmental conditions that are known (Tiku, 2020). In the present study, it has been observed that accumulation of tannin content in roots and shoots of milk thistle at both altitudes (i.e., Qta and Tbt) enhanced under Cd^{+2} stress. However, at Tbt, the tannins contents in roots were comparatively less than in Qta milk thistle plants, thus indicating environmental regime variation impact (**Figures 6E,F**).

Phenolics are donors of electrons that could mitigate the oxidative stress effect, which is an ultimate substrate for antioxidant enzymes, i.e., peroxidases (Posmyk et al., 2009). Migahid et al. (2019) reported that the total phenolic contents in milk thistle did not change under H_2O_2. However, our findings in the present study suggest that phenolics contents in the roots decrease significantly in control and Cd^{+2} conditions at both altitudes (i.e., Qta and Tbt), while phenolics contents in shoots significantly ($p < 0.05$) increased to a high level as compared to root phenolics, while, under Cd^{+2} stress, the respective treatments applied with a concentration of SA and H_2O_2 showed significant results (**Figures 6C,D**). Chaman et al. (2003) reported that SA increases the phenylalanine ammonia-lyase activity that is an essential enzyme being involved in phenolics compounds biosynthesis in the early stages. Zahra et al. (2021d) reported that, in milk thistle, it was perused that the alkaloid and anthocyanin contents enhanced under stress in comparison with control. It was also reported from the study of Khan et al. (2019) that foliar application of SA increased anthocyanin contents in seedlings of rice subjected to abiotic stress. The same tendency was observed in the present study, that anthocyanin contents in shoot significantly ($p < 0.05$) increased while, in roots, a non-significant ($p > 0.05$) increased under Cd^{+2} toxicity (**Figures 6A,B**). However, under control conditions, the contents of anthocyanin remain suppressed at both the altitudinal fields Qta and Tbt (**Figures 6A,B**), thus providing the evidence that the secondary metabolite increases and work as defense system under stressful environments.

CONCLUSION

The toxicity of heavy metal (Cd^{+2}) hampered the morphological and physiological attributes of milk thistle grown at two different altitudes. Data revealed that, under Cd^{+2} toxicity, morpho-physiological attributes were hampered. However, priming and foliar treatment of plant-signaling molecules SA and H_2O_2 showed a positive impact on alleviating the toxic effect of Cd^{+2}. The secondary metabolites showed improved tolerance to Cd^{+2} concentration supported the growth and development of milk thistle at both altitudes by modulating Cd^{+2}-induced changes, especially with the application of SA and H_2O_2. Milk thistle being a weed plant grown in areas, which are mostly heavy metal affected due to industrially released chemicals, mining, and cadmium present in soil; it would be very beneficial to grow these plants, which can tolerate heavy metal stress. The present research is thus helpful to conduct comparative studies of medicinal plants grown under varying altitudes and under cadmium/heavy metal stress. The study motivates to unveil the genes involved in ameliorating the heavy metal toxicity in the same plant across the altitudinal gradient as no such literature has yet been reported.

DATA AVAILABILITY STATEMENT

The original contributions presented in the study are included in the article/supplementary material, further inquiries can be directed to the corresponding authors.

AUTHOR CONTRIBUTIONS

MN and KS conceived and designed the research. MN, KS, and AS performed the experiment and wrote the initial draft of the manuscript. AR, NZ, and MBH assisted with the analysis, revised subsequent versions of the manuscript, and provided the technical guidance. AR, KS, QA, HMA, and MHS proofread and edited the final version. All authors have read and agreed to the published version of the manuscript.

FUNDING

The publication of this work was supported by the Researchers Supporting Project Number (RSP-2021/123), King Saud University, Riyadh, Saudi Arabia.

ACKNOWLEDGMENTS

We are thankful to all members of Department of Botany, University of Balochistan, Quetta, Pakistan, for providing research environment and support to conduct this study. Furthermore, we would like to extend their sincere appreciation to the Researchers Supporting Project No. RSP-2021/123, King Saud University, Riyadh, Saudi Arabia.

REFERENCES

Ali, B., Wang, B., Ali, S., Ghani, M., Hayat, M., Yang, C., et al. (2013). 5-Aminolevulinic acid ameliorates the growth, photosynthetic gas exchange capacity, and ultrastructural changes under cadmium stress in *Brassica napus* L. *J. Plant Growth Regul.* 32, 604–614. doi: 10.1007/s00344-013-9328-6

Andrade, A. F. M., Amaral Sobrinho, N. M. B., Santos, F. S., Magalhães, M. O. L., Tolón-Becerra, A., and Lima, L. S. (2014). EDTA-induced phytoextraction of lead and barium by brachiaria (B. decumbens cv. Basilisk) in soil contaminated by oil exploration drilling waste. *Acta Sci. Agron.* 36, 495–500. doi: 10.4025/actasciagron.v36i4.18172

Arnon, D. I. (1949). Copper enzymes in isolated chloroplasts. Polyphenoloxidase in *Beta vulgaris*. *Plant Physiol.* 24:1. doi: 10.1104/pp.24.1.1

Bai, X., Dong, Y., Kong, J., Xu, L., and Liu, S. (2015). Effects of application of salicylic acid alleviates cadmium toxicity in perennial ryegrass. *Plant Growth Regul.* 75, 695–706. doi: 10.1007/s10725-014-9971-3

Bijak, M. (2017). Silybin, a major bioactive component of milk thistle (Silybum marianum L. Gaernt.)—Chemistry, bioavailability, and metabolism. *Molecules* 22:1942. doi: 10.3390/molecules22111942

Bremner, J., and Mulvaney, C. (1982). "Total nitrogen," in *Methods of Soil Analysis. American Society of Agronomy and Soil Science*, eds A. L. Page, R. H. Miller, and D. R. Keeny (Madison, WI: American Society of Agronomy), 1119–1123.

Cai, Y., Cao, F., Wei, K., Zhang, G., and Wu, F. (2011). Genotypic dependent effect of exogenous glutathione on Cd-induced changes in proteins, ultrastructure and antioxidant defense enzymes in rice seedlings. *J. Hazard. Mater.* 192, 1056–1066. doi: 10.1016/j.jhazmat.2011.06.011

Cain, S., and Castro, G. (1959). *Manual of Vegetative Analysis*. New York, NY: Harper & Brothers, 325.

Chaman, M. E., Copaja, S. V., and Argandoña, V. H. (2003). Relationships between salicylic acid content, phenylalanine ammonia-lyase (PAL) activity, and resistance of barley to aphid infestation. *J. Agric. Food Chem.* 51, 2227–2231. doi: 10.1021/jf020953b

Dikilitas, M., Simsek, E., and Roychoudhury, A. (2020). Modulation of abiotic stress tolerance through hydrogen peroxide," in *Protective Chemical Agents in the Amelioration of Plant Abiotic Stress: Biochemical and Molecular Perspectives*, eds A. Roychoudhury, and D.K. Tripathi (Hoboken, NY: John Wiley & Sons), 147–173. doi: 10.1002/9781119552154.ch7

El Dakak, R. A., and Hassan, I. A. (2020). The alleviative effects of salicylic acid on physiological indices and defense mechanisms of maize (Zea Mays L. Giza 2) stressed with cadmium. *Environ. Process.* 7, 873–884.

Faraz, A., Faizan, M., Sami, F., Siddiqui, H., and Hayat, S. (2020). Supplementation of salicylic acid and citric acid for alleviation of cadmium toxicity to *Brassica juncea*. *J. Plant Growth Regul.* 39, 641–655. doi: 10.1007/s00344-019-10007-0

Ferreira, R. R., Fornazier, R. F., Vitória, A. P., Lea, P. J., and Azevedo, R. A. (2002). Changes in antioxidant enzyme activities in soybean under cadmium stress. *J. Plant Nutr.* 25, 327–342. doi: 10.1080/15226514.2017.1365346

Guo, B., Liu, C., Liang, Y., Li, N., and Fu, Q. (2019). Salicylic acid signals plant defence against cadmium toxicity. *Int. J. Mol. Sci.* 20:2960. doi: 10.3390/ijms20122960

Heath, R., and Packer, L. (1968). Photoperoxidation in isolated chloroplasts: I. Kinetics and stoichiometry of fatty acid peroxidation. *Arch. Biochem. Biophys.* 125, 189–198. doi: 10.1016/0003-9861(68)90654-1

Heidari, Z., Kamkar, B., and Masoud Sinaki, J. (2014). Determination of cardinal temperatures of milk thistle (Silybum marianum L.) germination. *Adv. Plants Agric. Res.* 1:28.

Julkunen-Tiitto, R. (1985). Phenolic constituents in the leaves of northern willows: methods for the analysis of certain phenolics. *J. Agric. Food Chem.* 33, 213–217. doi: 10.1021/jf00062a013

Karkanis, A., Bilalis, D., and Efthimiadou, A. (2011). Cultivation of milk thistle (*Silybum marianum* L. Gaertn.), a medicinal weed. *Ind. Crops Prod.* 34, 825–830. doi: 10.1016/j.indcrop.2011.03.027

Kaur, R., Yadav, P., Sharma, A., Thukral, A. K., Kumar, V., Kohli, S. K., et al. (2017). Castasterone and citric acid treatment restores photosynthetic attributes in *Brassica juncea* L. under Cd (II) toxicity. *Ecotoxicol. Environ. Saf.* 145, 466–475. doi: 10.1016/j.ecoenv.2017.07.067

Kaya, C., Okant, M., Ugurlar, F., Alyemeni, M. N., Ashraf, M., and Ahmad, P. (2019). Melatonin-mediated nitric oxide improves tolerance to cadmium toxicity by reducing oxidative stress in wheat plants. *Chemosphere* 225, 627–638. doi: 10.1016/j.chemosphere.2019.03.026

Khan, T. A., Yusuf, M., Ahmad, A., Bashir, Z., Saeed, T., Fariduddin, Q., et al. (2019). Proteomic and physiological assessment of stress sensitive and tolerant variety of tomato treated with brassinosteroids and hydrogen peroxide under low-temperature stress. *Food Chem.* 289, 500–511. doi: 10.1016/j.foodchem.2019.03.029

Khatamipour, M., Piri, E., Esmaeilian, Y., and Tavassoli, A. (2011). Toxic effect of cadmium on germination, seedling growth and proline content of Milk thistle (Silybum marianum). *Ann. Biol. Res.* 2, 527–532.

Kirk, J., and Allen, R. (1965). Dependence of chloroplast pigment on actidione. *Arch. Biochem. Biophys. Res. Commun.* 21, 523–530. doi: 10.1016/0006-291x(65)90516-4

Krantev, A., Yordanova, R., Janda, T., Szalai, G., and Popova, L. (2008). Treatment with salicylic acid decreases the effect of cadmium on photosynthesis in maize plants. *J. Plant Physiol.* 165, 920–931. doi: 10.1016/j.jplph.2006.11.014

Lindsay, W. L., and Norvell, W. A. (1978). Development of a DTPA soil test for zinc, iron, manganese, and copper. *Soil Sci. Soc. Am. J.* 42, 421–428. doi: 10.2136/sssaj1978.03615995004200030009x

Liu, Y., Zeng, G., Wang, X., Chen, B., Song, H., and Xu, L. (2010). Cadmium accumulation in Vetiveria zizanioides and its effects on growth, physiological and biochemical characters. *Bioresour. Technol.* 101, 6297–6303. doi: 10.1016/j.biortech.2010.03.028

Lu, Q., Zhang, T., Zhang, W., Su, C., Yang, Y., Hu, D., et al. (2018). Alleviation of cadmium toxicity in Lemna minor by exogenous salicylic acid. *Ecotoxicol. Environ. Saf.* 147, 500–508. doi: 10.1016/j.ecoenv.2017.09.015

Majumdar, S., Sachdev, S., and Kundu, R. (2020). Salicylic acid mediated reduction in grain cadmium accumulation and amelioration of toxicity in *Oryza sativa* L. cv Bandana. *Ecotoxicol. Environ. Saf.* 205:111167. doi: 10.1016/j.ecoenv.2020.111167

McLean, E. (1983). "Soil pH and lime requirement," in *Methods of Soil Analysis: Part 2 Chemical and Microbiological Properties*, Vol. 9, ed. A. L. Page (Madison, WI: American Society of Agronomy, Soil Science Society of America), 199–224.

Migahid, M., Elghobashy, R., Bidak, L., and Amin, A. (2019). Priming of Silybum marianum (L.) Gaertn seeds with H2O2 and magnetic field ameliorates seawater stress. *Heliyon* 5:e01886. doi: 10.1016/j.heliyon.2019.e01886

Mwamba, T., Islam, F., Ali, B., Lwalaba, J., Gill, R., Zhang, F., et al. (2020). Comparative metabolomic responses of low-and high-cadmium accumulating genotypes reveal the cadmium adaptive mechanism in *Brassica napus*. *Chemosphere* 250:126308. doi: 10.1016/j.chemosphere.2020.126308

Olsen, S., Cole, C., Watanabe, F., and Dean, L. (1954). *Estimation of Available Phosphorus in Soils by Extraction with Sodium Bicarbonate. USDA Circular No. 939.19*. Washington, DC: US Department of Agriculture.

Parida, A. K., and Jha, B. (2010). Antioxidative defense potential to salinity in the euhalophyte Salicornia brachiata. *J. Plant Growth Regul.* 29, 137–148. doi: 10.1007/s00344-009-9129-0

Podazza, G., Arias, M., and Prado, F. E. (2012). Cadmium accumulation and strategies to avoid its toxicity in roots of the citrus rootstock Citrumelo. *J. Hazard. Mater.* 215, 83–89. doi: 10.1016/j.jhazmat.2012.02.031

Popova, L., Maslenkova, L., Yordanova, R., Krantev, A., Szalai, G., and Janda, T. (2008). Salicylic acid protects photosynthesis against cadmium toxicity in pea plants. *Gen. Appl. Plant Physiol.* 34, 133–148.

Posmyk, M., Kontek, R., and Janas, K. (2009). Antioxidant enzymes activity and phenolic compounds content in red cabbage seedlings exposed to copper stress. *Ecotoxicol. Environ. Saf.* 72, 596–602. doi: 10.1016/j.ecoenv.2008.04.024

Raza, A., Habib, M., Charagh, S., and Kakavand, S. N. (2021a). "Genetic engineering of plants to tolerate toxic metals and metalloids," in *Handbook of Bioremediation*, eds M. Hasanuzzaman, and M. N. Vara Prasad (Amsterdam: Elsevier), 411–436. doi: 10.1016/b978-0-12-819382-2.00026-0

Raza, A., Habib, M., Kakavand, S. N., Zahid, Z., Zahra, N., Sharif, R., et al. (2020). Phytoremediation of cadmium: physiological, biochemical, and molecular mechanisms. *Biology* 9:177. doi: 10.3390/biology9070177

Raza, A., Hussain, S., Javed, R., Hafeez, M. B., and Hasanuzzaman, M. (2021b). "Antioxidant defense systems and remediation of metal toxicity in plants," in *Approaches to the Remediation of Inorganic Pollutants*, eds M. Hasanuzzaman (Berlin: Springer), 91–124. doi: 10.1007/978-981-15-6221-1_6

Raza, A., Tabassum, J., Mubarik, M. S., Anwar, S., Zahra, N., Sharif, Y., et al. (2021c). Hydrogen sulfide: an emerging component against abiotic stress in plants. *Plant Biol*. doi: 10.1111/plb.13368 [Epub ahead of print].

Raza, A., Tabassum, J., Zahid, Z., Charagh, S., Bashir, S., Barmukh, R., et al. (2022). Advances in "omics" approaches for improving toxic metals/metalloids tolerance in plants. *Front. Plant Sci.* 12:794373. doi: 10.3389/fpls.2021.794373

Rhoades, J. D. (1982). "Soluble salts," in *Methods of Soil Analysis, Part II. ASA Monograph No. 9*, 2nd Edn, ed. A. L. Page (Madison, WI: ASA), 167–179.

Richards, L. (1954). *Diagnosis and Improvement of Saline Sodic and Alkali Soils USDA Agric. Handbook 60*, Vol. 160. Washington, DC: US Department of Agriculture.

Salehi, H., Chehregani Rad, A., Raza, A., and Chen, J.-T. (2021). Foliar application of CeO2 nanoparticles alters generative components fitness and seed productivity in bean crop (*Phaseolus vulgaris* L.). *Nanomaterials* 11:862. doi: 10.3390/nano11040862

Shah, A. A., Khan, W. U., Yasin, N. A., Akram, W., Ahmad, A., Abbas, M., et al. (2020). Butanolide alleviated cadmium stress by improving plant growth, photosynthetic parameters and antioxidant defense system of *Brassica oleracea*. *Chemosphere* 261:127728. doi: 10.1016/j.chemosphere.2020.127728

Shaukat, K., Wahid, A., Zahra, N., and Basra, S. M. (2020). Metabolites adjustment is crucial to cross-locational adaptability of lemongrass populations from quetta and faisalabad: evidence from reciprocal swap study. *Int. J. Agric. Biol.* 24, 1855–1866.

Song, W. Y., Yang, H. C., Shao, H. B., Zheng, A. Z., and Brestic, M. (2014). The alleviative effects of salicylic acid on the activities of catalase and superoxide dismutase in malting barley (Hordeum uhulgare L.) seedling leaves stressed by heavy metals. *Clean Soil Air Water* 42, 88–97. doi: 10.1002/clen.201200310

Spitaler, R., Winkler, A., Lins, I., Yanar, S., Stuppner, H., and Zidorn, C. (2008). Altitudinal variation of phenolic contents in flowering heads of Arnica montana cv. ARBO: a 3-year comparison. *J. Chem. Ecol.* 34, 369–375. doi: 10.1007/s10886-007-9407-x

Strack, D., and Wray, V. (1989). "Anthocyanins," in *Methods in Plant Biochemistry*, ed. P. M. Dey (Amsterdam: Elsevier), 325–356.

Tiku, A. R. (2020). "Antimicrobial compounds (phytoanticipins and phytoalexins) and their role in plant defense," in *Co-Evolution of Secondary Metabolites*, eds J.-M. Merillon Kishan and G. Ramawat (Berlin: Springer), 845–868.

Valková, V., Ďúranová, H., Bilčíková, J., and Habán, M. (2021). Milk thistle (*Silybum marianum*): a valuable medicinal plant with several therapeutic purposes. *J. Microbiol. Biotechnol. Food Sci.* 2021, 836–843. doi: 10.15414/jmbfs.2020.9.4.836-843

Velikova, V., Yordanov, I., and Edreva, A. (2000). Oxidative stress and some antioxidant systems in acid rain-treated bean plants: protective role of exogenous polyamines. *Plant Sci.* 151, 59–66.

Wahid, A., Ghani, A., Ali, I., and Ashraf, M. (2007). Effects of cadmium on carbon and nitrogen assimilation in shoots of mungbean [Vigna radiata (L.) Wilczek] seedlings. *J. Agron. Crop sci.* 193, 357–365.

Walkley, A., and Black, I. A. (1934). An examination of the Degtjareff method for determining soil organic matter, and a proposed modification of the chromic acid titration method. *Soil Sci.* 37, 29–38. doi: 10.1097/00010694-193401000-00003

Wang, Q., Liang, X., Dong, Y., Xu, L., Zhang, X., Hou, J., et al. (2013a). Effects of exogenous nitric oxide on cadmium toxicity, element contents and antioxidative system in perennial ryegrass. *Plant Growth Regul.* 69, 11–20. doi: 10.1007/s10725-012-9742-y

Wang, Q., Liang, X., Dong, Y., Xu, L., Zhang, X., Kong, J., et al. (2013b). Effects of exogenous salicylic acid and nitric oxide on physiological characteristics of perennial ryegrass under cadmium stress. *J. Plant Growth Regul.* 32, 721–731. doi: 10.1007/s00344-013-9339-3

Xu, L., Dong, Y., Kong, J., and Liu, S. (2014). Effects of root and foliar applications of exogenous NO on alleviating cadmium toxicity in lettuce seedlings. *Plant Growth Regul.* 72, 39–50. doi: 10.1016/j.ecoenv.2018.08.064

Yang, W.-C., Bao, H.-Y., Liu, Y.-Y., Nie, Y.-Y., Yang, J.-M., Hong, P.-Z., et al. (2018). Depsidone derivatives and a cyclopeptide produced by marine fungus *Aspergillus unguis* under chemical induction and by its plasma induced mutant. *Molecules* 23:2245. doi: 10.3390/molecules23092245

Yu, Y., Zhou, X., Zhu, Z., and Zhou, K. (2018). Sodium hydrosulfide mitigates cadmium toxicity by promoting cadmium retention and inhibiting its translocation from roots to shoots in *Brassica napus*. *J. Agric. Food Chem.* 67, 433–440. doi: 10.1021/acs.jafc.8b04622

Zahra, N., Wahid, A., Hafeez, M. B., Shaukat, K., Shahzad, S., Shah, T., et al. (2021c). Plant growth promoters alleviate oxidative damages and improve the growth of milk thistle (Silybum marianum L.) under salinity stress. *J. Plant Growth Regul.* 1–26. doi: 10.1007/s00344-021-10498-w

Zahra, N., Hafeez, M. B., Shaukat, K., Wahid, A., and Hasanuzzaman, M. (2021a). Fe toxicity in plants: impacts and remediation. *Physiol. Plant.* 173, 201–222. doi: 10.1111/ppl.13361

Zahra, N., Wahid, A., Shaukat, K., Hafeez, M. B., Batool, A., and Hasanuzzaman, M. (2021d). Oxidative stress and tolerance potential of milk thistle ecotypes after supplementation of different plant growth-promoting agents under salinity. *Plant Physiol. Biochem.* 166, 53–65. doi: 10.1016/j.plaphy.2021.05.042

Zahra, N., Wahid, A., Arfan, M., and Basra, S. (2021b). Phenotypic plasticity for growth and nutrient uptake in milk thistle under salt stress: modulatory role of soil supplementations with plant growth promoters. *Int. J. Agric. Biol.* 25, 692–700.

Conflict of Interest: The authors declare that the research was conducted in the absence of any commercial or financial relationships that could be construed as a potential conflict of interest.

Publisher's Note: All claims expressed in this article are solely those of the authors and do not necessarily represent those of their affiliated organizations, or those of the publisher, the editors and the reviewers. Any product that may be evaluated in this article, or claim that may be made by its manufacturer, is not guaranteed or endorsed by the publisher.

Copyright © 2022 Nizar, Shaukat, Zahra, Hafeez, Raza, Samad, Ali, Siddiqui and Ali. This is an open-access article distributed under the terms of the Creative Commons Attribution License (CC BY). The use, distribution or reproduction in other forums is permitted, provided the original author(s) and the copyright owner(s) are credited and that the original publication in this journal is cited, in accordance with accepted academic practice. No use, distribution or reproduction is permitted which does not comply with these terms.

frontiers in Plant Science

ORIGINAL RESEARCH
published: 17 February 2022
doi: 10.3389/fpls.2021.831140

Genome-Wide Identification and Expression Profiling of Germin-Like Proteins Reveal Their Role in Regulating Abiotic Stress Response in Potato

Madiha Zaynab[1†], Jiaofeng Peng[2†], Yasir Sharif[3], Mahpara Fatima[4], Mohammed Albaqami[5], Rashid Al-Yahyai[6], Khalid Ali Khan[7,8,9], Saqer S. Alotaibi[10], Ibrahim A. Alaraidh[11], Hassan O. Shaikhaldein[11] and Shuangfei Li[1]*

[1] Shenzhen Key Laboratory of Marine Bioresource and Eco-Environmental Sciences, College of Life Sciences and Oceanography, Shenzhen University, Shenzhen, China, [2] Instrument Analysis Center, Shenzhen University, Shenzhen, China, [3] College of Plant Protection, Fujian Agriculture and Forestry University, Fuzhou, China, [4] College of Agriculture, Fujian Agriculture and Forestry University, Fuzhou, China, [5] Department of Biology, Faculty of Applied Science, Umm Al-Qura University, Makkah, Saudi Arabia, [6] Department of Plant Sciences, College of Agricultural and Marine Sciences, Sultan Qaboos University, Muscat, Oman, [7] Research Center for Advanced Materials Science (RCAMS), King Khalid University, Abha, Saudi Arabia, [8] Unit of Bee Research and Honey Production, Faculty of Science, King Khalid University, Abha, Saudi Arabia, [9] Department, Faculty of Science, King Khalid University, Abha, Saudi Arabia, [10] Department of Biotechnology, College of Science, Taif University, Taif, Saudi Arabia, [11] Botany and Microbiology Department, Science College, King Saud University, Riyadh, Saudi Arabia

Germin and germin-like proteins (GLPs) perform a significant role in plants against biotic and abiotic stress. To understand the role of GLPs in potato, a comprehensive genome-wide analysis was performed in the potato genome. This study identified a total of 70 *StGLPs* genes in the potato genome, distributed among 11 chromosomes. Phylogenetic analysis exhibited that *StGLPs* were categorized into six groups with high bootstrap values. *StGLPs* gene structure and motifs analysis showed a relatively well-maintained intron–exon and motif formation within the cognate group. Additionally, several *cis*-elements in the promoter regions of *GLPs* were hormones, and stress-responsive and different families of miRNAs target *StGLPs*. Gene duplication under selection pressure also exhibited positive and purifying selections in *StGLPs*. In our results, the *StGLP5* gene showed the highest expression in response to salt stress among all expressed *StGLPs*. Totally 19 *StGLPs* genes were expressed in response to heat stress. Moreover, three genes, *StGLP30*, *StGLP17*, and *StGLP14*, exhibited a relatively higher expression level in the potato after heat treatment. In total, 22 genes expressed in response to abscisic acid *(*ABA) treatment indicated that ABA performed an essential role in the plant defense or tolerance mechanism to environmental stress. RNA-Seq data validated by RT-qPCR also confirm that the *StGLP5* gene showed maximum expression among selected genes under salt stress. Concisely, our results provide a platform for further functional exploration of the *StGLPs* against salt and heat stress conditions.

Keywords: abiotic stress, gene expression, gene structure, miRNA, RNA-seq, stress responses

OPEN ACCESS

Edited by:
Mohammad Anwar Hossain, Bangladesh Agricultural University, Bangladesh

Reviewed by:
Naeem Iqbal, Muhammad Nawaz Shareef University of Agriculture, Pakistan
Faheem Shehzad Baloch, Sivas Bilim Ve Teknoloji Fakültesi, Turkey

***Correspondence:**
Shuangfei Li
sfli@szu.edu.cn

[†] These authors have contributed equally to this work

Specialty section:
This article was submitted to Plant Biotechnology, a section of the journal Frontiers in Plant Science

Received: *08 December 2021*
Accepted: *31 December 2021*
Published: *17 February 2022*

Citation:
Zaynab M, Peng J, Sharif Y, Fatima M, Albaqami M, Al-Yahyai R, Khan KA, Alotaibi SS, Alaraidh IA, Shaikhaldein HO and Li S (2022) Genome-Wide Identification and Expression Profiling of Germin-Like Proteins Reveal Their Role in Regulating Abiotic Stress Response in Potato. Front. Plant Sci. 12:831140. doi: 10.3389/fpls.2021.831140

INTRODUCTION

Germin-like proteins (GLPs) are pervasive proteins regarded as water-soluble glycoproteins present in either cell apoplast or its extracellular matrix (Lane et al., 1992; Dunwell et al., 2008). These proteins were first identified in wheat germinating embryos (Lu et al., 2010). At present, several proteins have been identified in different plant groups that exhibit 30–70% sequence homogeneity with wheat germin proteins (Finn et al., 2007).

Germin-like genes are expressed in embryos, leaves, stems, roots, flowers, and seeds of plants responding to various environmental stimuli based upon the species or genes under consideration (Wang et al., 2013). Abiotic and biotic stresses significantly affect plant growth and production worldwide (Raza et al., 2020; Qasim et al., 2021, 2018a; Raza, 2021). Various evidence has been given as an indication of *GLPs* involvement in defense and tolerance mechanisms of plants (Breen and Bellgard, 2010). Incidents like pathogen infections, insect infestation, or exposure to various chemicals such as salicylic acid, hydrogen peroxide, or ethylene may trigger the expression level of *GLPs* (Godfrey et al., 2007). Many internal elements have influenced the expression of germin, as in wheat, where the germin gene gf-2.8 is induced by hormone auxin (Schweizer et al., 1999). Transient overexpression and silencing of some *Hordeum vulgare GLP* genes have imparted enhanced resistance against fungal infection of powdery mildew (Schweizer et al., 1999). The promoter alternative of rice oxalate oxidase genes envisaged in the resistance against *Magnaporthe oryzae*. For some subfamilies, transitory and stable expression depicted the superoxide dismutase activity of the encoded protein (EC1.15.1.1) (Zimmermann et al., 2006). The silencing of GLPs in *Nicotiana attenuate* has proved fruitful in enhancing performance against herbivores (Lou and Baldwin, 2006). Fluctuation in the transcription of germin genes in *Brassica napus* and nearly associated *Arabidopsis* is found during the circadian cycle (Heintzen et al., 1994). These *GLPs* are associated with the protective mechanisms of cereals against the infection of fungal pathogens (Lane, 2000). Studies have revealed that the transfer of *GLPs* from soybean and sunflower to *Nicotiana tabacum* can increase its resistance against *Sclerotinia sclerotiorum* (Beracochea et al., 2015; Zhang et al., 2018). Transient-enhanced expression of *TaGLP4* and *HvGLP4* makes wheat and barley plants more resistant to *Blumeria graminis.* At the same time, the ephemeral gene that is silenced by utilizing RNA interference minimizes the basal resistance in cereals (Christensen et al., 2004, p. 4). A study is conducted to explore that the regulatory factors in various GLP gene promoters and several regulatory factors are associated with many essential roles with variable copy numbers and dispersed in locations of various positive or negative strands. Cotton GLP as *GhABP19* is involved in various essential tasks in the exhibition of resistance to *Verticillium* and *Fusarium wilt* in crops (Pei et al., 2019, p. 19). A few GLP subfamily members are intricated in a vast range of fungal disease resistance in the tissues of leaves (Davidson et al., 2009).

Germin-like protein genes have variable expression and multiple tasks in several tissues and at different phases of plant growth processes (Barman and Banerjee, 2015). This gene family is one of those gene families that are crucial and indispensable for the defense and stress tolerance mechanisms of plants. Expression of these genes varies against various abiotic stress such as salt (Wang et al., 2013), heavy metal (Berna and Bernier, 1999), and drought stress. Moreover, some purposes of *GLP* genes have been characterized in *Hordeum vulgare* (Zimmermann et al., 2006), *Arabidopsis thaliana* (Rietz et al., 2012), *Oryza sativa* (Li et al., 2016), and *Glycine max* (Wang et al., 2014). The expression levels of many rice *GLP* genes were altered under salt stress (Das et al., 2019). *OsGLP8-14* was found to be involved in salt stress response (Banerjee et al., 2017). Liao et al. (2021) reported the differential expression of *CsGLP* genes in response to salt, drought, and ABA treatments (Liao et al., 2021).

Potato (*Solanum tuberosum* L.) is an economically essential field crop and is widely grown as a basic food commodity worldwide. About 368,168,914 tons of potatoes were harvested in 2018 on 17,578,672 ha of land, and over 1 billion people consumed them (Rashid et al., 2021). Like other plant species, potato yield is also in jeopardy due to many biotic and abiotic environmental fluctuations (Zaynab et al., 2021d). To date, the expression analysis of *GLP* genes against abiotic stress has not been reported in potatoes. Therefore, this study used genome-wide analysis to find *GLP* genes in the potato genome. Furthermore, their evolutionary relationships, synteny analysis, gene structures, conserved motifs, *cis*-elements, and miRNA predictions were investigated. Expression profiling in many tissues/organs and response to various hormones and abiotic stresses have been substantially explored, enabling us to explore and understand these *GLPs* in extensive detail in the potato genome.

MATERIALS AND METHODS

Identification and Characterization of GLP Genes in Potato

In this study, we used two methods to identify *GLP* genes from the genome of the *Solanum tuberosum.* The first method was the Hidden Markov Model (HMM), and the second one was the BLASTP search (Raza et al., 2021; Zaynab et al., 2021d). Potato genome sequences were retrieved from JGI Phytozome 12.0[1] database (Goodstein et al., 2012). GLP amino acids sequences of *A. thaliana* were taken from TAIR[2] (Rhee, 2003) database and used as a query to run BLASTP search. The HMM file with Pfam ID PF00190 containing *GLP* genes was downloaded from Pfam[3] (El-Gebali et al., 2019) database. Moreover, a local HMMER 3.1[4] webserver was utilized to identify the *GLP* genes with default parameters (Finn et al., 2015). Eventually, a total of 70 *GLP* genes were identified from the genome of the potato. Non-redundant genes with conserved domains were serially named through *StGLP1–StGLP70* and used for further analysis.

[1]https://phytozome.jgi.doe.gov/pz/portal.html
[2]http://www.arabidopsis.org/
[3]http://pfam.xfam.org/
[4]http://www.hmmer.org/

TABLE 1 | List of identified putative *StGLPs* and their features.

Gene name	Transcript name	Gene start (bp)	Gene end (bp)	Chromosome name	Transcript end (bp)	Transcript start (bp)	No. of amino acids	Molecular weight	PI
StGLP1	PGSC0003DMT400040093	20,824,518	20,825,297	ST4.03ch02	20,825,297	20,824,518	228	24,389.04	7.79
StGLP2	PGSC0003DMT400032968	40,814,829	40,816,831	ST4.03ch02	40,816,831	40,814,829	515	61,094.18	5.12
StGLP3	PGSC0003DMT400081522	43,168,850	43,169,134	ST4.03ch00	43,169,134	43,168,850	94	10,650.29	7.99
StGLP4	PGSC0003DMT400057096	55,379,029	55,379,951	ST4.03ch07	55,379,951	55,379,029	201	22,001.22	7.71
StGLP5	PGSC0003DMT400033858	38,547,986	38,548,621	ST4.03ch07	38,548,621	38,547,986	211	22,055.77	5.84
StGLP6	PGSC0003DMT400000051	71,669,764	71,670,896	ST4.03ch01	71,670,896	71,669,764	313	34,015.31	6.9
StGLP7	PGSC0003DMT400034084	79,622,868	79,623,667	ST4.03ch01	79,623,667	79,622,868	228	24,491.01	5.62
StGLP8	PGSC0003DMT400017373	64,470,132	64,472,699	ST4.03ch01	64,472,699	64,470,132	188	19,878.96	8.52
StGLP9	PGSC0003DMT400034092	79,600,750	79,614,804	ST4.03ch01	79,601,534	79,600,750	228	24,517.12	5.88
StGLP10	PGSC0003DMT400046879	79,534,943	79,535,624	ST4.03ch01	79,535,624	79,535,115	169	18,065.87	9.74
StGLP11	PGSC0003DMT400017382	64,505,199	64,505,959	ST4.03ch01	64,505,959	64,505,199	225	24,736.65	5.51
StGLP12	PGSC0003DMT400061076	80,764,817	80,766,134	ST4.03ch01	80,766,134	80,764,817	362	38,977.83	5.75
StGLP13	PGSC0003DMT400053377	79,649,888	79,650,650	ST4.03ch01	79,650,650	79,649,888	216	23,186.36	5.36
StGLP14	PGSC0003DMT400047065	79,150,246	79,151,880	ST4.03ch01	79,151,880	79,150,246	210	22,228.7	8.44
StGLP15	PGSC0003DMT400017379	64,490,847	64,491,641	ST4.03ch01	64,491,641	64,490,847	225	24,708.72	9.28
StGLP16	PGSC0003DMT400046995	79,507,167	79,507,900	ST4.03ch01	79,507,900	79,507,167	228	24,625.34	6.17
StGLP17	PGSC0003DMT400047067	79,135,984	79,137,376	ST4.03ch01	79,137,376	79,135,984	211	22,272.7	7.8
StGLP18	PGSC0003DMT400053424	79,647,675	79,648,034	ST4.03ch01	79,648,034	79,647,675	119	13,318.31	6.9
StGLP19	PGSC0003DMT400046887	79,523,462	79,524,263	ST4.03ch01	79,524,263	79,523,462	230	24,753.47	8.55
StGLP20	PGSC0003DMT400000042	71,626,643	71,627,873	ST4.03ch01	71,627,873	71,626,643	348	38,041.87	5.74
StGLP21	PGSC0003DMT400088315	80,783,956	80,786,749	ST4.03ch01	80,786,749	80,783,956	207	22,017.21	7.69
StGLP22	PGSC0003DMT400061073	80,803,974	80,805,300	ST4.03ch01	80,805,300	80,803,974	362	38,986.74	6.04
StGLP23	PGSC0003DMT400017381	64,501,551	64,502,069	ST4.03ch01	64,502,069	64,501,551	128	14,095.21	5.42
StGLP24	PGSC0003DMT400017372	64,463,708	64,464,591	ST4.03ch01	64,464,591	64,463,714	222	24,245.05	6.95
StGLP25	PGSC0003DMT400046992	79,536,560	79,537,367	ST4.03ch01	79,537,367	79,536,560	228	24,522.09	6.49
StGLP26	PGSC0003DMT400053421	79,661,664	79,662,463	ST4.03ch01	79,662,463	79,661,664	174	18,975.74	8.89
StGLP27	PGSC0003DMT400000049	71,661,596	71,662,286	ST4.03ch01	71,662,286	71,661,596	192	21,734.96	5.39
StGLP28	PGSC0003DMT400017366	64,436,796	64,437,584	ST4.03ch01	64,437,584	64,436,796	225	24,725.77	8.77
StGLP29	PGSC0003DMT400088001	64,444,053	64,444,436	ST4.03ch01	64,444,436	64,444,053	127	14,195.59	9.43
StGLP30	PGSC0003DMT400053423	79,654,305	79,655,071	ST4.03ch01	79,655,071	79,654,305	228	24,429.06	6.49
StGLP31	PGSC0003DMT400017387	64,508,106	64,508,869	ST4.03ch01	64,508,869	64,508,106	162	17,779.49	5.19
StGLP32	PGSC0003DMT400017363	64,424,713	64,425,516	ST4.03ch01	64,425,516	64,424,713	225	24,860.8	8.94
StGLP33	PGSC0003DMT400046891	79,517,314	79,518,118	ST4.03ch01	79,518,118	79,517,314	230	24,628.3	8.55
StGLP34	PGSC0003DMT400017367	64,450,575	64,451,350	ST4.03ch01	64,451,350	64,450,575	225	24,878.8	8.4
StGLP35	PGSC0003DMT400058298	6,670,741	6,672,129	ST4.03ch05	6,672,129	6,670,741	211	22,544.89	8.58
StGLP36	PGSC0003DMT400030317	52,610,039	52,610,665	ST4.03ch12	52,610,665	52,610,039	208	21,643.96	6.82
StGLP37	PGSC0003DMT400019402	55,885,543	55,887,421	ST4.03ch06	55,887,421	55,885,543	459	51,649.76	8.95
StGLP38	PGSC0003DMT400019389	55,877,736	55,879,480	ST4.03ch06	55,879,480	55,877,736	458	51,627.42	7.32
StGLP39	PGSC0003DMT400008698	55,873,841	55,875,211	ST4.03ch06	55,875,211	55,873,841	374	42,039.48	9.33
StGLP40	PGSC0003DMT400019388	55,889,622	55,891,351	ST4.03ch06	55,891,351	55,889,622	455	51,137.24	9.1
StGLP41	PGSC0003DMT400019398	55,882,134	55,883,989	ST4.03ch06	55,883,989	55,882,134	457	51,399.11	6.04
StGLP42	PGSC0003DMT400044214	56,455,696	56,458,487	ST4.03ch09	56,458,487	56,455,696	520	58,788.33	6.59
StGLP43	PGSC0003DMT400044229	56,325,068	56,327,136	ST4.03ch09	56,327,136	56,325,068	226	24,986.91	5.77
StGLP44	PGSC0003DMT400026705	50,134,244	50,135,537	ST4.03ch09	50,135,537	50,134,244	371	41,766.35	6.43
StGLP45	PGSC0003DMT400044231	56,322,818	56,323,971	ST4.03ch09	56,323,971	56,322,818	224	23,985.76	5.49
StGLP46	PGSC0003DMT400049823	47,996,075	48,000,869	ST4.03ch09	48,000,869	47,996,075	451	50,927.94	9.05
StGLP47	PGSC0003DMT400044224	56,339,851	56,341,183	ST4.03ch09	56,341,183	56,339,851	225	24,724.45	5.72
StGLP48	PGSC0003DMT400082074	54,002,237	54,005,886	ST4.03ch09	54,005,886	54,002,237	567	65,780.62	7.54
StGLP49	PGSC0003DMT400026712	50,168,038	50,169,925	ST4.03ch09	50,169,925	50,168,038	481	54,427.26	6.82
StGLP50	PGSC0003DMT400096380	56,330,056	56,331,514	ST4.03ch09	56,331,514	56,330,056	226	25,186.3	9.17
StGLP51	PGSC0003DMT400044227	56,334,086	56,338,772	ST4.03ch09	56,338,772	56,337,621	383	43,087.09	4.46
StGLP52	PGSC0003DMT400026650	50,132,519	50,132,890	ST4.03ch09	50,132,890	50,132,519	123	13,673.41	6.72

(Continued)

TABLE 1 | (Continued)

Gene name	Transcript name	Gene start (bp)	Gene end (bp)	Chromosome name	Transcript end (bp)	Transcript start (bp)	No. of amino acids	Molecular weight	PI
StGLP53	PGSC0003DMT400063164	53,565,261	53,565,923	ST4.03ch03	53,565,923	53,565,261	220	23,470.25	6.5
StGLP54	PGSC0003DMT400036428	61,605,492	61,606,118	ST4.03ch03	61,606,118	61,605,492	208	21,519.77	5.83
StGLP55	PGSC0003DMT400053916	7,589,586	7,592,195	ST4.03ch03	7,592,195	7,589,586	450	51,300.84	7.77
StGLP56	PGSC0003DMT400063166	53,567,656	53,568,309	ST4.03ch03	53,568,309	53,567,656	217	23,201.87	6.27
StGLP57	PGSC0003DMT400034989	639,862	644,028	ST4.03ch03	644,028	639,862	430	48,782.81	8.28
StGLP58	PGSC0003DMT400067755	40,482,716	40,483,336	ST4.03ch11	40,483,336	40,482,716	206	21,854.14	5.51
StGLP59	PGSC0003DMT400061586	5,333,291	5,333,929	ST4.03ch11	5,333,929	5,333,291	212	23,300.94	6.41
StGLP60	PGSC0003DMT400067758	40,480,217	40,480,828	ST4.03ch11	40,480,828	40,480,217	203	21,650.87	6.91
StGLP61	PGSC0003DMT400067709	40,477,347	40,479,544	ST4.03ch11	40,479,544	40,477,347	303	32,003.43	6.34
StGLP62	PGSC0003DMT400003235	5,633,348	5,633,974	ST4.03ch11	5,633,974	5,633,348	208	22,581.1	9.36
StGLP63	PGSC0003DMT400040214	45,351,028	45,352,678	ST4.03ch11	45,352,678	45,351,028	356	38,205.97	6.15
StGLP64	PGSC0003DMT400070424	43,975,664	43,979,229	ST4.03ch11	43,979,229	43,975,664	509	57,013.7	5.67
StGLP65	PGSC0003DMT400040162	45,354,585	45,358,874	ST4.03ch11	45,358,874	45,354,585	513	56,512.04	6.58
StGLP66	PGSC0003DMT400092000	40,481,535	40,482,146	ST4.03ch11	40,482,146	40,481,535	203	21,422.5	6.26
StGLP67	PGSC0003DMT400029687	58,884,139	58,885,066	ST4.03ch10	58,885,066	58,884,139	217	22,866.41	7.72
StGLP68	PGSC0003DMT400092672	58,892,246	58,892,689	ST4.03ch10	58,892,689	58,892,246	147	16,028.43	6.16
StGLP69	PGSC0003DMT400029689	58,881,482	58,882,474	ST4.03ch10	58,882,474	58,881,482	217	23,082.58	7
StGLP70	PGSC0003DMT400087849	58,876,226	58,879,838	ST4.03ch10	58,879,838	58,876,226	429	45,493.44	6.45

CDS, coding sequence; pI, isoelectric point.

Physiochemical characteristics, including molecular weight and isoelectric points, were identified through ProtParam[5] (Gasteiger et al., 2005).

Phylogenetic, Gene Structure, Motif, and Synteny Analysis

In order to investigate the evolutionary history of the *StGLP* family genes, a phylogenetic tree was constructed among the amino acid sequences of *Solanum lycopersicum, S. tuberosum,* and *A. thaliana.* We used MEGA 7[6] (Kumar et al., 2018) for the construction of phylogenetic tree. The neighbor-joining method was applied to make a phylogenetic tree with 1,000 bootstrap values. TBtools software[7] was deployed to construct the gene structure of *StGLPs* (Chen et al., 2020). Conserved motifs present in *StGLPs* sequences were recognized through MEME[8] (Bailey et al., 2009) server. For comparative synteny analysis, Circoletto Tool[9] was used.

Chromosomal Locations, Selection Pressure, and *Cis*-Elements Analysis

Data related to the chromosomal location was taken from general feature format (GFF) files of *S. tuberosum* genome database (PGSC Ref seq v4.03) (The Potato Genome Sequencing Consortium, 2011). The localization of 70 identified genes on chromosomes was performed by utilizing TBtools (Chen et al., 2020). To explore the putative *cis*-elements in the promoter region of *StGLPs*, we extracted a sequence of 2 Kb upstream of start codons in the genome of *S. tuberosum*. Afterward, to analyze the promoter region of each gene, we deployed them to PlantCARE[10] (Lescot, 2002) and figures made by TBtools (Chen et al., 2020). Besides, the synonymous and non-synonymous substitution rate was computed by employing KaKs Calculator 2.0 software using the MYN procedure. Ks and Ka refer to the number of synonymous and non-synonymous substitutions concerning the synonymous non-synonymous site (Wang et al., 2010). Divergence time ($t = Ks/2r$) was estimated through exchange rate as ($r = 2.6 \times 10^{-9}$) (Li et al., 2019).

Prediction of miRNA and Protein–Protein Interactions

For identifying miRNA targeting *StGLPs,* psRNAtarget[11] was used with default parameters (Dai et al., 2018). For illustrating the protein–protein interaction network, the STRING 11.0[12] server was employed, and for reference, the genome of *S. tuberosum* was used. The exhibit specifications were propped as the confidence value is 0.9 for network; and 10 for edges evidence and maximum number of interaction.

Expression Profiling of StGLP Genes in Different Tissues

In order to investigate the expression of *StGLP* genes in various tissues and under various stress conditions, the transcriptome data were obtained from the available public database BioProject

[5]http://web.expasy.org/protparam/

[6]https://megasoftware.net/home

[7]https://github.com/CJ-Chen/TBtools

[8]https://meme-suite.org/meme/db/motifs

[9]tools.bat.infspire.org/circoletto/

[10]http://bioinformatics.psb.ugent.be/webtools/plantcare/html/

[11]https://www.zhaolab.org/psRNATarget/

[12]https://string-db.org/

ID: Project: PRJEB2430. For the expression analysis of *StGLP* genes in different tissues and under different stresses, fragments per kilobase million (FPKM) were observed (Zaynab et al., 2021d). The obtained data were arranged according to their expression in different tissues. The observed FPKM values were utilized to construct a heatmap through TBtools after the normalization of log2 values.

Potato Growth Conditions and Stress Treatment

The rooster variety of *S. tuberosum* was selected as the sample for these experiments, which were conducted at the experimental station of the National Institute for Genomics and Advanced Biotechnology (NIGAB), Islamabad, Pakistan. After 6 weeks of growth, the sample was treated with 150 mM NaCl for 0 and 24 h, respectively, for salt treatment. The first time point (0 h) served as a control. After NaCl treatment, leaves were taken, and samples were immediately frozen in liquid nitrogen and stored at −80°C for total RNA extraction.

RNA Extraction and RT-qPCR Analysis

Total RNA was extracted using TransZol Up Plus RNA Kit (TransGen Biotech, Beijing, China). For cDNA synthesis, cDNA Synthesis SuperMix was purchased from the above-mentioned Chinese company. Instructions given by manufacturers were followed during the whole process. The comprehensive knowledge about reactions of RT-qPCR has been reported in our earlier published work (Zaynab et al., 2021a). In our study, the expression data were evaluated by using the $2^{-\Delta\Delta CT}$ methods (Zaynab et al., 2021c), and the elongation factor 1-alpha was chosen as a housekeeping gene (Zaynab et al., 2021b). The primers used in this study are given in **Supplementary Table 1**.

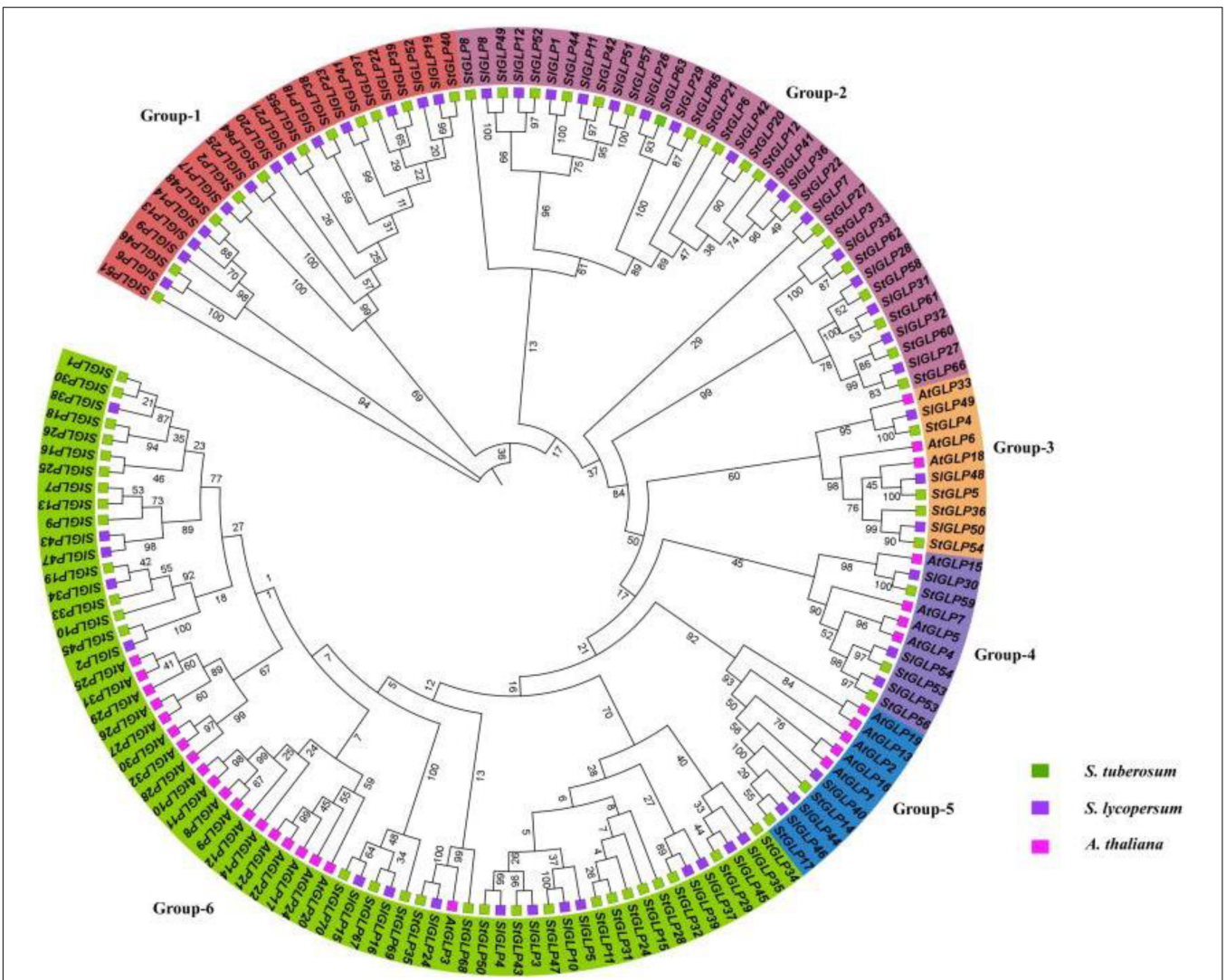


FIGURE 1 | Phylogenetic tree of GLP proteins from *Arabidopsis*, *S. lycoperiscum*, and *S. tuberosum*. The colored arcs indicate different groups. The stars colors represent proteins of *Arabidopsis*, *S. lycoperiscum*, and *S. tuberosum*.

RESULTS

Identification, Phylogenetic, Gene Structure, Motif Analysis of *GLP* Genes in Potato

A total of 70 *GLP* genes were identified in the potato genome by employing sequences of *A. thaliana* as a query (**Table 1**). In this study, Batch-CD and SMART were utilized to confirm the domain with Pfam ID (PF00190). All these 70 genes contain a domain with Pfam ID (PF00190). The protein sequences of *A. thaliana*, *S. lycopersicum*, and identified StGLPs are given in **Supplementary Table 2**. Amino acids length varied from 94 to 567, the molecular weight from 10.650 to 65.780 kDa, and the isoelectric point values from 4.46 to 9.74 (**Table 1**). A phylogenetic tree was constructed using the neighbor-joining method through MEGA7 to illustrate the phylogenetic relationship among *A. thaliana, S. lycoperiscum,* and *S. tuberosum*. This study results showed that the phylogenetic tree was divided into six groups. Group-6 is the largest group, and group-3 is the smallest among all groups (**Figure 1**). Exons and introns are two main determinants in the gene family evolution. The detailed analysis of the phylogenetic relationship and gene composition illustration corroborated our understanding of the structures of *StGLPs* genes (**Figure 2**). The

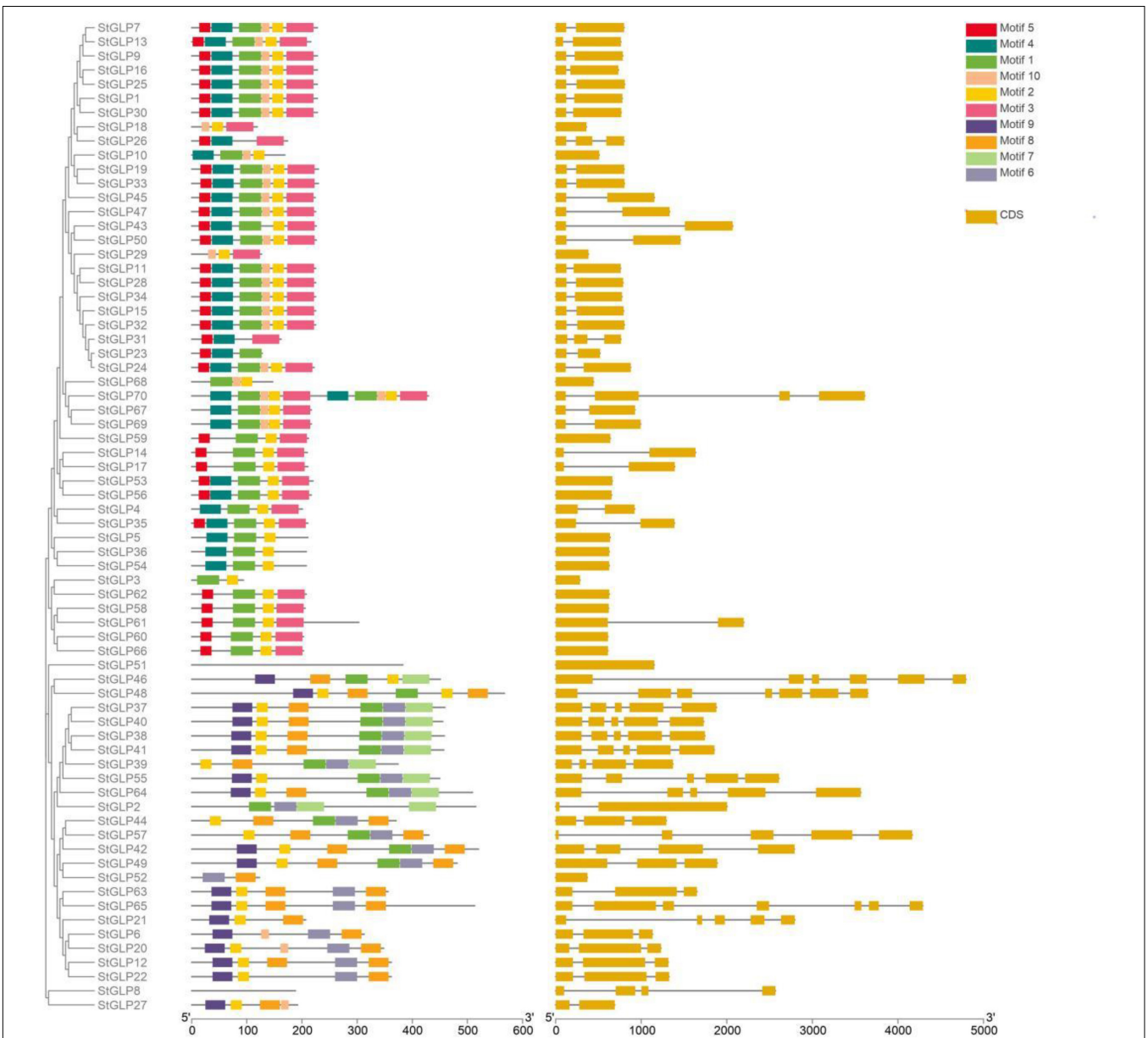


FIGURE 2 | Distribution of exons, introns, and untranslated regions (UTR) in *StGLP* gene sequences and distributions of *de novo* MEME motifs in the StGLP proteins.

results revealed that numerical attributes of exon and intron in *StGLP* genes possessed high inconsistency in numbers of exons and introns (**Figure 2**). In this study, the *StGLP46* gene possessed the most extended sequence. Some genes such as *StGLP41* and *StGLP38* exhibited similarities in exon numbers. Additionally, *StGLP21* and *StGLP57* genes were equal in exons numbers but differed in their sequence lengths. For determining structural diversification and functional characterization of these *StGLPs*, we analyzed full-length sequences of 70 StGLPs through MEME software to localize their conserved motifs. The motif results revealed that a total of ten motifs were identified (**Figure 2**). The sequences of predicted motifs are given in **Supplementary Table 3**. All of the *StGLPs* genes contained motif 1 except genes *StGLP StGLP18, StGLP26, StGLP29, StGLP31, StGLP51, StGLP52, StGLP63, StGLP65, StGLP21, StGLP6, StGLP20, StGLP12, StGLP22, StGLP8,* and *StGLP27*. The length of the motif was varied from 21 to 50 amino acids. The highest 50 amino acids were possessed by motif 3,7, and 10, while motif 2 and 5 contained the lowest 21 amino acids. In our results, motif 4 had 39 amino acids, motif 8 had 35 amino acids, while motifs 1 and 9 had 41 amino acids in their sequence. In short, the reliability of group organization was exceedingly encouraged by analyzing conserved motif conformation, genetic structures, and phylogenetic relationship, indicating that StGLP proteins possess enormously well-sustained amino acid members and remain inside a group. Thus, it can be inferred that proteins with identical motifs and structures may possess functional similarities.

Chromosomal Locations, Synteny, and Gene Duplication Analysis

Chromosomal distribution analysis of *StGLPs* depicted their unequal localization on all chromosomes (**Figure 3**). A maximum number of 29 genes were present on the 1st chromosome, while the 9th chromosome had 11 genes. There are 9 genes present on chromosome number 11. Only 2 genes are located on chromosome number 02 (**Figure 3**) in our results. Furthermore, there was no gene located on chromosome number 08. To determine the rate of molecular evolution of each gene pair that has been duplicated, the Ka to Ks (synonymous/non-synonymous substitution) ratios were calculated. When the value of the ratio is more than 1, then the selection effect will be positive; if its value is less than 1, then purifying selection will be exhibited, while when this ratio's value is equal to 1, then there will be the presence of neutral selection in gene pairs (Yang and Bielawski, 2000). The cosmic majority of *StGLPs* genes exhibited a value of Ks more than 0.52, and the corresponding deviation time may be more than 100 million years ago (MYA). In this study, duplicated genes (*StGLP4/StGLP35*) showed the Ks value 3.54 while its corresponding time may be 682.30 MYA (**Table 2**). Comparative synteny analysis was analyzed among *A. thaliana*, *S. tuberosum,* and *S. lycoperiscum* which exhibited a phenomenal relationship in the evolution expression, duplication, triplication, and function of genes. Genes sequence of *SlGLP17* exhibited synteny with the sequence of *StGLP2*. At the same time, two potato genes, *StGLP20* and *StGLP22*, showed synteny with the *SlGLP41* gene of tomato. The comparative synteny analysis

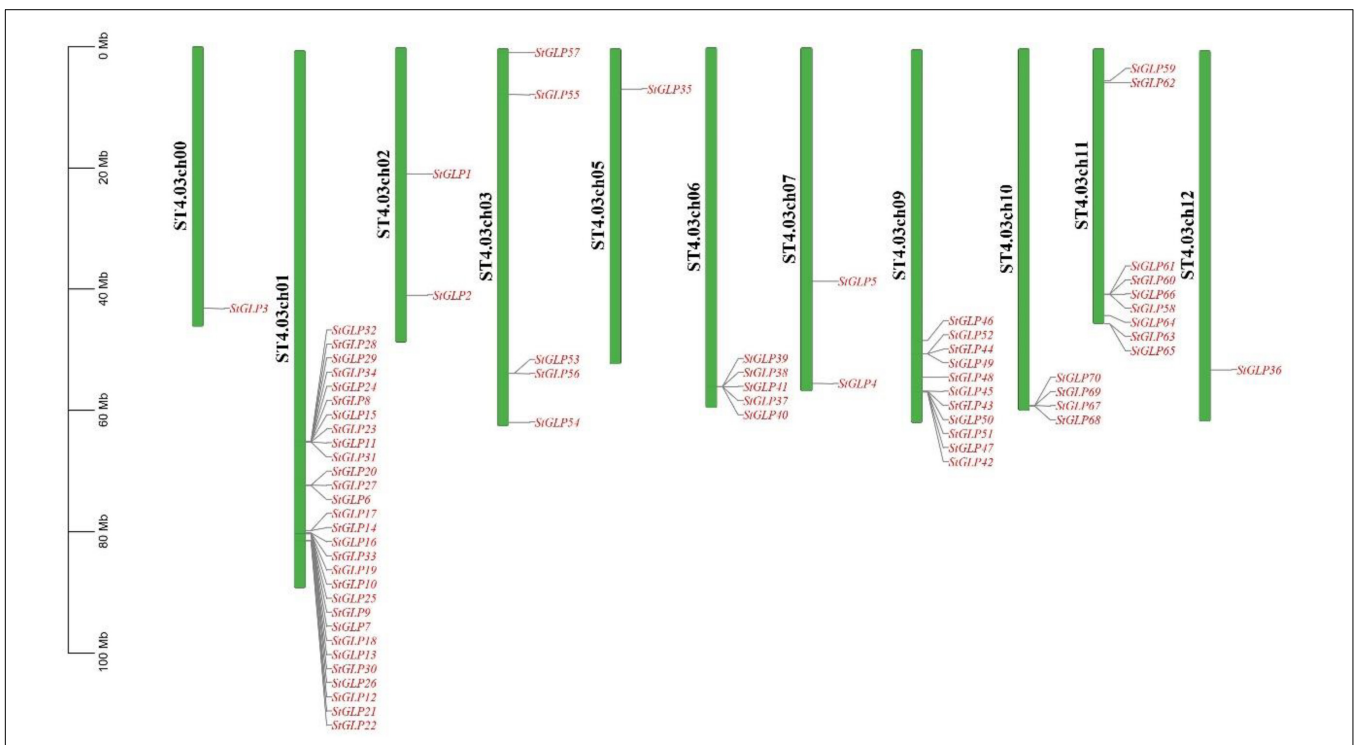


FIGURE 3 | Chromosomal distribution of *StGLP* genes. Green color shows chromosomes, red color shows *StGLP* genes, and black color shows the number of chromosomes.

TABLE 2 | Gene duplication and selection pressure of *StGLPs*.

Seq_1	Seq_2	Ka	Ks	Ka_Ks	Time (MYA)
StGLP6	*StGLP20*	0.00587159	0.019568986	0.300045672	3.763266576
StGLP12	*StGLP22*	0.059038628	0.193459314	0.305173356	37.20371428
StGLP63	*StGLP65*	0.047638432	0.282922672	0.168379692	54.40820612
StGLP42	*StGLP57*	0.321196935	1.332395831	0.241067202	256.2299675
StGLP39	*StGLP55*	0.237145767	0.571605039	0.41487697	109.924046
StGLP38	*StGLP41*	0.06693679	0.288679494	0.231872342	55.51528724
StGLP4	*StGLP35*	0.635162456	3.548006451	0.179019533	682.3089328
StGLP36	*StGLP54*	0.090222715	1.503069078	0.060025661	289.0517458
StGLP3	*StGLP62*	0.083490733	0.188993779	0.441764451	36.34495755
StGLP58	*StGLP61*	0.022084776	0.136249525	0.162090661	26.20183183
StGLP60	*StGLP66*	0.066557407	0.157685536	0.422089489	30.32414157
StGLP14	*StGLP17*	0.012705439	0.132943691	0.095570077	25.56609445
StGLP53	*StGLP56*	0.063376386	0.255022102	0.248513307	49.04271201
StGLP67	*StGLP70*	0.023344121	0.08530024	0.273670051	16.40389238
StGLP19	*StGLP33*	0.021457901	0.147797879	0.14518409	28.42266902
StGLP1	*StGLP30*	0.019660366	0.228158531	0.086169759	43.87664054
StGLP18	*StGLP26*	0.267626689	0.427706455	0.625725158	82.25124131
StGLP7	*StGLP13*	0.002038737	0.033904078	0.060132509	6.520014918
StGLP43	*StGLP50*	0.124561464	0.128964836	0.965856028	24.80093
StGLP11	*StGLP28*	0.149905888	0.166366256	0.901059457	31.99351068
StGLP31	*StGLP32*	0.119090894	0.142681101	0.834664809	27.43867323
StGLP29	*StGLP34*	0.206352764	0.292304449	0.7059515	56.21239411

Ka, number of non-synonymous substitutions per non-synonymous site; Ks, number of synonymous substitutions per synonymous site; MYA, million years ago.

revealed the conservation and duplication of inward and outward tangling events in ribbons, respectively (**Figure 4**).

Cis-Elements and *miRNA* Analysis

To observe the *StGLPs* gene function and their regulatory role, promoter *cis*-elements were analyzed using the PlantCARE database. The *cis*-elements that are associated with plant hormones were identified. As shown in **Figure 5**, the number of genes associated with phytohormones indicates the importance of these genes in phytohormone stress. Furthermore, the role of anaerobic, light, and low-temperature responsive factors in this study was discovered (**Figure 5**). Mainly several elements that are responsive to light were categorized to be extensively distributed in all genes, indicating the significant role of *StGLPs* in response to light stress. Generally, findings envisaged that diversification in the expression levels of various *StGLPs* might be attributed to different plant hormones and environmental stress. The Hormones- and stress-related cis-elements found in the promoter regions of StGLPs are given in **Supplementary Table 4**.

Many researchers have reported that microRNA mediated a significant role in enhancing stress response in plants (Su et al., 2021; Xu et al., 2021). Thus, for an in-depth comprehension of miRNA-triggered post-transcriptional modulations of *StGLPs*, we identified miRNAs targeting *StGLPs* genes. Several sites that are targeted by miRNA are illustrated in **Supplementary Table 1**. Our findings revealed that seven members of the miR166 family target six genes, including *StGLP8, StGLP54, StGLP23, StGLP24, StGLP38*, and *StGLP28*. A gene, *StGLP2,* was targeted by a single member of the miR169 family. Targets *StGLP51, StGLP48,* and *StGLP47* (**Figure 6** and **Supplementary Table 5**) are all three members of the miRNA gene family. The findings of our study revealed that two members of the miR8040 aimed at two genes, *StGLP51* and *StGLP62*. A gene *StGLP55* was the target of two members of the miR1886 family. Our results mainly estimated two genes, *StGLP40* and *StGLP8*, to target numerous miRNAs.

The protein–protein interaction network provided details about StGLPs in the genome of potatoes. The interaction network was observed among several proteins, including StGLP57, StGLP44, StGLP46, StGLP48, and StGLP2. These proteins depicted the concurrence, co-expression, fusion, and homology of genes. Likewise, another framework was also identified among StGLP53, StGLP63, and StGLP4 protein. Among all StGLPs, two proteins, StGLP48 and StGLP46, are responsible for framing a protein–protein interaction network, so these can be reputed as hub proteins of StGLPs (**Figure 7**).

Tissue-Specific Expression Profiling

Expression profiling of *StGLPs* revealed that many genes exhibited high expression in the tissues of roots than that in the tissues of stems and leaves. Some genes showed expression in some tissues, while some genes have no expression in others. For example, the *StGLP17* gene showed a higher expression level in the tissues of roots, leaves, and stems, while the *StGLP26* and *StGLP45* genes showed higher expression levels in the tissues of roots and stems. Furthermore, in the tissues of leaves, *StGLP5* genes showed the maximum expression in our results (**Figure 8**).

Expression Patterns of StGLP Genes in Response to Heat and Salt Stress

Transcriptional profiling of *GLPs* was performed when potato plants were subjected to heat stress. *StGLPs* may help potato plants cope better with high temperatures, according to some research. A total of 19 *StGLPs* genes were expressed in response to heat stress. Moreover, three genes, *StGLP30*, *StGLP17*, and *StGLP14,* exhibited a relatively higher expression level in potatoes after heat treatment (**Figure 9**). In our results, *StGLP30* gene expression was higher than *StGLP17* and *StGLP14*.

Furthermore, *StGLP16* genes showed the lowest expression compared with other expressed *StGLPs* after heat treatment. Likewise, 29 *GLPs* were expressed in response to salt treatment. This study showed that *StGLP54*, *StGLP12*, and *StGLP5* genes were highly expressed in potatoes after salt treatment (**Figure 9**), but the expression level of the *StGLP5* gene was relatively higher as compared to *StGLP12* and *StGLP54* genes in the potato genome.

Expression Patterns of StGLP Genes in Response to Phytohormones

Three hormones, abscisic acid (ABA), gibberellic acid (GA3), and indole acetic acid (IAA), were selected to evaluate the hormonal response of StGLPs.

This study results showed that 22 *StGLP* genes were expressed after the treatment of ABA. Similarly, in the case of IAA treatment, 24 *StGLP* genes were expressed. Furthermore, the

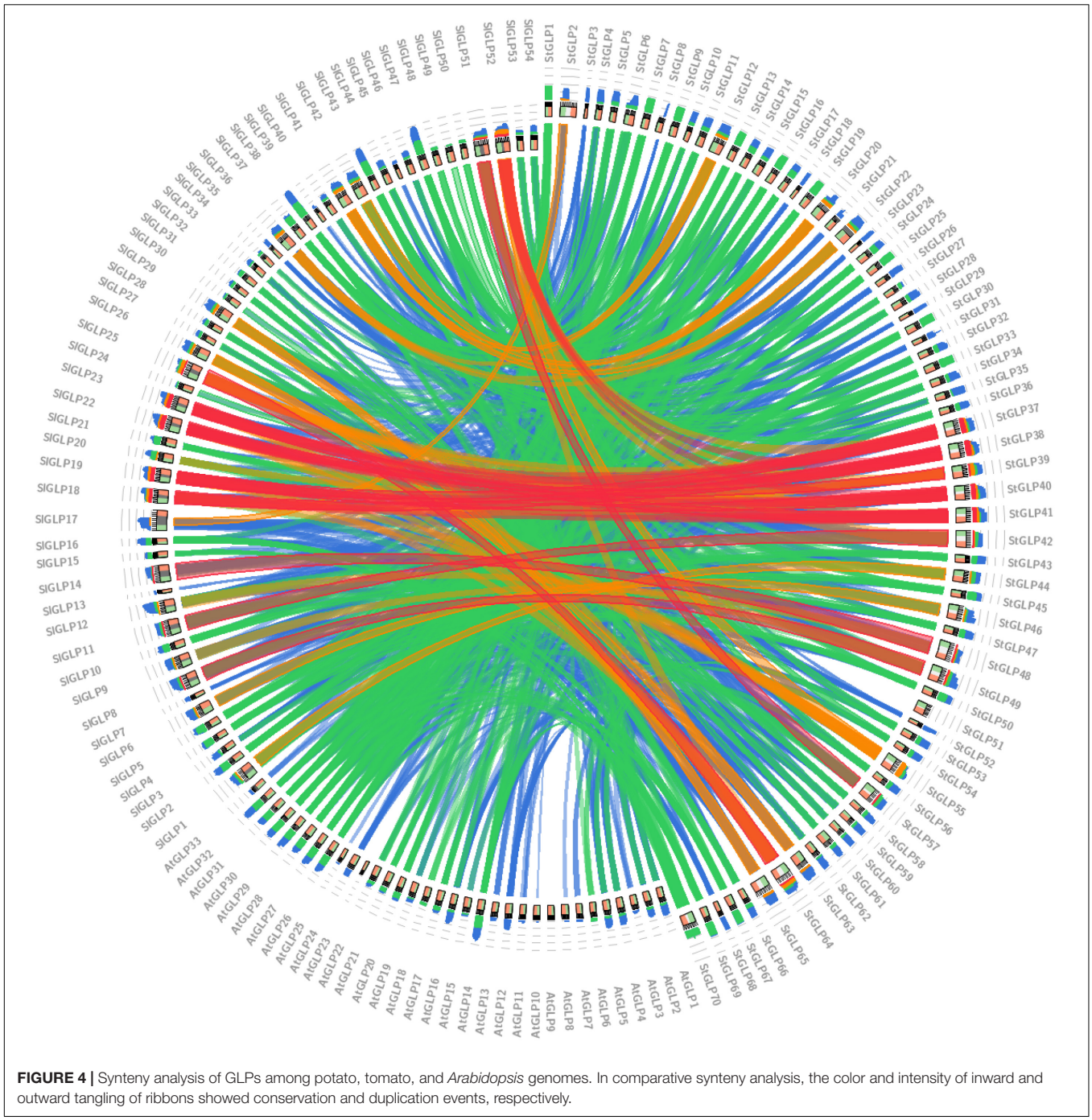


FIGURE 4 | Synteny analysis of GLPs among potato, tomato, and *Arabidopsis* genomes. In comparative synteny analysis, the color and intensity of inward and outward tangling of ribbons showed conservation and duplication events, respectively.

StGLP12 gene was highly expressed compared with others after the treatment of ABA, while *StGLP5* showed the highest expression after IAA treatment (**Figure 10**). Additionally, 27 *StGLPs* were expressed when treated with GA3, and the expression of gene *StGLP14* was highest among all 27 expressed genes (**Figure 10**). The upregulation of *StGLPs* after ABA, IAA, and GA3 treatment revealed the significant role of *StGLP* genes in mitigating the lethal effects of different hormonal and environmental stress.

RT-qPCR Analysis

Real-time-qPCR was performed to confirm the expression of five genes, namely, *StGLP63*, *StGLP17*, *StGLP51*, *StGLP14*, and *StGLP47*, in the tissues of roots, stems, and leaves (**Figure 11**). Two genes, namely, *StGLP17* and *StGLP14*, exhibited a comparatively higher expression level in the tissues of stems than that in the tissues of roots and leaves. In contrast, the expression of *StGLP47* was relatively more in the tissues of leaves than that in the tissues of roots and stems. Generally,

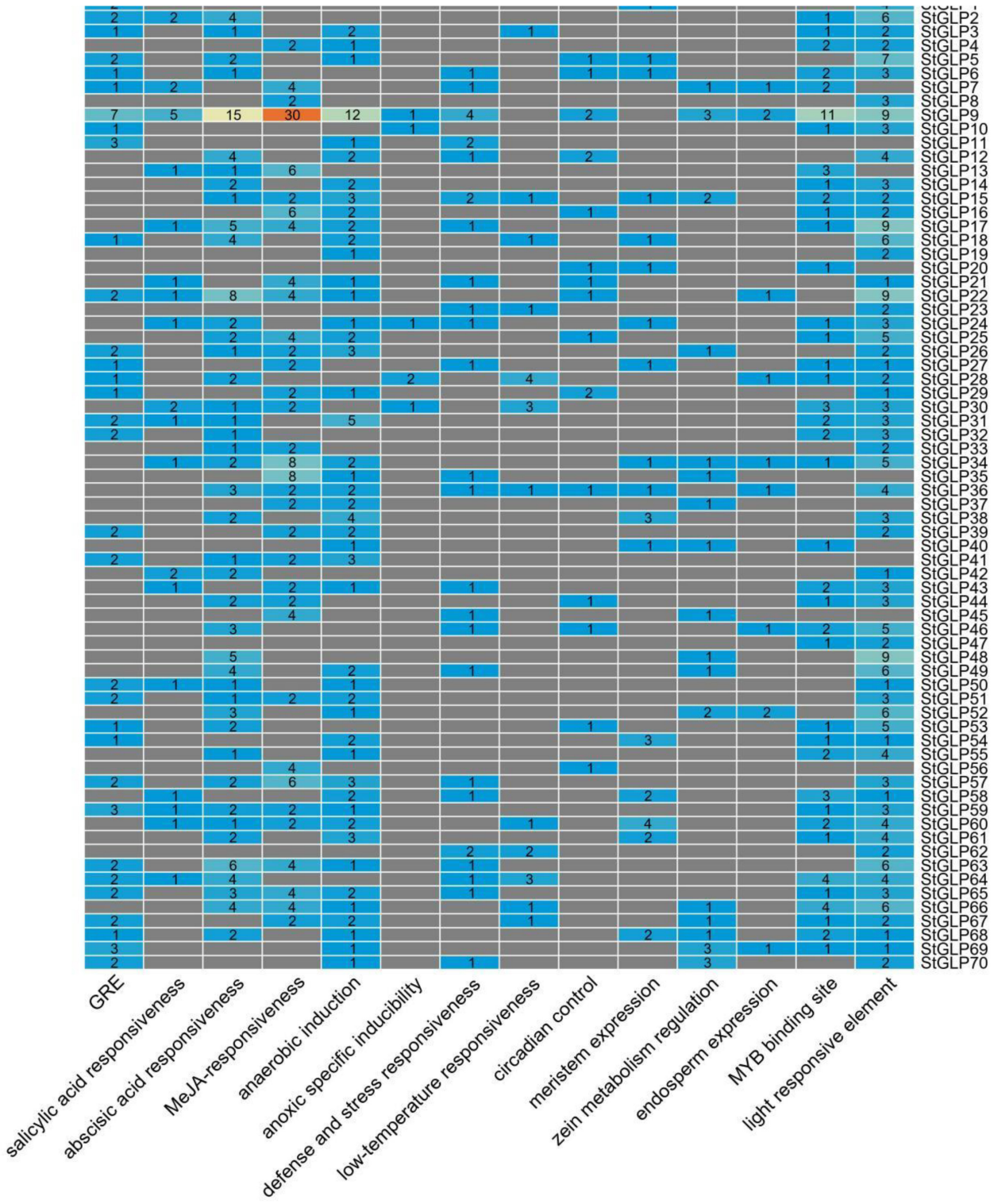


FIGURE 5 | *Cis*-acting elements distribution in the upstream regulatory regions of *StGLPs*.

findings depicted that *StGLP* genes may perform particular functions in potato plant growth and developmental process. Similarly, RT-qPCR was performed to confirm the expression of five genes, namely, *StGLP5*, *StGLP12*, *StGLP30*, *StGLP 36*, and *StGLP54,* in leaves treated with 150 mM NaCl. The results showed that the *StGLP5* genes showed the maximum

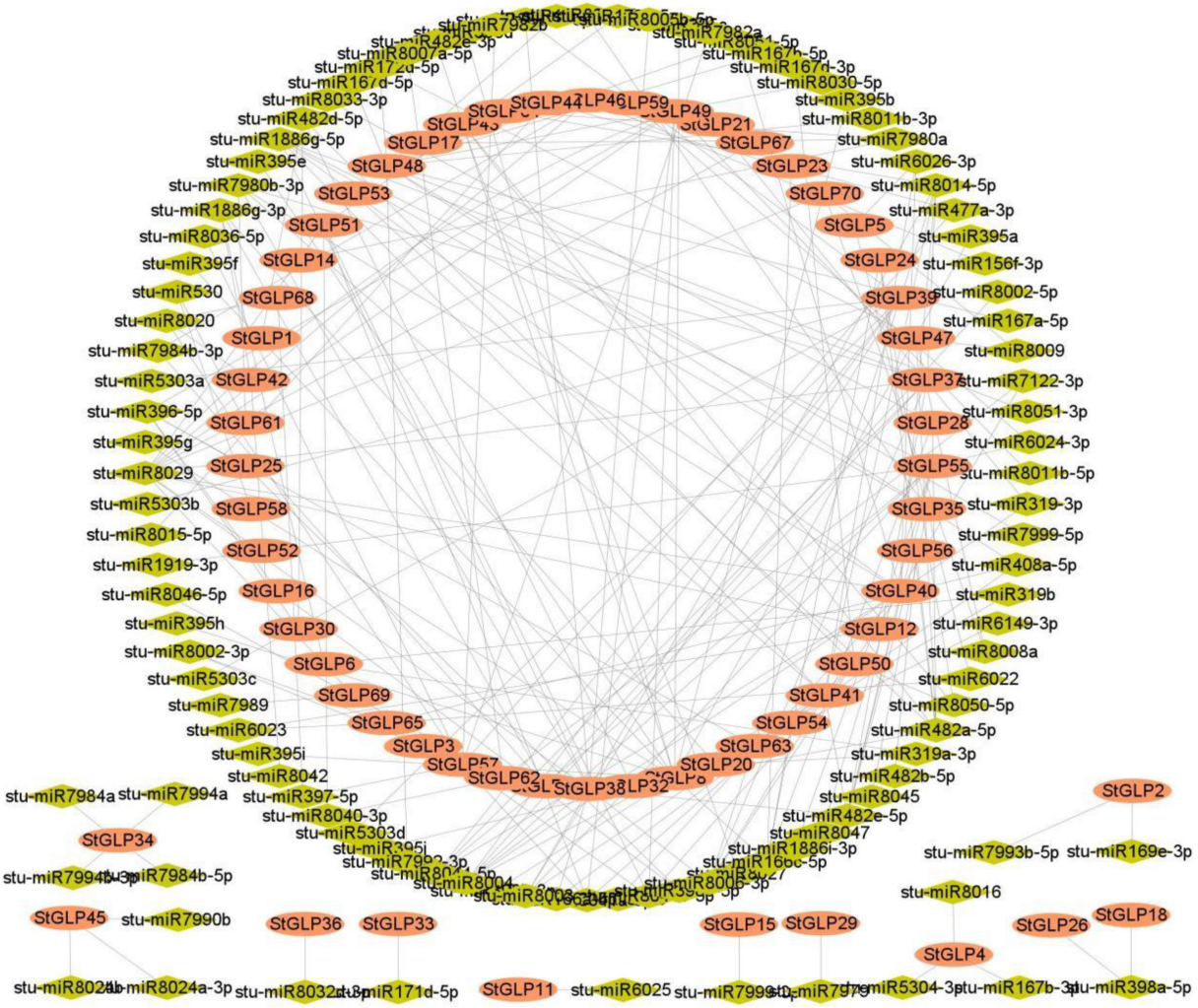


FIGURE 6 | miRNAs targeting *StGLP* genes. Network figure of anticipated miRNAs targeting the *StGLP* genes. Green color represents miRNAs, while orange color corresponds to the target *StGLP* gene.

expression after 24 h of NaCl stress. In addition, genes such as *StGLP12*, *StGLP 36,* and *StGLP54* were highly expressed with the extension of stress time. Moreover, *StGLP30* showed expression but low expression compared with the other four genes (**Figure 12**).

DISCUSSION

Potato is an integral part of the food chain worldwide (Zaynab et al., 2017b). Potato plants are subjected to different biotic and abiotic stresses (Zaynab et al., 2021b). *GLPs* have a significant role in plant signaling and response to various environmental stresses (Yuan et al., 2021). Members of *GLPs* show variations in their expression and possess considerable functions in several tissues at different phases of growth cycle of the plant (Barman and Banerjee, 2015). This crucial gene family carried out vital defense mechanisms and is an essential part of plant defense processes. The expression of the essential genes increases exponentially when plants encounter stress like salinity (Wang et al., 2013; Zaynab et al., 2021d), water shortage (Komatsu et al., 2010), heavy metals (Berna and Bernier, 1999), and heat stress (Qasim et al., 2018b). Various functions of *GLPs* have also been determined in different crops such as *Hordeum vulgare* (Zimmermann et al., 2006), *A. thaliana* (Rietz et al., 2012), *Oryza sativa* (Li et al., 2016), and *Glycine max* (Wang et al., 2014). But till now, there has been no considerable in-depth study of *GLPs* in the potato. These days, the whole-genomic sequence of potato is comfortably accessible, allowing us to conduct genome-wide analysis of the *GLP* genes family that may prove worthy for further research.

Structural analysis of *StGLPs* will prove beneficial for their functional characterization. The utilization of the evolutionary relic of *GLPs* has established that the evolution of genes has been affected by the arrangement of their exons and introns (Moore and Purugganan, 2005; Flagel and Wendel, 2009). This is in

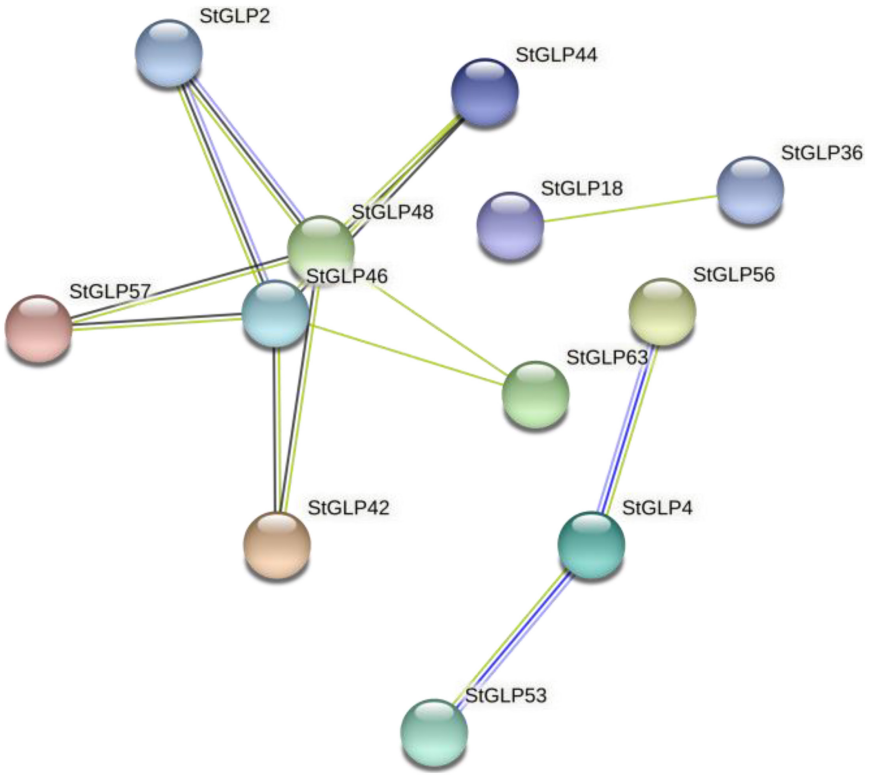


FIGURE 7 | Protein–protein interaction network of *StGLPs*.

correlation with previous scientists finding that genes with short introns or no introns are retained in the genomic systems of plants during the evolutionary process. At the same time, the expression levels of such genes are also low in plants (Mattick and Gagen, 2001). Moreover, the compact arrangement of genes favors the expression response of the *GLPs* against different exo or endogenous stimuli (Jeffares et al., 2008). Our findings through structural analysis of these genes inferred that those sequences of *StGLP* depicted a similar number of exons–introns with identical functional properties because they may have arisen through duplication events in the course of evolution (Waqas et al., 2019).

Studying the defense mechanisms employed by plants against various types of environmental stress, *cis*-elements were investigated in the promoter region of these genes. According to our findings, different *cis*-elements were identified that show their response against light and hormone stress. Several identified *cis*-elements were associated with ABA, SA, GA, MeJA, low temperature, anaerobic induction, and light. Earlier reports have attributed the stress response of plants to these *cis*-acting elements (Osakabe et al., 2014). *Cis*-factors are integral parts of plant stress response machinery as they regulate stress-responsive genes (Wu et al., 2014). So, these crucial *Cis*-acting sites of *StGLPs* indicate their behavior when different stresses are imposed.

All identified *StGLP* genes were classified into six clades. Similarly, phylogenetic grouping was also observed in other plants. The comparative phylogenetic analysis revealed that the organization of *S. lycoperiscum*, *S. tuberosum*, and *A. thaliana* proteins was relatively similar in six clades, indicating that all *StGLP* genes in these groups may have descended from a common ancestor. Previous studies (Li et al., 2016) reported the classification of *GLPs* into six clades in rice and *Arabidopsis*, supporting our results.

The size of the genome, duplication events in the genome, and the distribution of genes are major determinants of genetic variability in land plants. Genetic duplication property has long been recognized throughout the origins of evolutionary novelty, expression, and complexity of the gene families. We also noticed some duplications in *StGLPs* that may carry out vital roles in their amplification. As gene duplication is an imperative character in neofunctionalization, expansion, and variability among gene families (Lavin et al., 2005), similarly, the arrangement and localization of *StGLP* genes at chromosomes will enable breeders of potato to breed better varieties with desirable features.

Several types of research have depicted the response of plants to salinity and other abiotic stresses, and it is now well understood that miRNAs and their objects have direct impacts on the stress tolerance processes of plants (Li, 2015; Villanueva et al., 2016). This study recognized micro RNAs from various families targeting *StGLP* genes. Likewise, the unique role of miR156 has been widely documented during various abiotic stress in several plants (Cui et al., 2014; Kohli et al., 2014). Similarly, a study on cotton established a critical role of miR827 in response to saline stress (Covarrubias and Reyes, 2010); miR167 has also been

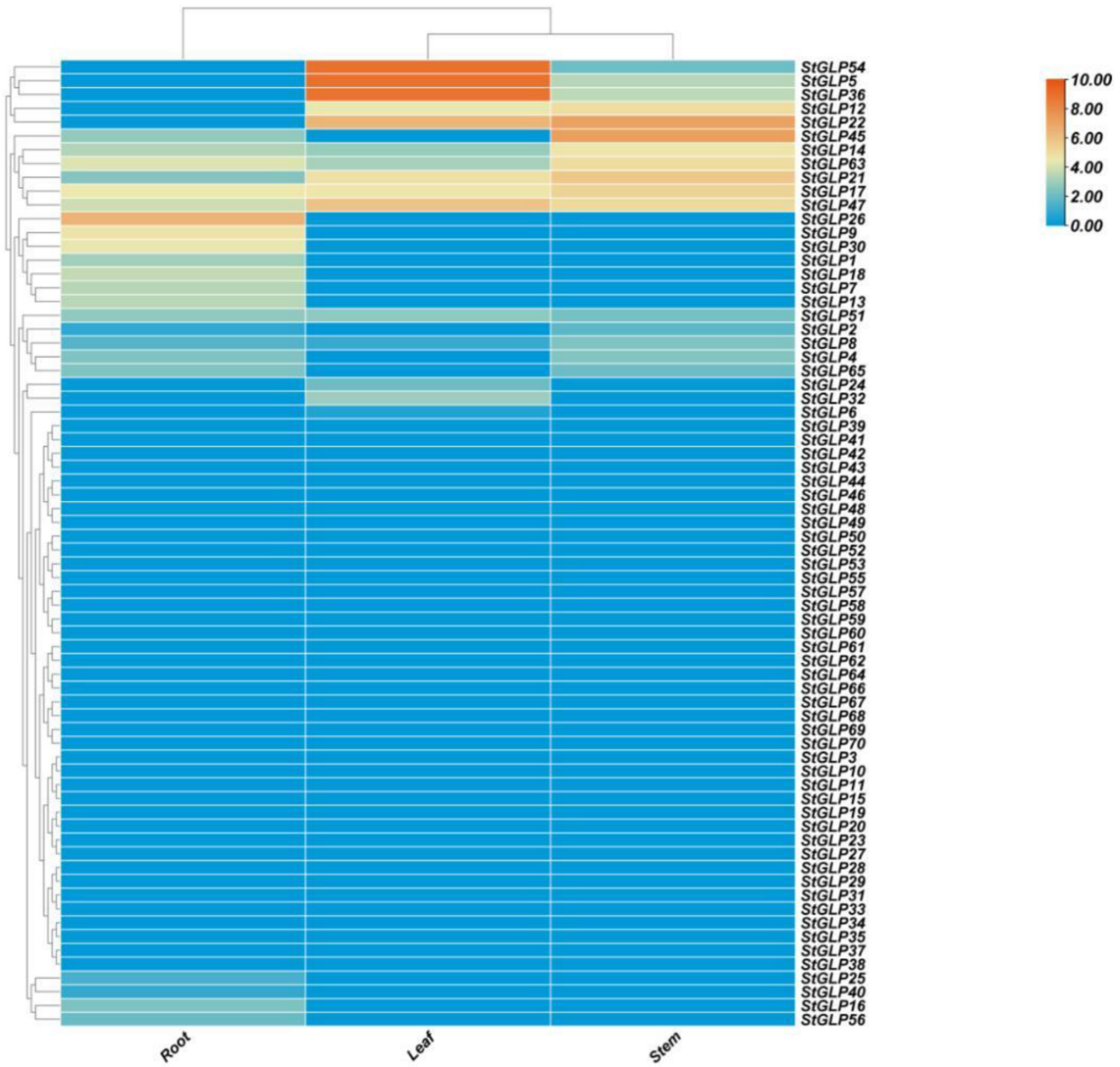


FIGURE 8 | Expression profiling of *StGLP* genes in leaves, roots, and stems. The orange and blue colors display high- to low-expression levels. The expression heat map was created by taking log10 normalized values of fragments per kilobase million (FPKM).

recognized as one of the significant role players in response to various stressed environmental conditions (Khraiwesh et al., 2012). Concisely, these results are in concordance with our findings that revealed that miR156, miR167, and miR827 are significant determinants of tolerance in plants against several stresses as they alter the expression of *StGLP* genes in the genome of potatoes.

Germin-like gene miRNAs are generally present in embryos, cotyledons, leaves, stems, flowers, roots, and seeds. Some are expressed in response to different environmental conditions; this depends upon genes under analysis or species in which they are expressed. Many authentications have indicated that various *GLPs* may have a critical role in the defense mechanisms of plants (Breen and Bellgard, 2010). So, the expression profiling of *GLPs* in the potato is helpful for their in-depth comprehension. Many genes exhibited a high level of expression in tissues, suggesting the putative role of these genes in potato growth and developmental processes. Our RT-qPCR findings revealed that the upregulation of genes in the tissues of roots and stems indicated the role of *GLP* in potato plant growth.

Furthermore, *GLPs* expression was observed in response to hormones and abiotic stress. These findings are following earlier reports that GLPs are an integral part of the defense system in saline tolerance (Wang et al., 2013), drought stress

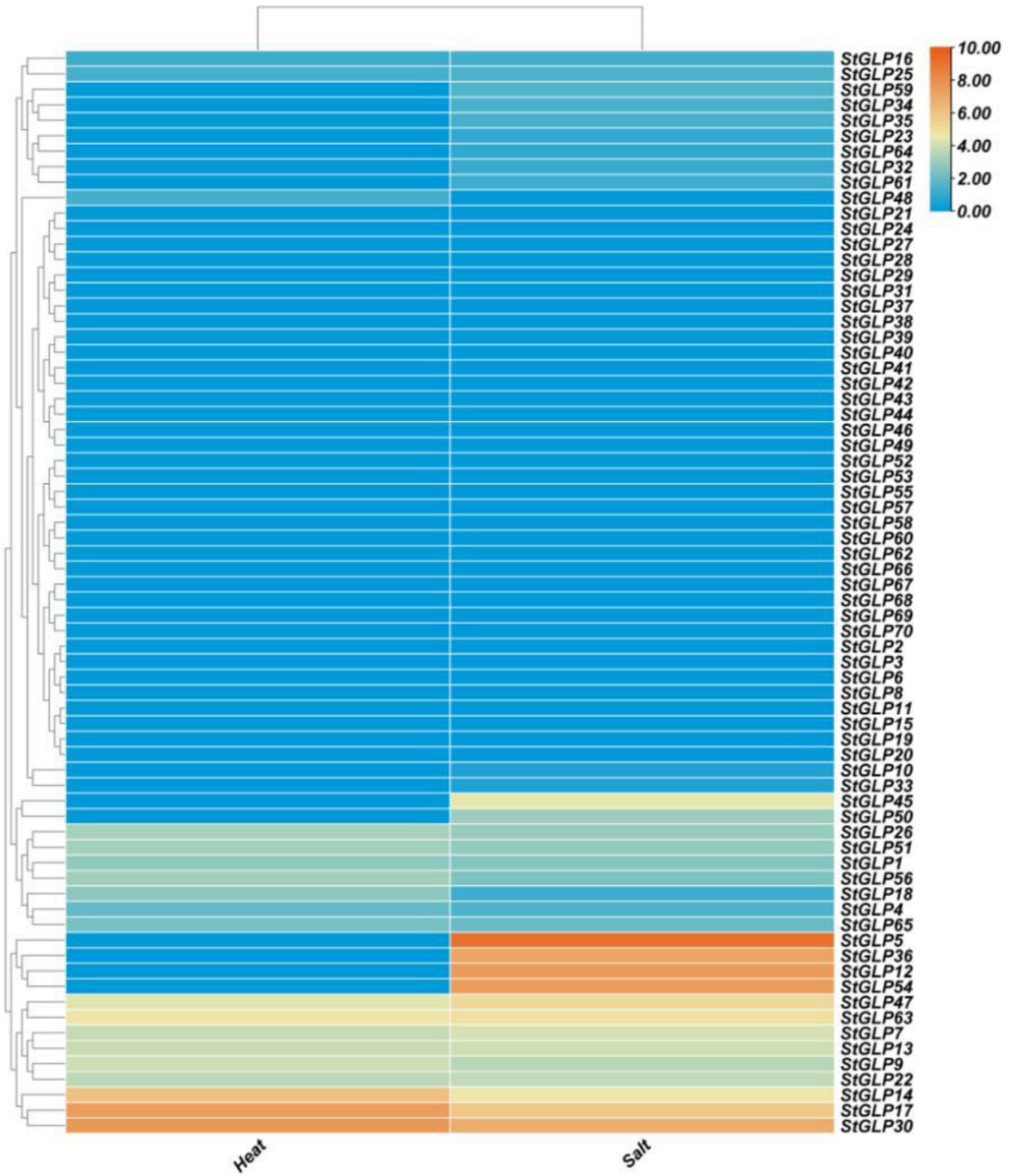


FIGURE 9 | Expression profiling of *StGLP* genes in response to salt and heat treatments. The orange and blue colors display high- to low-expression levels. The expression heat map was created by taking log10 of fragments per kilobase million (FPKM).

(Komatsu et al., 2010), cold tolerance, and heavy metals tolerance (Berna and Bernier, 1999). Up till now, numerous researches have depicted that *GLPs* are significant players of plant stress response mechanisms. In our results, *StGLP14*, *StGLP17*, and *StGLP30* are upregulated in response to heat stress, and *StGLP5*, *StGLP12*, and *StGLP54* are highly expressed

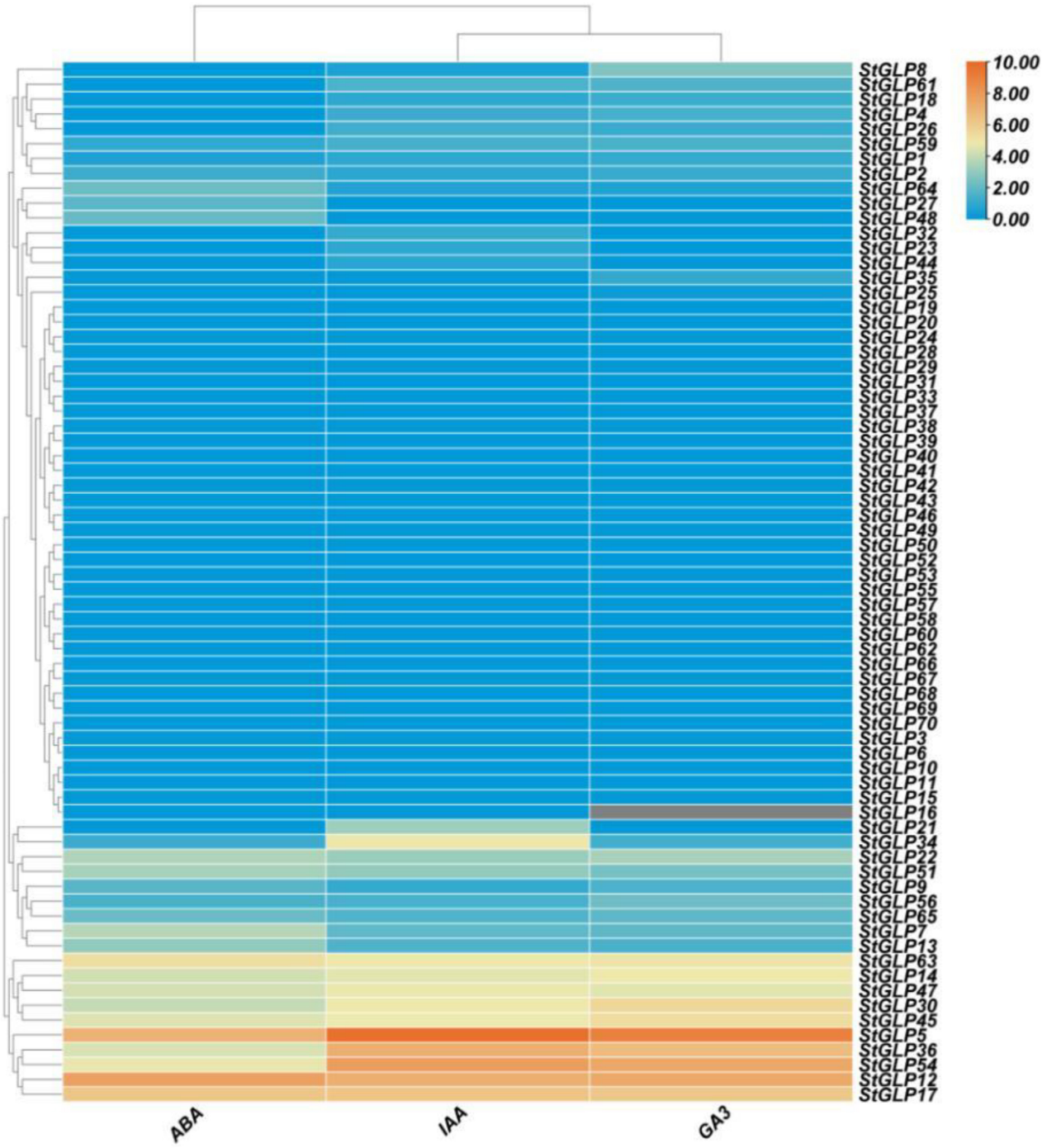


FIGURE 10 | Expression profiling of *StGLP* genes in response to ABA, IAA, and GA3. The orange and blue colors display high- to low-expression levels. The expression heat map was created by taking log10 of fragments per kilobase million (FPKM).

in response to salt stress supported by the findings of Wang et al. (2013). Hormones may alter the physio-biochemical pathways or metabolisms of plants by different pathways of signal transduction (Zaynab et al., 2017a; Fatima et al., 2021). ABA and IAA are major hormones of the immune system in plants. Several studies have established that besides being part of plant response to different stresses, GLPs also are involved in developing systems and hormonal signaling (Wang et al., 2020). To study how hormone signaling affects the production of StGLPs, leaves of potato were treated with ABA, GA3, and IAA, and the expression of genes was investigated. There was the induction of 22 genes on the treatment of

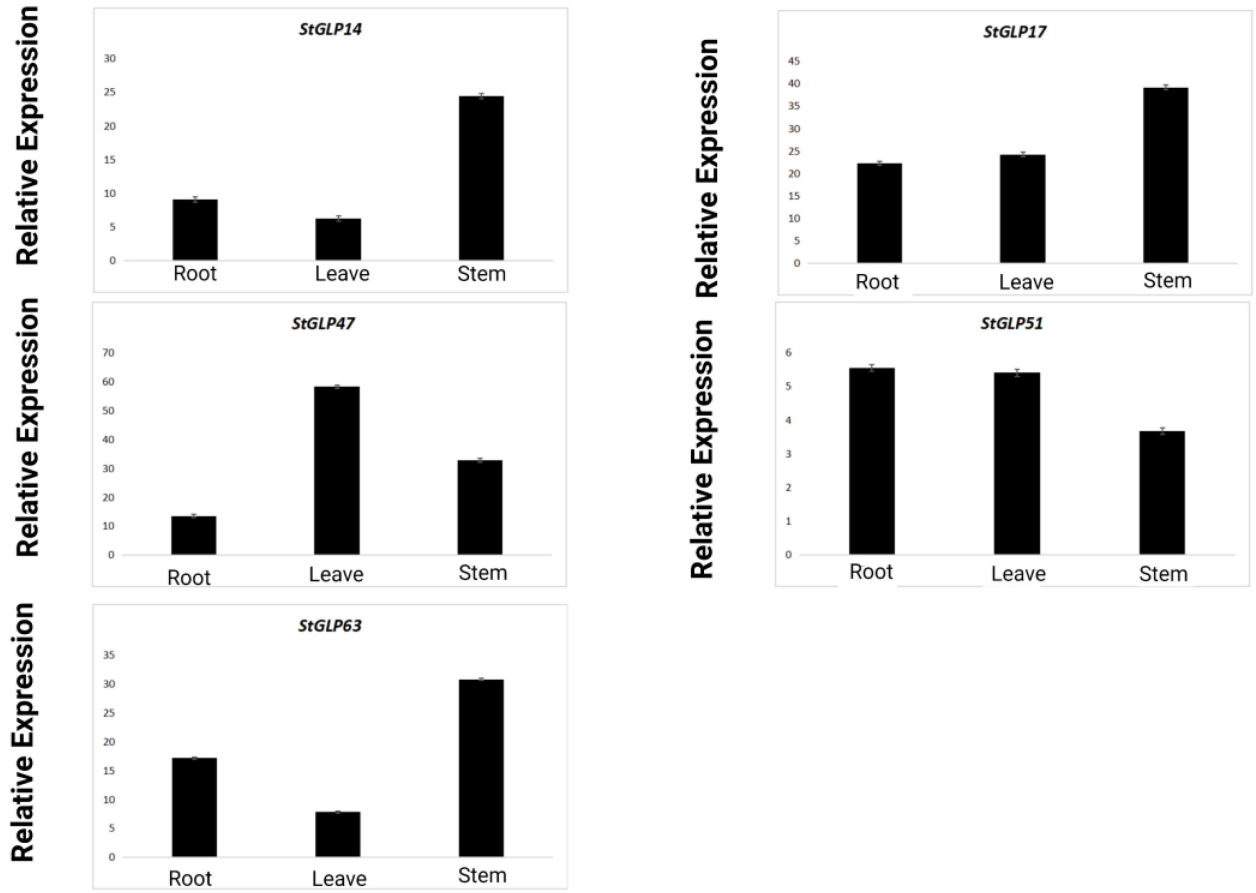


FIGURE 11 | Real-time relative expressions of *StGLPs* in leaves, roots, and stems.

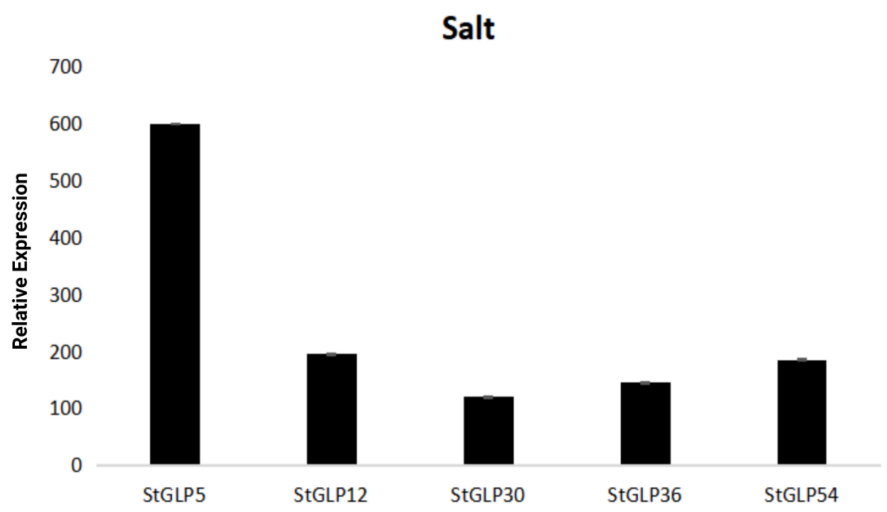


FIGURE 12 | Real-time relative expressions of *StGLPs* in salt treatment.

ABA, 24 genes on the treatment of IAA, and 27 genes on the treatment of GA3, suggesting that various members of *StGLPs* carry out crucial roles in the plant defense system induced by these hormones. When the treatment of ABA and IAA was made, increasing the expression level of potato GLPs exhibited that these hormones possess an essential part in this

defense mechanism, similar to the results obtained by Wang et al. (2020). The strong correlation between clusters of genes and their expression was noted under various stresses and tissues.

CONCLUSION

In this study, we identified 70 *GLPs* in the genome of the potato by genome-wide analysis. The gene structure, synteny, phylogenetic motifs, promotor, and miRNA analysis were performed to enhance our comprehension. The expression profiling after various stresses has been analyzed. The findings exhibited that *GLPs* genes responded significantly against hormonal and abiotic stresses, strengthening our comprehension. In our results, the *StGLP5* gene showed the highest expression in response to salt stress. So, further analysis is needed to corroborate the persistent role of *GLPs* genes in response to salt stress.

DATA AVAILABILITY STATEMENT

The original contributions presented in the study are included in the article/**Supplementary Material**, further inquiries can be directed to the corresponding author.

AUTHOR CONTRIBUTIONS

MZ, JP, and YS gave the idea. MF, MA, and RA-Y performed the experiments. KK and SA wrote the manuscript. SL revised the manuscript. All authors contributed to the article and approved the submitted version.

FUNDING

This work was supported by Shenzhen Special Project for Sustainable Development (KCXFZ20201221173211033). The authors appreciate the support of the Research Center for Advanced Materials Science (RCAMS) at King Khalid University Abha, Saudi Arabia, through a grant KKU/RCAMS/G002-21. Taif University Researchers Supporting Project number (TURSP-2020/38), Taif University, Taif, Saudi Arabia.

SUPPLEMENTARY MATERIAL

The Supplementary Material for this article can be found online at: https://www.frontiersin.org/articles/10.3389/fpls.2021.831140/full#supplementary-material

REFERENCES

Bailey, T. L., Boden, M., Buske, F. A., Frith, M., Grant, C. E., Clementi, L., et al. (2009). MEME SUITE: tools for motif discovery and searching. *Nucleic Acids Res.* 37, W202–W208. doi: 10.1093/nar/gkp335

Banerjee, J., Gantait, S., and Maiti, M. K. (2017). Physiological role of rice germin-like protein 1 (OsGLP1) at early stages of growth and development in indica rice cultivar under salt stress condition. *Plant Cell Tissue Organ. Cult.* 131, 127–137. doi: 10.1007/s11240-017-1270-z

Barman, A. R., and Banerjee, J. (2015). Versatility of germin-like proteins in their sequences, expressions, and functions. *Funct. Integr. Genomics* 15, 533–548. doi: 10.1007/s10142-015-0454-z

Beracochea, V. C., Almasia, N. I., Peluffo, L., Nahirñak, V., Hopp, E. H., Paniego, N., et al. (2015). Sunflower germin-like protein HaGLP1 promotes ROS accumulation and enhances protection against fungal pathogens in transgenic *Arabidopsis thaliana*. *Plant Cell Rep.* 34, 1717–1733. doi: 10.1007/s00299-015-1819-4

Berna, A., and Bernier, F. (1999). Regulation by biotic and abiotic stress of a wheat germin gene encoding oxalate oxidase, a H2O2-producing enzyme. *Plant Mol. Biol.* 39, 539–549. doi: 10.1023/A:1006123432157

Breen, J., and Bellgard, M. (2010). Germin-like proteins (GLPs) in cereal genomes: gene clustering and dynamic roles in plant defence. *Funct. Integr. Genomics* 10, 463–476. doi: 10.1007/s10142-010-0184-1

Chen, C., Chen, H., Zhang, Y., Thomas, H. R., Frank, M. H., He, Y., et al. (2020). TBtools: an integrative toolkit developed for interactive analyses of big biological data. *Mol. Plant* 13, 1194–1202. doi: 10.1016/j.molp.2020.06.009

Christensen, A. B., Thordal-Christensen, H., Zimmermann, G., Gjetting, T., Lyngkjær, M. F., Dudler, R., et al. (2004). The germinlike protein GLP4 exhibits superoxide dismutase activity and is an important component of quantitative resistance in wheat and barley. *MPMI* 17, 109–117. doi: 10.1094/MPMI.2004.17.1.109

Covarrubias, A. A., and Reyes, J. L. (2010). Post-transcriptional gene regulation of salinity and drought responses by plant microRNAs. *Plant Cell Environ.* 33, 481–489. doi: 10.1111/j.1365-3040.2009.02048.x

Cui, L. G., Shan, J. X., Shi, M., Gao, J. P., and Lin, H. X. (2014). The *miR156-SPL9-DFR* pathway coordinates the relationship between development and abiotic stress tolerance in plants. *Plant J.* 80, 1108–1117. doi: 10.1111/tpj.12712

Dai, X., Zhuang, Z., and Zhao, P. X. (2018). psRNATarget: a plant small RNA target analysis server (2017 release). *Nucleic Acids Res.* 46, W49–W54. doi: 10.1093/nar/gky316

Das, A., Pramanik, K., Sharma, R., Gantait, S., and Banerjee, J. (2019). In-silico study of biotic and abiotic stress-related transcription factor binding sites in the promoter regions of rice germin-like protein genes. *PLoS One* 14:e0211887. doi: 10.1371/journal.pone.0211887

Davidson, R. M., Reeves, P. A., Manosalva, P. M., and Leach, J. E. (2009). Germins: a diverse protein family important for crop improvement. *Plant Sci.* 177, 499–510. doi: 10.1016/j.plantsci.2009.08.012

Dunwell, J. M., Gibbings, J. G., Mahmood, T., and Saqlan Naqvi, S. M. (2008). Germin and germin-like proteins: evolution, structure, and function. *Crit. Rev. Plant Sci.* 27, 342–375. doi: 10.1080/07352680802333938

El-Gebali, S., Mistry, J., Bateman, A., Eddy, S. R., Luciani, A., Potter, S. C., et al. (2019). The Pfam protein families database in 2019. *Nucleic Acids Res.* 47, D427–D432. doi: 10.1093/nar/gky995

Fatima, M., Ma, X., Zhou, P., Zaynab, M., and Ming, R. (2021). Auxin regulated metabolic changes underlying sepal retention and development after pollination in spinach. *BMC Plant Biol.* 21:166. doi: 10.1186/s12870-021-02944-4

Finn, R. D., Clements, J., Arndt, W., Miller, B. L., Wheeler, T. J., Schreiber, F., et al. (2015). HMMER web server: 2015 update. *Nucleic Acids Res.* 43, W30–W38. doi: 10.1093/nar/gkv397

Finn, R. D., Tate, J., Mistry, J., Coggill, P. C., Sammut, S. J., Hotz, H.-R., et al. (2007). The Pfam protein families database. *Nucleic Acids Res.* 36, D281–D288. doi: 10.1093/nar/gkm960

Flagel, L. E., and Wendel, J. F. (2009). Gene duplication and evolutionary novelty in plants. *New Phytol.* 183, 557–564. doi: 10.1111/j.1469-8137.2009.02923.x

Gasteiger, E., Hoogland, C., Gattiker, A., Duvaud, S., Wilkins, M. R., Appel, R. D., et al. (2005). "Protein identification and analysis tools on the ExPASy server," in *The Proteomics Protocols Handbook*, ed. J. M. Walker (Totowa, NJ: Humana Press), 571–607.

Godfrey, D., Able, A. J., and Dry, I. B. (2007). Induction of a grapevine germin-like protein (VvGLP3) gene is closely linked to the site of erysiphe necator infection: a possible role in defense? *MPMI* 20, 1112–1125. doi: 10.1094/MPMI-20-9-1112

Goodstein, D. M., Shu, S., Howson, R., Neupane, R., Hayes, R. D., Fazo, J., et al. (2012). Phytozome: a comparative platform for green plant genomics. *Nucleic Acids Res.* 40, D1178–D1186. doi: 10.1093/nar/gkr944

Heintzen, C., Fischer, R., Melzer, S., Kappeler, S., Apel, K., and Staiger, D. (1994). Circadian oscillations of a transcript encoding a germin-like protein that is associated with cell walls in young leaves of the long-day plant *Sinapis alba* L. *Plant Physiol.* 106, 905–915. doi: 10.1104/pp.106.3.905

Jeffares, D. C., Penkett, C. J., and Bähler, J. (2008). Rapidly regulated genes are intron poor. *Trends Genet.* 24, 375–378. doi: 10.1016/j.tig.2008.05.006

Khraiwesh, B., Zhu, J.-K., and Zhu, J. (2012). Role of miRNAs and siRNAs in biotic and abiotic stress responses of plants. *Biochim. Biophys. Acta Gene Regul. Mech.* 1819, 137–148. doi: 10.1016/j.bbagrm.2011.05.001

Kohli, D., Joshi, G., Deokar, A. A., Bhardwaj, A. R., Agarwal, M., Katiyar-Agarwal, S., et al. (2014). Identification and characterization of wilt and salt stress-responsive microRNAs in chickpea through high-throughput sequencing. *PLoS One* 9:e108851. doi: 10.1371/journal.pone.0108851

Komatsu, S., Kobayashi, Y., Nishizawa, K., Nanjo, Y., and Furukawa, K. (2010). Comparative proteomics analysis of differentially expressed proteins in soybean cell wall during flooding stress. *Amino Acids* 39, 1435–1449. doi: 10.1007/s00726-010-0608-1

Kumar, S., Stecher, G., Li, M., Knyaz, C., and Tamura, K. (2018). MEGA X: molecular evolutionary genetics analysis across computing platforms. *Mol. Biol. Evol.* 35, 1547–1549. doi: 10.1093/molbev/msy096

Lane, B. G. (2000). Oxalate oxidases and differentiating surface structure in wheat: germins. *Biochem. J.* 349, 309–321. doi: 10.1042/bj3490309

Lane, B. G., Cuming, A. C., Fregeau, J., Carpita, N. C., Hurkman, W. J., Bernier, F., et al. (1992). Germin isoforms are discrete temporal markers of wheat development. Pseudogermin is a uniquely thermostable water-soluble oligomeric protein in ungerminated embryos and like germin in germinated embryos, it is incorporated into cell walls. *Eur. J. Biochem.* 209, 961–969. doi: 10.1111/j.1432-1033.1992.tb17369.x

Lavin, M., Herendeen, P. S., and Wojciechowski, M. F. (2005). Evolutionary rates analysis of leguminosae implicates a rapid diversification of lineages during the tertiary. *Syst. Biol.* 54, 575–594. doi: 10.1080/10635150590947131

Lescot, M. (2002). PlantCARE, a database of plant cis-acting regulatory elements and a portal to tools for in silico analysis of promoter sequences. *Nucleic Acids Res.* 30, 325–327. doi: 10.1093/nar/30.1.325

Li, G., Hou, M., Liu, Y., Pei, Y., Ye, M., Zhou, Y., et al. (2019). Genome-wide identification, characterization and expression analysis of the non-specific lipid transfer proteins in potato. *BMC Genomics* 20:375. doi: 10.1186/s12864-019-5698-x

Li, L., Xu, X., Chen, C., and Shen, Z. (2016). Genome-wide characterization and expression analysis of the germin-like protein family in rice and *Arabidopsis*. *IJMS* 17:1622. doi: 10.3390/ijms17101622

Li, S. (2015). The *Arabidopsis thaliana* TCP transcription factors: a broadening horizon beyond development. *Plant Signal. Behav.* 10:e1044192. doi: 10.1080/15592324.2015.1044192

Liao, L., Hu, Z., Liu, S., Yang, Y., and Zhou, Y. (2021). Characterization of germin-like proteins (GLPs) and their expression in response to abiotic and biotic stresses in cucumber. *Horticulturae* 7:412. doi: 10.3390/horticulturae7100412

Lou, Y., and Baldwin, I. T. (2006). Silencing of a germin-like gene in *Nicotiana attenuata* improves performance of native herbivores. *Plant Physiol.* 140, 1126–1136. doi: 10.1104/pp.105.073700

Lu, M., Han, Y.-P., Gao, J.-G., Wang, X.-J., and Li, W.-B. (2010). Identification and analysis of the germin-like gene family in soybean. *BMC Genomics* 11:620. doi: 10.1186/1471-2164-11-620

Mattick, J. S., and Gagen, M. J. (2001). The evolution of controlled multitasked gene networks: the role of introns and other noncoding RNAs in the development of complex organisms. *Mol. Biol. Evol.* 18, 1611–1630. doi: 10.1093/oxfordjournals.molbev.a003951

Moore, R. C., and Purugganan, M. D. (2005). The evolutionary dynamics of plant duplicate genes. *Curr. Opin. Plant Biol.* 8, 122–128. doi: 10.1016/j.pbi.2004.12.001

Osakabe, Y., Yamaguchi-Shinozaki, K., Shinozaki, K., and Tran, L. P. (2014). ABA control of plant macroelement membrane transport systems in response to water deficit and high salinity. *New Phytol.* 202, 35–49. doi: 10.1111/nph.12613

Pei, Y., Li, X., Zhu, Y., Ge, X., Sun, Y., Liu, N., et al. (2019). GhABP19, a novel germin-like protein from *Gossypium hirsutum*, plays an important role in the regulation of resistance to *Verticillium* and *Fusarium* wilt pathogens. *Front. Plant Sci.* 10:583. doi: 10.3389/fpls.2019.00583

Qasim, M., Baohua, W., Zou, H., Lin, Y., Dash, C. K., Bamisile, B. S., et al. (2018a). Phylogenetic relationship and genetic diversity of citrus psyllid populations from China and Pakistan and their associated *Candidatus bacterium*. *Mol. Phylogenet. Evol.* 126, 173–180. doi: 10.1016/j.ympev.2018.04.028

Qasim, M., Lin, Y., Dash, C. K., Bamisile, B. S., Ravindran, K., Islam, S. U., et al. (2018b). Temperature-dependent development of Asian citrus psyllid on various hosts, and mortality by two strains of Isaria. *Microb. Pathog.* 119, 109–118. doi: 10.1016/j.micpath.2018.04.019

Qasim, M., Xiao, H., He, K., Omar, M. A. A., Hussain, D., Noman, A., et al. (2021). Host-pathogen interaction between Asian citrus psyllid and entomopathogenic fungus (*Cordyceps fumosorosea*) is regulated by modulations in gene expression, enzymatic activity and HLB-bacterial population of the host. *Comp. Biochem. Physiol. C Toxicol. Pharmacol.* 248:109112. doi: 10.1016/j.cbpc.2021.109112

Rashid, M.-O., Li, J.-H., Liu, Q., Wang, Y., and Han, C.-G. (2021). Molecular detection and identification of eight potato viruses in Gansu province of China. *Curr. Plant Biol.* 25:100184. doi: 10.1016/j.cpb.2020.100184

Raza, A. (2021). Eco-physiological and biochemical responses of rapeseed (*Brassica napus* L.) to abiotic stresses: consequences and mitigation strategies. *J. Plant Growth Regul.* 40, 1368–1388. doi: 10.1007/s00344-020-10231-z

Raza, A., Ashraf, F., Zou, X., Zhang, X., and Tosif, H. (2020). "Plant adaptation and tolerance to environmental stresses: mechanisms and perspectives," in *Plant Ecophysiology and Adaptation under Climate Change: Mechanisms and Perspectives I*, ed. M. Hasanuzzaman (Singapore: Springer Singapore), 117–145.

Raza, A., Su, W., Gao, A., Mehmood, S. S., Hussain, M. A., Nie, W., et al. (2021). Catalase (CAT) gene family in rapeseed (*Brassica napus* L.): genome-wide analysis, identification, and expression pattern in response to multiple hormones and abiotic stress conditions. *IJMS* 22:4281. doi: 10.3390/ijms22084281

Rhee, S. Y. (2003). The *Arabidopsis* Information Resource (TAIR): a model organism database providing a centralized, curated gateway to Arabidopsis biology, research materials and community. *Nucleic Acids Res.* 31, 224–228. doi: 10.1093/nar/gkg076

Rietz, S., Bernsdorff, F. E. M., and Cai, D. (2012). Members of the germin-like protein family in *Brassica napus* are candidates for the initiation of an oxidative burst that impedes pathogenesis of *Sclerotinia sclerotiorum*. *J. Exp. Bot.* 63, 5507–5519. doi: 10.1093/jxb/ers203

Schweizer, P., Christoffel, A., and Dudler, R. (1999). Transient expression of members of the germin-like gene family in epidermal cells of wheat confers disease resistance. *Plant J.* 20, 541–552. doi: 10.1046/j.1365-313X.1999.00624.x

Su, W., Raza, A., Gao, A., Jia, Z., Zhang, Y., Hussain, M. A., et al. (2021). Genome-wide analysis and expression profile of superoxide dismutase (SOD) gene family in rapeseed (*Brassica napus* L.) under different hormones and abiotic stress conditions. *Antioxidants* 10:1182. doi: 10.3390/antiox10081182

The Potato Genome Sequencing Consortium (2011). Genome sequence and analysis of the tuber crop potato. *Nature* 475, 189–195. doi: 10.1038/nature10158

Villanueva, M. A., Islas-Flores, T., and Ullah, H. (2016). Signaling through WD-repeat proteins in plants. *Front. Plant Sci.* 7:1157. doi: 10.3389/fpls.2016.01157

Wang, D., Zhang, Y., Zhang, Z., Zhu, J., and Yu, J. (2010). KaKs_calculator 2.0: a toolkit incorporating gamma-series methods and sliding window strategies. *Genomics Proteomics Bioinform.* 8, 77–80. doi: 10.1016/S1672-0229(10)60008-3

Wang, H., Zhang, Y., Xiao, N., Zhang, G., Wang, F., Chen, X., et al. (2020). Rice GERMIN-LIKE PROTEIN 2-1 functions in seed dormancy under the control of abscisic acid and gibberellic acid signaling pathways. *Plant Physiol.* 183, 1157–1170. doi: 10.1104/pp.20.00253

Wang, T., Chen, X., Zhu, F., Li, H., Li, L., Yang, Q., et al. (2013). Characterization of peanut germin-like proteins, AhGLPs in plant development and defense. *PLoS One* 8:e61722. doi: 10.1371/journal.pone.0061722

Wang, X., Zhang, H., Gao, Y., Sun, G., Zhang, W., and Qiu, L. (2014). A comprehensive analysis of the cupin gene family in soybean (*Glycine max*). *PLoS One* 9:e110092. doi: 10.1371/journal.pone.0110092

Waqas, M., Azhar, M. T., Rana, I. A., Azeem, F., Ali, M. A., Nawaz, M. A., et al. (2019). Genome-wide identification and expression analyses of WRKY transcription factor family members from chickpea (*Cicer arietinum* L.) reveal their role in abiotic stress-responses. *Genes Genom.* 41, 467–481. doi: 10.1007/s13258-018-00780-9

Wu, J., Wang, J., Pan, C., Guan, X., Wang, Y., Liu, S., et al. (2014). Genome-wide identification of MAPKK and MAPKKK gene families in tomato and transcriptional profiling analysis during development and stress response. *PLoS One* 9:e103032. doi: 10.1371/journal.pone.0103032

Xu, T., Zhang, L., Yang, Z., Wei, Y., and Dong, T. (2021). Identification and functional characterization of plant MiRNA under salt stress shed light on salinity resistance improvement through MiRNA manipulation in crops. *Front. Plant Sci.* 12:665439. doi: 10.3389/fpls.2021.665439

Yang, Z., and Bielawski, J. P. (2000). Statistical methods for detecting molecular adaptation. *Trends Ecol. Evol.* 15, 496–503. doi: 10.1016/s0169-5347(00)01994-7

Yuan, B., Yang, Y., Fan, P., Liu, J., Xing, H., Liu, Y., et al. (2021). Genome-wide identification and characterization of germin and germin-like proteins (GLPs) and their response under powdery mildew stress in wheat (*Triticum aestivum* L.). *Plant Mol. Biol. Rep.* [Epub ahead of print]. doi: 10.1007/s11105-021-01291-w

Zaynab, M., Wang, Z., Hussain, A., Bahadar, K., Sajid, M., Sharif, Y., et al. (2021d). ATP-binding cassette transporters expression profiling revealed its role in the development and regulating stress response in *Solanum tuberosum*. *Mol. Biol. Rep.* [Epub ahead of print]. doi: 10.1007/s11033-021-06697-z

Zaynab, M., Chen, H., Chen, Y., Ouyang, L., Yang, X., Xu, W., et al. (2021a). Transcriptome analysis revealed transporter proteins role in the growth of *Labrenzia* sp. PO1 and SY1. *J. King Saud Univ. Sci.* 33:101433. doi: 10.1016/j.jksus.2021.101433

Zaynab, M., Hussain, A., Sharif, Y., Fatima, M., Sajid, M., Rehman, N., et al. (2021b). Mitogen-activated protein kinase expression profiling revealed its role in regulating stress responses in potato (*Solanum tuberosum*). *Plants* 10:1371. doi: 10.3390/plants10071371

Zaynab, M., Pan, D., Fatima, M., Sharif, Y., Chen, S., and Chen, W. (2021c). Proteomics analysis of *Cyclobalanopsis gilva* provides new insights of low seed germination. *Biochimie* 180, 68–78. doi: 10.1016/j.biochi.2020.10.008

Zaynab, M., Kanwal, S., Hussain, I., Qasim, M., Noman, A., Iqbal, U., et al. (2017b). Rice chitinase gene expression in genetically engineered potato confers resistance against *Fusarium solani* and *Rhizictonia solani*. *PSM Microbiol.* 2, 63–73.

Zaynab, M., Kanwal, S., Furqan, M., Islam, W., Noman, A., Ali, G. M., et al. (2017a). Proteomic approach to address low seed germination in *Cyclobalnopsis gilva*. *Biotechnol. Lett.* 39, 1441–1451. doi: 10.1007/s10529-017-2393-3

Zhang, Y., Wang, X., Chang, X., Sun, M., Zhang, Y., Li, W., et al. (2018). Overexpression of germin-like protein GmGLP10 enhances resistance to *Sclerotinia sclerotiorum* in transgenic tobacco. *Biochem. Biophys. Res. Commun.* 497, 160–166. doi: 10.1016/j.bbrc.2018.02.046

Zimmermann, G., Bäumlein, H., Mock, H.-P., Himmelbach, A., and Schweizer, P. (2006). The multigene family encoding germin-like proteins of barley. Regulation and function in basal host resistance. *Plant Physiol.* 142, 181–192. doi: 10.1104/pp.106.083824

Conflict of Interest: The authors declare that the research was conducted in the absence of any commercial or financial relationships that could be construed as a potential conflict of interest.

Publisher's Note: All claims expressed in this article are solely those of the authors and do not necessarily represent those of their affiliated organizations, or those of the publisher, the editors and the reviewers. Any product that may be evaluated in this article, or claim that may be made by its manufacturer, is not guaranteed or endorsed by the publisher.

Copyright © 2022 Zaynab, Peng, Sharif, Fatima, Albaqami, Al-Yahyai, Khan, Alotaibi, Alaraidh, Shaikhaldein and Li. This is an open-access article distributed under the terms of the Creative Commons Attribution License (CC BY). The use, distribution or reproduction in other forums is permitted, provided the original author(s) and the copyright owner(s) are credited and that the original publication in this journal is cited, in accordance with accepted academic practice. No use, distribution or reproduction is permitted which does not comply with these terms.

frontiers | Frontiers in Plant Science

CORRECTION
published: 23 May 2022
doi: 10.3389/fpls.2022.910487

Corrigendum: Genome-Wide Identification and Expression Profiling of Germin-Like Proteins Reveal Their Role in Regulating Abiotic Stress Response in Potato

Madiha Zaynab[1†], Jiaofeng Peng[2†], Yasir Sharif[3], Mahpara Fatima[4], Mohammed Albaqami[5], Rashid Al-Yahyai[6], Khalid Ali Khan[7,8,9], Saqer S. Alotaibi[10], Ibrahim A. Alaraidh[11], Hassan O. Shaikhaldein[11] and Shuangfei Li[1]*

[1] Shenzhen Key Laboratory of Marine Bioresource and Eco-Environmental Sciences, College of Life Sciences and Oceanography, Shenzhen University, Shenzhen, China, [2] Instrument Analysis Center, Shenzhen University, Shenzhen, China, [3] College of Plant Protection, Fujian Agriculture and Forestry University, Fuzhou, China, [4] College of Agriculture, Fujian Agriculture and Forestry University, Fuzhou, China, [5] Department of Biology, Faculty of Applied Science, Umm Al-Qura University, Makkah, Saudi Arabia, [6] Department of Plant Sciences, College of Agricultural and Marine Sciences, Sultan Qaboos University, Muscat, Oman, [7] Research Center for Advanced Materials Science (RCAMS), King Khalid University, Abha, Saudi Arabia, [8] Unit of Bee Research and Honey Production, Faculty of Science, King Khalid University, Abha, Saudi Arabia, [9] Department, Faculty of Science, King Khalid University, Abha, Saudi Arabia, [10] Department of Biotechnology, College of Science, Taif University, Taif, Saudi Arabia, [11] Botany and Microbiology Department, Science College, King Saud University, Riyadh, Saudi Arabia

Keywords: abiotic stress, gene expression, gene structure, miRNA, RNA-seq, stress responses

OPEN ACCESS

Approved by:
Frontiers Editorial Office, Frontiers Media SA, Switzerland

***Correspondence:**
Shuangfei Li
sfli@szu.edu.cn

[†]These authors have contributed equally to this work

Specialty section:
This article was submitted to Plant Biotechnology, a section of the journal Frontiers in Plant Science

Received: *01 April 2022*
Accepted: *28 April 2022*
Published: *23 May 2022*

Citation:
Zaynab M, Peng J, Sharif Y, Fatima M, Albaqami M, Al-Yahyai R, Khan KA, Alotaibi SS, Alaraidh IA, Shaikhaldein HO and Li S (2022) Corrigendum: Genome-Wide Identification and Expression Profiling of Germin-Like Proteins Reveal Their Role in Regulating Abiotic Stress Response in Potato. Front. Plant Sci. 13:910487. doi: 10.3389/fpls.2022.910487

A Corrigendum on

Genome-Wide Identification and Expression Profiling of Germin-Like Proteins Reveal Their Role in Regulating Abiotic Stress Response in Potato

by Zaynab, M., Peng, J., Sharif, Y., Fatima, M., Albaqami, M., Al-Yahyai, R., Khan, K. A., Alotaibi, S. S., Alaraidh, I. A., Shaikhaldein, H. O., and Li, S. (2022). Front. Plant Sci. 12:831140. doi: 10.3389/fpls.2021.831140

Ali Raza was included as an author in the submitted article. However, during proofing the authors submitted the authorship change form but the typesetter missed the author name removal request. The corrected Author Contributions Statement and Funding appears below.

Madiha Zaynab[1†], Jiaofeng Peng[2†], Yasir Sharif[3], Mahpara Fatima[4], Mohammed Albaqami[5], Rashid Al-Yahyai[6], Khalid Ali Khan[7,8,9], Saqer S. Alotaibi[10], Ibrahim A. Alaraidh[11], Hassan O. Shaikhaldein[11] and Shuangfei Li[1*]

[1] Shenzhen Key Laboratory of Marine Bioresource and Eco-Environmental Sciences, College of Life Sciences and Oceanography, Shenzhen University, Shenzhen, China
[2] Instrument Analysis Center, Shenzhen University, Shenzhen, China
[3] College of Plant Protection, Fujian Agriculture and Forestry University, Fuzhou, China
[4] College of Agriculture, Fujian Agriculture and Forestry University, Fuzhou, China
[5] Department of Biology, Faculty of Applied Science, Umm Al-Qura University, Makkah, Saudi Arabia
[6] Department of Plant Sciences, College of Agricultural and Marine Sciences, Sultan Qaboos University, Muscat, Oman

[7] Research Center for Advanced Materials Science (RCAMS), King Khalid University, Abha, Saudi Arabia
[8] Unit of Bee Research and Honey Production, Faculty of Science, King Khalid University, Abha, Saudi Arabia
[9] Department, Faculty of Science, King Khalid University, Abha, Saudi Arabia
[10] Department of Biotechnology, College of Science, Taif University, Taif, Saudi Arabia
[11] Botany and Microbiology Department, Science College, King Saud University, Riyadh, Saudi Arabia

AUTHOR CONTRIBUTIONS

MZ, JP, and YS gave the idea. MF, MA, and RA-Y performed the experiments. KK and SA wrote the manuscript. SL revised the manuscript. All authors contributed to the article and approved the submitted version.

FUNDING

This work was supported by Shenzhen Special Project for Sustainable Development (KCXFZ20201221173211033). The authors appreciate the support of the Research Center for Advanced Materials Science (RCAMS) at King Khalid University Abha, Saudi Arabia, through a grant KKU/RCAMS/G002-21. Taif University Researchers Supporting Project number (TURSP-2020/38), Taif University, Taif, Saudi Arabia.

The authors and production team apologize for this error and state that this does not change the scientific conclusions of the article in any way. The original article has been updated.

Publisher's Note: All claims expressed in this article are solely those of the authors and do not necessarily represent those of their affiliated organizations, or those of the publisher, the editors and the reviewers. Any product that may be evaluated in this article, or claim that may be made by its manufacturer, is not guaranteed or endorsed by the publisher.

Copyright © 2022 Zaynab, Peng, Sharif, Fatima, Albaqami, Al-Yahyai, Khan, Alotaibi, Alaraidh, Shaikhaldein and Li. This is an open-access article distributed under the terms of the Creative Commons Attribution License (CC BY). The use, distribution or reproduction in other forums is permitted, provided the original author(s) and the copyright owner(s) are credited and that the original publication in this journal is cited, in accordance with accepted academic practice. No use, distribution or reproduction is permitted which does not comply with these terms.

frontiers in Plant Science

ORIGINAL RESEARCH
published: 18 February 2022
doi: 10.3389/fpls.2022.842349

Zinc Oxide Nanoparticles Interplay With Physiological and Biochemical Attributes in Terminal Heat Stress Alleviation in Mungbean (*Vigna radiata* L.)

*Hafiz Abdul Kareem[1,2], Muhammad Farrukh Saleem[2], Sana Saleem[3], Shabir A. Rather[4,5], Shabir Hussain Wani[6], Manzer H. Siddiqui[7], Saud Alamri[7], Ritesh Kumar[8], Nikhil B. Gaikwad[9], Zhipeng Guo[1], Junpeng Niu[1] and Quanzhen Wang[1]**

[1] College of Grassland Agriculture, Northwest A&F University, Xianyang, China, [2] Department of Agronomy, University of Agriculture, Faisalabad, Pakistan, [3] Institute of Horticultural Sciences, University of Agriculture, Faisalabad, Pakistan, [4] Center of Integrative Conservation, Xishuangbanna Tropical Botanical Garden, Chinese Academy of Sciences, Mengla, China, [5] State Key Laboratory of Biocontrol and Guangdong Key Laboratory of Plant Resources, School of Life Sciences, Sun Yat-sen University, Guangzhou, China, [6] Mountain Research Centre for Field Crops, Khudwani, Sher-e-Kashmir University of Agricultural Sciences and Technology of Kashmir, Jammu and Kashmir, India, [7] Department of Botany and Microbiology, College of Science, King Saud University, Riyadh, Saudi Arabia, [8] Department of Agronomy, Kansas State University, Manhattan, KS, United States, [9] Department of Botany, Shivaji University, Kolhapur, India

OPEN ACCESS

Edited by:
Mohammad Anwar Hossain, Bangladesh Agricultural University, Bangladesh

Reviewed by:
Muhammad Azeem, Chinese Academy of Sciences (CAS), China
Josphat K. Saina, Fairy Lake Botanical Garden, Chinese Academy of Sciences (CAS), China

***Correspondence:**
Quanzhen Wang
wangquanzhen191@nwsuaf.edu.cn; wangquanzhen191@163.com

Specialty section:
This article was submitted to Plant Breeding, a section of the journal Frontiers in Plant Science

Received: *23 December 2021*
Accepted: *10 January 2022*
Published: *18 February 2022*

Citation:
Kareem HA, Saleem MF, Saleem S, Rather SA, Wani SH, Siddiqui MH, Alamri S, Kumar R, Gaikwad NB, Guo Z, Niu J and Wang Q (2022) Zinc Oxide Nanoparticles Interplay With Physiological and Biochemical Attributes in Terminal Heat Stress Alleviation in Mungbean (Vigna radiata L.). Front. Plant Sci. 13:842349. doi: 10.3389/fpls.2022.842349

Gradually rising atmospheric temperature is the vital component of the environment, which is anticipated as the riskiest abiotic stress for crop growth. Nanotechnology revolutionizing the agricultural sectors, notably, zinc oxide nanoparticles (nano-ZnO) has captured intensive research interests due to their distinctive properties and numerous applications against abiotic stresses. Mungbean (*Vigna radiata* L.), being a summer crop, is grown all over the world at an optimum temperature of 28–30°C. A rise in temperature above this range, particularly during the flowering stage, can jeopardize the potential performance of the plant. Hence, an outdoor study was performed to evaluate the effect of multiple suspensions of nano-ZnO (0, 15, 30, 45, and 60 mg l^{-1}) on physicochemical attributes and yield of mungbean crop under heat stress. Heat stress was induced by fine-tuning of sowing time as: S1 is the optimal sowing time having day/night temperatures <40/25°C and S2 and S3 are late sown that were above >40/25°C during the flowering stage. *In vitro* studies on Zn release from nano-ZnO by inductively coupled plasma mass spectroscopy (ICPMS) disclosed that the Zn release and particles uptake from nano-ZnO were concentration-dependent. Exogenous foliar application of nano-ZnO significantly upstreamed the production of antioxidants and osmolytes to attenuate the shocks of heat stress in S2 and S3. Likewise, nano-ZnO substantially rebated the production of reactive oxygen species in both S2 and S3 that was associated with curtailment in lipid peroxidation. Adding to that, foliar-applied nano-ZnO inflates not only the chlorophyll contents and gas exchange attributes, but also the seeds per pod (SPP) and pods per plant (PPP), which results in the better grain yield under heat stress. Thus, among all the sowing dates, S1 statistically

performed better than S2 and S3, although foliar exposure of nano-ZnO boosted up mungbean performance under both the no heat and heat-induced environments. Hence, foliar application of nano-ZnO can be suggested as an efficient way to protect the crop from heat stress-mediated damages with the most negligible chances of nanoparticles delivery to environmental compartments that could be possible in case of soil application.

Keywords: zinc oxide, nanoparticles, osmolytes, ICPMS, heat stress, antioxidants, mungbean

INTRODUCTION

Globally, it is forecasted that by the end of the twenty-first century, the air temperature will ascend by 0.2°C per decade, resulting in inflate of 1.8–4.0°C temperature more than the existing level (IPCC, 2014). Global warming has led to climate change, causing adverse effects on plant growth, as high temperatures have detrimental results on crop production worldwide (Ohama et al., 2017). Heat stress is known to alter several morphological and physicochemical processes in plants, reducing yield and disrupting cellular homeostasis (Bita and Gerats, 2013). Heat stress can disturb cellular homeostasis due to the excess production of reactive oxygen species (ROS) (Buttar et al., 2020). Under stress conditions, a substantial increase in the concentration of hydrogen peroxide (H_2O_2) and malondialdehyde (MDA) manifests high membrane permeability, which eventually ends up with enhanced lipid peroxidation (Bi et al., 2016; Irshad et al., 2021). Fortunately, to cope with ROS, plants have triggered specific mechanisms to reverse the decline in growth caused by heat stress, which include: (i) enzymatic and non-enzymatic antioxidant defense system and (ii) osmoregulation by producing compatible solutes (Hasanuzzaman et al., 2013). The antioxidant enzymes, such as superoxide dismutase (SOD), peroxidase (POD), and catalase (CAT) quench, and detoxify ROS from the plant cell (Hu et al., 2012; Sharma et al., 2012). When plants are exposed to stress conditions, antioxidant enzymes perform a vital role in maintaining plant growth and development and various studies have revealed a direct association between plant thermotolerance and ROS scavenging (Hameed et al., 2012). Different environmental conditions accompany different growth stages of plants. "The suitable sowing date" is one of the most imperative factors to obtain optimum yield. Plant growth is modified to a specific environmental condition at various growth stages; thus, a suitable selection of sowing dates inflates the photosynthetic efficiency (Ali et al., 2021). In Kharif season crops, during early growth stages, the temperature reaches more than 40°C. It caused a significant reduction in seed yield due to frequent flower drops, lack of fertilization, non-viability of pollen, and catalytic deactivation of rubisco activase, leading to complete enzyme failure (Perdomo et al., 2017). Heat stress harms the retention of flowering and pod formation. The primary flower shedding occurred up to 40°C temperature in mungbean and flower drop has been reported more than 79% (Kaur et al., 2015). The reproductive stage is the most sensitive stage to heat stress, resulting in loss of flower buds and seed yield (Kaushal et al., 2013; Sharma et al., 2016). Heat stress causes degradation of chlorophyll, disturbance in electron flow, disruption of photosystem II, and attenuation in carbon fixation that collectively inhibit the process of photosynthesis (Hussain et al., 2021; Li et al., 2021).

For the stability of proteins and biological membranes, Zn plays a vital role. It also facilitates maintaining ROS assembly and scavenging, as it acts as an SOD cofactor. Zn, being a part of Cu/Zn-SOD, is present within the cytosolic and chloroplast enzymes that have a crucial role against oxidative stress (Khan et al., 2021). Zn, a necessary micronutrient for all plants, takes part in numerous physiological activities, i.e., pollen performance, biosynthesis of chlorophyll, enzymes, proteins, and metabolic processes (Singh et al., 2018). It is a key component of the enzyme carbonic anhydrase, which catalyzes the exchange of CO_2 and HCO_3 in the mechanism of C4 photosynthesis (Faizan et al., 2021). Recent advances in nanotechnology have revolutionized agriculture and offer immense potential in enhancing abiotic stress tolerance, mainly through upregulating plant antioxidant activities (Rana et al., 2021). Nanoparticles (NPs) are atomic or molecular aggregates having at least one dimension between 1 and 100 nm that can significantly alter their physicochemical characteristics compared to the bulk material (Rastogi et al., 2017). NPs present a proficient way in an organized fashion to spray fertilizers and pesticides with the high site-specificity due to their small particles and large ratio of surface area to volume (Prasad et al., 2012; Kah et al., 2018). NPs play a pivotal role in stressed plants, which could help the plants to tolerate the abiotic stresses (Martínez-Fernández et al., 2015; Aghdam et al., 2016; Dimkpa et al., 2017). Nano-ZnO has recently captured the vast research struggles due to its distinctive quality and multiple applications in numerous fields (Sturikova et al., 2018). It has been documented that nano-ZnO is far more efficient in augmenting the productivity and absorption of Zn because of its high surface area to volume ratio (Khan et al., 2021). Under stress, NPs increase the potential of an antioxidant defense system for scavenging the free radicals by changing the microRNA expression and regulating the numerous morphological, physiological, and metabolic processes of the plant (Siddiqi and Husen, 2016; Kambe et al., 2021).

Mungbean seems to be a promising crop because it is nutritionally sound, fixes nitrogen, overgrows, and requires less water (Samson et al., 2020). As a critical pulse crop, mungbean is anticipated to be a vital component of ameliorating and diversifying cropping systems and worldwide diets. It provides vital vitamins, minerals, and amino acids (Schafleitner et al., 2015;

Vittal et al., 2018). Being an imperative leguminous summer-season crop, it is much responsive to biotic and abiotic stresses. In April and May, mungbean cultivation faces temperature >30°C, which can even go up to 45°C, particularly at the time of pod filling and flowers initiation to significantly influence the yield (Hanumantharao et al., 2016; Malaviarachchi et al., 2016; Kumari et al., 2021). Foliar application of nano-ZnO against sowing time-mediated heat stress was rarely studied in previous times. Therefore, it was hypothesized that Zn as NPs is an intelligent delivery system with a larger surface area, high sorption capacity, and slow-release kinetics to target areas, which can mitigate the deleterious effects of heat activating the physiochemical mechanisms of plants against oxidative stress. One of the suitable ways to study the effect of heat stress in field conditions is to extend the sowing dates that ensure high temperature (>40/25°C) during the reproductive stage. This also provides a fair insight to study the sensitivity of a crop against heat stress. Thus, this proposed study was planned in field conditions by adjusting different sowing dates to impose heat stress at the reproductive stage. The foliar-applied nano-ZnO was applied to study the physicochemical processes and yield attributes of mungbean crops under different sowing regimes generated heat stress.

MATERIALS AND METHODS

Characterization of Nano-ZnO

The ZnO-NPs were obtained from Alfa Aesar (Thermo Fisher Scientific, Shanghai, China), having a size range between 20 and 30 nm, density 5.606 g cm^{-3}, and 99% purity. Scanning electron microscopic (SEM) (Hitachi SU8010, Tokyo, Japan) analysis was further performed to identify nano-ZnO morphology. X-ray diffraction (XRD) was used to record the peaks patterns of nano-ZnO specimens by using a Siemens D5000 diffractometer. Additionally, a UV–visible spectrophotometer (Shimadzu, Kyoto, Japan) at a 200–800 nm wavelength range was performed to examine the intensity.

Study Site Description and Experimental Design

The planned research trial was conducted at the Agronomic Research Farm, University of Agriculture, Faisalabad, Pakistan in 2018 (73.06° E, 31.27° N). The climate of this region is semiarid and subtropical at an altitude of 184.4 m above sea level. The seeds of mungbean variety NM-2016 were acquired from the Nuclear Institute for Agriculture and Biology, Faisalabad, Pakistan. Mungbean seeds were treated by fungicide (azoxystrobin) and sown as a test crop in a well-prepared soil @ 20 kg ha^{-1}. The layout trial of plot size 3 m × 1.8 m, comprising three replications, was used in a randomized complete block design (RCBD) under a split-plot arrangement. The chemical and physical analysis of soil was carried out by taking the soil sample earlier than sowing of the crop (**Supplementary Table 1**). The seedbed was prepared with the help of a cultivator followed by planking to pulverize the soil. Distance between the lines was maintained at 30 cm. Thinning was done after 10 days of sowing to maintain 10 cm distance between the plants. All the irrigations were applied according to crop requirements in all the sowing dates. First irrigation after 3 weeks of germination, second irrigation at the flowering stage, and third irrigation at pod formation were applied. Application of fertilizer was done by using the sources of urea, diammonium phosphate (DAP), and potassium sulfate (SOP) to apply the recommended dose of N:P:K at the rate of 30:60:30 kg ha^{-1} before each sowing date. Uniform agronomic operations were performed for all the treatments. Crop protection measures were adapted to save the crop from the attack of various insects, pests, and diseases. After harvesting and threshing the crop manually, seed production was counted and weighed from every plot. Grain yield (GY) was calculated as kg ha^{-1}. During the mungbean growing season, data about weather details, such as daily maximum/minimum temperature, relative humidity, wind speed, and photoperiod, were obtained from the Meteorological Observatory, University of Agriculture, Faisalabad, Pakistan (**Supplementary Figures 1, 2**). The daily minimum and maximum temperatures were recorded and averaged each month (**Figure 1**).

Zinc Oxide Nanoparticles and Heat Treatments

Heat stress was induced by setting three different sowing times, as a main plot factor, with an interval of 3 weeks: (1) the optimal sowing time S1 on 1 March 2018, when the flowering stage has day/night temperatures around 36.8/26.5°; (2) late sown S2 on 21 March 2018, having day/night temperatures 39.7/28.5°; (3) late sown S3 on 11 April 2018, when the flowering stage has day/night temperatures around 44.1/33.2° (sown in such a way that flowering stage coincided with periods of heat stress) (**Figure 1**). Five levels of nano-ZnO: CK (0), ZnO-1 (15 mg l^{-1}), ZnO-2 (30 mg l^{-1}), ZnO-3 (45 mg l^{-1}), and ZnO-4 (60 mg l^{-1}) were kept as subplot factor. The doses of nano-ZnO were derived by previous studies (Dhoke et al., 2011; Liu and Lal, 2015). All the solutions were prepared with deionized water. The ultrasonication of suspensions was done for 30 min to increase the dispersion of NPs. Tween 20 (0.05%) was added in solution as a surfactant to ensure the uniform retention and coverage of solution on the leaf surface. Foliar application of nano-ZnO was made at the flowering stage to study dangerous effect of the heat stress. For three replicates, the total amount of nano-ZnO used per treatment was 1 L. Each plant was sprayed three times, with the nozzle of the sprayer calibrated to deliver 1 ml of nano-ZnO in each spray.

Biochemical Assays

After applying nano-ZnO at the flowering stage, within 24–36 h, five plants per plot were randomly selected and their entirely expanded young leaves were taken for biochemical analysis. After that, pestle and mortar were used to crush 0.5 g sample under chilled conditions at pH of 7.8. The enzyme extract was then added to 1 ml of phosphate buffer. It was centrifuged for 10 min at 4°C. After centrifugation, the residues were discarded, the supernatant was used to determine the enzymes, and the extracted material was kept at 4°C (Terras et al., 1993).

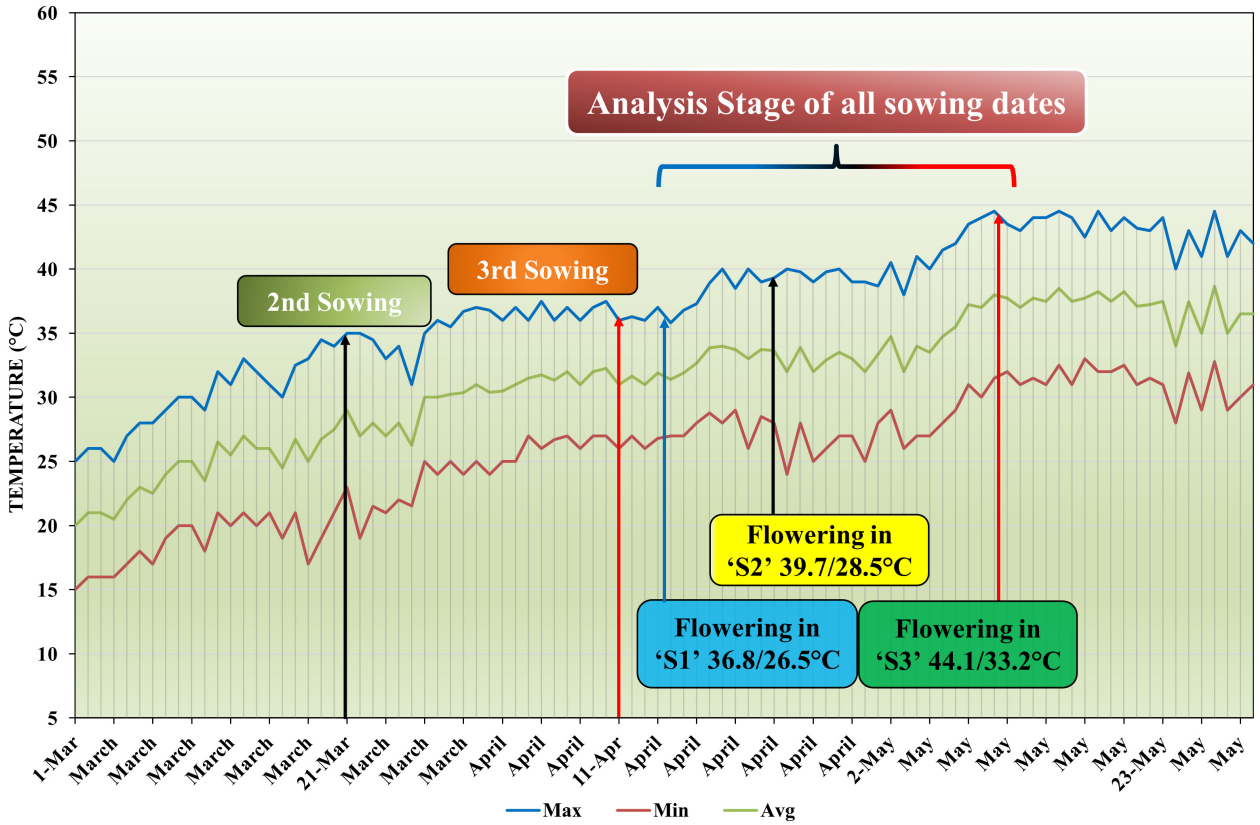


FIGURE 1 | Maximum, minimum, and average temperature profile during three sowing time situations in the growing season of mungbean.

Furthermore, for evaluation of enzymatic antioxidants, 96-well plates were used for pipetting of samples into it. A microplate reader was used for reading plates at different wavelengths.

Determination of Antioxidant Enzyme Activity

For enzyme activity, the samples were prepared by grinding 0.5 g of plant leaves with 5 ml of 0.1 M potassium phosphate buffer [phosphate-buffered saline (PBS)] (pH = 7.8). Then, homogenates were centrifuged at 12,000 × g at 4°C for 20 min and the supernatants were used for the determination of the activity of antioxidant enzymes. SOD (EC, 1.15.1.1) activity was calculated at 25°C under 4,000 W (light intensity) (Giannopolitis and Ries, 1977). POD (EC, 1.11.1.7) activity was measured by using guaiacol [1-hydroxy-2-methoxybenzene ($C_7H_8O_2$)] as an electron donor. CAT activity (EC, 1.11.1.6) was determined by measuring the conversion rate of H_2O_2 to water and oxygen molecules (Bianco and Defez, 2009).

Total Phenolic Contents

Total phenolic contents (TPCs) were measured in 10 ml 80% acetone 0.5 g leaf tissue by using the Folin-Ciocalteu reagent method (Rover and Brown, 2013). After that, absorbance was read at 765 nm. The calibration curve was developed by using gallic acid (10–100 mg l^{-1}) for TPC determination and results were presented as gallic acid equivalent (GAE) (Ainsworth and Gillespie, 2007).

Gas Exchange and Chlorophyll Determinations

For the determination of gas exchange parameters [photosynthesis rate (Pn), transpiration rate (E), stomatal conductance (gs), and intracellular CO_2 concentration (Ci)], fully expanded healthy apical leaves were used in photosynthesis apparatus Li-6400 (LI-COR Incorporation, Lincoln, Nebraska, United States). For chlorophyll determination, a 0.5 g subsample was collected of randomly taken green leaves from each experimental plot and soaked in 80% acetone overnight. 1.5 µl leaves extracts were taken to record absorbance at 663 and 645 nm in the ELISA plate. The chlorophyll a and b contents were calculated by using Eq. 1 and 2 (Arnon, 1949).

$$\text{Chl a (mg g} - \text{1FW)} = \frac{[12.7 \times \text{A663} - 2.69 \times \text{A645}] \times \text{V}}{1000 \times \text{W}} \quad (1)$$

$$\text{Chl b (mg g} - \text{1FW)} = \frac{[22.9 \times \text{A645} - 4.68 \times \text{A663}] \times \text{V}}{1000 \times \text{W}} \quad (2)$$

Where A: absorbance, V: volume of extract (ml), and W: weight of fresh leaves tissue.

Determination of Leaf Proline, Glycine Betaine, and Total Soluble Protein

For estimation of leaf proline (LP) content, we followed the method of Bates et al. (1973) and absorbance was recorded at 520 nm by using ELISA plates. Determination of glycine betaine (GB) was done by Grieve and Grattan (1983) method and absorbance was recorded by using an organic layer at 365 nm. Total soluble protein (TSP) was analyzed by using Bradford Reagent and were added to the ELISA plate to record absorbance at 595 nm (Bradford, 1976).

Lipid Peroxidation (Malondialdehyde) and H_2O_2

The concentration of H_2O_2 was estimated by the method of Velikova et al. (2000). For lipid peroxidation, the content of MDA was measured by incubating tissue extract with thiobarbituric acid (TBA) at boiling temperature (Dhindsa et al., 1981).

Yield Components

A number of pods per plant (PPP) were counted by taking five plants at random from each plot and then pods were manually measured from selected plants and then averaged. To calculate seeds per pod (SPP), five PPP were chosen randomly from each plot. In each selected plot, manually seeds were removed from every pod and averaged after counting. After manually harvesting and threshing the crop, seed production was measured and weighed from every plot. GY was calculated as kg ha^{-1}.

Inductively Coupled Plasma Mass Spectroscopy Study of Zn Dissolution

Zn release from N-ZnO was measured by inductively coupled plasma mass spectroscopy (ICPMS) (ELAN DRC-e, PerkinElmer, Waltham, Massachusetts, United States). For digestion of ultrapure HNO_3 suspension, we followed the standard techniques of Pradhan et al. (2013), which was subsequently tested by using a Zn standard solution in an ICPMS system. All the measurements were carried out in three replicates for every treatment.

Statistical Analysis

The collected data were statistically evaluated by using Fisher's ANOVA and differences among treatment means were compared using the honestly significant difference (HSD) test at a 5% probability level by using Statistical Package for the Social Sciences (SPSS) software version 7 (SPSS Incorporation, Chicago, IL, United States). Graphical illustrations of statistically analyzed data were prepared by using GraphPad Prism software version 7.00 (GraphPad Software Incorporation, San Diego, California, United States). Pictorial diagrams were drawn by using Adobe Photoshop 2020. The Pearson's correlation analyses were performed in R software version 3.6.1 to explain the correlation between plant yield and biochemical attributes with a foliar nano-ZnO application under sowing time generated heat stress.

RESULTS

Characterization of Nano-ZnO

The particle size of the sample is in the nanometer regime with an average length of 20 ± 5 nm. The XRD pattern for ZnO-NPs showed a single phase as peaks of other phases were not present and the highest peak appeared at 370 along the x-axis (**Figure 2A**). The UV–visible spectrophotometer results of ZnO-NPs showed that the bandgap remains almost the same (**Figure 2B**) as calculated by the equation:

$$Eg = \frac{hc}{\lambda} \quad (3)$$

The surface morphology of specimen ZnO-NPs was observed near nanospheres and some nanorod shapes as shown in **Figures 2D,E**. These SEM, XRD, and UV–visible spectrophotometer measurements were almost the same as purchased from the company.

Climatic Condition of the Studied Area

Daily maximum and minimum temperatures were recorded for all the sowing dates. The temperature at the flowering stage during day/night was 36.8/26.5°C for S1, 39.7/28.5°C for S2, and 44.1/33.2°C for S3 (**Figure 1**). Relative humidity recorded during the day/night fall between 62 and 94/20 and 52% for S1, 52 and 82/16 and 40% for S2, and 41 and 74/10 and 37% for S3 (**Supplementary Figure 1**). Photoperiod ranged fall between 12.8 and 13.7 in all the sowing dates.

Antioxidant Activities

Superoxide dismutase, POD, CAT, and TPC activities were decreased under heat stress plants of S2 and S3 over ambient conditions in S1 (**Figures 3A–D**). In S1, the antioxidant activities, such as SOD, POD, and TPC, were increased by 21, 23, and 29%, respectively, at 30 mg l^{-1}. CAT has increased by 23% at 45 mg l^{-1} doses foliar-applied nano-ZnO application compared with control. In S2, the more distant activities than control of SOD (31%), POD (37%), CAT (32%), and TPC (71%) were observed where 45 mg l^{-1} doses of nano-ZnO were applied. In S3, the activities of the enzymes, such as SOD, POD, CAT, and TPC, by 60, 39, 52, and 139%, respectively, were higher relative to control at 60 mg l^{-1} dose of foliar-applied nano-ZnO. The minimum antioxidant activities were found in control under all the three sowing times.

Osmoprotectants and Lipid Peroxidation

Sowing time generated heat stress in S2 and S3 manifested maximum decrement in TSP, GB, and LP over control (**Figures 4A–C**), whereas conversely, the maximum increment of MDA content and H_2O_2 were scrutinized in S3 followed by S2 and S1, which symbolizing boosted lipid peroxidation under stressed conditions (**Figures 5A,B**). Under stressful environment, 60 mg l^{-1} dose of nano-ZnO significantly rebated the H_2O_2 and MDA contents by 25%, and 20% in S3, by 32 and 30% in S2, relative to control, respectively. In S3, the accumulation

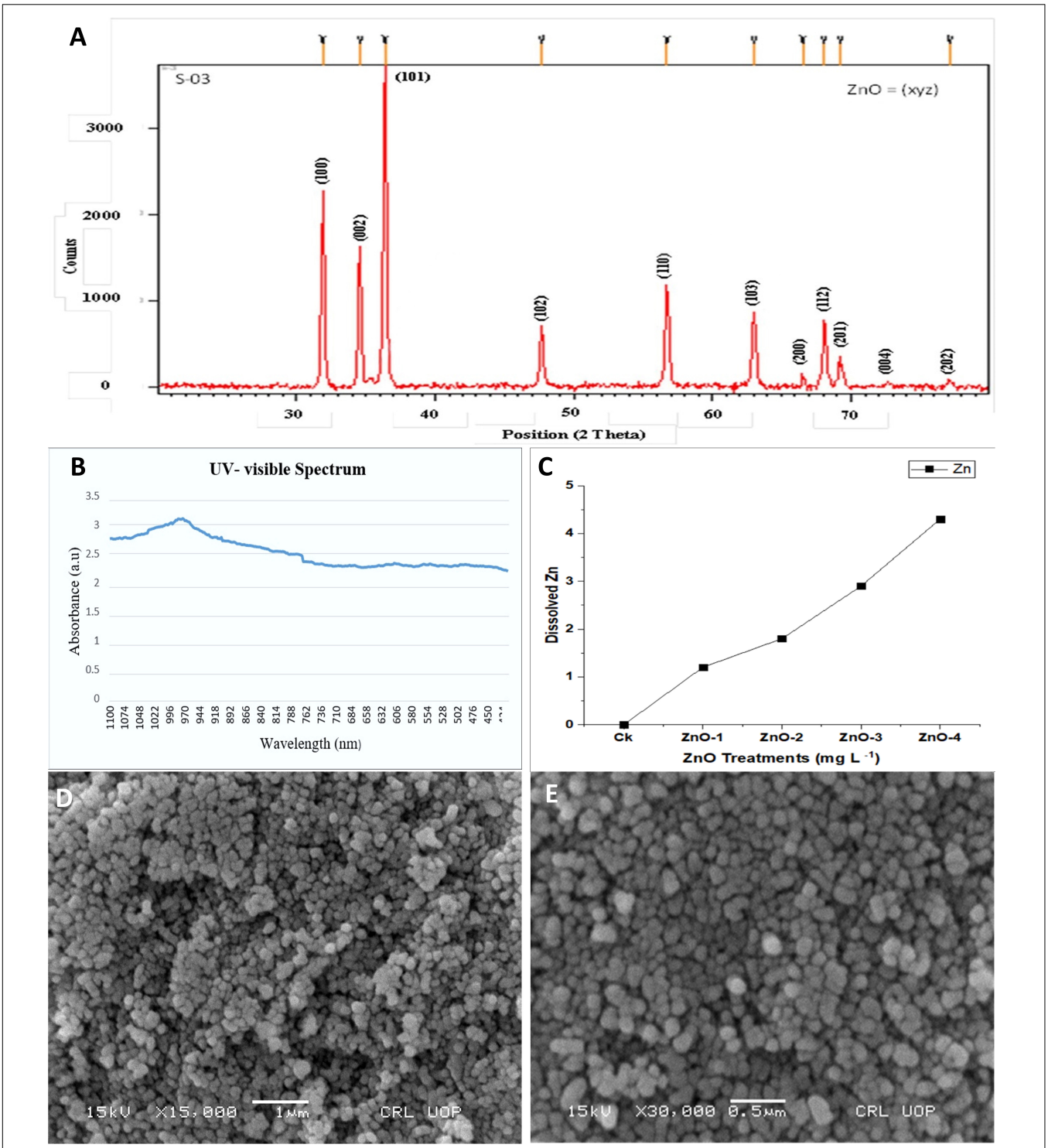


FIGURE 2 | Characterization of zinc oxide nanoparticles (ZnO-NPs) by using **(A)** X-ray diffraction (XRD) spectra, **(B)** UV-visible spectrum, **(C)** nano-ZnO dissolution pattern at different concentration (CK: control, ZnO-1: 15 mg l^{-1}, ZnO-2: 30 mg l^{-1}, ZnO-3: 45 mg l^{-1}, and ZnO-4: 45 mg l^{-1}), and **(D,E)** Scanning electron microscopy (SEM).

of osmolytes significantly augmented the LP, GB, and TSP by 79, 88, and 112% at 60 mg l^{-1} nano-ZnO concentration over control. Likewise, 30 and 45 mg l^{-1} levels of nano-ZnO showed better findings of osmolytes activities over control in S1 and S2, respectively. Foliar application of nano-ZnO significantly inflates the activities of osmolytes (PC, GB, and TSP) and attenuated lipid

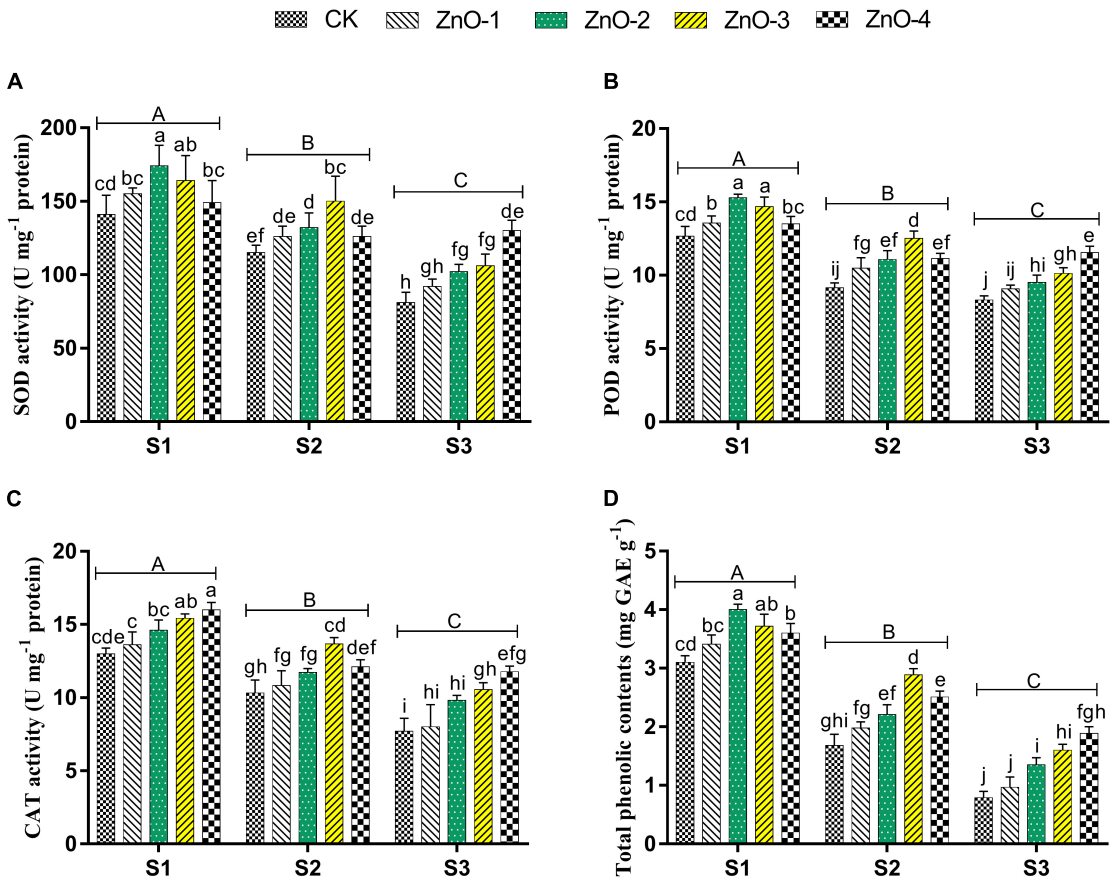


FIGURE 3 | Effect of foliar application of nano-ZnO on superoxide dismutase (SOD) **(A)**, peroxidase (POD) **(B)**, catalase (CAT) **(C)**, total phenolic contents, and **(D)** in *Vigna radiata* L. under sowing time generated heat stress. Nano-ZnO doses: CK (distilled water), ZnO-1 (15 mg l^{-1}), ZnO-2 (30 mg l^{-1}), ZnO-3 (45 mg l^{-1}), and ZnO-4 (60 mg l^{-1}). S1, First sowing-March 1 (recommended); S2, Second sowing-March 22 (late sown); S3, Third sowing-April 11 (late sown). Data are mean (±SE) of three replicates and different letters designate significant changes at Tukey's test ($p < 0.05$). In contrast, capital letters represent a significant difference among sowing time treatments and small letters represent a significant difference among the nano-ZnO treatments.

peroxidation (MDA and H_2O_2) compared to control among all the sowing dates.

Gaseous Exchange and Chlorophyll Contents

Heat stress in S3 and S2 caused a significant diminution of chlorophyll contents in mungbean plants compared with S1 (**Figure 4D**). Heat stress-mediated higher diminishment in chlorophyll contents was marked in S3, followed by S2 and S1. Although, foliar application of nano-ZnO at 30 mg l^{-1} significantly inflates the chlorophyll contents by 14, 11, and 25% in S1, S2, and S3, respectively, compared with control among all the sowing dates. In comparison with S1, sowing time generated heat stress in S2 and S3 resulted in a significant lessening of Pn by 40 and 54%, E by 47 and 61%, gs by 31 and 48%, and Ci by 20 and 35%, respectively, whereas, foliar application of nano-ZnO at 30 mg l^{-1} resulted in the significant rise of gas exchange determinations in all the sowing dates. As, in S1: Pn by 51%, E by 87%, Gs by 58%, and Ci by 32%, in S2: Pn by 81%, E by 84%, Gs by 60%, and Ci by 41%, and in S3: Pn by 75%, E by 154%, Gs by 102%, and Ci by 34%, it gets increased relative to control (**Table 1**).

Yield Attributes

Grain yield, SPP, and PPP were significantly decreased in heat-stressed treatments S2 and S3 relative to unstressed treatment S1. Bargains in GY, SPP (**Figures 5C,D**), and PPP (**Figure 6**) levels by 18, 21, and 45% were calculated at 30 mg l^{-1} dose of nano-ZnO in S1 relative to control, respectively, whereas, foliar application of 30 mg l^{-1} nano-ZnO also significantly mitigated heat stress impact and had the highest alleviating effect in GY, SPP, and PPP by 23, 42, and 30% in S2 and 35, 48, and 37% in S3, respectively, in comparison with control.

Inductively Coupled Plasma Mass Spectroscopy Study of Zn Release From Nano-ZnO

In *in vitro* ICPMS, after 24 h at pH 7.0, investigations on the Zn release from various concentrations of nano-ZnO of 0, 15, 30, 45, and 60 mg l^{-1} discovered that less Zn amount of 0, 1.1, 1.8, 2.9,

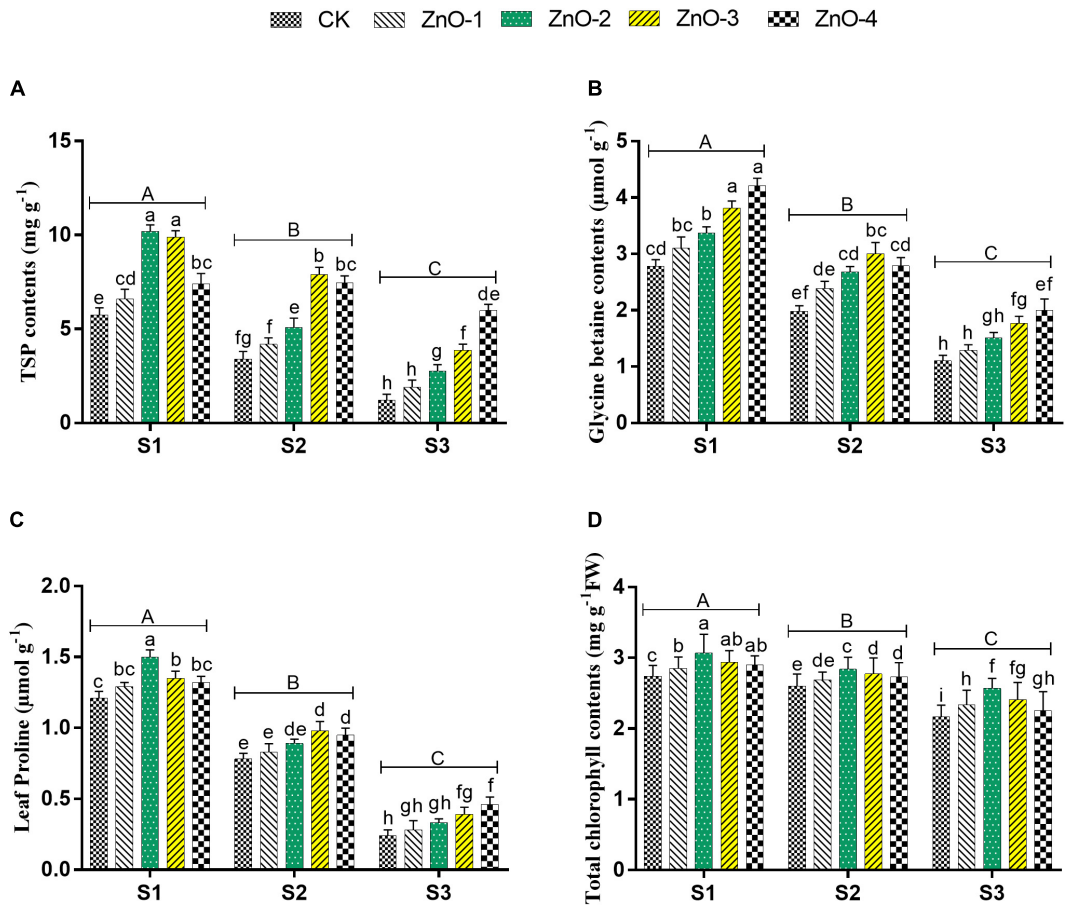


FIGURE 4 | Effect of foliar application of nano-ZnO on total soluble proteins (TSPs) **(A)**, glycine betaine **(B)**, leaf proline **(C)**, and total chlorophyll contents **(D)** in *Vigna radiata* L. under sowing time generated heat stress. Nano-ZnO doses: CK (distilled water), ZnO-1 (15 mg l^{-1}), ZnO-2 (30 mg l^{-1}), ZnO-3 (45 mg l^{-1}), and ZnO-4 (60 mg l^{-1}). S1, First sowing-March 1 (recommended); S2, Second sowing-March 22 (late sown); S3, Third sowing-April 11 (late sown). Data are mean (±SE) of three replicates and different letters designate significant changes at Tukey's test ($p < 0.05$). In contrast, capital letters represent a significant difference among sowing time treatments and small letters represent a significant difference among the nano-ZnO treatments.

and 4.2 mg l^{-1} was released, respectively (**Figure 2C**). ICPMS study revealed that Zn release and uptake from nano-ZnO were concentration-dependent.

Correlation Between Plant Yield and Biochemical Attributes With Foliar Nano-Zno Application Under Sowing Time Generated Heat Stress

We observed a strong positive correlation between PPP, SPP, and GY being this associated with an overall plant yield obtained by foliar application of nano-ZnO under sowing time generated heat stress. GY showed a strong positive correlation with total chlorophylls, antioxidants activity, and osmolytes production and SPP and PPP in nano-ZnO sprayed plants under heat stress. Total chlorophylls contents were also positively correlated with overall antioxidant response and osmolytes activities. Plant antioxidant responses (SOD, POD, CAT, and TPC) and osmolytes (TSP, GB, and LP) pose a strong positive correlation between them. SPP and PPP also exhibit a strong positive correlation with total chlorophylls contents along with antioxidants and osmolytes activity. On the other hand, MDA and H_2O_2 were found to be in strong negative correlation with antioxidants activity and osmolytes production, whereas a weak negative correlation was observed with GY, PPP, and SPP (**Figure 7**).

DISCUSSION

Heat stress is an excellent debacle for the growth and productivity of crop plants. Mungbean genotype, which is used in this study, is recommended to sow on 1 March (S1); to inflict heat stress (>40/25°C) at reproductive stage, this genotype was also late sown with 3 weeks interval as S2 and S3. Subsequently, the delayed sown plants encountered the issue of heat stress at the flowering stage. The temperature was 4–6°C higher than the optimal sowing, which seriously affected the biochemical attributes performance, particularly pod set reduction, PPP, SPP, and seed yield, implying heat sensitivity of mungbean (**Figure 1**). Our observations on the decline in seed yield were inlined

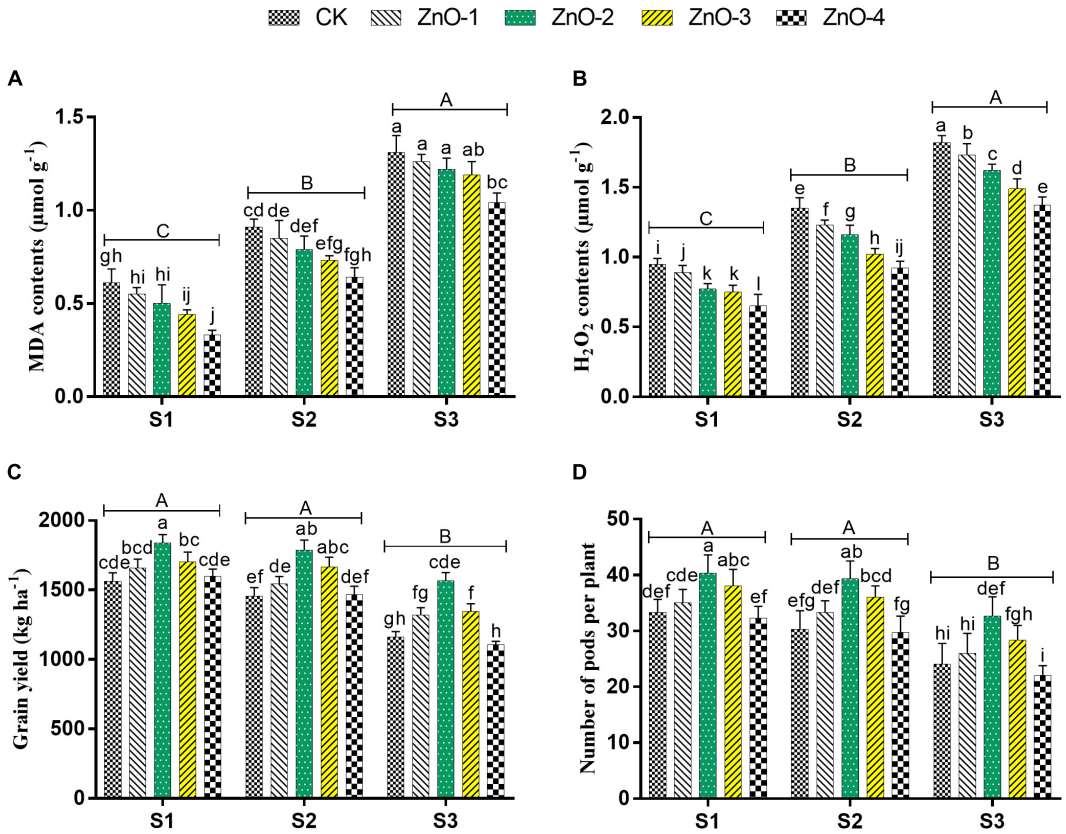


FIGURE 5 | Effect of foliar application of nano-ZnO on malondialdehyde (MDA) contents **(A)**, hydrogen peroxide (H_2O_2) contents **(B)**, grain yield **(C)**, number of pods per plant, and **(D)** in *Vigna radiata* L. under sowing time generated heat stress. Nano-ZnO doses: CK (distilled water), ZnO-1 (15 mg l^{-1}), ZnO-2 (30 mg l^{-1}), ZnO-3 (45 mg l^{-1}), and ZnO-4 (60 mg l^{-1}). S1, First sowing-March 1 (recommended); S2, Second sowing-March 22 (late sown); S3, Third sowing-April 11 (late sown). Data are mean (±SE) of three replicates and different letters designate significant changes at Tukey's test ($p < 0.05$). In contrast, capital letters represent a significant difference among sowing time treatments and small letters represent a significant difference among the nano-ZnO treatments.

with some previous studies, which demonstrated the inhibitive effects of heat stress on mungbean crops (Sanat et al., 2006; Malaviarachchi et al., 2016).

To combat abiotic stresses, plants deploy an antioxidant defensive mechanism to ameliorate the negative influence of heat stress-generated ROS (Buttar et al., 2020). In our findings, depressed antioxidant activities were observed in heat-stressed environments S2 and S3 relative to no heat environment S1. As the level of oxidative damage is raised, the efficiency of photosynthesis decreases, which influences the growth of mungbean (Bansal et al., 2014). A direct relationship between heat stress and nano-ZnO doses was observed. Zn plays a central role in the stability of biomembranes and protein because it is a cofactor in the SOD enzyme (Faizan et al., 2020). Therefore, as the level of heat stress gets increased, the activities of SOD, POD, CAT, and TPC also get increased, at various concentrations of nano-ZnO, relative to control (**Figure 3**). Cu/Zn-SOD production may increase due to foliar application of nano-ZnO, which favored the defensive mechanism in scavenging of ROS, as reported by Mansoor (2013). In this study, escalation in the total phenolic activity was also examined due to the function of zinc, which coincided with the finding of Yuan et al. (2016). A strong negative correlation between antioxidants activities and MDA and H_2O_2 confirmed the positive role of nano-ZnO application against ROS under heat stress (**Figure 7**).

Osmolytes, such as LP, GB, and TSP, are low-molecular weight substances utilized by plant cells and tissues under adverse environmental conditions to keep a steady water potential by accumulating them as organic solutes to create a hypotonic environment (Yancey, 2005). Heat stress triggered the breakdown of chlorophyll that caused a reduction in sucrose synthesis, which decreased the biosynthesis of LP, GB, and TSP. Foliar applications of nano-ZnO might inflate the biosynthesis of tryptophan, which is involved in photosynthesis; hence, it increased the synthesis of sucrose required for the biosynthesis of LP, GB, and TSP (**Supplementary Figure 1**). Hereafter, the biosynthesis of LP, GB, and TSP was increased in S2 and S3 by exogenous foliar application of nano-ZnO under heat stress relative to control (Waraich et al., 2012). In our finding, osmolytes (LP, GB, and TSP) were found to be positively correlated with antioxidants and chlorophylls (**Figure 7**).

Peroxidation of membrane lipid is a significant damaging effect of ROS and its extent in plants is detected by measuring MDA (Garg and Manchanda, 2009; Hussain et al., 2016;

TABLE 1 | Effect of foliar application of zinc oxide nanoparticles (nano-ZnO) on gas exchange determinations: photosynthetic rate (Pn), transpiration (E), stomatal conductance (gs), and intracellular CO_2 concentration (Ci) in *Vigna radiata* (L.) under sowing time generated heat stress.

Treatments	Gas exchange attributes			
	Pn (μ mol m^{-2} s^{-1})	E (mmol H_2O m^{-2} s^{-1})	gs (mmol H_2O m^{-2} s^{-1})	Ci (μ mol mol^{-1})
1st sowing (S1)				
Control/water spray (CK)	16.00 ± 0.57^{ef}	2.55 ± 0.27^{def}	0.113 ± 0.02^{def}	270.3 ± 10.9^{d}
15 mg L^{-1} zinc oxide (ZnO-1)	17.60 ± 0.31^{cd}	3.19 ± 0.35^{cd}	0.122 ± 0.02^{bcd}	290.0 ± 13^{cd}
30 mg L^{-1} zinc oxide (ZnO-2)	24.18 ± 0.83^{a}	4.78 ± 0.33^{a}	0.179 ± 0.03^{a}	358.0 ± 10.2^{a}
45 mg L^{-1} zinc oxide (ZnO-3)	22.11 ± 0.87^{ab}	3.77 ± 0.40^{b}	0.141 ± 0.01^{b}	321.7 ± 12.2^{b}
60 mg L^{-1} zinc oxide (ZnO-4)	20.22 ± 0.62^{bc}	3.30 ± 0.23^{bc}	0.134 ± 0.03^{bc}	303.7 ± 9.9^{c}
2nd sowing (S2)				
Control/water spray (CK)	9.56 ± 0.70^{hi}	1.34 ± 0.35^{hi}	0.078 ± 0.01^{gh}	213.7 ± 15.0^{ij}
15 mg L^{-1} zinc oxide (ZnO-1)	11.31 ± 0.50^{hi}	1.81 ± 0.24^{gh}	0.089 ± 0.01^{fgh}	238.7 ± 7.9^{gh}
30 mg L^{-1} zinc oxide (ZnO-2)	17.33 ± 0.60^{de}	3.34 ± 0.29^{c}	0.125 ± 0.02^{bc}	300.7 ± 15^{bc}
45 mg L^{-1} zinc oxide (ZnO-3)	15.97 ± 0.61^{ef}	2.41 ± 0.18^{def}	0.105 ± 0.02^{ef}	263.0 ± 6.8^{ef}
60 mg L^{-1} zinc oxide (ZnO-4)	14.49 ± 0.78^{efg}	2.18 ± 0.26^{fgh}	0.097 ± 0.02^{fgh}	248.3 ± 11.7^{fg}
3rd sowing (S3)				
Control/water spray (CK)	7.32 ± 0.46^{i}	0.98 ± 0.20^{i}	0.058 ± 0.01^{i}	175.0 ± 8.0^{k}
15 mg L^{-1} zinc oxide (ZnO-1)	8.70 ± 0.63^{i}	1.44 ± 0.24^{ghi}	0.071 ± 0.02^{hi}	198.0 ± 14.2^{jk}
30 mg L^{-1} zinc oxide (ZnO-2)	12.78 ± 0.75^{fgh}	2.96 ± 0.41^{de}	0.118 ± 0.01^{de}	$233.7 \pm 8.0h^{i}$
45 mg L^{-1} zinc oxide (ZnO-3)	10.14 ± 1.02^{ghi}	2.19 ± 0.23^{fg}	0.099 ± 0.02^{efg}	211.0 ± 15.1^{ij}
60 mg L^{-1} zinc oxide (ZnO-4)	10.33 ± 0.51^{hi}	1.99 ± 0.23^{fgh}	0.092 ± 0.01^{gh}	203.3 ± 7.2^{j}

S1, First sowing-March 1 (recommended); S2, Second sowing-March 22 (late sown); S3, Third sowing-April 11 (late sown). Data are mean (±SE) of three replicates and different letters designate significant changes at Tukey's test ($p < 0.05$).

Zafar et al., 2017). The curtailment in H_2O_2 with the escalation in foliar-applied nano-ZnO doses was noted because Zn is a part of the most abundantly found Cu/Zn-SOD in plant inflated antioxidant defense mechanism for the production of Cu/Zn-SOD to detoxify ROS (**Figure 8**). The findings of Disante et al. (2011) also supported the fact that under Zn deficiency, the production of Cu/Zn-SOD gets decreased, which leads to lipid peroxidation by increasing the ROS level. However, our findings showed that under S2 and S3 heat stress control conditions, the insidious effects of heat stress caused more significant lipid peroxidation by degrading biomembranes, which reduced the ability of plants to produce chlorophylls and osmolytes. Although diminution was studied in MDA contents under nano-ZnO application, Zn as a gene activator plays a crucial role in synthesizing protein and signaling. A strong negative correlation of MDA and H_2O_2 with antioxidants was also noted (**Figure 7**).

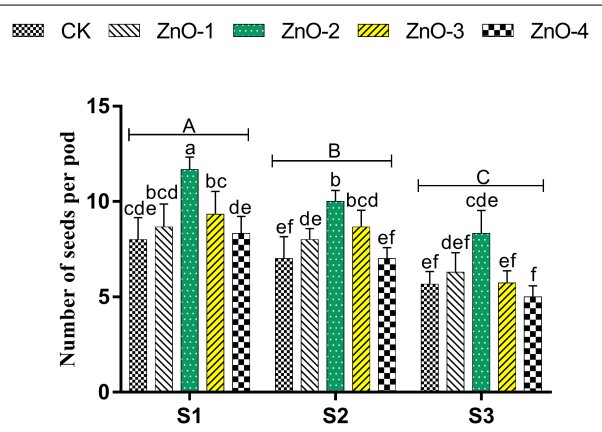


FIGURE 6 | Effect of foliar application of nano-ZnO on number of seeds per pod in *Vigna radiata* under sowing time generated heat stress. Nano-ZnO doses: CK (distilled water), ZnO-1 (15 mg l^{-1}), ZnO-2 (30 mg l^{-1}), ZnO-3 (45 mg l^{-1}), and ZnO-4 (60 mg l^{-1}). S1, First sowing-March 1 (recommended); S2, Second sowing-March 22 (late sown); S3, Third sowing-April 11 (late sown). Data are mean (±SE) of three replicates and different letters designate significant changes at Tukey's test ($p < 0.05$). In contrast, capital letters represent a significant difference among sowing time treatments and small letters represent a significant difference among the nano-ZnO treatments.

Chlorophyll is usually believed to be the most resistant pigment against heat stress. Higher temperatures eventually result in decreased photosynthesis by disrupting the function and structure of chloroplast (Faseela et al., 2020). Hence, similar findings were observed in this study, leading toward reduced chlorophyll contents (Zafar et al., 2017). Photosynthesis gets diminished due to stomatal closure as an early plant response toward heat stress, favoring better utilization of relative water contents (Tan et al., 2011). Heat stress-mediated decline in gs due to closing of stomata led to decreased Ci, which resulted in the reduction of Pn, E, pigment contents, and electron transportation to PSII (Pagter et al., 2005; Buttar et al., 2020). In this study, heat stress-mediated decrement in chlorophyll contents, Pn, E, gs, and Ci was significantly alleviated by the foliar application of nano-ZnO. As the size of applied ZnO-NPs was 20 ± 5 nm

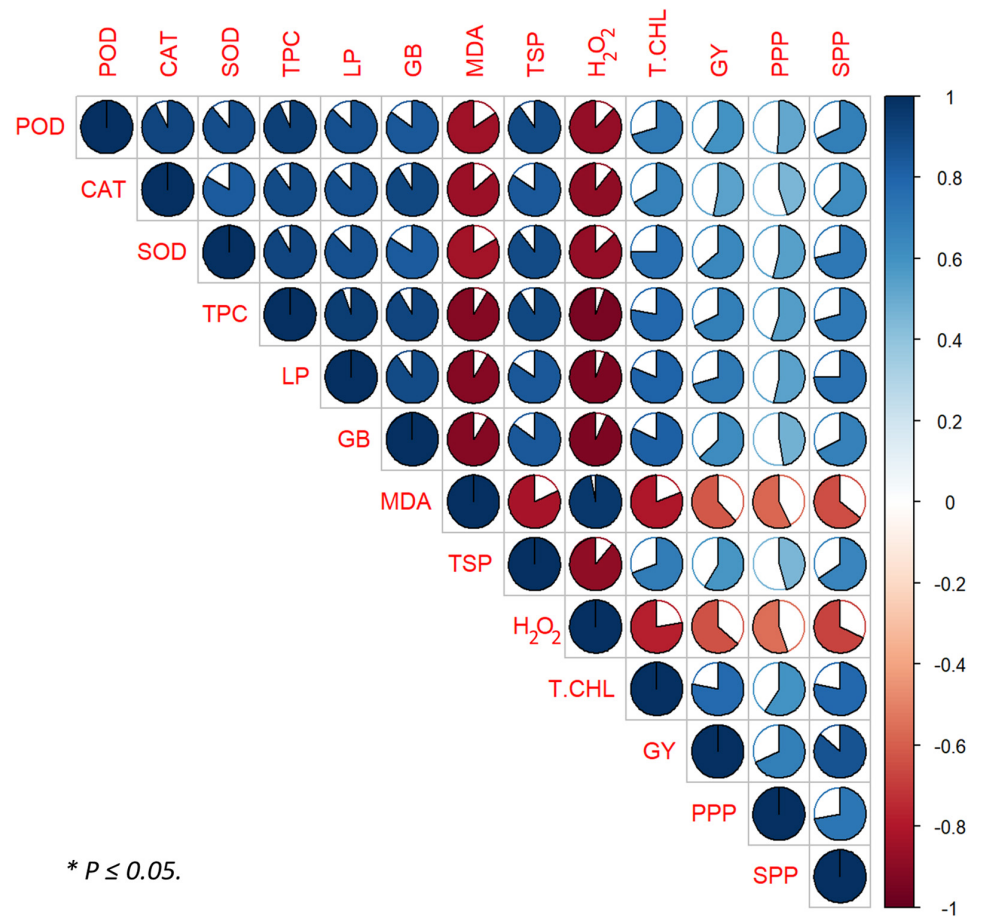


FIGURE 7 | Pearson's correlation matrix between plant yield and biochemical attributes with foliar-applied nano-ZnO under sowing time generated heat stress. Correlations are displayed in blue (positive) and red (negative); color intensity and circle size are proportional to the correlation coefficient. POD, peroxidase; CAT, catalase; SOD, superoxide dismutase; TPC, total phenolic content; LP, leaf proline; GB, glycine betaine; MDA, malondialdehyde; TSP, total soluble protein; H_2O_2, hydrogen peroxide; T.CHL, total chlorophyll; GY, grain yield; PPP, pods per plant; SPP, seeds per pod.

(**Figure 2C**), so they can easily find their way from stomatal pores to the phloem vessels *via* plasmodesmata (40 nm in diameter) and become readily available as observed by Kumar and Nagesh (2019). Hence, it was noted that nano-ZnO application potentially affected the gas exchange measures, which can be attributed to the upregulation of antioxidant defense mechanism and downregulation of ROS. Prasad et al. (2012) explicated that nano-ZnO was more effective to enhance the chlorophyll contents, flowering, and yield of pods in peanuts. Application of nano-ZnO increased the chlorophyll contents in the heat-stressed environment (S2 and S3) at specific concertation, as Zn is required for the production of chlorophyll that rebates the activity of chlorophyllase enzyme, which led to producing more chlorophyll contents in a leaf tissue as explained by Turan et al. (2009). Application of ZnO-NPs at low concentrations was found to be effective in alleviating various abiotic stresses and enhanced plant growth and development (Dhoke et al., 2011; Soliman et al., 2015). Therefore, at a higher concentration of nano-ZnO, degradation of chlorophyll led to a decrease in the overall performance of IRGA attributes. Although, the exogenous foliar applications of nano-ZnO at 30 mg l^{-1} inflated the biosynthesis of tryptophan amino acid, which is involved in photosynthesis that eventually increased the chlorophyll and growth of the plant (Waraich et al., 2012). Our findings revealed that the increased chlorophyll contents by nano-ZnO sprayed plants under heat stress was positively correlated with antioxidant enzymatic activity and osmoprotectants supporting its role in stress amelioration (**Figure 7**).

In contrast, earlier studies evaluating the effect of heat stress on mungbean plants grown in an outdoor environment at different intervals of time documented early shifting of phonological stages (Malaviarachchi et al., 2016). There was a phonological variation due to other sowing times in this study (**Figure 1**), which substantially decreased the flowering and podding duration, resulting in fewer flowers, pods, and seeds being produced. Pod set usually influenced pod and seed number, which is sensitive to heat stress in many crop species, including cotton (Snider et al., 2011), chickpea (Fang et al., 2010; Kumar et al., 2013), tomato (Li et al., 2013), and mungbean (Kaur et al., 2015).

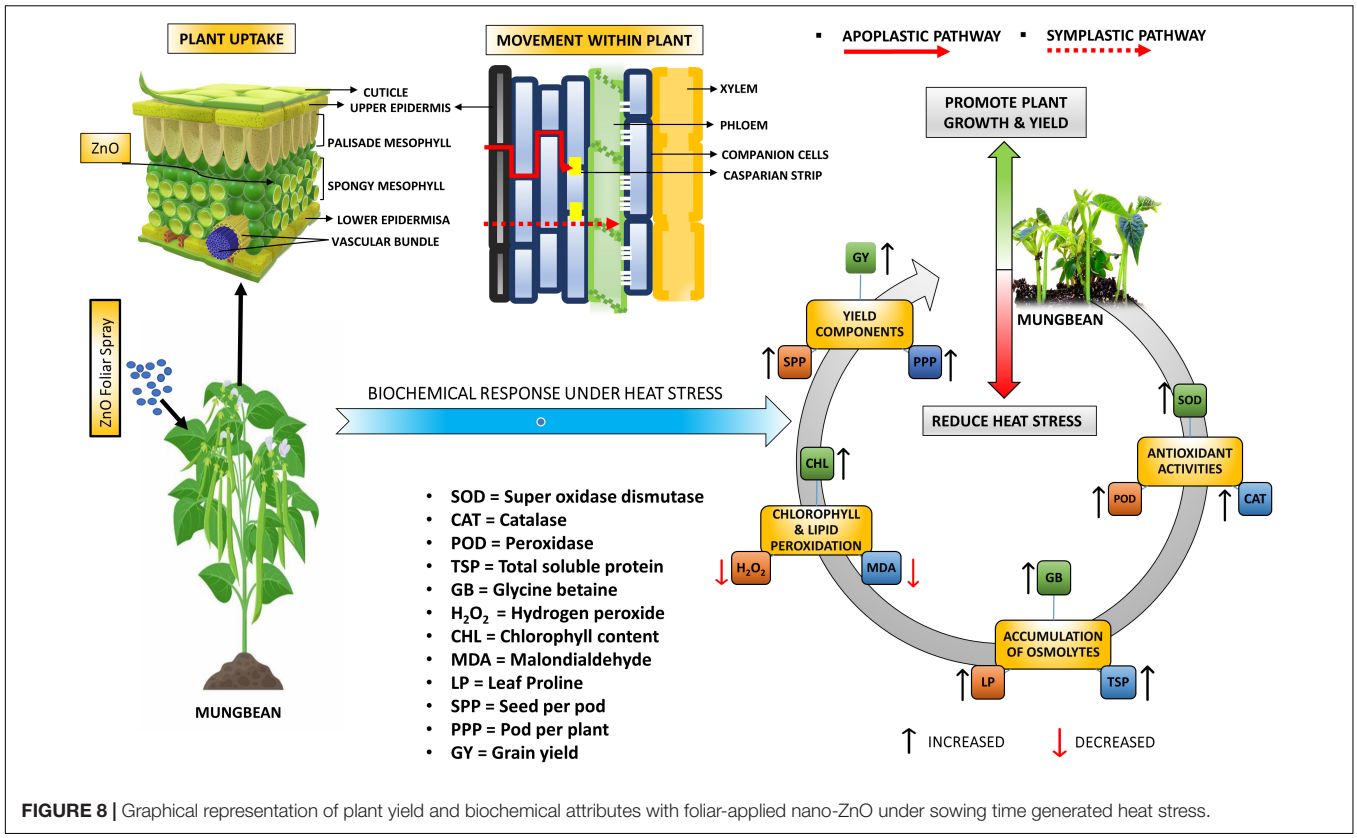


FIGURE 8 | Graphical representation of plant yield and biochemical attributes with foliar-applied nano-ZnO under sowing time generated heat stress.

Heat stress causes hindrance in the production of sucrose in leaves and creates an obstacle in its transport to reproductive organs (Prasad and Djanaguiraman, 2011; Li et al., 2012; Kaushal et al., 2013). Heat stress manifested significant diminution in PPP, SPP, and GY can be attributed to decreased chlorophyll contents, antioxidant activities, and osmolytes, leading to increased lipid peroxidation. The reduction in PPP and SPP caused by heat stress was reported in chickpea and soybean (Djanaguiraman et al., 2013). Many pods were aborted in heat-stressed mungbean plants of S2 and S3 as a result of limited sucrose import from the leaves. Hence, it causes a significant decrement in the number of filled pods as well as an increment in the number of infertile pods. Rainey and Griffiths (2005) demonstrated that heat stress in summers reduced yield because of pods and flowers abortion. Pod and seed diameters (data not given) were also significantly lower in S2 and S3 than in S1, indicating reduced sucrose translocation for developing sinks in heat-stressed S2 and S3 plants, as observed in chickpea (Awasthi et al., 2014) and tomato (Li et al., 2013). Although, under heat stress plants of S2 and S3, foliar-applied nano-ZnO increased PPP, SPP, and GY than control. This might be because Zn being an NPs, easily gets transported from the application site to the site of action through microcellular spaces, likely *via* plasmodesmata (Etxeberria et al., 2016). The entered nano-ZnO enhanced antioxidants competency against ROS in the plant system and produced more chlorophylls contents that ameliorate pollen performance, pollen germinability, and viability. This caused more fruit setting and eventually grew more PPP and SPP (Thakur et al., 2010; Prasad et al., 2012). Thus, nano-ZnO application in S2 and S3 ameliorated the functional aspects of reproductive organs and enhanced the antioxidant and osmolytes activities. This may be a primary cause of less pod abortion and, consequently, more pods and seeds per plant led toward more GY. Moreover, yield components (GY, SPP, and PPP) strongly correlated with chlorophyll contents, antioxidant activities, and osmoprotectants (**Figure 7**).

CONCLUSION

Among abiotic stresses, heat stress-mediated damage resulted in fluctuation and shrinkage of crop growth, development, and overall yield. Conclusively, under the umbrella of above-discussed facts and analysis, attenuation in antioxidants and osmolytes and escalation in MDA and H_2O_2 were witnessed during finely tuned sowing time generated heat stress imposition in S2 and S3. Antioxidant performance, osmolytes activities, and gas exchange measures improve with foliar application of nano-ZnO in all the sowing dates, which were obvious as reduced ROS accumulation. Upregulated antioxidants and osmoprotectants prevented oxidative damage justified the beneficial role of nano-ZnO supplementations to ameliorate tolerance mechanism against heat stress and, consequently, improved yield of mungbean crop. Particularly, 30 mg l^{-1} dose of nano-ZnO performed better in all the sowing dates and better ameliorate the negative impact of heat stress. Further study is needed to be

studied at the molecular level to unleash nano-ZnO-associated pathways and gene response about tolerance mechanism of heat-stressed mungbean plant.

DATA AVAILABILITY STATEMENT

The original contributions presented in the study are included in the article/**Supplementary Material**, further inquiries can be directed to the corresponding author.

AUTHOR CONTRIBUTIONS

HAK conceived the original research plans and wrote the original draft of the manuscript. MFS and QW designed and advised the research and agreed to serve as the author responsible for contact and ensure communication. HAK and JN performed the experiments. ZG assisted in microscopic experiments. SAR, SS, and SA analyzed the data and made a figure. MHS, SAR, and RK directed the experiments and revised the manuscript. NG, SW, SAR, and QW contributed to the editing and reviewing of the manuscript. All authors contributed to the article and approved the submitted version.

ACKNOWLEDGMENTS

Special thanks are given to QW for their skillful technical assistance and Peerwith expert "Gary Bentley" for native English language editing of the manuscript (http://peerwith.expert/garybentley). We would like to thank the management of the University of Agriculture, Faisalabad, Pakistan for providing all the facilities and financial support to conduct quality scientific research at the analytical laboratory, Department of Agronomy. The authors MFS and HAK also want to present his gratitude to the deanship of the Department of Biochemistry, University of Agriculture, Faisalabad, Pakistan for helping to buy good quality characterized nano-ZnO from a well-renowned company Alfa Aesar (Thermo Fisher Scientific, Shanghai, China). The authors would like to extend their sincere appreciation to the Researchers Supporting Project Number (RSP-2021/347), King Saud University, Riyadh, Saudi Arabia.

SUPPLEMENTARY MATERIAL

The Supplementary Material for this article can be found online at: https://www.frontiersin.org/articles/10.3389/fpls.2022.842349/full#supplementary-material

REFERENCES

Aghdam, M. T. B., Mohammadi, H., and Ghorbanpour, M. (2016). Effects of nanoparticulate anatase titanium dioxide on physiological and biochemical performance of *Linum usitatissimum* (Linaceae) under well-watered and drought stress conditions. *Rev. Brasil. Bot.* 39, 139–146. doi: 10.1007/s40415-015-0227-x

Ainsworth, E. A., and Gillespie, K. M. (2007). Estimation of total phenolic content and other oxidation substrates in plant tissues using Folin-Ciocalteu reagent. *Nat. Protoc.* 2, 875–877. doi: 10.1038/nprot.2007.102

Ali, A., Nadeem, M. A., Khan, B. A., and Ali, M. F. (2021). Optimizing the Growth and Yield of Mungbean (*Vigna radiata* L.) Cultivars by Altering Sowing Dates. *Pak. J. Agri. Res.* 3, 559–568. doi: 10.17582/journal.pjar/2021/34.3.559.568

Arnon, D. I. (1949). Copper Enzymes in Isolated Chloroplasts. Polyphenoloxidase in Beta Vulgaris. *Plant Physiol.* 24, 1–15. doi: 10.1104/pp.24.1.1

Awasthi, R., Kaushal, N., Vadez, V., Turner, N. C., Berger, J., Siddique, K. H. M., et al. (2014). Individual and combined effects of transient drought and heat stress on carbon assimilation and seed filling in chickpea. *Funct. Plant Biol.* 41, 1148–1167. doi: 10.1071/FP13340

Bansal, M., Kukreja, K., Suneja, S., and Dudeja, S. S. (2014). Symbiotic effectivity of high temperature tolerant mungbean (*Vigna radiata*) rhizobia under different temperature conditions. *Int. J. Curr. Microbiol. App. Sci.* 3, 807–821.

Bates, L. S., Waldren, R. P., and Teare, I. D. (1973). Rapid determination of free proline for water-stress studies. *Plant Soil* 39, 205–207.

Bi, A., Fan, J., Hu, Z., Wang, G., Amombo, E., Fu, J., et al. (2016). Differential acclimation of enzymatic antioxidant metabolism and photosystem II photochemistry in tall fescue under drought and heat and the combined stresses. *Front. Plant Sci.* 7:453. doi: 10.3389/fpls.2016.00453

Bianco, C., and Defez, R. (2009). Medicago truncatula improves salt tolerance when nodulated by an indole-3-acetic acid-overproducing *Sinorhizobium meliloti* strain. *J. Exp. Bot.* 60, 3097–3107. doi: 10.1093/jxb/erp140

Bita, C. E., and Gerats, T. (2013). Plant tolerance to high temperature in a changing environment: Scientific fundamentals and production of heat stress-tolerant crops. *Front. Plant Sci.* 4:1–18. doi: 10.3389/fpls.2013.00273

Bradford, M. (1976). A Rapid and Sensitive Method for the Quantitation of Microgram Quantities of Protein Utilizing the Principle of Protein-Dye Binding. *Anal. Biochem.* 72, 248–254. doi: 10.1006/abio.1976.9999

Buttar, Z. A., Wu, S. N., Arnao, M. B., Wang, C., Ullah, I., and Wang, C. (2020). Melatonin suppressed the heat stress-induced damage in wheat seedlings by modulating the antioxidant machinery. *Plants* 9, 1–17. doi: 10.3390/plants9070809

Dhindsa, R. S., Plumb-dhindsa, P., and Thorpe, T. A. (1981). Leaf Senescence: Correlated with Increased Levels of Membrane Permeability and Lipid Peroxidation, and Decreased Levels of Superoxide Dismutase and Catalase. *J. Exp. Bot.* 32, 93–101.

Dhoke, S. K., Mahajan, P., and Khanna, A. S. (2011). Effect of nano-ZnO particle suspension on growth of mung (*Vigna radiata*) and gram (*Cicer arietinum*) seedlings using plant agar method. *J. Nanotechnol.* 2011:696535. doi: 10.1155/2011/696535

Dimkpa, C. O., Bindraban, P. S., Fugice, J., Agyin-Birikorang, S., Singh, U., and Hellums, D. (2017). Composite micronutrient nanoparticles and salts decrease drought stress in soybean. *Agron. Sustain Dev.* 37, 1–13. doi: 10.1007/s13593-016-0412-8

Disante, K. B., Fuentes, D., and Cortina, J. (2011). Response to drought of Zn-stressed Quercus suber L. seedlings. *Environ. Exp. Bot.* 70, 96–103. doi: 10.1016/j.envexpbot.2010.08.008

Djanaguiraman, M., Prasad, P. V. V., Boyle, D. L., and Schapaugh, W. T. (2013). Soybean pollen anatomy, viability and pod set under high temperature stress. *J. Agron. Crop Sci.* 199, 171–177. doi: 10.1111/jac.12005

Etxeberria, E., Gonzalez, P., Bhattacharya, P., Sharma, P., and Ke, P. C. (2016). Determining the size exclusion for nanoparticles in citrus leaves. *Hortic. Sci.* 51, 732–737. doi: 10.21273/hortsci.51.6.732

Faizan, M., Faraz, A., Mir, A. R., and Hayat, S. (2021). Role of Zinc Oxide Nanoparticles in Countering Negative Effects Generated by Cadmium in Lycopersicon esculentum. *J. Plant Growth Regul.* 40, 101–115. doi: 10.1007/s00344-019-10059-2

Faizan, M., Hayat, S., and Pichtel, J. (2020). Effects of Zinc Oxide Nanoparticles on Crop Plants: A Perspective Analysis. [Preprint]. 83–99. doi: 10.1007/978-3-030-33996-8_4

Fang, X., Turner, N. C., Yan, G., Li, F., and Siddique, K. H. M. (2010). Flower numbers, pod production, pollen viability, and pistil function are reduced and flower and pod abortion increased in chickpea (Cicer arietinum L.) under terminal drought. *J. Exp. Bot.* 61, 335–345. doi: 10.1093/jxb/erp307

Faseela, P., Sinisha, A. K., Brestič, M., and Puthur, J. T. (2020). Chlorophyll a fluorescence parameters as indicators of a particular abiotistress in rice. *Photosynthetica* 58, 293–300. doi: 10.32615/ps.2019.147

Garg, N., and Manchanda, G. (2009). ROS generation in plants: Boon or bane? *Plant Biosyst. Int. J. Dealing Aspects Plant Biol.* 143, 81–96. doi: 10.1080/11263500802633626

Giannopolitis, C. N., and Ries, S. K. (1977). Superoxide dismutases: Occurrence in higher plants. *Plant Physiol.* 59, 309–314. doi: 10.1104/pp.59.2.309

Grieve, C. M., and Grattan, S. R. (1983). Rapid assay for determination of water soluble quaternary ammonium compounds. *Plant Soil* 70, 303–307. doi: 10.1007/BF02374789

Hameed, A., Goher, M., and Iqbal, N. (2012). Heat Stress-Induced Cell Death, Changes in Antioxidants, Lipid Peroxidation, and Protease Activity in Wheat Leaves. *J. Plant Growth Regul.* 31, 283–291. doi: 10.1007/s00344-011-9238-4

Hanumantharao, B., Nair, R. M., and Nayyar, H. (2016). Salinity and high temperature tolerance in mungbean [*Vigna radiata* (L.) Wilczek] from a physiological perspective. *Front. Plant Sci.* 7:1–20. doi: 10.3389/fpls.2016.00957

Hasanuzzaman, M., Nahar, K., Alam, M. M., Roychowdhury, R., and Fujita, M. (2013). Physiological, biochemical, and molecular mechanisms of heat stress tolerance in plants. *Int. J. Mol. Sci.* 14, 9643–9684. doi: 10.3390/ijms14059643

Hu, L., Huang, Z., Liu, S., and Fu, J. (2012). Growth response and gene expression in antioxidant-related enzymes in two bermudagrass genotypes differing in salt tolerance. *J. Am. Soc. Hortic. Sci.* 137, 134–143. doi: 10.21273/jashs.137.3.134

Hussain, S., Khan, F., Cao, W., Wu, L., and Geng, M. (2016). Seed priming alters the production and detoxification of reactive oxygen intermediates in rice seedlings grown under sub-optimal temperature and nutrient supply. *Front. Plant Sci.* 7:1–13. doi: 10.3389/fpls.2016.00439

Hussain, S., Ulhassan, Z., Brestic, M., Zivcak, M., Weijun Zhou, Allakhverdiev, S. I., et al. (2021). Photosynth Resunder climate change. *Photosynth. Res.* 150, 5–19. doi: 10.1007/s11120-021-00861-z

IPCC (2014). *IPCC (Intergovernmental panel on climate change) Fourth assessment report: climate change synthesis report*. Geneva: World Met Org.

Irshad, A., Naveed, R., Rehman, U., Abdul, H., Yang, P., and Hu, T. (2021). Addressing the challenge of cold stress resilience with the synergistic effect of Rhizobium inoculation and exogenous melatonin application in *Medicago truncatula*. *Ecotox. Environ. Safe.* 226:112816. doi: 10.1016/j.ecoenv.2021.112816

Kah, M., Kookana, R. S., Gogos, A., and Bucheli, T. D. (2018). A critical evaluation of nanopesticides and nanofertilizers against their conventional analogues. *Nat. Nanotechnol.* 13, 677–684. doi: 10.1038/s41565-018-0131-1

Kambe, T., Tsuji, T., Hashimoto, A., and Itsumura, N. (2021). Molecular roles of zinc transporters. *Zinc Homeostasis Metabol.* 2021, 749–784. doi: 10.1152/physrev.00035.2014

Kaur, R., Bains, T. S., Bindumadhava, H., and Nayyar, H. (2015). Responses of mungbean (*Vigna radiata* L.) genotypes to heat stress: Effects on reproductive biology, leaf function and yield traits. *Sci. Hortic. Amsterdam* 197, 527–541. doi: 10.1016/j.scienta.2015.10.015

Kaushal, N., Awasthi, R., Gupta, K., Gaur, P., Siddique, K. H. M., and Nayyar, H. (2013). Heat-stress-induced reproductive failures in chickpea (Cicer arietinum) are associated with impaired sucrose metabolism in leaves and anthers. *Funct. Plant Biol.* 40, 1334–1349. doi: 10.1071/FP13082

Khan, I., Awan, S. A., Ikram, R., Rizwan, M., Akhtar, N., Yasmin, H., et al. (2021). Effects of 24-epibrassinolide on plant growth, antioxidants defense system, and endogenous hormones in two wheat varieties under drought stress. *Physiol. Plant.* 172, 696–706. doi: 10.1111/ppl.13237

Kumar, A., and Nagesh, B. (2019). Foliar application of nanofertilizers in agricultural crops -A review Foliar application of nanofertilizers in agricultural crops – A review. *J. Farm Sci.* 32, 239–249.

Kumar, S., Thakur, P., Kaushal, N., Malik, J. A., Gaur, P., and Nayyar, H. (2013). Effect of varying high temperatures during reproductive growth on reproductive function, oxidative stress and seed yield in chickpea genotypes differing in heat sensitivity. *Arch. Agron. Soil Sci.* 59, 823–843. doi: 10.1080/03650340.2012.683424

Kumari, V. V., Roy, A., Vijayan, R., Banerjee, P., Verma, V. C., Nalia, A., et al. (2021). Drought and Heat Stress in Cool-Season Food Legumes in Sub-Tropical Regions: Consequences, Adaptation, and Mitigation Strategies. *Plants* 10:lants10061038. doi: 10.3390/plants10061038

Li, D., Wang, M., Zhang, T., Chen, X., Li, C., Liu, Y., et al. (2021). Glycinebetaine mitigated the photoinhibition of photosystem II at high temperature in transgenic tomato plants. *Photosynth. Res.* 147, 301–315. doi: 10.1007/s11120-020-00810-2

Li, Z., Palmer, W. M., Martin, A. P., Wang, R., Rainsford, F., Jin, Y., et al. (2012). High invertase activity in tomato reproductive organs correlates with enhanced sucrose import into, and heat tolerance of, young fruit. *J. Exp. Bot.* 63, 1155–1166. doi: 10.1093/jxb/err329

Li, Z., Zhang, L., Wang, A., Xu, X., and Li, J. (2013). Ectopic Overexpression of SlHsfA3, a Heat Stress Transcription Factor from Tomato, Confers Increased Thermotolerance and Salt Hypersensitivity in Germination in Transgenic Arabidopsis. *PLoS One* 8:0054880. doi: 10.1371/journal.pone.0054880

Liu, R., and Lal, R. (2015). Potentials of engineered nanoparticles as fertilizers for increasing agronomic productions. *Sci. Total Environ.* 514, 131–139. doi: 10.1016/j.scitotenv.2015.01.104

Malaviarachchi, M. A. P. W. K., de Costa, W. A. J. M., Kumara, J. B. D. A. P., Suriyagoda, L. D. B., and Fonseka, R. M. (2016). Response of Mung Bean (Vigna radiata (L.) R. Wilczek) to an Increasing Natural Temperature Gradient under Different Crop Management Systems. *J. Agron. Crop Sci.* 202, 51–68. doi: 10.1111/jac.12131

Mansoor, S. (2013). Effect of heat stress on lipid peroxidation and antioxidant enzymes in mung bean (*Vigna radiata* L.) seedlings. *Afr. J. Biotechnol.* 12, 3196–3203. doi: 10.4314/ajb.v12i21

Martínez-Fernández, D., Vítková, M., Bernal, M. P., and Komárek, M. (2015). Effects of nano-maghemite on trace element accumulation and drought response of *Helianthus annuus* L. in a contaminated mine soil. *Water Air Soil Poll.* 226:2365–y. doi: 10.1007/s11270-015-2365-y

Ohama, N., Sato, H., Shinozaki, K., and Yamaguchi-Shinozaki, K. (2017). Transcriptional Regulatory Network of Plant Heat Stress Response. *Trends Plant Sci.* 22, 53–65. doi: 10.1016/j.tplants.2016.08.015

Pagter, M., Bragato, C., and Brix, H. (2005). Tolerance and physiological responses of Phragmites australis to water deficit. *Aquat. Bot.* 81, 285–299. doi: 10.1016/j.aquabot.2005.01.002

Perdomo, J. A., Capó-Bauçà, S., Carmo-Silva, E., and Galmés, J. (2017). Rubisco and rubisco activase play an important role in the biochemical limitations of photosynthesis in rice, wheat, and maize under high temperature and water deficit. *Front. Plant Sci.* 8:00490. doi: 10.3389/fpls.2017.00490

Pradhan, S. Patra, P., Das, S., Chandra, S., Mitra, S., Dey, K. K., et al. (2013). Photochemical modulation of biosafe manganese nanoparticles on *Vigna radiata*: a detailed molecular, biochemical, and biophysical study. *Environ. Sci. Technol.* 47, 13122–13131. doi: 10.1021/es402659t

Prasad, P. V. V., and Djanaguiraman, M. (2011). High night temperature decreases leaf photosynthesis and pollen function in grain sorghum. *Funct. Plant Biol.* 38, 993–1003. doi: 10.1071/FP11035

Prasad, T. N. V. K. V., Sudhakar, P., Sreenivasulu, Y., Latha, P., Munaswamy, V., Raja Reddy, K., et al. (2012). Effect of nanoscale zinc oxide particles on the germination, growth and yield of peanut. *J. Plant Nutr.* 35, 905–927. doi: 10.1080/01904167.2012.663443

Rainey, K. M., and Griffiths, P. D. (2005). Differential response of common bean genotypes to high temperature. *J. Am. Soc. Hortic. Sci.* 130, 18–23. doi: 10.21273/jashs.130.1.18

Rana, R. A., Siddiqui, M. N., Skalicky, M., Brestic, M., Hossain, A., Kayesh, E., et al. (2021). Prospects of nanotechnology in improving the productivity and quality of horticultural crops. *Horticulturae* 7, 1–19. doi: 10.3390/horticulturae7100332

Rastogi, A., Zivcak, M., Sytar, O., Kalaji, H. M., He, X., Mbarki, S., et al. (2017). Impact of metal and metal oxide nanoparticles on plant: A critical review. *Front. Chem.* 5:1–16. doi: 10.3389/fchem.2017.00078

Rover, M. R., and Brown, R. C. (2013). Quantification of total phenols in bio-oil using the Folin-Ciocalteu method. *J. Anal. Appl. Pyrol.* 104, 366–371. doi: 10.1016/j.jaap.2013.06.011

Samson, B. K., Sengxua, P., Vorlason, S., Douangboupha, K., Eberbach, P., Vote, C., et al. (2020). Short-duration mungbean (*Vigna radiata* (L.) R. Wilczek) genotypes differ in performance, water use and apparent water-use efficiency in southern Lao PDR. *Field Crop Res.* 245:107662. doi: 10.1016/j.fcr.2019.107662

Sanat, G., Khattak, G., Saeed, I., and Muhammad, T. (2006). Breeding for heat tolerance in mungbean (Vigna radiata (L.) Wilczek). *Pak. J. Bot.* 38, 1539–1550.

Schafleitner, R., Nair, R. M., Rathore, A., Wang, Y. W., Lin, C. Y., Chu, S. H., et al. (2015). The AVRDC - The World Vegetable Center mungbean (Vigna radiata) core and mini core collections. *BMC Genomics* 16:1–11. doi: 10.1186/s12864-015-1556-7

Sharma, L., Priya, M., Bindumadhava, H., Nair, R. M., and Nayyar, H. (2016). Influence of high temperature stress on growth, phenology and yield performance of mungbean [*Vigna radiata* (L.) Wilczek] under managed growth conditions. *Sci. Hortic. Amsterdam* 213, 379–391. doi: 10.1016/j.scienta.2016.10.033

Sharma, P., Jha, A. B., Dubey, R. S., and Pessarakli, M. (2012). Reactive Oxygen Species, Oxidative Damage, and Antioxidative Defense Mechanism in Plants under Stressful Conditions. *J. Bot.* 2012:217037. doi: 10.1155/2012/217037

Siddiqi, K. S., and Husen, A. (2016). Engineered Gold Nanoparticles and Plant Adaptation Potential. *Nanoscale Res. Lett.* 2016:2. doi: 10.1186/s11671-016-1607-2

Singh, A., Singh, N. B., Afzal, S., Singh, T., and Hussain, I. (2018). Zinc oxide nanoparticles: a review of their biological synthesis, antimicrobial activity, uptake, translocation and biotransformation in plants. *J. Mater. Sci.* 53, 185–201. doi: 10.1007/s10853-017-1544-1

Snider, J. L., Oosterhuis, D. M., Loka, D. A., and Kawakami, E. M. (2011). High temperature limits in vivo pollen tube growth rates by altering diurnal carbohydrate balance in field-grown Gossypium hirsutum pistils. *J. Plant Physiol.* 168, 1168–1175. doi: 10.1016/j.jplph.2010.12.011

Soliman, A., Universit, C., Elfeky, S., and Darwish, E. (2015). Alleviation of salt stress on Moringa peregrina using foliar application of nanofertilizers. *J. Hortic. For.* 2015:0379. doi: 10.5897/JHF2014.0379

Sturikova, H., Krystofova, O., Huska, D., and Adam, V. (2018). Zinc, zinc nanoparticles and plants. *J. Hazard. Mater.* 349, 101–110. doi: 10.1016/j.jhazmat.2018.01.040

Tan, W., Brestic, M., Olsovska, K., and Yang, X. (2011). Photosynthesis is improved by exogenous calcium in heat-stressed tobacco plants. *J. Plant Physiol.* 168, 2063–2071. doi: 10.1016/j.jplph.2011.06.009

Terras, F. R. G., Torrekens, S., van Leuven, F., Osborn, R. W., Vanderleyden, J., Cammue, B. P. A., et al. (1993). A new family of basic cysteine-rich plant antifungal proteins from Brassicaceae species. *FEBS Letters.* 316, 233–240. doi: 10.1016/0014-5793(93)81299-F

Thakur, P., Kumar, S., Malik, J. A., Berger, J. D., and Nayyar, H. (2010). Cold stress effects on reproductive development in grain crops: An overview. *Environ. Exp. Bot.* 67, 429–443. doi: 10.1016/j.envexpbot.2009.09.004

Turan, M. A., Elkarim, A. H. A., Taban, N., and Taban, S. (2009). Effect of salt stress on growth, stomatal resistance, proline and chlorophyll concentrations on maize plant. *Afr. J. Agr. Res.* 4, 893–897.

Velikova, V., Yordanov, I., and Edreva, A. (2000). Oxidative stress and some antioxidant systems in acid rain-treated bean plants Protective role of exogenous polyamines. *Plant Sci.* 151, 59–66.

Vittal, R., Venugopal, U., Kumar, A., Kota, S., and Ramya, V. (2018). Article Chronicle: Background and Objectives. *Agric. Update* 12, 1567–1572. doi: 10.15740/HAS/AU/12

Waraich, E. A., Ahmad, R., Halim, A., and Aziz, T. (2012). Alleviation of temperature stress by nutrient management in crop plants: A review. *J. Soil Sci. Plant Nut.* 12, 221–244. doi: 10.4067/S0718-95162012000200003

Yancey, P. H. (2005). Organic osmolytes as compatible, metabolic and counteracting cytoprotectants in high osmolarity and other stresses. *J. Exp. Biol.* 208, 2819–2830. doi: 10.1242/jeb.01730

Yuan, M., Quan, L. N., Comin, R., Walters, G., Sabatini, R., Voznyy, O., et al. (2016). Perovskite energy funnels for efficient light-emitting diodes. *Nat. Nanotechnol.* 11, 872–877. doi: 10.1038/nnano.2016.110

Zafar, S., Hameed, A., Khan, S., and Ashraf, M. (2017). Heat shock induced morpho-physiological response in indica rice (*Oryza sativa* L.) at early seedling stage. *Pak. J. Bot.* 49, 453–463.

Conflict of Interest: The authors declare that the research was conducted in the absence of any commercial or financial relationships that could be construed as a potential conflict of interest.

Publisher's Note: All claims expressed in this article are solely those of the authors and do not necessarily represent those of their affiliated organizations, or those of the publisher, the editors and the reviewers. Any product that may be evaluated in this article, or claim that may be made by its manufacturer, is not guaranteed or endorsed by the publisher.

Copyright © 2022 Kareem, Saleem, Saleem, Rather, Wani, Siddiqui, Alamri, Kumar, Gaikwad, Guo, Niu and Wang. This is an open-access article distributed under the terms of the Creative Commons Attribution License (CC BY). The use, distribution or reproduction in other forums is permitted, provided the original author(s) and the copyright owner(s) are credited and that the original publication in this journal is cited, in accordance with accepted academic practice. No use, distribution or reproduction is permitted which does not comply with these terms.

frontiers in Plant Science

ORIGINAL RESEARCH
published: 03 March 2022
doi: 10.3389/fpls.2022.816858

The Combined Inoculation of *Curvularia lunata* AR11 and Biochar Stimulates Synthetic Silicon and Potassium Phosphate Use Efficiency, and Mitigates Salt and Drought Stresses in Rice

*Arjun Adhikari[1], Muhammad Aaqil Khan[1], Muhammad Imran[1], Ko-Eun Lee[1], Sang-Mo Kang[1], Jin Y. Shin[2], Gil-Jae Joo[3], Murtaza Khan[1], Byung-Wook Yun[1] and In-Jung Lee[1]**

[1] Department of Applied Biosciences, Kyungpook National University, Daegu, South Korea, [2] Department of Chemistry and Environmental Science, Medgar Evers College, The City University of New York, New York City, NY, United States, [3] Institute of Agricultural Science and Technology, Kyungpook National University, Daegu, South Korea

OPEN ACCESS

Edited by:
Shabir Hussain Wani, Sher-e-Kashmir University of Agricultural Sciences and Technology, India

Reviewed by:
Abbu Zaid, Government Degree College Doda, India
Ali Raza, Fujian Agriculture and Forestry University, China

***Correspondence:**
In-Jung Lee
ijlee@knu.ac.kr

Specialty section:
This article was submitted to Plant Biotechnology, a section of the journal Frontiers in Plant Science

Received: *17 November 2021*
Accepted: *01 February 2022*
Published: *03 March 2022*

Citation:
Adhikari A, Khan MA, Imran M, Lee K-E, Kang S-M, Shin JY, Joo G-J, Khan M, Yun B-W and Lee I-J (2022) The Combined Inoculation of Curvularia lunata AR11 and Biochar Stimulates Synthetic Silicon and Potassium Phosphate Use Efficiency, and Mitigates Salt and Drought Stresses in Rice. Front. Plant Sci. 13:816858. doi: 10.3389/fpls.2022.816858

Synthetic chemical fertilizers are a fundamental source of nutrition for agricultural crops; however, their limited availability, low plant uptake, and excessive application have caused severe ecological imbalances. In addition, the gravity of environmental stresses, such as salinity and water stress, has already exceeded the threshold limit. Therefore, the optimization of nutrient efficiency in terms of plant uptake is crucial for sustainable agricultural production. To address these challenges, we isolated the rhizospheric fungus *Curvularia lunata* ARJ2020 (AR11) and screened the optimum doses of biochar, silicon, and potassium phosphate (K_2HPO_4), and used them—individually or jointly—to treat rice plants subjected to salt (150 mM) and drought stress (20–40% soil moisture). Bioassay analysis revealed that AR11 is a highly halotolerant and drought-resistant strain with an innate ability to produce gibberellin (GA_1, GA_3, GA_4, and GA_7) and organic acids (i.e., acetic, succinic, tartaric, and malic acids). In the plant experiment, the co-application of AR11 + Biochar + Si + K_2HPO_4 significantly improved rice growth under both salt and drought stresses. The plant growth regulator known as abscisic acid, was significantly reduced in co-application-treated rice plants exposed to both drought and salt stress conditions. These plants showed higher Si (80%), P (69%), and K (85%) contents and a markedly low Na^+ ion (208%) concentration. The results were further validated by the higher expression of the Si-carrying gene *OsLSi1*, the salt-tolerant gene *OsHKT2,* and the *OsGRAS23*'s drought-tolerant transcriptome. Interestingly, the beneficial effect of AR11 was significantly higher than that of the co-application of Biochar + Si + K_2HPO_4 under drought. Moreover, the proline content

of AR11-treated plants decreased significantly, and an enhancement of plant growth-promoting characteristics was observed. These results suggest that the integrated co-application of biochar, chemical fertilizers, and microbiome could mitigate abiotic stresses, stimulate the bioavailability of essential nutrients, relieve phytotoxicity, and ultimately enhance plant growth.

Keywords: abiotic stress, environment, fertilizer, nutrient, physiology, PGPMs

INTRODUCTION

Sustainable agricultural practices have been recognized as a pragmatic economic approach to attain the goal of food security (Francis and Porter, 2011). However, one of the biggest challenges for the sustainability transitions is the management of chemical fertilizers and environmental stresses, such as drought and salinity (Butcher et al., 2016; Mark Ibekwe et al., 2017). Salinization-related reduction in crop yield in semiarid and arid region of world accounts to 18–43% and more than three percent of soil resources are affected globally (Singh, 2021). Similarly, the percentage of lands affected by drought has doubled in the last 40 years, affecting farmers more than any other natural hazards (FAO, 2021). It is predicted that, by the first half of the twenty first century, water drought events will dramatically worsen, reaching record levels never seen before in the history of mankind (Premanandh, 2011). Forecasts predict a 1.3-fold increase in water requirements in the agricultural sector by 2025 (Premanandh, 2011). In addition, the world's population is rapidly increasing and is expected to reach nine billion by 2050 (Fariduddin et al., 2019). In these scenarios, the mitigation of salt stress and droughts is crucial to overcome the probable risk of food insecurity (Zhai et al., 2019).

Understanding the physiological context of salt and water deficiency stresses is essential for their alleviation and to develop long-term management strategies (Dawood et al., 2021). In general, salt and drought stresses harm plant metabolism, causing ionic imbalance, osmotic stress, oxidative damage, damage of cellular structures, and a decrease in gas exchange rates, which ultimately lead to plant death (Bhusal et al., 2021; Khan et al., 2021; Nabi et al., 2021).

Plants acquire several strategies to cope with abiotic stresses and, among these, ionic adjustment such as Na^+/K^+ ratio, and endogenous phytohormones such as ABA regulation play a key role in modulating the overall physiological system (Garg and Bhandari, 2016; Zaid et al., 2021). Under salinity stress, plants accumulate toxic ions which causes ionic toxicity; in response, amassing of soluble osmolytes and synthesis of reducing agents occur which aids to osmotic adjustment and nutrients balance (Golldack et al., 2014; Dawood et al., 2021). Under drought stress, plants mobilize the ABA channel that activates guard cells to regulate stomatal conductance and sustain high moisture level, by influencing the leaf and soil water potential (Harb et al., 2010). It has been reported that the plants' ionic system is extensively regulated by the balanced presence of sodium, potassium, phosphorus, and silicon (Etesami, 2018). Bargaz et al. (2016) showed that the phosphorus (P) supply induced salt tolerance in *Phaseolus vulgaris* through the acquisition of K^+ and Ca^{++}. Similarly, the role of silicon (Si) in improving plant physiology, growth, and yield has been widely reported in numerous studies (Kim et al., 2014; Zhu and Gong, 2014). The enhancement of P, K, and Si uptake in plants was shown to mitigate several stresses in plants, including both biotic (e.g., pathogens) (Bakhat et al., 2018), and abiotic ones, such as heavy metal stress, water stress, thermal stress, and salt stress (Zaid et al., 2018). Therefore, it can be concluded that the proper utilization of Si, P, and K could improve plant metabolism and growth under diverse environmental conditions.

The nutritional sources of plants largely depend on synthetic fertilizers. According to the Food and Agriculture Organization (FAO) (Food and Agriculture Organization of the United Nations, 2017), the world consumption of nitrogen, phosphorus, and potassium (NPK) was estimated at about 186.67 million tonnes in 2016, and P demand specifically increased by 2.2% in 2020, but the utilization efficiency by plants is limited to 10–15% (Simpson et al., 2011). Soil nutrient depletion has been adversely affecting poverty-stricken farmers worldwide (Yang et al., 2009). The net accumulation of toxic elements in agriculture is increasing due to the overuse of synthetic chemicals and to industrialization, which result in water eutrophication and environmental hazards (Simpson et al., 2011; Bouraoui and Grizzetti, 2014; Ali et al., 2019). The scientific community has repeatedly warned that the long-term, continuous application of chemical fertilizers without adequate organic amendments may degrade soils to such an extent that they may become extremely low or non-responsive to inorganic fertilizers (Fofana et al., 2008; Tittonell and Giller, 2013; Tounkara et al., 2020).

Plant growth-promoting microorganisms (PGPMs) and biochar are the emerging alternatives to agrochemicals for the production sustainable food (Yang et al., 2009; Abhilash et al., 2016; Ali et al., 2017). PGPMs have been widely reported to enhance plant growth-promoting traits such as through abscisic acid (ABA) regulation (Cohen et al., 2009), gibberellin (GA) production (Bottini et al., 2004), and phosphate, potassium, and silicate solubilization (Adhikari et al., 2020a). Similarly, biochar has been widely reported to facilitate PGPM growth, prevent disease incidence, stabilize heavy metal concentrations, increase soil fertility, and mitigate severe biotic and abiotic stresses (Farhangi-Abriz and Torabian, 2017; Gavili et al., 2019). Under stress conditions, these biostimulants enhance plant physiology through the modulation of phytohormones, including ABA, jasmonic acid (JA), gibberellic acid (GA), and salicylic acid (SA) (Waqas et al., 2012). In addition, they were reported to strengthen the antioxidant system through the modulation of amino acids

under stress (Qadir et al., 2020). Moreover, biochar and PGPMs were shown to have a functional role in lowering Na^+ uptake and enhancing K^+ ion uptake in plants exposed to salt stress, while also enhancing the water holding capacity of soils and plants under drought stress (Ali et al., 2017; Khan et al., 2019a).

Salinity and drought were shown to be crucial limiting factors for the growth of major cereal crops such as rice (Kumar et al., 2013; Tang et al., 2019). Rice is the most important staple crop, consumed by billions of people globally, representing 75% of the total calorie intake in Asian countries (Xia et al., 2019). As mineral elements—such as Si, P, and K—play a key role in the increase of several biotic and abiotic stresses, an efficient strategy to boost their uptake efficiency in plants is still lacking. Hence, there is an urgent call for developing a sustainable agriculture contrivance in perspective of climate change, abiotic stresses, excess fertilizer demand, environmental pollution and high-production cost. To address these challenges, in the present study, we identified a highly drought- and salt-tolerant fungus and assessed its plant growth-promoting traits. The effects of this fungal species on the modulation of rice physiology under salt and drought stresses were elucidated along with those of biochar, inorganic silicon, phosphorous, and potassium.

MATERIALS AND METHODS

Fungus Isolation and Identification

A total of 120 different fungal colonies were isolated from the agriculture waste decomposing site at Kyungpook National University, Daegu, and their pathogenicity and plant growth-promoting traits were evaluated (**Supplementary Table 1** and **Figure 1**). The GA production of the isolates was tested through inoculation on the GA-deficient dwarf mutant rice strain *Waito-C,* in glucose agar media. The AR11 strain, which was shown to highly influence growth performance in *Waito-C* plants, was selected for further experiments (**Supplementary Figure 2**). The identification of AR11 was performed by sequencing the internal transcribed regions (ITS) using universal primer with ITS1 (5′-TCCGTAGGTGAACCTGCGG-3′) and ITS4 (5′-GCTGCGTTCTTCATCGATGC-3′).

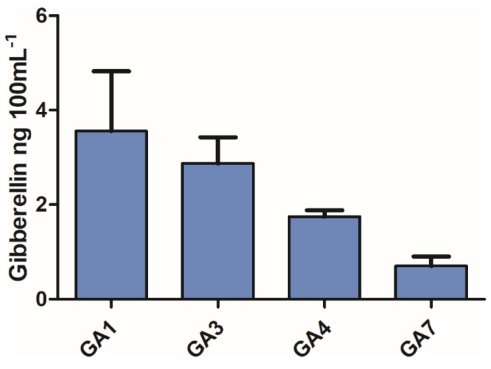


FIGURE 1 | Quantification of gibberellin content in the *Curvularia lunata* (AR11) pure culture.

Assessment of the Plant Growth Promoting-Traits of AR11

Growth Performance Test Under Stress

The AR11 fungal strain was grown under salt concentrations of 100, 200, 300, 400, and 500 mM; and at a polyethylene glycol (PEG 6000)-supplemented potato-dextrose Agar (PDA) media. The isolate growth was observed with different osmotic potentials (−0.05, −00.15, −00.3, −0.49, and −00.73 MPa). In addition, fungal growth on inorganic Si and K_2HPO_4 was also evaluated.

Gibberellic Acid, Organic Acids, and Amino Acid Quantification

- GA: GA was quantified based on the method described by Lee et al. (2015). In brief, 200 mL of 1-week-old AR11 culture broth was supplemented with the GA internal standard ($^2H_2$), and extraction was performed. The extract obtained was then subjected to chromatography and mass spectroscopy for GA detection and quantification.
- Organic acids: Organic acids, such as succinic, malic, acetic, and tartaric acid, were quantified based on the method described by Lee et al. (2019). In brief, after the fungal suspension culture was grown in a shaking incubator for a week, it was centrifuged and the supernatant was collected, filtered, and injected on high-performance liquid chromatography (HPLC, Waters 600, Milford, MA, United States) using a PL Hi-Plex H column (7.7 × 300 mm, Waters Co., Milford, MA, United States), detector refractive index (RI, Waters 410, Milford, MA, United States), and 5 mM H_2SO_4 was used as solvent in distilled water.
- Amino acids: Free amino acids were quantified on a 1-week-old fungal pure culture; the culture was centrifuged, and the supernatant was separated. The solution was then filtered and suspended with 5% trichloroacetic acid and was subjected to shaking for 2 h. The solvent was further centrifuged, and the supernatant was separated, filtered, and injected on an amino acid analyzer (L-8900; Hitachi, Tokyo, Japan).

Plant Material and Experiment

Two independent experiments were conducted on salt and drought stresses in rice. The experimental design is represented in **Table 1**. The statement of results is mostly written with the data compared with T2 (Control +ve) in the results section.

Soil and Pot Preparation

Before transplanting the plants, the soil was prepared, based on the above-mentioned experimental design. The screening of plant growth was performed with randomly selected, similar concentration of Si and K_2HPO_4 (1, 2, 3, 4, and 5 mM), and biochar (composition: charcoal 70%, Dolomite 10%, Zeolite 5%, Molasses 10%, and Peat 5%) at 1, 2, 3, 4, and 5% w/w. It was conducted under salt and drought stress conditions. The optimum dose of 2 mM for Si, 3 mM for K_2HPO_4 and 3% for biochar was selected based on plant growth observations. The biochar and fungal suspension were added before the transplantation of seedlings, whereas Si and K_2HPO_4 were supplied after it. Paddy soil (Peat moss: 5%, Cocopeat: 35.6%,

TABLE 1 | Outline of the experimental design for the independent experiment conducted under salt and drought stress conditions.

Treatment	Salt stress	Drought stress
T1	Control –ve (-S)	Control1 –ve (-D)
T2	Control +ve (-S)	Control2 +ve (-D)
T3	Si (-S)	Si (-D)
T4	KP (-S)	KP (-D)
T5	AR11 (-S)	AR11 (-D)
T6	Bio (-S)	Bio (-D)
T7	Si + KP (-S)	Si + KP (-D)
T8	Si + KP + AR11 (-S)	Si + KP + AR11 (-D)
T9	Si + KP + Bio (-S)	Si + KP + Bio (-D)
T10	Si + KP + AR11 (-S)	Si + KP + Bio + AR11 (-D)

(-S), salt stressed; (-D), drought stressed; –ve, only water (no stress); +ve, complete stress (no treatment); Si, silicon; KP, potassium phosphate (K_2HPO_4); AR11, Curvularia lunata AR11 fungal suspension; Bio, biochar.

Zeolite: 5%, Diatomaceous soil: 3%, Red clay: 8%, Fly ashes: 3%, Vermiculite: 40%, Fertilizer: 0.32%, pH: 0.05%, wetting agent: 0.03%, Manufacturer: Non-ghyup, Gyeongi-do, South Korea) was autoclaved twice and placed in a sealed bucket. Then, it was mixed with biochar and a quantity of 300 g soil was then transferred into each pot (diameter 3.93" × height 3.74"). The AR11 suspension was inoculated on the soil based on the previously mentioned **Table 1**. The soil was irrigated with autoclaved distilled water and kept in a growth chamber for 2 weeks.

Plant Experiment

The Japonica rice seeds *var*. "Jinbek" available in the Crop Physiology Laboratory of Kyungpook National University, were sterilized by washing with autoclaved distilled water containing 0.01% Tebuconazole and allowed to germinate in an incubator at 30°C for 4-days. The seeds were now sown in a 100 cells seedling trays using autoclaved paddy soil as mentioned in Section Soil and Pot Preparation and kept in a growth chamber for 3 weeks. Four equally sized, 3-week-old rice plants were transplanted in each pot as prepared in Section Soil and Pot Preparation. In the plant experiment, each treatment had eight replicates. After a week, 100 mL of Si (2 mM) and K_2HPO_4 (3 mM) were applied to each pot for 2 days, and the plants were normally irrigated for a week. Subsequently, they were subjected to drought and salt stresses. A volume of 20 mL of water per pot was supplied for the first 3 days, 25 mL/pot for the second 3 days, and 30 mL/pot for the last 4 days, to specifically produce drought stress. The soil moisture level was detected 20–40%, depending upon the treatments used which was estimated using the soil pH, and humidity tester (Model DM-5, Takemura Electric Works, LTD., Tokyo, Japan). Whereas, 150 mM NaCl (50 mL/pot) was applied to each pot for 3 days to induce salt stress. Adequate water was supplied for the following 7 days, after which sampling was conducted for further biochemical analysis. The entire experiment was carried out at controlled growth chamber conditions (day/night cycle: 12 h; 28°C/12 h; 22°C; relative humidity (RH) 68%; light intensity 1,000 $\mu mm^{-2}s$ Natrium lamps).

Biochemical Analysis of Plants

Quantification of Mineral Elements

Mineral elements (Si, P, K, Na) were quantified based on the method described by Adhikari et al. (2020a). In brief, 0.1 g of free-dried sample was suspended with HNO_3 reagent and processed using a microwave digestion system (MDS): Ultrawave (milestone). The sample was diluted with 2% HNO_3, and the solution obtained was injected and quantified through inductively coupled plasma mass spectrometry (ICP-MS, Optima 7300DV).

RNA Isolation and Quantitative Real Time-PCR Analysis

RNA isolation and quantitative real time-PCR (qRT-PCR) was performed following the method described by Al Azzawi et al. (2020). In brief, RNA was isolated using TRI-reagent; cDNA was synthesized with the RNA extract and subjected to qRT-PCR to analyze the expression of the gene *OsLSi1*, *OsHKT2,* and the *OsGRAS23*. Specifically, 1 μg RNA was used for cDNA synthesis using BioFACT RT-Kit (BIOFACT, Daejeon, South Korea) following the manufacturer's protocol. A two-step qRT-PCR was performed with Illumina ECO system (Illumina, San Diego, CA, United States). The primers used are listed in the (**Supplementary Table 2**).

Analysis of Abscisic Acid

The method described by Shahzad et al. (2017b) was followed to extract the ABA and quantify its content. In brief, 0.5 g of lyophilized ground samples was extracted with isopropanol and acetic acid (95:5 v/v). The ABA extracts were analyzed by GC-MS/SIM (6890N Network GC System and 5973 Network Mass Selective Detector: Agilent Technologies, Santa Clara, CA, United States). The peak obtained was compared to the standard curve derived from the ABA-internal standard [(±) −03, 5, 5, 7, 7, 7-d6].

Polyphenol and Proline Quantification

The quantification of proline was carried out following the method reported by Shahzad et al. (2017a) using automatic amino acid analyzer (HITACHI Corporation L-8900, Tokyo, Japan) attached to a HITACHI HPLC system (packed column with ion-exchanging resin, No. 2622 PF; 4.6 × 60 mm) and ultraviolet detector (VIS1: 570 nm, VIS2: 44 nm). Polyphenol contents were quantified based on the method described by Adhikari et al. (2018). Samples were extracted with 100% methanol and the wavelength was measured at 750nm using a spectrophotometer (Multiskan GO; Thermo Fischer Scientific, Vantaa, Finland).

Statistical Analysis

The results were analyzed in R (version 4.0.3). A least significant difference (LSD) test ($p < 0.05$) was used to determine significant differences among treatments. The mean and standard deviation were estimated in Microsoft Excel 2019, and the data were graphically presented using GraphPad Prism (version 6.01; San Diego, CA, United States).

RESULTS

Identification of Isolate AR11

Isolate AR11 was identified as a *Curvularia lunata* strain and was submitted to the NCBI database as *Curvularia lunata* ARJ2020, with accession number MZ145250.

Evaluation of the Plant Growth-Promoting Traits of AR11

The AR11 strain was shown to be highly halotolerant, drought and heavy metal resistant, and could efficiently grow on Si and K_2HPO_4 supplemented media. Inoculations with this strain significantly improved the growth of the GA-deficient rice mutant *Waito-C*. Moreover, GA quantification results showed that isolate AR11 could produce biologically active gibberellin, i.e., GA1, GA3, GA4, and GA7 (**Figure 1**). The AR11 pure culture presented a lower amount of free amino acids, whereas organic acids—such as succinic, acetic, malic, and tartaric acids—were detected in larger quantities (**Tables 2**, **3**). Under drought stress conditions, the AR11 strain forms a layer in the upper part of the soil which produces a mulching effect on plants, preserving the water potential and allowing the gradual release of water from the upper layer. A maximum of 40% soil moisture level was detected in AR11 treated soil, whereas on other treatment it was below 30%. The AR11 strain holds water for a long period of time and delivers it to the plant allowing it to thrive.

Evaluation of the Growth Parameters of Rice Plants

Exposure to salt and drought stresses caused adverse effects on the morphological attributes of the plants. Characteristics such as root and shoot weight were significantly reduced by approximately 50–70% in the +ve control plants compared to the −ve control ones. The application of Si, KP, AR11, and biochar increased shoot weight by 15, 13, 31, and 12%, respectively, under salt stress, and co-application of Si + KP, Si + KP + AR11, Si + KP + Bio, and Si + KP + Bio + AR11 further enhanced this trait by 51, 77, 89, and 112% respectively. A similar increasing trend was observed for root weight. However, under drought stress, the sole or combined application of Si, KP, and biochar without AR11 produced only minor differences in the improvement of plant growth characteristics. Interestingly, these were significantly improved by the presence of AR11, both in the sole and combined application. The sole AR11 application enhanced shoot weight by 69%, and the co-application of Si + KP + Bio + AR11 increased it by 98%. Similarly, these same sole and combined applications increased root weight by 133 and 180%, respectively (**Tables 4**, **5**). The results of study showed that the application of Si and KP along with biochar and *C. lunata* significantly improved the plants' physiological and morphological attributes. Interesting results were observed under drought stress conditions, as it was shown that the growth-promoting effect of AR11 alone was more efficient compared to that produced by the combined application of biochar, Si, and K_2HPO_4.

TABLE 2 | Quantification of organic acid content in AR11 suspension culture.

Organic acid content (ppm)	Succinic acid	Acetic acid	Tartaric acid	Malic acid
Control	500	ND	20	ND
Control	450	ND	15	ND
Control	360	ND	18	ND
AF1	1300	600	50	40
AF1	998	435	65	25
AF1	1036	202	35	21

TABLE 3 | Free amino acid intake potential of *Curvularia lunata* AR11.

Nomenclature	Control (μg/ml)	AR11 (μg/ml)
Phosphoserine	0	0
Taurine	0	0
Phospho ethanol amine	0	0
Urea	0	0
Aspartic acid	13.5	5.23
Threonine	7.07	3.70
Serine	7.48	3.04
Glutamic acid	38.6	12.93
Sarcosine	0	0
α-Amino asipic acid	0	0
Glycine	5.24	3.66
Alanine	27.59	12.23
Citrulline	1.10	1.10
α-Amino-n-butyric acid	0	0
Valine	14.76	7.16
Cystine	0	0
Methionine	3.94	1.20
Cystathionine	0.33	0.17
Isoleucine	10.90	4.22
Leucine	18.62	7.16
Tyrosine	3.14	1.83
Phenylalanine	11.93	4.84
β-Alanine	0.19	0.34
β-Amino isobutyric acid	0.87	0.75
γ-Amino-n-butyric acid	4.65	2.02
Ethanol amine	0	0.19
Ammonia	4.53	4.05
Hydroxylysine	0	0
Ornithine	2.97	1.00
Lysine	7.94	5.80
1-Methylhistidine	0	0
Histidine	1.25	0.95
3-Methylhistidine	0	0
Anserine	0	0
Carnosine	0	0
Arginine	8.83	3.78
Hydroxy proline	0	0
Proline	9.48	3.80

TABLE 4 | Effect of silicon, K_2HPO_4, AR11, and biochar on morphological attributes under drought stress.

Treatments	Root Wt-D	Shoot Wt-D
Control1 −ve (Dr)	2.74 ± 0.23a	3.82 ± 0.2a
Control2 +ve (Dr)	0.71 ± 0.07ef	1.47 ± 0.01e
Si (Dr)	1.12 ± 0.13d	1.77 ± 0.04de
KP (Dr)	0.54 ± 0.31f	1.60 ± 0.08e
AR11 (Dr)	1.66 ± 0.26c	2.5 ± 0.15c
Bio (Dr)	0.82 ± 0.06ef	2.04 ± 0.55d
Si + KP (Dr)	0.80 ± 0.07ef	1.74 ± 0.07de
Si + KP + AR11 (Dr)	1.85 ± 0.08bc	2.73 ± 0.05bc
Si + KP + Bio (Dr)	0.90 ± 0.01de	1.80 ± 0.066de
Si + KP + Bio + AR11 (Dr)	1.99 ± 0.13b	2.92 ± 0.06b

Each value represents the mean ± SD (n = 6). Different letters within the columns represent significant differences at P ≤ 0.05.

TABLE 5 | Effect of silicon, K_2HPO_4, AR11, and biochar morphological attributes under salt stress.

Treatments	Root Wt.-S	Shoot Wt.-S
Control1 −ve (NaCl)	2.7 ± 0.11a	3.83 ± 0.25a
Control2 +ve (NaCl)	0.76 ± 0.12g	1.59 ± 0.11g
Si (NaCl)	0.96 ± 0.04f	1.84 ± 0.37f
KP (NaCl)	0.87 ± 0.04fg	1.81 ± 0.06f
AR11 (NaCl)	1.22 ± 0.06de	2.1 ± 0.1e
Bio (NaCl)	0.92 ± 0.04f	1.8 ± 0.1fg
Si + KP (NaCl)	1.16 ± 0.05e	2.42 ± 0.1d
Si + KP + AR11 (NaCl)	1.37 ± 0.05de	2.83 ± 0.06c
Si + KP + Bio (NaCl)	1.41 ± 0.11c	3.02 ± 0.15c
Si + KP + Bio + AR11 (NaCl)	2.04 ± 0.17b	3.4 ± 0.1b

Each value represents the mean ± SD (n = 6). Different letters within the column represent significant differences at P ≤ 0.05.

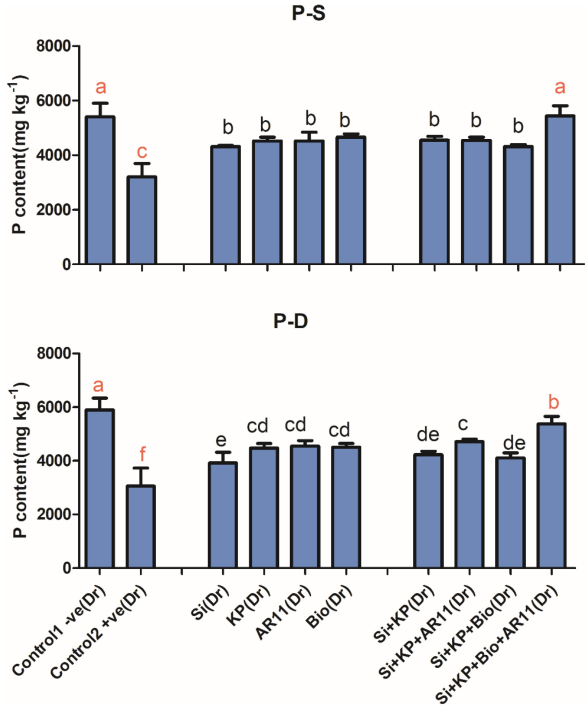


FIGURE 2 | Effects of AR11, Si, K_2HPO_4, and biochar inoculation on phosphorus content in rice shoots subjected to salt and drought stresses. (-S), salt; (-D), drought. Error bars represent standard deviations. Each data point represents the mean of at least three replications. Bars with different letters are significantly different from each other at $P \leq 0.05$.

Quantification of Mineral Elements in Plant Shoots

Phosphorous (P)

Salt and drought stress conditions caused a significant drop in P content in the +ve control, specifically by 40 and 48%, respectively, when compared to the −ve control. Under drought stress, the sole application of Si, KP, AR11, and biochar improved P uptake by 28, 46, 49, and 47%, respectively. The co-application of Si + KP, Si + KP + AR11, Si + KP + Bio, and Si + KP + Bio + AR11 enhanced the P content of plant shoots by 38, 54, 34, and 76%, respectively. A similar trend was observed under salt stress, where the sole application of Si, KP, AR11, and biochar enhanced P uptake by 34, 40, 41, and 45%, respectively. The co-application of Si + KP, Si + KP + AR11, Si + KP + Bio, and Si + KP + Bio + AR11 increased P uptake by 41, 41, 34, and 69%, respectively, when compared to the +ve control (**Figure 2**).

Silicon (Si)

The trend of Si uptake was similar to that of other elements. The Si content was significantly dropped under salt and drought stress in +ve control plants. However, the sole application of Si, KP, AR11, and biochar on increased Si content by 36, 27, 24, and 50%, respectively, under salt stress. Similarly, under drought stress, the sole application of Si, KP, AR11, and biochar enhanced Si content by 42, 2, 15, and 21%, respectively. The co-application of Si + KP, Si + KP + AR11, Si + KP + Bio, and Si + KP + Bio + AR11 increased Si content by 46%, 61%, 46% and 88%, respectively, under drought stress, and 50, 66, 58, and 80%, respectively, under salt stress when compared to the +ve control (**Figure 3**).

Sodium (Na)

Under salt stress, Na^+ ion content showed an approximate 27-fold increase in the +ve control compared to the −ve plants. However, treatment with Si, KP, AR11, and biochar lowered the ion content by 40, 39, 62, and 54%, respectively. Moreover, co-application caused a further decrease in Na^+ ion content by 67, 57, and 74% in the plants treated with Si + KP + AR11, Si + KP + Bio, and Si + KP + Bio + AR11, respectively. Under drought stress, Na^+ ion content dropped by 59% in the +ve control compared to the −ve control plants. Here, the plants treated with sole applications showed a higher Na^+ ion uptake, compared to those treated with co-applications. The sole application of Si, KP, AR11, and biochar increased the Na^+ ion level by 347, 264, 108, and 161%, respectively. However, co-application enhanced Na^+ ion content less than the sole applications did—Si + KP (85%), Si + KP + AR11 (14%), Si + KP + Bio (118%), and Si + KP + Bio + AR11 (208%)—when compared to the +ve control plants (**Figure 4**).

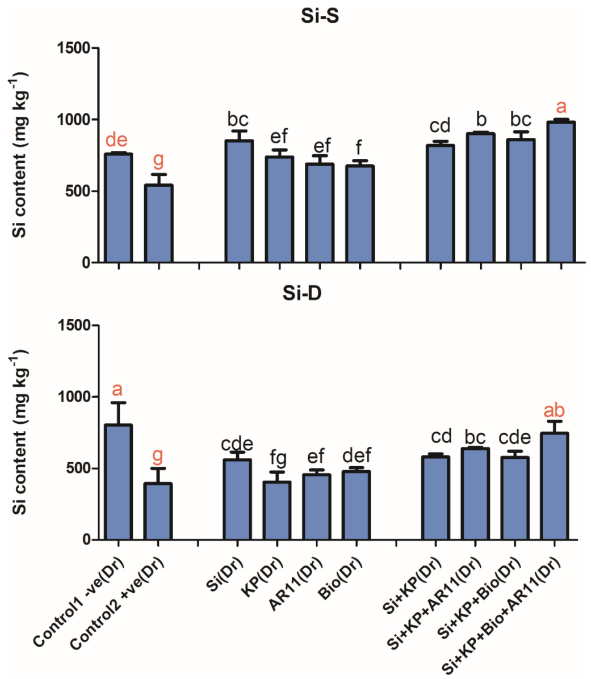


FIGURE 3 | Concentration of silicon in rice shoots subjected to salt and drought stresses following AR11, Si, K_2HPO_4, and biochar inoculation. (-S), salt; (-D), drought. Error bars represent standard deviations. Each data point represents the mean of at least three replications. Bars with different letters are significantly different from each other at $P \leq 0.05$.

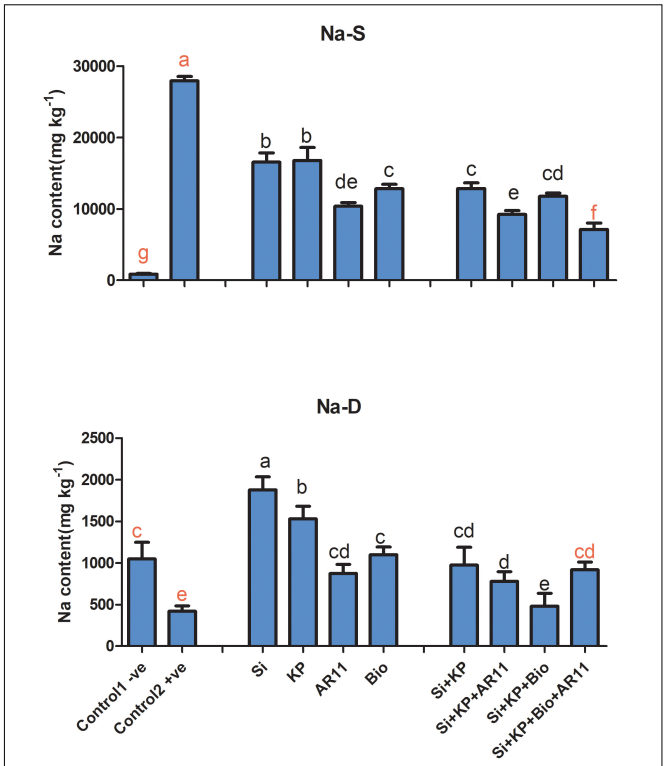


FIGURE 4 | Influx of Na^+ ion content in rice shoots subjected to salt and drought stresses following AR11, Si, K_2HPO_4, and biochar inoculation. (-S), salt; (-D), drought. Error bars represent standard deviations. Each data point represents the mean of at least three replications. Bars with different letters are significantly different from each other at $P \leq 0.05$.

These results validate the detoxification effect of co-application of AR11, biochar, Si, and K_2HPO_4.

Potassium (K)

The sole application of Si, KP, AR11, and biochar significantly enhanced K content in both salt and drought stress conditions. Under salt stress, K content in the +ve control significantly dropped by 54%. However, the treatment with Si, KP, AR11, and biochar enhanced K uptake in plant shoots by 95, 120, 105, and 107%, respectively. The uptake of K was further stimulated by the co-application of Si + KP (122%), Si + KP + AR11 (130%), Si + KP + Bio (126%), and Si + KP + Bio + AR11 (149%). Under drought stress, K content significantly dropped by 59% in the +ve control compared to the −0ve control plants. However, the application of Si, KP, AR11, and biochar enhanced K uptake by 12, 27, 64, and 16%, respectively. The co-application of Si + KP, Si + KP + AR11, Si + KP + Bio, and Si + KP + Bio + AR11 further increased it by 54, 61, 25, and 85%, respectively, when compared to the +ve control (**Figure 5**). Indeed, the sole application of synthetic KP and biochar alone had a very small effect in mineral uptake under salt and drought stresses.

Quantification of Abscisic Acid

Salt stress elevated the ABA level by 282% in +ve control plants compared to −0ve control. However, the ABA level significantly dropped by 59, 54, 60, 63, 65, 69, 61, and 69% with the treatment of Si, KP, AR11, Bio, Si + KP, Si + KP + AR11, Si + KP + Bio, and Si + KP + Bio + AR11 respectively.

Similarly, under drought stress, the ABA level significantly increased by 216% in the +ve control compared to the −0ve control. Sole treatments with Si, KP, AR11, and biochar significantly dropped the ABA level by 22, 26, 49, and 23%, respectively, when compared to the +ve control plants. The co-application of Si + KP, Si + KP + AR11, Si + KP + Bio, and Si + KP + Bio + AR11 significantly reduced the ABA level by 26, 63, 35, and 59%, respectively (**Figure 6**).

Analysis of Polyphenol Contents

Polyphenol contents in the +ve control plants significantly decreased by 50 and 60% under drought and salt stress, respectively. The application of Si, KP, AR11, and biochar under salt stress, significantly improved the polyphenol levels by 52, 46, 64, and 25%, respectively. However, minor differences were observed for the sole application of Si, KP, and biochar under drought stress. Interestingly, under drought stress, the sole application of AR11 produced higher polyphenol contents when compared with the co-application of Si + KP + Bio. Moreover, the co-application of Si + KP + Bio + AR11 significantly increased the polyphenol contents by 51%, compared to the +ve control (**Figure 7**).

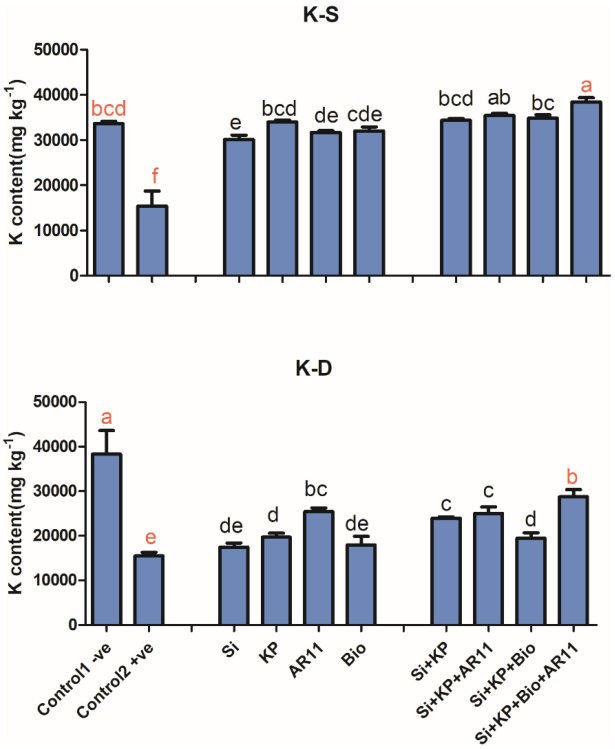


FIGURE 5 | Quantification of K^+ content in rice shoots subjected to salt and drought stresses following AR11, Si, K_2HPO_4, and biochar inoculation. (-S), salt; (-D), drought. Error bars represent standard deviations. Each data point represents the mean of at least three replications. Bars with different letters are significantly different from each other at $P \leq 0.05$.

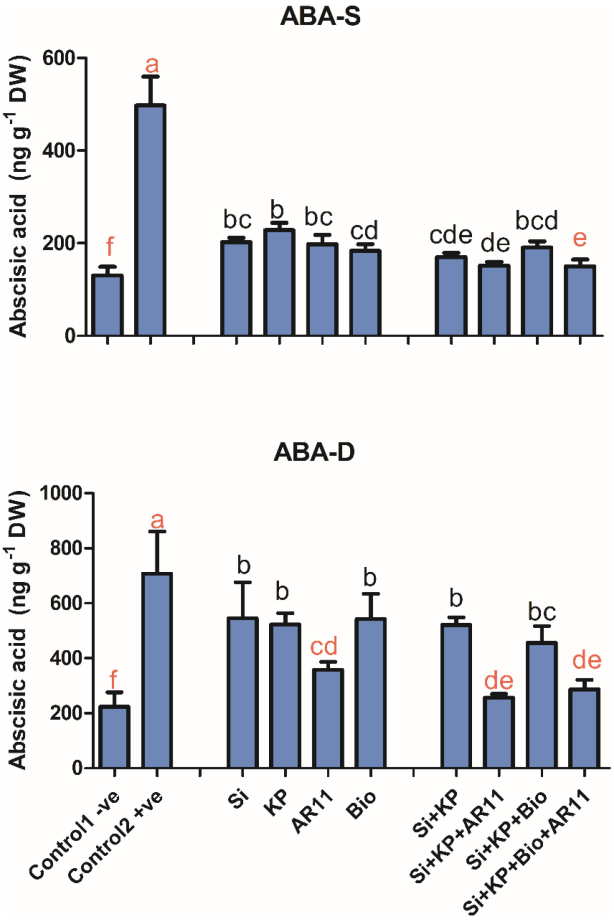


FIGURE 6 | Effect of co-application (AR11, Si, K_2HPO_4, and biochar) on the abscisic acid (ABA) level under salt and drought stresses. (-S), salt; (-D), drought. Error bars represent standard deviations. Each data point represents the mean of at least three replications. Bars with different letters are significantly different from each other at $P \leq 0.05$.

Proline Quantification

Proline content was significantly enhanced by 63 and 83% in +ve control plants exposed to salt and drought stresses, respectively, compared to the −0ve control. The sole application of Si, KP, AR11, and biochar decreased proline content by 14, 12, 24, and 15%, respectively, under salt stress when compared to +ve control. In addition, proline content dropped by 21, 31, 22, and 36% in plants shoot during treatment with Si + KP, Si + KP + AR11, Si + KP + Bio, and Si + KP + Bio + AR11, respectively, under salt stress.

Similarly, the content decreased by 17, 10, 35, and 27% with the sole application of Si, KP, AR11, and biochar respectively, under drought stress. Moreover, proline content decreased by 15, 34, 22, and 36% in plants treated with Si + KP, Si + KP + AR11, Si + KP + Bio, and Si + KP + Bio + AR11, respectively under drought stress, compared to the +ve control (**Figure 8**).

Analysis of Gene Expression in Rice Shoots

Potassium Transporter Gene *OsHKT2*

The results of the present study showed that the K transporter gene *OsHKT2* was significantly downregulated under salt stress. However, the application of Si, KP, AR11, and biochar produced a 7, 7, 9, and 3-fold enhancement of its expression level, respectively, and co-application of Si + KP, Si + KP + AR11, Si + KP + Bio, and Si + KP + Bio + AR11, produced a further 3, 10, 9, and 11-fold expression enhancement respectively. These results validated the quantification of K content in rice shoots exposed to salt stress (**Figure 9**).

Drought-Resistant Gene *OsGRAS23*

The expression value of the drought-resistant *OsGRAS23* transcriptome in rice shoots treated with Si, KP, AR11, and biochar experienced a significant 5, 3, 7, and 2-fold enhancement, respectively. The co-application of Si + KP, Si + KP + AR11, Si + KP + Bio, and Si + KP + Bio + AR11, produced a further 3, 6, 3, and 13-fold increase in the expression level, respectively, when compared to the +ve control (**Figure 9**).

Silicon Transporter Gene *OsLsi1*

In the present study, the silicon transporter gene *OsLsi1* was highly expressed in the co-application of Si + KP + Bio + AR11. This is further confirmed by the high Si content observed in

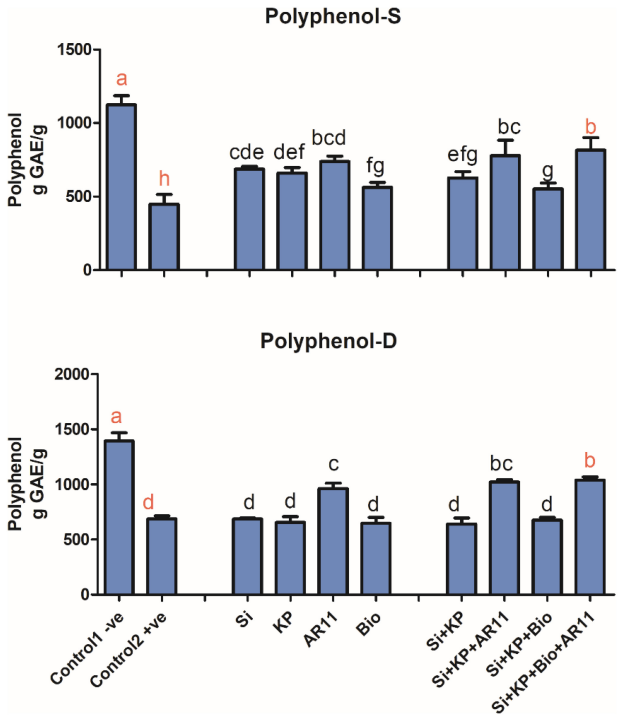


FIGURE 7 | Effect of co-application (AR11, Si, K_2HPO_4, and biochar) on the phenolic level of plant shoots under salt and drought stresses. (-S), salt; (-D), drought. Error bars represent standard deviations. Each data point represents the mean of at least three replications. Bars with different letters are significantly different from each other at $P \leq 0.05$.

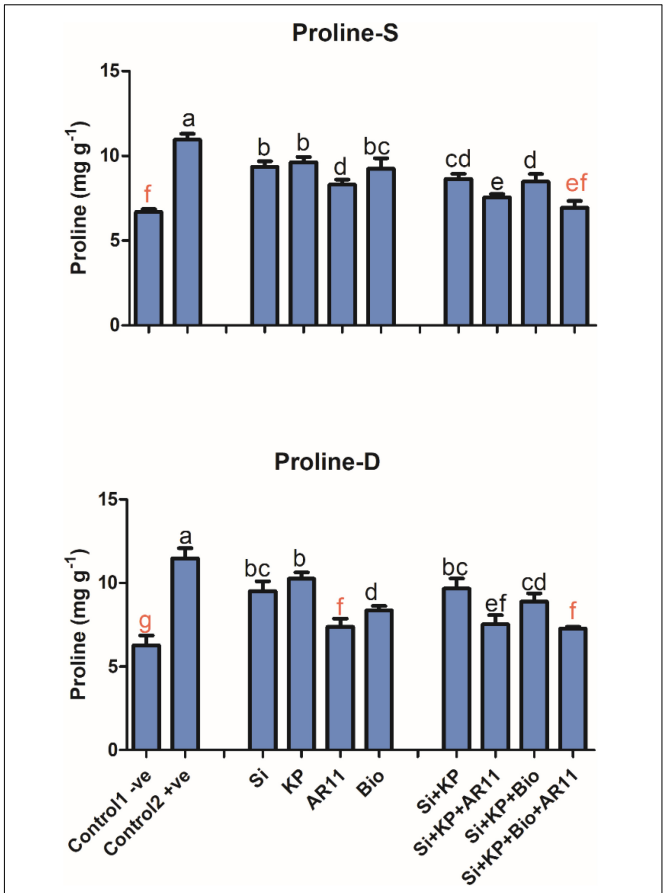


FIGURE 8 | Analysis of proline content in plant shoots subjected to salt and drought stresses. (-S), salt; (-D), drought. Error bars represent standard deviations. Each data point represents the mean of at least three replications. Bars with different letters are significantly different from each other at $P \leq 0.05$.

plants treated with co-application under both salt and drought stresses. Here, the application of Si, KP, AR11, and biochar caused a 10, 3, 8, and 5-fold upregulation of *OsLsi1* expression, respectively. The co-application of Si + KP, Si + KP + AR11, Si + KP + Bio, and Si + KP + Bio + AR11 stimulated a further 11, 13, 12, and 16-fold increase in the expression level of this gene, respectively, under salt stress.

A similar trend was observed under drought stress, where *OsLsi1* expression experienced 3, 12, 17, and 8-fold increase during treatments with Si, KP, AR11, and biochar, respectively. The plants treated with Si + KP, Si + KP + AR11, Si + KP + Bio, and Si + KP + Bio + AR11 co-applications showed a 13, 25, 22, and 40-fold increase in *OsLsi1* expression, respectively (**Figure 10**).

DISCUSSION

There is an urgent need to counteract the effects of environmental stresses, chemical pollution, climate change, and economic inflation on agriculture (Arif et al., 2019; Gupta et al., 2020). As biostimulants (biochar and PGPMs) are widely reported as ecologically safe agents for enhancing the efficiency of inorganic fertilizers and mitigating environmental stresses (Grobelak et al., 2015; Hossain et al., 2017; Zou et al., 2021), in the present study we elucidated how these agents mobilize synthetic Si, P, and K contents and modulate the internal physiology of rice plants exposed to drought and salt stress conditions. The use of PGPMs and biochar is a promising tool for crop improvement; biochar creates favorable condition for sustaining microbiomes which facilitates symbiotic association of PGPMs in plant rhizosphere (Zhang et al., 2018; Gorovtsov et al., 2020). As PGPMs are widely reported for producing secondary metabolites and mediating nutrient recycling; they would further intensify the nutrient assimilation that maintains various metabolic processes and confer stress tolerance in crops (Egamberdieva et al., 2018; Khan et al., 2019b; Kazerooni et al., 2021). In our experimental process, we observed combined application of Si, P, K, AR11, and biochar produced a symbiotic effect that downregulated the Na influx and enhanced the uptake of K, Si, and P contents by plants, therefore maintaining the ionic balance in their metabolic system.

Excessive salt concentrations cause ionic disturbances in plants, and drought further exacerbates the effect of salinity on crops causing osmotic stress, which may ultimately lead to cell death (Sahin et al., 2018). The results of the current study showed that the plant growth was tremendously improved with the combined application of Si, PK, AR11, and biochar. Previous

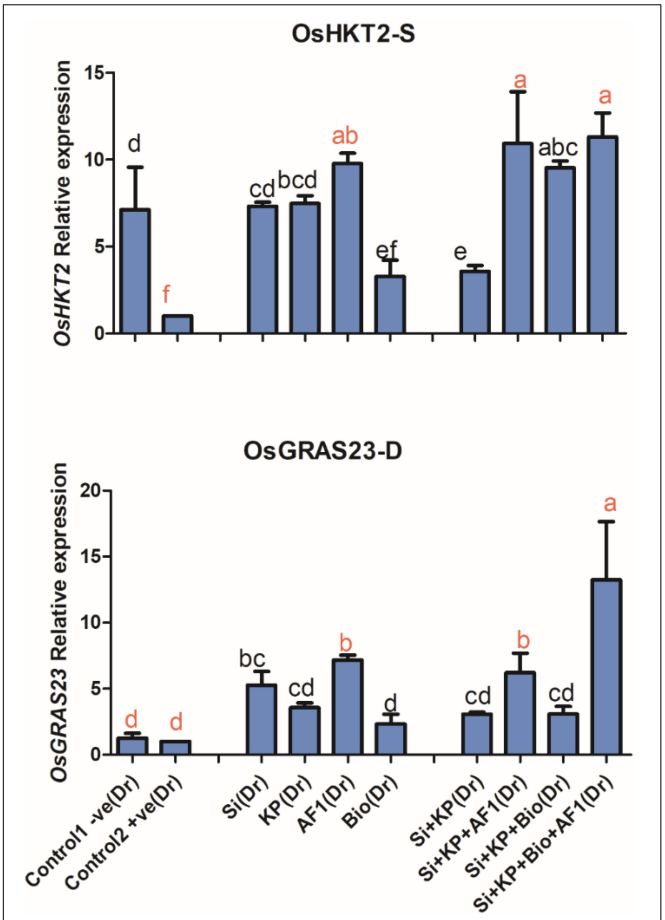


FIGURE 9 | Expression level of the potassium transporter gene *OsHKT2* and drought-resistant *OsGRAS23* transcriptome in rice shoots subjected to salt and drought stresses. (-S), salt; (-D), drought. Error bars represent standard deviations. Each data point represents the mean of at least three replications. Bars with different letters are significantly different from each other at $P \leq 0.05$.

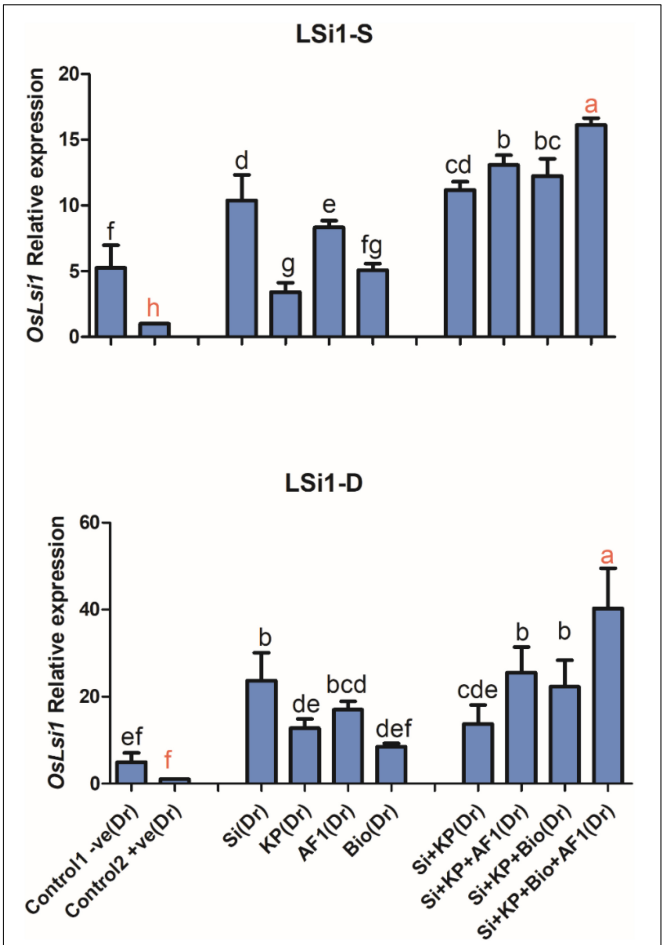


FIGURE 10 | Expression level of the silicon-carrying gene *OsLSi1* in rice shoots subjected to salt and drought stresses following the sole and co-application of AR11, Si, K_2HPO_4, and biochar. (-S), salt; (-D), drought. Error bars represent standard deviations. Each data point represents the mean of at least three replications. Bars with different letters are significantly different from each other at $P \leq 0.05$.

study has reported that GA producing microbes could play a key role in regulating endogenous phytohormones under salt and drought stress (Khan et al., 2015). Additionally, organic acid chelates ions, dissolutes the insoluble mineral ions and enhance bioavailability to plant uptake (Ullah et al., 2015). Since the *C. lunata* AR11 strain has the potential to spontaneously produce GA (GA_1, GA_3, GA_4, and GA_7), and organic acids that can possibly boost the uptake of essential elements under salt and drought stress conditions.

The researchers are now desperately conscientious in developing the approach of optimizing fertilizer use efficiency and mitigating stress for sustainable agriculture. Despite the efforts, limited success has been achieved in terms of improving the utilization efficiency of synthetic fertilizers (Tounkara et al., 2020). Thus, the main goal of the present study was based on enhancement of nutrient use efficiency. In our study, the application of AR11 and biochar significantly increased the uptake of Si, P, and K in rice plants. Ma et al. (2006) first succeeded in revealing a suppression of *OsLsi1* results in reduced silicon uptake in rice. Moreover, Ma et al. (2007) further discovered efflux transporter of silicon *OsLsi2* which revealed a unique phenomenon in nutrient transport in rice. Thus, a higher uptake values of Si in our results were further correlated with the higher expression of the Si transporter gene *OsLsi1*.

Moreover, the ABA stress hormone was observed to be low in the plants treated with co-application, under both stress conditions. As ABA regulates stomatal conductance, which in turn regulates the transpiration rate in plants, a higher ABA level or depletion represents a higher stress level (Chen et al., 2020; González-Guzmán et al., 2021). The results obtained in this study indicate the low-stress level present in plants, which is further validated by the higher expression of the stress-responsive genes *OsGRAS23* and *OSHKT2*. Our results are supported by various previous studies which have shown that the application of exogenous Si, K_2HPO_4, biochar, and plant growth-promoting microorganisms improved Si, K, and P contents and *OsLsi1* expression and decreased the ABA level in plants under abiotic

stress (Kim et al., 2014; Adhikari et al., 2020b; Khan et al., 2020). These results are further supported by findings reported in various previous studies, for example, Gong et al. (2006) and Gengmao et al. (2015) showed that Si reduced Na^+ uptake under salt stress. The combined effect of biochar and silicon was shown to improve several physiological traits, like seed yield and oil quality, in *Helianthus annuus* under water deficit stress (Seleiman et al., 2019).

Reactive oxygen species (ROS), a by-product of aerobic metabolism are recognized as oxygen radicals which are highly vulnerable for normal plant metabolic processes (Zaid and Wani, 2019). To neutralize these negative effects, plants activate antioxidant system to produce phenolic content (Bilal et al., 2018; Decros et al., 2019). Our results showed that AR11 application combined with biochar, silicon, and potassium phosphate significantly increased polyphenol contents. These results agree with Li et al. (2012), Hashem et al. (2015), and Ikram et al. (2018) who reported the role of biostimulants in strengthening the antioxidant system of plants under abiotic stresses.

Altogether, our results coincide with the findings of several authors: Danish and Zafar-ul-Hye (2019) showed biochar and PGPR co-application improved yield of wheat under drought stress, Asaf et al. (2018) reported GA producing fungus *Aspergillus flavus* conferred salt tolerance in *Glycine max*. Similarly, Biju et al. (2017) and Cui et al. (2021) reported Si application alleviated drought stress in crops by regulating enzymes, osmolytes, oxidative metabolism, and nutrient assimilation. Adnan et al. (2020) and Kaya et al. (2003) showed the supplementation of potassium and phosphorus coupled with phosphate solubilizing bacteria ameliorated salt stress in maize, pepper and cucumber plants. These evidence suggest that our methodology covers the magnitude of all of these stress mitigation tools with a single comprehensive approach.

CONCLUSION

To sum up, our study demonstrated that the co-application of Si (2 mM), K_2HPO_4 (3 mM) and biochar (3%) with isolate AR11 could significantly optimize the nutrient uptake efficiency of plants, modulate plant growth regulators and stress-responsive genes to confer salt (150 mM) and drought (20–40%) of soil moisture level] stress tolerance in rice. The strategies defined in this study could contribute to reducing the use of fertilizers, minimizing production costs and environmental pollution, decreasing food toxicity, and promoting sustainable agriculture.

DATA AVAILABILITY STATEMENT

The datasets presented in this study can be found in online repositories. The names of the repository/repositories and accession number(s) can be found at: https://www.ncbi.nlm.nih.gov/ and https://www.ncbi.nlm.nih.gov/nuccore/MZ145250.1/.

AUTHOR CONTRIBUTIONS

AA conceptualized the research and methodologies, conducted the experiment, and prepared the original draft. MAK, MI, S-MK, and K-EL helped in investigation. G-JJ and JYS provided the resource for investigation and managed the software. B-WY reviewed and edited the manuscript. S-MK and I-JL supervised, administered, and managed the funding. All authors contributed to the article and approved the submitted version.

FUNDING

This research was supported by Korea Basic Science Institute (National research Facilities and Equipment center) grant funded by the Ministry of Education (2021R1A6C101A416).

ACKNOWLEDGMENTS

We express our deep reverence for Department of Applied Biosciences, Kyungpook National University for providing us well-equipped resources to undergo our research activities.

SUPPLEMENTARY MATERIAL

The Supplementary Material for this article can be found online at: https://www.frontiersin.org/articles/10.3389/fpls.2022.816858/full#supplementary-material

REFERENCES

Abhilash, P. C., Dubey, R. K., Tripathi, V., Gupta, V. K., and Singh, H. B. (2016). Plant growth-promoting microorganisms for environmental sustainability. *Trends Biotechnol.* 34, 847–850. doi: 10.1016/j.tibtech.2016.05.005

Adhikari, A., Khan, M. A., Lee, K. E., Kang, S. M., Dhungana, S. K., Bhusal, N., et al. (2020a). The halotolerant Rhizobacterium—*Pseudomonas koreensis* MU2 enhances inorganic silicon and phosphorus use efficiency and augments salt stress tolerance in soybean (*Glycine max* L.). *Microorganisms* 8:1256. doi: 10.3390/microorganisms8091256

Adhikari, A., Lee, K. E., Khan, M. A., Kang, S. M., Adhikari, B., Imran, M., et al. (2020b). Effect of silicate and phosphate solubilizing Rhizobacterium *Enterobacter ludwigii* GAK2 on *Oryza sativa* L. under cadmium stress. *J. Microbiol. Biotechnol.* 30, 118–126. doi: 10.4014/jmb.1906.06010

Adhikari, B., Dhungana, S. K., Ali, M. W., Adhikari, A., Kim, I. D., and Shin, D. H. (2018). Resveratrol, total phenolic and flavonoid contents, and antioxidant potential of seeds and sprouts of Korean peanuts. *Food Sci. Biotechnol.* 27, 1275–1284. doi: 10.1007/s10068-018-0364-7

Adnan, M., Fahad, S., Zamin, M., Shah, S., Mian, I. A., Danish, S., et al. (2020). Coupling phosphate-solubilizing bacteria with phosphorus supplements improve maize phosphorus acquisition and growth under lime induced salinity stress. *Plants* 9:900. doi: 10.3390/plants9070900

Al Azzawi, T. N. I., Khan, M., Hussain, A., Shahid, M., Imran, Q. M., Mun, B. G., et al. (2020). Evaluation of Iraqi rice cultivars for their tolerance to drought stress. *Agronomy* 10:1782. doi: 10.3390/agronomy10111782

Ali, H., Khan, E., and Ilahi, I. J. (2019). Environmental chemistry and ecotoxicology of hazardous heavy metals: environmental persistence, toxicity, and bioaccumulation. *J. Chem.* 2019:6730305. doi: 10.1007/398_2019_38

Ali, S., Rizwan, M., Qayyum, M. F., Ok, Y. S., Ibrahim, M., Riaz, M., et al. (2017). Biochar soil amendment on alleviation of drought and salt stress in plants: a critical review. *Environ. Sci. Pollut. Res. Int.* 24, 12700–12712. doi: 10.1007/s11356-017-8904-x

Arif, M., Jan, T., Riaz, M., Fahad, S., Arif, M. S., Shakoor, M. B., et al. (2019). "Chapter 29 - advances in rice research for abiotic stress tolerance: agronomic approaches to improve rice production under abiotic stress," in *Advances in Rice Research for Abiotic Stress Tolerance*, eds M. Hasanuzzaman, M. Fujita, K. Nahar, and J. K. Biswas (Sawston: Woodhead Publishing), 585–614.

Asaf, S., Hamayun, M., Khan, A. L., Waqas, M., Khan, M. A., and Jan, R. (2018). Salt tolerance of *Glycine max*. L induced by endophytic fungus *Aspergillus flavus* CSH1, via regulating its endogenous hormones and antioxidative system. *Plant Physiol. Biochem.* 128, 13–23. doi: 10.1016/j.plaphy.2018.05.007

Bakhat, H. F., Bibi, N., Zia, Z., Abbas, S., Hammad, H. M., Fahad, S., et al. (2018). Silicon mitigates biotic stresses in crop plants: a review. *Crop Prot.* 104, 21–34. doi: 10.1016/j.cropro.2017.10.008

Bargaz, A., Nassar, R., Rady, M., Gaballah, M., Thompson, S., and Brestic, M. (2016). Improved salinity tolerance by phosphorus fertilizer in two *Phaseolus vulgaris* recombinant inbred lines contrasting in their P-efficiency. *J. Agron. Crop Sci.* 202, 497–507. doi: 10.1111/jac.12181

Bhusal, N., Lee, M., Lee, H., Adhikari, A., Han, A. R., Han, A., et al. (2021). Evaluation of morphological, physiological, and biochemical traits for assessing drought resistance in eleven tree species. *Sci. Total Environ.* 779:146466. doi: 10.1016/j.scitotenv.2021.146466

Biju, S., Fuentes, S., and Gupta, D. J. (2017). Silicon improves seed germination and alleviates drought stress in lentil crops by regulating osmolytes, hydrolytic enzymes and antioxidant defense system. *Plant Physiol. Biochem.* 119, 250–264. doi: 10.1016/j.plaphy.2017.09.001

Bilal, L., Asaf, S., Hamayun, M., Gul, H., Iqbal, A., Ullah, I., et al. (2018). Plant growth promoting endophytic fungi *Asprgillus fumigatus* TS1 and *Fusarium proliferatum* BRL1 produce gibberellins and regulates plant endogenous hormones. *Symbiosis* 76, 117–127. doi: 10.1007/s13199-018-0545-4

Bottini, R., Cassán, F., and Piccoli, P. J. (2004). Gibberellin production by bacteria and its involvement in plant growth promotion and yield increase. *Appl. Microbiol. Biotechnol.* 65, 497–503. doi: 10.1007/s00253-004-1696-1

Bouraoui, F., and Grizzetti, B. J. (2014). Modelling mitigation options to reduce diffuse nitrogen water pollution from agriculture. *Sci. Total Environ.* 468-469, 1267–1277. doi: 10.1016/j.scitotenv.2013.07.066

Butcher, K., Wick, A. F., DeSutter, T., Chatterjee, A., and Harmon, J. J. (2016). Soil salinity: a threat to global food security. *Agron. J.* 108, 2189–2200. doi: 10.2134/agronj2016.06.0368

Chen, K., Li, G. J., Bressan, R. A., Song, C. P., Zhu, J. K., and Zhao, Y. B. (2020). Abscisic acid dynamics, signaling, and functions in plants. *J. Integr. Plant Biol.* 62, 25–54. doi: 10.1111/jipb.12899

Cohen, A. C., Travaglia, C. N., Bottini, R., and Piccoli, P. N. (2009). Participation of abscisic acid and gibberellins produced by endophytic *Azospirillum* in the alleviation of drought effects in maize. *Botany* 87, 455–462. doi: 10.1139/b09-023

Cui, G., Xiao, X., Zhang, W., Lang, D., Li, Z., and Zhang, X. (2021). Exogenous silicon relieve drought stress and salt stress of *Glycyrrhiza uralensis* seedlings by regulating proline metabolism and nitrogen assimilation. *J. Hortic. Sci. Biotechnol.* 96, 728–737. doi: 10.1080/14620316.2021.1921624

Danish, S., and Zafar-ul-Hye, M. (2019). Co-application of ACC-deaminase producing PGPR and timber-waste biochar improves pigments formation, growth and yield of wheat under drought stress. *Sci. Rep.* 9:5999. doi: 10.1038/s41598-019-42374-9

Dawood, M., Zaid, A., and Latef, A. A. H. A. (2021). Salicylic acid spraying-induced resilience strategies against the damaging impacts of drought and/or salinity stress in two varieties of *Vicia faba* L. seedlings. *J. Plant Growth Regul.* 1–24. doi: 10.1007/s00344-021-10381-8

Decros, G., Baldet, P., Beauvoit, B., Stevens, R., Flandin, A., Colombié, S., et al. (2019). Get the balance right: ROS homeostasis and redox signalling in fruit. *Front. Plant Sci.* 10:1091. doi: 10.3389/fpls.2019.01091

Egamberdieva, D., Hua, M., Reckling, M., Wirth, S., and Bellingrath-Kimura, S. D. (2018). Potential effects of biochar-based microbial inoculants in agriculture. *Environ. Sustain.* 1, 19–24. doi: 10.1007/s42398-018-0010-6

Etesami, H. (2018). Can interaction between silicon and plant growth promoting rhizobacteria benefit in alleviating abiotic and biotic stresses in crop plants? *Agric. Ecosyst. Environ.* 253, 98–112. doi: 10.1016/j.agee.2017.11.007

FAO (2021). *Drought and Agriculture*. Available online at: https://www.fao.org/land-water/water/drought/droughtandag/en/ (accessed August 15, 2021).

Farhangi-Abriz, S., and Torabian, S. J. (2017). Antioxidant enzyme and osmotic adjustment changes in bean seedlings as affected by biochar under salt stress. *Ecotoxicol. Environ. Saf.* 137, 64–70. doi: 10.1016/j.ecoenv.2016.11.029

Fariduddin, Q., Zaid, A., and Mohammad, F. (2019). "Plant growth regulators and salt stress: mechanism of tolerance trade-off," in *Salt Stress, Microbes, and Plant Interactions: Causes and Solution: Volume 1*, ed. M. S. Akhtar (Singapore: Springer), 91–111. doi: 10.1007/978-981-13-8801-9_4

Fofana, B., Wopereis, M. C. S., Bationo, A., Breman, H., and Mando, A. J. (2008). Millet nutrient use efficiency as affected by natural soil fertility, mineral fertilizer use and rainfall in the West African Sahel. *Nutr. Cycl. Agroecosyst.* 81, 25–36. doi: 10.1007/s10705-007-9146-y

Food and Agriculture Organization of the United Nations (2017). *Food and Agriculture Organization of the United Nations*. Available Online at: http://www.fao.org/3/a-i6895e.pdf (accessed August 14, 2021).

Francis, C. A., and Porter, P. (2011). Ecology in sustainable agriculture practices and systems. *Crit. Rev. Plant Sci.* 30, 64–73. doi: 10.1080/07352689.2011.554353

Garg, N., and Bhandari, P. (2016). Silicon nutrition and mycorrhizal inoculations improve growth, nutrient status, K+/Na+ ratio and yield of *Cicer arietinum* L. genotypes under salinity stress. *Plant Growth Regul.* 78, 371–387. doi: 10.1007/s10725-015-0099-x

Gavili, E., Moosavi, A. A., and Kamgar Haghighi, A. A. (2019). Does biochar mitigate the adverse effects of drought on the agronomic traits and yield components of soybean? *Ind. Crops Prod.* 128, 445–454. doi: 10.1016/j.indcrop.2018.11.047

Gengmao, Z., Shihui, L., Xing, S., Yizhou, W., and Zipan, C. (2015). The role of silicon in physiology of the medicinal plant (*Lonicera japonica* L.) under salt stress. *Sci. Rep.* 5:12696. doi: 10.1038/srep12696

Golldack, D., Li, C., Mohan, H., and Probst, N. (2014). Tolerance to drought and salt stress in plants: unraveling the signaling networks. *Front. Plant Sci.* 5:151. doi: 10.3389/fpls.2014.00151

Gong, H. J., Randall, D. P., and Flowers, T. J. (2006). Silicon deposition in the root reduces sodium uptake in rice (*Oryza sativa* L.) seedlings by reducing bypass flow. *Plant Cell Environ.* 29, 1970–1979. doi: 10.1111/j.1365-3040.2006.01572.x

González-Guzmán, M., Gómez-Cadenas, A., and Arbona, V. (2021). Abscisic acid as an emerging modulator of the responses of plants to low oxygen conditions. *Front. Plant Sci.* 12:661789. doi: 10.3389/fpls.2021.661789

Gorovtsov, A. V., Minkina, T. M., Mandzhieva, S. S., Perelomov, L. V., Soja, G., Zamulina, I. V., et al. (2020). The mechanisms of biochar interactions with microorganisms in soil. *Environ. Geochem. Health* 42, 2495–2518. doi: 10.1007/s10653-019-00412-5

Grobelak, A., Napora, A., and Kacprzak, M. (2015). Using plant growth-promoting rhizobacteria (PGPR) to improve plant growth. *Ecol. Eng.* 84, 22–28. doi: 10.1016/j.ecoleng.2015.07.019

Gupta, A., Rico-Medina, A., and Caño-Delgado, A. I. (2020). The physiology of plant responses to drought. *Science* 368, 266–269. doi: 10.1126/science.aaz7614

Harb, A., Krishnan, A., Ambavaram, M. M., and Pereira, A. J. P. P. (2010). Molecular and physiological analysis of drought stress in Arabidopsis reveals early responses leading to acclimation in plant growth. *Plant Physiol.* 154, 1254–1271. doi: 10.1104/pp.110.161752

Hashem, A., Abd Allah, E. F., Alqarawi, A. A., Aldubise, A., and Egamberdieva, D. (2015). Arbuscular mycorrhizal fungi enhances salinity tolerance of *Panicum turgidum* Forssk by altering photosynthetic and antioxidant pathways. *J. Plant Interact.* 10, 230–242. doi: 10.1080/17429145.2015.1052025

Hossain, M. M., Sultana, F., and Islam, S. (2017). "Plant growth-promoting fungi (PGPF): phytostimulation and induced systemic resistance," in *Plant-Microbe Interactions in Agro-Ecological Perspectives, Volume 2: Microbial Interactions and Agro-Ecological Impacts*, eds D. Singh, H. Singh, and R. Prabha (Singapore: Springer), 135–191. doi: 10.1007/978-981-10-6593-4_6

Ikram, M., Ali, N., Jan, G., Jan, F. G., Rahman, I. U., Iqbal, A., et al. (2018). IAA producing fungal endophyte *Penicillium roqueforti* Thom., enhances stress tolerance and nutrients uptake in wheat plants grown on heavy

metal contaminated soils. *PLoS One* 13:e0208150. doi: 10.1371/journal.pone.0208150

Kaya, C., Higgs, D., Ince, F., Amador, B. M., Cakir, A., and Sakar, E. J. (2003). Ameliorative effects of potassium phosphate on salt-stressed pepper and cucumber. *J. Plant Nutr.* 26, 807–820. doi: 10.1081/pln-120018566

Kazerooni, E. A., Maharachchikumbura, S. S. N., Adhikari, A., Al-Sadi, A. M., Kang, S.-M., Kim, L.-R., et al. (2021). Rhizospheric *Bacillus amyloliquefaciens* protects *Capsicum annuum* cv. geumsugangsan from multiple abiotic stresses via multifarious plant growth-promoting attributes. *Front. Plant Sci.* 12:669693. doi: 10.3389/fpls.2021.669693

Khan, A. L., Hussain, J., Al-Harrasi, A., Al-Rawahi, A., and Lee, I.-J. (2015). Endophytic fungi: resource for gibberellins and crop abiotic stress resistance. *Crit. Rev. Biotechnol.* 35, 62–74. doi: 10.3109/07388551.2013.800018

Khan, M. A., Asaf, S., Khan, A. L., Adhikari, A., Jan, R., Ali, S., et al. (2019a). Halotolerant rhizobacterial strains mitigate the adverse effects of NaCl stress in soybean seedlings. *Biomed Res. Int.* 2019:9530963. doi: 10.1155/2019/9530963

Khan, M. A., Asaf, S., Khan, A. L., Adhikari, A., Jan, R., Ali, S., et al. (2020). Plant growth-promoting endophytic bacteria augment growth and salinity tolerance in rice plants. *Plant Biol.* 22, 850–862. doi: 10.1111/plb.13124

Khan, M. A., Asaf, S., Khan, A. L., Jan, R., Kang, S. M., Kim, K. M., et al. (2019b). Rhizobacteria AK1 remediates the toxic effects of salinity stress via regulation of endogenous phytohormones and gene expression in soybean. *Biochem. J.* 476, 2393–2409. doi: 10.1042/BCJ20190435

Khan, M. A., Sahile, A. A., Jan, R., Asaf, S., Hamayun, M., Imran, M., et al. (2021). Halotolerant bacteria mitigate the effects of salinity stress on soybean growth by regulating secondary metabolites and molecular responses. *BMC Plant Biol.* 21:176. doi: 10.1186/s12870-021-02937-3

Kim, Y. H., Khan, A. L., Waqas, M., Shim, J. K., Kim, D. H., Lee, K. Y., et al. (2014). Silicon application to rice root zone influenced the phytohormonal and antioxidant responses under salinity stress. *J. Plant Growth Regul.* 33, 137–149. doi: 10.1007/s00344-013-9356-2

Kumar, K., Kumar, M., Kim, S. R., Ryu, H., and Cho, Y. G. (2013). Insights into genomics of salt stress response in rice. *Rice* 6:27. doi: 10.1186/1939-8433-6-27

Lee, K.-E., Adhikari, A., Kang, S.-M., You, Y.-H., Joo, G.-J., Kim, J.-H., et al. (2019). Isolation and characterization of the high silicate and phosphate solubilizing novel strain *Enterobacter ludwigii* GAK2 that promotes growth in rice plants. *Agronomy* 9:144. doi: 10.3390/agronomy9030144

Lee, K. E., Radhakrishnan, R., Kang, S. M., You, Y. H., Joo, G. J., Lee, I. J., et al. (2015). *Enterococcus faecium* LKE12 cell-free extract accelerates host plant growth via gibberellin and indole-3-acetic acid secretion. *J. Microbiol. Biotechnol.* 25, 1467–1475. doi: 10.4014/jmb.1502.02011

Li, X., Bu, N., Li, Y., Ma, L., Xin, S., and Zhang, L. (2012). Growth, photosynthesis and antioxidant responses of endophyte infected and non-infected rice under lead stress conditions. *J. Hazard. Mater.* 213-214, 55–61. doi: 10.1016/j.jhazmat.2012.01.052

Ma, J. F., Tamai, K., Yamaji, N., Mitani, N., Konishi, S., Katsuhara, M., et al. (2006). A silicon transporter in rice. *Nature* 440, 688–691.

Ma, J. F., Yamaji, N., Mitani, N., Tamai, K., Konishi, S., Fujiwara, T., et al. (2007). An efflux transporter of silicon in rice. *Nature* 448, 209–212. doi: 10.1038/nature05964

Mark Ibekwe, A., Ors, S., Ferreira, J. F. S., Liu, X., and Suarez, D. L. (2017). Seasonal induced changes in spinach rhizosphere microbial community structure with varying salinity and drought. *Sci. Total Environ.* 579, 1485–1495. doi: 10.1016/j.scitotenv.2016.11.151

Nabi, R. B. S., Tayade, R., Hussain, A., Adhikari, A., Lee, I.-J., Loake, G. J., et al. (2021). A novel *DUF569* gene is a positive regulator of the drought stress response in Arabidopsis. *Int. J. Mol. Sci.* 22:5316. doi: 10.3390/ijms22105316

Premanandh, J. (2011). Factors affecting food security and contribution of modern technologies in food sustainability. *J. Sci. Food Agric.* 91, 2707–2714. doi: 10.1002/jsfa.4666

Qadir, M., Hussain, A., Hamayun, M., Shah, M., Iqbal, A., Husna, et al. (2020). Phytohormones producing rhizobacterium alleviates chromium toxicity in *Helianthus annuus* L. by reducing chromate uptake and strengthening antioxidant system. *Chemosphere* 258:127386. doi: 10.1016/j.chemosphere.2020.127386

Sahin, U., Ekinci, M., Ors, S., Turan, M., Yildiz, S., and Yildirim, E. (2018). Effects of individual and combined effects of salinity and drought on physiological, nutritional and biochemical properties of cabbage (*Brassica oleracea* var. capitata). *Sci. Hortic.* 240, 196–204. doi: 10.1016/j.scienta.2018.06.016

Seleiman, M. F., Refay, Y., Al-Suhaibani, N., Al-Ashkar, I., El-Hendawy, S., and Hafez, E. M. J. (2019). Integrative effects of rice-straw biochar and silicon on oil and seed quality, yield and physiological traits of *Helianthus annuus* L. grown under water deficit stress. *Agronomy* 9:637. doi: 10.3390/agronomy9100637

Shahzad, R., Khan, A. L., Bilal, S., Asaf, S., and Lee, I. J. (2017a). Plant growth-promoting endophytic bacteria versus pathogenic infections: an example of *Bacillus amyloliquefaciens* RWL-1 and *Fusarium oxysporum* f. sp. *lycopersici* in tomato. *PeerJ* 5:e3107. doi: 10.7717/peerj.3107

Shahzad, R., Khan, A. L., Bilal, S., Waqas, M., Kang, S.-M., and Lee, I.-J. (2017b). Inoculation of abscisic acid-producing endophytic bacteria enhances salinity stress tolerance in *Oryza sativa*. *Environ. Exp. Bot.* 136, 68–77.

Simpson, R. J., Oberson, A., Culvenor, R. A., Ryan, M. H., Veneklaas, E. J., Lambers, H., et al. (2011). Strategies and agronomic interventions to improve the phosphorus-use efficiency of farming systems. *Plant Soil* 349, 89–120.

Singh, A. (2021). Soil salinization management for sustainable development: a review. *J. Environ. Manag.* 277:111383. doi: 10.1016/j.jenvman.2020.111383

Tang, Y., Bao, X., Zhi, Y., Wu, Q., Guo, Y., Yin, X., et al. (2019). Overexpression of a MYB family gene, *OsMYB6*, increases drought and salinity stress tolerance in transgenic rice. *Front. Plant Sci.* 10:168. doi: 10.3389/fpls.2019.00168

Tittonell, P., and Giller, K. E. (2013). When yield gaps are poverty traps: the paradigm of ecological intensification in African smallholder agriculture. *Field Crops Res.* 143, 76–90. doi: 10.1016/j.fcr.2012.10.007

Tounkara, A., Clermont-Dauphin, C., Affholder, F., Ndiaye, S., Masse, D., and Cournac, L. (2020). Inorganic fertilizer use efficiency of millet crop increased with organic fertilizer application in rainfed agriculture on smallholdings in central Senegal. *Agric. Ecosyst. Environ.* 294:106878.

Ullah, A., Heng, S., Munis, M. F. H., Fahad, S., and Yang, X. (2015). Phytoremediation of heavy metals assisted by plant growth promoting (PGP) bacteria: a review. *Environ. Exp. Bot.* 117, 28–40. doi: 10.1016/j.envexpbot.2015.05.001

Waqas, M., Khan, A. L., Kamran, M., Hamayun, M., Kang, S. M., Kim, Y. H., et al. (2012). Endophytic fungi produce gibberellins and indoleacetic acid and promotes host-plant growth during stress. *Molecules* 17, 10754–10773. doi: 10.3390/molecules170910754

Xia, Q., Green, B. D., Zhu, Z., Li, Y., Gharibzahedi, S. M. T., Roohinejad, S., et al. (2019). Innovative processing techniques for altering the physicochemical properties of wholegrain brown rice (*Oryza sativa* L.) - opportunities for enhancing food quality and health attributes. *Crit. Rev. Food Sci. Nutr.* 59, 3349–3370. doi: 10.1080/10408398.2018.1491829

Yang, J., Kloepper, J. W., and Ryu, C. M. (2009). Rhizosphere bacteria help plants tolerate abiotic stress. *Trends Plant Sci.* 14, 1–4. doi: 10.1016/j.tplants.2008.10.004

Zaid, A., Ahmad, B., and Wani, S. H. (2021). "Medicinal and aromatic plants under abiotic stress: a crosstalk on phytohormones' perspective," in *Plant Growth Regulators: Signalling under Stress Conditions*, eds T. Aftab and K. R. Hakeem (Cham: Springer International Publishing), 115–132.

Zaid, A., Gul, F., Ahanger, M. A., and Ahmad, P. (2018). "Chapter 20 - silicon-mediated alleviation of stresses in plants," in *Plant Metabolites and Regulation Under Environmental Stress*, eds P. Ahmad, M. A. Ahanger, V. P. Singh, D. K. Tripathi, P. Alam, and M. N. Alyemeni (Cambridge, MA: Academic Press), 377–387. doi: 10.1016/b978-0-12-812689-9.00020-0

Zaid, A., and Wani, S. H. (2019). "Reactive oxygen species generation, scavenging and signaling in plant defense responses," in *Bioactive Molecules in Plant Defense: Signaling in Growth and Stress*, eds S. Jogaiah and M. Abdelrahman (Cham: Springer International Publishing), 111–132.

Zhai, M., Huang, G., Liu, L., Xu, X., and Li, J. (2019). Transfer of virtual water embodied in food: a new perspective. *Sci. Total Environ.* 659, 872–883. doi: 10.1016/j.scitotenv.2018.12.433

Zhang, L., Jing, Y., Xiang, Y., Zhang, R., and Lu, H. (2018). Responses of soil microbial community structure changes and activities to biochar addition: a meta-analysis. *Sci. Total Environ.* 643, 926–935. doi: 10.1016/j.scitotenv.2018.06.231

Zhu, Y., and Gong, H. J. (2014). Beneficial effects of silicon on salt and drought tolerance in plants. *Agron. Sustain. Dev.* 34, 455–472. doi: 10.1007/s13593-013-0194-1

Zou, Y. N., Wu, Q. S., and Kuča, K. (2021). Unravelling the role of arbuscular mycorrhizal fungi in mitigating the oxidative burst of plants under drought stress. *Plant Biol.* 23, 50–57. doi: 10.1111/plb.13161

Conflict of Interest: The authors declare that the research was conducted in the absence of any commercial or financial relationships that could be construed as a potential conflict of interest.

Publisher's Note: All claims expressed in this article are solely those of the authors and do not necessarily represent those of their affiliated organizations, or those of the publisher, the editors and the reviewers. Any product that may be evaluated in this article, or claim that may be made by its manufacturer, is not guaranteed or endorsed by the publisher.

Copyright © 2022 Adhikari, Khan, Imran, Lee, Kang, Shin, Joo, Khan, Yun and Lee. This is an open-access article distributed under the terms of the Creative Commons Attribution License (CC BY). The use, distribution or reproduction in other forums is permitted, provided the original author(s) and the copyright owner(s) are credited and that the original publication in this journal is cited, in accordance with accepted academic practice. No use, distribution or reproduction is permitted which does not comply with these terms.

frontiers in Plant Science

ORIGINAL RESEARCH
published: 09 March 2022
doi: 10.3389/fpls.2022.825829

Calcium Nanoparticles Impregnated With Benzenedicarboxylic Acid: A New Approach to Alleviate Combined Stress of DDT and Cadmium in *Brassica alboglabra* by Modulating Bioacummulation, Antioxidative Machinery and Osmoregulators

Samavia Mubeen[1], Iqra Shahzadi[2], Waheed Akram[3], Wajid Saeed[4], Nasim Ahmad Yasin[5,6], Aqeel Ahmad[7], Anis Ali Shah[8]*, Manzer H. Siddiqui[9] and Saud Alamri[9]*

[1] State Key Laboratory for Biocontrol, School of Life Sciences, Sun Yat-sen University, Guangzhou, China, [2] Hubei Key Laboratory of Biomass Resource Chemistry and Environmental Biotechnology, Hubei International Scientific and Technological Cooperation Base of Sustainable Resource and Energy, Hubei Engineering Center of Natural Polymersbased Medical Materials, School of Resource and Environmental Science, Wuhan University, Wuhan, China, [3] Department of Plant Pathology, Institute of Agricultural Sciences, University of the Punjab, Lahore, Pakistan, [4] Key Laboratory of Crop Cultivation and Farming System, Agriculture College, Guangxi University, Nanning, China, [5] Senior Superintendent Garden, University of the Punjab, Lahore, Pakistan, [6] Guangdong Key Laboratory for New Technology Research of Vegetables/Vegetable Research Institute, Guangdong Academy of Agricultural Sciences, Guangzhou, China, [7] Key Laboratory of Land Surface Pattern and Simulation, Institute of Geographic Sciences and Natural Resources Research, Chinese Academy of Sciences, Beijing, China, [8] Department of Botany, Division of Science and Technology, University of Education, Lahore, Pakistan, [9] Department of Botany and Microbiology, College of Science, King Saud University, Riyadh, Saudi Arabia

At present, the alleviation of stress caused by climate change and environmental contaminants is a crucial issue. Dichlorodiphenyltrichloroethane (DDT) is a persistent organic pollutant (POP) and an organochlorine, which causes significant health problems in humans. The stress caused by cadmium (Cd) and the toxicity of DDT have direct effects on the growth and yield of crop plants. Ultimately, the greater uptake and accumulation of DDT by edible plants affects human health by contaminating the food chain. The possible solution to this challenging situation is to limit the passive absorption of POPs into the plants. Calcium (Ca) is an essential life component mandatory for plant growth and survival. This study used impregnated Ca (Bd_{Ca}) of benzenedicarboxylic acid (Bd) to relieve abiotic stress in plants of *Brassica alboglabra*. Bd_{Ca} mitigated the deleterious effects of Cd and reduced DDT bioaccumulation. By increasing the removal efficacy (RE) up to 256.14%, Bd_{Ca} greatly decreased pollutant uptake (Cd 82.37% and DDT 93.64%) and supported photosynthetic machinery (86.22%) and antioxidant enzyme defenses (264.73%), in applied plants. Exogenously applied Bd also

OPEN ACCESS

Edited by:
Mohammad Anwar Hossain, Bangladesh Agricultural University, Bangladesh

Reviewed by:
Deepak Kumar, Banaras Hindu University, India
Mohd Asgher, Baba Ghulam Shah Badshah University, India
Satwinderjeet Kaur, Guru Nanak Dev University, India

***Correspondence:**
Aqeel Ahmad
aqeelahmad1@gmail.com
Anis Ali Shah
anisalibot@gmail.com

Specialty section:
This article was submitted to Plant Biotechnology, a section of the journal Frontiers in Plant Science

Received: *30 November 2021*
Accepted: *18 January 2022*
Published: *09 March 2022*

Citation:
Mubeen S, Shahzadi I, Akram W, Saeed W, Yasin NA, Ahmad A, Shah AA, Siddiqui MH and Alamri S (2022) Calcium Nanoparticles Impregnated With Benzenedicarboxylic Acid: A New Approach to Alleviate Combined Stress of DDT and Cadmium in Brassica alboglabra by Modulating Bioacummulation, Antioxidative Machinery and Osmoregulators. Front. Plant Sci. 13:825829. doi: 10.3389/fpls.2022.825829

successfully improved the antioxidant system and the physiochemical parameters of plants. However, impregnation with Ca further enhanced plant tolerance to stress. This novel study revealed that the combined application of Ca and Bd could effectively relieve individual and combined Cd stress and DDT toxicity in *B. alboglabra*.

Keywords: abiotic stress, bioaccumulation, *Brassica alboglabra*, cadmium uptake, DDT, heavy metal removal, organochlorine, persistent organic pollutant

INTRODUCTION

Dichlorodiphenyltrichloroethane (DDT), an organochlorine and a persistent organic pollutant (POP), was first synthesized in 1874 to control insect pests on large scales in the agriculture fields (Turusov et al., 2002). Its effectiveness evolved into the most abundantly used pesticide before it was banned by the Environmental Protection Agency (EPA) in the United States during 1972 (Jaga and Dharmani, 2003). It was famous for the long-term pest control, more effectiveness, easy manufacturing, and cost-effectiveness (Sadasivaiah et al., 2007). Besides, DDT is also released as a by-product of all the chemical industries dealing with or producing chlorinated chemicals/liquids. Because DDT has been used in bulk amounts worldwide and for long periods, it has become a high-ranked source of toxicity for the human population without any geographical discrimination. Some other chemical processes that involved chlorine (e.g., smelting of metals, bleaching of paper pulp, production of cement, impregnation of wood, and incineration of solid waste and sewage sludge) add a significant share in the DDT contents in the environment.

Cadmium (Cd) is among the most injurious metals imposing multiple detrimental effects on the growth and development of plants and concomitantly on humans (Sardar et al., 2022a). Rapid industrialization and excessive use of Cd based fungicides, herbicides, insecticides, and fertilizers are continuously contaminating soils and water (Sardar et al., 2022b). Cd-contaminated soils disturb enzymatic activities, metabolic processes, plant growth, and quality of the plant produce (Shah et al., 2021). The consumption of Cd-contaminated plant commodities may cause gastrointestinal and pulmonary disorders besides cancer. Soil Cd uptake is a primary source of food chain contamination. Cd is bioaccumulation in the foliage ($>$ 5–10 $\mu g\ g^{-1}$) and has harmful effects on the physiochemical activities of plants. Henceforward, it becomes indispensable to adopt some suitable strategies to lower Cd toxicity and reduce its uptake by plants growing in polluted sites.

Both Cd and DDT are readily absorbed in plant tissues, translocated between different tissues, and preserved in the lipid-rich areas. Complete avoidance of these pollutants is necessarily important, which seems impossible if the pollutants are part of our everyday diet. Therefore, limiting Cd and DDT contents in agri-food products can greatly assist in avoiding pollutant bioaccumulation in human tissues.

Brassica is an oil seed-producing plant famous for its consumption as a leafy vegetable and animal feed. Vegetables are perishable crops, therefore, mostly cultivated in agricultural lands situated near urban areas. In such regions, crops may be irrigated by water contaminated with industrial wastewater containing Cd and other metal contaminants (Rezapour and Samadi, 2011). Cost-effective DDT has been extensively used for the management of insect pests of several crops. Residues of DDT are still present in these soils (Mansouri et al., 2017). Growing such an important crop in a DDT- and Cd-polluted environment causes the pollutants to be absorbed, translocated, and preserved in the edible plant parts. Plant pollutants cause orchestration in the concentration of total soluble protein, soluble sugars, leaf water, and osmoprotectants besides the decline in the activity of antioxidant enzymes, including ascorbate peroxidase (APX), superoxide dismutase (SOD), and peroxidase (POD) in stressed plants (Yasin et al., 2018a; Ahmad et al., 2020b; Li et al., 2021). They severely affect plant growth, photosynthesis, chlorophyll activity, antioxidant activity, reactive oxygen species (ROS), and many other physiological attributes.

Benzenedicarboxylic acid (Bd) is well-documented for driving plant physiological responses toward a new equilibrium. It successfully induced antioxidant defenses, improved enzymatic activities, and augmented the nutritional quality of fruits (Ahmad et al., 2019). Considering its diverse physiological effects in plants, and potential to improve fruit quality, Bd was selected to inhibit DDT and Cd absorption from the surrounding environment. This is the first study that evaluates the molecule in limiting the absorption and translocation of plant stressors. Nevertheless, Bd is readily soluble in water. Therefore, it can be easily scavenged or washed off from plant surfaces during rain. Its molecules contain chromophores (with absorbance at wavelengths $>$290 nm), therefore, stay highly susceptible to photolysis by sunlight, and also degrade readily in water (Lu et al., 2002). Consequently, its stable, slow, and continuous release needs some safeguard agent for which calcium (Ca) impregnation could be a useful strategy.

Calcium nanoparticles are a family of inorganic layered materials (Ram Reddy et al., 2006; Xu et al., 2006; Reddy et al., 2008), which can be synthesized using a cost-effective protocol (Xu et al., 2006). The main feature of Ca includes its role in the formation of plant structure. The Ca can be applied to plants for increased growth and defense parameters (Thor, 2019). Several positive physiological impacts have already been documented on Ca application (Fletcher et al., 2020). Ca alleviates Cd and other abiotic stresses in applied plants (Sakouhi et al., 2021; Tong et al., 2021).

To reduce the accumulation level of Cd and DDT in crops, to ensure food safety, and to reduce human intake, this study found an additive that can effectively reduce the absorption of pollutants by crops. It was hypothesized that the combined application of Ca with Bd might have beneficial effects on plant stress alleviation and growth improvement. According to

our information, there is no study demonstrating the role of Bd and/or Ca in alleviating multiple environmental stresses. Henceforth, this study is designed to investigate the role of Bd-coated Ca (Bd_{Ca}) in alleviating multiple stress (DDT and Cd) conditions in Kale plants and their joint effect of controlling the bioaccumulation of the toxic organic contaminant. This study elucidates the role of Bd_{Ca} on growth, gas exchange attributes, and antioxidative system of *Brassica alboglabra* plants under DDT and temperature stress. Moreover, this study was deliberated to examine the potential of Bd_{Ca} in reducing the bioaccumulation of toxic organic contaminant, i.e., DDT.

MATERIALS AND METHODS

Plant Material and Growth Conditions

Seeds of *B. alboglarba* were surface sterilized by submerging in 0.1% potassium permanganate for 15 min and subsequent thorough washing by using deionized water. The 10 sterilized seeds were placed on 2 layers of 3-mm Whatman filter paper embedded in 9 cm glass jars supplemented with 10 ml of standard Davtyan (0.75 N) nutrient solution in ddH_2O (Daryadar et al., 2019). All aforementioned steps were performed beneath very low light. Then, these covered jars were randomly kept in a plant growth chamber in the dark at 25 ± 2°C for 5 days. After the growth of the initial 5 days, seedlings were transferred to pots (2 plants/pot) packed with 1 kg of Cd-contaminated UQ23 pot soil.

Bd_{Ca} Synthesis

The method by Mitter et al. (2017) was strictly followed to prepare Ca nanoparticles. The process included non-aqueous precipitation, heat treatment, purification step, and dispersion in water. The complete procedure yielded an average particle size of 45 nm, which were analyzed by a Nanosizer, Nano ZS instrument (Malvern Instruments) to obtain the *Z* average size and particle diameter (PdI). The chemical composition and crystal structure were verified by powder X-ray diffraction (XRD) with five Ca samples (Rigaku Miniflex X-Ray Diffractometer), Fourier-transform IR spectroscopy (Nicolet 6700 FTIR; Thermo Electron Corporation) with attenuated total reflection mode (Xu et al., 2006), and imaged by JEOL Transmission Electron Microscope, JSM-2010 (**Supplementary Data Set 1**).

Loading of Bd

To define optimal and complete loading of respective Bd into Ca nanoparticles, the ratio of Bd/Ca was adjusted to 1:10. A mixture of 10 ml of Bd and 100 ml of Ca was prepared and incubated at room temperature for 30 min with continuous agitation of 120 rpm. The quantification of the residual Bd was carried out using the standard method developed by Sun et al. (2020). High-performance liquid chromatography (HPLC) system equipped with ZORBAX-Eclipse XDB-C18 column (4.6 mm × 250 mm, 5 μm, Agilent) separated the free Bd molecule aqueous mobile phase of 40% methanol flowing at the rate of 0.4 ml min^{-1}. Samples of 10 μl were separately processed at 40°C, and absorbance readings were recorded at 210 nm. The stable release of Bd was also ensured at three different incubation temperatures of 0°C, 25°C, and 50°C for a period of 60 by using a method as described earlier (**Supplementary Data Set 1**).

Treatment Application

Bd ($C_{19}H_{22}O_6$) was purchased from the RPI Research Products International, CAS # 77-06-5. The growth regulator was initially dissolved in ethanol to prepare a stock concentration of 0.5 mM L^{-1} and then diluted with distilled sterilized water to attain a concentration of 5 μM L^{-1} as a working concentration recommended by Miao et al. (2017). Similarly, the Bd_{Ca} solution was prepared to get the final working concentration of 0.5 mM L^{-1} for Bd. However, the concentration of Ca was 1 g L^{-1}. The third treatment of Ca nanoparticles was also prepared (1 g L^{-1}). Each seedling received 0.5 ml of the respective spray treatment.

To elucidate the pathway-specific uptake of DDT into the plants, the experiment was designed to expose potted *B. alboglabra* plants to DDT through the use of incubation chambers (ICs). The ICs were designed and built using glass material by strictly following the method of a previous study (Zhu et al., 2016). There were two separate entry points for air and DDT into the chamber, powered with electric pumps and connected through polytetrafluoroethylene pipes. Chambers also have an air sampling system and a temperature regulation system. A separate chamber was used for each treatment. The potting soil was covered with a 2-cm layer of silica sand (150-380 μm) to minimize the DDT exchange between the soil and the air (Zhu et al., 2020). The DDT concentration in the air was adjusted to 1,000 mg m^{-3} as derived from its minimum toxic concentration of 582.4 mg m^{-3} and kept constant throughout the incubation period (Jarrell et al., 2002). To compensate for the loss of particulate on the plant surface over time, the POP dust-spraying step was repeated weekly. Later, the conditions of ICs were adjusted at 70-76% relative humidity and 500–550 mmol m^{-2} s^{-1} light with a 16-h photoperiod. Five replications were used for each treatment. Cd treatment was applied to the plants by strictly following the method developed by Li et al. (2021). All these dose treatments were adopted based on the previous literature and the highest quantity of pollutants recorded in the environment. Furthermore, the concentration of the pollutants was kept stable in the growth chamber.

Determination of Growth, Physiological, and Antioxidant Defense Parameters

After 8 weeks of incubation, entire plants were sampled randomly. The harvested plants were separated into the root, shoot, and leaf samples. These plant parts were kept individually in distilled water for 60 s. Later, plant parts were dried on blotting paper and stored at −80°C. The plant samples were processed for the estimation of Leaf Relative Water Content (LRWC), Photosynthetic pigments (Chl *a* and Chl *b*), Soluble Sugars, Gas Exchange Parameters, net Photosynthetic Rate (*Pn*), Estimation of Cd Contents, Metal Tolerance Index (MTI), Evaluation of Hydrogen Peroxide, Lipid Peroxidation, Electrolyte Leakage (EL), Leaf Osmotic Potential, Membrane Stability Index (MSI), Estimation of Water Potential, Proline Content, β-carotenoids

Contents, and the parameters of Oxidative and Antioxidant Enzymatic Activities using the standard optimized protocols (Khan et al., 2019).

Quantification of DDT

The DDT was quantified by gas chromatography-mass spectrometry (GC-MS), as described by Baumer et al. (2020). The system consisted of GC-MS (QP) by Shimadzu (Kyoto, Japan), coupled with a mass detector and a capillary column. Detailed specifications were 30 m DB-5, 0.1 μm film thickness, and 0.25 mm internal diameter of the capillary column used for the determination of DDT. Samples were injected using a splitless injection mode while keeping an ion source temperature of 250°C and using helium as the carrier gas at 0.75 ml/min flow rate. The oven temperature was ramped at the rate of 4°C min^{-1}, initializing its range from 120°C to 190°C, and at the rate of 32°C min^{-1} up to 270°C, which was kept constant for 4 min. By operating the mass spectrometer at scanning mode between 45 and 475 Da (*m*/*z*), DDT was detected in the sample size of 50 μl with a minimum limit of 1 mg kg^{-1}.

Calculation of Mobility, Distribution, and Remediation Efficiency

The translocation factor (TF) and avoidance efficiency (AE) were used to evaluate the ability of the plants to absorb, translocate, and/or avoid pollutants, according to the following equations (Xiao et al., 2019; Zeng et al., 2019):

(1) $TF = C_{substanceshoot}/C_{substanceleaf}$

(2) $AE = (C_{substanceshoot} \times M_{shoot} \times C_{substance\ leaf} \times M_{leaf})/(C_{substanceair} \times M_{air})$

where $C_{substance\ shoot}$, $C_{substance\ leaf}$, and $C_{substance\ air}$ are the contents of DDT ($mg \cdot kg^{-1}$) in shoots, roots, and air, respectively. However, the mass of one cubic meter of air was standardized as 1.29 kg during the experimentation.

Statistical Analysis

Randomized one-way ANOVA was used for the comparisons between different treatments. Means were compared using the all pairs Tukey's honestly significant difference test. Statistical calculations of ANOVA were performed using DSAASTAT statistics software.

RESULTS

Evaluation of Bd_{Ca}

Transmission electron micrograph revealed a single crystalline Ca (44 μm) impregnated with Bd. The comparison of the three FTIR spectra (i.e., Bd, Ca, and Bd_{Ca}) had one unique dejection at 2,237 in Bd_{Ca}, which was absent in Bd and Ca, showing a stable bond between them. The XRD assay came up with the two characteristic peaks in Bd, one in Ca, and three in Bd_{Ca}, showing the sustained identity of the two impregnated substances (**Figure 1**).

Determination of Growth Attributes

The results of this study showed that Bd alone had the potential to boost the growth parameters of the plants, i.e., root fresh weight, shoot fresh weight, root dry weight, and shoot dry weight under multiple stress conditions of DDT toxicity and Cd stress. All these growth credentials were improved 1.3–1.9 times after Bd treatment. However, another interesting finding was the positive support of C toward the plant growth parameters. Growth parameters were elevated by 1.3–1.6 times due to Ca use. The growth regulator Bd allowed *Brassica* plants to overcome DDT toxicity, introducing pollutant tolerance in them. Besides, it also elevated the plant growth parameters up to 162% (**Supplementary Figure 1**). However, Ca could enhance the plant growth, up to 131%, when exposed to DDT. The maximum growth enhancement (258%) was reported in the plants exposed to Bd_{Ca}, and it could be reduced up to 221% under DDT toxicity. In contrast, the toxic effects of DDT caused a 34–49% reduction in growth attributes and leaf area of the plants as opposed to control therapy. Bd, Ca, and Bd_{Ca} were proved successful in augmenting chlorophyll contents in *Brassica* plants. However, enhancement in chlorophyll contents was recorded as 139% by Bd application, 125% by Ca procedure, and 158% by Bd_{Ca}. DDT stress plants also displayed a substantial increase of 147% in chlorophyll contents when primed with Bd_{Ca}. Cd toxicity exerts deleterious effects on *Brassica* plants, retarding 18% of growth attributes, 21% of leaf area, and 15% chlorophyll contents (**Supplementary Figure 2**).

Estimation of Leaf Relative Water Content

The findings showed the impact of Cd and DDT on LRWC (53.24 and 18.61%, respectively) relative to the *Brassica* plant. The maximum LRWC was recorded in the negative Cd control treatments. However, as opposed to the control, the Bd treatment increased the value of LRWC (46.31%). Ca application to *Brassica* plants also increased LRWC by 36.98%, while under Bd_{Ca} treatment, a 51.76% increase in LRWC was evident. The treatment with DDT reduced *Pn* to 51.37%. A significant increase in *Pn* due to Bd and Ca was found at 25.61% and 22.13%, respectively. The Bd_{Ca} application reported a maximum *Pn* increase of 40.25%. As far as the photosystem-quenching Fv/Fm is concerned, the effect of Bd-impregnated Ca treatment was significantly higher than the individual effects of Ca and Bd (28.66%). Bd_{Ca} was the most successful plant treatment that produced the greatest improvement in stomatal conductance, *Ci*, and the rate of transpiration. However, all these physiological parameters were negatively affected by the stress caused by Cd and DDT toxicity. The cell physiology of *Brassica* was positively affected by both Bd and Ca (**Figure 2**).

Determination of Photosynthetic Pigments and Soluble Sugars

The DDT toxicity substantially decreased photosynthetic pigments by up to 46.31% as compared to the control treatment. Bd induced an elevation of 1.35 times in the pigments and Ca treatment of 1.24 times. Bd_{Ca} lied in the stronger support to the

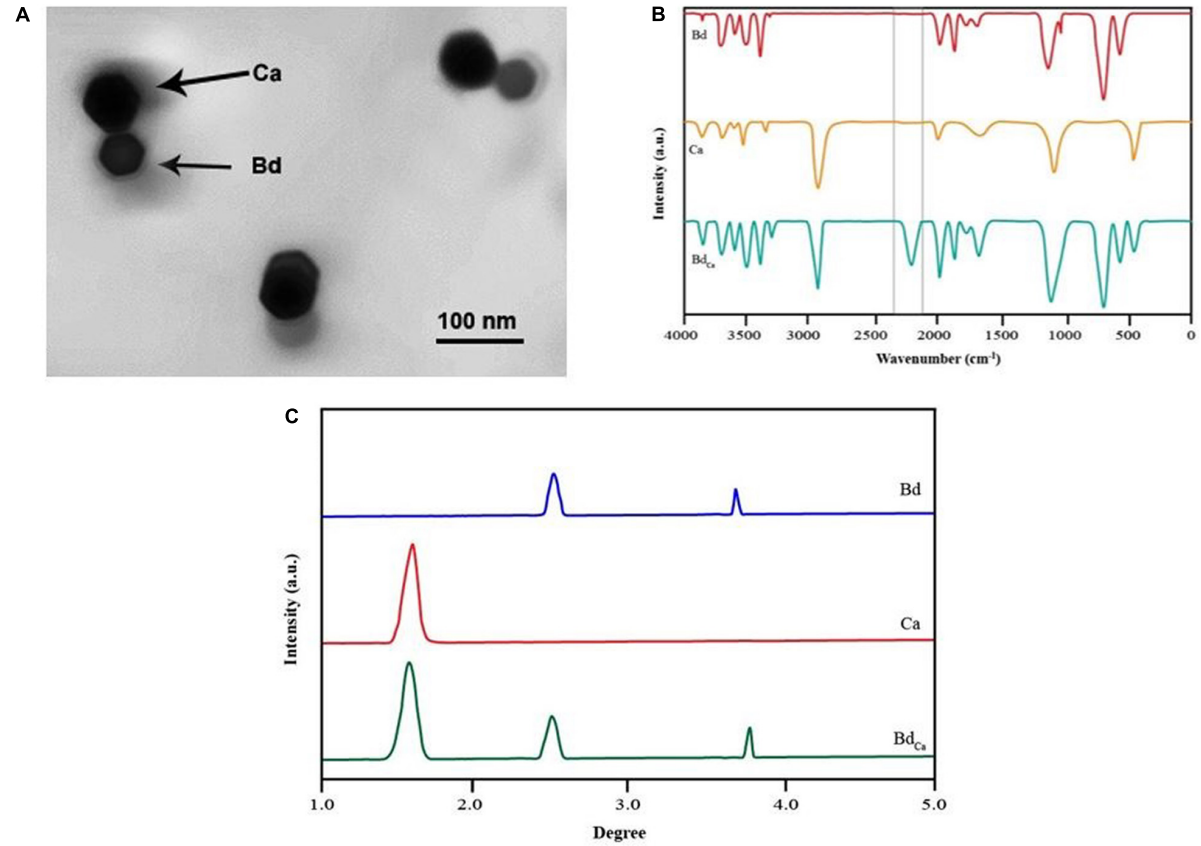


FIGURE 1 | Transmission elctron micrograph of Calcium (Cal) particles coupled with benzenedicarboxylic acid **(A)**. FTIR spectrum of benzendicarboxylic acid, calcium, and calcium impregnated with benzenedicarboxylic acid **(B)**, and X-ray diffraction pattern of benzendicarboxylic acid, calcium, and calcium impregnated with benzenedicarboxylic acid. Benzendicarboxylic acid (Bd), Calcium (Cal), and calcium impregnated with benzenedicarboxylic acid (Bd_{Cal}) **(C)**.

overall chlorophyll contents, raising it to 235.78%. A 17.92% reduction in chlorophyll in the Kale plants was caused by Cd. DDT was responsible for a substantial decrease in the soluble sugar content of 3.18 mg/g when compared to the control treatment of 5.48 mg/g. Bd (12.06 mg/g) and Ca treatment (9.92 mg/g) recorded the substantial mitigation of the soluble sugar contents. While, in the presence of DDT, Bd_{Ca} increased the soluble sugar content up to (12.38 mg/g), whereas, in the absence of toxic DDT, the contents were increased up to 14.69 mg/g. In terms of soluble sugars, Cd stress had deleterious effects on *Brassica* plants. However, Bd_{Ca} (mg/g) could successfully mitigate the detrimental effects of the plant stressors (**Table 1**).

Antioxidant Defenses

Nitrate reductase activity was significantly decreased by the toxic content of DDT and increased by the application of Bd and Ca. Bd_{Ca} resulted in the most successful mitigation, which increased the activity of the enzyme by 247.64%. The enzyme activity was adversely affected by Cd, and Bd_{Ca} significantly mitigated Cd and DDT toxicity, resulting in an increase in nitrate reductase activity of 218.39%. Similar patterns have been observed for other enzymes studied, such as catalase, POD, SOD, and carbon anhydrase. DDT toxicity and Cd variations adversely affected the activities of the enzymes. However, Bd_{Ca} effectively alleviated the hazardous effects and increased the activity of the enzymes by up to 227.36%, improving the antioxidant protection of the plant (**Figure 3**).

Electrolyte Leakage Malondialdehyde Content (MDA) and H_2O_2

The DDT toxicity and Cd stress boosted the EL. Due to DDT, an increase of 234.74% was reported in EL. However, in comparison with the control treatment, the increased EL due to Cd was significantly elevated. Under the toxic effects of DDT, malondialdehyde content (MDA) was also increased by more than two times. The H_2O_2 content was elevated by toxic DDT and Cd (223.54% and 208.36%, respectively) by strictly following the identical pattern. Successfully downregulated H_2O_2 contents by Bd and Ca treatments minimized the risk of oxidative harm to plant cells (**Figure 3**).

Enzymatic Analysis

The enzymatic content of monodehydroascorbate reductase (MDHAR), dehydroascorbate reductase (DHAR), glutathione-*S*-transferase (GST), glutathione peroxidase (GPX), glutathione reductase (GR), and APX in Kale plants was significantly

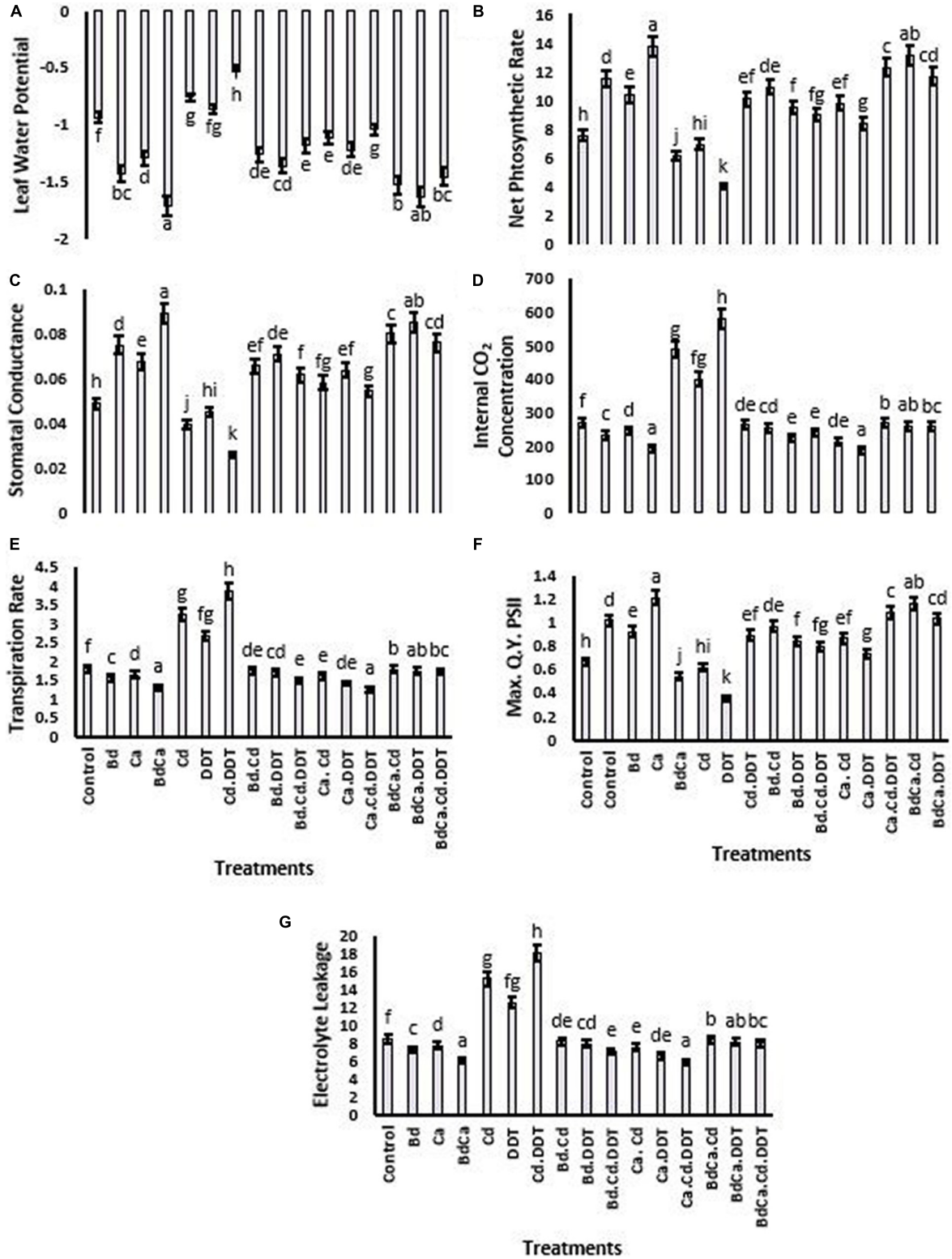


FIGURE 2 | Effect of benzenedicarboxylic acid (Bd) on photosynthesis-related parameters of *Brassica alboglabra* under toxic conditions of dichlorodiphenyltrichloroethane (DDT) and cadmium (Cd). Leaf relative water content **(A)**, net photosynthesis rate **(B)**, stomatal conductance **(C)**, internal CO_2 concentration **(D)**, transpiration rate **(E)**, maximum quality yield of PS-II **(F)**, and electrolyte leakage **(G)**. Values demonstrate means ± SD (n = 5). Different letters indicate a significant difference among the treatments ($P \leq 0.05$). Bd, benzenedicarboxylic acid; Cd, cadmium; DDT, dichlorodiphenyltrichloroethane; Bd_{Cal}, benzedicarboxylic acid doped calcium.

TABLE 1 | Effect of benzenedicarboxylic acid (Bd) and calcium nanoparticles (Ca) on chlorophyll *a*, chlorophyll *b*, total chlorophyll, and soluble sugars of *Brassica alboglabra* under Cd stress, temperature stress, and BDE-28 toxicity.

Treatments	Chl*a*	Chl*b*	Total Chlorophyll	Soluble Sugars (mg g^{-1})
Control	0.95 ± 0.05*i*	0.52 ± 0.08*h*	1.48 ± 0.16*i*	5.48 ± 0.19*h*
Bd	1.45 ± 0.04*c*	0.80 ± 0.04*b*	2.26 ± 0.48*bc*	12.06 ± 0.24*bc*
Ca	1.31 ± 0.05*e*	0.72 ± 0.03*d*	2.04 ± 0.029*e*	9.92 ± 0.11*d*
Bd_{Ca}	1.73 ± 0.03*a*	0.95 ± 0.01*a*	2.69 ± 0.36*a*	14.69 ± 0.19*a*
Cd	0.77 ± 0.04*kl*	0.42 ± 0.064*jk*	1.20 ± 0.54*kl*	2.79 ± 0.32*jk*
DDT	0.87 ± 0.03*k*	0.48 ± 0.04*j*	1.36 ± 0.049*k*	3.18 ± 0.41*j*
Cd.DDT	1.50 ± 0.02*l*	1.28 ± 0.04*k*	1.78 ± 0.075*l*	3.41 ± 0.17*l*
Bd.Cd	1.27 ± 0.04*e*	0.70 ± 0.03*de*	1.98 ± 0.067*e*	9.37 ± 0.18*de*
Bd.DDT	1.38 ± 0.06*ef*	0.75 ± 0.01*de*	2.15 ± 0.052*ef*	9.75 ± 0.21*de*
Bd.Cd.DDT	1.20 ± 0.03*h*	0.66 ± 0.07*fg*	1.86 ± 0.047*h*	7.07 ± 0.17*fg*
Ca. Cd	1.13 ± 0.04*g*	0.62 ± 0.06*fg*	1.76 ± 0.036*g*	7.23 ± 0.17*fg*
Ca.DDT	1.24 ± 0.03*gh*	0.68 ± 0.04*f*	1.92 ± 0.075*gh*	7.62 ± 0.16*f*
Ca.Cd.DDT	1.05 ± 0.05*ij*	0.58 ± 0.06*hi*	1.64 ± 0.15*ij*	4.93 ± 0.18*hi*
Bd_{Ca}.Cd	1.55 ± 0.08*b*	0.85 ± 0.07*bc*	2.41 ± 0.094*b*	12.00 ± 0.14*bc*
Bd_{Ca} DDT	1.65 ± 0.04*bc*	0.90 ± 0.03*b*	2.58 ± 0.042*bc*	12.38 ± 0.24*b*
Bd_{Ca}.Cd.DDT	1.47 ± 0.07*d*	0.81 ± 0.04*de*	2.29 ± 0.075*d*	9.70 ± 0.19*de*

Values demonstrate means ± SD (n = 5). Different letters indicate significant difference among the treatments (P ≤ 0.05). C, control; Cd,Cadmium; Ca, Calcium.

increased. The enzyme activities were also improved by Ca treatment alone, but the level of upregulation was significantly lower than that of Bd. The amounts of all these enzymes shared a common pattern of elevation after exposure to Ca and Bd. Whereas significant reductions in the enzyme activities were observed after their exposure to the plant stressors, i.e., Cd and DDT. The mitigating function of Bd_{Ca}, however, was dominant, and it mitigated all the stress effects of Cd and DDT on *B. alboglabra* (**Table 2**).

Proline, Lycopene, β-Carotene, and Lutein Contents

Proline contents showed significant retardation in the plants treated with DDT (43.71%). However, a positive effect of Bd was recorded on the proline, resulting in a significant elevation of 46.18% in its contents as compared to the control treatment. The positive results of Bd on proline contents were also comparable with the positive results of Ca. Cd toxicity negatively affected lycopene, β-carotene, and lutein. Cd and DDT jointly abridged the proline contents more severely. However, all these biochemicals were substantially improved by the three treatments, namely, Bd, Ca, and Bd_{Ca} (**Figure 4**).

Water Potential, Leaf Osmotic Potential, and MSI

Exogenously applied Bd caused the leaf water potential of Kale plants to increase by 153.620%. Kale plants are grown in a toxic DDT environment, which, however, had an 8.69% lower potential for leaf water. Similarly, Cd application negatively impacted the leaf water potential and caused a significant reduction, whereas Ca and Bd_{Ca} treatments have demonstrated significant improvements in leaf water potential. The treatments also mitigated the Cd and DDT toxicity effectively. The leaf osmotic potential and MSI were also found following a similar pattern. The stress effects of Cd and DDT toxicity were successfully mitigated by Bd_{Ca}, which was the best treatment used in the assays (**Table 3**).

Cd Contents

The Cd contents were recorded the highest in root tissues of the plants (22.21 μg/g), which were reduced to 20.41 μg/g in the shoots, 19.89 μg/g in the leaves, and ultimately 19.35 μg/g in the seeds when Kale plants were exposed to Cd. The TF value of Cd was 633.60, and MTI of Kale against Cd was 7.87, with a removal efficacy (RE) value of 13.09. DDT put the stress effects on Kale plants, significantly increasing the Cd contents in the plant tissues, elevated TF, decreased MTI, and reduced RE. The best performing treatment Bd_{Ca} showed reduced Cd content of 11.72 μg/g in the plant roots, 10.77 μg/g in shoots, 10.50 μg/g in leaves, and 10.21 μg/g in seeds under the influence of two stressors, namely, Cd and DDT. The treatment also showed a TF value of 334.40, an MTI value of 15.05, and an RE value of 71.61 (**Table 3**).

DDT Contents, TF, and Pollutant Tolerance Index

The DDT accumulation was higher in roots (8.39 μg/g) compared to shoots (5.59 μg/g), leaves (3.71 μg/g), and seeds (1.69 μg/g) under the DDT control treatment during the study. Meanwhile, the TF value was 182.04, along with the MTI value of 16.87 and the RE value of 173.28. Cd played the role of an enhancer for DDT accumulations (elevating DDT bioconcentration) in both plant tissues and seeds (2.44 μg/g). Both the Ca and Bd mitigated the stress caused by DDT and Cd and lowered down the DDT contents in plant tissues. The Cd application assisted the stress effects of DDT and caused a significant increase in its bioaccumulation in plant tissues. After the application of Bd, the DDT contents were recorded 5.33 μg/g

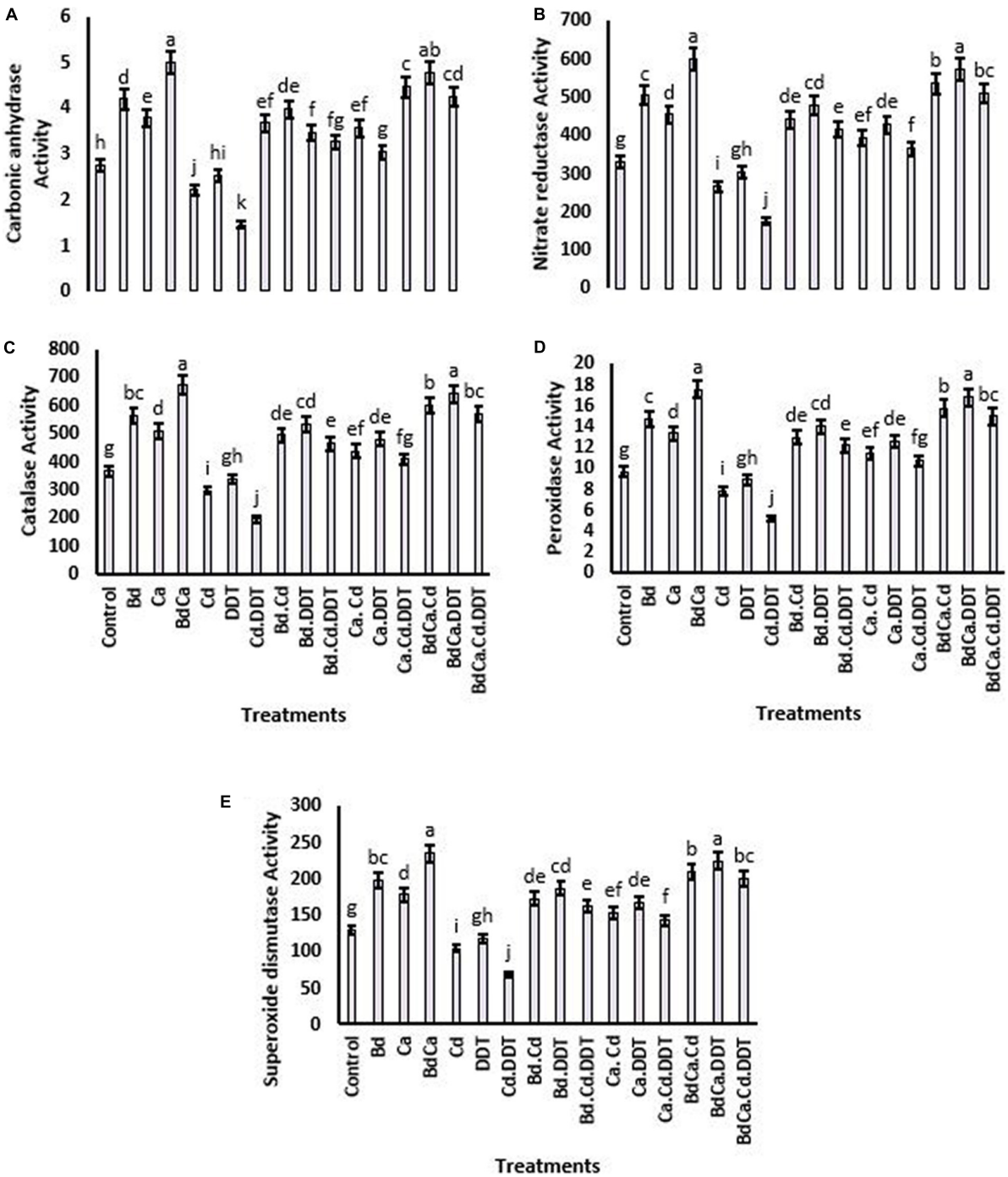


FIGURE 3 | Effect of benzenedicarboxylic acid (Bd) on antioxidant defense parameters of *Brassica alboglabra* under under toxic environment of dichlorodiphenyltrichloroethane (DDT) and cadmium (Cd). Carbonic anhydrase **(A)**, nitrate reductase activity **(B)**, catalase activity **(C)**, peroxidase activity **(D)**, and superoxide dismutase activity **(E)**. Values demonstrate means ± SD ($n = 5$). Different letters indicate a significant difference among the treatments ($P \leq 0.05$). Bd, benzenedicarboxylic acid; Cd, cadmium; DDT, dichlorodiphenyltrichloroethane; Bd_{Cal}, benzedicarboxylic acid doped calcium.

in roots, 3.55 μg/g in shoots, 2.36 μg/g in leaves, and 1.07 μg/g in seeds of the Kale plants. It could reduce the TF value up to 115.62, whereas it improved the MTI value up to 26.59 and the RE value up to 584.82. The most promising treatment was Bd_{Ca} that did not allow DDT contents to exceed 5.39 μg/g in the roots, 3.59 μg/g in the shoots, 2.38 μg/g in the leaves, and 1.08 μg/g in the seeds of the Kale plants. It recorded a TF value of 116.85 with improved MTI and RE values (**Table 4**). The overall observation

TABLE 2 | Effect of benzenedicarboxylic acid (Bd) and calcium nanoparticles (Ca) on dehydroascorbate reductase (DHAR), monodehydroascorbate reductase (MDHAR), glutathione-s-transferase (GST), glutathione reductase (GR), glutathione peroxidase (GPX), and ascorbate peroxidase (APX), in *Brassica alboglabra* under Cd stress, temperature stress, and BDE-28 toxicity.

Treatments	DHAR (nmol min^{-1} mg^{-1} protein)	MDHAR (nmol min^{-1} mg^{-1} protein)	GST (nmol g^{-1} FW)	GR (EU mg^{-1} protein)	GPX (μmol g^{-1} FW)	APX (EU mg^{-1} protein)
Control	103.00 ± 3.9*h*	54.20 ± 2.47*h*	37.10 ± 1.25*h*	3.98 ± 0.12*h*	53.14 ± 1.34*f*	2.21 ± 0.08*f*
Bd	157.59 ± 7.1*c*	82.93 ± 3.44*bc*	56.76 ± 1.27*bc*	6.09 ± 1.01*d*	81.30 ± 2.91*c*	3.38 ± 0.15*bc*
Ca	142.14 ± 5.61*d*	74.80 ± 2.1*d*	51.20 ± 1.87*d*	5.49 ± 0.13*e*	73.33 ± 1.75*d*	3.05 ± 0.05*d*
Bd_{Ca}	187.46 ± 2.8*a*	98.64 ± 1.11*a*	67.52 ± 1.9*a*	7.24 ± 0.03*a*	96.71 ± 0.99*a*	4.02 ± 0.02*a*
Cd	83.43 ± 3.67*jk*	43.90 ± 2.21*jk*	30.05 ± 0.81*jk*	3.22 ± 0.34*j*	43.04 ± 2.23*g*	1.79 ± 0.07*g*
DDT	94.76 ± 7.14*j*	49.86 ± 2.21*j*	34.13 ± 1.17*j*	3.66 ± 0.41*hi*	48.89 ± 1.43*fg*	2.03 ± 0.05*fg*
Cd.DDT	55.59 ± 3.1*k*	29.73 ± 1.14*k*	19.66 ± 0.99*k*	2.11 ± 0.05*k*	28.16 ± 0.64*h*	1.17 ± 0.08*h*
Bd.Cd	138.02 ± 8.62*de*	72.63 ± 2.32*de*	49.71 ± 1.14*de*	5.33 ± 0.28*ef*	71.21 ± 1.28*de*	2.96 ± 0.11*de*
Bd.DDT	149.35 ± 6.61*de*	78.59 ± 2.41*de*	53.80 ± 1.53*de*	5.77 ± 0.32*de*	77.05 ± 2.15*cd*	3.20 ± 0.08*cd*
Bd.Cd.DDT	129.78 ± 5.34*fg*	68.29 ± 2.14*fg*	46.75 ± 2.19*fg*	5.01 ± 0.31*f*	66.96 ± 3.17*e*	2.78 ± 0.06*e*
Ca. Cd	122.57 ± 4.74*fg*	64.50 ± 2.71*fg*	44.15 ± 1.22*fg*	4.74 ± 0.37*fg*	63.24 ± 1.98*e*	2.63 ± 0.09*e*
Ca.DDT	133.90 ± 3.67*f*	70.46 ± 1.34*f*	48.23 ± 1.77*f*	5.17 ± 0.61*ef*	69.08 ± 3.75*de*	2.87 ± 0.05*de*
Ca.Cd.DDT	114.33 ± 3.67*hi*	60.16 ± 3.11*hi*	41.18 ± 2.07*hi*	4.42 ± 1.01*g*	58.99 ± 1.63*a*	2.45 ± 0.09*g*
Bd_{Ca}.Cd	167.89 ± 3.67*b*	88.35 ± 2.49*bc*	60.47 ± 1.33*b*	6.49 ± 0.11*c*	86.62 ± 0.64*b*	3.60 ± 0.07*b*
Bd_{Ca} DDT	179.22 ± 3.67*c*	94.31 ± 2.42*b*	64.55 ± 2.16*bc*	6.93 ± 0.03*ab*	92.46 ± 1.38*ab*	3.85 ± 0.07*ab*
Bd_{Ca}.Cd.DDT	159.65 ± 3.67*de*	84.01 ± 2.21*de*	57.51 ± 2.84*de*	6.17 ± 0.34*cd*	82.40 ± 2.41*bc*	3.43 ± 0.06*bc*

Values demonstrate means ± SD (n = 5). Different letters indicate significant difference among the treatments (P ≤ 0.05). C, control; Cd, Cadmium; Ca, Calcium.

of the experiments was summarized in a schematic diagram to understand the positive effects of Bd_{Ca} and the mechanistic aspects behind them (**Figure 5**).

DISCUSSION

For the first time, the current investigation sets out a method for the sustainable exogenous delivery of Bd to a plant surface after Ca impregnation. Bd is a fungal metabolite primarily known for its role in the augmentation of cell defenses against pathogenic fungi (Ahmad et al., 2014a,b, 2019). The reaction of the plant to Bd is purely dose- and duration-dependent. The early studies reported that this compound improved the nutritional profiles of tomato fruits. However, with the high water solubility, it cannot be applied to plant surfaces in rainy and humid environments. To ensure the sustained availability of Bd at plant surfaces, a formulation development is necessary. This study remains an outstanding approach in the field of plant protection and cell physiology. In addition, Bd has a tendency to change the physiological processes and genetic controls of plants (Khan et al., 2019; Ahmad et al., 2020a).

Stress factors (e.g., DDT) induce metabolic imbalances and encourage EL and oxidative stress, contributing to the accumulation of solutes in the form of adaptive cellular responses (Jan et al., 2012; Shafique et al., 2014). This lays the basis for the increased coefficient of bioconcentration of DDT in various *Brassica* plant tissues. In addition, the analysis first defines the TF of DDT in Kale plants, elaborating the fate of the pollutant absorbed into the edible plant (Rignell-Hydbom et al., 2007; Khan et al., 2017). Bd is involved in initializing the expression of the genetic cascade associated with starch and sugar, which essentially determines the energy economy of the plant. This property of Bd has been used during stress conditions to harmonize the physiological balances. In addition, the scientific research investigated the mitigation actions of Ca and Bd through the reharmonization of stress markers, such as EL, LRWC, gaseous exchange, antioxidant defenses, and the activities of enzymes. The primary tools of environmental toxicants to slow plant growth and metabolism are EL, *Ci*, reduced *Pn*, and leaf water potential. Cd toxicity also exerts similar stress symptoms on the physiology of plants (Faiz et al., 2021). The study recommends Bd_{Ca}, which has the potential to rehabilitate cellular homeostasis, as an effective plant metabolism modulator. It was evident that Bd_{Ca} increased the photosynthetic pigments (Chl *a* and Chl *b*), *Pn*, and total soluble sugars, which demonstrated the full-swing rehabilitation of Kale photosynthetic function, which was reduced by Cd and DDT. During the current investigation, increased chlorophyll biosynthesis subsequently increased the photosynthetic activity and augmented development in Bd_{Ca}-applied plants.

The least objective of a plant is to ensure its survival through the devastating period of stress, and the least objective of a farmer is to get enough yield to cover the cultivation costs (Yasin et al., 2018b). Both of these objectives can be achieved by improving plant tolerance against stressors (Zaheer et al., 2016). Therefore, this study considered the tolerance index against both the pollutant DDT and the metal Cd. Both the stress mitigators (i.e., Ca, Bd) and their combined form (Bd_{Ca}) successfully achieved phoenix tolerance indices DDT and Cd. Removing the pollutants and heavy metals is the safest method for remediating environmental toxins and safeguarding the food chain for consumers, including humans (Shah et al., 2020). It also makes the toxins and pollutants to be exposed to environmental deteriorations for natural degradation (Liu et al., 2013; Abbas et al., 2020). This study introduced a unique technique based on

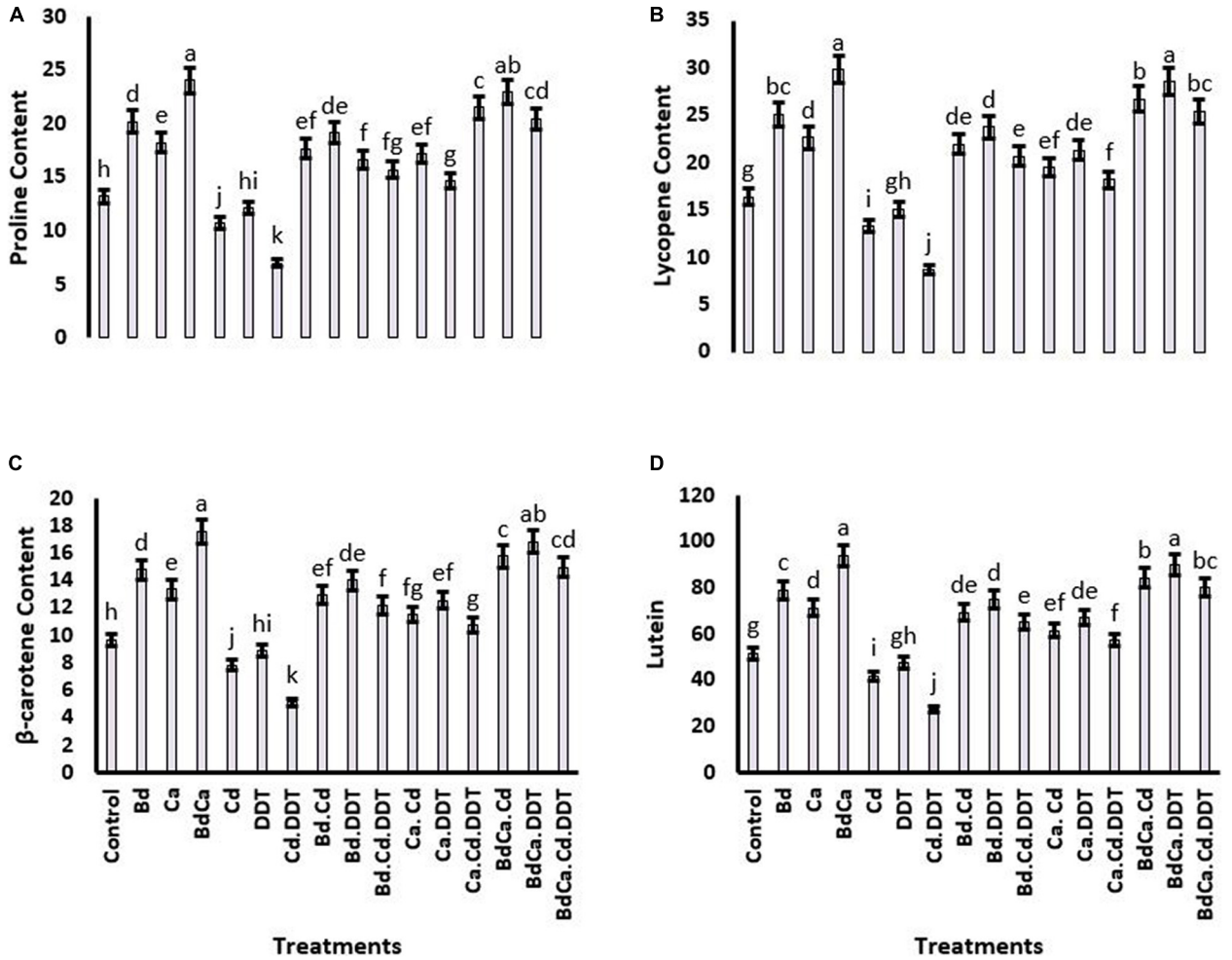


FIGURE 4 | Effect of benzenedicarboxylic acid (Bd) on physiological parameters of *Brassica alboglabra* under under toxic environment of dichlorodiphenyltrichloroethane (DDT) and cadmium (Cd). Proline content **(A)**, lycopene content **(B)**, β-carotene content **(C)**, and lutein content **(D)**. Values demonstrate means ± SD ($n = 5$). Different letters indicate a significant difference among the treatments ($P \leq 0.05$). Bd, benzenedicarboxylic acid; Cd, cadmium; DDT, dichlorodiphenyltrichloroethane; Bd_{Cal}, benzedicarboxylic acid doped calcium.

Bd-impregnated Ca, which successfully hampered the entry of DDT into the food chain, which would certainly be detoxified overtime under natural degradation.

In addition, the single and combined effect of Ca and Bd resulted in beneficial physiochemical changes in plant cells. A few studies have previously used Ca for topical delivery of RNAi to make plants immune to pathogens (Mitter et al., 2017). Even, there was no ultimate conclusion about how the application of nanoparticles will respond to plant growth. This study highlighted the supporting role of Ca nanoparticles in plant growth for the first time. All the tested growth parameters of the Kale plants were in favor of the technique. It also elevated the enzyme activities responsible for antioxidant defenses, metabolic processes, and other physiological responses without a negative effect on plant growth. The study showed that Ca had an enormous potential to be used under stress conditions as a plant growth enhancer. A beneficial aspect of Ca explored in this study is getting no adverse cross talk with Bd.

The importance of LRWC serves as a biomarker of plant-water relationships (Wang et al., 2019; Ahmad et al., 2021a). There are detrimental effects of Cd stress on both osmotic ability and water (Khan et al., 2018; Hafeez et al., 2020). The LRWC values of *Brassica* plants were also negatively impacted by Cd, suggesting decreased drought tolerance. All the three treatments, namely, Ca, Bd, and Bd_{Ca}, greatly improved LRWC during the current investigation, proving a good option for high precipitation areas and areas adversely affected by Cd contamination. Lipid peroxidation-induced membranous injuries deteriorate cell metabolic processes and serve as a biomarker of cellular injuries in stressed plants. Similarly, the increased amount of ROS triggers the necrosis of cells in stressed plants (Arshad et al., 2016; Tariq et al., 2021). However, under stress, Ca and Bd-applied plants showed a decreased synthesis

TABLE 3 | Effect of benzenedicarboxylic acid (Bd) and calcium nanoparticles (Ca) on water potential, leaf osmotic potential, membrane stability index (MSI), root and shoot Cd uptake, translocation factor (TF) of Cd and metal tolerance index (MTI) of Cd in *Brassica alboglabra* under Cd stress, temperature stress, and BDE-28 toxicity.

Treatments	Water potential	Leaf osmotic potential	MSI	Root Cd ($\mu g\ g^{-1}$)	Shoot Cd ($\mu g\ g^{-1}$)	Leaf Cd ($\mu g\ g^{-1}$)	Seed Cd ($\mu g\ g^{-1}$)	TF_{Cd}	MTI	RE_{Cd} (%)
Control	0.69 ± 0.04*h*	0.860 ± 0.04*h*	0.93 ± 0.03*f*	–	–	–	–	–	–	–
Bd	1.06 ± 0.19*d*	1.316 ± 0.03*d*	1.42 ± 0.04*c*	–	–	–	–	–	–	–
Ca	0.95 ± 0.03*e*	1.187 ± 0.02*e*	1.28 ± 0.01*d*	–	–	–	–	–	–	–
Bd_{Ca}	1.26 ± 0.1*a*	1.565 ± 0.04*a*	1.69 ± 0.01*a*	–	–	–	–	–	–	–
Cd	0.56 ± 0.03*j*	0.697 ± 0.01*j*	0.75 ± 0.01*g*	22.21 ± 0.15*b*	20.41 ± 0.03*b*	19.89 ± 0.15*b*	19.35 ± 0.03*b*	633.60 ± 5.01*b*	7.87 ± 3.5*b*	13.09 ± 0.08*b*
DDT	0.63 ± 0.04*hi*	0.791 ± 0.07*hi*	0.86 ± 0.04*fg*	–	–	–	–	–	–	–
Cd.DDT	0.37 ± 0.03*k*	0.456 ± 0.03*k*	0.49 ± 0.02*h*	26.41 ± 0.21*a*	24.27 ± 0.2*a*	23.65 ± 0.21*a*	23.01 ± 0.2*a*	753.28 ± 8.04*a*	5.15 ± 3.1*a*	8.085 ± 0.51*a*
Bd.Cd	0.92 ± 0.03*ef*	1.152 ± 0.04*ef*	1.25 ± 0.03*de*	11.97 ± 0.1*cd*	11.00 ± 0.1*cd*	10.72 ± 0.1*cd*	10.43 ± 0.1*cd*	341.44 ± 0.01*cd*	13.01 ± 6.9*cd*	67.76 ± 1.24*cd*
Bd.DDT	1.00 ± 0.03*de*	1.247 ± 0.03*de*	1.35 ± 0.02*cd*	–	–	–	–	–	–	–
Bd.Cd.DDT	0.87 ± 0.04*f*	1.084 ± 0.03*f*	1.17 ± 0.01*e*	10.24 ± 0.48*de*	9.41 ± 0.01*d*	9.17 ± 0.48*de*	8.92 ± 0.01*de*	292.16 ± 0.03*d*	12.23 ± 5.8*de*	49.28 ± 1.33*d*
Ca. Cd	0.82 ± 0.02*fg*	1.023 ± 0.01*fg*	1.11 ± 0.02*e*	10.98 ± 0.38*d*	10.09 ± 0.02*cd*	9.83 ± 0.38*d*	9.57 ± 0.02*d*	313.28 ± 0.01*cd*	11.55 ± 3.7*d*	55.055 ± 2.02*cd*
Ca.DDT	0.90 ± 0.04*ef*	1.118 ± 0.02*ef*	1.21 ± 0.01*de*	–	–	–	–	–	–	–
Ca.Cd.DDT	0.77 ± 0.04*g*	0.955 ± 0.02*g*	1.03 ± 0.01*a*	8.51 ± 0.19*f*	7.82 ± 0.01*e*	7.62 ± 0.19*f*	7.42 ± 0.21*f*	242.88 ± 0.01*e*	10.78 ± 6.1*f*	36.575 ± 1.14*e*
Bd_{Ca}.Cd	1.12 ± 0.03*c*	1.402 ± 0.02*c*	1.52 ± 0.01*b*	12.22 ± 0.38*c*	11.23 ± 0.21*c*	10.94 ± 0.38*c*	10.64 ± 0.03*c*	348.48 ± 0.03*c*	15.83 ± 2.96*c*	90.09 ± 2.35*c*
Bd_{Ca} DDT	1.20 ± 0.03*ab*	1.496 ± 0.01*ab*	1.62 ± 0.02*ab*	–	–	–	–	–	–	–
Bd_{Ca}.Cd.DDT	1.07 ± 0.03*cd*	1.333 ± 0.03*cd*	1.44 ± 0.02*bc*	11.72 ± 0.4*cd*	10.77 ± 0.03*cd*	10.50 ± 0.4*cd*	10.21 ± 0.01*cd*	334.40 ± 0.03*cd*	15.05 ± 6.3*cd*	71.61 ± 3.14*cd*

Values demonstrate means ± SD (n = 5). Different letters indicate significant difference among the treatments ($P \leq 0.05$). C, control; Cd, Cadmium; Ca, Calcium.

of ROS (H_2O_2). Furthermore, the amount of MDA, which is the final by-product of lipid peroxidation, was decreased by Bd_{Ca} supplementation. Similarly, oxidative damage to cells and lipid membranes is triggered by a higher H_2O_2 level in stressed plants (Farooq et al., 2013; Sattar et al., 2020). The EL caused by the weakened cell membrane decreases the development of plant growth and biomass. Several studies have shown that the upregulated antioxidant machinery activity decreases the synthesis of H_2O_2 in stressed plants (Farooq et al., 2013; Sattar et al., 2020; Ahmad et al., 2021b). Superoxide is detoxified by the action of SOD into a less injurious H_2O_2, which is eventually transformed by the activity of POD, catalse (CAT), and APX into H_2O. By improving the function of the antioxidative system in stressed plants, the exogenous application of Bd_{Ca} improved stress tolerance. In addition to the decreased level of EL, H_2O_2, and MDA, the upregulation in antioxidant machinery has highlighted the favorable role of Bd_{Ca} in reducing oxidative injuries and controlling redox homeostasis in stressed plants.

The SOD is known as one of the key antioxidant defenses of plant cells, which is essential for survival under the conditions of stress (Askary et al., 2017). While SOD and CAT are primarily localized in the plant cell peroxisomes and mitochondria, they have shown a significant response to stress conditions (Shereefa and Kumaraswamy, 2016). The stress responses in Kale plants, however, were mitigated by Bd_{Ca} treatment. A comprehensive interrelation between the enzyme activities of Bd, Ca, Bd_{Ca}, ROS, MDA, and antioxidants is given in the current investigation. It can be inferred that all three treatments (i.e., Bd, Ca, and Bd_{Ca}) have improved plant defenses against Cd stress and DDT toxicity by considering the overall physiological responses of the plant. However, in this respect, the most promising formulation was Bd_{Ca}. The scavenging of H_2O_2 was a primary feature of Kale plants thriving under stress conditions in the plant cells. The key source of ROS is H_2O_2, and one of the most important substrates for scavenging H_2O_2 is ascorbate (Ibrahim et al., 2016; Nahar et al., 2017). The greater biosynthesis of ROS than that which is scavenged (by the antioxidant system) contributes to irreversible oxidative damages to the plant cells. The non-enzymatic antioxidant protection mechanism contains ascorbate, glutathione, and carotenoids. However, the main components of the enzymatic antioxidant mechanism are GST, GR, GPX, DHAR, MDHAR, APX, SOD, and CAT. A dual role to improve the oxidative defense mechanism of Kale plants has been performed by Bd_{Ca}. It raised the activity of antioxidants to further increase the protective layers of plants against oxidative damages.

Researchers have long been involved in increasing the proline and carotenoid content of edible plants (i.e., β-carotene, lycopene, and lutein). The pigmented elements of plants that contribute to the photosynthetic machinery and perform a defensive role against photodamage are carotenoids (Tan and Norhaizan, 2019). Foods rich in carotenoids defend humans against age-related illnesses. Lycopene is a major carotenoid of Kale plants with a distinctive red color and unique antioxidant properties. Proline is a primary component of the machinery for protein biosynthesis that determines the cell structure, metabolism, profile of nutrition, wound healing, antioxidant reactions, and responses to protection (Wu et al., 2011;

TABLE 4 | Effect of benzenedicarboxylic acid (Bd) and calcium nanoparticles (Ca) on water potential, leaf osmotic potential, membrane stability index (MSI), root and shoot Cd uptake, translocation factor (TF) of Cd and pollutant tolerance index (PTI) of Cd in *Brassica alboglabra* under Cd stress, temperature stress, and BDE-28 toxicity.

Treatments	Root DDT ($\mu g\ g^{-1}$)	Shoot DDT ($\mu g\ g^{-1}$)	Leaf DDT ($\mu g\ g^{-1}$)	Seed DDT ($\mu g\ g^{-1}$)	TF_{DDT}	PTI	RE_{DDT} (%)
Control	–	–	–	–	–	–	–
Bd	–	–	–	–	–	–	–
Ca	–	–	–	–	–	–	–
Bd_{Ca}	–	–	–	–	–	–	–
Cd	–	–	–	–	–	–	–
DDT	8.39 ± 0.19*b*	5.59 ± 0.1*b*	3.71 ± 0.15*b*	1.69 ± 0.02*b*	182.04 ± 4.47*b*	16.87 ± 6.9*g*	173.28 ± 3.56*g*
Cd.DDT	12.13 ± 0.21*a*	8.09 ± 0.2*a*	5.37 ± 0.21*a*	2.44 ± 0.2*a*	263.22 ± 7.63*a*	9.72 ± 3.1*h*	75.81 ± 4.37*h*
Bd.Cd	–	–	–	–	–	–	–
Bd.DDT	5.33 ± 0.43*cd*	3.55 ± 0.01*cd*	2.36 ± 0.4*cd*	1.07 ± 0.01*cd*	115.62 ± 3.17*cd*	26.59 ± 6.3*c*	584.82 ± 4.74*c*
Bd.Cd.DDT	4.71 ± 0.48*d*	3.14 ± 0.01*d*	2.08 ± 0.48*cd*	0.95 ± 0.01*cd*	102.09 ± 4.03*d*	23.11 ± 5.8*de*	462.08 ± 5.31*de*
Ca. Cd	–	–	–	–	–	–	–
Ca.DDT	4.42 ± 0.38*de*	2.95 ± 0.03*de*	1.96 ± 0.38*d*	0.89 ± 0.03*d*	95.94 ± 2.13*de*	23.84 ± 6.1*d*	465.69 ± 9.11*d*
Ca.Cd.DDT	3.91 ± 0.1*e*	2.61 ± 0.21*e*	1.73 ± 0.38*de*	0.79 ± 0.21*de*	84.87 ± 1.17*e*	20.36 ± 3.5*f*	342.95 ± 8.06*f*
Bd_{Ca}.Cd	–	–	–	–	–	–	–
Bd_{Ca} DDT	5.44 ± 0.15*c*	3.63 ± 0.03*c*	2.41 ± 0.1*c*	1.09 ± 0.03*c*	118.08 ± 1.98*c*	31.91 ± 2.96*a*	794.2 ± 5.73*a*
Bd_{Ca}.Cd.DDT	5.39 ± 0.38*cd*	3.59 ± 0.02*cd*	2.38 ± 0.19*cd*	1.08 ± 0.1*cd*	116.85 ± 2.44*cd*	28.43 ± 3.7*b*	671.46 ± 4.24*b*

Values demonstrate means ± SD (n = 5). Different letters indicate significant difference among the treatments (P ≤ 0.05). C, control; Cd, Cadmium; Ca, Calcium.

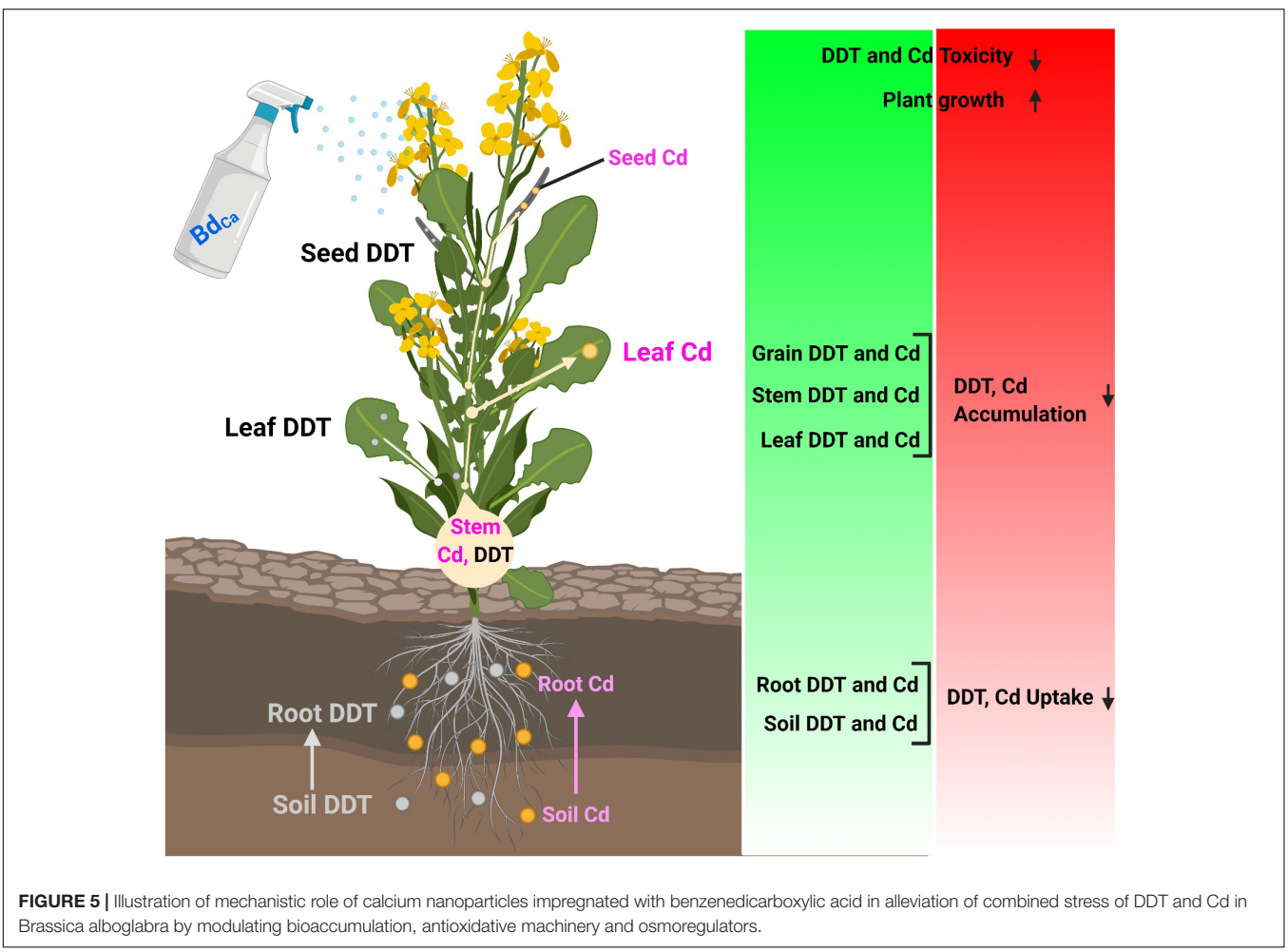


FIGURE 5 | Illustration of mechanistic role of calcium nanoparticles impregnated with benzenedicarboxylic acid in alleviation of combined stress of DDT and Cd in Brassica alboglabra by modulating bioaccumulation, antioxidative machinery and osmoregulators.

Shaddad et al., 2013). Proline has a pivotal role in the stability of the arrangement of macromolecules and the turgidity of the structure of the cell membrane in stressed plants. Proline scavenges ROS in plants and attenuates tension. Bd_{Ca} successfully increased the proline and carotenoid contents in Kale plants under various stress conditions during this study. It hardened the plants and made them tolerate DDT toxicity and Cd stress. The increased concentration of DDT in plant roots growing in a toxic DDT environment is because vacuole and root cell wall can accumulate and retain higher POP contents compared to the shoot cells. Due to modified homeostasis, the exogenous application of Bd_{Ca} decreased the DDT content in plants. Furthermore, all the advantages of reducing the content of DDT in Kale leaves and Kale seeds are the achievements of the study. Reducing the toxins and contaminants in the seeds of the Kale plants will be of much assistance to prevent humans from DDT. Given the essence of transfer, persistence, bioaccumulation, and lethal effects of DDT, the treatment of Bd_{Ca} achieved a hallmark of preventing the entry into the human food chain. In addition, the application of Bd_{Ca} decreased the bioaccumulation of the Kale roots, hampering the transfer of DDT from soil to food at the first level. The analysis can be established to look for the bioconcentration activity of POPs in other food plants.

This study discloses a novel strategy to grow healthier food crops in a contaminated environment. The large-scale production and application of Bd_{Ca} can mitigate chemical stress and heavy metal stress, and *Brassica* produces more crop yields with the least accumulation of POPs. It can be a very beneficial technique of crop cultivation in the contaminated soil and air. However, some detailed studies are required to verify the effects of Bd_{Ca} on some other crop plants.

CONCLUSION

It can be concluded that the growth and physiological attributes of Kale were successfully improved by Ca- and Bd-dependent Bd_{Ca} under various stress conditions caused by Cd and DDT pollution. By reducing the biosynthesis of ROS, enhancing the antioxidative mechanism, and modulating the synthesis of osmoregulators, the exogenously applied Bd_{Ca} increased plant resistance to the combined abiotic stressors. In addition, Bd_{Ca} inhibited the absorption of DDT in plant tissues and decreased its TF. Therefore, the novel treatment of Bd_{Ca} is recommended for relieving multiple stresses and for a stainable crop production system. However, further field experiments are compulsory to evaluate the efficacy of Bd_{Ca} in Kale plants and other crop plants.

DATA AVAILABILITY STATEMENT

The original contributions presented in the study are included in the article/**Supplementary Material**, further inquiries can be directed to the corresponding author/s.

AUTHOR CONTRIBUTIONS

SM and IS: perform experiments. AA and WA: design research. IS: perform WS statistical analysis. NY: writing. AS: review and drafting. MS and SA: writing and funding acquisition. All authors contributed to the article and approved the submitted version.

ACKNOWLEDGMENTS

The authors would like to extend their sincere appreciation to the Researchers Supporting Project Number (RSP-2021/194), King Saud University, Riyadh, Saudi Arabia.

SUPPLEMENTARY MATERIAL

The Supplementary Material for this article can be found online at: https://www.frontiersin.org/articles/10.3389/fpls.2022.825829/full#supplementary-material

REFERENCES

Abbas, H. M. K., Huang, H.-X., Wang, A.-J., Wu, T. Q., Xue, S. D., Ahmad, A., et al. (2020). Metabolic and transcriptomic analysis of two *Cucurbita moschata* germplasms throughout fruit development. *BMC Genomics* 21:365. doi: 10.1186/s12864-020-6774-y

Ahmad, A., Akram, W., Shahzadi, I., Wang, R., Hu, D., Bashir, Z., et al. (2019). Benzenedicarboxylic acid upregulates O48814 and Q9FJQ8 for improved nutritional contents of tomato and low risk of fungal attack. *J. Sci. Food Agric.* 99, 6139–6154. doi: 10.1002/jsfa.9836

Ahmad, A., Khan, T. A., Mubeen, S., Shahzadi, I., Akram, W., Saeed, T., et al. (2020a). Metabolic and proteomic perspectives of augmentation of nutritional contents and plant defense in *Vigna unguiculata*. *Biomolecules* 10:224. doi: 10.3390/biom10020224

Ahmad, A., Khan, W. U., Shah, A. A., Yasin, N. A., Naz, S., Ali, A., et al. (2020b). Synergistic effects of nitric oxide and silicon on promoting plant growth, oxidative stress tolerance and reduction of arsenic uptake in *Brassica juncea*. *Chemosphere* 2020:128384. doi: 10.1016/j.chemosphere.2020.128384

Ahmad, A., Khan, W. U., Shah, A. A., Yasin, N. A., Ali, A., Rizwan, M., et al. (2021a). Dopamine alleviates hydrocarbon stress in *Brassica oleracea* through modulation of physio-biochemical attributes and antioxidant defense systems. *Chemosphere* 270:128633. doi: 10.1016/j.chemosphere.2020.128633

Ahmad, A., Khan, W. U., Shah, A., Yasin, N. A., Naz, S., Ali, A., et al. (2021b). Synergistic effects of nitric oxide and silicon on promoting plant growth, oxidative stress tolerance and reduction of arsenic uptake in *Brassica juncea*. *Chemosphere* 262:128384. doi: 10.1016/j.chemosphere.2020.128384

Ahmad, A., Shafique, S., and Shafique, S. (2014a). Intracellular interactions involved in induced systemic resistance in tomato. *Sci. Hortic.* 176, 127–133. doi: 10.1016/j.scienta.2014.07.004

Ahmad, A., Shafique, S., and Shafique, S. (2014b). Molecular basis of antifungal resistance in tomato varieties. *Pakistan J. Agric. Sci.* 51, 683–687.

Arshad, M., Ali, S., Noman, A., Ali, Q., Rizwan, M., Farid, M., et al. (2016). Phosphorus amendment decreased cadmium (Cd) uptake and ameliorates chlorophyll contents, gas exchange attributes, antioxidants, and mineral nutrients in wheat (*Triticum aestivum* L.) under Cd stress. *Arch. Agron. Soil Sci.* 62, 533–546. doi: 10.1080/03650340.2015.1064903

Askary, M., Talebi, S. M., Amini, F., and Bangan, A. D. B. (2017). Effects of iron nanoparticles on *Mentha piperita* L. under salinity stress. *Biologija* 63:3476. doi: 10.6001/biologija.v63i1.3476

Baumer, A., Escher, B. I., Landmann, J., and Ulrich, N. (2020). Direct sample introduction GC-MS/MS for quantification of organic chemicals in mammalian

tissues and blood extracted with polymers without clean-up. *Anal. Bioanal. Chem.* 412, 7295–7305. doi: 10.1007/s00216-020-02864-6

Daryadar, M., Mairapetyan, K. H., Tovmasyan, A. H., Aleksanyan, J. S., Tadevosyan, A. H., Kalachyan, L. H., et al. (2019). Productivity of leafy green vegetable kale in soilless cultivation conditions. *J. Agric. Sci. Food Res.* 10:260. doi: 10.35248/2593-9173.19.10.260

Faiz, S., Shah, A. A., Naveed, N. H., Nijabat, A., Yasin, N. A., Batool, A. I., et al. (2021). Synergistic application of silver nanoparticles and indole acetic acid alleviate cadmium induced stress and improve growth of *Daucus carota* L. *Chemosphere* 290, 133200. doi: 10.1016/j.chemosphere.2021.133200

Farooq, M. A., Ali, S., Hameed, A., Ishaque, W., Mahmood, K., and Iqbal, Z. (2013). Alleviation of cadmium toxicity by silicon is related to elevated photosynthesis, antioxidant enzymes; suppressed cadmium uptake and oxidative stress in cotton. *Ecotoxicol. Environ. Saf.* 96, 242–249. doi: 10.1016/j.ecoenv.2013.07.006

Fletcher, S. J., Reeves, P. T., Hoang, B. T., and Mitter, N. A. (2020). Perspective on RNAi-based biopesticides. *Front. Plant Sci.* 11:51. doi: 10.3389/fpls.2020.00051

Hafeez, M., Liu, S., Yousaf, H. K., Jan, S., Wang, R.-L., Fernández-Grandon, G., et al. (2020). RNA interference-mediated knockdown of a cytochrome P450 gene enhanced the toxicity of α-cypermethrin in xanthotoxin-fed larvae of *Spodoptera exigua* (Hübner). *Pestic. Biochem. Physiol.* 162, 6–14. doi: 10.1016/J.PESTBP.2019.07.003

Ibrahim, A., Shahid, A. A., Noreen, S., and Ahmad, A. (2016). Physiological changes against meloidogyne incognita in rhizobacterial treated eggplant under organic conditions. *J. Anim. Plant Sci.* 26:196.

Jaga, K., and Dharmani, C. (2003). Global surveillance of DDT and DDE levels in human tissues. *Int. J. Occup. Med. Environ. Health* 16, 7–20.

Jan, S., Parween, T., Siddiqi, T. O., and Mahmooduzzafar (2012). Anti-oxidant modulation in response to gamma radiation induced oxidative stress in developing seedlings of *Psoralea corylifolia* L. *J. Environ. Radioact.* 113, 142–149. doi: 10.1016/j.jenvrad.2012.05.019

Jarrell, J. F., Gocmen, A., Akyol, D., and Brant, R. (2002). Hexachlorobenzene exposure and the proportion of male births in Turkey 1935-1990. *Reprod. Toxicol.* 16, 65–70. doi: 10.1016/S0890-6238(01)00196-4

Khan, T. A., Yusuf, M., Ahmad, A., Bashir, Z., Saeed, T., Fariduddin, Q., et al. (2019). Proteomic and physiological assessment of stress sensitive and tolerant variety of tomato treated with brassinosteroids and hydrogen peroxide under low-temperature stress. *Food Chem.* 289, 500–511. doi: 10.1016/j.foodchem.2019.03.029

Khan, W. U., Ahmad, S. R., Yasin, N. A., Ali, A., Ahmad, A., and Akram, W. (2017). Application of Bacillus megaterium MCR-8 improved phytoextraction and stress alleviation of nickel in *Vinca rosea*. *Int. J. Phytoremed.* 19, 813–824. doi: 10.1080/15226514.2017.1290580

Khan, W. U., Yasin, N. A., Ahmad, S. R., Ali, A., Ahmad, A., Akram, W., et al. (2018). Role of Burkholderia cepacia CS8 in Cd-stress alleviation and phytoremediation by *Catharanthus roseus*. *Int. J. Phytoremediat.* 20, 581–592. doi: 10.1080/15226514.2017.1405378

Li, G., Shah, A. A., Khan, W. U., Yasin, N. A., Ahamd, A., Abbas, M., et al. (2021). Hydrogen sulfide mitigates cadmium induced toxicity in Brassica rapa by modulating physiochemical attributes, osmolyte metabolism and antioxidative machinery. *Chemosphere* 263:127999. doi: 10.1016/j.chemosphere.2020.127999

Liu, C. Y., Jiang, X., Fan, J. L., and Ziadi, N. (2013). Hexachlorobenzene accumulation in rice plants as affected by farm manure and urea applications in dissimilar soils. *Can. J. Soil Sci.* 93, 631–638. doi: 10.4141/CJSS2013-001

Lu, G. H., Zhao, Y. H., Yang, S. G., and Cheng, X. J. (2002). Quantitative structure-biodegradability relationships of substituted benzenes and their biodegradability in river water. *Bull. Environ. Contam. Toxicol.* 69, 111–116. doi: 10.1007/s00128-002-0016-7

Mansouri, A., Cregut, M., Abbes, C., Durand, M. J., Landoulsi, A., and Thouand, G. (2017). The environmental issues of DDT pollution and bioremediation: a multidisciplinary review. *Appl. Biochem. Biotechnol.* 181, 309–339. doi: 10.1007/s12010-016-2214-5

Miao, H. Y., Wang, M. Y., Chang, J. Q., Tao, H., Sun, B., and Wang, Q. M. (2017). Effects of glucose and gibberellic acid on glucosinolate content and antioxidant properties of Chinese kale sprouts. *J. Zhejiang Univ. Sci. B* 18, 1093–1100. doi: 10.1631/jzus.B1700308

Mitter, N., Worrall, E. A., Robinson, K. E., Li, P., Jain, R. G., Taochy, C., et al. (2017). Clay nanosheets for topical delivery of RNAi for sustained protection against plant viruses. *Nat. Plants* 3:16207. doi: 10.1038/nplants.2016.207

Nahar, K., Hasanuzzaman, M., Suzuki, T., and Fujita, M. (2017). Polyamines-induced aluminum tolerance in mung bean: a study on antioxidant defense and methylglyoxal detoxification systems. *Ecotoxicology* 26, 58–73. doi: 10.1007/s10646-016-1740-9

Ram Reddy, M. K., Xu, Z. P., Lu, G. Q., and Diniz da Costa, J. C. (2006). Layered double hydroxides for CO 2 capture: structure evolution and regeneration. *Ind. Eng. Chem. Res.* 45, 7504–7509. doi: 10.1021/ie060757k

Reddy, M. K. R., Xu, Z. P., Lu, G. Q., and Diniz da Costa, J. C. (2008). Effect of SO x adsorption on layered double hydroxides for CO 2 capture. *Ind. Eng. Chem. Res.* 47, 7357–7360. doi: 10.1021/ie8004226

Rezapour, S., and Samadi, A. (2011). Soil quality response to long-term wastewater irrigation in Inceptisols from a semi-arid environment. *Nutr. Cycl. Agroecosyst.* 91, 269–280. doi: 10.1007/s10705-011-9460-2

Rignell-Hydbom, A., Rylander, L., and Hagmar, L. (2007). Exposure to persistent organochlorine pollutants and type 2 diabetes mellitus. *Hum. Exp. Toxicol.* 26, 447–452. doi: 10.1177/0960327107076886

Sadasivaiah, S., Tozan, Y., & Breman, J. G. (2007). Dichlorodiphenyltrichloroethane (DDT) for indoor residual spraying in Africa: how can it be used for malaria control?. *Am. J. Trop. Med. Hyg.* 77, 249–263. doi: 10.4269/ajtmh.2007.77.249

Sakouhi, L., Kharbech, O., Massoud, M. B., Gharsallah, C., Hassine, S. B., Munemasa, S., et al. (2021). Calcium and ethylene glycol tetraacetic acid mitigate toxicity and alteration of gene expression associated with cadmium stress in chickpea (*Cicer arietinum* L.) shoots. *Protoplasma* 258, 849–861. doi: 10.1007/s00709-020-01605-x

Sardar, R., Ahmed, S., Shah, A. A., and Yasin, N. A. (2022a). Selenium nanoparticles reduced cadmium uptake, regulated nutritional homeostasis and antioxidative system in *Coriandrum sativum* grown in cadmium toxic conditions. *Chemosphere* 287:132332. doi: 10.1016/j.chemosphere.2021.132332

Sardar, R., Ahmed, S., and Yasin, N. A. (2022b). Titanium dioxide nanoparticles mitigate cadmium toxicity in *Coriandrum sativum* L. through modulating antioxidant system, stress markers and reducing cadmium uptake. *Environ. Pollut.* 292:118373. doi: 10.1016/j.envpol.2021.118373

Sattar, A., Sher, A., Ijaz, M., Ul-Allah, S., Rizwan, M. S., Hussain, M., et al. (2020). Terminal drought and heat stress alter physiological and biochemical attributes in flag leaf of bread wheat. *PLoS One* 15:e0232974. doi: 10.1371/journal.pone.0232974

Shaddad, A. K., Abd El-Samad, H. M., and Mostafa, D. (2013). Role of gibberellic acid (GA 3) in improving salt stress tolerance of two wheat cultivars. *Int. J. Plant Physiol. Biochem.* 5, 50–57. doi: 10.5897/IJPPB11.055

Shafique, S., Ahmad, A., Shafique, S., Anjum, T., Akram, W., and Bashir, Z. (2014). Determination of molecular and biochemical changes in cotton plants mediated by mealybug. *NJAS Wageningen J. Life Sci.* 7, 39–45. doi: 10.1016/j.njas.2014.05.001

Shah, A. A., Aslam, S., Akbar, M., Ahmad, A., Khan, W. U., Yasin, N. A., et al. (2021). Combined effect of *Bacillus fortis* IAGS 223 and zinc oxide nanoparticles to alleviate cadmium phytotoxicity in *Cucumis melo*. *Plant Physiol. Biochem.* 158, 1–12. doi: 10.1016/j.plaphy.2020.11.011

Shah, A. A., Khan, W. U., Yasin, N. A., Akram, W., Ahmad, A., Abbas, M., et al. (2020). Butanolide alleviated cadmium stress by improving plant growth, photosynthetic parameters and antioxidant defense system of *Brassica oleracea*. *Chemosphere* 261:127728. doi: 10.1016/j.chemosphere.2020.127728

Shereefa, L. A. H., and Kumaraswamy, M. (2016). Reactive oxygen species and ascorbate–glutathione interplay in signaling and stress responses in *Sesamum orientale* L. against *Alternaria sesami* (Kawamura) Mohanty and Behera. *J. Saudi Soc. Agric. Sci.* 15, 48–56. doi: 10.1016/j.jssas.2014.04.007

Sun, W., Liu, C., Luo, J., Niu, C., Wang, J., Zheng, F., et al. (2020). Residue analysis of gibberellic acid isomer (iso-GA3) in brewing process and its toxicity evaluation in mice. *Regul. Toxicol. Pharmacol.* 110:104514. doi: 10.1016/j.yrtph.2019.104514

Tan, B. L., and Norhaizan, M. E. (2019). Carotenoids: how effective are they to prevent age-related diseases? *Molecules* 24:1801. doi: 10.3390/molecules24091801

Tariq, M., Shah, A. A., Yasin, N. A., Ahmad, A., and Rizwan, M. (2021). Enhanced performance of *Bacillus megaterium* OSR-3 in combination with putrescine

ammeliorated hydrocarbon stress in *Nicotiana tabacum*. *Int. J. Phytoremed.* 23, 119–129. doi: 10.1080/15226514.2020.1801572

Thor, K. (2019). Calcium—nutrient and messenger. *Front. Plant Sci.* 10:440. doi: 10.3389/fpls.2019.00440

Tong, T., Li, Q., Jiang, W., Chen, G., Xue, D., Deng, F., et al. (2021). Molecular evolution of calcium signaling and transport in plant adaptation to abiotic stress. *Int. J. Mol. Sci.* 22:12308. doi: 10.3390/ijms222212308

Turusov, V., Rakitsky, V., and Tomatis, L. (2002). Dichlorodiphenyltrichloroethane (DDT): ubiquity, persistence, and risks. *Environ. Health Perspect.* 110, 125–128. doi: 10.1289/ehp.02110125

Wang, Q., Zhao, R., Chen, Q., Teixeira Da Silva, J. A., Chen, L., and Yu, X. (2019). Physiological and biochemical responses of two herbaceous peony cultivars to drought stress. *HortScience* 54, 492–498. doi: 10.21273/HORTSCI13704-18

Wu, G., Bazer, F. W., Burghardt, R. C., Johnson, G. A., Kim, S. W., Knabe, D. A., et al. (2011). Proline and hydroxyproline metabolism: implications for animal and human nutrition. *Amino Acids* 40, 1053–1063. doi: 10.1007/s00726-010-0715-z

Xiao, R., Ali, A., Wang, P., Li, R., Tian, X., and Zhang, Z. (2019). Comparison of the feasibility of different washing solutions for combined soil washing and phytoremediation for the detoxification of cadmium (Cd) and zinc (Zn) in contaminated soil. *Chemosphere* 230, 510–518. doi: 10.1016/j.chemosphere.2019.05.121

Xu, Z. P., Stevenson, G. S., Lu, C.-Q. Q., Lu, G. Q., Bartlett, P. F., and Gray, P. P. (2006). Stable suspension of layered double hydroxide nanoparticles in aqueous solution. *J. Am. Chem. Soc.* 128, 36–37. doi: 10.1021/ja056652a

Yasin, N. A., Khan, W. U., Ahmad, S. R., Ahmad, A., Akram, W., and Ijaz, M. (2018a). Role of *Acinetobacter* sp. cs9 in improving growth and phytoremediation potential of catharanthus longifolius under cadmium stress. *Polish J. Environ. Stud.* 28, 435–443. doi: 10.15244/pjoes/80806

Yasin, N. A., Zaheer, M. M., Khan, W. U., Ahmad, S. R., Ahmad, A., Ali, A., et al. (2018b). The beneficial role of potassium in Cd-induced stress alleviation and growth improvement in *Gladiolus grandiflora* L. *Int. J. Phytoremed.* 20, 274–283. doi: 10.1080/15226514.2017.1374337

Zaheer, M. M., Yasin, N. A., Ahmad, S. R., Khan, W. U., Ahmad, A., Ali, A., et al. (2016). Amelioration of cadmium stress in gladiolus (*Gladiolus grandiflora* L.) by application of potassium and silicon. *J. Plant Nutr.* 41, 461–476. doi: 10.1080/01904167.2017.1385808

Zeng, H., Chen, L., Zhou, X., and Zeng, Q. (2019). Cadmium accumulation in winter crops and the assessment of paddy soil phytoremediation in southern China. *Environ. Sci. Pollut. Res.* 26, 17173–17182. doi: 10.1007/s11356-019-05054-9

Zhu, H., Sun, H., Zhang, Y., Xu, J., Li, B., and Zhou, Q. (2016). Uptake pathway, translocation, and isomerization of hexabromocyclododecane diastereoisomers by wheat in closed chambers. *Environ. Sci. Technol.* 50, 2652–2659. doi: 10.1021/acs.est.5b05118

Zhu, H., Wang, F., Li, B., Yao, Y., Wang, L., and Sun, H. (2020). Accumulation and translocation of polybrominated diphenyl ethers into plant under multiple exposure scenarios. *Environ. Int.* 143:105947. doi: 10.1016/j.envint.2020.105947

Conflict of Interest: The authors declare that the research was conducted in the absence of any commercial or financial relationships that could be construed as a potential conflict of interest.

Publisher's Note: All claims expressed in this article are solely those of the authors and do not necessarily represent those of their affiliated organizations, or those of the publisher, the editors and the reviewers. Any product that may be evaluated in this article, or claim that may be made by its manufacturer, is not guaranteed or endorsed by the publisher.

Copyright © 2022 Mubeen, Shahzadi, Akram, Saeed, Yasin, Ahmad, Shah, Siddiqui and Alamri. This is an open-access article distributed under the terms of the Creative Commons Attribution License (CC BY). The use, distribution or reproduction in other forums is permitted, provided the original author(s) and the copyright owner(s) are credited and that the original publication in this journal is cited, in accordance with accepted academic practice. No use, distribution or reproduction is permitted which does not comply with these terms.

frontiers in Plant Science

ORIGINAL RESEARCH
published: 10 March 2022
doi: 10.3389/fpls.2022.857980

Mechanistic Insights Into Trehalose-Mediated Cold Stress Tolerance in Rapeseed (*Brassica napus* L.) Seedlings

Ali Raza†‡, Wei Su†‡, Ziqi Jia, Dan Luo, Yi Zhang, Ang Gao, Muhammad Azhar Hussain, Sundas Saher Mehmood, Yong Cheng, Yan Lv and Xiling Zou**

Key Laboratory of Biology and Genetic Improvement of Oil Crops, Oil Crops Research Institute, Chinese Academy of Agricultural Sciences, Wuhan, China

OPEN ACCESS

Edited by:
Mohammad Anwar Hossain, Bangladesh Agricultural University, Bangladesh

Reviewed by:
Rajesh Singhal, Indian Grassland and Fodder Research Institute (ICAR), India
M. Nasir Khan, University of Tabuk, Saudi Arabia

***Correspondence:**
Yan Lv
lvyan01@caas.cn
Xiling Zou
zouxiling01@caas.cn

†ORCID:
Ali Raza
orcid.org/0000-0002-5120-2791
Wei Su
orcid.org/0000-0003-1289-4403

‡*These authors have contributed equally to this work*

Specialty section:
This article was submitted to Plant Breeding, a section of the journal Frontiers in Plant Science

Received: *19 January 2022*
Accepted: *14 February 2022*
Published: *10 March 2022*

Citation:
Raza A, Su W, Jia Z, Luo D, Zhang Y, Gao A, Hussain MA, Mehmood SS, Cheng Y, Lv Y and Zou X (2022) Mechanistic Insights Into Trehalose-Mediated Cold Stress Tolerance in Rapeseed (Brassica napus L.) Seedlings. Front. Plant Sci. 13:857980. doi: 10.3389/fpls.2022.857980

Cold stress (CS) severely affects several physiological, biochemical, and molecular mechanisms and limits the growth and production of rapeseed (*Brassica napus* L.). Trehalose (Tre) acts as a growth modulator, which is extensively used to improve the tolerance to multiple plant stresses. Further, Tre also serves as an external force in inducing plant signaling molecules, regulating the expression of stress-responsive genes, and enhancing the CS tolerance in plants. Nevertheless, the importance of exogenous Tre in improving the CS tolerance in rapeseed is still unclear. Therefore, the current study was designed to get mechanistic insights into Tre-mediated CS tolerance in rapeseed seedlings. To explore the Tre role, we designed four treatments [control (CK), CK + 20 mM L^{-1} Tre, Cold, and Cold + 20 mM L^{-1} Tre] and three CS conditions (4, 0, and −4°C). The results showed that Tre treatments significantly mitigated the adverse effects of CS on the seedlings and increased the survival rate of Tre-treated seedlings under CS conditions. The exogenous Tre dramatically increased the contents of osmoprotectants, including the soluble sugar (SS), soluble protein (SP), and proline (Pro), and the activities of antioxidant enzymes, such as catalase (CAT), peroxidase (POD), superoxide dismutase (SOD), and ascorbate peroxidase (APX) were also increased under CS conditions. Additionally, Tre decreased the malondialdehyde (MDA) contents to protect the rapeseed seedlings. Moreover, Tre also remarkably augmented the expression levels of antioxidant genes (*CAT12, POD34,* and *FSD7*), CS-responsive marker genes (*CBF1, CBF2, CBF4, COR6.6, COR15, COR25, COL1,* and *KIN1*), and Tre-biosynthesis genes (*TPS4, TPS8,* and *TPS9*). Briefly, exogenous Tre not only regulates the antioxidant and osmotic balance, but it also significantly participates in Tre metabolism and signaling network to improve the CS tolerance in rapeseed. Thus, Tre-induced supervisory connections between physiological or/and biochemical attributes provide information to dissect the mechanisms of Tre-mediated CS tolerance.

Keywords: abiotic stress, antioxidant defense system, gene expression, marker genes, osmoprotectants, trehalose metabolism, chilling stress

INTRODUCTION

Plants are constantly confronted by the changing climate, which leads to several environmental stresses. Amongst them, cold stress (CS) [(chilling (0–15°C) and freezing temperature (<0°C)] is a main abiotic factor that influences the productivity of the plants, restricts the geographical circulation, and lessens crop yields (He et al., 2021; Mehmood et al., 2021). Consequently, CS leads to alterations in the physiological, biochemical, and molecular mechanisms, as reviewed by Raza et al. (2021c) and Zahra et al. (2021). Short-term CS enhances the levels of reactive oxygen species (ROS) (He et al., 2021), triggers mitogen-activated protein kinase cascades (MAPKs/MPKs), activates down-stream C-repeat binding factor (CBF)-dependent or CBF-independent pathways (Lohani et al., 2020; Raza et al., 2021a), and eventually adjusts the expression levels of CS-responsive genes (Ding et al., 2019; Lei et al., 2019; He et al., 2021). On the contrary, long-term CS triggers the overproduction of ROS and redox imbalance (Ding et al., 2019; Hasanuzzaman et al., 2020; Mehmood et al., 2021). In contrast, the ROS accumulation damaged large molecules, including DNA, proteins, lipids, cell structure and membrane, and the physio-biochemical and metabolic processes (Hasanuzzaman et al., 2020). Subsequently, CS reduces the cell membrane fluidity, photosynthesis, crop productivity, and even leads to cell death (Ding et al., 2019).

During the previous two decades, several elements, such as messenger molecules (ROS calcium, and phytohormones), protein kinases and phosphatases (MAPKs/MPKs, CDPKs, CBLs, CIPKs, etc.), and transcription factors (CBF, COR, DREB, etc.) have been identified in the CS signaling pathways (Wang et al., 2017; Shi et al., 2018; Ding et al., 2019; Raza et al., 2021a). So far, ICE-CBF-COR signaling pathways have been best characterized under CS conditions. Mainly, *CBF* genes can quickly be induced by CS, and they play substantial roles in the cold acclimation phenomenon (Wang et al., 2017; Shi et al., 2018), whereas *COR* genes are mainly regulated by CS, including *COR, KIN, COL,* etc., (Shi et al., 2018). Interestingly, these genes encode cryoprotective and osmolyte proteins to protect plants from freezing damage (Shi et al., 2018). Moreover, *CBFs* can directly attach with the *COR* genes promoters and induce their expression levels, thus, improving the CS tolerance in plants (Liu et al., 1998).

In the recent past, several plant growth regulators have been extensively applied to improve the stress tolerance in crop plants (Mubarik et al., 2021; Raza et al., 2021d; Sabagh et al., 2021). Among them, trehalose (Tre) is a non-reducing disaccharide sugar that possesses two glucose molecules (Wingler, 2002). The Tre mainly exists in different organisms, including yeasts, bacteria, invertebrates, and in a smaller amount in plants, that alleviate osmoprotectant molecules and are easily absorbed by the plants (Wingler, 2002; Kosar et al., 2019). The endogenous Tre content was found to be very low in plants, such as rice and tobacco (Kretovich, 1980); nevertheless, it is greatly induced by numerous abiotic stresses, including CS (Kosar et al., 2019; Joshi et al., 2020; Zulfiqar et al., 2021a). A study has been concentrated on the clarification of Tre metabolism, especially in transgenic crops with stress tolerance (Schwarz and Van Dijck, 2017). A low amount of Tre is not merely because of the activity of Tre but also owes to strong modulation of trehalose-6-phosphate synthase (*TPS*) and trehalose-6-phosphate phosphatase (*TPP*) gene expression and enzyme activities (Delorge et al., 2014). Interestingly, Tre not only contributes to plant metabolisms but also contributes to signaling mechanisms (Paul et al., 2008). Furthermore, the exogenously sprayed Tre can quickly accumulate and be moved by the roots and the leaf tissues, showing significant roles as osmoprotectants (Luo et al., 2010). Previously, it has been documented that Tre regulates different osmotic substances in various plant species under stress conditions, e.g., osmotic pressure, chillness, drought, and heat stress (Luo et al., 2008; Liu et al., 2020; Zulfiqar et al., 2021a). Recently, Williams et al. (2015) described that Tre was extensively distinguished in CS-tolerant crop plants, such as *Tripogon loliiformis*, signifying that Tre was involved in developing CS tolerance in diverse plant species.

In the recent years, limited studies have been carried out using exogenous Tre to enhance CS tolerance in different plant species, such as tomato (*Solanum lycopersicum* L.) (Liu et al., 2020), rice (*Oryza sativa* L.) (Fu et al., 2020), wheat (*Tritum aestivum* L.) (Liang et al., 2021), melon (*Cucumis melo* L.) (Liu et al., 2021), etc., and the mechanisms mediating Tre effects have not been fully discovered. Most importantly, the effect of exogenous Tre in improving the CS tolerance in rapeseed (*Brassica napus* L.) is still unclear. Rapeseed is the third-leading oilseed crop in China that is frequently exposed to CS, mainly in the winter (He et al., 2021; Li et al., 2021; Raza, 2021; Su et al., 2021a). The CS significantly impairs rapeseed productivity and ultimately reduces biomass and seed harvest (Raza, 2021). Hence, the current experiment was designed to elucidate the positive role of exogenous Tre in improving the CS tolerance in rapeseed. To get insights into Tre-mediated CS tolerance, we examined the physiological and biochemical indices in the seedling treated with exogenous Tre. Furthermore, we also analyzed the expression levels of CS-responsive antioxidants and Tre-biosynthesis genes to identify the key effects of Tre application at the molecular level, which could be acting as an expressive approach for unraveling the mechanistic insights of Tre in enhancing the CS tolerance in rapeseed.

MATERIALS AND METHODS

Plant Material and Growth Conditions

The seeds of a widely cultivated rapeseed variety, "ZhongShang11 (ZS11)" (Sun et al., 2017), were supplied by the Oil Crops Research Institute, the Chinese Academy of Agricultural Sciences (CAAS), Wuhan, China. The vigorous seeds of ZS11 were grown on moist filter paper on petri dishes in a chamber (25°C day/night and 16 h/8 h light/dark cycle). After 7 days, the seedlings were moved to pots (10 cm, four plants pot^{-1}) containing a mixture of vermiculite and nutrient soil (2:1). The 21-day-old (four-leaf stage) seedlings were exposed to CS treatments.

Treatments and Sample Harvesting

The research was performed in a completely randomized design, including three biological replications. We designed four

treatments [control (CK), CK + Tre, Cold, and Cold + Tre] and three stress conditions (4, 0, and −4°C) to investigate the effects of exogenous Tre (CAS#99-20-7) on rapeseed that has CS tolerance. The Tre was purchased from Yuanye Bio-Tech Co., Ltd., (Shanghai, China). Before CS treatments, the whole plants were pretreated with 20 mM L^{-1} of Tre solution and distilled water at room temperature [25°C/18°C (day/night)]. The Tre concentration (20 mM L^{-1}) was selected based on previous studies (Ibrahim and Abdellatif, 2016; Samadi et al., 2019; Liu et al., 2020). The selected pots for Tre treatment were sprayed with 10 mL of Tre solution, and the CK seedlings were sprayed with 10 mL of distilled water. Every treatment was replicated three-times (three pots/replication) and arbitrarily organized. After 24 h, half of the seedlings were exposed to CS (4°C for 24 h, 0°C for 12 h, and −4°C for 6 h). The CK samples were kept at room temperature (25°C) with the corresponding treatment time. After CS treatments, the green leaves were harvested and immediately preserved in liquid nitrogen and kept at −80°C until the next analysis.

Measurements of Physiological and Biochemical Attributes

To analyze the physiological and biochemical alterations in rapeseed under CS, the contents of soluble sugar (SS), soluble protein (SP), proline (Pro), malondialdehyde (MDA), and hydrogen peroxide (H_2O_2) were measured using commercial kits following the manufacturer's guidelines. Similarly, the antioxidant defense enzymes activities, including catalase (CAT, EC 1.11.1.6), superoxide dismutase (SOD, EC 1.15.1.1), peroxidase (POD, EC 1.11.1.7), and ascorbate peroxidase (APX, EC 1.11.1.11), were measured using commercial kits following the manufacturer's guidelines. The kits for SS (G0501W), SP (G0418W), Pro (G0111W), MDA (G0109F), H_2O_2 (G0112F), CAT (G0105F), SOD (G0101F), POD (G0107F), and APX (G0203F) were bought from Suzhou Grace Biotechnology Co., Ltd., (Suzhou, Jiangsu, China). The detailed protocol manuals are freely available at the company profile[1] and can be extracted using the above-mentioned kit IDs. All the parameters were measured using three biological replications and a spectrophotometer microplate reader (Epoch, BioTek, Instruments, Inc., Winooski, VT, United States).

Gene Expression Analysis

To boost our understanding of Tre-mediated CS tolerance in rapeseed seedlings, we evaluated the expression levels of antioxidant genes, stress-related marker genes, and genes involved in Tre biosynthesis/metabolism (**Table 1**). Antioxidant and Tre genes were identified and randomly selected using keywords in the rapeseed genome[2]. Total RNA was extracted using TransZol Up Plus RNA Kit (TransGen Biotechnology, Beijing, China) following the manufacturer's guidelines. The RNA was treated and purified with TransScript One-Step gDNA Removal to eradicate the gDNA impurities. According to the manufacturer's guidelines, the cDNA was harmonized utilizing a complementary DNA (cDNA) Synthesis SuperMix kit (TransGen Biotechnology, Beijing, China). The quantitative real-time-PCR (qRT-PCR) reaction was accomplished with an ABI StepOne real-time fluorescence quantitative PCR instrument (Applied Biosystems, CA, United States) following the reported method (Raza et al., 2021b). Briefly, the *BnACTIN* gene was used as an internal control. The qRT-PCR reaction was executed as follows: at 94°C for 10 min, followed by 40 cycles of 94°C for 15 s, 60°C for 30 s, and 72°C for 10 s. Gene expression analysis was carried out with three technical replications. The information of genes and primers used for qRT-PCR analysis are shown in **Table 1**.

Statistical Data Analysis

The data were examined using GraphPad Prism Ver. 9 (Swift, 1997). The statistical significance was verified with a two-way ANOVA and Tukey's test at a significant level of $^{****}P < 0.0001$, $^{***}P \leq 0.001$, $^{**}P \leq 0.01$, $^{*}P \leq 0.05$. Pearson's correlation analysis was performed using the mcor function, and corrplots were prepared using corrplot package Ver. 0.89 (Wei et al., 2017) in RStudio (Allaire, 2012). Principal component analysis (PCA) was performed using fviz-pca function of the factoextra R package Ver. 1.0.7 (Kassambara and Mundt, 2020) in RStudio. All other graphs were prepared in GraphPad Prism.

RESULTS

Exogenous Tre Improves the Survival Rate of Cold-Stressed Rapeseed Seedlings

Cold stress (either freezing or/and chilling temperature) significantly impair the productivity of the rapeseed. Upon exposure to CS (4, 0, and −4°C), the rapeseed seedlings experienced a damaging phenomenon. Thus, the rapeseed seedlings were pretreated with Tre to evaluate their survival rate under CS conditions. Exogenous Tre significantly improved the survival rate compared to CK and cold-stressed seedlings, except for the chilling stress (0°C). For instance, under CS conditions, the Tre treatment showed a 100% survival rate at 4°C, and 97% survival rate at 0 and −4°C, which are significantly higher than CK seedlings without Tre application (**Figure 1**). Initially, the CS reduced the seedling growth, whereas the exogenous Tre significantly alleviated the survival rate of the rapeseed seedlings under freezing conditions (−4°C). Therefore, Tre pretreatment could be considered as a fascinating approach in mitigating the adverse effect of CS on rapeseed productivity.

Impact of Tre on the Physiological and Biochemical Indices

Tre Promotes the Levels of Osmoprotectant Substances in Cold-Stressed Rapeseed Seedlings

Cold stress increased the Pro contents in the leaves of rapeseed seedlings. Cold stress led to increased Pro content by 167% at 4°C, 164% at 0°C, and 189% at −4°C, compared to CK (**Figure 2A**). Under normal conditions, the exogenous Tre improves the Pro contents by 141, 150, and 159% compared to the CK seedlings

[1] http://www.geruisi-bio.com/pro

[2] http://cbi.hzau.edu.cn/bnapus/index.php

TABLE 1 | A list of primers used for the gene expression analysis.

Gene name	Gene ID/Accession number	Forward	Reverse
CBF1	BnaC07g39680D	CACCCAGTTTACAGAGGAGTTCG	ATCTCGGCTGTTAGGAAAGTACC
CBF2	BnaA03g13620D	TCTGAAATGTTGGGCTCCGA	CGCGTCTCCCGAAACTTCTT
CBF4	BnaA10g07630D	TTTCTCAGACTCGTTCCTCTCG	CTCCCTGCTCGTTTCTTCG
COR15	U14665.1	TCTCATTGGGATTGGTTCTTCTTT	ATGTTGCCGTCACCTTTATCG
COR25	HM187577.1	GGTCACAGCGAAAAACCAGAT	TCTTGGCGTGATAACCTGGAA
COR6.6	BnaA02g02910D	GGAGAAGGGTAATGTGCTGATGG	GCTACTTGTTCATGCCGGTCTT
COL1	BnaA02g02840D	CTTCTTGGTTGTTGCCTAGTTC	CATATGACATCCTGAGGACACA
KIN1	BnaAnng37980D	TCGTGCTGAGGAGAAGGGTA	CCGCCTCCGTTATCTTCTGT
CAT12	BnaC08T0260800ZS	AGCTTGCTTTCAACCCTGGT	CATTCACAGGCAGCTGGAGA
FSD7	BnaC03T0164000ZS	TTGATGCTCTAGAACCGCATAT	GATAGACTCCCAGAAGAACTCG
POD34	BnaC08g20820D	CGTGCTGATAACGTGTTAAGATTTG	CTCCCTTTGACTCCACCTTGT
TSP4	BnaA03g43320D	TTGTGGATTATGATGGGACGAT	AAACGATATTCTTGGGGTCACT
TSP8	BnaA07g24830D	CTAGCTGGACCTTCTCTCTAGA	GTCTTCTTTTAAGCAGCCTACG
TSP9	BnaA07g34230D	GACGTGATACAACACATGAAGG	GCGTTCTCCTCAAGAAACTTTT

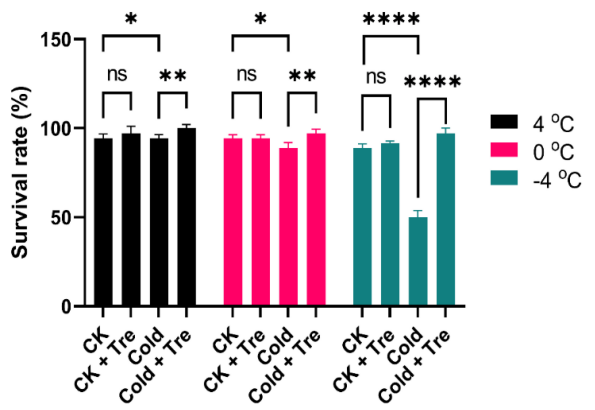


FIGURE 1 | Impact of Tre on the survival rate of rapeseed seedlings under four treatments [control (CK), CK + Tre, Cold, and Cold + Tre] and three cold stress conditions (4, 0, and –4°C). Tre indicates the application of 20 mM L^{-1} Tre. Data are expressed as the mean (± SD) from three biological replications for each sample and treatment. Asterisks show significant levels at ****$P < 0.0001$, **$P \leq 0.01$, *$P \leq 0.05$, and ns means non-significant.

treated with water (**Figure 2A**). Under CS conditions, the application of Tre significantly increased the Pro contents by 227, 224, and 248% at 4, 0, and −4°C compared to CK, respectively (**Figure 2A**). Likewise, the CS decreased the SS contents by 75% at 0°C and 52% at −4°C compared to CK (**Figure 2B**). However, the application of Tre increased the SS contents by 128, 115, and 141% at 4, 0, and −4°C compared to CK, respectively (**Figure 2B**). In addition, under CS conditions, the SS contents of seedlings with Tre application were significantly increased by 167% at 4°C, and 281% at −4°C compared to CK. Additionally, CS reduced the SP contents at 4°C (by 73%) and −4°C (by 87%) compared to CK (**Figure 2C**). Under normal conditions, with Tre application, the SP contents were remarkably increased by 115, 142, and 113% at 4, 0, and −4°C compared to CK, respectively (**Figure 2C**). Whereas, under CS conditions, the SP contents of seedlings with Tre application were significantly increased by 134, 142, and 131% at 4, 0, and −4°C compared to CK, respectively (**Figure 2C**). In short, the CS reduces the SS and SP contents, and exogenous Tre significantly increased the Pro, SS, and SP contents at CK and CS conditions.

Tre-Induced Malondialdehyde and H_2O_2 Levels in Cold-Stressed Rapeseed Seedlings

Under CS conditions, the MDA level was increased by 132, 177, and 172% at 4, 0, and −4°C compared to CK, respectively (**Figure 3A**). The CS also resulted in increased H_2O_2 levels by 155, 125, and 144% at 4, 0, and −4°C compared to CK, respectively (**Figure 3B**). Under normal conditions, the exogenous Tre significantly reduced the MDA contents by 82, 72, and 91% at 4, 0, and −4°C, compared to CK, respectively (**Figure 3A**). Likewise, the exogenous Tre application also reduced the H_2O_2 levels by 90, 85, and 92% at 4, 0, and −4°C compared to CK, respectively (**Figure 3B**). Whereas under CS conditions, the MDA content was declined significantly by 72% at 4°C, and 54% at −4°C compared to CK, respectively (**Figure 3A**). Under CS conditions (4 and −4°C), there was no considerable difference in the H_2O_2 levels compared to CK (**Figure 3B**). Notably, the H_2O_2 level was only reduced at 0°C (by 70%) than the CK (**Figure 3B**). Briefly, the exogenous Tre substantially reduced the MDA and H_2O_2 levels in cold-stressed and CK seedlings compared to CK.

Exogenous Tre Regulates the Antioxidant Enzyme Activities in Cold-Stressed Rapeseed Seedlings

Cold stress substantially increases the ROS production in plants compared to the CK plants. Thus, the improved activities of antioxidant enzymes, including CAT, POD, SOD, and APX, adjust the equilibrium of ROS production under CS conditions. In this research, the CS reduced the CAT activity by 59, 86, 80% at 4, 0, and −4°C compared to CK, respectively (**Figure 4A**). Under normal conditions, the exogenous Tre significantly increased the CAT activity by 114, 120, and 121% at 4, 0, and −4°C of rapeseed seedlings treated with Tre. Likewise, under CS conditions, the CAT activity was boosted by 102, 110, 117%

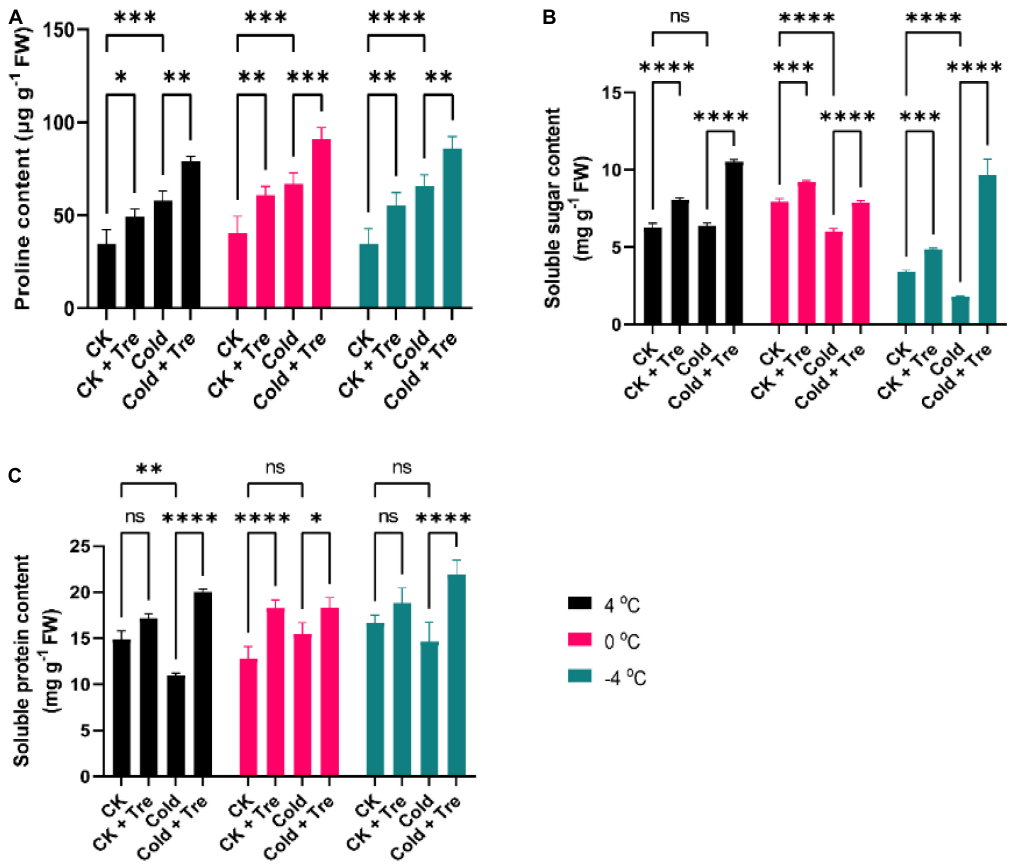


FIGURE 2 | Impact of Tre on the levels of osmoprotectant substances in rapeseed seedling under cold stress conditions. **(A)** Proline contents, **(B)** soluble sugar contents, and **(C)** soluble protein contents under four treatments [control (CK), CK + Tre, Cold, and Cold + Tre] and three stress conditions (4, 0, and –4°C). Tre indicates the application of 20 mM L^{-1} of Tre. Data are expressed as the mean (± SD) from three biological replications for each sample and treatment. Asterisks show significant levels at ****$P < 0.0001$, ***$P \leq 0.001$, **$P \leq 0.01$, *$P \leq 0.05$, and ns means non-significant.

at 4, 0, and −4°C compared to CK, respectively (**Figure 4A**). Cold increases the POD activity by 126% at 4°C, and 131% at 0°C compared to CK (**Figure 4B**). However, under normal conditions, the exogenous Tre significantly increased the POD activity by 139, 141, and 108% at 4, 0, and −4°C compared to CK, respectively (**Figure 4B**). Under CS conditions, the POD activity was substantially augmented by 190, 225, and 145% at 4, 0, and −4°C compared to CK, respectively (**Figure 4B**).

Under CS conditions (mainly at −4°C), the SOD activity was reduced by 84% compared to CK, whereas it was slightly improved at 4 and 0°C conditions (**Figure 4C**). The exogenous Tre increases the SOD activity by 152, 121, and 115% in CK seedlings with Tre application at 4, 0, and −4°C compared to CK, respectively (**Figure 4C**). Under CS conditions, the SOD activity was increased by 160, 140, and 132% at 4, 0, and −4°C compared to CK, respectively (**Figure 4C**). Under CS conditions, mainly at 0°C, and −4°C, the APX activity was substantially dropped by 84 and 61% compared to CK, respectively, whereas it was significantly increased by 202% at 4°C (**Figure 4D**). However, under normal conditions, the Tre application enhanced the APX activity by 168, 155, and 168% at 4, 0, and −4°C compared to CK, respectively (**Figure 4D**). Under CS conditions, the APX activity was significantly boosted by 216, 184, and 141% at 4, 0, and −4°C compared to CK, respectively (**Figure 4D**). Overall, our results showed that CS alone reduced the antioxidant enzyme activities. Therefore, the exogenous application of Tre remarkably increased the CAT, POD, SOD, and APX activities to cold-stressed and CK seedlings with the application of Tre. The highest activities were recorded with the Tre treatment throughout the CS conditions.

Impact of Tre on the Cold Stress-Responsive Marker and Tre-Biosynthesis Genes in Cold-Stressed Rapeseed Seedlings

Effect of Tre on the Expression Levels of Antioxidant Genes

In plants, the ROS production is mainly regulated by an antioxidant defense system (Hasanuzzaman et al., 2020). In this study, the exogenous Tre significantly increased the antioxidant enzyme activities (**Figure 4**). Therefore, we also evaluated the impact of Tre on the expression level of antioxidant-encoding genes (**Figure 5**). The exogenous Tre significantly increases the

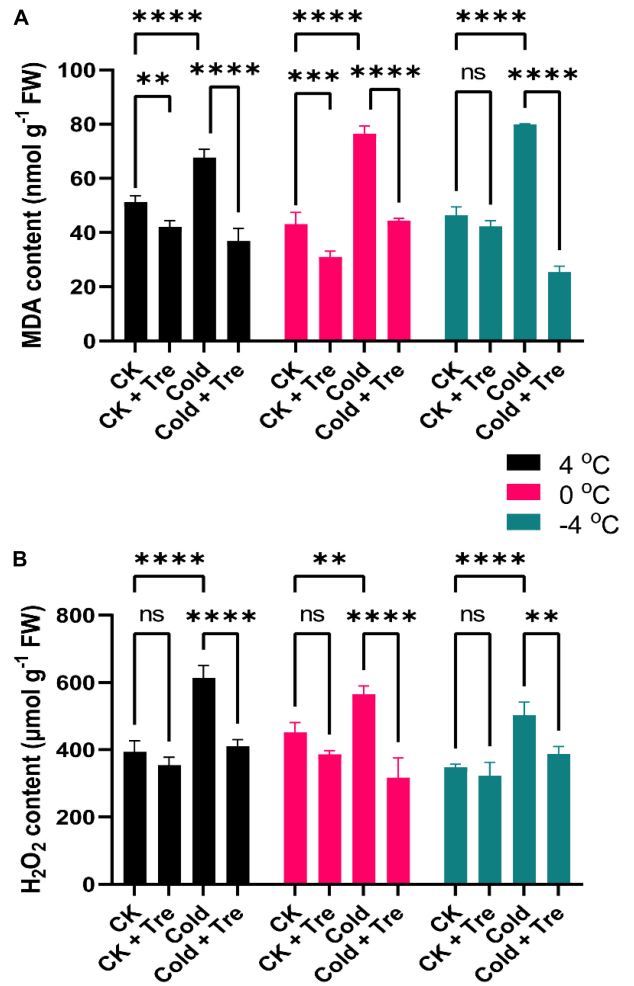


FIGURE 3 | Impact of Tre on the levels of malondialdehyde (MDA) and hydrogen peroxide (H_2O_2) in rapeseed seedling under cold stress conditions. **(A)** MDA contents, and **(B)** H_2O_2 contents under four treatments [control (CK), CK + Tre, Cold, and Cold + Tre] and three stress conditions (4, 0, and −4°C). Tre indicates the application of 20 mM L^{-1} of Tre. Data are expressed as the mean (± SD) from three biological replications for each sample and treatment. Asterisks show significant levels at $^{****}P < 0.0001$, $^{***}P \leq 0.001$, $^{**}P \leq 0.01$, and ns means non-significant.

expression level of the *CAT12* gene by 328, 275, and 235% at 4, 0, and −4°C compared to CK, respectively (**Figure 5A**). Under normal conditions, the Tre also slightly increases the *CAT12* expression (**Figure 5A**). Likewise, the *POD34* expression level was increased by 316% at 4°C, and 217% at 0°C in the seedlings treated with Tre compared to CK under normal conditions (**Figure 5B**). In cold-stressed seedlings, the *POD34* expression level of seedlings with Tre application was significantly boosted at 4, 0, and −4°C compared to CK, respectively (**Figure 5B**). Under CS conditions, the expression level of the Fe-SOD gene (*FSD7*) was dramatically increased at 4, 0, and −4°C compared to CK, respectively (**Figure 5C**). The maximum expression levels of *CAT12, POD34,* and *FSD7* were recorded in cold-stressed seedlings when treated with Tre (**Figure 5**).

Effect of Tre on the Expression Levels of Cold-Related Marker Genes

The *CBF* and *COR* genes participate in CS signaling in plants. Earlier, it was described that the promoter sections of *COR6.6*, *COR15,* and *COR25* genes comprise C-repeat/dehydration responsive element (CRT/DRE), which could be bound by *CBF* genes (Thomashow, 1999). To get further insights on the Tre-induced regulation of gene expressions, we observed the expression levels of *CBF* and *COR* genes (**Figure 6**). In cold-stressed seedlings, the exogenous Tre significantly induced the expressions of *CBF1*, *CBF2*, and *CBF4* at 4, 0, and −4°C compared to CK, respectively (**Figures 6A–C**). Likewise, the expressions of *COR6.6*, *COR15*, and *COR25* were substantially enhanced with Tre treatment in cold-stressed seedlings at 4, 0, and −4°C compared to CK, respectively (**Figures 6D–F**). Whereas at normal conditions, the expression levels of *COR6.6* and *COR25* were slightly induced by exogenous Tre than CK (**Figures 6D,F**). However, there was no considerable change in the *COL1* and *KIN1* expression levels under normal conditions with or without exogenous Tre. However, under CS conditions, the exogenous Tre remarkably boosted the expression levels of *COL1* and *KIN1* at 4, 0, and −4°C compared to CK, respectively (**Figures 6G,H**). Collectively, all the cold-related genes showed higher expression levels in the seedlings treated with exogenous Tre under CS conditions.

Effect of Tre on the Expression Levels of Tre-Biosynthesis Genes

To disclose further insights into the influence of Tre on the regulation of Tre-biosynthesis genes, we evaluated the expressions of Tre-biosynthesis genes in cold-stressed seedlings (**Figure 7**). The outcomes exhibited that the exogenous Tre significantly augmented the expression levels of *TPS4*, *TPS8*, and *TPS9* genes in the cold-stressed seedlings at 4, 0, and −4°C compared to CK, respectively (**Figures 7A–C**). With the application of Tre under normal conditions, there was no substantial change in the expression of the *TPS4* gene, but the expression of *TPS8* was reduced. On the other hand, the expression of *TPS9* was slightly increased by 138% at 4 and −4°C compared to CK (**Figures 7A–C**). The results showed that *TPS4, TPS8,* and *TPS9* also responded to CS greatly; however, the Tre treatment significantly boosted their expression levels in cold-stressed seedlings.

Correlation Analysis

A Pearson's correlation analysis was performed among different evaluated indices and genes of the rapeseed seedlings (**Figure 8**). The correlation analysis showed that SS, SP, and Pro were positively correlated with APX, CAT, POD, and SOD; meanwhile, it was negatively correlated with H_2O_2 and MDA (**Figure 8A**). Similarly, all the antioxidants (APX, CAT, POD, and SOD) were positively correlated with each other. Additionally, H_2O_2 and MDA were negatively correlated with APX, CAT, POD, and SOD (**Figure 8A**). Likewise, the gene correlation analysis showed that all the genes were strongly and positively correlated with each other (**Figure 8B**). This correlation represents a close relationship

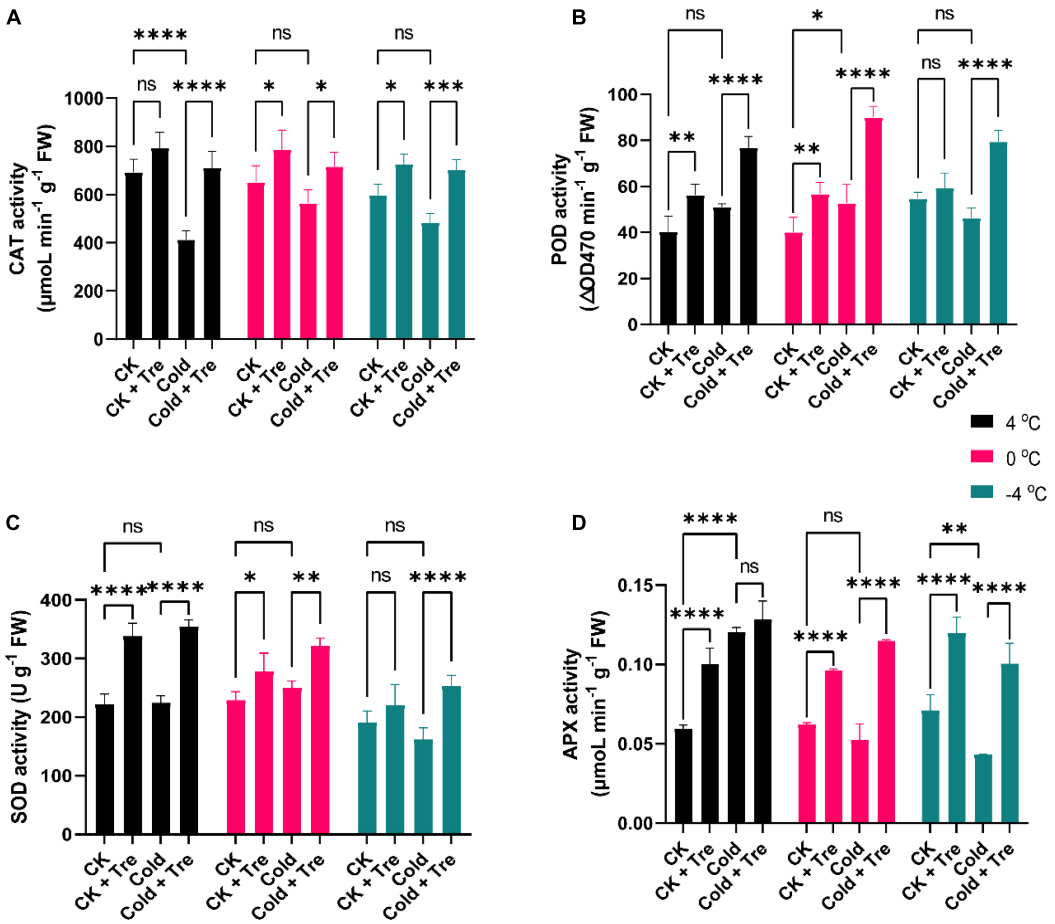


FIGURE 4 | Impact of Tre on antioxidant enzyme activities in rapeseed seedling under cold stress conditions. **(A)** Catalase (CAT) activity, **(B)** peroxidase (POD) activity, **(C)** superoxide dismutase (SOD) activity, and **(D)** ascorbate peroxidase (APX) activity under four treatments [control (CK), CK + Tre, Cold, and Cold + Tre] and three stress conditions (4, 0, and –4°C). Tre indicates the application of 20 mM L^{-1} of Tre. Data are expressed as the mean (± SD) from three biological replications for each sample and treatment. Asterisks show significant levels at ****$P < 0.0001$, ***$P \leq 0.001$, **$P \leq 0.01$, *$P \leq 0.05$, and ns means non-significant.

between osmoprotectants, antioxidants, stress-responsive genes, and Tre-induced CS tolerance in the rapeseed seedlings.

Principal Component Analysis

To evaluate the effect of Tre treatments on the studied indices of rapeseed seedlings, the score and loading graphs of PCA were executed (**Figure 9**). The first two components, such as Dim1 (PC1, 57.7%) and Dim2 (PC2, 18.7%) showed the greatest involvement and presented 76.4% of the total variance in the dataset. Concerning CS conditions, the same treatments at different temperatures were clustered nearby, whereas the different treatments were separated effectively by the first two components (**Figure 9A**). This separation of the treatments clearly indicated that the Tre treatment under CS had a substantial ameliorative impact on the studied indices of rapeseed seedlings compared to CK. The first group of the variables of PCA, i.e., PC1, is positively correlated, involving the variables like CAT, SOD, POD, APX, SP, SS, and Pro (**Figure 9B**). On the contrary, a significant negative correlation of PC1 variables involves H_2O_2 and MDA that are aligned with PC2 (**Figure 9B**).

DISCUSSION

Rapeseed is a vital oilseed crop worldwide; however, CS significantly affects its growth and production (He et al., 2021; Mehmood et al., 2021; Raza, 2021; Raza et al., 2021e; Su et al., 2021b). Exogenously applied plant growth regulators (phytohormones, osmolytes, neurotransmitters, etc.) can successfully improve the CS tolerance in different crop plants (Diao et al., 2017; Hu et al., 2017; Waqas et al., 2017; He et al., 2021). Among them, Tre is considered as the "sugar of life" due to its phenomenal protective role against numerous abiotic factors, including high salinity, drought, osmotic pressure, waterlogging, and extreme temperature (Kosar et al., 2019). However, the effect of exogenous Tre in improving the CS tolerance in the rapeseed is still uncertain. Therefore, in the present study, exogenous Tre (20 mM L^{-1}) significantly improved the survival rate of cold-stressed rapeseed seedlings (**Figure 1**). Cold stress alone reduces the growth of the seedlings, while the Tre application showed a protective role. These results are consistent with the previous findings, such as cold-stressed tomato plants showing

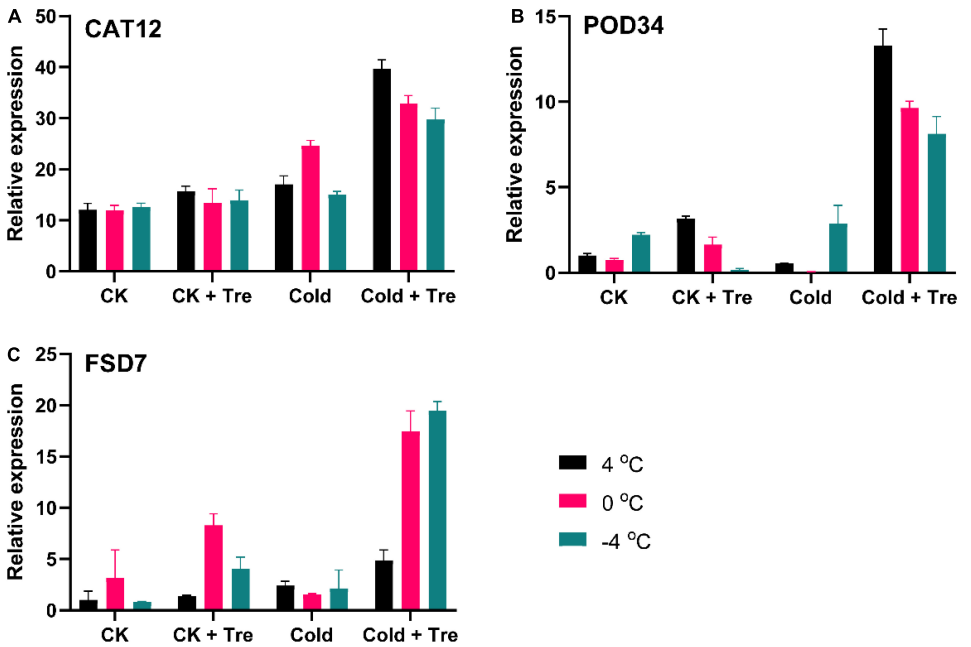


FIGURE 5 | Impact of Tre on the relative expression of antioxidant enzyme-encoding genes in rapeseed seedling under cold stress conditions. **(A)** the relative expression of catalase (*CAT12*) gene, **(B)** the relative expression of peroxidase (*POD34*) gene, and **(C)** the relative expression of superoxide dismutase (Fe-SOD/*FSD7*) gene under four treatments [control (CK), CK + Tre, Cold, and Cold + Tre] and three stress conditions (4, 0, and –4°C). Data are expressed as the mean (± SD) from three technical replications for each sample and treatment.

improved survival rate and growth attributes with 10 mM of Tre treatment (Liu et al., 2020). In another study, seed priming with Tre and Tre + spermidine significantly improved the seed vigor and the growth of the cold-stressed rice seedlings (Fu et al., 2020). In wheat, exogenous Tre inhibited floret degeneration and improved the floret fertility in the apical spikelets, thereby considerably lowering the grain number per spike under CS conditions (Liang et al., 2021). The report in the rapeseed also supports the protective role of Tre in advancing the plant growth and production under adverse environmental conditions, mainly under CS conditions.

Previous reports show a positive association between osmoprotectants and CS tolerance in plants (Fu et al., 2020; Liu et al., 2020; He et al., 2021). Shifting the osmotic stability is meant to be adequate to retain the veracity and strength of the cell membrane of the plants to adapt to stress conditions. Proline has important roles in osmotic alteration in the stress signal transduction, and it also functions as an antioxidant. The upsurge of the Pro level under various stresses was reported earlier (Kaur and Asthir, 2015; Fu et al., 2020). In this study, the Tre treatment increases the SP, SS, and Pro contents in cold-stressed seedlings than CK and improves the CS tolerance (**Figure 2**). These findings are in agreement with the previous results of Fu et al. (2020), who found that Tre-primed seedlings significantly increase the SS and Pro contents in rice under CS conditions. Drought-stressed *Alpinia zerumbet* plants also showed an increase in leaf-free Pro contents with the foliar application of Tre (Zulfiqar et al., 2021a). In another study, Xie et al. (2015a) reported that exogenous Tre increased the SS and SP contents in wheat plants and improved the CS tolerance in wheat. Under salt stress, the exogenously applied Tre also upsurges the SS contents in *Arabidopsis* plants (Yang et al., 2014). In a recent report, exogenous Tre improves the oxidative damage triggered by high temperature, coordinating the influence of wheat on heat stress by regulating the gene expression (Luo et al., 2021). These findings indicate that exogenous Tre plays a significant part in regulating the osmotic substances because Tre participates in sugar metabolism mainly under stress conditions which are important to minimize the adverse effect of multiple stresses.

Induction of oxidative stress is a common consequence of abiotic factors (Hasanuzzaman et al., 2020), and CS triggers the ROS overproduction and imbalanced the redox state (Mittler, 2017; Ding et al., 2019; Hasanuzzaman et al., 2020). Nonetheless, ROS are vital for several essential natural progressions, such as cellular proliferation and dierentiation (Mittler, 2017). The MDA is interpreted as an end product of lipid peroxidation, and the regulated MDA contents disclose the oxidative stress levels in the plants (Gaweł et al., 2004), whereas H_2O_2 is a vital signaling molecule in regulating the stress responses in plants (Neill et al., 2002). In this study, the CS increased the H_2O_2 and MDA contents by decreasing the temperature (from 4^oC to -4^oC). Interestingly, the Tre treatment decreased the MDA contents mainly at 4^oC and -4^oC, and decreased the H_2O_2 contents at 0^oC in cold-stressed rapeseed seedlings (**Figure 3**). However, alleviated or nearly no change in H_2O_2 contents at 4^o and -4^oC in the cold-stressed rapeseed seedlings was observed, indicating that Tre may have complex effects on the stressed

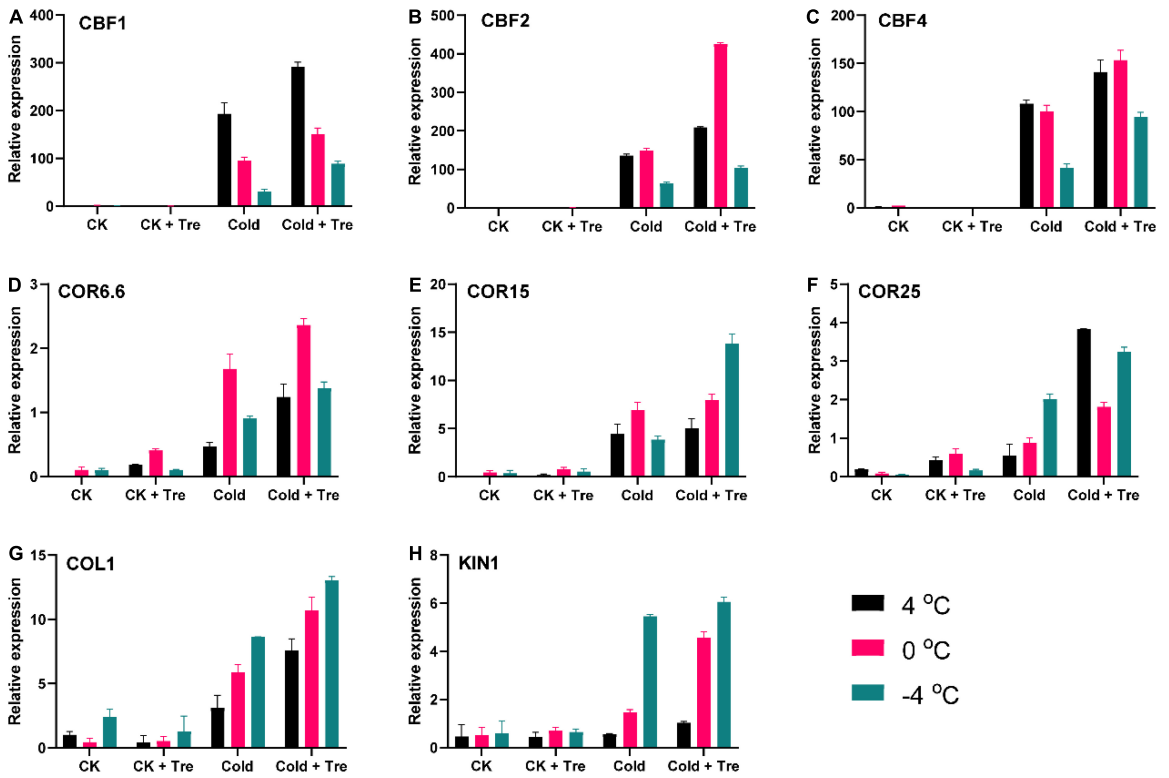


FIGURE 6 | Impact of Tre on the relative expression of cold stress-related marker genes in rapeseed seedling under cold stress conditions. **(A–C)** the relative expression of C-repeat/dehydration responsive element (CRT/DRE) binding factor (*CBF1, CBF2,* and *CBF4*) genes; **(D–F)** the relative expression of cold-regulated (*COR6.6, COR15,* and *COR25*) genes; **(G)** the relative expression of Collagen 1 (*COL1*) gene, and **(H)** the relative expression of *KIN1* gene under four treatments [control (CK), CK + Tre, Cold, and Cold + Tre] and three stress conditions (4, 0, and –4°C). Data are expressed as the mean (± SD) from three technical replications for each sample and treatment.

rapeseed (**Figure 3**). It has been known that the H_2O_2 and MDA contents were closely associated with the extent of CS, which act as a negative symbol of the CS tolerance in the rapeseed (Yan et al., 2019; He et al., 2021), and H_2O_2 also serves as a signaling component. Our results are in agreement with the previous study (Liu et al., 2020), which also found that CS increased the MDA contents, and Tre treatment reduces the MDA contents in cold-stressed tomato plants. Similarly, Tre treatment reduces the level of MDA and thus improves the CS tolerance in wheat plants (Xie et al., 2015a). Under drought stress, exogenous Tre reduces the H_2O_2 and MDA contents in sweet basil (*Ocimum basilicum* L.) and improves drought tolerance by mitigating the adverse effect of oxidative stress (Zulfiqar et al., 2021b). Under CS conditions, the H_2O_2 contents were reduced over time, whereas the Tre treatment increased it in the tomato plants (Liu et al., 2020). At certain time points, there was no considerable influence on the H_2O_2 contents in cold-stressed plants (Liu et al., 2020). These results support our findings as there was no major divergence in the H_2O_2 contents at 4^o and -4^oC. In a recent report, exogenous Tre induces the rise in H_2O_2 and nitric oxide levels in cold stressed melon plants (Liu et al., 2021). In plants, CS leads to ROS production, and antioxidative enzymes display crucial responsibilities in preserving the redox stability by ROS scavenging (Mittler, 2017; Hasanuzzaman et al., 2020). The enhanced activities of POD, CAT, SOD, and APX are generally considered as markers of CS tolerance in plants (Yan et al., 2019; Liu et al., 2020; He et al., 2021). In the current study, the SOD, CAT, POD, and APX activities were significantly decreased under CS conditions, except on a few occasions, such as SOD had no significant change at 4 and 0°C; POD activity was increased at 4 and 0°C in cold-stressed seedlings (**Figure 4**). The cold-stressed melon plants increase the SOD, APX, and glutathione reductase activities with Tre application compared to CK (Liu et al., 2021). Interestingly, the Tre treatment significantly improved the activities of CAT, SOD, POD, and APX in cold-stressed rapeseed seedlings and improved the freezing tolerance (**Figure 4**). These results are in agreement with the previous studies (Xie et al., 2015a; Liu et al., 2020). Foliar application of Tre increases the SOD, POD, and CAT activities in drought stressed-sweet basil and improves the overall growth and physiological attributes (Zulfiqar et al., 2021b). Previous studies have shown that Tre can lessen ROS production in plants under abiotic conditions (temperature, drought, salinity, and heavy metals) by improving the antioxidant defense systems (Kosar et al., 2020). It was further confirmed by the correlation analysis where SP, SS, and Pro were positively correlated with SOD, POD, CAT, and APX; meanwhile, they were negatively correlated with the H_2O_2 and MDA contents (**Figure 8**). These observations proved that Tre also serves as a

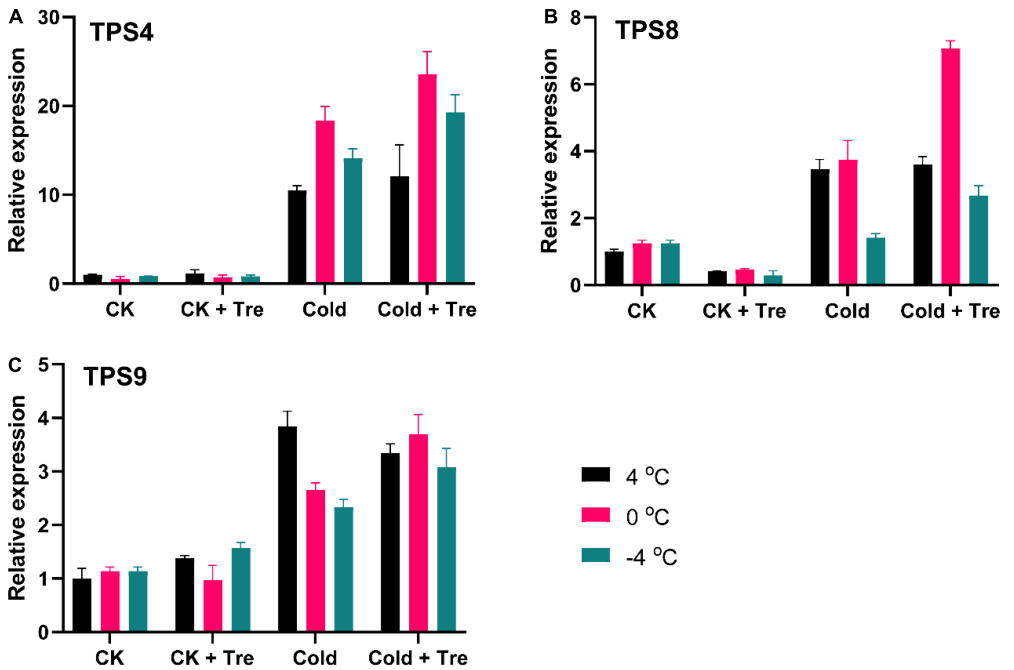


FIGURE 7 | Impact of Tre on the relative expression of trehalose-6-phosphate synthase (TPS)-biosynthesis genes in rapeseed seedling under cold stress conditions. **(A)** the relative expression of *TPS4* gene, **(B)** the relative expression of *TPS8* gene, and **(C)** the relative expression of *TPS9* gene under four treatments [control (CK), CK + Tre, Cold, and Cold + Tre] and three stress conditions (4, 0, and –4°C). Data are expressed as the mean (± SD) from three technical replications for each sample and treatment.

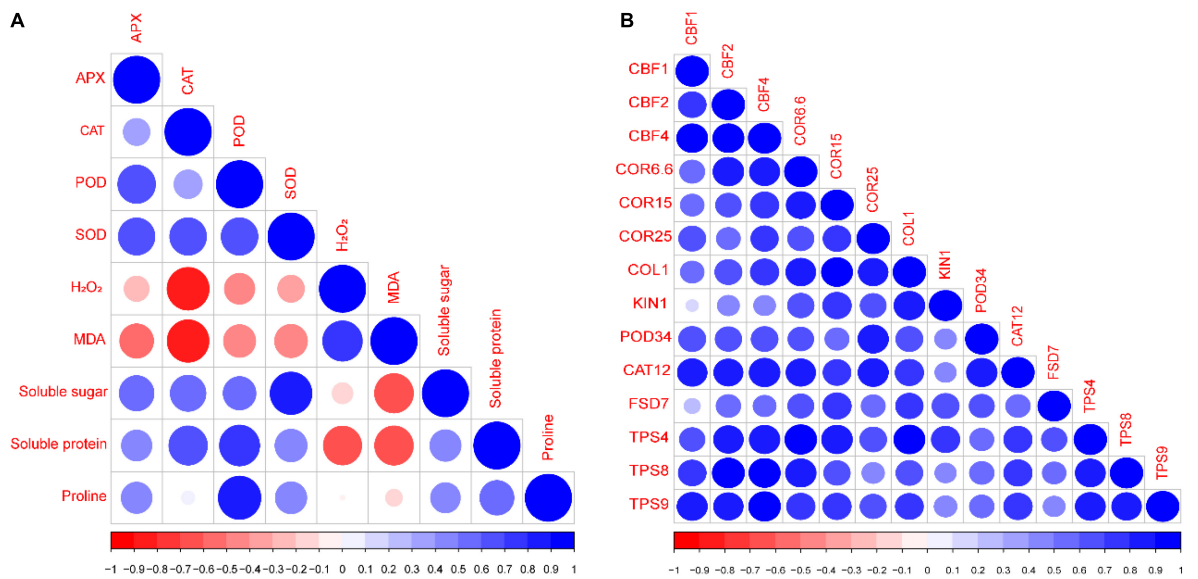


FIGURE 8 | Pearson's correlation analysis between **(A)** different studied indices and **(B)** stress-responsive genes of rapeseed seedlings grown under four treatments [control (CK), CK + Tre, Cold, and Cold + Tre] and three stress conditions (4, 0, and –4°C). Blue and red colors indicate positive and negative correlation, respectively.

booster for improving the defense mechanisms in plants, mainly under adverse abiotic stress conditions.

As antioxidant enzyme plays a substantial part in ROS scavenging and improving the CS tolerance with the help of exogenous Tre, we evaluated the expression levels of antioxidant genes (**Figure 5**). In this study, it was observed that the CS induced the activities of antioxidant defense systems and the expression level of the relative genes. On the contrary, the exogenous Tre increases the expression levels of *CAT12, POD34,* and *FSD7* genes in the cold-stressed seedlings (**Figure 5**),

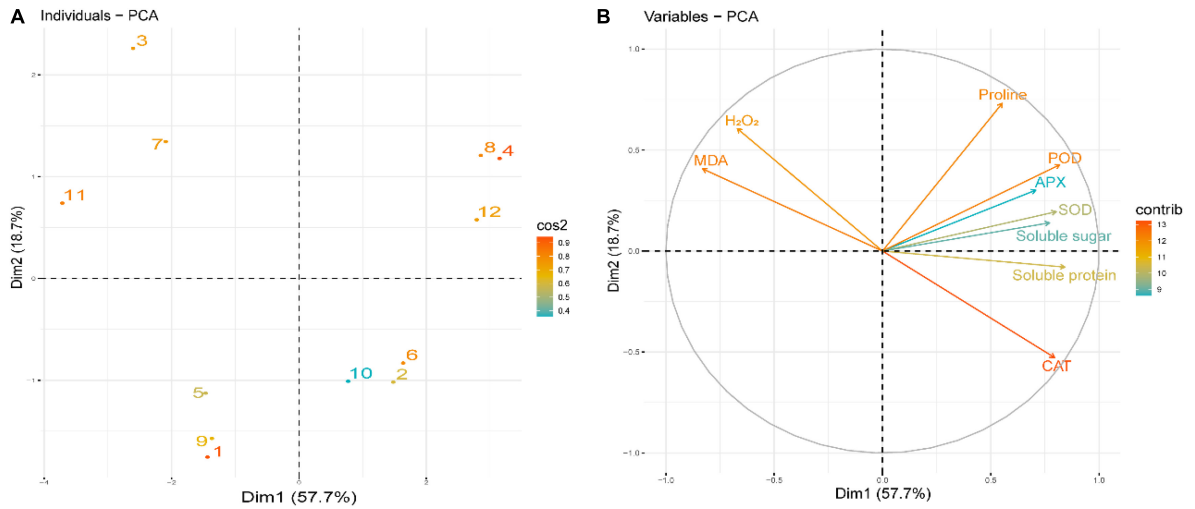


FIGURE 9 | Principal component analysis (PCA) of **(A)** individual treatments by PCA and **(B)** different studied indices of rapeseed seedlings grown under four treatments [control (CK), CK + Tre, Cold, and Cold + Tre] and three stress conditions (4, 0, and −4°C). **(A)** Score plot signifies the partition of treatments as (1) CK_4°C, (2) CK + Tre_4°C, (3) Cold_4°C, (4) Cold + Tre_4°C, (5) CK_0°C, (6) CK + Tre_0°C, (7) Cold_0°C, (8), Cold + Tre_0°C, (9) CK_−4°C, (10) CK + Tre_−4°C, (11), Cold_−4°C, and (12) Cold + Tre_−4°C. Other abbreviations are defined in the main text.

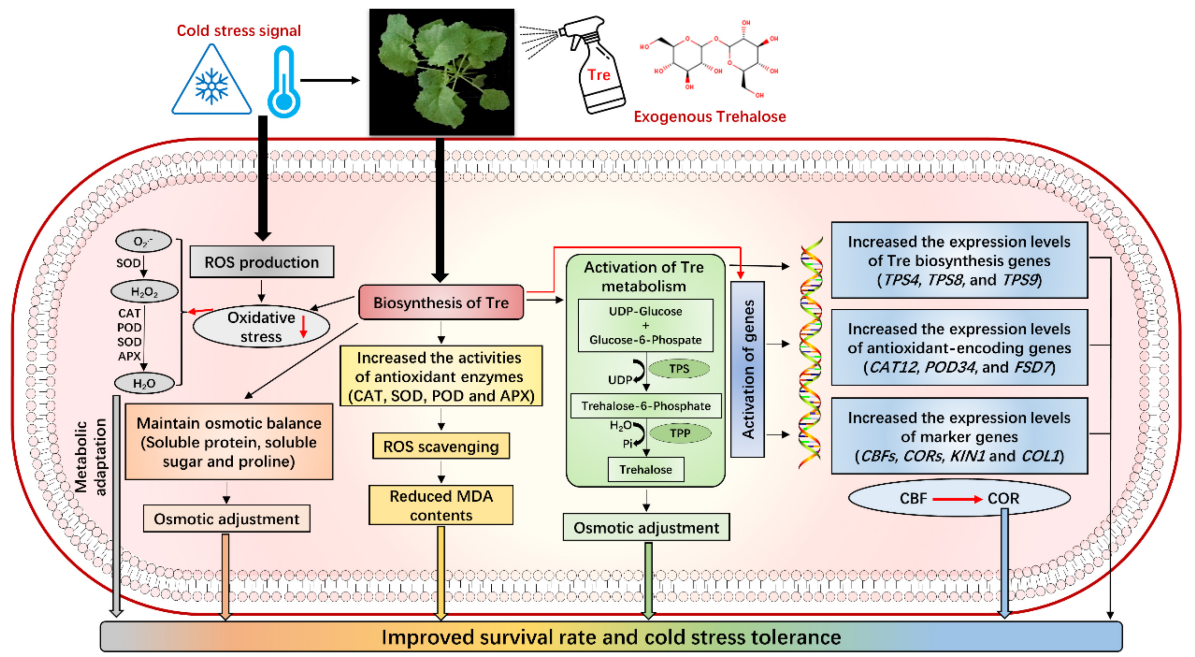


FIGURE 10 | Mechanism of Tre-induced cold stress tolerance in rapeseed seedlings. Exogenous Tre not only regulates the antioxidant defense system and osmotic adjustment, but it also significantly participates in the activation of Tre metabolism and signaling network to improve cold tolerance in rapeseed by regulating the expression levels of stress-responsive genes.

indicating that SOD catalyzed oxygen change into H_2O_2, which was then switched to water/oxygen through CAT/SOD in cold-stressed seedlings (Mittler, 2002). This could facilitate the CS response in rapeseed and eventually lead to CS tolerance (Yan et al., 2019; Liu et al., 2020; He et al., 2021). It can be concluded that the CS induced the activities of antioxidants and cannot entirely negotiate additional ROS production. The exogenous Tre boosts the expression levels of antioxidant enzyme-encoding genes in the rapeseed seedlings. Similar observations have also been reported by Liu et al. (2020), who reported the increased expressions of *Cu/Zn-SOD, APX5, CAT1,* and *GR1* genes with Tre treatments in the cold stressed tomato leaves.

Until now, ICE-CBF-COR signaling pathways have been clearly characterized under CS conditions (Wang et al., 2017; Shi et al., 2018; He et al., 2021). Thus, the expression levels of CS-responsive marker genes, including *CBFs, CORs, COL1,* and *KIN1,* were evaluated (**Figure 6**). The results showed that Tre treatment substantially enhanced the expression levels of *CBF1, CBF2, CBF4, COR6.6, COR15, COR25, COL1,* and *KIN1* genes in cold-stressed rapeseed seedlings compared to CK (**Figure 6**). It signified that Tre was involved in the transcriptional regulation, mainly by altering the expression levels of *CBFs* and *CORs* genes. Recently, it was described that the exogenous treatment with other plant growth regulators like melatonin improves the CS tolerance by adjusting the expression levels of *AtCBF1-AtCBF3* and *COR15a* genes in *Arabidopsis* (Shi et al., 2015). Similar results were recorded in the rapeseed plants under CS, where melatonin increases the expression levels of several CS-responsive marker genes, including *CBFs, CORs, COL1,* etc., (He et al., 2021). In the near future, more insightful studies are required to fully explore the Tre-induced increase in gene expression levels, mainly under CS conditions.

Further, the expression levels of Tre-biosynthesis genes were also evaluated (**Figure 7**). Recent findings showed that the *TPS* gene family mainly responds to several abiotic factors in plants (Yang et al., 2012; Xie et al., 2015b; Rahman et al., 2021). In the present study, we observed that *TPS4, TPS8,* and *TPS9* significantly responded to CS, whereas their expression levels increased with Tre treatments in cold-stressed rapeseed seedlings (**Figure 7**). The highest expression levels were detected at 0°C with Tre treatment. In a recent study, it was observed that the Tre treatments increased the expression levels of *OsTPP1* and *OsTPP2* genes in rice plants under CS conditions (Fu et al., 2020). Further, Joshi et al. (2020) reported that the increased Tre biosynthesis improves yield potential in rice plants under drought, saline, and sodic conditions. It was further confirmed by correlation analysis, where all the expression levels of investigated genes were positively correlated with each other (**Figure 8**) which helped the rapeseed plants to survive under CS conditions. Similarly, the overexpression of *TPS* genes also increased the endogenous Tre contents and improved the tolerance to multiple abiotic stress conditions, such as salinity (Ge et al., 2008; Lyu et al., 2013), cold (Liu et al., 2019), heat (Lyu et al., 2018), drought (Suárez et al., 2008; Lyu et al., 2013; Nuccio et al., 2015; Lin et al., 2019), and high light (Rathod et al., 2016). Therefore, we proposed that the high expression levels of Tre-biosynthesis genes could increase the endogenous Tre contents and stress tolerance.

CONCLUSION

In this study, exogenous Tre improved the CS tolerance in the rapeseed seedlings by maintaining the contents of osmoprotectants. Under CS conditions, Tre treatments also activate the antioxidant defense systems and the expression levels of antioxidant-encoding genes to cope with ROS production, thus eventually reducing the MDA damage and lessening the CS-induced growth inhibition. Additionally, Tre also contributed to the signaling network of CS tolerance by increasing the expression levels of markers genes (*CBFs, CORs, KIN1,* and *COL1*) and Tre-biosynthesis genes. It can be determined that the exogenous Tre not only regulates the antioxidant and osmotic balance but also significantly participates in sugar and Tre metabolism to improve CS tolerance in plants (**Figure 10**). Thus, the current study boosted our understanding of Tre-mediated CS response and tolerance in the rapeseed seedlings. In the near future, more in-depth studies are required to fully uncover the Tre-induced gene expression, leading to increased endogenous Tre contents and improving the stress tolerance under various stress conditions.

DATA AVAILABILITY STATEMENT

The original contributions presented in the study are included in the article/supplementary material, further inquiries can be directed to the corresponding author/s.

AUTHOR CONTRIBUTIONS

AR conceived the idea and wrote the manuscript. AR and WS performed the experiment. WS, ZJ, DL, YZ, AG, MH, and SM helped in literature search and data analysis. YC, XZ, and YL supervised the work, reviewed, and edited the manuscript. All authors have read and approved the final version of the manuscript.

FUNDING

This work was supported by the Science and Technology Innovation Project of the Chinese Academy of Agricultural Sciences (CAAS), China, and Fundamental Research Funds for the Central Nonprofit Scientific Institution (OCRI, CAAS, 1610172018010).

ACKNOWLEDGMENTS

AR conveys his special thanks to CAAS for providing Ph.D. Scholarship and research environment. We would also like to thank all the members of the Key Lab of Biology and Genetic Improvement of Oil Crops, Oil Crops Research Institute, the Chinese Academy of Agricultural Sciences (CAAS), Wuhan China for their support throughout the study.

REFERENCES

Allaire, J. (2012). *RStudio: Integrated Development Environment for R*, Vol. 770. Boston, MA: RStudio, 394.

Delorge, I., Janiak, M., Carpentier, S., and Van Dijck, P. (2014). Fine tuning of trehalose biosynthesis and hydrolysis as novel tools for the generation of abiotic stress tolerant plants. *Front. Plant Sci.* 5:147. doi: 10.3389/fpls.2014.00147

Diao, Q., Song, Y., Shi, D., and Qi, H. (2017). Interaction of polyamines, abscisic acid, nitric oxide, and hydrogen peroxide under chilling stress in tomato (Lycopersicon esculentum Mill.) seedlings. *Front. Plant Sci.* 8:203. doi: 10.3389/fpls.2017.00203

Ding, Y., Shi, Y., and Yang, S. (2019). Advances and challenges in uncovering cold tolerance regulatory mechanisms in plants. *N. Phytol.* 222, 1690–1704. doi: 10.1111/nph.15696

Fu, Y., Zhang, Z., Liu, J., Chen, M., Pan, R., Hu, W., et al. (2020). Seed priming with spermidine and trehalose enhances chilling tolerance of rice via different mechanisms. *J. Plant Growth Regul.* 39, 669–679.

Gaweł, S., Wardas, M., Niedworok, E., and Wardas, P. (2004). Malondialdehyde (MDA) as a lipid peroxidation marker. *Wiadomosci. Lekarskie (Warsaw, Poland: 1960)* 57, 453–455.

Ge, L.-F., Chao, D.-Y., Shi, M., Zhu, M.-Z., Gao, J.-P., and Lin, H.-X. (2008). Overexpression of the trehalose-6-phosphate phosphatase gene OsTPP1 confers stress tolerance in rice and results in the activation of stress responsive genes. *Planta* 228, 191–201. doi: 10.1007/s00425-008-0729-x

Hasanuzzaman, M., Bhuyan, M., Zulfiqar, F., Raza, A., Mohsin, S. M., Mahmud, J. A., et al. (2020). Reactive oxygen species and antioxidant defense in plants under abiotic stress: revisiting the crucial role of a universal defense regulator. *Antioxidants* 9:681. doi: 10.3390/antiox9080681

He, H., Lei, Y., Yi, Z., Raza, A., Zeng, L., Yan, L., et al. (2021). Study on the mechanism of exogenous serotonin improving cold tolerance of rapeseed (Brassica napus L.) seedlings. *Plant Growth Regul.* 94, 161–170.

Hu, Y., Jiang, Y., Han, X., Wang, H., Pan, J., and Yu, D. (2017). Jasmonate regulates leaf senescence and tolerance to cold stress: crosstalk with other phytohormones. *J. Exp. Bot.* 68, 1361–1369. doi: 10.1093/jxb/erx004

Ibrahim, H. A., and Abdellatif, Y. M. (2016). Effect of maltose and trehalose on growth, yield and some biochemical components of wheat plant under water stress. *Ann. Agric. Sci.* 61, 267–274.

Joshi, R., Sahoo, K. K., Singh, A. K., Anwar, K., Pundir, P., Gautam, R. K., et al. (2020). Enhancing trehalose biosynthesis improves yield potential in marker-free transgenic rice under drought, saline, and sodic conditions. *J. Exp. Bot.* 71, 653–668. doi: 10.1093/jxb/erz462

Kassambara, A., and Mundt, F. (2020). *Factoextra: Extract and Visualize the Results of Multivariate Data Analyses (Version R Package version 1.0. 7.) [Computer software]. Retrieved July 15, 2020*.

Kaur, G., and Asthir, B. (2015). Proline: a key player in plant abiotic stress tolerance. *Biol. Plantarum* 59, 609–619.

Kosar, F., Akram, N. A., Ashraf, M., Ahmad, A., Alyemeni, M. N., and Ahmad, P. (2020). Impact of exogenously applied trehalose on leaf biochemistry, achene yield and oil composition of sunflower under drought stress. *Physiol. Plant* 172, 317–333. doi: 10.1111/ppl.13155

Kosar, F., Akram, N. A., Sadiq, M., Al-Qurainy, F., and Ashraf, M. (2019). Trehalose: a key organic osmolyte effectively involved in plant abiotic stress tolerance. *J. Plant Growth Regul.* 38, 606–618. doi: 10.1007/s00344-018-9876-x

Kretovich, V. (1980). *Biochemistry of Plants*. Moscow: Vysshaya Shkola, 30–35.

Lei, Y., Shah, T., Cheng, Y., Yan, L., Zhang, X.-K., and Zou, X.-L. (2019). Physiological and molecular responses to cold stress in rapeseed (Brassica napus L.). *J. Integrat. Agric.* 18, 2742–2752.

Li, W., Huai, X., Li, P., Raza, A., Mubarik, M. S., Habib, M., et al. (2021). Genome-Wide Characterization of Glutathione Peroxidase (GPX) gene family in rapeseed (Brassica napus L.) revealed their role in multiple abiotic stress response and hormone signaling. *Antioxidants* 10:1481. doi: 10.3390/antiox10091481

Liang, Z., Luo, J., Wei, B., Liao, Y., and Liu, Y. (2021). Trehalose can alleviate decreases in grain number per spike caused by low-temperature stress at the booting stage by promoting floret fertility in wheat. *J. Agronomy Crop Sci.* 2017, 717–732.

Lin, Q., Yang, J., Wang, Q., Zhu, H., Chen, Z., Dao, Y., et al. (2019). Overexpression of the trehalose-6-phosphate phosphatase family gene AtTPPF improves the drought tolerance of Arabidopsis thaliana. *BMC Plant Biol.* 19:381. doi: 10.1186/s12870-019-1986-5

Liu, Q., Kasuga, M., Sakuma, Y., Abe, H., Miura, S., Yamaguchi-Shinozaki, K., et al. (1998). Two transcription factors, DREB1 and DREB2, with an EREBP/AP2 DNA binding domain separate two cellular signal transduction pathways in drought-and low-temperature-responsive gene expression, respectively, in Arabidopsis. *Plant Cell* 10, 1391–1406. doi: 10.1105/tpc.10.8.1391

Liu, T., Shi, J., Li, M., Ye, X., and Qi, H. (2021). Trehalose triggers hydrogen peroxide and nitric oxide to participate in melon seedlings oxidative stress tolerance under cold stress. *Environ. Exp. Bot.* 184:104379. doi: 10.1016/j.envexpbot.2021.104379

Liu, T., Ye, X., Li, M., Li, J., Qi, H., and Hu, X. (2020). H2O2 and NO are involved in trehalose-regulated oxidative stress tolerance in cold-stressed tomato plants. *Environ. Exp. Bot.* 171:103961.

Liu, X., Fu, L., Qin, P., Sun, Y., Liu, J., and Wang, X. (2019). Overexpression of the wheat trehalose 6-phosphate synthase 11 gene enhances cold tolerance in Arabidopsis thaliana. *Gene* 710, 210–217. doi: 10.1016/j.gene.2019.06.006

Lohani, N., Jain, D., Singh, M. B., and Bhalla, P. L. (2020). Engineering multiple abiotic stress tolerance in canola, Brassica napus. *Front. Plant Sci.* 11:3. doi: 10.3389/fpls.2020.00003

Luo, Y., Li, F., Wang, G., Yang, X., and Wang, W. (2010). Exogenously-supplied trehalose protects thylakoid membranes of winter wheat from heat-induced damage. *Biol. Plantarum* 54, 495–501.

Luo, Y., Li, W.-M., and Wang, W. (2008). Trehalose: protector of antioxidant enzymes or reactive oxygen species scavenger under heat stress? *Environ. Exp. Bot.* 63, 378–384. doi: 10.1016/j.envexpbot.2007.11.016

Luo, Y., Xie, Y., Li, W., Wei, M., Dai, T., Li, Z., et al. (2021). Physiological and transcriptomic analyses reveal exogenous trehalose is involved in the responses of wheat roots to high temperature stress. *Plants* 10:2644. doi: 10.3390/plants10122644

Lyu, J. I., Min, S. R., Lee, J. H., Lim, Y. H., Kim, J.-K., Bae, C.-H., et al. (2013). Overexpression of a trehalose-6-phosphate synthase/phosphatase fusion gene enhances tolerance and photosynthesis during drought and salt stress without growth aberrations in tomato. *Plant Cell Tissue Organ Culture (PCTOC)* 112, 257–262.

Lyu, J. I., Park, J. H., Kim, J.-K., Bae, C.-H., Jeong, W.-J., Min, S. R., et al. (2018). Enhanced tolerance to heat stress in transgenic tomato seeds and seedlings overexpressing a trehalose-6-phosphate synthase/phosphatase fusion gene. *Plant Biotechnol. Rep.* 12, 399–408. doi: 10.1007/s11816-018-0505-8

Mehmood, S. S., Lu, G., Luo, D., Hussain, M. A., Raza, A., Zafar, Z., et al. (2021). Integrated Analysis of Transcriptomics and Proteomics provides insights into the molecular regulation of cold response in *Brassica napus*. *Environ. Exp. Bot.* 187:104480.

Mittler, R. (2002). Oxidative stress, antioxidants and stress tolerance. *Trends Plant Sci.* 7, 405–410.

Mittler, R. (2017). ROS are good. *Trends Plant Sci.* 22, 11–19. doi: 10.1016/j.tplants.2016.08.002

Mubarik, M. S., Khan, S. H., Sajjad, M., Raza, A., Hafeez, M. B., Yasmeen, T., et al. (2021). A manipulative interplay between positive and negative regulators of phytohormones: a way forward for improving drought tolerance in plants. *Physiol. Plantarum* 172, 1269–1290. doi: 10.1111/ppl.13325

Neill, S., Desikan, R., and Hancock, J. (2002). Hydrogen peroxide signalling. *Curr. Opin. Plant Biol.* 5, 388–395.

Nuccio, M. L., Wu, J., Mowers, R., Zhou, H.-P., Meghji, M., Primavesi, L. F., et al. (2015). Expression of trehalose-6-phosphate phosphatase in maize ears improves yield in well-watered and drought conditions. *Nat. Biotechnol.* 33, 862–869. doi: 10.1038/nbt.3277

Paul, M. J., Primavesi, L. F., Jhurreea, D., and Zhang, Y. (2008). Trehalose metabolism and signaling. *Annu. Rev. Plant Biol.* 59, 417–441.

Rahman, M. M., Rahman, M. M., Eom, J.-S., and Jeon, J.-S. (2021). Genome-wide identification, expression profiling and promoter analysis of trehalose-6-phosphate phosphatase gene family in rice. *J. Plant Biol.* 64, 55–71.

Rathod, J. P., Prakash, G., Vira, C., and Lali, A. M. (2016). Trehalose phosphate synthase overexpression in Parachlorella kessleri improves growth and photosynthetic performance under high light conditions. *Preparat. Biochem. Biotechnol.* 46, 803–809. doi: 10.1080/10826068.2015.1135465

Raza, A. (2021). Eco-physiological and biochemical responses of rapeseed (*Brassica napus* L.) to abiotic stresses: consequences and mitigation strategies. *J. Plant Growth Regul.* 40, 1368–1388.

Raza, A., Tabassum, J., Kudapa, H., and Varshney, R. K. (2021c). Can omics deliver temperature resilient ready-to-grow crops? *Crit. Rev. Biotechnol.* 41, 1209–1232. doi: 10.1080/07388551.2021.1898332

Raza, A., Razzaq, A., Mehmood, S. S., Hussain, M. A., Wei, S., He, H., et al. (2021a). Omics: the way forward to enhance abiotic stress tolerance in *Brassica napus* L. *GM Crops Food* 12, 251–281. doi: 10.1080/21645698.2020.1859898

Raza, A., Tabassum, J., Mubarik, M., Anwar, S., Zahra, N., Sharif, Y., et al. (2021d). Hydrogen sulfide: an emerging component against abiotic stress in plants. *Plant Biol.* doi: 10.1111/plb.13368

Raza, A., Su, W., Gao, A., Mehmood, S. S., Hussain, M. A., Nie, W., et al. (2021b). Catalase (CAT) gene family in rapeseed (Brassica napus L.): genome-wide analysis, identification, and expression pattern in response to multiple hormones and abiotic stress conditions. *Inter. J. Mol. Sci.* 22:4281. doi: 10.3390/ijms22084281

Raza, A., Su, W., Hussain, M. A., Mehmood, S. S., Zhang, X., Cheng, Y., et al. (2021e). Integrated analysis of metabolome and transcriptome reveals insights for cold tolerance in rapeseed (*Brassica napus* L.). *Front. Plant Sci.* 12:721681. doi: 10.3389/fpls.2021.721681

Sabagh, A. E., Mbarki, S., Hossain, A., Iqbal, M., Islam, M., Raza, A., et al. (2021). Potential role of plant growth regulators in administering crucial processes against abiotic stresses. *Front. Agron.* 3:648694. doi: 10.3389/fagro.2021.648694

Samadi, S., Habibi, G., and Vaziri, A. (2019). Exogenous trehalose alleviates the inhibitory effects of salt stress in strawberry plants. *Acta Physiol. Plantarum* 41, 1–11.

Schwarz, S., and Van Dijck, P. (2017). Trehalose metabolism: a sweet spot for Burkholderia pseudomallei virulence. *Virulence* 8, 5–7. doi: 10.1080/21505594.2016.1216295

Shi, H., Qian, Y., Tan, D. X., Reiter, R. J., and He, C. (2015). Melatonin induces the transcripts of CBF/DREB1s and their involvement in both abiotic and biotic stresses in Arabidopsis. *J. Pineal Res.* 59, 334–342. doi: 10.1111/jpi.12262

Shi, Y., Ding, Y., and Yang, S. (2018). Molecular regulation of CBF signaling in cold acclimation. *Trends Plant Sci.* 23, 623–637. doi: 10.1016/j.tplants.2018.04.002

Su, W., Raza, A., Gao, A., Jia, Z., Zhang, Y., Hussain, M. A., et al. (2021a). Genome-wide analysis and expression profile of superoxide dismutase (SOD) gene family in rapeseed (*Brassica napus* L.) under Different Hormones and Abiotic Stress Conditions. *Antioxidants* 10:1182. doi: 10.3390/antiox10081182

Su, W., Raza, A., Zeng, L., Gao, A., Lv, Y., Ding, X., et al. (2021b). Genome-wide analysis and expression patterns of lipid phospholipid phospholipase gene family in Brassica napus L. *BMC Genomics* 22:548. doi: 10.1186/s12864-021-07862-1

Suárez, R., Wong, A., Ramírez, M., Barraza, A., Orozco, M. D. C., Cevallos, M. A., et al. (2008). Improvement of drought tolerance and grain yield in common bean by overexpressing trehalose-6-phosphate synthase in rhizobia. *Mol. Plant-Microbe Interact.* 21, 958–966. doi: 10.1094/MPMI-21-7-0958

Sun, F., Fan, G., Hu, Q., Zhou, Y., Guan, M., Tong, C., et al. (2017). The high-quality genome of Brassica napus cultivar 'ZS 11'reveals the introgression history in semi-winter morphotype. *Plant J.* 92, 452–468. doi: 10.1111/tpj.13669

Swift, M. L. (1997). GraphPad prism, data analysis, and scientific graphing. *J. Chem. Inform. Comput. Sci.* 37, 411–412.

Thomashow, M. F. (1999). Plant cold acclimation: freezing tolerance genes and regulatory mechanisms. *Annu. Rev. Plant Biol.* 50, 571–599. doi: 10.1146/annurev.arplant.50.1.571

Wang, D.-Z., Jin, Y.-N., Ding, X.-H., Wang, W.-J., Zhai, S.-S., Bai, L.-P., et al. (2017). Gene regulation and signal transduction in the ICE–CBF–COR signaling pathway during cold stress in plants. *Biochemistry (Moscow)* 82, 1103–1117. doi: 10.1134/S0006297917100030

Waqas, M. A., Khan, I., Akhter, M. J., Noor, M. A., and Ashraf, U. (2017). Exogenous application of plant growth regulators (PGRs) induces chilling tolerance in short-duration hybrid maize. *Environ. Sci. Pollut. Res.* 24, 11459–11471. doi: 10.1007/s11356-017-8768-0

Wei, T., Simko, V., Levy, M., Xie, Y., Jin, Y., and Zemla, J. (2017). Package 'corrplot'. *Statistician* 56:e24.

Williams, B., Njaci, I., Moghaddam, L., Long, H., Dickman, M. B., Zhang, X., et al. (2015). Trehalose accumulation triggers autophagy during plant desiccation. *PLoS Genet.* 11:e1005705. doi: 10.1371/journal.pgen.1005705

Wingler, A. (2002). The function of trehalose biosynthesis in plants. *Phytochemistry* 60, 437–440. doi: 10.1016/s0031-9422(02)00137-1

Xie, D., Wang, X., Fu, L., Sun, J., Li, Z., and Zheng, W. (2015a). Effect of exogenous trehalose on germ length and seedling freeze resistance of winter wheat under cold stress. *J. Triticeae Crops* 32, 215–223.

Xie, D., Wang, X., Fu, L., Sun, J., Zheng, W., and Li, Z. (2015b). Identification of the trehalose-6-phosphate synthase gene family in winter wheat and expression analysis under conditions of freezing stress. *J. Genet.* 94, 55–65. doi: 10.1007/s12041-015-0495-z

Yan, L., Shah, T., Cheng, Y., Yan, L., Zhang, X.-K., and Zou, X.-L. (2019). Physiological and molecular responses to cold stress in rapeseed (*Brassica napus* L.). *J. Integrat. Agric.* 18, 2742–2752.

Yang, H.-L., Liu, Y.-J., Wang, C.-L., and Zeng, Q.-Y. (2012). Molecular evolution of trehalose-6-phosphate synthase (TPS) gene family in Populus, Arabidopsis and rice. *PLoS One* 7:e42438. doi: 10.1371/journal.pone.0042438

Yang, L., Zhao, X., Zhu, H., Paul, M., Zu, Y., and Tang, Z. (2014). Exogenous trehalose largely alleviates ionic unbalance, ROS burst, and PCD occurrence induced by high salinity in Arabidopsis seedlings. *Front. Plant Sci.* 5:570. doi: 10.3389/fpls.2014.00570

Zahra, N., Shaukat, K., Hafeez, M. B., Raza, A., Hussain, S., Chaudhary, M. T., et al. (2021). "Physiological and molecular responses to high, chilling, and freezing temperature in plant growth and production: consequences and mitigation possibilities," in *Harsh Environment and Plant Resilience: Molecular and Functional Aspects*, ed. A. Husen (Cham: Springer), 235.

Zulfiqar, F., Chen, J., Finnegan, P. M., Nafees, M., Younis, A., Shaukat, N., et al. (2021a). Foliar application of trehalose or 5-Aminolevulinic acid improves photosynthesis and biomass production in drought stressed alpinia zerumbet. *Agriculture* 11:908.

Zulfiqar, F., Chen, J., Finnegan, P. M., Younis, A., Nafees, M., Zorrig, W., et al. (2021b). Application of trehalose and salicylic acid mitigates drought stress in sweet basil and improves plant growth. *Plants* 10:1078. doi: 10.3390/plants10061078

Conflict of Interest: The authors declare that the research was conducted in the absence of any commercial or financial relationships that could be construed as a potential conflict of interest.

Publisher's Note: All claims expressed in this article are solely those of the authors and do not necessarily represent those of their affiliated organizations, or those of the publisher, the editors and the reviewers. Any product that may be evaluated in this article, or claim that may be made by its manufacturer, is not guaranteed or endorsed by the publisher.

Copyright © 2022 Raza, Su, Jia, Luo, Zhang, Gao, Hussain, Mehmood, Cheng, Lv and Zou. This is an open-access article distributed under the terms of the Creative Commons Attribution License (CC BY). The use, distribution or reproduction in other forums is permitted, provided the original author(s) and the copyright owner(s) are credited and that the original publication in this journal is cited, in accordance with accepted academic practice. No use, distribution or reproduction is permitted which does not comply with these terms.

frontiers in Plant Science

REVIEW
published: 23 March 2022
doi: 10.3389/fpls.2022.819658

Multidimensional Role of Silicon to Activate Resilient Plant Growth and to Mitigate Abiotic Stress

Rakeeb Ahmad Mir[1], Basharat Ahmad Bhat[2], Henan Yousuf[3], Sheikh Tajamul Islam[2], Ali Raza[4]*, Masood Ahmad Rizvi[5], Sidra Charagh[6], Mohammed Albaqami[7], Parvaze A. Sofi[8] and Sajad Majeed Zargar[9]**

[1] Department of Biotechnology, School of Life Sciences, Central University of Kashmir, Ganderbal, India, [2] Centre of Research for Development, University of Kashmir, Srinagar, India, [3] Department of Biotechnology, School of Biosciences and Biotechnology, Baba Ghulam Shah Badshah University, Rajouri, India, [4] Key Laboratory of Ministry of Education for Genetics, Breeding and Multiple Utilization of Crops, Oil Crops Research Institute, Center of Legume Crop Genetics and Systems Biology/College of Agriculture, Fujian Agriculture and Forestry University (FAFU), Fuzhou, China, [5] Department of Chemistry, University of Kashmir, Srinagar, India, [6] State Key Laboratory of Rice Biology, China National Rice Research Institute, Chinese Academy of Agricultural Science, Hangzhou, China, [7] Department of Biology, Faculty of Applied Science, Umm Al-Qura University, Makkah, Saudi Arabia, [8] Division of Genetics and Plant Breeding, Sher-e-Kashmir University of Agricultural Sciences and Technology of Kashmir, Srinagar, India, [9] Proteomics Laboratory, Division of Plant Biotechnology, Sher-e-Kashmir University of Agricultural Sciences and Technology of Kashmir (SKUAST-K), Srinagar, India

Sustainable agricultural production is critically antagonistic by fluctuating unfavorable environmental conditions. The introduction of mineral elements emerged as the most exciting and magical aspect, apart from the novel intervention of traditional and applied strategies to defend the abiotic stress conditions. The silicon (Si) has ameliorating impacts by regulating diverse functionalities on enhancing the growth and development of crop plants. Si is categorized as a non-essential element since crop plants accumulate less during normal environmental conditions. Studies on the application of Si in plants highlight the beneficial role of Si during extreme stressful conditions through modulation of several metabolites during abiotic stress conditions. Phytohormones are primary plant metabolites positively regulated by Si during abiotic stress conditions. Phytohormones play a pivotal role in crop plants' broad-spectrum biochemical and physiological aspects during normal and extreme environmental conditions. Frontline phytohormones include auxin, cytokinin, ethylene, gibberellin, salicylic acid, abscisic acid, brassinosteroids, and jasmonic acid. These phytohormones are internally correlated with Si in regulating abiotic stress tolerance mechanisms. This review explores insights into the role of Si in enhancing the phytohormone metabolism and its role in maintaining the physiological and biochemical well-being of crop plants during diverse abiotic stresses. Moreover, in-depth information about Si's pivotal role in inducing abiotic stress tolerance in crop plants through metabolic and molecular modulations is elaborated. Furthermore, the potential of various high throughput technologies has also been discussed in improving Si-induced multiple stress tolerance. In addition, a special emphasis is engrossed in the role of Si in achieving sustainable agricultural growth and global food security.

Keywords: silicon, phytohormones, abiotic stress, sustainable agriculture, climate change, non-essential elements

OPEN ACCESS

Edited by:
Mohammad Anwar Hossain, Bangladesh Agricultural University, Bangladesh

Reviewed by:
Norollah Kheyri, Islamic Azad University of Gorgan, Iran
Adnan Mustafa, Academy of Sciences of the Czech Republic (ASCR), Czechia
Athar Mahmood, University of Agriculture Faisalabad, Pakistan

****Correspondence:***
Rakeeb Ahmad Mir
rakeebahmad@bgsbu.ac.in
Ali Raza
alirazamughal143@gmail.com
Sajad Majeed Zargar
smzargar@skuastkashmir.ac.in

Specialty section:
This article was submitted to Plant Breeding, a section of the journal Frontiers in Plant Science

Received: *22 November 2021*
Accepted: *31 January 2022*
Published: *23 March 2022*

Citation:
Mir RA, Bhat BA, Yousuf H, Islam ST, Raza A, Rizvi MA, Charagh S, Albaqami M, Sofi PA and Zargar SM (2022) Multidimensional Role of Silicon to Activate Resilient Plant Growth and to Mitigate Abiotic Stress. Front. Plant Sci. 13:819658. doi: 10.3389/fpls.2022.819658

INTRODUCTION

The reduction in crop productivity by 51–82% on a global scale is primarily influenced by abiotic stress factors, such as drought, salinity, heat, cold, toxic heavy metals, hypoxia and anoxia, waterlogging, and nutrient imbalance (Cooke and Leishman, 2016; Zahra et al., 2021; Raza et al., 2022). Contemporary climate change notably imparts drought and heat stress, two major abiotic stress factors resulting in crop loss and productivity (Zandalinas et al., 2018). For instance, studies report that about a 40% loss in yield in maize (*Zea mays* L.) and wheat (*Triticum aestivum* L.) is primarily due to drought stress (Daryanto et al., 2016). Therefore, it is evident that abiotic stress factors are the most severe constraints to global food production, leading to nutritional and food insecurity in the climate-changing era (Del Buono, 2021; Kamenya et al., 2021; Raza, 2022). The last few decades witnessed an increase in the prevalence of abiotic stressors primarily due to unpredictable weather changes induced by global climatic change (Del Buono, 2021; Kamenya et al., 2021; Raza, 2022). Abiotic stressors alter the homeostasis of the physiological, molecular, and biochemical setup of crop plants, such as water relations, nutrient uptake and assimilation, osmotic deregulation, loss of membrane integrity, impairment in enzyme activity, and the most notable decline in photosynthetic efficiency (Moradtalab et al., 2018; Ahanger et al., 2019; Raza, 2021; Raza et al., 2021e). Most of these impairments after exposure to the stress factors are associated with phytohormone production and their transport in underground and aerial parts of plants (Gangwar et al., 2014; Verma et al., 2016; Arif et al., 2021). Moreover, plants primarily respond to these abiotic stressors by producing reactive oxygen species (ROS), which, in turn, induce severe damage to the cellular structures, such as biomembranes and organelles (da Silva and Yücel, 2008; Hasanuzzaman et al., 2020).

To circumvent these harmful effects, plants respond through physiological and molecular mechanistic adjustments to mitigate the adverse impacts of abiotic stressors (Raza, 2021, 2022). Additionally, the defense response to these abiotic stressors includes synthesis of critical proteins linked to metabolism, activation of signal transduction, and regulatory pathways controlled by the expression of a large number of stress-tolerant genes, which, in turn, are regulated by diverse organic and inorganic molecules (da Silva and Yücel, 2008; Hasanuzzaman et al., 2020; Raza et al., 2021e). Among inorganic molecules, Si, formally categorized as the non-essential element, has been recently found to defend against the harmful effects of abiotic stressors in crop plants. The uptake of Si results in the activation of a diverse range of critical genes to mitigate stress conditions to regulate plant growth and development. Si is the second most abundant element found in the earth's crust (Luyckx et al., 2017; Atta et al., 2019; Zargar et al., 2019). Si is crystalline in structure and forms at least two stable oxide forms, *viz*. Si monoxide (SiO) and silica (SiO_2). Average soils contain about 28% Si by weight in silicates, alumina-silicates, and Si dioxide, most of which are unavailable to crop plants. Traces of monosilicic acid found in soil are the only form of Si available to plants (Pereira et al., 2013). A later form of Si is soluble in water and is weakly adsorbed by soil. The transport of Si into aerial parts of crop plants occurs through several specific and non-specific transporters. In several crop plants, such as maize, cucumber, rice, and barley; genes, such as *Lsi2*, *Lsi1*, and *Lsi6*, are responsible for uptake of Si in roots and aerial organs (Wang et al., 2015; Ouellette et al., 2017; Ratcliffe et al., 2017). Among these, *Lsi1* and *Lsi6* transporters belonging to aquaporins are abundantly distributed in shoot and root tissues, whereas *Lsi2*, an anion transporter, is found in membranes of root endodermis (Mitani et al., 2011).

Crop plants may grow well in the absence of Si, although in a few plants, such as rice and horsetail, the absence of Si may make them vulnerable to fungal infections (Law and Exley, 2011). Si has been reported to play numerous roles in mitigating abiotic stress conditions (Coskun et al., 2016; Luyckx et al., 2017; Rasoolizadeh et al., 2018; Zhu et al., 2019a; Alamri et al., 2020; Salim et al., 2021). For instance, Si mediates diverse strategies to sequester the metal ions by modulating soil pH, metal speciation, co-precipitation, and compartmentalization (Debona et al., 2017). Recent trends have proved the evolution of Si-based fertilizers to impart growth and developmental effects of crop plants, such as enhancing photosynthesis and regulating electrolytic leakage under stress conditions (Chen et al., 2011). For example, Si enhances photosynthesis in mango trees and increases water and nutrient uptake under abiotic stress conditions (Santos et al., 2014). Si is found in almost all the plants in variable amounts, imparting varying physiological effects (Cooke and Leishman, 2011). Apart from its critical role in stress tolerance imposed by excess salt and drought, uptake of Si results in enhanced mechanical support to shoots and leaf blades (Chen et al., 2011; Zhu et al., 2019a). Numerous reports reveal the application of Si in mitigating abiotic and biotic stresses in various plant species (Zargar et al., 2019; Gou et al., 2020). Moreover, Si plays a vital role in ameliorating metal toxicity in several crop plants (Chen et al., 2011; Singh et al., 2019; Wu et al., 2019). Moreover, Si helps to mitigate metal ion stresses like that of aluminum (Al) and manganese (Mn) stress in crop plants (Tripathi et al., 2016). Water uptake through aquaporins and root hydraulic conductance is upregulated by administering exogenous Si (Liu P. et al., 2015). For instance, supplementation of Si in Talh trees (*Acacia gerrardii* Benth) induces salinity tolerance, possibly through overproduction of glycine betaine and proline to conserve water in tissues, positively regulating metabolic activity (Al-Huqail et al., 2019). Inclusively, Si is critical to plant growth and metabolism under a diverse range of abiotic stress conditions (**Figure 1**; Song et al., 2014; Yin et al., 2016).

Phytohormones play a pivotal role in stress tolerance by modulating a wide range of physiological, cellular, and molecular responses by activating various signal transduction pathways critical to defense mechanisms (Fahad et al., 2015a; Fei et al., 2019; Mubarik et al., 2021; Sabagh et al., 2021). These critical phytohormone-controlled physiological processes during defense include osmotic adjustment, plant-water relations, source/sink transition, the adjustment in photosynthesis, nutrient allocation, and activation of antioxidant defense systems (Miura and Tada, 2014; Khan et al., 2020a). The main phytohormones proven to mitigate the stress conditions through physiological, biochemical, and molecular adjustments include auxin, CK, ETH,

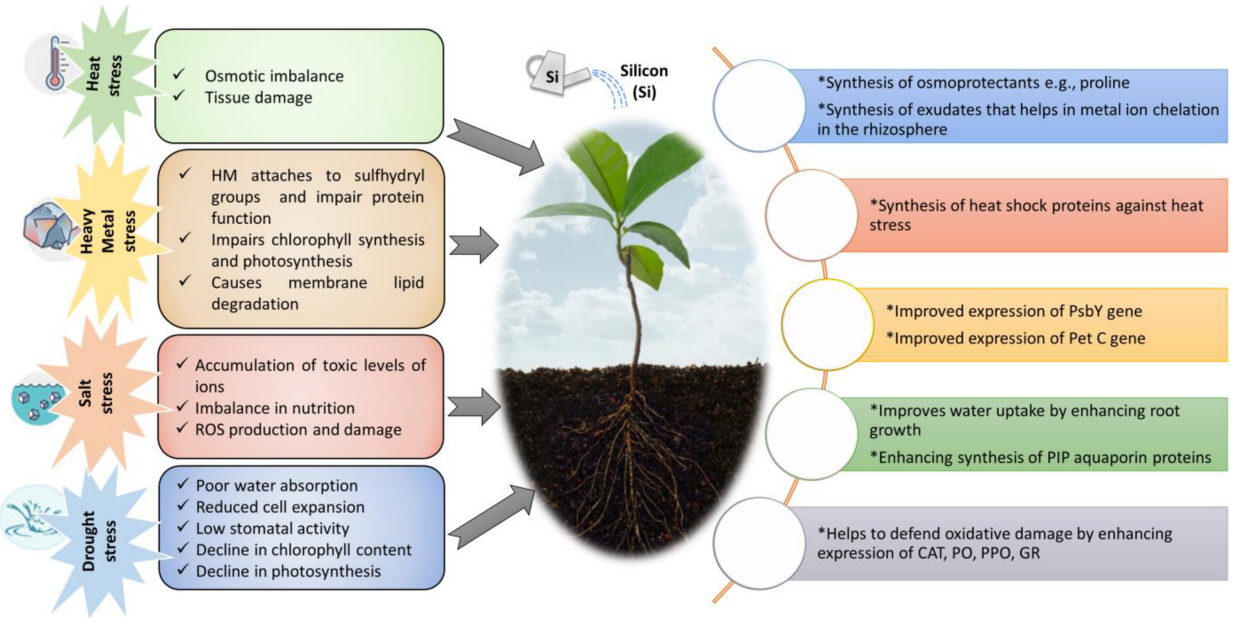


FIGURE 1 | Impact of abiotic stress on various aspects of plant growth and defense mechanisms evoked by application of Si.

GAs, SA, ABA, BRs, and JA (Khan et al., 2020a,b). The levels of phytohormones are reported to be enhanced upon exogenous Si supplementation under abiotic stress conditions (Kim et al., 2016). Considering the beneficial role of Si in alleviating the abiotic stress in crop plants, we believe it is the need of the hour to discuss its clinical properties at the physiological and molecular levels. Against this background, the current review is aimed to provide an in-depth account of the role of Si as a critical element in sustaining plant growth and productivity under abiotic stress conditions. We have also discussed the intervention of Si in triggering the phytohormone synthesis, regulating expression of genes in alleviating the abiotic stress conditions, and detailed the updated account on its role in enhancing growth and metabolism. We believe the current review will pave the way to further open the window of exploring this golden element and its frontline role in attaining global food security.

SILICON – A GOLDEN KEY ELEMENT TO ATTAIN SUSTAINABLE AGRICULTURE GROWTH

Population increase has put immense pressure on the agricultural system to overcome food insecurity. Even though diverse technological interventions increased the crop yield, at the same time, industrialization has triggered an increase in severity of environmental stresses, affecting crop production and, in turn, failure to achieve sustainable agriculture growth. Plants adjust to these factors by modulating their metabolic networks and inducing physiological changes (Raza et al., 2020a,b). Several reports suggest that Si plays an essential role in the production and yield of crops under extreme environmental conditions (Majeed Zargar et al., 2010; Liang et al., 2015b; Zargar et al., 2019; Salim et al., 2021). The growth and the metabolism of several monocots and dicot crops are enhanced by the active accumulation of Si in their organs in larger quantities (Liang et al., 2015c). High salinity results in reproductive disorders because higher Na^+ competes with the transport of K^+ and Ca^{2+} in the plasma membrane of cells (Zhu, 2016). Recent reports have suggested that Si alleviates Na^+ accumulation, oxidative damage, and osmotic stress (Zhu et al., 2015; Flam-Shepherd et al., 2018; Yin et al., 2019). Several defense pathways related to phytohormone synthesis and compatible solutes are triggered by Si against abiotic stressors (Majeed Zargar et al., 2012; Mir et al., 2020). Elevated proline accumulation is observed in salt-sensitive genotypes of okra (*Abelmoschus esculentus*) upon exogenous application of Si to withstand salinity stress (Abbas et al., 2015). Si induced overproduction of total free amino acids, including proline and glycine betaine, in two *Capsicum annuum* cultivars, enhancing tolerance to salt stress (Pereira et al., 2013). Further accumulation of Si in wheat and soybean results in a declined trend of proline content, hence proving the efficacy of Si to induce its own mechanism to mitigate the salt stress (Lee et al., 2010; Bybordi, 2015).

Si administration positively affects the growth, yield, and fruit quality of different fruit crops (Neumann and Zur Nieden, 2001). Si induces water and energy-saving capability, improvement in fruit quality, and an increase in yield. Due to the extent of differences in the Si accumulation, plants differ in their Si-based positive responses to abiotic stressors (Deren, 2001; Mitani and Ma, 2005; Keeping and Reynolds, 2009). Si is accumulated through specific transporters by major crop plants, including dicots like cotton, soybean, cucurbits, tomato, and monocots, such as rice, maize, and wheat, to alleviate different

stress factors (Zargar and Agnihotri, 2013; Liang et al., 2015a). Application of Si leads to the overexpression of defense-related genes and their activity, apart from its role in accumulating defensive compounds, such as phytoalexins, momi-lactones, and phenolics (Liang et al., 2003; Rémus-Borel et al., 2005; Rahman et al., 2015). For instance, in rice plants, the ROS scavenging activities are decreased upon supplementation of Si during exposure to stressful conditions (Kim et al., 2014c). A clue to adapt Si as a remedial measure for sustainable agriculture is evident from the role of Si in the upregulation of genes involved in several adaptations, such as phytohormone metabolism and cell wall synthesis under stressful conditions in canola (*Brassica napus*) (Haddad et al., 2019). A wide range of genes has been modulated against the abiotic stress factors upon Si supplementation (**Figure 2**). Exogenous supply of Si alleviates sulfur and osmotic stress by promoting root growth *via* increased root sucrose levels in barley (Maillard et al., 2018). Emamverdian et al. (2018) reported that Si is capable of heavy metal remediation by initiating different pathways through scavenging ROS. It is reported that Si enrichment improved the growth and development of plants through enhancements in nutrient use efficiency (NUE) in winter wheat (Neu et al., 2017). For instance, Si is reported to decrease metal ion toxicity by reducing the solubility of metals in the cell wall or by detoxifying the metal ions (Wu et al., 2019; Vaculík et al., 2020). Several reports strongly report the role of Si to enhance tolerance to UV-B radiation by activation of defense mechanisms, fortification of the cell wall, etc., in crop plants (Yao et al., 2011; Guntzer et al., 2012). These reports suggest that Si plays a significant role in maintaining plants' physiological and metabolic functions under drought stress conditions. In the preceding section, we have discussed the ameliorating effects of silicon on phytohormone-based resilience under extreme abiotic conditions.

SI-INDUCED DIFFERENTIAL PHYTOHORMONE SYNTHESIS UNDER ABIOTIC STRESS CONDITIONS: AN UPDATE

Phytohormones play a critical role in growth and development and are essential to circumventing a diverse range of environmental stressors (Sato et al., 2010; Raza et al., 2019;

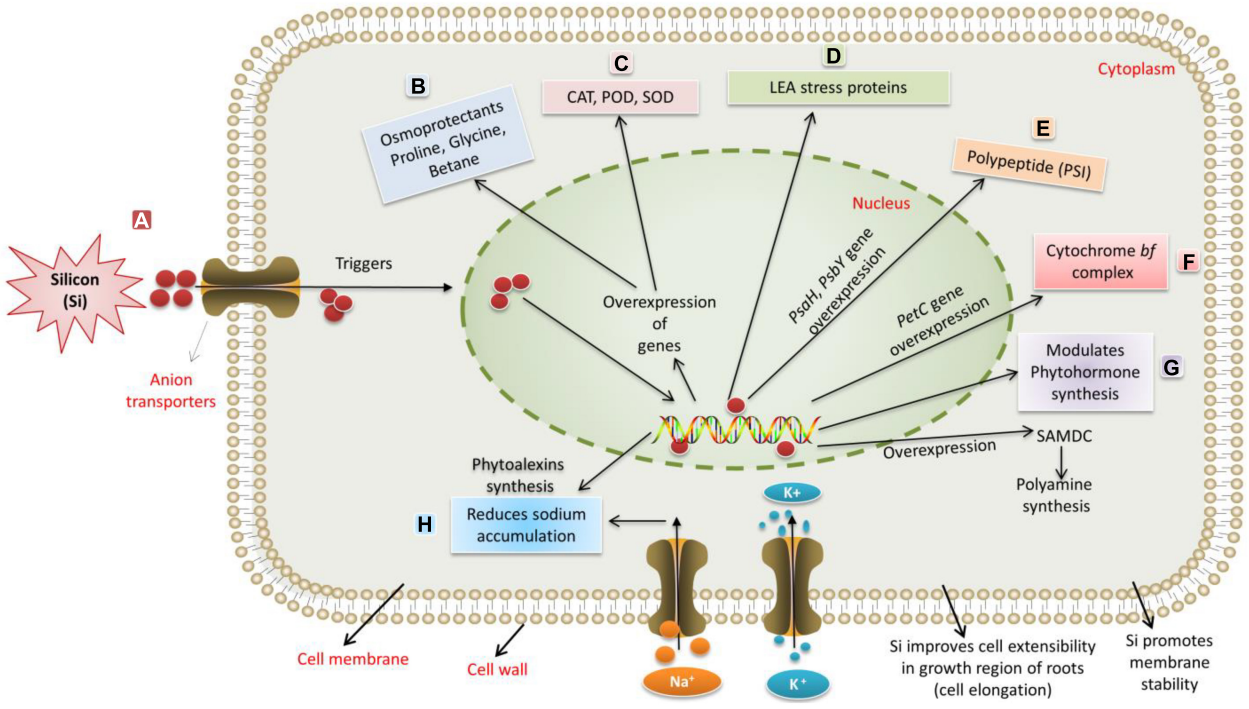


FIGURE 2 | The silicon-induced mechanism for regulating abiotic stresses. **(A)** Silicon is taken up through anion transporters. **(B)** Drought and salinity stress induce osmotic stress and osmotic imbalance. Si enhances the synthesis of osmoprotectants like proline, glycine, and betaine. **(C)** Stress induces the formation of ROS. Si enhances the expression of CAT, SOD, and POD for protection against oxidative damage. **(D–F)** Si supplementation results in transcriptional regulation of genes related to photosynthesis, such as overexpression of *PsaH,* which encodes essential polypeptide subunits of photosystem-I (PSI) dimer, the *PsbY* (*Os08g02530*) gene encoding polyprotein component of Photosystem II and the *PetC* gene, encoding Rieske Fe-S center-binding polypeptide of cytochrome bf complex. **(G)** Si modulates the synthesis of plant growth regulators to alleviate stress. Si induces the S-adenosyl-L-methionine decarboxylase (SAMDC) gene, encoding essential enzymes responsible for synthesizing polyamines. **(H)** Salinity stress negatively affects plant growth by increasing the accumulation of ions up to toxic levels. Due to a higher influx of NaCl, plants experience more severe oxidative and ionic stress. Sodium-ion accumulation up to toxic levels triggers ROS production, which, in turn, severely damages the cellular components and accelerates senescence in mature leaves, leading to reduced growth and metabolism. Si administration improves uptake of K^+, which, in turn, stimulates H+-ATPase enzymes in the plasma membrane that helps to overcome salt stress.

Hafeez et al., 2021b; Mubarik et al., 2021). Phytohormones, such as auxin, CK, ABA, GAs, and BR, are vital to growth and metabolism during normal and stressful conditions (Sato et al., 2010; Raza et al., 2019; Hafeez et al., 2021b; Mubarik et al., 2021). These hormones modulate a wide range of physiological networks at low concentrations, once transported directly to the corresponding cells or transported to distant tissues (Colebrook et al., 2014), thus resilience to environmental stressors. The combinatorial effects of phytohormonal regulation, such as JA, ABA, and SA, play a vital role in mediating heat and drought tolerance in crop plants (Ilyas et al., 2021; Mostofa et al., 2021). Upregulation of GAs can ameliorate the abiotic stress conditions to maintain the growth and development of plants. In addition, upon exogenous application of SA, plants exhibit tolerance to various abiotic stresses like drought, heat, chilling, and tolerance to other stressors like viral, fungal, and bacterial attacks (Prakash et al., 2021; Saleem et al., 2021). Phytohormones like ABA are upregulated during osmotic stress to enhance tolerance by expressing several genes (Al Murad et al., 2020). Even though ABA levels were increased under salt stress, reverse trends were observed once Si was applied in soybean plants (Lee et al., 2010). ABA induces stomatal closure to prevent water loss under extreme saline conditions (de Ollas et al., 2013). In addition, ABA biosynthetic genes *ZEP* and *NCED3* are reported to be upregulated under abiotic stresses (Ma et al., 2018; Müller, 2021). On the other hand, ETH also senses external stimuli to adjust plant metabolism as per environmental conditions. It helps ameliorate abiotic stress in corroboration with other phytohormones, such as SA and JA (Rai et al., 2020). ETH regulates numerous physiological responses, such as triple response in the etiolated seedlings of a pea, induction of flowering, and seed germination (Kim et al., 2011). Higher levels of ETH are attributed to stress tolerance in plants, particularly tolerance to heat stress (Huang et al., 2021; Poór et al., 2021; Chen et al., 2022). Moreover, significant genes are upregulated by ETH to mediate diverse beneficial functions to plants (Kazan, 2015; Poór et al., 2021).

On the other hand, Si interacts with several phytohormones and other signaling molecules, such as polyamines, hydrogen sulfide, and nitric oxide, in improving multiple abiotic stresses (**Figure 3**; Raza et al., 2021g; Sabagh et al., 2021; Tripathi et al., 2021). As a result, the interaction network improves the antioxidant defense system, reduces oxidative damage, and increases resistance to multiple abiotic stresses (**Figure 3**). In recent years, Si has been reported to enhance phytohormone synthesis to upregulate the physiological process of crop plants under extreme environmental conditions. Under abiotic stress conditions, Si enhanced the metabolism and synthesis of phytohormones in plants (Zhu and Gong, 2014; Kim et al., 2016). The major phytohormones upregulated by Si under abiotic stress conditions include ABA, JA, GA, ET, SA, BR, and IAA (Arif et al., 2021). Si-induced phytohormones synergistically regulate the growth, metabolism, and stress tolerance in pepper, as shown by *in silico* data analysis (Gómez-Merino et al., 2020). In tobacco and rice, Si regulates gene expression of plant hormones like ABA, JA, SA, and ETH to adjust metabolism against abiotic stress factors (**Table 1**). Lee et al. (2010), Kim et al. (2014c), Liang et al. (2015b) reported that Si-treated rice plants exposed to heavy metals increase ABA concentration, followed by a decrease after 14th day of treatment. In addition,

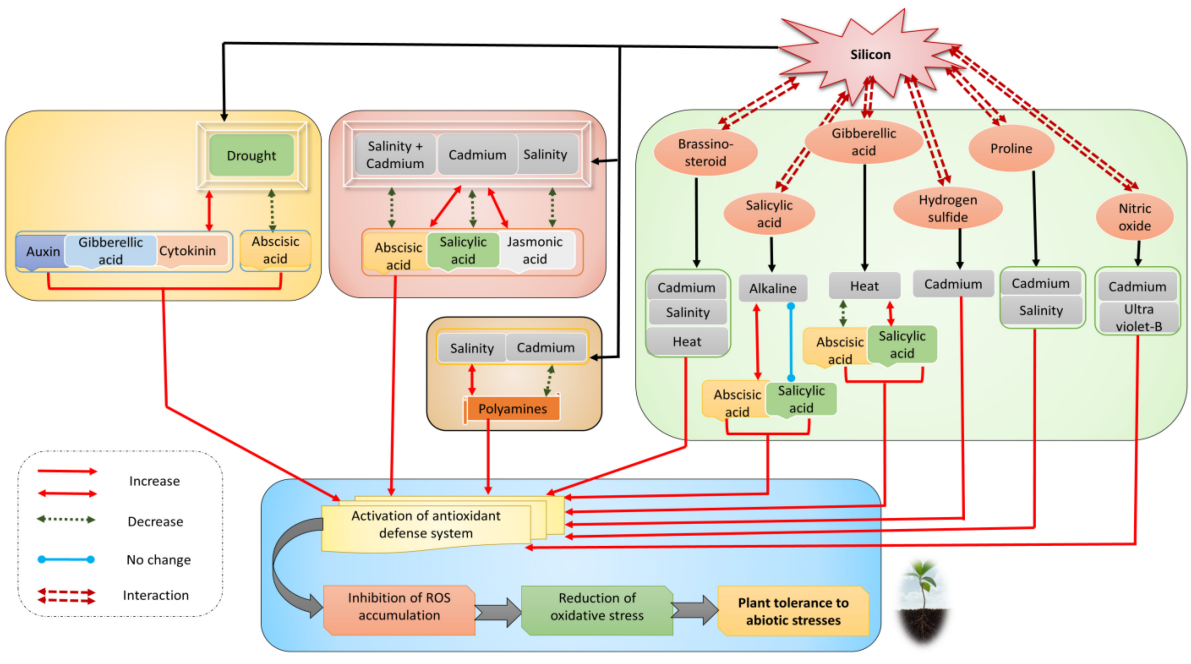


FIGURE 3 | Interaction and crosstalk network of silicon with phytohormones and other signaling molecules in response to various abiotic and oxidative stresses. Read the text for further information.

TABLE 1 | Silicon-induced gene expression in plants under various abiotic stress conditions.

Abiotic stress	Plant name	Genes	Gene function/Protein encoded	References
Drought stress	*Arabidopsis thaliana*	*At5g22460*	Esterase lipase thioesterase family protein Transporter gene	Li et al., 2008; Naz et al., 2021a
	Arabidopsis thaliana	*At5g59030*	Copper transporter gene	Li et al., 2008; Carneiro et al., 2017
	Oryza sativa	*AK070732*	Member of RING domain-containing protein family Regulatory gene	Khattab et al., 2014; Malik et al., 2021
	Oryza sativa	*AF300971*	Dehydration responsive element binding protein Regulatory gene	Khattab et al., 2014; Malik et al., 2021
	Oryza sativa	*AJ578494*	Choline monooxygenase Regulatory gene	Khattab et al., 2014; Malik et al., 2021
	Oryza sativa	*AB028184*	NAC regulons (No apical meristem (NAM), Arabidopsis thaliana activating factor [ATAF], and cup-shaped cotyledon [CUC]) Regulatory gene	Khattab et al., 2014; Manivannan and Ahn, 2017
	Oryza sativa	*NM-001074375*	Dehydrin Regulatory gene	Khattab et al., 2014
	Sorghum bicolor	*Sb02g025110*	S-Adenosyl-L-methionine decarboxylase Polyamine synthesis	Yin et al., 2016; Malik et al., 2021; Wang et al., 2021
	Sorghum bicolor	*Sb04g025720*	S-Adenosyl-Metdecarboxylase Polyamine synthesis	Yin et al., 2016
	Sorghum bicolor	*Sb06g021540*	S-Adenosyl-Metdecarboxylase Polyamine synthesis	Yin et al., 2016
	Sorghum bicolor	*Sb10g002070*	Arginine decarboxylase Polyamine synthesis	Yin et al., 2016
	Sorghum bicolor	*SbPIP1;6*	Plasma membrane intrinsic protein (PIP) 1;6 aquaporins	Liu P. et al., 2015
	Sorghum bicolor	*SbPIP2;6*	plasma membrane intrinsic protein (PIP) 2;6 aquaporins	Liu P. et al., 2015
	Sorghum bicolor	*SbPIP2;2*	plasma membrane intrinsic protein (PIP) 2;2 aquaporins	Liu P. et al., 2015
	Sorghum bicolor	*Sb04g021790*	N-Carbamoyl putrescine amidohydrolase Polyamine synthesis	Yin et al., 2016
	Oryza sativa	*OsRDCP1*	Oryza sativa RING domain-containing protein	Khattab et al., 2014
	Oryza sativa	*OsCMO*	Oryza sativa choline monooxygenase	Khattab et al., 2014; Rehman et al., 2021
	Oryza sativa	*LEA3*	Late Embryogenesis Abundance protein	Khattab et al., 2014
	Oryza sativa	*DREB2A*	Dehydration-responsive element-binding protein 2A	Khattab et al., 2014
	Oryza sativa	*OsRAB16b dehydrin*	Dehydrin RAB16B protein	Khattab et al., 2014
Cold stress	*Oryza sativa*	*SAMDC*	S-adenosyl-L-methionine decarboxylase	Pottosin and Shabala, 2014
	Arabidopsis	*DREB1A*	Dehydration-responsive element-binding protein 1A	Liu et al., 1998; Liang et al., 2021
	Arabidopsis	*DREB1B*	Dehydration-responsive element-binding protein 1B	Liu et al., 1998; Manivannan and Ahn, 2017
	Arabidopsis	*DREB1C*	Dehydration-responsive element binding protein 1C	Liu et al., 1998; Manivannan and Ahn, 2017
Salinity stress	*Lycopersicum esculentum*	*leDREB-1*	Lycopersicum esculentum Dehydration-responsive element binding-1 protein	Muneer and Jeong, 2015; Dhiman et al., 2021
	Lycopersicum esculentum	*leDREB-2*	Lycopersicum esculentum Dehydration-responsive element binding-2 protein	Muneer and Jeong, 2015
	Lycopersicum esculentum	*leDREB-3*	Lycopersicum esculentum Dehydration-responsive element binding-3 protein	Muneer and Jeong, 2015; Dhiman et al., 2021
	Oryza sativa	*ZEP*	zeaxanthin epoxidase	Kim et al., 2014c
	Oryza sativa	*NCED1*	9-cis-epoxicarotenoid oxygenase 1	Kim et al., 2014c
	Oryza sativa	*NCED4*	9-cis-epoxicarotenoid oxygenase 2	Kim et al., 2014c
	Lycopersicum esculentum	*leLsi-1*	Lycopersicum esculentum Low Si-1 transporter	Muneer and Jeong, 2015
	Lycopersicum esculentum	*leLsi-2*	Lycopersicum esculentum Low Si-2 transporter	Muneer and Jeong, 2015
	Lycopersicum esculentum	*leLsi-3*	Lycopersicum esculentum Low Si-3 transporter	Muneer and Jeong, 2015
	Lycopersicum esculentum	*leAPX*	Lycopersicum esculentum Ascorbate peroxidase	Muneer and Jeong, 2015
	Lycopersicum esculentum	*leSOD*	Lycopersicum esculentum Superoxide dismutase	Muneer and Jeong, 2015
	Lycopersicum esculentum	*leCAT*	Lycopersicum esculentum Catalase	Muneer and Jeong, 2015
	Glycine max	*TaLsi1*	Si-Influxer	Hwang et al., 2007
	Glycine max	*TaLsi2*	Si-effluxer	Hwang et al., 2007
	Oryza Sativa	*AOC*	Allene oxide cyclase	Kim et al., 2014c
	Oryza Sativa	*AOS*	13-Allene oxide synthase (13-AOS)	Kim et al., 2014c
	Oryza Sativa	*OPR3*	Opda reductase3	Kim et al., 2014c

(Continued)

TABLE 1 | (Continued)

Abiotic stress	Plant name	Genes	Gene function/Protein encoded	References
	Oryza Sativa	*LOX*	Lipoxygenase	Kim et al., 2014c
Metal ion stress	*Oryza Sativa*	*OsHMA3*	Oryza Sativa heavy metal ATPases	Kim et al., 2014a
	Oryza Sativa	*OsLsi-1*	Oryza Sativa Low Si Rice 1	Kim et al., 2014a
	Oryza Sativa	*OsLsi1*	Oryza Sativa Low Si Rice 2	Kim et al., 2014a
	Oryza Sativa	*OsHMA2*	Oryza Sativa heavy metal ATPases	Kim et al., 2014a
	Oryza sativa	*Os08g02630*	Subunit of oxygen evolving complex-PSII Photosynthesis	Song et al., 2014; Lesharadevi et al., 2021
	Oryza sativa	*Os05g48630*	Photosynthetic co8y stability maintenance Photosynthesis	Song et al., 2014; Lesharadevi et al., 2021
	Oryza sativa	*Os07g37030*	Maintenance of cytochrome Photosynthesis	Song et al., 2014
	Oryza sativa	*Os03g57120*	Ferrodoxin NADP + reductase Photosynthesis	Song et al., 2014; Lesharadevi et al., 2021
	Oryza sativa	*Os09g26810*	Subunit of LHC II complex Photosynthesis	Song et al., 2014; Lesharadevi et al., 2021
	Oryza sativa	*Os04g38410*	Subunit of LHC II complex Photosynthesis	Song et al., 2014; Lesharadevi et al., 2021
	Oryza Sativa	*PetC gene*	Rieske Fe-S center-binding polypeptide of cytochrome bf complex	Song et al., 2014; Lesharadevi et al., 2021
Heat stress	*Solanum lycopersicum* L.	*SlLsi1*	Low Si Rice 2	Khan et al., 2020b
	Solanum lycopersicum L.	*SlLsi2*	Low Si Rice 2	Khan et al., 2020b
	Solanum lycopersicum L.	*SlHsfA1a-b*	Heat Stress Transcription Factor	Khan et al., 2020b
	Solanum lycopersicum L.	*SlHsfA2-A3*	Heat Stress Transcription Factor	Khan et al., 2020b
	Solanum lycopersicum L.	*SlHsfA7*	Heat Stress Transcription Factor	Khan et al., 2020b
	Solanum lycopersicum L.	*SlDREB2*	dehydration-responsive element binding proteins	Khan et al., 2020b
Wound stress	*Lycopersicum esculentum*	*OsAOS1*	Allene oxide synthase-1	Kramell et al., 1995; Agrawal et al., 2003
	Lycopersicum esculentum	*OsAOS2*	Allene oxide synthase-1	Kramell et al., 1995; Agrawal et al., 2003
	Lycopersicum esculentum	*OsOPR3*	12-oxo-phytodienoic acid reductase	Kramell et al., 1995; Agrawal et al., 2003
	Lycopersicum esculentum	*OsLOX*	Lipoxygenase	Kramell et al., 1995; Agrawal et al., 2003
Chilling and drought	*Oryza sativa*	*OsDREB1*	*Oryza sativa* Dehydration-responsive element-binding protein 1A	Ito et al., 2006
Salinity and drought stress	*Arabidopsis*	*DREB2B*	Dehydration-responsive element-binding protein 2A	Islam and Wang, 2009
Sulfur deficiency and osmotic stress	*Hordeum vulgare*	*ZEP*	Zeaxanthin epoxidase	Maillard et al., 2018
Sulfur deficiency and osmotic stress	*Hordeum vulgare*	*NCED3*	9-cis-epoxicarotenoid oxygenase 1	Maillard et al., 2018
Salinity/ Drought stress	*Oryza sativa*	*NAC5*	NAC (NAM/ATAF/CUC) transcription factor	Khattab et al., 2014

reduction of SA's and JA's endogenous concentration has also been observed in these Si-treated rice plants. Various cellular and developmental processes, such as embryo development and dormancy, stomatal opening, and seed development, are regulated by ABA in plants (Sreenivasulu et al., 2012). Stress conditions trigger the upregulation of genes-encoding enzymes for the biosynthesis of ABA. In *Arabidopsis thaliana*, the signals from roots to regulate the decreased leaf water potential and conductance are accomplished by ABA triggered by the closure of stomata under drought stress (Hasan et al., 2021; Liu et al., 2021). ABA levels in Si-treated plants are decreased under salinity stress and increased when plants are exposed to heavy metals like cadmium (Cd) and copper (Cu) (Khan et al., 2021b; Mostofa et al., 2021; Tripathi et al., 2021).

Moreover, Si-treated plants ameliorate metal toxicity, leading to low production of ABA. Time-dependent effects of Si on ABA and JA synthesis were also reported under abiotic stressors (Kim et al., 2014c). Overexpression of Si transporter genes, such as *TaLsi1* (Si-Influxer) and *TaLsi2* (Si-effluxer), under salinity-induced ABA was reported upon supplementation of exogenous Si in wheat (Zia et al., 2021). Si-induced alteration of ABA-related genes glyceraldehydes-3-phosphate dehydrogenase (GAPDH), cyclophilin (CYC), ADP-ribosylation factor (ADP-RF1), and sulfur transporter (HsST1) alleviates sulfur deficiency and osmotic stress in crop plants (Maillard et al., 2018). Moreover, ABA levels are declined due to downregulation of genes by exogenous supplementation of Si to enhance the stress tolerance in barley (Maillard et al., 2018). It is reported that, in rice plants exposed to salt stress, Si upregulated expression of ABA biosynthesis genes, such as *ZEP*-encoding zeaxanthin epoxidase, *NCED1*-encoding 9-cis-epoxicarotenoid oxygenase 1, and *NCED4*-encoding 9-cis-epoxicarotenoid oxygenase 2

(Kim et al., 2014b). A versatile transcription factor, NAC encoded by *RD25* genes, was found to be induced by stress factors, such as salinity and drought, in addition to its induction upon treatment of crop plants by JA and ABA (Singh et al., 2021).

JA is another hormone critical to generate a response against a wide range of stress factors through activation of defense signaling pathways (Pieterse et al., 2012; Caarls et al., 2015). JA production is lowered upon exogenous treatment of Si; later, decline in JA can be correlated by low-stress levels exerted by Si treatment (Wang et al., 2020; Raza et al., 2021b). The reduction in the levels of JA induced by Si involves the modulation of several signaling pathways (Liu and Timko, 2021; Tripathi et al., 2021). Si application drastically improves the signaling of JA to initiate a defense system during wounding stress in rice plants (Hamayun et al., 2010). The expression of genes related to JA synthesis, like *LOX* and other genes, is upregulated when Si is administered to wound-stressed rice plants (Kim et al., 2011, 2014b). Under wound stress *via* feedforward activation, the *LOX* gene further amplifies the expression of JA in *A. thaliana* (Sato et al., 2010). Genes related to JA like *OsAOS1*, *OsAOS2*, *OsOPR3,* and *OsLOX* were downregulated upon exogenous application of Si during wound stress, highlighting the role of Si in triggering metabolic networks to heal the mechanical injuries in rice plants (Kim et al., 2014b). In addition, overexpression genes like *AOC, AOS, OPR3,* and *LOX* during early stages occurred during wound stress; downregulation of JA biosynthesis was also demonstrated in tomatoes. GAs are an important class of phytohormones critical to plants, such as seed germination and fruiting (Colebrook et al., 2014). The endogenous levels of GA are upregulated under salinity stress in *Glycine max* upon application of Si at 2.5-mM concentration (Arif et al., 2021; Dhiman et al., 2021). The Si-triggered upregulation of GA_1 and GA_4 content in cucumber plants helps to withstand drought and salinity stress (Hamayun et al., 2010). The combinatorial effect of Si and nitrogen on the growth and metabolism of two rice cultivars led to upregulation of GA_{20} and GA_1, initiating vegetative and anthesis stages (Lee et al., 2010). Moreover, the decreased levels of GA under salt stress were restored by applying Si in rice plants (Lee et al., 2010). In another study, Si-mediated increase in the synthesis of GA, such as GA_1 and GA_4 levels, profoundly enhanced salt tolerance in *Glycyrrhiza uralensis* Fisch (Zhang et al., 2018). Likewise, Si-treated plants enhanced GA concentration in saline conditions and reduced JA concentration under wound response (Lee et al., 2010; Kim et al., 2011).

Auxin is another phytohormone critical to a wide range of development and growth of plants (Du and Scheres, 2018). It has been reported in several studies that IAA plays an essential role in the tolerance of crop plants to salinity stress (Fahad et al., 2015b; Hussain et al., 2019). Activation and upregulation of numerous genes triggered by auxins have been reported in rice, soybean, and Arabidopsis, which are important for the development and growth of plants (Wani et al., 2016). It is reported that, upon administration of Si, IAA levels decreased in crop plants, resulting in a delay of leaf senescence in canola (*Brassica napus*) (Haddad et al., 2018). The synthesis of IAA and ABA was transcriptionally downregulated by Si supplementation, resulting in osmotic stress tolerance in barley (Maillard et al., 2018).

Likewise, Si applied to the rice plants having wound stress resulting in decreased ETH production compared to rice plants not treated with Si (Kim et al., 2011). The delaying of senescence was observed in crop plants upon Si supplementation through increased synthesis of CK biosynthesis in Arabidopsis and sorghum (Markovich et al., 2017). Si enhanced the growth and development of rice plants by its effect on endogenous ETH and JA levels, even though JA and JA show inverse correlation under wound stress (Kim et al., 2011). SA, another potential phytohormone, has important physiological implications on crop plants, such as transport and uptake of ions, photosynthetic metabolism, and membrane permeability during stress (Noreen et al., 2009). More importantly, SA is reported to outwit abiotic stressors like the generation of ROS, attacks by pathogens, salinity, and drought stress (Hara et al., 2012). Tolerance to stress conditions, such as salinity, is initiated by SA-based interplay of phytohormones (El-Mashad and Mohamed, 2012). Combinatorial supplementation of SA and Si reduces damage caused by boron toxicity through increased carotenoid, chlorophyll content, biomass production, and reduction in oxidative stress (Eraslan et al., 2008). A possible mechanism of stress tolerance induced by SA occurs through expression of several genes, such as those coding for pathogenesis-related proteins (PR-proteins) (Kidokoro et al., 2009). Exogenous application of SA helps in the resistance and adaptation of crop plants in various abiotic stress factors, such as drought, salinity, and iron deficiency (Mostofa et al., 2021; Tariq et al., 2022). In pea plants, abiotic stress, such as oxidative stress, was reported to be remedied by exogenous supplementation of Si and SA (Rahman et al., 2017). Moreover, soybean plants withstand salt stress through modulation of SA and JA upon treatment with Si (Kim et al., 2014a). In conclusion, the reports suggest that interplay of Si and phytohormones is critical to the growth and metabolism of plants under drought stress conditions.

PHYSIOLOGICAL BENEFITS OF SILICON UNDER ABIOTIC STRESS

The growth and the metabolism of plants are improved through their mechanisms to develop tolerance against abiotic stressors. Later attributes were primarily alleviated by supplementation of Si to withstand negative environmental stress factors (Arif et al., 2021; Souri et al., 2021). In sugarcane, Si has been attributed to enhancing leaves' rigidity and erectness, resulting in improved photosynthesis (Verma et al., 2019). Pfannschmidt and Yang (2012) reported overexpression of *PsaH*, which encodes essential polypeptide subunits of photosystem-I (PSI) dimer upon supplementation of Si. A comparative study showed that Si-administered cucumber exhibited increased perception of light, the enhanced concentration of chlorophyll pigments, and rough petioles (Adatia and Besford, 1986; Lozano-González et al., 2021; Meng et al., 2021). Several reports suggest that Si positively modulates the plant growth and yield in rice plants (Dorairaj et al., 2017; Garg and Singh, 2018). It has been demonstrated that Si positively modulates the growth, development, and metabolism in sugarcane (*Saccharum*

officinarum) (Verma et al., 2021), beans (*Phaseolus vulgaris*) (Zuccarini, 2008; Nosrati et al., 2014; El-Saadony et al., 2021), cotton, (*Gossypium hirsutum*) (Wang et al., 2001; dos Santos et al., 2020), rice (Hwang et al., 2007; Feng et al., 2011), and soybean (*Glycine max)* (Hamayun et al., 2010).

Moreover, Si has been shown to positively modulate the metabolism of several crop plants, such as spinach (*Spinacia oleracea*) (Eraslan et al., 2008), wheat (Gong et al., 2005; Sattar et al., 2019; Bukhari et al., 2021a), barley (Savant et al., 1999; Benslima et al., 2021; Sierra et al., 2021), and maize (Liang et al., 2005; El-Mageed et al., 2021). Shi et al. (2013) reported that tomato seedlings completely recover their growth and photosynthesis once exposed to Si under water stress conditions. Si can ameliorate the metal ion toxicity and, in turn, able to enhance the quality and quantity of biomass in *Phaseolus vulgaris* (Zuccarini, 2008; Artyszak, 2018). The application of Si detoxifies Na^+ through modification of the antioxidant defense system. Later effect positively modulates important biochemical and physiological metabolic networks in sunflower and sorghum under abiotic stresses, particularly salt stress, to increase shoot dry matter production (Hurtado et al., 2020). Si-treated rice plants significantly improved the shoot, and root morphology restored photosynthetic efficiency amid Cd toxicity (Bari et al., 2020). In addition, Si was reported to mediate a wide range of physiological benefits like enhanced growth, nutrient uptake, provision of mechanical strength, and resistance to biotic stressors like fungal diseases (Akhtar and Hussain, 2008; Bakhat et al., 2018; Souri et al., 2021). Moreover, Si helps to reduce lipid peroxidation in crop plants exposed to wound stress in rice plants (Kim et al., 2014b). The germination characteristics like the germination rate and percentage and shoot length are highly enhanced by applying Si under normal and drought and salinity stress conditions in tomatoes (Shi et al., 2014). In crop plants, such as maize, rice, wheat, tomato, and cucumber, Si enhanced shoot and root growth under salt stress (Wu et al., 2015). Water balance in cucumber is improved by exogenous supplementation of Si through its effect on increasing the root-shoot ratio under salt stress (Wang et al., 2015). For instance, the supplementation of Si leads to the overexpression of stress-responsive genes, such as *Oryza sativa* RING domain-containing protein *(OsRDCP1), Oryza sativa* choline monooxygenase (*OsCMO*), *DREB2A,* dehydrin *OsRAB16b*, and *NAC5,* under abiotic stress conditions (Khattab et al., 2014). Production of ROS is disastrous to crop plants as it induces lipid peroxidation (Gill and Tuteja, 2010). The foliar application of Si in okra leads to overexpression of ROS-scavenging genes coding for CAT, POD, and SOD during salinity stress. Later, enzymes help decrease the lipid peroxidation in okra plants (Abbas et al., 2015). Differentially enhanced activity of ROS-scavenging enzymes, such as APX, CAT, and POD in roots, shoots, and leaves, was reported in alfalfa under salinity stress by application of Si (Wang et al., 2010).

Moreover, Si reduces oxidative stress in tomato plants under salinity stress, indicating the effect of Si on the activity of antioxidant enzymes (Li et al., 2015). Similar results were also observed in rice plants grown under salinity stress when Si was applied (Kim et al., 2014c). Numerous studies back up the role of Si in alleviating abiotic stress in crop plants (Mir et al., 2019). The combined ameliorative effect of Si ad *Bacillus subtilis* fbl-10 was found to enhance tolerance to Pb (Lead) toxicity in brinjal (*Solanum melongena*) (Shah et al., 2021). Moreover, the effect of Si on delaying leaf senescence in mustard (*Brassica juncea*) under drought and salinity stress was accomplished by modulation of homeostasis of ions and antioxidative defensive systems (Alamri et al., 2020). It is reported that, after deposition, Si helps to thicken the xylem cell wall and the Casparian strips of endodermis to impede the metal ion transport in crop plants (da Cunha and do Nascimento, 2009; Mandlik et al., 2020; Souri et al., 2021). In combination with SA, in mung bean seeds, Si enhanced physiological parameters through the decreased accumulation of Na^+ and increased proliferation of K^+ (Lotfi and Ghassemi-Golezani, 2015). Several physiological parameters, such as the transpiration rate, stomatal conductance, chlorophyll levels, and membrane permeability, are maintained by Si during abiotic stress, particularly during salinity stress (Coskun et al., 2016). Besides, the adverse effects of heat stress in tomato plants are mitigated by exogenous application of Si, further enhancing biomass production and shoot length (Khan et al., 2020b). Plants overexpress several genes pertaining to transpiration, photosynthesis, synthesis of polyamines, and secondary metabolism in response to abiotic stressors (Abdel-Haliem et al., 2017). For instance, in sorghum, it is reported that, upon application of Si, the root growth was stimulated by root elongation due to cell wall extensibility in the growth region (Hattori et al., 2003; de Oliveira et al., 2019). Several reports suggest that Si induces modulation of phytohormones to delay senescence in rice and sorghum (Lee et al., 2010; Kim et al., 2014c; Yin et al., 2014). In chickpea cultivars, drought tolerance was regulated by supplementation of Si through improvement of various growth parameters. High salinity in rice and Mn, Al, Cu, and Cd toxicity in sorghum and wheat is alleviated by supplementation of Si (Kang et al., 2015; Keller et al., 2015; Rizwan et al., 2015).

A large number of stress-tolerant genes are upregulated by exposure of crop plants to Si. For instance, studies have reported Si results in transcriptional regulation of genes related to photosynthesis during zinc stress in rice plants (Song et al., 2014). In rice, wide ranges of stressful conditions are acclimatized by the expression of LEA genes-encoding stress tolerance LEA proteins (Lenka et al., 2011). Several studies report overexpression of the *OsNAC5* gene is attributed to alleviating the stress tolerance through the abundant expression of LEA3 in rice plants (Takasaki et al., 2010). Likewise, in rice, upregulation of *OsRDCP1* and *OsCMO* gene levels alleviated the dehydration stress upon supplementation of exogenous Si (Khattab et al., 2014). The overexpression of the S-adenosyl-L-methionine decarboxylase (*SAMDC*) gene, encoding vital enzymes responsible for the synthesis of polyamines, is augmented by supplementation of Si (Pottosin and Shabala, 2014). These polyamines are critical to withstand the onslaught by environmental stressors (Liu P. et al., 2015). The wonderful effects of Si under drought stress conditions have considerably shifted scientists' focus on its emerging role in maintaining the physiological hemostasis of crop plants. In the preceding sections, we have discussed the role of Si in alleviating

the stress tolerance of plants against salinity, drought, heavy metal, temperature, and other abiotic stressors.

SALINITY TOLERANCE MEDIATED BY SILICON

Agricultural crop production is grossly limited by salinity stress leading to a drastic decline in food production at the commercial and industrial levels (Munns and Gilliham, 2015). Plants are negatively affected by salinity through an increase in ionic and osmotic stress. On a global scale, almost 6% of cultivated land is graded as saline and is expected to increase by 2050 due to global climatic change, further worsening the scenario of crop production. Moreover, salinity stress induces a reduction in osmosis, imbalance in nutrient supply, and enhanced accumulation of ions up to toxic levels (Hasegawa et al., 2000; Hafeez et al., 2021a; Saddiq et al., 2021). Further, it is evident that salt stress is a major abiotic factor that inhibits crop plants' growth and metabolism, resulting in reduced crop yield (Han et al., 2021). The elevation of salt stress is further compounded by anthropogenic activities, such as saline water irrigation, pollution through industries, and higher use of chemical fertilizers (Zhu et al., 2019a). Sodium-ion accumulation up to toxic levels triggers the production of ROS, which, in turn, severely damages the cellular organelles, such as chloroplast, cell membrane, mitochondria, and peroxisomes, to impair the metabolic networks in crop plants (Munns and Gilliham, 2015).

Moreover, it is reported that the accumulation of Na^+ to toxic levels in older leaves accelerates senescence in mature leaves, leading to reduced growth and metabolism (Munns and Gilliham, 2015; Saddiq et al., 2021). Global production of agricultural food crops is reduced up to 20% by salinity stress among all the abiotic stresses (Kumar et al., 2017; Hussain et al., 2018). High salinity reduces the potential of plants to absorb the water, resulting in a reduction of cell expansion and low stomatal activity due to less inter- and intracellular water levels. Due to a higher influx of NaCl, plants experience more severe oxidative and ionic stress (Ferchichi et al., 2018). The salt stress is attenuated more frequently by Si administration (Etesami and Jeong, 2018; Liu et al., 2019). In maize, salinity stress is alleviated by exposure to Si through improvements in growth and maintaining ion homeostasis *via* decline in Na^+ uptake (Ali et al., 2021). Si improves uptake of K^+, which, in turn, stimulates H^+-ATPase enzymes in the plasma membrane to overcome salt stress in maize and other plants (Liang et al., 2005; Liu et al., 2019; Dhiman et al., 2021). Under salinity stress, the application of Si in rice was reported to decrease the accumulation of sodium and chloride ions through apoplastic transport (Shi et al., 2013). Hyper-accumulators of Si were found to form double cuticle layers, enhancing photosynthesis by preventing evapotranspiration. Moreover, Si influences starch metabolism, glycolytic pathways, and the Krebs cycle under osmotic stress in barley (Hosseini et al., 2017). In addition, cucumber seedlings could ameliorate the extreme oxidative stress upon the influx of Si (Gou et al., 2020). Declined chlorophyll content due to salinity stress was reported to be significantly ameliorated by the supplementation of exogenous Si to root zones or foliar in tomato (Al-aghabary et al., 2005), pea (Ahmad and Jhon, 2005), and cucumber (Hamayun et al., 2010) crop plants. In plants, Si accumulates and deposits in discrete silica bodies in the form of phytoliths, usually beneath the cell walls on different parts, such as roots, stems, and leaves. These phytoliths then bind with Na^+ to reduce their uptake and increase K^+ uptake to different regions of plants. Concomitantly, it is reported that Si induces greater H + -ATPase activity to lower the electrolyte leakage resulting in higher secretion of Na^+ from cells in *Puccinellia distans* (Soleimannejad et al., 2019). Furthermore, to avoid multiple abiotic stressors, Si deposition in leaf blades during salinity results in converting complexions to non-toxic stable ions to regulate ROS production (Mandlik et al., 2020; Ahire et al., 2021; Dhiman et al., 2021). Due to the deposition of Si in the cell walls of endodermis and rhizodermis, the transport of Na^+ is blocked through a reduction in apoplastic movement of Si across the root system, leading to a drastic decline in the transport of Si from roots to shoots, hence salinity tolerance (Khan et al., 2019). Moreover, negative impacts of higher salt levels are greatly tolerated by Si application through the production of glycine betaine to maintain metabolic activity to regulate water levels in plants (Al-Huqail et al., 2019). The compatible osmolytes, such as glycine betaine, are critical to the stability of membrane, functional proteins, protein complexes, and enzymes under saline conditions (Rajasheker et al., 2019). In addition, Si enhances proline content to induce salt tolerance in cucumber (Gou et al., 2020). Plants synthesize proline as major osmoprotectants that protect the integrity of membrane and protein stability under salinity stress (Ahanger et al., 2020a). Moreover, the variable concentration of Si resulted in enhanced activities of enzymes, such as glutamine synthetase (GS), nitrate reductase (NR), sucrose synthetase (SS), and sucrose phosphate synthetase (SPS), to enhance nitrogen and carbon metabolism under salinity stress in *Glycyrrhiza uralensis* Fisch (Cui et al., 2021). In tomato, several genes, such as *leDREB-1*, *leDREB-2*, *leDREB*-3, *leLsi*-1, *leLsi*-2, *leLsi*-3, *leAPX*, *leSOD*, and *leCAT*, are upregulated upon supplementation of Si upon exposure to salt stress (Ngwepe et al., 2019), whereas the exposure of *Arabidopsis* to salinity and dehydration resulted in transient expression of *DREB2A* and *DREB2B* (Liu et al., 1998; Sakuma et al., 2006; Manna et al., 2021; Singh and Chandra, 2021). The increase in contents of minerals, such as Ca and Mg in tomato leaves and Mg, K, Ca, and P in *Trifolium alexandrinum,* was reported upon supplementation of Si to regulate growth under salt stress (Abdalla, 2011; Li et al., 2015). Overall, Si plays a critical role in circumventing salt stress through the induction of diverse biochemical and physiological mechanisms (Al Murad et al., 2020). See **Table 2** for some recent examples of Si-induced salinity tolerance.

DROUGHT TOLERANCE MEDIATED BY SILICON

The normal growth and the metabolism of plants are severely affected by drought stress, and, additionally, it creates a

TABLE 2 | A summary of some recent reports on silicon-induced abiotic stress tolerance in crop plants.

Plant specie	Stress condition	Silicon dose	Protective role	References
Salinity				
Zea mays L.	80 mM NaCl; 160 mM NaCl	Si (Na_2SiO_3; 1 mM)	Si addition alleviated the salt toxicity by increasing RWC, MSI, CAT, SOD, APX, and POD activities	Ali et al., 2021
Oryza sativa L.	200 mM NaCl	2 mM K_2SiO_3	Si improves the rice growth and salinity tolerance by modulating the Salt-Overly Sensitive (SOS) pathway	Gupta et al., 2021
Medicago sativa L.	120 mM NaCl	Si 3 mM	Si application lowered the oxidative damage, modulated SOD, polyphenol oxidase activities, and improved flavonoid, total polyphenol, and carotenoid contents	El Moukhtari et al., 2021
Solanum tuberosum L.	NaCl 5, 8, and 12 dS m^{-1}	$NaSiO_3$- NPs 400 mg L^{-1}, SiO_2 1000 mg L^{-1}	Si application increases the proline content and leaf soluble carbohydrates than control Si treatment also lowered the Na^+/K^+ twice and induced antioxidant enzyme activities	Kafi et al., 2021
Oryza sativa L.	0, 25, 50, and 100 mM NaCl	Si, 2 mM	Si application improves the endogenous levels of polyamine by upregulating PAs biosynthetic enzymes While reducing GABA accumulation by downregulating PAs catabolism and maintaining functional GABA shunt, which may lower the oxidative damage	Das et al., 2021
Cucumis sativus L.	75 mM NaCl	1.5 mM Si	Si treatment increases the numerous growth-associated parameters and alleviates the adverse salinity effects. Si application reduces the chlorides (Cl^-) shoot concentration	Kaloterakis et al., 2021
Drought				
Arachis hypogaea L.	Solitary drought (i.e., 10% PEG and 15% PEG)	Na_2SiO_3 2 mM	Si treatment promotes mineral nutrient absorption improves RWC, leaf chlorophyll content, and biomass It also provides osmoprotection by accumulating metabolites and improving the JA, IAA, GA3, zeatin levels	Patel et al., 2021
Avena sativa L.	June, only 6 mm rainfall despite a 30-year average of 66.5 mm	Si 3.0 L ha^{-1}	Si treatment increased the synthesis rate (16.8–149.3%), transpiration (5.4–5.6%), air–leaf temperature difference (16.2–43.2%), Chl (1.0%) and carotenoid (2.5%) content	Kutasy et al., 2022
Zea mays L.	10% (w/v) PEG	1.0 mM Na_2SiO_3	Si treatment decreased the electrolyte leakage from 0.64 to 0.52% and increased membrane stability 12%, Chl a 35%, Chl b 31%, and carotenoids 51% than control	Bijanzadeh et al., 2022
Zea mays L.	Full irrigation 100% and deficit irrigation 80%	Na_2SiO_3 0, 2, and 4 mM at 40 and 60 days after planting	Si treatment improves plant growth, gaseous exchange, cell membrane integrity, water use efficiency, physiological performance, and maize productivity It also lowered the concentrations of Ni^{+2}, Cd^{+2}, and Cr^{+3} in leaves and grains of maize	El-Mageed et al., 2021
Triticum aestivum L.	Samples drying in an oven at 70°C for 72 h	Si, 6 mM	Si treatment alleviated the oxidative stress and negative drought impacts by increasing the antioxidant enzyme activities	Naz et al., 2021a
Cucumis melo L.	soil moisture regimes 100, 75, and 50% FC	H_4SiO_4, 0, 100, 200, and 400 kg ha^{-1}	Si treatments increased self-resistance to lodging and strengthened cell wall, restricted fungal disease, and insect infestations, reduced mutual shading, improved water balance, reduced transpiration, and water loss	Alam et al., 2021
Toxic metals/metalloids				
Triticum aestivum L.	Cd 25 mg kg^{-1}	3 mM Si	Si treatment reduced the Cd-mediated oxidative stress and improved photosynthetic pigments, net photosynthetic rate, strengthening the antioxidant defense system, enhancing metabolite accumulation, and improving plant nutrient status	Thind et al., 2020
Triticum aestivum L.	As(V) 25, 50, and 100 μM	5 mM Si	Si treatment mitigated the arsenate-induced effects and oxidative stress Si application also respiratory cycle, GABA synthesis, and its associated enzymes	Sil et al., 2018
Capsicum annuum L.	0.05 mM B, 2.0 mM BT	2.0 mM Si	Si treatment improves plant growth, proline content, and various antioxidant enzymes activities while lowering the MDA, H_2O_2 contents, and membrane leakage	Kaya et al., 2020
Poa annua L.	100 μM Cd	1 mM Si	Si application alleviated the Cd-toxicity, restored the activity of G6PDH and the expression of G6PDH, and lowered the oxidative stress induced by Cd	Li et al., 2017
Brassica napus L	0.5 and 1.0 mM $CdCl_2$	SiO_2, 1.0 mM	Si treatment reduced the H_2O_2 and MDA contents and improved antioxidant defense mechanisms through increasing the AsA and GSH pools and activities of AsA-GSH cycle and glyoxalase system enzymes and CAT	Hasanuzzaman et al., 2017
Zea mays L.	Ni 100 μM	2.5 mM Si	Si treatment mitigated the Ni-induced stress by enhancing membrane stability and influencing enzymatic (SOD, POX, and CAT) and non-enzymatic (Pro, and AsA) defense systems	Fiala et al., 2021
Salvia officinalis L.	400 μM Cu	0, 0.25, 0.5, and 1 mM Si	Si treatment alleviated the oxidative damage, increasing proline content, enhancing the CAT and SOD activities, and up-regulating the *SOD* gene expression	Pirooz et al., 2021
Temperature (cold/heat)				
Solanum lycopersicum L.	30°C to 43 ± 0.5°C	1 Mm Si	Si application provides thermotolerance by activating the antioxidant system, endogenous phytohormones, and heat shock proteins	Khan et al., 2020b

(Continued)

TABLE 2 | (Continued)

Plant specie	Stress condition	Silicon dose	Protective role	References
Triticum aestivum L.	37 ± 2°C	2 and 4 mM Si	Si application increased the Chl a, b, and a + b and carotenoids by improving the activities of enzymatic antioxidants, CAT, SOD, POD, and osmoprotectants	Mustafa et al., 2021
Triticum aestivum L.	45°C, 4 h	1.5 mM K_2SiO_3 and 1.66 mM Si NPs	Si treatments restored the heat stress-provoked ultrastructural distortions of chloroplasts and the nucleus and enhanced photosynthetic capacity Si treatment also stimulated the overexpression of *TaPIP1* and *TaNIP2* with an improvement in the RWC	Younis et al., 2020
Hordeum vulgare L.	25, 30, and 35°C	1.5 mM Si	Si application reduced HT-mediated oxidative stress by decreasing the concentration of MDA (39 and 49%) and H_2O_2 (14 and 56%) and increased shoot (49 and 46%) and root (40 and 34%) dry masses, Chl a (10 and 86%), Chl b (82 and 81%), and carotenoids (53 and 33%)	Hussain et al., 2019
Hordeum vulgare L	34°C	0.2, 0.4, and 0.6 mM $Na_2O_3Si.5H_2O$	Si treatment alleviated the detrimental impacts enhancing the antioxidant enzymes SOD, POD, CAT, and PPO, together with soluble sugars accumulation and free proline for osmotic adjustment	Naz et al., 2021b
Euphorbia pulcherrima L.	40°C	75 mg L^{-1} K_2SiO_3	Si treatment alleviates the temperature stress by regulating the stomata, photosynthesis, oxidative damage, and by lower production of H_2O_2 and MDA	Hu et al., 2020
Zea mays L.	12–14°C	40 mg H_4SiO_4 kg^{-1}	Si treatment related to an improved Zn and Mn status maintains a balanced hormonal (IAA, GA, and CK) status that restores plant growth and helps to increase the expression of enzymatic (SOD and POD) and non-enzymatic (phenolic antioxidants) defense systems	Moradtalab et al., 2018
Hordeum vulgare L.	5°C and −5°C	56 mg L^{-1} as Na2SiO3	Si treatment increased the activity of antioxidative enzymes and concentrations of soluble carbohydrates and proteins	Joudmand and Hajiboland, 2019
Aloe barbadensis L.	4°C	Si 500, 1000, 1500, and 2000 mg L^{-1}	Si treatment improved both enzymatic antioxidant activity and concentrations of soluble sugars	Azarfam et al., 2020
Phyllostachys praecox	5, 0, and −5°C	Si 0, 0.5, 1.0, 2.0, 4.0, or 8.0 g kg^{-1}	Si treatment stimulated antioxidant systems and the enzyme activities of SOD, CAT, and POD Whereas the MDA content and cell membrane permeability decreased with all Si treatments	Qian et al., 2019

negative impact on ecosystem balance and agricultural systems (Kutasy et al., 2022). Drought markedly inhibits photosynthesis rather than respiration in crop plants (Vanlerberghe et al., 2016). Several studies approved the role of Si to mitigate the adverse effects of drought stress to crop plants and, hence, to regulate normal metabolism, such as photosynthesis and alleviation of photoinhibition (Habibi and Hajiboland, 2013; Zhu and Gong, 2014; Alamri et al., 2020; Ahmad et al., 2021; Malik et al., 2021). Some recent examples of Si-induced drought tolerance are presented in **Table 2**. The crop plants respond to temperature and drought stress by activating regulons, such as dehydration-responsive element-binding protein (*DREB2*) (Nakashima et al., 2012). For instance, exogenous supplementation of Si in tomatoes helps cope with drought to regulate osmotic adjustment and accumulation of drought-induced ROS (Cao et al., 2020a). Moreover, it is reported that drought-mediated accumulation of ROS can be circumvented through supplementation of Si to promote energy dissipation in tomato crop plants (Cao et al., 2020a). In a recent study, Kaya et al. (2006) have reported that Si highly enhanced the growth of shoots in maize under water-scarce conditions. In addition, drought stress can be mitigated by accumulating mineral nutrients like K^+ ions induced by Si in wheat seedlings (Keller et al., 2015). Si results in enhanced uptake of macronutrient Ca, Mg, P, and K and micronutrients Cu, Mn, and Fe during drought stress in sunflower (Gunes et al., 2007). Water uptake was enhanced by Si-induced overexpression of *SbPIP1;6, SbPIP2;6*, and *SbPIP2;2*, encoding plasma membrane intrinsic protein (PIP) aquaporins in roots of *Sorghum bicolor* (Liu P. et al., 2015). Similar results were also displayed in rice where genes, such as *OsRDCP1*-encoding choline monooxygenase and dehydrin *OsRAB16b*, were upregulated under drought stress (Khattab et al., 2014). Several studies reported that Si supplementation enhanced root growth in crop plants under drought stress (Ahmed et al., 2011; Hameed et al., 2013).

Moreover, drought tolerance is incrementally enhanced by Si supplementation to alleviate the deficiency of minerals in plants (Habibi and Hajiboland, 2013; Bityutskii et al., 2017; Hosseini et al., 2017). Moreover, Verma et al. (2021) investigated that Si played a defensive role against drought stress in sugarcane. Another mechanism responsible for enhancing tolerance by Si depends on its capability to boost the binding of nutrients to plant tissues and also stimulates the translocation of nutrients from the root apoplast to the shoots (Greger et al., 2018). The versatility of Si to defend drought stress largely depends on its capability to induce the expression of genes to mitigate the stress. For instance, Kapoor et al. (2020) detailed the Si-regulated expression of genes coding for MYB, no apical meristem (NAC), C-repeat/dehydration-responsive element-binding factors (CBF/DREB), zinc-finger proteins (ZFPs), and cup-shaped cotyledon (CUC) to activate brought a tolerant-signaling cascade in plants. Additionally, Si also induces the expression of genes linked with flavonoid biosynthesis and elevation of genes pertaining to antioxidant

enzymes to enhance drought tolerance in plants (Ma et al., 2016; Bhardwaj and Kapoor, 2021). Recently, under water-deficit conditions, the foliar application of Si has enhanced the antioxidants activities, osmolytes contents, growth, flowering, and yield of squash plants (Salim et al., 2021). These studies clearly indicate that Si is a central player in mitigating drought stress and further opens the wide scope to explore the molecular and genetic mechanisms to have in-depth knowledge for its resilience mechanism against drought.

HEAVY METALS STRESS TOLERANCE MEDIATED BY SILICON

The frequently found heavy metals, such as Al, Cd, arsenic (As), lead (Pb), mercury (Hg), copper (Cu), and zinc (Zn), in cultivated crop plants available through irrigation greatly influence the dynamics of soils (Shimo et al., 2011; Nazli et al., 2020; Asaad Bashir et al., 2021; Mehmood et al., 2021; Haseeb et al., 2022; Raza et al., 2022). These heavy metals induce devastating impacts on crop production and are potentially toxic to human health. The accumulation of heavy metals, such as Cd and Cu, binds to sulfhydryl groups of proteins, resulting in inhibition of major metabolic networks, such as lipid peroxidation, photosynthesis, and electron transport chain (ETC) (Sudo et al., 2008; Raza et al., 2021a,c). Crop production may be primarily affected by heavy metal ion-mediated adverse effects on tissues, such as induction of necrosis, leaf chlorosis, impairment in the synthesis of chlorophyll, and membrane lipid breakage (Sharma and Dietz, 2009; Takahashi et al., 2011; Raza et al., 2021d, 2022). In the rhizosphere of crop plants, Si leads to exudates rich in chelated metal ions, hence reducing metal ion uptake (Khan et al., 2021a).

Additionally, due to the deposition of Si in the endodermis, a physical barrier is created to retard the uptake of metal ions through the xylem to reduce metal ion toxicity in wheat seedlings (Keller et al., 2015). The majority of crop plants like rice, barley, broad bean, summer squash, cucumber, and cowpea ameliorate Mn-based toxicity upon accumulation of Si (Liang et al., 2007). Si accumulators show considerably lower Mn toxicity, as they help reduce more than 90% of Mn in cell walls (Rogalla et al., 2002; Ahire et al., 2021; Mundada et al., 2021). The tolerance to Mn induced by Si is due to stronger affinity of Mn to cells walls of cucumber and cowpea (Iwasaki et al., 2002; Rogalla et al., 2002; Pavlovic et al., 2021). Moreover, Si is reported to enhance the tolerance of crop plants to salinity and heavy metals like Mn and Al (Liang et al., 2007). In addition, Si ameliorates the Cd toxicity in crop plants like wheat, cotton, rice, Bok choy, and peanut (Singh et al., 2019).

Additionally, Si mediates two critical functions in crop plants: reduced Cd uptake from shoots to grains and reduced uptake of Cd in plants (Fahad et al., 2015b). Moreover, it is documented that, in wheat plants, Si plays a vital role in Cd tolerance by augmenting the uptake of metals and inducing the translocation of metal-binding proteins associated with Cd (Greger et al., 2016). The concentration of Si ranging from 1.0–1.5 mM is reported to mitigate Cd toxicity in wheat, alfalfa, and rice. Liang et al. (2005) and Farooq et al. (2016) reported that tolerance to Cd in maize was obtained by administration of exogenous Si. Exogenous Si treatment in canola declined the adverse impacts of Cd on photosynthesis and other plant growth parameters (Baryla et al., 2001; Bukhari et al., 2021b). See **Table 2** for some recent examples of Si-induced metal tolerance.

The possible mechanism of counteracting the toxic effects of Cd and Cu through the application of Si was correlated with overexpression of metal ion transporter genes, such as *OsLsi* and *OsHMA3* (Kim et al., 2014b). Moreover, Si resulted in declined Al and Cr (Chromium) uptake through roots, stems, and leaves of peanut and rice seedlings, ameliorating toxic effects of these heavy metals (Ali et al., 2013; Shen et al., 2014; Tripathi et al., 2015). Si in the form of silica gel helps to shuttle the influx transporter (Lsi1) to transport Si rather than arsenic, reducing its toxicity in rice (Rizwan et al., 2015). Comparative studies reported that Si supplementation enhanced the transcription levels of the *PsbY* (*Os08g02530*) gene-encoding polyprotein component of Photosystem II, whereas Zn administration downregulates its transcription in rice plants (Song et al., 2014). Under Zn stress, it is reported that Si mediates overexpression of the *PetC* gene, encoding Rieske Fe-S center-binding polypeptide of cytochrome *bf* complex, an essential component of cytochromes in plant electron chain system (Song et al., 2014). Under metal toxicity, it was reported that Si supplementation mediated positive effects on plants through enhancing chlorophyll biosynthesis and, in turn, photosynthetic machinery (Adrees et al., 2015; Imtiaz et al., 2016). The stomatal conductance, net photosynthetic quotient, transpiration ratio increase by enhanced synthesis of carotenoids, chlorophyll a, and b upon administration of Si under heavy metal stress in cotton and wheat plants (Bharwana et al., 2013; Hussain et al., 2015; Tripathi et al., 2015). Si supplementation downregulated the expression of zinc (Zn) transporters under zinc toxicity in maize roots (Bokor et al., 2015).

WOUND STRESS TOLERANCE MEDIATED BY SILICON

Plant wound stress occurs due to physical injuries usually induced by wind or herbivory. The damaged cells/tissue injuries are easily excess to bacterial or fungal origin pathogens. To be very specific, most of the time, injuries to C_3 and C_4 plants are primarily caused due to lodging (Savatin et al., 2014). Apart from injuries, unsaturated fatty acids of the plasma membrane are also damaged by wound-induced oxidative stress and lipid peroxidation (Farmer, 2005). Later response, i.e., lipid peroxidation, initiates a defensive signaling pathway mediated by the triggering of JA biosynthesis. Therefore, it is evident that wounding stress markedly results in increased lipid peroxidation and JA synthesis as reported in *A. thaliana* (Gfeller et al., 2011). Several reports have demonstrated the role of Si in providing strength to plant membranes and protection against injury during extreme stress conditions in crop plants, such as in *Paeonia lactiflora* Pall (Liang et al., 2007; Zhao et al., 2013). In response to oxidative stress, Si-supplied rice plants

overexpress genes and activated oxidative enzymes, such as peroxidase (PO), catalase (CAT), and polyphenol oxidase (PPO), to alleviate the wound-induced oxidative damage (Kim et al., 2014b). Comparable trends were also observed in other crop plants, such as maize, wheat, and barley (Gong et al., 2005). In Si-administered crop plants, the silicified cells obstruct the pathogen entry at wound sites to impede the dissemination of infection (Ma et al., 2008). They may cause mandibular wear in grasshoppers due to abrasiveness in leaf tissue of rescue grass (Mir et al., 2019). The growth and the development of rice plants during the wound were maintained by exogenous supplementation of Si through enhancement of endogenous levels of ETH and JA.

TEMPERATURE STRESS TOLERANCE MEDIATED BY SILICON

Heat Stress

Crop production is deeply hindered by heat stress, resulting in the loss of economy and global food insecurity (Zhou et al., 2017; Raza, 2020). Furthermore, heat stress negatively affects tomato plant growth and production (Kumar and Kaushik, 2021; Ul Hassan et al., 2021). The rate of osmotic potential is impeached by heat stress, leading to an imbalance in water potential, resulting in the negative impact of biochemical pathways and tissue damage. To overcome the fluctuating temperatures, plants have evolved a diverse array of tolerance mechanisms, which include the production of heat shock proteins (HSPs), mechanisms to scavenge the ROS, and induction of specific phytohormones (Khan et al., 2020b; Haider et al., 2021a,b; Raza et al., 2021f). Khan et al. (2020b) reported that Si helps to induce thermotolerance by stimulating heat shock proteins, phytohormone production, and antioxidant system in tomatoes. Moreover, it is reported that small HSPs improve heat stress resistance in peanuts (Fragkostefanakis et al., 2016). Exogenous administration of Si was shown to enhance the tolerance to heat stress, resulting in improving shoot length and biomass production in sword fern, cucumber, and rice (Liu et al., 2009; Sivanesan et al., 2014). The heat tolerance in crop plants was inferred to Si-enhanced synthesis in photosynthetic pigments, such as chlorophyll a, chlorophyll b, and carotenoids in plants like grapevine and submerged macrophytes (Wang et al., 2010; Chalanika De Silva and Asaeda, 2017). The expression of *SlLsi1* and *SlLsi2* genes-encoding Si transporters was upregulated in Si-treated plants upon exposure to heat stress to improve heat tolerance in tomato plants (Khan et al., 2020b). See **Table 2** for some recent examples of Si-induced heat stress tolerance.

Studies reveal that Si significantly triggered overexpression of heat tolerance genes, such as *HSFA3*, *HSFA5,* and *HSF30* in date palm and *DREB2, MAPK1, HSFA1a*, *HSFA1b*, *HSFA2*, *HSFA3,* and *HSFA7* in tomatoes (Khan et al., 2020b; Saha et al., 2021). For instance, Janni et al. (2020) reviewed the detailed mechanistic response of plants to overcome heat stress through activation of conserved pathways, viz. overexpression of ABA-responsive genes, Ca^{2+}-sensing proteins, HSP-induced protein folding, and ROS-scavenging genes. Furthermore, it is reported that these signaling cascades lead to activation of *HSP* genes, such as *HSP18*, *HSP70,* and *HSP90,* through activation of HSFA2c to maintain folding and prevent non-specific protein formation under heat stress in tall fescue (Wang and Huang, 2017). Most remarkably, the activation of HSFs and HSPs interact with diverse signaling cascades triggered by Ca^{2+}, phospholipids, SA, ET, ABA, H_2O_2, and NO to circumvent the negative impacts of heat stress on crop plants (Liu J. et al., 2015; Sharma et al., 2020). Hence, these reports strongly suggest that Si-induced HSPs are at the forefront of establishing proper folding, preventing denaturation and aggregation of cellular proteins, and inducing stay green traits through phytohormones under heat-stress conditions (Abdelrahman et al., 2017).

Cold Stress

The cold stress, including the temperatures < 15°C referred to as chilling and below 0°C for freezing, drastically influences the development and growth of plants (Habibi, 2015). Cold stress damages lipids, proteins, carbohydrates, and nucleic acids through the production of ROS (Suzuki et al., 2012). To avoid this, plants have adopted several strategies to combat the cold stress for maintaining growth and development (Dey et al., 2022). Habibi (2015) reported that foliar-applied Si effectively alleviates the cold stress by maintaining the integrity of bio-membranes and decreasing photoinhibition in grapevine plants. Reports suggest that, upon Si treatment, plants modulate levels of phytohormones, such as JA, SA, and ABA, which, in turn, activate several cold tolerance-signaling pathways (Miura and Furumoto, 2013; Eremina et al., 2016; Rastogi et al., 2021). Moreover, Si helps to enhance the tolerance to cold stress by expressing a wide array of genes, most notably transcription factors. For instance, three cold-tolerant genes, viz. *DREB1A, DREB1B*, and *DREB1C,* transiently expressed during the cold stress in Arabidopsis to regulate growth (Liu et al., 1998; Lee et al., 2005; Gujjar et al., 2014). Subsequently, the overexpression of *OsDREB1* was reported to enhance tolerance to chilling and drought stress (Ito et al., 2006). Qian et al. (2019) reported that Si induced cold tolerance in *Phyllostachys praecox* by stimulating the activities of CAT, SOD, and POD during cold stress.

Similarly, Si enhances cold tolerance by affecting the hormonal balance and micronutrient homeostasis during early growth in maize plants (Bradáčová et al., 2016; Moradtalab et al., 2018). Earlier studies also reported that the Si-induced homeostasis of micronutrients is critical to protection under cold stress in maize (Imran et al., 2013; Bradáčová et al., 2016). Si alleviates the cold stress by modulating the concentration of metabolites and activity of apoplastic enzymes in leaf apoplasm in barley plants (Joudmand and Hajiboland, 2019). Recent reports have suggested that Si ameliorates the negative impacts of cold stress by regulating cellular redox homeostasis (Basu and Kumar, 2021; Mostofa et al., 2021). For instance, Hu et al. (2022) have recently reported that Si, in combination with selenium (Se), improves the yield, growth, and other physiological attributes of cucumber plants under field trails to circumvent extreme conditions, such as cold stress. See **Table 2** for some recent examples of Si-induced cold stress tolerance. All these reports strongly suggest that Si plays a pivotal role

in evading the negative impacts of cold stress on plants, even though scientists are still underway to explore the clear-cut molecular mechanism behind the resilience mediated by Si to alleviate cold stress.

OXIDATIVE STRESS TOLERANCE MEDIATED BY SILICON

The major consequence of environmental stress elevated by oxidative stress by augmenting ROS generation, which damages cellular proteins and biomembranes, hinders the host antioxidant system and impairs major metabolic activities (Bhardwaj and Kapoor, 2021). Against these reactive species, plants have evolved enzymatic as well as non-enzymatic antioxidant systems to protect against damage induced by oxidative stress (Hussain et al., 2016). For instance, Si-supplied plants withstand the harmful effects of ROS-induced oxidation of membrane lipids and other metabolic imbalances exposed to abiotic stresses, particularly heat stress (Chalanika De Silva and Asaeda, 2017; Li et al., 2018; Hussain et al., 2019; Merewitz and Liu, 2019). In a recent study, Abdelaal et al. (2020) have reported that sweet pepper Si alleviated the oxidative stress by accretion of protective proteins and decreasing the ion toxicity, hence enhancing the activity of oxidative enzymes and eliminating O^{2-} and H_2O_2 from cells. Si helps to enhance the activity of antioxidant enzymes, which, in turn, enhance the scavenging of ROS, declining lipid peroxidation (Liu P. et al., 2015; Coskun et al., 2019). Hasanuzzaman et al. (2020) reported that, even under optimal conditions, many metabolism processes produce ROS. Sorghum and sunflower were found to mitigate salt stress when Si was added to the growth medium (Liu P. et al., 2015; Yin et al., 2016; Hurtado et al., 2021). Foliar application of Si (150 mg L^{-1}) in okra was found to enhance salt tolerance through its positive effect on activities of an antioxidant enzyme, leading to the reduction of lipid peroxidation (Abbas et al., 2015, 2017). Moreover, Si-alleviated salt stress in several crop plants like sorghum, sunflower, rice, wheat, maize, and mungbean, when supplemented in a growth medium (Liu P. et al., 2015; Abdel-Haliem et al., 2017; Alzahrani et al., 2018; Bosnic et al., 2018; Flam-Shepherd et al., 2018; Ahmad et al., 2019; Khan et al., 2020b; Hurtado et al., 2021). The Si supplemented in salt stress conditions resulted in increased activity of the antioxidant enzyme, leading to a decrease in the generation of ROS and reduced lipid peroxidation (Coskun et al., 2019). The lipid peroxidation and the production of H_2O_2 were alleviated by overexpression of the *OsNAC5* gene upon supplementation of Si (Hu et al., 2008). The ROS-scavenging enzymes, such as SOD, CAT, and GR, are upregulated upon exogenous administration of Si in barley to stand oxidative stress (Liang et al., 2003). In sorghum, wheat, rice, tomato, grapes, and okra, water uptake through aquaporins is improved by foliar application of Si due to reduced production of H_2O_2 (Soylemezoglu et al., 2009; Liu P. et al., 2015; Abbas et al., 2017; Abdel-Haliem et al., 2017). Overall, these reports validate the pivotal role played by Si to mitigate the oxidative stress by accretion of defense proteins, enhancing activity of antioxidant enzymes, reduction in membrane damage, and overexpression of ROS-scavenging genes.

HIGH-THROUGHPUT APPROACHES TO INVESTIGATE SI-INDUCED TOLERANCE TO ABIOTIC STRESSORS

Even though conventional breeding programs for combating abiotic stressors are achievable, the process is slow and tedious. The transfer of traits between species is incompatible and involves multiple backcrossing to screen desired traits out of thousands of genes (Ahmad and Mukhtar, 2017; Parmar et al., 2017). The traditional breeding methods are surmounted by genetic engineering techniques to precisely modify the gene of interest and its transfer to desired organisms (Singh and Singh, 2014). The genetic engineering approaches are aided by the advent of omics approaches to understand and identify genes/traits linked with the metabolic pathways critical to stress response, hence facilitating the transfer of identified traits to develop stress-tolerant crop plants (Mohanta et al., 2017).

High-throughput techniques, such as transcriptomics, proteomics, microarray analysis, and ionomics, have been widely used to identify differentially expressed genes or proteins in crop plants under control and stress conditions (Zargar et al., 2016; Khan et al., 2018; Yang and Guo, 2018; Afzal et al., 2022). The role of Si in alleviating stress is now obvious and has been reported to have a beneficial effect on plant growth and development under salt stress. However, the mechanism involved is not fully understood.

Transcriptomic studies are grossly employed to investigate the role of Si through the identification of a wide array of genes whose expression is altered in response to Si treatment under stress conditions. These genes are reportedly involved in solute transport, hormone biosynthesis and signaling, and biotic and abiotic stress response. A good percentage of differentially expressed genes in response to Si treatment are transcription factors (Zhu et al., 2019b; Arif et al., 2021). Liu P. et al. (2015) and Manivannan and Ahn (2017) reported that Si-upregulated *SbPIP* gene coding plasma membrane intrinsic protein (PIP) is vital for maintaining uptake of water by positively regulating the aquaporin activity and additionally enhanced salt tolerance in sorghum. Similarly, upregulation of stress-tolerant genes, such as *Os03g57120*, *Os09g26810*, and enhanced activity of S-adenosyl-L-methionine decarboxylase (SAMDC), to increase the synthesis of polyamines by Si is essential in mitigating the abiotic stressors (Manivannan and Ahn, 2017). The Si-upregulated expression of the *OsRDCP1* gene led to a decrease in dehydration of plant cells, hence mitigating drought stress (Khattab et al., 2014).

Transcriptome studies revealed that Si mitigates stress by upregulating the expression of genes *PsbY*, *PsaH*, *PsII,* and *LHC* involved in modulating PSII, oxygen-evolving manganese subunit PSI, and light harvesting complex activities during the photosynthesis process (Song et al., 2014; Lesharadevi et al., 2021). In wheat, Si improves heavy metal stress tolerance by increasing gene expression of metallothionein synthase 1 (*TaMT1*) and phytochelatin synthase (*TaPCS1*), and, in

pea, Si application improves heavy metal stress tolerance by upregulating the expression of MTA (metallothionein) and GSH1 (a precursor of phytochelatin) genes in roots (Kaushik and Saini, 2019; Arif et al., 2021). Si upregulates the expression of transcription factors, such as dehydration-responsive element-binding protein (DREB2) and NAC, involved in mitigating osmotic stress *via* the ABA independent pathway (Manivannan and Ahn, 2017; Almutairi, 2019). Comparative transcriptome studies by Zhu et al. (2019b) suggested that Si acts as an elicitor to induce salt stress in cucumber. They reported that, among the genes whose expression was altered (708 upregulated and 774 downregulated) under salt stress, the majority of them (609 and 595, respectively) reverted to the normal expression levels upon Si treatment, shifting the transcriptome of salt-stressed cucumber back to normal.

The transcriptome analysis of different tissues, such as flag leaves (FLs), spikelets (SPs), and node Is (NIs) of Cd-exposed rice after Si application, revealed that the gene expression profiles associated with the Si-mediated alleviation of Cd stress were tissue-specific. Si may alter the expression pattern of genes associated with transport, biosynthesis and metabolism, and oxidation-reduction. In Cd-exposed rice, the expression of ATP-binding cassette (ABC)-transporters, essential nutrient transporters, carbohydrate, secondary metabolite biosynthesis, and cytochrome oxidase activity were mostly upregulated in FL and SP with Si treatment, while the expression of bivalent cation transporters was mostly downregulated, possibly to reduce Cd accumulation (Sun et al., 2022). In another study, Hao et al. (2021) used RNA-seq technology to identify DEGs in wheat seedlings treated with Si. They reported that 3,057 genes related to transcription factors, chaperons, phenylpropanoid biosynthesis, and protein processing were differentially expressed upon Si treatment. Approximately, 28 differentially expressed transcription factors from the MYB TF family were downregulated under Si treatment.

The proteomics offers a new approach to discovering a myriad of stress-inducible proteins that respond to abiotic stresses at transcriptional and translational levels to identify proteins and understand the pathways associated with stress tolerance (Kosová et al., 2011, 2018). Understanding the key metabolic proteins and pathways of stress tolerance can help in biotechnological interventions for the development of varieties with improved stress tolerance. Abiotic stresses interfere with protein synthesis and cause loss of protein. Si has been reported to efficiently lower stress by upregulating the synthesis of a protein associated with signal transduction processes and antioxidant defense machinery. Proteomics studies have identified that, upon exposure of plants to Si, 17% stress-tolerant proteins, 11% proteins related to cellular and hormone biosynthesis, RNA synthesis, and synthesis of secondary metabolites are upregulated to alleviate abiotic stressors (Al Murad et al., 2020). Likewise, proteomic studies have aided in tracing the upregulation of proteins, such as RNA polymerase mediator, homologs of transcription elongation (SPT4), MADS-box TF, TFs for elongation, tRNA-lysidine synthase, ribosomal protein L16, ribosome-recycling factor, and reverse transcriptase, by Si to confer tolerance against abiotic stress in plants (Muneer and Jeong, 2015; Al Murad et al., 2020).

Furthermore, proteomic studies have confirmed that Si mitigates environmental stressors, including salinity and thermal stresses by inducing synthesis of β-carotene synthesis protein carotene desaturase, chaperone protein, such as ClpC3, CF1α subunit of ATP-synthase, cupin family protein phosphoglycerate kinase, glutelin, and β-keto acyl reductase, plasma membrane intrinsic protein (PIP1), and nodulin 26-like intrinsic protein (NIP2) (Choi, 2009; Cao et al., 2020b; Younis et al., 2020). Like other grasses, rice accumulates Si and stores most of it in leaves. Study of change in leaf proteome in Si-induced Cd tolerance in rice has revealed that Si significantly regulated synthesis of proteins involved in photosynthesis, redox homeostasis, protein synthesis regulation, chaperone activity, and pathogen response, class III peroxidase, disulfide isomerase, an NADH-ubiquinone oxidoreductase alone, or in combination with Cd. It suggests a strong role of Si in induced tolerance (Nwugo and Huerta, 2011). A similar study on Si-induced salinity stress tolerance in *Capsicum annuum,* Manivannan et al. (2016) carried out proteomic analysis by two-dimensional gel electrophoresis (2DE), followed by matrix-assisted laser desorption/ionization time-of-flight mass spectrometry (MALDI-TOF-MS), revealed that Si treatment upregulated the accumulation of proteins with nucleotide-binding and transferase activity involved in several metabolic processes and also modulated the expression of vital proteins involved in the ubiquitin-mediated nucleosome pathway and carbohydrate metabolism (Manivannan et al., 2016).

Metabolomic studies helped to identify the accumulation of metabolites critical to the growth, sustenance, and development of plants under the influence of Si to mitigate adverse abiotic stress conditions (Jana et al., 2019; Raza, 2020). The Si upregulated the metabolites that include ascorbate, glutathione, phenol, tocopherol, and flavonoids to attenuate the harmful effects of abiotic stressors such that normal growth and metabolism will be sustained (Metwally et al., 2018). Recent ionomic studies have revealed that Si application induced the accumulation of critical cofactors of enzymes, such as Cu, Fe, and Zn, to mitigate stressors (Banerjee et al., 2021). Si application increases the accumulation of several nutrients, such as N, P, K, Mn, Fe, Na, Ca, and Mg, which reduce stress-induced ionic damage, increase drought tolerance, and enhance plant growth (Ahanger et al., 2020b; Pavlovic et al., 2021).

These omics reports serve as the backbone for applying genetic engineering approaches to mediate resilience in transgenic crop plants. For instance, the development of transgenic cultivars of rice plants through a transfer of the *Lsi1* gene modulated the physiological and molecular activities to mitigate arsenic stress upon exposure to Si (Boorboori et al., 2021). Likewise, overexpression of the *VyDOF8* transcription factor gene derived from Chinese wild grapevine was reported to mitigate drought stress in transgenic tobacco plants (Li et al., 2021). Similarly, *OsMADS57* TF was upregulated by Si, overexpressed in rice, and *A. thaliana* mitigated salinity stress. All these reports strongly suggest that genetic engineering technology speeds up the development of stress-resilient crop plants for food and nutritional security. The last few decades have witnessed shifting research on genome-editing technologies, such as ZFN, TALEN, and CRISPR/Cas systems, for higher accuracy and precision to

develop desired crop plants with tolerance to different abiotic stressors (Mushtaq et al., 2021; Pandita, 2021). For instance, Li et al. (2019) employed CRISPR/Cas9 to mediate mutagenesis of *SlNPR1* to enhance drought tolerance in tomatoes. Almost no other report is available on the editing of the Si-encoding genes; thus, in the future, the CRISPR/Cas system should be applied to Si-encoding genes to increase the tolerance against various abiotic stresses in major crop plants. We believe the application of high-throughput technologies will aid in speeding up the quest to develop stress-tolerant crop varieties for food and nutritional security (Varshney et al., 2018, 2020, 2021a,b; Pazhamala et al., 2021).

CONCLUSION AND FUTURE PERSPECTIVES

Even though the metabolic demand of Si is deficient, its presence in plant systems is critical to alleviating abiotic stress. Keeping in view the importance of Si to crop plants, the last decade witnessed many publications pertaining to its role in alleviating abiotic stress. Si is proven to play a vital role in combating abiotic stress conditions by positively modulating the physiological attributes of crop plants. Central to the role of Si is its upregulation of phytohormones and their signaling cascades operated to withstand abiotic stresses. Remarkably, Si is reported to impart more excellent resistance to abiotic stress factors through overexpression of genes regulating the synthesis of phytohormones. The stress tolerance mediated by Si-induced phytohormones is largely regulated through signal transduction pathways. Although the effect of Si to alleviate the abiotic stress in crop plants is variable, the multidimensional role of Si in plant development, such as the alleviation of sulfur deficiency, osmotic stress tolerance, alteration of genes related to glyceraldehydes-3-phosphate dehydrogenase, cyclophilin (CYC), ADP-Ribosylation Factor (ADP-RF1), and positively modulating metabolic pathways under abiotic stress, is well accustomed. The effect may vary concerning stress duration and intensity, *in vitro* methods of application, and cultivation. We conclude that Si can be integrated as a requisite part of fertilizers to benefit the crop plants in adverse ecological conditions. The focus on Si-based fertilizers may help to attain global sustainable agricultural growth.

The clear insights into the pivotal role of Si in circumventing the stress tolerance are still scanty, primarily due to a poor understanding of the molecular mechanism imparted by this multitalented element. Furthermore, extensive molecular investigation into the integrated effects of Si and phytohormones on alleviating the drought tolerance in plants is still at its early stage. In addition, the genes pertaining to the physiological improvements need to be further unveiled to authenticate the role of Si as the leading element in fertilizers for fortification and sustainable agricultural growth. Advanced omics technologies, such as transcriptomic, proteomic, and metabolomic studies, can further aid in-depth exploration of crosstalk of Si with phytohormones to unravel novel signaling molecules responsible for alleviating the stress tolerance in crop plants. In addition, special attention should be put on the role of Si in regulating signal transduction pathways under a wide range of abiotic stress conditions. Furthermore, shifting focus upon deciphering the role of Si in cop plants in felid trails rather than in controlled laboratory conditions is of dire need. In the future, the CRISPR/Cas system should be applied to Si-encoding genes to increase the tolerance against various abiotic stresses in major crop plants.

AUTHOR CONTRIBUTIONS

RM and SZ conceived the idea. RM, BB, HY, SI, MR, MA, PS, SC, and AR collected the literature and participated in writing. RM, BB, AR, SI, and SZ proofread and edited the final version. All authors have read and approved the final version of the manuscript.

FUNDING

SZ acknowledges the support of the National Mission on Himalayan Studies (NMHS) implemented by the Ministry of Environment, Forest and Climate Change (MoEFCC) vide project sanction No.: GBPNI/NMHS-2017-18/SG24/622. SZ and PS also acknowledge the Hon'ble Vice-Chancellor SKUAST-K (Prof. Nazir A. Ganai) for his support.

REFERENCES

Abbas, T., Balal, R. M., Shahid, M. A., Pervez, M. A., Ayyub, C. M., Aqueel, M. A., et al. (2015). Silicon-induced alleviation of NaCl toxicity in okra (Abelmoschus esculentus) is associated with enhanced photosynthesis, osmoprotectants and antioxidant metabolism. *Acta Physiol. Plant.* 37:6.

Abbas, T., Sattar, A., Ijaz, M., Aatif, M., Khalid, S., and Sher, A. (2017). Exogenous silicon application alleviates salt stress in okra. *Horticult. Environ. Biotechnol.* 58, 342–349. doi: 10.1007/s13580-017-0247-5

Abdalla, M. M. (2011). Impact of diatomite nutrition on two Trifolium alexandrinum cultivars differing in salinity tolerance. *Int. J. Plant Physiol. Biochem.* 3, 233–246.

Abdelaal, K. A. A., Mazrou, Y. S. A., and Hafez, Y. M. (2020). Silicon foliar application mitigates salt stress in sweet pepper plants by enhancing water status, photosynthesis, antioxidant enzyme activity and fruit yield. *Plants* 9:733. doi: 10.3390/plants9060733

Abdel-Haliem, M. E. F., Hegazy, H. S., Hassan, N. S., and Naguib, D. M. (2017). Effect of silica ions and nano silica on rice plants under salinity stress. *Ecol. Engine.* 99, 282–289.

Abdelrahman, M., El-Sayed, M., Jogaiah, S., Burritt, D. J., and Tran, L.-S. P. (2017). The "STAY-GREEN" trait and phytohormone signaling networks in plants under heat stress. *Plant Cell Rep.* 36, 1009–1025. doi: 10.1007/s00299-017-2119-y

Adatia, M. H., and Besford, R. T. (1986). The effects of silicon on cucumber plants grown in recirculating nutrient solution. *Ann. Bot.* 58, 343–351. doi: 10.1093/oxfordjournals.aob.a087212

Adrees, M., Ali, S., Rizwan, M., Zia-ur-Rehman, M., Ibrahim, M., Abbas, F., et al. (2015). Mechanisms of silicon-mediated alleviation of heavy metal toxicity in

plants: a review. *Ecotoxicol. Environ. Safety* 119, 186–197. doi: 10.1016/j.ecoenv.2015.05.011

Afzal, S., Chaudhary, N., Sharma, D., and Singh, N. K. (2022). Towards understanding abiotic stress physiological studies in plants: Conjunction of genomic and proteomic approaches. *Plant Perspect. Glob. Clim. Changes* 2022, 25–49. doi: 10.1016/b978-0-323-85665-2.00013-3

Agrawal, G. K., Jwa, N.-S., Agrawal, S. K., Tamogami, S., Iwahashi, H., and Rakwal, R. (2003). Cloning of novel rice allene oxide cyclase (OsAOC): mRNA expression and comparative analysis with allene oxide synthase (OsAOS) gene provides insight into the transcriptional regulation of octadecanoid pathway biosynthetic genes in rice. *Plant Sci.* 164, 979–992. doi: 10.1016/s0168-9452(03)00082-7

Ahanger, M. A., Aziz, U., Alsahli, A. A., Alyemeni, M. N., and Ahmad, P. (2020a). Influence of exogenous salicylic acid and nitric oxide on growth, photosynthesis, and ascorbate-glutathione cycle in salt stressed Vigna angularis. *Biomolecules* 10:42. doi: 10.3390/biom10010042

Ahanger, M. A., Bhat, J. A., Siddiqui, M. H., Rinklebe, J., and Ahmad, P. (2020b). Integration of silicon and secondary metabolites in plants: a significant association in stress tolerance. *J. Exp. Bot.* 71, 6758–6774. doi: 10.1093/jxb/eraa291

Ahanger, M. A., Qin, C., Maodong, Q., Dong, X. X., Ahmad, P., Abd_Allah, E. F., et al. (2019). Spermine application alleviates salinity induced growth and photosynthetic inhibition in Solanum lycopersicum by modulating osmolyte and secondary metabolite accumulation and differentially regulating antioxidant metabolism. *Plant Physiol. Biochem.* 144, 1–13. doi: 10.1016/j.plaphy.2019.09.021

Ahire, M. L., Mundada, P. S., Nikam, T. D., Bapat, V. A., and Penna, S. (2021). Multifaceted roles of silicon in mitigating environmental stresses in plants. *Plant Physiol. Biochem.* 169, 291–310. doi: 10.1016/j.plaphy.2021.11.010

Ahmad, A., Aslam, Z., Naz, M., Hussain, S., Javed, T., Aslam, S., et al. (2021). Exogenous salicylic acid-induced drought stress tolerance in wheat (Triticum aestivum L.) grown under hydroponic culture. *PLoS One* 16:e0260556. doi: 10.1371/journal.pone.0260556

Ahmad, N., and Mukhtar, Z. (2017). Genetic manipulations in crops: challenges and opportunities. *Genomics* 109, 494–505. doi: 10.1016/j.ygeno.2017.07.007

Ahmad, P., Ahanger, M. A., Alam, P., Alyemeni, M. N., Wijaya, L., Ali, S., et al. (2019). Silicon (Si) supplementation alleviates NaCl toxicity in mung bean [Vigna radiata (L.) Wilczek] through the modifications of physio-biochemical attributes and key antioxidant enzymes. *J. Plant Growth Regul.* 38, 70–82. doi: 10.1007/s00344-018-9810-2

Ahmad, P., and Jhon, R. (2005). Effect of salt stress on growth and biochemical parameters of Pisum sativum L. (Einfluss von Salzstress auf Wachstum und biochemische Parameter von Pisum sativum L.). *Arch. Agron. Soil Sci.* 51, 665–672.

Ahmed, M., Qadeer, U., and Aslam, M. A. (2011). Silicon application and drought tolerance mechanism of sorghum. *Afr. J. Agricult. Res.* 6, 594–607.

Akhtar, P., and Hussain, F. (2008). Salinity tolerance of three range grasses at germination and early growth stages. *Pak. J. Bot.* 40, 2437–2441.

Al Murad, M., Khan, A. L., and Muneer, S. (2020). Silicon in horticultural crops: cross-talk, signaling, and tolerance mechanism under salinity stress. *Plants* 9:460. doi: 10.3390/plants9040460

Al-aghabary, K., Zhu, Z., and Shi, Q. (2005). Influence of silicon supply on chlorophyll content, chlorophyll fluorescence, and antioxidative enzyme activities in tomato plants under salt stress. *J. Plant Nutrit.* 27, 2101–2115. doi: 10.1081/pln-200034641

Alam, A., Hariyanto, B., Ullah, H., Salin, K. R., and Datta, A. (2021). Effects of silicon on growth, yield and fruit quality of cantaloupe under drought stress. *Silicon* 13, 3153–3162. doi: 10.1007/s12633-020-00673-1

Alamri, S., Hu, Y., Mukherjee, S., Aftab, T., Fahad, S., Raza, A., et al. (2020). Silicon-induced postponement of leaf senescence is accompanied by modulation of antioxidative defense and ion homeostasis in mustard (Brassica juncea) seedlings exposed to salinity and drought stress. *Plant Physiol. Biochem.* 157, 47–59. doi: 10.1016/j.plaphy.2020.09.038

Al-Huqail, A. A., Alqarawi, A. A., Hashem, A., Malik, J. A., and Abd_Allah, E. F. (2019). Silicon supplementation modulates antioxidant system and osmolyte accumulation to balance salt stress in Acacia gerrardii Benth. *Saudi J. Biol. Sci.* 26, 1856–1864. doi: 10.1016/j.sjbs.2017.11.049

Ali, M., Afzal, S., Parveen, A., Kamran, M., Javed, M. R., Abbasi, G. H., et al. (2021). Silicon mediated improvement in the growth and ion homeostasis by decreasing Na+ uptake in maize (Zea mays L.) cultivars exposed to salinity stress. *Plant Physiol. Biochem.* 158, 208–218. doi: 10.1016/j.plaphy.2020.10.040

Ali, S., Farooq, M. A., Yasmeen, T., Hussain, S., Arif, M. S., Abbas, F., et al. (2013). The influence of silicon on barley growth, photosynthesis and ultra-structure under chromium stress. *Ecotoxicol. Environ. Safety* 89, 66–72. doi: 10.1016/j.ecoenv.2012.11.015

Almutairi, Z. M. T. (2019). Plant molecular defense mechanisms promoted by nanoparticles against environmental stress. *Int. J. Agric. Biol.* 21, 259–270. doi: 10.3390/ijms23041947

Alzahrani, Y., Kuşvuran, A., Alharby, H. F., Kuşvuran, S., and Rady, M. M. (2018). The defensive role of silicon in wheat against stress conditions induced by drought, salinity or cadmium. *Ecotoxicol. Environ. Safety* 154, 187–196. doi: 10.1016/j.ecoenv.2018.02.057

Arif, Y., Singh, P., Bajguz, A., Alam, P., and Hayat, S. (2021). Silicon mediated abiotic stress tolerance in plants using physio-biochemical, omic approach and cross-talk with phytohormones. *Plant Physiol. Biochem.* 166, 278–289. doi: 10.1016/j.plaphy.2021.06.002

Artyszak, A. (2018). Effect of silicon fertilization on crop yield quantity and quality—A literature review in Europe. *Plants* 7:54. doi: 10.3390/plants7030054

Asaad Bashir, M., Wang, X., Naveed, M., Mustafa, A., Ashraf, S., Samreen, T., et al. (2021). Biochar Mediated-Alleviation of Chromium Stress and Growth Improvement of Different Maize Cultivars in Tannery Polluted Soils. *Int. J. Environ. Res. Public Health* 18:4461. doi: 10.3390/ijerph18094461

Atta, B., Rizwan, M., Sabir, A. M., Gogi, M. D., and Ayub, M. A. (2019). Silicon mediated induced resistance in plants for the management of agricultural insect pests: A review. *World J. Biol. Biotechnol.* 4, 19–27. doi: 10.1016/j.pestbp.2020.104641

Azarfam, S., Nadian, H., Moezzi, A., and Gholami, A. (2020). Effect of silicon on phytochemical and medicinal properties of aloe vera under cold stress. *Appl. Ecol. Environ. Res.* 18, 561–575. doi: 10.15666/aeer/1801_561575

Bakhat, H. F., Bibi, N., Zia, Z., Abbas, S., Hammad, H. M., Fahad, S., et al. (2018). Silicon mitigates biotic stresses in crop plants: a review. *Crop Protect.* 104, 21–34.

Banerjee, A., Singh, A., Sudarshan, M., and Roychoudhury, A. (2021). Silicon nanoparticle-pulsing mitigates fluoride stress in rice by fine-tuning the ionomic and metabolomic balance and refining agronomic traits. *Chemosphere* 262:127826. doi: 10.1016/j.chemosphere.2020.127826

Bari, M. A., Prity, S. A., Das, U., Akther, M. S., Sajib, S. A., Reza, M. A., et al. (2020). Silicon induces phytochelatin and ROS scavengers facilitating cadmium detoxification in rice. *Plant Biol.* 22, 472–479. doi: 10.1111/plb.13090

Baryla, A., Carrier, P., Franck, F., Coulomb, C., Sahut, C., and Havaux, M. (2001). Leaf chlorosis in oilseed rape plants (Brassica napus) grown on cadmium-polluted soil: causes and consequences for photosynthesis and growth. *Planta* 212, 696–709. doi: 10.1007/s004250000439

Basu, S., and Kumar, G. (2021). Exploring the significant contribution of silicon in regulation of cellular redox homeostasis for conferring stress tolerance in plants. *Plant Physiol. Biochem.* 166, 393–404. doi: 10.1016/j.plaphy.2021.06.005

Benslima, W., Zorrig, W., Bagues, M., Abdelly, C., and Hafsi, C. (2021). Silicon mitigates potassium deficiency in Hordeum vulgare by improving growth and photosynthetic activity but not through polyphenol accumulation and the related antioxidant potential. *Plant Soil* 2021, 1–18.

Bhardwaj, S., and Kapoor, D. (2021). Fascinating regulatory mechanism of silicon for alleviating drought stress in plants. *Plant Physiol. Biochem.* 166, 1044–1053. doi: 10.1016/j.plaphy.2021.07.005

Bharwana, S. A., Ali, S., Farooq, M. A., Iqbal, N., Abbas, F., and Ahmad, M. S. A. (2013). Alleviation of lead toxicity by silicon is related to elevated photosynthesis, antioxidant enzymes suppressed lead uptake and oxidative stress in cotton. *J. Bioremed. Biodeg.* 4, 10–4172. doi: 10.1016/j.ecoenv.2013.07.006

Bijanzadeh, E., Barati, V., and Egan, T. P. (2022). Foliar application of sodium silicate mitigates drought stressed leaf structure in corn (Zea mays L.). *South Afr. J. Bot.* 147, 8–17. doi: 10.1016/j.sajb.2021.12.032

Bityutskii, N. P., Yakkonen, K. L., Petrova, A. I., and Shavarda, A. L. (2017). Interactions between aluminium, iron and silicon in Cucumber sativus L. grown under acidic conditions. *J. Plant Physiol.* 218, 100–108. doi: 10.1016/j.jplph.2017.08.003

Bokor, B., Bokorová, S., Ondoš, S., Švubová, R., Lukačová, Z., Hýblová, M., et al. (2015). Ionome and expression level of Si transporter genes (Lsi1, Lsi2, and Lsi6) affected by Zn and Si interaction in maize. *Environ. Sci. Poll. Res.* 22, 6800–6811. doi: 10.1007/s11356-014-3876-6

Boorboori, M. R., Lin, W., Jiao, Y., and Fang, C. (2021). Silicon Modulates Molecular and Physiological Activities in Lsi1 Transgenic and Wild Rice Seedlings under Arsenic Stress. *Agronomy* 11:1532. doi: 10.3390/agronomy11081532

Bosnic, P., Bosnic, D., Jasnic, J., and Nikolic, M. (2018). Silicon mediates sodium transport and partitioning in maize under moderate salt stress. *Environ. Exp. Bot.* 155, 681–687. doi: 10.1016/j.envexpbot.2018.08.018

Bradáčová, K., Weber, N. F., Morad-Talab, N., Asim, M., Imran, M., Weinmann, M., et al. (2016). Micronutrients (Zn/Mn), seaweed extracts, and plant growth-promoting bacteria as cold-stress protectants in maize. *Chem. Biol. Technol. Agricult.* 3, 1–10. doi: 10.1142/9781848160521_0001

Bukhari, M. A., Ahmad, Z., Ashraf, M. Y., Afzal, M., Nawaz, F., Nafees, M., et al. (2021a). Silicon mitigates drought stress in wheat (Triticum aestivum L.) through improving photosynthetic pigments, biochemical and yield characters. *Silicon* 13, 4757–4772. doi: 10.1007/s12633-020-00797-4

Bukhari, M. A., Sharif, M. S., Ahmad, Z., Barutçular, C., Afzal, M., Hossain, A., et al. (2021b). Silicon mitigates the adverse effect of drought in canola (Brassica napus L.) through promoting the physiological and antioxidants activity. *Silicon* 13, 3817–3826. doi: 10.1007/s12633-020-00685-x

Bybordi, A. (2015). Influence of exogenous application of silicon and potassium on physiological responses, yield, and yield components of salt-stressed wheat. *Commun. Soil Sci. Plant Anal.* 46, 109–122.

Caarls, L., Pieterse, C. M. J., and Van Wees, S. (2015). How salicylic acid takes transcriptional control over jasmonic acid signaling. *Front. Plant Sci.* 6:170. doi: 10.3389/fpls.2015.00170

Cao, B. L., Ma, Q., and Xu, K. (2020a). Silicon restrains drought-induced ROS accumulation by promoting energy dissipation in leaves of tomato. *Protoplasma* 257, 537–547.

Cao, F., Dai, H., Hao, P.-F., and Wu, F. (2020b). Silicon regulates the expression of vacuolar H+-pyrophosphatase 1 and decreases cadmium accumulation in rice (Oryza sativa L.). *Chemosphere* 240:124907.

Carneiro, J. M. T., Chacón-Madrid, K., Galazzi, R. M., Campos, B. K., Arruda, S. C. C., Azevedo, R. A., et al. (2017). Evaluation of silicon influence on the mitigation of cadmium-stress in the development of Arabidopsis thaliana through total metal content, proteomic and enzymatic approaches. *J. Trace Elements Med. Biol.* 44, 50–58.

Chalanika De Silva, H. C., and Asaeda, T. (2017). Effects of heat stress on growth, photosynthetic pigments, oxidative damage and competitive capacity of three submerged macrophytes. *J. Plant Interact.* 12, 228–236.

Chen, H., Bullock, D. A., Alonso, J. M., and Stepanova, A. N. (2022). To Fight or to Grow: The Balancing Role of Ethylene in Plant Abiotic Stress Responses. *Plants* 11:33.

Chen, W., Yao, X., Cai, K., and Chen, J. (2011). Silicon alleviates drought stress of rice plants by improving plant water status, photosynthesis and mineral nutrient absorption. *Biol. Trace Element Res.* 142, 67–76.

Choi, W.-G. (2009). *Nodulin 26-like Intrinsic Protein NIP2; 1 and NIP7; 1: Characterization of Transport Functions and Roles in Developmental and Stress Responses in Arabidopsis*. Knoxville, TN: University of Tennessee.

Colebrook, E. H., Thomas, S. G., Phillips, A. L., and Hedden, P. (2014). The role of gibberellin signalling in plant responses to abiotic stress. *J. Exp. Biol.* 217, 67–75.

Cooke, J., and Leishman, M. R. (2011). Is plant ecology more siliceous than we realise? *Trends Plant Sci.* 16, 61–68.

Cooke, J., and Leishman, M. R. (2016). Consistent alleviation of abiotic stress with silicon addition: a meta-analysis. *Funct. Ecol.* 30, 1340–1357.

Coskun, D., Britto, D. T., Huynh, W. Q., and Kronzucker, H. J. (2016). The role of silicon in higher plants under salinity and drought stress. *Front. Plant Sci.* 7:1072. doi: 10.3389/fpls.2016.01072

Coskun, D., Deshmukh, R., Sonah, H., Menzies, J. G., Reynolds, O., Ma, J. F., et al. (2019). The controversies of silicon's role in plant biology. *New Phytol.* 221, 67–85.

Cui, J., Zhang, E., Zhang, X., and Wang, Q. (2021). Silicon alleviates salinity stress in licorice (Glycyrrhiza uralensis) by regulating carbon and nitrogen metabolism. *Sci. Rep.* 11, 1–12.

Daryanto, S., Wang, L., and Jacinthe, P. A. (2016). Global synthesis of drought effects on maize and wheat production. *PloS one* 11:e0156362.

da Cunha, K. P. V., and do Nascimento, C. W. A. (2009). Silicon effects on metal tolerance and structural changes in maize (Zea mays L.) grown on a cadmium and zinc enriched soil. *Water Air Soil Poll.* 197, 323–330.

da Silva, J. A. T., and Yücel, M. (2008). Revealing response of plants to biotic and abiotic stresses with microarray technology. *Genes Genomes Genomics* 2, 14–48.

Das, P., Manna, I., Sil, P., Bandyopadhyay, M., and Biswas, A. K. (2021). Silicon augments salt tolerance through modulation of polyamine and GABA metabolism in two indica rice (Oryza sativa L.) cultivars. *Plant Physiol. Biochem.* 166, 41–52.

de Oliveira, R. L. L., de Mello Prado, R., Felisberto, G., and Cruz, F. J. R. (2019). Different sources of silicon by foliar spraying on the growth and gas exchange in sorghum. *J. Soil Sci. Plant Nutrit.* 19, 948–953.

de Ollas, C., Hernando, B., Arbona, V., and Gómez-Cadenas, A. (2013). Jasmonic acid transient accumulation is needed for abscisic acid increase in citrus roots under drought stress conditions. *Physiol. Plant.* 147, 296–306.

Debona, D., Rodrigues, F. A., and Datnoff, L. E. (2017). Silicon's role in abiotic and biotic plant stresses. *Annu. Rev. Phytopathol.* 55, 85–107.

Del Buono, D. (2021). Can biostimulants be used to mitigate the effect of anthropogenic climate change on agriculture? It is time to respond. *Sci. Total Environ.* 751:141763.

Deren, C. W. (2001). Plant genotype, silicon concentration, and silicon-related responses. *Stud. Plant Sci.* 8, 149–158.

Dey, P., Datta, D., Pattnaik, D., Dash, D., Saha, D., Panda, D., et al. (2022). Physiological, biochemical, and molecular adaptation mechanisms of photosynthesis and respiration under challenging environments. *Plant Perspect. Glob. Clim. Changes* 2022, 79–100.

Dhiman, P., Rajora, N., Bhardwaj, S., Sudhakaran, S. S., Kumar, A., Raturi, G., et al. (2021). Fascinating role of silicon to combat salinity stress in plants: An updated overview. *Plant Physiol. Biochem.* 162, 110–123.

Dorairaj, D., Ismail, M. R., Sinniah, U. R., and Kar Ban, T. (2017). Influence of silicon on growth, yield, and lodging resistance of MR219, a lowland rice of Malaysia. *J. Plant Nutrit.* 40, 1111–1124.

dos Santos, A. F. B., Teixeira, G. C. M., Campos, C. N. S., Baio, F. H. R., de Mello Prado, R., Teodoro, L. P. R., et al. (2020). Silicon increases chlorophyll and photosynthesis and improves height and NDVI of cotton (Gossypium hirsutum L. r. latifolium Hutch). *Res. Soc. Dev.* 9, e548973826–e548973826.

Du, Y., and Scheres, B. (2018). Lateral root formation and the multiple roles of auxin. *J. Exp. Bot.* 69, 155–167.

El Moukhtari, A., Carol, P., Mouradi, M., Savoure, A., and Farissi, M. (2021). Silicon improves physiological, biochemical, and morphological adaptations of alfalfa (Medicago sativa L.) during salinity stress. *Symbiosis* 2021, 1–20.

El-Mageed, A., Taia, A., Shaaban, A., El-Mageed, A., Shimaa, A., Semida, W. M., et al. (2021). Silicon defensive role in maize (Zea mays L.) against drought stress and metals-contaminated irrigation water. *Silicon* 13, 2165–2176.

El-Mashad, A. A. A., and Mohamed, H. I. (2012). Brassinolide alleviates salt stress and increases antioxidant activity of cowpea plants (Vigna sinensis). *Protoplasma* 249, 625–635.

El-Saadony, M. T., Desoky, E.-S. M., Saad, A. M., Eid, R. S. M., Selem, E., and Elrys, A. S. (2021). Biological silicon nanoparticles improve Phaseolus vulgaris L. yield and minimize its contaminant contents on a heavy metals-contaminated saline soil. *J. Environ. Sci.* 106, 1–14.

Emamverdian, A., Ding, Y., Xie, Y., and Sangari, S. (2018). Silicon mechanisms to ameliorate heavy metal stress in plants. *BioMed Res. Int.* 2018:8492898. doi: 10.1155/2018/8492898

Eraslan, F., Inal, A., Pilbeam, D. J., and Gunes, A. (2008). Interactive effects of salicylic acid and silicon on oxidative damage and antioxidant activity in spinach (Spinacia oleracea L. cv. Matador) grown under boron toxicity and salinity. *Plant Growth Regul.* 55, 207–219.

Eremina, M., Rozhon, W., and Poppenberger, B. (2016). Hormonal control of cold stress responses in plants. *Cell. Mol. Life Sci.* 73, 797–810.

Etesami, H., and Jeong, B. R. (2018). Silicon (Si): Review and future prospects on the action mechanisms in alleviating biotic and abiotic stresses in plants. *Ecotoxicol. Environ. Safety* 147, 881–896.

Fahad, S., Hussain, S., Bano, A., Saud, S., Hassan, S., Shan, D., et al. (2015a). Potential role of phytohormones and plant growth-promoting rhizobacteria in abiotic stresses: consequences for changing environment. *Environ. Sci. Poll. Res.* 22, 4907–4921.

Fahad, S., Hussain, S., Matloob, A., Khan, F. A., Khaliq, A., Saud, S., et al. (2015b). Phytohormones and plant responses to salinity stress: a review. *Plant Growth Regulat.* 75, 391–404.

Farmer, V. C. (2005). Forest vegetation does recycle substantial amounts of silicon from and back to the soil solution with phytoliths as an intermediate phase, contrary to recent reports. *Eur. J. Soil Sci.* 56, 271–272.

Farooq, M. A., Detterbeck, A., Clemens, S., and Dietz, K. J. (2016). Silicon-induced reversibility of cadmium toxicity in rice. *J. Exp. Bot.* 67, 3573–3585.

Fei, Q., Liang, L., Li, F., Zhang, L., Li, Y., Guo, Y., et al. (2019). Transcriptome profiling and phytohormone responses of Arabidopsis roots to different ambient temperatures. *J. Plant Interact.* 14, 314–323.

Feng, J., Yamaji, N., and Mitani-Ueno, N. (2011). Transport of silicon from roots to panicles in plants. *Proc. Jap. Acad. Ser. B* 87, 377–385.

Ferchichi, S., Hessini, K., Dell'Aversana, E., D'Amelia, L., Woodrow, P., Ciarmiello, L. F., et al. (2018). Hordeum vulgare and Hordeum maritimum respond to extended salinity stress displaying different temporal accumulation pattern of metabolites. *Funct. Plant Biol.* 45, 1096–1109.

Fiala, R., Fialová, I., Vaculík, M., and Luxová, M. (2021). Effect of silicon on the young maize plants exposed to nickel stress. *Plant Physiol. Biochem.* 166, 645–656.

Flam-Shepherd, R., Huynh, W. Q., Coskun, D., Hamam, A. M., Britto, D. T., and Kronzucker, H. J. (2018). Membrane fluxes, bypass flows, and sodium stress in rice: the influence of silicon. *J. Exp. Bot.* 69, 1679–1692.

Fragkostefanakis, S., Mesihovic, A., Simm, S., Paupière, M. J., Hu, Y., Paul, P., et al. (2016). HsfA2 controls the activity of developmentally and stress-regulated heat stress protection mechanisms in tomato male reproductive tissues. *Plant Physiol.* 170, 2461–2477.

Gangwar, S., Singh, V. P., Tripathi, D. K., Chauhan, D. K., Prasad, S. M., and Maurya, J. N. (2014). Plant responses to metal stress: the emerging role of plant growth hormones in toxicity alleviation. *Emerg. Technol. Manage. Crop Stress Toler.* 2014, 215–248.

Garg, N., and Singh, S. (2018). Arbuscular mycorrhiza Rhizophagus irregularis and silicon modulate growth, proline biosynthesis and yield in Cajanus cajan L. Millsp.(pigeonpea) genotypes under cadmium and zinc stress. *J. Plant Growth Regul.* 37, 46–63.

Gfeller, A., Baerenfaller, K., Loscos, J., Chételat, A., Baginsky, S., and Farmer, E. E. (2011). Jasmonate controls polypeptide patterning in undamaged tissue in wounded Arabidopsis leaves. *Plant Physiol.* 156, 1797–1807.

Gill, S. S., and Tuteja, N. (2010). Reactive oxygen species and antioxidant machinery in abiotic stress tolerance in crop plants. *Plant Physiol. Biochem.* 48, 909–930.

Gómez-Merino, F. C., Trejo-Téllez, L. I., García-Jiménez, A., Escobar-Sepúlveda, H. F., and Ramírez-Olvera, S. M. (2020). Silicon flow from root to shoot in pepper: a comprehensive in silico analysis reveals a potential linkage between gene expression and hormone signaling that stimulates plant growth and metabolism. *PeerJ* 8:e10053.

Gong, H., Zhu, X., Chen, K., Wang, S., and Zhang, C. (2005). Silicon alleviates oxidative damage of wheat plants in pots under drought. *Plant Sci.* 169, 313–321.

Gou, T., Chen, X., Han, R., Liu, J., Zhu, Y., and Gong, H. (2020). Silicon can improve seed germination and ameliorate oxidative damage of bud seedlings in cucumber under salt stress. *Acta Physiol. Plant.* 42, 1–11.

Greger, M., Kabir, A. H., Landberg, T., Maity, P. J., and Lindberg, S. (2016). Silicate reduces cadmium uptake into cells of wheat. *Environ. Poll.* 211, 90–97.

Greger, M., Landberg, T., and Vaculík, M. (2018). Silicon influences soil availability and accumulation of mineral nutrients in various plant species. *Plants* 7:41.

Gujjar, R. S., Akhtar, M., and Singh, M. (2014). Transcription factors in abiotic stress tolerance. *Ind. J. Plant Physiol.* 19, 306–316.

Gunes, A., Pilbeam, D. J., Inal, A., Bagci, E. G., and Coban, S. (2007). Influence of silicon on antioxidant mechanisms and lipid peroxidation in chickpea (Cicer arietinum L.) cultivars under drought stress. *J. Plant Interact.* 2, 105–113.

Guntzer, F., Keller, C., and Meunier, J.-D. (2012). Benefits of plant silicon for crops: a review. *Agron. Sustain. Dev.* 32, 201–213.

Gupta, B. K., Sahoo, K. K., Anwar, K., Nongpiur, R. C., Deshmukh, R., Pareek, A., et al. (2021). Silicon nutrition stimulates Salt-Overly Sensitive (SOS) pathway to enhance salinity stress tolerance and yield in rice. *Plant Physiol. Biochem.* 166, 593–604.

Habibi, G. (2015). Effects of soil-and foliar-applied silicon on the resistance of grapevine plants to freezing stress. *Acta Biol. Szegediensis* 59, 109–117.

Habibi, G., and Hajiboland, R. J. F. H. (2013). Alleviation of drought stress by silicon supplementation in pistachio (Pistacia vera L.) Plants. *Folia Horticult.* 25, 21–29.

Haddad, C., Arkoun, M., Jamois, F., Schwarzenberg, A., Yvin, J.-C., Etienne, P., et al. (2018). Silicon promotes growth of Brassica napus L. and delays leaf senescence induced by nitrogen starvation. *Front. Plant Sci.* 9:516. doi: 10.3389/fpls.2018.00516

Haddad, C., Trouverie, J., Arkoun, M., Yvin, J.-C., Caïus, J., Brunaud, V., et al. (2019). Silicon supply affects the root transcriptome of Brassica napus L. *Planta* 249, 1645–1651.

Hafeez, M. B., Zahra, N., Zahra, K., Raza, A., Khan, A., Shaukat, K., et al. (2021b). Brassinosteroids: molecular and physiological responses in plant growth and abiotic stresses. *Plant Stress* 2:100029.

Hafeez, M. B., Raza, A., Zahra, N., Shaukat, K., Akram, M. Z., Iqbal, S., et al. (2021a). Gene regulation in halophytes in conferring salt tolerance. *Handb. Bioremed.* 2021, 341–370.

Haider, S., Iqbal, J., Naseer, S., Yaseen, T., Shaukat, M., Bibi, H., et al. (2021a). Molecular mechanisms of plant tolerance to heat stress: current landscape and future perspectives. *Plant Cell Rep.* 2021, 1–25.

Haider, S., Rehman, S., Ahmad, Y., Raza, A., Tabassum, J., Javed, T., et al. (2021b). In Silico Characterization and Expression Profiles of Heat Shock Transcription Factors (HSFs) in Maize (Zea mays L.). *Agronomy* 11:2335.

Hamayun, M., Sohn, E. Y., Khan, S. A., Shinwari, Z. K., Khan, A. L., and Lee, I. J. (2010). Silicon alleviates the adverse effects of salinity and drought stress on growth and endogenous plant growth hormones of soybean (Glycine max L.). *Pak. J. Bot.* 42, 1713–1722.

Hameed, A., Sheikh, M. A., Jamil, A., and Basra, S. M. A. (2013). Seed priming with sodium silicate enhances seed germination and seedling growth in wheat (Triticum aestivum L.) under water deficit stress induced by polyethylene glycol. *Pak. J. Life Soc. Sci.* 11, 19–24.

Han, W., Jia, J., Hu, Y., Liu, J., Guo, J., Shi, Y., et al. (2021). Maintenance of root water uptake contributes to salt-tolerance of a wild tomato species under salt stress. *Arch. Agron. Soil Sci.* 67, 205–217.

Hao, L., Shi, S., Guo, H., Zhang, J., Li, P., and Feng, Y. (2021). Transcriptome analysis reveals differentially expressed MYB transcription factors associated with silicon response in wheat. *Sci. Rep.* 11, 1–9.

Hara, M., Furukawa, J., Sato, A., Mizoguchi, T., and Miura, K. (2012). Abiotic stress and role of salicylic acid in plants. *Abiotic Stress Responses Plants* 2021, 235–251.

Hasan, M. M., Gong, L., Nie, Z.-F., Li, F.-P., Ahammed, G. J., and Fang, X.-W. (2021). ABA-induced stomatal movements in vascular plants during dehydration and rehydration. *Environ. Exp. Bot.* 2021:104436.

Hasanuzzaman, M., Bhuyan, M. H. M., Zulfiqar, F., Raza, A., Mohsin, S. M., Mahmud, J. A., et al. (2020). Reactive oxygen species and antioxidant defense in plants under abiotic stress: revisiting the crucial role of a universal defense regulator. *Antioxidants* 9:681.

Hasanuzzaman, M., Nahar, K., Anee, T. I., and Fujita, M. (2017). Exogenous silicon attenuates cadmium-induced oxidative stress in Brassica napus L. by modulating AsA-GSH pathway and glyoxalase system. *Front. Plant Sci.* 8:1061. doi: 10.3389/fpls.2017.01061

Haseeb, M., Iqbal, S., Hafeez, M. B., Saddiq, M. S., Zahra, N., Raza, A., et al. (2022). Phytoremediation of nickel by quinoa: Morphological and physiological response. *PLoS One* 17:e0262309. doi: 10.1371/journal.pone.0262309

Hasegawa, P. M., Bressan, R. A., Zhu, J. K., and Bohnert, H. J. (2000). Plant cellular and molecular responses to high salinity. *Annu. Rev. Plant Biol.* 51, 463–499.

Hattori, T., Inanaga, S., Tanimoto, E., Lux, A., Luxová, M., and Sugimoto, Y. (2003). Silicon-induced changes in viscoelastic properties of sorghum root cell walls. *Plant Cell Physiol.* 44, 743–749.

Hosseini, S. A., Maillard, A., Hajirezaei, M. R., Ali, N., Schwarzenberg, A., Jamois, F., et al. (2017). Induction of Barley Silicon Transporter HvLsi1 and HvLsi2, increased silicon concentration in the shoot and regulated Starch and ABA Homeostasis under Osmotic stress and Concomitant Potassium Deficiency. *Front. Plant Sci.* 8:1359. doi: 10.3389/fpls.2017.01359

Hu, H., You, J., Fang, Y., Zhu, X., Qi, Z., and Xiong, L. (2008). Characterization of transcription factor gene SNAC2 conferring cold and salt tolerance in rice. *Plant Mol. Biol.* 67, 169–181.

Hu, J., Li, Y., and Jeong, B. R. (2020). Silicon alleviates temperature stresses in poinsettia by regulating stomata, photosynthesis, and oxidative damages. *Agronomy* 10:1419.

Hu, W., Su, Y., Zhou, J., Zhu, H., Guo, J., Huo, H., et al. (2022). Foliar application of silicon and selenium improves the growth, yield and quality characteristics of cucumber in field conditions. *Sci. Horticult.* 294:110776.

Huang, J., Zhao, X., Bürger, M., Wang, Y., and Chory, J. (2021). Two interacting ethylene response factors regulate heat stress response. *Plant Cell* 33, 338–357.

Hurtado, A. C., Chiconato, D. A., de Mello Prado, R., da Silveira Sousa Junior, G., Viciedo, D. O., Díaz, Y. P., et al. (2021). Silicon alleviates sodium toxicity in Sorghum and sunflower plants by enhancing ionic homeostasis in roots and shoots and increasing dry matter accumulation. *Silicon* 13, 475–486.

Hurtado, A. C., Chiconato, D. A., de Mello Prado, R., Junior, G. D. S. S., Gratão, P. L., Felisberto, G., et al. (2020). Different methods of silicon application attenuate salt stress in sorghum and sunflower by modifying the antioxidative defense mechanism. *Ecotoxicol. Environ. Safety* 203:110964.

Hussain, I., Ashraf, M. A., Rasheed, R., Asghar, A., Sajid, M. A., and Iqbal, M. (2015). Exogenous application of silicon at the boot stage decreases accumulation of cadmium in wheat (Triticum aestivum L.) grains. *Brazil. J. Bot.* 38, 223–234.

Hussain, I., Parveen, A., Rasheed, R., Ashraf, M. A., Ibrahim, M., Riaz, S., et al. (2019). Exogenous Silicon Modulates Growth, Physio-Chemicals and Antioxidants in Barley (Hordeum vulgare L.) Exposed to Different Temperature Regimes. *Silicon* 11, 2753–2762.

Hussain, M., Ahmad, S., Hussain, S., Lal, R., Ul-Allah, S., and Nawaz, A. (2018). Rice in saline soils: physiology, biochemistry, genetics, and management. *Adv. Agronomy* 148, 231–287.

Hussain, S., Khan, F., Hussain, H. A., and Nie, L. (2016). Physiological and biochemical mechanisms of seed priming-induced chilling tolerance in rice cultivars. *Front. Plant Sci.* 7:116. doi: 10.3389/fpls.2016.00116

Hwang, S.-J., Hamayun, M., Kim, H.-Y., Na, C.-I., Kim, K.-U., Shin, D.-H., et al. (2007). Effect of nitrogen and silicon nutrition on bioactive gibberellin and growth of rice under field conditions. *J. Crop Sci. Biotechnol.* 10, 281–286.

Ilyas, M., Nisar, M., Khan, N., Hazrat, A., Khan, A. H., Hayat, K., et al. (2021). Drought tolerance strategies in plants: A mechanistic approach. *J. Plant Growth Regul.* 40, 926–944.

Imran, M., Mahmood, A., Römheld, V., and Neumann, G. (2013). Nutrient seed priming improves seedling development of maize exposed to low root zone temperatures during early growth. *Eur. J. Agronomy* 49, 141–148.

Imtiaz, M., Rizwan, M. S., Mushtaq, M. A., Ashraf, M., Shahzad, S. M., Yousaf, B., et al. (2016). Silicon occurrence, uptake, transport and mechanisms of heavy metals, minerals and salinity enhanced tolerance in plants with future prospects: a review. *J. Environ. Manage.* 183, 521–529.

Islam, M. S., and Wang, M.-H. (2009). Expression of dehydration responsive element-binding protein-3 (DREB3) under different abiotic stresses in tomato. *BMB Rep.* 42, 611–616.

Ito, Y., Katsura, K., Maruyama, K., Taji, T., Kobayashi, M., Seki, M., et al. (2006). Functional analysis of rice DREB1/CBF-type transcription factors involved in cold-responsive gene expression in transgenic rice. *Plant Cell Physiol.* 47, 141–153.

Iwasaki, K., Maier, P., Fecht, M., and Horst, W. J. (2002). Leaf apoplastic silicon enhances manganese tolerance of cowpea (Vigna unguiculata). *J. Plant Physiol.* 159, 167–173.

Jana, G. A., Al Kharusi, L., Sunkar, R., Al-Yahyai, R., and Yaish, M. W. (2019). Metabolomic analysis of date palm seedlings exposed to salinity and silicon treatments. *Plant Signal. Behav.* 14:1663112.

Janni, M., Gullì, M., Maestri, E., Marmiroli, M., Valliyodan, B., Nguyen, H. T., et al. (2020). Molecular and genetic bases of heat stress responses in crop plants and breeding for increased resilience and productivity. *J. Exp. Bot.* 71, 3780–3802.

Joudmand, A., and Hajiboland, R. (2019). Silicon mitigates cold stress in barley plants via modifying the activity of apoplasmic enzymes and concentration of metabolites. *Acta Physiol. Plant.* 41:29.

Kafi, M., Nabati, J., Ahmadi-Lahijani, M. J., and Oskoueian, A. (2021). Silicon compounds and potassium sulfate improve salinity tolerance of potato plants through instigating the defense mechanisms, cell membrane stability, and accumulation of osmolytes. *Commun. Soil Sci. Plant Anal.* 52, 843–858. doi: 10.1080/00103624.2020.1869768

Kaloterakis, N., van Delden, S. H., Hartley, S., and De Deyn, G. B. (2021). Silicon application and plant growth promoting rhizobacteria consisting of six pure Bacillus species alleviate salinity stress in cucumber (Cucumis sativus L). *Sci. Horticult.* 288:110383. doi: 10.1016/j.scienta.2021.110383

Kamenya, S. N., Mikwa, E. O., Song, B., and Odeny, D. A. (2021). Genetics and breeding for climate change in Orphan crops. *Theoret. Appl. Genet.* 2021, 1–29.

Kang, J., Zhao, W., Zhao, M., Zheng, Y., and Yang, F. (2015). NaCl and Na 2 SiO 3 coexistence strengthens growth of the succulent xerophyte Nitraria tangutorum under drought. *Plant Growth Regulat.* 77, 223–232. doi: 10.1007/s10725-015-0055-9

Kapoor, D., Bhardwaj, S., Landi, M., Sharma, A., Ramakrishnan, M., and Sharma, A. (2020). The impact of drought in plant metabolism: how to exploit tolerance mechanisms to increase crop production. *Appl. Sci.* 10:5692. doi: 10.1111/pce.12417

Kaushik, P., and Saini, D. K. (2019). Silicon as a vegetable crops modulator—A review. *Plants* 8:148. doi: 10.3390/plants8060148

Kaya, C., Ashraf, M., Al-Huqail, A. A., Alqahtani, M. A., and Ahmad, P. (2020). Silicon is dependent on hydrogen sulphide to improve boron toxicity tolerance in pepper plants by regulating the AsA-GSH cycle and glyoxalase system. *Chemosphere* 257:127241. doi: 10.1016/j.chemosphere.2020.127241

Kaya, C., Tuna, L., and Higgs, D. (2006). Effect of silicon on plant growth and mineral nutrition of maize grown under water-stress conditions. *J. Plant Nutrit.* 29, 1469–1480.

Kazan, K. (2015). Diverse roles of jasmonates and ethylene in abiotic stress tolerance. *Trends Plant Sci.* 20, 219–229. doi: 10.1016/j.tplants.2015.02.001

Keeping, M. G., and Reynolds, O. L. (2009). Silicon in agriculture: new insights, new significance and growing application. *Ann. Appl. Biol.* 155:153. doi: 10.1111/j.1744-7348.2009.00358.x

Keller, C., Rizwan, M., Davidian, J. C., Pokrovsky, O. S., Bovet, N., Chaurand, P., et al. (2015). Effect of silicon on wheat seedlings (Triticum turgidum L.) grown in hydroponics and exposed to 0 to 30 μM Cu. *Planta* 241, 847–860. doi: 10.1007/s00425-014-2220-1

Khan, A., Bilal, S., Khan, A. L., Imran, M., Shahzad, R., Al-Harrasi, A., et al. (2020a). Silicon and Gibberellins: Synergistic Function in Harnessing ABA Signaling and Heat Stress Tolerance in Date Palm (Phoenix dactylifera L.). *Plants* 9:620. doi: 10.3390/plants9050620

Khan, A., Khan, A. L., Imran, M., Asaf, S., Kim, Y.-H., Bilal, S., et al. (2020b). Silicon-induced thermotolerance in Solanum lycopersicum L. via activation of antioxidant system, heat shock proteins, and endogenous phytohormones. *BMC Plant Biol.* 20:7. doi: 10.1186/s12870-020-02456-7

Khan, A., Khan, A. L., Muneer, S., Kim, Y.-H., Al-Rawahi, A., and Al-Harrasi, A. (2019). Silicon and salinity: crosstalk in crop-mediated stress tolerance mechanisms. *Front. Plant Sci.* 10:1429. doi: 10.3389/fpls.2019.01429

Khan, M. I. R., Ashfaque, F., Chhillar, H., Irfan, M., and Khan, N. A. (2021b). The intricacy of silicon, plant growth regulators and other signaling molecules for abiotic stress tolerance: An entrancing crosstalk between stress alleviators. *Plant Physiol. Biochem.* 162, 36–47. doi: 10.1016/j.plaphy.2021.02.024

Khan, I., Awan, S. A., Rizwan, M., Ali, S., Hassan, M. J., Brestic, M., et al. (2021a). Effects of silicon on heavy metal uptake at the soil-plant interphase: A review. *Ecotoxicol. Environ. Safety* 222:112510. doi: 10.1016/j.ecoenv.2021.112510

Khan, S.-A., Li, M.-Z., Wang, S.-M., and Yin, H.-J. (2018). Revisiting the role of plant transcription factors in the battle against abiotic stress. *Int. J. Mol. Sci.* 19:1634. doi: 10.3390/ijms19061634

Khattab, H. I., Emam, M. A., Emam, M. M., Helal, N. M., and Mohamed, M. R. (2014). Effect of selenium and silicon on transcription factors NAC5 and DREB2A involved in drought-responsive gene expression in rice. *Biol. Plant.* 58, 265–273.

Kidokoro, S., Maruyama, K., Nakashima, K., Imura, Y., Narusaka, Y., Shinwari, Z. K., et al. (2009). The phytochrome-interacting factor PIF7 negatively regulates DREB1 expression under circadian control in Arabidopsis. *Plant Physiol.* 151, 2046–2057. doi: 10.1104/pp.109.147033

Kim, Y. H., Khan, A. L., Waqas, M., Shim, J. K., Kim, D. H., Lee, K. Y., et al. (2014c). Silicon application to rice root zone influenced the phytohormonal and antioxidant responses under salinity stress. *J. Plant Growth Regul.* 33, 137–149. doi: 10.1007/s00344-013-9356-2

Kim, Y.-H., Khan, A. L., Waqas, M., Jeong, H.-J., Kim, D.-H., Shin, J. S., et al. (2014b). Regulation of jasmonic acid biosynthesis by silicon application during physical injury to Oryza sativa L. *J. Plant Res.* 127, 525–532. doi: 10.1007/s10265-014-0641-3

Kim, Y.-H., Khan, A. L., Kim, D.-H., Lee, S.-Y., Kim, K.-M., Waqas, M., et al. (2014a). Silicon mitigates heavy metal stress by regulating P-type heavy metal ATPases, Oryza sativa low silicon genes, and endogenous phytohormones. *BMC Plant Biol.* 14, 1–13. doi: 10.1186/1471-2229-14-13

Kim, Y.-H., Khan, A. L., and Lee, I.-J. (2016). Silicon: a duo synergy for regulating crop growth and hormonal signaling under abiotic stress conditions. *Crit. Rev. Biotechnol.* 36, 1099–1109. doi: 10.3109/07388551.2015.1084265

Kim, Y.-H., Khan, A. L., Hamayun, M., Kang, S. M., Beom, Y. J., and Lee, I.-J. (2011). Influence of short-term silicon application on endogenous physiohormonal levels of Oryza sativa L. under wounding stress. *Biol. Trace Element Res.* 144, 1175–1185. doi: 10.1007/s12011-011-9047-4

Kosová, K., Vítámvás, P., Prášil, I. T., and Renaut, J. (2011). Plant proteome changes under abiotic stress—contribution of proteomics studies to understanding plant stress response. *J. Proteom.* 74, 1301–1322. doi: 10.1016/j.jprot.2011.02.006

Kosová, K., Vítámvás, P., Urban, M. O., Prášil, I. T., and Renaut, J. (2018). Plant abiotic stress proteomics: the major factors determining alterations in cellular proteome. *Front. Plant Sci.* 9:122. doi: 10.3389/fpls.2018.00122

Kramell, R., Atzorn, R., Schneider, G., Miersch, O., Brückner, C., Schmidt, J., et al. (1995). Occurrence and identification of jasmonic acid and its amino acid conjugates induced by osmotic stress in barley leaf tissue. *J. Plant Growth Regul.* 14, 29–36. doi: 10.1007/bf00212643

Kumar, A., and Kaushik, P. (2021). *Heat Stress and its Impact on Plant Function: An Update*. [Preprint].

Kumar, J., Singh, S., Singh, M., Srivastava, P. K., Mishra, R. K., Singh, V. P., et al. (2017). Transcriptional regulation of salinity stress in plants: A short review. *Plant Gene* 11, 160–169.

Kutasy, E., Buday-Bódi, E., Virág, I. C., Forgács, F., Melash, A. A., Zsombik, L., et al. (2022). Mitigating the Negative Effect of Drought Stress in Oat (Avena sativa L.) with Silicon and Sulphur Foliar Fertilization. *Plants* 11:30. doi: 10.3390/plants11010030

Law, C., and Exley, C. (2011). New insight into silica deposition in horsetail (Equisetum arvense). *BMC Plant Biol.* 11:112. doi: 10.1186/1471-2229-11-112

Lee, B.-H., Henderson, D. A., and Zhu, J.-K. (2005). The Arabidopsis cold-responsive transcriptome and its regulation by ICE1. *Plant Cell* 17, 3155–3175. doi: 10.1105/tpc.105.035568

Lee, S. K., Sohn, E. Y., Hamayun, M., Yoon, J. Y., and Lee, I. J. (2010). Effect of silicon on growth and salinity stress of soybean plant grown under hydroponic system. *Agroforestry Syst.* 80, 333–340. doi: 10.1007/s10457-010-9299-6

Lenka, S. K., Katiyar, A., Chinnusamy, V., and Bansal, K. C. (2011). Comparative analysis of drought-responsive transcriptome in Indica rice genotypes with contrasting drought tolerance. *Plant Biotechnol. J.* 9, 315–327. doi: 10.1111/j.1467-7652.2010.00560.x

Lesharadevi, K., Parthasarathi, T., and Muneer, S. (2021). Silicon biology in crops under abiotic stress: A paradigm shift and cross-talk between genomics and proteomics. *J. Biotechnol.* 333, 21–38. doi: 10.1016/j.jbiotec.2021.04.008

Li, G., Xu, W., Jing, P., Hou, X., and Fan, X. (2021). Overexpression of VyDOF8, a Chinese wild grapevine transcription factor gene, enhances drought tolerance in transgenic tobacco. *Environ. Exp. Bot.* 190:104592. doi: 10.1016/j.envexpbot.2021.104592

Li, H., Zhu, Y., Hu, Y., Han, W., and Gong, H. (2015). Beneficial effects of silicon in alleviating salinity stress of tomato seedlings grown under sand culture. *Acta Physiol. Plant.* 37:71.

Li, J., Leisner, S. M., and Frantz, J. (2008). Alleviation of copper toxicity in Arabidopsis thaliana by silicon addition to hydroponic solutions. *J. Am. Soc. Horticult. Sci.* 133, 670–677. doi: 10.21273/jashs.133.5.670

Li, P., Zhao, C., Zhand, Y., Wang, X., Wang, J., Wang, F., et al. (2017). Silicon enhances the tolerance of Poa annua to cadmium by inhibiting its absorption and oxidative stress. *Biol. Plant.* 61, 741–750. doi: 10.1007/s10535-017-0731-x

Li, R., Liu, C., Zhao, R., Wang, L., Chen, L., Yu, W., et al. (2019). CRISPR/Cas9-Mediated SlNPR1 mutagenesis reduces tomato plant drought tolerance. *BMC Plant Biol.* 19, 1–13. doi: 10.1186/s12870-018-1627-4

Li, X., Wei, J.-P., Scott, E. R., Liu, J.-W., Guo, S., Li, Y., et al. (2018). Exogenous melatonin alleviates cold stress by promoting antioxidant defense and redox homeostasis in Camellia sinensis L. *Molecules* 23:165. doi: 10.3390/molecules23010165

Liang, Y., Nikolic, M., Bélanger, R., Gong, H., and Song, A. (2015b). Effect of silicon on crop growth, yield and quality. *Silicon Agricult.* 2015, 209–223. doi: 10.1007/978-94-017-9978-2_11

Liang, Y., Nikolic, M., Bélanger, R., Gong, H., and Song, A. (2015c). *Silicon in agriculture*, Vol. 10. Dordrecht: Springer, 978–994. doi: 10.1007/978-94-017-9978-2

Liang, X., Wang, H., Hu, Y., Mao, L., Sun, L., Dong, T., et al. (2015a). Silicon does not mitigate cell death in cultured tobacco BY-2 cells subjected to salinity without ethylene emission. *Plant Cell Rep.* 34, 331–343. doi: 10.1007/s00299-014-1712-6

Liang, Y., Chen, Q. I. N., Liu, Q., Zhang, W., and Ding, R. (2003). Exogenous silicon (Si) increases antioxidant enzyme activity and reduces lipid peroxidation in roots of salt-stressed barley (Hordeum vulgareL.). *J. Plant Physiol.* 160, 1157–1164. doi: 10.1078/0176-1617-01065

Liang, Y., Li, X., Yang, R., Gao, B., Yao, J., Oliver, M. J., et al. (2021). BaDBL1, a unique DREB gene from desiccation tolerant moss Bryum argenteum, confers osmotic and salt stress tolerances in transgenic Arabidopsis. *Plant Sci.* 313:111047. doi: 10.1016/j.plantsci.2021.111047

Liang, Y., Sun, W., Zhu, Y.-G., and Christie, P. J. E. (2007). Mechanisms of silicon-mediated alleviation of abiotic stresses in higher plants: a review. *Environ. Pollut.* 147, 422–428. doi: 10.1016/j.envpol.2006.06.008

Liang, Y., Wong, J., and Wei, L. J. C. (2005). Silicon-mediated enhancement of cadmium tolerance in maize (Zea mays L.) grown in cadmium contaminated soil. *Chemosphere* 58, 475–483. doi: 10.1016/j.chemosphere.2004.09.034

Liu, B., Soundararajan, P., and Manivannan, A. (2019). Mechanisms of silicon-mediated amelioration of salt stress in plants. *Plants* 8:307. doi: 10.3390/plants8090307

Liu, H., and Timko, M. P. (2021). Jasmonic Acid Signaling and Molecular Crosstalk with Other Phytohormones. *Int. J. Mol. Sci.* 22:2914. doi: 10.3390/ijms22062914

Liu, H., Shen, J., Yuan, C., Lu, D., Acharya, B. R., Wang, M., et al. (2021). The Cyclophilin ROC3 Regulates ABA-Induced Stomatal Closure and the Drought Stress Response of Arabidopsis thaliana. *Front. Plant Sci.* 12:668792. doi: 10.3389/fpls.2021.668792

Liu, P., Yin, L., Wang, S., Zhang, M., Deng, X., Zhang, S., et al. (2015). Enhanced root hydraulic conductance by aquaporin regulation accounts for silicon alleviated salt-induced osmotic stress in Sorghum bicolor L. *Environ. Exp. Bot.* 111, 42–51. doi: 10.1016/j.envexpbot.2014.10.006

Liu, J., Feng, L., Li, J., and He, Z. (2015). Genetic and epigenetic control of plant heat responses. *Front. Plant Sci.* 6:267. doi: 10.3389/fpls.2015.00267

Liu, J.-J., Lin, S.-H., Xu, P.-L., Wang, X.-J., and Bai, J.-G. (2009). Effects of exogenous silicon on the activities of antioxidant enzymes and lipid peroxidation in chilling-stressed cucumber leaves. *Agricult. Sci. China* 8, 1075–1086. doi: 10.1016/s1671-2927(08)60315-6

Liu, Q., Kasuga, M., Sakuma, Y., Abe, H., Miura, S., Yamaguchi-Shinozaki, K., et al. (1998). Two transcription factors, DREB1 and DREB2, with an EREBP/AP2 DNA binding domain separate two cellular signal transduction pathways in drought-and low-temperature-responsive gene expression, respectively, in Arabidopsis. *Plant Cell* 10, 1391–1406. doi: 10.1105/tpc.10.8.1391

Lotfi, R., and Ghassemi-Golezani, K. (2015). Influence of salicylic acid and silicon on seed development and quality of mung bean under salt stress. *Seed Sci. Technol.* 43, 52–61. doi: 10.15258/sst.2015.43.1.06

Lozano-González, J. M., Valverde, C., Hernández, C. D., Martin-Esquinas, A., and Hernández-Apaolaza, L. (2021). Beneficial Effect of Root or Foliar Silicon Applied to Cucumber Plants under Different Zinc Nutritional Statuses. *Plants* 10:2602. doi: 10.3390/plants10122602

Luyckx, M., Hausman, J.-F., Lutts, S., and Guerriero, G. (2017). Silicon and plants: current knowledge and technological perspectives. *Front. Plant Sci.* 8:411. doi: 10.3389/fpls.2017.00411

Ma, D., Sun, D., Wang, C., Qin, H., Ding, H., Li, Y., et al. (2016). Silicon application alleviates drought stress in wheat through transcriptional regulation of multiple antioxidant defense pathways. *J. Plant Growth Regul.* 35, 1–10. doi: 10.1007/s00344-015-9500-2

Ma, J., Yamaji, N. J. C., and Sciences, M. L. (2008). Functions and transport of silicon in plants. *Cell Mol. Life Sci.* 65, 3049–3057. doi: 10.1007/s00018-008-7580-x

Ma, Y., Cao, J., He, J., Chen, Q., Li, X., and Yang, Y. (2018). Molecular mechanism for the regulation of ABA homeostasis during plant development and stress responses. *Int. J. Mol. Sci.* 19:3643. doi: 10.3390/ijms19113643

Maillard, A., Ali, N., Schwarzenberg, A., Jamois, F., Yvin, J.-C., and Hosseini, S. A. (2018). Silicon transcriptionally regulates sulfur and ABA metabolism and delays leaf senescence in barley under combined sulfur deficiency and osmotic stress. *Environ. Exp. Bot.* 155, 394–410. doi: 10.1016/j.envexpbot.2018.07.026

Majeed Zargar, S., Ahmad Macha, M., Nazir, M., Kumar Agrawal, G., and Rakwal, R. (2012). Silicon: A Multitalented Micronutrient in OMICS Perspective–An Update. *Curr. Proteom.* 9, 245–254. doi: 10.2174/157016412805219152

Majeed Zargar, S., Nazir, M., Kumar Agrawal, G., Kim, D.-W., and Rakwal, R. (2010). Silicon in plant tolerance against environmental stressors: towards crop improvement using omics approaches. *Curr. Proteom.* 7, 135–143. doi: 10.2174/157016410791330507

Malik, M. A., Wani, A. H., Mir, S. H., Rehman, I. U., Tahir, I., Ahmad, P., et al. (2021). Elucidating the role of silicon in drought stress tolerance in plants. *Plant Physiol. Biochem.* 165, 187–195. doi: 10.1016/j.plaphy.2021.04.021

Mandlik, R., Thakral, V., Raturi, G., Shinde, S., Nikoliæ, M., Tripathi, D. K., et al. (2020). Significance of silicon uptake, transport, and deposition in plants. *J. Exp. Bot.* 71, 6703–6718. doi: 10.1093/jxb/eraa301

Manivannan, A., and Ahn, Y.-K. (2017). Silicon regulates potential genes involved in major physiological processes in plants to combat stress. *Front. Plant Sci.* 8:1346. doi: 10.3389/fpls.2017.01346

Manivannan, A., Soundararajan, P., Muneer, S., Ko, C. H., and Jeong, B. R. (2016). Silicon mitigates salinity stress by regulating the physiology, antioxidant enzyme activities, and protein expression in Capsicum annuum 'Bugwang'. *BioMed Res. Int.* 2016:076357. doi: 10.1155/2016/3076357

Manna, M., Thakur, T., Chirom, O., Mandlik, R., Deshmukh, R., and Salvi, P. (2021). Transcription factors as key molecular target to strengthen the drought stress tolerance in plants. *Physiol. Plant.* 172, 847–868. doi: 10.1111/ppl.13268

Markovich, O., Steiner, E., Kouøil, Š, Tarkowski, P., Aharoni, A., and Elbaum, R. (2017). Silicon promotes cytokinin biosynthesis and delays senescence in Arabidopsis and Sorghum. *Plant Cell Environ.* 40, 1189–1196. doi: 10.1111/pce.12913

Mehmood, S., Wang, X., Ahmed, W., Imtiaz, M., Ditta, A., Rizwan, M., et al. (2021). Removal mechanisms of slag against potentially toxic elements in soil and plants for sustainable agriculture development: a critical review. *Sustainability* 13:5255. doi: 10.3390/su13095255

Meng, X., Luo, S., Dawuda, M. M., Gao, X., Wang, S., Xie, J., et al. (2021). Exogenous silicon enhances the systemic defense of cucumber leaves and roots against CA-induced autotoxicity stress by regulating the ascorbate-glutathione cycle and photosystem II. *Ecotoxicol. Environ. Safety* 227:112879. doi: 10.1016/j.ecoenv.2021.112879

Merewitz, E. B., and Liu, S. (2019). Improvement in heat tolerance of creeping Bentgrass with melatonin, Rutin, and silicon. *J. Am. Soc. Horticult. Sci.* 144, 141–148. doi: 10.21273/jashs04643-19

Metwally, A. M., Radi, A. A., El-Shazoly, R. M., and Hamada, A. M. (2018). The role of calcium, silicon and salicylic acid treatment in protection of canola plants against boron toxicity stress. *J. Plant Res.* 131, 1015–1028. doi: 10.1007/s10265-018-1008-y

Mir, R. A., Bhat, K. A., Shah, A. A., and Zargar, S. M. (2020). Role of Silicon in Abiotic Stress Tolerance of Plants. *Improving Abiotic Stress Toler. Plants* 2020, 271–290. doi: 10.1201/9780429027505-15

Mir, S. H., Rashid, I., Hussain, B., Reshi, Z. A., Assad, R., and Sofi, I. A. (2019). Silicon supplementation of rescuegrass reduces herbivory by a grasshopper. *Front. Plant Sci.* 10:671. doi: 10.3389/fpls.2019.00671

Mitani, N., and Ma, J. F. (2005). Uptake system of silicon in different plant species. *J. Exp. Bot.* 56, 1255–1261. doi: 10.1093/jxb/eri121

Mitani, N., Yamaji, N., Ago, Y., Iwasaki, K., and Ma, J. F. (2011). Isolation and functional characterization of an influx silicon transporter in two pumpkin cultivars contrasting in silicon accumulation. *Plant J.* 66, 231–240. doi: 10.1111/j.1365-313X.2011.04483.x

Miura, K., and Furumoto, T. (2013). Cold signaling and cold response in plants. *Int. J. Mol. Sci.* 14, 5312–5337. doi: 10.3390/ijms14035312

Miura, K., and Tada, Y. (2014). Regulation of water, salinity, and cold stress responses by salicylic acid. *Front. Plant Sci.* 5:4. doi: 10.3389/fpls.2014.00004

Mohanta, T. K., Bashir, T., Hashem, A., and AbduAllah, E. F. (2017). Systems biology approach in plant abiotic stresses. *Plant Physiol. Biochem.* 121, 58–73. doi: 10.1016/j.plaphy.2017.10.019

Moradtalab, N., Weinmann, M., Walker, F., Höglinger, B., Ludewig, U., and Neumann, G. (2018). Silicon improves chilling tolerance during early growth of maize by effects on micronutrient homeostasis and hormonal balances. *Front. Plant Sci.* 9:420. doi: 10.3389/fpls.2018.00420

Mostofa, M. G., Rahman, M. M., Ansary, M. M. U., Keya, S. S., Abdelrahman, M., Miah, M. G., et al. (2021). Silicon in mitigation of abiotic stress-induced oxidative damage in plants. *Crit. Rev. Biotechnol.* 41, 918–934. doi: 10.1080/07388551.2021.1892582

Mubarik, M. S., Khan, S. H., Sajjad, M., Raza, A., Hafeez, M. B., Yasmeen, T., et al. (2021). A manipulative interplay between positive and negative regulators of phytohormones: A way forward for improving drought tolerance in plants. *Physiol. Plant.* 172, 1269–1290. doi: 10.1111/ppl.13325

Müller, M. (2021). Foes or friends: ABA and ethylene interaction under abiotic stress. *Plants* 10:448. doi: 10.3390/plants10030448

Mundada, P. S., Jadhav, S. V., Salunkhe, S. S., Gurme, S. T., Umdale, S. D., Barmukh, R. B., et al. (2021). Silicon and Plant Responses Under Adverse Environmental Conditions. *Plant Perform. Under Environ. Stress* 2021, 357–385. doi: 10.1007/978-3-030-78521-5_14

Muneer, S., and Jeong, B. R. (2015). Proteomic analysis of salt-stress responsive proteins in roots of tomato (Lycopersicon esculentum L.) plants towards silicon efficiency. *Plant Growth Regulat.* 77, 133–146. doi: 10.1007/s10725-015-0045-y

Munns, R., and Gilliham, M. J. (2015). Salinity tolerance of crops–what is the cost? *New Phytol.* 208, 668–673. doi: 10.1111/nph.13519

Mushtaq, M., Dar, A. A., Basu, U., Bhat, B. A., Mir, R. A., Vats, S., et al. (2021). Integrating CRISPR-Cas and Next Generation Sequencing in Plant Virology. *Front. Genet.* 12:735489. doi: 10.3389/fgene.2021.735489

Mustafa, T., Sattar, A., Sher, A., Ul-Allah, S., Ijaz, M., Irfan, M., et al. (2021). Exogenous application of silicon improves the performance of wheat under terminal heat stress by triggering physio-biochemical mechanisms. *Sci. Rep.* 11, 1–12. doi: 10.1038/s41598-021-02594-4

Nakashima, K., Takasaki, H., Mizoi, J., Shinozaki, K., and Yamaguchi-Shinozaki, K. J. B. (2012). NAC transcription factors in plant abiotic stress responses. *Biochim. Biophys. Acta* 1819, 97–103.

Naz, R., Batool, S., Shahid, M., Keyani, R., Yasmin, H., Nosheen, A., et al. (2021a). Exogenous silicon and hydrogen sulfide alleviates the simultaneously occurring drought stress and leaf rust infection in wheat. *Plant Physiol. Biochem.* 166, 558–571. doi: 10.1016/j.plaphy.2021.06.034

Naz, R., Gul, F., Zahoor, S., Nosheen, A., Yasmin, H., Keyani, R., et al. (2021b). Interactive effects of hydrogen sulphide and silicon enhance drought and heat tolerance by modulating hormones, antioxidant defence enzymes and redox status in barley (Hordeum vulgare L.). *Plant Biol.* 10, 1435–8603. doi: 10.1111/plb.13374

Nazli, F., Mustafa, A., Ahmad, M., Hussain, A., Jamil, M., Wang, X., et al. (2020). A Review on Practical Application and Potentials of Phytohormone-Producing Plant Growth-Promoting Rhizobacteria for Inducing Heavy Metal Tolerance in Crops. *Sustainability* 12:9056. doi: 10.3390/su12219056

Neu, S., Schaller, J., and Dudel, E. G. (2017). Silicon availability modifies nutrient use efficiency and content. C: N: P stoichiometry, and productivity of winter wheat. *Sci. Rep.* 7, 1–8. doi: 10.1038/srep40829

Neumann, D., and Zur Nieden, U. (2001). Silicon and heavy metal tolerance of higher plants. *Phytochemistry* 56, 685–692. doi: 10.1016/s0031-9422(00)00472-6

Ngwepe, R. M., Mashilo, J., Shimelis, H. J. G. R., and Evolution, C. (2019). Progress in genetic improvement of citron watermelon (Citrullus lanatus var. citroides): a review. *Genet. Resour. Crop Evol.* 66, 735–758. doi: 10.1007/s10722-018-0724-4

Noreen, S., Ashraf, M., Hussain, M., and Jamil, A. (2009). Exogenous application of salicylic acid enhances antioxidative capacity in salt stressed sunflower (Helianthus annuus L.) plants. *Pak. J. Bot.* 41, 473–479.

Nosrati, H., Roshandel, P., and Mohamadkhani, A. R. (2014). The role of silicon to increase salt tolerance in red and white varieties of bean (Phaseolus vulgaris L.). *J. Plant Sci. Res.* 30:81.

Nwugo, C. C., and Huerta, A. J. (2011). The effect of silicon on the leaf proteome of rice (Oryza sativa L.) plants under cadmium-stress. *J. Proteome Res.* 10, 518–528. doi: 10.1021/pr100716h

Ouellette, S., Goyette, M.-H., Labbé, C., Laur, J., Gaudreau, L., Gosselin, A., et al. (2017). Silicon transporters and effects of silicon amendments in strawberry under high tunnel and field conditions. *Front. Plant Sci.* 8, 1664–1462. doi: 10.3389/fpls.2017.00949

Pandita, D. (2021). "CRISPR/Cas-mediated genome editing for improved stress tolerance in plants," in Frontiers in Plant-Soil Interaction. *Elsevier* 2021, 259–291. doi: 10.1016/b978-0-323-90943-3.00001-8

Parmar, N., Singh, K. H., Sharma, D., Singh, L., Kumar, P., Nanjundan, J., et al. (2017). Genetic engineering strategies for biotic and abiotic stress tolerance and quality enhancement in horticultural crops: a comprehensive review. *3 Biotech* 7, 1–35. doi: 10.1007/s13205-017-0870-y

Patel, M., Fatnani, D., and Parida, A. K. (2021). Silicon-induced mitigation of drought stress in peanut genotypes (Arachis hypogaea L.) through ion homeostasis, modulations of antioxidative defense system, and metabolic regulations. *Plant Physiol. Biochem.* 166, 290–313. doi: 10.1016/j.plaphy.2021.06.003

Pavlovic, J., Kostic, L., Bosnic, P., Kirkby, E. A., and Nikolic, M. (2021). Interactions of silicon with essential and beneficial elements in plants. *Front. Plant Sci.* 12:1224. doi: 10.3389/fpls.2021.697592

Pazhamala, L. T., Kudapa, H., Weckwerth, W., Millar, A. H., and Varshney, R. K. (2021). Systems biology for crop improvement. *Plant Genome* 10, 1–23. doi: 10.1002/tpg2.20098

Pereira, T. S., da Silva Lobato, A. K., Tan, D. K. Y., da Costa, D. V., Uchoa, E. B., do Nascimento, et al. (2013). Positive interference of silicon on water relations, nitrogen metabolism, and osmotic adjustment in two pepper ('capsicum annuum') cultivars under water deficit. *Austral. J. Crop Sci.* 7, 1064–1071.

Pfannschmidt, T., and Yang, C. (2012). The hidden function of photosynthesis: a sensing system for environmental conditions that regulates plant acclimation responses. *Protoplasma* 249, 125–136. doi: 10.1007/s00709-012-0398-2

Pieterse, C. M. J., Van der Does, D., Zamioudis, C., Leon-Reyes, A., and Van Wees, S. C. M. (2012). Hormonal modulation of plant immunity. *Annu. Rev. Cell Dev. Biol.* 28, 489–521. doi: 10.1146/annurev-cellbio-092910-154055

Pirooz, P., Amooaghaie, R., Ahadi, A., and Sharififar, F. (2021). Silicon-induced nitric oxide burst modulates systemic defensive responses of Salvia officinalis under copper toxicity. *Plant Physiol. Biochem.* 162, 752–761. doi: 10.1016/j.plaphy.2021.02.048

Poór, P., Nawaz, K., Gupta, R., Ashfaque, F., and Khan, M. I. R. (2021). Ethylene involvement in the regulation of heat stress tolerance in plants. *Plant Cell Rep.* 13, 1–24. doi: 10.1007/s00299-021-02675-8

Pottosin, I., and Shabala, S. J. F. (2014). Polyamines control of cation transport across plant membranes: implications for ion homeostasis and abiotic stress signaling. *Front. Plant Sci.* 5:154. doi: 10.3389/fpls.2014.00154

Prakash, V., Singh, V. P., Tripathi, D. K., Sharma, S., and Corpas, F. J. (2021). Nitric oxide (NO) and salicylic acid (SA): A framework for their relationship in plant development under abiotic stress. *Plant Biol.* 23, 39–49. doi: 10.1111/plb.13246

Qian, Z. Z., Zhuang, S. Y., Li, Q., and Gui, R. Y. (2019). Soil Silicon Amendment Increases Phyllostachys praecox Cold Tolerance in a Pot Experiment. *Forests* 10:405. doi: 10.3390/f10050405

Rahman, A., Wallis, C. M., and Uddin, W. (2015). Silicon-induced systemic defense responses in perennial ryegrass against infection by Magnaporthe oryzae. *Phytopathology* 105, 748–757. doi: 10.1094/PHYTO-12-14-0378-R

Rahman, M. F., Ghosal, A., Alam, M. F., and Kabir, A. H. (2017). Remediation of cadmium toxicity in field peas (Pisum sativum L.) through exogenous silicon. *Ecotoxicol. Environ. Safety* 135, 165–172. doi: 10.1016/j.ecoenv.2016.09.019

Rai, K. K., Pandey, N., and Rai, S. P. (2020). Salicylic acid and nitric oxide signaling in plant heat stress. *Physiol. Plant.* 168, 241–255. doi: 10.1111/ppl.12958

Rajasheker, G., Jawahar, G., Jalaja, N., Kumar, S. A., Kumari, P. H., Punita, D. L., et al. (2019). Role and regulation of osmolytes and ABA interaction in salt and drought stress tolerance. *Plant Signal. Mol.* 2019, 417–436. doi: 10.1016/b978-0-12-816451-8.00026-5

Rasoolizadeh, A., Labbé, C., Sonah, H., Deshmukh, R. K., Belzile, F., Menzies, J. G., et al. (2018). Silicon protects soybean plants against Phytophthora sojae by interfering with effector-receptor expression. *BMC Plant Biol.* 18:7. doi: 10.1186/s12870-018-1312-7

Rastogi, A., Yadav, S., Hussain, S., Kataria, S., Hajihashemi, S., Kumari, P., et al. (2021). Does silicon really matter for the photosynthetic machinery in plants? *Plant Physiol. Biochem.* 169, 40–48. doi: 10.1016/j.plaphy.2021.11.004

Ratcliffe, S., Jugdaohsingh, R., Vivancos, J., Marron, A., Deshmukh, R., Ma, J. F., et al. (2017). Identification of a mammalian silicon transporter. *Am. J. Physiol. Cell Physiol.* 312, C550–C561. doi: 10.1152/ajpcell.00219.2015

Raza, A. (2020). Metabolomics: a systems biology approach for enhancing heat stress tolerance in plants. *Plant Cell Rep.* 2020, 1–23. doi: 10.1007/s00299-020-02635-8

Raza, A. (2021). Eco-physiological and Biochemical Responses of Rapeseed (Brassica napus L.) to Abiotic Stresses: Consequences and Mitigation Strategies. *J. Plant Growth Regul.* 40, 1368–1388. doi: 10.1007/s00344-020-10231-z

Raza, A. (2022). Plant biotechnological tools: Solutions for raising climate-resilient crop plants. *Modern Phytomorphol.* 15, 132–133.

Raza, A., Ashraf, F., Zou, X., Zhang, X., and Tosif, H. (2020a). Plant Adaptation and Tolerance to Environmental Stresses: Mechanisms and Perspectives. *Plant Ecophysiol. Adaptat. Under Clim. Change Mechanisms Perspect.* 1, 117–145. doi: 10.1007/978-981-15-2156-0_5

Raza, A., Charagh, S., Sadaqat, N., and Jin, W. (2020b). Arabidopsis thaliana: Model Plant for the Study of Abiotic Stress Responses. *Plant Fam. Brassicaceae* 2020, 129–180. doi: 10.1007/978-981-15-6345-4_3

Raza, A., Su, W., Hussain, M. A., Mehmood, S. S., Zhang, X., Cheng, Y., et al. (2021e). Integrated analysis of metabolome and transcriptome reveals insights for cold tolerance in rapeseed (Brassica napus L.). *Front. Plant Sci.* 12:721681. doi: 10.3389/fpls.2021.721681

Raza, A., Tabassum, J., Mubarik, M., Anwar, S., Zahra, N., Sharif, Y., et al. (2021g). Hydrogen sulfide: an emerging component against abiotic stress in plants. *Plant Biol.* 2021, 1435–8603. doi: 10.1111/plb.13368

Raza, A., Charagh, S., Zahid, Z., Mubarik, M. S., Javed, R., Siddiqui, M. H., et al. (2021b). Jasmonic acid: a key frontier in conferring abiotic stress tolerance in plants. *Plant Cell Rep.* 40, 1513–1541. doi: 10.1007/s00299-020-02614-z

Raza, A., Charagh, S., Najafi-Kakavand, S., and Siddiqui, M. H. (2021a). The Crucial Role of Jasmonates in Enhancing Heavy Metals Tolerance in Plants. *Jasmonates Salicylates Signal. Plants* 2021, 159–183. doi: 10.1007/s00299-017-2168-2

Raza, A., Habib, M., Charagh, S., and Kakavand, S. N. (2021c). Genetic engineering of plants to tolerate toxic metals and metalloids. *Handb. Bioremed.* 2021, 411–436. doi: 10.1016/b978-0-12-819382-2.00026-0

Raza, A., Hussain, S., Javed, R., Hafeez, M. B., and Hasanuzzaman, M. (2021d). Antioxidant Defense Systems and Remediation of Metal Toxicity in Plants. *Approaches Remediat. Inorganic Poll.* 2021, 91–124. doi: 10.1007/978-981-15-6221-1_6

Raza, A., Tabassum, J., Kudapa, H., and Varshney, R. K. (2021f). Can omics deliver temperature resilient ready-to-grow crops? *Crit. Rev. Biotechnol.* 41, 1209–1232. doi: 10.1080/07388551.2021.1898332

Raza, A., Mehmood, S. S., Tabassum, J., and Batool, R. (2019). Targeting plant hormones to develop abiotic stress resistance in wheat. *Wheat Product. Changing Environ.* 2019, 557–577. doi: 10.1007/978-981-13-6883-7_22

Raza, A., Tabassum, J., Zahid, Z., Charagh, S., Bashir, S., Barmukh, R., et al. (2022). Advances in "Omics" Approaches for Improving Toxic Metals/Metalloids Tolerance in Plants. *Front. Plant Sci.* 12:794373. doi: 10.3389/fpls.2021.794373

Rehman, M. U., Ilahi, H., Adnan, M., Wahid, F., Rehman, F. U., Ullah, A., et al. (2021). Application of Silicon: A Useful Way to Mitigate Drought Stress: An Overview. *Curr. Res. Agric. Farm.* 2, 9–17. doi: 10.18782/2582-7146.134

Rémus-Borel, W., Menzies, J. G., and Bélanger, R. R. (2005). Silicon induces antifungal compounds in powdery mildew-infected wheat. *Physiol. Mol. Plant Pathol.* 66, 108–115. doi: 10.1016/j.pmpp.2005.05.006

Rizwan, M., Ali, S., Ibrahim, M., Farid, M., Adrees, M., Bharwana, S. A., et al. (2015). Mechanisms of silicon-mediated alleviation of drought and salt stress in plants: a review. *Environ. Sci. Poll. Res.* 22, 15416–15431. doi: 10.1007/s11356-015-5305-x

Rogalla, H., Römheld, V. J. P., Cell, and Environment. (2002). Role of leaf apoplast in silicon-mediated manganese tolerance of Cucumis sativus L. *Plant Cell Environ.* 25, 549–555. doi: 10.1046/j.1365-3040.2002.00835.x

Sabagh, A. E., Mbarki, S., Hossain, A., Iqbal, M., Islam, M., Raza, A., et al. (2021). Potential Role of Plant Growth Regulators in Administering Crucial Processes Against Abiotic Stresses. *Front. Agronomy* 3:648694. doi: 10.3389/fagro.2021.648694

Saddiq, M. S., Afzal, I., Iqbal, S., Hafeez, M. B., and Raza, A. (2021). Low leaf sodium content improves the grain yield and physiological performance of wheat genotypes in saline-sodic soil. *Pesquisa Agropecuária Tropical* 51, e67663–e67663.

Saha, G., Mostofa, M. G., Rahman, M. M., and Tran, L.-S. P. (2021). Silicon-mediated heat tolerance in higher plants: a molecular outlook. *Plant Physiol. Biochem.* 166, 341–347. doi: 10.1016/j.plaphy.2021.05.051

Sakuma, Y., Maruyama, K., Osakabe, Y., Qin, F., Seki, M., Shinozaki, K., et al. (2006). Functional analysis of an Arabidopsis transcription factor, DREB2A,

involved in drought-responsive gene expression. *Plant Cell* 18, 1292–1309. doi: 10.1105/tpc.105.035881

Saleem, M., Fariduddin, Q., and Janda, T. (2021). Multifaceted role of salicylic acid in combating cold stress in plants: a review. *J. Plant Growth Regul.* 40, 464–485. doi: 10.1007/s00344-020-10152-x

Salim, B., Abou El-Yazied, A., Salama, Y., Raza, A., and Osman, H. S. (2021). Impact of silicon foliar application in enhancing antioxidants, growth, flowering and yield of squash plants under deficit irrigation condition. *Ann. Agricult. Sci.* 66, 176–183.

Santos, M. R. D., Martinez, M. A., Donato, S. L. R., and Coelho, E. F. (2014). 'Tommy Atkins' mango yield and photosynthesis under water deficit in semiarid region of Bahia. *Rev. Brasil. Engenharia Agrícola Ambiental* 18, 899–907.

Sato, M., Tsuda, K., Wang, L., Coller, J., Watanabe, Y., Glazebrook, J., et al. (2010). Network modeling reveals prevalent negative regulatory relationships between signaling sectors in Arabidopsis immune signaling. *PLoS Pathog.* 6:e1001011. doi: 10.1371/journal.ppat.1001011

Sattar, A., Cheema, M. A., Sher, A., Ijaz, M., Ul-Allah, S., Nawaz, A., et al. (2019). Physiological and biochemical attributes of bread wheat (Triticum aestivum L.) seedlings are influenced by foliar application of silicon and selenium under water deficit. *Acta Physiol. Plant.* 41, 1–11.

Savant, N. K., Korndörfer, G. H., Datnoff, L. E., and Snyder, G. H. (1999). Silicon nutrition and sugarcane production: a review. *J. Plant Nutrit.* 22, 1853–1903.

Savatin, D. V., Gramegna, G., Modesti, V., and Cervone, F. (2014). Wounding in the plant tissue: the defense of a dangerous passage. *Front. Plant Sci.* 5:470. doi: 10.3389/fpls.2014.00470

Shah, A. A., Yasin, N. A., Akram, K., Ahmad, A., Khan, W. U., Akram, W., et al. (2021). Ameliorative role of Bacillus subtilis FBL-10 and silicon against lead induced stress in Solanum melongena. *Plant Physiol. Biochem.* 158, 486–496. doi: 10.1016/j.plaphy.2020.11.037

Sharma, L., Priya, M., Kaushal, N., Bhandhari, K., Chaudhary, S., Dhankher, O. P., et al. (2020). Plant growth-regulating molecules as thermoprotectants: functional relevance and prospects for improving heat tolerance in food crops. *J. Exp. Bot.* 71, 569–594. doi: 10.1093/jxb/erz333

Sharma, S. S., and Dietz, K.-J. J. T. (2009). The relationship between metal toxicity and cellular redox imbalance. *Trends Plant Sci.* 14, 43–50. doi: 10.1016/j.tplants.2008.10.007

Shen, X., Xiao, X., Dong, Z., and Chen, Y. J. A. P. P. (2014). Silicon effects on antioxidative enzymes and lipid peroxidation in leaves and roots of peanut under aluminum stress. *Acta Physiol. Plant.* 36, 3063–3069.

Shi, Y., Wang, Y., Flowers, T. J., and Gong, H. (2013). Silicon decreases chloride transport in rice (Oryza sativa L.) in saline conditions. *J. Plant Physiol.* 170, 847–853. doi: 10.1016/j.jplph.2013.01.018

Shi, Y., Zhang, Y., Yao, H., Wu, J., Sun, H., and Gong, H. (2014). Silicon improves seed germination and alleviates oxidative stress of bud seedlings in tomato under water deficit stress. *Plant Physiol. Biochem.* 78, 27–36. doi: 10.1016/j.plaphy.2014.02.009

Shimo, H., Ishimaru, Y., An, G., Yamakawa, T., Nakanishi, H., and Nishizawa, N. K. J. J. (2011). Low cadmium (LCD), a novel gene related to cadmium tolerance and accumulation in rice. *J. Exp. Bot.* 62, 5727–5734. doi: 10.1093/jxb/err300

Sierra, M. J., Schmid, T., Guirado, M., Escolano, O., and Millán, R. (2021). How management practices affect silicon uptake by Hordeum vulgare grown in a highly calcareous soil. *Soil Use Manage.* 2021:12723.

Sil, P., Das, P., and Biswas, A. K. (2018). Silicon induced mitigation of TCA cycle and GABA synthesis in arsenic stressed wheat (Triticum aestivum L.) seedlings. *South Afr. J. Bot.* 119, 340–352.

Singh, H. P., and Singh, B. P. (2014). Genetic engineering of field, industrial and pharmaceutical crops. *Am. J. Plant Sci.* 5:3974.

Singh, K., and Chandra, A. (2021). DREBs-potential transcription factors involve in combating abiotic stress tolerance in plants. *Biologia* 76, 3043–3055.

Singh, S., Koyama, H., Bhati, K. K., and Alok, A. (2021). The biotechnological importance of the plant-specific NAC transcription factor family in crop improvement. *J. Plant Res.* 2021, 1–21.

Singh, S., Singh, V. P., Prasad, S. M., Sharma, S., Ramawat, N., Dubey, N. K., et al. (2019). Interactive effect of silicon (Si) and salicylic acid (SA) in maize seedlings and their mechanisms of cadmium (Cd) toxicity alleviation. *J. Plant Growth Regul.* 38, 1587–1597.

Sivanesan, I., Son, M. S., Soundararajan, P., and Jeong, B. R. (2014). Effect of Silicon on Growth and Temperature Stress Tolerance of *Nephrolepis exaltata*'Corditas'. *Horticult. Sci. Technol.* 32, 142–148.

Soleimannejad, Z., Abdolzadeh, A., and Sadeghipour, H. R. (2019). Beneficial effects of silicon application in alleviating salinity stress in halophytic puccinellia distans plants. *Silicon* 11, 1001–1010.

Song, A., Li, P., Fan, F., Li, Z., and Liang, Y. (2014). The effect of silicon on photosynthesis and expression of its relevant genes in rice (Oryza sativa L.) under high-zinc stress. *PLoS One* 9:e113782. doi: 10.1371/journal.pone.0113782

Souri, Z., Khanna, K., Karimi, N., and Ahmad, P. (2021). Silicon and plants: current knowledge and future prospects. *J. Plant Growth Regul.* 40, 906–925.

Soylemezoglu, G., Demir, K., Inal, A., and Gunes, A. (2009). Effect of silicon on antioxidant and stomatal response of two grapevine (Vitis vinifera L.) rootstocks grown in boron toxic, saline and boron toxic-saline soil. *Sci. Horticult.* 123, 240–246.

Sreenivasulu, N., Harshavardhan, V. T., Govind, G., Seiler, C., and Kohli, A. (2012). Contrapuntal role of ABA: does it mediate stress tolerance or plant growth retardation under long-term drought stress? *Gene* 506, 265–273. doi: 10.1016/j.gene.2012.06.076

Sudo, E., Itouga, M., Yoshida-Hatanaka, K., Ono, Y., and Sakakibara, H. J. J. (2008). Gene expression and sensitivity in response to copper stress in rice leaves. *J. Exp. Bot.* 59, 3465–3474. doi: 10.1093/jxb/ern196

Sun, L., Wang, R., Tang, W., Chen, Y., Zhou, J., Ma, H., et al. (2022). Robust identification of low-Cd rice varieties by boosting the genotypic effect of grain Cd accumulation in combination with marker-assisted selection. *J. Hazard. Mater.* 424:127703. doi: 10.1016/j.jhazmat.2021.127703

Suzuki, N., Koussevitzky, S., Mittler, R. O. N., and Miller, G. A. D. (2012). ROS and redox signalling in the response of plants to abiotic stress. *Plant Cell Environ.* 35, 259–270. doi: 10.1111/j.1365-3040.2011.02336.x

Takahashi, R., Ishimaru, Y., Senoura, T., Shimo, H., Ishikawa, S., Arao, T., et al. (2011). The OsNRAMP1 iron transporter is involved in Cd accumulation in rice. *J. Exp. Bot.* 62, 4843–4850. doi: 10.1093/jxb/err136

Takasaki, H., Maruyama, K., Kidokoro, S., Ito, Y., Fujita, Y., Shinozaki, K., et al. (2010). The abiotic stress-responsive NAC-type transcription factor OsNAC5 regulates stress-inducible genes and stress tolerance in rice. *Mol. Genet. Genomics* 284, 173–183. doi: 10.1007/s00438-010-0557-0

Tariq, R. M. S., Ahmad, T., Ayub, M. A., Dogar, W. A., Ahmad, Z., and Aslam, M. M. (2022). Management of Abiotic Stress Conditions by Salicylic Acid. *Plant Abiotic Stress Physiol.* 2:157.

Thind, S., Hussain, I., Ali, S., Hussain, S., Rasheed, R., Ali, B., et al. (2020). Physiological and biochemical bases of foliar silicon-induced alleviation of cadmium toxicity in wheat. *J. Soil Sci. Plant Nutrit.* 20, 2714–2730.

Tripathi, D. K., Singh, V. P., Ahmad, P., Chauhan, D. K., and Prasad, S. M. (2016). *Silicon in plants: advances and future prospects*. Florida, FL: CRC Press.

Tripathi, D. K., Singh, V. P., Prasad, S. M., Chauhan, D. K., Dubey, N. K., Rai, A. K. J. E., et al. (2015). Silicon-mediated alleviation of Cr (VI) toxicity in wheat seedlings as evidenced by chlorophyll florescence, laser induced breakdown spectroscopy and anatomical changes. *Ecotoxicol. Environ. Safety* 113, 133–144. doi: 10.1016/j.ecoenv.2014.09.029

Tripathi, D. K., Vishwakarma, K., Singh, V. P., Prakash, V., Sharma, S., Muneer, S., et al. (2021). Silicon crosstalk with reactive oxygen species, phytohormones and other signaling molecules. *J. Hazard. Mater.* 408:124820. doi: 10.1016/j.jhazmat.2020.124820

Ul Hassan, M., Rasool, T., Iqbal, C., Arshad, A., Abrar, M., Abrar, M. M., et al. (2021). Linking Plants Functioning to Adaptive Responses Under Heat Stress Conditions: A Mechanistic Review. *J. Plant Growth Regul.* 2021, 1–18.

Vaculík, M., Lukačová, Z., Bokor, B., Martinka, M., Tripathi, D. K., and Lux, A. (2020). Alleviation mechanisms of metal (loid) stress in plants by silicon: a review. *J. Exp. Bot.* 71, 6744–6757. doi: 10.1093/jxb/eraa288

Vanlerberghe, G. C., Martyn, G. D., and Dahal, K. (2016). Alternative oxidase: a respiratory electron transport chain pathway essential for maintaining photosynthetic performance during drought stress. *Physiol. Plant.* 157, 322–337. doi: 10.1111/ppl.12451

Varshney, R. K., Bohra, A., Roorkiwal, M., Barmukh, R., Cowling, W. A., Chitikineni, A., et al. (2021a). Fast-forward breeding for a food-secure world. *Trends Genet.* 37, 1124–1136. doi: 10.1016/j.tig.2021.08.002

Varshney, R. K., Bohra, A., Yu, J., Graner, A., Zhang, Q., and Sorrells, M. E. (2021b). Designing future crops: genomics-assisted breeding comes of age. *Trends Plant Sci.* 26, 631–649. doi: 10.1016/j.tplants.2021.03.010

Varshney, R. K., Singh, V. K., Kumar, A., Powell, W., and Sorrells, M. E. (2018). Can genomics deliver climate-change ready crops? *Curr. Opin. Plant Biol.* 45, 205–211. doi: 10.1016/j.pbi.2018.03.007

Varshney, R. K., Sinha, P., Singh, V. K., Kumar, A., Zhang, Q., and Bennetzen, J. L. (2020). 5Gs for crop genetic improvement. *Curr. Opin. Plant Biol.* 56, 190–196. doi: 10.1016/j.pbi.2019.12.004

Verma, K. K., Liu, X.-H., Wu, K.-C., Singh, R. K., Song, Q.-Q., Malviya, M. K., et al. (2019). The impact of silicon on photosynthetic and biochemical responses of sugarcane under different soil moisture levels. *Silicon* 2019, 1–13.

Verma, K. K., Song, X.-P., Tian, D.-D., Singh, M., Verma, C. L., Rajput, V. D., et al. (2021). Investigation of defensive role of silicon during drought stress induced by irrigation capacity in sugarcane: Physiological and biochemical characteristics. *ACS Omega* 6, 19811–19821. doi: 10.1021/acsomega.1c02519

Verma, V., Ravindran, P., and Kumar, P. P. (2016). Plant hormone-mediated regulation of stress responses. *BMC Plant Biol.* 16, 1–10. doi: 10.1186/s12870-016-0771-y

Wang, H., Li, C., and Liang, Y. (2001). Agricultural utilization of silicon in China. *Stud. Plant Sci.* 2001, 343–358.

Wang, J., Song, L., Gong, X., Xu, J., and Li, M. (2020). Functions of jasmonic acid in plant regulation and response to abiotic stress. *Int. J. Mol. Sci.* 21:1446. doi: 10.3390/ijms21041446

Wang, L.-J., Fan, L., Loescher, W., Duan, W., Liu, G.-J., Cheng, J.-S., et al. (2010). Salicylic acid alleviates decreases in photosynthesis under heat stress and accelerates recovery in grapevine leaves. *BMC Plant Biol.* 10, 1–10. doi: 10.1186/1471-2229-10-34

Wang, M., Wang, R., Mur, L. A. J., Ruan, J., Shen, Q., and Guo, S. (2021). Functions of silicon in plant drought stress responses. *Horticult. Res.* 8, 1–13. doi: 10.1038/s41438-021-00681-1

Wang, S., Liu, P., Chen, D., Yin, L., Li, H., and Deng, X. (2015). Silicon enhanced salt tolerance by improving the root water uptake and decreasing the ion toxicity in cucumber. *Front. Plant Sci.* 6:759. doi: 10.3389/fpls.2015.00759

Wang, X., and Huang, B. (2017). Lipid-and calcium-signaling regulation of HsfA2c-mediated heat tolerance in tall fescue. *Environ. Exp. Bot.* 136, 59–67.

Wani, S. H., Kumar, V., Shriram, V., and Sah, S. K. (2016). Phytohormones and their metabolic engineering for abiotic stress tolerance in crop plants. *Crop J.* 4, 162–176.

Wu, J., Guo, J., Hu, Y., and Gong, H. (2015). Distinct physiological responses of tomato and cucumber plants in silicon-mediated alleviation of cadmium stress. *Front. Plant Sci.* 6:453. doi: 10.3389/fpls.2015.00453

Wu, J., Mock, H.-P., Giehl, R. F. H., Pitann, B., and Mühling, K. H. (2019). Silicon decreases cadmium concentrations by modulating root endodermal suberin development in wheat plants. *J. Hazard. Mater.* 364, 581–590. doi: 10.1016/j.jhazmat.2018.10.052

Yang, Y., and Guo, Y. (2018). Elucidating the molecular mechanisms mediating plant salt-stress responses. *N. Phytol.* 217, 523–539. doi: 10.1111/nph.14920

Yao, X., Chu, J., Cai, K., Liu, L., Shi, J., and Geng, W. (2011). Silicon improves the tolerance of wheat seedlings to ultraviolet-B stress. *Biol. Trace Element Res.* 143, 507–517. doi: 10.1007/s12011-010-8859-y

Yin, J., Jia, J., Lian, Z., Hu, Y., Guo, J., Huo, H., et al. (2019). Silicon enhances the salt tolerance of cucumber through increasing polyamine accumulation and decreasing oxidative damage. *Ecotoxicol. Environ. Safety* 169, 8–17. doi: 10.1016/j.ecoenv.2018.10.105

Yin, L., Wang, S., Liu, P., Wang, W., Cao, D., Deng, X., et al. (2014). Silicon-mediated changes in polyamine and 1-aminocyclopropane-1-carboxylic acid are involved in silicon-induced drought resistance in Sorghum bicolor L. *Plant Physiol. Biochem.* 80, 268–277. doi: 10.1016/j.plaphy.2014.04.014

Yin, L., Wang, S., Tanaka, K., Fujihara, S., Itai, A., Den, X., et al. (2016). Silicon-mediated changes in polyamines participate in silicon-induced salt tolerance in S orghum bicolor L. *Plant Cell Environ.* 39, 245–258. doi: 10.1111/pce.12521

Younis, A., Khattab, H., and Emam, M. (2020). Impacts of silicon and silicon nanoparticles on leaf ultrastructure and TaPIP1 and TaNIP2 gene expressions in heat stressed wheat seedlings. *Biol. Plant.* 64, 343–352.

Zahra, N., Hafeez, M. B., Shaukat, K., Wahid, A., Hussain, S., Naseer, R., et al. (2021). Hypoxia and Anoxia Stress: Plant responses and tolerance mechanisms. *J. Agronomy Crop Sci.* 207, 249–284.

Zandalinas, S. I, Mittler, R., Balfagón, D., Arbona, V., and Gómez-Cadenas, A. (2018). Plant adaptations to the combination of drought and high temperatures. *Physiol. Plant.* 162, 2–12. doi: 10.1111/ppl.12540

Zargar, S. M., and Agnihotri, A. (2013). Impact of silicon on various agro-morphological and physiological parameters in maize and revealing its role in enhancing water stress tolerance. *Emirates J. Food Agricult.* 2013, 138–141.

Zargar, S. M., Gupta, N., Mir, R. A., and Rai, V. (2016). Shift from gel based to gel free proteomics to unlock unknown regulatory network in plants: a comprehensive review. *J. Adv. Res. Biotechnol.* 19:15226.

Zargar, S. M., Mahajan, R., Bhat, J. A., Nazir, M., and Deshmukh, R. (2019). Role of silicon in plant stress tolerance: opportunities to achieve a sustainable cropping system. *3 Biotech* 9:73. doi: 10.1007/s13205-019-1613-z

Zhang, X., Zhang, W., Lang, D., Cui, J., and Li, Y. (2018). Silicon improves salt tolerance of Glycyrrhiza uralensis Fisch. by ameliorating osmotic and oxidative stresses and improving phytohormonal balance. *Environ. Sci. Poll. Res.* 25, 25916–25932. doi: 10.1007/s11356-018-2595-9

Zhao, D., Hao, Z., Tao, J., and Han, C. (2013). Silicon application enhances the mechanical strength of inflorescence stem in herbaceous peony (Paeonia lactiflora Pall.). *Sci. Horticult.* 151, 165–172.

Zhou, R., Yu, X., Ottosen, C.-O., Rosenqvist, E., Zhao, L., Wang, Y., et al. (2017). Drought stress had a predominant effect over heat stress on three tomato cultivars subjected to combined stress. *BMC Plant Biol.* 17, 1–13. doi: 10.1186/s12870-017-0974-x

Zhu, J.-K. (2016). Abiotic stress signaling and responses in plants. *Cell* 167, 313–324.

Zhu, Y. X., Gong, H. J., and Yin, J. L. (2019a). Role of silicon in mediating salt tolerance in plants: a review. *Plants* 8:147. doi: 10.3390/plants8060147

Zhu, Y., and Gong, H. (2014). Beneficial effects of silicon on salt and drought tolerance in plants. *Agron. Sustain. Dev.* 34, 455–472.

Zhu, Y., Yin, J., Liang, Y., Liu, J., Jia, J., Huo, H., et al. (2019b). Transcriptomic dynamics provide an insight into the mechanism for silicon-mediated alleviation of salt stress in cucumber plants. *Ecotoxicol. Environ. Safety* 174, 245–254. doi: 10.1016/j.ecoenv.2019.02.075

Zhu, Y.-X., Xu, X.-B., Hu, Y.-H., Han, W.-H., Yin, J.-L., Li, H.-L., et al. (2015). Silicon improves salt tolerance by increasing root water uptake in Cucumis sativus L. *Plant Cell Rep.* 34, 1629–1646. doi: 10.1007/s00299-015-1814-9

Zia, A., Hegazy, H. S., Hassan, N. S., Naguib, D. M., and Abdel-Haliem, M. E. (2021). Biochemical responses of wheat to silicon application under salinity. *J. Plant Nutrit. Soil Sci.* 184, 255–262. doi: 10.1016/j.plaphy.2021.02.023

Zuccarini, P. (2008). Effects of silicon on photosynthesis, water relations and nutrient uptake of Phaseolus vulgaris under NaCl stress. *Biol. Plant.* 52, 157–160.

Conflict of Interest: The authors declare that the research was conducted in the absence of any commercial or financial relationships that could be construed as a potential conflict of interest.

Publisher's Note: All claims expressed in this article are solely those of the authors and do not necessarily represent those of their affiliated organizations, or those of the publisher, the editors and the reviewers. Any product that may be evaluated in this article, or claim that may be made by its manufacturer, is not guaranteed or endorsed by the publisher.

Copyright © 2022 Mir, Bhat, Yousuf, Islam, Raza, Rizvi, Charagh, Albaqami, Sofi and Zargar. This is an open-access article distributed under the terms of the Creative Commons Attribution License (CC BY). The use, distribution or reproduction in other forums is permitted, provided the original author(s) and the copyright owner(s) are credited and that the original publication in this journal is cited, in accordance with accepted academic practice. No use, distribution or reproduction is permitted which does not comply with these terms.

frontiers in Plant Science

ORIGINAL RESEARCH
published: 31 March 2022
doi: 10.3389/fpls.2022.817730

Effects on Photosynthetic Response and Biomass Productivity of *Acacia longifolia* ssp. *longifolia* Under Elevated CO_2 and Water-Limited Regimes

Muhammad Mansoor Javaid[1], Xiukang Wang[2]*, Singarayer K. Florentine[3], Muhammad Ashraf[4], Athar Mahmood[5], Feng-Min Li[6] and Sajid Fiaz[7]*

[1] Department of Agronomy, College of Agriculture, University of Sargodha, Sargodha, Pakistan, [2] College of Life Sciences, Yan'an University, Yan'an, China, [3] Future Regions Research Centre, Federation University Australia, Mount Helen, VIC, Australia, [4] Institute of Molecular Biology and Biotechnology, The University of Lahore, Lahore, Pakistan, [5] Department of Agronomy, University of Agriculture Faisalabad, Faisalabad, Pakistan, [6] State Key Laboratory of Grassland Agroecosystems, School of Life Sciences, Institute of Arid Agroecology, Lanzhou University, Lanzhou, China, [7] Department of Plant Breeding and Genetics, The University of Haripur, Haripur, Pakistan

OPEN ACCESS

Edited by:
Shabir Hussain Wani, Sher-e-Kashmir University of Agricultural Sciences and Technology, India

Reviewed by:
Awais Shakoor, Universitat de Lleida, Spain
Abbu Zaid, Govt. Degree College Doda, India

***Correspondence:**
Muhammad Mansoor Javaid
mmansoorjavaid@gmail.com
Xiukang Wang
wangxiukang@yau.edu.cn

Specialty section:
This article was submitted to Plant Breeding, a section of the journal Frontiers in Plant Science

Received: *18 November 2021*
Accepted: *15 February 2022*
Published: *31 March 2022*

Citation:
Javaid MM, Wang X, Florentine SK, Ashraf M, Mahmood A, Li F-M and Fiaz S (2022) Effects on Photosynthetic Response and Biomass Productivity of Acacia longifolia ssp. longifolia Under Elevated CO_2 and Water-Limited Regimes. Front. Plant Sci. 13:817730. doi: 10.3389/fpls.2022.817730

It is known that the impact of elevated CO_2 (eCO_2) will cause differential photosynthetic responses in plants, resulting in varying magnitudes of growth and productivity of competing species. Because of the aggressive invasive nature of *Acacia longifolia* ssp. *longifolia*, this study is designed to investigate the effect of eCO_2 on gas exchange parameters, water use efficiency, photosystem II (PSII) activities, and growth of this species. Plants of *A. longifolia* ssp. *longifolia* were grown at 400 ppm (ambient) and 700 ppm (elevated) CO_2 under 100 and 60% field capacity. Leaf gas exchange parameters, water use efficiency, intrinsic water use efficiency, instantaneous carboxylation efficiency, and PSII activity were measured for 10 days at 2-day intervals. eCO_2 mitigated the adverse effects of drought conditions on the aforementioned parameters compared to that grown under ambient CO_2 (aCO_2) conditions. *A. longifolia*, grown under drought conditions and re-watered at day 8, indicated a partial recovery in most of the parameters measured, suggesting that the recovery of this species under eCO_2 will be higher than that with aCO_2 concentration. This gave an increase in water use efficiency, which is one of the reasons for the observed enhanced growth of *A. longifolia* under drought stress. Thus, eCO_2 will allow to adopt this species in the new environment, even under severe climatic conditions, and foreshadow its likelihood of invasion into new areas.

Keywords: elevated CO_2, photosynthetic processes, water use efficiency, photosystem II, drought, *Acacia longifolia* ssp. *longifolia*

Abbreviations: aCO_2, ambient CO_2; eCO_2, elevated CO_2; PPFD, photosynthetic photon flux density; PSII, photosystem II; RuBP, ribulose 1,5-bishosphate.

INTRODUCTION

A substantial increase in atmospheric CO_2 level has already occurred since the Industrial Revolution, and it is predicted that it will approach 700 ppm by the year 2050 (IPCC, 2018). This increase in atmospheric CO_2 will cause global warming (Boucher et al., 2009) that leads to water scarcity, a key constraint of crop productivity. Despite that, elevated CO_2 (eCO_2) is believed to increase the photosynthetic rate and suppress their photorespiration (Li et al., 2019). eCO_2 increased the photosynthesis and stimulated biomass and yield parameters (Kirschbaum, 2011) along with decreased water use per unit area of vegetation by partial stomatal closure (Pastore et al., 2020). Studies have also shown that eCO_2 causes a 20–30% increase in net assimilation rate, together with an increase in dry matter and yield of crops (Cruz et al., 2018; Pan et al., 2018; Xie et al., 2018). Increasing atmospheric CO_2 has significant effects on physiological processes related to plant growth, even though responses will be modified under drought stress (Qaderi et al., 2006, 2013). It is well documented that enhanced biomass production and alteration in photosynthetic activity and water relation under eCO_2 are dependent on the availability of other limiting resources (Robredo et al., 2007). According to Elgawad et al. (2015), eCO_2 has been shown to mitigate the stress impact of drought, and they quote examples of how the reduction of drought stress affects barley and alfalfa crops. Despite these beneficial effects on crops, ongoing increases in atmospheric CO_2 may have important consequences for weed-crop competition, leading to subsequent yield losses (Ziska et al., 2019).

It has been noted that climate change further increases the risk of plant invasiveness by facilitating a change in the ecosystem through the increased competitiveness of the weed under eCO_2 conditions (Bradley et al., 2010; Le et al., 2019). Previous studies have shown that invasive plants exhibit greater climatic change tolerance in invaded habitats compared to native species due to evolutionary plasticity (Clements and Ditommaso, 2011; Davidson et al., 2011). In this respect, eCO_2 and water stress, sowing to climate change, can directly affect plant physiology and morphology (Lobell and Gourdji, 2012; Salazar-Parra et al., 2012). It is postulated that because invasive species benefit from eCO_2, this will enable them to acclimatize to their new environments in the future (Dukes et al., 2011; Pastore et al., 2020). It is predicted that rising atmospheric CO_2 may cause global warming, which could be the basis of change in precipitation patterns and drought occurrence, and could possibly affect those regions not currently subjected to drought (Robredo et al., 2007; Dai, 2013; Dai et al., 2018). It is also postulated that different plant species showed different responses with rising atmospheric CO_2 concentration under drought conditions (Pastore et al., 2020). Researchers have observed that plants are grown under eCO_2 and dry more slowly as water is withheld due to lower stomatal conductance and transpiration rate (Dikšaitytė et al., 2019; Pastore et al., 2020).

Acacia species, which are native to Australia, have been deliberately exported for some years to a number of temperate countries in order to stabilize degraded soil (especially sand dunes) for ornamental purposes and fuelwood (Kull et al., 2011). However, the aggressive growth properties of most of the *Acacia* species have made them particularly invasive (Corlett, 2010), with the result that these species are currently included in the Global Invasive Species Database. It is well established that invasive alien species affected the growth and wellbeing of native species by altering the ecosystem and introducing direct competition for resources (Werner et al., 2008; Alba et al., 2019). According to Blossey and Notzold (1995) hypothesis, competitive abilities can be maximized by increasing vegetative growth or reproductive growth for success in a particularly new environment. This alteration in the mix of biota presents environmental managers with an urgent challenge to stem the infiltration of invasive species in order to maintain indigenous biodiversity (Qaderi et al., 2013). In many situations, it is evident that these invasive plant species are considered to be the major cause of biodiversity loss and are also thought to contribute to global environmental change (Bellard et al., 2014).

Acacia longifolia ssp. *longifolia*, which is the focus of this article, belongs to the *Fabaceae* family and is commonly known as either Sydney golden wattle, long-leaved wattle, or shallow wattle (Marchante et al., 2010). It is indigenous to South Eastern Australia (Costermans, 1981), but currently it is widely distributed throughout Australia (Marchante et al., 2015). Whilst sandy coastal areas are the preferred habitat of *A. longifolia*, it also grows successfully in woodlands, grasslands, and along roadsides (Marchante et al., 2010). Its ability to fix nitrogen enables this species to colonize successfully in nutrient-poor soil (Sampaio, 2019). Due to its aggressive growth habit, this species is currently recognized as a problematic invasive plant in adjoining native areas in Australia, as well as in introduced environments in Portugal, Southern Africa, and Spain (Souza-Alonso et al., 2018). Many reports have indicated that this species can outcompete native plants by rapid growth even under disturbed conditions (Osunkoya et al., 2005; Marchante et al., 2015). This invasive character of *A. longifolia* ssp. *longifolia* can be attributed to its prolific annual seed production and physical seed dormancy due to its hard seed coat, which facilitates its soil seed bank persistence and its consequent emergence in times of stress (Welgama et al., 2019).

The interest of this article is that many species of *Acacia* respond to eCO_2 concentrations and record increased growth as a result of enhanced carbon assimilation (Evans et al., 2000; Le et al., 2019). In this respect, Evans et al. (2000) studied the effect of eCO_2 on photosynthetic activity of 10 *Acacia* species (i.e., *Acacia aneura*, *Acacia colei*, *Acacia coriacea*, *Acacia tetragonophylla*, *Acacia irrorata*, *Acacia dealbata*, *Acacia mearnsii*, *Acacia implexa*, *Acacia melanoxylon*, and *Acacia saligna*) under normal irrigation conditions. Except for *A. aneura*, results revealed that growth and gas exchange measurements of all species were enhanced under 700 ppm CO_2 compared to that under 350 ppm, with the degree of enhancement being species-specific. *A. longifolia* ssp. *longifolia* was not included in the previous study, but other studies have revealed a wealth of information on its ecology and biology. Nonetheless, more information about physiological processes and biomass production regarding *A. longifolia* ssp. *longifolia* will increase the understanding of the potential future impacts of

climate change on this species. As a consequence, this study was designed to investigate the effects of drought on *A. longifolia* ssp. *longifolia* under two atmospheric CO_2 concentrations (400 and 700 ppm), noting changes in physiological processes, water use efficiency, and growth.

MATERIALS AND METHODS

Experimental Site and Sowing Conditions

Experiments were conducted at Federation University, Mt Helen, Australia (37°37.39°S, 143°53.27°E) in two CO_2 chambers (2.1 m length, 2.1 m width, and 2.0 m height) (Steridium Pty Ltd., Brendale, QLD, Australia). One CO_2 chamber was set at 400 ppm CO_2 concentration [ambient CO_2 (aCO_2)], whilst the other was set at 700 ppm CO_2 concentration (eCO_2). The average chamber temperature was maintained at 22°C day/18°C night alternating temperature with 60% humidity. Mature seeds of *A. longifolia* ssp. *longifolia* were collected from the Grampians National Park Victoria (37°12.16°S, 142°23.35°E). Two moisture levels (well-watered and drought) were also maintained in each CO_2 chamber. Twenty plastic pots (13 cm wide and 14 cm height) were filled each with 800 g of 2:1 mixture of garden soil and commercially available potting mixture. The seeds of *A. longifolia* ssp. *longifolia* were surface-scarified with sandpaper No. 1000 to remove the physical dormancy, imposed by the seed coat. Five scarified seeds were sown in each pot.

Effects on Photosynthetic Response by Drought Conditions and Elevated CO_2 Levels

Out of 20 pots, 10 pots were placed in the chamber with aCO_2 concentration, and the remaining half were placed in the chamber with eCO_2 concentration. The pots were placed in large plastic trays, and water was added to these trays to reduce the disturbance of the potting mixture until emergence occurred. At the four-leaf stage, the seedlings were thinned to two per pot. After 30 days from sowing, the first measurements of gas exchange parameters were recorded, and these measurements were termed "zero-day." Subsequently, moisture treatments of well-watered and drought were commenced. The well-watered treatments were maintained at 100% field capacity and drought treatments at 60% field capacity. These water regimes were selected as different plant species showed variable responses with eCO_2 concentration under drought conditions. The water holding capacity of the soil used in the pots was calculated according to the method suggested by Bajwa et al. (2017). Of the 10 pots in each chamber, half were subjected to well-watered, and the remaining half were subjected to drought. The pots were weighed in order to maintain the field capacity levels, and the weight of the growing plant was much smaller than that of the soil in pot. There were five replications (one pot for each replication) for each treatment, and each replication consisted of two plants. In the drought treatments, water was withheld until day 8 in both CO_2 chambers, after which drought treatment pots were re-watered to investigate the recovery response of the *A. longifolia* ssp. *longifolia* plants. The amount of water added was calculated based on pot weight, and 60% field capacity was maintained till day 10. In the well-watered treatments, water was added on alternate days. To evaluate the effect of CO_2 and drought, physiological parameters were measured using the LI-COR portable infrared CO_2 gas analyzer (LI-6400 XT portable photosynthesis system, LI-COR, Biosciences, Lincoln, Nebraska, United States). Measurements were recorded with the following adjustments of LI-COR: block temperature was set at 20°C, photosynthetic photon flux density (PPFD) was 1,000 μmol m^{-2} s^{-1}, leaf cuvette area was set at 2 cm^2, and the flow rate was adjusted at 500 μmol m^{-2} s^{-1}. The CO_2 concentration in the chamber was noted before each measurement. Net photosynthetic rate, stomatal conductance, transpiration rate, and intercellular CO_2 concentration were measured on alternate days. Water use efficiency was calculated by dividing the net photosynthetic rate with transpiration rate, intrinsic water use efficiency was calculated by dividing the net photosynthetic rate with stomatal conductance, and instantaneous carboxylation efficiency was calculated by dividing the net photosynthetic rate by the intercellular CO_2 concentration. Photosystem II (PSII) activity, such as minimum fluorescence, maximum fluorescence, quantum yield of PSII, photochemical efficiency of PSII, photochemical quenching, non-photochemical quenching, and photosynthetic electron transport rate, was calculated according to the methods described by Maxwell and Johnson (2000).

Effects on Biomass Productivity by Drought Conditions and Elevated CO_2 Levels

Growth parameters, including plant height, number of leaves, number of branches, stem diameter, leaf thickness, leaf area, leaf fresh weight, dry weight, and root-shoot fresh and dry weights, were measured at the conclusion of the experiment on day 10. Plants were removed from pots, and the stem was cut from the roots. Root fresh weight was measured after careful washing and air drying. Stem, leaves, and roots were placed in a separate paper bag and dried in an oven at 70°C for 72 h.

Statistical Analysis

Data for gas exchange parameters were presented in graphs along with the SE of each mean, and the graphs were prepared using the SigmaPlot version 11 software. To investigate the effect of time of observation (time), water conditions (water), and CO_2 levels (CO_2), physiological parameters were analyzed with Statistix version 8.1 using three-way ANOVA. All the main effects and two- and three-way interactions were examined using the Tukey's honestly significant difference (HSD) test at a 5% probability level. Data of growth parameters were subjected to two-way ANOVA to assess the effect of CO_2 concentrations and water regimes on the growth of *A. longifolia* ssp. *longifolia*. Five replications (two plants per pot) were used for each combination of treatments. The significance among the treatment means was separated by using the Tukey's HSD at $p \leq 0.05$.

RESULTS

Effects on Photosynthetic Response by Drought Conditions and Elevated CO_2 Levels

Photosynthetic activities were measured for *A. longifolia* ssp. *longifolia* when grown under two moisture regimes (i.e., well-watered and drought) at 400 ppm CO_2 concentration (aCO_2 concentration) and 700 ppm CO_2 concentration (eCO_2 concentration). **Figure 1A** shows that eCO_2 concentration increased the net photosynthetic rate by 2–4 μmol CO_2 m^{-2} s^{-1} when compared to that with aCO_2 concentration under well-watered conditions. However, a variable response was noted with both CO_2 concentrations when *A. longifolia* ssp. *longifolia* was grown under drought conditions. At aCO_2 concentration, the net photosynthetic rate decreased to 0.07 μmol CO_2 m^{-2} s^{-1} at day 8, whilst plants under eCO_2 concentration recorded a net photosynthetic rate of 6.17 μmol CO_2 m^{-2} s^{-1} on the same day. After all these measurements, water was added to the drought treatments on day 8 to investigate the recovery response of the plants in terms of the net photosynthetic rate. Photosynthesis was recovered at a high rate with eCO_2 and increased from 6.17 to 9.8 μmol CO_2 m^{-2} s^{-1}, whilst under aCO_2 concentration, it increased from 0.17 to 5.1 μmol CO_2 m^{-2} s^{-1} (**Figure 1A**). The ANOVA results showed that time (p = 0.001), water ($p < 0.001$), CO_2 ($p < 0.001$), time × water (p = 0.001), and time × CO_2 (p = 0.001) were significant for photosynthetic rate of *A. longifolia*, whereas the interaction of water × CO_2 and time × water × CO_2 was non-significant (**Table 1**).

A. longifolia ssp. *longifolia* exhibited a significant difference in stomatal conductance under eCO_2 and aCO_2 concentrations (**Figure 1B**). eCO_2 inhibited the stomatal conductance compared to that with aCO_2 under well-watered conditions. Drought stress resulted in a progressive decline in stomatal conductance up to day 8 with aCO_2 (0.009 mol H_2O m^{-2} s^{-1}). However, this decline was less with eCO_2, since 0.027 mol H_2O m^{-2} s^{-1} stomatal conductance was recorded on day 8. After the addition of water to drought treatments on day 8, stomatal conductance recovered slightly, but this recovery was larger with eCO_2 than that with aCO_2. The results of ANOVA in **Table 1** indicate that the stomatal conductance *of A. longifolia* spp. *longifolia* in response to time, water, CO_2, and time × water was significant ($p < 0.04$).

The eCO_2 concentration inhibited the transpiration rate under well-watered conditions compared to that with aCO_2 (**Figure 1C**). The transpiration rate reduced progressively with an increase in the duration of drought under both CO_2 regimes.

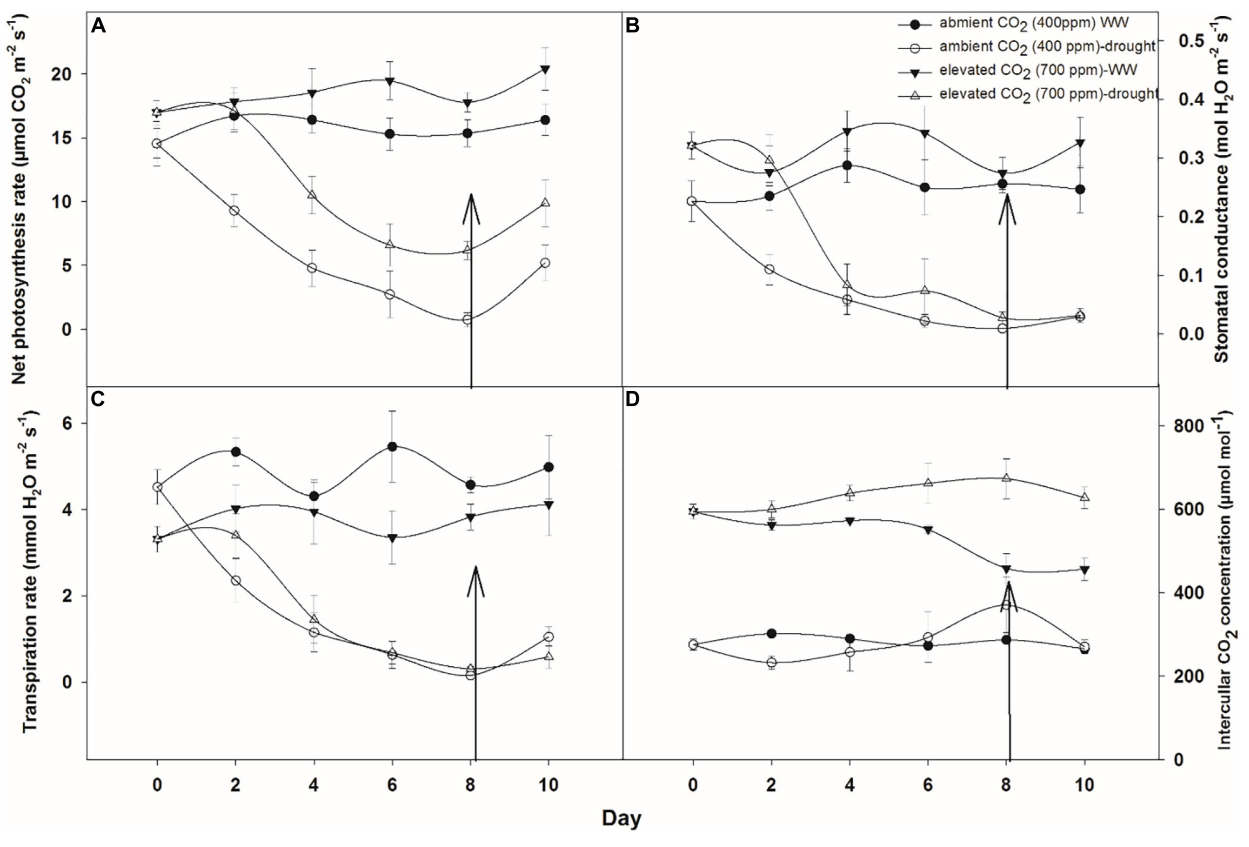


FIGURE 1 | Effect of CO_2 concentrations and moisture conditions on photosynthetic rate **(A)**, stomatal conductance **(B)**, transpiration rate **(C)**, and intercellular CO_2 concentration **(D)** of *A. longifolia* ssp. *longifolia*. Nail on the data point represents the SE of the mean, and vertical arrow line after day 8 represents the addition of water in the drought treatments. WW, well-watered.

TABLE 1 | Statistical significances for physiological parameters of *A. longifolia* ssp. *longifolia* in response to time of observation, water conditions, and CO_2 levels.

Parameter	Time		Water		CO_2		Time × water		Time × CO_2		Water × CO_2		Time × water × CO_2	
	p-value	HSD at 0.05	*p*-value	HSD at 0.05	*p*-value	HSD at 0.05	*p*-value	HSD at 0.05	*p*-value	HSD at 0.05	*p*-value	HSD at 0.05	*p*-value	HSD at 0.05
Photosynthetic rate	0.001	3.82	0.000	1.51	0.000	1.50	0.000	6.22	0.001	6.22	0.466	2.80	0.158	9.83
Stomatal conductance	0.000	0.06	0.000	0.02	0.196	0.03	0.000	0.11	0.372	0.10	0.062	0.05	0.005	0.17
Transpiration rate	0.000	0.95	0.000	0.37	0.580	0.38	0.000	1.55	0.383	1.55	0.010	0.70	0.033	2.45
Intercellular CO_2 concentration	0.000	74.6	0.000	29.41	0.000	29.41	0.000	121.55	0.000	121.55	0.000	54.80	0.000	192.15
Water use efficiency	0.050	23.19	0.791	9.14	0.041	9.13	0.045	37.76	0.123	37.75	0.107	17.03	0.231	59.70
Intrinsic water use efficiency	0.02	365.9	0.910	144.21	0.043	144.22	0.272	595.90	0.182	595.80	0.083	268.70	0.309	942.12
Instantaneous carboxylation efficiency	0.893	0.001	0.080	0.001	0.103	0.001	0.105	0.001	0.120	0.001	0.102	0.001	0.098	0.001
Photosynthetic electron transport rate	0.017	23.50	0.000	9.26	0.412	9.26	0.000	38.26	0.110	38.27	0.356	17.25	0.858	60.49
Minimum fluorescence	0.003	37.35	0.487	4.71	0.050	4.72	0.471	60.82	0.066	60.82	0.081	27.42	0.940	96.15
Maximum fluorescence	0.000	113.99	0.000	44.99	0.042	44.91	0.133	185.61	0.445	185.61	0.185	83.68	0.911	293.40
Quantum yield of PSII	0.016	0.55	0.000	0.02	0.040	0.02	0.000	0.09	0.011	0.09	0.359	0.04	0.852	0.14
Photochemical efficiency of PSII	0.000	0.05	0.000	0.02	0.050	0.02	0.024	0.08	0.621	0.09	0.160	0.03	0.916	0.13
Photochemical quenching	0.000	0.08	0.000	0.03	0.062	0.03	0.000	0.14	0.008	0.14	0.230	0.06	0.741	0.22
Non-photochemical quenching	0.000	0.24	0.000	0.09	0.310	0.09	0.037	0.39	0.618	0.39	0.880	0.17	0.674	0.62

During the initial days of drought stress, transpiration did not reduce significantly with eCO_2, whilst aCO_2 reduced the transpiration rate linearly, and it was measured at 0.6 mmol H_2O m^{-2} s^{-1} on the 8th day of observation. The addition of water to drought treatments after the 8th day of observation resulted in higher recovery (from 0.6 to 1.0 4 mmol H_2O m^{-2} s^{-1}) in the transpiration rate of *A. longifolia* ssp. *longifolia* with aCO_2, compared to that when grown under eCO_2. Response of transpiration rate of *A. longifolia* spp. *longifolia* to time, water, time × water, and water × CO_2 was significant (**Table 1**).

When *A. longifolia* ssp. *longifolia* was grown under well-watered conditions, eCO_2 caused an increase in intracellular CO_2 concentration, being recorded between 450 and 590 μmol mol^{-1} compared with aCO_2 where intercellular CO_2 concentration was between 270 and 300 μmol mol^{-1} (**Figure 1D**). Drought stress exerted significant effects on intercellular CO_2 concentration, and it increased with an increase in drought duration under both CO_2 concentrations, attaining maximum value on the 8th day of measurement. An increase in intracellular CO_2 concentration was higher with eCO_2 compared to that with aCO_2. The addition of water to drought treatments on the 8th day slightly reduced the value of intercellular CO_2 concentration, whilst it was significantly reduced under aCO_2 with the addition of water. The ANOVA results showed that the main effects (time, water, and CO_2) and two-way or three-way interactions for intracellular CO_2 concentration were significant ($p < 0.02$).

Under well-watered conditions, eCO_2 increased the water use efficiency by 0.76 mmol CO_2 mol^{-1} H_2O in comparison with that with aCO_2, whereas the effects of drought on water use efficiency of *A. longifolia* ssp. *longifolia* were different under both CO_2 concentrations. eCO_2 linearly increased the water use efficiency and recorded a maximum on the 8th day of measurement (21.6 mmol CO_2 mol^{-1} H_2O). Whilst drought conditions reduced the water use efficiency of *A. longifolia* ssp. *longifolia* when grown under aCO_2, the recorded minimum water use efficiency (0.038 mmol CO_2 mol^{-1} H_2O) was measured on the 8th day. The addition of water to drought treatments when grown under aCO_2 recovered the water use efficiency by 4.09 mmol CO_2 mol^{-1} H_2O till the 10th day of measurement. In contrast to aCO_2, the recovery in water use efficiency did not occur with eCO_2, and it was reduced with the addition of water to drought treatments when grown under eCO_2 concentration (**Figure 2A**). The ANOVA results showed that the effect of time, CO_2, and time × water on water use efficiency of *A. longifolia* spp. *longifolia* was significant (**Table 1**).

Intrinsic water use efficiency of *A. longifolia* ssp. *longifolia* was the same under both CO_2 concentrations when grown under well-watered conditions (**Figure 2B**). However, the effect of drought was different for intrinsic water use efficiency under

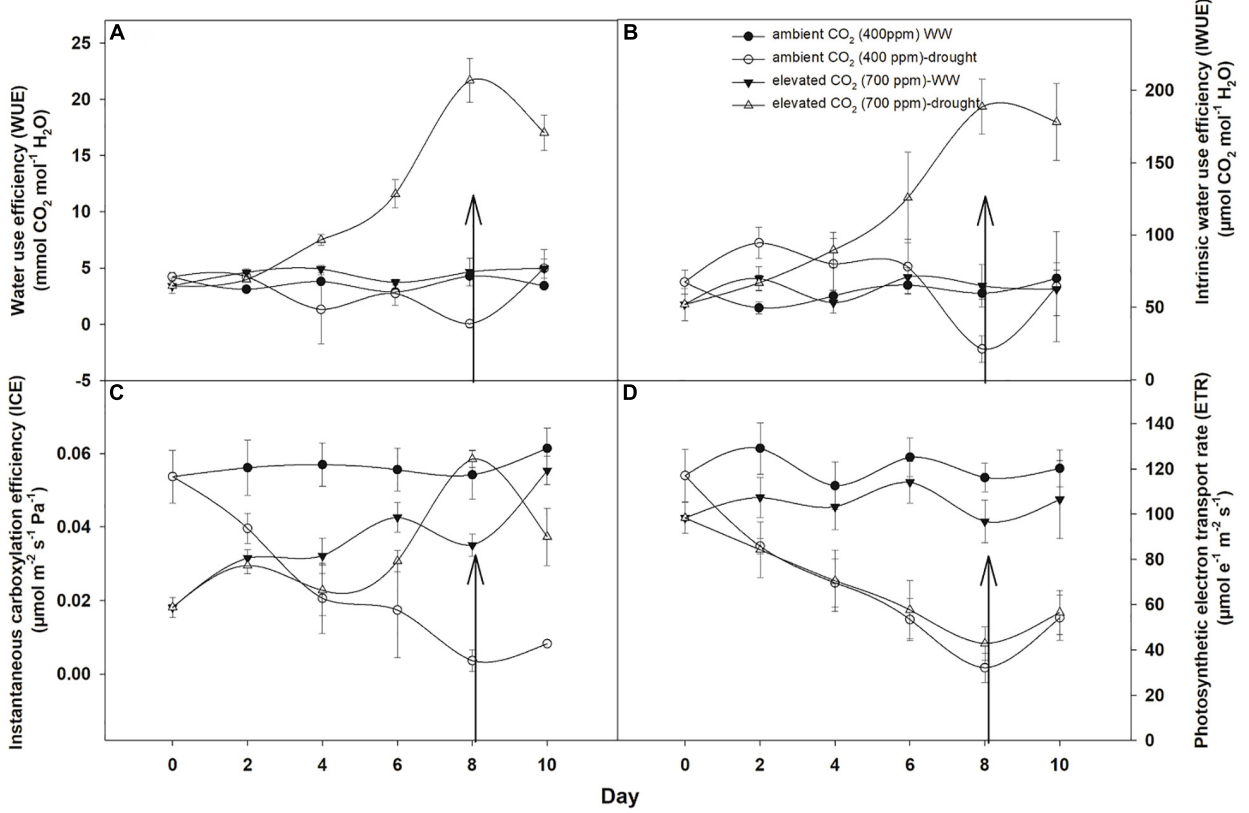


FIGURE 2 | Effect of CO_2 concentrations and moisture conditions on water use efficiency **(A)**, intrinsic water use efficiency **(B)**, instantaneous carboxylation efficiency **(C)**, and photosynthetic electron transport rate **(D)** of *A. longifolia* ssp. *longifolia*. Nail on the data point represents the SE of the mean, and vertical arrow line after day 8 represents the addition of water in the drought treatments. WW, well-watered.

both CO_2 concentrations. eCO_2 in drought conditions increased the intrinsic water use efficiency linearly up to the 8th day of measurement. Whilst aCO_2 sustained the intrinsic water use efficiency under drought conditions till the 6th day of measurement, after this time, the intrinsic water use efficiency decreased to a minimum value (21.1 µmol CO_2 mol^{-1} H_2O). The addition of water to the drought treatments had no effects in terms of recovery of intrinsic water use efficiency of *A. longifolia* ssp. *longifolia* when grown under eCO_2. In contrast, significant recovery in intrinsic water use efficiency was noted for aCO_2 with the addition of water on the 8th day of measurement (**Figure 2B**). The ANOVA showed that the effect of time ($p = 0.02$) and CO_2 ($p = 0.04$) on intrinsic water use efficiency was significant.

Instantaneous carboxylation efficiency of *A. longifolia* ssp. *longifolia* was higher with aCO_2 than that with eCO_2 when grown under well-watered conditions (**Figure 2C**). Drought stress had variable effects on instantaneous carboxylation efficiency under both CO_2 concentrations. eCO_2 under drought conditions had no effects on instantaneous carboxylation efficiency up to the 4th day of observation. Subsequently, it increased the instantaneous carboxylation efficiency and recorded the maximum value (0.05 µmol m^{-2} s^{-1} Pa^{-1}) on the 8th day of measurement. This contrasts with aCO_2 under drought conditions, which progressively decreased the instantaneous carboxylation efficiency with an increase in drought duration. The addition of water to drought treatments when grown under eCO_2 decreased the instantaneous carboxylation efficiency, while the addition of water to aCO_2 treatment did not affect instantaneous carboxylation efficiency (**Figure 2C**). According to the results of ANOVA, the effect of time, water, and CO_2 on instantaneous carboxylation efficiency was non-significant.

Under well-watered conditions, the photosynthetic electron transport rate was higher with aCO_2 concentration than that with eCO_2 concentration (**Figure 2D**). Drought significantly affected the photosynthetic electron transport efficiency with every increment in the drought days, and the photosynthetic electron transport rate reached a minimum value (32 µmol e^{-1} m^{-2} s^{-1} for aCO_2 and 42 µmol e^{-1} m^{-2} s^{-1} for eCO_2) on the 8th day of measurement under both CO_2 concentrations. The addition of water to drought treatments recovered the photosynthetic electron transport rate under both CO_2 concentrations. The photosynthetic electron transport rate of *A. longifolia* spp. *longifolia* was significant in response to time and CO_2; however, all the interactions were non-significant (**Table 1**).

The minimum and maximum fluorescence values of *A. longifolia* ssp. *longifolia* when grown under well-watered conditions were higher with eCO_2 compared to those with aCO_2

(**Figures 3A,B**). The effect of drought was more pronounced on minimum fluorescence under eCO_2 as fluorescence decreased linearly till the 8th day of observation with an increase in drought duration under eCO_2. In comparison, aCO_2 under drought conditions had no effects on minimum fluorescence till the 6th day of observation, and after that, it began to reduce on day 8 (**Figure 3A**). The addition of water to drought treatments recovered the minimum fluorescence for both CO_2 concentrations. Maximum fluorescence under drought conditions was higher with eCO_2 when compared to that with aCO_2, and a decline in maximum fluorescence occurred in both CO_2 concentrations with an increase in drought duration till the 8th day of measurement. The addition of water to drought treatments slightly recovered the maximum fluorescence in both CO_2 concentrations (**Figure 2D**). The effect of time ($p = 0.003$) and CO_2 ($p = 0.05$) on minimum fluorescence was significant, whereas the effect of time ($p < 0.001$), water ($p < 0.001$), and CO_2 ($p = 0.042$) on maximum fluorescence was significant (**Table 1**).

The quantum yield of PSII was relatively higher when *A. longifolia* ssp. *longifolia* was grown under aCO_2 in well-watered conditions (**Figure 3C**). Drought stress decreased the yield progressively in both CO_2 concentrations. eCO_2 slightly mitigated the adverse effects of drought on the quantum yield of PSII as the yield was 0.1 on the 8th day of measurement compared to that with aCO_2 where it was 0.07 on the same day (**Figure 3C**). The addition of water to drought treatments recovered the yield in the same way for both CO_2 concentrations. The ANOVA table showed that time ($p = 0.016$), water ($p < 0.001$), CO_2 ($p = 0.040$), time × CO_2 ($p < 0.001$), and time × water ($p = 0.011$) have significant effects on quantum yield of PSII (**Table 1**). Under well-watered conditions, the photochemical efficiency of PSII was significantly higher with eCO_2 compared to that with aCO_2 throughout the observation period (days 0–10) (**Figure 3D**). Data showed that eCO_2 mitigated the adverse effects of drought on the photochemical efficiency of PSII as no decline in photochemical efficiency of PSII occurred until day 4, and after that, the photochemical efficiency of PSII slightly reduced till the 8th day of observation. The drought had drastic effects on the photochemical efficiency of PSII under aCO_2 which decreased to 0.34. However, the addition of water to drought treatments when grown under aCO_2 recovered the photochemical efficiency of PSII significantly compared to that in eCO_2 (**Figure 3D**). The ANOVA table showed that time ($p < 0.001$), water ($p < 0.001$), CO_2 ($p = 0.050$), and time × CO_2 ($p = 0.024$) have significant effects on the photochemical efficiency of PSII (**Table 1**).

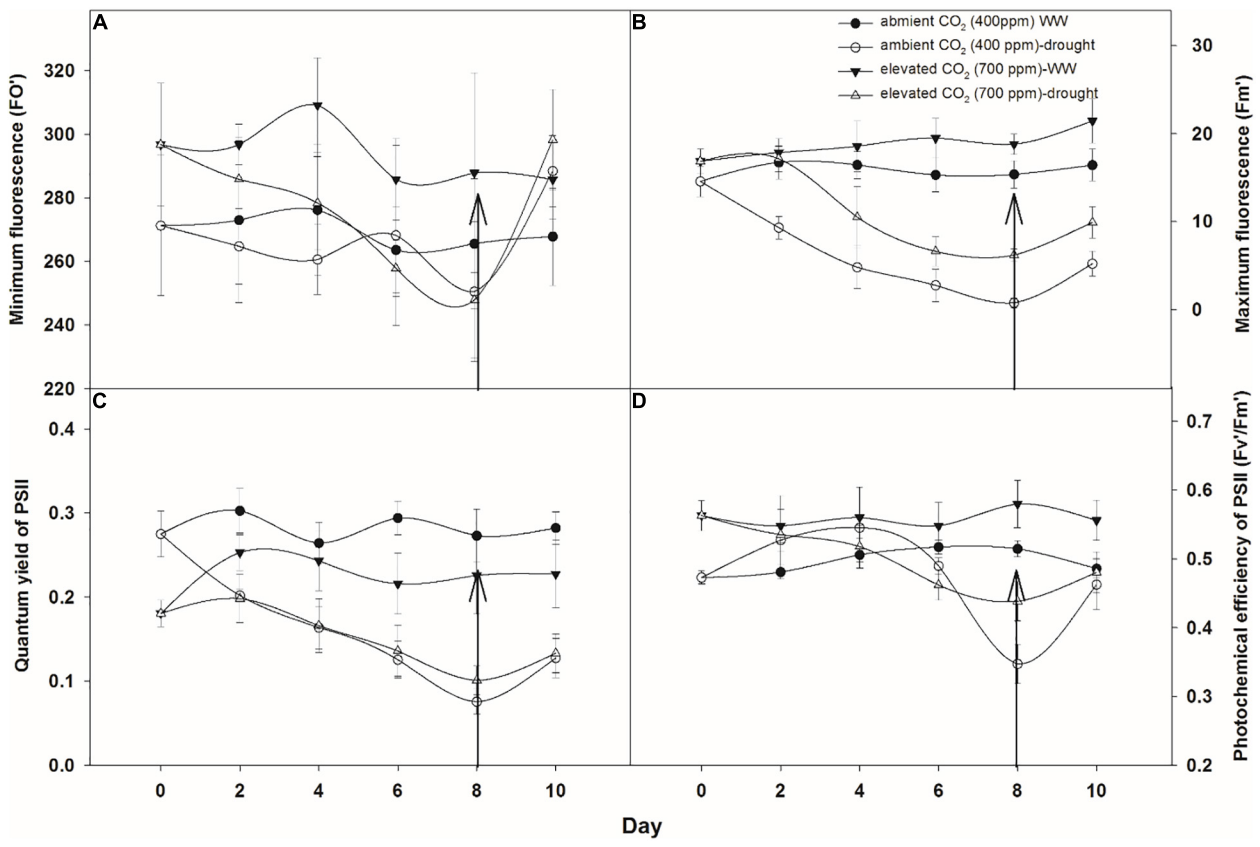


FIGURE 3 | Effect of CO_2 concentrations and moisture conditions on minimum fluorescence **(A)**, maximum fluorescence **(B)**, quantum yield of photosystem II (PSII) **(C)**, and photochemical efficiency of PSII **(D)** of *A. longifolia* ssp. *longifolia*. Nail on the data point represents the SE of the mean, and vertical arrow line after day 8 represents the addition of water in the drought treatments. WW, well-watered.

Photochemical and non-photochemical quenching was higher with aCO_2 when *A. longifolia* ssp. *longifolia* was grown under well-watered conditions (**Figures 4A,B**). eCO_2 mitigated the adverse effects of drought on photochemical quenching, and a decline in this parameter was less with an increase in drought duration as compared to that with aCO_2. eCO_2 had no effects on non-photochemical quenching under drought conditions. The addition of water to drought treatments recovered the photochemical and non-photochemical quenching under both CO_2 concentrations (**Figures 4A,B**). The results of ANOVA indicated that the effect of time, water, and time × water was significant on photochemical and non-photochemical quenching of *A. longifolia* (**Table 1**).

Effects on Biomass Productivity by Drought Conditions and Elevated CO_2 Levels

Plant height was significantly affected by water regimes and CO_2 concentrations (**Figure 5A**). eCO_2 produced 6.4 cm taller plants (25.1 cm) of *A. longifolia* ssp. *longifolia* under well-watered conditions compared with aCO_2 (18.7 cm). Under drought conditions, eCO_2 mitigated the adverse effects of drought on the height of *A. longifolia* ssp. *longifolia* and recorded 21.1 cm taller plants. Plants subjected to drought when grown under aCO_2 attained a height of only 13.6 cm. Under well-watered conditions, the number of leaves per plant was statistically the same with both CO_2 concentrations. Stem diameter was not improved with eCO_2 under well-watered conditions in comparison with aCO_2, whilst eCO_2 enhanced the stem diameter by 0.3 mm when grown under drought conditions (**Figure 5B**). Drought significantly affected the number of leaves per plant under both CO_2 concentrations, but eCO_2 slightly improved the number of leaves by mitigating the drought effects, hence, producing four more leaves than that with aCO_2 (**Figure 5C**). The number of branches was the same for both CO_2 concentrations under well-watered conditions (**Figure 5D**). However, eCO_2 mitigated the adverse effects of drought and produced a higher number of branches per plant (4.2) compared to that with aCO_2 where branches (3.2) were produced under drought conditions. Drought stress affected the leaf thickness and leaf area per plant under both CO_2 concentrations, and this effect was more when plants were grown under aCO_2 (**Figures 6A,B**). The effect of eCO_2 was significant for leaf thickness and non-significant for leaf area per plant when *A. longifolia* ssp. *longifolia* was grown under well-watered conditions. eCO_2 increased the plant height, stem diameter, number of leaves, and number of branches by 34, 12, 13, and 6%, respectively, over aCO_2 under well-watered conditions. In contrast, under drought conditions, an increase of 55, 10, 31, and 31% in plant height, stem diameter, number of leaves, and number of branches, respectively, was observed with eCO_2 over aCO_2 (data not shown).

Leaf fresh weight was significantly affected by water regimes, and drought caused the lowest fresh weight of leaves per plant (4.8 g) under aCO_2 (**Figure 6C**). Leaf dry weight was significantly affected by water regimes and CO_2 concentrations. eCO_2 produced higher leaf dry weight under both water conditions when compared to that with aCO_2 (**Figure 6D**). The effect of water regimes and CO_2 concentrations was significant for root fresh weight per plant of *A. longifolia* ssp. *longifolia* (**Figure 7A**). eCO_2 recorded maximum fresh weight of root when grown under well-watered conditions. However, eCO_2 did not enhance the root fresh weight under drought conditions in comparison with that of aCO_2. Root dry weight was also enhanced by eCO_2 when *A. longifolia* ssp. *longifolia* was grown under well-watered conditions (**Figure 7B**). The effect of water conditions and CO_2 concentrations was non-significant for the shoot fresh and shoot dry weights of *A. longifolia* ssp. *longifolia* (**Figures 7C,D**). eCO_2 increased the leaf fresh weight, leaf dry weight, root fresh weight, and root dry weight by 18, 19, 77, and 25% under well-watered conditions and 8, 57, 39, and 38% under drought conditions, respectively, over aCO_2 (data not shown).

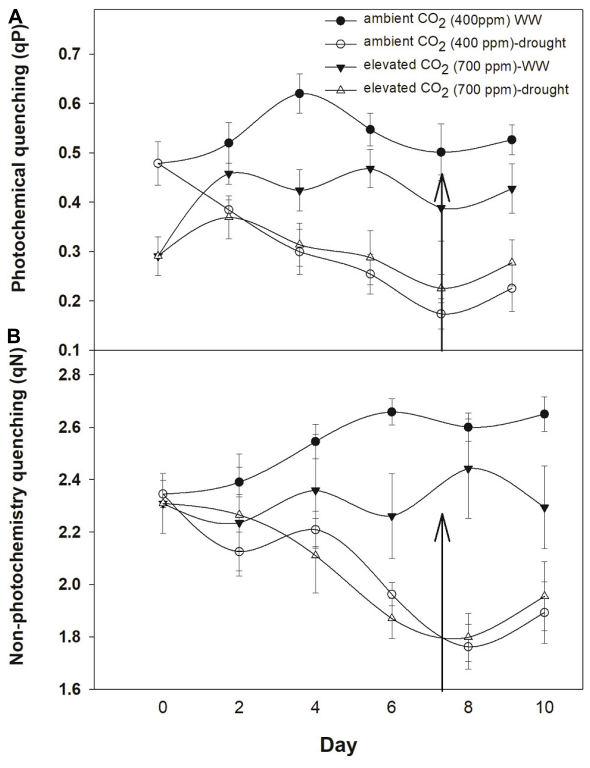


FIGURE 4 | Effect of CO_2 concentrations and moisture conditions on photochemical quenching **(A)** and non-photochemical quenching **(B)** of *A. longifolia* ssp. *longifolia*. Nail on the data point represents the SE of the mean, and vertical arrow line after day 8 represents the addition of water in the drought treatments. WW, well-watered.

DISCUSSION

eCO_2 and drought stress are the main components of climate change that directly affect the physiology and morphology of plants (Lobell and Gourdji, 2012; Salazar-Parra et al., 2012; Chadha et al., 2020; Dawood et al., 2021). This study exhibits that CO_2 concentrations (ambient at 400 ppm

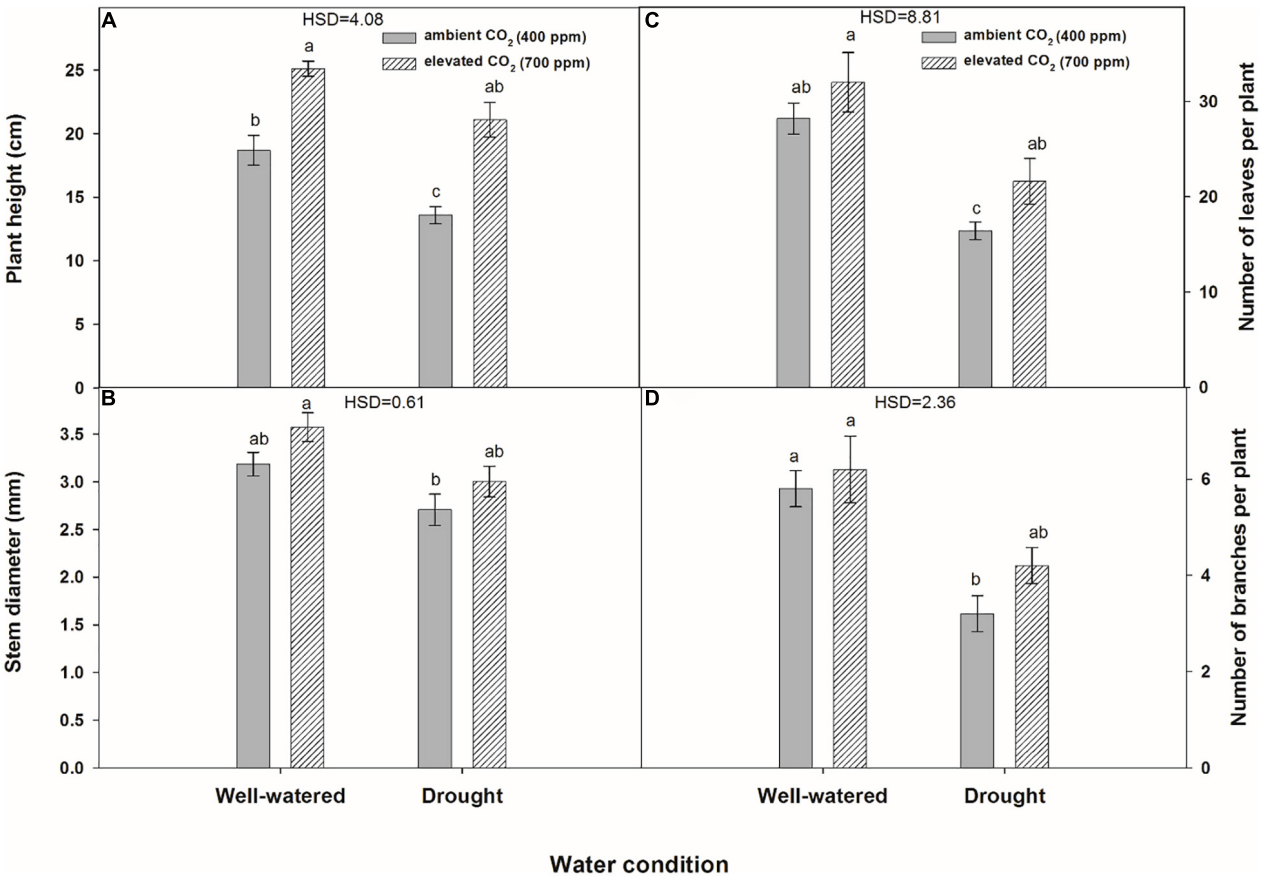


FIGURE 5 | Effect of CO_2 concentrations and moisture conditions on plant height **(A)**, stem diameter **(B)**, number of leaves per plant **(C)**, and number of branches per plant **(D)** of *A. longifolia* ssp. *longifolia*. Nail on the bar represents the SE of the mean.

and elevated at 700 ppm) had variable effects on gas exchange, water use efficiency, PSII activities, and growth of *A. longifolia* ssp. *longifolia* when grown under well-watered and drought conditions. Drought conditions had negative effects on photosynthetic activity, water use efficiency, and growth of *A. longifolia* ssp. *longifolia*, but eCO_2 mitigated the adverse effects of drought on the physiological and morphological parameters of this plant. Prior study showed that drought stress causes various responses of photosynthetic mechanisms depending upon species (Prieto et al., 2009; Weller et al., 2020). Furthermore, leaf photosynthesis is generally believed to increase with eCO_2 even under stressful environments (Meibaum et al., 2012). In our study, the net photosynthetic rate of *A. longifolia* ssp. *longifolia* leaves increased by 12% with eCO_2. According to Evans et al.'s (2000) study on growth and gas exchange, measurements of nine *Acacia* species were recorded to be enhanced under 700 $\mu l\ L^{-1}$ CO_2 concentration. A study by Ibrahim et al. (2020) reported that *Acacia mangium* was well adapted to higher temperatures and eCO_2 compared to native health forest species, including *Buchanania arborescens* Blume, *Dillenia suffruticosa* Martelli, *Calophyllum inophyllum* L., and *Ploiarium alternifolium* Melch. eCO_2 induced a low transpiration rate under well-watered and drought conditions. The decline in transpiration rate might have been due to the stomatal closure as a result of the effect of eCO_2 and drought. It is postulated that eCO_2 increases cytosolic-free calcium within guard cells, which may act as a messenger in the signal transduction pathway for maintaining the turgor pressure of the guard cells (Kim et al., 2010). Low transpiration rate and stomatal conductance of *A. longifolia* ssp. *longifolia* under eCO_2 conserve soil moisture (Habermann et al., 2019), and this increases the net photosynthetic rate and growth under eCO_2. Soil moisture conservation in other species exposed to eCO_2 has been observed (Wullschleger et al., 2002; Qaderi et al., 2013; Miranda-Apodaca et al., 2018; Dikšaitytė et al., 2019). According to Yu et al. (2012), plants grown under eCO_2 in drought conditions resulted in greater stomatal closure than that of the plants grown under aCO_2. A study by Weller et al. (2021) showed that stomatal conductance of *Amaranthus retroflexus* L. (redroot pigweed) was reduced under eCO_2. Furthermore, eCO_2 reduced the drought-induced damage, and plant recovery was notable upon re-watering the plants grown under water stress. However, in previous studies, it was noted that the degree of recovery depends upon species and duration of drought, as barley plants were not able to recover stomatal closure when plants were re-watered after 16 days of drought stress under eCO_2 (Robredo et al., 2007). In our study, stomatal conductance of *A. longifolia*

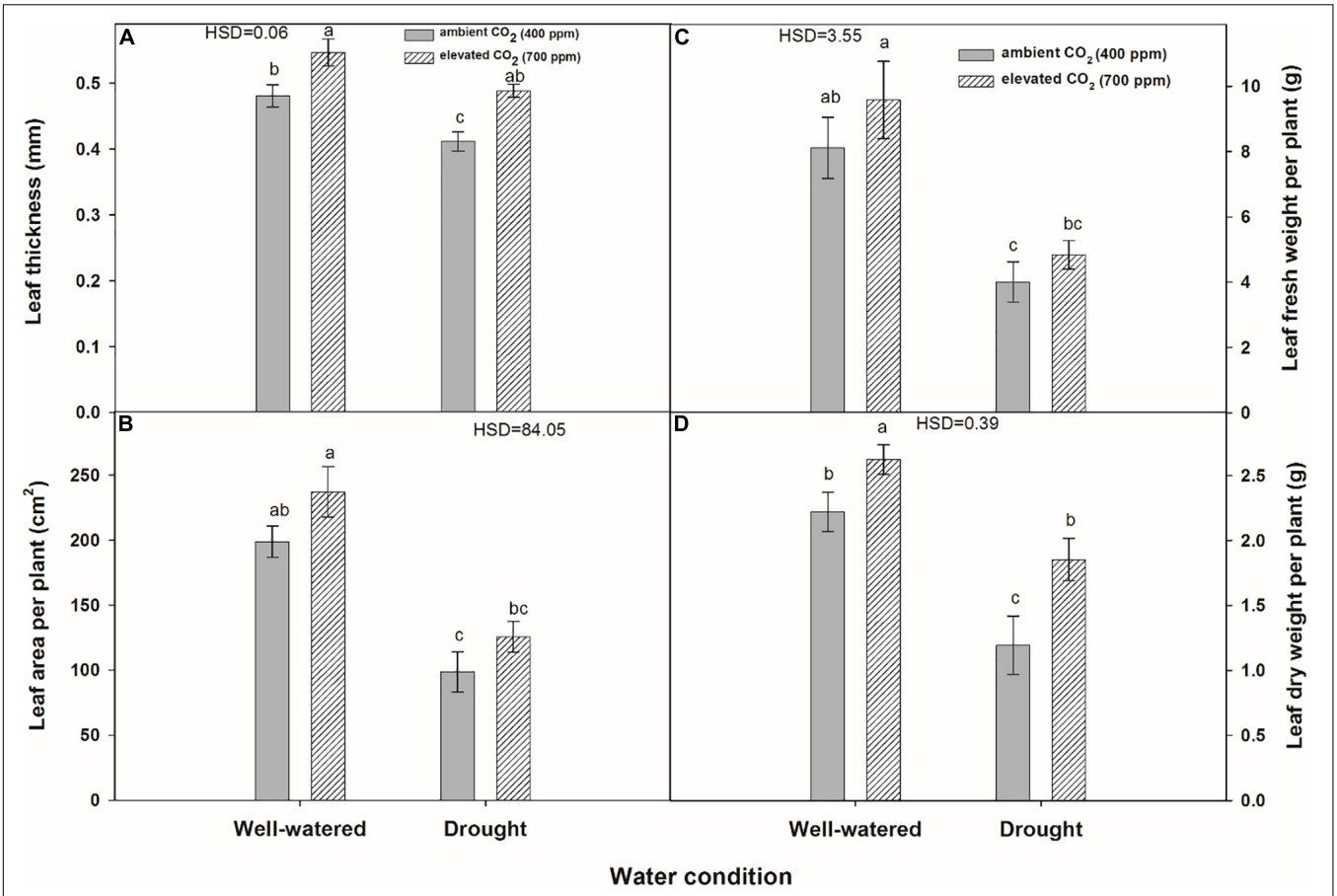


FIGURE 6 | Effect of CO_2 concentrations and moisture conditions on leaf thickness **(A)**, leaf area per plant **(B)**, leaf fresh weight per plant **(C)**, and leaf dry weight per plant **(D)** of *A. longifolia* ssp. *longifolia*. Nail on the bar represents the SE of the mean.

ssp. *longifolia* was recovered with the addition of water to drought-treated plants. In contrast, higher transpiration rate and stomatal conductance of *A. longifolia* ssp. *longifolia* under aCO_2 with both moisture conditions caused a faster decrease in soil moisture contents which affected the photosynthesis activity and growth of the plant. These findings share some similarities with tall fescue, in which a lower stomatal conductance was observed under drought conditions in the aCO_2 treatment (Yu et al., 2012). Furthermore, our findings are inconsistent with those of Robredo et al. (2007) who concluded that under eCO_2, water stress was developed more slowly due to a slower rate of moisture depletion. Intercellular CO_2 concentration was increased with an increase in drought duration, and this showed higher increase with eCO_2, which could have been due to the combined effect of eCO_2 and drought, thereby causing stomatal closure. Conversely, our findings are in line with those of Robredo et al. (2007) and Wang et al. (2015) who reported that eCO_2 caused stomatal closure with high intercellular CO_2 concentration at 700 ppm, which led to a higher rate of carbon assimilation.

Under well-watered conditions, water use efficiency of *A. longifolia* ssp. *longifolia* increased by 0.75 mmol CO_2 mol^{-1} H_2O under eCO_2 in comparison with that of aCO_2. Water use efficiency was seen to be further enhanced when plants were grown under drought conditions. This might have been the result of decreased transpiration rate under eCO_2. Previous studies have shown that eCO_2 increased water use efficiency by lowering the transpiration rate and moisture depletion at eCO_2 (Schmid et al., 2016; Tom-Dery et al., 2019; Hebbar et al., 2020; Ma et al., 2020). For example, photosynthetic activities and water use efficiency of invasive *A. mangium* were reported to be stimulated by eCO_2 when compared to that with native *B. arborescens* and *D. suffruticosa* (Ibrahim et al., 2020). Therefore, regarding the increase in water use efficiency of *A. longifolia* ssp. *longifolia* under eCO_2, our results are supported by Saxe et al. (1998) and Gilbert et al. (2011) who reported that intrinsic water use efficiency increased by 25–30% as a result of reduced stomatal conductance and enhanced photosynthetic rate under eCO_2. Soil moisture conservation due to eCO_2 concentration has been observed in other species (Wullschleger et al., 2002; Madhu and Hatfield, 2013; Kimball, 2016), and this may reduce the impact of limited water conditions on growth (Reddy et al., 2010). Our results are in accordance with the findings of Pérez-López et al. (2013) and Wang et al. (2015) who reported that instantaneous carboxylation efficiency declined with eCO_2.

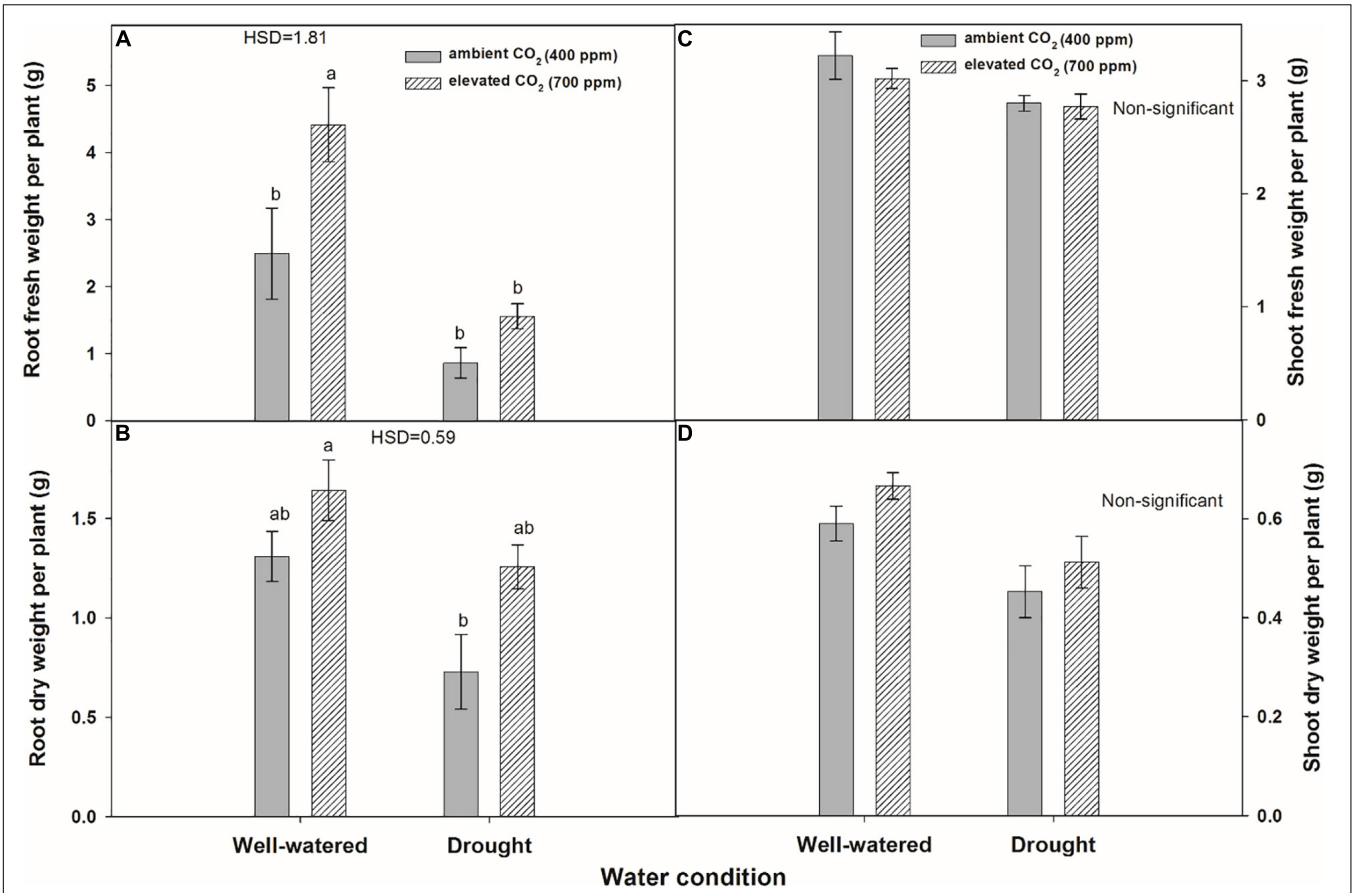


FIGURE 7 | Effect of CO_2 concentrations and moisture conditions on root fresh weight per plant **(A)**, root dry weight per plant **(B)**, shoot fresh weight per plant **(C)**, and shoot dry weight per plant **(D)** of *A. longifolia* ssp. *longifolia*. Nail on the bar represents the SE of the mean.

Drought significantly affected the photosynthetic electron transport rate under both CO_2 concentrations, but this decline was less marked with eCO_2. A higher rate of photosynthetic electron transport occurring in a drought stress environment coupled with eCO_2 was also reported by Kitao et al. (2007). Drought stress decreased the quantum yield of PSII, whilst eCO_2 mitigated the adverse effects of drought on the quantum yield of PSII in our study. Similarly, the photochemical efficiency of PSII was also increased with eCO_2, which led to the conclusion that a CO_2-enriched environment reduces the risk of damage by drought stress. These findings are also supported by Perveen et al. (2010), Zhao et al. (2010), and Wang et al. (2018) who showed that eCO_2 decreased the quantum yield of PSII and increased the photochemical efficiency of PSII. Drought stress caused a decline in photochemical quenching; however, eCO_2 reduced the rate of decline even with an increase in drought duration. This suggested that eCO_2 reduced the risk of photoinhibition (Arena et al., 2011).

Water stress generally has negative effects on plant growth, but under eCO_2, growth appears to have a positive effect (Serret et al., 2018). The interactive effect of drought and eCO_2 is important to consider when predicting the effects of climate change on plant species (Martínez-Carrasco et al., 2005; Battaglia and Bruce, 2017). Our results showed that eCO_2 significantly increased plant height, number of leaves, stem diameter, leaf thickness, leaf area, leaf dry weight, and root dry weight of *A. longifolia* ssp. *longifolia* when compared to aCO_2 under both moisture conditions. This enhanced growth with eCO_2 might have been due to increased photosynthesis and water use efficiency, and reduced stomatal conductance resulting in decreased transpiration rate. Ziska et al. (2019) predicted that plant biomass would increase as a result of increased photosynthetic rate and water use efficiency. The reports of Qaderi et al. (2006) showed that eCO_2 increased the availability of building blocks for the production of proteins and structural molecules, which increased the leaf area and specific leaf mass. This was supported by the observation that plants grown under aCO_2 and water stress had the lowest biomass productions. Previous studies have shown that eCO_2 alleviated the drought impacts by reinforcement in CO_2 uptake, decreasing the oxidative pressure in the chloroplast electron transport chain, changing the biomass accumulation, and altering the partitioning to favor water acquisition. All these changes enable the plants to cope more effectively with water shortages (Avila et al., 2020). Another study demonstrated that

drought-imposed limitations on photosynthesis were based on a significant decrease in stomatal conductance and intercellular concentration (Salmon et al., 2020). Given that the increased photosynthesis under eCO_2 resulted in more ATP use for ribulose 1,5-bishosphate (RuBP) regeneration (López-Calcagno et al., 2020). eCO_2 levels also improve the allometric adjustment linked to drought tolerance (Avila et al., 2020). The aggressive nature of *A. longifolia* ssp. *longifolia* for growth under eCO_2 will affect the growth and wellbeing of native species by altering the ecosystem and introducing direct competition for resources in a new environment.

CONCLUSION

This study reveals that eCO_2 improved the photosynthetic activity, water use efficiency, and general growth parameters of *A. longifolia* ssp. *longifolia* under both well-watered and drought conditions. Therefore, this species is able to compensate for a lack of soil moisture with greater growth of its root and shoot, and it takes an advantage of eCO_2 to increase overall biomass. This ability to grow under limited water availability with eCO_2 indicated that this species will be able to adapt to new environments even under severe variation in climatic conditions, and foreshadows its likelihood of invasion into new areas. This species has a potential threat to the ecosystem in future due to changing climatic conditions.

DATA AVAILABILITY STATEMENT

The raw data supporting the conclusions of this article will be made available by the authors, without undue reservation.

AUTHOR CONTRIBUTIONS

SKF conceived and designed the study. MMJ conducted the experiments. All authors were involved in writing, reviewing the manuscript.

FUNDING

This publication was supported by the Natural Science Basic Research Program of Shaanxi Province (Grant No. 2018JQ5218) and the National Natural Science Foundation of China (Grant No. 51809224) of the Top Young Talents of Shaanxi Special Support Program.

SUPPLEMENTARY MATERIAL

The Supplementary Material for this article can be found online at: https://www.frontiersin.org/articles/10.3389/fpls.2022.817730/full#supplementary-material

REFERENCES

Alba, C., Fahey, C., and Flory, S. L. (2019). Global change stressors alter resources and shift plant interactions from facilitation to competition over time. *Ecology* 100:e02859. doi: 10.1002/ecy.2859

Arena, C., Vitale, L., and De Santo, A. V. (2011). Influence of irradiance on photosynthesis and PSII photochemical efficiency in maize during short-term exposure at high CO_2 concentration. *Photosynthetica* 49, 267–274. doi: 10.1007/s11099-011-0034-y

Avila, R. T., de Almeida, W. L., Costa, L. C., Machado, K. L., Barbosa, M. L., de Souza, R. P., et al. (2020). Elevated air [CO_2] improves photosynthetic performance and alters biomass accumulation and partitioning in drought-stressed coffee plants. *Environ. Exper. Bot.* 177:104137. doi: 10.1016/j.envexpbot.2020.104137

Bajwa, A. A., Chauhan, B. S., and Adkins, S. (2017). Morphological, physiological and biochemical responses of two Australian biotypes of *Parthenium hysterophorus* to different soil moisture regimes. *Environ. Sci. Poll. Res.* 24, 16186–16194. doi: 10.1007/s11356-017-9176-1

Battaglia, M., and Bruce, J. (2017). Direct climate change impacts on growth and drought risk in blue gum (Eucalyptus globulus) plantations in Australia. *Aus. For.* 80, 216–227. doi: 10.1080/00049158.2017.1365403

Bellard, C., Leclerc, C., Leroy, B., Bakkenes, M., Veloz, S., Thuiller, W., et al. (2014). Vulnerability of biodiversity hotspots to global change. *Glob. Ecol. Biogeogr.* 23, 1376–1386.

Blossey, B., and Notzold, R. (1995). Evolution of increased competitive ability in invasive nonindigenous plants: a hypothesis. *J. Ecol.* 83, 887–889. doi: 10.1007/s004420050899

Boucher, O., Friedlingstein, P., Collins, B., and Shine, K. P. (2009). The indirect global warming potential and global temperature change potential due to methane oxidation. *Environ. Res. Lett.* 4:044007. doi: 10.1039/c2cs35095e

Bradley, B. A., Blumenthal, D. M., Wilcove, D. S., and Ziska, L. H. (2010). Predicting plant invasions in an era of global change. *Trends Ecol. Evol.* 25, 310–318. doi: 10.1016/j.tree.2009.12.003

Chadha, A., Florentine, S., Javaid, M., Welgama, A., and Turville, C. (2020). Influence of elements of climate change on the growth and fecundity of Datura stramonium. *Environ. Sci. Poll. Res.* 27, 35859–35869. doi: 10.1007/s11356-020-10251-y

Clements, D., and Ditommaso, A. (2011). Climate change and weed adaptation: can evolution of invasive plants lead to greater range expansion than forecasted? *Weed Res.* 51, 227–240. doi: 10.1111/j.1365-3180.2011.00850.x

Corlett, R. T. (2010). Invasive aliens on tropical East Asian islands. *Biodivers. Conserv.* 19, 411–423.

Costermans, L. F. (1981). *Native trees and shrubs of south-eastern Australia. Native trees and shrubs of south-eastern Australia*. Australia: New Holland Publishers

Cruz, J. L., LeCain, D. R., Alves, A. A., Coelho Filho, M. A., and Coelho, E. F. (2018). Elevated CO_2 reduces whole transpiration and substantially improves root production of cassava grown under water deficit. *Arch. Agro. Soil Sci.* 64, 1623–1634. doi: 10.1080/03650340.2018.1446523

Dai, A. (2013). Increasing drought under global warming in observations and models. *Nat. Clim. Change* 3, 52–58.

Dai, A., Zhao, T., and Chen, J. (2018). Climate change and drought: A precipitation and evaporation perspective. *Curr. Clim. Change Rep.* 4, 301–312. doi: 10.1007/s40641-018-0101-6

Davidson, A. M., Jennions, M., and Nicotra, A. B. (2011). Do invasive species show higher phenotypic plasticity than native species and, if so, is it adaptive? *Meta-Anal. Ecol. Lett.* 14, 419–431. doi: 10.1111/j.1461-0248.2011.01596.x

Dawood, M. F., Zaid, A., and Latef, A. A. H. A. (2021). Salicylic acid spraying-induced resilience strategies against the damaging impacts of drought and/or salinity stress in two varieties of Vicia faba L. Seedlings. *J. Plant Grow. Regul.* 41, 1–24.

Dikšaitytė, A., Viršilė, A., Žaltauskaitė, J., Januškaitienė, I., and Juozapaitienė, G. (2019). Growth and photosynthetic responses in Brassica napus differ during stress and recovery periods when exposed to combined heat, drought and elevated CO_2. *Plant Physiol. Biochem.* 142, 59–72. doi: 10.1016/j.plaphy.2019.06.026

Dukes, J. S., Chiariello, N. R., Loarie, S. R., and Field, C. B. (2011). Strong response of an invasive plant species (Centaurea solstitialis L.) to global environmental changes. *Ecol. Appl.* 21, 1887–1894. doi: 10.1890/11-0111.1

Elgawad, H., Farfan-Vignolo, E. R., de Vos, D., and Asard, H. (2015). Elevated CO_2 mitigates drought and temperature-induced oxidative stress differently in grasses and legumes. *Plant Sci.* 231, 1–10. doi: 10.1016/j.plantsci.2014.11.001

Evans, J. R., Schortemeyer, M., McFarlane, N., and Atkin, O. K. (2000). Photosynthetic characteristics of 10 Acacia species grown under ambient and elevated atmospheric CO_2. *Funct. Plant Biol.* 27, 13–25.

Gilbert, M. E., Zwieniecki, M. A., and Holbrook, N. M. (2011). Independent variation in photosynthetic capacity and stomatal conductance leads to differences in intrinsic water use efficiency in 11 soybean genotypes before and during mild drought. *J.Exper. Bot.* 62, 2875–2887. doi: 10.1093/jxb/erq461

Habermann, E., Dias, de Oliveira, E. A., Contin, D. R., San Martin, J. A., Curtarelli, L., et al. (2019). Stomatal development and conductance of a tropical forage legume are regulated by elevated [CO_2] under moderate warming. *Front. Plant Sci.* 10:609. doi: 10.3389/fpls.2019.00609

Hebbar, K., Apshara, E., Chandran, K., and Prasad, P. V. (2020). Effect of elevated CO_2, high temperature, and water deficit on growth, photosynthesis, and whole plant water use efficiency of cocoa (Theobroma cacao L.). *Int. J. Biometeorol.* 64, 47–57. doi: 10.1007/s00484-019-01792-0

Ibrahim, M. H., Sukri, R. S., Tennakoon, K. U., Le, Q.-V., and Metali, F. (2020). Photosynthetic Responses of Invasive Acacia mangium and Co-Existing Native Heath Forest Species to Elevated Temperature and CO_2 Concentrations. *J.Sustain. Forestry* 40, 1–21. doi: 10.1080/10549811.2020.1792317

IPCC (2018). *IPCC Special Report on Global Warming of 1.5°C. United Nations Intergovernmental Panel on Climate Change*. Switzerland: IPCC

Kim, T.-H., Böhmer, M., Hu, H., Nishimura, N., and Schroeder, J. I. (2010). Guard cell signal transduction network: advances in understanding abscisic acid, CO_2, and Ca2+ signaling. *Annu. Rev. Plant Biol.* 61, 561–591. doi: 10.1146/annurev-arplant-042809-112226

Kimball, B. A. (2016). Crop responses to elevated CO_2 and interactions with H_2O, N, and temperature. *Curr. Opin. Plant Biol.* 31, 36–43.

Kirschbaum, M. U. (2011). Does enhanced photosynthesis enhance growth? Lessons learned from CO_2 enrichment studies. *Plant Physiol.* 155, 117–124. doi: 10.1104/pp.110.166819

Kitao, M., Lei, T. T., Koike, T., Kayama, M., Tobita, H., and Maruyama, Y. (2007). Interaction of drought and elevated CO_2 concentration on photosynthetic down-regulation and susceptibility to photoinhibition in Japanese white birch seedlings grown with limited N availability. *Tree Physiol.* 27, 727–735. doi: 10.1093/treephys/27.5.727

Kull, C. A., Shackleton, C. M., Cunningham, P. J., Ducatillon, C., Dufour-Dror, J. M., Esler, K. J., et al. (2011). Adoption, use and perception of Australian acacias around the world. *Divers. Distrib.* 17, 822–836.

Le, Q.-V., Tennakoon, K. U., Metali, F., and Sukri, R. S. (2019). Photosynthesis in co-occurring invasive Acacia spp. and native Bornean heath forest trees at the post-establishment invasion stage. *J. Sustain. For.* 38, 230–243.

Li, D., Zhang, X., Li, L., Aghdam, M. S., Wei, X., Liu, J., et al. (2019). Elevated CO_2 delayed the chlorophyll degradation and anthocyanin accumulation in postharvest strawberry fruit. *Food Chem.* 285, 163–170. doi: 10.1016/j.foodchem.2019.01.150

Lobell, D. B., and Gourdji, S. M. (2012). The influence of climate change on global crop productivity. *Plant Physiol.* 160, 1686–1697. doi: 10.1104/pp.112.208298

López-Calcagno, P. E., Brown, K. L., Simkin, A. J., Fisk, S. J., Vialet-Chabrand, S., Lawson, T., et al. (2020). Stimulating photosynthetic processes increases productivity and water-use efficiency in the field. *Nat. Plants* 6, 1054–1063. doi: 10.1038/s41477-020-0740-1

Ma, Y., Wu, Y., and Song, X. (2020). Seasonal responses of maize growth and water use to elevated CO_2 based on a coupled device with climate chamber and weighing lysimeters. *Sci. Total Environ.* 140344. doi: 10.1016/j.scitotenv.2020.140344

Madhu, M., and Hatfield, J. (2013). Dynamics of plant root growth under increased atmospheric carbon dioxide. *Agro. J.* 105, 657–669.

Marchante, H., Freitas, H., and Hoffmann, J. H. (2010). Seed ecology of an invasive alien species, Acacia longifolia (Fabaceae), in Portuguese dune ecosystems. *Am. J. Bot.* 97, 1780–1790. doi: 10.3732/ajb.1000091

Marchante, H., Marchante, E., Freitas, H., and Hoffmann, J. H. (2015). Temporal changes in the impacts on plant communities of an invasive alien tree. Acacia longifolia. *Plant Ecol.* 216, 1481–1498.

Martínez-Carrasco, R., Pérez, P., and Morcuende, R. (2005). Interactive effects of elevated CO_2, temperature and nitrogen on photosynthesis of wheat grown under temperature gradient tunnels. *Environ. Exper. Bot.* 54, 49–59. doi: 10.1016/j.envexpbot.2004.05.004

Maxwell, K., and Johnson, G. N. (2000). Chlorophyll fluorescence: a practical guide. *J. Exper. Bot.* 51, 659–668. doi: 10.1093/jxb/51.345.659

Meibaum, B., Riede, S., Schröder, B., Manderscheid, R., Weigel, H.-J., and Breves, G. (2012). Elevated CO_2 and drought stress effects on the chemical composition of maize plants, their ruminal fermentation and microbial diversityin vitro. *Arch. Anim. Nutr.* 66, 473–489. doi: 10.1080/1745039x.2012.735080

Miranda-Apodaca, J., Pérez-López, U., Lacuesta, M., Mena-Petite, A., and Muñoz-Rueda, A. (2018). The interaction between drought and elevated CO_2 in water relations in two grassland species is species-specific. *J. Plant Physiol.* 220, 193–202. doi: 10.1016/j.jplph.2017.11.006

Osunkoya, O. O., Othman, F. E., and Kahar, R. S. (2005). Growth and competition between seedlings of an invasive plantation tree, Acacia mangium, and those of a native Borneo heath-forest species, Melastoma beccarianum. *Ecol. Res.* 20, 205–214.

Pan, C., Ahammed, G. J., Li, X., and Shi, K. (2018). Elevated CO_2 improves photosynthesis under high temperature by attenuating the functional limitations to energy fluxes, electron transport and redox homeostasis in tomato leaves. *Front. Plant Sci.* 9:1739.doi: 10.3389/fpls.2018.01739

Pastore, M. A., Lee, T. D., Hobbie, S. E., and Reich, P. B. (2020). Interactive effects of elevated CO_2, warming, reduced rainfall, and nitrogen on leaf gas exchange in five perennial grassland species. *Plant Cell Environ.*43:1862–1878 doi: 10.1111/pce.13783

Pérez-López, U., Miranda-Apodaca, J., Muñoz-Rueda, A., and Mena-Petite, A. (2013). Lettuce production and antioxidant capacity are differentially modified by salt stress and light intensity under ambient and elevated CO_2. *J. Plant Physiol.* 170, 1517–1525. doi: 10.1016/j.jplph.2013.06.004

Perveen, S., Shahbaz, M., and Ashraf, M. (2010). Regulation in gas exchange and quantum yield of photosystem II (PSII) in salt-stressed and non-stressed wheat plants raised from seed treated with triacontanol. *Pak. J. Bot.* 42, 3073–3081.

Prieto, P., Penuelas, J., Llusia, J., Asensio, D., and Estiarte, M. (2009). Effects of long-term experimental night-time warming and drought on photosynthesis, Fv/Fm and stomatal conductance in the dominant species of a Mediterranean shrubland. *Acta Physiol. Plantarum* 31, 729–739.

Qaderi, M. M., Kurepin, L. V., and Reid, D. M. (2006). Growth and physiological responses of canola (Brassica napus) to three components of global climate change: temperature, carbon dioxide and drought. *Physiol. Plantarum* 128, 710–721.

Qaderi, M. M., Lynch, A. L., Godin, V. J., and Reid, D. M. (2013). Single and interactive effects of temperature, carbon dioxide, and watering regime on the invasive weed black knapweed (Centaurea nigra). *Ecoscience* 20, 328–338.

Reddy, A. R., Rasineni, G. K., and Raghavendra, A. S. (2010). The impact of global elevated CO2 concentration on photosynthesis and plant productivity. *Curr. Sci.* 46–57.

Robredo, A., Pérez-López, U., de la Maza, H. S., González-Moro, B., Lacuesta, M., Mena-Petite, A., et al. (2007). Elevated CO_2 alleviates the impact of drought on barley improving water status by lowering stomatal conductance and delaying its effects on photosynthesis. *Environ. Exper. Bot.* 59, 252–263.

Salazar-Parra, C., Aguirreolea, J., Sánchez-Díaz, M., Irigoyen, J. J., and Morales, F. (2012). Photosynthetic response of Tempranillo grapevine to climate change scenarios. *Ann. Appl. Biol.* 161, 277–292.

Salmon, Y., Lintunen, A., Dayet, A., Chan, T., Dewar, R., Vesala, T., et al. (2020). Leaf carbon and water status control stomatal and nonstomatal limitations of photosynthesis in trees. *New Phytol.* 226, 690–703. doi: 10.1111/nph.16436

Sampaio, C. V. R. D. S. (2019). *Influence of Abiotic Factors on Growth and Nodulation of Acacia longifolia*. Ph.D Dissertation, Departamento De Biologia Animal, Faculdade De Ciencias, Universidade De Lisboa, Portugal.

Saxe, H., Ellsworth, D. S., and Heath, J. (1998). Tree and forest functioning in an enriched CO_2 atmosphere. *New Phytol.* 139, 395–436.

Schmid, I., Franzaring, J., Müller, M., Brohon, N., Calvo, O., Högy, P., et al. (2016). Effects of CO_2 enrichment and drought on photosynthesis, growth and yield of an old and a modern barley cultivar. *J. Agro. Crop Sci.* 202, 81–95.

Serret, M. D., Yousfi, S., Vicente, R., Piñero, M. C., Otálora-Alcón, G., Del Amor, F. M., et al. (2018). Interactive effects of CO_2 concentration and water regime on stable isotope signatures, nitrogen assimilation and growth in sweet pepper. *Front. Plant Sci.* 8:2180. doi: 10.3389/fpls.2017.02180

Souza-Alonso, P., González, L., López-Nogueira, A., Cavaleiro, C., and Pedrol, N. (2018). Volatile organic compounds of Acacia longifolia and their effects on germination and early growth of species from invaded habitats. *Chem. Ecol.* 34, 126–145.

Tom-Dery, D., Eller, F., Fromm, J., Jensen, K., and Reisdorff, C. (2019). Elevated CO_2 does not offset effects of competition and drought on growth of shea (Vitellaria paradoxa CF Gaertn.) seedlings. *Agrofor. Syst.* 93, 1807–1819.

Wang, A., Lam, S. K., Hao, X., Li, F. Y., Zong, Y., Wang, H., et al. (2018). Elevated CO_2 reduces the adverse effects of drought stress on a high-yielding soybean (Glycine max (L.) Merr.) cultivar by increasing water use efficiency. *Plant Physiol. Biochem.* 132, 660–665. doi: 10.1016/j.plaphy.2018.10.016

Wang, M., Xie, B., Fu, Y., Dong, C., Hui, L., Guanghui, L., et al. (2015). Effects of different elevated CO_2 concentrations on chlorophyll contents, gas exchange, water use efficiency, and PSII activity on C3 and C4 cereal crops in a closed artificial ecosystem. *Photosynth. Res.* 126, 351–362.

Welgama, A., Florentine, S., Marchante, H., Javaid, M. M., and Turville, C. (2019). The germination success of Acacia longifolia subsp. longifolia (Fabaceae): a comparison between its native and exotic ranges. *Aus. J. Bot.* 67, 414–424.

Weller, S., Florentine, S., Javaid, M. M., Welgama, A., Chadha, A., Chauhan, B. S., et al. (2021). Amaranthus retroflexus L.(Redroot Pigweed): Effects of elevated CO_2 and soil moisture on growth and biomass and the effect of radiant heat on seed germination. *Agronomy*, 11:728.

Weller, S. L., Javaid, M. M., and Florentine, S. K. (2020). Evaluation of the growth response of arid zone invasive species Salvia verbenaca cultivars to atmospheric carbon dioxide and soil moisture. *Rangeland J.* 42, 45–53.

Werner, C., Peperkorn, R., Máguas, C., and Beyschlag, W. (2008). *Competitive balance between the alien invasive Acacia longifolia and native Mediterranean species. Plant invasions: human perception, ecological impacts and management*. Leiden: Backhuys Publishers, 261–275.

Wullschleger, S., Tschaplinski, T., and Norby, R. (2002). Plant water relations at elevated CO_2, implications for water-limited environments. *Plant Cell Environ.* 25, 319–331. doi: 10.1073/pnas.1605036113

Xie, X., Li, R., Zhang, Y., Shen, S., and Bao, Y. (2018). Effect of elevated [CO_2] on assimilation, allocation of nitrogen and phosphorus by maize (*Zea Mays* L.). *Commun. Soil Sci. Plant Anal.* 49, 1032–1044.

Yu, J., Chen, L., Xu, M., and Huang, B. (2012). Effects of elevated CO_2 on physiological responses of tall fescue to elevated temperature, drought stress, and the combined stresses. *Crop Sci.* 52, 1848–1858.

Zhao, X., Mao, Z., and Xu, J. (2010). Gas exchange, chlorophyll and growth responses of Betula Platyphylla seedlings to elevated CO_2 and nitrogen. *Int. J. Biol.* 2, 143.

Ziska, L. H., Blumenthal, D. M., and Franks, S. J. (2019). Understanding the nexus of rising CO_2, climate change, and evolution in weed biology. *Invasive Plant Sci. Manag.* 12, 79–88.

Conflict of Interest: The authors declare that the research was conducted in the absence of any commercial or financial relationships that could be construed as a potential conflict of interest.

Publisher's Note: All claims expressed in this article are solely those of the authors and do not necessarily represent those of their affiliated organizations, or those of the publisher, the editors and the reviewers. Any product that may be evaluated in this article, or claim that may be made by its manufacturer, is not guaranteed or endorsed by the publisher.

Copyright © 2022 Javaid, Wang, Florentine, Ashraf, Mahmood, Li and Fiaz. This is an open-access article distributed under the terms of the Creative Commons Attribution License (CC BY). The use, distribution or reproduction in other forums is permitted, provided the original author(s) and the copyright owner(s) are credited and that the original publication in this journal is cited, in accordance with accepted academic practice. No use, distribution or reproduction is permitted which does not comply with these terms.

frontiers | Frontiers in Plant Science

REVIEW
published: 25 April 2022
doi: 10.3389/fpls.2022.868874

The Multifaceted Roles of MYC2 in Plants: Toward Transcriptional Reprogramming and Stress Tolerance by Jasmonate Signaling

Cheng Song[1†], Yunpeng Cao[2†], Jun Dai[1], Guohui Li[1], Muhammad Aamir Manzoor[3], Cunwu Chen[1] and Hui Deng[1]*

[1] College of Biological and Pharmaceutical Engineering, West Anhui University, Lu'an, China, [2] Wuhan Botanical Garden, Chinese Academy of Sciences, Wuhan, China, [3] College of Life Science, Anhui Agricultural University, Hefei, China

Environmental stress is one of the major restrictions on plant development and foodstuff production. The adaptive response in plants largely occurs through an intricate signaling system, which is crucial for regulating the stress-responsive genes. Myelocytomatosis (MYC) transcription factors are the fundamental regulators of the jasmonate (JA) signaling branch that participates in plant development and multiple stresses. By binding to the *cis*-acting elements of a large number of stress-responsive genes, JA-responsive transcription factors activate the stress-resistant defense genes. The mechanism of stress responses concerns myriad regulatory processes at the physiological and molecular levels. Discovering stress-related regulatory factors is of great value in disclosing the response mechanisms of plants to biotic or abiotic stress, which could guide the genetic improvement of plant resistance. This review summarizes recent researches in various aspects of MYC2-mediated JA signaling and emphasizes MYC2 involvement in plant growth and stress response.

Keywords: JA signaling, stress tolerance, transcriptional regulation, crosstalk, secondary metabolism

OPEN ACCESS

Edited by:
Mohammad Anwar Hossain, Bangladesh Agricultural University, Bangladesh

Reviewed by:
Ali Raza, Fujian Agriculture and Forestry University, China
Emilie Widemann, University of Western Ontario, Canada

***Correspondence:**
Hui Deng
dhup@qq.com

[†]These authors have contributed equally to this work

Specialty section:
This article was submitted to Plant Breeding, a section of the journal Frontiers in Plant Science

Received: *03 February 2022*
Accepted: *17 March 2022*
Published: *25 April 2022*

Citation:
Song C, Cao Y, Dai J, Li G, Manzoor MA, Chen C and Deng H (2022) The Multifaceted Roles of MYC2 in Plants: Toward Transcriptional Reprogramming and Stress Tolerance by Jasmonate Signaling. Front. Plant Sci. 13:868874. doi: 10.3389/fpls.2022.868874

INTRODUCTION

Phytohormones are a group of signaling molecules that are essential to perceive changes in the external environment, regulate their growth status, defend themselves against insects and maintain survival (Santner and Estelle, 2009; Dubois et al., 2018). JA is often used as a plant growth regulator as well as a signaling molecule for plant defense responses (Mao et al., 2017). Biotic and abiotic stresses have always been the vital factors in restricting the yield of food products. The adaptive responses are mainly achieved by simulating the transcription of a large number of downstream genes through complex signaling pathways (Sabagh et al., 2022). JA mediated plant development and a variety of biotic stresses caused by physical injury, pathogen attack, and insect feeding, as well as several abiotic challenges such as low temperature, drought, excessive salinity, and UV radiation (Verma et al., 2016; Yang et al., 2019). To protect against external invasion, plants perceive and transmit JA cascade signals through a variety of regulatory factors that are over-defensive and may hamper plant growth and development (Zander et al., 2020). MYC transcription factors could bind to the promoter regions of several targeted-genes, which affects their expression that help plants deal with stresses. In Arabidopsis, MYC2-mediated activation of JA signaling is precisely regulated by its repressor,

the JASMONATE-ZIM DOMAIN (JAZ) protein, and a subunit of the Mediator complex (MED25) protein (Wu et al., 2020). Jasmonic acid-isoleucine conjugate (JA-Ile), as an active molecule, binds to the subunit of the Skp1/Cullin/F-box (SCF^{COI1}) ubiquitin ligase and transmits downstream signaling (Wasternack and Xie, 2010). In the absence of external stress, JAZ protein binds to MYC2 and other transcription factors, rendering them inactive and devoid of triggering the transcription of downstream genes. MYC2 is repressed by JAZ, resulting in the closure of the downstream regulatory switch. Once JA-Ile is present as an activating signal, CORONATINE-INSENSITIVE 1 (COI1), JA-Ile and JAZ proteins form a co-receptor complex. COI1 regulates ubiquitin-dependent JAZ degradation via the 26S proteasome, releasing MYC2 from repression (Thines et al., 2007). Some studies demonstrated that MYC2-mediated JA signaling had an influence on the transcription reprogramming of a variety of stress-responsive genes (Zander et al., 2020). Given the critical role of MYC transcription factors, this review highlights the regulatory functions of MYCs at multiple levels and dwells on the activation and reduction mechanisms of JA signaling.

COMPONENTS AND STRUCTURAL FUNCTIONS OF MYC2 TRANSCRIPTION FACTORS

MYC proteins are the core transcription factors in JA signaling pathway. As a branch of the basic helix-loop-helix (bHLH) superfamily, the MYC family is widely present in bryophytes and angiospermae (Peñuelas et al., 2019). The MYC-related TFs between *Arabidopsis thaliana* and the liverwort *Marchantia polymorpha* had an early-diverging lineage. The evolutionary relationship suggested MYC function originally occurred in charophycean algae and hence predates the evolutionary appearance of any other jasmonate pathway component. Plants have a large number of bHLH family members that mainly involved in plant growth, stress response, and secondary metabolic processes (Heim et al., 2003; Toledo-Ortiz et al., 2003). Their bHLH genes are more closely related to the group B in the animal members. *AtbHLHs* were categorized into 12 families and then further classified based on conserved domains, with 14 new members found (Toledo-Ortiz et al., 2003). Currently, 158 and 173 bHLH transcription factors have been identified in *A. thaliana* and *O. sativa*, respectively (Pires and Dolan, 2010).

MYC-like transcription factors have three subfamilies, namely IIId, IIIe, and IIIf bHLHs. MYC2 belongs to the IIIe bHLH clade. In *A. thaliana*, IIIe bHLH members consist of *AtMYC2*, *AtMYC3*, *AtMYC4*, and *AtMYC5*. *AtMYC2* was discovered from the screening of *jasmonate-insensitive* (*jin*) mutants. Earlier study indicated that *jin1* and *jin4* mutant showed insensitivity to exogenous JA stimulation (Berger et al., 1996). AtMYC2 positively regulated both JA-mediated wounding response and negatively regulates JA-mediated resistance to saprophytic pathogens (Lorenzo et al., 2004). In addition to its high affinity for the canonical G-box, MYC2 binds to the G-box mutants 5′-CACATG-3′ and 5′-CACGTT-3′ with low affinity (Dombrecht et al., 2007). The base types at both ends of the G-box affect MYC2 binding, and the number of thymine residing at the C-terminus of the G-box could affect the binding ability of MYC2 (Figueroa and Browse, 2012).

MYC2 included a 60-amino acid conserved bHLH domain at the C-terminus, which was composed of a Basic and an HLH domain, along with a JID domain and a TAD domain at the N-terminus (Goossens et al., 2015). The Basic domain consists of 15–20 basic amino acids and is mainly responsible for binding the G-box. The HLH domain consists of a loop region connecting two α-helices composed of hydrophobic amino acids, which are responsible for forming homo- or heterodimers. The JID domain is responsible for interacting with JAZ proteins, while the TAD domain is responsible for transcriptional activation and interactions with MED25 (**Figure 1**). MYC2 functions by binding to DNA through its basic domain (Lian et al., 2017). The crystal structure of the bHLH domain of MYC2 protein combined with DNA shows that two homodimers form parallel shoulder-to-shoulder tetramers reversely arranged in the MYC2-DNA structure, while MYC3 can only form homodimers (Lian et al., 2017). In contrast to MYC3, MYC2 has a stronger activation capacity. This is because the tetramerized MYC2 can mediate the formation of DNA looping structures, which in turn increases the ability of MYC2 to bind DNA and activate gene expression (Kazan and Manners, 2013).

REGULATORY MECHANISMS OF MYC2 TRANSCRIPTION FACTORS IN THE JASMONATE SIGNALING PATHWAY

Although JA is the initiator that activates the JA signaling pathway, the real functional component is JA-Ile (Suza and Staswick, 2008). JA-Ile is synthesized by an ATP-dependent jasmonate-amino acid amidase encoded by *JASMONATE RESISTANT 1 (JAR1)* and whose product, (3R,7S)-jasmonoyl-L-isoleucine, is the most biologically active JA component. JAZ proteins, as a type of repressors, could interact with other transcription factors or co-repressors to block downstream signaling. The TIFY family included three subfamilies JAZ, Zinc-finger protein expressed in Inflorescence Meristem (ZIM) and PEAPOD (PPD), among which JAZ did not contain DNA binding domains and required reciprocal interactions to perform its functions (Bai et al., 2011). There were three conserved domains within JAZ, including NT, ZIM, and Jas (Zhang et al., 2017). The NT domain at the N-terminus interacted with the GIBBERELLIC ACID INSENSITIVE (DELLA) protein (Wager and Browse, 2012). The ZIM domain contained the TIFY conserved motif TIF[F/Y]XG, which was responsible for homo- or heterodimer formation of the JAZ protein and interacts with the co-repressor Novel Interactor of JAZ (NINJA) (Pauwels et al., 2010). The C-terminal Jas domain could directly interact with the JID domain of MYC2 or COI1, which was responsible for the degradation of JAZ. Some JAZ members also contained an EAR motif at the N-terminus, which interacted directly with its co-repressor TOPLESS (TPL). Those proteins that did not have an EAR motif could not

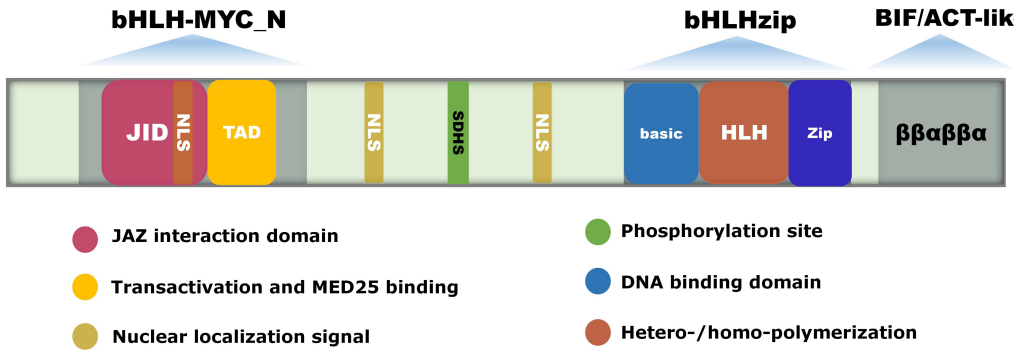


FIGURE 1 | The gene structure and conserved domains of MYC2. bHLH-MYC_N, bHLH-zip, and BIF/ACT-like are the three conserved domains of MYC2. The bHLH domain at the C-terminus is composed of the Basic and HLH domains, and the N-terminus contains the JID and TAD domains. The Basic domain is responsible for binding to the G-box in the promoter of the targeted gene. The HLH domain is responsible for forming homo- or heterodimers. The JID domain binds to the Jas domain of the JAZ protein, and the TAD domain is responsible for transactivation and interactions with the MED25 subunit. The BIF structural domain contains a ββαββα structure similar to the ACT domain, and is responsible for transactivation and homodimer formation. NSL is the nuclear localization signaling structure. The conserved amino acid SDHS is the phosphorylation site.

directly interact with TPL and required the participation of the NINJA protein. Due to the EAR motif in NINJA, JAZ, and TPL formed a JAZ-NINJA-TPL complex to exert its transcriptional repression. TPL protein is a member of the Gro/Tup1 family. Sixteen Groucho/Thymidine uptake 1 (Gro/Tup1) members from Arabidopsis are divided into two major groups. As co-repressors of MYC-regulon, TOPLESS/TOPLESS-Related/WUSCHELINTERACTING PROTEIN (TPL/TPR/WSIP) and LEUNIG/LEUNIG_HOMOLOG (LUG/LUH) participated in organ development, stem cell maintenance, environmental physiology, and so on (Ma et al., 2017). Although JAZ probably suppressed MYC function by interacting with MYC, some studies demonstrated that JAZ–TF transcriptional modules could control discrete branches of the JA-responsive genes in an MYC-independent manner (Cheng et al., 2011; Major et al., 2017). JASMONATE-ASSOCIATED MYC2-LIKE (JAM) and MYC2-TARGETED BHLH (MTB) from IIId bHLHs inhibited JA response by binding competitively to the promoters of MYC2-targeted genes (Sasaki-Sekimoto et al., 2013; Song et al., 2013; Wasternack, 2019).

JA-mediated MYC2 activation is fine-tuned by JAZ and the mediator complex MED25 (**Figure 2**). In addition to interacting with MYC2, MED25 also interacts with the receptor COI1 and a subset of JAZ repressors like NINJA and TPL (Zhai and Li, 2019; Zhai et al., 2020). In the repression phase, JAZ and its co-repressors compete with MED25 for the interaction with MYC2. In the activation phase, JA-Ile acts as molecular docking to facilitate the COI1–JAZ conjugation, which leads to proteasome-dependent degradation of JAZ repressors (Zhang F. et al., 2015). In the response phase, MED25 interacts with MYC2 and recruits HISTONE ACETYLTRANSFERASE OF THE CBP FAMILY1 (HAC1) as well as RNA polymerase II (Pol II) to the promoters of MYC2-targeted genes, thereby activating their expression (An et al., 2017). HAC1 regulates the transcription of JA-responsive genes by epigenetically controlling the H3K9 acetylation of MYC2-target genes. The Gro/Tup1 family members LUG and LUH activate MYC2-mediated transcription of *JAZ2* and *LOX2* through the mediator complex and HAC1 (You et al., 2019). LUH promotes JA-dependent enhancement of protein interactions between MYC2 and its coactivators MED25 and HAC1. MED25 recruits LUH to the promoter of the MYC2-targeted gene. MED25 and MYC2 can activate the expression of MYC2-TARGETED BHLH (MTB), which reduces the expression of JA-responsive genes. MTBs negatively regulate JA-responsive transcriptional reprogramming by weakening the stability of MYC2-MED25 complex (Liu et al., 2019). Accompanied by the deactivation of the JA signal, the status returns to the repression phase. MYC2-mediated transcription of downstream targets is not only dependent on the activation of MED25, but also associated with enhancers that assist the transcription of promoters, such as JA enhancers (JAEs) (Wang H. et al., 2019). JA mediates MED25 to regulate the chromatin looping formation between JAE and its promoter, while MYC2 uses the JAE element to regulate its own expression. The JAE (ME2 element) in the MYC2 locus positively regulates MYC2 expression in the short-term JA response and negatively regulates MYC2 in the persistent JA response. Recent studies had emerged CUL3-based E3 ubiquitin ligases($CUL3^{BPM}$) roles in the ubiquitination of MYC proteins (Chico et al., 2020). JA stabilized BPM3 to construct a negative feedback regulatory loop to mediate the expression of MYC.

Depending on the JID domain, AtMYC2 can interact with most JAZs, and SlMYC2 can interact with all JAZs in tomato (Fernández-Calvo et al., 2011; Du et al., 2017). MYC3 interacted with JAZ9 not only in the JID domain but also in the TAD domain. This suggests that MYC2 utilizes the same and overlapping regions to interact with JAZ and MED25. The result that JAZ9 competitively interacted with MED25 and MYC2 explained why JAZ and MED25 had both antagonistic and synergistic effects on MYC2 transcription (Zhang F. et al., 2015). Changes in conserved amino acids would bring MYC2 and MYC3 out of repression and increased their transcriptional activities (Goossens et al., 2015). The $MYC2^{D105N}$ mutant was constructed by introducing aspartic acid at position 105 of the MYC2

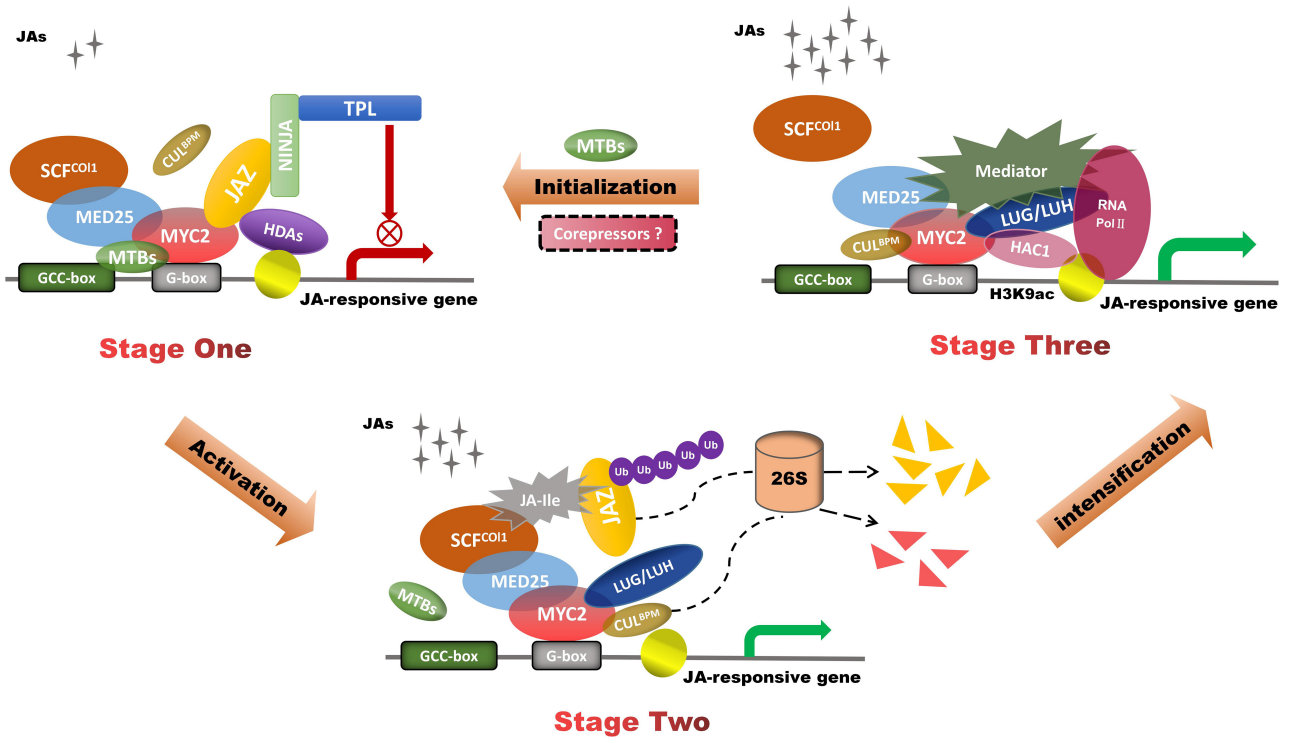


FIGURE 2 | JAZ and MED25 mutually regulate JA-induced transactivation of MYC2-targeted genes. In Stage one, the MED25–MYC2 interaction is relatively weak because JAZ competes with MED25 for interaction with MYC transcription factors. In Stage two, COI1–JAZ co-receptor complex leads to proteasome-dependent degradation of JAZ repressors, which participate in the degradation of JAZ by 26S proteasome. In Stage three, MED25 recruits Pol II and LUH to the promoter of the MYC2-targeted gene, thereby regulating their expression. LUH enhanced the interactions of MYC2 coupled with its co-activators MED25 and HAC1. MTBs competitively interact with MYC2-targeted genes and impair the MED25–MYC2 complex. CUL3^{BPM} reduce MYC levels by the ubiquitination of MYC TFs.

amino acid, which merely interacted with JAZ1 and JAZ10 with significantly reduced binding capacity. Compared with MYC2, MYC3, and MYC4 have overlapping roles and their uniqueness in response to JA signaling and downstream regulation. MYC3 and MYC4 could form heterodimers and tetramers with MYC2, respectively. The functional deletion of MYC3 and MYC4 partially attenuated the capacities of JA response, while increased the insensitivity in *myc2* mutants (Fernández-Calvo et al., 2011). In contrast to MYC3, MYC2 had a faster and higher levels of inducible response to JA (Lian et al., 2017). Taken together, MYC3 and MYC4 may play a part in the activation of JA signaling, which requires collaboration with MYC2 to regulate JA-mediated stress responses at different levels.

MYC2 IS INVOLVED IN THE REGULATION OF PLANT GROWTH AND DEVELOPMENT

MYC2 not only regulates JA-mediated growth, development and resistance, but also participates in light signaling, circadian rhythm and cross-talk with other hormones (**Figure 3**). MYC2 restrained leaf vein development by reducing auxin biosynthesis (Dombrecht et al., 2007; Huang et al., 2017). MYC2 negatively regulates the development of leaf veins. JA also mediates MYC2 to inhibit the cell division of the primary root meristem (Chen et al., 2011). MYC2 binds to the G-box promoter of *PLETHORA (PLT)* in response to JA signaling, resulting in the reduction of MYC2-targeted genes. JA-mediated root growth is suppressed by *MYC2*. MYC2 is also involved in seed size, seed weight, and the formation of seed storage proteins. AtMYC2 has been shown to be positively correlated with seed storage rate at various stages (Gao et al., 2016). A recent study has demonstrated that MYC2 could inhibit adventitious root initiation by suppressing *CYTOKININ OXIDASE/DEHYDROGENASE1* (*CKX1*) and enhancing the transcription of *APETALA2.6 LIKE* (*RAP2.6L*) (Dob et al., 2021). MYC2 and ETHYLENE INSENSITIVE3 (EIN3) synergistically controlled plant development and JA response (Zheng et al., 2017). MYC2 physically interacted with EIN3 to reduce *HOOKLESS1* (*HLS1*) expression or binding to the promoter of *EIN3 BINDING F-BOX PROTEIN1* (*EBF1*) to induce its expression (Zhang et al., 2014).

Light is indispensable for plant development and morphogenesis. MYC2 participated in photomorphogenesis by activating *phytochrome A* (*phyA*), which led to JA biosynthesis that recruited COI1 from the degradation of JAZ (Hsieh and Okamoto, 2014). Degradation of JAZ repressors results in the release of MYC transcription factors. At low R/FR ratios, *phyA* and *myc2* mutants both showed decreased hypocotyl inhibition, which suggested MYC2 was responsible for far-red

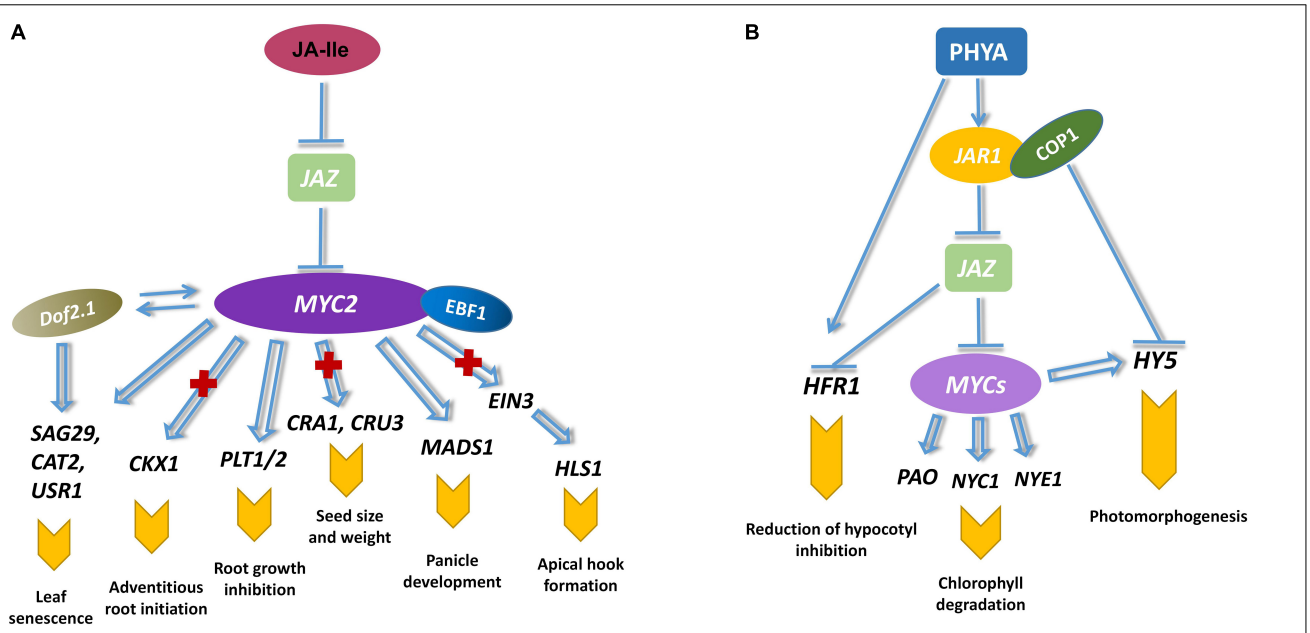


FIGURE 3 | MYC2 regulates plant growth and photomorphogenesis. **(A)** MYC2 mediates JA-regulated root growth and meristem development. MYC2 inhibits adventitious root initiation by reducing the expression of *CKX1* (Dob et al., 2021). JA-induced division and stem cell differentiation in meristematic tissue is mediated by MYC2, which interacts with PLT to suppress the expression of PLT-targeted genes (Chen et al., 2011). MYC2 restrains seed development by regulating the expression of seed storage protein CRA1 and CRU3 (Gao et al., 2016). MYC2 and EIN3 additionally controlled apical hook development by interacting with EBF1 and repressing the expression of *HLS1* (Zhang et al., 2014). Senescence-associated genes are mutually enhanced by MYC2 and Dof proteins (Zhuo et al., 2020). MYC2 accelerates leaf senescence by raising the transcription of *SAG29*, *CAT2*, and *USR1* (Qi et al., 2015b; Zhang Z. et al., 2020). **(B)** MYCs are involved in the photomorphogenesis of plants. PHYA regulates the downstream of JA signaling and ultimately affects the activation of MYCs (Chico et al., 2014). PHYA control the hypocotyl inhibition and chlorophyll reduction through JA-mediated HFR1 and HY5 (Chakraborty et al., 2019). MYCs regulate JA-induced Chl degradation by directly activating some Chl catabolic genes (*PAO, NYC1, NYE1*) (Zhu et al., 2015).

light response. Additionally, *myc2* and *phyA* mutants exhibited a significant hypocotyl elongation of sheltering effect (Chico et al., 2014). HYPOCOTYL 5 (HY5) is a basic leucine-zipper (bZIP) transcription factor involved in photomorphogenesis at different wavelengths. *hy5* mutants exhibit reduced hypocotyl elongation and chlorophyll accumulation. MYC2 and HY5 regulate seedling development under blue light irradiation (Chakraborty et al., 2019). MYC2 negatively regulates the expression of *HY5* by binding to the promoter E-box. HY5 acts toward *MYC2* in different patterns, implying that they coordinate seedling growth in a mutually antagonistic way. Chlorophyll (Chl) degradation is a characteristic event during green organ senescence or maturation. JA-induced Chl degradation could be mediated by directly activating some Chl catabolic genes, such as *pheophorbide a oxygenase* (*PAO*), *NON-YELLOW COLORING 1* (*NYC1*), and *NON-YELLOWING 1* (*NYE1*) (Zhu et al., 2015). The *myc* and *phyB* mutants exhibit similar phenotypes in delaying seed development and hypocotyl growth. Overexpression of *MYC2* in *phyB* mutants partially reduces the prolonged hypocotyl phenotype (Ortigosa et al., 2020). By binding to the promoter of *HY5*, MYC2 and MYC3 activate the expression of the red light-responsive gene *HY5*. In addition to light signaling, the expression of *MYC2* is regulated by circadian rhythm. MYC2 interacts with TIME FOR COFFEE (TIC) resulting in its degradation by the ubiquitination of 26S proteasome. The *tic* and *myc2* mutants exhibited opposite JA-responsive phenotypes (Shin et al., 2012).

Floral initiation is a sophisticated and complex process, and the timing of flowering is synergistically regulated by a variety of factors such as temperature, light, and hormones. MYC2 is involved in JA-mediated inhibition of flowering (Wang et al., 2017). The *myc2/3* and *myc2/4* double mutants exhibited an earlier flowering phenotype than the wild type under long-day conditions, whereas the *myc2*, *myc3*, and *myc4* single mutants and the *myc3/4* double mutant had similar flowering times to the wild type. MYC2 is also involved in the developmental regulation of the calyx (Qi et al., 2015a). The *myc2, myc3, myc4,* and *myc5* mutants displayed a failure to dehisce anther phenotype, delayed dehiscence, and low pollen grain survival, whereas the quadruple mutants had a delayed calyx development phenotype. Floral spike is an important component of the floral organ that affects reproductive growth and crop yield (Cai et al., 2014). EXTRA GLUME 1 and 2 (EG1 and EG2) were identified from spike deficient mutants of rice, where EG2 worked as a negative regulator to reduce MYC2-mediated floral morphogenesis. In the presence of JA signals, MYC2 promotes normal flowering spike by activating the flowering-related *MADS1*.

Ethylene is a regulatory molecule that promotes fruit ripening and organ senescence. In apples, JA induction and MYC2 can accelerate the expression of *1-AMINOCYCLOPROPANE-1-CARBOXYLATE OXIDASE* (*ACO*)

and *1-AMINOCYCLOPROPANE-1-CARBOXYLATE SYNTHASE* (*ACS*), on the other hand, ethylene production (Li et al., 2017). MYC2 not only bond to the promoters of *ACS1* and *ACO1* to increase their expression levels, but also simultaneously increased the activity of ERF3, which mediated the transcription regulation of *ACS1* (Hu et al., 2022). MYC2 suppressed the repressive effect of ERF2 on the *ACS1* promoter by interacting with ERF2, which prevented ERF2 from binding to ERF3 and produced large quantities of free ERF3 to activate the transcription of *ACS1* (Kazan, 2015; Li et al., 2016). Interestingly, the IIIe bHLHs and the IIIb bHLH transcription factors bHLH3, bHLH13, bHLH14, and bHLH17 have antagonistic roles in regulating physiological processes such as chlorophyll accumulation, photochemical efficiency of PHOTOSYSTEM II (PSII), and membrane ion permeation (Qi et al., 2015b).

Leaf senescence is regulated by a large number of internal and environmental factors. MYC2, MYC3, and MYC4 are capable of activating JA-induced leaf senescence and regulating the senescence process by binding to the promoter of *SENESCENCE-ASSOCIATED GENE29* (*SAG29*), whereas IIIb bHLHs bind to the *SAG29* promoter to reduce its expression (Qi et al., 2015b). H_2O_2 scavenging significantly inhibits JA-induced leaf senescence and the expression of *SAGs*. Some studies have shown the *myc2* mutant exhibits delayed leaf senescence with increased expression of *CATALASE 2* (*CAT2*) and lower H_2O_2 accumulation (Zhang Y. et al., 2020). Arabidopsis DNA binding-with-one-finger (Dof) proteins are associated with leaf senescence. *Dof2.1*, a JA-inducible gene, accelerated leaf senescence by increasing the expression of *MYC2*. MYC2 was also responsible for the JA-inducible expression of *Dof2.1* (Zhuo et al., 2020). U-box Senescence Related 1 (USR1) is involved in both age-dependent and dark-induced leaf senescence in Arabidopsis. The *usr1* mutant exhibited a delay in the age-dependent and dark-induced leaf senescence. JA treatments promoted the accumulation of *AtUSR1* by the activation function of MYC2 (Zhang Z. et al., 2020).

MYC2 PARTICIPATES IN THE BIOTIC STRESS RESPONSE

MYC2, MYC3, and MYC4 play analogous roles in regulating plant resistance to insects (**Figure 4**). The *myc2 myc3 myc4* triple mutant is more susceptible to *Spodoptera mauritia* and *Spodoptera exigua* Hiibner than the wild plant (Fernández-Calvo et al., 2011; Schweizer et al., 2013; Song et al., 2014). MYC2 regulates the associated mechanical injury caused by herbivorous insects to positively regulate the expression of *JASMONIC ACID2* (*JA2*) and *JASMONIC ACID2-LIKE* (*JA2L*), therefore controlling ABA biosynthesis and stomatal closure (Du et al., 2014). MYC2 promotes the transcription of the IAA biosynthesis gene *YUCCA* induced by the bite of the two-spotted spider mite *Tetranychus urticae* by binding to the tandem G-box in the promoter of *YUC8* and *YUC9* (Pérez-Alonso et al., 2021). MYC2, MYC3, and MYC4 promote the content of glucosinolates to enhance insect resistance. Glucosinolates are a class of thioglucosides containing nitrogen and sulfur, whose biosynthesis were governed by six R2R3-MYB transcription factors: MYB28, MYB29, MYB76, MYB34, MYB51, and MYB122. The interaction of MYCs and MYBs promotes the transcription of glucosinolate-related genes, resulting in increased GS levels (Schweizer et al., 2013). By forming a transcription factor complex with several MYB transcription factors, MYC2, MYC3, and MYC4 bond to the promoters of more than twenty glucosinolate biosynthesis genes, and directly regulated their expressions (Schweizer et al., 2013). In addition, MYC2 binds directly to the promoters of the *terpene synthases TPS10*, *TPS11*, and *TPS21*, and triggers their transcription. This could boost terpenoid production and provide independent resistance to insect attacks (Hong et al., 2012). Wounding-induced JA biosynthesis was relevant to the transcriptional reprogramming on the downstream of JA biosynthesis. JA catabolic genes, such as *allene oxide synthase* (*AOS*), *allene oxide cyclase1 (AOC1), cis-(+)-12-oxo- phytodienoic acid reductase 3(OPR3), lipoxygenase 2 (LOX2), JASMONATE RESISTANT 1 (JAR1), jasmonic acid carboxyl methyltransferase (JMT), jasmonate-induced oxygenases 2 (JOX2),* and *cytochrome P450 94B1 (CYP94B1)*, etc. are upregulated by MYC2 at different levels (Zhang C. et al., 2020). ET-induced ERF15 and ERF16 also regulate JA biosynthesis in tomato. ET triggered the transcription of MYC2 and ERF16 by regulating JA biosynthesis genes (Hu et al., 2021).

In contrast to its regulatory role in insect resistance, MYC2 serves as a negative regulator of plant pathogens (Zheng et al., 2017). MYC2 blocked the function of EIN3 by decreasing ethylene-mediated pathogen response. MYC2 interacts with EIN3 to antagonistically regulate the expression of *ERF*, which enhanced the expression of pathogen-induced *PDF1.2* (Song et al., 2014). The *myc2* mutants are more resistant to pathogens like *Botrytis cinerea* than the wild type, probably attributed to MYC2 reciprocally inhibiting the function of EIN3. Cytochrome P450 enzymes are required for camalexin biosynthesis. CYP79B2 or CYP79B3 convert Trp to indole-3-acetaldoxime. Pathogen infection or abiotic stresses could induce the expression of *CYP71A12* and *CYP71A13*, which dehydrate indole-3-acetaldoxime to produce indole-3-acetonitrile (IAN). IAN is subsequently activated, probably to indole cyanohydrin, and conjugated with glutathione to form GS-IAN. GS-IAN is degraded to Cys (IAN) via glutamyl peptidase 1 (GGP1), and Cys (IAN) is then converted to camalexin via *CYP71B15* (Koprivova et al., 2019; Mucha et al., 2019). MiSSP7, a fungal symbiotic effector from *Laccaria bicolor*, blocked the dimerization of Populus JAZs, which facilitated the release of MYC2-targeted genes (Plett et al., 2014; Daguerre et al., 2020). The *jin1* mutants are resistant to both *P. syringae* pv. tomato DC3000 and COR. The *JIN* gene is necessary for the inhibition of salicylic acid-dependent defenses in *P. syringae* infection. COR activates NAC transcription factors via MYC2, impairing the production of salicylic acid (SA) and weakening host immunity (Laurie-Berry et al., 2006). By phosphorylating and degrading MYC2, the receptor kinase FERONIA (FER) suppresses JA and COR signaling, hence positively regulating immunity (Guo et al., 2018). Transcriptional activation of the SA hormone defense sector acts as a critical barrier to biotrophic infections. In

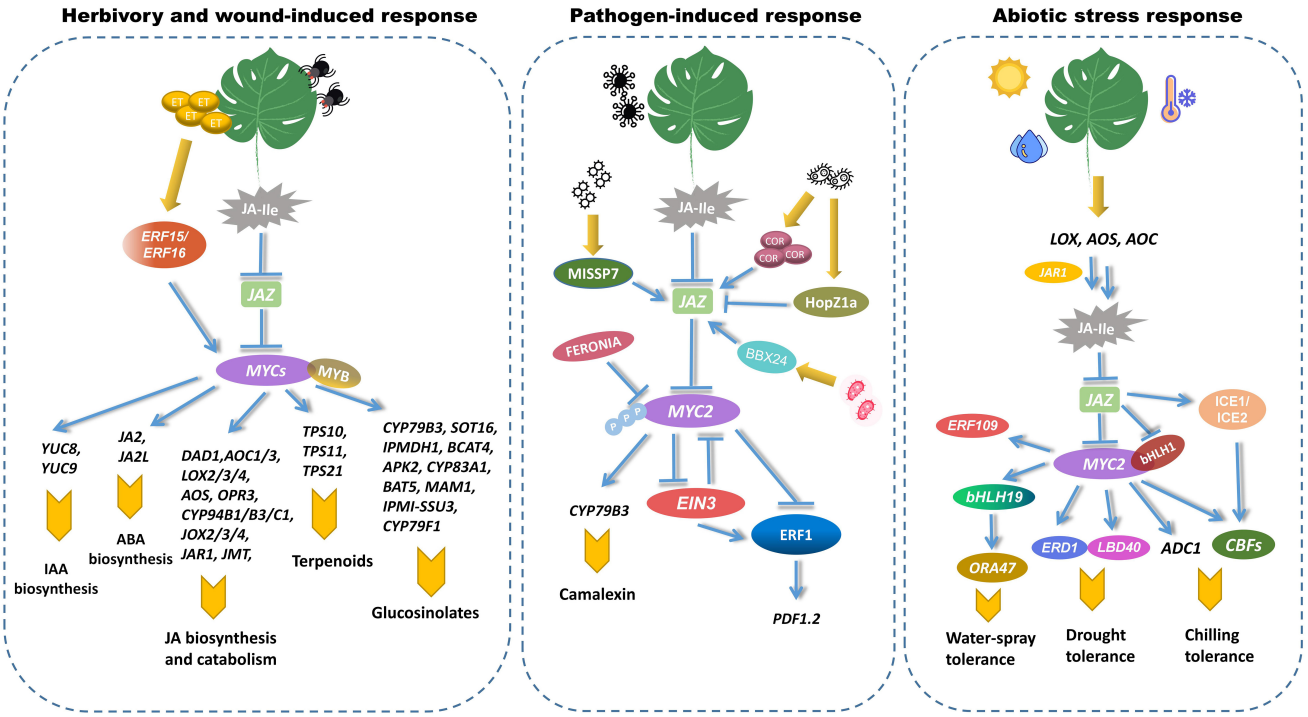


FIGURE 4 | MYCs regulate biotic and abiotic stress responses in plants. MYCs participate in the process of pathogen infection and wound responses. MYCs interact with MYB to control the expression of several glucosinolate-biosynthetic genes, such as *CYP79B3*, *SOT16*, *IPMDH1*, and *BCAT4,* etc. (Mikkelsen et al., 2003; Piotrowski et al., 2004; Knill et al., 2008; He et al., 2011). MYC2 promotes the production of terpenoid phytolexin by upregulating the expression of *TPS10, TPS11,* and *TPS21* (Hong et al., 2012). MYC2 regulates the associated mechanical injury of herbivorous insects by positively regulating the expression of *NAC019* and *JA2L*, which increase the expression level of *VSP1* and *TD* (Du et al., 2014, 2017). MYC2 enhanced the transcription of the IAA biosynthesis genes *YUC8* and *YUC9* (Pérez-Alonso et al., 2021). The transcription of multiple JA biosynthesis and catabolism genes are also mediated by MYC2 under wounding response. MYC2 interacts with EIN3 in ethylene signaling to antagonistically regulate the expression of *ERF*, which in turn regulates the expression of pathogen-related *PDF1.2* (Song et al., 2014). MiSSP7 and BBX24 inhibit MYC2-targeted gene expression by increasing their interaction with JAZ (Daguerre et al., 2020; Zhang H. et al., 2020). HopZ1a triggered AtJAZ1 degradation and increased the expression of JA-responsive genes (Jiang et al., 2013). MYC2 function is inhibited by FER via its phosphorylation (Guo et al., 2018). MYCs are engaged in abiotic stresses such as low temperature, water-spray and drought. Environmental stress can increase the transcription of *MYC2* and *bHLH1*, which in turn upregulate the expression of low-temperature stress-related *CBFs* and drought stress-related *ERD1* (Li Y. et al., 2019; Wang Y. et al., 2019). ICE1 and ICE2 upregulate the expression of *CBFs* (Kashyap and Deswal, 2019). MYC2 increased *ADC1* levels, which resulted in increased putrescine biosynthesis (Ding et al., 2021). Water spray-inducible MYC-regulon creates a hierarchical transcriptional network via interacting with bHLH19 and ERF109 (van Moerkercke et al., 2019). bHLH19 in turn directly activates the promoter of *ORA47* (Chen et al., 2016).

Arabidopsis effector-triggered immunity, the EDS1 complex in combination with PAD4 inhibits MYC2 to enhance the SA defense (Cui et al., 2018). *P. syringae* HopZ1a induced the degradation of AtJAZ1, and fostered JA-responsive gene expression during bacterial infection (Jiang et al., 2013). HopZ1a acetylated JAZs through a putative acetyltransferase catalysis. In recent studies, MYC2 has been implicated as a negative regulator of SA-mediated defense against bacterial infections. Overexpression of *MYC2* confers hyper-resistance to a wide range of virulent and avirulent bacterial pathogens (Gautam et al., 2021). IbBBX24, a transcription factor from the B-box (BBX) family, modulated JA responses in sweet potato by antagonistically binding to IbJAZ10, which interacted with IbMYC2 (Zhang H. et al., 2020). Overexpression of *IbBBX24* dramatically enhanced resistance to Fusarium wilt disease. Using the ChIP-seq approach, 665 MYC2-targeted binding genes in tomato were discovered (Du et al., 2017). These genes were found to be highly abundant under early JA stress, and one type of MYC2-targeted transcription factor (MTF) directly regulated the transcription of late defense genes.

MYC2 PARTICIPATES IN THE ABIOTIC STRESS RESPONSE

Beyond modulating biotic stress responses, MYC2 is engaged in abiotic resistance, such as cold and drought stress (**Figure 4**). To avoid freezing injury or death, plants bolster the expression of *C-repeat-binding factor* (*CBF*), *cold-regulated (COR), cold-induced (KIN)*, and *low-temperature-induced (LTI)*. The INDUCER OF CBF EXPRESSION (ICE)-CBF transcriptional cascade is critical for the plant cold stress response (Kashyap and Deswal, 2019). ICE1 and ICE2, two bHLH TFs from *A. thaliana*, upregulate the expression of *CBF* by binding to CANNTG motif in the promoter. At the normal temperature, JAZ1/4 interacts with ICE1 and ICE2 to block the ICE-CBF pathway. However,

Low-temperature conditions promote the expression of JA biosynthesis-related genes such as *AOS1*, *DAD1*, *AOC*, and *LOX2*, resulting in the production of JA-Ile and stimulation of COI1 to interact with JAZ1 (Zhu, 2016; Hu et al., 2017). Putrescine alleviated the oxidative damage caused by cold stress. Some research has demonstrated that inhibition of MYC2 decreased the expression of *arginine decarboxylase 1* (*ADC1*) and lowered putrescine accumulation (Ding et al., 2021). JA regulated chilling response in apple (Wang Y. et al., 2019). Exogenous application of MeJA could increase the expression of *bHLH1*, *CBF1*, *CBF2*, and *CBF3*. bHLH1 regulated the chilling resistance by interacting with JAZ1/4 and MYC2. MYC2 sharply increased the expression level of *CBFs*, whereas JAZ1/4 decreased the facilitation of MYC2 on chilling resistance. Furthermore, MYC2 participated in JA-mediated drought tolerance (Li Y. et al., 2019). In *A. thaliana*, the *coi1-2*, *JAZ1-Jas*, and *myc2-2* mutants exhibit drought sensitivity and regulate the stress caused by water deficit through the induction of *EARLY RESPONSIVE TO DEHYDRATION 1* (*ERD1*). MYC2 modulates drought-responsive genes by binding to the promoter of *ERD1*, which in turn enhances drought tolerance. JA and 12-OPDA could increase stomatal closure. The elevation in OPDA levels coordinated with the decreased stomatal aperture and the increased drought tolerance (Savchenko et al., 2014). OsbHLH148 binds to OsJAZ1 to induce the expression of *OsDREB1*, thereby enhancing the drought resistance in rice (Sarwat and Tuteja, 2017). Recent studies have demonstrated that the Arabidopsis BBD proteins are essential in the ABA-mediated interplay of ABA and JA against drought stresses. Overexpression of *AtBBD1* increased ABA sensitivity considerably and enhanced the expression of critical genes involved in the ABA-mediated drought cascade, particularly those related to ABA biosynthesis and downstream transcription factors (Mahmudul Huque et al., 2021). The LATERAL ORGAN BOUNDARIES DOMAIN (LBD)-containing protein isolated from tomato participates in JA-mediated drought tolerance (Liu et al., 2020). The knockout of *SlLBD40* improved the water-holding ability of tomatoes. Water spray-inducible MYC-regulon creates a hierarchical transcriptional network via interacting with bHLH19 and ERF109, which demonstrated that spray-induced jasmonate accumulation was transcriptionally regulated by an MYC2-controlled positive-feedback loop (van Moerkercke et al., 2019).

MYC2 REGULATES THE BIOSYNTHESIS OF PLANT SECONDARY METABOLITES

Plants have evolved over time to develop a variety of stress-responsive mechanisms, including the production of defense chemicals against external stimuli. When a plant is stressed or induced by hormones, numerous secondary metabolites arise and accumulate. JA regulates the expression of key enzymes involved in plant secondary metabolism by activating or suppressing the activity of relevant transcription factors, which influences the expression of key enzymes and, as a result, influences secondary metabolite accumulation (Chen et al., 2019). In general, different types of transcription factors specifically regulate the biosynthetic pathways of different secondary metabolites, and some transcription factors are usually capable of regulating multiple genes along the same route (**Figure 5**).

MYC-like transcription factors are involved in the regulation of secondary metabolites such as terpenoids, alkaloids, flavonoids, and thioglycosides (Afrin et al., 2015). Paclitaxel, artemisinin, and tanshinone are terpenoids, which are classified into monoterpenes, sesquiterpenes, diterpenes, and triterpenes based on the number of isoprenoid units. AtTPS21 and AtTPS11 are responsible for volatile sesquiterpene biosynthesis. AtMYC2 directly binds to the promoters of *TPS11* and *TPS21* to regulate their expressions (Hong et al., 2012). DELLA can interact with MYC2 to repress the transactivation of *TPS*. Artemisinin is a sesquiterpene lactone whose biosynthesis is restricted to the specific glandular trichome cells (Olsson et al., 2009). Artemisinin biosynthesis genes are regulated by octadecanoid-derivative responsive AP2-domain protein (AaORA), which is regulated by the glandular trichome-specific transcription factor *Artemisia annua* GST-specific WRKY1 (AaGSW1). Overexpression of *AaMYC2* resulted in large increases in *cytochrome P450–dependent hydroxylase (CYP71AV1)* and *double bond reductase 2* (*DBR2*) levels, as well as an elevation in artemisinin content (Yu et al., 2012). MYC2 and bZIP1 synergistically regulate the expression of *GSW1*, while GSW1 binds to the promoter of *TEOSINTE BRANCHED 1/CYCLOIDEA/PROLIFERATING CELL FACTOR15* (*TCP15*) to regulate its transcription. ORA interacts with TCP14/15 to enhance the expression and transactivation of *DBR2* and *ALDEHYDE DEHYDROGENASE 1* (*ALDH1*) via TCP14/15 (Ma et al., 2018, 2021). AabHLH1 was specifically expressed in glandular trichome, and overexpression of bHLH1 can increase the expression of *AMORPHA-4, 11-DIENE SYNTHASE* (*ADS*), and *CYP71AV1* (Li L. et al., 2019). AabZIP9 binds to the ACGT element on the promoters of *ADS* and *CYP71AV1* (Shen et al., 2019). Overexpression of AabZIP9 increased the expression of *ADS*, but had no significant effect on the expression of *CYP71AV1*, *DBR2*, and *ALDH1*.

Paclitaxel is a diterpene that is strongly triggered by JA. Extensive *in vitro* interaction studies revealed that MYCs were involved in the expression of several critical genes in the upstream of paclitaxel (Cui et al., 2019). TcMYC2a can interact with JAZ3 protein to mediate the expression of paclitaxel biosynthesis genes. By binding to T/G-box, G-box, and E-box, TcMYC2a affects the expression level of the *GUS* gene. Overexpression of *MYC2a* in the *Taxus chinensis* suspension cell line increases the expression of *taxadiene synthase* (*TASY*), *taxadiene-5α-ol-acetyltransferase* (*tat*), *30-N-dephenylated paclitaxel-N-benzoyltransferase* (*dbtnbt*), and *taxane 13-alpha-hydroxylase* (*t13h*), whereas TcMYC2a inhibits the expression of *TASY* through its interaction with TcERF12/15 (Zhang M. et al., 2015; Zhang et al., 2018b). JA-inducible MYC transcription factors (TcJAMYC1, TcJAMYC2, and TcJAMYC4) are a group of negative regulators induced by JA whose domains are highly homologous to AtMYC2 (Lenka et al., 2015). JAMYCs regulate paclitaxel

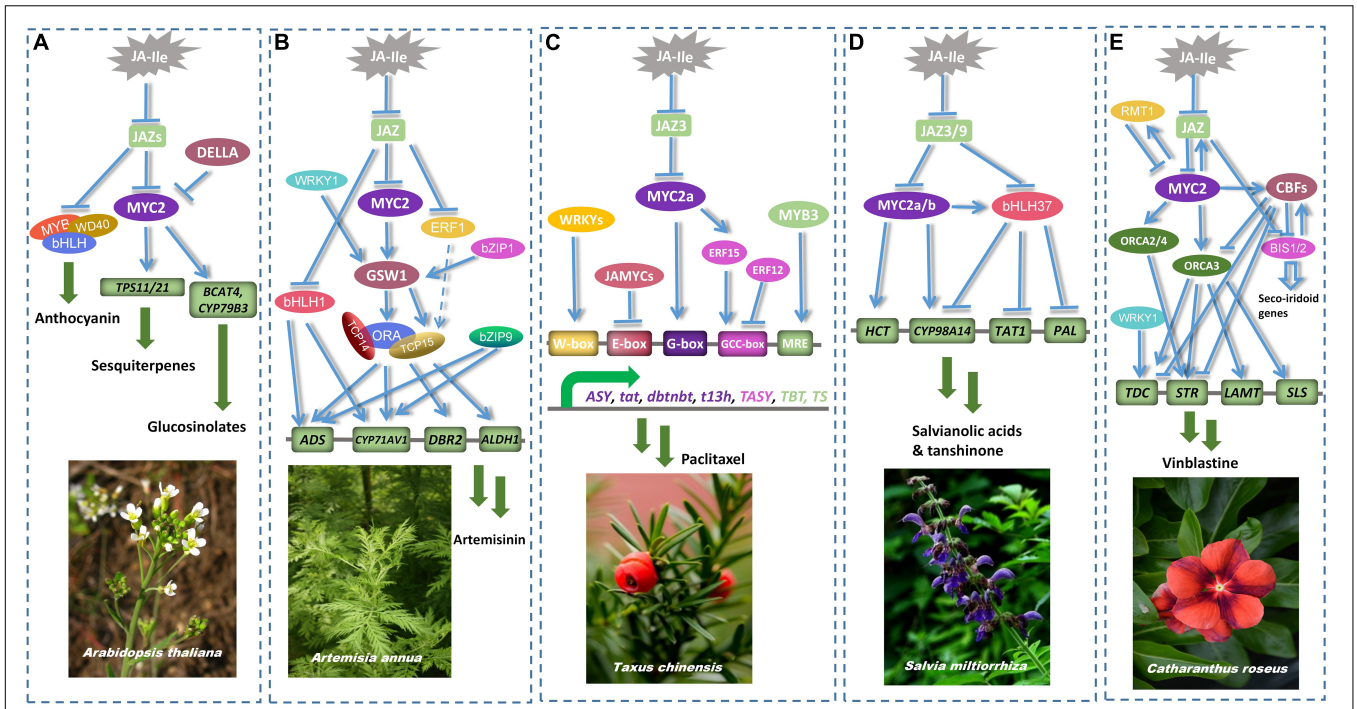


FIGURE 5 | MYC2 plays an important regulatory role in the formation of secondary metabolites in model plants. **(A)** AtMYC2 alone or together with the MYB/bHLH/WD40 complex regulates the expression of *CYP79B3*, *TPS11*, *TPS21* and anthocyanins accumulation (Xu et al., 2013; Wang L. et al., 2019). **(B)** AaMYC2 up-regulates the expression of *CYP71AV1*, by regulating the transcription of the glandular trichome-specific transcription factor AaGSW1 (Yu et al., 2012). AaMYC2 cooperates with ERFs, bHLHL1 and WRKY1 to jointly regulate the expression of *ADS* and *DBR2* (Ma et al., 2018; Li L. et al., 2019). **(C)** TcMYC2a interacts with JAZ3 protein to regulate the expression of *tat*, *dbtnbt*, *t13h*, and coordinates with ERF12/15 to control the expression of *TASY* (Zhang M. et al., 2015; Zhang et al., 2018b). TcMYC2 and TcJAMYCs antagonistically regulate key genes of paclitaxel biosynthetic pathway (Lenka et al., 2015). **(D)** SmMYC2 interacts with SmJAZ3/9 to competitively control the expression of *HCT6* and *CYP98A14* (Zhou et al., 2016). bHLHL37 and MYC2 synergistically regulate the synthesis of salvianolic acid B. Unlike MYC2, bHLHL37 negatively regulates the expression of *TAT1*, *PAL1,* and *CYP98A14* (Du et al., 2018). **(E)** CrMYC2 affects the expression of downstream genes *STR* and *TDC* by regulating the transcription of *ORCA2* and *ORCA3* (Van der Fits and Memelink, 2001; Zhang et al., 2011). In contrast, the negative regulators CBF1 and CBF2 competitively bind to MYC2-targeted genes thereby repressing the expression of TIA pathway genes (Sui et al., 2018).

biosynthesis via binding to the E-box on the promoters of paclitaxel-biosynthetic genes *TASY, taxadien-5α-ol by taxadien-5α-ol hydroxylase(T5aH), 10-deacetyl baccatinIII-10-O-acetyltransferase(DBAT), taxaneα-O-benzoyltransferase(DBBT), phenylalanine aminomutase (PAM), Baccatin III:3-amino, 3-phenylpropanoyl transferase(BAPT), 3-N-debenzoyl-2-deoxypaclitaxel-N-benzoyltransferase(DBTNBT)*. Overexpression of JAMYC negatively regulates the transcription of key genes related to paclitaxel biosynthesis. TcWRKYs regulate the expression of *TcERF12/15* and paclitaxel-biosynthetic genes at different levels (Zhang et al., 2018a). Overexpression of *WRKY8/20/26/47* positively regulates the expression of paclitaxel-biosynthetic genes. TmMYB3 increases the production of the paclitaxel precursor 10-deacetylbaccatin by binding to the MRE elements to upregulate the expression of *TBT* and *TS* (Yu et al., 2020).

Tanshinone is a representative diterpenoid. Tanshinone and salvianolic acid are two important active components in *Salvia miltiorrhiza*, whose biosynthesis is induced by JA. *SmMYC2a* and *SmMYC2b* participate in JA-mediated biosynthesis of tanshinone and salvianolic acid (Zhou et al., 2016). Hydroxy-cinnamoyl transferase6 (SmHCT6) and cytochrome P450 monooxygenase (SmCYP98A14) are key enzymes of the salvianolic acid biosynthesis pathway, whose expressions are induced by JA. MYC2a activates the expression of *HCT6* and *CYP98A14* by attaching to the promoter E-box of *HCT6* and *CYP98A14*. MYC2b regulates the expression of *CYP98A14* by binding to the E-box of *CYP98A14*. On the contrary, overexpression of *SmJAZ3* or *SmJAZ9* in *S. miltiorrhiza* hairy roots resulted in a significant decrease in tanshinone content, which might be attributed to the interaction of JAZ proteins with MYC2 to inhibit their transactivation. Tyrosine aminotransferase1(*TAT1*), phenylalanine ammonialyase1(*PAL1*) and *CYP98A14* are key genes for tanshinolate biosynthesis. *SmbHLHL37* and *SmMYC2* synergistically regulate the synthesis of salvianolic acid B (Du et al., 2018). The expression of *bHLHL37* is regulated by MYC2. It was found that MYC2 regulates the transcriptional activity of salvianolic acid B biosynthesis genes by binding to their promoters. bHLHL37 can dimerize and interact with JAZ3/8. Overexpression of *bHLHL37* decreases the synthesis of salvianolic acid B. bHLHL37 inhibits the production of salvianolic acid B by binding to the promoters of *SmTAT1*, *SmPAL1*, and *SmCYP98A14* to suppress their transcriptional activities.

Terpene alkaloids, especially terpene indole alkaloids (TIAs), have received more attention in *Catharanthus roseus*. JA is primarily responsible for inducing the production of these alkaloids. CrMYC1 was altered by fungal elicitor and JA in *C. roseus* suspension cells, indicating that CrMYC1 may be involved in the regulation of genes involved in JA signaling (Chatel et al., 2003). CrMYC2 is an early JA-responsive factor and regulates the expression of a series of TIA biosynthetic genes, by modulating the transcription of *octadecanoid-derivative responsive Catharanthus AP2-domain proteins* (*ORCA2* and *ORCA3*) (Zhang et al., 2011). Knockdown of *CrMYC2* by RNA interference significantly reduced the expression of *ORCA2* and *ORCA3*. MeJA induced the expression of *ORCA2* and *ORCA3* and was specifically bound to the JERE element in the *strictosidine synthase* (*STR*) promoter. This implies that CrMYC2 stimulates STR activity via binding to a G-box-like element on the promoter of *ORCA2/3*, triggering the production of ORCAs-targeted genes rather than directly to the *STR* promoter. CrMYC2 also controls the expression of TIA biosynthesis genes in collaboration with certain repressors. The G-box binding factors CrCBF1 and CrCBF2 act as negative regulators to repress the production of TIAs (Sui et al., 2018). Overexpression of *CrMYC2* increased the expression of *CrGBF* and eventually led to a reduction in alkaloid accumulation. CrGBF1 and CrGBF2 can form homo- and heterodimers to repress the activation of TIA pathway genes. CrGBF dimerizes with CrMYC2 and suppresses the transactivation of alkaloid-bisynthetic genes by competitively binding to the T/G-box of *CrMYC2* targeted genes. Like CrGBF, *CrRMT1* acts as a repressor of CrMYC2 that negatively regulates the MYC2-mediated transactivation of TIA-related genes (Patra et al., 2018). Nicotine is another well-studied alkaloid, featuring *NtCOI1*, *NtJAZ*, and *NtMYC2* involved in its production. Putrescine N-methyltransferase (NtPMT1a) is a key enzyme in nicotine production. NtMYC2 controls nicotine production via two regulatory mechanisms (Shoji and Hashimoto, 2011). The first directly binds to the G-box of the *PMT1a* promoter to regulate its transcriptional activation, and the second regulates the expression of *PMT1a* through interacting with ERF in the NIC2 region. NtMYC2a and NtMYC2b form a conjugated complex with NtJAZ1 that negatively regulates multiple steps of JA-induced nicotine biosynthesis (Zhang et al., 2012). Our research investigated the TIA-regulatory gene *MYC2* in *Dendrobium officinale* (Zhu et al., 2017). *DoMYC2* negatively regulates the upstream pathway of terpene alkaloids. The expression of *DoMYC2* could be induced by MeJA and chitosan in a short period. Overexpression of *DoMYC2* in Arabidopsis attenuated the expression levels of *HMG-CoA reductase* (*AtHMGR2*), *farnesyl diphosphate synthase* (*AtFPS1/AtFPS2*), and *isopentenyl transferases* (*AtIPTs*).

CONCLUSION AND FUTURE CHALLENGES

Since the discovery of JA receptor COl1, several regulatory factors in the JA signaling pathway have been uncovered one after another. JA plays an essential role in both maintaining normal development and protecting plants from environmental stresses. Plants have evolved a sophisticated negative feedback mechanisms to regulate the moderate onset of resistance responses during their continuous adaptation to the environment and various stresses. In this review, we encapsulate the diverse roles of MYC TFs and generalize a MYC-mediated JA signaling pathway. This gives our understanding of how JA works to maintain a balance between plant growth and adaptability to the external environment. The basic guidelines described here provide a framework for elucidating a cross-regulation between MYC2 and its co-regulons. As the core regulatory molecules of the JA signaling branch, MYC2 and its relatives directly target hundreds of JA-responsive genes, building a positive cascade of transcriptional reprogramming. The downstream TFs under MYC2 and its homologs directly targeted overlapping but separate cohorts of genes, indicating that they have different roles within the JA response. The intricacy within the MYC2-mediated JA signaling pathway in general is the presence of some feedforward and feedback loops that are simultaneously activated. However, relationships between these subnetworks through the dynamics and resilience of their regulatory effects on the broader network are not well understood. Uncoupling these subnetworks would be an effective way to assess how they socialize to drive a robust activation of JA signaling.

AUTHOR CONTRIBUTIONS

CS, YC, and HD discussed the writing plan. CS, YC, JD, and GL drafted the manuscript. CS, MM, and CC edited the manuscript. HD and CS acquired the funding. All authors have read, reviewed, and approved the submitted version.

FUNDING

This work was supported by the Natural Science Foundation of Anhui Province (1808085MH307), High-level Talents Research Initiation Funding Project of West Anhui University (WGKQ2022025), and Quality Engineering Project in Anhui Province (2020jyxm2137).

REFERENCES

An, C., Li, L., Zhai, Q., You, Y., Deng, L., Wu, F., et al. (2017). Mediator subunit MED25 links the jasmonate receptor to transcriptionally active chromatin. *Proc. Natl. Acad. Sci. U S A.* 114, E8930–E8939. doi: 10.1073/pnas.1710885114

Afrin, S., Huang, J. J., and Luo, Z. Y. (2015). JA-mediated transcriptional regulation of secondary metabolism in medicinal plants. *Sci. Bull.* 60, 1062–1072. doi: 10.1007/s11434-015-0813-0

Bai, Y., Meng, Y., Huang, D., Qi, Y., and Chen, M. (2011). Origin and evolutionary analysis of the plant-specific TIFY transcription factor family. *Genomics* 98, 128–136. doi: 10.1016/j.ygeno.2011.05.002

Berger, S., Bell, E., and Mullet, J. E. (1996). Two methyl jasmonate-insensitive mutants show altered expression of AtVsp in response to methyl jasmonate and wounding. *Plant Physiol.* 111, 525–531. doi: 10.1104/pp.111.2.525

Cai, Q., Yuan, Z., Chen, M., Yin, C., Luo, Z., Zhao, X., et al. (2014). Jasmonic acid regulates spikelet development in rice. *Nat. Commun.* 5:3476. doi: 10.1038/ncomms4476

Chakraborty, M., Gangappa, S. N., Maurya, J. P., Sethi, V., Srivastava, A. K., Singh, A., et al. (2019). Functional interrelation of MYC2 and HY5 plays an important role in *Arabidopsis* seedling development. *Plant J.* 99, 1080–1097. doi: 10.1111/tpj.14381

Chatel, G., Montiel, G., Pré, M., Memelink, J., Thiersault, M., Saint-Pierre, B., et al. (2003). CrMYC1, a Catharanthus roseus elicitor- and jasmonate-responsive bHLH transcription factor that binds the G-box element of the strictosidine synthase gene promoter. *J. Exp. Bot.* 54, 2587–2588. doi: 10.1093/jxb/erg275

Chen, H. Y., Hsieh, E. J., Cheng, M. C., Chen, C. Y., Hwang, S. Y., and Lin, T. P. (2016). ORA47 (octadecanoid-responsive AP2/ERF-domain transcription factor 47) regulates jasmonic acid and abscisic acid biosynthesis and signaling through binding to a novel cis-element. *New Phytol.* 211, 599–613. doi: 10.1111/nph.13914

Chen, Q., Sun, J., Zhai, Q., Zhou, W., Qi, L., Xu, L., et al. (2011). The basic helix-loop-helix transcription factor myc2 directly represses plethora expression during jasmonate-mediated modulation of the root stem cell niche in *Arabidopsis*. *Plant Cell* 23, 3335–3352. doi: 10.1105/tpc.111.089870

Chen, X., Wang, D. D., Fang, X., Chen, X. Y., and Mao, Y. B. (2019). Plant specialized metabolism regulated by jasmonate signaling. *Plant Cell Physiol.* 60, 2638–2647. doi: 10.1093/pcp/pcz161

Cheng, Z., Sun, L., Qi, T., Zhang, B., Peng, W., Liu, Y., et al. (2011). The bHLH transcription factor MYC3 interacts with the jasmonate ZIM-domain proteins to mediate jasmonate response in *Arabidopsis*. *Mol. Plant* 4, 279–288. doi: 10.1093/mp/ssq073

Chico, J. M., Fernández-Barbero, G., Chini, A., Fernández-Calvo, P., Díez-Díaz, M., and Solano, R. (2014). Repression of jasmonate-dependent defenses by shade involves differential regulation of protein stability of MYC transcription factors and their JAZ repressors in *Arabidopsis*. *Plant Cell* 26, 1967–1980. doi: 10.1105/tpc.114.125047

Chico, J. M., Lechner, E., Fernandez-Barbero, G., Canibano, E., García-Casado, G., Franco-Zorrilla, J. M., et al. (2020). CUL3BPM E3 ubiquitin ligases regulate MYC2, MYC3, and MYC4 stability and JA responses. *Proc. Natl. Acad. Sci. U. S. A.* 117, 6205–6215. doi: 10.1073/pnas.1912199117

Cui, H., Qiu, J., Zhou, Y., Bhandari, D. D., Zhao, C., Bautor, J., et al. (2018). Antagonism of transcription factor MYC2 by EDS1/PAD4 complexes bolsters salicylic acid defense in *Arabidopsis* effector-triggered immunity. *Mol. Plant* 11, 1053–1066. doi: 10.1016/j.molp.2018.05.007

Cui, Y., Mao, R., Chen, J., and Guo, Z. (2019). Regulation mechanism of MYC family transcription factors in jasmonic acid signalling pathway on taxol biosynthesis. *Int. J. Mol. Sci.* 20:1843. doi: 10.3390/ijms20081843

Daguerre, Y., Basso, V., Hartmann-Wittulski, S., Schellenberger, R., Meyer, L., Bailly, J., et al. (2020). The mutualism effector MiSSP7 of Laccaria bicolor alters the interactions between the poplar JAZ6 protein and its associated proteins. *Sci. Rep.* 10:20362. doi: 10.1038/s41598-020-76832-76836

Ding, F., Wang, C., Xu, N., Wang, M., and Zhang, S. (2021). Jasmonic acid-regulated putrescine biosynthesis attenuates cold-induced oxidative stress in tomato plants. *Sci. Hortic. (Amsterdam)* 288:110373. doi: 10.1016/j.scienta.2021.110373

Dob, A., Lakehal, A., Novak, O., and Bellini, C. (2021). Jasmonate inhibits adventitious root initiation through repression of CKX1 and activation of RAP2.6L transcription factor in *Arabidopsis*. *J. Exp. Bot.* 72, 7107–7118. doi: 10.1093/jxb/erab358

Dombrecht, B., Gang, P. X., Sprague, S. J., Kirkegaard, J. A., Ross, J. J., Reid, J. B., et al. (2007). MYC2 differentially modulates diverse jasmonate-dependent functions in *Arabidopsis*. *Plant Cell* 19, 2225–2245. doi: 10.1105/tpc.106.048017

Du, M., Zhai, Q., Deng, L., Li, S., Li, H., Yan, L., et al. (2014). Closely related NAC transcription factors of tomato differentially regulate stomatal closure and reopening during pathogen attack. *Plant Cell* 26, 3167–3184. doi: 10.1105/tpc.114.128272

Du, M., Zhao, J., Tzeng, D. T. W., Liu, Y., Deng, L., Yang, T., et al. (2017). MYC2 orchestrates a hierarchical transcriptional cascade that regulates jasmonate-mediated plant immunity in tomato. *Plant Cell* 29, 1883–1906. doi: 10.1105/tpc.16.00953

Du, T., Niu, J., Su, J., Li, S., Guo, X., Li, L., et al. (2018). SmbHLH37 functions antagonistically with smMYC2 in regulating jasmonate-mediated biosynthesis of phenolic acids in salvia miltiorrhiza. *Front. Plant Sci.* 871:1720. doi: 10.3389/fpls.2018.01720

Dubois, M., Van den Broeck, L., and Inzé, D. (2018). The pivotal role of ethylene in plant growth. *Trends Plant Sci.* 23, 311–323. doi: 10.1016/j.tplants.2018.01.003

Fernández-Calvo, P., Chini, A., Fernández-Barbero, G., Chico, J. M., Gimenez-Ibanez, S., Geerinck, J., et al. (2011). The *Arabidopsis* bHLH transcription factors MYC3 and MYC4 are targets of JAZ repressors and act additively with MYC2 in the activation of jasmonate responses. *Plant Cell* 23, 701–715. doi: 10.1105/tpc.110.080788

Figueroa, P., and Browse, J. (2012). The *Arabidopsis* JAZ2 promoter contains a G-box and thymidine-rich module that are necessary and sufficient for jasmonate-dependent activation by MYC transcription factors and repression by JAZ proteins. *Plant Cell Physiol.* 53, 330–343. doi: 10.1093/pcp/pcr178

Gao, C., Qi, S., Liu, K., Li, D., Jin, C., Li, Z., et al. (2016). MYC2, MYC3, and MYC4 function redundantly in seed storage protein accumulation in *Arabidopsis*. *Plant Physiol. Biochem.* 108, 63–70. doi: 10.1016/j.plaphy.2016.07.004

Gautam, J. K., Giri, M. K., Singh, D., Chattopadhyay, S., and Nandi, A. K. (2021). MYC2 influences salicylic acid biosynthesis and defense against bacterial pathogens in *Arabidopsis thaliana*. *Physiol. Plantarum* 173, 2248–2261. doi: 10.1111/ppl.13575

Goossens, J., Swinnen, G., Vanden Bossche, R., Pauwels, L., and Goossens, A. (2015). Change of a conserved amino acid in the MYC2 and MYC3 transcription factors leads to release of JAZ repression and increased activity. *New Phytol.* 206, 1229–1237. doi: 10.1111/nph.13398

Guo, H., Nolan, T. M., Song, G., Liu, S., Xie, Z., Chen, J., et al. (2018). FERONIA receptor kinase contributes to plant immunity by suppressing jasmonic acid signaling in *Arabidopsis thaliana*. *Curr. Biol.* 28, 3316–3324.e6. doi: 10.1016/j.cub.2018.07.078.

He, Y., Chen, L., Zhou, Y., Mawhinney, T. P., Chen, B., Kang, B. H., et al. (2011). Functional characterization of *Arabidopsis thaliana* isopropylmalate dehydrogenases reveals their important roles in gametophyte development. *New Phytol.* 189, 160–175. doi: 10.1111/j.1469-8137.2010.03460.x

Heim, M. A., Jakoby, M., Werber, M., Martin, C., Weisshaar, B., and Bailey, P. C. (2003). The basic helix-loop-helix transcription factor family in plants: a genome-wide study of protein structure and functional diversity. *Mol. Biol. Evol.* 20, 735–747. doi: 10.1093/molbev/msg088

Hong, G. J., Xue, X. Y., Mao, Y. B., Wang, L. J., and Chen, X. Y. (2012). *Arabidopsis* MYC2 interacts with DELLA proteins in regulating sesquiterpene synthase gene expression. *Plant Cell* 24, 2635–2648. doi: 10.1105/tpc.112.098749

Hsieh, H. L., and Okamoto, H. (2014). Molecular interaction of jasmonate and phytochrome a signalling. *J. Exp. Bot.* 65, 2847–2857. doi: 10.1093/jxb/eru230

Hu, C., Wei, C., Ma, Q., Dong, H., Shi, K., Zhou, Y., et al. (2021). Ethylene response factors 15 and 16 trigger jasmonate biosynthesis in tomato during herbivore resistance. *Plant Physiol.* 185, 1182–1197. doi: 10.1093/PLPHYS/KIAA089

Hu, Y., Jiang, Y., Han, X., Wang, H., Pan, J., and Yu, D. (2017). Jasmonate regulates leaf senescence and tolerance to cold stress: crosstalk with other phytohormones. *J. Exp. Bot.* 68, 1361–1369. doi: 10.1093/jxb/erx004

Hu, Y., Sun, H., Han, Z., Wang, S., Wang, T., Li, Q., et al. (2022). ERF4 affects fruit ripening by acting as a JAZ interactor between ethylene and jasmonic acid hormone signaling pathways. *Hortic. Plant J.* doi: 10.1016/j.hpj.2022.01.002

Huang, C. F., Yu, C. P., Wu, Y. H., Lu, M. Y. J., Tu, S. L., Wu, S. H., et al. (2017). Elevated auxin biosynthesis and transport underlie high vein density in C4 leaves. *Proc. Natl. Acad. Sci. U S A.* 114, E6884–E6891. doi: 10.1073/pnas.1709171114

Jiang, S., Yao, J., Ma, K. W., Zhou, H., Song, J., He, S. Y., et al. (2013). Bacterial effector activates jasmonate signaling by directly targeting JAZ transcriptional repressors. *PLoS Pathog* 9:e1003715. doi: 10.1371/journal.ppat.1003715

Kashyap, P., and Deswal, R. (2019). Two ICE isoforms showing differential transcriptional regulation by cold and hormones participate in *Brassica juncea* cold stress signaling. *Gene* 695, 32–41. doi: 10.1016/j.gene.2019.02.005

Kazan, K. (2015). Diverse roles of jasmonates and ethylene in abiotic stress tolerance. *Trends Plant Sci.* 20, 219–229. doi: 10.1016/j.tplants.2015.02.001

Kazan, K., and Manners, J. M. (2013). MYC2: the master in action. *Mol. Plant* 6, 686–703. doi: 10.1093/mp/sss128

Knill, T., Schuster, J., Reichelt, M., Gershenzon, J., and Binder, S. (2008). *Arabidopsis* branched-chain aminotransferase 3 functions in both amino acid and glucosinolate biosynthesis. *Plant Physiol.* 146, 1028–1039. doi: 10.1104/pp.107.111609

Koprivova, A., Schuck, S., Jacoby, R. P., Klinkhammer, I., Welter, B., Leson, L., et al. (2019). Root-specific camalexin biosynthesis controls the plant growth-promoting effects of multiple bacterial strains. *Proc. Natl. Acad. Sci. U S A.* 116, 15735–15744. doi: 10.1073/pnas.1818604116

Laurie-Berry, N., Joardar, V., Street, I. H., and Kunkel, B. N. (2006). The *Arabidopsis thaliana* JASMONATE INSENSITIVE 1 gene is required for suppression of salicylic acid-dependent defenses during infection by *Pseudomonas syringae*. *Mol. Plant-Microbe Interact.* 19, 789–800. doi: 10.1094/MPMI-19-0789

Lenka, S. K., Ezekiel Nims, N., Vongpaseuth, K., Boshar, R. A., Roberts, S. C., and Walker, E. L. (2015). Jasmonate-responsive expression of paclitaxel biosynthesis genes in Taxus cuspidata cultured cells is negatively regulated by the bHLH transcription factors TcJAMYC1, TcJAMYC2, and TcJAMYC4. *Front. Plant Sci.* 6:115. doi: 10.3389/fpls.2015.00115

Li, L., Hao, X., Liu, H., Wang, W., Fu, X., Ma, Y., et al. (2019). Jasmonic acid-responsive AabHLH1 positively regulates artemisinin biosynthesis in *Artemisia annua*. *Biotechnol. Appl. Biochem.* 66, 369–375. doi: 10.1002/bab.1733

Li, T., Jiang, Z., Zhang, L., Tan, D., Wei, Y., Yuan, H., et al. (2016). Apple (Malus domestica) MdERF2 negatively affects ethylene biosynthesis during fruit ripening by suppressing MdACS1 transcription. *Plant J.* 88, 735–748. doi: 10.1111/tpj.13289

Li, T., Xu, Y., Zhang, L., Ji, Y., Tan, D., Yuan, H., et al. (2017). The jasmonate-activated transcription factor MdMYC2 regulates ETHYLENE RESPONSE FACTOR and ethylene biosynthetic genes to promote ethylene biosynthesis during apple fruit ripening. *Plant Cell* 29, 1316–1334. doi: 10.1105/tpc.17.00349

Li, Y., Yang, X., and Li, X. (2019). Role of jasmonate signaling pathway in resistance to dehydration stress in *Arabidopsis*. *Acta Physiol. Plant.* 41:100. doi: 10.1007/s11738-019-2897-2897

Lian, T. F., Xu, Y. P., Li, L. F., and Su, X. D. (2017). Crystal structure of tetrameric *Arabidopsis* MYC2 reveals the mechanism of enhanced interaction with DNA. *Cell Rep.* 19, 1334–1342. doi: 10.1016/j.celrep.2017.04.057

Liu, L., Zhang, J., Xu, J., Li, Y., Guo, L., Wang, Z., et al. (2020). CRISPR/Cas9 targeted mutagenesis of SlLBD40, a lateral organ boundaries domain transcription factor, enhances drought tolerance in tomato. *Plant Sci.* 301:110683. doi: 10.1016/j.plantsci.2020.110683

Liu, Y., Du, M., Deng, L., Shen, J., Fang, M., Chen, Q., et al. (2019). Myc2 regulates the termination of jasmonate signaling via an autoregulatory negative feedback loop[open]. *Plant Cell* 31, 106–127. doi: 10.1105/tpc.18.00405

Lorenzo, O., Chico, J. M., Sánchez-Serrano, J. J., and Solano, R. (2004). JASMONATE-INSENSITIVE1 encodes a MYC transcription factor essential to discriminate between different jasmonate-regulated defense responses in *Arabidopsis*. *Plant Cell* 16, 1938–1950. doi: 10.1105/tpc.022319

Ma, H., Duan, J., Ke, J., He, Y., Gu, X., Xu, T. H., et al. (2017). A D53 repression motif induces oligomerization of TOPLESS corepressors and promotes assembly of a corepressor-nucleosome complex. *Sci. Adv.* 3:e1601217. doi: 10.1126/sciadv.1601217

Ma, Y. N., Xu, D. B., Li, L., Zhang, F., Fu, X. Q., Shen, Q., et al. (2018). Jasmonate promotes artemisinin biosynthesis by activating the TCP14-ORA complex in *Artemisia annua*. *Sci. Adv.* 4:eaas9357. doi: 10.1126/sciadv.aas9357

Ma, Y. N., Xu, D. B., Yan, X., Wu, Z. K., Kayani, S. I., Shen, Q., et al. (2021). Jasmonate- and abscisic acid-activated AaGSW1-AaTCP15/AaORA transcriptional cascade promotes artemisinin biosynthesis in *Artemisia annua*. *Plant Biotechnol. J.* 19, 1412–1428. doi: 10.1111/pbi.13561

Mahmudul Huque, A. K. M., So, W., Noh, M., You, M. K., and Shin, J. S. (2021). Overexpression of atbbd1, *Arabidopsis* bifunctional nuclease, confers drought tolerance by enhancing the expression of regulatory genes in aba-mediated drought stress signaling. *Int. J. Mol. Sci.* 22:2936. doi: 10.3390/ijms22062936

Major, I. T., Yoshida, Y., Campos, M. L., Kapali, G., Xin, X. F., Sugimoto, K., et al. (2017). Regulation of growth-defense balance by the JASMONATE ZIM-DOMAIN (JAZ)-MYC transcriptional module. *New Phytol.* 215, 1533–1547. doi: 10.1111/nph.14638

Mao, Y. B., Liu, Y. Q., Chen, D. Y., Chen, F. Y., Fang, X., Hong, G. J., et al. (2017). Jasmonate response decay and defense metabolite accumulation contributes to age-regulated dynamics of plant insect resistance. *Nat. Commun.* 8:13925. doi: 10.1038/ncomms13925

Mikkelsen, M. D., Petersen, B. L., Glawischnig, E., Jensen, A. B., Andreasson, E., and Halkier, B. A. (2003). Modulation of CYP79 genes and glucosinolate profiles in *Arabidopsis* by defense signaling pathways. *Plant Physiol.* 131, 298–308. doi: 10.1104/pp.011015

Mucha, S., Heinzlmeir, S., Kriechbaumer, V., Strickland, B., Kirchhelle, C., Choudhary, M., et al. (2019). The formation of a camalexin biosynthetic metabolon. *Plant Cell* 31, 2697–2710. doi: 10.1105/tpc.19.00403

Olsson, M. E., Olofsson, L. M., Lindahl, A. L., Lundgren, A., Brodelius, M., and Brodelius, P. E. (2009). Localization of enzymes of artemisinin biosynthesis to the apical cells of glandular secretory trichomes of *Artemisia annua* L. *Phytochemistry* 70, 1123–1128. doi: 10.1016/j.phytochem.2009.07.009

Ortigosa, A., Fonseca, S., Franco-Zorrilla, J. M., Fernández-Calvo, P., Zander, M., Lewsey, M. G., et al. (2020). The JA-pathway MYC transcription factors regulate photomorphogenic responses by targeting HY5 gene expression. *Plant J.* 102, 138–152. doi: 10.1111/tpj.14618

Patra, B., Pattanaik, S., Schluttenhofer, C., and Yuan, L. (2018). A network of jasmonate-responsive bHLH factors modulate monoterpenoid indole alkaloid biosynthesis in *Catharanthus roseus*. *New Phytol.* 217, 1566–1581. doi: 10.1111/nph.14910

Pauwels, L., Barbero, G. F., Geerinck, J., Tilleman, S., Grunewald, W., Pérez, A. C., et al. (2010). NINJA connects the co-repressor TOPLESS to jasmonate signalling. *Nature* 464, 788–791. doi: 10.1038/nature08854

Peñuelas, M., Monte, I., Schweizer, F., Vallat, A., Reymond, P., García-Casado, G., et al. (2019). Jasmonate-related MYC transcription factors are functionally conserved in marchantia polymorpha. *Plant Cell* 31, 2491–2509. doi: 10.1105/tpc.18.00974

Pérez-Alonso, M. M., Sánchez-Parra, B., Ortiz-García, P., Santamaría, M. E., Díaz, I., and Pollmann, S. (2021). Jasmonic acid-dependent myc transcription factors bind to a tandem g-box motif in the yucca8 and yucca9 promoters to regulate biotic stress responses. *Int. J. Mol. Sci.* 22:9768. doi: 10.3390/ijms22189768

Piotrowski, M., Schemenewitz, A., Lopukhina, A., Müller, A., Janowitz, T., Weiler, E. W., et al. (2004). Desulfoglucosinolate sulfotransferases from *Arabidopsis thaliana* catalyze the final step in the biosynthesis of the glucosinolate core structure. *J. Biol. Chem.* 279, 50717–50725. doi: 10.1074/jbc.M407681200

Pires, N., and Dolan, L. (2010). Origin and diversification of basic-helix-loop-helix proteins in plants. *Mol. Biol. Evol.* 27, 862–874. doi: 10.1093/molbev/msp288

Plett, J. M., Daguerre, Y., Wittulsky, S., Vayssierres, A., Deveau, A., Melton, S. J., et al. (2014). Effector MiSSP7 of the mutualistic fungus *Laccaria bicolor* stabilizes the Populus JAZ6 protein and represses jasmonic acid (JA) responsive genes. *Proc. Natl. Acad. Sci. U S A.* 111, 8299–8304. doi: 10.1073/pnas.1322671111

Qi, T., Huang, H., Song, S., and Xie, D. (2015a). Regulation of jasmonate-mediated stamen development and seed production by a bHLH-MYB complex in *Arabidopsis*. *Plant Cell* 27, 1620–1633. doi: 10.1105/tpc.15.00116

Qi, T., Wang, J., Huang, H., Liu, B., Gao, H., Liu, Y., et al. (2015b). Regulation of jasmonate-induced leaf senescence by antagonism between bHLH subgroup IIIe and IIId factors in *Arabidopsis*. *Plant Cell* 27, 1634–1649. doi: 10.1105/tpc.15.00110

Sabagh, A. E. L., Islam, M. S., Hossain, A., Battaglia, M., Ahmed, S., Rehman, A., et al. (2022). Phytohormones as growth regulators during abiotic stress tolerance in plants. *Front. Plant Sci.* 4:765068. doi: 10.3389/fagro.2022.765068

Santner, A., and Estelle, M. (2009). Recent advances and emerging trends in plant hormone signalling. *Nature* 459, 1071–1078. doi: 10.1038/nature08122

Sarwat, M., and Tuteja, N. (2017). Hormonal signaling to control stomatal movement during drought stress. *Plant Gene* 11, 143–153. doi: 10.1016/j.plgene.2017.07.007

Sasaki-Sekimoto, Y., Jikumaru, Y., Obayashi, T., Saito, H., Masuda, S., Kamiya, Y., et al. (2013). Basic helix-loop-helix transcription factors JASMONATE-ASSOCIATED MYC2-LIKE1 (JAM1), JAM2, and JAM3 are negative regulators

of jasmonate responses in *Arabidopsis*. *Plant Physiol.* 163, 291–304. doi: 10.1104/pp.113.220129

Savchenko, T., Kolla, V. A., Wang, C. Q., Nasafi, Z., Hicks, D. R., Phadungchob, B., et al. (2014). Functional convergence of oxylipin and abscisic acid pathways controls stomatal closure in response to drought. *Plant Physiol.* 164, 1151–1160. doi: 10.4161/psb.28304

Schweizer, F., Fernández-Calvo, P., Zander, M., Diez-Diaz, M., Fonseca, S., Glauser, G., et al. (2013). *Arabidopsis* basic helix-loop-helix transcription factors MYC2,MYC3, andMYC4 regulate glucosinolate biosynthesis, insect performance, and feeding behavior. *Plant Cell* 25, 3117–3132. doi: 10.1105/tpc.113.115139

Shen, Q., Huang, H., Zhao, Y., Xie, L., He, Q., Zhong, Y., et al. (2019). The transcription factor Aabzip9 positively regulates the biosynthesis of artemisinin in *Artemisia annua*. *Front. Plant Sci.* 10:1294. doi: 10.3389/fpls.2019.01294

Shin, J., Heidrich, K., Sanchez-Villarreal, A., Parker, J. E., and Davis, S. J. (2012). TIME FOR COFFEE represses accumulation of the MYC2 transcription factor to provide time-of-day regulation of jasmonate signaling in *Arabidopsis*. *Plant Cell* 24, 2470–2482. doi: 10.1105/tpc.111.095430

Shoji, T., and Hashimoto, T. (2011). Tobacco MYC2 regulates jasmonate-inducible nicotine biosynthesis genes directly and by way of the NIC2-Locus ERF genes. *Plant Cell Physiol.* 52, 1117–1130. doi: 10.1093/pcp/pcr063

Song, S., Huang, H., Gao, H., Wang, J., Wu, D., Liu, X., et al. (2014). Interaction between MYC2 and ETHYLENE INSENSITIVE3 modulates antagonism between jasmonate and ethylene signaling in *Arabidopsis*. *Plant Cell* 26, 263–279. doi: 10.1105/tpc.113.120394

Song, S., Qi, T., Fan, M., Zhang, X., Gao, H., Huang, H., et al. (2013). The bHLH Subgroup IIId factors negatively regulate jasmonate-mediated plant defense and development. *PLoS Genet.* 9:e1003653. doi: 10.1371/journal.pgen.1003653

Sui, X., Singh, S. K., Patra, B., Schluttenhofer, C., Guo, W., Pattanaik, S., et al. (2018). Cross-family transcription factor interaction between MYC2 and GBFs modulates terpenoid indole alkaloid biosynthesis. *J. Exp. Bot.* 69, 4267–4281. doi: 10.1093/jxb/ery229

Suza, W. P., and Staswick, P. E. (2008). The role of JAR1 in Jasmonoyl-l-isoleucine production during *Arabidopsis* wound response. *Planta* 227, 1221–1232. doi: 10.1007/s00425-008-0694-694

Thines, B., Katsir, L., Melotto, M., Niu, Y., Mandaokar, A., Liu, G., et al. (2007). JAZ repressor proteins are targets of the SCFCOI1 complex during jasmonate signalling. *Nature* 448, 661–665. doi: 10.1038/nature05960

Toledo-Ortiz, G., Huq, E., and Quail, P. H. (2003). The *Arabidopsis* basic/helix-loop-helix transcription factor family. *Plant Cell* 15, 1749–1770. doi: 10.1105/tpc.013839

Van der Fits, L., and Memelink, J. (2001). The jasmonate-inducible AP2/ERF-domain transcription factor ORCA3 activates gene expression via interaction with a jasmonate-responsive promoter element. *Plant J.* 25, 43–53. doi: 10.1046/j.1365-313X.2001.00932.x

van Moerkercke, A., Duncan, O., Zander, M., Simura, J., Broda, M., Bossche, R., et al. (2019). A MYC2/MYC3/MYC4-dependent transcription factor network regulates water spray-responsive gene expression and jasmonate levels. *Proc. Natl. Acad. Sci. U S A.* 116, 23345–23356. doi: 10.1073/pnas.1911758116

Verma, V., Ravindran, P., and Kumar, P. P. (2016). Plant hormone-mediated regulation of stress responses. *BMC Plant Biol.* 16:86. doi: 10.1186/s12870-016-0771-y

Wager, A., and Browse, J. (2012). Social network: JAZ protein interactions expand our knowledge of jasmonate signaling. *Front. Plant Sci.* 3:41. doi: 10.3389/fpls.2012.00041

Wang, H., Li, Y., Pan, J., Lou, D., Hu, Y., and Yu, D. (2017). The bHLH transcription factors MYC2, MYC3, and MYC4 are required for jasmonate-mediated inhibition of flowering in *Arabidopsis*. *Mol. Plant* 10, 1461–1464. doi: 10.1016/j.molp.2017.08.007

Wang, H., Li, S., Li, Y., Xu, Y., Wang, Y., Zhang, R., et al. (2019). MED25 connects enhancer-promoter looping and MYC2-dependent activation of jasmonate signalling. *Nat. Plants* 5, 616–625. doi: 10.1038/s41477-019-0441-449

Wang, L., Tang, W., Hu, Y., Zhang, Y., Sun, J., Guo, X., et al. (2019). A MYB/bHLH complex regulates tissue-specific anthocyanin biosynthesis in the inner pericarp of red-centered kiwifruit *Actinidia chinensis* cv. *Hongyang*. *Plant J.* 99, 359–378. doi: 10.1111/tpj.14330

Wang, Y., Xu, H., Liu, W., Wang, N., Qu, C., Jiang, S., et al. (2019). Methyl jasmonate enhances apple' cold tolerance through the JAZ-MYC2 pathway. *Plant Cell. Tissue Organ Cult.* 136, 75–84. doi: 10.1007/s11240-018-1493-1497

Wasternack, C. (2019). Termination in jasmonate signaling by MYC2 and MTBs. *Trends Plant Sci.* 24, 667–669. doi: 10.1016/j.tplants.2019.06.001

Wasternack, C., and Xie, D. (2010). The genuine ligand of a jasmonic acid receptor: improved analysis of jasmonates is now required. *Plant Signal. Behav.* 5, 337–340. doi: 10.4161/psb.5.4.11574

Wu, F., Deng, L., Zhai, Q., Zhao, J., Chen, Q., and Li, C. (2020). Mediator subunit MED25 couples alternative splicing of JAZ genes with fine-tuning of jasmonate signaling. *Plant Cell* 32, 429–448. doi: 10.1105/tpc.19.00583

Xu, W., Grain, D., Le Gourrierec, J., Harscoët, E., Berger, A., Jauvion, V., et al. (2013). Regulation of flavonoid biosynthesis involves an unexpected complex transcriptional regulation of TT8 expression, in *Arabidopsis*. *New Phytol.* 198, 59–70. doi: 10.1111/nph.12142

Yang, J., Duan, G., Li, C., Liu, L., Han, G., Zhang, Y., et al. (2019). The crosstalks between jasmonic acid and other plant hormone signaling highlight the involvement of jasmonic acid as a core component in plant response to biotic and abiotic stresses. *Front. Plant Sci.* 10:1349. doi: 10.3389/fpls.2019.01349

You, Y., Zhai, Q., An, C., and Li, C. (2019). Leunig_homolog mediates MYC2-dependent transcriptional activation in cooperation with the coactivators HAC1 and MED25. *Plant Cell* 31, 2187–2205. doi: 10.1105/TPC.19.00115

Yu, C., Luo, X., Zhang, C., Xu, X., Huang, J., Chen, Y., et al. (2020). Tissue-specific study across the stem of Taxus media identifies a phloem-specific TmMYB3 involved in the transcriptional regulation of paclitaxel biosynthesis. *Plant J.* 103, 95–110. doi: 10.1111/tpj.14710

Yu, Z. X., Li, J. X., Yang, C. Q., Hu, W. L., Wang, L. J., and Chen, X. Y. (2012). The jasmonate-responsive AP2/ERF transcription factors AaERF1 and AaERF2 positively regulate artemisinin biosynthesis in *Artemisia annua* L. *Mol. Plant* 5, 353–365. doi: 10.1093/mp/ssr087

Zander, M., Lewsey, M. G., Clark, N. M., Yin, L., Bartlett, A., Saldierna Guzmán, J. P., et al. (2020). Integrated multi-omics framework of the plant response to jasmonic acid. *Nat. Plants* 6, 290–302. doi: 10.1038/s41477-020-0605-607

Zhai, Q., and Li, C. (2019). The plant Mediator complex and its role in jasmonate signaling. *J. Exp. Bot.* 70, 3415–3424. doi: 10.1093/jxb/erz233

Zhai, Q., Deng, L., and Li, C. (2020). Mediator subunit MED25: at the nexus of jasmonate signaling. *Curr. Opin. Plant Biol.* 57, 78–86. doi: 10.1016/j.pbi.2020.06.006

Zhang, C., Lei, Y., Lu, C., Wang, L., and Wu, J. (2020). MYC2, MYC3, and MYC4 function additively in wounding-induced jasmonic acid biosynthesis and catabolism. *J. Integr. Plant Biol.* 62, 1159–1175. doi: 10.1111/jipb.12902

Zhang, F., Ke, J., Zhang, L., Chen, R., Sugimoto, K., Howe, G. A., et al. (2017). Structural insights into alternative splicing-mediated desensitization of jasmonate signaling. *Proc. Natl. Acad. Sci. U S A.* 114, 1720–1725. doi: 10.1073/pnas.1616938114

Zhang, F., Yao, J., Ke, J., Zhang, L., Lam, V. Q., Xin, X. F., et al. (2015). Structural basis of JAZ repression of MYC transcription factors in jasmonate signalling. *Nature* 525, 269–273. doi: 10.1038/nature14661

Zhang, H. B., Bokowiec, M. T., Rushton, P. J., Han, S. C., and Timko, M. P. (2012). Tobacco transcription factors NtMYC2a and NtMYC2b form nuclear complexes with the NtJAZ1 repressor and regulate multiple jasmonate-inducible steps in nicotine biosynthesis. *Mol. Plant* 5, 73–84. doi: 10.1093/mp/ssr056

Zhang, H., Hedhili, S., Montiel, G., Zhang, Y., Chatel, G., Pré, M., et al. (2011). The basic helix-loop-helix transcription factor CrMYC2 controls the jasmonate-responsive expression of the ORCA genes that regulate alkaloid biosynthesis in *Catharanthus roseus*. *Plant J.* 67, 61–71. doi: 10.1111/j.1365-313X.2011.04575.x

Zhang, H., Zhang, Q., Zhai, H., Gao, S., Yang, L., Wang, Z., et al. (2020). IbBBX24 promotes the jasmonic acid pathway and enhances fusarium wilt resistance in Sweet Potato. *Plant Cell* 32, 1102–1123. doi: 10.1105/TPC.19.00641

Zhang, M., Jin, X., Chen, Y., Wei, M., Liao, W., Zhao, S., et al. (2018b). TcMYC2a, a basic helix-loop-helix transcription factor, transduces JA-signals and regulates taxol biosynthesis in taxus chinensis. *Front. Plant Sci.* 9:863. doi: 10.3389/fpls.2018.00863

Zhang, M., Chen, Y., Nie, L., Jin, X., Liao, W., Zhao, S., et al. (2018a). Transcriptome-wide identification and screening of WRKY factors involved

in the regulation of taxol biosynthesis in *Taxus chinensis*. *Sci. Rep.* 8:5197. doi: 10.1038/s41598-018-23558-23551

Zhang, M., Li, S., Nie, L., Chen, Q., Xu, X., Yu, L., et al. (2015). Two jasmonate-responsive factors, TcERF12 and TcERF15, respectively act as repressor and activator of tasy gene of taxol biosynthesis in *Taxus chinensis*. *Plant Mol. Biol.* 89, 463–473. doi: 10.1007/s11103-015-0382-382

Zhang, X., Zhu, Z., An, F., Hao, D., Li, P., Song, J., et al. (2014). Jasmonate-activated MYC2 represses ETHYLENE INSENSITIVE3 activity to antagonize ethylene-promoted apical hook formation in *Arabidopsis*. *Plant Cell* 26, 1105–1117. doi: 10.1105/tpc.113.122002

Zhang, Y., Ji, T. T., Li, T. T., Tian, Y. Y., Wang, L. F., and Liu, W. C. (2020). Jasmonic acid promotes leaf senescence through MYC2-mediated repression of CATALASE2 expression in *Arabidopsis*. *Plant Sci.* 299:110604. doi: 10.1016/j.plantsci.2020.110604

Zhang, Z., Xu, M., and Guo, Y. (2020). Ring/U-Box protein AtUSR1 functions in promoting leaf senescence through JA signaling pathway in *Arabidopsis*. *Front. Plant Sci.* 11:608589. doi: 10.3389/fpls.2020.608589

Zheng, Y., Lan, Y., Shi, T., and Zhu, Z. (2017). Diverse contributions of MYC2 and EIN3 in the regulation of *Arabidopsis* jasmonate-responsive gene expression. *Plant Direct* 1:e00015. doi: 10.1002/pld3.15

Zhou, Y., Sun, W., Chen, J., Tan, H., Xiao, Y., Li, Q., et al. (2016). SmMYC2a and SmMYC2b played similar but irreplaceable roles in regulating the biosynthesis of tanshinones and phenolic acids in Salvia miltiorrhiza. *Sci. Rep.* 6:22852. doi: 10.1038/srep22852

Zhu, J.-K. (2016). Abiotic stress signaling and responses in plants. *Cell* 167, 313–324. doi: 10.1016/j.cell.2016.08.029

Zhu, X., Chen, J., Xie, Z., Gao, J., Ren, G., Gao, S., et al. (2015). Jasmonic acid promotes degreening via MYC2/3/4- and ANAC019/055/072-mediated regulation of major chlorophyll catabolic genes. *Plant J.* 84, 597–610. doi: 10.1111/tpj.13030

Zhu, Y., Meng, C., Zhu, L., Li, D., Jin, Q., Song, C., et al. (2017). Cloning and characterization of DoMYC2 from *Dendrobium officinale*. *Plant Cell. Tissue Organ Cult.* 129, 533–541. doi: 10.1007/s11240-017-1198-1193

Zhuo, M., Sakuraba, Y., and Yanagisawa, S. (2020). A jasmonate-activated MYC2-Dof2.1-MYC2 transcriptional loop promotes leaf senescence in *Arabidopsis*. *Plant Cell* 32, 242–262. doi: 10.1105/tpc.19.00297

Conflict of Interest: The authors declare that the research was conducted in the absence of any commercial or financial relationships that could be construed as a potential conflict of interest.

Publisher's Note: All claims expressed in this article are solely those of the authors and do not necessarily represent those of their affiliated organizations, or those of the publisher, the editors and the reviewers. Any product that may be evaluated in this article, or claim that may be made by its manufacturer, is not guaranteed or endorsed by the publisher.

Copyright © 2022 Song, Cao, Dai, Li, Manzoor, Chen and Deng. This is an open-access article distributed under the terms of the Creative Commons Attribution License (CC BY). The use, distribution or reproduction in other forums is permitted, provided the original author(s) and the copyright owner(s) are credited and that the original publication in this journal is cited, in accordance with accepted academic practice. No use, distribution or reproduction is permitted which does not comply with these terms.

frontiers | Frontiers in Plant Science

ORIGINAL RESEARCH
published: 25 April 2022
doi: 10.3389/fpls.2022.872263

Genome-Wide Identification and Expression Profiling of *KCS* Gene Family in Passion Fruit (*Passiflora edulis*) Under *Fusarium kyushuense* and Drought Stress Conditions

Hafiz Muhammad Rizwan[1†‡], Fang Shaozhong[2‡], Xiaoting Li[1], Muhammad Bilal Arshad[3], Ahmed Fathy Yousef[1,4], Yang Chenglong[2], Meng Shi[1], Mohammed Y. M. Jaber[5], Muhammad Anwar[6], Shuai-Ya Hu[7], Qiang Yang[1], Kaiwei Sun[1], Mohamed A. A. Ahmed[8], Zheng Min[9], Ralf Oelmüller[1,10], Lin Zhimin[2] and Faxing Chen[1]**

[1] College of Horticulture, Fujian Agriculture and Forestry University, Fuzhou, China, [2] Institute of Biotechnology, Fujian Academy of Agricultural Sciences, Fuzhou, China, [3] Department of Plant Breeding and Genetics, College of Agriculture, University of Sargodha, Sargodha, Pakistan, [4] Department of Horticulture, College of Agriculture, University of Al-Azhar, Assiut, Egypt, [5] Department of Plant Production and Protection, Faculty of Agriculture and Veterinary Medicine, An-Najah National University, Nablus, Palestine, [6] Guangdong Technology Research Center for Marine Algal Bioengineering, Guangdong Key Laboratory of Plant Epigenetics, College of Life Sciences and Oceanography, Shenzhen University, Shenzhen, China, [7] College of Horticulture, Academy for Advanced Interdisciplinary Studies, Nanjing Agriculture University, Nanjing, China, [8] Plant Production Department (Horticulture-Medicinal and Aromatic Plants), Faculty of Agriculture (Saba Basha), Alexandria University, Alexandria, Egypt, [9] Department of Horticulture, Fujian Agricultural Vocational College, Fuzhou, China, [10] Matthias Schleiden Institute, Plant Physiology, Friedrich-Schiller-University Jena, Jena, Germany*

Plant and fruit surfaces are covered with cuticle wax and provide a protective barrier against biotic and abiotic stresses. Cuticle wax consists of very-long-chain fatty acids (VLCFAs) and their derivatives. β-Ketoacyl-CoA synthase (*KCS*) is a key enzyme in the synthesis of VLCFAs and provides a precursor for the synthesis of cuticle wax, but the *KCS* gene family was yet to be reported in the passion fruit (*Passiflora edulis*). In this study, thirty-two *KCS* genes were identified in the passion fruit genome and phylogenetically grouped as *KCS1*-like, *FAE1*-like, *FDH*-like, and *CER6*-like. Furthermore, thirty-one *PeKCS* genes were positioned on seven chromosomes, while one *PeKCS* was localized to the unassembled genomic scaffold. The *cis*-element analysis provides insight into the possible role of *PeKCS* genes in phytohormones and stress responses. Syntenic analysis revealed that gene duplication played a crucial role in the expansion of the *PeKCS* gene family and underwent a strong purifying selection. All PeKCS proteins shared similar 3D structures, and a protein–protein interaction network was predicted with known *Arabidopsis* proteins. There were twenty putative ped-miRNAs which were also predicted that belong to nine families targeting thirteen *PeKCS* genes. Gene ontology (GO) and Kyoto Encyclopedia of Genes and Genomes (KEGG) annotation results were highly associated with fatty acid synthase and elongase activity, lipid metabolism, stress responses, and plant-pathogen interaction. The highly enriched transcription factors (TFs) including ERF, MYB, Dof, C2H2, TCP, LBD, NAC, and bHLH were predicted in *PeKCS* genes. qRT-PCR expression analysis

OPEN ACCESS

Edited by:
Mohammad Anwar Hossain, Bangladesh Agricultural University, Bangladesh

Reviewed by:
Rahat Sharif, Yangzhou University, China
Mohammad Irfan, Cornell University, United States

***Correspondence:**
Lin Zhimin
linzhimin@faas.cn
Faxing Chen
fxchen@fafu.edu.cn

†ORCID:
Hafiz Muhammad Rizwan
orcid.org/0000-0001-9645-3378

‡These authors have contributed equally to this work

Specialty section:
This article was submitted to Plant Biotechnology, a section of the journal Frontiers in Plant Science

Received: *09 February 2022*
Accepted: *03 March 2022*
Published: *25 April 2022*

Citation:
Rizwan HM, Shaozhong F, Li X, Bilal Arshad M, Yousef AF, Chenglong Y, Shi M, Jaber MYM, Anwar M, Hu S-Y, Yang Q, Sun K, Ahmed MAA, Min Z, Oelmüller R, Zhimin L and Chen F (2022) Genome-Wide Identification and Expression Profiling of KCS Gene Family in Passion Fruit (Passiflora edulis) Under Fusarium kyushuense and Drought Stress Conditions. Front. Plant Sci. 13:872263. doi: 10.3389/fpls.2022.872263

revealed that most *PeKCS* genes were highly upregulated in leaves including *PeKCS2, PeKCS4, PeKCS8, PeKCS13,* and *PeKCS9* but not in stem and roots tissues under drought stress conditions compared with controls. Notably, most *PeKCS* genes were upregulated at 9th dpi under *Fusarium kyushuense* biotic stress condition compared to controls. This study provides a basis for further understanding the functions of *KCS* genes, improving wax and VLCFA biosynthesis, and improvement of passion fruit resistance.

Keywords: very long chain fatty acids, wax biosynthesis, synteny, transcription factor, micro-RNA, gene anthology, stress conditions

INTRODUCTION

Plant growth and development are significantly affected by a variety of biotic and abiotic stresses including drought, salinity, high or low temperature, fungal, bacterial, and viral pathogens. These stress conditions directly affect the crop yield and cause huge economic losses (Raza et al., 2021; Sharif et al., 2021). To adapt and resist these stress conditions, most plants are covered with a hydrophobic protective layer commonly known as cuticle wax and is the first barrier between the environment and plants (Trivedi et al., 2019). Plant cuticle plays an important role in controlling non-stomatal water loss, regulating transpiration, and prevent from mechanical damages caused by fungal, bacterial, insects, ultraviolet (UV) light, and other environmental biotic and abiotic stresses (Lewandowska et al., 2020; Arya et al., 2021; Raza et al., 2022). The structure and composition of cuticle waxes vary between different tissues and between different plants. Different factors affect the biosynthesis and composition of cuticle wax including water, light, temperature, and genotype (Xue et al., 2017). The biosynthesis and transport pathways of cuticle wax are complicated and required the participation of different organelles and enzymes to complete (Fernández et al., 2016; Skalicky et al., 2021). Cuticle waxes are composed of very-long-chain fatty acids (VLCFAs) and their derivatives, such as alkanes, ketones, primary and secondary alcohols, aldehydes, esters, and triterpenes (Zhang et al., 2020). VLCFAs are long-chain fatty acids between C16 and C34 carbons and are the major constituents of sphingolipids, phospholipids, glycerophospholipids, sterol esters, triacylglycerols, and wax esters (Beaudoin et al., 2009). In *Arabidopsis*, sphingolipids containing VLCFAs describe as a secretory pathway for polar plasma membrane protein (Markham et al., 2011).

Biosynthesis of VLCFAs is accomplished in two pathways, including prokaryotic and eukaryotic pathways, involving the *de novo* synthesis of C16 and C18 fatty acids in plastids by fatty acid synthase (FAS) complex (prokaryotic pathway) and elongation of fatty acids from C16 andC18 chains to C26-C34 chains (eukaryotic pathway) via fatty acid elongase (*FAE*) complex in the endoplasmic reticulum (ER) (Bach and Faure, 2010; Xue et al., 2017). Elongation of fatty acids consists of four consecutive reactions in ER including condensation, reduction, dehydration, and secondary reduction and catalyzed by four major enzymes such as β-ketoacyl-CoA synthetase (*KCS*), trans-2,3-enoyl CoA reductase (*ECR*), 3-hydroxacyl-CoA dehydratase (*HCD*) and 3-ketoacyl-CoA reductase (*KCR*) (De Bigault Du Granrut and Cacas, 2016; Kogure et al., 2022). Each of these enzymes utilizes the product of the previous enzyme as a substrate in a cycle starting from the condensation of malonyl-CoA to long-chain acyl-CoA (De Bigault Du Granrut and Cacas, 2016).

β-Ketoacyl-CoA synthase is the key enzyme with distinct substrate specificity that catalyzes the fatty acid elongation and is involved in the synthesis of waxy component precursors during VLCFAs biosynthesis (Wang X. et al., 2017; Yang H. et al., 2021). The first member of *KCS* was identified and functionally characterized in *Arabidopsis* by James et al. (1995), who found *KCS* contributions in the production and storage of VLFACs in developing seeds and finally named as *FAE1*/*KCS18*. Later on, 21 members of the *KCS* gene family were identified and divided into four subfamilies including *KCS1*-like, *FDH*-like, *FAEl*-like, and *CER6* according to the homology of amino acid sequences (Joubès et al., 2008). The KCS proteins have two conserved domains including FAE1/Type III polyketide synthase-like protein domain (FAE1_CUT1_RppA) and 3-Oxoacyl-[acyl-carrier-protein (ACP)] synthase III C-terminal domain (ACP_syn_III_C) (Dai et al., 2021).

Several studies have been reported on the functional characterization of *KCS* genes in plants. It has been reported that five *KCS* genes including *KCS1*, *KCS2*, *CUT1*-CER6/*KCS6*, *KCS9*, and *KCS20* mainly involved in VLCFAs biosynthesis, precursors of cuticular wax and suberin (Lee and Suh, 2013). Beaudoin et al. (2009) reported the involvement of *KCS1* in VLCFAs synthesis, seed triacylglycerols (TAGs), root glycerolipids, and sphingolipids. Todd et al. (1999) reported the involvement of *KCS1* synthase in decarbonylation and acyl-reduction wax synthesis pathways. Overexpression of *KCS2* and *KCS20* increased the wax content in *Arabidopsis* (Lee et al., 2009). *KCS9* was found to be related to tetracosanoic acid as a precursor of epidermal waxes, suberin, sphingolipids, and phospholipids (Kim et al., 2013). *KCS16* was found to be involved in wax biosynthesis and leaf trichomes in *Arabidopsis* (Hegebarth et al., 2017). Yang H. et al. (2021) also reported the involvement of *CsKCS2* and *CsKCS11* in fruit cuticular wax biosynthesis, at the ripening stage in Citrinae species. *KCS* also involved in the cuticular wax synthesis of leaf rice (*Oryza sativa*) (Wang X. et al., 2017). In sunflower (*Helianthus annuus*), *HaKCS1* and *HaKCS2* were expressed in seeds and involved in the elongation of fatty

TABLE 1 | Physiochemical properties of *PeKCS* genes.

Gene ID	Gene name	Cr*	Genomic position	CDS (bp)	A.A* (bp)	M.W*	pI*	II*	Ai*	GR-AVY*	E:I*	SCL*
ZX.01G0003560	*PeKCS1*	1	11711497:11719406−	1311	436	46.68	5.94	31.71	99.36	0.084	9:8	pm
ZX.01G0013920	*PeKCS2*	1	21567509:21569083−	1575	524	58.98	9.17	40.3	91.56	−0.10	1:0	pm
ZX.01G0021050	*PeKCS3*	1	28056974:28058343+	1188	395	43.35	6.85	48.7	88.43	−0.23	2:1	pm
ZX.01G0024040	*PeKCS4*	1	30497870:30500240+	1533	510	57.44	9.38	40.92	95.37	−0.08	2:1	pm
ZX.01G0031680	*PeKCS5*	1	36909208:36910698+	1491	496	56.08	9.38	40.53	100.24	0.02	1:0	pm
ZX.01G0039870	*PeKCS6*	1	42004537:42005907+	1371	456	51.21	8.81	34.12	91.73	−0.06	1:0	pm
ZX.01G0043410	*PeKCS7*	1	43962364:43963095−	594	197	21.96	9.03	39.63	78.22	−0.38	4:3	pm
ZX.01G0060290	*PeKCS8*	1	58285499:58287979−	1677	558	63.18	8.5	44.07	85.11	−0.10	2:1	pm
ZX.01G0068830	*PeKCS9*	1	67253621:67261640−	3159	1052	118.05	9.21	36.2	93.62	−0.08	4:3	pm
ZX.01G0104390	*PeKCS10*	1	213114936:213116972+	1569	522	58.27	8.77	35.34	91.51	−0.07	2:1	pm
ZX.01G0109160	*PeKCS11*	1	216625662:216626789+	1128	375	41.52	8.78	45.41	89.44	−0.15	1:0	pm
ZX.01G0112910	*PeKCS12*	1	220335704:220337194+	1491	496	56.14	9.02	40.08	97.68	0.01	1:0	pm
ZX.01G0116460	*PeKCS13*	1	222578824:222581518+	1572	523	59.33	9.14	38.86	89.29	−0.14	2:1	pm
ZX.01G0132900	*PeKCS14*	1	259611759:259613042−	1284	427	48.22	8.81	35.71	91.57	−0.13	1:0	pm
ZX.01G0133040	*PeKCS15*	1	259664268:259665551+	1284	427	48.17	8.73	35.38	91.33	−0.12	1:0	pm
ZX.02G0008560	*PeKCS16*	2	44526547:44527829+	1185	394	43.01	6.04	40.8	92.59	−0.04	2:1	pm
ZX.02G0008600	*PeKCS17*	2	44614547:44615829+	1185	394	42.98	5.89	42.12	93.32	−0.02	2:1	pm
ZX.02G0008660	*PeKCS18*	2	44697815:44699045+	1122	373	40.87	6.41	41.76	91.02	−0.10	3:2	pm
ZX.03G0023030	*PeKCS19*	3	120077461:120078743−	1185	394	43.01	6.04	40.8	91.85	−0.05	2:1	pm
ZX.03G0023630	*PeKCS20*	3	121353658:121356221+	1242	413	46.55	8.99	34.32	83.58	−0.14	3:2	pm
ZX.04G0004320	*PeKCS21*	4	5525588:5532445+	1710	570	64.17	9.03	40.42	101.11	0.02	6:5	pm
ZX.04G0004390	*PeKCS22*	4	5557716:5565015+	1968	656	73.53	8.91	40.92	95.87	−0.06	5:4	pm
ZX.04G0006280	*PeKCS23*	4	9698999:9701865−	1536	511	57.30	8.83	38.9	100.33	0.04	3:2	pm
ZX.04G0021370	*PeKCS24*	4	76968245:76969643−	1185	394	43.60	6.57	30.01	97.26	−0.08	2:1	pm
ZX.04G0021390	*PeKCS25*	4	77032127:77033535−	1185	394	43.33	6.28	27.47	97.74	−0.06	2:1	pm
ZX.04G0023850	*PeKCS26*	4	85619890:85621186−	1173	390	42.93	6.28	28.46	98.49	−0.08	3:2	pm
ZX.06G0023310	*PeKCS27*	6	107833067:107834602−	1536	511	56.97	9.17	38.3	96.16	−0.01	1:0	pm
ZX.07G0008030	*PeKCS28*	7	59570657:59577025−	1209	402	42.43	6.45	38.95	92.96	0.06	8:7	pm
ZX.07G0016310	*PeKCS29*	7	93550083:93552388−	1170	389	42.81	6.42	38.35	92.21	−0.13	2:1	pm
ZX.08G0007160	*PeKCS30*	8	31405598:31406619−	963	320	36.20	9.14	48.39	81.34	−0.27	4:3	pm
ZX.08G0030480	*PeKCS31*	8	58887421:58888698+	1278	425	47.68	9.3	34.08	90.14	−0.25	1:0	pm
ZX.00000070	*PeKCS32*	Sca	300822:301919+	1098	365	39.07	6.06	37.08	93.1	0.08	1:0	pm

Cr-chromosome NO; A.A*-amino acid/protein length; M.W*-molecular weight (KDa); pI*-isoelectric point; II*-instability index; Ai*-aliphatic index; GRAVY*-grand average of hydropathicity; E:I*-No of Exon: Intron; SCL*-Sub-cellular localization; pm*-plasma membrane. Positive (+) and negative (–) signs indicate the presence of a gene on the positive and negative strands of that particular marker at the genome location.*

acids from C_{18} to C_{20}–C_{24} respectively (González-Mellado et al., 2019). Recently Wang et al. (2022) also reported the involvement of *CsKCS20* in VLCFAs elongation and cuticular wax biosynthesis.

Previous studies also reported the role of *KCS* in environmental stress responses including salt, drought, and biotic stresses. In *Arabidopsis*, *AtKCS*2 and *AtKCS*20 mutants showed higher expression patterns under osmotic stress conditions (Lee et al., 2009). Serra et al. (2009) found that silencing of *StKCS6* in potato (*Solanum tuberosum*) reduced the suberine chain length. Ectopic overexpression of apple (*Malus domestica*) *MdKCS*2 increased the wax contents and resistance to drought conditions in *Arabidopsis* plants (Lian et al., 2021). Yang Z. et al. (2020) reported that ectopic overexpression of grape (*Vitis vinifera*) *VvKCS* in *Arabidopsis* enhanced the tolerance to salt stress at germination and seedling stages. Overexpression of *AhKCS*1 in groundnut (*Arachis hypogaea*) (Lokesh et al., 2019) increased the cuticular waxes and reduced membrane damage under drought stress conditions. Overexpression of *BnKCS*1-1/*BnKCS*1-2 in rapeseed (*Brassica napus*) exhibited increased wax concentration and tolerance to drought under drought conditions (Wang Y. et al., 2020). However, Todd et al. (1999) reported that *AtKCS*1 mutants were less resistant to low humidity conditions at the young stage. Ectopic overexpression of navel orange (*Citrus sinensis*) *CsKCS6* in *Arabidopsis* plants increased the tolerance to drought and salt stress conditions (Guo et al., 2020). Weidenbach et al. (2015) found that the growth rate of barley (*Hordeum vulgare*) *HvKCS*6 mutants was improved underwater limitation conditions. Overexpression of *HvKCS*1 in barley improved the leaf waxes and resistance to barley powdery mildew fungus (Li et al., 2018). In cotton (*Gossypium hirsutum*), *GhKCS13* mutants regulated the cold response by modulating the lipids and oxylipin biosynthesis (Wang Q. et al., 2020).

Transcription factors (TFs) are sequence-specific DNA binding proteins that help recruit the transcriptional machinery to gene promoters, that play an important role in the regulatory

network of plant growth and development under normal and stress conditions (Samad et al., 2017). Different TFs have been reported to be involved in the regulation of VLCFAs and wax biosynthesis, including basic leucine zipper (bZIP), myeloblastosis (MYB), wax inducer (WIN), apetala2/ethylene response factor (AP2/ERF), NAC [no apical meristem (NAM), Arabidopsis transcription activation factor (ATAF1/2), and cup-shaped cotyledon (CUC2)], and PUCHI (Ois Roudier et al., 2010; Oshima et al., 2013; Trinh et al., 2019; Guyomarc'h et al., 2021; Han et al., 2022). In addition, the miRNAs (micro-RNAs) are non-coding single-stranded RNAs (approximately 21–30 nucleotides) and play an important role in numerous cellular mechanisms as well as in stress resistance through translational inhibition and/or cleavage of target mRNAs during or after transcription (Zhang et al., 2006; Ohtani, 2017). It has been reported that miRNAs were found to be involved in cuticular wax biosynthesis in *Arabidopsis* such as trans-acting small interfering RNA (tasiRNA) was involved in *CER3* silencing during stem wax production (Lam et al., 2015). Wang Z. et al. (2017) and Su et al. (2021b) conducted a genome-scale study in *Brassica napus* and discovered several miRNAs targeting the fatty acid and lipid metabolism enzymes that could regulate the fatty acid synthesis, lipid transport, and metabolism. Later on, Liu et al. (2019) proposed that the bna-miR165a-5p (*Brassica napus* miRNA) might be involved in the wax biosynthesis process by regulating the putative target BnaA06g40560D gene. Recently, Paul et al. (2020) also identified several miRNAs in passion fruit (*Passiflora edulis*) and predicted their involvement in different molecular and biological process, however, the specific mechanism of all the miRNAs are not clear in passion fruit and need further studies. Genes can be further classified according to their function using Gene Ontology (GO) terms such as biological processes (GO-BP), cellular component (GO-CC), and molecular function (GO-MF). The functional classification of genes can be achieved in species using advanced GO terms (Ashburner et al., 2000; Roncaglia et al., 2013). To understand the biological functions of the gene at the genome level, the Kyoto Encyclopedia of Genes and Genomes (KEGG) is a bioinformatics resource that provides functional information in network pathways (Kanehisa and Goto, 2000; Masoudi-Nejad et al., 2007).

Genome-wide identification of gene families facilitates the study of gene functions by providing a foundation for further functional analysis. Due to the availability of large-scale plant genome sequencing and widespread use of bioinformatics techniques, the *KCS* gene family has been identified in different plant species with diverse members including 21 *KCS* genes identified in *Arabidopsis* (*Arabidopsis thaliana*) (Joubès et al., 2008); 28 in maize (*Zea mays*) (Campbell et al., 2019); 30 in peanut (*Arachis hypogea*) (Huai et al., 2020); 58 in rapeseed (*Brassica napus*) (Xue et al., 2020); eight in grape (*Vitis vinifera*) (Guo et al., 2016); 58 in cotton (*Gossypium hirsutum*), 31 in *G. arboreum* and 33 in *G. raimondii* (Xiao et al., 2016); 33 in barley (*Hordeum vulgare*) (Tong et al., 2021); 96 *KCS* genes were identified in six Citrinae species including13 in *Atalantia buxifolia*, 16 in *Citrus ichangensis*, 21 in *C. medica,* 14 in *C. grandis*, 16 in *C. sinensis* and 16 in *C. clementina* (Yang H. et al., 2021) respectively. Whereas, the *KCS* gene family has not been identified in passion fruit (*Passiflora edulis*). Passion fruit is a perennial evergreen climbing vine and is usually cultivated throughout tropical and subtropical areas of the world. Passion fruit is an economically important fruit plant that is demanded its fresh juice, rich in aroma and distinctive nutritional values (Rizwan et al., 2021). Recently, the passion fruit genome has been sequenced and published (Ma et al., 2021), a comprehensive genome-wide study for the first time to determine the *KCS* gene family in passion fruit was conducted. Moreover, their *in silico* prediction of TFs, subcellular localization, evolutionary relationship *via* phylogenic and syntenic analysis, conserved motifs, gene structures, *cis*-regulatory-elements, prediction of putative miRNA, GO and KEGG annotation have been characterized. The gene expression profiles of several *KCS* genes in different passion fruit tissues under drought stress and *Fusarium kyushuense* fungal stress conditions were analyzed to gain insight into passion fruit *KCS* genes. Our findings will facilitate further functional analysis of *KCS* genes in terms of wax and VLCFA biosynthesis to facilitate genetic improvement of passion fruit against biotic and abiotic stresses.

MATERIALS AND METHODS

Identification of β-Ketoacyl-CoA Synthase Genes in Passion Fruit

To identify and characterize the *KCS* genes in the passion fruit (*Passiflora edulis*) genome, passion fruit proteins, CDS, gff3, genome files were downloaded from the passion fruit genome[1] (Ma et al., 2021). We performed two methods, which are Basic Local Alignment Search Tool for proteinsT (BLASTp) and Hidden Markov Models (HMMER) search tool, to identify the *KCS* genes in the passion fruit genome. All known KCS family protein sequences of *Arabidopsis thaliana* (*AtKCS*) (Joubès et al., 2008) were downloaded from The *Arabidopsis* Information Resource (TAIR) database[2], *M. domestica* (Apple) *MdKCS* (Lian et al., 2020) from apple genome[3], and *A. hypogaea* (Peanut) *AhKCS* (Huai et al., 2020) from peanut genome[4]. The BLASTp was performed in the passion fruit genome based on protein homology alignments with default mode using the known KCS protein sequences *via* the TBTools software package version 1.0986858 (Chen C. et al., 2018). The KCS domains were downloaded from the Pfam database[5] [PF08392 (FAE1/Type III polyketide synthase-like protein) and PF08541 (3-Oxoacyl-[acyl-carrier protein (ACP)] synthase III C terminal)]. hese domains were used for HMMER in passion fruit genome *via* TBTools with default mode. The results of the two methods were merged

[1]https://ftp.cngb.org/pub/CNSA/data3/CNP0001287/CNS0275691/CNA0017758/

[2]http://www.Arabidopsis.org

[3]https://iris.angers.inra.fr/gddh13/the-apple-genome-downloads.html

[4]https://www.peanutbase.org/download

[5]http://pfam.xfam.org/

and further analyzed by Web CD-Search Tool[6] and SMART[7] to confirm the domains in passion fruit KCS protein.

Physiochemical Properties, Alignment, and Phylogenetic Analyses of *PeKCS* Genes

The *PeKCS* genes' physical and chemical properties include molecular weight (M.W), amino acid (A.A) length, coding sequence (CDS) length, isoelectric point (pl), instability index (II), aliphatic index (Ai), number of an exon, and intron (E/I) were evaluated by using the ExPASY-Prot[8]. The online CELLO version 0.2.5[9] program was used to predict the subcellular localization of *PeKCS* genes. The phylogenetic analyses were performed by aligning the full-length KCS protein sequences of *P. edulis* (*PeKCS*), *A. thaliana* (*AtKCS*), *M. domestica* (*MdKCS*), and *A. hypogaea* (*AhKCS*) by Molecular Evolutionary Genetics Analyses (MEGA) software version 10.1.8[10]. The aligned sequences were subjected to neighbor-joining (NJ) tree construction using the MEGA software with 1,000 bootstrap replicates and all other parameters were set to default. The online web tool iTOL[11] was used to visualize the phylogenetic tree and divided it into four main groups and eight subgroups according to *AtKCS* (Joubès et al., 2008). The *PeKCS* genes distribution and mapping on all 9 assembled and 1 unassembled scaffold passion fruit chromosomes were investigated by using the passion fruit genomic and annotation files *via* Tbtools software (Chen C. et al., 2018). Moreover, the online Sequence Identity and Similarity (SIAS)[12] tool was used to perform a pairwise sequences identity between passion fruit *KCS* genes.

PeKCS Gene Structures and Motifs Analyses

The *PeKCS* genes structural organizations and chromosome locations were retrieved from passion fruit genomic files. The conserved motifs of PeKCS protein sequences were predicted by using the Multiple Expectation Maximization for Motif Elicitation (MEME) online tools[13] and the numbers of motifs were set to 10 motifs. The *PeKCS* gene structures and conserved motifs from the passion fruit were visualized by TBTools software.

Cis-Regulatory Element Analysis of *PeKCS* Genes

To predict the putative *cis*-regulatory elements in promoter regions of *PeKCS* genes, the upstream 2,000 bp sequences of all the *PeKCS* genes were extracted from the genomic DNA sequences. Moreover, the promoter sequence of each gene was subjected to the PlantCARE database[14] and the *cis*-regulatory elements figure was drawn by using TBTools software (Chen C. et al., 2018). Additionally, the numbers, functions, and sequences of putative *cis*-regulatory elements of *PeKCS* genes were summarized and highlighted into plant growth and development, phytohormones responses, and stress-responsive categories.

Synteny Analysis and Ka/Ks Values Calculation for *PeKCS* Genes

The tandem and segmental or whole-genome duplication (WGD) duplication provides a new understanding of family genes development and genome progression. The homologous *PeKCS* genes with only one intervening gene on the same passion fruit chromosome were considered to be tandem duplicated, while homologs on other chromosomes were considered to be segmental duplications. *PeKCS* duplicated genes were identified and visualized on their physical location on the chromosomes in the passion fruit genome. Gene duplication, synteny analysis, and Ka (non-synonymous)/Ks (synonymous) values calculation of *PeKCS* genes were performed in TBTools. The syntenic relationships of *KCS* genes between *P. edulis*, *A. thaliana,* and *M. domestica* were performed using the MCScanX toolkit, and *KCS* relationships between the target species were visualized by the Advance Circos package in the TBTools software (Chen C. et al., 2018). Furthermore, the multiple collinearity analysis of *KCS* genes in *P. edulis*, *A. thaliana*, *M. domestica,* and *A. hypogaea* whole genomes were also performed by Multiple synteny Plot packages in TBTools software. The Ka), Ks nucleotide substitution rates, and the Ka/Ks ratios of duplicated *PeKCS* genes were annotated using TBTools and divergence time (T, MYA; million years ago) was calculated by the following formula; T = Ks/2x ($x = 6.38 \times 10^{-9}$) (Ma et al., 2021).

Protein–Protein Network Interaction, Secondary Structure, and 3D Modeling of *PeKCS*

The online tool STRING version 11[15] was used to predict and construct the protein–protein interaction network of PeKCS proteins based on *Arabidopsis* homologous proteins. The STRING tool parameters were set as follows; network type-full STRING network; the meaning of network edges-evidence; the minimum required interaction score was set to medium confidence parameter (0.4) and max number of interaction display was no more than 10. The PeKCS proteins' secondary structures were predicted by SOPMA SECONDARY STRUCTURE PREDICTION METHOD[16]. Three-dimensional modeling (3D) of PeKCS protein was performed using the Phyre2 online tool[17] with default settings.

[6] https://www.ncbi.nlm.nih.gov/Structure/bwrpsb/bwrpsb.cgi
[7] http://smart.embl-heidelberg.de/
[8] https://web.expasy.org/protparam/
[9] http://cello.life.nctu.edu.tw
[10] https://www.megasoftware.net/
[11] https://itol.embl.de/login.cgi
[12] http://imed.med.ucm.es/Tools/sias.html
[13] http://meme-suite.org/index.html
[14] http:/bioinformatics.psb.ugent.be/webtools/plantcare/html/
[15] https://string-db.org/cgi/input.pl
[16] https://npsa-prabi.ibcp.fr/cgi-bin/npsa_automat.pl?page=npsa_sopma.html
[17] http://www.sbg.bio.ic.ac.uk/phyre2/html/

Prediction of Putative Micro-RNAs Targeting *PeKCS* Genes, Gene Ontology and Kyoto Encyclopedia of Genes and Genomes Annotation Analysis

To predict putative miRNA target sites in the *PeKCS* genes, at first, the mature sequences of passion fruit miRNAs were downloaded from published data (Paul et al., 2020). Moreover, the *PeKCS* CDS sequences were submitted to the online psRNATarget Server[18] with default parameters for prediction of potential miRNAs in *PeKCS* genes. The interaction network between the predicted miRNAs and *PeKCS* target genes was constructed and visualized by Cytoscape software version 3.9[19] (Kohl et al., 2011). Furthermore, the GO and KEGG annotation analyses were performed by submitting PeKCS protein sequences to the online database eggNOG[20] and their enrichment analysis were performed in TBTools software (Chen C. et al., 2018).

Transcription Factor Regulatory Network Analysis

The TFs' prediction and regulatory network analysis were performed according to Zheng et al. (2020) with slight modifications. The 1000 bp nucleotide sequences from upstream regions of *PeKCS* genes were extracted and were submitted to the Plant Transcriptional Regulatory Map (PTRM)[21] with p-value $\leq 1e^{-6}$ (Tian et al., 2020) for the prediction of TFs. Cytoscape version 3.9 software (Kohl et al., 2011) was used to construct and visualized the TF regulatory network.

Expression Analyses of *PeKCS* Genes in Various Tissues

The passion fruit RNA-Seq raw reads were downloaded from National Center for Biotechnology Information (NCBI) Sequence Read Archive (SRA) database[22] with the following accession numbers (SRP150688) and (PRJNA634206). The peel samples were from yellow (*P. edulis.* Flavicarpa cv Huangjin) and purple (*P. edulis.* Sims cv Tainong) passion fruit cultivars at the ripening stage, while pulp samples were from both cultivars at different fruit developmental stages. The root samples were from purple passion fruit Pingtan-1 cold-tolerant cultivar under two cultivation areas as limestone (L) and sandy dolomite (D) rocky desertification areas. The leave samples were from yellow Huangjinguo (HJG) cold-sensitive and purple Tainong-1 cold-tolerant cultivars under normal temperature (NT) and chilling stress (CS) conditions. The RNA-Seq raw reads were quality controlled and filtered by fastp package (Chen S. et al., 2018) and mapped to the passion fruit reference genome (Ma et al., 2021) with HISAT2 package (Kim and Langmead, 2015) in Ubuntu wsl v 20.04.3[23]. The sequence alignment map (SAM) files were transformed to binary alignment map (BAM) and sorted with Samtools packages (Li et al., 2009). Fragments per kilobase million (FPKM) values were calculated using the limma and edgeR (Law et al., 2016). Due to large differences in FPKM values among different tissues of passion fruit, the FPKM values were transformed to $\log^2$. Heatmaps were constructed using TB-Tools software (Chen C. et al., 2018) to visualize the expression profiles of *PeKCS* genes in different tissues.

Plant Material Under Drought and Fungal Stress Conditions

The *KCS* genes play an important role in VLCFA biosynthesis and plant resistance to biotic and abiotic stresses. The *PeKCS* genes expression profiles were studied by applying the drought stress (abiotic) and *Fusarium kyushuense* fungal pathogen (biotic) stressed conditions compared to controls of yellow and purple passion fruit cultivars. To prepare drought-stressed and normal condition samples for *PeKCS* genes expression analysis, seeds of two commercial passion fruit cultivars yellow (*P. edulis.* Flavicarpa cv Huangjin) and purple (*P. edulis.* Sims cv Tainong) were planted in plastic pots filled with peat moss and soil (2:1 ratio). Greenhouse conditions were set as follows; temperature $25 \pm 2°C$, photoperiod (16-h), and 75% relative humidity. One-month-old passion fruit plants were subjected to dehydration for 10 days and rewatered to study the qRT-PCR (Quantitative real-time polymerase chain reaction) expression profile of *PeKCS* selected genes under drought conditions. Leaves, root, and stem samples of both cultivars with three biological replicates were collected and quickly frozen in liquid nitrogen and were stored at $-80°C$ for further uses. The samples from normally watered plants were taken as controls. In order to prepare the fungal stress samples, fruits of both passion fruit cultivars were collected from a commercial orchard located in Fujian province, China (23°48035.200 N and 117°07008.100 E). Fruits were surface sterilized and infected with the *F. kyushuense* pathogenic fungus following the protocol mentioned in our previous publication (Rizwan et al., 2021). Peels from infected areas were collected after the 9th and 12th days post-inoculation (dpi), while uninfected fruit at 9th and 12th days were used controls.

RNA Extraction and Quantitative Real-Time Polymerase Chain Reaction Analysis

RNA was extracted from frozen samples using the Tiangen mini-RNA extraction kit (Tiangen, China) according to the manufacturer's instructions, and RNA was quantified with a Thermo Scientific NanoDrop 2000 UV-Vis Spectrophotometer (Thermo Scientific, United States). One μg of total RNA was used to synthesize the complementary DNA (cDNA) by Takara PrimeScript™ RT Kit with gDNA eraser (TAKARA, China) and cDNAs were diluted to 5x with deionized distilled water. qRT-PCR was performed on a LightCycler® 96 (Roche Applied Science, Penzberg, Germany) in 20 μL reaction mix consisting of 10 μL TB Green master mix solution (TAKARA), 1 μL of each forward and reverse primer (100 μM), 1 μL of cDNA and 7 μL of ddH_2O. Using *Pe*60s (Munhoz et al., 2015), As an internal reference gene, the qRT-PCR reactions were performed with the

[18] https://www.zhaolab.org/psRNATarget/

[19] https://cytoscape.org/download.html

[20] http://eggnog-mapper.embl.de/

[21] http://plantregmap.gao-lab.org/binding_site_prediction.php

[22] http://www.ncbi.nlm.nih.gov/sra

[23] https://ubuntu.com/wsl

conditions as; preincubation at 95°C for 30 s, followed by 45 cycles at 95°C for 10 s, and 60°C for 30 s. Three biological replicates were used for each reaction and the relative gene expression levels were calculated using the $2^{-\Delta\Delta CT}$ method (Schmittgen and Livak, 2008). The primer used in this study has been provided in **Supplementary Table 1**.

Subcellular Localization of *PeKCS2* Gene

The sub-cellular localization of *PeKCS* genes was hypothetically predicted by CELLO v.2.5 and for the validation, the transient expression assay was performed in onion epidermal cells by selecting a *PeKCS*2 candidate gene. To construct a vector for transient expression assays, the pCAMBIA1302 vector with cauliflower mosaic virus 35S (CaMV35S) promoter and green fluorescent protein (GFP) marker in the upstream region of the multiple cloning site (MCS) was used. The *PeKCS* full-length coding DNA sequences (CDS) without stop codon was amplified by PCR using the following primers: 5′-ACGGGGGACTCTTGACCATGGATGGATAGAGAAA GAGA TCTTTTGTCCACG-3′ (*Nco*I) and 5′-TCTCCTTTACTAGTC AGATCTCAGAGTCGCA GGAGGATATCTGT-3′ (*Bgl*II) (underlined are the restriction sites), and cloned into the pMD 19-T vector (Cat# 6013, TAKARA, Shiga, Japan) following the manufactures instructions. The positive clones were confirmed by sequencing (Sangon Biotech Co., Ltd, Shanghai, China), the gene fragment was digested with *Nco*I and *Bgl*II restriction enzymes and ligated into the *Nco*I-*Bgl*II digested pCAMBIA1302 vector using ClonExpress II One Step Cloning Kit (Cat# C112, Vazyme Biotech Co., Ltd., Nanjing, China) and then transferred to *Agrobacterium tumefaciens* EHA105 strain for the following infection. The resulting plasmids were named CaMV35S-*PeKCS2*-GFP and empty vector CaMV35S-GFP as control. These vectors were successfully transformed into onion epidermal cells by agroinfiltration method and GFP expressions were examined by laser scanning confocal microscopy (Olympus, Tokyo, Japan; FV1200) after 24–72 h of agroinfiltration (Xu et al., 2014).

Statistical Analysis

One-way ANOVA was performed for statistical analyses and Figures were generated by GraphPad Prism version 8.0.1[24]. The comparisons between treated and controlled samples were performed using Student's *t*-test and were considered statistically significant if $p < 0.05$.

RESULTS

Identification and Physiochemical Properties of β-Ketoacyl-CoA Synthase Genes in Passion Fruit

In this study, after removing redundant, repetitive, and unrecognized sequences from BLASTp and HMMR results, finally, thirty-two *KCS* genes in the passion fruit genome by computational tools were identified. Passion fruit *KCS* genes were named from *PeKCS1* to *PeKCS32* according to their chromosomal positions. Except for chromosomes numbers five and nine, all *PeKCS* genes were unevenly distributed on seven of the nine passion fruit chromosomes and *PeKCS32* was localized on an unassembled chromosome region. The largest number of *PeKCS* genes (14 genes) appeared on chromosome number one, followed by chromosome number four (5 genes), chromosome 2 (3 genes), chromosomes number three, seven, and eight (2 genes each), There is only one *PeKCS* gene on chromosome number six. *PeKCS*32 was found in the scaffold chromosome region, while no *PeKCS* gene was found on chromosomes 5 and 9 (**Figure 1A** and **Table 1**). Details of all 32 *PeKCS* genes can be found in **Table 1** and the protein sequences have been provided in **Supplementary Table 2**. CD and SMART search tools for domains verification was used and found that PeKCS proteins contained two domains such as ACP_syn_III_C ((PF08541) 3-Oxoacyl-[acyl-carrier protein (ACP)] synthase III C terminal domain) and FAE1_CUT1_RppA ((PF08392) FAE1/Type III polyketide synthase-like protein domain) (**Figure 1B**).

Most of the PeKCS proteins contained both proteins 68% (22 genes), 19% (6 genes) contained only FAE1_CUT1_RppA domains and 9% (3 genes) contained only ACP_syn_III_C domain respectively (**Figure 1B**). Furthermore, the results of physiochemical properties showed that *PeKCS* genes varied in their properties such as; the protein length varied from 197 bp (PeKCS7) to 1052 bp (PeKCS9), the CDS length ranged from594 bp (*PeKCS7*) to 3159 bp (*PeKCS*9), as well as the protein molecular weight (M.W), ranged from 21.96 KDa (*PeKCS7*) to 118.05 KDa (*PeKCS*9). The isoelectric point (pI) of PeKCS proteins also varied ranged from 5.89 (*PeKCS*17) to 9.38 (*PeKCS*4 and *PeKCS*5), protein instability index (II) varied from 27.47 (*PeKCS*25) to 48.7 (*PeKCS*2) and aliphatic index (Ai) ranged from 81.34 (*PeKCS*30) to 101.11 (*PeKCS*11). The grand average of hydropathicity (GRAVY) ranged from −0.38 (*PeCS7*) to 0.08 (*PeKCS*1). PeKCS protein also varied in number of exons ranged from 1 (PeKCS2, PeKCS5, PeKCS6, PeKCS10, PeKCS11, PeKCS14, PeKCS15, PeKCS27, PeKCS31, and PeKCS32) to 9 (PeKCS1). The proteins subcellular localization prediction showed that all the PeKCS proteins were associated with the plasma membrane (**Table 1**).

Multiple-Sequence Alignment and Phylogenetic Analysis of β-Ketoacyl-CoA Synthase Genes

Multiple sequence alignment and evolutionary tree analyses of identified passion fruit *KCS* genes were performed. The multiple sequences analysis between *AtKCS* and *PeKCS* genes exhibited two conserved domains FAE1_CUT1_RppA (**Supplementary Figure 1**, presented in red box) domain and the ACP_syn_III_C domain (**Supplementary Figure 1**, presented in the blue box). Both sequences were highly identical and conserved in both regions, indicating the importance of these domains for *KCS* gene functions (**Supplementary Figure 1**). Furthermore, the N-terminal deletion of the FAE1_CUT1_RppA domain in *PeKCS7* was pre*cis*e compared to other *PeKCS* genes, suggesting that *PeKCS7* may have a

[24]https://www.graphpad.com/scientific-software/prism

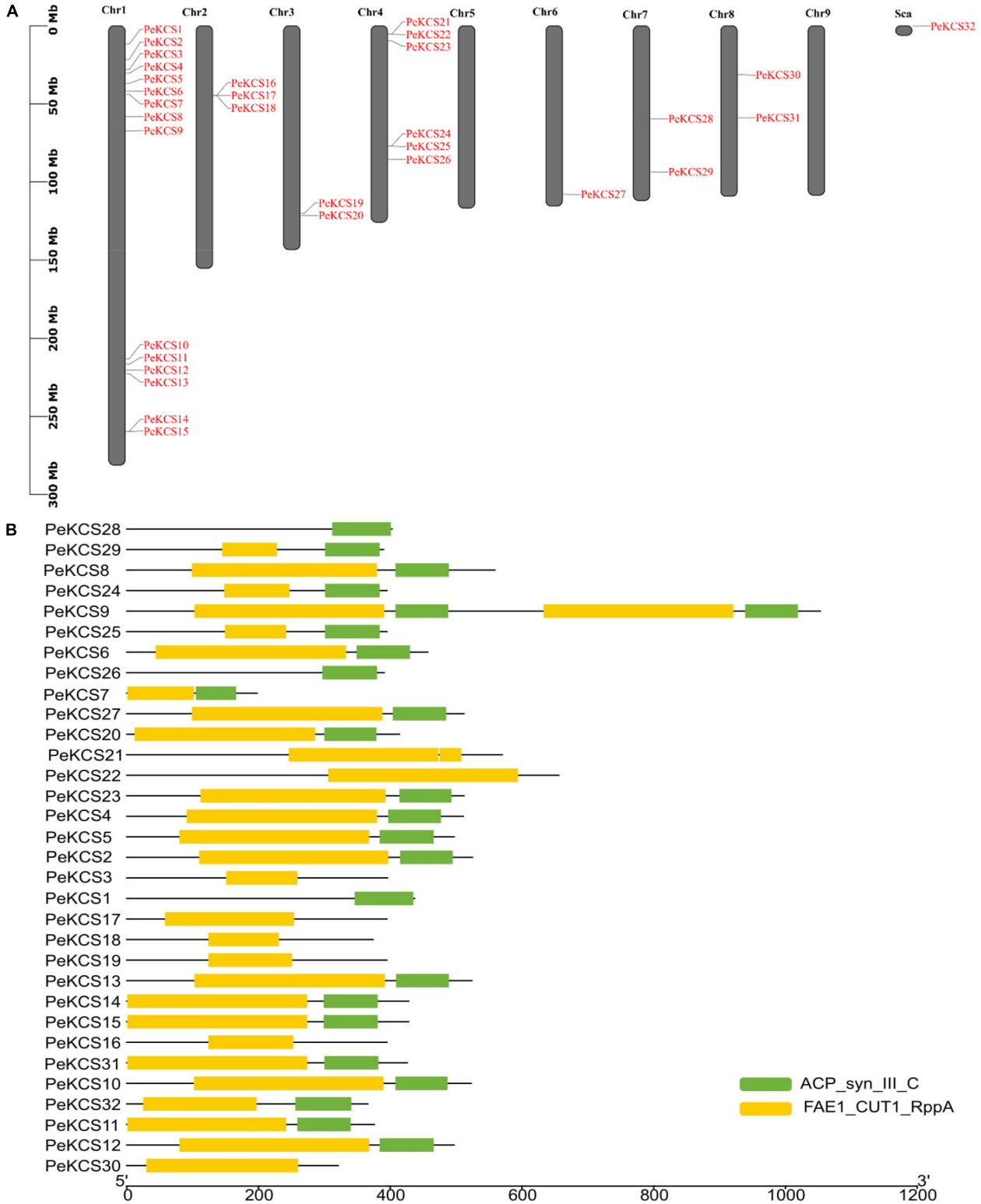


FIGURE 1 | Chromosome location and conserved domains of *PeKCS* in passion fruit. **(A)** Chromosomal location of PeKCS genes, the scale represents the 300 MB chromosomal distance and the PeKCS genes are represented in red color. **(B)** The two conserved domains of PeKCS genes in passion fruit named as FAE1_CUT1_RppA: FAE1 (PF08392); ACP_syn_III_C (PF08541) (readers are referred to the Web version of this article for the understanding of the references to color in this figure legend). Sca-scaffold chromosome.

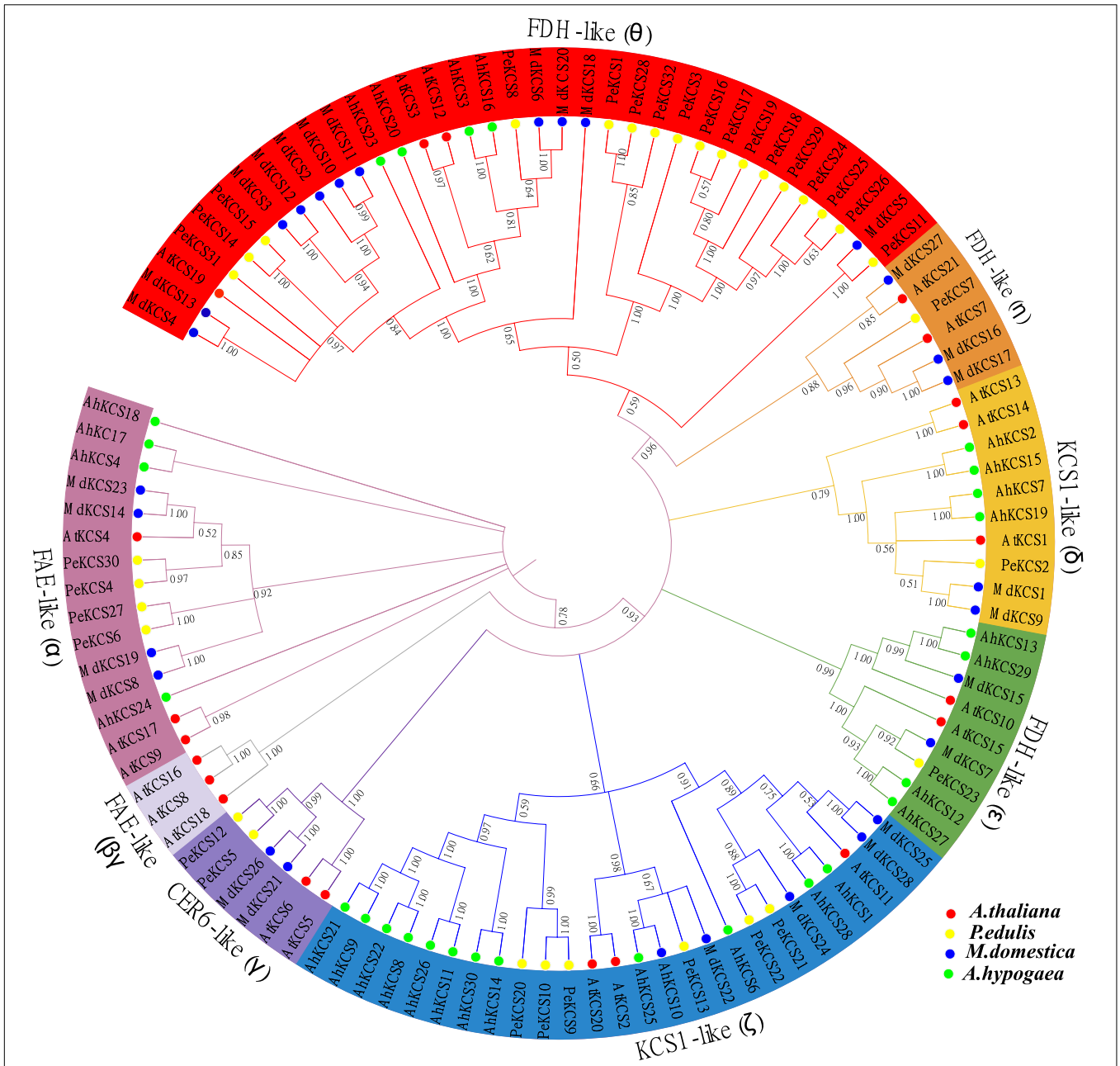


FIGURE 2 | An unrooted neighbor-joining (NJ) phylogenetic tree based on the amino acid sequences alignment among *A. thaliana, P. edulis, M. domestica, and A. hypogaea* KCS sequences with 1000 bootstraps. All the KCS members were divided into 8 groups and presented in different colors. The protein sequences of AtKCS, PeKCS, MdKCS, and AhKCS are represented by red, yellow, blue, and green color circles respectively.

unique function (**Supplementary Figure 1**). One hundred and eleven KCS protein sequences from *A. thaliana* (AtKCS), *P. edulis* (PeKCS), *M. domestica* (MdKCS), and *A. hypogaea* (AhKCS) species were used to assess the evolutionary relationship and unrooted phylogenetic tree (All the KCS protein sequences used in the phylogenetic tree have been provided in **Supplementary Table 2**. The KCS protein sequences were aligned and a neighbor-joining tree was constructed using MEGA software.

The phylogenetic tree was divided into four main groups (*FAE*-like, *FDH*-like, *KCS1*-like, and*CER6*-like) and eight subgroups including *FAE*-like (α), *FAE*-like (β), *CER6*-like (γ), *KCS1*-like (δ), *KCS1*-like (ζ), *FDH*-like (ε), *FDH*-like (η), and *FDH*-like (θ) (**Figure 2**) according to *AtKCS* (Joubès et al., 2008). Phylogenetic analysis showed that *FDH*-like (θ) subgroup consisted of 35 *KCS* genes (17 *PeKCS*, 3 *AtKCS*, 11 *MdKCS*, and 4 *AhKCS*) followed by *KCS1*-like (ζ) 26 genes (6 *PeKCS*, 3 *AtKCS*, 5 *MdKCS*, and 12 *AhKCS*), *FAE*-like

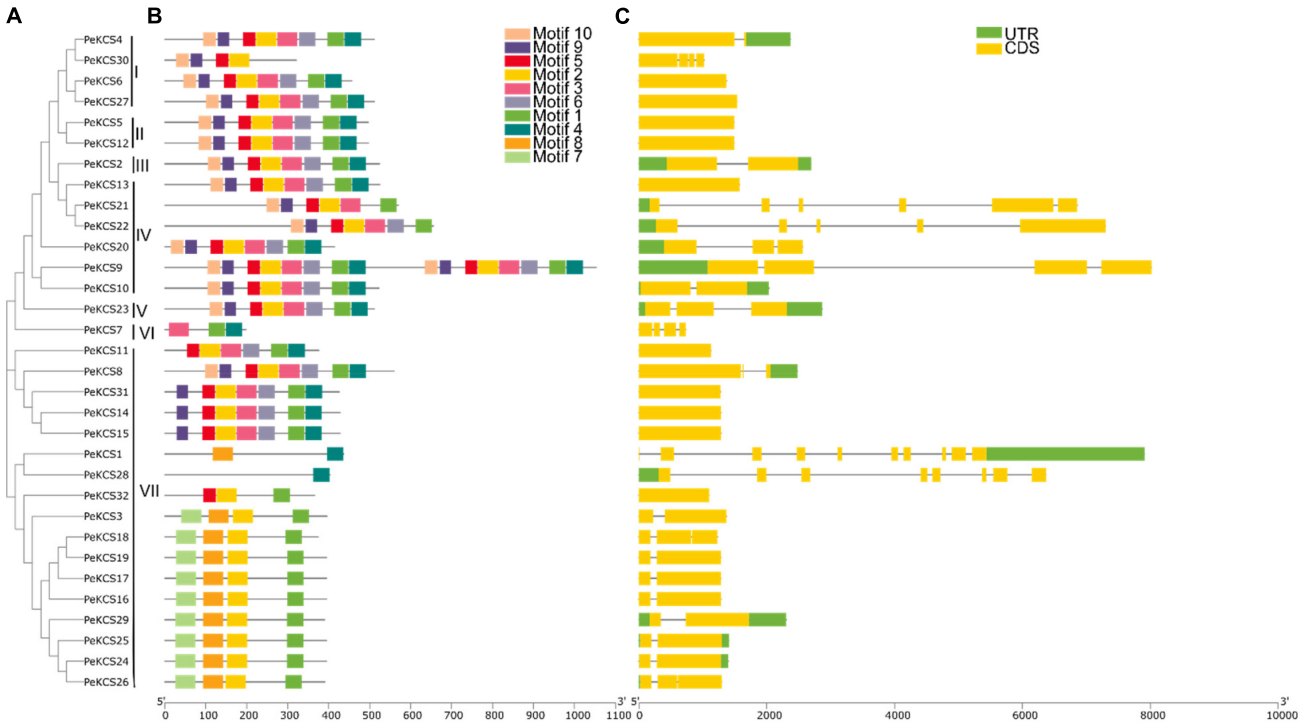


FIGURE 3 | The unrooted phylogenetic tree, conserved motifs and gene structure of *PeKCS* genes. **(A)** The neighbor-joining tree on the left comprised of 32 KCS proteins from passion fruit. **(B)** Conserved motifs were represented *via* boxes and different colors represents different motifs. **(C)** *PeKCS* genes structures, yellow color indicates the exons, the green color shows the untranslated 5′ and 3′-regions, and gray color indicates the introns.

(α) consists of 15 genes (4 *PeKCS*, 3 *AtKCS*, 4 *MdKCS*, and 4 *AhKCS*), *KCS1*-like (δ) consists of 10 genes (1 *PeKCS*, 3 *AtKCS*, 2 *MdKCS*, and 4 *AhKCS*), FDH-like (ε) consists of 9 genes (1 *PeKCS*, 2 *AtKCS*, 2 *MdKCS*, and 4 *AhKCS*), *FDH*-like (η) consists of 6 genes (1 *PeKCS*, 2 *AtKCS*, and 3 *MdKCS*), *CER6*-like (γ) consists of 6 genes (2 *PeKCS*, 2 *AtKCS*, and 2 *MdKCS*), and *FAE*-like (β) composed of only 3 *Arabidopsis KCS* genes (**Figure 2**). *FDH*-like (θ) was found to be the largest subgroup consisting of 35 *KCS* genes followed by *KCS1*-like (ζ) 26 genes and *FAE*-like (β) was the smallest subgroup containing only 3 *Arabidopsis KCS* genes. The number of *KCS* genes was similar in *FDH*-like (η) and *CER6*-like (γ). There were also differences in the uneven distribution of *PeKCS* genes between different subgroups, for example, the largest number of *PeKCS* genes (17 genes) was found in the *FDH*-like (θ) subgroup, followed by the *KCS1*-like (ζ) subgroup (6 genes), and only 1 *PeKCS* gene was found in the *KCS1*-like (δ), *FDH*-like (n), *FDH*-like (ε) subgroups and no any *PeKCS* gene was aligned in the *FAE*-like (β) subgroup (**Figure 2**). The results revealed that *P. edulis* KCS proteins shared greater homology with *M. domestica* (MdKCS) and *A. thaliana* (AtKCS) compared to *A. hypogaea* (AhKCS) (**Figure 2**). Furthermore, the pair-wise identity between *PeKCS* genes was performed to better understand the evolution and the result showed that the similarity varied from 22.71% (*PeKCS*1/*PeKCS*13) to 99.84% (*PeKCS*16/*PeKCS*17 and *PeKCS*17/*PeKCS*19) respectively (**Supplementary Table 3**). *PeKCS*17 showed the highest similarity of 99.84% with *PeKCS*16 and *PeKCS*19 genes. Pairwise similarity results were contrasted with phylogenetic tree results, where *PeKCS*16, *PeKCS*17, and *PeKCS*19 genes were grouped in the same *FDH*-like (θ) subgroup (**Figure 2** and **Supplementary Table 3**).

Gene Structure and Motifs Analyses of *PeKCS* Genes

The relationship between 32 *PeKCS* genes was investigated through the construction of a phylogenetic tree using the neighbor-joining (NJ) method and grouped from I-V11 (**Figure 3A**). The protein sequences of all *PeKCS* genes have been provided in **Supplementary Table 2**. According to the results, group VII was the largest group with 17 *PeKCS* genes followed by group 4 with 6 genes. The smallest groups were III, V, and VI with only one *PeKCS* gene (**Figure 3A**). To further understand the development and functions of *PeKCS* family genes, the conserved motifs and exon-intron configuration of *PeKCS* gene structure were analyzed (**Figures 3B,C**). Moreover, the conserved motifs among 32 *PeKCS* genes were predicted using the online MEME tool. The conserved motifs among PeKCS proteins vary ranged from 1 (*PeKCS*28) to 16 (*PeKCS*9) and overall, 10 conserved motifs were recognized in all PeKCS proteins (**Supplementary Table 4**). Most of the *PeKCS* genes (12 genes) have 8 motifs followed by 4 motifs (9 genes) and *PeKCS*28 have only one motif. *PeKCS*9 contained a maximum of 16 motifs. The motif distribution among group I-VII was also similar

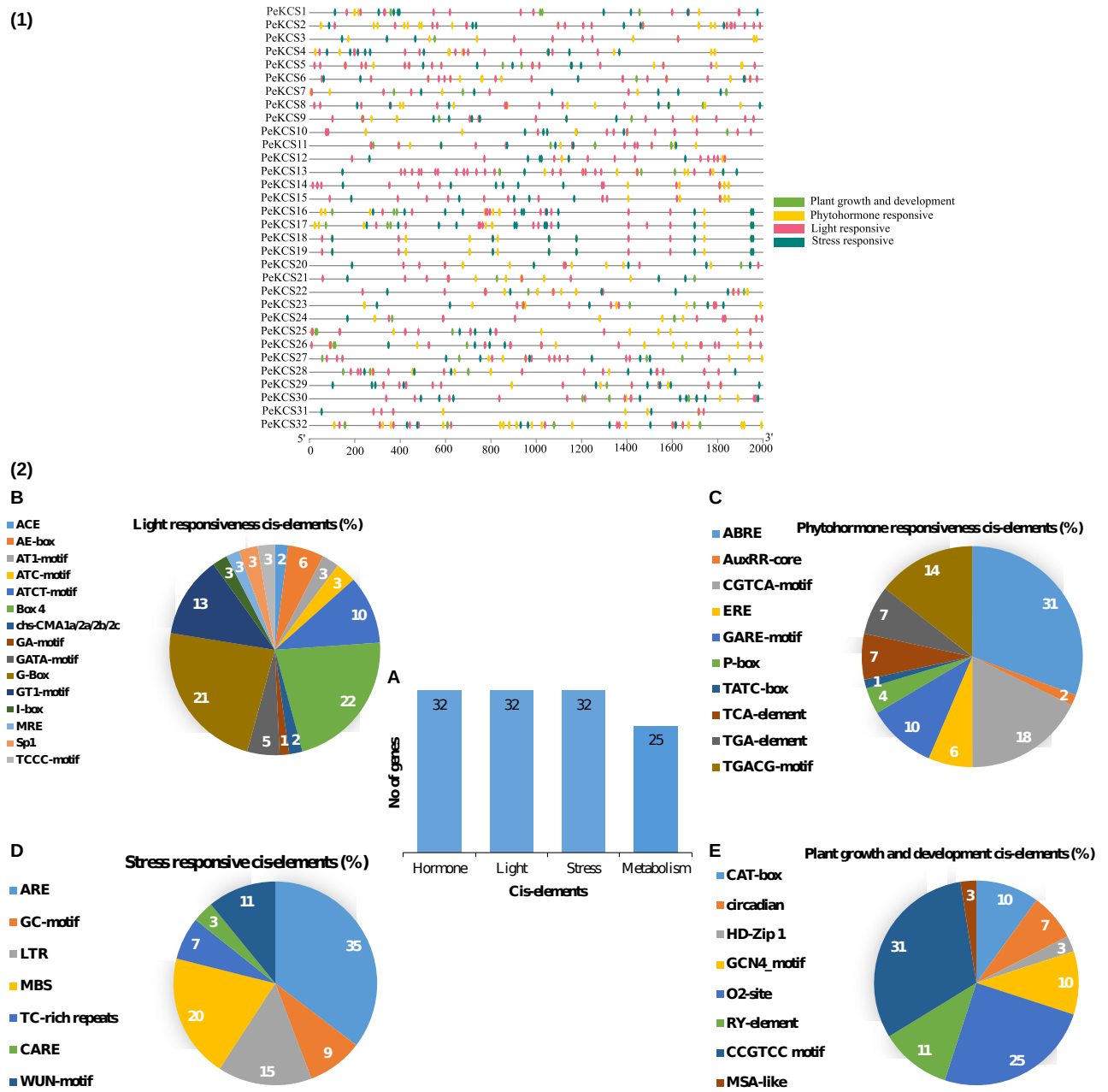


FIGURE 4 | The cis-regulatory element analysis in *PeKCS* genes **(1,2)**. **(A)** The sum number of *PeKCS* genes involved in four categories of cis-elements and the percentage (%) ratio of the numerous cis-elements from each category is presented in pie charts; **(B)** plant growth and development responsive **(C)** phytohormones-responsive, **(D)** light-responsive, and **(E)** stress-responsive. Different colors indicate different cis-acting elements and their ratio present in *PeKCS* genes.

such as groups I, II, III, and V contained 8 conserved motifs except for *PeKCS*30. Furthermore, the 9 members of group VII contained 4 conserved motifs (**Figures 3A,B**). Genomic structural analysis of exons in 32 *PeKCS* genes revealed that the number of exons identified in *PeKCS* varied from 1 to 9 (**Figure 3C**). Most *PeKCS* genes (11 genes) consist of 2 exons and 1 exon (10 genes). In addition, *PeKCS*1 contains up to 9 exons (**Figure 3C**). Group II has only 1 exon and no intron, group 1, III, IV, and V have 1 to 4 introns, group VI have 3 introns and group VII contained 1 to 9 introns except *PeKCS*11, *PeKCS*14, *PeKCS*15, and *PeKCS*32 genes have no introns (**Figure 3C**). Overall, groups I, II, III, and V showed similar exon-intron patterns whereas groups IV and VII had different exon-intron association patterns (**Figure 2C**). These results suggest that *PeKCS* genes within a group have remarkably similar gene structures consistent with their phylogenetic relationships

(**Figure 3**). In conclusion, after analyzing the composition of conserved motifs, gene structure, phylogenetic relationships, and group classification, the results indicated that *PeKCS* genes have highly conserved amino acids and genes within a group may have the same functions.

Cis-Regulatory Element Analysis of *PeKCS* Genes

The *cis*-regulatory element analysis of the *PeKCS* genes from the 2000 bp upstream promoter region was conducted to better understand the role of *PeKCS* genes in biotic and abiotic responses (**Figure 4** and **Supplementary Table 5**). Mainly four different categories of *cis*-regulatory elements were found in the *PeKCS* promoter regions including plant growth and development (8 different types of *cis*-elements), phytohormones (10 different types of *cis*-elements), light (15 different types of *cis*-elements), and stress (7 different types of *cis*-elements) responsiveness (**Figure 4.1**). Overall, a total of 969 *cis*-elements belonging to different categories were identified in 32 *PeKCS* genes, and when comparing between four different categories, the phytohormone-responsive category had the highest number of *cis*-elements at 40% (391/969), followed by light-responsive 37% (351/969), stress-responsive 15% (147/969) and the lowest number of *cis*-elements found in the plant growth and development response category 8.3% (80/969) (**Figure 4.2**). Furthermore, all the 32 *PeKCS* genes contained the phytohormone, light, and stress-responsive *cis*-elements, whereas only 25 *PeKCS* contained metabolism (plant growth and development) responsive *cis*-elements (**Figure 4.2**A).

The main four categories were further divided into subcategories based on different *cis*-elements. Light responsiveness category comprised of the 3-AF1 binding site, ACE, AE-box, AT1-motif, ATC-motif, ATCT-motif, TCT-motif, Box 4, chs-CMA1a/2a/2b/2c, GA-motif, GATA-motif, G-Box, GT1-motif, I-box, LAMP-element, MRE, Sp1, and TCCC-motif *cis*-elements (**Figure 4.2** and **Supplementary Table 5**). The highest light-responsive *cis*-elements consisted of Box-4 22% followed by G-Box 21%, while the GA-motif consisted of only 1% *cis*-elements (**Figure 4.2**B). The phytohormone responsive category further includes ABRE (abs*cis*ic acid-responsive), AuxRR-core (auxin-responsive), ERE (ethylene-responsive), GARE-motif, P-box, TATC-box (gibberellin responsive); TCA-element (salicylic acid-responsive); TGA-element and TGACG-motif (MeJA responsive) *cis*-elements. The highest number of *cis*-elements from the phytohormones category was ABRE 31% followed by CGTCA-motif 18%, while the AuxRR-core consisted of only 1% *cis*-elements (**Figure 4.2**C and **Supplementary Table 5**).

The stress response category further included ARE, GC-motif, LTR, MBS, TC-rich repeats, CARE, and WUN-motif *cis*-element. ARE accounted for the highest number 35% followed by MBS with 19%, and CARE with only 3% (**Figure 4.2**D and **Supplementary Table 5**). The plant growth and development category further include subcategories of meristem, metabolism, seed related, and circadian. Meristem associated *cis*-elements included CAT-box (10%) and GCN4-motifs (10%). Metabolism-related *cis*-elements included O2-sit (25%), seed and circadian-related *cis*-element included RY-element (11%), and only 3% of MSA-like *cis*-elements were found (**Figure 4.2**E and **Supplementary Table 5**). The information on developmental, light, stress, and hormone-related *cis*-elements suggested that the transcriptional profiling of *PeKCS* genes may vary in developmental, hormonal, and stressful contexts and require further investigation. Details on the *cis*-regulatory elements in the passion fruit *KCS* genes have been provided in **Supplementary Table 5**.

Synteny Analysis of *PeKCS* Genes

Synteny analysis was performed to further understand the evolution and expansion mechanism of the *PeKCS* gene family in the passion fruit genome and the genomes of other species. *PeKCS* gene duplications were assessed based on a tandem or segmental duplications. The results of gene duplication analysis indicate that there were 8 *PeKCS* gene pairs (**Figure 5A** and **Supplementary Table 6**), of which 3 gene pairs were segmentally duplicated on chromosomes 1, 2, 3, 6, and 8, whereas 5 gene pairs were tandem duplicated on chromosomes 1 and 4 in passion fruit genome. The duplicated genes belonged to different chromosomes, and chromosome 1 was found to have half of the duplicated genes (8 genes) (**Figure 5A** and **Supplementary Table 6**). These results suggest that gene duplication may play an important role in the development of the *PeKCS* gene family and the passion fruit genome. In addition, the Ka/Ks ratios were calculated in duplicated genes to assess the evolutionary rates and selection pressures (**Supplementary Table 6**). In general, a Ka/Ks ratio greater than 1 indicates that the gene was positively selected, a ratio less than 1 indicates a purifying selection, and a ratio equal to 1 indicates neutral selection. Details of the Ka, Ks values, and Ka/Ks ratios of the duplicated *PeKCS* gene pairs are provided in **Supplementary Table 6**. Overall, all duplicated *PeKCS* gene pairs showed a Ka/Ks ratio of less than 1, indicating that these genes had gone through purifying selection. Additionally, the divergence time between duplicated genes was measured as a substitution rate of 6.38×10^{-9} substitutions per site per year (Ma et al., 2021). The results of the divergence indicated that the duplication process between the tandem and segmental *PeKCS* genes was estimated to be between 0.30 and 27.64 million years ago (**Supplementary Table 6**). It can be concluded that the evolutionary mechanism of the *PeKCS* gene showed maintenance during the domestication of passion fruit.

Comprehensive synteny analyses of *KCS* genes between *P. edulis*, *A. thaliana,* and *M. domestica* species were performed and 45 *KCS* gene pairs were identified within these three species. Among the 32 *P. edulis KCS* genes, 15 *PeKCS* genes were paired with 26 *KCS* genes in *A. thaliana* (10 *AtKCS*) and *M. domestica* (16 *MdKCS*) (**Figure 5B** and **Supplementary Table 7**). Among species, 15 *KCS* gene pairs were found between *P. edulis* (8 *PeKCS*) and *A. thaliana* (10 *AtKCS*) species (**Supplementary Table 7**). On the other hand, 30 KCS gene pairs were found between *P. edulis* (15 *PeKCS*) and

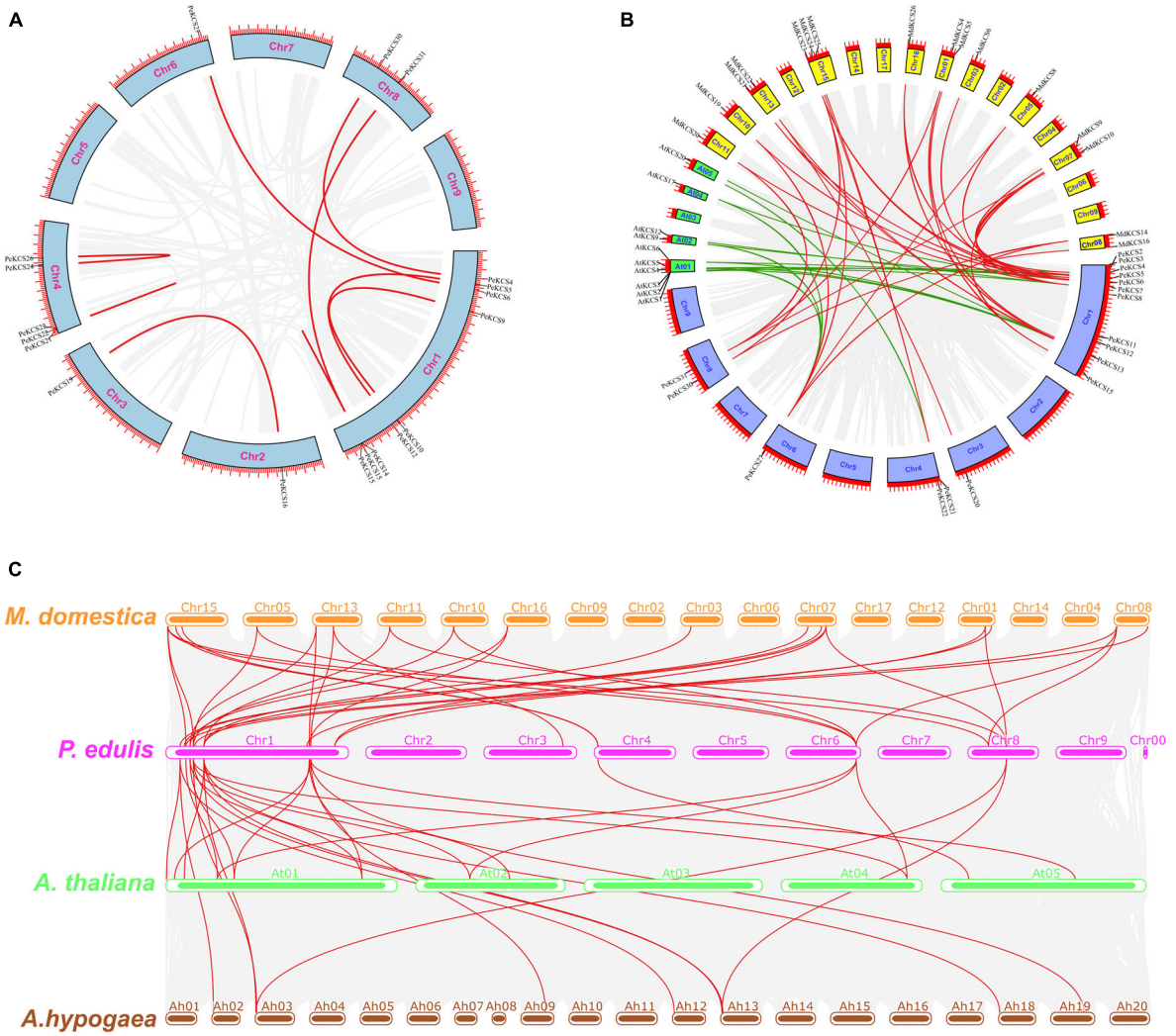


FIGURE 5 | Circos illustrations of the *PeKCS* genes duplication and multiple collinearity analysis of KCS genes between *P. edulis, A. thaliana, M. domestica,* and *A. hypogaea* species. **(A)** Gene duplication of *KCS* genes in *P. edulis*. The background gray lines show all the syntenic blocks in the passion fruit genome, and the red lines show the segmental or tandem duplication link regions among *PeKCS* genes. The approximately location of *PeKCS* genes are labeled with a short gray line outside with gene names. **(B)** Orthologous of *P. edulis KCS* genes with *A. thaliana (AtKCS)* and *M. domestica (MdKCS)* species. Chromosomes of *P. edulis are* represented with Chr1–Chr9, *A. thaliana* with At01-At05 and *M. domestica* with Chr01–Chr17. The background gray lines show all the syntenic blocks genomes of different species, green lines represented the syntenic relationship among *P. edulis* and *A. thaliana* KCS genes, red lines represented the syntenic relationship among *P. edulis* and *M. domestica KCS* genes, **(C)** Multiple collinearity analysis of *KCS* genes between *P. edulis, A. thaliana, M. domestica,* and *A. hypogaea* species. The red lines represent the *P. edulis KCS* genes orthologous in *A. thaliana*, *M. domestica,* and *A. hypogaea* species, the gray lines in the background represent the collinear blocks within *P. edulis* and other species genomes.

M. domestica (16 *MdKCS*) species (**Supplementary Table 7** and **Figure 5B**). Taken together, the *P. edulis* and *M. domestica KCS* genes showed a high degree of synteny compared with *A. thaliana*, suggesting that they may have originated from the same ancestors and performed the same functions, which required further study.

Multicollinearity analysis was performed to reveal robust orthologs of *KCS* genes between *P. edulis A. thaliana*, *M. domestica,* and *A. hypogaea* species (**Figure 5C** and **Supplementary Table 8**). The results showed that multiple collinear gene pairs between the four species were inferred as genetic copies with lineage-specific expansion. In general, 58 *P. edulis KCS* genes showed syntenic association with 31 *M. domestica* genes, 16 *A. thaliana* genes, and 11 *A. hypogaea* genes. Overall, the maximum collinear genes were found between *P. edulis* and *M. domestica* followed by *P. edulis* and *A. thaliana,* while the fewest were found between *P. edulis* and *A. hypogaea* species. *P. edulis* chromosome 1 shared the maximum collinear genes among *M. domestica* and *A. thaliana* (**Figure 5C** and **Supplementary Table 8**), suggesting that the *KCS* genes are conserved and may have the same ancestors besides with duplication or loss of *KCS* genes. Furthermore, many homologs from *A. thaliana*, *M. domestica,* and *A. hypogaea* species maintained a syntenic

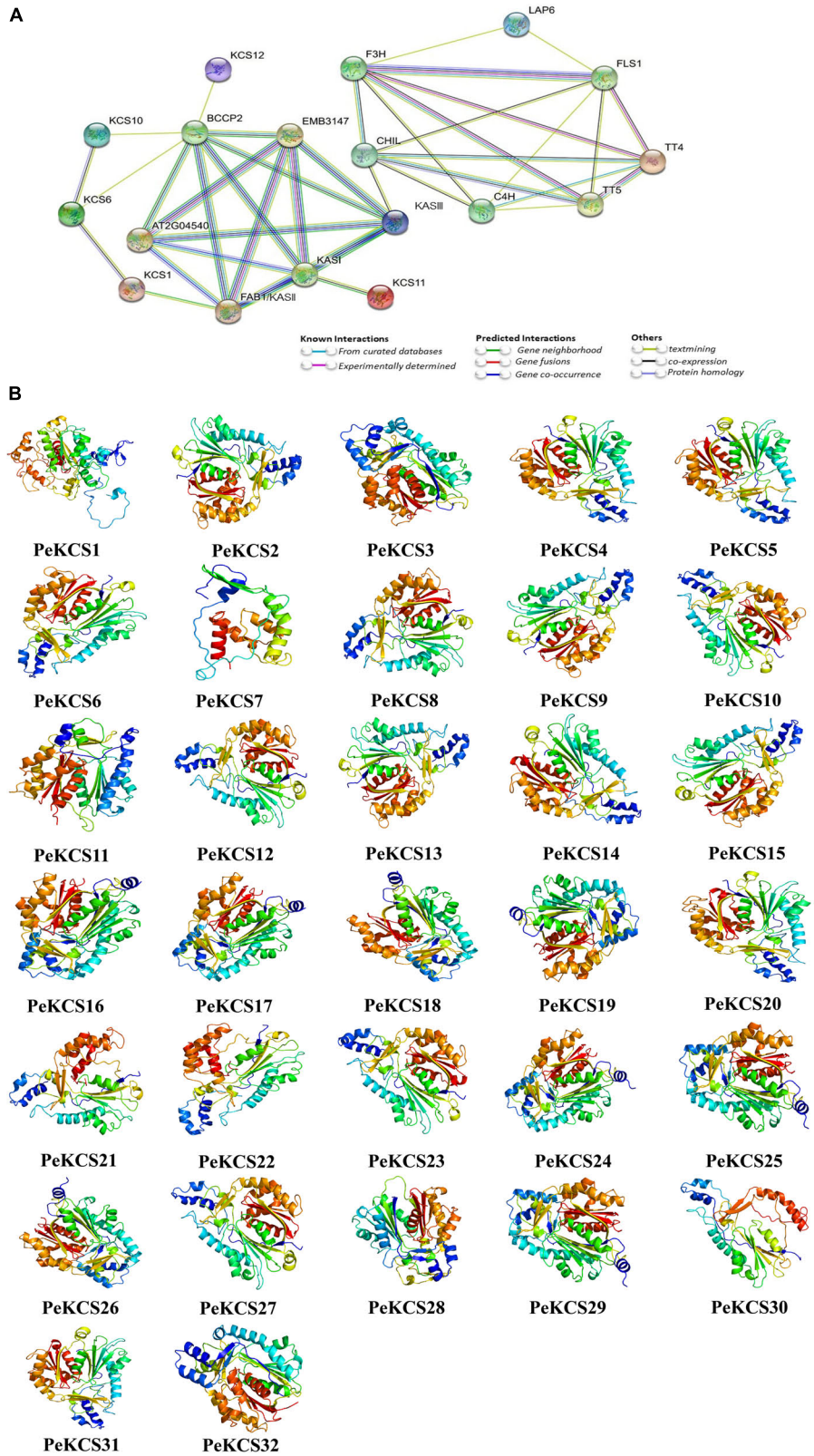


FIGURE 6 | Protein–protein interaction and predicted 3D models of *PeKCS* proteins. **(A)** The network was constructed using online STRING software. The proteins are displayed at network nodes with 3D structure of the proteins within nodes and the lines colors indicate different data sources. The higher the interaction coefficient, the thicker the network lines between proteins and vice versa. **(B)** 3D models were constructed using the online Phyre2 server with default mode.

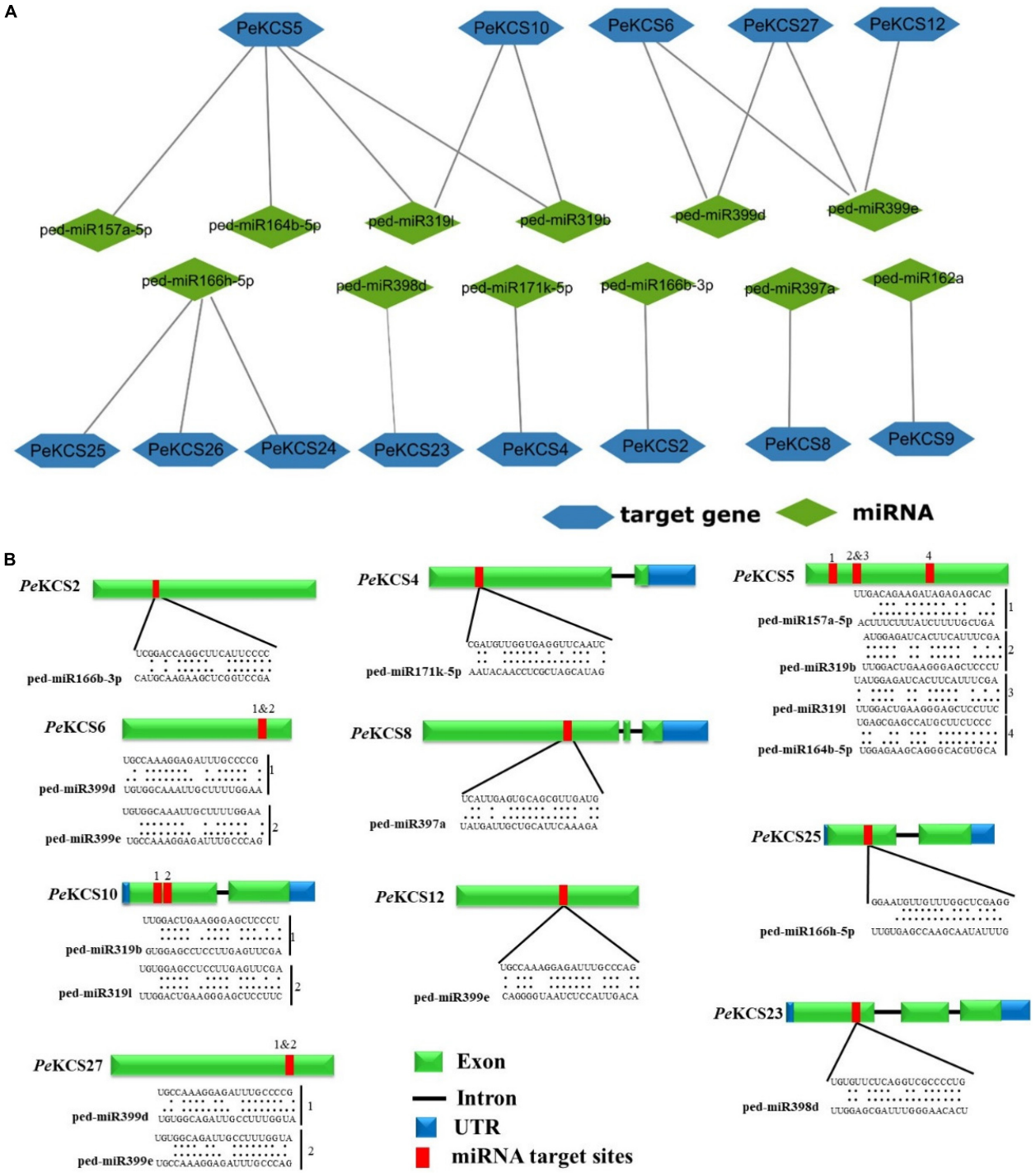


FIGURE 7 | Predicted miRNAs targeting *PeKCS* genes. **(A)** Network illustration of predicted miRNA targeted *PeKCS* genes. Green ellipse shapes represent the predicted miRNAs and bluish hexagon shapes represent targeted *PeKCS* genes. **(B)** The schematic diagram indicates the *PeKCS* targeted by miRNAs and the putative miRNAs sites are indicated by red color, upper sequences are from the gene region and lower sequences are from the miRNAs (**Supplementary Table 8** for detailed information of all the predicted miRNAs and targeted *PeKCS* genes).

association with the *P. edulis KCS* gene family suggesting that, in addition to segmental duplications, the whole-genome duplications also play an important role in the evolution of the *PeKCS* gene family.

Protein–Protein Interaction, Secondary Structure, and 3D Modeling of *PeKCS*

The protein–protein interaction network analysis of PeKCS proteins based on known *Arabidopsis* proteins was conducted.

PeKCS portions having higher homologous similarity with *Arabidopsis* proteins were selected as STRING proteins. Among all, 31 PeKCS proteins were associated with known *Arabidopsis* proteins (**Figure 6A** and **Supplementary Table 9**). PeKCS proteins belonging to different groups may have diverse functions in *Arabidopsis*. PeKCS1 and PeKCS28 were homologous with AtKASIII protein and have a strong interaction among AtKASI, AtEMB3147, AT2G04540, and AtBCCP2 proteins. PeKCS2 showed homology with AtKCS1 protein and interacts with AtFAB1/KASI and AtKCS6 proteins. PeKCS5, PeKCS11, and PeKCS12 were homologous with AtKCS6 and showed an interaction with AtKCS6 and AtKCS10 proteins. PeKCS23 shows homology with AtKCS10 and interacts with AtBCCP2 and AtKCS6 proteins. PeKCS8 was homologous with AtKCS12 and interacts with AtBCCP2 protein. PeKCS3 was homologous with AtLAP6 and interacts with AtFLS1 and AtF3H proteins. PeKCS9, PeKCS20, PeKCS21, and PeKCS22 were homologous with AtKCS11 and have a strong interaction with AtKASI protein. PeKCS16, PeKCS17, PeKCS18, PeKCS19, PeKCS24, PeKCS25, PeKCS26, and PeKCS29 were homologous with AtTTP4 and have an interaction among AtFLS1 and AtTT5 proteins. The PeKCS proteins that have strong interaction with *Arabidopsis* proteins might have similar functions as in *Arabidopsis*. The higher the interaction coefficient, the thicker the line between proteins and vice versa (**Figure 6A** and **Supplementary Table 9**).

The protein secondary structure generally consists of alpha helices, extended strands, beta turns, and random coils. The PeKCS protein secondary structure analysis was performed and found that in all PeKCS proteins, the alpha helix accounted for the largest percentage of secondary structures 49.6% (PeKCS5) followed by random coils 41.96% (PeKCS1) and extended strands 22.89% (PeKCS28), whereas the beta turns accounts only for 9.2% (PeKCS28). PeKCS28 showed the highest percentage in extended strands and beta turns might have a specific function that needs further studies (**Supplementary Table 10**). Additionally, the 3D models of all the PeKCS proteins were predicted by using the Phyre2 server with default mode (**Figure 6B**). The following templates were used for the predicted PeKCS protein models including nineteen PeKCS (PeKCS2, PeKCS4, PeKCS5, PeKCS6, PeKCS7, PeKCS8, PeKCS9, PeKCS10, PeKCS12, PeKCS13, PeKCS14, PeKCS15, PeKCS20, PeKCS21, PeKCS22, PeKCS23, PeKCS27, PeKCS30, and PeKCS31) protein models were predicted with c3vs9F template. Eight PeKCS (PeKCS16, PeKCS17, PeKCS18, PeKCS19, PeKCS24, PeKCS25, PeKCS26, and PeKCS29) protein models were predicted with c1cmlA template. Template c1u0mA in PeKCS32 model, template c2d3mA in PeKCS3 model, template c3gwaA in PeKCS28 model, template c3tsyA in PeKCS11 model and template c4b3yB in PeKCS1 respectively. All PeKCS proteins showed a flexible structure due to the presence of coils (**Figure 6B**). Our finding suggested that *PeKCS* genes from individual genomes may be ancestrally similar with each other or initially differ maybe stabilized during long-term domestication, leading to changes in protein structure and functions.

Prediction of Potential Micro-RNAs Targeting *PeKCS* Genes

MicroRNAs are a class of small non-coding regulatory RNAs that control gene expression by directing target mRNA cleavage or translational repression (Sunkar and Zhu, 2004). Over the past few decades, various studies have been reported that miRNAs induce the regulation of stress, plant development, and single transduction (Witkos et al., 2011). Therefore, to better understand the regulatory mechanism of miRNA involved in the regulation of *PeKCS* genes, the identification of putative miRNA in *PeKCS* genes was performed by using the mature sequences of known passion fruit miRNAs as described in the material section. Details of the putative miRNA targeting sites and the *PeKCS* genes have been provided in **Supplementary Table 11**. Twenty putative ped-miRNAs belonging to 9 different families were identified, targeting the 13 *PeKCS* genes (**Figure 7** and **Supplementary Table 11**). The results show that one member of the ped-miR157 family targeted one gene (*PeKCS*5); one member of the ped-miR162 family targeted one gene (*PeKCS*9); one member of ped-miR164 family targeted one gene (*PeKCS*5); two members of the ped-miR166 family targeted four genes (*PeKCS*2, *PeKCS*24, *PeKCS*25, and *PeKCS*26); one member of ped-miR171 family targeted one gene (*PeKCS*4); two members of ped-miR319 family targeted two genes (*PeKCS*5 and *PeKCS*10); one member of ped-miR397 family targeted one gene (*PeKCS*8); one member of ped-miR398 family targeted one gene (*PeKCS*23) and two members of ped-miR399 family targeted three genes (*PeKCS*12, *PeKCS*26, and *PeKCS*27) (**Figure 7** and **Supplementary Table 11**). Taken together, the results indicated that *PeKCS*5 was most targeted by four putative ped-miRNAs (ped-miR157a-5p, ped-miR164b-5, ped-miR319b, and ped-miR319l) belonging to four distant families, whereas the ped-miR166 family that targeted up to four *PeKCS* genes (*PeKCS*2, *PeKCS*24, *PeKCS*5, and *PeKCS*26) (**Figure 7A** and **Supplementary Table 11**). Network and schematic diagram of putative miRNA targeting sites of *PeKCS* genes shown in **Figures 7A,B**.

Prediction of Transcription Factor Regulatory Network of *PeKCS* Genes

The potential TFs in the upstream region of (1000bp) of *PeKCS* genes were predicted and constructed the TF regulatory networks (**Figure 8**). The results showed that, overall, 1701 TFs were identified in 32 *PeKCS* genes belonging to 38 different TF families including ERF, AP2, GRAS, ARF, MYB, Dof, C2H2, TCP, LBD, bHLH, MIKC_MADS, BBR-BPC, and NAC (**Figure 8** and **Supplementary Table 12**). The most abundant TF families were ERF (719 members), MYB (138 members), Dof (102 members), C2H2 (91 members), TCP (75 members), LBD (64 members), and bHLH (61 members) (**Supplementary Table 12**). Whereas the least abundant TF families were also identified contained only 1 member including WOX, EIL SRS, HSF, BES1, and S1Fa-like (**Supplementary Table 12**). All 32 *PeKCS* genes were predicted to be targeted by numerous TFs belonging to different families, for example, *PeKCS*32 was the most targeted with 547 TFs followed

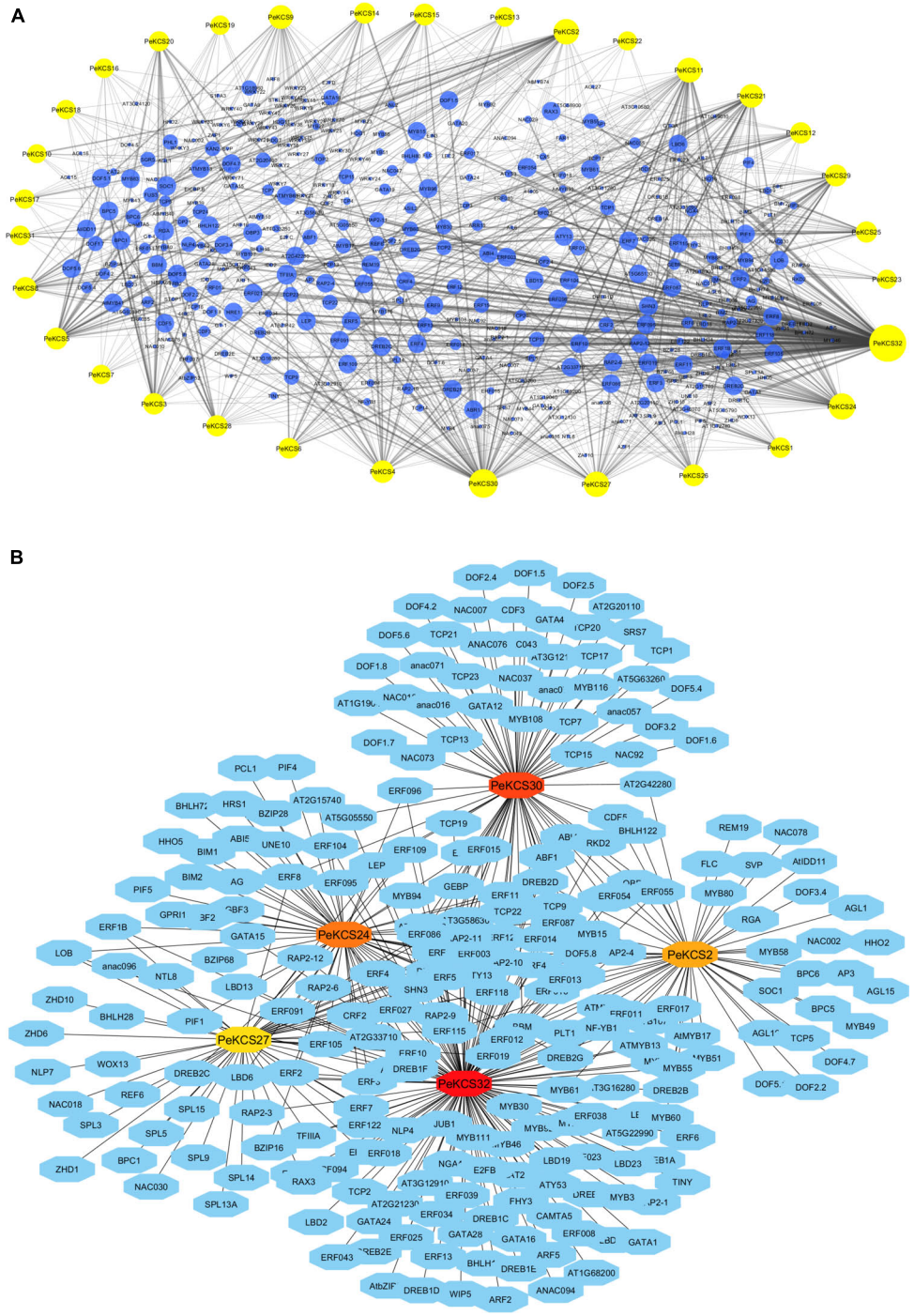


FIGURE 8 | The putative transcription factor regulatory network analysis of *PeKCS* genes. **(A)** Bluish circular nodes represent transcription factors; yellow octagonal nodes represent *PeKCS* genes and node size represents the degree of interaction between nodes based on degree value. **(B)** The top 5 highly enriched and targeted *PeKCS* genes are shown, darker the color shows highly enriched. Transcriptional factors were predicted by PTRM online program and regulatory network was constructed using the Cytoscape 3.9 software.

by *PeKCS*30 with 113, *PeKCS*24 with 76, *PeKCS*2 with 72, and *PeKCS*27 with 64 TFs. Whereas *PeKCS*10 and *PeKCS*22 were minimally targeted genes with only 10 and 9 TFs respectively (**Figure 8** and **Supplementary Table 12**).

Furthermore, a regulatory network of TFs for the top five *PeKCS* genes was constructed based on their degree of interaction, and the results showed that *PeKCS*32 was highly targeted, followed by *PeKCS*30, *PeKCS*24, *PeKCS*2, and *PeKCS*27

(**Figure 8B** and **Supplementary Table 12**). *PeKCS* genes were targeted with numerous members of different TF families such as *PeKCS*32 was enriched in ERF (412), LBD (40), and MYB (27) family members, *PeKCS*30 was enriched in ERF (38), TCP (20), and NAC (16) family members. *PeKCS*2 has enriched ERF (17), MYB (14), and MIKC_MADS (13) family members (**Figure 8B** and **Supplementary Table 12**). Overall, the ERF family was found to be dominant in all TF families. The TFs regulatory network of all the 32 *PeKCS* genes are shown in **Figure 8A**, and the networks of the top five highly enriched *PeKCS* genes are shown in **Figure 8B, respectively** and **more** details can be found in **Supplementary Table 12**. The different fatty acids and defense-related TFs belonging to different families were identified in the present study including ERF, AP2, bHLH, WRKY, and MYB. TFs involved in plant growth and development including TCP, bHLH, BBR-BPC, WRKY, LBD, and AP2 were also found in *PeKCS* genes. In addition, phytohormone-related TFs were also identified, including ERF and ARF. Interestingly, ERF, MYB, and AP2 TFs were shown to be universally distributed in most of the *PeKCS* genes (**Figure 8** and **Supplementary Table 12**).

Gene Ontology and Kyoto Encyclopedia of Genes and Genomes Enrichment Analysis of *PeKCS* Genes

Gene ontology and KEGG annotation analysis of the *PeKCS* gene was performed to further understand the possible roles of *PeKCS* genes in molecular function (MF), cellular component (CC), and biological process (BP) at the molecular levels. The details of annotation results and numerous significantly enriched terms for MF, CC, and BP have been provided in **Supplementary Tables 13a,b**. Seventeen terms were identified in 32 *PeKCS* genes belonging to GO-MF class, among which four terms were highly enriched including fatty acid synthase activity (GO:0004312), fatty acid elongase activity (GO:0009922), and acyltransferase activity (GO:0016746, GO:001674747) (**Figure 9A** and **Supplementary Table 13**). The GO enrichment analysis showed that GO-CC class exhibited thirty-one terms in 32 *PeKCS* genes, and seven terms were highly enriched including endoplasmic reticulum (GO:0005783), endomembrane system (GO:0012505), obsolete cytoplasmic part (GO:0044444), membrane-bounded organelle (GO:0043227), and organelle membrane (GO:0031090) (**Figure 9A** and **Supplementary Table 13**).

For instance, the maximum number of sixty-seven terms were identified in GO-BP class and six terms were highly enriched including response to cold (GO:0009409), response to temperature stimulus (GO:0009266), response to light stimulus (GO:0009416), response to radiation (GO:0009314), response to abiotic stimulus (GO:0009628) and response to stress (GO:0006950) (**Figure 9A** and **Supplementary Table 13**). Taken together, the enrichment and annotation results revelated that biological class terms were highly enriched followed by the cellular class in *PeKCS* genes. In addition, KEGG pathway enrichment analysis revealed that 15 pathways were predicted to be involved in different functions among the 32 *PeKCS* genes. Among the predicted KEGG pathways, the highly enriched pathways are presented in **Figure 9B**, including metabolism (A09100), lipid metabolism (B09103), environmental adaptation (B09159), organismal systems (A09150), polyketide biosynthesis proteins (01008), plant-pathogen interaction (04626), fatty acid elongation (00062) and circadian rhythm (04712) respectively (**Figure 9B** and **Supplementary Table 4**). In conclusion, the GO and KEGG enrichment analysis suggests that *PeKCS* genes may play important roles in different biological, molecular, and cellular processes including metabolism, fatty acid biosynthesis, and responses to different biotic and abiotic stresses.

Subcellular Localization of *PeKCS*2 Gene

The subcellular localization of all 32 *PeKCS* genes was hypothetically predicted using the online CELLO version 2.5 program. All 32 *PeKCS* genes were expected to localize to the plasma membrane (**Table 1**). To validate the hypothesized predicted results, *PeKCS*2 was used to perform a transient expression assay in onion epidermal cells. The CaMV35S-*PeKCS*2-GFP fusion construct was transformed into onion epidermal cells by the agroinfiltration method for transient expression assays (Xu et al., 2014). GFP expression was observed and results showed that GFP signals were highly expressed in the plasma membrane (**Figures 10d–f**). However, the empty vector CaMV35S-GFP was used as a control and the results showed that the GFP was dispersed throughout the cell (**Figures 10a–c**). The *PeKCS*2 subcellular localization results were consistent with the hypothesized predictions.

Expression Profiles of *PeKCS* Genes at Different Fruit Developmental Stages

The expression profiles of all 32 *PeKCS* genes in the pulp tissue of yellow and purple cultivars at different fruit development stages (fruitlet stage, green stage, veraison stage, and ripening stage) based on FPKM values were evaluated. The FPKM expression values have been provided in **Supplementary Table 15**. The FPKM values were transformed to $\log^2$ and a circular heatmap was generated by Tbtools software (**Figure 11A** and **Supplementary Table 15**). The expression profiles of *PeKCS* genes varied at different fruit developmental stages among both cultivars. Overall, 30 of the 32 *PeKCS* genes were expressed during different fruit developmental stages in both cultivars except *PeKCS*31 and *PeKCS*32. In the yellow cultivar, out of the 30 *PeKCS* expressed genes, 28 (87%), 27 (84%), 24 (75%), and 22 (68%) genes were expressed at fruitlet, green, veraison, and ripening stages. In terms of expression patterns, 14 (50%) genes were highly expressed (FPKM $>$ 10) at the fruitlet stage, 5 (18%) genes at the green stage, 8 (20%) genes at the veraison stage, and 10 (18%) genes at ripening stage. In the comparison of different developmental stages and genes, the expression pattern of *PeKCS*30 (FPKM = 356.7) was highest at the green stage, followed by *PeKCS*10 (FPKM = 324.52) at the fruitlet stage, *PeKCS*30 (FPKM = 233.51) at veraison, and *PeKCS*30 (FPKM = 96.12) at the ripening stage. Only one *PeKCS*13 gene expression was constantly increased during fruitlet (FPKM = 4.71) to ripening stage (FPKM = 23.68), while the expression patterns of five

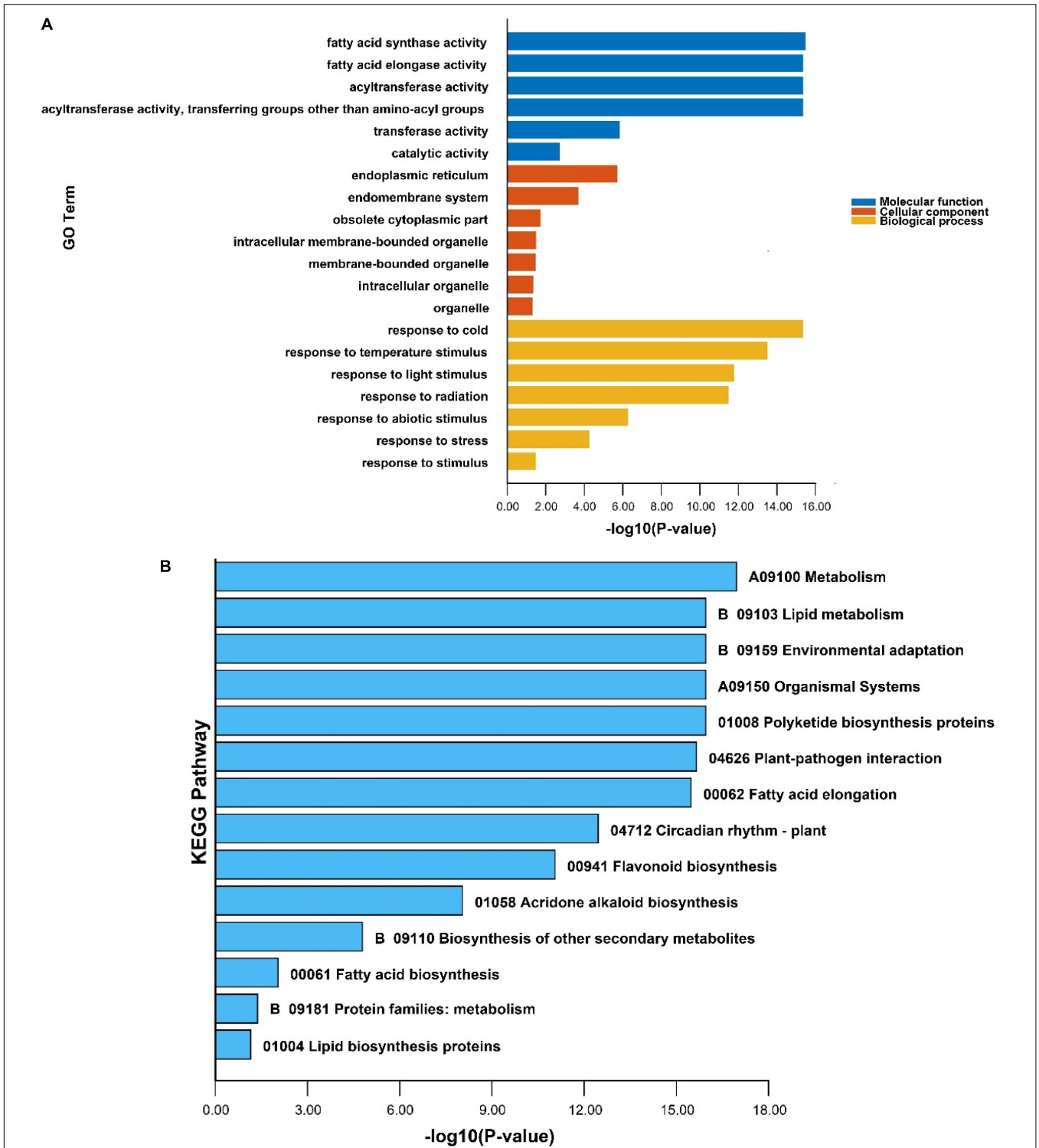


FIGURE 9 | GO and KEGG enrichment analysis of *PeKCS* genes. **(A)** The highly enriched GO terms in *PeKCS* genes. **(B)** The highly enriched KEGG pathways in *PeKCS* genes. Details about GO annotation, enrichment and terms of MF, CC, BP, and KEGG pathways can be found in **Supplementary Tables 11**, **13a,b**.

genes (*PeKCS*17, *PeKCS*19, *PeKCS*21, *PeKCS*22, and *PeKCS*28) decreased during fruitlet (FPKM = 69.22, 24.43, 13.16, 14.11, and 20.59) to ripening stages (FPKM = 2.77, 0.6, 3.72, 3.6, and 3.68) (**Figure 11A** and **Supplementary Table 15**). Interestingly, three genes had a constant high expression pattern in the four fruit development stages of yellow cultivar, including

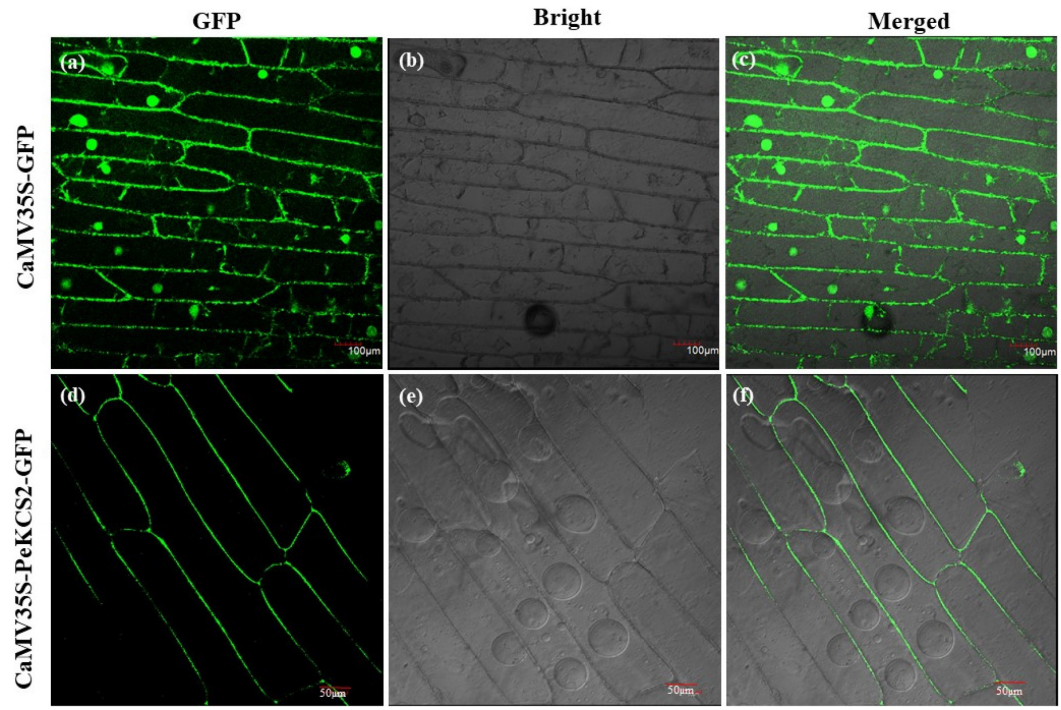


FIGURE 10 | Subcellular localization of GFP-fused *PeKCS*2 protein based on transient expression in onion epidermal cells. **(a–c)** Onion cells transformed with CaMV35S–GFP as control (scale bar = 100 μm). **(d–f)** Onion cells transformed with CaMV35S-*PeKCS*2-GFP (scale bar = 50 μm). **(b,e)** Onion epidermal cells under bright light. **(a–d)** GFP signal under dark field. **(c,f)** represent merged of **(a,b)**, and **(d,e)**, respectively. The transiently expressed in inner epidermis of onion was observed by laser scanning confocal microscopy (Olympus, Japan) after 24 h.

*PeKCS*1 (FPKM = 17–55.62), *PeKCS*10 (FPKM = 13.73–324.52), and *PeKCS*30 (FPKM = 96.12–356.70) (**Figure 11A** and **Supplementary Table 15**).

In the purple cultivar, overall, 30 (93%) *PeKCS* genes were expressed at the fruitlet stage, 25 (78%) at the green stage, 27 (84%) at veraison and ripening stages. Among them, 8 (26%) genes were highly expressed (FPKM > 10) at fruitlet, 5 (20%) at the green, 9 (33%) at veraison, and 7 (26%) at ripening stages. *PeKCS*10 exhibited the highest expression pattern (FPKM = 231.18) at the fruitlet stage, followed by green stage (FPKM = 130.89), *PeKCS*29 (FPKM = 74.68) at the veraison stage, and *PeKCS*1 (FPKM = 43.24) at the ripening stage. The expression patterns of 6 genes (*PeKCS*13, *PeKCS*16, *PeKCS*17, *PeKCS*18, *PeKCS*19, and *PeKCS*19) showed an increased trend from small fruitlet (FPKM = 0.1–1.1) to ripening stage (FPKM = 7.0–74.68), while 3 genes (*PeKCS*10, *PeKCS*27, and *PeKCS*28) decreased expression pattern from fruitlet (FPKM = 23.07–231.18) to ripening stage (FPKM = 0.11–2.3). Remarkably, *PeKCS*1 had a constant high expression pattern in the four fruit development stages of the purple cultivar (FPKM = 25.96–42.53) (**Figure 11A** and **Supplementary Table 15**).

In the comparison of *PeKCS* genes between the tested stages, *PeKCS*1 and *PeKCS*30 showed similar higher expressions (FPKM > 10) (**Figure 11A** and **Supplementary Table 15**). In the yellow cultivar, the green stage exhibits to have the highest expressions (FPKM = 324.52), whereas in purple the fruitlet stage showed the highest expressions (FPKM = 231.18). Overall, the yellow cultivar had higher expression levels and maximum genes with higher expression patterns compared to the purple cultivar. In addition, the yellow cultivar had decreased an expression pattern (5 genes) from fruitlet to ripening, while purple had increased expression patterns (6 genes) from fruitlet to ripening stages. These findings suggest that *PeKCS* genes may have significant roles in fruit development and ripening stages in both cultivars and further research is still needed (**Figure 11A** and **Supplementary Table 15**).

Expression Pattern of *PeKCS* Genes in Different Passion Fruit Tissues

The expression profiles of *PeKCS* genes in the root, stem, and peel tissues of yellow and purple passion fruit cultivars under different conditions were evaluated in FPKM values, and have been provided in **Supplementary Table 16**. The expression profiles of *PeKCS* genes in root tissue of the purple, leaf, and peel tissues of yellow cultivars were evaluated in FPKM values and visualized in circular heatmaps by converting to log2 values (**Figure 11B** and **Supplementary Table 16**). The expression profiles of *PeKCS* genes varied in different tissues among both cultivars. Overall, out of 32 *PeKCS* genes, 19 (59%) *PeKCS* genes were expressed in purple L and D root tissues, and 15 (46%) *PeKCS* genes were expressed in yellow and purple peel tissues. In contrast, 23 (72%) *PeKCS* genes were expressed in purple

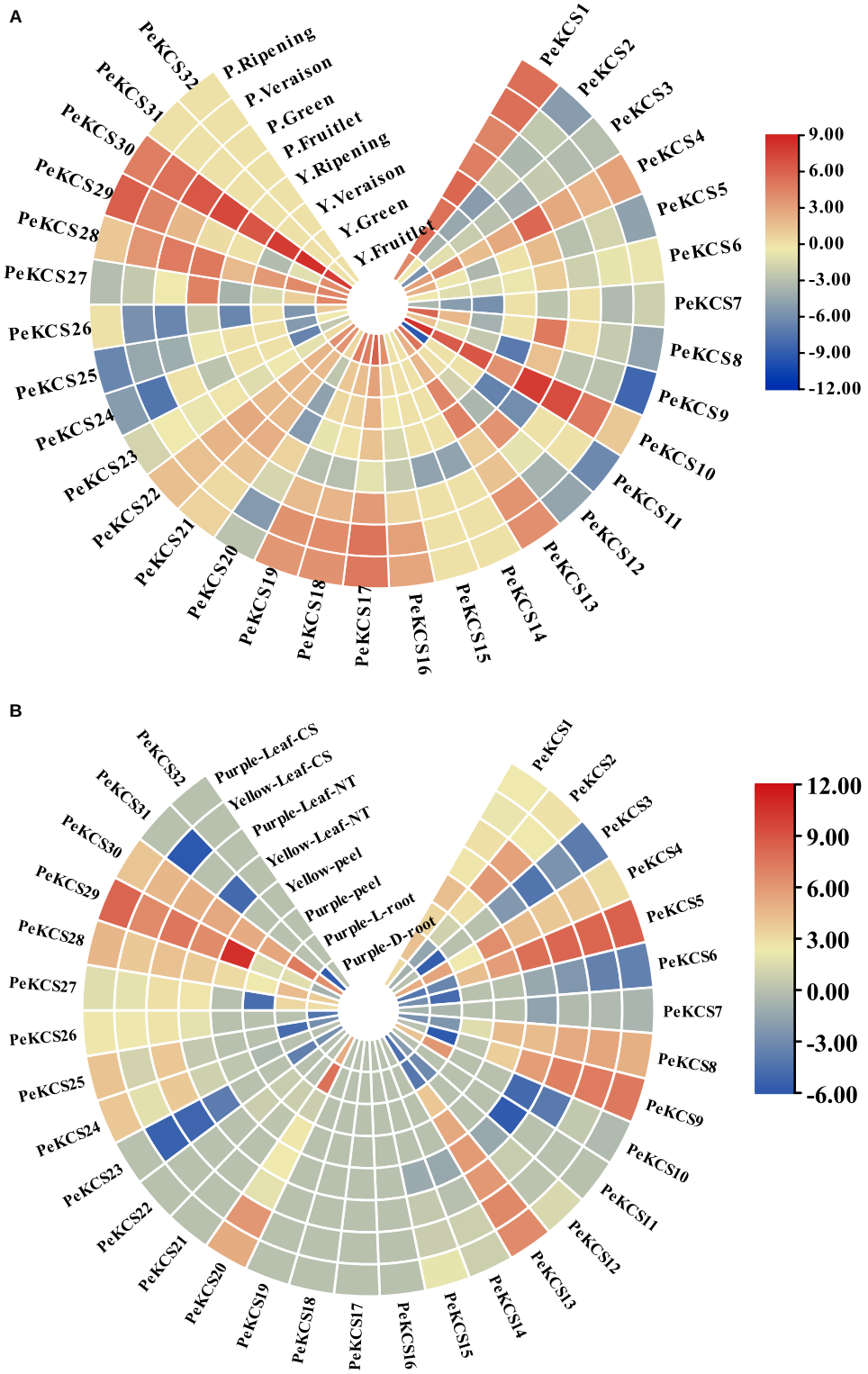


FIGURE 11 | Circular heatmap showing the expression profiles of *PeKCS* genes in pulp, root, peel, and leave tissues of yellow and purple cultivar under different conditions. **(A)** PeKCS expressions in pulp of yellow and purple passion fruit cultivars at different developmental stages. **(B)** *PeKCS* genes expressions in root, peel, and leaves of yellow and purple passion fruit cultivars under different conditions. Y and L represents the yellow (Y) and purple (P) passion fruit cultivars. L and D represents the samples from limestone (L) and sandy dolomite (D) rocky desertification areas. The NT and CS indicate the normal temperature (NT) and chilling stress (CS) conditions. Fragments per kilobase per million (FPKM) values of *PeKCS* genes all tissues were transformed by log2 and heatmap was constructed by TBTools software (the red color shows the highest and the blue color shows lowest expression levels in expression bar).

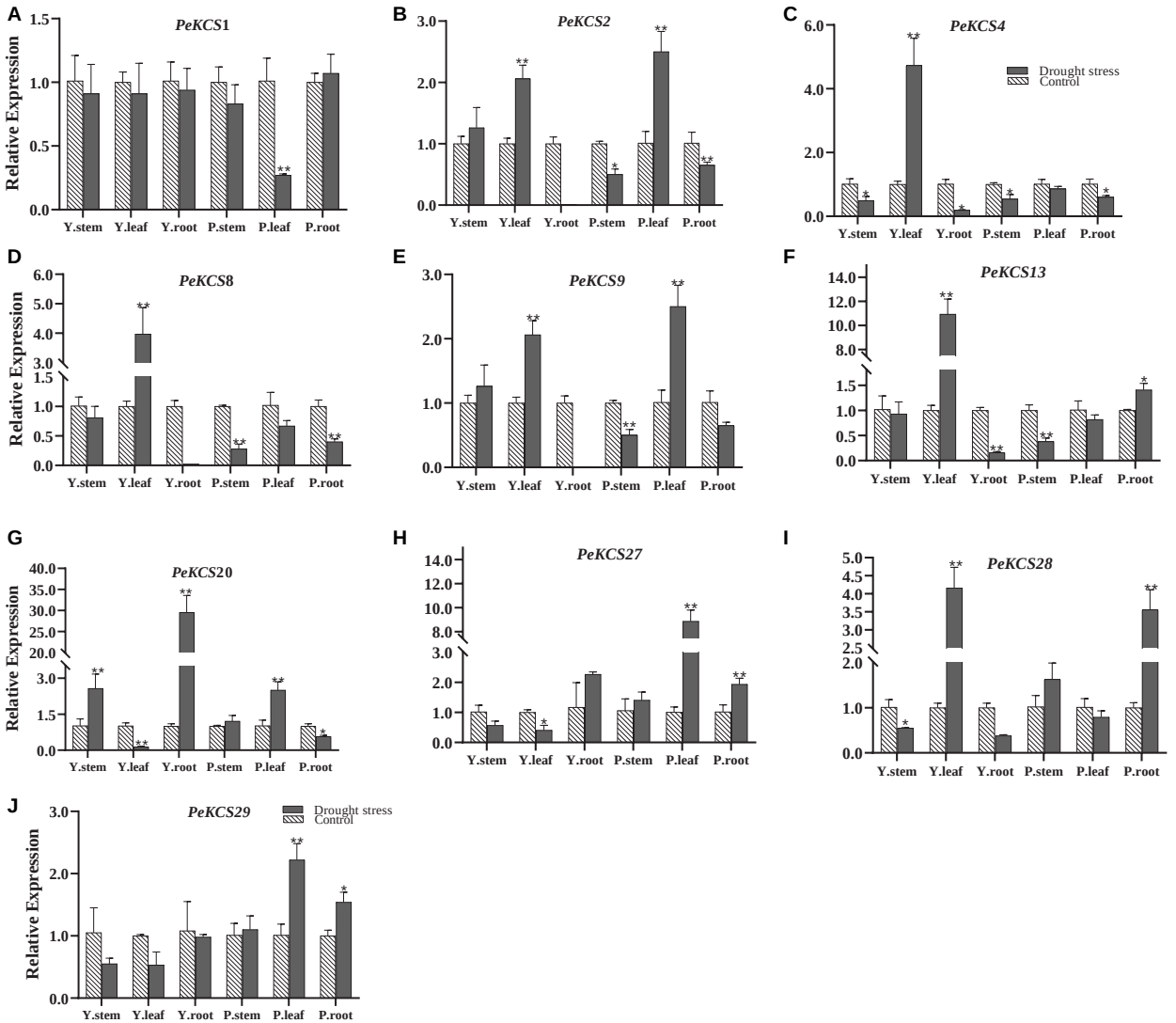


FIGURE 12 | The relative expressions of *PeKCS* genes in stem, root and leave tissues of yellow and purple passion fruit plants under control and drought stress conditions. The relative gene expression levels were calculated using the $2^{-\Delta\Delta ct}$. Plants with regular watering were taken as control. Vertical bars represent means ± SD ($n = 3$). The * and ** shows significance at $p \leq 0.05$ and $p \leq 0.01$, respectively, among control and drought stress condition according to Students *t*-test. Y, yellow passion fruit; P, purple passion fruit.

leaf NT condition, 25 (78%) in yellow leaf NT, 22 (69%) in purple leaf CS, and 24 (75%) genes were expressed in yellow leaf CS conditions respectively (**Figure 11B** and **Supplementary Table 16**). Among the expressed *PeKCS* genes in roots, 6 (31%) and 5 (26%) genes were highly expressed (FPKM > 10) in L and D roots. Roots under the L condition had the highest expression (*PeKCS*20, FPKM = 213.63) compared to roots in the L condition (FPKM = 82.58, *PeKCS*30) (**Figure 11B** and **Supplementary Table 16**).

Among the genes expressed in the peel, 8 (53%) and 3 (20%) *PeKCS* genes showed high expressions (FPKM > 10) in purple and yellow peels. Whereas, the purple peel was highly expressed (*PeKCS*29, FPKM = 1692.94) compared to yellow peel (*PeKCS*30, FPKM = 41.97). Under two different conditions (NT and CS), the expression profiles of *PeKCS* genes varied in leaf tissue of both cultivars such as 11 (48%) genes were highly expressed (FPKM > 10) in purple leaf-NT condition, 9 (36%) genes in yellow leaf-NT, 10 (45%) genes in purple leaf-CS and 9 (37%) genes in yellow leaf-CS conditions. Comparing both cultivars under NT and CS conditions, purple leaves under CS had the highest expression (FPKM = 359.34, *PeKCS*5), followed by yellow CS leaves (FPKM = 306.76, *PeKCS*5), purple NT leaves (FPKM = 303.78, *PeKCS*5), and yellow NT leaves (FPKM = 226.04, *PeKCS*5) (**Figure 11B** and **Supplementary Table 16**). Taken together, purple had the higher expression in all the tested tissues, whereas, in comparison between tissues, the peel was found to have the highest expression (FPKM = 1692.94, *PeKCS*29) followed by leave tissues

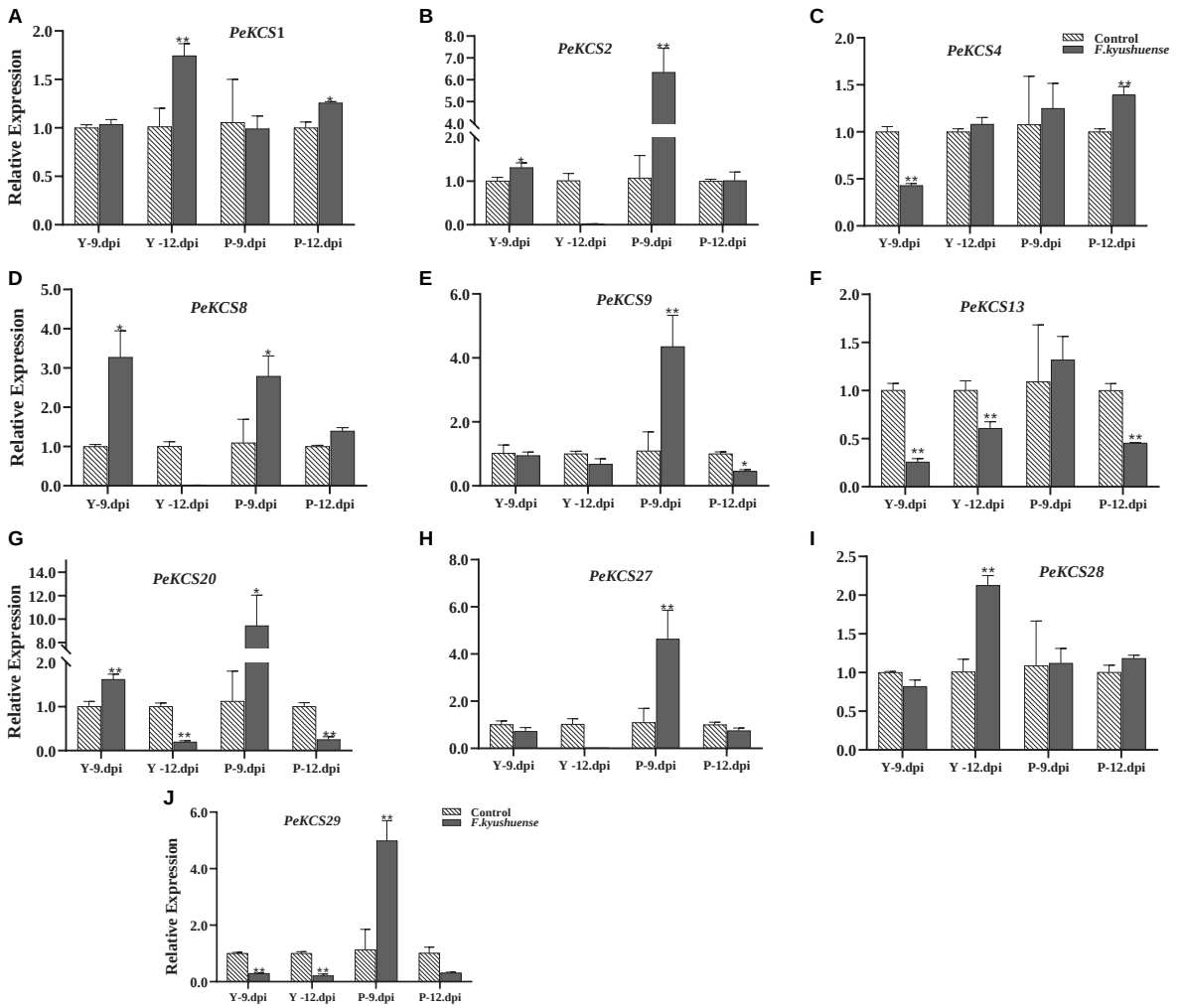


FIGURE 13 | The relative expressions of *PeKCS* genes in peel tissues of yellow and purple passion fruit plants under *F. kyushuense* fungal biotic stress and control conditions. The relative gene expression levels were calculated using the $2^{-\Delta\Delta ct}$. Vertical bars represents means ± SD ($n = 3$). The * and ** shows significance at $p \leq 0.05$ and $p \leq 0.01$, respectively, among control and biotic stress conditions according to Students *t*-test. Y, yellow passion fruit; P, purple passion fruit; dpi, days post inoculation.

(FPKM = 359.34, *PeKCS*5) and root (FPKM = 213.63, *PeKCS*20) (**Figure 11B** and **Supplementary Table 16**). Five genes (*PeKCS*16, *PeKCS*17, *PeKCS*18, *PeKCS*19, and *PeKCS*32) were not expressed in all tissues (leave, peel and root) indicating that they might not involve in passion fruit growth and development. These results indicate that *PeKCS* genes have specific expression patterns in all tested tissues and genes with the highest expressions (*PeKCS*5, *PeKCS*29, and *PeKCS*30) might play an important role in specific functions, but further research is required. These genotype-based tissue expression patterns provide ideas for further study of the *PeKCS* gene family in passion fruit.

Expression Profiles of *PeKCS* Genes Under Drought Stress Condition

The functional characterization of *KCS* genes has not been studied in passion fruit. Gene expression profiles can provide a reflection of gene function. In the current study, the expression profiles of ten candidate *PeKCS* genes were evaluated by qRT-PCR under drought stress conditions (**Figure 12**). In general, the expression profiles of all candidate *PeKCS* genes showed different expression levels in the stem, leave and root tissues of yellow and purple cultivars under drought conditions. Overall, the results showed that the expression levels of most genes were increased under drought conditions in leave and root tissues compared to controls. The relative expression level of the *PeKCS*20 gene was highest with a more than 29-fold increase in yellow roots under drought conditions (**Figure 12G**). However, under drought conditions, the relative expression levels of *PeKCS*13 and *PeKCS*27 in yellow and purple leaves increased by more than 10 and 8-folds, respectively (**Figures 12F,H**). Whereas, relative expressions of *PeKCS*1 decreased in most tissues under drought conditions (**Figure 12A**). On the contrary, the relative expression levels

of *PeKCS*4 and *PeKCS*8 increased by more than 4 and 3-folds in yellow leaves, and all other tissues decreased. Interestingly, *PeKCS*2 showed an increased relative expression in yellow and purple leaves more than 2.5 folds under drought (**Figure 12B**). Except for *PeKCS*9 and *PeKCS*20, the relative expression levels of most genes decreased in the stem tissue of the yellow cultivar. The relative expression of *PeKCS*28 was increased by more than 4 and 3-folds in yellow leaves and purple roots under drought conditions (**Figure 12I**). All the yellow tissues showed decreased relative expression levels in *PeKCS*29, while increased in purple tissues under drought conditions (**Figure 12J**). The leave tissue showed the highest expression consistent with the FPKM expression values (**Figure 12** and **Supplementary Table 16**). Taken together, the results indicated that *PeKCS* genes responded to external drought stress conditions by increasing or decreasing their expression levels in different tissues of the two cultivars, which provided evidence for further functional studies.

Expression Profiles of *PeKCS* Genes *F. kyushuense* Fungal Biotic Stress Condition

The functional characterization of *KCS* genes against fungal pathogens has not been studied in passion fruit. To gain insight into the potential functional role of *PeKCS* genes at expression levels in passion fruit defense against fungal pathogens as biotic stress, in the current study, the expression profiles of ten candidate *PeKCS* genes were assessed by qRT-PCR under *F. kyushuense* fungal stress (biotic stress) condition in peel tissues of yellow and purple cultivars at 9th and 12th days post-inoculation (dpi) (**Figure 13**). Overall, all *PeKCS* genes were expressed and showed increased or decreased expression levels under biotic stress conditions in yellow and purple cultivars compared to controls (**Figure 13**).

All the tested genes showed higher expression levels under biotic stress in purple 9th dpi (P-9.dpi) except *PeKCS*1 (**Figure 13A**) and *PeKCS28* (**Figure 13I**) compared to yellow 9th dpi (Y-9.dpi) (**Figure 13**). Among them, *PeKCS20* (**Figure 13G**) showed an increased expression level by more than 9-fold, followed by *PeKCS*2 more than 6-fold, *PeKCS*9, *PeKCS*27, and *PeKCS*29 more than 4-fold, *PeKCS*8 more than 2.5-fold, and *PeKCS*4 and *PeKCS*13 more than 1-fold at 9th dpi in purple cultivar (**Figure 13**). In yellow cultivar at 9th dpi, Only the expression levels of *PeKCS*8, *PeKCS*2, and *PeKCS*20 were found to be increased by 3-fold and more than 1-fold, while the expression level of all other genes decreased at Y-9.dpi (**Figure 13**). Interestingly, *PeKCS*1 and *PeKCS*28 expression levels were increased by 1.7- and 2.1-folds at 12th dpi in yellow cultivar (**Figure 13**). Overall, the results showed that *PeKCS* genes expression was increased under biotic stress conditions in purple at 9th dpi compared to controls (**Figure 13**). Taken together, the results showed that *PeKCS* genes have responded to fungal biotic stress by increasing or decreasing their expression levels at different time points of two cultivars providing evidence for further functional studies.

Validation of RNA-Seq Expression Data by Quantitative Real-Time Polymerase Chain Reaction

According to RNA-Seq FPKM expression data (**Supplementary Tables 15**, **16**), the *PeKCS*1, *PeKCS*2, *PeKCS*4, *PeKCS*9, *PeKCS*10, *PeKCS*13, *PeKCS*20, *PeKCS*27, *PeKCS*28, and *PeKCS*29 have relative higher FPKM expressions in purple peels compared to yellow. The FPKM expression values were further validated by qRT-PCR analysis using *PeKCS*1, *PeKCS*2, *PeKCS*4, *PeKCS*8, *PeKCS*9, *PeKCS*13, *PeKCS*20, *PeKCS*27, *PeKCS*28, and *PeKCS*29 genes in yellow and purple passion fruit peel tissues (The primer details can be found in **Supplementary Table 1**). After normalization with Pe60s reference genes, all the tested *PeKCS* genes showed a trend line consistent with the RNA-Seq expression values (**Figure 14**). These results revealed that RNA-Seq expression values provided an appropriate expression result for all the tested tissues among both passion fruit cultivars.

DISCUSSION

The plant cuticle wax is the first barrier between the environment and plants to protect them from biotic and abiotic stresses (Trivedi et al., 2019). Plant cuticle consists of a combination of VLCFAs and their derivatives (Yeats and Rose, 2013). VLCFAs are fatty acids consisting of C_{16} to C_{40} carbons that play important roles in plant development and are essential for the synthesis of seed storage triacylglycerols, epicuticular waxes, and sphingolipids (Roudier et al., 2010). Elongation of C_{16} and C_{18} fatty acids to VLCFAs (C_{20} to C_{40}) consists of four enzymes in the endoplasmic reticulum (ER) such as *KCS*, *KCR*, *ECR*, and *HCD* (Raffaele et al., 2009). Among them, *KCS* is known to be the key enzyme for VLCFAs biosynthesis (Wang X. et al., 2017; Yang H. et al., 2021). Due to the important roles of *KCS* in plant cuticle synthesis and other biological processes, the genome-wide identification of the *KCS* gene family has been reported in various plant species including *Arabidopsis thaliana* (Joubès et al., 2008), *Zea mays* (Campbell et al., 2019), *Arachis hypogea* (Huai et al., 2020), *Brassica napus* (Xue et al., 2020), *Vitis vinifera* (Guo et al., 2016), *Gossypium hirsutum*, *G. arboreum*, *G. raimondii* (Xiao et al., 2016), *Hordeum vulgare* (Tong et al., 2021), *Atalantia buxifolia*, *Citrus ichangensis*, *C. medica, C. grandis*, *C. Sinensis*, and *C. clementina* (Yang H. et al., 2021) ranging from 16 to 58 *KCS* members. In addition, the *KCS* family members have been functionally characterized in *Arabidopsis* (Lee et al., 2009; Kim et al., 2013; Hegebarth et al., 2017), *C. sinensis* (Yang H. et al., 2021; Wang et al., 2022), *O. sativa* (Wang X. et al., 2017), *H. annuus* (González-Mellado et al., 2019), *S. tuberosum* (Serra et al., 2009), *M. domestica* (Lian et al., 2021), *V. vinifera* (Yang Z. et al., 2020), and *A. hypogaea* (Lokesh et al., 2019). However, information about the *KCS* gene family in passion fruit was unknown and the availability of the passion fruit genome (Ma et al., 2021) made it possible to study on genomic levels. Therefore, identification and analyzing the physicochemical properties, structure, and

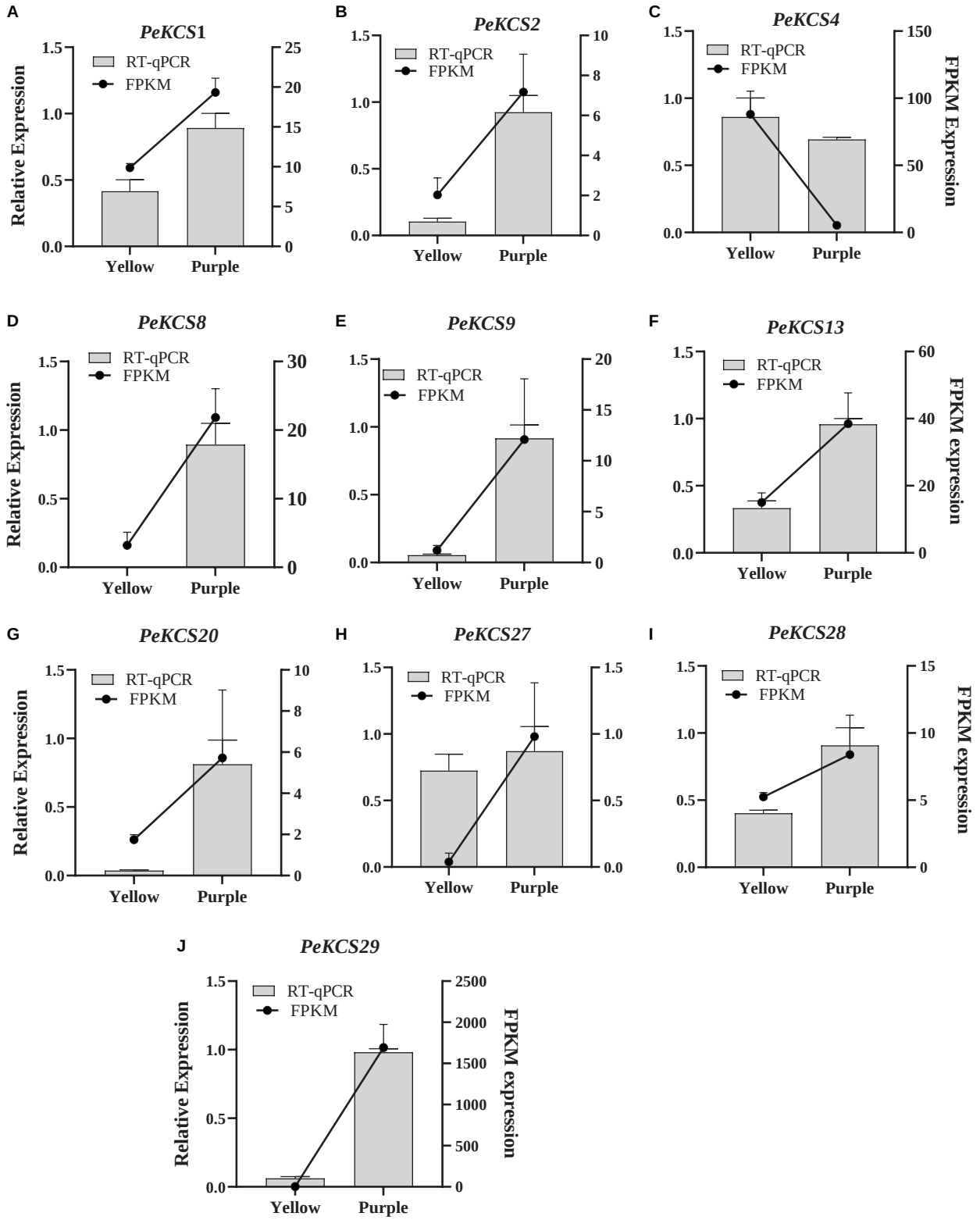


FIGURE 14 | Validation of RNA-seq expression data by qRT-PCR. Histograms show the qPCR results of 10 *PeKCS* genes in peel tissues of yellow and purple cultivars at ripening stage. Black line charts show the FPKM values of *PeKCS* genes on and vertical gray bars show the qPCR results ($2^{-\Delta\Delta ct}$) and represents mean ± SD. The left *Y*-axis represents the relative expression levels by qPCR and the right *Y*-axis indicates the FPKM values of RNA-seq data.

function of the passion fruit *KCS* gene at the genome level could provide a theoretical basis for functional characterization to improve the stress resistance and genetic improvement of passion fruit.

In the current study, a total of 32 *PeKCS* genes were identified in the passion fruit genome by BLASTp and HMMER search basis (**Table 1** and **Figure 1A**). The number of identified *KCS* genes in the passion fruit genome was relatively higher (32 *PeKCS* genes) compared with *Arabidopsis* (21 *AtKCS* genes) (Joubès et al., 2008), which may be due to large differences in genome size and a high number of repeated sequences. Our results are inconsistent with rapeseed (58 *BnKCS* genes) and barley (33 *HvKCS*) (Tong et al., 2021), in which they also identified a higher number of KCS genes (Xue et al., 2020) compared to *AtKCS*. The two domains (FAE1_CUT1_RppA and ACP_syn_III_C) were conserved in PeKCS proteins such as 22 PeKCS proteins have both domains, 6 PeKCS proteins have only FAE1_CUT1_RppA domain and 3 PeKCS proteins contained only ACP_syn_III_C domain (**Figure 1B**). Abbadi et al. (2000) also reported that the ACP_syn_III_C domain is important for initiating the fatty acid synthase chain reactions in plants and bacteria. KCS protein members with the FAE1_CUT1_RppA domain are described as 3-ketoacyl-CoA synthases and contain the active motifs involved in substrate binding and might be related to the substrate specificity of the *KCS* enzyme (Sagar et al., 2015). These reports support our results, that genes with ACP_syn_III_C and FAE1_CUT1_RppA domains identified in this study belong to the *KCS* gene family. Later on, multiple sequences alignment analysis between *AtKCS* and *PeKCS* genes was performed and found the two conserved domains regions indicating the importance of these domains to *KCS* gene functions (**Supplementary Figure 1**). Similar results were found by Lian et al. (2021) in *M. domestica* and Lokesh et al. (2019) in *A. hypogaea*.

The phylogenetic tree was constructed among KCS protein sequences of AtKCS, PeKCS, MdKCS, and AhKCS species (**Figure 3**) and exhibited into four subfamilies and eight clades including *FAE*-like (α), *FAE*-like (β), *CER6*-like (γ), *KCS1*-like (δ), *KCS1*-like (ζ), *FDH*-like (ε), *FDH*-like (η), and *FDH*-like (θ), which are consistent with previously published reports (Joubès et al., 2008; Lokesh et al., 2019; Lian et al., 2021). However, all the 32 *PeKCS* genes were grouped into seven clades and no *PeKCS* gene was found in FAE-like (β) clade (**Figure 3**). *PeKCS* genes in the KCS1-like (δ) clade were closely related to *AtKCS*1, which were involved in decarbonylation and acyl-reduction wax synthesis pathways (Todd et al., 1999). *PeKCS* genes in *KCS1*-like (ζ) clade were grouped with *AtKCS*2 and *AtKCS*20, which were involved in wax biosynthesis and tolerant to osmotic stress conditions (Lee et al., 2009). *PeKCS* genes in *FAE*-like (α) clade were grouped with *AtKCS*9 and *AtKCS*4, which were involved in VLCFAs, waxes, suberin, sphingolipids, and phospholipids (Kim et al., 2013, 2021). *FAE*-like (β) clade contained the *AtKCS*16, which were involved in the elongation of C_{34}-C_{36} and C_{38} VLCFA required for wax biosynthesis and leaf trichomes in *Arabidopsis* (Hegebarth et al., 2017). *PeKCS* genes in *FDH*-like (ε) clade were grouped with *AtKCS*10, which were involved in organ development (Yang T. et al., 2021). These findings suggested that genes present in the same clade might perform similar functions (Liu et al., 2018).

Differences in protein functions can be described by predicting conserved motifs during the development of different gene families (Wong et al., 2015). Furthermore, the conserved motifs in *PeKCS* genes were evaluated and found a diverse motif pattern ranging from 1–16 motifs, whereas, 10 conserved motifs were recognized in all 32 *PeKCS* genes. The motif distribution contrasts with different groups of the evolutionary tree, suggesting that these conserved motifs may be functionally distinct (**Figure 2B**). Our results are similar to Lian et al. (2021) who also reported a different distribution of motifs and identified 15 conserved motifs in *MdKCS*s. The existence of exons and introns in gene structure (especially intron) provides an important source for determining gene family variation, function, and expressions (Xu et al., 2012). Additionally, the intron number and length negatively correlated with the expression level of corresponding genes (Eghbalnia et al., 2020; Su et al., 2021a). In the current study, a quite different number of introns among 32 *PeKCS* genes ranging from 0 to9 introns were identified and group II was found with having no introns, whereas groups 1, III, IV, and V have 1 to 4 introns, group VI has 3 introns and group VII contained 1 to 9 introns except *PeKCS*11. *PeKCS*14, *PeKCS*15 and *PeKCS*32 genes have no introns (**Figure 2C**). Similar results for exon/intron were also reported by Lian et al. (2021) and Tong et al. (2021), where different intron and exon patterns were found in the *KCS* genes. These findings suggest that the *PeKCS* gene ancestor may have undergone several rounds of intron loss and gain during development (Frugoli et al., 1998).

The *cis*-regulatory element analysis in *PeKCS* genes was performed and found numerous *cis*-elements that were involved in different plant developmental and stress responses. The *cis*-elements including ABRE, G-Box, Box 4, CGTCA-motif, TGACG-motif, GARE-motif, and ARE were abundant (**Figure 4**), indicating that *KCS* genes may play an important role in plant hormone response and stresses (Porto et al., 2014). *PeKCS cis*-element results were consistent with the qRT-PCR expression analysis, as genes containing the larger number of stress-related *cis*-elements were highly upregulated under stress conditions, including *PeKSC2*, *PeKCS9*, *PeKCS13,* and *PeKCS28* genes were highly upregulated in drought stress condition (**Figure 12**), while *PeKCS2*, *PeKCS8*, *PeKCS9,* and *PeKCS27* genes were highly upregulated under F. kyushuense fungal biotic stress condition (**Figure 13**) Kim et al. (2011) reported that the promoter ABRE sequence was involved in the expression of the DREB2A gene under osmotic stress conditions. Sibéril et al. (2001) proposed that G-BOX might involve in the transduction pathway that regulates the gene expression in the nucleus. These results suggest that genes containing the above-mentioned *cis*-elements might involve in different plant developmental and stress responses as reported earlier (Wingender et al., 1990; Wang et al., 2011; Liu et al., 2016; Xiong et al., 2020). Different species such as *Arabidopsis*, peanut, apple, grape, rapeseed, cotton, sunflower have different numbers of chromosomes and *KCS*

genes, suggesting that they might have gone through lineage-specific genome duplication, which is a prominent feature of plant genomes that can lead to evolution and functional novelty from existing genes (Flagel and Wendel, 2009). Guo et al. (2016) reported that the WGD/segmental duplication plays a major role in the expansion of plant *KCS* genes. WGD/segmental and tandem duplications may lead to a sudden increase in the size of the genome and the entire gene sets by generating two gene copies (Van de Peer et al., 2009).

Synteny analysis was performed and calculated *PeKCS* genes divergence rate and found less than 1 Ka/Ks values, suggesting that *PeKCS* genes have gone through purifying selection and the duplication process among tandem and segmental *PeKCS* genes was estimated to be 0.30 to 27.64 mya (**Supplementary Table 6**), which is inconsistent with Xia et al. (2021), who reported that, the passion fruit experienced a two WGD between 12 mya and 65 mya. *PeKCS* gene duplication analysis showed 3 segmental and 5 tandems duplicated *PeKCS* genes within passion fruit genome (**Figure 5A** and **Supplementary Table 6**), correspondence with *Arabidopsis KCS* duplication by Joubès et al. (2008). Furthermore, comprehensive *KCS* gene duplication showed a higher number of KCS duplications were between *PeKCS* and *MdKCS* compared to *AtKCS* (**Figure 5B** and **Supplementary Table 7**). The multiple collinearity analysis between *P. edulis A. thaliana*, *M. domestica,* and *A. hypogaea* species (**Figure 5C** and **Supplementary Table 8**) also revealed the higher number of orthologous between *P.* edulis and *M. domestica*. Similar results were reported by Santos et al. (2014) that compared to the dicot genomes the number of repetitive elements between *P. edulis* and *M.domestica* genomes was 42.4%. These findings indicate that these orthologous might have the same ancestors and retain corresponding functions.

Protein–protein interaction networks for specific gene families provide evidence of the relationship between known family members (Piya et al., 2014). In the current study, 31 PeKCS proteins showed homology and interaction with known *Arabidopsis* proteins (**Figure 6A** and **Supplementary Table 9**). The results showed that PeKCS proteins had homology and interaction with AtKASI, AtLAP, AtKASIII, AtKCS, AtBCCP, AtTTP4. Our results are consistent with published reports suggesting that PeKCS have similar functions, such as Chen et al. (2009) revealed that BCCP (Biotin carboxyl carrier protein) was involved in the fatty acid biosynthesis pathway. Wu and Xue (2010) reported that *KAS* (β-Ketoacyl-acyl carrier protein synthase) catalyzes the elongation of *de novo* fatty acid synthesis and plays a role in chloroplast division and embryo development. Su et al. (2018) stated that *KASII* (Fatty acid biosynthesis I (FAB1)/3-oxoacyl-acyl-carrier-protein synthase II) catalyzes the fatty acid synthesis by conferring resistance to low temperatures by maintaining the integrity of chloroplast membranes. *KCS* is the key enzyme involved in VLCFA biosynthesis and cuticle wax biosynthesis pathways (Lee et al., 2009; Wang X. et al., 2017). Dobritsa et al. (2010) stated that LAP5/LAP6 (Less adhesive pollen) are multifunctional enzymes that might play role in pollen fatty acids and exine phenolic. Xuan et al. (2018) stated that TT4/TT5 (Transparent Testa) encodes chalcone synthase (CHS), a key enzyme involved in the biosynthesis of flavonoids and auxin transport. The proteins' secondary structures are the physical arrangement of amino acid sequences and are highly conserved between homologous proteins. The amino acid order directly affects the protein folding, 3D structure, and functions (Ridout et al., 2010).

Protein secondary structure analysis revealed that the alpha helix accounts for the largest percentage of secondary structures 49.6%, followed by random coils 41.96%, and extended strands 22.89% (**Supplementary Table 10**). Similar results have been reported by Lian et al. (2020) in the apple *KCS* gene family. In addition, 3D models of all the PeKCS proteins showed similar structures among them (**Figure 6B**), indicating that the identified PeKCS proteins were conserved and consistent with the domains, motif, and gene structure analysis (Lian et al., 2020). Recently, different miRNAs have been identified in numerous species including *Brassica napus* (Su et al., 2021b; Wen et al., 2021), maize (*Zea mays*) (Aravind et al., 2017), in cowpea (*Vigna unguiculata*) (Barrera-Figueroa et al., 2011), soybean (*Glycine max*) (Song et al., 2011), *Arachis hypogaea* (Zhao et al., 2015) and passion fruit (Paul et al., 2020), and involved in different metabolism, development, and environmental stresses. In this study, twenty putative ped-miRNAs belonging to nine different families were identified and targeted the 13 *PeKCS* genes (**Figure 7** and **Supplementary Table 11**). These miRNAs included ped-miR157, ped-miR162, ped-miR164, ped-miR166, ped-miR171, ped-miR319, ped-miR397, ped-miR398 and ped-miR399, respectively. Ped-miR166 family targeted up to four *PeKCS* genes and miR166 has been reported to be involved in drought stress in maize (Aravind et al., 2017), cowpea (Barrera-Figueroa et al., 2011); soybean (*Glycine max*) seed development (Song et al., 2011); peanut disease resistant (Zhao et al., 2015); plant growth, development and stress response in apple (Varkonyi-Gasic et al., 2010). miR171 has been reported to be involved in the development, metabolism, photosynthesis in grapevine (*Vitis vinifera*) (Han et al., 2014); coffee (*Coffea Arabica*) (Chaves et al., 2015); tea (*Camellia sinensis*) stress response (Zhang et al., 2014); passion fruit development and defense (Paul et al., 2020). miR399 involved in drought stress response in sugarcane (*Saccharum officinarum*) (Zanca et al., 2010); phosphate homeostasis, signaling, transport in apple (Pant et al., 2008) and sorghum (*Sorghum bicolor*) phosphate deficiency (Katiyar et al., 2012a). These findings suggest that these ped-miRNAs may play key roles in multiple developments and stress processes by altering the transcriptional level of *KCS* genes in passion fruit. The functions and expression levels of these predicted miRNAs and their target genes need to be further examined in the passion fruit.

Plant TFs have been reported to be involved in the regulation of fatty acids and wax biosynthesis under different conditions (Hao et al., 2017). The TFs in the promoter regions of 32 *PeKCS* genes were predicted and proposed a regulatory network interacting with *PeKCS* genes (**Figure 8** and **Supplementary Table 12**). The most abundant TF families were ERF, MYB, Dof, C2H2, TCP, LBD, NAC, and bHLH (**Supplementary Table 12**). Go et al. (2014) reported that wax biosynthesis in

Arabidopsis was negatively regulated under AP2/ERF-type TFs. Overexpression of AP2/ERF-type TFs increased the wax load and drought resistance in *Arabidopsis* and tobacco (*Nicotiana tabacum*) (Yang S. U. et al., 2020). MYB TFs regulate VLCFAs biosynthesis, plant development, metabolism, and response to stresses (Raffaele et al., 2008; Katiyar et al., 2012b; Ambawat et al., 2013). Zhang et al. (2019) stated that the MYB30 TF is involved in cuticular wax biosynthesis and resistance against pathogens. Wen et al. (2016) found that *CsDof* TF might play a role against biotic stresses in cucumber (*Cucumis sativus*). Rojas-Gracia et al. (2019) stated the SIDOF10 TF involved regulation of vascular tissue in tomatoes (*Solanum lycopersicum*). C2H2 TF regulates abiotic stress responses in plants (Han et al., 2020). TCP TFs regulate plant growth, development, and stress response (Li, 2015; Danisman, 2016). LBD TFs play role in anthocyanin and nitrogen metabolisms, pollen development, and pathogen response (Grimplet et al., 2017). NAC TF promoted cuticle wax biosynthesis in citrus (Yang H. et al., 2022). bHLH TF is involved in plant growth, metabolism, light signal transduction, cuticle development (Li et al., 2016; Sun et al., 2018). the qRT-PCR expression analysis was performed and found that the expression levels of *PeKCS* genes were positively or negatively regulated under stress conditions containing numerous TFs (**Figures 12**, **13**). Our results are consistent with previous reports suggesting a role for *PeKCS* TFs in regulating of VLCFAs, wax biosynthesis, and plant stress responses, while wax regulation analysis requires further investigation.

Gene ontology and KEGG annotation results of *PeKCS* genes revealed that highly enriched GO terms were associated with fatty acid synthase and elongase activity, acyltransferase activity, endoplasmic reticulum, and response to stresses, while KEGG pathways included fatty acid elongation, lipid metabolism, and plant-pathogen interaction (**Figure 9**). Our GO results were consistent with qRT-PCR expression analysis, for example, *PeKCS2*, *PeKCS9,* and *PeKCS13* (**Figure 12**) were highly upregulated under drought stress conditions compared to controls, and these genes contained stress-responsive GO-BP terms (**Supplementary Tables 13a,b**). It has been reported that *KCS* genes take part in different processes including fatty acid elongase Todd et al. (1999), pathogen interaction (Xue et al., 2020), and lipid metabolism in the endoplasmic reticulum (De Bigault Du Granrut and Cacas, 2016). *KCS* genes have been reported to play important roles in VLCFA and wax biosynthesis as well as biotic and abiotic stresses (Kim et al., 2013; Lee and Suh, 2013; Lokesh et al., 2019; Yang Z. et al., 2020; Lian et al., 2021). The expression profiles of *KCS* genes in different tissues have been described earlier in numerous plant species and exhibited a diverse expression pattern among them. For example, in *C. sinensis,* Cs8g17800 and Cs4g04880 exhibited higher expression levels in flowers. Cs7g13310 and Cs7g28170 showed higher expression levels in the leaf. Cs7g04850 was expressed in flower and embryo. Cs4g17260 and Cs6g02360 were mainly expressed in flavedo. Cs2g16470 was universally expressed in the fruit. The expression levels of Cs2g16470, Cs8g17800, Cs4g17260, Cs6g02360, and orange1.1t00556 genes steadily increased along with fruit ripening (Yang H. et al., 2021).

In apple, *MdKCS*6 showed higher expression in leaves whereas, *MdKCS*1 was highly expressed in the peel. Overall, the highest expression levels were found in most of the *MdKCS* genes in apple peels (Lian et al., 2020). In *Arabidopsis KCS*6 and *KSC10* were highly expressed compared in roots, stems, flowers, and siliques. *KCS19* was not expressed in leaves and stems (Joubès et al., 2008). In the current study, the following genes exhibited higher expression patterns throughout the fruit developmental stages including *PeKCS*1 (FPKM = 17–55.62), *PeKCS*10 (FPKM = 13.73–324.52), and *PeKCS*30 (FPKM = 96.12–356.7) (**Figure 11A**). *PeKCS*20 showed the highest expression (FPKM = 213.63) in L conditioned root. *PeKCS* 29, showed the highest expression (FPKM = 1692.94) in the peel. *PeKCS*5 showed the highest expression (FPKM = 359.34) under NT and CS leaves (FPKM = 306.76, *PeKCS5*) (**Figure 11B**). *PeKCS*31 and *PeKCS*32 were not expressed in all pulp tissues, whereas four genes (*PeKCS*16, *PeKCS*17, *PeKCS*18, and *PeKCS*19) were not expressed in leaves, peel, and root tissues, indicating that they might not involve in passion fruit growth and development. These diverse expression results indicate that *PeKCS* genes have specific expression patterns in all tested tissues and may play important roles in specific functions, but further research is required.

Consistent with the findings of other studies, *KCS* has been reported to be involved in regulating plant responses to drought and biotic stresses (Li et al., 2018; Lokesh et al., 2019; Guo et al., 2020; Wang Y. et al., 2020). The expression patterns of *PeKCS* genes under drought stress and *F. kyushuense* fungal biotic stress conditions (**Figures 12**, **13**) were analyzed. Most of the genes were positively or negatively regulated under stress conditions. Among them, *PeKCS*20 was up-regulated (29-fold) in yellow roots, *PeKCS*27 and *PeKCS*13 were up-regulated (8 to10-fold) in yellow and purple leaves under drought conditions. *PeKCS*1 was down-regulated in all tissues (root, stem, and leaves), indicating that its expression was inhibited by drought conditions. Relative expressions of *PeKCS*4 and *PeKCS*8 were up-regulated (4 and 3-folds) in yellow leaves but down-regulated in roots and stems (**Figure 12**). The expression profiles of *PeKCS* genes under biotic stress conditions (*F. kyushuense* fungal stress) showed that all *PeKCS* genes were expressed at different expression levels and most of the *PeKCS* genes were upregulated under biotic stress in purple 9th dpi except *PeKCS*1 compared to yellow 9th dpi (**Figure 13**). *PeKCS*20 was upregulated up to 9 folds, *PeKCS*2 > 6 folds, *PeKCS*9, *PeKCS*27, and *PeKCS*29 > 4 folds, *PeKCS*8 > 2.5-fold, *PeKCS*4 and *PeKCS*13 > 1-fold at 9th.dpi in purple cultivar. Whereas in yellow cultivar, *PeKCS*8, *PeKCS*2 and *PeKCS*20 were upregulated > 1- 3folds at 9th dpi. Only two gens *PeKCS*1 and *PeKCS*28 were upregulated > 1–2 folds at 12th dpi in the yellow cultivar.

Similar results were found by Lian et al. (2020) in apple *MdKCS* genes, eight *MdKCS* genes showed fluctuated (down-up-down-regulation) trend under drought conditions. *MdKCS*12 and *MdKCS*24 showed upregulated expressions (5 to 10-folds) under drought conditions. *MdKCS*6 expression was downregulated most of the time under drought conditions. The expressions of *KCS20* and *KCS2*/*DAISY* genes were upregulated in *Arabidopsis* stem under drought stress (Lee et al., 2009). *HvKCS*1 improved the barley leaf waxes and resistance to barley

powdery mildew fungus (Li et al., 2018). Previous reports indicate that the accumulation of cuticular wax and VLCFAs increases under stress conditions (Seo et al., 2011; Budke and Goffinet, 2016; Wang Y. et al., 2020). Our expression results suggest that positive or negative regulations of *PeKCS* genes may be due to the increase or decrease of cuticle wax and VLCFAs under drought and fungal stress conditions, but further studies are required.

CONCLUSION

In this study, comprehensive analyses were performed and identified 32 *PeKCS* genes in the passion fruit genome. All identified *PeKCS* genes were subjected to physio-chemical features, evolutionary relationships, motifs, gene structures, *cis*-regulatory elements, protein–protein interaction, syntenic analysis, TFs regulatory network analysis, GO, KEGG annotation, and putative micro-RNAs prediction analysis. The *KCS* gene family was expanded and subjected to purification screening. The hypothetically predicted subcellular localization of *PeKCS* genes was validated by a transient expression assay of *the PeKCS2* gene in the onion epidermis cell. Plant TFs families including ERF, MYB, and Dof were identified, and a regulatory network associated with the *PeKCS* genes was performed. FPKM-based gene expression profiles of *PeKCS* exhibited a diverse expression in the root, peel, leaves, and pulp tissues. The qRT-PCR based expressions suggested that most of the *PeKCS* genes were highly upregulated in leaves under drought and at 9th dpi under fungal (*F. kyushuense*) stresses conditions, specifically for genotype compared to controls. These findings provide a basis for future studies on the functions of *KCS* genes in passion fruit. Attempting to breed passion fruit cultivars susceptible to biotic or abiotic stress by overexpressing or inhibiting *KCS* gene expression in passion fruit tissues may provide new clues for the selection of passion fruit resistant cultivars. In future studies, we will further explore the role of *PeKCS* genes in VLCFA and cuticle wax biosynthesis on transcriptomics and metabolomic levels of passion fruit.

DATA AVAILABILITY STATEMENT

The original contributions presented in the study are included in the article/**Supplementary Material**, further inquiries can be directed to the corresponding author/s.

AUTHOR CONTRIBUTIONS

FC and HMR convinced the idea. HMR, FS, XL, AFY, MS, QY, YC, and KS performed the formal analysis and qRT-PCR. MB, HMR, and S-YH performed the bioinformatics analysis and wrote the manuscript. FC, RO, MYMJ, MA, MAAA, ZM, and LZ revised and edited the manuscript. All authors have read and agreed to the published version of the manuscript.

FUNDING

FC's research project was funded by the Department of Science and Technology, Fujian Province, China (2020N0004 and 2020S0056) and the Engineering Research Center of Fujian Province University (G2-KF2006).

SUPPLEMENTARY MATERIAL

The Supplementary Material for this article can be found online at: https://www.frontiersin.org/articles/10.3389/fpls.2022.872263/full#supplementary-material

REFERENCES

Abbadi, A., Brummel, M., Schütt, B. S., Slabaugh, M. B., Schuch, R., and Spener, F. (2000). Reaction mechanism of recombinant 3-oxoacyl-(acyl-carrier-protein) synthase III from *Cuphea wrightii* embryo, a fatty acid synthase type II condensing enzyme. *Biochem. J.* 345, 153–160. doi: 10.1042/bj3450153

Ambawat, S., Sharma, P., Yadav, N. R., and Yadav, R. C. (2013). MYB transcription factor genes as regulators for plant responses: an overview. *Physiol. Mol. Biol. Plants* 19, 307–321. doi: 10.1007/s12298-013-0179-1

Aravind, J., Rinku, S., Pooja, B., Shikha, M., Kaliyugam, S., Mallikarjuna, M. G., et al. (2017). Identification, characterization, and functional validation of drought-responsive microRNAs in subtropical maize inbreds. *Front. Plant Sci.* 8:941. doi: 10.3389/fpls.2017.00941

Arya, G. C., Sarkar, S., Manasherova, E., Aharoni, A., and Cohen, H. (2021). The plant cuticle: an ancient guardian barrier set against longstanding rivals. *Front. Plant Sci.* 12:1264. doi: 10.3389/fpls.2021.663165

Ashburner, M., Ball, C. A., Blake, J. A., Botstein, D., Butler, H., Cherry, J. M., et al. (2000). Gene ontology: tool for the unification of biology. *Nat. Genet.* 25, 25–29.

Bach, L., and Faure, J.-D. (2010). Role of very-long-chain fatty acids in plant development, when chain length does matter. *Comptes Rendus Biol.* 333, 361–370. doi: 10.1016/j.crvi.2010.01.014

Barrera-Figueroa, B. E., Gao, L., Diop, N. N., Wu, Z., Ehlers, J. D., Roberts, P. A., et al. (2011). Identification and comparative analysis of drought-associated microRNAs in two cowpea genotypes. *BMC Plant Biol.* 11:127. doi: 10.1186/1471-2229-11-127

Beaudoin, F., Wu, X., Li, F., Haslam, R. P., Markham, J. E., Zheng, H., et al. (2009). Functional characterization of the *Arabidopsis* β-ketoacyl-coenzyme A reductase candidates of the fatty acid elongase. *Plant Physiol.* 150, 1174–1191. doi: 10.1104/pp.109.137497

Budke, J. M., and Goffinet, B. (2016). Comparative cuticle development reveals taller sporophytes are covered by thicker calyptra cuticles in mosses. *Front. Plant Sci.* 7:832. doi: 10.3389/fpls.2016.00832

Campbell, A. A., Stenback, K. E., Flyckt, K., Hoang, T., Perera, M. A. D., and Nikolau, B. J. (2019). A single-cell platform for reconstituting and characterizing fatty acid elongase component enzymes. *PLoS One* 14:e0213620. doi: 10.1371/journal.pone.0213620

Chaves, S., Fernandes-Brum, C., Silva, G., Ferrara-Barbosa, B., Paiva, L., Nogueira, F., et al. (2015). New insights on Coffea miRNAs: features and evolutionary conservation. *Appl. Biochem. Biotechnol.* 177, 879–908. doi: 10.1007/s12010-015-1785-x

Chen, C., Chen, H., He, Y., and Xia, R. (2018). TBtools, a toolkit for biologists integrating various biological data handling tools with a user-friendly interface. *BioRxiv* [Preprint]. doi: 10.1101/289660v2

Chen, M., Mooney, B. P., Hajduch, M., Joshi, T., Zhou, M., Xu, D., et al. (2009). System analysis of an *Arabidopsis mutant* altered in de novo fatty acid synthesis

reveals diverse changes in seed composition and metabolism. *Plant Physiol.* 150, 27–41. doi: 10.1104/pp.108.134882

Chen, S., Zhou, Y., Chen, Y., and Gu, J. (2018). fastp: an ultra-fast all-in-one FASTQ preprocessor. *Bioinformatics* 34, i884–i890. doi: 10.1093/bioinformatics/bty560

Dai, H., Zhang, Y.-Y., Jin, P., Song, F.-P., Xu, W., Liu, A.-Z., et al. (2021). Identification of KCS gene family and functional analysis of FAE-like genes from *Malania oleifera*. *Oil Crop Sci.* 6, 35–40. doi: 10.1016/j.ocsci.2021.03.003

Danisman, S. (2016). TCP transcription factors at the interface between environmental challenges and the plant's growth responses. *Front. Plant Sci.* 7:1930. doi: 10.3389/fpls.2016.01930

De Bigault Du Granrut, A., and Cacas, J.-L. (2016). How very-long-chain fatty acids could signal stressful conditions in plants? *Front. Plant Sci.* 7:1490. doi: 10.3389/fpls.2016.01490

Dobritsa, A. A., Lei, Z., Nishikawa, S.-I., Urbanczyk-Wochniak, E., Huhman, D. V., Preuss, D., et al. (2010). LAP5 and LAP6 encode anther-specific proteins with similarity to chalcone synthase essential for pollen exine development in *Arabidopsis*. *Plant Physiol.* 153, 937–955. doi: 10.1104/pp.110.157446

Eghbalnia, H. R., Wilfinger, W. W., Mackey, K., and Chomczynski, P. (2020). Coordinated analysis of exon and intron data reveals novel differential gene expression changes. *Sci. Rep.* 10, 1–13. doi: 10.1038/s41598-020-72482-w

Fernández, V., Guzmán-Delgado, P., Graça, J., Santos, S., and Gil, L. (2016). Cuticle structure in relation to chemical composition: re-assessing the prevailing model. *Front. Plant Sci.* 7:427. doi: 10.3389/fpls.2016.00427

Flagel, L. E., and Wendel, J. F. (2009). Gene duplication and evolutionary novelty in plants. *New Phytol.* 183, 557–564. doi: 10.1111/j.1469-8137.2009.02923.x

Frugoli, J. A., Mcpeek, M. A., Thomas, T. L., and Mcclung, C. R. (1998). Intron loss and gain during evolution of the catalase gene family in angiosperms. *Genetics* 149, 355–365. doi: 10.1093/genetics/149.1.355

Go, Y. S., Kim, H., Kim, H. J., and Suh, M. C. (2014). *Arabidopsis* cuticular wax biosynthesis is negatively regulated by the DEWAX gene encoding an AP2/ERF-type transcription factor. *Plant Cell* 26, 1666–1680. doi: 10.1105/tpc.114.123307

González-Mellado, D., Salas, J. J., Venegas-Calerón, M., Moreno-Pérez, A. J., Garcés, R., and Martínez-Force, E. (2019). Functional characterization and structural modelling of *Helianthus annuus* (sunflower) ketoacyl-CoA synthases and their role in seed oil composition. *Planta* 249, 1823–1836. doi: 10.1007/s00425-019-03126-1

Grimplet, J., Pimentel, D., Agudelo-Romero, P., Martinez-Zapater, J. M., and Fortes, A. M. (2017). The LATERAL ORGAN BOUNDARIES Domain gene family in grapevine: genome-wide characterization and expression analyses during developmental processes and stress responses. *Sci. Rep.* 7, 1–18. doi: 10.1038/s41598-017-16240-5

Guo, H.-S., Zhang, Y.-M., Sun, X.-Q., Li, M.-M., Hang, Y.-Y., and Xue, J.-Y. (2016). Evolution of the KCS gene family in plants: the history of gene duplication, sub/neofunctionalization and redundancy. *Mol. Genet. Genom.* 291, 739–752. doi: 10.1007/s00438-015-1142-3

Guo, W., Wu, Q., Yang, L., Hu, W., Liu, D., and Liu, Y. (2020). Ectopic expression of CsKCS6 from navel orange promotes the production of very-long-chain fatty acids (VLCFAs) and increases the abiotic stress tolerance of *Arabidopsis thaliana*. *Front. Plant Sci.* 11:564656. doi: 10.3389/fpls.2020.564656

Guyomarc'h, S., Boutté, Y., and Laplaze, L. (2021). AP2/ERF transcription factors orchestrate very long chain fatty acid biosynthesis during *Arabidopsis* lateral root development. *Mol. Plant* 14, 205–207. doi: 10.1016/j.molp.2021.01.004

Han, G., Lu, C., Guo, J., Qiao, Z., Sui, N., Qiu, N., et al. (2020). C2H2 zinc finger proteins: master regulators of abiotic stress responses in plants. *Front. Plant Sci.* 11:115.

Han, J., Fang, J., Wang, C., Yin, Y., Sun, X., Leng, X., et al. (2014). Grapevine microRNAs responsive to exogenous gibberellin. *BMC Genomics* 15:111. doi: 10.1186/1471-2164-15-111

Han, X., Wei, X., Lu, W., Wu, Q., Mao, L., and Luo, Z. (2022). Transcriptional regulation of KCS gene by bZIP29 and MYB70 transcription factors during ABA-stimulated wound suberization of kiwifruit (*Actinidia deliciosa*). *BMC Plant Biol.* 22:23. doi: 10.1186/s12870-021-03407-6

Hao, S., Ma, Y., Zhao, S., Ji, Q., Zhang, K., Yang, M., et al. (2017). McWRI1, a transcription factor of the AP2/SHEN family, regulates the biosynthesis of the cuticular waxes on the apple fruit surface under low temperature. *PLoS One* 12:e0186996. doi: 10.1371/journal.pone.0186996

Hegebarth, D., Buschhaus, C., Joubès, J., Thoraval, D., Bird, D., and Jetter, R. (2017). *Arabidopsis* ketoacyl-CoA synthase 16 (KCS16) forms C36/C38 acyl precursors for leaf trichome and pavement surface wax. *Plant Cell Environ.* 40, 1761–1776. doi: 10.1111/pce.12981

Huai, D., Xue, X., Li, Y., Wang, P., Li, J., Yan, L., et al. (2020). Genome-wide identification of peanut KCS genes reveals that AhKCS1 and AhKCS28 are involved in regulating VLCFA contents in seeds. *Front. Plant Sci.* 11:406. doi: 10.3389/fpls.2020.00406

James, D. W. Jr., Lim, E., Keller, J., Plooy, I., Ralston, E., and Dooner, H. K. (1995). Directed tagging of the *Arabidopsis* FATTY ACID ELONGATION1 (FAE1) gene with the maize transposon activator. *Plant Cell* 7, 309–319. doi: 10.1105/tpc.7.3.309

Joubès, J., Raffaele, S., Bourdenx, B., Garcia, C., Laroche-Traineau, J., Moreau, P., et al. (2008). The VLCFA elongase gene family in *Arabidopsis thaliana*: phylogenetic analysis, 3D modelling and expression profiling. *Plant Mol. Biol.* 67, 547–566. doi: 10.1007/s11103-008-9339-z

Kanehisa, M., and Goto, S. (2000). KEGG: kyoto encyclopedia of genes and genomes. *Nucleic Acids Res.* 28, 27–30.

Katiyar, A., Smita, S., Chinnusamy, V., Pandey, D. M., and Bansal, K. (2012a). Identification of miRNAs in sorghum by using bioinformatics approach. *Plant Signal. Behav.* 7, 246–259. doi: 10.4161/psb.18914

Katiyar, A., Smita, S., Lenka, S. K., Rajwanshi, R., Chinnusamy, V., and Bansal, K. C. (2012b). Genome-wide classification and expression analysis of MYB transcription factor families in rice and *Arabidopsis*. *BMC Genom.* 13:544. doi: 10.1186/1471-2164-13-544

Kim, D., and Langmead, B. (2015). Salzberg SLHISAT. A fast spliced aligner with low memory requirements. *Nat. Methods* 12, 357–360. doi: 10.1038/nmeth.3317

Kim, J., Jung, J. H., Lee, S. B., Go, Y. S., Kim, H. J., Cahoon, R., et al. (2013). *Arabidopsis* 3-ketoacyl-coenzyme a synthase9 is involved in the synthesis of tetracosanoic acids as precursors of cuticular waxes, suberins, sphingolipids, and phospholipids. *Plant Physiol.* 162, 567–580. doi: 10.1104/pp.112.210450

Kim, J., Lee, S. B., and Suh, M. C. (2021). *Arabidopsis* 3-ketoacyl-CoA synthase 4 is essential for root and pollen tube growth. *J. Plant Biol.* 64, 155–165. doi: 10.1007/s12374-020-09288-w

Kim, J.-S., Mizoi, J., Yoshida, T., Fujita, Y., Nakajima, J., Ohori, T., et al. (2011). An ABRE promoter sequence is involved in osmotic stress-responsive expression of the DREB2A gene, which encodes a transcription factor regulating drought-inducible genes in *Arabidopsis*. *Plant Cell Physiol.* 52, 2136–2146. doi: 10.1093/pcp/pcr143

Kogure, K., Watanabe, A., and Ito, Y. (2022). Interaction of ONION2 ketoacyl CoA synthase with ketoacyl CoA reductase of rice. *Mol. Biol. Rep.* 49, 1643–1647. doi: 10.1007/s11033-021-07060-y

Kohl, M., Wiese, S., and Warscheid, B. (2011). "Cytoscape: software for visualization and analysis of biological networks," in *Data Mining in Proteomics*, eds M. Hamacher, M. Eisenacher, and C. Stephan (Cham: Springer), 291–303. doi: 10.1007/978-1-60761-987-1_18

Lam, P., Zhao, L., Eveleigh, N., Yu, Y., Chen, X., and Kunst, L. (2015). The exosome and trans-acting small interfering RNAs regulate cuticular wax biosynthesis during *Arabidopsis* inflorescence stem development. *Plant Physiol.* 167, 323–336. doi: 10.1104/pp.114.252825

Law, C. W., Alhamdoosh, M., Su, S., Dong, X., Tian, L., Smyth, G. K., et al. (2016). RNA-seq analysis is easy as 1-2-3 with limma, Glimma and edgeR. *F1000Research* 5:ISCBCommJ-1408. doi: 10.12688/f1000research.9005.3

Lee, S. B., Jung, S. J., Go, Y. S., Kim, H. U., Kim, J. K., Cho, H. J., et al. (2009). Two *Arabidopsis* 3-ketoacyl CoA synthase genes, KCS20 and KCS2/DAISY, are functionally redundant in cuticular wax and root suberin biosynthesis, but differentially controlled by osmotic stress. *Plant J.* 60, 462–475. doi: 10.1111/j.1365-313X.2009.03973.x

Lee, S. B., and Suh, M. C. (2013). Recent advances in cuticular wax biosynthesis and its regulation in *Arabidopsis*. *Mol. Plant* 6, 246–249. doi: 10.1093/mp/sss159

Lewandowska, M., Keyl, A., and Feussner, I. (2020). Wax biosynthesis in response to danger: its regulation upon abiotic and biotic stress. *New Phytol.* 227, 698–713. doi: 10.1111/nph.16571

Li, C., Haslam, T. M., Krüger, A., Schneider, L. M., Mishina, K., Samuels, L., et al. (2018). The β-ketoacyl-CoA synthase Hv KCS1, encoded by Cer-zh, plays a key

role in synthesis of barley leaf wax and germination of barley powdery mildew. *Plant Cell Physiol.* 59, 811–827. doi: 10.1093/pcp/pcy020

Li, H., Handsaker, B., Wysoker, A., Fennell, T., Ruan, J., Homer, N., et al. (2009). The sequence alignment/map format and SAMtools. *Bioinformatics* 25, 2078–2079. doi: 10.1093/bioinformatics/btp352

Li, S. (2015). The *Arabidopsis thaliana* TCP transcription factors: a broadening horizon beyond development. *Plant Signal Behav.* 10:e1044192. doi: 10.1080/15592324.2015.1044192

Li, S., Wang, X., He, S., Li, J., Huang, Q., Imaizumi, T., et al. (2016). CFLAP1 and CFLAP2 are two bHLH transcription factors participating in synergistic regulation of AtCFL1-mediated cuticle development in *Arabidopsis*. *PLoS Genet.* 12:e1005744. doi: 10.1371/journal.pgen.1005744

Lian, X.-Y., Gao, H.-N., Jiang, H., Liu, C., and Li, Y.-Y. (2021). MdKCS2 increased plant drought resistance by regulating wax biosynthesis. *Plant Cell Rep.* 40, 2357–2368. doi: 10.1007/s00299-021-02776-4

Lian, X.-Y., Wang, X., Gao, H.-N., Jiang, H., Mao, K., You, C.-X., et al. (2020). Genome wide analysis and functional identification of MdKCS genes in apple. *Plant Physiol. Biochem.* 151, 299–312. doi: 10.1016/j.plaphy.2020.03.034

Liu, C., Wright, B., Allen-Vercoe, E., Gu, H., and Beiko, R. (2018). Phylogenetic clustering of genes reveals shared evolutionary trajectories and putative gene functions. *Genome Biol. Evol.* 10, 2255–2265. doi: 10.1093/gbe/evy178

Liu, L., Xu, W., Hu, X., Liu, H., and Lin, Y. (2016). W-box and G-box elements play important roles in early senescence of rice flag leaf. *Sci. Rep.* 6, 1–9. doi: 10.1038/srep20881

Liu, T., Tang, J., Chen, L., Zeng, J., Wen, J., Yi, B., et al. (2019). Differential expression of miRNAs and their targets in wax-deficient rapeseed. *Sci. Rep.* 9, 1–12. doi: 10.1038/s41598-019-48439-z

Lokesh, U., Venkatesh, B., Kiranmai, K., Nareshkumar, A., Amarnathareddy, V., Rao, G. L., et al. (2019). Overexpression of ß-Ketoacyl Co-A Synthase1 gene improves tolerance of drought susceptible groundnut (*Arachis hypogaea* L.) cultivar K-6 by increased leaf epicuticular wax accumulation. *Front. Plant Sci.* 9:1869. doi: 10.3389/fpls.2018.01869

Ma, D., Dong, S., Zhang, S., Wei, X., Xie, Q., Ding, Q., et al. (2021). Chromosome-level reference genome assembly provides insights into aroma biosynthesis in passion fruit (*Passiflora edulis*). *Mol. Ecol. Resour.* 21, 955–968. doi: 10.1111/1755-0998.13310

Markham, J. E., Molino, D., Gissot, L., Bellec, Y., Hématy, K., Marion, J., et al. (2011). Sphingolipids containing very-long-chain fatty acids define a secretory pathway for specific polar plasma membrane protein targeting in *Arabidopsis*. *Plant Cell* 23, 2362–2378. doi: 10.1105/tpc.110.080473

Masoudi-Nejad, A., Goto, S., Endo, T. R., and Kanehisa, M. (2007). "KEGG bioinformatics resource for plant genomics research," in *Plant Bioinformatics*, ed. D. Edwards (Cham: Springer), 437–458. doi: 10.1007/978-1-59745-535-0_21

Munhoz, C., Santos, A., Arenhart, R., Santini, L., Monteiro-Vitorello, C., and Vieira, M. (2015). Analysis of plant gene expression during passion fruit–Xanthomonas axonopodis interaction implicates lipoxygenase 2 in host defence. *Ann. Appl. Biol.* 167, 135–155. doi: 10.1111/aab.12215

Ohtani, M. (2017). Transcriptional regulation of snRNAs and its significance for plant development. *J. Plant Res.* 130, 57–66. doi: 10.1007/s10265-016-0883-3

Ois Roudier, F., Gissot, L., De Ric Beaudoin, F., Haslam, R., Michaelson, L., Marion, J., et al. (2010). Very-long-chain fatty acids are involved in polar auxin transport and developmental patterning in *Arabidopsis*. *Plant Cell* 22, 364–375.

Oshima, Y., Shikata, M., Koyama, T., Ohtsubo, N., Mitsuda, N., and Ohme-Takagi, M. (2013). MIXTA-like transcription factors and WAX INDUCER1/SHINE1 coordinately regulate cuticle development in *Arabidopsis* and *Torenia fournieri*. *Plant Cell* 25, 1609–1624. doi: 10.1105/tpc.113.110783

Pant, B. D., Buhtz, A., Kehr, J., and Scheible, W. R. (2008). MicroRNA399 is a long-distance signal for the regulation of plant phosphate homeostasis. *Plant J.* 53, 731–738. doi: 10.1111/j.1365-313X.2007.03363.x

Paul, S., De La Fuente-Jiménez, J. L., Manriquez, C. G., and Sharma, A. (2020). Identification, characterization and expression analysis of passion fruit (*Passiflora edulis*) microRNAs. *3 Biotech* 10, 1–9. doi: 10.1007/s13205-019-2000-5

Piya, S., Shrestha, S. K., Binder, B., Stewart, C. N. Jr., and Hewezi, T. (2014). Protein-protein interaction and gene co-expression maps of ARFs and Aux/IAAs in *Arabidopsis*. *Front. Plant Sci.* 5:744. doi: 10.3389/fpls.2014.00744

Porto, M., Pinheiro, M., Batista, V., Dos Santos Filho, R., Filho Pde, A., and de Lima, L. M. (2014). Plant promoters: an approach of structure and function. *Mol. Biotechnol.* 56, 38–49. doi: 10.1007/s12033-013-9713-1

Raffaele, S., Leger, A., and Roby, D. (2009). Very long chain fatty acid and lipid signaling in the response of plants to pathogens. *Plant Signal. Behav.* 4, 94–99. doi: 10.4161/psb.4.2.7580

Raffaele, S., Vailleau, F., Léger, A., Joubès, J., Miersch, O., Huard, C., et al. (2008). A MYB transcription factor regulates very-long-chain fatty acid biosynthesis for activation of the hypersensitive cell death response in *Arabidopsis*. *Plant Cell* 20, 752–767. doi: 10.1105/tpc.107.054858

Raza, A., Tabassum, J., Mubarik, M., Anwar, S., Zahra, N., Sharif, Y., et al. (2021). Hydrogen sulfide: an emerging component against abiotic stress in plants. *Plant Biol.* [Epub ahead of print]. doi: 10.1111/plb.13368

Raza, A., Tabassum, J., Zahid, Z., Charagh, S., Bashir, S., Barmukh, R., et al. (2022). Advances in "omics" approaches for improving toxic metals/metalloids tolerance in plants. *Front. Plant Sci.* 12:794373. doi: 10.3389/fpls.2021.794373

Ridout, K. E., Dixon, C. J., and Filatov, D. A. (2010). Positive selection differs between protein secondary structure elements in *Drosophila*. *Genome Biol. Evol.* 2, 166–179. doi: 10.1093/gbe/evq008

Rizwan, H. M., Zhimin, L., Harsonowati, W., Waheed, A., Qiang, Y., Yousef, A. F., et al. (2021). Identification of fungal pathogens to control postharvest passion fruit (*Passiflora edulis*) decays and multi-omics comparative pathway analysis reveals purple is more resistant to pathogens than a yellow cultivar. *J. Fungi* 7:879. doi: 10.3390/jof7100879

Rojas-Gracia, P., Roque, E., Medina, M., López-Martín, M. J., Cañas, L. A., Beltrán, J. P., et al. (2019). The DOF transcription factor SlDOF10 regulates vascular tissue formation during ovary development in tomato. *Front. Plant Sci.* 10:216. doi: 10.3389/fpls.2019.00216

Roncaglia, P., Martone, M. E., Hill, D. P., Berardini, T. Z., Foulger, R. E., Imam, F. T., et al. (2013). The Gene Ontology (GO) cellular component ontology: integration with SAO (Subcellular Anatomy Ontology) and other recent developments. *J. Biomed. Semant.* 4, 1–11. doi: 10.1186/2041-1480-4-20

Roudier, F., Gissot, L., Beaudoin, F., Haslam, R., Michaelson, L., Marion, J., et al. (2010). Very-long-chain fatty acids are involved in polar auxin transport and developmental patterning in *Arabidopsis*. *Plant Cell* 22, 364–375. doi: 10.1105/tpc.109.071209

Sagar, M., Pandey, N., Qamar, N., Singh, B., and Shukla, A. (2015). Domain analysis of 3 Keto Acyl-CoA synthase for structural variations in *Vitis vinifera* and *Oryza brachyantha* using comparative modelling. *Interdiscip. Sci. Comput. Life Sci.* 7, 7–20. doi: 10.1007/s12539-013-0017-8

Samad, A. F., Sajad, M., Nazaruddin, N., Fauzi, I. A., Murad, A., Zainal, Z., et al. (2017). MicroRNA and transcription factor: key players in plant regulatory network. *Front. Plant Sci.* 8:565. doi: 10.3389/fpls.2017.00565

Santos, A. A., Penha, H. A., Bellec, A., De Freitas Munhoz, C., Pedrosa-Harand, A., Bergès, H., et al. (2014). Begin at the beginning: a BAC-end view of the passion fruit (*Passiflora*) genome. *BMC Genomics* 15:816. doi: 10.1186/1471-2164-15-816

Schmittgen, T. D., and Livak, K. J. (2008). Analyzing real-time PCR data by the comparative CT method. *Nat. Protoc.* 3, 1101–1108. doi: 10.1038/nprot.2008.73

Seo, P. J., Lee, S. B., Suh, M. C., Park, M.-J., Go, Y. S., and Park, C.-M. (2011). The MYB96 transcription factor regulates cuticular wax biosynthesis under drought conditions in *Arabidopsis*. *Plant Cell* 23, 1138–1152. doi: 10.1105/tpc.111.083485

Serra, O., Soler, M., Hohn, C., Franke, R., Schreiber, L., Prat, S., et al. (2009). Silencing of StKCS6 in potato periderm leads to reduced chain lengths of suberin and wax compounds and increased peridermal transpiration. *J. Exp. Bot.* 60, 697–707. doi: 10.1093/jxb/ern314

Sharif, R., Raza, A., Chen, P., Li, Y., El-Ballat, E. M., Rauf, A., et al. (2021). HD-ZIP gene family: potential roles in improving plant growth and regulating stress-responsive mechanisms in plants. *Genes* 12:1256. doi: 10.3390/genes12081256

Sibéril, Y., Doireau, P., and Gantet, P. (2001). Plant bZIP G-box binding factors. Modular structure and activation mechanisms. *Eur. J. Biochem.* 268, 5655–5666. doi: 10.1046/j.0014-2956.2001.02552.x

Skalicky, M., Karademir, E., Rahim, J., Islam, M. S., Sytar, O., Ahmed, S., et al. (2021). Potential role of plant growth regulators in administering crucial

processes against abiotic stresses. *Front. Agron.* 3:648694. doi: 10.3389/fagro.2021.648694

Song, Q.-X., Liu, Y.-F., Hu, X.-Y., Zhang, W.-K., Ma, B., Chen, S.-Y., et al. (2011). Identification of miRNAs and their target genes in developing soybean seeds by deep sequencing. *BMC Plant Biol.* 11:5. doi: 10.1186/1471-2229-11-5

Su, C., Chen, K., Ding, Q., Mou, Y., Yang, R., Zhao, M., et al. (2018). Proteomic analysis of the function of a novel cold-regulated multispanning transmembrane protein COR413-PM1 in *Arabidopsis*. *Int. J. Mol. Sci.* 19:2572. doi: 10.3390/ijms19092572

Su, W., Raza, A., Gao, A., Jia, Z., Zhang, Y., Hussain, M. A., et al. (2021a). Genome-wide analysis and expression profile of superoxide dismutase (SOD) gene family in rapeseed (*Brassica napus* L.) under different hormones and abiotic stress conditions. *Antioxidants* 10:1182. doi: 10.3390/antiox10081182

Su, W., Raza, A., Zeng, L., Gao, A., Lv, Y., Ding, X., et al. (2021b). Genome-wide analysis and expression patterns of lipid phospholipid phospholipase gene family in *Brassica napus* L. *BMC Genomics* 22:548. doi: 10.1186/s12864-021-07862-1

Sun, X., Wang, Y., and Sui, N. (2018). Transcriptional regulation of bHLH during plant response to stress. *Biochem. Biophys. Res. Commun.* 503, 397–401. doi: 10.1016/j.bbrc.2018.07.123

Sunkar, R., and Zhu, J.-K. (2004). Novel and stress-regulated microRNAs and other small RNAs from *Arabidopsis*. *Plant Cell* 16, 2001–2019. doi: 10.1105/tpc.104.022830

Tian, F., Yang, D.-C., Meng, Y.-Q., Jin, J., and Gao, G. (2020). PlantRegMap: charting functional regulatory maps in plants. *Nucleic Acids Res.* 48, D1104–D1113. doi: 10.1093/nar/gkz1020

Todd, J., Post-Beittenmiller, D., and Jaworski, J. G. (1999). KCS1 encodes a fatty acid elongase 3-ketoacyl-CoA synthase affecting wax biosynthesis in *Arabidopsis thaliana*. *Plant J.* 17, 119–130. doi: 10.1046/j.1365-313x.1999.00352.x

Tong, T., Fang, Y.-X., Zhang, Z., Zheng, J., Zhang, X., Li, J., et al. (2021). Genome-wide identification and expression pattern analysis of the KCS gene family in barley. *Plant Growth Regul.* 93, 89–103. doi: 10.1007/s10725-020-00668-3

Trinh, D.-C., Lavenus, J., Goh, T., Boutté, Y., Drogue, Q., Vaissayre, V., et al. (2019). PUCHI regulates very long chain fatty acid biosynthesis during lateral root and callus formation. *Proc. Natl. Acad. Sci. U.S.A.* 116, 14325–14330. doi: 10.1073/pnas.1906300116

Trivedi, P., Nguyen, N., Hykkerud, A. L., Häggman, H., Martinussen, I., Jaakola, L., et al. (2019). Developmental and environmental regulation of cuticular wax biosynthesis in fleshy fruits. *Front. Plant Sci.* 10:431. doi: 10.3389/fpls.2019.00431

Van de Peer, Y., Maere, S., and Meyer, A. (2009). The evolutionary significance of ancient genome duplications. *Nat. Rev. Genet.* 10, 725–732. doi: 10.1038/nrg2600

Varkonyi-Gasic, E., Gould, N., Sandanayaka, M., Sutherland, P., and Macdiarmid, R. M. (2010). Characterisation of microRNAs from apple (*Malus domestica* 'Royal Gala') vascular tissue and phloem sap. *BMC Plant Biol.* 10:159. doi: 10.1186/1471-2229-10-159

Wang, Q., Du, X., Zhou, Y., Xie, L., Bie, S., Tu, L., et al. (2020). The β-ketoacyl-CoA synthase KCS13 regulates the cold response in cotton by modulating lipid and oxylipin biosynthesis. *J. Exp. Bot.* 71, 5615–5630. doi: 10.1093/jxb/eraa254

Wang, Y., Jin, S., Xu, Y., Li, S., Zhang, S., Yuan, Z., et al. (2020). Overexpression of BnKCS1-1, BnKCS1-2, and BnCER1-2 promotes cuticular wax production and increases drought tolerance in *Brassica napus*. *Crop J.* 8, 26–37. doi: 10.1016/j.cj.2019.04.006

Wang, X., Guan, Y., Zhang, D., Dong, X., Tian, L., and Qu, L. Q. (2017). A β-ketoacyl-CoA synthase is involved in rice leaf cuticular wax synthesis and requires a CER2-LIKE protein as a cofactor. *Plant Physiol.* 173, 944–955. doi: 10.1104/pp.16.01527

Wang, Z., Qiao, Y., Zhang, J., Shi, W., and Zhang, J. (2017). Genome wide identification of microRNAs involved in fatty acid and lipid metabolism of *Brassica napus* by small RNA and degradome sequencing. *Gene* 619, 61–70. doi: 10.1016/j.gene.2017.03.040

Wang, Y., Liu, G.-J., Yan, X.-F., Wei, Z.-G., and Xu, Z.-R. (2011). MeJA-inducible expression of the heterologous JAZ2 promoter from *Arabidopsis* in *Populus trichocarpa* protoplasts. *J. Plant Dis. Protect.* 118, 69–74. doi: 10.1007/bf03356384

Wang, Y., Yang, X., Chen, Z., Zhang, J., Si, K., Xu, R., et al. (2022). Function and transcriptional regulation of CsKCS20 in the elongation of very-long-chain fatty acids and wax biosynthesis in *Citrus sinensis* flavedo. *Hortic. Res.* 9:uhab027. doi: 10.1093/hr/uhab027

Weidenbach, D., Jansen, M., Bodewein, T., Nagel, K. A., and Schaffrath, U. (2015). Shoot and root phenotyping of the barley mutant kcs6 (3-ketoacyl-CoA synthase6) depleted in epicuticular waxes under water limitation. *Plant Signal. Behav.* 10:e1003752. doi: 10.1080/15592324.2014.1003752

Wen, C.-L., Cheng, Q., Zhao, L., Mao, A., Yang, J., Yu, S., et al. (2016). Identification and characterisation of Dof transcription factors in the cucumber genome. *Sci. Rep.* 6, 1–11. doi: 10.1038/srep23072

Wen, Y., Raza, A., Chu, W., Zou, X., Cheng, H., Hu, Q., et al. (2021). Comprehensive in silico characterization and expression profiling of TCP gene family in rapeseed. *Front. Genet.* 12:794297. doi: 10.3389/fgene.2021.794297

Wingender, R., Röhrig, H., Höricke, C., and Schell, J. (1990). cis-regulatory elements involved in ultraviolet light regulation and plant defense. *Plant Cell* 2, 1019–1026. doi: 10.1105/tpc.2.10.1019

Witkos, M. T., Koscianska, E., and Krzyzosiak, W. J. (2011). Practical aspects of microRNA target prediction. *Curr. Mol. Med.* 11, 93–109. doi: 10.2174/156652411794859250

Wong, A., Gehring, C., and Irving, H. R. (2015). Conserved functional motifs and homology modeling to predict hidden moonlighting functional sites. *Front. Bioeng. Biotechnol.* 3:82. doi: 10.3389/fbioe.2015.00082

Wu, G.-Z., and Xue, H.-W. (2010). *Arabidopsis* β-ketoacyl-[acyl carrier protein] synthase I is crucial for fatty acid synthesis and plays a role in chloroplast division and embryo development. *Plant Cell* 22, 3726–3744. doi: 10.1105/tpc.110.075564

Xia, Z., Huang, D., Zhang, S., Wang, W., Ma, F., Wu, B., et al. (2021). Chromosome-scale genome assembly provides insights into the evolution and flavor synthesis of passion fruit (*Passiflora edulis* Sims). *Hortic. Res.* 8, 1–14. doi: 10.1038/s41438-020-00455-1

Xiao, G. H., Wang, K., Huang, G., and Zhu, Y. X. (2016). Genome-scale analysis of the cotton KCS gene family revealed a binary mode of action for gibberellin A regulated fiber growth. *J. Integr. Plant Biol.* 58, 577–589. doi: 10.1111/jipb.12429

Xiong, J., Liu, L., Ma, X., Li, F., Tang, C., Li, Z., et al. (2020). Characterization of PtAOS1 promoter and three novel interacting proteins responding to drought in *Poncirus trifoliata*. *Int. J. Mol. Sci.* 21:4705. doi: 10.3390/ijms21134705

Xu, G., Guo, C., Shan, H., and Kong, H. (2012). Divergence of duplicate genes in exon–intron structure. *Proc. Natl. Acad. Sci. U.S.A.* 109, 1187–1192. doi: 10.1073/pnas.1109047109

Xu, K., Huang, X., Wu, M., Wang, Y., Chang, Y., Liu, K., et al. (2014). A rapid, highly efficient and economical method of Agrobacterium-mediated in planta transient transformation in living onion epidermis. *PLoS One* 9:e83556. doi: 10.1371/journal.pone.0083556

Xuan, L., Zhang, C., Yan, T., Wu, D., Hussain, N., Li, Z., et al. (2018). TRANSPARENT TESTA 4-mediated flavonoids negatively affect embryonic fatty acid biosynthesis in *Arabidopsis*. *Plant Cell Environ.* 41, 2773–2790. doi: 10.1111/pce.13402

Xue, D., Zhang, X., Lu, X., Chen, G., and Chen, Z.-H. (2017). Molecular and evolutionary mechanisms of cuticular wax for plant drought tolerance. *Front. Plant Sci.* 8:621. doi: 10.3389/fpls.2017.00621

Xue, Y., Jiang, J., Yang, X., Jiang, H., Du, Y., Liu, X., et al. (2020). Genome-wide mining and comparative analysis of fatty acid elongase gene family in *Brassica napus* and its progenitors. *Gene* 747:144674. doi: 10.1016/j.gene.2020.144674

Yang, H., Mei, W., Wan, H., Xu, R., and Cheng, Y. (2021). Comprehensive analysis of KCS gene family in Citrinae reveals the involvement of CsKCS2 and CsKCS11 in fruit cuticular wax synthesis at ripening. *Plant Sci.* 310:110972. doi: 10.1016/j.plantsci.2021.110972

Yang, T., Li, Y., Liu, Y., He, L., Liu, A., Wen, J., et al. (2021). The 3-ketoacyl-CoA synthase WFL is involved in lateral organ development and cuticular wax synthesis in *Medicago truncatula*. *Plant Mol. Biol.* 105, 193–204. doi: 10.1007/s11103-020-01080-1

Yang, H., Zhu, Z., Zhang, M., Li, X., Xu, R., Zhu, F., et al. (2022). CitWRKY28 and CitNAC029 promote the synthesis of cuticular wax by activating CitKCS gene expression in citrus fruit. *Plant Cell Rep.* [Epub ahead of print]. doi: 10.1007/s00299-021-02826-x

Yang, S. U., Kim, H., Kim, R. J., Kim, J., and Suh, M. C. (2020). AP2/DREB transcription factor RAP2. 4 activates cuticular wax biosynthesis in *Arabidopsis* leaves under drought. *Front. Plant Sci.* 11:895. doi: 10.3389/fpls.2020.00895

Yang, Z., Yang, X., Dong, S., Ge, Y., Zhang, X., Zhao, X., et al. (2020). Overexpression of β-ketoacyl-CoA synthase from Vitis vinifera L. Improves salt tolerance in *Arabidopsis thaliana*. *Front. Plant Sci.* 11:1687. doi: 10.3389/fpls.2020.564385

Yeats, T. H., and Rose, J. K. (2013). The formation and function of plant cuticles. *Plant Physiol.* 163, 5–20. doi: 10.1104/pp.113.222737

Zanca, A. S., Vicentini, R., Ortiz-Morea, F. A., Del Bem, L. E., Da Silva, M. J., Vincentz, M., et al. (2010). Identification and expression analysis of microRNAs and targets in the biofuel crop sugarcane. *BMC Plant Biol.* 10:260. doi: 10.1186/1471-2229-10-260

Zhang, B., Pan, X., Cobb, G. P., and Anderson, T. A. (2006). Plant microRNA: a small regulatory molecule with big impact. *Dev. Biol.* 289, 3–16. doi: 10.1016/j.ydbio.2005.10.036

Zhang, Y., Zhu, X., Chen, X., Song, C., Zou, Z., Wang, Y., et al. (2014). Identification and characterization of cold-responsive microRNAs in tea plant (*Camellia sinensis*) and their targets using high-throughput sequencing and degradome analysis. *BMC Plant Biol.* 14:271. doi: 10.1186/s12870-014-0271-x

Zhang, Y.-L., You, C.-X., Li, Y.-Y., and Hao, Y.-J. (2020). Advances in biosynthesis, regulation, and function of apple cuticular wax. *Front. Plant Sci.* 11:1165. doi: 10.3389/fpls.2020.01165

Zhang, Y.-L., Zhang, C.-L., Wang, G.-L., Wang, Y.-X., Qi, C.-H., Zhao, Q., et al. (2019). The R2R3 MYB transcription factor MdMYB30 modulates plant resistance against pathogens by regulating cuticular wax biosynthesis. *BMC Plant Biol.* 19:362. doi: 10.1186/s12870-019-1918-4

Zhao, C., Xia, H., Cao, T., Yang, Y., Zhao, S., Hou, L., et al. (2015). Small RNA and degradome deep sequencing reveals peanut microRNA roles in response to pathogen infection. *Plant Mol. Biol. Rep.* 33, 1013–1029. doi: 10.1007/s11105-014-0806-1

Zheng, Y., Chen, X., Wang, P., Sun, Y., Yue, C., and Ye, N. (2020). Genome-wide and expression pattern analysis of JAZ family involved in stress responses and postharvest processing treatments in *Camellia sinensis*. *Sci. Rep.* 10, 1–13. doi: 10.1038/s41598-020-59675-z

Conflict of Interest: The authors declare that the research was conducted in the absence of any commercial or financial relationships that could be construed as a potential conflict of interest.

Publisher's Note: All claims expressed in this article are solely those of the authors and do not necessarily represent those of their affiliated organizations, or those of the publisher, the editors and the reviewers. Any product that may be evaluated in this article, or claim that may be made by its manufacturer, is not guaranteed or endorsed by the publisher.

Copyright © 2022 Rizwan, Shaozhong, Li, Bilal Arshad, Yousef, Chenglong, Shi, Jaber, Anwar, Hu, Yang, Sun, Ahmed, Min, Oelmüller, Zhimin and Chen. This is an open-access article distributed under the terms of the Creative Commons Attribution License (CC BY). The use, distribution or reproduction in other forums is permitted, provided the original author(s) and the copyright owner(s) are credited and that the original publication in this journal is cited, in accordance with accepted academic practice. No use, distribution or reproduction is permitted which does not comply with these terms.

frontiers | Frontiers in Plant Science

ORIGINAL RESEARCH
published: 25 April 2022
doi: 10.3389/fpls.2022.849477

Exogenous Methyl Jasmonate Application Improved Physio-Biochemical Attributes, Yield, Quality, and Cadmium Tolerance in Fragrant Rice

Adam Sheka Kanu[1,2,3], Umair Ashraf[1,4], Lamin R. Mansaray[3,5], Farhat Abbas[6], Sajid Fiaz[7], Sikandar Amanullah[8], Christen Shaka Charley[2] and Xiangru Tang[1]**

[1] Department of Crop Science and Technology, College of Agriculture, South China Agricultural University, Guangzhou, China, [2] Sierra Leone Agricultural Research Institute (SLARI)-Rokupr Agricultural Research Centre (RARC), Freetown, Sierra Leone, [3] Agro-Geo Services (SL) Limited, Freetown, Sierra Leone, [4] Department of Botany, Division of Science and Technology, University of Education, Lahore, Pakistan, [5] Institute of Geography and Development Studies, School of Environmental Sciences, N'jala University, Njala, Sierra Leone, [6] College of Horticulture, South China Agricultural University, Guangzhou, China, [7] Department of Plant Breeding and Genetics, The University of Haripur, Haripur, Pakistan, [8] College of Horticulture and Landscape Architecture, Northeast Agricultural University, Harbin, China

OPEN ACCESS

Edited by:
Shabir Hussain Wani, Sher-e-Kashmir University of Agricultural Sciences and Technology, India

Reviewed by:
Abbu Zaid, Government Degree College Doda, India
Mohammad Nauman Khan, Huazhong Agricultural University, China

***Correspondence:**
Adam Sheka Kanu
skanuadam@yahoo.com
Xiangru Tang
tangxr@scau.edu.cn

Specialty section:
This article was submitted to Plant Breeding, a section of the journal Frontiers in Plant Science

Received: *06 January 2022*
Accepted: *16 February 2022*
Published: *25 April 2022*

Citation:
Kanu AS, Ashraf U, Mansaray LR, Abbas F, Fiaz S, Amanullah S, Charley CS and Tang X (2022) Exogenous Methyl Jasmonate Application Improved Physio-Biochemical Attributes, Yield, Quality, and Cadmium Tolerance in Fragrant Rice. Front. Plant Sci. 13:849477. doi: 10.3389/fpls.2022.849477

Cadmium (Cd) has detrimental effects on crop plants, whereas, jasmonates (JAs) play a vital role in abiotic stress tolerance in plants. The present study investigated the effects of exogenous application of methyl jasmonate (MeJa) on the physio-biochemical attributes, yield, and quality of two fragrant rice cultivars, i.e., Xiangyaxiangzhan and Meixiangzhan-2 under Cd stress. The experiment was comprised of four treatments, i.e., CK, control (normal conditions); Cd: 100 mg Cd kg^{-1} of soil; MeJa: exogenous application of MeJa at 20 mM; and Cd + MeJa: 100 mg Cd kg^{-1} of soil + exogenous MeJa application at 20 mM. Results depicted that Cd toxicity resulted in a substantial reduction of enzymatic activities and non-enzymatic antioxidants, chlorophyll contents, while enhanced oxidative damage in the terms of lipid peroxidation (higher malondialdehyde (MDA) contents), H_2O_2, and electrolyte leakage. Proline contents were found higher whereas protein and soluble sugars were lower under Cd stress as compared with Ck and Cd + MeJa. Exogenous MeJa application further improved the panicles per pot, spikelets per panicle, seed setting (%), 1,000 grain weight, and yield per pot under Cd stress conditions as compared with non-MeJa applied plant under Cd stress. In addition, exogenous MeJa application enhanced the accumulation of macro (N, P, K, Mg, and Ca) and micronutrients (Mn, Zn, Fe, and Cr) in both cultivars under Cd stress, while reduced the Cd contents in different plant parts. Overall, the contents of Cd in different plant organs were recorded as: root > stem > leaves > grains for all treatments. Comparing both cultivars, the grain Cd contents were higher in Meixiangzhan 2 than Xiangyaxianzhan under Cd contaminated conditions. Conclusively, Cd toxicity impaired growth in rice by affecting physio-biochemical attributes, however, Xiangyaxiangzhan performed better than Meixiangzhan-2 cultivar.

Keywords: antioxidants, cadmium, yield, quality, fragrant rice

INTRODUCTION

Increasing the soil deposition of heavy metals and its associated toxic effects on crop plants has attracted global attention among researchers and farmers (Zaid et al., 2019; Huang J. et al., 2020). Cadmium (Cd) is among the most toxic heavy metals posing threats to crop production, grain quality, and human and animal health (Kanu et al., 2017a; Quddus et al., 2021). Cd is being deposited in arable lands through various sources, such as emission of pollutants from industries, discharge waste from anthropogenic sources, metal smelting, ore mining, and use of synthetic agrochemicals by farmers (Ashraf et al., 2015; Huang and Hartemink, 2020; Huang S. et al., 2020). Cd is known to be easily taken up by plant roots and then translocated to aerial parts, thus, obstructing plant growth and several physiological activities. Cd further interferes with nutrient uptake and its assimilation, photosynthesis, chlorophyll biosynthesis, respiration, and regulates plant signaling mechanism (Anjum et al., 2008; Rao et al., 2019). Moreover, Cd inhibits plant morphological growth, biomass accumulation, yield, and related attributes as well as interferes with plant-nutrient uptake within the rhizosphere in rice (Srivastava et al., 2014). Furthermore, Cd in rice plant primarily disturbs the cellular redox environment and thus causing oxidative stress by the excessive production of reactive oxygen species (ROS) (Farooq et al., 2015). Cd causes cardiac failure, anemia, cancer, hypertension, cerebrovascular infarction, damages the lungs, renal dysfunction in the eyes, osteoporosis, and finally deaths in humans (Cao et al., 2014).

Fragrant rice is famous and desired by consumers due to its special aromatic and cooking characters (Bryant and McClung, 2010). In South-East Asia, it is the most widely desired rice for cultivation among farmers because of its high demand by consumers (Kanu et al., 2017b). The aroma profile is not only necessary to fulfill the consumer demand but also it defend plants from external stimuli (Abbas et al., 2017, 2019, 2020). Therefore, the efforts in producing fragrant rice genotypes with minimum/negligible Cd contamination become eminent especially in a region like South China, where rapid industrial development coupled with less pollution control measures have contributed to the increased heavy metals (HMs) contamination in agricultural lands (Ji et al., 2000). Results from soil survey performed by Zhang and Huang (2000) revealed that a minimum of 13,000 ha of agricultural land in 11 provinces in China were contaminated by varying degrees of Cd, whereas soils in "Zhangtu" and "Sheyang" provinces, that were found to be highly contaminated with HMs in which Cd concentration in both rice grains and soils were above the maximum permissible limits (Huang et al., 2004).

During early grain filling stage in rice, many essential nutrients are remobilized from different plant organs toward grains (Kobayashi et al., 2013). Cd and other mineral elements are generally accumulated in rachises of panicles that form the bases for the termination of vascular bundles in the stem (Fujimaki et al., 2010). Moreover, elements in rachises are then transported to the glumes and developing rice grains through channels and transporters found in the husk around the cells' embryo and endosperm (Pinto and Ferreira, 2015). The transport rates of ions from rachises to grains were found greatly different among cultivars as well as the type of the element (Sarwar et al., 2010). Therefore, enhancing the Cd inhibition capacity of rice grains based on agronomic practices could provide a promising approach to reduce grain Cd toxicity to ensure food safety.

Jasmonic acid (JA) has been identified to play a significant role as a potential growth regulator which includes the induction of trichome and seed formation, regulation in the reproductive organ development, modulation in seed germination, root growth and development, and regulation in plant responses to various biotic and abiotic stresses (Wasternack and Hause, 2013; Campos et al., 2014). So far, JA application has received much attention due to its multi-functional and stress-alleviatory roles in plants under various abiotic stress conditions (Yan et al., 2010; Ahmad et al., 2015; Kaya and Doganlar, 2016; Ali et al., 2018);

Recent research on MeJa application in Cd mitigation has reported the reduction of chilling injury effects in a number of horticultural crops, such as mango, tomato, fruit, and sweet pepper (Doganlar et al., 2016; Ali et al., 2018) however, the role of MeJa under Cd stress conditions in cereals especially fragrant rice is rarely investigated. The present study was therefore conducted to assess the roles of exogenous JA application on morpho-physiological, yield, and quality aspects of fragrant rice grown under Cd contaminated soil.

MATERIALS AND METHODS

Experimental Site and Conditions

The experiment was conducted in rain protected wirehouse under open-air conditions at the Experimental Research Farm, College of Agriculture, South China Agricultural University, Guangzhou city (23°14′ N, 113°37′ E, 20 M altitude) during the 2017–2018 cropping years. Paddy soil from the research farm was collected to a depth of 20 cm and then air-dried, sieved through a 4 mm sieve, mixed thoroughly, and filled in plastic pots (30 cm height) with 10 kg in each pot. The experimental soil was comprised of 4.96 mg/kg Cd, 18.73 g/kg organic matter, 0.81, 0.9, and 16.79 g/kg total NPK, and 69.15, 10.15, and 109.62 mg/kg, available NPK, respectively, with 5.92 soil pH.

Crop Husbandry and Treatment Application

The seeds of two fragrant rice cultivars, i.e., "Xiangyaxiangzhan" (Xiangsimiao126 × Xiangyaruanzhan, an indica type of fragrant rice cultivar with a maturity period of about 112–114 days), and "Meixiangzhan-2" (Lemont × Fengaozhan, indica type of fragrant rice cultivar with expected maturity period of 145–147 days), were collected from the Department of Crop Science and Technology, College of Agriculture, South China Agricultural University, Guangzhou, China. The seeds were soaked in a container with deionized water and kept at 25–30°C for 48 h to complete the germination process. Sprouted seeds were then sown in trays containing soil parachute. The trays were placed on leveled paddy field and protected with a plastic sheet in early March to prevent the chilling effect. The 21-day old seedlings were then transplanted to soil containing

plastic pots with 3–4 seedlings per hill and 5 hills per pot. Then, 1 week after transplanting, the damaged and affected seedlings were replaced with the healthy ones to get a good stand establishment. Fertilizer was applied with 2.25 g N (urea 46%), 3.33 g P (superphosphate 12% P_2O_5), and 1.35 g K (potassium chloride 60% K_2O) in each pot. Further, 2 weeks before nursery transplantation, Cd in the form of $CdCl_2 2.5\ H_2O$ was added to the soil to obtain the required Cd levels for each treatment in solution form. The experimental treatments were comprised of: Ck, control (normal conditions); Cd: 100 mg Cd kg^{-1} of soil; MeJa: exogenous application of MeJa at 20 mM; and Cd + MeJa: 100 mg Cd kg^{-1} of soil + exogenous MeJa application at 20 mM. The MeJa was uniformly applied two times, i.e., at vegetative and the reproductive stages. The pots were kept in submerged conditions by maintaining a water level of 2–3 cm above the soil surface to create fully anaerobic conditions within the pots.

Sampling and Measurements

The crop was observed throughout the growth period and plant samples were collected at panicle heading stages and stored at –80°C for physio-biochemical assays while yield components and quality were recorded at the maturity stage after harvesting.

Photosynthetic Pigments and Physio-Biochemical Assay

Photosynthetic pigments were determined according to Arnon (1949). The fresh leaf samples (0.3 g) at the panicle heading stage were extracted with 15 ml of 95% ethanol and placed in a dark place overnight. The absorbance was read at 665, 649, and 470 nm.

For determining the antioxidant enzymes, the fresh leaf samples (0.3 g) were ground in liquid-N_2 and homogenized in 6 ml containing 50 mM sodium phosphate buffer (pH 7.8) using mortar and pestle in an ice bath and homogenate were centrifuged at 10,000 *g* for 20 min at 4°C and the supernatant was used to record the enzymatic activities. The activities of superoxide dismutase (SOD) were assayed according to Zhang et al. (2008) following the inhibition of photochemical reduction due to nitro blue tetrazolium (NBT). The SOD activity per unit was defined as the amount of enzyme required to inhibit NBT photochemical reduction to 50% as an activity unit (U). The peroxidase (POD) activity was measured by using the guaiacol method with minor modifications in Lück (1965). The reactions mixture containing 1 ml of sodium phosphate buffer (pH 7.8), 0.2% of 0.95 ml guaiacol, 1 ml of 0.3% H_2O_2, and 0.05 ml aliquot of enzyme extract was used and the absorbance was read at 470 nm. Then, 1 unit of POD activity was recorded as the amount of enzyme that caused the decomposition of 1 μg substrate at 470 nm. The catalase activity (CAT) was assayed according to Aebi (1984) whereas 1 unit of enzyme activity (U) was the decomposition of 1 M H_2O_2 at A_{240} nm within 1 min in 1 g of fresh leaves samples. The ascorbate peroxidase (APX) activity was estimated by using the "APX determination kit" obtained from Nanjing Jiancheng Bioengineering Institute, China. The manufacturer's procedure was followed carefully and the absorbance was read at 290 nm. The contents of malondialdehyde (MDA) were determined by following the methods devised by Hodges et al. (1999). Hydrogen peroxide (H_2O_2) contents were determined following Velikova et al. (2000). To determine electrical conductivity (EC), the fresh leaf samples were washed with distilled water and then cut into smaller pieces. Leaf disks (0.3 g) were placed in 10 ml of deionized water and incubated at 25°C for 6 h and the (EC1) was recorded with an EC meter (SX650, Sansin, China). Samples were further incubated at 90°C for 2 h, then cool down to 25°C for recording the second EC (EC2). The EC of leaves samples was calculated as: EC (%) = (EC1/EC2) × 100. The protein contents in fresh leaf samples were determined according to Bradford (1976) at panicle heading stage using G-250. The proline contents in fresh leaves samples were determined according to Bates et al. (1973) using ninhydrin. The soluble sugar contents were determined at panicle heading stage following the methods of Zhang et al. (2008). For the reduced glutathione (GSH) and oxidized glutathione (GSSG), estimation was done by using the enzyme-built kits (A006-1 for GSH and A061-2 for GSSG), purchased from the Nanjing Jiancheng Bioengineering Institute, China[1]. The instructions were strictly followed and the absorbance was read at 420 and 412 nm, respectively. Total glutathione was the addition of both GSH and GSSG (GSH + GSSG) contents.

Grain Yield and Yield Components

At maturity, three pots from each treatment were randomly selected and rice plants from each pot were manually harvested using a sickle and then threshed, the paddy was sun-dried to the required moisture content and grain yield per pot was determined and expressed in grams per pot (g pot^{-1}). Total panicles per pot were counted for each treatment and averaged. Filled and unfilled grains were separated and counted manually from each panicle to obtain a total number of filled and unfilled grains per panicle. The 1,000-grain weight was recorded by weighing a random sample of 1,000 filled grains and averaged.

Grain Quality Attributes

Rice quality attributes were determined from the harvested grains stored at an appropriate moisture content. Brown rice rate was calculated as: (brown rice weight/paddy weight) × 100. The brown rice was then milled using a Jingmi testing rice miller (Zhejiang, China) and the milling recovery was recorded as: (milled rice weight/original weight) × 100. Milling degree was calculated as: (milled rice weight/brown rice weight) × 100. Head rice rate was calculated by separating whole milled grains from 100 grains and head rice rate was calculated on a percentage basis. Grain chalkiness percentage and chalkiness degree were assessed using an SDE-A lightbox (Guangzhou, China). Grain chalkiness is the grains with opaque spots either on the dorsal and or in the center of the grain. Grain moisture, amylose, and protein contents were determined by using an Infratec 1241 (FOSS-TECATOR) grain analyzer.

Determination of Grain Mineral and Cd Contents in Different Plant Parts

To determine the grain mineral and Cd contents in different plant parts, the plant samples were ground into powder form and

[1]http://www.njjcbio.com

digested with HNO_3 and $HClO_4$ in 4:1 (V/V) and the contents were estimated by atomic absorption spectrometer (AAS 6300C, Shimadzu, Japan).

Experimental Design and Statistical Analyses

The research was a two-factor factorial and pots were arranged in a randomized complete block design (RCBD), placing them so as to allow enough space to avoid shading, each treatment had 15 pots for sampling, yield, and quality analysis. The data were analyzed by using the statistical software "Statistix 8" (Analytical Software, Tallahassee, Florida, Unied Satse) while difference among treatments was separated using the least significant difference (LSD) test at $p < 0.05$.

RESULTS

Antioxidant Enzymes

Both Cd toxicity and MeJa affected the activities of SOD, POD, CAT, and APX in both rice cultivars. The SOD activity was substantially reduced under Cd toxic conditions for both rice cultivars, however, maximum toxicity was observed in the Cd treatment and SOD activities were reduced when compared with the control treatment for both varieties. In Xiangyaxiangzhan, comparing the control treatment with exogenous MeJa application, 4.85 and 5.92% increase in SOD activities were observed for MeJa and MeJa + Cd treatments, respectively, whereas, 1.1% decrease in SOD activities was observed in the Cd treatment when compared with the control treatment. In Meixiangzhan-2 cultivar, exogenous MeJa application increased SOD activities by 3.85, 30.12, and 37.35% for Cd, MeJa, and MeJa + Cd treatments, respectively. Both Xiangyaxiangzhan and Meixiangzhan-2 cultivars experienced a 2.95 and 14.14% decrease, respectively, in the POD activities in the Cd treatments. For MeJa and MeJa + Cd treatments, 15.38 and 20.07% increase were observed for Xiangyaxiangzhan, respectively, while 3.74 and 38.84% increase were observed for Meixiangzhan-2 cultivar, respectively, when compared with the control treatment. The activities of CAT were decreased by 13.72 and 12.9% for the Cd treatments in both Xiangyaxiangzhan and Meixiangzhan-2 cultivars, respectively, while maximum increased CAT activity (28.41%) was observed in the MeJa + Cd treatment for Xiangyaxiangzhan cultivar. The APX activities saw significant reduction (60.37 and 34.58%) in the Cd treatment for Xiangyaxiangzhan and Meixiangzhan-2 cultivars, respectively; while MeJa addition augmented APX activities in the MeJa + Cd treatment for both cultivars (**Table 1**).

Chlorophyll Pigments

Cadmium stress significantly affected photosynthetic pigments, i.e., Chl a, Chl b, total chlorophyll contents (Chl a + b), and carotenoids while MeJa supplementation augmented photosynthetic pigments in both cultivars. In comparison with the control treatment, maximum increased Chl a (63.9 and 88.93%), Chl b (51.59 and 146.65%), and total chlorophyll contents (58.81 and 111.36%) were observed in the MeJa + Cd treatment for Xiangyaxiangzhan and Meixiangzhan-2 cultivars, respectively (**Figure 1**).

Reduced and Oxidized Glutathione Contents

In the Cd treatments, the levels of GSH, i.e., 20.16 and 15.3% were higher in Xiangyaxiangzhan and Meixiangzhan-2, respectively. Maximum GSSG content (41.7%) was observed in the MeJa + Cd treatment for Meixiangzhan-2 cultivar. Total glutathione (GSH + GSSG) were recorded for the two cultivars studied and the increased levels were higher in Xiangyaxiangzhan than in Meixiangzhan-2 cultivar. The exogenous supplementation of MeJa reduced contents of GSH, GSSG, and total glutathione (GSH + GSSG) in Cd-affected plants.

Oxidative Damage

The MDA contents in the leaves of both rice cultivars were substantially increased under Cd stress conditions. Exogenous MeJa application and MeJa + Cd reduced the amount of MDA by about 31.8 and 50% for Xiangyaxiangzhan and Meixiangzhan-2 cultivars, respectively. In addition, H_2O_2 was

TABLE 1 | The effects of exogenous methyl jasmonate (MeJa) application on superoxide dismutase (SOD), peroxidase (POD), catalase (CAT), and ascorbate peroxidase (APX) in two fragrant rice cultivars under cadmium (Cd) stress.

Variety	Treatment	SOD(U min^{-1} g^{-1} FW)	POD(U min^{-1} g^{-1} FW)	CAT(U min^{-1} g^{-1} FW)	APX(U min^{-1} g^{-1} FW)
Xiangyaxiangzhan	CK	371.00 ± 1.00Ab	214.00 ± 0.15Ac	145.47 ± 1.44Ac	0.35 ± 0.02Ab
	Cd	366.93 ± 0.21Ab	207.67 ± 0.02Ad	125.50 ± 0.21Ad	0.14 ± 0.01Ac
	MeJa	389.00 ± 0.52Aa	246.83 ± 1.01Ab	165.60 ± 0.70Ab	0.35 ± 0.02Ab
	MeJa + Cd	393 ± 0.30Aa	256.97 ± 0.17Aa	186.80 ± 0.33Aa	0.64 ± 0.01Aa
Meixiangzhan-2	CK	305.77 ± 0.13Bd	195.67 ± 0.20Bc	165.10 ± 0.49Bb	0.23 ± 0.01Bb
	Cd	317.57 ± 0.23Bc	168.00 ± 0.73Bd	143.80 ± 1.11Bc	0.15 ± 0.72Bc
	MeJa	397.87 ± 0.47Bb	203.00 ± 0.15Bb	172.27 ± 0.65Ba	0.23 ± 0.38Bb
	MeJa + Cd	420.00 ± 0.58Ba	271.67 ± 0.85Ba	174.50 ± 0.82Ba	0.39 ± 0.02Ba

Three replicated means (± SE) were calculated for each treatment. Values with different letters indicate significant difference between cultivars and treatments at $p < 0.05$ least significant difference (LSD). CK; control (normal conditions); Cd:100 mg Cd kg^{-1} of soil, MeJa: exogenous application of MeJa at 20 mM, and Cd + MeJa: 100 mg Cd kg^{-1} of soil + exogenous MeJa application at 20 mM.

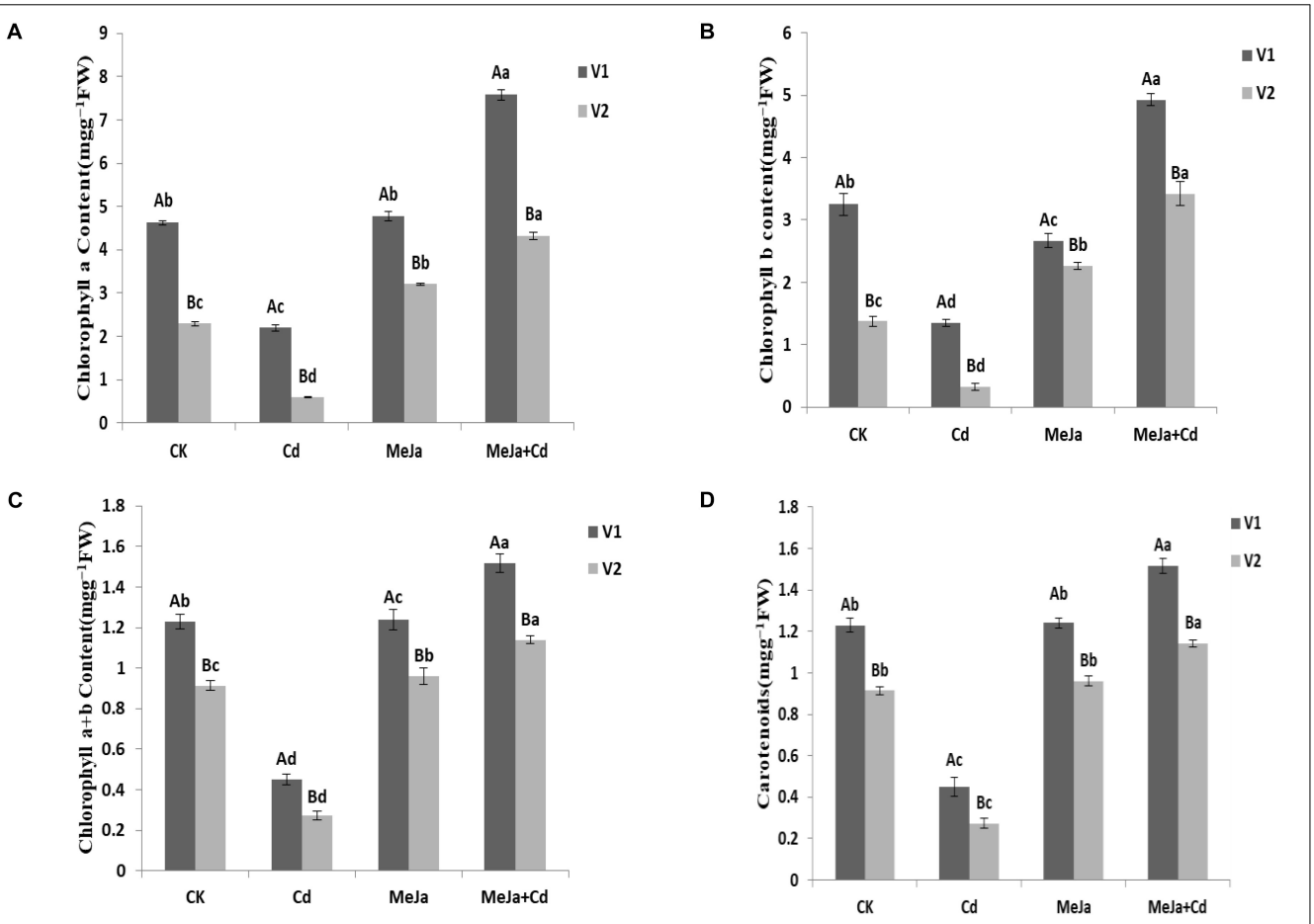


FIGURE 1 | The effects of MeJa on **(A)** Chl a, **(B)** Chl b, **(C)** Chl a + b, and **(D)** carotenoids in two rice cultivars under Cd stress. The values are representative of three replicated means per treatment ± SE. Different letters indicate significant differences between cultivars and treatments at $p < 0.05$, LSD (V1 = Xiangyaxiangzhan and V2 = Meixiangzhan-2).

found to increase by 45.32 and 35.12% in the Cd treatments for Xiangyaxiangzhan and Meixiangzhan-2 cultivars, respectively. Plants treated with only Cd showed increased H_2O_2 content, but decreased significantly with MeJa application. In comparison with the control treatment, a significant reduction in H_2O_2 content, i.e., 34.14 and 52.87% was recorded for MeJa + Cd treatments for both Xiangyaxiangzhan and Meixiangzhan-2, respectively. Furthermore, significant reduction of electrolyte leakage (EL) was recorded in plants under MeJa + Cd treatment.

Proline, Protein, and Soluble Sugar Contents

The proline content increased by 36 and 27% for Xiangyaxiangzhan and Meixiangzhan-2 cultivars, respectively, under Cd stress conditions whereas the proline contents were lowered by 28 and 49% in the MeJa + Cd treatments for Xiangyaxiangzhan and Meixiangzhan-2, respectively. Significant reduction in protein contents, i.e., 14.52 and 38.71% was observed in the MeJa + Cd treatments for Xiangyaxiangzhan and Meixiangzhan-2, respectively. Soluble sugar contents were found to increase almost 36% in the MeJa + Cd for both rice cultivars.

Yield and Yield Related Components

Cadmium stress reduced the rice yield and its components while an application of MeJa improved yield and its related attributes. In Xiangyaxiangzhan, compared with CK, the maximum number of panicles per pot was recorded in the MeJa + Cd treatment, while the minimum number was recorded in the Cd treatment. Similarly, spikelet number and seed setting rate were reduced under Cd treatment while increased under MeJa and MeJa + Cd treatments. Significant differences were not observed in the 1,000 grain weight in all treatments except for the MeJa + Cd treatment which had a maximum 1,000 grain weight (23.19 g). Furthermore, grain yield was 53.47% higher in MeJa + Cd than Cd treatment. For Meixiangzhan, the highest number of panicles per pot was recorded in MeJa treatment, followed by MeJa + Cd treatment whereas, the least number of panicles per pot were recorded in Cd treatment. In the terms of spikelet number per panicle and 1,000 grains weight, no significant differences were noted except in the MeJa + Cd treatment. Moreover, grain yield in MeJa + Cd treatment was 51.88% higher than Cd treatment. Overall, Cd has negative impacts on grain yield while exogenous MeJa

application enhanced the grain yield under Cd stress conditions (**Table 2**).

Grain Quality Attributes

Cadmium toxicity was found to affect grain quality traits while significant improvements were observed in quality-related attributes for both rice cultivars augmented with MeJa. For Xiangyaxiangzhan cultivar, brown rice was reduced under Cd treatment by (7.36%) but increased by (5.28%) in MeJa + Cd treatments. Maximum reduction in amylose contents, i.e., 22.71% was recorded for MeJa + Cd treatment, whereas the highest grain chalkiness, i.e., 43.49% was recorded in Cd treatment. Moreover, the maximum reduction in milled and head rice rate, i.e., 20.85 and 21.15%, respectively, was recorded under Cd treatment. Reduced protein content was recorded in the Cd-induced treatment while increased in the treatment with supplemented MeJa.

In Meixiangzhan 2, the Cd was found to have obstructed grain quality while MeJa improved grain quality attributes. For example, protein contents, brown rice rate, and milled rice rate were remained higher under MeJa + Cd than Cd treatment. Moreover, the maximum grain chalkiness (43.49%) and chalkiness degree (27.32%) and minimum brown rice rate (41.54%), head rice rate (52.13%), protein contents (29.39%), and milled rice rate (10.23%) were observed in the Cd treatment. Overall, all grain quality attributes were relatively affected by Cd toxicity and the application of MeJa improved the grain quality of both Xiangyaxiangzhan and Meixiangzhan 2 cultivars (**Table 3**).

Grain Mineral Elements

Significant differences were observed in grain mineral contents among treatments. For instance, in Xiangyaxiangzhan, the mineral elements were decreased in the Cd treatment while the application of MeJa enhanced the grain mineral content. Compared with CK, there were 52.32, 40.94, 95.28, 67.45, 67.13, 20.92, 35.98, 35.74, and 62.85% decrease in N, P, K, Mg, Ca, Mn, Zn, Fe, and Cr contents, respectively, in the Cd treatment, while in the MeJa + Cd treatment, the contents of N, P, K, Mg, Ca, Mn, Zn, Fe, and Cr increased by 11.76, 4.74, 11.73, 24.12, 8.53, 8.84,14.53, 16.47, and 41.83%, respectively. Similar trends were observed in Meixiangzhan 2 cultivar, in which Cd induced treatment severely affected grain mineral contents but with MeJa application, grain mineral contents were augmented (**Table 4**).

Cadmium Accumulation in Different Plant Parts

Cadmium accumulation in the various organs, i.e., roots, stems, leaves, and grains were substantially higher in Cd treatment, while lower in MeJa applied treatment (**Table 2**). Exogenous application of MeJa reduced Cd uptake and accumulation in the rice roots and shoots. In the combined treatment (MeJa + Cd), Cd uptake was substantially reduced in the roots, stems, leaves, and grains of Xiangyaxiangzhan by 72.41, 157, 109, and 70%, respectively, while in Meixiangzhan 2, there were 32.75, 119.68, 162.21, and 601.50% decrease in Cd contents of roots, stems, leaves, and grains, respectively. On average, Cd accumulation was in the descending order: root > stem > leaves > grains for all treatments. In summary, Cd uptake and translocation were higher in the roots than stems, leaves, and grains for all the cultivars. However, the grain Cd contents in Xiangyaxiangzhan were substantially lower in Cd + MeJa than Cd treatment whereas found statistically similar ($p > 0.05$) for Meixiangzhan 2.

DISCUSSION

Recently, the excess application of untreated wastewater and industrial effluents to agricultural lands severely contaminate the soils and build pools of heavy metals. In recent years, the role of jasmonates (JAs) has received considerable attention among researchers due to its involvement in the growth regulation under stress conditions (Welch and Graham, 2002). In this study, we have explored the possible role of exogenous application of MeJa as plant growth regulators on physio-biochemical attributes, oxidative status, yield, and quality traits as well as mineral elements and Cd accumulation in different plant parts of fragrant rice.

The activities of antioxidant enzymes were found reduced under Cd stress conditions while the MeJa application increased antioxidant enzymes activities, i.e., SOD, POD, CAT, and APX in both rice cultivars, though such increment was higher in Xiangyaxiangzhan than Meixiangzhan-2 (**Table 1**). Similarly, the GSH and GSSG contents were higher in Cd + MeJa

TABLE 2 | The effects of exogenous MeJa application on yield and related components in two fragrant rice cultivars under Cd stress.

Variety	Treatments	Panicles/pot	Spikelet/panicle	Seed Setting (%)	1000 Grain Weight(g)	Yield(g/pot)
Xiangyaxiangzhan	CK	29Ac	112.58Aa	90.61Aa	19.02Bb	75.53Ab
	Cd	26cAd	101.22Ac	76.54Ab	18.23Bb	36.73Ad
	MeJa	35Ab	106.71Ab	92.95Aa	21.56Bb	87.22Aa
	MeJa + Cd	41Aa	98.38Bc	93.23Aa	23.19Aa	56.37Ac
Meixiangzhan-2	CK	27Bb	100.11Ba	86.38Bb	18.81Bc	53.96Bb
	Cd	21Bc	96.00Bab	78.45Bc	18.28Bc	28.91Bd
	MeJa	30Ba	97.55Bab	88.98Bb	20.24Bb	65.46Ba
	MeJa + Cd	29Bab	109.93Aa	92.24Ba	22.25Aa	43.91Bc

The values are representative of three replicated means per treatment ± SE. Different letters indicate significant differences between cultivars and treatments at $p < 0.05$, LSD. CK, control (normal conditions); Cd, 100 mg Cd kg^{-1} of soil; MeJa, exogenous application of MeJa at 20 mM; and Cd + MeJa, 100 mg Cd kg^{-1} of soil + exogenous MeJa application at 20 mM.

than Cd treatment whereas the GSH and GSSG contents were comparatively higher in Xiangyaxiangzhan than Meixiangzhan 2 (**Table 5**). The increased activity of antioxidant enzymes in response to MeJa application may be attributed to the direct interaction of MeJa with ROS as reported by Chen et al. (2014). In addition, the increased antioxidant enzymes activity due to MeJa supplementation in Cd-stressed plants has been reported by other researchers (Keramat et al., 2009; Yan et al., 2015; Per et al., 2016). Similarly, in *Mentha arvensis* L., the application of plant growth regulators improve the growth, photosynthesis, mineral nutrient, and antioxidant system under cadmium stress (Zaid et al., 2020). Increased SOD, POD, CAT, and APX activity in MeJa supplemented treatments under Cd stress. Strengthening the antioxidant defense system by MeJa supplementation might reduce ROS production and their consequent effects resulting in the alleviation of Cd-induced oxidative stress in Xiangyaxiangzhan than Meixiangzhan-2 rice cultivars. Similarly, the mitigating role of exogenous MeJa

TABLE 3 | The effects of exogenous MeJa application on grain quality attributes in two fragrant rice cultivars under Cd stress.

Cultivar	Grain Quality Parameters	CK	Cd	MeJa	MeJa + Cd
Xiangyaxiangzhan	Brown rice rate (%)	79.83 ± 0.28Ac	74.36 ± 0.52Ad	82.55 ± 0.44Ab	84.28 ± 0.32Aa
	Milled rice rate (%)	87.45 ± 0.05Ac	72.36 ± 0.13Ad	88.60 ± 0.07Ab	89.59 ± 0.09Aa
	Head rice rate (%)	81.36 ± 0.05Ac	65.53 ± 0.12Ad	83.45 ± 0.10Ab	86.55 ± 0.13Aa
	Chalkiness rate (%)	27.39 ± 0.04Ab	48.47 ± 0.10Aa	23.52 ± 0.13Bc	19.55 ± 0.14Ad
	Chalkiness degree (%)	11.36 ± 0.04Ab	15.6 ± 0.11Aa	10.53 ± 0.12Bc	7.65 ± 0.11Bd
	Moisture contents (%)	10.50 ± 0.03Ab	12.45 ± 0.01Aa	9.59 ± 0.19Bcd	8.94 ± 8.81Bd
	Amylose contents (%)	20.36 ± 0.09Ab	23.64 ± 0.12Aa	19.84 ± 0.03Bc	16.59 ± 0.19Bd
	Protein contents (%)	10.49 ± 0.04Ab	8.58 ± 0.06Ad	9.56 ± 0.05Ac	11.48 ± 0.14Aa
Meixiangzhan 2	Bbrown rice rate (%)	74.75 ± 0.24Bb	52.81 ± 0.26Bd	75.22 ± 0.23Bb	76.16 ± 0.28Ba
	Milled rice rate (%)	76.56 ± 0.15Bb	69.46 ± 0.05Bc	77.00 ± 0.06Ba	76.95 ± 0.03Ba
	Head rice rate (%)	76.87 ± 0.01Bb	50.53 ± 0.12Bd	75.52 ± 0.23Bc	78.49 ± 0.04Ba
	Chalkiness rate (%)	31.68 ± 0.15Bb	54.45 ± 0.14Ba	30.19 ± 0.03Ac	27.61 ± 0.11Ad
	Chalkiness regree (%)	12.66 ± 0.12Bb	17.42 ± 0.02Ba	11.66 ± 0.11Ac	9.97 ± 0.28Ad
	Moisture contents (%)	11.34 ± 0.07Bb	14.44 ± 0.09Ba	10.47 ± 0.03Ac	10.01 ± 0.03Ad
	Amylose contents (%)	21.49 ± 0.03Bb	22.35 ± 6.66Ba	20.04 ± 0.13Ac	19.41 ± 0.29Ad
	Protein contents (%)	9.43 ± 0.07Bb	7.29 ± 0.02Bd	7.92 ± 0.03Bc	9.94 ± 0.03Ba

The values are representative of three replicated means per treatment ± SE. Different letters indicate significant differences between cultivars and treatments at $p < 0.05$, LSD. CK; control (normal conditions); Cd:100 mg Cd kg^{-1} of soil, MeJa: exogenous application of MeJa at 20 mM, and Cd + MeJa: 100 mg Cd kg^{-1} of soil + exogenous MeJa application at 20 mM.

TABLE 4 | The effects of exogenous MeJa application on grain mineral elements (mg/kg) in two fragrant rice cultivars under Cd stress.

		Treatments			
Cultivars	**Elements**	**CK**	**Cd**	**MeJa**	**MeJa + Cd**
Xiangyaxiangzhan	N	52.43 ± 0.18Ab	34.42 ± 0.13Ac	53.77 ± 1.49Ab	59.42 ± 0.13Aa
	P	27.33 ± 0.17Ab	19.39 ± 0.04Ad	22.39 ± 0.04Ac	28.69 ± 0.16Aa
	K	2321.3 ± 4.89Ab	1188.7 ± 6.53Ad	2150.1 ± 1.77Ac	2629.9 ± 1.18Aa
	Mg	1246.7 ± 9.40Ac	744.5 ± 5.47Ad	1284.8 ± 3.10Ab	1643 ± 1.61Aa
	Ca	72.74 ± 0.24Ac	43.53 ± 0.15Ad	75.04 ± 0.41Ab	79.53 ± 0.04Aa
	Mn	63.57 ± 0.15Ab	52.57 ± 0.25Ac	63.72 ± 0.32Ab	69.74 ± 0.29Aa
	Zn	30.46 ± 0.04Ac	22.4 ± 0.06Ad	31.86 ± 0.20Ab	35.64 ± 0.10Aa
	Fe	21.95 ± 0.34Ac	16.17 ± 0.25Ad	23.34 ± 0.12Ab	26.28 ± 0.25Aa
	Cr	0.57 ± 0.02Ac	0.35 ± 8.81Ad	0.63 ± 0.02Ab	0.98 ± 0.01Aa
Meixiangzhan 2	N	47.36 ± 0.05Bb	26.52 ± 0.19Bc	47.29 ± 0.08Bb	49.56 ± 0.04Ba
	P	22.54 ± 0.03Bb	15.34 ± 8.81Bc	23.03 ± 0.36Bab	23.18 ± 0.02Ba
	K	2047.6 ± 1.34Bc	1023.8 ± 0.81Bd	2136.1 ± 1.65Bb	2441.9 ± 1.51Ba
	Mg	1111.8 ± 0.29Bd	5414.3 ± 1.16Ba	1133.9 ± 0.94Bc	1285.8 ± 1.43Bb
	Ca	66.16 ± 0.20Bb	32.01 ± 0.40Bc	66.51 ± 0.10Bb	69.43 ± 0.15Ba
	Mn	55.16 ± 0.41Bbc	28.98 ± 0.25Bd	56.08 ± 0.37Bb	57.86 ± 0.24Ba
	Zn	22.35 ± 0.10Bc	17.7 ± 0.32Bd	23.58 ± 0.23Bb	29.74 ± 0.19Ba
	Fe	17.42 ± 0.03Bc	11.08 ± 0.15Bd	18.03 ± 0.14Bb	21.31 ± 0.04Ba
	Cr	0.51 ± 3.33Bc	0.24 ± 0.01Bd	0.56 ± 0.02Bb	0.6 ± 0.01Ba

The values are representative of three replicated means per treatment. Different letters indicate significant differences between cultivars and treatments at $p < 0.05$, LSD. CK, control (normal conditions); Cd,100 mg Cd kg^{-1} of soil; MeJa, exogenous application of MeJa at 20 mM; and Cd + MeJa: 100 mg Cd kg^{-1} of soil + exogenous MeJa application at 20 mM.

application with increased antioxidant enzyme activities under Cd stress conditions has been reported in various plants, i.e., *Solanum nigrum* (Yan et al., 2015), *Brassica juncea* (Per et al., 2016), *Kandelia obovata* (Chen et al., 2014), and *Glycine max* (Keramat et al., 2009). Several previous studies have revealed that MeJa alleviate cadmium stress by regulating ROS detoxification and physio-biochemical damages (Zaid and Mohammad, 2018). In addition, the higher levels of GSH reduced Cd-induced phytotoxic effects and redox regulation and hormonal balancing in *Brassica napus* (Kim et al., 2021) and rice (Kanu et al., 2019) under Cd toxic condition. Furthermore, Cd accumulation led to the substantial reduction in Chl a, b, total Chl, and carotenoid contents with maximum reduction in Meixiangzhan-2 (**Figure 1**) that may be associated with its sensitivity to Cd stress. The accumulation of Cd in leaves might damage the chlorophyll biosynthesis and thus resulted in reduced chlorophyll contents. In addition, Farooq et al. (2022) reported that Cd stress led to substantial reduction in chlorophyll contents in different rice varieties whereas exogenous MeJa improved the leaf chlorophyll contents (Anjum et al., 2007). Similarly, MeJa application substantially alleviate cadmium toxicity by eliminating the Cd-induced effects on the growth of capsicum (Yan et al., 2013).

In our study, the increased production of MDA, H_2O_2, and EL were observed in both cultivars under Cd stress, however, exogenous MeJa provided relieve against oxidative stress (**Table 6**). Moreover, free proline, protein, and soluble sugar contents in both rice cultivars were found higher in Cd treatments (**Figure 2**). In plants generally, proline directly act as an antioxidant providing protection for the cell against free radical damages for enabling a more favorable environment to reduce Cd sequestration (Shah and Nongkynrih, 2007). In addition, the yield and related traits were substantially reduced under Cd toxic conditions whereas foliar MeJa application improved the panicles/pot, spikelet/panicle, seed setting (%), 1,000-grain weight, and grain yield (**Table 2**). Higher grain yield under MeJa treatment might be associated with the improved yield related attributes of both rice cultivars. Substantial reduction in yield and other agronomic attributes were noticed in Cd exposed rice plants (Majumdar et al., 2020), whereas MeJa alleviate the toxic effects of Cd by modulating the signaling mechanism in rice (Verma et al., 2020). Our findings corroborate with White and Broadley (2005), who concluded that exogenous application of plant growth regulators increased rice growth and yield under Cd stress conditions. Rice grain quality were affected by Cd toxicity and the exogenous application of MeJa improved grain quality attributes. External factors affecting plant led to significant changes in rice quality attributes especially aromatic rice. Reductions in rice quality attributes (brown and milled rice rates as well as head milled rice rate) were found in both rice cultivars under Cd toxicity whereas MeJa

TABLE 5 | The effects of exogenous MeJa application on reduced glutathione (GSH), oxidized glutathione (GSSG), total glutathione (GSH + GSSG), and GSH/GSSG in two fragrant rice cultivars under Cd stress.

Variety	Treatments	GSH(μmolg^{-1}FW)	GSSG(μmolg^{-1}FW)	GSH + GSSG(μmolg^{-1}FW)	GSH/GSSG(μmolg^{-1}FW)
Xiangyaxiangzhan	CK	269.63 ± 0.16Ab	68.17 ± 0.44Aa	337.80 ± 0.98Ab	3.96 ± 0.04Ac
	Cd	324.00 ± 0.17Aa	25.36 ± 0.49Ad	349.37 ± 0.72Aa	12.78 ± 0.27Aa
	MeJa	255.70 ± 0.13Ac	55.30 ± 0.81Ab	311.00 ± 1.00Ac	4.62 ± 0.05Ab
	MeJa + Cd	142.37 ± 0.73Ad	45.70 ± 0.85Ac	188.07 ± 0.31Ad	3.12 ± 0.11Ad
Meixiangzhan-2	CK	249.00 ± 0.73Bb	49.87 ± 1.07Bb	298.87 ± 0.74Bb	4.99 ± 0.07Ba
	Cd	287.00 ± 0.52Ba	88.13 ± 0.47Ba	375.13 ± 0.95Ba	3.25 ± 0.06Bc
	MeJa	250.00 ± 0.53Bb	50.90 ± 0.66Bb	300.90 ± 0.17Bb	4.91 ± 0.03Ba
	MeJa + Cd	127.00 ± 0.31Bc	29.06 ± 0.97Bc	156.07 ± 0.14Bc	4.38 ± 0.09Bb

The values are representative of three replicated means per treatment ± SE. Different letters indicate significant differences between cultivars and treatments at $p < 0.05$, LSD. CK, control (normal conditions); Cd,100 mg Cd kg^{-1} of soil; MeJa, exogenous application of MeJa at 20 mM; and Cd + MeJa, 100 mg Cd kg^{-1} of soil + exogenous MeJa application at 20 mM.

TABLE 6 | The effects of exogenous MeJa application on malondialdehyde (MDA), H_2O_2, and electrolyte leakage (EL) in two fragrant rice cultivars under Cd stress.

Variety	Treatments	MDA (μmolg^{-1} FW)	H_2O_2 (μmolg^{-1} FW)	EL (%)
Xiangyaxiangzhan	CK	5.77 ± 0.19Bb	16.40 ± 0.15Bb	32.55 ± 0.84Bb
	Cd	10.47 ± 0.17Ba	23.83 ± 0.12Ba	58.43 ± 0.29Ba
	MeJa	6.06 ± 0.08Bb	16.77 ± 0.16Bb	32.13 ± 0.46Bb
	MeJa + Cd	3.93 ± 0.12Bc	10.80 ± 0.15Bc	21.40 ± 0.21Bc
Meixiangzhan-2	CK	7.80 ± 0.11Ab	19.16 ± 0.08Ab	43.91 ± 0.26Ab
	Cd	12.86 ± 0.08Aa	25.90 ± 0.12Aa	63.27 ± 0.15Aa
	MeJa	7.27 ± 0.11Ac	18 ± 0.26Ab	38.59 ± 0.54Ac
	MeJa + Cd	3.90 ± 0.12Ad	9.03 ± 0.61Ac	24.46 ± 0.17Ad

The values are representative of three replicated means per treatment ± SE. Different letters indicate significant differences between cultivars and treatments at $p < 0.05$, LSD. CK, control (normal conditions); Cd,100 mg Cd kg^{-1} of soil; MeJa, exogenous application of MeJa at 20 mM; and Cd + MeJa, 100 mg Cd kg^{-1} of soil + exogenous MeJa application at 20 mM.

supplementation improved the grain quality characters (**Table 3**). Similarly, Ashraf et al. (2017) and Ashraf and Tang (2017) reported the deterioration in rice grain quality attributes under heavy metal toxicity. It has been demonstrated that exogenous hormone application improves plant fitness *via* maximizing the transcriptional level of related biosynthesis pathway genes in plants (Abbas et al., 2021a,b). Mineral elements contents were increased in treatments with applied MeJa, while under Cd stressed treatments, mineral elements contents reduced greatly. Rice plants require macro- and micronutrients (K, Ca, Mg, Fe, Cu, Mn, Ni, and Zn) for the growth, development, and increased productivity (Pinto and Ferreira, 2015). Various forms of interactions among plants exist during the uptake and accumulation of mineral elements (Du et al., 2013; Pinto and Ferreira, 2015), since Cd compete with important mineral nutrients uptake by plant as reported by Nazar et al. (2012) and Asgher et al. (2014). The present study revealed that the Cd accumulation in rice plants considerably reduced the uptake of essential mineral nutrients (**Table 4**) whereas MeJa application mitigated such competition by restoring the root-to-shoot translocation mechanism of key mineral elements. Similar observations have been reported by Gómez et al. (2010)

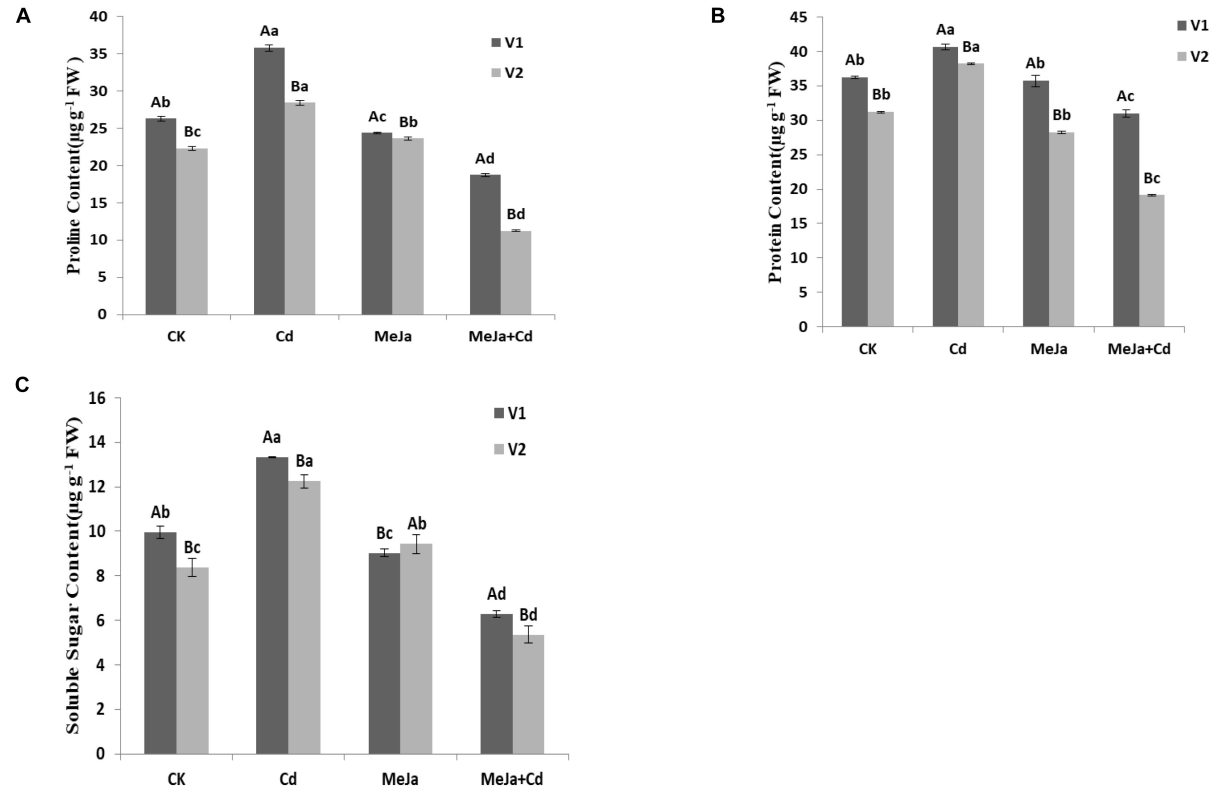


FIGURE 2 | The effects of MeJa on **(A)** proline, **(B)** protein, and **(C)** soluble sugars in two rice cultivars under Cd stress. The values are representative of three replicated means per treatment ± SE. Different letters indicate significant differences between cultivars and treatments at $p < 0.05$, LSD (V1 = Xiangyaxiangzhan and V2 = Meixiangzhan-2).

TABLE 7 | The effects of exogenous MeJa application on Cd contents in different plant parts (μg/g dry weight) in two fragrant rice cultivars under Cd stress.

Cultivar	Treatments	Roots	Stems	Leaves	Grains
Xiangyaxiangzhan	CK	3.5 ± 0.03Bb	0.74 ± 0.02Bc	0.23 ± 0.01Bc	0.01 ± 3.52Bc
	Cd	369.41 ± 1.18Ba	16.36 ± 0.04Ba	4.27 ± 0.05Ba	1.15 ± 0.19Ba
	MeJa	2.55 ± 0.12Bb	0.53 ± 0.01Bc	0.18 ± 0.02Bc	0.01 ± 3.00Bc
	MeJa + Cd	352.03 ± 0.04Ba	10.29 ± 0.01Bb	3.11 ± 5.77Bb	0.51 ± 5.77Bb
Meixiangzhan 2	CK	4.62 ± 2.47Ab	0.96 ± 0.18Ab	0.32 ± 0.01Ab	0.09 ± 0.05Ab
	Cd	471.47 ± 0.07Aa	34.59 ± 0.06Aa	3.56 ± 0.01Aa	2.88 ± 0.01Aa
	MeJa	4.04 ± 0.11Ab	0.88 ± 0.06Ab	0.33 ± 0.32Ab	0.06 ± 3.33Ab
	MeJa + Cd	473.48 ± 0.11Aa	31.43 ± 0.06Aa	3.12 ± 0.01Aa	2.01 ± 3.33Aa

The values are representative of three replicated means per treatment ± SE. Different letters indicate significant differences between cultivars and treatments at $p < 0.05$, LSD.

for *Solanum lycopersicum* and Kováčik et al. (2011) for *Scenedesmus quadricauda*. Furthermore, phloem sap in rachis forms the closest source for supplying elements to stimulate grains development, therefore, the concentration of Cd and other elements between rachises and grains shows the extent of grains ability to accumulate different elements. Our study revealed genotypic differences in mineral elements accumulation in grains. Additionally, Cai et al. (2010) revealed that exogenous application of growth regulator increased certain mineral nutrient uptake, i.e., Zn, Cu, and Mn, while Cd uptake was decreased in rice in concentration and a genotype-dependent manner. Previous studies have shown that many quantitative trait loci (QTLs) aiding the mineral accumulation in rice grains exist and are largely dependent on the environment (Du et al., 2013). Hence, rice cultivated under Cd stress conditions continuously faces a reduction in the accumulation of grain mineral elements. Furthermore, genes and QTLs for mineral elements accumulation have been reported to mediate transporting several elements at the same time (Gill et al., 2013). Improvements in rice yields and grain micro-nutrients' accumulation might be the result of plants higher nutrients absorption ability from the soils enriched with a suitable growth regulator, hence, increased the nutrient use efficiencies (Farooq et al., 2015).

Substantial Cd contents were noticed in different plant parts, i.e., root, stem, leaves, and grains under Cd treatment, however, the relative Cd contents were lower under MeJa treatment (**Table 7**). Rice plants treated with MeJa had less Cd in all plants part as MeJa mediates in binding Cd into other complexes which cannot be easily taken up by the plants. On the other hand, Cd uptake is found to be largely influenced by rice genotypic character for metal accumulation and speciation in different plant parts. In this study, genotypic differences existed in Cd accumulation with Xiangyaxiangzhan cultivar accumulating less Cd in different plant parts compared with Meixiangzhan-2 under the same conditions and agronomic practices. Further studies are recommended to further explore the understanding of genotypic variations regarding Cd accumulation in rice since it is very difficult to select inheritable low-heavy-metal accumulation traits in rice plants as suggested by Tan and Barrington (2005).

CONCLUSION

Cadmium toxicity has negative consequences on physio-biochemical attributes, rice yield, grain quality, and mineral nutrient accumulation in grains whereas exogenous MeJa improved the overall performance of both rice cultivars. MeJa application led to improved anti-oxidant activity, chlorophyll contents, while reduced oxidative damage under Cd stress conditions. Moreover, rice roots can accumulate higher Cd than shoots, however, transport in above ground plant parts may vary among cultivars. Overall, Xiangyaxiangzhan variety performed better than Meixiangzhan 2 under Cd toxic conditions. Further studies are needed to examine the involvement of MeJa in Cd stress tolerance and regulation mechanism in fragrant rice.

DATA AVAILABILITY STATEMENT

The original contributions presented in the study are included in the article/supplementary material, further inquiries can be directed to the corresponding author/s.

AUTHOR CONTRIBUTIONS

AK and UA designed and performed experiment. AK, UA, LM, and FA perform the experiments. SF, SA and CC help in formal analysis. AK, UA, FA, and XT drafted the manuscript. All authors approved the final version of the manuscript.

FUNDING

This work was supported by the Natural Science Foundation of China (31271646), the Guangdong Province Natural Science Foundation (8151064201000017), the Guangdong Province Agricultural Research Projects (2011AO20202001), and the Guangdong Province Agricultural Standardization Project (4100 F10003).

REFERENCES

Abbas, F., Ke, Y., Yu, R., and Fan, Y. (2019). Functional characterization and expression analysis of two terpene synthases involved in floral scent formation in *Lilium* 'Siberia'. *Planta* 249, 71–93. doi: 10.1007/s00425-018-3006-7

Abbas, F., Ke, Y., Yu, R., Yue, Y., Amanullah, S., Jahangir, M. M., et al. (2017). Volatile terpenoids: multiple functions, biosynthesis, modulation and manipulation by genetic engineering. *Planta* 246, 803–816. doi: 10.1007/s00425-017-2749-x

Abbas, F., Ke, Y., Zhou, Y., Ashraf, U., Li, X., Yu, Y., et al. (2020). Molecular cloning, characterization and expression analysis of *LoTPS2* and *LoTPS4* involved in floral scent formation in oriental hybrid *Lilium* variety 'Siberia'. *Phytochemistry* 173:112294. doi: 10.1016/j.phytochem.2020.112294

Abbas, F., Ke, Y., Zhou, Y., Yu, Y., Waseem, M., Ashraf, U., et al. (2021a). Genome-wide analysis reveals the potential role of MYB transcription factors in floral scent formation in *Hedychium coronarium*. *Front. Plant Sci.* 12:623742. doi: 10.3389/fpls.2021.623742

Abbas, F., Zhou, Y., He, J., Ke, Y., Qin, W., Yu, R., et al. (2021b). Metabolite and transcriptome profiling analysis revealed that melatonin positively regulates floral scent production in *Hedychium coronarium*. *Front. Plant Sci.* 12:808899. doi: 10.3389/fpls.2021.808899

Aebi, H. (1984). Catalase in-vitro. *Meth. Enzymol.* 105, 121–126. doi: 10.1016/s0076-6879(84)05016-3

Ahmad, P., Sarwat, M., Bhat, N. A., Wani, M. R., Kazi, A. G., and Tran, L.-S. P. (2015). Alleviation of cadmium toxicity in brassica juncea L. (Czern. & Coss.) by calcium application involves various physiological and biochemical strategies. *PLoS One* 10:e0114571. doi: 10.1371/journal.pone.0114571

Ali, E., Hussain, N., Shamsi, I. H., Jabeen, Z., Siddiqui, M. H., and Jiang, L. X. (2018). Role of jasmonic acid in improving tolerance of rapeseed (*Brassica napus* L.) to Cd toxicity. *J. Zhejiang Univ.-Sci. B* 19, 130–146. doi: 10.1631/jzus.B1700191

Anjum, N. A., Umar, S., Ahmad, A., Iqbal, M., and Khan, N. A. (2007). Ontogenic variation in response of Brassica campestis L. to cadmium toxicity. *J. Plant Interact.* 3, 189–198. doi: 10.1080/17429140701823164

Anjum, N. A., Umar, S., Ahmad, A., Iqbal, M., and Khan, N. A. (2008). Sulphur protects mustard (*Brassica campestris L.*) from cadmium toxicity by improving leaf ascorbate and glutathione. *Plant Growth Regul.* 54, 271–279.

Arnon, D. T. (1949). Copper enzyme in isolated chloroplasts polyphenoloxidase in Beta vulgaris. *Plant Physiol.* 24, 1–15. doi: 10.1104/pp.24.1.1

Asgher, M., Khan, M. I. R., Anjum, N. A., and Khan, N. A. (2014). Minimising toxicity of cadmium in plants—role of plant growth regulators. *Protoplasma* 252, 399–413. doi: 10.1007/s00709-014-0710-4

Ashraf, U., Hussain, S., Anjum, S. A., Abbas, F., Tanveer, M., Noor, M. A., et al. (2017). Alterations in growth, oxidative damage, and metal uptake of five aromatic rice cultivars under lead toxicity. *Plant Physiol. Biochem.* 115, 461–471. doi: 10.1016/j.plaphy.2017.04.019

Ashraf, U., Kanu, A. S., Mo, Z., Hussain, S., Anjum, S. A., Khan, I., et al. (2015). Lead toxicity in rice: effects, mechanisms, and mitigation strategies-a mini review. *Environ. Sci. Pollut. Res.* 22, 18318–18332. doi: 10.1007/s11356-015-5463-x

Ashraf, U., and Tang, X. (2017). Yield and quality responses, plant metabolism and metal distribution pattern in aromatic rice under lead (Pb) toxicity. *Chemosphere* 176, 141–155. doi: 10.1016/j.chemosphere.2017.02.103

Bates, L. S., Waldren, R. P., and Teare, I. D. (1973). Rapid determination of free proline for water-stress studies. *Plant Soil* 39, 205–207. doi: 10.1007/BF00018060

Bradford, M. N. (1976). A rapid and sensitive method for the quantitation of microgram quantities of protein utilizing the principle of protein-dye binding. *Anal. Chem.* 72, 248–254. doi: 10.1016/0003-2697(76)90527-3

Bryant, R. J., and McClung, A. M. (2010). Volatile profiles of aromatic and non-aromatic rice cultivars using SPME/GCMS. *Food Chem.* 124, 501–513. doi: 10.1016/j.foodchem.2010.06.061

Cai, Y., Lin, L., Cheng, W., Zhang, G., and Wu, F. (2010). Genotypic dependent effect of exogenous glutathione on Cd-induced changes in cadmium and mineral uptake and accumulation in rice seedlings (*Oryza sativa*). *Plant Soil Environ.* 56, 524–533. doi: 10.17221/107/2010-PSE

Campos, M. L., Kang, J. H., and Howe, G. A. (2014). Jasmonate-triggered plant immunity. *J. Chem. Ecol.* 40, 657–675. doi: 10.1007/s10886-014-0468-3

Cao, F., Wang, R., Cheng, W., Zeng, F., Ahmed, I. M., Hu, X., et al. (2014). Genotypic and environmental variation in cadmium, chromium, lead and copper in rice and approaches for reducing the accumulation. *Sci. Total Environ.* 496, 275–281. doi: 10.1016/j.scitotenv.2014.07.064

Chen, J., Yan, Z., and Li, X. (2014). Effect of methyl jasmonate on cadmium uptake and antioxidative capacity in Kandeliaobovata seedlings under cadmium stress. *Ecotoxicol. Environ. Saf.* 104, 349–356. doi: 10.1016/j.ecoenv.2014.01.022

Doganlar, O., Doganlar, Z. B., Muranlı, F. D. G., and Guner, U. (2016). Genotoxic effect and carcinogenic potential of a mixture of as and cd in zebrafish at permissible maximum contamination levels for drinking water. *Water Air Soil Pollut.* 227, 1–16.

Du, Y., Hu, X. F., Wu, X. H., Shu, Y., Jiang, Y., and Yan, X. J. (2013). Affects of mining activities on Cd pollution to the paddy soils and rice grain in Hunan province, Central South China. *Environ. Monit. Assess.* 185, 9843–9856. doi: 10.1007/s10661-013-3296-y

Farooq, H., Asghar, H. N., Khan, M. Y., Saleem, M., and Zahir, Z. A. (2015). Auxin mediated growth of rice in cadmium contaminated soil. *Turk J. Agric. For.* 39, 272–276. doi: 10.3906/tar-1405-54

Farooq, M. U., Ishaaq, I., Barutcular, C., Skalicky, M., Maqbool, R., Rastogi, A., et al. (2022). Mitigation effects of selenium on accumulation of cadmium and morpho-physiological properties in rice varieties. *Plant Physiol. Biochem.* 170, 1–13. doi: 10.1016/j.plaphy.2021.11.035

Fujimaki, S., Suzui, N., Ishioka, N. S., Kawachi, N., Ito, S., Chino, M., et al. (2010). Tracing cadmium from culture to spikelet: noninvasive imaging and quantitative characterization of absorption, transport, and accumulation of cadmium in an intact rice plant. *Plant Physiol* 152, 1796–1806. doi: 10.1104/pp.109.151035

Gill, N. A., Anjum, M., Hasanuzzaman, R., Gill, D. K., Trivedi, I., Ahmad, E., et al. (2013). Glutathione and glutathione reductase: a boon in disguise for plant abiotic stress defense operations. *Plant Physiol. Biochem.* 70, 204–212. doi: 10.1016/j.plaphy.2013.05.032

Gómez, S., Ferrieri, R. A., Schueller, M., and Orians, C. M. (2010). Methyl jasmonate elicits rapid changes in carbon and nitrogen dynamics in tomato. *New Phytol.* 188, 835–844.

Hodges, D. M., DeLong, J. M., Forney, C. F., and Prange, R. K. (1999). Improving the thiobarbituric acid-reactive-substances assay for estimating lipid peroxidation in plant tissues containing anthocyanin and other interfering compounds. *Planta* 207, 604–611. doi: 10.1007/s004250050524

Huang, X. D., El-Alawi, Y., Penrose, D. M., Glick, B. R., and Greenberg, B. M. (2004). A multi-process phytoremediation system for removal of polycyclic aromatic hydrocarbons from contaminated soils. *Environ. Pollut.* 130, 465–476.

Huang, J., and Hartemink, A. E. (2020). Soil and environmental issues in sandy soils. *Earth-Sci. Rev.* 208:103295.

Huang, J., Wang, C., Qi, L., Zhang, X., Tang, G., Li, L., et al. (2020). Phosphorus is more effective than nitrogen in restoring plant communities of heavy metals polluted soils. *Environ. Pollut.* 266:115259. doi: 10.1016/j.envpol.2020.115259

Huang, S., Rao, G., Ashraf, U., He, L., Zhang, Z., Zhang, H., et al. (2020). Application of inorganic passivators reduced Cd contents in brown rice in oilseed rape-rice rotation under Cd contaminated soil. *Chemosphere* 259:127404. doi: 10.1016/j.chemosphere.2020.127404

Ji, G. L., Wang, J. H., and Zhang, X. N. (2000). "Environmental problems in soil and groundwater induced by acid rain and management strategies in China," in *Soils and Groundwater Pollution and Remediation: Asia, Africa and Oceania*, eds P. M. Huang and I. K. Iskandar (London: CRC Press), 201–224.

Kanu, A. S., Ashraf, U., Mo, Z., Baggie, I., Charley, C. S. K., and Tang, X. (2019). Calcium amendment improved the performance of fragrant rice and reduced metal uptake under cadmium toxicity. *Environ. Sci. Pollut. Res.* 26, 24748–24757. doi: 10.1007/s11356-019-05779-7

Kanu, A. S., Ashraf, U., Mo, Z., Fuseini, I., Mansaray, L. R., Duan, M., et al. (2017a). Cadmium uptake and distribution in fragrant rice genotypes and related consequences on yield and grain quality traits. *J. Chem.* 2017:1405878. doi: 10.1155/2017/1405878

Kanu, A. S., Ashraf, U., Bangura, A., Yang, D. M., Ngaujah, A. S., and Tang, X. (2017b). Cadmium (Cd) stress in rice; phyto-availability, toxic effects, and mitigation measures-a critical review. *IOSR-JESTFT* 11, 7–23. doi: 10.9790/2402-1112010723

Kaya, A., and Doganlar, Z. B. (2016). Exogenous jasmonic acid induces stress tolerance in tobacco (*Nicotiana tabacum*) exposed to imazapic. *Ecotoxicol. Environ. Saf.* 124, 470–479. doi: 10.1016/j.ecoenv.2015.11.026

Keramat, B., Kalantari, K. M., and Arvin, M. J. (2009). Effects of methyl jasmonate in regulating cadmium induced oxidative stress in soybean plant (*Glycine max* L.). *Afr. J. Microbiol. Res.* 3, 240–244.

Kim, H. S., Lee, H. J., Jung, W. Y., Weon, J. I., Shin, D. Y., Jang, Y., et al. (2021). Integrative comparison of cadmium and iron oxide as yellow pigment in terms of cellular stress and genotoxicity in vitro and in vivo. *Mol. Cell. Toxicol.* 17, 99–109.

Kobayashi, N. I., Tanoi, K., Hirose, A., and Nakanishi, T. M. (2013). Characterization of rapid intervascular transport of cadmium in rice stem by radioisotope imaging. *J. Exp. Bot.* 64, 507–517. doi: 10.1093/jxb/ers344

Kováčik, J., Klejdus, B., Štork, F., Hedbavny, J., and Baèkor, M. (2011). Comparison of methyl jasmonate and cadmium effect on selected physiological parameters in *Scenedesmus quadricauda* (Chlorophyta, Chlorophyceae). *J. Phycol.* 47, 1044–1049. doi: 10.1111/j.1529-8817.2011.01027.x

Lück, H. (1965). "Catalase," in *Methods of Enzymatic Analysis*, ed. H. U. Bergmeyer (London: Academic press), 885–894.

Majumdar, S., Sachdev, S., and Kundu, R. (2020). Salicylic acid mediated reduction in grain cadmium accumulation and amelioration of toxicity in *Oryza sativa* L. cv Bandana. *Ecotoxicol. Environ. Saf.* 205:111167. doi: 10.1016/j.ecoenv.2020.111167

Nazar, R., Iqbal, N., Masood, A., Khan, M. I. R., Syeed, S., and Khan, N. A. (2012). Cadmium toxicity in plants and role of mineral nutrients in its alleviation. *Am. J. Plant Sci.* 03, 1476–1489.

Per, T. S., Khan, N. A., Masood, A., and Fatma, M. (2016). Methyl jasmonate alleviates cadmium-induced photosynthetic damages through increased S-assimilation and glutathione production in mustard. *Front. Plant Sci.* 7:1933. doi: 10.3389/fpls.2016.01933

Pinto, E., and Ferreira, I. M. (2015). Cation transporters/channels in plants: tools for nutrient biofortification. *J. Plant Physiol.* 179, 64–82. doi: 10.1016/j.jplph.2015.02.010

Quddus, A., Yimer, N., Basit, M. A., Khan, S., and Amir, M. (2021). Review of antioxidant-rich natural dietary products as protective and therapeutic factors

against cadmium toxicity in living organisms. *Pertanika J. Trop. Agric. Sci.* 44, 83–105.

Rao, G., Huang, S., Ashraf, U., Mo, Z., Duan, M., Pan, S., et al. (2019). Ultrasonic seed treatment improved cadmium (Cd) tolerance in *Brassica napus* L. *Ecotoxicol. Environ. Saf.* 185:109659. doi: 10.1016/j.ecoenv.2019.109659

Sarwar, N., Saifullah, M. S. S., Zia, M. H., Naeem, A., Bibi, S., and Farid, G. (2010). Role of mineral nutrition in minimizing cadmium accumulation by plants. *J. Sci. Food Agric.* 90, 925–937. doi: 10.1002/jsfa.3916

Shah, K., and Nongkynrih, J. M. (2007). Metal hyperaccumulation and bioremediation. *Biologiaplantarum* 51, 618–634. doi: 10.1007/s10535-007-0134-5

Srivastava, R. K., Pandey, P., Rajpoot, R., Rani, A., and Dubey, R. S. (2014). Cadmium and lead interactive e?ects on oxidative stress and antioxidative responses in rice seedlings. *Protoplasma* 251, 1047–1065. doi: 10.1007/s00709-014-0614-3

Tan, F. H., and Barrington, S. (2005). Zinc and copper uptake by plants under two transpirationrates. Part 1. Wheat (*Triticum aestivum* L). *Environ. Pollut.* 138, 538–547. doi: 10.1016/j.envpol.2004.06.005

Velikova, V., Yordanov, I., and Edreva, A. (2000). Oxidative stress and some antioxidant systems in acid rain-treated bean plants: protective role of exogenous polyamines. *Plant Sci.* 151, 59–66.

Verma, G., Srivastava, D., Narayan, S., Shirke, P. A., and Chakrabarty, D. (2020). Exogenous application of methyl jasmonate alleviates arsenic toxicity by modulating its uptake and translocation in rice (*Oryza sativa* L.). *Ecotoxicol. Environ. Saf.* 201:110735. doi: 10.1016/j.ecoenv.2020.110735

Wasternack, C., and Hause, B. (2013). Jasmonates: biosynthesis, perception, signal transduction and action in plant stress response, growth and development. an update to the 2007 review in Annals of Botany. *Ann. Bot.-Lond.* 111, 1021–1058. doi: 10.1093/aob/mct067

Welch, R. M., and Graham, R. D. (2002). Breeding crops for enhanced micronutrient content. *Plant Soil* 245, 205–214. doi: 10.1023/A:1020668100330

White, P. J., and Broadley, M. R. (2005). Biofortifying crops with essential mineral elements. *Trends Plant Sci.* 10, 586–593. doi: 10.1016/j.tplants.2005.10.001

Yan, Y. F., Choi, D. H., Kim, D. S., and Lee, B. W. (2010). Genotypic variation of cadmium accumulation and distribution in rice. *J. Crop. Sci. Biotechnol.* 13, 69–73. doi: 10.1007/s12892-010-0036-5

Yan, Z., Chen, J., and Li, X. (2013). Methyl jasmonate as modulator of Cd toxicity in *Capsicum frutescens* var. fasciculatum seedlings. *Ecotoxicol. Environ. Saf.* 98, 203–209. doi: 10.1016/j.ecoenv.2013.08.019

Yan, Z., Zhang, W., Chen, J., and Li, X. (2015). Methyl jasmonate alleviates cadmium toxicity in *Solanum nigrum* by regulating metal uptake and antioxidative capacity. *Biol. Plant* 59, 373–381. doi: 10.1007/s10535-015-0491-4

Zaid, A., Bhat, J. A., Wani, S. H., and Masoodi, K. Z. (2019). Role of nitrogen and sulfur in mitigating cadmium induced metabolism alterations in plants. *J. Plant Sci. Res.* 35, 121–141.

Zaid, A., and Mohammad, F. (2018). Methyl jasmonate and nitrogen interact to alleviate cadmium stress in *Mentha arvensis* by regulating physio-biochemical damages and ROS detoxification. *J. Plant Growth Regul.* 37, 1331–1348. doi: 10.1007/s00344-018-9854-3

Zaid, A., Mohammad, F., and Fariduddin, Q. (2020). Plant growth regulators improve growth, photosynthesis, mineral nutrient and antioxidant system under cadmium stress in menthol mint (*Mentha arvensis* L.). *Physiol. Mol. Biol. Plants* 26, 25–39. doi: 10.1007/s12298-019-00715-y

Zhang, J. B., and Huang, W. N. (2000). Advances on physiological and ecological effects of cadmium on plants. *Chin. J. Acta Ecol. Sin.* 20, 514–523.

Zhang, W. F., Zhang, F., Raziuddin, R., Gong, H. J., Yang, Z. M., Lu, L., et al. (2008). E?ects of 5-aminolevulinic acid on oilseed rape seedling growth under herbicide toxicity stress. *J. Plant Growth Regul.* 27, 159–169. doi: 10.1007/s00344-008-9042-y

Conflict of Interest: AK and LM were employed by Agro-Geo Services (SL) Limited.

The remaining authors declare that the research was conducted in the absence of any commercial or financial relationships that could be construed as a potential conflict of interest.

Publisher's Note: All claims expressed in this article are solely those of the authors and do not necessarily represent those of their affiliated organizations, or those of the publisher, the editors and the reviewers. Any product that may be evaluated in this article, or claim that may be made by its manufacturer, is not guaranteed or endorsed by the publisher.

Copyright © 2022 Kanu, Ashraf, Mansaray, Abbas, Fiaz, Amanullah, Charley and Tang. This is an open-access article distributed under the terms of the Creative Commons Attribution License (CC BY). The use, distribution or reproduction in other forums is permitted, provided the original author(s) and the copyright owner(s) are credited and that the original publication in this journal is cited, in accordance with accepted academic practice. No use, distribution or reproduction is permitted which does not comply with these terms.

frontiers | Frontiers in Plant Science

ORIGINAL RESEARCH
published: 27 April 2022
doi: 10.3389/fpls.2022.855900

Melatonin Rescues Photosynthesis and Triggers Antioxidant Defense Response in *Cucumis sativus* Plants Challenged by Low Temperature and High Humidity

*Bakht Amin[1], Muhammad Jawaad Atif[1,2], Huanwen Meng[1], Muhammad Ali[1], Shuju Li[3], Hesham F. Alharby[4,5], Ali Majrashi[6], Khalid Rehman Hakeem[4,5,7] and Zhihui Cheng[1]**

[1] College of Horticulture, Northwest A&F University, Yangling, China, [2] Horticultural Research Institute, National Agricultural Research Centre, Islamabad, Pakistan, [3] Tianjin Kerun Cucumber Research Institute, Tianjin, China, [4] Department of Biological Sciences, Faculty of Science, King Abdulaziz University, Jeddah, Saudi Arabia, [5] Princess Dr. Najla Bint Saud Al-Saud Center for Excellence Research in Biotechnology, King Abdulaziz University, Jeddah, Saudi Arabia, [6] Department of Biology, College of Science, Taif University, Taif, Saudi Arabia, [7] Department of Public Health, Daffodil International University, Dhaka, Bangladesh

OPEN ACCESS

Edited by:
Shabir Hussain Wani, Sher-e-Kashmir University of Agricultural Sciences and Technology, India

Reviewed by:
Noushina Iqbal, Jamia Hamdard University, India
Muhammad Ali, Zhejiang University, China

***Correspondence:**
Zhihui Cheng
chengzh@nwafu.edu.cn

Specialty section:
This article was submitted to Plant Breeding, a section of the journal Frontiers in Plant Science

Received: *16 January 2022*
Accepted: *28 February 2022*
Published: *27 April 2022*

Citation:
Amin B, Atif MJ, Meng H, Ali M, Li S, Alharby HF, Majrashi A, Hakeem KR and Cheng Z (2022) Melatonin Rescues Photosynthesis and Triggers Antioxidant Defense Response in Cucumis sativus Plants Challenged by Low Temperature and High Humidity. Front. Plant Sci. 13:855900. doi: 10.3389/fpls.2022.855900

Environmental factors such as low temperature (LT) and high humidity (HH) hinder plant growth and development in plastic tunnels and solar greenhouses in the cold season. In this study, we examined the effect of melatonin (MT) on shoot-based tolerance to LT and HH conditions in cucumber (*Cucumis sativus*) seedlings and explored its underlying mechanism. LT and HH stress inhibited growth and biomass accumulation, produced leaf chlorosis, led to oxidative stress, lowered chlorophyll and carotenoid contents, reduced photosynthetic and photosystem II (PSII) activities, and increased the level of intercellular carbon dioxide and the non-photochemical quenching of photosystem I (PSI) and PSII. However, foliar application of MT significantly improved the morphological indices and photosynthetic efficiency of cucumber seedlings, which entailed the elevation of electrolyte leakage, lipid peroxidation, and reactive oxygen species accumulation by boosting the antioxidant enzyme defense system under LT and HH conditions. Additionally, the measurement of nitrogen (N), magnesium (Mg), and iron (Fe) contents in roots and leaves showed that MT significantly augmented the nutrient uptake of cucumber seedlings exposed to LT and HH stresses. Furthermore, MT application increased the transcripts levels of genes encoding antioxidant enzymes under LT and HH conditions, whereas treatment with LT and HH suppressed these genes, suggesting that MT application increases the LT and HH tolerance of cucumber seedlings. Overall, our results suggest that MT application increases the tolerance

of cucumber seedlings to LT and HH stress by enhancing the plant morphometric parameters, regulating PSI and PSII, and activating the antioxidant defense mechanism. Thus, the exogenous application of MT could be potentially employed as a strategy to improve the LT and HH tolerance of cucumber.

Keywords: antioxidant enzyme, cucumber, high-humidity, low-temperature, melatonin

INTRODUCTION

The growth and productivity of plants are negatively impacted by numerous abiotic stresses, which occur throughout the plant life cycle in the natural environment. Tropical plants are susceptible to environmental factors such as low temperature (LT) (Zhao et al., 2017) and high humidity (HH) (Han et al., 2019), which hamper plant growth and impose physiological stress. Any compromise of plant growth parameters can eventually lead to food scarcity, as has been observed recently in many plant species in response to global climatic changes (Han et al., 2019; Zhang et al., 2021). Weather-related changes and frequent fluctuations in temperature have been shown to affect the growth, development, and biochemical and physiological attributes of crop plants (Sakina et al., 2019).

Photosynthesis is the main physiological process affected by chilling stress. Physiological changes observed in plants under cold conditions are mainly the result of a disturbance in biochemical reactions operating in the photosynthetic machinery, which eventually impedes plant growth. Cold stress leads to growth modifications that limit energy usage and inhibit photosynthesis (Ruelland and Zachowski, 2010). Previous studies reported that an increase in temperature and humidity impairs photosynthesis by reducing turgor and limiting carbon dioxide (CO_2) availability because of stomatal closure and damage to photosystem I (PSI) and photosystem II (PSII) components (Yang et al., 2012; Han et al., 2019). Stressed plants have been shown to accumulate reactive oxygen species (ROS) such as hydrogen peroxide (H_2O_2) and superoxide anion (O_2^-) in the cellular and subcellular compartments, which damages cells, leading to programmed cell death (PCD) and a reduction in plant growth and development (Marta et al., 2016; Raja et al., 2017). To escape the detrimental effects of oxidative stress caused by unfavorable abiotic conditions, plants have evolved several mechanisms, one of which involves an increase in the endogenous levels of antioxidant enzymes such as superoxide dismutase (SOD), catalase (CAT), peroxidase (POD), ascorbate POD (APX), glutathione reductase (GR), monodehydroascorbate reductase (MDHAR), and dehydroascorbate reductase (DHAR) (Gupta et al., 2016; Mehla et al., 2017; Hasanuzzaman et al., 2020).

Numerous studies have shown that low temperature (LT) stress impairs plant nutrient uptake and accumulation, photosynthesis, and the antioxidant defense system (Anwar et al., 2018; Ciura and Kruk, 2018). The most innovative strategy for protecting plants against individual and concurrent abiotic stresses is to use plant bio stimulators or hormones that can help the plant to adapt to and evade the stress (Eremina et al., 2016; Li et al., 2016). Plants detect cooling signals *via* hormones, which cause biochemical and physiological changes. Melatonin (MT) (N-acetyl-5-methoxytryptamine) is a recent addition to the list of phytohormones in angiosperms. MT is a small molecule first discovered in the bovine pineal gland (Lerner et al., 1958). This discovery led to the investigation of the impacts of MT on animal biology, including physiological processes such as circadian rhythm, sleep, body temperature, physical activity, retinal physiology, sexual activity, seasonal reproduction, and the immune system (Zhang et al., 2021). Recently, Erdal (2019) revealed that MT plays a critical role in plants as well. MT has been found to stimulate vegetative growth in plants by promoting the formation of lateral roots and increasing the shoot length and leaf area. MT has also been reported to function as a signaling molecule that protects plants from adverse environmental conditions (Shi et al., 2015; Li et al., 2016; Arora and Bhatla, 2017). Lei and colleagues used MT in carrot suspension cells to reverse the damage caused by freezing stress (Lei et al., 2004). Furthermore, MT has been found to enhance cucumber (*Cucumis sativus* L.) seed germination by preventing the peroxidation of membrane lipids during cold stress (Posmyk et al., 2009). Zhao et al. (2016) and Anwar et al. (2018) found that MT and 5-aminolevulinic acid (ALA) improve antioxidant defense, regulate photosynthesis and nutrient uptake, and accelerate ROS scavenging in cucumber plants exposed to cold stress. Although cucumber is an all-season salad crop with huge commercial importance, the impact of LT and high humidity (HH) stress on this important plant species has not been carried out in a systematic way.

Cucumber (Cucurbitaceae) is a well-known vegetable crop grown all over the world. Today, cucumber is cultivated commercially in all seasons in fields and nurseries in different agroclimatic zones throughout the year. Cucumber plants require adequate water and moderate temperature for proper growth. Although many new cucumber cultivars have been developed for different seasons, LT has a negative impact on the growth and productivity of all cultivars (Lee et al., 2002). A previous study demonstrated that cold stress causes physiological injury to cucumber seedlings, particularly when grown in plastic tunnels and under greenhouse conditions during the winter season. Cucumber plants grown under such conditions produce small fruits with low yields (Cabrera and Saltveit, 1990). Although it has been demonstrated that MT is critical for antioxidant defense and photosynthesis in cucumber seedlings exposed to LT, the optimal dose of MT and its impact on LT and HH tolerance have not been thoroughly investigated. In this study, we investigated the impact of exogenous MT application on the morphophysiological characteristics of cucumber plants and on the antioxidant defense mechanisms under LT and HH stress. We observed that MT could improve LT and HH tolerance, and found that MT applied at a concentration of 200 μm was the most effective. To the

best of our knowledge, this is the first report on the effect of MT on the LT and HH tolerance of cucumber plants and the underlying mechanisms.

MATERIALS AND METHODS

Plant Materials and Growth Conditions

Cucumber (*Cucumis sativus* L.) cultivar Zhongnong 37 was used in this study, in the controlled growth chamber at College of Horticulture Northwest A&F University, China. The seeds were soaked first in hot water at 55°C for 15 min and then in room-temperature water for 6–8 h, before being placed in an incubator at 25 ± 1°C for sprouting. Following germination on moist filter paper in Petri dishes, the sprouted seeds were shifted to a 32-hole plug tray filled with nutrient medium, and incubated under controlled conditions: 25°C/18°C day/night temperature, 80% relative humidity, 12-h light/12-h dark photoperiod, and 2,000 Lx photosynthetically active radiation. The seedlings were routinely managed. When the cotyledons were fully opened, uniform-sized seedlings were transferred to plastic pots. Cucumber seedlings at the fully developed 2-leaf stage were divided into two groups; 50% of the seedlings were sprayed with 200 μm MT once a day at 8 p.m. for 5 days, and the remaining 50% were sprayed with distilled water at the same frequency. The optimum concentration of MT was selected based on a preliminary experiment (unpublished data). Both the water and MT treated groups were divided into two sets. One set of plants was placed in a growth chamber under LT and HH (LTHH) stress conditions (15/10°C day/night temperature and 95% humidity), whereas the other set was placed under control conditions (25/18°C day/night temperature and 80% humidity). The experiment was repeated three times (n = 3), and each replication comprised 20 plants. Thus, four treatments were conducted overall: (i) Control, seedlings incubated under control conditions; (ii) Control + MT, seedlings subjected to control conditions and then sprayed with MT; (iii) LTHH, seedlings subjected to LT and HH; (iv) LTHH + MT, seedlings subjected to LT and HH conditions and then sprayed with MT.

Sampling

The morphological parameters of cucumber seedlings were measured 6 days after treatment (DAT). Leaves were sampled at 0, 2, 4, and 6 DAT to monitor dynamic changes. Photosynthetic parameters were evaluated in intact leaves.

Morphometric Studies

The plant height and root length were measured using a scale, while the shoot fresh weight (FW), shoot dry weight (DW), and total DW were determined using a digital balance (Mettler Toledo, model PL303, United States). The strong seedling index (SSI) was calculated by the following equation:

$$Strong\ Seedling\ Index = \left(\frac{Stem\ diameter}{Plant\ height} + \frac{Root\ DW}{Shoot\ DW}\right) \times Total\ DW$$

Leaf Photosynthetic Gas Exchange Parameters

Gas exchange parameters including, photosynthesis (pn), stomatal conductance (Gs), intercellular CO_2 concentration (Ci), and transpiration rate (E) were measured using a portable photosynthesis system (LI-COR 6800XT, Lincoln, NE, United States). To measure these parameters, seedlings of the same size and with intact leaves were chosen from each treatment and maintained under control conditions for 1 h (from 11 a.m. to 12 p.m.) (Anwar et al., 2018).

Chlorophyll Fluorescence Parameters

The chlorophyll fluorescence indices were measured using multispectral fluorescence imaging technology (FC800 FluorCam, PSI Czech). To measure the maximum quantum yield (F_v/F_m), non-photochemical quenching (NPQ), photochemical quenching (qP), and electron transport rate (ETR), plants were dark-adapted for 30 min post-treatment. Maximum fluorescence was recorded using a 0.8-s pulsed light at 4,000 μmol s^{-1} m^{-2}. F_v/F_m was determined for each plant using a whole leaf as the area of interest (Zhang et al., 2020).

Preparation of Enzyme Extract

Leaf samples (0.5 g FW) were homogenized at 4°C in 5 ml of pre-cooled 50 mm potassium phosphate buffer (pH 7.8) containing 0.2 mM EDTA-Na_2, and 1% (w/w) insoluble polyvinylpyrrolidone (PVP). The homogenate was centrifuged at 15,000 × g for 20 min at 4°C, and the supernatant was used for measuring antioxidant enzyme activity and malondialdehyde (MDA) content.

Antioxidant Enzyme Activity Assay

To conduct antioxidant enzyme activity assays, samples were prepared as described previously (Amin et al., 2021). To measure the SOD (EC 1.15.1.1) activity, nitro blue tetrazolium (NBT) was added to the enzyme extract and exposed to fluorescent light for 20 min, after 20 min, the absorbance of the reaction mixture was measured using a spectrophotometer at 560 nm (Stewart and Bewley, 1980). The activity of POD (EC 1.11.1.7) was measured as described previously (Polle et al., 1994). Briefly, a 20-μl aliquot of the enzyme extract was mixed with 3 ml of the POD reaction mixture (0.1 mm phosphate buffer [pH 6.0], 16 mm guaiacol, and 19 μl of 10% (w/v) H_2O_2), and POD activity was recorded at 30-s intervals for 3 min at a wavelength of 470 nm. The activity of CAT (EC 1.11.1.6) was measured *via* H_2O_2 reduction, as described previously (Chance and Maehly, 1955). Briefly, a 50-μl aliquot of enzyme extract was mixed with 2.5 ml of the reaction mixture [0.1 mM phosphate buffer (pH 7.0) and 0.1 mm H_2O_2], and absorbance was measured at 240 nm. The activity of APX was determined by adding 0.2 ml of enzyme extract to the reaction buffer containing 50 mm phosphate buffer (pH 7.0), 0.1 mm EDTA, 0.5 mm AsA, and 1.0 mm H_2O_2, followed by measuring the absorbance with a spectrophotometer at 290 nm (Nakano and Asada, 1981). GR activity was measured according to the method of Rao et al. (1996). Briefly, 1 ml of reaction buffer (100 mM phosphate buffer, 0.5 mM GSSG, 2 mm EDTA, and

0.2 mM nicotinamide adenine dinucleotide phosphate (NADPH) was added to 0.25 ml of enzyme extract, shaken thoroughly, and incubated at 100°C for 10 min. Activities of MDHAR and DHAR were assayed using the protocol of Ma and Cheng (2004). To assay the MDHAR activity, the reaction buffer containing 925 μl of 50 mm 1-piperazineethanesulfonic acid (HEPES) phosphate buffer (pH 7.6), 10 μl of 25 mm NADPH, and 10 μl of 250 mM AsA was mixed with 1 ml of enzyme solution, and absorbance was noted at 340 nm. To determine DHAR activity, 20 μl of enzyme extract was added to a mixture containing 50 μl of 4 mm DHA and 25 μl of 100 mm GSH. Then, 905 μl of 0.1 M phosphate buffer (pH 7) was added to the reaction mixture, and absorbance was recorded at 265 nm.

Determination of Chlorophyll and Carotenoid Content

According to Shah et al. (2019) leaf pigments were estimated by acetone under dim light. A 0.25 g leaf sample was ground by using TissueLyzer, then added 5 ml of 80% acetone before centrifugation at 10,000 × *g* for 5 min. After centrifugation, the supernatant was collected, and the absorbance for chlorophyll and carotenoid contents were noted at 663.6 and 646.6 nm wavelength, respectively.

Determination of Malondialdehyde Content and Electrolyte Leakage

The MDA content was measured as described previously (Tiwari et al., 2010). Briefly, 2 ml of thiobarbituric acid (TBA) and 1 ml of enzyme extract were mixed with 5% TCA (v/v), and the mixture was heated in a water bath for 15 min. Subsequently, the reaction mixture was incubated at room temperature for a while, and absorbance was measured through a spectrophotometer at 450, 532, and 600 nm. A standard curve was used to calculate the MDA content.

To detect electrolyte leakage (EL), 20 leaf discs were immersed in test tubes containing deionized water. Electrical conductivity (EC) was measured before and after heating the samples in a water bath at 50°C for 25 min. Then, the tubes were heated again at 100°C for 10 min, and electrolyte leakage (%) was used determined using the following equation (Jan et al., 2018):

$$Electrolyte\ leakage\ =\ \frac{EC_b - EC_a}{EC_c}\ \times\ 100$$

where EC_a, EC_b, and EC_c represent the EC of samples before heating, heated at 25°C, and heated at 100°C, respectively.

Measurement of O_2^- and H_2O_2 Contents

The contents of O_2^- and H_2O_2 were measured as described previously (Zhang et al., 2010). To determine the O_2- concentration, a 0.2-g sample was ground in phosphate buffer (pH 7.8) and centrifuged at 10,000 × *g* for 10 min. The reaction mixture contained 75 μl phosphate buffer (pH 7.8), and 25 μl 10 mm was mixed with the upper phase, and incubated for 20 min. Subsequently, 100 μl of the supernatant was mixed with 1 ml of 7 mm α-naphthalene diamine hydrochloride, 1 ml of 17 mM sulphanilamide (in 30% acetic acid), and 3 ml of ether, and centrifuged at 5,000 × *g* for 10 min. After centrifugation, the absorbance of each sample was measured at 240 nm, and the O_2^- content was calculated using a standard curve.

To determine the H_2O_2 content, a 0.5-g sample was ground in 5 ml of acetone, and the sample was centrifuged at 5,000 × *g* for 5 min at 4°C. Then, 200 μl of ammonia solution and 100 μl of titanium tetrachloride were added to 1 ml of supernatant. The mixture was centrifuged at 12,000 × *g* for 10 min, and absorbance was measured at 410 nm.

Determination of Nutrient Contents

The leaves and roots of the cucumber seedlings were separately dried at 65°C for 2 days and then milled into powder using a TissueLyser. A microwave digestion system (MARS6; CEM, United States) was used to digest 0.1–0.2 g of the powdered tissue with 4 ml of nitric acid and 1 ml of H_2O_2. The digested sample was filtered through a 0.45-μm Millipore filter, and stored in plastic vials for further analysis. An Induced Couple Plasma Mass Spectrometer (ICP-MS, NexION 300X; PerkinElmer: NexION 300X, NY, United States) was used to determine the iron (Fe) and magnesium (Mg) contents (Anwar et al., 2018). The total nitrogen (N) content of the root and leaf tissues was measured using the Kjeldahl method.

RNA Extraction and Gene Expression Analysis

Total RNA was extracted from cucumber leaf samples using an RNA Isolation Kit (Omega Bio-Tek, Doraville, GA, United States) according to the manufacturer's instructions. The quality of the RNA samples was assessed using a NanoDrop spectrometer:

TABLE 1 | Effect of melatonin on cucumber seedling morphology under low-temperature and high-humidity

Treatment	Plant height (cm)	Shoot fresh weight (g plant^{-1})	Shoot dry weight (g plant^{-1})	Root length (cm)	SSI	Total dry weight (g plant^{-1})
Control	6.80 ± 0.2a	10.93 ± 0.04a	0.86 ± 0.07b	26.66 ± 1.52a	0.83 ± 0.02a	1.02 ± 0.05a
Control + MT	6.93 ± 0.15a	11.56 ± 0.75a	0.89 ± 0.09a	26.66 ± 2.51a	0.83 ± 0.02a	1.05 ± 0.07b
LTHH	5.30 ± 0.10c	8.32 ± 0.04c	0.65 ± 0.04d	17.33 ± 0.57c	0.62 ± 0.01c	0.73 ± 0.04d
LTHH + MT	6.03 ± 0.15b	9.71 ± 0.32b	0.72 ± 0.09c	21.33 ± 1.57b	0.69 ± 0.02b	0.81 ± 0.06c

Control (25/18°C); Control + MT (200 μM melatonin, 25/18°C); LTHH (15/10°C, 95%); LTHH + MT (200 μM melatonin, 15/10°C, 95%). SSI (strong seedling index). Same letters represent no significant differences, while different letters represent significant differences among treatments (P > 0.05 was non-significant). Data are means ± SD of three replicates.

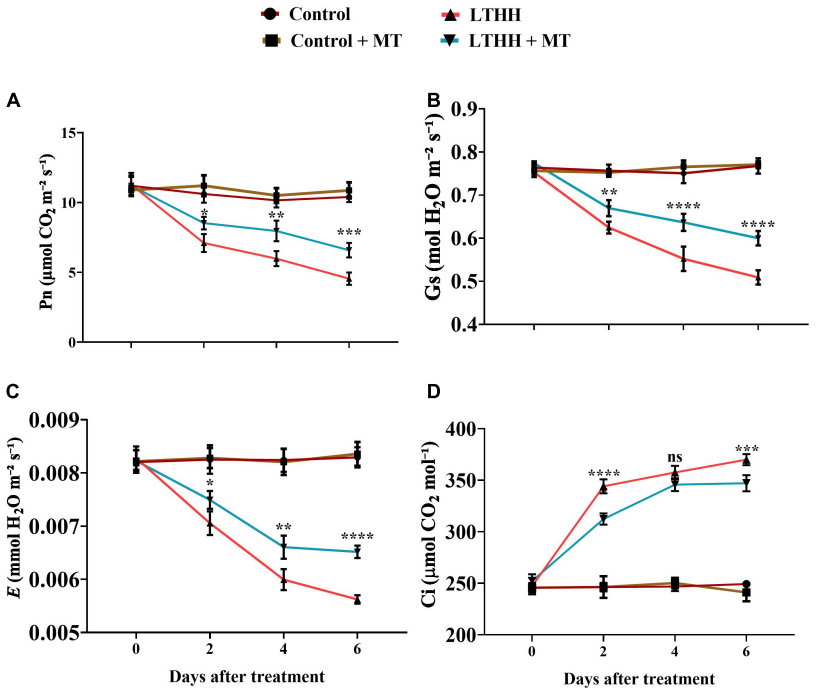


FIGURE 1 | Effect of exogenous melatonin on net photosynthesis **(A)**, stomatal conductance **(B)**, transpiration rate **(C)**, and intercellular concentration of carbon dioxide rate **(D)** of cucumber seedling under low-temperature and high-humidity stress. Control (25/18°C); Control + MT (200 μM melatonin, 25/18°C); LTHH (15/10°C, 95%); LTHH + MT (200 μM melatonin, 15/10°C, 95%). Results were presented as means ± SD (n = 3), significance values were presented as: *P < 0.05; **P < 0.01; ***P < 0.001; ****P < 0.0001; while non-significant (ns) (P > 0.05).

(1000 spectrophotometer NanoDrop Technologies, Wilmington, DE, United States). First-strand complementary DNA (cDNA) was synthesized from 1 μg total RNA using a PrimeScript RT Reagent Kit with a gDNA Eraser (Takara Bio, Shiga, Japan). The resulting cDNA was quantified and diluted to 200 μg. To analyze gene expression, primers were designed using Primer3web (version 4.1) (**Supplementary Table 1**), and real-time quantitative PCR (RT-qPCR) was performed on the Bio-Rad CFX 134 Connect Real-Time PCR Detection System using a SYBR Green qPCR Kit: TaKaRa, United States. A cucumber *ACTIN* gene was used for data normalization. Three technical replications were performed, and relative gene expression was calculated using the $2^{-\Delta\Delta Ct}$ method (Zhang et al., 2021).

Statistical Analysis

The data were presented as mean ± SD, and statistically analyzed using Tukey's multiple comparison test with GraphPad PRISM version 8.00: Two-way ANOVA followed by Tukey's multiple comparisons test was performed using GraphPad Prism version 8.0.0 for Windows, GraphPad Software, San Diego, California, United States.[1] Significant differences were indicated with asterisks, as follows: *P < 0.05, **P < 0.01, ***P < 0.001, ****P < 0.0001. Differences with P > 0.05 were considered non-significant (ns).

[1]www.graphpad.com

RESULTS

Morphometric Study

In the present study, we examined the effect of MT dose on the LT and HH tolerance of cucumber seedlings. At 6 DAT, we measured the seedling height, total FW, total DW, shoot FW and DW, root length, and SSI. The LTHH treatment significantly reduced seedling height, shoot FW, shoot DW, root length, SSI, and total DW by 22.05, 23.86, 24.26, 35, 25.48, and 27.98%, respectively, compared with seedlings grown under normal (control) conditions. On the other hand, pretreatment with MT (LTHH + MT) significantly ameliorated the damaging effect of LTHH conditions and increased seedling height, shoot FW, shoot DW, root length, SSI, and total DW by 11.27, 11.16, 16.74, 20, 17.19, and 20.50%, respectively, compared with control plants (**Table 1**).

Leaf Photosynthetic Gas Exchange

Next, we monitored the gas exchange parameters. Plants treated with or without MT showed no significant changes in gas exchange parameters under control conditions (**Figure 1**). However, in the LTHH treatment, the values of Pn, Gs, and E decreased significantly, and the decline was more prominent in the later stages than in the early stages of growth. Compared with the control plants, the values of Pn, Gs, and E in LTHH treated plants decreased by 59.39, 33.35, and 31.47%, respectively, at 6 DAT, while that of Ci increased by 51.51%. However,

exogenous MT application significantly mitigated this decline; at 6 DAT, values of Pn, Gs, and E, were increased by 37.93, 20.69, and 21%, respectively, in the LTHH + MT treatment compared with the water pretreatment, while that of Ci decreased by 40.94% (**Figure 1**).

Chlorophyll Fluorescence

Next, we sought to determine the chlorophyll fluorescence indices, including Fv/Fm, qP, NPQ, and ETR, in cucumber seedling leaves to elucidate whether MT can alleviate the effects of LT and HH stress on photosynthesis-related parameters (**Figure 2**). Under control conditions, no significant changes were observed between plants treated with and without MT. However, compared with the water pretreatment, the LTHH treatment significantly reduced Fv/Fm, qP, and ETR by 63.42, 65.71, and 66.73%, respectively, at 6 DAT, and increased the NPQ by 157.97% (**Figure 2**). The LTHH + MT treatment alleviated the photochemical reaction and balanced the PSII efficiency in cucumber plants. The LTHH + MT treatment significantly increased Fv/Fm, qP, and ETR, by 35.98, 46.01, and 50.75%, respectively, while that of NPQ was decreased by 127.11%, at 6 DAT compared with the control (**Figures 2A–D**).

Antioxidant Enzyme Activity

We measured the activities of antioxidant enzymes in cucumber seedlings under LT and HH conditions. Statistical analysis of the data revealed considerable differences in enzyme activities among the different treatments (**Figure 3**). In the LTHH treatment, enzyme activities initially increased and then declined at 6 DAT. At 4 DAT, the activities of SOD, POD, CAT, APX, MDHAR, DHAR, and GR increased by 97.67, 188.85, 496.97, 166, 401.67, 289.58, and 164.61%, respectively, in the LTHH treatment compared with the control. Then, the enzyme activities gradually decreased before peaking at 6 DAT. In the LTHH + MT treatment, the activities of SOD, POD, CAT, APX, MDHAR, DHAR, and GR were increased by 201.3, 213.92, 477.63, 205.54, 434.47, 385.52, and 224%, respectively, at 4 DAT.

Expression of Antioxidant Enzyme-Encoding Genes

The expression profile of the genes involved in the antioxidant defense mechanism was studied under LT and HH conditions. In the LTHH treatment, the antioxidant enzyme-encoding genes including *CsSOD, CsPOD, CsCAT, CsAPX, CsMDHAR, CsDHAR*, and *CsGR* were significantly upregulated at 2 and 4 DAT but downregulated 6 DAT (**Figure 4**). Compared with the LTHH treatment, the expression of these genes was upregulated in the LTHH + MT treatment at all time points. Additionally, MT significantly upregulated the expression levels of *CsSOD, CsPOD*, and *CsGR* by 69.25, 95.33, and 3.38%, respectively, at 4 DAT, and those of *CsAPX, CsMDHAR,* and *CsDHAR* by 92.54, 4.12, 23.21%, respectively, at 2 DAT. *CsCAT* was only the gene upregulated in the LTHH + MT treatment (by 166.53%) at 6 DAT compared with the LTHH treatment (**Figures 4D–F**).

Chlorophyll Content

Low temperature and HH stress can reduce photosynthesis and damage chlorophyll pigments; both these traits are interconnected with each other. The contents of chlorophyll a and chlorophyll b were significantly affected by the LTHH treatment (**Figure 5**). Compared with plants grown under control conditions, those treated with LTHH exhibited decreased levels of chlorophyll a and chlorophyll b at various time points, beginning at 2 DAT (**Figures 5A,B**). At 6 DAT, the contents of chlorophyll a and chlorophyll b were decreased by 42.90 and 46.03%, respectively, in the LTHH treatment compared with the control. However, in the LTHH + MT treatment, chlorophyll a and b contents were significantly increased by 30.86 and 19.44%, respectively, at 6 DAT (**Figure 5**). This suggests that MT application reduces the degradation of chlorophyll pigments in cucumber seedlings under LT and HH conditions.

Carotenoid Content

Photosynthesis is extremely sensitive to LTHH stress, which can impede photosynthesis regulation by reducing plant chlorophyll and carotenoid contents. In this study, the content of carotenoid was significantly lower in the LTHH treatment at 2 DAT compared with the control and control + MT treatments (**Figure 6**). However, in the LTHH + MT treatment, the contents of carotenoid, polar carotenoid, and non-polar carotenoid were significantly increased at each time point (**Figure 6**). At 6 DAT, the carotenoid, polar carotenoid, and non-polar carotenoid contents were significantly lower in the LTHH treatment (by 48.60, 61.98, and 83.99%, respectively) than in the control treatment. Exogenous MT application to LTHH treated cucumber seedlings alleviated the reduction in their carotenoid contents, and the carotenoid, polar carotenoid, and non-polar carotenoid contents were increased by 38.84, 39.75, and 58.88%, respectively, at 6 DAT.

Nutrient Contents

The LTHH treatment significantly affected nutrient uptake in cucumber seedlings. Compared with the control, the LTHH treatment reduced the contents of N, Mg, and Fe in leaves at each time point; the N, Mg, and Fe concentrations were reduced in leaves by 48.85, 70.89, and 49.24%, respectively, at 6 DAT (**Figures 7A,C,E**). However, pretreatment with MT in the LTHH + MT treatment significantly increased the N, Mg, and Fe concentrations in leaves by 25.88, 34.54, and 27.17%, respectively, at 6 DAT. Additionally, under LTHH conditions, the root N, Mg, and Fe concentrations were decreased by 58.19, 65.90, and 82.58%, respectively, at 6 DAT compared with the control treatment; however, MT pretreatment increased these nutrients by 36.46, 46.07, and 53.84%, respectively, at 6 DAT (**Figures 7B,D,F**).

MDA, Electrolyte Leakage, H_2O_2, and O_2^- Contents

We also measured MDA and EL in the leaf samples to investigate whether MT alleviates LTHH stress that induces damage in cucumber seedlings. The LTHH treatment increased EL and

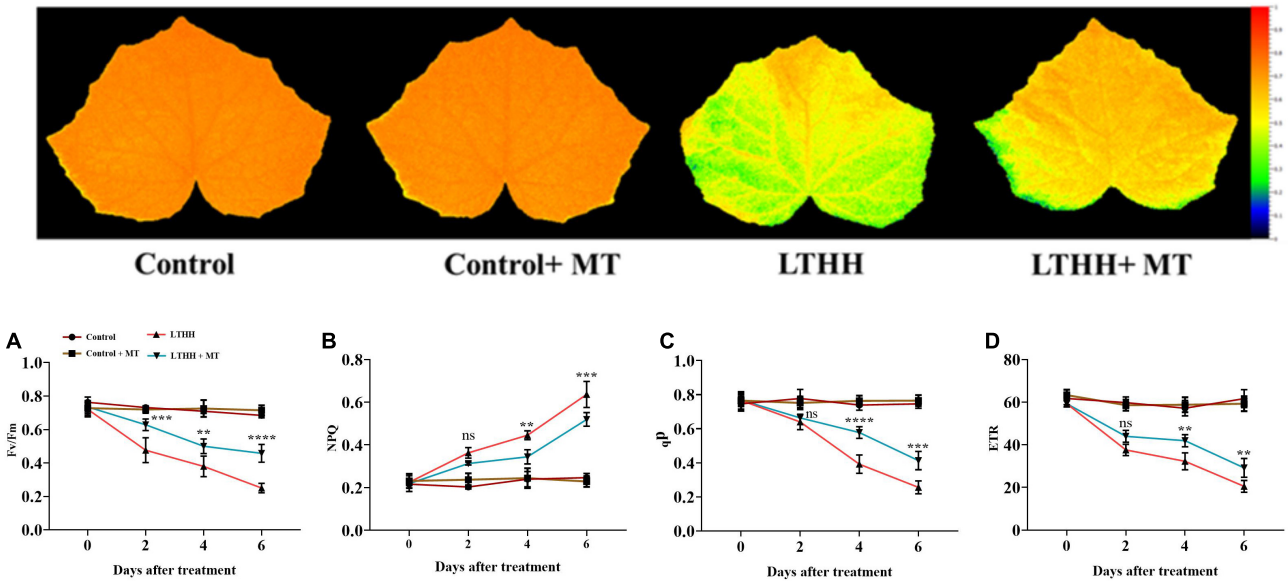


FIGURE 2 | Effect of exogenous melatonin on chlorophyll fluorescence parameters PSII maximum efficiency **(A)**, non-photochemical quenching **(B)**, photochemical quenching **(E)**, and electron transport rate **(D)** of cucumber seedling under low-temperature and high-humidity stress. Control (25/18°C); Control + MT (200 μM melatonin, 25/18°C); LTHH (15/10°C, 95%); LTHH + MT (200 μM melatonin, 15/10°C, 95%). Results were presented as means ± SD (n = 3), significance values were presented as: *P < 0.05; **P < 0.01; ***P < 0.001; ****P < 0.0001; while non-significant (ns) (P > 0.05).

induced dramatic accumulations of MDA in cucumber seedlings compared with the control treatment. A dramatic increase was observed in EL and MDA content between 2 and 4 DAT, and the increase continued until 6 DAT. A significant increase in MDA content and EL (431.37 and 362.23%, respectively) was observed at 6 DAT in the LTHH treatment. However, in the LTHH + MT treatment, the MDA content and EL were decreased by 246.1 and 167.58%, respectively, at 6 DAT (**Figures 8A,B**).

To investigate the degree of LT- and HH-induced oxidative damage to cell membranes, we measured the H_2O_2 and O_2^- contents. The H_2O_2 content showed a sharp increase at 4 DAT, followed by a slight increase at 6 DAT. However, MT pretreatment (LTHH + MT) significantly reduced this increase, especially at 2 and 4 DAT (**Figure 8C**). A marked increase was observed in O_2^- generation rate over time under the LTHH conditions (**Figure 8D**), whereas the LTHH + MT treatment significantly suppressed the production of O_2^- at all time points.

DISCUSSION

Because of its economic significance, cucumber is increasingly being cultivated in various countries including China. In recent years, high tunnels have been preferred for planting cucumber to meet the market demand. However, because of the LT in northern regions, both LT and HH pose a considerable threat to the growth and development of cucumber plants. Therefore, strategies for improving the stress tolerance potential of cucumber plants are urgently needed. Such approaches would help to increase cucumber yield and quality and ensure global food security (Ahanger et al., 2020). MT has been implicated in plant tolerance to various environmental stresses, including LT, heavy metal toxicity, high salinity, and drought (Bajwa et al., 2014; Zuo et al., 2014; Li et al., 2016; Arora and Bhatla, 2017). However, no report is available on the role of MT in reducing the stress imposed by LT and HH in cucumber. In this study, we show that MT application improves cucumber seedling growth under LT and HH stress by regulating seedling morphology and improving photosynthesis, antioxidant enzyme defense, and nutrient uptake. Consistent with our recent report (Amin et al., 2021), LT and HH obstructed cucumber seedling growth by negatively affecting the plant morphological traits and biomass accumulation, and foliar application of MT effectively alleviated these inhibitory effects of LTHH stress. These results are also in agreement with the study of Li et al. (2017), which showed that the growth and biomass of plants reflect their sensitivity or resistance to abiotic stresses. The reduction in morphological traits might be related to photosynthesis and the antioxidant defense system. LT and HH affect photosynthesis by impacting carbon (C) fixation and electron transport in thylakoids (Amin et al., 2021). LT and HH damage photosynthesis by affecting energy production. Ninety-five percent of the dry matter content of plants is derived from photosynthesis and forms the basis of crop yield (Zhang et al., 2021). The decline in photosynthetic efficiency is the main reason for the reduction in plant biomass under LT and HH conditions (Amin et al., 2021). Photosynthesis is a complex process that involves numerous biological pathways. Environmental stressors, such as cold, salinity, and drought, impair photosynthetic C metabolism in plants, resulting in stunted plants and reduced yield (Hutchison et al., 2000; Ding et al., 2017b; Wang et al., 2020). In the photosystem reaction center, an extreme

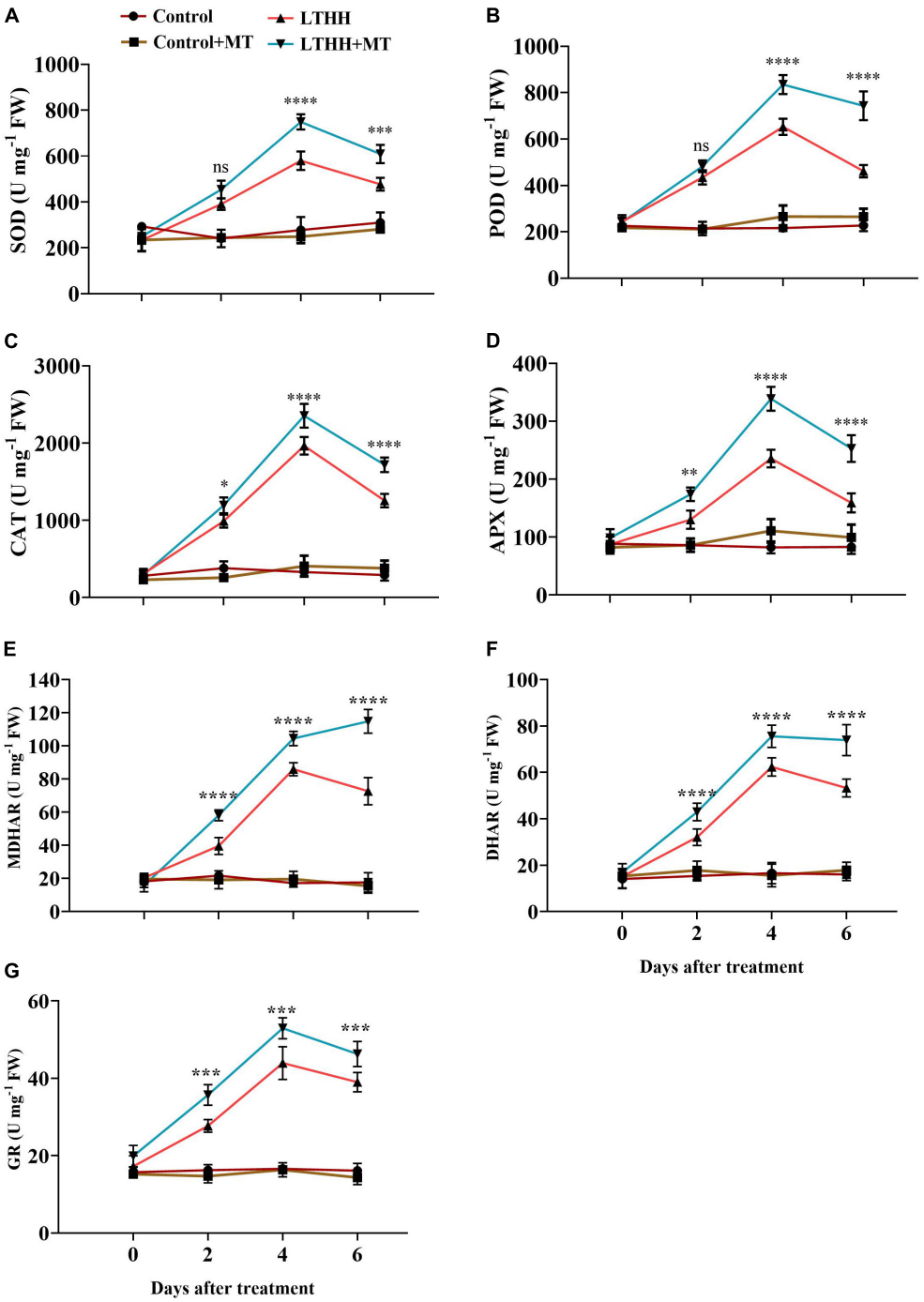


FIGURE 3 | Effect of exogenous melatonin on superoxide dismutase **(A)**, peroxidase **(B)**, catalase **(C)**, ascorbate peroxidase **(D)** monodehydroascorbate reductase **(E)**, dehydroascorbate reductase **(F)**, and glutathione reductase **(G)**, activities of cucumber seedling under low-temperature and high-humidity stress. Control (25/18°C); Control + MT (200 μM melatonin, 25/18°C); LTHH (15/10°C, 95%); LTHH + MT (200 μM melatonin, 15/10°C, 95%). Results were presented as means ± SD (n = 3), significance values were presented as: *P < 0.05; **P < 0.01; ***P < 0.001; ****P < 0.0001; while non-significant (ns) (P > 0.05).

stress environment causes severe photoinhibition. When the dissipation mechanism fails, plants utilize excess energy, which damages the photosystem reaction center (Jahan et al., 2021). In this study, we evaluated the parameters of PSI and PSII to unveil the damaging effects of LT and HH on photosynthesis, PSII activity, and the role of MT in plant defense (**Figure 1**). MT application triggers many genes and enzymes associated with C and N metabolism, which in turn improves photosynthesis

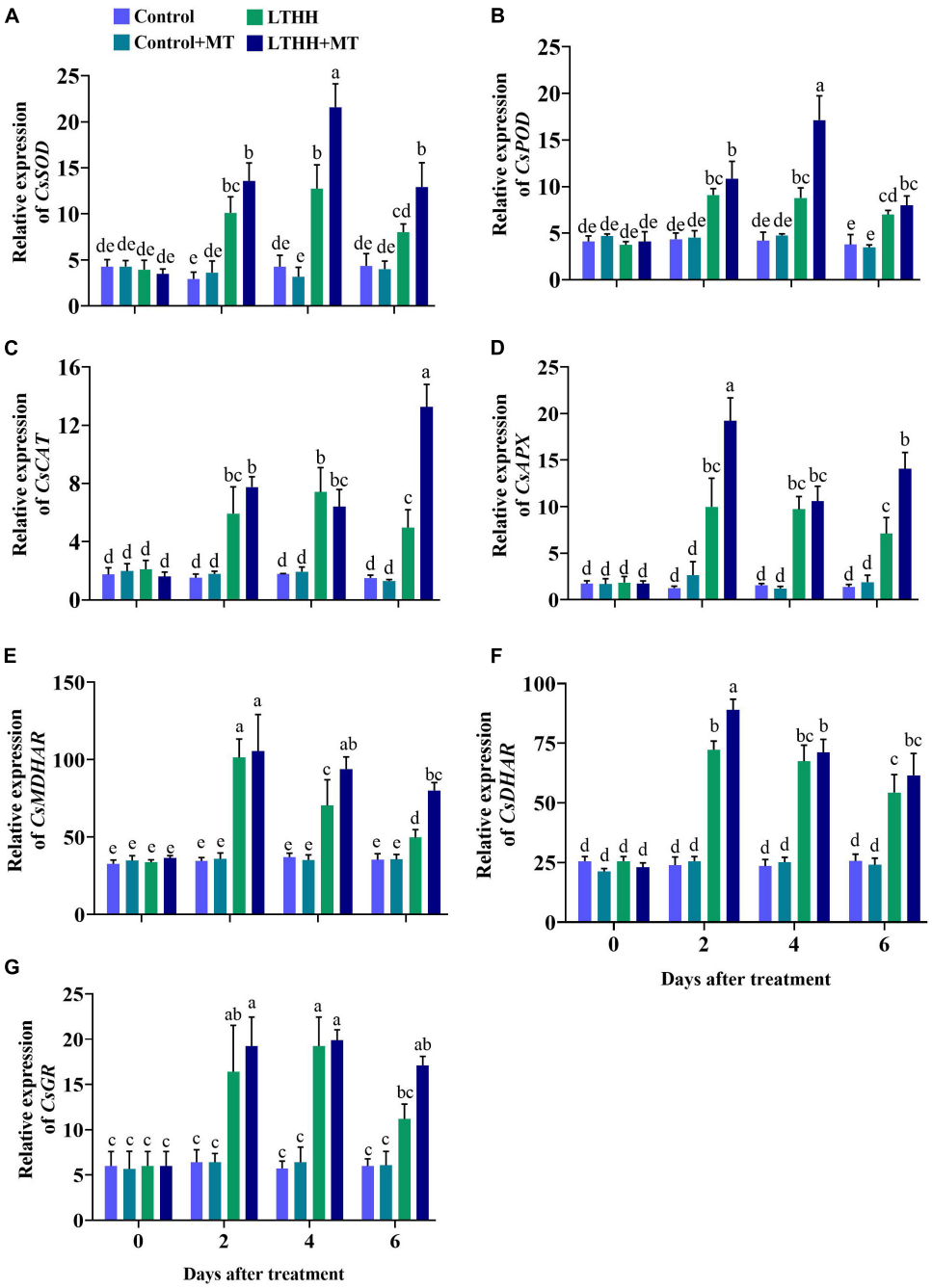


FIGURE 4 | Effect of exogenous melatonin on relative expression of SOD **(A)**, POD **(B)**, CAT **(C)**, APX **(D)**, MDHAR **(E)**, DHAR **(F)**, and GR **(G)** in cucumber seedling under low-temperature and high-humidity stress. Control (25/18°C); Control + MT (200 μM melatonin, 25/18°C); LTHH (15/10°C, 95%); LTHH + MT (200 μM melatonin, 15/10°C, 95%). Same letters on the bars represent no significant differences, while different letters represent significant differences among treatments ($P > 0.05$ was non-significant). Data are means ± SD of three replicates ($n = 3$).

and consequently promotes plant growth and development under abiotic stress conditions (Ren et al., 2021). We found that Pn, Gs, and E, were markedly reduced by LTHH stress, which is consistent with previous studies (Ding et al., 2017a, 2018) in which exogenous application of MT enhanced photosynthesis under cold stress. The resumption of photosynthesis and plant growth is important for survival under stress conditions (Wang et al., 2020). In this study, MT application facilitated the recovery of photosynthesis after LTHH-treated cucumber seedlings were reverted to normal growth conditions. Moreover, evidence related to the regulatory mechanisms underlying the beneficial effect of MT on photosynthesis under LT and HH conditions,

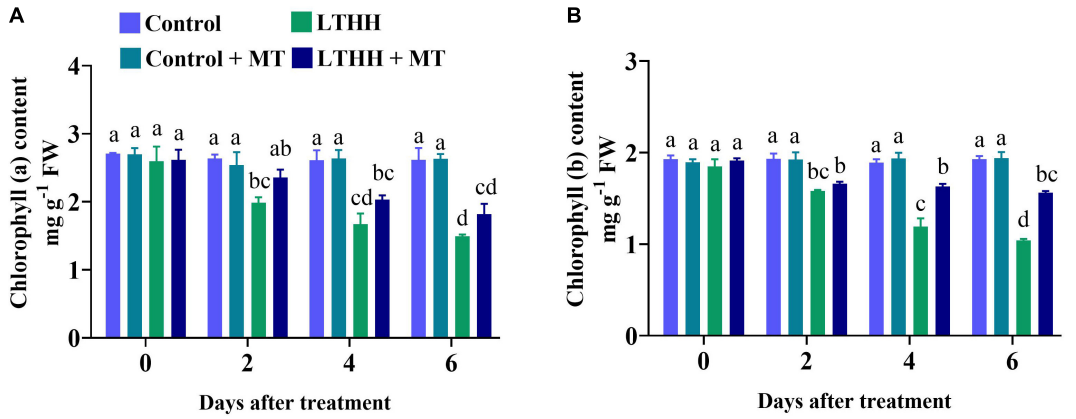


FIGURE 5 | Effect of exogenous melatonin on chlorophyll *a* **(A)**, and chlorophyll *b* **(B)** content of cucumber seedling under low-temperature and high-humidity stress. Control (25/18°C); Control + MT (200 μM melatonin, 25/18°C); LTHH (15/10°C, 95%); LTHH + MT (200 μM melatonin, 15/10°C, 95%). Same letters on the bars represent no significant differences, while different letters represent significant differences among treatments ($P > 0.05$ was non-significant). Data are means ± SD of three replicates ($n = 3$).

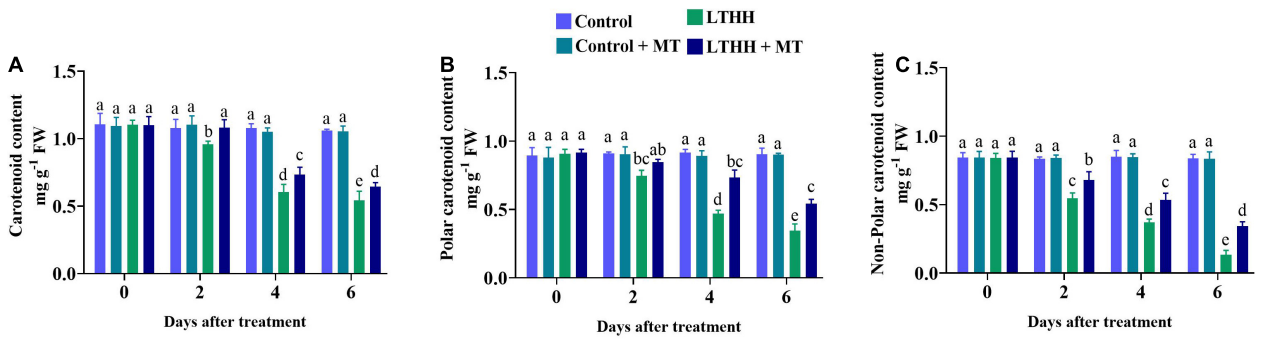


FIGURE 6 | Effect of exogenous melatonin on carotenoid **(A)**, polar carotenoid **(B)**, and non-polar carotenoid **(C)** content of cucumber seedling under low-temperature and high-humidity stress. Control (25/18°C); Control ± MT (200 μM melatonin, 25/18°C); LTHH (15/10°C, 95%); LTHH + MT (200 μM melatonin, 15/10°C, 95%). Same letters on the bars represent no significant differences, while different letters represent significant differences among treatments ($P > 0.05$ was non-significant). Data are means ± SD of three replicates ($n = 3$).

particularly in chilling-sensitive crop species, is limited. Previous studies showed that the decline in photosynthesis during chilling stress is mainly caused by a reduction in the activity of photosynthetic enzymes, PSII, and PSI (Bi et al., 2015). Consistently, we found that LT and HH reduced the values of Fv/Fm, qP, and ETR (**Figure 2**); however, PSII activity was higher in cucumber seedlings subjected to the foliar application of MT than in those subjected to the LTHH conditions. Investigation of the PSII reaction center and its donor and acceptor sites is considered important for PSII activity in plants, especially under abiotic stress conditions (Li et al., 2005). Chlorophyll is essential for harvesting light during photosynthesis. Both LT and HH severely retard or inhibit the synthesis of chlorophyll, which directly impacts plant growth and yield (Zhang et al., 2021). Cold stress degrades photosynthetic pigments by upregulating chlorophyllase activity and downregulating enzymes involved in chlorophyll biosynthesis, thus directly affecting photosynthesis and chlorophyll fluorescence (Jahan et al., 2021). Chlorophyll is essential for photosynthesis and is highly sensitive to cold stress (Amin et al., 2021), which disrupts all key mechanisms of photosynthesis. In the current study, we verified that MT pretreatment reduces LT and HH stress-induced chlorophyll degradation and carotenoid biosynthesis, suggesting that MT can effectively stimulate chlorophyll synthesis in stressful environments.

Low temperature causes oxidative stress, which affects cell membrane function. Lipid peroxidation and EL are the primary indicators of cellular damage. In cucumber plants exposed to LTHH stress conditions, a dramatic increase in MDA and EL was detected, suggesting severe lipid peroxidation and plasma membrane damage. MT application effectively alleviated the LTHH stress-induced damage in cucumber plants (**Figures 8A,B**), suggesting that MT rescues cucumber seedlings from LTHH-induced oxidative stress. Our results are consistent with previous studies, in which exogenous MT application increased the LT tolerance of cucumber (Zhao et al., 2016), watermelon (Li et al., 2016), and Bermudagrass (Fan et al., 2015) by reducing the MDA content and EL. A reduction in

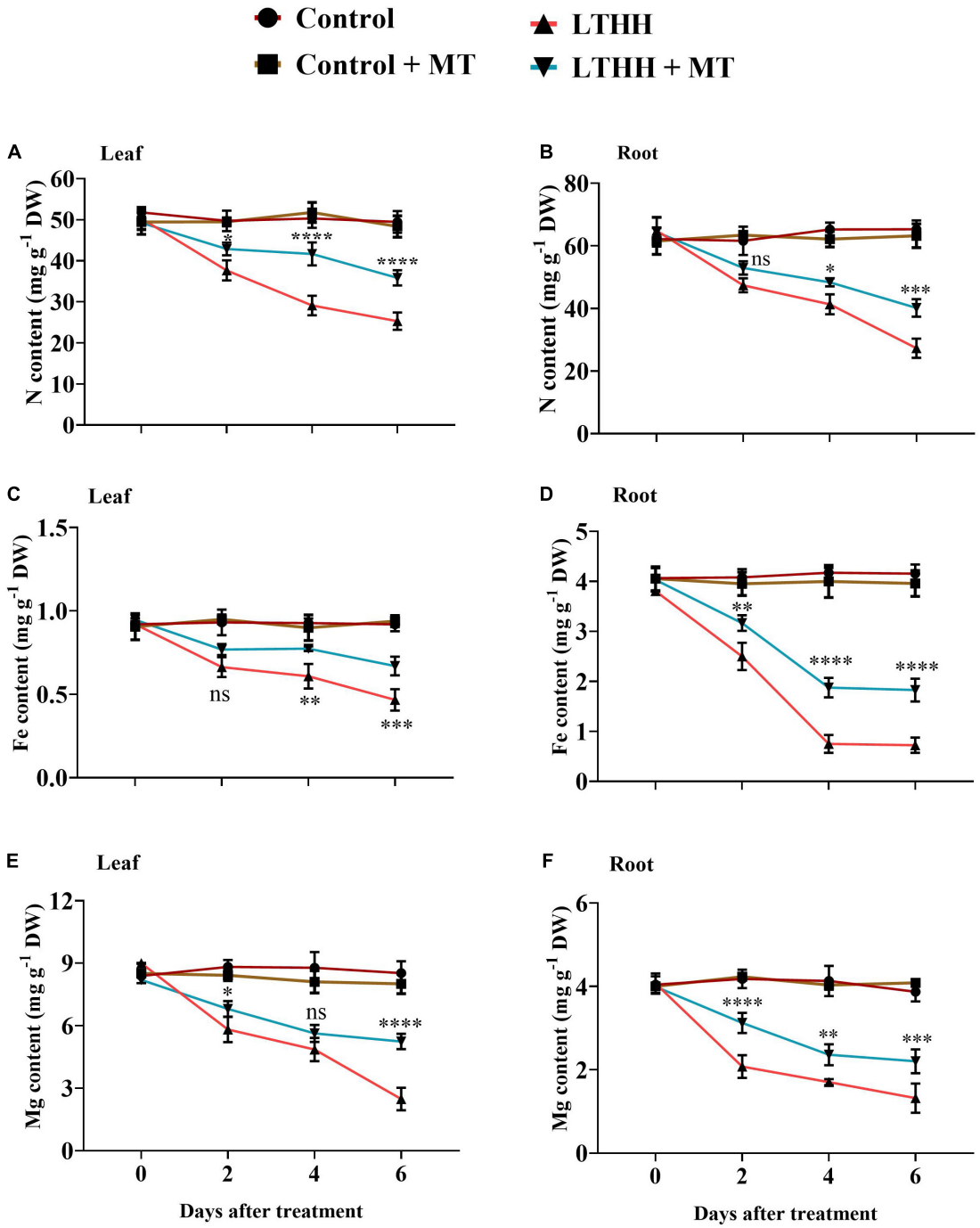


FIGURE 7 | Effect of exogenous melatonin on nitrogen content **(A,B)**, iron content **(C,D)**, and magnesium content **(E,F)**, in root and leaves of cucumber seedling under low-temperature and high-humidity stress. Control (25/18°C); Control + MT (200 μM melatonin, 25/18°C); LTHH (15/10°C, 95%); LTHH + MT (200 μM melatonin, 15/10°C, 95%). Results were presented as means ± SD ($n = 3$), significance values were presented as: *$P < 0.05$; **$P < 0.01$; ***$P < 0.001$; ****$P < 0.0001$; while non-significant (ns) ($P > 0.05$).

MDA content and EL in MT-treated plants indicate reduced oxidative damage to cell membranes. We assume that ROS concentration in MT treated seedlings was lower than that in untreated seedlings under LTHH stress conditions because lower MDA content and EL represent the alleviation of oxidative damage to cell membranes. Several studies have shown that ROS accumulation is directly related to lipid peroxidation, cell integrity, and cell death (Zhao et al., 2020). The degree of oxidative injury to the cell membrane due to LT and HH was investigated by measuring the ROS content. H_2O_2 is a

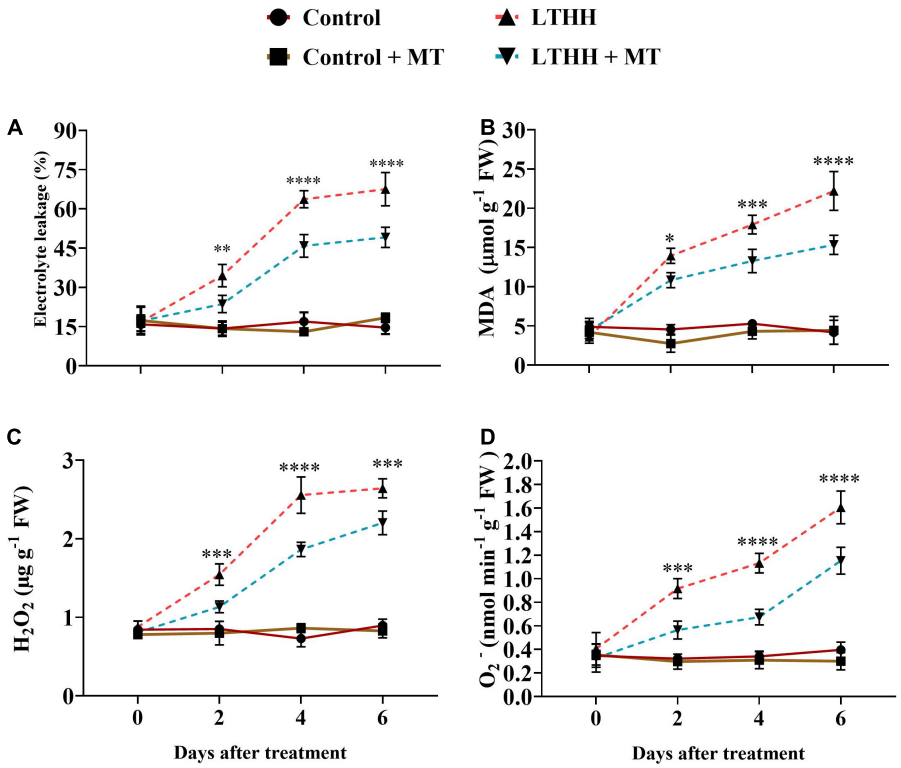


FIGURE 8 | Effect of exogenous melatonin on electrolyte leakage **(A)**, malondialdehyde **(B)**, hydrogen peroxide **(C)**, and superoxide anion **(D)** content of cucumber seedling under low-temperature and high-humidity stress. Control (25/18°C); Control + MT (200 μM melatonin, 25/18°C); LTHH (15/10°C, 95%); LTHH + MT (200 μM melatonin, 15/10°C, 95%). Results were presented as means ± SD ($n = 3$), significance values were presented as: *$P < 0.05$; **$P < 0.01$; ***$P < 0.001$; ****$P < 0.0001$; while non-significant (ns) ($P > 0.05$).

crucial ROS in plants and is generated under stress conditions. Accumulation of ROS hastens cell membrane lipoylation and leads to the production of MDA, thereby increasing plant membrane permeability and compromising membrane structural integrity. The application of MT reduced ROS accumulation in the present study. MT acts as an antioxidant in plants under harsh environmental conditions (Wang et al., 2020). In our experiment, cucumber seedlings exposed to LTHH stress exhibited oxidative stress compared with those grown under control conditions; however, the foliar spray of MT reduced the production of ROS (**Figures 8C,D**). MT is considered a free radical scavenger and an antioxidant that can eliminate H_2O_2 for maintaining cellular homeostasis (Tan et al., 2007); this phenomenon has been reported in apple (Wang et al., 2012) and cucumber (Marta et al., 2016).

Reactive oxygen species are directly or indirectly linked with the antioxidant defense system and affect antioxidant enzymes. Many researchers have argued that exogenous MT application strengthens the endogenous antioxidant defense mechanism against climate change (Kingston-Smith et al., 1997; Cano et al., 2003; Wang et al., 2020). To cope with oxidative stress induced by adverse environmental conditions, higher plants have developed an antioxidant defense system that includes antioxidant enzymes (Zhang et al., 2014). SOD, POD, CAT, and APX are four crucial enzymes in the plant defense system. SOD can reduce O_2^- to produce H_2O_2, which is subsequently completely decomposed by POD and CAT, producing H_2O and O_2 and attenuating membrane damage (Jun et al., 2008). Furthermore, except for the scavenging antioxidant enzymes mentioned above, a number of other enzymes detected in various subcellular compartments also play a role in maintaining redox homeostasis by directly scavenging specific ROS. Such antioxidant enzymes include DHAR, MDHAR, and GR. These enzymes work together to perform synergistic functions *via* the ascorbate–glutathione cycle, which operates in plant cell organelles (Gupta et al., 2018). MT boosts the plant antioxidant defense mechanism against abiotic stresses by enhancing antioxidant activity and the expression of corresponding genes (Sun et al., 2019). In a previous study, foliar application of MT enhanced the antioxidant enzyme defense mechanism and reduced the accumulation of ROS in wheat seedlings exposed to cold stress (Li et al., 2018). Consistently, in the current study, we found that exogenous application of MT dramatically elevated the activity of antioxidant enzymes and relative messenger RNA (mRNA) abundance at all time points, thus enabling plants to eliminate excess ROS (**Figures 3**, **4**). Exogenous application of MT treatment significantly increased the expression levels of *CsSOD*, *CsPOD*, *CsCAT*, *CsAPX*, *CsMDHAR*, *CsDHAR*, and *CsGR*, and decreased the oxidative damage (**Figure 4**). Similar trends were reported in watermelon and in cucumber seedlings

grown under chilling and drought stress conditions (Liu et al., 2015; Zhang et al., 2021). We speculate that MT exerts a positive influence on the activity of antioxidant enzymes. Interestingly, MT pretreatment enhanced the activities of these enzymes, thus maintaining low H_2O_2 content during the LTHH stress. This was also confirmed in trials with apple and watermelon plants, where MT directly scavenged H_2O_2 and boosted the activities of antioxidant enzymes to detoxify H_2O_2 in plants treated with cold stress (Li et al., 2017) or drought stress (Wang et al., 2013). These arguments suggest that MT plays a crucial role in plant stress mitigation.

Nutrient uptake and compartmentalization are important not only for normal plant growth and development but also for maintaining plant health under unfavorable environmental conditions that disrupt ion homeostasis (Zhang et al., 2017). LT stress has been shown to inhibit the uptake and transport of macro- and micro-nutrients in cucumbers (Anwar et al., 2018). Among the various plant nutrients, N, Mg, and Fe are responsible for chlorophyll biosynthesis as well as for other physicochemical reactions associated with plant growth and development. A deficiency of these elements can decrease photosynthetic activity (Zhang et al., 2017). In this study, we noted that the LTHH treatment decreased the N, Mg, and Fe contents of cucumber seedlings in underground and aboveground plant parts (roots and leaves). However, the MT pretreatment of stressed plants promoted the uptake of N, Mg, and Fe and their translocation from roots and leaves. The enhanced concentrations of N, Mg, and Fe in MT-treated plants suggest that MT has a positive influence on plant growth and development (Anwar et al., 2018). MT defends against chlorophyll degradation and increases plant growth under stressful environments, perhaps because it upregulates the accumulation of N, Mg, and Fe under such conditions (Ahammed et al., 2020).

CONCLUSION

The findings of this study revealed that MT mitigates the damaging effects of LT and HH on cucumber seedlings. LT and HH affected the morphological attributes of cucumber seedlings, inhibited photosynthesis, and affected nutrient uptake by increasing ROS contents, lipid peroxidation, and electrolyte leakage in cucumber seedlings. However, MT rescued the growth of cucumber seedlings under LT and HH conditions by improving morphometric traits, increasing antioxidant enzyme activities and transcript levels, regulating PSI and PSII, enhancing nutrient uptake, and alleviating oxidative damage. Our findings demonstrate that the foliar application of MT reestablishes cucumber seedling growth under LT and HH stress conditions. Our work provides a case study that exogenous application of melatonin may serve as a practical approach to improve LT and HH tolerance in cucumber production. Future studies should include the integrity of chloroplast structure and molecular characterization of cucumber to improve understanding of the underlying mechanisms of LTHH stress and melatonin response.

DATA AVAILABILITY STATEMENT

The raw data supporting the conclusions of this article will be made available by the authors, without undue reservation.

AUTHOR CONTRIBUTIONS

BA, ZC, HM, and SL: conceptualization. BA, MJA, HFA, AM, and KRH: methodology. BA and HFA: software. BA, AM, KRH, and MA: validation. BA: formal analysis, investigation, and writing—original draft preparation. MJA and ZC: writing—review and editing. ZC: resources, supervision, project administration, and funding acquisition. All authors contributed to the article and approved the submitted version.

FUNDING

This work was supported by the National Key R&D Project (2018YFD0100701).

ACKNOWLEDGMENTS

The authors would like to thank the Deanship of Scientific Research At Taif University to the Researchers Supporting Project (TURSP2020/110); Taif University. Taif, Saudi Arabia.

SUPPLEMENTARY MATERIAL

The Supplementary Material for this article can be found online at: https://www.frontiersin.org/articles/10.3389/fpls.2022.855900/full#supplementary-material

REFERENCES

Ahammed, G. J., Wu, M., Wang, Y., Yan, Y., Mao, Q., Ren, J., et al. (2020). Melatonin alleviates iron stress by improving iron homeostasis, antioxidant defense and secondary metabolism in cucumber. *Sci. Hortic.* 265:109205. doi: 10.1016/j.scienta.2020.109205

Ahanger, M. A., Aziz, U., Alsahli, A. A., Alyemeni, M. N., and Ahmad, P. (2020). Influence of exogenous salicylic acid and nitric oxide on growth, photosynthesis, and ascorbate-glutathione cycle in salt stressed *Vigna angularis*. *Biomolecules* 10:42. doi: 10.3390/biom10010042

Amin, B., Atif, M. J., Wang, X., Meng, H., Ghani, M. I., Ali, M., et al. (2021). Effect of low temperature and high humidity stress on physiology of cucumber at different leaf stages. *Plant Biol.* 23, 785–796. doi: 10.1111/plb.13276

Anwar, A., Yan, Y., Liu, Y., Li, Y., and Yu, X. (2018). 5-aminolevulinic acid improves nutrient uptake and endogenous hormone accumulation, enhancing low-temperature stress tolerance in cucumbers. *Int. J. Mol. Sci.* 19:3379. doi: 10.3390/ijms19113379

Arora, D., and Bhatla, S. C. (2017). Melatonin and nitric oxide regulate sunflower seedling growth under salt stress accompanying differential expression of

Cu/Zn SOD and Mn SOD. *Free Radic. Biol. Med.* 106, 315–328. doi: 10.1016/j.freeradbiomed.2017.02.042

Bajwa, V. S., Shukla, M. R., Sherif, S. M., Murch, S. J., and Saxena, P. K. (2014). Role of melatonin in alleviating cold stress in *Arabidopsis thaliana*. *J. Pineal Res.* 56, 238–245. doi: 10.1111/jpi.12115

Bi, H., Dong, X., Wu, G., Wang, M., and Ai, X. (2015). Decreased TK activity alters growth, yield and tolerance to low temperature and low light intensity in transgenic cucumber plants. *Plant Cell Rep.* 34, 345–354. doi: 10.1007/s00299-014-1713-5

Cabrera, R. M., and Saltveit, M. E. (1990). Physiological response to chilling temperatures of intermittently warmed cucumber fruit. *J. Am. Soc. Hortic. Sci.* 115, 256–261. doi: 10.21273/jashs.115.2.256

Cano, A., Alcaraz, O., and Arnao, M. B. (2003). Free radical-scavenging activity of indolic compounds in aqueous and ethanolic media. *Anal. Bioanal. Chem.* 376, 33–37. doi: 10.1007/s00216-003-1848-7

Chance, B., and Maehly, A. (1955). [136] Assay of catalases and peroxidases. *Methods Enzymol.* 2, 764–775. doi: 10.1016/s0076-6879(55)02300-8

Ciura, J., and Kruk, J. (2018). Phytohormones as targets for improving plant productivity and stress tolerance. *J. Plant Physiol.* 229, 32–40.

Ding, F., Liu, B., and Zhang, S. (2017a). Exogenous melatonin ameliorates cold-induced damage in tomato plants. *Sci. Hortic.* 219, 264–271. doi: 10.1016/j.scienta.2017.03.029

Ding, F., Wang, M., Liu, B., and Zhang, S. (2017b). Exogenous melatonin mitigates photoinhibition by accelerating non-photochemical quenching in tomato seedlings exposed to moderate light during chilling. *Front. Plant Sci.* 8:244. doi: 10.3389/fpls.2017.00244

Ding, F., Wang, G., and Zhang, S. (2018). Exogenous melatonin mitigates methyl viologen-triggered oxidative stress in poplar leaf. *Molecules* 23:2852. doi: 10.3390/molecules23112852

Erdal, S. (2019). Melatonin promotes plant growth by maintaining integration and coordination between carbon and nitrogen metabolisms. *Plant Cell Rep.* 38, 1001–1012. doi: 10.1007/s00299-019-02423-z

Eremina, M., Rozhon, W., and Poppenberger, B. (2016). Hormonal control of cold stress responses in plants. *Cell. Mol. Life Sci.* 73, 797–810. doi: 10.1007/s00018-015-2089-6

Fan, J., Hu, Z., Xie, Y., Chan, Z., Chen, K., Amombo, E., et al. (2015). Alleviation of cold damage to photosystem II and metabolisms by melatonin in Bermudagrass. *Front. Plant Sci.* 6:925. doi: 10.3389/fpls.2015.00925

Gupta, D. K., Palma, J. M., and Corpas, F. J. (2016). *Redox State as a Central Regulator of Plant-Cell Stress Responses*. Cham: Springer.

Gupta, D. K., Palma, J. M., and Corpas, F. J. (2018). *Antioxidants and Antioxidant Enzymes in Higher Plants*. Cham: Springer.

Han, W., Yang, Z., Huang, L., Sun, C., Yu, X., and Zhao, M. (2019). Fuzzy comprehensive evaluation of the effects of relative air humidity on the morpho-physiological traits of Pakchoi (*Brassica chinensis* L.) under high temperature. *Sci. Hortic.* 246, 971–978. doi: 10.1016/j.scienta.2018.11.079

Hasanuzzaman, M., Bhuyan, M., Zulfiqar, F., Raza, A., Mohsin, S. M., Mahmud, J. A., et al. (2020). Reactive oxygen species and antioxidant defense in plants under abiotic stress: revisiting the crucial role of a universal defense regulator. *Antioxidants* 9:681. doi: 10.3390/antiox9080681

Hutchison, R. S., Groom, Q., and Ort, D. R. (2000). Differential effects of chilling-induced photooxidation on the redox regulation of photosynthetic enzymes. *Biochemistry* 39, 6679–6688. doi: 10.1021/bi000 1978

Jahan, M. S., Guo, S., Sun, J., Shu, S., Wang, Y., Abou El-Yazied, A., et al. (2021). Melatonin-mediated photosynthetic performance of tomato seedlings under high-temperature stress. *Plant Physiol. Biochem.* 167, 309–320. doi: 10.1016/j.plaphy.2021.08.002

Jan, S., Alyemeni, M. N., Wijaya, L., Alam, P., Siddique, K. H., and Ahmad, P. (2018). Interactive effect of 24-epibrassinolide and silicon alleviates cadmium stress *via* the modulation of antioxidant defense and glyoxalase systems and macronutrient content in *Pisum sativum* L. seedlings. *BMC Plant Biol.* 18:146. doi: 10.1186/s12870-018-1359-5

Jun, T., Ju, Y., Li-Qing, Y., Jia-Le, S., and Cai-Hong, Z. (2008). Effects of short-term high temperature stress on antioxidant system in poinsettia. *Acta Hortic. Sin.* 35:1681.

Kingston-Smith, A. H., Harbinson, J., Williams, J., and Foyer, C. H. (1997). Effect of chilling on carbon assimilation, enzyme activation, and photosynthetic electron transport in the absence of photoinhibition in maize leaves. *Plant Physiol.* 114, 1039–1046. doi: 10.1104/pp.114.3.1039

Lee, S. H., Singh, A. P., Chung, G. C., Kim, Y. S., and Kong, I. B. (2002). Chilling root temperature causes rapid ultrastructural changes in cortical cells of cucumber (*Cucumis sativus* L.) root tips. *J. Exp. Bot.* 53, 2225–2237. doi: 10.1093/jxb/erf071

Lei, X. Y., Zhu, R. Y., Zhang, G. Y., and Dai, Y. R. (2004). Attenuation of cold-induced apoptosis by exogenous melatonin in carrot suspension cells: the possible involvement of polyamines. *J. Pineal Res.* 36, 126–131. doi: 10.1046/j.1600-079x.2003.00106.x

Lerner, A. B., Case, J. D., Takahashi, Y., Lee, T. H., and Mori, W. (1958). Isolation of melatonin, the pineal gland factor that lightens melanocyteS1. *J. Am. Chem. Soc.* 80, 2587–2587. doi: 10.1021/ja01543a060

Li, G., Ma, J., Tan, M., Mao, J., An, N., Sha, G., et al. (2016). Transcriptome analysis reveals the effects of sugar metabolism and auxin and cytokinin signaling pathways on root growth and development of grafted apple. *BMC Genomics* 17:150. doi: 10.1186/s12864-016-2484-x

Li, H., Chang, J., Chen, H., Wang, Z., Gu, X., Wei, C., et al. (2017). Exogenous melatonin confers salt stress tolerance to watermelon by improving photosynthesis and redox homeostasis. *Front. Plant Sci.* 8:295. doi: 10.3389/fpls.2017.00295

Li, H., Dong, Y., Chang, J., He, J., Chen, H., Liu, Q., et al. (2016). High-throughput microRNA and mRNA sequencing reveals that microRNAs may be involved in melatonin-mediated cold tolerance in *Citrullus lanatus* L. *Front. Plant Sci.* 7:1231. doi: 10.3389/fpls.2016.01231

Li, J., Li, Y., Tian, Y., Qu, M., Zhang, W., and Gao, L. (2017). Melatonin has the potential to alleviate cinnamic acid stress in cucumber seedlings. *Front. Plant Sci.* 8:1193. doi: 10.3389/fpls.2017.01193

Li, M. Q., Hasan, M. K., Li, C. X., Ahammed, G. J., Xia, X. J., Shi, K., et al. (2016). Melatonin mediates selenium-induced tolerance to cadmium stress in tomato plants. *J. Pineal Res.* 61, 291–302. doi: 10.1111/jpi.12346

Li, P.-M., Gao, H.-Y., and Strasser, R. J. (2005). Application of the fast chlorophyll fluorescence induction dynamics analysis in photosynthesis study. *Zhi Wu Sheng Li Yu Fen Zi Sheng Wu Xue Xue Bao* 31, 559–566.

Li, X., Brestic, M., Tan, D. X., Zivcak, M., Zhu, X., Liu, S., et al. (2018). Melatonin alleviates low PS I-limited carbon assimilation under elevated CO 2 and enhances the cold tolerance of offspring in chlorophyll b-deficient mutant wheat. *J. Pineal Res.* 64:e12453. doi: 10.1111/jpi.12453

Liu, J., Wang, W., Wang, L., and Sun, Y. (2015). Exogenous melatonin improves seedling health index and drought tolerance in tomato. *Plant Growth Regul.* 77, 317–326. doi: 10.1007/s10725-015-0066-6

Ma, F., and Cheng, L. (2004). Exposure of the shaded side of apple fruit to full sun leads to up-regulation of both the xanthophyll cycle and the ascorbate-glutathione cycle. *Plant sci.* 166, 1479–1486. doi: 10.1016/j.plantsci.2004.01.024

Marta, B., Szafrańska, K., and Posmyk, M. M. (2016). Exogenous melatonin improves antioxidant defense in cucumber seeds (*Cucumis sativus* L.) germinated under chilling stress. *Front. Plant Sci.* 7:575. doi: 10.3389/fpls.2016.00575

Mehla, N., Sindhi, V., Josula, D., Bisht, P., and Wani, S. H. (2017). "An introduction to antioxidants and their roles in plant stress tolerance," in *Reactive oxygen Species and Antioxidant Systems in Plants: Role and Regulation Under Abiotic Stress*, eds M. Khan and N. Khan (Singapore: Springer), 1–23. doi: 10.1007/978-981-10-5254-5_1

Nakano, Y., and Asada, K. (1981). Hydrogen peroxide is scavenged by ascorbate-specific peroxidase in spinach chloroplasts. *Plant Cell Physiol.* 22, 867–880.

Polle, A., Otter, T., and Seifert, F. (1994). Apoplastic peroxidases and lignification in needles of Norway spruce (*Picea abies* L.). *Plant Physiol.* 106, 53–60. doi: 10.1104/pp.106.1.53

Posmyk, M. M., Bałabusta, M., Wieczorek, M., Sliwinska, E., and Janas, K. (2009). Melatonin applied to cucumber (*Cucumis sativus* L.) seeds improves germination during chilling stress. *J. Pineal Res.* 46, 214–223. doi: 10.1111/j.1600-079X.2008.00652.x

Rao, M. V., Paliyath, G., and Ormrod, D. P. (1996). Ultraviolet-B- and ozoneinduced biochemical changes in antioxidant enzymes of *Arabidopsis thaliana*. *Plant Physiol.* 110, 125–136. doi: 10.1104/pp.110.1.125

Raja, V., Majeed, U., Kang, H., Andrabi, K. I., and John, R. (2017). Abiotic stress: interplay between ROS, hormones and MAPKs. *Environ. Exp. Bot.* 137, 142–157. doi: 10.1016/j.envexpbot.2017.02.010

Ren, J., Yang, X., Ma, C., Wang, Y., and Zhao, J. (2021). Melatonin enhances drought stress tolerance in maize through coordinated regulation of carbon and nitrogen assimilation. *Plant Physiol. Biochem.* 167, 958–969. doi: 10.1016/j.plaphy.2021.09.007

Ruelland, E., and Zachowski, A. (2010). How plants sense temperature. *Environ. Exp. Bot.* 69, 225–232. doi: 10.1016/j.envexpbot.2010.05.011

Sakina, A., Wani, W., Mushtaq, M., Wani, S. H., and Shikari, A. B. (2019). "Omics approaches for cold stress tolerance in plants," in *Recent Approaches in Omics for Plant Resilience to Climate Change*, ed. S. Wani (Cham: Springer), 331–356. doi: 10.1007/s00299-016-2073-0

Shah, K., Amin, N. U., Ahmad, I., Ara, G., Rahman, M. U., Zuo, X., et al. (2019). Cement dust induce stress and attenuates photosynthesis in *Arachis hypogaea*. *Environ. Sci. Pollut. Res.* 26, 19490–19501. doi: 10.1007/s11356-019-04861-4

Shi, H., Jiang, C., Ye, T., Tan, D.-X., Reiter, R. J., Zhang, H., et al. (2015). Comparative physiological, metabolomic, and transcriptomic analyses reveal mechanisms of improved abiotic stress resistance in bermudagrass [*Cynodon dactylon* (L). Pers.] by exogenous melatonin. *J. Exp. Bot.* 66, 681–694. doi: 10.1093/jxb/eru373

Stewart, R. R., and Bewley, J. D. (1980). Lipid peroxidation associated with accelerated aging of soybean axes. *Plant Physiol.* 65, 245–248. doi: 10.1104/pp.65.2.245

Sun, Y., Liu, Z., Lan, G., Jiao, C., and Sun, Y. (2019). Effect ofexogenous melatonin on resistance of cucumber to downy mildew. *Sci. Hortic.* 255, 231–241. doi: 10.1016/j.scienta.2019.04.057

Tan, D.-X., Manchester, L. C., Helton, P., and Reiter, R. J. (2007). Phytoremediative capacity of plants enriched with melatonin. *Plant Signal. Behav.* 2, 514–516. doi: 10.4161/psb.2.6.4639

Tiwari, J. K., Munshi, A. D., Kumar, R., Pandey, R. N., Arora, A., Bhat, J. S., et al. (2010). Effect of salt stress on cucumber: Na+–K+ ratio, osmolyte concentration, phenols and chlorophyll content. *Acta Physiol. Plant.* 32, 103–114. doi: 10.1007/s11738-009-0385-1

Wang, M., Zhang, S., and Ding, F. (2020). Melatonin mitigates chilling-induced oxidative stress and photosynthesis inhibition in tomato plants. *Antioxidants* 9, 218. doi: 10.3390/antiox9030218

Wang, P., Sun, X., Li, C., Wei, Z., Liang, D., and Ma, F. (2013). Long-term exogenous application of melatonin delays drought-induced leaf senescence in apple. *J. Pineal Res.* 54, 292–302. doi: 10.1111/jpi.12017

Wang, P., Yin, L., Liang, D., Li, C., Ma, F., and Yue, Z. (2012). Delayed senescence of apple leaves by exogenous melatonin treatment: toward regulating the ascorbate–glutathione cycle. *J. Pineal Res.* 53, 11–20. doi: 10.1111/j.1600-079X.2011.00966.x

Yang, Y., Chen, J., Liu, Q., Ben, C. C., Todd, C. D., Shi, J., et al. (2012). Comparative proteomic analysis of the thermotolerant plant *Portulaca oleracea* acclimation to combined high temperature and humidity stress. *J. Proteome Res.* 11, 3605–3623. doi: 10.1021/pr300027a

Zhang, H. J., Zhang, N., Yang, R. C., Wang, L., Sun, Q. Q., Li, D. B., et al. (2014). Melatonin promotes seed germination under high salinity by regulating antioxidant systems, ABA and GA 4 interaction in cucumber (*Cucumis sativus* L.). *J. Pineal Res.* 57, 269–279. doi: 10.1111/jpi.12167

Zhang, R., Sun, Y., Liu, Z., Jin, W., and Sun, Y. (2017). Effects of melatonin on seedling growth, mineral nutrition, and nitrogen metabolism in cucumber under nitrate stress. *J. Pineal Res.* 62:e12403. doi: 10.1111/jpi.12403

Zhang, T., Shi, Z., Zhang, X., Zheng, S., Wang, J., and Mo, J. (2020). Alleviating effects of exogenous melatonin on salt stress in cucumber. *Sci. Hortic.* 262:109070. doi: 10.13287/j.1001-9332.201706.005

Zhang, X., Feng, Y., Jing, T., Liu, X., and Bi, H. (2021). Melatonin promotes chilling tolerance of cucumber seedlings by regulating antioxidant systems and relieving photoinhibition. *Front. Plant Sci.* 12:789617. doi: 10.3389/fpls.2021.789617

Zhang, Y.-J., Zhang, X., Chen, C.-J., Zhou, M.-G., and Wang, H.-C. (2010). Effects of fungicides JS399-19, azoxystrobin, tebuconazloe, and carbendazim on the physiological and biochemical indices and grain yield of winter wheat. *Pestic. Biochem. Physiol.* 98, 151–157. doi: 10.1016/j.pestbp.2010.04.007

Zhao, H., Ye, L., Wang, Y., Zhou, X., Yang, J., Wang, J., et al. (2016). Melatonin increases the chilling tolerance of chloroplast in cucumber seedlings by regulating photosynthetic electron flux and the ascorbate-glutathione cycle. *Front. Plant Sci.* 7:1814. doi: 10.3389/fpls.2016.01814

Zhao, H., Zhang, K., Zhou, X., Xi, L., Wang, Y., Xu, H., et al. (2017). Melatonin alleviates chilling stress in cucumber seedlings by up-regulation of CsZat12 and modulation of polyamine and abscisic acid metabolism. *Sci. Rep.* 7:4998. doi: 10.1038/s41598-017-05267-3

Zhao, Y., Han, Q., Ding, C., Huang, Y., Liao, J., Chen, T., et al. (2020). Effect of low temperature on chlorophyll biosynthesis and chloroplast biogenesis of rice seedlings during greening. *Int. J. Mol. Sci.* 21:1390. doi: 10.3390/ijms21041390

Zuo, B., Zheng, X., He, P., Wang, L., Lei, Q., Feng, C., et al. (2014). Overexpression of MzASMT improves melatonin production and enhances drought tolerance in transgenic *Arabidopsis thaliana* plants. *J. Pineal Res.* 57, 408–417. doi: 10.1111/jpi.12180

Conflict of Interest: The authors declare that the research was conducted in the absence of any commercial or financial relationships that could be construed as a potential conflict of interest.

Publisher's Note: All claims expressed in this article are solely those of the authors and do not necessarily represent those of their affiliated organizations, or those of the publisher, the editors and the reviewers. Any product that may be evaluated in this article, or claim that may be made by its manufacturer, is not guaranteed or endorsed by the publisher.

Copyright © 2022 Amin, Atif, Meng, Ali, Li, Alharby, Majrashi, Hakeem and Cheng. This is an open-access article distributed under the terms of the Creative Commons Attribution License (CC BY). The use, distribution or reproduction in other forums is permitted, provided the original author(s) and the copyright owner(s) are credited and that the original publication in this journal is cited, in accordance with accepted academic practice. No use, distribution or reproduction is permitted which does not comply with these terms.

frontiers | Frontiers in Plant Science

SYSTEMATIC REVIEW
published: 27 April 2022
doi: 10.3389/fpls.2022.825309

Effects of Fallow Management Practices on Soil Water, Crop Yield and Water Use Efficiency in Winter Wheat Monoculture System: A Meta-Analysis

Muhammad Adil[1†], Shaohong Zhang[1,2†], Jun Wang[1,2], Adnan Noor Shah[1,3], Mohsin Tanveer[4] and Sajid Fiaz[5]*

[1] Shaanxi Key Laboratory of Earth Surface System and Environmental Carrying Capacity, College of Urban and Environmental Science, Northwest University, Xi'an, China, [2] State Key Laboratory of Soil Erosion and Dryland Farming on the Loess Plateau, Institute of Soil and Water Conservation, Chinese Academy of Sciences and Ministry of Water Resources, Yangling, China, [3] Department of Agricultural Engineering, Khwaja Fareed University of Engineering and Information Technology, Rahim Yar Khan, Pakistan, [4] Tasmanian Institute of Agriculture, University of Tasmania, Hobart, TAS, Australia, [5] Department of Plant Breeding and Genetics, The University of Haripur, Haripur, Pakistan

OPEN ACCESS

Edited by:
Shabir Hussain Wani,
Sher-e-Kashmir University of Agricultural Sciences and Technology, India

Reviewed by:
Giuseppe Badagliacca,
Mediterranea University of Reggio Calabria, Italy
QaSim Ali,
University of Florida, United States

***Correspondence:**
Jun Wang
wangj@nwu.edu.cn

[†]These authors share first authorship

Specialty section:
This article was submitted to Plant Breeding, a section of the journal Frontiers in Plant Science

Received: 30 November 2021
Accepted: 07 February 2022
Published: 27 April 2022

Citation:
Adil M, Zhang S, Wang J, Shah AN, Tanveer M and Fiaz S (2022) Effects of Fallow Management Practices on Soil Water, Crop Yield and Water Use Efficiency in Winter Wheat Monoculture System: A Meta-Analysis. Front. Plant Sci. 13:825309. doi: 10.3389/fpls.2022.825309

Winter wheat monoculture is a predominant cropping system for agricultural production in dry areas. However, fallow management effects on soil water conservation and crop yield and water use have been inconsistent among studies. We selected 137 studies and performed a meta-analysis to test the effects of tillage and mulching during the fallow period on precipitation storage efficiency (PSE), soil water storage at wheat planting (SWSp), crop yield, evapotranspiration (ET), and water use efficiency (WUE). Compared to conventional tillage (CT), conservation tillage during fallow period overall increased PSE, SWSp and wheat yield by 31.0, 6.4, and 7.9%, respectively, but did not affect ET and WUE. No tillage (NT) had a better performance on soil water conservation during fallow period but a similar effect on wheat yield and WUE compared to reduced tillage (RT) and subsoil tillage (ST). Compared to no mulching, fallow mulching practices overall increased PSE by 19.4%, but had a non-significant impact on SWSp, wheat yield, and ET. Compared to straw mulching, film mulching, and stubble mulching during fallow period, cover cropping as a biological mulching decreased SWSp, wheat yield, and WUE significantly. Wheat WUE was improved by straw mulching but not affected by film mulching and stubble mulching. Strong interactions between tillage method and mulching practices were found for most variables. NT with fallow mulching or with no mulching exhibited a greater impact on soil water conservation during fallow period compared to other combinations. The effects of tillage and mulching during fallow period on soil water conservation and wheat yield and water use also varied with soil and climatic conditions. Overall, NT in combination with straw mulching significantly increased SWSp, PSE, wheat yield, and WUE and can be the best fallow management practice for winter wheat production in varying edaphic and climatic conditions.

Keywords: wheat mono-cropping system, fallow, tillage, mulching, soil water conservation

INTRODUCTION

Wheat (*Triticum aestivum* L.) is one of the most important cereal crops throughout the world (Bruning et al., 2020; Bukhari et al., 2021). It is planted on more than 2.2 million acres in the inland Pacific Northwest of the USA alone (Schillinger and Papendick, 2008) and an additional 4.3 million hectares in the Chinese Loess Plateau, providing 40% of the food grains in China (Tong et al., 2003). In the arid and semiarid regions where water and heat resources are limited, wheat is generally cultivated in mono-culture following with a short or long fallow period. A short 3-month summer fallow between the harvest in late June and planting in late September of winter wheat, is adopted on the Loess Plateau of China (Shangguan et al., 2002; Wang et al., 2011) while a long fallow of more than 14 months, growing one crop in two years, is generally practiced in the western United States (Smiley and Uddin, 1993; Peterson et al., 1996; Tanaka and Anderson, 1997; Nielsen and Vigil, 2010). Improving precipitation storage efficiency (PSE) during the fallow period could significantly increase wheat yield and profitability of the winter wheat mono-culture system in dryland areas.

After harvesting winter wheat at the beginning of the rainy season in the drylands, local farmers generally plow the soil to increase soil moisture retention through dust-mulch effects (Shah et al., 2017). Although such conventional tillage (CT) can increase water permeability temporarily, but it could increase water loss due to evaporation compared to undisturbed soil (Jin et al., 2007). Compared to CT, conservation tillage practices including subsoil tillage (ST), reduced tillage (RT), and no tillage (NT) have been widely adopted to save water during the fallow period (Rasmussen, 1999; Schillinger, 2001; Lampurlanes et al., 2002; Wang et al., 2003; Li et al., 2007; He et al., 2009). Changes in soil water-related properties acquired with NT depend on several factors, including initial soil properties, land management history, weather conditions, and type and tillage intensity (Mahboubi et al., 1993). RT improved soil infiltration, reduced surface runoff and evaporation, and ultimately increased soil water content (Zhai et al., 1990). According to Patrignani et al. (2012), the effect of conservation tillage on soil water recharge during the fallow period varied with climatic and soil conditions (Mahboubi et al., 1993). Conservation tillage increased PSE with a 27% higher value compared to CT in Ohio and 25% higher in Colorado, USA (Farahani et al., 1998). Similarly, NT and ST increased SWSp by 10.2 and 11.5%, respectively, in northwestern China (Hou et al., 2012). The PSE increased by 81% and soil water storage at planting (SWSp) by 188 mm under NT than CT in the Great Plains (Nielsen and Vigil, 2010), and the PSE increased by 43% at North Platte (Smika and Wicks, 1968), and by 38% at Sidney, MT (Tanaka and Aase, 1987).

In dryland agriculture, soil surface cover management determines soil moisture loss, water storage, and crop productivity. Covering the soil surface with plastic film has become a broadly used technique to improve crop productivity in arid regions of China (Xie et al., 2005), including covering all or part of the soil surface (ridge mulching and planting in furrows) during the whole year or part of the growing period (Li et al., 1999). Wang et al. (2018) reported that straw mulching increased PSE by 13–16% compared to no mulching during summer fallow. Straw mulching significantly increased soil water content and wheat yield by 23% each and water use efficiency (WUE) by 33% (Zhang et al., 2015). Similarly, straw mulching enhanced winter wheat grain yield and WUE by 13–25% compared to no mulching (Chakraborty et al., 2010). Film mulching during summer fallow increased SWSp by 13% (He et al., 2016) and 56% (Ren et al., 2019), making it the highest soil-water storage (50 mm) in winter wheat cropping system. Wheat grain yield was significantly lower with cover cropping than bare fallow in the first year of study (Zhang et al., 2015). However, more information is needed to understand whether different mulching and tillage methods can always increase water storage and crop yields under different soil types and climatic conditions.

A meta-analysis is a valuable tool that uses the effect size of individual studies combining the data from different management practices originating from different soil and climate conditions (Hedges et al., 1999; Hungate et al., 2009). In this study, we collected the data available in the literature and conducted a meta-analysis to check the overall and individual effect of conservation tillage and mulching methods on soil and plant parameters compared to conventional tillage and bare fallow cropping patterns under different edaphic and climate conditions. We hypothesized that conservation tillage and mulching would improve PSE, SWSp, winter wheat yield, and WUE compared to conventional tillage and bare fallow. Relative effects on soil water parameters may differ within tillage practices, mulching methods, and edaphic and climatic conditions.

MATERIALS AND METHODS

Data Collection

Peer-reviewed journal articles published between 1968 and 2021 were searched in Google Scholar[1] and Web of Science[2] to evaluate the effects of fallow tillage and mulching methods on soil water and crop yield and water use in mono-culture winter wheat system. We used soil water, precipitation storage efficiency, wheat yield, and WUE along with conventional tillage, conservation tillage, bare fallow, and mulching as keywords. Initially, about 1,326 publications were collected and then screened using criteria as follows:

- Tillage and/or mulching studies should be carried out in the mono-culture winter wheat cropping system experiments in a field.
- Each study should have a control treatment, e.g., conventional tillage (for tillage comparison) and bare fallow (for mulching comparison) with similar edaphic and climatic conditions.
- SWSp, PSE, yield, ET, and WUE should be compared between conservation tillage methods (NT, RT, and ST) and

[1]https://scholar.google.com/

[2]https://www.webofknowledge.com/

CT or between straw mulching, plastic film mulching, cover cropping (as a biological mulching), stubble mulching, and a bare fallow without mulching. All crop residues should be removed immediately at harvest of the main crop, and the land kept bare during the whole fallow period as a control treatment for mulching.

- Experiments should be conducted in a rain-fed system with no irrigation applied during the entire experimental period. The simulation model and multi-cropping studies were excluded.

A brief description of tillage and mulching practices used in this meta-analysis is provided in **Table 1**, which further clarifies search criteria. Finally, 2,187 observations for tillage and 1,655 observations for mulching were collected from 137 studies from 76 sites, covering 15 countries (**Figure 1**). Group homogenization of the data was accomplished according to different tillage and mulching methods. Data from the figures were extracted by using GetData graph digitizer 2.20 software.[3] By using standard error (*SE*) value, we calculated the standard deviation (*SD*) value by using the following formula:

$$SD = SE \times \sqrt{n} \quad (1)$$

Where "*n*" represents the number of samples.

In publications where PSE, ET, or WUE were not calculated, but the SWS and fallow precipitation were available, we manually calculated these variables using the following equations (Tanaka and Anderson, 1997; Nielsen and Vigil, 2010; Zhang et al., 2015).

$$PSE = \frac{\Delta SWS}{P_f} \quad (2)$$

Where ΔSWS is the difference in SWSp and harvest during the fallow period, and P_f is the precipitation during the fallow period.

Wheat WUE was calculated as:

$$WUE = \frac{Yield}{ET} \quad (3)$$

Where ET is evapotranspiration, whereas ET was determined by following soil water balance equation:

$$ET = \Delta SWS + P_g \quad (4)$$

Where ΔSWS is the change in soil water storage during wheat growing season and P_g represents the precipitation during the growing season.

Mean annual precipitation (MAP), mean annual air temperature (MAT), along with soil texture of the experimental plots, were also recorded for each study. If the information about soil properties, and climatic conditions were not found in the study, then these observations were searched in an online search engine.[4] Soil textures were categorized into three groups: fine (clay, clay loam, silty clay loam, and silty clay), medium (silt, loam, silt loam, and sandy silt loam) and coarse (sandy loam, sandy clay loam, loamy sand and sand) according to the USDA soil classification system. MAP was classified into <400 mm, 400–600 mm, and >600 mm, and MAT was grouped into frigid (<8°C), mesic (8–15°C), and thermic (>15°C) (Knorr et al., 2005).

TABLE 1 | Description of tillage and mulching practices used for fallow management in a wheat monoculture system.

Management practices	Brief description
Tillage	
Conventional tillage (CT)	The field is tilled using a tractor-mounted moldboard plow to a depth of 20–25 cm for 4–6 times during a fallow period (with or without mulching).
No-tillage (NT)	Land remained bare and undisturbed during the entire fallow period until the next planting, mostly no-till planter was used to plant the main crop.
Reduced tillage (RT)	Soil was inverted and plowed to a depth of 25–30 cm combined with generally harrowing at a depth of 5–8 cm in the primary tillage.
Subsoil tillage (ST)	Soil is plowed by a deep soil chisel to a depth of 30–35 cm, with its adjustable wings making the distance between two ends by at least 60 cm.
Mulching	
Bare fallow (control)	At winter wheat harvest, all the residual straw was removed, and the land was kept fallow until sowing of the next wheat crop (by keeping tillage constant).
Straw mulching	Wheat straw was evenly distributed over the soil surface at an average rate of 6 t ha^{-1} during the entire fallow period.
Film mulching	A plastic film of generally 0.008 mm thickness was used as mulching during the whole fallow period.
Cover cropping	Growing of cover crops during the entire fallow period.
Stubble mulching	All of the residual straw of wheat was kept in place during the entire fellow period.

Data Analysis

The effects of conservation tillage compared to CT and of fallow mulching compared to no mulching were determined with the help of response ratio (RR) and the natural log of RR taken as effect size (Hedges et al., 1999):

$$RR = Ln\left(\frac{X_{COT}}{X_{CT}}\right) = Ln\left(X_{COT}\right) - Ln\left(X_{CT}\right) \quad (5)$$

$$RR = Ln\left(\frac{X_{NM}}{X_{M}}\right) = Ln\left(X_{NM}\right) - Ln\left(X_{M}\right) \quad (6)$$

Where X_{COT} and X_{CT} exhibits arithmetic mean fluxes of soil and plant parameters (SWSp, PSE, yield, ET, and WUE) with conservation tillage and CT, respectively. The comparison between CT and COT was determined separately for each experiment studied. X_{NM} and X_M exhibit arithmetic mean fluxes with no mulching and fallow mulching practices, respectively. For each experiment studied, the comparison between fallow mulching and no mulching was determined separately.

[3] http://getdata-graph-digitizer.com/index.php

[4] www.whatsmygps.com

Error variance (V) within each experiment studied was calculated with the following formula (Hedges et al., 1999).

$$V = \frac{S_{COT}^2}{N_{COT}X_{COT}^2} + \frac{S_{CT}^2}{N_{CT}X_{CT}^2} \quad (7)$$

$$V = \frac{S_M^2}{N_M X_M^2} + \frac{S_{NM}^2}{N_{NM}X_{NM}^2} \quad (8)$$

Where S_{COT} and S_{CT} are SD values for conservation tillage and CT, N_{COT} and N_{CT} indicate number of replications for conservation tillage and CT, and X_{COT} and X_{CT} are mean for conservation tillage and CT, S_M and S_{NM} are SD values for fallow mulching and no mulching, N_M and N_{NM} are number of replications for fallow mulching and no mulching, and X_M and X_{NM} are water storage with no mulching and fallow mulching, respectively.

The reciprocal of the variance (V) taken as the weight (W) for each RR was determined by the following formula (Lucas et al., 2011):

$$W = \frac{1}{V} \quad (9)$$

Studies with more variance are weighed less heavily during analysis than those with less variance, a method given by Hedges et al. (1999). Individual RR value of conventional and conservation tillage was used to calculate the overall mean response ratio (RR_{E++}) as follows:

$$RR_{E++} = \frac{\sum_{i=1}^{n}\sum_{j=1}^{m} W_{ij}RR_{ij}}{\sum_{i=1}^{n}\sum_{j=1}^{m} W_{ij}} \quad (10)$$

Within each category, "n" represents the number of treatments while "m" is the number of comparisons. The standard error of RR_{E++} was calculated as:

$$SE(RR_{E++}) = \sqrt{\frac{1}{\sum_{i=1}^{n}\sum_{j=1}^{m} W_{ij}}} \quad (11)$$

In order to analyze the impact of conservation tillage methods on soil and crop parameters (SWSp, PSE, yield, ET, and WUE), random model MetaWin 2.1 (Sinaure Associate Inc., Sunderland, United Kingdom) was used to calculate the mean effect size of bias-based bootstrap at 95% confidence Interval. The impact of the conservation tillage methods was measured significant if the 95% confidence interval did not overlap with the zero line. Correlations of the RRs of wheat yield, ET, and WUE to that of SWSp were conducted using the Origin 2018 software (OriginLab Corporation, United States).

RESULTS

Tillage Effect on Precipitation Storage Efficiency and Soil Water Storage at Wheat Planting

We collected 267 paired observations for PSE and 754 for SWSp (**Figures 2A,B**). Data exhibited high heterogeneities as indicated by high Qt values of 256 and 767 for PSE and SWSp, respectively. Conservation tillage methods overall increased PSE by 31.0% ($P < 0.05$) compared to CT (**Figure 2A**). Among conservation tillage methods, the highest increase in PSE was observed with NT (42.5%), followed by RT (15.2%) and ST (7.0%). The effect of PSE to NT also varied with mulching practices. The RR of PSE was greater with NT cover cropping than NT straw mulching. However, no significant differences among mulching practices in the RRs of PSE were found under RT and ST compared to CT. The RR of PSE to conservation tillage methods compared to CT did not vary with soil textures (**Figure 3A**). The enhancement of conservation tillage on PSE was greater when MAP was 400–600 mm than < 400 and > 600 mm. Conservation tillage also increased PSE in the regions when MAT was 8–15℃ and had no significant effect when MAT was > 15℃.

Compare to CT, conservation tillage overall increased SWSp by 6.4% ($P < 0.05$, **Figure 2B**). However, such positive effect on SWSp varied with tillage methods. NT increased SWSp by 10.5%, but ST decreased by 12.5%. Strong interactions were found between tillage methods and mulching practices. All conservation tillage methods increased SWSp with mulching practices except for cover cropping. Both NT and RT decreased SWSp with cover cropping but increased with other mulching practices. The RR of SWSp for ST was positive with cover cropping but negative with stubble mulching. The RR of SWSp to conservation tillage to CT was negative in fine soils, but positive in medium and coarse soils (**Figure 3B**). The effect of Conservation tillage on SWSp did not vary with MAP, and was positive when MAT was 8–15℃ but not significant when MAT was <8 and > 15℃.

Tillage Effect on Winter Wheat Yield, Evapotranspiration, and Water Use Efficiency

Overall, 708 observations were measured for winter wheat yield, 69 for ET, and 389 for WUE. Data was heterogeneous for yield (Qt = 689) and WUE (Qt = 372), but not for ET (Qt = 70) (**Figures 2C–E**). Conservation tillage methods increased winter wheat yield by 7.9% compared to CT ($P < 0.05$, **Figure 2C**). The categorical meta-analysis showed that NT, RT, and ST increased winter wheat yield by 7.3, 9.2, and 8.3%, respectively. When combined with mulching practices, however, winter wheat yield was only enhanced by NT no mulching, NT straw mulching, RT no mulching, ST straw mulching, and ST film mulching. The RR of wheat yield to conservation tillage compared to CT was consistent with soil textures, MAP, and MAT, although conservation tillage had a non-significant impact on wheat yield when MAT was > 15℃ (**Figure 3C**).

There was no significant effect of overall conservation tillage methods on winter wheat ET. However, NT no mulching decreased ET by 9.1% and ST no mulching increased by 6.3% ($P < 0.05$, **Figure 2D**). With all other management practices, ET remained non-significant. Conservation tillage increased ET in coarse soils, but its effect on ET was not significant in fine and medium soils (**Figure 3D**). The RR of ET to conservation tillage compared to CT was also positive when MAP was 400–600 mm, but non-significant when MAP was < 400 mm. Conservation

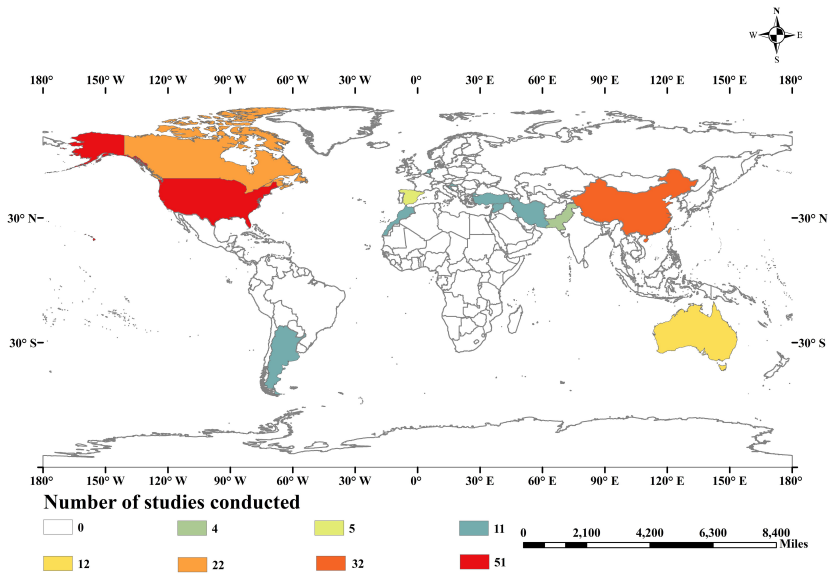


FIGURE 1 | Distribution of 137 experimental sites around the globe from where the data was collected for the meta-analysis.

tillage increased ET when MAT was < 15°C but and decreased it when MAT was > 15°C.

Winter wheat WUE was also not significant for conservation tillage during fallow period (**Figure 2E**). However, strong interactions with mulching practices were found for NT, RT, and ST. Compared to CT, NT increased wheat WUE by 13.3%, and 5.6% with no mulching and straw mulching, respectively, but decreased by 22.4% with cover cropping. Similarly, RT increased wheat WUE by 8.4% with no mulching but decreased by 8.5% with stubble mulching. ST also increased wheat WUE by 5.8% with no mulching. Winter wheat WUE increased with conservation tillage during fallow period in fine and coarse soils, but decreased in medium soils (**Figure 3E**). The RR of wheat WUE to conservation tillage compared to CT was negative when MAP was 400–600 mm, but not significant when MAP was over the range. Wheat WUE RR was also negative when MAT was < 8 and > 15°C but negative when MAT 8–15°C.

Mulching Effect on Precipitation Storage Efficiency and Soil Water Storage at Wheat Planting

We collected 204 and 552 paired observations for PSE and SWSp with fallow mulching practices (**Figures 4A,B**), respectively. High heterogeneities were found for the data as indicated by the high *Qt* values (211 and 516 for PSE and SWSp, respectively). Compared to no mulching, fallow mulching practices overall increased PSE by 19.4% ($P < 0.05$) compared to no mulching (**Figure 4A**). The categorical meta-analysis showed that all fallow mulching practices exhibited a positive effect on PSE, with increases of 23.9, 30.8, 19.1, and 10.8% ($P < 0.05$) for straw mulching, film mulching, cover cropping, and stubble mulching, respectively. Strong interactions with tillage were found for all fallow mulching practices except for film mulching. Cover cropping effect on PSE compared to no mulching was neutral with CT but positive with NT. Similarly, compared to no mulching, fallow stubble mulching had no effect on PSE with CT and RT, but increased PSE with NT and ST. Fallow mulching had no effect on PSE in medium soils, but increased PSE in fine and coarse soils with a greater RR value in coarse than fine soils (**Figure 5A**). The RR of PSE to fallow mulching compared to no mulching was not different with MAP and greater when MAT was <8°C than 8–15°C.

Not like PSE, the overall effect of fallow mulching practices on SWSp was not significant compared to no mulching (**Figure 4B**). Straw mulching, film mulching, and stubble mulching increased SWSp by 12.6, 10.2, and 13.4% over no mulching fallow ($P < 0.05$), respectively. However, cover cropping decreased SWSp by 16.3% ($P < 0.05$) compared to no mulching during fallow period. Effects of fallow mulching practices on SWSp were not interacted with tillage methods, and no significant differences were found in the RRs of SWSp among tillage methods for each mulching practice. The RRs of SWSp to fallow mulching were not significant in soil textures (**Figure 5B**). Fallow mulching increased SWSp when MAP was < 400 and > 600 mm but decreased when it was 400–600 mm. Positive effect of fallow mulching on SWSp was only observed when MAT was > 15°C.

Mulching Effect on Winter Wheat Yield, Evapotranspiration, and Water Use Efficiency

The mulching responses were variable on 400 observations for wheat yield, 97 for ET, and 402 for WUE (**Figures 4C–E**). Data exhibited high heterogeneities with *Qt* values of 388, 98, and 406 for wheat yield, ET, and WUE, respectively. The mulching practices showed negative to positive RR on wheat yield, exhibiting an overall non-significant effect (**Figure 4C**).

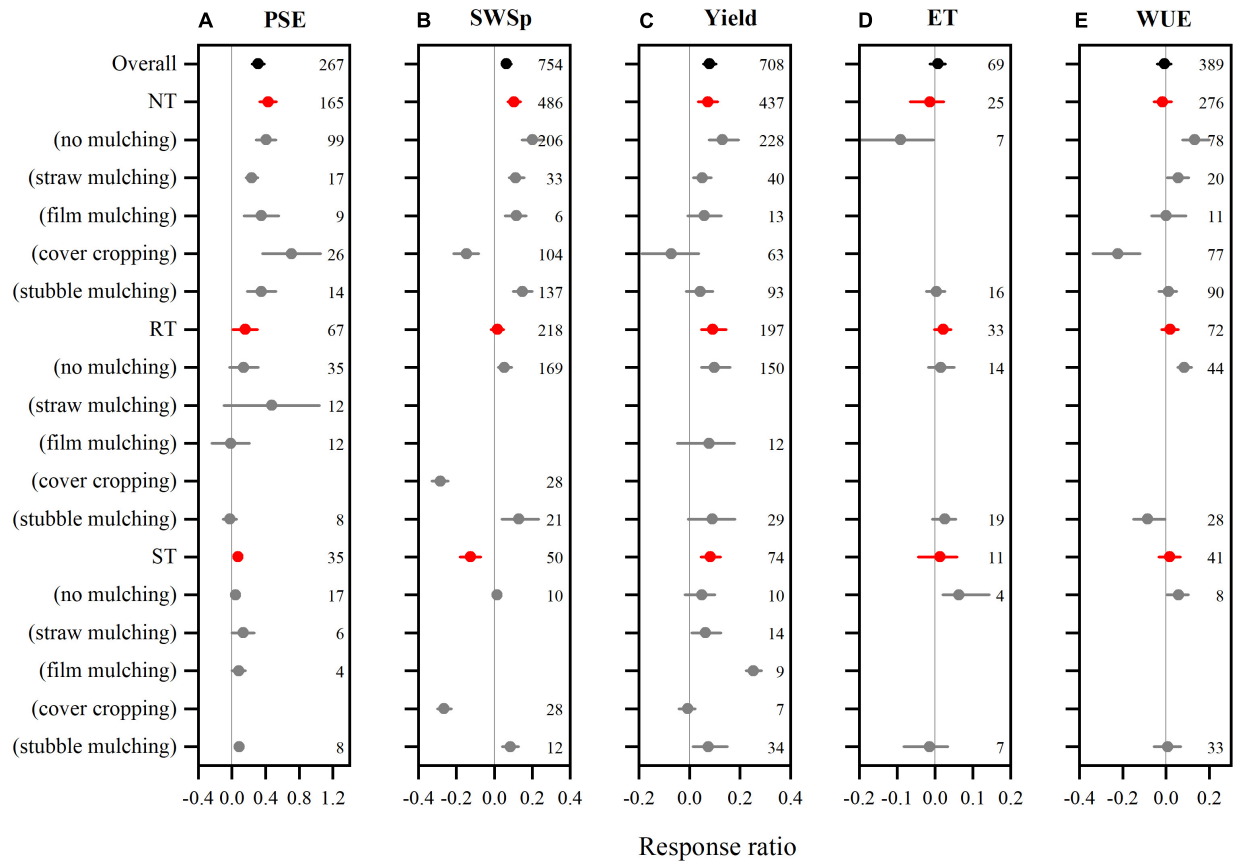


FIGURE 2 | The mean response ratios of precipitation storage efficiency (PSE, **A**), soil water storage at wheat planting (SWSp, **B**), winter wheat grain yield **(C)**, evapotranspiration (ET, **D**), and water use efficiency (WUE, **E**) to conservation tillage methods during fallow period compared to conventional tillage (CT) and their interactions with fallow mulching practices. The horizontal line represents the bootstrapped 95% confidence interval. Conservation tillage methods are no tillage (NT), reduced tillage (RT), subsoil tillage (ST). The reference line (RR = 0) specifies no variation between conservation tillage and conventional tillage. Numbers accompanying the bootstrapped 95% confidence intervals designate the number of observations for comparisons.

Compared to no mulching during fallow, straw mulching, film mulching, and stubble mulching increased winter wheat yield by 4.2, 6.2, and 5.5% ($P < 0.05$), respectively, while cover cropping decreased wheat yield by 7.0% ($P < 0.05$). Strong interaction with tillage methods was found for straw mulching. Straw mulching significantly decreased winter wheat yield with CT, but increased with NT and ST. Fallow mulching also decreased wheat yield in medium soil, but increased in fine and coarse soils (**Figure 5C**). The RR of wheat yield to fallow mulching compared to no mulching was only positive when MAP was < 400 mm and MAT < 8℃ but not significant for other climatic conditions.

Fallow mulching overall had a neutral effect on ET compared to no mulching (**Figure 4D**). This is true for all mulching practices. Also, no interactions were found between mulching practices with tillage methods. Fallow mulching decreased ET in fine soil, but increased in coarse soil (**Figure 5D**). The RR of ET to fallow mulching compared to no mulching did not vary with MAP, and was positive when MAT was < 8℃ but negative when MAT was > 15℃.

Winter wheat WUE was overall 12.8% lower with mulching than no mulching during fallow period (**Figure 4E**). Straw mulching increased wheat WUE by 4.4%, while cover cropping decreased by 26.3% compared to no mulching. Both film mulching and stubble mulching had no effect on wheat WUE. When combined with tillage methods, however, film mulching increased WUE with NT, and stubble mulching decreased with RT. Fallow mulching also decreased wheat WUE in fine and medium soils but had a neutral effect in coarse soil (**Figure 5E**). The RR of wheat WUE to fallow mulching compared to no mulching was not significant with MAP, and negative when MAT was >8℃.

Correlations of Winter Wheat Yield, Evapotranspiration, and Water Use Efficiency to Soil Water Storage at Planting

The RR of winter wheat yield increased with increase of the RR of SWSp linearly for both tillage and mulching management practices (**Figures 6A,B**). About 7 and 36% increases in the RR of wheat yield can be explained by the increase of the RR of SWSp for tillage and mulching management practices, respectively.

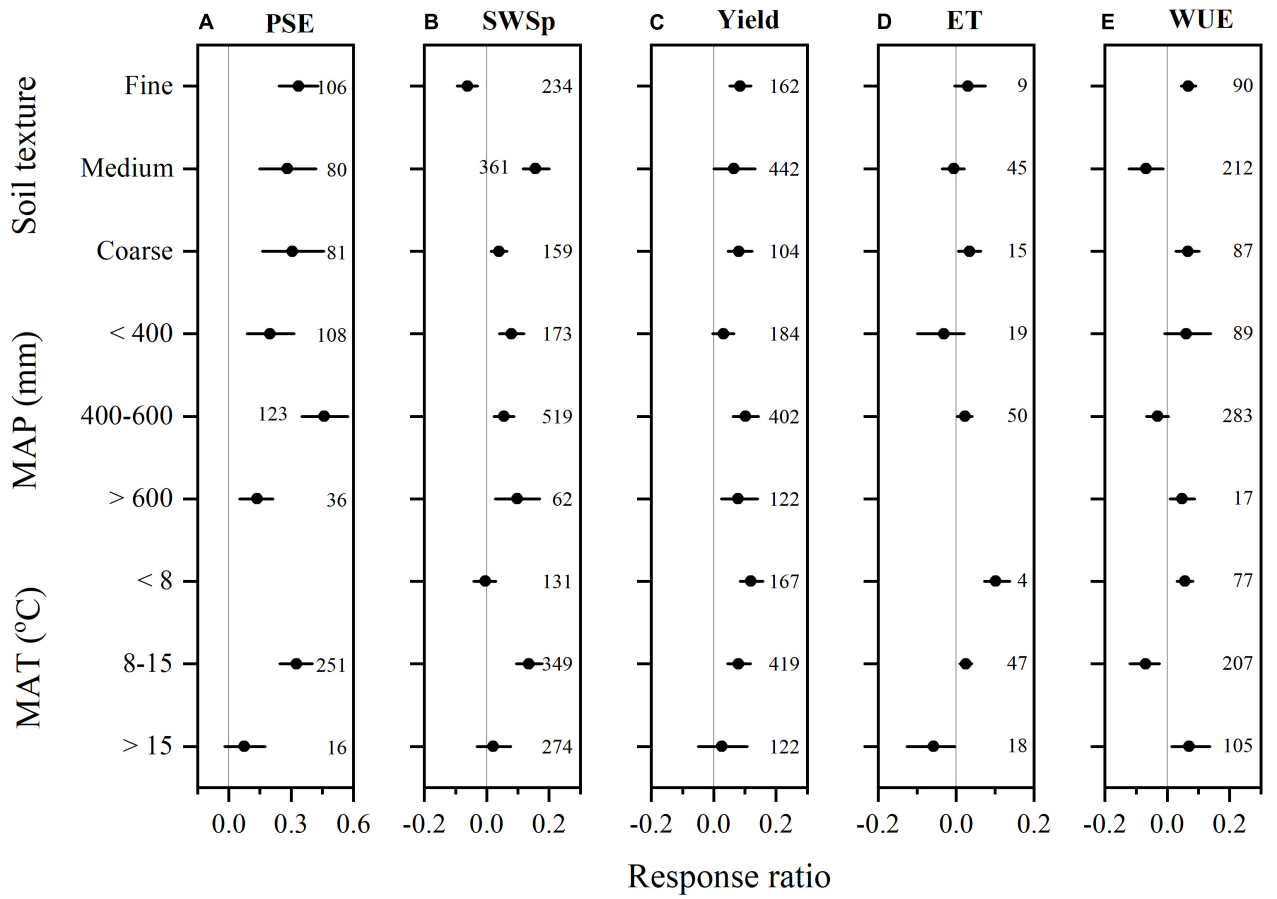


FIGURE 3 | The mean response ratios of precipitation storage efficiency (PSE, **A**), soil water storage at wheat planting (SWSp, **B**), winter wheat grain yield **(C)**, evapotranspiration (ET, **D**), and water use efficiency (WUE, **E**) to conservation tillage methods during fallow period compared to conventional tillage and their bootstrapped 95% confidence intervals (Horizontal line) as affect by soil texture, mean annual precipitation (MAP), and mean annual air temperature (MAT). The reference line (RR = 0) specifies no variation between conservation tillage and conventional tillage. Numbers accompanying the bootstrapped 95% confidence intervals designate the number of observations for comparisons.

Similarly, The RR of ET was also related to with that of SWSp, and about 42 and 9% increases in the RR of ET can be explained by the increase of the RR of SWSp for tillage and mulching during fallow period. No correlation was found between the RR of wheat WUE and that of SWSp.

DISCUSSION

Responses of Soil Water Storage to Fallow Tillage and Mulching Practices

Soil water storage during fallow is one of the critical factors affecting winter wheat yield in winter wheat monoculture system (Wang et al., 2018). Conservation tillage overall showed promises because of increased PSE and SWSp (**Figures 2A,B**), confirming our first hypothesis that conservation tillage methods improve soil water storage in fallow periods. The positive effects of conservation tillage on soil water conservation are probably due to the reduced soil disturbance, reduced soil bulk density, and improved aggregate stability by conservation tillage and mulching methods (Oyedele et al., 1999; Zhang et al., 2007). Previous studies also demonstrate water conservation benefits, although the relative effects on yield and water use vary with conservation tillage systems (Yan et al., 2005; Jin et al., 2007). However, the effect of conservation tillage during fallow period on soil water varied with tillage methods (**Figures 2A,B**). NT had a greater impact on PSE and SWSp than other conservation tillage practices during fallow, while RT had no impact on SWSp and ST significantly decreased SWSp compared to CT. Halvorson et al. (2000) and Jin et al. (2007) also reported that NT was the best tillage practice in fallow period for water conservation. During a 3-year study, soil water storage improved to varying degrees with different tillage practices irrespective of the volume of fallow period rainfall, but NT was more effective in fallow precipitation storage by increasing SWS and PSE compared to CT (Hou et al., 2012). Although some researchers reported that RT or ST after winter wheat harvest is useful to retain the rain water by increasing water infiltration and reducing runoff and evaporation (Jin et al., 2007; Hou et al., 2012), this meta-analysis suggests that they may not be efficient to conserve soil water during fallow

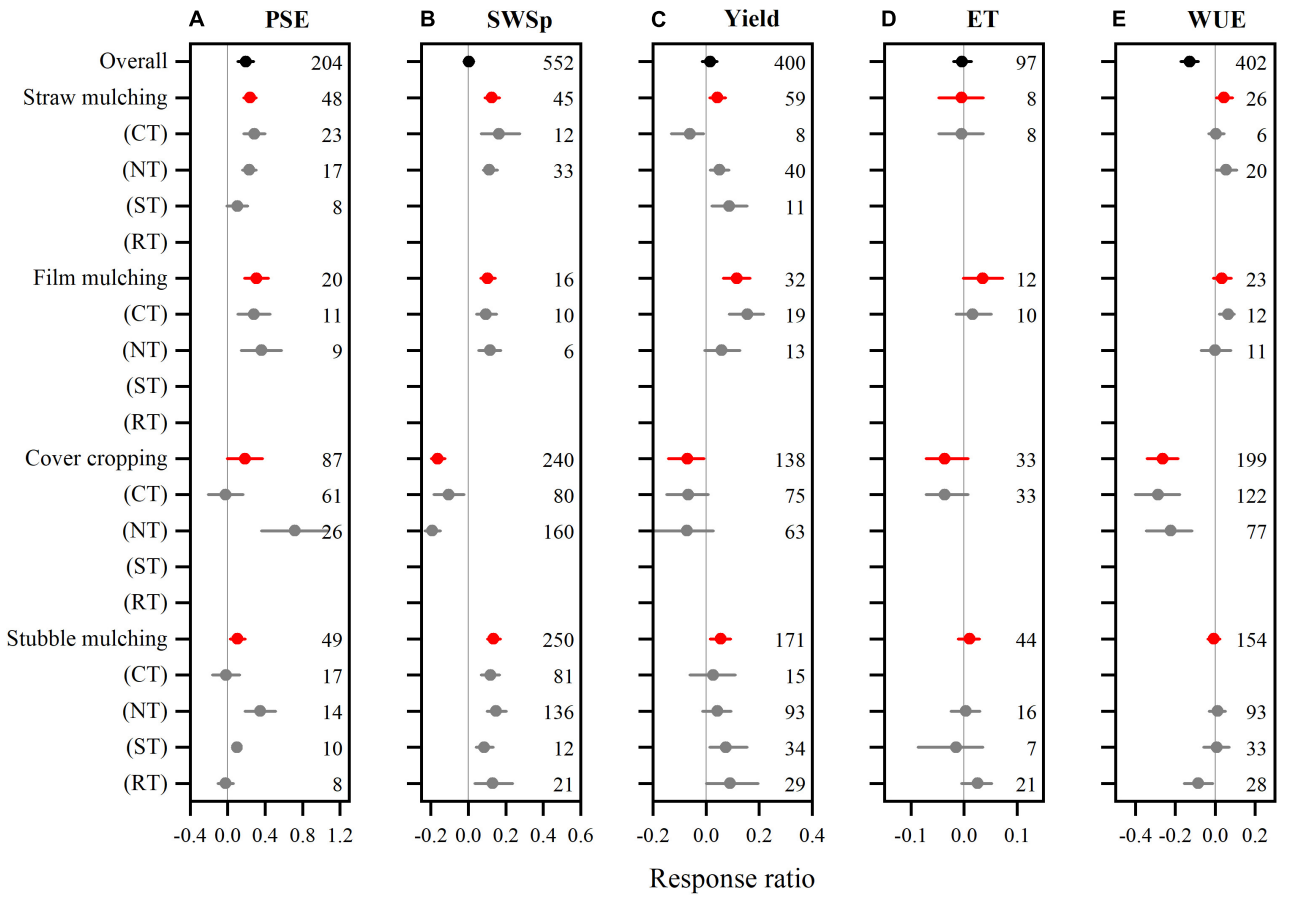


FIGURE 4 | The mean response ratios of precipitation storage efficiency (PSE, **A**), soil water storage at wheat planting (SWSp, **B**), winter wheat grain yield **(C)**, evapotranspiration (ET, **D**), and water use efficiency (WUE, **E**) to fallow mulching practices compared to no mulching and their interactions with tillage methods. The horizontal line represents the bootstrapped 95% confidence interval. Conservation tillage methods are no tillage (NT), reduced tillage (RT), subsoil tillage (ST). The reference line (RR = 0) specifies no variation between conservation tillage and conventional tillage. Numbers accompanying the bootstrapped 95% confidence intervals designate the number of observations for comparisons.

period. We also found that the effect of NT on SWSp compared to CT interacted with mulching practices during fallow period. NT no mulching, NT straw mulching, and NT stubble mulching increased SWSp (**Figure 2B**), but NT cover cropping significantly decreased SWSp although it had a positive impact on PSE. This confirms the recent meta-analysis by Wang et al. (2021), who reported that SWSp of succeeding main crops reduced after cover cropping during fallow. Including cover crops during fallow period may consume more water for their establishment and growth (Ward et al., 2012; Wang et al., 2021).

Not like conservation tillage, mulching practice during fallow period overall had a neutral impact on SWSp despite its positive effect on PSE (**Figures 4A,B**). Such non-significant effect may not be conclusive since the positive effects of straw mulching, film mulching, and stubble mulching were neutralized by the negative impact of cover cropping, which is considered as a practice of biological mulching. Compared to no mulching, surface mulching with crop straw, stubble and plastic film can conserve soil water during fallow period through reducing soil moisture loss caused by evaporation (Fan et al., 2007; Gao et al., 2009), improving water penetration, saturated hydraulic conductivity, and soil water sorption (Blanco-Canqui and Lal, 2007), and lowering potential runoff (Jin et al., 2007). Cover cropping also tended to increase PSE due to increased soil water-related properties (Blanco-Canqui and Ruis, 2020), especially with NT. However, water loss through cover crop transpiration, combined with the potential water loss during the interval between cover crop termination and winter wheat planting, may lead to a reduction in SWSp with cover cropping (**Figure 4B**).

Responses of Wheat Yield and Water Use to Fallow Tillage and Mulching Practices

Winter wheat grain yield overall increased with conservation tillage but remained non-significant with mulching practices during fallow period, which partly confirms our hypothesis. Hou et al. (2012) reported significant differences in wheat yield among conservation and conventional tillage systems with the grain yield increased by 9.6 and 10.7% with NT and ST compared

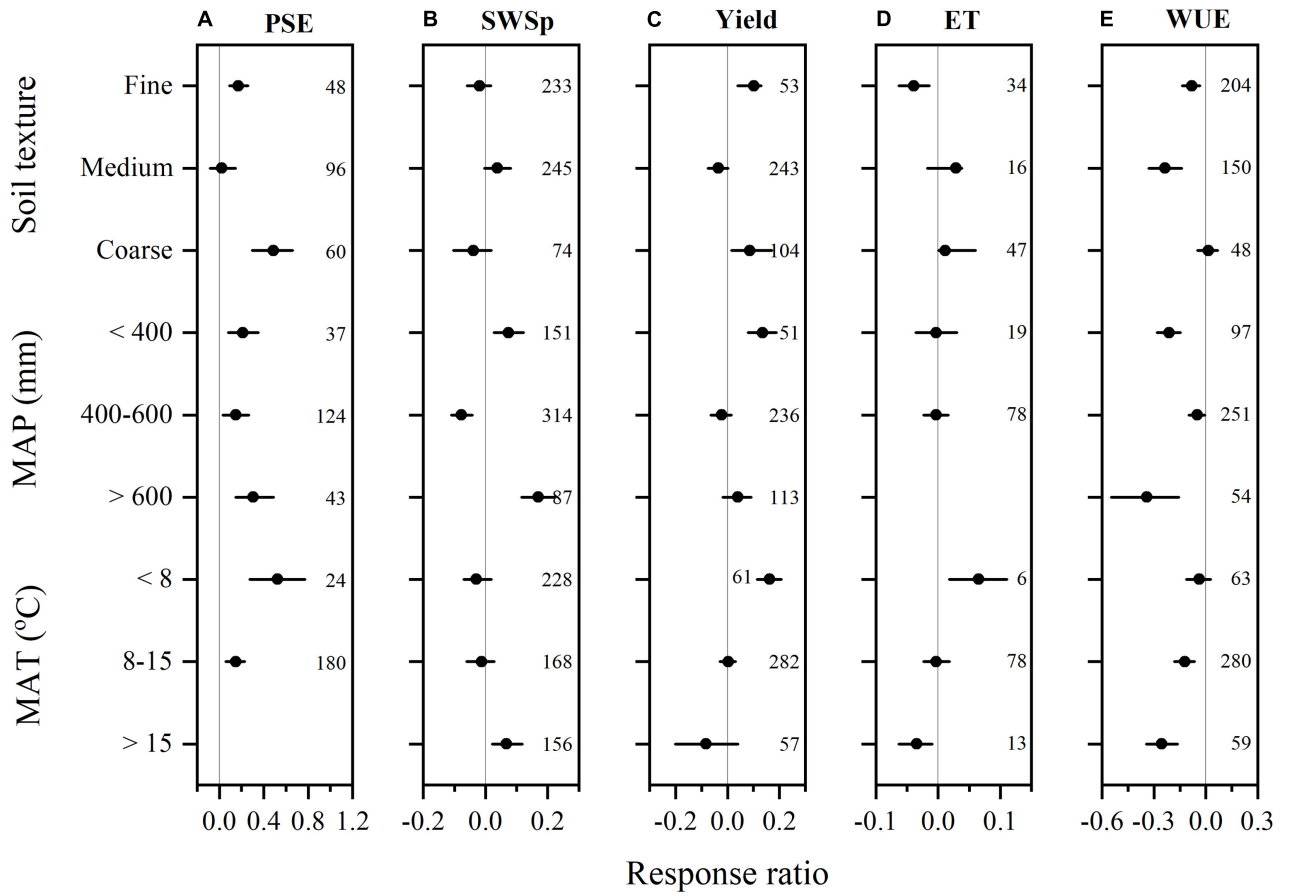


FIGURE 5 | The mean response ratios of precipitation storage efficiency (PSE, **A**), soil water storage at wheat planting (SWSp, **B**), winter wheat grain yield **(C)**, evapotranspiration (ET, **D**), and water use efficiency (WUE, **E**) to fallow mulching practices compared to no mulching and their bootstrapped 95% confidence intervals (Horizontal line) as affect by soil texture, mean annual precipitation (MAP), and mean annual air temperature (MAT). The reference line (RR = 0) specifies no variation between conservation tillage and conventional tillage. Numbers accompanying the bootstrapped 95% confidence intervals designate the number of observations for comparisons.

to CT. Higher winter wheat yield with conservation tillage than CT was due to improved soil physical and chemical properties (Fabrizzi et al., 2005). Compared to CT, conservation tillage reduced soil disturbance, improved aggregate stability (Zhang et al., 2007) and water holding capacity (Hillel, 1998), which would be helpful to conserve soil water at wheat planting and correspondingly provide a buffer against short droughts during the growing season and increase wheat crop yield (Pikul and Aase, 1999; Pikul and Aase, 2003; Verhulst et al., 2011). Interestingly, conservation tillage requires less manpower and energy for agricultural production (Zhang et al., 2009), and provide long-term benefits such as improved soil structure, reduced farm traffic and soil erosion (Wang et al., 2008). The non-significant yield response to fallow mulching, however, might be a result of counteraction between cover cropping and other mulching practices as discussed above. Strong correlations between the RR of wheat yield and that of SWSp for both tillage and mulching practices (**Figure 6**), indicate that enhancement of soil water storage during fallow through proper fallow management can increase wheat yield. Similarly, Wang et al. (2021) also reported a significant correlation between the RR of succeeding crop yield and that of SWSp under cover cropping systems, which emphasizes the importance of SWSp for crop production. In improved SWS conditions, crops would consume more soil water stimulating their growth (Wang et al., 2004). Strong interaction between tillage and mulching was also found for wheat yield in this study. NT no mulching, NT straw mulching, RT no mulching and ST film mulching increased wheat yield compared to other combinations, indicating that residue cover or with reduced tillage with NT and RT can store more soil moisture by minimizing rainfall water loss and soil surface evaporation and eventually increase crop yield (Wang et al., 2011).

The overall effect of conservation tillage methods on ET was negligible (**Figure 2D**). This is in consistent with the finding by López and Arrúe (1997), who reported that the total ET was generally similar for all tillage treatments. A large proportion of ET lost as evaporation could explain this lack of differences, and decreased ET under conservation tillage during vegetative growth of crop, demonstrating the treatment's inability to meet

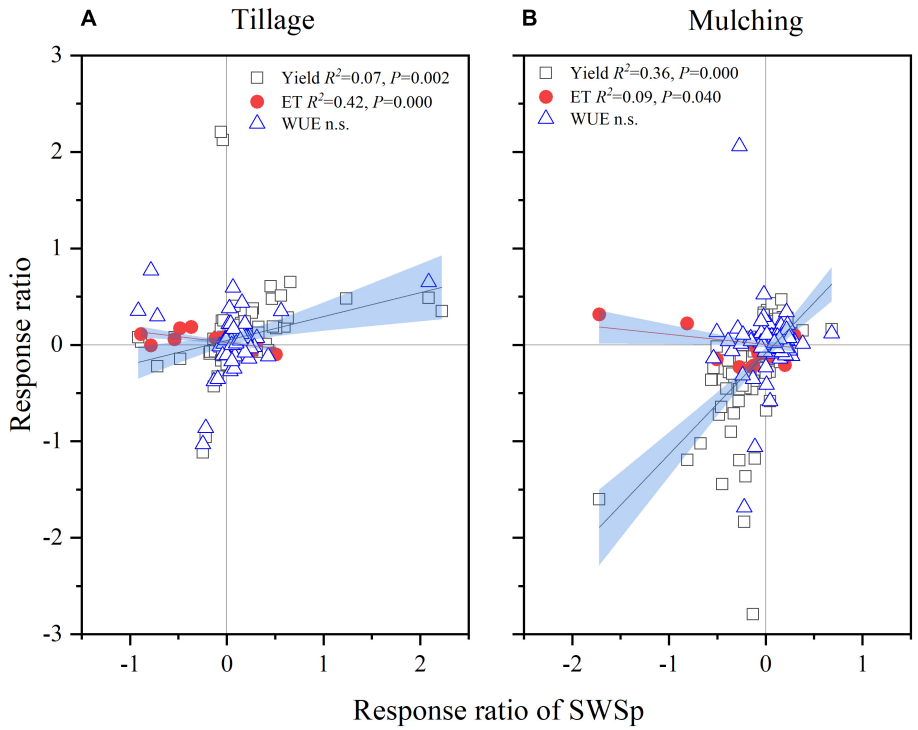


FIGURE 6 | Correlations of the response ratio of winter wheat grain yield, evapotranspiration (ET), and water use efficiency (WUE) to that of soil water storage at wheat planting (SWSp) **(A,B)**.

crop water needs in the rainfed cropping systems. The reduced ET with conservation tillage may relate to higher levels of soil strength (Schmidt and Belford, 1994) and/or insufficient amounts of crop residues on the soil surface (Gibson et al., 1992). Our meta-analysis also showed that fallow mulching overall did not affect ET but cover cropping tended to decrease it (**Figure 4D**). Similarly, He et al. (2016) reported that planting legume and straw-legume as cover crops during fallow decreased winter wheat ET. The reduced ET due to cover cropping could be explained by lower soil water storage at wheat planting, which could result in less accessible soil moisture supply, reducing water evaporation from the soil surface and limiting winter wheat transpiration (Zhang et al., 2007).

Wheat WUE was not affected by conservation tillage methods (**Figure 2E**) but decreased by fallow mulching practices (**Figure 4E**). Crop water use depends on both SWSp and the amount and distribution of precipitation in crop growing season (Hemmat and Eskandari, 2004, 2006; Huang et al., 2006). This study indicates that the water conservation during fallow period due to conservation tillage may not always lead to a better water use in cases of no more precipitation occurred during growing season. Although a linear relationship between wheat grain yield and WUE has been reported by several researches (Huang et al., 2005; Lenssen et al., 2014), our findings contradicted previous reports of higher WUE with mulching than without in rainfed agriculture systems (Deng et al., 2006; Chakraborty et al., 2010). However, straw mulching during fallow period exhibited a positive impact on wheat WUE, indicating that straw mulching could be a better choice for wheat water use compared to other mulching practices (Wang et al., 2018).

Variances With Soil Textures and Climatic Conditions

The effects of tillage methods and mulching practices during fallow period on soil water conservation and wheat yield and water use also varied with soil textures and climatic conditions (**Figures 3**, **5**). Soil texture generally affects the hydraulic properties of soil, which may affect the water loss with different fallow management practices (Hammel et al., 1981; Gajri et al., 2002). The positive impact of conservation tillage on SWSp and wheat yield and WUE in coarse soil was in accordance to previous finding by Carter and Tavernetti (1968), who revealed that crop yield response to conservation tillage was directly linked with soil strength in California (United States). Similarly, there is significant evidence that conservation tillage in coarse-textured soils creates a continuous low-strength slit for root expansion, providing interim relief to crops, and resulted in a significant increase in wheat yield (Gajri et al., 1991). Compared to no mulching, fallow mulching also increased PSE and wheat yield in fine and coarse-textured soils. The results support the findings of Gajri et al. (1994) who revealed that mulching increased grain yield in coarse-textured soils for all the 10 years studied. Similarly, Triplett et al. (1970) reported that mulching increased crop yield in coarse-textured soils, but decreased crop yield on the

medium-textured soils. Gajri et al. (1994) found that mulching with conservation tillage increased grain yield in coarse-textured soils. Conservative tilled or mulched soils could help plants to scavenge water and nutrients from the subsoil more efficiently (Arora et al., 1991).

Climate variables might bring positive or negative influences on crop yield (Saddique et al., 2020). In Pacific Northwest (United States), most of the water loss occurs in fallow land in a dry layer of 10 cm or more in thickness, while large variations in diurnal temperature occur in the upper 15 cm of soil may affect the dry layer vapor flow (Papendick et al., 1973). The fallow duration under winter wheat monoculture generally ranges from 3 months (Wang et al., 2011) to 24 months (Huang et al., 2015). Using the data for MAP instead of the precipitation occurred during fallow period or growing season may have led to some bias in this meta-analysis study, as wheat production is affected by not only SWSp but also water supply during growing season (Brown and Rosenberg, 1997; Wang et al., 2011; Maitah et al., 2021). In Eastern United States, where the relationship between crop yield and precipitation revealed that moisture scarcity, however, herded crop yield (Huang et al., 2015). Fallow mulching can maintain an even soil temperature, increase soil moisture (Barman et al., 2008), and reduce soil evaporation (Liu et al., 2002). Mean annual temperature (MAT) significantly affected PSE and wheat yield, and maximum PSE and yield were obtained at 8–15°C with tillage (**Figure 3**), and at < 8°C with mulching (**Figure 5**), which can be explained by the crop yields normally decrease with increasing temperature because of the shorter phenological phases (Brown and Rosenberg, 1997).

CONCLUSION

This meta-analysis summarized the effects of conservation tillage methods and mulching practices during fallow period on soil water storage, crop yield and water use under winter wheat mono-cropping systems and demonstrated NT with straw mulching as the most suitable practice for soil water conservation and dryland crop production. Conservation tillage during fallow period overall increased PSE, SWSp and wheat yield but did not affect ET and WUE. NT is more efficient to conserve soil water during fallow period compared to RT and ST. Fallow mulching practices overall increased PSE but had a non-significant impact on SWSp, wheat yield, and ET. Compared to straw mulching, film mulching, and stubble mulching during fallow period, cover cropping as a biological mulching decreased SWSp, wheat yield, and WUE significantly. Wheat WUE was significantly enhanced by fallow straw mulching. The effects of tillage method and mulching practices were strongly interacted for soil water conservation and wheat yield and water use, and varied with soil textures and climatic conditions. NT in combination with straw mulching significantly increased SWSp, PSE, wheat yield, and WUE and can be the best fallow management practice for winter wheat production in varying edaphic and climatic conditions.

DATA AVAILABILITY STATEMENT

The original contributions presented in the study are included in the article/supplementary material, further inquiries can be directed to the corresponding author/s.

AUTHOR CONTRIBUTIONS

MA, SZ, JW, and AS conceived the review, drafted, and finalized the manuscript. MT and SF helped to improve the draft by providing useful suggestions and information. All authors contributed to the article and approved the submitted version.

FUNDING

The study was supported by the Chinese Academy of Sciences "Light of West China" Program for Introduced Talent in the West, the National Natural Science Foundation of China (Grant No. 31570440), the Key International Scientific and Technological Cooperation and Exchange Project of Shaanxi Province, China (Grant No. 2020KWZ-010), and the Shaanxi Agricultural Science and Technology Innovation-Driven Project (Grant No. NYKJ-2021-XA-005).

REFERENCES

Arora, V. K., Gajri, P. R., and Prihar, S. S. (1991). Tillage effects on corn in sandy soils in relation to water retentivity, nutrient and water management, and seasonal evaporativity. *Soil Tillage Res.* 21, 1–21. doi: 10.1016/0167-1987(91)90002-F

Barman, K. K., Khankhane, P. J., and Varshney, J. G. (2008). Effect of mulching on weed infestation and tuber yield of potato in black cotton soil. *Ind. J. Weed Sci.* 40, 136–139.

Blanco-Canqui, H., and Lal, R. (2007). Soil structure and organic carbon relationships following 10 years of wheat straw management in no-till. *Soil Tillage Res.* 95, 240–254. doi: 10.1016/j.still.2007.01.004

Blanco-Canqui, H., and Ruis, S. J. (2020). Cover crop impacts on soil physical properties: a review. *Soil Sci. Soc. Am. J.* 84, 1527–1576. doi: 10.1002/saj2.20129

Brown, R. A., and Rosenberg, N. J. (1997). Sensitivity of crop yield and water use to change in a range of climatic factors and CO_2 concentrations: a simulation study applying EPIC to the central United States. *Agric. For. Meteorol.* 83, 171–203. doi: 10.1016/s0168-1923(96)02352-0

Bruning, B., Berger, B., Lewis, M., Liu, H., and Garnett, T. (2020). Approaches, applications, and future directions for hyperspectral vegetation studies: an emphasis on yield-limiting factors in wheat. *Plant Phenome J.* 3:e20007. doi: 10.1002/ppj2.20007

Bukhari, M. A., Shah, A. N., Fahad, S., Iqbal, J., Nawaz, F., Manan, A., et al. (2021). Screening of wheat (*Triticum aestivum L.*) genotypes for drought tolerance using polyethylene glycol. *Arab. J. Geosci.* 14:2808. doi: 10.1007/s12517-021-09073-0

Carter, L. M., and Tavernetti, J. R. (1968). Influence of precision tillage and soil compaction on cotton yields. *Trans. ASAE.* 11, 65–0067. doi: 10.13031/2013.39334

Chakraborty, D., Garg, R., Tomar, R., Singh, R., Sharma, S., Singh, R., et al. (2010). Synthetic and organic mulching and nitrogen effect on winter wheat (Triticum aestivum L.) in a semi-arid environment. *Agric. Water Manag.* 97, 738–748. doi: 10.1016/j.agwat.2010.01.006

Deng, X. P., Shan, L., Zhang, H., and Turner, N. C. (2006). Improving agricultural water use efficiency in arid and semiarid areas of China. *Agric. water Manag.* 80, 23–40. doi: 10.1016/j.agwat.2005.07.021

Fabrizzi, K., Garcıa, F., Costa, J., and Picone, L. (2005). Soil water dynamics, physical properties and corn and wheat responses to minimum and no-tillage systems in the southern Pampas of Argentina. *Soil Tillage Res.* 81, 57–69. doi: 10.1016/j.still.2004.05.001

Fan, X. W., Pang, J. M., and Fan, H. F. (2007). Study on Mulch Effect and Toxic Action of Polyvinyl Chloride (PVC) Film. *J. Shanxi Agric. Sci.* 5, 46–50.

Farahani, H., Peterson, G., Westfall, D., Sherrod, L., and Ahuja, L. (1998). Soil water storage in dryland cropping systems: the significance of cropping intensification. *Soil Sci. Soc. Am. J.* 62, 984–991. doi: 10.2136/sssaj1998.03615995006200040020x

Gajri, P., Arora, V. K., and Prihar, S. S. (2002). *Tillage for Sustainable Cropping*. Binghamton: Food Products Press. doi: 10.1079/PGR20036

Gajri, P. R., Arora, V. K., and Chaudhary, M. R. (1994). Maize growth responses to deep tillage, straw mulching and farmyard manure in coarse textured soils of NW India. *Soil Use Manag.* 10, 15–19. doi: 10.1111/j.1475-2743.1994.tb00451.x

Gajri, P. R., Prihar, S. S., Cheema, H. S., and Kapoor, A. (1991). Irrigation and tillage effects on root development, water use and yield of wheat on coarse textured soils. *Irrig. Sci.* 12, 161–168. doi: 10.1007/BF00192288

Gao, Y., Li, Y., Zhang, J., Liu, W., Dang, Z., Cao, W., et al. (2009). Effects of mulch, N fertilizer, and plant density on wheat yield, wheat nitrogen uptake, and residual soil nitrate in a dryland area of China. *Nutr. Cycl. Agroecosyst.* 85, 109–121. doi: 10.1007/s10705-009-9252-0

Gibson, G., Radford, B. J., and Nielsen, R. G. H. (1992). Fallow management, soil water, plant-available soil nitrogen and grain sorghum production in south west Queensland. *Aust. J. Exp. Agric.* 32, 473–482. doi: 10.1071/EA9920473

Halvorson, A. D., Black, A. L., Krupinsky, J. M., Merrill, S. D., Wienhold, B. J., and Tanaka, D. L. (2000). Spring wheat response to tillage and nitrogen fertilization in rotation with sunflower and winter wheat. *Agron. J.* 92, 136–144. doi: 10.1007/s100870050016

Hammel, J., Papendick, R., and Campbell, G. (1981). Fallow tillage effects on evaporation and seedzone water content in a dry summer climate. *Soil Sci. Soc. Am. J.* 45, 1016–1022. doi: 10.2136/sssaj1981.03615995004500060003x

He, G., Wang, Z., Li, F., Dai, J., Li, Q., Xue, C., et al. (2016). Soil water storage and winter wheat productivity affected by soil surface management and precipitation in dryland of the Loess Plateau, China. *Agric. Water Manag.* 171, 1–9. doi: 10.1016/j.agwat.2016.03.005

He, J., Kuhn, N., Zhang, X., Zhang, X., and Li, H. (2009). Effects of 10 years of conservation tillage on soil properties and productivity in the farming–pastoral ecotone of Inner Mongolia, China. *Soil Use Manag.* 25, 201–209. doi: 10.1111/j.1475-2743.2009.00210.x

Hedges, L. V., Gurevitch, J., and Curtis, P. S. (1999). The meta-analysis of response ratios in experimental ecology. *Ecology* 80, 1150–1156. doi: 10.2307/177062

Hemmat, A., and Eskandari, I. (2004). Conservation tillage practices for winter wheat–fallow farming in the temperate continental climate of northwestern Iran. *Field Crops Res.* 89, 123–133. doi: 10.1016/j.fcr.2004.01.019

Hemmat, A., and Eskandari, I. (2006). Dryland winter wheat response to conservation tillage in a continuous cropping system in northwestern Iran. *Soil Tillage Res.* 86, 99–109. doi: 10.1016/j.still.2005.02.003

Hillel, D. (1998). *Environmental Soil Physics: Fundamentals, Applications, and Environmental Considerations*. Amsterdam: Elsevier.

Hou, X., Li, R., Jia, Z., Han, Q., Wang, W., and Yang, B. (2012). Effects of rotational tillage practices on soil properties, winter wheat yields and water-use efficiency in semi-arid areas of north-west China. *Field Crops Res.* 129, 7–13. doi: 10.1016/j.fcr.2011.12.021

Huang, C., Duiker, S. W., Deng, L., Fang, C., and Zeng, W. (2015). Infuence of precipitation on maize yield in the eastern United States. *Sustainability* 7, 5996–6010. doi: 10.3390/su7055996

Huang, G.-B., Guo, Q.-Y., Zhang, R.-Z., Pang, L., Li, G., Chan, K. Y., et al. (2006). Effects of conservation tillage on soil moisture and crop yield in a phased rotation system with spring wheat and field pea in dryland. *Acta Ecol. Sin.* 26, 1176–1185.

Huang, H. C., Tan, Y. C., Liu, C. W., and Chen, C. H. (2005). A novel hysteresis model in unsaturated soil. *Hydrol. Process.* 19, 1653–1665. doi: 10.1002/hyp.5594

Hungate, B. A., Van Groenigen, K. J., Six, J., Jastrow, J. D., Luo, Y., De Graaff, M. A., et al. (2009). Assessing the effect of elevated carbon dioxide on soil carbon: a comparison of four meta-analyses. *Glob. Change Biol.* 15, 2020–2034. doi: 10.1111/j.1365-2486.2009.01866.x

Jin, K., Cornelis, W. M., Schiettecatte, W., Lu, J., Yao, Y., Wu, H., et al. (2007). Effects of different management practices on the soil–water balance and crop yield for improved dryland farming in the Chinese Loess Plateau. *Soil Tillage Res.* 96, 131–144. doi: 10.1016/j.still.2007.05.002

Knorr, M., Frey, S. D., and Curtis, P. S. (2005). Nitrogen additions and litter decomposition: a meta-analysis. *Ecology* 86, 3252–3257. doi: 10.1890/05-0150

Lampurlanes, J., Angas, P., and Cantero-Martınez, C. (2002). Tillage effects on water storage during fallow, and on barley root growth and yield in two contrasting soils of the semi-arid Segarra region in Spain. *Soil Tillage Res.* 65, 207–220. doi: 10.1016/S0167-1987(01)00285-9

Lenssen, A. W., Sainju, U. M., Jabro, J. D., Iversen, W. M., Allen, B. L., and Evans, R. G. (2014). Crop diversification, tillage, and management system influence spring wheat yield and water use. *Agron. J.* 106:1445. doi: 10.2134/agronj14.0119

Li, F.-M., Guo, A.-H., and Wei, H. (1999). Effects of clear plastic film mulch on yield of spring wheat. *Field Crops Res.* 63, 79–86. doi: 10.1016/s0378-4290(99)00027-1

Li, H., Gao, H., Wu, H., Li, W., Wang, X., and He, J. (2007). Effects of 15 years of conservation tillage on soil structure and productivity of wheat cultivation in northern China. *Soil Res.* 45, 344–350. doi: 10.1071/SR07003

Liu, C., Zhang, X., and Zhang, Y. (2002). Determination of daily evaporation and evapotranspiration of winter wheat and maize by large-scale weighing lysimeter and micro-lysimeter. *Agric. For. Meteorol.* 111, 109–120. doi: 10.1016/S0168-1923(02)00015-1

López, M. V., and Arrúe, J. L. (1997). Growth, yield and water use efficiency of winter barley in response to conservation tillage in a semi-arid region of Spain. *Soil Tillage Res.* 44, 35–54. doi: 10.1016/S0167-1987(97)00030-5

Lucas, R., Klaminder, J., Futter, M., Bishop, K. H., Egnell, G., Laudon, H., et al. (2011). A meta-analysis of the effects of nitrogen additions on base cations: implications for plants, soils, and streams. *For. Ecol. Manag.* 262, 95–104. doi: 10.1016/j.foreco.2011.03.018

Mahboubi, A., Lal, R., and Faussey, N. (1993). Twenty-eight years of tillage effects on two soils in Ohio. *Soil Sci. Soc. Am. J.* 57, 506–512. doi: 10.2136/sssaj1993.03615995005700020034x

Maitah, M., Malec, K., and Maitah, K. (2021). Influence of precipitation and temperature on maize production in the Czech Republic from 2002 to 2019. *Sci. Rep.* 11:10467. doi: 10.1038/s41598-021-89962-2

Nielsen, D. C., and Vigil, M. F. (2010). Precipitation storage efficiency during fallow in wheat-fallow systems. *Agron. J.* 102, 537–543. doi: 10.2134/agronj2009.0348

Oyedele, D. J., Schjønning, P., Sibbesen, E., and Debosz, K. (1999). Aggregation and organic matter fractions of three Nigerian soils as affected by soil disturbance and incorporation of plant material. *Soil Tillage Res.* 50, 105–114. doi: 10.1016/S0167-1987(98)00200-1

Papendick, R., Lindstrom, M., and Cochran, V. (1973). Soil mulch effects on seedbed temperature and water during fallow in eastern Washington. *Soil Sci. Soc. Am. J.* 37, 307–314. doi: 10.2136/sssaj1973.03615995003700020039x

Patrignani, A., Godsey, C., Ochsner, T., and Edwards, J. (2012). Soil water dynamics of conventional and no-till wheat in the Southern Great Plains. *Soil Sci. Soc. Am. J.* 76, 1768–1775. doi: 10.2136/sssaj2012.0082

Peterson, G. A., Schlegel, A. J., Tanaka, D. L., and Jones, O. R. (1996). Precipitation use efficiency as affected by cropping and tillage systems. *J. Prod. Agric.* 9, 180–186. doi: 10.2134/jpa1996.0180

Pikul, J. Jr., and Aase, J. (1999). Wheat response and residual soil properties following subsoiling of a sandy loam in eastern Montana. *Soil Tillage Res.* 51, 61–70. doi: 10.1016/S0167-1987(99)00031-8

Pikul, J. L., and Aase, J. K. (2003). Water infiltration and storage affected by subsoiling and subsequent tillage. *Soil Sci. Soc. Am. J.* 67, 859–866. doi: 10.2136/sssaj2003.8590

Rasmussen, K. (1999). Impact of ploughless soil tillage on yield and soil quality: a Scandinavian review. *Soil Tillage Res.* 53, 3–14. doi: 10.1016/S0167-1987(99)00072-0

Ren, A., Sun, M., Xue, L., Deng, Y., Wang, P., Lei, M., et al. (2019). Spatio-temporal dynamics in soil water storage reveals effects of nitrogen inputs on soil water consumption at different growth stages of winter wheat. *Agric. Water Manag.* 216, 379–389. doi: 10.1016/j.agwat.2019.01.023

Saddique, Q., Khan, M. I, Habib ur Rahman, M., Jiatun, X., Waseem, M., Gaiser, T., et al. (2020). Effects of elevated air temperature and CO2 on maize production and water use efficiency under future climate change scenarios in Shaanxi Province, China. *Atmosphere* 11:843. doi: 10.3390/atmos11080843

Schillinger, W. F. (2001). Minimum and delayed conservation tillage for wheat–fallow farming. *Soil Sci. Soc. Am. J.* 65, 1203–1209. doi: 10.2136/sssaj2001.6541203x

Schillinger, W. F., and Papendick, R. I. (2008). Then and now: 125 years of dryland wheat farming in the Inland Pacific Northwest. *Agron. J.* 100, S–166–S–182. doi: 10.2134/agronj2007.0027c

Schmidt, C. P., and Belford, R. K. (1994). Increasing the depth of soil disturbance increases yields of direct drilled wheat on the sandplain soils of Western Australia. *J. Exp. Agric.* 34, 777–781. doi: 10.1071/EA9940777

Shah, A. N., Tanveer, M., Shahzad, B., Yang, G., Fahad, S., Ali, S., et al. (2017). Soil compaction effects on soil health and cropproductivity: an overview. *Environ. Sci. Pollut. Res.* 24, 10056–10067. doi: 10.1007/s11356-017-8421-y

Shangguan, Z., Shao, M., Lei, T., and Fan, T. (2002). Runoff water management technologies for dryland agriculture on the Loess. *Int. J. Sustain. Dev. World Ecol.* 9, 341–350. doi: 10.1080/13504500209470129

Smika, D., and Wicks, G. (1968). Soil water storage during fallow in the Central Great Plains as influenced by tillage and herbicide treatments. *Soil Sci. Soc. Am. J.* 32, 591–595. doi: 10.2136/sssaj1968.03615995003200040046x

Smiley, R., and Uddin, W. (1993). Influence of soil temperature on Rhizoctonia root rot (*R. solani AG-8 and R. oryzae*) of winter wheat. *Phytopathology* 83, 777–785. doi: 10.1094/phyto-83-777

Tanaka, D., and Aase, J. (1987). Fallow method influences on soil water and precipitation storage efficiency. *Soil Tillage Res.* 9, 307–316. doi: 10.1016/0167-1987(87)90056-0

Tanaka, D., and Anderson, R. (1997). Soil water storage and precipitation storage efficiency of conservation tillage systems. *J. Soil Water Conserv.* 52, 363–367. doi: 10.1016/j.heliyon.2021.e06308

Tong, C., Hall, C. A., and Wang, H. (2003). Land use change in rice, wheat and maize production in China (1961–1998). *Agric. Ecosyst. Environ.* 95, 523–536. doi: 10.1016/S0167-8809(02)00182-2

Triplett, G. B., Van Doren, D. M., and Johnson, W. H. (1970). Response of tillage systems as influenced by soil type. *Trans. ASAE.* 13, 765–767.

Verhulst, N., Nelissen, V., Jespers, N., Haven, H., Sayre, K. D., Raes, D., et al. (2011). Soil water content, maize yield and its stability as affected by tillage and crop residue management in rainfed semi-arid highlands. *Plant Soil* 344, 73–85. doi: 10.1007/s11104-011-0728-8

Wang, C.-R., Tian, X.-H., and Li, S.-X. (2004). Effects of cultivation by mulching and rain harvesting on yield and nutrient uptake of winter wheat. *Agric. Res. Arid Areas* 22, 108–111.

Wang, J., Ghimire, R., Fu, X., Sainju, U. M., and Liu, W. (2018). Straw mulching increases precipitation storage rather than water use efficiency and dryland winter wheat yield. *Agric. Water Manag.* 206, 95–101. doi: 10.1016/j.agwat.2018.05.004

Wang, J., Liu, W., and Dang, T. (2011). Responses of soil water balance and precipitation storage efficiency to increased fertilizer application in winter wheat. *Plant Soil* 347, 41–51. doi: 10.1007/s11104-011-0764-4

Wang, J., Zhang, S., Sainju, U. M., Ghimire, R., and Zhao, F. (2021). A meta-analysis on cover crop impact on soil water storage, succeeding crop yield, and water-use efficiency. *Agric. Water Manag.* 256:107085. doi: 10.1016/j.agwat.2021.107085

Wang, Q., Bai, Y., Gao, H., He, J., Chen, H., Chesney, R. C., et al. (2008). Soil chemical properties and microbial biomass after 16 years of no-tillage farming on the Loess Plateau, China. *Geoderma* 144, 502–508. doi: 10.1016/j.geoderma.2008.01.003

Wang, X., Cai, D., Jin, K., Wu, H., Bai, Z., Zhang, C., et al. (2003). Water availability for winter wheat affected by summer fallow tillage practices in sloping dryland. *Agric. Sci. China* 2, 773–778.

Ward, P., Flower, K., Cordingley, N., Weeks, C., and Micin, S. (2012). Soil water balance with cover crops and conservation agriculture in a Mediterranean climate. *Field Crops Res.* 132, 33–39. doi: 10.1016/j.fcr.2011.10.017

Xie, Z. K., Wang, Y.-J., and Li, F.-M. (2005). Effect of plastic mulching on soil water use and spring wheat yield in arid region of northwest China. *Agric. Water Manag.* 75, 71–83. doi: 10.1016/j.agwat.2004.12.014

Yan, J., Deng, L.-J., and Huang, J. (2005). Effect of conservation tillage on soil physicochemical properties and crop yields. *Chin. Agric. Mech.* 2, 31–34. doi: 10.1038/s41598-020-61650-7

Zhai, R., Kachanoski, R., and Voroney, R. (1990). Tillage effects on the spatial and temporal variations of soil water. *Soil Sci. Soc. Am. J.* 54, 186–192. doi: 10.2136/sssaj1990.03615995005400010029x

Zhang, G., Chan, K., Oates, A., Heenan, D., and Huang, G. (2007). Relationship between soil structure and runoff/soil loss after 24 years of conservation tillage. *Soil Tillage Res.* 92, 122–128. doi: 10.1016/j.still.2006.01.006

Zhang, G., Hu, X., Zhang, X., and Li, J. (2015). Effects of plastic mulch and crop rotation on soil physical properties in rain-fed vegetable production in the mid-Yunnan plateau, China. *Soil Tillage Res.* 145, 111–117. doi: 10.1016/j.still.2014.09.010

Zhang, S., Lövdahl, L., Grip, H., Tong, Y., Yang, X., and Wang, Q. (2009). Effects of mulching and catch cropping on soil temperature, soil moisture and wheat yield on the Loess Plateau of China. *Soil Tillage Res.* 102, 78–86. doi: 10.1016/j.still.2008.07.019

Conflict of Interest: The authors declare that the research was conducted in the absence of any commercial or financial relationships that could be construed as a potential conflict of interest.

Publisher's Note: All claims expressed in this article are solely those of the authors and do not necessarily represent those of their affiliated organizations, or those of the publisher, the editors and the reviewers. Any product that may be evaluated in this article, or claim that may be made by its manufacturer, is not guaranteed or endorsed by the publisher.

Copyright © 2022 Adil, Zhang, Wang, Shah, Tanveer and Fiaz. This is an open-access article distributed under the terms of the Creative Commons Attribution License (CC BY). The use, distribution or reproduction in other forums is permitted, provided the original author(s) and the copyright owner(s) are credited and that the original publication in this journal is cited, in accordance with accepted academic practice. No use, distribution or reproduction is permitted which does not comply with these terms.

frontiers | Frontiers in Plant Science

REVIEW
published: 09 May 2022
doi: 10.3389/fpls.2022.847175

Melatonin-Mediated Abiotic Stress Tolerance in Plants

Wen Zeng[1], *Salma Mostafa*[1,2], *Zhaogeng Lu*[1]* *and Biao Jin*[1]*

[1]College of Horticulture and Plant Protection, Yangzhou University, Yangzhou, China, [2]Department of Floriculture, Faculty of Agriculture, Alexandria University, Alexandria, Egypt

Melatonin is a multi-functional molecule that is ubiquitous in all living organisms. Melatonin performs essential roles in plant stress tolerance; its application can reduce the harmful effects of abiotic stresses. Plant melatonin biosynthesis, which usually occurs within chloroplasts, and its related metabolic pathways have been extensively characterized. Melatonin regulates plant stress responses by directly inhibiting the accumulation of reactive oxygen and nitrogen species, and by indirectly affecting stress response pathways. In this review, we summarize recent research concerning melatonin biosynthesis, metabolism, and antioxidation; we focus on melatonin-mediated tolerance to abiotic stresses including drought, waterlogging, salt, heat, cold, heavy metal toxicity, light and others. We also examine exogenous melatonin treatment in plants under abiotic stress. Finally, we discuss future perspectives in melatonin research and its applications in plants.

Keywords: melatonin, abiotic stress, stress tolerance, exogenous applications, biosynthesis, metabolism, antioxidants, molecular signaling

OPEN ACCESS

Edited by:
Guo-Liang Jiang,
Virginia State University,
United States

Reviewed by:
Xin Li,
Tea Research Institute (CAAS), China
Mirza Hasanuzzaman,
Sher-e-Bangla Agricultural University,
Bangladesh

***Correspondence:**
Zhaogeng Lu
zglu@yzu.edu.cn
Biao Jin
bjin@yzu.edu.cn

Specialty section:
This article was submitted to Plant Breeding, a section of the journal Frontiers in Plant Science

Received: *01 January 2022*
Accepted: *19 April 2022*
Published: *09 May 2022*

Citation:
Zeng W, Mostafa S, Lu Z and Jin B (2022) Melatonin-Mediated Abiotic Stress Tolerance in Plants. Front. Plant Sci. 13:847175. doi: 10.3389/fpls.2022.847175

INTRODUCTION

Plants encounter various environmental stresses throughout their lives. As sessile organisms, plants have evolved multiple response mechanisms to cope with adverse conditions, thus ensuring their survival and reproductive success. N-acetyl-5-methoxytryptamine (melatonin), an indolic compound derived from tryptophan, is a universal abiotic stress regulator in plants (Wang et al., 2018). Melatonin was first identified in the bovine pineal gland in 1958 (Lerner et al., 1958). It was later characterized as an essential animal hormone that is involved in multiple biological processes, including antioxidation, circadian rhythms, seasonal reproduction, sleep, sexual behavior, mood, temperature homeostasis, retina physiology, and immunological enhancement (Lerner et al., 1958; Shi et al., 2015b). In 1995, melatonin was first identified in plants (Dubbels et al., 1995; Hattori et al., 1995). Since then, melatonin has been shown to participate in various abiotic stress responses as a pleiotropic signaling molecule. In addition, it is an efficient scavenger of both reactive oxygen species (ROS) and reactive nitrogen species (RNS; Arnao and Hernández-Ruiz, 2019b). Melatonin is present in the leaves, roots, stems, petals, flower buds, fruits and seeds of various plant species. Its biosynthesis typically occurs in chloroplasts and mitochondria (Tan and Reiter, 2020).

Since the discovery of melatonin, numerous studies have been conducted to examine its functions in plants, thus revealing its protective roles against both biotic and abiotic stresses. In adverse environments, melatonin regulates plant growth and development by promoting seed germination, boosting lateral root generation, controlling flowering time and delaying

leaf senescence (Arnao and Hernández-Ruiz, 2019a, 2020). Melatonin acts as a direct regulator by scavenging ROS and RNS. It also acts as an indirect regulator by regulating gene expression *via* stress-responsive transcription factors. Melatonin also functions as an auxin-like regulator, sharing a precursor molecule with auxin. It can mimic auxin activity, acting upstream of the auxin pathway to alter the expression profiles of various auxin-related transcription factors (e.g., WRKY, NAC, MYB, bHLH, and HD-ZIP family transcription factors; Liang et al., 2017; Tan and Reiter, 2020). Melatonin may also interact with other plant hormones such as indoleacetic acid (IAA), gibberellic acid (GA), cytokinin (CK), abscisic acid (ABA), ethylene (ET), salicylic acid (SA), jasmonic acid (JA), brassinosteroid (BR), strigolactones, and polyamines (Arnao and Hernández-Ruiz, 2020). Moreover, the exogenous application of melatonin can enhance plant tolerance (e.g., to drought, salt, heat, cold, waterlogging, and heavy metal toxicity) by modulating the biosynthesis of endogenous melatonin and the activities of antioxidative enzymes (Weeda et al., 2014; Zhang et al., 2015; Moustafa-Farag et al., 2020; Sun et al., 2021).

Considering its protective functions, melatonin has attracted increasing research attention in recent years because of the increasing harmful effects of climate change, soil salinization, and industrial pollution on agriculture, crop production, and food chain security. Over the past decade, considerable progress has been made in the general understanding of melatonin in plants. Therefore, an updated review highlighting recent findings in melatonin-mediated abiotic stress tolerance is needed. In this review, we have summarized the biosynthetic and catabolic pathways of melatonin. We have also focused on the defensive roles of melatonin against various abiotic stresses, as well as its applications for improving plant stress tolerance.

BIOSYNTHESIS AND METABOLISM OF PHYTOMELATONIN

Biosynthetic Pathway

Melatonin, which is ubiquitous among most plant species, has a low molecular weight and a stable structure (Wu Y. et al., 2021). Its biosynthetic pathways in model animals and plants have been elucidated. In animals, four main enzymes participate in the classic melatonin biosynthetic pathway. First, tryptophan hydroxylase converts tryptophan into 5-hydroxytryptophan, which is then decarboxylated by aromatic amino acid decarboxylase to form 5-hydroxytryptamine (serotonin). Next, arylalkylamine N-acetyltransferase, also known as serotonin N-acetyltransferase (SNAT), acetylates serotonin to form N-acetyl-5-hydroxytryptamine (N-acetylserotonin). Finally, hydroxyindole-O-methyltransferase, also known as N-acetylserotonin methyltransferase (ASMT), O-methylates N-acetyl-5-hydroxytryptamine to generate melatonin (Axelrod and Weissbach, 1960; Weissbach et al., 1960; Tan et al., 2016).

The melatonin biosynthetic pathway in plants differs from the pathway in animals. It involves at least six biosynthetic enzymes including tryptophan decarboxylase (TDC), tryptophan hydroxylase, tryptamine 5-hydroxylase (T5H), SNAT, ASMT, and caffeic acid O-methyltransferase (COMT; **Figure 1**; Back et al., 2016; Sun et al., 2021). Among them, SNAT is a key rate-limiting enzyme (Liao et al., 2021). SNAT plant knockout strains exhibit altered phenotypes and become more sensitive to some abiotic stresses (Lee et al., 2019). ASMT and COMT were likely involved in plant terrestrialization. COMT first appeared in bryophytes and is presume to have evolved from ASMT. The increased activity of COMT compared to ASMT may have enhanced melatonin production in plants. In higher plants, COMT acquired an additional function in lignin biosynthesis (Zhao et al., 2021). Moreover, other hormonal pathways influence the expression of key melatonin biosynthesis genes. For example, ET insensitive protein 3 (*CcEIN3*) activates the expression of *CcTDC* and *CcASMT1* in hickory (Chen W. et al., 2021).

The first two biosynthesis steps in the plant melatonin pathway are the reverse of the first two steps in animals. In plants, tryptophan is decarboxylated by TDC in the first step, after which tryptamine is hydroxylated by T5H (Tan et al., 2016). SNAT and ASMT/COMT catalyze the final two biosynthesis steps, the order of which alternates depending on the environmental conditions (Byeon et al., 2015a). Under abiotic stress, the expression of different ASMT isoforms is induced, so serotonin is first O-methylated to form 5-methoxytryptamine by ASMT, and then acetylated to form melatonin (Ye et al., 2019; Tan and Reiter, 2020). In contrast, under standard conditions, the dominant pathway involves serotonin acetylation to form N-acetyl-5-hydroxytryptamine and then O-methylation to form melatonin (Ye et al., 2019; **Figure 1**).

In animals, melatonin is biosynthesized in the pineal gland. The specific organs in which melatonin is synthesized in plants are currently unknown. However, melatonin can be transported from roots to shoots as a long-distance signal in some plant species (Mukherjee et al., 2014; Li H. et al., 2017). The cellular location of melatonin biosynthesis in plants is clear. Tan et al. (2013) hypothesized that mitochondria and chloroplasts are the sites of melatonin biosynthesis in plants. The key melatonin synthetase, SNAT, is mainly localized to the chloroplasts in plants such as rice, cucumber, and tomato (Byeon et al., 2014; Wang et al., 2020). COMT and ASMT can be highly expressed in the chloroplast and their overexpression results in enhanced melatonin production (Choi et al., 2017). Taken together, this evidence suggests that the chloroplast may be the main site of melatonin biosynthesis. In addition to chloroplasts, mitochondria are regarded as sites of melatonin biosynthesis. The apple *MzSNAT5* gene, which is localized to mitochondria, is more closely related to animal SNAT than to the chloroplast-localized *MzSNAT9* or SNATs present in rice, *Arabidopsis*, or cyanobacteria (Wang et al., 2017; Tan and Reiter, 2020).

Mitochondria and chloroplasts are the biosynthetic sites of melatonin because of their evolutionary histories Hardeland, 2019. Melatonin is produced by several bacterial taxa, including cyanobacteria and α-proteobacteria. Mitochondria evolved from ingested α-proteobacteria, while chloroplasts originated from photosynthetic cyanobacteria. Throughout evolution, both organelles likely retained their ability to produce melatonin (Zhao et al., 2019). Moreover, there is evidence

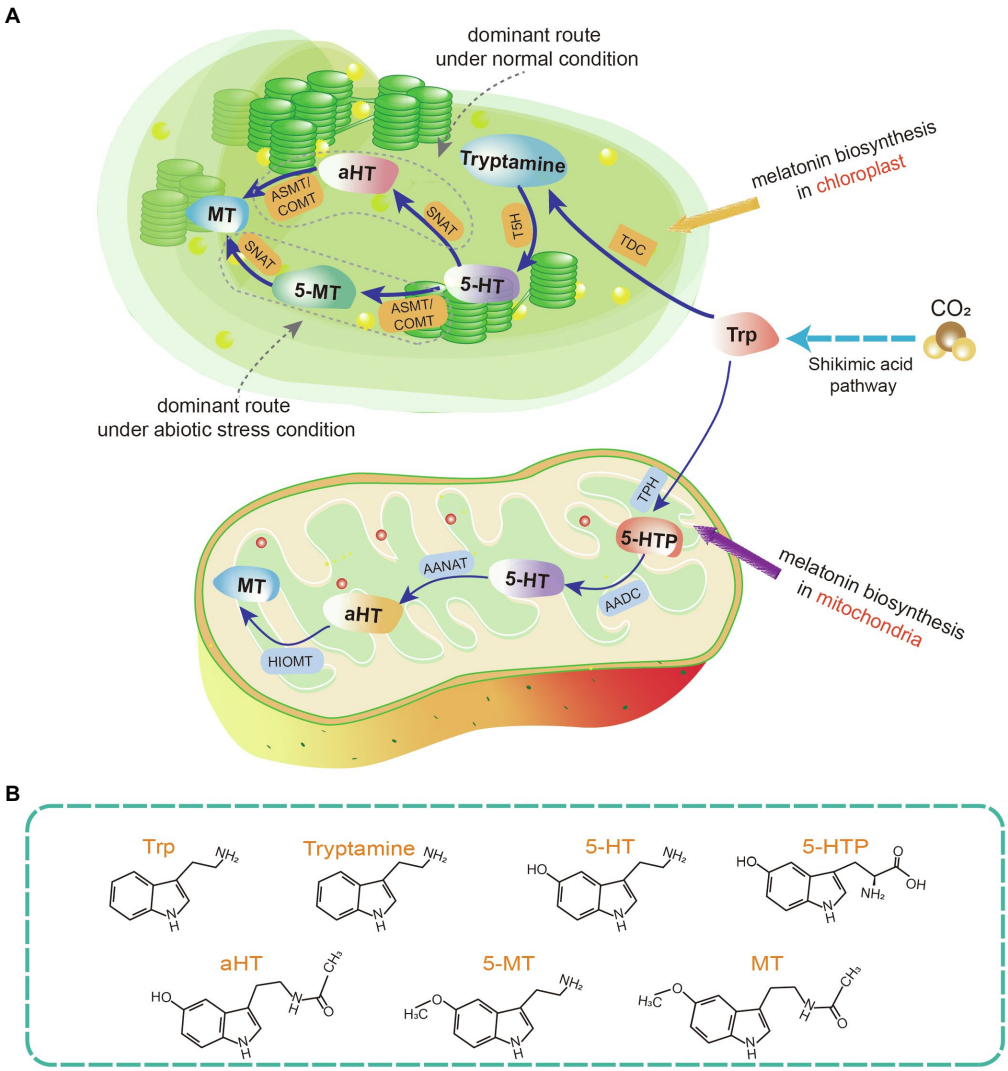


FIGURE 1 | Phytomelatonin biosynthetic pathway in chloroplasts and mitochondria. **(A)** Schematic of melatonin biosynthetic pathways. **(B)** Molecular structures of key intermediate products in the melatonin biosynthetic pathway. Plants usually synthesize melatonin in chloroplasts under normal conditions. If this pathway is blocked, melatonin biosynthesis may be switched to the mitochondria. Trp, tryptophan; 5-HT, 5-hydroxytryptamine; 5-HTP, 5-hydroxytryptophan; aHT, N-acetyl-5-hydroxytryptamine; 5-MT, 5-methoxytryptamine; MT, melatonin; TDC, tryptophan decarboxylase; T5H, tryptamine 5-hydroxylase; SNAT, serotonin N-acetyltransferase; ASMT, N-acetylserotonin-O-methyltransferase (plant type SNATs and ASMTs appear to have origins distinct from the origins in animals); COMT, caffeic acid O-methyltransferase; TPH, tryptophan hydroxylase; AADC, aromatic amino acid decarboxylase; AANAT, arylalkylamine N-acetyltransferase (also known as arylamine N-acetyltransferase); and HIOMT, hydroxyindole-O-methyltransferase (also known as N-acetylserotonin O-methyltransferase).

to suggest that plants preferentially perform melatonin biosynthesis in chloroplasts under normal conditions. When the chloroplast pathway is blocked, melatonin biosynthesis takes place in the mitochondria (Tan and Reiter, 2020; **Figure 1**).

Metabolic Pathway

Melatonin can be degraded *via* enzymatic and non-enzymatic transformation routes (Tan et al., 2012; Hardeland, 2015; Back, 2021). In the enzymatic transformation route of animals, melatonin is metabolized into 6-hydroxymelatonin (6-OHM) by P450 enzymes. 6-OHM is then sulfated into 6-sulfatoxymelatonin and N1-acetyl-N2-formyl-5-methoxykynuramine (AFMK) by several enzymes (e.g., indoleamine 2,3-dioxygenase; Ma et al., 2005; Semak et al., 2005; Hardeland, 2017). 6-OHM is the major product of enzymatic melatonin degradation in animals. In non-enzymatic transformation routes, melatonin is degraded by free radicals or other oxidants. Examples of melatonin metabolites include cyclic 3-OHM (c3-OHM), 4-OHM, 2-OHM, AFMK, and N-acetyl-5-methoxykynuramine, which are produced non-enzymatically through interactions with ROS and RNS (Hardeland, 2017; Back, 2021).

The enzymatic degradation of melatonin in plants shares some common features with such degradation in vertebrates

and other eukaryotes (Sun et al., 2021). For example, indoleamine 2,3-dioxygenase, which converts melatonin to AFMK, was identified in water hyacinth (*Eichhornia crassipes*) and other phototrophs such as phaeophytes, dinoflagellates, and chlorophyceae (Tan et al., 2007; Hardeland et al., 2009; Okazaki et al., 2010; Hardeland, 2015). Similarly, 2-OHM and c3-OHM are two melatonin hydroxylation metabolites present in the plant metabolic pathway. They are generated by melatonin 2-hydroxylase (M2H) and melatonin 3-hydroxylase (M3H), respectively (Byeon and Back, 2015; Byeon et al., 2015c; Lee et al., 2016; Choi and Back, 2019). Notably, M2H-1, a 2-oxoglutarate-dependent dioxygenase (2-ODD) isogene in rice, is localized to chloroplasts and has a major role in 2-OHM biosynthesis. Other 2-ODD isogenes with moderate M2H activity are expressed in the cytoplasm. The M2H pathway is the most important catabolic pathway, with crucial roles in modulating physiological and biochemical processes under biotic and abiotic stresses (Byeon et al., 2015b; Sun et al., 2021). There is evidence that endogenously triggered 2-OHM production, as well as exogenously applied 2-OHM, can improve plant tolerance to various adverse stresses such as cold, drought, metal stress, and pathogen attack (Lee and Back, 2016a; Shah et al., 2020; Tan and Reiter, 2020).

The gene responsible for producing c3-OHM, another important melatonin hydroxylation metabolite, has been cloned in rice (Lee et al., 2016). c3-OHM production is catalyzed by M3H, which belongs to the 2-ODD superfamily. It is located in the cytoplasm. Of note, c3-OHM levels exhibit a diurnal rhythm in rice (Choi and Back, 2019). Additionally, M2H and M3H are endemic to terrestrial plants, suggesting that the functions of their enzymatic products are specific to land plants (Lee and Back, 2019). Generally, c3-OHM and 2-OHM are the predominant hydroxylated forms of melatonin found in plants, in contrast to the 6-OHM mainly found in animals. Moreover, 5-methoxytryptamine is another bioactive metabolite. It is formed from melatonin by N-acetylserotonin deacetylase (ASDAC) and from serotonin by ASMT in rice seedlings (Back, 2021). For non-enzymatic melatonin degradation, melatonin can be nitrosated at the nitrogen atom of its indole ring, resulting in the formation of N-nitrosomelatonin (Blanchard et al., 2000; Mukherjee, 2019). The melatonin metabolites beta-hydroxymelatonin, cyclic beta-hydroxymelatonin, and cyclic melatonin are also present in corn and cucumber. They may be produced because of interactions between melatonin and oxidizing agents such as ROS and RNS (Kołodziejczyk et al., 2015; Manchester et al., 2015; **Figure 2**).

Melatonin coexists with its major metabolites (3-OHM, 2-OHM, and 5-methoxytryptamine) in plant cells (Lee and Back, 2019). Both endogenous melatonin and its metabolisms may be affected by exogenous melatonin (Back, 2021). After exogenous melatonin application in plants, the resulting physiological and biochemical changes and stress responses may differ depending on the changed level of melatonin metabolites and endogenous melatonin (Lee and Back, 2016a). Endogenous levels of melatonin metabolites are generally high in plants, where they exhibit high antioxidant activity.

Many melatonin-mediated abiotic stress responses (e.g., to drought, salt, and heat) and physiological process (e.g., flowering, senescence, somatic embryogenesis, sugar metabolism and secondary metabolism) are related to the mitogen-activated protein kinase (MAPK) cascade pathway, melatonin metabolism (Erland et al., 2018; Kobylińska et al., 2018; Qi et al., 2018; Huang et al., 2019; Liu et al., 2019; Zhang H. et al., 2019; Back, 2021), and other more complicated signaling pathways (hormones, ROS, and Ca^{2+}; Arnao and Hernández-Ruiz, 2018; Zhang Y. et al., 2021). Melatonin metabolites can reduce oxidative damage by balancing the redox state (Galano and Reiter, 2018; Yu et al., 2018). However, the signaling pathways of melatonin metabolites in plants have not been fully elucidated.

MELATONIN FUNCTIONS AS AN ANTIOXIDANT IN PLANTS

Melatonin as a ROS and RNS Scavenger

Reactive oxygen species are byproducts in plant aerobic metabolic processes (Apel and Hirt, 2004). ROS consist of radical and non-radical oxygen species. They may be as simple as molecules of superoxide or more complex molecules, like hydrogen peroxide (H_2O_2) and hydroxyl radical (OH·; Ray et al., 2012). In plants, H_2O_2, $O_2^{\bullet-}$, OH·, and $^1O_2$ are the most common ROS. They are mainly generated in chloroplasts, mitochondria, and peroxisomes under stresses. In chloroplasts, ROS generation depends on the interaction of chlorophyll (chl) and light (Hasanuzzaman et al., 2020). The light energy is captured in photosystem II (PSII) to cause photosynthetic electron transfer. During light-driven photosynthetic electron transport, highly reactive singlet oxygen ($^1O_2$) is formed by transferring the absorbed energy to ground-state oxygen of O_2 (Li and Kim, 2021). ^{3}Chl and ^{3}P680 are involved in this process. In addition, $O_2^{\bullet-}$ is produced in photosystem I (PSI) by Mehler reaction. $O_2^{\bullet-}$ can be transferred to H_2O_2 and O_2 by SOD, thus generating OH· *via* the interaction of H_2O_2 with transition metal ions (Fe^{2+} and Cu^+; Hasanuzzaman et al., 2020; Li and Kim, 2021). In mitochondria, Complex I and Complex III are two components of the mitochondrial electron transport chain (mtETC) to covert O_2 to $O_2^{\bullet-}$. Then, Mn-SOD and Cu-Zn-SOD catalyze $O_2^{\bullet-}$ to H_2O_2 (Huang et al., 2016; Hasanuzzaman et al., 2020). In addition, oxidative metabolism also exits in peroxisomes. A number of enzymes are implicated in active metabolism of ROS in peroxisomes such as glycolate oxidase, xanthine oxidase and NADPH oxidase (Del Río and López-Huertas, 2016; Kerchev et al., 2016). Peroxisome is also one of the main cellular sites of NO production that exerts a regulatory function of ROS metabolism.

Damage caused by environmental stress in plants typically occurs because of oxidant stress, which manifests as a loss of equilibrium between oxidant and antioxidant chemical species in the cell, thus altering redox homeostasis and accelerating ROS accumulation (Nguyen et al., 2018). ROS can cause oxidative modification of proteins in chloroplasts under stress conditions. For example, excess $^1O_2$ is reported to oxidize PSII core proteins, polyunsaturated fatty acids (PUFAs) and some

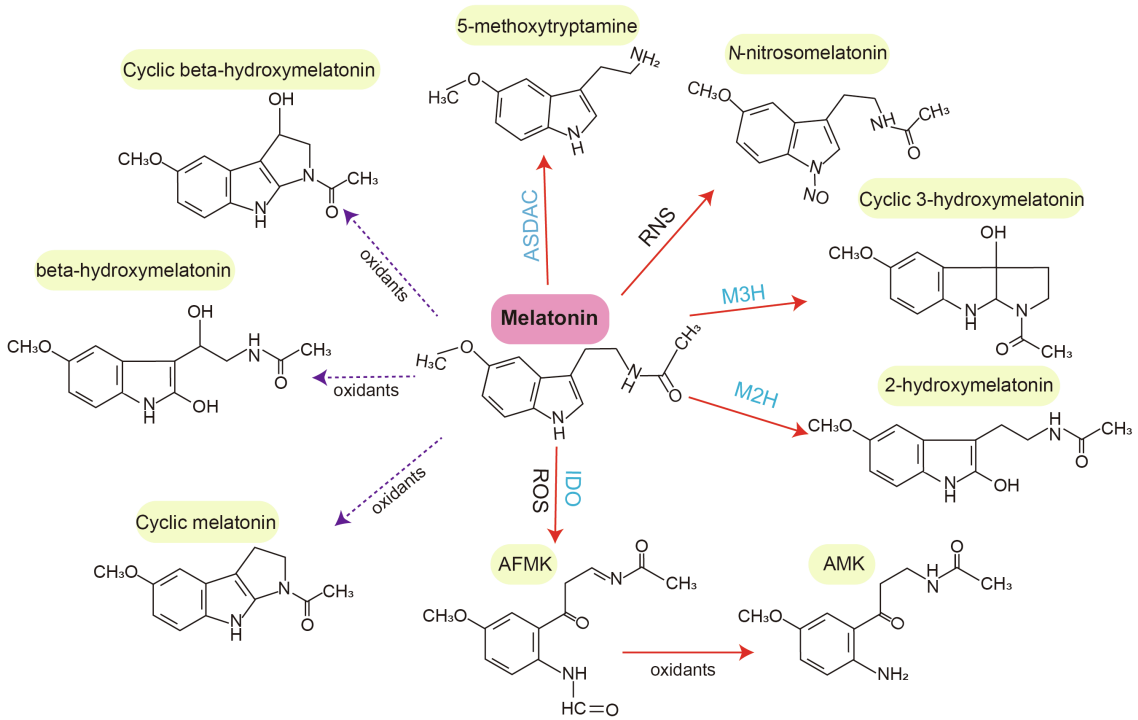


FIGURE 2 | Degradation (catabolism) of melatonin in plants. Melatonin is typically degraded into various metabolites through enzymatic (M3H, M2H, ASDAC, and IDO) and non-enzymatic (oxidants, ROS, and RNS) transformation routes. Red solid arrows indicate confirmed melatonin metabolites. Purple broken arrows indicate potential melatonin metabolites. AFMK, N1-acetyl-N2-formyl-5-methoxykynuramine; AMK, N-acetyl-5-methoxykynuramine; IDO, indoleamine 2,3-dioxygenase; M2H, melatonin 2-hydroxylase; M3H, melatonin 3-hydroxylase; and ASDAC, N-acetylserotonin deacetylase.

specific amino acid residues like tryptophan (Trp), tyrosine (Tyr), phenylalanine (Phe), histidine (His), methionine (Met), and cysteine (Cys; Li and Kim, 2021). $O_2^{\bullet-}$ and OH· can oxidize tyrosine (Y) 246 in the D1 protein (Kumar et al., 2021). α-tocopherol plays a significant role in preventing oxidative modification of the D1-Y246 residue (Li and Kim, 2021). $^1O_2$ can also oxidize a disulfide bond (DSB), thus forming a disulfide crosslink with thiol-containing proteins (Jiang et al., 2021; Li and Kim, 2021). In addition, ROS are utilized as signaling agents by plants and trigger a series of responses that protect the plant against stress factors (Nabi et al., 2019). Among ROS signaling pathways, operational retrograde signaling (ORS) pathways are generally associated with stress. ORS pathways can be mediated by β-cyclocitra (βCC), 3′ (2′)-phosphoadenosine-5′-phosphate (PAP), methylerythritol cyclodiphosphate (MEcPP), and EXECUTER1 (EX1; Kim, 2020; Li and Kim, 2021). Moreover, various hormones (JA, SA, ABA) participate in the crosstalk with ROS to active ROS detoxification under environmental stresses (Lemos et al., 2016; Lv et al., 2019; Postiglione and Muday, 2020; Wang Y. et al., 2021). In addition to hormones, trehalose and anthocyanins are also reported to regulate ROS metabolism (Naing and Kim, 2021; Yang et al., 2022).

NO is an important molecular signal and regulates ROS metabolism (Corpas et al., 2019). Interactions between nitric oxide (NO) and ROS induce radical and non-radical RNS generation under unfavorable conditions. This process is known as nitrosative stress (Corpas and Barroso, 2013; Saddhe et al., 2019). RNS include nitroxyl anion (NO^-), nitrosonium cation (NO^+), higher oxides of nitrogen (NO, NO_2 and higher valence), S-nitrosothiols, and dinitrosyl iron complexes (DNICs; Martínez and Andriantsitohaina, 2009). RNS modify protein activity *via* nitrosylation and interactions between NO and other biomolecules (ferrous heme and catalase; Arora et al., 2016). Moreover, peroxynitrite (ONOO-) and S-nitrosoglutathione (GSNO) derived from NO can modulate the ROS metabolism of peroxisomes through protein posttranslational modifications (Corpas et al., 2019). RNS can also interact with various signaling cascades, such as Ca^{2+}-dependent and phytohormone signaling pathways (Arora et al., 2016; Hasanuzzaman et al., 2018). ROS and RNS have dual roles in plant cells. At low levels, they act as intracellular signaling agents and induce a positive response within the antioxidant system. At high levels, they become toxic and damage both cells and proteins. In plants, the genes of receptor kinase, annexin, and peroxisome biogenesis can be induced by ROS (Apel and Hirt, 2004). ROS and RNS can be neutralized or scavenged by a diverse array of enzymatic and non-enzymatic antioxidants (Arnao and Hernández-Ruiz, 2019b). Enzymatic antioxidant agents include superoxide dismutase (SOD), catalase (CAT), ascorbate peroxidase (APX), glutathione (GSH) peroxidase, GSH S-transferase, monodehydroascorbate reductase (MDHAR), peroxidase, and peroxiredoxin. Non-enzymatic compounds

include polyphenols, flavonoids, polyamines, ascorbic acid (AsA), GSH, cysteine, alkaloids, proline, carotenoids, tocopherols, and plastoquinone.

Melatonin is one of ROS-regulated molecules (Pardo-Hernández et al., 2020). It is well known for ROS detoxification and an ecologically friendly antioxidant compound. Melatonin neutralizes free radical species *via* single-electron and hydrogen transfer (Galano and Reiter, 2018). It can directly interact with ROS to enhance plant resistance to various stresses by scavenging ROS ($O_2^{\bullet-}$, OH·), RNS (nitric oxide and dioxide radicals, azide radicals and peroxynitrite radicals) and other oxidative agents. The most reactive free radical among ROS is the hydroxyl radical (OH·), which is mainly responsible for the oxidative damage to DNA (Chatgilialoglu et al., 2009; Galano and Alvarez-Idaboy, 2009). Furthermore, melatonin has superior OH· scavenging activity, compared to mannitol and GSH (Arnao and Hernández-Ruiz, 2019b). Melatonin reduced nickel-induced oxidative damage by decreasing $O_2^{\bullet-}$ and hydrogen peroxide (H_2O_2) production in tomato leaves and roots (Jahan et al., 2020). Melatonin improved high light tolerance of *Arabidopsis* by scavenging H_2O_2 and $O_2^{\bullet-}$ (Yang et al., 2021). Under different abiotic stresses, exogenous melatonin can trigger the biosynthesis of endogenous melatonin to suppress the accumulation of H_2O_2, $O_2^{\bullet-}$ and MDA, thus alleviating cell membrane damage and improving photosynthesis (Chen Y. et al., 2021; Imran et al., 2021). In addition, melatonin derivatives such as c3-OHM and AFMK exhibit high OH· and hydroperoxyl radical scavenging efficiency (Galano et al., 2014; Galano and Reiter, 2018). Therefore, melatonin and its metabolites act as direct ROS and RNS scavengers in plants under stress.

Melatonin as a Signaling Molecule

Melatonin functions as a signaling molecule. Under stress conditions, melatonin can directly enhance antioxidant enzyme activity and indirectly activates the gene expression of stress response systems and antioxidative systems (**Figure 3**). The expression of antioxidant enzymes (e.g., CAT, POD, and SOD, which detoxify excess H_2O_2) is induced by melatonin to restore redox homeostasis and control ROS levels. A number of antioxidant enzyme-related genes are induced by melatonin. For example, melatonin can alleviate oxidative damage caused by salt stress through the enhancement of antioxidant enzyme activity and removal of H_2O_2 in cotton (Zhang Y. et al., 2021). However, melatonin induces the expression of respiratory burst oxidase homologs (RBOH) that generate $O_2^{\bullet-}$, causing an increase in H_2O_2 levels (Chen et al., 2017; Arnao and Hernández-Ruiz, 2019a). In plants, melatonin signaling triggers abiotic and biotic stress responses by acting on ROS- and RNS-mediated pathways. It also modulates various antioxidant pathways such as the AsA-GSH cycle (Erland et al., 2017). Melatonin can regulate hydrogen peroxide-mediated signaling pathway to detoxify excess ROS (Imran et al., 2021). In addition, Ca^{2+} signal pathway participates in melatonin-mediated abiotic stress tolerance *via* the regulation of Ca^{2+} signal genes like *CIPK3* and *CIPK9* (Gu et al., 2020). ROS generating enzymes (NADPH oxidase and GOX) are suppressed by the combined application of melatonin and Ca^{2+} (Zhang Y. et al., 2021). Moreover, melatonin regulates stress-related gene expression. For example, melatonin induced the expression of *HSFA2* and heat *HSP90*, which enhance thermotolerance in tomato seedlings (Jahan et al., 2019). In salt stress, ion-response gene expressions (*GhNHX1*, *GhSOS1* and *GhAKT1*) were upregulated by melatonin treatment for better salt tolerance of cotton (Shen et al., 2021). In tomato, carbohydrate metabolism is also demonstrated to be regulated by melatonin treatment (Iqbal et al., 2021). Carbon starvation-induced chlorophyll degradation and leaf senescence were alleviated by exogenous melatonin through upregulating transcript levels of miR171b, thus suppressing the expression of *α-glucan water dikinase* (*GWD*) gene (Wang et al., 2022).

Melatonin can also mediate the NOS-like system to exert physiological functions and benefit plants under stress conditions (Arnao and Hernández-Ruiz, 2018). For example, it interacts with NO to activate the SA-dependent pathway and MAPK cascades in response to biotic stresses (He and He, 2020). In *Arabidopsis*, pathogen attack-induced melatonin biosynthesis can activate MAPK kinase kinases such as oxidative signal-induced kinase 1, followed by the MAPK kinase 4/5/7/9 and MAPK3/6 cascades. This upregulates the expression of several defense genes such as pathogenesis-related protein 1 (*PR1*), isochorismate synthase 1 (*ICS1*), GSH S-transferase 1 (*GST1*), and *APX1* (Lee et al., 2015; Lee and Back, 2016b, 2017). Similar to melatonin, some melatonin metabolites such as 2-OHM and AFMK can activate MAPKs. However, the induction of MAPK pathways by c3-OHM has not yet been reported (Lee and Back, 2016b).

A controversial topic of melatonin research is the regulation of other plant hormones by melatonin. Melatonin regulates the gene expression of multiple enzymes, receptors, and transcription factors that are associated with the biosynthesis and catabolism of IAA, GA, CK, ABA, ET, JA, SA, and BR. These relationships indicate possible crosstalk between melatonin and other phytohormones (Weeda et al., 2014; Arnao and Hernández-Ruiz, 2019a; **Figure 3**). Melatonin and IAA are structurally related and have the same precursor, tryptophan. Melatonin also upregulates the expression of auxin signaling and efflux genes (*PIN1*, *PIN3*, and *PIN7*), along with adventitious root formation in tomato (Wen et al., 2016). It also influences the biosynthesis and catabolism of ABA in response to various abiotic stresses (e.g., salt, drought, heat, and cold), possibly acting upstream of the ABA pathway (Li et al., 2015; Fu et al., 2017; Li H. et al., 2017; Arnao and Hernández-Ruiz, 2018). In addition, melatonin reprograms the biosynthesis and metabolism of ET and polyamine biosynthesis to improve waterlogging tolerance in alfalfa (Zhang Q. et al., 2019; Gu et al., 2020). Although there is increasing evidence of crosstalk between melatonin and other plant hormones, details regarding the underlying mechanisms are largely unknown.

ROLES OF MELATONIN IN PLANT ABIOTIC STRESS RESPONSES

Melatonin has important roles in plant responses to abiotic stress. In this section, recent research concerning melatonin-mediated responses to several major abiotic stress factors will be discussed.

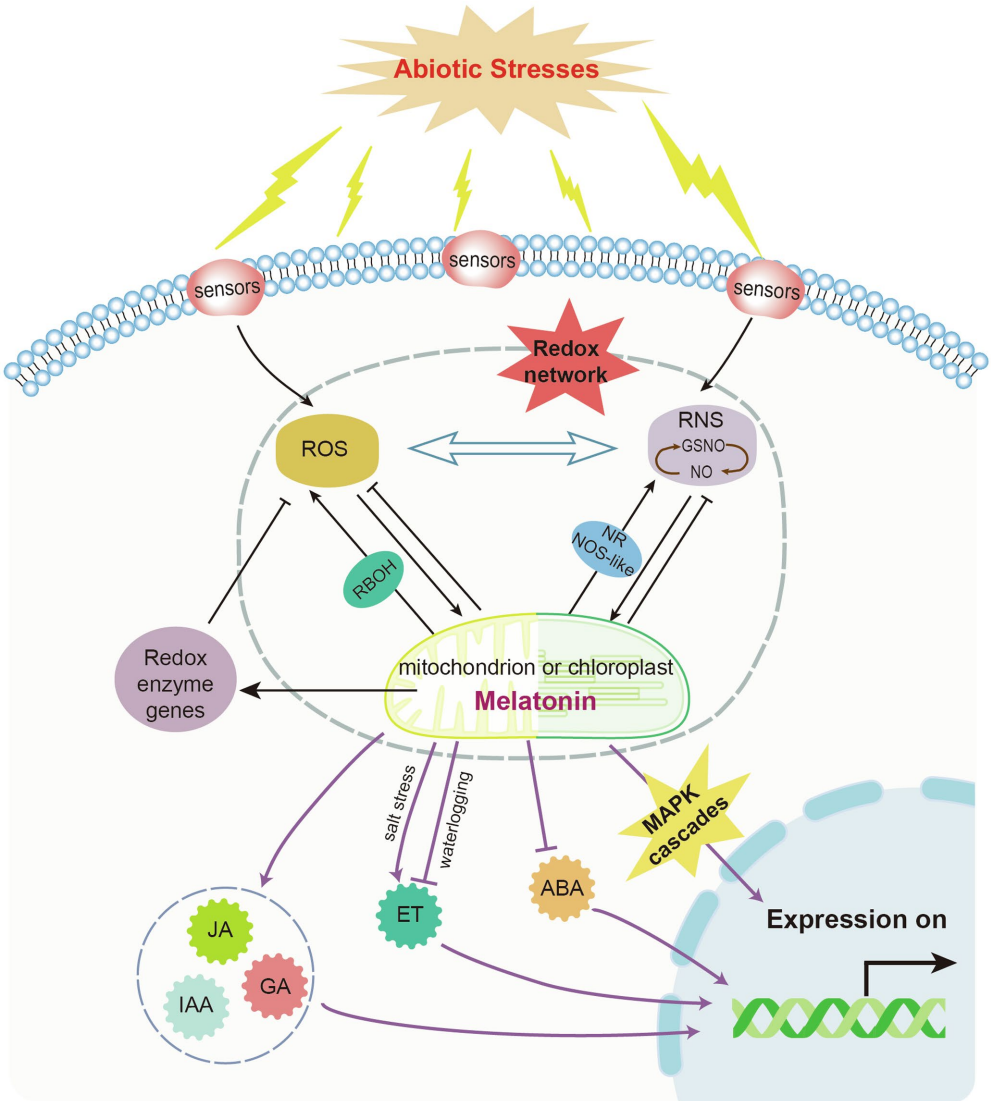


FIGURE 3 | Endogenous melatonin-modulated feedback mechanism in plants under abiotic stresses. Abiotic stresses induce the accumulation of reactive oxygen species (ROS) and reactive nitrogen species (RNS), thus triggering the biosynthesis of endogenous melatonin. RNS and ROS can be scavenged by plant melatonin. Their levels can also be controlled by melatonin-mediated induction of redox enzymes. Mitogen-activated protein kinase (MAPK) cascades and other phytohormone signals are involved in melatonin-modulated transcriptional feedback mechanisms under abiotic stresses. NOS, nitric oxide synthase; GSNO, S-nitrosoglutathione; and RBOH, respiratory burst oxidase homolog.

Drought Stress

Drought restricts plant growth and development. It is also a severe threat to crop productivity and quality because of alterations to the morphological, physiological, biochemical, and molecular features of plants (Cherono et al., 2021). Drought induces oxidative stress and activates stress signaling pathways mediated by ROS, Ca^{2+}, and hormones. In addition, drought stress can activate transcription factors such as NACs, MYBs, AP2/EREBPs, bZIPs, HDs, and bHLHs (Zhang J. et al., 2014). Melatonin has an important role in drought response and resistance in plants. Typically, water deficiency promotes melatonin biosynthesis (Shi et al., 2015a). Endogenous melatonin levels change during water deprivation because melatonin biosynthesis genes (e.g., *TDC*, *ASMT*, *COMT*, and *SNAT*) are upregulated. Drought-induced melatonin biosynthesis has been reported in *Arabidopsis*, barley, bermudagrass, apple, grapevine, and rice (Moustafa-Farag et al., 2020).

Exogenous melatonin treatment can trigger an increase in endogenous melatonin levels, thereby improving turgor pressure, cell stability, chlorophyll recovery, and photosynthetic machinery stability under drought stress (Meng et al., 2014; Ding et al., 2018). Furthermore, melatonin treatment can promote seed germination, lateral root formation, hypocotyl elongation, vegetative growth, and fruit quality during drought (Hosseini et al., 2021; Sun et al., 2021). In rapeseed, seed priming with melatonin improves stomatal and ultrastructural traits, as well

as osmotic adjustment, thus improving drought tolerance (Khan et al., 2019). Melatonin pretreatment in tomato improves dehydration resistance and promotes vegetative growth by decreasing the compatible solute content (e.g., of proline and soluble sugars) and increasing photosynthetic efficiency (Liu et al., 2015; Ibrahim et al., 2020). In lemon verbena plants, melatonin treatment alleviates the adverse effects of drought, while improving growth and essential oil yields by regulating mineral homeostasis and osmolyte accumulation (Hosseini et al., 2021). Moreover, melatonin-mediated drought tolerance in soybean is associated with glucose metabolism.

Melatonin treatment can also alleviate drought-induced oxidative damage in plant species such as apple, tomato, alfalfa, and wheat (Li et al., 2015; Antoniou et al., 2017; Cui et al., 2017). During oxidative stress, antioxidative enzymes such as APX, CAT, SOD, peroxide dismutase, peroxidase, dehydroascorbate reductase (DHAR) and GSH reductase are activated by melatonin, which suppresses ROS accumulation in drought environments (Alharby and Fahad, 2020; Sadak and Bakry, 2020). In *Medicago sativa*, melatonin serves as a priming agent by modulating nitro-oxidative and osmoprotective homeostasis to resist drought stress (Sun et al., 2021). After melatonin treatment, the AsA-GSH cycle, an integral antioxidant system, is enhanced through the upregulation of related genes (*APX*, *MDHAR*, and *DHAR*) to improve drought stress tolerance (Cui et al., 2017; Tiwari et al., 2021). In addition, MAPKs and transcription factors that improve drought tolerance are regulated by melatonin (Tiwari et al., 2021). In oat seedlings, the expression levels of MAPKs (e.g., *Asmap1* and *Aspk11*) and transcription factor genes (e.g., *WRKY1*, *DREB2*, and *MYB*) are upregulated by melatonin treatment (Gao et al., 2018).

Crosstalk between melatonin and other phytohormones is another crucial drought stress regulatory mechanism. The application of melatonin may alleviate drought-induced suppression of flowering in plants by inducing GA biosynthesis (Tiwari et al., 2020). Drought tolerance is enhanced by interactions between melatonin and ABA, which regulate stomatal closure (Chen et al., 2020; Qi et al., 2021). Melatonin downregulates ABA biosynthesis genes and upregulates ABA catabolism genes (*MdCYP707A1* and *MdCYP707A2*) to maintain stomatal function during drought stress (Li et al., 2015).

Waterlogging Stress

Waterlogging can affect crop survival, growth, and productivity. This phenomenon severely limits gas diffusion, which results in hypoxic stress caused by anaerobic respiration in the roots, thereby promoting ROS accumulation (Zhang Q. et al., 2019; Gu et al., 2020; Wu Q. et al., 2021). This burst of excessive ROS production causes roots to rot and leaves to wilt (Hossain et al., 2009). Melatonin participates in the regulation of plant responses to waterlogging. When plants are faced with waterlogging stress, their endogenous melatonin levels increase because melatonin biosynthesis genes (e.g., *TDC*, *T5H*, *ASMT*, *COMT*, and *SNAT*) are upregulated (Moustafa-Farag et al., 2020).

Endogenous melatonin levels are positively correlated with waterlogging resistance. Treatment with exogenous melatonin markedly enhances seedling vitality in peach, apple, and alfalfa by regulating endogenous melatonin levels under waterlogging conditions (Zheng et al., 2017; Zhang Q. et al., 2019; Gu et al., 2020). Additionally, melatonin treatment abates stomatal closure, chlorophyll and photosynthesis reduction, and leaf senescence (Zhang Q. et al., 2019; Gu et al., 2020). In *Malus baccata*, exogenous melatonin application induces the post-transcriptional regulation of endogenous melatonin levels during waterlogging (Zheng et al., 2017). In addition, waterlogging-induced oxidative damage is alleviated by melatonin treatment. Melatonin application enhanced the activities of several antioxidant enzymes and reduced H_2O_2 concentrations in both leaves and roots of peach seedlings to maintain redox homeostasis under waterlogging stress (Gu et al., 2020).

Additionally, melatonin plays a beneficial role in the regulation of waterlogging-induced hypoxia stress by optimizing metabolism in roots and regulating hypoxia-related genes (e.g., ET response factors and calcineurin B-like protein-interacting protein kinase) in peach seedlings (Gu et al., 2020). ET is an important signal associated with hypoxia stress. ET synthesis and signaling is affected by melatonin, which inhibits the expression of 1-aminocyclopropane-1-carboxylate synthase, 1-aminocyclopropane-1-carboxylic acid oxidase, and ET response factor (Zhang Q. et al., 2019; Gu et al., 2020). Notably, waterlogging induced-ET production is suppressed by treatment with moderate amounts of melatonin, whereas ET biosynthesis is induced by treatment with high concentrations of melatonin (Zheng et al., 2017). Therefore, the crosstalk between melatonin and ET has an important regulatory role in waterlogging stress tolerance.

Salt Stress

Salt stress has become a severe global problem, limiting agricultural production and leading to substantial economic losses worldwide (Su et al., 2021). Salt has two detrimental effects on plants: osmotic stress and ion poisoning (Van Zelm et al., 2020). Salt stress alters gene expression, mRNA stability, and translational regulation, thus altering the abundances of proteins in plants (Sharma and Dietz, 2009; Van Zelm et al., 2020). Plant phospholipid signals, protein kinase signals, and ABA are involved in responses to salt stress.

Salt tolerance is enhanced by melatonin in various plants such as maize, wheat, cucumber, tomato, cotton, and rice (Liang et al., 2015; Zhou et al., 2016; Chen et al., 2018; Ke et al., 2018; Zhang Y. et al., 2021). Salt stress can affect the expression patterns of key melatonin biosynthetic enzymes and increase endogenous melatonin content (Arnao and Hernández-Ruiz, 2009). Moreover, the overexpression of *SNAT* can significantly improve plant salt tolerance. For example, *VvSNAT1* overexpression *Arabidopsis* lines exhibit greener leaves, enhanced growth, and higher germination rates under salt stress, compared with wild-type lines (Wu Y. et al., 2021). In contrast, SNAT inhibition lowers endogenous melatonin levels, thereby increasing the sensitivity of rice to salt stress (Byeon and Back, 2016).

Exogenous melatonin treatment helps to protect plants against salt stress by regulating antioxidant enzyme expression and activity, polyamine metabolism, and NO signaling (Zhan et al., 2019). The activation of major antioxidant enzymes decreases

salinity-induced ROS and H_2O_2 levels. In addition, crosstalk between melatonin and NO regulates redox equilibrium *via* the differential expression of *copper/zinc-SOD* and *manganese-SOD*, and by modulating both GSH levels and GSH reductase activity in cotyledons under salt stress (Arora and Bhatla, 2017). Moreover, melatonin induces crosstalk between NO and hydrogen sulfide, thus improving salt stress tolerance in pepper (Kaya et al., 2020). Molecular hydrogen triggers melatonin signaling by activating SNAT-dependent melatonin production in *Arabidopsis* (Su et al., 2021).

Ion homeostasis is vital for plant survival under salt stress. There is evidence that melatonin assists with ion homeostasis maintenance, particularly concerning K^+ and Na^+. Melatonin-mediated ion homeostasis is associated with the expression of *NHX* and *AKT*, which encode two important ion channels (Li et al., 2012). The NHX family is related to K^+ and Na^+ antiporters. Na^+ accumulates in vacuoles when *NHX* is upregulated (Munns and Tester, 2008). Under salt stress, the salt overly sensitive signaling pathway is triggered to transport Na^+ out of the cells, or to activate an unknown transporter that confines Na^+ to the vacuole.

Exogenous melatonin treatment leads to triacylglycerol breakdown, fatty acid β-oxidation, and energy turnover to maintain the activity of the plasma membrane H^+-ATPase. These processes mediate K^+/Na^+ homeostasis and provide evidence for the mediation of seed germination by melatonin in cucumber under salt stress (Zhang N. et al., 2017). In addition, Na^+ and Cl^- accumulation is inhibited in rice roots and leaves after exogenous melatonin application by enhancing the transcription of *OsSOS1* in roots and of *OsCLC1* and *OsCLC2* in roots and leaves (Li X. et al., 2017).

ET biosynthesis is promoted by exogenous melatonin treatment during salt stress in grapevine. Endogenous ET enhancement is regulated by *MYB108A* expression, which activates the expression of the ET biosynthesis-related gene *ACS1* (Xu et al., 2019). GA and ABA, as well as antioxidant enzymes, are involved in melatonin-mediated seed germination under high salt conditions in cucumber (Zhang H. et al., 2014). Melatonin coordinates with BR during salt stress by regulating genes involved in BR biosynthesis and signal transduction in cotton. In addition, the Ca^{2+} signal transduction pathway has a pivotal role in melatonin-mediated salt tolerance (Zhang Y. et al., 2021).

Cold (Chilling) Stress

Cold stress exerts destructive effects on crop growth and productivity. It can lead to redox imbalance and induce excessive ROS accumulation. In response to cold stress, plants increase ABA synthesis, thus activating the C-repeat binding factor pathway (Knight et al., 2004). Extreme cold environments typically induce melatonin accumulation to protect plants against fatal injuries. Increasing endogenous melatonin levels can improve plant cold tolerance. For example, *SNAT* transgenic rice are less sensitive to cold than wild-type plants, indicating the protective role of melatonin in cold resistance (Kang et al., 2010). There is evidence that melatonin functions as a long-distance signal that can be transported from roots to shoots (Tan et al., 2007). In grafted watermelons, melatonin improves cold tolerance *via* root-to-shoot communication and transportation (Li H. et al., 2021).

Exogenous melatonin treatment can maintain the quality of fruits, vegetables, and cut flowers by conferring chilling tolerance under cold storage. For example, pre-storage treatment of loquat fruit with melatonin triggers the accumulation of phenolic compounds and a reduction in lignin, thereby alleviating flavor and nutrition loss induced by chilling injury under cold storage (Wang D. et al., 2021). Melatonin treatment in Bermuda grass can improve the levels of secondary metabolites including amino acids, organic acids, carbohydrates, and sugars, thereby enhancing cold tolerance (Hu et al., 2016). The application of 2-hydroxymelatonin, a metabolite of melatonin, may also improve cold and drought tolerances in tobacco, tomato, and cucumber (Lee and Back, 2019).

Similar to its effects in the context of other stress factors, exogenous melatonin application can alleviate cold damage through the activation of antioxidant enzymes, as well as reductions of both ROS accumulation and lipid peroxidation (Hu et al., 2016). For example, cut flowers treated with melatonin had lower H_2O_2 concentrations and increased 2,2-diphenyl-1-picrylhydrazyl (DPPH) scavenging capacity under cold stress than did untreated flowers (Aghdam et al., 2019). Chilling tolerance in tomato increases because of arginine-dependent NO accumulation after melatonin treatment. Under cold stress, melatonin upregulates genes related to stress responsive pathways such as C-repeat binding factor/dehydration-responsive element-binding protein (CBF/DREB), *cold regulated 15a* (*COR15a*), *calmodulin binding transcription activator 1* (*CAMTA1*), and zinc finger transcription factors 10 and 12 (ZAT 10 and ZAT 12; Zhao et al., 2017; Guo et al., 2018; Wang et al., 2018). The rhythmic expression patterns of circadian clock genes are also altered by melatonin supplementation in hulless barley seedlings, regulating their growth and enhancing cold resistance (Chang et al., 2021).

Additionally, the expression patterns of phytohormone biosynthesis genes are modulated by exogenous melatonin. For example, the expression levels of a key gene (*ClAOC1*) in JA biosynthesis, and a key gene (*ClAMI1*) in IAA biosynthesis are upregulated in watermelon leaves after melatonin application under cold stress (Chang et al., 2020; Li H. et al., 2021). Consequently, the JA and IAA contents increase, thus improving photosynthesis and redox homeostasis (Chang et al., 2021).

Heat Stress

Heat stress is becoming a global concern because of global warming. Frequent heat waves have a profound impact on terrestrial plants. Heat stress affects plants at the physiological (e.g., photosynthesis, cell membrane thermostability, and oxidative damage), transcriptional, post-transcriptional (e.g., non-coding RNAs), and epigenetic (e.g., DNA methylation, histone modification, and chromatin remodeling) levels (Zhao et al., 2020). During heat stress, endogenous melatonin levels increase, thereby improving plant thermotolerance. In tomato, *COMT1* and *TDC* silencing aggravates high temperature-induced oxidative damage by suppressing endogenous melatonin biosynthesis (Ahammed et al., 2019). Furthermore, *ASMT* and *SNAT* overexpression significantly

improves thermotolerance by increasing endogenous melatonin (Xu et al., 2016; Wang et al., 2020).

Under heat stress, exogenous melatonin treatment can enhance plant antioxidant defense systems *via* control of ROS accumulation and enhancement of proline metabolism. In tomato seedlings, melatonin treatment promotes thermotolerance by balancing redox homeostasis, while modulating polyamine and nitric oxide biosynthesis (Jahan et al., 2019). In wheat, photosynthetic potential is maintained by interactions between melatonin and hydrogen sulfide under heat stress (Iqbal et al., 2021). Upon exposure to high temperatures, exogenous melatonin treatment can alleviate heat damage in plants by mediating the activity of HSFs, which are the master mediators of heat responses. In *Arabidopsis*, melatonin-mediated thermotolerance was associated with the upregulation of *HSFA2* and *HSA32*, as well as *HSP90* and *HSP101* (Shi et al., 2015b). In tomato, melatonin treatment upregulated *HSP* gene expression and increases HSP production, which then repaired denatured or damaged proteins after heat exposure (Xu et al., 2016). Furthermore, *HSP40* interacted with *SlSNAT* to regulate melatonin biosynthesis and promote thermotolerance by maintaining Rubisco enzyme stability under heat stress (Wang et al., 2020). In addition, heat-induced leaf senescence is suppressed by melatonin treatment, which regulates ABA and CK biosynthesis and signaling pathways (Zhang J. et al., 2017). Exogenous melatonin reduces heat-induced damage by upregulating SA production and downregulating ABA levels in soybean seedlings (Imran et al., 2021).

Heavy Metal Toxicity

Heavy metals are toxic to plants. Heavy metal stress can repress root growth and promote the leaf senescence by inducing ROS accumulation and damaging chloroplasts. In addition, Calvin cycle enzymes, photosynthesis, and carbohydrate metabolism are also inhibited by heavy mental toxicity (Hasan et al., 2015, 2019; Ni et al., 2018). Toxicity caused by lead (Pb), copper, vanadium, and aluminum can disrupt redox homeostasis and accelerate the accumulation of redox agents (Nagajyoti et al., 2010).

Melatonin treatment can alleviate heavy metal-induced suppression of root growth and activity (Ni et al., 2018; Jahan et al., 2020). Endogenous melatonin production can be induced by treatment with exogenous melatonin to strengthen heavy metal tolerance. In wheat seedlings, melatonin treatment promoted endogenous melatonin biosynthesis in shoots and roots. The enhancement of endogenous melatonin alleviated cadmium (Cd) toxicity by balancing H_2O_2 homeostasis and activating antioxidant enzymes (Ni et al., 2018). Exogenous melatonin treatment also enhances the antioxidant potential of plants and reduces lipid peroxidation under aluminum stress (Sun et al., 2020). In tomato, melatonin effectively ameliorated Cd-induced toxicity by enhancing H^+-ATPase activity, increasing GSH and phytochelatin contents, and facilitating Cd sequestration in plant cells (Hasan et al., 2015). In addition, melatonin treatment alleviates nickel phytotoxicity by improving gas exchange, while increasing the contents of photosynthetic pigments, minerals, nutrients, and secondary metabolites (Jahan et al., 2020). NO signaling is involved in melatonin-induced antioxidant defenses. NO has a vital role in re-establishing redox homeostasis in plants under heavy metal stress. Crosstalk between melatonin and NO improves Pb and Cd stress tolerance (Kaya et al., 2019; Okant and Kaya, 2019).

In addition to regulating antioxidant levels, melatonin mediates heavy metal tolerance by enhancing heavy metal uptake and sequestration. Cd, vanadium, and copper are excluded from or sequestered in plant cells after exogenous melatonin treatment (Nawaz et al., 2018; Cao et al., 2019; Hasan et al., 2019). Notably, melatonin treatment balances endogenous GA and ABA levels and improves thiol-mediated detoxification in two indica rice. Furthermore, melatonin reduces Pb damage in radish plants *via* DNA demethylation of metal transporters and antioxidant genes (Tang et al., 2021).

Light Stress

Light is dispensable to plants. However, it is also an environmental stressor that causes photodamage and overaccumulation of ROS in plants. Ultraviolet (UV) light can induce the generation of free radicals in plants (Demarsy et al., 2018; Nazir et al., 2020). Exposure to high UV radiation for a long time can result in damage of the nuclear membrane and generally cause changes in the ultrastructure of various cellular components in many plant species.

One important regulator of melatonin biosynthesis is light (Tan et al., 2007; Zhang H. et al., 2019). In plants, it was observed that the concentration of endogenous melatonin was increased after UV-B treatment for short time, suggesting that endogenous melatonin is involved in UV-B response (Afreen et al., 2006; Wei et al., 2019). Exogenous melatonin increased the content isoflavone monomers in 4-day-old germinated soybeans under UV-B stress (Yin et al., 2022). In *Arabidopsis*, melatonin also participated in UV-B signaling pathway by delaying and subsequently enhancing expression of *COP1*, *HY5*, *HYH*, and *RUP1/2* to mediate UV-B stress tolerance (Yao et al., 2021). Under high light stress, melatonin can improve photosynthesis, alleviate inhibitory effect of stomatal apertures and relieve the oxidative damage to cells by regulating redox state (Wei et al., 2019; Haskirli et al., 2021; Yang et al., 2021). In contrast, snat1 knockout mutants of *Arabidopsis* failed to induce melatonin biosynthesis and lower expression of ROS-responsive genes, resulting in sensitivity to high light stress (Lee and Back, 2018). In addition, melatonin may regulate flavonoids to mediate light tolerance (Wei et al., 2019; Nazir et al., 2020). Flavonoids are also important antioxidants (Shen et al., 2022), however, the interaction of melatonin and flavonoids need further investigation.

Other Abiotic Stresses

Melatonin functions on other abiotic stress factors have been discussed. Potassium deficiency tolerance is a vital problem to crop production. Melatonin can enhance potassium content in *Malus* under different stress conditions and promote potassium deficiency tolerance in wheat (Li et al., 2016; Li G. et al., 2021). *TaHAK1* regulated by *TaNAC71* played an important role in MT-mediated potassium deficiency tolerance in wheat (Li G. et al., 2021). In addition, plastic pollution has received

TABLE 1 | Exogenous melatonin application to plants under abiotic stresses.

Species	Stress level	Melatonin level	Main effects	References
Drought stress				
Glycine max	Drought stress (45% soil water), 72 h	100 μM	Promote sugar metabolism and production and repair the membrane damage by regulating gene expression and enzyme activities (sucrose phosphate synthase, sucrose synthase, sucrose invertase, β-amylase) of sugar metabolism	Cao et al., 2021
Zea mays	Drought stress (40%–45% soil water), 7 days	100 μM	Improve resistance to drought stress by enhancing the activity of SOD, CAT, POD, APX, enhancing the levels of osmo-protectants and controlling root growth	Ahmad et al., 2021
Zea mays	Drought stress (50% soil water), 6 days	100 μM	Enhance leaf gas exchange, regulate carbon and nitrogen metabolism *via* promoting the activity of SPS, AGPase, PEPC, CS, NR, NiR, GS, and GOGAT	Alharby and Fahad, 2020
Zea mays	Withholding water, 8 days	1 mM	Exert a protective effect on drought tolerance by regulating ABA and JA, improving photosystem II efficiency and photochemistry	Fleta-Soriano et al., 2017
Gossypium hirsutum	Drought stress (45 ± 5% soil water), 9 days	200 μM	Improve antioxidative capacity by promoting the expression of *Cu/ZnSOD*, *CAT*, *POD* and increasing AsA content and the activity of APX, GR and DHAR	Hu et al., 2021
Lippia citriodora	Drought stress (50% and 25% soil water), 45 days	100 μM	Minimize drought effects by enhancing antioxidative capacity, keeping mineral balance and regulating ABA content	Hosseini et al., 2021
Medicago sativa	Withholding water, 7 days	10 μM	Improve nitro-oxidative homeostasis through regulating RNS metabolic enzymes, limit cellular redox disruption through the regulation of the mRNA levels of antioxidant and redox-related components	Antoniou et al., 2017
Waterlogging stress				
Sorghum bicolor	Place seedlings into pots lacking holes for drainage, 14 days	100 μM	Strengthen waterlogging tolerance by increasing soluble protein contents and improving the activity of POD, CAT, APX	Zhang R. et al., 2021
Prunus persica	Keep water levels at 2 cm above the soil surface, 12 days	200 μM	Improve antioxidant enzyme activities, control anaerobic respiration in roots through enhancing aerenchym, regulating the Ca^{2+} signal genes (*CIPK3* and *CIPK9*), metabolism-related genes (*ADH6*, *PDC2*, and *LDHa*) and ethylene synthesis genes (*ACS* and *ACO*)	Gu et al., 2020
Medicago sativa	Keep water levels at 1 cm above the soil surface, 10 days	100 μM	Alleviate growth inhibition and membrane damage by enhancing polyamines (Put, Spd and Spm) content, decreasing MDA content regulating the expression of key genes involved in polyamine metabolism (*SAMDC*, *SPDS*, *SPMS*, *ADC*, *DAO* and *PAO*) and decreasing ethylene levels	Zhang Q. et al., 2019
Salt stress				
Oryza sativa	150 mM NaCl solution treatment, 7 days	200 μM	Reduce membrane damage and improve antioxidant capacity by enhancing antioxidant enzyme activity (SOD, CAT, POD, APX, GR) and antioxidant content (proline, glycine betaine, flavonoid, total phenol)	Yan et al., 2021
Oryza sativa	Two salt treatments (150 and 200 mM NaCl), 7 days	75 μM	Strengthen root vigor by enhancing antioxidant enzyme activity, reducing contents of Na^+ and Cl^- and increasing transcription of *OsSOS1* in roots	Li X. et al., 2017
Gossypium hirsutum	100 mM NaCl treatment, 8 days	1 μM	Enhance photosynthetic capacity and osmotic regulation by enhancing antioxidant system and ion-response gene expression (*GhNHX1*, *GhSOS1* and *GhAKT1*)	Shen et al., 2021
Gossypium hirsutum	100 mM NaCl treatment, 12 h	20 μM	Strengthen salt tolerance by scavenging ROS and Ca^+ signal transduction	Zhang Y. et al., 2021
Brassica juncea	150 mM NaCl treatment, 16 days	1 μM	Recover salinity-damaged plants by improving amino acid, protein, and SA contents; decreasing ABA content	Park et al., 2021
Zea mays	100 mM NaCl treatment, 8 days	1 μM	Achieve salt tolerance by regulating the content of sucrose, fructose and proline, suppressing the accumulation of H_2O_2 and MDA for better osmotic adjustment and ion balance	Ren et al., 2020
Hevea brasiliensis	1% NaCl treatment, 3 days	100 μM	Enhance photosynthesis and salt tolerance by increasing flavonoid content and suppressing H_2O_2 accumulation	Yang et al., 2019
Vitis vinifera	100 mM NaCl treatment, 3 days	50 μM	Improve salt tolerance by increasing ACC content and ethylene biosynthesis mediated by *MYB108A*	Xu et al., 2019
Brassica napus	125 mM NaCl treatment, 24 h	1 μM	Promote salinity tolerance through reestablished redox and ion homeostasis, modulated antioxidant defense related genes and the regulation of *NHX1* and *SOS2* expression	Zhao et al., 2018

(Continued)

TABLE 1 | Continued

Species	Stress level	Melatonin level	Main effects	References
Heat stress				
Triticum aestivum	40°C for 15 days at 6 h time duration every day	100 μM	Protect heat stress-induced photosynthetic inhibition *via* a crosstalk with H_2S that regulates carbohydrate metabolism	Iqbal et al., 2021
Glycine max	42°C, 7 days	100 μM	Increase total phenolic and flavonoid contents, enhance PA and SA biosynthesis, decrease ABA content *via* down-regulation of the *gmNCED3* and up-regulation of catabolic genes (*CYP707A1* and *CYP707A2*) and promote ROS detoxification *via* the hydrogen peroxide-mediated signaling pathway	Imran et al., 2021
Solanum lycopersicum	42°C, 24 h	100 μM	Improve antioxidant activities by regulating their related gene expression and the ascorbate-glutathione cycle, detoxify excess ROS *via* hydrogen peroxide-mediated signaling pathway (induction of *RBOH*, *P5CS*, *HSP90*), increase PA and NO contents	Jahan et al., 2019
Actinidia deliciosa	45°C, 8 h	200 μM	Enhance antioxidant enzyme activities (POD, CAT, SOD) and regulate key AsA-GSH cycle enzymes (APX, MDHAR, DHAR, GR)	Liang et al., 2018
Lolium perenne	38/33°C day/night, 28 days	20 μM	Increase t-ZR contents by regulating CK biosynthesis (*LpIPT2*, *LpLOG1*) and signaling gene (*LpARR1*, *LpARR10*, *LpARR5*, *LpARR17*), decrease ABA content by regulating biosynthesis (*LpZEP*, *LpNCED1*) and signaling genes (*LpABI3*, *LpABI5*)	Zhang J. et al., 2017
Cold (chilling) stress				
Cucumis sativus	5°C, 72 h	100 μM	Increase NR activity and NO content, upregulate NR-relative mRNA expression and induce chilling response genes (*ICE1*, *CBF1* and *COR47*)	Feng et al., 2021
Cucumis sativus	15/8°C day/night, 8 days	200 μM	Upregulate *CsZat12* expression, modulate the PA (Put, Spd and Spm) metabolism and ABA metabolism *via* the regulation of *CsNCED1*, *CsNCED2*, *CsCYP707A1* and *CsCYP707A2*	Zhao et al., 2017
Citrullus lanatus	4°C, 24 h	150 μM	Increase MeJA content	Li H. et al., 2021
Citrullus lanatus	4°C, 72 h	1.5 μM	Enhance photosystem II and AsA-GSH cycle; mediate CBF-responsive pathway by upregulating *ClCBF1* expression; increase IAA content and decrease ABA content	Chang et al., 2020
Capsicum annuum	4°C ± 0.5°C, 20 days	100 μM	Reduce cell structure damage; increase membrane lipid and proline contents, keep higher unsaturated: saturated fatty acid ratio	Kong et al., 2020
Lycopersicon esculentum	4°C ± 0.5°C, 28 days	100 μM	Enhance H-ATPase, Ca-ATPase, cytochrome c oxidase (CCO), and succinate dehydrogenase (SDH) enzyme activity, inhibit the transcription of *CaNAC1*, increase unSFA/SFA ratio	Jannatizadeh et al., 2019
Heavy mental stress				
Oryza sativa	150 μM sodium arsenate (As), 2 days	20 μM	Decrease arsenic bioaccumulation *via* modulating the expression levels of selected arsenic transporters (*OsNramp1*, *OsPT2*, *OsPT8*, *OsLsi1*) and controlling endogenous phytohormone homeostasis	Samanta et al., 2021
Raphanus sativus var. *radculus pers*	200 mg L^{-1} $Pb(NO_3)_2$ treatment	50 μM	DNA demethylation of metal transporters n (e.g., *RsABCF5*, *RsYSL7* and *RsHMT*) and antioxidant genes (e.g., *RsAPX2*, *RsPOD52* and *RsGST*)	Tang et al., 2021
Triticum aestivum	30 mM $AlCl_3$, 12 h	/	Alleviate Al toxicity by augmenting oxidants, enhance exclusion of Al from root apex by altering cell wall polysaccharides and increasing pectin methylesterase (PME) activity	Sun et al., 2020
Triticum aestivum	200 mM for $CdCl_2$, 12 h	50 mM	Balance hydrogen peroxide homeostasis *via* maintaining the hydrogen peroxide homeostasis and the regulation of the antioxidant systems	Ni et al., 2018
Medicago truncatula	7.52 g L^{-1} Pb solution, 12 weeks	10 μM	Improve AM symbiosis and induce *MtPT4* expression by inhibiting Pb uptake, make a synergistic effect on Pb stress tolerance	Zhang et al., 2020
Malus baccata	30 μM Cd, 20 days	100 μM	Regulate Cd uptake, transport, and detoxification by altering the mRNA levels of several genes (*HA7*, *NRAMP1*, *NRAMP3*, *HMA4*, *PCR2*, *NAS1*, *MT2*, *ABCC1*, and *MHX*)	He et al., 2020
Solanum lycopersicum	Nickel chloride ($NiCl_2{\cdot}6H_2O$), 14 days	100 μM	Enhance photosynthesis, improve secondary metabolism (total phenols, flavonoids and anthocyanins) and alters the detoxification related gene expression (*SOD*, *CAT*, *APX*, *GR*, *GST*, *MDHAR*, and *DHAR*)	Jahan et al., 2020

(Continued)

TABLE 1 | Continued

Species	Stress level	Melatonin level	Main effects	References
Solanum lycopersicum	100 μM Cd, 15 days	100 μM	Regulate sulfur metabolism by suppressing sulfate transporter *(SUT)1* and *SUT2* genes and decreasing transcript levels of the *ATPS*, *APSR*, *SiR* and *OASTL* genes to enhance Cd detoxification	Hasan et al., 2019
Carthamus tinctorius	50 μM $Pb(NO_3)_2$, 14 days	100/150/200/300 μM	Alleviate Pb toxicity by reducing Pb uptake and its root-to-shoot translocation along with stimulating activity of SOD, APX, CAT, GPX and GR	Namdjoyan et al., 2019
Arabidopsis thaliana	8% w/v $NaClO_3$, 15 min	1 μM	Increase root growth by interfering with NO-mediated reduction of cell division cycle progression	Zhang J. et al., 2019
Zea mays	$PbCl_2$·2.5 H_2O, 4 weeks	0.05/0.1 mM	Alleviate Pb toxicity by increasing proline levels, NO levels and antioxidant enzyme activities (SOD, CAT and POD)	Okant and Kaya, 2019
Nicotiana tabacum	100 μM Cd ($CdCl_2$), 7 days	100 μM	Weaken Cd uptake by regulating genes expression of *IRT1*, *Nramp1*, *HMA2*, *HMA4* and *HMA3*	Wang et al., 2019
Cucumis sativus	80 μmol·L^{-1} Cu^{2+} ($CuSO_4$), 2 weeks	10 nM	Enhance the cell wall capacity for binding copper by increasing the gene expression of *CesA*, *CSL*, *PME* and *XTH*, maintain nutrient elements homoeostasis, activate carbon metabolism *via* the upregulation of *ADH*, *ALDO*, *ENO*, *GAPDH*, *GPI*, *PDC and PGK*	Cao et al., 2019
Citrullus lanatus	50 mg/L Vanadium, 7 days	0.1 μM	Enhanced the activity of SOD and CAT, regulate relative transcript expression of respiratory burst oxidase genes (*Cla000765* and Cla001877) and chlorophyll degradation related genes (*Cla013675*, and *Cla006037*)	Nawaz et al., 2018
Light stress				
Glycine max	40 μW/cm^2 UV-B radiation, 2 and 4 days	25 μM	Remove UV-B stress by regulating isoflavone metabolism-related enzyme activities (PAL, C4H, 4CL) and enhancing the content of total flavonoids and isoflavone monomers	Yin et al., 2022
Arabidopsis thaliana	0.7 μmol·m^{-2}·s^{-1} UV-B, 6 h	100 μM	Mediate UV-B signaling pathway by delaying and enhancing expression of *COP1*, *HY5*, *HYH*, *and RUP1/2*	Yao et al., 2021
Arabidopsis thaliana	UV-B (46 and 92 kJ·m^{-2}·d^{-1}), 90 and 180 min	100 μM	Regulate the expression of *glutathione peroxidase 2* (*GPX2*) and *GPX7*, decrease the expression of *alternative oxidase 1a* (*AOX1a*) and *AOX1d*	Haskirli et al., 2021
Arabidopsis thaliana	High light (1,000 μmol·m^{-2}·s^{-1}), 3 h	100 μM	Protected photosystem protein by inhibiting the accumulation of H_2O_2 and promoting the activity of SOD, POD, APX and GPX	Yang et al., 2021
Malus hupehensis	UV-B dosage of 0.24 W·m^{-2} and UV-B dosage of 0.45 W·m^{-2}	1 μM	Improve UV-B tolerance by suppressing H_2O_2 accumulation and increasing phenolic compounds (chlorogenic acid, phloridzin and quercetin-3-galactoside)	Wei et al., 2019

a great concern worldwide. Melatonin was reported to reduce the nanoplastic uptake by roots and their translocation to shoots by regulating the expression of genes associated with aquaporin (*TIP2-9*, *PIP2*, *PIP3*, *PIP1-5* and *PIP1.2*). Melatonin enhanced the tolerance to nanoplastic toxicity by maintaining a better redox homeostasis and ameliorating the negative effects of nanoplastics on carbohydrate metabolism (Li S. et al., 2021).

EXOGENOUS MELATONIN APPLICATION

Exogenous melatonin treatment can improve the tolerance of plants to various abiotic stresses (e.g., salt, drought, waterlogging, heat, cold, and heavy metal toxicity) in several plant species. These improvements in stress tolerance are largely associated with the induction of endogenous melatonin production after exogenous melatonin treatment. In addition, these improvements are typically dose-dependent. Treatment with low melatonin concentrations typically induces stronger stress tolerance responses than does treatment with high melatonin concentrations (Zhang et al., 2015).

Overall, melatonin has great potential for use as an anti-stress agent in agricultural crop production applications. Recent reports of exogenous melatonin treatment for abiotic stresses are summarized in **Table 1**.

CONCLUSIONS AND FUTURE PERSPECTIVES

Plant melatonin is important for alleviating damage caused by various abiotic stresses. In this review, we summarized the regulatory mechanisms that drive melatonin-mediated abiotic stress tolerance in plants. Plant tolerance is typically enhanced by melatonin *via* the following pathways. Melatonin can act as a direct scavenger of ROS and RNS to improve antioxidant capacity. It also acts as a signaling molecule, regulating the expression of genes involved in stress responses, antioxidant production, and phytohormone pathways (e.g., ABA, ET, and JA; **Figure 4**). Moreover, melatonin affects the redox network. It can interact with NO to regulate redox homeostasis, thus maintaining antioxidant potential during abiotic stress.

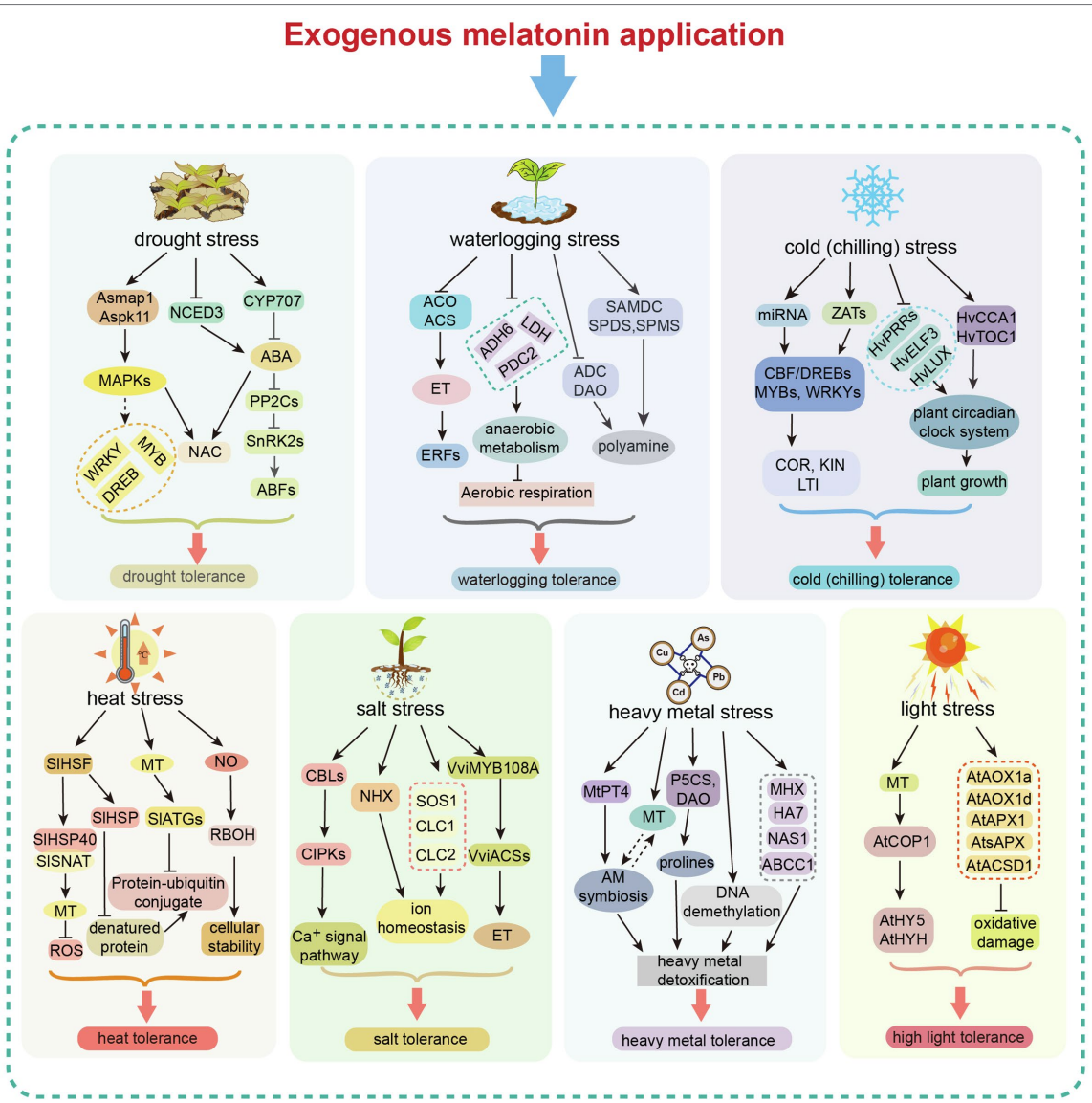


FIGURE 4 | Exogenous melatonin-mediated regulation in response to different abiotic stresses. Exogenous melatonin application induces changes in gene expression in different abiotic stress response pathways, resulting in enhanced tolerance to major abiotic stresses (drought, waterlogging, heat, cold, salt, heavy metal toxicity and light). MAPK, mitogen-activated protein kinase; NCED3, nine-cis-epoxycarotenoid dioxygenase 3; NAC, N-acetylcysteine; DREB, dehydration responsive element binding; CYP, cytochrome P450; PP2C, protein phosphatase 2C; SnRK, sucrose non-fermenting–related related kinase; ABF, abscisic acid responsive element-binding factor; ABA, abscisic acid; ACO, acyl-CoA oxidase; ACS, acetyl-CoA synthetase; ET, ethylene; ERF, ETS2 repressor factor; ADH, alcohol dehydrogenase; LDH, lactate dehydrogenase; PDC2, pyruvate decarboxylase-2; SAMDC, S-adenosylmethionine decarboxylase; SPDS, spermidine synthase; SPMS, spermine synthase; ADC, arginine decarboxylase; DAO, di-amine acid oxidase; CBF/DREB, dehydration responsive element binding/C-repeat binding factor; ZAT, zinc transporter; COR, cold-regulated gene; KIN, Kin17 DNA and RNA binding protein; LTI, low-temperature-induced genes; PRRs, pseudo-response regulators; ELF3, E74 like ETS transcription factor 3; CCA1, circadian colck associated 1; TOC1, timing of CAB expression 1; HSF, heat shock facter; HSP, heat shock protein; SNAT, serotonin N-acetyltransferase; MT, melatonin; RBOH, respiratory burst oxidase homolog; ATG, autophagy-related; CBL, calcineurin B-like proteins; CIPK, CBL-interacting protein kinases; NHX, Na^+/H^+ exchanger protein; SOS1, SOS Ras/Rac guanine nucleotide exchange factor 1; CLC, chloride channel; PT4, phosphate transporter 4; AM, arbuscular mycorrhizal; P5CS, delta 1-pyrroline-5-carboxylate synthase; DAO, D-amino acid oxidase; MHX, magnesium/proton exchanger; NAS1, nicotianamine synthase 1; nicotianamine synthase 1; COP1, constitutive photomorphogenic 1; HY5, elongated hypocotyl 5; HYHAPX, hy5 homolog; APX, ascorbate peroxidase; AOX, aldehyde oxidase; and ACSD, 2-amino-3-carboxymuconate-6-semialdehyde decarboxylase.

The key melatonin biosynthetic enzymes (TDC, T5H, SNAT, ASMT, COMT) have been identified. The melatonin biosynthetic pathway has been characterized in several plant species. Under normal conditions, the chloroplast is the main biosynthetic site of plant melatonin. Mitochondria are also sites of melatonin biosynthesis in plants when the chloroplast pathway is blocked. The melatonin catabolic pathway and its metabolites have received increasing research attention in recent years because of their beneficial effects on plant resistance to environmental stresses. Exogenous melatonin application can regulate plant

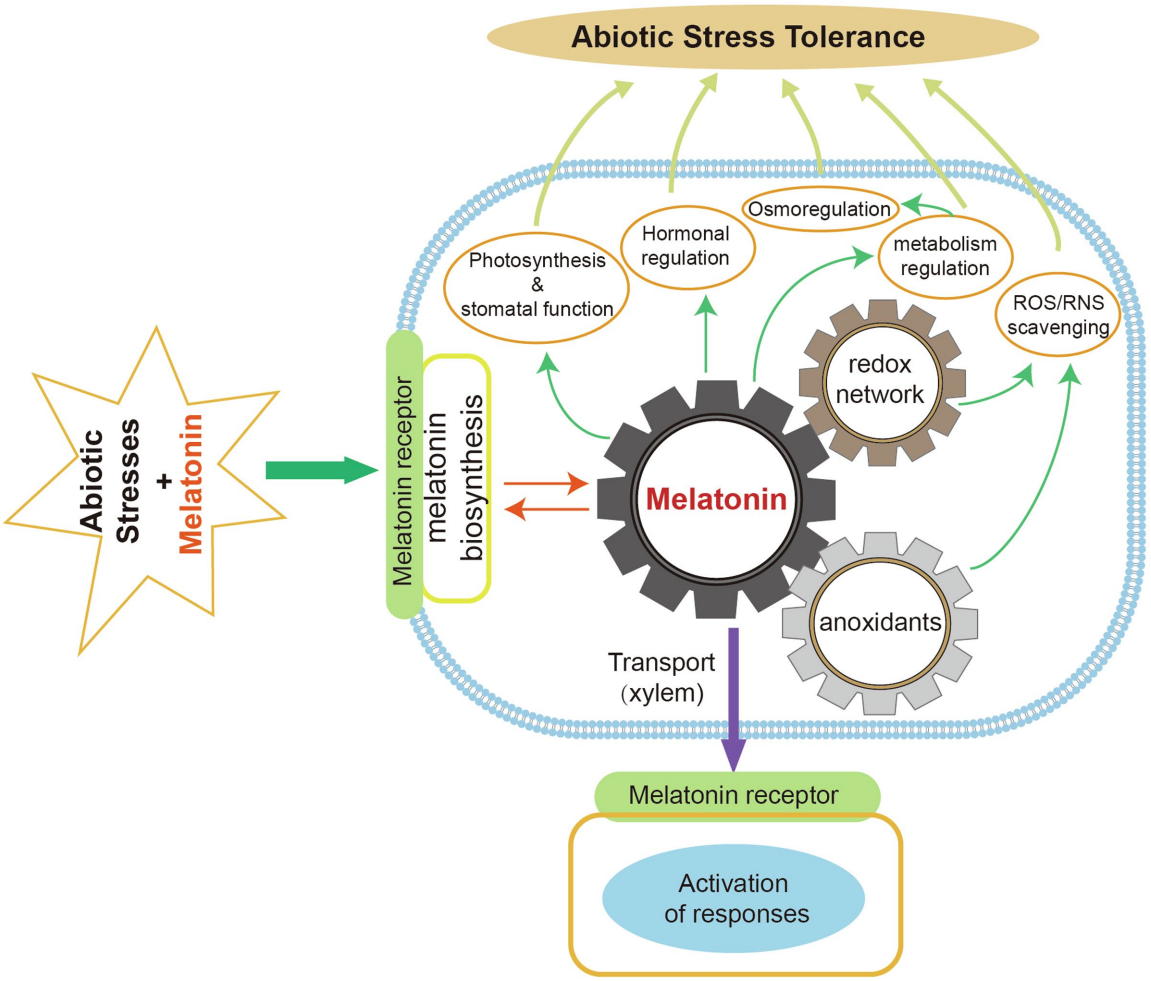


FIGURE 5 | Roles of melatonin in improving plant abiotic stress tolerance. Exogenous melatonin can remove ROS and RNS by interacting with melatonin receptors to induce endogenous melatonin production and increased antioxidant levels. Melatonin facilitates photosynthesis and stomatal functions. It also regulates plant hormones, osmosis, and metabolism in response to abiotic stresses. Melatonin can be transported to various plant organs *via* the xylem and then activate stress responses.

physiological and biochemical processes to enhance stress tolerance (**Figure 5**).

Several studies have demonstrated the powerful effects of exogenous melatonin on plant stress tolerance enhancement. However, the precise signaling, transcriptional, and epigenetic mechanisms of melatonin remain unclear and require further characterization. Although melatonin can influence the biosynthesis and signaling of other phytohormones, some mechanisms by which melatonin interacts with other phytohormones remain elusive. Furthermore, most melatonin-mediated stress tolerance studies have been performed using model plant systems, as well as some important crops. However, the transferability of these findings to other plant species should be investigated. Considering the role of melatonin in abiotic stress tolerance in plants, melatonin-related transgenic technologies could be developed to enhance stress resistance in plants.

Exogenous melatonin treatment has mainly been applied under laboratory-scale conditions. However, large-scale commercial and agricultural applications of melatonin have rarely been performed. Furthermore, the potential detrimental effects of melatonin treatment on plants grown under standard conditions must be investigated. Therefore, field studies are required to determine the effects of melatonin treatment on final crop yield and quality under regular conditions.

AUTHOR CONTRIBUTIONS

WZ and BJ: conceptualization. WZ and ZL: writing—original preparation. WZ, SM, and BJ: writing—review and editing. All authors contributed to the article and approved the submitted version.

ACKNOWLEDGMENTS

We apologize for not being able to cite all the relevant publications in the literature due to space limitations.

REFERENCES

Afreen, F., Zobayed, S. M., and Kozai, T. (2006). Melatonin in *Glycyrrhiza uralensis*: response of plant roots to spectral quality of light and UV-B radiation. *J. Pineal Res.* 41, 108–115. doi: 10.1111/j.1600-079X.2006.00337.x

Aghdam, M. S., Jannatizadeh, A., Nojadeh, M. S., and Ebrahimzadeh, A. (2019). Exogenous melatonin ameliorates chilling injury in cut anthurium flowers during low temperature storage. *Postharvest Biol. Technol.* 148, 184–191. doi: 10.1016/j.postharvbio.2018.11.008

Ahammed, G. J., Xu, W., Liu, A., and Chen, S. (2019). Endogenous melatonin deficiency aggravates high temperature-induced oxidative stress in *Solanum lycopersicum* L. *Environ. Exp. Bot.* 161, 303–311. doi: 10.1016/j.envexpbot.2018.06.006

Ahmad, S., Muhammad, I., Wang, G. Y., Zeeshan, M., Yang, L., Ali, I., et al. (2021). Ameliorative effect of melatonin improves drought tolerance by regulating growth, photosynthetic traits and leaf ultrastructure of maize seedlings. *Plant Biol.* 21:368. doi: 10.1186/s12870-021-03160-w

Alharby, H. F., and Fahad, S. (2020). Melatonin application enhances biochar efficiency for drought tolerance in maize varieties: modifications in physio-biochemical machinery. *Agron. J.* 112, 2826–2847. doi: 10.1002/agj2.20263

Antoniou, C., Chatzimichail, G., Xenofontos, R., Pavlou, J. J., Panagiotou, E., Christou, A., et al. (2017). Melatonin systemically ameliorates drought stress-induced damage in *Medicago sativa* plants by modulating nitro-oxidative homeostasis and proline metabolism. *J. Pineal Res.* 62:e12401. doi: 10.1111/jpi.12401

Apel, K., and Hirt, H. (2004). Reactive oxygen species: metabolism, oxidative stress, and signal transduction. *Annu. Rev. Plant Biol.* 55, 373–399. doi: 10.1146/annurev.arplant.55.031903.141701

Arnao, M. B., and Hernández-Ruiz, J. (2009). Chemical stress by different agents affects the melatonin content of barley roots. *J. Pineal Res.* 46, 295–299. doi: 10.1111/j.1600-079X.2008.00660.x

Arnao, M. B., and Hernández-Ruiz, J. (2018). Melatonin and its relationship to plant hormones. *Ann. Bot.* 121, 195–207. doi: 10.1093/aob/mcx114

Arnao, M. B., and Hernández-Ruiz, J. (2019a). Melatonin: a new plant hormone and/or a plant master regulator? *Trends Plant Sci.* 24, 38–48. doi: 10.1016/j.tplants.2018.10.010

Arnao, M. B., and Hernández-Ruiz, J. (2019b). Melatonin and reactive oxygen and nitrogen species: a model for the plant redox network. *Melatonin Res.* 2, 152–168. doi: 10.32794/11250036

Arnao, M., and Hernández-Ruiz, J. (2020). Melatonin in flowering, fruit set and fruit ripening. *Plant Reprod.* 33, 77–87. doi: 10.1007/s00497-020-00388-8

Arora, D., and Bhatla, S. C. (2017). Melatonin and nitric oxide regulate sunflower seedling growth under salt stress accompanying differential expression of cu/Zn SOD and Mn SOD. *Free Radic. Biol. Med.* 106, 315–328. doi: 10.1016/j.freeradbiomed.2017.02.042

Arora, D., Jain, P., Singh, N., Kaur, H., and Bhatla, S. C. (2016). Mechanisms of nitric oxide crosstalk with reactive oxygen species scavenging enzymes during abiotic stress tolerance in plants. *Free Radic. Res.* 50, 291–303. doi: 10.3109/10715762.2015.1118473

Axelrod, J., and Weissbach, H. (1960). Enzymatic O-methylation of N-acetylserotonin to melatonin. *Science* 131:1312. doi: 10.1126/science.131.3409.1312

Back, K. (2021). Melatonin metabolism, signaling and possible roles in plants. *Plant J.* 105, 376–391. doi: 10.1111/tpj.14915

Back, K., Tan, D. X., and Reiter, R. J. (2016). Melatonin biosynthesis in plants: multiple pathways catalyze tryptophan to melatonin in the cytoplasm or chloroplasts. *J. Pineal Res.* 61, 426–437. doi: 10.1111/jpi.12364

Blanchard, B., Pompon, D., and Ducrocq, C. (2000). Nitrosation of melatonin by nitric oxide and peroxynitrite. *J. Pineal Res.* 29, 184–192. doi: 10.1034/j.1600-079X.2000.290308.x

Byeon, Y., and Back, K. (2015). Molecular cloning of melatonin 2-hydroxylase responsible for 2-hydroxymelatonin production in rice (*Oryza sativa*). *J. Pineal Res.* 58, 343–351. doi: 10.1111/jpi.12220

Byeon, Y., and Back, K. (2016). Low melatonin production by suppression of either serotonin N-acetyltransferase or N-acetylserotonin methyltransferase in rice causes seedling growth retardation with yield penalty, abiotic stress susceptibility, and enhanced coleoptile growth under anoxic conditions. *J. Pineal Res.* 60, 348–359. doi: 10.1111/jpi.12317

Byeon, Y., Choi, G. H., Lee, H. Y., and Back, K. (2015a). Melatonin biosynthesis requires N-acetylserotonin methyltransferase activity of caffeic acid O-methyltransferase in rice. *J. Exp. Bot.* 66, 6917–6925. doi: 10.1093/jxb/erv396

Byeon, Y., Lee, H. Y., Hwang, O. J., Lee, H. J., Lee, K., and Back, K. (2015b). Coordinated regulation of melatonin synthesis and degradation genes in rice leaves in response to cadmium treatment. *J. Pineal Res.* 58, 470–478. doi: 10.1111/jpi.12232

Byeon, Y., Lee, H. Y., Lee, K., Park, S., and Back, K. (2014). Cellular localization and kinetics of the rice melatonin biosynthetic enzymes SNAT and ASMT. *J. Pineal Res.* 56, 107–114. doi: 10.1111/jpi.12103

Byeon, Y., Tan, D. X., Reiter, R. J., and Back, K. (2015c). Predominance of 2-hydroxymelatonin over melatonin in plants. *J. Pineal Res.* 59, 448–454. doi: 10.1111/jpi.12274

Cao, Y. Y., Qi, C. D., Li, S., Wang, Z., Wang, X., Wang, J., et al. (2019). Melatonin alleviates copper toxicity via improving copper sequestration and ROS scavenging in cucumber. *Plant Cell Physiol.* 60, 562–574. doi: 10.1093/pcp/pcy226

Cao, L., Qin, B., and Zhang, Y. X. (2021). Exogenous application of melatonin may contribute to enhancement of soybean drought tolerance via its effects on glucose metabolism. *Biotechnol. Biotechnol. Equip.* 35, 964–976. doi: 10.1080/13102818.2021.1941254

Chang, J., Guo, Y., Zhang, Z., Wei, C., Zhang, Y., Ma, J., et al. (2020). CBF-responsive pathway and phytohormones are involved in melatonin-improved photosynthesis and redox homeostasis under aerial cold stress in watermelon. *Acta Physiol. Plant.* 42:159. doi: 10.1007/s11738-020-03147-4

Chang, T., Zhao, Y., He, H., Xi, Q., Fu, J., and Zhao, Y. (2021). Exogenous melatonin improves growth in hulless barley seedlings under cold stress by influencing the expression rhythms of circadian clock genes. *Peer J.* 9:e10740. doi: 10.7717/peerj.10740

Chatgilialoglu, C., D'Angelantonio, M., Guerra, M., Kaloudis, P., and Mulazzani, Q. G. (2009). A reevaluation of the ambident reactivity of the guanine moiety towards hydroxyl radicals. *Angew. Chem. Int. Ed. Eng.* 48, 2214–2217. doi: 10.1002/anie.200805372

Chen, Z., Gu, Q., Yu, X., Huang, L., Xu, S., Wang, R., et al. (2018). Hydrogen peroxide acts downstream of melatonin to induce lateral root formation. *Ann. Bot.* 121, 1127–1136. doi: 10.1093/aob/mcx207

Chen, K., Li, G. J., Bressan, R. A., Song, C. P., Zhu, J. K., and Zhao, Y. (2020). Abscisic acid dynamics, signaling, and functions in plants. *J. Integr. Plant Biol.* 62, 25–54. doi: 10.1111/jipb.12899

Chen, Y., Li, R., Ge, J., Liu, J., Wang, W., Xu, M., et al. (2021). Exogenous melatonin confers enhanced salinity tolerance in rice by blocking the ROS burst and improving Na^+/K^+ homeostasis. *Environ. Exp. Bot.* 189:104530. doi: 10.1016/j.envexpbot.2021.104530

Chen, Z., Xie, Y., Gu, Q., Zhao, G., Zhang, Y., Cui, W., et al. (2017). The AtrbohF-dependent regulation of ROS signaling is required for melatonin-induced salinity tolerance in *Arabidopsis*. *Free Radic. Biol. Med.* 108, 465–477. doi: 10.1016/j.freeradbiomed.2017.04.009

Chen, W., Zhang, J., Zheng, S., Wang, Z., Xu, C., Zhang, Q., et al. (2021). Metabolite profiling and transcriptome analyses reveal novel regulatory mechanisms of melatonin biosynthesis in hickory. *Hortic. Res.* 8:196. doi: 10.1038/S41438-021-00631-X

Cherono, S., Ntini, C., Wassie, M., Mollah, M. D., Belal, M. A., Ogutu, C., et al. (2021). Exogenous application of melatonin improves drought tolerance in coffee by regulating photosynthetic efficiency and oxidative damage. *J. Am. Soc. Hortic. Sci.* 146, 24–32. doi: 10.21273/JASHS04964-20

Choi, G. H., and Back, K. (2019). Cyclic 3-hydroxymelatonin exhibits diurnal rhythm and cyclic 3-hydroxymelatonin overproduction increases secondary tillers in rice by upregulating *MOC1* expression. *Melatonin Res.* 2, 120–138. doi: 10.32794/11250034

Choi, G. H., Lee, H. Y., and Back, K. (2017). Chloroplast overexpression of rice caffeic acid O-methyltransferase increases melatonin production in chloroplasts via the 5-methoxytryptamine pathway in transgenic rice plants. *J. Pineal Res.* 63:e12412. doi: 10.1111/jpi.12412

Corpas, F. J., and Barroso, J. B. (2013). Nitro-oxidative stress vs oxidative or nitrosative stress in higher plants. *New Phytol.* 199, 633–635. doi: 10.1111/nph.12380

Corpas, F. J., Río, L. A. D., and Palma, J. M. (2019). Impact of nitric oxide (NO) on the ROS metabolism of peroxisomes. *Plan. Theory* 8:37. doi: 10.3390/plants8020037

Cui, G., Zhao, X., Liu, S., Sun, F., Zhang, C., and Xi, Y. (2017). Beneficial effects of melatonin in overcoming drought stress in wheat seedlings. *Plant Physiol. Biochem.* 118, 138–149. doi: 10.1016/j.plaphy.2017.06.014

Del Río, L. A., and López-Huertas, E. (2016). ROS generation in peroxisomes and its role in cell signaling. *Plant Cell Physiol.* 57, 1364–1376. doi: 10.1093/pcp/pcw076

Demarsy, E., Goldschmidt-Clermont, M., and Ulm, R. (2018). Coping with 'dark sides of the sun' through photoreceptor signaling. *Trends Plant Sci.* 23, 260–271. doi: 10.1016/j.tplants.2017.11.007

Ding, F., Wang, G., Wang, M., and Zhang, S. (2018). Exogenous melatonin improves tolerance to water deficit by promoting cuticle formation in tomato plants. *Molecules* 23:1605. doi: 10.3390/molecules23071605

Dubbels, R., Reiter, R., Klenke, E., Goebel, A., Schnakenberg, E., Ehlers, C., et al. (1995). Melatonin in edible plants identified by radioimmunoassay and by high performance liquid chromatography-mass spectrometry. *J. Pineal Res.* 18, 28–31. doi: 10.1111/j.1600-079X.1995.tb00136.x

Erland, L. A., Saxena, P. K., and Murch, S. J. (2017). Melatonin in plant signalling and behaviour. *Funct. Plant Biol.* 45, 58–69. doi: 10.1071/FP16384

Erland, L. A. E., Shukla, M. R., Singh, A. S., Murch, S. J., and Saxena, P. K. (2018). Melatonin and serotonin: mediators in the symphony of plant morphogenesis. *J. Pineal Res.* 64:e12452. doi: 10.1111/jpi.12452

Feng, Y., Fu, X., Han, L., Xu, C., Liu, C., Bi, H., et al. (2021). Nitric oxide functions as a downstream signal for melatonin-induced cold tolerance in cucumber seedlings. *Front. Plant Sci.* 12:686545. doi: 10.3389/fpls.2021.686545

Fleta-Soriano, E., Díaz, L., Bonet, E., and Munné-Bosch, S. (2017). Melatonin may exert a protective role against drought stress in maize. *J. Agron. Crop Sci.* 203, 286–294. doi: 10.1111/jac.12201

Fu, J., Wu, Y., Miao, Y., Xu, Y., Zhao, E., Wang, J., et al. (2017). Improved cold tolerance in Elymus nutans by exogenous application of melatonin may involve ABA-dependent and ABA-independent pathways. *Sci. Rep.* 7:39865. doi: 10.1038/srep39865

Galano, A., and Alvarez-Idaboy, J. R. (2009). Guanosine + OH radical reaction in aqueous solution: a reinterpretation of the UV-vis data based on thermodynamic and kinetic calculations. *Org. Lett.* 11, 5114–5117. doi: 10.1021/ol901862h

Galano, A., and Reiter, R. J. (2018). Melatonin and its metabolites vs oxidative stress: from individual actions to collective protection. *J. Pineal Res.* 65:e12514. doi: 10.1111/jpi.12514

Galano, A., Tan, D. X., and Reiter, R. J. (2014). Cyclic 3-hydroxymelatonin, a key metabolite enhancing the peroxyl radical scavenging activity of melatonin. *RSC Adv.* 4, 5220–5227. doi: 10.1039/c3ra44604b

Gao, W., Zhang, Y., Feng, Z., Bai, Q., He, J., and Wang, Y. J. (2018). Effects of melatonin on antioxidant capacity in naked oat seedlings under drought stress. *Molecules* 23:1580. doi: 10.3390/molecules23071580

Gu, X., Xue, L., Lu, L., Xiao, J., Song, G., Xie, M., et al. (2020). Melatonin enhances the waterlogging tolerance of *Prunus persica* by modulating antioxidant metabolism and anaerobic respiration. *J. Plant Growth Regul.* 40, 2178–2190. doi: 10.1007/s00344-020-10263-5

Guo, X., Liu, D., and Chong, K. (2018). Cold signaling in plants: insights into mechanisms and regulation. *J. Integr. Plant Biol.* 60, 745–756. doi: 10.1111/jipb.12706

Hardeland, R. (2015). Melatonin in plants and other phototrophs: advances and gaps concerning the diversity of functions. *J. Exp. Bot.* 66, 627–646. doi: 10.1093/jxb/eru386

Hardeland, R. (2017). Taxon-and site-specific melatonin catabolism. *Molecules* 22:2015. doi: 10.3390/molecules22112015

Hardeland, R. (2019). Melatonin in the evolution of plants and other phototrophs. *Melatonin Res.* 2, 10–36. doi: 10.32794/mr11250029

Hardeland, R., Tan, D. X., and Reiter, R. J. (2009). Kynuramines, metabolites of melatonin and other indoles: the resurrection of an almost forgotten class of biogenic amines. *J. Pineal Res.* 47, 109–126. doi: 10.1111/j.1600-079X.2009.00701.x

Hasan, M. K., Ahammed, G. J., Sun, S., Li, M., Yin, H., and Zhou, J. (2019). Melatonin inhibits cadmium translocation and enhances plant tolerance by regulating sulfur uptake and assimilation in *Solanum lycopersicum* L. *J. Agric. Food Chem.* 67, 10563–10576. doi: 10.1021/acs.jafc.9b02404

Hasan, M. K., Ahammed, G. J., Yin, L., Shi, K., Xia, X., Zhou, Y., et al. (2015). Melatonin mitigates cadmium phytotoxicity through modulation of phytochelatins biosynthesis, vacuolar sequestration, and antioxidant potential in *Solanum lycopersicum* L. *Front. Plant Sci.* 6:601. doi: 10.3389/fpls.2015.00601

Hasanuzzaman, M., Bhuyan, M. H. M. B., Parvin, K., Bhuiyan, T. F., Anee, T. I., Nahar, K., et al. (2020). Regulation of ROS metabolism in plants under environmental stress: a review of recent experimental evidence. *Int. J. Mol. Sci.* 21:8695. doi: 10.3390/ijms21228695

Hasanuzzaman, M., Oku, H., Nahar, K., Bhuyan, M., Mahmud, J. A., Baluska, F., et al. (2018). Nitric oxide-induced saltstress tolerance in plants: ROS metabolism, signaling, and molecular interactions. *Plant Biotechnol. Rep.* 12, 77–92. doi: 10.1007/s11816-018-0480-0

Haskirli, H., Yilmaz, O., Ozgur, R., Uzilday, B., and Turkan, I. (2021). Melatonin mitigates UV-B stress via regulating oxidative stress response, cellular redox and alternative electron sinks in *Arabidopsis thaliana*. *Phytochemistry* 182:112592. doi: 10.1016/j.phytochem.2020.112592

Hattori, A., Migitaka, H., Iigo, M., Itoh, M., Yamamoto, K., Ohtani-Kaneko, R., et al. (1995). Identification of melatonin in plants and its effects on plasma melatonin levels and binding to melatonin receptors in vertebrates. *Biochem. Mol. Biol. Int.* 35, 627–634. PMID: 7773197

He, H., and He, L. F. (2020). Crosstalk between melatonin and nitric oxide in plant development and stress responses. *Physiol. Plant.* 170, 218–226. doi: 10.1111/ppl.13143

He, J., Zhuang, X., Zhou, J., Sun, L., Wan, H., Li, H., et al. (2020). Exogenous melatonin alleviates cadmium uptake and toxicity in apple rootstocks. *Tree Physiol.* 40, 746–761. doi: 10.1093/treephys/tpaa024

Hossain, Z., López-Climent, M. F., Arbona, V., Pérez-Clemente, R. M., and Gómez-Cadenas, A. (2009). Modulation of the antioxidant system in citrus under waterlogging and subsequent drainage. *J. Plant Physiol.* 166, 1391–1404. doi: 10.1016/j.jplph.2009.02.012

Hosseini, M. S., Samsampour, D., Zahedi, S. M., Zamanian, K., Rahman, M. M., Mostofa, M. G., et al. (2021). Melatonin alleviates drought impact on growth and essential oil yield of lemon verbena by enhancing antioxidant responses, mineral balance, and abscisic acid content. *Physiol. Plant.* 172, 1363–1375. doi: 10.1111/ppl.13335

Hu, Z., Fan, J., Xie, Y., Amombo, E., Liu, A., Gitau, M. M., et al. (2016). Comparative photosynthetic and metabolic analyses reveal mechanism of improved cold stress tolerance in bermudagrass by exogenous melatonin. *Plant Physiol. Biochem.* 100, 94–104. doi: 10.1016/j.plaphy.2016.01.008

Hu, W., Zhang, J., Yan, K., Zhou, Z., Zhao, W., Zhang, X., et al. (2021). Beneficial effects of abscisic acid and melatonin in overcoming drought stress in cotton (*Gossypium hirsutum* L.). *Physiol. Plant.* 173, 2041–2054. doi: 10.1111/ppl.13550

Huang, B., Chen, Y. E., Zhao, Y. Q., Ding, C. B., Liao, J. Q., Hu, C., et al. (2019). Exogenous melatonin alleviates oxidative damages and protects photosystem II in maize seedlings under drought stress. *Front. Plant Sci.* 10:677. doi: 10.3389/fpls.2019.00677

Huang, S., VanAken, O., Schwarzländer, M., Belt, K., and Millar, A. H. (2016). The roles of mitochondrial reactive oxygen species in cellular signaling and stress responses in plants. *Plant Physiol.* 171, 1551–1559. doi: 10.1104/pp.16.00166

Ibrahim, M. F. M., Elbar, O. H. A., Farag, R., Hikal, M., El-Kelish, A., El-Yazied, A. A., et al. (2020). Melatonin counteracts drought induced oxidative damage and stimulates growth, productivity and fruit quality properties of tomato plants. *Plan. Theory* 9:1276. doi: 10.3390/plants9101276

Imran, M., Aaqil Khan, M., Shahzad, R., Bilal, S., Khan, M., Yun, B.-W., et al. (2021). Melatonin ameliorates thermotolerance in soybean seedling through balancing redox homeostasis and modulating antioxidant defense, phytohormones and polyamines biosynthesis. *Molecules* 26:5116. doi: 10.3390/molecules26175116

Iqbal, N., Fatma, M., Gautam, H., Umar, S., Sofo, A., D'ippolito, I., et al. (2021). The crosstalk of melatonin and hydrogen sulfide determines photosynthetic performance by regulation of carbohydrate metabolism in wheat under heat stress. *Plan. Theory* 10:1778. doi: 10.3390/plants10091778

Jahan, M. S., Guo, S., Baloch, A. R., Sun, J., Shu, S., Wang, Y., et al. (2020). Melatonin alleviates nickel phytotoxicity by improving photosynthesis, secondary metabolism and oxidative stress tolerance in tomato seedlings. *Ecotoxicol. Environ. Saf.* 197:110593. doi: 10.1016/j.ecoenv.2020.110593

Jahan, M. S., Shu, S., Wang, Y., Chen, Z., He, M., Tao, M., et al. (2019). Melatonin alleviates heat-induced damage of tomato seedlings by balancing redox homeostasis and modulating polyamine and nitric oxide biosynthesis. *Plant Biol.* 19:414. doi: 10.1186/s12870-019-1992-7

Jannatizadeh, A., Aghdam, M. S., Luo, Z., Razavi, F. J. F., and Technology, B. (2019). Impact of exogenous melatonin application on chilling injury in tomato fruits during cold storage. *Food Bioprocess Technol.* 12, 741–750. doi: 10.1007/s11947-019-2247-1

Jiang, S., Carroll, L., Mariotti, M., Hagglund, P., and Davies, M. J. (2021). Formation of protein cross-links by singlet oxygen-mediated disulfide oxidation. *Redox Biol.* 41:101874. doi: 10.1016/j.redox.2021.101874

Kang, K., Lee, K., Park, S., Kim, Y. S., and Back, K. (2010). Enhanced production of melatonin by ectopic overexpression of human serotonin N-acetyltransferase plays a role in cold resistance in transgenic rice seedlings. *J. Pineal Res.* 49, 176–182. doi: 10.1111/j.1600-079X.2010.00783.x

Kaya, C., Higgs, D., Ashraf, M., Alyemeni, M. N., and Ahmad, P. (2020). Integrative roles of nitric oxide and hydrogen sulfide in melatonin-induced tolerance of pepper (*Capsicum annuum* L.) plants to iron deficiency and salt stress alone or in combination. *Physiol. Plant.* 168, 256–277. doi: 10.1111/ppl.12976

Kaya, C., Okant, M., Ugurlar, F., Alyemeni, M. N., Ashraf, M., and Ahmad, P. (2019). Melatonin-mediated nitric oxide improves tolerance to cadmium toxicity by reducing oxidative stress in wheat plants. *Chemosphere* 225, 627–638. doi: 10.1016/j.chemosphere.2019.03.026

Ke, Q., Ye, J., Wang, B., Ren, J., Yin, L., Deng, X., et al. (2018). Melatonin mitigates salt stress in wheat seedlings by modulating polyamine metabolism. *Front. Plant Sci.* 9:914. doi: 10.3389/fpls.2018.00914

Kerchev, P., Waszczak, C., Lewandowska, A., Willems, P., Shapiguzov, A., and Li, Z. (2016). Lack of GLYCOLATE OXIDASE1, but not GLYCOLATE OXIDASE2, attenuates the photorespiratory phenotype of CATALASE2-deficient *Arabidopsis*. *Plant Physiol.* 171, 1704–1719. doi: 10.1104/pp.16.00359

Khan, M. N., Zhang, J., Luo, T., Liu, J., Rizwan, M., Fahad, S., et al. (2019). Seed priming with melatonin coping drought stress in rapeseed by regulating reactive oxygen species detoxification: antioxidant defense system, osmotic adjustment, stomatal traits and chloroplast ultrastructure perseveration. *Ind. Crop. Prod.* 140:112165. doi: 10.1016/j.indcrop.2019.111597

Kim, C. (2020). ROS-driven oxidative modification: its impact on chloroplasts-nucleus communication. *Front. Plant Sci.* 10:1729. doi: 10.3389/fpls.2019.01729

Knight, H., Zarka, D. G., Okamoto, H., Thomashow, M. F., and Knight, M. (2004). Abscisic acid induces CBF gene transcription and subsequent induction of cold-regulated genes via the CRT promoter element. *Plant Physiol.* 135, 1710–1717. doi: 10.1104/pp.104.043562

Kobylińska, A., Borek, S., and Posmyk, M. M. (2018). Melatonin redirects carbohydrates metabolism during sugar starvation in plant cells. *J. Pineal Res.* 64:e12466. doi: 10.1111/jpi.12466

Kołodziejczyk, I., Bałabusta, M., Szewczyk, R., and Posmyk, M. M. J. A. P. P. (2015). The levels of melatonin and its metabolites in conditioned corn (*Zea mays* L.) and cucumber (*Cucumis sativus* L.) seeds during storage. *Acta Physiol. Plant.* 37:105. doi: 10.1007/s11738-015-1850-7

Kong, X. M., Ge, W. Y., Wei, B. D., Zhou, Q., Zhou, X., Zhao, Y. B., et al. (2020). Melatonin ameliorates chilling injury in green bell peppers during storage by regulating membrane lipid metabolism and antioxidant capacity. *Postharvest Biol. Technol.* 170:111315. doi: 10.1016/j.postharvbio.2020.111315

Kumar, A., Prasad, A., Sedlarova, M., Kale, R., Frankel, L. K., Sallans, L., et al. (2021). Tocopherol controls D1 amino acid oxidation by oxygen radicals in photosystem II. *Proc. Natl. Acad. Sci. U. S. A.* 118:e2019246118. doi: 10.1073/pnas.2019246118

Lee, H. J., and Back, K. (2016a). 2-Hydroxymelatonin promotes the resistance of rice plant to multiple simultaneous abiotic stresses (combined cold and drought). *J. Pineal Res.* 61, 303–316. doi: 10.1111/jpi.12347

Lee, H. Y., and Back, K. (2016b). Mitogen-activated protein kinase pathways are required for melatonin-mediated defense responses in plants. *J. Pineal Res.* 60, 327–335. doi: 10.1111/jpi.12314

Lee, H. Y., and Back, K. (2017). Melatonin is required for H_2O_2-and NO-mediated defense signaling through MAPKKK3 and OXI1 in *Arabidopsis thaliana*. *J. Pineal Res.* 62:e12379. doi: 10.1111/jpi.12379

Lee, H. Y., and Back, K. (2018). Melatonin induction and its role in high light stress tolerance in *Arabidopsis thaliana*. *J. Pineal Res.* 65:e12504. doi: 10.1111/jpi.12504

Lee, H. J., and Back, K. (2019). 2-Hydroxymelatonin confers tolerance against combined cold and drought stress in tobacco, tomato, and cucumber as a potent anti-stress compound in the evolution of land plants. *Melatonin Res.* 2, 35–46. doi: 10.32794/mr11250020

Lee, H. Y., Byeon, Y., Tan, D. X., Reiter, R. J., and Back, K. (2015). *Arabidopsis* serotonin N-acetyltransferase knockout plants exhibit decreased melatonin and salicylic acid levels resulting in susceptibility to an avirulent pathogen. *J. Pineal Res.* 58, 291–299. doi: 10.1111/jpi.12214

Lee, H. Y., Lee, K., and Back, K. (2019). Knockout of *Arabidopsis* serotonin N-acetyltransferase-2 reduces melatonin levels and delays flowering. *Biomol. Ther.* 9:712. doi: 10.3390/biom9110712

Lee, K., Zawadzka, A., Czarnocki, Z., Reiter, R. J., and Back, K. (2016). Molecular cloning of melatonin 3-hydroxylase and its production of cyclic 3-hydroxymelatonin in rice (*Oryza sativa*). *J. Pineal Res.* 61, 470–478. doi: 10.1111/jpi.12361

Lemos, M., Xiao, Y., Bjornson, M., Wang, J. Z., Hicks, D., Souza, A., et al. (2016). The plastidial retrograde signal methyl erythritol cyclopyrophosphate is a regulator of salicylic acid and jasmonic acid crosstalk. *J. Exp. Bot.* 67, 1557–1566. doi: 10.1093/jxb/erv550

Lerner, A. B., Case, J. D., Takahashi, Y., Lee, T. H., and Mori, W. (1958). Isolation of melatonin, the pineal gland factor that lightens melanocytes. *J. Am. Chem. Soc.* 80:2587. doi: 10.1021/ja01543a060

Li, H., Chang, J., Zheng, J., Dong, Y., Liu, Q., Yang, X., et al. (2017). Local melatonin application induces cold tolerance in distant organs of *Citrullus lanatus* L. via long distance transport. *Sci. Rep.* 7:40858. doi: 10.1038/srep40858

Li, H., Guo, Y., Lan, Z., Xu, K., Chang, J., Ahammed, G. J., et al. (2021). Methyl jasmonate mediates melatonin-induced cold tolerance of grafted watermelon plants. *Hortic. Res.* 8:57. doi: 10.1038/S41438-021-00496-0

Li, S., Guo, J., Wang, T., Gong, L., Liu, F., Brestic, M., et al. (2021). Melatonin reduces nanoplastic uptake, translocation, and toxicity in wheat. *J. Pineal Res.* 71:e12761. doi: 10.1111/jpi.12761

Li, M., and Kim, C. (2021). Chloroplast ROS and stress signaling. *Plant Commun.* 3:100264. doi: 10.1016/j.xplc.2021.100264

Li, C., Liang, B., Chang, C., Wei, Z., Zhou, S., and Ma, F. (2016). Exogenous melatonin improved potassium content in *Malus* under different stress conditions. *J. Pineal Res.* 61, 218–229. doi: 10.1111/jpi.12342

Li, G. Z., Liu, J., Chen, S. J., Wang, P. F., Liu, H. T., Dong, J., et al. (2021). Melatonin promotes potassium deficiency tolerance by regulating HAK1 transporter and its upstream transcription factor NAC71 in wheat. *J. Pineal Res.* 70:e12727. doi: 10.1111/jpi.12727

Li, C., Tan, D. X., Liang, D., Chang, C., Jia, D., and Ma, F. (2015). Melatonin mediates the regulation of ABA metabolism, free-radical scavenging, and stomatal behaviour in two *Malus* species under drought stress. *J. Exp. Bot.* 66, 669–680. doi: 10.1093/jxb/eru476

Li, C., Wang, P., Wei, Z., Liang, D., Liu, C., Yin, L., et al. (2012). The mitigation effects of exogenous melatonin on salinity-induced stress in *Malus hupehensis*. *J. Pineal Res.* 53, 298–306. doi: 10.1111/j.1600-079X.2012.00999.x

Li, X., Yu, B., Cui, Y., and Yin, Y. (2017). Melatonin application confers enhanced salt tolerance by regulating Na^+ and Cl^- accumulation in rice. *Plant Growth Regul.* 83, 441–454. doi: 10.1007/s10725-017-0310-3

Liang, D., Gao, F., Ni, Z., Lin, L., Deng, Q., Tang, Y., et al. (2018). Melatonin improves heat tolerance in kiwifruit seedlings through promoting antioxidant enzymatic activity and glutathione S-Transferase transcription. *Molecules* 23:584. doi: 10.3390/molecules23030584

Liang, C., Li, A., Yu, H., Li, W., Liang, C., Guo, S., et al. (2017). Melatonin regulates root architecture by modulating auxin response in rice. *Front. Plant Sci.* 8:134. doi: 10.3389/fpls.2017.00134

Liang, C., Zheng, G., Li, W., Wang, Y., Hu, B., Wang, H., et al. (2015). Melatonin delays leaf senescence and enhances salt stress tolerance in rice. *J. Pineal Res.* 59, 91–101. doi: 10.1111/jpi.12243

Liao, L., Zhou, Y., Xu, Y., Zhang, Y., Liu, X., Liu, B., et al. (2021). Structural and molecular dynamics analysis of plant serotonin N-Acetyltransferase reveal an acid/base-assisted catalysis in melatonin biosynthesis. *Angew. Chem. Int. Ed. Eng.* 133, 12127–12133. doi: 10.1002/ange.202100992

Liu, D. D., Sun, X. S., Liu, L., Shi, H. D., Chen, S. Y., and Zhao, D. K. (2019). Overexpression of the melatonin synthesis-related gene SlCOMT1 improves the resistance of tomato to salt stress. *Molecules* 24:1514. doi: 10.3390/molecules24081514

Liu, J., Wang, W., Wang, L., and Sun, Y. (2015). Exogenous melatonin improves seedling health index and drought tolerance in tomato. *Plant Growth Regul.* 77, 317–326. doi: 10.1007/s10725-015-0066-6

Lv, R., Li, Z., Li, M., Dogra, V., Lv, S., Liu, R., et al. (2019). Uncoupled expression of nuclear and plastid photosynthesis-associated genes contributes to cell death in a lesion mimic mutant. *Plant Cell* 31, 210–230. doi: 10.1105/tpc.18.00813

Ma, X., Idle, J. R., Krausz, K. W., and Gonzalez, F. J. (2005). Metabolism of melatonin by human cytochromes p450. *Drug Metab. Dispos.* 33, 489–494. doi: 10.1124/dmd.104.002410

Manchester, L. C., Coto-Montes, A., Boga, J. A., Andersen, L. P. H., Zhou, Z., Galano, A., et al. (2015). Melatonin: an ancient molecule that makes oxygen metabolically tolerable. *J. Pineal Res.* 59, 403–419. doi: 10.1111/jpi.12267

Martínez, M. C., and Andriantsitohaina, R. (2009). Reactive nitrogen species: molecular mechanisms and potential significance in health and disease. *Antioxid. Redox Signal.* 11, 669–702. doi: 10.1089/ars.2007.1993

Meng, J., Xu, T., Wang, Z., Fang, Y., Xi, Z., and Zhang, Z. (2014). The ameliorative effects of exogenous melatonin on grape cuttings under water-deficient stress: antioxidant metabolites, leaf anatomy, and chloroplast morphology. *J. Pineal Res.* 57, 200–212. doi: 10.1111/jpi.12159

Moustafa-Farag, M., Mahmoud, A., Arnao, M. B., Sheteiwy, M. S., Dafea, M., Soltan, M., et al. (2020). Melatonin-induced water stress tolerance in plants: recent advances. *Antioxidants* 9:809. doi: 10.3390/antiox9090809

Mukherjee, S. (2019). Recent advancements in the mechanism of nitric oxide signaling associated with hydrogen sulfide and melatonin crosstalk during ethylene-induced fruit ripening in plants. *Nitric Oxide* 82, 25–34. doi: 10.1016/j.niox.2018.11.003

Mukherjee, S., David, A., Yadav, S., Baluška, F., and Bhatla, S. (2014). Salt stress-induced seedling growth inhibition coincides with differential distribution of serotonin and melatonin in sunflower seedling roots and cotyledons. *Physiol. Plant.* 152, 714–728. doi: 10.1111/ppl.12218

Munns, R., and Tester, M. (2008). Mechanisms of salinity tolerance. *Annu. Rev. Plant Biol.* 59, 651–681. doi: 10.1146/annurev.arplant.59.032607.092911

Nabi, R. B. S., Tayade, R., Hussain, A., Kulkarni, K. P., Imran, Q. M., Mun, B. G., et al. (2019). Nitric oxide regulates plant responses to drought, salinity, and heavy metal stress. *Environ. Exp. Bot.* 161, 120–133. doi: 10.1016/j.envexpbot.2019.02.003

Nagajyoti, P. C., Lee, K. D., and Sreekanth, T. V. M. (2010). Heavy metals, occurrence and toxicity for plants: a review. *Environ. Chem. Lett.* 8, 199–216. doi: 10.1007/s10311-010-0297-8

Naing, A. H., and Kim, C. K. (2021). Abiotic stress-induced anthocyanins in plants: their role in tolerance to abiotic stresses. *Physiol. Plant.* 172, 1711–1723. doi: 10.1111/ppl.13373

Namdjoyan, S., Soorki, A. A., Elyasi, N., Kazemi, N., and Simaei, M. (2019). Melatonin alleviates lead-induced oxidative damage in safflower (*Carthamus tinctorius* L.) seedlings. *Ecotoxicology* 29, 108–118. doi: 10.1007/s10646-019-02136-9

Nawaz, M. A., Jiao, Y., Chen, C., Shireen, F., Zheng, Z., Imtiaz, M., et al. (2018). Melatonin pretreatment improves vanadium stress tolerance of watermelon seedlings by reducing vanadium concentration in the leaves and regulating melatonin biosynthesis and antioxidant-related gene expression. *J. Plant Physiol.* 220, 115–127. doi: 10.1016/j.jplph.2017.11.003

Nazir, M., Asad Ullah, M., Mumtaz, S., Siddiquah, A., Shah, M., Drouet, S., et al. (2020). Interactive effect of melatonin and UV-C on phenylpropanoid metabolite production and antioxidant potential in callus cultures of purple basil (*Ocimum basilicum* L. var. purpurascens). *Molecules* 25:1072. doi: 10.3390/molecules25051072

Nguyen, H., Lin, K., Ho, S., Chiang, C., and Yang, C. (2018). Enhancing the abiotic stress tolerance of plants: from chemical treatment to biotechnological approaches. *Physiol. Plant.* 164, 452–466. doi: 10.1111/ppl.12812

Ni, J., Wang, Q., Shah, F. A., Liu, W., Wang, D., Huang, S., et al. (2018). Exogenous melatonin confers cadmium tolerance by counterbalancing the hydrogen peroxide homeostasis in wheat seedlings. *Molecules* 23:799. doi: 10.3390/molecules23040799

Okant, M., and Kaya, C. (2019). The role of endogenous nitric oxide in melatonin-improved tolerance to lead toxicity in maize plants. *Environ. Sci. Pollut. Res. Int.* 26, 11864–11874. doi: 10.1007/s11356-019-04517-3

Okazaki, M., Higuchi, K., Aouini, A., and Ezura, H. (2010). Lowering intercellular melatonin levels by transgenic analysis of indoleamine 2, 3-dioxygenase from rice in tomato plants. *J. Pineal Res.* 49, 239–247. doi: 10.1111/j.1600-079X.2010.00788.x

Pardo-Hernández, M., López-Delacalle, M., and Rivero, R. M. (2020). ROS and NO regulation by melatonin under abiotic stress in plants. *Antioxidants* 9:1078. doi: 10.3390/antiox9111078

Park, H. S., Kazerooni, E. A., Kang, S. M., Al-Sadi, A. M., and Lee, I. J. (2021). Melatonin enhances the tolerance and recovery mechanisms in *Brassica juncea* (L.) Czern. Under saline conditions. *Front. Plant Sci.* 12:593717. doi: 10.3389/fpls.2021.593717

Postiglione, A. E., and Muday, G. K. (2020). The role of ROS homeostasis in ABA-induced guard cell signaling. *Front. Plant Sci.* 11:968. doi: 10.3389/fpls.2020.00968

Qi, Z. Y., Wang, K. X., Yan, M. Y., Kanwar, M. K., Li, D. Y., Wijaya, L., et al. (2018). Melatonin alleviates high temperature-induced pollen abortion in *Solanum lycopersicum*. *Molecules* 23:386. doi: 10.3390/molecules23020386

Qi, H., Xia, F. N., and Xiao, S. (2021). Autophagy in plants: physiological roles and post-translational regulation. *J. Integr. Plant Biol.* 63, 161–179. doi: 10.1111/jipb.12941

Ray, P. D., Huang, B. W., and Tsuji, Y. (2012). Reactive oxygen species (ROS) homeostasis and redox regulation in cellular signaling. *Cell. Signal.* 24, 981–990. doi: 10.1016/j.cellsig.2012.01.008

Ren, J., Ye, J., Yin, L., Li, G., Deng, X., and Wang, S. (2020). Exogenous melatonin improves salt tolerance by mitigating osmotic, ion, and oxidative stresses in maize seedlings. *Agronomy* 10:663. doi: 10.3390/agronomy10050663

Sadak, M. S., and Bakry, B. A. (2020). Alleviation of drought stress by melatonin foliar treatment on two flax varieties under sandy soil. *Physiol. Mol. Biol. Plants* 26, 907–919. doi: 10.1007/s12298-020-00789-z

Saddhe, A. A., Malvankar, M. R., Karle, S. B., and Kumar, K. (2019). Reactive nitrogen species: paradigms of cellular signaling and regulation of salt stress in plants. *Environ. Exp. Bot.* 161, 86–97. doi: 10.1016/j.envexpbot.2018.11.010

Samanta, S., Banerjee, A., and Roychoudhury, A. (2021). Exogenous melatonin regulates endogenous phytohormone homeostasis and thiol-mediated detoxification in two indica rice cultivars under arsenic stress. *Plant Cell Rep.* 40, 1585–1602. doi: 10.1007/s00299-021-02711-7

Semak, I., Naumova, M., Korik, E., Terekhovich, V., Wortsman, J., and Slominski, A. (2005). A novel metabolic pathway of melatonin: oxidation by cytochrome C. *Biochemistry* 44, 9300–9307. doi: 10.1021/bi050202d

Shah, A. A., Ahmed, S., Ali, A., and Yasin, N. A. (2020). 2-Hydroxymelatonin mitigates cadmium stress in cucumis sativus seedlings: modulation of antioxidant enzymes andpolyamines. *Chemosphere* 243:125308. doi: 10.1016/j.chemosphere.2019.125308

Sharma, S. S., and Dietz, K. J. (2009). The relationship between metal toxicity and cellular redox imbalance. *Trends Plant Sci.* 14, 43–50. doi: 10.1016/j.tplants.2008.10.007

Shen, J., Chen, D., Zhang, X., Song, L., Dong, J., Xu, Q., et al. (2021). Mitigation of salt stress response in upland cotton (*Gossypium hirsutum*) by exogenous melatonin. *J. Plant Res.* 134, 857–871. doi: 10.1007/s10265-021-01284-6

Shen, N., Wang, T., Gan, Q., Liu, S., Wang, L., and Jin, B. (2022). Plant flavonoids: classification, distribution, biosynthesis, and antioxidant activity. *Food Chem.* 383:132531. doi: 10.1016/j.foodchem.2022.132531

Shi, H., Jiang, C., Ye, T., Tan, D. X., Reiter, R. J., Zhang, H., et al. (2015a). Comparative physiological, metabolomic, and transcriptomic analyses reveal mechanisms of improved abiotic stress resistance in bermudagrass [*Cynodon dactylon* (L). Pers.] by exogenous melatonin. *J. Exp. Bot.* 66, 681–694. doi: 10.1093/jxb/eru373

Shi, H., Tan, D. X., Reiter, R. J., Ye, T., Yang, F., and Chan, Z. J. (2015b). Melatonin induces class A1 heat-shock factors (HSFA1s) and their possible involvement of thermotolerance in *Arabidopsis*. *J. Pineal Res.* 58, 335–342. doi: 10.1111/jpi.12219

Su, J., Yang, X., Shao, Y., Chen, Z., and Shen, W. (2021). Molecular hydrogen–induced salinity tolerance requires melatonin signalling in *Arabidopsis thaliana*. *Plant Cell Environ.* 44, 476–490. doi: 10.1111/pce.13926

Sun, C., Liu, L., Wang, L., Li, B., Jin, C., and Lin, X. (2021). Melatonin: a master regulator of plant development and stress responses. *J. Integr. Plant Biol.* 63, 126–145. doi: 10.1111/jipb.12993

Sun, C., Lv, T., Huang, L., Liu, X., Jin, C., and Lin, X. (2020). Melatonin ameliorates aluminum toxicity through enhancing aluminum exclusion and reestablishing redox homeostasis in roots of wheat. *J. Pineal Res.* 68:e12642. doi: 10.1111/jpi.12642

Tan, D. X., Hardeland, R., Back, K., Manchester, L. C., Alatorre-Jimenez, M. A., and Reiter, R. J. (2016). On the significance of an alternate pathway of melatonin synthesis via 5-methoxytryptamine: comparisons across species. *J. Pineal Res.* 61, 27–40. doi: 10.1111/jpi.12336

Tan, D. X., Hardeland, R., Manchester, L. C., Korkmaz, A., Ma, S., Rosales-Corral, S., et al. (2012). Functional roles of melatonin in plants, and perspectives in nutritional and agricultural science. *J. Exp. Bot.* 63, 577–597. doi: 10.1093/jxb/err256

Tan, D. X., Manchester, L. C., Di Mascio, P., Martinez, G. R., Prado, F. M., and Reiter, R. J. (2007). Novel rhythms of N1-acetyl-N2-formyl-5-methoxykynuramine and its precursor melatonin in water hyacinth: importance for phytoremediation. *FASEB J.* 21, 1724–1729. doi: 10.1096/fj.06-7745com

Tan, D. X., Manchester, L. C., Liu, X., Rosales-Corral, S. A., Acuna-Castroviejo, D., and Reiter, R. J. (2013). Mitochondria and chloroplasts as the original sites of melatonin synthesis: a hypothesis related to melatonin's primary function and evolution in eukaryotes. *J. Pineal Res.* 54, 127–138. doi: 10.1111/jpi.12026

Tan, D. X., and Reiter, R. J. (2020). An evolutionary view of melatonin synthesis and metabolism related to its biological functions in plants. *J. Exp. Bot.* 71, 4677–4689. doi: 10.1093/jxb/eraa235

Tang, M., Xu, L., Wang, Y., Dong, J., Zhang, X., Wang, K., et al. (2021). Melatonin-induced DNA demethylation of metal transporters and antioxidant genes alleviates lead stress in radish plants. *Hortic. Res.* 8:124. doi: 10.1038/s41438-021-00561-8

Tiwari, R. K., Lal, M. K., Kumar, R., Chourasia, K. N., Naga, K. C., Kumar, D., et al. (2021). Mechanistic insights on melatonin-mediated drought stress mitigation in plants. *Physiol. Plant.* 172, 1212–1226. doi: 10.1111/ppl.13307

Tiwari, R. K., Lal, M. K., Naga, K. C., Kumar, R., Chourasia, K. N., Subhash, S., et al. (2020). Emerging roles of melatonin in mitigating abiotic and biotic stresses of horticultural crops. *Sci. Hortic.* 272:109592. doi: 10.1016/j.scienta.2020.109592

Van Zelm, E., Zhang, Y., and Testerink, C. (2020). Salt tolerance mechanisms of plants. *Annu. Rev. Plant Biol.* 71, 403–433. doi: 10.1146/annurev-arplant-050718-100005

Wang, K., Cai, S., Xing, Q., Qi, Z., Fotopoulos, V., Yu, J., et al. (2022). Melatonin delays dark-induced leaf senescence by inducing miR171b expression in tomato. *J. Pineal Res.* 72:e12792. doi: 10.1111/jpi.12792

Wang, D., Chen, Q., Chen, W., Guo, Q., Xia, Y., Wu, D., et al. (2021). Melatonin treatment maintains quality and delays lignification in loquat fruit during cold storage. *Sci. Hortic.* 284:110126. doi: 10.1016/j.scienta.2021.110126

Wang, M., Duan, S., Zhou, Z., Chen, S., and Wang, D. (2019). Foliar spraying of melatonin confers cadmium tolerance in *Nicotiana tabacum* L. *Ecotoxicol. Environ. Saf.* 170, 68–76. doi: 10.1016/j.ecoenv.2018.11.127

Wang, L., Feng, C., Zheng, X., Guo, Y., Zhou, F., Shan, D., et al. (2017). Plant mitochondria synthesize melatonin and enhance the tolerance of plants to drought stress. *J. Pineal Res.* 63:e12429. doi: 10.1111/jpi.12429

Wang, Y., Mostafa, S., Zeng, W., and Jin, B. (2021). Function and mechanism of jasmonic acid in plant responses to abiotic and biotic stresses. *Int. J. Mol. Sci.* 22:8568. doi: 10.3390/ijms22168568

Wang, Y., Reiter, R. J., and Chan, Z. (2018). Phytomelatonin: a universal abiotic stress regulator. *J. Exp. Bot.* 69, 963–974. doi: 10.1093/jxb/erx473

Wang, X., Zhang, H., Xie, Q., Liu, Y., Lv, H., Bai, R., et al. (2020). *SlSNAT* interacts with *HSP40*, a molecular chaperone, to regulate melatonin biosynthesis and promote thermotolerance in tomato. *Plant Cell Physiol.* 61, 909–921. doi: 10.1093/pcp/pcaa018

Weeda, S., Zhang, N., Zhao, X., Ndip, G., Guo, Y., Buck, G. A., et al. (2014). *Arabidopsis* transcriptome analysis reveals key roles of melatonin in plant defense systems. *PLoS One* 9:e93462. doi: 10.1371/journal.pone.0093462

Wei, Z., Li, C., Gao, T., Zhang, Z., Liang, B., Lv, Z., et al. (2019). Melatonin increases the performance of *Malus hupehensis* after UV-B exposure. *Plant Physiol. Biochem.* 139, 630–641. doi: 10.1016/j.plaphy.2019.04.026

Weissbach, H., Redfield, B. G., and Axelrod, J. (1960). Biosynthesis of melatonin: enzymic conversion of serotonin to N-acetylserotonin. *Biochim. Biophys. Acta* 43, 352–353. doi: 10.1016/0006-3002(60)90453-4

Wen, D., Gong, B., Sun, S., Liu, S., Wang, X., Wei, M., et al. (2016). Promoting roles of melatonin in adventitious root development of Solanum lycopersicum L. by regulating auxin and nitric oxide signaling. *Front. Plant Sci.* 7:718. doi: 10.3389/fpls.2016.00718

Wu, Y., Fan, X., Zhang, Y., Jiang, J., Sun, L., Rahman, F. U., et al. (2021). VvSNAT1 overexpression enhances melatonin production and salt tolerance in transgenic *Arabidopsis*. *Plant Physiol. Biochem.* 166, 485–494. doi: 10.1016/j.plaphy.2021.06.025

Wu, Q., Su, N., Huang, X., Cui, J., Shabala, L., Zhou, M., et al. (2021). Hypoxia-induced increase in GABA content is essential for restoration of membrane potential and preventing ROS-induced disturbance to ion homeostasis. *Plant Commun.* 2:100188. doi: 10.1016/j.xplc.2021.100188

Xu, W., Cai, S. Y., Zhang, Y., Wang, Y., Ahammed, G. J., Xia, X. J., et al. (2016). Melatonin enhances thermotolerance by promoting cellular protein protection in tomato plants. *J. Pineal Res.* 61, 457–469. doi: 10.1111/jpi.12359

Xu, L., Xiang, G., Sun, Q., Ni, Y., Jin, Z., Gao, S., et al. (2019). Melatonin enhances salt tolerance by promoting MYB108A-mediated ethylene biosynthesis in grapevines. *Hortic. Res.* 6:114. doi: 10.1038/s41438-019-0197-4

Yan, F., Wei, H., Ding, Y., Li, W., Liu, Z., Chen, L., et al. (2021). Melatonin regulates antioxidant strategy in response to continuous salt stress in rice seedlings. *Plant Physiol. Biochem.* 165, 239–250. doi: 10.1016/j.plaphy.2021.05.003

Yang, H., Dai, L., Wei, Y., Deng, Z., and Li, D. (2019). Melatonin enhances salt stress tolerance in rubber tree (*Hevea brasiliensis*) seedlings. *Ind. Crop. Prod.* 145:111990. doi: 10.1016/j.indcrop.2019.111990

Yang, S. J., Huang, B., Zhao, Y. Q., Hu, D., Chen, T., Ding, C. B., et al. (2021). Melatonin enhanced the tolerance of *Arabidopsis thaliana* to high light through improving anti-oxidative system and photosynthesis. *Front. Plant Sci.* 12:752584. doi: 10.3389/fpls.2021.752584

Yang, Y., Yao, Y., Li, J., Zhang, J., Zhang, X., Hu, L., et al. (2022). Trehalose alleviated salt stress in tomato by regulating ROS metabolism, photosynthesis, osmolyte synthesis, and trehalose metabolic pathways. *Front. Plant Sci.* 13:772948. doi: 10.3389/fpls.2022.772948

Yao, J. W., Ma, Z., Ma, Y. Q., Zhu, Y., Lei, M. Q., Hao, C. Y., et al. (2021). Role of melatonin in UV-B signaling pathway and UV-B stress resistance in *Arabidopsis thaliana*. *Plant Cell Environ.* 44, 114–129. doi: 10.1111/pce.13879

Ye, T., Yin, X., Yu, L., Zheng, S. J., Cai, W. J., Wu, Y., et al. (2019). Metabolic analysis of the melatonin biosynthesis pathway using chemical labeling coupled with liquid chromatography-mass spectrometry. *J. Pineal Res.* 66:e12531. doi: 10.1111/jpi.12531

Yin, Y., Tian, X., Yang, J., Yang, Z., Tao, J., and Fang, W. (2022). Melatonin mediates isoflavone accumulation in germinated soybeans (*Glycine max* L.) under ultraviolet-B stress. *Plant Physiol. Biochem.* 175, 23–32. doi: 10.1016/j.plaphy.2022.02.001

Yu, Y., Lv, Y., Shi, Y., Li, T., Chen, Y., Zhao, D., et al. (2018). The role of phyto-melatonin and related metabolites in response to stress. *Molecules* 23:1887. doi: 10.3390/molecules23081887

Zhan, H., Nie, X., Zhang, T., Li, S., Wang, X., Du, X., et al. (2019). Melatonin: a small molecule but important for salt stress tolerance in plants. *Int. J. Mol. Sci.* 20:709. doi: 10.3390/ijms20030709

Zhang, J. Y., Cruz De Carvalho, M. H., Torres-Jerez, I., Kang, Y., Allen, S. N., Huhman, D. V., et al. (2014). Global reprogramming of transcription and metabolism in Medicago truncatula during progressive drought and after rewatering. *Plant Cell Environ.* 37, 2553–2576. doi: 10.1111/pce.12328

Zhang, Y., Fan, Y., Rui, C., Zhang, H., Xu, N., Dai, M., et al. (2021). Melatonin improves cotton salt tolerance by regulating ROS scavenging system and Ca^{2+} signal transduction. *Front. Plant Sci.* 12:693690. doi: 10.3389/fpls.2021.693690

Zhang, J., Li, D., Wei, J., Ma, W., Kong, X., Rengel, Z., et al. (2019). Melatonin alleviates aluminum-induced root growth inhibition by interfering with nitric oxide production in *Arabidopsis*. *Environ. Exp. Bot.* 161, 157–165. doi: 10.1016/j.envexpbot.2018.08.014

Zhang, Q., Liu, X., Zhang, Z., Liu, N., Li, D., and Hu, L. (2019). Melatonin improved waterlogging tolerance in alfalfa (*Medicago sativa*) by reprogramming polyamine and ethylene metabolism. *Front. Plant Sci.* 10:44. doi: 10.3389/fpls.2019.00044

Zhang, J., Shi, Y., Zhang, X., Du, H., Xu, B., and Huang, B. (2017). Melatonin suppression of heat-induced leaf senescence involves changes in abscisic acid and cytokinin biosynthesis and signaling pathways in perennial ryegrass

(*Lolium perenne* L.). *Environ. Exp. Bot.* 138, 36–45. doi: 10.1016/j.envexpbot.2017.02.012

Zhang, N., Sun, Q., Zhang, H., Cao, Y., Weeda, S., Ren, S., et al. (2015). Roles of melatonin in abiotic stress resistance in plants. *J. Exp. Bot.* 66, 647–656. doi: 10.1093/jxb/eru336

Zhang, H., Wang, L., Shi, K., Shan, D., Zhu, Y., Wang, C., et al. (2019). Apple tree flowering is mediated by low level of melatonin under the regulation of seasonal light signal. *J. Pineal Res.* 66:e12551. doi: 10.1111/jpi.12551

Zhang, R., Yue, Z., Chen, X., Wang, Y., Zhou, Y., Xu, W., et al. (2021). Foliar applications of urea and melatonin to alleviate waterlogging stress on photosynthesis and antioxidant metabolism in sorghum seedlings. *Plant Growth Regul.* 1–10. doi: 10.1007/s10725-021-00705-9

Zhang, N., Zhang, H. J., Sun, Q. Q., Cao, Y. Y., Li, X., Zhao, B., et al. (2017). Proteomic analysis reveals a role of melatonin in promoting cucumber seed germination under high salinity by regulating energy production. *Sci. Rep.* 7:503. doi: 10.1038/s41598-017-00566-1

Zhang, H., Zhang, N., Yang, R., Wang, L., Sun, Q., Li, D., et al. (2014). Melatonin promotes seed germination under high salinity by regulating antioxidant systems, ABA and GA 4 interaction in cucumber (*Cucumis sativus* L.). *J. Pineal Res.* 57, 269–279. doi: 10.1111/jpi.12167

Zhang, X., Zhang, H., Zhang, H., and Tang, M. (2020). Exogenous melatonin application enhances rhizophagus irregularis symbiosis and induces the antioxidant response of Medicago truncatula under lead stress. *Front. Microbiol.* 11:516. doi: 10.3389/fmicb.2020.00516

Zhao, J., Lu, Z., Wang, L., and Jin, B. (2020). Plant responses to heat stress: physiology, transcription, noncoding RNAs, and epigenetics. *Int. J. Mol. Sci.* 22:117. doi: 10.3390/ijms22010117

Zhao, D., Yao, Z., Zhang, J., Zhang, R., Mou, Z., Zhang, X., et al. (2021). Melatonin synthesis genes N-acetylserotonin methyltransferases evolved into caffeic acid O-methyltransferases and both assisted in plant terrestrialization. *J. Pineal Res.* 71:e12737. doi: 10.1111/jpi.12737

Zhao, D., Yu, Y., Shen, Y., Liu, Q., Zhao, Z., Sharma, R., et al. (2019). Melatonin synthesis and function: evolutionary history in animals and plants. *Front. Endocrinol.* 10:249. doi: 10.3389/fendo.2019.00249

Zhao, H., Zhang, K., Zhou, X., Xi, L., Wang, Y., Xu, H., et al. (2017). Melatonin alleviates chilling stress in cucumber seedlings by up-regulation of CsZat12 and modulation of polyamine and abscisic acid metabolism. *Sci. Rep.* 7:4998. doi: 10.1038/s41598-017-05267-3

Zhao, G., Zhao, Y., Yu, X., Kiprotich, F., Han, H., Guan, R., et al. (2018). Nitric oxide is required for melatonin-enhanced tolerance against salinity stress in rapeseed (*Brassica napus* L.) seedlings. *Int. J. Mol. Sci.* 19:1912. doi: 10.3390/ijms19071912

Zheng, X., Zhou, J., Tan, D. X., Wang, N., Wang, L., Shan, D., et al. (2017). Melatonin improves waterlogging tolerance of *Malus baccata* (Linn.) Borkh. Seedlings by maintaining aerobic respiration, photosynthesis and ROS migration. *Front. Plant Sci.* 8:483. doi: 10.3389/fpls.2017.00483

Zhou, X., Zhao, H., Cao, K., Hu, L., Du, T., Baluska, F., et al. (2016). Beneficial roles of melatonin on redox regulation of photosynthetic electron transport and synthesis of D1 protein in tomato seedlings under salt stress. *Front. Plant Sci.* 7:1823. doi: 10.3389/fpls.2016.01823

Conflict of Interest: The authors declare that the research was conducted in the absence of any commercial or financial relationships that could be construed as a potential conflict of interest.

Publisher's Note: All claims expressed in this article are solely those of the authors and do not necessarily represent those of their affiliated organizations, or those of the publisher, the editors and the reviewers. Any product that may be evaluated in this article, or claim that may be made by its manufacturer, is not guaranteed or endorsed by the publisher.

Copyright © 2022 Zeng, Mostafa, Lu and Jin. This is an open-access article distributed under the terms of the Creative Commons Attribution License (CC BY). The use, distribution or reproduction in other forums is permitted, provided the original author(s) and the copyright owner(s) are credited and that the original publication in this journal is cited, in accordance with accepted academic practice. No use, distribution or reproduction is permitted which does not comply with these terms.

frontiers | Frontiers in Plant Science

ORIGINAL RESEARCH
published: 18 May 2022
doi: 10.3389/fpls.2022.810991

Silicon Supplementation Modulates Physiochemical Characteristics to Balance and Ameliorate Salinity Stress in Mung Bean

Musa Al Murad[1,2] *and Sowbiya Muneer*[1]*

[1]*Horticulture and Molecular Physiology Lab, School of Agricultural Innovations and Advanced Learning, Vellore Institute of Technology, Vellore, India,* [2]*School of Biosciences and Technology, Vellore Institute of Technology, Vellore, India*

Mung bean is a low-cost high-protein legume that is sensitive to salinity. Salt stress has been demonstrated to be mitigated by silicon (Si). In legumes, the potential for silicon (Si)-mediated abiotic stress reduction has mainly been ignored. Moreover, there is little information on the specific role of comparable Si (sodium silicate) concentrations in salinity stress reduction. As a result, the current study investigated the impact of two distinct Si concentrations (1 and 5 mM) on the physiochemical features of the "mung bean," one of the most extensively cultivated legumes, when exposed to salinity (10, 20, and 50 mM NaCl). Salinity stress reduced growth variables such as biomass, nodule formation, plant length, height, and photosynthetic measures, which were mitigated by silicon supplementation at 5 mM sodium silicate. The inclusion of silicon increased the expression of photosynthetic proteins such as PSI, PSII, and LHCs under salt stress. Salinity stress also caused oxidative damage in the mung bean in the form of hydrogen peroxide (H_2O_2) and superoxide radical (O_2^-), leading in increased lipid peroxidation (MDA) and electrolyte leakage. In contrast, 5 mM sodium silicate tends to scavenge free radicals, reducing lipid peroxidation (MDA) and electrolyte loss. This was linked to significant silica deposition in the leaf epidermis, which eventually functioned as a mechanical barrier in mitigating the deleterious effects of salt stress. Si supplementation also decreased Na^+ uptake while increasing K^+ uptake. Silicon, specifically 5 mM sodium silicate, was found to minimize salinity stress in mung bean by altering physio-chemical parameters such as photosynthetic machinery, Na^+/K^+ homeostasis, mechanical barriers, osmolyte production, and oxidative stress.

Keywords: amelioration, physiochemical characteristics, mung bean, salinity stress, silicon

OPEN ACCESS

Edited by:
Shabir Hussain Wani, Sher-e-Kashmir University of Agricultural Sciences and Technology, India

Reviewed by:
Mohsin Tanveer, University of Tasmania, Australia
Anis Ali Shah, University of Education Lahore, Pakistan

***Correspondence:**
Sowbiya Muneer
sowbiya.muneer@vit.ac.in;
sobiyakhan126@gmail.com

Specialty section:
This article was submitted to Plant Biotechnology, a section of the journal Frontiers in Plant Science

Received: *08 November 2021*
Accepted: *12 April 2022*
Published: *18 May 2022*

Citation:
Al Murad M and Muneer S (2022) Silicon Supplementation Modulates Physiochemical Characteristics to Balance and Ameliorate Salinity Stress in Mung Bean. Front. Plant Sci. 13:810991. doi: 10.3389/fpls.2022.810991

INTRODUCTION

Salinity is one of the major abiotic stresses that has reportedly affected around 20% of the irrigated land accounting to 60 million hectares worldwide, thus arising concerns about its negative ecological and socio-economic outcomes (Munns and Tester, 2008; Islam et al., 2016; Sehrawat et al., 2018). This problem is expected to worsen in the coming years, due to

continued global warming, extreme climate fluctuations, and unmonitored use of fertilizers, industrial pollution, and irrigation with saline water (Zhu et al., 2019; Meng et al., 2020).

Salinity stress inhibits plant growth and development by decreasing osmotic potential in soil solutions and increasing ion toxicity, particularly of Na^+ and Cl^- ions (Ashraf and Akram, 2009; Daoud et al., 2018). The buildup of Na^+ and Cl^- at exceptionally high levels during salinity stress largely impedes plant nutrient uptake (Ahanger and Agarwal, 2017). Salinity stress also causes a decrease in the Calvin cycle, a decrease in CO_2 intake, and a decrease in photosynthetic pigments such as chlorophyll concentration, all of which have an effect on the net photosynthesis rate (Sairam et al., 2002; Munns et al., 2020). By increasing the Na^+/K^+ ratio, salinity stress slows various other metabolic processes in crops, including transpiration, stomatal conductance, and PSII quantum yield (Gupta and Huang, 2014). In fact, photoinhibition caused by salinity stress results in the accumulation of untapped energy, which destroys the photosynthetic apparatus, leading in the production of reactive oxygen species (ROS; Nishiyama and Murata, 2014; Gururani et al., 2015; Tokarz et al., 2021). Excessive ROS concentrations in cells weaken the antioxidant apparatus, resulting in lipid peroxidation (MDA), which affects the cell membrane structure and permeability (Davey et al., 2005) and also damages lipids, proteins, and nucleic acid (Tanveer, 2020). As a result, the worrying biochemical and physiological changes that result in diminished plant growth and development might be related to salinity stress.

Mung bean (*Vigna radiata* L.) is an important legume crop that supplies a significant quantity of protein (24.5%), carbs (59.9%), fatty acids (1.2%), and fibers (4.5%), as well as vital amino acids (Fuller, 2007; Khattak et al., 2008; Aasim et al., 2019). Around 3 million tons of this economic crop are produced annually, accounting for 5% of the total pulse production worldwide (World Vegetable Centre, 2018). Due to its high nutritional value and global production, mung bean remains a staple source of protein for millions of people in developing countries (Sehrawat et al., 2013). However, legumes such as mung bean are cultivated in arid and semi-arid regions which are prone to salt stress and hence are considered salt-sensitive crops (Sprent and Gehlot, 2010). It has been reported that salinity limits the yield of mung bean to almost 70% at 50 mM NaCl and exerts a negative effect on the quality of the crop (Saha et al., 2010; Sehrawat et al., 2013). Besides, salinity also affects its seed germination, seedling development, radicle length (Dutta and Bera, 2014; Sehrawat et al., 2014), whole plant growth, biomass (Ahmed, 2009), nutrient accumulation (Naher and Alam, 2010), photosynthesis (Koyro, 2006), ROS formation, relative water content, membrane stability index, chlorophyll and carotenoid content (Sehrawat et al., 2015), nodulation, nodule respiration, and root hair formation (Swaraj and Bishnoi, 1999; Naher and Alam, 2010). As a result, there is an urgent need to develop a robust and long-term strategy for conferring salt tolerance on the mung bean, which is an important leguminous and food crop.

The upgradation of silicon (Si) from a "nonessential" substance to the status of a "beneficial substance" by the International Nutrition Institute (IPNI) in 2015 has established the fact that Si is not directly involved in plant growth, function or metabolic processes, but ameliorates the negative effects of biotic and abiotic stresses, and in turn reflects on the improvements in plant growth, function, and metabolic processes (Gao et al., 2011; Coskun et al., 2018; Flam-Shepherd et al., 2018). For example, several studies have shown Si-mediated alleviation of salinity stress in crops like capsicum (Manivannan et al., 2016; Abdelaal et al., 2020), tomato (Muneer and Jeong, 2015; Hoffmann et al., 2020), sorghum (Liu et al., 2015), okra (Abbas et al., 2015), cucumber (Zhu et al., 2004; Yin et al., 2019), wheat (Alzahrani et al., 2018; Javaid et al., 2019), rice (Shi et al., 2013), basil (Farouk et al., 2020), alfalfa (Meng et al., 2020), and soybean (Chung et al., 2019). The mechanisms by which Si infers salinity stress tolerance to plants include: (a) retention of water content at optimal levels (Zhu and Gong, 2014), (b) improving physiological attributes such as leaf area expansion, light interception leading to increased photosynthetic rates (Ma et al., 2006), (c) limiting the oxidative stress by regulating ion toxicity, (d) regulation of compatible solutes such as betaine, glycine, and proline which stabilize important membrane proteins (Etesami and Jeong, 2018), (e) accumulation of polyamines which prevent Na^+ and K^+ flow *via* non-selective cationic channels (Zhao et al., 2007), and (f) increasing performance of antioxidant enzymes and efficiency of PSII (Al-Aghabary et al., 2004).

Despite the fact that various studies on Si-mediated stress mitigation in plants have been conducted, the effect of Si supplementation in legumes has mainly been overlooked. The Poaceae family receives the majority of silicon research (42%), whereas the Fabaceae family receives only 7% (Putra et al., 2021), emphasizing the urgent need to enhance the focus of Si research on legumes as well. Also, no report on a comparison analysis of two distinct concentrations of the same source of Si (sodium silicate) in any crop/plant has been published to date. Variable impacts of Si sources have been reported among plant species. However, it would be fascinating to determine if or not the effects of Si-mediated stress reduction are concentration dependent. As a result, we attempted to evaluate the impacts of two different sodium silicate concentrations on the physiochemical characteristics of mung bean exposed to salt stress in our study. The present study depicted that silicon (sodium silicate) ameliorates and balances the salinity stress by modulating physiochemical characteristics in mung bean. Moreover, a significant physiological mechanism was also inculcated on silicon can alleviate salinity stress in mung bean.

MATERIALS AND METHODS

Plant Materials, Growth Conditions, and Treatments

Seeds of mung bean (*Vigna radiata* L.) collected from local growers were surface-sterilized with 5% (*v*/*v*) sodium hypochlorite solution for 30 min and further washed with distilled water. The seeds were then sown in pots filled with sterilized red soil, sand, and vermicompost in the ratio 1:1:1 and grown in polyhouse of VIT School of Agricultural Innovations and Advanced Learning

(VAIAL), VIT, Vellore, India. The pots had a diameter and height of 13 and 17 cm, respectively. Four seedlings were sown in each pot. The temperature of the greenhouse was maintained between 27 and 30°C with a relative humidity of 60–70% (monitored with the help of digital temperature sensor; Richie HTC infrared/Optical thermometer). After 30 days, the pots were divided randomly for salinity and silicon treatments. For silicon treatment, two concentrations of sodium silicate were used in the experiment, *viz.* 1 mM (Si_1) and 5 mM (Si_2). Our experiment was comprised of the following eight different treatments: (i) control (T1) (ii) −NaCl+Si (1 mM/5 mM) (T2), (iii) 10 mM NaCl/−Si (T3), (iv) 10 mM NaCl/+ Si (1 mM/5 mM) (T4), (v) 20 mM NaCl/−Si (T5), (vi) 20 mM NaCl/+Si (1 mM/5 mM) (T6), (vii) 50 mM NaCl/−Si (T7), (viii) 50 mM NaCl/+Si (1 mM/5 mM) (T8) (**Figure 1**). The experiments were designed in a completely randomized manner with four replicates for each treatment. For silicon treatment, the plants were irrigated with sodium silicate (1 mM/5 mM) solution followed by intermittent irrigation with normal water for the period of 10 days. Leaf samples were collected after 5 and 10 days of treatments, respectively, and stored at −80°C for further experimentation.

Plant Growth and Biomass Yield

Plants were uprooted from pots, washed with distilled water, and then weighed in a digital weighing balance for fresh biomass measurement. For measuring dry biomass, plant samples were placed in a hot air oven for 48 h at 65–75°C and then weighed subsequently. The lengths of shoot and root were measured using a measuring scale.

Determination of Gaseous Exchange Parameters and Quantum Yield of PSII

The net photosynthesis rate, stomatal conductance, and transpiration rate were measured using a portable SPAD meter (Konica Minolta, Tokyo, Japan). A mini-PAM 2000 chlorophyll fluorescence meter (Heinz Walz GmbH) was used to measure the chlorophyll fluorescence (F_v/F_m). The leaves were adapted to dark conditions 30 min before measurement. The maximum PSII quantum yield (F_v/F_m) was calculated as $F_v/F_m = (F_m - F_0)/F_m$ (Yang et al., 2013).

Determination of Pigments

The content of the photosynthetic pigments, *viz.* chlorophyll and carotenoid, was determined according to the method of Hiscox and Israelstam (1979). Briefly, 1 g of leaf samples was immersed in 5 ml of dimethyl sulfoxide (DMSO) and incubated in a hot water bath (65°C) for 1 h for the pigments to leach out. Following incubation, the absorbance of the samples was determined using an UV-VIS spectrophotometer at wavelengths 410, 510, 663, and 445 nm, respectively. The content of chlorophyll and carotenoid was then calculated using the formulae given by Arnon and Israelstam (1949).

Analysis of Multiprotein Complex Proteins in Thylakoids (1D-BN-PAGE)

Blue native polyacrylamide gel electrophoresis (BN-PAGE) of integral thylakoid proteins was performed according to Muneer et al. (2014) with minor modifications. Two grams of fresh leaf tissues was homogenized in liquid nitrogen, followed by extraction of thylakoid proteins using an extraction buffer (pH 7.8) containing

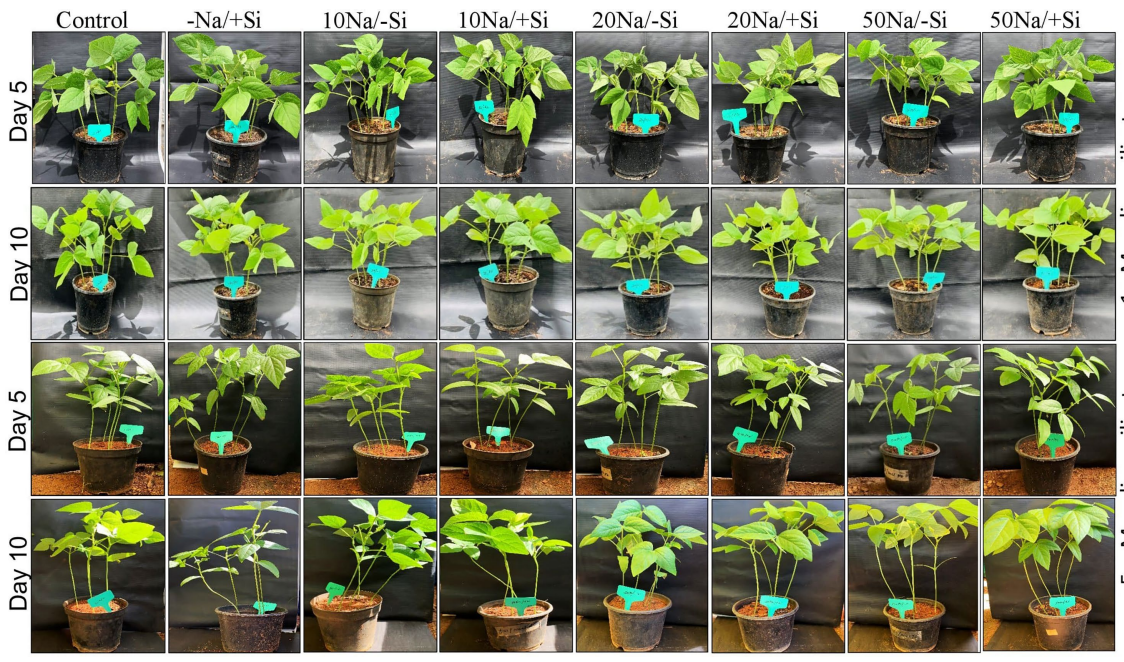


FIGURE 1 | Experimental setup of mung bean (*Vigna radiata*) under 1 mM (Si_1) and 5 mM (Si_2) Si supply and salinity stress after eight treatments: (i) control (T1), (ii) −NaCl+Si (1 mM/5 mM) (T2), (iii) 10 mM NaCl/−Si (T3), (iv) 10 mM NaCl/+Si (1 mM/5 mM) (T4), (v) 20 mM NaCl/−Si (T5), (vi) 20 mM NaCl/+Si (1 mM/5 mM) (T6), (vii) 50 mM NaCl/−Si (T7), and (viii) 50 mM NaCl/+Si (1 mM/5 mM) (T8) for a period of 10 days.

20 mM Tricine-NaOH, 70 mM sucrose and 5 mM $MgCl_2$, which was then filtered through Mira cloth, followed by centrifugation at 4,500 rpm for 10 min. The thylakoid pellets were re-suspended in the above buffer (pH 7.8) and centrifuged again at the same parameters. The pellet containing the thylakoid membrane was then washed with washing buffer (pH 7.0) containing 330 mM sorbitol, 50 mM Bis-Tris-HCl, pH 7.0, and 0.1 mg ml^{-1} pefabloc. An equal volume of re-suspension buffer and solubilization buffer were then added to the pellet, and membrane proteins were allowed to solubilize in ice for 2–3 min. Insoluble material was removed by centrifugation at 18,000 rpm for 15 min. The supernatant was then mixed with 0.1% loading dye (5% CBB-G250, 100 mM Bis-Tris-HCl, pH 7.0, 30% *w*/*v* sucrose, and 500 mM ε-amino-*n*-caproic acid) and loaded onto a 5–12.5% acrylamide gradient gel with a constant voltage of 70 V for 15–20 min and followed by 120 V until completion.

Determination of Relative Water Content (RWC %)

The RWC % was estimated according to Turner and Kramer (1980). Fresh leaves were washed carefully, and their fresh weight (FW) was measured. The leaves were then soaked in distilled water for 4 h at room temperature (25°C) to determine the turgid weight (TW) and further incubated in hot air oven (80°C) for 24 h. The dry weight (DW) of the leaves was then measured. The relative water content (RWC) was measured as follows:

$$\mathrm{RWC\%} = \left(\mathrm{FW} - \mathrm{TW}\right) / \left(\mathrm{DW} - \mathrm{TW}\right) \times 100$$

where fresh weight (FW); turgid weight (TW); dry weight (DW).

Determination of Proline Content

Proline content was determined according to Bates et al. (1973). For this, 0.3 g of leaf samples was homogenized in 10 ml of 3% sulfosalicylic acid and was centrifuged at 3,300 rpm for 10 min. Approximately 2 ml of supernatant was taken, to which 2 ml of acid ninhydrin solution and 2 ml of glacial acetic acid were added. The reaction mixture was incubated in hot water bath (100°C) for 1 h and then terminated in ice bath. Further, 4 ml of toluene was added to the mixture with vigorous stirring and the absorbance of the solvent layer was determined at 520 nm.

Determination of Lipid Peroxidation Level (MDA Content)

The MDA content in leaves was determined according to Heath and Packer (1968). Briefly, 0.5 g of leaf samples was homogenized in 0.1% trichloroacetic acid (TCA) and then centrifuged at 7,000 rpm for 10 min. The supernatant was collected; to it 4 ml of 0.5% thiobarbituric acid (TBA) dissolved in 20% TCA was added. The mixture was then incubated in hot water bath (95°C) for 30 min. Finally, the reaction mixture was placed in ice bath to terminate the reaction. The absorbance was determined at 532 nm and corrected for unspecific turbidity by subtracting the values obtained at 600 nm.

Determination of Electrolyte Leakage Percentage

The procedure used to determine electrolyte leakage percentage was based on the method of Lutts et al. (1996). Leaf samples were washed with distilled water three times to remove surface contaminants and were then placed in individual stoppered vials containing 10 ml of distilled water. The samples were incubated at room temperature (25°C) on a shaker (100 rpm) for 24 h. After incubation, the electrical conductivity of the bathing solution (EC1) was measured using a conductivity meter (EC tester 11+, Fieldscout, 2265FS). Samples were then incubated in a hot water bath (95°C) for 15 min, and the electrical conductivity (EC2) of the bathing solution was read after cooling it down to the room temperature. ELP was calculated as EC1/EC2 and expressed as %.

In situ Localization of Oxidative Stress Markers (H_2O_2 and O_2^-)

The histochemical staining of hydrogen peroxide (H_2O_2) and superoxide radicle (O_2^-) was performed according to Muneer et al. (2013).

For H_2O_2 localization, fresh leaf samples were immersed in 0.1% solution of 3, 3′-diaminobenzidine (DAB) in Tris-HCl buffer (pH 6.5). The samples were vacuum infiltrated for 5 min and then incubated for 12 h in dark. The leaves were then submerged and bleached in boiling ethanol (95%) to visualize the brown spots and photographed using digital camera.

For O_2^- localization, fresh leaf samples were immersed in a 0.1% solution of nitro blue tetrazolium chloride (NBT), in K-phosphate buffer (pH 6.4), containing 10 mM sodium azide. The remaining steps were carried out as in the case of H_2O_2 localization. The formation of blue formazan precipitate was visualized and then photographed using a digital camera.

Measurement of Tissue Ion Concentration

Around 10 expanded leaves were chosen randomly from each pot. Each treatment group consisted of four replicates. Leaves were dried in a hot air oven for 48 h at 80°C and ground to fine powder. Around 100 mg of leaf samples was acidified with HNO_3 for 12 h and digested further using a microwave digestion system for elemental analysis. Elemental concentrations were measured using an inductively coupled plasma optical emission spectrometer (PERKIN ELMER OPTIMA 5300 DV ICP-OES; Muneer et al., 2014).

Histochemical Staining of Silica Body

The histochemical staining of silica bodies in leaf epidermis was carried out according to Yokoyama et al. (2015). Briefly, leaf samples were fixed in FAA solution (formamide, 80% ethanol, and 100% acetic acid) in the ratio 90:5:5 for 24 h in room temperature (RT). This was followed by dehydration treatments with 80, 90, and 100% ethanol for 20 min each at RT. Washing of the dehydrated samples was done with 10, 20, 30, 40, 50, 60, 70, 80, 90, and 100% benzene (in ethanol) for 20 min each at RT. Benzene equilibrated samples were then stained in 0.1% crystal violet lactone solution (in benzene) to

visualize the silica bodies in a phase contrast microscope (Model: MT4300L, MEIJI TECHNO CO., LTD., Made in Japan).

RESULTS

Si Improved the Formation of Root Nodules in Mung Bean Under Salinity Stress

Because legumes have the unique ability to form root nodules for nitrogen fixation, it is thought to be a significant component in legume output. As a result, we looked into whether Si can help with the formation of root nodules under salt stress. According to our observations, the number of nodules formed was relatively limited in the early stages of salt stress (5th day), indicating a more severe loss of root nodules in the later stages of salinity stress (**Figures 2A,B**). Si_1 supplementation significantly improved root nodulation on days 5 and 10 of salt stress treatments. The greatest increases in T8 and T6 were 62.07% on day 10 and 58.11% on day 5. Similarly, Si_2 supplementation increased root nodule formation on days 5 and 10 of salinity stress treatments, with Si_2 alone showing a significant increase in nodule formation when compared to the control.

Si Improved the Growth Factors of Mung Bean During Salinity Stress

On day 5 of treatment, different levels of salinity stress reduced plant root and shoot length (**Figures 3A,B**). On the fifth day of salinity treatment, however, the application of Si_1 (1 mM Si) significantly increased root and shoot length. On day 5 of treatment, the increase in root length was found to be around 32% in T8, and the increase in shoot length was found to be 29.33 and 31.13% in T6 and T8, respectively. On the tenth day of salinity treatment, the addition of Si_1 had no effect on root and shoot length. Similarly, Si_1 supplementation increased plant fresh and dry biomass on the fifth day of salinity stress but had no effect on biomass on the tenth day of treatment (**Figures 3C,D**).

However, Si_2 (5 mM sodium silicate) supplementation resulted in maximum recovery (T4, T6, and T8) across all levels of salinity stress treatments (T3, T5, and T7) on both salinity treatment days (5th and 10th; **Figures 3D,E**). The root length increased by 44.55 and 40.6% in T6 after 5 and 10 days of silicon treatment, respectively. In the case of shoot length after Si_2 supplementation, a similar trend was observed. Si_2 supplementation also resulted in an increase (T4, T6, and T8) in fresh and dry biomass of plants on days 5 and 10 of salinity stress treatment (**Figures 3F,G,H**). Si supplementation (T2) alone had a positive effect on mung bean growth characteristics during salinity stress.

Si Improved the Gaseous Exchange Parameters and PSII Quantum Yield During Salinity Stress

Except for net photosynthesis rate, which was improved by 34.01 and 7.8% in T4 and T6 on day 5 and by 30.29% in T8 on day 10, the addition of Si_1 to salinity-treated mung bean did not show much difference in stomatal conductance and transpiration rate (**Figures 4A–C**). The fluorescence of chlorophyll was also unaffected by Si_1 addition (**Figure 4D**).

In contrast, applying Si_2 to mung bean plants under salinity stress increased their net photosynthesis rate by 41.15, 38.82, and 29.97% on day 10 compared to day 5 (**Figure 5A**). A similar trend was observed in stomatal conductance, which was uniformly improved by Si_2 on day 10, but there was no significant difference in transpiration rate under salinity stress and/or with Si supplementation (**Figures 5B,C**). However, Si_2 addition significantly improved the quantum yield of PSII (F_v/F_m) on day 10 compared to day 5 of salinity stress treatments (**Figure 5D**).

Si Increased the Photosynthetic Pigments in Leaves During Salinity Stress

On day 10 of salinity treatment, the chlorophyll content increased by 29.7, 8.40, and 40.71% in T4, T6, and T8, respectively, with Si_1 supplementation (**Figure 6A**). The application of Si_2 had a greater impact on improving pigment content on day 5 of salinity treatment than on day 10, with an increase in chlorophyll content of 5.64, 18.1, and 25.8% in T4, T6, and T8, respectively (**Figure 6B**). A similar pattern was observed in the increase in carotenoid content during salinity stress as seen in the case of chlorophyll content, with Si_1 efficiently increasing the carotenoid levels in day 5 and day 10 of treatments and Si_2 also exerting its beneficial role in improving the carotenoid level more efficiently in day 5 as compared to that in day 10 of treatment (**Figures 6C,D**).

Si Improved the Expression of Thylakoid Membrane Proteins Under Salinity Stress

Since then, Si_2 has been shown to positively modulate photosynthetic parameters under salinity stress. As a result, we only used Si_2-treated samples to examine the expression levels of important photosynthetic proteins in order to validate the results obtained from photosynthetic physiological modulations. For salinity-stressed mung bean supplemented with Si_2, the Blue Native PAGE technique (BN-PAGE) was used (**Figure 7**). On both days 5 and 10 of treatment, BN-PAGE revealed an increase in the expression levels of PSII monomers in salinity-stressed plants supplemented with Si_2. Light harvesting complex proteins (LHC II) assembly trimer expression levels were also increased in Si_2 supplemented groups. Light harvesting complex proteins (LHC II) assembly monomer, ATPase, and PSI core dimer were also found but did not differ significantly between treatment and control groups.

Si Improved the Leaf Water Status During Salinity Stress

The induction of salinity stress had an effect on the relative water content of leaves (**Figures 8A,B**). Si supplementation, on the other hand, was found to be effective in restoring the RWC. However, Si_1 supplementation only reversed the effects of salinity stress in T6 and T8 on the fifth day and had no effect on RWC on the tenth day. On the 5th and 10th days

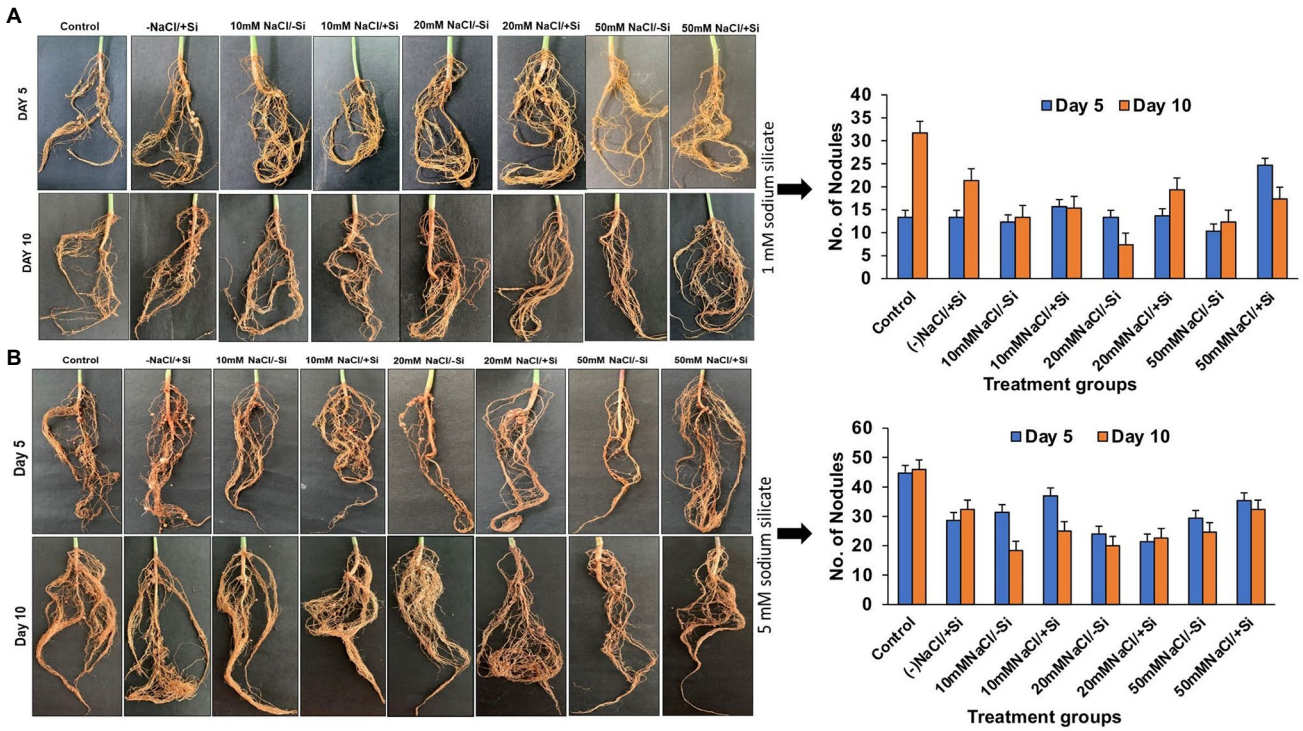


FIGURE 2 | Changes in the formation of root nodules of mung bean (*Vigna radiata*) under **(A)** 1 mM (Si_1) and **(B)** 5 mM (Si_2) Si supply and salinity stress after eight treatments: (i) control (T1), (ii) −NaCl+Si (1 mM/5 mM) (T2), (iii) 10 mM NaCl/−Si (T3), (iv) 10 mM NaCl/+ Si (1 mM/5 mM) (T4), (v) 20 mM NaCl/−Si (T5), (vi) 20 mM NaCl/+Si (1 mM/5 mM) (T6), (vii) 50 mM NaCl/−Si (T7), and (viii) 50 mM NaCl/+Si (1 mM/5 mM) (T8) for a period of 5 and 10 days. Vertical bars indicate Mean ± SE of the means for $n = 4$. Means denoted by the different letters are significantly different at $p \leq 0.05$ according to the Tukey's studentized range test.

of salinity stress, Si_2 supplementation was more effective than Si_1 in restoring water status.

Si Increased the Levels of Proline Accumulation Under Salinity Stress

The accumulation of protective osmolytes such as proline is an important indicator of the "plant stress-response strategy" that confers salinity stress tolerance. On the fifth and tenth days after treatment, we observed a decrease in proline content and an increase in salinity levels (**Figures 9A,B**). However, Si_2 supplementation increased proline levels in all plants exposed to salinity stress for 5 and 10 days. After 5 days of salinity stress, the content of proline increased by 69.5, 75.6, and 69.2% in T4, T6, and T8, respectively, and by 25.3, 54.9, and 54.1% in T4, T6, and T8, respectively, after 10 days of salinity stress. Supplementation of Si_1 was also able to increase the proline content in few treatment groups, but the effect was considered inconsistent as compared to the beneficial effects of Si_2.

Si Decreased the Lipid Peroxidation (MDA) Levels During Salinity Stress

Lipid peroxidation (MDA), expressed as malondialdehyde (MDA) content, was found to increase with levels of salinity (**Figures 10A,B**). However, supplementation of Si to the salinity-stressed mung bean resulted in a decrease in the lipid peroxidation (MDA) levels, with Si_2 decreasing the lipid peroxidation (MDA) levels more efficiently up to 27.2, 15.52, and 41.14% with the increasing levels of salinity stress, respectively. Si_2 was also seen to reduce the lipid peroxidation (MDA) levels under salinity stress, but was not as efficient as Si_1.

Si Reduced Electrolyte Leakage During Salinity Stress

Excessive permeability of ions and electrolytes is caused by increased lipid peroxidation (MDA) during salinity stress (**Figures 10C,D**). As a result, under salinity stress, electrolyte leakage potential increased significantly, which was countered by Si supplementation. When compared to Si_1, which was partially effective, supplementation with Si_2 reduced electrolyte leakage potential by 10, 50.64, and 0.625% with increasing levels of salinity stress, respectively.

Si Alleviated Oxidative Stress in the Form of H_2O_2 and O_2^- During Salinity Stress

The accumulation of ROS such as hydrogen peroxide and superoxide radical is caused by an increase in lipid peroxidation (MDA) and electrolyte leakage. During salinity stress, the histochemical test revealed that H_2O_2 and O_2^- were localized on leaves as dark brown and dark blue spots, respectively. The localization of H_2O_2 was observed in all plants after the 5th and 10th days of salinity stress treatments, with an increase in H_2O_2 localization with increasing salinity levels

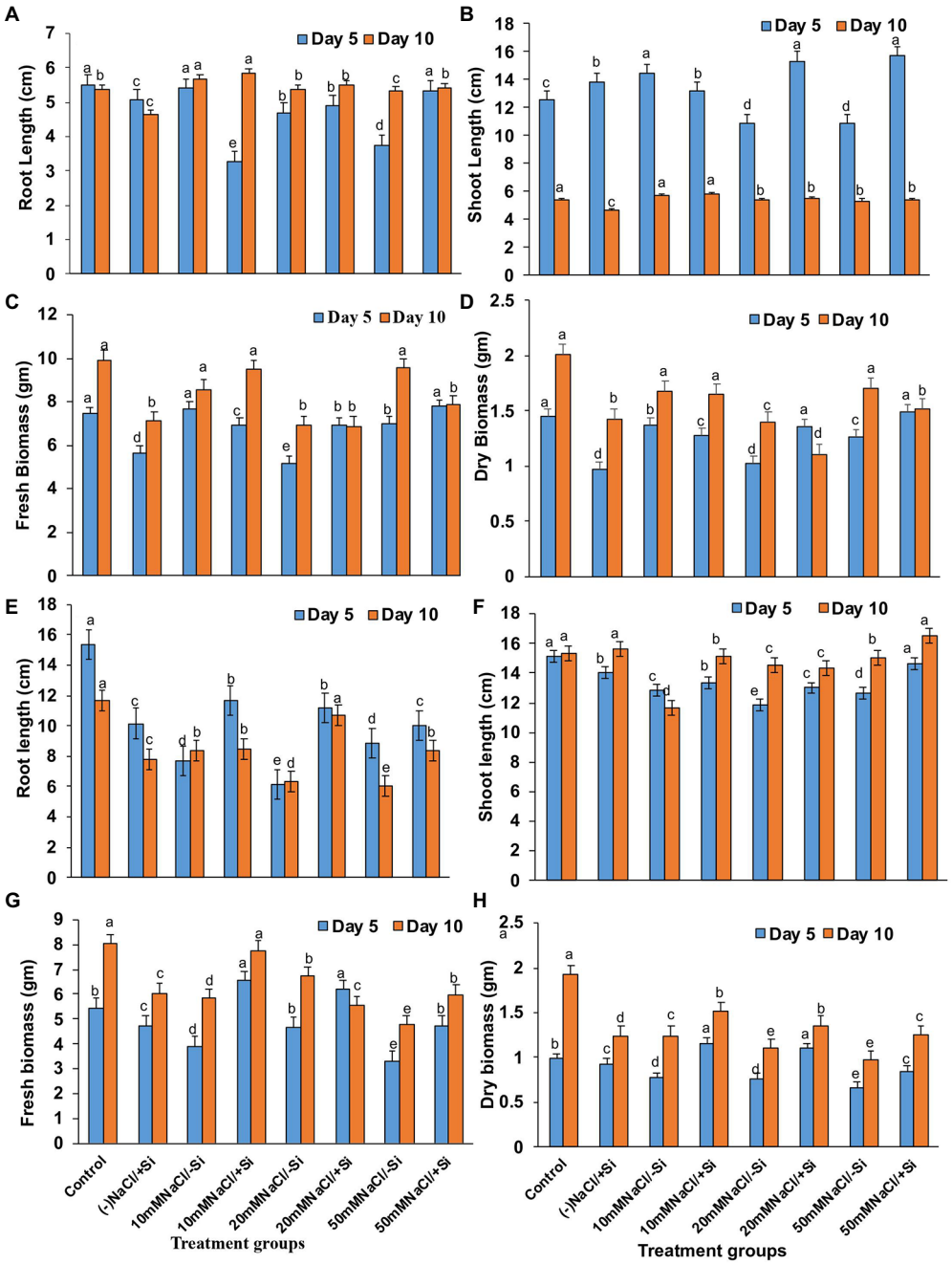


FIGURE 3 | Changes in **(A,E)** root length, **(B,F)** shoot length, **(C,G)** fresh biomass, and **(D,H)** dry biomass of mung bean (*Vigna radiata*) under 1 mM (Si_1) Si supply and salinity stress after eight treatments: (i) control (T1), (ii) −NaCl+Si (1 mM/5 mM) (T2), (iii) 10 mM NaCl/−Si (T3), (iv) 10 mM NaCl/+Si (1 mM/5 mM) (T4), (v) 20 mM NaCl/−Si (T5), (vi) 20 mM NaCl/+Si (1 mM/5 mM) (T6), (vii) 50 mM NaCl/−Si (T7), and (viii) 50 mM NaCl/+Si (1 mM/5 mM) (T8) for a period of 5 and 10 days. Vertical bars indicate Mean ± SE of the means for $n = 4$. Means denoted by the different letters are significantly different at $p \leq 0.05$ according to the Tukey's studentized range test.

(**Figures 11A,B**). Both Si_1 and Si_2 reduced the oxidative stress generated by varying degrees of salt on the 5th and 10th days following treatment, as seen as brown patches, with Si_2 having the upper hand in the "oxidative stress mitigation" role.

The formation of O_2^-, which is characterized by a blue spot (due to formazan produced during reaction with NBT), was seen to be more prominent in 10 days compared to the 5th day under salinity stress (**Figures 12A,B**). However, Si_2 could scavenge/neutralize the free radical formed, as is evident by the reduction of blue spots in treatment groups T4, T6, and T8 when compared to salinity stress-treated plant groups T3, T5, and T7. Si_1 was also able to scavenge the O_2^- radical

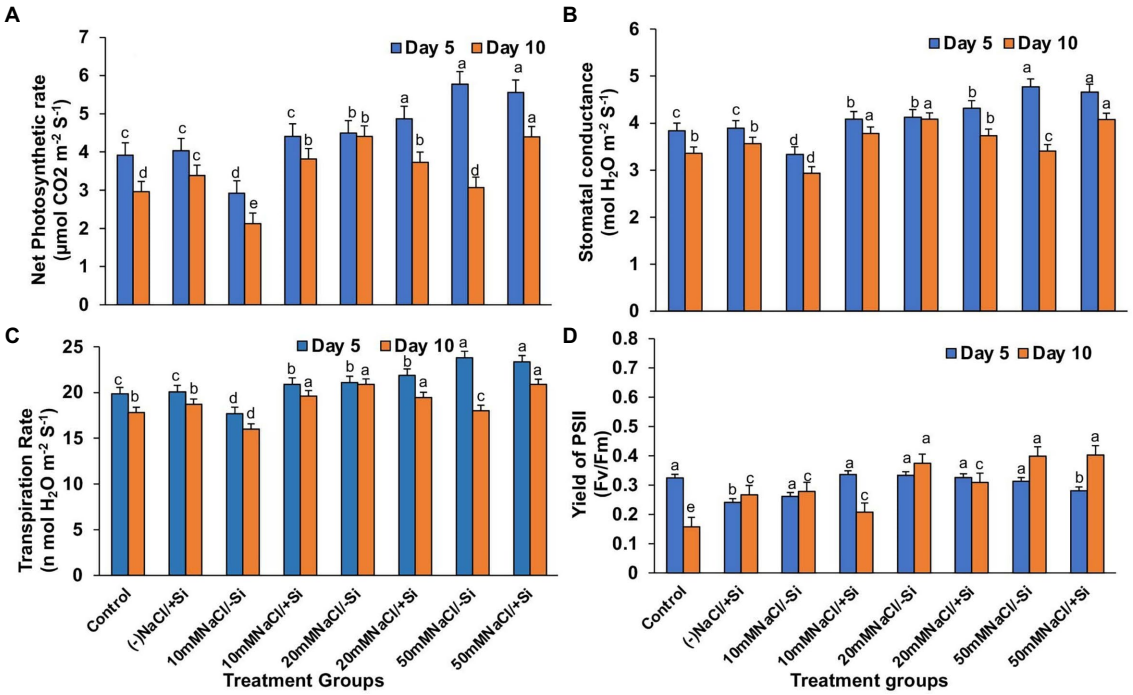


FIGURE 4 | Changes in **(A)** net photosynthesis, **(B)** stomatal conductance, **(C)** transpiration rate, and **(D)** PSII quantum yield of mung bean (*Vigna radiata*) under 1 mM (Si_1) Si supply and salinity stress after eight treatments: (i) control (T1), (ii) −NaCl+Si (1 mM) (T2), (iii) 10 mM NaCl/−Si (T3), (iv) 10 mM NaCl/+ Si (1 mM) (T4), (v) 20 mM NaCl/−Si (T5), (vi) 20 mM NaCl/+Si (1 mM) (T6), (vii) 50 mM NaCl/−Si (T7), and (viii) 50 mM NaCl/+Si (1 mM) (T8) for a period of 5 and 10 days. Vertical bars indicate Mean ± SE of the means for $n = 4$. Means denoted by the different letters are significantly different at $p \leq 0.05$ according to the Tukey's studentized range test.

on both 5th and 10th days after treatment, but the level of mitigation was not as significant as seen in Si_1 supplementation.

Si Reduced the Na^+ Uptake and Increased K^+ Uptake During Salinity Stress

The concentration of Na^+ in salinity-stressed plants increased with increasing levels of salinity, with the highest concentration of Na^+ observed in T7 (50 mM NaCl) as compared to control (**Figures 13A,B**). However, Si-mediated obstruction to Na^+ uptake was reported in the salinity-stressed plants. Si_1 supplementation decreased the concentration of Na^+ in treatment groups T6 and T8 by 88 and 42.4%, respectively, whereas the application of Si_2 decreased the Na^+ concentration in T4, T6, and T8 evenly, with the greatest decrease in T8 by 393%. The application of Si_1 and Si_2 alone also significantly lowers Na^+ concentration as compared to control. The concentration of K^+ in salinity-treated plants did not show much difference with or without supplementation with Si_1 and Si_2. However, supplementation Si_1/Si_2 alone has shown a higher concentration of K^+ as compared to control.

Si Uptake and Its Deposition Acts as a Mechanical Barrier During Salinity Stress

Supplementation of Si_1 to mung bean plants subjected to different levels of salinity could lead to the efficient deposition of silica body in treatment groups T4 and T6 on day 5 of treatment and in treatment groups T6 and T8 on day 10 of salinity treatment (**Figure 14A**). When Si_1 alone was applied to mung bean plants, a considerable amount of silica deposition was observed in the leaf epidermis, cortex and vascular bundle. In contrast, Si_2 supplementation to salinity-stressed plants resulted in an increased uptake of silicon and its subsequent deposition in the epidermis, cortical region and vascular bundle of leaves on both day 5 and day 10 of salinity treatments, as compared to control. When mung bean was subjected to different levels of salinity stress (T3, T5, and T7) alone, the deposition of silica was found to be nearly negligible on both day 5 and day 10 of salinity treatment. However, Si_2 supplementation alone has shown significant silica deposition in leaves on day 5 and day 10 of salinity treatments. With Si_2 supplementation showing more silica deposition on day 10 of treatment, similarly, the uptake of Si_2 on day 10 of treatment was found to be significantly improved in salinity-stressed plants supplemented with Si_2 (**Figure 14B**). Silicon uptake was increased by 57.9% in T6 and by 6.6% in T8, respectively. Si_2 supplementation alone increased the silicon uptake by 53.3% as compared to control.

DISCUSSION

Most of the Si research has been done on the Poaceae family, thus ignoring the potential role of Si in plant functional groups such as legumes (Fabaceae). Legumes are well known for fixing

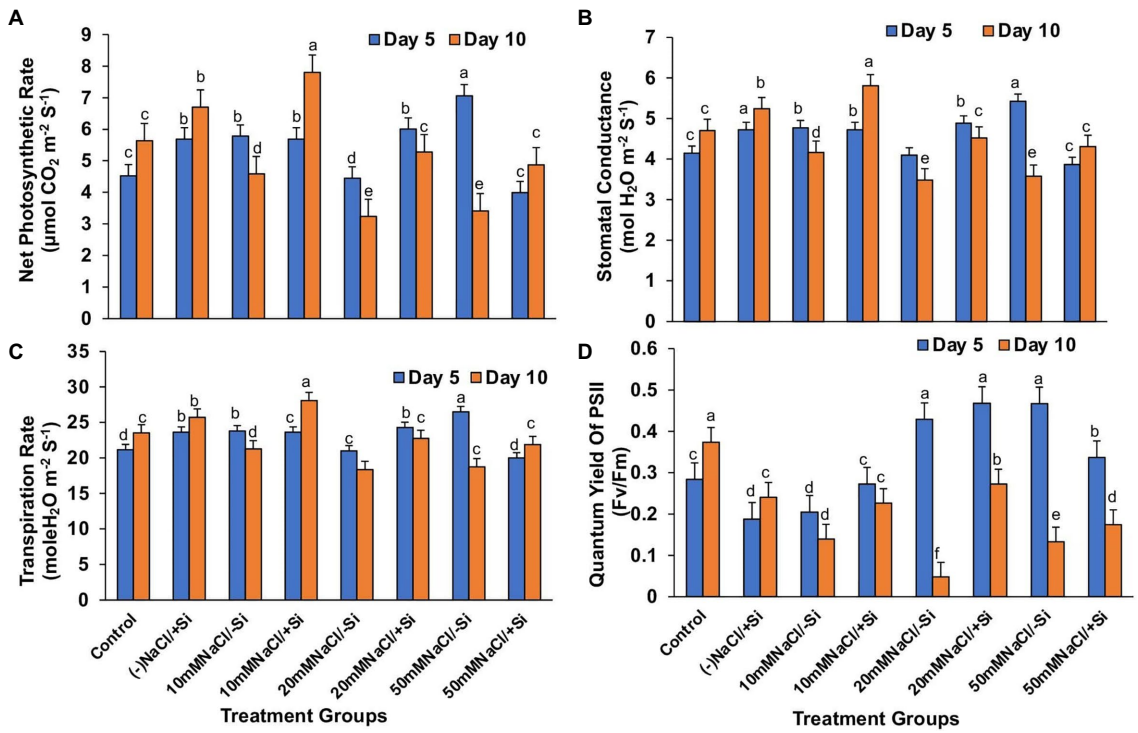


FIGURE 5 | Changes in **(A)** net photosynthesis, **(B)** stomatal conductance, **(C)** transpiration rate, and **(D)** PSII quantum yield of mung bean (*Vigna radiata*) under 5 mM (Si_2) Si supply and salinity stress after eight treatments: (i) control (T1), (ii) −NaCl+Si (5 mM) (T2), (iii) 10 mM NaCl/−Si (T3), (iv) 10 mM NaCl/+Si (5 mM) (T4), (v) 20 mM NaCl/−Si (T5), (vi) 20 mM NaCl/+Si (5 mM) (T6), (vii) 50 mM NaCl/−Si (T7), and (viii) 50 mM NaCl/+Si (5 mM) (5 mM) (T8) for a period of 5 and 10 days. Vertical bars indicate Mean ± SE of the means for $n = 4$. Means denoted by the different letters are significantly different at $p \leq 0.05$ according to the Tukey's studentized range test.

atmospheric nitrogen in root nodules by forming symbiotic relationship with nitrogen-fixing bacteria (Putra et al., 2020). However, it has been reported that the process of root nodulation in *Lotus japonicus* (López et al., 2006) and *Phaseolus vulgaris* (Faghire et al., 2011) was severely affected by salinity stress. Similarly, in our study, we found that the number of root nodules in mung bean was significantly reduced with increasing levels of salinity. In contrast, on Si supplementation, the nodulation has been found to be drastically improved across all the salinity-treated plant groups, in particular with Si_2 supply (**Figures 2A,B**). Our findings are in accordance with Kurdali et al. (2018), who showed that silicon had a more prominent effect on root nodulation during salinity stress in *Sesbania aculeata*. Application of Si to *Glycine max* under stress conditions also increased the nodule numbers when compared to unstressed plants (Steiner et al., 2018). Nelwamondo and Dakora (1999) also reported the beneficial effects of Si supplementation on nodule formation and their function. This increase in nodulation may be attributed to the role of Si in enhancing solute and gas exchange between soil and plant (Putra et al., 2020), structural modulations in nodules by increasing the bacteroids and symbiosomes (Nelwamondo et al., 2001), increased silicification leading to changes in signaling of flavonoids necessary for establishment of symbiosis (Zhang et al., 2013). The results obtained from our study showed that silicon (sodium silicate) particularly 5 mM improved the formation of root nodules in mung bean and depicted that its supplementation can alleviate the negative impact on root nodule formation.

Salinity stress is known for its negative effects on plant growth and performance, where plant biomass remains a crucial indicator for plant stress tolerance (Wei et al., 2017). Our present study suggested that salinity significantly reduced the growth features (root length, shoot length, fresh biomass, and dry biomass) of mung bean, hinting toward inhibition of cell division and inhibition (**Figure 3**). The decrease in biomass was due to increased NaCl uptake, causing ROS formation, consequently disturbing plasma membrane and ionic imbalance, thus, inhibiting metabolic processes and growth (Mittler et al., 2011). However, the plant growth and biomass were improved by the supplementation of Si. From our results, we observed that Si was able to ameliorate the negative effects of salinity stress on growth, in particular when Si_2 was supplemented. These findings are in agreement with previous reports of Si-mediated recovery of plant growth in *Cucumis sativus* (Zhu et al., 2020), *Ocimum basilicum* (Farouk et al., 2020), *Sorghum bicolor* (Yin et al., 2013) under salinity stress. The Si-mediated amelioration could be attributed to maintain the integrity of the plasma membrane by efficient Na^+/K^+ homeostasis, gene expression stimulation, and enhancement of ROS scavenging machinery (Kim et al., 2014; Daoud et al., 2018).

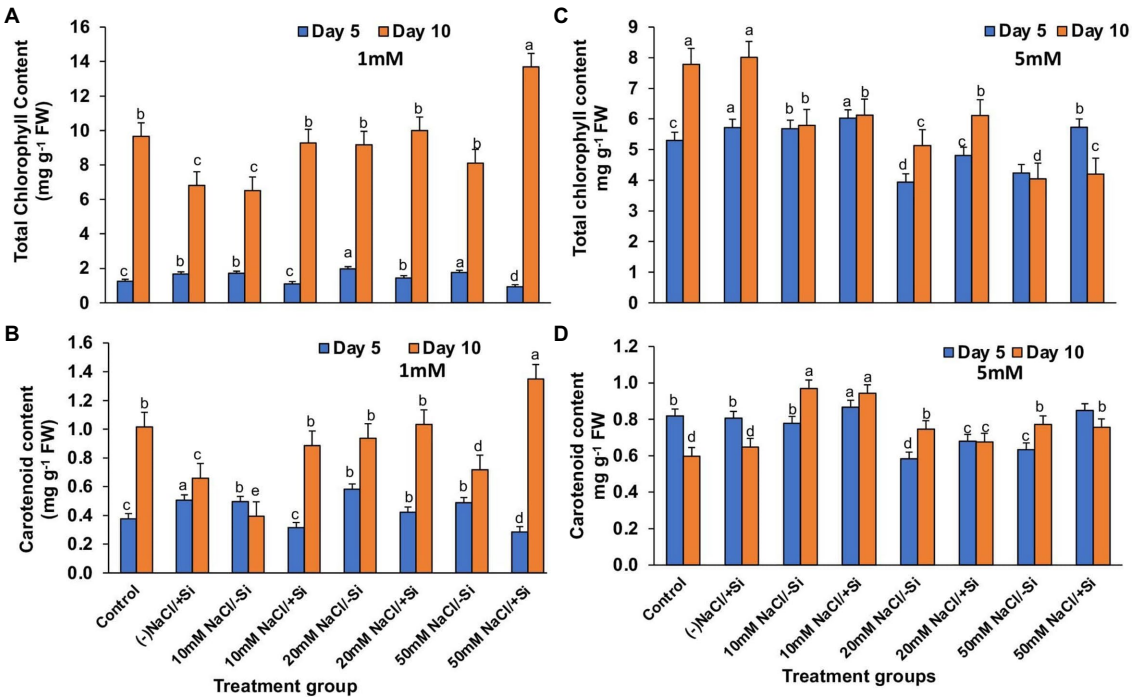


FIGURE 6 | Changes in **(A,C)** total chlorophyll, **(B,D)** carotenoid content of mung bean (*Vigna radiata*) under 1 mM (Si_1) and 5 mM (Si_2) Si supply and salinity stress after eight treatments: (i) control (T1), (ii) –NaCl+Si (1 mM/5 mM) (T2), (iii) 10 mM NaCl/–Si (T3), (iv) 10 mM NaCl/+Si (1 mM/5 mM) (T4), (v) 20 mM NaCl/–Si (T5), (vi) 20 mM NaCl/+Si (1 mM/5 mM) (T6), (vii) 50 mM NaCl/–Si (T7), and (viii) 50 mM NaCl/+Si (1 mM/5 mM) (T8) for a period of 5 and 10 days. Vertical bars indicate Mean ± SE of the means for $n = 4$. Means denoted by the different letters are significantly different at $p \leq 0.05$ according to the Tukey's studentized range test.

Salinity stress affects chlorophyll pigment concentrations, lowering photosynthetic rate and reducing plant development. The loss of membrane integrity and the development of enzymes like chlorophyllase, which is proteolytic in nature, cause chlorophyll degradation under stress conditions, may be responsible for the decrease in chlorophyll content (Sabater and Rodriquez, 1978; Tuna et al., 2007). In our study, the gaseous exchange parameters showed a reduction on exposure to salinity stress (**Figures 4A–D, 5A–D**). Simultaneously, the chlorophyll and carotenoid content were also found to be reduced under salinity stress (**Figures 6A–D**). In our study, supplementation of Si was prudent in improving the chlorophyll and carotenoid pigment, in particular with Si_2, which is in line with reports described on *Cucumis sativus* (Feng et al., 2009), *Zea mays* (Khan et al., 2017), *Lactuca sativa* (Lemos Neto et al., 2020). Si confers protection to chlorophyll due to cell wall deposition of Si resulting in leaf erection leading to higher light interception for photosynthesis (Ma and Yamaji, 2006). The chlorosis and necrosis recorded during salinity stress is stipulated to have reduced the stomatal density, which ultimately affected the stomatal conductance and transpiration rate. However, Si supplementation induced recovery form the detrimental effects on chlorophyll pigment and stomata, leading to the induction of optimal photosynthetic measurements and pigment content. Similarly, Si-mediated improvement of photosynthetic measurements was also reported in *Solanum lycopersicum* (Muneer et al., 2014), *Zinnia elegans* (Manivannan et al., 2015), *Abelmoschus esculentus* (Abbas et al., 2015), which may be attributed to the formation of a double-layered cuticle in leaves that confers mechanical support and maintains photosynthesis in plants (Ma and Yamaji, 2006). The present study also showed a decline in the quantum yield of PSII (F_v/F_m) in mung bean plants during salinity treatments, which is supposedly due to reduction in transfer of energy between antennae and reaction centers (Ghassemi-Golezani and Lotfi, 2015). A reduction in F_v/F_m is an indicator of damage to PSII which affects the photosynthetic rate in turn reducing the plant growth and yield (Rosenqvist and van Kooten 2003). However, Si supplementation was found to be efficient in increasing the F_v/F_m values causing recovery of PSII damage and consequent improvement in chlorophyll fluorescence due to less photoinhibition. The role of Si in maintaining F_v/F_m has also been reported in *Zea Mays* (Khan et al., 2017), *Solanum lycopersicum* (Al-Aghabary et al., 2004), and *Pistacia vera* (Habibi and Hajiboland, 2013). It is hypothesized that the detoxification of ROS mediated by Si leads to an increase in chlorophyll content which leads to the improvement of F_v/F_m (Oukarroum et al., 2015).

The photosynthetic measurements, *viz.* photosynthetic pigments, PSII quantum yield, net photosynthetic rate,

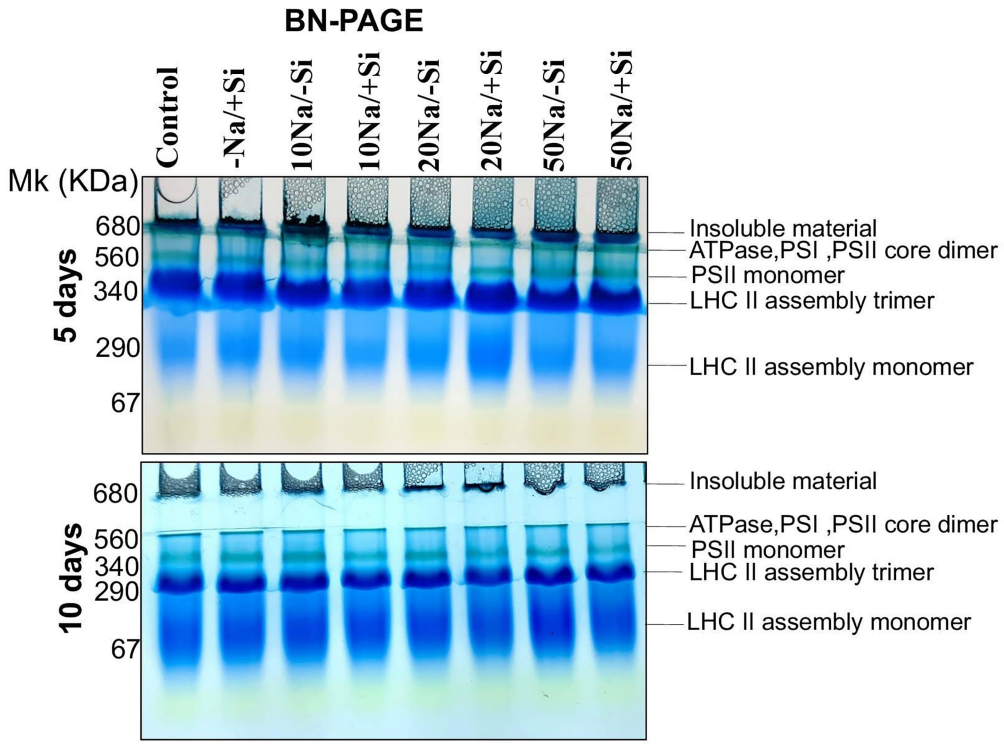


FIGURE 7 | First dimension BN-PAGE of mung bean (*Vigna radiata*) under 5 mM (Si_2) Si supply and salinity stress after eight treatments: (i) control (T1), (ii) –NaCl+Si (5 mM) (T2), (iii) 10 mM NaCl/–Si (T3), (iv) 10 mM NaCl/+Si (5 mM) (T4), (v) 20 mM NaCl/–Si (T5), (vi) 20 mM NaCl/+Si (5 mM) (T6), (vii) 50 mM NaCl/–Si (T7), and (viii) 50 mM NaCl/+Si (5 mM) (T8) for a period of 5 and 10 days. For first dimension BN-PAGE fresh thylakoid membranes were solubilized in 1% BDM at chlorophyll concentration of 1 $\mu g\,\mu l^{-1}$, and the protein sample was separated by 7–12.5% gradient BN-PAGE.

transpiration, and stomatal conductance, showed a varied reduction in mung bean under salinity stress which was mitigated by supplementation of Si. From these results, we also depicted that Si_2 (5 mM sodium silicate) showed more positive effects compared to Si_1 supply (1 mM Si); thus, we selected the plants for expression analysis of photosynthetic proteins treated with (Si_2) 5 mM of silicon (sodium silicate) and salinity stress (**Figure 7**). In our study, we found a reduction in PSI, PSII, monomer and LHC II assembly trimer complex with the exception of LHC-II assembly monomer, under salinity stress. However, supplementation of Si reduced the loss of thylakoid protein complexes. Muneer et al. (2014) reported a similar reduction in thylakoid protein expression in *Solanum lycopersicum* under salinity stress, which was upregulated on Si-supplementation. The damage control of PSI by Si could increase the excitation energy required for NADPH generation from $NADP^+$, thus leading to optimal functioning of the photosystem complexes.

The maintenance of metabolic activities during osmotic adjustments under salinity stress is possible when a good water status is maintained in cells and tissues. In our study, leaf water status (RWC) was found to be affected during salinity stress in mung bean (**Figures 8A,B**). However, application of Si (sodium silicate) was found to restore the RWC in leaves to optimal levels. de Oliveira et al. (2019) also reported that Si (sodium silicate) decreases the water loss by reducing the transpiration rate in Sorghum bicolor. Similarly, Si-mediated osmotic adjustments are touted to be the reason for stress tolerance in *Solanum lycopersicum* (Romero-Aranda et al., 2006), *Sorghum bicolor* (Sonobe et al., 2009), *Zea mays* (Tahir et al., 2012).

During abiotic stress, plants generate and accumulate osmoprotectant as compatible solutes to uphold water for physio-chemical functions in cell (Liang et al., 2018). Proline, a compatible solute, is known to play a crucial role in osmotic adjustments and other protective roles such as protection of protein and membrane structure, scavenging of ROS and cellular homeostasis (Bhaskara et al., 2015). In our study, we found the levels of proline increased with the supplementation of Si to salinity-stressed plants, thus conferring salinity tolerance to mung bean plants (**Figure 9**). Si-mediated proline accumulation under salinity stress has been reported in *Glycyrrhiza uralensis* (Zhang et al., 2017), *Cucumis sativus* (Zhu et al., 2020) and *Phaseolus vulgaris* (Rady et al., 2019). However, whether an increase or decrease in proline accumulation leads to Si-mediated salinity resistance needs further investigation, as the current knowledge is insufficient.

In plants, reactive oxygen species in low concentrations are needed for the regulation of growth, development and

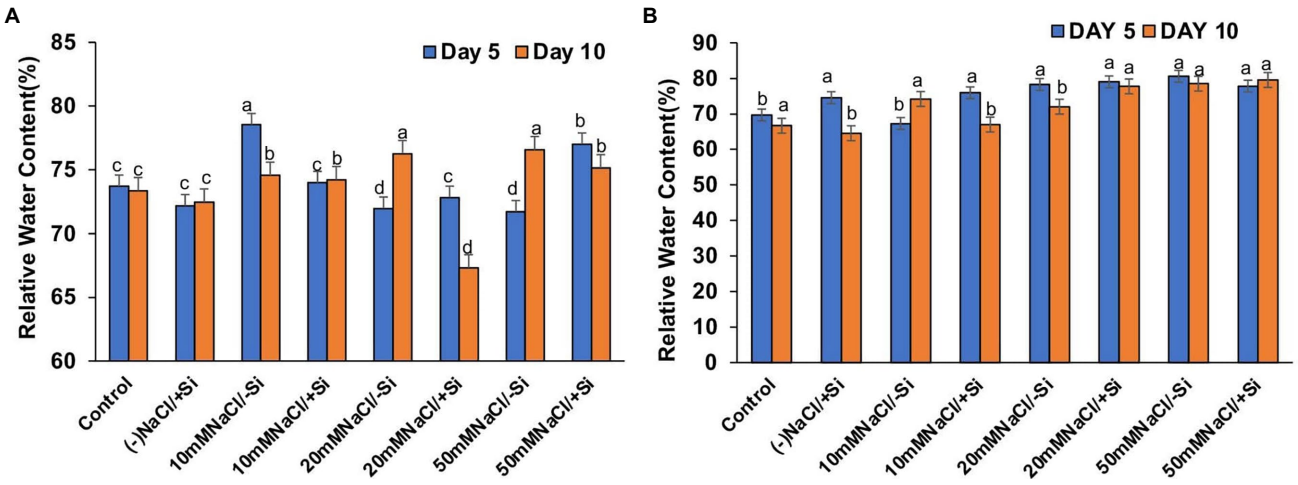


FIGURE 8 | Changes in relative water content of mung bean (*Vigna radiata*) under **(A)** 1 mM (Si_1), **(B)** 5 mM (Si_2) Si supply and salinity stress after eight treatments: (i) control (T1), (ii) −NaCl+Si (1 mM/5 mM) (T2), (iii) 10 mM NaCl/−Si (T3), (iv) 10 mM NaCl/+Si (1 mM/5 mM) (T4), (v) 20 mM NaCl/−Si (T5), (vi) 20 mM NaCl/+Si (1 mM/5 mM) (T6), (vii) 50 mM NaCl/−Si (T7), and (viii) 50 mM NaCl/+Si (1 mM/5 mM) (T8) for a period of 5 and 10 days. Vertical bars indicate Mean ± SE of the means for $n = 4$. Means denoted by the different letters are significantly different at $p \leq 0.05$ according to the Tukey's studentized range test.

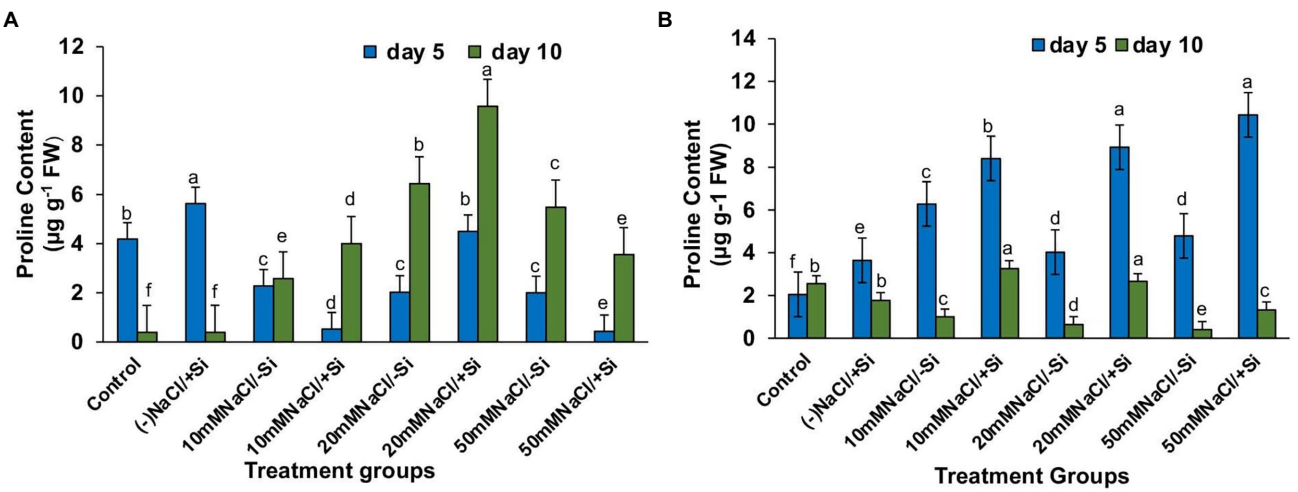


FIGURE 9 | Changes in proline of mung bean (*Vigna radiata*) under **(A)** 1 mM (Si_1), **(B)** 5 mM (Si_2) Si supply and salinity stress after eight treatments: (i) control (T1), (ii) −NaCl+Si (1 mM/5 mM) (T2), (iii) 10 mM NaCl/−Si (T3), (iv) 10 mM NaCl/+Si (1 mM/5 mM) (T4), (v) 20 mM NaCl/−Si (T5), (vi) 20 mM NaCl/+Si (1 mM/5 mM) (T6), (vii) 50 mM NaCl/−Si (T7), and (viii) 50 mM NaCl/+Si (1 mM/5 mM) (T8) for a period of 5 and 10 days. Vertical bars indicate Mean ± SE of the means for $n = 4$. Means denoted by the different letters are significantly different at $p \leq 0.05$ according to the Tukey's studentized range test.

signaling, whereas excessive levels of ROS are synonymous with causing oxidation of membrane lipids, denaturation of proteins, DNA alteration and mutation (Møller et al., 2007; Choudhury et al., 2013). The rate of detoxification is exceeded by the generation of ROS during abiotic stress. Studies have reported that salinity interferes with the process of ROS production and removal, thereby causing more ROS to accumulate, damaging tissue structure and cellular metabolism (Zhu et al., 2015). In our study, salinity stress resulted in an increase in lipid peroxidation (MDA) and electrolyte leakage (**Figures 10A–D**). Solute leakage is thus associated with a change in membrane lipid composition (Lemos Neto et al., 2020). However, Si supplementation reduces lipid peroxidation (MDA) and electrolyte leakage, which is attributed to the minimum membrane damage as compared to that during salinity stress. Salinity stress also resulted in an oxidative burst, which was seen in the form of H_2O_2 and O_2^- significantly localized in the leaves of mung bean

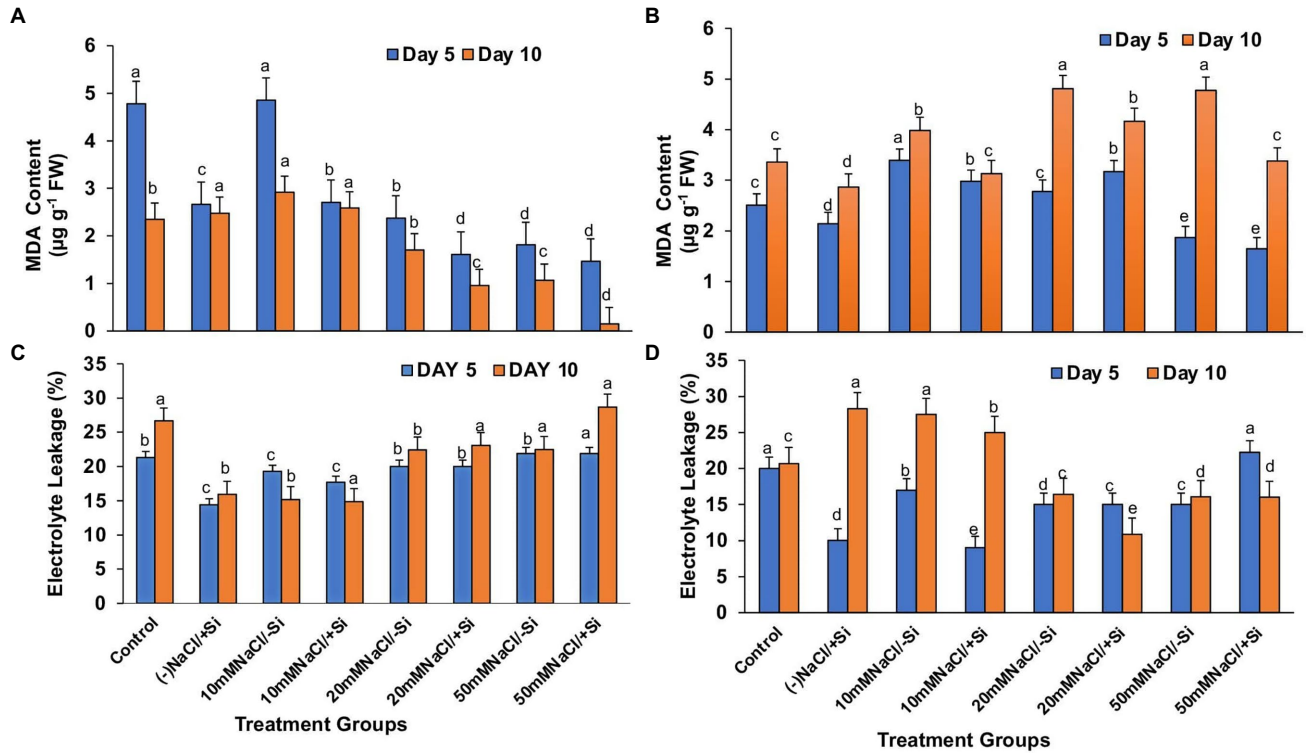


FIGURE 10 | Changes in **(A,B)** malondialdehyde content and **(C,D)** electrolyte leakage of mung bean (*Vigna radiata*) under 1 mM (Si_1) and 5 mM (Si_2) Si supply and salinity stress after eight treatments: (i) control (T1), (ii) −NaCl+Si (1 mM/5 mM) (T2), (iii) 10 mM NaCl/−Si (T3), (iv) 10 mM NaCl/+Si (1 mM/5 mM) (T4), (v) 20 mM NaCl/−Si (T5), (vi) 20 mM NaCl/+Si (1 mM/5 mM) (T6), (vii) 50 mM NaCl/−Si (T7), and (viii) 50 mM NaCl/+Si (1 mM/5 mM) (T8) for a period of 5 and 10 days. Vertical bars indicate Mean ± SE of the means for $n = 4$. Means denoted by the different letters are significantly different at $p \leq 0.05$ according to the Tukey's studentized range test.

during salinity stress (**Figures 11A,B, 12A,B**). However, on supplementation of Si the oxidative stress was significantly mitigated. Previous research on salinity-stressed plants such as *Capsicum annuum* (Manivannan et al., 2016), *Lycopersicon esculentum* (Muneer and Jeong, 2015), *Lactuca sativa* (Lemos Neto et al., 2020), and *Medicago sativa* (Xiong et al., 2018; Meng et al., 2020) supported our findings. The Si-mediated amelioration of oxidative stress may be due to (a) Si transport and its deposition in the epidermis of cells or in the cortex of vascular tissue, leading to hardening of the cell wall, consequently, preventing the plant from external abiotic stresses (Liang et al., 2003), (b) improved cell turgidity and cell wall extension due to Si polymerization, leading to better transpiration and simultaneous opening and closing of stomata, and (c) activation of antioxidant enzymes to scavenge ROS produced by salinity stress (Tripathi et al., 2017).

Salinity stress negatively affects ion homeostasis in plants, which leads to the accumulation of various toxic ions, leading to ion toxicity and consequently affecting plant growth (Sofy et al., 2020). In our study, salinity stress resulted in an increase in the Na^+ concentration and simultaneous decrease in K^+ concentration in mung bean leaves, ultimately affecting the K^+/Na^+ ratio (**Figures 13A,B**). The decrease in K^+ concentration may be attributed to its physicochemical similarity with Na^+, leading to competition between Na^+ and K^+ ions for binding sites, since the uptake of Na^+ from roots is facilitated through non-selective K^+ channels and high affinity K^+ transporters (Azooz et al., 2015; Miranda et al., 2017; Shahzad et al., 2021). However, we found that Si supplementation resulted in a decrease in Na^+ content and increased the K^+ content in mung bean during salinity stress. Reduction of Na^+ and increment of K^+ content by Si supplementation were also reported in *Triticum aestivum* (Gong et al., 2005), *Hordeum vulgare* (Liang et al., 2003), *Cucumis sativus* (Wang et al., 2015), *Lycopersicon esculentum* (Muneer and Jeong, 2015), and *Ocimum basilicum* (Farouk et al., 2020). The reduction of Na^+ content can be attributed to Si deposition in the inner region of the root endodermis, thereby causing obstruction of the apoplastic Na^+ absorption by roots during salinity stress (Liu et al., 2015). Moreover, our findings on silica deposition in leaf epidermis of mung bean under salinity stress and Si-supplementation further supports this phenomenon. The counteractive uptake of K^+ against Na^+ during Si supplementation is due to the activation of plasma membrane H^+-ATPases of the roots (Karmollachaab and Gharineh, 2015).

The incorporation of Si within plant tissues occurs as amorphous hydrated opaline silica ($SiO_2 \times nH_2O$), the process



FIGURE 11 | Histochemical localization of H_2O_2 in mung bean (*Vigna radiata*) under **(A)** 1 mM (Si_1) and **(B)** 5 mM (Si_2) Si supply and salinity stress after eight treatments: (i) control (T1), (ii) −NaCl+Si (1 mM/5 mM) (T2), (iii) 10 mM NaCl/−Si (T3), (iv) 10 mM NaCl/+Si (1 MM/5 mM) (T4), (v) 20 mM NaCl/−Si (T5), (vi) 20 mM NaCl/+Si (1 mM/5 mM) (T6), (vii) 50 mM NaCl/−Si (T7), and (viii) 50 mM NaCl/+Si (1 mM/5 mM) (T8) for a period of 5 and 10 days.



FIGURE 12 | Histochemical localization of O_2^- in mung bean (*Vigna radiata*) under **(A)** 1 mM (Si_1) and **(B)** 5 mM (Si_2) Si supply and salinity stress after eight treatments: (i) control (T1), (ii) −NaCl+Si (1 mM/5 mM) (T2), (iii) 10 mM NaCl/−Si (T3), (iv) 10 mM NaCl/+Si (1 mM/5 mM) (T4), (v) 20 mM NaCl/−Si (T5), (vi) 20 mM NaCl/+Si (1 mM/5 mM) (T6), (vii) 50 mM NaCl/−Si (T7), and (viii) 50 mM NaCl/+Si (1 mM/5 mM) (T8) for a period of 5 and 10 days.

of which is widely termed as silicification (Guerriero et al., 2020). Although numerous researches have been carried out to establish the mitigating role of Si during abiotic and biotic stresses, very few reports have been published on imaging silica deposition in plants, and the ones that have been published are from the early 2000s and 2010s. In our study, imaging silica deposition served as a complementary result to the physiological and biochemical data, as it provided spatial information (**Figure 14A**). We found that silica deposition is more prominent in salinity-treated groups when supplemented with Si. The deposition of silica in leaf improves the leaf rigidity and strength, thereby making the plant more resistant to abiotic stresses in general. Si accumulation varies from species to species with some plants being Si-accumulator and other being Si excluder (Coskun et al., 2018). However, we found significant accumulation of Si in salinity-stressed mung bean which may be due to the deposition of Si on leaf epidermis, indicating that mung bean is a Si accumulator (**Figure 14B**). The enhanced accumulation of Si in plants under salinity stress have also been reported (Tuna et al., 2007; Muneer et al., 2014; Lemos Neto et al., 2020). The uptake of Si from the soil and its subsequent transport to the leaves and further accumulation of Si in leaf epidermis are the key events which facilitate the overall Si-mediated salinity tress tolerance in mung bean. However, these results are not conclusive and more research into Si transporters at molecular level would enable us to understand the status of mung bean as a Si accumulator or not.

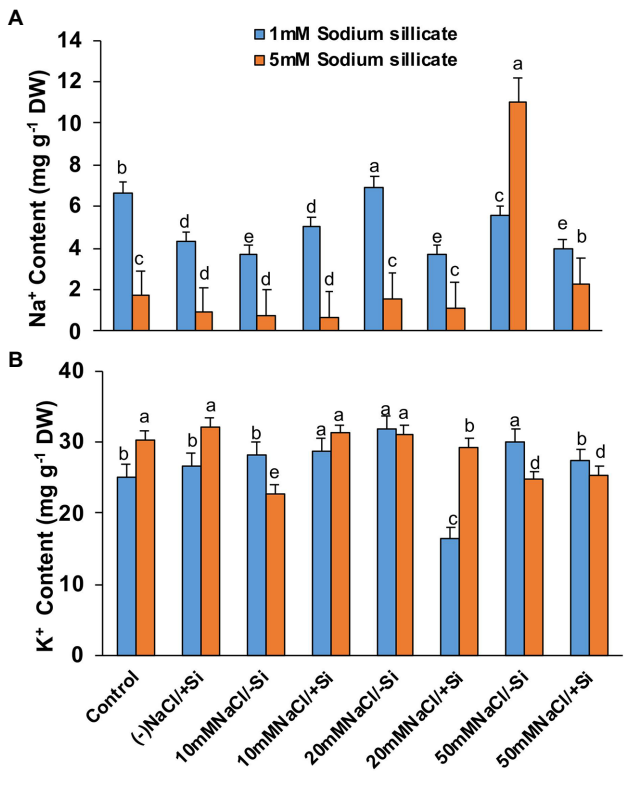


FIGURE 13 | Changes in **(A)** Na^+ content **(B)** K^+ of mung bean (*Vigna radiata*) under 1 mM (Si_1) and 5 mM (Si_2) Si supply and salinity stress after eight treatments: (i) control (T1), (ii) –NaCl+Si (1 mM/5 mM) (T2), (iii) 10 mM NaCl/–Si (T3), (iv) 10 mM NaCl/+Si (1 mM/5 mM) (T4), (v) 20 mM NaCl/–Si (T5), (vi) 20 mM NaCl/+Si (1 mM/5 mM) (T6), (vii) 50 mM NaCl/–Si (T7), and (viii) 50 mM NaCl/+Si (1 mM/5 mM) (T8) for a period of 10 days. Vertical bars indicate Mean ± SE of the means for $n = 4$. Means denoted by the different letters are significantly different at $p \leq 0.05$ according to the Tukey's studentized range test.

CONCLUSION

Pulses are a classic example of the challenge of low returns in a growing market that India's cash crops are experiencing. Modern markets are all about turning crop shortage into abundance. Hence, the world urgently needs an agricultural approach that is both efficient and climate change resistant. Mung bean is one of the most productive leguminous crops, yet abiotic stressors pose a significant threat to its yield. Due to poor soil and irrigation water quality, salinity stress has long been a key stumbling block for this leguminous crop's growth and development. Silicon, on the other hand, is regarded as a quasi-essential element for reducing abiotic stressors such as salt. However, there has been a limited number of researches on leguminous crops under salinity stress, with one in particular being a comparison study. In this work, mung bean was investigated under lower (10 mM), intermediate (20 mM), and higher (50 mM) salinity concentrations with two distinct doses of Si, "Si_1" (1 mM Si) and "Si_2" (5 mM sodium silicate). Our physio-chemical experiments revealed that Si, in particular the Si_2 (5 mM sodium silicate) supply, can alleviate salinity stress in mung-bean. Using Si as a supplement, our simulated studies will be able to boost mung bean output regardless of salinity stress.

DATA AVAILABILITY STATEMENT

The raw data supporting the conclusions of this article will be made available by the authors, without undue reservation.

AUTHOR CONTRIBUTIONS

SM conceptualized, supervised, edited, and finalized the manuscript. MA performed the experiments and wrote the manuscript. All authors contributed to the article and approved the submitted manuscript.

FUNDING

The research was funded by VIT Seed grant (Project no. SG20210182).

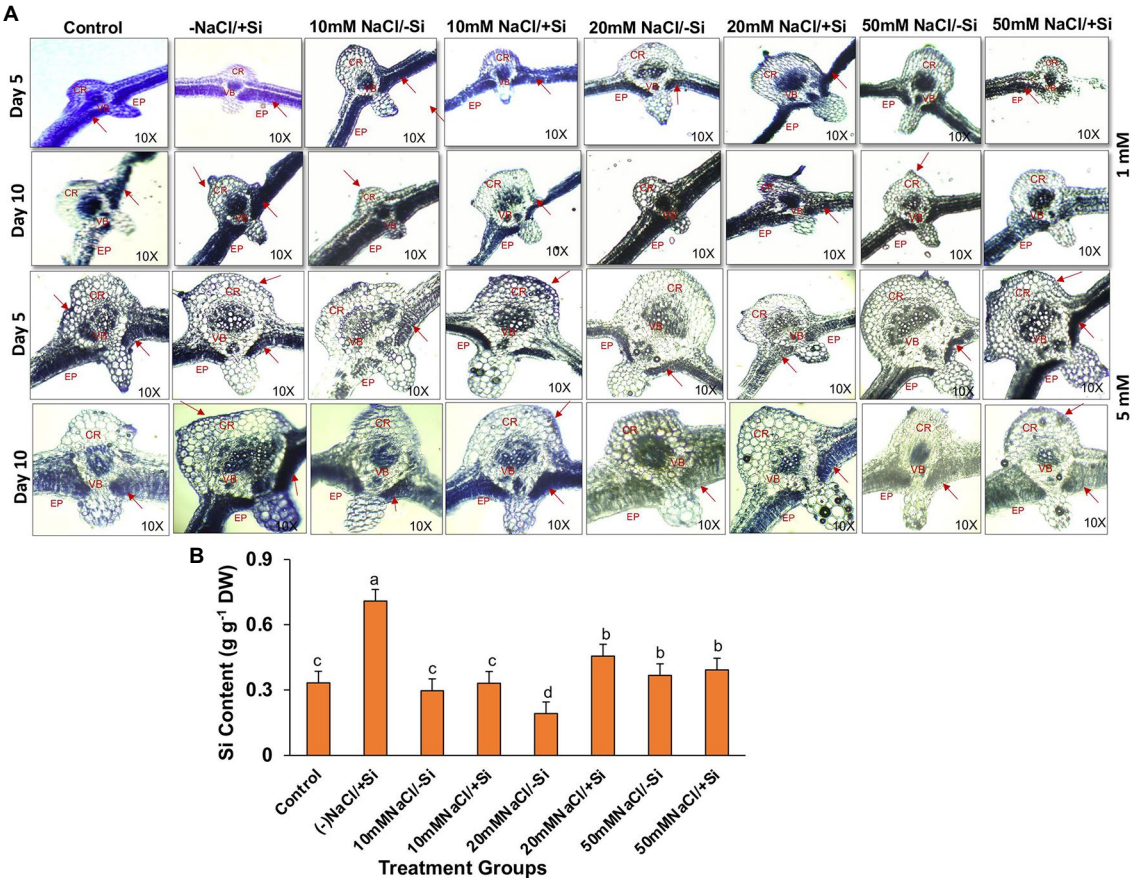


FIGURE 14 | (A) Silica deposition in mung bean (*Vigna radiata*) under 1 mM (Si_1) and 5 mM (Si_2) Si supply and salinity stress after eight treatments: (i) control (T1), (ii) –NaCl+Si (1 mM/5 mM) (T2), (iii) 10 mM NaCl/–Si (T3), (iv) 10 mM NaCl/+Si (1 mM/5 mM) (T4), (v) 20 mM NaCl/–Si (T5), (vi) 20 mM NaCl/+Si (1 mM/5 mM) (T6), (vii) 50 mM NaCl/–Si (T7), and (viii) 50 mM NaCl/+Si (1 mM/5 mM) (T8) for a period of 5 and 10 days. EP indicates epidermis; CR indicates cortex; VB indicates vascular bundles. **(B)** Silicon concentration in mung bean (*Vigna radiata*) under 5 mM (Si_2) Si supply and salinity stress after 10 days of treatment. Vertical bars indicate Mean ± SE of the means for $n = 4$. Means denoted by the different letters are significantly different at $p \leq 0.05$ according to the Tukey's studentized range test.

REFERENCES

Aasim, M., Barpete, S., Usta, A., and Sevinc, C. (2019). An insight into agrobacterium tumafaciens-mediated genetic transformation studies in mung bean (*Vigna radiata* L. Wilczek). *J. Glob. Innov. Agric. Soc. Sci.* 7, 47–51. doi: 10.22194/JGIASS/7.855

Abbas, T., Balal, R. M., Shahid, M. A., Pervez, M. A., Ayyub, C. M., Aqueel, M. A., et al. (2015). Silicon-induced alleviation of NaCl toxicity in okra (*Abelmoschus esculentus*) is associated with enhanced photosynthesis, osmoprotectants and antioxidant metabolism. *Acta Physiol. Plant.* 37, 1–15. doi: 10.1007/s11738-014-1768-5

Abdelaal, K. A. A., Mazrou, Y. S. A., and Hafez, Y. M. (2020). Silicon foliar application mitigates salt stress in sweet pepper plants by enhancing water status, photosynthesis, antioxidant enzyme activity and fruit yield. *Plan. Theory* 9:733. doi: 10.3390/plants9060733

Ahanger, M. A., and Agarwal, R. M. (2017). Salinity stress induced alterations in antioxidant metabolism and nitrogen assimilation in wheat (*Triticum aestivum* L) as influenced by potassium supplementation. *Plant Physiol. Biochem.* 115, 449–460. doi: 10.1016/j.plaphy.2017.04.017

Ahmed, S. (2009). Effect of soil salinity on the yield and yield components of mungbean. *Pak. J. Bot.* 41, 263–268.

Al-Aghabary, K., Zhu, Z., and Shi, Q. (2004). Influence of silicon supply on chlorophyll content, chlorophyll fluorescence and anti-oxidative enzyme activities in tomato plants under salt stress. *J. Plant Nutr.* 27, 2101–2115.

Alzahrani, Y., Kuşvuran, A., Alharby, H. F., Kuşvuran, S., and Rady, M. M. (2018). The defensive role of silicon in wheat against stress conditions induced by drought, salinity or cadmium. *Ecotoxicol. Environ. Saf.* 154, 187–196. doi: 10.1016/j.ecoenv.2018.02.057

Arnon, J. D., and Israelstam, G. F. (1949). Copper enzymes in isolated chloroplast oxidase in *Beta vulgaris*. *Plant Physiol.* 42, 287–292.

Ashraf, M., and Akram, N. A. (2009). Improving salinity tolerance of plants through conventional breading and genetic engineering: an analytical comparison. *Biotechnol. Adv.* 27, 744–752. doi: 10.1016/j.biotechadv.2009.05.026

Azooz, M. M., Metwally, A., and Abou-Elhamd, M. F. (2015). Jasmonate-induced tolerance of Hassawi okra seedlings to salinity in brackish water. *Acta Physiol. Plant.* 37:77. doi: 10.1007/s11738-015-1828-5

Bates, L. S., Waldren, R. P., and Teare, I. D. (1973). Rapid determination of free Proline for water-stress studies. *Plant Soil* 39, 205–207. doi: 10.1007/BF00018060

Bhaskara, G. B., Yang, T., and Verslues, P. E. (2015). Dynamic proline metabolism: importance and regulation in water limited environments. *Front. Plant Sci.* 6:484. doi: 10.3389/fpls.2015.00484

Choudhury, S., Panda, P., Sahoo, L., and Panda, S. K. (2013). Reactive oxygen species signaling in plants under abiotic stress. *Plant Signal. Behav.* 8:e23681. doi: 10.4161/psb.23681

Chung, Y. S., Kim, K. S., Hamayun, M., and Kim, Y. (2019). Silicon confers soybean resistance to salinity stress through regulation of reactive oxygen and reactive nitrogen species. *Front. Plant Sci.* 10:1725. doi: 10.3389/fpls.2019.01725

Coskun, D., Deshmukh, R., Sonah, H., Menzies, J. G., Reynolds, O., Ma, J. F., et al. (2018). The controversies of silicon's role in plant biology. *New Phytol.* 221, 67–85. doi: 10.1111/nph.15343

Daoud, A. M., Hemada, M. M., and Seber, N. (2018). Effect of silicon on the tolerance of wheat (*Triticum aestivum* L.) to salt stress at different growth stages: case study for the management of irrigation water. *Plan. Theory* 04:29. doi: 10.21767/2471-9889-C5-019

Davey, M. W., Stals, E., Panis, B., Keulemans, J., and Swennen, R. L. (2005). High-throughput determination of malondialdehyde in plant tissues. *Anal. Biochem.* 347, 201–207. doi: 10.1016/j.ab.2005.09.041

de Oliveira, R. L. L., de Mello Prado, R., Felisberto, G., and Cruz, F. J. R. (2019). Different sources of silicon by foliar spraying on the growth and gas exchange in sorghum. *J. Soil Sci. Plant Nutr.* 19, 948–953. doi: 10.1007/s42729-019-00092-1

Dutta, P., and Bera, A. K. (2014). Effect of NaCl salinity on seed germination and seedling growth of mungbean cultivars. *Legum. Res.* 37, 161–164. doi: 10.5958/j.0976-0571.37.2.024

Etesami, H., and Jeong, B. R. (2018). Silicon (Si): review and future prospects on the action mechanisms in alleviating biotic and abiotic stresses in plants. *Ecotoxicol. Environ. Saf.* 147, 881–896. doi: 10.1016/j.ecoenv.2017.09.063

Faghire, M., Bargaz, A., Farissi, M., Palma, F., Mandri, B., Lluch, C., et al. (2011). Effect of salinity on nodulation, nitrogen fixation and growth of comMon bean (*Phaseolus vulgaris*) inoculated with rhizobial strains isolated from the Haouz region of Morocco. *Symbiosis* 55, 69–75. doi: 10.1007/s13199-011-0144-0

Farouk, S., Elhindi, K. M., and Alotaibi, M. A. (2020). Silicon supplementation mitigates salinity stress on *Ocimum basilicum* L. via improving water balance, ion homeostasis, and antioxidant defense system. *Ecotoxicol. Environ. Saf.* 206:111396. doi: 10.1016/j.ecoenv.2020.111396

Feng, J., Shi, Q., Wang, X., Wei, M., Yang, F., and Xu, H. (2009). Silicon supplementation ameliorated the inhibition of photosynthesis and nitrate metabolism by cadmium (Cd) toxicity in *Cucumis sativus* L. *Sci. Hortic.* 123, 521–530. doi: 10.1016/j.scienta.2009.10.013

Flam-Shepherd, R., Huynh, W. Q., Coskun, D., Hamam, A. M., Britto, D. T., and Kronzucker, H. J. (2018). Membrane fluxes, bypass flows, and sodium stress in rice: the influence of silicon. *J. Exp. Bot.* 69, 1679–1692. doi: 10.1093/jxb/erx460

Fuller, D. Q. (2007). Contrasting patterns in crop domestication and domestication rates: recent archaeobotanical insights from the old world. *Ann. Bot.* 100, 903–924. doi: 10.1093/aob/mcm048

Gao, D., Cai, K., Chen, J., Luo, S., Zeng, R., Yang, J., et al. (2011). Silicon enhances photochemical efficiency and adjusts mineral nutrient absorption in *Magnaporthe oryzae* infected rice plants. *Acta Physiol. Plant.* 33, 675–682. doi: 10.1007/s11738-010-0588-5

Ghassemi-Golezani, K., and Lotfi, R. (2015). The impact of salicylic acid and silicon on chlorophyll a fluorescence in mung bean under salt stress. *Russ. J. Plant Physiol.* 62, 611–616. doi: 10.1134/S1021443715040081

Gong, H., Zhu, X., Chen, K., Wang, S., and Zhang, C. (2005). Silicon alleviates oxidative damage of wheat plants in pots under drought. *Plant Sci.* 169, 313–321. doi: 10.1016/j.plantsci.2005.02.023

Guerriero, G., Stokes, I., Valle, N., Hausman, J.-F., and Exley, C. (2020). Visualising silicon in plants: histochemistry, silica sculptures and elemental imaging. *Cells* 9:1066. doi: 10.3390/cells9041066

Gupta, B., and Huang, B. (2014). Mechanism of salinity tolerance in plants: physiological, biochemical and molecular characterization. *Int. J. Genom.* 2014:701596. doi: 10.1155/2014/701596

Gururani, M. A., Venkatesh, J., and Tran, L. S. P. (2015). Regulation of photosynthesis during abiotic stress-induced photoinhibition. *Mol. Plant* 8, 1304–1320. doi: 10.1016/j.molp.2015.05.005

Habibi, G., and Hajiboland, R. (2013). Alleviation of drought stress by silicon supplementation in pistachio (*Pistacia vera* L.) plants. *Folia Hortic.* 25, 21–29. doi: 10.2478/fhort-2013-0003

Heath, R. L., and Packer, L. (1968). Photoperoxidation in isolated chloroplast I. Kinetics and stoichiometry of fatty acid peroxidation. *Arch. Biochem. Biophys.* 125, 189–198. doi: 10.1016/0003-9861(68)90654-1

Hiscox, J. D., and Israelstam, G. F. (1979). A method for the extraction of chlorophyll from leaf tissue without maceration. *Can. J. Bot.* 57, 1332–1334. doi: 10.1139/b80-044

Hoffmann, J., Berni, R., Hausman, J. F., and Guerriero, G. (2020). A review on the beneficial role of silicon against salinity in non-accumulator crops: tomato as a model. *Biomol. Ther.* 10:1284. doi: 10.3390/biom10091284

Islam, F., Yasmeen, T., Arif, M. S., Ali, S., Ali, B., Hameed, S., et al. (2016). Plant growth promoting bacteria confer salt tolerance in *Vigna radiata* by up-regulating antioxidant defense and biological soil fertility. *Plant Growth Regul.* 80, 23–36. doi: 10.1007/s10725-015-0142-y

Javaid, T., Farooq, M. A., Akhtar, J., Saqib, Z. A., and Anwar-ul-Haq, M. (2019). Silicon nutrition improves growth of salt-stressed wheat by modulating flows and partitioning of Na^+, Cl^- and mineral ions. *Plant Physiol. Biochem.* 141, 291–299. doi: 10.1016/j.plaphy.2019.06.010

Karmollachaab, A., and Gharineh, M. H. (2015). Effect of silicon application on wheat seedlings growth under water-deficit stress induced by polyethylene glycol. *Iran Agric. Res.* 34, 31–38. doi: 10.22099/IAR.2015.3040

Khan, W. D., Aziz, T., Hussain, I., Ramzani, P. M. A., and Reichenauer, T. G. (2017). Silicon: a beneficial nutrient for maize crop to enhance photochemical efficiency of photosystem II under salt stress. *Arch. Agron. Soil Sci.* 63, 599–611. doi: 10.1080/03650340.2016.1233322

Khattak, G. S. S., Saeed, I., and Shah, S. A. (2008). Breeding high yielding and disease resistant mung bean (*Vigna radiata* (L.) Wilczek) genotypes. *Pak. J. Bot.* 40, 1411–1417.

Kim, Y. H., Khan, A. L., Waqas, M., Shim, J. K., Kim, D. H., Lee, K. Y., et al. (2014). Silicon application to rice root zone influenced the photo hormonal and antioxidant responses under salinity stress. *J. Plant Growth Regul.* 33, 137–149. doi: 10.1007/s00344-013-9356-2

Koyro, H. W. (2006). Effect of salinity on growth, photosynthesis, water relations and solute composition of the potential cash crop halophyte *Plantago coronopus* (L.). *Environ. Exp. Bot.* 56, 136–146. doi: 10.1016/j.envexpbot.2005.02.001

Kurdali, F., Al-ChamMaa, M., and Al-Ain, F. (2018). Growth and N_2-fixation in saline and/or water stressed *Sesbania aculeata* plants in response to silicon application. *SILICON* 11, 781–788. doi: 10.1007/s12633-018-9884-2

Lemos Neto, H. S., de Almeida Guimarães, M., Mesquita, R. O., Edelky Sousa Freitas, W., de Oliveira, A. B., da Silva Dias, N., et al. (2020). Silicon supplementation induces physiological and biochemical changes that assist lettuce salinity tolerance. *SILICON* 13, 4075–4089. doi: 10.1007/s12633-020-00715-8

Liang, Y., Chen, Q., Liu, Q., Zhang, W., and Ding, R. (2003). Exogenous silicon (Si) increases antioxidant enzyme activity and reduces lipid peroxidation in roots of salt-stressed barley (*Hordeum vulgare* L.). *J. Plant Physiol.* 160, 1157–1164. doi: 10.1078/0176-1617-01065

Liang, W., Ma, X., Wan, P., and Liu, L. (2018). Plant salt-tolerance mechanism: a review. *Biochem. Biophys. Res. Commun.* 495, 286–291. doi: 10.1016/j.bbrc.2017.11.043

Liu, P., Yin, L., Wang, S., Zhang, M., Deng, X., Zhang, S., et al. (2015). Enhanced root hydraulic conductance by aquaporin regulation accounts for silicon alleviated salt-induced osmotic stress in *Sorghum bicolor* L. *Environ. Exp. Bot.* 111, 42–51. doi: 10.1016/j.envexpbot.2014.10.006

López, M., Herrera-Cervera, J. A., Lluch, C., and Tejera, N. A. (2006). Trehalose metabolism in root nodules of the model legume *Lotus japonicus* in response to salt stress. *Physiol. Plant.* 128, 701–709. doi: 10.1111/j.1399-3054.2006.00802.x

Lutts, S., Kinet, J. M., and Bouharmont, J. (1996). NaCl-induced senescence in leaves of Rice (*Oryza sativa* L.) cultivars differing in salinity resistance. *Ann. Bot.* 78, 389–398. doi: 10.1006/anbo.1996.0134

Ma, J. F., Tamai, K., Yamaji, N., Mitani, N., Konishi, S., Katsuhara, M., et al. (2006). A silicon transporter in rice. *Nature* 440, 688–691. doi: 10.1038/nature04590

Ma, J. F., and Yamaji, N. (2006). Silicon uptake and accumulation in higher plants. *Trends Plant Sci.* 11, 392–397. doi: 10.1016/j.tplants.2006.06.007

Manivannan, A., Soundararajan, P., Arrum, L. S., Ko, C. H., Muneer, S., and Jeong, B. R. (2015). Silicon-mediated enhancement of physiological and biochemical characteristics of *Zinnia elegans* 'dreamland yellow' green under salinity stress. *Hortic. Environ. Biotechnol.* 56, 721–731. doi: 10.1007/s13580-015-1081-2

Manivannan, A., Soundararajan, P., Muneer, S., Ko, C. H., and Jeong, B. R. (2016). Silicon mitigates salinity stress by regulating the physiology, antioxidant enzyme activities, and protein expression in *Capsicum annuu*m 'Bugwang'. *Biomed. Res. Int.* 2016:3076357. doi: 10.1155/2016/3076357

Meng, Y., Yin, Q., Yan, Z., Wang, Y., Niu, J., Zhang, J., et al. (2020). Exogenous silicon enhanced salt resistance by maintaining K^+/Na^+ homeostasis and antioxidant performance in alfalfa leaves. *Front. Plant Sci.* 11:1183. doi: 10.3389/fpls.2020.01183

Miranda, R. S., Mesquita, R. O., Costa, J. H., Alvarez-Pizarro, J. C., Prisco, J. T., and Gomes-Filho, E. (2017). Integrative control between proton pumps and SOS1 antiporters in roots is crucial for maintaining low Na^+ accumulation and salt tolerance in amMonium supplied Sorghum bicolor. *Plant Cell Physiol.* 58, 522–536. doi: 10.1093/pcp/pcw231

Mittler, R., Vanderauwera, S., Suzuki, N., Miller, G., Tognetti, V. B., Vandepoele, K., et al. (2011). ROS signaling: the new wave? *Trends Plant Sci.* 16, 300–309. doi: 10.1016/j.tplants.2011.03.007

Møller, I. M., Jensen, P. E., and Hansson, A. (2007). Oxidative modifications to cellular components in plants. *Annu. Rev. Plant Biol.* 58, 459–481. doi: 10.1146/annurev.arplant.58.032806.103946

Muneer, S., and Jeong, B. R. (2015). Proteomic analysis of salt-stress responsive proteins in roots of tomato (*Lycopersicon esculentum* L.) plants towards silicon efficiency. *Plant Growth Regul.* 77, 133–146. doi: 10.1007/s10725-015-0045-y

Muneer, S., Lee, B. R., Bae, D. W., and Kim, T. H. (2013). Changes in expression of proteins involved in alleviation of Fe-deficiency by sulfur nutrition in *Brassica napus L. Acta Physiol. Plant.* 35, 3037–3045. doi: 10.1007/s11738-013-1336-4

Muneer, S., Park, Y. G., Manivannan, A., Soundararajan, P., and Jeong, B. R. (2014). Physiological and proteomic analysis in chloroplasts of *Solanum lycopersicum* L. under silicon efficiency and salinity stress. International journal of molecular. *Science* 15, 21803–21824. doi: 10.3390/ijms151221803

Munns, R., Day, D. A., Fricke, W., Watt, M., Arsova, B., Barkla, B. J., et al. (2020). Energy costs of salt tolerance in crop plants. *New Phytol.* 225, 1072–1090. doi: 10.1111/nph.15864

Munns, R., and Tester, M. (2008). Mechanisms of salinity tolerance. *Annu. Rev. Plant Biol.* 59, 651–681. doi: 10.1146/annurev.arplant.59.032607.092911

Naher, N., and Alam, A. K. (2010). Germination, growth and nodulation of mungbean (*Vigna radiata* L.) as affected by sodium chloride. *Int. J. Sustain. Crop Prod.* 5, 8–11.

Nelwamondo, A., and Dakora, F. D. (1999). Silicon promotes nodule formation and nodule function in symbiotic cowpea (*Vigna unguiculata*). *New Phytol.* 142, 463–467. doi: 10.1046/j.1469-8137.1999.00409.x

Nelwamondo, A., Jaffer, M. A., and Dakora, F. D. (2001). Subcellular organization of N_2-fixing nodules of cowpea (*Vigna unguiculata*) supplied with silicon. *Protoplasma* 216, 94–100. doi: 10.1007/BF02680136

Nishiyama, Y., and Murata, N. (2014). Revised scheme for the mechanism of photoinhibition and its application to enhance the abiotic stress tolerance of the photosynthetic machinery. *Appl. Microbiol. Biotechnol.* 98, 8777–8796. doi: 10.1007/s00253-014-6020-0

Oukarroum, A., Bussotti, F., Goltsev, V., and Kalaji, H. M. (2015). Correlation between reactive oxygen species production and photochemistry of photosystems I and II in *Lemna gibba* L. plants under salt stress. *Environ. Exp. Bot.* 109, 80–88. doi: 10.1016/j.envexpbot.2014.08.005

Putra, R., Powell, J. R., Hartley, S. E., and Johnson, S. N. (2020). Is it time to include legumes in plant silicon research? *Funct Ecol.* doi: 10.1111/1365-2435.13565

Putra, R., Vandegeer, R. K., Karan, S., Powell, J. R., Hartley, S. E., and Johnson, S. N. (2021). Silicon enrichment alters functional traits in legumes depending on plant genotype and symbiosis with nitrogen-fxing bacteria. *Funct Ecol.* 35, 2856–2869. doi: 10.1111/1365-2435.13912

Rady, M. M., Kuşvuran, A., Alharby, H. F., Alzahrani, Y., and Kuşvuran, S. (2019). Pretreatment with proline or an organic bio-stimulant induces salt tolerance in wheat plants by improving antioxidant redox state and enzymatic activities and reducing the oxidative stress. *J. Plant Growth Regul.* 38, 449–462. doi: 10.1007/s00344-018-9860-5

Romero-Aranda, M. R., Jurado, O., and Cuartero, J. (2006). Silicon alleviates the deleterious salt effect on tomato plant growth by improving plant water status. *J. Plant Physiol.* 163, 847–855. doi: 10.1016/j.jplph.2005.05.010

Rosenqvist, E., and van Kooten, O. (2003). "Chlorophyll Fluorescence: A general description and nomenclature," in *Practical Applications of Chlorophyll Fluorescence in Plant Biology*. eds. J. R. DeEll and P. M. A. Toivonen (Kluwer: Academic Publishers), 31–37.

Sabater, B., and Rodriquez, M. I. (1978). Control of chlorophyll degradation in detached leaves of barley and oat through effect of kinetin on chlorophyllase levels. *Physiol. Plant.* 43, 274–276. doi: 10.1111/j.1399-3054.1978.tb02577.x

Saha, P., Chatterjee, P., and Biswas, A. K. (2010). NaCl pretreatment alleviates salt stress by enhancement of antioxidant defense and osmolyte accumulation in mungbean (*Vigna radiata* L. Wilczek). *Indian J. Exp. Biol.* 48, 593–600. PMID: 20882762

Sairam, R. K., Rao, K. V., and Srivastava, G. C. (2002). Differential response of wheat genotypes to long term salinity stress in relation to oxidative stress, antioxidant activity and osmolyte concentration. *Plant Sci.* 163, 1037–1046. doi: 10.1016/S0168-9452(02)00278-9

Sehrawat, N., Bhat, K. V., Sairam, R. K., and Jaiwal, P. K. (2013). Identification of salt resistant wild relatives of mungbean (*Vigna radiata* (L.) Wilczek). *Asian J. Plant Sci. Res.* 3, 41–49.

Sehrawat, N., Yadav, M., Bhat, K. V., Sairam, R. K., and Jaiwal, P. K. (2014). Evaluation of mungbean genotypes for salt tolerance at early seedling growth stage. *Biocatal. Agric. Biotechnol.* 3, 108–113. doi: 10.1016/j.bcab.2014.07.009

Sehrawat, N., Yadav, M., Bhat, K. V., Sairam, R. K., and Jaiwal, P. K. (2015). Effect of salinity stress on mungbean [*Vigna radiata* (L.) wilczek] during consecutive sumMer and spring seasons. *J. Agric. Sci. Serbia* 60, 23–32. doi: 10.2298/JAS1501023S

Sehrawat, N., Yadav, M., Sharma, A. K., Kumar, V., and Bhat, K. V. (2018). Salt stress and mung bean [*Vigna radiata* (L.) Wilczek]: effects, physiological perspective and management practices for alleviating salinity. *Arch. Agron. Soil Sci.* 65, 1287–1301. doi: 10.1080/03650340.2018.1562548

Shahzad, B., Rehman, A., and Tanveer, M. (2021). Salt stress in brassica: effects, tolerance mechanisms, and management. *J. Plant Growth Regul.* 41, 781–795. doi: 10.1007/s00344-021-10338-x

Shi, Y., Wang, Y., Flowers, T. J., and Gong, H. (2013). Silicon decreases chloride transport in rice (*Oryza sativa* L.) in saline conditions. *J. Plant Physiol.* 170, 847–853. doi: 10.1016/j.jplph.2013.01.018

Sofy, M. R., Elhindi, K. M., Farouk, S., and Alotaibi, M. A. (2020). Zinc and paclobutrazol mediated regulation of growth, upregulating antioxidant aptitude and plant productivity of pea plants under salinity. *Plants* 9:1197. doi: 10.3390/plants9091197

Sonobe, K., Hattori, T., An, P., Tsuji, W., Eneji, E., Tanaka, K., et al. (2009). Diurnal variations in photosynthesis, stomatal conductance and leaf water relation in sorghum grown with or without silicon under water stress. *J. Plant Nutr.* 32, 433–442. doi: 10.1080/01904160802660743

Sprent, J. I., and Gehlot, H. S. (2010). Nodulated legumes in arid and semi-arid environments: are they important? *Plant Ecol. Divers.* 3, 211–219. doi: 10.1080/17550874.2010.538740

Steiner, F., Zuffo, A. M., Bush, A., and Santos, D. M. D. S. (2018). Silicate fertilization potentiates the nodule formation and symbiotic nitrogen fixation in soybean. *Pesqui. Agropecu. Trop.* 48, 212–221. doi: 10.1590/1983-40632018v4851472

Swaraj, K., and Bishnoi, N. R. (1999). Effect of salt stress on nodulation and nitrogen fixation in legumes. *Indian J. Exp. Biol.* 37, 843–848. PMID: 10687277

Tahir, M. A., Aziz, T., Farooq, M., and Sarwar, G. (2012). Silicon-induced changes in growth, ionic composition, water relations, chlorophyll contents and membrane permeability in two salt-stressed wheat genotypes. *Arch. Agron. Soil Sci.* 58, 247–256. doi: 10.1080/03650340.2010.518959

Tanveer, M. (2020). Tissue-specific reactive oxygen species signalling and ionic homeostasis in *Chenopodium quinoa* and *Spinacia oleracea* in the context of salinity stress tolerance. doctoral dissertation. University of Tasmania.

Tokarz, K. M., Wesołowski, W., Tokarz, B., Makowski, W., Wysocka, A., Jędrzejczyk, R. J., et al. (2021). Stem photosynthesis—A key element of grass pea (*Lathyrus sativus* L.) acclimatisation to salinity. *Int. J. Mol. Sci.* 22:685. doi: 10.3390/ijms22020685

Tripathi, D. K., Singh, S., Singh, V. P., Prasad, S. M., Dubey, N. K., and Chauhan, D. K. (2017). Silicon nanoparticles more effectively alleviated UV-B stress than silicon in wheat (*Triticum aestivum*) seedlings. *Plant Physiol. Biochem.* 110, 70–81. doi: 10.1016/j.plaphy.2016.06.026

Tuna, A. L., Kaya, C., Ashraf, M., Altunlu, H., Yokas, I., and Yagmur, B. (2007). The effects of calcium sulphate on growth, membrane stability and nutrient uptake of tomato plants grown under salt stress. *Environ. Exp. Bot.* 59, 173–178. doi: 10.1016/j.envexpbot.2005.12.007

Turner, N. C., and Kramer, P. J. (1980). *Adaptation of Plant to Water and High Temperature Stress*. New York, NY, USA: Wiley Interscience Pub, 207–230.

Wang, S., Liu, P., Chen, D., Yin, L., Li, H., and Deng, X. (2015). Silicon enhanced salt tolerance by improving the root water uptake and decreasing the ion toxicity in cucumber. *Front. Plant Sci.* 6:759. doi: 10.3389/fpls.2015.00759

Wei, L. X., Lv, B. S., Li, X. W., Wang, M. M., Ma, H. Y., Yang, H. Y., et al. (2017). Priming of rice (*Oryza sativa* L.) seedlings with abscisic acid enhances

seedling survival, plant growth, and grain yield in saline-alkaline paddy fields. *Field Crop Res.* 203, 86–93. doi: 10.1016/j.fcr.2016.12.024

World Vegetable Centre, (2018). Shanhua, Tainan, Taiwan 74151. Available at: avrdc.org

Xiong, X., Liu, N., Wei, Y., Bi, Y., Luo, J., Xu, R., et al. (2018). Effects of non-uniform root zone salinity on growth, ion regulation, and antioxidant defense system in two alfalfa cultivars. *Plant Physiol. Biochem.* 132, 434–444. doi: 10.1016/j.plaphy.2018.09.028

Yang, L., Tian, D., Todd, C. D., Luo, Y., and Hu, X. (2013). Comparative proteome analyses reveal that nitric oxide is an important signal molecule in the response of rice to aluminium toxicity. *J. Proteome Res.* 12, 1316–1330. doi: 10.1021/pr300971n

Yin, J., Jia, J., Lian, Z., Hu, Y., Guo, J., Huo, H., et al. (2019). Silicon enhances the salt tolerance of cucumber through increasing polyamine accumulation and decreasing oxidative damage. *Ecotoxicol. Environ. Saf.* 169, 8–17. doi: 10.1016/j.ecoenv.2018.10.105

Yin, L., Wang, S., Li, J., Tanaka, K., and Oka, M. (2013). Application of silicon improves salt tolerance through ameliorating osmotic and ionic stresses in the seedling of *Sorghum bicolor*. *Acta Physiol. Plant.* 35, 3099–3107. doi: 10.1007/s11738-013-1343-5

Yokoyama, R., Kido, N., Yamamoto, T., Furukawa, J., Iwai, H., Satoh, S., et al. (2015). Histochemical staining of silica body in rice leaf blades. *Bio Protocol.* 5:e1609. doi: 10.21769/BioProtoc.1609

Zhang, G., Cui, Y., Ding, X., and Dai, Q. (2013). Stimulation of phenolic metabolism by silicon contributes to rice resistance to sheath blight. *J. Plant Nutr. Soil Sci.* 176, 118–124. doi: 10.1002/jpln.201200008

Zhang, W., Xie, Z., Wang, L., Li, M., Lang, D., and Zhang, X. (2017). Silicon alleviates salt and drought stress of *Glycyrrhiza uralensis* seedling by altering antioxidant metabolism and osmotic adjustment. *J. Plant Res.* 130, 611–624. doi: 10.1007/s10265-017-0927-3

Zhao, F., Song, C. P., He, J., and Zhu, H. (2007). Polyamines improve K^+/Na^+ homeostasis in barley seedlings by regulating root ion channel activities. *Plant Physiol.* 145, 1061–1072. doi: 10.1104/pp.107.105882

Zhu, Y., and Gong, H. (2014). Beneficial effects of silicon on salt and drought tolerance in plants. *Agron. Sustain. Dev.* 34, 455–472. doi: 10.1007/s13593-013-0194-1

Zhu, Y., Gong, H., and Yin, J. (2019). Role of silicon in mediating salt tolerance in plants: a review. *Plan. Theory* 8, 147–168. doi: 10.3390/plants8060147

Zhu, Y., Jiang, X., Zhang, J., He, Y., Zhu, X., Zhou, X., et al. (2020). Silicon confers cucumber resistance to salinity stress through regulation of proline and cytokinins. *Plant Physiol. Biochem.* 156, 209–220. doi: 10.1016/j.plaphy.2020.09.014

Zhu, Z. J., Wei, G. Q., Li, J., Qian, Q. Q., and Yu, J. Q. (2004). Silicon alleviates salt stress and increases antioxidant enzymes activity in leaves of salt-stressed cucumber (*Cucumis sativus* L.). *Plant Sci.* 167, 527–533. doi: 10.1016/j.plantsci.2004.04.020

Zhu, Y. X., Xu, X. B., Hu, Y. H., Han, W. H., Yin, J. L., Li, H. L., et al. (2015). Silicon improves salt tolerance by increasing root water uptake in *Cucumis sativus* L. *Plant Cell Rep.* 34, 1629–1646. doi: 10.1007/s00299-015-1814-1819

Conflict of Interest: The authors declare that the research was conducted in the absence of any commercial or financial relationships that could be construed as a potential conflict of interest.

Publisher's Note: All claims expressed in this article are solely those of the authors and do not necessarily represent those of their affiliated organizations, or those of the publisher, the editors and the reviewers. Any product that may be evaluated in this article, or claim that may be made by its manufacturer, is not guaranteed or endorsed by the publisher.

Copyright © 2022 Al Murad and Muneer. This is an open-access article distributed under the terms of the Creative Commons Attribution License (CC BY). The use, distribution or reproduction in other forums is permitted, provided the original author(s) and the copyright owner(s) are credited and that the original publication in this journal is cited, in accordance with accepted academic practice. No use, distribution or reproduction is permitted which does not comply with these terms.

frontiers | Frontiers in Plant Science

ORIGINAL RESEARCH
published: 19 May 2022
doi: 10.3389/fpls.2022.836063

Expression of Potato *StDRO1* in Arabidopsis Alters Root Architecture and Drought Tolerance

*Chao Sun[1], Wenjun Liang[1], Kan Yan[2], Derong Xu[1], Tianyuan Qin[1], Sajid Fiaz[3], Philip Kear[4], Zhenzhen Bi[1], Yuhui Liu[1], Zhen Liu[1], Junlian Zhang[1] and Jiangping Bai[1]**

[1] Gansu Provincial Key Laboratory of Arid Land Crop Science, College of Agronomy, Gansu Agricultural University, Lanzhou, China, [2] School of Biological and Pharmaceutical Engineering, Lanzhou Jiaotong University, Lanzhou, China, [3] Department of Plant Breeding and Genetics, The University of Haripur, Haripur, Pakistan, [4] International Potato Center (CIP), CIP China Center for Asia Pacific (CCCAP), Beijing, China

OPEN ACCESS

Edited by:
Shabir Hussain Wani, Sher-e-Kashmir University of Agricultural Sciences and Technology, India

Reviewed by:
Ali Raza, Fujian Agriculture and Forestry University, China
Jeshima K. Yasin, Indian Council of Agricultural Research (ICAR), India
Muhammad Azhar Nadeem, Sivas University of Science and Technology, Turkey

***Correspondence:**
Jiangping Bai
baijp@gsau.edu.cn

Specialty section:
This article was submitted to Plant Biotechnology, a section of the journal Frontiers in Plant Science

Received: *15 December 2021*
Accepted: *20 April 2022*
Published: *19 May 2022*

Citation:
Sun C, Liang W, Yan K, Xu D, Qin T, Fiaz S, Kear P, Bi Z, Liu Y, Liu Z, Zhang J and Bai J (2022) Expression of Potato StDRO1 in Arabidopsis Alters Root Architecture and Drought Tolerance. Front. Plant Sci. 13:836063. doi: 10.3389/fpls.2022.836063

Potato (*Solanum tuberosum* L) is the third important crop for providing calories to a large human population, and is considered sensitive to moderately sensitive to drought stress conditions. The development of drought-tolerant, elite varieties of potato is a challenging task, which can be achieved through molecular breeding. Recently, the *DEEPER ROOTING 1* (*DRO1*) gene has been identified in rice, which influences plant root system and regulates grain yield under drought stress conditions. The potato StDRO1 protein is mainly localized in the plasma membrane of tobacco leaf cells, and overexpression analysis of *StDRO1* in Arabidopsis resulted in an increased lateral root number, but decreased lateral root angle, lateral branch angle, and silique angle. Additionally, the drought treatment analysis indicated that *StDRO1* regulated drought tolerance and rescued the defective root architecture and drought-tolerant phenotypes of *Atdro1*, an Arabidopsis *AtDRO1* null mutant. Furthermore, *StDRO1* expression was significantly higher in the drought-tolerant potato cultivar "Unica" compared to the drought-sensitive cultivar "Atlantic." The transcriptional response of *StDRO1* under drought stress occurred significantly earlier in Unica than in Atlantic. Collectively, the outcome of the present investigation elucidated the role of DRO1 function in the alternation of root architecture, which potentially acts as a key gene in the development of a drought stress-tolerant cultivar. Furthermore, these findings will provide the theoretical basis for molecular breeding of drought-tolerant potato cultivars for the farming community.

Keywords: molecular breeding, root system, branch angle, abiotic stress, food security

INTRODUCTION

Potato (*Solanum tuberosum*) is indispensable for food security around the globe and the fourth largest food crop in China (Cao et al., 2020). The world potato catalog contains information on approximately 4,500 cultivable varieties from around the globe.[1] These potato cultivars vary by various morphological, physiological, biochemical, and pathological attributes under

[1] www.euroseeds.eu/potatoes

ever-changing environmental conditions (Pieczynski et al., 2018). Several classical and molecular studies have been undertaken to understand the genomic regions controlling traits with agricultural and economic importance using diploid and tetraploid potato plants. Kondrák et al. (2012) developed a transgenic White Lady potato cultivar, which expressed the *trehalose-6-phosphate synthase* gene exhibiting drought tolerance. Similarly, Zaki and Radwan (2022) investigated a set of 21 commercial potato cultivars representing genetic diversity in the Middle East and screened drought tolerance based on morpho-physiological traits and tuber production under *in vitro* and field trails. The results displayed the upregulation of *DRO, ERECTA, ERF, DREB*, and *StMYB* genes in drought-tolerant cultivars, indicating the possible role of these genes in future molecular breeding programs. Recently, the availability of genome sequence data for most crops, e.g., Arabidopsis (Weigel and Mott, 2009), rice (3,000 rice genomes project, 2014), wheat (Walkowiak et al., 2020), soybean (Xie et al., 2019), maize (Vicki and Volker, 2002), and potato (Leisner et al., 2018; Hoopes et al., 2022) has enabled to understand and improve both quantitative and qualitative traits, especially genes governing abiotic stress tolerance.

Drought is considered the major abiotic stress for crop plants (Sun et al., 2021). The availability of irrigation water will continue to decrease across the globe owing to a surge in human population from 7 to 9 billion by 2050 (Edmeades, 2013). Therefore, it is imperative to use agricultural mechanization and cultivation water-saving techniques, as well as to develop high-yield and high-quality varieties with better resistance to biotic and abiotic stresses to improve agricultural production (Weber et al., 2014; Brito et al., 2016). Potato, being a shallow root crop, is relatively more sensitive to drought stress than other staple crops (Deblonde and Ledent, 2001; Schafleitner et al., 2007). Long-term or seasonal drought seriously affects the yield and commercial quality of potato (Walworth and Carling, 2002). Moreover, it is notable that some major potato production areas are located in arid and semiarid regions (Porter et al., 1999; Fabeiro et al., 2001). Accelerating global climate change and associated drought is a threat to potato production (Kumar et al., 2007; Li et al., 2019). Roots are integral in performing a variety of functions, e.g., nutrients and water uptake, serving as a storage organ and helping the plant to anchor in the soil (Smith and De Smet, 2012). The variable interactions of plant roots with the environment depends on root components and root architecture (Lynch and Brown, 2012).

Root architecture defines the spatial configuration of roots and helps the plant to respond to ever-changing environmental conditions. Understating root architecture is important for agricultural productivity because mostly soils have an uneven distribution of resources (Zhao et al., 2018). The spatial distribution of roots allow the plant to exploit available soil resources efficiently. Plant roots function in the absorption and transport of water and nutrients, and root architecture is known to strongly contribute for plant's ability to tolerate abiotic stresses, especially drought condition (Manschadi et al., 2006; Mansoorkhani et al., 2014; Bartlett et al., 2022; Ranjan et al., 2022; Rasool et al., 2022). Several studies have shown that drought (or the lack of irrigation in the topsoil) can promote the formation of deeper roots to allow crops to access water and nutrients from the deeper soil (Shahnazari et al., 2007; Chimungu et al., 2014). In recent years, extensive efforts have been observed to harness deep rooting architecture as a screening and evaluation index for drought-tolerance breeding in some cereal crops (Wasson et al., 2012; Lynch, 2013; Liao et al., 2022). Genetic information focused on root architecture, and its role to counter abiotic stresses especially drought in tuber crops is less available (Villordon et al., 2014a).

In rice, a major quantitative trait locus, *OsDRO1* (*DEEPER ROOTING 1*), was functionally characterized by map-based cloning of two varieties with apparent differences in their root architecture. The DRO1 protein was shown to regulate both root angle and drought tolerance (Uga et al., 2012, 2013; Arai-Sanoh et al., 2014). Subsequently, *DRO1* orthologs in Arabidopsis (*Arabidopsis thaliana*), plum (*Prunus domestica*), and wheat (*Triticum aestivum*) were also found to function in regulating root architecture; however, it is notable that the specific root traits regulated by this gene were distinct in these plants (Hollender and Dardick, 2015; Ge and Chen, 2016, 2019; Guseman et al., 2017; Taniguchi et al., 2017; Ashraf et al., 2019; Furutani et al., 2020; Waite et al., 2020). In addition, *DRO1* orthologs in Arabidopsis were placed within the larger *IGT* gene family, with the *LAZY* and *TILLER ANGLE CONTROL* genes (Yoshihara et al., 2013; Hollender and Dardick, 2015; Guseman et al., 2017; Taniguchi et al., 2017; Ge and Chen, 2019). Keeping in view, the present study was designed to analyze the role of *DRO1* orthologs in potato (*S. tuberosum*) exerting similar functions, we initially cloned *StDRO1* and conducted a series of functional analyses to study the function of *StDRO1* for the alternation of root architecture and improvement for the drought stress tolerance.

MATERIALS AND METHODS

Plant Materials and Mutant Detection

Arabidopsis ecotype Columbia (Col.) was used for the present investigation. The Arabidopsis T-DNA insertion mutant (SALK_201221C, Col. background) *Atdro1* was obtained from the Arabidopsis Biological Resource Center (Ohio State University, United States). Heterozygous mutants of *AtDRO1* were first identified, and the homozygous mutants were obtained from self-crossed progenies of the heterozygous parent. The gene-specific primers of left genomic primer (LP) and right genomic primer (RP) were utilized for genotyping; moreover, LBa1 was used as border primer of T-DNA (**Supplementary Table 1**). The potato cultivars Atlantic and Unica for tissue culture seedlings were provided by the Key Laboratory of Crop Genetic Improvement and the Germplasm Innovation of Gansu Agricultural University whereas, virus-free potato mini-tubers of both drought-sensitive "Atlantic" and drought-tolerant "Unica" cultivars were provided by the Dingxi Academy of Agricultural Sciences, the Gansu province.

Cloning, Vector Construction, and Subcellular Localization Analysis of *StDRO1*

Gene-cloning primers of *StDRO1* were designed according to the potato reference sequence available in the NCBI[2] database (LOC102585440 and XM_006361272.2), gateway technology (Invitrogen, Thermo Fisher Scientific) was employed to clone *StDRO1* into the expression vector (**Supplementary Table 1**). The full-length coding sequence of *StDRO1* fragments was amplified and cloned into the pDONR/Zeo entry clone vector, and the sequence was verified. Later, *StDRO1* was cloned into the expression vector *pBIB-BASTA-35s-GWR-GFP* and the sequence was verified. StDRO1-green fluorescent protein (GFP) fusion protein and GFP control were transiently expressed in tobacco (*Nicotiana tabacum*) leaves mediated by *Agrobacterium* GV3101. Fluorescence signals were observed under a laser confocal microscope (Zeiss LSM800).

Transgenic Plant Generation

The expression vector *pBIB-BASTA-35s-StDRO1-GFP* was transferred into the Col. and *Atdro1* mutant by the floral dip method (Clough and Bent, 1998). Polymerase chain reaction (PCR) was used to identify T_1 transgene-positive lines, forward primer was designed according to the 35 s promoter and *StDRO1* gene-specific as reverse primer (**Supplementary Table 1**). T_1-positive lines were harvested individually and further sown in isolated pots to develop T_2 and T_3 generations, genotyping was carried out for each generation. Stable homozygous transgenic lines were identified and studied for subsequent phenotypic observation and drought tolerance analysis.

Phenotype Observation and Determination of Physiological and Biochemical Indexes of Transgenic Plants

Root Phenotype Observation

Arabidopsis seeds were surface-sterilized with 75% (v/v) ethanol for 40 s, followed by 1% (v/v) NaClO for an additional 8 min and then washed with desterilized water six times. The washed seeds were placed on one-half-strength MS plates containing 0.8% (w/v) agar and 1% (w/v) sucrose. Seeds were vernalized at 4°C for 3 days and transferred to a growth chamber under a long-day condition (16 h of light and 8 h of dark) at 22°C. After 2 weeks of growth, the images of the root system were taken. All measurements were carried out using ImageJ.[3]

Determination of Physiological and Biochemical Indexes Under Drought Stress

Arabidopsis seeds were surface-sterilized with the similar procedure as described above and placed at one-half-strength MS plates with 0.8% (w/v) agar, 1% (w/v) sucrose, and 75 mM mannitol to simulate drought stress conditions (Murashige and Skoog, 1962). After 2 weeks of growth, physiological and biochemical indexes were determined. The activities of superoxide dismutase (SOD), peroxidase (POD), and catalase (CAT) were measured by the nitrogen blue tetrazolium photoreduction method, guaiacol colorimetric method, and ultraviolet absorption method (Beauchamp and Fridovich, 1971), respectively. In addition, the proline (Pro) content was determined by the acid ninhydrin color method (Irigoyen et al., 1992).

Phenotypic Observation of Aerial Parts

Nutrient soil and vermiculite were mixed at a 2:1 volume ratio and supplied to 10-cm diameter pots. Sterilized and vernalized Arabidopsis seeds were sown in pots containing nutrient soils, and the pots were placed in a greenhouse under a long-day condition (16 h of light and 8 h of dark) at 22°C. After 5 weeks of growth, aerial parts' images were taken.

RNA Extraction and Quantitative Real-Time Polymerase Chain Reaction of *StDRO1*

Potted Potato Growth Conditions

Nutrient soil and vermiculite were mixed at a 2:1 volume ratio and put into a 38-cm diameter pot. Virus-free mini-tubers were sown 5 cm below the soil surface. The pots were placed under field conditions at Gansu Agricultural University, normal agronomic practices were carried out throughout the growing period. After 65 days of growth, the whole plant, including roots, was carefully uprooted from the soil. Various tissues were quickly frozen in liquid nitrogen and stored at −80°C. The same procedure was repeated for all plants under investigation.

Potato Tissue Culture Growth and Treatment Condition

Stems (approximately 2 cm) of 1-month-old tissue culture plantlets were cut and transferred to sterilized glass jars containing MS medium. The jars were placed in a greenhouse under long-day conditions (16 h of light and 8 h of dark) at 22°C. After 4 weeks of growth, potato seedlings were collected and grown with 200 mM mannitol in liquid medium for 0, 2, 6, 12, and 24 h. After treatment, seedlings were quickly frozen in liquid nitrogen and stored at − 80°C.

RNA Extraction and Quantitative Real-Time Polymerase Chain Reaction

The RNA extraction kit (Tiangen) was used for the extraction of total RNAs from various potato tissues. About 5 μg of RNA was transcribed to cDNA using the ReverTra Ace® qPCR RT Master Mix kit (TOYOBO). The resulting cDNAs, corresponding to 100 ng of total RNA, were then used as templates for quantitative real-time PCR by the StepOnePlus™ Real-Time PCR System (Applied Biosystems) utilizing the TB Green® Premix Ex Taq II kit (Takara). The relative expression level was calculated utilizing the $-\Delta\Delta$Ct method, and ACTIN2 was used as an internal control. The primers used for real-time PCR are listed in **Supplementary Table 1**. The experimental procedures were the same as those reported previously by Sun et al. (2017).

[2]https://www.ncbi.nlm.nih.gov/

[3]http://rsb.info.nih.gov/ij/

Statistical Data Analysis

All experiments were repeated independently at least three times, and each sampling was analyzed separately. SPSS 20.0 software was used for statistical analyses, and statistically significant differences were measured by using Student's *t*-test at * $p < 0.05$; ** $p < 0.01$; *** $p < 0.001$.

RESULTS

Subcellular Localization and Tissue-Specific Expression Analysis of *StDRO1*

In the model plant Arabidopsis and some other plant species, *DRO1* was found to play an integral role for regulating the growth and development of the root system; however, its function in potatoes has not been reported (Uga et al., 2012; Guseman et al., 2017; Ashraf et al., 2019). The potato *StDRO1* was cloned, and an overexpression vector containing a StDRO1-GFP fusion was constructed. The vector was transiently transformed into tobacco leaves, and the GFP signals were observed under a laser confocal microscope. The StDRO1-GFP fusion protein was mainly located at the plasma membrane, whereas GFP control appeared in both the plasma membrane and the nucleus (**Figure 1A**). Moreover, the yeast two-hybrid assay displayed no interaction between potato *StDRO1* (or StDRO1ΔEAR) and StTOPLESS (**Supplementary Figure 1**).

We also evaluated *StDRO1* expression in the roots, stems, and leaves of the drought-tolerant potato cultivar (Unica) and the drought-sensitive potato cultivar (Atlantic). In both Atlantic and Unica, *StDRO1* expression was observed to be non-significant in leaves, whereas approximately 1.5-fold higher expression was observed in the stem of the Unica cultivar. However, the *StDRO1* expression level in the roots of Unica was highly significantly more than Atlantic ($p < 0.001$; *t*-test) (**Figure 1B**).

StDRO1 Regulates Plant Root Architecture

To investigate the capacity of potato *StDRO1* to affect root architecture, we first obtained the Arabidopsis T-DNA insertion mutant *Atdro1* (Col. background) and confirmed the homozygous mutant (**Figure 2A**). Compared with Col. plants, *Atdro1* plants showed a significant increase in lateral root angle and a significant decrease in lateral root number, confirming that *AtDRO1* regulates root architecture. Moreover, we overexpressed *StDRO1* in both wild-type (Col.) and *Atdro1* mutant plants (**Figure 2B**). The results displayed that overexpressed *StDRO1* homozygous plants had significant reductions in lateral root angle and a significant increase in the number of lateral roots compared to Col [$p < 0.05$; analysis of variance (ANOVA)] (**Figures 2C–E**). In addition, we found complementary *Atdro1* mutant plants based on transgenic overexpression of *StDRO1* rescued root phenotypes as wild-type [$p < 0.05$; analysis of variance (ANOVA)] (**Figures 2C–E**). Thus, beyond confirming that Arabidopsis *AtDRO1* regulates root architecture, the results also indicated that potato *StDRO1* can regulate the angle and number of lateral roots.

Therefore, we observed the aerial organs of the different transgenic plants and found that the overexpression of *StDRO1* in the Col. background caused a significant decrease in the lateral

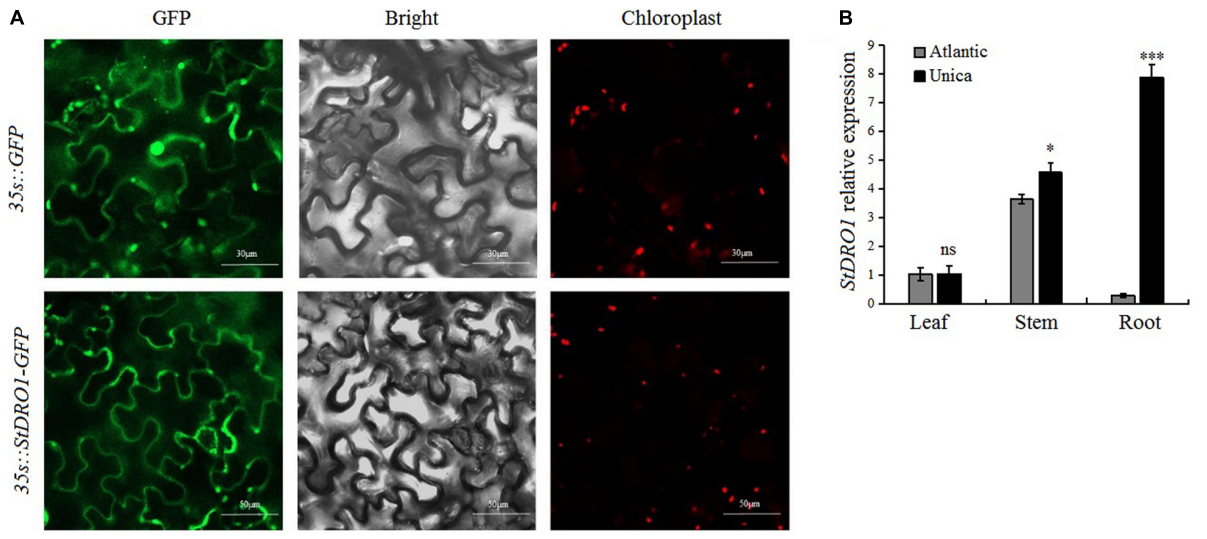


FIGURE 1 | Subcellular localization and tissue-specific expression analysis of *StDRO1*. **(A)** Tobacco leaves transiently transformed with pBIB-BASTA-35s-StDRO1-GFP, the green fluorescent protein (GFP) fluorescence was mainly visible in the plasma membrane under a confocal laser scanning microscope. In tobacco leaves transformed with pBIB-35s-BASTA-GFP (control), GFP fluorescence was also visible in the cell nucleus. Left, GFP fluorescence; center, DIC images; right, chloroplast autofluorescence. **(B)** The expression level of *StDRO1* in the different tissues of potato cultivars. Sixty-five-day-old plant tissues of one drought-tolerant potato cultivar (Unica) and one drought-sensitive potato cultivar (Atlantic) were used. *StACTIN2* was used as a reference gene. Error bars represent SD ($n = 3$). Student's *t*-tests were carried out to evaluate the significance of differences between the potato cultivar Atlantic and Unica for each examined organ. *$p < 0.05$; ***$p < 0.001$; and ns, not significant.

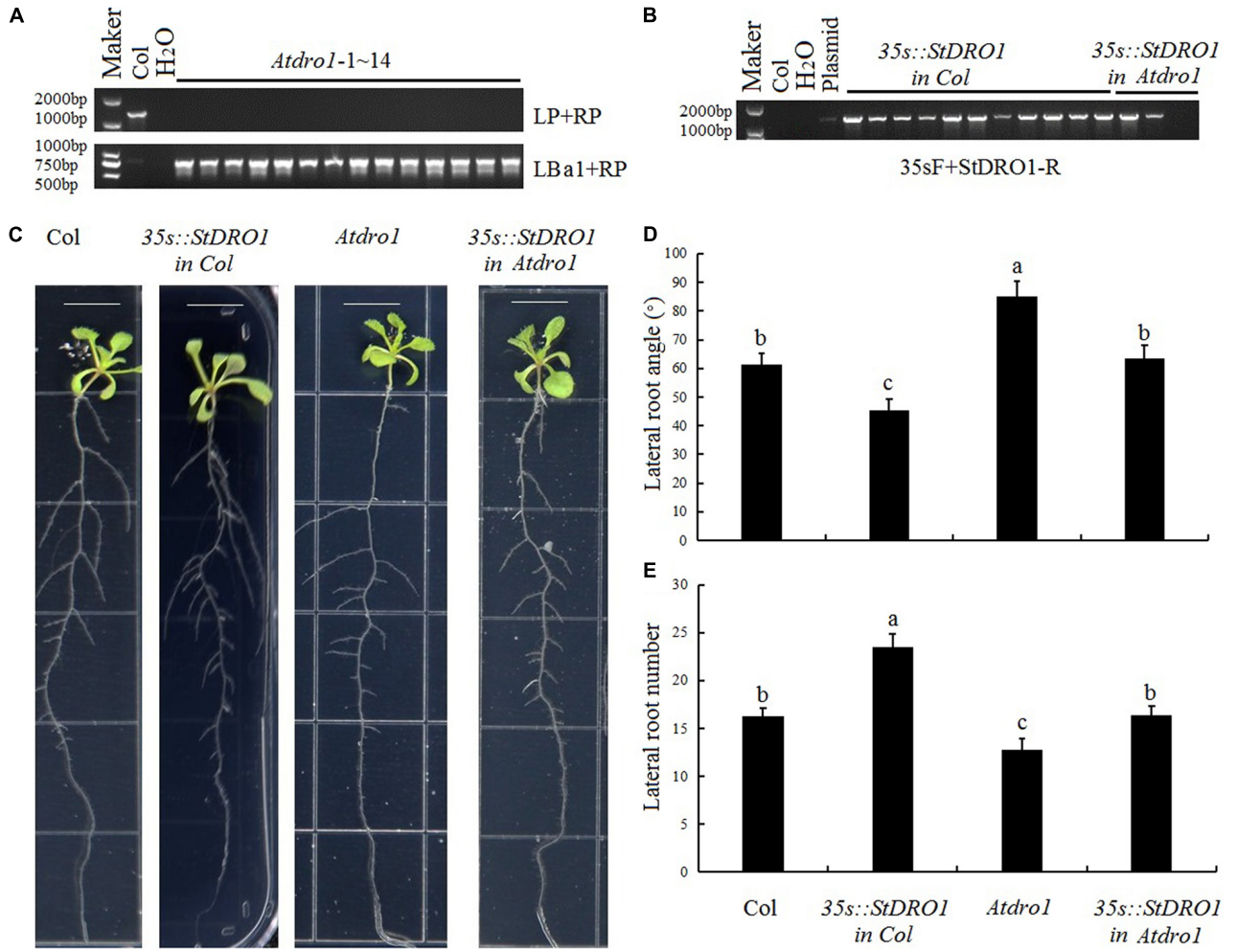


FIGURE 2 | *StDRO1* regulates plant root architecture. **(A,B)** Genotyping of materials for four genotypes: Col. (negative control), *Atdro1* (here, 14 homozygous T-DNA insertion mutant individuals), *35s:StDRO1 in Col.* (11 positive transgenic lines for *StDRO1* expression in the Col. background), and *35s:StDRO1 in Atdro1* (2 positive transgenic lines for *StDRO1* expression in the *Atdro1* background). H_2O was used as an additional negative control; the plasmid was used as a positive control; **(C–E)** Images **(C)** and quantified lateral root angles **(D)** and numbers **(E)** of 2-week-old long-day-grown seedlings of Col., homozygous of *35s:StDRO1 in Col.*, *Atdro1*, and homozygous of *35s:StDRO1 in Atdro1*; the ruler length is 1 cm; Statistical tests (ANOVA) were carried out to evaluate the significance of differences among these four genotypes. Different letters indicate significant differences ($p < 0.05$).

branch angle and silique angle ($p < 0.05$; ANOVA) (**Figure 3**). In addition, *Atdro1* showed larger angles of side branches and siliques as compared to Col. Background, and genetic complementation analysis showed that the overexpression of *StDRO1* could successfully rescue the aerial organ phenotypes of *Atdro1* to the wild-type level ($p < 0.05$; ANOVA) (**Figure 3**).

StDRO1 Regulates the Drought Tolerance of Plants

It has been reported that *OsDRO1* regulates the root architecture of rice and also influence rice to develop drought tolerance (Uga et al., 2013). Therefore, to examine the role of potato *StDRO1* in drought tolerance, we measured physiological and biochemical indicators of stress tolerance, including the activities of the antioxidant enzymes SOD, POD, and CAT, along with the Pro content of the four aforementioned Arabidopsis genotypes, under both normal growth conditions and drought treatments (75 mM mannitol in the growth medium). For Col. plants, drought stress increased the activities of the examined antioxidant enzymes and increased the Pro content ($p < 0.05$; *t*-test) (**Figure 4**). It was noteworthy that drought stress caused an increase in four indicators, namely, SOD, POD, CAT, and Pro content, and a highly significant increase in these indicators was observed in *StDRO1* overexpression line (35s:StDRO1 in Col.) plants than in Col. ($p < 0.05$; *t*-test). Moreover, our analysis of *Atdro1* plants showed no differences for SOD, POD, and CAT activities under normal and drought stress conditions; however, it detected a slight increase in Pro content in drought-stressed plants ($p < 0.05$; *t*-test). In contrast, complementation of *Atdro1* mutant plants based on transgenic *StDRO1* overexpression rescued the response for SOD, POD, CAT, and Pro content ($p < 0.05$;

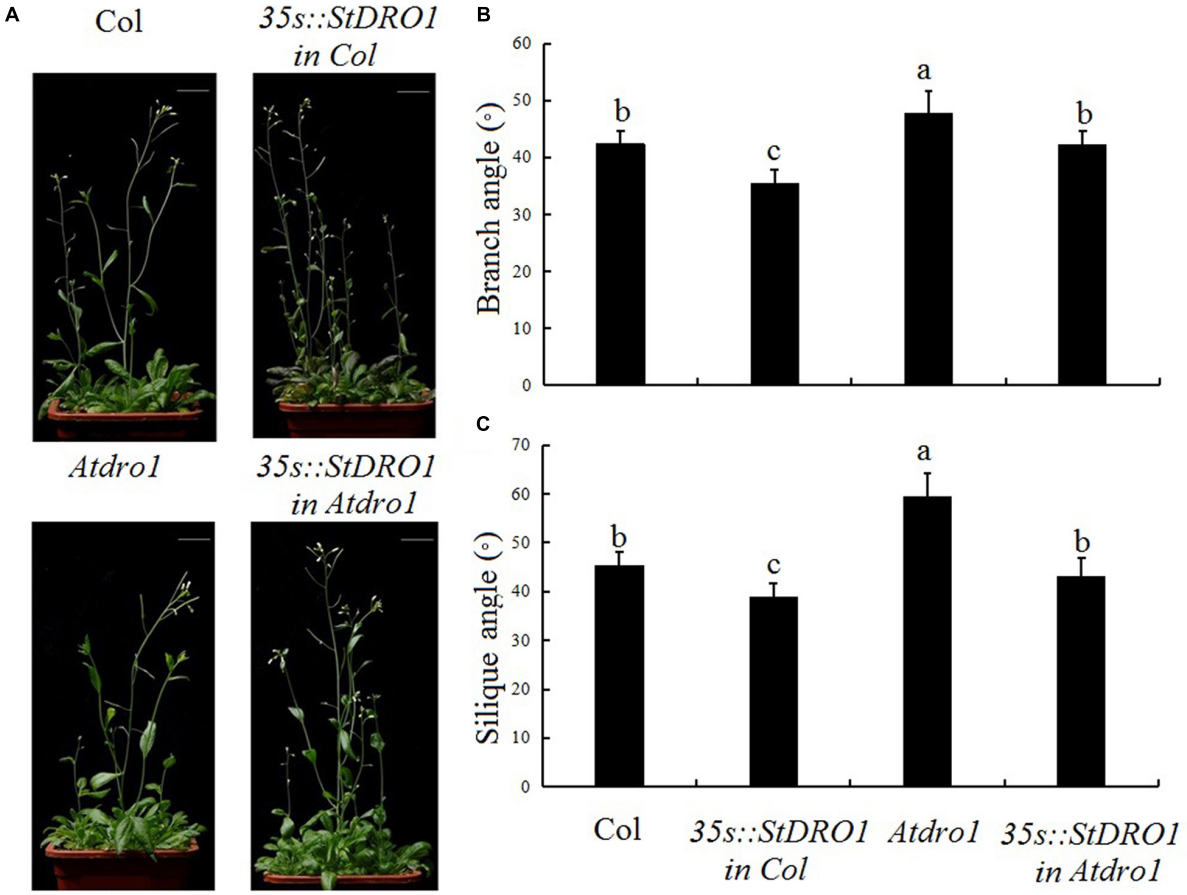


FIGURE 3 | *StDRO1* regulates the branch angle of plant aerial organs. Images of **(A)** quantified branch angles **(B)** and silique angles **(C)** of 5-week-old plants of Col., homozygous of *35s:StDRO1 in Col.*, *Atdro1*, and homozygous of *35s:StDRO1 in Atdro1*. Statistical analysis (ANOVA) was carried out to evaluate the significance of differences between these four genotypes. Different letters indicate significant differences ($p < 0.05$).

t-test) (**Figure 4**). These finding established the loss of *AtDRO1* function influences drought stress responses in Arabidopsis. The data also indicated that potato *StDRO1* can regulate drought tolerance in plants.

StDRO1 Gene Expression Is Induced by Drought Stress

Based on the recorded observation, *StDRO1* can regulate drought tolerance, we further expanded our research objective to investigate *StDRO1* gene expression under induced drought stress conditions. The real-time quantitative PCR (qRT-PCR) analysis results showed that drought treatment (mannitol), coupled with increasing treatment time, caused a slow elevation in the expression level of *StDRO1* for drought-sensitive Atlantic cultivar plants; however, it gradually increased by 10-fold with an additional 24-h sampling time point (**Figure 5**). In contrast, the drought-tolerant cultivar Unica showed that the expression level of *StDRO1* first increased and decreased subsequently, reaching its maximum at 6 h (with a 4-fold increase) (**Figure 5**). Thus, the *StDRO1* expression response to drought stress occurs earlier in the drought-tolerant cultivar Unica compared to the drought-sensitive cultivar Atlantic, and a significant difference of *StDRO1* expression at 6 h was detected between the two cultivars, ($p < 0.01$, *t*-test) (**Figure 5**).

DISCUSSION

Potato tubers are rich in starch, protein, vitamin C, crude fiber, potassium, calcium, and have an excellent nutritional profile (Zaheer and Akhtar, 2016; Robertson et al., 2018). Potatoes are grown worldwide and are of great significance for global nutrition and food security (Friedman, 2006). A series of studies have indicated that the spatial distribution of crop roots largely determines the ability of plants to obtain soil resources, regulating crop water, and nutrient use efficiency as well as crop adaptability to abiotic stress conditions (Malekpoor et al., 2014). In cereal crops, root traits have been extensively studied as an informative breeding index (Wasson et al., 2012; Lynch, 2013; Henry et al., 2014). In recent years, research on tuber crops has found that the optimization of root system architecture can confer substantial yield increases (Villordon et al., 2014b). However, drought is one of the principal abiotic stress limiting potato production around

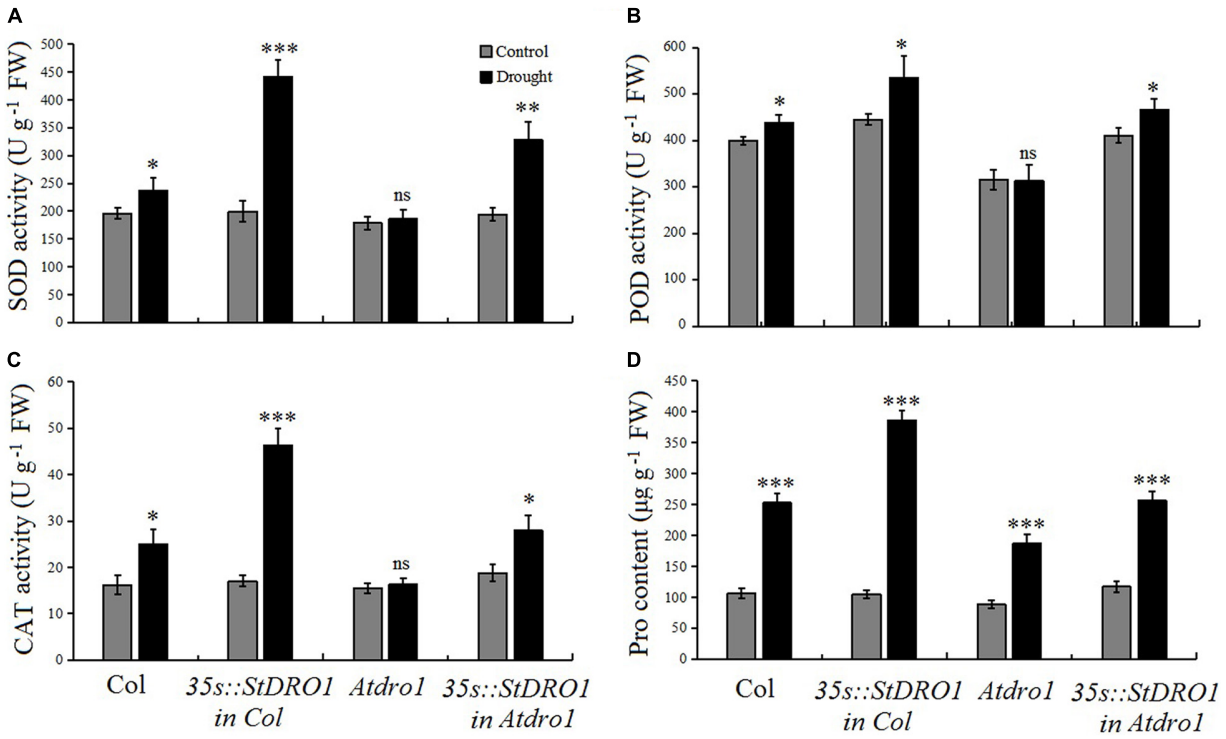


FIGURE 4 | *StDRO1* regulates plant drought tolerance. **(A–D)** Responses of SOD, POD, and CAT activity along with proline (Pro) content under drought stress treatment. Two-week-old seedling of Col., homozygous *35s:StDRO1 in Col.*, *Atdro1*, and homozygous of *35s:StDRO1 in Atdro1* grown with or without 75 mM mannitol were used. Student's *t*-test was carried out to evaluate the significant difference among control and drought treatment. $*p < 0.05$; $**p < 0.01$; $***p < 0.001$; and ns, not significant.

the globe (Deblonde and Ledent, 2001; Toubiana et al., 2020). For instance, the lack of water in the upper soil layers caused by irregular rainfall and high-intensity sunlight is common for rainfed potato planting areas. Therefore, maintaining tuber yield and commercial quality under such production conditions that have uneven distribution of water resources across different soil layers has been hotspot among researchers (Fabeiro et al., 2001; Liu et al., 2006; Kifle and Gebretsadikan, 2016; Li et al., 2019). In addition to studying and developing water-retaining and efficient cultivation techniques, researchers have sought to identify genes that help optimize root architecture and improve drought tolerance, which can be used in future potato molecular breeding programs.

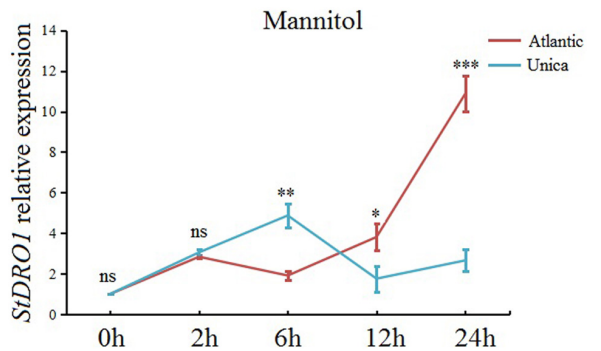


FIGURE 5 | *StDRO1* gene expression is induced by drought stress. At the indicated time point, the effect of drought stress (by mannitol treatment) on *StDRO1* gene expression. Four-week-old seedlings of the drought-tolerant potato cultivar (Unica) and the drought-sensitive potato cultivar (Atlantic) grown under long-day-condition treated with or without 200 mM mannitol were used. *StACTIN2* was used as a reference gene. Error bars represent SD ($n = 3$). Student's *t*-test was carried out to evaluate significance at each time point between Unica and Atlantic. *, $p < 0.05$; **, $p < 0.01$; ***, $p < 0.001$; and ns, not significant.

In a study, map-based cloning was conducted on the shallow root rice variety "IR64" and the deep root variety "KP" for the *DRO1* gene, sequencing analysis revealed that a nucleotide deletion mutation occurred in the *DRO1* gene of "IR64" that caused premature cessation of DRO1 protein translation causing the deletion of C-terminal EAR motif (Uga et al., 2013; Guseman et al., 2017). For further verification, the near-isogenic line DRO1-NIL was constructed (having the "KP" *DRO1* allele in the "IR64" genetic background). Compared with "IR64," DRO1-NIL has significantly smaller root angles at different growth stages, and higher yield under drought conditions without affecting root dry weight. The outcome of the study supported the hypothesis that *OsDRO1* participates in regulating the root angle and drought tolerance of rice (Uga et al., 2013). Furthermore, another group examined Arabidopsis and reported that single-gene mutations of *AtDRO1* can enlarge

lateral root angles, showing that *AtDRO1* overexpression causes smaller lateral root and lateral branch angles. Taken together, this could indicate that *AtDRO1* regulates root architecture in Arabidopsis. The C-terminal EAR motif of the AtDRO1 protein was proven to be an essential element controlling root architecture (Guseman et al., 2017).

The construction, screening, and identification of transgenic lines in potato may took considerably longer time compared to Arabidopsis, therefore the *Atdro1* (Col. background) mutant was used to assess the potato *StDRO1* gene function. We found that the expression of potato *StDRO1* reduced the angles of lateral roots, side branches, and siliques; however, *StDRO1* expression increased lateral root numbers. In addition, transgenic expression of *StDRO1* could successfully rescue the defective phenotype of *Atdro1* mutant plants. We also observed that, under drought stress, the ability of *Atdro1* mutants to activate antioxidant enzymes and osmotic stress protection decreased, indicating that *AtDRO1* functions in drought stress responses in Arabidopsis, a result that has not been reported in previous studies.

Our findings based on transient expression in tobacco leaves indicated that the DRO1 protein is mainly localized at the plasma membrane. This membrane localization for *StDRO1* was reported in *OsDRO1* (rice) and *TaDRO1* (wheat) (**Figure 1A**) (Uga et al., 2013; Ashraf et al., 2019). A recent study reported that for *Atdro1* null mutant plants complemented with a VENUS-tagged *AtDRO1* driven by the native *AtDRO1* promoter, the reporter protein was localized in the nuclei of root tip cells (Waite et al., 2020). Further, the deletion of the EAR motif of DRO1 was reported to alter the localization of this protein in rice protoplasts (cell membrane with the full-length protein; cell nucleus and cytoplasm with the ΔEAR mutant variant) (Uga et al., 2013; Weber et al., 2014). EAR motifs are present in numerous transcriptional co-repressor proteins in plants, some of which have been shown to function by recruiting TOPLESS, a repressor of auxin-regulated, root-promoting genes (Kell, 2011). Previous reports in wheat complemented the interaction of TaDRO1-like with TaTOPLESS through the EAR motif with *in vitro* experiments (Ashraf et al., 2019). However, in the present investigation, the yeast two-hybrid assay displayed no interaction between potato StDRO1 (or StDRO1ΔEAR) and StTOPLESS, indicating that *DRO1* can putatively exert distinct molecular functions in different plant species. The detailed function and molecular mechanism of *StDRO1* in potato need to be further analyzed.

It is noteworthy to mention that in rice, Arabidopsis, and wheat, *DRO1* is mainly expressed in the root tips and basal part of shoots; however, in the present investigation we observed that *StDRO1* expression was low in leaves whereas it was strong in the stem part of the plant. In potato roots, the *StDRO1* expression level of the drought-tolerant cultivar Unica was significantly higher than that of the drought-sensitive cultivar Atlantic. Moreover, we also observed that the gene expression of *StDRO1* could be induced by drought stress, the transcriptional response of *StDRO1* to drought stress occurred significantly earlier in Unica than in the Atlantic cultivar. The findings were consistent with previous studies (Schafleitner et al., 2007; Kashiwagi et al., 2015; Li et al., 2019). These results strongly imply that *StDRO1* exerts the function of drought tolerance in potato; however, related molecular mechanism(s) await further characterization. Previous studies on Arabidopsis indicated that other members of the *IGT* gene family (to which DRO1 belongs) are involved in the regulation of root and shoot branching angles (Yoshihara et al., 2013; Taniguchi et al., 2017; Yoshihara and Spalding, 2017; Ge and Chen, 2019). Thus, our findings showing that the function of potato *StDRO1* for the regulation of root architecture and drought stress tolerance further support that *StDRO1* can be considered as an attractive gene for molecular breeding efforts to obtain robust-rooting and drought-tolerant potato varieties.

CONCLUSION

In this study, DRO1 function for the regulation of root architecture and drought tolerance was investigated. In addition, *StDRO1* expression was several-fold higher in the stem and root of the Unica (drought-tolerant) cultivar, whereas, overexpression rescued the aerial organ and root phenotypes of the Arabidopsis *Atdro1* null mutant. The ectopic expression of *StDRO1* in Arabidopsis revealed a significant increase in biochemical indicators (e.g., SOD, POD, and CAT), along with Pro content under drought stress conditions, indicating that *StDRO1* is potentially a key player for potato drought stress tolerance. These results provide additional evidence that *StDRO1* functions during drought stress, thus laying a foundation for future studies focusing on *DRO1* and related genes in the drought responses of other crops under drought stress conditions.

DATA AVAILABILITY STATEMENT

The original contributions presented in the study are included in the article/**Supplementary Material**, further inquiries can be directed to the corresponding author.

AUTHOR CONTRIBUTIONS

CS designed the experiments and wrote the original draft of this manuscript and revision. CS, WL, KY, DX, and TQ performed the experiments and analyzed the data. SF, PK, ZB, YL, ZL, and JZ contributed to the review and editing. JB developed the research concept and managed the funding for the publication. All authors have read and agreed to the published version of this manuscript.

FUNDING

This work was supported by the National Natural Science Foundation of China (32060502 and 31960442), the Gansu Science and Technology fund (21JR7RA804 and 20JR10RA225), and the Lanzhou Science and Technology Project (2017-RC-39).

SUPPLEMENTARY MATERIAL

The Supplementary Material for this article can be found online at: https://www.frontiersin.org/articles/10.3389/fpls.2022.836063/full#supplementary-material

REFERENCES

Arai-Sanoh, Y., Takai, T., Yoshinaga, S., Nakano, H., Kojima, M., Sakakibara, H., et al. (2014). Deep rooting conferred by DEEPER ROOTING 1 enhances rice yield in paddy fields. *Sci. Rep.* 4:5563. doi: 10.1038/srep05563

Ashraf, A., Rehman, O. U., Muzammil, S., Léon, J., Naz, A. A., Rasool, F., et al. (2019). Evolution of Deeper Rooting 1-like homoeologs in wheat entails the C-terminus mutations as well as gain and loss of auxin response elements. *PLoS One* 14:e0214145. doi: 10.1371/journal.pone.0214145

Bartlett, M. K., Sinclair, G., Fontanesi, G., Knipfer, T., Walker, M. A., and McElrone, A. J. (2022). Root pressure-volume curve traits capture rootstock drought tolerance. *Ann. Bot.* 129, 389–402. doi: 10.1093/aob/mcab132

Beauchamp, C., and Fridovich, I. (1971). Superoxide dismutase: improved assays and an assay applicable to acrylamide gels. *Anal. Biochem.* 44, 276–287. doi: 10.1016/0003-2697(71)90370-8

Brito, G. G., Fagundes, P. R. R., Telo, G. M., Abreu, A. G., Magalhães, A. M. Jr., Franco, D. F., et al. (2016). Impact of Supra-Optimal Temperatures Onphysiology and Yield in Rice Field. *J. Agri. Sci.* 8:27. doi: 10.5539/jas.v8n2p27

Cao, M., Hengzhi, L., Chao, Z., Dongdong, W., Xiaofang, L., and Qin, C. (2020). Functional Analysis of StPHT1;7, a *Solanum tuberosum* L. Phosphate Transporter Gene, in Growth and Drought Tolerance. *Plants* 9:1384. doi: 10.3390/plants9101384

Chimungu, J. G., Brown, K. M., and Lynch, J. P. (2014). Large root cortical cell size improves drought tolerance in maize. *Plant Phys.* 166, 2166–2178. doi: 10.1104/pp.114.250449

Clough, S. J., and Bent, A. F. (1998). Floral dip: a simplified method for *Agrobacterium*-mediated transformation of Arabidopsis thaliana. *Plant J.* 16, 735–743. doi: 10.1046/j.1365-313x.1998.00343.x

Deblonde, P., and Ledent, J. F. (2001). Effects of moderate drought conditions on green leaf number, stem height, leaf length and tuber yield of potato cultivars. *Eur. J. Agron.* 14, 31–41. doi: 10.1016/s1161-0301(00)00081-2

Edmeades, G. O. (2013). *) Progress in Achieving and Delivering Drought Tolerance in Maize-An Update*. Ithaca, NY: ISAAA.

Fabeiro, C., Olalla, F., and Juan, J. (2001). Yield and size of deficit irrigated potatoes. *Agric. Water Manag.* 48, 255–266. doi: 10.3389/fpls.2017.01400

Friedman, M. (2006). Potato glycoalkaloids and metabolites: roles in the plant and in the diet. *J. Agric. Food Chem.* 54, 8655–8681. doi: 10.1021/jf061471t

Furutani, M., Hirano, Y., Nishimura, T., Nakamura, M., Taniguchi, M., Suzuki, K., et al. (2020). Polar recruitment of RLD by LAZY1-like protein during gravity signaling in root branch angle control. *Nat. Commun.* 11:76. doi: 10.1038/s41467-019-13729-7

Ge, L., and Chen, R. (2016). Negative gravitropism in plant roots. *Nat. Plants* 2:16155. doi: 10.1038/nplants.2016.155

Ge, L., and Chen, R. (2019). Negative gravitropic response of roots directs auxin flow to control root gravitropism. *Plant Cell Environ.* 42, 2372–2383. doi: 10.1111/pce.13559

Guseman, J. M., Webb, K., Srinivasan, C., and Dardick, C. (2017). DRO1 influences root system architecture in Arabidopsis and Prunus species. *Plant J.* 89, 1093–1105. doi: 10.1111/tpj.13470

Henry, A., Dixit, S., Mandal, N. P., Anantha, M. S., Torres, R., and Kumar, A. (2014). Grain yield and physiological traits of rice lines with the drought yield QTL qDTY(12.1) showed different responses to drought and soil characteristics in upland environments. *Funct. Plant Biol.* 41, 1066–1077. doi: 10.1071/fp13324

Hollender, C. A., and Dardick, C. (2015). Molecular basis of angiosperm tree architecture. *New Phytol.* 206, 541–556. doi: 10.1111/nph.13204

Hoopes, G., Meng, X., Hamilton, J. P., Achakkagari, S. R., de Alves Freitas, Guesdes, F., et al. (2022). Phased, chromosome-scale genome assemblies of tetraploid potato reveal a complex genome, transcriptome, and predicted proteome landscape underpinning genetic diversity. *Mol. Plant* 15, 520–536. doi: 10.1016/j.molp.2022.01.003

Irigoyen, J. J., Emerich, D. W., and Sanchez-Diaz, M. (1992). Water stress induced changes in concentrations of proline and total soluble sugars in nodulated alfalfa (*Medicago sativa*) plants. *Physiol. Plant* 84, 55–60. doi: 10.1034/j.1399-3054.1992.840109.x

Kashiwagi, J., Krishnamurthy, L., Purushothaman, R., Upadhyaya, H. D., and Varshney, R. K. (2015). Scope for improvement of yield under drought through the root traits in chickpea (*Cicer arietinum* L.). *Field Crops Res.* 170, 47–54. doi: 10.1016/j.fcr.2014.10.003

Kell, D. B. (2011). Breeding crop plants with deep roots: their role in sustainable carbon, nutrient and water sequestration. *Annal. Bot.* 108, 407–418. doi: 10.1093/aob/mcr175

Kifle, M., and Gebretsadikan, T. G. (2016). Yield and water use efficiency of furrow irrigated potato under regulated deficit irrigation, Atsibi-Wemberta, North Ethiopia. *Agric. Water Manag.* 170, 133–139. doi: 10.1016/j.agwat.2016.01.003

Kondrák, M., Marincs, F., Antal, F., Juhasz, Z., and Banfalvi, Z. (2012). Effects of yeast trehalose-6-phosphate synthase 1 on gene expression and carbohydrate contents of potato leaves under drought stress conditions. *BMC Plant Biol.* 12:74. doi: 10.1186/1471-2229-12-74

Kumar, S., Asrey, A., and Mandal, G. (2007). Effect of differential irrigation regimes on potato (*Solanum tuberosum* L.) yield and post-harvest attributes. *Indian J. Agric. Sci.* 77, 366–368.

Leisner, C. P., Hamilton, J. P., Crisovan, E., Manrique-Carpintero, N. C., Marand, A. P., Newton, L., et al. (2018). Genome sequence of M6, a diploid inbred clone of the high-glycoalkaloid-producing tuber-bearing potato species Solanum chacoense, reveals residual heterozygosity. *Plant J.* 94, 562–570. doi: 10.1111/tpj.13857

Li, X., Ramírez, D. A., Qin, J., Dormatey, R., Bi, Z., Sun, C., et al. (2019). Water restriction scenarios and their effects on traits in potato with different degrees of drought tolerance. *Sci. Hortic.* 256:108525. doi: 10.1016/j.scienta.2019.05.052

Liao, Q., Chebotarov, D., Islam, M. S., Quintana, M. R., Natividad, M. A., De Ocampo, M., et al. (2022). Aus rice root architecture variation contributing to grain yield under drought suggests a key role of nodal root diameter class. *Plant Cell Environ.* 45, 854–870. doi: 10.1111/pce.14272

Liu, F., Ali, S., Andersen, M. N., Sven-Erik, J., and Jensen, C. R. (2006). Physiological responses of potato (*Solanum tuberosum* L.) to partial root-zone drying: ABA signalling, leaf gas exchange, and water use efficiency. *J. Exp. Bot.* 57, 3727–3735. doi: 10.1093/jxb/erl131

Lynch, J. P. (2013). Steep, cheap and deep: an ideotype to optimize water and N acquisition by maize root systems. *Annals Bot.* 112, 34–357. doi: 10.1093/aob/mcs293

Lynch, J. P., and Brown, K. M. (2012). Topsoil foraging-An architectural adaptation of plants to low phosphorus availability. *Plant Soil* 237, 225–237. doi: 10.1023/A:1013324727040

Malekpoor, M. F., Seymour, G. B., Swarup, R., Moeiniyan, B. H., Ramsey, R. J., and Thompson, A. J. (2014). Environmental, developmental, and genetic factors controlling root system architecture. *Biotechnol. Genet. Eng. Rev.* 30, 95–112. doi: 10.1080/02648725.2014.995912

Manschadi, A. M., Christopher, J., Devoil, P., and Hammer, G. L. (2006). The role of root architectural traits in adaptation of wheat to water-limited environments. *Fun. Plant Biol.* 33, 823–837. doi: 10.1071/FP06055

Mansoor-khani, F. M., Seymour, G. B., Swarup, R., Bagheri, H. M., Ramsey, R., and Thompson, A. J. (2014). Environmental, developmental, and genetic factors controlling root system architecture. *Biotechnol. Gen. Eng. Rev.* 30, 95–112.

Murashige, T., and Skoog, F. (1962). A revised medium for rapid growth and bio assays with tobacco tissue cultures. *Physiol. Plant* 15, 473–497. doi: 10.1111/j.1399-3054.1962.tb08052.x

Pieczynski, M., Wyrzykowska, A., Milanowska, K., Boguszewska-Mankowska, D., Zagdanska, B., Karlowski, W., et al. (2018). Genome wide identification of genes involved in the potato response to drought indicates functional evolutionary conservation with Arabidopsis plants. *Plant Biotechnol. J.* 16, 603–614. doi: 10.1111/pbi.12800

Porter, G. A., Opena, G. B., Bradbury, W. B., McBurnie, J. C., and Sisson, J. A. (1999). Soil management and supplemental irrigation effects on potato: I. Soil properties, tuber yield, and quality. *Agron. J.* 91, 416–425. doi: 10.2134/agronj1999.00021962009100030010x

Ranjan, A., Sinha, R., Singla-Pareek, S. L., Pareek, A., and Singh, A. K. (2022). Shaping the Root System Architecture in Plants for Adaptation to Drought Stress. *Physiol. Plant* 174:e13651. doi: 10.1111/ppl.13651

Rasool, F., Khan, M. R., Schneider, M., Uzair, M., Aqeel, M., Ajmal, W., et al. (2022). Transcriptome unveiled the gene expression patterns of root architecture in drought-tolerant and sensitive wheat genotypes. *Plant Physiol. Biochem.* 178, 20–30. doi: 10.1016/j.plaphy.2022.02.025

Robertson, T. M., Alzaabi, A. Z., Robertson, M. D., and Fielding, B. A. (2018). Starchy Carbohydrates in a Healthy Diet: The Role of the Humble Potato. *Nutrients* 10:1764. doi: 10.3390/nu10111764

Schafleitner, R., Gutierrez, R., Espino, R., Gaudin, A., Pérez, J., Martínez, M., et al. (2007). Field Screening for Variation of Drought Tolerance in *Solanum tuberosum* L. by Agronomical, Physiological and Genetic Analysis. *Potato Res.* 50, 71–85. doi: 10.1007/s11540-007-9030-9

Shahnazari, A., Liu, F., Andersen, M. N., Jacobsen, S. E., and Jensen, C. R. (2007). Effects of partial root-zone drying on yield, tuber size and water use efficiency in potato under field conditions. *Field Crops Res.* 100, 117–124. doi: 10.1016/j.fcr.2006.05.010

Smith, S., and De Smet, I. (2012). Root system architecture: insights from Arabidopsis and cereal crops. *Philos. Trans. R. Soc. B. Biol. Sci.* 367, 1441–1452. doi: 10.1098/rstb.2011.0234

Sun, C., Ali, K., Yan, K., Fiaz, S., Dormatey, R., Bi, Z., et al. (2021). Exploration of Epigenetics for Improvement of Drought and Other Stress Resistance in Crops: A Review. *Plants* 10:1226. doi: 10.3390/plants10061226

Sun, C., Yan, K., Han, J. T., Tao, L., Lv, M. H., Shi, T., et al. (2017). Scanning for New BRI1 Mutations via TILLING Analysis. *Plant Physiol.* 174, 1881–1896. doi: 10.1104/pp.17.00118

Taniguchi, M., Furutani, M., Nishimura, T., Nakamura, M., Fushita, T., Iijima, K., et al. (2017). The arabidopsis LAZY1 family plays a key role in gravity signaling within statocytes and in branch angle control of roots and shoots. *Plant Cell* 29, 1984–1999. doi: 10.1105/tpc.16.00575

3,000 rice genomes project (2014). The 3,000 rice genomes project. *Gigascience* 3:7.

Toubiana, D., Cabrera, R., Salas, E., Maccera, C., Franco Dos Santos, G., Cevallos, D., et al. (2020). Morphological and metabolic profiling of a tropical-adapted potato association panel subjected to water recovery treatment reveals new insights into plant vigor. *Plant J.* 103, 2193–2210. doi: 10.1111/tpj.14892

Uga, Y., Hanzawa, E., Nagai, S., Sasaki, K., and Sato, Y. T. (2012). Identification of qSOR1, a major rice QTL involved in soil-surface rooting in paddy fields. *Theor. Appl. Gen.* 124, 175–186. doi: 10.1007/s00122-011-1688-3

Uga, Y., Sugimoto, K., Ogawa, S., Rane, J., Ishitani, M., Hara, N., et al. (2013). Control of root system architecture by DEEPER ROOTING 1 increases rice yield under drought conditions. *Nat. Genet.* 45:1097. doi: 10.1038/ng.2725

Vicki, L. C., and Volker, B. (2002). The Maize Genome Sequencing Project. *Plant Phys.* 130, 1594–1597. doi: 10.1104/pp.015594

Villordon, A. Q., Ginzberg, I., and Firon, N. (2014a). Root architecture and root and tuber crop productivity. *Trends Plant Sci.* 19, 419–425. doi: 10.1016/j.tplants.2014.02.002

Villordon, A. Q., Ginzberg, I., and Firon, N. (2014b). Root architecture and root and tuber crop productivity. *Trend. Plant Sci.* 19, 419–425.

Waite, J. M., Collum, T. D., and Dardick, C. (2020). AtDRO1 is nuclear localized in root tips under native conditions and impacts auxin localization. *Plant Mol. Biol.* 103, 197–210. doi: 10.1007/s11103-020-00984-2

Walkowiak, S., Gao, L., Monat, C., Haberer, G., Kassa, M. T., Brinton, J., et al. (2020). Multiple wheat genomes reveal global variation in modern breeding. *Nature* 588, 277–283. doi: 10.1038/s41586-020-2961-x

Walworth, J. L., and Carling, D. E. (2002). Tuber initiation and development in irrigated and non-irrigated potatoes. *Am. J. Potato Res.* 79, 387–395. doi: 10.1007/bf02871683

Wasson, A. P., Richards, R. A., Chatrath, R., Misra, S. C., Prasad, S. V., Rebetzke, G. J., et al. (2012). Traits and selection strategies to improve root systems and water uptake in water-limited wheat crops. *J. Exp. Bot.* 63, 3485–3498. doi: 10.1093/jxb/ers111

Weber, R. L. M., Wiebke-Strohm, B., Bredemeier, C., Margis-Pinheiro, M., de Brito, G. G., Rechenmacher, C., et al. (2014). Expression of an Osmotin-Like Protein from *Solanum nigrum* Confers Drought Tolerance in Transgenic Soybean. *BMC Plant Biol.* 14:343. doi: 10.1186/s12870-014-0343-y

Weigel, D., and Mott, R. (2009). The 1001 Genomes Project for *Arabidopsis thaliana*. *Genome Biol.* 10:107. doi: 10.1186/gb-2009-10-5-107

Xie, M., Chung, C. Y., Li, M. W., Wong, F. L., Wang, X., Liu, A., et al. (2019). A reference-grade wild soybean genome. *Nat. Commun.* 10:1216. doi: 10.1038/s41467-019-09142-9

Yoshihara, T., and Spalding, E. P. (2017). LAZY Genes Mediate the Effects of Gravity on Auxin Gradients and Plant Architecture. *Plant Physiol.* 175, 959–969. doi: 10.1104/pp.17.00942

Yoshihara, T., Spalding, E. P., and Iino, M. (2013). AtLAZY1 is a signaling component required for gravitropism of the Arabidopsis thaliana inflorescence. *Plant J.* 74, 267–279. doi: 10.1111/tpj.12118

Zaheer, K., and Akhtar, M. H. (2016). Potato Production, Usage, and Nutrition–A Review. *Crit. Rev. Food Sci. Nutr.* 56, 711–721. doi: 10.1080/10408398.2012.724479

Zaki, H. E. M., and Radwan, K. S. A. (2022). Response of potato (*Solanum tuberosum* L.) cultivars to drought stress under in vitro and field conditions. *Chem. Biol. Technol. Agric.* 9:1.

Zhao, J., Zhan, X., Jiang, Y., and Xu, J. (2018). Variations in climatic suitability and planting regionalization for potato in northern China under climate change. *PLoS One* 13:e0203538. doi: 10.1371/journal.pone.0203538

Conflict of Interest: The authors declare that the research was conducted in the absence of any commercial or financial relationships that could be construed as a potential conflict of interest.

Publisher's Note: All claims expressed in this article are solely those of the authors and do not necessarily represent those of their affiliated organizations, or those of the publisher, the editors and the reviewers. Any product that may be evaluated in this article, or claim that may be made by its manufacturer, is not guaranteed or endorsed by the publisher.

Copyright © 2022 Sun, Liang, Yan, Xu, Qin, Fiaz, Kear, Bi, Liu, Liu, Zhang and Bai. This is an open-access article distributed under the terms of the Creative Commons Attribution License (CC BY). The use, distribution or reproduction in other forums is permitted, provided the original author(s) and the copyright owner(s) are credited and that the original publication in this journal is cited, in accordance with accepted academic practice. No use, distribution or reproduction is permitted which does not comply with these terms.

frontiers | Frontiers in Plant Science

MINI REVIEW
published: 19 May 2022
doi: 10.3389/fpls.2022.870626

Research Progress in the Field of Microbial Mitigation of Drought Stress in Plants

Shifa Shaffique[1†], Muhamad Aaqil Khan[1†], Muhamad Imran[1], Sang-Mo Kang[1], Yong-Sung Park[1], Shabir Hussain Wani[2] and In-Jung Lee[1]*

[1] Department of Applied Biosciences, Kyungpook National University, Daegu, South Korea, [2] Mountain Research Center for Field Crops Khudwani, Sher-e-Kashmir University of Agriculture Sciences and Technology of Jammu, Srinagar, India

Plants defend themselves against ecological stresses including drought. Therefore, they adopt various strategies to cope with stress, such as seepage and drought tolerance mechanisms, which allow plant development under drought conditions. There is evidence that microbes play a role in plant drought tolerance. In this study, we presented a review of the literature describing the initiation of drought tolerance mediated by plant inoculation with fungi, bacteria, viruses, and several bacterial elements, as well as the plant transduction pathways identified *via* archetypal functional or morphological annotations and contemporary "omics" technologies. Overall, microbial associations play a potential role in mediating plant protection responses to drought, which is an important factor for agricultural manufacturing systems that are affected by fluctuating climate.

Keywords: microbes, mitigate, drought, stress, plants

OPEN ACCESS

Edited by:
David W. M. Leung, University of Canterbury, New Zealand

Reviewed by:
Manzer H. Siddiqui, King Saud University, Saudi Arabia

***Correspondence:**
In-Jung Lee
ijlee@knu.ac.kr

[†] These authors have contributed equally to this work

Specialty section:
This article was submitted to Plant Biotechnology, a section of the journal Frontiers in Plant Science

Received: *07 February 2022*
Accepted: *14 April 2022*
Published: *19 May 2022*

Citation:
Shaffique S, Khan MA, Imran M, Kang S-M, Park Y-S, Wani SH and Lee I-J (2022) Research Progress in the Field of Microbial Mitigation of Drought Stress in Plants. Front. Plant Sci. 13:870626. doi: 10.3389/fpls.2022.870626

INTRODUCTION

Despite several advances in agricultural technology, drought is a major environmental stress for plants. Interventions with microbes can mitigate drought stress (Hossain et al., 2016; Li and Liu, 2016; Salehi-Lisar and Bakhshayeshan-Agdam, 2016; Shinozaki et al., 2016). In this review, we summarized drought stress mitigation using microbes, current control tactics, and unconventional control approaches. We also discussed possible alternative strategies for more effective drought-stress management.

Drylands are used to evaluate drought stress in biomes because of their limited agricultural productivity. Given the importance of water as a macromolecule for the physiological growth and development of plants, water scarcity and deprivation are phenomena that commonly cause drought stress (Siddique et al., 2000; Bartels and Phillips, 2010; Farooq et al., 2012; Askari-Khorasgani et al., 2021). This is a major environmental constraint that limits crop production; indeed, drought stress affects physiological, biochemical, and molecular levels. In response to such stress, plants enter avoidance, tolerance, or adaptation phases (Palmer, 1965; Svoboda et al., 2002; Farooq et al., 2009; Basu et al., 2016). Lack of water affects the water-plant relationship, arrests the

Abbreviations: AMF, Arbuscular mycorrhizal fungi; MDA, Malondialdehyde; LB, Lysogeny broth; PGPR, Plant-growth-promoting rhizobacteria; PGPB, Plant-growth-promoting bacteria; RIDER, Rhizobacteria-induced drought endurance and resilience; SOD, Superoxide dismutase; ROS, Reactive oxygen species; TPP, Trehalose-6-phosphate phosphatases; ABA, Abscisic acid; IAA, Indole acetic acid; ACC, Aminocyclopropane-1-carboxylic acid; VOC, Volatile oil compounds.

plant growth, and causes a reduction in the leaf size, stem extension, and root proliferation. Arrested plant growth leads to reduced carbon dioxide assimilation, which subsequently damages membrane potential. This damage leads to the accumulation of reactive oxygen species (ROS), with free radical accumulation leading to oxidative stress and disturbances in adenosine triphosphate synthesis (Anjum et al., 2011; Van Loon, 2015). Drought stress can be reduced through breeding, mass screening, and exogenous phytohormone production (Siddiqui et al., 2022). Plants can autoregulate to minimize stress by producing phytohormones [e.g., abscisic acid (ABA) and gibberellins] and low-molecular-weight osmolytes (e.g., amino acids and polyols) and by modifying succulent leaves to reduce transpiration loss (Seki et al., 2007; Farooq et al., 2009; Rahdari and Hoseini, 2012).

Microbes can promote plant growth both directly and indirectly (**Figure 1**). The indirect activation of plant growth involves a series of events by which microbes prevent the inhibition of plant growth and development induced by pathogens (Ahmad et al., 2021). During direct activation, microbes biosynthesize bacterial compounds that promote the uptake of nutrients from the soil and stimulate plant growth and development (Berg, 2009; Choudhary et al., 2016). Microbes induce local or systemic stress mitigation response mechanisms that help plants survive under abiotic stress conditions (**Figure 2**), such as drought stress, and help plants sustain growth and development through the fixation, mobilization, and/or production of nutrients, hormones, and organic phytostimulants (Martins et al., 2018; Yadav and Yadav, 2018; Kour and Yadav, 2020). In this study, we summarized the currently known implications of using microbes for drought tolerance, including their fundamental mechanisms of action (**Figure 3**). This review adds to previously published reviews by addressing the implementation of mitigation strategies to prevent adverse effects of drought stress.

MOLECULAR MECHANISM OF ACTION OF MICROBES IN PLANTS UNDER DROUGHT STRESS

Microbial Production of Phytohormone

Phytohormones such as gibberellins, ethylene, indole acetic acid (IAA), ABA, and cytokinin are chemical messengers that are organic in nature, synchronize cellular events in plants, and play key roles in plant progression and drought stress (Kefeli et al., 2003; Khan et al., 2012; Jogawat et al., 2021).

Phytohormones are produced by plants and, in some cases, by microorganisms that interact with plants. Auxin mitigates drought stress in a secondary manner *via* cumulative root growth and modification of root design and/or root hairs, which absorb water and nutrients from the soil. Auxins are produced *via* tryptophan-dependent pathways (Vanneste and Friml, 2009; Zhao, 2010). They produce indole-3-acetamide, which is converted into indole-3-acetaldoxime and tryptamine to give the final product, i.e., indole-3-pyruvic acid (Skubacz et al., 2016). Several studies have provided evidence to support the role of IAA in inducing drought-related signaling pathways when plants are exposed to osmotic stress (Fahad et al., 2015; Yu et al., 2020). These adaptations are interrelated with higher auxin amalgamation in microbe-treated plants; auxin has the capacity to elongate the stems and coleoptiles of plants under stress conditions (Raheem et al., 2018; Ullah et al., 2019).

The application of microbes also enhances the production of plant gibberellins, which are diterpeniods that cause hyperactive elongation of stems in response to stress. Gibberellins are associated with two bioactive components, namely, carotenes and isoprene (Davies, 1995; Alagoz et al., 2018). Carotenes can stimulate photosynthesis and protect plant cells from harmful photodynamic reactions, whereas isoprene maintains turgor pressure and stabilizes the cell membrane structure (Jeon et al., 2003; Mollah and Pratiwi, 2020).

In response to abiotic stress, cytokinin biosynthesis increases in plants in association with auxin and regulation of developmental responses. Cytokinin can transfer the phosphoryl group $P^{+}O_3{}^{2-}$. In addition, cytokinin helps in the phosphorylation of sugar molecules, which leads to their accumulation in cells and prevents reverse diffusion (Mok and Mok, 2001). Competitive phosphorylation helps plant cells combat stress, and cytokinin protects plant cells from oxidative stress (Werner and Schmülling, 2009; Wybouw and De Rybel, 2019).

Ethylene is an important hormone that regulates not only plant growth but also senescence of growth attributes. It frequently interacts with other hormones. Ethylene is a second messenger hormone that regulates various developmental processes, ranging from germination to the plant life cycle (Kanellis et al., 2012; Wen, 2014).

Abscisic acid is a particularly important hormone that is secreted when plants are subjected to stress; thus, it is known as a universal stress hormone. ABA plays an important role in mitigating stress because it causes stomatal closure and is a powerful inhibitor of stomatal opening (Bright et al., 2006). ABA also regulates genes responsible for desiccation tolerance (Sakata et al., 2014).

The ability of these rhizobacteria to synthesize and produce phytohormones is the first key factor in mitigating stress through a complex signaling network in plants to respond to environmental conditions and maintain the plant inner environment through regulation of these hormones, antioxidants, and osmolytes to enhance stress tolerance.

Microbial Production of Aminocyclopropane-1-Carboxylate Deaminase

Aminocyclopropane-1-carboxylic acid (ACC) is a precursor of ethylene, the production of which increases in plants under ecological stress. Numerous microorganisms have been reported to produce ACC deaminase, which reduces ACC, thereby lowering the increased levels of ethylene in host plants (Campbell, 1995; Houda et al., 2013). Under drought stress, plants enhance their ethylene production, which inhibits plant growth by

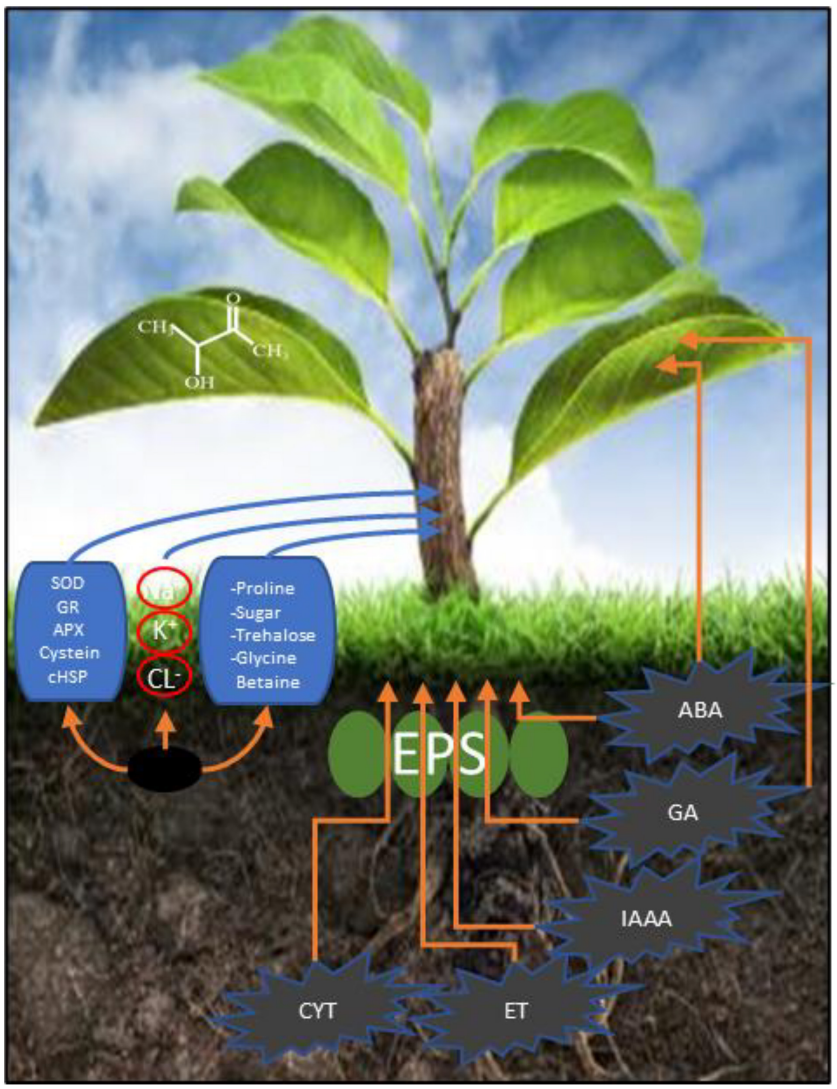


FIGURE 1 | Mechanism of action of microbial mitigation of drought stress.

affecting seed germination and root enlargement. Higher ACC levels are induced to combat severe drought stress (Dikarev et al., 2016; Ustiatik et al., 2021).

Beneficial microbes can produce ACC deaminase. ACC regulates plant growth and development by sequestering and cleaving plant-produced ACC and lowering the level of ethylene in plants.

Osmotic Amendment

When plants are subjected to abiotic stress, a sudden loss of osmolytes occurs, which can shock the plant. However, microbial interactions lead to osmotic adjustments. Plant–microbe interactions are facilitated by secreted metabolites; plants upregulate the production of metabolites such as proline, sugars, glycine, organic acids, trehalose, betaine, potassium, calcium, and chloride ions as an adaptive response to drought stress. As one of the most important osmolytes, proline accumulates in plants under osmotic stress and facilitates the maintenance and osmotic adjustment of cellular components in plant cells to overcome stress. Some rhizosphere bacteria produce proline (Yamada et al., 2005; Mohammadkhani and Heidari, 2008; Dobra et al., 2010).

Glycine betaine is a secondary metabolite that helps plants maintain growth and development. Trehalose is a safe, non-reducing sugar that contains two glucose molecules and stores energy for use under stress conditions. Microbes can accelerate trehalose biosynthesis through the TPS/trehalose-6-phosphate phosphatases (TPS/TPP) pathway, maintain osmolytes concentrations, and stabilize turgor pressure in plant cells (Iordachescu and Imai, 2011; Kahraman et al., 2019). The application of microbes to plant cells increases the secretion of organic acids (e.g., oxalic acid, citric acid, and malic acid) and minerals (e.g., chlorine, sodium, and potassium), which are important for nutrient availability, metabolic reactions, and the

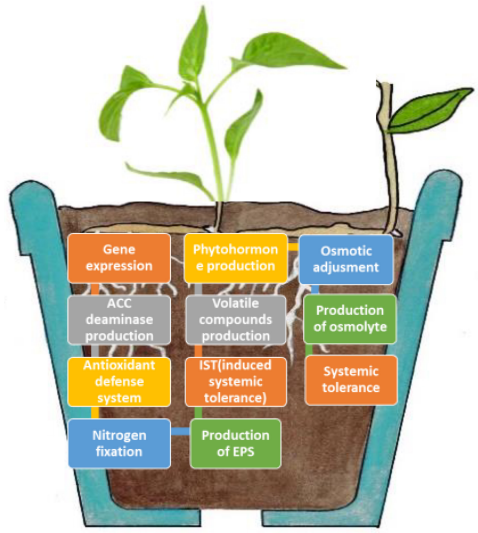


FIGURE 2 | Plant–microbial interactions involved in the mitigation of drought stress.

maintenance of osmoregulation in plant cells (Kirst, 1996; Chen and Jiang, 2010).

The ability to regulate osmotic amendment of plant-growth-promoting rhizobacteria (PGPR) in plant cells is due to generating a low water gradient potential in the cytosol. They maintain the turgor pressure and osmotic adjustment and improve stress tolerance.

Microbial Production of Exopolysaccharides for Drought Stress Mitigation

Exopolysaccharides are macromolecules composed of long-chain polymers of repeating sugar units such as glucose, galactose, and rhannose in different ratios (Ilyas et al., 2020; Bhagat et al., 2021). Exopolysaccharides form hydrophilic biofilms that offer protection against aridness during osmotic stress by enhancing the water-retaining potential of the soil and regulating the distribution of biological carbon sources. Microbes form sheaths to protect roots from dehydration and maintain the moisture content (Sandhya et al., 2009; Nadeem et al., 2021). Exopolysaccharides can be released into soil as slime ingredients comprising cation hydrogen bridges, van der Waals linkages, and anion adsorption interactions, which act as defensive capsules around the soil and improve the biological properties of the soil by increasing aggregation and macroporosity (Ilyas et al., 2020). Overall, exopolysaccharide production helps plants cope with abiotic stress (Naseem et al., 2018).

The vital interaction of the plant and microbes facilitates the production of a biofilm that allows microbes to attach with plant roots, provides a shield to the roots, and imparts a strong root adhering capability.

Effects of Microbial Volatile Organic Compounds Against Osmotic Stress

The application of beneficial microbes produces volatile compounds that can increase growth, development, photosynthesis, iron uptake, and crop productivity, while reducing the incidence of plant diseases and death. For example, stress-induced volatile compounds such as 3-hydroxy-2-butanone (acetoin), 2,3-butanediol, and 2-pentylfuran play a role in plant growth and development (Seco et al., 2015; Ali et al., 2017). These volatile compounds are also insect repellents owing to their strong odor and help boost plant growth. Under stress conditions, these compounds cause stomatal closure and impart systemic stress resistance to plants, highlighting their role in plant growth and development under stress conditions (Liu and Zhang, 2015; Mohammadipanah and Zamanzadeh, 2019).

Plant–microbial interactions emit volatile oil compounds (VOCs), which mitigate stress tolerance through the expression of genes and scavenge free radicals.

Microbial Induction of Antioxidant Machinery in Plants

Osmotic stress induces the production of ROS in plants, including superoxide, radicals, singlet oxygen, hydrogen peroxide (H_2O_2), superoxide anion radicals, and alkoxy radicals. ROS react with lipids, proteins, and DNA, thereby causing oxidative damage and affecting redox regulation in plants (Tambussi et al., 2000; Ahmad et al., 2014). To protect against oxidative damage during osmotic stress, plants induce antioxidant defense systems involving enzymatic and non-enzymatic pathways (Chai et al., 2005). Enzymatic antioxidant pathways involve enzymes such as glutathione reductase, superoxide dismutase (SOD), catalase, and ascorbate peroxidase, whereas non-enzymatic components include ABA, cysteine, and glutathione (Chai et al., 2005; Ahmad et al., 2014; Li B. et al., 2020). The presence and exogenous inoculation of microbes in the soil can confer drought tolerance by inducing antioxidant systems. Various microbes, such as *Actinomycetes*, fungi, and algae, contain phenolic components that are secreted when plants are subjected to stress (Kaushal and Wani, 2016; Ilyas et al., 2021).

The ROS scavenging ability of PGPR regulates the antioxidant enzymes and may provide a solid barrier against abiotic stress. The plant–microbial interaction ensures that there is always a homeostatic balance between ROS and removal machinery, which mitigates stress tolerance in plants.

Stimulation of Stress-Response Genes by Plant–Microbe Interactions

Stress tolerance can be enhanced by treating plants with microbes because this induces stress-response genes that regulate plant stress. The expression of such genes is modulated in plants under drought stress, which helps optimize plant growth and development. Stress-related genes and proteins involved in plant–microbe interactions include *CaPR-10*, *sHSP*, Δ1-pyrroline-5-carboxylate reductase (*P5CR*), dehydrin-like protein (*Cadhn*), vacuolar ATPase (*VA*), and pyrroline-5-carboxylate dehydrogenase (*P5CDH*)

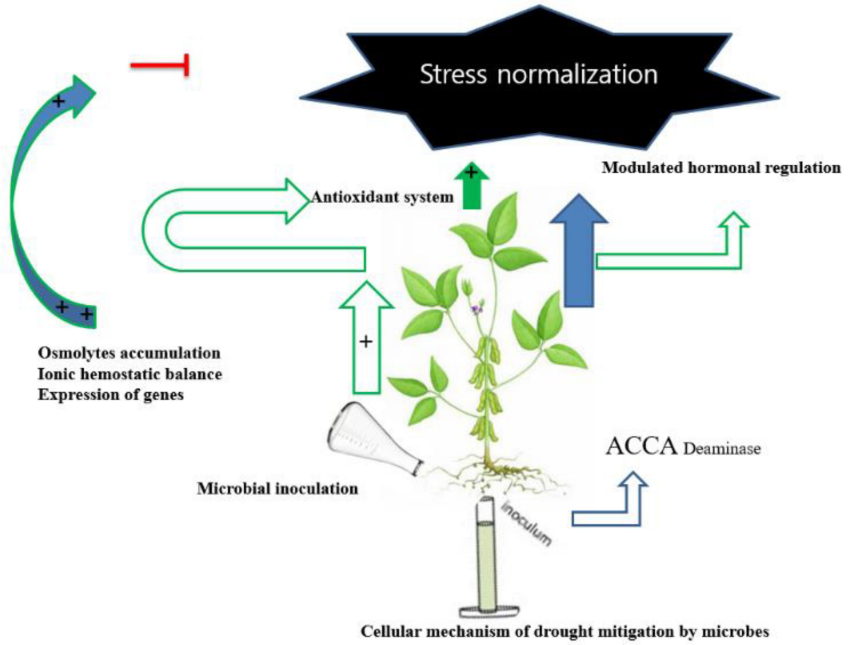


FIGURE 3 | Cellular mechanism of drought mitigation by microbes.

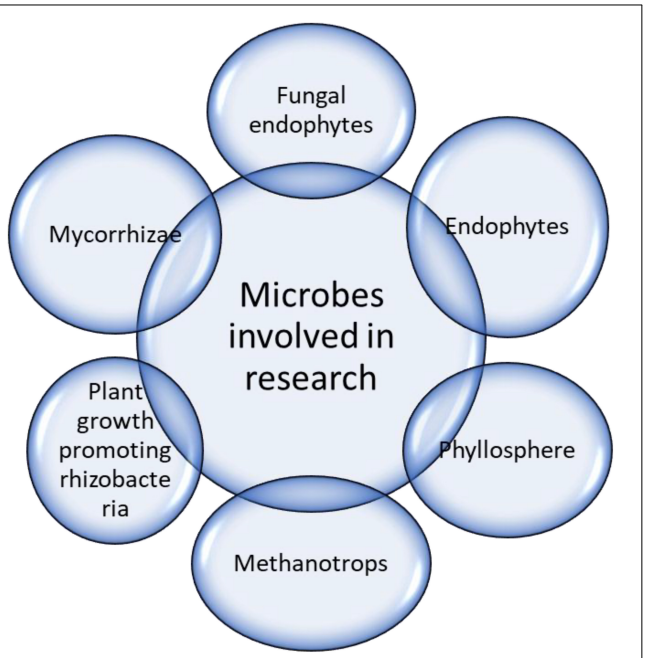


FIGURE 4 | Microbes involved in drought stress mitigation.

(Shinozaki and Yamaguchi-Shinozaki, 1998, 2007). Microarray studies have suggested that gene expression can be categorized into functional or regulatory proteins depending on the role of the encoded protein. Regulatory proteins include transcription factors, protein phosphate kinases, and ABA biosynthetic factors. Functional proteins include detoxification enzymes, water channel transporters, proteases, osmolyte biosynthesis enzymes, and macromolecule protection factors. Genes and transcription factors can encode sustainable agricultural products (Shinozaki and Yamaguchi-Shinozaki, 1998, 2007; Kavar et al., 2008).

The expression and upregulation of stress-related genes in response to drought stress can be used as a powerful tool for mitigating and enhancing drought tolerance in plants.

Microbes and Mineral Uptake

Drought stress causes an imbalance between the mineral and ion exchange. It disturbs the levels of Na^+, Cl^-, and K^+, which are responsible for plant growth. Plant–microbial interactions are able to maintain the ionic balance by scavenging the NHXI protein in the plant cytosol (Mukerji et al., 2006; Banfield and Nealson, 2018).

Beneficial microbial populations produce large numbers of organic components that can be used as signaling molecules and nutritional components for plants under drought stress. Various microbiota, such as fungi, cyanobacteria, and plant growth-promoting rhizobacteria, play important roles in mineral uptake and rehabilitation of the nutritional status (Teotia et al., 2016; Zhu et al., 2016). They mediate the solubilization of phosphosulfate compounds, nitrogen fixation, denitrification, and siderophore production. There are two pathways for mineral uptake, namely, direct and indirect (Zhu et al., 2016; Kapadia et al., 2021). Phosphate is present in the ecosystem mostly in the form of inositol phosphate; therefore, microbes solubilize phosphorus into the most soluble form by synthesizing low-molecular-weight components such as citric acid and gluconic

acid. This is an example of an indirect pathway: in direct pathways, phosphorus is solubilized by lowering the pH of the external environment and turns into low-molecular-weight organic compounds (Hupfauf et al., 2016; Sharma et al., 2020).

Therefore, a microbial population that interacts with plants in a beneficial environment can provide hemostasis for ionic exchange in the cytosol by maintaining the nutritional status of plants under drought stress.

MICROBES THAT MITIGATE DROUGHT STRESS

Endophytes

Endophytes are microscopic organisms (i.e., bacteria, fungi, and viruses) that exhibit symbiotic relationships with plants (**Figure 4**). They have been comprehensively investigated because of their beneficial effects on environmental stress (Cheng et al., 2021; Meena et al., 2021; Verma et al., 2021). Endophytes can amplify biomass accumulation (fresh and dry) in host plants under stressful conditions (Zhang et al., 2006; Barman et al., 2016). The stress mitigation effects of the endophytes were comparable among different plant species. Under drought conditions in the presence of endophytes, eudicots and C4 plant species showed increased biomass compared with monocots and C3 species. Evidence of endophyte-mediated plant stress attenuation has been established in recent decades (Strobel, 2003; Rodriguez et al., 2009).

Microbes are beneficial for reducing stress, which would otherwise limit the crop yield. When plants are under stress, they experience difficulty in sustaining their normal growth. In a previous study (Singh et al., 2020), rice crops were subjected to drought stress, and various characteristics, such as growth limitation and metabolite content, were recorded. These plants were inoculated with a combination of *Trichoderma T42* and *Pseudomonas*, which significantly improved their metabolic ability during drought stress. Microbial induction increases the total polyphenolic content and activates antioxidant enzymes to reduce oxidative stress. Inoculation also led to overexpression of *PAL*, a gene responsible for combating drought stress. These results were significant compared with those of uninoculated plants (Singh et al., 2020).

In a comparative analysis, two groups were experimentally compared, namely, untreated red rice seedlings and red rice seedlings inoculated with *Gluconacetobacter diazotrophicus* strain Pal5 (Filgueiras et al., 2020). Both seedling types were grown under water constraints of 30–35, 50–55, 70–75, or 100% field capacity for 15 days. Physical, chemical, and molecular evaluations of the plants were subsequently conducted. Leaves were found to contain increased levels of osmoprotectants, such as osmolytes (e.g., proline and glycine betaine), which help combat drought stress. Omics analysis showed the relative gene expression of *gor*, *cat*, *P5CR*, *sod*, and *BADH*. Overall, this study suggests that *G. diazotrophicus* is effective at combating the effects of drought stress.

Currently, water scarcity is a major challenge; however, rhizobacteria can facilitate plant growth under water stress. A study conducted in India involved the inoculation of great millet plants with strains of *Streptomyces laurentii* (EU-LWT3-69) and *Penicillium* sp. (EU-DSF-10), which was followed by exposure to drought stress (Kour et al., 2020a). Under drought stress, plants experience various issues, including reduced bioavailability of phosphorus, which is an important component of the soil present in its active form in microbes that are precursors to the initiation of the phosphorus availability cycle. Both the tested bacterial strains, namely, EU-DSF-10 and EU-LWT3-69, tended to solubilize phosphorus, which increased its availability to plants. These two bacterial strains are also known to solubilize phosphorus. Phosphorus-solubilizing microbes also increased the chlorophyll content, proline levels, and glycine betaine levels while reducing lipid peroxidation. Overall, the results of this study suggest that inoculated plants show better growth and defense under drought conditions than those of uninoculated plants (Kour et al., 2020a). In a study (Bilal et al., 2020), the combined effects of LHL10 and LHL06 inoculation on *Glycine max* were investigated. The microbes produced a significant synergistic effect, with observable increases in the dry biomass, roots, shoot length, and leaf area. The genomic analysis revealed an increase in *HSP90* expression levels, while the biochemical analysis revealed that lipid peroxidation increased by 24.8–141.6%. Additionally, increased calcium levels and phosphate-solubilizing potential were observed. In conclusion, the synergistic effects were remarkably effective against combined stresses, as shown in **Table 1** (Bilal et al., 2020).

In another study conducted by Kang et al. (2021), two *Enterobacter ludwigii* strains, namely, AFFR02 and Mj1212, were isolated and inoculated into alfalfa plants; subsequently, their growth attributes, hormones, and mineral concentrations were assessed. The data showed that bacterial inoculation significantly rescued plants from drought stress. The stalk diameter, fresh and dry biomass, and root/shoot elongation were all significantly higher in the treated plants than in the untreated plants. In addition, treated plants have higher levels of ABA, flavonoids, and minerals than those of untreated plants (Kang et al., 2021).

Silambarasan et al. (2019) mixed the *Rhodotorula mucilaginosa* strain CAM4 with sawdust at a ratio of 1–5%, and the formulation was applied to *Lactuca sativa*. The inoculated microbial formulations displayed tolerance to drought stress at various developmental stages. An increase in the content of chlorophyll (48–65%), carotenoids (12–54%), and proline was observed. Proline is an important precursor for maintaining the cell structure and clearing oxidative stress. Plant growth and development were observed for 24 weeks, and growth, dry biomass, root proliferation, and stem elongation were all significantly improved in the treated group compared with those in the untreated group. Furthermore, malondialdehyde (MDA) levels decreased, indicating lipid peroxidation. Overall, the formulation was suitable for reducing aluminum, drought, and salinity stress and reduced oxidative stress by activating antioxidant enzymes (Silambarasan et al., 2019).

Fungal Endophytes

Desert plants use fungal endophytes to mitigate salinity and drought stresses in arid environments. In a study conducted by

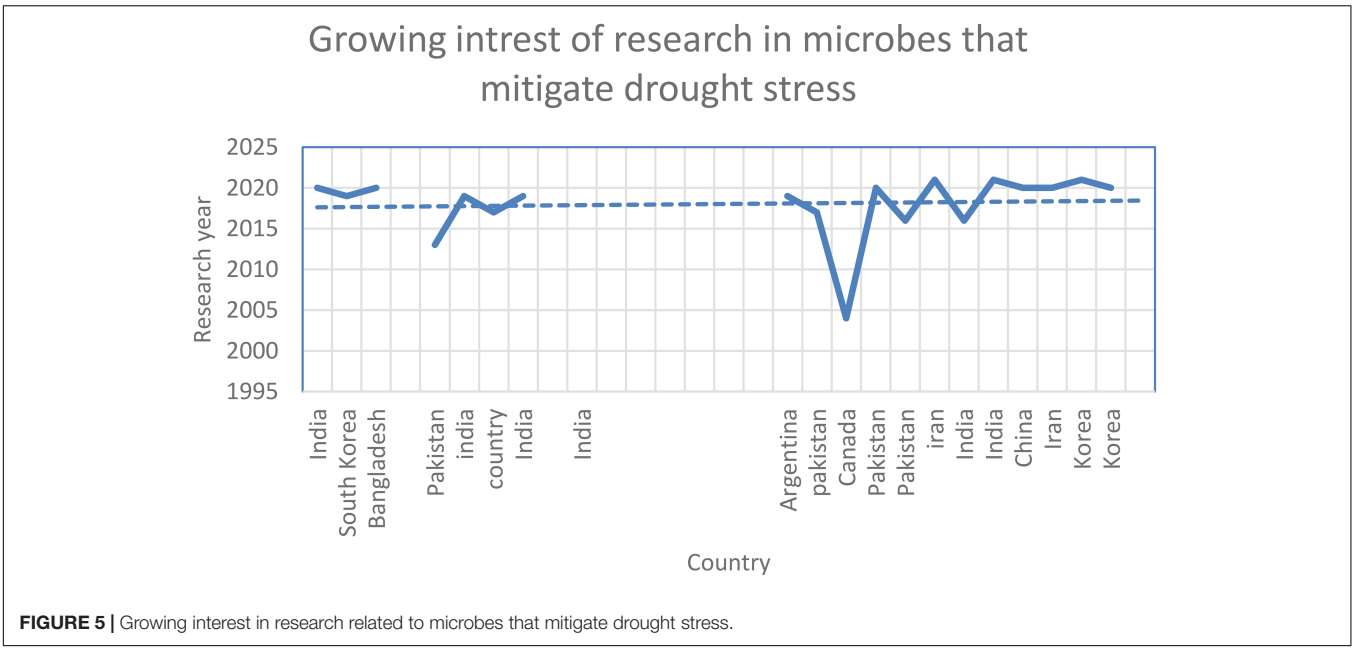


FIGURE 5 | Growing interest in research related to microbes that mitigate drought stress.

Jain et al. (2020), tomato and cucumber seedlings were exposed to fungal endophytes for 96 days. These include halotolerant microbes, such as *Neocamarosporium chichastianum, Neocamarosporium goegapense,* and *Periconia macrospinosa*, which mitigate stress by increasing the levels of proline, antioxidant enzymes, and chlorophyll, as well as enhancing growth attributes. Among these, *P. macrospinosa* significantly reduced drought and salinity stress. Thus, some endophytes can adapt to particular habitats and act as biofertilizers and ecofriendly protectors against stress (Jain et al., 2020).

When the bacterial strain YNA59 was inoculated into a broccoli plant (Kim et al., 2020), a remarkable increase in hormone levels (e.g., ABA, jasmonate, and salicylic acid) was observed. Inoculated plants also showed significant enhancement in antioxidant enzyme levels, including SOD, catalase, and ascorbate peroxidase levels (Kim et al., 2020). Another study conducted to determine the role of the fungal endophyte *Neotyphodium coenophialum* when inoculated into *Lolium arundinaceum* under drought stress revealed that the mechanism of drought tolerance was dependent on the osmotic balance and increased water uptake efficiency, which enhanced photosynthesis and altered gene expression. In addition, endophytes isolated from a *Nicotiana* plant and inoculated into *Nicotiana benthamiana* increased the ability of the plant to tolerate drought stress (Dastogeer et al., 2020; **Table 2**).

Under low-water conditions, endophytic microorganisms associated with plants have the potential to enhance resistance by maintaining water status, ion homeostasis, and nutrient uptake to induce oxidative stress and enhance stress tolerance.

Phyllosphere

Phyllosphere microbes are present above the ground surface of plants. These bacterial strains can promote plant growth (**Figure 4**). In one study, rice plant seedlings were selected and subjected to drought stress, and the plants were inoculated with the phyllosphere bacterial strains PB50, PB46, and PB3 based on their significant plant-growth-promoting activities in PEG 6000 plants subjected to drought (Arun et al., 2020). Growth attributes, such as root and shoot length, leaf area, and stem extension, were measured, and the biochemical analysis of the plants revealed their remarkable potential to solubilize important nutrients, including potassium, phosphorus, and zinc. Nutrient availability enables plant hydration under drought stress. In addition, the biochemical analysis revealed an increase in the levels of exopolysaccharides, phytohormones, soluble sugars, chlorophyll, total protein, and sugars, which improved plant survival under conditions of water constraints (Arun et al., 2020). In another study (Devarajan et al., 2021), rice phyllosphere bacterial strains (e.g., *Bacillus endophyticus* PB3, *Bacillus altitudinis* PB46, and *Bacillus megaterium* PB50) were inoculated into *Oryza sativa* pots in a greenhouse experiment. Drought tolerance was moderately minimized in strain PB50, resulting in significant tolerance to drought. Additionally, biochemical and morphological traits were observed and compared; inoculated plants showed higher expression of *LEA*, *SNAC1*, *HSP70*, *RAB16B*, and *bZIP23* as well as osmolyte accumulation, which helped combat drought (Devarajan et al., 2021; **Table 3**).

These beneficial microorganisms reside on the ground surface of plants. Phyllosphere microbiota enhance drought tolerance by promoting plant growth and protecting plants.

Plant-Growth-Promoting Rhizobacteria

Plant-growth-promoting rhizobacteria can ameliorate drought stress and improve agronomic sustainability (Kanwal et al., 2017; Vanamala et al., 2021; Aslam et al., 2022). PGPR alleviate

TABLE 1 | Endophytic microbes mitigate drought stress.

Country, year, references	Microbes	Host plant	Effect on drought stress	Mechanism of action	Isolation
India, 2020, Singh et al. (2020)	*Trichoderma* T42 and *Pseudomonas*	*Oryza sativa* L.	Reduce	*PAL* expression, polyphenols	GenBank Accession No. JN128894; Banaras Hindu University, Varanasi, India
India, 2020, Kour et al. (2020c)	EU- LRNA-72 and EU-FTF-6	Foxtail millet	Mitigate	↑Glycine betaine, chlorophyll a and b, proline, and sugars ↓LPO	Rhizosphere soil, Himachal Pradesh, India
Brazil, 2019, Filgueiras et al. (2020)	*Gluconacetobacter diazotrophicus* Pal5	*Oryza sativa* L.	Defense	Expression of *gor*, *cat*, *P5CR*, *sod*, and *BADH* ↑proline ↑glycine betaine	Sugarcane, sweet potato
India, 2020, Kour et al. (2020a)	*Streptomyces laurentii EU*-LWT3-69 and *Penicillium sp.* strain EU-DSF-10	*Sorghum bicolor* L.	Adaptation	↑osmolytes ↑ACC and deaminase ↑solubilize P ↓LPO ↑chlorophyll content	Rhizosphere, hamaliyah soil
Chile, 2019, Silambarasan et al. (2019)	CAM4	*Lactuca sativa*	Mitigate	↓MDA ↑proline ↑chlorophyll a and b and carotenoids	Rhizosphere soil, Araucania region, Southern Chile
South Korea, 2019, Bilal et al. (2020)	Endophytes (LHL10 and LHL06)	*Glycine max*	Drought protection	↑*GmHsp90A2* and *GmHsp90A1* expression ↑SOD ↓LPO	Endophytic microbes
Brazil, 2018, Martins et al. (2018)	UFGS1, UFGS2, UFGRB2, and UFGRB3	*Glycine max*	Reduce	Gmdreb1a ↑stomatal conductance ↑transpiration ↑Fv/Fm	Rhizosphere, Goiania, Goiás, Brazil

The ↑ and ↓ represent increase and decrease the response of specific mechanism.

TABLE 2 | Fungal endophytes mitigate drought tolerance.

Country, year, references	Microbes	Host plant	Effect on drought stress	Mechanism of action	Isolation
Korea, 2020, Kim et al. (2020)	YNA59	Broccoli	Mitigate	↑ABA, ↑sugar content ↑protein, ↑chlorophyll content, ↑JA, and ↑SA	Daehaw-myeon, Gang won-do, Republic of Korea
Bangladesh, 2020, Dastogeer et al. (2020)	*Neotyphodium coenophialum*	*Lolium arundinaceum Nicotiana benthamiana*	Drought tolerant	↑gaseous exchange ↑antioxidant enzyme Altered gene expression and osmotic balance	Endophytic fungi from ferns, grasses, mosses, and pteridophytes

The ↑ and ↓ represent increase and decrease the response of specific mechanism.

drought stress *via* rhizobacteria-induced drought endurance and resilience (RIDER), which induces biochemical changes (Rubin et al., 2017; Khan et al., 2018; Ansari and Ahmad, 2019). Various RIDER mechanisms include optimization of the antioxidant defense system, bacterial exopolysaccharides, phytohormone production, and cyclic metabolic pathway conventions that are involved in the deposition of several carbon-based components (**Figure 1**), such as sugars, amino acids, and polyamines, as well as the production of heat-shock proteins (Figueiredo et al., 2010; Monteiro et al., 2021; Sinha et al., 2021).

Plant-growth-promoting rhizobacteria can effectively mitigate drought stress in wheat and *Zea mays* grass. In one study (Jochum et al., 2019), two microbial strains, namely, *Bacillus* sp. 12D6 and *Enterobacter* sp. 16i, were used to combat drought stress. Plant growth attributes, hormones, and metabolite contents were analyzed. The results suggest that *Bacillus* sp. 12D6 was more effective in mitigating drought stress by increasing the root length, surface area, and plant productivity. The phytohormones IAA and salicylic acid were also found to be partly responsible for drought stress tolerance (Jochum et al., 2019). Bano et al.

TABLE 3 | Phyllosphere mitigates drought stress.

Country, year, references	Microbes	Host plant	Effect on drought stress	Mechanism of action	Isolation
India, 2020, Arun et al. (2020)	Phyllosphere bacteria (PB50, PB46, and PB3)	Rice plant *[R(4), PMK3]*	Tolerant	↑chlorophyll, carotenoids, proteins, soluble sugar, and exopolysaccharides	Leaf surface of drought-tolerant plant
India, 2021, Devarajan et al. (2021)	Rice phyllosphere bacteria *(Bacillus endophyticus PB3, Bacillus altitudinis* PB46, and *Bacillus megaterium* PB50)	*Oryza sativa* L.	Moderate	Overexpression of genes (↑*ABF*, *OsbZIP23*, and *bZIP23*) Minimal oxidative damage Osmolyte accumulation	Rice phyllosphere

The ↑ and ↓ represent increase and decrease the response of specific mechanism.

(2013) inoculated *Azospirillum* (GQ255950) into *Z. mays* plants. Microbes were isolated from water-restricted environments and inoculated into plants during the vegetative phase. After inoculation, the plants were subjected to drought conditions, and their growth attributes were recorded. Inoculation increased the root length, fresh biomass, and shoot length by 2.69–9.70%. Inoculation also increased the levels of proline, soluble sugars (63.15%), amino acids (54.54%), and osmoticum. Overall, inoculated plants can cope better with drought stress than uninoculated plants (Bano et al., 2013).

Drought is an important biotic stress factor that negatively affects crop yield. In a previous study, wheat plants were inoculated with *Pseudomonas libanensis* EU-LWNA-33, and the measurement of growth attributes revealed that the root length and biomass increased following inoculation. Furthermore, the biochemical analysis showed that proline levels increased by up to twofold, whereas glycine betaine levels increased by up to 1.2-fold at 75% stress. Proline and glycine betaine levels affect osmoregulation, as well as the solubilization and uptake of phosphorus, which is an important macronutrient with limited availability in plants. The inoculated strains effectively solubilized phosphorus (Kour et al., 2020b).

Drought stress can alter microbial interactions; for example, in a greenhouse experiment, three types of soil obtained from California valley rice fields were subjected to drought stress (Santos-Medellín et al., 2017). Water restriction altered the microbial interactions in all soil types. The altered patterns comprised enriched *Actinobacteria* and *Chloroflexi* and loss of *Acidobacteria* and *Deltaproteobacteria*. Compartment-specific restructuring results in plant survival under drought conditions (Santos-Medellín et al., 2017).

Plant-growth-promoting bacteria (PGPB) can help mitigate drought stress in various ways. Phytohormone production, 1-aminocyclopropane-1-carboxylate deaminase exopolysaccharide activation, solute production, chlorophyll synthesis, and increased mineral solubilization can help reduce stress. Such bacteria are safe, eco-friendly, and help sustain drought-tolerant crops (Priyanka et al., 2019). In a previous study (Chiappero et al., 2019), PGPR were isolated from soil, inoculated on Lysogeny broth (LB) medium plates, and cultured for 24 h in an incubator. After 1 day, the plate media contained colonies of *Pseudomonas fluorescens* WCS417r and *Bacillus amyloliquefaciens* GB03, both of which were evaluated for their effects on drought stress. Peppermint was selected, drought stress was induced, and plants were inoculated with microbes. The results demonstrated that drought stress was significantly reduced by the upregulation of the antioxidant defense system. Bioassay results revealed the hallmarks of phenolic components (Chiappero et al., 2019). In addition, the roots of *Acacia arabica* plants have been shown to be enriched with rhizosphere bacteria.

Plant-growth-promoting rhizobacteria such as *Bacillus*, *Enterobacter*, *Moraxella*, and *Pseudomonas* have been isolated and inoculated into drought-stressed wheat plants. The analysis of physiological and biochemical markers in these plants revealed increased levels of auxin, which help plants mitigate stress and enhance drought tolerance, thereby overcoming drought-related crop loss. *Bacillus* species can significantly improve auxin production to 25.9 $\mu g\ ml^{-1}$, which, in turn, improves field capacity by 10% and crop yield by 34% (Raheem et al., 2018). PGPR strains such as *Pseudomonas putida* (i.e., NBRIRA) and *B. amyloliquefaciens* (i.e., NBRISN13) have been isolated from alkaline soils in Uttar Pradesh, India (Kumar et al., 2016). These two strains were simultaneously inoculated into chickpea plants to observe their combined effects in *in vivo* greenhouse and *in vitro* experiments. Their combination in plants led to an increased chlorophyll content, photosynthesis, osmolyte content, and biomass compared with those in single-strain treatments. Thus, PGPB are ecofriendly biofertilizers that can alleviate drought stress (Kumar et al., 2016). Various studies on several microbes have provided a basis for studies on microbial interactions. These studies have investigated the dynamics of microbial interactions to reveal their combined effects on stress tolerance in plants. In a field study, *Azospirillum brasilense* Sp245 was inoculated into wheat seedlings, and comparisons were made between inoculated and uninoculated seedlings (Creus et al., 2004). The inoculated seeds contained a higher mineral content, with increased levels of Mg, K, and Ca, and showed improved water regulation. Overall, a 12.4% improvement in grain yield was observed after inoculation.

Actinomycetes are Gram-positive anaerobic unicellular microbes that mitigate drought stress. However, research on this topic is scarce. In a previous study involving *Actinomycetes*, *Streptomyces pactum* Act12 was inoculated into the wheat

TABLE 4 | Plant-growth-promoting rhizobacteria and drought tolerance.

Country, year, references	Microbes	Host plant	Effect on drought stress	Mechanism of action	Isolation
India, 2020, Kour et al. (2020c)	*Acinetobacter calcoaceticus* EU-LRNA-72 and EU-FTF-6	Foxtail millet	Mitigate	↑glycine betaine, chlorophyll a and b, proline, and sugars ↓LPO	Rhizosphere, Himachal Pradesh, India
Brazil, 2018, Martins et al. (2018)	*Bacillus* strains UFGS1, UFGS2, UFGRB2, and UFGRB3	Soybean	Reduce	Gmdreb1a ↑stomatal conductance ↑transpiration ↑ Fv/Fm	Rhizosphere, Goiania, Goiás, Brazil
United States, 2019, Jochum et al. (2019)	*Bacillus* sp. (12D6) and *Enterobacter* sp. (16i)	*Triticum aestivum* and *Zea mays*	Tolerate	↑IAA ↑SA	Rhizosphere El Paso, TX, United States
Pakistan, 2013, Bano et al. (2013)	*Azospirillum* (GQ255950)	*Zea mays*	Mitigate	↑amino acids, proline, and sugar	Water-stressed condition
India, 2019, Kour et al. (2020b)	*Pseudomonas libanensis* EU-LWNA-33	Wheat	Sustain	↑ACC deaminase ↑osmolytes ↑P solubilization	Baru Sahib Valley of Divine Peace
Unites States, 2017, Santos-Medellín et al. (2017)	Compartment-specific restructuring	*Oryza sativa* and *Oryza glaberrima*	Survival	↑*Actinobacteria* ↑*Chloroflexi* ↓*Deltaproteobacteria* ↓*Acidobacteria*	California Central Valley fields
India, 2019, Priyanka et al. (2019)	*Azospirillum*	Wheat (*Triticum aestivum*)	Tolerant	↑phytohormone ↑solute formation ↑exopolysaccharide production	Rhizosphere soil, India
	Azospirillum brasilense	*Phaseolus vulgaris*	↑ACC deaminase ↑overexpression of *Cadhn*, *VA*, *sHSP*, and *CaPR-10*		
	Achromobacter piechaudii	*Lycopersicon esculentum* and *Capsicum annuum*			
	Azospirillum brasilense	*Zea mays*			
	Bacillus licheniformis K11	*Capsicum annuum*			
	Achromobacter piechaudii ARV8	*Lycopersicon esculentum* and *Capsicum annuum*	↓ethylene ↑ACC deaminase ↑root and shoot length ↑chlorophyll synthesis ↓ethylene ↓ACC deaminase		
	Enterobacter cancerogenus	*Jatropha curcas*			
Argentina, 2019, Chiappero et al. (2019)	PGPR (*Pseudomonas fluorescens* WCS417↑r and *Bacillus amyloliquefaciens* GB03)	*Mentha piperita*	Mitigate	↑phenolic compounds Antioxidant defense	Rhizosphere soil
Pakistan, 2017, Raheem et al. (2018)	PGPR (*Bacillus, Enterobacter, Moraxella,* and *Pseudomonas*)	*Triticum aestivum* L.	Mitigate	↑auxin	Root system of *Acacia arabica*
Canada, 2004, Creus et al. (2004)	*Azospirillum brasilense* Sp245	*Triticum aestivum*	Minimize	↑mineral content ↑elastic adjustment	N/A

(Continued)

TABLE 4 | (Continued)

Country, year, references	Microbes	Host plant	Effect on drought stress	Mechanism of action	Isolation
China, 2020, Li H. et al. (2020)	*Streptomyces pactum* Act12	Wheat	Resistance	Overexpression of *EXPA2*, *EXPA6*, *P5CS*, and *SnRK2* ↑root length, ↑shoot length, ↑sugar content, ↑MDA, and ↑ABA	Alpine meadow in the Sanjiangyuan region
India, 2016, Kumar et al. (2016)	PGPR (*Pseudomonas putida* NBRIRA and *Bacillus amyloliquefaciens* NBRISN13)	Chickpea	Tolerate	↑chlorophyll ↑antioxidant enzymes ↑protein content	Alkaline soil of Uttar Pradesh, India

The↑ and ↓ represent increase and decrease the response of specific mechanism.

TABLE 5 | Methanotrophs mitigate drought stress.

Country, year, references	Microbes	Host plant	Effect on drought stress	Mechanism of action	Isolation
India, 2019, Kumar et al. (2019)	Methylotrophic bacteria (*Methylarcula, Methylobacillus, Methylobacterium, Methylocapsa, Methylocella, Methyloferula, Methylohalomonas, Methylomonas, Methylophilus, Methylopila, Methylosinus, Methylotenera,* and *Methylovirgula*)	*Glycine max*	Tolerant	↑auxin and cytokines ↑nitrogen fixation ↑ethylene ↑ACC deaminase ↑mineral solubilization	Phyllospheres of cotton and maize and earthworms in Tamil Nadu soil
Pakistan, 2020, Danish et al. (2020)	*Pseudomonas aeruginosa, Enterobacter cloacae, Achromobacter xylosoxidans,* and *Leclercia adecarboxylata*	*Zea mays*	Tolerant	↑ACC deaminase	Maize rhizosphere

The ↑ and ↓ represent increase and decrease the response of specific mechanism.

plant cultivar Xinong 979 (Li H. et al., 2020). This inoculation significantly increased the overexpression of *EXPA6*, *P5CS*, *EXPA2*, and *SnRK2* and increased the root length by 13.6%, shoot length by 10.3%, and fresh biomass by 21.3%. Chemical assays also revealed that the exposed seedlings showed stress reduction through an increase in the levels of sugars and antioxidant enzymes.

Water shortages can be a major challenge in agricultural systems because they negatively affect the quality and quantity of crops. An experiment was conducted on foxtail millet crops that were subjected to drought stress, followed by inoculation with *Acinetobacter calcoaceticus* EU-LRNA-72 and *Penicillium* sp. EU-FTF-6 (Kour et al., 2020c). Plant growth attributes were measured, which showed mitigation of drought stress and physiological growth due to inoculation. In this study, drought stress was mitigated by the accumulation of osmolytes, proline, and glycine betaine, as well as by increased levels of chlorophyll a and b. An increased chlorophyll content resulted in plant growth and development, whereas increased proline and glycine betaine levels improved osmotic adjustment and membrane integrity, respectively. These results demonstrated that inoculation with microbes efficiently combats drought stress (Kour et al., 2020c). In a randomized controlled trial (Martins et al., 2018), soybean was inoculated with *Bacillus subtilis* (i.e., UFGS1), *Bacillus thuringiensis* (i.e., UFGS2 and UFGRB2), and *Bacillus cereus* (i.e., UFGRB3) strains. The strains were selected based on their growth under water stress on media plates. *B. thuringiensis* UFGRB2 maintained the quantum efficiency of PSII; *B. thuringiensis* and *B. cereus* maintained the photosynthetic rates of the plants, while *B. thuringiensis* sustained the transpiration rate and stomatal conductance. These physiological features demonstrate the improved growth observed in inoculated plants compared with that of uninoculated plants. Additionally, the genomic analysis showed that overexpression of *Gmdreb1a* contributed to drought stress tolerance (Martins et al., 2018; **Table 4**).

Plant-growth-promoting rhizobacteria enhance the growth, development, and disease resistance of plants through a wide range of mechanisms. These are the most common microbes that mitigate drought stress. They secrete compounds of

TABLE 6 | Mycorrhizae mitigate drought stress.

Country, year, references	Microbes	Host plant	Effect on drought stress	Mechanism of action	Isolation
Iran, 2021, Moradtalab et al. (2019)	Arbuscular mycorrhizal fungus	*Fragaria* × *ananassa* Duch.	Mitigate	↑Zn ↑AA enzyme ↑water uptake	Pal Axel Lab, Lund University, Sweden
Argentina, 2014, Grümberg et al. (2015)	Arbuscular mycorrhizal fungi	*Glycine max*	Tolerance	↑osmoprotectants ↑proline, glycine, and soluble sugars ↓MDA	Ecosystem, experimental field Central Argentina
China, 2021, Cheng et al. (2021)	*Funneliformis mosseae*	*Trifoliate orange*	Stress modulation	↑phenolic contents ↑terpenes ↑root exudate ↑coumarins ↓alkanes, ester, and amides	Rhizosphere Jingzhou, China
Italy, 2017, Bernardo et al. (2017)	Arbuscular mycorrhizal fungus (*Glomus mosseae*)	*Triticum* spp.	Tolerance	↓6-SFT ↓SOD ↑genetic diversity ↓sulfur metabolism	MycAgro Lab (Techno pole Agro-Environment, Bretenière, France)
Saudi Arabia, 2020, Al-Arjani et al. (2020)	AMF (*Glomus etunicatum*, *Glomus intraradices*, and *Glomus mosseae*)	*Ephedra foliata* Boiss	Tolerance	↑gene expression ↑mineral solubilization ↑phytohormone production ↑transport protein expression ↑osmolytes ↑antioxidant enzyme	Rhizosphere of *Acacia gerrardii*

The ↑ and ↓ represent increase and decrease the response of specific mechanism.

valuable potential biostimulants and play a pivotal role in plant stress responses.

Methanotrophs

To sustain biofertilization in India, an attempt was made to isolate and inoculate a methylotrophic bacterial community (e.g., *Methylarcula*, *Methyloferula*, *Methylobacterium*, *Methylotenera*, *Methylobacillus*, *Methylophilus*, *Methylocapsa*, *Methylocella*, *Methylohalomonas*, *Methylomonas*, *Methylopila*, *Methylosinus*, and *Methylovirgula*) (Kumar et al., 2019). Bacteria were isolated from the phyllospheres of cotton, maize, earthworms, and rhizosphere soil in Tamil Nadu, India. Methylotrophs increased the levels of auxin and cytokines, and the increased levels of phytohormones promoted germination and growth. In addition to increasing the ACC deaminase activity, these bacteria enhance nitrogen fixation and mineral solubilization. The novelty of this microbial community is that it is composed of type 1 and type 2 methanotrophs that have the potential to tolerate stress (Kumar et al., 2019). In another study (Danish et al., 2020), rhizosphere bacteria were collected from *Z. mays* and reinoculated into plants; data (submitted to National Center for Biotechnology Information (NCBI)) indicated the presence of *Pseudomonas aeruginosa*, *Enterobacter cloacae*, *Achromobacter xylosoxidans,* and *Leclercia adecarboxylata.* Additionally, bioassays demonstrated the significant involvement of ACC deaminase. Among these microbes, *E. cloacae* significantly increased grain yield by up to 73% owing to the ACC deaminase activity (**Table 5**).

Methanotrophs metabolize methane from carbon molecules and produce sulfate, nitrate, and oxidation energy. They require only a single carbon atom for survival; therefore, their survival rate is higher.

Mycorrhizae

Mycorrhizae are microbial symbiotes that maintain a symbiotic association with plants. They are host-specific and have interspecific functionality (Sheteiwy et al., 2021). Arbuscular mycorrhizae facilitate host plant survival by increasing water and nutrient absorption from the rhizosphere (Agapitos et al., 2008), whereas endophytes do so by providing phytohormones and inducing defense-related secondary metabolism within the plants (Barman et al., 2016; Cheng et al., 2021; Kozjek et al., 2021).

In a study on soybean, which is highly sensitive to abiotic stress, plants were inoculated with arbuscular mycorrhizal fungi (AMF); the isolates were obtained from Argentina (Grümberg et al., 2015). After inoculation, the plants were subjected to drought conditions, and their physiological, biochemical, and molecular characteristics were evaluated. The quantitative analysis showed increased levels of proline, soluble sugars, and glycine betaine and reduced levels of MDA. MDA is a product of polyunsaturated fatty acids in cells and serves as the gold standard for identifying oxidative stress. The fungal strains *Septoglomus constrictum, Glomus* sp., and *Glomus aggregatum* effectively increase the levels of osmoprotectants in plant leaves and provide potential protection against drought stress (Grümberg et al., 2015).

Apart from abiotic stress, drought stress is the leading cause of plant diseases and limits crop production. In a randomized trial conducted by Cheng et al. (2021), *Funneliformis mosseae* was used to colonize trifoliate orange. After treatment for 8 weeks, a dramatic increase was observed in the leaf number, leaf area, stem elongation, and root microenvironment of the plants. Additionally, the qualitative analysis revealed increased phenolic, coumarin, and terpene contents in the root exudates. Phenolic components are key elements of drought stress tolerance, as they reduce oxidative stress (Cheng et al., 2021). In another study, two cultivars of wheat bread and durum wheat were selected and inoculated with *Glomus mosseae*, a strain of mycorrhizal fungi, and then subjected to water restriction (Bernardo et al., 2017). In a randomized controlled trial, analyses of growth parameters and proteomics were conducted to determine the mechanisms of drought tolerance. The results suggest that inoculation increased the accumulation of aboveground dry biomass. Furthermore, an increased genotype diversity is related to stress tolerance. Various genes modulate the signaling pathways of sulfur and oxylipin metabolism, which inhibits ethylene formation. Ethylene causes plant stress and damages cell integrity and osmotic pressure. Downregulation of 6-SFT expression was also noted. The upregulation of osmolytes in the cellular components of plants was significant, indicating that oxidation–reduction mechanism is associated with drought tolerance (Bernardo et al., 2017).

Microbes can be ecofriendly and aid in stress tolerance in plants. Drought stress involves a cascade of events that cause oxidative damage. Thus, the plant antioxidant defense system is activated by the induction of gene expression to combat ROS. For example, inoculation of two AMF strains of *Gigaspora margarita* and *Glomus intraradices* in host plants resulted in the expression of *GmarCuZnSOD, GintPDX1, GintMT1,* and *GintSOD*. In addition, the mechanism for tolerating drought stress involves the reduction of cytoplasmic protein levels and regulation of redox status *via* pyridoxamine synthesis (Zou et al., 2021).

Drought stress negatively affects the crop quality and quantity. However, this can be mitigated through the inoculation of three species of AMF, namely, *G. mosseae, Glomus etunicatum*, and *G. intraradices*. Al-Arjani et al. (2020) isolated these three species from the rhizosphere of *Acacia gerrardii* and applied them to *Ephedra foliata* Boiss plants. Consequently, plants were preserved under restricted water conditions (used to induce drought stress). Specifically, compared with control plants, the inoculated plants were more likely to show photoassimilation, which increased the chlorophyll and carotenoid contents. Additionally, increased levels of sucrose-phosphate synthase were observed in the carbon pool. Furthermore, increased osmolytes are among other factors attributed to drought stress tolerance (Al-Arjani et al., 2020). In another study, AMF and silicon were inoculated with 1-week-old strawberry seedlings to observe their synergistic effects against drought stress (Moradtalab et al., 2019). Following a randomized trial over 4 weeks, AMF and silicone were found to increase the biomass, water uptake, and mineral content and promote the antioxidant defense system. Thus, the two are beneficial for combating drought stress when combined (Moradtalab et al., 2019; **Table 6**).

Mycorrhiza form a symbiotic relationship between fungi and plants. The term mycorrhiza refers to the role of the fungus in the plant axis; mycorrhizae play a significant role in plant growth, nutrition, soil biochemistry, and stress tolerance.

GROWING INTEREST

There is an increasing trend in publications related to this topic, which will likely continue to increase owing to the need to identify adaptive solutions that can determine the effects of climate change on crops. Notably, several studies have used a mixture of diverse microbial strains, and it has been speculated that a consortium would be more archetypal of the original microbiome, which would include numerous strains that can provide distinctive synergistic benefits compared with individual strains (**Figure-5**).

CONCLUSION AND FUTURE PERSPECTIVES

Plants have evolved in a sophisticated manner with microbes to overcome drought stress and its adverse effects within cells. Microbes strengthen the intrinsic stress tolerance mechanisms of plants by producing exopolysaccharides, phytohormones, ACC deaminase, osmolytes, and volatile compounds. In addition, cells synthesize diverse molecules that regulate redox damage and overcome antioxidant damage.

This review highlights a variety of adverse effects of drought stress on plant growth and reveals how such effects can be mitigated using microbes. Previous reviews have focused on drought mitigation by using a group of microbes. However, this review discusses a variety of microbes that mitigate drought stress, their fundamental mechanisms of action, and the changes that they produce at the molecular level. Microbial intervention has led to substantial progress in drought tolerance. Future investigations should evaluate whether acute and chronic effects are beneficial to plant phenotypes. Although known microbial interventions are promising, their dose, frequency, and timing warrant practical validation.

AUTHOR CONTRIBUTIONS

SS and MAK contributed to the original draft writing. MI and S-MK helped with review and graphical representation. Y-SP and SHW helped in formatting the manuscript. I-JL helped with funding. All authors contributed to the article and approved the submitted version.

FUNDING

This work was supported by the National Research Foundation of Korea (NRF) grant funded by the Korean Government (MSIT) (No. 2022R1A2C1008993).

REFERENCES

Agapitos, A., Togelius, J., Lucas, S. M., Schmidhuber, J., and Konstantinidis, A. (2008). "Generating diverse opponents with multiobjective evolution," in *Proceedings of the IEEE Symposium On Computational Intelligence and Games, 2008. CIG'08*, (Piscataway, NJ: IEEE), 135–142.

Ahmad, A., Aslam, Z., Naz, M., Hussain, S., Javed, T., Aslam, S., et al. (2021). Exogenous salicylic acid-induced drought stress tolerance in wheat (*Triticum aestivum* L.) grown under hydroponic culture. *PLoS One* 16:e0260556. doi: 10.1371/journal.pone.0260556

Ahmad, P., Jamsheed, S., Hameed, A., Rasool, S., Sharma, I., Azooz, M., et al. (2014). "Drought stress induced oxidative damage and antioxidants in plants," in *Oxidative Damage to Plants*, ed. P. Ahmad (New York, NY: Elsevier), 345–367.

Alagoz, Y., Nayak, P., Dhami, N., and Cazzonelli, C. I. (2018). Cis-carotene biosynthesis, evolution and regulation in plants: the emergence of novel signaling metabolites. *Arch. Biochem. Biophys.* 654, 172–184. doi: 10.1016/j.abb.2018.07.014

Al-Arjani, A.-B. F., Hashem, A., and Abd_Allah, E. F. (2020). Arbuscular mycorrhizal fungi modulates dynamics tolerance expression to mitigate drought stress in *Ephedra foliata* Boiss. *Saudi J. Biol. Sci.* 27, 380–394. doi: 10.1016/j.sjbs.2019.10.008

Ali, F., Bano, A., and Fazal, A. (2017). Recent methods of drought stress tolerance in plants. *Plant Growth Regul.* 82, 363–375. doi: 10.1007/s10725-017-0267-2

Anjum, S. A., Xie, X.-Y., Wang, L.-C., Saleem, M. F., Man, C., and Lei, W. (2011). Morphological, physiological and biochemical responses of plants to drought stress. *Afr. J. Agricult. Res.* 6, 2026–2032.

Ansari, F. A., and Ahmad, I. (2019). "Alleviating drought stress of crops through PGPR: mechanism and application," in *Microbial Interventions in Agriculture and Environment*, eds D. P. Singh, V. K. Gupta, and R. Prabha (Singapore: Springer), 341–358. doi: 10.1007/978-981-13-8383-0_11

Arun, K. D., Sabarinathan, K. G., Gomathy, M., Kannan, R., and Balachandar, D. (2020). Mitigation of drought stress in rice crop with plant growth-promoting abiotic stress-tolerant rice phyllosphere bacteria. *J. Basic Microbiol.* 60, 768–786. doi: 10.1002/jobm.202000011

Askari-Khorasgani, O., Pardo, F. B. F., and Pessarakli, M. (2021). "Drought stress sensing-signaling in plants," in *Handbook of Plant and Crop Physiology*, ed. M. Pessarakli (Boca Raton, FL: CRC Press), 465–481. doi: 10.1201/9781003093640-30

Aslam, M. M., Idris, A. L., Zhang, Q., Weifeng, X., Karanja, J. K., and Wei, Y. (2022). Rhizosphere microbiomes can regulate plant drought tolerance. *Pedosphere* 32, 61–74. doi: 10.1016/s1002-0160(21)60061-9

Banfield, J. F., and Nealson, K. H. (2018). *Geomicrobiology: Interactions between Microbes and Minerals*. Berlin: Walter de Gruyter GmbH & Co KG.

Bano, Q., Ilyas, N., Bano, A., Zafar, N., Akram, A., and Hassan, F. (2013). Effect of *Azospirillum* inoculation on maize (*Zea mays* L.) under drought stress. *Pak. J. Bot.* 45, 13–20.

Barman, J., Samanta, A., Saha, B., and Datta, S. (2016). Mycorrhiza. *Resonance* 21, 1093–1104.

Bartels, D., and Phillips, J. (2010). "Drought stress tolerance," in *Genetic Modification of Plants*, eds F. Kempken and C. Jung (Berlin: Springer), 139–157.

Basu, S., Ramegowda, V., Kumar, A., and Pereira, A. (2016). Plant adaptation to drought stress. *F1000Research* 5:1554. doi: 10.12688/f1000research.7678.1

Berg, G. (2009). Plant–microbe interactions promoting plant growth and health: perspectives for controlled use of microorganisms in agriculture. *Appl. Microbiol. Biotechnol.* 84, 11–18. doi: 10.1007/s00253-009-2092-7

Bernardo, L., Morcia, C., Carletti, P., Ghizzoni, R., Badeck, F. W., Rizza, F., et al. (2017). Proteomic insight into the mitigation of wheat root drought stress by arbuscular mycorrhizae. *J. Proteomics* 169, 21–32. doi: 10.1016/j.jprot.2017.03.024

Bhagat, N., Raghav, M., Dubey, S., and Bedi, N. (2021). Bacterial exopolysaccharides: insight into their role in plant abiotic stress tolerance. *J. Microbiol. Biotechnol.* 31, 1045–1059. doi: 10.4014/jmb.2105.05009

Bilal, S., Shahzad, R., Imran, M., Jan, R., Kim, K. M., and Lee, I.-J. (2020). Synergistic association of endophytic fungi enhances *Glycine max* L. resilience to combined abiotic stresses: heavy metals, high temperature and drought stress. *Industr. Crops Prod.* 143:111931. doi: 10.1016/j.indcrop.2019.111931

Bright, J., Desikan, R., Hancock, J. T., Weir, I. S., and Neill, S. J. (2006). ABA-induced NO generation and stomatal closure in *Arabidopsis* are dependent on H2O2 synthesis. *Plant J.* 45, 113–122. doi: 10.1111/j.1365-313X.2005.02615.x

Campbell, B. G. (1995). *Isolation and Molecular Characterisation of Two Pseudomonas sp. ACC Deaminase Genes*. Cape Town: University of Cape Town.

Chai, T.-T., Fadzillah, N., Kusnan, M., and Mahmood, M. (2005). Water stress-induced oxidative damage and antioxidant responses in micropropagated banana plantlets. *Biol. Plant.* 49, 153–156. doi: 10.1007/s00000-005-3156-9

Chen, H., and Jiang, J.-G. (2010). Osmotic adjustment and plant adaptation to environmental changes related to drought and salinity. *Environ. Rev.* 18, 309–319. doi: 10.1139/a10-014

Cheng, H.-Q., Giri, B., Wu, Q.-S., Zou, Y.-N., and Kuèa, K. (2021). Arbuscular mycorrhizal fungi mitigate drought stress in citrus by modulating root microenvironment. *Arch. Agron. Soil Sci.* Online ahead of Print,

Chiappero, J., Del Rosario Cappellari, L., Alderete, L. G. S., Palermo, T. B., and Banchio, E. (2019). Plant growth promoting rhizobacteria improve the antioxidant status in *Mentha piperita* grown under drought stress leading to an enhancement of plant growth and total phenolic content. *Industr. Crops Prod.* 139:111553. doi: 10.1016/j.indcrop.2019.111553

Choudhary, D. K., Varma, A., and Tuteja, N. (2016). *Plant-Microbe Interaction: An Approach to Sustainable Agriculture*. Berlin: Springer.

Creus, C. M., Sueldo, R. J., and Barassi, C. A. (2004). Water relations and yield in Azospirillum-inoculated wheat exposed to drought in the field. *Can. J. Bot.* 82, 273–281. doi: 10.1139/b03-119

Danish, S., Zafar-Ul-Hye, M., Mohsin, F., and Hussain, M. (2020). ACC-deaminase producing plant growth promoting rhizobacteria and biochar mitigate adverse effects of drought stress on maize growth. *PLoS One* 15:e0230615. doi: 10.1371/journal.pone.0230615

Dastogeer, K. M. G., Chakraborty, A., Sarker, M. S. A., and Akter, M. A. (2020). Roles of fungal endophytes and viruses in mediating drought stress tolerance in plants. *Int. J. Agricult. Biol.* 24, 1497–1512.

Davies, P. J. (1995). "The plant hormone concept: concentration, sensitivity and transport," in *Plant Hormones Davies*, ed. P.J. Davies (Dordrecht: Springer), 13–38. doi: 10.1007/978-94-011-0473-9_2

Devarajan, A. K., Muthukrishanan, G., Truu, J., Truu, M., Ostonen, I., Panneerselvam, P., et al. (2021). The foliar application of rice phyllosphere bacteria induces drought-stress tolerance in *Oryza sativa* (L.). *Plants* 10:387. doi: 10.3390/plants10020387

Dikarev, A., Dikarev, V., Geras'kin, S. A., and Dikareva, N. (2016). Plant tolerance. *Biochem. Physiol. Traits* 51, 89–99.

Dobra, J., Motyka, V., Dobrev, P., Malbeck, J., Prasil, I. T., Haisel, D., et al. (2010). Comparison of hormonal responses to heat, drought and combined stress in tobacco plants with elevated proline content. *J. Plant Physiol.* 167, 1360–1370.

Fahad, S., Nie, L., Chen, Y., Wu, C., Xiong, D., Saud, S., et al. (2015). "Crop plant hormones and environmental stress," in *Sustainable Agriculture Reviews*, ed. E. Lichtfouse (Cham: Springer), 371–400. doi: 10.1007/978-3-319-09132-7_10

Farooq, M., Hussain, M., Wahid, A., and Siddique, K. (2012). "Drought stress in plants: an overview," in *Plant Responses to Drought Stress*, ed. R. Aroca (Berlin: Springer), 1–33.

Farooq, M., Wahid, A., Kobayashi, N., Fujita, D., and Basra, S. (2009). Plant drought stress: effects, mechanisms and management. *Sustain. Agricult.* 29, 153–188.

Figueiredo, M. D. V. B., Seldin, L., De Araujo, F. F., and Mariano, R. D. L. R. (2010). "Plant growth promoting rhizobacteria: fundamentals and applications," in *Plant Growth and Health Promoting Bacteria*, ed. D. Maheshwari (Berlin: Springer), 21–43. doi: 10.1007/978-3-642-13612-2_2

Filgueiras, L., Silva, R., Almeida, I., Vidal, M., Baldani, J. I., and Meneses, C. H. S. G. (2020). Gluconacetobacter diazotrophicus mitigates drought stress in *Oryza sativa* L. *Plant Soil* 451, 57–73. doi: 10.1007/s11104-019-04163-1

Grümberg, B. C., Urcelay, C., Shroeder, M. A., Vargas-Gil, S., and Luna, C. M. (2015). The role of inoculum identity in drought stress mitigation by arbuscular mycorrhizal fungi in soybean. *Biol. Fertil. Soils* 51, 1–10. doi: 10.1007/s00374-014-0942-7

Hossain, M. A., Wani, S. H., Bhattacharjee, S., Burritt, D. J., and Tran, L.-S. P. (2016). *Drought Stress Tolerance in Plants, Vol 2: Molecular and Genetic Perspectives*. Berlin: Springer.

Houda, T., Issam, B. S., and Naïma, K. B. (2013). Effectiveness of the plant growth-promoting rhizobacterium Pantoea sp. *Soil Sci.* 158, 442–453.

Hupfauf, S., Bachmann, S., Juárez, M. F.-D., Insam, H., and Eichler-Löbermann, B. (2016). Biogas digestates affect crop P uptake and soil microbial community composition. *Sci. Total Environ.* 542, 1144–1154. doi: 10.1016/j.scitotenv.2015.09.025

Ilyas, M., Nisar, M., Khan, N., Hazrat, A., Khan, A. H., Hayat, K., et al. (2021). Drought tolerance strategies in plants: a mechanistic approach. *J. Plant Growth Regul.* 40, 926–944.

Ilyas, N., Mumtaz, K., Akhtar, N., Yasmin, H., Sayyed, R., Khan, W., et al. (2020). Exopolysaccharides producing bacteria for the amelioration of drought stress in wheat. *Sustainability* 12:8876. doi: 10.3390/su12218876

Iordachescu, M., and Imai, R. (2011). "Trehalose and abiotic stress in biological systems," in *Abiotic Stress in Plants-Mechanisms and Adaptations*, eds A. K. Shanker and B. Venkateswarlu (Croatia: Intech), 215–234.

Jain, D., Phurailatpam, L., and Mishra, S. (2020). "Microbes-mediated mitigation of drought stress in plants: recent trends and future challenges," in *Advances in Plant Microbiome and Sustainable Agriculture*, eds A. Yadav, A. Rastegari, N. Yadav, and D. Kour (Singapore: Springer), 199–218. doi: 10.1007/978-981-15-3204-7_9

Jeon, J.-S., Lee, S.-S., Kim, H.-Y., Ahn, T.-S., and Song, H.-G. (2003). Plant growth promotion in soil by some inoculated microorganisms. *J. Microbiol.* 41, 271–276.

Jochum, M. D., Mcwilliams, K. L., Borrego, E. J., Kolomiets, M. V., Niu, G., Pierson, E. A., et al. (2019). Bioprospecting plant growth-promoting rhizobacteria that mitigate drought stress in grasses. *Front. Microbiol.* 10:2106. doi: 10.3389/fmicb.2019.02106

Jogawat, A., Yadav, B., Lakra, N., Singh, A. K., and Narayan, O. P. (2021). Crosstalk between phytohormones and secondary metabolites in the drought stress tolerance of crop plants: a review. *Physiol. Plant.* 172, 1106–1132. doi: 10.1111/ppl.13328

Kahraman, M., Sevim, G., and Bor, M. (2019). "The role of proline, glycinebetaine, and trehalose in stress-responsive gene expression," in *Osmoprotectant-Mediated Abiotic Stress Tolerance in Plants*, eds M. Hossain, V. Kumar, D. Burritt, M. Fujita, and P. Mäkelä (Cham: Springer), 241–256. doi: 10.1007/978-3-030-27423-8_11

Kanellis, A., Chang, C., Klee, H., Bleecker, A., Pech, J., and Grierson, D. (2012). *Biology and Biotechnology of the Plant Hormone Ethylene II*. Berlin: Springer Science & Business Media.

Kang, S.-M., Khan, M.-A., Hamayun, M., Kim, L.-R., Kwon, E.-H., Kang, Y.-S., et al. (2021). Phosphate-Solubilizing Enterobacter ludwigii AFFR02 and *Bacillus megaterium* Mj1212 rescues Alfalfa's growth under post-drought stress. *Agriculture* 11:485. doi: 10.3390/agriculture11060485

Kanwal, S., Ilyas, N., Batool, N., and Arshad, M. (2017). Amelioration of drought stress in wheat by combined application of PGPR, compost, and mineral fertilizer. *J. Plant Nutr.* 40, 1250–1260. doi: 10.1080/01904167.2016.1263322

Kapadia, C., Sayyed, R., El Enshasy, H. A., Vaidya, H., Sharma, D., Patel, N., et al. (2021). Halotolerant microbial consortia for sustainable mitigation of salinity stress, growth promotion, and mineral uptake in tomato plants and soil nutrient enrichment. *Sustainability* 13:8369. doi: 10.3390/su13158369

Kaushal, M., and Wani, S. P. (2016). Plant-growth-promoting rhizobacteria: drought stress alleviators to ameliorate crop production in drylands. *Ann. Microbiol.* 66, 35–42. doi: 10.1007/s13213-015-1112-3

Kavar, T., Maras, M., Kidrič, M., Šuštar-Vozlič, J., and Meglič, V. (2008). Identification of genes involved in the response of leaves of *Phaseolus vulgaris* to drought stress. *Mol. Breed.* 21, 159–172. doi: 10.1007/s11032-007-9116-8

Kefeli, V. I., Kefeli, V., Kalevitch, M., and Borsari, B. (2003). *Natural Growth Inhibitors and Phytohormones in Plants and Environment*. Berlin: Springer Science & Business Media.

Khan, N. A., Nazar, R., Iqbal, N., and Anjum, N. A. (2012). *Phytohormones and Abiotic Stress Tolerance in Plants*. Berlin: Springer Science & Business Media.

Khan, N., Bano, A., Shahid, M. A., Nasim, W., and Babar, M. A. (2018). Interaction between PGPR and PGR for water conservation and plant growth attributes under drought condition. *Biologia* 73, 1083–1098. doi: 10.2478/s11756-018-0127-1

Kim, Y.-N., Khan, M. A., Kang, S.-M., Hamayun, M., and Lee, I.-J. (2020). Enhancement of drought-stress tolerance of *Brassica oleracea* var. italica L. by newly isolated *Variovorax sp*. YNA59. *J. Microbiol. Biotechnol.* 30, 1500–1509. doi: 10.4014/jmb.2006.06010

Kirst, G. (1996). "Osmotic adjustment in phytoplankton and macroalgae," in *Biological and Environmental Chemistry of DMSP and Related Sulfonium Compounds*, eds R. P. Kiene, P. T. Visscher, M. D. Keller, and G. O. Kirst (New York, NY: Springer), 121–129. doi: 10.1007/978-1-4613-0377-0_11

Kour, D., and Yadav, A. N. (2020). Microbe mediated mitigation of drought stress in crops. *Agric. Lett.* 1, 79–82.

Kour, D., Rana, K. L., Kaur, T., Sheikh, I., Yadav, A. N., Kumar, V., et al. (2020a). Microbe-mediated alleviation of drought stress and acquisition of phosphorus in great millet (*Sorghum bicolour* L.) by drought-adaptive and phosphorus-solubilizing microbes. *Biocatal. Agricult. Biotechnol.* 23:101501.

Kour, D., Rana, K. L., Sheikh, I., Kumar, V., Yadav, A. N., Dhaliwal, H. S., et al. (2020b). Alleviation of drought stress and plant growth promotion by *Pseudomonas* libanensis EU-LWNA-33, a drought-adaptive phosphorus-solubilizing bacterium. *Proc. Natl. Acad. Sci. India B Biol. Sci.* 90, 785–795. doi: 10.1007/s40011-019-01151-4

Kour, D., Rana, K. L., Yadav, A. N., Sheikh, I., Kumar, V., Dhaliwal, H. S., et al. (2020c). Amelioration of drought stress in Foxtail millet (*Setaria italica* L.) by P-solubilizing drought-tolerant microbes with multifarious plant growth promoting attributes. *Environ. Sustainability* 3, 23–34. doi: 10.1007/s42398-020-00094-1

Kozjek, K., Kundel, D., Kushwaha, S. K., Olsson, P. A., Ahrén, D., Fliessbach, A., et al. (2021). Long-term agricultural management impacts arbuscular mycorrhizal fungi more than short-term experimental drought. *Appl. Soil Ecol.* 168:104140. doi: 10.1016/j.apsoil.2021.104140

Kumar, M., Kour, D., Yadav, A. N., Saxena, R., Rai, P. K., Jyoti, A., et al. (2019). Biodiversity of methylotrophic microbial communities and their potential role in mitigation of abiotic stresses in plants. *Biologia* 74, 287–308. doi: 10.2478/s11756-019-00190-6

Kumar, M., Mishra, S., Dixit, V., Kumar, M., Agarwal, L., Chauhan, P. S., et al. (2016). Synergistic effect of *Pseudomonas putida* and *Bacillus amyloliquefaciens* ameliorates drought stress in chickpea (*Cicer arietinum* L.). *Plant Signal. Behav.* 11:e1071004. doi: 10.1080/15592324.2015.1071004

Li, B., Feng, Y., Zong, Y., Zhang, D., Hao, X., and Li, P. (2020). Elevated CO2-induced changes in photosynthesis, antioxidant enzymes and signal transduction enzyme of soybean under drought stress. *Plant Physiol. Biochem.* 154, 105–114. doi: 10.1016/j.plaphy.2020.05.039

Li, H., Guo, Q., Jing, Y., Liu, Z., Zheng, Z., Sun, Y., et al. (2020). Application of Streptomyces pactum Act12 enhances drought resistance in wheat. *J. Plant Growth Regul.* 39, 122–132. doi: 10.1007/s00344-019-09968-z

Li, X., and Liu, F. (2016). "Drought stress memory and drought stress tolerance in plants: biochemical and molecular basis," in *Drought Stress Tolerance in Plants, Vol 1*, eds I. M. A. Hossain, S. H. Wani, S. Bhattacharjee, D. J. Burritt, and L.-S. P. Tran (Berlin: Springer), 17–44. doi: 10.1007/978-3-319-28899-4_2

Liu, X.-M., and Zhang, H. (2015). The effects of bacterial volatile emissions on plant abiotic stress tolerance. *Front. Plant Sci.* 6:774. doi: 10.3389/fpls.2015.00774

Martins, S. J., Rocha, G. A., De Melo, H. C., De Castro Georg, R., Ulhôa, C. J., De Campos Dianese, É, et al. (2018). Plant-associated bacteria mitigate drought stress in soybean. *Environ. Sci. Pollut. Res.* 25, 13676–13686. doi: 10.1007/s11356-018-1610-5

Meena, K. K., Bitla, U., and Sorty, A. M. (2021). "Root-endophytes and their contribution to plant abiotic stress tolerance," in *Microbial Management of Plant Stresses*, eds A. Kumar and S. Droby (Elsevier), 119–129. doi: 10.1016/b978-0-323-85193-0.00002-4

Mohammadipanah, F., and Zamanzadeh, M. (2019). "Bacterial mechanisms promoting the tolerance to drought stress in plants," in *Secondary Metabolites of Plant Growth Promoting Rhizomicroorganisms*, eds H. B. Singh, C. Keswani, M. S. Reddy, E. Sansinenea, and C. García-Estrada (Singapore: Springer), 185–224. doi: 10.1007/978-981-13-5862-3_10

Mohammadkhani, N., and Heidari, R. (2008). Drought-induced accumulation of soluble sugars and proline in two maize varieties. *World Appl. Sci. J.* 3, 448–453.

Mok, D. W., and Mok, M. C. (2001). Cytokinin metabolism and action. *Annu. Rev. Plant Biol.* 52, 89–118. doi: 10.1146/annurev.arplant.52.1.89

Mollah, A., and Pratiwi, E. (2020). Application of various types of local microorganisms to the growth and production of two rice varieties. *IOP Conf. Ser. Earth Environ. Sci.* 575:012148. doi: 10.1088/1755-1315/575/1/012148

Monteiro, G., Nogueira, G., Neto, C., Nascimento, V., and Freitas, J. (2021). "Promotion of nitrogen assimilation by plant growth-promoting rhizobacteria," in *Nitrogen in Agriculture-Physiological, Agricultural and Ecological Aspects*, eds T. Ohyama and K. Inubushi (London: IntechOpen).

Moradtalab, N., Hajiboland, R., Aliasgharzad, N., Hartmann, T. E., and Neumann, G. (2019). Silicon and the association with an arbuscular-mycorrhizal fungus (*Rhizophagus clarus*) mitigate the adverse effects of drought stress on strawberry. *Agronomy* 9:41. doi: 10.3390/agronomy9010041

Mukerji, K. G., Manoharachary, C., and Singh, J. (2006). *Microbial Activity in the Rhizosphere*. Berlin: Springer Science & Business Media.

Nadeem, S. M., Ahmad, M., Tufail, M. A., Asghar, H. N., Nazli, F., and Zahir, Z. A. (2021). Appraising the potential of EPS-producing rhizobacteria with ACC-deaminase activity to improve growth and physiology of maize under drought stress. *Physiol. Plant.* 172, 463–476. doi: 10.1111/ppl.13212

Naseem, H., Ahsan, M., Shahid, M. A., and Khan, N. (2018). Exopolysaccharides producing rhizobacteria and their role in plant growth and drought tolerance. *J. Basic microbiol.* 58, 1009–1022. doi: 10.1002/jobm.201800309

Palmer, W. C. (1965). *Meteorological Drought*. Washington, DC: US Department of Commerce Weather Bureau.

Priyanka, J. P., Goral, R. T., Rupal, K. S., and Saraf, M. (2019). "Rhizospheric microflora: a natural alleviator of drought stress in agricultural crops," in *Plant Growth Promoting Rhizobacteria for Sustainable Stress Management*, ed. R. Z. Sayyed (Singapore: Springer), 103–115. doi: 10.1007/978-981-13-6536-2_6

Rahdari, P., and Hoseini, S. (2012). Drought stress: a review. *Int. J. Agron. Plant Production* 3, 443–446.

Raheem, A., Shaposhnikov, A., Belimov, A. A., Dodd, I. C., and Ali, B. (2018). Auxin production by rhizobacteria was associated with improved yield of wheat (*Triticum aestivum* L.) under drought stress. *Arch. Agron. Soil Sci.* 64, 574–587. doi: 10.1080/03650340.2017.1362105

Rodriguez, R., White, J. Jr., Arnold, A., and Redman, A. R. A. (2009). Fungal endophytes: diversity and functional roles. *N. Phytol.* 182, 314–330. doi: 10.1111/j.1469-8137.2009.02773.x

Rubin, R. L., Van Groenigen, K. J., and Hungate, B. A. (2017). Plant growth promoting rhizobacteria are more effective under drought: a meta-analysis. *Plant Soil* 416, 309–323. doi: 10.1007/s11104-017-3199-8

Sakata, Y., Komatsu, K., and Takezawa, D. (2014). "ABA as a universal plant hormone," in *Progress in Botany*, eds U. Lüttge, W. Beyschlag, and J. Cushman (Berlin: Springer), 57–96. doi: 10.1007/978-3-642-38797-5_2

Salehi-Lisar, S. Y., and Bakhshayeshan-Agdam, H. (2016). "Drought stress in plants: causes, consequences, and tolerance," in *Drought Stress Tolerance in Plants*, Vol. 1, eds M. Hossain, S. Wani, S. Bhattacharjee, D. Burritt, and L. S. Tran (Cham: Springer), 1–16. doi: 10.1007/978-3-319-28899-4_1

Sandhya, V., Sk, Z. A., Grover, M., Reddy, G., and Venkateswarlu, B. (2009). Alleviation of drought stress effects in sunflower seedlings by the exopolysaccharides producing *Pseudomonas putida* strain GAP-P45. *Biol. Fertil. Soils* 46, 17–26. doi: 10.1007/s00374-009-0401-z

Santos-Medellín, C., Edwards, J., Liechty, Z., Nguyen, B., and Sundaresan, V. (2017). Drought stress results in a compartment-specific restructuring of the rice root-associated microbiomes. *MBio* 8:e00764-17. doi: 10.1128/mBio.00764-17

Seco, R., Karl, T., Guenther, A., Hosman, K. P., Pallardy, S. G., Gu, L., et al. (2015). Ecosystem-scale volatile organic compound fluxes during an extreme drought in a broadleaf temperate forest of the Missouri Ozarks (central USA). *Glob. Change Biol.* 21, 3657–3674. doi: 10.1111/gcb.12980

Seki, M., Umezawa, T., Urano, K., and Shinozaki, K. (2007). Regulatory metabolic networks in drought stress responses. *Curr. Opin. Plant Biol.* 10, 296–302. doi: 10.1016/j.pbi.2007.04.014

Sharma, V., Salwan, R., and Tawfeeq, L. (2020). *Molecular Aspects of Plant Beneficial Microbes in Agriculture*. Cambridge, MA: Academic Press.

Sheteiwy, M. S., Ali, D. F. I., Xiong, Y.-C., Brestic, M., Skalicky, M., Hamoud, Y. A., et al. (2021). Physiological and biochemical responses of soybean plants inoculated with Arbuscular mycorrhizal fungi and *Bradyrhizobium* under drought stress. *BMC Plant Biol.* 21:195. doi: 10.1186/s12870-021-02949-z

Shinozaki, K., and Yamaguchi-Shinozaki, K. (1998). *Molecular Responses to Drought Stress*. Amsterdam: Elsevier Science.

Shinozaki, K., and Yamaguchi-Shinozaki, K. (2007). Gene networks involved in drought stress response and tolerance. *J. Exp. Bot.* 58, 221–227. doi: 10.1093/jxb/erl164

Shinozaki, K., Urano, K., Maruyama, K., and Takahashi, F. (2016). Drought stress. *Plant Physiol. Dev.* 1, 8–15.

Siddique, M., Hamid, A., and Islam, M. (2000). Drought stress effects on water relations of wheat. *Bot. Bull. Acad. Sin.* 41, 35–39.

Siddiqui, M. H., Khan, M. N., and Singh, V. P. (2022). *Hot and Dry: How Plants can Thrive in Future Climates*. Berlin: Springer.

Silambarasan, S., Logeswari, P., Cornejo, P., Abraham, J., and Valentine, A. (2019). Simultaneous mitigation of aluminum, salinity and drought stress in *Lactuca sativa* growth via formulated plant growth promoting *Rhodotorula mucilaginosa* CAM4. *Ecotoxicol. Environ. Saf.* 180, 63–72. doi: 10.1016/j.ecoenv.2019.05.006

Singh, D. P., Singh, V., Gupta, V. K., Shukla, R., Prabha, R., Sarma, B. K., et al. (2020). Microbial inoculation in rice regulates antioxidative reactions and defense related genes to mitigate drought stress. *Sci. Rep.* 10:4818. doi: 10.1038/s41598-020-61140-w

Sinha, D., Mukherjee, S., and Mahapatra, D. (2021). "Multifaceted potential of Plant Growth Promoting Rhizobacteria (PGPR): an overview," in *Handbook of Research on Microbial Remediation and Microbial Biotechnology for Sustainable Soil*, ed. J. Ahmad Malik (Pennsylvania: IGI Global), 205–268. doi: 10.4018/978-1-7998-7062-3.ch008

Skubacz, A., Daszkowska-Golec, A., and Szarejko, I. (2016). The role and regulation of ABI5 (ABA-Insensitive 5) in plant development, abiotic stress responses and phytohormone crosstalk. *Front. Plant Sci.* 7:1884. doi: 10.3389/fpls.2016.01884

Strobel, G. A. (2003). Endophytes as sources of bioactive products. *Microbes Infect.* 5, 535–544. doi: 10.1016/s1286-4579(03)00073-x

Svoboda, M., Lecomte, D., Hayes, M., Heim, R., Gleason, K., Angel, J., et al. (2002). The drought monitor. *Bull. Am. Meteorol. Soc.* 83, 1181–1190.

Tambussi, E. A., Bartoli, C. G., Beltrano, J., Guiamet, J. J., and Araus, J. L. (2000). Oxidative damage to thylakoid proteins in water-stressed leaves of wheat (*Triticum aestivum*). *Physiol. Plant.* 108, 398–404. doi: 10.1034/j.1399-3054.2000.108004398.x

Teotia, P., Kumar, V., Kumar, M., Shrivastava, N., and Varma, A. (2016). "Rhizosphere microbes: potassium solubilization and crop productivity–present and future aspects," in *Potassium Solubilizing Microorganisms for Sustainable Agriculture*, eds V. S. Meena, B. R. Maurya, J. P. Verma, and R. S. Meena (Berlin: Springer), 315–325. doi: 10.1007/978-81-322-2776-2_22

Ullah, A., Nisar, M., Ali, H., Hazrat, A., Hayat, K., Keerio, A. A., et al. (2019). Drought tolerance improvement in plants: an endophytic bacterial approach. *Appl. Microbiol. Biotechnol.* 103, 7385–7397. doi: 10.1007/s00253-019-10045-4

Ustiatik, R., Nuraini, Y., Suharjono, S., Jeyakumar, P., Anderson, C. W. N., and Handayanto, E. (2021). Mercury resistance and plant growth promoting traits of endophytic bacteria isolated from mercury-contaminated soil. *Bioremediat. J.* 1–20. doi: 10.1080/10889868.2021.1973950

Van Loon, A. F. (2015). Hydrological drought explained. *Wiley Interdiscip. Rev.* 2, 359–392. doi: 10.1002/wat2.1085

Vanamala, P., Sultana, U., Sindhura, P., and Gul, M. Z. (2021). "Plant Growth-Promoting Rhizobacteria (PGPR): a unique strategy for sustainable agriculture," in *Handbook of Research on Microbial Remediation and Microbial Biotechnology for Sustainable Soil*, ed. J. Ahmad Malik (Pennsylvania: IGI Global), 332–357. doi: 10.4018/978-1-7998-7062-3.ch012

Vanneste, S., and Friml, J. (2009). Auxin: a trigger for change in plant development. *Cell* 136, 1005–1016. doi: 10.1016/j.cell.2009.03.001

Verma, H., Kumar, D., Kumar, V., Kumari, M., Singh, S. K., Sharma, V. K., et al. (2021). The potential application of endophytes in management of stress from drought and salinity in crop plants. *Microorganisms* 9:1729. doi: 10.3390/microorganisms9081729

Wen, C.-K. (2014). *Ethylene in Plants*. Berlin: Springer.

Werner, T., and Schmülling, T. (2009). Cytokinin action in plant development. *Curr. Opin. Plant Biol.* 12, 527–538. doi: 10.1016/j.pbi.2009.07.002

Wybouw, B., and De Rybel, B. (2019). Cytokinin–a developing story. *Trends Plant Sci.* 24, 177–185. doi: 10.1016/j.tplants.2018.10.012

Yadav, A. N., and Yadav, N. (2018). Stress-adaptive microbes for plant growth promotion and alleviation of drought stress in plants. *Acta Sci. Agric.* 2, 85–88.

Yamada, M., Morishita, H., Urano, K., Shiozaki, N., Yamaguchi-Shinozaki, K., Shinozaki, K., et al. (2005). Effects of free proline accumulation in petunias under drought stress. *J. Exp. Bot.* 56, 1975–1981. doi: 10.1093/jxb/eri195

Yu, Z., Duan, X., Luo, L., Dai, S., Ding, Z., and Xia, G. (2020). How plant hormones mediate salt stress responses. *Trends Plant Sci*. 25, 1117–1130. doi: 10.1016/j.tplants.2020.06.008

Zhang, H. W., Song, Y. C., and Tan, R. X. (2006). Biology and chemistry of endophytes. *Nat. Prod. Rep.* 23, 753–771. doi: 10.1039/b609472b

Zhao, Y. (2010). Auxin biosynthesis and its role in plant development. *Annu. Rev. Plant Biol.* 61, 49–64. doi: 10.1146/annurev-arplant-042809-112308

Zhu, Q., Riley, W. J., Tang, J., and Koven, C. D. (2016). Multiple soil nutrient competition between plants, microbes, and mineral surfaces: model development, parameterization, and example applications in several tropical forests. *Biogeosciences* 13, 341–363. doi: 10.5194/bg-13-341-2016

Zou, Y. N., Wu, Q. S., and Kuèa, K. (2021). Unravelling the role of arbuscular mycorrhizal fungi in mitigating the oxidative burst of plants under drought stress. *Plant Biol.* 23, 50–57. doi: 10.1111/plb.13161

Conflict of Interest: The authors declare that the research was conducted in the absence of any commercial or financial relationships that could be construed as a potential conflict of interest.

Publisher's Note: All claims expressed in this article are solely those of the authors and do not necessarily represent those of their affiliated organizations, or those of the publisher, the editors and the reviewers. Any product that may be evaluated in this article, or claim that may be made by its manufacturer, is not guaranteed or endorsed by the publisher.

Copyright © 2022 Shaffique, Khan, Imran, Kang, Park, Wani and Lee. This is an open-access article distributed under the terms of the Creative Commons Attribution License (CC BY). The use, distribution or reproduction in other forums is permitted, provided the original author(s) and the copyright owner(s) are credited and that the original publication in this journal is cited, in accordance with accepted academic practice. No use, distribution or reproduction is permitted which does not comply with these terms.

frontiers | Frontiers in Plant Science

ORIGINAL RESEARCH
published: 01 June 2022
doi: 10.3389/fpls.2022.869072

Leaf Functional Traits of Invasive Grasses Conferring High-Cadmium Adaptation Over Natives

Muhammad Ilyas[1,2,3], Sakhawat Shah[4], Ya-Wen Lai[2], Jan Sher[5], Tao Bai[6], Fawad Zaman[2], Farkhanda Bibi[7], Monika Koul[8], Shabir Hussain Wani[9], Ali Majrashi[10], Hesham F. Alharby[11,12], Khalid Rehman Hakeem[11,12,13], Yong-Jian Wang[2] and Shabir A. Rather[5]**

[1] CAS Key Laboratory of Tropical Forest Ecology, Xishuangbanna Tropical Botanical Garden, Chinese Academy of Sciences, Menglun, China, [2] College of Horticulture and Forestry Sciences/Hubei Engineering Technology Research Centre for Forestry Information, Huazhong Agricultural University, Wuhan, China, [3] University of Chinese Academy of Sciences, Beijing, China, [4] Hubei Insect Resources Utilization and Sustainable Pest Management Key Laboratory, College of Plant Science and Technology, Huazhong Agricultural University, Wuhan, China, [5] Center for Integrative Conservation, Xishuangbanna Tropical Botanical Garden, Chinese Academy of Sciences, Menglun, China, [6] Hubei Ecology Polytechnic College, Wuhan, China, [7] CAS Key Laboratory of Tropical Plant Resources and Sustainable Use, Xishuangbanna Tropical Botanical Garden, Chinese Academy of Sciences, Menglun, China, [8] Department of Botany, Hansraj College, University of Delhi, New Delhi, India, [9] Mountain Research Centre for Field Crops, Khudwani, Sher-e-Kashmir University of Agricultural Sciences and Technology of Kashmir, Jammu and Kashmir, India, [10] Department of Biology, College of Science, Taif University, Taif, Saudi Arabia, [11] Department of Biological Sciences, Faculty of Science, King Abdulaziz University, Jeddah, Saudi Arabia, [12] Princess Dr. Najla Bint Saud Al- Saud Center for Excellence Research in Biotechnology, King Abdulaziz University, Jeddah, Saudi Arabia, [13] Department of Public Health, Daffodil International University, Dhaka, Bangladesh

OPEN ACCESS

Edited by:
Rafaqat Ali Gill, Oil Crops Research Institute (CAAS), China

Reviewed by:
Aadil Yousuf Tantray, University of Aberdeen, United Kingdom
Haris Khurshid, Pakistan Agricultural Research Council, Pakistan

***Correspondence:**
Tao Bai
taobai1982@yeah.net
Shabir A. Rather
rathershabir100@gmail.com; shabir@xtbg.ac.cn

Specialty section:
This article was submitted to Plant Breeding, a section of the journal Frontiers in Plant Science

Received: *03 February 2022*
Accepted: *25 April 2022*
Published: *01 June 2022*

Citation:
Ilyas M, Shah S, Lai Y-W, Sher J, Bai T, Zaman F, Bibi F, Koul M, Wani SH, Majrashi A, Alharby HF, Hakeem KR, Wang Y-J and Rather SA (2022) Leaf Functional Traits of Invasive Grasses Conferring High-Cadmium Adaptation Over Natives. Front. Plant Sci. 13:869072. doi: 10.3389/fpls.2022.869072

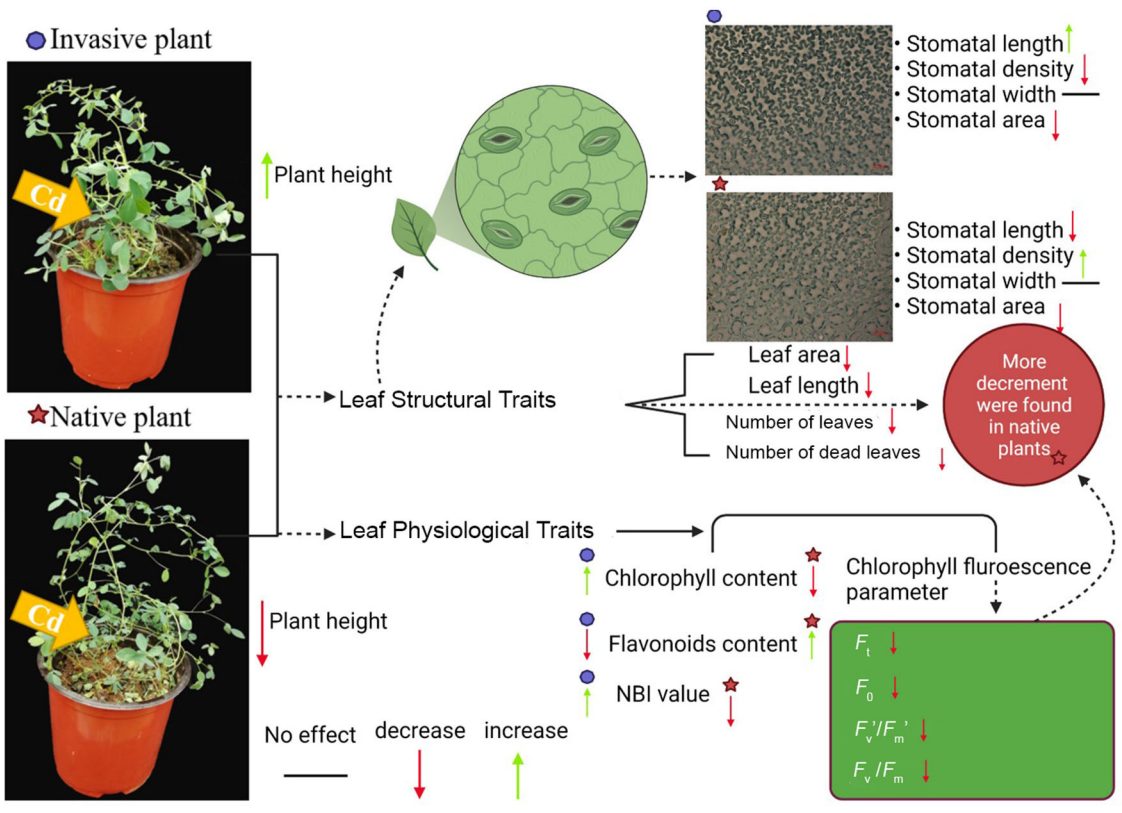
Heavy metal (HM) contamination resulting from industrialization and urbanization during the Anthropocene along with plant invasion can severely threaten the growth and adaptation of local flora. Invasive alien plant species generally exhibit a growth pattern consistent with their functional traits in non-contaminated environments in the introduced range. However, it remains unclear whether invasive alien plants have an advantage over native plants in contaminated environments and whether this growth pattern is dependent on the adaptation of their leaf functional traits. Here, we selected two congeneric pairs of invasive alien and native grasses that naturally co-exist in China and are commonly found growing in contaminated soil. To evaluate the effect of cadmium (Cd) on the structural and physiological leaf traits, we grew all four species in soil contaminated without or with 80 mg/kg Cd. Invasive plants contained significantly higher concentrations of Cd in all three organs (leaf, stem, and root). They displayed a higher transfer factor and bioconcentration factor (BCF) of shoot and root than natives, indicating that invasive species are potential Cd hyperaccumulators. Invasive plants accumulated polyphenol oxidase (PPO) to higher levels than natives and showed similar patterns of leaf structural and physiological traits in response to changes in Cd bioconcentration. The quantifiable leaf structural traits of invasive plants were significantly greater (except for stomatal density and number of dead leaves) than native plants. Leaf physiological traits, chlorophyll content, and flavonoid content were also significantly higher in invasive plants than in natives under Cd stress conditions after 4 weeks, although nitrogen balance index (NBI) showed no significant difference between the two species. Chlorophyll fluorescence parameters decreased, except for

the quantum yield of photosystem II (ΦPSII) and the proportion of open photosystem II (qP), which increased under Cd stress conditions in both species. However, invasive plants exhibited higher fluorescence parameters than natives under Cd stress, and the decrement observed in invasive plants under Cd stress was greater than that in natives. High Cd adaptation of invasive grasses over natives suggests that invasive plants possess optimal leaf structural and physiological traits, which enable them to adapt to stressful conditions and capture resources more quickly than natives. This study further emphasizes the potential invasion of alien plants in contaminated soil environments within the introduced range. To a certain extent, some non-invasive alien plants might adapt to metalliferous environments and serve as hyperaccumulator candidates in phytoremediation projects in contaminated environments.

Keywords: bioconcentration factor, cadmium, leaf functional traits, phytoremediation, physiological response

INTRODUCTION

Heavy metal (HM) contamination, which occurred in Anthropocene, has the potential to severely threaten biodiversity and human health, especially in developing countries (Li et al., 2014; Duan et al., 2016). In the last few decades, the HM contamination of soil has spread extensively throughout the globe (Huamain et al., 1999; Dong et al., 2001). The increment of soil HM contamination is one of the common and severe threats to urban flora and fauna communities (Bi et al., 2013; Li et al., 2014). HM can greatly impact plant growth, reproduction, and migration (Deng et al., 2007). Plants lack the ability to deliberately migrate away from a polluted area, and the only way to increase their chance of survival in adverse environments is to trigger defense mechanisms and evolve tolerance-inducing genes (Chmielowska-Bak et al., 2014). When exposed to cadmium



GRAPHICAL ABSTRACT | Higher structural and physiological leaf traits in invasive than in native plants.

(Cd) stress, plants display signs of injury in the form of chlorosis, growth inhibition, root tip browning, and eventually death (Mohanpuria et al., 2007; Ali H. et al., 2013; Ali et al., 2014). HM stress inhibits biological processes such as photosynthesis, cell division, and water absorption, thus reducing plant growth and canopy cover (Jadia and Fulekar, 2009; Taiz and Zeiger, 2010).

Elevated Cd concentration can cause many disturbances in the morphological, anatomical, and physiological processes of plants. A recent study reported that HM reduces leaf chlorophyll index, leaf area, and various other metabolic processes in plants (Hatamian et al., 2020). Several mechanisms are involved in delaying plant development under HM stress. Cell division and leaf morphological features are adversely affected by lead (Pb) and Cd toxicity (Hatamian et al., 2020). Plants regulate their morphological, physiological, and ecological adaptation to environmental fluctuations and change the leaf functional traits under unfavorable conditions (Dwyer et al., 2014; Meng et al., 2014). Functional traits directly or indirectly affect plant adaptability through their effects on plant development, survival, and reproduction (Marteinsdóttir and Eriksson, 2014).

Plant functional traits are expected to represent general adaptation under stress (Dwyer et al., 2014; Marteinsdóttir and Eriksson, 2014; Ilyas et al., 2021). Specific leaf area (SLA) is an outstanding indicator of plant functional traits and explains the changes in plant species in response to any changes in the available resources (Kardel et al., 2010; Scheepens et al., 2010). Besides leaf size, and shape, chlorophyll content is an important functional trait of leaves, which accurately describes the plant resource use strategy (Wang et al., 2016). The competitive ability of plants for resource acquisition, especially sunlight, is influenced by plant height (Gross et al., 2007; Thomson et al., 2011). Similarly, the leaf dry weight, leaf number, and plant height significantly decreased under Cd (Farooq et al., 2016). Related or even identical environmental stresses, such as habitat filtering, can also affect the leaf functional traits (Gross et al., 2007). Furthermore, invasive plant species exhibit a higher leaf shape index than native species to increase their resource capturing efficiency and enhance their competitiveness (Liu et al., 2017). Moreover, under stress conditions, invasive plants grow significantly taller than native plants, which enables them to capture more light energy and transport more water (Ishii and Asano, 2010; Wang et al., 2017). Wang et al. (2018b) reported that HM treatments negatively affected the functional traits of invasive and native plants; however, invasive plants showed an increase in height and leaf shape index compared with native plants. Cd has a major impact on the survival and physiological efficiency of native plants. Moreover, it has been proposed that biotic stresses, such as enemy release, superior competitor, and allelopathy, benefit invasive species over resident species (Bakker and Wilson, 2001; Maron and Vilà, 2001; Keane and Crawley, 2002; Callaway and Ridenour, 2004). Many invasive plants exhibit a greater ability to use water and nutrients under stress conditions (Blicker et al., 2003), implying that the adaptation or tolerance to stressful environments may be an important trait of invasive plant species. However, well-established invasive plant populations may pay a high fitness cost during subsequent bouts of admixture with native populations (Pantoja et al., 2018). Invasive plant species demonstrate local adaptation as frequently as and at least as effectively as native plant species (Oduor et al., 2016). Previous studies confirmed that, given their functional traits, invasive plants can grow and adapt to metalliferous environments more effectively than native plants (Arredondo et al., 2006; Murtaza et al., 2017). The growth pattern and leaf functional traits of invasive alien plants are generally consistent with those observed under limited light, limited water, and limited nutrient environments or under altitude stress in the introduced range (Liu et al., 2017, 2022; Wang et al., 2017, 2019). However, whether invasive alien plants have an advantage over native plants in contaminated environments is poorly understood.

Invasive plant species invade the ecosystem and change their functions and processes by affecting nutrient cycling and reducing the biodiversity of native flora (Ehrenfeld, 2010; Simberloff et al., 2013). However, rather than getting eliminated from the ecosystem, these species are used for ecosystem restoration and the bioremediation of contaminated soil (Ewel and Putz, 2004; Pandey, 2012). In previous studies, invasive alien plant species such as *Chromolaena odorata* and *Praxelis clematidea* significantly enhanced soil nutrient levels (Koné et al., 2012; Wei et al., 2017). Therefore, some alien plant species may be useful for the restoration of degraded ecosystems. Comparatively, invasive plant species have higher adaptability to stressful environments (Ehrenfeld, 2010; Bai et al., 2020). According to previous studies, the high adaptability rate of invasive plants makes them a potentially better choice for removing soil pollutants (Tanhan et al., 2007; Sun et al., 2009; Pandey, 2012). Chlorophyll fluorescence parameters are the significant determinants of the performance and adaptability of plants in stressed environments. Fluorescence parameters such as maximum potential quantum efficiency of photosystem II (PSII; F_v/F_m) and quantum yield of PSII (ΦPSII) decreased under HM stress (Chen et al., 2015), and parameters including variable fluorescence (F_v) and F_v/F_m decreased in plants exposed to high Cd concentration (Li et al., 2015). In contrast, parameters including minimum fluorescence (F_0) and non-photochemical quenching (NPQ) increased, whereas maximum fluorescence (F_m) was not significantly affected in Purslane plants under Cd stress (Yaghoubian et al., 2016). Joshi and Mohanty (2004) reported that different concentrations of Cd had a major impact on chlorophyll a, chlorophyll b, and carotenoids contents, F_0 and chlorophyll fluorescence in *Amaranthus caudatus* L.; however, changes in chlorophyll fluorescence parameters F_0 and F_m were dependent on the experimental conditions such as the plant growth stage and metal ion exposure of plants (Joshi and Mohanty, 2004).

In this study, we aimed to understand the effect of Cd toxicity on the leaf functional traits (structural and physiological traits) of invasive and native plant species and the accumulation of Cd in different parts of these species. We hypothesized that (1) Cd stress has more negative impacts on native grasses than on invasive grasses, and invasive species exhibit greater stress resistance than native species; and (2) leaf functional traits

confer better physiological response, plant adaptation, and Cd accumulation ability (i.e., high Cd adaptation) compared to invasive with grasses than to natives under stress conditions. This study provides a solid theoretical base and practical applications for the control and prevention of invasion under HM stress.

MATERIALS AND METHODS

Species Selection and Cultivation

Two invasive (*Pennisetum purpureum* and *Paspalum dilatatum*) and two native (*Pennisetum alopecuroides* and *Paspalum distichum*) grasses, which are commonly found co-occurring in the grasslands of China, were included in this study (**Supplementary Table 1**). More than 100 ramets of each species were collected from the Hubei Province of China in 2014. To increase the likelihood of sampling ramets from different genets (i.e., genotypes), ramets spaced at least 500 m apart were collected. After collection, the ramets were vegetatively cultivated for 1 year in a glasshouse at Huazhong Agricultural University in Wuhan (Hubei Province, China) to produce enough new clonal fragments.

Experimental Design

Experiments were conducted in a plastic greenhouse at Huazhong Agricultural University, Wuhan, China. A factorial design was applied, with two levels of HM contamination in the soil (0 and 80 mg/kg). Cd was used in this study because it is one of the most important HMs found in China and was added to the soil at a concentration of 80 mg/kg (Alaboudi et al., 2018). 3.8 g of $CdCl_2 \cdot 2.5H_2O$ was prepared into 10 and 240 mg/ml water respectively. Before transplanting, soil samples were collected to determine the initial index of the soil. Subsequently, plants were transplanted in disposable plastic pots (30 cm diameter × 20 cm height) filled with 9.5 L of a mixture of sand and yellow-brown soil (1:1, v/v) collected from Shizishan Mountain in Wuhan, Hubei Province, China. The nutrient concentration of the soil mixture was quite low, with total N, P, and K contents of 0.23 ± 0.03, 0.32 ± 0.04, and 14.27 ± 1.25 g kg^{-1}, respectively (mean ± SE, $n = 10$). Each pot contained one invasive and one native plant, which were planted in the center of the pot (**Figure 1**). Two weeks after transplanting, weed management and daily watering were carried out until the end of the experiment. Relevant data, including chlorophyll and flavonoid contents, nitrogen balance index (NBI), number of total leaves and dead leaves, and plant height, were measured one time a week for 8–10 weeks. Four replicate pots were used for each treatment. The experiment was terminated 10 weeks after the start of the treatments.

Measurements of Leaf Structural Traits

To measure leaf structural traits, samples were collected at the end of the experimental period. All samples were collected at 9:00 a.m. and 11:00 a.m. on sunny days from August to September 2020. Mature leaves were randomly collected from each plant in three replicates, with each replicate containing three leaves. After collection, all leaf samples were preserved in an ice bag for transfer from the greenhouse to the laboratory for further processing. The leaves were fixed in formaldehyde-alcohol-acetic acid (FAA) for 1–2 min to measure stomatal traits. Then, the leaves were removed from the FAA and excess FAA was blotted with a filter paper. Subsequently, nail polish was applied to the adaxial and abaxial side of the leaf. After air-drying for 40 seconds, the nail polish marks were removed with transparent adhesive tape, and leaves were placed on a microscopic glass slides. To determine the density and size of the stomata in the lower epidermis, these were photographed under a light microscope (AxioPlan, Zeiss, Jena, Germany). The images were then used to determine the pore number and size. The x (long) and y (short) axes of each pore were measured using (https://imagej.net). The size of at least 30 pores was measured from each leaf sample. To determine pore density, all the pores within a 309.81-mm^2 area were counted. Plant height and leaf length were also measured with the scale. The number of total leaves and dead leaves per plant was counted carefully. To determine the leaf area, fully expanded leaves were selected from the plants and measured using Image-Pro Plus version 6.0 (Media Cybernetics, USA). All measurements were taken in triplicate, within a 1% measurement error.

Estimation of Chlorophyll Content, Flavonoid Content, and NBI

All representative plants in the control and Cd treatments with four replicates were selected and subjected to proximal sensing using the Dualex 4 sensor (Force-A, Orsay, France). The plant samples and sensor readings were obtained 3 weeks after planting. The Dualex values were measured on the adaxial side of leaves at six growth points: topmost, second, and third leaves before tasseling and leaves above and below the panicle as well as the panicle leaf at the tasseling stage. The Dualex readings (chlorophyll and flavonoid contents and NBI) were recorded one time a week for up to 7 weeks from leaves at the same position for each plant species.

Measurement of Chlorophyll Fluorescence Parameters

Chlorophyll fluorescence was measured with a portable fluorometer (PAM-2500, Walz, Germany), as described previously (Genty et al., 1989). To measure fluorescence parameters, the light intensity was maintained at 200 μmol m^{-2} s^{-1}. The leaf samples were dark-adapted for 30 min using leaf-clip holders (2030-B, Walz). Values of F_0 and F_m were measured in dark-adapted leaves. The variable fluorescence ΦPSII quantum yield of PSII, ΦPSII qP proportion of open PSII, and ΦPSII F_v/F_m maximum quantum yield of PSII were calculated as shown in Equations (1)–(3), respectively (Schreiber et al., 1986). Values of F_0', F_m', and steady-state fluorescence (F_t) were measured using leaves adapted to actinic

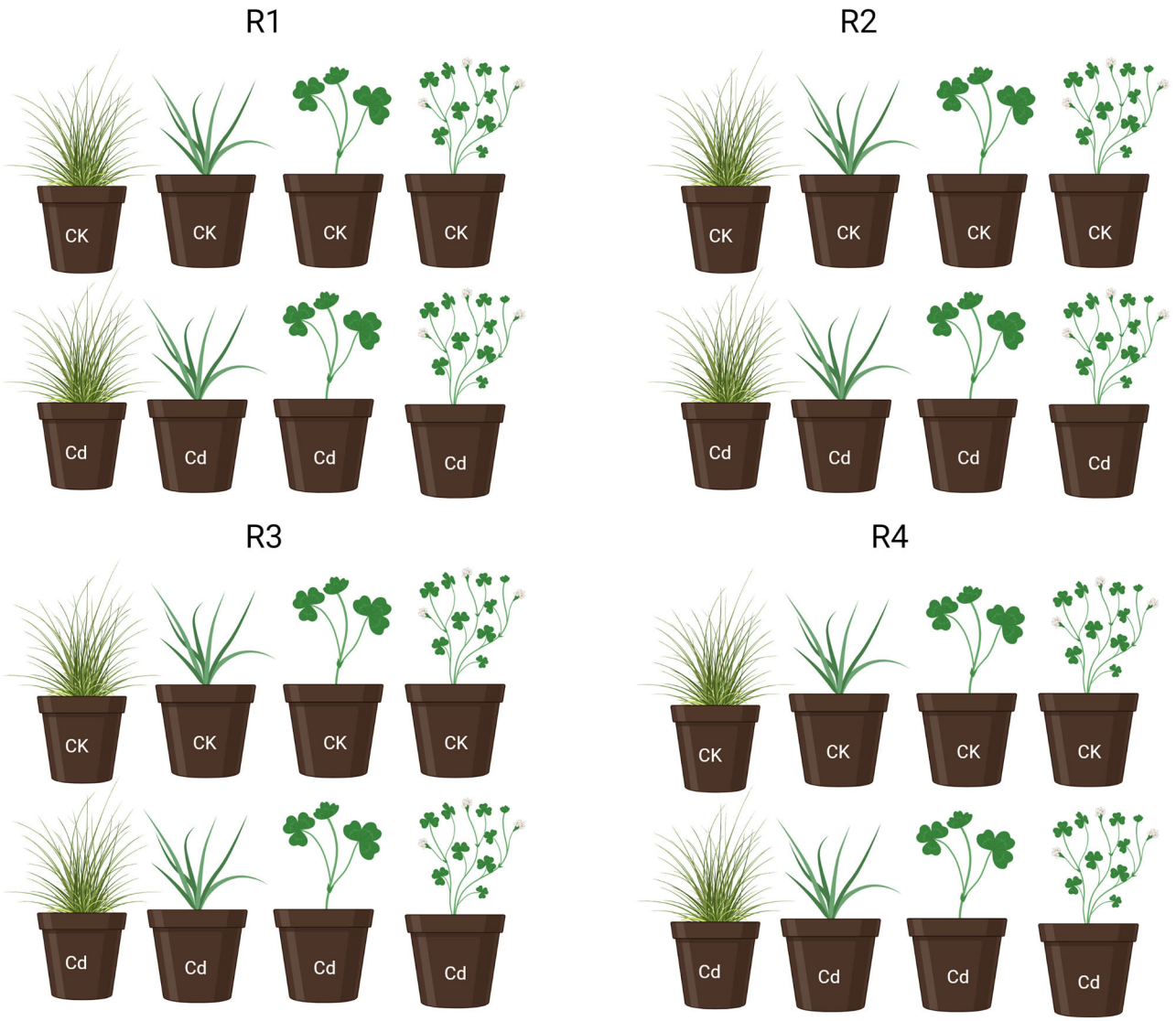


FIGURE 1 | Experimental design. Notes, CK, control, Cd, cadmium stress. Experimental layout. R1-4 mean replicates.

light (Klughammer and Schreiber, 2008).

$$\Phi\text{PSII} = (F'_m - F'_t)/F_m \quad (1)$$

$$\Phi\text{PSII} = (F'_m - F_t)/(F'_m - F'_0) \quad (2)$$

$$\Phi\text{PSII} = (F_m - F_0)/F_m \quad (3)$$

Measurements of Cd Concentration and Polyphenol Oxidase Activity

The activity of PPO was measured in leaves and roots of plants treated with and without Cd stress, as described previously (Webb et al., 2014). Additionally, the Cd removal efficiency of all four plant species was quantified using a combination of shoot bioconcentration factor (shoot BCF), root BCF, and transfer factor (Wei et al., 2018; Bai et al., 2020). Shoot and root BCFs were calculated by dividing the shoot and root Cd concentrations, respectively, with soil Cd concentration at the end of the incubation period, as shown in Equations (4) and (5):

$$\text{Shoot BCF} = (\text{Cd}_{\text{stem}} + \text{Cd}_{\text{leaf}})/\text{Cd}_{\text{soil}} \quad (4)$$

$$\text{Root BCF} = \text{Cd}_{\text{root}}/\text{Cd}_{\text{soil}} \quad (5)$$

where Cd_{root}, Cd_{stem}, Cd_{leaf}, and Cd_{soil} represent Cd concentrations (mg kg^{-1}) in the root, stem, leaf, and soil, respectively.

The transfer factor, which indicates the capacity of a plant to transport Cd from the root system to aboveground organs (stem

and leaf), was calculated using Equation (6):

$$\text{Transfer factor} = \frac{Cd_{stem} + Cd_{leaf}}{Cd_{root}} \quad (6)$$

Statistical Analysis

Two-way analysis of variance (ANOVA) was used to test the effects of soil Cd concentration (0 and 80 mg/kg) and species origin (invasive alien and native) on leaf functional (structural and physiological) traits of plants. If a significant effect of Cd contamination or species origin was detected, then Tukey's honestly significant difference (HSD) test was conducted to compare the means of different treatment combinations. Additionally, two-way repeated measures ANOVA was used to examine the effects of soil Cd concentration, species origin, and time (different experimental periods) on leaf functional traits. Data are presented as mean ± standard error (SE). Significant differences among different traits were determined using SPSS 13.0 (SPSS Inc., Chicago, IL, USA, 2016) and indicated using asterisks ($^{*}p < 0.05$, $^{**}p < 0.01$, $^{***}p < 0.001$). All figures were drawn with OriginPro 7.0 and GraphPad Prism 8 (Graph-Pad Software Inc., San Diego, CA, USA). The relationship among different functional traits of invasive and native species was analyzed with a correlation matrix using the R software (version 4.0.3; R Development Core Team 2012).

RESULTS

Effects of Cd Stress on the Morphological Traits of Invasive and Native Plants

Morphological traits of invasive and native plant species were significantly affected by Cd stress. However, from 3 to 5 weeks, the total leaf number of invasive and native plant species under Cd stress was significantly lower than that of control plants ($p < 0.05$). Moreover, native species showed fewer leaves than invasive species under Cd stress (**Figure 2B**). Cd-treated native species produced the greatest amount of leaf litter, followed by Cd-treated invasive species. Leaf litter under Cd stress was significantly higher than that in the control treatment for both invasive and native species ($p < 0.05$). However, in the Cd stress treatment, the leaf litter of native species increased from 3 to 7 weeks, whereas that of invasive plant species increased from 5 to 7 weeks (**Figure 2A**). During the experimental period, the plant height of invasive and native species was similar between the control and Cd stress treatments from 1 to 3 weeks but dramatically decreased from 4 to 7 weeks. The height of invasive and native plant species under Cd stress was significantly lower than that of their control counterparts ($p < 0.05$). Under Cd stress, the plant height of invasive species was greater than that of native species, indicating that the height of native plants was affected by soil contamination to a greater extent than that of invasive plants (**Figure 2C**). These findings suggest that leaf litter and leaf abscission are higher in native plants than in invasive plants in a metalliferous environment. This indicates that invasive species are more tolerant to HM stress and can potentially survive in a metalliferous environment.

Effects of Cd Stress on the Leaf Structural Traits of Invasive and Native Plants

Effects on Leaf Morphological Traits

All quantifiable leaf structural traits of invasive plants, except stomatal density and number of dead leaves, were significantly greater than those of native plants. Among the invasive and native plants, species had significant effects on all leaf and stomatal traits. Overall, the species effects were highly significant for stomatal and leaf traits ($p \leq 0.001$). Cd stress had significant effects on leaf length, stomatal area, stomatal length, and stomatal width ($p \leq 0.001$) but non-significant effects on leaf area and stomatal density. The interaction between species origin and Cd stress had a significant effect ($p \leq 0.001$) on stomatal and leaf traits, except for stomatal density and leaf area (**Table 1**).

The stomatal traits of invasive and native plants showed different responses to Cd stress. The stomatal density of native species was higher in the control treatment than in the Cd treatment, whereas invasive species were similar under both conditions (**Figure 3A**). Moreover, the stomatal length of all species decreased following Cd treatment, and the decline observed in stomatal length was greater in native plants than in invasive plants (**Figure 3B**). The stomatal area data showed similar trends (**Figure 3D**). The stomatal width of both invasive and native plants was slightly lower in the Cd treatment than in the control treatment (**Figure 3C**). These results suggest that stomatal traits were affected by Cd stress, and the stomatal traits of invasive plant species respond better than that of native species in metalliferous environments.

Overall, the leaf area and leaf length of invasive and native species were lower under Cd stress than under control conditions (**Figure 4**). Under Cd stress, the leaf area of native plants was lower than that of invasive plants (**Figure 4A**). The leaf length data showed similar trends (**Figure 4B**). These results suggest that the leaf traits of native plants are affected by Cd stress to a greater extent than those of invasive plants.

Effects on Stomatal Morphology

Exposure to Cd stress-induced clear morphological changes in the shape of epidermal cells on the abaxial leaf surface in invasive and native plants (**Figure 5**); however, no visible changes were observed in stomatal depth (i.e., how deep the stomata are inserted in the leaf epidermis). Under Cd stress, the stomata guard cells were affected more in native plants than in invasive plants. Additionally, Cd stress decreased stomatal length and width in invasive and native plants, although the decrease in both these parameters was greater in native plants than in invasive plants (**Figure 5**). These results demonstrate that the morphology of epidermal and guard cells changes under Cd stress, which increases stomatal density but decreases stomatal length, width, and area.

Effects of Cd Stress on the Physiological Parameters of Invasive and Native Plants

Under Cd stress, the leaf chlorophyll and flavonoid contents of invasive species were significantly higher than those of native

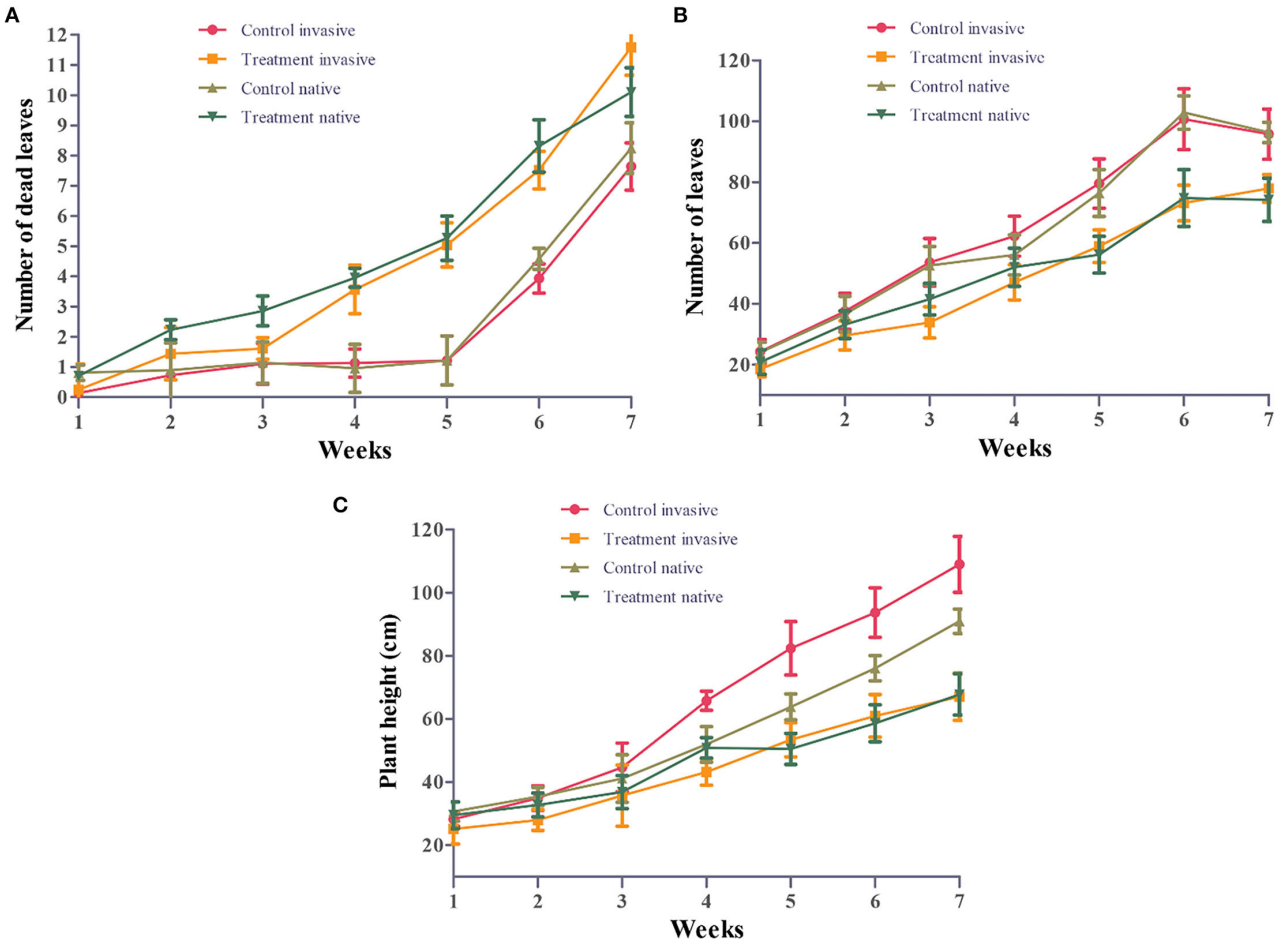


FIGURE 2 | Number of leaves **(A)**, number of dead leaves **(B)** and plant height **(C)** of invasive and native plants during cadmium (Cd) stress. Control: uncontaminated soil + native and invasive: Treatment Cd contaminated soil (80 mg/kg) +native and invasive. Error bars depict the SE of the mean of four independent replicates.

TABLE 1 | Two-way ANOVA analysis of effects of Cd stress on leaf functional traits of invasive and native plants.

Effect		Leaf area		Leaf length		Stomatal area	
	Df	F ratio	*P*	F ratio	*P*	F ratio	*P*
Species	3	17.17	**0.001*** **	38.60	**0.001*** **	3.43	**0.001*** **
Cd	1	0.20	0.658ns	10.84	**0.001*** **	8.33	**0.001*** **
Species*Cd	3	0.72	0.715ns	4.15	**0.003***	1.43	**0.001*** **
Effect		**Stomatal length**		**Stomatal width**		**Stomatal density**	
	Df	**F ratio**	***P***	**F ratio**	***P***	**F ratio**	***P***
Species	3	2.63	**0.001*** **	1.33	**0.001*** **	4.23	**0.001*** **
Cd	1	6.73	**0.001*** **	2.82	**0.001*** **	0.56	0.456ns
Species*Cd	3	4.81	**0.001*** **	7.33	**0.001*** **	0.40	0.94ns

*Cd, cadmium Significant effects are indicated in boldface as follows: ***p ≤ 0.001, *p ≤ 0.05. ns: no significance.*

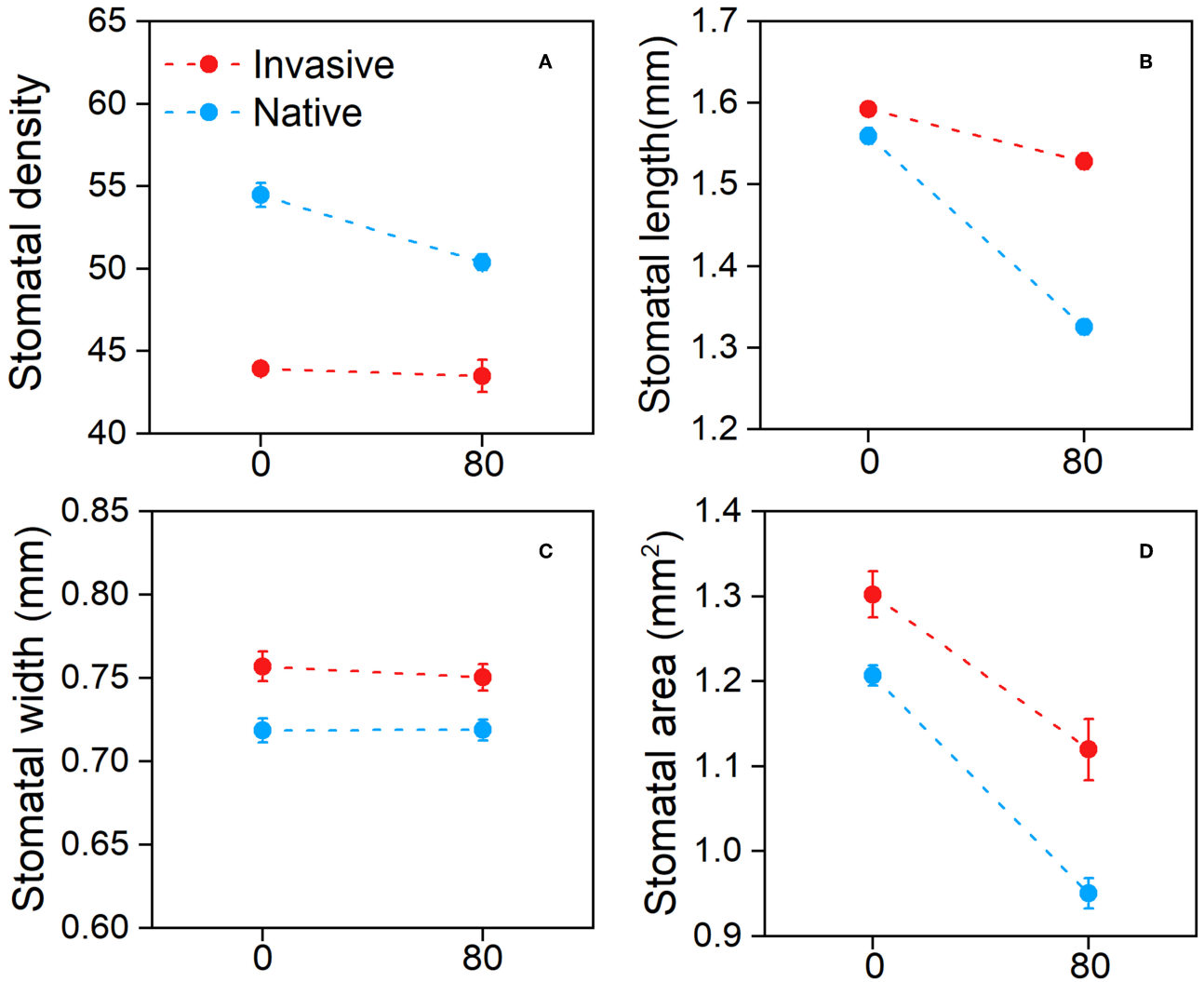


FIGURE 3 | Stomatal density **(A)**, stomatal length **(B)**, stomatal width **(C)**, and stomatal area **(D)** of the invasive and native plants in response to cadmium (Cd). Values are means ± standard error (SE).

species after 4 weeks, although the NBI showed a significant difference between the two groups of plant species. We also investigated the effects of Cd stress on the leaf chlorophyll content of invasive and native species at different time points. The results showed that chlorophyll content of both plant groups was lower under Cd stress than under control conditions at different time points (1–7 weeks; **Figure 6A**). At 2–3 weeks, chlorophyll content showed a greater reduction in native species than in invasive species. The chlorophyll content of invasive and native plant species was significantly lower under Cd stress than under control conditions. Under Cd stress, the flavonoid contents of invasive and native plants increased dramatically from 1 to 7 weeks. The flavonoid content of invasive species was higher under Cd stress than in the control treatment and was higher than that of native plants under both Cd stress and control conditions (**Figure 6B**). The NBI values of invasive and native plants fluctuated during the experimental period. The NBI values of Cd-treated plants were lower than those of control samples. During week 1, the NBI values showed no significant difference among treatments. From weeks 2–7, the NBI values of Cd-treated native and invasive plants were lower than those of their control counterparts. However, the NBI values of invasive species were significantly higher than those of native species at some time points, particularly during weeks 3 and 4 (**Figure 6C**). These findings suggest that Cd stress decreased the chlorophyll content and NBI values of both invasive and native plant groups but had a greater negative impact on the flavonoid content of native species than that of invasive species.

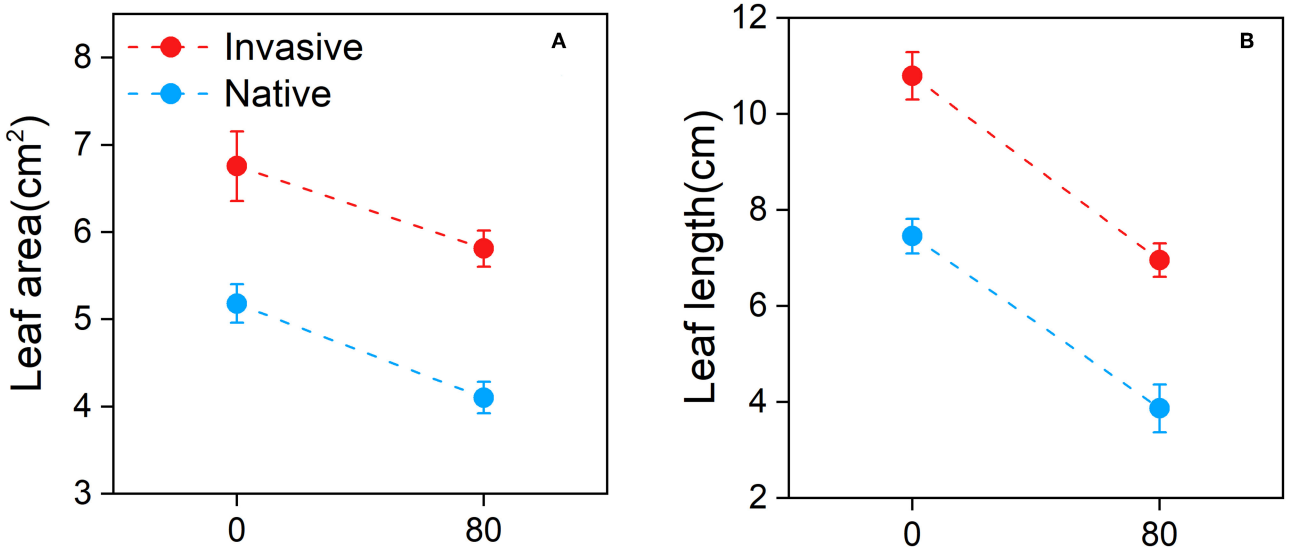


FIGURE 4 | Leaf area **(A)** and leaf length **(B)** of the invasive and native plants in response to cadmium (Cd). Values are means ± standard error (SE).

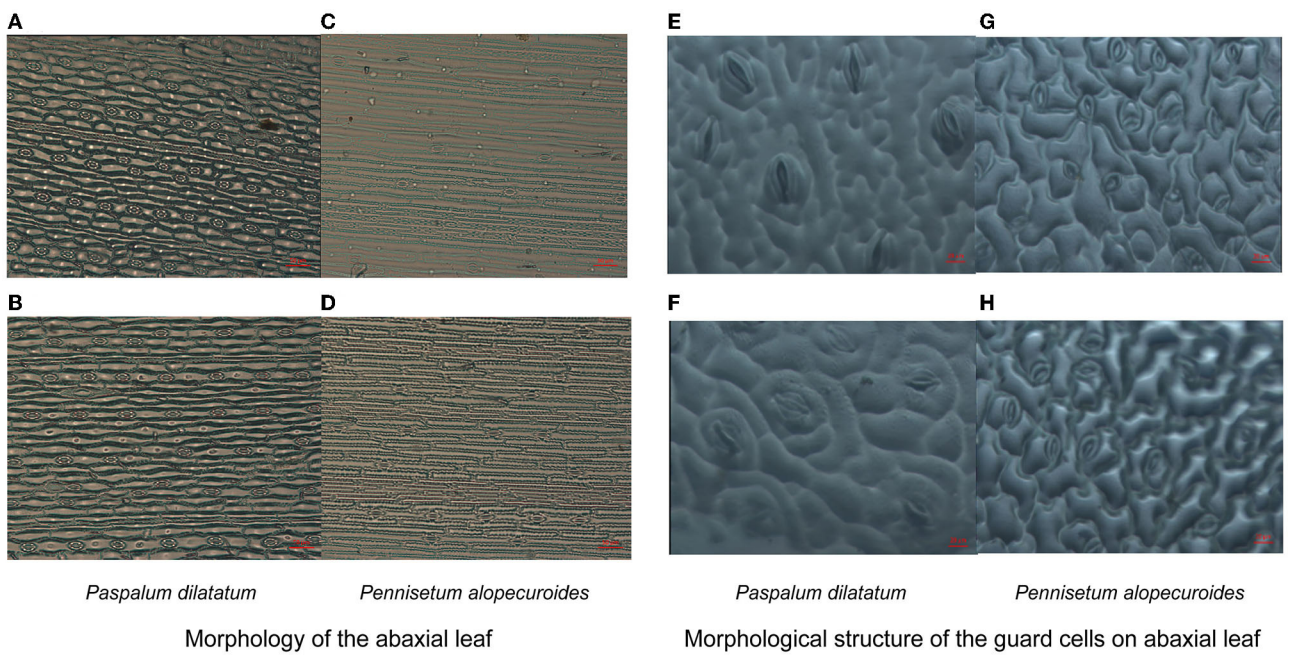


FIGURE 5 | Morphology of the abaxial leaf **(A–D)** and structure of the guard cells on abaxial surface **(E–H)** of the invasive (*Paspalum dilatatum*) and native plant (*Pennisetum alopecuroides*) in control and Cd stress treatments. Images were taken by light microscope for stomatal density with 50-μm scale and for guard cells with 20-μm scale.

Effects of Cd Stress on the Fluorescence Parameters of Invasive and Native Plants

The chlorophyll fluorescence parameters of native and invasive plants decreased under Cd stress; the only exceptions were ΦPSII and qP, which increased under Cd stress. The values of fluorescence parameters were higher in invasive species than natives under Cd stress.

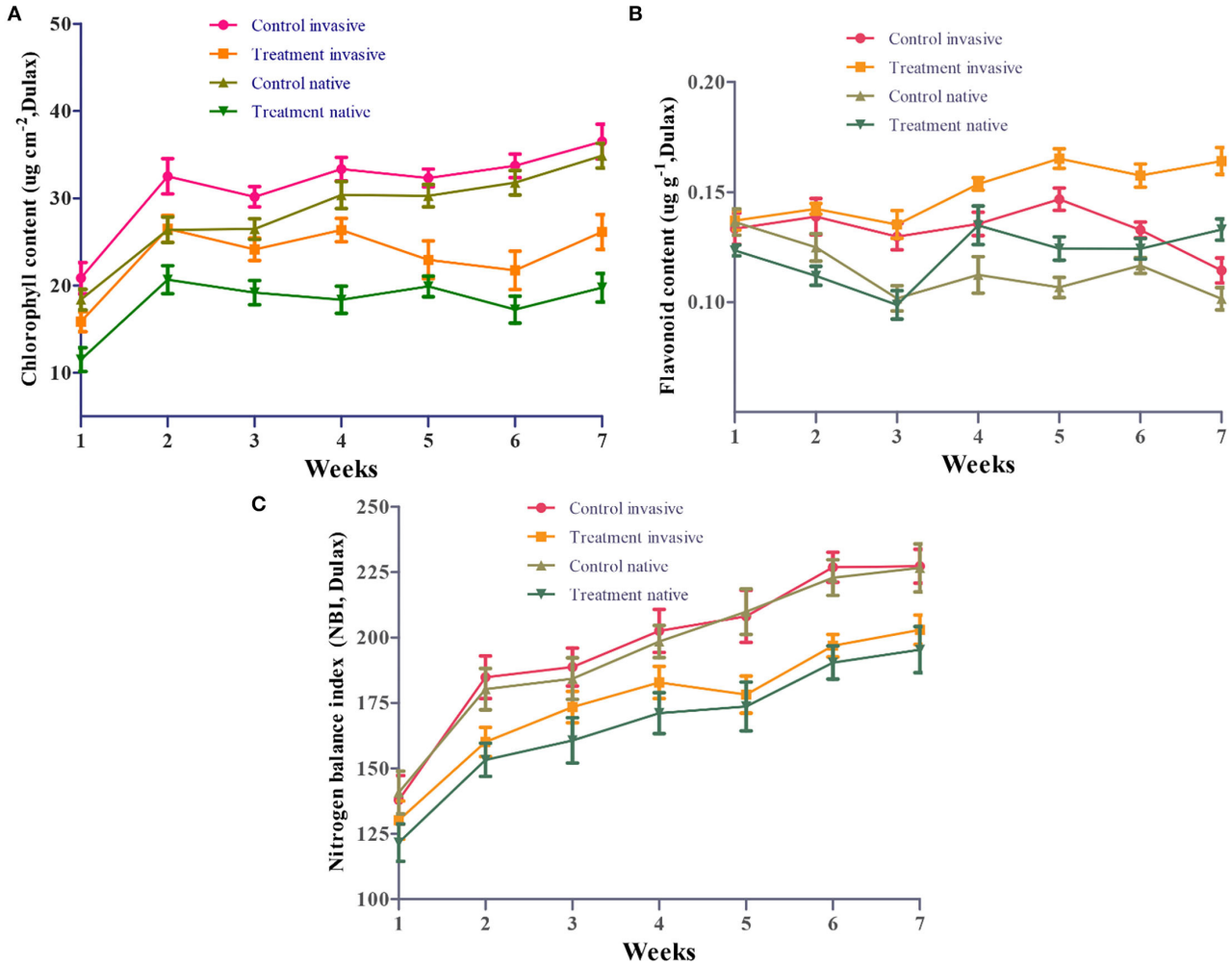


FIGURE 6 | Effect of cadmium (Cd) on chlorophyll content **(A)**, flavonoids content **(B)** and NBI **(C)** of leaves in invasive and native plants during stress conditions. Control: uncontaminated soil + native and invasive plants: Treatment Cd contaminated soil (80 mg/kg) +native and invasive. Error bars depict the SE of the mean of four independent replicates.

Effects on Chlorophyll Fluorescence Parameters

Chlorophyll fluorescence parameters of invasive and native plants were significantly affected by Cd stress (**Figures 7A,B**). Values of F_t in invasive and native plants were lower under Cd stress than under control conditions. The F_0 values of invasive and native plants were similar in the control treatment and decreased in the Cd treatment; however, the magnitude of reduction was greater in invasive plants than in native plants. Under Cd stress conditions, values of F_v'/F_m' and F_v/F_m decreased in both plants, whereas the higher decrement was found in native plants than in invasive plants (**Figures 7C,D**). This finding shows that invasive plants exhibit greater photosynthetic efficiency than native plants under Cd stress.

Effect on Photochemical and Non-Photochemical Chlorophyll Fluorescence Parameters

Values of ΦPSII and F_v/F_m of invasive and native plants were lower under Cd stress than under control conditions. Both parameters showed a greater decline in native plants than in invasive plants under Cd stress (**Figures 8A–C**). In comparison, an improvement in Cd treatment in both plant species was identified in the proportion of open photosystem II, and a further increase was detected in invasive plants simultaneously. These findings suggest that the chlorophyll fluorescence parameters of native plants are more negatively affected by Cd stress than those of invasive plants.

Correlation Between the Chlorophyll Fluorescence Parameters of Native and Invasive Plants

The photochemical and non-photochemical chlorophyll fluorescence parameters, including F_v'/F_m'-NPQ, F_v/F_m-QN, and NPQ-QN, showed significant positive correlations (1, 0.84, and 0.84, respectively) between invasive and native plants. Additionally, two chlorophyll fluorescence parameters, F_0- ΦPSII and F_t- ΦPSII qP, showed extremely negative correlations (−1 and −0.84, respectively) between invasive and native plants. Thus, the results of correlation analysis

revealed that some chlorophyll fluorescence parameters were positively correlated, whereas others were negatively correlated between invasive and native plants under Cd stress conditions (**Figure 9**).

Response of Leaf Functional Traits of Invasive and Native Plants to Cd Stress

The exposure of invasive and native plants to Cd stress in greenhouse experiments resulted in a significant change in stomatal and leaf traits (**Table 2**). The leaf area of invasive species, *Pennisetum purpureum schum* (13.977 ± 0.970 cm^2) and *Paspalum dilatatum* (6.229 ± 0.459 cm^2), was greater than that of native species, *Pennisetum alopecuroides* (5.745 ± 0.577 cm^2) and *Paspalum distichum* (3.879 ± 0.372 cm^2). The leaf length of *Pennisetum purpureum* was the highest (28.150 ± 1.488 cm), while that of *Paspalum distichum* was the lowest (6.133 ± 1.484 cm). Similarly, *P. purpureum* showed the highest stomatal area (1.59 ± 0.120 mm^2), and *P. distichum* showed the lowest leaf area (0.8713 ± 0.122 mm^2). By contrast, stomatal density was the highest in *P. distichum* (48.167 ± 5.954 mm^2) and the lowest *in P. dilatatum* (24.500 ± 5.549 mm^2). The highest stomatal length and width (1.7110 ± 0.077 and 0.9180 ± 0.0301 mm, respectively) were observed in *P. purpureum*. In contrast, the lowest values of stomatal length (1.393 ± 0.077) and width (0.670 ± 0.040 mm) were observed in *P. alopecuroides* and *P. distichum*, respectively. Overall, all leaf functional traits of the two invasive plant species were higher than those of the two native plant species, except stomatal density. This suggests that invasive plants showed better adaptation to metalliferous conditions than native plants.

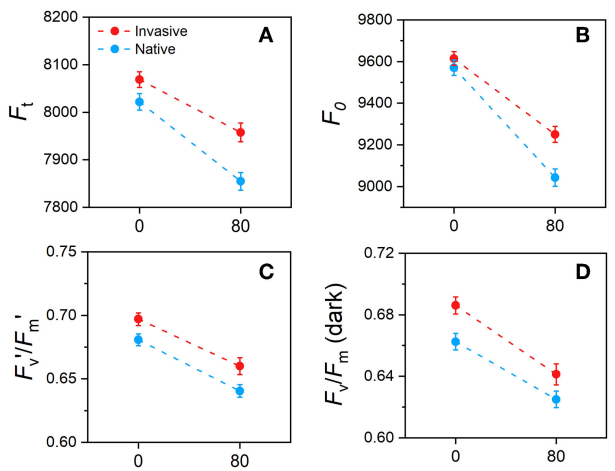


FIGURE 7 | Changes in chlorophyll fluorescence parameters in young-mature (i.e., just after reaching their final size) leaves of invasive and native plants during long term stress and acclimation in response to cadmium (Cd) treatment **(A)** F_t, ground fluorescence in the light-adapted state **(B)** F_0, ground fluorescence in the dark-adapted **(C)** F_v'/F_m', maximum chlorophyll fluorescence in the light-adapted **(D)** F_v/F_m maximum chlorophyll fluorescence in the dark-adapted state. Values are means ± standard error (SE). Notes, 0, control 80, Cd concentration mg/kg.

Cd Bioaccumulation and Translocation in Different Organs of Invasive and Native Plants

Invasive plant species contained a significantly higher concentration of Cd in all three organs (leaf, stem, and root) and showed higher transfer factor and shoot and root BCFs than natives, indicating that invasive species are potential Cd hyperaccumulators. Moreover, invasive plants accumulated a higher level of PPO to adapt to Cd stress than natives. At the end of the Cd treatment, the leaf Cd concentration of invasive plants was higher (97.62 ± 6.02 mg^{-1}) than that of native plants (33.72 ± 3.9 mg^{-1}) (**Figure 10A**). Similarly, the stem and root tissues of invasive species contained more Cd (194.20 ± 11.16 and 334.43 ± 17.44 mg^{-1}, respectively) than those of native plants (118.67 ± 9.09 and 257.46 ± 21.35 mg^{-1}, respectively) (**Figures 10B,C**). Surprisingly, the highest difference in Cd concentration between

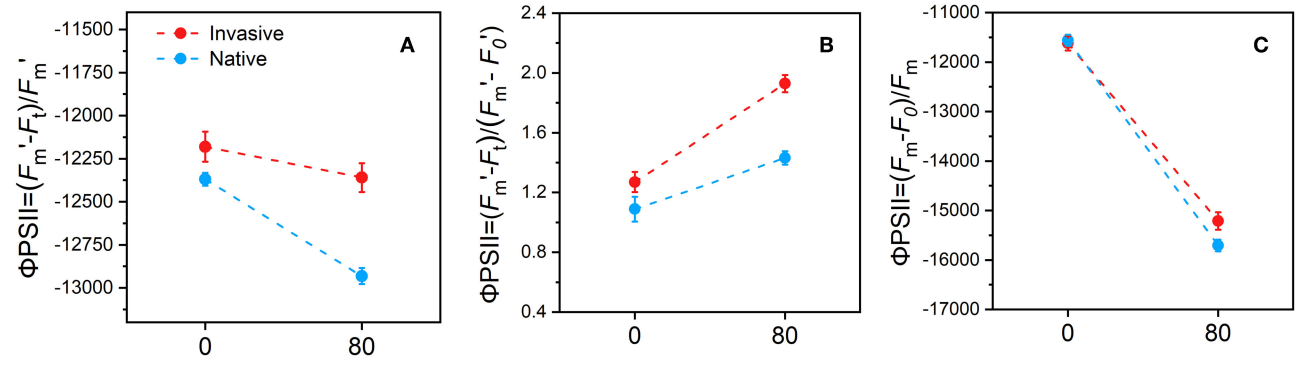


FIGURE 8 | Changes in chlorophyll fluorescence parameters in young-mature (i.e., just after reaching their final size) leaves of invasive and native plants during stress and long-term acclimation in response to cadmium (Cd) treatments **(A)** ΦPSII quantum yield of photosystem II **(B)** ΦPSII qP proportion of open photosystem II **(C)** ΦPSII F_v/F_m maximum quantum yield of photosystem II. Values are means ± standard error (SE).

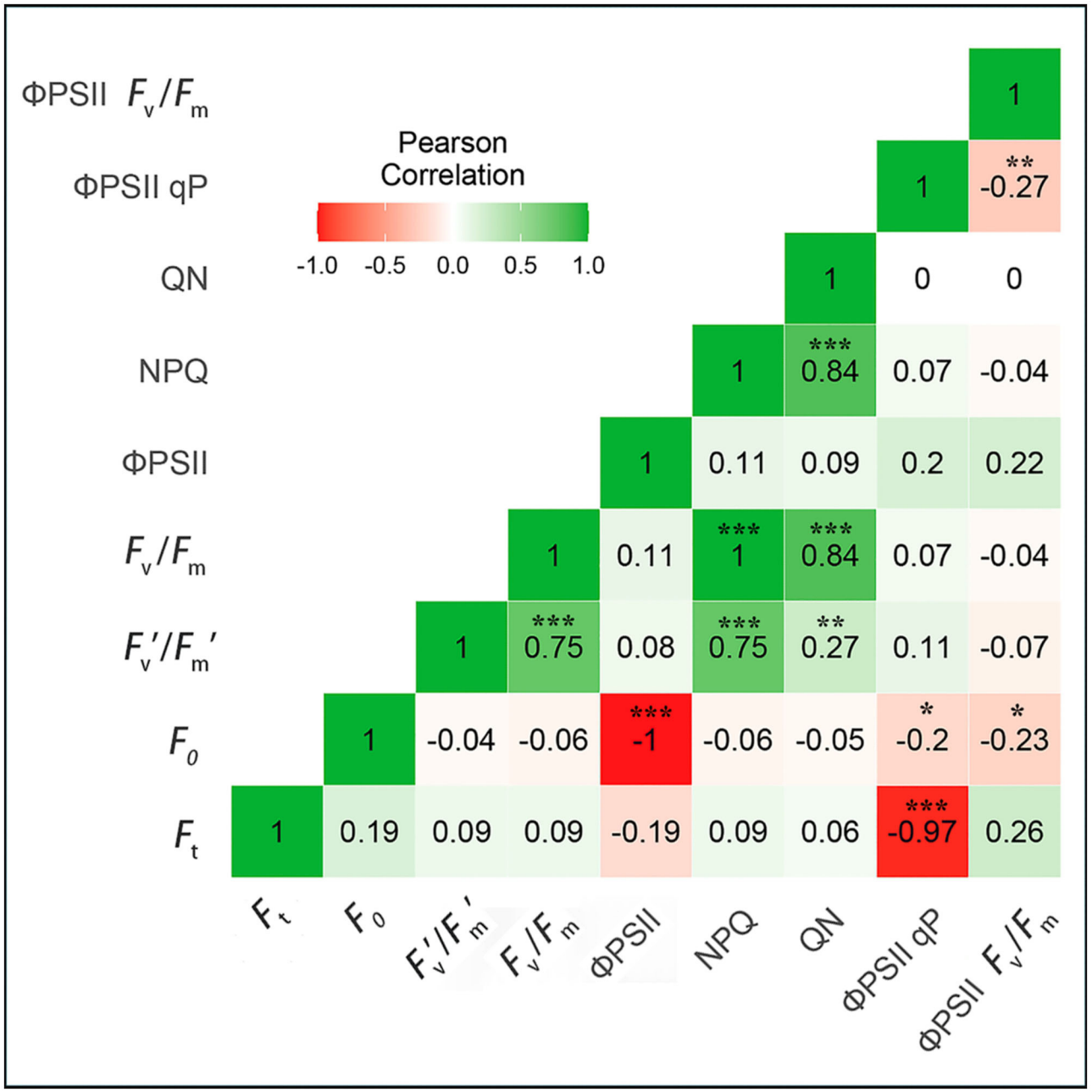


FIGURE 9 | Correlation matrix of chlorophyll fluorescence parameters in young-mature leaves of invasive and native plant species, the labels were similar in **Table 1**. The colored gradient legends represent coefficients of correlation r values from +1.0 (green) to −1.0 (red). The significant correlation at a level ($p^{***} < 0.001$), ($p^{**} < 0.001$), ($P^{*} < 0.05$). All coefficients were computed by the Pearson correlation for possible pairs of variables in the matrix.

invasive and native plants was found in the leaf compared with other plant parts (**Figure 10**).

The shoot BCF of invasive plants (3.64 ± 0.21) was higher than that of native plants (1.90 ± 0.16) under Cd stress and decreased with the increase in soil Cd concentration in both plants (**Figure 11A**). Similarly, the root BCF and average transfer factor of invasive species (4.18 ± 0.21 and 0.87 ± 0.08, respectively) were greater than those of native species (3.21 ± 0.26 and 0.59 ± 0.05, respectively) (**Figures 11B,C**). These results suggest that invasive plant species are either Cd tolerant or Cd bioaccumulators.

Compared with the control, the Cd stress treatment increased activity of PPO in the leaf and root tissues of invasive and native plants. Under Cd stress, PPO enzyme activity in the leaf of

TABLE 2 | The effects of Cd stress on leaf functional traits of each invasive and native plant.

Plant species	Leaf area		Leaf length		Stomatal area	
	CK	Cd stress	CK	Cd stress	CK	Cd stress
Pennisetum purpureum (invasive)	15.543 ± 0.992a	13.977 ± 0.970a	27.241 ± 1.318a	28.150 ± 1.488a	1.171 ± 0.086ab	1.590 ± 0.120a
Pennisetum alopecuroides (native)	5.245 ± 0.474c	5.745 ± 0.577c	11.757 ± 0.823bc	9.350 ± 1.483c	1.146 ± 0.108ab	1.152 ± 0.1220c
Paspalum dilatatum (invasive)	6.434 ± 0.451b	6.229 ± 0.459b	13.799 ± 1.132b	11.533 ± 1.438b	1.049 ± 0.096b	1.166 ± 0.120b
Paspalum distichum (native)	5.776 ± 0.336c	3.879 ± 0.372d	11.526 ± 1.215bc	6.133 ± 1.484d	1.343 ± 0.109a	0.871 ± 0.122d
Plant species	**Stomatal density**		**Stomatal length**		**Stomatal width**	
	CK	Cd stress	CK	Cd stress	CK	Cd stress
Pennistem purpureum (invasive)	50.333 ± 5.373b	44.000 ± 5.949b	1.461 ± 0.047b	1.7110 ± 0.077a	0.832 ± 0.027a	0.918 ± 0.030a
Pennisetum alopecuroides (native)	49.124 ± 4.977b	42.500 ± 5.9549b	1.392 ± 0.034b	1.393 ± 0.077c	0.822 ± 0.019a	0.828 ± 0.030ab
Paspalum dilatatum (invasive)	27.252 ± 1.242c	24.500 ± 5.549c	1.292 ± 0.021c	1.410 ± 0.097b	0.663 ± 0.018c	0.808 ± 0.020ab
Paspalum distichum (native)	62.231 ± 5.551a	48.167 ± 5.954a	1.547 ± 0.053a	1.289 ± 0.079d	0.775 ± 0.019b	0.670 ± 0.040d

Data points are mean ± standard error; different letter was (a, b, c, d) shown as significant differences among different plants were determined by a multiple comparisons Tukey's test.

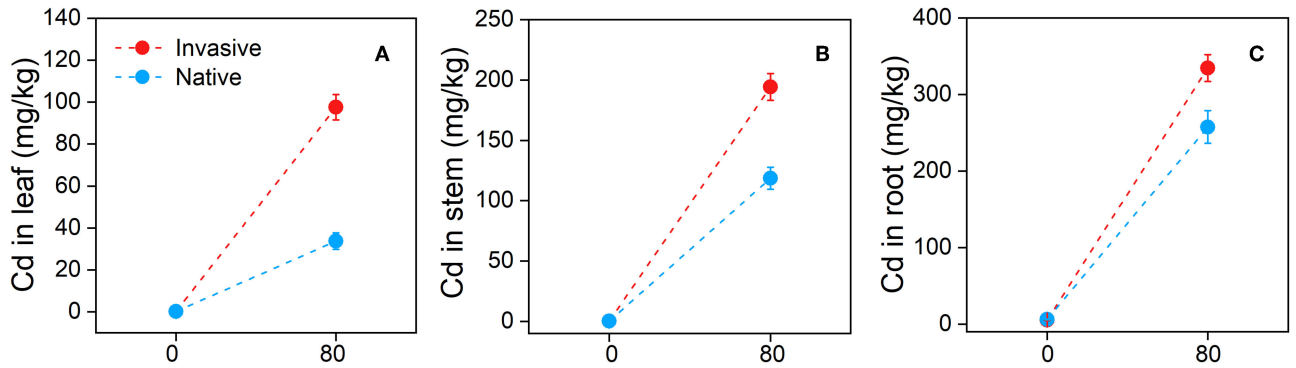


FIGURE 10 | Cd (Cadmium) concentrations in leaf **(A)**, stem **(B)**, and root **(C)** of the two group of invasive and native species under Cd 80 mg/kg level. Values are means ± standard error (SE).

invasive plants (4.44 ± 0.31) was higher than that in the leaf of native plants (2.32 ± 0.19) (**Figure 12A**). Similarly, PPO enzyme was active in the invasive plant root (0.85 ± 0.06) which was higher than that in the native plant root (0.45 ± 0.05) under Cd stress conditions. Overall, PPO enzyme activity in the leaf and root tissues of invasive plants was significantly higher than that in the corresponding tissues of native plants in contaminated soil. Therefore, this study suggests that invasive plants exhibit more effective defense against stresses, such as pathogens, HM, and herbivores, than native plants.

DISCUSSION

Our study showed that Cd stress significantly decreased the leaf functional traits and altered the physiological parameters of both groups of plants, which showed a different response to Cd stress. Overall, invasive plant species showed better growth and higher adaptation of leaf functional (structural and physiological) traits to Cd stress than native plants.

Response of Plant Physiological Parameters to Cd Toxicity

Chlorophyll is an important pigment required for maintaining plant growth. In this study, we investigated the effects of Cd toxicity on the chlorophyll content of invasive and native plant species at different time points for up to 7 weeks. The Cd treatment significantly decreased the chlorophyll content of both plant groups compared with the control (**Figure 6A**). This result is consistent with a previous study (Qian et al., 2009), which showed that Cd stress decreased plant chlorophyll and carotenoid contents because of the inhibitory effect of Cd on enzymes involved in pigment biosynthesis. Additionally, the chlorophyll content of leaves decreased significantly upon Cd application, which is consistent with previous studies showing that Cd inhibited chlorophyll biosynthesis and induced a form of senescence (Fang et al., 1998; Nada et al., 2007; Qian et al., 2009; Gill et al., 2012). Thus, the reduction in chlorophyll content of leaves indicated that Cd stress is a major factor responsible for plant injury. In this study, the negative effect

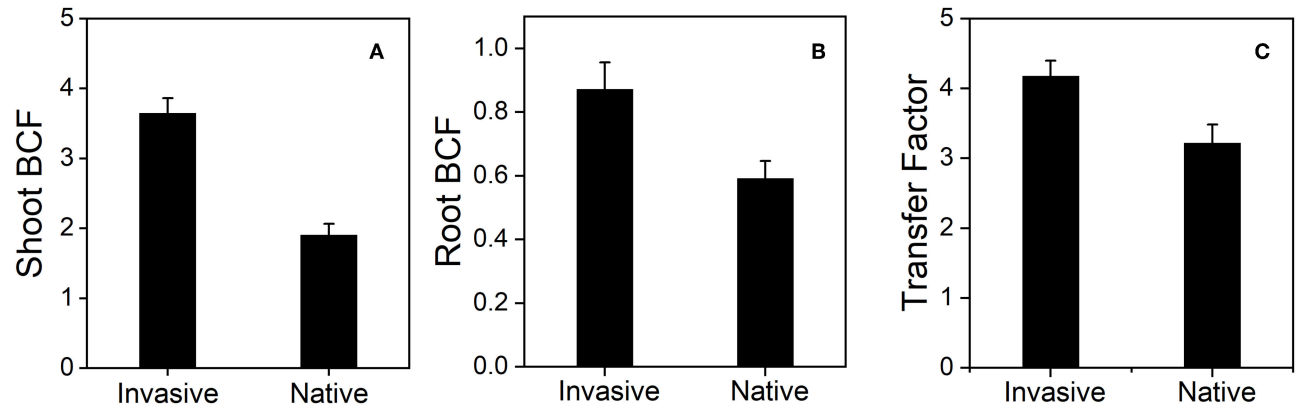


FIGURE 11 | Shoot BCF (bioconcentration factor) **(A)**, Root BCF (bioconcentration factor) **(B)**, and transfer factor **(C)**, the two group of invasive and native species under Cd 80 mg/kg level. Values are means ± standard error (SE).

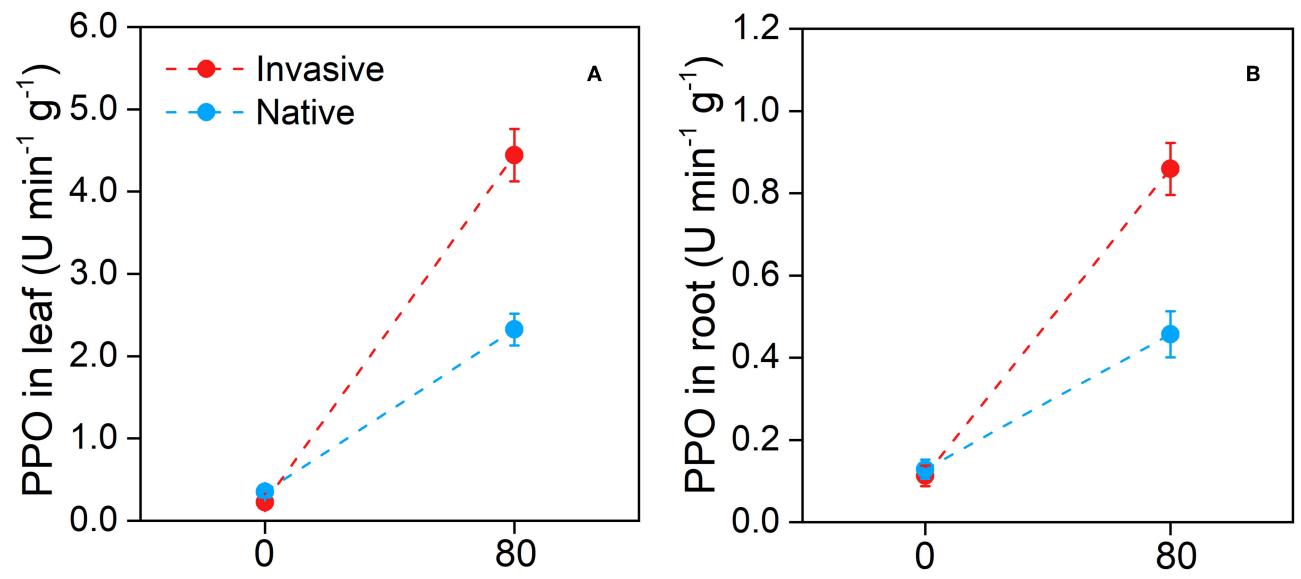


FIGURE 12 | Polyphenol oxidase in leaf **(A)** and in root **(B)** in the two group of invasive and native species under Cd 80 mg/kg level. Values are means ± standard error (SE).

of Cd on leaf chlorophyll content was less in invasive plants than in native plants, which suggests that invasive plants have high physiological adaptation to Cd stress. This result was also in line with the higher Cd accumulation in invasive plants, particularly in the roots. Similarly, *Ageratina adenophora*, a widely invasive plant species, can quickly accumulate Cd in its roots in metal-contaminated areas (Lux et al., 2011; Dai et al., 2020). These results indicate that invasive plants exhibit greater resistance to high Cd levels than native plants. Besides, Cd serves as a non-biological inducer of flavonoid synthesis in plants (Ibrahim et al., 2017). Previous research has shown that Cd present in the soil has a major impact on the content of flavonoids in the leaves of *Robinia pseudoacacia* seedlings, implying that the effect of Cd on flavonoid biosynthesis is species-specific. Furthermore, an important association between total flavonoid and soluble sugar contents in leaves revealed that Cd regulates the main metabolites and increases the total flavonoid content of leaves (Zhang et al., 2021). Similarly, flavonoid content increased dramatically at different time points during the experimental period (1–7 weeks). However, invasive plant species showed a greater increment in flavonoid content than native species (**Figure 6B**). The effect of Cd on flavonoid synthesis is species-dependent (Gondor et al., 2014; Zoufan et al., 2020). As a result, our findings indicate that invasive plant species with higher

total flavonoid content and activity can endure Cd stress better than native plant species. Enrichment of HM in the root affects the accumulation of N, which further alters the NBI (Yadav et al., 2015). Consistent with this finding, the NBI values of invasive and native plants were reduced under Cd stress in this study (**Figure 6C**). The effect of change in plant photosynthetic activity on NBI values has been observed at the elevated level of HM in soil (Chapin III and Eviner, 2003). The NBI values are closely linked to C and N metabolism, and these nutrients allow plants to potentially growth and development (Zheng, 2009). Therefore, these results indicate that NBI can be used to predict plant growth.

Response of the Leaf Functional Traits of Invasive and Native Plants to Cd Stress

The height and other morphological characteristics of plants play the important roles in determining their competitive ability in stress environments (Gross et al., 2007; Thomson et al., 2011). Our results showed that invasive plants grew taller than native plants when exposed to Cd stress (**Figure 2C**), which is consistent with the previous studies (Wang et al., 2018a,b). Greater height may confer a higher competitive ability to invasive plants for resource acquisition, especially for sunlight, one of the most important ecological factors required for plant growth, reproduction, and survival (Meng et al., 2014; DeMalach et al., 2017). Consequently, invasive plants exhibited superior functional traits, such as plant height and leaf shape in a metalliferous environment, which facilitated their spread and successful invasion. Furthermore, the number of leaves of invasive and native plants decreased with the increase in Cd concentration, and native plants showed a greater reduction in leaf number than invasive plants (**Figure 2A**). High Cd concentrations result in brownish or yellowish leaves and dry shoots, resulting in leaf litter, which is positively associated with plant biomass production (Gomes et al., 2011; Mirshekali et al., 2012). In a previous study, high Cd concentration in soil caused chlorosis, development inhibition, and leaf senescence (Mohanpuria et al., 2007). Similarly, we observed that high Cd concentration increased the senescence rates of leaves in both native and invasive species, although to a greater extent in native plants than in invasive plants (**Figure 2B**). Moreover, Cd stress affected the leaf traits to a greater level in native plants than in invasive plants (**Figures 4A,B**). As recorded in studies on *Avena sativa*, *Hordeum vulgare*, *Brassica campestris,* and *Apium graveolens*, high HM content in soil changed the morphological and functional traits of leaves, reducing plant growth and biomass (Gross et al., 2007). Additionally, under HM stress, plants exhibited phytotoxicity symptoms such as chlorosis, leaf necrosis, and decreased production of plant roots, stems, and leaves (Bini et al., 2000). Therefore, our results indicate that leaf traits of invasive plants ensure better survival in metalliferous conditions compared with native plants (**Table 2**). Similarly, invasive plants exhibited superior leaf functional traits and performed better than native plants under HM stress, which could accelerate their subsequent invasion ability by improving resource acquisition (Bai et al., 2020).

Response of the Physiological Fluorescence Parameters of Invasive and Native Plants to Cd Stress

Plant growth is commonly inhibited because of reduction in leaf photosynthetic rate under stress conditions. This inhibition of photosynthesis is caused by the damage to chlorophyll fluorescence parameters (Tanyolaç et al., 2007; Rodríguez-Serrano et al., 2009). In this study, chlorophyll fluorescence parameters, including F_v'/F_m' and F_v/F_m, of invasive and native plant species, were significantly affected by Cd stress (**Figure 7**). High foliar Cd concentration dramatically decreased the chlorophyll fluorescence parameters in a previous study (Baumann et al., 2009). Consistently, values of F_t, F_0, F_v/F_m, and F_v'/F_m' decreased significantly under Cd stress conditions in this study (**Figures 7A,D**). Furthermore, previous studies showed that F_0 reduced PSII (photochemical ability) and was correlated with the leaf chlorophyll content (Calatayud et al., 2006; Fu et al., 2012). Therefore, a greater decline observed in the chlorophyll fluorescence parameters of native plants compared with invasive plants indicates that physiological traits of invasives are tolerant to Cd stress.

The ΦPSII values represent the performance and photochemistry of plants at different photosynthetic photon flux density (PPFDs) (Maxwell and Johnson, 2000; Baker and Rosenqvist, 2004). F_v/F_m, qP, and NPQ have been extensively used to investigate PSII activities in plants (Liu et al., 2014). In our study, plants exhibited relatively low values of F_v/F_m and ΦPSII in the Cd treatment, indicating that electron transfer at the acceptor side of PSII was impeded under Cd stress. This suggests that Cd stress causes great damage to the photosynthetic apparatus in leaves and increases ΦPSII and qP (**Figures 8A,C**). However, we found that chlorophyll fluorescence parameters including (F_v'/F_m' – NPQ), (F_v/F_m – QN), and (NPQ – QN) were significantly positively correlated under Cd stress, whereas (F_0 – ΦPSII) and (F_t – ΦPSII qP) were extremely negatively correlated (**Figure 9**). Previous studies also reported negative correlations among qP, NPQ, ΦPSII, and NPQ (Massacci et al., 2008; Fu et al., 2012). Our results are consistent with a previous study on cucumber (Jin et al., 2017). Moreover, the reduction in NPQ and QN values, accompanied by an increase in ΦPSII and qP values, in the Cd stress treatment was in line with the results of a previous study (Gururani et al., 2015). This approach could be used to increase the photochemical competence of plants and protect them from photo-oxidation under stress conditions. Therefore, our results indicate that the photosynthetic parameters of plants are severely affected by Cd stress.

Response of the Morphological and Structural Traits of Invasive and Native Plants to Cd Stress

Cd stress had a significant effect on stomatal traits, i.e., stomatal area, length, and width ($p \leq 0.001$) (**Table 1**). Previous research

has shown that plants in metalliferous environments have less stomatal areas than those in non-metalliferous environments (Khosropour et al., 2019). We found that the stomatal traits of invasive and native species were negatively affected by Cd stress, although invasive plants showed a better response than native plants (**Figure 3**). The greater decline in the stomatal density and stomatal area of native plants indicates that the development and growth of stomata were affected to a greater extent in native plants than in invasive plants in metalliferous environments (Dineva, 2004). Additionally, in contaminated environments, changes in stomatal traits and structure have been reported in various plant species (Ghouse et al., 1980; Baruah et al., 2014). Stomatal length was found to be negatively linked to increasing stress exposure in a recent study (Aasamaa et al., 2001). In this study, both native and invasive plant groups showed a clear increment in stomatal density under Cd stress, although the increase in stomatal density was greater in native than in invasive plants (**Figure 5**). This result demonstrates that contamination levels alter stomatal density as an adaptation (Verma et al., 2006; Shiv and Ila, 2014). Moreover, previous studies demonstrated that stomatal density increased whereas the length and width of stomata decreased under HM contamination (Alves et al., 2008; Gostin, 2009). Therefore, this study results suggest that the morphological structure of epidermal cells and guard cells changes under Cd stress.

Cd Bioaccumulation and Translocation in Invasive and Native Plants

Our results suggest that invasive species could potentially be used for the phytoremediation of Cd-contaminated soil. Invasive plants showed high bioaccumulation of Cd (**Figure 10**) and high shoot BCF, root BCF, and transfer factor (**Figure 11**). The high shoot and root BCFs are the two important indicators that reflect the pertinence of species for phytoremediation. The transfer factor shows the competence of plants to transfer HM from belowground organs to aboveground plant parts (Marques et al., 2009; Rascio and Navari-Izzo, 2011). However, in previous studies, plant species with shoot BCF and transfer factor > 1 have been accepted as HM hyperaccumulators. In our study, invasive plants exhibited greater BCF and transfer factors than natives. The shoot and root BCF were 3.64 for invasive plants and 1.90 for native plants, whereas the transfer factor values were 0.87 and 0.59 for invasive and native species, respectively (**Figure 11**). The shoot and root BCF were greater than the commonly recognized threshold (Marques et al., 2009; Ali B. et al., 2013). Additionally, higher PPO activity in invasive plant species suggest that plants exhibit great defense in response to Cd stress (**Figure 12**). Similarly, in a previous study, *Salicornia* plants were found to be more resistant to HM stress than other plants based on the PPO activity (Adamski et al., 2012; Khalilzadeh et al., 2020). These results suggest that invasive plant species are more effective in bioaccumulating and translocating Cd and avoiding Cd stress.

CONCLUSION

This study revealed that invasive plant species could be employed as potential Cd hyperaccumulators as they had higher Cd levels in all three plant parts (leaf, stem, and root) and showed higher shoot and root BCF than native plant species. Similarly, the increased activity of PPO in invasive plants may comprise the adaptive defense system against Cd toxicity, which shows that invasive plants are hyperaccumulators of HMs and more resistant to metalliferous conditions. The quantifiable leaf functional traits of invasive plants were significantly higher than that of native plants under Cd stress which indicates that invasive plants can spread further as their ability to capture resources increases. This is particularly true as they have more access to sunlight and soil nutrients as the length of the plant parts shows increasing trend both in root and shoot system. Furthermore, chlorophyll fluorescence parameters provide additional insights into the responses of invasive and native plants to HM and can identify a variety of conditions suitable for the partial reversal of photo-inhibitory damage. However, native plants showed a greater decline in chlorophyll fluorescence parameters than invasive plants. This implies that elevated Cd concentrations reduce the photosynthetic ability of native plants and impact their physiological and biochemical processes. We conclude that invasive plants grow better and show greater adaptation to metalliferous environments than native plants. Based on our results, we propose that *Pennisetum purpureum* and *Paspalum dilatatum* are the bioaccumulators of Cd and can be recommended for plantation in Cd-contaminated soil. Our study further emphasizes that the potential invasion by alien plants in contaminated soil environments is occurring within the introduced range. Therefore, alien non-invasive plants and native plants should be recommended to facilitate land phytoremediation in contaminated environments.

DATA AVAILABILITY STATEMENT

The original contributions presented in the study are included in the article/**Supplementary Material**, further inquiries can be directed to the corresponding author/s.

AUTHOR CONTRIBUTIONS

MI, Y-JW, and MK: conceptualization. MI, TB, and Y-JW: methodology. SS and Y-WL: software. JS, FB, FZ, and SW: validation. SAR and MI: formal analysis, investigation, and writing—original draft preparation. AM, HFA, KRH, and SAR writing, reviewing, and editing. Y-JW: resources, supervision, project administration, and funding acquisition. All authors contributed to the article and approved the submitted version.

FUNDING

This research was supported by NSFC (32171510, 31770449, 32071527), the Fundamental Research Funds for the Central Universities (2662020YLPY016),

and Hubei Forestry Scientific Research Project (2020-LYKJ1).

ACKNOWLEDGMENTS

The authors would like to thank Yuan-Yuan Liu, Cong-Ying Zhao, and Amir Hamid for their help with the experiments. The authors would like to thank the Deanship of Scientific Research at Taif University to the Researchers Supporting Project (TURSP2020/110); Taif University, Taif, Saudi Arabia.

SUPPLEMENTARY MATERIAL

The Supplementary Material for this article can be found online at: https://www.frontiersin.org/articles/10.3389/fpls.2022.869072/full#supplementary-material

REFERENCES

Aasamaa, K., Sõber, A., and Rahi, M. (2001). Leaf anatomical characteristics associated with shoot hydraulic conductance, stomatal conductance and stomatal sensitivity to changes of leaf water status in temperate deciduous trees. *Funct. Plant Biol.* 28, 765–774. doi: 10.1071/PP00157

Adamski, J. M., Danieloski, R., Deuner, S., Braga, E. J. B., de Castro, L. A. S., and Peters, J. A. (2012). Responses to excess iron in sweet potato: impacts on growth, enzyme activities, mineral concentrations, and anatomy. *Acta Physiol. Plant.* 34, 1827–1836. doi: 10.1007/s11738-012-0981-3

Alaboudi, K. A., Ahmed, B., and Brodie, G. (2018). Phytoremediation of Pb and Cd contaminated soils by using sunflower (Helianthus annuus) plant. *Ann. Agric. Sci.* 63, 123–127. doi: 10.1016/j.aoas.2018.05.007

Ali, B., Gill, R. A., Yang, S., Gill, M. B., Ali, S., Rafiq, M. T., et al. (2014). Hydrogen sulfide alleviates cadmium-induced morpho-physiological and ultrastructural changes in *Brassica napus*. *Ecotoxicol. Environ. Saf.* 110, 197–207. doi: 10.1016/j.ecoenv.2014.08.027

Ali, B., Tao, Q., Zhou, Y., Gill, R. A., Ali, S., Rafiq, M. T., et al. (2013). 5-Aminolevolinic acid mitigates the cadmium-induced changes in *Brassica napus* as revealed by the biochemical and ultra-structural evaluation of roots. *Ecotoxicol. Environ. Saf.* 92, 271–280. doi: 10.1016/j.ecoenv.2013.02.006

Ali, H., Khan, E., and Sajad, M. A. (2013). Phytoremediation of heavy metals—concepts and applications. *Chemosphere* 91, 869–881. doi: 10.1016/j.chemosphere.2013.01.075

Alves, E. S., Tresmondi, F., and Longui, E. L. (2008). Leaf anatomy of *Eugenia uniflora* L. (Myrtaceae) in urban and rural environments, São Paulo State, Brazil. *Acta Bot. Brasilica* 22, 241–248. doi: 10.1590/S0102-33062008000100023

Arredondo, M., Martinez, R., Nunez, M. T., Ruz, M., and Olivares, M. (2006). Inhibition of iron and copper uptake by iron, copper and zinc. *Biol. Res.* 39, 95–102. doi: 10.4067/S0716-97602006000100011

Bai, T., Liu, Y.-Y., Muhammad, I., Yang, X., Yin, X.-J., Bai, L., et al. (2020). Mixed nitrogen form addition facilitates the growth adaptation of legume plant to heavy metal contamination in degraded mining areas. *Glob. Ecol. Conserv.* 24, e01387. doi: 10.1016/j.gecco.2020.e01387

Baker, N. R., and Rosenqvist, E. (2004). Applications of chlorophyll fluorescence can improve crop production strategies: an examination of future possibilities. *J. Exp. Bot.* 55, 1607–1621. doi: 10.1093/jxb/erh196

Bakker, J., and Wilson, S. (2001). Competitive abilities of introduced and native grasses. *Plant Ecol.* 157, 119–127. doi: 10.1023/A:1013972403293

Baruah, P., Saikia, R. R., Baruah, P. P., and Deka, S. (2014). Effect of crude oil contamination on the chlorophyll content and morpho-anatomy of *Cyperus brevifolius* (Rottb.) Hassk. *Environ. Sci. Pollut. Res.* 21, 12530–12538. doi: 10.1007/s11356-014-3195-y

Baumann, H. A., Morrison, L., and Stengel, D. B. (2009). Metal accumulation and toxicity measured by PAM—chlorophyll fluorescence in seven species of marine macroalgae. *Ecotoxicol. Environ. Saf.* 72, 1063–1075. doi: 10.1016/j.ecoenv.2008.10.010

Bi, X., Pan, X., and Zhou, S. (2013). Soil security is alarming in China's main grain producing areas. *Environ. Sci. Technol.* 47, 7593–7594.

Bini, C., Casaril, S., and Pavoni, B. (2000). Fertility gain and heavy metal accumulation in plants and soil, studied by means of a compost amended cultivation of *Taraxacum officinale*. *Toxicol. Environ. Chem.* 77, 131–142.

Blicker, P. S., Olson, B. E., and Wraith, J. M. (2003). Water use and water-use efficiency of the invasive Centaurea maculosa and three native grasses. *Plant Soil* 254, 371–381. doi: 10.1023/A:1025530315788

Calatayud, A., Roca, D., and Martínez, P. F. (2006). Spatial-temporal variations in rose leaves under water stress conditions studied by chlorophyll fluorescence imaging. *Plant Physiol. Biochem.* 44, 564–573. doi: 10.1016/j.plaphy.2006.09.015

Callaway, R. M., and Ridenour, W. M. (2004). Novel weapons: invasive success and the evolution of increased competitive ability. *Front. Ecol. Environ.* 2, 436–443. doi: 10.1890/1540-9295(2004)002[0436:NWISAT]2.0.CO;2

Chapin, F. S. III, and Eviner, V. T. (2003). Biogeochemistry of terrestrial net primary production. *Treatise Geochem.* 8, 682.doi: 10.1016/B0-08-043751-6/08130-5

Chen, Y.-E., Cui, J.-M., Yang, J.-C., Zhang, Z.-W., Yuan, M., Song, C., et al. (2015). Biomonitoring heavy metal contaminations by moss visible parameters. *J. Hazard. Mater.* 296, 201–209. doi: 10.1016/j.jhazmat.2015.04.060

Chmielowska-Bak, J., Gzyl, J., Rucińska-Sobkowiak, R., Arasimowicz-Jelonek, M., and Deckert, J. (2014). The new insights into cadmium sensing. *Front. Plant Sci.* 5, 245. doi: 10.3389/fpls.2014.00245

Dai, Z.-C., Cai, H.-H., Qi, S.-S., Li, J., Zhai, D.-L., Wan, J. S. H., et al. (2020). Cadmium hyperaccumulation as an inexpensive metal armor against disease in Crofton weed. *Environ. Pollut.* 267, 115649. doi: 10.1016/j.envpol.2020.115649

DeMalach, N., Zaady, E., and Kadmon, R. (2017). Light asymmetry explains the effect of nutrient enrichment on grassland diversity. *Ecol. Lett.* 20, 60–69. doi: 10.1111/ele.12706

Deng, J., Liao, B., Ye, M., Deng, D., Lan, C., and Shu, W. (2007). The effects of heavy metal pollution on genetic diversity in zinc/cadmium hyperaccumulator Sedum alfredii populations. *Plant Soil* 297, 83–92. doi: 10.1007/s11104-007-9322-5

Dineva, S. B. (2004). Comparative studies of the leaf morphology and structure of white ash *Fraxinus americana* L. and London plane tree *Platanus acerifolia* Willd growing in polluted area. *Dendrobiology* 52, 3–8.

Dong, W. Q. Y., Cui, Y., and Liu, X. (2001). Instances of soil and crop heavy metal contamination in China. *Soil Sediment Contam.* 10, 497–510. doi: 10.1080/20015891109392

Duan, Q., Lee, J., Liu, Y., Chen, H., and Hu, H. (2016). Distribution of heavy metal pollution in surface soil samples in China: a graphical review. *Bull. Environ. Contam. Toxicol.* 97, 303–309. doi: 10.1007/s00128-016-1857-9

Dwyer, J. M., Hobbs, R. J., and Mayfield, M. M. (2014). Specific leaf area responses to environmental gradients through space and time. *Ecology* 95, 399–410. doi: 10.1890/13-0412.1

Ehrenfeld, J. G. (2010). Ecosystem consequences of biological invasions. *Annu. Rev. Ecol. Evol. Syst.* 41, 59–80. doi: 10.1146/annurev-ecolsys-102209-144650

Ewel, J. J., and Putz, F. E. (2004). A place for alien species in ecosystem restoration. *Front. Ecol. Environ.* 2, 354–360. doi: 10.1890/1540-9295(2004)002[0354:APFASI]2.0.CO;2

Fang, Z., Bouwkamp, J. C., and Solomos, T. (1998). Chlorophyllase activities and chlorophyll degradation during leaf senescence in non-yellowing mutant and wild type of *Phaseolus vulgaris* L. *J. Exp. Bot.* 49, 503–510. doi: 10.1093/jxb/49.320.503

Farooq, M. A., Ali, S., Hameed, A., Bharwana, S. A., Rizwan, M., Ishaque, W., et al. (2016). Cadmium stress in cotton seedlings: physiological, photosynthesis and oxidative damages alleviated by glycinebetaine. *South African J. Bot.* 104, 61–68. doi: 10.1016/j.sajb.2015.11.006

Fu, W., Li, P., and Wu, Y. (2012). Effects of different light intensities on chlorophyll fluorescence characteristics and yield in lettuce. *Sci. Hortic.* 135, 45–51. doi: 10.1016/j.scienta.2011.12.004

Genty, B., Briantais, J.-M., and Baker, N. R. (1989). The relationship between the quantum yield of photosynthetic electron transport and quenching of chlorophyll fluorescence. *Biochim. Biophys. Acta General Subj.* 990, 87–92. doi: 10.1016/S0304-4165(89)80016-9

Ghouse, A. K. M., Zaidi, H., and Attique, A. (1980). Effect of air pollution on the foliar organs of *Callistemon citrinus* Stapf. *J Sci Res* 2, 207–209.

Gill, S. S., Khan, N. A., and Tuteja, N. (2012). Cadmium at high dose perturbs growth, photosynthesis and nitrogen metabolism while at low dose it up regulates sulfur assimilation and antioxidant machinery in garden cress (*Lepidium sativum* L.). *Plant Sci.* 182, 112–120. doi: 10.1016/j.plantsci.2011.04.018

Gomes, M. P., Nogueira, M., de, O. G., Castro, E. M. de, and Soares, Â. M. (2011). Ecophysiological and anatomical changes due to uptake and accumulation of heavy metal in Brachiaria decumbens. *Sci. Agric.* 68, 566–573. doi: 10.1590/S0103-90162011000500009

Gondor, O. K., Szalai, G., Kovács, V., Janda, T., and Pál, M. (2014). Impact of UV-B on drought-or cadmium-induced changes in the fatty acid composition of membrane lipid fractions in wheat. *Ecotoxicol. Environ. Saf.* 108, 129–134. doi: 10.1016/j.ecoenv.2014.07.002

Gostin, I. N. (2009). Air pollution effects on the leaf structure of some Fabaceae species. *Not. Bot. Horti Agrobot. Cluj Napoca* 37, 57–63. doi: 10.15835/nbha3723078

Gross, N., Suding, K. N., Lavorel, S., and Roumet, C. (2007). Complementarity as a mechanism of coexistence between functional groups of grasses. *J. Ecol.* 95, 1296–1305. doi: 10.1111/j.1365-2745.2007.01303.x

Gururani, M. A., Venkatesh, J., Ganesan, M., Strasser, R. J., Han, Y., Kim, J.-I., et al. (2015). In vivo assessment of cold tolerance through chlorophyll-a fluorescence in transgenic zoysiagrass expressing mutant phytochrome A. *PLoS ONE* 10, e0127200. doi: 10.1371/journal.pone.0127200

Hatamian, M., Rezaei Nejad, A., Kafi, M., Souri, M. K., and Shahbazi, K. (2020). Interaction of lead and cadmium on growth and leaf morphophysiological characteristics of European hackberry (*Celtis australis*) seedlings. *Chem. Biol. Technol. Agric.* 7, 1–8. doi: 10.1186/s40538-019-0173-0

Huamain, C., Chunrong, Z., Cong, T. U., and Yongguan, Z. (1999). Heavy metal pollution in soils in China: status and countermeasures. *Ambio* 28, 130–134.

Ibrahim, M. H., Chee Kong, Y., and Mohd Zain, N. A. (2017). Effect of cadmium and copper exposure on growth, secondary metabolites and antioxidant activity in the medicinal plant Sambung Nyawa (*Gynura procumbens* (Lour.) Merr). *Molecules* 22, 1623. doi: 10.3390/molecules22101623

Ilyas, M., Liu, Y.-Y., Shah, S., Ali, A., Khan, A. H., Zaman, F., et al. (2021). Adaptation of functional traits and their plasticity of three ornamental trees growing in urban environment. *Sci. Hortic.* 286, 110248. doi: 10.1016/j.scienta.2021.110248

Ishii, H., and Asano, S. (2010). The role of crown architecture, leaf phenology and photosynthetic activity in promoting complementary use of light among coexisting species in temperate forests. *Ecol. Res.* 25, 715–722. doi: 10.1007/s11284-009-0668-4

Jadia, C. D., and Fulekar, M. H. (2009). Phytoremediation of heavy metals: recent techniques. *Afr. J. Biotechnol.* 8, 921–928.

Jin, L., Che, X., Zhang, Z., Li, Y., Gao, H., and Zhao, S. (2017). The mechanisms by which phenanthrene affects the photosynthetic apparatus of cucumber leaves. *Chemosphere* 168, 1498–1505. doi: 10.1016/j.chemosphere.2016.12.002

Joshi, M. K., and Mohanty, P. (2004). "Chlorophyll a fluorescence as a probe of heavy metal ion toxicity in plants," in *Chlorophyll a Fluorescence*, eds G. C. Papageorgiou, and R. Govindjee (Dordrecht: Springer), 637–661.

Kardel, F., Wuyts, K., Babanezhad, M., Vitharana, U. W. A., Wuytack, T., Potters, G., et al. (2010). Assessing urban habitat quality based on specific leaf area and stomatal characteristics of *Plantago lanceolata* L. *Environ. Pollut.* 158, 788–794. doi: 10.1016/j.envpol.2009.10.006

Keane, R. M., and Crawley, M. J. (2002). Exotic plant invasions and the enemy release hypothesis. *Trends Ecol. Evol.* 17, 164–170. doi: 10.1016/S0169-5347(02)02499-0

Khalilzadeh, R., Pirzad, A., Sepehr, E., Khan, S., and Anwar, S. (2020). Long-term effect of heavy metal–polluted wastewater irrigation on physiological and ecological parameters of *Salicornia europaea* L. *J. Soil Sci. Plant Nutr.* 20, 1574–1587. doi: 10.1007/s42729-020-00299-7

Khosropour, E., Attarod, P., Shirvany, A., Pypker, T. G., Bayramzadeh, V., Hakimi, L., et al. (2019). Response of *Platanus orientalis* leaves to urban pollution by heavy metals. *J. For. Res.* 30, 1437–1445. doi: 10.1007/s11676-018-0692-8

Klughammer, C., and Schreiber, U. (2008). Complementary PS II quantum yields calculated from simple fluorescence parameters measured by PAM fluorometry and the Saturation Pulse method. *PAM Appl. Notes* 1, 201–247.

Koné, A. W., Edoukou, E. F., Gonnety, J. T., Aurélie, N. A., Assémien, L. F. E., Angui, P. K. T., et al. (2012). Can the shrub *Chromolaena odorata* (Asteraceae) be considered as improving soil biology and plant nutrient availability? *Agrofor. Syst.* 85, 233–245. doi: 10.1007/s10457-012-9497-5

Li, S., Yang, W., Yang, T., Chen, Y., and Ni, W. (2015). Effects of cadmium stress on leaf chlorophyll fluorescence and photosynthesis of Elsholtzia argyi—a cadmium accumulating plant. *Int. J. Phytoremed.* 17, 85–92. doi: 10.1080/15226514.2013.828020

Li, Z., Ma, Z., van der Kuijp, T. J., Yuan, Z., and Huang, L. (2014). A review of soil heavy metal pollution from mines in China: pollution and health risk assessment. *Sci. Total Environ.* 468, 843–853. doi: 10.1016/j.scitotenv.2013.08.090

Liu, J. H., Yong, X. H., Han, Q., Ali, A., and Wang, Y. J. (2017). Response of plant functional traits to species origin and adaptive reproduction in weeds. *Plant Biosyst.* 151, 323–330. doi: 10.1080/11263504.2016.1174171

Liu, M., Zhang, Z., Gao, H., Yang, C., Fan, X., and Cheng, D. (2014). Effect of leaf dehydration duration and dehydration degree on PSII photochemical activity of papaya leaves. *Plant Physiol. Biochem.* 82, 85–88. doi: 10.1016/j.plaphy.2014.05.003

Liu, Y., Li, Z., Xu, L., Fu, Q., and Wang, Y. (2022). Effects of region and elevation on adaptation of leaf functional traits of an invasive plant *Erigeron annuus* in China. *Phyton Int. J. Exp. Bot.* 91, 115–128. doi: 10.32604/phyton.2022.015395

Lux, A., Martinka, M., Vaculík, M., and White, P. J. (2011). Root responses to cadmium in the rhizosphere: a review. *J. Exp. Bot.* 62, 21–37. doi: 10.1093/jxb/erq281

Maron, J. L., and Vilà, M. (2001). When do herbivores affect plant invasion? Evidence for the natural enemies and biotic resistance hypotheses. *Oikos* 95, 361–373. doi: 10.1034/j.1600-0706.2001.950301.x

Marques, A. P. G. C., Rangel, A. O. S. S., and Castro, P. M. L. (2009). Remediation of heavy metal contaminated soils: phytoremediation as a potentially promising clean-up technology. *Crit. Rev. Environ. Sci. Technol.* 39, 622–654. doi: 10.1080/10643380701798272

Marteinsdóttir, B., and Eriksson, O. (2014). Plant community assembly in semi-natural grasslands and ex-arable fields: a trait-based approach. *J. Veg. Sci.* 25, 77–87. doi: 10.1111/jvs.12058

Massacci, A., Nabiev, S. M., Pietrosanti, L., Nematov, S. K., Chernikova, T. N., Thor, K., et al. (2008). Response of the photosynthetic apparatus of cotton (Gossypium hirsutum) to the onset of drought stress under field conditions studied by gas-exchange analysis and chlorophyll fluorescence imaging. *Plant Physiol. Biochem.* 46, 189–195. doi: 10.1016/j.plaphy.2007.10.006

Maxwell, K., and Johnson, G. N. (2000). Chlorophyll fluorescence—a practical guide. *J. Exp. Bot.* 51, 659–668. doi: 10.1093/jexbot/51.345.659

Meng, F., Cao, R., Yang, D., Niklas, K. J., and Sun, S. (2014). Trade-offs between light interception and leaf water shedding: a comparison of shade- and sun-adapted species in a subtropical rainforest. *Oecologia* 174, 13–22. doi: 10.1007/s00442-013-2746-0

Mirshekali, H., Hadi, H., Amirnia, R., and Khodaverdiloo, H. (2012). Effect of zinc toxicity on plant productivity, chlorophyll and Zn contents of sorghum (*Sorghum bicolor*) and common lambsquarter (*Chenopodium album*). *Int. J. Agric. Res. Rev.* 2, 247–254.

Mohanpuria, P., Rana, N. K., and Yadav, S. K. (2007). Cadmium induced oxidative stress influence on glutathione metabolic genes of *Camellia sinensis* (L.) O. Kuntze. *Environ. Toxicol. An Int. J.* 22, 368–374. doi: 10.1002/tox.20273

Murtaza, G., Javed, W., Hussain, A., Qadir, M., and Aslam, M. (2017). Soil-applied zinc and copper suppress cadmium uptake and improve the performance of cereals and legumes. *Int. J. Phytoremediation* 19, 199–206. doi: 10.1080/15226514.2016.1207605

Nada, E., Ferjani, B. A., Ali, R., Bechir, B. R., Imed, M., and Makki, B. (2007). Cadmium-induced growth inhibition and alteration of biochemical parameters

in almond seedlings grown in solution culture. *Acta Physiol. Plant.* 29, 57–62. doi: 10.1007/s11738-006-0009-y

Oduor, A. M. O., Leimu, R., and van Kleunen, M. (2016). Invasive plant species are locally adapted just as frequently and at least as strongly as native plant species. *J. Ecol.* 104, 957–968. doi: 10.1111/1365-2745.12578

Pandey, V. C. (2012). Invasive species based efficient green technology for phytoremediation of fly ash deposits. *J. Geochemical Explor.* 123, 13–18. doi: 10.1016/j.gexplo.2012.05.008

Pantoja, P. O., Paine, C. E. T., and Vallejo-Marín, M. (2018). Natural selection and outbreeding depression suggest adaptive differentiation in the invasive range of a clonal plant. *Proc. R. Soc. B Biol. Sci.* 285, 20181091. doi: 10.1098/rspb.2018.1091

Qian, H., Li, J., Sun, L., Chen, W., Sheng, G. D., Liu, W., et al. (2009). Combined effect of copper and cadmium on *Chlorella vulgaris* growth and photosynthesis-related gene transcription. *Aquat. Toxicol.* 94, 56–61. doi: 10.1016/j.aquatox.2009.05.014

Rascio, N., and Navari-Izzo, F. (2011). Heavy metal hyperaccumulating plants: how and why do they do it? And what makes them so interesting? *Plant Sci.* 180, 169–181. doi: 10.1016/j.plantsci.2010.08.016

Rodríguez-Serrano, M., Romero-Puertas, M. C., Pazmino, D. M., Testillano, P. S., Risueño, M. C., Luis, A., et al. (2009). Cellular response of pea plants to cadmium toxicity: cross talk between reactive oxygen species, nitric oxide, and calcium. *Plant Physiol.* 150, 229–243. doi: 10.1104/pp.108.131524

Scheepens, J. F., Frei, E. S., and Stöcklin, J. (2010). Genotypic and environmental variation in specific leaf area in a widespread Alpine plant after transplantation to different altitudes. *Oecologia* 164, 141–150. doi: 10.1007/s00442-010-1650-0

Schreiber, U., Schliwa, U., and Bilger, W. (1986). Continuous recording of photochemical and non-photochemical chlorophyll fluorescence quenching with a new type of modulation fluorometer. *Photosynth. Res.* 10, 51–62. doi: 10.1007/BF00024185

Shiv, K., and Ila, P. (2014). Stomatal analysis in Cassia occidentalis L. in response to automobile pollution along roadsides in Meerut city, India. *Int. Res. J. Sci. Eng.* 2, 167–170.

Simberloff, D., Martin, J.-L., Genovesi, P., Maris, V., Wardle, D. A., Aronson, J., et al. (2013). Impacts of biological invasions: what's what and the way forward. *Trends Ecol. Evol.* 28, 58–66. doi: 10.1016/j.tree.2012.07.013

Sun, Y., Zhou, Q., Wang, L., and Liu, W. (2009). Cadmium tolerance and accumulation characteristics of Bidens pilosa L. as a potential Cd-hyperaccumulator. *J. Hazard. Mater.* 161, 808–814. doi: 10.1016/j.jhazmat.2008.04.030

Taiz, L., and Zeiger, E. (2010). *Plant Physiology, Chapter 19*. Auxin: The Growth Hormone.

Tanhan, P., Kruatrachue, M., Pokethitiyook, P., and Chaiyarat, R. (2007). Uptake and accumulation of cadmium, lead and zinc by Siam weed [*Chromolaena odorata* (L.) King & Robinson]. *Chemosphere* 68, 323–329. doi: 10.1016/j.chemosphere.2006.12.064

Tanyolaç, D., Ekmekçi, Y., and Ünalan, S. (2007). Changes in photochemical and antioxidant enzyme activities in maize (*Zea mays* L.) leaves exposed to excess copper. *Chemosphere* 67, 89–98. doi: 10.1016/j.chemosphere.2006.09.052

Thomson, F. J., Moles, A. T., Auld, T. D., and Kingsford, R. T. (2011). Seed dispersal distance is more strongly correlated with plant height than with seed mass. *J. Ecol.* 99, 1299–1307. doi: 10.1111/j.1365-2745.2011.01867.x

Verma, R. B., Siddiqi, T. O., and Iqbal, M. (2006). Foliar response of Ipomea pes-tigridis L. to coal-smoke pollution. *Turk. J. Botany* 30, 413–417.

Wang, C., Liu, J., Xiao, H., and Zhou, J. (2016). Differences in leaf functional traits between *Rhus typhina* and native species. *CLEAN Soil Air Water* 44, 1591–1597. doi: 10.1002/clen.201600144

Wang, C., Wu, B., Jiang, K., and Zhou, J. (2018a). Differences in functional traits between invasive and native Amaranthus species under simulated acid deposition with a gradient of pH levels. *Acta Oecologica* 89, 32–37. doi: 10.1016/j.actao.2018.04.006

Wang, C., Wu, B., Jiang, K., and Zhou, J. (2018b). Effects of different types of heavy metal pollution on functional traits of invasive redroot pigweed and native red amaranth. *Int. J. Environ. Res.* 12, 419–427. doi: 10.1007/s41742-018-0101-3

Wang, Y. J., Chen, D., Yan, R., Yu, F. H., and van Kleunen, M. (2019). Invasive alien clonal plants are competitively superior over co-occurring native clonal plants. *Perspect. Plant Ecol. Evol. Syst.* 40, 125484. doi: 10.1016/j.ppees.2019.125484

Wang, Y. J., Müller-Schärer, H., van Kleunen, M., Cai, A. M., Zhang, P., et al. (2017). Invasive alien plants benefit more from clonal integration in heterogeneous environments than natives. *New Phytologist* 216, 1072–1078. doi: 10.1111/nph.14820

Webb, K. J., Cookson, A., Allison, G., Sullivan, M. L., and Winters, A. L. (2014). Polyphenol oxidase affects normal nodule development in red clover (*Trifolium pratense* L.). *Front. Plant Sci.* 5, 700. doi: 10.3389/fpls.2014.00700

Wei, H., Huang, M., Quan, G., Zhang, J., Liu, Z., and Ma, R. (2018). Turn bane into a boon: application of invasive plant species to remedy soil cadmium contamination. *Chemosphere* 210, 1013–1020. doi: 10.1016/j.chemosphere.2018.07.129

Wei, H., Xu, J., Quan, G., Zhang, J., and Qin, Z. (2017). Effects of Praxelis clematidea invasion on soil nitrogen fractions and transformation rates in a tropical savanna. *Environ. Sci. Pollut. Res.* 24, 3654–3663. doi: 10.1007/s11356-016-8127-6

Yadav, A., Ram, A., Majithiya, D., Salvi, S., Sonavane, S., Kamble, A., et al. (2015). Effect of heavy metals on the carbon and nitrogen ratio in Avicennia marina from polluted and unpolluted regions. *Mar. Pollut. Bull.* 101, 359–365. doi: 10.1016/j.marpolbul.2015.10.020

Yaghoubian, Y., Siadat, S. A., Telavat, M. R. M., and Pirdashti, H. (2016). Quantify the response of purslane plant growth, photosynthesis pigments and photosystem II photochemistry to cadmium concentration gradients in the soil. *Russ. J. plant Physiol.* 63, 77–84. doi: 10.1134/S1021443716010180

Zhang, C., Jia, X., Zhao, Y., Wang, L., Cao, K., Zhang, N., et al. (2021). The combined effects of elevated atmospheric CO2 and cadmium exposure on flavonoids in the leaves of *Robinia pseudoacacia* L. seedlings. *Ecotoxicol. Environ. Saf.* 210, 111878. doi: 10.1016/j.ecoenv.2020.111878

Zheng, Z.-L. (2009). Carbon and nitrogen nutrient balance signaling in plants. *Plant Signal. Behav.* 4, 584–591. doi: 10.4161/psb.4.7.8540

Zoufan, P., Azad, Z., Ghahfarokhie, A. R., and Kolahi, M. (2020). Modification of oxidative stress through changes in some indicators related to phenolic metabolism in *Malva parviflora* exposed to cadmium. *Ecotoxicol. Environ. Saf.* 187, 109811. doi: 10.1016/j.ecoenv.2019.109811

Conflict of Interest: The authors declare that the research was conducted in the absence of any commercial or financial relationships that could be construed as a potential conflict of interest.

Publisher's Note: All claims expressed in this article are solely those of the authors and do not necessarily represent those of their affiliated organizations, or those of the publisher, the editors and the reviewers. Any product that may be evaluated in this article, or claim that may be made by its manufacturer, is not guaranteed or endorsed by the publisher.

Copyright © 2022 Ilyas, Shah, Lai, Sher, Bai, Zaman, Bibi, Koul, Wani, Majrashi, Alharby, Hakeem, Wang and Rather. This is an open-access article distributed under the terms of the Creative Commons Attribution License (CC BY). The use, distribution or reproduction in other forums is permitted, provided the original author(s) and the copyright owner(s) are credited and that the original publication in this journal is cited, in accordance with accepted academic practice. No use, distribution or reproduction is permitted which does not comply with these terms.

frontiers | Frontiers in Plant Science

ORIGINAL RESEARCH
published: 10 June 2022
doi: 10.3389/fpls.2022.890550

Integration of Metabolomics and Transcriptomics for Investigating the Tolerance of Foxtail Millet (*Setaria italica*) to Atrazine Stress

Lifang Sun[1], Libin Liu[1], Yuting Wang[1], Yanfei Feng[1], Wei Yang[1], Di Wang[1], Shuren Gao[1], Xingfen Miao[1] and Wentao Sun[2]**

[1] Key Laboratory of Crop Germplasm Improvement and Cultivation in Cold Regions, Key Laboratory of Low Carbon Green Agriculture of Northeast Plain in Ministry of Agriculture and Rural Affairs, Agronomy College of Heilongjiang Bayi Agricultural University, Daqing, China, [2] Heilongjiang HYHC Company, Daqing, China

Foxtail millet (*Setaria italica*) is a monotypic species widely planted in China. However, residual atrazine, a commonly used maize herbicide, in soil, is a major abiotic stress to millet. Here, we investigated atrazine tolerance in millet based on the field experiments, then obtained an atrazine-resistant variety (Gongai2, GA2) and an atrazine-sensitive variety (Longgu31, LG31). To examine the effects of atrazine on genes and metabolites in millet plants, we compared the transcriptomic and metabolomic profiles between GA2 and LG31 seedling leaves. The results showed that 2,208 differentially expressed genes (DEGs; 501 upregulated, 1,707 downregulated) and 192 differentially expressed metabolites (DEMs; 82 upregulated, 110 downregulate) were identified in atrazine-treated GA2, while in atrazine-treated LG31, 1,773 DEGs (761 upregulated, 1,012 downregulated) and 215 DEMs (95 upregulated, 120 downregulated) were identified. The bioinformatics analysis of DEGs and DEMs showed that many biosynthetic metabolism pathways were significantly enriched in GA2 and LG31, such as glutathione metabolism (oxiglutatione, γ-glutamylcysteine; *GSTU6*, *GSTU1*, *GSTF1*), amino acid biosynthesis (L-cysteine, N-acetyl-L-glutamic acid; *ArgB*, *GS*, *hisC*, *POX1*), and phenylpropanoid biosynthesis [*trans*-5-o-(4-coumaroyl)shikimate; *HST*, *C3′H*]. Meanwhile, the co-expression analysis indicated that GA2 plants had enhanced atrazine tolerance owing to improved glutathione metabolism and proline biosynthesis, and the enrichment of scopoletin may help LG31 plants resist atrazine stress. Herein, we screened an atrazine-resistant millet variety and generated valuable information that may deepen our understanding of the complex molecular mechanism underlying the response to atrazine stress in millet.

Keywords: ***Setaria italica*, atrazine, metabolomics, transcriptomics, stress**

OPEN ACCESS

Edited by:
Mohammad Anwar Hossain, Bangladesh Agricultural University, Bangladesh

Reviewed by:
Ling Xu, Zhejiang Sci-Tech University, China
Awdhesh Kumar Mishra, Yeungnam University, South Korea

***Correspondence:**
Xingfen Miao
byndmxf@126.com
Wentao Sun
wt_suns@126.com

Specialty section:
This article was submitted to Plant Breeding, a section of the journal Frontiers in Plant Science

Received: *06 March 2022*
Accepted: *16 May 2022*
Published: *10 June 2022*

Citation:
Sun L, Liu L, Wang Y, Feng Y, Yang W, Wang D, Gao S, Miao X and Sun W (2022) Integration of Metabolomics and Transcriptomics for Investigating the Tolerance of Foxtail Millet (Setaria italica) to Atrazine Stress. Front. Plant Sci. 13:890550. doi: 10.3389/fpls.2022.890550

INTRODUCTION

Atrazine (2-chloro-4-ethylamino-6-isopropylamino-1,3,5-triazine) is a synthetic herbicide that has been extensively applied for the control of broadleaf and grass weeds in field-planted sorghum, wheat, and maize (Gast, 1970; Lebaron et al., 2011; Daniele and Maggi, 2017; Felisbino et al., 2018). However, atrazine residue can remain for up to 231 days in the environment (Karlsson et al., 2016),

and previous studies have shown that increased atrazine concentrations in the soil are related to exponentially increased accumulated rainfall in the soil. These studies showed that under the most severe drought conditions, injury to cereal crops could occur up to 3 years after atrazine application at 1.2–1.5 kg/ha (Moyer and Blackshaw, 1993). In addition, the application of atrazine over years may lead to its accumulation in the soil, which not only damages plants but also harms the health of humans, animals, and aquatic organisms (Contreras et al., 2020). Therefore, the toxicity of atrazine and its implications have consequently been the focus of considerable attention.

The mechanisms of toxicity of atrazine to plants have been studied, and it appears that atrazine can cause oxidative damage to plants and decrease the efficiency of photosynthesis. Erinle et al. (2018) found that the levels of malondialdehyde (MDA) and reactive oxygen species (ROS) in pearl millet significantly increased with increasing atrazine concentrations in the soil, whereas antioxidant gene expression was significantly suppressed, reaching its lowest when atrazine was applied at 50 mg/kg. The content of thiobarbituric acid reactive substances in the roots of pearl millet exposed to atrazine for 6 days increased 26% compared with the treatment that was exposed for 2 days, and the ROS also increased (Zhang Y. et al., 2021). The activities of antioxidases in the leaf and root of *Pennisetum americanum* L. were increased to protect the plant from atrazine-induced oxidative damage (Jiang et al., 2016). In addition, atrazine can suppress electron transport at both the donor and receptor sides and acts on the absorption, transfer, and utilization of light energy by damaging the photosystem II reaction center of the microalga *Chlorella* sp. (Sun C. et al., 2020). The effective quantum yield of photosystem II and the electron transport rate of photosynthesis in *Handroanthus heptaphyllus* (Vell.) were gradually reduced by the action of atrazine (Barbosa et al., 2021). These studies suggest that the mechanism of atrazine toxicity is complex and depends on numerous molecular changes.

Metabolomics, as a new discipline, can well analyze all low molecular weight metabolites in a given organism or tissue (Goodacre et al., 2004). Based on the Liquid Chromatography-Mass Spectrometer (LC-MS) and/or Gas Chromatography-Mass Spectrometer (GC-MS) technologies, it has been widely performed to identify and assess the expression levels of multiple metabolites in various studies, all of which obtained valuable results in areas such as human diseases (Zhang K. H. et al., 2021), plant nutrition (Cao et al., 2020), plant microorganism (Skliros et al., 2018), and plant development (Zhang et al., 2019). In addition, high-throughput sequencing technology (RNA-Seq) has become an important tool for transcriptome analysis to detect differentially expressed genes among samples (Shan et al., 2021). Recently, metabolomics combined with transcriptome sequencing has provided a powerful way to study the metabolic phenotype of organisms and related genes for further understanding the molecular and biological mechanisms of functional genomics (Li et al., 2018; Sun J. H. et al., 2020; Zhang et al., 2020).

Foxtail millet (*Setaria italica* L.) is an ancient crop that is widely planted in China because it is rich in protein and crude fat. However, millet is sensitive to herbicides, thereby creating the need for manual weeding. The continuous planting of maize leads to the accumulation of atrazine residue in the soil, as is apparent in the Heilongjiang province of China, and seriously affects the cultivation of millet as a rotation crop. Therefore, the aims of this study were to screen atrazine resistant millet varieties and to evaluate the expression of specific genes and metabolites at the seedling stage using transcriptomics and metabolomics profiles. These data will be valuable for providing basic information to understand the potential biological processes that are relevant to the mechanism of atrazine stress on millet plants.

MATERIALS AND METHODS

Plant Materials and Atrazine Treatment in Field

Based on the stress results of atrazine in the germination stage by Wang et al. (2021), 20 different resistant millet varieties, widely planted in China, were selected for field experiments to further verify their responses to atrazine (**Table 1**). The experiment was conducted in 2019 at the 5th management zone of Yinlang Farm (124° 44′ 13.89″ E, 56° 29′ 53.60″ N) in Daqing City, Heilongjiang Province, China. This site had an average annual temperature of 4.6°C, an active accumulated temperature of >2800°C, annual average sunshine of 2782.5 h, and a frost-free period of 136 days.

The experiment was conducted using a completely randomized design with three replications. The plot size was 9.75 m^2, with 5-m rows, 0.65-m row spacing, and 3 lines per repeat. The sowing density was 600000 plants/hm^2. Following the experimental screening results of atrazine stress in the germination stage by Wang et al. (2021), a mixture of approximately 13.55 ml of 38% fully mixed atrazine suspension and 800 ml of water (approximately 11 μmol/L) was sprayed evenly on each plot after sowing for 1 day. Water was used as the control. Additionally, 37.5 kg/hm^2 urea, 225 kg/hm^2 diammonium phosphate, and 120 kg/hm^2 potassium sulfate were applied as base fertilizers, after which approximately 120 kg/hm^2 urea was applied at the heading stage. Jinan Tianbang Chemical Co., Ltd., Jinan, Shandong province, China, provided the 38% atrazine suspension.

Determination Indicators and Methods

At the 3-leaf seedling stage, fresh leaf tissues were used to determine the physiological and biochemical indexes, including the chlorophyll content through ethanol extraction and colorimetric methods described by Liu et al. (2020), malondialdehyde (MDA) content using the thiobarbituric acid method as described by Akbulut and Yigit (2010), and soluble protein content using the coomassie brilliant blue G-250-binding method as described by Bradford (1976), with some modifications. Briefly, the whole plant at the 3-leaf seedling stage was transferred into paper bags, heated at 105°C for 30 min, then dried at 80°C to constant weight, and weighed using a 1/10000 gram balance with three biological repetitions. Subsequently, the average was taken after each determination.

TABLE 1 | Varieties used in the field experiment.

No.	Varieties	Response to atrazine	No.	Varieties	Response to atrazine
1	Jingu 26 (JG26)	MR	11	Nenxuan 15 (NX15)	HS
2	Fenxuan 3 (FX3)	HR	12	Longgu 25 (LG25)	HS
3	Zigengu (ZGG)	HR	13	Zuantoubai (ZTB)	MS
4	Jingu 40 (JG40)	MR	14	Jinsuihuangjin (JSHJ)	HS
5	Dabaigu (DBG)	MR	15	Longgu 31 (LG31)	HS
6	Gongai 2 (GA2)	HR	16	Huangjindungu (HJDG)	MS
7	Shandongliushan (SDLS)	MR	17	Gongai 5 (GA5)	MS
8	Shanxiwugu (SXWG)	HR	18	Yangu 2 (YG2)	HS
9	Hebeixianggu (HBXG)	HR	19	Zigenbai (ZGB)	MS
10	Caogu (CG)	HR	20	Baigenhongniangu (BGHNG)	MS

HR, high resistant; MR, middle resistant; MS, middle sensitive; HS, high sensitive.

At the 7–8-leaf seedling stage, fully expanded young leaves of 3 plants with the same growth pattern were selected for each treatment. Subsequently, we measured net photosynthetic rates, transpiration rates, and stomatal conductance of their inverter clovers using a LI-COR 6400 portable photosynthetic instrument (LI-COR Inc., Lincoln, NE, United States) on sunny days (9:00 to 11:00 h) at 1500 μmol m^{-2} s^{-1} PPFD. Ambient water vapor pressure, CO_2 concentration, and leaf temperature were maintained at 1.2 $\pm$ 0.1 kPa, 400 μmol m^{-2} s^{-1}, and 25 $\pm$ 1.0°C, respectively. The average values were taken for data analysis.

At maturity, five panicles were randomly selected from each treatment to determine the grain weight per panicle. The average value was taken for data analysis.

Statistical Analyses

All measurements conducted were repeated at least in triplicate. Relative values between the treatment and control were used in the data analysis through repetitions to avoid differences in genotypes. Data analysis was conducted using SPSS-26.0 (SPSS, Chicago, IL, United States) to determine the weight value of each indicator through principal component analysis (PCA), as described by Dong et al. (2016). The standardized principal component (PC) scores were extracted from the correlation matrix, and those PCs with eigenvalues of $\geq$1.00 were selected. It should be emphasized that to make the trend of each index consistent, the relative value of MDA should be converted to its reciprocal. Ultimately, the subordinate function method was used to comprehensively evaluate the resistance of different millet genotypes to stress.

RNA Sequencing, Annotation, and Expression Analysis

Material Preparation

All seeds of the resistant and tolerant millet varieties were sterilized in 0.1% NaClO (v/v) and sown in germination boxes (20-cm diameter and 15-cm height; 5 holes and 5 plants per hole) containing approximately 0.5 kg of soil, flint, and perlite in a 3:2:1 ratio. We set up two treatments [control (water) and atrazine] in four boxes each. The concentration of atrazine was consistent with the germination stage, according to Wang et al. (2021). Subsequently, all pots were placed in a greenhouse (25 $\pm$ 1.5°C during the day and 20 $\pm$ 1.5°C at night) with a photoperiod of 14:10 h (light/dark). These pots were watered using 1/2 concentration of the Hoagland nutrient solution once a day. At the 3-leaf seedling stage, the leaves were harvested and stored at −80°C for further analysis.

RNA Extraction

A total of 12 samples (3 biological repetitions per treatment group of each variety) were used for transcriptome sequencing. Total RNA was extracted from leaves using the RNAiso Reagent Plant Kit (Takara, Dalian, China) (Sun et al., 2012) following the manufacturer's protocols. The quality and quantity of RNA were assessed using a NanoDrop 1000 spectrophotometer and Agilent 2100 bio-analyzer before constructing a cDNA library at Beijing Biomarker Biotechnology Co., Ltd., Beijing, China[1].

cDNA Library Construction and Illumina Sequencing

Total RNA was treated with DNase I, following which oligo(dT) magnetic beads were used to enrich Poly (A+) RNA for digestion using RNA Fragmentation buffer. The first-strand cDNAs were synthesized using the mRNA fragments as templates with random hexamer primers. Subsequently, the second strands were synthesized using dNTPs, DNA polymerase I, and RNase H; purified using QIAquick PCR purification kit (Qiagen, Hilden, Germany); and then resolved into EB buffer for end reparation and single nucleotide A (adenine) addition. The short fragments were then connected with adapters. Fragments suitable for PCR amplification were selected through agarose gel electrophoresis. During qPCR, the quantity and quality of the sample library were assessed using Agilent 2100 bio-analyzer and ABI StepOnePlus Real-Time PCR Systems. Subsequently, the library was sequenced using Illumina HiSeq 4000 or other sequencers, as necessary, at Beijing Biomarker Biotechnology Co., Ltd. (see text footnote 1).

De novo Assembly and Data Analysis

After sequencing, the raw reads were filtered to remove low-quality, adaptor-polluted, and >10% unknown base (N) reads to obtain clean reads. The clean reads of each library were then mapped to a reference genome[2] using the HISAT2 method (Kim et al., 2015). The unique mapped reads were assembled *de novo* to obtain reconstructed transcripts using StringTie (Pertea et al., 2015) after genome mapping. The novel transcripts in

[1] www.biomarker.com.cn

[2] https://phytozome.jgi.doe.gov/pz/portal.html#!info?alias=Org_Sitalica

our samples were identified by comparing the reconstructed transcripts with genome annotation information according to cuffcompare, a tool of cufflinks (Trapnell et al., 2012). Subsequently, the coding potentials of novel transcripts were predicted using CPC methods (Kong et al., 2007) to merge with reference transcripts for obtaining a complete reference for further analysis.

Gene Expression Level Analysis

The gene expression level of each sample was calculated based on the expected number of fragments per kilobase of transcript sequence per millions fragments mapped after mapping the clean reads to the reference genome using Bowtie 2 (Langmead and Salzberg, 2012). The differentially expressed genes (DEGs) between the two samples were also analyzed using DESeq two methods with adjusted *p*-values. The DEGs were identified using the following parameters: false discovery rate (FDR) of <0.01 and absolute fold change of ≥ 2. Gene Ontology (GO) and Kyoto Encyclopedia of Genes and Genomes (KEGG) pathway enrichment analyses of DEGs were further performed based on the major public database (Kanehisa, 2008).

Ultra-Performance Liquid Chromatography/Tandem Mass Spectrometry-Based Metabolomics Analysis

Metabolite Extraction

Fully ground tissue samples were first dissolved in extract solution (volume ratio of methanol to acetonitrile = 1:1, internal standard concentration 2 mg/L). Then, the samples were treated with ultrasound for 10 min in an ice bath, followed by storage at −20°C for 1 h and centrifugation at 12000 × *g* for 15 min at 4°C. Next, 500 μl of the supernatant was transferred into a new 1.5-ml tube for drying, followed by the addition of 160 μl of extract solution (volume ratio of acetonitrile to water = 1:1). The solution was vortexed for 30 s and subjected to ultrasound for 10 min in an ice bath for redissolution. Afterward, the suspension was allowed to stand for 30 min at 4°C before centrifugation (12000 × *g* at 4°C for 15 min) to obtain supernatants ready for injection. This yielded 12 samples (4 treatment groups, including GCK, GT, LCK, and LT, each with 3 biological replicates) using the same method. A quality control (QC) sample was prepared by combining equal aliquots from each sample. All samples were stored at 4°C for analyses within 3 days.

Ultra-Performance Liquid Chromatography/Tandem Mass Spectrometry Analysis

Millet extracts were analyzed using an ACQUITY UPLC I-Class PLUS system (Waters Corporation, Milford, MA, United States) coupled to a Xevo G2-XS QTof system (Waters Corporation, Milford, MA, United States) with an electrospray ionization (ESI) source under positive and negative modes. In the ESI+ and ESI− modes, mobile phases A and B were 0.1% formic acid aqueous solution and 0.1% formic acid acetonitrile, respectively. The injection volume was 1 μL. Chromatographic separation was achieved using an ACQUITY UPLC HSS T3 column (2.1 mm × 100 mm, 1.8 μm; Waters Pacific Pte. Ltd, Milford, MA, United States) at a flow rate of 400 μL/min using the following gradient: 98% A and 2% B for 0.25 min, decreased to 2% A and increased to 98% B within 13 min, and then increased to 98% A and decreased to 2% B in the last 2 min.

A Waters Xevo G2-XS QTOF high-resolution mass spectrometer can collect primary and secondary mass spectrometry data in the MSe mode under the control of the acquisition software (MassLynx V4.2, Waters Corporation, Milford, MA, United States). In each data acquisition cycle, it can simultaneously conduct dual-channel data acquisition for low and high collision energies. The low collision energy was 2 V, the high collision energy range was 10–40 V, and the scanning frequency was 0.2 s.

Data Preprocessing and Analysis

The collected raw data were processed using the Progenesis QI software for peak extraction, peak alignment, and other data processing operations. Metabolite quantification and theoretical fragment identification were conducted based on the online METLIN[3] database of the Progenesis QI software and self-built library of Beijing Biomarker Biotechnology Co., Ltd. Theoretical fragment identification parameters and mass deviation were all within 100 ppm.

The follow-up analysis was conducted after normalizing the original peak area information with the total peak area. PCA and Spearman's correlation analysis were performed to assess the repeatability of the test and quality control samples. According to the grouping information, we calculated and compared different multiples. First, the *t*-test was used to assess significant differences (*p*-value) between the compounds. The variable importance in the projection (VIP) value of the model was calculated using multiple cross validation. The differentially expressed metabolites (DEMs) were identified using the following screening criteria: absolute fold change (FC) of ≥ 1.5 and VIP of ≥ 1. The DEMs were queried to classify pathway information based on KEGG and human metabolome databases (HMDB). The extraction, identification, and quantification of metabolites were conducted at Beijing Biomarker Biotechnology Co., Ltd. (see text footnote 1).

Coexpression Network Analysis of Transcriptome and Metabolome

According to the fold changes of each DEG and DEM, the Pearson's correlation coefficient was calculated. Before calculating the correlation, the data were preprocessed using the *Z*-value transformation method. Correlations corresponding to a coefficient of $R^2 > 0.8$ and *p*-value of <0.05 were selected. The relationship between the metabolome and transcriptome was illustrated using BMKCloud (see text footnote 1).

Real-Time Quantitative Reverse Transcription PCR Validation of Differentially Expressed Genes

The leaves of the millet plant were used for real-time quantitative reverse transcription PCR (qRT-PCR). The method used followed

[3]http://metlin.scripps.edu

the procedures described in a previous report (Sun et al., 2018). The primers were designed and synthesized according to the gene sequences in the millet sequence database (see text footnote 2) and the 25S RNA sequence was used as the endogenous control (**Supplementary Table 1**). At the end of the PCR for each sample, based on the fluorescence logarithmic graph, the appropriate threshold was chosen and the Ct values were obtained to analyze the transcript levels of each gene using the $2^{-\Delta\Delta Ct}$ method (Livak and Schmittgen, 2001). The Bio-Rad CFX96 Real-Time System (Bio-Rad, Hercules, CA, United States) and CFX Manager System software version 2.0 were used in following the manufacturer's instructions in this study.

RESULTS

Acquisition of Resistant/Tolerant Millet Varieties Under Atrazine Stress

To analyze the sensitivity of different millet varieties to atrazine, eight indicators in different growth stages were detected and the data were subjected to PC factor analysis. Kaiser–Meyer–Olkin (KMO) and Bartlett's ball tests were conducted on the relative value data of each trait using SPSS (**Supplementary Table 2**). The results showed that the KMO test value was $0.819 > 0.5$ and the probability of significance in Bartlett's ball test was $p < 0.05$, indicating that the test data conformed to spherical distribution (**Table 2**). Therefore, the experimental data of this study were suitable for factor analysis.

In **Table 3**, the eigenvalues of the first three PCs were >1, and the cumulative contribution rate reached 76.722%, reflecting most of the information of the 8 indexes. Therefore, the first three PCs were selected to evaluate the eight indexes of atrazine tolerance in millet. The confidence level of the evaluation was 76.722%. Based on PCA, the weight value of each indicator was calculated. Results are shown in **Table 3**. Ultimately, the comprehensive values of atrazine tolerance in 20 foxtail millet varieties were calculated (**Table 4**). This result showed that the *T* value of Gongai 2 (GA2) was the highest (0.91), whereas that of Longgu 31 (LG31) was the lowest (0.09), indicating that GA2 was not sensitive to atrazine, whereas LG31 was sensitive to atrazine. Therefore, GA2 and LG31 varieties were used further analysis.

TABLE 2 | Kaiser–Meyer–Olkin (KMO) and Bartlett's test.

Kaiser–Meyer–Olkin measure of sampling adequacy		**0.819**
Bartlett's test of sphericity	Approx. chi-square	58.013
	df	28
	Sig.	0.001

TABLE 3 | First three principal components (PCs) of variable project, eigenvalues, variability (%), cumulative (%), and weight value.

Variable	PC1	PC2	PC3	Weight value
MDA	0.605	−0.382	0.433	0.10
Soluble protein	0.157	0.814	0.471	0.14
Chlorophyll content	0.817	−0.126	−0.299	0.10
Net photosynthetic rate	0.803	−0.070	−0.303	0.10
Transpiration rate	0.752	0.348	−0.046	0.15
Stomatal conductance	0.832	0.220	0.059	0.16
Dry matter	0.880	0.009	−0.161	0.15
Grain weight per panicle	0.440	−0.430	0.634	0.09
Eigenvalue	3.929	1.184	1.025	
Variance contribution (%)	49.111	14.804	12.807	
Cumulative variance contribution (%)	49. 111	63.915	76.722	

Transcriptome Analysis of Millet Under Atrazine Stress

For a deeper understanding of the molecular mechanisms occurring in the millet plant under atrazine stress, its leaves (**Figure 1**) were used for RNA-Seq, and the raw data of RNA-Seq were uploaded to the NCBI website. With three biological replicates, a total of 87.16 Gb of clean data with 94.31% of bases scoring Q30 were obtained. Of the total clean reads, 93.54–94.91% were unique matches with the *Setaria italic* L. reference genome and 35,747 unique genes were expressed in the millet leaves, of which 1,163 were novel genes and only 856 genes were successfully annotated (**Supplementary Table 3**).

The expression levels of the transcripts for each sample were calculated to analyze the different resistant and sensitive millet varieties. A total of 3,981 DEGs were identified in the samples of both varieties: 2,208 (501 upregulated and 1,707 downregulated) genes in the Gongai variety and 1,773 (761 upregulated and 1,012 downregulated) genes in the Longgu variety (FC $\geq$ 2 and FDR < 0.01; **Table 5**). The detailed information of the genes is presented in **Supplementary Table 4**. The results also showed that the number of downregulated genes (1,707 in GA2 and 1,012 in LG31) was significantly higher than the number of upregulated genes (501 in GA2 and 761 in LG31) under atrazine stress. The results demonstrated that atrazine could induce changes in transcript levels in millet leaves and that the expression of most genes may be inhibited to adapt to atrazine stress.

Functional Analysis of Differentially Expressed Genes in Millet Under Atrazine Stress

To classify the functions of DEGs, GO, and KEGG analyses were performed to clarify the biological pathways and functions in millet leaves affected by atrazine. The results showed that the significantly enriched GO categories were "metabolic process," "cellular process," and "single-organism process" in the resistant and sensitive millet varieties (**Supplementary Figure 1**). However, the KEGG analysis results implied that the resistant and sensitive millet varieties had different metabolic pathways (**Supplementary Table 4**). Based on the results presented in **Figure 2A**, when comparing GT with GCK, the DEGs enriched in "phenylalanine biosynthesis," "flavonoid biosynthesis," "flavone and flavonol biosynthesis," "ribosome biogenesis," and "ribosome" showed remarkable downregulation, whereas those enriched in "lysine biosynthesis," "arginine and proline metabolism," "fructose and mannose metabolism," "pentose phosphate pathway," and "terpenoid backbone biosynthesis"

TABLE 4 | Comprehensive evaluation of foxtail millet under atrazine stress.

Varieties	MDA	Soluble pro.	Chlorophyll content	Net photosynthetic rate	Transpiration rate	Stomatal conductance	Dry matter	Grain weight per panicle	*T* value	Ranking
JG26	0.99	0.35	0.75	0.72	0.26	0.28	0.88	0.85	0.59	7
FX3	0.67	0.19	0.99	1.00	1.00	0.91	0.95	0.73	0.80	2
ZGG	0.21	0.06	0.46	0.34	0.31	0.35	0.34	0.48	0.31	16
JG40	0.67	0.37	0.35	0.13	0.18	0.41	0.23	0.49	0.30	17
DBG	0.00	0.53	0.87	0.58	0.59	0.47	0.56	0.52	0.52	10
GA2	0.99	0.58	0.99	0.99	0.99	1.00	0.92	0.84	0.91	1
SDLS	0.89	0.30	0.89	0.62	0.73	0.90	0.86	0.78	0.74	4
SXWG	0.17	0.80	0.39	0.65	0.46	0.82	0.70	0.00	0.54	9
HBXG	0.05	0.59	0.52	0.79	0.94	0.51	0.78	0.56	0.62	5
CG	0.66	0.43	0.80	0.95	0.70	1.02	1.00	0.85	0.80	3
NX15	0.28	0.61	0.13	0.45	0.11	0.25	0.00	1.00	0.32	14
LG25	0.31	0.00	0.20	0.17	0.52	0.35	0.04	0.54	0.26	19
ZTB	0.48	1.00	0.17	0.20	0.72	0.78	0.34	0.78	0.59	6
JSHJ	0.34	0.22	0.06	0.63	0.43	0.28	0.09	0.53	0.31	15
LG31	0.15	0.08	0.00	0.00	0.00	0.07	0.16	0.30	0.09	20
HJDG	0.77	0.23	0.63	0.86	0.40	0.90	0.37	0.35	0.56	8
GA5	0.29	0.49	0.60	0.69	0.57	0.37	0.29	0.36	0.45	12
YG2	0.19	0.16	0.88	0.83	0.22	0.74	0.54	0.74	0.52	11
ZGB	0.51	0.16	0.13	0.65	0.42	0.46	0.45	0.80	0.43	13
BGHNG	0.27	0.28	0.60	0.12	0.20	0.00	0.42	0.43	0.27	18

T is the comprehensive value of atrazine tolerance in different varieties.

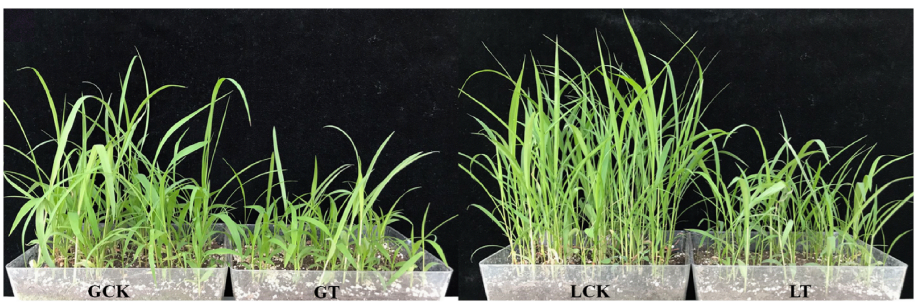


FIGURE 1 | Phenotypes of resistant/sensitive millet under atrazine stress at the seedling stage. GCK, GA2 (Gongai 2) treated with water; GT, GA2 treated with atrazine; LCK, LG31 (Longgu 31) treated with water; LT, LG31 treated with atrazine.

were significantly upregulated. In the "LCK vs. LT" comparison, except for the "ribosome," "ribosome biogenesis in eukaryotes," and "vitamin B6 metabolism" pathways, the other metabolic pathways with DEGs were significantly upregulated (**Figure 2B**).

Metabolome Analysis of Millet Under Atrazine Stress

For an overview of the metabolomic changes induced by atrazine treatment in millet, the widely targeted metabolomics was analyzed using LC–MS/MS. A total of 636 metabolites were obtained from all samples (**Figure 3A** and **Supplementary Table 5**) and divided into four groups according to PCA (**Figure 3B**). On the basis of FC of ≥1.5, the numbers of upregulated and downregulated metabolites in GCK and GT and LCK and LT were 82 and 95 and 110 and 120, respectively (**Supplementary Table 5**). Moreover, these DEMs were identified into 65 species and were mainly involved in phenylpropanoid biosynthesis (18), biosynthesis of secondary metabolites (59), metabolic pathways (82), glutathione metabolism (4), flavonoid biosynthesis (7), carbon metabolism (13), arginine and proline metabolism (8), glutathione metabolism (4), glyoxylate and dicarboxylate metabolism (7), purine metabolism (8), and others (**Figure 3C** and **Supplementary Table 6**). The DEMs related to proline metabolism, glutathione metabolism, and flavonoid metabolism were significantly accumulated in GCK and GT and LCK and LT. The results implied that atrazine can induce changes in antioxidant levels in millet leaves.

TABLE 5 | DEGs under atrazine stress in millet leaves.

Samples	Total of DEGs	Up	Down
GCK and GT	2208	501	1707
LCK and LT	1773	761	1012

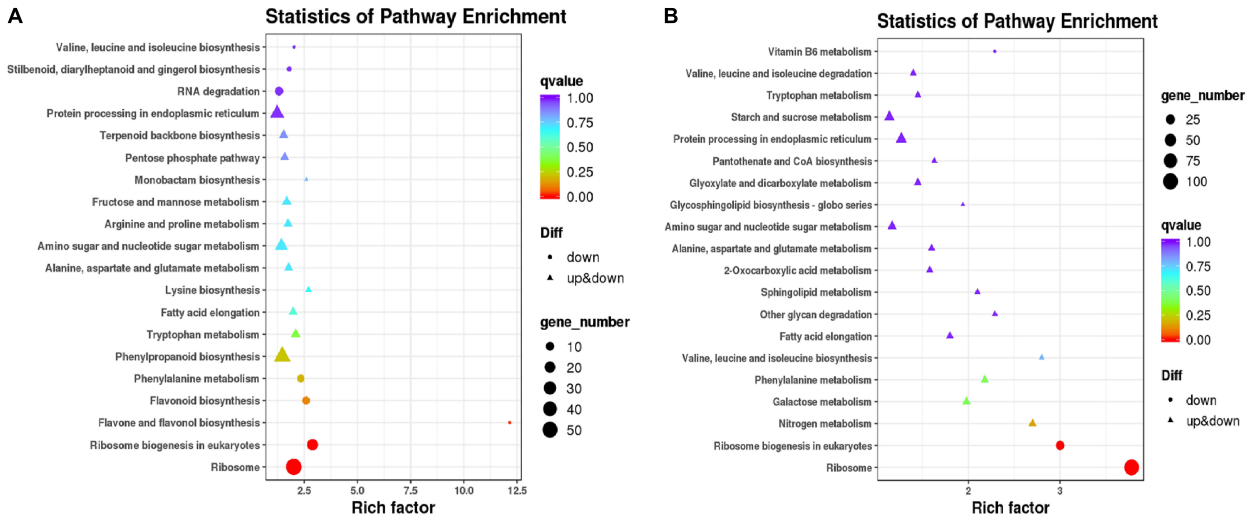


FIGURE 2 | Venn diagram and KEGG analysis of differentially expressed genes in resistant/sensitive millet. Venn diagram of DEGs between two samples: **(A)** GCK and GT; **(B)** LCK and LT.

Relationship Analysis Between Differentially Expressed Genes and Differentially Expressed Metabolites in Millet Under Atrazine Stress

To analyze the relationship between DEGs and DEMs under atrazine stress in millet, a coexpression network analysis of DEGs and DEMs was performed (Pearson's coefficient $R^2 > 0.8$ and $p < 0.05$; **Supplementary Table 7**). The results of the KEGG analysis between the DEGs and DEMs are presented in **Supplementary Figure 2**. The results implied that GA2 and LG31 millet varieties have different regulation mechanisms under atrazine stress. For example, the DEGs and DEMs in GCK vs. GT were mainly involved in flavonoid biosynthesis, glutathione metabolism, amino acid biosynthesis, and fructose/mannose metabolism (**Supplementary Figure 2A**). However, in LCK vs. LT, the galactose, starch and sucrose, and thiamine metabolisms were mainly enriched (**Supplementary Figure 2B**).

To further examine the relationship between DEGs and DEMs in millet under atrazine stress, a coexpression network analysis was conducted. Oxiglutatione, L-cysteine, and γ-glutamylcysteine were found to be related to glutathione metabolism (ko00480, **Supplementary Figure 3** and **Figures 4A,B**) and more highly regulated in GCK vs. GT than in LCK vs. LT (**Table 6**). By contrast, except for glutathione synthesis, *trans*-5-o-(4-coumaroyl)shikimate and scopolin were highly enriched in LCK vs. LT and were correlated with phenylpropanoid biosynthesis (ko00940, **Supplementary Figure 3** and **Figures 4C,D**). Moreover, the coexpression network of DEGs and DEMs in GCK vs. GT was mainly enriched in the biosynthesis of amino acids (ko01230, **Supplementary Figure 3** and **Figure 4E**), such as L-cysteine, and N-acetyl-L-glutamic acid was more highly regulated in GCK vs. GT than in LCK vs. LT (**Table 6**).

Integrated Analysis of Genes and Metabolites Involved in Glutathione Biosynthesis in Millet Under Atrazine Stress

To further analyze the effects of atrazine on genes and metabolites involved in glutathione biosynthesis in millet, the networks of DEGs and DEMs involved in glutathione metabolism pathway (ko00480) were analyzed (**Figure 5A** and **Supplementary Table 8**). The results showed that 12 and 4 genes were differentially expressed in GA2 and LG31 at transcriptional levels, respectively. Compared with the CK group, the expression of all genes, except Seita.9G06450 and Seita.4G241000, was downregulated in the treatment group. The functions of all these genes were related to glutathione S-transferase (EC: 2.5.1.18). In addition, other genes in this pathway, such as *GCLC* (encoding for glutamate cysteine ligase catalytic subunit, Seita.3G050000), *GGT* (encoding for γ-glutamyl transpeptidase, Seita.5G104100), and *G6PDH* (encoding for glucose-6-phosphate 1-dehydrogenase, Seita.9G424300), were downregulated, whereas *GSS* (encoding for glutathione synthase, Seita.3G348900) was upregulated in GA2 (**Supplementary Table 9**). DEMs such as oxiglutatione, L-cysteine, and γ-glutamylcysteine were related to glutathione metabolism and more highly regulated in GCK vs. GT than in LCK vs. LT. The results showed that the DEGs and DEMs related to glutathione metabolism in GA2 were involved in the response to atrazine stress.

Integrated Analysis of Genes and Metabolites Involved in Amino Acid Biosynthesis in Millet Under Atrazine Stress

To investigate the effect of atrazine stress on the expressions of genes and metabolites involved in amino acid biosynthesis,

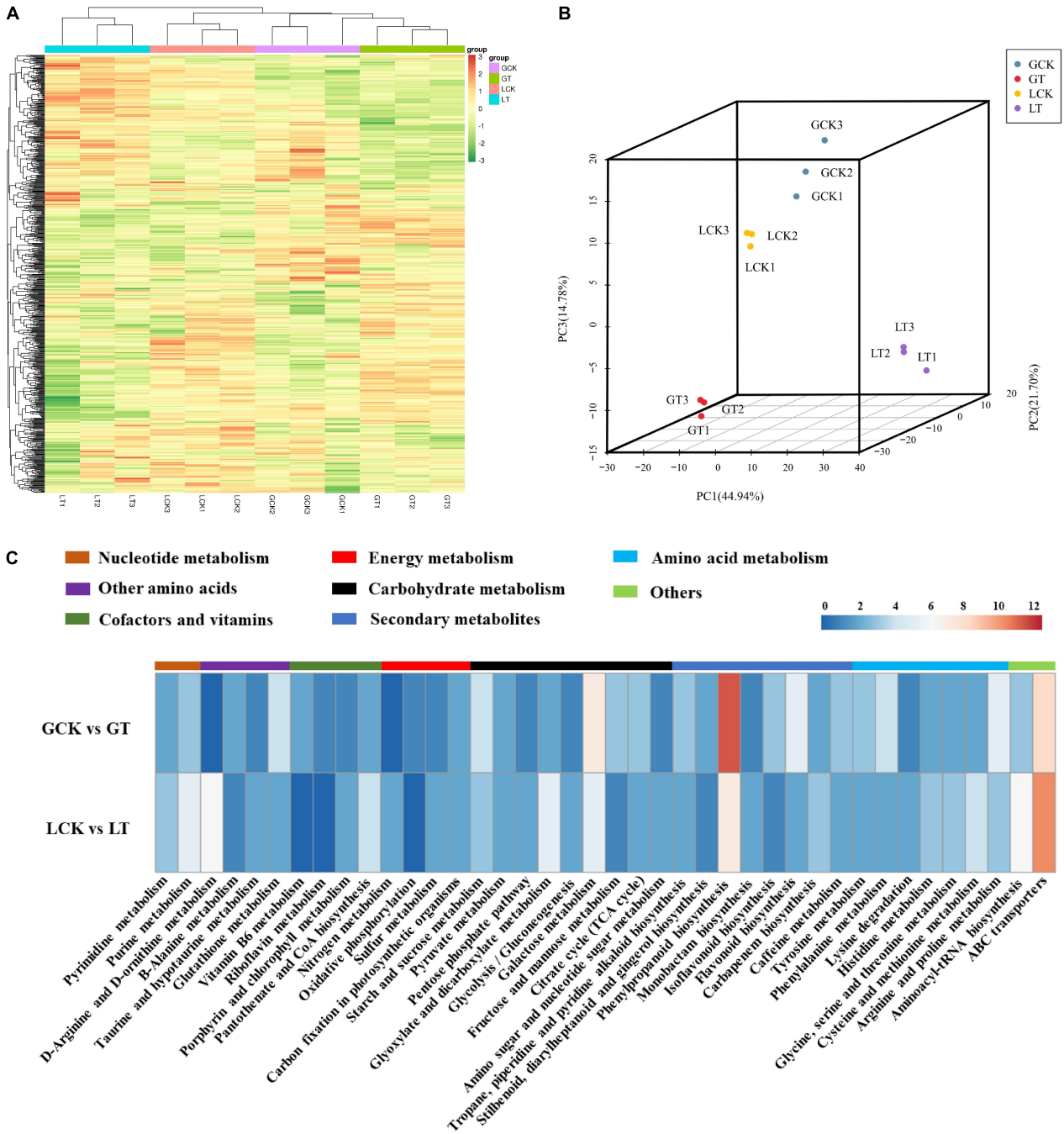


FIGURE 3 | Metabolite analysis using the leaves of resistant/sensitive millet varieties under atrazine stress. **(A)** Heat map visualization of metabolites. Each metabolite is represented by a single row and each example is visualized in a single column; red indicates upregulation and green indicates downregulation. **(B)** PCA of metabolites. PC1, the first principal component; PC2, the second principal component; PC3, the third principal component. **(C)** Distribution of pathways of DEMs annotated in the KEGG data library of resistant/sensitive (GA2/LG31) millet varieties.

the interaction of DEGs and DEMs involved in amino acid biosynthesis (ko01230) was analyzed (**Figure 5B** and **Supplementary Table 10**). We found that the expression of the DEMs N-acetyl-L-glutamic acid and L-proline was more highly regulated in GCK vs. GT than in LCK vs. LT. However, almost all DEGs related to this pathway were downregulated in GA2 (**Supplementary Table 9**), including the genes that may be regulated by enzymes related to the two abovementioned metabolites, such as *NAGS* (encoding for N-acetyl-L-glutamate synthetase, Seita.7G188800) and *P5CS* (encoding for delta-1-pyrroline-5-carboxylate synthetase, Seita.3G220500), except for *ArgC* (encoding for N-acetyl-gamma-glutamyl-phosphate

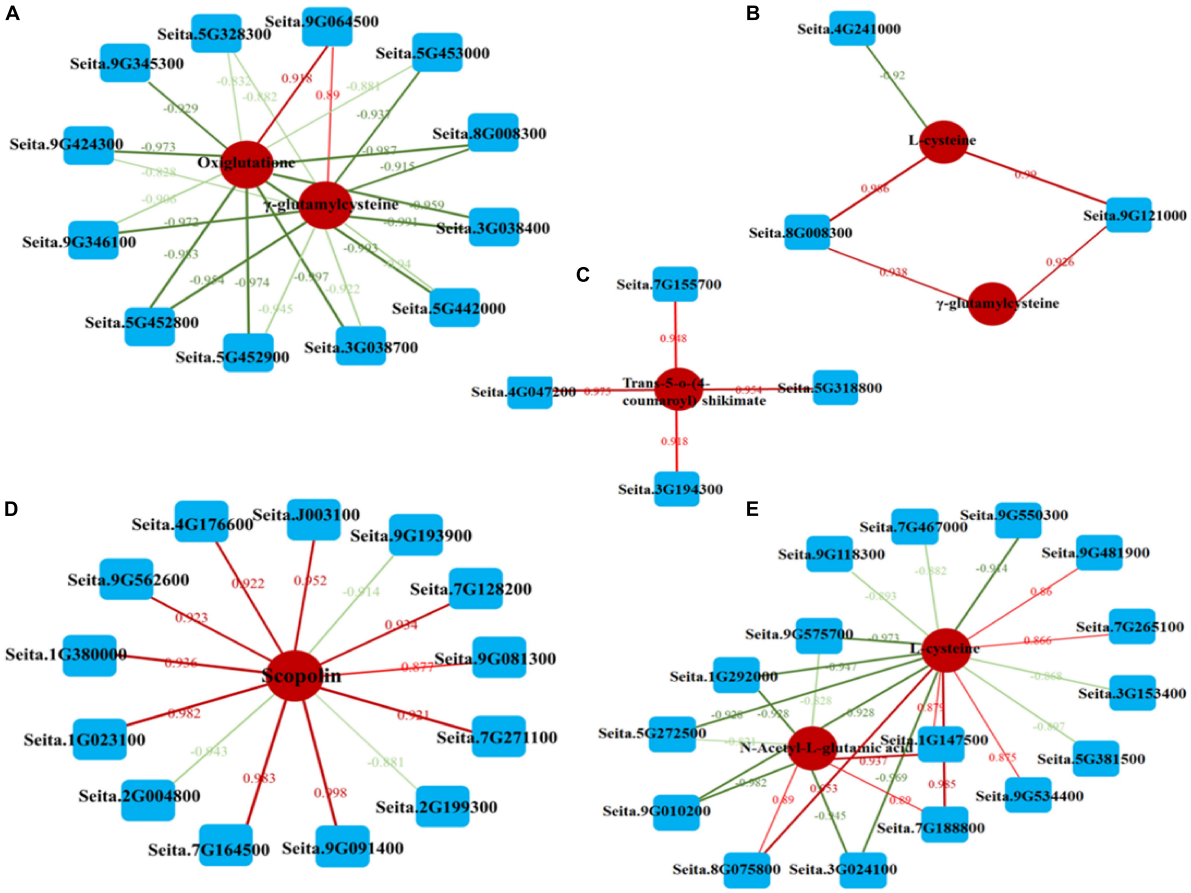


FIGURE 4 | Coexpression analysis of DEGs and DEMs based on Pearson's correlation. **(A,B)** Interaction network of DEGs and DEMs involved in glutathione biosynthesis (ko00480) in GCK vs. GT and LCK vs. LT. **(C,D)** Interaction network of DEGs and DEMs involved in phenylpropanoid biosynthesis (ko00940) in GCK vs. GT and LCK vs. LT. **(E)** Interaction network of DEGs and DEMs involved in amino acid biosynthesis (ko01230) in LCK vs. LT. Lines colored in "red" and "green" display positive and negative correlation, respectively, according to Pearson's correlation coefficient of >0.8 or <–0.8, respectively.

reductase, Seita.9G167800). The results showed that the DEGs and DEMs related to amino acid biosynthesis in GA2 were involved in the response to atrazine stress.

Integrated Analysis of Genes and Metabolites Involved in Phenylpropanoid Biosynthesis in Millet Under Atrazine Stress

To examine the effects of atrazine stress on the expression of genes and metabolites involved in phenylpropanoid biosynthesis, the interaction of DEGs and DEMs involved in amino acid biosynthesis was analyzed (**Figure 5C** and **Supplementary Table 10**). DEGs such as *ToGT1* (encoding for scopoletin glucosyltransferase, Seita.5G239500) and *C3′H* [encoding for 5-o-(4-coumaroyl)-D-quinate 3′-monooxygenase, Seita.3G194300] were upregulated in LG31 (**Supplementary Table 9**). Moreover, the DEMs *trans*-5-o-(4-coumaroyl)shikimate and scopolin were highly enriched in LCK vs. LT and were correlated to phenylpropanoid biosynthesis (ko00940). The results showed that the DEGs and DEMs related to phenylpropanoid biosynthesis in LG31 were jointly involved in the response to atrazine stress.

Real-Time Quantitative Reverse Transcription PCR Validation of Differentially Expressed Genes in Millet Under Atrazine Stress

To validate the accuracy of the RNA-Seq data, the expression levels of approximately 34 DEGs (**Supplementary Table 11**) that were related to glutathione, phenylpropanoid, and amino acid biosyntheses, such as *GSTU6*, *HST*, *GLN1-3*, and GSTF1, were measured using qRT-PCR. The results were similar to those of RNA-Seq (log_2FC), which verified the reproducibility and credibility of the RNA-Seq data.

DISCUSSION

In recent years, the rapid increase in the use of the herbicide atrazine in field-planted maize has resulted in a serious impact on

TABLE 6 | Regulation of metabolites in the two samples under atrazine stress.

No.	Meta ID	Meta name	GCK vs. GT	LCK vs. LT
1	pmb3264	Oxiglutatione	Up	Unchanged
2	pme2563	γ-glutamylcysteine	Up	Down
3	pmb0751	*Trans*-5-o-(4-coumaroyl)shikimate	Down	Up
4	mws1077	Scopolin	Down	Up
5	pme0195	L-cysteine	Up	Down
6	pme0075	N-Acetyl-L-glutamic acid	Up	Down
7	pme0006	L-Proline	Up	Down

the next rotation crop and environment. Considering that millet is a suitable rotation crop for maize, it is important to screen and obtain atrazine-tolerant varieties of millet for maize rotation. In this study, we analyzed the effects of atrazine stress on glutathione metabolism and amino acid and phenylpropanoid biosyntheses by performing an integrated analysis of the transcriptome and metabolome. The results showed that millet plants can be damaged by atrazine stress.

Glutathione Biosynthesis Was Enhanced in GA2 Millet Variety Under Atrazine Stress

several studies indicated that atrazine stress can lead to excessive accumulation of ROS in plant cells, resulting in the peroxidation of membrane lipids and oxidative damage to the cell membrane, proteins, and DNA (Bai et al., 2015; Baxter et al., 2015; Erinle et al., 2018; Singh et al., 2018). However, to avoid damage caused by ROS, plants have evolved a complex detoxification system (Yuan et al., 2007). For example, plants can use ROS scavenging enzymes (Superoxide Dismutase, Peroxidases, and Catalase) and non-enzymatic antioxidants (glutathione, glutathione reductase, and glutathione-Px) to scavenge excess ROS (Sharif et al., 2018). If the excess ROS is not eliminated by detoxification system, which could be marked by the accumulation of MDA (Bai et al., 2015). Sathish et al. (2022) found MDA content in *Zea mays* L. was significantly increased by water deficit stress. In the present study,

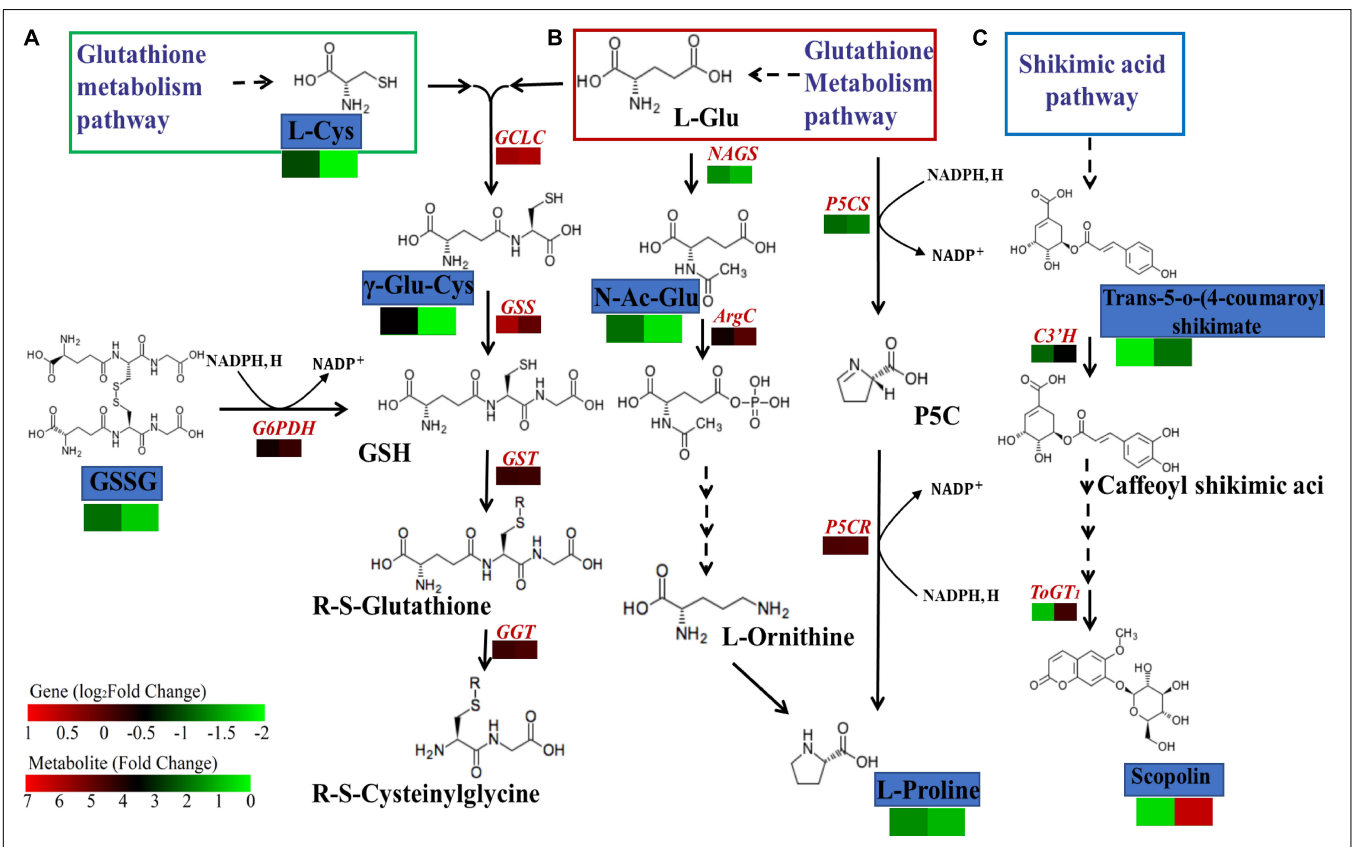


FIGURE 5 | DEGs and DEMs involved in glutathione biosynthesis **(A)**, amino acid biosynthesis **(B)**, and shikimic acid **(C)** metabolism pathway in response to atrazine stress. The rectangles are divided into two equal parts, the left part represents DEGs or DEMs in GA2, whereas the right part represents DEGs or DEMs in LG31. The colors in the rectangles represent the genes or metabolites that were regulated under atrazine stress (red indicates upregulation; black indicates no changes; and green indicates downregulation). *GCLC*, glutamate cysteine ligase catalytic subunit; *GSS*, glutathione synthase; *GST*, glutathione S-transferase; *GGT*, γ-glutamyltranspeptidase; *G6PDH*, glucose-6-phosphate 1-dehydrogenase; *ToGT1*, scopoletin glucosyltransferase; *C3′H*, 5-o-(4-coumaroyl)-D-quinate 3′-monooxygenase; *NAGS2*, N-acetyl-L-glutamate synthetase; *ArgC*, N-acetyl-gamma-glutamyl-phosphate reductase; *P5CS*, delta-1-pyrroline-5-carboxylate synthetase; *P5CR*, pyrroline-5-carboxylate reductase.

the MDA content in GA2 was lower than that in LG31 under atrazine stress, indicating that the degree of peroxidation damage caused by atrazine in GA2 was less to maintain relatively better membrane stability. Moreover, the activities of ROS scavenging enzymes were not well detected in this study. These results indicate that ROS scavenging in millet plants mainly occurs by increasing the levels of non-enzymatic antioxidants, which corroborates the findings of a previous study on fulvic acid used for alleviating drought stress in tea plants (Sun J. H. et al., 2020).

Glutathione is a thiol tripeptide with a low molecular weight that widely exists in all kinds of cells and functions as a non-enzymatic antioxidant that scavenges for H_2O_2, $^1O_2$, $OH^{\bullet}$, and $O_2^{\bullet-}$ and protects different biomolecules to maintain ROS homeostasis (Das and Roychoudhury, 2014). Glutathione S-transferases (GSTs) can convert various herbicides using glutathione into non-toxic and water-soluble forms, making the plant resistant and reducing the damage to crops caused by herbicides (Shimabukuro et al., 1970). In this study, glutathione levels were not significantly different in the atrazine-resistant GA2 and atrazine-sensitive LG31 variety. Oxidized glutathione (GSSG) levels were increased in GA2, but showed no change in LG31. These results imply that the dynamic equilibrium between glutathione and GSSG may fluctuate because glutathione participates in resistance to environmental stress in GA2. Moreover, a previous study reported that maize and grain sorghum, as crops naturally tolerant to atrazine, showed rapid detoxification resulting from the high constitutive activity of GSTs (Timmerman, 1989). Similarly, studies on *Lolium rigidum* in Australia and *Alopecurus myosuroides* in the United Kingdom have also proved the detoxification mechanisms of GST (Cummins et al., 2013; Yu and Powles, 2014). In the present study, nine genes with functions related to GST were detected in GA2, but the expressions of the GST genes in the atrazine treatment group were downregulated at the transcriptional level. The reason for this may be that gene transcription occurs before substance metabolism. Therefore, we deduced that the glutathione pathway plays an important role in the resistance of GA2 to atrazine stress.

Proline Levels Increased in the GA2 Millet Variety Under Atrazine Stress

Proline, an osmotic regulator, is the main amino acid for the stabilization and protection of cell membranes and proteins under certain stress conditions, such as drought, salinity, and low and high temperatures (Rivero et al., 2014; Hasanuzzaman et al., 2019). The biosynthesis of proline mainly depends on glutamate, and the rate-limiting step in this pathway is catalyzed by pyrroline-5-carboxylate synthetase (P5CS; Rejeb et al., 2014). Previous studies reported that *P5CS1* expression can be induced by drought, salt, abscisic acid (ABA), light, nitric oxide, and pathogens to improve the concentration of proline in Arabidopsis (Savouré et al., 1995; Strizhov et al., 1997; Hayashi et al., 2000; Fabro et al., 2004; Zhao et al., 2009). In general, tolerant genotypes of crop plants accumulated more osmoprotectants with high concentrations than sensitive genotypes under stress. For example, a near-isogenic line of spring barley genotypes (NIL143) that contains the wild allele *pyrroline-5-carboxylate synthase 1-P5cs1* was observed higher proline concentrations in leaf and root and less severe symptoms of drought compared with any other genotypes under reduced water availability conditions (Frimpong et al., 2021).

In our study, we found the DEGs related to the proline biosynthesis pathway were all downregulated, including *P5CS* (Seita.3G220500). While proline was significantly accumulated in the GA2 group under atrazine stress. Many researchers also suggested that proline can not only improve osmotic tolerance in plants cell but also reduce ROS generation and scavenge excessive free ROS (Smirnoff and Cumbes, 1989; Alia et al., 1991; Shalata and Neumann, 2001). Recent studies also showed a positive correlation between proline and ROS levels under abiotic stress or exogenous treatment with H_2O_2 (Yang et al., 2009; Lopez-Delacalle et al., 2020). Previous studies showed that many metabolic mechanisms are involved in the response of plants to abiotic stress, including the production of signal molecules, activation and inactivation of gene expression, and synthesis of functional proteins (Zushi et al., 2014; Zandalinas et al., 2020). Among these, gene expression is rapid and occurs before protein synthesis. Thus, we only detected significantly increased levels of proline in the atrazine-tolerant GA2 variety, suggesting that proline may help in scavenging excessive ROS produced by atrazine stress and protecting cells from damage.

Scopoletin Levels Increased in the LG31 Millet Variety Under Atrazine Stress

To protect plant themselves from various environmental stress factors, plant cells have developed an inducible defense mechanism that involves the production of toxic chemicals or antimicrobial compounds, such as secondary metabolites (Kliebenstein and Osbourn, 2012; Tiku, 2018). Scopoletin and its glucoside scopolin are coumarins, which are one of the secondary metabolite classes (Kai et al., 2006). The biosynthesis of scopoletin mostly occurs via the shikimic acid pathway (Bayoumi et al., 2008). Previous studies reported that treatment with $CuCl_2$, shortwave UV, and Triton X-100 induces scopoletin accumulation in sunflower leaves (Gutierrez et al., 1995). Scopoletin is also produced in leaves in response to pathogen attack (Barón et al., 2016). Moreover, its role in abiotic stress may be as an antioxidant for scavenging ROS to reduce oxidative stress in plant cells (Chong et al., 2002; Döll et al., 2018). In this study, DEMs and DEGs in the synthesis pathways of scopolin and metabolites [scopolin and *trans*-5-o-(4-coumaroyl)shikimate] as well as genes (*ToGT1* and *C3′H*) were significantly upregulated in LG31 and downregulated in GA2. These results showed that scopolin may be accumulated in LG31 as an antioxidant to scavenge excessive ROS produced by atrazine stress.

CONCLUSION

In summary, we systematically analyzed the effects of the mechanisms of atrazine stress on millet plants by using metabolomics and transcriptomics approaches. Our results showed that many biological metabolic pathways are affected by atrazine stress in millet leaves, such as glutathione metabolism, amino acid biosynthesis, and phenylpropanoid biosynthesis.

Meanwhile, our results also revealed that the GA2 variety enhanced atrazine tolerance probably by changing glutathione metabolism and amino acid biosynthesis. Moreover, the accumulation of scopolin in LG31 may play an important role in the response to atrazine stress.

DATA AVAILABILITY STATEMENT

The datasets presented in this study can be found in online repositories. The names of the repository/repositories and accession number(s) can be found below: National Center for Biotechnology Information (NCBI) BioProject database under accession number PRJNA751769.

AUTHOR CONTRIBUTIONS

XM and SG were responsible for the conceived and designed the experiments. WS was responsible for designed the experiments and revised the manuscript. LS was responsible for the data analysis, literature search, and manuscript preparation. LL, YW, and WY performed the experiments and data analysis. YF and DW contributed to reagents, materials, and analysis tools. All authors read and approved the final version of the manuscript.

FUNDING

This work was supported by the Post-doctoral funding of Heilongjiang Province in China (LBH-Q17140 and LBH-Q18101), Key research and development projects of Heilongjiang Province in China (GA21B009-5) and Special Funds from the Central Finance to Support the Development of Local Universities in China (2022010005).

SUPPLEMENTARY MATERIAL

The Supplementary Material for this article can be found online at: https://www.frontiersin.org/articles/10.3389/fpls.2022.890550/full#supplementary-material

REFERENCES

Akbulut, G. B., and Yigit, E. (2010). The changes in some biochemical parameters in *Zea mays* cv. "Martha F1" treated with atrazine. *Ecotoxicol. Environ. Saf.* 73, 1429–1432. doi: 10.1016/j.ecoenv.2010.05.023

Alia, P. S. P., Pardha, S. P., and Mohanty, P. (1991). Proline enhances primary photochemical activities in isolated thylakoid membranes of *Brassica juncea* by arresting photoinhibitory damage. *Biochem. Biophys. Res. Commun.* 181, 1238–1244. doi: 10.1016/0006-291X(91)92071-Q

Bai, X., Sun, C., Xie, J., Song, H., Zhu, Q., Su, Y., et al. (2015). Effects of atrazine on photosynthesis and defense response and the underlying mechanisms in *Phaeodactylum tricornutum*. *Environ. Sci. Pollut. Res. Int.* 22, 17499–17507. doi: 10.1007/s11356-015-4923-7

Barbosa, F., Costa, A. C., Megguer, C. A., Lima, J. S., Martins, D. A., Almeida, G. M., et al. (2021). Atrazine toxicity to Handroanthus heptaphyllus, a nontarget species from a Brazilian biome threatened by agriculture. *Environ. Qual. Manag.* 3, 1–9. doi: 10.1002/tqem.21726

Barón, M., Pineda, M., and Pérez-Bueno, M. L. (2016). Picturing pathogen infection in plants. *Zeitsch. Naturforschung. C J. Biosci.* 71, 355–368. doi: 10.1515/znc-2016-0134

Baxter, L., Brain, R. A., Hosmer, A. J., Nema, M., Müller, K. M., Solomon, K. R., et al. (2015). Effects of atrazine on egg masses of the yellow-spotted salamander (*Ambystoma maculatum*) and its endosymbioltic alga (*Oophila amblystomatis*). *Environ. Pollut.* 206, 324–331. doi: 10.1016/j.envpol.2015.07.017

Bayoumi, S., Rowan, M. G., Blagbrough, I. S., and Beeching, J. R. (2008). Biosynthesis of scopoletin and scopolin in cassava roots during post-harvest physiological deterioration: the e-z-isomerisation stage. *Phytochemistry* 69, 2928–2936. doi: 10.1016/j.phytochem.2008.09.023

Bradford, M. M. (1976). A rapid method for the quantitation of microgram quantities of protein utilizing the principle of protein-dye binding. *Anal. Biochem.* 72, 248–254.

Cao, Y. W., Qu, R. J., Tang, X. Q., Sun, L. Q., Chen, Q. Q., and Miao, Y. J. (2020). UPLC-Triple TOF-MS/MS based metabolomics approach to reveal the influence of nitrogen levels on Isatis indigotica seedling leaf. *Sci. Horticult.* 266:109280.

Chong, J., Baltz, R., Schmitt, C., Beffa, R., Fritig, B., and Saindrenan, P. (2002). Downregulation of a pathogen-responsive tobacco UDP-Glc: phenylpropanoid glucosyltransferase reduces scopoletin glucoside accumulation, enhances oxidative stress, and weakens virus resistance. *Plant Cell* 14, 1093–1107. doi: 10.1021/cen-v077n039.p064

Contreras, M. B. C., Camacho, J. V., Fernandez-Morales, F. J., Canizares, P. C., and Rodrigo, M. A. R. (2020). Biodegradability improvement and toxicity reduction of soil washing effluents polluted with atrazine by means of electrochemical pre-treatment: influence of the anode material. *J. Environ. Manag.* 255, 109895.1–109895.7. doi: 10.1016/j.jenvman.2019.109895

Cummins, I., Wortley, D. J., Sabbadin, F., He, Z., Coxon, C. R., Straker, et al. (2013). Key role for a glutathione transferase in multiple herbicide resistance in grass weeds. *Proc. Natl. Acad. Sci. U.S.A.* 110, 5812–5817. doi: 10.1073/pnas.1221179110

Daniele, L. C., and Maggi, F. (2017). In-situ atrazine biodegradation dynamics in wheat (*Triticum*) crops under variable hydrologic regime. *J. Contaminant Hydrol.* 203:104. doi: 10.1016/j.jconhyd.2017.05.004

Das, K., and Roychoudhury, A. (2014). Reactive oxygen species (ROS) and response of antioxidants as ROS-scavengers during environmental stress in plants. *Front. Environ. Sci.* 2:1–13. doi: 10.3389/fenvs.2014.00053

Döll, S., Kuhlmann, M., Rutten, T., Mette, M. F., Scharfenberg, S., Petridis, A., et al. (2018). Accumulation of the coumarin scopolin under abiotic stress conditions is mediated by the *Arabidopsis thaliana* THO/TREX complex. *Plant J.* 93, 431–444. doi: 10.1111/tpj.13797

Dong, W. J., Chen, Y. M., and Meng, P. (2016). The determining weight method of the influence factors of PM2.5 based on principal component analysis. *J. Guangdong Polytech. Norm. Univ. China* 37, 25–28. doi: 10.13408/j.cnki.gjsxb.2016.11.007

Erinle, K. O., Jiang, Z., Ma, B., Ur-Rehman, K., Shahla, A., and Zhang, Y. (2018). Physiological and molecular responses of pearl millet seedling to atrazine stress. *Int. J. Phytoremed.* 20, 1–10. doi: 10.1080/15226514.2017.1393385

Fabro, G., Kovács, I., Pavet, V., Szabados, L., and Alvarez, M. E. (2004). Proline accumulation and AtP5CS2 gene activation are induced by plant-pathogen incompatible interactions in *Arabidopsis*. *Mole. Plant Microbe Interact.* 17, 343–350. doi: 10.1094/MPMI.2004.17.4.343

Felisbino, K., Santos-Filho, R., Piancini, L. D. S., Cestari, M. M., and Leme, D. M. (2018). Mesotrione herbicide does not cause genotoxicity, but modulates the genotoxic effects of Atrazine when assessed in mixture using a plant test system (*Allium cepa*). *Pestic. Biochem. Physiol.* 150, 83–88. doi: 10.1016/j.pestbp.2018.07.009

Frimpong, F., Anokye, M., Windt, C. W., Naz, A. A., Frei, M., Du, et al. (2021). Proline-mediated drought tolerance in the barley (*Hordeum vulgare* L.) isogenic line is associated with lateral root growth at the early seedling stage. *Plants* 10: 2177. doi: 10.3390/plants10102177

Gast, A. (1970). "Use and performance of triazine herbicides on major crops and major weeds throughout the world," in *Residue Reviews: The Triazine*

Herbicides, eds F. A. Gunther and J. D. Gunther (New York, NY: Springer), 11–18. doi: 10.1007/978-1-4615-8464-3_2

Goodacre, R., Vaidyanathan, S., Dunn, W. B., Harrigan, G. G., and Kell, D. B. (2004). Metabolomics by numbers: acquiring and understanding global metabolite data. *Trends Biotechnol.* 22, 245–252. doi: 10.1016/j.tibtech.2004.03.007

Gutierrez, M. C., Parry, A., Tena, M., Jorrin, J., and Edwards, R. (1995). Abiotic elicitation of coumarin phytoalexins in sunflower. *Phytochemistry* 38, 1185–1191. doi: 10.1016/0031-9422(94)00808-7

Hasanuzzaman, M., Anee, T. I., Bhuiyan, T. F., Nahar, K., and Fujita, M. (2019). Emerging role of osmolytes in enhancing abiotic stress tolerance in rice. *Adv. Rice Res. Abiotic Stress Tolerance* 13, 677–708. doi: 10.1016/B978-0-12-814332-2.00033-2

Hayashi, F., Ichino, T., Osanai, R., and Wada, K. (2000). Oscillation and regulation of proline content by P5CS and ProDH gene expressions in the light/dark cycles in *Arabidopsis thaliana* L. *Plant Cell Physiol.* 41, 1096–1101. doi: 10.1093/pcp/pcd036

Jiang, Z., Ma, B. B., Erinle, K. O., Cao, B., Liu, X., Ye, S., et al. (2016). Enzymatic antioxidant defense in resistant plant: *Pennisetum americanum* (L.) K. Schum during long-term atrazine exposure. *Pesticide Biochem. Physiol.* 133, 59–66. doi: 10.1016/j.pestbp.2016.03.003

Kai, K., Shimizu, B., Mizutani, M., Watanabe, K., and Sakata, K. (2006). Accumulation of coumarins in *Arabidopsis thaliana*. *Phytochemistry* 67, 379–386. doi: 10.1016/j.phytochem.2005.11.006

Kanehisa, M. (2008). *The KEGG Database[M]'In Silico' Simulation of Biological Processes*. Hoboken, NJ: Wiley-Blackwell.

Karlsson, A. S., Weihermüller, L., Tappe, W., Mukherjee, S., and Spielvogel, S. (2016). Field scale boscalid residues and dissipation half-life estimation in a sandy soil. *Chemosphere* 145, 163–173. doi: 10.1016/j.chemosphere.2015.11.026

Kim, D., Langmead, B., and Salzberg, S. L. (2015). HISAT: a fast spliced aligner with low memory requirements. *Nat. Methods* 12, 357–360. doi: 10.1038/nmeth.3317

Kliebenstein, D. J., and Osbourn, A. (2012). Making new molecules - evolution of pathways for novel metabolites in plants. *Curr. Opin. Plant Biol.* 15, 415–423. doi: 10.1016/j.pbi.2012.05.005

Kong, L., Zhang, Y., Ye, Z. Q., Liu, X. Q., Zhao, S. Q., Wei, L., et al. (2007). CPC: assess the protein-coding potential of transcripts using sequence features and support vector machine. *Nucleic Acids Res.* 35(suppl_2), W345–W349. doi: 10.1093/nar/gkm391

Langmead, B., and Salzberg, S. (2012). Fast gapped-read alignment with Bowtie 2. *Nat. Methods* 9, 357–359. doi: 10.1038/nmeth.1923

Lebaron, H. M., McFarland, J. E., and Burnside, O. C. (2011). *The Triazine Herbicides*. San Diego, CA: Elsevier.

Li, Y., Fang, J., Qi, X., Lin, M., Zhong, Y., Sun, L., et al. (2018). Combined analysis ofthe fruit metabolome and transcriptome reveals candidate genes involved in flavonoid biosynthesis in *Actinidia argute*. *Inte. J. Mol. Sci.* 19, 1471. doi: 10.3390/ijms19051471

Liu, B. H., Zhao, D. C., Zhang, P. Y., Liu, F. C., Jia, M., and Liang, J. (2020). Seedling evaluation of six walnut rootstock species originated in China based on principal component analysis and cluster analysis. *Sci. Horticult.* 265:109212. doi: 10.1016/j.scienta.2020.109212

Livak, K. J., and Schmittgen, T. D. (2001). Analysis of relative gene expression data using real-time quantitative PCR and the 2-ΔΔCT method. *Methods* 25, 402–408. doi: 10.1006/meth.2001.1262

Lopez-Delacalle, M., Silva, C. J., Mestre, T. C., Martinez, V., and Rivero, R. M. (2020). Synchronization and interaction of proline, ascorbate and oxidative stress pathways under abiotic stress combination in tomato plants. *bioRxiv* [Preprint] doi: 10.1101/2020.06.30.179770

Moyer, J. R., and Blackshaw, R. E. (1993). Effect of soil moisture on atrazine and cyanazine persistence and injury to subsequent cereal crops in southern Alberta. *Weed Technol.* 7, 988–994. doi: 10.1111/j.1365-3180.1993.tb01958.x

Pertea, M., Pertea, G. M., Antonescu, C. M., Chang, T. C., Mendell, J. T., and Salzberg, S. L. (2015). StringTie enables improved reconstruction of a transcriptome from RNA-seq reads. *Nat. Biotechnol.* 33, 290–295. doi: 10.1038/nbt.3122

Rejeb, K. B., Abdelly, C., and Savouré, A. (2014). How reactive oxygen species and proline face stress together. *Plant Physiol. Biochem.* 80, 278–284. doi: 10.1016/j.plaphy.2014.04.007

Rivero, R. M., Mestre, T. C., Mittler, R., Rubio, F., Garcia-Sanchez, F., and Martinez, V. (2014). The combined effect of salinity and heat reveals a specific physiological, biochemical and molecular response in tomato plants. *Plant Cell Environ.* 37, 1059–1073. doi: 10.1111/pce.12199

Sathish, P., Vanaja, M., Lakshmi, N. J., Sarkar, B., Kumar, G. V., Vagheera, P., et al. (2022). Impact of water deficit stress on traits influencing the drought tolerance and yield of maize (*Zea mays* L.) genotypes. *Plant Physiol. Rep.* 27, 109–118. doi: 10.1007/s40502-021-00640-x

Savouré, A., Jaoua, S., Hua, X. J., Ardiles, W., Van Montagu, M., and Verbruggen, N. (1995). Isolation, characterization, and chromosomal location of a gene encoding the DELTA-1pyrroline-5-carboxylate synthetase in *Arabidopsis thaliana*. *FEBS Lett.* 372, 13–19. doi: 10.1016/0014-5793(95)00935-3

Shalata, A., and Neumann, P. M. (2001). Exogenous ascorbic acid (Vitamin C) increases resistance to salt stress and reduces lipid peroxidation. *J. Exp. Bot.* 52, 2207–2211. doi: 10.1093/jexbot/52.364.2207

Shan, T. Y., Yin, M. Z., Wu, J. X., Yu, H. W., Liu, M. L., Xu, R., et al. (2021). Comparative transcriptome analysis of tubers, stems, and flowers of *Gastrodia elata* Blume reveals potential genes involved in the biosynthesis of phenolics. *Fitoterapia* 153: 104988. doi: 10.1016/j.fitote.2021.104988

Sharif, R., Xie, C., Zhang, H., Arnao, M. B., Ali, M., Ali, Q., et al. (2018). Melatonin and its effects on plant systems. *Molecules* 23:2352. doi: 10.3390/molecules23092352

Shimabukuro, R. H., Frear, D. S., Swanson, H. R., and Walsh, W. C. (1970). Glutathione conjugation: an enzymatic basis for atrazine resistance in corn. *Plant Physiol.* 47, 10–14. doi: 10.1104/pp.46.1.103

Singh, S., Kumar, V., Chauhan, A., Datta, S., Wani, A. B., Singh, N., et al. (2018). Toxicity, degradation and analysis of the herbicide atrazine. *Environ. Chem. Lett.* 16, 211–237. doi: 10.1007/s10311-017-0665-8

Skliros, D., Kalloniati, C., Karalias, G., Skaracis, G. N., Rennenberg, H., and Flemetakis, E. (2018). Global metabolomics analysis reveals distinctive tolerance mechanisms in different plant organs of lentil (*Lens culinaris*) upon salinity stress. *Plant Soil* 429, 451–468. doi: 10.1007/s11104-018-3691-9

Smirnoff, N., and Cumbes, Q. J. (1989). Hydroxyl radical scavenging activity of compatible solutes. *Phytochemistry* 28, 1057–1060. doi: 10.1016/0031-9422(89)80182-7

Strizhov, N., Abraham, E., Okresz, L., Blickling, S., Zilberstein, A., Schell, J., et al. (1997). Differential expression of two P5CS genes controlling proline accumulation during salt-stress requires ABA and is regulated by ABA1, ABI1 and AXR2 in *Arabidopsis*. *Plant J.* 12, 557–569. doi: 10.1111/j.0960-7412.1997.00557.x

Sun, L. F., Wu. Y., Su, S. Z., Liu, H. K., Yang, G., Li, S. P., et al. (2012). Differential gene expression of maize (*Zea mays* L.) inbred line H99 during somatic embryogenesis. *Plant Cell Tissue Organ. Cult.* 109, 271–286. doi: 10.1007/s11240-011-0093-6

Sun, C., Xu, Y., Hu, N., Ma, J., Sun, S., Cao, W., et al. (2020). To evaluate the toxicity of atrazine on the freshwater microalgae *Chlorella* sp. using sensitive indices indicated by photosynthetic parameters. *Chemosphere* 244:125514. doi: 10.1016/j.chemosphere.2019.125514

Sun, J. H., Qiu, C., Ding, Y. Q., Wang, Y., Sun, L. T., Fan, K., et al. (2020). Fulvic acid ameliorates drought stressinduced damage in tea plants by regulating the ascorbate metabolism and flavonoids biosynthesis. *BMC Genomics* 21:411. doi: 10.1186/s12864-020-06815-4

Sun, L. F., Miao, X. F., Cui, J., Deng, J., Wang, X., Wang, Y. F., et al. (2018). Genome-wide high-resolution mapping of DNA methylation identifies epigenetic variation across different salt stress in maize (*Zea mays L.*). *Euphytica* 214, 1–15. doi: 10.1007/s10681-017-2076-0

Tiku, A. R. (2018). "Antimicrobial compounds and their role in plant defense," in *Molecular Aspects of Plant-Pathogen Interaction*, eds A. Singh and I. Singh (Singapore: Springer), 283–307. doi: 10.1007/978-981-10-7371-7_13

Timmerman, K. P. (1989). Molecular characterization of corn glutathione S-transferase isozymes involved in herbicide detoxification. *Physiol. Plant.* 77, 465–471. doi: 10.1111/j.1399-3054.1989.tb05668.x

Trapnell, C., Roberts, A., Goff, L., Pertea, G., Kim, D., Kelley, D. R., et al. (2012). Differential gene and transcript expression analysis of RNA-seq experiments with TopHat and Cufflinks. *Nat. Protoc.* 7:562. doi: 10.1038/nprot.2012.016

Wang, Y. T., Miao, X. F., and Wang, D. (2021). Screening and evaluation of atrazine-resistant germplasm resources of Foxtail Millet at germination stage. *J. Crops China* 5, 194–204. doi: 10.16035/j.issn.1001-7283.2021.05.030

Yang, S. L., Lan, S. S., and Gong, M. (2009). Hydrogen peroxide-induced proline and metabolic pathway of its accumulation in maize seedlings. *J. Plant Physiol.* 166, 1694–1699. doi: 10.1016/j.jplph.2009.04.006

Yu, Q., and Powles, S. (2014). Metabolism-based herbicide resistance and cross resistance in crop weeds: a threat to herbicide sustainability and global crop production. *Plant Physiol.* 166, 1106–1118. doi: 10.1104/pp.114.242750

Yuan, J. S., Tranel, P. J., and Stewart, C. N. (2007). Non-target-site herbicide resistance: a family business. *Trends Plant Sci.* 12, 6–13. doi: 10.1016/j.tplants.2006.11.001

Zandalinas, S. I., Fritschi, F. B., Mittler, R., and Lawson, T. (2020). Signal transduction networks during stress combination. *J. Exp. Bot.* 71, 1734–1741. doi: 10.1093/jxb/erz486

Zhang, K. H., Yao, Y. F., Wang, M. Q., Liu, F. L., Wang, Q., Ma, H. H., et al. (2021). A UPLC-MS/MS-based metabolomics analysis of the pharmacological mechanisms of rabdosia serra against cholestasis. *Phytomedicine* 91, 153683. doi: 10.1016/j.phymed.2021.153683

Zhang, L. B., Ma, C., Chao, H. B., Long, Y., Wu, J. S., Li, Z. Y., et al. (2019). Integration of metabolome and transcriptome reveals flavonoid accumulation in the intergeneric hybrid between Brassica rapa and *Raphanus sativus*. *Sci. Rep.* 9:18368. doi: 10.1038/s41598-019-54889-2

Zhang, Q., Wang, L., Liu, Z. G., Zhao, Z. H., Zhao, J., Wang, Z. T., et al. (2020). Transcriptome and metabolome profiling unveil the mechanisms of *Ziziphus jujuba* Mill. Peel coloration. *Food Chem.* 312:125903. doi: 10.1016/j.foodchem.2019.125903

Zhang, Y., Jiang, D., Yang, C., Deng, S. J., Lv, X. Y., Chen, R. F., et al. (2021). The oxidative stress caused by atrazine in root exudation of *Pennisetum americanum* (L.) K. Schum. *Ecotoxicol. Environ. Saf.* 211, 111943. doi: 10.1016/j.ecoenv.2021.111943

Zhao, M. G., Chen, L., Zhang, L. L., and Zhang, W. H. (2009). Nitric reductase-dependent nitric oxide production is involved in cold acclimation and freezing tolerance in *Arabidopsis*. *Plant Physiol.* 151, 755–767. doi: 10.1104/pp.109.140996

Zushi, K., Ono, M., and Matsuzoe, N. (2014). Light intensity modulates antioxidant systems in salt-stressed tomato (*Solanum lycopersicum* L. cv. Micro-Tom) fruits. *Sci. Horticult.* 165, 384–391. doi: 10.1016/j.scienta.2013.11.033

Conflict of Interest: WS was employed by Heilongjiang HYHC Company.

The remaining authors declare that the research was conducted in the absence of any commercial or financial relationships that could be construed as a potential conflict of interest.

Publisher's Note: All claims expressed in this article are solely those of the authors and do not necessarily represent those of their affiliated organizations, or those of the publisher, the editors and the reviewers. Any product that may be evaluated in this article, or claim that may be made by its manufacturer, is not guaranteed or endorsed by the publisher.

Copyright © 2022 Sun, Liu, Wang, Feng, Yang, Wang, Gao, Miao and Sun. This is an open-access article distributed under the terms of the Creative Commons Attribution License (CC BY). The use, distribution or reproduction in other forums is permitted, provided the original author(s) and the copyright owner(s) are credited and that the original publication in this journal is cited, in accordance with accepted academic practice. No use, distribution or reproduction is permitted which does not comply with these terms.

frontiers | Frontiers in Plant Science

ORIGINAL RESEARCH
published: 22 June 2022
doi: 10.3389/fpls.2022.877016

NAC Transcription Factor *TwNAC01* Positively Regulates Drought Stress Responses in Arabidopsis and Triticale

*Meng Wang[1,2], Li-Tong Ren[3], Xiao-Yong Wei[1], Yue-Ming Ling[1], Hai-Tao Gu[1], Shan-Shan Wang[1], Xue-Feng Ma[4] and Guang-Chao Kong[1]**

[1]Key Laboratory of Oasis Eco-Agriculture, Xinjiang Production and Construction Corps, Agriculture College of Shihezi University, Shihezi, China, [2]Institute of Economic Crops, Xinjiang Academy of Agricultural Sciences, Urumqi, China, [3]School of Chemistry and Chemical Engineering of Shihezi University, Shihezi, China, [4]Forage Genetics International, West Salem, WI, United States

OPEN ACCESS

Edited by:
Mohammad Anwar Hossain, Bangladesh Agricultural University, Bangladesh

Reviewed by:
Ali Raza, Fujian Agriculture and Forestry University, China
Sadhana Singh, International Crops Research Institute for the Semi-Arid Tropics (ICRISAT), India

***Correspondence:**
Guang-Chao Kong
kgch_agr@shzu.edu.cn

Specialty section:
This article was submitted to Plant Biotechnology, a section of the journal Frontiers in Plant Science

Received: *16 February 2022*
Accepted: *02 June 2022*
Published: *22 June 2022*

Citation:
Wang M, Ren L-T, Wei X-Y, Ling Y-M, Gu H-T, Wang S-S, Ma X-F and Kong G-C (2022) NAC Transcription Factor TwNAC01 Positively Regulates Drought Stress Responses in Arabidopsis and Triticale. Front. Plant Sci. 13:877016. doi: 10.3389/fpls.2022.877016

The NAC transcription factors play important roles in regulating plant growth, development, and senescence, and responding to biotic and abiotic stressors in plants. A novel coding sequence (1,059 bp) was cloned from hexaploid triticale in this study. The putative protein (352 amino acids) encoded by this sequence was over 95% similar to the amino acid sequence of a NAC protein from *Aegilops tauschii* (XP020161331), and it formed a clade with *Ae. tauschii*, durum wheat, and barley. The putative protein contained a conserved nature actomyosin (NAM) domain (129 consecutive amino acids) between the 20th and 148th amino acids at the N-terminus and three transcription activation regions at the C-terminus. The novel gene was identified as a triticale *NAC* gene localized in the nucleus and designated as *TwNAC01* (GenBank accession MG736919). The expression levels of *TwNAC01* were the highest in roots, followed by leaves and stems when triticale lines were exposed to drought, polyethylene glycol 6,000 (PEG6000), NaCl, cold, methyl jasmonate (MeJA), and abscisic acid (ABA). Transgenic *Arabidopsis thaliana* overexpressing *TwNAC01* had significantly lower leaf water loss rates and longer roots than wild-type (WT) *A. thaliana.* Virus-induced silencing of the *TwNAC01* gene in triticale delayed root development and decreased length of primary root. Under drought stress, leaves of *TwNAC01*-silenced triticale had higher levels of malondialdehyde (MDA) and hydrogen peroxide (H_2O_2), but lower relative water content (RWC), net photosynthetic rate, stomatal conductance, intercellular CO_2 concentration, and transpiration rate than the leaves of the WT. Gene overexpression and silencing experiments suggested that TwNAC01 improves plant stress tolerance by increasing root length, regulating the water content of plant leaves by reducing MDA and H_2O_2 content, and adjusting respiration rate. The results suggest that *TwNAC01* is a novel NAC transcription factor gene that can be exploited for triticale and cereal improvement.

Keywords: gene cloning, gene silencing, NAC transcription factor, Triticale, gene function analyses

INTRODUCTION

Triticale (× *Triticosecale* Wittmack) is a new allopolyploid crop derived from the intergeneric hybridization between wheat (*Triticum*) and rye (*Secale*), followed by chromosome doubling (Zillinsky, 1974). This crop, which can be used as both a food crop and a forage crop, inherits the high grain yield and quality characteristics of wheat with the stress-resistant traits of rye (Sun, 2002; Cao and Kong, 2011). Since triticale exhibits good stress tolerance and it is an important genetic resource for improving wheat and other cereal species, exploring its resistant or tolerant genes against various biotic and abiotic stresses is important for improving not only triticale, but also wheat and other cereals.

During growth and development, plants are often affected by a variety of adverse environmental factors, such as high temperature, drought, salinity, and extreme weather conditions. To overcome these challenges, plants use a series of defense mechanisms against a variety of biotic and abiotic stresses (Cramer, 2010; Pinheiro and Chaves, 2011). By binding to cis-acting elements of the target gene promoter, transcription factors act as molecular switches for gene expression by activating or inhibiting gene expression in response to stress conditions (Nakashima et al., 2012; Puranik et al., 2012). Many transcription factor families, including NAC, WRKY, DREB, and MYB have been found in plants (Puranik et al., 2012). Of these, the plant-specific NAC transcription factor family has the most members (Kim et al., 2004; Pérez-Rodríguez et al., 2010). Several studies have shown that NAC transcription factors play important roles in a variety of plant processes, including growth and development, leaf senescence, hormone increase and decrease, and regulation of defense response to biotic and abiotic stresses (Nakashima et al., 2012; Puranik et al., 2012). For example, in *Arabidopsis thaliana,* overexpression of the *AtNAC2* gene improved lateral root elongation (He et al., 2005). In addition, Jensen et al. (2013) reported that *Arabidopsis* overexpressing *ATAF1 s*howed obvious dwarfism and flowering delay; the endogenous ABA content of the transgenic *Arabidopsis* overexpressing *ATAF1* was also significantly greater (a 6–8-fold increase) than that of the wild-type (WT) counterpart, which improved the drought tolerance of the transgenic lines. Similarly, overexpression of the *OsNAC10* gene, which is specifically expressed in rice roots, increased the diameter of rice roots, improved drought tolerance of rice, and significantly increased rice yield under drought stress (Jeong et al., 2010). Also in rice, overexpression of the *SNAC1* gene improved drought and salt tolerance in field and greenhouse; transgenic plants overexpressing *SNAC1* also had lower water loss rates and were more sensitive to ABA stress than WT plants (Xiong et al., 2001). Overexpression of the wheat genes *TaNAC2* and *TaNAC67* in *A. thaliana* significantly improved tolerance to salt, drought and cold stress (Mao et al., 2012). Indeed, RT-PCR analysis showed that *TaNAC4* and *TaNAC8* were induced by phytohormones (e.g., salicylic acid, SA; methyl jasmonate, MeJA; and abscisic acid, ABA), pathogens (stripe rust), abiotic stressors (salinity and cold), and mechanical injury (Kang et al., 2010). Transgenic wheat overexpressing the *TaNAC69* gene had greater biomass and longer roots than the control, and thus had a better survival rate under salt and drought stresses (Xue et al., 2011). These studies demonstrated that *NAC* genes can be induced by biotic and abiotic stresses under a variety of conditions, and thus are likely to play critical roles in stress tolerance in plant. However, little is known about *NAC* genes in triticale. To address this knowledge gap, we aimed to identify and characterize *NAC* genes in triticale.

In this study, a novel *NAC* transcription factor gene, *TwNAC01*, from triticale was cloned. Gene expression characteristics demonstrated that *TwNAC01* responded to various abiotic stresses. We characterized the gene in detail for further exploration of triticale and cereal improvement.

MATERIALS AND METHODS

Plant Materials

A drought tolerant triticale cultivar., "Xinxiaoheimai 3" (developed and kindly provided by the Wheat Crop Research Institute of Shihezi University, Xinjiang, China; Li et al., 2008) was used for this study. After cleaning and disinfection, the seeds were planted in an arid lot with irrigation at the Experimental Station of the Agricultural College of Shihezi University (85° 59′ 50″ N, 44° 18′ 58″ E, Xinjiang, China). The experiment station is located at an altitude about 437–450 m with an annual rainfall of 208 mm, on average, and an evaporation capacity of about 1,660 mm, a typical continental climate suitable for irrigated agriculture. The soil type was calcaric fluvisol, a sandy loam soil texture with 19.5% clay, 32.1% silt, and 38.5% sand. The soil bulk (0–20-cm depth) property was characterized as 1.34 g cm^{-3} in density with 15.3 g kg^{-1} organic matter, 1.0 g kg^{-1} total *N*, 19.3 mg kg^{-1} Olsen P and 194 mg kg^{-1} total K.

To eliminate the effects of rainfall, a rain shelter was built over the drought stress plots. Plants flowering at the same time were selected during the flowering stage. In drought-stressed plots, irrigation was stopped when the triticale developed at the heading stage, and the control was irrigated normally. The plots were laid out randomly with three replications in both irrigated and drought-stressed areas. Proline, MDA and electrical conductivity levels in the plant leaves were assessed daily as described previously (Chen and Wang, 2002). Roots, stems, flag leaves, and immature grains of both the stressed and control plants were collected at a point when the proline, MDA and electrical conductivity increased (67.30%, 42.12%, and 37.67%, respectively) significantly, and the soil moisture content decreased (37.32%) significantly in the stressed plots.

Full-Length 5′- and 3′-Race

RNA was extracted from the above-mentioned triticale leaves using Hipure HP Plant RNA Mini Kits (Magen). Using these RNA as templates, we performed reverse transcriptase PCR (RT-PCR) to synthesize cDNA sequences using SMARTScribe

genome Reverse Transcriptase (TaKaRa, Dalian, China). Synthesized cDNA was stored at −20°C before being sequenced. Based on RNA-Seq sequencing results, the sequence of Unigene c51971 (708 bp) was studied in this research, and specific primers for 5′- and 3′-RACE using SMARTer RACE kits (**Supplementary Table S1**) were designed. The RACE procedure was as follows: 94°C for 2 min, 94°C for 30 s, 55°C for 30 s, 72°C for 1 min, 72°C for 35 min, and 16°C for 10 min. The PCR products were recovered and purified using 1.0% agarose gel electrophoresis. The purified PCR products were ligated to the pMD19-T vector (TaKaRa, Dalian, China) and transformed into TOPO10 cells (TIANGEN, China). Positive clones were identified and sequenced. The open reading frame (ORF) of the full-length cDNA sequence was obtained by splicing the sequencing results using an online tool CAP3[1] (Shang et al., 2019) and the National Center for Biotechnology Information Basic Local Alignment Search Tool (NCBI-BLAST). Sequence alignment analysis preliminarily identified the sequence as a triticale *NAC* gene, which was preliminarily designated *TwNAC01*.

Analysis of the Triticale *TwNAC01* Sequence

The NCBI ORF Finder[2] was used to identify sequences homologous to the ORF and coding sequences of *TwNAC01* (GenBank: MG736919). Conserved structures in the TwNAC01 gene were identified using Smart[3] and the ProtParam tool.[4] Physical and chemical properties of the predicted TwNAC01 protein were analyzed, as well as its hydrophobicity[5] using the ExPASy server.[6] Multi-alignment of TwNAC01 with other NAC proteins in different species was conducted using DNAMAN. Subcellular location of the protein was predicted using Protcomp and TargetP 1.1.[7] The relevant sequences were aligned using MEGA (version 10.0; Shang et al., 2019) and MegAlign (DNAStar).

Real-Time Fluorescence Quantitative PCR

The RNA samples used for real-time fluorescence quantitative PCR (qRT-PCR) were from two sources, the drought-stressed triticale plants from stressed plots as mentioned above in plant materials, and seedlings treated with 20% PEG6000 (osmotic potential of about −0.50 MPa; Michel and Kaufmann, 1973; Michel et al., 1983), 200-mM NaCl, cold (4°C), 100-μM MeJA, or 100-μM ABA as follows (Huang et al., 2015). The triticale seedlings were cultured at 25°C with a normal watering regime, under a 12-h light/12-h dark cycle in a growth chamber. The seedlings were transplanted in hydroponic boxes when they had two leaves and one main shoot. Three hydroponic boxes were allocated to each treatment; each box had 12 holes with 5 seedlings in each hole. After transplantation, seedlings were allowed to acclimate for 5 days. After acclimation, one set of boxes was transferred to a cold room (4°C). Other boxes were treated with each of the followings: 1 L of 20% PEG6000 (osmotic potential of about −0.50 MPa; Michel and Kaufmann, 1973; Michel et al., 1983), 200-mM NaCl, 100-μM MeJA, and 100-μM ABA, respectively. In all treatments, plant roots were soaked and leaves were sprayed with the same solution. Roots and leaves were collected after 0, 1, 3, 6, 12, and 24 h of treatment. Collected samples were frozen in liquid nitrogen and then transferred to a freezer at −80°C. The relative expression levels of target genes were calculated with the $2^{-\Delta\Delta Ct}$ method (Livak and Schmittgen, 2001).

RNA was extracted from the triticale materials collected from each of the six treatments (field drought, 20% PEG6000, 200-mM NaCl, cold (4°C), 100-μM MeJA, and 100-μM ABA) using Hipure HP Plant RNA Mini Kits (Magen, China), and cDNA was synthesized using 5X All-ln-One RT MasterMix (Applied Biological Materials, Canada) with specific primers (qRT-PCR primer pair in **Supplementary Table S1**). The wheat actin gene, *TaActin*, was used as internal reference for real-time qPCR (**Supplementary Table S1**). qPCR was performed using SuperReal PreMixPlus (SYBR Green) kits (Tiangen, China). Each 10-μl qPCR volume contained 6 μl 2× SuperReal PreMixPlus, 0.25-μl forward primer, 0.25-μl reverse primer, 1-μl cDNA template, and sufficient ddH_2O to make 10 μl. qRT-PCR amplifications were performed using a Roche Light-Cycler 480R with the following cycling conditions: pre-denaturation at 95°C for 15 min, followed by 40 cycles of denaturation at 95°C for 10 s, annealing at 61°C for 30 s, and amplification at 72°C for 30 s. All reactions were performed in triplicate, and relative gene expression levels were determined using the $2^{-\Delta\Delta Ct}$ method (Livak and Schmittgen, 2001).

Subcellular Localization of the TwNAC01 Protein

The coding sequence of the *TwNAC01* gene was cloned into the plant subcellular expression vector pCAMBIA1301S Enhanced Green Fluorescent Protein (EGFP; GenBank accession E17099). Insertion primers containing *Bam*HI-*Xba*I restriction sites (**Supplementary Table S1**) were designed and ligated using a ClonExpressII one-step cloning kit (TaKaRa, Dalian, China). After verification *via* sequencing, the recombinant plasmid and the empty vector control (VC) were transformed into *Agrobacterium tumefaciens* GV3101 (TaKaRa, Dalian, China; Mao et al., 2014). GV3101 carrying the recombinant plasmid or the empty vector (TaKaRa, Dalian, China) was cultured on Luria-Bertani (LB) medium containing Kan + and Rif+. When the OD600 of the bacterial solution reached 0.5–0.6, the bacterial solution was collected and re-suspended in infection buffer [10-mM $MgCl_2$, 10-mM fatty acid methyl ester sulfonate (MES), 150-μM surfactant-AS, pH 5.7].

Subcellular location was visualized in tobacco leaves. Tobacco seeds were planted in a growth chamber and cultured at 23°C,

[1]http://doua.prabi.fr/software/cap3
[2]https://www.ncbi.nlm.nih.gov/orffinder/
[3]http://smart.embl-heidelberg.de/
[4]https://web.expasy.org/protparam/
[5]https://web.expasy.org/cgi-bin/protparam/protparam
[6]https://web.expasy.org
[7]http://www.cbs.dtu.dk/services/TargetP

with 60% relative humidity and a 16-h light/8-h dark cycle, for 3 weeks prior to vector inoculation. The cultured *A. tumefaciens* solution was then injected into tobacco leaves with 5-ml needleless sterile syringe, and tobacco seedlings were then cultured in darkness for 36 h. Tobacco leaves exhibiting normal growth after inoculation were selected for examination. The area of each selected leaf around the infection site was excised. Enhanced Green Fluorescent Protein (EGFP) fluorescence signals in the tobacco leaves were observed using a Fluo-View confocal microscope (FV300, Olympus, Japan).

Generation of Transgenic *Arabidopsis* Overexpressing *TwNAC01*

To obtain transgenic *Arabidopsis* plants, the coding sequence containing the stop codon of *TwNAC01* was amplified by RT-PCR and cloned into the *Kpn*I and *Xba*I restriction sites of the pCAMBIA1300-35S vector (TaKaRa, Dalian, China) under the control of the 35S promoter of the cauliflower mosaic virus (CMV). The primers containing the *Kpn*I and *Xba*I restriction sites are listed in **Supplementary Table S1**. The recombinant vector pCAMBIA1300-35S-TwNAC01 and the empty vector pCAMBIA1300-35S-VC were introduced into *A. tumefaciens* strain GV3101 (TaKaRa, Dalian, China). Finally, transgenic *Arabidopsis* plants were generated using the *A. tumefaciens*-mediated floral dipping method (Clough and Bent, 1998). To generate homozygous progeny, T1 and T2 seeds were selected on kanamycin (50 mg l^{-1}) plates. T3 transgenic and WT plants of *A. thaliana* were watered once at the rosette stage and then subjected to drought stress for 25 days. RNA was then extracted from the leaves and roots of both transgenic and WT *A. thaliana* using Hipure HP Plant RNA Mini Kits (Magen, China). *TwNAC01* gene expression levels were then measured using semi-quantitative analysis with gene-specific primers (**Supplementary Table S1**) following the same qPCR protocol. Representative lines overexpressing *TwNAC01* were used for further analysis.

Drought Tolerance of Transgenic *Arabidopsis thaliana* Overexpressing *TwNAC01*

We then measured various stress-related physiological indexes in 35-day-old transgenic *A. thaliana* overexpressing *TwNAC01*, mock-transformed *A. thaliana*, and WT *A. thaliana*. Leaf relative water content (RWC) was determined following the methods of Flexas et al. (2006), leaf electrical conductivity was measured following Chen and Wang (2002), leaf MDA content was estimated following Chen and Wang (2002), and leaf H_2O_2 content was determined using an H_2O_2 measurement kit (China Nanjing Jiancheng Science and Technology Co., Ltd). The concentration of hydrogen peroxide was estimated according to a standard formulae as: H_2O_2 (mmol/gprot) = (OD_{tissue} − OD_{blank})/($OD_{standard}$ − OD_{blank}) * standard concentration (163 mmol/l), where H_2O_2 (mmol/gprot) is the hydrogen peroxide concentration measured from the testing tissue, OD_{tissue} is the OD value measured from the testing tissue, OD_{blank} is the OD value measured from the blank control, and $OD_{standard}$ is the OD value of the kit standard. We also determined the rate of water loss in leaves. Five rosette leaves from each group of *A. thaliana* plants (WT, VC, and the three *TwNAC01*-overexpression lines) were collected, transferred to filter paper, and placed in a constant temperature incubator at 25°C. Leaves were weighed every hour for 8 h and photographed at three time points (2, 5, and 8 h). Water loss was characterized based on weight loss and the degree of leaf curl. Water loss rate measurements were replicated six times. After growing for 55 days, plants of all *A. thaliana* lines were carefully removed from the nutrient soil and washed. The length of the main root system of each plant was measured.

Virus-Induced Gene Silencing of the Triticale *TwNAC01* Gene

Specific primers were designed for PCR amplification of silencing fragments based on the 3′-UTR region of the *TwNAC01* gene (**Supplementary Table S1**), and the barley stripe mosaic virus (BSMV) vector was constructed using ligation-independent cloning (LIC) as previously described (Lee et al., 2015). The BSMV-*γb* vector was digested with the *Apa*I restriction enzyme and the vector skeleton was recovered. The PCR fragments were then treated with T4 DNA polymerase in a reaction mixture containing 1-mM deoxythymidine triphosphate (dTTP). The mixture was subjected to react for 30 min at room temperature. After the completion of the reaction, the system was heated to 75°C for 10 min to inactivate the T4 DNA polymerase. The treated fragments (200 ng) and the BSMV vector (20 ng) were mixed, heated to 66°C for 2 min, and then cooled slowly to room temperature. We transformed 10 μl of the mixture into *Escherichia coli* using the heat shock method. Positive clones were screened using colony PCR and verified *via* sequencing. The positive clones were shaken, and the plasmids were extracted for follow-up experiments. The extracted viral vector plasmids were transferred into *A. tumefaciens* GV3101 for triticale inoculation.

Stress Tolerance of Triticale After *TwNAC01* Gene Silencing

A. tumefaciens carrying BSMV-phytoene desaturase BSMV::asTaPDS constructs (BSMV-*PDS*) induce photobleaching or yellow–orange coloration in the silenced tissue due to depletion of enzymes involved in biosynthesis of carotenoid pigments or chlorophyll, respectively (Lee et al., 2015). Thus, these constructs may be used as positive controls for gene silencing. Triticale plants were inoculated with BSMV-*PDS*, BSMV-*γb*, or BSMV-*TwNAC01* for about a week (two to three leaves were treated per plant). After an additional 2 weeks of growth, white stripes began to appear on the leaves due to the expression of the indicator gene. At this point, samples of the leaves were taken and stored at −80°C. Total RNA was extracted from these samples for quantitative reverse transcription PCR (qRT-PCR). The RWC of the leaves was determined following the methods of Flexas et al. (2006), MDA content in the leaves was estimated following Chen and Wang (2002), and H_2O_2 content in the

leaves was determined using an H_2O_2 measurement kit (Nanjing Jiancheng Science and Technology Co., Ltd). Stomatal conductance, net photosynthesis rate, transpiration rate, and intercellular CO_2 concentration were measured using a LI-6400 portable photosynthesis meter (Li-Cor). All these physiological parameters were determined in four replications, respectively.

Statistical Analysis

Microsoft Excel was used for data analysis, and one-way ANOVA was conducted using SPSS Statistics 22.0 software to assess significance of differences. The data were analyzed using Student's *t*-test and the difference was considered significant statistically at $p < 0.05$.

RESULTS

The Full-Length *TwNAC01* Gene

Using primers designed based on the sequence of Unigene c51971 (GSP-R/F in **Supplementary Table S1**), we amplified an intermediate sequence from the extracted triticale RNA (**Supplementary Figure S1A**) that was 502-bp long (**Supplementary Figure S1B**). Based on this intermediate sequence, we used 5′-RACE to amplify the 224 bp 5′ sequence (**Supplementary Figure S1C**), and 3′-RACE to amplify the 557 bp 3′ sequence (**Supplementary Figure S1D**). Splicing of the 5′ and 3′ sequences based on the intermediate sequence (Unigene c51971) yielded a fill-length ORF of 1,059 bp. Using specific primers designed out of this ORF sequence, we successfully amplified the gene (**Supplementary Figure S1E**). Transformation of this gene fragment into *E. coli via* the pMD19-T vector confirmed the expression of a 1,059-bp sequence (**Supplementary Figure S1F**). The predicted amino acid sequence of the gene was 352-bp long and had over 95% homology with the NAC amino acid sequences from barley, wheat, and other plants. We thus inferred that the cloned gene was a triticale *NAC* gene, which was designated *TwNAC01*. This gene has been submitted to GenBank (accession number MG736919).

Gene Sequence Analysis

The molecular formula of the encoded protein was predicted to be $C_{1722}H_{2642}N_{464}O_{522}S_{19}$, with a predicted molecular weight of 38805.86 kDa, and a theoretical isoelectric point of 5.44. The total number of positive/negative charge residues predicted in this protein were 46/37, and the atomic composition was C_{1722}, H_{2642}, N_{464}, O_{522}, and S_{19}. The extinction coefficient of the predicted protein was 46,996, and its absorbance at a wavelength of 280 nm was 1.2111 g^{-1} cm^{-1}. The total average hydrophobic coefficient of the predicted protein was −0.494, indicating that the putative protein was hydrophilic.

A NJ phylogenetic tree based on sequence similarity showed that the triticale TwNAC01 protein formed a clade with NAC proteins from *Aegilops tauschii* (XP-020161331), and *Hordeum vulgare* (KAE8777325 and CBZ41151; **Figure 1A**). In particular, the amino acid sequence of TwNAC01 was more than 97% similar to *Ae. tauschii* protein AtNAC92 (XP20161331.1; **Figure 1B**). The predicted TwNAC01 sequence contained a conserved NAM-superfamily domain composed of 129 consecutive amino acids at the N-terminus (between amino acid 20 and 148) and three transcriptional activation domains at the C-terminus (**Figure 1C**).

Subcellular Localization in the Nucleus

Localization prediction analysis indicated that the TwNAC01 protein was not located in the chloroplasts or mitochondria. This protein was unlikely to be a chloroplast transport peptide, mitochondrial transport peptide, or signal peptide. The target protein was found in other organelles secretory pathways. Further study with the Protcomp analysis indicated that the predicted protein was located in the nucleus. The shear site was the 62th amino acids with the maximum value of 0.113, and the comprehensive splicing site was the 62th amino acids with the maximum value of 0.107 (No signal peptide; **Table 1**). The shear site was consistent with the predicted upper transmembrane region and signal peptide (**Table 1**). In the control group (35S:EGFP), the EGFP localization signal was dispersed throughout the cell, with the strongest signals originating primarily from the cell membrane and nucleus (**Figure 2**). In the treatment group (35S:TwNAC01-EGFP), the EGFP protein signal was restricted to the nucleus (**Figure 2**). This suggested that the fusion protein was located in the nucleus, as was predicted by our bioinformatics analysis.

Analysis of *TwNAC01* Gene Expression in Triticale Under Drought Stress

The *TwNAC01* gene was significantly upregulated ($p < 0.01$) in triticale roots and grains of drought-stressed plants as compared to the control (**Figure 3A**); *TwNAC01* was also upregulated with respect to the control in the leaves ($p < 0.05$), but upregulated insignificantly with respect to the control in the stems. This suggested that the triticale *TwNAC01* gene was upregulated in response to drought stress, with the strongest upregulation found in the grain, followed by the root, leaf, and stem.

After 1- and 24-h NaCl treatment, *TwNAC01* expression was significantly more upregulated in the roots than in the leaves (**Figure 3B**). In contrast, after 24 h of cold and PEG6000-induced dehydration stress, *TwNAC01* was significantly upregulated in the leaves as compared to the roots (although *TwNAC01* was significantly upregulated in the roots as compared to the leaves after 12-h PEG6000 treatment; **Figures 3C,D**). After 24 h of MeJA and ABA stress, *TwNAC01* was significantly upregulated in the roots as compared to the leaves; in response to these stressors, *TwNAC01* expression levels appeared to increase over time (**Figures 3E,F**). After ABA treatment, *TwNAC01* gene expression levels in roots were significantly higher than those in leaves throughout the time course (**Figure 3F**). Overall, the data indicated that the *TwNAC01* gene played a role in the stress response of the triticale roots and leaves.

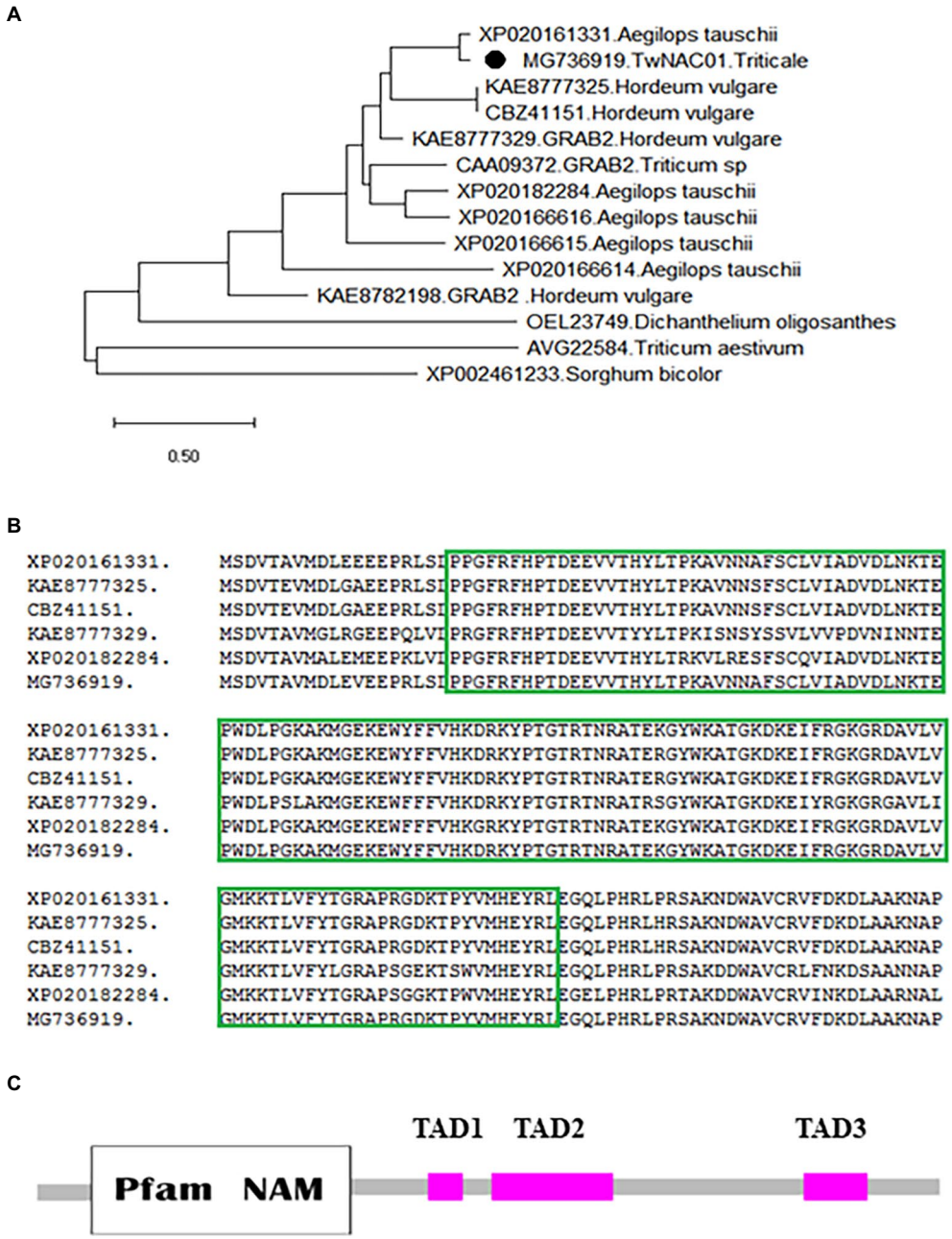


FIGURE 1 | Phylogenetic relationships among NAC proteins in plants, and the conserved NAM superfamily of *TwNAC01*. **(A)** Neighbor-joining phylogenetic relationships between the TwNAC01 and other NAC proteins in plants; **(B)** Amino acid sequence alignment analysis showing the conserved homeodomain regions of *TwNAC01* with its closest homologs from barley, wheat, *Aegilopsis tauschii*, and durum wheat; **(C)** The conserved NAM superfamily domain in the TwNAC01 protein. TAD, transcription activation domain.

Confirmation of Transgenic *Arabidopsis thaliana* Lines Overexpressing *TwNAC01*

PCR analysis of *E. coli* transformed with the pCAMBIA1300-35S overexpression vector recovered a 1,059-bp band, indicating that transformation had been successful and that the target gene was ligated to the vector (**Supplementary Figure S2A**). After restriction endonuclease digestion, the vector skeleton (10 kb) and a band slightly longer than 1,000 bp were obtained (**Supplementary Figure S2B**), again indicating that the recombinant expression plasmid containing the target gene were successfully constructed. The *A. tumefaciens* solution containing the expression vector plasmid was also analyzed using PCR, and a 1,059-bp band was confirmed (**Supplementary Figure S2C**). After the plasmid was introduced into *A. thaliana* inflorescences using the floral dip method, three T_0 plants expressing *TwNAC01* were identified *via* 1/2

TABLE 1 | Subcellular localization scores.

[a]Position	cTP	mTP	SP	Other	Loc	RC	TPlen
Positioning score	0.09	0.104	0.171	0.887	_	2	_
[b]Position	Nucleus	Cell membrane	Extracellular	Mitochondria	Chloroplast	Bubble	
Positioning score	8.26	1.01	0.04	0.01	0.11	0.48	

[a]*cTP, chloroplast transit peptide; mTP, mitochondrial transit peptide; SP, signal peptide; RC, reliability level; Tplen, Other organelles.*
[b]*Scores were obtained online using the Target P1.1 Server (http://www.cbs.dtu.dk/services/TargetP/).*

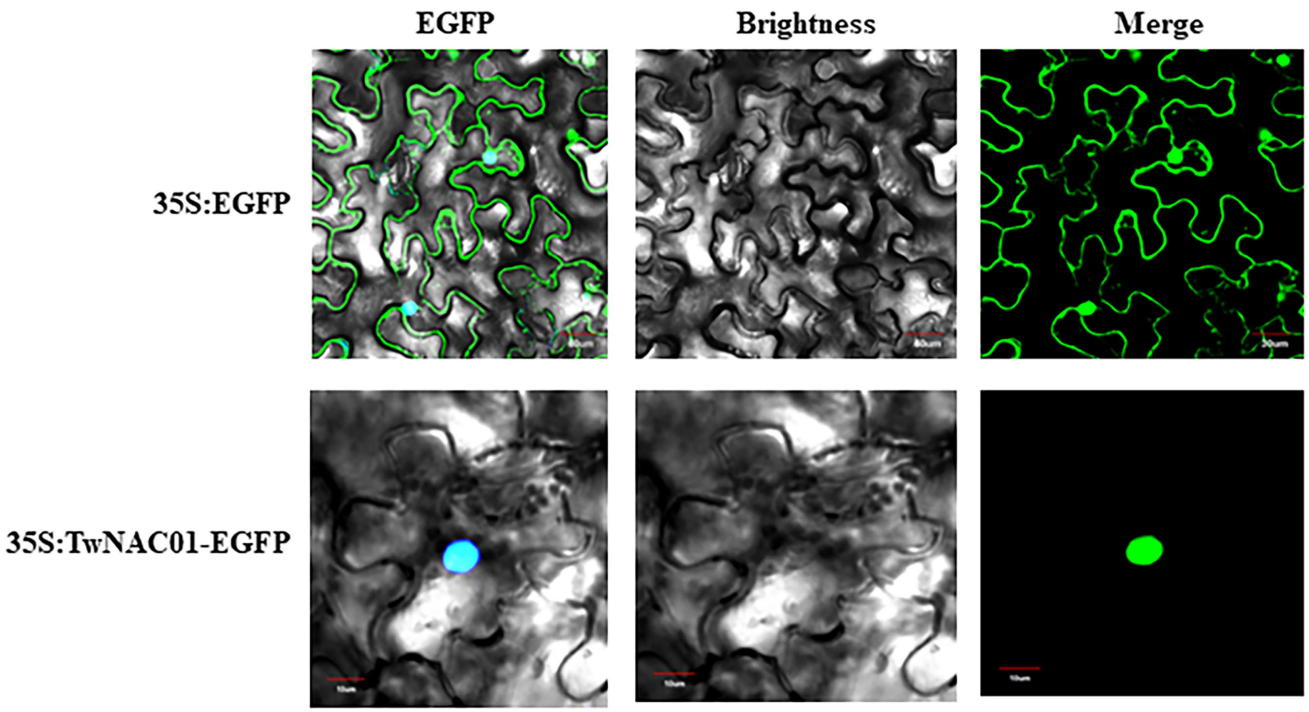


FIGURE 2 | Subcellular localization of the TwNAC01 protein in the nuclei of tobacco cells.

MS Kan + medium followed by PCR verification. Derived from these T_0 lines, three T_3 lines were confirmed to express *TwNAC01*.

Root Length and Leaf Water Loss Rate in Transgenic *Arabidopsis* Overexpressing *TwNAC01*

After 2 h of treatment at 25°C, while the leaves of *A. thaliana* WT and those expressing the VC had curled slightly, the leaves of the transgenic *A. thaliana* lines overexpressing *TwNAC01* (TwNAC01-1, TwNAC01-2, and TwNAC01-3) exhibited no obvious curling (**Figure 4A**). After 5 h at 25°C, the leaves of the WT and VC plants were obviously curled, while the leaves of the *TwNAC01*-overexpressing lines were only slightly curled. After 8 h of dehydration, the leaves of the WT and VC plants were noticeably withered and crumpled in appearance; although the leaves of the transgenic lines were also somewhat withered, the observed degree of dehydration was much less severe (**Figure 4A**).

However, the three transgenics slowed down water loss (29.90%–49.30%) significantly, especially during the first 2 h. As drying continued, water loss rates increased almost linearly in all lines (**Figure 4B**). The overall data indicated that water loss rates in the transgenic lines were significantly ($p < 0.05$) lower (16.77%–58.77%) than those in the WT (31.02%–68.18%) and VC (27.07%–62.86%) lines (**Figure 4B**). This result should attribute to the longer roots (9.90 ± 0.03–10.20 ± 0.24 cm) in transgenic lines relative to the WT (6.52 ± 0.41 cm) and VC (8.18 ± 0.17 cm) counterparts (differences of 1.5-fold and 1.2-fold, respectively; **Figures 5A,B**).

Physiological Indexes of Stress Tolerance in *Arabidopsis thaliana* Overexpressing *TwNAC01*

Although the relative leaf water contents (62.03%–64.70%) of the three transgenic *Arabidopsis* lines were slightly higher than those of VC (55.92%) and WT (48.09%) lines, these

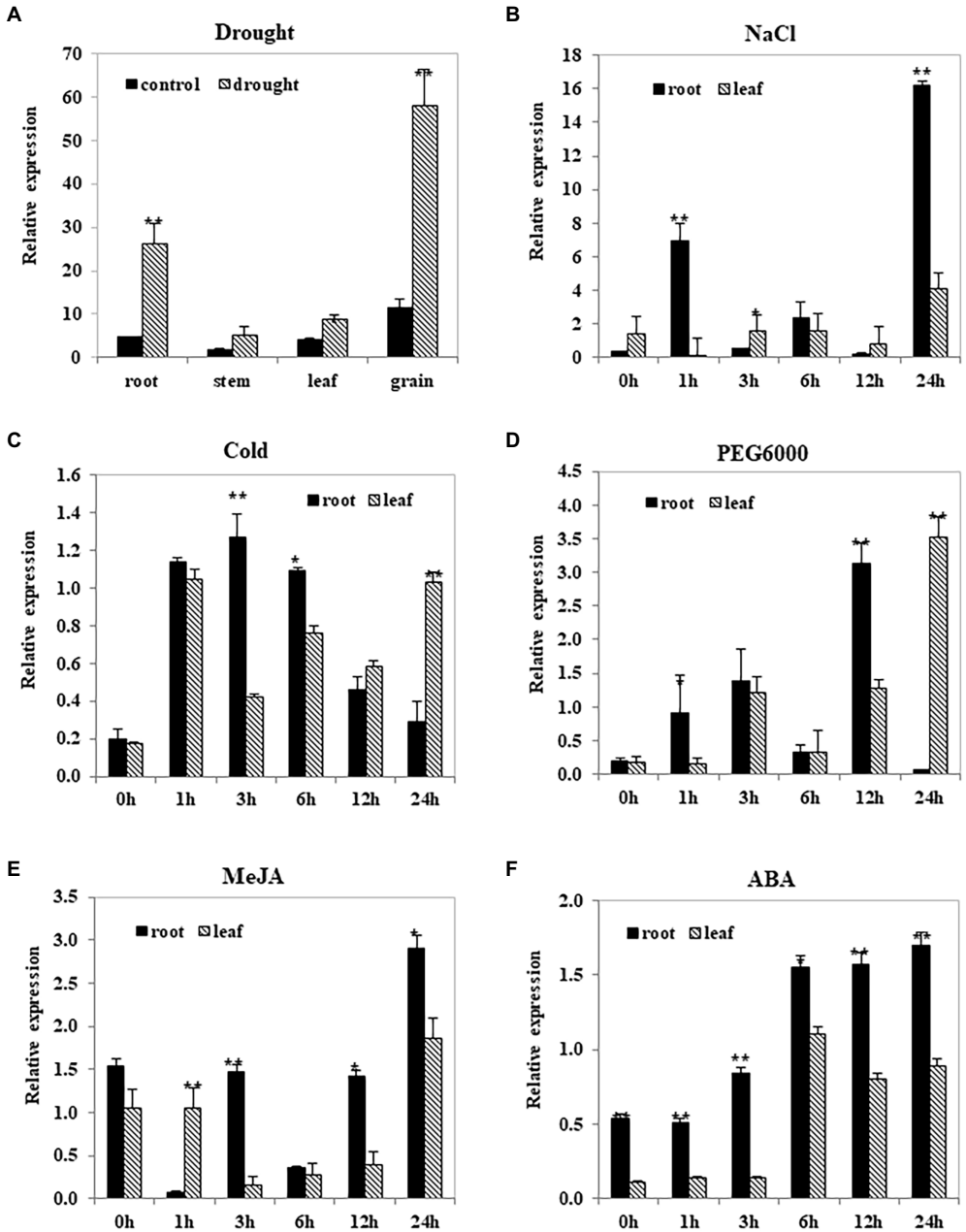


FIGURE 3 | *TwNAC01* gene expression patterns in triticale after stress treatments. Triticale plants were subjected to one of the following treatments: **(A)** drought, **(B)** 200-mM NaCl, **(C)** cold (4°C), **(D)** 20% PEG6000, **(E)** 100-μM MeJA, or **(F)** 100-μM ABA. Relative expression levels in the plant tissues were determined using qRT-PCR and the $2^{-\Delta\Delta CT}$ method. Transcript levels were normalized to the wheat actin genes (*TaActin*). Values shown are the means ± SE of three replicates of three independent samples. * and ** indicates significant difference at 0.05% and 0.01% level, respectively.

differences were not significant (**Figure 6A**). However, leaf electrical conductivity (reflecting electrolyte leakage and thus membrane damage) was significantly greater in the VC (63.67%) and WT (71.60%) lines as compared to the transgenic lines (32.07%–32.60%; **Figure 6B**). Hydrogen peroxide (18.29 μmol g^{-1} FW) and MDA (6.27 μmol g^{-1} FW) levels were significantly greater in the leaves of the WT line as compared to all other lines; there were no significant differences in H_2O_2 or MDA levels between the VC plants (14.37 μmol g^{-1} FW and 5.81 μmol g^{-1} FW) and any of the transgenic lines (11.85–12.12 μmol g^{-1} FW and 2.32–2.66 μmol g^{-1} FW; **Figures 6C,D**).

After drought stress, *TwNAC01* was upregulated in the roots and leaves of the transgenic plants as compared to the VC and WT plants; in all three transgenic lines, *TwNAC01* gene expression was significantly greater in the

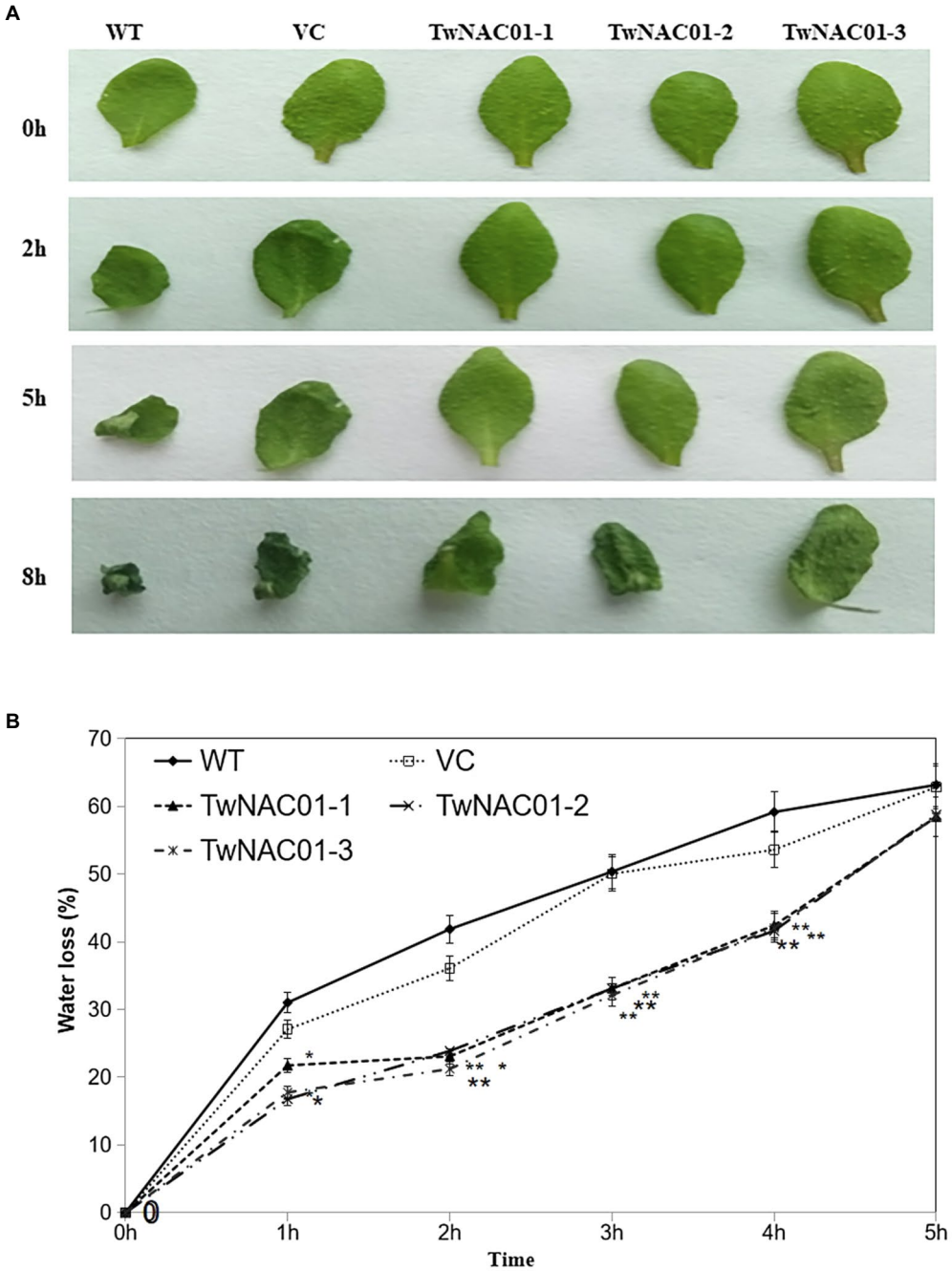


FIGURE 4 | Three lines overexpressing *TwNAC01* (TwNAC01-1, TwNAC01-2, and TwNAC01-3) in Arabidopsis exhibit reduced rates of water loss in the leaves compared to WT (wild type) and VC (vector control). **(A)** Leaves of various Arabidopsis lines after 0–8 h of dehydration; **(B)** Rates of moisture loss in the leaves of various Arabidopsis lines. Values are means ± SE of three replicates. * and **indicates significant difference at 0.05% and 0.01% level, respectively.

roots than it in the leaves (**Figure 6E**). On average, *TwNAC01* gene expression levels in the transgenic *A. thaliana* lines were 8-fold and 38-fold greater than in the VC and WT plants, respectively. Thus, in response to drought stress, *TwNAC01* was upregulated in transgenic *A. thaliana* overexpressing *TwNAC01* as compared to mock-transformed and WT controls.

Expression of *TwNAC01* After Virus-Induced Gene Silencing in Triticale Under Drought Stress

A 327-bp sequence was amplified from the triticale cDNA as mentioned above using the virus-induced gene silencing (VIGS) primers (**Supplementary Figure S3A**). After transformation of the amplified sequence into *E. coli*, positive clones were identified

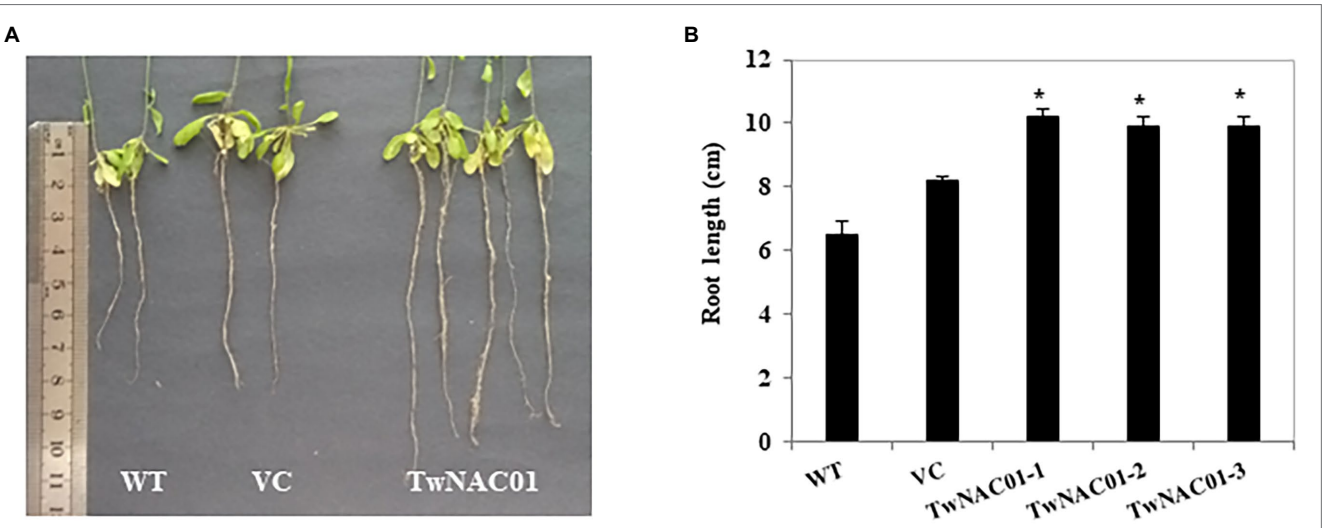


FIGURE 5 | Root growth of the WT (wild type), VC (vector control), and transgenic Arabidopsis lines overexpressing *TwNAC01*. **(A)** Primary root length of WT, VC, and transgenic plants grown for 55 d; **(B)** Statistical analysis of the root growth. Values shown are the means ± SE of three replicates of three independent samples. * and **indicates significant difference at 0.05% and 0.01% level, respectively.

via PCR amplification (**Supplementary Figures S3B,C**). After drought stress, *TwNAC01* gene expression levels in the control were significantly greater than those in the *TwNAC01*-silenced plants (BSMV-*TwNAC01*; **Figure 7**). In contrast, drought stress significantly upregulated *TwNAC01* in the empty vector (BSMV-*γb*) and indicator-gene (BSMV-*PDS*) plants as compared to the control. This indicated that drought stress upregulated the triticale *TwNAC01* gene; *TwNAC01* was downregulated significantly even under drought conditions when it was silenced (**Figure 7**).

Phenotypic Implications of *TwNAC01* Gene Silencing in Triticale

About 2 weeks after inoculation with the BSMV vectors, the indicator-gene (BSMV-*PDS*) plants began to exhibit symptoms of stripe mosaic virus. On the 20th day after inoculation, large areas of the leaves of the BSMV-*PDS* plants were bleached, while the leaves of empty vector (BSMV-*γb*) and *TwNAC01*-silenced (BSMV-TwNAC01) plants showed slight bleaching (**Figure 8A**). In general, the growth potential of each of the inoculated groups (BSMV-*γb*, BSMV-*PDS*, and BSMV-*TwNAC01*) was weaker than that of the control (**Figures 8B,C**). The mean RWC (57.64%) of the leaves of BSMV-*TwNAC01* was significantly lower than that of the leaves of the control (71.63%; **Figure 8D**). The roots of the *TwNAC01*-silenced plants were significantly shorter (3.95 cm) than those of the control (5.58 cm), BSMV-*γb* (5.04 cm), and indicator-gene plants (4.95 cm; **Figures 8E,F**). The results indicated that *TwNAC01* gene silencing inhibits triticale root development and significantly reduced triticale growth.

Physiological Indexes of Drought Stress and Photosynthesis in *TwNAC01*-Silenced Triticale

After drought stress, levels of H_2O_2 (54.17 μmol g^{-1} FW) and MDA (41.49 μmol g^{-1} FW) in the leaves of BSMV-*TwNAC01* plants were significantly higher (**Figures 9A,B**), while RWC was significantly lower (57.64%; **Figure 9C**) than those in the leaves of uninfected control plants (65.51%–71.63%). This result demonstrated that the triticale leaves were more stressed by drought when the *TwNAC01* gene was silenced, i.e., the stress-resistant ability of the plant decreased after silencing the *TwNAC01* gene. The data suggested that *TwNAC01* played an important role in coping with stress. Furthermore, net photosynthetic rate, stomatal conductance to H_2O, intracellular CO_2 level, and transpiration rate were significantly lower in the BSMV-*TwNAC01* leaves as compared to the control (**Figures 9D–G**). Net photosynthetic rate and intracellular CO_2 level were significantly lower than the control in the BSMV-*γb* and BSMV-*PDS* leaves (**Figures 9D,F**), while transpiration rate was significantly lower than the control in the BSMV-*PDS* leaves (**Figure 9G**).

DISCUSSION

NAC transcription factors are considered the most important family of transcription factors in plants; these transcription factors play various important roles in stress response, as well as in the regulation of plant growth and development (Xu et al., 2015). Stress-related NAC transcription factors have been well examined in wheat, rice, and *Leymus triticoides*. Here, we used RACE RNA-seq and RT-PCR to clone the first putative *NAC* gene from hexaploid triticale. This putative *NAC* gene had over 95% similarity with known *NAC* genes from other crops, including common wheat, *Aegilops*, and durum wheat. These findings were consistent with our phylogenetic analysis. In addition, the predicted protein sequence of the putative *NAC* gene included a conserved NAM domain between the 20th and 148th amino acids at

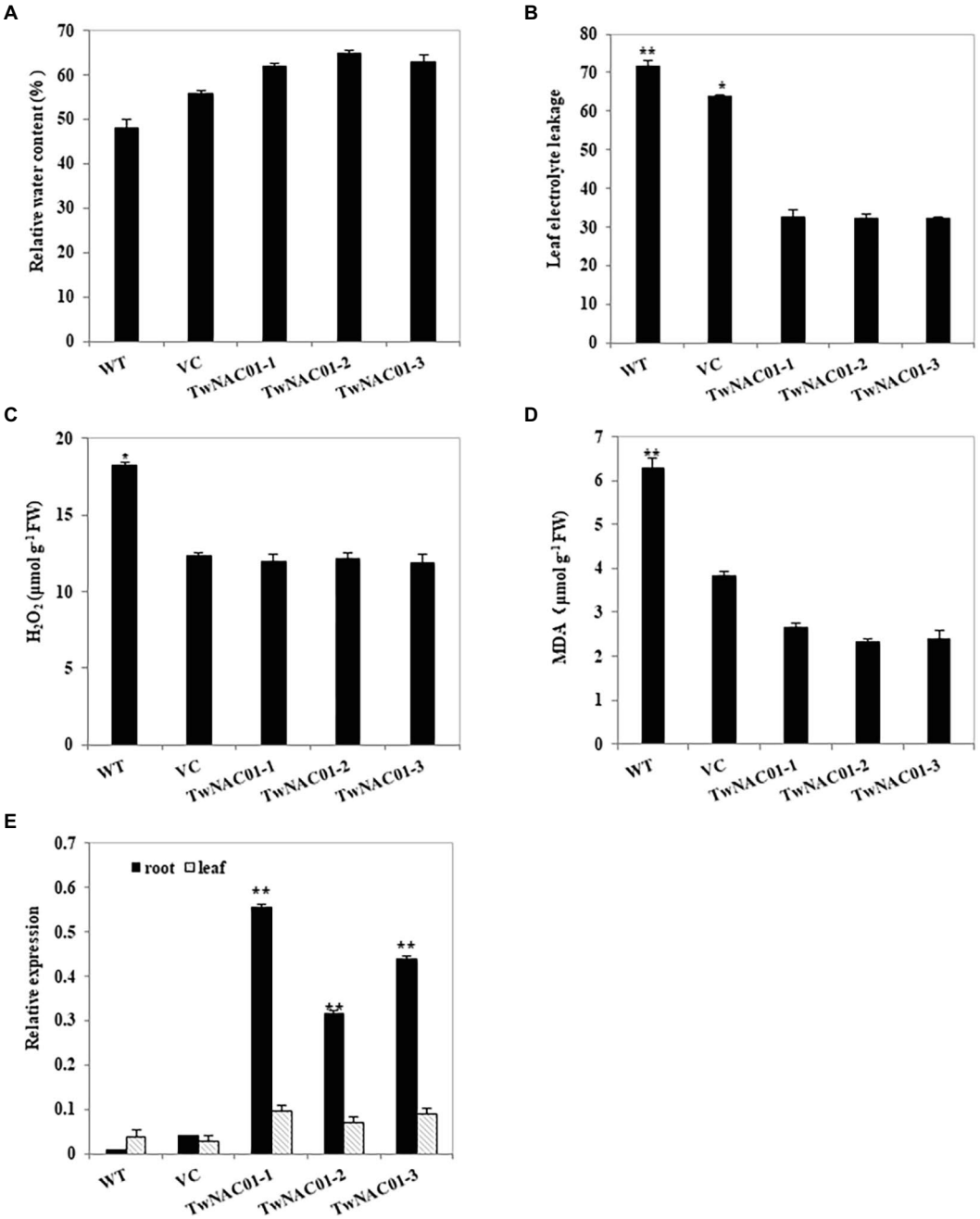


FIGURE 6 | Analysis of physiological indexes of the transgenic Arabidopsis lines overexpressing *TwNAC01* under drought stress conditions. Analyses of leaf relative water content (%) **(A)** leaf electrolyte leakage **(B)**, H_2O_2 content (μmol g^{-1} FW; **C**), and MDA content (μmol g^{-1} FW; **D**) in WT (wild type) and transgenic lines overexpressing *TwNAC01* lines under drought-stressed conditions. Relative expression of *TwNAC01* in the roots and leaves of transgenic *Arabidopsis thaliana* lines **(E)**. Values are means ± SE of three replicates. * and **indicates significant difference at 0.05% and 0.01% level, respectively.

the N-terminus, as well as three transcriptional activation regions at the C-terminus. We thus concluded that the putative gene was indeed an *NAC* gene. This gene was designated *TwNAC01*.

Our results showed that *TwNAC01* was upregulated by a variety of abiotic stressors and signal molecules, including salinity, drought, PEG6000, and ABA. Several studies have shown that about 20%–25% of plant *NAC* genes respond to stress treatments and participate in stress alleviation (Fang et al., 2008; Nuruzzaman et al., 2010; Puranik et al., 2012). In addition, *A. thaliana* overexpressing the wheat *NAC* genes *TaNAC2* and *TaNAC67* exhibited significantly improved tolerance to drought, salinity, and cold as compared to the WT control (Mao et al., 2014). Similarly, overexpression of

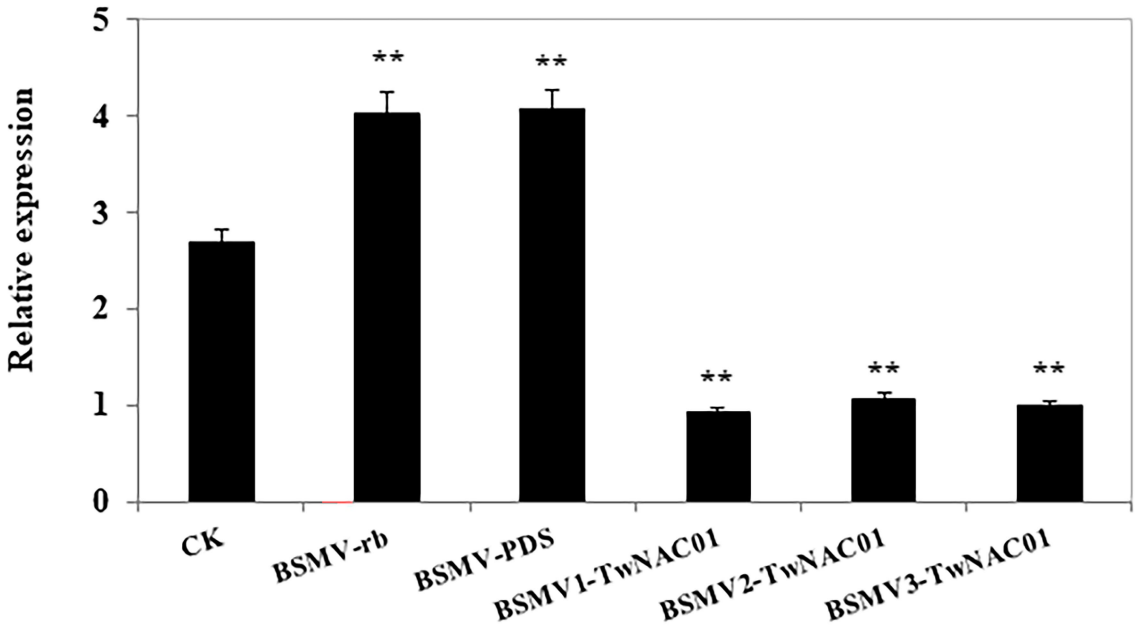


FIGURE 7 | Relative *TwNAC01* expression patterns in triticale after silencing the *TwNAC01* gene, as determined using qRT-PCR and the $2^{-\Delta\Delta CT}$ method. Transcript levels were normalized to *TaActin*. CK, wide type control; BSMV-*γb*, empty vector control; BSMV-*PDS*, BSMV with indicator gene; BSMV-*TwNAC01*, vector carrying silenced *TwNAC01*. Values shown are the means ± SE of three replicates of three independent samples. **indicates significant difference at 0.01% level.

the wheat *NAC* genes (*TaNAC2a, TaNAC4a, TaNAC6, TaNAC7, TaNAC13,* and *TaNTL5*) in tobacco significantly improved drought tolerance (Tang et al., 2012). Previous studies have also shown that *NAC* gene expression increases in response to drought stress (Nakashima et al., 2007; Wu et al., 2009; Chen et al., 2014). In this study of triticale, *TwNAC01* expression was significantly upregulated in the drought-stressed plant roots and young grains as compared to unstressed controls. This suggested that *TwNAC01* expression is induced by drought stress, and it plays an important role in response to drought in triticale. *NAC* genes have also been shown to be upregulated in aging plant tissues, by treatment with plant signal molecules (e.g., ABA, ethephon, JA, and SA; Bu et al., 2008; Jensen et al., 2010; Xia et al., 2010; Tang et al., 2012), and by exposure to ethylene and methyl jasmonate (Scharrenberg et al., 2003). The upregulation of *TwNAC01* in response to stress was stronger in roots than in leaves, which was in agreement with a previous study in wheat showing that *TaNAC4* was more strongly upregulated in wheat roots compared to leaves and stems (Jensen et al., 2007; Xia et al., 2010). The data suggest that *TwNAC01* is upregulated in triticale roots first in response to stress, in order to promote the development of plant roots and reduce the damage caused by adverse conditions.

The mechanisms by which *NAC* transcription factors alleviate drought stress in plants have been well studied. For example, overexpression of the *NAC* gene *ATAF1* in *A. thaliana* decreased transpiration rate and increased drought tolerance (Christiansen et al., 2011). Similarly, rice overexpressing *OsNAP* had lower water loss rates during vegetative growth, increased sensitivity to exogenous ABA, and improved tolerance to salt, drought, and low temperature stress (Negi et al., 2018). Also in rice, NAC transcription factors regulate the expression of *OsSRO1c* genes, which are primarily expressed in guard cells; the overexpression of *OsSRO1c* increases H_2O_2 accumulation in guard cells and reduces the number of completely open stomata, thus reducing water loss *via* transpiration (You et al., 2013). Finally, the *SNAC3* gene in rice targets a ROS-scavenging gene, and *SNAC3* overexpression upregulates this target gene (Fang et al., 2015). Previous studies suggest that, when plants are under stress, the NAC family act as transcriptional activators or repressors of their downstream genes, such as NAC regulatory network interactions with jasmonic acid-, salicylic acid- and ethylene-mediated stress responses *via* both ABA-dependent and independent pathways by binding to the promoter of Early Response to Dehydration 1 (ERD1; Figueroa et al., 2021). These regulatory networks can reduce transpiration rate by promoting plant root elongation, reducing H_2O_2 and MDA accumulation, and increasing leaf water content. Ultimately, these factors enhance plant adaptability to adversity. In this study, *TwNAC01* expression was successfully silenced in triticale BSMV-*TwNAC01* plants: *TwNAC01* expression levels in the triticale BSMV-*TwNAC01* plants were significantly lower than those in the control, BSMV-*γb*, and BSMV-*PDS* plants. In general, the growth potential of the *TwNAC01*-silenced plants was significantly lower than that of the other lines. In particular, the *TwNAC01*-silenced plants had shorter roots and reduced water content as compared to the other plants. Under drought conditions, indexes of physiological stress (i.e., MDA and H_2O_2 levels) were significantly increased in *TwNAC01*-silenced plants as

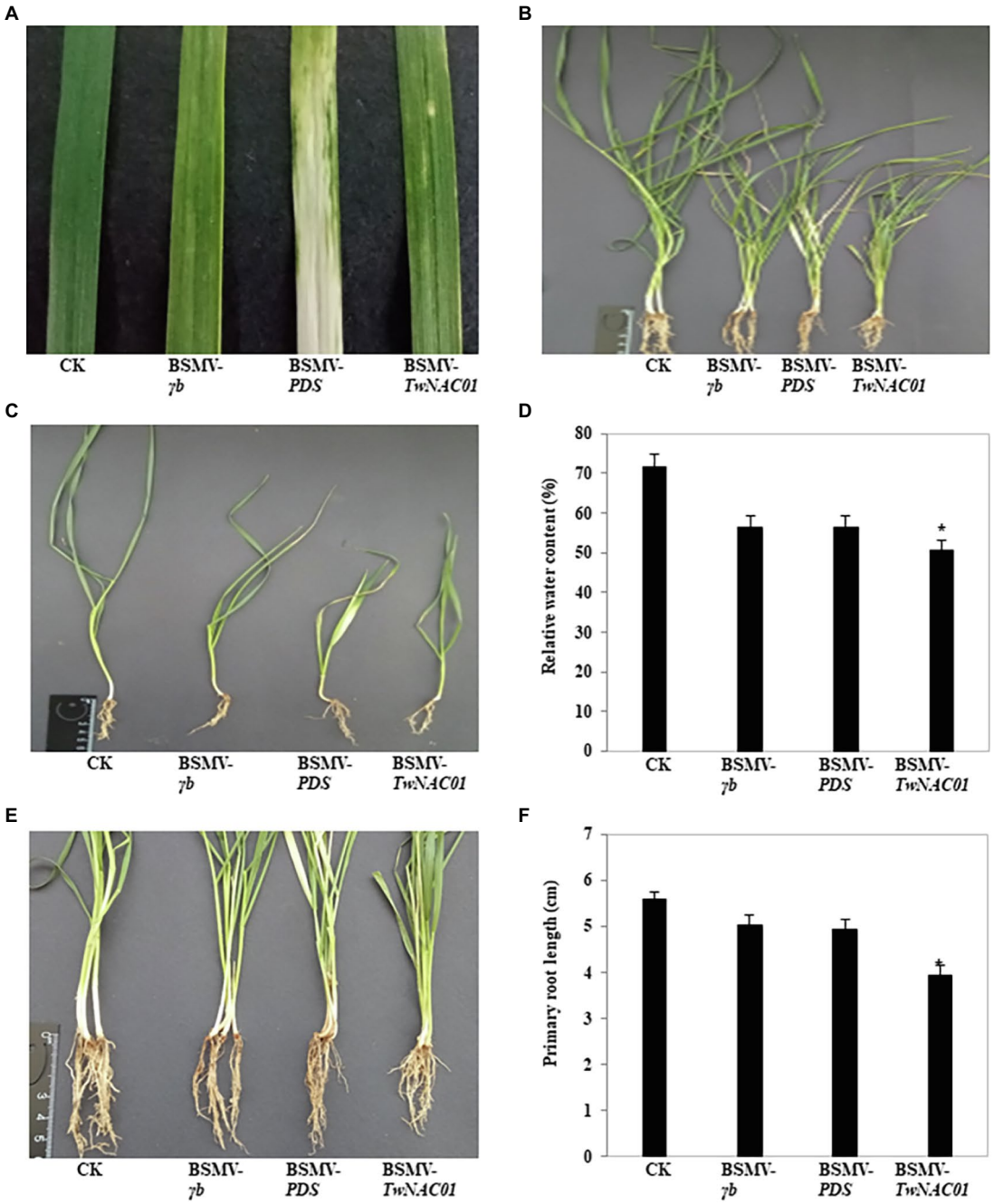


FIGURE 8 | Phenotypic differences among triticale plants inoculated with different BSMV vectors for the VIGS of *TwNAC01*. **(A)** Leaves showing viral infection; **(B,C)** Biomass comparison; **(D)** Relative water contents (%); **(E)** Visual comparison of root lengths; **(F)** Root length quantification. Values shown are means ± SE of three replicates. *indicates significant difference at 0.05% level. CK, control; BSMV-*γb*, empty vector; BSMV-*PDS*, BSMV with indicator gene; BSMV-*TwNAC01*, vector carrying silenced *TwNAC01*.

compared to the controls, while relative water content and indexes of photosynthetic activity (net photosynthetic rate, stomatal conductance, transpiration rate, and intercellular CO_2 concentration) were significantly reduced. The observed changes in these physiological indexes suggested that triticale growth and stress tolerance were substantially impaired by *TwNAC01* silencing.

CONCLUSION

In conclusion, overexpression of the triticale *TwNAC01* gene in *A. thaliana* improved drought tolerance of *A. thaliana* by increasing the water retention capacity of leaves, reducing cellular membrane damage, decreasing production of ROS in the leaves, and promoting root elongation. In

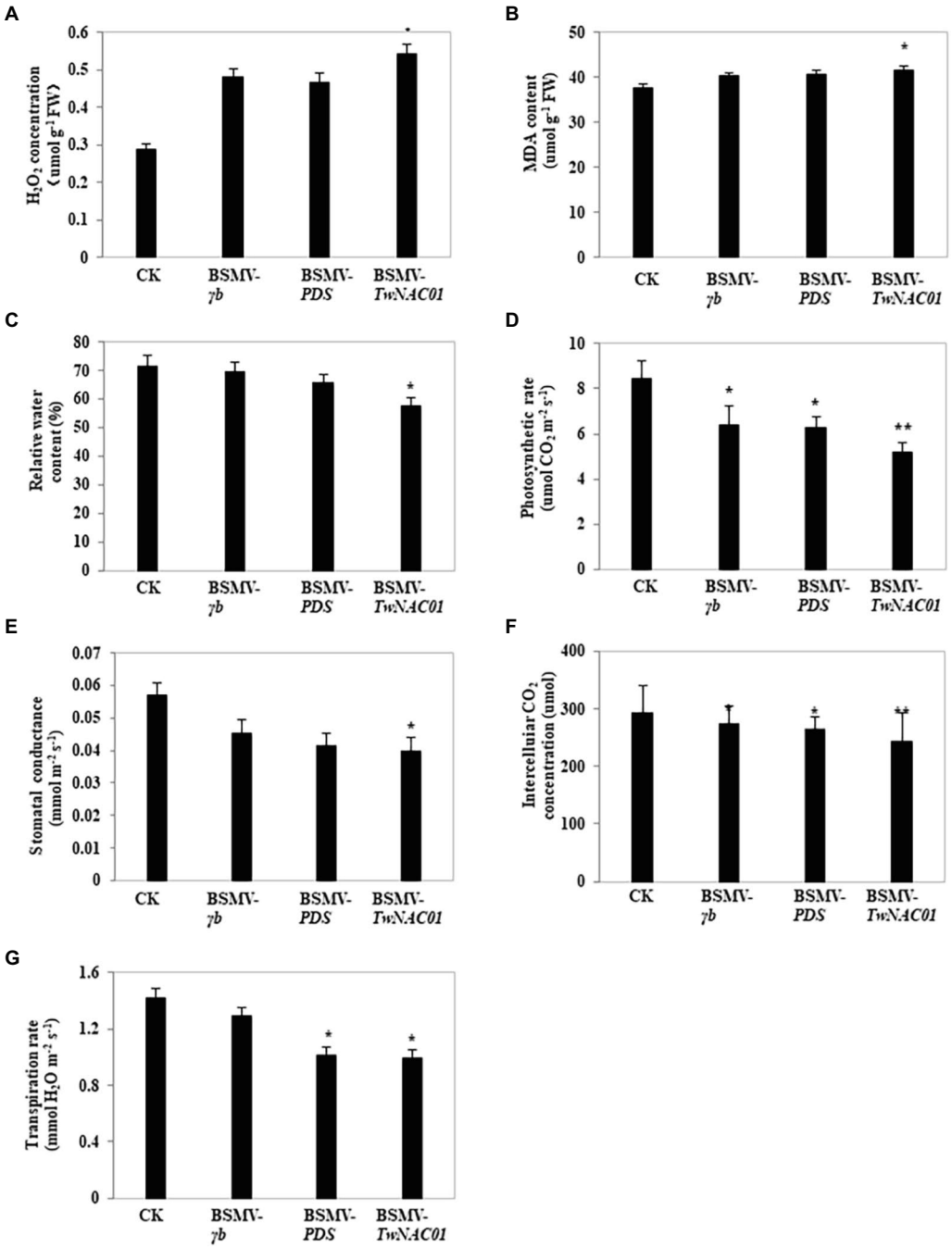


FIGURE 9 | Physiological indexes of drought stress and photosynthesis in triticale leaves after virus-induced gene silencing using BSMV. **(A)** H_2O_2 concentration (μmol g^{-1} FW); **(B)** MDA content (μmol g^{-1} FW); **(C)** Relative water content (RWC; %); **(D)** Photosynthetic rate (μmol CO_2 m^{-2} s^{-1}); **(E)** Stomatal conductance to H_2O (mmol m^{-2} s^{-1}); **(F)** Intercellular CO_2 concentration (μmol); **(G)** Transpiration rate (mmol H_2O m^{-2} s^{-1}). Values shown are means ± SE of three replicates. * and **, indicates significant difference at $p < 0.05$, 0.01, respectively. CK, control; BSMV-*γb*, empty vector; BSMV-*PDS*, BSMV with indicator gene; BSMV-*TwNAC01*, vector carrying silenced *TwNAC01*.

TwNAC01-silenced triticale, leaf relative water content and root length were significantly decreased as compared to the control, while leaf H_2O_2 and MDA levels were significantly increased. Leaf net photosynthetic rate, stomatal conductance, intercellular CO_2 concentration, and transpiration rate were also significantly lower in the *TwNAC01*-silenced plants as compared to the control. These results indicated that *TwNAC01* silencing decreased drought tolerance of triticale, suggesting that the *TwNAC01* gene plays an important role in response to drought stress in triticale.

DATA AVAILABILITY STATEMENT

The datasets presented in this study can be found in online repositories. The names of the repository/repositories and accession number(s) can be found at: https://www.ncbi.nlm.nih.gov/nuccore/1545818062.

AUTHOR CONTRIBUTIONS

G-CK planned and designed the research and wrote the main manuscript text. MW performed most of the experiments and data acquisition and participated in figure preparation and manuscript organization. L-TR, X-YW, H-TG, S-SW, and Y-ML helped with experiments and data analysis. X-FM reviewed and revised the manuscript. All authors contributed to the article and approved the submitted version.

FUNDING

This study was supported by the National Natural Science Foundation of China (31860376 and 31360333) and the Ministry of Agriculture 948 project (2013-Z75).

SUPPLEMENTARY MATERIAL

The Supplementary Material for this article can be found online at: https://www.frontiersin.org/articles/10.3389/fpls.2022.877016/full#supplementary-material

REFERENCES

Bu, Q., Jiang, H., Li, C. B., Zhai, Q., Zhang, J., Wu, X., et al. (2008). Role of the *Arabidopsis thaliana* NAC transcription factors ANAC019 and ANAC055 in regulating jasmonic acid-signaled defense responses. *Cell Res.* 18, 756–767. doi: 10.1038/cr.2008.53

Cao, L. P., and Kong, G. C., (2011). *Research and Application of Physiology Ecology and Genetics of Triticale*. Beijing: Economic Management Press.

Chen, J. X., and Wang, X. F., (2002). *Plant Physiology Experiment Guide*. Guangzhou: South China University of Technology Press. 124.

Chen, X., Wang, Y., Lv, B., Li, J., Luo, L., Lu, S., et al. (2014). The NAC family transcription factor OsNAP confers abiotic stress response through the ABA pathway. *Plant Cell Physiol.* 55, 604–619. doi: 10.1093/pcp/pct204

Christiansen, M. W., Holm, P. B., and Gregersen, P. L. (2011). Characterization of barley (*Hordeum vulgare* L.) NAC transcription factors suggests conserved functions compared to both monocots and dicots. *BMC. Res. Notes* 4, 1–13. doi: 10.1186/1756-0500-4-302

Clough, S. J., and Bent, A. F. (1998). Floral dip: a simplified method for Agrobacterium-mediated transformation of *Arabidopsis thaliana*. *Plant J.* 16, 735–743. doi: 10.1046/j.1365-313x.1998.00343.x

Cramer, G. R. (2010). Abiotic stress and plant responses from the whole vine to the genes. *Aust. J. Grape Wine Res.* 16, 86–93. doi: 10.1111/j.1755-0238.2009.00058.x

Fang, Y., Liao, K., Du, H., Xu, Y., Song, H., Li, X., et al. (2015). A stress-responsive NAC transcription factor SNAC3 confers heat and drought tolerance through modulation of reactive oxygen species in rice. *J. Exp. Bot.* 66, 6803–6817. doi: 10.1093/jxb/erv386

Fang, Y., You, J., Xie, K., Xie, W., and Xiong, L. (2008). Systematic sequence analysis and identification of tissue-specific or stress-responsive genes of NAC transcription factor family in rice. *Mol. Genet. Genomics* 280, 547–563. doi: 10.1007/s00438-008-0386-6

Figueroa, N., Lodeyro, A. F., Carrillo, N., Gómez, R., and Lodeyro, A. F. (2021). Meta-analysis reveals key features of the improved drought tolerance of plants overexpressing NAC transcription factors. *Environ. Exp. Bot.* 186:104449. doi: 10.1016/j.envexpbot.2021.104449

Flexas, J., Ribas-Carbó, M., Bota, J., Galmés, J., Henkle, M., Martínez-Cañellas, S., et al. (2006). Decreased Rubisco activity during water stress is not induced by decreased relative water content but related to conditions of low stomatal conductance and chloroplast CO2 concentration. *New Phytol.* 172, 73–82. doi: 10.1111/j.1469-8137.2006.01794.x

He, X. J., Mu, R. L., Cao, W. H., Zhang, Z. G., Zhang, J. S., and Chen, S. Y. (2005). AtNAC2, a transcription factor downstream of ethylene and auxin signaling pathways, is involved in salt stress response and lateral root development. *Plant J.* 44, 903–916. doi: 10.1111/j.1365-313X.2005.02575.x

Huang, Q. J., Wang, Y., Li, B., Chang, J. L., Chen, M. J., Li, K. X., et al. (2015). TaNAC29, a NAC transcription factor from wheat, enhances salt and drought tolerance in transgenic Arabidopsis. *BMC Plant Biol.* 15:268. doi: 10.1186/s12870-015-0644-9

Jensen, M. K., Kjaersgaard, T., Nielsen, M. M., Galberg, P., Petersen, K., O'shea, C., et al. (2010). The *Arabidopsis thaliana* NAC transcription factor family: structure–function relationships and determinants of ANAC019 stress signalling. *Biochem. J.* 426, 183–196. doi: 10.1042/BJ20091234

Jensen, M. K., Lindemose, S., De Masi, F., Reimer, J. J., Nielsen, M., Perera, V., et al. (2013). ATAF1 transcription factor directly regulates abscisic acid biosynthetic gene NCED3 in *Arabidopsis thaliana*. *FEBS Open Bio.* 3, 321–327. doi: 10.1016/j.fob.2013.07.006

Jensen, M. K., Rung, J. H., Gregersen, P. L., Gjetting, T., Fuglsang, A. T., Hansen, M., et al. (2007). The HvNAC6 transcription factor: a positive regulator of penetration tolerance in barley and Arabidopsis. *Plant Mol. Biol.* 65, 137–150. doi: 10.1007/s11103-007-9204-5

Jeong, J. S., Kim, Y. S., Baek, K. H., Jung, H., Ha, S. H., Do Choi, Y., et al. (2010). Root-specific expression of OsNAC10 improves drought tolerance and grain yield in rice under field drought conditions. *Plant Physiol.* 153, 185–197. doi: 10.1104/pp.110.154773

Kang, S. G., Price, J., Lin, P. C., Hong, J. C., and Jang, J. C. (2010). The Arabidopsis bZIP1 transcription factor is involved in sugar signaling, protein networking, and DNA binding. *Mol. Plant* 3, 361–373. doi: 10.1093/mp/ssp115

Kim, C. K., Chung, J. D., Park, S. H., Burrell, A. M., Kamo, K. K., and Byrne, D. H. (2004). *Agrobacterium tumefaciens*-mediated transformation of Rosa hybrida using the green fluorescent protein (GFP) gene. *Plant Cell Tiss. Org. Cult.* 78, 107–111. doi: 10.1023/B:TICU.0000022529.16697.90

Lee, W. S., Rudd, J. J., and Kanyuka, K. (2015). Virus induced gene silencing (VIGS) for functional analysis of wheat genes involved in Zymoseptoria tritici susceptibility and tolerance. *Fungal Genet. Biol.* 79, 84–88. doi: 10.1016/j.fgb.2015.04.006

Li, C. Y., Li, C., Ainiwar, J., Kong, G. C., Hu, X. B., and Cao, L. P. (2008). Evaluation on drought resistance of spring forage triticale. *J. Triticeae Crops* 28, 1080–1085.

Livak, K. J., and Schmittgen, T. D. (2001). Analysis of relative gene expression data using real-time quantitative PCR and the $2^{-\Delta\Delta CT}$ method. *Methods* 25, 402–408. doi: 10.1006/meth.2001.1262

Mao, X., Chen, S., Li, A., Zhai, C., and Jing, R. (2014). Novel NAC transcription factor TaNAC67 confers enhanced multi-abiotic stress tolerances in Arabidopsis. *PLoS One* 9:e84359. doi: 10.1371/journal.pone.0084359

Mao, X., Zhang, H., Qian, X., Li, A., Zhao, G., and Jing, R. (2012). TaNAC2, a NAC-type wheat transcription factor conferring enhanced multiple abiotic stress tolerances in Arabidopsis. *J. Exp. Bot.* 63, 2933–2946. doi: 10.1093/jxb/err462

Michel, B. E., and Kaufmann, M. R. (1973). The osmotic potential of polyethylene glycol 6000. *Plant Physiol.* 51, 914–916. doi: 10.1104/pp.51.5.914

Michel, B. E., Wiggins, O. K., and Outlaw, W. H. (1983). A guide to establishing water potential of aqueous two-phase solutions (polyethylene glycol plus dextran) by amendment with mannitol. *Plant Physiol.* 72, 60–65. doi: 10.1104/pp.72.1.60

Nakashima, K., Takasaki, H., Mizoi, J., Shinozaki, K., and Yamaguchi-Shinozaki, K. (2012). NAC transcription factors in plant abiotic stress responses. *Biochim. Biophys. Acta* 1819, 97–103. doi: 10.1016/j.bbagrm.2011.10.005

Nakashima, K., Tran, L. S. P., Van Nguyen, D., Fujita, M., Maruyama, K., Todaka, D., et al. (2007). Functional analysis of a NAC-type transcription factor OsNAC6 involved in abiotic and biotic stress-responsive gene expression in rice. *Plant J.* 51, 617–630. doi: 10.1111/j.1365-313X.2007.03168.x

Negi, S., Tak, H., and Ganapathi, T. R. (2018). A banana NAC transcription factor (MusaSNAC1) impart drought tolerance by modulating stomatal closure and H_2O_2 content. *Plant Mol. Biol.* 96, 457–471. doi: 10.1007/s11103-018-0710-4

Nuruzzaman, M., Manimekalai, R., Sharoni, A. M., Satoh, K., Kondoh, H., Ooka, H., et al. (2010). Genome-wide analysis of NAC transcription factor family in rice. *Gene* 465, 30–44. doi: 10.1016/j.gene.2010.06.008

Pérez-Rodríguez, P., Riano-Pachon, D. M., Corrêa, L. G. G., Rensing, S. A., Kersten, B., and Mueller-Roeber, B. (2010). PlnTFDB: updated content and new features of the plant transcription factor database. *Nucleic Acids Res.* 38, D822–D827. doi: 10.1093/nar/gkp805

Pinheiro, C., and Chaves, M. M. (2011). Photosynthesis and drought: can we make metabolic connections from available data? *J. Exp. Bot.* 62, 869–882. doi: 10.1093/jxb/erq340

Puranik, S., Sahu, P. P., Srivastava, P. S., and Prasad, M. (2012). NAC proteins: regulation and role in stress tolerance. *Trends Plant Sci.* 17, 369–381. doi: 10.1016/j.tplants.2012.02.004

Scharrenberg, C., Falk, J., Quast, S., Haussühl, K., Humbeck, K., and Krupinska, K. (2003). Isolation of senescence-related cDNAs from flag leaves of field grown barley plants. *Physiol. Plant.* 118, 278–288. doi: 10.1034/j.1399-3054.2003.00098.x

Shang, B., Zang, Y., Zhao, X., Zhu, J., Fan, C., Guo, X., et al. (2019). Functional characterization of GhPHOT2 in chloroplast avoidance of *Gossypium hirsutum*. *Plant Physiol. Biochem.* 135, 51–60. doi: 10.1016/j.plaphy.2018.11.027

Sun, Y. (2002). *Research and Application of Chinese Triticale Genetic Breeding*. Hangzhou: Zhejiang Science and Technology Press

Tang, Y., Liu, M., Gao, S., Zhang, Z., Zhao, X., Zhao, C., et al. (2012). Molecular characterization of novel TaNAC genes in wheat and overexpression of TaNAC2a confers drought tolerance in tobacco. *Physiol. Plant.* 144, 210–224. doi: 10.1111/j.1399-3054.2011.01539.x

Wu, Y., Deng, Z., Lai, J., Zhang, Y., Yang, C., Yin, B., et al. (2009). Dual function of Arabidopsis ATAF1 in abiotic and biotic stress responses. *Cell Res.* 19, 1279–1290. doi: 10.1038/cr.2009.108

Xia, N., Zhang, G., Liu, X. Y., Deng, L., Cai, G. L., Zhang, Y., et al. (2010). Characterization of a novel wheat NAC transcription factor gene involved in defense response against stripe rust pathogen infection and abiotic stresses. *Mol. Biol. Rep.* 37, 3703–3712. doi: 10.1007/s11033-010-0023-4

Xiong, L., Ishitani, M., Lee, H., and Zhu, J. K. (2001). The Arabidopsis LOS5/ABA3 locus encodes a molybdenum cofactor sulfurase and modulates cold stress–and osmotic stress–responsive gene expression. *Plant Cell* 13, 2063–2083. doi: 10.1105/TPC.010101

Xu, Z., Wang, C., Xue, F., Zhang, H., and Ji, W. (2015). Wheat NAC transcription factor TaNAC29 is involved in response to salt stress. *Plant Physiol. Biochem.* 96, 356–363. doi: 10.1016/j.plaphy.2015.08.013

Xue, G. P., Way, H. M., Richardson, T., Drenth, J., Joyce, P. A., and McIntyre, C. L. (2011). Overexpression of TaNAC69 leads to enhanced transcript levels of stress up-regulated genes and dehydration tolerance in bread wheat. *Mol. Plant* 4, 697–712. doi: 10.1093/mp/ssr013

You, J., Zong, W., Li, X., Ning, J., Hu, H., Li, X., et al. (2013). The SNAC1-targeted gene OsSRO1c modulates stomatal closure and oxidative stress tolerance by regulating hydrogen peroxide in rice. *J. Exp. Bot.* 64, 569–583. doi: 10.1093/jxb/ers349

Zillinsky, F. J. (1974). The Development of triticale. *Adv. Agron.* 26, 315–348. doi: 10.1016/S0065-2113(08)60875-5

Conflict of Interest: X-FM was employed by the company Forage Genetics International, West Salem, WI, United States.

The remaining authors declare that the research was conducted in the absence of any commercial or financial relationships that could be construed as a potential conflict of interest.

Publisher's Note: All claims expressed in this article are solely those of the authors and do not necessarily represent those of their affiliated organizations, or those of the publisher, the editors and the reviewers. Any product that may be evaluated in this article, or claim that may be made by its manufacturer, is not guaranteed or endorsed by the publisher.

Copyright © 2022 Wang, Ren, Wei, Ling, Gu, Wang, Ma and Kong. This is an open-access article distributed under the terms of the Creative Commons Attribution License (CC BY). The use, distribution or reproduction in other forums is permitted, provided the original author(s) and the copyright owner(s) are credited and that the original publication in this journal is cited, in accordance with accepted academic practice. No use, distribution or reproduction is permitted which does not comply with these terms.

frontiers | Frontiers in Plant Science

ORIGINAL RESEARCH
published: 27 June 2022
doi: 10.3389/fpls.2022.898307

Comprehensive Genome-Wide Identification and Expression Profiling of *Eceriferum* (*CER*) Gene Family in Passion Fruit (*Passiflora edulis*) Under *Fusarium kyushuense* and Drought Stress Conditions

Hafiz Muhammad Rizwan[1], *Abdul Waheed*[2], *Songfeng Ma*[1], *Jiankun Li*[1], *Muhammad Bilal Arshad*[3], *Muhammad Irshad*[4], *Binqi Li*[1], *Xuelian Yang*[1], *Ahmad Ali*[5], *Mohamed A. A. Ahmed*[6], *Nusrat Shaheen*[7], *Sandra S. Scholz*[8], *Ralf Oelmüller*[1,8], *Zhimin Lin*[9]* *and Faxing Chen*[1]*

[1] College of Horticulture, Fujian Agriculture and Forestry University, Fuzhou, China, [2] Key Laboratory for Bio Pesticide and Chemical Biology, Ministry of Education, Fujian Agriculture and Forestry University, Fuzhou, China, [3] Department of Plant Breeding and Genetics, College of Agriculture, University of Sargodha, Sargodha, Pakistan, [4] College of Horticulture, The University of Agriculture, Peshawar, Pakistan, [5] National Engineering Research Center for Sugarcane, Fujian Agriculture and Forestry University, Fuzhou, China, [6] Plant Production Department (Horticulture-Medicinal and Aromatic Plants), Faculty of Agriculture (Saba Basha), Alexandria University, Alexandria, Egypt, [7] Department of Chemistry, Abbottabad University of Science and Technology, Abbottabad, Pakistan, [8] Matthias Schleiden Institute, Plant Physiology, Friedrich-Schiller-University Jena, Jena, Germany, [9] Institute of Biotechnology, Fujian Academy of Agricultural Sciences, Fuzhou, China

Plant surfaces are covered with cuticle wax and are the first barrier between a plant and environmental stresses. *Eceriferum* (*CER*) is an important gene family involved in wax biosynthesis and stress resistance. In this study, for the first time, 34 *CER* genes were identified in the passion fruit (*Passiflora edulis*) genome, and PeCER proteins varied in physicochemical properties. A phylogenetic tree was constructed and divided into seven clades to identify the evolutionary relationship with other plant species. Gene structure analyses revealed that conserved motifs ranged from 1 to 24, and that exons ranged from 1 to 29. The *cis*-element analysis provides insight into possible roles of *PeCER* genes in plant growth, development and stress responses. The syntenic analysis revealed that segmental (six gene pairs) and tandem (six gene pairs) gene duplication played an important role in the expansion of *PeCER* genes and underwent a strong purifying selection. In addition, 12 putative ped-miRNAs were identified to be targeting 16 *PeCER* genes, and *PeCER6* was the most targeted by four miRNAs including ped-miR157a-5p, ped-miR164b-5p, ped-miR319b, and ped-miR319l. Potential transcription factors (TFs) such as ERF, AP2, MYB, and bZIP were predicted and visualized in a TF regulatory network interacting with *PeCER* genes. GO and KEGG annotation analysis revealed that *PeCER* genes were highly related to fatty acid, cutin, and wax biosynthesis, plant-pathogen interactions, and stress response pathways. The hypothesis that most PeCER proteins were predicted to localize to the plasma membrane was validated by transient expression assays of

OPEN ACCESS

Edited by:
Mohammad Anwar Hossain, Bangladesh Agricultural University, Bangladesh

Reviewed by:
Muhammad Azhar Nadeem, Sivas University of Science and Technology, Turkey
Neftali Ochoa-Alejo, Centro de Investigación y de Estudios Avanzados del Instituto Politécnico Nacional, Mexico

***Correspondence:**
Zhimin Lin
linzhimin@faas.cn
Faxing Chen
fxchen@fafu.edu.cn

Specialty section:
This article was submitted to Plant Biotechnology, a section of the journal Frontiers in Plant Science

Received: *17 March 2022*
Accepted: *27 April 2022*
Published: *27 June 2022*

Citation:
Rizwan HM, Waheed A, Ma S, Li J, Arshad MB, Irshad M, Li B, Yang X, Ali A, Ahmed MAA, Shaheen N, Scholz SS, Oelmüller R, Lin Z and Chen F (2022) Comprehensive Genome-Wide Identification and Expression Profiling of Eceriferum (CER) Gene Family in Passion Fruit (Passiflora edulis) Under Fusarium kyushuense and Drought Stress Conditions. Front. Plant Sci. 13:898307. doi: 10.3389/fpls.2022.898307

PeCER32 protein in onion epidermal cells. qRT-PCR expression results showed that most of the *PeCER* genes including *PeCER1*, *PeCER11*, *PeCER15*, *PeCER17,* and *PeCER32* were upregulated under drought and *Fusarium kyushuense* stress conditions compared to controls. These findings provide a foundation for further studies on functions of *PeCER* genes to further facilitate the genetic modification of passion fruit wax biosynthesis and stress resistance.

Keywords: cuticle wax biosynthesis, synteny, gene ontology, micro-RNA, stress conditions

INTRODUCTION

Plant growth and development are significantly affected by different environmental factors such as biotic and abiotic stresses (Pandey et al., 2017; Raza, 2021; Sharif et al., 2021). The plant cuticle is a hydrophobic protective layer covering plant epidermis and is the first barrier between the environment and plants. Epicuticle wax is composed of very-long-chain fatty acids (VLCFAs) and their derivatives such as alkanes, ketones, primary and secondary alcohols, aldehydes, esters, and triterpenes (Zhang et al., 2020). The wax of plant cuticles play an important role in controlling non-stomatal water loss and preventing mechanical damages, ultraviolet (UV) light, pathogens, and other environmental biotic and abiotic stresses (Lewandowska et al., 2020). Plant leaves without wax tend to have high transpiration rate, low chlorophyll content, and inferior CO_2 assimilation ability (Medeiros et al., 2017). According to reports, fruit quality and shelf life are also associated with the development and structure of wax on fruit surfaces (Lara et al., 2019; Ding et al., 2020; Zhang et al., 2021).

Eceriferum (*CER*) genes play an important role in VLCFAs and wax biosynthesis pathways, and have been thoroughly investigated in numerous plant species (Li et al., 2021). The first member, the *CER1* gene, was molecularly characterized in *Arabidopsis* (*AtCER1*) and was discovered to be responsible for the conversion of ultra-long-chain aldehydes into ultra-long-chain alkanes and stimulated under biotic and abiotic stresses (Aarts et al., 1995; Wang et al., 2021). The overexpression of *OsCER1* in rice (*Oryza sativa*) involved the biosynthesis of VLCFAs and alkanes, differentiation of plastids, and pollen development (Ni et al., 2018). Wang et al. (2020) also pointed out that *BnCER1-2* in overexpressed rapeseed (*Brassica napus*) plants stimulated the production of alkanes and improved the tolerance to drought. Sakuradani et al. (2013) found that the *CER22* gene, an allele of *CER1*, was involved in the biosynthesis of cuticular wax alkanes in *Arabidopsis*. *AtCER2* was found to be involved in VLCFA biosynthesis and acyltransferase in C_{28} elongation process (Pascal et al., 2013) as well as in pollen coat and cuticle formation (Haslam et al., 2015). *CER3* was found to be involved in epidermal wax biosynthesis in response to changes in humidity in *Arabidopsis*. *CER3* interacts with *CER1* and catalyzes redox-dependent VLCFAs from very long chain acyl-CoA (Rowland et al., 2007; Kim et al., 2019). *CER4* encodes fatty acyl-CoA that forms alcohol reductase and is involved in the ester reduction pathway for production of *Arabidopsis* epidermal wax. *CER4* has been reported to be expressed in different plant tissues including plant stem, roots, flowers, leaves, and siliques (Rowland et al., 2006). Adenosine triphosphate-binding cassette (ABC) proteins are transporters in endogenous substrates across the plasma and intracellular membranes (Sharom et al., 2011). Epicuticular wax is produced in epidermal cells and transported to the cuticle *via* ABC transporters. Pighin et al. (2004) reported that the *Arabidopsis CER5* gene encodes an ABC transporter, which is required for wax export to the cuticle and localized in the plasma membrane of epidermal cells. The overexpression of the *CER6* gene in *Arabidopsis* showed a significant increase in the production of stem wax (Hooker et al., 2002), as well as in the production of fatty acids from C_{26} to C_{28} (Tresch et al., 2012).

Arabidopsis CER7 mutants participate in wax biosynthesis by reducing the expression level of *CER3/WAX2* and promoting cellular procedures (Hooker et al., 2007). Lü et al. (2009) reported that the *Arabidopsis CER8/LACS* (long-chain acyl-CoA-synthetase-1) mutant showed an overlapping function with *LACS2* in cuticle wax biosynthesis. *CER9* was involved in cuticle biosynthesis and maintained plant water level by encoding the putative E3 ubiquitin ligase in *Arabidopsis* and participating in the signal transduction of abscisic acid (ABA) in seeds and seedlings (Zhao et al., 2014). Zheng et al. (2005) reported that *CER10* was involved in VLCFA biosynthesis, and later on, Ensing et al. (2016) further identified that the *CER10* mutant exhibited an increase in non-stomatal water loss and was tolerant to drought conditions. Pascal et al. (2013) demonstrated that the CER26 and CER2-like proteins were involved in the elongation of VLCFAs and wax biosynthesis. The overexpression of *CER26* mutants exhibited a glossy stem phenotype and C_{30} carbon leading to cuticle wax biosynthesis. *CER60* was involved in VLCFA, which prolonged C_{28} to C_{30} activity and produces trace amounts of VLCFA after expressed in yeast (Hooker et al., 2002; Trenkamp et al., 2004).

Cuticular wax plays an important role in plant biotic and abiotic stresses. Drought is the main type of abiotic stress, limiting the growth and productivity of plants and leading to global food security and terrestrial health (Kumar et al., 2021). The expression levels of *CER* genes were upregulated in response to drought, osmotic, and ABA responses (Xue et al., 2017). The ectopic overexpression of *AtCER1* and *AtCER3* genes in tobacco improved the cuticle wax and reduced water loss under drought stress conditions (Cameron et al., 2006). Wang et al. (2015) reported that the overexpression of cucumber (*Cucumis sativus*) *CsWAX2* homologous to *CER3* increased resistance to drought and pathogens. The biosynthesis of cuticle wax is mediated by different transcription factors

(TFs) and the coordinated expression of multiple related genes (Al-Abdallat et al., 2014). Different TFs have been reported to be involved in the biosynthesis of fatty acids and wax including AP2/ERF (APETALA2/ETHYLENE RESPONSIVE FACTOR), WIN1 (WAX INDUCER1), SHN1 (SHINE1), and WRI1 (WRINKLED1) (Hao et al., 2017).

In addition, micro-RNAs (miRNAs) are non-coding single-stranded RNAs (∼21–30 nucleotides) found in plants and animals. It has been reported that miRNAs play an important role in numerous cellular mechanisms as well as in stress resistance by translational inhibition and/or cleavage of target mRNAs during or after transcription (Yadav et al., 2020). The miRNA, such as trans-acting small interfering RNA (tasiRNA) in *Arabidopsis thaliana* has been reported to be involved in *CER3* silencing during stem wax production (Lam et al., 2015). Similarly, Liu et al. (2019) mentioned that brassica miRNA (bna-miR165a-5p) may be involved in the synthesis of wax by regulating the *BnaA06g40560D* gene. These findings suggested that miRNA might have a significant role in wax biosynthesis by modulating targeted genes. Gene Ontology (GO) is a collection of ideas described in terms that aimed to classify genes on the basis of function and consists of three main classifications, biological processes (GO-BP), cellular component (GO-CC), and molecular function (GO-MF). Using advanced GO terms, functional classification of genes can be conducted on species (Ashburner et al., 2000; Raza et al., 2022). The Kyoto Encyclopedia of Genes and Genomes (KEGG) is a bioinformatics resource for understanding biological functions at genomic levels, and contains network information to present functions in pathways (Masoudi-Nejad et al., 2007).

The *CER* gene family has been identified in different plant species including 29 *CER* family members in jujuba (*Ziziphus jujuba* Mill.) (Li et al., 2021), 10 *CER* family members in apple (*Malus domestica*) (Qi et al., 2019a), and 37 *CER* family members in sunflower (*Helianthus annuus*) (Ahmad et al., 2021). However, the *CER* gene family has not been identified in passion fruit (*Passiflora edulis*). Passion fruit is a perennial climbing vine and is usually cultivated throughout tropical and subtropical regions of the world. Passion fruit is an economically important fruit plant and is well-known for its fresh juice, rich aroma, and distinctive nutritional values (Rizwan et al., 2021). Recently, the passion fruit genome (Ma et al., 2021) has been published. For the first time, a comprehensive genome-wide study was conducted to identify the *CER* genes in the passion fruit genome. Moreover, their *in-silico* prediction of TFs, subcellular localization, evolutionary relationship *via* phylogenic and syntenic analysis, conserved motifs, gene structures, *cis*-regulatory elements, prediction of putative miRNA, and functional annotation analyses were performed. qRT-PCR expression profiles in different passion fruit tissues under drought stress (abiotic stress) and *Fusarium kyushuense* fungal stress (biotic stress) conditions were identified to gain insight into passion fruit *CER* genes. This study provides a foundation for further functional studies on candidate passion fruit *CER* genes to further genetic improvement of passion fruit.

MATERIALS AND METHODS

Passion Fruit CER Gene Identification

In order to perform the genome-wide identification of *CER* genes in passion fruit, all known CER family protein sequences of *Arabidopsis thaliana* (AtCER) were downloaded from The *Arabidopsis* Information Resource (TAIR) database (http://www.Arabidopsis.org), *Malus domestica* (apple, MdCER) (Qi et al., 2019a) from the Phytozome database (https://data.jgi.doe.gov/refine-download/phytozome?organism=Mdomestica&expanded=491), and *Helianthus annuus* (sunflower, HaCER) (Ahmad et al., 2021) and *Ziziphus jujuba* (jujuba, ZjCER) (Li et al., 2021) from National Center for Biotechnology Information (NCBI) (https://www.ncbi.nlm.nih.gov/). The passion fruit protein, CDS (coding DNA sequence), gff, and genome sequence files were downloaded from the passion fruit genome (http://ftp.cngb.org/pub/CNSA/data3/CNP0001287/CNS0275691/CNA0017758/) (Ma et al., 2021). To identify the homologous *CER* genes in the passion fruit genome, BLASTp (Basic Local Alignment Search Tool for proteins) was performed in default mode using the protein sequences in TBtools software package v 1.098726 (https://github.com/CJ-Chen/TBtools/releases/tag/1.098726) (Chen C. et al., 2020).

Physicochemical Features and Phylogenetic Analyses of *PeCER* Genes

Physicochemical features such as molecular weight (MW), CDS length, amino acid (AA) length, instability index (II), aliphatic index (AI), isoelectric point (pl), number of exons and introns (E/I) of *PeCER* genes were evaluated using the ExPASY-Prot online tool (https://web.expasy.org/protparam/) (Gasteiger et al., 2005). Subcellular localization of *PeCER* genes was predicted using CELLO v.2.5 (http://cello.life.nctu.edu.tw) (Yu et al., 2004). Full-length protein sequences of the *CER* genes of *P. edulis*, *A. thaliana*, *M. domestica*, *H. annus*, and *Z. jujuba* were aligned with Molecular Evolutionary Genetics Analyses (MEGA) software v 10.1.8 (https://www.megasoftware.net/) (Kumar et al., 2008) and were used for phylogenetic analyses. A neighbor-joining (NJ) tree was constructed using the MEGA software with 1,000 bootstrap replicates, and all other parameters were set to default. The iTOL web tool (https://itol.embl.de/login.cgi) (Letunic and Bork, 2007) was used to visualize the phylogenetic tree and divide it into clades. Passion fruit genomic files were used to investigate the distribution of *PeCER* genes on all passion fruit chromosomes with the TBtools software (Chen C. et al., 2020). Moreover, the online SIAS (Sequence Identity and Similarity) (http://imed.med.ucm.es/Tools/sias.html) tool was used to perform pairwise sequence identification on passion fruit *CER* genes.

Determination of *PeCER* Gene Structures and Motifs Analyses

Gene structure annotations for candidate *CER* genes were retrieved from passion fruit gff genomic files. Conserved motifs of PeCER proteins were recognized by employing the MEME (Multiple Expectation Maximization for Motif Elicitation) online tool (http://meme-suite.org/index.html)

(Bailey et al., 2006), and the number of motifs was set to fifteen. The TBtools software was used to merge and visualize *PeCER* gene structures and conserved motifs from passion fruit.

PeCER Gene *cis*-Regulatory Element Analysis

Two-thousand-bp sequences of upstream regions of all *PeCER* genes were extracted from genomic DNA sequences for the prediction of putative *cis*-regulatory elements. Furthermore, the extracted sequences (2,000 bp) were subjected to the online PlantCARE database (https://bioinformatics.psb.ugent.be/webtools/plantcare/html/) (Lescot, 2002), and a figure was drawn using the TBtools software (Chen C. et al., 2020). The numbers, functions, and sequences of putative *cis*-acting elements of *PeCER* genes were summarized and highlighted into different categories including plant growth and development, phytohormone responses, and stress responses.

PeCER Gene Synteny Analysis and Calculation of Ka/Ks Values

Segmental and tandem duplication provides new insight into family gene development and genome progression. Homologous *PeCER* genes on the same passion fruit chromosome with no more than one intervention gene were considered tandem duplicates, while on other chromosomes were considered segmental duplicates. *PeCER* gene duplicates were identified and visualized according to their physical position on chromosomes in the passion fruit genome. Gene duplication, synteny, and non-synonymous (Ka)/synonymous (Ks) analysis of *CER* genes were performed with the TBtools software (Chen C. et al., 2020). The syntenic relationships of CER genes between *P. edulis, A. thaliana, M. domestica, H. annus*, and *Z. jujuba* were performed by TBtools software using MCScanX toolkit package (Chen C. et al., 2020). Ka and Ks nucleotide substitution rates and Ka/Ks ratios were annotated using TBtools, and divergence time (mya = millions year ago) was calculated as follows: time = Ks/2x (x = 6.38×10^{-9}) (Ma et al., 2021).

PeCER Protein-Protein Interaction, Secondary Structure Prediction, and 3D Modeling

The PeCER protein-protein interaction network was predicted using the online tool STRING 11.0 (https://string-db.org/cgi/input.pl), and the interaction was constructed based on known *Arabidopsis* proteins. The parameters for the STRING tool were set as follows: network type-full STRING network: the meaning of network edge evidence; minimum required interaction score was set to medium confidence parameter (0.4), and the maximum number of interactors to show was no more than 10. The protein secondary structures of PeCER were predicted using SOPMA SECONDARY STRUCTURE PREDICTION METHOD (https://npsa-prabi.ibcp.fr/cgi-bin/npsa_automat.pl?page=npsa_sopma.html) (Geourjon and Deleage, 1995). All 34 PeCER proteins were three-dimensionally modeled (3D) using Phyre2 with default mode (http://www.sbg.bio.ic.ac.uk/phyre2/html/) (Kelley et al., 2015).

Putative miRNAs Targeting *PeCER* Gene Prediction and GO and KEGG Annotation Analyses

The potential miRNA target sites in *PeCER* genes were predicted by the following steps; first, the published mature sequences of passion fruit miRNAs were downloaded (Paul et al., 2020), later the CDS sequences of all the 34 PeCER genes were submitted to the psRNATarget server with default parameters (https://www.zhaolab.org/psRNATarget/) for the prediction of potential miRNAs in PeCER genes. Cytoscape software V 3.9 (https://cytoscape.org/download.html) was used to visualize the interaction network between the predicted miRNAs and *PeCER* target genes. The GO and KEGG annotation analyses were performed by submitting all the 34 PeCER protein sequences to the online database eggNOG (http://eggnog-mapper.embl.de/), and their enrichment and annotation analysis were performed with the TBtools software (Chen C. et al., 2020).

Plant Transcription Factor Regulatory Network Analysis of *PeCER* Genes

The plant TF prediction and regulatory network analysis were performed as described by Zheng et al. (2020) with slight modifications. In order to predict the TFs in the upstream regions of PeCER genes, 1,000-bp nucleotide sequences from the upstream promoter region of *PeCER* genes were extracted from the passion fruit genome and submitted to Plant Transcriptional Regulatory Map (PTRM) (http://plantregmap.gao-lab.org/binding_site_prediction.php) with $p \leq$ 1e-6 (Tian et al., 2020). The transcription factor regulatory network was constructed and visualized with the Cytoscape 3.9 software (Kohl et al., 2011).

PeCER Genes Expression Analyses of Different Tissues

The expression profiles of the 34 identified *PeCER* genes in different tissues of yellow and purple passion fruit cultivars were evaluated through the available public data. The RNA-Seq raw reads were downloaded from the NCBI Sequence Read Archive database (http://www.ncbi.nlm.nih.gov/sra) with the following accession numbers: SRP150688 (Xu et al., 2019) and PRJNA634206 (Wu et al., 2021). The passion fruit sample information for the NCBI raw reads was as follows: peel tissue samples were from yellow (*P. edulis*. Flavicarpa cv Huangjin) and purple (*P. edulis*. Sims cv Tainong) cultivars in the ripening stage, and pulp samples were from fruit developmental stages (fruitlet, green, version, and ripening stages). Root tissue samples were from the purple passion fruit Pingtan-1 cold-tolerant cultivar in two cultivation areas: limestone (L) and sandy dolomite (D) rocky desertification areas. Leaf tissue samples were from yellow Huangjinguo (HJG) cold-sensitive and purple Tainong-1 cold-tolerant cultivars under normal temperature (NT) and chilling stress (CS) conditions.

RNA-Seq raw reads were quality-controlled and filtered with the fastp package (Chen S. et al., 2018) and mapped to the passion fruit reference genome (Ma et al., 2021) using the HISAT2 package (Kim and Langmead, 2015) in Ubuntu wslv 20.04.3 (https://ubuntu.com/wsl). The sequence alignment map (SAM) files were transformed to binary alignment map (BAM) and sorted with the Samtools package (Li et al., 2009). Fragments per kilobase of exon per million mapped fragments (FPKM) values were calculated using the limma and edgeR (Law et al., 2016). Since the FPKM expression values of different tissues of passion fruit were quite different, the FPKM values were converted to $\log^2$FC (FC = fold change), and heatmaps were constructed using the TBtools software.

Plant Material

To study the expression profiles of selected *PeCER* genes under drought stress and normal conditions, seeds of two commercial passion fruit cultivars yellow (*P. edulis.* Flavicarpa cv Huangjin) and purple (*P. edulis.* Sims cv Tainong) were grown in plastic pots filled with peat moss and soil (2:1 ratio). Greenhouse temperature was 25 ± 2°C, photoperiod was 16/8 h, light/dark, and relative humidity was 75%. One-month-old passion fruit seedlings were subjected to dehydration for 10 days and rewatered. Leaf, root, and stem samples from each cultivar with three biological replicates were taken and immediately frozen in liquid nitrogen and were stored at −80°C for further use. Samples from normally watered plants were taken as control. For *F. kyushuense* fungal biotic stress samples, fruits of both cultivars were obtained from a commercial orchard located in Fujian province, China (23°48035.200 N and 117°07008.100 E). Fruits were surface-sterilized and inoculated with *F. kyushuense* pathogenic fungus by following the protocol mentioned in our previous publication (Rizwan et al., 2021). Peel samples from the infected areas were collected at 9th and 12th day post-inoculation (dpi), and fruits without infections were used as control.

RNA Extraction and qRT-PCR Analysis

Total RNA was isolated from frozen samples using a Tiangen mini-RNA extraction kit (Tiangen, China) following the manufacturer's instructions and was quantified with a Thermo Fisher Scientific NanoDrop 2000 UV-Vis spectrophotometer (United States). The first strand of complementary DNA (cDNA) was synthesized using 1 μg of total RNA by Takara PrimeScript™ RT Reagent Kit with a gDNA eraser (TAKARA, China), and cDNA was diluted five times with double distilled water (ddH_2O). The quantitative real-time polymerase chain reaction (qRT-PCR) was carried out on LightCycler® 96 (Roche Applied Science, Penzberg, Germany) in a 20-μl total reaction mixture, which was composed of 10 μl of a TB Green premixed enzyme solution (TAKARA, China), 1 μl each of the forward and reverse primers (100 μM), 1 μl cDNA, and 7 μl ddH_2O. Passion fruit genes encoding *Pe60S*, *PeTIF* (transcription initiation factor), and histone were used as the reference genes for internal control (Munhoz et al., 2015). The qRT-PCR reaction was performed as described below, including preincubation at 95°C for 30 s, followed by 45 cycles at 95°C for 10 s, and 60°C for 30 s. Each reaction was performed with three biological replicates, and relative gene expression levels were normalized with the *Pe60S* gene and calculated using the $2^{-\Delta\Delta CT}$ method (Schmittgen and Livak, 2008). The details of all the primers used in this study can be found in **Supplementary Table S1**.

Subcellular Localization of PeCER32 Protein

To validate the predicted results of the subcellular localization of PeCER proteins, a transient expression assay of the PeCER32 protein was performed in onion epidermal cells with a pCAMBIA1302 vector containing a cauliflower mosaic virus 35S (CaMV35S) promoter and a green fluorescent protein (GFP) tag in the upstream region of the multiple cloning sites (MCS). The full-length CDS (930 bp) of PeCER32 without stop codon was amplified by PCR using the following primers: 5′-ACGGGGGACTCTTGACCATGGATGAAGGTGACTGTAGTTTCTCGC-3′ (*NcoI*) and 5′- TCTCCTTTACTAGTCAGATCTCAGGAATGGGGGCAGTATAATCCA-3′ (*BglII*) (restriction sites are underlined), and cloned into the pMD™ 19-T vector (Cat# 6013; TAKARA, Shiga, Japan). Sequencing (Sangon Biotech Co., Ltd., Shanghai, China) was performed to confirm the positive clones, which were digested with *NcoI* and *BglII* restriction enzymes (TAKARA, China). ClonExpress II One Step Cloning Kit (Cat# C112; Vazyme Biotech Co., Ltd., Nanjing, China) was used for ligation into the *NcoI*-*BglII*-digested pCAMBIA1302 vector and transferred to *Agrobacterium tumefaciens* EHA105 strain for subsequent infection. The resulting plasmids were named CaMV35S-PeCER32-GFP and empty vector CaMV35S-GFP, and they were successfully transformed into onion epidermal cells with the agroinfiltration method. GFP signals were detected and visualized with a laser scanning confocal microscope (Olympus, Tokyo, Japan; FV1200) after 24-72 h of agroinfiltration (Xu et al., 2014).

Statistical Analysis

All statistical analyses were performed by one-way analysis of variance (ANOVA) and figures were generated with GraphPad Prism 8.0.1 (https://www.graphpad.com/scientific-software/prism). Student's *t*-test ($p < 0.05$) was conducted to compare the samples of yellow and purple passion fruits tissues under controlled and stressed condition.

RESULTS

Identification and Physicochemical Properties of *CER* Genes in Passion Fruit

In this study, the known CER protein sequences from different species were blasted with passion fruit genome proteins and after removing redundant, repetitive, and unrecognized sequences, finally, 34 *CER* genes were identified in the passion fruit genome with computational tools. The passion fruit *CER* genes were named from *PeCER*1 to *PeCER*34 based on their positions on chromosomes (**Table 1**). The *PeCER* genes were unevenly distributed on eight out of nine passion fruit chromosomes. Chromosome number 1 contained a comparatively high number of *PeCER* genes (12 genes) followed by chromosome 6 (6 genes), chromosome 5 (5 genes), chromosomes 2 and 8 (4 genes on

TABLE 1 | Physicochemical features of *PeCER* genes.

Gene ID	Gene name	Chr*	Genomic position	CDS (bp)	A.A* (bp)	M.W*	pI*	II*	Ai*	GR-AVY*	E:I*	SCL*
*PeCER*1	ZX.01G0006120	1	16013784:16016240-	741	246	28.2	7.4	46.1	96.8	0.02	5:4	pm
*PeCER*2	ZX.01G0019790	1	26796949:26798567+	846	281	32.6	10.1	32.1	84.0	−0.41	6:5	mit
*PeCER*3	ZX.01G0019860	1	26843466:26844659+	849	282	32.0	9.8	30.1	104.4	−0.10	5:4	mit
*PeCER*4	ZX.01G0024040	1	30497870:30500240+	1,533	510	57.4	9.4	40.9	95.4	−0.08	2:01	pm
*PeCER*5	ZX.01G0024770	1	31123019:31125903+	774	257	29.7	7.3	37.3	101.6	0.15	2:1	pm
*PeCER*6	ZX.01G0031680	1	36909208:36910698+	1,491	496	56.1	9.4	40.5	100.2	0.02	1:00	pm
*PeCER*7	ZX.01G0039150	1	41610479:41619444–	4,395	1,464	163.5	6.1	43.1	104.6	0.21	21:19	pm
*PeCER*8	ZX.01G0039870	1	42004537:42005907+	1,371	456	51.2	8.8	34.1	91.7	−0.06	1:00	pm
*PeCER*9	ZX.01G0112910	1	220335704:220337194+	1,491	496	56.1	9.0	40.1	97.7	0.01	1:00	pm
*PeCER*10	ZX.01G0116460	1	222578824:222581518+	1,572	523	59.3	9.1	38.9	89.3	−0.14	2:01	pm
*PeCER*11	ZX.01G0124790	1	231570306:231574170–	879	292	33.8	6.6	41.5	90.8	0.03	5:4	pm
*PeCER*12	ZX.01G0136790	1	267272100:267274802–	933	310	36.0	9.6	51.4	86.4	−0.11	4:03	pm
*PeCER*13	ZX.02G0014730	2	59578861:59589952+	5,157	1,718	199.3	8.8	39.0	93.3	−0.07	28–29	pm
*PeCER*14	ZX.02G0015130	2	59791229:59797692–	2,367	788	90.9	7.0	40.4	85.1	−0.21	14:13	pm
*PeCER*15	ZX.02G0015160	2	59820344:59821338–	549	182	20.6	9.5	38.9	107.6	−0.17	5:4	mit
*PeCER*16	ZX.02G0018030	2	61499311:61505027+	1,698	565	63.6	8.6	40.5	78.2	−0.25	9:8	pm
*PeCER*17	ZX.03G0021830	3	111603305:111606334+	711	236	27.4	8.8	37.6	86.7	0.14	6:5	pm
*PeCER*18	ZX.04G0004390	4	5557716:5565015+	1,968	655	73.5	8.9	40.9	95.9	−0.06	5:04	pm
*PeCER*19	ZX.04G0008120	4	18732041:18739420+	1,584	527	59.4	6.1	47.5	104.3	0.01	11:10	pm
*PeCER*20	ZX.04G0030740	4	111909920:111921418–	4,173	1,390	155.2	8.9	44.6	93.3	0.08	19:18	pm
*PeCER*21	ZX.04G0031300	4	113389251:113392492+	1,263	420	48.4	8.8	43.5	101.0	0.38	8:7	pm
*PeCER*22	ZX.04G0031310	4	113392969:113394946+	675	224	25.0	8.5	33.4	93.1	−0.06	5:4	cyt
*PeCER*23	ZX.05G0019760	5	112330539:112336467+	2,028	675	76.2	5.9	35.7	86.5	−0.21	19:18	cyt
*PeCER*24	ZX.06G0000900	6	3463805:3474069–	2,904	967	108.4	9.9	51.1	84.7	−0.21	16:15	pm
*PeCER*25	ZX.06G0022930	6	107622892:107626542–	1,905	634	73.8	8.5	36.1	95.0	0.01	10:9	pm
*PeCER*26	ZX.06G0022950	6	107650045:107652816–	1,644	547	63.5	8.8	34.3	94.4	−0.03	7:6	pm
*PeCER*27	ZX.06G0023310	6	107833067:107834602–	1,536	511	57.0	9.2	38.3	96.2	−0.01	1:00	pm
*PeCER*28	ZX.06G0024510	6	108511963:108517390–	3,390	1,129	126.0	5.9	36.8	110.1	0.34	8:07	pm
*PeCER*29	ZX.06G0027150	6	110954426:110966330–	4,227	1,408	157.6	9.1	45.9	91.1	0.07	15:14	pm
*PeCER*30	ZX.08G0019030	8	49562396:49563948+	738	245	27.9	9.7	52.2	82.1	−0.04	5:4	pm
*PeCER*31	ZX.08G0019680	8	50041436:50043895–	1,080	359	42.4	8.8	48.5	95.9	0.00	4:3	pm
*PeCER*32	ZX.08G0029780	8	57784308:57787580–	933	310	36.2	9.6	48.7	85.5	−0.08	4:03	pm
*PeCER*33	ZX.08G0032230	8	61391202:61394104–	738	245	28.2	7.2	37.6	92.3	0.05	3:2	pm
*PeCER*34	ZX.09G0020720	9	69749686:69754295–	711	236	27.5	9.0	37.6	82.5	0.10	6:5	pm

Chr, chromosome NO; A.A*, amino acid/protein length; M.W*, molecular weight (KDa); pI*, isoelectric point; II*, instability index; Ai*, aliphatic index; GRAVY*, grand average of hydropathicity; E:I*, number of exons:introns; SCL*, subcellular localization; pm*, plasma membrane; mit, mitochondrial; cyt, cytoplasmic. Positive (+) and negative (–) signs indicate the presence of a gene on the positive and negative strands of that particular marker at genome location.*

each); chromosomes 3, 5, and 9 contained only one *PeCER* gene (**Table 1**, **Supplementary Figure S1**). The detailed information of all the 34 *PeCER* genes is available in **Table 1**, and protein sequences have been provided in **Supplementary Table S2**. The protein analysis shows that the length of the PeCER protein varied from 182 (PeCER15) to 1,718 bp (PeCER13), that the CDS length ranged from 549 (*PeCER*15) to 5,157 bp (*PeCER*13), and that the protein molecular weight ranged from 20.64 (PeCER15) to 199.26 KDa (PeCER13) (**Table 1**). The isoelectric point of proteins ranged from 5.92 (PeCER23) to 10.07 (PeCER2), the protein instability index varied from 30.11 (PeCER3) to 52.21 (PeCER30), and the aliphatic index of proteins varied from 82.11 (PeCER30) to 110.12 (PeCER28). The GRAVY ranged from −0.25 (PeCER16) to 0.383 (PeCER21). The number of exons varied from 1 (PeCER6, PeCER8, and PeCER9) to 28 (PeCER13). The subcellular location prediction showed that most of the PeCER proteins were associated with the plasma membrane except for PeCER2, PeCER3 and PeCER15 (mitochondrial), and PeCER22 and PeCER23 (cytoplasmic) (**Table 1**).

Phylogenetic Analysis of *CER* Genes

One hundred and forty-four CER protein sequences from *P. edulis* (PeCER), *A. thaliana* (AtCER), *M. domestica (*MdCER), *H. annus* (HaCER), and *Z. jujuba* (ZjCER) were used to assess the evolutionary relationship and construct the phylogenetic tree (all the protein sequences used for the phylogenetic tree has been provided in **Supplementary Table S2**). The protein sequences were aligned, and a neighbor-joining tree was constructed by grouping into seven clades based on sunflower *HaCER* (Ahmad et al., 2021) (**Figure 1A**). The results showed that clade 1 comprised of 24 *CER* genes (3 *PeCER*s, 4 *AtCERs*, 7 *HaCERs*, 6 *MdCERs*, and 4 *ZjCERs*); clade 2 comprised of 16 genes (3 *PeCER*s, 4 *AtCERs*, 1 *ZjCERs*, 3 *MdCERs*, and 5 *HaCERs*); clade 3 comprised of 37 genes (7 *PeCER*s, 6 *AtCERs*, 4 *HaCERs*, 7 *MdCERs*, and 13 *ZjCERs*); clade 4 comprised of 12 genes (6 *PeCER*s and 6 *ZjCERs*); clade 5 comprised of 22 genes (8 *PeCER*s, 6 *AtCERs*, 6 *HaCERs*, and 2 *ZjCERs*); clade 6 comprised of 15 genes (6 *PeCER*s, 4 *HaCERs*, 2 *AtCERs*, and 3 *ZjCERs*); clade 7 comprised of 18 genes (1 *PeCER*, 9 *AtCERs*, 7 *HaCERs*, and 1 *MdCER*) (**Figure 1A**). Each clade varied in the number of genes; among them, clade 2 was found to be the largest group containing the highest number of *CER* genes (37 genes) followed by clade 1 (24 genes), whereas clade 4 was the smallest group that contained only 12 *CER* genes (**Figure 1A**). *PeCER* genes also varied in their unequal distribution among the different clades such as the highest number of *PeCER* genes (8 genes) found in clade 5 followed by clade 3 (7 genes), and clade 7 contained only 1 *PeCER* gene (**Figure 1A**). These alignment and evolutionary results revealed that the PeCER proteins shared greater homology with *A. thaliana* and *Z. jujuba* compared with *H. annus* and *M. domestica* CER proteins (**Figure 1A**). In terms of pairwise gene similarity percentage index in the *PeCER* genes, the similarity index also varied from 2.66 (*PeCER*7/*PeCER*22) to 91.54% (*PeCER*6/*PeCER*9). The results showed that the PeCER6 and PeCER9 proteins showed the highest similarity of 91.54% and were consistent with the phylogenetic results as grouped in the same clade 5 (**Figure 1A**, **Supplementary Table S3**).

PeCER Gene Structure and Motif Analyses

The conserved motifs and exon-intron organization of gene structure were analyzed to further understand the development of the *PeCER* gene family. Furthermore, the conserved motifs among 34 *PeCER* genes were predicted using the online MEME suit, and the range of conserved motifs varied from 1 to 24 (**Figure 1B**). Overall, a total of 15 conserved motifs were predicted among the 34 PeCER proteins (**Supplementary Table S4**). The majority of *PeCER* genes (12 genes) have 8 motifs followed by 3 motifs (4 genes). *PeCER*7 contains 11 motifs, and *PeCER* 15 and *PeCER*16 contain 9 motifs. A maximum of 24 and 10 motifs were recognized in *PeCER*13 and *PeCER*14 respectively, whereas *PeCER*1, *PeCER*17, *PeCER*23, *PeCER*28, *PeCER*30, and *PeCER*31 contained only 1 motif (**Figure 1B**, **Supplementary Table S4**). The genomic structural analysis for exon-intron position in the 34 *PeCER* genes revealed that the number of exon-intron in the identified *PeCER* genes varied from 1 to 29 (**Figure 1C**). Most of the *PeCER* genes contained more than 5 exons, whereas genes such as *PeCER*13, *PeCER*7, *PeCER*20, and *PeCER*24 contained 29, 21, 19, and 16 exons, respectively. For instance, the *PeCER*6, *PeCER*8, and *PeCER*9 genes contained only 1 exon and no intron (**Figure 1C**). These findings stated that variation of motifs and exon-intron during the evolutionary process occurred instantaneously in *PeCER* gene family development, and that *PeCER* genes that contain the same features may have the same function.

PeCER Gene *cis*-Regulatory Element Analyses

To further understand the possible role of *PeCER* genes in response to biotic and abiotic stresses, the *cis*-regulatory elements of *PeCER* genes from 2,000 bp upstream promoter regions were analyzed (**Figure 2**). The promoters of *PeCER* genes mainly comprised four categories of *cis*-regulatory elements including plant growth- and development-responsive (six different types of *cis*-elements including CAT-box, circadian, GCN4-motif, O2-site, RY-element, and CCGTCC motif), phytohormone-responsive (twelve different types of *cis*-elements including ABRE, AuxRR-core, CGTCA-motif, ERE, GARE-motif, P-box, TATC-box, TCA-element, TGA-box, TGA-element, JERE, and TGACG-motif), light-responsive (nineteen different types of *cis*-elements including 3-AF1 binding site, ACE, AE-box, AT1-motif, ATC-motif, ATCT-motif, TCT-motif, Box 4, chs-CMA1a/2a/2b/2c, GA-motif, GATA-motif, G-Box, GT1-motif, GTGGC motif, I-box, LAMP-element, MRE, Sp1, and TCCC-motif), and stress-responsive including anaerobic induction, MYB binding site, and wound and temperature-responsive, (eight different types of *cis*-elements: ARE, GC-motif, LTR, MBS, TC-rich repeats, CARE, WUN-motif, and CCAAT-box) elements (**Figure 2A**, **Supplementary Table S5**). In terms of *cis*-element categories, the light-responsive category contains the maximum number of *cis*-elements followed by phytohormone-responsive and stress-responsive, while the lowest number of *cis*-elements was found in the plant growth and development-responsive

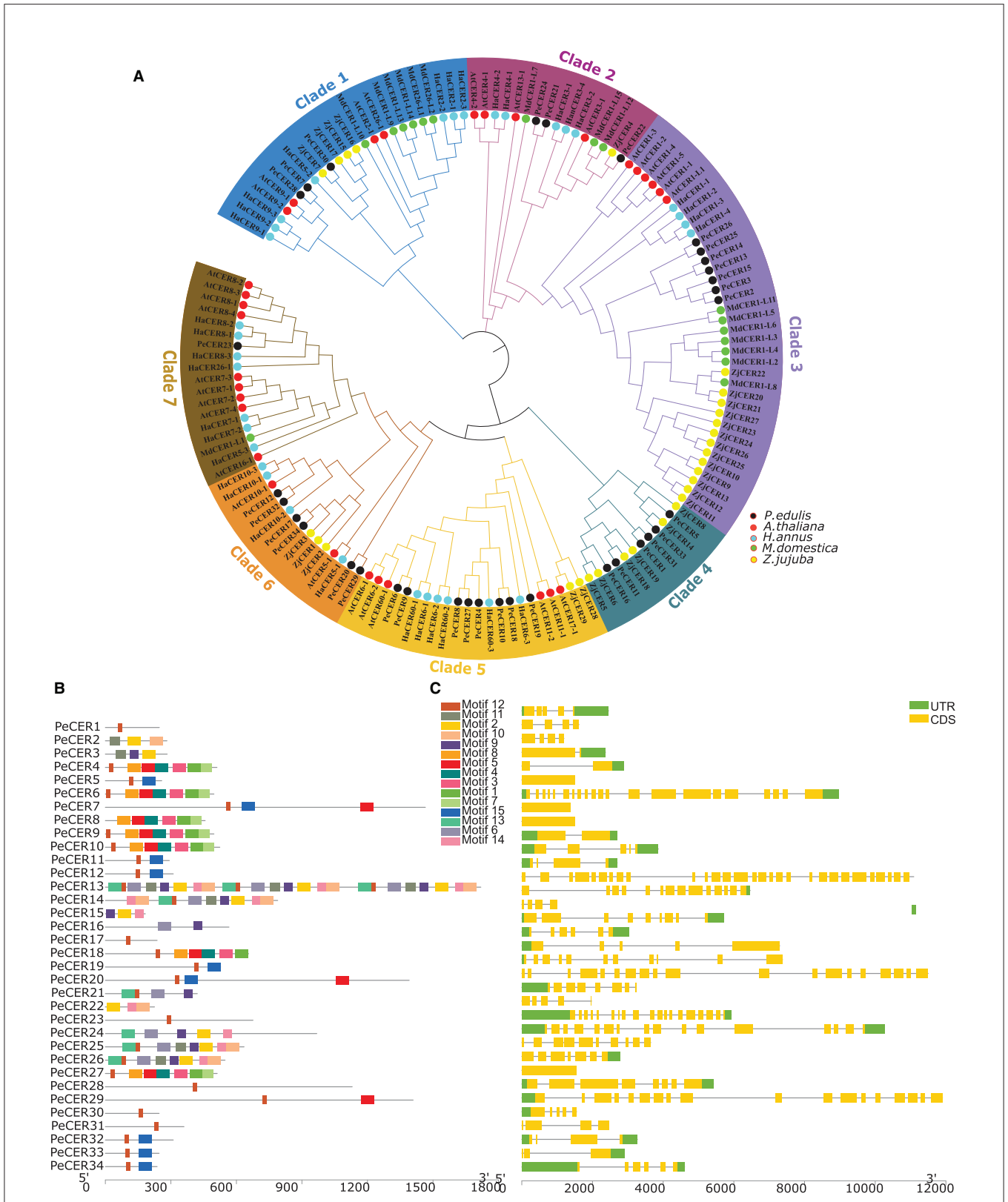


FIGURE 1 | (A) Unrooted neighbor-joining phylogenetic tree among *P. edulis, A. thaliana, M. domestica, H. annus,* and *Z. jujuba* CER amino acid sequences with 1,000 bootstraps constructed with MEGA software v10.1.8. The protein sequences of PeCER, AtCER, HaCER, MdCER, and ZjCER are represented by black, red, aqua, green, and yellow color circles, respectively. **(B)** Conserved motifs were represented *via* boxes, and different colors represent different motifs. **(C)** *PeCER* gene structures; yellow color indicates the exons, green color shows the untranslated 5′ and 3′-regions, and gray color indicates the introns.

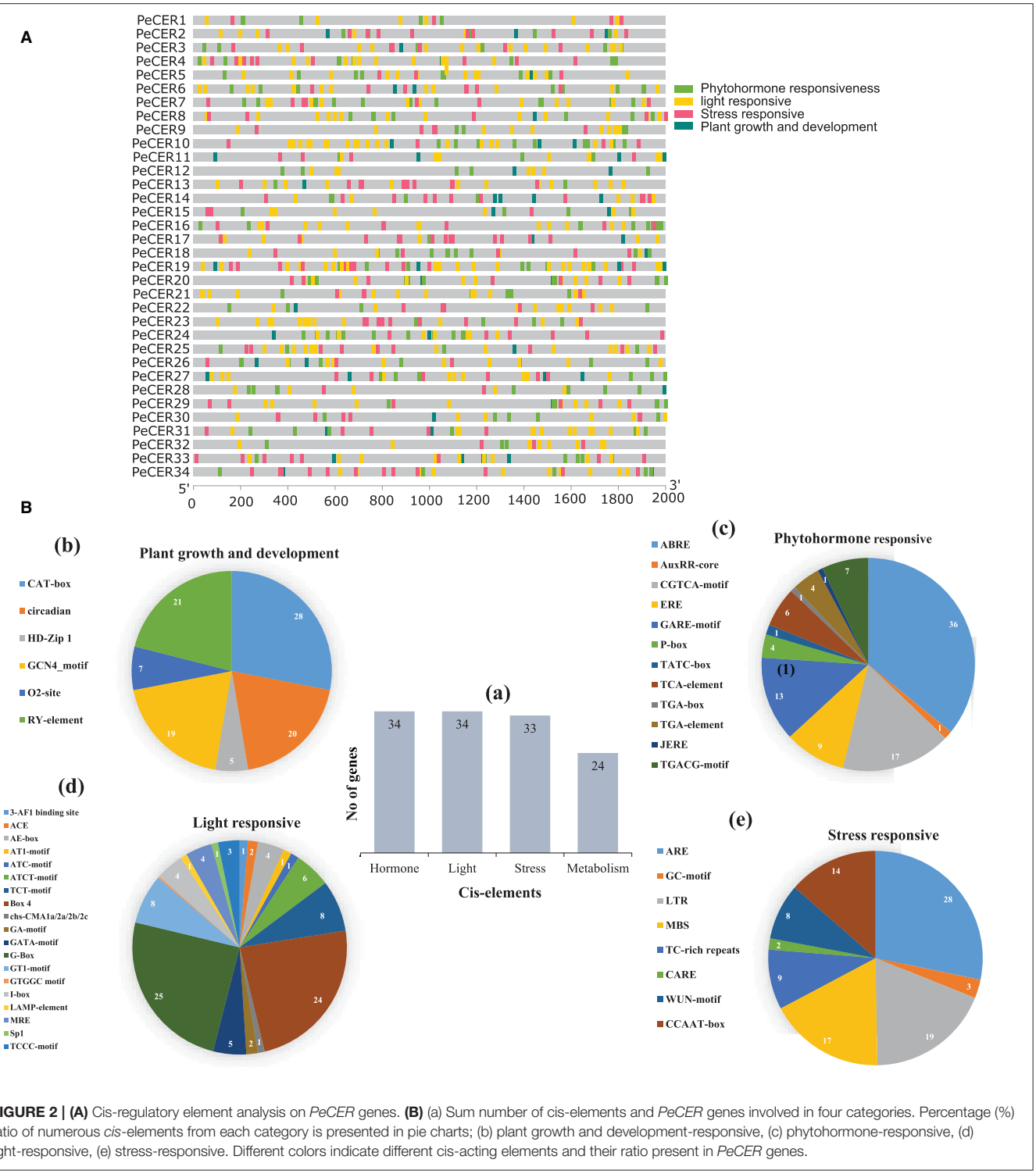


FIGURE 2 | (A) Cis-regulatory element analysis on *PeCER* genes. **(B)** (a) Sum number of cis-elements and *PeCER* genes involved in four categories. Percentage (%) ratio of numerous *cis*-elements from each category is presented in pie charts; (b) plant growth and development-responsive, (c) phytohormone-responsive, (d) light-responsive, (e) stress-responsive. Different colors indicate different cis-acting elements and their ratio present in *PeCER* genes.

category (**Figure 2B**). In addition, the *PeCER* genes were classified based on the number of genes involved in each category (**Figure 2B**a). It was found that all the 34 *PeCER* genes were involved in phytohormones and light-responsive, 33 *PeCER* genes were involved in stress-responsive, while only 24 *PeCER* genes were involved in plant growth and development responsiveness (**Figure 2B**a). These results proposed that transcript profiling of *PeCER* may vary among hormones and stress-responsive. The plant growth and development category was further classified into four subcategories (meristem,

metabolism, seed related, and circadian). Meristem-related *cis*-elements include CAT-box and GCN4-motifs, which belong to meristem expression.

The metabolism-related *cis*-element includes O2-sit and seed, and the circadian-related *cis*-element includes RY-element. In the plant growth and development category, the highest number of cis-elements (28%) consisted of CAT-box, followed by circadian (20%), and the lowest (5%) consisted of HDzip1 (**Figure 2B**b). The phytohormone-responsive category comprised of ABRE (abs*cis*ic acid-responsive), AuxRR-core (auxin-responsive), ERE (ethylene-responsive), GARE-motif, P-box, TATC-box (gibberellin responsive); TCA-element (salicylic acid-responsive); TGA-element and TGACG-motif (methyl jasmonate responsive) *cis*-elements. The highest number of *cis*-elements from the phytohormone category comprised of ABRE at 36% followed by CGTCA-motif at 17%, whereas the AuxRR-core, TATC box, and TGA box were the lowest, containing only 1% *cis*-elements (**Figure 2B**c). The light-responsive category contained the 3-AF1 binding site, ACE, AE-box, AT1-motif, ATC-motif, ATCT-motif, TCT-motif, Box 4, chs-CMA1a/2a/2b/2c, GA-motif, GATA-motif, G-Box, GT1-motif, I-box, LAMP-element, MRE, Sp1, and TCCC-motif *cis*-elements. The highest light-responsive category comprised of only G-Box (25%) followed by Box-4 (24%), while AT1-motif and ATC-motif were the lowest and comprised of only 1% (**Figure 2B**d). The stress-responsive category contained ARE, GC-motif, LTR, MBS, TC-rich repeats, CARE, WUN-motif, and CCAAT-box *cis*-elements; among which, ARE comprised the highest number (28%) followed by LTR and MBS (19 and 17%), while CARE contained only 2% (**Figure 2B**e). The detailed information about *cis*-regulatory elements in the passion fruit *CER* genes has been provided in **Supplementary Table S5**.

Synteny Analysis of *PeCER* Genes

The expansion and evolutionary mechanism of the *PeCER* gene family in the passion fruit genome and genomes of other species were further investigated by synteny analysis. The tandem and segmental duplication analysis of the *PeCER* genes was performed to elucidate the duplication of the *PeCER* genes. There were eight duplicated *PeCER* gene pairs, among which six gene pairs were segmentally duplicated on chromosomes 1, 2, 4, 6, and 8, whereas two *PeCER* gene pairs were tandem-duplicated on chromosomes 1 and 2. *PeCER*13 and *PeCER*25 were duplicated twice (**Figure 3A**, **Supplementary Table S6**). These findings suggested that gene duplication has played an important role in *PeCER* gene family development in the passion fruit genome.

To determine the selection pressure and evolution rate among duplicated genes, Ka/Ks ratio is an indicator. Generally, if Ka/Ks ratio is more than 1, it indicates that genes have undergone a positive selection, a ratio <1 indicates purifying selection, while a ratio equal to 1 indicates neutral selection. The details about Ka and Ks values and Ka/Ks ratios of duplicated *PeCER* gene pairs are shown in **Supplementary Table S6**. Overall, all the segmental and tandem duplicated *PeCER* gene pairs exhibited a Ka/Ks ratio <1, indicating that all the duplicated *PeCER* genes underwent purifying selection (**Supplementary Table S6**). Furthermore, the time of divergence among the duplicated genes was measured based on a substitution rate of 6.38×10^{-9} substitutions per site per year (Ma et al., 2021). The results showed that the rate of divergence process among the tandem and segmental *PeCER* genes was estimated to be 1.12 to 20.78 mya (**Supplementary Table S6**). It can be concluded that the evolutionary mechanism of *PeCER* genes shows maintenance in the process of passion fruit domestication.

In addition, a comprehensive synteny analysis of *P. edulis CER* genes with *CER* genes of other species, including *A. thaliana*, *M. domestica,* and *Z. jujuba,* was performed by alignment and chromosomal localization (**Supplementary Table S7**). The results showed that out of the 34 *PeCER* genes, 10 *PeCER* were paired with 12 *CER* genes from the above-mentioned species, and that the 10 *PeCER* genes were located on passion fruit chromosomes 1, 6, and 8 (**Figure 3B**, **Supplementary Table S8**). The presence of six *PeCER* gene pairs with *AtCER* (*PeCER*9:*AtCER60*-1, *PeCER*9:*AtCER6*-1, *PeCER*6:*AtCER6*-1, *PeCER*6:*AtCER60*-1, and *PeCER*32:*AtCER10*-1) (**Figure 3B**, **Supplementary Table S8**), three *PeCER* gene pairs with *MdCER* (*PeCER*3:*MdCER1*-L2, *PeCER*2:*MdCER1*-L6, and *PeCER*24:*MdCER1*-L12), and five *PeCER* gene pairs with *ZdCER* (*PeCER*3:ZjCER9, *PeCER*5:ZjCER8, *PeCER*30:ZjCER7, *PeCER*33:ZjCER14, and *PeCER*30:ZjCER15) was detected and visualized with Circos (**Figure 3B**, **Supplementary Table S8**). Overall, the *PeCER* and *AtCER* genes showed a greater degree of synteny than the other species, indicating that they might belong to the same ancestors with the same functions, which required further study.

Furthermore, a multicollinearity analysis of *P. edulis CER* genes with genomes of *A. thaliana*, *M. domestica, H. annus,* and *Z. jujuba* species was performed to reveal the robust orthologs in the genomes of these species. Multiple collinear gene pairs between the aforementioned species were found to be inferred and have undergone lineage-specific amplification of genetic copies (**Figure 4**). The multicollinearity results showed that the highest collinearity was found between *P. edulis* with *M. domestica* (43 collinear genes) followed by *P. edulis* with *H. annus* and *A. thaliana* (26 collinear genes), whereas the least collinearity was found between *P. edulis* with *Z. jujuba* (16 collinear genes) (**Figure 4**, **Supplementary Table S9**). *P. edulis* chromosome 1 shared the maximum collinear genes among *M. domestica* (20 genes), *H. annus* (14 genes), *A. thaliana* (13 genes), and *Z. jujuba* (7 genes) (**Figure 4**, **Supplementary Table S9**). These findings suggest that the *CER* genes were conserved and might have the same ancestors besides the duplication or loss of *CER* genes.

Protein-Protein Interaction and 3D Modeling of PeCER

The PeCER protein-protein interaction network was constructed based on *Arabidopsis* orthologous proteins. PeCER proteins with highest homologous similarity to *Arabidopsis* proteins were selected as STRING proteins. All the 34 PeCER proteins have an association with known *Arabidopsis* proteins (**Figure 5A**, **Supplementary Table S10**). PeCER proteins belonging to different groups may have diverse functions. PeCER2,

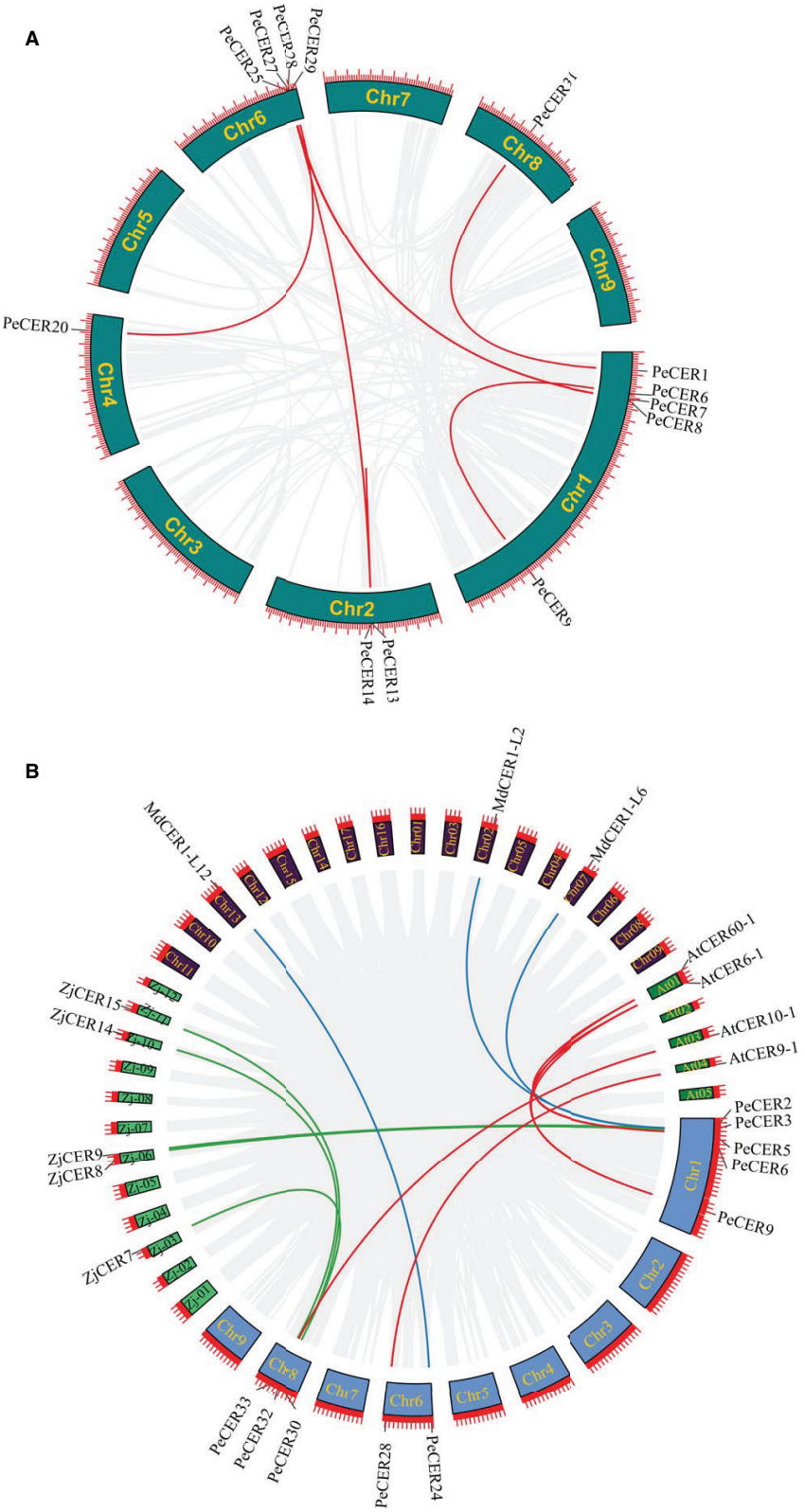


FIGURE 3 | Circos illustrations of *PeCER* gene duplication. **(A)** Gene duplication of *CER* genes in *P. edulis*. The background gray lines show all the syntenic blocks in the passion fruit genome, and the red lines show segmental or tandem duplication link regions among the *PeCER* genes. The approximate location of *PeCER* genes were labeled with a short gray line outside with gene names. **(B)** Orthologous of *P. edulis CER* genes with *A. thaliana*, *M. domestica*, and *Z. jujuba CER* genes.

(Continued)

FIGURE 3 | Chromosomes of *P. edulis are* represented with Chr1-Chr9, *A. thaliana* with At01-At05, *M. domestica* with Chr01-Chr17, and *Z. jujuba* with Zj-01 to Zj-12. The background gray lines show all the syntenic blocks in different genomes, blue lines represent the syntenic relationship among *P. edulis* and *M. domestica CER* genes, red lines represent the syntenic relationship among *P. edulis* and *A. thaliana* genes, and green lines represent the syntenic relationship among *P. edulis* and *Z. jujuba* genes.

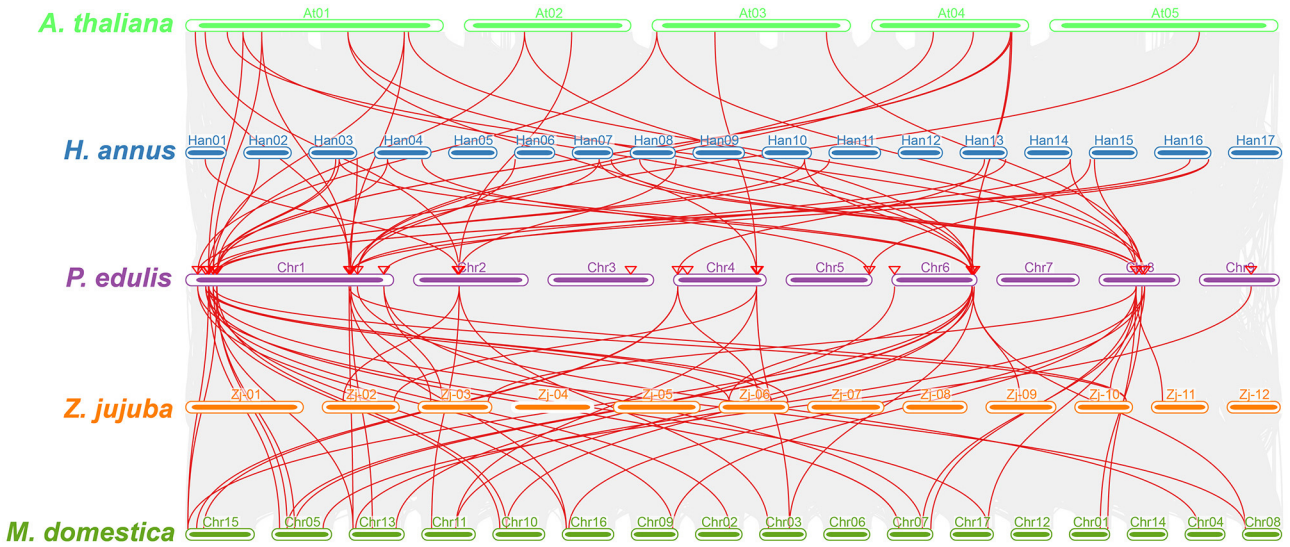


FIGURE 4 | Multicollinearity analysis of the P. edulis CER genes with genomes of the *A. thaliana*, *M. domestica*, *H. annus*, and *Z. jujuba* species. The red lines represent the CER syntenic genes among *P. edulis*, *A. thaliana*, *M. domestica*, *H. annus*, and *Z. jujube* genomes, and the gray lines in the background represent all orthologous genes from the genomes of *P. edulis* and other species.

PeCER3, PeCER13, PeCER14, PeCER15, PeCER25, and PeCER26 were homologous with AtCER1; PeCER21 and PeCER28 with AtCER9; PeCER32 with AtCER10; PeCER 23 with AtLACS1; PeCER22 and PeCER24 with AtCER3, and they all had a strong interaction among them. PeCER1 and PeCER31 were homologous with AtSTE1 and interacted with AtDWF1, AtDWF5, AtSMO2-1, AtSMO2-2, AtSMO2-3, and AtFAH1/T29F13.2 (**Figure 5A**). PeCER2, PeCER3, PeCER14, PeCER15, PeCER25, and PeCER26 were homologous with AtCER1; PeCER4 and PeCER8 were homologous with AtKCS4; PeCER6 and PeCER9 with AtKCS6; PeCER18 with AtKCS11; PeCER10 with AtKCS20, and they had a strong interaction between them (**Figure 5A**). PeCER5 and PeCER33 showed homology with AtSBH1 and interacted with AtCER10, AtDWF5 and AtFAH1/T29F13.2. PeCER proteins and that showed a strong interaction with known *Arabidopsis* proteins and might have similar functions as in *Arabidopsis*. The higher the interaction coefficient, the thicker the line between proteins and vice versa (**Figure 5A**, **Supplementary Table S10**).

A protein secondary structure analysis was performed, which generally consists of alpha helices, extended strands, beta turns, and random coils (**Supplementary Table S11**). Among all the 34 PeCER proteins, alpha helix accounted for the largest percentage of secondary structures ranging from 31.96 to 57.2% (PeCER13, PeCER19) followed by random coils from 25.19 to 40.95% (PeCER19, PeCER24), and extended strands from 11.43 to 25.68% (PeCER33 and PeCER15), whereas beta turns ranged from 1.95 to 9.29% (PeCER28 and PeCER15) (**Supplementary Table S11**). Additionally, the 3D structures and models of all the 34 PeCER proteins were predicted by the Phyre2 online server with default mode (**Figure 5B**).

Templates were used for the predicted PeCER protein models such as template c4zr0A was used in the PeCER1, PeCER5, PeCER11, PeCER17, PeCER30, PeCER31 and PeCER33 protein models; template c6jzuA was used in the PeCER2, PeCER3, PeCER13, PeCER14, PeCER15, PeCER21, PeCER22, PeCER24, PeCER25, and PeCER26 protein models; template c4jatB was used in the PeCER6 and PeCER9 protein models; template c4zr0A in the PeCER34 model; template c5mstA in the PeCER23 model; template c7c83A in the PeCER12 and PeCER29 models; template d2cq0a1 in the PeCER16 model; template c1u0mA in the PeCER10 model; templatec6hb2B in the PeCER19 model; template c2d8sA in the PeCER7 and PeCER28 models; template c3wy0A in the PeCER8 model; template c4jatB in the PeCER4 and PeCER27 models; template c7p06A in the PeCER20 model; template c7c83A in the PeCER32 model; template c6z00B in the PeCER18 model. All the PeCER proteins had flexible structures due to the existence of coils (**Figure 5B**). Based on our results, it was proposed that *CER* genes from individual genomes might be ancestrally similar to each other or initial differences may have been stabilized during long-term domestication, leading to changes in protein structure and function.

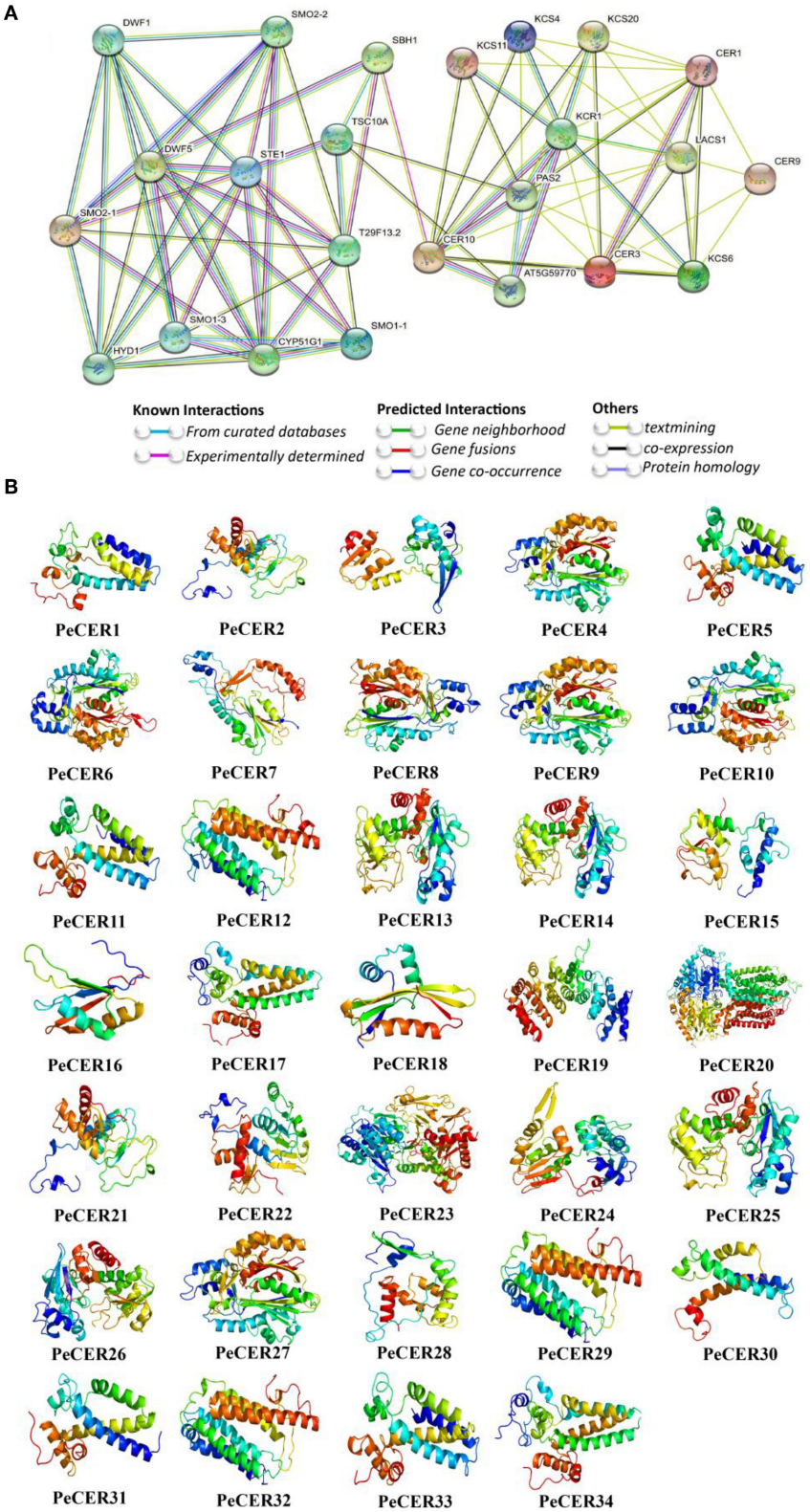


FIGURE 5 | Protein-protein interaction of PeCER proteins based on known *Arabidopsis* protein orthologous. **(A)** The network was constructed using the online STRING software. The proteins were displayed at network nodes with 3D structure of the proteins in nodes, and the line colors indicate different data sources. **(B)** Predicted 3D models of PeCER proteins. 3D models were constructed using the online Phyre2 server with default mode.

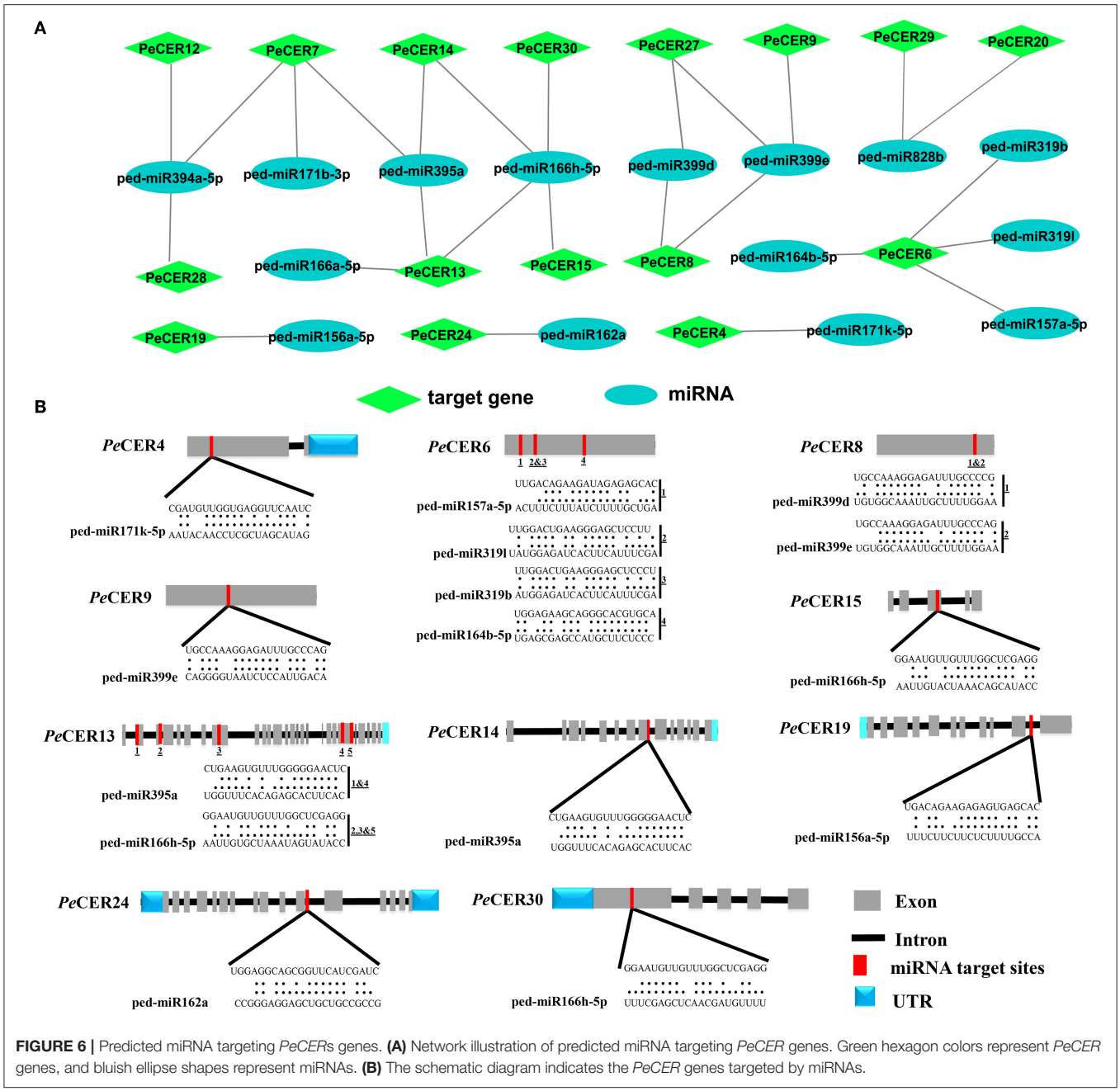


FIGURE 6 | Predicted miRNA targeting *PeCER*s genes. **(A)** Network illustration of predicted miRNA targeting *PeCER* genes. Green hexagon colors represent *PeCER* genes, and bluish ellipse shapes represent miRNAs. **(B)** The schematic diagram indicates the *PeCER* genes targeted by miRNAs.

Genome-Wide Prediction of Potential miRNAs Targeting *PeCER* Genes

During the past few decades, various investigations have reported that the miRNAs induced the regulation of stresses, plant development, and signal transduction. Therefore, to better understand the regulatory mechanism of miRNAs involved in the regulation of *PeCER* genes, 12 putative miRNAs targeting 16 *PeCER*s genes were identified, as shown in the network illustration (**Figure 6A**) and the schematic diagrams indicating the *PeCER* genes targeted by miRNAs (**Figure 6B**). The detailed information on the putative miRNA targeting sites and the *PeCER* genes has been provided in **Supplementary Table S12**. The results showed that two members of the ped-miR171 family targeted two genes including *PeCER4* and *PeCER7*; one member of the ped-miR157 family targeted one gene, *PeCER6*; one member of the ped-miR164 family targeted one gene, *PeCER6*; two members of the ped-miR319 family targeted one gene, *PeCER6*; one member of the ped-miR395 family targeted three gene including, *PeCER7*, *PeCER13*, and *PeCER14*; one member of the ped-miR394 family targeted three gene

including, *PeCER*7, *PeCER*12, and *PeCER*28; two members of the ped-miR399 family targeted three gene including, *PeCER*8, *PeCER*9, and *PeCER*27; two members of the ped-miR166 family targeted three gene including, *PeCER*13, *PeCER*14, *PeCER*15, and *PeCER*30; one member of the ped-miR828 family targeted two gene including, *PeCER*20 and *PeCER*29; one member of the ped-miR162 family targeted only *PeCER24* gene (**Figures 6A,B**, **Supplementary Table S12**).

Overall, the prediction results show that the *PeCER7* gene was targeted by three miRNA families including, ped-miR395a, ped-miR394a-5p, and ped-miR171b-3p; similarly, the *PeCER*13 gene was also targeted by three miRNA families including, ped-miR166h-5p, ped-miR395a, and ped-miR166a-5, whereas the *PeCER*6 gene was targeted by four miRNA families including, ped-miR157a-5p, ped-miR164b-5p, ped-miR319b, and ped-miR319l (**Figures 6A,B**, **Supplementary Table S12**). The expression levels of these predicted miRNAs and their target *PeCER* genes require further studies to better understand their functions in passion fruit.

Transcription Factor Regulatory Network of *PeCER* Genes

The potential TF regulatory network of the *PeCER* genes was identified by extracting 1,000-bp upstream sequences from all the 34 *PeCER* genes, and was analyzed using the PTRM online database. The results showed that there were 2402 TFs from numerous TF families including ERF, TCP, MYB, NACWRKY, BBR-BPC and bHLH, which were involved in the regulation of the 34 *PeCER* genes (**Supplementary Table S13**). Among all the predicted TFs, the most abundant members belonged to the ERF family (1,122), followed by the BBR-BPC (221), TCP (121), MYB (117), and NAC (101) TF families (**Figure 7A**). The least-targeted TF family members belonged to ARR-B (2), EIL (2), VOZ (2), S1Fa-like (1), and NF-YB (1) (**Figure 7A**). All the *PeCER* genes were targeted by numerous TFs families members such as *PeCER*33 that interacts with 108, *PeCER*14 with 83, *PeCER*15 with 81, and *PeCER*27 with 56 TF families. In addition, the *PeCER33* gene was the one targeted by most TFs (762), followed by *PeCER15* (267). Among the targeted TF families, the ERF family was dominated by 680 and 216 members in *PeCER33* and *PeCER15* genes (**Figure 7B**). The TF regulatory network of all the 34 *PeCER* genes are shown in **Figure 7A**, and the networks of the top five highly targeted *PeCER* genes are shown in **Figure 7B**, respectively. Fatty acids and wax biosynthesis-related TFs belonging to different TF families were also predicted in this study including ERF, AP2, bHLH, and MYB. Different TFs involved in plant growth and development including TCP, bHLH, BBR-BPC, WRKY, LBD, and AP2 were also found in the *PeCER* genes. In addition, phytohormone-related TFs were also identified, including ERF and ARF. Interestingly, ERF and AP2 TFs were shown to be universally distributed in most of the *PeCER* genes (**Figure 7**, **Supplementary Table S13**).

GO and KEGG Enrichment Analyses of *PeCER* Genes

GO and KEGG function annotation and enrichment analyses of passion fruit *PeCER* genes were performed. The GO function annotation and enrichment analysis was classified into the molecular function (MF), cellular component (CC), and biological process (BP) classes. The detailed annotation results and highly enriched terms of MF, CC, and BP have been provided in **Supplementary Tables S14A,B**. The results showed that the highest 200 terms were found in the GO-BP class, followed by 90 terms in GO-MF and at least 29 terms in the GO-CC class (**Supplementary Table S14A**). In terms of high enrichment analysis, there were 27 highly enriched terms in the GO-BP class inducing metabolic process (GO:0008152), lipid metabolic process (GO:0006629), organic substance biosynthetic process (GO:1901576), fatty acid derivative biosynthetic process (GO:1901570), wax metabolic process (GO:0010166), wax biosynthetic process (GO:0010025), cuticle development (GO:0042335), response to cold (GO:0009409), response to temperature stimulus (GO:0009266), and response to light stimulus (GO:0009416). Six terms were highly enriched in the GO-MF class including catalytic activity (GO:0003824), oxidoreductase activity (GO:0016491), fatty acid elongase activity (GO:0009922), fatty acid synthase activity (GO:0004312), and acyltransferase activity (GO:0016746-47). The GO-CC enrichment results exhibited 20 highly enriched terms including endoplasmic reticulum (GO:0005783), endomembrane system (GO:0012505), obsolete cytoplasmic part (GO:0044444), membrane-bounded organelle (GO:0043227), and organelle membrane (GO:0031090) (**Figure 8A**, **Supplementary Table S14B**).

The KEGG pathway analysis revealed that there were 31 KEGG pathways predicted in the 34 *PeCER* genes; among them, the highly enriched pathways are shown in **Figure 8B** including metabolism (A09100), lipid metabolism (B09103), fatty acid elongation (00062), cutin, suberine, and wax biosynthesis (00073), plant-pathogen interaction (04626), environmental adaptation (B09159), and organismal systems (A09150) (**Figure 8B**, **Supplementary Table S15**). Overall, the GO and KEGG enrichment analyses show that the *PeCER* genes might play an important role in several biological, molecular, and cellular processes such as plant metabolism, fatty acid and wax biosynthesis as well as in response to biotic and abiotic stress.

Subcellular Localization of PeCER32 Protein

Most of the PeCER proteins were hypothetically predicted to be localized to the plasma membrane (**Table 1**). The validation of predicted subcellular localization was performed by selecting a PeCER32 protein, which were strongly evolved in various predicted functions including metabolism, organ-specific, organ developmental, and different stress responses. A transient expression assay was carried out by transformation with the CaMV35S-PeCER32-GFP fusion construct (**Figure 9A**a) and empty vector CaMV35S-GFP (**Figure 9A**b) into onion epidermal cells with the agroinfiltration method. The results showed that GFP signals were highly expressed in the plasma membrane (**Figures 9B**d–f). The empty vector CaMV35S-GFP was used as control, and the results showed a dispersed pattern of GFPs throughout the whole cell (**Figures 9B**a–c). The subcellular localization results of PeCER32 protein were consistent with the most preferential prediction.

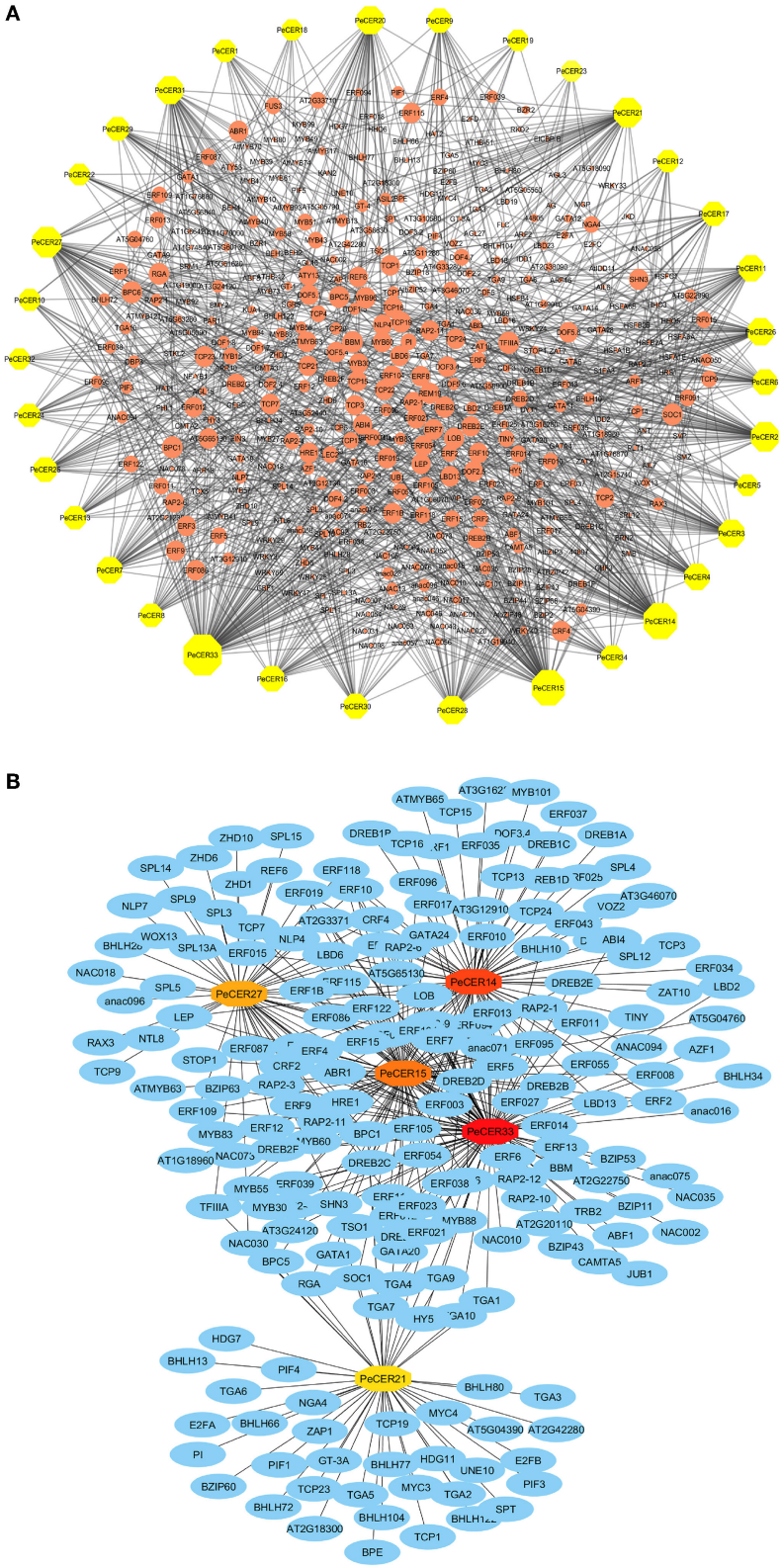


FIGURE 7 | Putative transcription factor regulatory network analysis of the *PeCER* genes. **(A)** Orange peel circular nodes represent transcription factors; yellow octagonal nodes represent *PeCER* genes, and node size represents the degree of interaction between nodes based on degree value. **(B)** Top 5 highly enriched and targeted *PeCER* genes with TFs are shown, blue nodes represent the TFs, dark red to light red colors show the *PeCER* genes, and darker *PeCER* node color shows highly enriched and vice versa.

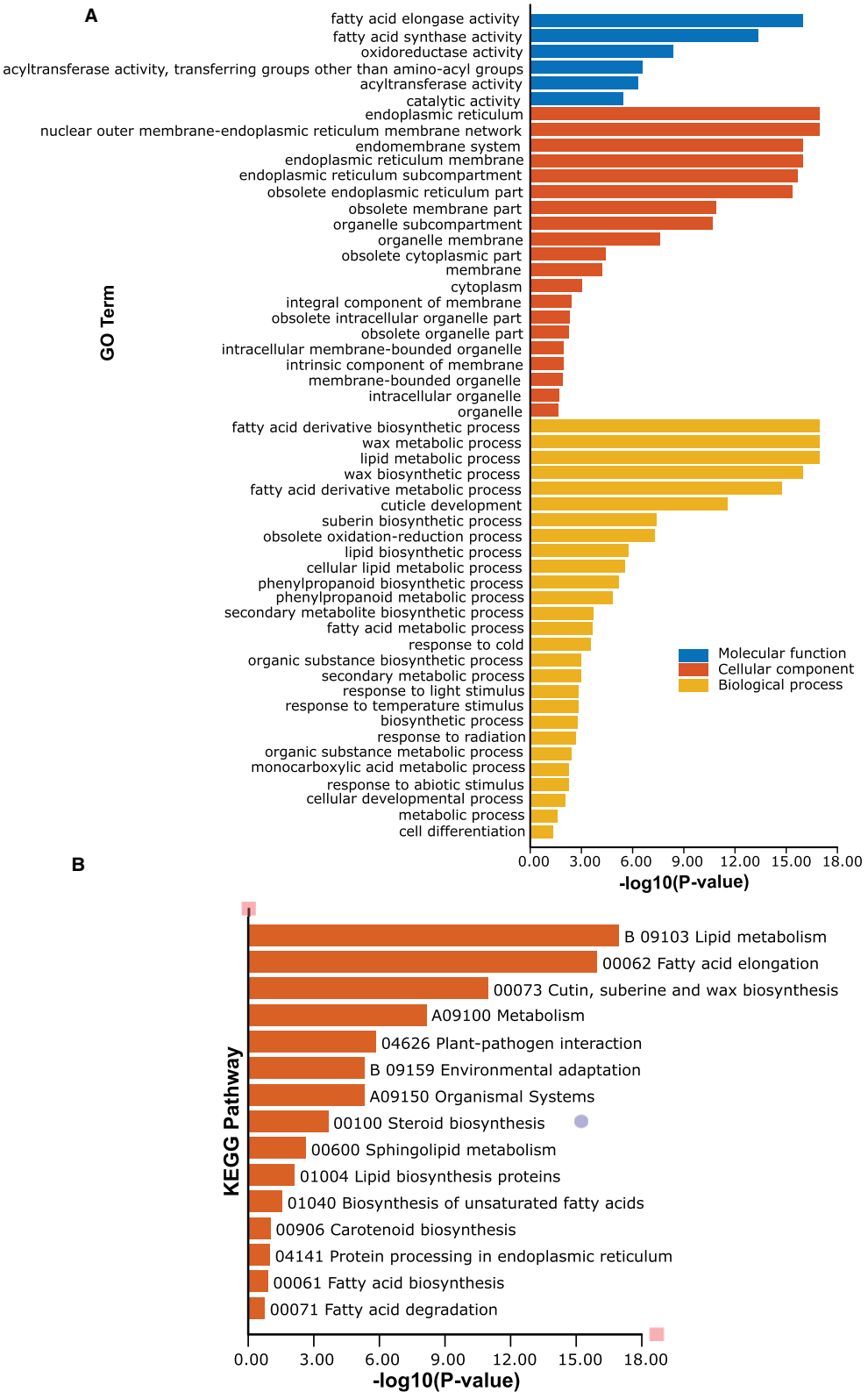


FIGURE 8 | Gene Ontology (GO) and Kyoto Encyclopedia of Genes and Genomes (KEGG) enrichment analyses of *PeCER*s genes. **(A)** Highly enriched GO terms in *PeCER* genes. **(B)** Highly enriched KEGG pathways in *PeCER* genes. Further detailed annotation results and numerous significantly enriched terms of MF, CC, BP, and KEGG pathways can be found in **Supplementary Tables S14A**, **S15**.

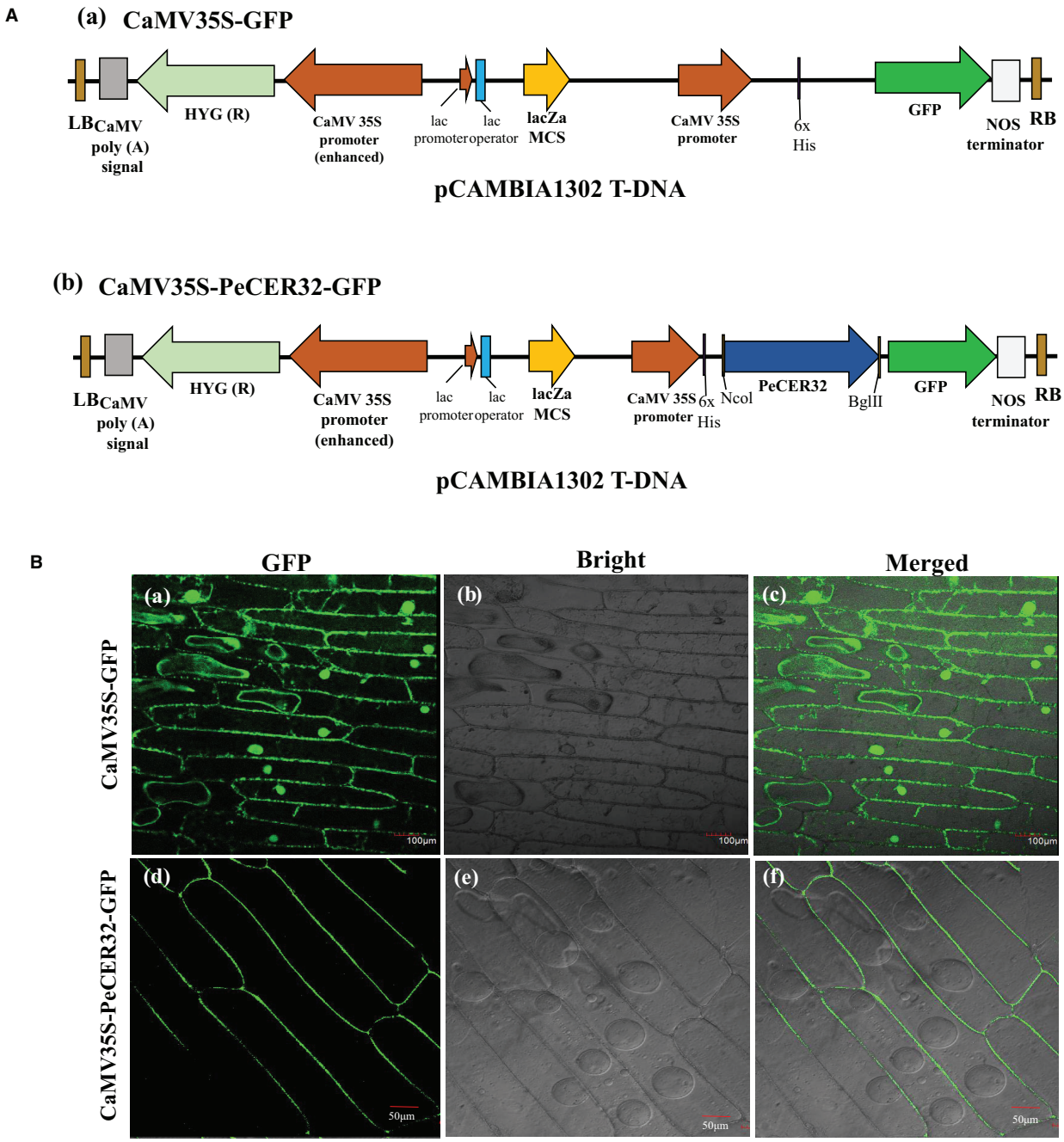


FIGURE 9 | Subcellular localization of GFP-fused PeCER32 protein based on transient expression assays in onion epidermal cells. **(A)** (a) Structure of CaMV35S-GFP as empty vector. (b) Structure of CaMV35S-*PeCER32*-GFP as construct. **(B)** (a–c) Onion cells transformed with CaMV35S-GFP as control (scale bar = 100 μm). (d–f) Onion cells transformed with CaMV35S-*PeCER32*-GFP (scale bar = 50 μm). (a,d) GFP signals visualized under dark field. (b,e) Onion epidermal cells under bright light. (c,f) represent merging of (a,b,d,e).

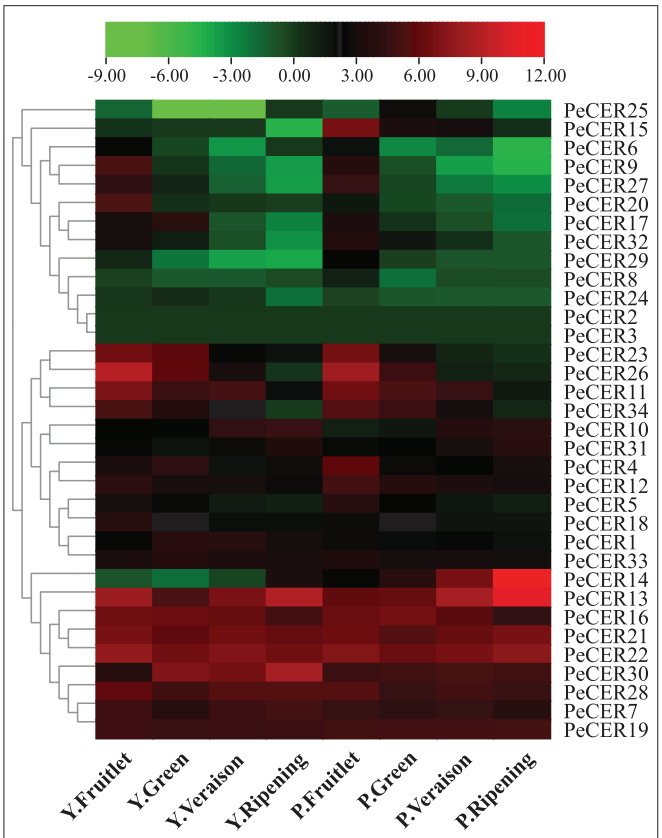


FIGURE 10 | Expression profiles of *PeCER* genes in pulp tissue of yellow and purple passion fruit cultivars in four fruit development stages. Y and L represent the yellow (Y) and purple (P) passion fruit cultivars. FPKM values were transformed by log2, and heatmap was constructed with the TBTools software. The red color shows the highest and the blue color shows the lowest expression levels in expression bar.

Expression Profiles of *PeCER* Genes in Different Fruit Development Stages

The expression profiles of the 34 *PeCER* genes in pulp tissues of yellow and purple passion fruit cultivars were further evaluated based on FPKM expression levels in four fruit development stages. The FPKM expression values have been provided in **Supplementary Table S16**. The FPKM values were transformed to $\log^2$FC, and a heatmap was generated with the TBtools software. The expression profiles of *PeCER* genes varied between both cultivars and developmental stages. Taken together, the results showed that 32 (94%) of the 34 (100%) *PeCER* genes were expressed during fruit development and ripening in both cultivars (**Figure 10**, **Supplementary Table S16**).

PeCER2 and *PeCER3* were not expressed in all the tissues, indicating that they might not be involved in fruit development. In the yellow passion fruit cultivar, 32 (94%), 31 (91%), 31 (91%), and 30 (88%) *PeCER* genes were expressed in the fruitlet, green, veraison, and ripening stages. Among the expressed genes, 17 (53%), 16 (51%), 11 (35%), and 10 (33%) *PeCER* genes were highly expressed (FPKM > 10) in the fruit development and ripening stages. In addition, 9 genes (*PeCER*7, *PeCER*13, *PeCER*16, *PeCER*19, *PeCER*21, *PeCER*22, *PeCER*28, *PeCER*29, and *PeCER*30) showed an increased expression pattern (FPKM = 13.97 to 440.13) throughout the fruit development and ripening stages. However, another 9 genes (*PeCER*9, *PeCER*11, *PeCER*12, *PeCER*18, *PeCER*20, *PeCER*23, *PeCER*26, *PeCER*27, and *PeCER*34) showed decreased expression level (FPKM = 489.71 to 0.07) from fruit development to ripening stages (**Figure 10**, **Supplementary Table S16**).

In the purple passion fruit cultivar, overall 32 (94%) *PeCER* genes were expressed in the fruitlet, green, veraison, and ripening stages. Among the 32 expressed genes, 19 (59%), 13 (41%), 11 (34%), and 11 (34%) *PeCER* genes exhibited high expression levels (FPKM > 10) in all tested stages,. Furthermore, 8 genes (*PeCER*7, *PeCER*13, *PeCER*16, *PeCER*19, *PeCER*21, *PeCER*22, *PeCER*28, and *PeCER*30) showed constantly high expressions (FPKM = 14.59 to 1575.51) through out all the tested stages, whereas 10 genes (*PeCER*4, *PeCER*5, *PeCER*11, *PeCER*12, *PeCER*15, *PeCER*23, *PeCER*26, *PeCER*27, *PeCER*32, and *PeCER*34) exhibited reduced expression levels (FPKM = 271.84 to 0.11) during fruit development to ripening stages. Comparing the *PeCER* expression profiles of both cultivars in fruit development and ripening stages, the results showed that 7 genes (*PeCER*7, *PeCER*13, *PeCER*16, *PeCER*21, *PeCER*22, *PeCER*28, and *PeCER*30) were found to have similar expression between both cultivars in all the tested stages (FPKM > 10). Overall, the purple cultivar had higher expression (FPKM = 3123.21, *PeCER14*) than the yellow (FPKM = 489.7, *PeCER26*). The highest expression level in the purple cultivar was observed during the stage of ripening (FPKM = 3123.22), followed by the veraison (FPKM = 321.01) > fruitlet > (FPKM = 99.3) and green (FPKM = 94.78) stages. In the yellow cultivar, the highest expression patterns were observed in the stage of fruitlet (FPKM = 489.70), followed by ripening (FPKM = 440.13) > veraison (FPKM = 127.38) and green stage (FPKM = 89.90) (**Figure 10**, **Supplementary Table S16**). These FPKM expression-based findings suggest that the *PeCER* genes may have significant roles in fruit development and ripening in the yellow and purple passion fruit cultivars, and further research is still needed.

Expression Pattern of *PeCER* Genes in Different Passion Fruit Tissues

The *PeCER* gene expression patterns in roots of the purple cultivar, and leaves and peel tissues of the yellow and purple cultivars were evaluated based on FPKM values. The FPKM expression values have been provided in **Supplementary Table S17**. The FPKM values were transformed to $\log^2$FC, and a heatmap was constructed with TBtools (**Figure 11**, **Supplementary Table S17**). Among all the 34 *PeCER* genes, 26 (76.47%) genes were expressed in purple L and D roots; 28 (82%) genes were expressed in yellow and purple leaves under NT and CS conditions; whereas, 29 (85%) genes were expressed in yellow and purple peel tissues, respectively. Among the expressed *PeCER* genes in the L and D roots, 12 (46%) and 11 (42%) genes were highly expressed (FPKM > 10). Comparing the expression levels of *PeCER* genes in L and D roots, the

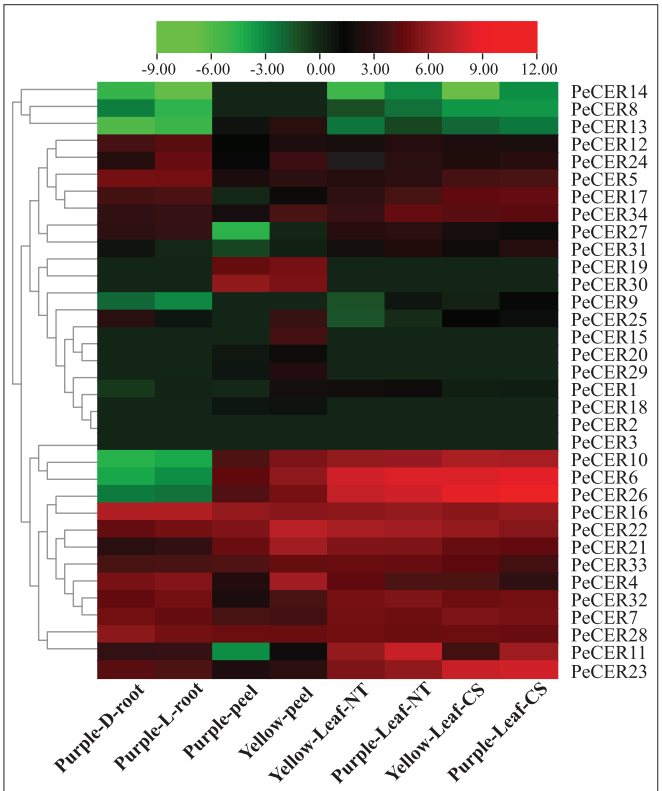


FIGURE 11 | Expression profiles of *PeCER* genes in roots, peels, and leaves of yellow and purple passion fruit cultivars under different conditions. L and D represent the samples from limestone (L) and sandy dolomite (D) rocky desertification areas. NT and CS indicate the normal temperature (NT) and chilling stress (CS) conditions. FPKM values were transformed by log2, and heatmap was constructed with the TBTools software. The red color shows the highest and the blue color shows the lowest expression levels in expression bar.

expression levels of root genes in L conditions (FPKM = 120.04, *PeCER16*) had the higher expression than those in D conditions (FPKM = 119.09, *PeCER16*). Among the expressed *PeCER* genes in purple and yellow peels, 11 (39%) and 16 (55%) *PeCER* genes showed highest expressions (FPKM > 10) in the yellow and purple peels. The purple peels showed highest expression level in *PeCER*22 (FPKM = 144.42) compared with yellow *PeCER*30 (FPKM = 58) (**Figure 11**, **Supplementary Table S17**).

The expression pattern in leaf tissues of the two cultivars under CS and NT conditions showed that 15 (58%), 13 (50%), 15 (58%), and 16 (61%) *PeCER* genes were highly expressed (FPKM > 10) in purple leaf-NT, yellow leaf-NT, purple leaf-CS, and yellow leaf-CS conditions. Comparing the leaf expressions of the two cultivars under CS and NT conditions, the highest expression was found in purple leaf-CS (FPKM = 647.01, *PeCER26*), followed by yellow leaf-CS (FPKM = 394.1, *PeCER26*), purple leaf-NT (FPKM = 303.78, *PeCER6*), and yellow leaf-NT (FPKM = 266.04, *PeCER6*). Taken together, the purple cultivar showed the highest expression in all the tested tissues such as purple leaf-CS > yellow leaf-CS > purple leaf-NT > yellow leaf-NT followed by purple L-root > purple D-root, and the lowest expression was found in the yellow peel (**Figure 11**, **Supplementary Table S17**). *PeCER2* and *PeCER3* were not expressed in all the tested tissues, indicating that they might not be involved in fruit or plant development, whereas *PeCER6* and *PeCER16* showed the highest expression, indicating that these genes might have important roles for specific functions in all the tissues, but further research is needed. These genotype-based tissue expression patterns provide ideas for further studies on plant and fruit development of the *PeCER* gene family in passion fruit.

Expression Profiles of *PeCER* Genes Under Drought Stress Conditions

CER genes have been reported to play important roles in drought stress conditions; to evaluate the expression profile of the *PeCER* genes under drought stress conditions, seven passion fruit *PeCER* genes were selected based on their significantly different FPKM expressions, *cis*-elements, and GO terms to participate in various stress responses and other functions. A qRT-PCR expression analysis was performed on the seven selected *PeCER* genes (**Figure 12**). Overall, all the seven *PeCER* genes exhibited diverse expression patterns in stems, leaves, and root tissues of the yellow and purple passion fruit cultivars under drought stress conditions. The results showed that the expression levels of most of the genes were upregulated in cultivars subjected to drought stress conditions as compared to the controls (**Figure 12**).

Overall all the seven *PeCER* genes were highly upregulated in leaf tissues compared with stem and root tissues (**Figure 12**). The *PeCER*25 gene showed the highest expression level (8.29-fold) in the leaf tissue of the yellow cultivar (**Figure 12E**), followed by *PeCER*34 (7.73-fold) in the stem tissue of the purple cultivar (**Figure 12G**) under drought conditions compared with the controls. *PeCER*15 showed higher expression levels (6.51-fold) in yellow cultivar leaves and purple cultivar root tissues (4.99-fold), while downregulated in both cultivar stem tissues under drought stress conditions compared to the control (**Figure 12C**). The *PeCER*17 gene showed consistent expression levels in yellow and purple leaves and root tissues among genotypes (**Figure 12D**). In the comparison of expression levels in tissues of the two genotypes, the stem tissues of the purple cultivar showed the highest expression level (1.7-fold) (**Figure 12B**), whereas the leaves (8.29-fold) (**Figure 12E**) and root (4.16-fold) (**Figure 12A**) tissues of the yellow cultivar showed highest expressions under drought stress conditions compared to the controls. These findings indicated the importance of *PeCER* genes under drought stress conditions and provide a foundation for further functional studies.

Expression Profiles of *PeCER* Genes Under Biotic Stress Conditions

CER genes have been reported to play important roles under biotic stress conditions, and the qRT-PCR expression profiles of the seven selected passion fruit *PeCER* genes under *F. kyushuense* (biotic stress) stress conditions were investigated (**Figure 13**). The *PeCER* gene expression in peel tissues of the yellow and purple passion fruit cultivars at 9^{th} and 12^{th} days post-inoculation (dpi) of the pathogenic fungus *F. kyushuense*

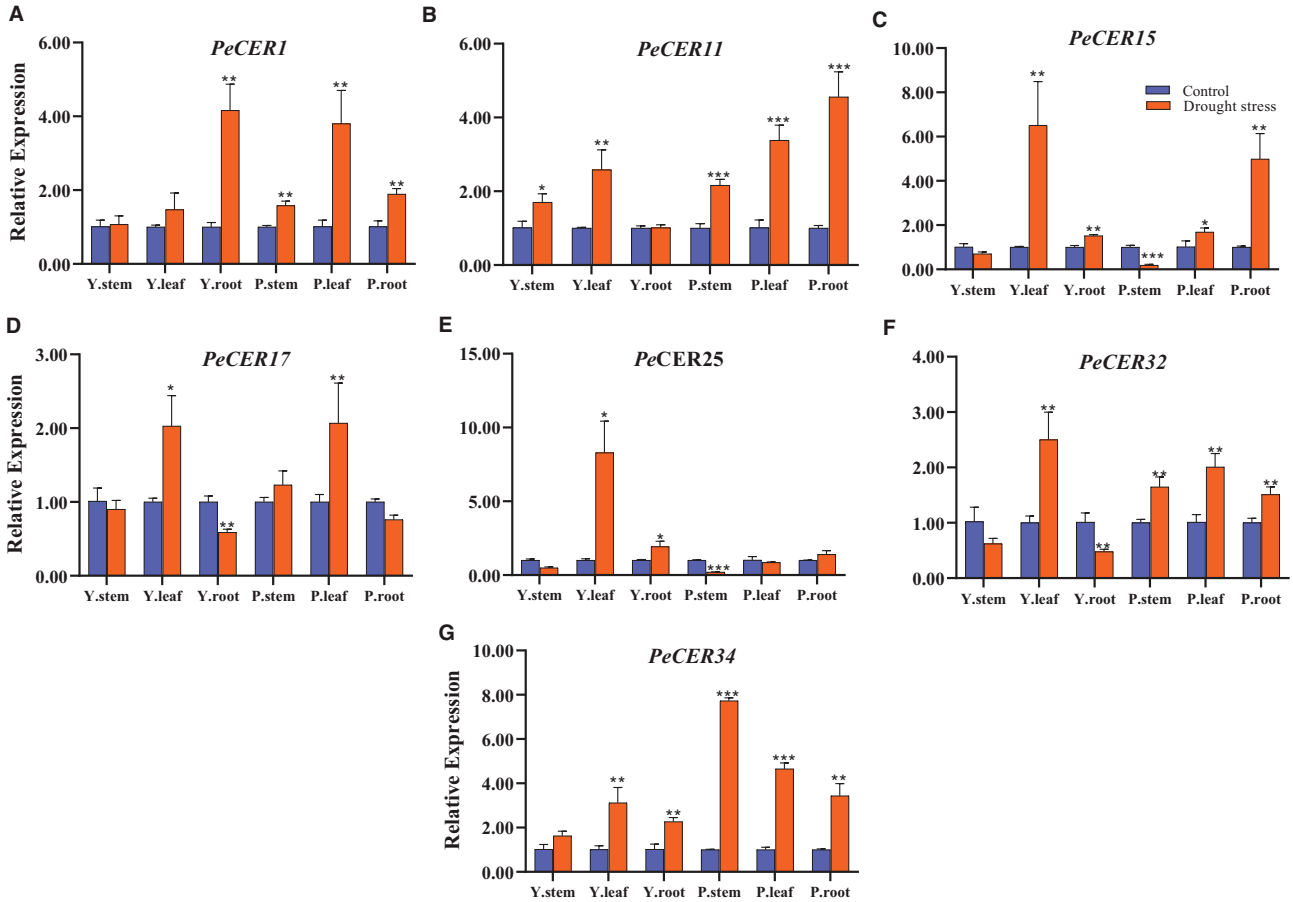


FIGURE 12 | Relative expressions of *PeCER* genes **(A–G)** in stem, root, and leaf tissues of yellow and purple passion fruit plants under control and drought stress conditions. Relative gene expression levels were calculated using $2^{-\Delta\Delta ct}$. Plants with regular watering were taken as control. Vertical bars represent means ± SD ($n = 3$). *, **, and *** show significance at $p \leq 0.05$, $p \leq 0.01$, and $p \leq 0.001$, respectively, under control and drought stress condition according to Students *t*-test. Y represents yellow passion fruit, and P represents purple passion fruit.

was analyzed by comparing with the controls (**Figure 13**). Overall, all the *PeCER* genes exhibited different expression levels under biotic stress conditions in the yellow and purple cultivars compared to the controls. *PeCER*32 showed the highest expression (4.03-fold) in purple 9 dpi (**Figure 13F**).

In comparison between the two cultivars at 9th and 12th dpi, the results showed that the expression levels of all the *PeCER* genes were downregulated under *F. kyushuense* stress conditions in the yellow cultivar except for the *PeCER*17 gene and were upregulated in the purple cultivar compared to the controls (**Figure 13**). The expression of the *PeCER*17 gene was upregulated in yellow (2.87-fold) 12 dpi compared with the control (**Figure 13D**). The *PeCER*1, *PeCER*11, *PeCER*15, *PeCER*17, and *PeCER*32 genes were highly upregulated (1.42, 2.76, 3.3, 1.80, and 4.03 folds) in the purple cultivars at 9th dpi compared to the controls (**Figure 13**). However, the *PeCER*15 and *PeCER*17 genes at 12th dpi were downregulated in the purple cultivar compared with the controls (**Figures 13C,D**). Altogether, the results show that the *PeCER* genes in the passion fruit purple cultivars presented high expressions in cultivars at 9th and 12th dpi samples compared with the yellow cultivar (**Figure 13**). These results suggest that genes with significantly higher expression levels including *PeCER1*, *PeCER*11, *PeCER*15, *PeCER*17, and *PeCER*32 may have important roles, and the purple cultivar with highly upregulated expressions under biotic stress provides basic information for further studies on the genetic improvement in passion fruit (**Figure 13**).

Validation of FPKM Expression Data by qRT-PCR

According to FPKM expression values, the *PeCER1, PeCER11, PeCER17, PeCER25, PeCER32,* and *PeCER34* genes were significantly expressed in most of the roots, leaves, pulp, and peel tissues, especially in the purple cultivar compared to yellow (**Figures 12**, **13**). The FPKM expression data were further validated by qRT-PCR analysis using the above-mentioned *PeCER* genes in yellow and purple passion fruit peel tissues. After normalization with *Pe*60S, all the tested *PeCER* genes showed a trend line consistent with the FPKM expression values

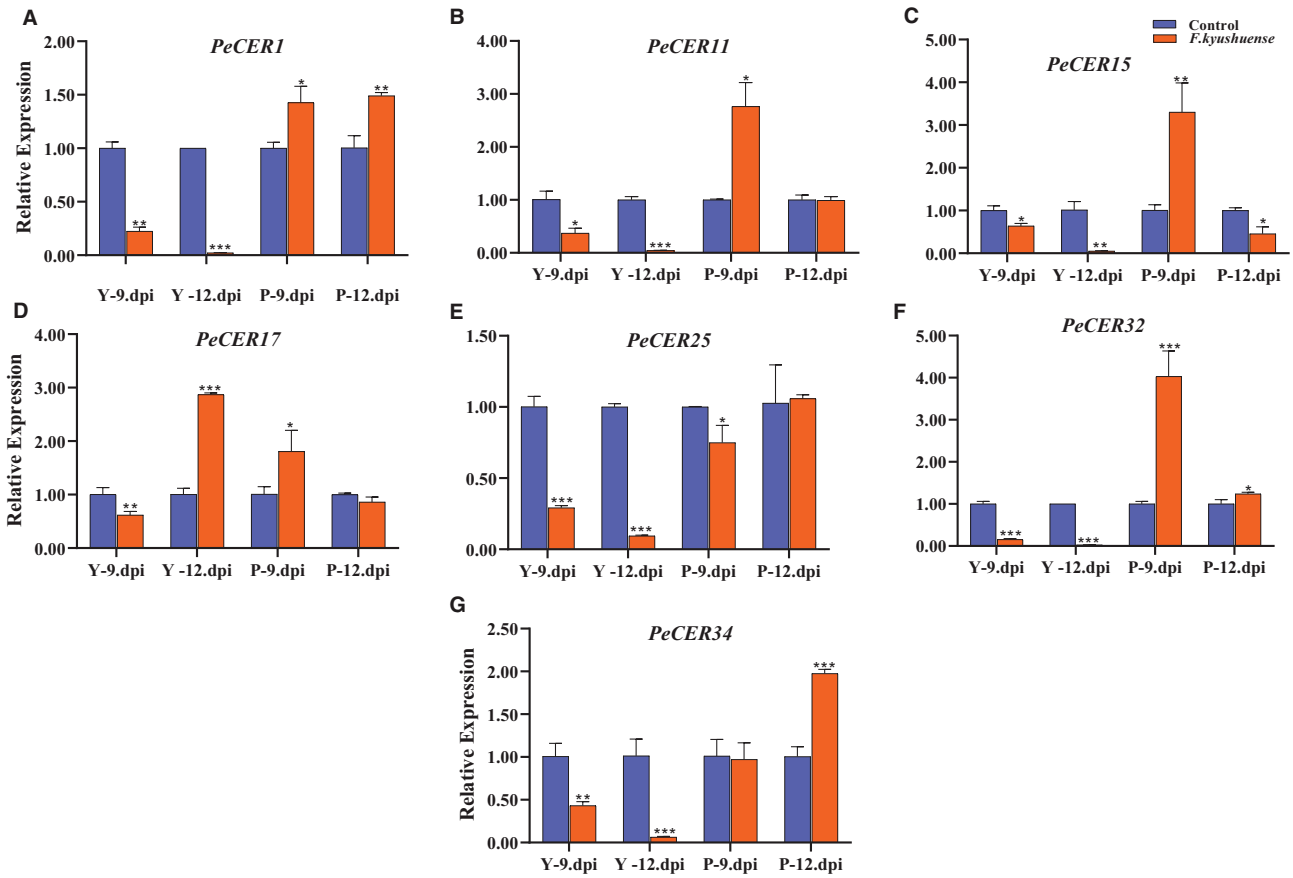


FIGURE 13 | qRT-PCR expression profiles of *PeCER* genes **(A–G)** in peel tissues of yellow and purple passion fruit cultivars under *F. kyushuense* biotic stress and control conditions. Relative gene expression levels were calculated using $2^{-\Delta\Delta ct}$. Vertical bars represents means ± SD ($n = 3$). *, **, and *** show significance at $p \leq 0.05$, $p \leq 0.01$, and $p \leq 0.001$, respectively, under control and biotic stress conditions according to Students *t*-test. Y, yellow passion fruit; P, purple passion fruit; dpi, days post inoculation.

(**Figure 14**). These results revealed that FPKM expression values provided an appropriate expression result for all the tested tissues between both passion fruit cultivars.

DISCUSSION

The cuticle of plants is a hydrophobic layer and is the first barrier between the environment and plants to protect them from biotic and abiotic stresses. It is composed of VLCFAs and their derivatives (Yeats and Rose, 2013). Wax biosynthesis has been described in different plant species including *B. napus* (Wang et al., 2020), *O. sativa* (Ni et al., 2018), *A. thaliana* (Aarts et al., 1995; Hooker et al., 2002; Trenkamp et al., 2004; Rowland et al., 2007; Pascal et al., 2013; Kim et al., 2019; Yang et al., 2020b), *Mangifera indica* (Tafolla-Arellano et al., 2017), *Sichuan kumquat* (Yang et al., 2022), *P. pratensis* (Wang et al., 2021), and *M. domestica* (Zhang et al., 2019a, 2020). Different genes are involved in cuticular wax biosynthesis and have been previously reported including *CER* (Bourdenx et al., 2011), KCS (Wang et al., 2020), KCR (beta-ketoacyl-CoA reductase) (Gan et al., 2016), FAR (fatty acyl-CoA reductase) (Wang et al., 2017), LACS (Schnurr et al., 2004), CUT1 (Millar et al., 1999), and FAE (fatty acid elongase) (Millar and Kunst, 1997). *CER* is one of the main gene families involved in cuticle wax biosynthesis and stress response (Bourdenx et al., 2011). The genome-wide identification of *CER* family genes has been reported in different plant species including *Z. jujuba* Mill (Li et al., 2021), *M. domestica* (Qi et al., 2019a), and *H. annuus* (Ahmad et al., 2021) and has been functionally characterized in *A. thaliana* (Aarts et al., 1995; Hooker et al., 2002; Trenkamp et al., 2004; Rowland et al., 2007; Pascal et al., 2013; Kim et al., 2019; Yang et al., 2020b), *P. pratensis* (Wang et al., 2021), *O. sativa* (Ni et al., 2018), *B. napus* (Wang et al., 2020), and *Brachypodium distachyon* (Wu et al., 2019). Information on *CER* genes in *P. edulis* remained unknown, but the availability of the passion fruit genome (Ma et al., 2021) made it possible studies on genomic levels.

In this study, 34 *PeCER* genes were identified in the passion fruit genome and were unevenly distributed across eight chromosomes, with the largest number of genes located on chromosome 1 (**Table 1**, **Supplementary Figure S1**). Ahmad et al. (2021) mentioned that the diversity of genes in the same family on different chromosomes may be due to their

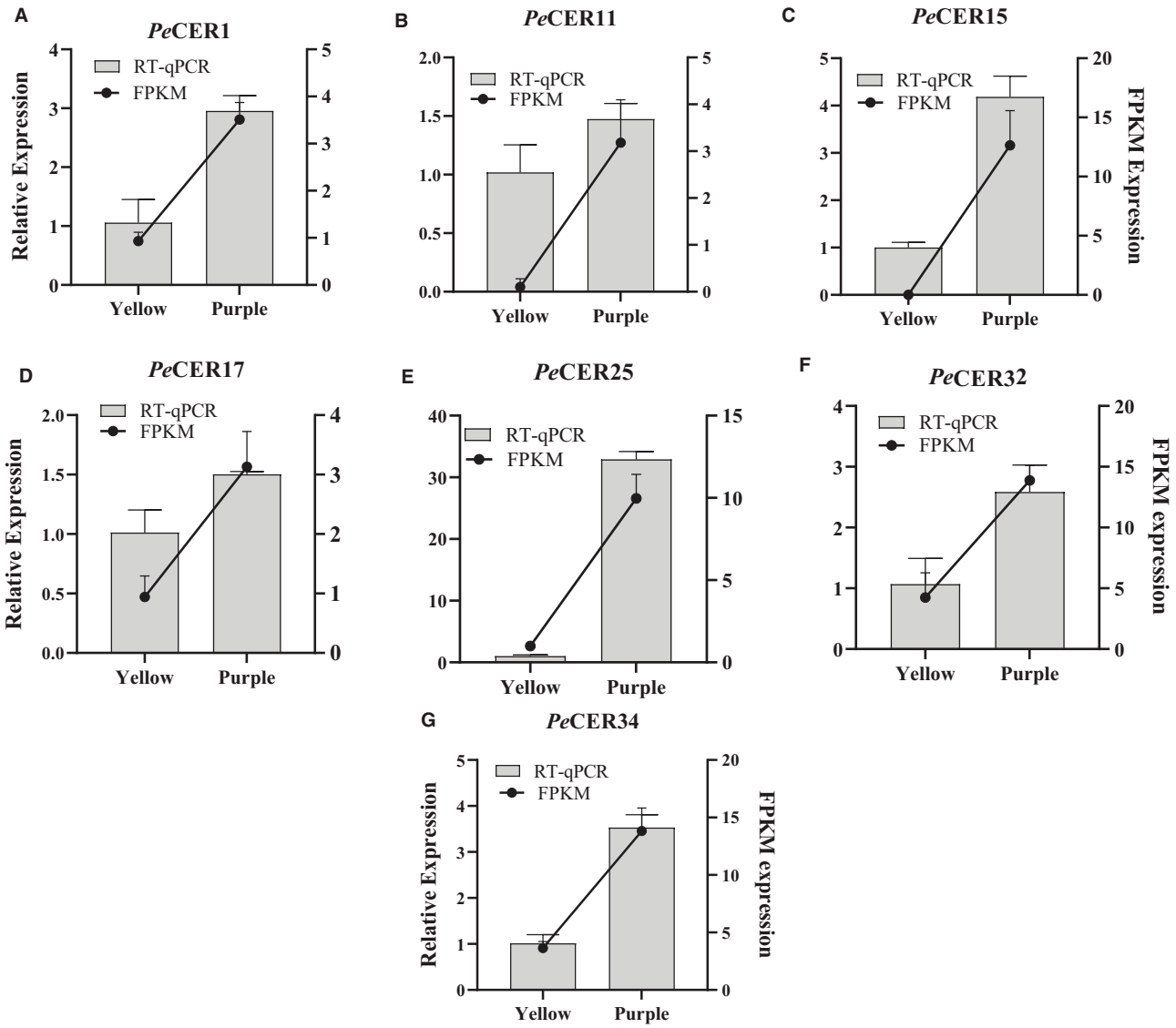


FIGURE 14 | Validation of FPKM expression data by qRT-PCR. **(A–G)** Histograms show the qPCR results of seven PeCER genes in peel tissues of yellow and purple passion fruit cultivars at the ripening stage. Black line charts show the FPKM values of PeCER genes, and vertical gray bars show the qPCR results ($2^{-\Delta\Delta ct}$) and represent mean ± SD. The left Y-axis represents the qPCR relative expression levels, and the right Y-axis indicates the FPKM expression values.

involvement in various functions. The 34 identified *PeCER* genes in the passion fruit genome were relatively similar in terms of number to sunflower *CER* (thirty-seven genes) (Ahmad et al., 2021), jujuba *CER* (twenty-nine) (Li et al., 2021), while some species have fewer *CER* genes including apple, which has 10 *CER* genes (Qi et al., 2019a); the difference in gene number may be due to differences in genome size. The phylogenetic tree was constructed among *P. edulis*, *A. thaliana*, *M. domestica*, *H. annus*, and *Z. jujuba* proteins and divided into 7 clades according to sunflower *CER* (Ahmad et al., 2021) (**Figure 1A**). Liu et al. (2018) pointed out that genes present in the same clade might perform similar functions. Differences in protein functions can be described by identifying conserved motifs during the development of different gene families (Wong et al., 2015). Furthermore, conserved motifs were predicted in PeCER proteins and a diverse motif pattern ranging from 1 to 24 motifs was found, indicating that PeCER proteins have a remarkably conserved protein structure (**Figure 1B**). Our results are inconsistent with Li et al. (2021), who also found similar motif results in jujuba.

Differences between the number of exons and introns provide an important source for gene family variation and determine the different functions and expressions of genes (Xu et al., 2012). In this study, a quite different number of introns were found in the *PeCER* genes ranging from 0 to 28 introns. The *PeCER*6, *PeCER*8, and *PeCER*9 genes have no introns, and similar results have been

reported previously for intron-less genes such as *AtCER6*-2 and *HanCER6*-2 (Ahmad et al., 2021), while *PeCER*13 contained 28 introns (**Figure 1C**). These results indicate that ancestors of the *PeCER* genes might have gone through several rounds of intron loss and gain during development (Frugoli et al., 1998).

The *cis*-regulatory element analysis of *PeCER* genes revealed that ABRE, CGTCA-motif, GARE-motif, G-Box, Box 4, and ARE *cis*-elements were found in abundance (**Figure 2**), indicating that *PeCER* might be involved in different plant developmental and stress responses (Wingender et al., 1990; Wang et al., 2011; Xiong et al., 2020). Fujita et al. (2013) demonstrated the important roles of the ABRE element in ABA and stress responses. Kaur et al. (2017) reported the involvement of GARE *cis*-elements in hormone responsiveness. Liu et al. (2016) reported the involvement of W-box and G-box elements in early senescence of rice flag leaf. Gene duplication is a prominent feature of plant genomics that could lead to evolutionary and functional novelties that arise from existing genes (Flagel and Wendel, 2009). The differences in *CER* genes and chromosome numbers among passion fruit, apple, sunflower, jujuba, and *Arabidopsis* species suggest that they have gone through lineage-specific genome duplication. Whole-genome duplication (WGD) consists of tandem and segmental duplications that cause a sudden increase in the size of a genome and entire gene sets by generating two gene copies (Van De Peer et al., 2009). The results of the synteny analysis and calculation of Ka/Ks values in *PeCER* genes showed that the duplication process between the tandem and segmental *PeCER* genes was estimated to be 1.12 to 20.78 mya (**Supplementary Table S6**), which is consistent with a published report on passion fruit, indicating that passion fruit has gone through WGD twice (12 and 65 mya) (Xia et al., 2021).

Six segmental and two tandem duplicate *CER* genes in the passion fruit genome (**Figure 3A**, **Supplementary Table S6**) were identified, which is consistent with Xia et al. (2021) who also found two tandem repeats in the passion fruit TPS-b subfamily. Furthermore, the synteny analysis of *P. edulis CER* genes with *A. thaliana*, *M. domestica,* and *Z. jujuba CER* genes identified 10 *PeCER* genes as orthologous to 12 *CER* genes from the above species (**Figure 3B**). The multicollinearity analysis of the *P. edulis CER* genes revealed the highest collinearity between *P. edulis* and *M. domestica* (43 collinear genes). Santos et al. (2014) reported that compared to dicot genomes, the number of repetitive elements between *P. edulis* and *M. domestica* genomes was 42.4% (**Figure 4**), suggesting that these orthologous may share the same ancestors and retain corresponding functions.

The protein--to-protein interaction network of a particular gene family provides evidence of the relationship between members (Piya et al., 2014). The protein-to-protein interaction results of PeCER proteins showed that seven PeCER proteins were homologous with AtCER1 (**Figure 5A**). Bernard and Joubès (2013) reported that AtCER1 dynamically contributes to wax biosynthesis and actively responds to biotic and abiotic stresses. Two PeCER proteins showed homology with AtCER3, and it has been reported that AtCER3 interacts with AtCER1 and catalyzes the redox-dependent VLCAs from very long-chain-Acyl-CoAs (Wu et al., 2019). Two PeCER proteins showed homology with AtSTE1 and interact with AtDWF1 and AtDWF5. Silvestro et al. (2013) stated that AtSTE1 (Delta(7)-sterol-C5(6)-desaturase1) is a precursor of growth-promoting brassinosteroids and is involved in sitosterol and campesterol biosynthesis. Choe et al. (2000) stated that AtDWF57-dehydrocholesterol reductase was involved in cholesterol production. Some PeCER proteins showed homology with AtKCS. Batsale et al. (2021) described that AtKCS was involved in the biosynthesis of VLCFAs and essential for cuticular wax and suberine biosynthesis. Two PeCER proteins showed interaction with AtSBH (sphingoid base hydroxylases). Shu et al. (2015) stated that AtSBH is involved in sphingolipid trihydroxy long-chain base (4-hydroxysphinganine) biosynthesis and response to high humidity and temperature stress. The PeCER protein-to-protein interaction results suggest that the homology and interaction with known *Arabidopsis* proteins may have the same functions such as wax biosynthesis, plant development, and stress responses, but further studies are required (**Figure 5A**).

The protein's secondary structures are the physical arrangement of amino acid sequences and are highly conserved between homologous proteins. The order of amino acids directly affects protein folding, 3D structure, and functions (Ridout et al., 2010). The results of PeCER protein secondary structure and 3D modeling indicate that the alpha helix accounts for the largest percentage of secondary structures (57.2%), followed by random coils (40.95%) and extended strands (25.68%) (**Supplementary Table S11**), and our results are identical to those of Lian et al. (2020), who also found the largest percentage of secondary structures followed by random coils and extended strands. In terms of 3D modeling, most of the PeCER proteins showed similar 3D structures except for a few of them (**Figure 5B**), indicating that the identified PeCER proteins were conserved and consistent with motif and gene structure analysis. Ridout et al. (2010) pointed out that protein structures, similar or different, may be due to differences in amino acid sequence size or arrangement.

In recent times, different miRNAs have been identified in numerous species, such as maize (*Zea mays*) (Aravind et al., 2017), cowpea (*Vigna unguiculata*) (Barrera-Figueroa et al., 2011), soybean (*Glycine max*) (Song et al., 2011), peanut (*Arachis hypogaea*) (Zhao et al., 2015), and passion fruit, that are involved in different metabolism, development, and environmental stresses (Paul et al., 2020). In this study, 12 putative miRNAs targeting 16 *PeCER* genes were identified (**Figure 6**, **Supplementary Table S12**), and two members of the ped-miR166 family targeted four *PeCER* genes. miR166 has been reported to be involved in drought stress in maize (Aravind et al., 2017) and cowpea (Barrera-Figueroa et al., 2011), seed development in soybean (Song et al., 2011), disease resistance in peanut (Zhao et al., 2015), development of protein metabolic process, shoot apical meristem in passion fruit (Paul et al., 2020), plant growth, development, and stress response in apple (Varkonyi-Gasic et al., 2010).

Two members of the ped-miR171 family targeted two *PeCER* genes, and miR171 has been reported to be involved in development, metabolism, and photosynthesis in grapevine

(*Vitis vinifera*) (Han et al., 2014), in coffee (*Coffea Arabica*) (Chaves et al., 2015); stress response in tea plant (*Camellia sinensis*) (Zhang et al., 2014), and development and defense responses in passion fruit (Paul et al., 2020). One member of the ped-miR395 family targeted three *PeCER* genes. miR395 was found to be involved in abiotic stress in wheat (*Triticum aestivum*) (Han et al., 2013), starch metabolism in cassava (*Manihot esculenta*) (Patanun et al., 2013), development and stress response in sorghum (*Sorghum bicolor*) (Katiyar et al., 2012a; Su et al., 2021), and salt stress tolerance in cotton (*Gossypium hirsutum*) (Wang et al., 2013). Two members of the ped-miR399 family targeted three *PeCER* genes and have been stated to be involved in drought stress response in barley (*Hordeum vulgare*), sugarcane (*Saccharum officinarum*) (Zanca et al., 2010), phosphate homeostasis, signaling, transport in apple (Pant et al., 2008), and phosphate deficiencyin sorghum (Katiyar et al., 2012a). These findings proposed that the identified ped-miRNAs may play key roles in combating multiple stresses by modifying the transcriptional level of *CER* genes in passion fruit but requires further studies.

Plant TFs have been reported to be involved in regulation of fatty acids and wax biosynthesis, as well as stress responses under different conditions (Hao et al., 2017). In this study, various TFs targeting the 34 *PeCER* genes were predicted and their regulatory network interactions with the *PeCER* genes were constructed (**Figure 7**, **Supplementary Table S13**). The ERF TF family was found to be the most abundant, followed by BBR-BPC, TCP, MYB, NAC, and AP2, indicating their positive or negative roles in wax and fatty acid biosynthesis and different stresses. Go et al. (2014) found that wax biosynthesis in *Arabidopsis* was negatively regulated by AP2/ERF-type TFs. The overexpression of AP2/ERF-type TFs in *Arabidopsis* and tobacco increased the load of wax and drought resistance (Yang et al., 2020a). BBR-BPC TFs response to cytokinin and control flower development, brassinosteroid signaling, size of stem cells, and seed development (Shanks et al., 2018; Theune et al., 2019). TCP TFs regulate plant growth, development, and stress response (Li, 2015; Danisman, 2016; Mir et al., 2022). MYB TFs regulate VLCFA biosynthesis, plant development, metabolism, and response to stresses (Raffaele et al., 2008; Katiyar et al., 2012b; Ambawat et al., 2013). Zhang et al. (2019b) reported that the MYB30 TF played an important role in cuticular wax biosynthesis and resistance to pathogens. NAC TFs play an important role in plant immunity and biotic and abiotic stresses (Nuruzzaman et al., 2013). Our results are consistent with previous reports indicating that the role of TFs in *PeCER* genes may be to regulate plant stress resistance, while the wax regulation analysis requires further investigation.

GO aims to functionally classify genes into distinct terms, which can be further classified into three ontology categories at the genome level: GO-BP, GO-CC, and GO-MF (Ashburner et al., 2000). KEGG bioinformatics resources can be used to obtain genome-level biological functions in pathway maps (Masoudi-Nejad et al., 2007). GO and KEGG annotation and enrichment analyses were also performed on the *PeCER* genes (**Figure 8**, **Supplementary Tables S14**, **S15**). Most of the GO terms were related to organelle membrane, fatty acid synthase, wax and lipid metabolic process, organic substance, and stress response. Highly enriched KEGG pathways among the *PeCER* genes include lipid and fatty acid metabolism, cutin, suberine and wax biosynthesis, and plant-pathogen interaction. Our results are consistent with previous reports (Ni et al., 2016; Qi et al., 2019b), which also found similar GO terms and KEGG pathways related to wax and fatty acid biosynthesis, plant-pathogen interaction, and different stress responses. Cuticular wax plays an important role in plant biotic and abiotic stress tolerance. *CER* genes play an important role in VLCFA and wax biosynthesis (Li et al., 2021). *CER10* is involved in VLCFA biosynthesis (Zheng et al., 2005), and the *CER10* mutant exhibits increase in non-stomatal water loss and tolerance to drought conditions (Ensing et al., 2016). The expression of *AtCER1* and *AtCER3* improved the cuticle wax and reduced water loss under drought stress conditions in tobacco (Cameron et al., 2006). The FPKM expression results showed that the *PeCER* genes were differentially and constitutively expressed in different passion fruit tissues under different conditions (**Figures 13**, **14**).

The FPKM expression results showed that compared with NT leaves, the expression levels of *PeCER* genes were higher in CS leaves, which were consistent with qRT-PCR expression results that the expressions of *PeCER* genes in drought-stressed leaves were higher compared to the control group (**Figures 13**, **14**). Similarly, Wang et al. (2021) also found that the expression of *PpCER1*-2 was higher in drought-stressed leaves than in watered leaves. Wang et al. (2020) also pointed out that the *BnCER1*-2 in brassica-overexpressed plants stimulates the production of alkanes and improves tolerance to drought. *Pp*CER1-2 was constitutively expressed in multiple tissues, with high expression in stems and leaves but very low expression in root tissues (Wang et al., 2021). In rice, *OsCER1* was highly expressed in the tapetum and bicellular pollen cells but lower in vegetative organs, suggesting a role in organ development. Based on the FPKM and qRT-PCR expression results between different tissues and *PeCER* genes, the results showed diverse expressions such as *PeCER*1, *PeCER*11, *PeCER*15, and *PeCER*32 were highly expressed in roots and leaves but not in stem tissues. Similar results were found in Pascal et al. (2013), where *CER26* was highly expressed in leaves but not in stems, *CER2* was expressed in all tissues, and *CER26*-like was highly expressed in flowers but low in all other tissues.

Rowland et al. (2006) also found that *CER4* was involved in the production of *Arabidopsis* epidermal wax and expressed in different plant tissues such as plant stems, roots, flowers, leaves, and siliques. Furthermore, cuticle wax also played an important role in plant defense against bacterial and fungal pathogens. The qRT-PCR expression results of *F. kyushuense* (biotic stress) showed that the *PeCER* genes under biotic stress conditions were upregulated in the purple cultivar compared with the controls, and are consistent with Bourdenx et al. (2011) who demonstrate that *CER1* was involved in alkane biosynthesis and was highly correlated with responses to biotic and abiotic stresses. Wang et al. (2015) also reported that the overexpression of cucumber *CsWAX2* homologous to *CER3* showed a significant increase in resistance to drought and pathogens. The qRT-PCR expression results of *PeCER* genes were also consistent with the predicted TF results that the expression levels of *PeCER* genes containing

numerous wax- and VLCFA-related transcription factors (EFR) were upregulated under stress conditions compared to the controls. Overall, these results suggest that the *PeCER* genes showed an important role by positive or negative regulation under stress conditions. In future studies, the identified *PeCER* genes could be used for further functional studies on wax biosynthesis and stress associated with the purpose of genetic improvement of passion fruit.

CONCLUSION

In this study, comprehensive analyses were performed, and 34 *PeCER* genes in the passion fruit genome were identified. All the *PeCER* genes were subjected to physio-chemical features, evolutionary relationships, chromosomal mapping, motifs, gene structures, *cis*-regulatory elements, protein-protein interaction, syntenic analysis, TFs regulatory network analysis, GO andKEGGannotation, and putative miRNA prediction analysis. The *PeCER* genes were expanded and subjected to purification selection. The predicted subcellular localization was validated by transient expression assay of the PeCER32 in onion epidermal cells. Different TFs including ERF, TCP, MYB, and NAC were identified, and a TF regulatory network associated with the *PeCER* genes was constructed. Diverse FPKM expression profiles of the *PeCER* genes were found in the roots, peels, leaves, and pulp tissues under different conditions. The qRT-PCR expression results revealed that *PeCER1, PeCER11, PeCER15, PeCER17,* and *PeCER32* were highly upregulated under drought and *F. kyushuense* stress conditions compared to the controls but varied in the yellow and purple passion fruit cultivars. These findings provide preliminary information for future functional studies on the *PeCER* genes for the genetic improvement of passion fruit, and the genes including *PeCER1, PeCER11, PeCER15, PeCER17*, and *PeCER32* that were highly expressed under stress may play important roles in wax biosynthesis and stress response, but further functional studies are needed.

DATA AVAILABILITY STATEMENT

The original contributions presented in the study are included in the article/**Supplementary Materials**, further inquiries can be directed to the corresponding authors.

AUTHOR CONTRIBUTIONS

FC and HMR: conceptualization and validation. AW, SM, MBA, JL, MI, and BL: methodology. HMR and AA: software. HMR, NS, MAAA, and XY: formal analysis. HMR: data curation and writing and original draft preparation. FC, SSS, and RO: review and editing. FC: supervision. ZL and FC: funding acquisition. All the authors have read and agreed to the published version of the manuscript.

FUNDING

FC research project was funded by the Department of Science and Technology, Fujian Province, China (2020N0004 and 2020S0056) and the Engineering Research Center of Fujian Province University (G2-KF2006). ZL research project was funded by Enterprise Technology Development (Contract: 2020-3501-04-001995).

SUPPLEMENTARY MATERIAL

The Supplementary Material for this article can be found online at: https://www.frontiersin.org/articles/10.3389/fpls.2022.898307/full#supplementary-material

REFERENCES

Aarts, M., Keijzer, C. J., Stiekema, W. J., and Pereira, A. (1995). Molecular characterization of the CER1 gene of Arabidopsis involved in epicuticular wax biosynthesis and pollen fertility. *Plant Cell* 7, 2115–2127. doi: 10.1105/tpc.7.12.2115

Ahmad, H. M., Wang, X., Fiaz, S., Nadeem, M. A., Khan, S. A., Ahmar, S., et al. (2021). Comprehensive genomics and expression analysis of eceriferum (CER) genes in sunflower (*Helianthus annuus*). *Saudi J. Biol. Sci.* 28, 6884–6896. doi: 10.1016/j.sjbs.2021.07.077

Al-Abdallat, A. M., Al-Debei, H. S., Ayad, J. Y., and Hasan, S. (2014). Over-expression of SlSHN1gene improves drought tolerance by increasing cuticular wax accumulation in tomato. *Int. J. Mol. Sci.* 15, 19499–19515. doi: 10.3390/ijms151119499

Ambawat, S., Sharma, P., Yadav, N. R., and Yadav, R. C. (2013). MYB transcription factor genes as regulators for plant responses: an overview. *Physiol. Mol. Biol. Plants* 19, 307–321. doi: 10.1007/s12298-013-0179-1

Aravind, J., Rinku, S., Pooja, B., Shikha, M., Kaliyugam, S., Mallikarjuna, M. G., et al. (2017). Identification, characterization, and functional validation of drought-responsive microRNAs in subtropical maize inbreds. *Front. Plant Sci.* 8, 941. doi: 10.3389/fpls.2017.00941

Ashburner, M., Ball, C. A., Blake, J. A., Botstein, D., Butler, H., Cherry, J. M., et al. (2000). Gene ontology: tool for the unification of biology. *Nat. Genet.* 25, 25–29. doi: 10.1038/75556

Bailey, T. L., Williams, N., Misleh, C., and Li, W. W. (2006). MEME: discovering and analyzing DNA and protein sequence motifs. *Nucleic Acids Res.* 34, W369–W373. doi: 10.1093/nar/gkl198

Barrera-Figueroa, B. E., Gao, L., Diop, N. N., Wu, Z., Ehlers, J. D., Roberts, P. A., et al. (2011). Identification and comparative analysis of drought-associated microRNAs in two cowpea genotypes. *BMC Plant Biol.* 11, 1–11. doi: 10.1186/1471-2229-11-127

Batsale, M., Bahammou, D., Fouillen, L., Mongrand, S., Joubès, J., and Domergue, F. (2021). Biosynthesis and functions of very-long-chain fatty acids in the responses of plants to abiotic and biotic *stresses.Cells* 10, 1284. doi: 10.3390/cells10061284

Bernard, A., and Joubès, J. (2013). Arabidopsis cuticular waxes: advances in synthesis, export and regulation. *Prog. Lipid Res.* 52, 110–129. doi: 10.1016/j.plipres.2012.10.002

Bourdenx, B., Bernard, A., Domergue, F., Pascal, S., Léger, A., Roby, D., et al. (2011). Overexpression of ArabidopsisECERIFERUM1 promotes wax

verylong-chain alkane biosynthesis and influences plant response to biotic and abiotic stresses. *Plant Physiol.* 156, 29–45. doi: 10.1104/pp.111.172320

Cameron, K. D., Teece, M. A., and Smart, L. B. (2006). Increased accumulation of cuticular wax and expression of lipid transfer protein in response to periodic drying events in leaves of tree tobacco. *Plant Physiol.* 140, 176–183. doi: 10.1104/pp.105.069724

Chaves, S., Fernandes-Brum, C., Silva, G., Ferrara-Barbosa, B., Paiva, L., Nogueira, F., et al. (2015). New insights on Coffea miRNAs: features and evolutionary conservation. *Appl. Biochem. Biotechnol.* 177, 879–908. doi: 10.1007/s12010-015-1785-x

Chen, C., Chen, H., Zhang, Y., Thomas, H. R., Frank, M. H., He, Y., and Xia, R. (2020). TBtools: an integrative toolkit developed for interactive analyses of big biological data. *Mol. Plant* 13, 1194–1202. doi: 10.1016/j.molp.2020.06.009

Chen, S., Zhou, Y., Chen, Y., and Gu, J. (2018). fastp: an ultra-fast all-in-one FASTQ preprocessor. *Bioinformatics* 34, i884–i890. doi: 10.1093/bioinformatics/bty560

Choe, S., Tanaka, A., Noguchi, T., Fujioka, S., Takatsuto, S., Ross, A. S., et al. (2000). Lesions in the sterol Δ7 reductase gene of Arabidopsis cause dwarfism due to a block in brassinosteroid biosynthesis. *Plant J.* 21, 431–443. doi: 10.1046/j.1365-313x.2000.00693.x

Danisman, S. (2016). TCP transcription factors at the interface between environmental challenges and the plant's growth responses. *Front. Plant Sci.* 7, 1930. doi: 10.3389/fpls.2016.01930

Ding, S., Zhang, J., Yang, L., Wang, X., Fu, F., Wang, R., et al. (2020). Changes in cuticle components and morphology of 'Satsuma'Mandarin (Citrus unshiu) during ambient storage and their potential role on Penicillium digitatum infection. *Molecules* 25, 412. doi: 10.3390/molecules25020412

Ensing, A., Gerson, E., Hofer, K., and Tanuseputra, O. (2016). The effect of water deficit on the growth rate of cer10 *Arabidopsis thaliana* mutants. *Expedition* 6. Available online at: https://ojs.library.ubc.ca/index.php/expedition/article/view/189104

Flagel, L. E., and Wendel, J. F. (2009). Gene duplication and evolutionary novelty in plants. *New Phytol.* 183, 557–564. doi: 10.1111/j.1469-8137.2009.02923.x

Frugoli, J. A., Mcpeek, M. A., Thomas, T. L., and Mcclung, C. R. (1998). Intron loss and gain during evolution of the catalase gene family in angiosperms. *Genetics* 149, 355–365. doi: 10.1093/genetics/149.1.355

Fujita, Y., Yoshida, T., and Yamaguchi-Shinozaki, K. (2013). Pivotal role of the AREB/ABF-SnRK2 pathway in ABRE-mediated transcription in response to osmotic stress in plants. *Physiol. Plant.* 147, 15–27. doi: 10.1111/j.1399-3054.2012.01635.x

Gan, L., Wang, X., Cheng, Z., Liu, L., Wang, J., Zhang, Z., et al. (2016). Wax crystal-sparse leaf 3 encoding a β-ketoacyl-CoA reductase is involved in cuticular wax biosynthesis in rice. *Plant Cell Rep.* 35, 1687–1698. doi: 10.1007/s00299-016-1983-1

Gasteiger, E., Hoogland, C., Gattiker, A., Wilkins, M. R., Appel, R. D., and Bairoch, A. (2005). "Protein identification and analysis tools on the ExPASy server," in *The Proteomics Protocols Handbook*, ed J. M. Walker (Totowa, NJ: Humana Press Inc), 571–607. doi: 10.1385/1-59259-890-0:571

Geourjon, C., and Deleage, G. (1995). SOPMA: significant improvements in protein secondary structure prediction by consensus prediction from multiple alignments. *Bioinformatics* 11, 681–684. doi: 10.1093/bioinformatics/11.6.681

Go, Y. S., Kim, H., Kim, H. J., and Suh, M. C. (2014). Arabidopsis cuticular wax biosynthesis is negatively regulated by the DEWAX gene encoding an AP2/ERF-type transcription factor. *Plant Cell* 26, 1666–1680. doi: 10.1105/tpc.114.123307

Han, J., Fang, J., Wang, C., Yin, Y., Sun, X., Leng, X., et al. (2014). Grapevine microRNAs responsive to exogenous gibberellin. *BMC Genom.* 15, 1–17. doi: 10.1186/1471-2164-15-111

Han, J., Kong, M., Xie, H., Sun, Q., Nan, Z., Zhang, Q., et al. (2013). Identification of miRNAs and their targets in wheat (*Triticum aestivum* L.) by EST analysis. *Genet. Mol. Res.* 12, 805. doi: 10.4238/2013.September.19.11

Hao, S., Ma, Y., Zhao, S., Ji, Q., Zhang, K., Yang, M., et al. (2017). McWRI1, a transcription factor of the AP2/SHEN family, regulates the biosynthesis of the cuticular waxes on the apple fruit surface under low temperature. *PLoS ONE* 12, e0186996. doi: 10.1371/journal.pone.0186996

Haslam, T. M., Haslam, R., Thoraval, D., Pascal, S., Delude, C., Domergue, F., et al. (2015). ECERIFERUM2-LIKE proteins have unique biochemical and physiological functions in very-long-chain fatty acid elongation. *Plant Physiol.* 167, 682–692. doi: 10.1104/pp.114.253195

Hooker, T. S., Lam, P., Zheng, H., and Kunst, L. (2007). A core subunit of the RNA-processing/degrading exosome specifically influences cuticular wax biosynthesis in Arabidopsis. *Plant Cell* 19, 904–913. doi: 10.1105/tpc.106.049304

Hooker, T. S., Millar, A. A., and Kunst, L. (2002). Significance of the expression of the CER6 condensing enzyme for cuticular wax production in Arabidopsis. *Plant Physiol.* 129, 1568–1580. doi: 10.1104/pp.003707

Katiyar, A., Smita, S., Chinnusamy, V., Pandey, D. M., and Bansal, K. (2012a). Identification of miRNAs in sorghum by using bioinformatics approach. *Plant Signal. Behav.* 7, 246–259. doi: 10.4161/psb.18914

Katiyar, A., Smita, S., Lenka, S. K., Rajwanshi, R., Chinnusamy, V., and Bansal, K. C. (2012b). Genome-wide classification and expression analysis of MYB transcription factor families in rice and Arabidopsis. *BMC Genom.* 13, 1–19. doi: 10.1186/1471-2164-13-544

Kaur, A., Pati, P. K., Pati, A. M., and Nagpal, A. K. (2017). *In-silico* analysis of cis-acting regulatory elements of pathogenesis-related proteins of *Arabidopsis thaliana* and *Oryza sativa*. *PLoS ONE* 12, e0184523. doi: 10.1371/journal.pone.0184523

Kelley, L. A., Mezulis, S., Yates, C. M., Wass, M. N., and Sternberg, M. J. (2015). The Phyre2 web portal for protein modeling, prediction and analysis. *Nat. Protoc.* 10, 845–858. doi: 10.1038/nprot.2015.053

Kim, D., and Langmead, B. (2015). Salzberg SLHISAT. A fast spliced aligner with low memory requirements. *Nat. Methods* 12, 357–360. doi: 10.1038/nmeth.3317

Kim, H., Yu, S.-I., Jung, S. H., Lee, B.-H., and Suh, M. C. (2019). The F-box protein SAGL1 and ECERIFERUM3 regulate cuticular wax biosynthesis in response to changes in humidity in Arabidopsis. *Plant Cell* 31, 2223–2240. doi: 10.1105/tpc.19.00152

Kohl, M., Wiese, S., and Warscheid, B. (2011). "Cytoscape: software for visualization and analysis of biological networks," in *Data Mining in Proteomics*, eds M. Hamacher, M. Eisenacher, and C. Stephan (Totowa, NJ: Humana Press), 291–303. doi: 10.1007/978-1-60761-987-1_18

Kumar, M., Patel, M. K., Kumar, N., Bajpai, A. B., and Siddique, K. H. (2021). Metabolomics and molecular approaches reveal drought stress tolerance in plants. *Int. J. Mol. Sci.* 22, 9108. doi: 10.3390/ijms22179108

Kumar, S., Nei, M., Dudley, J., and Tamura, K. (2008). MEGA: a biologist-centric software for evolutionary analysis of DNA and protein sequences. *Brief Bioinform.* 9, 299–306. doi: 10.1093/bib/bbn017

Lam, P., Zhao, L., Eveleigh, N., Yu, Y., Chen, X., and Kunst, L. (2015). The exosome and trans-acting small interfering RNAs regulate cuticular wax biosynthesis during Arabidopsis inflorescence stem development. *Plant Physiol.* 167, 323–336. doi: 10.1104/pp.114.252825

Lara, I., Heredia, A., and Domínguez, E. (2019). Shelf life potential and the fruit cuticle: the unexpected player. *Front. Plant Sci.* 10, 770. doi: 10.3389/fpls.2019.00770

Law, C. W., Alhamdoosh, M., Su, S., Dong, X., Tian, L., Smyth, G. K., et al. (2016). RNA-seq analysis is easy as 1-2-3 with limma, Glimma and edgeR. *F1000Research* 5: ISCB Comm J-1408. doi: 10.12688/f1000research.9005.3

Lescot, M. (2002). Patrice D hais, Gert Thijs, Kathleen Marchal, Yves Moreau, Yves Van de Peer, Pierre Rouz and Stephane Rombauts. *Nucleic Acids Res.* 30, 325–327. doi: 10.1093/nar/30.1.325

Letunic, I., and Bork, P. (2007). Interactive Tree Of Life (iTOL): an online tool for phylogenetic tree display and annotation. *Bioinformatics* 23, 127–128. doi: 10.1093/bioinformatics/btl529

Lewandowska, M., Keyl, A., and Feussner, I. (2020). Wax biosynthesis in response to danger: its regulation upon abiotic and biotic stress. *New Phytol.* 227, 698–713. doi: 10.1111/nph.16571

Li, H., Handsaker, B., Wysoker, A., Fennell, T., Ruan, J., Homer, N., et al. (2009). The sequence alignment/map format and SAMtools. *Bioinformatics* 25, 2078–2079. doi: 10.1093/bioinformatics/btp352

Li, N., Li, X., Song, Y., Yang, S., and Li, L. (2021). Genome-wide identification, characterization, and expression profiling of the ECERIFERUM (CER) gene family in *Ziziphus jujube*. *Russian J. Plant Physiol.* 68, 828–837. doi: 10.1134/S1021443721050101

Li, S. (2015). The *Arabidopsis thaliana* TCP transcription factors: a broadening horizon beyond development. *Plant Signal. Behav.* 10, e1044192. doi: 10.1080/15592324.2015.1044192

Lian, X.-Y., Wang, X., Gao, H.-N., Jiang, H., Mao, K., You, C.-X., et al. (2020). Genome-wide analysis and functional identification of MdKCS genes in apple. *Plant Physiol. Biochem.* 151, 299–312. doi: 10.1016/j.plaphy.2020.03.034

Liu, C., Wright, B., Allen-Vercoe, E., Gu, H., and Beiko, R. (2018). Phylogenetic clustering of genes reveals shared evolutionary trajectories and putative gene functions. *Genome Biol. Evol.* 10, 2255–2265. doi: 10.1093/gbe/evy178

Liu, L., Xu, W., Hu, X., Liu, H., and Lin, Y. (2016). W-box and G-box elements play important roles in early senescence of rice flag leaf. *Sci. Rep.* 6, 1–9. doi: 10.1038/srep20881

Liu, T., Tang, J., Chen, L., Zeng, J., Wen, J., Yi, B., et al. (2019). Differential expression of miRNAs and their targets in wax-deficient rapeseed. *Sci. Rep.* 9, 1–12. doi: 10.1038/s41598-019-48439-z,

Lü, S., Song, T., Kosma, D. K., Parsons, E. P., Rowland, O., and Jenks, M. A. (2009). Arabidopsis CER8 encodes LONG-CHAIN ACYL-COA SYNTHETASE 1 (LACS1) that has overlapping functions with LACS2 in plant wax and cutin synthesis. *Plant J.* 59, 553–564. doi: 10.1111/j.1365-313X.2009.03892.x,

Ma, D., Dong, S., Zhang, S., Wei, X., Xie, Q., Ding, Q., et al. (2021). Chromosome-level reference genome assembly provides insights into aroma biosynthesis in passion fruit (*Passiflora edulis*). *Mol. Ecol. Resour.* 21, 955–968. doi: 10.1111/1755-0998.13310

Masoudi-Nejad, A., Goto, S., Endo, T. R., and Kanehisa, M. (2007). "KEGG bioinformatics resource for plant genomics research," in *Plant Bioinformatics*, ed D. Edwards (Totowa, NJ: Humana Press), 437–458.

Medeiros, C., Falcão, H., Almeida-Cortez, J., Santos, D., Oliveira, A., and Santos, M. (2017). Leaf epicuticular wax content changes under different rainfall regimes, and its removal affects the leaf chlorophyll content and gas exchanges of Aspidosperma pyrifolium in a seasonally dry tropical forest. *South Afr. J. Bot.* 111, 267–274. doi: 10.1016/j.sajb.2017.03.033

Millar, A. A., Clemens, S., Zachgo, S., Giblin, E. M., Taylor, D. C., and Kunst, L. (1999). CUT1, an Arabidopsis gene required for cuticular wax biosynthesis and pollen fertility, encodes a very-long-chain fatty acid condensing enzyme. *Plant Cell* 11, 825–838. doi: 10.1105/tpc.11.5.825

Millar, A. A., and Kunst, L. (1997). Very-long-chain fatty acid biosynthesis is controlled through the expression and specificity of the condensing enzyme. *Plant J.* 12, 121–131. doi: 10.1046/j.1365-313X.1997.12010121.x

Mir, R. A., Bhat, B. A., Yousuf, H., Islam, S. T., Raza, A., Rizvi, M. A., et al. (2022). Multidimensional role of silicon to activate resilient plant growth and to mitigate abiotic stress. *Front. Plant Sci.* 13, 819658. doi: 10.3389/fpls.2022.819658

Munhoz, C., Santos, A., Arenhart, R., Santini, L., Monteiro-Vitorello, C., and Vieira, M. (2015). Analysis of plant gene expression during passion fruit-Xanthomonas axonopodis interaction implicates lipoxygenase 2 in host defense. *Ann. Appl. Biol.* 167, 135–155. doi: 10.1111/aab.12215

Ni, E., Zhou, L., Li, J., Jiang, D., Wang, Z., Zheng, S., et al. (2018). OsCER1 plays a pivotal role in verylong-chain alkane biosynthesis and affects plastid development and programmed cell death of tapetum in rice (*Oryza sativa* L.). *Front. Plant Sci.* 9, 1217. doi: 10.3389/fpls.2018.01217

Ni, Y., Guo, N., Zhao, Q., and Guo, Y. (2016). Identification of candidate genes involved in wax deposition in Poa pratensis by RNA-seq. *BMC Genom.* 17, 1–12. doi: 10.1186/s12864-016-2641-2

Nuruzzaman, M., Sharoni, A. M., and Kikuchi, S. (2013). Roles of NAC transcription factors in the regulation of biotic and abiotic stress responses in plants. *Front. Microbiol.* 4, 248. doi: 10.3389/fmicb.2013.00248

Pandey, P., Irulappan, V., Bagavathiannan, M. V., and Senthil-Kumar, M. (2017). Impact of combined abiotic and biotic stresses on plant growth and avenues for crop improvement by exploiting physio-morphological traits. *Front. Plant Sci.* 8, 537. doi: 10.3389/fpls.2017.00537

Pant, B. D., Buhtz, A., Kehr, J., and Scheible, W. R. (2008). MicroRNA399 is a long-distance signal for the regulation of plant phosphate homeostasis. *Plant J.* 53, 731–738. doi: 10.1111/j.1365-313X.2007.03363.x

Pascal, S., Bernard, A., Sorel, M., Pervent, M., Vile, D., Haslam, R. P., et al. (2013). The Arabidopsis cer26 mutant, like the cer2 mutant, is specifically affected in the very long-chain fatty acid elongation process. *Plant J.* 73, 733–746. doi: 10.1111/tpj.12060

Patanun, O., Lertpanyasampatha, M., Sojikul, P., Viboonjun, U., and Narangajavana, J. (2013). Computational identification of microRNAs and their targets in cassava (*Manihot esculenta* Crantz.). *Mol. Biotechnol.* 53, 257–269. doi: 10.1007/s12033-012-9521-z

Paul, S., De La Fuente-Jiménez, J. L., Manriquez, C. G., and Sharma, A. (2020). Identification, characterization and expression analysis of passion fruit (*Passiflora edulis*) microRNAs. *3 Biotech* 10, 1–9. doi: 10.1007/s13205-019-2000-5

Pighin, J. A., Zheng, H., Balakshin, L. J., Goodman, I. P., Western, T. L., Jetter, R., et al. (2004). Plant cuticular lipid export requires an ABC transporter. *Science* 306, 702–704. doi: 10.1126/science.1102331

Piya, S., Shrestha, S. K., Binder, B., Stewart C. N. Jr., and Hewezi, T. (2014). Protein-protein interaction and gene co-expression maps of ARFs and Aux/IAAs in Arabidopsis. *Front. Plant Sci.* 5, 744. doi: 10.3389/fpls.2014.00744

Qi, C., Jiang, H., Zhao, X., Mao, K., Liu, H., Li, Y., et al. (2019a). The characterization, authentication, and gene expression pattern of the MdCER family in *Malus domestica*. *Horticultural Plant J.* 5, 1–9. doi: 10.1016/j.hpj.2018.11.003

Qi, X., Ogden, E. L., Die, J. V., Ehlenfeldt, M. K., Polashock, J. J., Darwish, O., et al. (2019b). Transcriptome analysis identifies genes related to the waxy coating on blueberry fruit in two northern-adapted rabbiteye breeding populations. *BMC Plant Biol.* 19, 1–15. doi: 10.1186/s12870-019-2073-7

Raffaele, S., Vailleau, F., Léger, A., Joubès, J., Miersch, O., Huard, C., et al. (2008). A MYB transcription factor regulates very-long-chain fatty acid biosynthesis for activation of the hypersensitive cell death response in Arabidopsis. *Plant Cell* 20, 752–767. doi: 10.1105/tpc.107.054858

Raza, A. (2021). Eco-physiological and biochemical responses of rapeseed (*Brassica napus* L.) to abiotic stresses: consequences and mitigation strategies. *J. Plant Growth Regul.* 40, 1368–1388. doi: 10.1007/s00344-020-10231-z

Raza, A., Tabassum, J., Zahid, Z., Charagh, S., Bashir, S., Barmukh, R., et al. (2022). Advances in "omics" approaches for improving toxic metals/metalloids tolerance in plants. *Front. Plant Sci.* 2:2949. doi: 10.3389/fpls.2021.794373

Ridout, K. E., Dixon, C. J., and Filatov, D. A. (2010). Positive selection differs between protein secondary structure elements in Drosophila. *Genome Biol. Evol.* 2, 166–179. doi: 10.1093/gbe/evq008

Rizwan, H. M., Zhimin, L., Harsonowati, W., Waheed, A., Qiang, Y., Yousef, A. F., et al. (2021). Identification of fungal pathogens to control postharvest passion fruit (*Passiflora edulis*) decays and multi-omics comparative pathway analysis reveals purple is more resistant to pathogens than a yellow cultivar. *J. Fungi* 7, 879. doi: 10.3390/jof7100879

Rowland, O., Lee, R., Franke, R., Schreiber, L., and Kunst, L. (2007). The CER3 wax biosynthetic gene from *Arabidopsis thaliana* is allelic to WAX2/YRE/FLP1. *FEBS Lett.* 581, 3538–3544. doi: 10.1016/j.febslet.2007.06.065

Rowland, O., Zheng, H., Hepworth, S. R., Lam, P., Jetter, R., and Kunst, L. (2006). CER4 encodes an alcohol-forming fatty acyl-coenzyme A reductase involved in cuticular wax production in Arabidopsis. *Plant Physiol.* 142, 866–877. doi: 10.1104/pp.106.086785

Sakuradani, E., Zhao, L., Haslam, T. M., and Kunst, L. (2013). The CER22 gene required for the synthesis of cuticular wax alkanes in *Arabidopsis thaliana* is allelic to CER1. *Planta* 237, 731–738. doi: 10.1007/s00425-012-1791-y

Santos, A. A., Penha, H. A., Bellec, A., De Freitas Munhoz, C., Pedrosa-Harand, A., Bergès, H., et al. (2014). Begin at the beginning: a BAC-end view of the passion fruit (Passiflora) genome. *BMC Genom.* 15, 1–16. doi: 10.1186/1471-2164-15-816

Schmittgen, T. D., and Livak, K. J. (2008). Analyzing real-time PCR data by the comparative CT method. *Nat. Protoc.* 3, 1101–1108. doi: 10.1038/nprot.2008.73

Schnurr, J., Shockey, J., and Browse, J. (2004). The acyl-CoA synthetase encoded by LACS2 is essential for normal cuticle development in Arabidopsis. *Plant Cell* 16, 629–642. doi: 10.1105/tpc.017608

Shanks, C. M., Hecker, A., Cheng, C. Y., Brand, L., Collani, S., Schmid, M., et al. (2018). Role of BASIC PENTACYSTEINE transcription factors in a subset of cytokinin signaling responses. *Plant J.* 95, 458–473. doi: 10.1111/tpj.13962

Sharif, R., Raza, A., Chen, P., Li, Y., El-Ballat, E. M., Rauf, A., et al. (2021). HD-ZIP gene family: potential roles in improving plant growth and regulating stress-responsive mechanisms in plants. *Genes* 12, 1256. doi: 10.3390/genes12081256

Sharom, F. J., Kretzschmar, T., Burla, B., Lee, Y., Martinoia, E., and Nagy, R. (2011). Functions of ABC transporters in plants. *Essays Biochem.* 50, 145–160. doi: 10.1042/bse0500145

Shu, Y., Tao, Y., Wang, S., Huang, L., Yu, X., Wang, Z., et al. (2015). GmSBH1, a homeobox transcription factor gene, relates to growth and development and

involves in response to high temperature and humidity stress in soybean. *Plant Cell Rep.* 34, 1927–1937. doi: 10.1007/s00299-015-1840-7

Silvestro, D., Andersen, T. G., Schaller, H., and Jensen, P. E. (2013). Plant sterol metabolism. Δ7-sterol-C5-desaturase (STE1/DWARF7), Δ5, 7-sterol-Δ7-reductase (DWARF5) and Δ24-sterol-Δ24-reductase (DIMINUTO/DWARF1) show multiple subcellular localizations in *Arabidopsis thaliana* (Heynh) L. *PLoS ONE* 8, e56429. doi: 10.1371/journal.pone.0056429

Song, Q.-X., Liu, Y.-F., Hu, X.-Y., Zhang, W.-K., Ma, B., Chen, S.-Y., et al. (2011). Identification of miRNAs and their target genes in developing soybean seeds by deep sequencing. *BMC Plant Biol.* 11, 1–16. doi: 10.1186/1471-2229-11-5

Su, W., Raza, A., Gao, A., Jia, Z., Zhang, Y., Hussain, M. A., et al. (2021). Genome-wide analysis and expression profile of superoxide dismutase (SOD) gene family in rapeseed (*Brassica napus* L.) under different hormones and abiotic stress conditions. *Antioxidants* 10, 1182. doi: 10.3390/antiox10081182

Tafolla-Arellano, J. C., Zheng, Y., Sun, H., Jiao, C., Ruiz-May, E., Hernández-Oñate, M. A., et al. (2017). Transcriptome analysis of mango (*Mangifera indica* L.) fruit epidermal peel to identify putative cuticle-associated genes. *Sci. Rep.* 7, 1–13. doi: 10.1038/srep46163

Theune, M. L., Bloss, U., Brand, L. H., Ladwig, F., and Wanke, D. (2019). Phylogenetic analyses and GAGA-motif binding studies of BBR/BPC proteins lend to clues in GAGA-motif recognition and a regulatory role in brassinosteroid signaling. *Front. Plant Sci.* 10, 466. doi: 10.3389/fpls.2019.00466

Tian, F., Yang, D.-C., Meng, Y.-Q., Jin, J., and Gao, G. (2020). PlantRegMap: charting functional regulatory maps in plants. *Nucleic Acids Res.* 48, D1104–D1113. doi: 10.1093/nar/gkz1020

Trenkamp, S., Martin, W., and Tietjen, K. (2004). Specific and differential inhibition of very-long-chain fatty acid elongases from *Arabidopsis thaliana* by different herbicides. *Proc. Nat. Acad. Sci. U.S.A.* 101, 11903–11908. doi: 10.1073/pnas.0404600101

Tresch, S., Heilmann, M., Christiansen, N., Looser, R., and Grossmann, K. (2012). Inhibition of saturated very-long-chain fatty acid biosynthesis by mefluidide and perfluidone, selective inhibitors of 3-ketoacyl-CoA synthases. *Phytochemistry* 76, 162–171. doi: 10.1016/j.phytochem.2011.12.023

Van De Peer, Y., Maere, S., and Meyer, A. (2009). The evolutionary significance of ancient genome duplications. *Nat. Rev. Genet.* 10, 725–732. doi: 10.1038/nrg2600

Varkonyi-Gasic, E., Gould, N., Sandanayaka, M., Sutherland, P., and Macdiarmid, R. M. (2010). Characterization of microRNAs from apple (Malus domestic royal Gala') vascular tissue and phloem sap. *BMC Plant Biol.* 10, 1–15. doi: 10.1186/1471-2229-10-159

Wang, D., Ni, Y., Liao, L., Xiao, Y., and Guo, Y. (2021). Poa pratensis ECERIFERUM1 (PpCER1) is involved in wax alkane biosynthesis and plant drought tolerance. *Plant Physiol. Biochem.* 159, 312–321. doi: 10.1016/j.plaphy.2020.12.032

Wang, M., Wang, Q., and Zhang, B. (2013). Response of miRNAs and their targets to salt and drought stresses in cotton (*Gossypium hirsutum* L.). *Gene* 530, 26–32. doi: 10.1016/j.gene.2013.08.009

Wang, M., Wu, H., Xu, J., Li, C., Wang, Y., and Wang, Z. (2017). Five fatty acyl-coenzyme a reductases are involved in the biosynthesis of primary alcohols in Aegilops tauschiileaves. *Front. Plant Sci.* 8, 1012. doi: 10.3389/fpls.2017.01012

Wang, W., Liu, X., Gai, X., Ren, J., Liu, X., Cai, Y., et al. (2015). Cucumis sativus L. WAX2 plays a pivotal role in wax biosynthesis, influencing pollen fertility and plant biotic and abiotic stress responses. *Plant Cell Physiol.* 56, 1339–1354. doi: 10.1093/pcp/pcv052

Wang, Y., Jin, S., Xu, Y., Li, S., Zhang, S., Yuan, Z., et al. (2020). Overexpression of BnKCS1-1, BnKCS1-2, and BnCER1-2 promotes cuticular wax production and increases drought tolerance in *Brassica napus*. *Crop J.* 8, 26–37. doi: 10.1016/j.cj.2019.04.006

Wang, Y., Liu, G.-J., Yan, X.-F., Wei, Z.-G., and Xu, Z.-R. (2011). MeJA-inducible expression of the heterologous JAZ2 promoter from Arabidopsis in Populus trichocarpa protoplasts. *J. Plant Dis. Protect.* 118, 69–74. doi: 10.1007/BF03356384

Wingender, R., Röhrig, H., Höricke, C., and Schell, J. (1990). cis-regulatory elements are involved in ultraviolet light regulation and plant defense. *Plant Cell* 2, 1019–1026. doi: 10.1105/tpc.2.10.1019

Wong, A., Gehring, C., and Irving, H. R. (2015). Conserved functional motifs and homology modeling to predict hidden moonlighting functional sites. *Front. Bioeng. Biotechnol.* 3, 82. doi: 10.3389/fbioe.2015.00082

Wu, H., Shi, S., Lu, X., Li, T., Wang, J., Liu, T., et al. (2019). Expression analysis and functional characterization of CER1 family genes involved in very-long-chain alkanes biosynthesis in Brachypodium distachyon. *Front. Plant Sci.* 10, 1389. doi: 10.3389/fpls.2019.01389

Wu, Y., Huang, W., Tian, Q., Liu, J., Xia, X., Yang, X., et al. (2021). Comparative transcriptomic analysis reveals the cold acclimation during chilling stress in sensitive and resistant passion fruit (*Passiflora edulis*) cultivars. *PeerJ* 9, e10977. doi: 10.7717/peerj.10977

Xia, Z., Huang, D., Zhang, S., Wang, W., Ma, F., Wu, B., et al. (2021). Chromosome-scale genome assembly provides insights into the evolution and flavor synthesis of passion fruit (*Passiflora edulis* Sims). *Horticult. Res.* 8, 1–14. doi: 10.1038/s41438-020-00455-1

Xiong, J., Liu, L., Ma, X., Li, F., Tang, C., Li, Z., et al. (2020). Characterization of PtAOS1 promoter and three novel interacting proteins responding to drought in Poncirus trifoliata. *Int. J. Mol. Sci.* 21, 4705. doi: 10.3390/ijms21134705

Xu, G., Guo, C., Shan, H., and Kong, H. (2012). Divergence of duplicate genes in exon-intron structure. *Proc. Nat. Acad. Sci. U.S.A.* 109, 1187–1192. doi: 10.1073/pnas.1109047109

Xu, K., Huang, X., Wu, M., Wang, Y., Chang, Y., Liu, K., et al. (2014). A rapid, highly efficient, and economical method of Agrobacterium-mediated in planta transient transformation in living onion epidermis. *PLoS ONE* 9, e83556. doi: 10.1371/journal.pone.0083556

Xu, M., Li, A., Teng, Y., Sun, Z., and Xu, M. (2019). Exploring the adaptive mechanism of *Passiflora edulis* in karst areas via integrative analysis of nutrient elements and transcriptional profiles. *BMC Plant Biol.* 19, 1–16. doi: 10.1186/s12870-019-1797-8

Xue, D., Zhang, X., Lu, X., Chen, G., and Chen, Z.-H. (2017). Molecular and evolutionary mechanisms of cuticular wax for plant drought tolerance. *Front. Plant Sci.* 8, 621. doi: 10.3389/fpls.2017.00621

Yadav, V., Arif, N., Singh, V. P., Deshmukh, R., Sahi, S., Shivaraj, S., et al. (2020). "Roles of microRNAs in plant development and stress tolerance," in *Plant Life Under Changing Environment*, eds D. Kumar Tripathi, V. Pratap Singh, N. Ramawat et al. (Cambridge, MA: Academic Press), 719–733.

Yang, L., Qiu, L., Liu, D., Kuang, L., Hu, W., and Liu, Y. (2022). Changes in the crystal morphology, chemical composition, and key gene expression of'Suichuan'kumquat cuticular waxes after hot water dipping. *Sci. Hortic.* 293, 110753. doi: 10.1016/j.scienta.2021.110753

Yang, S. U., Kim, H., Kim, R. J., Kim, J., and Suh, M. C. (2020a). AP2/DREB transcription factor RAP2. 4 activates cuticular wax biosynthesis in Arabidopsis leaves under drought. *Front. Plant Sci.* 11, 895. doi: 10.3389/fpls.2020.00895

Yang, X., Feng, T., Li, S., Zhao, H., Zhao, S., Ma, C., et al. (2020b). CER16 inhibits post-transcriptional gene silencing of CER3 to regulate alkane biosynthesis. *Plant Physiol.* 182, 1211–1221. doi: 10.1104/pp.19.01002

Yeats, T. H., and Rose, J. K. (2013). The formation and function of plant cuticles. *Plant Physiol.* 163, 5–20. doi: 10.1104/pp.113.222737

Yu, C. S., Lin, C. J., and Hwang, J. K. (2004). Predicting subcellular localization of proteins for Gram-negative bacteria by support vector machines based on n-peptide compositions. *Protein Sci.* 13, 1402–1406. doi: 10.1110/ps.03479604

Zanca, A. S., Vicentini, R., Ortiz-Morea, F. A., Del Bem, L. E., Da Silva, M. J., Vincentz, M., et al. (2010). Identification and expression analysis of microRNAs and targets in the biofuel crop sugarcane. *BMC Plant Biol.* 10, 1–13. doi: 10.1186/1471-2229-10-260

Zhang, M., Zhang, P., Lu, S., Ou-Yang, Q., Zhu-Ge, Y., Tian, R., et al. (2021). Comparative analysis of cuticular wax in various grape cultivars during berry development and after storage. *Front. Nutr.* 1272:1272. doi: 10.3389/fnut.2021.817796

Zhang, Y., Zhu, X., Chen, X., Song, C., Zou, Z., Wang, Y., et al. (2014). Identification and characterization of cold-responsive microRNAs in tea plant (*Camellia sinensis*) and their targets using high-throughput sequencing and degradome analysis. *BMC Plant Biol.* 14, 1–18. doi: 10.1186/s12870-014-0271-x

Zhang, Y.-L., You, C.-X., Li, Y.-Y., and Hao, Y.-J. (2020). Advancesin biosynthesis, regulation, and function of apple cuticular wax. *Front. Plant Sci.* 11:1165. doi: 10.3389/fpls.2020.01165

Zhang, Y.-L., Zhang, C.-L., Wang, G.-L., Wang, Y.-X., Qi, C.-H., You, C.-X., et al. (2019a). Apple AP2/EREBP transcription factor MdSHINE2 confers drought resistance by regulating wax biosynthesis. *Planta* 249, 1627–1643. doi: 10.1007/s00425-019-03115-4

Zhang, Y.-L., Zhang, C.-L., Wang, G.-L., Wang, Y.-X., Qi, C.-H., Zhao, Q., et al. (2019b). The R2R3 MYB transcription factor MdMYB30 modulates plant resistance against pathogens by regulating cuticular wax biosynthesis. *BMC Plant Biol.* 19, 1–14. doi: 10.1186/s12870-019-1918-4

Zhao, C., Xia, H., Cao, T., Yang, Y., Zhao, S., Hou, L., et al. (2015). Small RNA and degradome deep sequencing reveals peanut microRNA roles in response to pathogen infection. *Plant Mol. Biol. Rep.* 33, 1013–1029. doi: 10.1007/s11105-014-0806-1

Zhao, H., Zhang, H., Cui, P., Ding, F., Wang, G., Li, R., et al. (2014). The putative E3 ubiquitin ligase ECERIFERUM9 regulates abscisic acid biosynthesis and response during seed germination and postgermination growth in Arabidopsis. *Plant Physiol.* 165, 1255–1268. doi: 10.1104/pp.114.239699

Zheng, H., Rowland, O., and Kunst, L. (2005). Disruptions of the Arabidopsis enoyl-CoA reductase gene reveal an essential role for verylong-chain fatty acid synthesis in cell expansion during plant morphogenesis. *Plant Cell* 17, 1467–1481. doi: 10.1105/tpc.104.030155

Zheng, Y., Chen, X., Wang, P., Sun, Y., Yue, C., and Ye, N. (2020). Genome-wide and expression pattern analysis of JAZ family involved in stress responses and postharvest processing treatments in *Camellia sinensis*. *Sci. Rep.* 10, 1–13. doi: 10.1038/s41598-020-59675-z

Conflict of Interest: The authors declare that the research was conducted in the absence of any commercial or financial relationships that could be construed as a potential conflict of interest.

Publisher's Note: All claims expressed in this article are solely those of the authors and do not necessarily represent those of their affiliated organizations, or those of the publisher, the editors and the reviewers. Any product that may be evaluated in this article, or claim that may be made by its manufacturer, is not guaranteed or endorsed by the publisher.

Copyright © 2022 Rizwan, Waheed, Ma, Li, Arshad, Irshad, Li, Yang, Ali, Ahmed, Shaheen, Scholz, Oelmüller, Lin and Chen. This is an open-access article distributed under the terms of the Creative Commons Attribution License (CC BY). The use, distribution or reproduction in other forums is permitted, provided the original author(s) and the copyright owner(s) are credited and that the original publication in this journal is cited, in accordance with accepted academic practice. No use, distribution or reproduction is permitted which does not comply with these terms.

frontiers | Frontiers in Plant Science

ORIGINAL RESEARCH
published: 05 July 2022
doi: 10.3389/fpls.2022.895427

Salicylic Acid Priming Regulates Stomatal Conductance, Trichome Density and Improves Cadmium Stress Tolerance in *Mentha arvensis* L.

Abbu Zaid[1,2*†], *Firoz Mohammad*[1] *and Kadambot H. M. Siddique*[3*]

[1]*Plant Physiology and Biochemistry Section, Department of Botany, Aligarh Muslim University, Aligarh, India,* [2]*Department of Botany, Government Degree College Doda, Doda, India,* [3]*The UWA Institute of Agriculture, The University of Western Australia, Perth, WA, Australia*

OPEN ACCESS

Edited by:
Mohammad Anwar Hossain, Bangladesh Agricultural University, Bangladesh

Reviewed by:
Tetiana Kalachova, Academy of Sciences of the Czech Republic, Czechia
Anis Ali Shah, University of Education Lahore, Pakistan

***Correspondence:**
Abbu Zaid
zaidabbu19gmail.com
Kadambot H. M. Siddique
kadambot.siddique@uwa.edu.au

†ORCID:
Abbu Zaid
orcid.org/0000-0002-2090-0212

Specialty section:
This article was submitted to Plant Breeding, a section of the journal Frontiers in Plant Science

Received: *13 March 2022*
Accepted: *06 June 2022*
Published: *05 July 2022*

Citation:
Zaid A, Mohammad F and Siddique KHM (2022) Salicylic Acid Priming Regulates Stomatal Conductance, Trichome Density and Improves Cadmium Stress Tolerance in Mentha arvensis L. Front. Plant Sci. 13:895427. doi: 10.3389/fpls.2022.895427

The application of phytohormones through seed priming could enhance quality of important medicinal and aromatic plants (MAPs) under heavy metal stress. We evaluated the potential of salicylic acid (SA) priming for overcoming the adverse effects of cadmium stress in *Mentha arvensis* L. plants. Suckers of plants were primed with SA before transplanting them into soil. At 30 days after transplanting, two doses (50 and 100 μm) of $CdCl_2$ were applied to the soil. Both Cd treatments altered plant growth, photosynthetic pigments, leaf gas exchange attributes, and mineral nutrient contents. The 50 and 100 μm Cd treatments increased endogenous Cd content by 97.95 and 98.03%, electrolyte leakage (EL) by 34.21 and 44.38%, hydrogen peroxide (H_2O_2) by 34.71 and 55.80%, malondialdehyde (MDA) by 53.08 and 63.15%, and superoxide content ($O_2^{-\bullet}$) by 24.07 and 38.43%, respectively. Cd triggered the up-regulation of antioxidant enzyme activities (superoxide dismutase, SOD; catalase, CAT; ascorbate peroxidase, APX; and glutathione reductase GR) and increased osmolyte biosynthesis and, interestingly, secondary metabolite (SM) accumulation. The presence of SA and Cd had an additive effect on these parameters. Nevertheless, plants primed with SA regulated stomatal conductance under Cd stress. SA priming to menthol mint plants under Cd stress overcome the effects of Cd stress while increasing SMs.

Keywords: cadmium stress, *Mentha arvensis*, photosynthesis, salicylic acid, secondary metabolites

INTRODUCTION

Heavy metal (HM) contamination is ubiquitous in all the spheres of the environment, *viz.* biosphere, lithosphere, atmosphere, hydrosphere, and anthroposphere. The plant–soil interface acts as a channel for different HMs to circulate into different environmental compartments and ultimately reach humans and plants through the food chain. In particular, cadmium (Cd) is a potent and noteworthy environmental contaminant. In most soils, Cd is present as a trace

element. However, due to high industrialization and sophisticated anthropogenic activities, such as the discharge of sewage sludge, mining, phosphorous fertilizers, and industrial effluents, excessive amounts of Cd are bio-available in vast tracts of lands (Zhang et al., 2009; He et al., 2015; Gao et al., 2018; Zaid et al., 2019a; Shah et al., 2020a,b). Cd pollution is the representative HM contamination in soil, as Cd^{2+} ions are readily absorbed by crop plants (DalCorso et al., 2008; Rizwan et al., 2018). In plants, Cd can close stomata, generate reactive oxygen species (ROS), oxidize membranes, lipids and proteins, and decrease photosynthetic potential, subsequently disturbing plant growth and development (Zaid and Mohammad, 2018; Bari et al., 2019; Pourghasemian et al., 2019).

Menthol mint (*Mentha avensis* L.) is a wild mint variety widely cultivated for its phytopharmaceutical importance (Nigam et al., 2019). Soil Cd enrichment is posing a major threat to its productivity by inducing oxidative stress. *M. arvensis* L. owes its aromatic properties to the presence of an essential oil (EO) rich in SMs and volatile constituents, including menthol, menthone, methyl acetate, and carvacrol, that impart its characteristic mint flavor (Tiwari, 2016). Advances in *M. arvensis* trichome research, stomatal conductance, and SMs biosynthesis under Cd stress have received little attention. Till date, no study has reported plant growth regulator (PGR)-mediated mechanisms of action for enhancing tolerance to Cd stress and SM production in *M. arvensis*.

Plant stress physiologists have attempted to reduce Cd contamination in soils and crop plants using various organic and inorganic molecules (Rizwan et al., 2016, 2017, 2019b; Zaid and Mohammad, 2018). The application of PGRs to reduce Cd uptake and alleviate Cd toxicity and to boost yield and quality attributes might be a cost-effective, practical, sustainable strategy for MAPs. External supplementation of PGRs is considered an effective practice for reducing the toxic effects of Cd contamination in different crop plants (Rizwan et al., 2016; Zaid and Mohammad, 2018). We recently showed that the external application of PGRs and mineral nutrients had a synergistic effect on alleviating the negative effect of Cd stress on menthol mint plants (Zaid and Mohammad, 2018; Zaid et al., 2020). The incorporation of *M. arvensis* biochar in the soil increased HM tolerance in *M. arvensis* in terms of improving yield and nutrient uptake (Nigam et al., 2019). The concomitant application of depolymerized polysaccharides and PGRs modulated physiological activities, active constituents, and EO production in menthol mint plants (Naeem et al., 2017). Bose et al. (2013) studied the synergistic effect of PGRs and diterpenoid on growth attributes, trichome size, density, and number, EO biosynthesis and the expression of some oil biosynthetic pathway genes. The effect of exogenous treatment of SA on growth, photosynthetic traits and EO production of peppermint plants exposed to soil-applied Cd was studied and the results advocated the ameliorative role of SA (Ahmad et al., 2018).

Seed priming before sowing is an important strategy to ensure optimum hydration for seeds without enabling radical emergence (Hussain et al., 2019b). Priming tends to enhance plant tolerance to abiotic stress by improving plant growth and cellular homeostasis under various stress conditions (Jisha et al., 2013; Savvides et al., 2016). SA is a potent PGR known to impart stress resistance in diverse crop plants (Khan et al., 2015; Ahmad et al., 2019; Santisree et al., 2020). Studies have shown that priming with PGRs is a promising field in plant stress physiology and crop stress management, which can overcome the toxic impacts of abiotic stresses in plants (Lal et al., 2018; Moulick et al., 2018; Panuccio et al., 2018; Sheteiwy et al., 2018). Priming with PGRs is regarded as an eco-friendly, cost-effective, and sustainable practice for reducing the effects of HM stress in plants (Sytar et al., 2018). Hassan and Mansoor (2017) showed that seed priming with PGRs alleviated Cd toxicity in mungbean. Priming with SA could boost growth, photosynthetic capacity and ameliorate the ill effects of HM stress in plants. For example in maize, Zanganeh et al. (2018) studied the coordinated role of seed priming with SA and sodium hydrosulfide under Pb stress. Shahnawaz et al. (2017) studied the impact of Al toxicity on barley cultivars and its alleviation through seed priming with ascorbic acid and SA. In a recent study, we identified the potential of exogenous SA for overcoming nickel stress in Indian mustard plants (Zaid et al., 2019b). However, the role of SA *via* priming under Cd stress in *M. arvensis* in relation to SM modulation and physio-biochemical traits has not been evaluated till date. Therefore, the present study aimed to determine (a) the effects of Cd stress on growth traits, photosynthetic potential, stomatal conductance, and yield and quality traits, (b) the potential of priming suckers with SA to mitigate the adverse impacts of Cd stress, and (c) whether SA priming enhances SM production in menthol mint plants in Cd-contaminated soils.

MATERIALS AND METHODS

Sucker Priming and Stress Treatment

The experiment was performed in a net house at the Botany Department, Aligarh Muslim University Aligarh, India (27°52′N, 78°51′E, 187.45 m altitude), with average day/night temperatures of 26 ± 3/14 ± 2°C, 65 ± 5% relative humidity, 815 ± 20 μmol m^{-2} s^{-1} photosynthetically active radiation (PAR), and 10–12 h critical photoperiod. Uniform suckers of *M. arvensis* Linn. "Kushal" were hand-picked for surface sterilization with 5% NaOCl solution for 6 min, followed by repeated washing with deionized and double distilled water (DDW). The suckers were primed with a solution of SA (10^{-6} M) in the dark at room T for 30 min and then transplanted to earthen pots. Each pot (25 × 25 cm) contained a 5 kg mixture of soil and farmyard manure (4:1). The physicochemical characteristics of the soil were sandy loam texture, pH (1:2) 7.9, EC (1:2) 0.58 mmhos cm^{-1}, and 96.8, 9.6, and 158.91 mg kg^{-1} soil available N, P, and K, respectively. A basal dose of N, P, and K ($N_{100}P_{50}K_{50}$; Khanuja et al., 2006) was applied, being 44.6 mg N, 22.3 mg P_2O_5, and 27.3 mg K_2O kg^{-1} soil as urea, single superphosphate and muriate of potash, respectively. After germination, plants were thinned, and three healthy seedlings were maintained in each pot. Thirty days after transplanting (DAT), two Cd treatments (50 and 100 μm) were applied to pots. A dilute

stock aqueous solution of cadmium chloride ($CdCl_2$) was prepared by dissolving 1.63 g of $CdCl_2$ in 100 ml of DDW and then the required quantity prepared by further diluting the stock solution with DDW. Control plants were provided with DDW only. The experimental pots were positioned in a randomized complete block design. In all, there were six treatments with five replications ($n = 5$): Control (CN; 0 µm Cd + 0 M SA); Salicylic acid (SA 10^{-6} M + Cd 0 µm); Cadmium (50 µm + 0 M SA); Cadmium + Salicylic acid (50 µm + 10^{-6} M SA); Cadmium (100 µm + 0 M SA); Cadmium + Salicylic acid (100 µm + 10^{-6} M SA). The plants were harvested at 100 DAT. Biochemical parameters and antioxidant enzyme activities of the menthol mint plants were determined in the topmost fully expanded young leaves.

Determination of Growth Parameters

Plant height (PH) was measured with a scale. Plant fresh and dry weights were weighed by using an electronic balance (Verbal 100 Super, Varanasi, Balance Works, Varanasi, India). After recording fresh weight, samples were oven-dried for dehydration at 70°C for 24 h and then weighed. The number of leaves per pot was counted manually. Leaf area was determined using a leaf area meter (AM 350, ADC Bioscientific, Hoddesdon, Herts, United Kingdom).

Determination of Photosynthetic Pigments

Photosynthetic pigment determination followed the protocol of Lichtenthaler and Buschmann (2001). Fresh leaf tissue (100 mg) was harvested and ground with 100% acetone (v/v) using a deep freezer cooled mortar and pestle. The absorbance of the pigment solution was recorded at 663, 645, and 470 nm to determine the contents of chlorophyll a, chlorophyll b, and carotenoids, respectively, using a spectrophotometer (ELICO SL 171 MINI SPEC) and dimethyl sulfoxide (DMSO) as a blank. Total chlorophyll (Chl) content was estimated by adding the contents of chlorophyll a and b. All pigments were expressed as mg g^{-1} leaf FW.

Determination of Leaf Gas Exchange Attributes

Leaf gas exchange measurements [net photosynthetic rate (P_N), stomatal conductance (g_s), carbon dioxide assimilation rate (*Ci*), and water use efficiency (WUE)] were measured on the uppermost fully expanded leaves in full and bright sunlight between 10:00 h and 12:00 h using IRGA (Li-COR 6400, Li-COR, Lincoln, NE, United States).

Determination of Oxidative Stress Biomarkers

The superoxide ($O_2^{-\bullet}$) content was determined by estimating nitrite production from the reaction of hydroxylamine with superoxide anions by adopting the standard method of Wang and Luo (1990). A 1 g leaf sample was homogenized in phosphate buffer (50 mm, pH 7.8) and polyvinylpyrrolidone solution and centrifuged for 20 min at 4°C. The supernatant was mixed with potassium phosphate buffer and hydroxylamine hydrochloride (50 mm, pH 7.8), then dissolved in a 3-aminobenzenesulphonic acid (17 mm) and 1-naphthylamine (7 mm) and incubated for 20 min at room T. The absorbance was measured at 530 nm and the $O_2^{-\bullet}$ generation rate calculated from the standard curve of sodium nitrite and expressed as µmol g^{-1} leaf FW.

Thiobarbituric acid reactive substances (TBARS) content was determined by estimating the MDA equivalents following the method of Hodges et al. (1999). Liquid N_2 frozen leaf tissue (0.5 g) was homogenized in 80% ethanol. The homogenate was centrifuged at 3000 *g* for 10 min. The supernatant (1 ml) was removed and added to an equal volume of 20% trichloroacetic acid (TCA), 0.65% thiobarbituric acid (TBA), and 0.01% butylated hydroxytoluene. The samples were heated at 90°C for 30 min, followed by gradual cooling to room T. Absorbance of the samples was read at 440, 532, and 600 nm, relative to a blank sample with no TBA present, to record MDA concentration.

The method of Sullivan and Ross (1979) was used to determine electrolyte leakage (EL); the detailed protocols described in Zaid and Mohammad (2018). Electrolyte leakage was calculated as follows:

$$\text{Electrolyte leakage } (\%) = [(ECb - ECa)/(ECc) \times 100].$$

The standard method of Jana and Choudhari (1981) was used for H_2O_2 determination. A fresh leaf sample (500 mg) was homogenized in 3.0 ml of phosphate buffer (50 mm and pH 6.8) and centrifuged at 6000 *g* for 30 min. After that, 3.0 ml of extract was removed and 1 ml of 0.1% titanium chloride in 20% (v/v) H_2SO_4 added to it. Centrifugation was carried out at 6000 *g* for 15 min. The absorbance of the reaction mixture was read at 410 nm on a spectrophotometer (ELICO SL 171 MINI SPEC, India).

Estimation of Antioxidant Activities

Freshly collected leaf material (500 mg) was frozen and ground to a powder using liquid N_2 in a pre-chilled mortar and pestle. After then, the samples were centrifuged at 12,000 *g* for 30 min at 4°C. The pellet was discarded and the supernatant used to determine different enzyme activities.

Superoxide dismutase activity (SOD, EC1.15.1.1) was measured using the nitroblue tetrazolium (NBT) reduction method (Kono, 1978). Catalase (CAT, 1.11.1.6) activity was determined by monitoring the disappearance of H_2O_2 for 2 min at 240 nm (Aebi, 1984). The complete methodology for SOD and CAT determination is described elsewhere (Khanam and Mohammad, 2018). Ascorbate peroxidase (APX, 1.11.1.11) activity was determined using the protocol of Nakano and Asada (1981). Glutathione reductase (GR, 1.6.4.2) activity was measured according to the method of Smith et al. (1988). Enzyme activities were expressed in enzyme units g^{-1} FM. All spectrophotometric analyses were conducted with a spectrophotometer (ELICO SL 171 MINISPEC).

Determination of Proline, Glycine Betaine, and Leaf Mineral Nutrients

Proline (Pro) and glycine betaine (GB) contents were determined according to the methods of Bates et al. (1973) and Grieve and Grattan (1983), respectively.

For mineral nutrient determinations, oven-dried leaf material (100 mg) was added to a 50 ml Kjeldahl flask containing an acid-peroxide solution and heated on a dry block heater. Aliquots of this solution were used to determine leaf N, P, and K contents. Leaf N content was determined using the protocol of Lindner (1944). The absorbance of the reaction mixture was read at 525 nm. Leaf P content was determined following the methodology of Fiske and Subbarow (1925). The intensity of the blue color formed was recorded at 620 nm. Leaf K content was determined by flame emission spectroscopy using a flame photometer (Model, ELICO, CL22D, India), running at 10 psi pressure (Hald, 1947).

Scanning Electron Microscopy and Energy Dispersive X-ray Analyzer

The method of Zaid and Mohammad (2018) was used for scanning electron microscopy (SEM) and energy dispersive X-ray analyzer (EDX) analysis. Fresh leaves from axillary positions were collected and fixed with 2.5% glutaraldehyde plus 2% paraformaldehyde in 0.1 M phosphate buffer (pH 7.0) for 4 h. This was followed by a second fixing with 1% osmium tetroxide in P buffer (pH 7.0) for 1 hand washing with P buffer for 20 min. Fixation was followed by alcohol dehydration in a graded series of ethanol (50, 70, 80, 90, 95, and 100%). Fixed and dehydrated leaves were dehydrated in a Carl Zeiss EVO 40 (Germany) scanning electron microscope critical point dryer with liquid CO_2. The leaf samples were coated with gold–palladium and observed under a Carl Zeiss EVO 40 (Germany) scanning electron microscope at high voltage (15 kV) and magnifications of 4,000× for stomata and 100× for peltate glandular trichomes (PGT).

Estimation of Essential Oil Content and Secondary Metabolites by Gas Chromatography

Essential oil (EO) content was determined following the hydro-distillation technique of Guenther (1972), whereby 50 g of freshly collected leaves were allowed for 3 h distillation. The oil was collected in vials of Clevenger apparatus and weighed. The oil percentage was calculated as follows: EO percentage = oil content/leaf weight × 100. Secondary metabolite (menthol, menthone, and methyl acetate) contents of the EO were determined by gas chromatography (GC) using the known peak area in the chromatogram (Adams, 2007). The estimation of SMs used a gas chromatograph (Nucon 5,700, New Delhi, India) equipped with an AT-1000 stainless steel column, flame ionization detector, and integrator. N gas was used as the carrier. N, H, and O flow rates were adjusted at 0.5, 0.5, and 5 mLs^{-1}, respectively. The sample size was 2 µl. The T recorded was 160°C oven, 250°C detector, and 250°C injector.

Statistical Analysis

Data were analyzed following one-way analysis of variance (ANOVA) using SPSS software version 17. The values presented are means ± SE ($n = 5$). Different letters indicate significant differences between treatments at $p \leq 0.05$. Principal component analysis was performed using Minitab Mtb EXE (2) software (Minitab Inc., State College PA, United States).

RESULTS

Effect of Salicylic Acid on Plant Growth Parameters Under Cadmium Stress

The Cd treatments significantly decreased ($p \leq 0.05$) plant fresh and dry weights, by 18.16 and 40.84% at 50 µm and 8.52 and 26.13% at 100 µm, respectively, relative to the control (**Table 1**). The SA + Cd treatments increased plant fresh weights by 7.57 and 26.66% and dry weights by 20.94 and 12.08% at 50 and 100 µM, respectively, relative to the respective Cd-only treatments. PH declined significantly ($p \leq 0.05$) by 10.25 and 17.70%, relative to the control plants. Priming with SA increased PH in Cd-stressed plants by 6.56 and 7.37% at 50 and 100 µm, respectively, relative to the respective Cd-only treatments (**Table 1**).

Leaf number declined by 13.15 and 48.68% at 50 and 100 µm, respectively, relative to the control plants. Priming with SA increased leaf number by 14.28 and 38.09% at 50 and 100 µm, respectively, relative to the respective Cd-only treatments. Leaf area also declined significantly ($p \leq 0.05$) by 22.45 and 39.35% at 50 and 100 µm, respectively, relative to the control plants. Priming with SA increased leaf area by 22.15 and 27.01% at 50 and 100 µm, respectively, relative to the respective Cd-only treatments (**Table 1**).

Salicylic Acid Restored Photosynthetic Pigments and Gas Exchange Attributes

The Cd treatments had a negative effect on photosynthetic pigments (Chl a, b, total Chl, and carotenoids). Chl a and b contents declined by 7.94 and 5.71% at 50 µm and 15.23 and 20% at 100 µm, respectively, relative to the control plants. Total Chl and carotenoid content also declined by 7.52 and 16.12% at 50 µm and 3.22 and 16.12% at 100 µm, respectively, relative to the control plants (**Table 2**). Priming with SA restored the photosynthetic pigment inhibition, increasing Chl a by 2.79 and 3.03%, Chl b by 13.15 and 12.50%, total Chl by 4.79 and 4.87%, and Caro content by 6.25 and 7.14% at 50 and 100 µm, respectively, relative to the respective Cd-only treatments (**Table 2**).

The Cd treatments reduced P_N by 29.47 and 55.88% at 50 and 100 µm, respectively, relative to the control plants. Priming with SA significantly improved P_N by 16.83 and 13.23% at 50 and 100 µm, respectively, relative to the respective Cd-only treatments (**Figure 1A**). Priming with SA reversed the decline in *gs* and Ci caused by Cd stress to values 3.35 and 1.89% at 50 µm and 3.85 and 1.83% at 100 µm higher than the respective Cd-only treatments (**Figures 1B,C**). The 50 and 100 µm Cd treatments decreased WUE by 24.44 and 46.66%, respectively, relative to the control plants. Priming with SA increased WUE by 24.44 and 25% at 50 and 100 µm, respectively, relative to the respective Cd-only treatments (**Figure 1D**).

TABLE 1 | Plant fresh and dry weights (g), plant height (cm), and leaf number and area per plant, of *Mentha arvensis* cultivar "Kushal" grown under 50 and 100 μm Cd levels and primed with or without salicylic acid.

Treatments	Plant fresh weight (g)	Plant dry weight (g)	Plant height (cm)	Leaf/plant	Area/leaf (cm^2)
CN	65.00 ± 2.90b	26.29 ± 1.29ab	79.93 ± 1.63b	15.20 ± 0.91b	7.75 ± 1.17b
SA (10^{-6} M)	75.90 ± 1.22a	31.47 ± 1.43a	88.04 ± 1.35a	20.00 ± 1.88a	9.31 ± 1.18a
Cd 50 (μm)	53.19 ± 0.69c	24.05 ± 1.03bc	71.73 ± 1.03c	13.20 ± 1.47b	6.01 ± 0.56cd
Cd 50 (μm) + SA (10^{-6} M)	57.55 ± 2.22c	30.42 ± 0.89a	76.77 ± 1.43b	15.40 ± 1.51b	7.72 ± 1.01b
Cd 100 (μm)	38.45 ± 2.57d	19.42 ± 1.29c	65.78 ± 1.48d	7.80 ± 1.21c	4.70 ± 0.77d
Cd 100 (μm) + SA (10^{-6} M)	52.43 ± 1.88c	22.09 ± 1.31bc	71.02 ± 0.92c	12.60 ± 1.06b	6.44 ± 1.07bc

Data are presented as treatments mean ± SE (n = 5). Data followed by the same letters are not significantly different by Duncan multiple range test at $p \leq 0.05$.

TABLE 2 | Contents of chlorophyll a, b, total chlorophyll, and carotenoids (mg g^{-1}FW) of *Mentha arvensis* cultivar "Kushal" grown under 50 and 100 μm Cd levels and primed with or without salicylic acid.Data are presented as treatments mean ± SE (*n* = 5).

Treatments	Chlorophyll a (mg g^{-1}FW)	Chlorophyll b (mg g^{-1}FW)	Total Chlorophyll (mg g^{-1}FW)	Carotenoids (mg g^{-1}FW)
CN	1.51 ± 0.01b	0.35 ± 0.07b	1.86 ± 0.04b	0.31 ± 0.01b
SA (10^{-6} M)	1.62 ± 0.02a	0.40 ± 0.07a	2.02 ± 0.01a	0.37 ± 0.01a
Cd 50 (μm)	1.39 ± 0.01c	0.33 ± 0.05bc	1.72 ± 0.01c	0.30 ± 0.07bc
Cd 50 (μm) + SA (10^{-6} M)	1.43 ± 0.02c	0.38 ± 0.09a	1.81 ± 0.03b	0.32 ± 0.07b
Cd 100 (μm)	1.28 ± 0.01d	0.28 ± 0.01d	1.56 ± 0.01e	0.26 ± 0.00c
Cd 100 (μm) + SA (10^{-6} M)	1.32 ± 0.02d	0.32 ± 0.07c	1.64 ± 0.01d	0.28 ± 0.02bc

Data followed by the same letters are not significantly different by Duncan multiple range test at $p \leq 0.05$.

Salicylic Acid Reduced Thiobarbituric Acid Reactive Substance, Electrolyte Leakage, Hydrogen Peroxide Content, and Superoxide Ion Production Under Cadmium Stress

The Cd treatments increased TBARS content, EL, H_2O_2 content, and $O_2^{-\bullet}$ production by 53.08, 34.21, 34.71 and 24.07% at 50 μM, respectively, relative to the control (**Figures 2A–D**), which was intensified further at 100 μM. Priming with SA significantly reduced TBARS content by 32.98%, EL by 32.83%, H_2O_2 content by 19.06%, and $O_2^{-\bullet}$ production by 25.58% in the 50 μm Cd treatment, relative to respective Cd-only treatment. At 100 μm Cd, SA priming decreased TBARS content by 30.33%, EL by 10.47%, in H_2O_2 content by 18.60% and $O_2^{-\bullet}$ production by 26.77%, relative to respective Cd-only treatment (**Figures 2A–D**).

Salicylic Acid Enhanced Antioxidant Enzyme Activities

The Cd treatments increased the activities of SOD, CAT, APX, and GR by 3.27 and 7.90%, 7.27 and 11.79%, 40.73 and 67.47%, 30.32 and 56.57% at 50 and 100 μm, respectively, relative to the control plants. Priming with SA had an additive impact on SOD, CAT, APX, and GR activities, which increased by 2.18 and 2.88%, 2.13 and 3.09%, 23.20 and 25.16%, and 9.23 and 12.88% at 50 and 100 μm, respectively, relative to the respective Cd-only treatments (**Figures 3A–D**).

Effect of Salicylic Acid and Cadmium on Osmoprotectants and Mineral Nutrient Contents

The Cd treatments triggered the accumulation of pro and GB in the presence or absence of SA. The pro and GB contents increased significantly ($p \leq 0.05$) by 1.39-fold and 1.83-fold, and 2.69-fold and 2.98-fold, at 50 μm and 100, respectively, relative to the control plants. Priming with SA increased pro and GB contents by 1.41-fold and 1.29-fold at 50 μm and 1.39-fold and 1.41-fold at 100 μm, relative to the respective Cd-only treatments (**Figures 4A,B**).

The Cd treatments decreased the mineral nutrient (N, P, and, K) contents, relative to the control plants. Priming with SA increased N content by 28.42%, P by 23.68%, and K by 13.55% at 50 μm and N by 28.20%, P by 16.94% and K (not significant) by 16.66% at 100 μm, relative to the respective Cd-only treatments (**Figures 4E,F**).

Salicylic Acid Reduced Cadmium Content as Evidenced by EDX

The plants in the 50 and 100 μm Cd treatments accumulated 97.95 and 98.03% more Cd, respectively, than the control plants. Priming with SA reduced Cd content by 79.59 and 29.41% at 50 and 100 μm, respectively, relative to the respective Cd-only treatments (**Figure 5D**).

Salicylic Acid and Cadmium Enhanced Essential Oil Content and Secondary Metabolite Production

The Cd treatments increased EO content and EO yield. Priming with SA had an additive effect, increasing EO content by 4.76% and EO yield by 8.16% at 50 and 100 μm, respectively, relative to the respective Cd-only treatments (**Figures 4C,D**).

Priming with SA triggered the production of SM in menthol mint plants in both Cd treatments; 50 μm Cd increased menthol content by 6.40% and menthone by 13.94% but decreased methyl acetate, and 100 μm Cd increased menthol content by

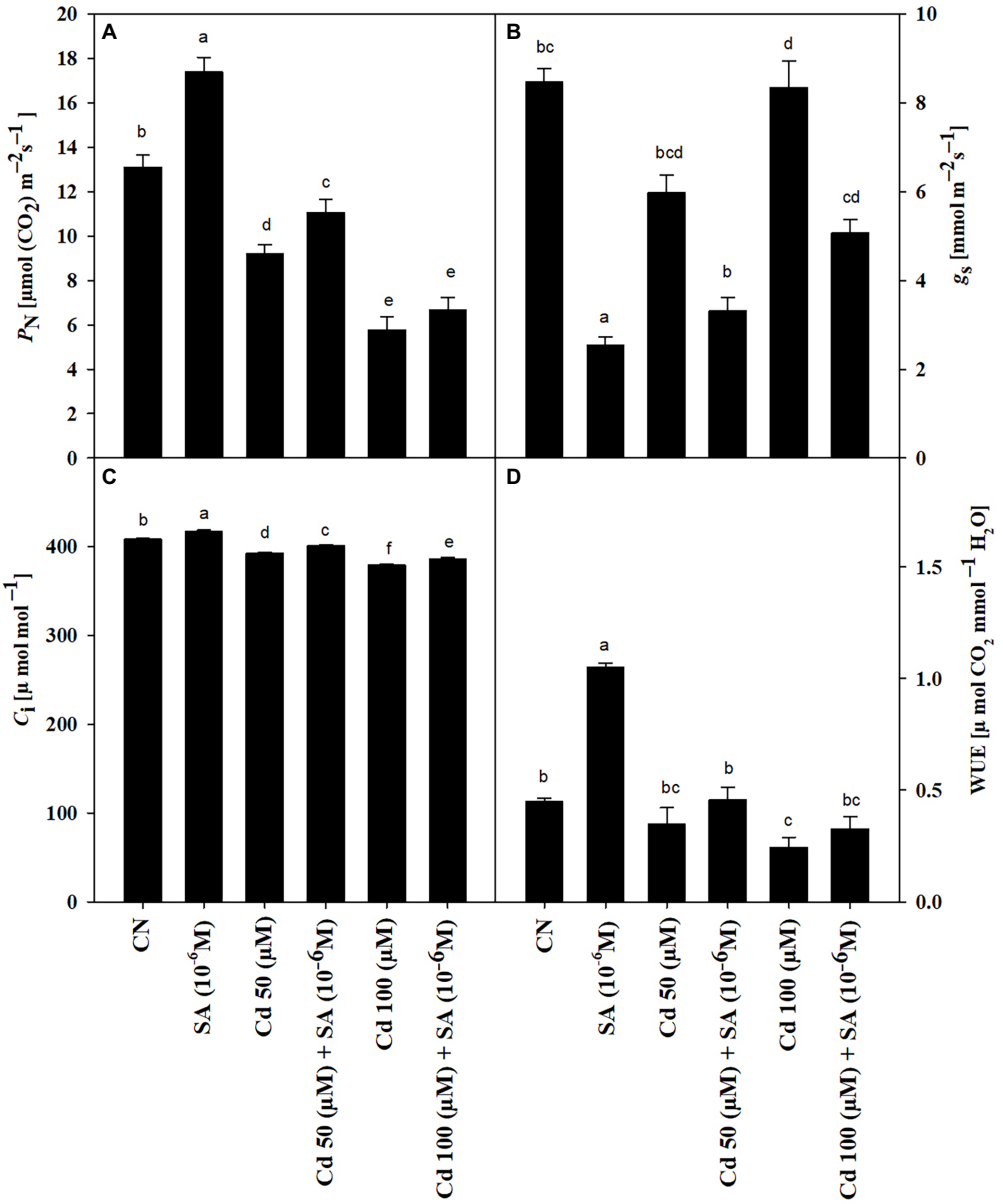


FIGURE 1 | (A) Net photosynthetic rate, P_N (µmol CO_2 m^{-2} s^{-1}), **(B)** stomatal conductance, g_s (mmol m^{-2} s^{-1}), **(C)** intercellular CO_2 concentration, C_i (µmol mol^{-1}), and **(D)** water use efficiency, WUE (µmol CO_2 $mmol^{-1}$ H_2O) of *Mentha arvensis* cultivar "Kushal" grown under 50 and 100 µm Cd levels and primed with or without salicylic acid. Data are presented as treatments mean ± SE ($n = 5$). Data followed by the same letters are not significantly different by Duncan multiple range test at $p \leq 0.05$.

8.70%, menthone by 13.64%, and methyl acetate by 24.15%, relative to the respective Cd-only treatments (**Figure 6**).

Effect of Salicylic Acid and Cadmium on Stomatal Response and Peltate Glandular Trichome Density Under Electron Microscopy

SA enriched the number of PGT in menthol mint plants, progressively from the control to the 100 µm Cd + SA treatment (**Figure 5A**).

Analysis of SEM showed that the Cd treatments induced stomatal closure. The control plants had a normal and open stomatal aperture with 3.08 µm pore size and characteristic guard cells, while the stomata in the 50 and 100 µm Cd treatments had partially closed with 0.25 µm and 1.52 µm pore size, respectively. Priming with SA decreased the Cd effects to open stomata with 1.68 µm and 2.73 µm pore size in the 50 and 100 µm Cd treatments, respectively (**Figure 5A**).

DISCUSSION

Cadmium contamination of agricultural land has become a principal constraint to crop production (Zaid and Mohammad, 2018;

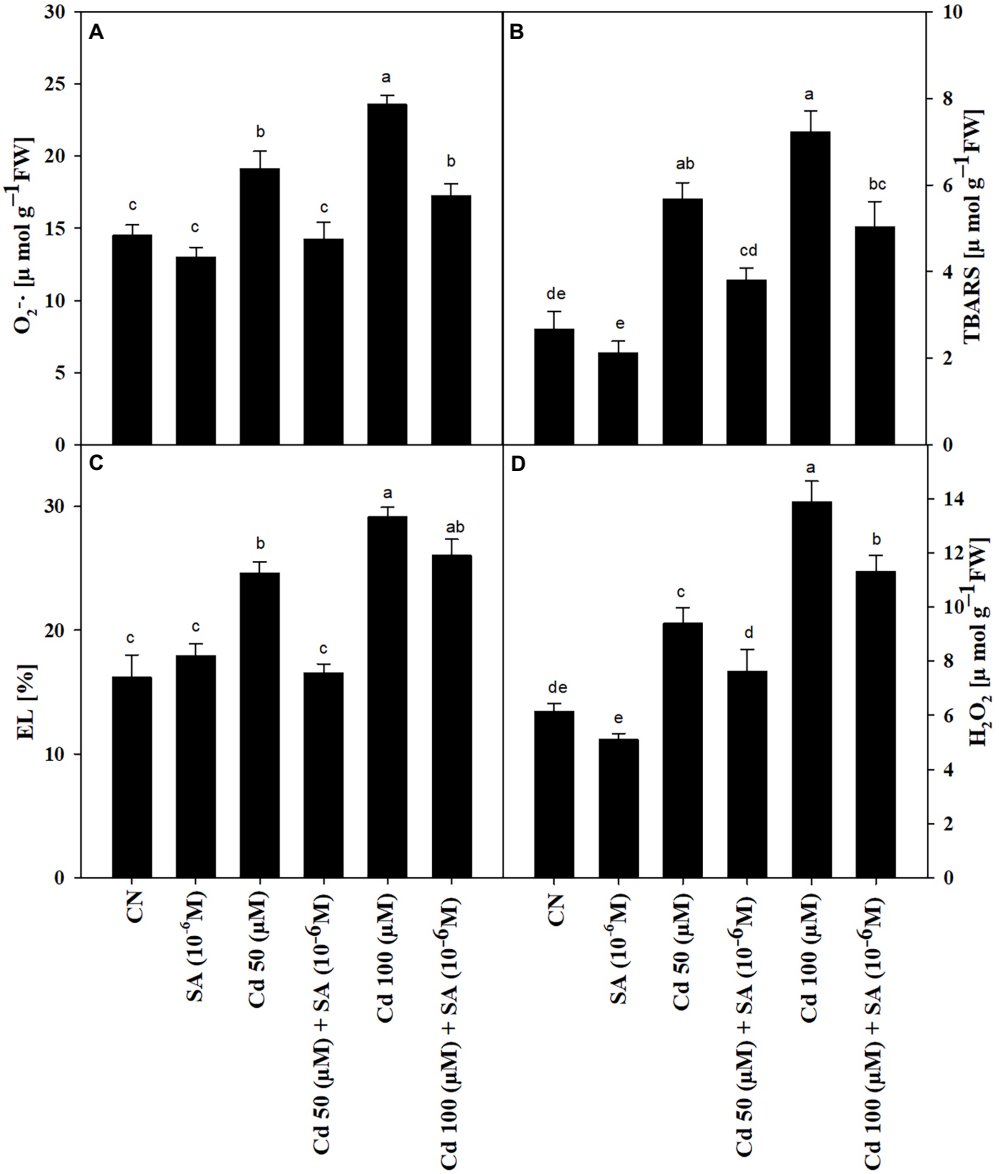


FIGURE 2 | (A) Superoxide, O_2^{-} (µmol g^{-1} FW), **(B)** thiobarbituric acid reactive substances, TBARS (µmol g^{-1} FW), **(C)** electrolyte leakage, EL (%), and **(D)** hydrogen peroxide, H_2O_2 (µmol g^{-1} FW) of *Mentha arvensis* cultivar "Kushal" grown under 50 and 100 µm Cd levels and primed with or without salicylic acid. Data are presented as treatments mean ± SE ($n = 5$). Data followed by the same letters are not significantly different by Duncan multiple range test at $p \leq 0.05$.

Hussain et al., 2019a; Rizwan et al., 2019a) as it substantially increases oxidative stress, thereby reducing nutritional homeostasis, growth and metabolism, photosynthetic yield, and quality and quantity of crops (Rizwan et al., 2016, 2019b; Zaid and Mohammad, 2018; Greco et al., 2019). This study was conducted on menthol mint plants to unravel various mechanisms underlying priming with SA that improve Cd-inhibited growth, photosynthesis and yield, and quality attributes.

Significant alterations in growth and photosynthesis parameters were observed in menthol mint plants under Cd stress. Similarly, reduced growth and photosynthesis under Cd stress have been observed in peppermint (Ahmad et al., 2018), wheat (Hussain et al., 2019b), tomato (Alyemeni et al., 2018), and *Lolium perenne* (Zhang et al., 2018). Plant height, fresh and dry weights, and leaf number and area declined in the Cd treatments. The reduced growth and biomass in Cd-treated plants might be because Cd obstructs the progression of the cell cycle and irreversibly alters the proton pumps thereby disrupting membrane permeability (Gomes-Junior et al., 2006; Liu et al., 2015). Thus, the Cd-induced disruptions in membrane permeability may have hindered ion absorption, as reflected in the reduced N, P, and K contents, and thereby hampered plant growth. Priming with SA overcame the Cd-induced growth inhibition. Under Cd stress, SA-induced

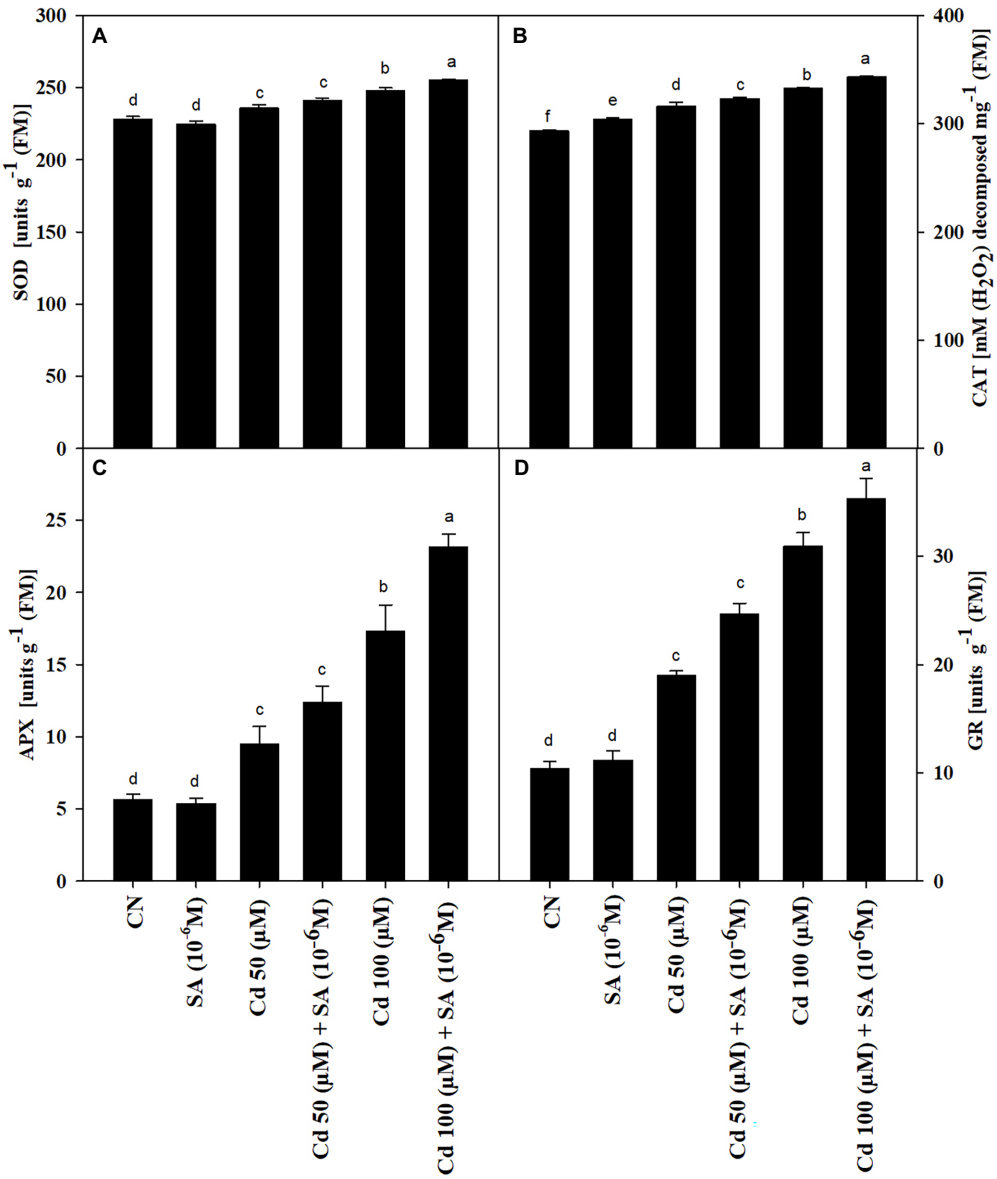


FIGURE 3 | Activities of **(A)** superoxide dismutase, SOD (units g^{-1} FM), **(B)** catalase, CAT (units g^{-1} FM), **(C)** ascorbate peroxidase, APX (units g^{-1} FM), and **(D)** glutathione reductase, GR (units g^{-1} FM) of *Mentha arvensis* cultivar "Kushal" grown under 50 and 100 µm Cd levels and primed with/without salicylic acid. Data are presented as treatments mean ± SE ($n = 5$). Data followed by the same letters are not significantly different by Duncan multiple range test at ($p \leq 0.05$).

expression of genes and maintains optimum endogenous SA accumulation that potentiated the Cd-induced growth inhibition (Wang et al., 2019). SA can also reduce the endogenous Cd content and various ROS (Zhang et al., 2015). Thus, the optimum redox balance maintained by SA in the present study under Cd stress increased growth and biomass yield in menthol mint plants.

The values of photosynthetic pigments (Chl a, b, total Chl, and Caro contents) and leaf gas exchange attributes (P_N, gs, Ci, and WUE) progressively declined with increasing levels of soil-applied Cd, relative to the control plants (**Table 2**; **Figure 1**). The Cd-induced inhibition of chlorophyll biosynthesis is due to the retention of Cd^{2+} ions in the thylakoids and stroma of the chloroplasts (Lysenko et al., 2018), and the substitution of Mg^{2+} bound into the chlorophyll molecule (Rydzyński et al., 2018). The reduction in leaf gas exchange attributes at both levels of Cd stress was due to stomatal inhibition (**Figure 5A**) that restricted gas exchange between the environment and menthol mint plants, and these results are in line with those of Zaid and Mohammad (2018). Priming with SA increased the leaf gas exchange values and nullified the reduction in photosynthesis. Under Cd stress, continuous gas exchange (**Figure 5A**) due to SA priming induced stomatal recovery to maintain proper gas flow.

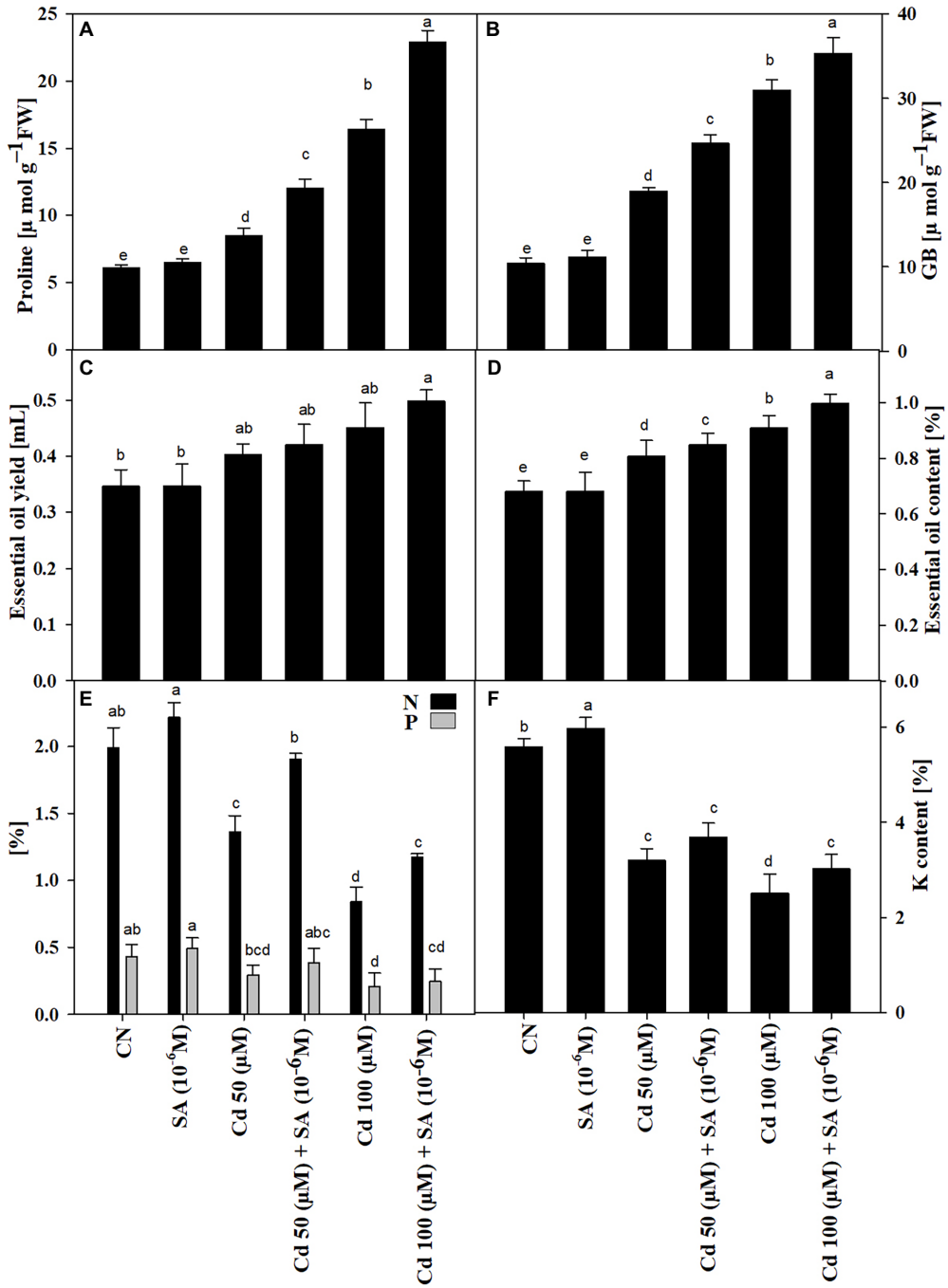


FIGURE 4 | Contents of **(A)** proline (µmolg^{-1} FW), **(B)** glycine betaine, GB (µmolg^{-1} FW), **(C)** essential oil yield, EO (mL), **(D)** essential oil content, EO (%), **(E)** nitrogen and phosphorous (%), and **(F)** potassium content (%) of *Mentha arvensis* cultivar "Kushal" grown under 50 and 100 µm Cd levels and primed with or without salicylic acid. Data are presented as treatments mean ± SE ($n = 5$). Data followed by the same letters are not significantly different by Duncan multiple range test at $p \leq 0.05$.

The increased Cd content (**Figure 5D**) under Cd stress declined substantially with SA priming, which was reflected in the increased activity of antioxidant enzymes and biosynthesis of osmolytes (proline and GB; **Figures 4A,B**). The application of SA decreased the accumulation of Cd in two melon cultivars (Zhang et al., 2015). Karimi and Ghasempour (2019) reported that SA restrained Ni content in *Alyssum inflatum*. Cd levels in the present study causes a state of oxidative stress by orchestrating the production of ROS (H_2O_2 and $O_2^{-\bullet}$ **Figures 2A,D**), ion leakage (EL, **Figure 2C**) and lipid oxidation (TBARS, **Figure 2B**). However, there is an increment in the activities of antioxidants (SOD,

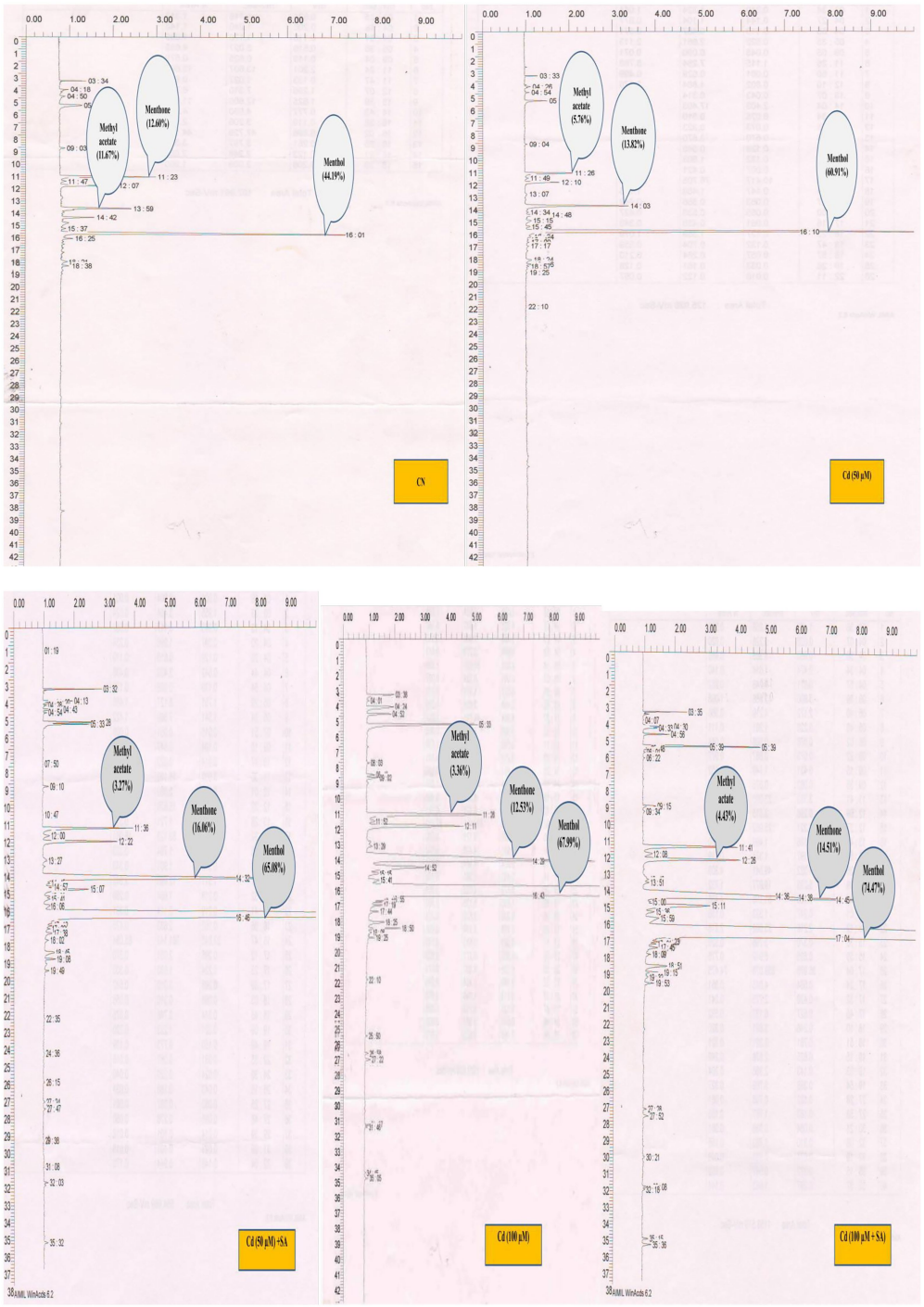


FIGURE 5 | Cadmium-mediated effect of salicylic acid (SA) sucker priming on menthol, menthone and methyl acetate content (GC graph) of *Mentha arvensis* cultivar "Kushal" in different treatments. GC chromatograms showing the peaks of different components of the essential oil. Abbreviations: CN, control; Cd, cadmium.

CAT, APX, and GR) (**Figures 3A–D**), which scavenge Cd-induced excess ROS and maintain an optimum redox homeostatic state (Zaid and Mohammad, 2018). Under Cd stress, SA triggered the expression of selected genes related to ROS and SA to regain the redox state (Li et al., 2019), which in turn enhanced the tolerance of menthol mint plants to Cd stress. Exogenous supplements of SA under Cd stress can increase endogenous SA (Wang et al., 2019); the enhanced biosynthesis of SA in the present study might have scavenged excess ROS and thus lowered TBARS and

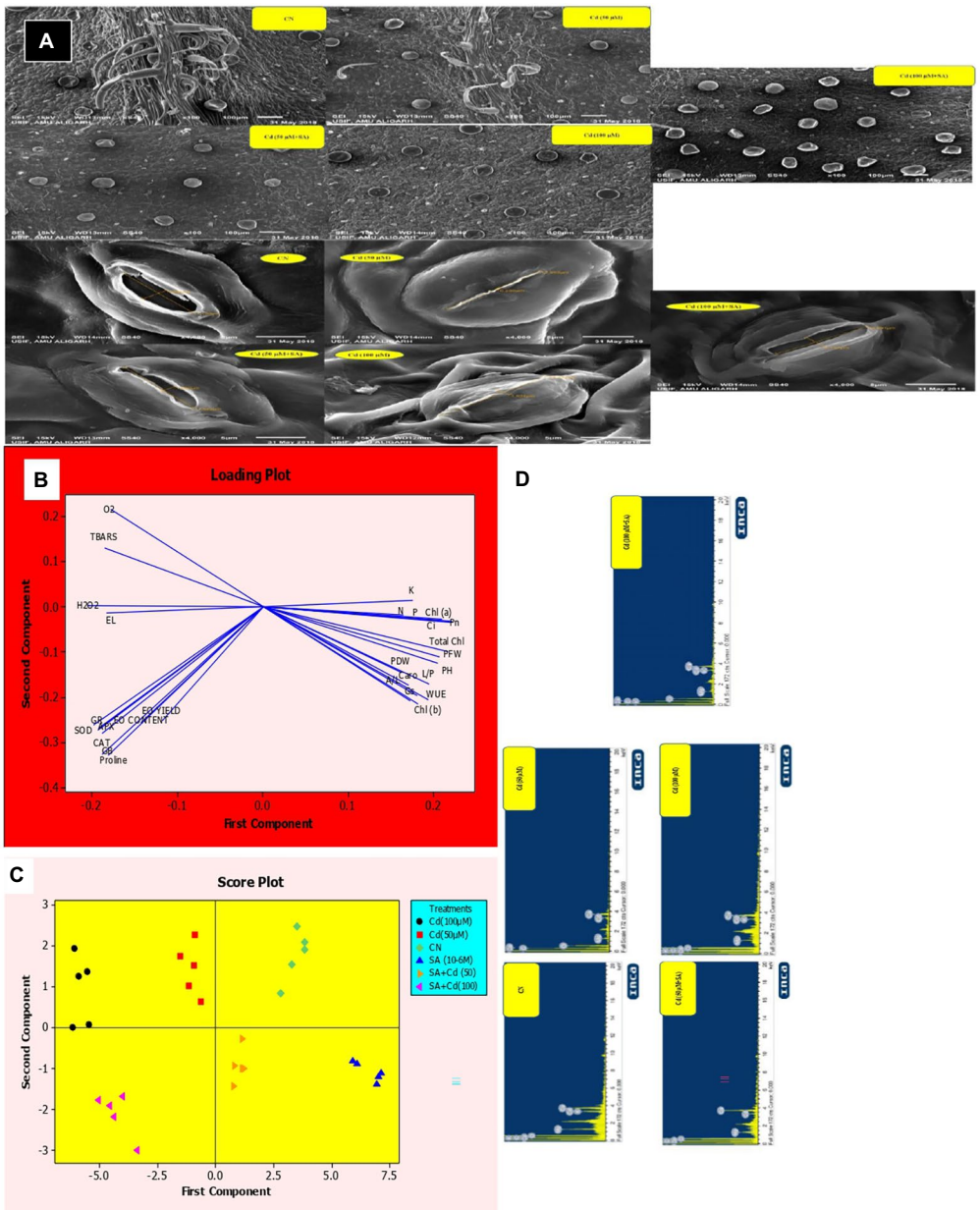


FIGURE 6 | A: Cadmium-mediated effect of salicylic acid (SA) sucker priming on peltate glandular trichome (PGT) density of *Mentha arvensis* cultivar "Kushal" at different treatments. Abbreviations: CN, control; Cd, cadmium. Stomatal behavior of *M. arvensis* leaves in different treatments. The opening and closing of stomatal behavior were observed under a scanning electron microscope at 4000 × magnification in *M. arvensis* leaves treated with 50 and 100 µm $CdCl_2$ at 30 days after transplantation (DAT). A single representative of each treatment is shown. Principal component analysis (PCA) of various parameters of menthol mint plants under cadmium (Cd) and salicylic priming (SA), **(B)** Loading plot of different parameters showing positive and negative correlations, **(C)** Score plot differentiating the treatments. PFW, plant fresh weight; PDW, plant dry weight; PH, plant height; L/P, number of leaves per plant; A/L, area per leaf; Chl (a), chlorophyll a; Chl (b), chlorophyll b; Total Chl, total chlorophyll; Caro, carotenoids; P_N, net photosynthetic rate; *gs*, stomatal conductance; *Ci*, intercellular CO_2 concentration; WUE, water use efficiency; O_2, superoxide ion; TBARS, thiobarbituric acid reactive substances; EL, electrolyte leakage; H_2O_2, hydrogen peroxide; SOD, superoxide dismutase activity; CAT, catalase; APX, ascorbate peroxidase; GR, glutathione reductase; GB, glycine betaine; EO, essential oil; N, nitrogen; P, phosphorous; K, potassium, and **(D)** EDX spectrum showing the content of Cd of *M. arvensis* cultivar "Kushal" at different treatments. Abbreviations: CN, control; Cd, cadmium.

EL levels in the Cd treatments (**Figures 2B,C**). Similarly, pre-soaking mungbean seeds in SA solution alleviated Cd-induced toxicity (Roychoudhury et al., 2016). Interestingly, low Cd content in SA-treated plants (**Figure 5D**) further reduced Cd-induced stress, indicating that the induced up-regulation of redox-related enzymes by SA priming under Cd stress plays a crucial role in scavenging intracellular ROS, thus, highlighting the importance PGRs priming in maintaining redox equilibrium under elevated levels of Cd in menthol mint plants.

Osmolytes, such as proline and GB, are compatible cytosolutes with modulatory roles in plants exposed to metal stress, including detoxifying ROS and chelating HM ions (Ashraf and Foolad, 2007; Bharwana et al., 2014; Zouari et al., 2016). Priming with SA increased the biosynthesis of osmolytes under Cd stress, which was maintained at 100 μM Cd (**Figures 4A,B**). Increased accumulation of osmolytes with SA priming resulted in the detoxification of ROS and chelation of Cd^{2+} ions as evidenced by EDX (**Figure 5D**). Similar SA-mediated increases in osmolytes under metal stress have been reported in crop plants including *Alyssum inflatum* (Karimi and Ghasempour, 2019), *Melissa officinalis* (Soltani Maivan et al., 2017), *Triticum aestivum* (Alamri et al., 2018), and *Zea mays* (Zanganeh et al., 2018).

Mineral nutrient contents (N, P, and, K) decreased as Cd levels increased from 50 to 100 μm (**Figures 4E,F**). Cd restricts the uptake of these important mineral elements (Zaid and Mohammad, 2018). In the present study, Cd contamination increased the endogenous Cd content that restricts mineral uptake because excess Cd^{2+} ions impose antagonistic effects on ion uptake (Nazar et al., 2012). Priming with SA restored mineral contents by either directly increasing their content or indirectly decreasing Cd^{2+} ions. Our study corroborates the findings of Ahmad et al. (2011). In bean plants exposed to short-term Cd stress, nutrient concentrations also increased in the SA treatment (Saidi et al., 2013).

Plants produce myriad of SMs, which protect against various environmental pressures (Berini et al., 2018). PGRs, especially SA, mediate a tolerance trade-off by eliciting SM production in plants (Singh and Dwivedi, 2018). HMs alter the production of SMs in plants; we observed significant modulation in menthol, menthone, and methyl acetate under Cd stress (**Figure 6**). Similarly, Paeizi et al. (2018) observed marked changes in medicinal alkaloid production in response to metal stress under PGR in *Catharanthus roseus*. We also observed an overall increase in EO and SM production with SA priming, which agrees with the findings of Darvizheh et al. (2018) in *Echinacea purpurea*. The increase in SMs by SA was due to an increase in PGT density. As observed in **Figure 5A**, SA increased the density of PGT under Cd, with the maximum density observed at 100 μM Cd; hence, increased PGT density is directly responsible for increasing EO and SM biosynthesis. SA also triggered SM biosynthesis in a *Taxus baccata* callus culture under glucose-mediated alterations (Sarmadi et al., 2018). In a recent study, Mohammadi et al. (2019) reported SA-induced modulations in EO constituents in different ecotypes of *Thymus* species under water stress. Exogenous PGR-mediated increases in SM production under Cd stress are also due to the up-regulation of transcriptional expressions of genes responsible for their biosynthesis (Chen et al., 2017). Moreover, the sustained increments in growth, photosynthesis, and mineral content of SA-treated plants under Cd stress are likely to culminate in maximized EO and SM contents in menthol mint plants.

Principal component analysis (PCA) identified the relationships between the studied traits, their variation, and whether SA priming can improve Cd-stress resistance and differentiate between the various treatments according to their toxicity and amelioration. Both of the Cd treatments affected plant growth, photosynthetic traits and mineral nutrient contents and they were positively correlated; however, oxidative stress biomarkers, antioxidant enzymes, and EO yield and content, which increased with Cd levels, were also positively correlated and clustered opposite the growth, photosynthetic and nutrient content parameters (**Figure 5B**). Our hypothesis was further confirmed that Cd-mediated oxidative stress induced repressions in menthol mint plants by affecting growth, photosynthetic traits, and mineral nutrient contents. The most toxic treatment was 100 μm Cd, followed by 50 μm Cd, and both were clustered next to each other. The score plot in PCA distinguishes various treatments according to their toxicities (**Figure 6C**). Starting from left side, SA under CN was the best treatment. It was followed by CN, SA + Cd (50), Cd (50), SA + Cd (100), and Cd (100). Priming plants with SA ameliorated the Cd-induced overall repressions in menthol mint plants.

CONCLUSION

In summary priming of menthol mint with SA plants can act as a low-cost, sustainable option in not only overcoming the Cd-induced adverse effects but also increasing its yield and quality attributes. A representation of the present work that how SA priming can overcome Cd stress and increase yield and quality attributes in menthol mint is presented in graphical abstract.

DATA AVAILABILITY STATEMENT

The original contributions presented in the study are included in the article/supplementary material; further inquiries can be directed to the corresponding authors.

AUTHOR CONTRIBUTIONS

AZ and FM designed the experiment. AZ carried out the experimental analysis, wrote the draft, and revised the manuscript. FM corrected the draft and overall supervised the work. KS critically analyzed the manuscript and edited it for language. All authors contributed to the article and approved the submitted version.

ACKNOWLEDGMENTS

AZ is grateful to UGC (New Delhi) India and Aligarh Muslim University, Aligarh, India, for providing the research fellowship. We thank the University Sophisticated Instrumentation Facility (USIF) A.M.U., Aligarh for SEM and EDX analysis. The results reported are part of Ph.D Thesis of Dr. Abbu Zaid.

REFERENCES

Adams, R. P. (2007). *Identification of Essential oil Components by gas Chromatography/mass Spectrometry. 4th Edn.* Carol Stream, USA: Allured Publishing Corporation.

Aebi, H. (1984). Catalase in vitro. *Methods Enzymol.* 105, 121–126. doi: 10.1016/S0076-6879(84)05016-3

Ahmad, B., Jaleel, H., Sadiq, Y., Khan, M. M. A., and Shabbir, A. (2018). Response of exogenous salicylic acid on cadmium induced photosynthetic damage, antioxidant metabolism and essential oil production in peppermint. *Plant Growth Regul.* 86, 273–286. doi: 10.1007/s10725-018-0427-z

Ahmad, P., Nabi, G., and Ashraf, M. (2011). Cadmium-induced oxidative damage in mustard [(*Brassica juncea* L.) Czern. & Coss.] plants can be alleviated by salicylic acid. *South Afr. J. Bot.* 77, 36–44. doi: 10.1016/j.sajb.2010.05.003

Ahmad, B., Zaid, A., Sadiq, Y., Bashir, S., and Wani, S. H. (2019). "Role of selective exogenous elicitors in plant responses to abiotic stress tolerance," in *Plant abiotic Stress Tolerance*. eds. M. Hasanuzzaman, K. Hakeem, K. Nahar and H. Alharby (Cham: Springer), 273–290.

Alamri, S. A. D., Siddiqui, M. H., Al-Khaishany, M. Y., Ali, H. M., Al-Amri, A., and AlRabiah, H. K. (2018). Exogenous application of salicylic acid improves tolerance of wheat plants to lead stress. *Adv. Agric. Sci.* 6, 25–35.

Alyemeni, M. N., Ahanger, M. A., Wijaya, L., Alam, P., Bhardwaj, R., and Ahmad, P. (2018). Selenium mitigates cadmium-induced oxidative stress in tomato (*Solanum lycopersicum* L.) plants by modulating chlorophyll fluorescence, osmolyte accumulation, and antioxidant system. *Protoplasma* 255, 459–469. doi: 10.1007/s00709-017-1162-4

Ashraf, M. F. M. R., and Foolad, M. (2007). Roles of glycine betaine and proline in improving plant abiotic stress resistance. *Environ. Exp. Bot.* 59, 206–216. doi: 10.1016/j.envexpbot.2005.12.006

Bari, M. A., Akther, M. S., Reza, M. A., and Kabir, A. H. (2019). Cadmium tolerance is associated with the root-driven coordination of cadmium sequestration, iron regulation, and ROS scavenging in rice. *Plant Physiol. Biochem.* 136, 22–33. doi: 10.1016/j.plaphy.2019.01.007

Bates, L. S., Waldren, R. P., and Teare, I. D. (1973). Rapid determination of free proline for water-stress studies. *Plant Soil* 39, 205–207. doi: 10.1007/BF00018060

Berini, J. L., Brockman, S. A., Hegeman, A. D., Reich, P. B., Muthukrishnan, R., Montgomery, R. A., et al. (2018). Combinations of Abiotic Factors Differentially Alter Production of Plant Secondary Metabolites in Five Woody Plant Species in the Boreal-Temperate Transition Zone. *Front. Plant Sci.* 9:1257. doi: 10.3389/fpls.2018.01257

Bharwana, S. A., Ali, S., Farooq, M. A., Iqbal, N., Hameed, A., Abbas, F., et al. (2014). Glycine betaine-induced lead toxicity tolerance related to elevated photosynthesis, antioxidant enzymes suppressed lead uptake and oxidative stress in cotton. *Turk. J. Bot.* 38, 281–292. doi: 10.3906/bot-1304-65

Bose, S. K., Yadav, R. K., Mishra, S., Sangwan, R. S., Singh, A. K., Mishra, B., et al. (2013). Effect of gibberellic acid and calliterpenone on plant growth attributes, trichomes, essential oil biosynthesis and pathway gene expression in differential manner in *Mentha arvensis* L. *Plant Physiol. Biochem.* 66, 150–158. doi: 10.1016/j.plaphy.2013.02.011

Chen, Q., Wu, K., Tang, Z., Guo, Q., Guo, X., and Wang, H. (2017). Exogenous ethylene enhanced the cadmium resistance and changed the alkaloid biosynthesis in *Catharanthus roseus* seedlings. *Acta Physiol. Plant.* 39:267. doi: 10.1007/s11738-017-2567-6

DalCorso, G., Farinati, S., Maistri, S., and Furini, A. (2008). How plants cope with cadmium: staking all on metabolism and gene expression. *J. Integr. Plant Biol.* 50, 1268–1280. doi: 10.1111/j.1744-7909.2008.00737.x

Darvizheh, H., Zahedi, M., Abaszadeh, B., and Razmjoo, J. (2018). Effects of irrigation regime and foliar application of salicylic acid and Spermine on the contents of essential oil and Caffeic acid derivatives in *Echinacea purpurea* L. *J. Plant Growth Regul.* 37, 1267–1285. doi: 10.1007/s00344-018-9874-z

Fiske, C. H., and Subbarow, Y. (1925). The colorimetric determination of phosphorus. *J. Biol. Chem.* 66, 375–400. doi: 10.1016/S0021-9258(18)84756-1

Gao, M., Zhou, J., Liu, H., Zhang, W., Hu, Y., Liang, J., et al. (2018). Foliar spraying with silicon and selenium reduces cadmium uptake and mitigates cadmium toxicity in rice. *Sci. Total Environ.* 631, 1100–1108. doi: 10.1016/j.scitotenv.2018.03.047

Gomes-Junior, R. A., Moldes, C. A., Delite, F. S., Pompeu, G. B., Gratão, P. L., Mazzafera, P., et al. (2006). Antioxidant metabolism of coffee cell suspension cultures in response to cadmium. *Chemosphere* 65, 1330–1337. doi: 10.1016/j.chemosphere.2006.04.056

Greco, M., Sáez, C. A., Contreras, R. A., Rodríguez-Rojas, F., Bitonti, M. B., and Brown, M. T. (2019). Cadmium and/or copper excess induce interdependent metal accumulation, DNA methylation, induction of metal chelators and antioxidant defences in the seagrass *Zostera marina*. *Chemosphere* 224, 111–119. doi: 10.1016/j.chemosphere.2019.02.123

Grieve, C. M., and Grattan, S. R. (1983). Rapid assay for determination of water soluble quaternary ammonium compounds. *Plant Soil* 70, 303–307. doi: 10.1007/BF02374789

Guenther, E. (1972). *The Essential Oils. History-origin in Plants-Production-Analysis. Vol. 1*. Malabar, Florida: Kreiger Publishing Company.

Hald, P. M. (1947). The flame photometer for the measurement of sodium and potassium in biological materials. *J. Biol. Chem.* 167, 499–510. doi: 10.1016/S0021-9258(17)31003-7

Hassan, M., and Mansoor, S. (2017). Priming seeds with phytohormones alleviates cadmium toxicity in mungbean (*Vigna radiate* L.Wilczek) seedlings. *Pak. J. Bot.* 49, 2071–2078.

He, S., He, Z., and Yang, X. (2015). Soil biogeochemistry, plant physiology and phytoremediation of cadmium-contaminated soils. *Adv. Agron.* 134, 135–225. doi: 10.1016/bs.agron.2015.06.005

Hodges, D. M., DeLong, J. M., Forney, C. F., and Prange, R. K. (1999). Improving the thiobarbituric acid-reactive-substances assay for estimating lipid peroxidation in plant tissues containing anthocyanin and other interfering compounds. *Planta* 207, 604–611. doi: 10.1007/s004250050524

Hussain, A., Ali, S., Rizwan, M., ur Rehman, M. Z., Qayyum, M. F., Wang, H., et al. (2019a). Responses of wheat (*Triticum aestivum*) plants grown in a cd contaminated soil to the application of iron oxide nanoparticles. *Ecotoxicol. Environ. Saf.* 173, 156–164. doi: 10.1016/j.ecoenv.2019.01.118

Hussain, A., Rizwan, M., Ali, Q., and Ali, S. (2019b). Seed priming with silicon nanoparticles improved the biomass and yield while reduced the oxidative stress and cadmium concentration in wheat grains. *Environ. Sci. Pollut. Res.* 26, 7579–7588. doi: 10.1007/s11356-019-04210-5

Jana, S., and Choudhari, M. A. (1981). Glycolate metabolism of three submerged aquatic angiosperms during ageing. *Aquat. Bot.* 12, 345–354. doi: 10.1016/0304-3770(82)90026-2

Jisha, K. C., Vijayakumari, K., and Puthur, J. T. (2013). Seed priming for abiotic stress tolerance: an overview. *Acta Physiol. Plant.* 35, 1381–1396. doi: 10.1007/s11738-012-1186-5

Karimi, N., and Ghasempour, H. R. (2019). Salicylic acid and jasmonic acid restrains nickel toxicity by ameliorating antioxidant defense system in shoots of metallicolous and non-metallicolous *Alyssum inflatum* Náyr. *Populations. Plant Physiol. Biochem.* 135, 450–459. doi: 10.1016/j.plaphy.2018.11.015

Khan, M. I. R., Fatma, M., Per, T. S., Anjum, N. A., and Khan, N. A. (2015). Salicylic acid-induced abiotic stress tolerance and underlying mechanisms in plants. *Front. Plant Sci.* 6:462. doi: 10.3389/fpls.2015.00462

Khanam, D., and Mohammad, F. (2018). Plant growth regulators ameliorate the ill effect of salt stress through improved growth, photosynthesis, antioxidant system, yield and quality attributes in *Mentha piperita* L. *Acta Physiol. Plant.* 40:188. doi: 10.1007/s11738-018-2769-6

Khanuja, S. P. S., Kalra, A., Singh, A., Patra, D. D., Patra, N. K., Tondon, S., et al. (2021). *Form Bulletin: Menthol Mint Cultivation.* Central Institute of Medicinal and Aromatic Plants, Lucknow, India.

Kono, Y. (1978). Generation of superoxide radical during autoxidation of hydroxylamine and an assay for superoxide dismutase. *Arch. Biochem. Biophys.* 186, 189–195. doi: 10.1016/0003-9861(78)90479-4

Lal, S. K., Kumar, S., Sheri, V., Mehta, S., Varakumar, P., Ram, B., et al. (2018). "Seed Priming: An Emerging Technology to Impart Abiotic Stress Tolerance in Crop Plants," in *Advances in Seed Priming*. eds. A. Rakshit and H. Singh (Singapore: Springer), 41–50.

Li, Q., Wang, G., Wang, Y., Yang, D., Guan, C., and Ji, J. (2019). Foliar application of salicylic acid alleviate the cadmium toxicity by modulation the reactive oxygen species in potato. *Ecotoxicol. Environ. Saf.* 172, 317–325. doi: 10.1016/j.ecoenv.2019.01.078

Lichtenthaler, H. K., and Buschmann, C. (2001). "Chlorophylls and carotenoids: measurement and characterization by UV Vis spectroscopy," in *Current Protocols in Food Analytical Chemistry*. eds. R. E. Wrolstad, T. E. Acree, H.

An, E. A. Decker, M. H. Penner, D. S. Reid et al. (New York, NY, USA: John Wiley and Sons), F4.3.1–F4.3.8.

Lindner, R. (1944). Rapid analytical methods for some of the more common inorganic constituents of plant tissues. *Plant Physiol.* 19, 76–89. doi: 10.1104/pp.19.1.76

Liu, S., Yang, R., Pan, Y., Ma, M., Pan, J., Zhao, Y., et al. (2015). Nitric oxide contributes to minerals absorption, proton pumps and hormone equilibrium under cadmium excess in *Trifolium repens* L. plants. *Ecotoxicol. Environ. Saf.* 119, 35–46. doi: 10.1016/j.ecoenv.2015.04.053

Lysenko, E. A., Klaus, A. A., Kartashov, A. V., and Kusnetsov, V. V. (2018). Distribution of cd and other cations between the stroma and thylakoids: a quantitative approach to the search for cd targets in chloroplasts. *Photosynth. Res.* 139, 1–22. doi: 10.1007/s11120-018-0528-6

Mohammadi, H., Amirikia, F., Ghorbanpour, M., Fatehi, F., and Hashempour, H. (2019). Salicylic acid induced changes in physiological traits and essential oil constituents in different ecotypes of *Thymus kotschyanus* and *Thymus vulgaris* under well-watered and water stress conditions. *Ind. Crop. Prod.* 129, 561–574. doi: 10.1016/j.indcrop.2018.12.046

Moulick, D., Santra, S. C., and Ghosh, D. (2018). Seed priming with se mitigates as-induced phytotoxicity in rice seedlings by enhancing essential micronutrient uptake and translocation and reducing As translocation. *Environ. Sci. Pollut. Res.* 25, 26978–26991. doi: 10.1007/s11356-018-2711-x

Naeem, M., Aftab, T., Idrees, M., Singh, M., Ali, A., Khan, M. M. A., et al. (2017). Modulation of physiological activities, active constituents and essential oil production of *Mentha arvensis* L. by concomitant application of depolymerised carrageenan, triacontanol and 28-homobrassinolide. *J. Essent. Oil Res.* 29, 179–188. doi: 10.1080/10412905.2016.1213188

Nakano, Y., and Asada, K. (1981). Hydrogen peroxide is scavenged by ascorbate-specific peroxidase in spinach chloroplasts. *Plant Cell Physiol.* 22, 867–880.

Nazar, R., Iqbal, N., Masood, A., Khan, M. I. R., Syeed, S., and Khan, N. A. (2012). Cadmium toxicity in plants and role of mineral nutrients in its alleviation. *Amer. J. Plant Sci.* 3, 1476–1489. doi: 10.4236/ajps.2012.310178

Nigam, N., Khare, P., Yadav, V., Mishra, D., Jain, S., Karak, T., et al. (2019). Biochar-mediated sequestration of Pb and cd leads to enhanced productivity in *Mentha arvensis*. *Ecotoxicol. Environ. Saf.* 172, 411–422. doi: 10.1016/j.ecoenv.2019.02.006

Paeizi, M., Karimi, F., and Razavi, K. (2018). Changes in medicinal alkaloids production and expression of related regulatory and biosynthetic genes in response to silver nitrate combined with methyl jasmonate in *Catharanthus roseus* in vitro propagated shoots. *Plant Physiol. Biochem.* 132, 623–632. doi: 10.1016/j.plaphy.2018.10.015

Panuccio, M. R., Chaabani, S., Roula, R., and Muscolo, A. (2018). Bio-priming mitigates detrimental effects of salinity on maize improving antioxidant defense and preserving photosynthetic efficiency. *Plant Physiol. Biochem.* 132, 465–474. doi: 10.1016/j.plaphy.2018.09.033

Pourghasemian, N., Landberg, T., Ehsanzadeh, P., and Greger, M. (2019). Different response to cd stress in domesticated and wild safflower (Carthamus spp.). *Ecotoxicol. Environ. Saf.* 171, 321–328. doi: 10.1016/j.ecoenv.2018.12.052

Rizwan, M., Ali, S., Abbas, T., Zia-ur-Rehman, M., Hannan, F., Keller, C., et al. (2016). Cadmium minimization in wheat: a critical review. *Ecotoxicol. Environ. Saf.* 130, 43–53. doi: 10.1016/j.ecoenv.2016.04.001

Rizwan, M., Ali, S., Akbar, M. Z., Shakoor, M. B., Mahmood, A., Ishaque, W., et al. (2017). Foliar application of aspartic acid lowers cadmium uptake and cd-induced oxidative stress in rice under cd stress. *Environ. Sci. Pollut. Res.* 24, 21938–21947. doi: 10.1007/s11356-017-9860-1

Rizwan, M., Ali, S., Ali, B., Adrees, M., Arshad, M., Hussain, A., et al. (2019b). Zinc and iron oxide nanoparticles improved the plant growth and reduced the oxidative stress and cadmium concentration in wheat. *Chemosphere* 214, 269–277. doi: 10.1016/j.chemosphere.2018.09.120

Rizwan, M., Ali, S., ur Rehman, M. Z., Rinklebe, J., Tsang, D. C., Bashir, A., et al. (2018). Cadmium phytoremediation potential of Brassica crop species: a review. *Sci. Total Environ.* 631, 1175–1191. doi: 10.1016/j.scitotenv.2018.03.104

Rizwan, M., Ali, S., Zia urRehman, M., Adrees, M., Arshad, M., Qayyum, M. F., et al. (2019a). Alleviation of cadmium accumulation in maize (*Zea mays* L.) by foliar spray of zinc oxide nanoparticles and biochar to contaminated soil. *Environ. Pollut.* 248, 358–367. doi: 10.1016/j.envpol.2019.02.031

Roychoudhury, A., Ghosh, S., Paul, S., Mazumdar, S., Das, G., and Das, S. (2016). Pre-treatment of seeds with salicylic acid attenuates cadmium chloride-induced oxidative damages in the seedlings of mung bean (*Vigna radiate* L.Wilczek). *Acta Physiol. Plant.* 38:11. doi: 10.1007/s11738-015-2027-0

Rydzyński, D., Piotrowicz-Cieślak, A. I., Grajek, H., and Michalczyk, D. J. (2018). Chlorophyll degradation by tetracycline and cadmium in spinach (*Spinacia oleracea* L.) leaves. *Int. J. Environ. Sci. Technol.* 16, 6301–6314. doi: 10.1007/s13762-018-2142-8

Saidi, I., Ayouni, M., Dhieb, A., Chtourou, Y., Chaïbi, W., and Djebali, W. (2013). Oxidative damages induced by short-term exposure to cadmium in bean plants: protective role of salicylic acid. *South Afr. J. Bot.* 85, 32–38. doi: 10.1016/j.sajb.2012.12.002

Santisree, P., Jalli, L. C. L., Bhatnagar-Mathur, P., and Sharma, K. K. (2020). Emerging roles of salicylic acid and jasmonates in plant abiotic stress responses. Protective chemical agents in the amelioration of plant abiotic stress. *Biochem. molecular perspect.* 1, 342–373. doi: 10.1002/9781119552154.ch17

Sarmadi, M., Karimi, N., Palazón, J., Ghassempour, A., and Mirjalili, M. H. (2018). The effects of salicylic acid and glucose on biochemical traits and taxane production in a *Taxus baccata* callus culture. *Plant Physiol. Biochem.* 132, 271–280. doi: 10.1016/j.plaphy.2018.09.013

Savvides, A., Ali, S., Tester, M., and Fotopoulos, V. (2016). Chemical priming of plants against multiple abiotic stresses: mission possible? *Trends Plant Sci.* 21, 329–340. doi: 10.1016/j.tplants.2015.11.003

Shah, A. A., Ahmed, S., Ali, A., and Yasin, N. A. (2020a). 2-Hydroxymelatonin mitigates cadmium stress in *cucumis sativus* seedlings: modulation of antioxidant enzymes and polyamines. *Chemosphere* 243:125308. doi: 10.1016/j.chemosphere.2019.125308

Shah, A. A., Bibi, F., Hussain, I., Yasin, N. A., Akram, W., Tahir, M. S., et al. (2020b). Synergistic effect of *bacillus thuringiensis* iags 199 and putrescine on alleviating cadmium-induced phytotoxicity in *capsicum annum*. *Plan. Theory* 9:1512. doi: 10.3390/plants9111512

Shahnawaz, M. D., Chouhan, R., and Sanadhya, D. (2017). Impact of aluminium toxicity on physiological aspects of barley (*Hordeum vulgare* L.) cultivars and its alleviation through ascorbic acid and salicylic acid seed priming. *Int. J. Curr. Microbiol. App. Sci.* 6, 875–891. doi: 10.20546/ijcmas.2017.605.098

Sheteiwy, M. S., Gong, D., Gao, Y., Pan, R., Hu, J., and Guan, Y. (2018). Priming with methyl jasmonate alleviates polyethylene glycol-induced osmotic stress in rice seeds by regulating the seed metabolic profile. *Environ. Exp. Bot.* 153, 236–248. doi: 10.1016/j.envexpbot.2018.06.001

Singh, A., and Dwivedi, P. (2018). Methyl-jasmonate and salicylic acid as potent elicitors for secondary metabolite production in medicinal plants: A review. *J. Pharma. Phytochem.* 7, 750–757.

Smith, L. K., Vierheller, T. L., and Thorne, C. A. (1988). Assay of glutathione reductase in crude tissue homogenates using 5,5-thiobis (2-nitro benzoic acid). *Ann. Biochem.* 175, 408–413. doi: 10.1016/0003-2697(88)90564-7

Soltani Maivan, E., Radjabian, T., Abrishamchi, P., and Talei, D. (2017). Physiological and biochemical responses of *Melissa officinalis* L. to nickel stress and the protective role of salicylic acid. *Arch. Agron. Soil Sci.* 63, 330–343. doi: 10.1080/03650340.2016.1207241

Sullivan, C. Y., and Ross, W. M. (1979). "Selecting the drought and heat resistance in grain sorghum," in *Physiology in crop Plants*. eds. H. Mussel and R. C. Staples (New York: Wiley), 263–328.

Sytar, O., Kumari, P., Yadav, S., Brestic, M., and Rastogi, A. (2018). Phytohormone priming: regulator for heavy metal stress in plants. *J. Plant Growth Regul.* 38, 739–752. doi: 10.1007/s00344-018-9886-8

Tiwari, P. (2016). Recent advances and challenges in trichome research and essential oil biosynthesis in *Mentha arvensis* L. *Ind. Crop. Prod.* 82, 141–148. doi: 10.1016/j.indcrop.2015.11.069

Wang, A. G., and Luo, G. H. (1990). Quantitative relation between the reaction of hydroxylamine and superoxide anion radicals in plants. *Plant Physiol. Commun.* 6, 55–57.

Wang, Y. Y., Wang, Y., Li, G. Z., and Hao, L. (2019). Salicylic acid-altering Arabidopsis plant response to cadmium exposure: underlying mechanisms affecting antioxidation and photosynthesis-related processes. *Ecotoxicol. Environ. Saf.* 169, 645–653. doi: 10.1016/j.ecoenv.2018.11.062

Zaid, A., Bhat, J. A., Wani, S. H., and Masoodi, K. Z. (2019a). Role of nitrogen and sulfur in mitigating cadmium induced metabolism alterations in plants. *The J. Plant Sci. Res.* 35, 121–141. doi: 10.32381/JPSR.2019.35.01.11

Zaid, A., and Mohammad, F. (2018). Methyl jasmonate and nitrogen interact to alleviate cadmium stress in *Mentha arvensis* by regulating physio-biochemical

damages and ros detoxification. *J. Plant Growth Regul.* 37, 1331–1348. doi: 10.1007/s00344-018-9854-3

Zaid, A., Mohammad, F., and Fariduddin, Q. (2020). Plant growth regulators improve growth, photosynthesis, mineral nutrient and antioxidant system under cadmium stress in menthol mint (*Mentha arvensis* L.). *Physiol. Mol. Biol. Plants* 26, 25–39. doi: 10.1007/s12298-019-00715-y

Zaid, A., Mohammad, F., Wani, S. H., and Siddique, K. M. (2019b). Salicylic acid enhances nickel stress tolerance by up-regulating antioxidant defense and glyoxalase systems in mustard plants. *Ecotoxicol. Environ. Saf.* 180, 575–587. doi: 10.1016/j.ecoenv.2019.05.042

Zanganeh, R., Jamei, R., and Rahmani, F. (2018). Impacts of seed priming with salicylic acid and sodium hydrosulfide on possible metabolic pathway of two amino acids in maize plant under lead stress. *Mol. Biol. Res. Comm.* 7:83. doi: 10.22099/mbrc.2018.29089.1317

Zhang, J., Sun, W., Li, Z., Liang, Y., and Song, A. (2009). Cadmium fate and tolerance in rice cultivars. *Agr. Sus. Devel.* 29, 483–490. doi: 10.1051/agro/2009008

Zhang, H., Xu, N., Li, X., Long, J., Sui, X., Wu, Y., et al. (2018). Arbuscular Mycorrhizal Fungi (Glomus mosseae) improves growth, photosynthesis and protects photosystem II in leaves of *Lolium perenne* L. in cadmium contaminated soil. *Front. Plant Sci.* 9:01156. doi: 10.3389/fpls.2018.01156

Zhang, Y., Xu, S., Yang, S., and Chen, Y. (2015). Salicylic acid alleviates cadmium-induced inhibition of growth and photosynthesis through upregulating antioxidant defense system in two melon cultivars (*Cucumis melo* L.). *Protoplasma* 252, 911–924. doi: 10.1007/s00709-014-0732-y

Zouari, M., Elloumi, N., Ahmed, C. B., Delmail, D., Rouina, B. B., Abdallah, F. B., et al. (2016). Exogenous proline enhances growth, mineral uptake, antioxidant defense, and reduces cadmium-induced oxidative damage in young date palm (*Phoenix dactylifera* L.). *Ecol. Eng.* 86, 202–209. doi: 10.1016/j.ecoleng.2015.11.016

Conflict of Interest: The authors declare that the research was conducted in the absence of any commercial or financial relationships that could be construed as a potential conflict of interest.

Publisher's Note: All claims expressed in this article are solely those of the authors and do not necessarily represent those of their affiliated organizations, or those of the publisher, the editors and the reviewers. Any product that may be evaluated in this article, or claim that may be made by its manufacturer, is not guaranteed or endorsed by the publisher.

Copyright © 2022 Zaid, Mohammad and Siddique. This is an open-access article distributed under the terms of the Creative Commons Attribution License (CC BY). The use, distribution or reproduction in other forums is permitted, provided the original author(s) and the copyright owner(s) are credited and that the original publication in this journal is cited, in accordance with accepted academic practice. No use, distribution or reproduction is permitted which does not comply with these terms.

frontiers | Frontiers in Plant Science

TYPE Original Research
PUBLISHED 28 July 2022
DOI 10.3389/fpls.2022.921668

Check for updates

OPEN ACCESS

EDITED BY
Shabir Hussain Wani,
Sher-e-Kashmir University of Agricultural Sciences and Technology, India

REVIEWED BY
Sunny Ahmar,
University of Silesia in Katowice, Poland
Muhammad Adnan,
Fujian Agriculture and Forestry University, China

*CORRESPONDENCE
Baber Ali
baberali@bs.qau.edu.pk
Romina Alina Marc
romina.vlaic@usamvcluj.ro

†These authors share first authorship

SPECIALTY SECTION
This article was submitted to Plant Biotechnology, a section of the journal Frontiers in Plant Science

RECEIVED 16 April 2022
ACCEPTED 30 June 2022
PUBLISHED 28 July 2022

CITATION
Ali B, Hafeez A, Ahmad S, Javed MA, Sumaira, Afridi MS, Dawoud TM, Almaary KS, Muresan CC, Marc RA, Alkhalifah DHM and Selim S (2022) *Bacillus thuringiensis* PM25 ameliorates oxidative damage of salinity stress in maize *via* regulating growth, leaf pigments, antioxidant defense system, and stress responsive gene expression.
Front. Plant Sci. 13:921668.
doi: 10.3389/fpls.2022.921668

COPYRIGHT
© 2022 Ali, Hafeez, Ahmad, Javed, Sumaira, Afridi, Dawoud, Almaary, Muresan, Marc, Alkhalifah and Selim. This is an open-access article distributed under the terms of the Creative Commons Attribution License (CC BY). The use, distribution or reproduction in other forums is permitted, provided the original author(s) and the copyright owner(s) are credited and that the original publication in this journal is cited, in accordance with accepted academic practice. No use, distribution or reproduction is permitted which does not comply with these terms.

Bacillus thuringiensis PM25 ameliorates oxidative damage of salinity stress in maize *via* regulating growth, leaf pigments, antioxidant defense system, and stress responsive gene expression

Baber Ali[1*†], Aqsa Hafeez[1†], Saliha Ahmad[1], Muhammad Ammar Javed[2], Sumaira[3], Muhammad Siddique Afridi[4], Turki M. Dawoud[5], Khalid S. Almaary[5], Crina Carmen Muresan[6], Romina Alina Marc[6*], Dalal Hussien M. Alkhalifah[7] and Samy Selim[8]

[1]Department of Plant Sciences, Quaid-i-Azam University, Islamabad, Pakistan, [2]Institute of Industrial Biotechnology, Government College University, Lahore, Pakistan, [3]Department of Biotechnology, Quaid-i-Azam University, Islamabad, Pakistan, [4]Department of Plant Pathology, Federal University of Lavras (UFLA), Lavras, MG, Brazil, [5]Department of Botany and Microbiology, College of Science, King Saud University, Riyadh, Saudi Arabia, [6]Food Engineering Department, Faculty of Food Science and Technology, University of Agricultural Science and Veterinary Medicine Cluj-Napoca, Cluj-Napoca, Romania, [7]Department of Biology, College of Science, Princess Nourah Bint Abdulrahman University, Riyadh, Saudi Arabia, [8]Department of Clinical Laboratory Sciences, College of Applied Medical Sciences, Jouf University, Sakaka, Saudi Arabia

Soil salinity is the major abiotic stress that disrupts nutrient uptake, hinders plant growth, and threatens agricultural production. Plant growth-promoting rhizobacteria (PGPR) are the most promising eco-friendly beneficial microorganisms that can be used to improve plant responses against biotic and abiotic stresses. In this study, a previously identified *B. thuringiensis* PM25 showed tolerance to salinity stress up to 3 M NaCl. The Halo-tolerant *Bacillus thuringiensis* PM25 demonstrated distinct salinity tolerance and enhance plant growth-promoting activities under salinity stress. Antibiotic-resistant Iturin C (*ItuC*) and bio-surfactant-producing (*sfp* and *srfAA*) genes that confer biotic and abiotic stresses were also amplified in *B. thuringiensis* PM25. Under salinity stress, the physiological and molecular processes were followed by the over-expression of stress-related genes (APX and SOD) in *B. thuringiensis* PM25. The results detected that *B. thuringiensis* PM25 inoculation substantially improved phenotypic traits, chlorophyll content, radical scavenging capability, and relative water content under salinity stress. Under salinity stress, the inoculation of *B. thuringiensis* PM25 significantly increased antioxidant enzyme levels in inoculated maize as compared to uninoculated plants. In addition, *B. thuringiensis* PM25-inoculation dramatically increased soluble sugars, proteins, total phenols, and flavonoids in maize as compared to uninoculated plants. The inoculation of *B. thuringiensis* PM25 significantly reduced oxidative burst in inoculated maize under salinity stress, compared

to uninoculated plants. Furthermore, *B. thuringiensis* PM25-inoculated plants had higher levels of compatible solutes than uninoculated controls. The current results demonstrated that *B. thuringiensis* PM25 plays an important role in reducing salinity stress by influencing antioxidant defense systems and abiotic stress-related genes. These findings also suggest that multi-stress tolerant *B. thuringiensis* PM25 could enhance plant growth by mitigating salt stress, which might be used as an innovative tool for enhancing plant yield and productivity.

KEYWORDS

abiotic stress, antioxiants, qRT-PCR, plant-microbe interactions, PGPR—plant growth-promoting rhizobacteria

Introduction

Abiotic factors, such as cold, heat, drought (Wahab et al., 2022), heavy metals (Nawaz et al., 2022), salt concentration (Hussain et al., 2022), and nutrient deficiency (Ahmad et al., 2022) drastically affect crop yield and productivity. Salinity stress is the most detrimental threat to agricultural yield (Daliakopoulos et al., 2016). The high salt concentration of farming lands costs a loss of 27 billion US dollars annually (Singh et al., 2020). It affects about 20–33% of the irrigated and cultivated land worldwide, and by the year 2050, these pernicious effects are anticipated to rise to 50% (Machado and Serralheiro, 2017).

Excessive salt concentration significantly interferes with the plants' physiological functions, such as nitrogen fixation, ion homeostasis, lipid metabolism, photosynthesis, and protein synthesis (Li and Jiang, 2017). Salinity causes the excessive generation of toxic ions by producing water-deficient conditions, i.e., osmotic stress, culminating in producing toxic free radicals that foster oxidative damage (Islam et al., 2016). This osmotic stress results in delayed or poor germination and post-germination growth anomalies (Munns and Tester, 2008). The overabundance of ethylene and Na^+ in high-salt stress inhibits macronutrient uptake and contrarily affects plant growth (Chen et al., 2007; Shibli et al., 2007). High salinity also fazes root growth by restricting plant cell division and elongation (Egamberdieva et al., 2017). Gaseous exchange, rate of transpiration, and photosynthesis are altered by infelicitous opening and closing of stomata under salinity stress. Furthermore, the uptake of necessary ions required for enzymatic and metabolic activities is also altered by high salt concentrations in soil (Hanin et al., 2016).

Certain reclamation techniques have been improvised to cope with excessive salt concentrations in soil. Some physical strategies, i.e., profile inversion, horizon mixing, deep plowing, channeling irrigation, sanding, and sub-soiling, can be implied, but their use is limited by their cost (Shrivastava and Kumar, 2015). The chemicals like gypsum, sulfur, and sulfuric acid can also be mixed with soil, but in dense soils, they can revert the reclamation process and increase salt concentration (Zia-ur-Rehman et al., 2016). The laboratory analysis and field applications have also supported electrodialysis, but the presence of insoluble compounds like $CaSO_4$ limits its efficacy (Mosavat et al., 2012). Other than conventional methods, traditional plant breeding methods for introducing favorable traits into elite varieties have been used to produce stress-tolerant plants for a long time (Meena et al., 2017). The availability of genetic tools for salinity tolerance in crop plants, as well as reliable screening methods, recognition of genetic components of tolerance, and active genetic modification of required genetic backgrounds, are all crucial factors in breeding for inducing salinity tolerance in crop plants (Arzani and Ashraf, 2016). Similarly, genetic engineering approaches have been used to impart salt tolerance in plants. Despite all the promising studies, improving salt tolerance by engineering ion transport channels is a complicated and challenging task, particularly for improving salt tolerance while still requiring a high yield. To the best of our knowledge, no genetically modified (GM) crops with salt resistance have ever been commercialized (Fita et al., 2015). At the ground level, there has not been any success.

Plant growth-promoting rhizobacteria (PGPR) are the microorganisms that dwell around the plant roots establishing symbiotic relations and promoting the growth and development of the plant directly or indirectly. Numerous researchers have anticipated the role of PGPR in mitigating abiotic stress, especially their effectiveness in reducing the perilous effects of salt stress (Sharma et al., 2017). The implementation of useful PGPR in soil enhances plant growth, development, and salt stress tolerance through various mechanisms. They promulgate growth and stress tolerance in plants by accumulating osmolytes (OS), phosphate, and potassium solubilization, boosting nutrient uptake, nitrogen fixation, increasing water

absorption capacity, siderophore sequestration, and enhancing antioxidant enzymes (AEs) activity (Islam et al., 2016; Hatran et al., 2021). They contain 1-aminoacyclopropane-1-carboxylic acid deaminase (ACCD), which curtails ethylene levels under salt stress by hydrolyzing ethylene precursor, which is 1-aminoacyclopropane-1-carboxylic acid (ACC) (Glick, 2014). These PGPR can also chelate excessive Na^+ and minimize its availability by secreting exopolysaccharides (EPS) under salinity stress (Choudhary et al., 2016). Furthermore, they can also produce phytohormones, which alleviate the deleterious effects of saline stress (Dodd and Pérez-Alfocea, 2012). *Arthrobacter aurescens, Bacillus atrophaeus, Enterobacter asburiae,* and *Pseudomonas fluorescens* were the most effective plant growth-promoting bacteria (PGPB). These salt-tolerant rhizobia with plant growth-promoting traits would help wheat plants grow in saline conditions (Sharma et al., 2016).

Maize (*Zea mays* L.) is one of the most imperative cereal crops worldwide and the 3rd most cultivated crop after wheat and rice in Pakistan (Sharma et al., 2017). Maize is moderately susceptible to salinity stress, and Pakistan is the 8th largest salt-affected country (FAO, 2018). Therefore, alternative eco-friendly and significant strategies are needed to sustain crops in saline soils all over the globe. The application of plant growth-promoting rhizobacteria onto maize fields has shown substantial potential under saline conditions (Kumawat et al., 2022). These PGPR can mitigate the inimical effects of salt stress by modulating phytohormone regulations, enhancing proline content, nutrient acquisition, and antioxidant enzyme production, preventing transportation of salt ions into the plant tissues, and overexpression of stress-tolerant genes (Li et al., 2020; Mehmood et al., 2021b).

The hypothesis of the current study shows that *B. thuringiensis* PM25 mitigates the adverse effects of salinity stress on maize and reveals the physiological and molecular mechanisms of PM25-induced salinity stress tolerance in plants. This strain can be more scientifically applied as a biological inoculant to improve the productivity of crops in saline soils. This study investigated the PGP activities of rhizospheric bacteria, identified as *Bacillus thuringiensis* PM25, and its tolerance potential against salinity stress in maize plants. This study was aimed (i) to characterize *B. thuringiensis* PM25 based on its PGP traits and activity of extracellular enzymes; (ii) to assess the ability of *B. thuringiensis* PM25 to increase seedlings biomass under salinity stress, (iii) to reveal the impact of PGPR candidates on chlorophyll content, antioxidant enzyme activity, compatible solutes, oxidative stress markers, and osmolytes in bacterized *in-vitro*-grown maize supplemented with increasing NaCl concentrations, and (iv) to analyze the principal mechanisms of PGPR in plant growth promotion and salinity stress alleviation.

Materials and methods

Acquirement of bacteria

All bacterial strains (PM21, PM22, PM23, PM26, PM27, PM28, B29, B30, B31, B32, B33, and B38) were obtained from Plant-Microbe Interactions Lab, Quaid-i-Azam University, Islamabad, Pakistan. The strains were evaluated against salinity tolerance potential (Afridi et al., 2019). *B. thuringiensis* PM25 showed the best salinity tolerance potential under different concentrations of NaCl (0, 1, 2, and 3 M). The *B. thuringiensis* PM25 sustained up to 3 M NaCl and grew significantly.

Salinity tolerance characteristics of bacteria

The salinity tolerance of *B. thuringiensis* PM25 was estimated based on the population density under salinity stress (0, 300, 600, and 900 mM NaCl) in a tryptic soy broth (TSB) medium. Sterilized flasks containing 100 ml of TSB medium with different salt concentrations were used for analyzing the bacteria. The TSB medium was inoculated with 10 μl of freshly prepared bacterial broth of *B. thuringiensis* PM25 and incubated at 26 ± 2°C and 150 rpm in a shaking incubator. About 10 ml of sterilized broth with both salt concentrations was incubated as an uninoculated control. After 24 h of incubation, the optical density of the culture was measured at $\lambda = 600$ nm using a spectrophotometer (Agilent 8453 UV-visible Spectroscopy System), and the growth was compared with uninoculated control at a particular stress level (Afridi et al., 2019).

To estimate bacterial flocculation, *B. thuringiensis* PM25 was grown in a TSB medium with 0, 300, 600, and 900 mM NaCl for 72 h at 30°C. The flocculation was collected using Whatman No. 1 filter paper and oven-dried at 60°C. After 2 h, the dry weight of the floc yield was measured (Molina et al., 2021).

The bacterial strain *B. thuringiensis* PM25 was screened for sodium uptake capacity at different NaCl concentrations. The bacterium *B. thuringiensis* PM25 was grown overnight at 30°C in a TSB medium containing salinity stress (0, 300, 600, and 900 mM NaCl). The 24 h old bacterial cells were then centrifuged and harvested by centrifugation, and the bacterial pellet was washed with sterilized distilled water to remove the traces of medium. Before being digested overnight, the washed pellet was in 0.1 N HCl at room temperature. Centrifugation was performed to obtain the supernatant, and a flame photometer was used to assess bacterial sodium absorption (Shultana et al., 2020).

The biofilm-forming capacity of *B. thuringiensis* PM25 was quantitatively analyzed by measuring the number of cells attached to a glass disk incorporated within the Petri dish containing the bacterial culture under salinity stress (0, 300, 600, and 900 mM NaCl) (Prouty et al., 2002), using the crystal violet

staining method proposed by O'Toole and Kolter (O'Toole and Kolter, 1998). The glass was taken under aseptic conditions at each exposure time, washed with 1 ml of NaCl (0.9% w/v), and treated with 1 ml of crystal violet indicator (0.1% w/v) over 20 min. Then, the glasses were washed three times with NaCl (0.9% w/v). Biofilm formation was quantified by adding 1 ml of 95% ethanol to each crystal violet stained glass. Biofilm was quantified at 506/570 nm using a UV spectrophotometer (752 N UV-VIS, Beijing, China).

Estimation of plant growth-promoting traits

Indole-3-acetic acid production (IAA) production

The colorimetric method was followed to estimate (IAA) production (Loper and Schroth, 1986). A nutrient broth amended with 0.1% L-tryptophan and NaCl (0, 300, 600, and 900 mM) was inoculated with 1 ml of overnight-grown bacterial culture. The culture broth was incubated in the shaker at 180 rpm for 48 h in the dark at 28 ± 2°C. The bacterial culture was centrifuged at 10,000 rpm for 10 min at 4°C. The supernatant (1 ml) was mixed with 4 ml Salkowski reagent and the appearance of a pink color indicated the production of IAA (Gordon and Weber, 1951). The absorbance of the final pink color solution was measured after 30 min at 535 nm in a UV/Visible spectrophotometer and compared with the standard curve. The standard curve of IAA (Serva, Islandia, USA) was made in the range of 10–100 μg/ml to estimate IAA concentration.

Siderophore production

The screening of *B. thuriniensis* PM25 for siderophore production was performed using CAS (Chrome azurol S) agar media (Schwyn and Neilands, 1987). For the preparation of CAS agar, 60.5 mg of CAS was dissolved in 50 ml of distilled water. Furthermore, 10 ml of Fe^{+3} solution (1 mM $FeCl_3.6H_2O$) and 40 ml of HDTMA (Hexadecyl trimethylammonium bromide) (72.9 mg in 40 ml dH_2O) were dissolved in a previously made CAS solution. Agar (15 g) was added to the resultant dark blue solution and was autoclaved. After the inoculation of the bacteria, plates were placed in an incubator for 7 d at 28°C. The development of orange zones around the bacterial inoculation revealed positive results for siderophore production. To estimate siderophore production, the protocol of Mehmood et al. (2021a) was followed. At 630 nm, optical density was observed and siderophore was estimated as percent siderophore unit (PSU) using the following formula:

$$PSU = Ar - \frac{As}{Ar} \times 100$$

Where, As is inoculated sample absorbance and Ar is a reference (un-inoculated broth + CAS reagent + salt conc.).

1-aminocyclopropane-1-carboxylate deaminase activity

The method of Zainab et al. (2021) was used to quantify the ACC deaminase. To quantify ACCD production by bacterial cultures, they were grown in Tryptic Soy Broth medium (TSB) for 24–48 h. The bacterial cells were harvested and centrifuged pellets were then washed with 0.1 M Tris HCl (pH = 7.5). The washed pellets were suspended in 2 ml of DF media containing 3 mM ACC supplemented with salinity stress (0, 300, 600, and 900 mM) and incubated in the cultures for 24–48 h again at 32°C. The bacterial cells were collected after 48 h by centrifugation at 300 rpm for 5 min, and pellets were washed with 2 ml of 0.1 M Tris HCl (pH = 7.5) and resuspended in 200 μl of 0.1 M Tris HCl (pH = 8.5). The bacterial pellets were labeled by adding 5% (v/v) toluen and then vortexed for 30 s. Then, 50 μl of each sample was incubated with 5 μl of 0.3 M ACC at 28°C for 30 min. Negative control had 50 μl of toluene labeled cells without ACC. Blank included 50 μl of toluene-labeled cells with 0.3 M 1-aminocyclopropane-1-carboxylate (ACC). Samples were mixed with 500 μl of 0.56 M HCl and centrifuged at 12,000 rpm for 5 min. Each 500 μl sample was taken from negative and blank in a glass test tube and added 400 μl of 0.56 N HCl, followed by 150 μl of 0.2% DNF solution and incubated for 30 min at 28°C. Before taking absorbance at 540 nm, 1 ml of 2 N NaOH was added. The activity was estimated by the hydrolysis of ACC into α- ketobutyrate. A standard curve of α- ketobutyrate was drawn ranging between 10 and 200 μmol and compared with absorbance taken at 540 nm of sample to determine μmol of α-ketobutyrate produced.

EPS production

The Exopolysaccharides quantification assay was performed following the method described by Ali et al. (2022a). The strain *B. thuringiensis* PM25 was grown in 50 ml ATCC no. 14-liquid medium: 0.2 g KH_2PO_4; 0.8 g K_2HPO_4; 0.2 g $MgSO_4$ $0.7H_2O$; 0.1 g $CaSO_4$ $0.2H_2O$; 2 mg $FeCl_3$; Na $2MoO_4$ $0.2H_2O$ (trace); 0.5 g yeast extract, 20 g sucrose; with pH of 7.2 by using sucrose as a carbon source (Ehsan et al., 2014) supplemented with NaCl (0, 300, 600, and 900 mM). The bacterium *B. thuringiensis* PM25 was also grown in 50 ml liquid medium ATCC no. 14 and incubated in a shaker for 3 days at 28°C with 200 rpm rotation. At the end of incubation, bacterial cells were harvested in pellet form by adding 1 mM EDTA, homogenized by shaking, and centrifuged for 10 min at 9,000 rpm. The supernatant containing EPS was separated and coupled with cold acetone with a proportion of 1:3. The mixture was again centrifuged at 15,000 rpm for 3 min. Deposition of EPS biomass was observed

and washed with distilled water and dried until dry weights were fixed. The EPS was estimated as mg/mL of the dried weight.

Soil analysis and seed inoculation

The soil was collected from the Quaid-i-Azam University, Islamabad, Pakistan (33.7470°N, 73.1371°E). The soil was first air-dried in the laboratory, and then it was crushed, sieved, and sterilized to get rid of all microbes and fungal spores (Afridi et al., 2019). The physio-chemical properties of the soil were assessed.

Certified maize seeds (SG-2002 variety) were collected from National Agricultural Research Center (NARC), Pakistan. Seeds were disinfected by serial washing with 70% ethyl alcohol for 5 min and 0.1% $HgCl_2$ for 1 min. After disinfection, all seeds were rinsed three times with autoclaved distilled water. The strain *B. thuringiensis* PM25 was cultured in 250-ml flasks containing LB broth. After 48 h, the culture was taken and centrifuged for 10 min at 10,000 rpm to collect the pellet. The pellet was washed with 0.85% of NaCl, suspended in deionized water to maintain the absorbance at 0.5, and obtained a homogenous bacterial population [10^8 colony-forming units (CFU) ml^{-1}]. Seeds were dipped in bacterial solution for 2–4 h, while uninoculated seeds were soaked in sterilized water taken as control (Ali et al., 2022b).

Experimental design

The Certified maize seeds (SG-2002 variety) were sown (6 surfaces of sterilized seeds per pot) in plastic pots containing 200 g of sterilized soil. Salinity stress was applied to the plants after 5 days of germination once a day with 80, 120, and 180 mM NaCl increments to the plants until reaching final concentrations of 300, 600, and 900 mM NaCl to avoid osmotic shock stress. The experimental design was summarized in Supplementary Table 1. Seeds were infected with bacteria and immersed in sterilized water for 2–4 h, whereas uninoculated seeds were used as a control.

The pots were placed in a growth chamber (CU-36L6, Iowa, USA) for 21 days. Each treatment received 20 ml of bacterial suspension after seed sowing within 7 days of the interval (7, 14 days), while the control was treated with 20 ml sterilized broth medium. Pots were rinsed with 50 ml of distilled water daily to maintain moisture for plant growth. Throughout the experiment, EC and the pH of the substrate in each pot were kept constant. The same quantity of water was sprayed regularly to maintain 60–70% of water holding capacity, balancing NaCl levels in each pot. Photosynthetic photon flux density (PPFD) levels were maintained up to 350 μmol. Humidity was maintained up to 60–80% in the growth chamber, the light duration for day and night was 12 h, and the temperature range was 32 and 20°C for day and night, respectively.

Zea mays L. plants were harvested, and their roots were wiped under running tap water after a 21 day pot experiment to eliminate soil particles from the root surface. The soil was removed from the roots, bagged plants, and taken to the lab for further testing.

Estimation of phenotypic traits

After 21 days of the experiment, three randomly selected plants from each treatment and control were investigated for phenotypic traits, such as plant height, shoot, root length, and fresh and dry biomass. All plants were dried for 24 h in an 80°C hot air oven before being weighed. The total leaf area was calculated with the help of scale by using the formula L × B × K, where L denotes leaf length, B; leaf breadth, and K; Kemp's constant (For Monocot 0.9) (Shi et al., 2021).

Estimation of photosynthetic pigments, relative water, and radical scavenging capacity of leaves

Photosynthetic pigments were extracted by homogenizing 0.1 g of fresh leaves with 6 ml of 80% ethanol. The extract was centrifuged, and the supernatant was taken in test tubes. A spectrophotometer (752 N UV-VIS, Beijing, China) was used to evaluate the optical density of chlorophyll *a*, *b*, and carotenoids at 663, 645, 510, and 480 nm, respectively (El-Esawi et al., 2018).

$$\text{Chlorophyll a} = (12.7 \times A663) - (2.49 \times A645)$$

$$\text{Chlorophyll b} = (12.9 \times A645) - (4.7 \times A663)$$

$$\text{Total chlorophyll} = \text{Chl a} + \text{Chl b}$$

$$\text{Carotenoids} = [(7.6 \times OD480) - 1.49(OD510)] \times [(\text{Final volume of filtrate}/1,000) \times 0.5)]$$

The relative water content (RWC) of green leaves was calculated by determining the turgid weight of fresh leaf samples and drying them in a hot air oven until they reached a consistent weight (Ali et al., 2021). A 0.5 g (FW) leaf was placed in a Petri dish filled with distilled water and left overnight in the dark. The turgid weight of the leaf was determined. After being heated at 72°C overnight, the leaf's dry weight (DW) was obtained.

$$RWC\ (\%) = [FW - DW/TW - DW] \times 100$$

FW = Fresh Leaf weight; TW = Turgid leaf weight; DW = Dry leaf weight

Radical scavenging activity or 2, 2-diphenyl-1-picrylhydrazyl (DPPH) of the extracts was evaluated according to the protocol of Asgari et al. (2021). Fresh leaves (100 mg) were crushed in 80% methanol, centrifuged at 10,000 rpm, and

collected the supernatant. A suitable volume of supernatant (2 ml) was mixed with 180 μl of DPPH (Aldrich Chemistry, Burlington, US) solution (0.1 mM). After 30 min, the mixture was discolored, and optical density (OD) was measured with a spectrophotometer (752 N UV-VIS, Beijing, China) at 517 nm.

$$I\ (\%) = Ac - \frac{As}{Ac} \times 100$$

Where A_c = Control; A_s = Sample's absorbance

Antioxidant enzymatic assays

Antioxidant activities (APX, SOD, and POD) were assessed in fresh leaves following the protocols of Hossain et al. (1984) and Afridi et al. (2019).

Fresh leaf samples (0.2 g) were crushed in a 2 ml extraction buffer (potassium phosphate, pH 7.5) and ascorbic acid (1 mM) to determine the APX level. The crushed materials were centrifuged for 20 min at 4°C and 13,000 rpm. The OD was obtained at 290 nm to evaluate APX. A standard curve was used to measure the activity in units/mg of proteins by estimating the decrement of ascorbate.

Using a precooled motor and pestle, freshly procured plant tissues (0.20 g) were crushed in 3 ml of 100 mM phosphate buffer (PB) for the POD assay. To separate the homogenate, the sample extract was centrifuged at 4°C and 10,000 rpm for 15 min. To determine peroxidase, an OD at 470 nm was obtained. One unit of POD is defined as the amount of enzyme that increases by 0.100 of absorbance at 436 nm/min.

To estimate SOD, the plant material was crushed in 4 ml of solution (1 g PVP, 0.0278 g Na_2EDTA) and centrifuged at 10,000 rpm. A reaction mixture (400 μl H_2O + 350 μl phosphate buffer + 100 μl methionine + 50 μl NBT + 50 μL enzyme extract + 50 μl riboflavin) was prepared to measure the activity of the SOD enzyme. The mixture was then exposed to light for 15 min, with the decrease in absorbance measured at 560 nm. A blank was made by omitting the enzyme extract. The activities of SOD were then calculated and expressed in milligrams per milligram of total soluble protein.

El-Saadony et al.'s (2021) methodology was used to assess the amount of ascorbic acid (AsA) in fresh leaves. The results were derived using an ascorbic acid (Sigma-Aldrich, St. Louis, USA) standard curve and expressed as mg/g FW.

Total soluble sugars and proteins

The Grad technique was used to calculate total soluble sugars (TSS) (Grad et al., 2021). Fresh leaves (0.1 g) were homogenized with 3–5 ml 80% ethanol to eliminate all traces of soluble sugars and centrifuged for 10 min at 10,000 rpm. The supernatant was collected and processed to calculate TSS. A freshly prepared anthrone solution (3 ml) and 0.1 mL of alcoholic extract were mixed in test tubes. All test tubes were heated for 12 min in boiling water and then iced for 10 min before being incubated for 20 min at 25°C. The optical density of the solution was measured at 625 nm using a spectrophotometer (752 N UV-VIS, Beijing, China). The total soluble sugars were estimated in μg/mL of fresh weight using the glucose standard curve.

The protein content of fresh maize leaves was determined using Bovine Serum Albumin (BSA) (Sigma-Aldrich, St. Louis, MO, USA) as a reference, as described by Mendez and Kwon (2021). Fresh leaves (0.1 g) were crushed in a mortar and pestle with 1 ml of phosphate buffer (pH 7.5) and centrifuged for 10 min at 3,000 rpm. The total volume of supernatant (0.1 ml) in test tubes was increased to 1 ml by adding distilled water. Reagent C (Solution a and b in 50:1 ratio) (Solution a: 2% Na_2CO_3, 1% Na-K, 0.4% 0.1 N NaOH; Solution b: 0.5% $CuSO_4.5H_2O$ in dH_2O) (1 ml) was added, mixed for 10 min and then 0.1 ml of reagent D (Folin phenol: distill water in a 1:1 ratio) was added. Different concentrations (20, 40, 60, 80, 320, and 640 mg) of the BSA solution were prepared, then the absorbance of all samples was measured at 650 nm after 30 min of incubation.

Total flavonoids and phenols

The total flavonoid content was determined using the aluminum chloride colorimetric assay (Woisky and Salatino, 1998). Fresh leaves (100 mg) were homogenized in 3 ml of 80% methanol for TFC estimation (Kim et al., 2005). In each tube, 0.50 ml of the extract was mixed with 1.50 ml of 95% ethanol and, 0.10 ml of 10% $AlCl_3$. At room temperature, the absorbance was measured at 415 nm with a UV-Vis spectrophotometer (UV-9200, Beijing, China) after 30 min of incubation. The calibration curve was generated using quercetin (Sigma, St. Louis, USA). The quantitative evaluation was performed using a calibration curve with quercetin 1:1 (w/v) dissolved in absolute methanol as a reference and, results were computed in milligrams of Quercetin equivalents per 100 g fresh mass (mg QE/100).

The total phenolic content was determined spectrophotometrically using the Folin-phenolic Ciocalteau's reagent (Merck, Taufkirchen, Germany) (Tawaha et al., 2007). Folin-reagent (0.5 ml) and 0.45 ml of 7.5% (w/v) saturated sodium carbonate solution were added to methanol extracted samples (20 μl). After a 2-h incubation period at 25°C, the samples' absorbance was measured at 765 nm using a UV-VIS spectrophotometer (UV-9200, Beijing, China). Total phenolic compounds were computed and represented as mg gallic acid equivalent (mg GAE/100 g) sample using gallic acid (Sigma-Aldrich, St. Louis, USA) as a reference (100–800 mg/L). The absorbance at 750 nm of the reaction mixture was measured spectrophotometrically.

Valuation of oxidative burst and osmolytes

The leakage of electrolytes from leaf disks was evaluated by determining the membrane stability index (Nisar et al., 2021). Leaf disks (0.10 g) of all treatments were placed in test tubes containing double distilled water. The EC of leaves was determined (C_1) after 30 min in the water bath at 40°C. The same leaf sample was subsequently maintained in a water bath at 100°C for 10 min, and the EC has measured again (C_2).

$$\text{Membrane Stability Index} = [1 - C1/C2] \times 100$$

The methods of Li et al. (2013) and Kapoor et al. (2021) were followed to determine endogenous H_2O_2 and malondialdehyde (MDA) content, respectively. The fresh leaves (0.10 g) were homogenized with 3 m of 0.1% trichloroacetic acid (TCA) in an ice bath and centrifuged at 12,000 rpm for 15 min to determine H_2O_2 concentration. Then, 1 M potassium iodide (1 ml) and 10 mM potassium phosphate (0.50 m) buffer (pH 7.00) were added to the supernatant. The absorbance of the supernatant was measured (at 390 nm). On a standardized curve, the content of H_2O_2 was expressed.

In a cooled mortar and pestle containing 2 ml of 1% (w/v) trichloroacetic acid (TCA), a fresh leaf sample (0.2 g) was crushed. After centrifugation of 10 min at 15,000 rpm, 2 ml of the supernatant was removed and 4 ml of 0.5% thiobarbituric acid (TBA) was added to it. The mixture was heated to 95°C and then allowed to cool. The absorbance, at 532 and 600 nm, of all treated samples was determined. The quantity of TBA was calculated using the absorption coefficient of 1.55 mmol/cm.

$$\text{MDA} = \Delta(\text{OD532} - \text{OD600})/1.56 \times 10^5$$

The ninhydrin method published by Shafiq et al. (2021) was used to determine free amino acids. The dried samples (200 mg) were homogenized in 5 ml of 80% alcohol and warmed for 15 min in a water bath. After that, the extract was centrifuged for 20 min at 2,000 rpm. In a water bath, a 0.20 ml sample of the reaction mixture was heated with 3.80 ml of ninhydrin reagent. The reaction mixture was cooled until it became purple-blue. At 570 nm, absorbance was measured. The standard curve was constructed using leucine amino acid and, findings were reported in mg of amino acid per gram of dry tissue.

The glycine betaine (GB) level was measured using a previously reported procedure (Luo et al., 2021). For glycine betaine quantification, the extract was made by homogenizing 500 mg of dried leaves with 5 ml distilled water and 0.05% toluene, placed for 24 h. The reaction mixture was filtered using 0.20-mm micropore filters before centrifuging for 5 min at 6,000 rpm. About 1 ml of HCl (2 N) and 0.10 ml of KI were stirred well with 0.50 ml of this extract. The mixture was chilled for 2 h and then violently agitated. Ice-cold water (2 ml) and 10 ml 1, 2-dichloroethane, or dichloromethane were carefully mixed with this extract. After removing the upper aqueous layer, the bottom, pink-colored layer was used to record optical density at 365 nm. The glycine betaine content in μg/gm dry weight was estimated through the betaine hydrochloride standard curve.

The method of Parveen and Siddiqui (2021) was utilized to determine proline content in shoots. Fresh shoot material (0.2 g) was crushed in 3 ml of 3% sulphosalicylic acid and stored at 5°C overnight. The obtained suspension was centrifuged for 5 min at 3,000 rpm. The supernatant (2 ml) was blended with an acidic ninhydrin reagent after centrifugation. This reagent was prepared by dissolving 1.25 g ninhydrin in 20 ml phosphoric acid (6 M) and 30 ml glacial acetic acid (1 M H_3PO_4 = 3 N H_3PO_4) with constant stirring. The reagent was kept stable for 24 h. The tubes carrying the contents were heated for 1 h in a water bath at 100°C. After cooling, the mixture was extracted with 4-ml toluene in a separate funnel. At 520 nm, optical density was determined using toluene as a blank.

$$\text{Proline } \mu g/g = K \times DF \times \text{Absorbance/FW}$$

K = 17.52; Dilution factor = 2; Fresh weight = 0.5 g.

Amplification of multi-stress related genes

The universal primers (Supplementary Table 2) were used to detect the Iturin C (*ItuC*) gene (Baysal et al., 2008). PCR reaction was done in a 25 μl reaction mixture. Thermal cycling conditions were initial activation at 95°C for 15 min, 35 cycles of 95°C for 1 min, 58°C for 1 min, and 72°C for 1.5 min, and at 72°C for 7 min.

The primers (Supplementary Table 2) were used for amplification of the *sfp* (Swaathy et al., 2014) and *srfAA* gene (Chung et al., 2008). The thermal cycler was set for an initial denaturation cycle of 1 min at 94°C, followed by 25 cycles of 1 min denaturation at 94°C, 30-sec annealing at 46°C, 1-min extension at 72°C, and a 10-min final extension at 72°C (Swaathy et al., 2014). The annealing temperature of the primer was adjusted to 58–60°C for the *srfAA* gene. The PCR result was examined using 2% of agarose gel during electrophoresis. The Gel Doc technique revealed distinct bands of the aforementioned genes.

Antioxidant (APX and SOD) gene expression

The expression level of antioxidant genes (APX and SOD) was quantified by using quantitative real-time PCR (qRT-PCR) in the presence and absence of *B. thuriniensis* PM25 under salinity stress (0, 300, 600, and 900 mM NaCl). The Qiagen

Rneasy Plant Mini kit (cat. Nos. 74903, Hilden, Germany) was used to isolate total RNA from maize plants and to remove the contaminated DNA. First-strand cDNA was synthesized using the Qiagen Reverse Transcription kit. The cDNA was then diluted to a final volume of 500 µl with ddH_2O and real-time assays were performed with SYBR Green I Master (Roche, Basel, Switzerland) according to the manufacturer's recommendations. Reaction efficiency values were calculated by running each primer set on serial dilutions of a cDNA mixture comprising stressed and control plants. Real-time quantitative PCR (RT-qPCR) was carried out using the Qiagen Rneasy Plant Mini kit (cat. Nos. 74903, Hilden, Germany) with gene-specific primers designed for SOD (F: 5′-ACATTTGCTACCTCTCCCTCACCT-3′; R: 3′-TCGGGTAAGACATCGTCGGTATGT-5′), and APX (F: 5′-AAACCCAAGCTCAGAGAGCCTCAT-3′; R: 3′-TACTTCACGGTGCTTCTTGGTGGA-5′). Reaction mixture recipes were described in Supplementary Table 3. PCR amplification conditions were set up as described by Hu et al. (2018). PCRs were performed in a thermal cycler programmed as follows: an initial denaturing step at 95°C for 3 min, followed by 45 cycles of 94°C for 10 s, 20 s annealing for different primer at 50–55 and 72°C for 20 s, with a final elongation at 72°C for 5 min. The amplified products were applied to 1.2% (w/v) agarose gel and stained in ethidium bromide (0.5 µg ml^{-1}). The strength of the fluorescent signal derived from ethidium bromide in each lane was determined by the Gel Doc system. The housekeeping gene Actin was used, and the amount of gene expression was measured using the $2^{-\Delta\Delta Ct}$ technique (Livak and Schmittgen, 2001).

Statistical analysis

Experimental data was calculated by computing standard errors and means values. The Statistix 8.1 software was used to analyze all the collected data by applying analysis of variance (ANOVA) and a pairwise comparison between all mean values was computed by using the Least Significant Difference (LSD) test ($p = 0.05$). R-software was used for Principal Component Analysis (PCA) and Pearson correlation analysis for calculated data.

Results

Bacterial growth curve analysis

Salinity negatively affects biological activity by high osmotic strength (low water potential), which can be attributed to the toxic effect on microbial growth, except for tolerant halophytic bacteria. The salinity tolerance potential of *Bacillus thuringiensis* PM25 revealed its ability to grow in various salt concentrations applied (0, 1, 2, and 3 M). It was investigated that in Luria-Bertani (LB) medium, *B. thuringiensis* PM25 could tolerate salt stress up to 3 M NaCl concentration. A log phase is revealed on the 4th day of incubation in growth curve analysis (Figure 1).

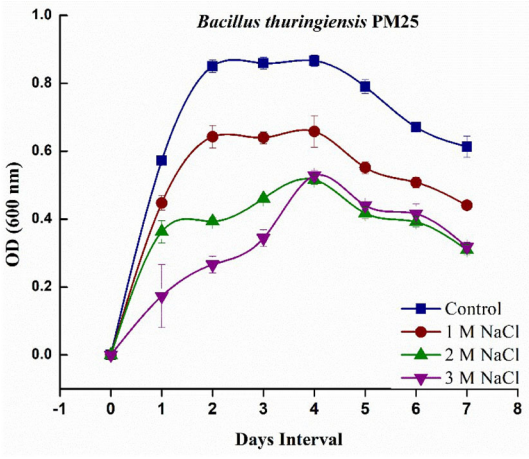


FIGURE 1
Growth curve analysis of *Bacillus thuringiensis* PM25 under salinity stress (0, 1, 2, and 3 M NaCl).

Salinity tolerance characteristics of bacteria

Bacterial survivability

The bacterial population in the culture medium plate was calculated with the number of colony-forming units (CFUs). The bacterial population was inversely proportional to salinity stress and a substantial drop in population (48.80%) of *B. thuringiensis* PM25 was observed at 900 mM NaCl while compared to control (Figure 2A).

Bacterial flocculation

In the case of bacterial flocculation yield, a direct relation was observed under salinity stress (Figure 2B). The flocculation yield increased significantly (76.45%) at 900 mM NaCl while compared to control (Figure 2B).

Bacterial sodium uptake

Accumulation of EPS-producing bacteria in the root zone of the plant reduces the accessibility of Na^+ ions in the rhizospheric region and alleviates salinity stress. The sodium absorption of

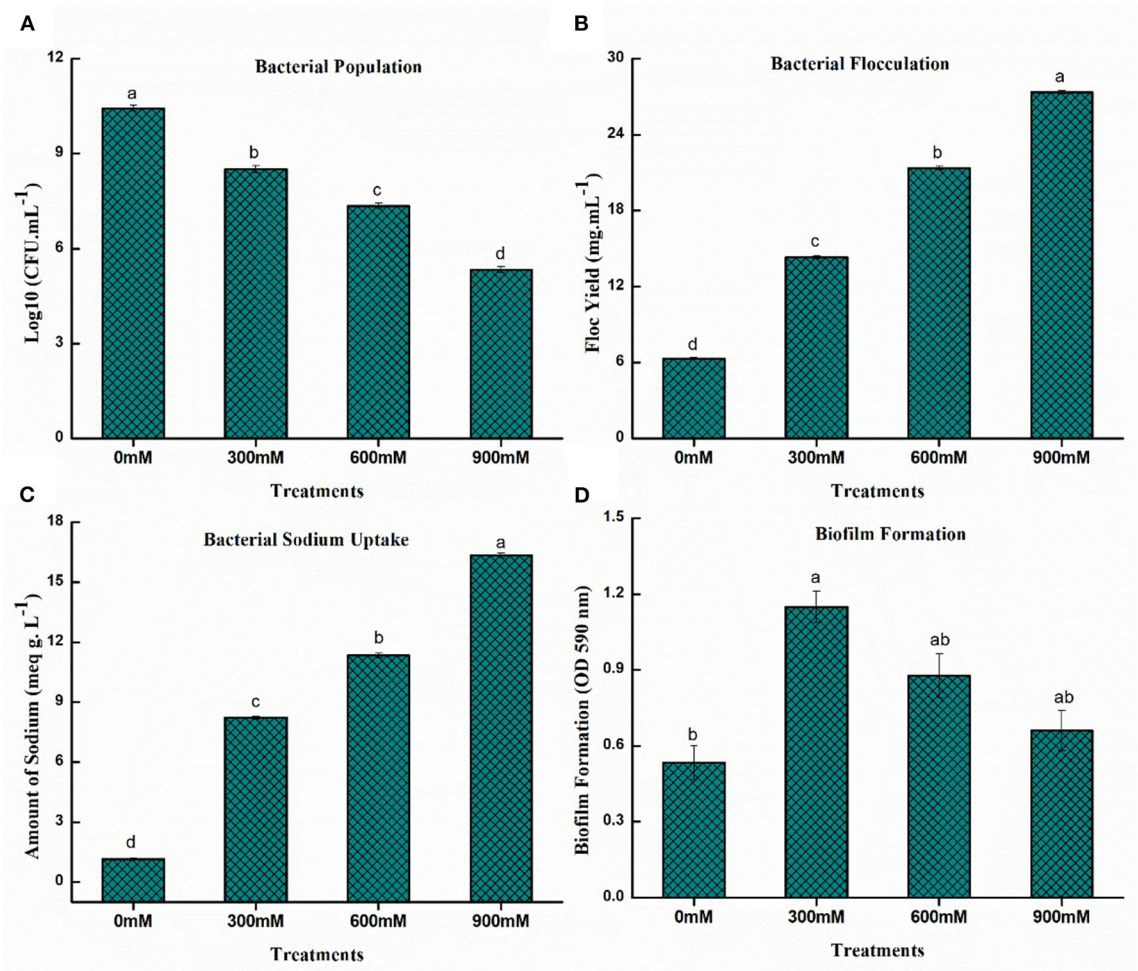


FIGURE 2
Effects of NaCl on salinity tolerance traits of PM25 **(A)** Bacterial population **(B)** Flocculation yield **(C)** Bacterial Na+ uptake **(D)** Biofilm formation. Bars sharing different letter (s) for each parameter are significantly different from each other according to the Least Significant Difference (LSD) test ($p \leq 0.05$). All the data represented are the average of three replications ($n = 3$). Error bars represent the standard errors (SE) of three replicates.

B. thuringiensis PM25 followed a similar pattern as floc yield. The Na^+ uptake was directly proportional to the increasing salinity stress (Figure 2C). The bacterial sodium uptake was significantly increased (93.01%) at 900 mM NaCl while compared to control (Figure 2C).

Biofilm formation

Salt-tolerant halophilic bacteria mainly form biofilms that confer salt-stress resistance. Biofilms contain exopolysaccharides (EPSs), which can protect bacterial cells against high salinity. The production of biofilm is specifically correlated to the production of EPS. The biofilm production *of B. thuringiensis* PM25 was significantly increased (19.69%) at 900 mM NaCl while compared to control (Figure 2D).

Quantification of PGP traits of bacteria

The PGPR exhibits beneficial traits in mitigating the toxic effects of high salt concentrations on morphological, physiological, and biochemical processes in plants, resulting in the significant rescue of yield loss. PGPR mitigates salinity stress symptoms by producing exopolysaccharides (EPS), improving ion homeostasis, decreasing ethylene levels through enzyme 1-aminocyclopropane-1-carboxylate (ACC) deaminase, and synthesizing phytohormones. The quantitative estimation of PGP traits for *B. thuringiensis* PM25 revealed increased production with increasing salinity stress (Figure 3). Significantly higher values were observed for all PGP traits under salinity stress (900 mM NaCl). Maximum increment for IAA, siderophore, ACC deaminase, and EPS were 43.02, 42, 75.33, and 46.15%, respectively, at 900 mM NaCl while comparing to control (Figure 3).

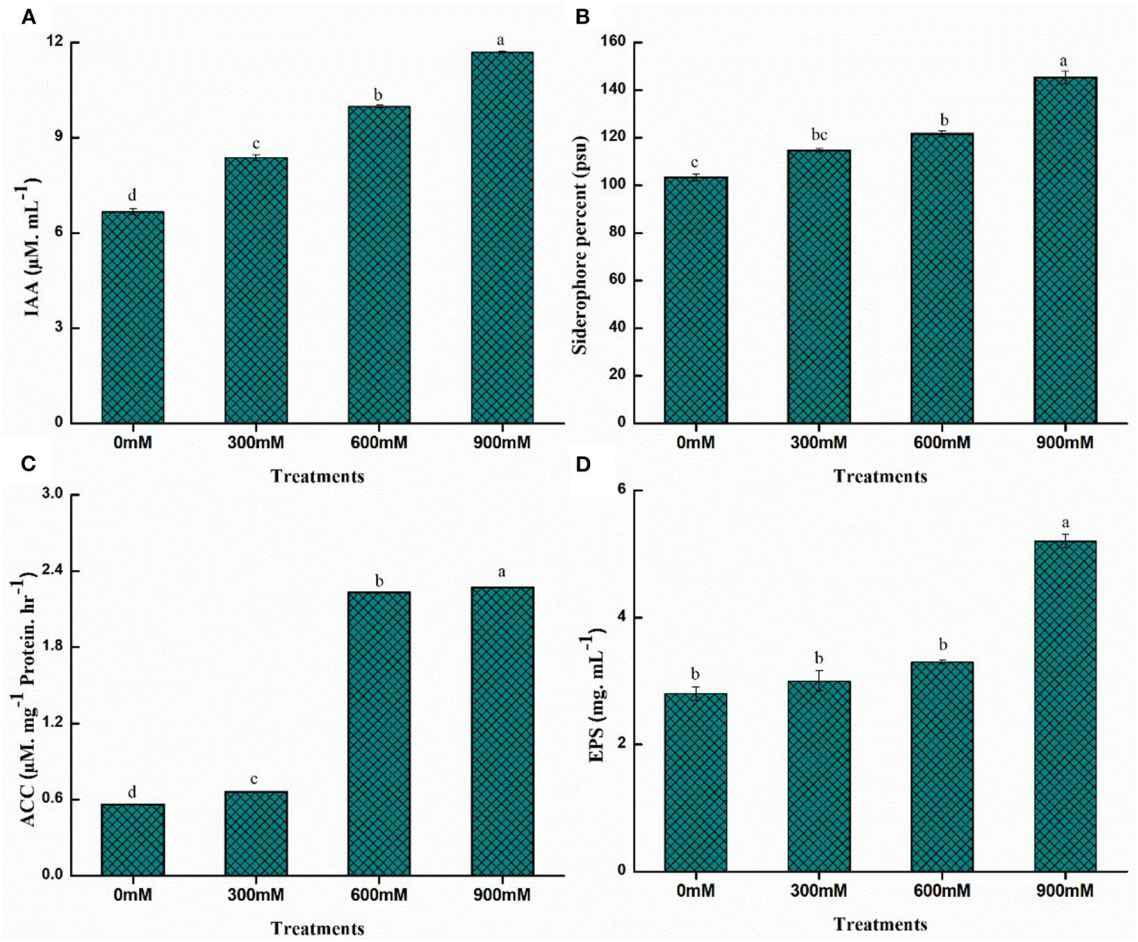


FIGURE 3
Quantitative estimation of PGP traits of PM25 under salinity stress: **(A)** IAA **(B)** Siderophore **(C)** ACCD **(D)** EPS. Bars sharing different letter (s) for each parameter are significantly different from each other according to the LSD test ($p \leq 0.05$). All the data represented are the average of three replications ($n = 3$). Error bars represent the standard errors (SE) of three replicates.

Pre-sowing and post-harvesting soil analysis

Table 1 shows the physicochemical parameters of soil. Pre-sowing and Post-harvesting soils had a loamy texture and mild alkalinity, with electrical conductivities of 1.53 and 4.49 dS/m, respectively. In pre-sowing soil, there was more organic matter and saturation than in post-harvested soil. Similarly, pre-sowing soil had higher phosphate and potassium levels than post-harvested soil (Table 1).

TABLE 1 Physio-chemical properties of soil.

Soil parameters	Soil 1 (pre-sowing)	Soil 2 (post-harvesting)
Soil texture	Loamy	Loamy
pH	7.94	7.87
Electrical conductivity (dS/m)	1.53	4.49
Organic matter (%)	3.49	1.88
Available phosphorus (mg/kg)	45.62	33.85
Available potassium (mg/kg)	601	124
Saturation (%)	44	43

Pot experiment under controlled conditions

A pot experiment was conducted for 21 days, and maize plants were then carefully harvested. The experiment evaluated the effect of *B. thuringiensis* PM25, as a halotolerant PGP strain, on growth parameters of *Zea mays* L.

Phenotypic traits of maize

High salinity significantly affects plant growth and physio-biochemical aspects, resulting in a decrease in germination rate (GRA), fresh and dry matters, photosynthetic pigments, essential nutrients uptake, and, most importantly, the loss of final crop yields. The co-cultivation of plant growth-promoting bacteria and plants in saline soils may reduce the severity of salinity stress, together with enhancing plant growth and crop yield. Before the application of *B. thuringiensis* PM25, the effect of salinity stress was determined. A significant reduction in shoot and root length was observed (Table 2). Plants that had been injected with bacteria, on the other hand, had longer shoots and roots than plants that had not been inoculated (Table 2). The results demonstrated that inoculating maize plants with *B. thuringiensis* PM25 had promising effects on all metrics under normal and salt stress conditions from 300 to 900 mM NaCl. By treating maize plants with *B. thuringiensis* PM25 under salinity stress, the shoot (17–41%), root length (33–48%), plant height (23–41%), fresh weight (55–69%), dry weight (53–59%), and leaf surface area (26–34%) grew significantly as compared to respective controls (Tables 2, 3). With and without salt stress, the PM25-inoculated plant showed an increase in all parameters, resulting in enhanced growth and biomass (Tables 2, 3).

Relative water content and DPPH activity of maize

Bacterial EPS and biofilm have promising water retention capacity. Therefore, EPS-producing PGPR shows significant tolerance to abiotic stress like drought and salinity. Leaves of maize plants were further subjected to the analysis for RWC under salinity stress and results showed a significant decrease, along with increasing concentrations of NaCl (Table 3). Under control conditions (0 mM), the *B. thuringiensis* PM25 inoculated maize plants have shown a rise in RWC. Under salinity stress, a significantly higher RWC was noted at 600 mM (28%) and 900 mM (29%) than 300 mM NaCl (26%) in inoculated maize plants as compared to the respective control (Table 3). The radical scavenging capacity was analyzed at 0, 300, 600, and 900 mM NaCl in *B. thuringiensis* PM25 inoculated and un-inoculated plants (Table 3). Under salinity stress, PM25-inoculated plants had greater DPPH than uninoculated plants. However, the increment was significant (20%) at 900 mM NaCl compared to the control (Table 3).

Estimation of photosynthetic pigments of plants

Salinity stress causes unrepairable damage to the photosynthetic apparatus at any development stage of a plant's life as it alters the structure of the chloroplasts, degrades the chloroplast envelope, and triggers chloroplast protrusions. Three different treatments were designed to analyze the positive effect of *B. thuringiensis* PM25 on pigments (Table 4). This experiment showed that salinity stress causes a negative effect on all photosynthetic pigments. The amount of pigmented content decreased under salinity stress (Table 4). The *B. thuringiensis* PM25-inoculated plants revealed a positive effect on pigments as compared to un-inoculated counterparts. The more promising increase was observed in chl *a* (33%), chl *b* (58%), total chlorophyll (42%), and carotenoids (53%) by inoculation of *B. thuringiensis* PM25 under salinity stress (900 mM NaCl) while comparing to respective control (Table 4).

Antioxidant enzymatic assays

Antioxidants help to reduce oxidative damage by decreasing the formation of reactive oxygen species (ROS) under saline soil. Oxidation of membrane proteins, lipids, or DNA is prevented by scavenging enzymes, including catalase, superoxide dismutase,

TABLE 2 Maize growth, biomass, and leaf surface area in the presence and absence of *Bacillus thuringiensis* PM25 under salinity stress.

NaCl (mM)	*B. thuringiensis* PM25	Shoot length (cm)	Root length (cm)	Plant height (cm)	Leaf area (cm^2)
0 mM	–PM25	31.33 ± 1.25^{b}	13.36 ± 0.60^{bcd}	44.7 ± 0.68^{bc}	16.01 ± 1.11^{bc}
	+PM25	38 ± 1.34^{a}	20 ± 1.66^{a}	58 ± 2.93^{a}	23.55 ± 1.30^{a}
300 mM	–PM25	28.83 ± 0.88^{bc}	10 ± 0.53^{cde}	38.83 ± 1.40^{cd}	14.89 ± 0.82^{bcd}
	+PM25	34.73 ± 1.23^{ab}	16.5 ± 1.30^{ab}	51.23 ± 1.41^{ab}	20.16 ± 1.24^{ab}
600 mM	–PM25	24.53 ± 0.46^{c}	8.07 ± 0.50^{de}	32.60 ± 0.78^{de}	12.13 ± 0.53^{cd}
	+PM25	32.33 ± 0.30^{ab}	15.51 ± 0.73^{abc}	47.85 ± 1.02^{abc}	16.75 ± 1.05^{bc}
900 mM	–PM25	17.26 ± 0.69^{d}	6.13 ± 0.39^{e}	23.4 ± 1.07^{e}	9.02 ± 0.60^{d}
	+PM25	29.33 ± 1.36^{bc}	10 ± 1.06^{cde}	39.33 ± 1.96^{cd}	13.63 ± 0.82^{cd}

Growth was measured at 21 days after seed owing under different salt concentration regimes. The treatments exhibit dissimilar letters within rows that represent a significant ($p \leq 0.05$) level.

TABLE 3 Biomass, leaf surface area, relative water content, and antioxidant activity of maize in the presence and absence of *Bacillus thuringiensis* PM25 under salinity stress.

NaCl (mM)	*B. thuringiensis* PM25	Fresh weight (g)	Dry weight (g)	RWC (%)	DPPH (IC_{50}) %
0 mM	–PM25	1.14 ± 0.16^{bcd}	0.37 ± 0.06^{bc}	47.76 ± 0.74^{bc}	35.14 ± 1.63^{e}
	+PM25	3.22 ± 0.08^{a}	0.78 ± 0.05^{a}	61.58 ± 1.01^{a}	45.15 ± 1.16^{cd}
300 mM	–PM25	0.80 ± 0.12^{cd}	0.31 ± 0.06^{bc}	43.39 ± 1.17^{cd}	38.48 ± 1.91^{de}
	+PM25	1.78 ± 0.20^{b}	0.71 ± 0.04^{a}	58.82 ± 0.71^{a}	49.34 ± 1.00^{bc}
600 mM	–PM25	0.57 ± 0.09^{d}	0.27 ± 0.05^{bc}	37.88 ± 0.95^{de}	43.30 ± 0.85^{cd}
	+PM25	1.75 ± 0.05^{b}	0.59 ± 0.05^{ab}	52.51 ± 0.79^{b}	53.33 ± 0.27^{b}
900 mM	–PM25	0.46 ± 0.07^{b}	0.21 ± 0.02^{c}	34.22 ± 0.79^{e}	48.41 ± 0.50^{bc}
	+PM25	1.49 ± 0.04^{bc}	0.51 ± 0.03^{abc}	47.95 ± 0.81^{bc}	60.63 ± 0.20^{a}

Growth was measured at 21 days after seed owing under different salt concentration regimes. RWC–Relative water content, DPPH–Radical scavenging activity of leaves. The treatments exhibit dissimilar letters within rows that represent a significant ($p \leq 0.05$) level.

TABLE 4 Pigmented content of maize in the presence and absence of *Bacillus thuringiensis* PM25 under salinity stress.

NaCl (mM)	*B. thuringiensis* PM25	Chl *a* (mg/g FW)	Chl *b* (mg/g FW)	Total Chl (mg/g FW)	Carotenoids (mg/g FW)
0 mM	–PM25	13.63 ± 0.58^{bcd}	6.16 ± 0.48^{bcd}	19.8 ± 1.06^{bcd}	6.67 ± 0.35^{bcd}
	+PM25	20.27 ± 1.19^{a}	11.23 ± 0.80^{a}	31.51 ± 1.75^{a}	11.36 ± 0.66^{a}
300 mM	–PM25	11.38 ± 0.46^{cd}	5.32 ± 0.39^{cd}	16.70 ± 0.84^{cd}	5.96 ± 0.47^{cde}
	+PM25	17.16 ± 0.93^{ab}	9.50 ± 0.61^{ab}	26.67 ± 1.07^{ab}	9.47 ± 0.66^{ab}
600 mM	–PM25	9.75 ± 0.92^{d}	4.4 ± 0.46^{cd}	14.15 ± 1.15^{d}	4.10 ± 0.54^{de}
	+PM25	15.53 ± 1.17^{abc}	8.25 ± 0.66^{abc}	23.79 ± 1.83^{abc}	8.19 ± 0.55^{abc}
900 mM	–PM25	8.60 ± 0.56^{d}	2.95 ± 0.45^{d}	11.56 ± 1.01^{d}	3.25 ± 0.39^{e}
	+PM25	12.86 ± 0.80^{bcd}	7.02 ± 0.93^{bcd}	19.89 ± 1.73^{bcd}	6.86 ± 0.40^{bcd}

Growth was measured at 21 days after seed owing under different salt concentration regimes. The treatments exhibit dissimilar letters within rows that represent a significant ($p \leq 0.05$) level.

and ascorbate peroxidase. Under salinity stress, the antioxidant defense system was analyzed. There was an increase in enzymatic antioxidants while a decrease in non-enzymatic antioxidants with increasing salinity stress (Figure 4). In comparison with uninoculated control plants, maize plants with *B. thuringiensis* PM25 accumulated more of these enzymes (APX: 25–34%; POD: 34–44%; SOD: 17–33%) at all concentrations (0, 300, 600, and 900 mM NaCl) (Figure 4). Ascorbic acid content declined as salinity stress increased, but inoculation of *B. thuringiensis* PM25 resulted in a considerable increment (48-60%) in AsA concentration under salinity while comparing to uninoculated maize plants (Figure 4).

Soluble sugars and protein content of maize

Plants protect themselves from salinity and drought stress by accumulating compatible solutes, such as sugars and proteins, to osmotically adjust themselves. The maize plants showed a significant decrease in total soluble sugars (TSS) and a significant increase in total protein content under salinity stress while compared to controlled plants (Figure 5). As 900-mM-NaCl stress was applied, the highest decrease in TSS and a considerable increase in total protein content were recorded compared to the control plants. Furthermore, PM25-treated plants had increased levels of total soluble sugars and proteins compared to uninoculated plants (Figure 5). The application of *B. thuringiensis* PM25 in maize plants significantly enhanced total soluble sugars (18–20%) and total protein content (49–59%) under salinity stress while compared to respective controls (Figure 5).

Total flavonoids and phenolic content

The effects of *B. thuringiensis* PM25 on the levels of flavonoids and phenolic content of maize plants were studied (Figure 5). The Flavonoids and phenolic content were reduced under salinity stress while compared to controlled plants. A significant decrement in flavonoid and phenolic contents was recorded at 900 mM NaCl (Figure 5). On the other hand, by the inoculation of *B. thuringiensis* PM25, *Zea mays* L. plants proclaimed significant enhancement in total flavonoid (9.24%)

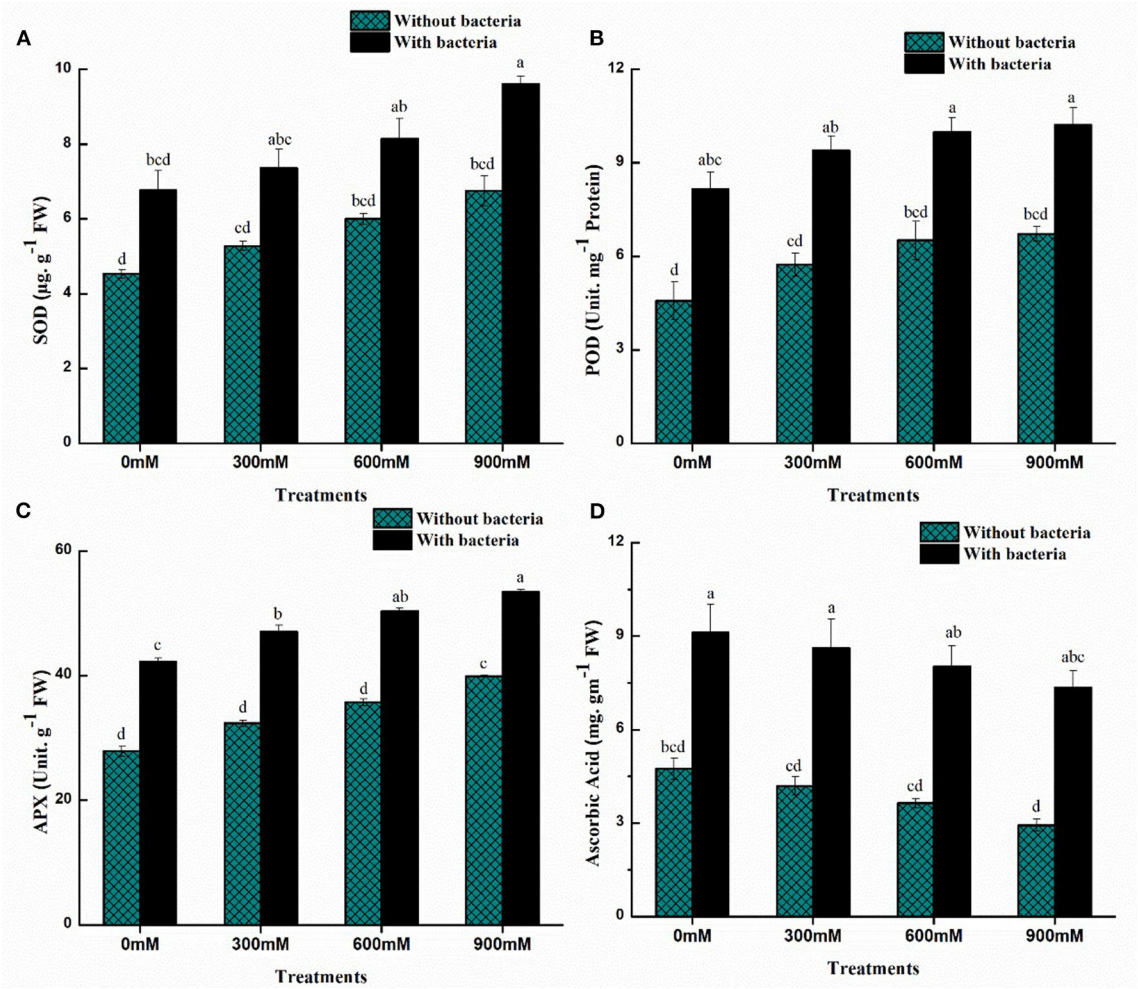


FIGURE 4
Effects of *Bacillus thuringiensis* PM25 on levels of enzymatic and non-enzymatic antioxidants: **(A)** APX **(B)** POD **(C)** SOD **(D)** Ascorbic Acid. Bars sharing different letter (s) for each parameter are significantly different from each other according to the LSD test ($p \leq 0.05$). All the data represented are the average of three replications ($n = 3$). Error bars represent the standard errors (SE) of three replicates.

and phenolic content (39%) at 900 mM NaCl as compared to uninoculated plants (Figure 5).

Estimation of oxidative burst and osmolytes

The PGPR aids to alleviate salinity stress in plants by reducing oxidative burst (electrolyte leakage, H_2O_2, and MDA content) and accumulating osmolytes (OS) (e.g., free amino acids, glycine betaine, and proline). Oxidative stress indicators [electrolyte leakage (ELL), hydrogen peroxide (H_2O_2), and malondialdehyde content (MDA)] and osmolyte [Free amino acids (FAA), glycine betaine (GB), and Proline] levels were greatly influenced by salinity (Tables 5, 6). While comparing to the control plants, the oxidative stress markers (ELL, H_2O_2, and MDA content) and osmolytes (FAA, GB, and Proline) in maize plants increased significantly under increasing salinity stress (Tables 5, 6). A significant increase was also observed in oxidative stress markers at 900-mM-salinity stress (Table 5). On the other hand, electrolyte leakage, hydrogen peroxide, and malondialdehyde content were significantly reduced (Table 5), while levels of compatible solutes were increased in bacterial inoculated plants while compared to uninoculated ones (Table 6). The application of *B. thuringiensis* PM25-inoculated maize plants showed a characteristic reduction in ELL (14–19%), H_2O_2 (28–54%), and MDA content (9–18%) (Table 5), while significant elevation in levels of FAA (42–47%), GB (45–52%), and proline (30–36%) under salinity stress as compared to respective controls (Table 6).

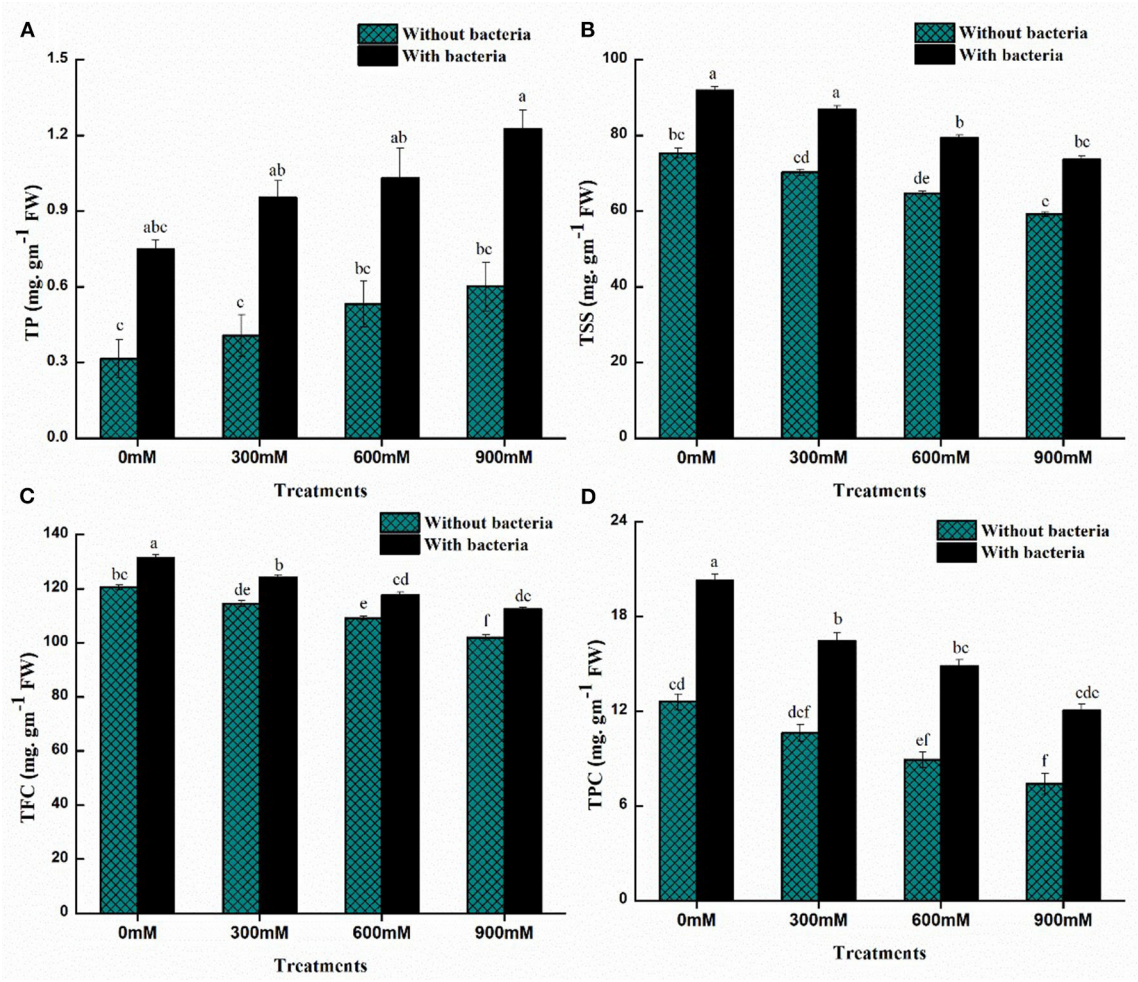


FIGURE 5
Effects of *Bacillus thuringiensis* PM25 on **(A)** Total soluble sugars **(B)** Protein content **(C)** Flavonoid content **(D)** Phenolic content. Bars sharing different letter (s) for each parameter are significantly different from each other according to the LSD test ($p \leq 0.05$). All the data represented are the average of three replications ($n = 3$). Error bars represent the standard errors (SE) of three replicates.

TABLE 5 Level of oxidative stress markers in the presence and absence of *Bacillus thuringiensis* PM25 under salinity stress.

NaCl (mM)	*B. thuringiensis* PM25	ELL (%)	H_2O_2 (μmol/g FW)	MDA (nmol/g FW)
0 mM	–PM25	36.06 ± 0.68^{cd}	36.17 ± 0.72^{de}	21.06 ± 0.67^{bc}
	+PM25	29.23 ± 0.68^{e}	33.09 ± 1.06^{e}	9.75 ± 1.10^{d}
300 mM	–PM25	41 ± 0.79^{c}	41.58 ± 1.61^{cd}	23.21 ± 0.77^{b}
	+PM25	33.06 ± 1.01^{de}	36.8 ± 0.66^{de}	12.61 ± 0.66^{d}
600 mM	–PM25	48.43 ± 0.87^{b}	49.05 ± 1.09^{ab}	26.02 ± 0.60^{ab}
	+PM25	39.4 ± 1.20^{c}	42.29 ± 1.25^{bcd}	15.23 ± 0.80^{cd}
900 mM	–PM25	54.76 ± 0.54^{a}	55.3 ± 0.96^{a}	29.57 ± 1.12^{a}
	+PM25	46.9 ± 0.46^{b}	45.23 ± 1.19^{bc}	21.26 ± 1.34^{b}

Growth was measured at 21 days after seed owing under different salt concentration regimes. ELL–Electrolyte leakage, H_2O_2-Hydrogen peroxide, MDA–Malondialdehyde. The treatments exhibit dissimilar letters within rows that represent a significant ($p \leq 0.05$) level.

TABLE 6 Level of osmolytes in the presence and absence of *Bacillus thuringiensis* PM25 under salinity stress.

NaCl (mM)	*B. thuringiensis* PM25	Free amino acid (mg/g DW)	Glycine betaine (μg/g DW)	Proline (μmol/g FW)
0 mM	–PM25	15.72 ± 0.58^{e}	10.68 ± 0.97^{f}	50.48 ± 1.59^{f}
	+PM25	27.76 ± 0.85^{bc}	22.18 ± 0.68^{cd}	77.76 ± 0.78^{c}
300 mM	–PM25	18.97 ± 0.93^{de}	13.82 ± 0.77^{ef}	53.54 ± 1.51^{ef}
	+PM25	32.83 ± 0.68^{b}	25.61 ± 0.39^{bc}	83.44 ± 0.66^{bc}
600 mM	–PM25	21.25 ± 1.05^{de}	15.77 ± 0.97^{e}	57.07 ± 0.80^{e}
	+PM25	39.83 ± 1.33^{a}	28.92 ± 0.54^{ab}	87.93 ± 0.36^{ab}
900 mM	–PM25	24.42 ± 0.78^{cd}	17.44 ± 0.85^{de}	65.19 ± 0.81^{d}
	+PM25	44.08 ± 1.06^{a}	32.48 ± 0.67^{a}	93.37 ± 0.61^{a}

Growth was measured at 21 days after seed owing under different salt concentration regimes. The treatments exhibit dissimilar letters within rows that represent a significant ($p \leq 0.05$) level.

Stress-related gene amplification

The multi-stress-related genes were amplified in *B. thuringiensis* PM25. The universal primers were used for PCR amplification of the *ItuC* (506 bp), *sfp* (675 bp), and *srfAA* (268 bp) genes of halo-tolerant *B. thuringiensis* PM25 and exhibited sharp bands at respective base pair (bp) (Supplementary material 1).

Expression level of antioxidant (APX and SOD) genes

Plants inoculated with PGPB under high salt conditions produces antioxidant genes that are involved in maintaining levels of ROS and confirm the role of PGPB in free radicals scavenging under salinity stress condition. Under control conditions, *B. thuringiensis* PM25 inoculation enhanced the expression of the two antioxidant genes (APX and SOD) in relation to uninoculated controls (Figure 6). Furthermore, *B. thuringiensis* PM25-inoculated plants revealed a higher expression level of antioxidant genes compared to uninoculated maize plants under salinity stress (Figure 6).

Principal component and Pearson correlation analysis

There was a correlation among multiple variables under salinity regimes and *B. thuringiensis* PM25 treatment in the principal component Biplot analysis. Significantly correlated variables were grouped in quadrates. Biplot indicated an 81.5% variance ($PC_1 = 59\%$; $PC_2 = 22.5\%$) (Figure 7). There was a positive correlation between antioxidants, agro-morphological traits, pigmented content, relative water content, and compatible solutes of maize. The antioxidant activity of leaves (DPPH) and oxidative stress indices were adversely interrelated with others.

Plant biomass was examined using Pearson's correlation of antioxidants and biochemical characteristics (Figure 8). In maize plants, pigmented content was found to have a substantial productive correlation with SL, FW, and RL. Increasing these features is significantly interrelated to a dramatic rise in plant biomass production (Figure 8). Total soluble sugar, pigmented content, RWC, total phenolic content, and carotenoids were all strongly related to SL, FW, and RL. The increment in biomass (SL, RL, and FW) and pigmented content resulted in elevated levels of FAA, SOD, APX, GB, TP, POD, and proline. All plant biomass parameters had a high negative connection with H_2O_2 MDA, EL, and DPPH. On the other hand, electrolyte leakage, total soluble sugars total flavonoid content, the antioxidants, and radical scavenging capacity glycine betaine, total protein, hydrogen peroxide, total phenolic content, free amino acids, malondialdehyde, antioxidant enzymes, and radical scavenging capacity were found to have a strong negative relationship. Under various treatments, lowering antioxidants causes a decrease in plant biomass (Figure 8).

Discussion

Sustainable agriculture needs crop yield and quality while ameliorating abiotic constraints (Amna et al., 2021). Nowadays, food security is a critical issue owing to the increasing population (Fróna et al., 2019). This can be accomplished by successfully introducing putative abiotic stress tolerance and PGPR. Keeping this in mind, the current work aims to investigate the potential of halo-tolerant *Bacillus thuringiensis* PM25 on maize growth promotion and salinity stress alleviation.

The potential of halo-tolerant *B. thuringiensis* PM25 against salinity stress was tested in this study. This halo-tolerant *B. thuringiensis* PM25 showed strong resilience to salinity (3 M NaCl) stress (Figure 1). The bacterial survival was steadily reduced under salinity stress (Figure 2A), which correlates with

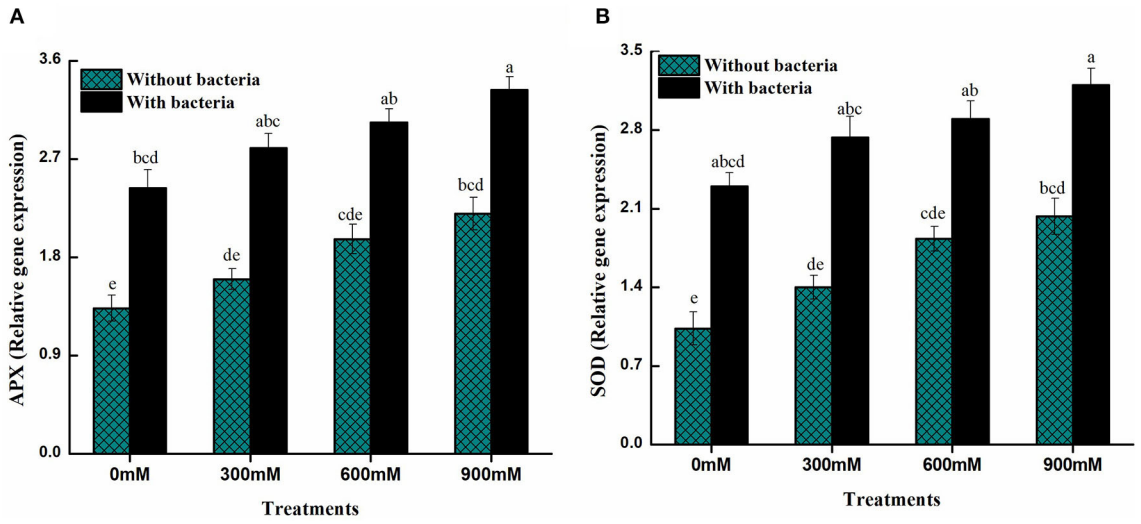


FIGURE 6
Expression levels of antioxidant genes of maize in the absence and presence of *B. thuringiensis* PM25 under salinity stress **(A)** Ascorbate peroxidase (APX) **(B)** Superoxide dismutase (SOD). Bars sharing different letter (s) for each parameter are significantly different from each other according to the LSD test ($p \leq 0.05$). All the data represented are the average of three replications ($n = 3$). Error bars represent the standard errors (SE) of three replicates.

previous results (Ali et al., 2022b). The bacterial population was reduced due to osmotic and water imbalance caused by salinity (Ali et al., 2022a).

Under salinity stress, the halo-tolerant *B. thuringiensis* PM25 developed much more floc production, biofilm, and Na^+ absorption (Figures 2B–D). Increased EPS-producing bacteria availability improves food and water uptake in the rhizosphere (Kalam et al., 2020). By raising water content in plants, the EPS can lessen the detrimental effects of osmotic stress and, hence, increase the plant's biomass (Ghosh et al., 2019). As a barrier between the cells and salinity stress, biofilm protects bacterial cells inside the EPS layer. Due to EPS production, bacteria uptake Na^+ while retaining a high population. The EPS-producing bacteria in this study reduced the amount of available Na^+ in the soil, hence, mitigating saline stress. The UPMRB9 produced a lot of EPS and biofilm at 1.5-M salinity (Shultana et al., 2020). Hong et al. (2017), reported that the adhesive qualities of EPS helped bacteria combine with soil particles and Na^+, lowering salt toxicity in plants. According to Basu et al. (2021), bacteriological polysaccharides are acidic and have a strong attraction for specific ions. A higher level of NaCl increased biofilm development in *Bacillus* spp., according to Kasim et al. (2016), with the largest peak occurring at 500 mM NaCl.

Under salinity stress, the PGPR, *B. thuringiensis* PM25 produced considerable amounts of IAA, siderophore, ACC deaminase, and EPS (Figure 3). Indole acetic acid (IAA) aids seed germination and the formation of longer roots with more root hairs, which aids nutrient intake indirectly. It also has a lot of potential for large-scale cereal crop production (Khan et al., 2016; Aloo et al., 2019; Bensidhoum and Nabti, 2019). It has been claimed that IAA produced by bacteria aids root growth by inducing cell elongation and/or responding to cell division (Vimal et al., 2019). The IAA production is linked to root development and structural alterations in response to stress (Abbas et al., 2018). Previous research found that PGPB synthesis of IAA increased plant growth in *Bacillus* sp., *Enterobacter* sp., *Bacillus thuringiensis*, *Bacillus tequilensis*, and *Bacillus mycoides* (Guerrero-Barajas et al., 2020).

Under salinity stress, *B. thuringiensis* PM25 followed a similar pattern as IAA (Figure 3) and enhanced plant growth by siderophore production. The presence of siderophore-producing PGPR in the rhizosphere can minimize the effect of salinity on Fe availability in the soil (Ferreira et al., 2019). Plants acquired iron from the soil and used siderophore-producing bacteria to suppress phytopathogens. Plants' chlorophyll biosynthesis, photosynthetic electron transport, and respiratory chain functioning were all influenced by iron chelation (Saha et al., 2016). The iron chelation increased the production and repair of DNA and RNA (Ferreira et al., 2019). During plant growth, many siderophore-producing endophytic bacterial communities, such as *Sphingomonas*, *Pseudomonas*, *Enterobacter*, and *Burkholderia* alternated (Ferrarezi et al., 2022).

Under salinity stress, *B. thuringiensis* PM25 degraded ACC into ammonia and α-ketobutyrate in roots, redirected ethylene production routes, and limited ethylene biosynthesis (Figure 3). Another technique for dealing with salt stress is for rhizospheric

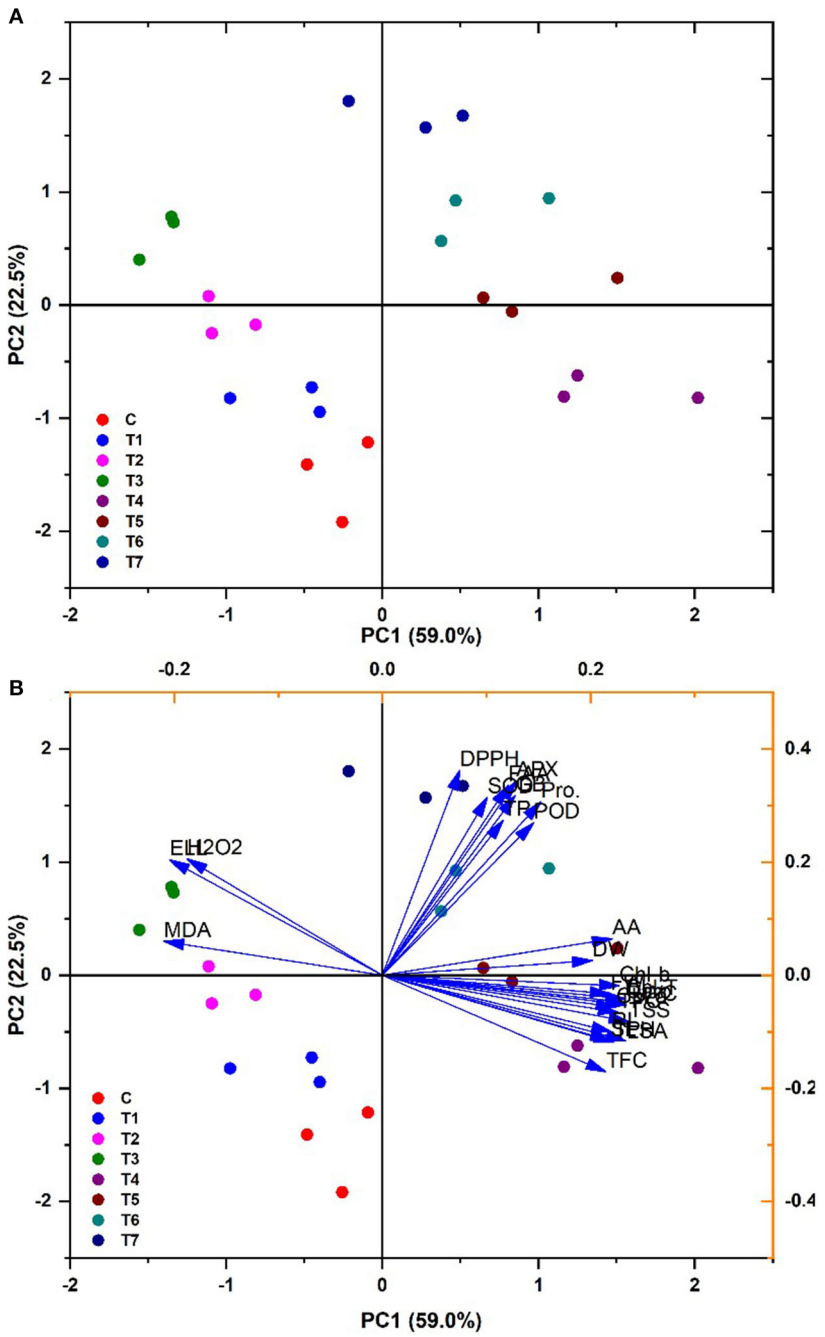


FIGURE 7
PCA biplot showing the categorization of PM25 based on its effects on maize growth-promoting characteristics under salinity stress **(A)** Cluster analysis **(B)** PCA Biplot analysis.

bacteria to have ACC deaminase activity (Gamalero and Glick, 2015). Under saline/sodic stress, ethylene production increased, inhibiting seed germination and plant growth (Koevoets et al., 2016). However, recruitment of ACC deaminase-producing bacteria to seedling roots metabolized ACC into ammonia and α-ketobutyrate, redirecting ethylene production pathways. As a result, the negative effects of ethylene are mitigated (Carlos et al., 2016; Sarkar et al., 2018), and germination is improved, leading to better plant growth under saline conditions (Kumari et al., 2018; Marag and Suman, 2018).

Some plant growth-promoting rhizobacteria (PGPR) produce exopolysaccharides (EPS) or surface polysaccharides.

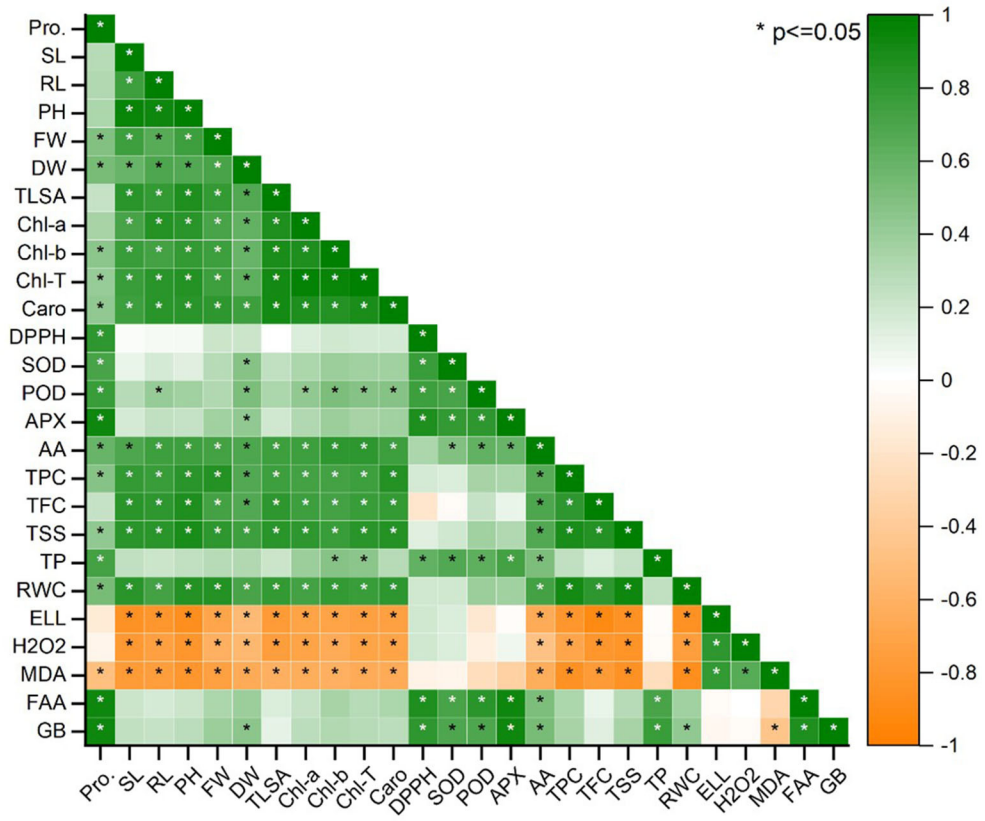


FIGURE 8
Pearson correlation between antioxidants and biochemical traits with plant biomass parameters under salinity stress; Pro, (Proline), SL (Shoot length), RL (Root length), PH (Plant height), FW (Fresh weight), DW (Dry weight), LA (Leaf area), Chl a (Chlorophyll a), Chl b (Chlorophyll b), T. Chl (Total chlorophyll), Caro (Carotenoids), DPPH (Radical scavenging capacity), SOD (Superoxide dismutase), POD (Peroxidases), APX (Ascorbate peroxidase), AA (Ascorbic acid), TPC (Total phenolic content), TFC (Total flavonoid content), TSS (Total soluble sugars), TP (Total Protein), RWC (Relative water content), EL (Electrolyte leakage), H_2O_2 (Hydrogen peroxide), MDA (Malondialdehyde), FAA (Free amino acids), GB (Glycine betaine). The treatments exhibit (*) within rows that represent a significance ($p \leq 0.05$) level.

Under salinity stress, *B. thuringiensis* PM25 produced significant EPS while compared to control (Figure 3). The EPS-producing PGPR strains increase soil salinity tolerance, improve soybean (*Glycine maxima*) plant growth (Zhang et al., 2022), and restrict Na^+ absorption by wheat roots (Souza et al., 2015). These EPS aids in the formation of bacterial aggregates, which enhances soil aeration, water infiltration, and root growth (Bhise and Dandge, 2019).

Salinity is one of the most significant abiotic constraints in agricultural production, particularly in dry and semi-arid regions. It reduces the amount of water available to plants, which has disastrous consequences for both growth and productivity (Hussain et al., 2019). Our results showed that the *B. thuringiensis* PM25 used in the current study promoted the vegetative growth of maize plants. It was worth mentioning that *B. thuringiensis* PM25 improved agro-morphological traits compared to uninoculated plants (Tables 2, 3). In comparison to control maize plants, PM25-inoculation overcame the unfavorable effects of salinity stress on growth and yield and promoted phenotypic traits of maize under salinity stress (Tables 2, 3). Inoculating wheat plants with PGPB increased the agro-morphological features in a pot experiment in saline soil (Paredes-Páliz et al., 2016; Bakka and Challabathula, 2020). Plant growth-promoting rhizobacteria (PGPR) modulate root architecture by establishing extended rhizo-sheaths, preventing salt uptake *via* roots by confining Na^+ ions in the EPS matrix, assisting the plant in maintaining ionic equilibrium. The increased growth of inoculated plants under a controlled and stressful environment is most likely due to IAA synthesis by the PGPR (Abbas et al., 2018).

Salinity causes osmotic stress, one of the most evident signs of a drop in leaf relative to water (Silambarasan et al., 2019). Under salinity stress, bacterial-inoculated maize plants had a greater RWC than the controls (Table 3)). PGPR significantly increases the roots and development of salt-stressed plants by

boosting water usage efficiency and improving the RWC (Singh and Jha, 2016; Nosheen et al., 2021).

Our results demonstrated that co-inoculation of *B. thuringiensis* PM25 augmented maize plants' radical scavenging potential (Table 3). Increased ROS scavenging ability has previously been reported in canola (Li et al., 2017), rice (Sarkar et al., 2018), chickpea (El-Esawi et al., 2019), sunflower (Gupta et al., 2019), and lettuce plants (Silambarasan et al., 2019) under abiotic stress by inoculating a plant with PGP microorganisms.

The reduction in plant growth was based on an increase in Na^+ ion levels and oxidative stress, which reduced photosynthetic efficiency, ion imbalance, and membrane integrity (Desoky et al., 2020). Inoculating maize with *B. thuringiensis* PM25 overcomes the negative impacts of salinity stress and increased physiological attributes, such as chlorophyll content (Table 4). Our findings backed up a prior study that found that PGPB inoculation increased chlorophyll synthesis and accelerated radish plant development (Al Kahtani et al., 2021). Tomato plants infected with PGPB, *Achromobacter piechaudii* ARV8, increased photosynthetic activity in salinity-stressed plants (Shrivastava and Kumar, 2015). According to Enebe and Babalola (2018), PGPR assists in the stability of photosynthetic pigments.

Low molecular weight antioxidants are produced by plants to impart salinity stress tolerance (Xu et al., 2015). Under salinity stress, inoculating maize plants with *B. thuringiensis* PM25 significantly enhanced enzymatic (APX, POD, SOD) and non-enzymatic (Ascorbic acid) antioxidants (Figure 4). Antioxidant activity was increased by the application of PGPB (Hashem et al., 2016). Furthermore, 5-aminolevulinic acid-producing bacteria reduced H_2O_2 production and boosted APX, POD, and SOD antioxidant activities in salinity-stressed rice (Kantachote et al., 2016; Wu et al., 2018). Ascorbic acid (AsA) is an excellent ROS scavenger due to its ability to activate enzymatic and non-enzymatic processes that influence H_2O_2 and maintain cell membranes (Akram et al., 2017).

For instance, total protein content (TP) and total soluble sugars (TSS) in plants under saline stress are important defensive strategies to cope with salt stress. Under salinity stress, the inoculation of halo-tolerant *B. thuringiensis* PM25 increased total soluble sugars and protein content (Figure 5). Plants inoculated with PGPR could increase the production of soluble proteins and soluble carbohydrates in high-salinity environments, allowing them to withstand oxidative and osmotic stressors (Qu et al., 2016; Bhise and Dandge, 2019). Previous studies have also shown that inoculating wheat seeds with the *Bacillus aquimaris* strain increases soluble sugars in saline circumstances, improving plants' growth and biomass (Upadhyay and Singh, 2015).

Under salinity stress, *B. thuringiensis* PM25 showed a considerable increase in flavonoid and polyphenol content (Figure 5). For instance (Sofy et al., 2021) discovered that inoculating pea plants with PGPB increases the phenolic content to reduce salt stress. Under salinity stress, the significant increase of flavonoids and phenolic content in halo-tolerant PGPB-treated plants may help in the inactivation of ROS and the breakdown of H_2O_2 to alleviate oxidative stress (Gago et al., 2016).

In this study, electrolyte leakage (ELL) and ROS levels (MDA and H_2O_2 content) were increased under salinity stress (Table 5). However, inoculation with PGPR (*B. thuringiensis* PM25) decreases the ROS levels in maize plants (Table 5). Likewise, maize inoculated with PGPR remarkably declined the ELL, MDA, and H_2O_2 levels under NaCl stress conditions (El-Esawi et al., 2018). Plant beneficial microbes of the rhizosphere can help to improve the integrity of plant cell membrane by inhibiting oxidative damage (Abadi and Sepehri, 2016). These findings are consistent with (Pinedo et al., 2015; Abd Allah et al., 2018), in which PGPB-inoculated maize and white clover plants lowered oxidative stress indicators under salinity.

Salinity stress raised the level of osmolytes considerably (Table 6). The present findings showed that PGPR inoculation (*B. thuringiensis* PM25) increased the levels of osmolytes under salinity stress (Table 6). Compatible organic solutes regulate leaf water potential and protect plants against osmotic imbalance (Upadhyay and Singh, 2015; Iqbal et al., 2016). Wheat treated with PGPR maintains growth under saline stress by accumulating compatible solutes (Xu et al., 2017). PGPR application significantly enhanced wheat yield under saline conditions (Akhtar et al., 2015; Farooq et al., 2015; Naili et al., 2018).

In the current investigation, surfactant-producing *sfp* and *srfAA* and while Iturin C (*ItuC*) gene, which encodes antibiotic synthesis, was amplified in *B. thuringiensis* PM25 (Supplementary material 1). The bio-surfactants improve colonization and yield by strengthening the interface between rhizobacteria that promote plant growth and roots (Khare and Arora, 2021; Kumar et al., 2021). Because the bacterial strain improved maize's growth and tolerance to salinity, this bacteria can be used as a bio-fertilizer and multi-stress resistant substance for plants.

Furthermore, inoculating *B. thuringiensis* PM25 massively improved the gene expression associated with salt tolerance and antioxidant enzymes (Figure 6). By regulating SOD and APX genes, salinity stress was alleviated in chickpeas (Elkelish et al., 2019). Salinity stress was mitigated in rice seedlings where levels of antioxidants were increased by inoculating PGPB (Ji et al., 2020).

Conclusion

In the recent scenario of the increasing global population and changing climatic conditions, sustainable agricultural methods are of immediate need. The current study found that inoculating maize plants with halo-tolerant *B. thuringiensis*

PM25 enhanced their resistance to salinity stress. The treatment of *B. thuringiensis* PM25 substantially alleviates salinity stress. This halo-tolerant bacteria *B. thuringiensis* PM25 has plant growth-promoting features and, in liquid formulations, it stimulated maize growth and biomass under salinity stress. This rhizospheric *B. thuringiensis* PM25 was critical in relieving salinity stress in maize plants by modifying the antioxidant defense system, lowering oxidative burst, and accumulating compatible solutes. According to the findings of the current study, halo-tolerant *B. thuringiensis* PM25 has the potential to be used as a viable alternative and environmentally acceptable for facilitating maize production and mitigating salinity stress. A pot experiment with *B. thuringiensis* PM25-inoculation at various salinity stress gives a baseline for analyzing potential PGPR under salinity stress. However, more study on natural saline soil under field circumstances is necessary. The use of PGPR in the agriculture field is a green option to increase productivity and crop yield.

Data availability statement

The original contributions presented in the study are included in the article/Supplementary material, further inquiries can be directed to the corresponding authors.

Author contributions

AH and BA: conceptualization. TD, KA, and MJ: data curation. AH, SA, S, and MA: formal analysis. RM, CM, TD, and KA: funding acquisition. S, RM, CM, AH, and MJ: software. BA and AH: investigation and methodology. BA, AH, and SA: writing—original draft. BA, AH, SA, MJ, S, MA, TD, KA, CM, RM, SS, and DA: writing—review and editing. AH, BA, TD, KA, RM, SS, DA, and CM: visualization. TD and KA: validation. All authors approved the final version of the manuscript.

Funding

The authors extend their appreciation to the Researchers supporting project number (RSP-2021/197), King Saud University, Riyadh, Saudi Arabia. The publication was supported by funds from the National Research Development Projects to finance excellence (PFE)-14/2022-2024 granted by the Romanian Ministry of Research and Innovation.

Conflict of interest

The authors declare that the research was conducted in the absence of any commercial or financial relationships that could be construed as a potential conflict of interest.

Publisher's note

All claims expressed in this article are solely those of the authors and do not necessarily represent those of their affiliated organizations, or those of the publisher, the editors and the reviewers. Any product that may be evaluated in this article, or claim that may be made by its manufacturer, is not guaranteed or endorsed by the publisher.

Supplementary material

The Supplementary Material for this article can be found online at: https://www.frontiersin.org/articles/10.3389/fpls.2022.921668/full#supplementary-material

References

Abadi, V. A. J. M., and Sepehri, M. (2016). Effect of *Piriformospora indica* and *Azotobacter chroococcum* on mitigation of zinc deficiency stress in wheat (*Triticum aestivum* L.). *Symbiosis* 69, 9–19. doi: 10.1007/s13199-015-0361-z

Abbas, H., Patel, R. M., and Parekh, V. B. (2018). Culturable endophytic bacteria from halotolerant *Salicornia brachata* L.: isolation and plant growth promoting traits. *Indian J. Appl. Microbiol.* 21, 10–21. doi: 10.46798/ijam.2018.v21i01.002

Abd Allah, E. F., Alqarawi, A. A., Hashem, A., Radhakrishnan, R., Al-Huqail, A. A., Al-Otibi, F. O. N., et al. (2018). Endophytic bacterium *Bacillus subtilis* (BERA 71) improves salt tolerance in chickpea plants by regulating the plant defense mechanisms. *J. Plant Interact.* 13, 37–44. doi: 10.1080/17429145.2017.1414321

Afridi, M. S., Amna, S., Mahmood, T., Salam, A., Mukhtar, T., et al. (2019). Induction of tolerance to salinity in wheat genotypes by plant growth promoting endophytes: involvement of ACC deaminase and antioxidant enzymes. *Plant Physiol. Biochem.* 139, 569–577. doi: 10.1016/j.plaphy.2019.03.041

Ahmad, M., Ishaq, M., Shah, W. A., Adnan, M., Fahad, S., Saleem, M. H., et al. (2022). Managing phosphorus availability from organic and inorganic sources for optimum wheat production in calcareous soils. *Sustainability* 14, 7669. doi: 10.3390/su14137669

Akhtar, S. S., Andersen, M. N., Naveed, M., Zahir, Z. A., and Liu, F. (2015). Interactive effect of biochar and plant growth-promoting bacterial endophytes on ameliorating salinity stress in maize. *Funct. Plant Biol.* 42, 770–781. doi: 10.1071/FP15054

Akram, N. A., Shafiq, F., and Ashraf, M. (2017). Ascorbic acid-a potential oxidant scavenger and its role in plant development and abiotic stress tolerance. *Front. Plant Sci.* 8, 613. doi: 10.3389/fpls.2017.00613

Al Kahtani, M., Hafez, Y., Attia, K., Al-Ateeq, T., Ali, M. A. M., Hasanuzzaman, M., et al. (2021). *Bacillus thuringiensis* and silicon modulate antioxidant metabolism and improve the physiological traits to confer salt tolerance in lettuce. *Plants* 10, 1025. doi: 10.3390/plants10051025

Ali, B., Wang, X., Saleem, M. H., Azeem, M. A., Afridi, M. S., Nadeem, M., et al. (2022a). Bacillus mycoides PM35 reinforces photosynthetic efficiency, antioxidant

defense, expression of stress-responsive genes, and ameliorates the effects of salinity stress in maize. *Life* 12, 219. doi: 10.3390/life12020219

Ali, B., Wang, X., Saleem, M. H., Hafeez, A., Afridi, M. S., Khan, S., et al. (2022b). PGPR-mediated salt tolerance in maize by modulating plant physiology, antioxidant defense, compatible solutes accumulation and bio-surfactant producing genes. *Plants* 11, 345. doi: 10.3390/plants11030345

Ali, J., Ali, F., Ahmad, I., Rafique, M., Munis, M. F. H., Hassan, S. W., et al. (2021). Mechanistic elucidation of germination potential and growth of *Sesbania sesban* seedlings with *Bacillus anthracis* PM21 under heavy metals stress: an *in vitro* study. *Ecotoxicol. Environ. Saf.* 208, 111769. doi: 10.1016/j.ecoenv.2020.111769

Aloo, B. N., Makumba, B. A., and Mbega, E. R. (2019). The potential of Bacilli rhizobacteria for sustainable crop production and environmental sustainability. *Microbiol. Res.* 219, 26–39.

Amna, A. B., Azeem, M. A., Qayyum, A., Mustafa, G., Ahmad, M. A., Javed, M. T., et al. (2021). Bio-Fabricated silver nanoparticles: a sustainable approach for augmentation of plant growth and pathogen control. *Sustain. Agric. Rev.* 53, 345–371. doi: 10.1007/978-3-030-86876-5_14

Arzani, A., and Ashraf, M. (2016). Smart engineering of genetic resources for enhanced salinity tolerance in crop plants. *Crit. Rev. Plant Sci.* 35, 146–189. doi: 10.1080/07352689.2016.1245056

Asgari, H. T., Es-haghi, A., and Karimi, E. (2021). Anti-angiogenic, antibacterial, and antioxidant activities of nanoemulsions synthesized by *Cuminum cyminum* L. tinctures. *J. Food Meas. Charact.* 15, 3649–3659. doi: 10.1007/s11694-021-00947-1

Bakka, K., and Challabathula, D. (2020). "Amelioration of salt stress tolerance in plants by plant growth-promoting rhizobacteria: insights from 'omics' approaches," in *Plant Microbe Symbiosis*, eds A. Varma, S. Tripathi, R. Prasad (Cham: Springer), 303–330. doi: 10.1007/978-3-030-36248-5_16

Basu, A., Prasad, P., Das, S. N., Kalam, S., Sayyed, R. Z., Reddy, M. S., et al. (2021). Plant growth promoting rhizobacteria (PGPR) as green bioinoculants: recent developments, constraints, and prospects. *Sustainability*. 13, 1140.

Baysal, Ö., Çalişkan, M., and Yeşilova, Ö. (2008). An inhibitory effect of a new *Bacillus subtilis* strain (EU07) against *Fusarium oxysporum* f. sp. radicis-lycopersici. *Physiol. Mol. Plant Pathol.* 73, 25–32. doi: 10.1016/j.pmpp.2008.11.002

Bensidhoum, L., and Nabti, E. (2019). "Plant growth-promoting bacteria for improving crops under saline conditions," in *Microorganisms in Saline Environments: Strategies and Functions*, eds B. Giri, and A. Varma (Cham: Springer), 329–352. doi: 10.1007/978-3-030-18975-4_14

Bhise, K. K., and Dandge, P. B. (2019). Mitigation of salinity stress in plants using plant growth promoting bacteria. *Symbiosis* 79, 191–204. doi: 10.1007/s13199-019-00638-y

Carlos, M.-H. J., Stefani, P.-V. Y., Janette, A.-M., Melani, M.-S. S., and Gabriela, P.-O. (2016). Assessing the effects of heavy metals in ACC deaminase and IAA production on plant growth-promoting bacteria. *Microbiol. Res.* 188, 53–61. doi: 10.1016/j.micres.2016.05.001

Chen, Z., Pottosin, I. I., Cuin, T. A., Fuglsang, A. T., Tester, M., Jha, D., et al. (2007). Root plasma membrane transporters controlling K+/Na+ homeostasis in salt-stressed barley. *Plant Physiol.* 145, 1714–1725. doi: 10.1104/pp.107.110262

Choudhary, D. K., Kasotia, A., Jain, S., Vaishnav, A., Kumari, S., Sharma, K. P., et al. (2016). Bacterial-mediated tolerance and resistance to plants under abiotic and biotic stresses. *J. Plant Growth Regul.* 35, 276–300. doi: 10.1007/s00344-015-9521-x

Chung, S., Kong, H., Buyer, J. S., Lakshman, D. K., Lydon, J., Kim, S.-D., et al. (2008). Isolation and partial characterization of *Bacillus subtilis* ME488 for suppression of soilborne pathogens of cucumber and pepper. *Appl. Microbiol. Biotechnol.* 80, 115–123. doi: 10.1007/s00253-008-1520-4

Daliakopoulos, I. N., Tsanis, I. K., Koutroulis, A., Kourgialas, N. N., Varouchakis, A. E., Karatzas, G. P., et al. (2016). The threat of soil salinity: a European scale review. *Sci. Total Environ.* 573, 727–739. doi: 10.1016/j.scitotenv.2016.08.177

Desoky, E.-S. M., Saad, A. M., El-Saadony, M. T., Merwad, A.-R. M., and Rady, M. M. (2020). Plant growth-promoting rhizobacteria: potential improvement in antioxidant defense system and suppression of oxidative stress for alleviating salinity stress in *Triticum aestivum* (L.) plants. *Biocatal. Agric. Biotechnol.* 30, 101878. doi: 10.1016/j.bcab.2020.101878

Dodd, I. C., and Pérez-Alfocea, F. (2012). Microbial amelioration of crop salinity stress. *J. Exp. Bot.* 63, 3415–3428. doi: 10.1093/jxb/ers033

Egamberdieva, D., Wirth, S., Jabborova, D., Räsänen, L. A., and Liao, H. (2017). Coordination between bradyrhizobium and pseudomonas alleviates salt stress in soybean through altering root system architecture. *J. Plant Interact.* 12, 100–107. doi: 10.1080/17429145.2017.1294212

Ehsan, S., Ali, S., Noureen, S., Mahmood, K., Farid, M., Ishaque, W., et al. (2014). Citric acid assisted phytoremediation of cadmium by *Brassica napus* L. *Ecotoxicol. Environ. Saf.* 106, 164–172. doi: 10.1016/j.ecoenv.2014.03.007

El-Esawi, M. A., Alaraidh, I. A., Alsahli, A. A., Alzahrani, S. M., Ali, H. M., Alayafi, A. A., et al. (2018). Serratia liquefaciens KM4 improves salt stress tolerance in maize by regulating redox potential, ion homeostasis, leaf gas exchange and stress-related gene expression. *Int. J. Mol. Sci.* 19, 3310. doi: 10.3390/ijms19113310

El-Esawi, M. A., Al-Ghamdi, A. A., Ali, H. M., and Alayafi, A. A. (2019). Azospirillum lipoferum FK1 confers improved salt tolerance in chickpea (*Cicer arietinum* L.) by modulating osmolytes, antioxidant machinery and stress-related genes expression. *Environ. Exp. Bot.* 159, 55–65. doi: 10.1016/j.envexpbot.2018.12.001

Elkelish, A. A., Soliman, M. H., Alhaithloul, H. A., and El-Esawi, M. A. (2019). Selenium protects wheat seedlings against salt stress-mediated oxidative damage by up-regulating antioxidants and osmolytes metabolism. *Plant Physiol. Biochem.* 137, 144–153. doi: 10.1016/j.plaphy.2019.02.004

El-Saadony, M. T., Desoky, E.-S. M., Saad, A. M., Eid, R. S. M., Selem, E., and Elrys, A. S. (2021). Biological silicon nanoparticles improve *Phaseolus vulgaris* L. yield and minimize its contaminant contents on a heavy metals-contaminated saline soil. *J. Environ. Sci.* 106, 1–14. doi: 10.1016/j.jes.2021.01.012

Enebe, M. C., and Babalola, O. O. (2018). The influence of plant growth-promoting rhizobacteria in plant tolerance to abiotic stress: a survival strategy. *Appl. Microbiol. Biotechnol.* 102, 7821–7835. doi: 10.1007/s00253-018-9214-z

FAO (2018). *Food and Agriculture Organization of the United Nations. FAO in Pakistan.* Food Agriculture Pakistan. Available online at: https://www.fao.org/pakistan/our-office/pakistan-at-a-glance/en/ (accessed November 8, 2021).

Farooq, M., Hussain, M., Wakeel, A., and Siddique, K. H. M. (2015). Salt stress in maize: effects, resistance mechanisms, and management. A review. *Agron. Sustain. Dev.* 35, 461–481. doi: 10.1007/s13593-015-0287-0

Ferrarezi, J. A., de Almeida Carvalho-Estrada, P., Batista, B. D., Aniceto, R. M., Tschoeke, B. A. P., de Maia Andrade, P. A., et al. (2022). Effects of inoculation with plant growth-promoting rhizobacteria from the Brazilian Amazon on the bacterial community associated with maize in field. *Appl. Soil Ecol.* 170, 104297. doi: 10.1016/j.apsoil.2021.104297

Ferreira, M. J., Silva, H., and Cunha, A. (2019). Siderophore-producing rhizobacteria as a promising tool for empowering plants to cope with iron limitation in saline soils: a review. *Pedosphere* 29, 409–420. doi: 10.1016/S1002-0160(19)60810-6

Fita, A., Rodríguez-Burruezo, A., Boscaiu, M., Prohens, J., and Vicente, O. (2015). Breeding and domesticating crops adapted to drought and salinity: a new paradigm for increasing food production. *Front. Plant Sci.* 6, 978. doi: 10.3389/fpls.2015.00978

Fróna, D., Szenderák, J., and Harangi-Rákos, M. (2019). The challenge of feeding the world. *Sustainability* 11, 5816. doi: 10.3390/su11205816

Gago, J., Daloso, D., M., Figueroa, C. M., Flexas, J., Fernie, A. R., et al. (2016). Relationships of leaf net photosynthesis, stomatal conductance, and mesophyll conductance to primary metabolism: a multispecies meta-analysis approach. *Plant Physiol.* 171, 265–279. doi: 10.1104/pp.15.01660

Gamalero, E., and Glick, B. R. (2015). Bacterial modulation of plant ethylene levels. *Plant Physiol.* 169, 13–22. doi: 10.1104/pp.15.00284

Ghosh, D., Gupta, A., and Mohapatra, S. (2019). A comparative analysis of exopolysaccharide and phytohormone secretions by four drought-tolerant rhizobacterial strains and their impact on osmotic-stress mitigation in *Arabidopsis thaliana*. *World J. Microbiol. Biotechnol.* 35, 1–15. doi: 10.1007/s11274-019-2659-0

Glick, B. R. (2014). Bacteria with ACC deaminase can promote plant growth and help to feed the world. *Microbiol. Res.* 169, 30–39. doi: 10.1016/j.micres.2013.09.009

Gordon, S. A., and Weber, R. P. (1951). Colorimetric estimation of indoleacetic acid. *Plant Physiol.* 26, 192. doi: 10.1104/pp.26.1.192

Grad, W. E., Kandil, S. H., Kenawy, E., and Massoud, M. I. (2021). The potential of sugarcane bagasse polymer composite for sustainable of *Stevia rebaudiana* productivity under deficit irrigation. *SVU Int. J. Agric. Sci.* 3, 22–36. doi: 10.21608/svuijas.2021.62483.1081

Guerrero-Barajas, C., Constantino-Salinas, E. A., Amora-Lazcano, E., Tlalapango-Ángeles, D., Mendoza-Figueroa, J. S., Cruz-Maya, J. A., et al. (2020). Bacillus mycoides A1 and *Bacillus tequilensis* A3 inhibit the growth of a member of the phytopathogen colletotrichum gloeosporioides species complex in avocado. *J. Sci. Food Agric.* 100, 4049–4056. doi: 10.1002/jsfa.10450

Gupta, P., Kumar, V., Usmani, Z., Rani, R., Chandra, A., and Gupta, V. K. (2019). A comparative evaluation towards the potential of *Klebsiella* sp. and *Enterobacter* sp. in plant growth promotion, oxidative stress tolerance and chromium uptake in *Helianthus annuus* (L.). *J. Hazard. Mater.* 377, 391–398. doi: 10.1016/j.jhazmat.2019.05.054

Hanin, M., Ebel, C., Ngom, M., Laplaze, L., and Masmoudi, K. (2016). New insights on plant salt tolerance mechanisms and their potential use for breeding. *Front. Plant Sci.* 7, 1787. doi: 10.3389/fpls.2016.01787

Hashem, A., Abd Allah, E. F., Alqarawi, A. A., Al-Huqail, A. A., Wirth, S., and Egamberdieva, D. (2016). The interaction between arbuscular mycorrhizal fungi and endophytic bacteria enhances plant growth of *Acacia gerrardii* under salt stress. *Front. Microbiol.* 7, 1089. doi: 10.3389/fmicb.2016.01089

Ha-tran, D. M., Nguyen, T. T. M., Hung, S. H., Huang, E., and Huang, C. C. (2021). Roles of plant growth-promoting rhizobacteria (Pgpr) in stimulating salinity stress defense in plants: a review. *Int. J. Mol. Sci.* 22, 1–38. doi: 10.3390/ijms22063154

Hong, B. H., Joe, M. M., Selvakumar, G., Kim, K. Y., Choi, J. H., and Sa, T. M. (2017). Influence of salinity variations on exocellular polysaccharide production, biofilm formation and flocculation in halotolerant bacteria. *J. Environ. Biol.* 38, 657. doi: 10.22438/jeb/38/4/MRN-284

Hossain, M. A., Nakano, Y., and Asada, K. (1984). Monodehydroascorbate reductase in spinach chloroplasts and its participation in regeneration of ascorbate for scavenging hydrogen peroxide. *Plant Cell Physiol.* 25, 385–395.

Hu, H., Jung, K., Wang, Q., Saif, L. J., and Vlasova, A. N. (2018). Development of a one-step RT-PCR assay for detection of pancoronaviruses (α-, β-, γ-, and δ-coronaviruses) using newly designed degenerate primers for porcine and avianfecal samples. *J. Microbiol. Methods.* 256, 116–122.

Hussain, S., Rasheed, M., Hamzah Saleem, M., Ahmed, Z., Hafeez, A., Jilani, G., et al. (2022). Salt tolerance in maize with melatonin priming to achieve sustainability in yield in salt affected soils. *Pak. J. Bot.* 55. doi: 10.30848/PJB2023-1(27)

Hussain, S., Shaukat, M., Ashraf, M., Zhu, C., Jin, Q., and Zhang, J. (2019). Salinity stress in arid and semi-arid climates: effects and management in field crops. *Clim. Chang. Agric.* 13, 87982. doi: 10.5772/intechopen.87982

Iqbal, M. S., Hafeez, M. N., Wattoo, J. I., Ali, A., Sharif, M. N., Rashid, B., et al. (2016). Prediction of host-derived miRNAs with the potential to target PVY in potato plants. *Front. Genet.* 7, 159. doi: 10.3389/fgene.2016.00159

Islam, F., Yasmeen, T., Arif, M. S., Ali, S., Ali, B., Hameed, S., et al. (2016). Plant growth promoting bacteria confer salt tolerance in *Vigna radiata* by up-regulating antioxidant defense and biological soil fertility. *Plant Growth Regul.* 80, 23–36. doi: 10.1007/s10725-015-0142-y

Ji, J., Yuan, D., Jin, C., Wang, G., Li, X., and Guan, C. (2020). Enhancement of growth and salt tolerance of rice seedlings (*Oryza sativa* L.) by regulating ethylene production with a novel halotolerant PGPR strain *Glutamicibacter* sp. YD01 containing ACC deaminase activity. *Acta Physiol. Plant.* 42, 1–17. doi: 10.1007/s11738-020-3034-3

Kalam, S., Basu, A., Ahmad, I., Sayyed, R. Z., El-Enshasy, H. A., Dailin, D. J., et al. (2020). Recent understanding of soil acidobacteria and their ecological significance: a critical review. *Front. Microbiol.* 11, 580024. doi: 10.3389/fmicb.2020.580024

Kantachote, D., Nunkaew, T., Kantha, T., and Chaiprapat, S. (2016). Biofertilizers from *Rhodopseudomonas palustris* strains to enhance rice yields and reduce methane emissions. *Appl. Soil Ecol.* 100, 154–161. doi: 10.1016/j.apsoil.2015.12.015

Kapoor, R. T., Alyemeni, M. N., and Ahmad, P. (2021). Exogenously applied spermidine confers protection against cinnamic acid-mediated oxidative stress in *Pisum sativum*. *Saudi J. Biol. Sci.* 28, 2619–2625. doi: 10.1016/j.sjbs.2021.02.052

Kasim, W. A., Gaafar, R. M., Abou-Ali, R. M., Omar, M. N., and Hewait, H. M. (2016). Effect of biofilm forming plant growth promoting rhizobacteria on salinity tolerance in barley. *Ann. Agric. Sci.* 61, 217–227. doi: 10.1016/j.aoas.2016.07.003

Khan, A., Sirajuddin., Zhao, X. Q., Javed, M. T., Khan, K. S., Bano, A., et al. (2016). *Bacillus pumilus* enhances tolerance in rice (*Oryza sativa* L.) to combined stresses of NaCl and high boron due to limited uptake of Na+. *Environ. Exp. Bot.* 124, 120–129. doi: 10.1016/j.envexpbot.2015.12.011

Khare, E., and Arora, N. K. (2021). Biosurfactant based formulation of *Pseudomonas guariconensis* LE3 with multifarious plant growth promoting traits controls charcoal rot disease in Helianthus annus. *World J. Microbiol. Biotechnol.* 37, 1–14. doi: 10.1007/s11274-021-03015-4

Kim, S.-Y., Lim, J.-H., Park, M.-R., Kim, Y.-J., Park, T.-I., Seo, Y.-W., et al. (2005). Enhanced antioxidant enzymes are associated with reduced hydrogen peroxide in barley roots under saline stress. *BMB Rep.* 38, 218–224. doi: 10.5483/BMBRep.2005.38.2.218

Koevoets, I. T., Venema, J. H., Elzenga, J. T., and Testerink, C. (2016). Roots withstanding their environment: exploiting root system architecture responses to abiotic stress to improve crop tolerance. *Front. Plant Sci.* 7, 1335. doi: 10.3389/fpls.2016.01335

Kumar, A., Singh, S. K., Kant, C., Verma, H., Kumar, D., Singh, P. P., et al. (2021). Microbial biosurfactant: a new frontier for sustainable agriculture and pharmaceutical industries. *Antioxidants* 10, 1472. doi: 10.3390/antiox10091472

Kumari, M. E. R., Gopal, A. V., and Lakshmipathy, R. (2018). Effect of stress tolerant plant growth promoting rhizobacteria on growth of blackgram under stress condition. *Int. J. Curr. Microbiol. App. Sci.* 7, 1479–1487. doi: 10.20546/ijcmas.2018.701.180

Kumawat, K. C., Nagpal, S., and Sharma, P. (2022). Potential of plant growth-promoting rhizobacteria-plant interactions in mitigating salt stress for sustainable agriculture: a review. *Pedosphere* 32, 223–245. doi: 10.1016/S1002-0160(21)60070-X

Li, H., Lei, P., Pang, X., Li, S., Xu, H., Xu, Z., et al. (2017). Enhanced tolerance to salt stress in canola (*Brassica napus* L.) seedlings inoculated with the halotolerant *Enterobacter cloacae* HSNJ4. *Appl. Soil Ecol.* 119, 26–34. doi: 10.1016/j.apsoil.2017.05.033

Li, H. Q., and Jiang, X. W. (2017). Inoculation with plant growth-promoting bacteria (PGPB) improves salt tolerance of maize seedling. *Russ. J. Plant Physiol.* 64, 235–241. doi: 10.1134/S1021443717020078

Li, X., Sun, P., Zhang, Y., Jin, C., and Guan, C. (2020). A novel PGPR strain Kocuria rhizophila Y1 enhances salt stress tolerance in maize by regulating phytohormone levels, nutrient acquisition, redox potential, ion homeostasis, photosynthetic capacity and stress-responsive genes expression. *Environ. Exp. Bot.* 174, 104023. doi: 10.1016/j.envexpbot.2020.104023

Li, Y., Zhang, S., Jiang, W., and Liu, D. (2013). Cadmium accumulation, activities of antioxidant enzymes, and malondialdehyde (MDA) content in Pistia stratiotes L. *Environ. Sci. Pollut. Res. Int.* 20, 1117–1123.

Livak, K. J., and Schmittgen, T. D. (2001). Analysis of relative gene expression data using real-time quantitative PCR and the 2-11CT method. *Methods* 25, 402–408. doi: 10.1006/meth.2001.1262

Loper, J. E., and Schroth, M. N. (1986). Influence of bacterial sources of indole-3-acetic acid on root elongation of sugar beet. *Phytopathology* 76, 386–389. doi: 10.1094/Phyto-76-386

Luo, X., Dai, Y., Zheng, C., Yang, Y., Chen, W., Wang, Q., et al. (2021). The ABI4-RbohD/VTC2 regulatory module promotes reactive oxygen species (ROS) accumulation to decrease seed germination under salinity stress. *New Phytol.* 229, 950–962. doi: 10.1111/nph.16921

Machado, R. M., and Serralheiro, R. P. (2017). Soil salinity: effect on vegetable crop growth. Management practices to prevent and mitigate soil salinization. *Horticulturae* 3, 30. doi: 10.3390/horticulturae3020030

Marag, P. S., and Suman, A. (2018). Growth stage and tissue specific colonization of endophytic bacteria having plant growth promoting traits in hybrid and composite maize (*Zea mays* L.). *Microbiol. Res.* 214, 101–113. doi: 10.1016/j.micres.2018.05.016

Meena, K. K., Sorty, A. M., Bitla, U. M., Choudhary, K., Gupta, P., Pareek, A., et al. (2017). Abiotic stress responses and microbe-mediated mitigation in plants: the omics strategies. *Front. Plant Sci.* 8, 172. doi: 10.3389/fpls.2017.00172

Mehmood, S., Khatoon, Z., Amna., Ahmad, I., Muneer, M. A., Kamran, M. A., et al. (2021a). *Bacillus* sp. PM31 harboring various plant growth-promoting activities regulates fusarium dry rot and wilt tolerance in potato. *Arch. Agron. Soil Sci.* 1–15. doi: 10.1080/03650340.2021.1971654

Mehmood, S., Muneer, M. A., Tahir, M., Javed, M. T., Mahmood, T., Afridi, M. S., et al. (2021b). Deciphering distinct biological control and growth promoting potential of multi-stress tolerant *Bacillus subtilis* PM32 for potato stem canker. *Physiol. Mol. Biol. Plants* 27, 2101–2114. doi: 10.1007/s12298-021-01067-2

Mendez, R. L., and Kwon, J. Y. (2021). Effect of extraction condition on protein recovery and phenolic interference in Pacific dulse (*Devaleraea mollis*). *J. Appl. Phycol.* 33, 2497–2509. doi: 10.1007/s10811-021-02467-3

Molina, R., López, G., Coniglio, A., Furlan, A., Mora, V., Rosas, S., et al. (2021). Day and blue light modify growth, cell physiology and indole-3-acetic acid production of *Azospirillum brasilense* Az39 under planktonic growth conditions. *J. Appl. Microbiol.* 130, 1671–1683. doi: 10.1111/jam.14869

Mosavat, N., Oh, E., and Chai, G. (2012). A review of electrokinetic treatment technique for improving the engineering characteristics of low permeable problematic soils. *Geomate J.* 2, 266–272. doi: 10.21660/2012.4.3i

Munns, R., and Tester, M. (2008). Mechanisms of salinity tolerance. *Annu. Rev. Plant Biol.* 59, 651–681. doi: 10.1146/annurev.arplant.59.032607.092911

Naili, F., Neifar, M., Elhidri, D., Cherif, H., Bejaoui, B., Aroua, M., et al. (2018). Optimization of the effect of PGPR–based biofertlizer on wheat growth and yield. *Biom. Biostat. Int. J.* 7, 226–232. doi: 10.15406/bbij.2018.07.00213

Nawaz, H., Ali, A., Saleem, M. H., Ameer, A., Hafeez, A., Alharbi, K., et al. (2022). Comparative effectiveness of EDTA and citric acid assisted phytoremediation of Ni contaminated soil by using canola (*Brassica napus*). *Brazilian J. Biol.* 82, e261785. doi: 10.1590/1519-6984.261785

Nisar, S., Dar, R. A., Bhat, A. A., Farooq, Z., and Tahir, I. (2021). Some important biochemical changes orchestrating flower development and senescence

in *Nicotiana plumbaginifolia* viv. and *Petunia hybrida* vilm. flowers. *J. Hortic. Sci. Biotechnol.* 96, 759–769. doi: 10.1080/14620316.2021.1932613

Nosheen, S., Ajmal, I., and Song, Y. (2021). Microbes as biofertilizers, a potential approach for sustainable crop production. *Sustainability* 13, 1868. doi: 10.3390/su13041868

O'Toole, G. A., and Kolter, R. (1998). Initiation of biofilm formation in *Pseudomonas fluorescens* WCS365 proceeds via multiple, convergent signalling pathways: a genetic analysis. *Mol. Microbiol.* 28, 449–461. doi: 10.1046/j.1365-2958.1998.00797.x

Paredes-Páliz, K. I., Caviedes, M. A., Doukkali, B., Mateos-Naranjo, E., Rodríguez-Llorente, I. D., and Pajuelo, E. (2016). Screening beneficial rhizobacteria from *Spartina maritima* for phytoremediation of metal polluted salt marshes: comparison of gram-positive and gram-negative strains. *Environ. Sci. Pollut. Res.* 23, 19825–19837. doi: 10.1007/s11356-016-7184-1

Parveen, A., and Siddiqui, Z. A. (2021). Zinc oxide nanoparticles affect growth, photosynthetic pigments, proline content and bacterial and fungal diseases of tomato. *Arch. Phytopathol. Plant Prot.* 54, 1519–1538. doi: 10.1080/03235408.2021.1917952

Pinedo, I., Ledger, T., Greve, M., and Poupin, M. J. (2015). Burkholderia phytofirmans PsJN induces long-term metabolic and transcriptional changes involved in *Arabidopsis thaliana* salt tolerance. *Front. Plant Sci.* 6, 466. doi: 10.3389/fpls.2015.00466

Prouty, A. M., Schwesinger, W. H., and Gunn, J. S. (2002). Biofilm formation and interaction with the surfaces of gallstones by *Salmonella* spp. *Infect. Immun.* 70, 2640–2649. doi: 10.1128/IAI.70.5.2640-2649.2002

Qu, L., Huang, Y., Zhu, C., Zeng, H., Shen, C., Liu, C., et al. (2016). Rhizobia-inoculation enhances the soybean's tolerance to salt stress. *Plant Soil* 400, 209–222. doi: 10.1007/s11104-015-2728-6

Saha, M., Sarkar, S., Sarkar, B., Sharma, B. K., Bhattacharjee, S., and Tribedi, P. (2016). Microbial siderophores and their potential applications: a review. *Environ. Sci. Pollut. Res.* 23, 3984–3999. doi: 10.1007/s11356-015-4294-0

Sarkar, A., Ghosh, P. K., Pramanik, K., Mitra, S., Soren, T., Pandey, S., et al. (2018). A halotolerant Enterobacter sp. displaying ACC deaminase activity promotes rice seedling growth under salt stress. *Res. Microbiol.* 169, 20–32. doi: 10.1016/j.resmic.2017.08.005

Schwyn, B., and Neilands, J. B. (1987). Universal chemical assay for the detection and determination of siderophores. *Anal. Biochem.* 160, 47–56. doi: 10.1016/0003-2697(87)90612-9

Shafiq, F., Iqbal, M., Ali, M., and Ashraf, M. A. (2021). Fullerenol regulates oxidative stress and tissue ionic homeostasis in spring wheat to improve net-primary productivity under salt-stress. *Ecotoxicol. Environ. Saf.* 211, 111901. doi: 10.1016/j.ecoenv.2021.111901

Sharma, I. P., Chandra, S., Kumar, N., and Chandra, D. (2017). "PGPR: heart of soil and their role in soil fertility," in *Agriculturally Important Microbes for Sustainable Agriculture* (Singapore: Springer), 51–67. doi: 10.1007/978-981-10-5589-8_3

Sharma, S., Kulkarni, J., and Jha, B. (2016). Halotolerant rhizobacteria promote growth and enhance salinity tolerance in peanut. *Front. Microbiol.* 7, 1600. doi: 10.3389/fmicb.2016.01600

Shi, P.-J., Li, Y.-R., Niinemets, Ü., Olson, E., and Schrader, J. (2021). Influence of leaf shape on the scaling of leaf surface area and length in bamboo plants. *Trees* 35, 709–715. doi: 10.1007/s00468-020-02058-8

Shibli, R. A., Kushad, M., Yousef, G. G., and Lila, M. A. (2007). Physiological and biochemical responses of tomato microshoots to induced salinity stress with associated ethylene accumulation. *Plant Growth Regul.* 51, 159–169. doi: 10.1007/s10725-006-9158-7

Shrivastava, P., and Kumar, R. (2015). Soil salinity: a serious environmental issue and plant growth promoting bacteria as one of the tools for its alleviation. *Saudi J. Biol. Sci.* 22, 123–131. doi: 10.1016/j.sjbs.2014.12.001

Shultana, R., Kee Zuan, A. T., Yusop, M. R., and Saud, H. M. (2020). Characterization of salt-tolerant plant growth-promoting rhizobacteria and the effect on growth and yield of saline-affected rice. *PLoS ONE* 15, e0238537. doi: 10.1371/journal.pone.0238537

Silambarasan, S., Logeswari, P., Cornejo, P., Abraham, J., and Valentine, A. (2019). Simultaneous mitigation of aluminum, salinity and drought stress in Lactuca sativa growth via formulated plant growth promoting *Rhodotorula mucilaginosa* CAM4. *Ecotoxicol. Environ. Saf.* 180, 63–72. doi: 10.1016/j.ecoenv.2019.05.006

Singh, R. P., and Jha, P. N. (2016). Alleviation of salinity-induced damage on wheat plant by an ACC deaminase-producing halophilic bacterium *Serratia* sp. SL-12 isolated from a salt lake. *Symbiosis* 69, 101–111. doi: 10.1007/s13199-016-0387-x

Singh, V. K., Mishra, A., Haque, I., and Jha, B. (2020). Author correction: a novel transcription factor-like gene SbSDR1 acts as a molecular switch and confers salt and osmotic endurance to transgenic tobacco. *Sci. Rep.* 10, 1. doi: 10.1038/s41598-020-62996-8

Sofy, M. R., Aboseidah, A. A., Heneidak, S. A., and Ahmed, H. R. (2021). ACC deaminase containing endophytic bacteria ameliorate salt stress in *Pisum sativum* through reduced oxidative damage and induction of antioxidative defense systems. *Environ. Sci. Pollut. Res.* 28, 40971–40991. doi: 10.1007/s11356-021-13585-3

Souza, R., de Ambrosini, A., and Passaglia, L. M. P. (2015). Plant growth-promoting bacteria as inoculants in agricultural soils. *Genet. Mol. Biol.* 38, 401–419. doi: 10.1590/S1415-475738420150053

Swaathy, S., Kavitha, V., Sahaya Pravin, A., Sekaran, G., Mandal, A. B., and Gnanamani, A. (2014). Phylogenetic framework and biosurfactant gene expression analysis of marine *Bacillus* spp. of Eastern Coastal Plain of Tamil Nadu. *Int. J. Bacteriol.* 2014, 860491. doi: 10.1155/2014/860491

Tawaha, K., Alali, F. Q., Gharaibeh, M., Mohammad, M., and El-Elimat, T. (2007). Antioxidant activity and total phenolic content of selected jordanian plant species. *Food Chem.* 104, 1372–1378. doi: 10.1016/j.foodchem.2007.01.064

Upadhyay, S. K., and Singh, D. P. (2015). Effect of salt-tolerant plant growth-promoting rhizobacteria on wheat plants and soil health in a saline environment. *Plant Biol.* 17, 288–293. doi: 10.1111/plb.12173

Vimal, S. R., Patel, V. K., and Singh, J. S. (2019). Plant growth promoting *Curtobacterium albidum* strain SRV4: an agriculturally important microbe to alleviate salinity stress in paddy plants. *Ecol. Indic.* 105, 553–562. doi: 10.1016/j.ecolind.2018.05.014

Wahab, A., Abdi, G., Saleem, M. H., Ali, B., Ullah, S., Shah, W., et al. (2022). Plants' physio-biochemical and phyto-hormonal responses to alleviate the adverse effects of drought stress: a comprehensive review. *Plants* 11, 1620. doi: 10.3390/plants11131620

Woisky, R. G., and Salatino, A. (1998). Analysis of propolis: some parameters and procedures for chemical quality control. *J. Apic. Res.* 37, 99–105. doi: 10.1080/00218839.1998.11100961

Wu, Y., Jin, X., Liao, W., Hu, L., Dawuda, M. M., Zhao, X., et al. (2018). 5-Aminolevulinic acid (ALA) alleviated salinity stress in cucumber seedlings by enhancing chlorophyll synthesis pathway. *Front. Plant Sci.* 9, 635. doi: 10.3389/fpls.2018.00635

Xu, H., Tie, C. A., Wang, Z., and He, M. (2015). Physiological basis for the differences of productive capacity among tillers in winter wheat. *J. Integr. Agric.* 14, 1958–1970. doi: 10.1016/S2095-3119(15)61094-2

Xu, L., Wang, A., Wang, J., Wei, Q., and Zhang, W. (2017). Piriformospora indica confers drought tolerance on *Zea mays* L. through enhancement of antioxidant activity and expression of drought-related genes. *Crop J.* 5, 251–258. doi: 10.1016/j.cj.2016.10.002

Zainab, N., Khan, A. A., Azeem, M. A., Ali, B., Wang, T., Shi, F., et al. (2021). PGPR-mediated plant growth attributes and metal extraction ability of *Sesbania sesban* L. in industrially contaminated soils. *Agronomy* 11, 1820. doi: 10.3390/agronomy11091820

Zhang, H., Qian, Y., Fan, D., Tian, Y., and Huang, X. (2022). Biofilm formed by *Hansschlegelia zhihuaiae* S113 on root surface mitigates the toxicity of bensulfuron-methyl residues to maize. *Environ. Pollut.* 292, 118366. doi: 10.1016/j.envpol.2021.118366

Zia-ur-Rehman, M., Murtaza, G., Qayyum, M. F., Rizwan, M., Ali, S., Akmal, F., et al. (2016). "Degraded soils: origin, types and management," in *Soil Science: Agricultural and Environmental Prospectives*, eds K. Hakeem, J. Akhtar, M. Sabir (Cham: Springer), 23–65. doi: 10.1007/978-3-319-34451-5_2

frontiers | Frontiers in Plant Science

TYPE Original Research
PUBLISHED 02 September 2022
DOI 10.3389/fpls.2022.975852

Check for updates

OPEN ACCESS

EDITED BY
Mohammad Anwar Hossain,
Bangladesh Agricultural University,
Bangladesh

REVIEWED BY
Anuj Kumar,
Dalhousie University,
Canada
Sheikh Mansoor,
Sher-e-Kashmir University of Agricultural Sciences and Technology of Jammu, India

*CORRESPONDENCE
Raheela Jabeen
drraheela.9054@wum.edu.pk
Faisal Zulfiqar
ch.faisal.zulfiqar@gmail.com
Kadambot H. M. Siddique
kadambot.siddique@uwa.edu.au

SPECIALTY SECTION
This article was submitted to Plant Biotechnology, a section of the journal Frontiers in Plant Science

RECEIVED 23 June 2022
ACCEPTED 10 August 2022
PUBLISHED 02 September 2022

CITATION
Jabeen R, Iqbal A, Deeba F, Zulfiqar F, Mustafa G, Nawaz H, Habiba U, Nafees M, Zaid A and Siddique KHM (2022) Isolation and characterization of peroxidase P7-like gene and Rab-GDI like gene from potential medicinal plants: A step toward understanding cell defense signaling. *Front. Plant Sci.* 13:975852. doi: 10.3389/fpls.2022.975852

COPYRIGHT
© 2022 Jabeen, Iqbal, Deeba, Zulfiqar, Mustafa, Nawaz, Habiba, Nafees, Zaid and Siddique. This is an open-access article distributed under the terms of the Creative Commons Attribution License (CC BY). The use, distribution or reproduction in other forums is permitted, provided the original author(s) and the copyright owner(s) are credited and that the original publication in this journal is cited, in accordance with accepted academic practice. No use, distribution or reproduction is permitted which does not comply with these terms.

Isolation and characterization of peroxidase P7-like gene and Rab-GDI like gene from potential medicinal plants: A step toward understanding cell defense signaling

Raheela Jabeen[1]*, Atia Iqbal[2], Farah Deeba[1], Faisal Zulfiqar[3]*, Ghulam Mustafa[4], Haq Nawaz[5], Ume Habiba[2], Muhammad Nafees[3], Abbu Zaid[6] and Kadambot H. M. Siddique[7]*

[1]Department of Biochemistry and Biotechnology, The Women University Multan, Multan, Punjab, Pakistan, [2]Department of Microbiology and Molecular Genetics, The Women University Multan, Multan, Punjab, Pakistan, [3]Department of Horticultural Sciences, Faculty of Agriculture and Environment, The Islamia University of Bahawalpur, Bahawalpur, Pakistan, [4]Department of Biochemsitry, Government College University Faisalabad, Faisalabad, Punjab, Pakistan, [5]Department of Biochemistry, Bahauddin Zakariya University, Multan, Punjab, Pakistan, [6]Aligarh Muslim University, Aligarh, Uttar Pradesh, India, [7]University of Western Australia, Perth, WA, Australia

Defensin genes form part of a plant's defense system and are activated when exposed to biotic or abiotic stress. They play a vital role in controlling many signaling pathways involved in various plant defense mechanisms. This research aimed to isolate and characterize novel defensin genes from selected medicinally important plants to explore their signaling mechanisms and defense associated roles for breeding. The DNA of *Albizia lebbeck* and *Moringa oleifera* was subjected to PCR amplification using gene-specific primers of defensin genes. Two novel defensin genes were isolated in each species, with sequence lengths of 300bp in *A. lebbeck* and 150bp in *M. oleifera*. *In-silico* analysis undertaken to retrieve and align their orthologous sequences revealed 100% similarity of the *A. lebbeck* gene with the *Musa acuminate* peroxidase P7-like gene and 85% similarity of the *M. oleifera* gene with the *Manihot esculenta* GDP dissociation inhibitor gene. The reliability, stability and physiochemical properties of homology models of these sequences was confirmed through online computational studies. This preliminary study confirmed the presence of novel genes with peroxidase P7 and Rab GDP dissociation inhibitor gene-like activity in *A. lebbeck* and *M. oleifera*, respectively, and their potential defense role in plants. Thus, the defensin genes of both species could be used in the synthesis of transgenic self-defensive plants with increased disease resistance and as potential candidates for improved crop production and thraputic formulation in the future.

KEYWORDS

defensin gene, *Albizia lebbeck*, *Moringa oleifera*, *in silico* analysis, plant defense system

Introduction

Plants are often exposed to biotic and abiotic stresses and use their natural defense system to circumvent them (Chojak-Koźniewska et al., 2018), producing several metabolites and secondary messengers to guard against these assaults (Reichling, 2018). Once the stress is detected, signaling pathways are triggered that induce gene expression to help plants acclimate to these conditions (Novaković et al., 2018). Among these, antimicrobial peptides (AMPs) form the first line of defense in a plant's protective mechanisms (Mahlapuu et al., 2016) and are higly important part of innate immunity (Zharkova et al., 2019), serving an antimicrobial function (Rawat et al., 2017). Defensins belong to the predominant families of AMPs. They are small (45–55 amino acids), non-acidic, rich in cysteine residues, and highly similar to peptides in many other organisms (Al Akeel et al., 2014). Plant defensins involve mechanisms to inhibit fungi and bacteria, reportedly by the structural targets in the cell membrane of microbes by producing reactive oxygen species (Parisi et al., 2019). They can also protect the host by inducing and potentiating several other plant-defending mechanisms (Souza et al., 2017). The isolation and characterization of these defensins are vital for developing economically and medically important substances. Analysis of sequenced plant genomes revealed that defensins are present as multigene families and overrepresented in the genomes of some plant species (Kovaleva et al., 2017). Cowpea defensin Cp-thionin II was isolated and characterized, with its antifungal activity checked against *F. culmorum* (Schmidt et al., 2019). Similarly, two tomato defensin genes (*SlyDF1* and *SlyDF2*) were cloned and characterized from *Solanum lycopersicum* (Cui et al., 2018). The AMPs are not only have their importance in plant defense system, but animals have also AMPs as their part of immune system, e.g., three novel β-defensin AMPs were also characterized in rainbow trout (*Oncorhynchus mykiss*; Casadei et al., 2009).

With the wealth of defensin nucleotide sequences available, gene isolation strategies coupled with recombinant production are used increasingly to characterize closely related plant defensin peptides. Many public databases and tools are available to study the structure and physicochemical properties of plant genes and transcriptomes (Lakshmi Priya and Sabu, 2015).

Albizzia lebbeck and *Moringa oleifera* have therapeutic potential against several diseases. *Albizzia lebbeck* bark extract is very much effective against speck disease (Arasu et al., 2022). The aquous extract of the same plant have reported anti-inflammatory activity (Kamala Lakshmi and Valarmathi, 2020). similarly the plant also possesses antidiabetic and anti lipedemic effect (Azam et al., 2022). *Moringa oleifera* also have several medicinal properties like anti diabetic, anti cancerous and anti inflammatory etc. (Kumar, 2017). Considering the importance of these medicinal plants, this study resulted in isolation and characterizion of defensin genes from leaf samples of *Albizia lebbeck* and *Moringa oleifera*. *In silico* analysis of these isolates revealed the properties and functional similarty of these novel genes with peroxidase P7 and Rab GDP dissociation inhibitor like gene activities, respectively. Physiochemical and homology modeling characterization studies revealed high similarity index of 100% and 85% for genes from *A. lebbeck* and *M. oleifera* with reliable structural stability properties. This preliminary study provides the data which may help us to understand the defense mechanism and transgenic plant breed optimization. Future experimental study of these genes may provide a pipeline for drug discovery project.

Materials and methods

Isolation and characterization of peroxidase P7-like gene and Rab-GDI like gene from potential medicinal plants.

Plant sample collection

Leaf samples of *A. lebbeck* and *M. oleifera* were procured, identified, and confirmed from the Department of Botany, The Women University Multan, Pakistan.

Extraction of genomic DNA

Genomic DNA from leaf samples of two plant species was extracted using Thermo Scientific GeneJet Plant Genomic DNA Purification Mini kit and stored at −20°C for further investigation (Long et al., 2019). The extracted DNA was analyzed by agarose gel electrophoresis on 1% agarose gel in 1X TAE buffer.

Amplification of defensin genes from total DNA template through PCR

DNA fragments of plants were amplified by PCR using forward primer 5′-CGCTGCCCCGACGCTTAC-3′ and reverse primer 5′-GACGACTTGGTAGTTGCTGT-3′ using an open reading frame of acknowledged plant defensin genes. The PCR profile for gene amplification was set as follows: 95°C for 3 min followed by 35 cycles of denaturation at 95°C for 1 min, annealing at 48°C for 1 min, extension at 72°C for 1 min, and a final extension at 72°C for 7 min. The PCR products were resolved on 1% agarose gel using 1X TAE buffer at 80 V, followed by ethidium bromide staining. PCR products were purified using a Thermo Scientific GeneJET Gel Extraction Kit. Purified PCR products were sequenced at the DNA sequencing facility of the Center for Applied Molecular Biology, Lahore, Pakistan, under the Access to the Scientific Instrumentation Program of the Higher Education Commission of Pakistan.

In silico analysis

All sequencing results were compiled using DNA Dragon software[1] (Hepperle, 2011). The consensus sequences obtained from DNA Dragon were checked for their homology with reported sequences presenting nucleotide database using BLASTn and BLASTx programs of NCBI BLAST[2] (Ingti et al., 2017). The sequences showing significant similarity with query sequences were retrieved and aligned using online Multiple Sequence Alignment tool CLUSTALW[3] (Thompson et al., 1994). Phylogenetic diversity was analyzed using the neighbor-joining method (Kumar et al., 2016) in the Molecular Evolutionary Genetics Analysis (MEGA) Program, version X (Newman et al., 2016). The predicted amino acid sequence of plant defensin genes was subjected to the ProtParam tool[4] on the ExPASy server to compute the physicochemical properties (Lim and Yoon, 2018).

The three-dimensional structures of defensin proteins were predicted using I-TASSER, SWISS-MODEL and RaptorX web tools (Fahim et al., 2018). The rough models obtained were subjected to GROMOS96 43B1 executed using Swiss-pdbViewer version 4.0.1 for energy minimization (Amir et al., 2019). PROCHECK and ProSA (Protein Structure Analysis) were used to assess the reliability of the homology models (Kumar et al., 2018). Possible docking sites and ligands were predicted using RaptorX (Wu et al., 2018). CD search and pfam analysis tools were used for the detection of structural and functional domains in plant defensins (Marchler-Bauer et al., 2017; Mistry et al., 2021).

Statistical analysis

The data were analyzed by simple regression rational analysis (Douwes et al., 2008).

Results

DNA purification and amplification of defensin genes

A good quality DNA (Figure 1A) from leaf samples of both plants were used for defensen gene amplification by PCR. Amplicons appeared as unique bright bands on the agarose gel (Figure 1B). The gene sequence length was ~150 bp for *Moringa oleifera* and >300 bp for *Albizia lebbeck*, as expected.

Sequence features and phylogenetic analysis of defensin genes

The sequenced fragments of *A. lebbeck* and *M. oleifera* were 300 bp and 317 bp in length containing open reading frames of 204 bp and 174 bp, respectively. Consensus sequences of both fragments were analyzed for their homology with sequences in the NCBI database using BLASTN and BLASTX on the BLAST server.[5] The *A. lebbeck* defensin gene showed 100% similarity with predicted *Musa acuminata* subsp. *malaccensis* peroxidase P7-like gene (accession number XM_009390426.2) and protein sequence (accession number XP_009388701.1) and the *M. oleifera* defensin gene showed 85% and 91% similarity with predicted *Manihot esculenta* GDP dissociation inhibitor gene sequence (accession number XM_021748685.1) and protein sequence (accession number XP_021604377.1), respectively. The orthologous sequences of *A. lebbeck* and *M. oleifera* defensins were retrieved and subjected to multiple sequence alignment using the online CLUSTALW tool. Phylogenetic analyses retrieved the orthologous polypeptide sequences. Figure 2 shows the phylogenetic trees of *A. lebbeck* and *M. oleifera* defensins. For the defensin-deduced amino acid sequences, 14 published homologous sequences from different plants were used to construct a phylogenetic tree by neighbor-joining distance analysis. For *A. lebbeck*, the topology showed that the polypeptides from four different branches were highly homologous sequences. The *A. lebbeck* polypeptide is clustered with predicted *Musa acuminata* peroxidase P7-like protein, indicating that it is the most recent ancestor of *A. lebbeck* defensin (Figure 2A). The analysis for *M. oleifera* showed clustering of the *M. oleifera* defensin polypeptide with *Manihot esculenta* GDP dissociation inhibitor 1 (Figure 2B). As DNA sequences with more than 75% similarity and protein sequences with more than 25% similarity are considered homologous sequences, we retrieved the sequences of homologous proteins of *A. lebbeck* (*M. acuminata* peroxidase P7-like) and *M. oleifera* defensins (*M. esculenta* GDP dissociation inhibitor 1) to check the properties and structure prediction of novel defensins from understudied medicinal plants.

Computational analysis of physicochemical properties of *Musa acuminata* peroxidase P7-like and *Manihot esculenta* GDP dissociation inhibitor 1

Table 1 summarizes the ProtParam analysis of physicochemical properties of *M. acuminata* peroxidase P7-like and *M. esculenta* GDP dissociation inhibitor 1. *Musa acuminata* peroxidase P7-like peptide had a predicted molecular weight of ~48 kDa and is neutral with an isoelectric point of 7.02, whereas *M. esculenta* GDP dissociation inhibitor 1 had a molecular weight

1 http://www.dna-dragon.com/
2 http://blast.ncbi.nlm.nih.gov/Blast.cgi
3 http://www.genome.jp/tools/clustalw/
4 https://web.expasy.org/protparam/
5 https://blast.ncbi.nlm.nih.gov/Blast.cgi

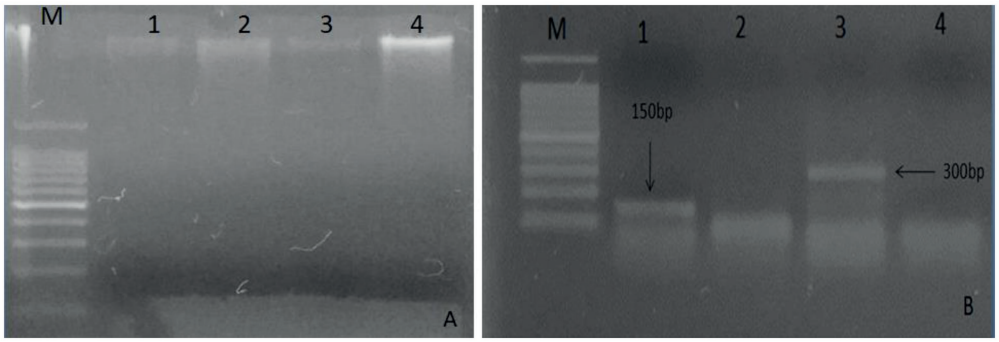


FIGURE 1
Analysis of total DNA extracted on 1% agarose from plant leaves. **(A)** Lane M: marker 100bp, lanes 1 and 3 show DNA bands of *Moringa oleifera*, and lanes 2 and 4 show bands of *Albizia lebbeck*; **(B)** Lane M indicates 100bp DNA ladder, lane 1 shows 150bp gene of *Moringa oleifera*, and lane 3 shows 300bp gene of *Albizia lebbeck*.

of ~50 kDa with an acidic isoelectric point of 5.53. Protein low instability and high aliphatic index values predicted that these proteins are heat stable. The grand average of hydropathicity (GRAVY) index indicated that *M. esculenta* GDP dissociation inhibitor 1 is more hydrophilic and has more surface accessibility to interact with water than *M. acuminata* peroxidase P7-like.

Prediction of three-dimensional structure of *Musa acuminata* peroxidase P7-like and *Manihot esculenta* GDP dissociation inhibitor 1

The I-TASSER server with diverse threading templates was used for comparative homology modeling of *M. acuminata* peroxidase P7-like and *M. esculenta* GDP dissociation inhibitor 1. In I-TASSER, the C-score is used to evaluate the result from the consensus of top structural suits. The template modeling score (TM score) is used to measure the homology between structures of templates and models and determine the sequence identity in the structurally aligned area.

For *M. acuminata* peroxidase P7-like protein, the predicted TM score of the selected model was 0.49 ± 0.15, and RMSD (root mean square deviation) score was 11.6 ± 4.5 Å, observed in the correct configuration. Stereochemical properties were stabilized by energy minimization using Swiss-pdbViewer.[6] Thepredicted homology model was authenticated using the ProSA and PROCHECK server. Figure 3A shows the Ramachandran plot in which% residues in the core allowed and disallowed regions tells about the acceptability of predicted structure. The maximum likelihood of finding protein residues (>90%) in the core/allowed regions indicatesthat the model built by I-TASSER was the good predicted structure. Figures 3B,C show the final modeled structure of *M. acuminata* peroxidase P7-like. Superimposition of predicted structure with template structure is represented in Figure 3D. PROCHECK and SWISS-MODEL revealed that all residues are in the core/allowed region, with none in the disallowed region, indicating the acceptability of Ramachandran plots (Table 2).

The structure of *M. acuminata* peroxidase P7-like protein was further evaluated using ProSA that mainly considers two predicted structure features: z-score and residue energies plot. Z-score reveals information on the model's quality, which can be used to measure the amount of total energy of the structure deviating from the energy distribution derived from random conformations. Z-scores outside a range characteristic for native proteins indicate erroneous structures *M. acuminata* peroxidase P7-like had a z-score of −7.29 (Figure 4A), similar to the scores obtained for similar-sized proteins, indicating structure reliability. The residue energy plot depicted the local model quality by plotting energies as a function of amino acid sequence position. The negative values of the *M. acuminata* peroxidase P7-like structure indicates that the predicted model is error-free and acceptable (Figure 4B). To identify the presence of domain in *M. acuminata* protein, pfam and CD search was performed which showed the presence of secretory protein domain (Figure 4C).

The binding site of the targeted protein was predicted using the raptorX tool, with the 3D structure of *M. acuminata* peroxidase 7 shown in Figure 5. The input sequence was processed in two domains, with six binding pockets predicted. Possible ligands that bind with these pockets are HEM, pyridine, Ca, Na, and K. HEM and Ca bind to pockets in both domains, while pyridine, Na, and K bind to pockets in domain 1 only.

The selected model of *M. esculenta* GDP dissociation inhibitor 1 had a predicted TM score of 0.89 ± 0.07 and RMSD score of 4.4 ± 2.9 Å, observed in the correct configuration. Stereochemical properties were stabilized by energy minimization using Swiss-pdbViewer. The predicted homology model was authenticated using ProSA and PROCHECK. Figure 6A shows the Ramachandran plot and % of the residues in the core allowed and disallowed regions. The maximum likelihood of finding protein

6 https://spdbv.unil.ch/

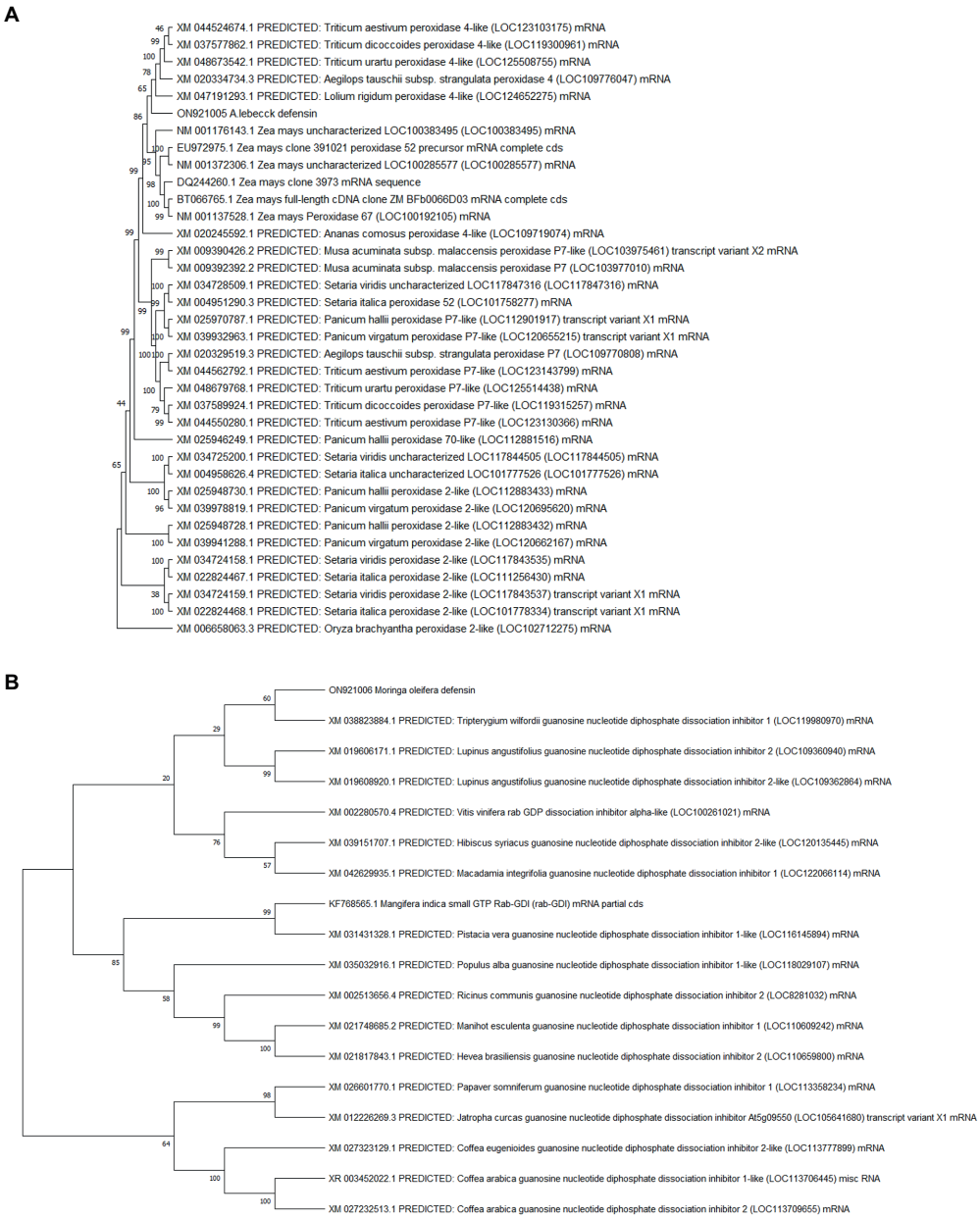


FIGURE 2
The phylogenetic analysis of **(A)** *A. lebbeck* defensin and **(B)** *M. oleifera* defensin with other plant species by MEGA X from CLUSTAL W alignment. The neighbor-joining method was used to construct the tree with p-distance.

residues (>90%) in the core/allowed regions indicates that the predicted model is of good stereochemical quality. PROCHECK revealed that all residues are in the core/allowed region, with none in the disallowed region, indicating the acceptability of Ramachandran plots (Table 3).

Figures 6B,C show the final modeled structure of *M. esculenta* GDP dissociation inhibitor 1, which was further evaluated using ProSA. Superimposition of predicted structure with template structure is represented in Figure 6D. *Manihot esculenta* GDP dissociation inhibitor 1 had a z-score of −10.11 (Figure 7A), similar to the scores of similar-sized proteins, indicating structure reliability. The residue energy plot depicted local model quality by plotting energies as a function of amino acid sequence position. The negative values of the residue energy plot of *M. esculenta* GDP dissociation inhibitor 1 structure indicate that predicted model is error-free and acceptable (Figure 7B). To identify the presence of domain in *M. esculenta* GDP dissociation inhibitor, pfam and CD search was performed which showed the presence of GDI domain (Figure 7C).

The binding site of the targeted protein was predicted using the raptorX tool, with the 3D structure of *M. esculenta* GDP dissociation inhibitor 1 shown in Figure 8. The input sequence was processed, with four binding pockets predicted.

Possible ligands that bind with these pockets are dihydroflavine-adenine dinucleotide (FDA), sulfate ion (SO_4^{2-}), chloride ion (Cl^-), and galactose-uridine-5′-diphosphate (GDU).

Discussion

Plants have the ability to integrate divergent signaling pathways to allow appropriate defense responses against various stresses (Brenner et al., 2012; Overmyer et al., 2018) Therefore, overexpression of a single gene can have a negative (i.e., susceptibility) or positive effect (i.e., tolerance) on the plant response to other stresses. These genes also serve as a promising source for engineering disease resistance traits in plants, enhancing self-defense mechanisms and reducing the requirement for supplementary chemical microbicides (Boukhatem et al., 2014). In this study, *in vitro* and *in silico* methods were used to isolate and characterize novel plant defending family-specific

TABLE 1 Physicochemical properties of *M. acuminata* peroxidase 7 like and *M. esculenta* GDP dissociation inhibitor 1 by ProtParam.

S. No.	Parameters	*M. acuminata* peroxidase 7 like	*M. esculenta* GDP dissociation inhibitor 1
1	Sequence length	451	444
2	Molecular weight	48,137.46	49,833.88
3	Theoretical isoelectric point	7.02	5.53
4	Instability index	36.39	33.44
5	Aliphatic index	83.41	86.49
6	GRAVY	0.003	−0.254

TABLE 2 Ramachandran plot statistics for *M. acuminata* peroxidase 7-like.

	No. residues	Percentage
Most favored regions [A, B, L]	232	90.6%
Additional allowed regions [a, b, l, p]	24	9.4%
Generously allowed regions [~a, ~b, ~l, ~p]	0	0%
Disallowed regions [XX]	0	0%
Non-glycine and non-proline residues	256	100%
Glycine residues	22	
Proline residues	12	
Total number of residues	292	

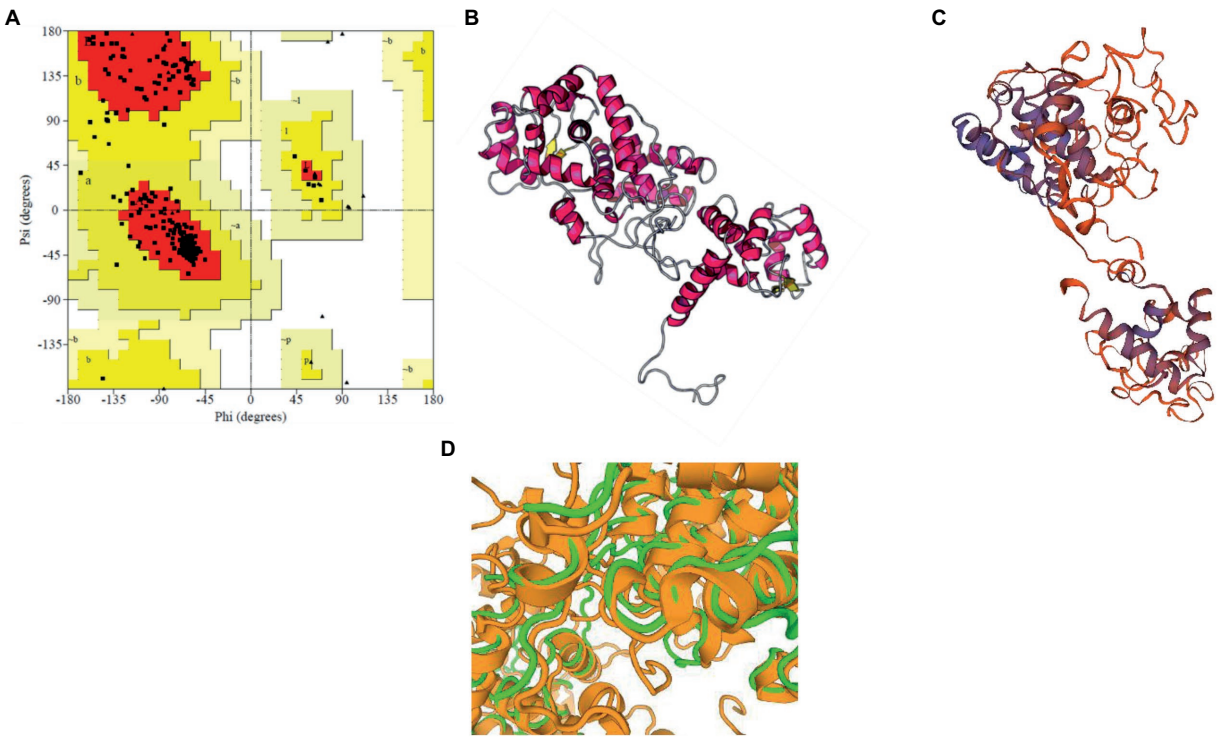


FIGURE 3
Prediction and validation of 3D structure of *M. acuminata* peroxidase P7-like protein. **(A)** Shows the Ramachandran plot and % residues in the core allowed and disallowed regions. **(B,C)** Show the final modeled structure of *M. acuminata* peroxidase P7-like predicted using I-Tasser and SWISS-MODEL, respectively. **(D)** The 3D structure superposition of template structure and predicted model is shown.

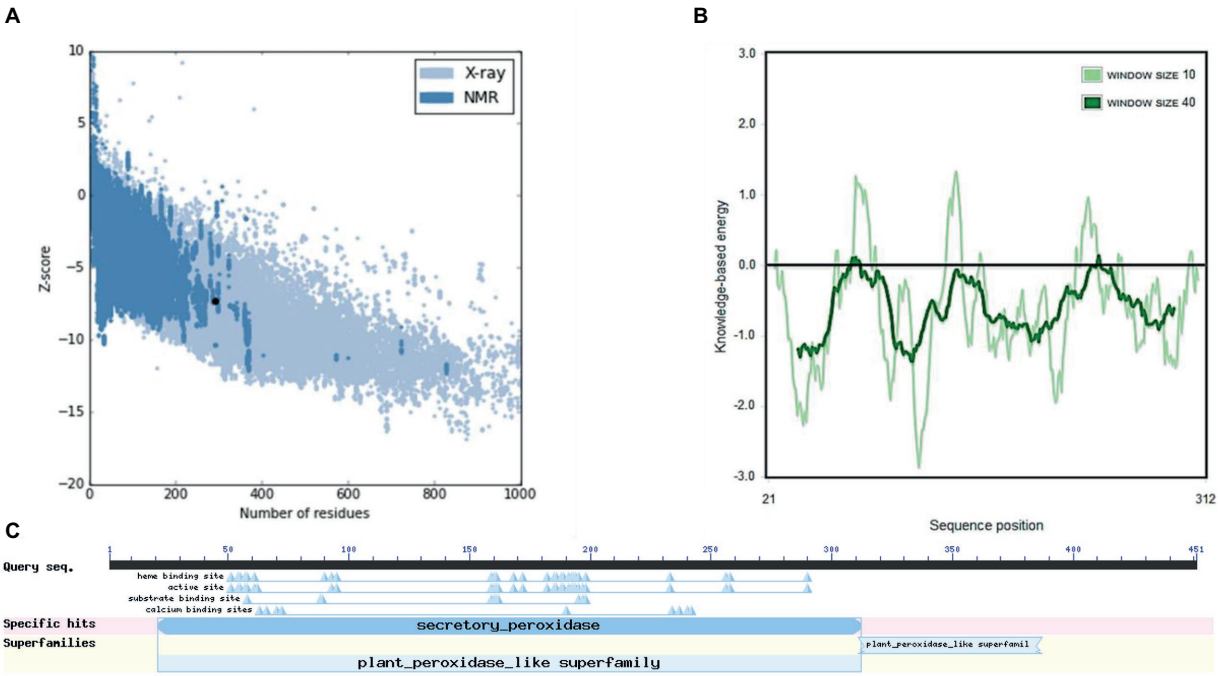


FIGURE 4
ProSA-web service analysis and domain search of *M. acuminata* peroxidase P7-like protein. **(A)** ProSA-web z-scores of the protein chains present in the Protein Data Bank refer to their length. Light and dark blue colors correspond to X-ray crystallography and NMR spectroscopy, respectively. Large dots highlight the z-scores of *M. acuminata* peroxidase P7-like protein. **(B)** Energy plot of *M. acuminata* peroxidase P7-like protein. **(C)** CD search and Pfam search shows the presence of secretory peroxidase domain in *M. acuminata* peroxidase P7-like protein.

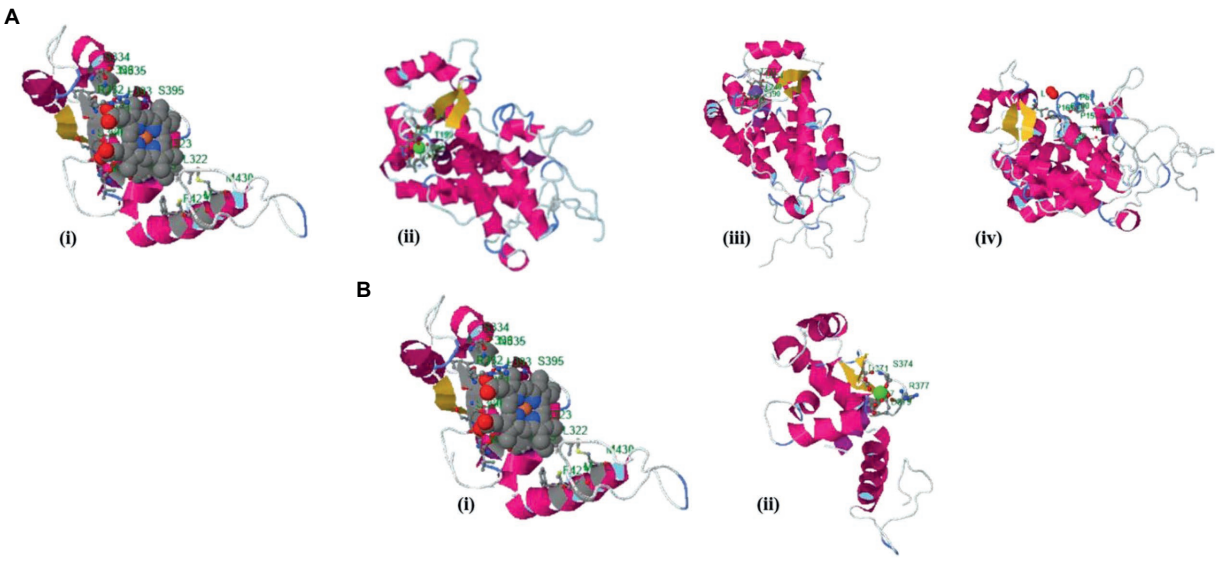


FIGURE 5
Identified binding sites of *M. acuminata* peroxidase P7-like 3D structure using the raptorX tool. **(A)** Ligand binding pockets identified in domain 1: (I) HEM; (ii) Calcium; (Ca) (iii) Potassium (K); (iv) Pyridine. **(B)** Binding pockets identified in domain 2: (i) HEM; (ii) Calcium (Ca).

antimicrobial genes from *Albizia lebecck* and *Moringa oleifera*. Same kind of study on defensin gene isolation from *Saccharum officinarum* was done by De-Paula and colleagues, who analyzed six sugar cane putative defensins (De-Paula et al., 2008). In our study, primers were designed on a consensus sequence of 3–5 aligned sequences retrieved from the NCBI database. Highly similar sequences that exhibited 75%–100% similarity with the primary sequence were selected for alignment through the BLAST

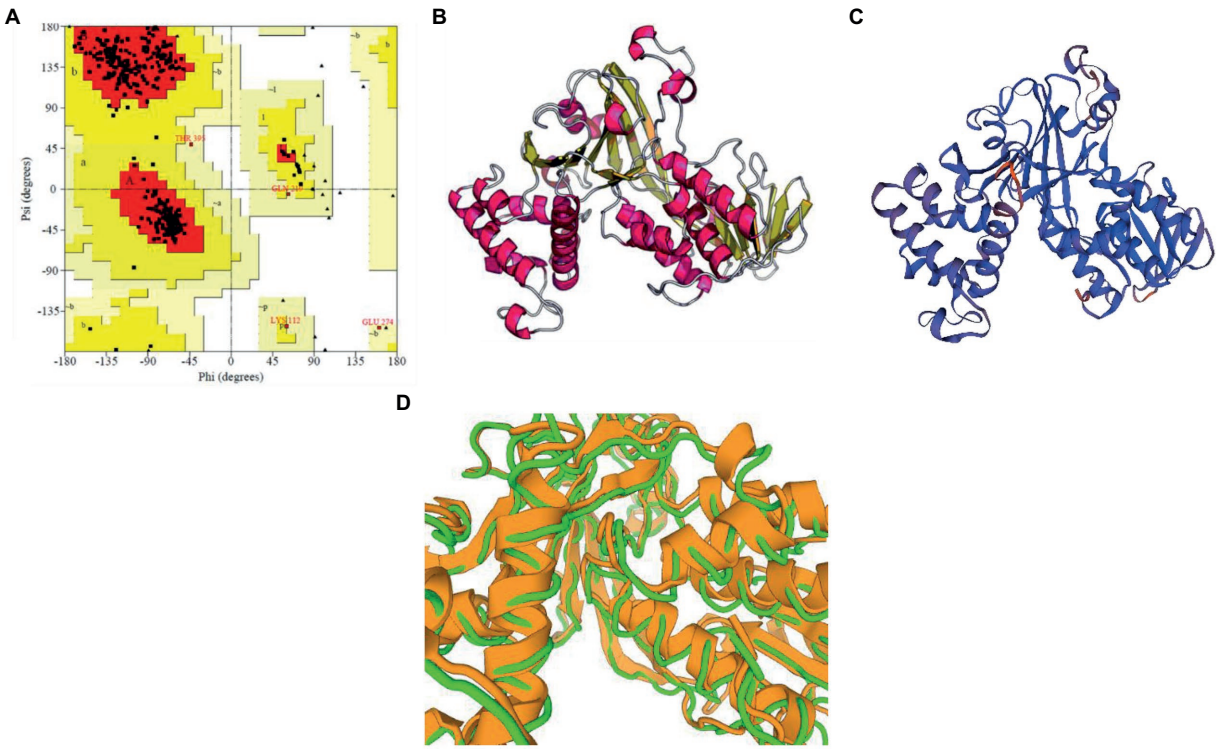


FIGURE 6
Prediction and validation of 3D structure of *M. esculenta* GDP dissociation inhibitor 1. **(A)** Ramachandran plot of *M. esculenta* GDP dissociation inhibitor 1 protein. The plot calculations for the 3D models were computed in PROCHECK. The most favored regions are in *red*, additional allowed, generously allowed, and disallowed regions are indicated in *yellow*, *light yellow*, and *white*, respectively. **(B,C)** The final 3D structure of *M. esculenta* GDP dissociation inhibitor 1 predicted using I-tasser and SWISS-MODEL, respectively. The α-helix is represented by *red helix*, β-sheet by *yellow arrows*, and loops by *gray lines* **(D)**.

TABLE 3 Ramachandran plot statistics for *M. esculenta* GDP dissociation inhibitor 1.

	No. residues	Percentage
Most favored regions [A, B, L]	365	93.8%
Additional allowed regions [a, b, l, p]	20	5.1%
Generously allowed regions [~a, ~b, ~l, ~p]	4	1%
Disallowed regions [XX]	0	0%
Non-glycine and non-proline residues	389	100%
Glycine residues	31	
Proline residues	22	
Total number of residues	444	

tool. In a recent study on one class of defensin genes—biodefensin—Rawat et al. (2017) isolated the full length of this gene encoding about 80 amino acids from *Brassica juncea* (family Brassicaceae). The authors reported that the gene had high levels of similarity with gamma thionin and knottin families of plant AMPs. Our isolates also showed that the biodefensin had similarities with defense genes in other plants. Studies have shown that gene transcription is significantly enhanced under stress, confirming the inducible defense response of AMP in plants (Rawat et al., 2017). The plant defensins Rs-AFP1 and Rs-AFP2 from radish (*Raphanus sativus*) is an example of potent antifungal proteins. The exact process involved in the antifungal function of these genes needs further study, but they likely target the cell membranes of microbes. These genes may also initiate other mechanisms involved in plant defense (Souza et al., 2017).

We used many online bioinformatics tools to study the physicochemical and functional properties, and also structural analyses of our novel defensin genes. Same kind of comparative analysis on Kisspeptin Receptors and their physicochemical characterization was done by Mukesh Kumar and his co-workers (Kumar et al., 2018). We predicted the 3-D structures of defensin proteins using I-TASSER and RaptorX web tools. Our novel gene, isolated from *Moringa oleifera* that showing homology with the GDP dissociation inhibitor gene, may function in membrane transport, as found in the GDP dissociation inhibitor (Palme, 1997; Zarsky et al., 1997). The GDP dissociation inhibitor gene regulates nucleotide states and subcellular localization of Rab/Ypt proteins (Ueda et al., 1998). Rab3a-GDI (Rab guanosine nucleotide diphosphate dissociaton inhibitor protein), first isolated from bovine cytosol (Sasaki et al., 1991), inhibits the dissociation of GDP to Rab3a and the binding of GTP to Rab3a, and thus has a potential function in regulating Rab GTPases (Burstein and Macara, 1992)

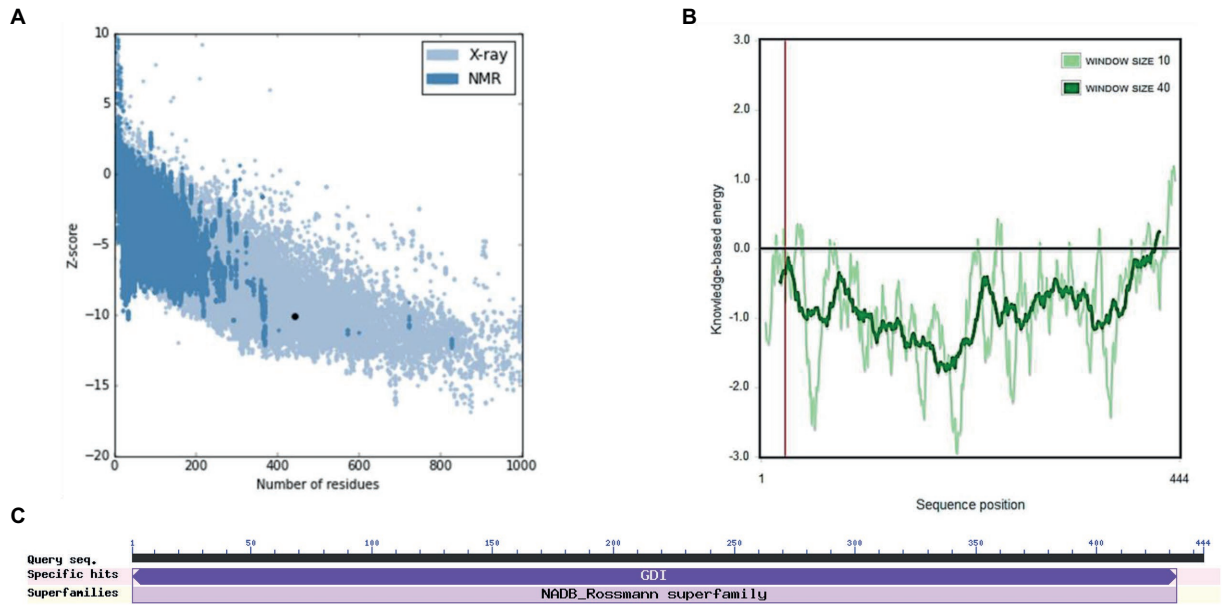


FIGURE 7
ProSA-web service analysis and domain search of *M. esculenta* GDP dissociation inhibitor 1. **(A)** ProSA-web z-scores of all protein chains present in the Protein Data Bank refer to their length. Light and dark blue colors correspond to X-ray crystallography and NMR spectroscopy, respectively. Large dots highlight the z-scores of *M. esculenta* GDP dissociation inhibitor 1. **(B)** Energy plot of *M. esculenta* GDP dissociation inhibitor 1. **(C)** CD search and Pfam search shows the presence of GDI domain in *M. esculenta* GDP dissociation inhibitor 1.

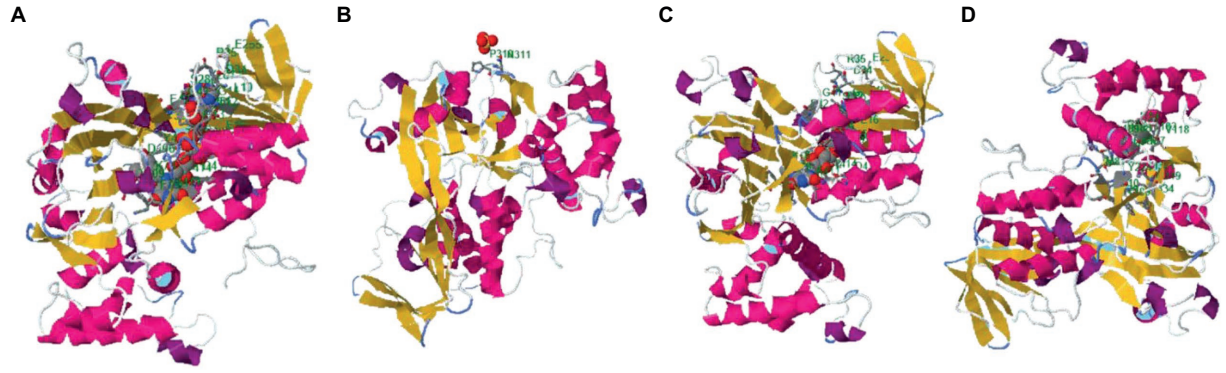


FIGURE 8
Identified binding sites of *M. esculenta* GDP dissociation inhibitor 1 using the raptorX tool. Four binding pockets were identified: **(A)** Dihydroflavine-adenine dinucleotide (FDA), **(B)** sulfate ion (SO_4^{2-}), **(C)** chloride ion (Cl^-), and **(D)** galactose-uridine-5′-diphosphate (GDU).

and secretory pathways (Andreeva et al., 1997). While we have not tested the function of our novel gene, but its homology with GDP dissociation inhibitor and function in membrane vesicular transport strongly suggest that it will also inhibit the entry of microbes across the membrane, thus preventing infection. Our other novel gene, isolated from *Albizzia lebecck* showed 100% similarity with predicted *Musa acuminata* subsp. *malaccensis* peroxidase P7-like gene. In a cold tolerance study of *Musa* spp. 'Dajiao', He et al. (2018) found that membrane-bound peroxidases potentially decrease lipid peroxidation and play a role in maintaining leaf cell water potential, contributing to plant defense against cold stress. Other researchers also found that membrane peroxidases are involved in the H_2O_2 scavenging system and ROS signaling networks (Passardi et al., 2004). The role of peroxidases in plant defense is elaborated by their activity on cell walls through the oxidation of phenolic compounds by reducing H_2O_2 under normal and stressed conditions (Almagro et al., 2009). Another study identified three defense enzymes—phenylalanine ammonia-lyase (PAL), peroxidase (PO), and polyphenol oxidase (PPO)—involved in phenol synthesis and oxidation in banana roots infected with *Radopholussimilis*, which strengthened cell walls. Wounded roots had significantly higher PO levels than control roots, they also reported enhanced PO activity in banana roots inoculated with fungus within 24 h of infection (Wuyts et al., 2006).

These results and the homology of our isolated gene with *Musa acuminata* subsp. *malaccensis* peroxidase P7-like gene strongly suggests that Albizzin has the same functional potential in the defense mechanism of plants and can serve its function against fungal diseases.

Conclusion

No doubt huge efforts are being made on genetic researches all over the world to discover more potent medicinal plants with beneficial gene products. However, still a large number of medicinal plants are at the need to be investigated for their possible defensive values. This study suggests a strategy for isolation of effective candidate genes that are part of signal transduction and defense system of plants. Examining the efficiency of these genes in practice is key to understand its role in defense mechanism. Screening of defensin gene from *M. oliefera* and *A. lebecck* resulted in isolation of GDP dissociation inhibitor like gene and peroxidase P7-like gene, respectively. These genes are very important as their role in membrane transport, regulation of nucleotide states, subcellular localization, free radical sacavenging properties and signaling of ROS. Further investigation on physical characterization and interaction of gene with downstream stress-responsive and growth and developmental-related genes of plant breeds with these genes would be worth examining whether these plants have enhanced resistance or tolerance to multiple biotic and abiotic stresses. Hence these genes would be potential candidate for breeding of plants with high resistance and strong defense. Structural characterization and biological interactions of GDP dissociation inhibitor and peroxidase P7-like gene from *M. oliefera* and *A. lebecck* respectively, revealed in this study conclude that these genes can serve for the synthesis of transgenic plants that will be more stress resistant and can give better crop yield in the future.

Data availability statement

The original contributions presented in the study are publicly available. This data can be found at: ON921005, ON921006.

Author contributions

Research work was supervised by RJ and AI. Material preparation, data collection, and analysis were performed by UH, RJ, and FD. The manuscript was finalized by HN and GM. Article review, editing, and proof reading was done by FZ, MN, AZ, and KS. All authors contributed to the article and approved the submitted version.

Funding

The research leading to these results received funding from Higher Education Commission, Government of Pakistan under grant agreement no. 21-1603/SRGP/R&D/HEC/2017.

Acknowledgments

We are highly thankful to the Higher Education Commission Pakistan. We heartily acknowledge The Women University Multan and Higher Education Commission Pakistan for the completion of this research and giving a platform to do this research work.

Conflict of interest

The authors declare that the research was conducted in the absence of any commercial or financial relationships that could be construed as a potential conflict of interest.

Publisher's note

All claims expressed in this article are solely those of the authors and do not necessarily represent those of their affiliated organizations, or those of the publisher, the editors and the reviewers. Any product that may be evaluated in this article, or claim that may be made by its manufacturer, is not guaranteed or endorsed by the publisher.

References

Al Akeel, R., Al-Sheikh, Y., Mateen, A., Syed, R., Janardhan, K., and Gupta, V. (2014). Evaluation of antibacterial activity of crude protein extracts from seeds of six different medical plants against standard bacterial strains. *Saudi J. Biol. Sci.* 21, 147–151. doi: 10.1016/j.sjbs.2013.09.003

Almagro, L., Gómez Ros, L. V., Belchi-Navarro, S., Bru, R., Ros Barceló, A., and Pedreño, M. A. (2009). Class III peroxidases in plant defence reactions. *J. Exp. Bot.* 60, 377–390. doi: 10.1093/jxb/ern277

Amir, A., Kapoor, N., and Kumar, H. T. (2019). Target protein in human herpes virus 8 (HHV8). *Biotech. Today Int. J. Biol. Sci.* 9, 41–48. doi: 10.5958/2322-0996.2019.00005.X

Andreeva, A. V., Kutuzov, M. A., Evans, D. E., and Hawes, C. R. (1997). Rab-GDP dissociation inhibitor isoforms in *Arabidopsis thaliana*. *J. Exp. Bot.* 48, 2109–2110. doi: 10.1093/jxb/48.12.2109

Arasu, M. V., Al-Dhabi, N. A., Choi, K. C., Bensy, A. D., and Rajaselvam, J. (2022). Bioactive potential of *Albizia lebbeck* extract against phytopathogens and protective properties on tomato plant against speck disease in greenhouse. *Physiol. Mol. Plant Pathol.* 117:101750. doi: 10.1016/j.pmpp.2021.101750

Azam, S., Latif, A., Hussain, K., Shahbaz, H., Perveen, S., Ashfaq, I., et al. (2022). Anti-diabetic and anti-lipidepmic effect of *Albizia lebbeck* seeds against HepG2 cells. *Pak. J. Pharm. Sci.* 35, 793–800.

Boukhatem, M. N., Ferhat, M. A., Kameli, A., Saidi, F., and Kebir, H. T. (2014). Lemon grass (*Cymbopogon citratus*) essential oil as a potent anti-inflammatory and antifungal drugs. *Libyan J. Med.* 9:25431. doi: 10.3402/ljm.v9.25431

Brenner, W. G., Ramireddy, E., Heyl, A., and Schmulling, T. (2012). Gene regulation by cytokinin in arabidopsis. *Front. Plant Sci.* 3:8. doi: 10.3389/fpls.2012.00008

Burstein, E. S., and Macara, I. G. (1992). Characterization of a guanine nucleotide-releasing factor and a GTPase-activating protein that are specific for the ras-related protein p25rab3A. *Proc. Natl. Acad. Sci.* 89, 1154–1158. doi: 10.1073/pnas.89.4.1154

Casadei, E., Wang, T., Zou, J., Vecino, J. L., Wadsworth, S., and Secombes, C. J. (2009). Characterization of three novel β-defensin antimicrobial peptides in rainbow trout (*Oncorhynchus mykiss*). *Mol. Immunol.* 46, 3358–3366. doi: 10.1016/j.molimm.2009.07.018

Chojak-Koźniewska, J., Kuźniak, E., and Zimny, J. (2018). The effects of combined abiotic and pathogen stress in plants: insights from salinity and pseudomonas syringae pv lachrymans interaction in cucumber. *Front. Plant Sci.* 9:1691. doi: 10.3389/fpls.2018.01691

Cui, J., Jiang, N., Meng, J., Hou, X., Yang, G., and Luan, Y. (2018). Identification and characterization of defensin genes conferring *Phytophthora infestans* resistance in tomato. *Physiol. Mol. Plant. Path* 103, 28–35. doi: 10.1016/j.pmpp.2018.04.003

De-Paula, V., Razzera, G., Medeiros, L., Miyamoto, C., Almeida, M., Kurtenbach, E., et al. (2008). Evolutionary relationship between defensins in the Poaceae family strengthened by the characterization of new sugarcane defensins. *Plant Mol. Biol.* 68, 321–335. doi: 10.1007/s11103-008-9372-y

Douwes, E., Crouch, N. R., Edwards, T. J., and Mulholland, D. A. (2008). Regression analysis of southern African ethnomedicinal plants: informing the targeted selection of bioprospecting and pharmacological screening subjects. *J. Ethnopharmacol.* 119, 356–364. doi: 10.1016/j.jep.2008.07.040

Fahim, A., Rehman, Z., Bhatti, M. F., Ali, A., Virk, N., Rashid, A., et al. (2018). Structural insights and characterization of human Npas4 protein. *PeerJ* 6:e4978. doi: 10.7717/peerj.4978

He, W. D., Gao, J., Dou, T. X., Shao, X. H., Bi, F. C., Sheng, O., et al. (2018). Early cold-induced peroxidases and aquaporins are associated with high cold tolerance in Dajiao (*Musa* spp.'Dajiao'). *Front. Plant Sci.* 9:282. doi: 10.3389/fpls.2018.00282

Hepperle, D. (2011). DNA dragon 1.4. 1-DNA sequence contig assembler software. Available at: www.Dna-dragon.Com (Accessed November 15, 2020).

Ingti, B., Laskar, M. A., Choudhury, S., Maurya, A. P., Paul, D., Talukdar, A. D., et al. (2017). Molecular and in silico analysis of a new plasmid-mediated AmpC β-lactamase (CMH-2) in clinical isolates of *Klebsiella pneumoniae*. *Infect. Genet. Evol.* 48, 34–39. doi: 10.1016/j.meegid.2016.12.009

Kamala Lakshmi, B., and Valarmathi, S. (2020). In vitro anti-inflammatory activity of aqueous extract of *Albizia lebbeck* leaf (l.). *J. Phytopharmacol.* 9, 356–360. doi: 10.31254/phyto.2020.9511

Kovaleva, V., Yusypovych, Y., and Gout, R. (2017). Scots pine defensins: structure, properties and biological functions. *Біологічнистудії* 11, 66–67.

Kumar, S. (2017). Medicinal importance of *Moringa oleifera*: drumstick plant. *Indian J. Sci. Res.* 1, 129–133.

Kumar, M., Basumatary, G., Ram, R. K., Singh, D. K., and Udit, U. K. (2018). Comparative studies on Kisspeptin receptor and their physicochemical characterization. *Int. J. Curr. Microbiol. App. Sci.* 7, 43–47.

Kumar, A., Kumar, S., and SubirKundu, M. D. (2016). Homology modeling of outer membrane lipoprotein of *Salmonella typhi*. *Res. Environ. Life Sci.* 9, 900–902.

Lakshmi Priya, P. M., and Sabu, K. K. (2015). In Silico analysis of Transcriptomes of *Catharanthus roseus* and *Rauvolfia serpentina*, two potent medicinal plants using a pipeline developed from publicly available tools. *Am. J. Bioinform. Res.* 5, 21–25. doi: 10.5923/j.bioinformatics.20150502.01

Lim, S., and Yoon, T. (2018). "Genomic comparison of four Metapneumovirus strains using decision tree, Apriori algorithm, ClustalW, and phylogenetic reconstruction," in *Proceedings of the 2018 5th International Conference on Bioinformatics Research and Applications*, 95–100.

Long, D. D., Bach, N. X., Thao, N. T., Nhung, P. T., Thom, V. T., and Huyen, P. T. (2019). Comparative analysis of different DNA extraction methods and preliminary analysis of genetic diversity of *Hedera nepalensis* K. Koch. in Vietnam based on GBSSI Marker. VNU J. Sci. Med. Pharmaceu Sci. 35, 88–95. doi: 10.25073/2588-1132/vnumps.4165

Mahlapuu, M., Håkansson, J., Ringstad, L., and Björn, C. (2016). Antimicrobial peptides: an emerging category of therapeutic agents. *Front. Cell. Infect. Microbiol.* 6:194. doi: 10.3389/fcimb.2016.00194

Marchler-Bauer, A., Bo, Y., Han, L., He, J., Lanczycki, C. J., Lu, S., et al. (2017). CDD/SPARCLE: functional classification of proteins via subfamily domain architectures. *Nucleic Acids Res.* 45, D200–D203. doi: 10.1093/nar/gkw1129

Mistry, J., Chuguransky, S., Williams, L., Qureshi, M., Salazar, G. A., Sonnhammer, E. L. L., et al. (2021). Pfam: the protein families database in 2021. *Nucleic Acids Res.* 49, D412–D419. doi: 10.1093/nar/gkaa913

Newman, L., Duffus, A. L., and Lee, C. (2016). Using the free program MEGA to build phylogenetic trees from molecular data. *Am. Biol. Teach.* 78, 608–612. doi: 10.1525/abt.2016.78.7.608

Novaković, L., Guo, T., Bacic, A., Sampathkumar, A., and Johnson, K. L. (2018). Hitting the wall—sensing and signaling pathways involved in plant cell wall remodeling in response to abiotic stress. *Plan. Theory* 7:89. doi: 10.3390/plants7040089

Overmyer, K., Vuorinen, K., and Brosche, M. (2018). Interaction points in plant stress signaling pathways. *Physiol. Plant.* 162, 191–204. doi: 10.1111/ppl.12639

Palme, K. (1997). At-GDI1 from *Arabidopsis thaliana* encodes a rab-specific GDP dissociation inhibitor that complements the sec19 mutation of. *FEBS Lett.* 403, 303–308. doi: 10.1016/S0014-5793(97)00072-0

Parisi, K., Shafee, T. M., Quimbar, P., van der Weerden, N. L., Bleackley, M. R., and Anderson, M. A. (2019). The evolution, function and mechanisms of action for plant defensins. *Semin. Cell. Dev. Biol.* 88, 107–118. doi: 10.1016/j.semcdb.2018.02.004

Passardi, F., Penel, C., and Dunand, C. (2004). Performing the paradoxal: how plant peroxidases modify the cell wall. *Trends Plant Sci.* 9, 534–540. doi: 10.1016/j.tplants.2004.09.002

Rawat, S., Ali, S., Nayankantha, N. C., Chandrashekar, N., Mittra, B., and Grover, A. (2017). Isolation and expression analysis of defensin gene and its promoter from *Brassica juncea*. *J. Plant Dis. Prot.* 124, 591–600. doi: 10.1007/s41348-017-0103-y

Reichling, J. (2018). Plant–microbe interactions and secondary metabolites with antibacterial, antifungal and antiviral properties. *Annual Plant Rev.* 15, 214–347. doi: 10.1002/9781119312994.apr0420

Sasaki, T., Kaibuchi, K., Kabcenell, A. K., Novick, P. J., and Takai, Y. (1991). A mammalian inhibitory GDP/GTP exchange protein (GDP dissociation inhibitor) for smg p25A is active on the yeast SEC4 protein. *Mol. Cell. Biol.* 11, 2909–2912.

Schmidt, M., Arendt, E. K., and Thery, T. L. (2019). Isolation and characterisation of the antifungal activity of the cowpea defensin Cp-thionin II. *Food Microbiol.* 82, 504–514. doi: 10.1016/j.fm.2019.03.021

Souza, T. P., Dias, R. O., and Silva-Filho, M. C. (2017). Defense-related proteins involved in sugarcane responses to biotic stress. *Genet. Mol. Biol.* 40, 360–372. doi: 10.1590/1678-4685-gmb-2016-0057

Thompson, J. D., Higgins, D. G., and Gibson, T. J. (1994). CLUSTAL W: improving the sensitivity of progressive multiple sequence alignment through sequence weighting, position-specific gap penalties and weight matrix choice. *Nucleic Acids Res.* 22, 4673–4680. doi: 10.1093/nar/22.22.4673

Ueda, T., Yoshizumi, T., Anai, T., Matsui, M., Uchimiya, H., and Nakano, A. (1998). AtGDI2, a novel Arabidopsis gene encoding a Rab GDP dissociation inhibitor. *Gene* 206, 137–143. doi: 10.1016/S0378-1119(97)00584-2

Wu, Q., Peng, Z., Zhang, Y., and Yang, J. (2018). COACH-D: improved protein–ligand binding sites prediction with refined ligand-binding poses through molecular docking. *Nucleic Acids Res.* 46, W438–W442. doi: 10.1093/nar/gky439

Wuyts, N., Swennen, R., and De Waele, D. (2006). Activity of phenylalanine ammoni-lyase, peroxidise and polyphenol oxidase in roots of banana(Musa acuminate AAA, cvs Grande Naine and Yangambi km5) before and after infection with Radopholus similis. *Nematol* 8, 201–209. doi: 10.1163/156854106777998674

Zarsky, V., Cvrckova, F., BischoffF, F., and Palme, K. (1997). At-GDI1 from *Arabidopsis thaliana* encodes a Rab-specific GDP dissociation inhibitor that complements the sec19 mutation of Saccharomyces cerevisiae. *FEBS Lett.* 403, 303–308. doi: 10.1016/S0014-5793(97)00072-0

Zharkova, M. S., Orlov, D. S., Golubeva, O. Y., Chakchir, O. B., Eliseev, I. E., Grinchuk, T. M., et al. (2019). Application of antimicrobial peptides of the innate immune system in combination with conventional antibiotics—a novel way to combat antibiotic resistance? *Front. Cell. Infect. Microbiol.* 9:128. doi: 10.3389/fcimb.2019.00128

frontiers | Frontiers in Plant Science

TYPE Review
PUBLISHED 15 September 2022
DOI 10.3389/fpls.2022.899464

Check for updates

OPEN ACCESS

EDITED BY
Shabir Hussain Wani,
Sher-e-Kashmir University
of Agricultural Sciences
and Technology of Kashmir, India

REVIEWED BY
Sheikh Mansoor,
Sher-e-Kashmir University
of Agricultural Sciences
and Technology of Jammu, India
Durgesh K. Jaiswal,
Savitribai Phule Pune University, India
Rohit Joshi,
Institute of Himalayan Bioresource
Technology (CSIR), India

*CORRESPONDENCE
Gustavo Santoyo
gustavo.santoyo@umich.mx

SPECIALTY SECTION
This article was submitted to
Plant Biotechnology,
a section of the journal
Frontiers in Plant Science

RECEIVED 18 March 2022
ACCEPTED 08 August 2022
PUBLISHED 15 September 2022

CITATION
Afridi MS, Javed MA, Ali S,
De Medeiros FHV, Ali B, Salam A,
Sumaira, Marc RA, Alkhalifah DHM,
Selim S and Santoyo G (2022) New
opportunities in plant microbiome
engineering for increasing agricultural
sustainability under stressful
conditions.
Front. Plant Sci. 13:899464.
doi: 10.3389/fpls.2022.899464

COPYRIGHT
© 2022 Afridi, Javed, Ali, De Medeiros,
Ali, Salam, Sumaira, Marc, Alkhalifah,
Selim and Santoyo. This is an
open-access article distributed under
the terms of the Creative Commons
Attribution License (CC BY). The use,
distribution or reproduction in other
forums is permitted, provided the
original author(s) and the copyright
owner(s) are credited and that the
original publication in this journal is
cited, in accordance with accepted
academic practice. No use, distribution
or reproduction is permitted which
does not comply with these terms.

New opportunities in plant microbiome engineering for increasing agricultural sustainability under stressful conditions

Muhammad Siddique Afridi[1], Muhammad Ammar Javed[2], Sher Ali[3], Flavio Henrique Vasconcelos De Medeiros[1], Baber Ali[4], Abdul Salam[5], Sumaira[6], Romina Alina Marc[7], Dalal Hussien M. Alkhalifah[8], Samy Selim[9] and Gustavo Santoyo[10]*

[1]Department of Plant Pathology, Federal University of Lavras (UFLA), Lavras, MG, Brazil, [2]Institute of Industrial Biotechnology, Government College University, Lahore, Pakistan, [3]Department of Food Engineering, Faculty of Animal Science and Food Engineering, University of São Paulo (USP), São Paulo, Brazil, [4]Department of Plant Sciences, Quaid-i-Azam University, Islamabad, Pakistan, [5]Zhejiang Key Laboratory of Crop Germplasm, Department of Agronomy, College of Agriculture and Biotechnology, Zhejiang University, Hangzhou, China, [6]Department of Biotechnology, Quaid-i-Azam University, Islamabad, Pakistan, [7]Food Engineering Department, Faculty of Food Science and Technology, University of Agricultural Sciences and Veterinary Medicine of Cluj-Napoca, Cluj-Napoca, Romania, [8]Department of Biology, College of Science, Princess Nourah Bint Abdulrahman University, Riyadh, Saudi Arabia, [9]Department of Clinical Laboratory Sciences, College of Applied Medical Sciences, Jouf University, Sakaka, Saudi Arabia, [10]Instituto de Investigaciones Químico-Biológicas, Universidad Michoacana de San Nicolás de Hidalgo, Morelia, Mexico

Plant microbiome (or phytomicrobiome) engineering (PME) is an anticipated untapped alternative strategy that could be exploited for plant growth, health and productivity under different environmental conditions. It has been proven that the phytomicrobiome has crucial contributions to plant health, pathogen control and tolerance under drastic environmental (a)biotic constraints. Consistent with plant health and safety, in this article we address the fundamental role of plant microbiome and its insights in plant health and productivity. We also explore the potential of plant microbiome under environmental restrictions and the proposition of improving microbial functions that can be supportive for better plant growth and production. Understanding the crucial role of plant associated microbial communities, we propose how the associated microbial actions could be enhanced to improve plant growth-promoting mechanisms, with a particular emphasis on plant beneficial fungi. Additionally, we suggest the possible plant strategies to adapt to a harsh environment by manipulating plant microbiomes. However, our current understanding of the microbiome is still in its infancy, and the major

perturbations, such as anthropocentric actions, are not fully understood. Therefore, this work highlights the importance of manipulating the beneficial plant microbiome to create more sustainable agriculture, particularly under different environmental stressors.

KEYWORDS

plant microbiome, fungi, sustainable agriculture, biotic and abiotic constraints, PGPR – plant growth-promoting rhizobacteria

Introduction

Different researchers have highlighted that by 2050, it is expected that the world population will reach 10 billion people. The massive surge in population will increase the amount of food necessary for the entire planet to be fed. However, food could be a problem for this drastically increased population. Even today, approximately 9% of the world's population (690 million people) go to bed with an empty stomach each night (Sakschewski et al., 2014). Combining these challenges without compromising the environment and human health is a major issue in the agricultural production sector and the forefront of many plant scientists.

To achieve this goal, it will be obligatory to engage two closely associated goals. The first is to improve crop yield, especially for cereal crops, which can be accomplished through different procedures, such as genetic modification, selective breeding, avoiding waste in irrigation as well as fertilization regimes (Beddington, 2010; Godfray et al., 2010; Singh et al., 2022). Second, curtail crop losses due to pests and diseases, which have been causing losses on the order of 20–40%, in addition to the indirect effects on livelihoods and the environment (Oerke, 2006; Beddington, 2010; Godfray et al., 2010; Savary et al., 2012; McDonald and Stukenbrock, 2016).

Implementing strategies to attain the latter is challenging, particularly because the elements that corroborate plant maladies are extremely complex and multivariate (Savary et al., 2012). Moreover, cereal crops are affected by several different organisms, e.g., a variety of bacteria, fungi, oomycetes, nematodes, and viruses (Dean et al., 2012).

Fungal species competence to survive in soil mainly invade the plant roots, causing various notorious diseases in plants while simultaneously undermining the host plant of its nutrients; this is the case for wheat disease caused by *Gaeumannomyces graminis var. triciti,* which in some cases can eradicate an entire wheat crop. Thus, worldwide, the take-all of wheat is considered the most important root ailment of wheat (Coombs, 2004; Kwak and Weller, 2013; Cook et al., 2015; Hernández-Restrepo et al., 2016; Ahmad M. et al., 2022). Plant-parasitic nematodes living in the same vicinity as plant roots are among the most destructive plant pathogens, causing estimated damage of more than US$100 billion per year. An expert-based assessment of crop health listed nematodes as among the most damaging pests and pathogens for different crops (Savary et al., 2012).

To avoid crop losses due to maladies, chemical pesticides are routinely applied on crops, with the main goal of eradicating or lessening the disease invasion, infection or severity. However, it is becoming increasingly clear that long-term chemical pesticide usage poses several adverse effects on the environment and human health (Sanyal and Shrestha, 2008; Kortekamp, 2011). For instance, a myriad of pesticides can cause acute and chronic toxicity in humans, and they are progressively being shown to cause widespread damage to the broader ecosystem, affecting non-target organisms, such as pollinator species, and soil pollution and water (Arora and Sahni, 2016; Grewal et al., 2017; Anwar et al., 2023). These non-target effects can also extend to reduce the beneficial microbial diversity within soil, which in turn refrains and suppresses the available populations of pathogens from competition and elevates the risks of pathogen invasion and colonization of plant tissues (Jacobsen and Hjelmsø, 2014). Additionally, plant pathogen genetic evolution and resistance against various resistant bread crop varieties can be devastating outcomes of the continuous application of pesticides, that pathogens can rapidly evoke plant host resistance mechanisms, especially when only a single gene is responsible for resistance. In certain circumstances, there are many crop species for which resistant cultivars are unavailable. For instance, every 2–3 years, rice cultivars that are usually resistant to *M. oryzae* typically become ineffective. These combined issues have opened up ways to search for another alternative.

Plant-associated microbiomes have essential functions in improving plant nutrition acquisition and provide protection against biotic and abiotic stressors. Nutrient acquisition has been thoroughly studied for plant symbioses with arbuscular mycorrhizal fungi (AMF) and Rhizobium bacteria (Bergelson et al., 2019; Trivedi et al., 2020). Additionally, these diverse microbial communities of plant microbiome perform multiple functions such as nitrogen fixation, nutrient solubilization, (Adnan et al., 2022; Khan et al., 2023) protection against devastating plant pathogens and production of phytohormones

(Haider et al., 2022) like indole acetic acid, auxin, gibberellin, abscisic acid, aminocyclopropane-1-carboxylate deaminase, antibiotics, development of induced resistance to pathogens in plants, and promotion of the population of other helpful microorganisms (Afridi et al., 2019, 2021; Mehmood et al., 2021a; Zainab et al., 2021).

Manipulation of the soil microbiome for plant growth and protection is considered one of the possible avenues in previous decades. The soil microbiome has complex interactions with the plant and its roots, helping to remove contaminants, provide nutrients, and proliferate growth (Liu et al., 2019). Continued research into this subject matter is necessary to elucidate the complex interactions that occur so that manipulating these relations may be used to help feed 10 billion people. Therefore, this review aimed to highlight the beneficial services of the plant-associated microbiome to be manipulated and optimized, resulting in better agricultural production, even under non-optimal conditions.

Defining the plant microbiome

Plants are associated with a diverse group of microbes, such as bacteria, oomycetes, fungi, archaea, and viruses, through three major associations, the rhizosphere (root-attached soil), endosphere (internal tissue), and phyllosphere (aboveground parts), which execute significant activities that influence host health and fitness and inhabit a well-defined area of plant microbiome. Among them, the rhizosphere is the most complex and diverse niche of microbial communities (Lakshmanan et al., 2014; Bandyopadhyay et al., 2017).

Plants have evolved to form complex, beneficial relationships with the microorganisms in their surroundings. Although the plant microbiome includes bacteria, fungi, archaea, protists and viruses, the majority of research has focused on bacterial and fungal communities (Trivedi et al., 2020). These organisms play important roles in the health and productivity of crops by forming complex co-association with plants (Fitzpatrick et al., 2018). In particular, plant-associated microbiota and plants form a 'holobiont,' and evolutionary selection among microbes and plants contributes to the stability of the ecosystem (Hamonts et al., 2018; Xu et al., 2018a).

Recently, developed culture-independent high-throughput sequencing has accelerated the identification of microbial communities inhabiting the surrounding spaces, as well as inside tissues and surfaces of plants, and demonstrated the existence of microbial lineage subsets, termed 'core microbiota,' which reproducibly make contacts with host plants across a wide range of environmental conditions (Bergelson et al., 2019).

In terms of therapeutic or diagnostic benefits and technical advancements, the study of the microbial community has been a leading interest amongst scientific society. In addition to compensation, all or some of these microbes actively support plant improvement (Parray and Shameem, 2019). In accordance with distribution, these microbes can be found in the phyllosphere (above the ground–stem and tissues), endosphere (underground–tissues within the plant) and rhizosphere (roots alongside growth layers) of the host (**Figure 1**). This is because the plant anatomy represents and provides a remarkably suitable environment for these microbes (Schlaeppi and Bulgarelli, 2015). Over the past decades, individual microbes from these microbiomes have displayed exceptional features (Rani et al., 2019; Gupta et al., 2020) containing their interactions with the host. The symbiotic association has been determined to be pathogenic and/or non-pathogenic to the host plants, including nitrogen fixation, development, bioremediation and stress tolerability (Roth and Paszkowski, 2017; Li et al., 2019). To overview an extended mutualistic to parasitic and commensalism dealing, plants correlated with the microbiota cover a large portion. Additionally, the study of this connection may lead to in-depth knowledge and could provide appreciative outputs.

According to the growth of the global population, a sustainable environment of high food security is urgently needed, which is achieved mostly by strengthening crop practices. In this regard, the microbial system has been a key technology in such progress. Since ∼300 BC, this goal has been founded by the manipulation of the soil microbiome (Vessey, 2003), which is a key to the green revolution (Parnell et al., 2016). It is interesting to note that soil microbiomes are now touted as a cornerstone of the next green revolution.

The plant microbiome at work

The microbiome, as a 'second genome' of organisms, including plants, has a mutualistic relation with health and general well-being. Taking this into consideration, **Figure 1** depicts a holistic overview of the plant microbiome with some attributes, signaling and cross-talk between the plant and its relevant biota. This mutualism can be direct and/or indirect; plant–plant, microbe–microbe, plant–microbe, and/or with some microbe–microbe and macrosoil eukaryote interactions (Tarkka et al., 2008). In addition, these interactions could be classified into competition, parasitism, mutualism and commensalism. Being more common, the latter two interactions provide major benefits to one or both interacting species.

Microbial services

Within this context, the manipulation of the phytomicrobiome can be of greater interest to boost diagnostics and therapies in plants, which are extendable to animals and humans in the future (Zmora et al., 2016). However, the phytomicrobiome is generally associated

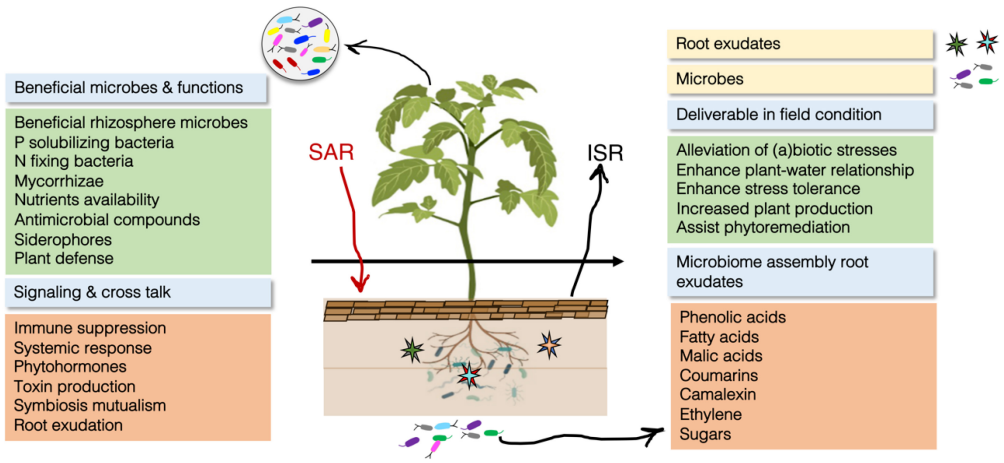


FIGURE 1
The holistic overview of plant microbiome compositions, the interaction between plant and its associated microbes, function and its positive effect on plant growth and development under extreme conditions. Plant recruit and assembly beneficial microbes via exudation and constitute a healthy and beneficial microbial community. This microbiome improves plant health, alleviates abiotic stresses and provides a safeguard to the host exhibiting various direct and indirect mechanisms.

with multiple microorganisms that are major factors for agricultural production and play a critical function. Agricultural sustainability has been a major proposal in the world and has been completed by the implementation of many microorganisms. In fact, some of these microbes colonized the plant roots, improve plant growth and regulate vital functions against detrimental pathogens and thereby lead to plant productivity (van der Heijden and Hartmann, 2016; Cordovez et al., 2019; Rafique et al., 2019). The world is transitioning to ecologically safe and economically effective approaches that could be used to promote agricultural productivity. Therefore, a balanced farming system is critical in terms of the survival of Earth. In this regard, crop output per unit area of land must be raised to fulfill the demand for food (Doran, 2002). As per recommendations, an equivalent improvement in plant health could be achieved via various strategies. Among them, PGPR, as probiotics for plant roots and prebiotic substrates/additives, can be used to cause compositional alterations in the phytomicrobiome and are termed soil amendments. The plant microbiome has a strong influence on nutrient availability and the growth and development of the host (Carvalhais et al., 2013). Accordingly, plants on the basis of natural exudate recruit and "engineer" a local microbiome (Kumar et al., 2018; Rojas-Solís et al., 2018) and make this habitat fit to their survival.

Signaling and cross-talk

In general, plants of the local habitat are in cross-talk with numerous surrounding stimuli incorporating the microbial communities (**Figure 1**); therefore, this is termed the homeostatic photomicrobiome. In such a homeostatic phytomicrobiome, plants are allowed to sense and properly respond to any interactive stimulus of the system. However, after microbial substance recognition, they can ultimately lead to mutualism or immunity. Furthermore, communicatory signaling is an important phenomenon responsible for healthy lifestyles and the survival of organisms (Cook et al., 2015; Müller et al., 2016). This communicatory network can be predicted for any of the micro- or macroorganisms living on the planet, such as quorum sensing bacteria (Cornforth et al., 2014), whales (Parks et al., 2015) and those across the tree of life. Such communicating circuitry plays a decisive role in the evolution of the life of associated organisms (West et al., 2015). Overlooking such a communicatory web, chemical signaling is highly vital and participates in perception and modulation in stationary organisms, such as plants. However, plants use these chemical bases as signals to maintain mutual links with presided microbes either on the aerial (trunk, shoots, leaves, etc.) and/or the underground parts (roots). As per estimation, approximately 5–20% photosynthetically fixed carbon has been an active ingredient in plant rhizosphere-inducing microbes for healthier microbial community formation (Marschner, 1995). In addition to carbon, microorganisms discharge many more signaling chemical substances to the rhizosphere. Through them, the most prominent are phytohormones, extracellular enzymes, organic acids, antibiotics, volatile contents and surface factors, e.g., immunomodulatory precursors such as flagellins and lipopolysaccharides in Pseudomonas (Ping, 2004; Dangl et al., 2013). As a signaling molecule, quorum sensing, e.g., *N*-acyl-homoserine lactones (AHLs), when secreted, is used to regulate gene expression by plant-associated bacteria (Berendsen et al., 2012). However, AHLs have been major

precursors affecting root development in a model plant of Arabidopsis (Ortíz-Castro et al., 2008). Moreover, AHLs have the tendency to elicit "systemic resistance" (ISR) that allows plants to evade lethal pathogens without requiring bacterial factors. This effect can be a systemic mechanism because the roots are inoculated with manifold plant growth-promoting rhizobacteria (PGPR), such as *Pseudomonas*, *Burkholderia*, and *Bacillus* sp. that turn host plants non-susceptible to invaders (Schuhegger et al., 2006; Choudhary et al., 2007; Tarkka et al., 2008). In line, such a microbial combination is essential and responsible for fitness and plant health and beyond fulfilling fundamental demands (water, nutrients, etc.), they increase the tolerability of plants against any of the (a)biotic stressors (van der Heijden and Hartmann, 2016; Cordovez et al., 2019). This association provides the main benefits to soil biochemistry to suppress soil-borne diseases and detrimental pathogens. It is noteworthy that these pathogens may still be present but in an inactive state that would not be able to cause soil-borne diseases or damage their resident host, while this setup can be termed "soil suppression."

The relevant role of plant-associated fungi and bacteria

Plants can be associated with an immense diversity of microorganisms, including fungi. There is sufficient evidence that some fungi, such as AMF, can provide broad benefits to the plant in a type of symbiotic interaction. AMF are obligate biotrophic organisms that supply mineral nutrients to the host plant and, in return, receive carbon derived from photosynthesis. In this same sense, AMF can modulate carbon distribution in plants by modifying the expression and activity of key enzymes for the synthesis, transport and/or catabolism of carbon compounds, such as sucrose. Since sucrose can be essential for the maintenance of all metabolic and physiological processes, the modifications addressed by AMF can significantly affect plant development and responses to stress. Additionally, the interaction between AMF and plants can also host lipid biosynthesis to acquire storage reserves and generate biomass.

Other fungal species that provide various services to the plant are *Trichoderma* spp. richoderma (teleomorph Hypocrea) is a fungal genus that inhabits many ecosystems, including those involved in agricultural and production practices. There are several examples of how Trichoderma is part of microbial bioinoculants, either individually or carrying out synergistic interactions with other microorganisms, such as plant growth-promoting bacteria or PGPB. *Trichoderma* species, such as *T. harzianum*, *T. viride*, and *T. virens*, among many more species, can ameliorate the severity of plant diseases by inhibiting the growth of phytopathogens in the soil (mainly), since they exhibit antagonistic and mycoparasitic activities. Additionally, it has been reported that *Trichoderma* spp. It is also capable of interacting directly with the roots, which leads to promoting the growth and development of vegetable crops, as well as of course, stimulating resistance to diseases and tolerance to multiple types of environmental stress, such as salinity or drought to name a few. To further explore topics on the importance of plant-associated fungi and their beneficial role, readers are directed literature (Santoyo et al., 2021).

The root surfaces tightly adhering to the rhizosphere's soil interface colonize these PGPR (Jain, 2016). PGPR-mediated biocontrol processes are wide-ranging, like availability of nutrients and ecological niches, synthesis of allelochemicals including enzymes and antibiotics, development of induced resistance to pathogens in plants, and promotion of the population of other helpful microorganisms (**Table 1**). The best-known PGPR that colonizes in the rhizosphere strains are *Bacillus, Rhizobium, Acinetobacter, Alcaligenes, Arthrobacter, Enterobacter, Pseudomonas, Serratia,* and *Burkholderia* (Vinayarani and Prakash, 2018; Mehmood et al., 2021b) successfully induce disease resistance against the bacterial pathogen in plants, including *R. solanacearum* (Cao et al., 2018), *E. carotovora* (Chandrasekaran and Chun, 2016), *D. solani*, *E. amylovora,* and *P. carotovorum* (Vega et al., 2019). Both growth promotion and biological control can regulate by the same strain of PGPR. Generally, biological control of these bacteria relies on direct or indirect modes of action; however, all these mechanisms are highly influenced by the type of host plants (Dey et al., 2004; Singh et al., 2019). In direct mechanism, pathogens directly affected by the production of metabolites, for instance, antibiotics, hydrogen cyanide (HCN), iron-chelating siderophores, pyoluteorin, tensin, 2,4- diacetylphloroglucinol, phenazines, viscosinamide, and other cell wall-degrading enzymes, while another mechanism is known as induced systemic resistance, this happens by the intervention of an inducing agent that systemically stimulates the chemical or physical defensive mechanisms of the host plant, resulting in decreased symptoms of pathogens that invade tissues distal to the inducer (**Table 1**; Khatoon et al., 2020; Raj et al., 2020).

Why engineer the plant microbiome?

In light of the intensification of cropping practices and changing climatic conditions, nourishing a growing global population requires optimizing environmental sustainability and reducing the ecosystem impacts of food production. The use of microbiological systems to ameliorate agricultural production in a sustainable and eco-friendly way is widely accepted as a future key technology. The manipulation of soil microbiomes to optimize crop productivity is an ancient practice; records can be traced to ∼ 300 BC (Vessey, 2003). It is interesting to

TABLE 1 Plant growth promoting microbes underpinning plant growth and enhance tolerance against biotic and abiotic stresses employing various mechanisms.

Host species	PGPR	Functions/Response	References
Arabidopsis thaliana	*B. phytofirmans* PsJN	Abscisic acid signaling, proline and ROS production	Pinedo et al., 2015
Arabidopsis thaliana	*B. subtilis* GB03	Import of Sodium ions in root	Wang et al., 2016
Arabidopsis thaliana	*P. yonginensis* DCY84T	ROS Detoxification, Sodium ion homeostasis	Sukweenadhi et al., 2015
Abelmoschus esculentus	*Enterobacter* sp. UPMR18	ROS pathway Antioxidant enzymes production	Habib et al., 2016
Glycine max	*P. simiae strain* AU	Antioxidant enzymes Production	Vaishnav et al., 2016
Glycine max	*B. firmus* SW5	Production of antioxidant enzymes, salinity tolerance,	El-Esawi et al., 2018
Gossypium hirsutum	*Brucella* sp. PS4	Pesticide degradation	Ahmad S. et al., 2022
Puccinellia tenuiflora	*B. subtilis* GB03	Modulation of Na^+ homeostasis	Niu et al., 2016
Saccharum officinarum	*B. xiamenensis*	Phytoremediation	Zainab et al., 2021
Solanum lycopersicum	*B. megaterium*	Metallothionein Glutathione reductase enzyme synthesis	Zameer et al., 2016
Solanum lycopersicum	*E. cloacae* PM23	ROS Detoxification, Sodium ion homeostasis	Ali et al., 2022b
Solanum lycopersicum	*B. safensis* (SCAL1)	Heat Stress	Mukhtar et al., 2022
Solanum lycopersicum	*B. anthracis* PM21	Phytoremediation	Ali et al., 2021
Solanum tuberosum	*B. subtilis* PM32	Fungal diseases biocontrol	Mehmood et al. (2021a)
Solanum tuberosum	*B. mycoides* PM35	Proline production, and ROS scavenging	Ali et al., 2022a;
Solanum lycopersicum L.	*B. safensis* Strain SCAL1	Produced exopolysaccharide and ACC deaminase	Mukhtar et al., 2022
Zea mays L.	*B. amyloliquefaciens* SQR9	Photosynthesis, Na^+ export, and sequestration	Chen L. et al., 2016
Lettuce microcosms	*T. hamatum GD12*	*N-acetyl*-β-D-glucosaminidase genes	Ryder et al., 2012
Curcuma longa L	*T. harzianum* TharDOB-31	Indole-3-acetic acid hydrogen cyanide production	Vinayarani and Prakash, 2018
Solanum lycopersicum	*A. pullulans 490*	Produces biosurfactants, biocontrol activity	Köhl et al., 2020
Solanum lycopersicum	*C. rosea 016*	Produces biosurfactants, biocontrol activity	Köhl et al., 2020
Capsicum annuum L	*Beauveria bassiana*	Niche or resources and antibiosis	Jaber and Alananbeh, 2018
Pinus radiata	*F. circinatum*	Antagonism,	Martínez-Álvarez et al., 2016
Poncirus trifoliata	*F. mosseae*	Drought stress, Hyphal water absorption rate	Zhang et al., 2018
Triticum aestivum	*G. mosseae*	Drought stress, osmotic potential, antioxidant enzymes	Rani, 2016
Triticum aestivum L.	*R. irregularis*	Heat stress, nutrient allocation nutrient composition in root	Cabral et al., 2016
Zea mays	*R. intraradices*	High temperature, enhanced transpiration photosynthetic rate	Mathur et al., 2016
Solanum lycopersicum	*R. irregulari*	High temperature, Enhanced photosynthetic phosphorylation	Calvo-Polanco et al., 2016
Cucumis sativus L.	*G. intraradices*	Salinity stress, enhanced antioxidant enzymes, biomass	Hashem et al., 2018
Solanum lycopersicum L.	*R. irregularis*	Salinity stress, Enhanced biomass and growth hormones	Khalloufi et al., 2017

note that soil microbiomes are now touted as a cornerstone of the next green revolution (Parnell et al., 2016). In addition, the continuous growth of the world population demands that the global availability of food be one of the major concerns in the near future. According to the projected data (DESA, 2019), if this increment continues, in turn, the demands for food will reciprocally increase by 8.5 billion in 2030, 9.7 billion in 2050, and 11 billion by 2100. However, the fulfillment of such demand must be ascertained with green and innovative technologies incorporating plant and microbial resources.

Environmental stressors have caused major alterations in plant physiology and biochemistry that lead to significant reductions in plant yield and production. In accordance with previous reports 30–50% of agricultural losses have been impacted by unfavorable environmental conditions. Agronomic loss coupled with continual population growth demands at least a 60% boost in agrarian production to meet food demand on a larger scale (Wild, 2003). Often, the agricultural production has mostly been supplemented with pesticides. Consistently, approximately 2 million tons of pesticides are globally administered to reduce causative pests, aiming for maximum crop production (Foong et al., 2020). Concurrently, the use of agrochemicals influences biodiversity and soil fertility, biochemistry, agricultural sustainability, food safety and nutritional security, among others. However, excessive use of pesticides not only produces environmental pollution, but over time, their drastic chemical substances can cause diseases in humans and livestock (Sharma et al., 2010; Fu et al., 2022). Additionally, they kill beneficial microbes and reduce nutrient availability, which are essential elements for plant growth and productivity (Meena et al., 2020).

Thus, the plant microbiome contributes to the basic functions of microbial ecosystem services in agriculture, plant production and performance, nutrition, improved quality of

the soil, and tolerance to (a)biotic stresses (**Figure 1**; Quiza et al., 2015; Vandenkoornhuyse et al., 2015; Enebe and Babalola, 2018; Ojuederie et al., 2019). The plant microbiome supports plants through the mechanisms of regulating hormones, specific antagonistic metabolite (rhizobitoxine) production that induces resistance against drastic pathogens, suppression of soil-borne disease, antibiosis, and competition for nutrients in the rhizosphere (Choudhary et al., 2007; Penton et al., 2014; Reitz et al., 2015; Zhang et al., 2019; Rodríguez et al., 2020).

Therefore, plant microbiome engineering is an alternative but an untapped strategy that can be exploited for plant health, growth, and productivity under extreme conditions. Recently, a number of accessible approaches have been proposed for plant microbiome engineering (**Figure 2**; Arif et al., 2020; Kumar and Dubey, 2020). An interesting avenue is to harness variations in exudation patterns to enhance the beneficial rhizosphere microbiome (Quiza et al., 2015). The microbiome can be engineered by traditionally amending soil with (in)organic supplementation and agricultural practices to promote microbial diversity, functions and interactions with the targeted host (**Figure 2**; Sankar Ganesh et al., 2017; Saeid and Chojnacka, 2019). Therefore, the living components of the rhizosphere can be engineered to promote plant health and growth, two features that strongly depend upon the interactions of living organisms with their environment (Dessaux et al., 2016). Thus, aiming at viable agronomic production, several innovative tools could play a central role by improving microbial bioengineering that is beneficial to replace lethal agrochemical substances.

Engineering the plant microbiome for green agricultural production

In addition to protection, plant microbiomes provide key benefits regarding better health, with improved growth and production and plant environmental adaptation (Haney et al., 2015; Berg et al., 2016). Most microorganisms are found in such a biome that they tend to cause physiological alterations and allow plants to survive detrimental invasions (Dubey et al., 2019; Santoyo et al., 2021). Within the microbiome, these microbes are clustered on the surface and tissues of the host plants. The bimodal association thereby allows nutrient acquisition, promoting the growth and resilience of the host against environmental stressors (van der Heijden and Hartmann, 2016; Cordovez et al., 2019).

The traits displayed by the microbiome community are of high relevance to plant health, yet they are influenced by microbial diversity, unwanted conditions and even host plant species (Jain et al., 2020). The entire microbiome is not involved in corresponding functions; however, they are performed by unique microbial species because of synergistic effects between two or more strains (Rojas-Solís et al., 2018). The manipulation of the bacterial microbiome and the production of bioinoculants have enabled scientists to control and properly monitor plant health and production (Adesemoye et al., 2009).

In this regard, several strategies, including soil amendment, artificial microbial consortia and host-dependent microbiome engineering, have been proposed that could strengthen stress tolerance, disease resistance and nutrient acquisition in host plants (**Figure 2**) A traditional method of soil engineering or amendments is adding (in)organic substances directly to soil or using alternative agricultural tools. Any of these sources guide farmers to manipulate plant–microbiome interactions to increase crop production (Wang et al., 2015; Sankar Ganesh et al., 2017).

Conforming reported data, a host-mediated microbiome engineering approach is a host-based indirect selection of proper microbes and leveraging out those that are influential to the microbiome in context (Mueller and Sachs, 2015). In addition, an "artificial microbial consortium (AMC)" has also been used in microbiome engineering.

A recent example of biostimulant consortium application in phytomicrobiome for enhancement productivity of chickpea and soil health was conducted by Mukherjee et al. (2022). These experiments were carried out in two different locations like Banaras Hindu University Varanasi, and Sarai Dangri village, Uttar Pradesh, India. Microbial strains BHUJPCS-15 and BHUJPVCRS-1 were isolated from chickpea seed and chickpea rhizosphere soil respectively. This study depicts that consortium significantly increased yield NPK, microbial counts and soil enzymes. Interestingly, the results showed that microbiome manipulation via potential biostimulant consortium directly influenced the yields and soil health. Recently Glick and Gamalero (2021) explored in their article that mostly plant attract and beneficial microbes. This study further highlighted that bacterial consortia assist plants in various ways such as promoting plant growth and providing protection to hosts from a wide range of direct and indirect environmental stresses. This study also suggests that the microbiome could be engineered by engineering plant seeds to contain desired bacterial strains. It is unquestioned that Phytomicrobiome is an untapped source which might be potentially resolved the current and future challenges of sustainable agriculture and food security. But at the same time biotic and abiotic constraints substantially imbalance the functionality of phytomicrobiome and we are unable to overlook them (Chouhan et al., 2021). This study also recommends and shaded light on the potential of Culturable PGPR and endophytes that could be harnessed for resilient microbiome engineering.

However, in this functional consortium, an established complex interactive network of different microbes in the rhizosphere environment has been essential (Kumar et al., 2018). Other than the rhizosphere, microbes can also be found in the root part that permits only useful

microbes to access plants as endophytes (Rojas-Solís et al., 2018). As a key benefit, AMC via microbiome engineering can be used to modify the respective phytomicrobiome. An ideal AMC fabrication is based on a systematic method that can contain a series of crucial steps. Similarly, active microbe selection and regulation of their mutual interactions, excavation along the culturing core microbiota to evaluate consortium efficacy (Kong et al., 2018), are major parts of the process utilized in AMC production (**Figure 2**).

Additionally, genotype-dependent host microbiome engineering has been harnessed for microbiome engineering to enhance host functions and induce resistance in diverse environments. The genetic bases of plants are fundamental for the shaping and functioning of microcosms (Arif et al., 2020), such as *Pseudomonas simiae* WCS417r, for improved biomass production in Arabidopsis (Wintermans et al., 2016). This indicates a genetic relation of Arabidopsis loci (controlling plant defense and cell wall integrity) with phyllospheric bacteria (Horton et al., 2014). It has also been proven that plants can expel bacterial species into the rhizosphere, but the mechanisms by which useful or harmful microbes exchange with related holobionts are unknown.

Improving plant growth-promoting mechanisms

The microbiome is composed of several different types of organisms, including bacteria, fungi, protozoa, archaea, and viruses (Mueller and Sachs, 2015). This array of microbial communities plays a pivotal role in the functioning of plants by influencing their physiology and development (Mendes et al., 2013). Plant microbiomes can play a beneficial role, protecting the plant from potential pathogens, improving plant growth and fitness and inducing tolerance to abiotic stresses (Haney et al., 2015; Berg et al., 2016).

Unsurprisingly, the rhizosphere microbiome also inherits soil-borne plant pathogens that colonize plant roots and successfully hack plant innate immunity by breaking the preventive microbial shield of beneficial microbes and causing disease (Mendes et al., 2013). However, it has been proven in various studies that plants secrete small molecules for the recruitment of actively beneficial microflora to assist their conformation under extreme conditions (Busby et al., 2014). It is well known that plants and associated microbes establish symbiotic relationships that facilitate nutrient acquisition and induce resistance in unfavorable environments. However, the plant unable to distinguish beneficial microbes and restrict the formation of pathogenic associations is still unknown (Zipfel and Oldroyd, 2017).

It is well documented that the interactions between plants and their microbiomes are mediated by metabolic signaling. Plant release 20–35% photosynthetic carbon into the rhizosphere in the form of metabolites that recruit beneficial microbes (**Figure 1**). These microbes symbiotically associate with host plants and underpin them under adverse conditions (Arif et al., 2020; Trivedi et al., 2020). However, concomitantly, the rhizosphere is also a playground and battlefield for soil-borne pathogens that establish parasitic relationships with host plants. Moreover, the diversity and population ratio of plant pathogens and beneficial microorganisms are linked to the amount and quality of plant root exudates and microbial interactions in the rhizosphere (Somers et al., 2004; Raaijmakers et al., 2009). For example, the model plant *Sorghum bicolor* secretes specific metabolites, which facilitates bacterial ATP-binding cassette transporter gene expression and, in turn, modifies the root-associated microbiome composition by promoting the abundance and activity of monoderm bacteria, which has a positive impact on the growth and development of *Sorghum bicolor* plants facing drought stress (Xu et al., 2018b). This is a potential blueprint for developing SynComs from such plant-associated microbiomes to increase crop productivity in arid areas with low precipitation and poor irrigation systems. Understanding the substantial role of metabolites and biotechnological approaches might help to unravel the mechanisms underlying beneficial microbe recruitment for microbiome engineering.

Enhancing phytoremediation activities

Phytoremediation is an environmentally friendly, solar-powered and cost-effective soil remediation technology. Based on plant ability, this technology has to do with the already existing contamination in the system biome, where it intercepts, takes up, accumulates and translocates contaminants (Pilon-Smits, 2005). The efficiency of phytoremediation depends on plants (Vangronsveld et al., 2009), contaminant concentration, soil pH, nutrients and oxidoreduction (Sessitsch et al., 2013) as well as those microorganisms that are associated with soil and plants, respectively. Phytoremediation, instead of a better technology, has often been observed with non-uniform results at the field scale, slow and incomplete degradation, and long clean-up processes (Vangronsveld et al., 2009; Stephenson and Black, 2014). To date, the improvement in soil, contaminant availability and accessibility (de La Torre-Roche et al., 2012), plant growth (Sessitsch et al., 2013), and exploration for the exploitation of soil and plant-associated organisms in phytoremediation (Barac et al., 2004; Abhilash et al., 2012) have been main topics of interest. In recent decades, many approaches have been focused on individual organisms rather than on integrated meta-organisms, while in such regards, the potential impact has been limited. Improved phytoremediation necessitates a central understanding of plant–microbe interactions, and responses to pollutants can be of high relevance. In line, the comprehension of how the

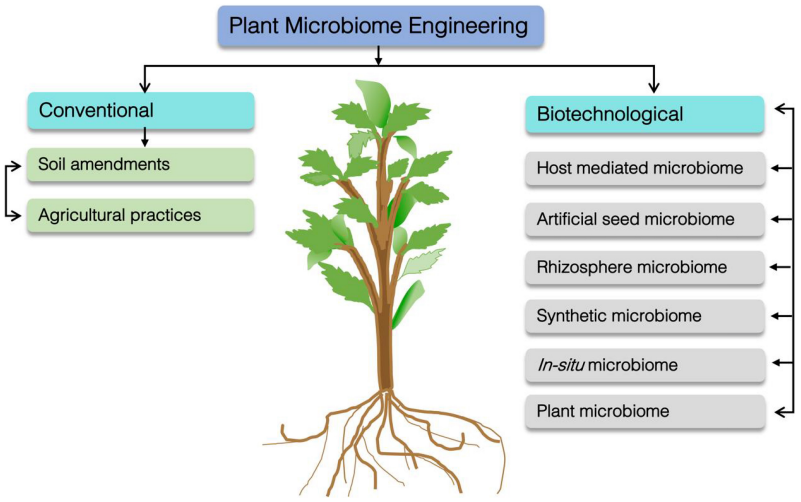


FIGURE 2
Plant microbiome engineering via biotechnological and conventional approaches. Host-mediated microbiome (indirectly selection of microbiome through utilization of host phenotype), artificial seed microbiome (artificial selection of microbiome and its integration/inoculation with seeds. This establish microbiome may evolve during the development and germination that consequently impact plant microbiome structure and function), Rhizosphere microbiome (bacterial competitiveness engineering) Synthetic microbiome (genetically engineered microbes inoculation to host plant) *In situ* microbiome (manipulation of native microbial community in their native context) Plant mycobiome (optimization and improvement of beneficial plant–fungal interactions).

host combines the beneficial microbiome and its function under contaminant stress is unavoidable. Molecular data and ecological models in this regard have clarified the assemblage of fewer insects (Scheuring and Yu, 2012), respectively.

Beyond plants and related microorganisms, the metaorganism has shown successful improvement in agriculture practices (Mendes et al., 2013; Berg et al., 2014) and disease mitigation (Berendsen et al., 2012) and has uncovered mutual interactions between plants and unlimited degradative microbial taxa. It has been declared that the plant microbiome can be helpful in extending the functional potential of targeted hosts. Therefore, such a microbiome enables regulation of the expression of traits in plants, thus strengthening physiological state and tolerance (Mendes et al., 2013). However, it can be emphasized that the phytoremediation is microbiome dependent. Moreover, it is accepted that hosts assemble non-random sets of microbial symbionts with a higher proportion of beneficial microbes than expected. With respect to polluted soil, a host plant is free to choose microbes with degradative genes within a pool of candidates in bulk soil (Siciliano et al., 2001), but a full understanding of how hosts carry the process is lacking. Expressively, hosts can be found with a mutualistic symbiosis of PGPR and mycorrhizal fungi. Within this symbiotic association, plants provide root exudates and produce a microbial habitat, while PGPR degradative bacteria and mycorrhiza sponsor plant growth and detoxify the environment. In the presence of contamination, the rhizosphere and root microbial communities are strongly damaged (Siciliano et al., 2001).

Ameliorating plant stress

The plant microbiome presents a complex interrelationship among many environmental factors and bacterial communities. In particular, under open field conditions, the possible bias in laboratory experiments is emphasized due to the lack of variability in environmental changes. Extreme environmental stresses, mainly climatic changes, can influence microbial communities. The soil microbiome can be affected by these stresses directly from drought-, salt- or heat-tolerant taxa (Martiny et al., 2017; Naylor et al., 2017) and indirectly by altering soil chemistry or diffusion rates (Liptzin et al., 2011).

The impact of salinity can be alleviated by the implementation of halo-tolerant synthetic microbiomes in saline soil systems. As the majority of microbes are halo-sensitive, some halophytic plant-associated members are halotolerant and can be considered potential targets for developing synthetic microbiomes. It has been demonstrated that inoculated halotolerant rhizobacteria improve the native microbial community's resilience to salinity stress and, as a result, can improve plant growth and stability in saline states (Bharti et al., 2015; Ali et al., 2022c). An engineered microbiome approach is recommended for use in areas with saline water irrigation systems.

Drought is among the worst obstacles to agricultural productivity. Plant stress tolerance must be improved to allow acceptable crop production in limited resources of water under drought situations (Liu et al., 2019; Salam et al., 2022). Drought stress tolerance in plants based on root-associated bacteria

has also been reported. In addition, molecular compositions (such as root exudates) have shown promising potential in the relevant scenario of plant microbiome perturbations. Studies have better explored an example of the biosynthetic salicylic acid in *A. thaliana* that collects a normal root microbiome (Lundberg et al., 2012). This study has shown that central regulators in the immune system of plants have an impact on root microbiome composition. Moreover, such regulators can be adapted to amend the microbial community, which, in addition to improved productivity, can increase resilience against unwanted stressors. Most studies on the plant microbiome have considered model plants, particularly *A. thaliana*. All information attained could be extrapolated to other plant communities. Therefore, more effort should be directed to microbiome engineering to enhance crop characteristics, such as tolerance against drought and diseases, thus allowing sustainable agricultural production (Dola et al., 2022). However, this technology has recently demonstrated its potential for the root microbiome of *S. bicolor*, for which drought conditions have caused the enrichment of a set of root microbes. Drought-based induced upgradation with metabolic shift was observed for the plants and microbes, revealing it to be a potential blueprint in handling the microbiome to strengthen crop fitness and upsurge production (Xu et al., 2018a).

Stimulating antagonistic and biocontrol activities

Plant diseases are the cause of major economic losses for farmers worldwide. The FAO estimated that pests and diseases are responsible for approximately 25% of crop loss (Dean et al., 2005). There are regional differences reported: it is estimated that diseases typically reduce crop yields by 10% every year in more developed countries, but yield loss due to diseases often exceeds 20% in less developed areas. To avoid crop losses due to maladies, chemical pesticides are routinely applied on crops, with the main goal of eradicating or lessening the disease invasion, infection, or severity (McMichael et al., 2007). However, it is becoming increasingly clear that long-term chemical pesticide usage poses several adverse effects on the environment and human health (Rani et al., 2021).

Plants harbor a diverse array of microbes in the rhizosphere that establish beneficial relationships with their hosts, guarding from plant pathogens and influencing their health and fitness through direct and indirect mechanisms. Competition, hyperparasitism, antibiosis, production of extracellular enzymes, and induction of resistance are well documented mechanisms (**Figure 1**; Raymaekers et al., 2020). All these beneficial microbes associated with the roots of crop plants exert beneficial effects on their hosts and are referred to as plant growth-promoting biocontrol agents. Various studies have proven that plants secrete small molecules for the recruitment of actively beneficial microflora to assist their conformation under extreme conditions (Busby et al., 2014). This array of microbes possesses various biological control traits, such as competition for food space and colonization (Hunziker et al., 2015; Lloyd and Allen, 2015; Santhanam et al., 2015), antibiosis (Gómez Expósito et al., 2017), hyperparasitism (McNeely et al., 2017) and the production of degradative enzymes. In addition, these microorganisms associated with plants form a mutual association that impacts the host plant-associated microbiome and hosts an innumerable wealth of bacterial taxa, many of which promote tolerance to abiotic and biotic stresses and plant growth, suppress plant diseases, degrade xenobiotic compounds, and positively affect yields (Berg et al., 2016). This immense microbial diversity can be a target of manipulation by employing artificial microbial consortia, providing new synergistic opportunities for enhancing disease management (Poudel et al., 2016).

Current challenges

Difficulties in isolating and characterizing microbiomes

Firmicutes, Bacteroidetes, Proteobacteria, and Actinobacteria are the major rhizobacterial phyla that are compliant with cultivation. Several studies have been conducted for their isolation, genome sequencing and characterization of their phenotypes (Bai et al., 2015; Mauchline et al., 2015; Levy et al., 2018). Experiments are performed in laboratories mimicking their natural interaction with plants to find the key features of plant–microbe relations. These studies enable scientists to understand the microbial recruitment behavior in the rhizosphere as microorganisms take part in the growth and tolerance of the plant (Bai et al., 2015; Niu et al., 2017). Isolation makes the assembly and sequencing of individual genomes simpler. Moreover, it provides more resolved data compared to assembling metagenomes. Furthermore, the isolation step also confirmed the presence of isolates in the rhizospheric community and their interaction with the host plant (Levy et al., 2018). After isolation, strains can be easily detected for key enzymes and molecular mechanisms involved, e.g., the proteomic or transcriptomic response of a single fungus or bacterium to nutrient stress or the plant microbiome enlightens the plant growth promoting (PGP) potential of microorganisms. This helps discover novel traits of the microorganisms related to their PGP activities (Bruto et al., 2014; Lidbury et al., 2016). The phenotypes embarked with the plants for PGP traits are not revealed by *in vitro* screening methods. In this regard, fast and large-scale screening can be performed by genome sequencing, which also encourages the discovery of novel PGP traits or genes (Finkel et al., 2017). The knowledge of interactions between plants and microorganisms and the role of PGP traits

or genes in enabling these interactions can be improved by combining these strategies with complementary molecular approaches, i.e., bioreporter and mutagenic expression systems (Wetmore et al., 2015).

Efforts to assign functions to microbes

The task of assigning a specific function to an individual microbiome or a group of microbiomes is often challenging, as a completely different lifestyle is evident in species of even a particular genus. It varies from mutualist to pathogen and vice versa depending upon the transfer of functional genes between distantly related species or the environmental conditions (Qiu et al., 2009; Hacquard et al., 2016). The desired traits, such as phosphate mobilization in microbial phenotypes, are altered by this changeability (Lidbury et al., 2016). Therefore, there is a need to find more sensitive methods for the characterization of bacterial species beyond the genus level, and large-scale throughput methods are required for better functional characterization of each species (Schlaeppi and Bulgarelli, 2015). Advancement in technology, combined with modeling/computational techniques, can be very auspicious. For example, a combination of metagenomics products with the environment i.e., the adaptation of metagenomics to metaphenomics takes into account all the parameters that may sway the plant–microbiome interaction within a community or environment (Jansson and Hofmockel, 2018). This transition makes metagenomics more powerful and widens its functional capabilities, such as carbohydrate utilization or secondary metabolite production (Bulgarelli et al., 2015). Moreover, these new advancements also enable researchers to gain more specific insights into the specific taxa responsible for imparting key functional characteristics. Ready-to-use commercial kits facilitate DNA extraction from a sample easily (Prosser, 2015).

In soils, most of the microbial biomass (>90%) is dormant or inactive (Fierer, 2017), but in the rhizosphere, this number drops significantly as most of the microorganisms are made metabolically active in these habitats by plant-mediated factors (Bulgarelli et al., 2013). Microorganisms from these niches have been isolated, and their RNA is extracted to identify the mechanisms involved in inducing responses to microbial or plant stimuli (Yergeau et al., 2014). Similarly, 13C-labeled CO_2 enrichment is combined with metatranscriptomics to study the response of microorganisms to plant exudates released in the rhizosphere and to better understand the plant-microbiome relation (Haichar et al., 2016). Exoproteins are more stable in the environment than RNA, which has short turnover times, reducing the robustness and simplicity of sampling efficiency and making sampling more prone to errors (Prosser, 2015). Metaproteomics also enables an intriguing possibility of studying metabolic activities, as it gives the profiles of expressed proteins (Heyer et al., 2015). The ecologically important proteins for nutrient uptake and microbial–host and microbial–microbial relationships (e.g., transporter systems and extracellular hydrolytic enzymes) are enriched by exometaproteomics or exoproteomics (Lidbury et al., 2016). However, the need for enough starting material (up to 100 g of soil) (Johnson-Rollings et al., 2014), accurate peptide profiles, and adequate computational power limit the applications of metaproteomics (Muth et al., 2016). These might be the reasons that restrict the use of meta(exo)proteomics in rhizosphere research.

Omics approaches to unveil plant-associated microbiota

Recently, the advent of omics tools, gene-editing techniques, and sequencing technology has allowed us to unravel the entangled webs of plant-microbes interactions, enhancing plant fitness and tolerance to biotic and abiotic challenges. Genomics is an effective tool for studying and predicting the interactions of microbes and plants and developing pathogen stress tolerance in plants (Frantzeskakis et al., 2020).

High genetic variability in the soil microbiome can be confirmed by multiple sequencing methodologies, such as prokaryotic16S, fungal ITS (internal transcribed spacer regions), and/or metagenomic analysis. Describing who is associated with the plant is relevant to unveiling their functions, so these microorganisms can become the extended genome partner of the host (Berendsen et al., 2012). More reports on genome engineering, gene editing, and advanced plant–microbe interaction technologies have been discussed (Frantzeskakis et al., 2019; Sharma et al., 2020). The microbiome composition can be altered by environmental factors such as soil conditions and temperature. However, plant biochemistry and the immune system also play key roles in determining the variability of the microbiome (Turner et al., 2013). Although plants bring beneficial microorganisms, such as PGPR and disease-suppressing microorganisms, it has been evident that they can also bring phytopathogens as well as human pathogenic bacteria. These harmful bacteria may enter the food chain, can cause plant disease, and can alter the entire microbiome composition (Gorshkov et al., 2020). Therefore, tools such as metagenomics, for example, offer a promising strategy to diagnose these phytopathogens (Chiu and Miller, 2019). Currently, nanopore sequencing using Oxford Nanopore Technologies (ONT) is the most encouraging technology for the identification of pathogens by metagenome sequencing (Jain et al., 2016). It is fast and is a direct sequencing method requiring no amplification step. It can be used even if we lack any prior knowledge of pathogens, as it can directly detect and identify all pathogens except RNA viruses. Moreover, it can also reconstruct the functional pathways in the microbiome and can foresee its composition. A high error rate limits the use of ONT (Rang et al., 2018).

Therefore, it can be combined with Illumina technologies to enhance the sequence assembly quality (Sevim et al., 2019). MinON^{TM} has already been used for metagenomics sequencing of bacterial, fungal and viral pathogens on several crops (Jongman et al., 2020; Mechan Llontop et al., 2020). Low sequencing cost and high quality suggest that direct sequencing is likely to be the future of metagenomics (Ciuffreda et al., 2021). An increasing number of propositions are becoming feasible because of the expanding information in metagenomics. It was first proposed that the initial molecular assessment of the soil and soil microbiome could help in the improvement of agricultural treatments (Schlaeppi and Bulgarelli, 2015). Conversely, the complimentary response of the host toward beneficial microbes should also be a part of the engineering program because the host is also involved in bringing the interaction. It would enable the plant cultivars to interact efficaciously with natural as well as acquired microorganisms (Bulgarelli et al., 2013). The drawback of genomic analysis is that it does not provide knowledge about the functional states of biological objects; therefore, a metagenomics approach can be used in combination with a transcriptomic approach to evaluate key traits in plant-microbiome interactions.

Next Generation Sequencing (NGS)-based transcriptomics is another approach used to unravel the molecular mechanisms involved in plant–microbiome interactions. It is usually applied in plant pathology and stress studies. It reveals the physiological response of plants to pathogens and characterizes the signaling events taking place in the rhizosphere. Although we can predict community function from multi-omics data alone to some extent, validation of interactions requires the complementary work with cultured isolates that can be interrogated in the laboratory (Terekhov et al., 2018; Kehe et al., 2019). For example, the resistance of barley to *Blumeria graminis* by the gene network has been uncovered by NGS (Li et al., 2020). It also revealed the underlying mechanism of resistance against *Pectobacterium atrosepticum* (Tsers et al., 2020). Moreover, the characteristic interactions between Phytophthora infestans and potato plants have been revealed by gene expression patterns or NGS (Duan et al., 2020). NGS can also be used to study plant interactions with non-infectious microbes and plant responses to abiotic stresses. For example, the tolerance of tomato to hypoxia (Safavi-Rizi et al., 2020), changes in the gene expression pattern of orchard grass due to short-term flooding (Qiao et al., 2020), and gene expression changes in Arabidopsis because of high ultraviolet stress (Huang et al., 2019) have been revealed by NGS. However, the vast data profiles generated by NGS are too enormous to be efficaciously translated into simple language. This makes the interpretation of NGS transcriptomic data difficult for higher plants (Murat et al., 2012). Moreover, in most cases, the expression level is not restricted to a single gene (Das et al., 2020). Therefore, the focus of transcriptomic studies has shifted from the individual gene level to the gene set level. Significant impact of anthropogenic activities on the plant microbiome.

Over the past few decades, industrialization and urbanization have caused an increase in carbon dioxide and temperature, which affect the climate globally. These changes cause erratic events worldwide, such as a decrease in moisture level, an increase in temperature, excessive greenhouse gas emissions, and an increase in snowfall and rainfall. Climate change, range shift and urbanization are key factors that affect plant microbial interactions in the rhizosphere (**Figure 3**). Soil microbial community determines the soil, and plant health and prerequisite for external constraints. Soil microbial ecosystem functions and diversity are significantly influenced by anthropogenic activities These activities produce a diverse array of hazardous substances including pesticides, heavy metals (Ma et al., 2022a) and organic pollutants and put tremendous pressure on soil microbiomes. Heavy metals notoriously imbalance the microbial population, diversity and seriously decline their activities (Abdu et al., 2017; Fajardo et al., 2019; Li et al., 2020).

Climate change

Abrupt changes in climate and weather patterns have become a global dilemma among researchers and farmers (Amna et al., 2021; Wahab et al., 2022). Anthropogenic activities such as global warming, deforestation, the greenhouse effect, and urbanization have made these climate changes inevitable. Excessive fertilizer and pesticide use, livestock farming, nitrous oxide emissions, and fossil fuel combustion are the other contributors to climate change. The development of plants is affected by different climatic factors, such as CO_2 levels in the atmosphere, temperature (Saeed et al., 2022), drought (Wahab et al., 2022), salinity (Mehmood et al., 2021a; Hussain et al., 2022), heavy metals (Ma et al., 2022b; Nawaz et al., 2022), and rainfall patterns. However, the impact of climate change on the variety of microfauna is also worthy of attention because microorganisms are also influenced by these changes as they perform carbon and nutrient cycling. Abrupt changes in climate can disrupt the microbial population above and below ground and can have a negative impact on plant development. For example, global warming affects microbial respiration and therefore directly alters the microbial composition (Classen et al., 2015). Temperature plays a key role in defining the microbial community of plants and is also decisive in plant phenological characteristics and development (Kashyap et al., 2017). In the past few decades, emissions of greenhouse gases (CO_2, CH_4, water vapor, etc.) due to rapid urbanization and industrialization has elevated the temperature. According to Compant et al. (2010), the average temperature is expected to rise by 1.8–3.6°C by 2100, which would lead to water scarcity and droughts (Farooq et al., 2022). Several studies have

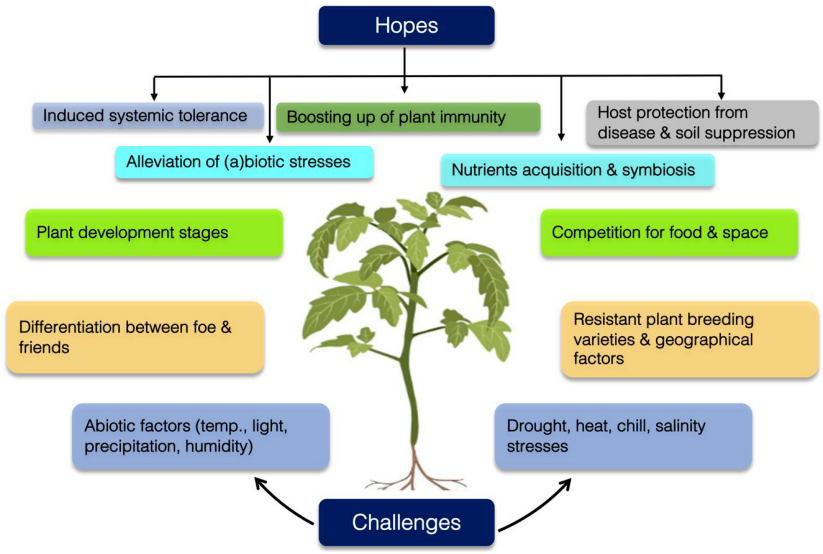


FIGURE 3
Plant Microbiome provides key functions for plant health and its protection. Plant microbiome offers vital services for plant health. It facilitates biogeochemical cycling of plant nutrients, assist plant growth under biotic and abiotic conditions, induces systemic acquired resistance (SAR) and induces systemic resistance (ISR) in plant against plant pathogen. Inversely, Plant microbiome synchronously encounters biotic and abiotic stresses which are the substantial drivers that influence or alter microbiome diversity and functionality.

been performed to describe the effects of elevated temperature on plant morphology (Chen et al., 2021). Similarly, elevated temperature also influences the activities and composition of microorganisms in the rhizosphere. An increase in temperature increases the growth rate of microorganisms with altered respiration (**Figure 3**; Classen et al., 2015). Karhu et al. (2014) reported an exponential increase in soil respiration with increasing temperature. Additionally, organic matter utilization by microorganisms is also dependent on temperature (Frey et al., 2013). Temperature alterations are also correlated with the pathogenicity of microbes. Increased temperature increases the growth of *Glomus mossae* and *Glomus intraradices* (Monz et al., 1994). Disease incidences in plants by certain seed-borne microbes that degrade cell walls and *Pectobacterium atrosepticum* causing soft rot can be increased by an increase in temperature (Hasegawa et al., 2005). Drought conditions pose a threat to plant carbohydrate exchange and nutrient uptake in the rhizosphere by AFM (Newsham et al., 1995). In mountainous soil, the warming effect is amplified when heat waves combined with elevated temperature increase the C and N cycling of microorganisms (Donhauser et al., 2021). However, other factors, such as UV radiation and moisture, also affect microbial communities. AFM cannot colonize plants under drought conditions (Staddon et al., 2004). The bacterial population is also reduced in the rhizosphere of sorghum roots under drought conditions (Xu et al., 2018c).

The allocation of carbon in the rhizosphere is regulated by atmospheric carbon dioxide. Therefore, atmospheric CO_2 regulates the root exudate composition in soil, which defines the microbial community in the rhizosphere (Williams et al., 2018). Microorganisms are the key factors in the net exchange of carbon in soil. They perform this function in various ways by altering the nutrient status of the soil, forming symbiotic or pathogenic interactions with plants, respiration and organic matter decomposition. Therefore, high levels of CO_2 can alter the microbial population directly or indirectly by altering plant physiology and metabolism. Elevated CO_2 levels alter the root exudate composition and nutrient availability in soil (Compant et al., 2010). Some fungi have the potential to assimilate more carbon than bacteria; therefore, they can store carbon than mobilization. Thus, the microbial population in soil is stimulated by excessive emission of carbon by roots. This microbial propagation eventually reduces nitrogen availability for plants because of nitrogen immobilization in the soil. Soil respiration is also increased by elevated CO_2 levels. Microorganisms respond differently to elevated CO_2 levels in soil. No significant effect was observed by Gavito et al. (2000) in AMF of *Pisum sativum* with an increase of 700 ppm of CO_2, while only with an increase of 7 ppm CO_2 was an increase in mycorrhizal colonization observed by Tang et al. (2009) in Barnyard grass. The 18S RNA sequencing-based Illumina MiSeq technique revealed a significant decrease in the populations of Glomus and Claroideoglomus species after long-term CO_2 (550 ppm) exposure in paddy fields (Panneerselvam et al., 2020). In *Pinus strobus* and *Boswellia papyrifera* plants, an increase in CO_2 (700 ppm) concentration increased the ectomycorrhizal fungi (ECM) population (Godbold and Berntson, 1997). Similarly, a threefold increase in ECM

mycelia was observed in *P. sylvestris* with an increase in CO_2 concentration (Fransson et al., 2005). PGPB are also influenced by the CO_2 concentrations in the soil. Several studies have been performed to observe the effect of CO_2 elevation on plant microbe interactions (Thakur et al., 2019; Yu and Chen, 2019; Prescott et al., 2020; Terrer et al., 2021). A threefold increase in *R. leguminosarum* was observed by Schortemeyer in the rhizosphere of white clover by an increase in CO_2 (600 ppm) concentration (Schortemeyer et al., 1996). In addition, more efforts are required to understand the behavior of plant–microbial interactions under elevated CO_2 levels to engineer the desired beneficial microorganisms for plant development.

Range shifts

Human activities have introduced new species to the new habitats (Essl et al., 2011) and have caused environmental warming that expands the potential survival capabilities of these species in the habitats where they could never survive before or have contracted their habitat (Walther et al., 2009). These two reasons have triggered the shifting ranges. Plant–microbial interactions have gone through unforeseen impacts because of these range shifts. The elevation gradient provides a practical system to evaluate the effect of abiotic and biotic factors on plant–microbe interactions, microbial composition and distribution. Cobian et al. (2019) revealed that a parabolic relationship was followed by leaf fungal endophyte specialization, where specialization was maximum at the center of tree species ranges and reduced toward edges. Balsam poplars' fungal community has higher diversity when relocated to the upper edges of the elevation gradient because they experience higher abiotic stresses (Bálint et al., 2015). Compared to fungi, leaf bacterial communities are less affected by changes in elevation gradients because fungi are more sensitive to temperature changes (Vacher et al., 2016). Along the elevation gradient, plant community dynamics also face a turn from competition to facilitation. However, a vast majority of research is required to study the positive and negative effects of elevation gradient shifts on plant-microbial interactions. Plant–soil feedback (PSF) is a mechanism by which plants influence abiotic and biotic factors in soil, and feedbacks influence their development and growth (van der Putten et al., 2016). PSF and microorganisms negatively affect native species (Bever, 2003). Previously established communities of microorganisms are reestablished by the novel soil biota through species range expansion, e.g., negative interactions develop between the soil biota and *Centaurea maculosa* in native ranges, while in North America, they develop positive interactions with microorganisms in soil (Callaway et al., 2004). The survival of non-native species in novel environments is favored by the dearth of natural enemies. A significant reduction in foliar and floral pathogens has been evident in invasive plants (Ramirez et al., 2019). In comparison, seed germination of *Acer saccharum was* reduced in soil beyond its native range limits even though the abiotic conditions were sufficient (Carteron et al., 2020). A variety of microbial interactions can influence species range shifts; however, thorough research is needed in this sector to evaluate the contrasting roles of microorganisms in driving plant range shifts.

Urbanization

Urbanization has been a source of various airborne pollutants. The use of chemicals and micro- and macronutrients influences local vegetation, eventually altering plant-microbial interactions (Annamalai and Namasivayam, 2015). Moreover, these anthropogenic activities also have the impact of the microbial population, which has the potential to remediate air pollution. The phyllosphere communities of bacteria and fungi are distinct in rural and urban trees (Smets et al., 2016; Laforest-Lapointe et al., 2017). A 10% increase in alpha-bacteria was observed by Laforest-Lapointe et al. (2017) and Imperato et al. (2019) in urban tree leaves. Espenshade et al. (2019) also observed the impact of traffic patterns and urban density on the bacterial composition of tree leaves, which was associated with black carbon and ultrafine particulate matter. A lower diversity of fungi was observed on urban trees by Jumpponen and Jones (2010). However, a higher fungal load was observed by Imperato et al. (2019). Moreover, traffic levels also influenced the phyllosphere community of bacteria (Smets et al., 2016). These findings enable the need to better understand the elements that bring changes in the phyllosphere of urban trees and to check the varying changes that take place within microbial functions.

Recent investigations have started to generate a link between the impact of urbanization on the genetic and functional changes of the phyllosphere microbiota. For instance, a higher number of bacteria was observed in urban trees. These bacteria have genes encoding enzymes for aromatic degradation that impart PGP traits to plants (Imperato et al., 2019). Additionally, it has also been observed that hydrocarbon-degrading bacteria are selected by plants when hydrocarbon levels increase in the atmosphere (Gandolfi et al., 2017). This phenomenon is termed phytoremediation, and plant-microbial interactions play a pivotal role in efficacious phytoremediation. Endophytes can remediate soil and water contaminants and promote the growth of plants (Siciliano et al., 2001; Mukhtar et al., 2018). Soil contaminants increase the prevalence of catabolic genes in endophytes, and this phenomenon can be artificially introduced in bacteria. The introduction of toluene-degrading genes in endophytic bacteria can enhance toluene degradation in soil, thus reducing phytotoxicity and toluene evapotranspiration through the leaves by up to 70% (Barac et al., 2004). A number of

studies have been performed to evaluate the contaminant-degrading capabilities of bacteria (Hong et al., 2018; Undugoda et al., 2018; Ben-Israel, 2020). However, the true potential of microorganisms and plants in degrading air and soil pollutants has yet to be discovered. In addition, these findings suggest that we need to determine the influence of urbanization on plant-microbial interactions if we want to engineer the microbiome of plants.

Conclusion

Chemical fertilizers and pesticides have been used for a long time among agricultural platforms. The goal of using such sources is to attain better crop production as per the demand of the growing human population. Excessive implementation of these chemical means may not be an acceptable choice for sustainable ecosystems. In such a way, this review, in addition to unveiling the complexities of the plant-microbiome interactions, as well as the wide possibilities to manipulate them under stressful conditions, has unraveled vital factors that are relevant to generate sustainable agriculture. Therefore, the engineering of the microbiome is a highly fundamental approach dedicated to the betterment of the health, growth and functions of plants. Studies aiming to grasp this interplay at the community level can enhance the understanding of factors that control the microbiome assemblage with its relevant feedback to a host plant. Such goals are obtainable with the support of modern tools such as "omics," yet combining such an innovative approach with additional efforts in rhizosphere microbiome engineering can interestingly provide new insights. Similarly, an optimized phytomicrobiome meta-organism may result in a sustainable ecosystem with better agricultural production and can similarly diminish greenhouse gas emissions and soil pollution. As the microbes in the rhizosphere are scarcely investigated, further efforts are required to monitor and engineer the arrangement and activities of this microbiome. A large body of research covered the various aspects of phytomicrobiome engineering. In the last decade, massive progress has been made in plant microbiome studies but some gaps are still needed to address and fulfilled. Understanding the importance of the plant microbiome, (1) the influence of secondary metabolites of microorganisms on beneficial microbes of the plant microbiome, (2) The alteration of continuous environmental condition and their impact on the host and its associated microbial communities, (3) to investigate the ability of host plant to refrain pathogenic microbes, (4) the integration of agronomic practices with synthetic biology and their optimization and compatibility to each other.

As per demand, further elaboration can support the comprehension of the mutual association of many microbes with their host plant based on their molecular and genetic basis under any environmental constraints, which beyond can open up new avenues to advance biological and ecological practices. Future studies are directed to explore the identified gaps and, based on current knowledge, should mainly focus on classifying those biotic and abiotic factors that responsibly influence the diversity, functions and association of the microbial communities with hosts in extreme habitats. Therefore, novel findings can lead us to better understand the ecological connections between plant and underground microbes.

Author contributions

MA, MJ, SA, FD, and BA: conceptualization. AS, Sumaira, RM, DA, and SS: data curation. AS, Sumaira, and RM: formal analysis. GS: funding acquisition. FD, RM, DA, and SS: software. MA, MJ, SA, FD, and BA: writing – original draft. MA, MJ, SA, FD, BA, AS, Sumaira, RM, DA, SS, and GS: writing – review and editing. All the authors have reviewed, edited, and approved the manuscript before submission.

Funding

This work was supported by CONACYT-México, Proposal: A1-S-15956, granted to GS.

Acknowledgments

We acknowledge the collaboration and assistance of all team members and the Brazilian funding agencies CNPq acknowledge the receipt of fellowship under "TWAS-CNPq Postgraduate Fellowship Programme (grant number 147998/2017-4)" for doctoral studies.

Conflict of interest

The authors declare that the research was conducted in the absence of any commercial or financial relationships that could be construed as a potential conflict of interest.

Publisher's note

All claims expressed in this article are solely those of the authors and do not necessarily represent those of their affiliated organizations, or those of the publisher, the editors and the reviewers. Any product that may be evaluated in this article, or claim that may be made by its manufacturer, is not guaranteed or endorsed by the publisher.

References

Abdu, N., Abdullahi, A. A., and Abdulkadir, A. (2017). Heavy metals and soil microbes. *Environ. Chem. Lett.* 15, 65–84. doi: 10.1007/s10311-016-0587-x

Abhilash, P. C., Powell, J. R., Singh, H. B., and Singh, B. K. (2012). Plant–microbe interactions: Novel applications for exploitation in multipurpose remediation technologies. *Trends Biotechnol.* 30, 416–420. doi: 10.1016/j.tibtech.2012.04.004

Adesemoye, A. O., Torbert, H. A., and Kloepper, J. W. (2009). Plant Growth-Promoting Rhizobacteria Allow Reduced Application Rates of Chemical Fertilizers. *Microb. Ecol.* 58, 921–929. doi: 10.1007/s00248-009-9531-y

Adnan, M., Fahad, S., Saleem, M. H., Ali, B., Mussart, M., Ullah, R., et al. (2022). Comparative efficacy of phosphorous supplements with phosphate solubilizing bacteria for optimizing wheat yield in calcareous soils. *Sci. Rep.* 12:11997. doi: 10.1038/s41598-022-16035-3

Afridi, M. S., Amna, Sumaira, Mahmood, T., Salam, A., Mukhtar, T., et al. (2019). Induction of tolerance to salinity in wheat genotypes by plant growth promoting endophytes: Involvement of ACC deaminase and antioxidant enzymes. *Plant Physiol. Biochem.* 139, 569–577. doi: 10.1016/j.plaphy.2019.03.041

Afridi, M. S., van Hamme, J. D., Bundschuh, J., Sumaira, Khan, N., and Salam, A. (2021). Biotechnological approaches in agriculture and environmental management - bacterium Kocuria rhizophila 14ASP as heavy metal and salt-tolerant plant growth- promoting strain. *Biologia* 76, 3091–3105. doi: 10.1007/s11756-021-00826-6

Ahmad, M., Ishaq, M., Shah, W. A., Adnan, M., Fahad, S., Saleem, M. H., et al. (2022). Managing phosphorus availability from organic and inorganic sources for optimum wheat production in calcareous soils. *Sustainability* 14:7669. doi: 10.3390/su14137669

Ahmad, S., Chaudhary, H. J., and Damalas, C. A. (2022). Microbial detoxification of dimethoate through mediated hydrolysis by Brucella sp. PS4: Molecular profiling and plant growth-promoting traits. *Environ. Sci. Pollut. Res.* 29, 2420–2431. doi: 10.1007/s11356-021-15806-1

Ali, J., Ali, F., Ahmad, I., Rafique, M., Munis, M. F. H., Hassan, S. W., et al. (2021). Mechanistic elucidation of germination potential and *growth of Sesbania sesban* seedlings with *Bacillus anthracis* PM21 under heavy metals stress: An in vitro study. *Ecotoxicol. Environ. Saf.* 208:111769.

Ali, B., Hafeez, A., Ahmad, S., Javed, M. A., Sumaira, and Afridi, M. S. (2022c). *Bacillus thuringiensis* PM25 Ameliorates Oxidative Damage of Salinity Stress in Maize via Regulating Growth, Leaf Pigments, Antioxidant Defense System, and Stress Responsive Gene Expression. *Front. Plant Sci.* 13:921668. doi: 10.3389/fpls.2022.921668

Ali, B., Wang, X., Saleem, M. H., Hafeez, A., Afridi, M. S., Khan, S., et al. (2022b). PGPR-mediated salt tolerance in maize by modulating plant physiology, antioxidant defense, compatible solutes accumulation and bio-surfactant producing genes. *Plants* 11:345. doi: 10.3390/plants11030345

Ali, B., Wang, X., Saleem, M. H., Azeem, M. A., Afridi, M. S., Nadeem, M., et al. (2022a). *Bacillus mycoides* PM35 reinforces photosynthetic efficiency, antioxidant defense, expression of stress-responsive genes, and ameliorates the effects of salinity stress in maize. *Life* 12:219. doi: 10.3390/life12020219

Amna, Ali, B., Azeem, M. A., Qayyum, A., Mustafa, G., Ahmad, M. A., et al. (2021). "Bio-Fabricated Silver Nanoparticles: A Sustainable Approach for Augmentation of Plant Growth and Pathogen Control," in *Sustainable Agriculture Reviews*, eds M. Faizan, S. Hayat, and F. Yu (Berlin: Springer), 345–371.

Annamalai, J., and Namasivayam, V. (2015). Endocrine disrupting chemicals in the atmosphere: Their effects on humans and wildlife. *Environ. Int.* 76, 78–97.

Anwar, T., Qureshi, H., Parveen, N., Mahmood, S., Haider, M. Z., Mumtaz, S., et al. (2023). Herbicidal effectiveness of wild poisonous plant Rhazya stricta using different media by the sandwich method. *Pak. J. Bot.* 55. doi: 10.30848/PJB2023-2(10) [Epub ahead of print].

Arif, I., Batool, M., and Schenk, P. M. (2020). Plant Microbiome Engineering: Expected Benefits for Improved Crop Growth and Resilience. *Trends Biotechnol.* 38, 1385–1396. doi: 10.1016/j.tibtech.2020.04.015

Arora, S., and Sahni, D. (2016). Pesticides effect on soil microbial ecology and enzyme activity- An overview. *J. Appl. Nat. Sci.* 8, 1126–1132.

Bai, Y., Müller, D. B., Srinivas, G., Garrido-Oter, R., Potthoff, E., Rott, M., et al. (2015). Functional overlap of the Arabidopsis leaf and root microbiota. *Nature* 528, 364–369.

Bálint, M., Bartha, L., O'Hara, R. B., Olson, M. S., Otte, J., Pfenninger, M., et al. (2015). Relocation, high-latitude warming and host genetic identity shape the foliar fungal microbiome of poplars. *Mol. Ecol.* 24, 235–248. doi: 10.1111/mec.13018

Bandyopadhyay, P., Bhuyan, S. K., Yadava, P. K., Varma, A., and Tuteja, N. (2017). Emergence of plant and rhizospheric microbiota as stable interactomes. *Protoplasma* 254, 617–626. doi: 10.1007/s00709-016-1003-x

Barac, T., Taghavi, S., Borremans, B., Provoost, A., Oeyen, L., Colpaert, J. V., et al. (2004). Engineered endophytic bacteria improve phytoremediation of water-soluble, volatile, organic pollutants. *Nat. Biotechnol.* 22, 583–588. doi: 10.1038/nbt960

Beddington, J. (2010). Food security: Contributions from science to a new and greener revolution. *Philos. Trans. R. Soc. Lond. B* 365, 61–71.

Ben-Israel, M. (2020). *Performance Evaluation of Microbe and Plant-Mediated Processes in Phytoremediation of Toluene in Fractured Bedrock Using Hybrid Poplars*, Ph.D thesis, Guelph: The University of Guelph.

Berendsen, R. L., Pieterse, C. M. J., and Bakker, P. A. H. M. (2012). The rhizosphere microbiome and plant health. *Trends Plant Sci.* 17, 478–486. doi: 10.1016/j.tplants.2012.04.001

Berg, G., Grube, M., Schloter, M., and Smalla, K. (2014). Unraveling the plant microbiome: Looking back and future perspectives. *Front. Microbiol.* 5:148. doi: 10.3389/FMICB.2014.00148/FULL

Berg, G., Rybakova, D., Grube, M., and Köberl, M. (2016). The plant microbiome explored: Implications for experimental botany. *J. Exp. Bot.* 67, 995–1002. doi: 10.1093/jxb/erv466

Bergelson, J., Mittelstrass, J., and Horton, M. W. (2019). Characterizing both bacteria and fungi improves understanding of the Arabidopsis root microbiome. *Sci. Rep.* 9:24. doi: 10.1038/s41598-018-37208-z

Bever, J. D. (2003). Soil community feedback and the coexistence of competitors: Conceptual frameworks and empirical tests. *New Phytol.* 157, 465–473. doi: 10.1046/j.1469-8137.2003.00714.x

Bharti, N., Barnawal, D., Maji, D., and Kalra, A. (2015). Halotolerant PGPRs Prevent Major Shifts in Indigenous Microbial Community Structure Under Salinity Stress. *Microb. Ecol.* 70, 196–208. doi: 10.1007/s00248-014-0557-4

Bruto, M., Prigent-Combaret, C., Muller, D., and Moënne-Loccoz, Y. (2014). Analysis of genes contributing to plant-beneficial functions in plant growth-promoting rhizobacteria and related *Proteobacteria*. *Sci. Rep.* 4:6261. doi: 10.1038/srep06261

Bulgarelli, D., Garrido-Oter, R., Münch, P. C., Weiman, A., Dröge, J., Pan, Y., et al. (2015). Structure and function of the bacterial root microbiota in wild and domesticated barley. *Cell Host Microbe* 17, 392–403. doi: 10.1016/j.chom.2015.01.011

Bulgarelli, D., Schlaeppi, K., Spaepen, S., Van Themaat, E. V. L., and Schulze-Lefert, P. (2013). Structure and functions of the bacterial microbiota of plants. *Annu. Rev. Plant Biol.* 64, 807–838.

Busby, P. E., Newcombe, G., Dirzo, R., and Whitham, T. G. (2014). Differentiating genetic and environmental drivers of plant-pathogen community interactions. *J. Ecol.* 102, 1300–1309. doi: 10.1111/1365-2745.12270

Cabral, C., Sabine, R., Ivanka, T., and Bernd, W. (2016). Arbuscular mycorrhizal fungi modify nutrient allocation and composition in wheat (*Triticum aestivum* L.) subjected to heat-stress. *Plant Soil* 408, 385–399. doi: 10.1007/s11104-016-2942-x

Callaway, R. M., Thelen, G. C., Rodriguez, A., and Holben, W. E. (2004). Soil biota and exotic plant invasion. *Nature* 427, 731–733.

Calvo-Polanco, M., Sanchez-Romera, B., Aroca, R., Asins, M. J., Declerck, S., Dodd, I. C., et al. (2016). Exploring the use of recombinant inbred lines in combination with beneficial microbial inoculants (AM fungus and PGPR) to improve drought stress tolerance in tomato. *Environ. Exp. Bot.* 131, 47–57. doi: 10.1016/j.envexpbot.2016.06.015

Cao, Y., Pi, H., Chandrangsu, P., Li, Y., Wang, Y., Zhou, H., et al. (2018). Antagonism of Two Plant-Growth Promoting *Bacillus* velezensis Isolates Against *Ralstonia solanacearum* and *Fusarium oxysporum*. *Sci. Rep.* 8:4360.

Carteron, A., Parasquive, V., Blanchard, F., Guilbeault-Mayers, X., Turner, B. L., Vellend, M., et al. (2020). Soil abiotic and biotic properties constrain the establishment of a dominant temperate tree into boreal forests. *J. Ecol.* 108, 931–944.

Carvalhais, L. C., Muzzi, F., Tan, C.-H., Hsien-Choo, J., and Schenk, P. M. (2013). Plant growth in Arabidopsis is assisted by compost soil-derived microbial communities. *Front. Plant Sci.* 4:235. doi: 10.3389/fpls.2013.00235

Chandrasekaran, M., and Chun, S. C. (2016). Expression of PR-protein genes and induction of defense-related enzymes by *Bacillus subtilis* CBR05 in

tomato (*Solanum lycopersicum*) plants challenged with *Erwinia carotovora* subsp. *carotovora*. *Biosci. Biotechnol. Biochem*. 80, 2277–2283. doi: 10.1080/09168451.2016.1206811

Chen, J., Liu, Q., Yu, L., Korpelainen, H., Niinemets, Ü, and Li, C. (2021). Elevated temperature and CO2 interactively modulate sexual competition and ecophysiological responses of dioecious Populus cathayana. *For. Ecol. Manag.* 481:118747.

Chen, L., Liu, Y., Wu, G., Veronican Njeri, K., Shen, Q., Zhang, N., et al. (2016). Induced maize salt tolerance by rhizosphere inoculation of *Bacillus* amyloliquefaciens SQR9. *Physiol. Plant.* 158, 34–44. doi: 10.1111/ppl.12441

Chiu, C. Y., and Miller, S. A. (2019). Clinical metagenomics. *Nat. Rev. Genet.* 20, 341–355.

Choudhary, D. K., Prakash, A., and Johri, B. N. (2007). Induced systemic resistance (ISR) in plants: Mechanism of action. *Indian J. Microbiol.* 47, 289–297. doi: 10.1007/s12088-007-0054-2

Chouhan, G. K., Verma, J. P., Jaiswal, D. K., Mukherjee, A., Singh, S., de Araujo Pereira, A. P., et al. (2021). Phytomicrobiome for promoting sustainable agriculture and food security: Opportunities, challenges, and solutions. *Microbiol. Res.* 248:126763. doi: 10.1016/j.micres.2021.126763

Ciuffreda, L., Rodríguez-Pérez, H., and Flores, C. (2021). Nanopore sequencing and its application to the study of microbial communities. *Comput. Struct. Biotechnol. J.* 19, 1497–1511. doi: 10.1016/j.csbj.2021.02.020

Classen, A. T., Sundqvist, M. K., Henning, J. A., Newman, G. S., Moore, J. A. M., Cregger, M. A., et al. (2015). Direct and indirect effects of climate change on soil microbial and soil microbial-plant interactions: What lies ahead? *Ecosphere* 6, 1–21.

Cobian, G. M., Egan, C. P., and Amend, A. S. (2019). Plant–microbe specificity varies as a function of elevation. *ISME J.* 13, 2778–2788.

Compant, S., Van Der Heijden, M. G. A., and Sessitsch, A. (2010). Climate change effects on beneficial plant–microorganism interactions. *FEMS Microbiol. Ecol.* 73, 197–214.

Cook, D. E., Mesarich, C. H., and Thomma, B. P. H. J. (2015). Understanding Plant Immunity as a Surveillance System to Detect Invasion. *Annu. Rev. Phytopathol.* 53, 541–563. doi: 10.1146/annurev-phyto-080614-120114

Coombs, W. T. (2004). Impact of Past Crises on Current Crisis Communication: Insights From Situational Crisis Communication Theory. *J. Bus. Commun.* 41, 265–289. doi: 10.1177/0021943604265607

Cordovez, V., Dini-Andreote, F., Carrión, V. J., and Raaijmakers, J. M. (2019). Ecology and Evolution of Plant Microbiomes. *Annu. Rev. Microbiol.* 73, 69–88. doi: 10.1146/annurev-micro-090817-062524

Cornforth, D. M., Popat, R., McNally, L., Gurney, J., Scott-Phillips, T. C., Ivens, A., et al. (2014). Combinatorial quorum sensing allows bacteria to resolve their social and physical environment. *Proc. Natl. Acad. Sci. U.S.A.* 111, 4280–4284.

Dangl, J. L., Horvath, D. M., and Staskawicz, B. J. (2013). Pivoting the Plant Immune System from Dissection to Deployment. *Science* 341, 746–751. doi: 10.1126/science.1236011

Das, S., McClain, C. J., and Rai, S. N. (2020). Fifteen years of gene set analysis for high-throughput genomic data: A review of statistical approaches and future challenges. *Entropy* 22:427. doi: 10.3390/e22040427

de La Torre-Roche, R., Hawthorne, J., Deng, Y., Xing, B., Cai, W., Newman, L. A., et al. (2012). Fullerene-Enhanced Accumulation of p, p ’-DDE in Agricultural Crop Species. *Environ. Sci.Technol.* 46, 9315–9323. doi: 10.1021/es301982w

Dean, R. A., Talbot, N. J., Ebbole, D. J., Farman, M. L., Mitchell, T. K., Orbach, M. J., et al. (2005). The genome sequence of the rice blast fungus Magnaporthe grisea. *Nature* 434, 980–986. doi: 10.1038/nature03449

Dean, R., van Kan, J. A. L., Pretorius, Z. A., Hammond-Kosack, K. E., di Pietro, A., Spanu, P. D., et al. (2012). The Top 10 fungal pathogens in molecular plant pathology. *Mol. Plant Pathol.* 13, 414–430. doi: 10.1111/j.1364-3703.2011.00783.x

DESA (2019). *World Population Prospects 2019: Highlights | Multimedia Library - United Nations Department of Economic and Social Affairs*. New York, NY: DESA.

Dessaux, Y., Grandclément, C., and Faure, D. (2016). Engineering the Rhizosphere. *Trends Plant Sci.* 21, 266–278. doi: 10.1016/j.tplants.2016.01.002

Dey, R., Pal, K. K., Bhatt, D. M., and Chauhan, S. M. (2004). Growth promotion and yield enhancement of peanut (*Arachis hypogaea* L.) by application of plant growth-promoting rhizobacteria. *Microbiol. Res.* 159, 371–394. doi: 10.1016/j.micres.2004.08.004

Dola, D. B., Mannan, M. A., Sarker, U., Mamun, M. A. A., Islam, T., Ercisli, S., et al. (2022). Nano-iron oxide accelerates growth, yield, and quality of Glycine max seed in water deficits. *Front. Plant Sci*. 13:992535.

Donhauser, J., Qi, W., Bergk-Pinto, B., and Frey, B. (2021). High temperatures enhance the microbial genetic potential to recycle C and N from necromass in high-mountain soils. *Glob. Change Biol.* 27, 1365–1386. doi: 10.1111/gcb.15492

Doran, J. W. (2002). Soil health and global sustainability: Translating science into practice. *Agric. Ecosyst. Environ.* 88, 119–127. doi: 10.1016/S0167-8809(01)00246-8

Duan, Y., Duan, S., Armstrong, M. R., Xu, J., Zheng, J., Hu, J., et al. (2020). Comparative transcriptome profiling reveals compatible and incompatible patterns of potato toward Phytophthora infestans. *G3* 10, 623–634. doi: 10.1534/g3.119.400818

Dubey, A., Malla, M. A., Khan, F., Chowdhary, K., Yadav, S., Kumar, A., et al. (2019). Soil microbiome: A key player for conservation of soil health under changing climate. *Biodivers. Conserv.* 28, 2405–2429. doi: 10.1007/s10531-019-01760-5

El-Esawi, M. A., Alaraidh, I. A., Alsahli, A. A., Alamri, S. A., Ali, H. M., and Alayafi, A. A. (2018). *Bacillus* firmus (SW5) augments salt tolerance in soybean (Glycine max L.) by modulating root system architecture, antioxidant defense systems and stress-responsive genes expression. *Plant Physiol. Biochem.* 132, 375–384. doi: 10.1016/j.plaphy.2018.09.026

Enebe, M. C., and Babalola, O. O. (2018). The influence of plant growth-promoting rhizobacteria in plant tolerance to abiotic stress: A survival strategy. *Appl. Microbiol. Biotechnol.* 102, 7821–7835. doi: 10.1007/s00253-018-9214-z

Espenshade, J., Thijs, S., Gawronski, S., Bové, H., Weyens, N., and Vangronsveld, J. (2019). Influence of urbanization on epiphytic bacterial communities of the platanus× hispanica tree leaves in a biennial study. *Front. Microbiol.* 10:675. doi: 10.3389/fmicb.2019.00675

Essl, F., Dullinger, S., Rabitsch, W., Hulme, P. E., Hülber, K., Jarošík, V., et al. (2011). Socioeconomic legacy yields an invasion debt. *Proc. Natl. Acad. Sci. U.S.A.* 108, 203–207. doi: 10.1073/pnas.1011728108

Fajardo, C., Costa, G., Nande, M., Botías, P., García-Cantalejo, J., and Martín, M. (2019). Pb, Cd, and Zn soil contamination: Monitoring functional and structural impacts on the microbiome. *Appl. Soil Ecol.* 135, 56–64. doi: 10.1016/j.apsoil.2018.10.022

Farooq, T. H., Rafay, M., Basit, H., Shakoor, A., Shabbir, R., Riaz, M. U., et al. (2022). Morpho-physiological growth performance and phytoremediation capabilities of selected xerophyte grass species toward Cr and Pb stress. *Front. Plant Sci.* 13:997120.

Fierer, N. (2017). Embracing the unknown: Disentangling the complexities of the soil microbiome. *Nat. Rev. Microbiol.* 15, 579–590. doi: 10.1038/nrmicro.2017.87

Finkel, O. M., Castrillo, G., Paredes, S. H., González, I. S., and Dangl, J. L. (2017). Understanding and exploiting plant beneficial microbes. *Curr. Opin. Plant Biol.* 38, 155–163.

Fitzpatrick, C. R., Copeland, J., Wang, P. W., Guttman, D. S., Kotanen, P. M., and Johnson, M. T. J. (2018). Assembly and ecological function of the root microbiome across angiosperm plant species. *Proc. Natl. Acad. Sci. U. S.A.* 115:E1157–E1165. doi: 10.1073/pnas.1717617115

Foong, S. Y., Ma, N. L., Lam, S. S., Peng, W., Low, F., Lee, B. H. K., et al. (2020). A recent global review of hazardous chlorpyrifos pesticide in fruit and vegetables: Prevalence, remediation and actions needed. *J. Hazard. Mater.* 400:123006. doi: 10.1016/j.jhazmat.2020.123006

Fransson, P., Taylor, A. F. S., and Finlay, R. D. (2005). Mycelial production, spread and root colonisation by the ectomycorrhizal fungi Hebeloma crustuliniforme and Paxillus involutus under elevated atmospheric CO2. *Mycorrhiza* 15, 25–31. doi: 10.1007/s00572-003-0289-7

Frantzeskakis, L., di Pietro, A., Rep, M., Schirawski, J., Wu, C.-H., and Panstruga, R. (2020). Rapid evolution in plant-microbe interactions - a molecular genomics perspective. *New Phytol.* 225, 1134–1142. doi: 10.1111/nph.15966

Frantzeskakis, L., Kusch, S., and Panstruga, R. (2019). The need for speed: Compartmentalized genome evolution in filamentous phytopathogens. *Mol. Plant Pathol.* 20, 3–7. doi: 10.1111/mpp.12738

Frey, S. D., Lee, J., Melillo, J. M., and Six, J. (2013). The temperature response of soil microbial efficiency and its feedback to climate. *Nat. Clim. Change* 3, 395–398.

Fu, H., Tan, P., Wang, R., Li, S., Liu, H., Yang, Y., et al. (2022). Advances in organophosphorus pesticides pollution: Current status and challenges in ecotoxicological, sustainable agriculture, and degradation strategies. *J. Hazard. Mater.* 424:127494. doi: 10.1016/j.jhazmat.2021.127494

Gandolfi, I., Canedoli, C., Imperato, V., Tagliaferri, I., Gkorezis, P., Vangronsveld, J., et al. (2017). Diversity and hydrocarbon-degrading potential of epiphytic microbial communities on Platanus x acerifolia leaves in

an urban area. *Environ. Pollut.* 220, 650–658. doi: 10.1016/j.envpol.2016.10.022

Gavito, M. E., Curtis, P. S., Mikkelsen, T. N., and Jakobsen, I. (2000). Atmospheric CO2 and mycorrhiza effects on biomass allocation and nutrient uptake of nodulated pea (*Pisum sativum* L.) plants. *J. Exp. Bot.* 51, 1931–1938. doi: 10.1093/jexbot/51.352.1931

Glick, B. R., and Gamalero, E. (2021). Recent developments in the study of plant microbiomes. *Microorganisms* 9:1533. doi: 10.3390/microorganisms9071533

Godbold, D. L., and Berntson, G. M. (1997). Elevated atmospheric CO2 concentration changes ectomycorrhizal morphotype assemblages in Betula papyrifera. *Tree Physiol.* 17, 347–350.

Godfray, H. C. J., Beddington, J. R., Crute, I. R., Haddad, L., Lawrence, D., Muir, J. F., et al. (2010). Food Security: The Challenge of Feeding 9 Billion People. *Science* 327, 812–818. doi: 10.1126/science.1185383

Gómez Expósito, R., de Bruijn, I., Postma, J., and Raaijmakers, J. M. (2017). Current Insights into the Role of Rhizosphere Bacteria in Disease Suppressive Soils. *Front. Microbiol.* 8:2529. doi: 10.3389/fmicb.2017.02529

Gorshkov, V., Osipova, E., Ponomareva, M., Ponomarev, S., Gogoleva, N., Petrova, O., et al. (2020). Rye snow mold-associated Microdochium nivale strains inhabiting a common area: Variability in genetics, morphotype, extracellular enzymatic activities, and virulence. *J. Fungi* 6:335. doi: 10.3390/jof6040335

Grewal, A. S., Singla, A., Kamboj, P., and Dua, J. S. (2017). Pesticide Residues in Food Grains, Vegetables and Fruits: A Hazard to Human Health. *J. Med. Chem. Toxicol.* 2, 40–46. doi: 10.15436/2575-808X.17.1355

Gupta, P., Kumar, V., Usmani, Z., Rani, R., Chandra, A., and Gupta, V. K. (2020). Implications of plant growth promoting Klebsiella sp. CPSB4 and *Enterobacter* sp. CPSB49 in luxuriant growth of tomato plants under chromium stress. *Chemosphere* 240:124944. doi: 10.1016/j.chemosphere.2019.124944

Habib, S. H., Kausar, H., and Saud, H. M. (2016). Plant Growth-Promoting Rhizobacteria Enhance Salinity Stress Tolerance in Okra through ROS-Scavenging Enzymes. *BioMed Res. Int.* 2016:6284547. doi: 10.1155/2016/6284547

Hacquard, S., Kracher, B., Hiruma, K., Münch, P. C., Garrido-Oter, R., Thon, M. R., et al. (2016). Survival trade-offs in plant roots during colonization by closely related beneficial and pathogenic fungi. *Nat. Commun.* 7:11362.

Haichar, F., Heulin, T., Guyonnet, J. P., and Achouak, W. (2016). Stable isotope probing of carbon flow in the plant holobiont. *Curr. Opin. Biotechnol.* 41, 9–13. doi: 10.1016/j.copbio.2016.02.023

Haider, M. W., Nafees, M., Ahmad, I., Ali, B., Maryam, Iqbal, R., et al. (2022). Postharvest dormancy-related changes of endogenous hormones in relation to dierent dormancy-breaking methods of potato (*Solanum tuberosum L.*) tubers. *Front. Plant Sci.* 13:945256. doi: 10.3389/fpls.2022.945256

Hamonts, K., Trivedi, P., Garg, A., Janitz, C., Grinyer, J., Holford, P., et al. (2018). Field study reveals core plant microbiota and relative importance of their drivers. *Environ. Microbiol.* 20, 124–140. doi: 10.1111/1462-2920.14031

Haney, C. H., Samuel, B. S., Bush, J., and Ausubel, F. M. (2015). Associations with rhizosphere bacteria can confer an adaptive advantage to plants. *Nat. Plants* 1:15051. doi: 10.1038/nplants.2015.51

Hasegawa, H., Chatterjee, A., Cui, Y., and Chatterjee, A. K. (2005). Elevated temperature enhances virulence of Erwinia carotovora subsp. carotovora strain EC153 to plants and stimulates production of the quorum sensing signal, N-acyl homoserine lactone, and extracellular proteins. *Appl. Environ. Microbiol.* 71, 4655–4663. doi: 10.1128/AEM.71.8.4655-4663.2005

Hashem, A., Alqarawi, A. A., Radhakrishnan, R., Al-Arjani, A. F., Aldehaish, H. A., Egamberdieva, D., et al. (2018). Arbuscular mycorrhizal fungi regulate the oxidative system, hormones and ionic equilibrium to trigger salt stress tolerance in Cucumis sativus L. *Saudi J. Biol. Sci.* 25, 1102–1114. doi: 10.1016/j.sjbs.2018.03.009

Hernández-Restrepo, M., Groenewald, J. Z., Elliott, M. L., Canning, G., McMillan, V. E., and Crous, P. W. (2016). Take-all or nothing. *Stud. Mycol.* 83, 19–48. doi: 10.1016/j.simyco.2016.06.002

Heyer, R., Kohrs, F., Reichl, U., and Benndorf, D. (2015). Metaproteomics of complex microbial communities in biogas plants. *Microb. Biotechnol.* 8, 749–763.

Hong, S. U. N., Ya-guang, Z., Hui, L. I., and Yang, L. I. (2018). Phyllosphere bacterial community structure of Osmanthus fragrans and Nerium indicum in different habitats. *Ying Yong Sheng Tai Xue Bao* 29, 1653–1659. doi: 10.13287/j.1001-9332.201805.036

Horton, M. W., Bodenhausen, N., Beilsmith, K., Meng, D., Muegge, B. D., Subramanian, S., et al. (2014). Genome-wide association study of Arabidopsis thaliana leaf microbial community. *Nat. Commun.* 5:5320. doi: 10.1038/ncomms6320

Huang, J., Zhao, X., and Chory, J. (2019). The Arabidopsis transcriptome responds specifically and dynamically to high light stress. *Cell Rep.* 29, 4186–4199. doi: 10.1016/j.celrep.2019.11.051

Hunziker, L., Bönisch, D., Groenhagen, U., Bailly, A., Schulz, S., and Weisskopf, L. (2015). *Pseudomonas* Strains Naturally Associated with Potato Plants Produce Volatiles with High Potential for Inhibition of Phytophthora infestans. *Appl. Environ. Microbiol.* 81, 821–830. doi: 10.1128/AEM.02999-14

Hussain, S. Q., Rasheed, M., Saleem, M. H., Ahmed, Z. I., Hafeez, A., Jilani, G., et al. (2022). Salt tolerance in maize with melatonin priming to achieve sustainability in yield on salt affected soils. *Pak. J. Bot.* 55.

Imperato, V., Kowalkowski, L., Portillo-Estrada, M., Gawronski, S. W., Vangronsveld, J., and Thijs, S. (2019). Characterisation of the Carpinus betulus L. phyllomicrobiome in urban and forest areas. *Front. Microbiol.* 10:1110. doi: 10.3389/fmicb.2019.01110

Jaber, L. R., and Alananbeh, K. M. (2018). Fungal entomopathogens as endophytes reduce several species of Fusarium causing crown and root rot in sweet pepper (*Capsicum annuum* L.). *Biol. Control* 126, 117–126.

Jacobsen, C. S., and Hjelmsø, M. H. (2014). Agricultural soils, pesticides and microbial diversity. *Curr. Opin. Biotechnol.* 27, 15–20. doi: 10.1016/j.copbio.2013.09.003

Jain, A. (2016). Insight into the Interaction between Plants and Associated Fluorescent *Pseudomonas* spp. *Int. J. Agron.* 2016:4269010. doi: 10.1155/2016/4269010

Jain, M., Olsen, H. E., Paten, B., and Akeson, M. (2016). The Oxford Nanopore MinION: Delivery of nanopore sequencing to the genomics community. *Genome Biol.* 17:239.

Jain, S., Jain, J., and Singh, J. (2020). "The Rhizosphere Microbiome: Microbial Communities and Plant Health," in *Plant Microbiome Paradigm*, eds A. Varma, S. Tripathi, and R. Prasad (Berlin: Springer International Publishing), 175–190. doi: 10.1007/978-3-030-50395-6_10

Jansson, J. K., and Hofmockel, K. S. (2018). The soil microbiome—from metagenomics to metaphenomics. *Curr. Opin.in Microbiol.* 43, 162–168. doi: 10.1016/j.mib.2018.01.013

Johnson-Rollings, A. S., Wright, H., Masciandaro, G., Macci, C., Doni, S., Calvo-Bado, L. A., et al. (2014). Exploring the functional soil-microbe interface and exoenzymes through soil metaexoproteomics. *ISME J.* 8, 2148–2150. doi: 10.1038/ismej.2014.130

Jongman, M., Carmichael, P. C., and Bill, M. (2020). Technological advances in phytopathogen detection and metagenome profiling techniques. *Curr. Microbiol.* 77, 675–681. doi: 10.1007/s00284-020-01881-z

Jumpponen, A., and Jones, K. L. (2010). Seasonally dynamic fungal communities in the Quercus macrocarpa phyllosphere differ between urban and nonurban environments. *New Phytol.* 186, 496–513. doi: 10.1111/j.1469-8137.2010.03197.x

Karhu, K., Auffret, M. D., Dungait, J. A. J., Hopkins, D. W., Prosser, J. I., Singh, B. K., et al. (2014). Temperature sensitivity of soil respiration rates enhanced by microbial community response. *Nature* 513, 81–84.

Kashyap, A. S., Pandey, V. K., Manzar, N., Kannojia, P., Singh, U. B., and Sharma, P. K. (2017). "Role of plant growth-promoting rhizobacteria for improving crop productivity in sustainable agriculture," in *Plant-Microbe Interactions in Agro-Ecological Perspectives*, eds D. Singh, H. Singh, R. Prabha (Berlin: Springer), 673–693.

Kehe, J., Kulesa, A., Ortiz, A., Ackerman, C. M., Thakku, S. G., Sellers, D., et al. (2019). Massively parallel screening of synthetic microbial communities. *Proc. Natl. Acad. Sci. U.S.A.* 116, 12804–12809. doi: 10.1073/pnas.1900102116

Khalloufi, M., Martínez-Andújar, C., Lachaâl, M., Karray-Bouraoui, N., Pérez-Alfocea, F., and Albacete, A. (2017). The interaction between foliar GA3 application and arbuscular mycorrhizal fungi inoculation improves growth in salinized tomato Solanum lycopersicum L. plants by modifying the hormonal balance. *J. Plant Physiol.* 214, 134–144. doi: 10.1016/j.jplph.2017.04.012

Khan, M. A., Adnan, M., Basir, A., Fahad, S., Hafeez, A., Saleem, M. H., et al. (2023). Impact of tillage and potassium levels and sources on growth, yield and yield attributes of *wheat. Pak. J. Bot*. 55. doi: 10.30848/PJB2023-1(30) [Epub ahead of print].

Khatoon, Z., Huang, S., Rafique, M., Fakhar, A., Kamran, M. A., and Santoyo, G. (2020). Unlocking the potential of plant growth-promoting rhizobacteria on soil health and the sustainability of agricultural systems. *J. Environ. Manag.* 273:111118. doi: 10.1016/j.jenvman.2020.111118

Köhl, J., Medeiros, F. H., Lombaers-van der Plas, C., Groenenboom-de Haas, L., and van den Bosch, T. (2020). Efficacies of bacterial and fungal isolates in biocontrol of Botrytis cinerea and *Pseudomonas* syringae pv. tomato and growth promotion in tomato do not correlate. *Biol. Control* 150:104375. doi: 10.1016/j.biocontrol.2020.104375

Kong, Z., Hart, M., and Liu, H. (2018). Paving the Way From the Lab to the Field: Using Synthetic Microbial Consortia to Produce High-Quality Crops. *Front. Plant Sci.* 9:1467. doi: 10.3389/fpls.2018.01467

Kortekamp, A. (2011). *Herbicides and Environment*. London: In Tech, doi: 10.5772/550

Kumar, A., and Dubey, A. (2020). Rhizosphere microbiome: Engineering bacterial competitiveness for enhancing crop production. *J. Adv. Res.* 24, 337–352. doi: 10.1016/j.jare.2020.04.014

Kumar, A., Vyas, P., Kumar, D., and Dubey, A. (2018). Screening and Characterization of Achromobacter xylosoxidans isolated from rhizosphere of *Jatropha curcas* L. (Energy Crop) for plant-growth-promoting traits. *J. Adv. Res. Biotechnol.* 3, 1–8. doi: 10.15226/2475-4714/3/1/00134

Kwak, Y.-S., and Weller, D. M. (2013). Take-all of Wheat and Natural Disease Suppression: A Review. *Plant Pathol. J.* 29, 125–135. doi: 10.5423/PPJ.SI.07.2012.0112

Laforest-Lapointe, I., Messier, C., and Kembel, S. W. (2017). Tree leaf bacterial community structure and diversity differ along a gradient of urban intensity. *mSystems* 2:e00087–17. doi: 10.1128/mSystems.00087-17

Lakshmanan, V., Selvaraj, G., and Bais, H. P. (2014). Functional Soil Microbiome: Belowground Solutions to an Aboveground Problem. *Plant Physiol.* 166, 689–700. doi: 10.1104/pp.114.245811

Levy, A., Gonzalez, I. S., Mittelviefhaus, M., Clingenpeel, S., Paredes, S. H., Miao, J., et al. (2018). Genomic features of bacterial adaptation to plavnts. *Nat. Genet.* 50, 138–150.

Li, Q., You, P., Hu, Q., Leng, B., Wang, J., Chen, J., et al. (2020). Effects of co-contamination of heavy metals and total petroleum hydrocarbons on soil bacterial community and function network reconstitution. *Ecotoxicol. Environ. Saf.* 204:111083. doi: 10.1016/j.ecoenv.2020.111083

Li, Y., Zhang, J., Zhang, J., Xu, W., and Mou, Z. (2019). Characteristics of Inorganic Phosphate-Solubilizing Bacteria from the Sediments of a Eutrophic Lake. *Int. J. Environ. Res. Public Health* 16:2141. doi: 10.3390/ijerph16122141

Lidbury, I. D. E. A., Murphy, A. R. J., Scanlan, D. J., Bending, G. D., Jones, A. M. E., Moore, J. D., et al. (2016). Comparative genomic, proteomic and exoproteomic analyses of three *Pseudomonas* strains reveals novel insights into the phosphorus scavenging capabilities of soil bacteria. *Environ. Microbiol.* 18, 3535–3549. doi: 10.1111/1462-2920.13390

Liptzin, D., Silver, W. L., and Detto, M. (2011). Temporal Dynamics in Soil Oxygen and Greenhouse Gases in Two Humid Tropical Forests. *Ecosystems* 14, 171–182. doi: 10.1007/s10021-010-9402-x

Liu, X., Li, Q., Li, Y., Guan, G., and Chen, S. (2019). *Paenibacillus* strains with nitrogen fixation and multiple beneficial properties for promoting plant growth. *PeerJ* 7:e7445. doi: 10.7717/peerj.7445

Lloyd, D. P., and Allen, R. J. (2015). Competition for space during bacterial colonization of a surface. *J. R. Soc. Interface* 12:20150608. doi: 10.1098/rsif.2015.0608

Lundberg, D. S., Lebeis, S. L., Paredes, S. H., Yourstone, S., Gehring, J., Malfatti, S., et al. (2012). Defining the core Arabidopsis thaliana root microbiome. *Nature* 488, 86–90. doi: 10.1038/nature11237

Ma, J., Saleem, M. H., Ali, B., Rasheed, R., Ashraf, M. A., Aziz, H., et al. (2022a). Impact of foliar application of syringic acid on tomato (*Solanum lycopersicum L.*) under heavy metal stress-insights into nutrient uptake, redox homeostasis, oxidative stress, and antioxidant defense. *Front. Plant Sci*. 13:950120. doi: 10.3389/fpls.2022.950120

Ma, J., Saleem, M. H., Yasin, G., Mumtaz, S., Qureshi, F. F., Ali, B., et al. (2022b). Individual and combinatorial eects of SNP and NaHS on morpho-physio-biochemical attributes and phytoextraction of chromium through Cr-stressed spinach (*Spinacia oleracea L.*). *Front. Plant Sci*. 13:973740. doi: 10.3389/fpls.2022.973740

Marschner, H. (1995). *Mineral Nutrition of Higher Plants*. Amsterdam: Elsevier, doi: 10.1016/B978-0-12-473542-2.X5000-7

Martínez-Álvarez, P., Fernández-González, R. A., Sanz-Ros, A. V., Pando, V., and Diez, J. J. (2016). Two fungal endophytes reduce the severity of pitch canker disease in Pinus radiata seedlings. *Biol. Control* 94, 1–10.

Martiny, J. B., Martiny, A. C., Weihe, C., Lu, Y., Berlemont, R., Brodie, E. L., et al. (2017). Microbial legacies alter decomposition in response to simulated global change. *ISME J.* 11, 490–499. doi: 10.1038/ismej.2016.122

Mathur, S., Sharma, M. P., and Jajoo, A. (2016). Improved photosynthetic efficacy of maize Zea mays plants with arbuscular mycorrhizal fungi (AMF) under high temperature stress. *J. Photochem. Photobiol. B* 180, 149–154. doi: 10.1016/j.jphotobiol.2018.02.002

Mauchline, T. H., Chedom-Fotso, D., Chandra, G., Samuels, T., Greenaway, N., Backhaus, A., et al. (2015). An analysis of P seudomonas genomic diversity in take-all infected wheat fields reveals the lasting impact of wheat cultivars on the soil microbiota. *Environ. Microbiol.* 17, 4764–4778. doi: 10.1111/1462-2920.13038

McDonald, B. A., and Stukenbrock, E. H. (2016). Rapid emergence of pathogens in agro-ecosystems: Global threats to agricultural sustainability and food security. *Philos. Trans. R. Soc. Lond. B* 371:20160026. doi: 10.1098/rstb.2016.0026

McMichael, A. J., Powles, J. W., Butler, C. D., and Uauy, R. (2007). Food, livestock production, energy, climate change, and health. *Lancet* 370, 1253–1263. doi: 10.1016/S0140-6736(07)61256-2

McNeely, D., Chanyi, R. M., Dooley, J. S., Moore, J. E., and Koval, S. F. (2017). Biocontrol of *Burkholderia cepacia* complex bacteria and bacterial phytopathogens by *Bdellovibrio bacteriovorus*. *Can. J. Microbiol.* 63, 350–358. doi: 10.1139/cjm-2016-0612

Mechan Llontop, M. E., Sharma, P., Aguilera Flores, M., Yang, S., Pollok, J., Tian, L., et al. (2020). Strain-level identification of bacterial tomato pathogens directly from metagenomic sequences. *Phytopathology* 110, 768–779. doi: 10.1094/PHYTO-09-19-0351-R

Meena, R., Kumar, S., Datta, R., Lal, R., Vijayakumar, V., Brtnicky, M., et al. (2020). Impact of Agrochemicals on Soil Microbiota and Management: A Review. *Land* 9:34. doi: 10.3390/land9020034

Mehmood, S., Khatoon, Z., Amna, Ahmad, I., Muneer, M. A., Kamran, M. A., et al. (2021a). *Bacillus* sp. PM31 harboring various plant growth-promoting activities regulates Fusarium dry rot and wilt tolerance in potato. *Arch. Agron. Soil Sci.* 1–15.

Mehmood, S., Muneer, M. A., Tahir, M., Javed, M. T., Mahmood, T., Afridi, M. S., et al. (2021b). Deciphering distinct biological control and growth promoting potential of multi-stress tolerant *Bacillus subtilis* PM32 for potato stem canker. *Physiol. Mol. Biol. Plants* 27, 2101–2114. doi: 10.1007/s12298-021-01067-2

Mendes, R., Garbeva, P., and Raaijmakers, J. M. (2013). The rhizosphere microbiome: Significance of plant beneficial, plant pathogenic, and human pathogenic microorganisms. *FEMS Microbiol. Rev.* 37, 634–663. doi: 10.1111/1574-6976.12028

Monz, C. A., Hunt, H. W., Reeves, F. B., and Elliott, E. T. (1994). The response of mycorrhizal colonization to elevated CO2 and climate change in Pascopyrum smithii and Bouteloua gracilis. *Plant Soil* 165, 75–80.

Mueller, U. G., and Sachs, J. L. (2015). Engineering Microbiomes to Improve Plant and Animal Health. *Trends Microbiol.* 23, 606–617. doi: 10.1016/j.tim.2015.07.009

Mukherjee, A., Singh, S., Gaurav, A. K., Chouhan, G. K., Jaiswal, D. K., de Araujo Pereira, A. P., et al. (2022). Harnessing of phytomicrobiome for developing potential biostimulant consortium for enhancing the productivity of chickpea and soil health under sustainable agriculture. *Sci. Total Environ.* 836:155550. doi: 10.1016/j.scitotenv.2022.155550

Mukhtar, T., Afridi, M. S., McArthur, R., Van Hamme, J. D., Rineau, F., Mahmood, T., et al. (2018). Draft genome sequence of *Bacillus* pumilus SCAL1, an endophytic heat-tolerant plant growth-promoting bacterium. *Genome Announc.* 6:e306–e318. doi: 10.1128/genomeA.00306-18

Mukhtar, T., Ali, F., Rafique, M., Ali, J., Afridi, M. S., Smith, D., et al. (2022). Biochemical Characterization and Potential of *Bacillus* safensis Strain SCAL1 to Mitigate Heat Stress in Solanum lycopersicum L. *J. Plant Growth Regul.* 1–16. doi: 10.1007/s00344-021-10571-4

Müller, D. B., Vogel, C., Bai, Y., and Vorholt, J. A. (2016). The Plant Microbiota: Systems-Level Insights and Perspectives. *Annu. Rev. Genet.* 50, 211–234. doi: 10.1146/annurev-genet-120215-034952

Murat, F., Van de Peer, Y., and Salse, J. (2012). Decoding plant and animal genome plasticity from differential paleo-evolutionary patterns and processes. *Genome Biol. Evol.* 4, 917–928. doi: 10.1093/gbe/evs066

Muth, T., Renard, B. Y., and Martens, L. (2016). Metaproteomic data analysis at a glance: Advances in computational microbial community proteomics. *Expert Rev. Proteomics* 13, 757–769. doi: 10.1080/14789450.2016.1209418

Nawaz, H., Ali, A., Saleem, M. H., Ameer, A., Hafeez, A., Alharbi, K., et al. (2022). Comparative effectiveness of EDTA and citric acid assisted phytoremediation of Ni contaminated soil by using canola (*Brassica napus*). *Braz. J. Biol.* 82:e261785. doi: 10.1590/1519-6984.261785

Naylor, D., DeGraaf, S., Purdom, E., and Coleman-Derr, D. (2017). Drought and host selection influence bacterial community dynamics in the grass root microbiome. *ISME J.* 11, 2691–2704. doi: 10.1038/ismej.2017.118

Newsham, K. K., Fitter, A. H., and Watkinson, A. R. (1995). Multi-functionality and biodiversity in arbuscular mycorrhizas. *Trends Ecol.Evol.* 10, 407–411. doi: 10.1016/s0169-5347(00)89157-0

Niu, B., Paulson, J. N., Zheng, X., and Kolter, R. (2017). Simplified and representative bacterial community of maize roots. *Proc. Natl. Acad. Sci. U.S.A.* 114:E2450–E2459. doi: 10.1073/pnas.1616148114

Niu, S.-Q., Li, H.-R., Paré, P. W., Aziz, M., Wang, S.-M., Shi, H., et al. (2016). Induced growth promotion and higher salt tolerance in the halophyte grass Puccinellia tenuiflora by beneficial rhizobacteria. *Plant Soil* 407, 217–230. doi: 10.1007/s11104-015-2767-z

Oerke, E.-C. (2006). Crop losses to pests. *J. Agric. Sci.* 144, 31–43. doi: 10.1017/S0021859605005708

Ojuederie, O., Olanrewaju, O., and Babalola, O. (2019). Plant Growth Promoting Rhizobacterial Mitigation of Drought Stress in Crop Plants: Implications for Sustainable Agriculture. *Agronomy* 9:712. doi: 10.3390/agronomy9110712

Ortíz-Castro, R., Valencia-Cantero, E., and López-Bucio, J. (2008). Plant growth promotion by *Bacillus megaterium* involves cytokinin signaling. *Plant Signal. Behav.* 3, 263–265. doi: 10.4161/psb.3.4.5204

Panneerselvam, P., Kumar, U., Senapati, A., Parameswaran, C., Anandan, A., Kumar, A., et al. (2020). Influence of elevated CO2 on arbuscular mycorrhizal fungal community elucidated using Illumina MiSeq platform in sub-humid tropical paddy soil. *Appl. Soil Ecol.* 145:103344.

Parks, S. E., Cusano, D. A., Stimpert, A. K., Weinrich, M. T., Friedlaender, A. S., and Wiley, D. N. (2015). Evidence for acoustic communication among bottom foraging humpback whales. *Sci. Rep.* 4:7508. doi: 10.1038/srep07508

Parnell, J. J., Berka, R., Young, H. A., Sturino, J. M., Kang, Y., Barnhart, D. M., et al. (2016). From the Lab to the Farm: An Industrial Perspective of Plant Beneficial Microorganisms. *Front. Plant Sci.* 7:1110. doi: 10.3389/fpls.2016.01110

Parray, J., and Shameem, N. (2019). *Sustainable Agriculture: Advances in Plant Metabolome and Microbiome*. Cambridge: Academic Press.

Penton, C. R., Gupta, V. V. S. R., Tiedje, J. M., Neate, S. M., Ophel-Keller, K., Gillings, M., et al. (2014). Fungal Community Structure in Disease Suppressive Soils Assessed by 28S LSU Gene Sequencing. *PLoS One* 9:e93893. doi: 10.1371/journal.pone.0093893

Pilon-Smits, E. (2005). Phytoremediation. *Annu. Rev. Plant Biol.* 56, 15–39. doi: 10.1146/annurev.arplant.56.032604.144214

Pinedo, I., Ledger, T., Greve, M., and Poupin, M. J. (2015). Burkholderia phytofirmans PsJN induces long-term metabolic and transcriptional changes involved in Arabidopsis thaliana salt tolerance. *Front. Plant Sci.* 6:466. doi: 10.3389/fpls.2015.00466

Ping, L. (2004). Signals from the underground: Bacterial volatiles promote growth in Arabidopsis. *Trends Plant Sci.* 9, 263–266. doi: 10.1016/j.tplants.2004.04.008

Poudel, R., Jumpponen, A., Schlatter, D. C., Paulitz, T. C., Gardener, B. B. M., Kinkel, L. L., et al. (2016). Microbiome Networks: A Systems Framework for Identifying Candidate Microbial Assemblages for Disease Management. *Phytopathology§* 106, 1083–1096. doi: 10.1094/PHYTO-02-16-0058-FI

Prescott, C. E., Grayston, S. J., Helmisaari, H.-S., Kaštovská, E., Körner, C., Lambers, H., et al. (2020). Surplus carbon drives allocation and plant–soil interactions. *Trends Ecol.Evol.* 35, 1110–1118. doi: 10.1016/j.tree.2020.08.007

Prosser, J. I. (2015). Dispersing misconceptions and identifying opportunities for the use of'omics' in soil microbial ecology. *Nat. Rev. Microbiol.* 13, 439–446. doi: 10.1038/nrmicro3468

Qiao, D., Zhang, Y., Xiong, X., Li, M., Cai, K., Luo, H., et al. (2020). Transcriptome analysis on responses of orchardgrass (*Dactylis glomerata* L.) leaves to a short term flooding. *Hereditas* 157:20. doi: 10.1186/s41065-020-00134-0

Qiu, X., Kulasekara, B. R., and Lory, S. (2009). "Role of horizontal gene transfer in the evolution of *Pseudomonas aeruginosa* virulence," in *Microbial Pathogenomics*, eds H. de Reuse and S. Bereswill (Berlin: Karger Publishers), 126–139.

Quiza, L., St-Arnaud, M., and Yergeau, E. (2015). Harnessing phytomicrobiome signaling for rhizosphere microbiome engineering. *Front. Plant Sci.* 6:507. doi: 10.3389/fpls.2015.00507

Raaijmakers, J. M., Paulitz, T. C., Steinberg, C., Alabouvette, C., and Moënne-Loccoz, Y. (2009). The rhizosphere: A playground and battlefield for soilborne pathogens and beneficial microorganisms. *Plant Soil* 321, 341–361. doi: 10.1007/s11104-008-9568-6

Rafique, M., Ortas, I., Ahmed, I. A., Rizwan, M., Afridi, M. S., Sultan, T., et al. (2019). Potential impact of biochar types and microbial inoculants on growth of onion plant in differently textured and phosphorus limited soils. *J. Environ. Manag.* 247, 672–680. doi: 10.1016/j.jenvman.2019.06.123

Raj, M., Kumar, R., Lal, K., Sirisha, L., Chaudhary, R., and Patel, S. K. (2020). Dynamic role of plant growth promoting rhizobacteria (PGPR) in agriculture. *Int. J. Chem. Stud.* 8, 105–110. doi: 10.22271/chemi.2020.v8.i5b.10284

Ramirez, K. S., Snoek, L. B., Koorem, K., Geisen, S., Bloem, L. J., Ten Hooven, F., et al. (2019). Range-expansion effects on the belowground plant microbiome. *Nat. Ecol. Evol.* 3, 604–611.

Rang, F. J., Kloosterman, W. P., and de Ridder, J. (2018). From squiggle to basepair: Computational approaches for improving nanopore sequencing read accuracy. *Genome Biol.* 19, 1–11. doi: 10.1186/s13059-018-1462-9

Rani, B. (2016). *Effect of Arbuscular Mycorrhiza Fungi on Biochemical Parameters in Wheat Triticum Aestivum L. Under Drought Conditions*, Ph.D thesis, Hisar: CCSHAU.

Rani, L., Thapa, K., Kanojia, N., Sharma, N., Singh, S., Grewal, A. S., et al. (2021). An extensive review on the consequences of chemical pesticides on human health and environment. *J. Clean. Prod.* 283:124657. doi: 10.1016/j.jclepro.2020.124657

Rani, R., Kumar, V., Usmani, Z., Gupta, P., and Chandra, A. (2019). Influence of plant growth promoting rhizobacterial strains *Paenibacillus* sp. IITISM08, *Bacillus* sp. PRB77 and *Bacillus* sp. PRB101 using Helianthus annuus on degradation of endosulfan from contaminated soil. *Chemosphere* 225, 479–489. doi: 10.1016/j.chemosphere.2019.03.037

Raymaekers, K., Ponet, L., Holtappels, D., Berckmans, B., and Cammue, B. P. A. (2020). Screening for novel biocontrol agents applicable in plant disease management – A review. *Biol. Control* 144:104240. doi: 10.1016/j.biocontrol.2020.104240

Reitz, M. U., Gifford, M. L., and Schäfer, P. (2015). Hormone activities and the cell cycle machinery in immunity-triggered growth inhibition. *J. Exp. Bot.* 66, 2187–2197. doi: 10.1093/jxb/erv106

Rodríguez, M., Torres, M., Blanco, L., Béjar, V., Sampedro, I., and Llamas, I. (2020). Plant growth-promoting activity and quorum quenching-mediated biocontrol of bacterial phytopathogens by *Pseudomonas* segetis strain P6. *Sci. Rep.* 10:4121. doi: 10.1038/s41598-020-61084-1

Rojas-Solís, D., Zetter-Salmón, E., Contreras-Pérez, M., Rocha-Granados, M., del, C., Macías-Rodríguez, L., et al. (2018). *Pseudomonas* stutzeri E25 and *Stenotrophomonas Maltophilia* CR71 endophytes produce antifungal volatile organic compounds and exhibit additive plant growth-promoting effects. *Biocatal. Agric. Biotechnol.* 13, 46–52. doi: 10.1016/j.bcab.2017.11.007

Roth, R., and Paszkowski, U. (2017). Plant carbon nourishment of arbuscular mycorrhizal fungi. *Curr. Opin. Plant Biol.* 39, 50–56. doi: 10.1016/j.pbi.2017.05.008

Ryder, L. S., Harris, B. D., Soanes, D. M., Kershaw, M. J., Talbot, N. J., and Thornton, C. R. (2012). Saprotrophic competitiveness and biocontrol fitness of a genetically modified strain of the plant-growth-promoting fungus *Trichoderma hamatum* GD12. *Microbiology* 158, 84–97. doi: 10.1099/mic.0.051854-0

Saeed, S., Ullah, A., Ullah, S., Noor, J., Ali, B., Khan, M. N., et al. (2022). Validating the Impact of Water Potential and Temperature on Seed Germination of Wheat (*Triticum aestivum* L.) via Hydrothermal Time Model. *Life* 12:983. doi: 10.3390/life12070983

Saeid, A., and Chojnacka, K. (2019). "Fertlizers," in *Organic Farming*, eds S. Chandran, M. R. Unni, and S. Thomas (Sawston: Woodhead Publishing), 91–116. doi: 10.1016/B978-0-12-813272-2.00004-5

Safavi-Rizi, V., Herde, M., and Stöhr, C. (2020). RNA-Seq reveals novel genes and pathways associated with hypoxia duration and tolerance in tomato root. *Sci. Rep.* 10, 1–17.

Sakschewski, B., von Bloh, W., Huber, V., Müller, C., and Bondeau, A. (2014). Feeding 10 billion people under climate change: How large is the production gap of current agricultural systems? *Ecol. Model.* 288, 103–111. doi: 10.1016/j.ecolmodel.2014.05.019

Salam, A., Ali, A., Afridi, M. S., Ali, S., and Ullah, Z. (2022). "Agrobiodiversity: Effect of drought stress on the eco-physiology and morphology of wheat," in *Biodiversity, conservation and sustainability in asia*, eds M. Öztürk, S. M. Khan, V. Altay, R .Efe, D. Egamberdieva, and F. O. Khassanov (Cham: Springer), doi: 10.1007/978-3-030-73943-0_33

Sankar Ganesh, K., Sundaramoorthy, P., Nagarajan, M., and Lawrence Xavier, R. (2017). "Role of Organic Amendments in Sustainable Agriculture," in *Sustainable Agriculture towards Food Security*, ed. A. Dhanarajan (Singapore: Springer Singapore), 111–124. doi: 10.1007/978-981-10-6647-4_7

Santhanam, R., Luu, V. T., Weinhold, A., Goldberg, J., Oh, Y., and Baldwin, I. T. (2015). Native root-associated bacteria rescue a plant from a sudden-wilt disease that emerged during continuous cropping. *Proc. Natl. Acad. Sci.* 112:E5013–E5120. doi: 10.1073/pnas.1505765112

Santoyo, G., Gamalero, E., and Glick, B. R. (2021). Mycorrhizal-Bacterial Amelioration of Plant Abiotic and Biotic Stress. *Front. Sustain. Food Syst.* 5:139. doi: 10.3389/fsufs.2021.672881

Sanyal, D., and Shrestha, A. (2008). Direct Effect of Herbicides on Plant Pathogens and Disease Development in Various Cropping Systems. *Weed Sci.* 56, 155–160. doi: 10.1614/WS-07-081.1

Savary, S., Ficke, A., Aubertot, J.-N., and Hollier, C. (2012). Crop losses due to diseases and their implications for global food production losses and food security. *Food Secur.* 4, 519–537. doi: 10.1007/s12571-012-0200-5

Scheuring, I., and Yu, D. W. (2012). How to assemble a beneficial microbiome in three easy steps. *Ecol. Lett.* 15, 1300–1307. doi: 10.1111/j.1461-0248.2012.01853.x

Schlaeppi, K., and Bulgarelli, D. (2015). The Plant Microbiome at Work. *Mol. Plant Microbe Interact.§* 28, 212–217. doi: 10.1094/MPMI-10-14-0334-FI

Schortemeyer, M., Hartwig, U. A., Hendrey, G. R., and Sadowsky, M. J. (1996). Microbial community changes in the rhizospheres of white clover and perennial ryegrass exposed to free air carbon dioxide enrichment (FACE). *Soil Biol. Biochem.* 28, 1717–1724.

Schuhegger, R., Ihring, A., Gantner, S., Bahnweg, G., Knappe, C., Vogg, G., et al. (2006). Induction of systemic resistance in tomato by N-acyl-L-homoserine lactone-producing rhizosphere bacteria. *Plant Cell Environ.* 29, 909–918. doi: 10.1111/j.1365-3040.2005.01471.x

Sessitsch, A., Kuffner, M., Kidd, P., Vangronsveld, J., Wenzel, W. W., Fallmann, K., et al. (2013). The role of plant-associated bacteria in the mobilization and phytoextraction of trace elements in contaminated soils. *Soil Biol. Biochem.* 60, 182–194. doi: 10.1016/j.soilbio.2013.01.012

Sevim, V., Lee, J., Egan, R., Clum, A., Hundley, H., Lee, J., et al. (2019). Shotgun metagenome data of a defined mock community using Oxford Nanopore, PacBio and Illumina technologies. *Sci. Data* 6:285. doi: 10.1038/s41597-019-0287-z

Sharma, D., Nagpal, A., Pakade, Y. B., and Katnoria, J. K. (2010). Analytical methods for estimation of organophosphorus pesticide residues in fruits and vegetables: A review. *Talanta* 82, 1077–1089. doi: 10.1016/j.talanta.2010.06.043

Sharma, M., Sudheer, S., Usmani, Z., Rani, R., and Gupta, P. (2020). Deciphering the Omics of Plant-Microbe Interaction: Perspectives and New Insights. *Curr. Genomics* 21, 343–362. doi: 10.2174/1389202921999200515140420

Siciliano, S. D., Fortin, N., Mihoc, A., Wisse, G., Labelle, S., Beaumier, D., et al. (2001). Selection of Specific Endophytic Bacterial Genotypes by Plants in Response to Soil Contamination. *Appl. Environ. Microbiol.* 67, 2469–2475. doi: 10.1128/AEM.67.6.2469-2475.2001

Singh, D., Dhillon, T. S., Javed, T., Singh, R., Dobaria, J., Dhankhar, S. K., et al. (2022). Exploring the genetic diversity of carrot genotypes through phenotypically and genetically detailed germplasm collection. *Agronomy* 12:1921. doi: 10.3390/agronomy12081921

Singh, M., Singh, D., Gupta, A., Pandey, K. D., Singh, P. K., and Kumar, A. (2019). "Chapter Three - Plant Growth Promoting Rhizobacteria: Application in Biofertilizers and Biocontrol of Phytopathogens," in *PGPR Amelioration in Sustainable Agriculture*, eds A. K. Singh, A. Kumar, and P. K. Singh (Sawston: Woodhead Publishing), 41–66. doi: 10.1016/B978-0-12-815879-1.00003-3

Smets, W., Wuyts, K., Oerlemans, E., Wuyts, S., Denys, S., Samson, R., et al. (2016). Impact of urban land use on the bacterial phyllosphere of ivy (Hedera sp.). *Atmos. Environ.* 147, 376–383.

Somers, E., Vanderleyden, J., and Srinivasan, M. (2004). Rhizosphere Bacterial Signalling: A Love Parade Beneath Our Feet. *Crit. Rev. Microbiol.* 30, 205–240. doi: 10.1080/10408410490468786

Staddon, P. L., Gregersen, R., and Jakobsen, I. (2004). The response of two Glomus mycorrhizal fungi and a fine endophyte to elevated atmospheric CO2, soil warming and drought. *Glob. Change Biol.* 10, 1909–1921.

Stephenson, C., and Black, C. R. (2014). One step forward, two steps back: The evolution of phytoremediation into commercial technologies. *Biosci. Horiz.* 7:hzu009–hzu009. doi: 10.1093/biohorizons/hzu009

Sukweenadhi, J., Kim, Y.-J., Choi, E.-S., Koh, S.-C., Lee, S.-W., Kim, Y.-J., et al. (2015). *Paenibacillus* yonginensis DCY84T induces changes in Arabidopsis thaliana gene expression against aluminum, drought, and salt stress. *Microbiol. Res.* 172, 7–15. doi: 10.1016/j.micres.2015.01.007

Tang, J., Xu, L., Chen, X., and Hu, S. (2009). Interaction between C4 barnyard grass and C3 upland rice under elevated CO2: Impact of mycorrhizae. *Acta Oecol.* 35, 227–235.

Tarkka, M., Schrey, S., and Hampp, R. (2008). "Plant Associated Soil Microorganisms," in *Molecular Mechanisms of Plant and Microbe Coexistence. Soil Biology*, eds C. S. Nautiyal and P. Dion (Berlin: Springer), 3–51. doi: 10.1007/978-3-540-75575-3_1

Terekhov, S. S., Smirnov, I. V., Malakhova, M. V., Samoilov, A. E., Manolov, I., Nazarov, A. S., et al. (2018). Ultrahigh-throughput functional profiling of microbiota communities. *Proc. Natl. Acad. Sci. U.S.A.* 115, 9551–9556. doi: 10.1073/pnas.1811250115

Terrer, C., Phillips, R. P., Hungate, B. A., Rosende, J., Pett-Ridge, J., Craig, M. E., et al. (2021). A trade-off between plant and soil carbon storage under elevated CO2. *Nature* 591, 599–603. doi: 10.1038/s41586-021-03306-8

Thakur, M. P., Del Real, I. M., Cesarz, S., Steinauer, K., Reich, P. B., Hobbie, S., et al. (2019). Soil microbial, nematode, and enzymatic responses to elevated CO2, N fertilization, warming, and reduced precipitation. *Soil Biol. Biochem.* 135, 184–193.

Trivedi, P., Leach, J. E., Tringe, S. G., Sa, T., and Singh, B. K. (2020). Plant–microbiome interactions: From community assembly to plant health. *Nat. Rev. Microbiol.* 18, 607–621. doi: 10.1038/s41579-020-0412-1

Tsers, I., Gorshkov, V., Gogoleva, N., Parfirova, O., Petrova, O., and Gogolev, Y. (2020). Plant soft rot development and regulation from the viewpoint of transcriptomic profiling. *Plants* 9:1176. doi: 10.3390/plants9091176

Turner, T. R., James, E. K., and Poole, P. S. (2013). The plant microbiome. *Genome Biol.* 14:209. doi: 10.3390/microorganisms9010188

Undugoda, L. J. S., Kandisa, R. V., Kannangara, S., and Sirisena, D. M. (2018). Plasmid Encoded Toluene and Xylene Degradation by Phyllosphere Bacteria. *J. Environ. Anal. Toxicol.* 8:559.

Vacher, C., Cordier, T., and Vallance, J. (2016). Phyllosphere fungal communities differentiate more thoroughly than bacterial communities along an elevation gradient. *Microb. Ecol.* 72, 1–3. doi: 10.1007/s00248-016-0742-8

Vaishnav, A., Kumari, S., Jain, S., Varma, A., Tuteja, N., and Choudhary, D. K. (2016). PGPR-mediated expression of salt tolerance gene in soybean through volatiles under sodium nitroprusside. *J. Basic Microbiol.* 56, 1274–1288. doi: 10.1002/jobm.201600188

van der Heijden, M. G. A., and Hartmann, M. (2016). Networking in the Plant Microbiome. *PLoS Biol.* 14:e1002378. doi: 10.1371/journal.pbio.1002378

van der Putten, W. H., Bradford, M. A., Pernilla Brinkman, E., van de Voorde, T. F. J., and Veen, G. F. (2016). Where, when and how plant–soil feedback matters in a changing world. *Funct. Ecol.* 30, 1109–1121.

Vandenkoornhuyse, P., Quaiser, A., Duhamel, M., le Van, A., and Dufresne, A. (2015). The importance of the microbiome of the plant holobiont. *New Phytol.* 206, 1196–1206. doi: 10.1111/nph.13312

Vangronsveld, J., Herzig, R., Weyens, N., Boulet, J., Adriaensen, K., Ruttens, A., et al. (2009). Phytoremediation of contaminated soils and groundwater: Lessons from the field. *Environ. Sci. Pollut. Res.* 16, 765–794. doi: 10.1007/s11356-009-0213-6

Vega, C., Rodríguez, M., Llamas, I., Béjar, V., and Sampedro, I. (2019). Silencing of Phytopathogen Communication by the Halotolerant PGPR Staphylococcus equorum Strain EN21. *Microorganisms* 8:42. doi: 10.3390/microorganisms8010042

Vessey, J. K. (2003). Plant growth promoting rhizobacteria as biofertilizers. *Plant Soil* 255, 571–586. doi: 10.1023/A:1026037216893

Vinayarani, G., and Prakash, H. (2018).Growth promoting rhizospheric and endophytic bacteria from *Curcuma longa L.* as biocontrol agents against rhizome rot and leaf blight diseases. *Plant Pathol. J.* 34:218. doi: 10.5423/PPJ.OA.11.2017.0225

Wahab, A., Abdi, G., Saleem, M. H., Ali, B., Ullah, S., Shah, W., et al. (2022). Plants' Physio-Biochemical and Phyto-Hormonal Responses to Alleviate the Adverse Effects of Drought Stress: A Comprehensive Review. *Plants* 11:1620. doi: 10.3390/plants11131620

Walther, G.-R., Roques, A., Hulme, P. E., Sykes, M. T., Pyšek, P., Kühn, I., et al. (2009). Alien species in a warmer world: Risks and opportunities. *Trends Ecol. Evol.* 24, 686–693. doi: 10.1016/j.tree.2009.06.008

Wang, B., Zhai, H., He, S., Zhang, H., Ren, Z., Zhang, D., et al. (2016). A vacuolar Na+/H+ antiporter gene, IbNHX2, enhances salt and drought tolerance in transgenic sweetpotato. *Sci. Hortic.* 201, 153–166.

Wang, S., Tan, Y., Fan, H., Ruan, H., and Zheng, A. (2015). Responses of soil microarthropods to inorganic and organic fertilizers in a poplar plantation in a coastal area of eastern China. *Appl. Soil Ecol.* 89, 69–75. doi: 10.1016/j.apsoil.2015.01.004

West, S. A., Fisher, R. M., Gardner, A., and Kiers, E. T. (2015). Major evolutionary transitions in individuality. *Proc. Natl. Acad. Sci. U.S.A.* 112, 10112–10119. doi: 10.1073/pnas.1421402112

Wetmore, K. M., Price, M. N., Waters, R. J., Lamson, J. S., He, J., Hoover, C. A., et al. (2015). Rapid quantification of mutant fitness in diverse bacteria by sequencing randomly bar-coded transposons. *mBio* 6:e00306–15. doi: 10.1128/mBio.00306-15

Wild, A. (2003). *Soils, Land and Food: Managing the Land During the Twenty-First Century*. Cambridge: Cambridge University Press.

Williams, A., Pétriacq, P., Beerling, D. J., Cotton, T. E., and Ton, J. (2018). Impacts of atmospheric CO2 and soil nutritional value on plant responses to rhizosphere colonization by soil bacteria. *Front. Plant Sci.* 9:1493. doi: 10.3389/fpls.2018.01493

Wintermans, P. C. A., Bakker, P. A. H. M., and Pieterse, C. M. J. (2016). Natural genetic variation in Arabidopsis for responsiveness to plant growth-promoting rhizobacteria. *Plant Mol. Biol.* 90, 623–634. doi: 10.1007/s11103-016-0442-2

Xu, J., Zhang, Y., Zhang, P., Trivedi, P., Riera, N., Wang, Y., et al. (2018a). The structure and function of the global citrus rhizosphere microbiome. *Nat. Commun.* 9:4894. doi: 10.1038/s41467-018-07343-2

Xu, L., Naylor, D., Dong, Z., Simmons, T., Pierroz, G., Hixson, K. K., et al. (2018b). Drought delays development of the sorghum root microbiome and enriches for monoderm bacteria. *Proc. Natl. Acad. Sci. U.S.A.* 115:E4284–E4293. doi: 10.1073/pnas.1717308115

Xu, L., Naylor, D., Dong, Z., Simmons, T., Pierroz, G., Hixson, K. K., et al. (2018c). Drought delays development of the sorghum root microbiome and enriches for monoderm bacteria. *Proc. Natl. Acad. Sci. U.S.A.* 115: E4284–E4293.

Yergeau, E., Sanschagrin, S., Maynard, C., St-Arnaud, M., and Greer, C. W. (2014). Microbial expression profiles in the rhizosphere of willows depend on soil contamination. *ISME J.* 8, 344–358. doi: 10.1038/ismej.2013.163

Yu, T., and Chen, Y. (2019). Effects of elevated carbon dioxide on environmental microbes and its mechanisms: A review. *Sci. Total Environ.* 655, 865–879.

Zainab, N., Amna, Khan, A. A., Azeem, M. A., Ali, B., Wang, T., et al. (2021). PGPR-Mediated Plant Growth Attributes and Metal Extraction Ability of *Sesbania sesban* L. in Industrially Contaminated Soils. *Agronomy* 11:1820.

Zameer, M., Zahid, H., Tabassum, B., Ali, Q., Nasir, I. A., Saleem, M., et al. (2016). PGPR Potentially Improve Growth of Tomato Plants in Salt-Stressed Environment. *Turk. J. Agric. Food Sci. Technol.* 4, 455–463. doi: 10.24925/turjaf.v4i6.455-463.614

Zhang, F., Jia-Dong, H. E., Qiu-Dan, N. I., Qiang-Sheng, W. U., and Zou, Y. N. (2018). Enhancement of drought tolerance in trifoliate orange by mycorrhiza: Changes in root sucrose and proline metabolisms. *Not. Bot. Horti. Agrobot. Cluj-Napoca* 46:270. doi: 10.15835/nbha46110983

Zhang, J., Liu, Y.-X., Zhang, N., Hu, B., Jin, T., Xu, H., et al. (2019). NRT1.1B is associated with root microbiota composition and nitrogen use in field-grown rice. *Nat. Biotechnol.* 37, 676–684. doi: 10.1038/s41587-019-0104-4

Zipfel, C., and Oldroyd, G. E. D. (2017). Plant signalling in symbiosis and immunity. *Nature* 543, 328–336. doi: 10.1038/nature22009

Zmora, N., Zeevi, D., Korem, T., Segal, E., and Elinav, E. (2016). Taking it Personally: Personalized Utilization of the Human Microbiome in Health and Disease. *Cell Host Microbe* 19, 12–20. doi: 10.1016/j.chom.2015.12.016

frontiers | Frontiers in Plant Science

TYPE Original Research
PUBLISHED 15 September 2022
DOI 10.3389/fpls.2022.871331

Check for updates

OPEN ACCESS

EDITED BY
Mohammad Anwar Hossain,
Bangladesh Agricultural University, Bangladesh

REVIEWED BY
Catherine Rayon,
University of Picardie Jules Verne, France
Ghazala Mustafa,
Quaid-i-Azam University, Pakistan

*CORRESPONDENCE
Saroj Kumar Sah
saroj1021@gmail.com
K. Raja Reddy
krreddy@pss.msstate.edu

†PRESENT ADDRESSES
Saroj Kumar Sah,
Biology Department, Brookhaven National Laboratory, Upton, NY, United States
Salah Jumaa,
Department of Field Crop Science, Tikrit University, Tikrit, Iraq

SPECIALTY SECTION
This article was submitted to Plant Biotechnology, a section of the journal Frontiers in Plant Science

RECEIVED 08 February 2022
ACCEPTED 05 August 2022
PUBLISHED 15 September 2022

CITATION
Sah SK, Jumaa S, Li J and Reddy KR (2022) Proteomic analysis response of rice (*Oryza sativa*) leaves to ultraviolet-B radiation stress. *Front. Plant Sci.* 13:871331. doi: 10.3389/fpls.2022.871331

COPYRIGHT
© 2022 Sah, Jumaa, Li and Reddy. This is an open-access article distributed under the terms of the Creative Commons Attribution License (CC BY). The use, distribution or reproduction in other forums is permitted, provided the original author(s) and the copyright owner(s) are credited and that the original publication in this journal is cited, in accordance with accepted academic practice. No use, distribution or reproduction is permitted which does not comply with these terms.

Proteomic analysis response of rice (*Oryza sativa*) leaves to ultraviolet-B radiation stress

Saroj Kumar Sah[1*†], Salah Jumaa[2†], Jiaxu Li[1] and K. Raja Reddy[2*]

[1]Department of Biochemistry, Molecular Biology, Entomology, and Plant Pathology, Mississippi State University, Mississippi State, MS, United States, [2]Department of Plant and Soil Sciences, Mississippi State University, Mississippi State, MS, United States

Rice (*Oryza sativa*) is a human staple food and serves as a model organism for genetic and molecular studies. Few studies have been conducted to determine the effects of ultraviolet-B (UV-B) stress on rice. UV-B stress triggers morphological and physiological changes in plants. However, the underlying mechanisms governing these integrated responses are unknown. In this study, we conducted a proteomic response of rice leaves to UV-B stress using two-dimensional gel electrophoresis and identified the selected proteins by mass spectrometry analysis. Four levels of daily biologically effective UV-B radiation intensities were imposed to determine changes in protein accumulation in response to UV-B stress: 0 (control), 5, 10, and 15 kJ m^{-2} d^{-1}in two cultivars, i.e., IR6 and REX. To mimic the natural environment, we conducted this experiment in Sunlit Soil-Plant-Atmosphere-Research (SPAR) chambers. Among the identified proteins, 11% of differentially expressed proteins were found in both cultivars. In the Rex cultivar, only 45% of proteins are differentially expressed, while only 27.5% were expressed in IR6. The results indicate that REX is more affected by UV-B stress than IR6 cultivars. The identified protein TSJT1 (spot 16) in both cultivars plays a crucial role in plant growth and development during stress treatment. Additionally, we found that UV-B stress altered many antioxidant enzymes associated with redox homeostasis and cell defense response. Another enzyme, the glyceraldehyde-3-phosphate dehydrogenase (GAPDH), has been identified as spot 15, which plays an essential role in glycolysis and cellular energy production. Another vital protein identified is glycosyl hydrolase (GH) as spot 9, which catalyzes the hydrolysis of glycosidic bonds in cell wall polymers and significantly affects cell wall architecture. Some identified proteins are related to photosynthesis, protein biosynthesis, signal transduction, and stress response. The findings of our study provide new insights into understanding how rice plants are tailored to UV-B stress *via* modulating the expression of UV-B responsive proteins, which will help develop superior rice breeds in the future to combat UV-B stress. Data are available *via* ProteomeXchange with identifier PXD032163.

KEYWORDS

***Oryza sativa*, ultraviolet-B stress, leaf-proteome, two-dimensional gel electrophoresis, mass spectrometry**

Introduction

Sunlight emits a broad spectrum of radiation: visible light, ultraviolet (UV), and infrared radiation, which reaches the Earth's surface (Kumar et al., 2016). Among these radiations, UV rays have direct and indirect effects at every level of the biological organization of plant molecules, affecting all ecosystems. The UV is divided into three different forms based on their wavelengths such as UV-A (320–400 nm), UV-B (280–320 nm), and UV-C (100–280 nm). Among them, UV-C is the most dangerous radiation, entirely absorbed by the ozone layer in the atmosphere. In contrast, UV-A radiation is unaffected, though such radiation does not harm plants. However, the UV-B radiation intensity is affected mainly by the thickness of the stratospheric ozone layer and is most harmful to plants (Sztatelman et al., 2015). The amount of UV-B radiation has increased due to stratospheric ozone (O3) depletion caused by anthropogenic chlorofluorocarbons. The increased doses of UV-B radiation cause severe biological effects on plants and other organisms. UV-B damages the cells at many levels, including altering DNA, proteins, and lipids (Brown and Jenkins, 2008). The UV-B also damages the photosynthetic pigments in plants because DNA and proteins can absorb the UV spectrum, declining the plants' photosynthetic efficiency (Wu et al., 2011). Besides these, a high level of UV-B enhances the production of reactive oxygen species (ROS), which activates stress signaling pathways (Brown and Jenkins, 2008). Mainly, UV-B radiation directly damages the DNA by forming dimers between adjacent pyrimidines in DNA strands, blocking DNA polymerase's progress and leading to cell death (Rastogi et al., 2010; Santos et al., 2012). Some genes are identified as UV-B dependent genes and are responsible for synthesizing UV screening compounds, DNA repairs, and activation of oxidative enzymes (Brosche and Strid, 2003). In addition, UV radiation causes downregulation of photosynthesis-related proteins, such as light-harvesting Chl a/b binding protein, whereas it upregulates protective proteins such as pathogen-related protein-1 (PR-1) at the mRNA level (Surplus et al., 1998). UV-B radiation also negatively affects leaf, hypocotyl, and seedling growth (Robson and Aphalo, 2012; Biever et al., 2014; Fina et al., 2017). The effects of UV-B have been studied in different crops like *Glycine max* (Liang et al., 2006; Peng and Zhou, 2009; Iii et al., 2013), *Triticum aestivum* (Agrawal and Rathore, 2007), *Hordeum vulgare* (Fedina et al., 2003), *Pisum sativum* (Qu et al., 2006), *Zea mays* (Casati et al., 2005; Reddy et al., 2013), and *Arabidopsis thaliana* (Sztatelman et al., 2015). Rice (*Oryza sativa* L.) is one of the most important staple food crops for human consumption and a model plant for genetic and molecular study. Some studies have been conducted on the physiological response of UV-B stress on rice (He et al., 1993; Dai et al., 1994; Roy and Roy, 2013); however, only a few studies (Du et al., 2011; Wu et al., 2011) have been conducted on the UV-B stress on protein levels. Therefore, the UV-B-induced proteomic study on rice will provide new insight into understanding the mechanisms underlying injurious and protective responses of crops during UV-B stress.

Nowadays, a proteomic approach to revealing the mechanisms of plants under stress has become the method of choice. Mass spectrometry is an essential tool in proteomic research (Li and Assmann, 2000). Innovation in mass spectrometry has significantly improved the study of protein structure and function. Especially when the genome sequence is unavailable, amino acid sequencing is required for protein identification. Amino acid sequence information can be determined by mass spectrometry, which allows homology searching and cloning or database identification of the corresponding gene (Shevchenko et al., 1997). In the past, Li and Assmann showed that the de novo peptide sequencing of a low-abundance broad bean (*Vicia faba*) protein isolated from two-dimensional gels illustrates the power of mass spectrometry for protein identification (Li and Assmann, 2000). In this study, the proteome analysis of the rice leaves was determined for two different varieties (*Japonica* REX and *Indica* IR6) irradiated by artificial UV-B radiation. IR6 and REX are more popular than other *Indica* and *Japonica* rice cultivars and are cultivated widely, especially in the United States. Both were considered tolerant stress to temperature and drought. Previously, we studied the effect of day/night temperatures on rubisco activity and electron transport in these two varieties (Singh et al., 2019). Moreover, our previous studies showed that IR6 performed very well under low and high temperatures (Reddy et al., 2021). Thus, we want to see how both these varieties perform under UV-B stress. Both varieties showed significant changes in the number and expression of various proteins using mass spectrometry analysis. Specific novel UV-B proteins were identified, and their role in UV-B stress was implicated. The findings of this study may provide new insights into understanding how rice plants adapt to UV-B stress by modulating the expression of UV-B responsive proteins and the relevant genes, which may provide information for cultivating superior rice breeds in the future.

Materials and methods

Plant materials and experimental conditions

This experiment used two varieties of rice: *Japonica* Rex and *Indica* IR6. The rice varieties were obtained from Dr. Ed Rodona, Rice Breeder, Delta Research and Extension Center, Stoneville, MS, USA. This study was conducted in sunlit Soil-Plant-Atmosphere-Research (SPAR) chambers located at the Rodney Foil Plant Research Center, Mississippi State University, Mississippi State (33°28′ N, 88°47′ W), USA. All the SPAR chambers are made up of a steel soil bin (1-m deep by 2 m long by 0.5 m wide) to accommodate the root system and a

Plexiglas chamber (2.5 m tall by 2.5 m long by 1.5 m wide) to accommodate aerial plant parts, a heating and cooling system, and an environmental monitoring and control system. The Plexiglas allows 97% of the visible solar radiation to pass without spectral variability in absorption and is opaque to solar UV-B radiation (280–320 nm) but transmits 12% of UV-A radiation (wavelength 320–400 nm). The lamps were wrapped with pre-solarized 0.07 mm cellulose diacetate film (JCS Industries Inc., La Mirada, CA) to avoid the germicidal effects of UV-C radiation. During these experiments, the measured minimum, maximum, and mean of daily solar radiation were 7.96, 31.22, and 22.34 ± 0.63 MJ m^{-2} d^{-1}, respectively. Temperatures in all SPAR units were maintained at 29/21°C (day/night) and CO_2 410 μmol mol^{-1} during the experimental period. Air temperature in all the SPAR units was documented and adjusted every 10 seconds within set points of 30/22°C (day/night) ± 0.5°C. The daytime temperature was initiated at sunrise and returned to the nighttime temperature 1 h after sunset (Reddy et al., 2013).

Growth conditions and treatments

Plant culture

Two varieties of rice seeds (Rex and IR6) were sown on May 10, 2017, in polyvinyl chloride pots (6" diameter by 12" high) filled with sand with a layer of gravel at the bottom. Each pot had a small hole at the bottom for excess water drainage. A total of 48 pots were used in the study. Six replicates per treatment for each variety were used. For each treatment, different SPAR chambers were used. Six pots per cultivar were arranged as a completely randomized design in six rows with two pots per row in each SPAR chamber (Supplementary Figure 1). Initially, four seeds were sown in each pot, and 11 days after emergence, the plants were thinned to one plant per pot. To ensure promising water and nutrients for growth, plants were irrigated three times a day with full-strength Hoagland's nutrient solution delivered at 08:00, 12:00, and 17:00 h through an automated and computer-controlled drip system.

UV-B radiation treatments

In the beginning, all the chambers were maintained at a 0 kJ m^{-2} d^{-1} UV-B level. Fifteen days after planting (15DAP), four levels of daily biologically effective UV-B radiation intensities, 0 (control), 5, 10, and 15 kJ m^{-2} d^{-1} were imposed and continued until harvest. The expected UV-B radiation dosage was provided by the square-wave UV-B supplementation system under near-ambient photosynthetically active radiation. The UV-B radiation was delivered daily from 08:00 to 16:00 h by eight fluorescent UV-313 lamps (Q-Panel Company, Cleveland, OH, USA) attached horizontally on a metal frame inside each chamber, powered by 40 W dimmable ballasts. However, the same setup was used in the control unit to simulate equal shading; however, the lamps were kept unilluminated. To filter out UV-C (<280 nm), we wrapped individual lamps with solarized 0.07 mm cellulose diacetate films (JCS Industries Inc., La Mirada, CA, USA), and these were replaced as needed to maintain the particular UV-B radiation treatment. The distance from the lamps to the plant canopy was maintained at 0.5 m and adjusted to match the plant height throughout the experiment. The anticipated UV-B level was supplied to the top of the plant canopy and was checked daily at 09:00 h with a UVX digital radiometer (UVP, Inc., San Gabriel, CA, USA) and standardized against an Optronic Laboratory Model 754 Spectroradiometer (Orlando, FL, USA) that was used initially to quantify lamp output. To ensure the plants received the exact UV-B dosage, we took the respective UV-B measurements at three locations, 50 cm apart, in each SPAR chamber. The measured average daily biologically effective UV-B radiation doses during the experimental period were 5.08 ± 0.13 for 5 KJ, 10.08 ± 0.14 for 10 kJ, and 15.9 ± 0.63 for 15 kJ of UV-B treatments.

Protein sample preparation

The second uppermost leaf of the treated rice plants was collected on the 20th day after UV-B exposure, control treatment, and 35 days after transplanting (35DAP). The samples were immediately frozen in liquid nitrogen and stored at −80°C for further use. Samples were ground to a fine powder in liquid nitrogen, and total proteins were extracted from rice leaves using the method of Wang et al. (2006), with slight modification. First, the 0.3–0.4 g fine powder was transferred into a 2 ml Eppendorf tube and filled with chilled 10% trichloroacetic acid (TCA)/acetone (Sigma-Aldrich, ≥ 99.0%). The mixture was vortexed and then centrifugated at 4°C for 3 mins at 16,000 x g, and the supernatant was discarded without touching the pellet with a glass pipette. The pellet was washed by adding 80% methanol plus 0.1 M ammonium acetate (Sigma, ∼98%) and further washed with 80% acetone at 4°C for 3 mins at 16,000 × g to remove residual TCA and contaminants. The pellet was air-dried in the hood for at least 10 mins to remove residual acetone. The pellet was suspended in a 1:1 ratio of phenol (pH 8.0) and sodium dodecyl sulfate (SDS) buffer [30% sucrose, 2% SDS (Bio-Rad, 1610302), 0.1 M Tris-HCl] supplemented with 5% 2-mercaptoethanol (Thermo-Fisher) and vortex for 30 s and then incubated at room temperature for 5–10 mins. The mixture was centrifuged at 16,000 × g for 3 mins at room temperature. The upper phenol phase (about 300 μl) was transferred into a new 2-ml Eppendorf tube, filled with five volumes of cold methanol plus 0.1 M ammonium acetate, and incubated at −20°C for about 2 h. After incubation, the mixture was centrifuged at 16,000 × g for 5 mins at 4°C, and

the supernatant was discarded without disturbing the pellet. The tube containing the pellet was filled with methanol plus 0.1 M ammonium acetate and centrifuged at 16,000 × g for 5 mins at 4°C. After centrifugation, the supernatant was discarded without disturbing the pellet. Finally, the pellet was washed with 80% acetone by centrifugation at 16,000 × g for 5 mins. The supernatant was discarded and pellet were air-dried to remove any remaining acetone, and the dried pellet (proteins) was stored in the tube at −80°C for further use.

Protein solubilization and quantification

The protein pellet was resuspended in an appropriate volume (about 150 μl) of rehydration buffer [9% urea, 4% 3-[(3-cholamidopropyl)dimethylammonium]-1-propanesulfonate (CHAPS) (GoldBio, 75621033), 50 mM Dithiothreitol (DTT; GoldBio, 27565419) supplemented with BioLyte 3/10 Ampholyte (Bio-Rad, 1632094). After gentle mixing, the mixture was incubated for 1 h with agitation. The protein samples were centrifuged at 16,000 xg at room temperature for 3 mins. The protein content in the supernatant was quantified using the modified Bradford assay (Bradford, 1976).

Two-dimensional gel (2-DE) electrophoresis

The 2-DE was performed using the precast immobilized pH gradient (IPG) strips (Bio-Rad Laboratories) in the first dimension by using an isoelectric focusing (IEF) system (PROTEAN IEF Cell, Bio-Rad Laboratories) according to the manufacturer's instructions. Rice leaf proteins (400 μg) in rehydration buffer (9 M urea, 4% CHAPS, 50 mM dithiothreitol, 0.1% Bio-Lyte Ampholyte) were added to individual channels of an IPG focusing tray (Bio-Rad Laboratories). The Bio-Rad IPG strips (pH 4–7, 11 cm) were then placed over the protein solutions in the channels of the IPG focusing tray. The protein samples were rehydrated in the IPG focusing tray at 50 Volt for 1 h. After rehydration, the samples were run at 250 Volt for 15 mins, then ramped to 8,000 Volt over 2.5 h, and kept at 8,000 Volt for 13 to 15 h. After isoelectric focusing, the IPG strips were equilibrated in equilibration buffer I (6 M urea, 0.375 M Tris-HCl, pH 8.8, 2% SDS, 20% glycerol, and 100 mM dithiothreitol) for 10 mins at room temperature and then placed in equilibration buffer II (100 mg Iodoacetamide, 6 M urea, 0.375 M Tris-HCl, pH 8.8, 2%SDS, 20% glycerol, and 0.01% bromophenol blue) for 10 mins. After incubation, the strips were directly placed on 12% polyacrylamide-SDS slab gels for second-dimension separation. Second-dimension gels were run at 8 mA per gel using a vertical gel electrophoresis system (R. Shadel Inc.). The same gel was stained with colloidal Coomassie blue or silver nitrate, and then the sensitivity in detecting different proteins between colloidal Coomassie staining and silver staining was compared. The results also showed that silver staining is more sensitive than colloidal Coomassie staining and provides better resolution of the spots (Supplementary Figure 2). After that, all the gels were then stained with silver staining, as described by Shevchenko et al. (1996), with minor modifications.

Image analysis

After staining, the 2-DE images were obtained with a ChemiDoc Touch imaging system (Bio-Rad Laboratories), and protein spots were detected and analyzed with Image Lab 6.0 (Bio-Rad Laboratories). Silver-stained gels were stored in a 1% acetic acid solution at 4°C until further analysis.

Protein digestion and mass spectrometry analysis

Protein spots on stained 2-DE gels were cut into ∼1 mm^3 pieces. Gel pieces were then subjected to a modified in-gel trypsin digestion procedure (Shevchenko et al., 1996). The samples were reduced by using DTT (1 mM concentration in 50 mM ammonium bicarbonate) for 30 mins at 60°C. The samples were then cooled to room temperature, and iodoacetamide (5 mM) was added for 15 mins in the dark at room temperature. DTT (5 mM) was then added to quench the reaction. Then sequence grade trypsin (Promega, Madison, WI) 5 ng/μl was added. After 45 mins, the excess trypsin solution was removed and replaced with a 50 mM ammonium bicarbonate solution to cover the gel pieces. The digestion was performed overnight at 37°C. Peptides were later extracted by removing the ammonium bicarbonate solution, followed by one wash with a solution containing 50% acetonitrile and 1% formic acid. The extracts were then dried in a speed-vac (∼1 h). The samples were then stored at 4°C until analysis. On the analysis day, the samples were reconstituted in 5–10 μl of HPLC solvent A (2.5% acetonitrile, 0.1% formic acid). A nano-scale reverse-phase HPLC capillary column was created by packing 2.6 μm C18 spherical silica beads into a fused silica capillary (100 μm inner diameter × ∼30 cm length) with a flame-drawn tip (Peng and Gygi, 2001). After equilibrating the column, each sample was loaded onto the column *via* a famous autosampler (LC Packings, San Francisco, CA). A gradient was formed, and peptides were eluted with increasing concentrations of solvent B (97.5% acetonitrile, 0.1% formic acid). As peptides were eluted, they were subjected to electrospray ionization and then entered into an LTQ Orbitrap Velos Pro ion-trap mass spectrometer (Thermo Fisher Scientific, Waltham, MA). Peptides were detected, isolated, and fragmented to produce a tandem mass spectrum of

specific fragment ions for each peptide. Peptide sequences (and hence protein identity) were determined by matching protein databases (http://www.uniprot.org/proteomes/?query=taxonomy:39947) with the acquired fragmentation pattern by the software program, Sequest (Thermo Fisher Scientific, Waltham, MA) (Eng et al., 1994). All databases include a reversed version of all the sequences, and the data were filtered to between a one and two percent peptide false discovery rate.

Functional analysis

Gene ontology(GO) annotation was performed *via* the Gene Ontology Database at (http://systemsbiology.cau.edu.cn/agriGOv2/) (Tian et al., 2017). The GO function of the identified proteins was classified into three categories, i.e., biological process, molecular process, and cellular component. The annotated GO term was plotted *via* a web tool, WEGO 2.0 (https://wego.genomics.cn/) (Ye et al., 2018). The pathway analysis was performed using the database RiceNetDB (http://bis.zju.edu.cn/ricenetdb/). The annotation was performed using the Kyoto Encyclopedia of Genes and Genomes (KEGG) (Liu et al., 2013). The gene functions were categorized based on databases, including the Rice Annotation Project Database (RAP-DB) build 5.0 (Sakai et al., 2013) by the International Rice Genome Sequencing Project (IRGSP), the MSU Rice Genome Annotation Database (Ouyang et al., 2007), and the Oryzabase Integrated Rice Science Database (https://shigen.nig.ac.jp/rice/oryzabase/).

Results

Morphological effects of UV-B on rice plants

In this study, the seedlings of two rice cultivars (REX, IR6) were treated with UV-B irradiation of 5, 10, and 15 kJ m^{-2} d^{-1} for 8 h daily. There is no morphological damage to plants, except for the fact that plants were shorter than the control (Figure 1). The plant height in both cultivars significantly differs between the treatments and cultivars. The UV-B effects on plant height in Rex cultivars are more severe than IR6 (Figure 1A). While increasing the UV-B dose, the plants become shorter in both varieties (Figure 1A). IR6 has more tillers than Rex, but there is no effect of UV-B stress on tiller number per plant in both cultivars compared to control (Figure 1B). The highly significant decreasing pattern in leaf numbers in both varieties is observed as UV-B stress dose increases compared to control (Figure 1C).

Differentially expressed protein in rice cultivars under UV-B stress

Proteomic analysis of rice leaves 2D-GE carried out the protein of two varieties modulated by UV-B stress. Each 2D-GE gel had ∼1,000 protein spots covering a 4.0–7.0 pH range and a molecular weight of 4–120 KDa, based on their isoelectric points. Seventeen spots, labeled 1 to 17, showed significant changes in the IR6 varieties under three different levels of UV-B stress compared to their respective controls (Figure 2A). Similarly, 23 spots labeled 18 to 40 exhibited significant changes in the rice Rex varieties compared to control in UV-B stress (Figure 2B). Figure 2 shows the representative 2D-GE gel images of IR6 and Rex. By comparing the gels produced in the three different doses of UV-B treatment, the 18 spots in the IR6 variety displayed significant changes in expression. These protein spots exhibited altered expression profiles (1, 2, 4–11, 14–18, 21, 34, and 37; Figure 2) were successfully identified by mass spectrometry (Table 1). Similarly, there are 30 spots in Rex varieties in the different UV-B treatment, i.e., spot 1, 4–6, 14–16, 1–40 (Table 1). Among these spots, 11 spots were identified in both varieties. These spots were No. 1, 4–6, 14–16, 17, 21, 34, 37, and 40 (Table 1). Out of 11 spots, six spots (No. 4, 5, 14, 16, 21, and 37) showed a similar expression pattern in both the varieties in all the different levels of UV-B treatment (Table 2). Altogether, in both varieties, 40 spots were identified. The Venn diagram showed the differentially expressed proteins in both the cultivars (Figure 3A). A total of 45% of proteins were differentially expressed in the Rex cultivar, whereas only 27.5% were expressed in the IR6 cultivar. Moreover, 11% of differentially expressed proteins were common in both cultivars (Figure 3A). These results suggest that REX is more affected by UV-B stress than IR6 cultivars.

Functional classification of protein spots

Forty protein spots exhibited altered expression profiles in both rice varieties (Figure 2). Among them, spot 12, 35, 16, and 39 were the same protein (Table 1). We next conducted a functional analysis of all identified proteins by mass spectrometry. Go enrichment analysis showed that proteins are involved in the metabolic and cellular processes in the subcategory of biological processes (Figure 3B). In addition, most of the proteins are also associated with molecular functions such as catalytic activity and binding (Figure 3B).

We did a pathway analysis further to understand the potential roles and significance of identified proteins. The KEGG analysis showed that most of the proteins are involved in metabolic pathways (Supplementary Table 2), which suggests that UV-B stress has a potential role in metabolic pathway regulation. Moreover, the cellular component analysis

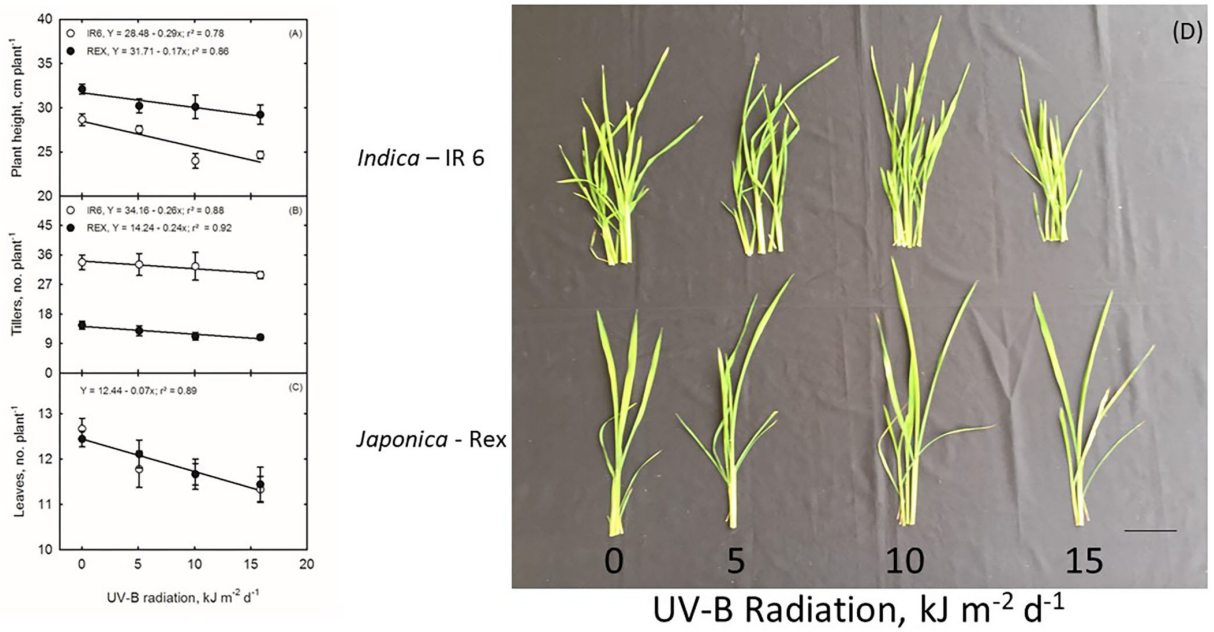


FIGURE 1
(A–D) Ultraviolet-B Effects on Rice Plants. Scale bar 2 cm.

showed that the identified proteins mainly resided in the cell, cell part, or as a part of protein-containing complexes (Figure 3B).

Most identified proteins are involved in metabolism, photosynthesis, protein biosynthesis, and redox homeostasis (Table 2). Few proteins—such as peptidyl-prolyl cis-trans isomerase, eukaryotic translation initiation factor 5A, glycin-rich protein two—were involved in signal transduction. Three proteins are detected, i.e., universal stress protein domain-containing protein, gibberellin receptor, and expressed protein (Table 2) implicated in stress response. There are 7 spots identified in metabolism (i.e., spots 37, 15, 14, 8,13, 9, and 19). Spots 37 is identified as a triosephosphate isomerase (TPI), a glycolytic enzyme that catalyzes the reversible interconversion of dihydroxyacetone phosphate to glyceraldehyde-3-phosphate. In both the cultivars, TPI is upregulated at 5, 10, and 15 kJ m^{-2} d^{-1} UV-B levels compared to control (Table 2). Another important protein is identified as spot 15, which is glyceraldehyde-3-phosphate dehydrogenase (GAPDH). GAPDH expression is decreased in both the cultivars under 5 and 10 kJ m^{-2} d^{-1} UV-B levels compared to control, whereas the expression is high in IR6 under 15 kJ m^{-2} d^{-1} UV-B levels compared to control. Similarly, fructose-bisphosphate aldolase, putative, is identified as spot 14, which is downregulated in both the cultivars under all the UV-B dose levels compared to control. Dehydrogenase and NAD(P) binding domain-containing protein were only detected in IR6 at 5 kJ m^{-2} d^{-1} UV-B levels compared to control. Similarly, glycosyl hydrolases (i.e., spot 9) are upregulated only in IR6 under all the UV-B dose levels compared to control. Likewise, spot 19 is identified as an uncharacterized oxidoreductase, upregulated in IR6 under all the UV-B dose levels compared to control (Table 2).

Like in metabolism, seven proteins have been identified in the photosynthesis process. In this functional category, the same protein identified in two spots (i.e., spots 12 and 35) belongs to the family of light-harvesting complex chlorophyll a/b-binding proteins. Spots 35 were only detected in REX, not in the IR6 cultivar. Under 5 and 15 kJ m^{-2} d^{-1} UV-B level, chlorophyll a/b-binding protein is upregulated in REX cultivars, whereas the expression is decreased under 10 kJ m^{-2} d^{-1} UV-B level. However, in IR6, this protein is detected at the 5 kJ m-2 d-1 UV-B level, whose expression is also upregulated like in another cultivar (Table 2). Similarly, another protein in the same family is identified as spot 40, only detected in the REX cultivar. Photosystem II, CP43 reaction center protein, is recognized as spot 18. It is upregulated in both the cultivars at 5 and 10 kJ m^{-2} d^{-1} UV-B levels as compared to the control. However, this protein is downregulated in both the cultivars at the 15 kJ m^{-2} d^{-1} UV-B level as compared to the control (Table 2). Oxygen-evolving enhancer protein 1 is identified as two spots, i.e., 17 and 23, and expression is decreased under all levels of UV-B dose as compared to the control and only detected in the REX cultivar (Table 2). The 60 kDa chaperonin alpha subunit is identified as spot 1 and is noticed in both cultivars. At the 5 kJ m^{-2} d^{-1} UV-B level, expression of chaperonin protein

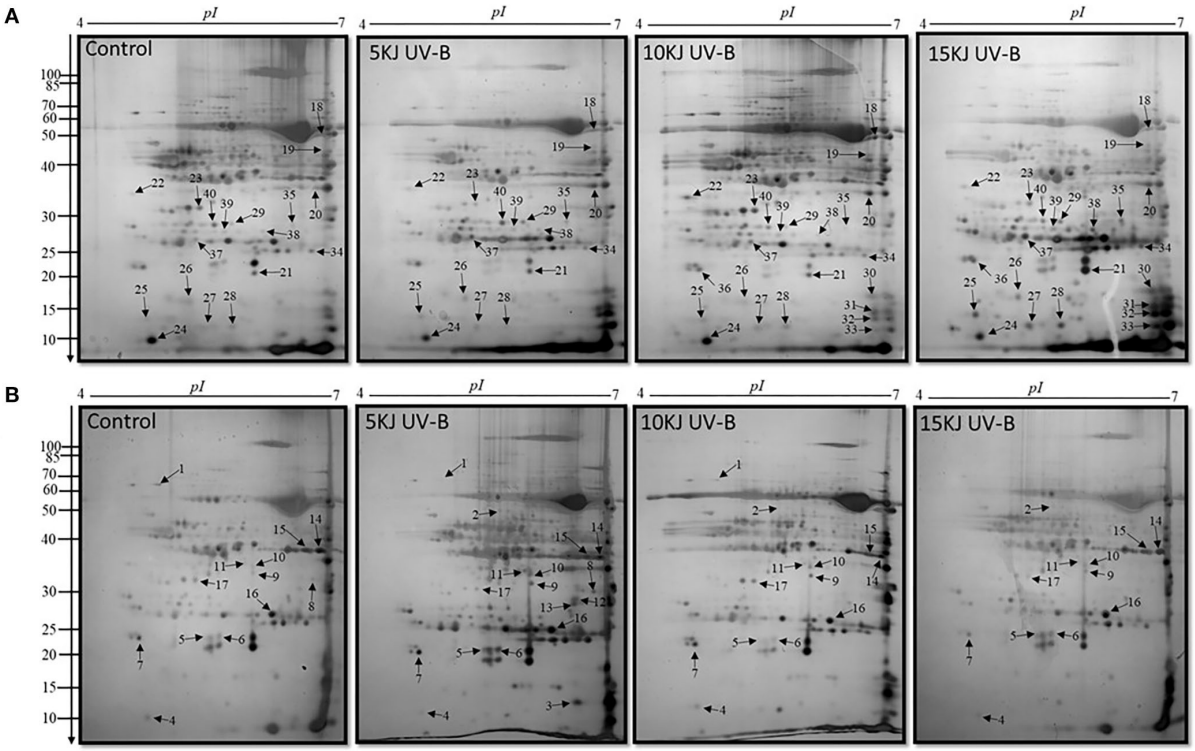


FIGURE 2
2D-GE maps of rice leaves proteins during 5, 10, and 15 kJ m^{-2} d^{-1} UV-B exposure along with control **(A)** cultivar REX **(B)** cultivar IR6. Quantitative image analysis revealed 40 differential spots were up and downregulated with silver staining. The black arrowheads showed the number of proteins identified. The numbers at the left of each panel are molecular masses in kilodaltons.

is high in Rex but decreased in IR6; however, at the 10 kJ m^{-2} d^{-1} UV-B level, expression of this protein was reduced in both the cultivars (Table 2). Three proteins have been identified in the stress response category, i.e., spots 21, 22, and 29, and the expression level is high under all levels of UV-B dose in the REX cultivar, whereas only spot 21 has been detected in the IR6 cultivar, whose expression is high at the 5 and 10 kJ m^{-2} d^{-1} UV-B level but low at the 15 kJ m^{-2} d^{-1} UV-B levels as compared to control. UV-B also played a significant role in plant growth and development. Two spots (i.e., spots 16 and 39) have been identified in this category as the same protein, which is stem-specific protein TSJT1. TSJT1 expression levels are increased in both cultivars, which may explain why the plants look shorter after the UV-B treatment. Likewise, in stress response, there are three proteins identified in the signal transduction category as spots 7, 26, and 34 (Table 2). Another category is redox homeostasis, in which there are eight proteins identified, i.e., spots 6, 10, 24, 25, 27, 28, 30, and 38. Only one protein identified in the storage protein category, spot 5, is recognized as a germin-like protein. In addition, seven proteins have been identified in the protein biosynthesis category. In these categories, ribosomal proteins are the most predominant proteins (Table 2).

Discussion

Unlike studies conducted in greenhouses, this research is carried out in (SPAR) chambers, which are closer to the natural environment. In this study, two varieties were used to compare the three levels of UV-B stress (5, 10, and 15 kJ m^{-2} d^{-1}) to control. In this work, we discovered 38 distinct proteins that were differentially expressed in both cultivars at different UV-B exposure levels compared to controls. We found 38 proteins, including previously known proteins. We also identified some novel proteins. According to identified proteins and their expression levels, the REX cultivar is more sensitive to UV-B damage than IR6 (Figures 2, 3A).

Effect of UV-B on plant growth and development-related proteins

Our studies identified the TSJT1 protein as spot 16 in both cultivars. After applying the UV-B stress, the expression of TSJT1 increases in both the cultivars compared to the control. Only a few studies have been conducted on the TSJT1 protein. In plants, internode elongation is correlated with cell elongation

TABLE 1 List of proteins in rice leaves under UV-B stress identified by mass spectrometry.

Spot no.	Protein description	Accession no.	pI	Mw	% Sequence coverage	FDR
1	60 kDa chaperonin alpha subunit	LOC_Os12g17910.1	5.12	61,129.76	39.62	0.000
2	Histidinol dehydrogenase, chloroplast precursor	LOC_Os01g13190.1	6.03	50,566.08	9.51	0.000
3	Ubiquitin-conjugating enzyme, putative, expressed	LOC_Os12g41220.1	6.42	16,664.90	32.19	0.000
4	Glycine Cleavage system H proten, mitochondrial	LOC_Os10g37180.1	4.92	17,367.31	8.54	0.000
5	Germin-like protein 8-14/Cupin domain containing protein	LOC_Os08g35760.1	6.01	21,861.22	9.39	0.000
6	Glyoxalase family protein, expressed	LOC_Os05g22970.1	5.84	21,329.11	32.8	0.000
7	Peptidyl-prolyl cis-trans isomerase, putative expressed	LOC_Os02g02890.1	8.61	18,360.98	18.02	0.000
8	dehydrogenase, putative, expressed	LOC_Os01g53910.1	6.52	32,019.87	35.44	0.000
9	glycosyl hydrolase, putative, expressed	LOC_Os05g15770.1	6.08	32,548.96	13.13	0.000
10	26S proteasome non-ATPase regulatory subunit 14	LOC_Os01g16190.1	6.12	34,338.55	17.59	0.000
11	ubiquinone biosynthesis protein COQ9, mitochondrial precursor	LOC_Os03g29180.1	5.82	34,328.53	10.67	0.000
12	chlorophyll A-B binding protein, putative	LOC_Os01g64960.1	6.41	27,903.34	26.87	0.000
13	expressed protein	LOC_Os03g60740.1	6.34	27,910.55	31.13	0.000
14	Fructose-bisphosphate aldolase	LOC_Os08g02700.1	6.62	38,393.58	3.87	0.000
15	glyceraldehyde-3-phosphate dehydrogenase, putative, expressed	LOC_Os04g40950.1	6.34	36,772.98	6.53	0.000
16	Stem-specific protein TSJT1, putative, expressed	LOC_Os03g53270.1	6.05	26,432.92	25.9	0.000
17	oxygen-evolving enhancer protein 1, chloroplast precursor	LOC_Os01g31690.1	6.08	34,861.42	57.96	0.000
18	Photosystem II CP43 reaction center protein	LOC_Os04g16874.1	6.71	52,076.13	14.59	0.000
19	uncharacterized oxidoreductase, putative, expressed	LOC_Os10g26400.2	6.51	41,013.19	26.84	0.000
20	Peroxidase precursor, putative, expressed	LOC_Os03g22010.1	6.51	33,426.69	21.56	0.000
21	Ethylene-responsive protein-like	LOC_Os02g47840.1	5.96	19,874.78	19.21	0.000
22	gibberellin receptor, putative, expressed	LOC_Os09g28630.1	4.95	33,240.63	16.19	0.000
23	oxygen-evolving enhancer protein 1, chloroplast precursor	LOC_Os01g31690.1	6.08	34,861.42	63.36	0.000
24	glyoxalase family protein	LOC_Os02g17920.1	4.32	8,982.11	40.24	0.000
25	pathogenesis-related Bet v I family protein, putative, expressed	LOC_Os12g36880.1	4.88	16,687.92	13.92	0.000
26	Eukaryotic translation initiation factor 5A	LOC_Os07g02210.2	5.45	17,765.89	17.9	0.000
27	Glyoxalase family protein, expressed	LOC_Os03g45720.1	5.47	15,174.04	53.19	0.000
28	Superoxide dismutase [Cu-Zn], chloroplastic	LOC_Os08g44770.1	5.79	21,300.99	36.02	0.000
29	expressed protein	LOC_Os08g16570.1	5.89	31,852.54	42.52	0.000
30	osmotin, putative, expressed	LOC_Os12g38170.1	6.27	23,787.37	20.17	0.000
31	30S ribosomal protein S7, chloroplastic	LOC_Os10g21372.1	11.82	17,628.78	26.28	0.000
32	40S ribosomal protein S16	LOC_Os12g03090.1	10.58	16,818.90	27.52	0.000
33	40S ribosomal protein S19	LOC_Os03g31090.1	10.04	16,386.81	23.97	0.000
34	Cold shock domain protein 1	LOC_Os02g02870.1	6.64	22,723.36	12.03	0.000
35	chlorophyll A-B binding protein, putative, expressed	LOC_Os01g64960.1	6.41	27,903.34	11.19	0.000
36	ubiquitin-conjugating enzyme E2-22 kDa, putative, expressed	LOC_Os01g70140.1	4.95	21,323.19	26.15	0.000
37	Triosephosphate isomerase, cytosolic	LOC_Os01g05490.1	5.38	27,062.95	35.57	0.000
38	Proteasome subunit alpha type-3/peptidase, T1 family	LOC_Os01g59600.2	5.74	27,238.06	34.14	0.000
39	stem-specific protein TSJT1, putative, expressed	LOC_Os03g53270.1	6.05	26,432.92	20.72	0.000
40	chlorophyll A-B binding protein, putative, expressed	LOC_Os03g39610.1	5.62	28,495.40	15.97	0.000

Spot No. corresponds to the spot numbers on the gels in Figure 2. MW, Calculated molecular mass in kilodalton (kD) and pI, isoelectric point based on protein sequence annotated in the UniProt database.

and cell division. Hu and coworkers reported that TSJT1 might act as a negative regulator in castor internode development (Hu et al., 2016). Another study demonstrated that the abundance of TSJT1 was decreased in the dwarf variety Zhebi 100 compared to Zhebi 26. Zhebi 26 suggests that TSJT1 plays a role in node development. Additionally, the expression of the TSJT1 protein demonstrated higher drought stress in roots and leaves in two cassava cultivars—SC124 and Arg7—which were identified in proteomic analysis (Zhao et al., 2015). Our study also observed that the plant height decreases after applying UV-B stress, and

10.3389/fpls.2022.871331

TABLE 2 Functional classification and expression pattern of proteins in rice leaves under different levels of UV-B response.

Functions	Spot no.	Protein spots description	Change pattern in REX				Change pattern in IR6			
			C	5	10	15	C	5	10	15
Cell defense	11	Ubiquinone biosynthesis protein COQ9, mitochondrial precursor	ND	ND	ND	ND	+	↑	↑	↓
	20	Peroxidase precursor, putative, expressed	+	↑	↑	↑	ND	ND	ND	ND
Growth and development	16	Stem-specific protein TSJT1, putative, expressed	+	↑	↑	↑	+	↑	↑	↑
	39	Stem-specific protein TSJT1, putative, expressed	+	↑	↑	↑		ND	ND	ND
Metabolism	37	Triosephosphate isomerase, cytosolic	ND	↑	↑	↑	+	↑	↑	↑
	15	Glyceraldehyde-3-phosphate dehydrogenase, putative, expressed	+	↓	↓	↓	+	↓	↓	↑
	14	Fructose-bisphosphate aldolase	+	↓	↓	↓	+	↓	↓	↓
	8	Dehydrogenase, putative, expressed	ND	ND	ND	ND	+	↑	ND	ND
	13	NAD(P)-binding domain containing protein expressed protein	ND	ND	ND	ND	ND	+	ND	ND
	9	Clycosyl hydrolase, putative, expressed	ND	ND	ND	ND	+	↑	↑	↑
	19	Uncharacterized oxidoreductase, putative, expressed	ND	↑	↑	↓	ND	ND	ND	ND
Photosynthesis	35	Chlorophyll A-B binding protein, putative, expressed	+	↑	↓	↑	ND	ND	ND	ND
	12	Chlorophyll A-B binding protein, putative	ND	ND	ND	ND	ND	+	ND	ND
	40	Chlorophyll A-B binding protein, putative, expressed	+	↓	↓	↓	ND	ND	ND	ND
	18	Photosystem II CP43 reaction center protein	+	↑	↑	↓	+	↑	↑	↓
	17	Oxygen-evolving enhancer protein 1, chloroplast precursor	ND	ND	ND	ND	+	↓	↓	↓
	23	Oxygen-evolving enhancer protein 1, chloroplast precursor	ND	ND	ND	ND	+	↓	↓	↓
	1	60 kDa chaperonin alpha subunit	+	↑	↓	↓	+	↓	↓	ND
Protein biosynthesis	3	Ubiquitin-conjugating enzyme, putative, expressed	ND	ND	ND	ND		ND	ND	ND
	2	Histidinol dehydrogenase, chloroplast precursor	ND	ND	ND	ND	ND	↑	↓	↓
	4	Glycine Cleavage system H proten, mitochondrial	+	↓	↑	↓	+	↓	↑	↓
	31	30S ribosomal protein S7, chloroplastic	ND	ND	↑	↑	ND	ND	ND	ND
	32	40S ribosomal protein S16	ND	ND	↑	↑	ND	ND	ND	ND
	33	40S ribosomal protein S19	ND	ND	↑	↑	ND	ND	ND	ND
	36	Ubiquitin-conjugating enzyme E2-22 kDa, putative, expressed	ND	ND	↑	↑	ND	ND	ND	ND
Redox Homeostasis	28	Superoxide dismutase [Cu-Zn], chloroplastic	+	↑	↑	↑	ND	ND	ND	ND
	10	26S proteasome non-ATPase regulatory subunit 14	ND	ND	ND	ND	+	↑	↑	↑
	38	Proteasome subunit alpha type-3/peptidase, T1 family	+	↑	↓	↑		ND	ND	ND
	6	Glyoxalase family protein, expressed	+	↓	↓	↑	+	↑	↓	↑
	24	Glyoxalase family protein	+	↓	↑	↓	ND	ND	ND	ND
	25	Pathogenesis-related Bet v I family protein, putative, expressed	+	↑	↑	↑	ND	ND	ND	ND
	27	Glyoxalase family protein, expressed	+	↑	↓	↑	ND	ND	ND	ND
	30	Osmotin (pathogen-related protein 5), putative, expressed	ND	ND	↑	↑	ND	ND	ND	ND
Signal transduction	7	Peptidyl-prolyl cis-trans isomerase, putative expressed	ND	ND	ND	ND	+	↑	↑	↓
	26	Eukaryotic translation initiation factor 5A	+	↑	↓	↑	ND	ND	ND	ND
	34	Glycine-rich protein 2, putative expressed	+	↓	↓	↑	+	↑	↓	↓
Storage Protein	5	Germin-like protein 8-14/Cupin domain containing protein	+	↑	↓	↑	+	↑	↓	↑
Stress response	21	Universal stress protein domain containing protein	+	↑	↑	↑	+	↑	↑	↑
	22	Gibberellin receptor, putative, expressed	+	↑	↑	↑	ND	ND	ND	ND
	29	Expressed protein	+	↑	↑	↑	ND	ND	ND	ND

"ND" indicates not detected protein spots; "+" indicates "detected" protein spots in control; The up arrow "↑" indicates upregulated protein spots related to the control, and the down arrow "↓" indicates down-regulated protein spots related to the control.

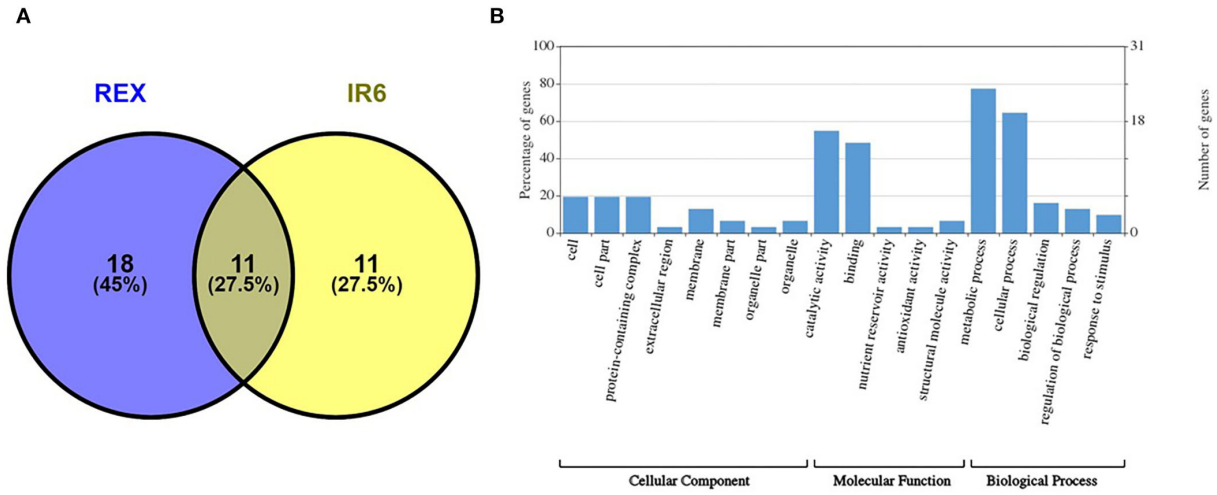


FIGURE 3
(A) Venn diagram showing the differentially expressed proteins in the cultivars REX and IR6 **(B)** GO enrichment analysis of identified proteins. The number of proteins enriched with each GO term in one of the three categories, including biological process, molecular function, and cellular component, is shown.

TSJT1 expression increases as UV-B stress is imposed. These results imply that TSJT1 inhibits plant growth and development when exposed to stress.

Effect of UV-B on cell defense and redox homeostasis-related proteins

Reactive oxygen species (ROS) play a dual role as critical regulators of growth, development, and defense pathways and toxic byproducts of aerobic metabolism (Mittler et al., 2004). The production of ROS is associated with the loosening of the plant cell wall during cell elongation. Rapid plant growth is characterized by an increase in antioxidation capacity since excessive ROS generation might damage cells (Cui et al., 2012; Hu et al., 2016). An alternative method, such as ROS scavenging by superoxide dismutase, can control ROS levels in plants (Goossens et al., 2003). In our study, UV-B stress caused changes in a number of antioxidation enzymes related to redox homeostasis and cell defense response proteins. In this study, UV-B stress treatment in cultivar REX increased the abundance of superoxide dismutase (spot 28), pathogenesis-related Bet V I family protein (spot 25), osmotin (pathogen-related protein 5) (spot 30), and peroxidase precursor (spot 20) as compared to control. Hu et al. (2016) also reported that—in the castor bin (high stalk variety Zhebi 100)—peroxidase precursor, and superoxide dismutase abundance were increased. The results presented above, including previously published data, suggest that the enhanced abundance of these proteins may also imply that the anti-oxidative defense system and resistance to UV-B stress are increased in cultivar REX as compared to control. These proteins were not detected in IR6.

Effect of UV-B on metabolism-related proteins

Glyceraldehyde-3-phosphate dehydrogenase (GAPDH) is an important enzyme involved in glycolysis and cellular energy production associated with plant development (Giegé et al., 2003). The primary function of GAPDH is to catalyze the conversion of glyceraldehyde-3-phosphate to 1,3-bisphosphoglycerate within the glycolytic pathways; therefore, it plays a crucial role in energy metabolism (Voss et al., 2007). Voss et al. (2007) used GAPDH as a model protein to study oxidative damage caused by irradiation such as UV-A, UV-B, and infrared (IR). They showed that only UV-B irradiation was more aggressive and that UV-B acted on specific amino acids, such as arginine, proline, and tyrosine (Voss et al., 2007). Our study identified that GAPDH (spot 15) and fructose-bisphosphate aldolase (spot 14) were decreased under UV-B stress. This agrees with an earlier report on cyanobacteria under UV-B stress using two-dimensional gel electrophoresis and matrix-assisted laser desorption/ionization-time of flight mass spectrometry (MALDI-TOF MS) (Babele et al., 2015). The enzyme fructose-bisphosphate aldolase occupies a central position in glycolysis and gluconeogenesis (Ziveri et al., 2017). Fructose-1,6 bisphosphate aldolase is an essential enzyme that converts fructose-1, 6-bis phosphate to glyceraldehyde-3-phosphate and dihydroxyacetone 3-phosphate. Under the stress conditions, glyceraldehyde-3-phosphate and fructose-1,

6 bis phosphate may be converted to glucose-6-phosphate to carry out the pentose phosphate pathway for NADPH synthesis (Nakahara et al., 2003). This may explain why both enzymes were downregulated in our study during UV-B stress. Fructose-bisphosphate aldolase is essential for bacterial multiplication and participates in the control of host redox homeostasis and the inflammatory immune response (Ziveri et al., 2017). This study also identified triosephosphate isomerase (OsTPI1.1) as spot 37. Interestingly, we found that OsTPI1.1 is upregulated in both cultivars under UV-B stress. The triosephosphate isomerase enzyme catalyzes the interconversion of dihydroxyacetone phosphate (DHAP) and GAPDH during glycolysis and gluconeogenesis. OsTPI1.1 also modulates ROS production as a resistance mechanism against *Xanthomonas oryzae pv oryzae (Xoo)* (Liu et al., 2018). *Xoo* causes severe damage to rice production worldwide (Liu et al., 2018). The above results, including our finding, suggest that UV-B plays a role in metabolic pathways, cell defense, and transcriptional regulation.

Effect of UV-B on cell wall architecture

Moreover, in this study, we identified glycosyl hydrolase (GH) as spot 9, whose expression has increased in IR6. However, GH was not detected in the REX cultivar. The primary function of GH is to catalyze the hydrolysis of glycosidic bonds in cell wall polymers and can have significant effects on cell wall architecture (Sharma et al., 2013). In rice, 437 GH genes are classified into 34 families. They identified 138 GH genes that are highly diverged between monocots and dicots, 57 of which have diverged further in rice as compared with four monocot genomes. They found two-thirds of GH genes in rice are upregulated in response to biotic and abiotic stress treatments (Sharma et al., 2013). In our study, GH is also upregulated, suggesting that UV-B stress treatment plays a role in abiotic and biotic stress adaptation and cell wall architecture. So far, GH has not been identified in the UV-B stress study. GH is the new protein we identified in UV-B stress treatment, suggesting that it may have a new function in cell wall architecture under UV-B stress.

Effect of UV-B on photosynthesis-related proteins

Photosynthesis and protein biosynthesis have a significant function in plant growth and development. UV-B responses on plant species and even genotypes within species are different (Yuan et al., 2000). Under UV-B stress, *Oryza sativa* cultivar Lemont, produced more water-soluble proteins without any harmful effects on rice leaf photosynthetic properties, which suggests that it might be related to its UV-B tolerance. However, in the same dose, it caused damage to pea plants (He et al., 1993). The net photosynthesis rate increased under moderate UV-B irradiation in *Pseudotsuga menziesii* (Bassman et al., 2002). The photosynthesis rate of *Acorus calamus* L. (sweet flag) plants was increased under low UV-B treatment, which led to increased biomass (Kumari et al., 2009). Similarly, all proteins associated with photosynthetic processes—such as oxygen evolution complex protein 1, RuBisCO, and carbonic anhydrase—were altered in *Oryza sativa* (Wu et al., 2011). In our study also, photosynthesis-related proteins such as chlorophyll A-B binding protein (12,35,40), photosystem II CP43 reaction center protein (spot 18), and oxygen-evolving enhancer protein (spot 17 and 23) were altered. Chlorophyll A-B binding protein is only detected in the cultivar REX. Spot 35 increases under lower and high doses but decreases under moderate doses. However, spot 40 proteins decreased under all levels of UV-B stress. Some proteins are represented by more than one spot. These spots may represent different products of two very closely related genes or post-translational modifications of a single protein. We also find that the expression level is also different, suggesting that there are probably different isoforms regulated in opposite ways or that one isoform is post-translationally regulated (Casati et al., 2011). Chlorophyll A-B binding proteins are part of the light-harvesting complex (LHC). The LHC functions as a light receptor that captures and delivers excitation energy to photosystems I and II. Chlorophyll A-B binding proteins are the most abundant membrane proteins in nature (Xu et al., 2011). The overexpression of chlorophyll A-B binding proteins enhances the stomatal sensitivity to ABA, whereas downregulation of chlorophyll A-B reduces the responsiveness of stomatal movement to ABA, which results in a decrease in plant tolerance to drought stress in Arabidopsis (Xu et al., 2011).

Similarly, we also identified photosystem II C43 reaction center protein (spot 18). CP43 is one of the components of the core complex of photosystem II (PSII). PSII is a large pigment-protein complex embedded in the thylakoid membrane of all oxygenic photosynthetic organisms. This pigment-protein complex contains the PSII core antenna proteins CP47 and CP43. These two proteins are the most dominant and long-lived proteins compared to other core RC proteins—D1 and D2 (Weisz et al., 2019). CP43 is increased in low and middle doses of UV-B but decrease in high dose of UV-B in both cultivars. We also identified oxygen-evolving enhancer protein 1 (OEE1) (spots 17 and 23) in both cultivars. The OEE1 is decreased in the cultivar IR6 but not detected in the REX cultivar. This protein's primary function is to stabilize the manganese cluster, the primary water-splitting site. Under drought and heat stress, OEE1 interacts with a dnaK family protein (HSP70, 4332413) in maize (Hu et al., 2015). The expression of OEE1 is also altered upon cytokine treatment (Talla et al., 2016). Recently, Zhao et al. (2021) reported that photoinactivation of the OEE regulates the photosynthetic strategy of the seagrass *Zostera marina* (Zhao et al., 2021). These data showed that UV-B plays a

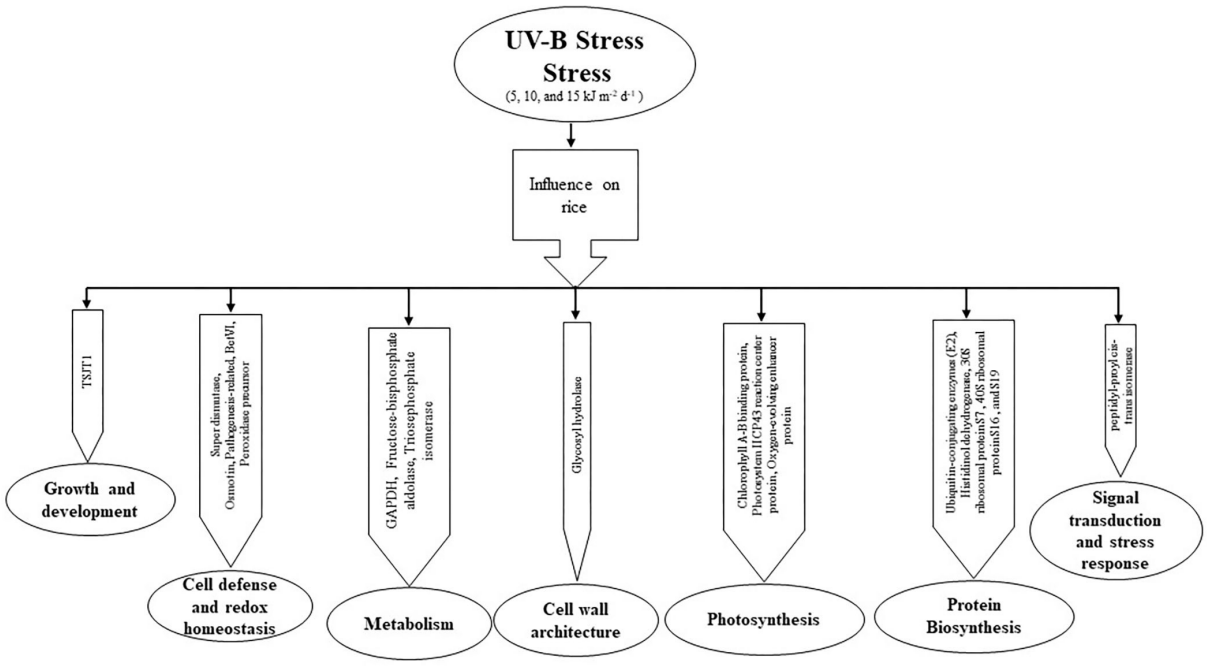


FIGURE 4
The pathway of UV-B induced protein expression in the proteomic response of rice leaves to cultivars IR6 and REX.

role in photosynthesis and ABA signaling partly by modulating ROS homeostasis.

Effect of UV-B on protein biosynthesis-related proteins

In protein biosynthesis, the ubiquitin-proteasome pathway is essential for regulating cell physiology and a cellular signaling system because it removes most abnormal and short-lived peptides and proteins. Ubiquitin-conjugating enzymes (E2) play a significant role in transporting ubiquitin from the ubiquitin-activating enzyme (E1) to the ubiquitin-ligase enzyme (E3) and the substrate (Liu et al., 2020). This study identified ubiquitin-conjugating enzymes (E2), which are upregulated under UV-B stress. However, ubiquitin-conjugating enzyme (UBC) gene family expression was reduced in rice (E et al., 2015). Jeon et al. (2012) isolated a novel E2 ubiquitin-conjugating enzyme from wild rice plants and found it highly expressed in leaves treated with salicylic acid and UV-B. And they also showed that UBC1 confers disease resistance and UV-B tolerance in transgenic Arabidopsis plants (Jeon et al., 2012). In our study, E2 enzymes were only identified in REX cultivars—not in IR6. The expression of E2 is higher than wild type under moderate and high doses of UV-B. These results suggest that the REX cultivar has more UV-B tolerance than IR6.

Similarly, we identified histidinol dehydrogenase (spot 2). Histidinol dehydrogenase is the first enzyme characterized by plants. Histidinol dehydrogenase enzyme catalyzes the NAD-linked four-electron dehydrogenase reaction leading from histidinol to His (Nagai and Scheidegger, 1991). Histidinol dehydrogenase was upregulated in transplastomic Arabidopsis lines, suggesting that histidine should be accumulated in the transplastomic lines (Stavridou et al., 2019). Glutamate can also be metabolized to produce histidine *via* reactions catalyzed by histidinol phosphate phosphatase and histidinol dehydrogenase (Stepansky and Leustek, 2006). These results suggest that histidinol dehydrogenase plays a role in protein biosynthesis, which is also affected by UV-B stress. In this study, we also identified 3 different ribosomal proteins. Ribosomal proteins are well-known for their role in mediating protein synthesis and maintaining the stability of the ribosomal complex. All three identified proteins, 30S ribosomal protein S7 (spot 31), 40S ribosomal protein S16 (spot 32), and S19 (spot 33), are upregulated under UV-B stress in cultivar REX. These three proteins are novel and have not been identified under UV-B stress. Some other ribosomal proteins in maize and Arabidopsis, such as RPL10A and RPL10C, were significantly upregulated under UV-B stress (Casati and Walbot, 2003; Ferreyra et al., 2010). These results suggest that UV-B plays a role in protein biosynthesis. Additionally, this study provides a resource for subsequent exploitation of RPL genes to improve abiotic and

biotic stress conditions in rice and some other crops in the future.

Effect of UV-B on signal transduction and stress response-related proteins

This study identified peptidyl-proyl cis-trans isomerase (PPIases) (spot 7). PPIases accelerate the folding of proteins. PPIases of rice OsIAA11 catalyzed by LATERAL ROOTLESS2 (LRT2), which is a cyclophilin-type peptidyl-prolyl cis/trans isomerase, directly regulates the stability of OsIAA11 (Jing et al., 2015). Knockdown of OsIAA11 expression partially rescues the LRT2 mutant phenotype in lateral root development. These results showed that cyclophilin-catalyzed peptidyl-prolyl isomerization promotes Aux/IAA degradation to regulate auxin signaling in rice (Jing et al., 2015; Acevedo et al., 2019). Plant cyclophilins have essential cellular functions in stress survival and the initiation of lateral root development (Kang et al., 2013). PPIase overexpressed under a low and moderate level of UV-B stress, whereas it was downregulated under a high level of UV-B doses in cultivar IR6 compared to control. So far, PPIase has not been identified in UV-B stress. Similarly, we also identified eukaryotic translation initiation factor 5A (eIF5A), which is upregulated in low and high doses of UV-B, whereas it was downregulated in the middle dose of UV-B. TaeIF5A1 from *Tamarix androssowii*, TaWRKY, and RAV protein share very similar expression patterns, and all stress-responsive genes are involved in the ABA signaling pathway (Wang et al., 2012). eIF5A-2 from Arabidopsis played a crucial role in plant growth and development by regulating cell division, cell growth, and cell death (Feng et al., 2007). This eIF5A has not been studied under UV-B stress. This study also identified glycine-rich protein 2, also called cold shock domain protein. In Arabidopsis, cold shock domain protein 2 negatively regulates seed germination by controlling ABA and GA levels (Sasaki et al., 2015). These results suggest that UV-B plays a role in signal transduction as well as the stress response.

In conclusion, we found that protein expression under different levels of UV-B stress seems to differ in both cultivars. The REX cultivar is more affected by UV-B stress than the IR6 cultivar. The differentially expressed proteins are related to plant growth and development, cell defense and redox homeostasis, metabolism, cell wall architecture, photosynthesis, signal transduction, stress response, and ABA signaling (Figure 4). Morphological and physiological studies are further required to understand the function of this protein in detail. This study helped develop the molecular marker in rice's molecular breeding to enhance the production during excessive UV-B exposure.

Data availability statement

The datasets presented in this study can be found in online repositories. The names of the repository/repositories and accession number(s) can be found below: The mass spectrometry proteomics data have been deposited to the ProteomeXchange Consortium *via* the PRIDE (Perez-Riverol et al., 2022) partner repository with the dataset identifier PXD032163.

Author contributions

SS: conceptualization, data curation, formal analysis, methodology, visualization, and writing–original draft and editing. SJ: data collection and review. JL: supervision, funding, review, and editing. KR: conceptualization, methodology, supervision, funding, review, and editing. All authors have read and approved the manuscript.

Funding

This research is partially funded by the National Institute of Food and Agriculture, NIFA 2019-34263-30552 and MIS 043050, and the MAFES SRI.

Acknowledgments

We thank David Brand for technical assistance and Dr. Ed Rodona, Rice Breeder, Delta Research, and Extension Center, Stoneville, MS, the USA, for providing the seed materials. SS was supported by a MAFES/FWRC Directors' Doctoral Fellowship awarded to JL and KR.

Conflict of interest

The authors declare that the research was conducted in the absence of any commercial or financial relationships that could be construed as a potential conflict of interest.

Publisher's note

All claims expressed in this article are solely those of the authors and do not necessarily represent those of their affiliated organizations, or those of the publisher, the editors and the reviewers. Any product that may be evaluated in this article, or claim that may be made by its manufacturer, is not guaranteed or endorsed by the publisher.

Supplementary material

The Supplementary Material for this article can be found online at: https://www.frontiersin.org/articles/10.3389/fpls.2022.871331/full#supplementary-material

SUPPLEMENTARY FIGURE 1
Schematic illustration of the layout of experiments.

SUPPLEMENTARY FIGURE 2
Comparison of staining method in 2 D Gel analysis of control rice leaves samples **(A)** Colloidal coomassie staining and **(B)** Silver staining. The arrow indicates the protein spots detected only in silver staining, not coomassie staining.

SUPPLEMENTARY TABLE 1
GO enrichment analysis of identified proteins. The number of proteins enriched with each GO term in one of the three categories, including biological process, molecular function, and cellular component, is shown. The number in BG/RF refers to the annotated number in the background/reference. MSU7.0 gene ID (TIGR) was used as a reference.

SUPPLEMENTARY TABLE 2
Pathway analysis of identified proteins through mass spectrometry under different levels of UV-B stress.

References

Acevedo, L. A., Kwon, J., and Nicholson, L. K. (2019). Quantification of reaction cycle parameters for an essential molecular switch in an auxin-responsive transcription circuit in rice. *Proc. Natl. Acad. Sci.* 116, 2589 LP–94. doi: 10.1073/pnas.1817038116

Agrawal, S., and Rathore, D. (2007). Changes in oxidative stress defense system in wheat (Triticum aestivum L.) and mung bean (Vigna radiata L.) cultivars grown with and without mineral nutrients and irradiated by supplemental ultraviolet-B. *Environ. Exp. Bot.* 59, 21–33. doi: 10.1016/j.envexpbot.2005.09.009

Babele, P. K., Singh, G., Kumar, A., and Tyagi, M. B. (2015). Induction and differential expression of certain novel proteins in Anabaena L31 under UV-B radiation stress. *Front. Microbiol.* 6, 1–14. doi: 10.3389/fmicb.2015.00133

Bassman, J. H., Edwards, G. E., and Robberecht, R. (2002). Long-term exposure to enhanced UV-B radiation is not detrimental to growth and photosynthesis in douglas-fir. *New Phytol.* 154, 107–120. doi: 10.1046/j.1469-8137.2002.00354.x

Biever, J. J., Brinkman, D., and Gardner, G. (2014). UV-B inhibition of hypocotyl growth in etiolated Arabidopsis thaliana seedlings is a consequence of cell cycle arrest initiated by photodimer accumulation. *J. Exp. Bot.* 65, 2949–2961. doi: 10.1093/jxb/eru035

Bradford, M. M. (1976). A rapid and sensitive method for the quantitation of microgram quantities of protein utilizing the principle of protein-dye binding. *Anal. Biochem.* 72, 248–254. doi: 10.1016/0003-2697(76)90527-3

Brosche, M., and Strid, A. (2003). Molecular events following perception of ultraviolet-B radiation by plants. *Physiol. Plant.* 117, 1–10. doi: 10.1034/j.1399-3054.2003.1170101.x

Brown, B. A., and Jenkins, G. I. (2008). UV-B Signaling pathways with different fluence-rate response profiles are distinguished in mature arabidopsis leaf tissue by requirement for UVR8, HY5, and HYH 1. *Plant Physiol.* 146, 576–588. doi: 10.1104/pp.107.108456

Casati, P., Campi, M., Morrow, D. J., Fernandes, J. F., and Walbot, V. (2011). Transcriptomic, proteomic and metabolomic analysis of UV-B signaling in maize. *BMC Genomics* 12, 321. doi: 10.1186/1471-2164-12-321

Casati, P., and Walbot, V. (2003). Gene expression profiling in response to ultraviolet radiation in maize genotypes with varying flavonoid content. *Plant Physiol.* 132, 1739–1754. doi: 10.1104/pp.103.022871

Casati, P., Zhang, X., Burlingame, A. L., and Walbot, V. (2005). Analysis of leaf proteome after UV-B irradiation in maize lines differing in sensitivity. *Mol. Cell. Proteomics* 4, 1673–1685. doi: 10.1074/mcp.M500173-MCP200

Cui, K., He, C., Zhang, J., Duan, A., and Zeng, Y. (2012). Temporal and spatial profiling of internode elongation-associated protein expression in rapidly growing culms of bamboo. *J. Proteome Res.* 11, 2492–2507. doi: 10.1021/pr2011878

Dai, Q., Shaobing, P., Chavez, A. Q., and Vergara, B. S. (1994). Intraspecific responses of 188 rice cultivars to enhanced UVB radiation. *Environ. Exp. Bot.* 34, 433–442. doi: 10.1016/0098-8472(94)90026-4

Du, H., Liang, Y., Pei, K., and Ma, K. (2011). UV radiation-responsive proteins in rice leaves: a proteomic analysis. *Plant Cell Physiol.* 52, 306–316. doi: 10.1093/pcp/pcq186

E, Z., Zhang, Y., Li, T., Wang, L., and Zhao, H. (2015). Characterization of the ubiquitin-conjugating enzyme gene family in rice and evaluation of expression profiles under abiotic stresses and hormone treatments. *PLoS ONE* 10, e0122621. doi: 10.1371/journal.pone.0122621

Eng, J. K., McCormack, A. L., and Yates, J. R. (1994). An approach to correlate tandem mass spectral data of peptides with amino acid sequences in a protein database. *J. Am. Soc. Mass Spectrom.* 5, 976–989. doi: 10.1016/1044-0305(94)80016-2

Fedina, I. S., Grigorova, I. D., and Georgieva, K. M. (2003). Response of barley seedlings to UV-B radiation as affected by NaCl. *J. Plant Physiol.* 160, 205–208. doi: 10.1078/0176-1617-00760

Feng, H., Chen, Q., Feng, J., Zhang, J., Yang, X., and Zuo, J. (2007). Functional characterization of the Arabidopsis eukaryotic translation initiation factor 5A-2 that plays a crucial role in plant growth and development by regulating cell division, cell growth, and cell death. *Plant Physiol.* 144, 1531–1545. doi: 10.1104/pp.107.098079

Ferreyra, M. L. F., Pezza, A., Biarc, J., Burlingame, A. L., and Casati, P. (2010). Plant L10 ribosomal proteins have different roles during development and translation under ultraviolet-B stress. *Plant Physiol.* 153, 1878–1894. doi: 10.1104/pp.110.157057

Fina, J., Casadevall, R., AbdElgawad, H., Prinsen, E., Markakis, M. N., Beemster, G. T., et al. (2017). UV-B inhibits leaf growth through changes in growth regulating factors and gibberellin levels. *Plant physiol.* 174, 1110–1126. doi: 10.1104/pp.17.00365

Giegé, P., Heazlewood, J. L., Roessner-Tunali, U., Millar, A. H., Fernie, A. R., Leaver, C. J., et al. (2003). Enzymes of glycolysis are functionally associated with the mitochondrion in Arabidopsis cells. *Plant Cell* 15, 2140–2151. doi: 10.1105/tpc.012500

Goossens, A., Häkkinen, S. T., Laakso, I., Seppänen-Laakso, T., Biondi, S., De Sutter, V., et al. (2003). A functional genomics approach toward the understanding of secondary metabolism in plant cells. *Proc. Natl. Acad. Sci.* 100, 8595–8600. doi: 10.1073/pnas.1032967100

He, J., Huang, L., Chow, W., Whitecross, M., and Anderson, J. (1993). Effects of supplementary ultraviolet-B radiation on rice and pea plants. *Aust. J. Plant Physiol.* 20, 129. doi: 10.1071/PP9930129

Hu, W., Chen, L., Qiu, X., Lu, H., Wei, J., Bai, Y., et al. (2016). Morphological, physiological and proteomic analyses provide insights into the improvement of castor bean productivity of a dwarf variety in comparing with a high-stalk variety. *Front. Plant Sci.* 7, 1473. doi: 10.3389/fpls.2016.01473

Hu, X., Wu, L., Zhao, F., Zhang, D., Li, N., Zhu, G., et al. (2015). Phosphoproteomic analysis of the response of maize leaves to drought, heat and their combination stress. *Front. Plant Sci.* 6, 298. doi: 10.3389/fpls.2015.00298

Iii, D. C. G., Britz, S. J., and Sullivan, J. H. (2013). Effect of ambient UV-B on stomatal density, conductance and Isotope discrimination in four field grown soybean [*Glycine max* (L.) Merr.] isolines. *Am. J. Plant Sci.* 4, 100–108. doi: 10.4236/ajps.2013.412A3012

Jeon, E. H., Pak, J. H., Kim, M. J., Kim, H. J., Shin, S. H., Lee, J. H., et al. (2012). Ectopic expression of ubiquitin-conjugating enzyme gene from wild rice, OgUBC1, confers resistance against UV-B radiation and Botrytis infection in Arabidopsis thaliana. *Biochem. Biophys. Res. Commun.* 427, 309–314. doi: 10.1016/j.bbrc.2012.09.048

Jing, H., Yang, X., Zhang, J., Liu, X., Zheng, H., Dong, G., et al. (2015). Peptidyl-prolyl isomerization targets rice Aux/IAAs for proteasomal degradation during auxin signalling. Nat. *Commun.* 6, 7395. doi: 10.1038/ncomms8395

Kang, B., Zhang, Z., Wang, L., Zheng, L., Mao, W., Li, M., et al. (2013). OsCYP2, a chaperone involved in degradation of auxin-responsive proteins, plays crucial roles in rice lateral root initiation. *Plant J.* 74, 86–97. doi: 10.1111/tpj.12106

Kumar, J., Babele, P. K., Singh, D., and Kumar, A. (2016). UV-B radiation stress causes alterations in whole cell protein profile and expression of certain genes in the rice phyllospheric bacterium enterobacter cloacae. *Front. Microbiol.* 7, 1440. doi: 10.3389/fmicb.2016.01440

Kumari, R., Singh, S., and Agrawal, S. B. (2009). Effects of supplemental ultraviolet-b radiation on growth and physiology of *Acorus calamus* L. (sweet flag). *Acta Biol. Cracoviensia Ser. Bot.* 51, 19–27.

Li, J., and Assmann, S. M. (2000). Mass spectrometry. an essential tool in proteome analysis. *Plant Physiol.* 123, 807–809. doi: 10.1104/pp.123.3.807

Liang, C. J., Huang, X. H., and Qingll, Z. (2006). Effect of cerium on photosynthetic characteristics of soybean seedling exposed to supplementary ultraviolet-B radiation. *J. Environ. Sci.* 18, 1147–1141. doi: 10.1016/S1001-0742(06)60053-3

Liu, L., Mei, Q., Yu, Z., Sun, T., Zhang, Z., and Chen, M. (2013). An integrative bioinformatics framework for genome-scale multiple level network reconstruction of rice. *J. Integr. Bioinform.* 10, 223. doi: 10.1515/jib-2013-223

Liu, W., Tang, X., Qi, X., Fu, X., Ghimire, S., Ma, R., et al. (2020). The ubiquitin conjugating enzyme: an important ubiquitin transfer platform in ubiquitin-proteasome system. *Int. J. Mol. Sci.* 21, 2894. doi: 10.3390/ijms21082894

Liu, Y., Cao, Y., Zhang, Q., Li, X., and Wang, S. (2018). A cytosolic triosephosphate isomerase is a key component in Xa3/XA26-medIated Resistance. *Plant Physiol.* 178, 923–935. doi: 10.1104/pp.18.00348

Mittler, R., Vanderauwera, S., Gollery, M., and Van Breusegem, F. (2004). Reactive oxygen gene network of plants. *Trends Plant Sci.* 9, 490–498. doi: 10.1016/j.tplants.2004.08.009

Nagai, A., and Scheidegger, A. (1991). Purification and characterization of histidinol dehydrogenase from cabbage. *Arch. Biochem. Biophys.* 284, 127–132. doi: 10.1016/0003-9861(91)90274-M

Nakahara, K., Yamamoto, H., Miyake, C., and Yokota, A. (2003). Purification and characterization of class-I and class-II fructose-1,6-bisphosphate aldolases from the cyanobacterium Synechocystis sp. PCC6803. *Plant Cell Physiol.* 44, 326–333. doi: 10.1093/pcp/pcg044

Ouyang, S., Zhu, W., Hamilton, J., Lin, H., Campbell, M., Childs, K., et al. (2007). The TIGR Rice Genome Annotation Resource: Improvements and new features. *Nucleic Acids Res.* 35, D883–D887. doi: 10.1093/nar/gkl976

Peng, J., and Gygi, S. P. (2001). Proteomics: the move to mixtures. *J. Mass Spectrom,.* 36, 1083–1091. doi: 10.1002/jms.229

Peng, Q., and Zhou, Q. (2009). Influence of lanthanum on chloroplast ultrastructure of soybean leaves under ultraviolet-B stress. *J. Rare Earths* 27, 304–307. doi: 10.1016/S1002-0721(08)60238-0

Perez-Riverol, Y., Bai, J., Bandla, C., Hewapathirana, S., García-Seisdedos, D., Kamatchinathan, S., et al. (2022). The PRIDE database resources in 2022: A hub for mass spectrometry-based proteomics evidences. *Nucleic Acids Res.* 50, D543–D552. doi: 10.1093/nar/gkab1038

Qu, Y., Feng, H., Wang, Y., Zhang, M., Cheng, J., Wang, X., et al. (2006). Nitric oxide functions as a signal in ultraviolet-B induced inhibition of pea stems elongation. *Plant Sci.* 170, 994–1000. doi: 10.1016/j.plantsci.2006.01.003

Rastogi, R. P., Richa, K., A., Tyagi, M. B., and Sinha, R.P. (2010). Molecular mechanisms of ultraviolet radiation-induced DNA damage and repair. *J. Nucleic Acids* 2010, 1–32. doi: 10.4061/2010/592980

Reddy, K. R., Seghal, A., Jumaa, S., Bheemanahalli, R., Kakar, N., Redoña, E. D., et al. (2021). Morpho-physiological characterization of diverse rice genotypes for seedling stage high-and low-temperature tolerance. *Agronomy*, 11, 112. doi: 10.3390/agronomy11010112

Reddy, K. R., Singh, S. K., Koti, S., Kakani, V. G., Zhao, D., Gao, W., et al. (2013). Quantifying the effects of corn growth and physiological responses to ultraviolet-b radiation for modeling. *Publ. Agron. J.* 105, 1367–1377. doi: 10.2134/agronj2013.0113

Robson, T. M., and Aphalo, P. J. (2012). Species-specific effect of UV-B radiation on the temporal pattern of leaf growth. *Physiol. Plant* 144, 146–160. doi: 10.1111/j.1399-3054.2011.01546.x

Roy, S. C., and Roy, T. (2013). Peptide mass fingerprinting of rice (Oryza sativa L.) leaves during UV-B induced stress at seedling stage: a proteom analysis. *Indian J. Biotechnol.* 12, 504–508.

Sakai, H., Lee, S. S., Tanaka, T., Numa, H., Kim, J., Kawahara, Y., et al. (2013). Rice annotation project database (RAP-DB): An integrative and interactive database for rice genomics. *Plant Cell Physiol.* 54, e6. doi: 10.1093/pcp/pcs183

Santos, A. L., Gomes, N. C. M., Henriques, I., Almeida, A., Correia, A., and Cunha, Â. (2012). Contribution of reactive oxygen species to UV-B-induced damage in bacteria. *J. Photochem. Photobiol. B Biol.* 117, 40–46. doi: 10.1016/j.jphotobiol.2012.08.016

Sasaki, K., Kim, M. H., Kanno, Y., Seo, M., Kamiya, Y., and Imai, R. (2015). Arabidopsis cold shock domain protein 2 influences ABA accumulation in seed and negatively regulates germination. *Biochem. Biophys. Res. Commun.* 456, 380–384. doi: 10.1016/j.bbrc.2014.11.092

Sharma, R., Cao, P., Jung, K., Sharma, M. K., and Ronald, P. C. (2013). Construction of a rice glycoside hydrolase phylogenomic database and identification of targets for biofuel research. *Front. Plant Sci.* 4, 1–15. doi: 10.3389/fpls.2013.00330

Shevchenko, A., Wilm, M., and Mann, M. (1997). Peptide sequencing by mass spectrometry for homology searches and cloning of genes. *J. Protein Chem.* 16, 481–490. doi: 10.1023/A:1026361427575

Shevchenko, A., Wilm, M., Vorm, O., and Mann, M. (1996). Mass spectrometric sequencing of proteins from silver-stained polyacrylamide gels. *Anal. Chem.* 68, 850–858. doi: 10.1021/ac950914h

Singh, B., Chastain, D. R., Jumaa, S., Wijewardana, C., Redoña, E. D., Gao, W., et al. (2019). Projected day/night temperatures specifically limits rubisco activity and electron transport in diverse rice cultivars. *Environ. Exp. Bot.* 159, 191–199. doi: 10.1016/j.envexpbot.2018.12.018

Stavridou, E., Michailidis, M., Gedeon, S., Ioakeim, A., Kostas, S., Chronopoulou, E., et al. (2019). Tolerance of transplastomic tobacco plants overexpressing a theta class glutathione transferase to abiotic and oxidative stresses. *Front. Plant Sci.* 9, 1–17. doi: 10.3389/fpls.2018.01861

Stepansky, A., and Leustek, T. (2006). Histidine biosynthesis in plants. *Amino Acids* 30, 127–142. doi: 10.1007/s00726-005-0247-0

Surplus, S. L., Jordan, B. R., Murphy, A. M., Carr, J. P., and Thomas, B. (1998). Ultraviolet-B-induced responses in Arabidopsis thaliana : role of salicylic acid and reactive oxygen species in the regulation of transcripts encoding photosynthetic and acidic pathogenesis-related proteins. *Plant Cell Environ.* 21, 685–694. doi: 10.1046/j.1365-3040.1998.00325.x

Sztatelman, O., Grzyb, J., Gabryś, H., and Banaś, A. K. (2015). The effect of UV-B on Arabidopsis leaves depends on light conditions after treatment. *BMC Plant Biol.* 15, 281. doi: 10.1186/s12870-015-0667-2

Talla, S. K., Panigrahy, M., Kappara, S., Nirosha, P., Neelamraju, S., and Ramanan, R. (2016). Cytokinin delays dark-induced senescence in rice by maintaining the chlorophyll cycle and photosynthetic complexes. *J. Exp. Bot.* 67, 1839–1851. doi: 10.1093/jxb/erv575

Tian, T., Liu, Y., Yan, H., You, Q., Yi, X., Du, Z., et al. (2017). AgriGO v2.0: A GO analysis toolkit for the agricultural community, 2017 update. *Nucleic Acids Res.* 45, W122–W129. doi: 10.1093/nar/gkx382

Voss, P., Hajimiragha, H., Engels, M., Ruhwiedel, C., Calles, C., Schroeder, P., et al. (2007). Irradiation of GAPDH: a model for environmentally induced protein damage. *Biol. Chem.* 388, 583–592. doi: 10.1515/BC.2007.068

Wang, L., Xu, C., Wang, C., and Wang, Y. (2012). Characterization of a eukaryotic translation initiation factor 5A homolog from Tamarix androssowii involved in plant abiotic stress tolerance. *BMC Plant Biol.* 12, 118. doi: 10.1186/1471-2229-12-118

Wang, W., Vignani, R., Scali, M., and Cresti, M. (2006). A universal and rapid protocol for protein extraction from recalcitrant plant tissues for proteomic analysis. *Electrophoresis* 27, 2782–2786. doi: 10.1002/elps.200500722

Weisz, D. A., Johnson, V. M., Niedzwiedzki, D. M., Shinn, M. K., Liu, H., Klitzke, C. F., et al. (2019). A novel chlorophyll protein complex in the repair cycle of photosystem II. *Proc. Natl. Acad. Sci.* 116, 21907 LP—21913. doi: 10.1073/pnas.1909644116

Wu, X. C., Fang, C. X., Chen, J. Y., Wang, Q. S., Chen, T., Lin, W. X., et al. (2011). A Proteomic analysis of leaf responses to enhanced ultraviolet-b radiation in two rice (Oryza sativa L.) cultivars differing in UV sensitivity. *J. Plant Biol.* 54, 251–261. doi: 10.1007/s12374-011-9162-y

Xu, Y. H., Liu, R., Yan, L., Liu, Z. Q., Jiang, S. C., Shen, Y. Y., et al. (2011). Light-harvesting chlorophyll a/b-binding proteins are required for stomatal response to abscisic acid in Arabidopsis. *J. Exp. Bot.* 63, 1095–1106. doi: 10.1093/jxb/err315

Ye, J., Zhang, Y., Cui, H., Liu, J., Wu, Y., Cheng, Y., et al. (2018). WEGO 2.0: a web tool for analyzing and plotting GO annotations, 2018 update. *Nucleic Acids Res.* 46, 71–75. doi: 10.1093/nar/gky400

Yuan, L., Yan-qun, Z., Haiyan, C., Jianjun, C., Jilong, Y., and Zhide, H. (2000). Intraspecific responses in crop growth and yield of 20 wheat cultivars to enhanced ultraviolet-B radiation under field conditions. *Field Crop Res.* 67, 25–33. doi: 10.1016/S0378-4290(00)00080-0

Zhao, P., Liu, P., Shao, J., Li, C., Wang, B., Guo, X., et al. (2015). Analysis of different strategies adapted by two cassava cultivars in response to drought stress: ensuring survival or continuing growth. *J. Exp. Bot*. 66, 1477–1488. doi: 10.1093/jxb/eru507

Zhao, W., Yang, X. Q., Zhang, Q. S., Tan, Y., Liu, Z., Ma, M. Y., et al. (2021). Photoinactivation of the oxygen-evolving complex regulates the photosynthetic strategy of the seagrass Zostera marina. *J. Photochem. Photobiol. B Biol*. 222, 112259. doi: 10.1016/j.jphotobiol.2021.112259

Ziveri, J., Tros, F., Guerrera, I. C., Chhuon, C., Audry, M., Dupuis, M., et al. (2017). The metabolic enzyme fructose-1,6-bisphosphate aldolase acts as a transcriptional regulator in pathogenic Francisella. *Nat. Commun*. 8, 853. doi: 10.1038/s41467-017-00889-7

frontiers | Frontiers in Plant Science

TYPE Review
PUBLISHED 28 September 2022
DOI 10.3389/fpls.2022.952759

Check for updates

OPEN ACCESS

EDITED BY
Shabir Hussain Wani,
Sher-e-Kashmir University of Agricultural Sciences and Technology, India

REVIEWED BY
Sunny Ahmar,
University of Silesia in Katowice, Poland
Sikandar Amanullah,
Northeast Agricultural University, China

*CORRESPONDENCE
Muhammad Azhar Nadeem
azharjoiya22@gmail.com
Yong Suk Chung
yschung@jejunu.ac.kr

SPECIALTY SECTION
This article was submitted to Plant Breeding, a section of the journal Frontiers in Plant Science

RECEIVED 25 May 2022
ACCEPTED 12 August 2022
PUBLISHED 28 September 2022

CITATION
Ali A, Altaf MT, Nadeem MA, Karaköy T, Shah AN, Azeem H, Baloch FS, Baran N, Hussain T, Duangpan S, Aasim M, Boo K-H, Abdelsalam NR, Hasan ME and Chung YS (2022) Recent advancement in OMICS approaches to enhance abiotic stress tolerance in legumes. *Front. Plant Sci.* 13:952759. doi: 10.3389/fpls.2022.952759

COPYRIGHT
© 2022 Ali, Altaf, Nadeem, Karaköy, Shah, Azeem, Baloch, Baran, Hussain, Duangpan, Aasim, Boo, Abdelsalam, Hasan and Chung. This is an open-access article distributed under the terms of the Creative Commons Attribution License (CC BY). The use, distribution or reproduction in other forums is permitted, provided the original author(s) and the copyright owner(s) are credited and that the original publication in this journal is cited, in accordance with accepted academic practice. No use, distribution or reproduction is permitted which does not comply with these terms.

Recent advancement in OMICS approaches to enhance abiotic stress tolerance in legumes

Amjad Ali[1], Muhammad Tanveer Altaf[1], Muhammad Azhar Nadeem[1]*, Tolga Karaköy[1], Adnan Noor Shah[2], Hajra Azeem[3], Faheem Shehzad Baloch[1], Nurettin Baran[4], Tajamul Hussain[5], Saowapa Duangpan[5], Muhammad Aasim[1], Kyung-Hwan Boo[6], Nader R. Abdelsalam[7], Mohamed E. Hasan[8] and Yong Suk Chung[9]*

[1]Faculty of Agricultural Sciences and Technologies, Sivas University of Science and Technology, Sivas, Turkey, [2]Department of Agricultural Engineering, Khwaja Fareed University of Engineering and Information Technology, Rahim Yar Khan, Pakistan, [3]Department of Plant Pathology, Faculty of Agricultural Sciences & Technology, Bahauddin Zakariya University, Multan, Pakistan, [4]Bitkisel Uretim ve Teknolojileri Bolumu, Uygulamali Bilimler Faku Itesi, Mus Alparslan Universitesi, Mus, Turkey, [5]Laboratory of Plant Breeding and Climate Resilient Agriculture, Agricultural Innovation and Management Division, Faculty of Natural Resources, Prince of Songkla University, Hat Yai, Thailand, [6]Subtropical/Tropical Organism Gene Bank, Department of Biotechnology, College of Applied Life Science, Jeju National University, Jeju, South Korea, [7]Agricultural Botany Department, Faculty of Agriculture (Saba Basha), Alexandria University, Alexandria, Egypt, [8]Bioinformatics Department, Genetic Engineering and Biotechnology Research Institute, University of Sadat City, Sadat City, Egypt, [9]Department of Plant Resources and Environment, Jeju National University, Jeju, South Korea

The world is facing rapid climate change and a fast-growing global population. It is believed that the world population will be 9.7 billion in 2050. However, recent agriculture production is not enough to feed the current population of 7.9 billion people, which is causing a huge hunger problem. Therefore, feeding the 9.7 billion population in 2050 will be a huge target. Climate change is becoming a huge threat to global agricultural production, and it is expected to become the worst threat to it in the upcoming years. Keeping this in view, it is very important to breed climate-resilient plants. Legumes are considered an important pillar of the agriculture production system and a great source of high-quality protein, minerals, and vitamins. During the last two decades, advancements in OMICs technology revolutionized plant breeding and emerged as a crop-saving tool in wake of the climate change. Various OMICs approaches like Next-Generation sequencing (NGS), Transcriptomics, Proteomics, and Metabolomics have been used in legumes under abiotic stresses. The scientific community successfully utilized these platforms and investigated the Quantitative Trait Loci (QTL), linked markers through genome-wide association studies, and developed KASP markers that can be helpful for the marker-assisted breeding of legumes. Gene-editing techniques have been successfully proven for soybean, cowpea, chickpea, and model legumes such as *Medicago truncatula* and *Lotus japonicus*. A number of efforts have been made to perform gene editing in legumes. Moreover, the scientific community did a great job of identifying various genes involved in the metabolic pathways and utilizing the resulted information in the development of climate-resilient legume cultivars at a rapid pace. Keeping in view, this

review highlights the contribution of OMICs approaches to abiotic stresses in legumes. We envisage that the presented information will be helpful for the scientific community to develop climate-resilient legume cultivars.

KEYWORDS

legumes, climate change, drought stress, marker-assisted breeding, marker-trait association

Introduction

The grand challenge facing scientists in the twenty-first century is to optimize climate change adaptation, agricultural productivity, food security, and environmental protection. Climate-related changes will likely boost the severity of both sole and joint abiotic stresses, especially drought, cold, salinity, and heat (Pandey et al., 2017; Anwar et al., 2022). These climate-change vulnerabilities pose a high threat to global food and nutritional security. Crops that can help overcome the effects of climate change are urgently needed. Legumes may prove to be one such suitable group of crops with promising future possibilities. Legumes being the members of Fabaceae family have a great value for their versatile usage and demand for humans and livestock. Legumes are a staple food for millions of people all over the world and serve as a cheap source of high-quality protein. As a result of its higher global consumption, this family ranks second after Gramineae and is the third largest flowering plant family followed by Asteraceae and Orchidaceae (Çakir et al., 2019). Presently, 88% of species of these families are examined and 750 genera consisting of 17,000–18,000 species play a significant role as food grains, pasture, and agroforestry to maintain the environments (Gupta and Pandey, 2021). Legumes are nutritionally used as staples worldwide. Legumes are a low-cost and good source of vitamins, carbohydrates, protein, and fiber. Concerning global distribution, chickpeas, pigeon pea, and lentils are widely cultivated in South Asian countries; faba beans are primarily cultivated in North Africa, China, and the Mediterranean countries; cowpeas in West African (WA) countries; soybean and other oilseed crops predominantly found in Indonesia, China and Japan while the Central and South America (C&SA) is also famous for the cultivations of beans (Joshi and Rao, 2017). The origins of legume crops are shown in Figure 1.

The consumption of legumes in different forms is common, with a beneficial aspect for the human diet, aiding good health. Legumes are full of substantial elements of diets including necessary proteins, minerals, complex carbohydrates, amino acids, dietary fibers, and vitamins such as riboflavin, vitamins B complex, tocopherols, pyridoxine, thiamine, and folates (Mefleh et al., 2022). Phaseolin is the major globulin in domesticated *Phaseolus* beans. Phaseolin is a protein containing a neutral sugar, usually mannan, and it is organized into three subunits, each of which possesses different molecular weights, isoelectric points, and glycosylation degrees. The legumes contain low saturated fats, and for that reason can be considered cholesterol-free. Protein is the main element for good health and is found high in legumes (40%) as compared to cereals (17%) (Kamau et al., 2020). Legumes seeds contain manyproteins such as oligomeric globulins, albumins, glutelins, and prolamins. These proteins are generally synthesized in the seed, and provide support for seedling germination. The amino acid analysis of legumes revealed a moderate quantity of sulfur-containing L-tryptophan and amino acids but high content of the primary Lysine. The carbohydrate is present in the form of starch, galactose ribose, á-galactosides, glucose, maltose, sucrose, and fructose as well as fermentable fibers in legumes seeds, and plants. The presences of amylopectin and amylose in dry grains and lignin, oligosaccharides, hemicellulose, cellulose, and pectin in plants are a vital source of carbohydrates that help in digestion. A significant amount of micronutrients is also present in legume crops. The micronutrients such as calcium, potassium, selenium, iron, magnesium, copper, and zinc are reported in mung bean, common bean, faba beans, chickpeas, lupins, and lentils which collectively play a vital role in body development (Roorkiwal et al., 2021). The nutritional comparison among food legumes is given in Table 1.

Despite their commercial and economic importance, legumes have not received the same level of attention as cereals to increase crop productivity. The legumes crop is threatened by a series of biotic diseases especially caused by fungi and nematodes. The fungal diseases such as ascochyta blight (*Ascochyta rabiei*), charcoal rot (*Macrophomina phaseolina*), powdery mildew (*Erysiphcpoiygoni*), alternaria blight (*Alternaria alternate*), botrytis gray mold (*Botrytis cinerea*), cercospora leaf spot (*Cercospora canescens*), collar rot (*Sclerotium rolfsii*), phytophthora blight (*Phytophthora drechsleri*), stemphylium blight (*Stemphylium* sp), fusarium wilt (*Fusarium oxysporum* f. sp. *ciceris*), wet root rot (*Rhizoctonia solani*), vascular wilt (*F. oxysporum* f. sp. *lentis*) are contributed to major yield loss in legumes crops as compared to all others (Sampaio et al., 2020; Mahmoud, 2021; Pandey and Basandrai, 2021; Urva, 2021). Nematodes (Cyst and root-knot) are also a major factor of yield loss in legumes (Zwart et al., 2019).

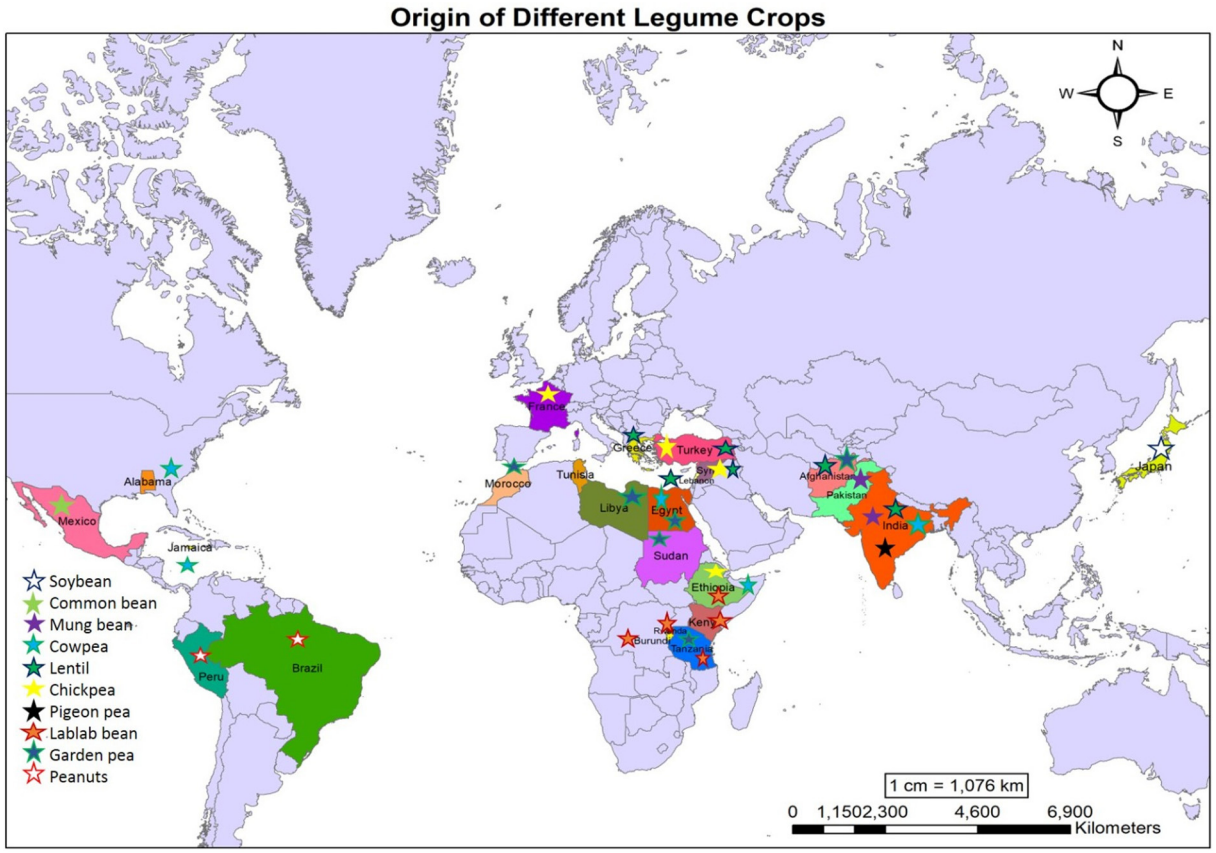


FIGURE 1
Origin centers of various legume crops.

TABLE 1 Nutritional comparison among food legumes.

Crops	Cowpea	Chickpea	Lentil	Mung bean	Kidney bean	Pigeon pea	Soybean	Moth-bean
Protein (%)	24	21	25	24	24	22	37	23
Dietary fiber (%)	11	12	11	16	25	15	9	–
Carbohydrate (%)	60	63	63	63	60	63	30	62
Lipids (%)	2	6	1	1	1	2	20	2
K ($\mu g\ g^{-1}$)	13,750	7,180	6,770	12,460	14,060	13,920	17,970	11,910
Zn ($\mu g\ g^{-1}$)	61	28	33	27	51	28	50	19
Ca ($\mu g\ g^{-1}$)	850	570	350	1,320	1,430	1,300	2,770	1,500
Na ($\mu g\ g^{-1}$)	80	240	60	150	240	170	20	300
Fe ($\mu g\ g^{-1}$)	100	43	65	67	82	52	157	109
P ($\mu g\ g^{-1}$)	4,380	2,520	2,810	3,670	4,070	3,670	7,040	4,890
Mg ($\mu g\ g^{-1}$)	3,330	790	470	1,890	1,400	1,830	2,800	3,810
Vitamin A (IU)	33	67	39	114	0	28	22	32
Vitamin C ($\mu g\ g^{-1}$)	15	40	45	48	45	0	60	40
vitamin B6 ($\mu g\ g^{-1}$)	4	5	4	4	4	3	4	4
Vitamin E ($\mu g\ g^{-1}$)	0	8	5	5	2	0	9	0
Thiamin ($\mu g\ g^{-1}$)	7	5	9	6	5	6	9	6

Similarly, crops are susceptible to insects, weeds, and diseases, which are also responsible for devastating yield losses (Reddy et al., 2004).

Globally, 55 developing countries having semiarid and tropical areas are affected by abiotic stress where mainly cultivation consists of grain legumes. In abiotic stress, multiple stresses are involved like drought, waterlogging, chilling, salinity, and high temperature are the main cause of the decrease in crop production annually (Ozturk Gokce et al., 2020). The cultivated land faced about 90% environmental stresses. Temperature plays a significant role in the survival of plant and their growth along with root nodules development. The rise in high-temperature result in poor pollination, and cause a significant reduction in the crop yield (Settele et al., 2016). Drought is an important abiotic stress issue that terribly affects crop production. Drought hinders the legume symbiotic routine, slowing down the growth, and eventually leading to decreased crop yield (Anjum et al., 2017). However, the influence of drought on the exposed plant is mainly dependent on the long drought period and magnitude of the stress. Cold-induced stress negatively affects photosynthetic pigments and capacity, antioxidant defense mechanisms, and mineral nutrient uptake; it alters metabolic and hormonal processes, and it disturbs plant developmental stages from seed germination to maturation. Plants exposed to low temperatures can increase the accumulation of reactive oxygen species (ROS), including superoxide anion radicals ($O_2^{-\bullet}$), singlet oxygen ($_1O^2$), hydrogen peroxide (H_2O_2), and hydroxyl ions (OH^-), which damage mitochondria and chloroplasts and can lead to cell death (Gill and Tuteja, 2010). Salinity is also an important abiotic stress issue that is proved as harmful to the survival of legumes (Shabala and Munns, 2012). In newly emerging leaves, the abscisic acid (ABA) level rises in the transpiration portion due to sodium chloride (Badhan et al., 2018). In the leaf veins and root, an ATP binding cassette (ABC) carrier was expressed that play a fundamental role toward ABC by showing hypersensitivity in plants regarding seedling and germination phase. Genetically designed plants were upregulated for ABA expression from separated leave have displayed a reduction in water loss as well as higher lead temperature than the normal plants (Raza et al., 2019).

Enhancement of already existing germplasm through focused evolution needs tracking of the desired traits to combine them. Previously, phenotype assisted in tracking the qualities of a plant in better ways that are nowadays exchanged in more meaningful ways in sense of DNA markers. Combinations of molecular studies and other breeding tools have moved into deeper knowledge to study the possible traits of a selected plant, including genomic and gene regulatory traits (Dhaliwal et al., 2020). The whole bunch of genes quantitative trait loci (QTLs) are studied along with the molecular markers that are connected with traits for trustworthy marker-aided breeding. The marker technology development in legumes is relatively slower as compared to cereals, giving them the label of an orphan crop (Gresta et al., 2016). The gradual development of molecular markers proceeds includes first-generation markers i.e., Restriction fragment length polymorphism (RFLP), amplified fragment length polymorphism (AFLP), random amplification of polymorphic DNA (RAPD), producing data of various loci in a single turn, mainly used in the study of diversity in pigeon pea, winged bean, cowpea, cluster bean, and dolichos bean (Chapman, 2015; Kumar et al., 2020). Furthermore, sequence-oriented markers, specifically, single nucleotide polymorphism (SNPs), simple sequence repeats (SSRs), and their alternation to increase reproducibility and reliability, efficiently working in trait mapping, fine mapping as well as linkage mapping studies (Choi, 2019) have also been documented. Simple sequence repeats (SSRs)markers have been used for the assessment of genetic diversity.

SSR markers have been used in cluster bean, pigeon pea, cowpea, and winged bean, whereas inter-species SSRs have been employed in lablab for the assessment of diversity and other purposes. SSRs markers have also been used in many dolichos bean studies for the assessment of genetic diversity (Keerthi et al., 2018; Singh et al., 2021). SNPs are desired markers due to their pervasive nature and lavishness in the genetic material. SNPs have been recognized as effective and used in genetic material-aided breeding of cluster bean, pigeon pea, winged bean, cowpea, and dolichos bean. As the desired markers are recognized, it provides us a pathway for mapping traits of concern going toward cloning as well as fine mapping (Bohra et al., 2019; Nawaz and Chung, 2020). This review article will provide a brief overview of multi-omics techniques and their uses for abiotic stress research on legumes.

Legumes genetic resources

Genetic diversity is essential for fulfilling the basic dietary and nutritional needs of an ever-increasing population, and it also serves as the foundation for selection response. Information on crop genetic resources, including pulse crops conserved in national and international gene banks, is available online at global portals such as Genesys (https://www.genesys-pgr.org/) and GRIN (https://www.ars-grin.gov/), as well as in a 1996 FAO publication titled "The second report on the state of the world's plant genetic resources for food and agriculture" (https://www.fao.org/3/i1500e/i1500e00.htm). According to the FAO report, CG centers hold 35,891 common bean accessions, 33,359 chickpea accessions, 15,588 cowpea accessions, 13,289 pigeonpea accessions, 10,864 lentil accessions, 9,186 faba bean accessions, 6,129 field pea accessions, and 3,225 grass pea accessions in trust (Table 2). Since then, the ICARDA gene bank has grown to include 50,968 accessions of pulse crops, including 15,749 chickpeas, 14,597 lentils, 10,034 faba beans, 6,131 peas,

TABLE 2 Legume germplasm holdings in major gene banks.

Crop	Global status	CG center	USDA	NBPGR,/India
Chickpea	98,285	33,359	7,000	14,704
Lentil	58,405	10,864	–	9,989
Vigna species	–	–	–	5,549
Common bean	261,963	35,891	–	1,514
Grass pea	26,066	3,225	–	2,797
Field pea	94,001	6,129	6,161	3,070
Cowpea	65,323	15,588	1,287	3,317
Pigeonpea	40,820	13,289	4,806	12,859
Faba bean	43,695	9,186	–	–
Others	183,078	13,690	–	19,579
Total	1,069,897	141,221		73,378

CG, Crop Genebanks; NBPGR, National Bureau of Plant Genetic Resources, India; USDA, United States Department of Agriculture.

and 4,457 grass peas. Similarly, ICRISAT holds 20,764 and 13,783 accessions of chickpea and pigeonpea, respectively. CIAT, IITA, and AVRDC hold 37,938, 16,460, and 10,946 accessions of Phaseolus beans, cowpea, and Vigna species, respectively. To facilitate accessibility and better use of the germplasm available with gene banks, various sets of core (Frankel, 1984; Brown, 1989), mini-core (Upadhyaya and Ortiz, 2001), focused identification of germplasm strategy (FIGS) (Mackay et al., 2004), and reference (Odong et al., 2011) germplasm have been developed. The FIGS strategy (https://www.icarda.org/research/innovations/focused-identification-germplasm-strategy-figs) is being pursued at ICARDA, which has proved effective for various adaptive traits such as heat, drought, cold, and salt tolerance, as well as insect pest and disease resistance. FIGS sets for chickpea, lentils, grass pea, and faba bean have recently been released, which can be used to find and apply valuable genes in preferred agronomic environments. Similarly, ICRISAT-developed mini-core sets of chickpea, pigeonpea, and groundnut provide a rich source of variety for desired traits in breeding operations (Upadhyaya et al., 2013). Except for a few features, the present germplasm of pulse crops contains sufficient variety for crucial economic traits. The creation of structured and representative collections of germplasm from the worldwide collection increases the efficiency with which beneficial alleles/traits can be identified and used.

OMICS approaches in the technological era

Omics is a fast-evolving technique that provides the methodology, technological proficiency, and interdisciplinary and transdisciplinary advancement needed to improve awareness and identification of all the plant's genomic and transcriptomic processes. Omics is a beneficial aid for understanding the change in plant metabolism as a consequence of contact with the external environment (Kumar et al., 2021). Transcriptomic, metabolomic, and genomic tools scan and give gene - expression and protein expression levels immediately, so in the advanced era these play a vital role in plant improvements (Jha et al., 2020). Omics technology not just increases our awareness, but also gives us new insights into how plants react when stressed. Whenever, a small change occurs in genetics, nutrients, or fluctuation in the external environment, a wide range of technologies is used to perceive these variations in plants. In the recent and modern era, these advanced tools are providing support to understand the whole plant genome, and the biggest example of this is *Arabidopsis thaliana*. Innovation in the modern era started with the complete genome sequencing of this model plant. Rice, maize, and soybeans are among the main crop plants whose genomes are complicated but have been fully sequenced. The introduction of high-throughput "Omics" methodologies has ushered in a time of successful plant molecular tools for responding to environmental changes. Rapid innovations and advancements in "omics" regarding the post-genomic epoch such as molecular characterization, next-generation sequencing, modeling of various molecular and physiological knowledge, and association of these assertions with plant establishment have contributed to a successful transition to resilience and efficiency under abiotic stress conditions (Pandey et al., 2021). With the invention of next-generation sequencing techniques, it become feasible and reliable to sequence plant species. Furthermore, current omics tools such as proteomics and transcriptomics aids to understand the level of genes and protein. Different results from reported studies showed that not all the genes are turned on or off at the same time; for that reason, the metabolism adopts a complex phenotype that cannot be determined by genotype (Jha et al., 2019; Singh et al., 2020). As a result, the successful integration of genomics, transcriptomics, phonemics, proteomics, epigenomics, metabolomics, interact omics, and ionomics would aid breeders in identifying promising candidates' genes and optimal features for generating and improving the productivity of legume crops under abiotic stresses (Kumar et al., 2022). Figure 2 is showing different omics approaches for the improvement of plant growth.

Contribution of OMICs approaches in legumes for abiotic stresses

The genome size of the legumes is large and some of them are polyploidy (Stai et al., 2019). As a result, model systems have been established to better recognize the legume biology and their modeling system that is developed for genetics studies regarding nodule formation and some dynamic processes like

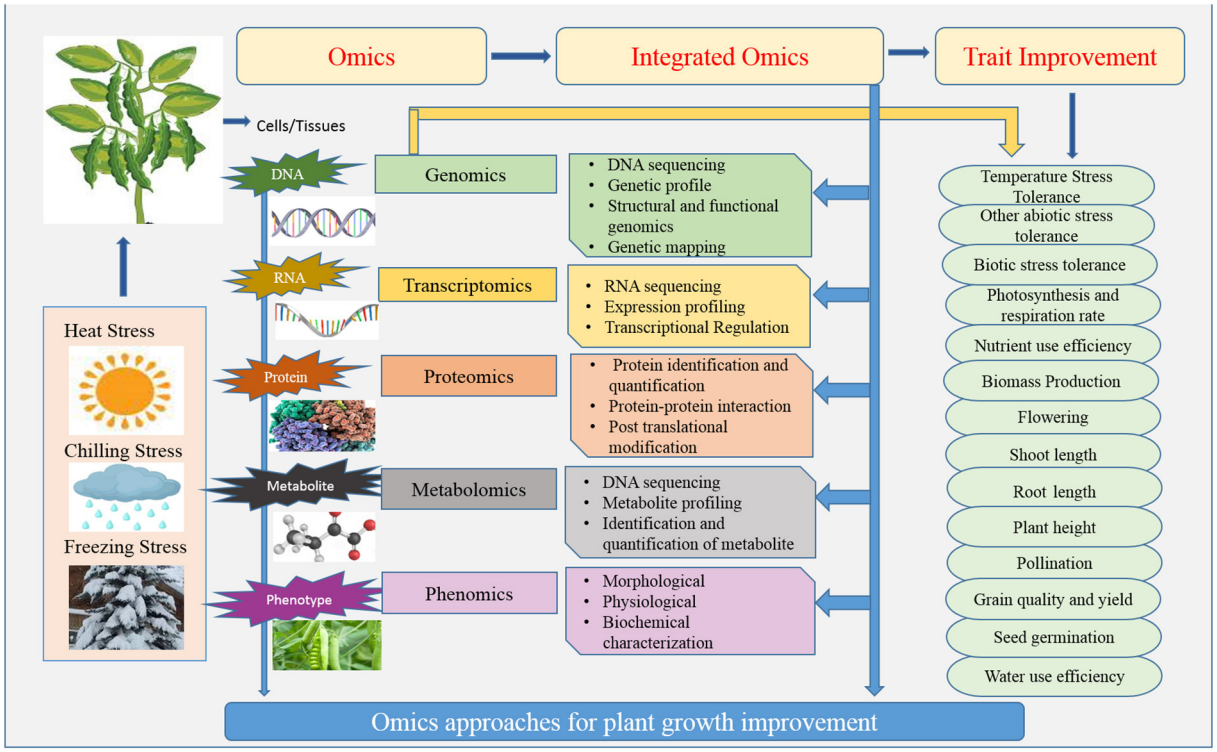


FIGURE 2
Schematic visualizing the contribution of OMIC's approaches for legume plant improvement.

active tolerance, resistance, and susceptibility toward numerous stresses. Figure 3 provide a brief information about the effects of various a biotic stress on the growth of legumes. The basic research on legumes is performed on plant model systems, most frequently *Lotus japonicas* and *Medicago truncatula*, because of their diploid small genome, short life cycle, and enormous production of seed (Cook, 1999; Cervantes et al., 2019). The implementation of all these models has significantly enhanced the genetic and genomic datasets regarding legumes, and the similarity between distinct legume genomes has indeed augmented the data's usefulness (Stracke et al., 2004). In addition, the genome sequencing of soybean and their higher similarity to model legume species may greatly assist many genetic methods for investigation, like positional cloning. The genome sequence data is extremely valuable and serve as a great initial point, it is insufficient to understand gene activity, and the numerous metabolic reactions and regulatory responses get stimulated as the stress condition prolongs in the legumes. New suitable approaches and methods for overcoming these barriers to biotic stresses including the study of quantitative and qualitative traits are essential for checking gene expression (Wan et al., 2017). These must be done through the use of transcriptome, proteomic, and metabolomic levels study with an understanding of the use of genetically modifying crops and marker-assisted screening (Dita et al., 2006). Genomic, metabolomics, transcriptomics, transgenomics, proteomics, phenomics, and functional genomics fall under 'omics' and are admired as omics tools. Significant advancements within those distinct omics (Figure 4 and Table 3) have played an important role in the better understanding of stress responses at the molecular as well as genetic levels (Langridge and Fleury, 2011).

Genomics advances for abiotic stress tolerance in legumes

Genomics focuses on the physical integrity of the genome, with the goal of recognizing, diagnosing, and regulating genomic features throughout the chromosomes. Now we deliberate some genomic advancements to apprehend the abiotic stress endurance in legumes (Chandrashekharaiah et al., 2021).

Molecular marker resources

The advent of genomic research has opened up new possibilities for genetic improvement of complex traits like salinity and drought endurance. In comparison to traditional breeding, a combination of genomic techniques and MAS

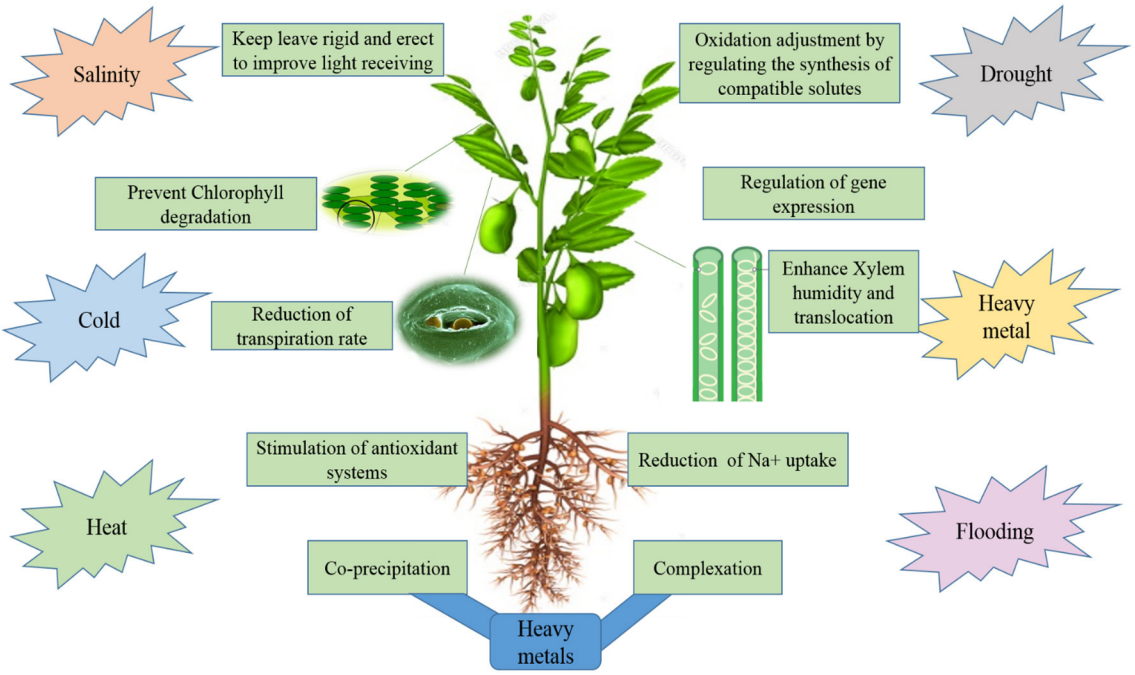


FIGURE 3
Exploring the effect of abiotic stresses on the growth of legume crops.

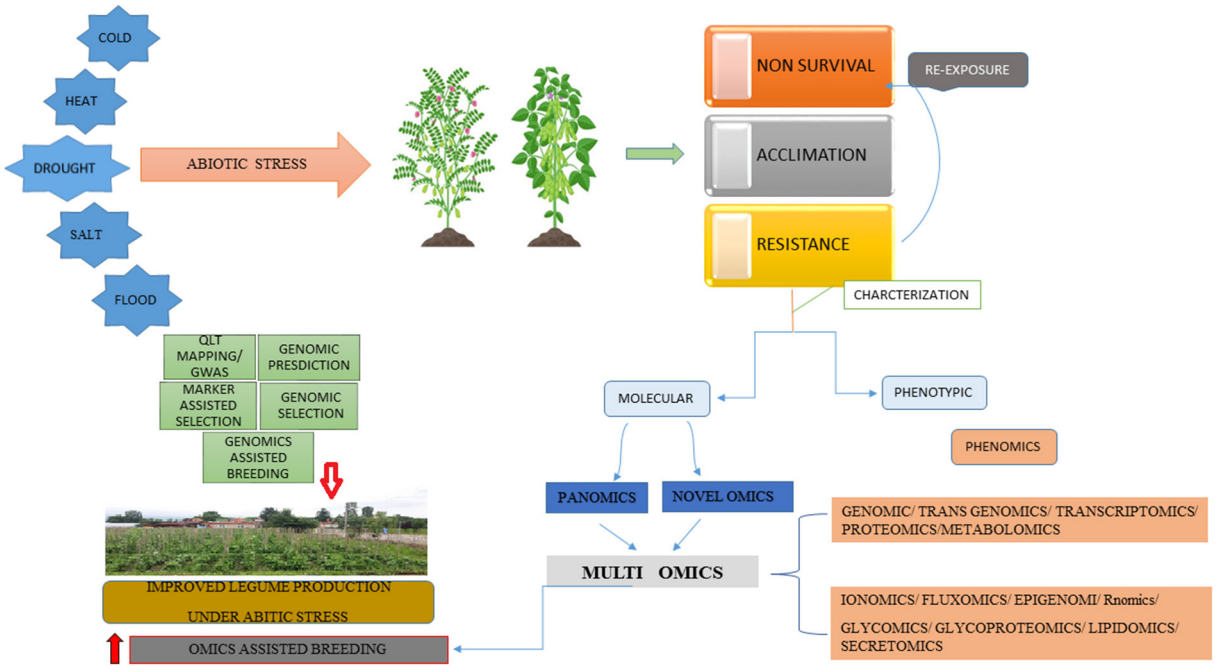


FIGURE 4
Improved abiotic stress tolerance in legumes using integrated multi-omics techniques.

TABLE 3 Novel omics approaches for legumes breeding.

Legumes	Abiotic stress	Omics technology	Details	References
Cowpea	Drought	Phosphoproteomics	Protein phosphorylation is induced by a gradual water deficiency.	Subba et al., 2013
		Secretomics	Dehydration, the stress-responsive secretome, and the highly complex metabolic network activity in the extracellular matrix have all been studied in depth.	Gupta et al., 2015
	Oxidative	Secretomics	CaFer1's role in iron buffering and oxidative stress adaption under different weather conditions.	Parveen et al., 2016
Common bean	Chlorpyrifos	Lipidomics	Triacylglycerol levels in pods and seeds are decreasing.	Fernandes et al., 2018
Soybean	Heat	Lipidomics	Reduced expression of fatty acid desaturase results in lower quantities of lipids with 18:3 acyl chains.	Narayanan et al., 2020
	Low phosphorus	Lipidomics	Under low-phosphorus circumstances, lipid remodeling occurs.	Okazaki et al., 2017
	Flooding	Phosphoproteomics	During flood stress, the ethylene signaling pathway was critical for protein phosphorylation in root tips.	Yin et al., 2014
		Glycoproteomics	Protein N-glycosylation was negatively affected by flooding.	Showalter et al., 2016

can contribute to the identification of individual-specific genes in breeding populations at a considerably faster rate (Saade et al., 2016). SNPs are excellent for distinguishing complex traits employing massively multiplexed marker oligonucleotides like the Affymetrix GeneChip, as these are fast, high-throughput, co-dominant, highly abundant, cost-effective, and sequence-tagged (Missanga et al., 2021; Thudi et al., 2021). High throughput Axiom® SNP array genotyping is an efficient and cost-effective method for genotyping and the development of high-density linkage maps. Recently "Axiom® *CicerSNP* Array" has been developed for genotyping of Recombinant inbred lines of chickpea (Roorkiwal et al., 2018).

Quantitative trait loci mapping for abiotic stresses in legumes

The heredity of abiotic stress resistance is a complex phenomenon, and QTL mapping is the most popular method of discovering QTL, as well as genetic and linkage mapping of genomic regions related to tolerance. QTL analysis allows researchers to examine the genetic structure of a characteristic. QTLs can identify genomic areas linked to the expression of the trait being researched (Kushwah et al., 2021). Strong linkage maps might be used for spatial replication of important genes. Because they are comprised of a sequence-tagged marker therefore these can also be used in functional genomics to analyze chromosomal arrangement and evolutionary purposes. Markers are successful in determining the QTLs for specific traits from various regions of chromosomes, for identifying genotypes against the different biotic stresses and multifunctional. QTLs were previously identified from the many legume crops by using linked markers (Luo et al., 2021; Zate, 2021). Advancements in phenomics and genomics now allowed us to better characterize the QTLs that influence a certain trait, admired as QTLome (Salvi and Tuberosa, 2015). Breeders have a responsibility to use QTLome's immense knowledge effectively because of its vastness. Improved QTL meta-analysis, estimations of QTL impact, and crop modeling will enable the QTLome to be used effectively against the abiotic stress of legumes. Several studies have been conducted to dissect QTLs in legumes crop for abiotic stresses. The identification of these QTLs against abiotic stress in various legumes are helpful for breeders during breeding activities. We have provided QTLs based studies in legumes against abiotic stress in Table 4.

Genome-wide association studies (GWAS) for abiotic stresses in legumes

Genome wide-association mapping is another beneficial tool to mitigate the constraints which provides the benefits from the historical meiosis of the diversity panel but may also offer better precision (Breria et al., 2020). In comparison to bi-parental mapping, association mapping is much more viable and cost-effective (Narayana and von Wettberg, 2020). Experimental architecture and statistical assessments in association mapping are continually changing to reduce the effects of influencing variables, reduce false positives, and regulate minor allele consequences. Due to genetic linkage and population structure, marker-trait relationships are muddled, creating a state of instability lacking real correlations. Numerous diagnostics or efficient statistical methods were developed to reduce false positives as well as minor allele QTL influences. Investigations of developmental genes including vernalization decreased height,

TABLE 4 QTLs identified against abiotic stresses for various legumes crops.

Crop	Abiotic stress	Associated marker (s)	Population type	Parental lines	Linkage group(s)/QTLs	References
Chickpea	Salinity	SSR (135)	RILs	JG-62 × ICCV 2	LG3, LG6, and LG4	Vadez et al., 2012
	Salinity	SSRs (28) and SNPs (28)	RILs	JG 11 × ICCV 2	CaLG05 and 07	Pushpavalli et al., 2015
	Salinity	SSRs (150)	F2	Vignaluteola oblonga× Vignaluteola	LG1	Chankaew et al., 2014
	Heat	SNPs (271)	RILs	ICC 15,614 × ICC 4,567	CaLG05 and 06	Paul et al., 2018
	Cold	SNPs (747)	RILs	PI 489,777 and ICC 4,958	CTCa3.1 and 8.1	Mugabe et al., 2019
	Drought	SSRs (97)	RILs	ILC 3,279 × ILC 588	Q1-1 and Q3-1	Rehman et al., 2011
	Salinity	SSRs (150)	F2	Vignaluteola oblonga× Vignaluteola	LG1	Chankaew et al., 2014
Cowpea	Heat	SNPs (8)	RILs	IT82E-18 × CB27	Cht 5	Lucas et al., 2013
	Drought	AFLP (306)	RILs	CB46 × IT93K503-1	10 QTL (Dro)	Muchero et al., 2009
	Salinity	SSRs (32) and RFLPs (116)	F2:5	Tokyo × S-100	LG N	Lee et al., 2004
	Aluminum toxicity	SSRs, FLP, and AFLP (2,639)	RILs	Huaxia 3 × Zhonghuang 24	qAAC_04 and qRRE_04	Wang et al., 2019a
Soybean	Aluminum toxicity	DNA markers (14)	RILs	Forrest × Essex	LG F	Sharma et al., 2011
	Aluminum toxicity	SSRs (11)	RILs	NN1138-2 × KF No.1	LG B1	Korir et al., 2013
	Drought	SNPs (4,117)	RILs	Magellan × PI 567,731, PI 567,690 × Pana	Gm09, 05, 10, 06, 19, and 12	Ye et al., 2020
Pea	Salinity	SNPs (705)	RILs	Parafield × Parafield	Ps III and Ps VII	Leonforte et al., 2013
	Frost/cold	SNPs (258)	RILs	Terese × Champagne	LG5 and 6	Dumont et al., 2009
	Drought	SSRs (6) and SNPs (2)	RILs	cv Messire × P665	AA175, AB141, PsAAP2_SNP4, and A6	Iglesias-García et al., 2015
	Heat	SSRs (7)	F2	PDL-1 × E-153 and PDL-2 × JL-3	qHt_ps and qHt_ss	Singh et al., 2017a
Lentil	Frost/cold	AFLP (94), RAPD (56), and ISSR (106)	RILs	Precoz × WA8649090	LG4	Kahraman et al., 2004
	Drought	SNPs (220) and AFLPs (180)	RILs	ILL 5,888 × ILL 6,002	QRSAVII: 21.94 QSL12IV: 103.83, QSL22VII: 21.94, QSPADVIII: 72.15 and QDRWVII: 21.93	Idrissi et al., 2016
Faba bean	Frost/cold1	SNPs (5)	RILs	Bean Gottingen Winter and Bean Pure Line 4628	LG-01, LG-02, LG-03, LG-04, LG-08, and LG-10	Sallam et al., 2016
Mung Bean	Drought	SSRs (313)	RILs	ZL × VC2917	qMLA2A and qPH5A	Liu et al., 2017
Common Bean	Drought	AFLP (53), RAPD (2), SSRs (42), and SNPs (127)	RILs	BAT 881 × G21212	Pv01 and 08	Diaz et al., 2018

and photoperiod response has been conducted at the exact genomic regions that are employed as a standard of comparison to integrate phenotypic variation with markers (Plewiński et al., 2020; Gondalia et al., 2022). These identified genes, being a strong genetic basis, can adjust the legumes plants under stress by changing heading time, plant height, and maturity time. In legumes, association mapping/GWAS is gaining popularity due to its capability to improve QTL discovery precision without investing additional resources in population growth. GWAS has made it possible to access functional genetic variations

TABLE 5 Application of GWAS approach to identify the genomic regions associated with abiotic stresses in legumes.

Crop	Abiotic stress	Markers used	Chromosomes/region/gene	References
Common bean	Drought stress	SNPs (8,657) and SilicoDArT (3,213)	Chr. 6, 7, 10, and 11	Valdisser et al., 2020
	Drought tolerance	SNPs (3,724,159)	Chr. 01 and 06	Wu et al., 2021
	Drought tolerance	SNPs(3,832,340)	Chr. 10/*PvXIP1;2*	Wu et al., 2022
	Drought tolerance	SNPs (5,389)	Chr. 02, 03, 04, 06,09, 10, and 11	Dramadri et al., 2021
	Aluminum toxicity	SNPs (13,906)	Chr. 1, 4, 5, 6, 11	Ambachew and Blair, 2021
	Aluminum toxicity	SNPs (5,389)	Chr. 02, 04, 06, 07, 09, and 10	Njobvu et al., 2020
Mung bean	Salt and drought stress	SNPs	Chr.1, 7, 9, and 11	Breria et al., 2020
Alfalfa	Salt stress	SNPs (4,653)	All chromosomes except 2	Liu et al., 2017
Phaseolus vulgaris L.	Drought stress	SNPs	Pv01 and Pv02	Trapp et al., 2015
	Drought and heat stress	SNPs	Chr. 1, 2, 3, 11	Oladzad et al., 2019
	Flooding tolerance	SNP (~203 K)	Pv07 and Pv08	Soltani et al., 2018
	Heat stress	SNP (23,373)	Chr. 1–11	Assefa et al., 2019
Glycine max (L.)	Salinity stress	SNPs	Chr. 3	Patil et al., 2016
	Flooding tolerance	Multi-locus random-SNP	QTN	Yu et al., 2019
	Flooding tolerance	SNPs	Chr 03, 4, 07, 13, and 19	Wu et al., 2020
	Flooding tolerance	SNPs (34,718)	*Glyma.01G198000, Glyma.05G008000, and Glyma.08G348500*	Sharmin et al., 2021
	Drought tolerance	SNPs (12,316)	Chr. 01–15	Sertse et al., 2021
Cicer arietinum L.	Salinity stress	DArTseq markers (1,856)	Chr. Ca4 and Ca2	Ahmed et al., 2021
	Drought tolerance	SNPs (144,777)	Chr. 01–08	Li et al., 2018
Vicia faba L	Heat tolerances	SNPs (10,749)	Chr. 9 and Chr. 11	Maalouf et al., 2022
Macrotyloma uniflorum	Drought stress	SNPs (20,241)	–	Choudhary et al., 2022
Camelina sativa	Salt tolerance	SNPs (17)	Chr. 1, 7, and 20	Luo et al., 2020
Pea	Frost tolerance	SNP (11366)	LGI, LGII, LGIII, LGV, LGVI	Beji et al., 2020

for salt tolerance traits in grain legume germplasms with greater accuracy and allelic richness (Hoyos-Villegas et al., 2017). Table 5 provide comprehensive information about the application of GWAS approach for the identification of genomic regions associated with abiotic stresses in legumes.

Genomic selection in legumes

With the development of model-based linkages with the widespread accessibility of genetic markers emerges a new concept called genomic selection which is developed to evaluate genotype pairing potential (Heffner et al., 2009). This method is used to overcome the limitations of map-based scientific studies of genetics, which only identify a few QTLs to explain the diversity in selected characteristics. Populations with much more allelic diversity of desired characteristics have a more accurate analysis of the QTL effect than a population that is strongly linked. Connection instability is regularly overstated in inter-mating individuals and it fades in subsequent meiotic activities (Nawaz and Chung, 2020). The genomic breeding potential is usually anticipated through genomic choice by altering marker-assisted selection using markers. The established model evaluated by genotypic and phenotypic facts of the research population will be applied to measure the phenotypic diversity of the selected respondent based solely on genetic makeup. This will increase yield potential in comparison to both QTL and phenotype trait selection (Shu et al., 2013; Sandhu et al., 2021). Statistical techniques are applied to create genomic selection models which depict the characteristics of many traits along with markers (Jannink et al., 2010). An optimum streamlined genome that is nonbiased assesses the genetic similarity between individuals based on molecular marker relatedness as well as evaluates the phenotypic

TABLE 6 Genomic selection studies in legumes.

Legume crop	Population size	Marker type	Traits	*Genomic selection models	References
Soybean	301	GBS	Grain yield	G-BLUP model	Jarquín et al., 2014
	5,000	4,236 SNPs	Yield, protein content, and height	DualCNN, deepGS, RR-BLUP	Liu et al., 2019
	249	23,279 SNPs	Amino acid	RR-BLUP model	Qin et al., 2019
	5,600	4,600 SNPs	Yield	G-BLUP	Howard and Jarquin, 2019
Alfalfa	190	GBS (10,000 SNPs)	Single harvest biomass Total biomass	RR-BLUP model	Chapman, 2015
	278 (adapted to two different environments)	GBS	Dry matter yield	RR-BLUP model	Annicchiarico et al., 2017
Pea	372	331 SNP	Date of flowering Number of seeds per plant and Thousand seed weight	LASSO PLS SPLS Bayes A, Bayes B, and G-BLUP	Burstin et al., 2015
	339	9,824 SNPs (GenoPea 13.2 K SNP Array)	Date of flowering Number of seeds per plant Thousand seed weight	(kPLSR), LASSO, G-BLUP, Bayes A, and Bayes B	Tayeh et al., 2015
Chickpea	320	3,000 DArT markers	Seed yield 100 seed weight Days to 50% flowering, Days to maturity	RR-BLUP, kinship GAUSS, Bayes Cπ, Bayes B, Bayesian LASSO, Random Forest (RF)	Roorkiwal et al., 2016
	320	8,900 SNPs	Seed weight, harvest index and biomass	Reaction norm models	Roorkiwal et al., 2018
	132	144,777 SNPs	Seed number and grain yield	BL and BRR	Li et al., 2018
Groundnut	188	2,356 DArT markers	Days to flowering, seed weight, and pod yield	RR-BLUP, kinship GAUSS, Bayes Cπ, Bayes B, Baysian LASSO and RF	Pandey et al., 2014
	340	13,355 SNPs	Seed wight, yield and days to maturity	Reaction norm models	Pandey et al., 2020
	281	493 SNPs	Leaf let length, days to maturity and 100 seed weight	RR-BLUP	Akohoue et al., 2020
Common bean	**481**	**5,820 SNPs**	**Grain yield and days to maturity**	**G-BLUP**	Keller et al., 2020

efficiency (Nadaf et al., 2012). These models are near to the assessment of breeding value (BV) from heredity as well as physical competence of associated genetic makeup in a pedigree. According to statistical assessments, forward or mixed sort regression models can eliminate markers associated with different substantial impacts. Ridge regression also includes a penalized factor in markers design that is more than the statistically allowed number (Annicchiarico et al., 2017). The use of genomic selection (GS) in legumes began with the goal of enhancing yield and agronomic traits in soybeans. GBS was used to genotype 301 elite breeding lines, which were then phenotyped for grain yield in several localities (Jarquín et al., 2014). Several genomic selection studies have been conducted for legumes and some of them are given in Table 6.

Transcriptome profiling for abiotic stress tolerance in legumes

Transcriptomics is a strong approach for quantifying gene expression along with the accurate image of a target cell or tissue. Transcriptomics properly identifies the gene regulatory pathway as well as candidate genes that are responsible for abiotic stress resilience in legumes and help

in crop breeding (Afzal et al., 2020). Serial analysis of gene expression (SAGE) and microarrays might be used to determine extensive transcriptome information due to advanced technology like high-throughput analysis. Differential gene expression (DGEs) is usually evaluated by sequencing of nucleic acid (RNA-seq). A relatively newer invented technique known as digital gene expression (DGE) is used for the quantified gene expression measurement. RNA-seq is a low-cost, high-throughput sequencing technique for evaluating vast quantities of transcriptome data. This method has various advantages over microarray technology, including the fact that it should not need genomic data to create probe sets and can detect unique transcripts (Lowe et al., 2017). This method has been used in many studies to identify the gene regulatory process which is responsible for the tolerance to abiotic stress, particularly on pulse crops (Table 7). Using the NGS method, a transcriptome process has been generated under stressful circumstances like drought in soybean (Libault et al., 2010). The transcriptional alterations in drought-tolerant as well as drought-sensitive soybean cultivars have been documented using a comparative transcriptome process (Wang et al., 2018). Different varieties of common bean genotype which are vulnerable to biotic and abiotic conditions such as drought, aluminum toxicity, low phosphorous, and heat were evaluated for paternal polymorphism, functional and molecular genomic data association by single nucleotide polymorphisms (SNPs) markers, that was obtained from Sanger sequencing along with Illumina's GoldenGate method (Blair et al., 2013). Das et al. (2017) explained that the metabolomics monitoring of nitrogen or sugar metabolism and phytochemical metabolic activity are all important during water shortage situations in soybean. Singh et al. (2017b) identified potential genes involved in drought stress during lentil seedlings predicated on a transcriptome study, while Pandey et al. (2008) discovered dehydration-responsive proteins in chickpeas. Molina et al. (2008) detected 80,238 labels indicating 17,493 distinct transcripts in chickpea transcriptomes with drought conditions by employing SuperSAGE and deep SuperSAGE. The rapid generation of jasmonate into chickpea roots in drought situations was revealed by root transcriptome profiling of particularly oxylipin production genes. Future potential breeding initiatives may benefit from the use of RNA-seq to better comprehend the genes expressed under stress conditions (Dai et al., 2021).

Metabolomics, proteomics, and ion-omics advances for abiotic stress in legumes

Abiotic stress has a significant impact on plants' metabolomes and proteomes, besides the change in genetic makeup and nucleotide sequences which are actively engaged in defense mechanisms against various stresses (Arbona et al., 2013). The proteome of an individual, which serves as a link between both the transcriptome and the metabolome more accurately represents the current level of proliferation and differentiation than Genetic markers. The transcriptome's assessment of cellular mRNA is not an exact representation of transcriptional activations (Min et al., 2019). The synthesis protein has played a role in cell signaling pathways and is implicated in stress adaption, stress repair, and also involved with other functions of the host plant. As a result, they aid the plant's recuperation from stress damage as well as make its survival much better in challenging situations (Hakeem et al., 2012). Conversely, metabolites, as opposed to mRNA or proteins, are a depiction of the transcriptional interactions that are involved in the regulation of gene expression throughout adverse conditions and have intimate linkages to the phenotype (Wienkoop et al., 2008). Metabolomics has been the most cross-functional of all systems biology and is present in many of the functions discussed (Arbona et al., 2013). Finally, detailed investigations proved that the metabolic networks participating in the growth and development of plants under a variety of environmental factors are critical for plant growth. Previously, metabolomics and proteomics were used to evaluate the molecular characteristics of legumes against abiotic stressors, as shown in Table 8. Ionomics is the science of a single tissue or the entire organism which encompasses the assessment of all elemental components in response to physiological functions or their alterations. Lahner et al. (2003) were the first who described an "ionome" as the metals, nonmetals, and metalloids present in an organism. Eventually, the terminology "ionome" was expanded to a "metallome" to relate to a collection of ecologically essential non-metals like nitrogen (N), sulfur (S), and phosphorus (P) (Salt et al., 2008). Ions play an important role in maintaining a plant's homeostasis under a variety of environmental situations. Ion transporters are also essential for the regular functioning of metabolic processes as well as managing stress. Particularly compared to various other grain crops, the ionomics technique has been widely employed in model legume plants (*Lotus japonicus*) and commercial legume crops including soybean (Chen et al., 2009). At the commercial level, the soybean genotypes with modified seed chemistry were found using this technique. Rapid innovations in ionomics have opened up new avenues for obtaining a precise description of the macro-and micronutrients or even the chemical compositions of legume grains in timely and cost-effective ways. Ionomics can be employed in this sense for attaining global food and nutritional security while also addressing the "hidden" starvation caused by micronutrient deficiencies (Hacisalihoglu and Settles, 2017; Ziegler et al., 2018). Finally, the ionome evidence can be used in experiments on the accessibility of micronutrients in fundamental pulses. Ionomics involves a thorough understanding of the transcriptional regulation concerned with homeostasis to assess the abiotic-stress-responsive

TABLE 7 Transcriptome profiling of legumes crops under abiotic stress using RNA-Seq.

Legumes crops	Abiotic stress	Plant parts	Seq. platform	*Details	References
Chickpea	Drought	Roots and Shoots	Illumina HiSeq 2500	Identification of transcription factors linked with drought tolerance	Mahdavi Mashaki et al., 2018
		Root	Illumina HiSeq 2500	Identification of drought-resistant transcription factors Bhlh, C3H, NAC, AP2-EREBP, and MYB.	Shukla et al., 2006
		Leaf	Illumina HiSeq 3000	1,562 genes were differentially expressed in the tolerant genotype based on RNA extracted from leaf tissues. Genes that respond to drought were elevated in the tolerant genotype.	Badhan et al., 2018
	Salinity and Drought	Root apex	Roche 454 FLX	Under transcriptome profiling, miRNA-mediated post-transcriptional regulation of genes involved in lateral root development and re-patterning of root hair cells, as well as genes with a high affinity for K+ absorption. The root apex was used to dissect salt and water deprivation situations.	Khandal et al., 2017
Common bean	Drought	Leaf	Illumina GAIIx	During drought stress drought-sensitive genes were detected.	Wu et al., 2014
	Drought	Leaf and root	Illumina platforms (GAII and HiSeq 2000)	Data from transcriptomes showed novel genes associated with the drought stress response.	Confortin et al., 2017
	Salinity	Cotyledon, hypocotyl, and radicle	Illumina HiSeq 2500 PE 150	During the sprouting stage under salt stress, the role of zinc finger proteins (C3H) was discovered.	Zhang et al., 2020
		Root	Illumina HiSeq TM 2000	Transcriptome analysis revealed a total of 2,678 transcription factors, 441 of which were involved in salinity tolerance.	Hiz et al., 2014
Cowpea	Drought	Leaf	Illumina deep sequencing technology	There were just drought-responsive miRNAs identified.	Barrera-Figueroa et al., 2011
	Drought	Leaf		For drought-responsive genes, an SSH database (http://sshdb.bi.up.ac.za/, viewed on 3 August 2021) was generated.	Coetzer et al., 2010
	Cold (Chilling)	Pods	Illumina HiSeq 2500	Many sRNAs and miRNAs are implicated in the response to chilling, according to sRNAomic and transcriptome analyses.	Zuo et al., 2018
		Leaf	Illumina HiSeq 4000	During the vegetative and blooming stages, a total of 538 and 642 putative Transcription factors were found, respectively.	Khan et al., 2019a
Faba bean	Drought	Root	Illumina HiSeq 4000	New DEGs with altered expression during drought were discovered.	Alghamdi et al., 2018
	Salinity	Cotyledons	Illumina HiSeq 4000	A total of 1,410 salinity-responsive genes were discovered, with the salt-tolerant genotype showing considerable up-regulation of these genes.	Yang et al., 2020

(Continued)

TABLE 7 (Continued)

Legumes crops	Abiotic stress	Plant parts	Seq. platform	*Details	References
Lentil	Drought	Leaf	Illumina HiSeq 2500	Drought-tolerant genotypes had more severe upregulation of genes involved in oxidation-reduction processes, TCA cycle, organ senescence, and stomatal conductance decrease than drought-sensitive genotypes.	Razzaq et al., 2021
	Heat	Leaf	Illumina HiSeq 2000	The cell wall and secondary metabolite pathways were both found to be significantly affected.	Singh et al., 2019
Mung bean	Desiccation	Seed	Illumina HiSeq 2500 with PE125	Many transcription factors (AP2, NAC, MYB, and methyltransferase and histone genes were discovered to be differently expressed.)	Tian et al., 2016

*AP2-EREBP, APETALA2/Ethylene-Responsive Element Binding Protein; bHLH, beta Helix Loop Helix; bZIP, beta Leucine Zipper; DEGs, Differentially expressed genes; HSPs, Heat shock proteins; LEA, Late embryogenesis associated; MADS, minichromosome maintenance factor1, agamous, deficiens, and serum response factor; miRNA, MicroRNA; MYB, myeloblastosis; NAC, NAM/ATAF1/CUC2; RNA, Ribonucleic acid; SSH, Suppression subtractive hybridization; sRNA, small RNA; TCA, Tricarboxylic acid cycle; TFs, Transcription factors.

TABLE 8 Combating abiotic stresses in legumes using proteomics and metabolomics approaches.

Crop	Abiotic stress	Omics approach	Details	References
Chickpea	Drought	Proteomics	Potential resources for improving drought tolerance were identified.	Vessal et al., 2020
	Drought	Comparative proteomics	A total of 75 proteins were found to be differentially expressed in roots.	Gupta et al., 2020
	Drought	Comparative proteomics	MALDI-TOF/TOF-MS/MS analyses revealed 24 differently expressed proteins in leaves under drought stress.	Çevik et al., 2019
	Drought	Metabolomics	Effect of PGPRs under drought stress was identified using UPLC-HRMS analysis	Khan et al., 2019b
	Heat	Comparative proteomics	A total of 482 heat-responsive proteins were found to be engaged in heat stress tolerance.	Parankusam et al., 2017
	Salinity	Comparative proteomics	Various proteins were found to be engaged in salinity tolerance.	Arefian et al., 2019
	Drought	Metabolomics	Effect of PGPRs under drought stress was identified using UPLC-HRMS analysis	Khan et al., 2019b
Cowpea	Drought	Metabolomics	GC-TOF-MS profiling of primary metabolites and LC-DAD profiling of secondary metabolites under drought stress. Prolonged stress irrespective of the developmental stage affected the metabolome.	Goufo et al., 2017
Faba bean	Drought	Proteomics	Proteins including chitinase, Bet, and glutamate–glyoxylate aminotransferase were found to be upregulated in leaves under drought stress.	Li et al., 2018
	Salinity	Metabolomics	Molecules such as myo-inositol, allantoin, and glycerophosphoglycerol were found to be up-regulated in roots in response to salt stress.	Richter et al., 2019
	Drought and heat	Metabolomics	Upregulation of nitrogen and metabolism under combined heat and drought stress.	Das et al., 2017
Soybean	Salinity	Comparative metabolomics	A total of 47 different metabolites were found to be responsible for salt tolerance.	Li et al., 2017
	Aluminum	Comparative proteomics	MALDI TOF analysis revealed differential protein expression in roots under Al stress.	Duressa et al., 2011

ion transporters, genetic mutations compounds, and other constituents. Combining ionomics with other pan-omics tools, such as metabolomics and proteomics, will expand the possibilities for evaluating the impacts of abiotic stresses in legumes and their implementations helps in increasing legume productivity (Singh et al., 2021).

Phenomics prospective in legumes

The phenotype of an organism seems to be an observable biophysical property like appearance, behavior, and development (Pratap et al., 2019). Phenomics is a research area that involves high-throughput phenotyping analysis. Phenotype results from a complex combination of genetic capability among an organism and its environment (Deshmukh et al., 2014). Understanding any biological process needs precise phenotyping. A specific phenotype is often employed in plant and animal studies (like symptoms) to comprehend the biological condition, including disease, pest infestation, or physiological disorders. Genetic resources are employed for phenotype-based assessment of genetic markers, which arise as a result of technological advancements; known as "genetic symptoms." The performance of genomics is determined by the consistency with which a genetic marker and phenotype are connected (Varshney et al., 2018). Plant breeding is using omics approaches to improve genetics to obtain an ideal phenotype that will provide a greater and more consistent yield under a variety of environmental situations. As a result, phenomics combined with certain other omics methods holds the most hope in plant breeding (Biswas et al., 2021). Abiotic stress tolerance seems to be a critical feature in terms of yield persistence and potential. Some traits which correlate to stress tolerance in legumes can be evaluated in a controlled condition at the time of sowing. The closing of stomata is one of the primary reasons for saline occurring in plants due to the osmotic effect of soluble compounds which are directly up taken by plant roots from groundwater. As a result, the photosynthesis process becomes slow. Therefore, an alternative measure can be exploited for stomatal responses and photosynthetic under osmotic tensity, which can also be stretched to legumes (Munns, 2010). Phenotyping concedes the imaging of characters of curiosity in real-time. NIRS (near-Infrared Spectroscopy) is one of the very dynamic techniques in advanced phenotyping study among plant breeding. For example, Jakubowski et al. (2017) chose various forage legume crops relying on their improved N_2 fixation from the atmosphere by using this NIRS technique. The plants were evaluated based on the highest tissue N levels, which were proven to increase N_2 fixation in the plant from the atmosphere. This depicts how phenotypic scanning would be used to assess and selected plants. The technique can be implemented to various legumes as well as more aspects.

Genome editing of legume crops against abiotic stress

Multiple candidate genes which are associated with response to abiotic stress are being explored using genome editing methods. To date, numerous biotechnological tools are present to identify these genes. Somaclonal variations, tissue culture, marker-assisted breeding, mutagenesis, wide hybridization, double haploids, and genetic transformation are the main tools of genome editing (Aasim et al., 2018). Genetic transformation (GT) is a famous biotechnological technique used to address the biotic or abiotic stresses of legume plants. Yet, no meaningful progress has been made so far anyway. Kumar and Fladung (2002) explained the genetic transformation process and revealed that the AMT (Agrobacterium Meditated Transformation) is the most useful and powerful technique applied in legumes for genome editing followed by microprojectile bombardment (MP), direct gene transfer to protoplast (DGTP), and electroporation (EP).

Genetic transformation in legumes

In the modern era, the insertion of exotic genes from wild plants to legumes and other important field crops through GT technology has become more significant (Somers et al., 2003). The reliability of transgenic germplasms for reproducing has been proven to be extremely low. Transgenic approaches aid in the production of more durable, genetically engineered germplasm with increased vigor and tolerance to different abiotic challenges, as well as enhanced crop productivity and quality (Chandra and Pental, 2003). The invention of transgenic tools has aided in the identification of mechanisms behind the transcriptional activation linked to abiotic stress resilience. The cultivation of genetically modified legume crops with better agronomic practices has been a great achievement (Aasim et al., 2013). Vadez et al. (2008) described that little progress has been made due to the complicated genetic pathways which are involved to produce crops tolerant to abiotic stress. Previously, a lot of studies revealed that genetically modified legume plants have shown more resilience to abiotic stressors such as salinity, drought, and metals (Atkinson and Urwin, 2012; Sita and Kumar, 2020).

Genome editing in legume crops

To reduce food insecurity, many strategies are being used to build a sustainable agriculture system. Genome editing (GE) for crop enhancement is one such technology that has the potential to build a climate-resilient agriculture system on a worldwide scale (Liu et al., 2013; Abdelrahman et al., 2018). Plant breeding techniques have been significantly influenced by GE technology, including novel strategies for making rapid and precise modifications in crop genomes to defend plants from diverse threats and improve crop yields (Taranto et al., 2018). Site-specific endonucleases such as zinc-finger nucleases (ZFNs), transcription activator-like effector nucleases (TALENs), and CRISPR-Cas9 are employed in genome editing approaches

(Zhu et al., 2017). There are many studies of genome editing that have been conducted on major legume crops.

Soybeans are rich in oil and protein, and an escalating demand requires genetic development with gene-editing tools to meet rising needs and cope with fluctuating climate (Bao et al., 2020). Curtin et al. (2011) targeted the green fluorescent protein (GFP) coding region in soybean with a ZFN array developed *via* context-sensitive selection strategies. This approach designed two independent ZFN pairs by deleting up to 71 base pairs on the target. Curtin et al. (2016) also focused on disturbing miRNA maturation and miRNA gene expression regulation. Accordingly, two ZFN pairs were designed to target Dicer-like 1a (DCL1a) and Dicer-like 1b (DCL1b) genes in soybean. Moreover, Curtin et al. (2018) generated a suite of combinatorial mutant plants using TALENs within the G. max Dicer-like2 gene by whole-genome sequencing. In CRISPR-Cas conditions, different sites of two endogenous soybean genes (GmFEI2 and GmSHR) were targeted by a transgene (bar) and six sgRNAs, and a sgRNA was designed that resulted in mutations in the targeted DNA of hairy roots (Cai et al., 2015). Di et al. (2019) CRISPR/Cas9 system was enhanced by highly active 5 U6 promoters targeting Glyma03g36470, Glyma14g04180, and Glyma06g136900 genes. Consequently, nucleotide insertion, deletion, and substitution mutations occurred. The following year, to target 102 candidate genes Bai et al. (2020) constructed 70 CRISPR-Cas9 vectors and obtained 407 T0 sgRNAs mutant lines with 59.2% mutagenesis frequency, and 35.6% lines carrying multiplex mutations. As a result, increased nodulation of gmric1/gmric2 double mutants and gmrdn1-1/1-2/1-3 triple mutant lines with decreased nodulation were detected.

L. japonicus a model organism for legume crops with similar features to *M. truncatula*, organizes determinate nodules, like soybean and cowpea. In *L. japonicus*, CRISPR/ Cas9 can perform SNF (symbiotic nitrogen fixation)-related gene mutations with hairy root transformation (Wang et al., 2016). Cai et al. (2018a) edited cytokinin receptor Lotus histidine kinaz I-interacting protein (LjCZF1) to disclose the process of cytokinin signaling regulation of rhizobia-legume symbiosis. They found mutant lines with reduced infection threads and nodules, indicating that LjCZF1 is a better regulator of nodulation. Later, CRISPR/Cas9 technology revealed that leghemoglobin (Lbs) in *L. japonicus* resulted in early nodule senescence (Wang et al., 2019b).

Chickpea (*C. arietinum*) is a commercially important crop worldwide, and gene-editing tools can be used to eliminate the problems in its production. Badhan et al. (2021) performed a study that targeted drought tolerance-associated genes, 4-coumarate ligase (4CL) and Reveille 7 (RVE7), for CRISPR/Cas9 editing in chickpea protoplast and the knock-out of the RVE7 gene showed high-efficiency editing *in vivo*. These results showed that CRISPR/Cas9 DNA-free gene editing can be used for genes associated with drought tolerance in chickpea by utilizing protoplast. To date, this was the first and only study that used CRISPR/Cas9 gene editing in chickpea.

Cowpea (*V. unguiculata L.*) Walp., with high nutrition content and health benefits, has tolerance to low rainfall, symbiotic nitrogen fixation (SNF) capability, and low fertilization requirements that make it commercially important (Ji et al., 2019; Che et al., 2021). Ji et al. (2019) targeted the SNF genes by CRISPR/ Cas9-mediated genome editing in non-inheritable mutated hairy roots in cowpea and found restricted nodule formation in the mutants with disrupted alleles. Following them, Juranić et al. (2020) used CRISPR/Cas9 gene editing and identified three cowpea meiosis genes; REC8 (encodes meiotic recombination protein), SPO11-1 (encodes SPO11 protein; an initiator of meiotic double-stranded breaks), and OSD1 (encodes Ophiostoma scytalone dehydratase protein promoting meiotic progression) to induce cowpea asexual seed formation. They found defects in meiosis due to biallelic mutations in exon 1 and exon 3 of the SPO11-1 gene. Recently, Che et al. (2021) also used CRISPR/Cas9 and noticed mutations at the target leading to inhibition of cowpea meiosis gene VuSPO11-1.

Lentils are a type of pulse crop that is consumed all over the world, being a good source of protein, minerals, carbohydrates, vitamins, dietary fiber, and secondary metabolites like phenolic compounds. Explants from various lentil tissues, such as shoot apices, epicotyls, nodal segments, embryo axes, cotyledonary nodes, and roots, have been explored for *in vitro* plant regeneration for genetic modification (Mahmoudian et al., 2002; Sarker et al., 2003; Akcay et al., 2009). As the number of shoots regenerated per explant greatly affect the transformation efficiency and success of CRISPR/Cas9-based gene editing, optimization of the protocol with an appropriate combination of mineral media and hormones is required in the near future. Gene disruption to improve lentils may be made simpler, less expensive, and more accurate by gene editing.

Mung bean is a warm-season, self-pollinated and diploid ($2n = 2x = 22$) legume crop with a small genome size (Parida et al., 1990; Nair et al., 2013; Kang et al., 2014). One of the first legumes to have a genetic linkage map was the mung bean in the early 1990s (Fatokun et al., 1992, 1993). In the past, molecular methods with an emphasis on yield, nutrient improvement, and disease resistance have been used to improve mung beans. These methods included random amplified polymorphic DNA (RAPD), restriction fragment length polymorphism (RFLP), SNP, and SSR markers (Fatokun et al., 1993; Chankaew et al., 2011; War et al., 2017). In mung bean breeding projects, CRISPR/Cas9 gene editing has a lot of potential. A symbiosis receptor-like kinase gene was recently successfully targeted using CRISPR/Cas9 gene editing to stop symbiotic nitrogen fixation in cowpea (V. unguiculata) (Ji et al., 2019). The achievement of CRISPR/Cas9 in a Vigna system shows that gene editing can be used for other species including mung bean. Quality attributes and disease resistance would be some of the initial targets for gene editing in mung beans. Developing mung bean varieties

TABLE 9 Application of transgenic tools for genome editing in legumes for abiotic stresses.

Legume crop	Performance of transgenic	Gene	Sources	Protein coded	Promoter used	References
Mung bean	Salt and drought stress	Coda	*A. globiformis*	Choline oxidase A	CaMV35S	Baloda and Madanpotra, 2017
	Salt stress	gly I	*Brassica juncea*	Glyoxalate	CaMV35S and CmYLCV	Bhomkar et al., 2008
	Salinity and drought stress	ALDRXV4	–	Osmoprotection and detoxification	CaMV35S	Singh et al., 2016
Phseolus vulgaris	Drought stress	HVA1 and bar	*Hordeum vulgare*	Late embryogenesis protein	CaMV35S	Nguyen and Sticklen, 2012
Medicago sativa	Salt tolerance	GmDREB1	*G. max*	DRE-binding protein	*A. thaliana* RD29A	Jin et al., 2019
	Drought stress	WXP1	*Medicago truncatula*	AP2 domain	CaMV35S	Zhang et al., 2005
	Freezing stress	Fe-SOD	*Nicotiana plumbaginifolia*	Fe-superoxide Dismutase	CaMV35S	McKersie et al., 2000
	Aluminum toxicity stress	Malate dehydrogenase	*M. sativa*	Malate dehydrogenase	CaMV35S	Tesfaye et al., 2001
	Freezing stress	Mn-SOD	*N. plumbaginifolia*	Mn-superoxide dismutas	CaMV35S	Song et al., 2019
	Freezing stress	SOD	*P. sativum and N. plumbaginifolia*	Superoxide dismutase	CaMV35S	McKersie et al., 1993
C. Arietinum	Oxidative stress	Cod A	*Arthrobacter globiformis*	Choline oxidase A	CaMV35S	Sharmila et al., 2009
	Osmotic and drought stress	p5cs	*Vigna aconitifolia*	O1-pyrroline 5-carboxylate synthase	CaMV35S	Bhatnagar-Mathur et al., 2009
Arachis hypogea	Drought stress	Alfin1, PDH45, and PgHSF4	Alfaalfa and Pea	–	CaMV35S	Ramu et al., 2016
	Drought stress	DREB1A	*A. thaliana*	DRE-binding protein	*A. thaliana* RD29A	Mathur et al., 2014
	Drought stress	MuNAC4	*Macrotyloma uniflorum*	NAC	CaMV35S	Pandurangaiah et al., 2014
	Drought stress	DREB1A	*A. thaliana*	DRE-binding protein	*A. thaliana* RD29A	Vadez et al., 2013
	Drought and SALINITY stress	MuWRKY3	*Macrotyloma uniflorum*	WRKY	CaMV35S	Kiranmai et al., 2018
	Drought and salinity stress	AtHDG11	*A. thaliana*	Transcription factor	*A. thaliana* RD29A	Banavath et al., 2018
	Drought and salinity stress	SBASR-1	*S. chiata*	Abscisic acid stress	CaMV35S	Tiwari et al., 2015
	Drought and salinity stress	AtNAC2	*A. thaliana*	NAC	CaMV35S	Patil et al., 2014
	Drought and salinity stress	AtDREB2A and AtABF3	*A. thaliana*	DRE-binding protein	CaMV35S	Pruthvi et al., 2014
	Drought and salinity stress	SbVPPase	*Sorghum bicolor*	Vacuolar proton pyrophosphatase	CaMV35S	Puli et al., 2021
	Salinity stress	SbNHXLP	*S. bicolor*	Na1/H1 antiporterlikeprotein	CaMV35S	Kavi Kishor et al., 2018
	Salt stress	SbpAPX	*Salicornia brachiata*	Peroxisomalascorbate peroxidase	CaMV35S	Singh et al., 2014
	Salt stress	PDH45	*Pisumsativum*	DNA helicase 45	CaMV35S	Manjulatha et al., 2014
Glycine max	Drought and salinity stress	NTR1	*Bactris campestris*	Jasmonic acid	CaMV35S	Xue and Zhang, 2007

that can withstand changing weather patterns would help in the further expansion of mung bean cultivation worldwide.

Faba bean is a diploid ($2n = 2x = 12$) and one of the most important cool-season grain legumes with high protein content, antioxidants, and a rich source of fiber (Ray and Georges, 2010; Sudheesh et al., 2019). A reference genome of faba bean is still lacking; however, significant progress has been made in creating genetic and genomic resources to facilitate molecular breeding. Application of CRISPR/Cas gene editing is hampered by the lack of an annotated reference genome for the intricate faba bean genome, especially when designing specific gRNA-targeted genes of interest. To date, no CRISPR/Cas9 studies have been reported for this crop.

Genome editing, particularly CRISPR/Cas9 is an effective technology for abiotic stress tolerance in legumes, which is still rarely used. Similarly, there are limited studies in the literature on the implementation of genome editing for abiotic stress tolerance in other crops (Debbarma et al., 2019). In legumes, Soybean genome editing using the CRISPR/Cas9 system has been reported to be successful (Bao et al., 2019). For example, using the CRISPR/Cas9 approach, the soybean gene GmFT2a (FT-Flower Locus T) related to flowering time was knocked out, resulting in GmFT2a mutants with delayed flowering (Cai et al., 2018b). The roles of GmHsp90A2 (Heat shock protein 90s) in soybean have recently been studied using stable transgenic lines overexpressing GmHsp90A2 as well as mutant lines produced using the CRISPR/Cas9 genome editing technique (Huang et al., 2019). Hsp90s is a stable and abundant protein chaperone involved in the protective stress response, and overexpression of GmHsp90A2 in the *Arabidopsis thaliana* model resulted in greater tolerance to heat stress in a prior study (Xu et al., 2013). The CRISPR/Cas9 deletion of the endogenous soybean GmHsp90A2 gene was verified up to the T1 generation in the study of Huang et al. (2019). Although there are fewer scientific studies on using accurate and targeted genome editing for abiotic stress tolerance in Fabaceae can be found, these approaches have immense potential for future use in legume molecular breeding. Here, we compiled a list of reports on the application of transgenic tools in legumes to abiotic stress resilience (Table 9).

Conclusion and future recommendations

Agriculture is dependent on the climate, and changes in climate are resulting in various stresses and causing significantl production losses each year. Legumes are multi-beneficial crops and can mitigate our food scarcity problems by providing high-quality food with low inputs. During the last two decades, significant progress has been made in utilizing state-of-the-art "OMICs" approaches to develop climate-smart legume cultivars. A huge number of legumes are conserved at the gene banks and also present in the small farmer's field and are yet to be characterized. Efforts should be done to characterize those unexplored legumes' genetic resources at both phenotypic and molecular levels to identify genetic variations that can be used for the development of improved cultivars. Nevertheless, a good number of efforts have been made to identify the genomic regions associated with abiotic stresses. However, fewer attempts have been made to validate the identified genomic region to speed up marker-assisted breeding. Therefore, it is a present-day need to develop KASP markers for speed breeding. Recent advancements in genomic resources for legumes have provided the basis to perform transformative breeding approaches like genomic selection and genome editing for crop improvement. However, these efforts are still few compared to cereals. It is very important to harness CRISPR/Cas9-based gene-editing technology for the targeted improvement of traits in legume crops.

Author contributions

MN conceived the idea and perform editing to the manuscript. MN, NB, and MA collected the literature. AA, MTA, AS, HA, and TH contributed to writing the original draft of the manuscript. AA, MTA, HA, NB, K-HB, and TK designed the tables and figures. MN, FB, MA, AS, SD, TH, and TK reviewed and edited the manuscript. MN, FB, YC, NA, and MH contributed to addressing comments raised by the reviewers. MN, FB, and YC provided resources. All authors have read and approved the final version of the manuscript.

Funding

The authors are very grateful to the Scientific Research Unit of Sivas University of Science and Technology for providing a research grant to MN through his project (Project Number: 2021-GENL-TBT-0003). Basic Science Research Program supported this research through the National Research Foundation of Korea (NRF), funded by the Ministry of Education (2019R1A6A1A11052070).

Conflict of interest

The authors declare that the research was conducted in the absence of any commercial or financial relationships that could be construed as a potential conflict of interest.

Publisher's note

All claims expressed in this article are solely those of the authors and do not necessarily represent those of their affiliated

organizations, or those of the publisher, the editors and the reviewers. Any product that may be evaluated in this article, or claim that may be made by its manufacturer, is not guaranteed or endorsed by the publisher.

References

Aasim, M., Baloch, F. S., Nadeem, M. A., Bakhsh, A., Sameeullah, M., and Day, S. (2018). "Fenugreek (*Trigonella foenum-graecum* L.): an underutilized edible plant of modern world," in *Global Perspectives on Underutilized Crops* (Cham: Springer), 381–408.

Aasim, M., Day, S., Rezaei, F., and Hajyzadeh, M. (2013). Multiple shoot regeneration of plumular apices of Chickpea. *Turk J. Agric. For.* 37, 33–39. doi: 10.3906/tar-1204-38

Abdelrahman, M., Al-Sadi, A. M., Pour-Aboughadareh, A., Burritt, D. J., and Tran, L. S. P. (2018). Genome editing using CRISPR/Cas9–targeted mutagenesis: an opportunity for yield improvements of crop plants grown under environmental stresses. *Plant Physiol. Biochem.* 131, 31–36. doi: 10.1016/j.plaphy.2018.03.012

Afzal, M., Alghamdi, S. S., Migdadi, H. H., Khan, M. A., Mirza, S. B., and El-Harty, E. (2020). Legume genomics and transcriptomics: from classic breeding to modern technologies. *Saudi J. Biol. Sci.* 27, 543–555. doi: 10.1016/j.sjbs.2019.11.018

Ahmed, S. M., Alsamman, A. M., Jighly, A., Mubarak, M. H., Al-Shamaa, K., Istanbuli, T., et al. (2021). Genome-wide association analysis of chickpea germplasms differing for salinity tolerance based on DArTseq markers. *PLoS ONE.* 16, e0260709. doi: 10.1371/journal.pone.0260709

Akcay, U. C., Mahmoudian, M., Kamci, H., Yucel, M., and Oktem, H. (2009). *Agrobacterium tumefaciens*-mediated genetic transformation of a recalcitrant grain legume, lentil (Lens culinaris Medik). *Plant Cell Rep.* 28, 407–417. doi: 10.1007/s00299-008-0652-4

Akohoue, F., Achigan-Dako, E. G., Sneller, C., Van Deynze, A., and Sibiya, J. (2020). Genetic diversity, SNP-trait associations and genomic selection accuracy in a west African collection of Kersting's groundnut [Macrotyloma geocarpum (Harms) Maréchal & Baudet]. *PLoS ONE* 15, e0234769. doi: 10.1371/journal.pone.0234769

Alghamdi, S. S., Khan, M. A., Ammar, M. H., Sun, Q., Huang, L., Migdadi, H. M., et al. (2018). Characterization of drought stress-responsive root transcriptome of Faba bean (*Vicia faba* L.) using RNA sequencing. *3 Biotech.* 8, 1–19. doi: 10.1007/s13205-018-1518-2

Ambachew, D., and Blair, M. W. (2021). Genome wide association mapping of root traits in the andean genepool of common bean (*Phaseolus vulgaris* L.) grown with and without aluminum toxicity. *Front. Plant Sci.* 12, 825. doi: 10.3389/fpls.2021.628687

Anjum, S. A., Ashraf, U., Zohaib, A., Tanveer, M., Naeem, M., Ali, I., et al. (2017). Growth and development responses of crop plants under drought stress: a review. *Zemdirbyste* 104, 267–276. doi: 10.13080/z-a.2017.104.034

Annicchiarico, P., Nazzicari, N., Wei, Y., Pecetti, L., and Brummer, E. C. (2017). Genotyping-by-sequencing and its exploitation for forage and cool-season grain legume breeding. *Front. Plant Sci.* 8, 679. doi: 10.3389/fpls.2017.00679

Anwar, A., Sinha, A., Sharif, A., Siddique, M., Irshad, S., Anwar, W., et al. (2022). The nexus between urbanization, renewable energy consumption, financial development, and CO2 emissions: Evidence from selected Asian countries. *Environ. Dev. Sustain.* 24, 6556–6576. doi: 10.1007/s10668-021-01716-2

Arbona, V., Manzi, M., Ollas, C. D., and Gómez-Cadenas, A. (2013). Metabolomics as a tool to investigate abiotic stress tolerance in plants. *Int. J. Mol. Sci.*14, 4885–4911. doi: 10.3390/ijms14034885

Arefian, M., Vessal, S., Malekzadeh-Shafaroudi, S., Siddique, K. H., and Bagheri, A. (2019). Comparative proteomics and gene expression analyses revealed responsive proteins and mechanisms for salt tolerance in Chickpea genotypes. *BMC Plant Biol.* 19, 1–26. doi: 10.1186/s12870-019-1793-z

Assefa, T., Assibi Mahama, A., Brown, A. V., Cannon, E. K., Rubyogo, J. C., Rao, I. M., et al. (2019). A review of breeding objectives, genomic resources, and marker-assisted methods in Common bean (*Phaseolus vulgaris* L.). *Mol. Breed.* 39, 1–23. doi: 10.1007/s11032-018-0920-0

Atkinson, N. J., and Urwin, P. E. (2012). The interaction of plant biotic and abiotic stresses: from genes to the field. *J.Exp. Bot.* 63, 3523–3543. doi: 10.1093/jxb/ers100

Badhan, S., Ball, A. S., and Mantri, N. (2021). First report of CRISPR/Cas9 mediated DNA-free editing of 4CL and RVE7 genes in chickpea protoplasts. *Int. J. Mol. Sci.* 22, 396. doi: 10.3390/ijms22010396

Badhan, S., Kole, P., Ball, A., and Mantri, N. (2018). RNA sequencing of leaf tissues from two contrasting chickpea genotypes reveals mechanisms for drought tolerance. *Plant Physiol. Biochem.* 129, 295–304. doi: 10.1016/j.plaphy.2018.06.007

Bai, M., Yuan, J., Kuang, H., Gong, P., Li, S., Zhang, Z., et al. (2020). Generation of a multiplex mutagenesis population via pooled CRISPR -Cas9 in soyabean. *Plant Biotechnol. J.* 18, 721–731. doi: 10.1111/pbi.13239

Baloda, A., and Madanpotra, S. (2017). Transformation of mungbean plants for salt and drought tolerance by introducing a gene for an osmoprotectant glycine betaine. *J. Plant Stress Physiol.* 3, 5–11. doi: 10.19071/jpsp.2017.v3.3148

Banavath, J. N., Chakradhar, T., Pandit, V., Konduru, S., Guduru, K. K., Akila, C. S., et al. (2018). Stress inducible overexpression of AtHDG11 leads to improved drought and salt stress tolerance in Peanut (*Arachis hypogaea* L.). *Front. Chem.* 6, 34. doi: 10.3389/fchem.2018.00034

Bao, A., Zhang, C., Huang, Y., Chen, H., Zhou, X., and Cao, D. (2020). Genome editing technology and application in soybean improvement. *Oil Crop Sci.* 5, 31–40. doi: 10.1016/j.ocsci.2020.03.001

Bao, Z., Yang, Z., Huang, Z., Zhou, Y., Cui, Q., and Dong, D. (2019). LncRNADisease 2.0: an updated database of long non-coding RNA-associated diseases. *Nucleic Acids Res.* 47, D1034–D1037. doi: 10.1093/nar/gky905

Barrera-Figueroa, B. E., Gao, L., Diop, N. N., Wu, Z., Ehlers, J. D., Roberts, P. A., et al. (2011). Identification and comparative analysis of drought-associated microRNAs in two Cowpea genotypes. *BMC Plant Biol.* 11, 1–11. doi: 10.1186/1471-2229-11-127

Beji, S., Fontaine, V., Devaux, R., Thomas, M., Negro, S. S., Bahrman, N., et al. (2020). Genome-wide association study identifies favorable SNP alleles and candidate genes for frost tolerance in Pea. *BMC Genom.* 21, 1–21. doi: 10.1186/s12864-020-06928-w

Bhatnagar-Mathur, P., Vadez, V., Jyostna Devi, M., Lavanya, M., Vani, G., and Sharma, K. K. (2009). Genetic engineering of Chickpea (*Cicer arietinum* L.) with the P5CSF129A gene for osmoregulation with implications on drought tolerance. *Mol. Breed.* 23, 591–606. doi: 10.1007/s11032-009-9258-y

Bhomkar, P., Upadhyay, C. P., Saxena, M., Muthusamy, A., Shiva Prakash, N., Pooggin, M., et al. (2008). Salt stress alleviation in transgenic *Vigna mungo* (L.) Hepper (blackgram) by overexpression of the glyoxalase I gene using a novel *Cestrum Yellow Leaf Curling Virus* (CmYLCV) promoter. *Mol. Breed.* 22, 169–181. doi: 10.1007/s11032-008-9164-8

Biswas, A., Andrade, M. H. M. L., Acharya, J. P., de Souza, C. L., Lopez, Y., De Assis, G., et al. (2021). Phenomics-assisted selection for herbage accumulation in Alfalfa (*Medicago sativa* L.). *Front. Plant Sci.* 12, 756768–756768. doi: 10.3389/fpls.2021.756768

Blair, M. W., Cortés, A. J., Penmetsa, R. V., Farmer, A., Carrasquilla-Garcia, N., and Cook, D. R. (2013). A high-throughput SNP marker system for parental polymorphism screening, and diversity analysis in common bean (*Phaseolus vulgaris* L.). *Theor. Appl. Genet.* 126, 535–548. doi: 10.1007/s00122-012-1999-z

Bohra, A., Bharadwaj, C., Radhakrishnan, T., Singh, N. P., and Varshney, R. K. (2019). Translational genomics and Mol. Breed for enhancing precision and efficiency in crop improvement programs: some examples in legumes. *Indian J. Genet. Plant Breed* 79, 227–240. doi: 10.31742/IJGPB.79S.1.13

Breria, C. M., Hsieh, C.-H., Yen, T.-B., Yen, J.-Y., Noble, T. J., and Schafleitner, R. (2020). A SNP-based genome-wide association study to mine genetic loci associated to salinity tolerance in mungbean (*Vigna radiata* L.). *Gene* 11, 759. doi: 10.3390/genes11070759

Brown, A. D. H. (1989). *Size and Structure of Collection: The Case for Core Collection. The Use of Plant Genetic Resources.* Chichester: John Wiley & Sons, Baffins Lane, 136–156.

Burstin, J., Salloignon, P., Chabert-Martinello, M., Magnin-Robert, J.-B., Siol, M., Jacquin, F., et al. (2015). Genetic diversity and trait genomic prediction in a pea diversity panel. *BMC Genom.* 16, 1–17. doi: 10.1186/s12864-015-1266-1

Cai, K., K., Yin, J., Chao, H., Ren, Y., Jin, L., et al. (2018a). A C3HC4-type RING finger protein regulates rhizobial infection and nodule organogenesis in lotus japonicus. *J. Integr. Plant Biol.* 60, 878–896. doi: 10.1111/jipb.12703

Cai, Y., Chen, L., Liu, X., Guo, C., Sun, S., Wu, C., et al. (2018b). CRISPR/Cas9-mediated targeted mutagenesis of GmFT2a delays flowering time in soya bean. *Plant Biotechnol. J.* 16, 176–185. doi: 10.1111/pbi.12758

Cai, Y., Chen, L., Liu, X., Sun, S., Wu, C., Jiang, B., et al. (2015). CRISPR/Cas9-mediated genome editing in soybean hairy roots. *PLoS ONE* 10, e0136064. doi: 10.1371/journal.pone.0136064

Çakir, Ö., Uçarli, C., Tarhan, Ç., Pekmez, M., and Turgut-Kara, N. (2019). Nutritional and health benefits of legumes and their distinctive genomic properties. *Food Sci. Technol.* 39, 1–12. doi: 10.1590/fst.42117

Cervantes, E., Saadaoui, E., Tocino, Á., and Gómez, J. J. M. (2019). "Seed shape quantification in the model legumes: Methods and applications," in *The Model Legume Medicago Truncatula* (New Jersey: John Wiley & Sons), 92–98.

Çevik, S., Akpinar, G., Yildizli, A., Kasap, M., Karaosmanoglu, K., and Ünyayar, S. (2019). Comparative physiological and leaf proteome analysis between drought-tolerant chickpea Cicer reticulatum and drought-sensitive chickpea *C. arietinum*. *J. Biosci.* 44, 1–13. doi: 10.1007/s12038-018-9836-4

Chandra, A., and Pental, D. (2003). Regeneration and genetic transformation of grain legumes: an overview. *Curr. Sci.* 84, 381–387.

Chandrashekharaiah, P., Paul, V., Kushwaha, S., Sanyal, D., and Dasgupta, S. (2021). "Biotechnological approaches for enhancing stress tolerance in legumes," in *Sustainable Agriculture Reviews 51*, eds P. Guleria, V. Kumar, and E. Lichtfouse (Springer), 247–293.

Chankaew, S., Isemura, T., Naito, K., Ogiso-Tanaka, E., Tomooka, N., Somta, P., et al. (2014). QTL mapping for salt tolerance and domestication-related traits in Vigna marina subsp. oblonga, a halophytic species. *Theor. Appl. Genet.* 127, 691–702. doi: 10.1007/s00122-013-2251-1

Chankaew, S., Somta, P., Sorajjapinun, W., and Srinives, P. (2011). Quantitative trait loci mapping of Cercospora leaf spot resistance in mungbean, Vigna radiata (L.) Wilczek. *Mol. Breed.* 28, 255–264. doi: 10.1007/s11032-010-9478-1

Chapman, M. A. (2015). Transcriptome sequencing and marker development for four underutilized legumes. *Appl. Plant Sci.* 3, 1400111. doi: 10.3732/apps.1400111

Che, P., Chang, S., Simon, M. K., Zhang, Z., Shaharyar, A., Ourada, J., et al. (2021). Developing a rapid and highly efficient cowpea regeneration, transformation and genome editing system using embryonic axis explants. *Plant J.* 106, 817–830. doi: 10.1111/tpj.15202

Chen, Z., Watanabe, T., Shinano, T., Okazaki, K., and Osaki, M. (2009). Rapid characterization of plant mutants with an altered ion-profile: a case study using Lotus japonicus. *New Phytol.* 181, 795–801. doi: 10.1111/j.1469-8137.2008.02730.x

Choi, H.-K. (2019). Translational genomics and multi-omics integrated approaches as a useful strategy for crop breeding. *Genes Genom.* 41, 133–146. doi: 10.1007/s13258-018-0751-8

Choudhary, S., Isobe, S., and Chahota, R. K. (2022). Elucidation of drought tolerance potential of horsegram (*Macrotyloma uniflorum* Var.) germplasm using genome wide association studies. *Gene* 819, 146241. doi: 10.1016/j.gene.2022.146241

Coetzer, N., Gazendam, I., Oelofse, D., and Berger, D. K. (2010). SSHscreen and SSHdb, generic software for microarray based gene discovery: application to the stress response in Cowpea. *Plant Methods* 6, 1–20. doi: 10.1186/1746-4811-6-10

Confortin, S. C., Meneghini, V., Ono, L. M., Schneider, I. J., Barbosa, A. R., and D'orsi, E. (2017). Anthropometric indicators as a screening tool for sarcopenia in older adults from Florianópolis, Santa Catarina: EpiFloripa Ageing study. *Revista de Nutrição*. 30, 287–296. doi: 10.1590/1678-98652017000300002

Cook, D. R. (1999). Medicago truncatula-a model in the making! *Curr. Opin. Plant Biol.* 2, 301–304. doi: 10.1016/S1369-5266(99)80053-3

Curtin, S. J., Michno, J.-M., Campbell, B. W., Gil-Humanes, J., Mathioni, S. M., Hammond, R., et al. (2016). MicroRNA maturation and MicroRNA target gene expression regulation are severely disrupted in soybean dicer-like1 double mutants. *G3* 6, 423–433. doi: 10.1534/g3.115.022137

Curtin, S. J., Xiong, Y., Michno, J.-M., Campbell, B. W., Stec, A. O., Cermák, T., et al. (2018). CRISPR/Cas9 and TALENs generate heritable mutations for genes involved in small RNA processing of *Glycine max* and *Medicago Truncatula*. *Plant Biotechnol. J.* 16, 1125–1137. doi: 10.1111/pbi.12857

Curtin, S. J., Zhang, F., Sander, J. D., Haun, W. J., Starker, C., Baltes, N. J., et al. (2011). Targeted mutagenesis of duplicated genes in soybean with zinc-finger nucleases. *Plant Physiol.* 156, 466–473. doi: 10.1104/pp.111.172981

Dai, X., Zhuang, Z., Boschiero, C., Dong, Y., and Zhao, P. X. (2021). LegumeIP V3: from models to crops—an integrative gene discovery platform for translational genomics in legumes. *Nucleic Acids Res.* 49, D1472–D1479. doi: 10.1093/nar/gkaa976

Das, A., Rushton, P.J., and Rohila, J. S. (2017). Metabolomic profiling of soybeans (*Glycine max* L.) reveals the importance of sugar and nitrogen metabolism under drought and heat stress. *Plants* 6, 21.

Debbarma, J., Sarki, Y. N., Saikia, B., Boruah, H. P. D., Singha, D. L., and Chikkaputtaiah, C. (2019). Ethylene response factor (ERF) family proteins in abiotic stresses and CRISPR–Cas9 genome editing of ERFs for multiple abiotic stress tolerance in crop plants: a review. *Mol. Biotechnol.* 61, 153–172. doi: 10.1007/s12033-018-0144-x

Deshmukh, R., Sonah, H., Patil, G., Chen, W., Prince, S., Mutava, R., et al. (2014). Integrating omic approaches for abiotic stress tolerance in soybean. *Front. Plant Sci.* 5, 244. doi: 10.3389/fpls.2014.00244

Dhaliwal, S. K., Talukdar, A., Gautam, A., Sharma, P., Sharma, V., and Kaushik, P. (2020). Developments and prospects in imperative underexploited vegetable legumes breeding: a review. *Int. J. Mol. Sci.* 21, 9615. doi: 10.3390/ijms21249615

Di, Y. H., Sun, X. J., Hu, Z., Jiang, Q. Y., Song, G. H., Zhang, B., et al. (2019). Enhancing the CRISPR/Cas9 system based on multiple GmU6 promoters in soybean. *Biochem. Biophysical Res. Commun*. 519, 819–823. doi: 10.1016/j.bbrc.2019.09.074

Diaz, L. M., Ricaurte, J., Tovar, E., Cajiao, C., Teran, H., Grajales, M., et al. (2018). QTL analyses for tolerance to abiotic stresses in a common bean (*Phaseolus vulgaris* L.) population. *PLoS ONE* 13, e0202342. doi: 10.1371/journal.pone.0202342

Dita, M. A., Rispail, N., Prats, E., Rubiales, D., and Singh, K. B. (2006). Biotechnology approaches to overcome biotic and abiotic stress constraints in legumes. *Euphytica* 147, 1–24. doi: 10.1007/s10681-006-6156-9

Dramadri, I. O., Nkalubo, S. T., Kramer, D. M., and Kelly, J. D. (2021). Genome-wide association analysis of drought adaptive traits in common bean. *Crop Sci.* 61, 3232–3253. doi: 10.1002/csc2.20484

Dumont, E., Fontaine, V., Vuylsteker, C., Sellier, H., Bodèle, S., Voedts, N., et al. (2009). Association of sugar content QTL and PQL with physiological traits relevant to frost damage resistance in pea under field and controlled conditions. *Theor. Appl. Genet.* 118, 1561–1571. doi: 10.1007/s00122-009-1004-7

Duressa, D., Soliman, K., Taylor, R., and Senwo, Z. (2011). Proteomic analysis of soybean roots under aluminum stress. *Int. J. Plant Genom.* 2011, 282531. doi: 10.1155/2011/282531

Fatokun, C. A., Danesh, D., Young, N. D., and Stewart, E. L. (1993). Molecular taxonomic relationships in the genus Vigna based on RFLP analysis. *Theoret. Appl. Genet.* 86, 97–104. doi: 10.1007/BF00223813

Fatokun, C. A., Menancio-Hautea, D. I., Danesh, D., and Young, N. D. (1992). Evidence for orthologous seed weight genes in Cowpea and Mung bean based on RFLP mapping. *Genetics* 132, 841–846. doi: 10.1093/genetics/132.3.841

Fernandes, C., Figueira, E., Tauler, R., and Bedia, C. (2018). Exposure to chlorpyrifos induces morphometric, biochemical and lipidomic alterations in Greenbeans (*Phaseolus vulgaris*). *Ecotoxicol. Environ. Saf. Eco. Environ. Safe* 156, 25–33. doi: 10.1016/j.ecoenv.2018.03.005

Frankel, O. H. (1984). Genetic perspectives of germplasm conservation. *Genet Manipul Impact Man Soc.* 161, 170.

Gill, S. S., and Tuteja, N. (2010). Reactive oxygen species and antioxidant machinery in abiotic stress tolerance in crop plants. *Plant. Physiol. Biochem.* 48, 909–930. doi: 10.1016/j.plaphy.2010.08.016

Gondalia, N., Vashi, R., Barot, V., Sharma, F., Anishkumar, P., Chatterjee, M., et al. (2022). "Genomic designing for abiotic stress tolerance in pea (*Pisum Sativum* L.)," in *Genomic Designing for Abiotic Stress Resistant Pulse Crops*, ed C. Kole (Springer), 45–113.

Goufo, P., Moutinho-Pereira, J. M., Jorge, T. F., Correia, C. M., Oliveira, M. R., Rosa, E. A., et al. (2017). Cowpea (*Vigna unguiculata* L. Walp.) metabolomics: osmoprotection as a physiological strategy for drought stress resistance and improved yield. *Front. Plant Sci.* 8, 586. doi: 10.3389/fpls.2017.00586

Gresta, F., Mercati, F., Santonoceto, C., Abenavoli, M. R., Ceravolo, G., Araniti, F., et al. (2016). Morpho-agronomic and AFLP characterization to explore guar (*Cyamopsis tetragonoloba* L.) genotypes for the Mediterranean environment. *Ind. Crops Prod.* 86, 23–30. doi: 10.1016/j.indcrop.2016.03.038

Gupta, S., Mishra, S. K., Misra, S., Pandey, V., Agrawal, L., Nautiyal, C. S., et al. (2020). Revealing the complexity of protein abundance in chickpea root under drought-stress using a comparative proteomics approach. *Plant Physiol. Biochem.* 151, 88–102. doi: 10.1016/j.plaphy.2020.03.005

Gupta, S., and Pandey, S. (2021). "Exploiting the potential of plant growth-promoting rhizobacteria in legume production," in *Abiotic Stress and Legumes*, eds V. P. Singh, S. Singh, and D. K. Chauhan (Elsevier), 1–32.

Gupta, S., Wardhan, V., Kumar, A., Rathi, D., Pandey, A., Chakraborty, S., et al. (2015). Secretome analysis of chickpea reveals dynamic extracellular remodeling and identifies a Bet v1-like protein, CaRRP1 that participates in stress response. *Sci. Rep.* 5, 1–14. doi: 10.1038/srep18427

Hacisalihoglu, G., and Settles, A. M. (2017). Quantification of seed ionome variation in 90 diverse soybean (*Glycine max*) lines. *J. Plant Nutr.* 40, 2808–2817. doi: 10.1080/01904167.2017.1382528

Hakeem, K. R., Chandna, R., Ahmad, P., Iqbal, M., and Ozturk, M. (2012). Relevance of proteomic investigations in plant abiotic stress physiology. *OMICS J. Integr. Biol.* 16, 621–635. doi: 10.1089/omi.2012.0041

Heffner, E. L., Sorrells, M. E., and Jannink, J. L. (2009). Genomic selection for crop improvement. *Crop Sci.* 49, 1–12. doi: 10.2135/cropsci2008.08.0512

Hiz, M. C., Canher, B., Niron, H., and Turet, M. (2014). Transcriptome analysis of salt tolerant common bean (*Phaseolus vulgaris* L.) under saline conditions. *PLoS ONE* 9, e92598. doi: 10.1371/journal.pone.0092598

Howard, R., and Jarquin, D. (2019). Genomic prediction using canopy coverage image and genotypic information in soybean via a hybrid model. *Evol. Bioinform.* 15, 1176934319840026. doi: 10.1177/1176934319840026

Hoyos-Villegas, V., Song, Q., and Kelly, J. D. (2017). Genome-wide association analysis for drought tolerance and associated traits in common bean. *Plant Genome* 10, 0122. doi: 10.3835/plantgenome2015.12.0122

Huang, H., Ullah, F., Zhou, D.-X., Yi, M., and Zhao, Y. (2019). Mechanisms of ROS regulation of plant development and stress responses. *Front. Plant Sci.* 10, 800. doi: 10.3389/fpls.2019.00800

Idrissi, O., Udupa, S. M., De Keyser, E., McGee, R. J., Coyne, C. J., Saha, G. C., et al. (2016). Identification of quantitative trait loci controlling root and shoot traits associated with drought tolerance in a lentil (Lens culinaris Medik.) recombinant inbred line population. *Front. Plant Sci.* 7, 1174. doi: 10.3389/fpls.2016.01174

Iglesias-García, R., Prats, E., Fondevilla, S., Satovic, Z., and Rubiales, D. (2015). Quantitative trait loci associated to drought adaptation in Pea (*Pisum Sativum* L.). *Plant Mol. Biol. Rep.* 33, 1768–1778. doi: 10.1007/s11105-015-0872-z

Jakubowski, A. R., Casler, M. D., and Jackson, R. D. (2017). Legume addition to perennial warm-season grass swards increases harvested biomass. *Crop Sci.* 57, 3343–3351. doi: 10.2135/cropsci2017.04.0266

Jannink, J.-L., Lorenz, A. J., and Iwata, H. (2010). Genomic selection in plant breeding: from theory to practice. *Brief Funct. Geno.* 9, 166–177. doi: 10.1093/bfgp/elq001

Jarquín, D., Kocak, K., Posadas, L., Hyma, K., Jedlicka, J., Graef, G., et al. (2014). Genotyping by sequencing for genomic prediction in a soybean breeding population. *BMC Genom.* 15, 1–10. doi: 10.1186/1471-2164-15-740

Jha, U. C., Bohra, A., Jha, R., and Parida, S. K. (2019). Salinity stress response and 'omics' approaches for improving salinity stress tolerance in major grain legumes. *Plant Cell Rep.* 38, 255–277. doi: 10.1007/s00299-019-02374-5

Jha, U. C., Bohra, A., and Nayyar, H. (2020). Advances in "omics" approaches to tackle drought stress in grain legumes. *Plant Breed.* 139, 1–27. doi: 10.1111/pbr.12761

Ji, J., Zhang, C., Sun, Z., Wang, L., Duanmu, D., and Fan, Q. (2019). Genome editing in cowpea vigna unguiculata using CRISPR-Cas9. *Int. J. Mol. Sci.* 20, 2471. doi: 10.3390/ijms20102471

Jin, X., Yin, X., Ndayambaza, B., Zhang, Z., Min, X., Lin, X., et al. (2019). Genome-wide identification and expression profiling of the ERF gene family in *Medicago sativa* (L.) under various abiotic stresses. *DNA and Cell Biol.* 38, 1056–1068. doi: 10.1089/dna.2019.4881

Joshi, P., and Rao, P. P. (2017). Global pulses scenario: status and outlook. *Ann. N. Y. Acad. Sci.* 1392, 6–17. doi: 10.1111/nyas.13298

Juranić, M., Nagahatenna, D. S. K., Salinas-Gamboa, R., Hand, M. L., SánchezLeón, N., Leong, W. H., et al. (2020). A detached leaf assay for testing transient gene expression and gene editing in Cowpea (*Vigna Unguiculata* [L.] Walp.). *Plant Methods* 16, 88. doi: 10.1186/s13007-020-00630-4

Kahraman, A., Kusmenoglu, I., Aydin, N., Aydogan, A., Erskine, W., and Muehlbauer, F. J. (2004). QTL mapping of winter hardiness genes in lentil. *Crop Sci*. 44, 13–22. doi: 10.2135/cropsci2004.1300

Kamau, E. H., Nkhata, S. G., and Ayua, E. O. (2020). Extrusion and nixtamalization conditions influence the magnitude of change in the nutrients and bioactive components of cereals and legumes. *Food Sci. Nutr.* 8, 1753–1765. doi: 10.1002/fsn3.1473

Kang, Y. J., Kim, S. K., Kim, M. Y., Lestari, P., Kim, K. H., Ha, B. K., et al. (2014). Genome sequence of mungbean and insights into evolution within Vigna species. *Nat. Commun.* 5, 1–9. doi: 10.1038/ncomms6443

Kavi Kishor, P., Venkatesh, K., Amareshwari, P., Hima Kumari, P., Punita, D., Anil Kumar, S., et al. (2018). Genetic engineering for salt and drought stress tolerance in Peanut (*Arachis hypogaea* L.). *Indian J. Plant Physiol.* 23, 647–652. doi: 10.1007/s40502-018-0421-5

Keerthi, C. M., Ramesh, S., Byregowda, M., and Vaijayanthi, P. V. (2018). Simple Sequence Repeat (SSR) Marker assay-based genetic diversity among dolichos bean (Lablab purpureus L. Sweet) advanced breeding lines differing for productivity per se traits. *Int. J. Curr. Microbiol. Appl. Sci.* 7, 3736–3744. Available online at: https://www.ijcmas.com/7-5-2018/C.M.%20Keerthi,%20et%20al.pdf

Keller, B., Ariza-Suarez, D., de la Hoz, J., Aparicio, J. S., Portilla-Benavides, A. E., Buendia, H. F., et al. (2020). Genomic prediction of agronomic traits in common bean (phaseolus vulgaris l.) under environmental stress. *Front. Plant Sci.* 11, 1001. doi: 10.3389/fpls.2020.01001

Khan, M. A., Alghamdi, S. S., Ammar, M. H., Sun, Q., Teng, F., Migdadi, H. M., et al. (2019a). Transcriptome profiling of faba bean (*Vicia faba* L.) drought-tolerant variety hassawi-2 under drought stress using RNA sequencing. *Electron. J. Biotechnol.* 39, 15–29. doi: 10.1016/j.ejbt.2019.02.004

Khan, N., Bano, A., Rahman, M. A., Guo, J., Kang, Z., and Babar, M. (2019b). Comparative physiological and metabolic analysis reveals a complex mechanism involved in drought tolerance in chickpea (*Cicer arietinum* L.) induced by PGPR and PGRs. *Sci. Rep.* 9, 1–19. doi: 10.1038/s41598-019-38702-8

Khandal, H., Parween, S., Roy, R., Meena, M. K., and Chattopadhyay, D. (2017). MicroRNA profiling provides insights into post-transcriptional regulation of gene expression in Chickpea root apex under salinity and water deficiency. *Sci. Rep.* 7, 1–14. doi: 10.1038/s41598-017-04906-z

Kiranmai, K., Lokanadha Rao, G., Pandurangaiah, M., Nareshkumar, A., Amaranatha Reddy, V., Lokesh, U., et al. (2018). A novel WRKY transcription factor, MuWRKY3 (Macrotyloma uniflorum Lam. Verdc.) enhances drought stress tolerance in transgenic Groundnut (*Arachis hypogaea* L.) plants. *Front. Plant Sci.* 9, 346. doi: 10.3389/fpls.2018.00346

Korir, P. C., Zhang, J., Wu, K., Zhao, T., and Gai, J. (2013). Association mapping combined with linkage analysis for aluminum tolerance among soybean cultivars released in Yellow and Changjiang River Valleys in China. *Theor. Appl. Genet.* 126, 1659–1675. doi: 10.1007/s00122-013-2082-0

Kumar, J., Sen Gupta, D., Djalovic, I., Kumar, S., and Siddique, K. H. (2021). Root-omics for drought tolerance in cool-season grain legumes. *Physiol. Planta.* 172, 629–644. doi: 10.1111/ppl.13313

Kumar, P., Choudhary, M., Halder, T., Prakash, N. R., Singh, V., Sheoran, S., et al. (2022). Salinity stress tolerance and omics approaches: revisiting the progress and achievements in major cereal crops. *Heredity* 1–22. doi: 10.1038/s41437-022-00516-2

Kumar, S., and Fladung, M. (2002). "Gene targeting in plants," in *Molecular Techniques in Crop Improvement*, eds S. Mohan Jain, D. S. Brar, and B. S. Ahloowalia (Springer), 481–499.

Kumar, S., Palve, A. S., Patel, S. K., Selvanayagam, S., Sharma, R., and Rathore, A. (2020). Development of genomic microsatellite markers in cluster bean using next-generation DNA sequencing and their utility in diversity analysis. *Curr. Plant Biol.* 21, 100134. doi: 10.1016/j.cpb.2019.100134

Kushwah, A., Bhatia, D., Rani, U., Yadav, I. S., Singh, I., Bharadwaj, C., et al. (2021). Molecular mapping of quantitative trait loci for ascochyta blight and botrytis grey mould resistance in an inter-specific cross in chickpea (*Cicer arietinum* L.) using genotyping by sequencing. *Breed. Sci.* 71, 229–239. doi: 10.1270/jsbbs.20085

Lahner, B., Gong, J., Mahmoudian, M., Smith, E. L., Abid, K. B., Rogers, E. E., et al. (2003). Genomic scale profiling of nutrient and trace elements in *Arabidopsis thaliana*. *Nat. Biotechnol.*21, 1215–1221. doi: 10.1038/nbt865

Langridge, P., and Fleury, D. (2011). Making the most of 'omics' for crop breeding. *Trends Biotechnol.* 29, 33–40. doi: 10.1016/j.tibtech.2010.09.006

Lee, G., Boerma, H., Villagarcia, M., Zhou, X., Carter, T., Li, Z., et al. (2004). A major QTL conditioning salt tolerance in S-100 soybean and descendent cultivars. *Theor. Appl. Genet.* 109, 1610–1619. doi: 10.1007/s00122-004-1783-9

Leonforte, A., Sudheesh, S., Cogan, N. O., Salisbury, P. A., Nicolas, M. E., Materne, M., et al. (2013). SNP marker discovery, linkage map construction and identification of QTLs for enhanced salinity tolerance in field pea (*Pisum Sativum* L.). *BMC Plant Biol.* 13, 1–14. doi: 10.1186/1471-2229-13-161

Li, M., Guo, R., Jiao, Y., Jin, X., Zhang, H., and Shi, L. (2017). Comparison of salt tolerance in Soja based on metabolomics of seedling roots. *Front. Plant Sci.* 8, 1101. doi: 10.3389/fpls.2017.01101

Li, Y., Ruperao, P., Batley, J., Edwards, D., Khan, T., Colmer, T. D., et al. (2018). Investigating drought tolerance in chickpea using genome-wide association mapping and genomic selection based on whole-genome resequencing data. *Front. Plant Sci.* 9, 190. doi: 10.3389/fpls.2018.00190

Libault, M., Farmer, A., Joshi, T., Takahashi, K., Langley, R. J., Franklin, L. D., et al. (2010). An integrated transcriptome atlas of the crop model *Glycine max*, and its use in comparative analyses in plants. *Plant J.* 63, 86–99. doi: 10.1111/j.1365-313X.2010.04222.x

Liu, C., Wu, J., Wang, L., Fan, B., Cao, Z., Su, Q., et al. (2017). Quantitative trait locus mapping under irrigated and drought treatments based on a novel genetic linkage map in mungbean (Vigna radiata L.). *Theor. Appl. Genet.* 130, 2375–2393. doi: 10.1007/s00122-017-2965-6

Liu, W., Yuan, J. S., and Stewart, C. N. Jr. (2013). Advanced genetic tools for plant biotechnology. *Nat. Rev. Genet*. 14, 781–793. doi: 10.1038/nrg3583

Liu, Y., Wang, D., He, F., Wang, J., Joshi, T., and Xu, D. (2019). Phenotype prediction and genome-wide association study using deep convolutional neural network of soybean. *Front. Genet*. 10, 1091doi: 10.3389/fgene.2019.01091

Lowe, R., Shirley, N., Bleackley, M., Dolan, S., and Shafee, T. (2017). Transcriptomics technologies. *PLoS Comput. Biol.* 13, e1005457. doi: 10.1371/journal.pcbi.1005457

Lucas, M. R., Ehlers, J. D., Huynh, B.-L., Diop, N.-N., Roberts, P. A., and Close, T. J. (2013). Markers for breeding heat-tolerant cowpea. *Mol. Breed.* 31, 529–536. doi: 10.1007/s11032-012-9810-z

Luo, H., Guo, J., Yu, B., Chen, W., Zhang, H., Zhou, X., et al. (2021). Construction of ddRADseq-based high-density genetic map and identification of quantitative trait loci for trans-resveratrol content in Peanut seeds. *Front. Plant Sci.* 12, 438. doi: 10.3389/fpls.2021.644402

Luo, Z., Szczepanek, A., and Abdel-Haleem, H. (2020). Genome-wide association study (GWAS) analysis of Camelina seedling germination under salt stress condition. *Agronomy*. 10, 1444. doi: 10.3390/agronomy10091444

Maalouf, F., Abou-Khater, L., Babiker, Z., Jighly, A., Alsamman, A. M., Hu, J., et al. (2022). Genetic dissection of heat stress tolerance in faba bean (*Vicia faba* L.) using GWAS. *Plants* 11, 1108. doi: 10.3390/plants11091108

Mackay, M. C., Street, K., Mitrofanova, O., Zuev, E., Strelchenko, P., and Pertziger, F. (2004). "Focused identification of germplasm strategy–FIGS," in *Proceedings 11th Wheat Breeding Assembly*, 20–24.

Mahdavi Mashaki, K., Garg, V., Nasrollahnezhad Ghomi, A. A., Kudapa, H., Chitikineni, A., Zaynali Nezhad, K., et al. (2018). RNA-Seq analysis revealed genes associated with drought stress response in kabuli chickpea (*Cicer arietinum* L.). *PLoS ONE* 13, e0199774. doi: 10.1371/journal.pone.0199774

Mahmoud, G. A.-E. (2021). "Biotic stress to legumes: fungal diseases as major biotic stress factor," in *Sustainable Agriculture Reviews 51*, eds P. Guleria, V. Kumar, and E. Lichtfouse (Springer), 181–212.

Mahmoudian, M., Yücel, M., and Öktem, H. A. (2002). Transformation of lentil (Lens culinaris M.) cotyledonary nodes by vacuum infiltration of *Agrobacterium tumefaciens*. *Plant Mol. Biol. Repor*. 20, 251–257. doi: 10.1007/BF02782460

Manjulatha, M., Sreevathsa, R., Kumar, A. M., Sudhakar, C., Prasad, T., Tuteja, N., et al. (2014). Overexpression of a pea DNA helicase (PDH45) in peanut (*Arachis hypogaea* L.) confers improvement of cellular level tolerance and productivity under drought stress. *Mol. Biotechnol.* 56, 111–125. doi: 10.1007/s12033-013-9687-z

Mathur, S., Agrawal, D., and Jajoo, A. (2014). Photosynthesis: response to high temperature stress. *J. Photochem. Photobiol. B Biol.* 137, 116–126. doi: 10.1016/j.jphotobiol.2014.01.010

McKersie, B. D., Chen, Y., de Beus, M., Bowley, S. R., Bowler, C., Inzé, D., et al. (1993). Superoxide dismutase enhances tolerance of freezing stress in transgenic alfalfa (*Medicago sativa* L.). *Plant Physiol.* 103, 1155–1163. doi: 10.1104/pp.103.4.1155

McKersie, B. D., Murnaghan, J., Jones, K. S., and Bowley, S. R. (2000). Iron-superoxide dismutase expression in transgenic alfalfa increases winter survival without a detectable increase in photosynthetic oxidative stress tolerance. *Plant Physiol.* 122, 1427–1438. doi: 10.1104/pp.122.4.1427

Mefleh, M., Pasqualone, A., Caponio, F., and Faccia, M. (2022). Legumes as basic ingredients in the production of dairy-free cheese alternatives: a review. *J. Sci. Food Agric.* 102, 8–18. doi: 10.1002/jsfa.11502

Min, C. W., Gupta, R., Agrawal, G. K., Rakwal, R., and Kim, S. T. (2019). Concepts and strategies of soybean seed proteomics using the shotgun proteomics approach. *Expert Rev. Proteom.* 16, 795–804. doi: 10.1080/14789450.2019.1654860

Missanga, J. S., Venkataramana, P. B., and Ndakidemi, P. A. (2021). Recent developments in Lablab purpureus genomics: a focus on drought stress tolerance and use of genomic resources to develop stress-resilient varieties. *Legume Sci.* 3, e99. doi: 10.1002/leg3.99

Molina, C., Rotter, B., Horres, R., Udupa, S. M., Besser, B., Bellarmino, L., et al. (2008). SuperSAGE: the drought stress-responsive transcriptome of chickpea roots. *BMC Genom.* 9, 1–28. doi: 10.1186/1471-2164-9-553

Muchero, W., Ehlers, J. D., Close, T. J., and Roberts, P. A. (2009). Mapping QTL for drought stress-induced premature senescence and maturity in Cowpea [*Vigna unguiculata* (L.) Walp.]. *Theor. Appl. Genet.* 118, 849–863. doi: 10.1007/s00122-008-0944-7

Mugabe, D., Coyne, C. J., Piaskowski, J., Zheng, P., Ma, Y., Landry, E., et al. (2019). Quantitative trait loci for cold tolerance in chickpea. *Crop Sci.* 59, 573–582. doi: 10.2135/cropsci2018.08.0504

Munns, R. (2010). "Approaches to identifying genes for salinity tolerance and the importance of timescale," in *Plant Stress Tolerance*, ed R. Sunkar (Springer), 25–38.

Nadaf, J., Riggio, V., Yu, T.-P., and Pong-Wong, R. (2012). "Effect of the prior distribution of SNP effects on the estimation of total breeding value," in *BMC Proceedings* (BioMed Central), 1–6.

Nair, R. M., Yang, R. Y., Easdown, W. J., Thavarajah, D., Thavarajah, P., Hughes, J., et al. (2013). Biofortification of mungbean (Vigna radiata) as a whole food to enhance human health. *J. Sci. Food Agric*. 93, 1805–1813. doi: 10.1002/jsfa.6110

Narayana, P. K., and von Wettberg, E. J. (2020). "GWAS and genomic approaches in legumes, an expanding toolkit for examining responses to abiotic stresses," in *The Plant Family Fabaceae*, eds M. Hasanuzzaman, S. Araújo, S. S. Gill (Springer), 161–180.

Narayanan, S., Zoong-Lwe, Z. S., Gandhi, N., Welti, R., Fallen, B., Smith, J. R., et al. (2020). Comparative lipidomic analysis reveals heat stress responses of two soybean genotypes differing in temperature sensitivity. *Plants* 9, 457. doi: 10.3390/plants9040457

Nawaz, M. A., and Chung, G. (2020). Genetic improvement of cereals and grain legumes. *Genes*. 11, 1255. doi: 10.3390/genes11111255

Nguyen, T., and Sticklen, M. (2012). Genetic transformation of common bean (*Phaseolus vulgaris* L.) with the gus color marker, the bar herbicide resistance, and the barley (Hordeum vulgare) HVA1 drought tolerance genes. *Int. J. Agron.* 2012, 198960. doi: 10.1155/2012/198960

Njobvu, J., Hamabwe, S. M., Munyinda, K., Kelly, J. D., and Kamfwa, K. (2020). Quantitative trait loci mapping of resistance to aluminum toxicity in common bean. *Crop Sci.* 60, 1294–1302. doi: 10.1002/csc2.20043

Odong, T. L., Van Heerwaarden, J., Jansen, J., van Hintum, T. J., and Van Eeuwijk, F. A. (2011). Determination of genetic structure of germplasm collections: are traditional hierarchical clustering methods appropriate for molecular marker data?. *Theoret. Appl. Genet.* 123, 195–205. doi: 10.1007/s00122-011-1576-x

Okazaki, Y., Takano, K., and Saito, K. (2017). Lipidomic analysis of soybean leaves revealed tissue-dependent diference in lipid remodeling under phosphorus-limited growth conditions. *Plant Biotechnol (Tokyo)*. 34, 57–63. doi: 10.5511/plantbiotechnology.17.0113a

Oladzad, A., Porch, T., Rosas, J. C., Moghaddam, S. M., Beaver, J., Beebe, S. E., et al. (2019). Single and multi-trait GWAS identify genetic factors associated with production traits in common bean under abiotic stress environments. *G3 Genes Genomes Genet.* 9, 1881–1892. doi: 10.1534/g3.119.400072

Ozturk Gokce, Z. N., Akbas, S., Ayten, S., Azimi, M. H., Das, R., Guven, S. B., et al. (2020). "Abiotic stress tolerance in field crops: integration of Omics approaches," in *Agronomic Crops*, ed M. Hasanuzzaman (Springer), 503–526.

Pandey, A., Chakraborty, S., Datta, A., and Chakraborty, N. (2008). Proteomics approach to identify dehydration responsive nuclear proteins from Chickpea (*Cicer arietinum* L.). *Mol. Cell. Proteom.* 7, 88–107. doi: 10.1074/mcp.M700314-MCP200

Pandey, A. K., and Basandrai, A. K. (2021). Will Macrophomina phaseolina spread in legumes due to climate change? A critical review of current knowledge. *J. Plant Dis. Prot.* 128, 9–18. doi: 10.1007/s41348-020-00374-2

Pandey, A. K., Rubiales, D., Wang, Y., Fang, P., Sun, T., Liu, N., et al. (2021). Omics resources and omics-enabled approaches for achieving high productivity and improved quality in Pea (*Pisum Sativum* L.). *Theor. Appl. Genet.* 134, 755–776. doi: 10.1007/s00122-020-03751-5

Pandey, M. K., Chaudhari, S., Jarquin, D., Janila, P., Crossa, J., Patil, S. C., et al. (2020). Genome-based trait prediction in multi-environment breeding trials in groundnut. *Theor. Appl. Genet.* 133, 3101–3117. doi: 10.1007/s00122-020-03658-1

Pandey, M. K., Upadhyaya, H. D., Rathore, A., Vadez, V., Sheshshayee, M., Sriswathi, M., et al. (2014). Genomewide association studies for 50 agronomic traits in peanut using the 'reference set'comprising 300 genotypes from 48 countries of the semi-arid tropics of the world. *PLoS ONE* 9, e105228. doi: 10.1371/journal.pone.0105228

Pandey, R., Aretano, R., Gupta, A. K., Meena, D., Kumar, B., and Alatalo, J. M. (2017). Agroecology as a climate change adaptation strategy for smallholders of Tehri-Garhwal in the Indian Himalayan region. *Small Scale Forest.* 16, 53–63. doi: 10.1007/s11842-016-9342-1

Pandurangaiah, M., Lokanadha Rao, G., Sudhakarbabu, O., Nareshkumar, A., Kiranmai, K., Lokesh, U., et al. (2014). Overexpression of horsegram (*Macrotyloma uniflorum* Lam. Verdc.) NAC transcriptional factor (MuNAC4) in groundnut confers enhanced drought tolerance. *Mol. Biotechnol.* 56, 758–769. doi: 10.1007/s12033-014-9754-0

Parankusam, S., Bhatnagar-Mathur, P., and Sharma, K. K. (2017). Heat responsive proteome changes reveal molecular mechanisms underlying heat tolerance in Chickpea. *Environ. Exp. Bot.* 141, 132–144. doi: 10.1016/j.envexpbot.2017.07.007

Parida, A., Raina, S. N., and Narayan, R. K. J. (1990). Quantitative DNA variation between and within chromosome complements of Vigna species (Fabaceae). *Genetica* 82, 125–133. doi: 10.1007/BF00124642

Parveen, S., Gupta, D. B., Dass, S., Kumar, A., Pandey, A., Chakraborty, S., et al. (2016). Chickpea ferritin CaFer1 participates in oxidative stress response and promotes growth and development. *Sci. Rep.* 6, 1–14. doi: 10.1038/srep31218

Patil, G., Do, T., Vuong, T. D., Valliyodan, B., Lee, J.-D., Chaudhary, J., et al. (2016). Genomic-assisted haplotype analysis and the development of high-throughput SNP markers for salinity tolerance in soybean. *Sci. Rep.* 6, 1–13. doi: 10.1038/srep19199

Patil, M., Ramu, S., Jathish, P., Sreevathsa, R., Reddy, P. C., Prasad, T., et al. (2014). Overexpression of AtNAC2 (ANAC092) in groundnut (*Arachis hypogaea* L.) improves abiotic stress tolerance. *Plant Biotechnol. Rep.* 8, 161–169. doi: 10.1007/s11816-013-0305-0

Paul, P. J., Samineni, S., Thudi, M., Sajja, S. B., Rathore, A., Das, R. R., et al. (2018). Molecular mapping of QTLs for heat tolerance in chickpea. *Int. J. Mol. Sci.* 19, 2166. doi: 10.3390/ijms19082166

Plewiński, P., Cwiek-Kupczyńska, H., Rudy, E., Bielski, W., Rychel-Bielska, S., Stawiński, S., et al. (2020). Innovative transcriptome-based genotyping highlights environmentally responsive genes for phenology, growth and yield in a non-model grain legume. *Plant Cell Environ.* 43, 2680–2698. doi: 10.1111/pce.13880

Pratap, A., Gupta, S., Nair, R. M., Gupta, S., Schafleitner, R., Basu, P., et al. (2019). Using plant phenomics to exploit the gains of genomics. *Agronomy* 9, 126. doi: 10.3390/agronomy9030126

Pruthvi, V., Narasimhan, R., and Nataraja, K. N. (2014). Simultaneous expression of abiotic stress responsive transcription factors, AtDREB2A, AtHB7 and AtABF3 improves salinity and drought tolerance in peanut (Arachis hypogaea L.). *PLoS ONE* 9, e111152. doi: 10.1371/journal.pone.0111152

Puli, C. O. R., Akila, C. S., Pandit, V., Konduru, S., Kandi, S. R., and Chinta, S. (2021). "Peanut (*Arachis hypogaea* L.) transgenic plants for abiotic stress tolerance," in *Genetically Modified Crops*, eds P. B. K. Kishor, M. V. Rajam, and T. Pullaiah (Springer), 139–173.

Pushpavalli, R., Krishnamurthy, L., Thudi, M., Gaur, P. M., Rao, M. V., Siddique, K. H., et al. (2015). Two key genomic regions harbour QTLs for salinity tolerance in ICCV 2× JG 11 derived chickpea (*Cicer arietinum* L.) recombinant inbred lines. *BMC Plant Biol.* 15, 1–15. doi: 10.1186/s12870-015-0491-8

Qin, J., Shi, A., Song, Q., Li, S., Wang, F., Cao, Y., et al. (2019). Genome wide association study and genomic selection of amino acid concentrations in soybean seeds. *Front. Plant Sci.* 10, 1445. doi: 10.3389/fpls.2019.01445

Ramu, V. S., Swetha, T. N., Sheela, S. H., Babitha, C. K., Rohini, S., Reddy, M. K., et al. (2016). Simultaneous expression of regulatory genes associated with specific drought-adaptive traits improves drought adaptation in peanut. *Plant Biotechnol. J.* 14, 1008–1020. doi: 10.1111/pbi.12461

Ray, H., and Georges, F. (2010). A genomic approach to nutritional, pharmacological and genetic issues of faba bean (*Vicia faba* L.): Prospects for genetic modifications. *GM Crops* 1, 99–106. doi: 10.4161/gmcr.1.2.11891

Raza, A., Razzaq, A., Mehmood, S. S., Zou, X., Zhang, X., Lv, Y., et al. (2019). Impact of climate change on crops adaptation and strategies to tackle its outcome: a review. *Plants* 8, 34. doi: 10.3390/plants8020034

Razzaq, M. K., Aleem, M., Mansoor, S., Khan, M. A., Rauf, S., Iqbal, S., et al. (2021). Omics and CRISPR-Cas9 approaches for molecular insight, functional gene analysis, and stress tolerance development in crops. *Int. J. Mol. Sci.* 22, 1292. doi: 10.3390/ijms22031292

Reddy, A. R., Chaitanya, K. V., and Vivekanandan, M. (2004). Drought-induced responses of photosynthesis and antioxidant metabolism in higher plants. *J. Plant Physiol.* 161, 1189–1202. doi: 10.1016/j.jplph.2004.01.013

Rehman, A., Malhotra, R., Bett, K., Tar'An, B., Bueckert, R., and Warkentin, T. (2011). Mapping QTL associated with traits affecting grain yield in chickpea (*Cicer arietinum* L.) under terminal drought stress. *Crop Sci.* 51, 450–463. doi: 10.2135/cropsci2010.03.0129

Richter, J. A., Behr, J. H., Erban, A., Kopka, J., and Zörb, C. (2019). Ion-dependent metabolic responses of *Vicia faba* L. to salt stress. *Plant Cell Environ.* 42, 295–309. doi: 10.1111/pce.13386

Roorkiwal, M., Jain, A., Kale, S. M., Doddamani, D., Chitikineni, A., Thudi, M., et al. (2018). Development and evaluation of high-density Axiom® Cicer SNP Array for high-resolution genetic mapping and breeding applications in chickpea. *Plant Biotechnol.* 16, 890–901. doi: 10.1111/pbi.12836

Roorkiwal, M., Pandey, S., Thavarajah, D., Hemalatha, R., and Varshney, R. K. (2021). Molecular mechanisms and biochemical pathways for micronutrient acquisition and storage in legumes to support biofortification for nutritional security. *Front. Plant Sci.* 12, 682842. doi: 10.3389/fpls.2021.682842

Roorkiwal, M., Rathore, A., Das, R. R., Singh, M. K., Jain, A., Srinivasan, S., et al. (2016). Genome-enabled prediction models for yield related traits in chickpea. *Front. Plant Sci.* 7, 1666. doi: 10.3389/fpls.2016.01666

Saade, S., Maurer, A., Shahid, M., Oakey, H., Schmöckel, S. M., Negrão, S., et al. (2016). Yield-related salinity tolerance traits identified in a nested association mapping (NAM) population of wild barley. *Sci. Rep.* 6, 1–9. doi: 10.1038/srep32586

Sallam, A., Arbaoui, M., El-Esawi, M., Abshire, N., and Martsch, R. (2016). Identification and verification of QTL associated with frost tolerance using linkage mapping and GWAS in winter faba bean. *Front. Plant Sci.* 7, 1098. doi: 10.3389/fpls.2016.01098

Salt, D. E., Baxter, I., and Lahner, B. (2008). Ionomics and the study of the plant ionome. *Annu. Rev. Plant Biol.* 59, 709–733. doi: 10.1146/annurev.arplant.59.032607.092942

Salvi, S., and Tuberosa, R. (2015). The crop QTLome comes of age. *Curr. Opin. Biotechnol.* 32, 179–185. doi: 10.1016/j.copbio.2015.01.001

Sampaio, A. M., Araújo, S.,d,.S., Rubiales, D., and Vaz Patto, M.C. (2020). Fusarium wilt management in legume crops. *Agronomy* 10, 1073. doi: 10.3390/agronomy10081073

Sandhu, K. S., Merrick, L. F., Sankaran, S., Zhang, Z., and Carter, A. H. (2021). Prospectus of genomic selection and phenomics in cereal, legume and oilseed breeding programs. *Front. Genet.* 12, 829131. doi: 10.3389/fgene.2021.829131

Sarker, R. H., Biswas, A., Mustafa, B. M., Mahbub, S., and Hoque, M. I. (2003). Agrobacterium-mediated transformation of lentil (Lens culinaris Medik.). *Plant Tissue Cult.* 13, 1–12.

Sertse, D., You, F. M., Ravichandran, S., Soto-Cerda, B. J., Duguid, S., and Cloutier, S. (2021). Loci harboring genes with important role in drought and related abiotic stress responses in flax revealed by multiple GWAS models. *Theor. Appl. Genet.* 134, 191–212. doi: 10.1007/s00122-020-03691-0

Settele, J., Bishop, J., and Potts, S. (2016). Climate change impacts on pollination. *Nat. Plants* 2, 16092. doi: 10.1038/nplants.2016.92

Shabala, S., and Munns, R. (2012). Salinity stress: physiological constraints and adaptive mechanisms. *Plant Stress Physiol.* 1, 59–93. doi: 10.1079/9781845939953.0059

Sharma, A. D., Sharma, H., and Lightfoot, D. A. (2011). The genetic control of tolerance to aluminum toxicity in the 'Essex'by 'Forrest'recombinant inbred line population. *Theor. Appl. Genet.* 122, 687–694. doi: 10.1007/s00122-010-1478-3

Sharmila, P., Phanindra, M., Anwar, F., Singh, K., Gupta, S., and Saradhi, P. P. (2009). Targeting prokaryotic choline oxidase into chloroplasts enhance the potential of photosynthetic machinery of plants to withstand oxidative damage. *Plant Physiol. Biochem.* 47, 391–396. doi: 10.1016/j.plaphy.2009.01.001

Sharmin, R. A., Karikari, B., Chang, F., Al Amin, G., Bhuiyan, M. R., Hina, A., et al. (2021). Genome-wide association study uncovers major genetic loci associated with seed flooding tolerance in soybean. *BMC Plant Biol.* 21, 1–17. doi: 10.1186/s12870-021-03268-z

Showalter, A. M., Keppler, B. D., Liu, X., Lichtenberg, J., and Welch, L. R. (2016). Bioinformatic identification and analysis of hydroxyproline-rich glycoproteins in Populus trichocarpa. *BMC Plant Biol.* 16, 1–34. doi: 10.1186/s12870-016-0912-3

Shu, Y., Yu, D., Wang, D., Bai, X., Zhu, Y., and Guo, C. (2013). Genomic selection of seed weight based on low-density SCAR markers in soybean. *Genet. Mol. Res.* 12, 2178–2188. doi: 10.4238/2013.July.3.2

Shukla, R. K., Raha, S., Tripathi, V., and Chattopadhyay, D. (2006). Expression of CAP2, an APETALA2-family transcription factor from chickpea, enhances growth and tolerance to dehydration and salt stress in transgenic tobacco. *Plant Physiol.* 142, 113–123. doi: 10.1104/pp.106.081752

Singh, A., Pratap Singh, A., and Ramaswamy, H. S. (2016). A controlled agitation process for improving quality of canned green beans during agitation thermal processing. *J. Food Sci.* 81, E1399–E1411. doi: 10.1111/1750-3841.13308

Singh, D., Chaudhary, P., Taunk, J., Singh, C. K., Singh, D., Tomar, R. S. S., et al. (2021). Fab advances in fabaceae for abiotic stress resilience: from 'omics' to artificial intelligence. *Int. J. Mol. Sci.*22, 10535. doi: 10.3390/ijms221910535

Singh, D., Singh, C. K., Singh Tomar, R. S., and Pal, M. (2017a). Genetics and molecular mapping of heat tolerance for seedling survival and pod set in lentil. *Crop Sci.* 57, 3059–3067. doi: 10.2135/cropsci2017.05.0284

Singh, D., Singh, C. K., Taunk, J., Jadon, V., Pal, M., and Gaikwad, K. (2019). Genome wide transcriptome analysis reveals vital role of heat responsive genes in regulatory mechanisms of lentil (Lens culinaris Medikus). *Sci. Rep.* 9, 1–19. doi: 10.1038/s41598-019-49496-0

Singh, D., Singh, C. K., Taunk, J., Tomar, R. S. S., Chaturvedi, A. K., Gaikwad, K., et al. (2017b). Transcriptome analysis of lentil (*Lens culinaris Medikus*) in response to seedling drought stress. *BMC Genom.* 18, 1–20. doi: 10.1186/s12864-017-3596-7

Singh, N., Mishra, A., and Jha, B. (2014). Ectopic over-expression of peroxisomal ascorbate peroxidase (SbpAPX) gene confers salt stress tolerance in transgenic peanut (*Arachis hypogaea*). *Gene* 547, 119–125. doi: 10.1016/j.gene.2014.06.037

Singh, N., Rai, V., and Singh, N. K. (2020). Multi-omics strategies and prospects to enhance seed quality and nutritional traits in pigeonpea. *Nucleus* 63, 249–256. doi: 10.1007/s13237-020-00341-0

Sita, K., and Kumar, V. (2020). Role of Gamma Amino Butyric Acid (GABA) against abiotic stress tolerance in legumes: a review. *Plant Physiol. Rep.* 25, 654–663. doi: 10.1007/s40502-020-00553-1

Soltani, A., MafiMoghaddam, S., Oladzad-Abbasabadi, A., Walter, K., Kearns, P. J., Vasquez-Guzman, J., et al. (2018). Genetic analysis of flooding tolerance in an Andean diversity panel of Dry bean (*Phaseolus vulgaris* L.). *Front. Plant Sci.* 9, 767. doi: 10.3389/fpls.2018.00767

Somers, D. A., Samac, D. A., and Olhoft, P. M. (2003). Recent advances in legume transformation. *Plant Physiol.* 131, 892–899. doi: 10.1104/pp.102.017681

Song, Y., Lv, J., Ma, Z., and Dong, W. (2019). The mechanism of alfalfa (*Medicago sativa* L.) response to abiotic stress. *Plant Growth Regul.* 89, 239–249. doi: 10.1007/s10725-019-00530-1

Stai, J. S., Yadav, A., Sinou, C., Bruneau, A., Doyle, J. J., Fernández-Baca, D., et al. (2019). Cercis: a non-polyploid genomic relic within the generally polyploid legume family. *Front. Plant Sci.* 10, 345. doi: 10.3389/fpls.2019.00345

Stracke, S., Sato, S., Sandal, N., Koyama, M., Kaneko, T., Tabata, S., et al. (2004). Exploitation of colinear relationships between the genomes of Lotus japonicus, *Pisum Sativum* and *Arabidopsis thaliana*, for positional cloning of a legume symbiosis gene. *Theor. Appl. Genet.* 108, 442–449. doi: 10.1007/s00122-003-1438-2

Subba, P., Barua, P., Kumar, R., Datta, A., Soni, K. K., Chakraborty, S., et al. (2013). Phosphoproteomic dynamics of chickpea (*Cicer arietinum* L.) reveals shared and distinct components of dehydration response. *J. Proteome Res.* 12, 5025–5047. doi: 10.1021/pr400628j

Sudheesh, S., Kimber, R., Braich, S., Forster, J., Paull, J., and Kaur, S. (2019). Construction of an integrated genetic linkage map and detection of quantitative trait loci for Ascochyta blight resistance in faba bean (*Vicia faba* L.). *Euphytica* 215, 42. doi: 10.1007/s10681-019-2365-x

Taranto, F., Nicolia, A., Pavan, S., De Vita, P., and D'Agostino, N. (2018). Biotechnological and digital revolution for climate-smart plant breeding. *Agronomy* 8, 277. doi: 10.3390/agronomy8120277

Tayeh, N., Aluome, C., Falque, M., Jacquin, F., Klein, A., Chauveau, A., et al. (2015). Development of two major resources for pea genomics: the GenoPea 13.2 K SNP Array and a high-density, high-resolution consensus genetic map. *Plant J.* 84, 1257–1273. doi: 10.1111/tpj.13070

Tesfaye, M., Temple, S. J., Allan, D. L., Vance, C. P., and Samac, D. A. (2001). Overexpression of malate dehydrogenase in transgenic alfalfa enhances organic acid synthesis and confers tolerance to aluminum. *Plant Physiol.* 127, 1836–1844. doi: 10.1104/pp.010376

Thudi, M., Palakurthi, R., Schnable, J. C., Chitikineni, A., Dreisigacker, S., Mace, E., et al. (2021). Genomic resources in plant breeding for sustainable agriculture. *J. Plant Physiol.* 257, 153351. doi: 10.1016/j.jplph.2020.153351

Tian, X., Li, S., Liu, Y., and Liu, X. (2016). Transcriptomic profiling reveals metabolic and regulatory pathways in the desiccation tolerance of Mungbean (*Vigna radiata* [L.] R. *Wilczek). Front. Plant Sci.* 7, 1921. doi: 10.3389/fpls.2016.01921

Tiwari, V., Chaturvedi, A. K., Mishra, A., and Jha, B. (2015). Introgression of the SbASR-1 gene cloned from a halophyte Salicornia brachiata enhances salinity and drought endurance in transgenic groundnut (*Arachis hypogaea*) and acts as a transcription factor. *PLoS ONE* 10, e0131567. doi: 10.1371/journal.pone.0131567

Trapp, J. J., Urrea, C. A., Cregan, P. B., and Miklas, P. N. (2015). Quantitative trait loci for yield under multiple stress and drought conditions in a dry bean population. *Crop Sci.* 55, 1596–1607. doi: 10.2135/cropsci2014.11.0792

Upadhyaya, H. D., and Ortiz, R. (2001). A mini core subset for capturing diversity and promoting utilization of chickpea genetic resources in crop improvement. *Theoret. Appl. Genet.* 102, 1292–1298. doi: 10.1007/s00122-001-0556-y

Upadhyaya, H. D., Wang, Y. H., Gowda, C. L. L., and Sharma, S. (2013). Association mapping of maturity and plant height using SNP markers with the sorghum mini core collection. *Theoret. Appl. Genet.* 126, 2003–2015. doi: 10.1007/s00122-013-2113-x

Urva, P. (2021). Detection and classification of grain crops and legumes disease: a survey. *Sparklinglight Transact Artif Intell Quantum Comp.* 1, 41–55. doi: 10.55011/STAIQC.2021.1105

Vadez, V., Krishnamurthy, L., Thudi, M., Anuradha, C., Colmer, T. D., Turner, N. C., et al. (2012). Assessment of ICCV 2× JG 62 chickpea progenies shows sensitivity of reproduction to salt stress and reveals QTL for seed yield and yield components. *Mol. Breed.* 30, 9–21. doi: 10.1007/s11032-011-9594-6

Vadez, V., Rao, J. S., Bhatnagar-Mathur, P., and Sharma, K. (2013). DREB1A promotes root development in deep soil layers and increases water extraction under water stress in groundnut. *Plant Bio.* 15, 45–52. doi: 10.1111/j.1438-8677.2012.00588.x

Vadez, V., Rao, S., Kholova, J., Krishnamurthy, L., Kashiwagi, J., Ratnakumar, P., et al. (2008). Root research for drought tolerance in legumes: Quo vadis? *J. Food Legumes* 21, 77–85.

Valdisser, P. A. M. R., Müller, B. S., de Almeida Filho, J. E., Morais Junior, O. P., Guimarães, C. M., Borba, T. C., et al. (2020). Genome-wide association studies detect multiple QTLs for productivity in Mesoamerican diversity panel of common bean under drought stress. *Front. Plant Sci.* 1563, 574674. doi: 10.3389/fpls.2020.574674

Varshney, R. K., Thudi, M., Pandey, M. K., Tardieu, F., Ojiewo, C., Vadez, V., et al. (2018). Accelerating genetic gains in legumes for the development of prosperous smallholder agriculture: integrating genomics, phenotyping, systems modelling and agronomy. *J. Exp. Bot.* 69, 3293–3312. doi: 10.1093/jxb/ery088

Vessal, S., Arefian, M., and Siddique, K. H. (2020). Proteomic responses to progressive dehydration stress in leaves of chickpea seedlings. *BMC Genom.* 21, 1–15. doi: 10.1186/s12864-020-06930-2

Wan, Q., Chen, S., Shan, Z., Yang, Z., Chen, L., Zhang, C., et al. (2017). Stability evaluation of reference genes for gene expression analysis by RT-qPCR in soybean under different conditions. *PLoS ONE* 12, e0189405. doi: 10.1371/journal.pone.0189405

Wang, L., Dong, S., Liu, L., Ma, Y., Li, S., and Zu, W. (2018). Transcriptome profiling reveals PEG-simulated drought, heat and combined stress response mechanisms in soybean. *Comput. Biol. Chem.* 77, 413–419. doi: 10.1016/j.compbiolchem.2018.09.012

Wang, L., Rubio, M. C., Xin, X., Zhang, B., Fan, Q., Wang, Q., et al. (2019b). CRISPR/Cas9 knockout of leghemoglobin genes in lotus japonicusuncovers their synergistic roles in symbiotic nitrogen fixation. *New Phytol.* 224, 818–832. doi: 10.1111/nph.16077

Wang, L., Wang, L., Tan, Q., Fan, Q., Zhu, H., Hong, Z., et al. (2016). Efficient inactivation of symbiotic nitrogen fixation related genes in lotus japonicus using CRISPR-Cas9. *Front. Plant Sci.* 7, 1333. doi: 10.3389/fpls.2016.01333

Wang, X., Cheng, Y., Yang, C., Yang, C., Mu, Y., Xia, Q., et al. (2019a). QTL mapping for aluminum tolerance in RIL population of soybean (*Glycine max* L.) by RAD sequencing. *PLoS ONE* 14, e0223674. doi: 10.1371/journal.pone.0223674

War, A. R., Murugesan, S., Naresh, B., Ramasamy, S., and Nair, R. (2017). Mechanism of resistance in mungbean [Vigna radiata (L.) R. Wilczek var. radiata] to bruchids, Callosobruchus spp. (Coleoptera: Bruchidae). *Front. Plant Sci.* 8, 1031. doi: 10.3389/fpls.2017.01031

Wienkoop, S., Morgenthal, K., Wolschin, F., Scholz, M., Selbig, J., and Weckwerth, W. (2008). Integration of metabolomic and proteomic phenotypes: analysis of data covariance dissects starch and RFO metabolism from low and high temperature compensation response in *Arabidopsis thaliana*. *Mol. Cell. Proteom.* 7, 1725–1736. doi: 10.1074/mcp.M700273-MCP200

Wu, C., Mozzoni, L. A., Moseley, D., Hummer, W., Ye, H., Chen, P., et al. (2020). Genome-wide association mapping of flooding tolerance in soybean. *Mol. Breed.* 40, 1–14. doi: 10.1007/s11032-019-1086-0

Wu, J., Wang, L., Li, L., and Wang, S. (2014). De novo assembly of the common bean transcriptome using short reads for the discovery of drought-responsive genes. *PLoS ONE* 9, e109262. doi: 10.1371/journal.pone.0109262

Wu, L., Chang, Y., Wang, L., Wang, S., and Wu, J. (2021). Genome-wide association analysis of drought resistance based on seed germination vigor and germination rate at the bud stage in common bean. *Agronomy* 113, 2980–2990. doi: 10.1002/agj2.20683

Wu, L., Chang, Y., Wang, L., Wang, S., and Wu, J. (2022). The aquaporin gene PvXIP1; 2 conferring drought resistance identified by GWAS at seedling stage in common bean. *Theoret. Appl. Genet.* 135, 485–500. doi: 10.1007/s00122-021-03978-w

Xu, J., Xue, C., Xue, D., Zhao, J., Gai, J., Guo, N., et al. (2013). Overexpression of GmHsp90s, a heat shock protein 90 (Hsp90) gene family cloning from soybean, decrease damage of abiotic stresses in *Arabidopsis thaliana*. *PLoS ONE* 8, e69810. doi: 10.1371/journal.pone.0069810

Xue, R., and Zhang, B. (2007). Increased endogenous methyl jasmonate altered leaf and root development in transgenic soybean plants. *J. Genet. Genom.* 34, 339–346. doi: 10.1016/S1673-8527(07)60036-8

Yang, F., Chen, H., Liu, C., Li, L., Liu, L., Han, X., et al. (2020). Transcriptome profile analysis of two Vicia faba cultivars with contrasting salinity tolerance during seed germination. *Sci. Rep.* 10, 1–10. doi: 10.1038/s41598-020-64288-7

Ye, H., Song, L., Schapaugh, W. T., Ali, M. L., Sinclair, T. R., Riar, M. K., et al. (2020). The importance of slow canopy wilting in drought tolerance in soybean. *J. Exp. Bot.* 71, 642–652. doi: 10.1093/jxb/erz150

Yin, X., Sakata, K., and Komatsu, S. (2014). Phosphoproteomics reveals the effect of ethylene in soybean root under flooding stress. *J. Proteome Res.* 13, 5618–5634. doi: 10.1021/pr500621c

Yu, Z., Chang, F., Lv, W., Sharmin, R. A., Wang, Z., Kong, J., et al. (2019). Identification of QTN and candidate gene for seed-flooding tolerance in soybean [*Glycine max* (L.) Merr.] using genome-wide association study (GWAS). *Gene* 10, 957. doi: 10.3390/genes10120957

Zate, Z. Z. (2021). Quantitative Trait Loci mapping of agronomic traits in a Cowpea (*Vigna unguiculata* L.) bi-parental cross. *J. Sustain. Dev.* 9, 39–58. doi: 10.20372/au.jssd.9.1.2021.0258

Zhang, J. Y., Broeckling, C. D., Blancaflor, E. B., Sledge, M. K., Sumner, L. W., and Wang, Z. Y. (2005). Overexpression of WXP1, a putative Medicago truncatula AP2 domain-containing transcription factor gene, increases cuticular wax accumulation and enhances drought tolerance in transgenic Alfalfa (*Medicago sativa*). *Plant J.* 42, 689–707. doi: 10.1111/j.1365-313X.2005.02405.x

Zhang, Q., Zhang, W.-J., Yin, Z.-G., Li, W.-J., Zhao, H.-H., Zhang, S., et al. (2020). Genome-and transcriptome-wide identification of C3Hs in common bean (*Phaseolus vulgaris* L.) and structural and expression-based analyses of their functions during the sprout stage under salt-stress conditions. *Front. Genet.* 1080, 564607. doi: 10.3389/fgene.2020.564607

Zhu, C., Bortesi, L., Baysal, C., Twyman, R. M., Fischer, R., Capell, T., et al. (2017). Characteristics of genome editing mutations in cereal crops. *Trends Plant Sci.* 22, 38–52. doi: 10.1016/j.tplants.2016.08.009

Ziegler, G., Nelson, R., Granada, S., Krishnan, H. B., Gillman, J. D., and Baxter, I. (2018). Genomewide association study of ionomic traits on diverse Soybean populations from germplasm collections. *Plant Direct.* 2, e00033. doi: 10.1002/pld3.33

Zuo, J., Wang, Y., Zhu, B., Luo, Y., Wang, Q., and Gao, L. (2018). sRNAome and transcriptome analysis provide insight into chilling response of cowpea pods. *Gene* 671, 142–151. doi: 10.1016/j.gene.2018.05.064

Zwart, R. S., Thudi, M., Channale, S., Manchikatla, P. K., Varshney, R. K., and Thompson, J. P. (2019). Resistance to plant-parasitic nematodes (PPNs) in Chickpea: current status and future perspectives. *Front. Plant Sci.* 10, 966. doi: 10.3389/fpls.2019.00966

frontiers | Frontiers in Plant Science

TYPE Original Research
PUBLISHED 30 September 2022
DOI 10.3389/fpls.2022.965765

Check for updates

OPEN ACCESS

EDITED BY
Mohammad Anwar Hossain,
Bangladesh Agricultural University, Bangladesh

REVIEWED BY
Hesham Alharby,
King Abdulaziz University, Saudi Arabia
Shyamal Krishna Talukder,
Texas A&M University, United States

*CORRESPONDENCE
Mohammad Moneruzzaman Khandaker
moneruzzaman@unisza.edu.my

SPECIALTY SECTION
This article was submitted to Plant Biotechnology, a section of the journal Frontiers in Plant Science

RECEIVED 10 June 2022
ACCEPTED 02 August 2022
PUBLISHED 30 September 2022

CITATION
Khandaker MM, Jamaludin R, Majrashi A, Rashid ZM, Karim SMR, Al-Yasi HM, Badaluddin NA, Alenazi MM and Mohd KS (2022) Enhancing *Rubisco* gene expression and metabolites accumulation for better plant growth in *Ficus deltoidea* under drought stress using hydrogen peroxide. *Front. Plant Sci.* 13:965765. doi: 10.3389/fpls.2022.965765

COPYRIGHT
© 2022 Khandaker, Jamaludin, Majrashi, Rashid, Karim, Al-Yasi, Badaluddin, Alenazi and Mohd. This is an open-access article distributed under the terms of the Creative Commons Attribution License (CC BY). The use, distribution or reproduction in other forums is permitted, provided the original author(s) and the copyright owner(s) are credited and that the original publication in this journal is cited, in accordance with accepted academic practice. No use, distribution or reproduction is permitted which does not comply with these terms.

Enhancing *Rubisco* gene expression and metabolites accumulation for better plant growth in *Ficus deltoidea* under drought stress using hydrogen peroxide

Mohammad Moneruzzaman Khandaker[1]*, Rosnah Jamaludin[1], Ali Majrashi[2], Zalilawati Mat Rashid[3], Sarker Mohammad Rezaul Karim[4], Hatim M. Al-Yasi[2], Noor Afiza Badaluddin[1], Mekhled Mutiran Alenazi[5] and Khamsah Suryati Mohd[1]

[1]School of Agriculture Science and Biotechnology, Faculty of Bioresources and Food Industry, Universiti Sultan Zainal Abidin, Terengganu, Malaysia, [2]Department of Biology, College of Science, Taif University, Taif, Saudi Arabia, [3]School of Food Industry, Faculty of Bioresources and Food Industry, Universiti Sultan Zainal Abidin, Terengganu, Malaysia, [4]Department of Crop Science, Faculty of Agriculture, Universiti Putra Malaysia, Seri Kembangan, Malaysia, [5]Plant Production Department, College of Food and Agricultural Sciences, King Saud University, Riyadh, Saudi Arabia

Growth improvement of the medicinal plant, *Ficus deltoidea* (Mas Cotek) under drought conditions is a vital issue in Malaysia since it is a slow-growing plant and disposed to leaf damage under the stresses of drought. Therefore, investigation was done to examine the outcomes of hydrogen peroxide (H_2O_2) application on *Rubisco* gene expression and metabolites accumulation of stressed *F. deltoidea* plants, and thereby to record the changes in leaf histology, photosynthesis, biochemical properties, and the growth of the plant. H_2O_2 at the rates of 0, 5, 10, 15, and 20 mM were foliar sprayed biweekly on the drought stressed plants using a hand sprayer. The application of 20 mM H_2O_2 amplified leaf number, tallness, stomatal conductance, and photosynthetic yield by 143, 24, 88, and 18%, respectively, over the control plant. A reduced transpiration rate and improved chlorophyll fluorescence were also noted in H_2O_2-treated plants. The treatment produced a greater amount of chlorophyll *a*, total phenols, total flavonoids, sugar content, and antioxidant activities by 1.61-, 1.30-, 1.98-, 1.92-, and 1.53-fold, respectively. Application of 15 mM H_2O_2 enhanced net photosynthetic rate and internal CO_2 concentrations by 1.05- and 1.25-fold, respectively. Additionally, H_2O_2 treatments promoted stomatal closure, increased stomata size, the number of stomata, improved vein structure, and reduced the damage of the leaf margin and mesophyll cells of drought stressed plants. The application of H_2O_2 also accumulated significantly higher contents of sodium (Na^+), calcium (Ca^{2+}), potassium (K^+), magnesium (Mg^+), and iron (Fe^{2+}) in stressed plants. Although the amount of Arsenic (As^+) and Antimony (Sb^{3+}) increased to some

extent, the increases were not at a toxic level. The use of H_2O_2 enhanced the *Rubisco* gene expression to a greater level and the ratio of *Rubisco* expression increased up to 16-fold. Finally, thirteen (13) identified and five (5) unmatched volatile compounds with a quality score above 70% were identified by gas chromatography-mass spectrometry (GCMS). The GCMS analysis showed that the foliar application of H_2O_2 accumulates a higher percentage of volatile components in plants which helps to mitigate the negative effects of drought stress. It is concluded that under drought stressed conditions the *F. deltoidea* plants should be treated with 10–15 mM of H_2O_2 twice a week to improve leaf histology, photosynthesis, the level of *Rubisco* gene expression and volatile compounds accumulation, and plant growth and development.

KEYWORDS

***Ficus deltoidea*, H_2O_2, drought, growth, physiology, *Rubisco*, metabolites**

Introduction

An important medicinal plant in Malaysia, *Ficus deltoidea* (Mas Cotek) is a C3 plant of the Moraceae family that can be found in Malaysia, Indonesia, Thailand, The Philippines, South Asia, and Africa (Starr et al., 2003; Hasham et al., 2013; Badron et al., 2014). The plant is grown as a house plant in cooler regions and is also cultivated in various parts of the world in abundance along the peat soil, beaches, and forest areas up to 3,000 m above sea level (Starr et al., 2003; Musa, 2005). It is used in traditional medicinal practices due to its various medical properties and functions. It is effective for healing, is used as a palliative agent, antinociceptive, antioxidant, anti-proliferative, and as preventive medicine which treats postpartum depression and assists in contracting and healing the muscles of the uterus and vaginal canal (Fasihuddin and Din, 2002). Tea from the leaves of *F. deltoidea* contain a considerable amount of magnesium, manganese, potassium, sodium, iron, and zinc, which are used to fulfill human daily nutrient requirements (Nihayah et al., 2012). *F. deltoidea* extracts are used to reduce diabetes complications, increase HDL levels, decrease LDL levels, improve sex life, assist the contraction of the vagina after delivery in addition to having anti-cancer and antimicrobial properties (Aris et al., 2009; Dramant et al., 2012). The plant contains phenols, flavonoids, tannins, triterpenoids and proanthocyanins (Aris et al., 2009; Nazarni et al., 2018). All these phenols and flavonoids display high antioxidant properties, with bioactive compounds vitexin and isovitexin from *F. deltoidea* displaying α-glucosidase inhibition (Nazarni et al., 2018; Nurdiana et al., 2018).

Currently the pharmaceutical industry uses plant-based sources to produce bioactive compounds and secondary metabolites. *F. deltoidea* as a medicinal herb is gaining popularity in local markets for the preparation of herbal tea and capsules (Misbah et al., 2013). This is a slow growing medicinal herb with low photosynthetic capacity since direct sunlight does not enhance its growth resulting in low biomass accumulation. The biomass accumulation in plants is very important for its commercialization. This herb also cannot bear drought stress as it needs plenty of water (6–8% soil moisture) to ensure its optimum growth and development. *F. deltoidea* plant is prone to an unexpected loss of leaves under drought conditions. Drought stress reduces cell division and enlargement, root differentiation, leaf area expansion, plant height, altered stomatal opening and closing, water use efficiency, and decreased plant yield and quality (Kumawat and Sharma, 2018). Due to the closing of the stomata, the activity of photosynthesis decreases, increasing production of reactive oxygen species (ROS), inducing membrane injury and altered function of several enzymes which are associated with ATP synthesis (Kumawat and Sharma, 2018; Sharma et al., 2020). To overcome all these problems in the *F. deltoidea* plant, this study proposes to use H_2O_2 to increase photosynthetic capacity, nutrients absorption, improve leaf histology, metabolites accumulation, and improve drought tolerance.

Drought stresses create interruption in plant growth, reduce plant productivity, and in severe cases, lead to plant death. The plant under drought stress produces signals for new structural and metabolic capabilities through gene expression for immediate survival and acclimatization (Bohnert and Sheveleva, 1998). Hydrogen peroxide (H_2O_2) may act as a messenger molecule to adapt signaling which triggers anti-susceptibility under abiotic stresses when it orchestrates a programmed cell death (Cheeseman, 2007; Ismail et al., 2015). Kar (2011) reported that the drought stress generates reactive oxygen species (ROS) leading to cellular damage. But H_2O_2 is a highly stable ROS at optimum concentration, which acts as a second messenger and sends signals to molecules for the promotion of plant growth, enhancement of photosynthetic activity, and increase in sugar content (Ozaki et al., 2009; Khandaker et al., 2012). Ozaki et al. (2009) also stated that

H_2O_2 (<50 mM concentration) produced stimulatory effects on plant growth and development of melon plants. A higher concentration of H_2O_2 initiates programmed cell death, damage chloroplast and the photosynthesis process, however, findings of Orabi et al. (2015) determined that a lower level of H_2O_2 stimulated growth regulators (auxins, gibberellin, and ABA) and enzyme activity. The foliar application of H_2O_2 maintains the leaf water content in soybean plants and enables them to avoid drought stress (Ishibashi et al., 2011). Many physiological processes in plants are controlled by H_2O_2 such as ABA-induced stomatal opening and closing, stomatal movement, hypersensitive responses, gene expression, programmed cell death, etc. (Neill et al., 2002).

H_2O_2 is produced in different enzymatic reactions in plants, which is transported through liquid flow in the plant body. It acts as a growth regulator in several selected plants. It was used in this study as the chemical promoter to overcome the early phase slow growth problem of *F. deltoidea* and to counteract the drought stress effects introduced to *F. deltoidea* plants. Attention was given through investigation to the regulatory effects of H_2O_2 in *Rubisco* (*rbcL*) gene expression and metabolite accumulation in *F. deltoidea* under drought stressed conditions to improve biochemical properties, leaf histology, photosynthesis, and plant growth. It was proposed that under drought stress conditions, foliar spraying of H_2O_2 could modulate the plant's growth and could mitigate the unfriendly effects of drought in this experimental plant, *F. deltoidea*. The findings of this study will be beneficial in mitigating the negative effects of drought stress in *F. deltoidea* as well as other medicinal herb plants.

Materials and methods

Experimental site and preparation of experimental plants

The study was conducted at Universiti Sultan Zainal Abidin, Terengganu, Malaysia during the period from December 2014 to February 2020. The experimental plant *Ficus deltoidea* var. *deltoidea* (FD 156) was collected from Kampung Sungai Nibong, Batu Pahat, Malaysia. The plants were propagated first in the university farm using stem cutting 8.0 inches in size and were used later for treatment application. For preparation of experimental plants, 25 stem cuttings were transplanted into an prepared planting media, each polybag contained 15 kg planting media. Cocoa peat, paddy husk, and perlite were mixed in the ratio of 2:1:1 to prepare the media. Side dressing with 2.5 g of NPK fertilizer (10:10:20) was done once a month. To simulate drought stress conditions in all experimental plants, less water (about 1.5 liters of water for 25 plants per spray) was applied three times per week using a watering can maintaining the moisture content at 40% of field capacity. One hundred eighty (180) ml of water was applied per plant to maintain drought stress of the experimental plants. The experimental plants were grown under a hoop house which provided the plants with direct sunlight and an average temperature about 30–35°C. The maximum PAR was between 300–700 $\mu Em^{-2}s^{-1}$ and relative humidity was 30–60% (Figure 2A).

Treatments application

The plants were sprayed twice a week manually with 10 ml of hydrogen peroxide (H_2O_2) at the concentrations of 5, 10, 15, 20 mM and 0 (water as control). The H_2O_2 concentration was selected based on previous studies reported by Ozaki et al. (2009) and Khandaker et al. (2012). The spraying was done at the dry leaf stage around 11:00 am, from the vegetative to flowering stage completing 15 foliar sprays during the experimental period. The treatments were applied following a completely randomized design (CRD) with five replications.

Data collection

Growth and physiological parameters

The number of leaves, the tallness of the plant, and the leaf area were recorded. A Leaf Area Meter (Model Portable Laser CI-202, CID Bio-science, USA) was used to quantify leaf area. A measuring tape was used to measure plant height (from base of plant to top of youngest shoot). The SPAD 502 Plus Meter of Konica Minolta; Opti-science, USA was used to record chlorophyll content. A Handy PEA meter (Hansatech-Instrument, UK) was used to record the data on chlorophyll fluorescence in three levels, F0, Fv, and Fv/Fm on sunny days, once a month. The CI-340 handheld Photosynthesis System (Bio-Science, USA) was used to record other physiological parameters, e.g., net photosynthetic rate (*Pn*), transpiration rate (*tr*), internal CO_2 concentration, and stomatal conductance ($g_s w$). As per Khandaker et al. (2012), growth and physiological parameters of treated and untreated plants were recorded eight (8) times and, for each time, data was recorded 2 days after the treatment application. A series of experiments were carried out for the repeated measurements of physiological and growth parameters, nutrient elements and biochemical analysis, gene expression studies, and major compound identifications from leaf extracts of drought stressed plants.

Biochemical properties and mineral nutrient analysis

First, the methanolic extract was developed using treated and untreated leaves of *F. deltoidea* for biochemical analysis. Harvested leaves (3 days after the treatment application) were dried for 3 days at 45°C in a dryer. The dried leaves were ground properly in a grinding machine and 10 g of leaf powder

were soaked in 70% methanol extract for 3 days and then transferred to an orbitary shaker for mixing. Filtration of the contents was done using Whatsman No. 1 filter paper. The crude methanolic extract was prepared by evaporating the filtrate into a rotary evaporator.

Dubois et al. (1956) method was referred to when measuring the sugar content in the crude methanolic extract. The standard method of Singleton and Rossi (1965) was used to estimate the total phenolic content of the extract. Gallic acid, as a standard chemical was used to express the phenolic content as mg/GAE/g [milligram gallic acid equivalents (GAE) per gram] of dry extract. The Aluminum Chloride colorimetric analysis (Chang et al., 2002) was used to determine the total flavonoid content as mg/QE/g [milligram quercetin equivalents (QE) per gram] dry weight since quercetin was used as a standard chemical. The antioxidant properties of the plants were ascertained by carrying an ABTS assay following the guidelines of the ABTS kit's manual (Sigma-aldrich). The formulae of Arnon (1949) were used to determine the contents of chlorophyll *a, b* and carotenoid. The leaves and syconium of treated and untreated plants were collected at 1 day after the treatment application for mineral nutrients analysis. The Neutron Activation Analysis (NAA) method was used to analyze the mineral accumulation in leaves and syconium, which was described by Nashriyah et al. (2006). The Sodium (Na^{+}), Potassium (K^{+}), Calcium (Ca^{2+}), Magnesium (Mg^{+}), Iron (Fe^{2+}), Arsenic (As^{+}), and Antimoni (Sb^{3+}) were analyzed at the Malaysian Nuclear Agency, Bangi, Kajang, Selangor.

Leaf histology

A histological examination was carried out at the Electron Microscope Scanning laboratory, Institute of Oceanography and Environment (INOS), Universiti Malaysia Terengganu (UMT), Terengganu with the help of a Scanning Electron Microscopy (SEM) (Model JEOL JSm-636OLA) as per methodology of Rohini et al. (2016). The prepared samples were arranged accordingly on the stub for gold coating and the samples were ready to be observed under the SEM. The parts of the leaves that were focused on in this study were the leaf cross section, leaf margin, stomata at lower and upper surfaces of the leaves, as well as stomatal size, and leaf vascular bundle.

Rubisco gene expression

The RNA extraction was done according to the procedure described by Wang et al. (2015) in the manual of SV RNA Isolation System kit (Promega) and the centrifugation was used at 12,000–14,000 rpm. Yield of RNA obtained was determined by using a Spectrophotometer at 260 nm wavelength. The manual of Takara Prime Script 1st strand cDNA synthesis kit was consulted to synthesize the cDNA. The reaction tubes were incubated in heat-block at 70°C for 15 mins to inactivate the reverse transcriptase before doing the PCR and amplification. Aliquots of the single strand cDNA of the treated plants either at 0, 15, or 20 mM were subjected to quantitative RT-PCR analysis on the *rbcL* gene. The expression of the *Co-GAPDH* (glyceraldehydes-3-phosphate-dehydrogenase) gene was considered as the internal control. Using a Rotor-Gene 6000 Series Software 1.7 (Build 65), the expression data were evaluated.

Gas chromatography-mass spectrometry

Agilent Technologies 7890A/5975C MSD Gas Chromatograph Mass spectrometry system, equipped with HP-5MS Ultra inert capillary column (30 m × 0.25 mm inner diameter, 0.25 μm film thickness) was used to identify the major compounds in the leaf extracts of H_2O_2 treated and untreated *F. deltoidea*. Helium was used as the carrier gas and conditioned at 8.2317 psi pressure with a flow rate at 1 ml min^{-1}. The samples were injected into the GCMS system with the injector and transfer line temperature conditioned at 250°C. The oven temperature was programmed at 60°C (10 min), 60°C to 180°C at the rate of 3°C/min and 180°C (15 min). The sample was injected into a split mode of front inlet with split ratio 50:1. Compounds present in the samples with quality of the probability score above 70% were selected and identified using the Wiley7Nist05.L and HPCH2205.L Mass Spectral Library.

Statistical analysis

A completely randomized design was followed to assign the treatments replicated five times. The SPSS-17 statistical software was referred to analyze the data as per the procedure of one-way ANOVA to know the significant difference between the parameters and the Tukey's test (HSD) was used to compare different concentrations of H_2O_2 in their effects on the parameters studied at $p = 0.05$.

Results

Impacts of H_2O_2 on growth and physiological parameters

The regulatory effects of various concentrations of liquid H_2O_2 and water were observed on drought-stressed *Ficus deltoidea* plants. The number of leaves were significantly influenced by the treatments, with the highest number of leaves recorded in the 20 mM treated plants. The plant height was 143% higher with the 20 mM H_2O_2 treatment as compared to

TABLE 1 The effects of H_2O_2 treatment on plant growth and photosynthetic characteristics of drought stressed *F. deltoidea* plants.

Treat (mM H_2O_2)	Number of leaves	Plant height (cm)	Leaf area (cm^2)	Photosynthetic rate ($\mu mol/m^2$ /s)	Transpiration rate ($mmol/m^2$ /s)	Stomatal conductance ($mmol/m^2$ /s)
0	234.05 ± 24.5a	47.05 ± 2.09a	6.02 ± 0.90a	2.64 ± 0.54a	0.30 ± 0.05a	32.92 ± 1.85a
5	297.07 ± 35.1a	47.70 ± 2.95a	6.61 ± 0.76a	2.68 ± 0.62a	0.25 ± 0.04a	39.95 ± 2.03b
10	309.47 ± 45.6a	51.33 ± 2.81a	6.78 ± 0.85a	2.69 ± 0.43a	0.25 ± 0.06a	45.32 ± 2.55c
15	458.03 ± 65.9b	57.10 ± 3.78a	6.85 ± 0.79a	2.73 ± 0.40b	0.22 ± 0.06a	61.76 ± 2.90d
20	568.43 ± 81.9c	58.45 ± 3.64a	7.32 ± 0.98a	2.76 ± 0.55b	0.20 ± 0.04a	62.07 ± 3.07e

Mean values in the same column with the different letters are significantly different according to Tukey's HSD test at p value 0.05.

TABLE 2 The effects of H_2O_2 treatment on leaf chlorophyll content (SPAD) and chlorophyll fluorescence of *F. deltoidea* plants under drought conditions.

Treat (mM H_2O_2)	Internal CO_2 (ppm)	Chlo. content (SPAD)	Lower chlo fluo. (F0)	Higher chlo fluo. (Fm)	Variable fluo. (Fv)	Photosynthetic yield (Fv/Fm)
0	63.40 ± 4.54b	51.90 ± 4.98a	702 ± 30.2a	2198 ± 209a	1496.1 ± 245c	0.61 ± 0.05a
5	57.45 ± 3.87ab	54.07 ± 2.88ab	707 ± 22.5a	2271 ± 225ab	1563.8 ± 215b	0.62 ± 0.04a
10	52.85 ± 3.90ab	55.51 ± 1.77ab	710 ± 35.0a	2533 ± 190ab	1828.3 ± 157a	0.69 ± 0.03ab
15	91.77 ± 4.80c	56.99 ± 2.69ab	728 ± 8.88a	2538 ± 225ab	1809.9 ± 150a	0.71 ± 0.03ab
20	47.84 ± 3.05a	57.82 ± 2.63b	721 ± 39.3a	2655 ± 259b	1934.19 ± 169a	0.72 ± 0.02b

Mean values in the same column with the different letters are significantly different according to Tukey's HSD test at p value 0.05.

the control plants, meaning that H_2O_2 application stimulated plant height of *F. deltoidea* in drought conditions although the differences were insignificant (Table 1). The leaf area was also not affected significantly with different treatments of H_2O_2.

The net photosynthetic rate was significantly higher in all H_2O_2 treatments under drought stress. The application of H_2O_2 at 15- and 20-mM concentrations produced higher photosynthesis rates which were 1.05- and 1.03-fold higher than the control plant. The lowest photosynthesis rate was found in the untreated plants at 2.64 $\mu molCO_2/m^2/s$. Therefore, the results indicated that H_2O_2 treatment could be a factor that promotes better photosynthetic rate in drought conditions (Table 1). For stressed plants, the highest transpiration rate was observed in the control plants with 0.3 $\mu molCO_2/m^2/s$ and the lowest transpiration rates were noted in the treatments of 20 and 15 mM H_2O_2. These were 33% and 27% lower than the control plants. These results signify that stomatal conductance was influenced differently between the treated and untreated plants under drought stressed conditions. Therefore, application of H_2O_2 is a method to reduce transpiration rate in stressed plants under drought conditions (Table 1).

The lowest stomatal conductance was observed in untreated plants at 32 mmol $CO_2/m^2/s$ (Table 1) but it was 1.88- and 1.87-fold higher in the 20 mM and 15 mM H_2O_2 treated plants, respectively (Table 1). The internal CO_2 was also influenced by different treatments of H_2O_2 (Table 2). The lowest internal CO_2 was detected in control plants at 618 ppm, ambient CO_2. Plants under the treatments of 15 mM and 20 mM H_2O_2 had significantly higher internal CO_2 levels, which were 1.24- and 1.28-fold respectively, greater than the control plants. Leaf chlorophyll content (estimated by SPAD value) increased by at least 10% due to the different treatments of H_2O_2 (Table 2).

The chlorophyll fluorescence value (F_0) and relative variable fluorescence (Fv) were significantly increased when H_2O_2 was applied to drought-stressed *F. deltoidea* plants. Plants treated with 20 mM of H_2O_2 produced a 20% higher Fm value compared to the control group. The photosynthetic yield increased 1.18-fold due to the application of 20 mM H_2O_2 (Table 2). The growth and plant physiological parameters of H_2O_2 treated plants were significantly positively correlated to each other except for the internal CO_2 concentration (Figure 1). Additionally, the results show that the number of leaves, plant height, and leaf area were positively correlated with net photosynthetic rate, transpiration rate, stomatal conductance, chlorophyll content, and photosynthetic yield of H_2O_2 treated *F. deltoidea* plants under drought stressed conditions (Figure 1).

Effects of H_2O_2 on biochemical properties

The chlorophyll content of leaves increased in the treated plants (Table 3) and this was highest for the treatment of 20 mM. Plants treated with 20 mM and 15 mM H_2O_2

10.3389/fpls.2022.965765

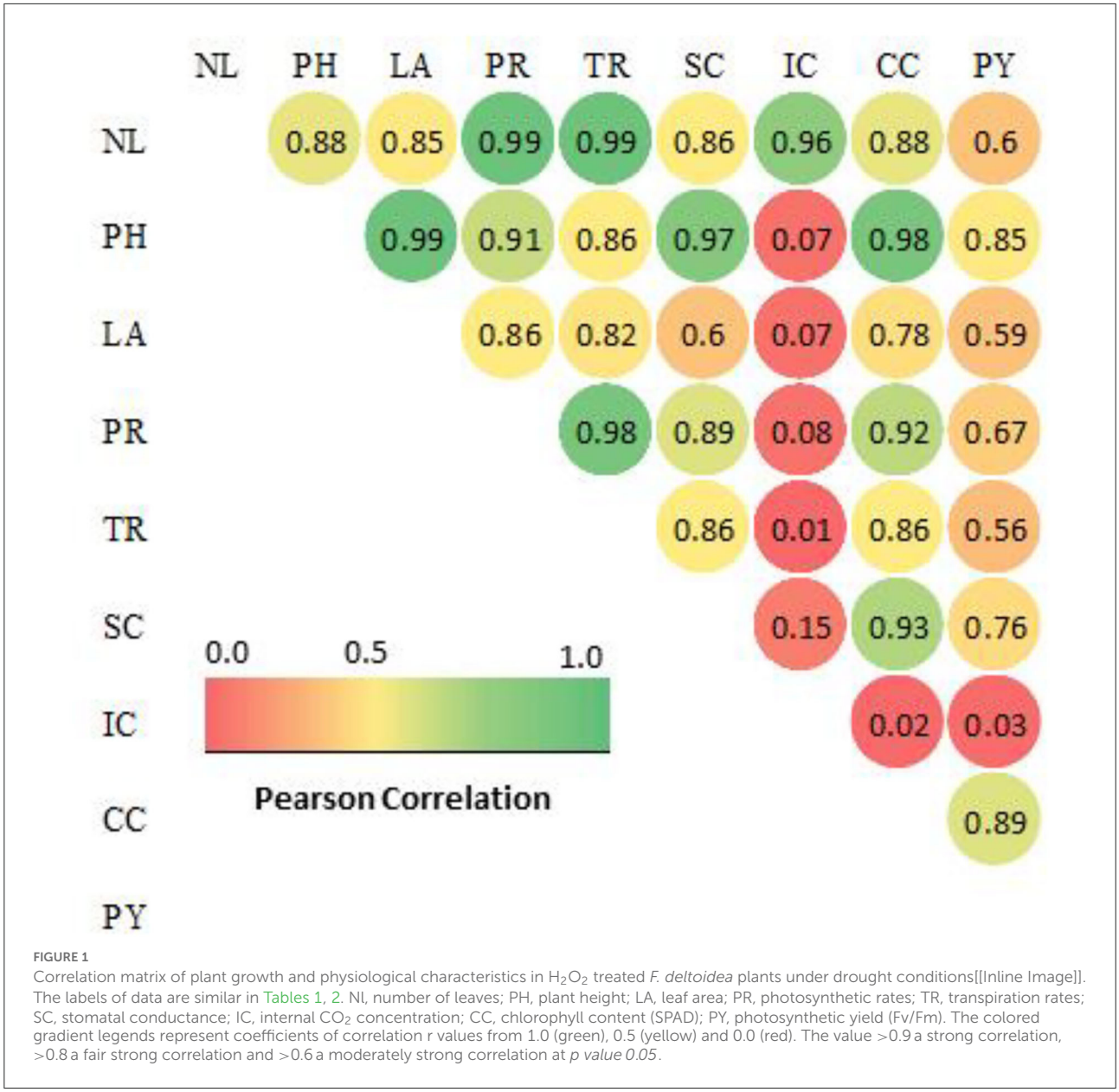


FIGURE 1
Correlation matrix of plant growth and physiological characteristics in H_2O_2 treated *F. deltoidea* plants under drought conditions[[Inline Image]]. The labels of data are similar in Tables 1, 2. Nl, number of leaves; PH, plant height; LA, leaf area; PR, photosynthetic rates; TR, transpiration rates; SC, stomatal conductance; IC, internal CO_2 concentration; CC, chlorophyll content (SPAD); PY, photosynthetic yield (Fv/Fm). The colored gradient legends represent coefficients of correlation r values from 1.0 (green), 0.5 (yellow) and 0.0 (red). The value >0.9 a strong correlation, >0.8 a fair strong correlation and >0.6 a moderately strong correlation at *p value 0.05*.

yielded 1.67- and 1.59- fold higher chlorophyll *b* content (Table 3). The lowest carotenoid content was recorded in fresh leaves extract in control (22% lower) compared to the 20 mM treated plants (Table 3). Therefore, application of H_2O_2 on drought-stressed Mas Cotek plants had a significant effect to increase carotenoid content of the plants (Table 3).

The content of total phenolic (TPC) and total flavonoid (TFC) also increased with the treatment of H_2O_2 (Table 3). An amount of 1.30- and 1.26- fold higher TPC and TFC content were produced with the application of 15 mM and 20 mM H_2O_2 to the drought-stressed plants (Table 3). The production of TFC under the treatment of 20 mM H_2O_2 was 98% higher than in the control plants (Table 3). The lowest TFC was determined in control plants with 12.2 mg quercetin equivalent (QE) per gram of dry leaf extract. Similarly, the total sugar content (TSC) also increased in the leaf extract of treated plants of *F. deltoidea* (Table 3). The lowest TSC was determined in untreated plants at 2.1 μmol glucose equivalent (GE) per gram of dried leaf extract. The increment of TSC in 15 mM and 20 mM H_2O_2 treated plants was 1.88- and 1.92-fold higher, respectively (Table 3). The results of ABTS assay test indicates an increment of 49 and 54%, respectively, antioxidant activity in a *F. deltoidea* methanolic leaf extract under the treatments of 15 and 20 mM in comparison to quercetin as a positive control. However, the differences between the treatments were immaterial (Table 3).

10.3389/fpls.2022.965765

TABLE 3 The effects of H_2O_2 on chlorophyll content, biochemical properties, and antioxidant activities of drought stressed *Ficus deltoidea* plants.

Treat (H_2O_2) (mM)	Chlorophyll a (mg/L FE)	Chlorophyll b (mg/L FE)	Carotenoid (μg/g FE)	TPC (mgGAE/g DE)	TFC (mgQE/g DE)	TSC (GE μmol/g DE)	ABTS (mMTrolox/g DE)
0	11.54 ± 0.01a	4.61 ± 0.28a	1.66 ± 0.04a	99 ± 10a	12.2 ± 0.2a	2.3 ± 0.02a	2.24 ± 0.28a
5	13.81 ± 0.13b	6.15± 0.13b	1.32 ± 0.001a	101 ±1.2a	16.32 ± 0.29b	2.71 ± 0.01b	2.44 ± 0.29a
10	14.75 ± 0.06c	6.93 ± 0.3bc	1.71 ± 0.02b	117 ± 0.88b	19.69 ± 0.1c	2.85 ± 0.01b	2.84 ± 0.20a
15	18.1 ± 0.06d	7.33 ± 0.13c	2.03 ± 0.01c	125 ± 1.53c	21.42 ± 0.15d	4.33 ± 0.06c	3.34 ± 0.18a
20	18.61 ± 0.09e	7.72 ± 0.01c	2.13 ± 0.03c	129 ± 1.33c	24.23 ± 0.22e	4.43 ± 0.03c	3.44 ± 0.15a

Means (±SE) within the same column followed by the same letter do not differ significantly according to the Tukey HSD test at p value 0.05.

TABLE 4 The effects of H_2O_2 on macro mineral uptake and accumulation of *F. deltoidea* plants under drought stressed conditions.

Treat (mM)	Na (μg/g)		K (%)		Ca (%)		Mg
	Leaf	Syconium	Leaf	Syconium	Leaf	Syconium	Leaf
0	81.3± 0.25ab	260 ± 0.18a	2.37± 0.22b	3.24± 0.23a	1.74 ± 0.12 a	1.34± 0.22b	0.59± 0.06a
5	85.0± 0.18ab	360 ± 0.18a	1.91± 0.17a	3.15± 0.22a	2.12 ± 0.28 a	0.56± 0.19a	0.55± 0.18a
10	85.0± 0.11ab	810 ± 0.24b	2.04± 0.21b	3.98± 0.17b	2.44 ± 0.16 b	0.71± 0.14a	0.51± 0.21a
15	95.0 ± 0.17b	410 ± 0.19ab	1.96± 0.16a	3.30± 0.19a	2.41 ± 0.16 b	0.74± 0.27a	0.64± 0.18a
20	70.0 ± 0.25a	290 ± 0.23a	1.90± 0.16a	4.12± 0.24b	2.26 ± 0.19 a	0.72± 0.31a	0.52± 0.22a

Mean values in the same column with the different letters are significantly different according to Tukey's HSD test at p value 0.05.

Effects of H_2O_2 on nutrient uptakes

Mineral uptake and accumulation in the H_2O_2-treated plants under stressed conditions was positively influenced. The results of Neutron Activation Analysis (NAA) showed that the application of H_2O_2 promoted sodium (Na) intake into the plants. The highest Na content in a leaf was detected in the 15 mM H_2O_2 treated plants with 95 μg per gram of dried leaf extract. The lowest Na content was detected in the 20 mM H_2O_2 treated plants with a value of 70 μg per gram of dried leaf extract, which was significantly less than the 15 mM treated plants (Table 4). The Na content in the treated *F. deltoidea* syconium was different from the untreated plants. The lowest Na content was observed on control plants with only 260 μg per gram syconium dried extract, meanwhile the highest Na content was detected in the 10 mM H_2O_2 treated plants with 810 μg per gram syconium dried extract. Hence, the application of H_2O_2 showed stimulative effects on Na uptake by the plants as all treated plants had higher Na content than the control plants (Table 4). On the other hand, the trend of potassium (K) content in *F. deltoidea* leaves was different from the Na content, with the highest found in the control and 10 mM H_2O_2 treated plants (2.37 and 2.04% K) (Table 4). The lowest K content in *F. deltoidea* leaves was in the 20 mM H_2O_2 treated plants. The opposite pattern was observed in K content of *F. deltoidea* syconium. It was marked that the lowest K content was in the control and 5 mM H_2O_2 treated plants, but the highest K content was observed in the plants treated with the highest concentration of H_2O_2. Hence, it can be said that H_2O_2 promoted K uptake especially in syconium rather than in *F. deltoidea* leaves (Table 4).

The spraying of H_2O_2 produced higher (1.74%) calcium (Ca) content in *F. deltoidea* leaves than in the control plants (1.74%), while the highest amount was determined in the 10 and 15 mM H_2O_2-treated plants (2.44 and 2.41%) (Table 4). The opposite trend of Ca content was observed in the syconium. The untreated plants produced the highest Ca content (1.34%) in the syconium while the lowest Ca content was found in the 5 mM H_2O_2 treated plants. Generally, calcium content is higher in plant leaves than in the syconium of the plants, but the study indicates different results (Table 4). The same pattern of stimulative effect was observed in magnesium (Mg) uptake in treated plants under drought-stressed conditions. It was determined that the highest Mg content was in the 15 mM H_2O_2 treated plants with 0.64 μg per gram of dried leaf extract while the control plants contained a lower Mg content of 0.59 μg per gram of dried leaf extract (Table 4). On the other hand, the control plants had the highest Mg content in *F. deltoidea* syconium with 0.41 μg per gram of syconium dried extract (Table 4). Our results confirmed that the 15 mM H_2O_2-treated plants gave positive impacts on Mg uptake in plant leaves, but Mg uptake and

10.3389/fpls.2022.965765

TABLE 5 The effects of H_2O_2 on micro mineral uptake and accumulation of *F. deltoidea* plants under drought stressed conditions.

Treat (mM)	Mg (μg/g)	As (μg/g)		Sb (μg/g)		Fe (μg/g)	
	Syconium	Leaf	Syconium	Leaf	Syconium	Leaf	Syconium
0	0.41 ± 0.21b	0.50 ± 0.18a	0.73 ± 0.11b	0.03± 0.01a	0.02 ± 0.06a	60.8 ± 0.19a	59.6 ± 0.10a
5	0.34 ± 0.12a	0.50 ± 0.23a	0.72 ± 0.21b	0.07± 0.05a	0.02 ± 0.20a	77.6 ± 0.21a	51.0 ± 0.18a
10	0.26 ± 0.04a	1.2 ± 0.18b	0.34 ± 0.18a	0.10± 0.10a	0.14 ± 0.17b	63.3 ± 0.09a	110 ± 0.10b
15	0.30 ± 0.20a	0.78±0.11ab	0.59 ± 0.19b	0.07± 0.17a	0.06 ± 0.01a	136 ± 0.21b	94.2 ± 0.23b
20	0.35 ± 0.21a	0.65 ± 0.04a	0.19 ± 0.18a	0.20± 0.05b	0.02 ± 0.02a	65.2 ± 0.05a	68.8 ± 0.06a

Mean values in the same column with the different letters are significantly different according to Tukey's HSD test at p value 0.05.

accumulation was higher in the syconium of control plants (Table 5).

The lowest arsenic (As) content in *F. deltoidea* leaves was detected in the control and 5 mM treated plants with 0.5 μg per gram of dried leaf extract, and the highest As content was noticed in the plants when treated with 10 mM H_2O_2 with 1.2 μg per gram of dried leaf extract (Table 5). On the other hand, the higher arsenic content in the syconium were detected in the control and 5 mM H_2O_2 treated plants and the lowest As content in the plant syconium was determined in the 20 mM H_2O_2 treated plants with only 0.19 μg per gram syconium dried extract. So, it can be said that the exogenous H_2O_2 application promoted arsenic accumulation in plant leaves, while it suppressed the As uptake in the plant syconium (Table 5). Antimony (Sb) content was present in *F. deltoidea* leaves only at trace amount. The Sb content in leaves was 6.67-fold higher in 20 mM H_2O_2 treated plants compared to the control plants and their differences were statistically significant (Table 5). The same increasing trend of Sb content was found in the syconium. This shows that 10–20 mM H_2O_2 were the best concentrations to promote Sb intake in both plant leaves and syconium (Table 5).

The iron (Fe) content in *F. deltoidea* leaves was observed at the lowest level in the control plants with 60.8 μg per gram of dried leaf extract, meanwhile the highest Fe content was detected in the 15 mM H_2O_2 treated plants with 136 μg per gram of dried leaf extract, which was significantly greater than the untreated plants (Table 5). In the syconium, the Fe content was also 1.58 times higher in treated plants compared to the control plants and their difference was statistically significant (Table 5). Therefore, H_2O_2 at the concentration of 15 mM was the best dose in promoting iron uptake in both plant leaves and syconium under drought stressed conditions (Table 5).

Regulatory effects of hydrogen peroxide on leaf histology

Several parts of leaves were examined under SEM to determine H_2O_2's effect on leaf histology of stressed *F. deltoidea* plants. H_2O_2 treatments under drought stress promoted stomatal closure of *F. deltoidea* leaves in a dose-dependent manner. The control treatment (H_2O_2 at 0 mM) had the widest leaf stomatal closure which was 2.7 μm. The smallest stomatal closure was observed in the highest H_2O_2 treated leaves (20 mM H_2O_2) which was 1.1 μm (Figure 2). It could be speculated that the application of exogenous H_2O_2 acts as an intermediary to promote guard cell closure under severe drought conditions in the presence of ABA.

The application of H_2O_2 produced significant changes on stomatal size in the upper and lower surfaces of the leaf (Figures 3, 4). The stomatal opening found on the upper surface was smaller. The control plant had 1.6–3.1 μm of a stomatal opening but the size increased when applied with H_2O_2 (Figure 3). Plants treated with 20 mM H_2O_2 had the lowest stomatal size of 0.8–1.5, which were significantly different from the untreated plants. Therefore, it is clear that the stomatal opening or closure is stimulated by H_2O_2 under stressed field conditions (Figure 3).

The lower leaf surface contained more numbers of stomata, and the largest stomatal size (1.14–4.1 μm) was recorded with the 20 mM H_2O_2 treatment (Figure 4). The H_2O_2 application also had a stimulatory effect on the stomatal size under stressed conditions. Treated plants with 5 and 10 mM of H_2O_2 had stomatal sizes of 3.0–3.4 μm and 2.0–3.0 μm, respectively. The smallest stomatal sizes (1.7–2.0 μm) were observed in the 15 mM H_2O_2 treated leaves (Figure 4), with the possibility that 15 mM H_2O_2 concentration is the best concentration to promote stomatal closure under drought stressed field conditions. Although slight damage appeared on the leaf margin of the control plants and the plants treated with a low dose, 5 mM H_2O_2, under drought-stressed conditions (Figure 5), no damage was spotted on the leaf margin of *F. deltoidea* plants treated with higher doses, e.g., 10, 15, and 20 mM H_2O_2. The results confirm that spraying H_2O_2 could protect the leaf margin of *F. deltoidea* plants from damage caused by drought stress (Figure 5).

Figure 5 demonstrates the cross section of treated and untreated leaves of *F. deltoidea* plants. It was noticed that the application of H_2O_2 reduced the damage to mesophyll

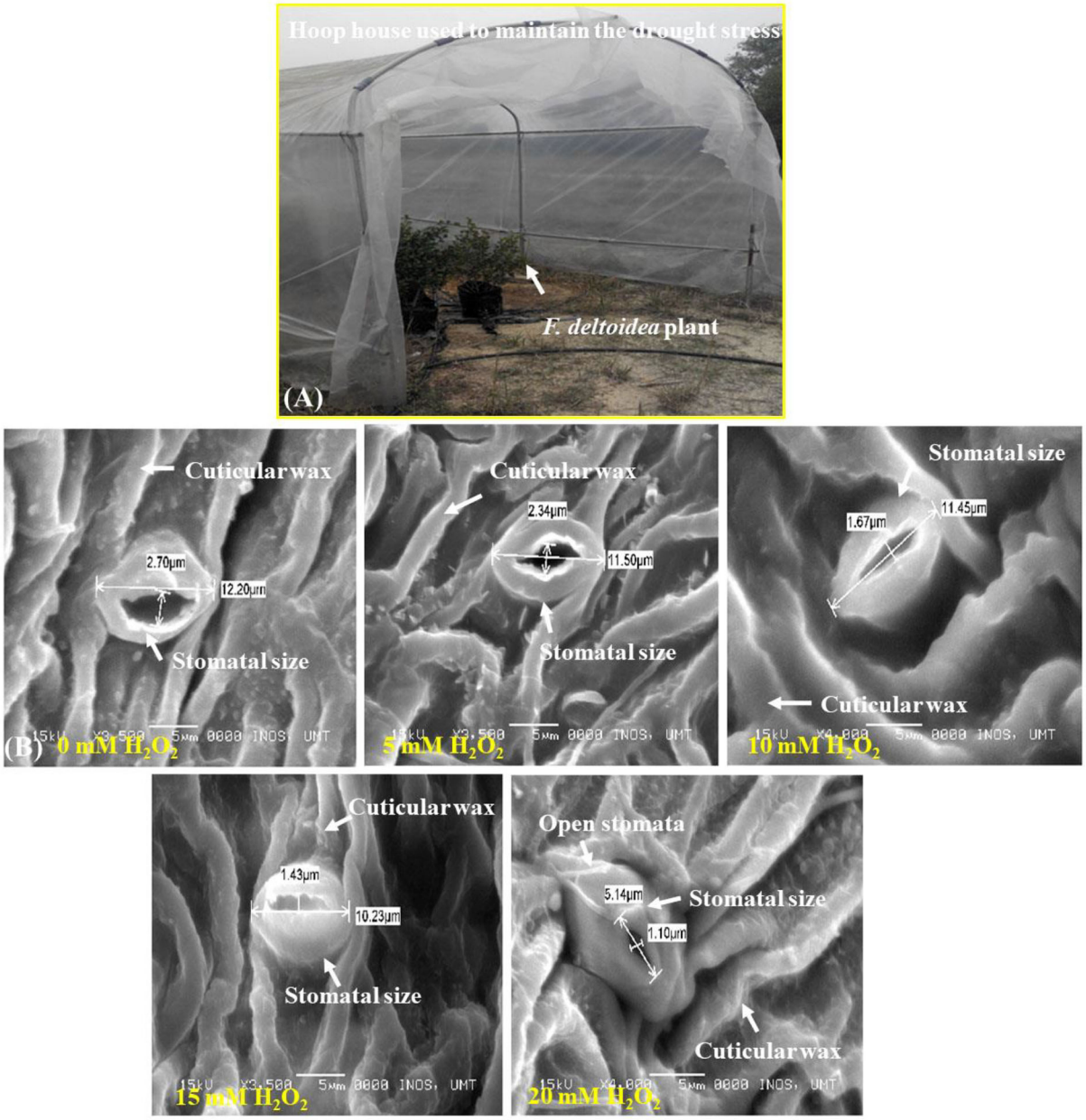


FIGURE 2
(A) A hoop house was used to maintain drought conditions to the experimental plants. **(B)** Scanning Electron Microscopy (SEM) photographs of stomatal closure at lower surface of treated and untreated leaves of *F. deltoidea* plants. Stomatal closure was the widest in control plants whereas the smallest stomatal closure was recorded in the 20 mM H_2O_2 treated plants. Deformed stoma and guard cell are visible at the leaf of control plants.

cells in the stressed plants. Treated leaves with 5, 10, 15, and 20 mM H_2O_2 had finer spongy and palisade mesophyll layers than the control plants. This might be related to the function of H_2O_2 in alleviating stress in the plants (Figure 6). When the cross section of the leaf vein was examined, a similar kind of positive effect, as noticed in mesophyll cells, was observed. All the treated plants had better vein structure than the untreated plants (Figure 7). It was observed that untreated plants had more or less a compact structure of xylem and phloem, whereas H_2O_2, treated plants had more turgid cells of tracheid in xylem and well-developed phloem tissue. It was also detected that the tracheid and vessel's cells in the vascular bundle were well developed and organized in the treated plants (Figure 7).

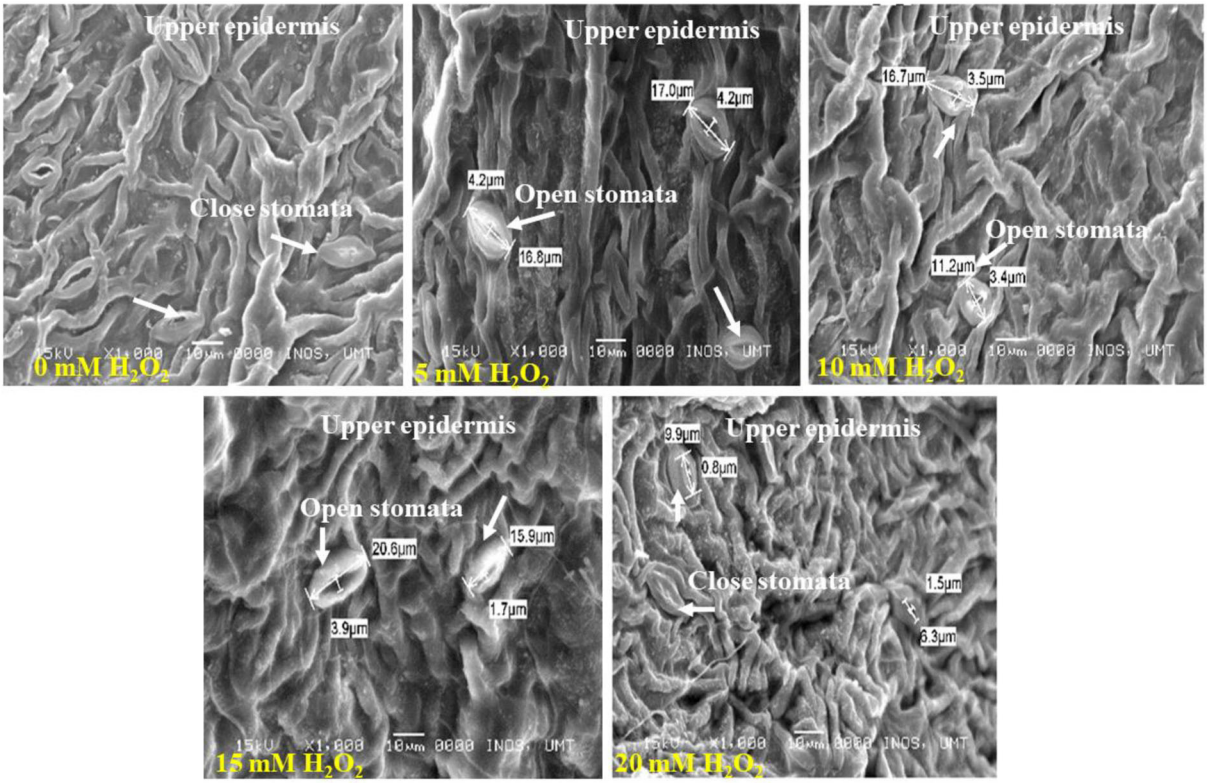


FIGURE 3
SEM photographs of stomatal opening at leaf's upper surface of H_2O_2 treated and untreated plants. Stomata are closed at control treatment, but the stomatal opening or size increased with H_2O_2 treatment (5 mM–15 mM H_2O_2). Stomatal size starts to decrease again with a higher concentration of H_2O_2. Less number of stomata contained at the upper surface of the leaves.

Effect of hydrogen peroxide on *Rubisco* gene expression

The effects of H_2O_2 on *Rubisco* gene expression in *F. deltoidea* plants were more visible in the study. H_2O_2 also regulated the *rbcL* gene expression in drought-stressed plants of *F. deltoidea*. In earlier studies, it was reported that the spraying of H_2O_2 at the concentrations of 15 and 20 mM produced the highest stimulative effects on a leaf histology, photosynthesis, biochemical properties, and plant growth, under drought-stressed conditions. In this study, 0 (control), 15, and 20 mM H_2O_2 treatments allow us to see the H_2O_2 effects on the rubisco gene expression and fold change, and determine the best treatment compared to the control. Based on plant growth and physiological performance we selected these three treatments for the *rbcL* gene expression study. The Real-Time PCR (RT-PCR) test confirmed the stimulative effects on the *rbcL* gene expression observed in a gel electrophoresis. Figure 8A displays the presence of the *rbcL* gene in both the leaves treated with 15 mM and 20 mM H_2O_2 and also in the leaves of control plants when compared with the housekeeping gene (Co-GAPDH). The fold change of *rbcL* gene was also calculated following *Pfaffl* and $2^{-\Delta\Delta CT}$ methods in comparison to 0 mM H_2O_2 as the control gene. Quantitative analysis indicated that the *rbcL* gene expression ratio was the highest 0.8649- (*Pfaffl* method) and 10.23-fold higher ($2^{-\Delta\Delta CT}$method) in the treatment of 15 mM H_2O_2 when compared to the control plants (Figure 8B). However, the plants treated with 20 mM of H_2O_2 had a slightly lower fold change of *rbcL* gene in comparison to the 15 mM H_2O_2 treatment, but it was still higher than the control. Therefore, application of 15 mM H_2O_2 promotes the expression of the *rbcL* gene at a better rate than 20 mM H_2O_2 treatments under drought stressed field conditions (Figure 8). The *rbcL* gene fold change was the lowest in the control gene (0 mM H_2O_2).

Gas chromatography-mass spectrometry analysis

GC-MS analysis was carried out to analyze the effects of hydrogen peroxide (H_2O_2) treatments (T1, 5 mM; T2, 10 mM; T3, 15 mM; T4, 20 mM) on drought stressed *F. deltoidea* for the major compounds in the leaf extracts compared to the

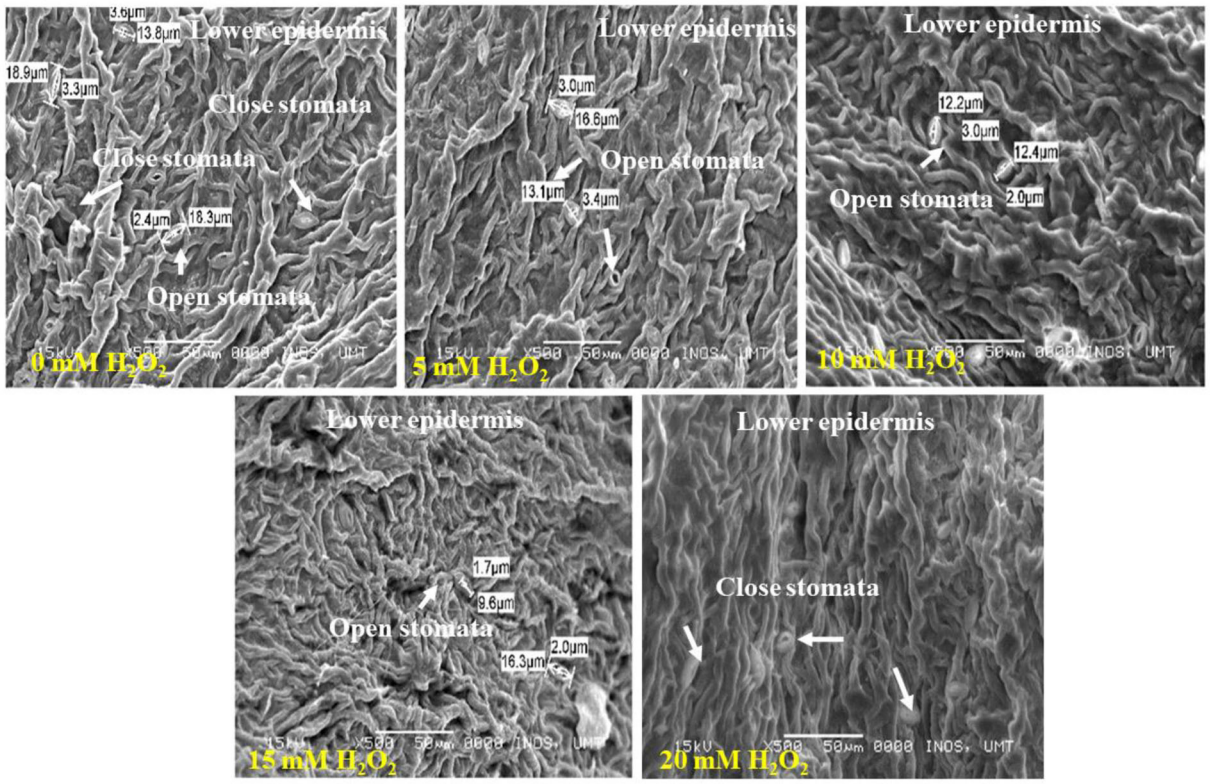


FIGURE 4
SEM photographs of stomatal closure at lower surface of the *F. deltoidea* leaves. Lower leaf surface contained a higher number of stomata than the upper surface. The smallest stoma size was observed in the 15 mM H_2O_2 treatment and stoma size started to decrease with an H_2O_2 concentration increase under drought stress.

untreated (T0) plants. The retention time (RT) and relative abundance (%) were recorded in this study. The comparison of total ion chromatograms of the control and treated groups (Figure 9) revealed the differences in percentages of 18 volatile compounds in the leaves following *F. deltoidea* treatment with H_2O_2. Thirteen (13) identified compounds with a quality score above 70% were identified, while five unmatched compounds were labeled as U1–U5 (Table 6). In this study, the aromatic volatile components detected in the native leaf extracts (T0) were mainly (E)-Caryophyllene (38.88%) at minute (min) 34.72, followed by α-Humulene (12.70%) at min 36.28, while the least amount was (E)-β-Ocimene (0.50%) at min 14.66. Other compounds detected were α-trans-Bergamotene (5.42%), α-Ylangene (3.38%), (E, E)-α-farnesene (2.94%), α-copaene (2.37%), and Germacrene D (1.26%). The volatile components detected in the leaves of the 5 mM H_2O_2 (T1) treated plants were mainly (*E*)-β-Ocimene (23.08%) at minute 14.66, followed by Germacrene D (15.86%) at minute 37.52, (*E*)-Caryophyllene (15.36) at minute 34.72, δ-Selinene (6.73%) at minute 37.75, and α-Copaene (1.96%) at minute 32.69, respectively (Table 6). On the other hand, the volatile components detected in the leaves of the 10 mM H_2O_2 (T2) treated plants were mainly Germacrene D (32.90%) at minute 37.52, followed by (*E*)-Caryophyllene (20.21%) at minute 34.72, α-Copaene (5.07%) at minute 32.69, δ-Cadinene (3.07%) at minute 39.38, and α-Guaiene (2.04%) at minute 38.15, respectively (Table 6). There were five (5) unidentified compounds which were also detected in the H_2O_2 treated plants under drought stressed conditions.

Heat map clustering analysis showed increasing average percentages of certain compounds (pattern; red > white > blue). These compounds were found to occur, be absent and/or increase in *F. deltoidea* leaf extracts corresponding to H_2O_2 treatments (Figure 10). As a result, a significant increase of (E)-β-Ocimene was clearly shown after the plant underwent T1 (23.08%) and T3 (71.80%) treatments, but the percentage was lessened to trace amounts for the T4 application. Besides, T1 and T2 treatments resulted in a higher abundance of Germacrene D with respective 15.86% and 32.90% compared to the native (control) plant. Following T4, the Germacrene D amount was found to be slightly less (26.50%). T1 also ensued the occurrence of several other volatile compounds including δ-Selinene (6.73%), while T2 resulted in a higher amount of α-Guaiene (2.04%), and δ-Cadinene (3.07%). Unidentified compound abundances also occur more intensely after T1

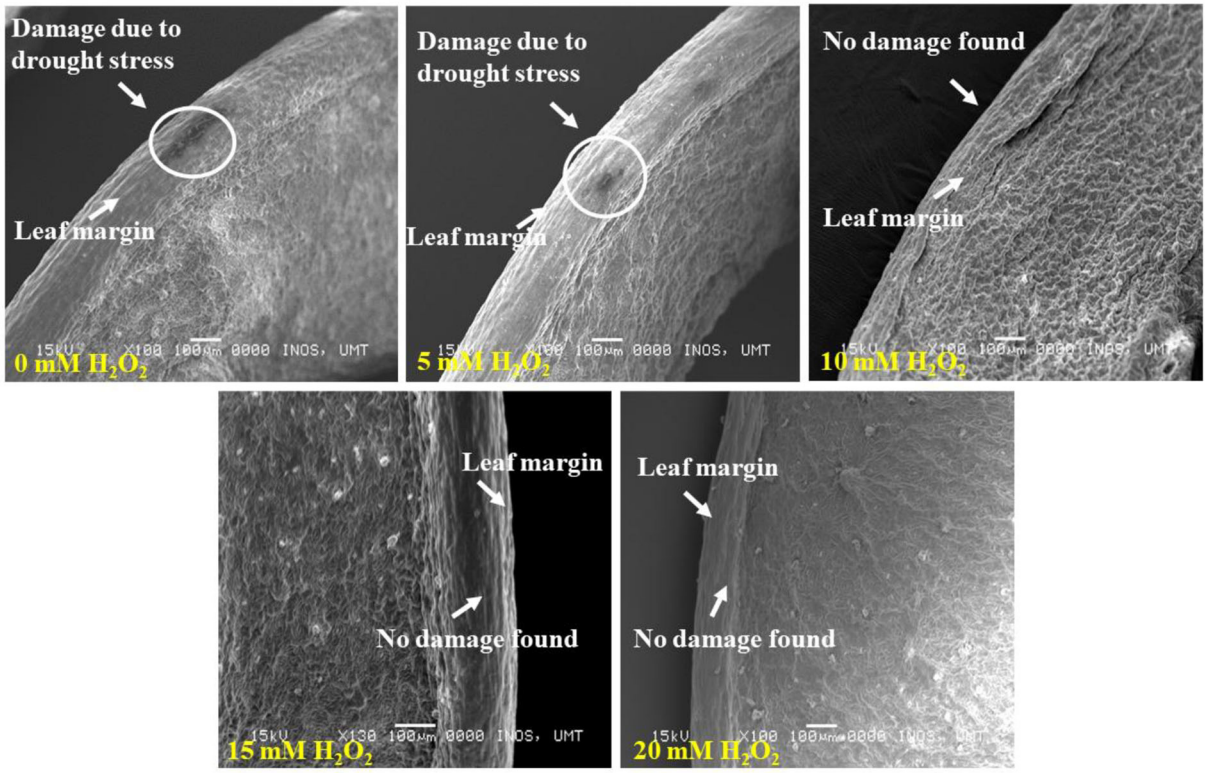


FIGURE 5
SEM photographs showing the leaf margin of *F. deltoidea* plants. Damaged appeared in the leaf margin of the control and 5 mM H_2O_2 treated plants. No damage was found in the 10–20 mM H_2O_2 treated plants and it is proven that exogenous H_2O_2 can protect leaf structure from oxidative damage induced by drought stress.

such as presented by U1 and U3. However, some compounds including (E)-Caryophyllene, α-Humulene, α-Ylangene, and ethyl acetate were found to have decreased. Following T4, δ-Cadinene (3.38%), (E, E)-α-Farnesene (4.40%), and U4 (23.94%) relative abundance were found to be higher than the control plant without treatment.

Discussion

Drought stress induces negative effects in plants including morphological, physiological, molecular, and metabolic changes which need to be improved by different means for better growth and development. Our results indicate that the number of leaves increased significantly with the application of H_2O_2 during drought conditions. This was due to the role of H_2O_2 in protein initiation, as well as in plant signaling and development (Barba-Espín et al., 2011; Ralmi et al., 2021). The treatments produced enhancing effects on plant height and leaf area of the *F. deltoidea,* although the results were not significant. H_2O_2 plays a role in increasing endogenous levels or to regulate relative gene expression. Liu et al. (2013) reported that the application of H_2O_2 positively influenced the plant metabolism and antioxidant enzyme production leading to better plant growth. It can be noted that drought stress leads to a decrease in photosynthetic activity due to stomatal closure. This study proved that the rate of photosynthesis was significantly improved with the application of H_2O_2 on stressed *F. deltoidea* plants. H_2O_2 is a signaling molecule, which creates a positive response under abiotic stress, such as drought (Ashraf et al., 2015). It is obvious in this study that exogenous H_2O_2 enhanced drought resistance by protecting the structures of organelle under drought stress conditions. In addition, H_2O_2 protects chloroplast/mesophyll ultra-structure, modulates the expression of the rubisco gene, and increases the actions of antioxidant enzymes to preserve photosynthesis during drought stress conditions (Liao et al., 2012).

H_2O_2 application reduces the transpiration rate in stressed *F. deltoidea* plants to some extent, which has been confirmed from this study. The reduced transpiration rate is an indicator of high water-use efficiency. Sofo et al. (2005) reported that H_2O_2, being an important signaling molecule, may increase water use efficiency, the recovery of net transpiration rate, and the net photosynthetic rate of plants. Increase in stomatal conductance

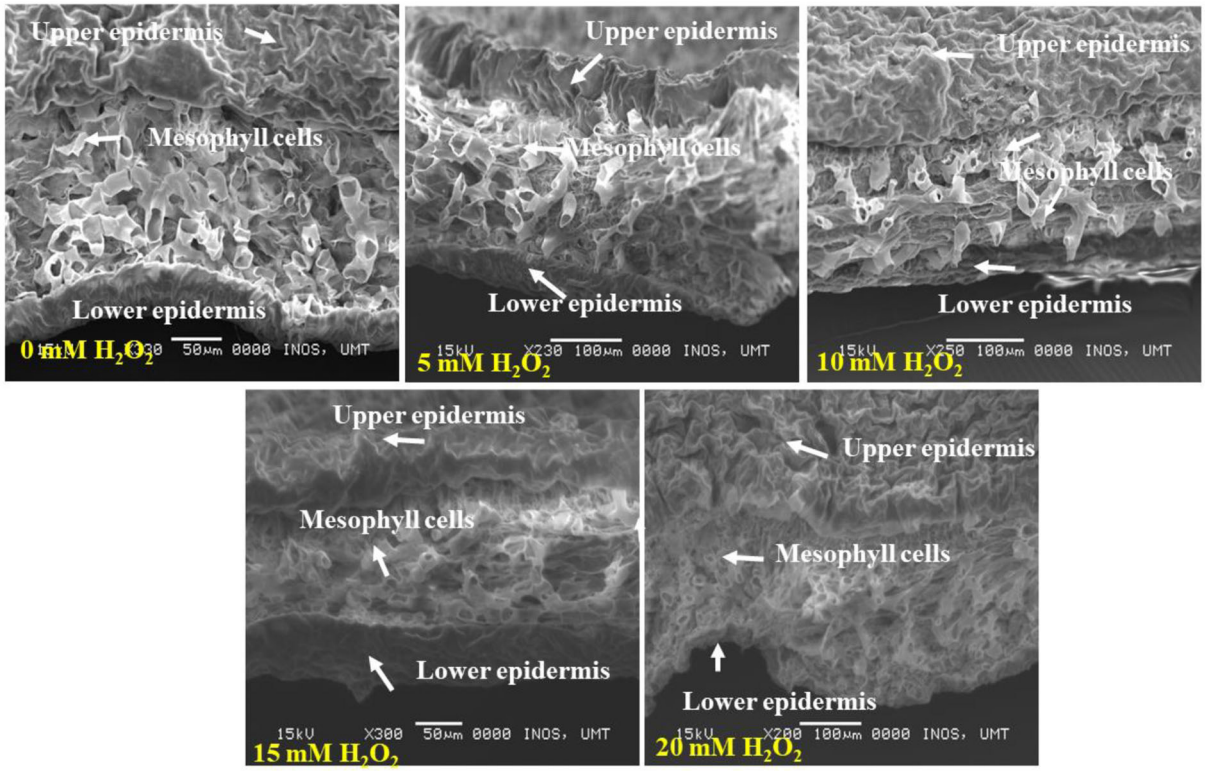


FIGURE 6
SEM photographs show the cross section of *F. deltoidea* leaves under drought stressed condition. The photographs show upper and lower leaf surfaces, each surface consists of an epidermis layer, cuticular wax, and mesophyll cells. Well-developed mesophyll cells are visible in 5 mM and 10 mM H_2O_2 treated plant leaves.

with the application of H_2O_2 is a tool to mitigate drought stress since it helps to control adaptive transpiration as reported by Hessini et al. (2008). Lawlor (1995) stated that when increasing the stress when the stomata is closed the presence of inner leaf CO_2 also declines. The opening and closing of the stomata is a mechanism in plants which regulates the water loss by sacrificing CO_2 uptake, especially when the environmental conditions are disparaging as reported by Arve et al. (2011). However, the results obtained from this study opposed these statements, and noted that the spraying of H_2O_2 at the concentrations of 15 and 20 mM could significantly improve the CO_2 content in stressed *F. deltoidea* plants. H_2O_2 also plays a vital role in brassinosteroid-regulated stomatal movement (Shi et al., 2015).

As per reports of others (Santos, 2004) under abiotic stresses the leaf chlorophyll content decreases due to an inhibited synthesis of 5-aminolaevulinic acid, but this study indicates a significant increase of chlorophyll content with H_2O_2 treatment in the *F. deltoidea* plants. It has been proclaimed by Steffens et al. (2013) that the withdrawal of the negative impacts of stresses through the application of H_2O_2 promoted plant chlorophyll content. Improved chlorophyll content might be due to the non-enzymatic defense mechanism especially due to activity of ROS-scavenging proteins under stress conditions. It is also speculated that this might be caused by the role of H_2O_2 itself as a signal of oxidative stress since it changed the redox status to antioxidative status of the surrounding cells (Sairam and Srivastava, 2000). Our study indicates that relative variable fluorescence and photosynthetic yield were significantly higher in treated plants under drought field conditions. This higher photosynthetic yield is also an indication of stress removal in the presence of exogenous H_2O_2. Our results showed that all the plant growth and physiological parameters were positively correlated with each other in H_2O_2 treated *F. deltoidea* plants. Improved plant physiological parameters create significant effects on plant growth and development under drought-stressed conditions.

Carotenoid content of pea seedlings was reduced when they were subjected to drought conditions (Moran et al., 1994). Our results show that carotenoid content was significantly improved with the spraying of 15 and 20 mM of H_2O_2 on *F. deltoidea* stressed plants. Total phenolic and flavonoid contents were also significantly improved with the application of H_2O_2 in *F. deltoidea* plants. The possible reason for higher phenolic and flavonoid content in treated plants was probably due to

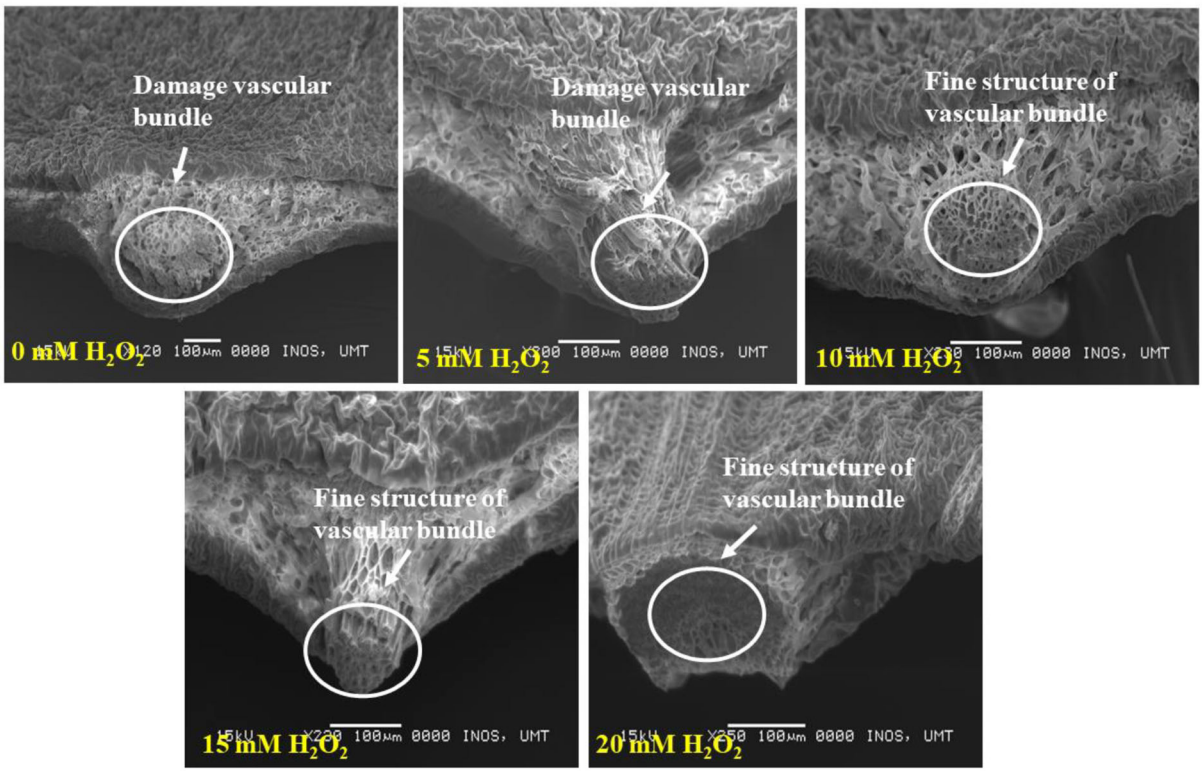


FIGURE 7
SEM photographs show the cross section of drought stressed *F. deltoidea* leaf veins. Fine structure of the vascular bundle (xylem and phloem tissues) is visible in the 10–20 mM H_2O_2 treated plant leaves. Damaged leaf vascular tissues are found in the control and 5 mM H_2O_2 treated plants.

the fact that H_2O_2 acted as a signaling molecule in phenolic synthesis (Zhang et al., 2013; Jamaludin et al., 2020). Chen et al. (2007) reported that the accumulation of proline, sugars, and polyols are responsible for plant survival under abiotic stresses. Soluble sugars also take part in signaling to regulate molecules in numerous plant growth and developmental processes. Our results demonstrate that the total sugar content of stressed *F. deltoidea* plants was significantly amended with the application of H_2O_2. The sucrose phosphate synthase (SPS) activity might be improved due to the regulatory effects of H_2O_2, and it regulated the manufacture of sucrose from triose phosphates during photosynthesis (Uchida et al., 2002).

We found that the spraying of H_2O_2 improved antioxidant activity in *F. deltoidea* plants under drought stress conditions. H_2O_2 may alleviate the level of antioxidants in plants by activating PAL, CHS, and stilbene enzymes (Nyathi and Baker, 2006). Zhang et al. (2001) suggested that under stressed conditions, when guard cells are amended with ABA, it may close the stomata through the production of H_2O_2, and H_2O_2 plays a role as intermediate in ABA signaling. This is in parallel with our results which indicate that the application of H_2O_2 promoted stomatal closure of *F. deltoidea* plants. The stomatal closure during drought stress is also related to the maintenance of xylem integrity (Jones and Sutherland, 1991).

The application of H_2O_2 improved the sodium (Na^+) content in both leaves and syconium under drought stress. The beneficial effects of Na^+ are the same as nitrogen (NO_3^- and NH_4^+) or K^+, which regulates plant growth by improving leaf chlorophyll content, net photosynthetic rates, water use efficiency, nitrate reductase activity and relative growth rate (Brownell and Jackman, 1966; Smith et al., 1980; Redondo-Gómez et al., 2010; Gattward et al., 2012). Nitrate reductase enzyme catalyzes the reduction of nitrate N to organic forms and reflects the level of nitrogen (N) activity in plant leaves (Lane et al., 1975). Na^+ also enhances nitrate uptake by roots and increases assimilation of nitrate in leaves (Ohta et al., 1989). The improved level of Na content may increase the activity of N in plants which stimulates plant growth and development in drought conditions. The photosynthetic capacity of leaves is interconnected with the nitrogen content, predominantly because the proteins of the Calvin cycle and thylakoids exemplify most of the leaf nitrogen (John, 1989). The treatment of 20 mM H_2O_2 produced the highest amount of K content in the plant syconium. The elevated level of K is essential in regulating the

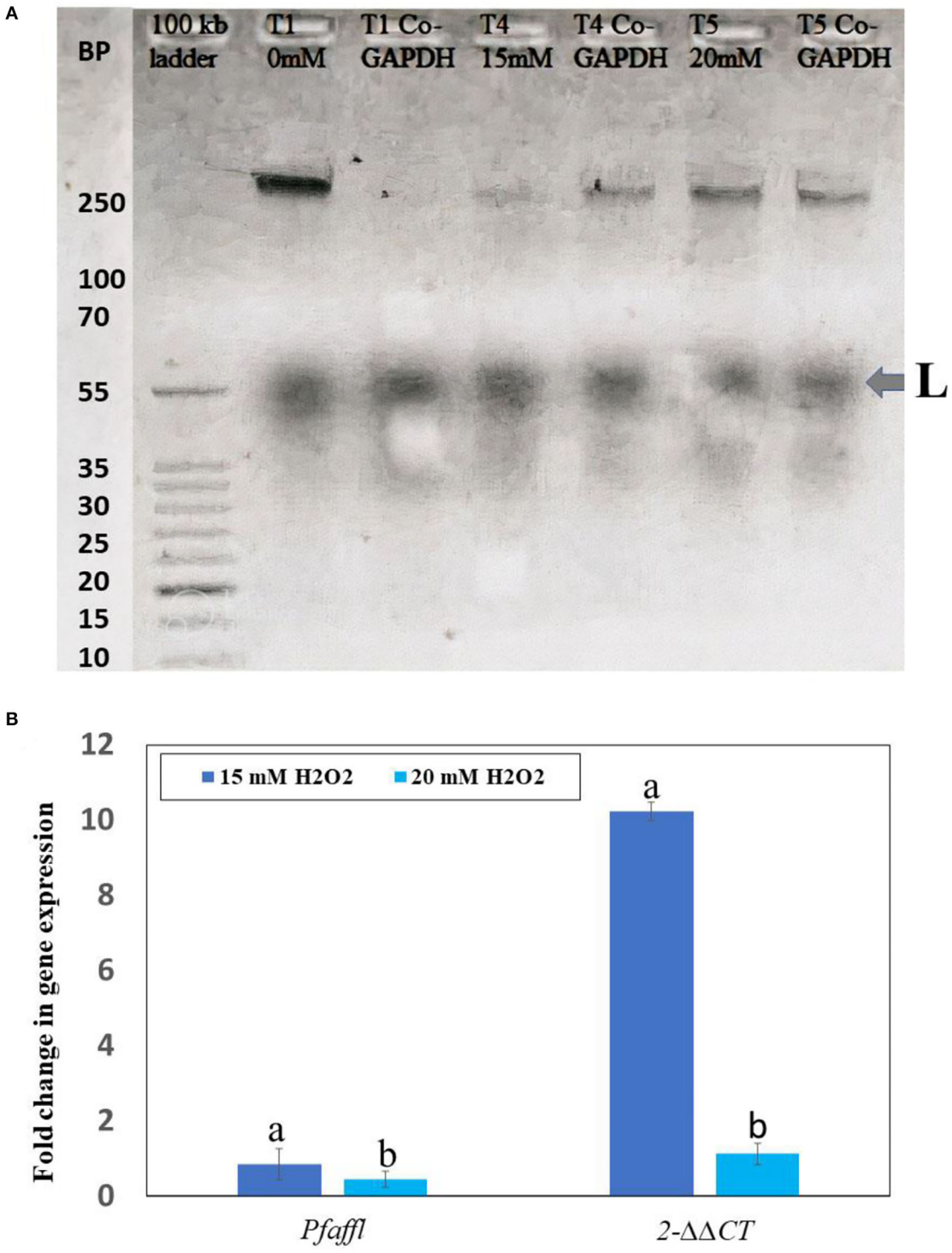


FIGURE 8
The result of RT-PCR when viewed under gel electrophoresis **(A)**. The *Pfaffi* and $2^{-\Delta\Delta CT}$ methods were used to analyze the fold change in *rubisco* (*rbcL*) gene expression in the control, 15 mM and 20 mM H_2O_2 treated plants **(B)**. Bars indicate (± S. E.). Means followed by the same lower case letters within the column are not significantly different according to Tukey's HSD-test (n = 3, $p \leq 0.05$).

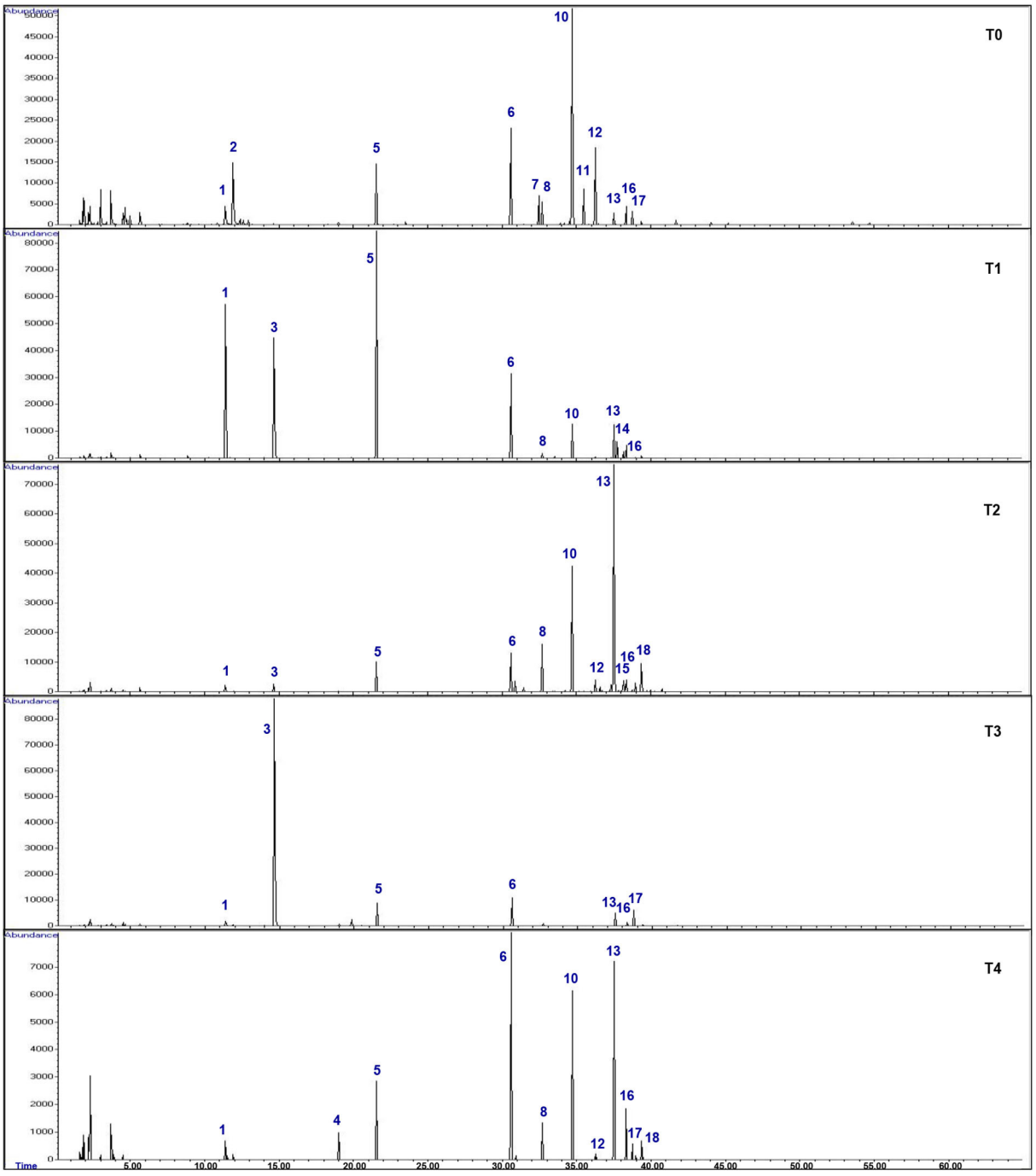


FIGURE 9
Gas chromatography mass spectrometry (GCMS) total ion chromatograms (TIC) of the leaf extracts of H_2O_2 treated and untreated *F. deltoidea* plants under drought stress. Thirteen (13) identified and five (5) unmatched volatile compounds with a quality score above 70% were identified, which are responsible for drought stress mitigation.

osmotic potential and water uptake in water-stressed plants. Since H_2O_2 is related to stomatal closure, it helps to adjust to drought stress in escalating plant resistance (WHO Regional Office for Europe, 2000). Moreover, the nutrient K, helps in galvanizing different enzyme systems and thereby regulates water movement and water use efficiency, nitrogen uptake and protein building and photosynthesis [Risk Assessment Studies (RAS), 2004]. In a study with broad beans, Kazerouni et al.

10.3389/fpls.2022.965765

TABLE 6 Retention time (RT) and relative abundance (%) of the volatile compounds (identified and unknown) in the leaf extracts of drought stressed *F. deltoidea* plants treated and untreated with H_2O_2.

Pk#	RT	Compound	% Content				
			T0	T1	T2	T3	T4
1	11.39	U1	2.71	9.32	3.04	1.74	2.30
2	11.92	(*E*)-3-Hexenyl acetate	5.33	0.00	0.00	0.13	0.64
3	14.66	(*E*)-β-Ocimene	0.50	23.08	2.32	71.80	0.00
4	19.02	U2	1.07	0.00	0.00	0.00	2.12
5	21.55	U3	8.62	13.85	13.90	10.93	11.11
6	30.59	U4	12.71	8.22	13.15	8.47	23.94
7	32.48	α-Ylangene	3.38	0.00	0.00	0.00	0.00
8	32.69	α-Copaene	2.37	1.96	5.07	0.58	3.70
9	33.52	β-Elemene	0.00	0.71	0.00	0.00	0.00
10	34.72	(*E*)-Caryophyllene	38.88	15.36	20.21	0.04	16.73
11	35.50	α-*trans*-Bergamotene	5.42	0.00	0.00	0.00	0.00
12	36.28	α-Humulene	12.70	0.54	1.03	0.00	0.64
13	37.52	Germacrene D	1.26	15.86	32.90	3.18	26.50
14	37.75	δ-Selinene	0.00	6.73	0.00	0.00	0.00
15	38.15	α-Guaiene	0.00	1.76	2.04	0.00	0.00
16	38.35	U5	2.12	1.57	3.23	1.01	4.55
17	38.76	(*E,E*)-α-Farnesene	2.94	0.04	0.04	2.13	4.40
18	39.38	δ-Cadinene	0.00	1.01	3.07	0.00	3.38

Pk#, peak number; T0, untreated control; T1, treatment with 5 mM hydrogen peroxide (H_2O_2); T2, treatment with 10 mM H_2O_2; T3, treatment with 15 mM hydrogen peroxide (H_2O_2); T4, treatment with 20 mM H_2O_2.

(2001) observed that potassium improved the water content in the plant leaves, and it increased the tolerance to water stress. Hence, under environmental stress conditions the enhancement of K content of plants is important for the survival of crops (Cakmak, 2005).

The higher amount of Ca is a good indicator of improved plant condition under stressed conditions. The elevated level of Ca^{2+} in a cell acts as a signal carrier and transporter into appropriate biological responses by downstream effectors. In this study, the amount of Ca content in the leaves was found to be greater in 10 mM H_2O_2 treated plants. The higher amount of Ca in plants helps to alleviate the adverse effects of drought stress. The exogenous application of Ca^{2+} and H_2O_2 also recovered the physiological damage of *Brassica* seedlings under drought stress (Khan et al., 2017). Pei et al. (2000) reported that, H_2O_2 production by induction of ABA and the H_2O_2-activated Ca^{2+} channels are significant for ABA-induced stomatal closing under stress conditions. Our results indicate that magnesium (Mg) content in the leaves was significantly higher in 15 mM H_2O_2 treated plants. The leaf magnesium plays a decisive role in the process of photosynthesis and is one of the major contributing factors of biomass formation (Tränkner et al., 2016). Liu and Porterfield (2014) explained the role of H_2O_2 in alleviating the effects of stresses as they demonstrated the use of magnesium peroxide for flooded corn as an effective oxygen buffer, which generated H_2O_2 and released biological oxygen for the stressed plants.

Our results indicate that arsenic (As) content was increased in the 10 mM H_2O_2 treated leaves while the highest As content in the syconium was present in the control plants. Higher doses of arsenate reduce seed germination, plant biomass accumulation, and produce oxidative damage (Mascher et al., 2002; Shri et al., 2009). But our results showed a positive result in plant growth and development, it was suggested that the application of foliar H_2O_2 promoted As uptake but not to a harmful level. The antimony (Sb) content in leaves was the highest in the 20 mM H_2O_2 treatment, while the 10 mM H_2O_2 treated plants had the highest Sb content in the plant syconium. Kabata and Pendias (2001) suggested that 5–10 mg kg^{-1} of Sb in plant tissue are phytotoxic, but as per reports of Eikmann and Kloke (1993) 5 mg kg^{-1} Sb in plants is at a tolerable level. Pan et al. (2010) also noticed the reduced plant growth and biomass accumulation due to Sb pollution. Thus, although the application of H_2O_2 improved Sb uptake, it was not up to its toxicity level in the plants.

Our results indicate that iron (Fe) accumulation was significantly improved in the leaves and syconium with the application of H_2O_2. Fe deficiency leads to severe chlorosis and reduction in yield and also the nutritional content of the plants (Marschner, 2002; Curie and Briat, 2003). Additionally, Fe is

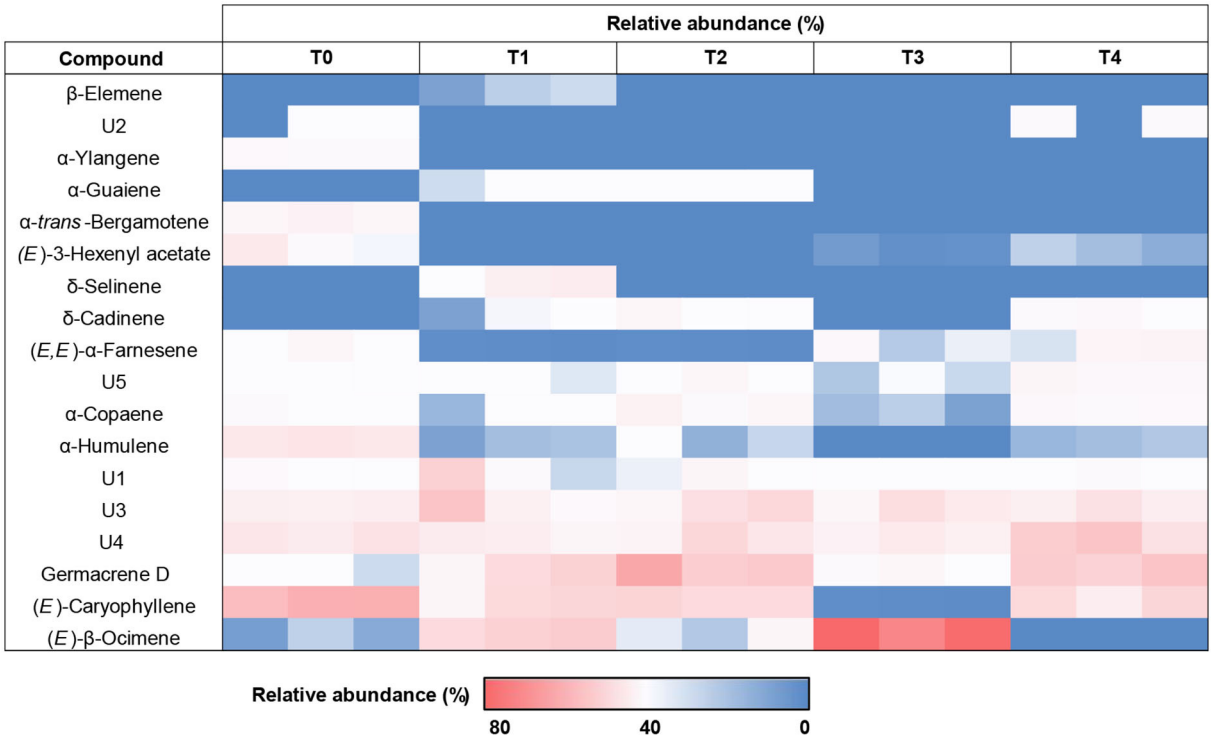


FIGURE 10
Clustered heat map based on increasing average relative abundance (%) of the volatile compounds (identified and unknown) in the leaf extracts of H_2O_2 treated *F. deltoidea* and untreated plants under drought stress.

helpful in many physiological processes such as photosynthesis, plant respiration, sulfate assimilation, synthesis of hormones, nitrogen fixation, DNA synthesis (Hell and Stephan, 2003; Puig et al., 2007). The improved physiological activities of treated plants may be due to the higher level of Fe in the plants. Ravet et al. (2009) demonstrated that ferritin protein in plants is responsible for controlling the levels of ROS, enzymatic activity is involved in ROS detoxification, which is a crucial role for the protection against oxidative damage in plants.

The distribution of stomata was found more frequent on the abaxial surface of leaves in treated *F. deltoidea* plants in comparison to the adaxial surface of the leaves, which is located on the epidermal layer of the leaf. Fu et al. (2013) testified that under drought stress conditions, stomatal density in eggplants at the abaxial surface increased by 20.39% compared to well-watered plants. As per reports of Liu et al. (2009) usually the stomatal numbers and pore aperture numbers would decrease during the periods of water stress, which is a common occurrence in *Arabidopsis* and grass species. Nonetheless, in some plant species it was disclosed that a decreased water level led to an increased stomatal density (Fraser et al., 2009). Moderate drought stress enhances the leaf thickness which may produce more guard cells for a given leaf area and increase stomatal density. Other than that, we suggest that the application of H_2O_2 could protect the leaf's margin from damage. This observation might be correlated to the function of H_2O_2 as a protective and signaling molecule which mediates the negative effects of drought stress in plants. Asad et al. (1998) suggested that H_2O_2 induced safety against lethal and mutagenic effects in *Escherichia coli* cells. Rose and Swift (2014) described the scorching of leaves which could appear as a spot or a burn along the leaf margin under drought stress. Hence, spraying the right amount of H_2O_2 could reduce the damage caused by water deficiency as shown in our results.

Thicker palisade parenchyma cells and a higher number of stomata make plants resistant to drought conditions. Moreover, our results indicate that the application of H_2O_2 reduced the damage of mesophyll cells in stressed plants by causing thicker mesophyll cells when compared to the untreated plants. In opposition, Sun et al. (2012) stated that tomato plants under mild stress conditions displayed a reduced palisade and spongy tissue thickness. Baum et al. (2000) noticed that abiotic stress affects the thickness of xylem and phloem cells, which regulates the xylem and phloem transport. The application of H_2O_2 in this study improved the leaf vein structure under drought stress field conditions. It is expected that the treated plants work better at carbon and water transportation as in plants with an improved structure of phloem and xylem.

Nasir et al. (2021) also reported that a lower concentration of H_2O_2 improved the tracheary elements and vascular cell of Mas Cotek leaves. Additionally, treated *F. deltoidea* plants might lead to better cross-linking of the cells and tissue of xylem and phloem. Hamann (2012) recorded that the strength and rigidity of the cell walls are improved by the cross-linking process which is an important mechanism in plants to mitigate environmental stresses.

Rubisco is a major enzyme which assimilates atmospheric CO_2 into the biosphere and is the most imperative target for improving the efficiency of photosynthesis in vascular plants (Parry et al., 2013). The progressive down-regulation of *rubisco* directs to a reduced RuBP content in plants during severe drought thereby inhibiting photosynthetic CO_2 assimilation (Flexas and Medrano, 2002). Our results indicate that the *Rubisco* gene expression was upregulated because of exogenous H_2O_2, and we suggest that it contributed to better adaptation of the *F. deltoidea* var. *deltoidea* plants by increasing photosynthetic rates and photosynthates accumulation under drought-stress. The results also show that the *rbcL* gene expression ratio was the highest in the 15 mM treatment compared to the 20 mM and 0 mM H_2O_2 treatments. Better *rbcL* gene expression in the 15 mM H_2O_2 treatment may trigger plant growth and development in drought stress conditions. It can be speculated that the exogenous H_2O_2 improved the levels of gene expression leading to better relative stability in the plants (Liu et al., 2010). This indication is supported by this study, that the net photosynthetic rate of all H_2O_2-treated plants increased in drought stress conditions. H_2O_2 as a ROS growth promoting chemicals induced the largest changes in the gene expression levels in various plants and this was probably due to its relative stability (Li et al., 2009).

In this study a total of 18 volatile compounds were detected from H_2O_2 treated and untreated *F. deltoidea* plants under drought conditions. These compounds were reported to be responsible for the aroma of *F. deltoidea* as well as other *Ficus* species (Grison-Pigé et al., 2002). Among the unidentified compounds, U4 peak at min 30.59 with a significantly high relative abundance (12.71%) is suggested to be the linalool which is reported as among the major essential oils in *F. deltoidea*. U4 is also less volatile, and thus detected later than ocimene which corresponds to the reported linalool (Grison-Pigé et al., 2002; Lee et al., 2011). The results of heat map clustering analysis showed that the percentage of certain compounds in treated leaves increasingly corresponded to H_2O_2 treatment under drought conditions. This finding indicates that treatment of *F. deltoidea* with H_2O_2 influences the accumulation of the volatile oils. Such similar occurrence was reported focusing on accumulation of volatile oils mediated by H_2O_2 production (Wang et al., 2011).

Drought stress affects synthesis of photosynthetic pigments and protein content, electron transfer chain (ETC), rubisco and sucrose phosphate synthase (SPS) enzyme activity, and the percentage of aromatic or volatile oils of plants (Bakshi et al., 2019). Our results show that exogenous H_2O_2 improved plant growth processes, protected cellular structure of leaves from damage, increased mineral accumulation and the level of *Rubisco* gene expression under drought stress. The percentage of volatile oils content in leaves of treated plants increased significantly compared to the control plants. The reduction of volatile oils in the control plants in this study may be due to the disturbance of the photosynthesis process and reduction of photosynthates accumulation in plants under drought stress, which suppresses plant growth and development (Flexas and Medrano, 2002). The disrupted function of the Calvin cycle and depletion of leaf area due to drought stress reduces the biosynthesis of volatile oils. The reduction of volatile oils in plant parts is a consequence of drought stress (Razmjoo et al., 2008). H_2O_2 is a non-radicle reactive oxygen species, which due to its stability and diffusion through the plasma membrane acts as a secondary messenger and regulates the flow of Ca^{+2}, protein synthesis and gene expression (Bienert et al., 2006).

Volatile oils belong to the group of terpenoids and are synthesized *via* the cytosolic mevalonic acid (MVA) pathway or methylerythritol phosphate (MEP) plasticity pathway (Perreca et al., 2020). Monoterpenes (synthesis by MEP pathway) and Sesquiterpenes (synthesis by MVA pathway) are the main constituents of volatile oils that play a role in synthesis of photosynthetic pigments, aroma, flavor, plant defense system and antioxidant activities (Pavela et al., 2021). H_2O_2 elevates the level of expression of saponin synthesis (SS), squalene epoxidase (SE) and β-amyrin synthase (β-AS) enzymes which regulate the biosynthesis of volatile oils (Hu et al., 2002, 2004; Kim et al., 2006). H_2O_2 also acts as a signaling molecule which mediates the biosynthesis of saponin in response to oligogalacturonic acid (OGA) and jasmonic acid (JA) (Zhao et al., 2010). In this study, the optimum concentrations of H_2O_2 (10–15 mM) may mediate the biosynthesis of volatile oils in *F. deltoidea* plants under drought conditions. The improved level of volatile oils plays a significant role in mitigating the negative effects of drought as well as other abiotic stresses of plants.

Conclusion

It is concluded that foliar applications of 10–15 mM of H_2O_2 should be applied biweekly to increase plant growth, photosynthesis, stomatal conductance, and chlorophyll fluorescence in *F. deltoidea* plants grown in drought stress conditions. In addition, chlorophyll, carotene, total phenols, total flavonoids, sugar content, and antioxidant activities of stressed plants are increased significantly with the H_2O_2 treatments leading to sustainable plant growth under drought-stressed conditions. The enhancement of macro nutrients content in the treated plants alleviates the negative effects of drought stress by improving plant physiological activities.

A slight increase of arsenic and antimony at safe levels in the treated plants contributes to stress mitigation as well. Furthermore, foliar applications of H_2O_2 improved the cellular and vein structure of the leaves and reduced the damage in leaves caused by drought stress. Similarly, the application of 15 mM H_2O_2 should be done to up-regulate the expression of the *Rubisco* gene in stressed *F. deltoidea* plants to catalyze the assimilation of CO_2 and increase net photosynthesis. Foliar application of H_2O_2 increased the accumulation of volatile oils in the plants, and the improved level of volatile oils mitigates the negative effects of drought stress. All these effects and influences help to alleviate the undesirable effects of drought stress. Our findings suggest that a foliar application of H_2O_2 is a novel technique to reduce the negative effects of drought stress in plants.

Data availability statement

The original contributions presented in the study are included in the article/supplementary material, further inquiries can be directed to the corresponding author.

Author contributions

MK: conceptualization, funding acquisition, supervision, data curation, and writing—original draft and editing. RJ: data curation, writing—original draft, and statistical analysis. AM, ZR, and SK: review and language editing. HA-Y, NB, MA, and KM: review, editing, and validation. All authors contributed to the article and approved the submitted version.

Funding

This research was funded by the Kementerian Pengajian Tinggi (KPT), Fundamental Research Grant Scheme (Project Code: FRGS/2/2014/SG03/UNISZA/02/1).

Acknowledgments

The authors wish to thank the Center for Research Excellence and Incubation Management (CREIM), Universiti Sultan Zainal Abidin, Campus Gong Badak, Terengganu, Malaysia, and FRGS/1/2019/WAB01/UNISZA/02/2 for the publication support. We also kindly acknowledge Taif University researchers supporting project numbers (TURSP-2020/199), Taif University, Taif, Saudi Arabia for providing partial publication support.

Conflict of interest

The authors declare that the research was conducted in the absence of any commercial or financial relationships that could be construed as a potential conflict of interest.

Publisher's note

All claims expressed in this article are solely those of the authors and do not necessarily represent those of their affiliated organizations, or those of the publisher, the editors and the reviewers. Any product that may be evaluated in this article, or claim that may be made by its manufacturer, is not guaranteed or endorsed by the publisher.

References

Aris, S. R. S., Mustafa, S., Ahmat, N., Jaafar, F. M., and Ahmad, R. (2009). Phenolic content and antioxidant activity of fruits of *Ficus deltoidea* var Angustifolia sp. *Malay. J. Anal. Sci.* 13, 146–150. Available online at: https://www.researchgate.net/publication/256089022_Phenolic_content_and_antioxidant_activity_of_fruits_of_Ficus_deltoidea_var_angustifolia_sp (accessed September 20, 2022).

Arnon, D. I. (1949). Copper enzymes in isolated chloroplasts, polyphenoxidase in *Beta vulgaris*. *Plant Physiol.* 24, 1–15. doi: 10.1104/pp.24.1.1

Arve, L. E., Torre, S., Olsen, J. E., and Tanino, K. K. (2011). *Stomatal Responses to Drought Stress and Air Humidity. Biochemistry, Genetics and Molecular Biology. Abiotic Stress in Plants—Mechanisms and Adaptations.* London: IntechOpen.

Asad, N. R., Asad, L. M. B. O., Silva, A. B., Felzenszwal, I., and Leitão, A. C. (1998). Hydrogen peroxide induces protection against lethal effects of cumene hydrogen peroxide in *Escherichia coli* cells: an Ahp independent but OxyR dependent system? *Mutat. Res.* 407, 253–259. doi: 10.1016/S0921-8777(98)00010-X

Ashraf, M. A., Rasheed, R., Hussain, I., Iqbal, M., Haider, M. Z., Parveen, S., et al. (2015). Hydrogen peroxide modulates antioxidant system and nutrient relation in maize (*Zea mays* L.) under water-deficit conditions. *Arch. Agron. Soil Sci.* 61, 507–523. doi: 10.1080/03650340.2014.938644

Badron, U. H., Talip, N., Mohamad, A. L., Affenddi, A. E. A., and Ahmad Juhari, A. A. (2014). Studies on leaf venation in selected taxa of the genus *Ficus* L. (Moraceae) in peninsular Malaysia. *Trop. Life Sci. Res.* 25, 111–125.

Bakshi, A., Moin, M., Madhav, M. S., and Kirti, P. B. (2019). Target of Rapamycin, a master regulator of multiple signalling pathways and a potential candidate gene for crop improvement. *Plant Biol. (Stuttg)* 21, 190–205. doi: 10.1111/plb.12935

Barba-Espín, G., Diaz-Vivancos, P., Job, D., Belghazi, M., Job, C., and Hernández, J. A. (2011). Understanding the role of H_2O_2 during pea seed germination: a combined proteomic and hormone profiling approach. *Plant Cell Environ.* 34, 1907–1919. doi: 10.1111/j.1365-3040.2011.02386.x

Baum, S. F., Phong, N. T., and Wendy, K. S. (2000). Effects of salinity on xylem structure and water use in growing leaves of sorghum. *New Phytol.* 146, 119–127. doi: 10.1046/j.1469-8137.2000.00625.x

Bienert, G. P., Schjoerring, J. K., and Jahn, T. P. (2006). Membrane transport of hydrogen peroxide'. *Biochem. Biophys. Acta* 1758, 994–1003. doi: 10.1016/j.bbamem.2006.02.015

Bohnert, H. J., and Sheveleva, E. (1998). Plant stress adaptations making metabolism move. *Curr. Opin. Plant Biol.* 1, 267–274. doi: 10.1016/S1369-5266(98)80115-5

Brownell, P. F., and Jackman, M. E. (1966). Changes during recovery from sodium deficiency in Atriplex. *Plant Physiol.* 41, 617–622. doi: 10.1104/pp.41.4.617

Cakmak, I. (2005). The role of potassium in alleviating detrimental effects of abiotic stresses in plants. *J. Plant Nutri. Soil Sci.* 168, 521–530. doi: 10.1002/jpln.200420485

Chang, C, Yang, M., Wen, H., and Chern, J. (2002). Estimation of total flavonoid content in propolis by two complementary colorimetric methods. *J. Food Drug. Anal.* 10, 178–182. doi: 10.38212/2224-6614.2748

Cheeseman, J. (2007). Hydrogen peroxide and plant stress: a challenging relationship. *Plant Stress* 1, 4–15. Available online at: https://www.life.illinois.edu/cheeseman/main/publications/peroxidePubs/PlStressH2O2review.pdf (accessed September 20, 2022).

Chen, Z., Cuin, T. A., Zhou, M., Twomey, A., Naidu, B. P., and Shabala, S. (2007). Compatible solute accumulation and stress-mitigating effects in barley genotypes contrasting in their salt tolerance. *J. Exp. Bot.* 58, 4245–4255. doi: 10.1093/jxb/erm284

Curie, C., and Briat, J. F. (2003). Iron transport and signaling in plants. *Ann. Rev. Plant Biol.* 54, 183–206. doi: 10.1146/annurev.arplant.54.031902.135018

Dramant, S., Aris, M. A. M., Akter, S. F. U., Azlina, H., Nor Azlina, A. R., and Norazlanshah, H. (2012). *F. deltoidea*: a possible supplement for type II diabetes: (a pilot study). *Pertanika J. Trop. Agril. Sci.* 35, 93–102. Available online at: http://www.pertanika.upm.edu.my/pjtas/browse/regular-issue?article=JTAS-0211-2009 (accessed September 20, 2022).

Dubois, M, K., Gilles, J., Hamilton, K., Robers, P. A., and Smith, F. (1956). A colorimetric method for the determination of sugar and related substances. *Anal. Chem.* 28, 350–356. doi: 10.1021/ac60111a017

Eikmann, T., and Kloke, A. (1993). "Nutzungs- und schutzgutbezogene Orientierungswerte fur (Schad-) stoffe in Boden," in *Bodenschutz. Ergänzbares Handbuch der Maßnahmen und Empfehlungen für Schutz, Pflege und Sanierung von Böden, Landschaft und Grundwasser-1, Band, 14 Lfg X/93*, eds D. Rosenkranz, G. Bachmann, G. Einsele, H. M. Harress (Berlin: Erich Schmidt).

Fasihuddin, B. A., and Din, L. B. (2002). *Medicinal Plants Used by Various Ethnic Groups in sabah.* Paper Presented at the French Malaysian-Symposium on Natural Products. Dept. of Chemistry, University of Malaya, Kuala Lumpur, p. 85

Flexas, J., and Medrano, H. (2002). Drought-inhibition of photosynthesis in C3 plants: stomatal and non-stomatal limitations revisited. *Anal. Bot.* 89, 183–189. doi: 10.1093/aob/mcf027

Fraser, L. H., Carlyle, C., Turkington, R., and Friedman, C. R. (2009). Adaptive phenotypic plasticity of Pseudoroegneria spicata: response of stomatal density, leaf area and biomass to changes in water supply and increased temperature. *Ann Bot.* 103, 769–775. doi: 10.1093/aob/mcn252

Fu, Q. S., Yang, R. C., Wang, H. S., Zhao, B., Zhou, C. L., Ren, S. X., et al. (2013). Leaf morphological and ultrastructural performance of eggplant (*Solanum melongena* L.) in response to water stress. *Photosynthetica* 51, 109–114. doi: 10.1007/s11099-013-0005-6

Gattward, J. N., Almeide, A. A. F., Souza, J. O., Gomes, F. P., and Kronzucker, H. J. (2012). Sodium-potassium synergism in *Theobroma cacao*: stimulation of photosynthesis, water-use efficiency and mineral nutrition. *Physiol. Plant.* 146, 350–362. doi: 10.1111/j.1399-3054.2012.01621.x

Grison-Pigé, L., Hossaert-McKey, M., and Bessiere, J. M. (2002). Fig volatile compounds—a first comparative study. *Phytochemistry* 61, 61–71. doi: 10.1016/S0031-9422(02)00213-3

Hamann, T. (2012). Plant cell wall integrity maintenance as an essential component of biotic stress response mechanisms. *Front. Plant Sci.* 3, 77. doi: 10.3389/fpls.2012.00077

Hasham, R., Choi, H. K., Sarmidi, M. R., and Park, C. S. (2013). Protective effects of a *Ficus deltoidea* extract against UVB-induced photo ageing in skin cells. *Biotechnol. Bioprocess Eng.* 18, 185–193. doi: 10.1007/s12257-012-0353-2

Hell, R., and Stephan, U. W. (2003). Iron uptake, trafficking and homeostasis in plants. *Planta*. 216, 541–551. doi: 10.1007/s00425-002-0920-4

Hessini, K., Ghandour, M., Albouchi, A., Soltani, A., Werner, K. H., and Abdelly, C. (2008). Biomass production, photosynthesis, and leaf water relations of Spartina alterniflora under moderate water stress. *J. Plant Res.* 121, 311–318. doi: 10.1007/s10265-008-0151-2

Hu, X. Y., Fang, J. Y., Cai, W. M., and Tang, Z. C. (2004). Oxygen burst and saponin synthesis of Panax ginseng cells induced by chitosan mediated by mitogen-activated protein kinase. *Sci. China Series C Life Sci.* 34, 3l—40. doi: 10.1360/03yc0074

Hu, X. Y., Zhang, W. Q., Fang, J. Y., Cai, W. M., and Tang, Z. C. (2002). Chitosan treatment raises the accumulation of saponin and the transcriptional level of genes encoding the key enzymes of saponin synthesis in cultured Panax ginseng cells. *J. Plant Physiol. Mol. Biol*. 28, 485–490. Available online at: https://europepmc.org/article/cba/539300 (accessed September 20, 2022).

Ishibashi, Y., Yamaguchi, H., Yuasa, T., Iwaya-Inoue, M., Arima, S., and Zheng, S. H. (2011). Hydrogen peroxide spraying alleviate drought stress in soybean plants. *J. Plant Physiol.* 168, 1562–1567. doi: 10.1016/j.jplph.2011.02.003

Ismail, S. Z., Khandaker, M. M., Mat, N., and Boyce, A. N. (2015). Effects of hydrogen peroxide on growth, development and quality of fruits: a review. *J. Agronomy* 14, 331–336. doi: 10.3923/ja.2015.331.336

Jamaludin, R., Mat, N., Mohd, K. S., Badaluddin, N. A., Mahmud, K., Sajili, M. H., et al. (2020). Influence of exogenous hydrogen peroxide on plant physiology, leaf anatomy and rubisco gene expression of the *Ficus deltoidea* Jack var. Deltoidea. *Agronomy* 10, 497. doi: 10.3390/agronomy10040497

John, R. E. (1989). Photosynthesis and nitrogen relationships in leaves of C3 plants. *Aecologia* 78, 9–19. doi: 10.1007/BF00377192

Jones, H. G., and Sutherland, R. A. (1991). Stomatal control of xylem embolism. *Plant Cell. Environ.* 14, 607–612. doi: 10.1111/j.1365-3040.1991.tb01532.x

Kabata, P. A., and Pendias, H. (2001). *Trace elements in Soils and Plants. 3rd edn*. Boca Raton, FL: CRC Press.

Kar, R. K. (2011). Plant responses to water stress: role of reactive oxygen species. *Plant Signal. Behav.* 6, 1741–1745. doi: 10.4161/psb.6.11.17729

Kazerouni, N., Sinha, R., Che-Han, H., Greenberg, A., and Rothman, N. (2001). Analysis of 200 items for benzo[a]pyrene and estimation of its intake in an epidemiologic study. *Food Chem. Toxicol.* 39, 423–436. doi: 10.1016/S0278-6915(00)00158-7

Khan, A., Anwar, Y., Hasan, M. M., Iqbal, A., Ali, M., Alharby, H. F., et al. (2017). Attenuation of Drought Stress in Brassica Seedlings with Exogenous Application of Ca_{2+} and H_2O_2. *Plants* 6, 20. doi: 10.3390/plants6020020

Khandaker, M. M., Boyce, A. N., and Osman, N. (2012). The influence of hydrogen peroxide on the growth, development and quality of wax apple (*Syzygium samarangense*, [Blume] Merrill & L. M. Perry var. jambu madu) fruits. *Plant Physiol. Biochem.* 53, 101–110. doi: 10.1016/j.plaphy.2012.01.016

Kim, Y. S., Cho, J. H., Ahn, J., and Hwang, B. (2006). Upregulation of isoprenoid pathway genes during enhanced saikosaponin biosynthesis in the hairy roots of *Bupleurum falcatum*. Mol. *Cells* 22, 269–274.

Kumawat, K. R., and Sharma, N. K. (2018). Effect of drought stress on plants growth. *Popular Kheti* 6, 239–241.

Lane, H. C., Thompson, A. C., Hesketh, J. D., and Sloane, C. (1975). "Some observations on nitrate reduction in cotton. III," in *Proc. Beltwide Cotton Production Res. Conf.* ed J. Brown (Memphis, TN: National Cotton Council)

Lawlor, D. W. (1995). "The effects of water deficit on photosynthesis," in *Environment and Plant Metabolism. Flexibility and Acclimation*, ed N. Smirnoff (Oxford: BIOS Scientific Publishers).

Lee, S. W., Wee, W., Yong, J. F. S., and Syamsumir, D. F. (2011). Characterization of antioxidant, antimicrobial, anticancer property and chemical of *Ficus deltoidea* Jack leaf extract. *J. Biol. Active Products Nat.* 1, 1–6. doi: 10.1080/22311866.2011.10719067

Li, Z., Wakao, S., Fischer, B. B., and Niyogi, K. K. (2009). Sensing and responding to excess light. *Ann. Rev. Plant Biol.* 60, 239–260. doi: 10.1146/annurev.arplant.58.032806.103844

Liao, W. B., Huang, G. B., Yu, J. H., and Zhang, M. L. (2012). Nitric oxide and hydrogen peroxide alleviate drought stress in marigold explants and promote its adventitious root development. *Plant Physiol. Biochem.* 58, 6–15. doi: 10.1016/j.plaphy.2012.06.012

Liu, G., and Porterfield, D. M. (2014). Oxygen enrichment with magnesium peroxide for minimizing hypoxic stress of flooded corn. *J. Plant Nutr. Soil Sci.* 177, 733–740. doi: 10.1002/jpln.201300424

Liu, J., Macarisin, D., Wisniewski, M., Sui, Y., By, S., and Norelli, J., et al. (2013). Production of hydrogen peroxide and expression of ros-generating genes in peach flower petals in response to host and non-host fungal pathogens. *Plant Pathol.* 62, 820–828. doi: 10.1111/j.1365-3059.2012.02683.x

Liu, T., Ohashi-Ito, K., and Bergmann, D. C. (2009). Orthologs of *Arabidopsis thaliana* stomatal bHLH genes and regulation of stomatal development in grasses. *Development* 136, 2265–2276. doi: 10.1242/dev.032938

Liu, Y., Ye, N., Liu, R., Chen, M., and Zhang, J. (2010). H_2O_2 mediates the regulation of ABA catabolism and GA biosynthesis in Arabidopsis seed dormancy and germination. *J. Exp. Bot.* 61, 2979–2990. doi: 10.1093/jxb/erq125

Marschner, H. (2002). *Mineral Nutrition in Higher Plants.* London: Academic Press.

Mascher, R., Lippmann, B., Holzinger, S., and Bergmann, H. (2002). Arsenate toxicity: effects on oxidative stress response molecules and enzymes in red clover plants. *Plant Sci*. 163, 961–969. doi: 10.1016/S0168-9452(02)00245-5

Misbah, H., Abdul Aziz, A., and Aminudin, N. (2013). Antidiabetic and antioxidant properties of *F. deltoidea* fruit extracts and fractions. *BMC Complement. Altern. Med*. 13, 118. doi: 10.1186/1472-6882-13-118

Moran, J. F., Manuel, B., Iñaki, I. O., Silvia, F., Robert, V. K., and Pedro, A. T. (1994). Drought induces oxidative stress in pea plants. *Planta* 194, 346–352. doi: 10.1007/BF00197534

Musa, Y. (2005). Variability in morphology and agronomy of mas cotek accessions found in Kelantan and Terengganu. *Bul. Teknol. Tanam*. 2, 35–48. Available online at: http://hari-inovasi.mardi.gov.my/2020/docu/Pemenang/New%20MSTE%20Extended%20Abstract%20.pdf (accessed September 20, 2022).

Nashriyah, M., Zaini, H., Mazleha, M., and Abdul, K. W. (2006). Mineral uptake by taro (*Colocasia esculenta*) in swamp agroecosystem following gramoxone® (paraquat) herbicide spraying. *J. Nuclear Related Technol*. 3, 59–68. Available online at: https://www.researchgate.net/publication/235951060_MINERAL_UPTAKE_BY_TARO_COLOCASIA_ESCULENTA_IN_SWAMP_AGROECOSYSTEM_FOLLOWING_GRAMOXONE_R_PARAQUAT_HERBICIDE_SPRAYING (accessed September 20, 2022).

Nasir, N. N. N. M., Khandaker, M. M., Mohd, K. S., Badaluddin, N. A., Osman, N., and Mat, N. (2021). Effect of hydrogen peroxide on plant growth, photosynthesis, leaf histology and rubisco gene expression of the *Ficus deltoidea* Jack Var. deltoidea Jack. *J. Plant Growth Regul*. 40, 1950–1971. doi: 10.1007/s00344-020-10243-9

Nazarni, C. I. M., Ajit, A., Naila, A., and Sulaiman, A. Z. (2018). Effect of microwave assisted hydro-distillation extraction on extracts of Ficus deltoidea. *Mater. Today Proc*. 2018, 5, 21772–21779. doi: 10.1016/j.matpr.2018.07.031

Neill, S., Desikan, R., and Hancock, J. (2002). Hydrogen peroxide signalling. *Curr. Opin. Plant Biol*. 5, 388–395. doi: 10.1016/S1369-5266(02)00282-0

Nihayah, M., Yong, K. W., and Faizah, A. B. (2012). Determination of mineral content in the *Ficus deltoidea* leaves. *J. Sci. Health Malaysia*. 10, 25–29. Available online at: http://journalarticle.ukm.my/6365/1/25-29.pdf (accessed September 20, 2022).

Nurdiana, S., Goh, Y. M., Hafandi, A., Dom, S. M., Nur Syimal'ain, A., Noor Syaffinaz, N. M., et al. (2018). Improvement of spatial learning and memory, cortical gyrification patterns and brain oxidative stress markers in diabetic rats treated with Ficus deltoidea leaf extract and vitexin. *J. Trad. Complement. Med*. 8, 190–202. doi: 10.1016/j.jtcme.2017.05.006

Nyathi, Y., and Baker, A. (2006). Plant peroxisomes as a source of signaling molecules. *Biochim. Biophys. Acta* 1763,1478–1495. doi: 10.1016/j.bbamcr.2006.08.031

Ohta, D., Yasuoka, S., Matoh, T., and Takahashi, E. (1989). Sodium stimulates growth of *Amaranthus tricolor* L. plants through enhanced nitrate assimilation. *Plant Physiol*. 89, 1102–1105. doi: 10.1104/pp.89.4.1102

Orabi, S. A., Dawood, M. G., and Salman, S. R. (2015). Comparative study between the physiological role of hydrogen peroxide and salicylic acid in alleviating the harmful effect of low temperature on tomato plants grown under sand-ponic culture. *Sci. Agric*. 9, 49–59. doi: 10.15192/PSCP.SA.2015.1.9.4959

Ozaki, K., Uchida, A., Takabe, T., Shinagawa, F., Tanaka, Y., Takabe, T., et al. (2009). Enrichment of sugar content in melon fruits by hydrogen peroxide treatment. *Plant Physiol*. 166, 569–578. doi: 10.1016/j.jplph.2008.08.007

Pan, X., Zhang, D., Chen, X., Bao, A., and Li, L. (2010). Antimony accumulation, growth performance, antioxidant defense system and photosynthesis of zea mays in response to antimony pollution in soil. *Water, Air Soil Poll*. 215, 517–523. doi: 10.1007/s11270-010-0496-8

Parry, M. A. J., Andralojc, P. J., Scales, J. C., Salvucci, M. E., Carmo-Silva, A. E., Alonso, H., et al. (2013). Rubisco activity and regulation as targets for crop improvement. *J. Exp. Bot*. 64, 717–730. doi: 10.1093/jxb/ers336

Pavela, R., Maggic, F., Giordanid, C., Cappellaccic, L., Petrellic, R., Canalee, A., et al. (2021). Insecticidal activity of two essential oils used in perfumery (ylang and frankincense). *Nat. Prod. Res*. 108, 137–147. doi: 10.1080/14786419.2020.1715403

Pei, Z. M., Murata, Y., Benning, G., Thomine, S., Klusener, B., Allen, G. J., et al. (2000). Calcium channels activated by hydrogen peroxide mediate abscisic acid signalling in guard cells. *Nature* 406, 731–734. doi.10.1038/35021067doi: 10.1038/35021067

Perreca, E., Rohwer, J., González-Cabanelas, D., Loreto, F., Schmidt, A., Gershenzon, J., et al. (2020). Effect of drought on the methylerythritol 4-phosphate (MEP) pathway in the isoprene emitting conifer Picea glauca. *Front. Plant Sci*. 11, 546295. doi: 10.3389/fpls.2020.546295

Puig, S., Andres-Colas, N., Garcia-Molina, A., and Pefiarrubia, L. (2007). Copper and iron homeostasis in Arabidopsis: responses to metal defincies, interactions and biotechnological applications. *Plant Cell Environ. 30, 27–290*. doi: 10.1111/j.1365-3040.2007.01642.x

Ralmi, N. H. A. A., Khandaker, M. M., Mohd, K. S., Majrashi, A., Fallatah, A. M., Badaluddin, N. A., et al. (2021). Influence of rhizopheric H_2O_2 on growth, mineral absorption, root anatomy and nematode infection of *Ficus deltoidea*. *Agronomy* 11, 704. doi: 10.3390/agronomy11040704

Ravet, K., Touraine, B., Boucherez, J., Briat, J. F., Gaymard, F., and Cellier, F. (2009). Ferritins control interaction between iron homeostasis and oxidative stress in Arabidopsis. *Plant J*. 57, 400–412. doi: 10.1111/j.1365-313X.2008.03698.x

Razmjoo, K., Heydarizadeh, P., and Sabzalian, M. R. (2008). Effect of salinity and drought stresses on growth parameters and essential oil content of *Matricaria chamomila*. *Int. J. Agric. Biol*. 10, 451–454. doi: 10.63/ASB/2008/10-4-451-454

Redondo-Gómez, S., Mateos-Naranjo, E., Figueroa, M. E., and Davy, A. J. (2010). Salt stimulation of growth and photosynthesis in an extreme halophyte, *Arthrocnemum macrostachyum*. *Plant Biol*. 12, 79–87. doi: 10.1111/j.1438-8677.2009.00207.x

Risk Assessment Studies (RAS) (2004). *Polycyclic Aromatic Hydrocarbons in Barbecued Meat. Report No., 14*. Food and Environmental Hygiene Department, the Government of the Hong Kong Special Administrative Region.

Rohini, G. H. G., Hariprasad, P., Brijesh, S. S., and Niranjana, S. R. (2016). Biological control of Phomopsis leaf blight of brinjal (*Solanum melongena* L.) with combining phylloplane and rhizosphere colonizing beneficial bacteria. *Biol. Cont*. 101, 123–129. doi: 10.1016/j.biocontrol.2016.05.007

Rose, S., and Swift, C. E. (2014). *Leaf Scorch—Colorado State University Extension*. Available online at: https://extension.colostate.edu/docs/pubs/garden/02911.pdf (accessed May 24, 2022).

Sairam, R. K., and Srivastava, G. C. (2000). Induction of oxidative stress and antioxidant activity by hydrogen peroxide treatment in tolerant and susceptible wheat genotypes. *Biol. Plant*. 43, 381–386. doi: 10.1023/A:1026730008917

Santos, C. V. (2004). Regulation of chlorophyll biosynthesis and degradation by salt stressed in sunflower leaves. *Sci. Hort*. 103, 93–99. doi: 10.1016/j.scienta.2004.04.009

Sharma, A., Kumar, V., Shahzad, B., Ramakrishnan, M., Sidhu, G. P. S., Bali, A. S., et al. (2020). Photosynthetic response of plants under different abiotic stresses: a review. *J. Plant Growth Regul*. 39, 509–531. doi: 10.1007/s00344-019-10018-x

Shi, K., Li, X., Zhang, H., Zhang, G., Liu, Y., Zhou, Y., et al. (2015). Guard cell hydrogen peroxide and nitric oxide mediate elevated CO_2-induced stomatal movement in tomato. *New Phytol*. 208, 342–353. doi: 10.1111/nph.13621

Shri, M., Kumar, S., Prabodh, D. C., Trivedi, K., Mallick, S., Misra, P., et al. (2009). Effect of arsenic on growth, oxidative stress, and antioxidant system in rice seedlings. *Ecotoxicol. Environ. Safety* 72, 1102–1110. doi: 10.1016/j.ecoenv.2008.09.022

Singleton, V., and Rossi, J. A. J. (1965). Colorimetry of total phenolic with phosphomolybdic—phosphotungstic acid reagents. *Am. J. Enol. Viticult*. 16, 144–158.

Smith, G. S., Middleton, K. R., and Edmonds, A. S. (1980). Sodium nutrition of pasture plants. II. Effects of sodium chloride on growth, chemical composition and reduction of nitrate nitrogen. *New Phytol*. 84, 613–622. doi: 10.1111/j.1469-8137.1980.tb04775.x

Sofo, A., Tuzio, A. C., Dichio, B., and Xiloyannis, C. (2005). Influence of water deficit and rewatering on the components of the ascorbate-glutathione cycle in four interspecific *Prumus hybrids*. *Plant Sci*. 169, 403–412. doi: 10.1016/j.plantsci.2005.04.004

Starr, F., Starr, K., and Loope, L. (2003). *Ficus deltoidea*. Maui, HI: United States Geological Survey-Biological Resources Division, Haleakala Field Station.

Steffens, B., Steffen-Heins, A., and Sauter, M. (2013). Reactive oxygen species mediate growth and death in submerged plants. *Front. Plant Sci*. 4, 1–7. doi: 10.3389/fpls.2013.00179

Sun, S. J., Li, J. M., Zong, W. J., Yao, Y. Z., and Chen, K. L. (2012). Effects of sub-low temperature and drought stress on root morphology and leaf structure of tomato seedlings. *Ying Yong Sheng Tai Xue Bao*. 23, 3027–3032.

Tränkner, M., Jákli, B., Tavakol, E., Geilfus, C. M., Cakmak, I., Dittert, K., et al. (2016). Magnesium deficiency decreases biomass water-use efficiency and increases leaf water-use efficiency and oxidative stress in barley plants. *Plant Soil* 406, 409–423. doi: 10.1007/s11104-016-2886-1

Uchida, A., Jagendorf, A. T., Hibino, T., Takabe, T., and Takabe, T. (2002). Effects of hydrogen peroxide and nitric oxide on both salt and heat stress tolerance in rice. *Plant Sci*. 163, 515–523. doi: 10.1016/S0168-9452(02)00159-0

Wang, B., Chen, J., Chen, L., Wang, X., Wang, R., Ma, L., et al. (2015). Combined drought and heat stress in *Camellia oleifera* cultivars: leaf characteristics, soluble

sugar and protein contents, and Rubisco gene expression. *Trees* 29,1483–1492. doi: 10.1007/s,00468-015-1229-9

Wang, Y., Dai, C. C., Zhao, Y. W., and Peng, Y. (2011). Fungal endophyte-induced volatile oil accumulation in Atractylodes lancea plantlets is mediated by nitric oxide, salicylic acid and hydrogen peroxide. *Process Biochem*. 46, 730–735. doi: 10.1016/j.procbio.2010.11.020

WHO Regional Office for Europe (2000). *Air Quality Guidelines, 2nd Edn*. Denmark: WHO.

Zhang, F., Wan, X., and Zhong, Y. (2013). Nitrogen as an important detoxification factor to cadmium stress in poplar plants. *J. Plant Interact*. 9, 249–258. doi: 10.1080/17429145.2013.819944

Zhang, X., Lin, Z., Facai, D., Junfeng, G., David, W. G., and Chun-Peng, S. (2001). Hydrogen peroxide is involved in abscisic acid-induced stomatal closure in *Vicia faba*. *Plant Physiol*. 126, 1438–1448. doi: 10.1104/pp.126.4.1438

Zhao, C. L., Cuib, X. M., Chena, Y. P., and Lianga, Q. (2010). Key enzymes of triterpenoid saponin biosynthesis and the induction of their activities and gene expressions in plants. *Nat. Prod. Com*. 5, 1147–58. doi: 10.1177/1934578X1000500736

frontiers | Frontiers in Plant Science

TYPE Original Research
PUBLISHED 21 October 2022
DOI 10.3389/fpls.2022.1023723

Check for updates

OPEN ACCESS

EDITED BY
Mohammad Anwar Hossain,
Bangladesh Agricultural University,
Bangladesh

REVIEWED BY
Syed Shabbar Hussain Shah,
Nagasaki University, Japan
Muhammad Qaswar,
University of Ghent, Belgium

*CORRESPONDENCE
Tu Jumin
jtu@zju.edu.cn
Seung Hwan Yang
ymichigan@jnu.ac.kr

SPECIALTY SECTION
This article was submitted to Plant Breeding, a section of the journal Frontiers in Plant Science

RECEIVED 20 August 2022
ACCEPTED 22 September 2022
PUBLISHED 21 October 2022

CITATION
Shah G, Fiaz S, Attia KA, Khan N, Jamil M, Abbas A, Yang SH and Jumin T (2022) Indole pyruvate decarboxylase gene regulates the auxin synthesis pathway in rice by interacting with the indole-3-acetic acid–amido synthetase gene, promoting root hair development under cadmium stress. *Front. Plant Sci.* 13:1023723. doi: 10.3389/fpls.2022.1023723

COPYRIGHT
© 2022 Shah, Fiaz, Attia, Khan, Jamil, Abbas, Yang and Jumin. This is an open-access article distributed under the terms of the Creative Commons Attribution License (CC BY). The use, distribution or reproduction in other forums is permitted, provided the original author(s) and the copyright owner(s) are credited and that the original publication in this journal is cited, in accordance with accepted academic practice. No use, distribution or reproduction is permitted which does not comply with these terms.

Indole pyruvate decarboxylase gene regulates the auxin synthesis pathway in rice by interacting with the indole-3-acetic acid–amido synthetase gene, promoting root hair development under cadmium stress

Gulmeena Shah[1], Sajid Fiaz[2], Kotb A. Attia[3], Naeem Khan[4], Muhammad Jamil[5], Adeel Abbas[6], Seung Hwan Yang[7]* and Tu Jumin[1]*

[1]Institute of Crop Science, College of Agriculture and Biotechnology, Zhejiang University, Hangzhou, China, [2]Department of Plant Breeding and Genetics, The University of Haripur, Haripur, Pakistan, [3]Department of Biochemistry, College of Science, King Saud University, Riyadh, Saudi Arabia, [4]Department of Agronomy, Institute of Food and Agricultural Sciences, Florida University, Gainesville, FL, United States, [5]Department of Biotechnology and Genetic Engineering, Kohat University of Science and Technology, Kohat, Pakistan, [6]Institute of Environment and Ecology, School of Environment and Safety Engineering, Jiangsu University, Zhenjiang, China, [7]Department of Biotechnology, Chonnam National University, Yeosu, South Korea

This research focused on cadmium (Cd), which negatively affects plant growth and auxin hemostasis. In plants, many processes are indirectly controlled through the expression of certain genes due to the secretion of bacterial auxin, as indole-3-acetic acid (IAA) acts as a reciprocal signaling molecule in plant–microbe interaction. The aim of current studies was to investigate responsible genes in rice for plant–microbe interaction and lateral root development due to the involvement of several metabolic pathways. Studies revealed that *GH3-2* interacts with endogenous IAA in a homeostasis manner without directly providing IAA. In rice, indole-3-pyruvate decarboxylase (*IPDC*) transgenic lines showed a 40% increase in lateral roots. Auxin levels and YUCCA (auxin biosynthesis gene) expression were monitored in *osaux1* mutant lines inoculated with *Bacillus cereus* exposed to Cd. The results showed an increase in root hairs (RHs) and lateral root density, changes in auxin levels, and expression of the YUCCA gene. *B. cereus* normalizes the oxidative stress caused by Cd due to the accumulation of O_2^- and H_2O_2 in *osaux1* mutant lines. Furthermore, the inoculation *of B. cereus* increases DR5:GUS expression,

indicating that bacterial species have a positive role in auxin regulation. Thus, the current study suggests that *B. cereus* and *IPDC* transgenic lines increase the RH development in rice by interacting with IAA synthetase genes in the host plant, alleviating Cd toxicity and enhancing plant defense mechanisms.

KEYWORDS

plant-microbe interaction, IpdC gene, auxin signaling pathway, cadmium toxicity, root hair development

Introduction

Plant-promoting rhizobacteria (PGPR) are the microbes that act as an efficient source of nutrition and are present in the plants' close vicinity, especially in the rhizosphere (Esitken et al., 2010; Malusá et al., 2012). Some of these microbes significantly influence root morphogenesis and architecture (Yu et al., 2016; Grover et al., 2021). *Azospirillum brasilense*, as a PGPR, triggers the proliferation of lateral roots rather than stimulation of lateral root growth under unfavorable conditions (Grover et al., 2021). Cadmium (Cd) alters many essential processes (photosynthetic activity, carbon fixation, transpiration, destruction of biomolecules and organelles) in the plant; averted growth and chlorosis are generic symptoms caused by Cd. Furthermore, Cd interferes with the transport and uptake of P, Ca, Mn, Mg, Zn, K, and Fe in the root, resulting in leaf chlorosis and inhibiting plant growth (Xu et al., 2017; Haider et al., 2021). In rice, overaccumulation of Cd in vacuoles moderately limits the translocation to roots and shoots (Tezuka et al., 2010; Miyadate et al., 2011). Based on our previous study on the pleiotropic effect of rhizospheric bacteria plant response to different bacterial classes, *Bacillus cereus* pathogenic bacteria as a model microbe of Cd toxicity alleviator were used to study the phenomena of lateral root development (Jan et al., 2019). The microbial community responsible for nitrogen fixation and production of phytohormones was found as a key factor for plant growth development by PGPR and for the development of proficient root architecture for enhanced nutrient and water uptake (Mia and Shamsuddin, 2010; Egorshina et al., 2012; Meldau et al., 2012; Rajendran et al., 2012; Yu et al., 2016).

Auxin moves within the plant through polar and nonpolar auxin transport (Kramer and Bennett, 2006) and includes influx transporters of the AUXIN1/LIKE AUX1 (AUX1/LAX) family (Swarup et al., 2008); AUX1 mediates the transport of IAA and influences lateral root development (Marchant et al., 2002). Several rhizospheric bacteria such as pathogenic bacteria, PGPR, *Bacillus* sp., *Enterobacter* sp., *Azospirillum* sp., *Rhizobium* sp., and *Pseudomonas* sp. (El-Hadi et al., 2009; Khan and Doty, 2009; Merzaeva and Shirokikh, 2010; Roy et al., 2010; Celloto et al., 2012; Xu et al., 2018) can produce IAA. In microorganisms, the majority of the phytohormone-producing bacteria have been found to produce IAA. Auxin production in microorganisms is not only limited to pathogenic PGPRs but also includes plant growth-promoting fungi and endophytic bacteria that produce IAA (García Sánchez, 2018; Vázquez-Chimalhua et al., 2021). A few species of rhizospheric bacteria are known to produce IAA and act as signaling molecules for communication between bacteria to coordinate their activities (Xu et al., 2018). Many plant processes are indirectly controlled through the expression of certain genes due to the secretion of bacterial auxin (Olatunji et al., 2017; Hsu et al., 2021). The biosynthesis of bacterial IAA helps to promote plant growth *via* the indole-3-pyruvate decarboxylase enzyme, encoded by the indole-3-pyruvate decarboxylase (IpdC) gene, catalyzes the conversion of indole-3-pyruvate (IPyA) to indole-3-acetaldehyde (IAAId) (Sgroy et al., 2009). The indole acetamide pathway is a key route for the production of IAA in phytopathogenic strains. Indole-3-acetamide synthesis from tryptophan is catalyzed by tryptophan-2-monooxygenase. In PGPR, IAA biosynthesis proceeds through intermediate indole-pyruvic acid (Won et al., 2011), while in tryptophan-dependent pathway, a precursor gene ipdC to IAAId is followed by IAA formation (Wang and Fu, 2011; Duca and Glick, 2020). The roots exudate tryptophan, which acts as a precursor for auxin production and influences IAA synthesis in the majority of IAA-producing PGPR (Merzaeva and Shirokikh, 2010).

Cd modifies auxin homeostasis by negatively regulating specific auxin-related genes, resulting in altered cell differentiation and inhibiting root growth (Ronzan et al., 2018). In plants, the phenomena of IAA production in roots and interaction with IAA-producing PGPRs are not clear at the molecular level due to the existence of different metabolic pathways and genes involved in the synthesis of IAA in plants and PGPRs, evoking the question of which genes are responsible and how they interact with each other for the development of IAA and enhancing lateral root development. The current work

Abbreviations: IpdC, indole-3-pyruvate decarboxylase; *GH3-2*, indole-3-acetic acid–amido synthetase gene; IPyA, indole-3-pyruvic acid; IAA, indole-3-acetic acid, Cd, cadmium.

was designed to find the responsible genes in rice root and *B. cereus* and the interaction between them that influences the plant and lateral root development.

Material and method

Bacterial growth conditions

The *Bacillus cereus* strain was first cultured on nutrient agar medium by the spread plate method containing 1% tryptophan, 2% yeast extract, 1% NaCl, and 1.5% agar A (w/v) for 24 h at 28° C. For inoculum preparation, a single colony was picked and cultivated in a liquid medium. Bacteria were grown aerobically for 24 h on a rotary shaker (120 rpm) at 28°C to attain the bacterial exponential phase. At 3,000 rpm, centrifugation was done for 8 min at 25°C for pelleting bacterial cells, washed thrice, and further resuspended in a sterile liquid medium as reported in previous studies by Jan et al. (2019).

Construction and transformation of IPDC gene

For the 35S:IPDC transgenes, the ORF of the indole-3-pyruvate *decarboxylase* gene from the *Bacillus cereus* strain ((*ATCC*-14579) NC_004722.1) was cloned along with the 35S promoter into pCAMBIA1300 using the primers listed (Supplementary Table S1). Agrobacterium strain EHA105 was used to introduce 35S:IPDC and was transformed into the Japonica cultivar Dongjin, as previously reported by Hiei et al. (1994).

OsAUX1 mutant's identification

The identification of three independent T-DNA integration sites of auxin mutants (*osaux1*, *osaux1*-2, and *osaux1*-3) was analyzed by comparison with the SIGnAL database at http://signal.salk.edu/cgi-bin/RiceGE database as described by Yu et al. (2015). OsAUX1-specific T-DNA border primers were designed and used to confirm the insertion.

Plant growth conditions

WT/Dongjin, *osaux1-1*, *osaux1-2*, *osaux1-3* mutant, and *IPDC* transgenic lines were germinated in $MS^{1/2}$ medium at pH 5.8–6.2, as previously described by Wang et al. (2014). The Cd treatment was performed by using 200 μM of Cd for 4 to 7 days; the duration of Cd treatments is indicated in the legends of figures for each experiment.

RNA extraction and quantitative RT-PCR

Total RNA was extracted from roots using the Trizol plant RNA extracting method as described by Wang et al. (2010a). To analyze of the Aux1 expression of *osaux1* mutant, reverse transcriptase PCR (RT-PCR) was performed using the Takara kit (http://www.takara-bio.com) as per manufacturer's instructions previously described by Wang et al. (2014). The primers used in this study are listed in Supplementary Table S1.

Subcellular localization of OsAux1

35S:IPDC:sGFP and 35S:*OsGH3* fusion construct was transiently expressed by agrobacterium-mediated transformation in rice protoplast, as previously described by Yoo et al. (2007). Confocal microscopy (Olympus fluoview fv300) was used to acquire images.

GUS staining and analysis of GUS activity

For GUS, staining wild-type and *osaux1* mutant seedlings transformed with *DR5:GUS* were primed with *B. cereus*, and GUS was performed as described by Ulmasov et al. (1997). After staining, roots were socked with 70% ethanol to remove the extra dye. Jefferson et al. (1987) method was used for the quantification of Gus activity by scrutinizing cleavage of 4-methylumbelliferyl-β-D-glucuronide (https://www.sangon.com). Canon EOS 800D was used to acquire GUS images.

Analysis of auxin and tryptophan

For analysis of IAA concentration, 15 to 20 mg FW of 5-day-old seedling of wild-type and *osaux1* mutant inoculated with or without *B. cereus* was washed with deionized water three to five times and ground into a fine powder using liquid nitrogen. The extraction of free IAA was performed as described by Wang et al. (2014), while gas chromatography was performed for purification and quantification as described by Ljung et al. (2005). Salkowski reagent was used for the analysis of IAA content by bacterial strain, and *ipdc* mutant was performed as described by Sarwar et al. (1992). For measurement of tryptophan content, the free amino acid was extracted from 5-day-old seedlings of wild-type and *osaux1* mutant inoculated with or without *B. cereus* as described by Muller and Touraine

(1992). Roots were kept in 80% ethanol for 12 h at 4°C, 1 h in 60% ethanol, and 24 h in deionized water at 4°C. The supernatant was fractioned and kept at −20°C, and tryptophan content was determined by using HPLC (Shimadzu, LC-20A series Japan).

Cd localization and quantification

To visualize the distribution of Cd (200 μM) in the root zone of wild-type and *osaux1-3* mutant with or without *B. cereus* inoculation from 7-day-old seedlings was determined by using the method mentioned by Jan et al. (2019). Roots were first washed with deionized water and then with 0.01 μM of EDTA solution, dried at 80°C until the material reached constant weight. In total, 100 mg of root sample was digested with sulfuric acid and nitric acid mixture. Digested samples were diluted with 20 ml of deionized distilled water and filtered using Whatman filter paper. Cd content was measured using a Synergy H1 atomic absorption spectroscope. For Cd analysis in bacterial culture, *B. cereus* was grown in an LB medium. After 18 h, *B. cereus* was treated with 400 μl of $Cdcl_2$ and grown for a further 4 h. The image was micro-graphed using the Nikon Eclipse DS-Ri2 microscope.

Quantification of H_2O_2 content and cell death detection by Evans blue, Hoechst 33342

In roots, H_2O_2 levels were measured using the methodology described by Jana and Choudhuri (1982). The roots were homogenized in 6 ml of 50 mmol/l PBS (pH 6.5). The absorbance was read at 410 nm with a Synergy H1 atomic absorption spectroscope. The primary roots of 7-day-old seedlings treated with 200μM $CdCl_2$ were excised from 20 seedlings of each wild-type and *osaux1* mutant with or without *B. cereus* inoculation and stained in 0.025% (w/v) Evans blue solution for 20 min at 25°C and washed with ddH_2O to eradicate excess dye. Root tips were immersed in 1% SDS and 50% methanol for 1 h at 50°C. The absorbance was measured at 600 nm with a microtiter plate using the protocol of Baker and Mock (1994). To see the cell wall integrity between wild-type and mutant line, roots were stained with propidium iodide for 20 min and then washed three to five times with 0.85% NaCl and micrographed using confocal microscopy. To study the nucleus in interphase cells, roots were washed three times with PBS solution (pH 7.4) and immersed in Hoechst labeling solution (http://cshprotocols.cshlp.org/) 1:100 solution for 30min at 25°C. The labeling solution was aspirated from the roots, washed three times with PBS, and micrographed at 483 nm with a Nikon Eclipse DS Ri2 microscope.

Results

Characterization of AUX1 and loss of function lines

The Salk database (http://signal.salk.edu/cgi-bin/RiceGE) led to the identification of three T-DNA integration sites for auxin mutant (*osaux1*-1, *osaux1*-2, and *osaux1*-3) in the Dongjin (DJ) background. A homozygous loss of function mutant was identified by PCR using DNA and RNA levels (Figure 1A). The RT-PCR analysis regarding auxin mutants analogous to the insertion sites did not detect any transcript of the *osaux1-3* mutant (Figure 1B). To study the role of *B. cereus* on root architecture of lateral root development, 5-day-old germinated wild-type and *osaux1* mutants inoculated with and without bacterial strain were transferred to fresh agar medium for an additional 4 days in the presence of Cd at 200 μM (Figures 1C–E). Under noninoculated conditions, auxin mutants exhibit lowered primary root length and root count as compared to wild-type seedlings, which are dramatically reduced in Cd-treated seedlings (Figure 1F). The inoculation with *B. cereus* amended the number of lateral roots in wild-type and mutant plants, and the density of lateral roots (LR) became higher in both auxin mutant and wild-type under Cd exposure (Figure 1C), confirming that *B. cereus* had a positive role in indusial growth rate.

OsAux1 expression in the PRs, LRs, and RHs of rice

To understand the molecular mechanism of plant–microbe interaction, transgenic lines of IPDC and *osaux1-1* mutant were visualized phenotypically or morphologically. The expression pattern of free IAA in the *ipdc* mutant line shows a strong reduction in IAA content (Figure 2A) in comparison to the control (*B. cereus*). From root surface examination, we found that the *Osaux1-3* mutant lines had shorter outer sheath or dermic cells in comparison to wild-type (Figure 2B). In response to Cd exposure, the LRs were much shorter as compared to wild-type, and the RH density decreased 35.5% in *Osaux1-3* but only 25.5% in wild-type. Interestingly, the RH density in IPDC transgenic lines was greater than 60% (Figures 2C, D), indicating that the auxin-dependent precursor of bacterial species influences the RH growth and density. In roots, IPDC transgenic line showed higher expression as compared to the shoots (Figure 2E).

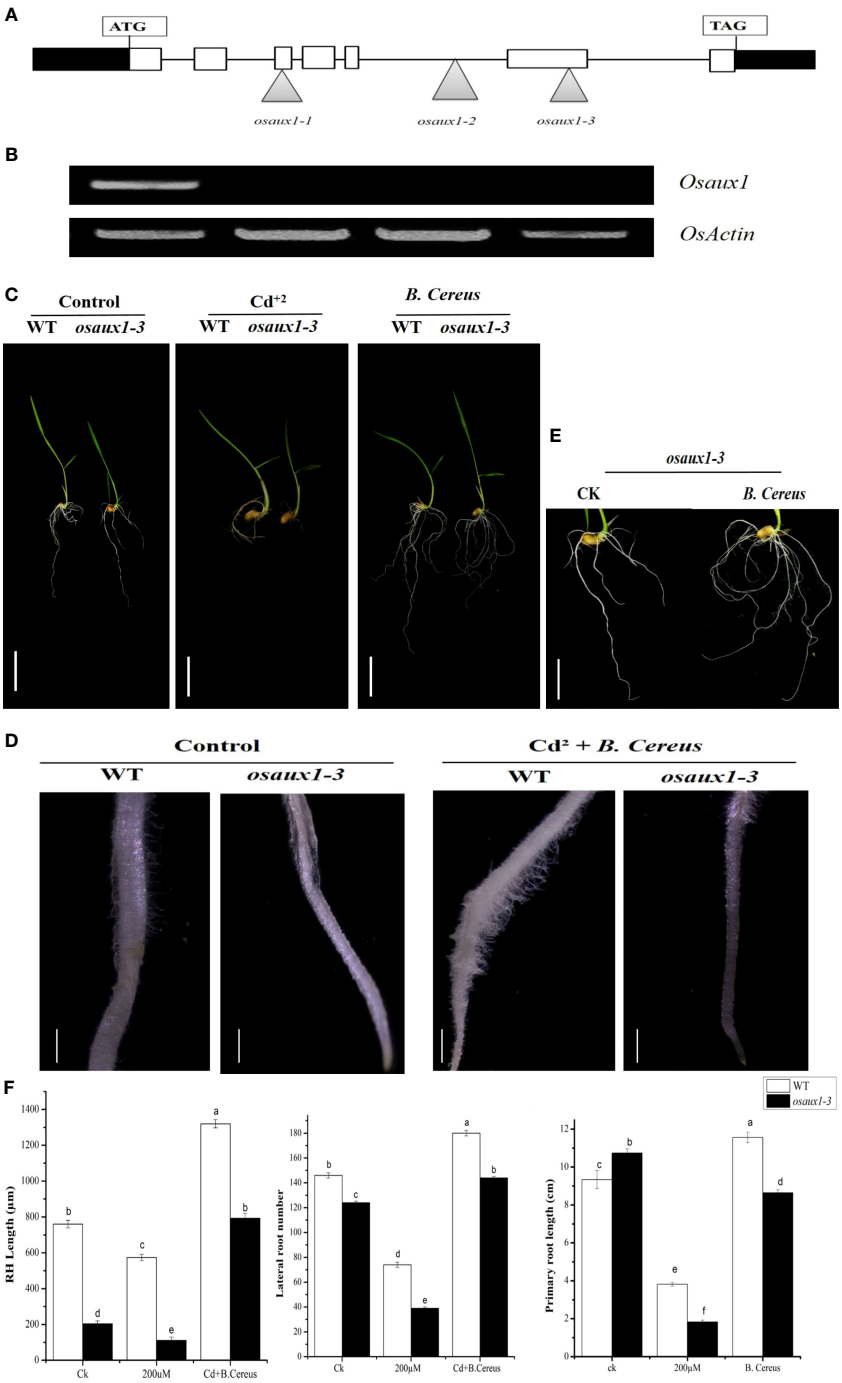


FIGURE 1
Three T-DNA insertion lines were identified in the *OsAux1* gene. **(A)** Schematic representation of T-DNA insertion mutations in *osaux1*-1, *osaux1*-2, and *osaux1-3* in the *OsAux1* gene. The open arrow heads represent T-DNA insertion positions. Filled white boxes represent exons; black boxes represent untranslated region; black lines represent introns. **(B)** Detection of RT-PCR of *OsAuxX1* transcripts in WT (Dongjin) *osaux1-1*, *osaux1-2*, and *osaux1-3*; actin transcripts were amplified as a control. **(C)** Seven-day phenotypic comparison of grown seedlings of wild-type (Dongjin), mutant lines *osaux1-3*, and **(B)** *cereus*-inoculated under Cd treatment. Scale bar, 1 cm. **(D)** Root hair morphology of **(B)** *cereus*-inoculated and noninoculated wild-type and *osaux1-3* after 3 days of treatment with 200 μM $CdCl_2$ using Nikon AZ100. Scale bar, 1 mm. **(E)** Focused image of *osaux1-3* mutant under control. **(F)** Root phenotype quantification of PR length, LR root number, and RH length in wild-type and mutant lines grown in Cd bacterial-inoculated and noninoculated (controlled) conditions. Five seedlings from each of three replicates were assessed and grown for 10 days. Lowercase letters indicate significant differences between means, determined using Duncan's multiple range mean comparisons.

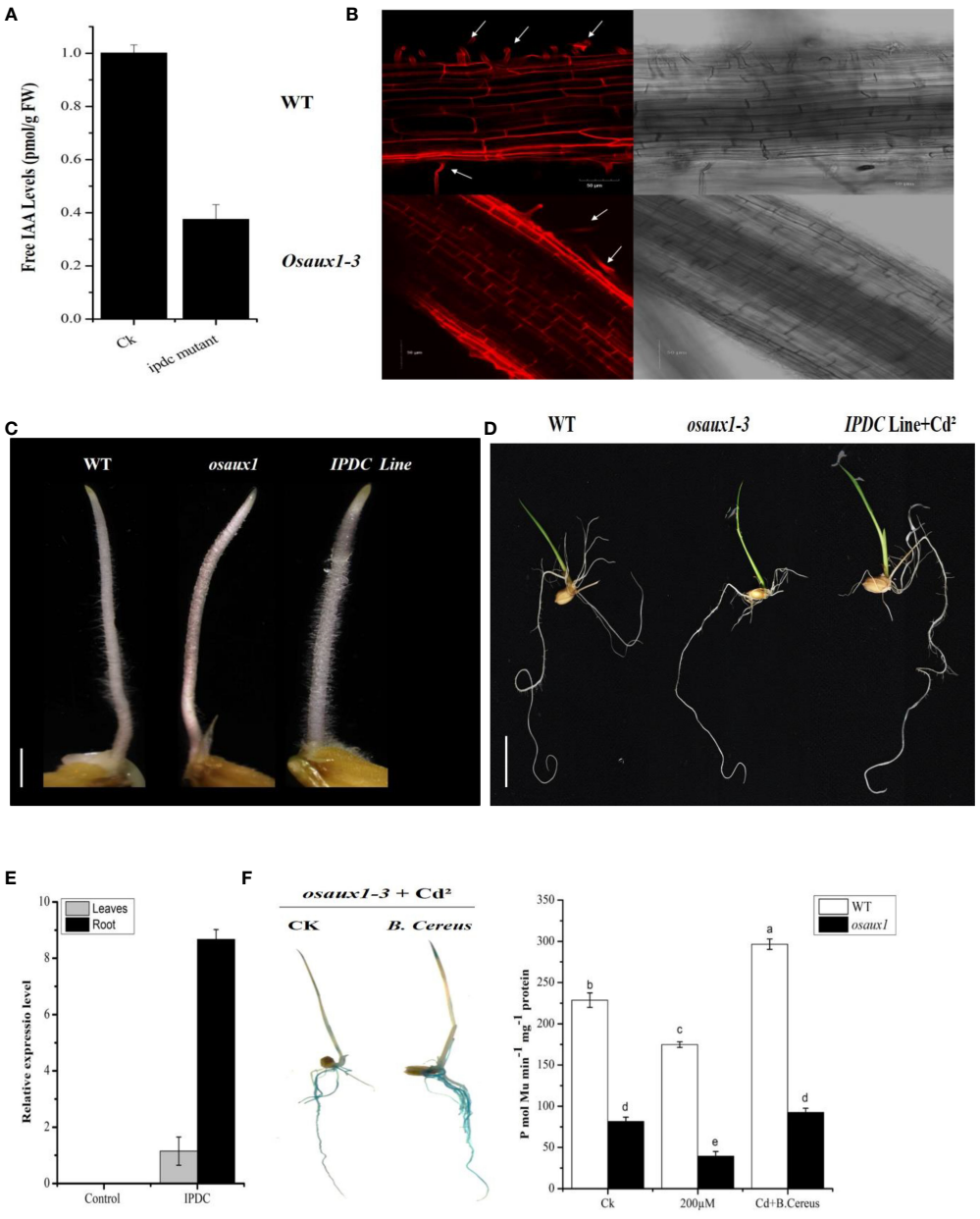


FIGURE 2
(A) Expression of indole-3-acetic acid by **(B)** *cereus* and an *ipdc* mutant. **(B)** Confocal micrographs showing propidium iodide staining of the cell wall of wild-type and *osaux1-3* mutant from the lateral root tips of *Oryza sativa*. L. Micrographic representation of cell size of the wild-type (above row) and *osaux1-3* mutant (below row). Arrow indicates the RHS development. Right, the bright field with a scale bar of 50 μm. **(C, D)** Phenotypic comparison between wild-type (Dongjin), mutant lines *Osaux1-3*, and *IPDC transgenic line* after 3 to 7 days of germination. Scale bar, 1 cm. **(E)** Relative expression of IPDC transgenic lines in root and shoot. Scale bar, 1 cm. **(F)** *osaux1-3* inoculated and noninoculated with **(B)** *cereus* expression in 10-day-old seedlings treated with 200 μM $CdCl_2$; DR5:*GUS* was transformed into the rice. Ten positive transgenic lines were observed. *ProDR5*:GUS activity is shown in **(F)**. Lowercase letters indicate significant differences between means, determined using Duncan's multiple range mean comparisons.

Auxin expression in root cell and localization in the nuclear membrane

To further investigate the auxin involvement in response to bacterial interaction, *osaux1-3* mutant negatively affects the LR development in response to Cd, which was promisingly upregulated in the inoculated mutant line (Figure 1F). By using the GUS assay, we examine the molecular mechanism of AUX1, which regulates RH development in rice. DR5:*GUS* staining in rice plants demonstrated that Cd reduced

expression in PR, LR, and root hair in the *osaux1-3* mutant line, but increased dramatically in *B. cereus*-inoculated rice seedlings, indicating that *B. cereus* interacts in the rhizosphere and plays a positive role in auxin regulation (Figure 2F). To further understand the plant–microbe interaction of AUX1 and *B. cereus*, the colocalization of *OsGH3-2* revealed that GH3s are most consistently localized to the ER membrane by using RFP:HDEL (ER marker) (Figure 3A) in rice protoplast. Protein interaction was localized transiently in ER membrane with *YFP^n-IPDC* and *OsGH3*-CFP^c expression vectors in the rice protoplast (Figure 3B), indicating that *Bacterial* spp. produce ipdC protein exogenously that further interacts with indole-3-acetic acid–amido synthetase gene protein (*GH3-2*) precursor and increases auxin content in roots, resulting in an increase in lateral roots and root hair.

OsAux1 mutants are sensitive to Cd stress and induced cell death

H_2O_2, O_2^-, and cell death were quantified to fully understand the augmented compassion towards the Os*AUX1* under Cd stress. As compared to wild-type, the amount of O_2 produced by the mitochondrial electron transport chain was determined in *osaux1-3* mutants under Cd treatment. At 200 μM of Cd treatment, H_2O_2 content in the *osaux1-3* mutant was high as compared to wild-type, while it became considerably low in bacterial-inoculated seedlings (Figure 4A). Moreover, Hoechst 33342 staining was used to quantify the cell integrity in rice root tips. Results revealed that the root tips of *osaux1* mutant showed lower cell integrity as compared to wild-type in response to Cd stress, while in bacterial-treated *osaux1* mutants (Figure 4B), the accumulation of Hoechst 33342 staining was high as compared to noninoculated seedlings, thus indicating that in *osaux1* mutant, cell death is most likely caused by Cd stress. The death rate was also high in bacterial culture in response to 200 μM of Cd treatment with Hoechst 33342 and propidium iodide staining (Figure 4C).

Metal absorption effect Cd, AUX1, and tryptophan content

We examined the Cd augmentation in root tips by transmission electron microscopy (TEM) (Figure 5) and by quantifying the Cd content in root tips (Figure 6A). The Cd content in the *osaux1* mutant was insignificantly high as compared to the wild-type as quantified by using the Synergy H1 spectroscope. The TEM qualification assay showed damaging results in *osaux1* mutants as compared to wild-type and *Bacillus*-inoculated root tips. The nucleolus gradually becomes invisible in Cd-treated seedlings of *osaux1* mutants and wild-type, indicating that Cd penetrates roots by cell rupturing (Figure 5). Tryptophan serves as a precursor for the biosynthesis of IAA. In the *osaux1* mutant, the free IAA content was less upon exposure to Cd (Figure 6B) whereas tryptophan content was higher (Figure 6C), while bacterial-inoculated seedlings resulted in normalizing the free IAA content in roots.

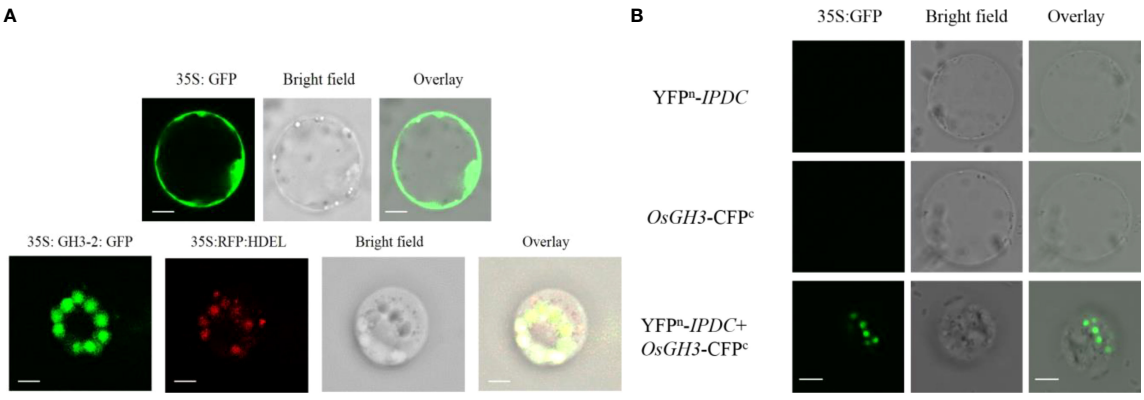


FIGURE 3
(A) Subcellular localization of 35S:*GH3-2*:GFP using rice protoplast 35S; green fluorescent protein (GFP) was used as a positive control. Left to right: green fluorescent protein of OsGH3-sGFP is shown in green color; red fluorescence shows RFP:HDEL (ER marker), bright field, and overlay microscope images. GH3s are most consistently localized to the ER membrane. Scale bars = 10 μm. **(B)** Protein interaction of *GH3* and *ipdc* using rice protoplasts. Scale bars = 10 μm.

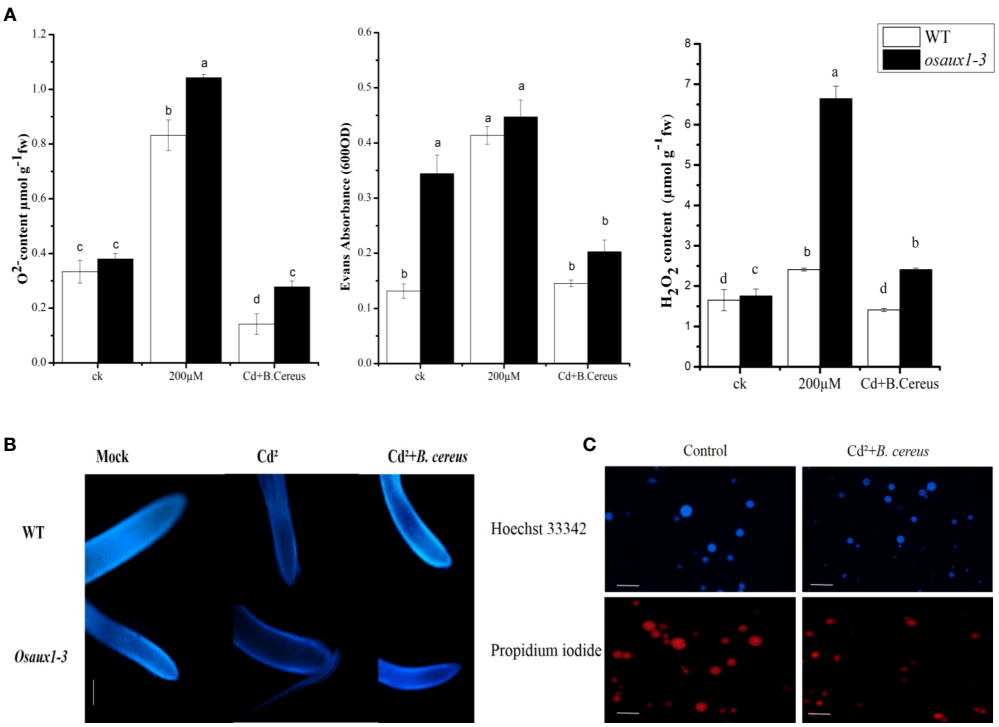


FIGURE 4
(A) Effect of Cd augmentation on H_2O_2, O_2, and cell death in rice. Accumulation of O_2^- and H_2O_2 was measured in wild-type and *osaux1-3* mutant exposed to 200 µM of $CdCl_2$ for 7 days. Cell death was also assessed after days of wild-type and *osaux1-3* by Evans Blue staining exposed to 200 µM of $CdCl_2$ for 7 days. **(B)** Histochemical detection of **(B)** *cereus*-inoculated and noninoculated wild-type and *osaux1-3* root tips exposed to 200 µM of $CdCl_2$ with Hoechst 33342 staining image was visualized after 7 days of stress using Nikon Eclipse DS Ri2 microscope. Scale bars = 2µm. **(C)** Cultural staining of **(B)** *cereus with* Hoechst 33342 and propidium iodide in the presence of Cd. The bacterial culture was grown in an LB medium with 10^8 CFU. Lowercase letters indicate significant differences between means, determined using Duncan's multiple range mean comparisons.

Expression of biosynthesis and transport genes

Upon inoculation with *B. cereus*, the level of YUCCA and AUX1 triggered and showed upregulation in response to the Cd treatment in both wild-type and *osaux1* mutants (Figures 6D, E). Other genes such as TSA, TSB, and ASA involved in the biosynthesis of tryptophan, IAA, and glucosinolate synthesis were stimulated two- to threefold (data not shown). The overall picture indicated that *B. cereus* strongly influences the root IAA production.

Discussion

In monocotyledonous species such as rice, lateral roots are essential organs that increase the absorbing capacity of water (Zhao et al., 2015). In early reports, *AUX1* and *LAX3* in *Arabidopsis* serve as LR and RH regulators (Jones et al., 2009). Biosynthetic signaling pathways get activated by auxins secreted by PGPR (Roy et al., 2010). Root morphology changes due to the disruption of the *AUX1* inhibited gene upon inoculation of rhizobacteria suggest that IAA is the main factor in plant–microbe interaction. Heavy metal uptake in roots mainly causes cell rupturing and infects plant integrity (Jan et al., 2019). When plants are exposed to high levels of toxic compounds, the roots are the primary part severely affected by such a level of abiotic stress. In our previous study, we found *B. cereus* is involved in plant growth development under Cd stress and acts as a PGPR (Jan et al., 2019). In the current study, we further investigated the involvement of auxin influx and signal transduction pathways in rice's LR and RH development in response to *B. cereus*. In *Arabidopsis*, auxin is not only expressed in root hair but also regulates root hair development. *AUX1* has been reported as an essential expressing gene during lateral root primordia initiation (Yu et al., 2016). In recent years, scientists have started paying close attention to auxin signaling and heavy metal response (Tamás et al., 2015). In our study, the *osaux1* mutant showed a significant decrease in the lateral root number, and root hair indicated that *AUX1* plays a key role in lateral root

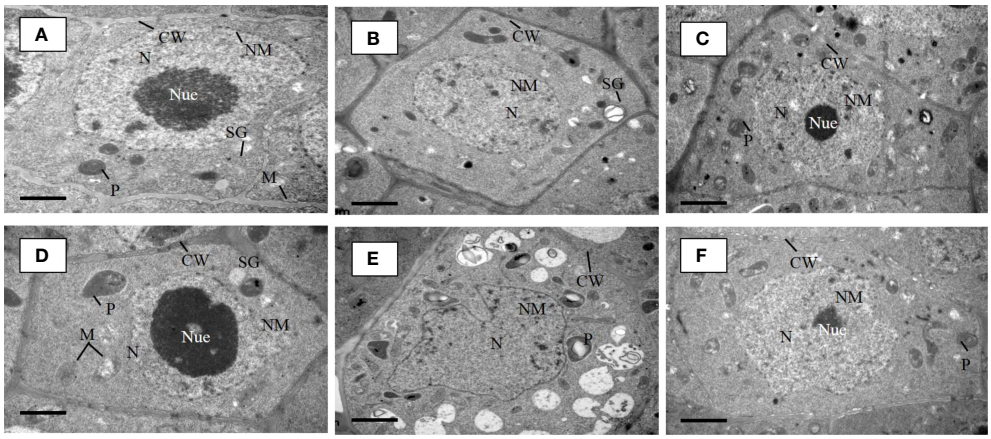


FIGURE 5
TEM micrographs of lateral root tip cells of 7-day wild-type **(A)** and *osaux1-3* **(D)** mutant under control condition, 200 μM $CdCl_2$ **(B, E)**, and 200 μM $CdCl_2$ with *B. cereus* inoculated **(C, F)**. **(A)** Root tip cells of Dongjin as a wild-type cultivar and **(D)** *osaux1-3* mutant under control **(CK)** show well-developed cell wall (CW), oval-shaped and clear mitochondria (M), starch grain (SG), plastids (P), nucleus (N), nuclear membrane (NM), and nucleolus (Nue). TEM micrographs of root tip cells of **(B)** wild-type and **(E)** *osaux1-3* under 200 μM Cd show immature nucleus (N), plastids (P), and scattered nucleolus (Nue) and a discontinue cell wall (CW). TEM micrographs of root tip cells of **(C)** wild-type and **(F)** *osaux1-3* under combined 200 μM Cd and bacterial treatment show well-developed cell wall (CW) and nucleus (N) along with a recovered nucleolus (Nue).

development in rice. Interestingly, the inoculation with rhizospheric bacteria showed an increase in primary and lateral root density in *osaux1* mutant under control (Dongjin wild-type) and 200 μM of Cd treatment, suggesting that Aux1 might be able to control or activate lateral root formation due to IAA accumulation in roots, similar to the finding of Zhao (2010) and Casanova-Sáez et al. (2021). Different microbial pathways exist for IAA synthesis (Spaepen et al., 2007). The indole-3-pyruvate pathway is one of the predominant pathways for plant root development in rhizobacteria like *Azospirillum brasilense*. An increase in the level of exogenous IAA in the rhizosphere by bacterial strains showed similar results to IPDC transgenic lines, suggesting that ipdc as precursor gene of auxin biosynthesis decisively affects plant development. It is therefore conjectured that bacterial auxin produced by PGPR may amend the level of auxin and affect the auxin-regulated physiological processes. Similar findings were also reported by Jasim et al. (2014) and Jijón-Moreno et al. (2015) that ipdC encodes the PPDC gene, which is a key enzyme in producing IAA growth hormone. Furthermore, the rate-limiting step is catalyzed by ipdC, and the mutation of ipdC leads to a strong reduction of IAA, similar to the finding of Baudoin et al. (2010). In bacterial *ipdc* knockout mutant, the level of IAA was not significantly higher than that of *B. cereus*, demonstrating that the ipdc gene plays a role in both Trp-dependent and Trp-independent biosynthesis pathways, with an average of 61 nmol g^{-1} FW tryptophan measured in the Cd treatment *osaux1-3* mutant, which increased significantly with bacterial inoculation. Tryptophan serves as a precursor for the biosynthesis of IAA (Zhao et al., 2015). Results revealed that bacterial inoculation significantly increases the level and distribution of IAA in response to Cd in the roots of *osaux1-3* than that of noninoculated one. Zhang et al. (2007) also provided similar evidence that PGPR can elicit changes in endogenous plant auxin homeostasis without providing microbial-originating auxin. In roots, the transcriptional level of IAA biosynthesis genes increases or remains unchanged upon inoculation. However, in primary and lateral root meristems, DR5::GUS transgenic plants revealed higher auxin levels, signifying that the tissue distribution of auxin or its polar transport is affected by the bacterium. Zhang et al. (2007) also reported that GB03 exposed DR5::GUS plants to *B. subtilis* led to the proposal that the PGPR strain not only affects auxin biosynthesis but also tissue homeostasis and polar transport.

Auxin as an auxin reflux carrier is supposed to be in *Arabidopsis*; auxin transport charged IAA to the cytoplasm (Péret et al., 2012). In rice, auxin is localized to the plasma membrane (Yu et al., 2015). Auxin-responsive genes in monocots include three families: Aux/IAAs, GH3s, and small auxin-up RNAs (SAURs) (Wang et al., 2010b). Previous studies also demonstrated that most of the group II GH3 subfamily members are IAA–amido synthetases that maintain endogenous auxin homeostasis by conjugating excess auxin with amino acids (Khan and Stone, 2007; Fu et al., 2011). Results showed that in rice, the GH3-2 gene localizes to the ER membrane. According to these findings, the interaction of the *OsGH3-2* gene with the ipdc gene showed positive signals in rice protoplast toward

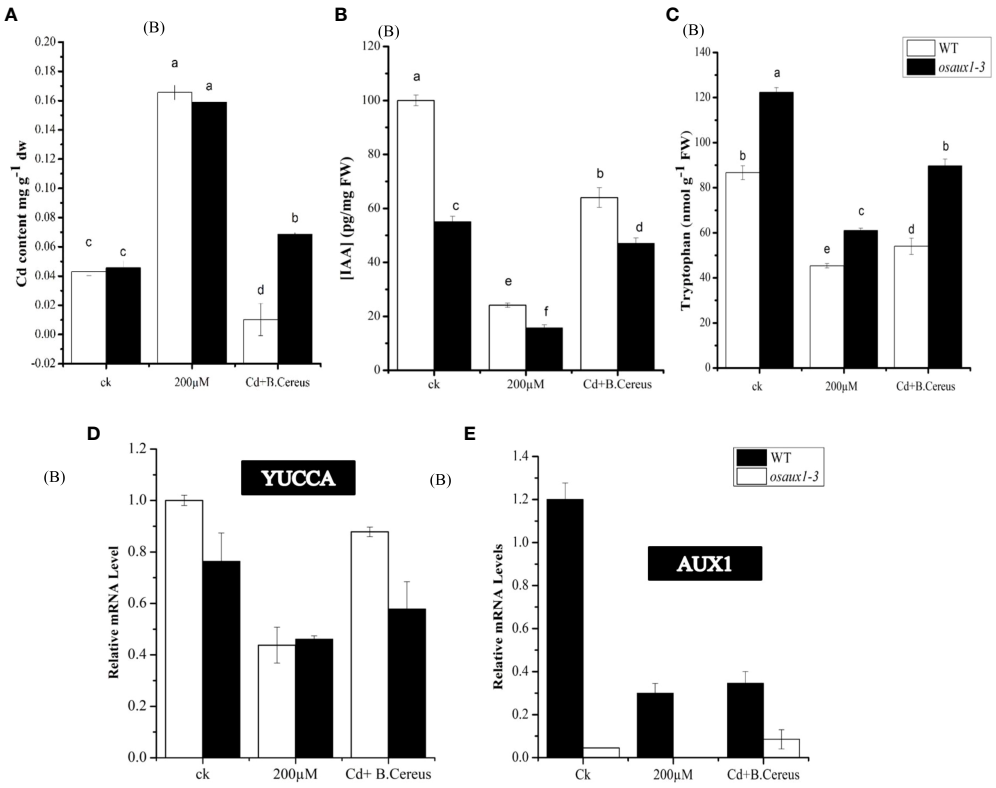


FIGURE 6
Effect of Cd on IAA and tryptophan content in wild-type and *osaux1-3* content. **(A)** Cadmium content was measured in root **(B)**, indole 3-acetic acid (IAA) **(C)**, and tryptophan content in WT and *osaux1-3*. Rice seedlings were inoculated with or without **(B)** *cereus* and 200 μM $CdCl_2$ for 4 days in three biological repeats. **(D, E)** Relative mRNA levels of YUCCA and AUX1 in roots of wild-type and *osaux1-3* after 3 days of treatment with 200 μM $CdCl_2$ and **(B)** *cereus*. Three biological repeats were included for quantitative RT-PCR analysis. Lowercase letters indicate significant differences between means, determined using Duncan's multiple range mean comparisons.

plant–microbe interaction; it can be assumed that the interaction of the *ipdc* gene with the GH3-2 synthetase gene influences IAA biosynthesis, resulting in enhanced LR and RHs.

Cd also affects the distribution and metabolism by interrupting auxin homeostasis in *Arabidopsis* (Hu et al., 2013). Cd sensitivity was increased by a reduction in auxin content. A study on *osaux1-3* mutant lines revealed that PR, LR, and HR are more sensitive to Cd than wild-type. The death rate of root cells becomes higher in *osaux1* mutants exposed to Cd stress, as determined by histochemical staining with Hoechst 33342 and propidium iodide. In the *osaux1* mutant, the Cd content was higher as compared to the wild-type, while upon inoculation with bacterial strain, the level of Cd content became lower under stress conditions. Results also demonstrated that the death rate of the bacterial cells was not significantly high or that Cd did not completely retard the growth rate of *B. cereus*, suggesting that *B. cereus* has a survival capability in response to Cd stress. Our findings are consistent with those of Sabater and Martín (2013); Souza et al. (2015), and Dubey et al. (2014), who reported that the production of reactive oxygen species causes plant cell death under stress conditions. Ecological stress generates several ROS. O_2^- is a primary reactive oxygen species for toxic heavy metals and triggers the generation of $OH^{\cdot}$ and O^2 as ROS (Das and Roychoudhury, 2014). The H_2O_2 concentration in the wild-type increased significantly after 3 days of Cd exposure, similar to the findings of Krishnamurthy and Rathinasabapathi (2013) in *Arabidopsis* under Cd treatment. O_2^- and H_2O_2 accumulation is the cause of oxidative stress. In *osaux1*, O_2^- and H_2O_2 are expressed at higher levels than in the wild-type under stress conditions. Through reactive oxygen species-mediating signaling, it can be assumed that in rice, auxin transport through *osaux1-3* H_2O_2 has a regulating role during tolerance to Cd stress conditions. Previous studies have already reported that in *Arabidopsis*, under unfavorable conditions, cell cycle regulation and auxin signaling function regulate root development (De Smet et al., 2010; Olanrewaju et al., 2017). Despite the effect of *B. cereus* on IAA biosynthesis and transport, IAA genes showed downregulation in the transcript level of *osaux1-3* compared to wild-type.

Conclusion

Our results indicate that a functional IAA signaling pathway is required for root architecture and lateral root development in response to *Bacillus cereus*. Although the action of PGPR on roots due to the involvement of auxin has long been said to originate from bacteria, it is the first key step of the auxin transduction pathway required in plant response. We showed that PGPR strains in the host plant affect the endogenous IAA homeostasis in a complex manner by interacting with the *GH3-2* gene without directly providing IAA. Nevertheless, the mechanism of ipdc, the precursor gene of IAA in bacterial strains, and GH3-2 in host–plant interaction is not clearly understood. Therefore, further research is required at the domain level to understand their mode of function and how they interact with each other in response to root development.

Data availability statement

The original contributions presented in the study are included in the article/Supplementary Material. Further inquiries can be directed to the corresponding authors.

Author contributions

TJ conceived of the research idea and supervised the research. GS conducted the research, collected data, and did a formal analysis of the data. MJ and GS wrote the original draft of the manuscript. SF, KA and NK provided technical expertise to strengthen the research concept. SF and SY helped in the funding acquisition. All authors contributed to the article and approved the submitted version.

Funding

This work was carried out with the support of CooperativeResearch Program for Agriculture Science and Technology Development (Project No. PJ017068032022) Rural Development Administration, Republic of Korea.

Acknowledgments

The authors extend their appreciation to the Researchers Supporting Project number (RSP-2021/369), King Saud University, Riyadh, Saudi Arabia. We would like to thank Dr. Adeel Abbas, Dr. Rashida Hameed and Dr. Muhammad Sajid for their help and guidance for this work and reviewing of the manuscript.

Conflict of interest

The authors declare that the research was conducted in the absence of any commercial or financial relationships that could be construed as a potential conflict of interest.

Publisher's note

All claims expressed in this article are solely those of the authors and do not necessarily represent those of their affiliated organizations, or those of the publisher, the editors and the reviewers. Any product that may be evaluated in this article, or claim that may be made by its manufacturer, is not guaranteed or endorsed by the publisher.

Supplementary material

The Supplementary Material for this article can be found online at: https://www.frontiersin.org/articles/10.3389/fpls.2022.1023723/full#supplementary-material

References

Baker, C. J., and Mock, N. M. (1994). An improved method for monitoring cell death in cell suspension and leaf disc assays using Evans blue. *Plant Cell Tissue Organ Cult.* 39 (1), 7–12. doi: 10.1007/BF00037585

Baudoin, E., Lerner, A., Mirza, M. S., El Zemrany, H., Prigent-Combaret, C., Jurkevich, E., et al. (2010). Effects of azospirillum brasilense with genetically modified auxin biosynthesis gene ipdC upon the diversity of the indigenous microbiota of the wheat rhizosphere. *Res. Microbiol.* 161 (3), 219–226. doi: 10.1016/j.resmic.2010.01.005

Casanova-Sáez, R., Mateo-Bonmatí, E., and Ljung, K. (2021). Auxin metabolism in plants. *Cold Spring Harbor Perspect. Biol.* 13 (3), a039867. doi: 10.1101/cshperspect.a039867

Celloto, V. R., Oliveira, A. J., Gonçalves, J. E., Watanabe, C. S., Matioli, G., and Gonçalves, R. A. (2012). Biosynthesis of indole-3-acetic acid by new klebsiella oxytoca free and immobilized cells on inorganic matrices. *Sci. World J.* 2012, 1–7. doi: 10.1100/2012/495970

Das, K., and Roychoudhury, A. (2014). Reactive oxygen species (ROS) and response of antioxidants as ROS-scavengers during environmental stress in plants. *Front. Environ. Sci.* 2, 53. doi: 10.3389/fenvs.2014.00053

De Smet, I., Lau, S., Voß, U., Vanneste, S., Benjamins, R., Rademacher, E. H., et al. (2010). Bimodular auxin response controls organogenesis in arabidopsis. *Proc. Natl. Acad. Sci.* 107 (6), 2705–2710. doi: 10.1073/pnas.0915001107

Dubey, S., Shri, M., Misra, P., Lakhwani, D., Bag, S. K., Asif, M. H., et al. (2014). Heavy metals induce oxidative stress and genome-wide modulation in transcriptome of rice root. *Funct. Integr. Genomics* 14 (2), 401–417. doi: 10.1007/s10142-014-0361-8

Duca, D. R., and Glick, B. R. (2020). Indole-3-acetic acid biosynthesis and its regulation in plant-associated bacteria. *Appl. Microbiol. Biotechnol.* 104 (20), 8607–8619. doi: 10.1007/s00253-020-10869-5

Egorshina, A., Khairullin, R., Sakhabutdinova, A., and Luk'yantsev, M. (2012). Involvement of phytohormones in the development of interaction between wheat seedlings and endophytic bacillus subtilis strain 11BM. *Russian J. Plant Physiol.* 59 (1), 134–140. doi: 10.1134/S1021443711050062

El-Hadi, N., El-Ala, H. A., and El-Azim, W. A. (2009). Response of some mentha species to plant growth promoting bacteria (PGPB) isolated from soil rhizosphere. *Aust. J. Basic Appl. Sci.* 3 (4), 4437–4448.

Esitken, A., Yildiz, H. E., Ercisli, S., Donmez, M. F., Turan, M., and Gunes, A. (2010). Effects of plant growth promoting bacteria (PGPB) on yield, growth and nutrient contents of organically grown strawberry. *Sci. Hortic.* 124 (1), 62–66. doi: 10.1016/j.scienta.2009.12.012

Fu, J., Yu, H., Li, X., Xiao, J., and Wang, S. (2011). Rice GH3 gene family: regulators of growth and development. *Plant Signaling Behav.* 6 (4), 570–574. doi: 10.4161/psb.6.4.14947

García Sánchez, J. (2018). Identificación de bacterias productoras de giberelinas presentes en plantas de stanophea tigrina con efecto promotor de crecimiento vegetal. *Benemérita Universidad Autónoma Puebla*.

Grover, M., Bodhankar, S., Sharma, A., Sharma, P., Singh, J., and Nain, L. (2021). PGPR mediated alterations in root traits: way toward sustainable crop production. *Front. Sustain. Food Syst.* 4, 618230. doi: 10.3389/fsufs.2020.618230

Haider, F. U., Liqun, C., Coulter, J. A., Cheema, S. A., Wu, J., Zhang, R., et al. (2021). Cadmium toxicity in plants: Impacts and remediation strategies. *Ecotoxicol. Environ. Saf.* 211, 111887. doi: 10.1016/j.ecoenv.2020.111887

Hiei, Y., Ohta, S., Komari, T., and Kumashiro, T. (1994). Efficient transformation of rice (Oryza sativa l.) mediated by agrobacterium and sequence analysis of the boundaries of the T-DNA. *Plant J.* 6 (2), 271–282. doi: 10.1046/j.1365-313X.1994.6020271.x

Hsu, S.-H., Shen, M.-W., Chen, J.-C., Lur, H.-S., and Liu, C.-T. (2021). The photosynthetic bacterium rhodopseudomonas palustris strain PS3 exerts plant growth-promoting effects by stimulating nitrogen uptake and elevating auxin levels in expanding leaves. *Front. Plant Sci.* 12, 573634. doi: 10.3389/fpls.2021.573634

Hu, Y. F., Zhou, G., Na, X. F., Yang, L., Nan, W. B., Liu, X., et al. (2013). Cadmium interferes with maintenance of auxin homeostasis in arabidopsis seedlings. *J. Plant Physiol.* 170 (11), 965–975. doi: 10.1016/j.jplph.2013.02.008

Jana, S., and Choudhuri, M. A. (1982). Glycolate metabolism of three submersed aquatic angiosperms during ageing. *Aquat. Bot.* 12, 345–354. doi: 10.1016/0304-3770(82)90026-2

Jan, M., Shah, G., Masood, S., Iqbal Shinwari, K., Hameed, R., Rha, E., et al. (2019). Bacillus cereus enhanced phytoremediation ability of rice seedlings under cadmium toxicity. *BioMed. Res. Int.* 2019, 1–12. doi: 10.1155/2019/8134651

Jasim, B., Jimtha John, C., Shimil, V., Jyothis, M., and Radhakrishnan, E. (2014). Studies on the factors modulating indole-3-acetic acid production in endophytic bacterial isolates from p iper nigrum and molecular analysis of ipdc gene. *J. Appl. Microbiol.* 117 (3), 786–799. doi: 10.1111/jam.12569

Jefferson, R. A., Kavanagh, T. A., and Bevan, M. W. (1987). GUS fusions: beta-glucuronidase as a sensitive and versatile gene fusion marker in higher plants. *EMBO J.* 6 (13), 3901–3907. doi: 10.1002/j.1460-2075.1987.tb02730.x

Jijón-Moreno, S., Marcos-Jiménez, C., Pedraza, R. O., Ramírez-Mata, A., de Salamone, I. G., Fernández-Scavino, A., et al. (2015). The ipdC, hisC1 and hisC2 genes involved in indole-3-acetic production used as alternative phylogenetic markers in azospirillum brasilense. *Antonie Van Leeuwenhoek* 107 (6), 1501–1517. doi: 10.1007/s10482-015-0444-0

Jones, A. R., Kramer, E. M., Knox, K., Swarup, R., Bennett, M. J., Lazarus, C. M., et al. (2009). Auxin transport through non-hair cells sustains root-hair development. *Nat. Cell Biol.* 11 (1), 78. doi: 10.1038/ncb1815

Khan, Z., and Doty, S. L. (2009). Characterization of bacterial endophytes of sweet potato plants. *Plant Soil* 322 (1-2), 197–207. doi: 10.1007/s11104-009-9908-1

Khan, S., and Stone, J. M. (2007). Arabidopsis thalianaGH3. 9 influences primary root growth. *Planta* 226 (1), 21–34. doi: 10.1007/s00425-006-0462-2

Kramer, E. M., and Bennett, M. J. (2006). Auxin transport: A field in flux. *Trends Plant Sci.* 11 (8), 382–386. doi: 10.1016/j.tplants.2006.06.002

Krishnamurthy, A., and Rathinasabapathi, B. (2013). Auxin and its transport play a role in plant tolerance to arsenite-induced oxidative stress in a rabidopsis thaliana. *Plant Cell Environ.* 36 (10), 1838–1849. doi: 10.1111/pce.12093

Ljung, K., Hull, A. K., Celenza, J., Yamada, M., Estelle, M., Normanly, J., et al. (2005). Sites and regulation of auxin biosynthesis in arabidopsis roots. *Plant Cell* 17 (4), 1090–1104. doi: 10.1105/tpc.104.029272

Malusá, E., Sas-Paszt, L., and Ciesielska, J. (2012). Technologies for beneficial microorganisms inocula used as biofertilizers. *Sci. World J.* 2012, 1–12. doi: 10.1100/2012/491206

Marchant, A., Bhalerao, R., Casimiro, I., Eklöf, J., Casero, P. J., Bennett, M., et al. (2002). AUX1 promotes lateral root formation by facilitating indole-3-acetic acid distribution between sink and source tissues in the arabidopsis seedling. *Plant Cell* 14 (3), 589–597. doi: 10.1105/tpc.010354

Meldau, D. G., Long, H. H., and Baldwin, I. T. (2012). A native plant growth promoting bacterium, bacillus sp. B55, rescues growth performance of an ethylene-insensitive plant genotype in nature. *Front. Plant Sci.* 3, 112. doi: 10.3389/fpls.2012.00112

Merzaeva, O., and Shirokikh, I. (2010). The production of auxins by the endophytic bacteria of winter rye. *Appl. Biochem. Microbiol.* 46 (1), 44–50. doi: 10.1134/S0003683810010072

Mia, M. B., and Shamsuddin, Z. (2010). Rhizobium as a crop enhancer and biofertilizer for increased cereal production. *Afr. J. Biotechnol.* 9 (37), 6001–6009.

Miyadate, H., Adachi, S., Hiraizumi, A., Tezuka, K., Nakazawa, N., Kawamoto, T., et al. (2011). OsHMA3, a P1B-type of ATPase affects root-to-shoot cadmium translocation in rice by mediating efflux into vacuoles. *New Phytol.* 189 (1), 190–199. doi: 10.1111/j.1469-8137.2010.03459.x

Muller, B., and Touraine, B. (1992). Inhibition of NO⊟ 3 uptake by various phloem-translocated amino acids in soybean seedlings. *J. Exp. Bot.* 43 (5), 617–623. doi: 10.1093/jxb/43.5.617

Olanrewaju, O. S., Glick, B. R., and Babalola, O. O. (2017). Mechanisms of action of plant growth promoting bacteria. *World J. Microbiol. Biotechnol.* 33 (11), 1–16. doi: 10.1007/s11274-017-2364-9

Olatunji, D., Geelen, D., and Verstraeten, I. (2017). Control of endogenous auxin levels in plant root development. *Int. J. Mol. Sci.* 18 (12), 2587. doi: 10.3390/ijms18122587

Péret, B., Swarup, K., Ferguson, A., Seth, M., Yang, Y., Dhondt, S., et al. (2012). AUX/LAX genes encode a family of auxin influx transporters that perform distinct functions during arabidopsis development. *Plant Cell* 24 (7), 2874–2885. doi: 10.1105/tpc.112.097766

Rajendran, G., Patel, M. H., and Joshi, S. J. (2012). Isolation and characterization of nodule-associated exiguobacterium sp. from the root nodules of fenugreek (Trigonella foenum-graecum) and their possible role in plant growth promotion. *Int. J. Microbiol.* 2012, 1–8. doi: 10.1155/2012/693982

Ronzan, M., Piacentini, D., Fattorini, L., Della Rovere, F., Eiche, E., Riemann, M., et al. (2018). Cadmium and arsenic affect root development in oryza sativa l. negatively interacting with auxin. *Environ. Exp. Bot.* 151, 64–75. doi: 10.1016/j.envexpbot.2018.04.008

Roy, B., Deb, B., and Sharma, G. (2010). Role of acetic acid bacteria in biological nitrogen fixation. *Biofrontiers* 2, 47–57.

Sabater, B., and Martín, M. (2013). Hypothesis: increase of the ratio singlet oxygen plus superoxide radical to hydrogen peroxide changes stress defense response to programmed leaf death. *Front. Plant Sci.* 4, 479. doi: 10.3389/fpls.2013.00479

Sarwar, M., Arshad, M., Martens, D. A., and Frankenberger, W. (1992). Tryptophan-dependent biosynthesis of auxins in soil. *Plant Soil* 147 (2), 207–215. doi: 10.1007/BF00029072

Sgroy, V., Cassán, F., Masciarelli, O., Del Papa, M. F., Lagares, A., and Luna, V. (2009). Isolation and characterization of endophytic plant growth-promoting (PGPB) or stress homeostasis-regulating (PSHB) bacteria associated to the halophyte prosopis strombulifera. *Appl. Microbiol. Biotechnol.* 85 (2), 371–381. doi: 10.1007/s00253-009-2116-3

Souza, R. D., Ambrosini, A., and Passaglia, L. M. (2015). Plant growth-promoting bacteria as inoculants in agricultural soils. *Genet. Mol. Biol.* 38, 401–419. doi: 10.1590/S1415-475738420150053

Spaepen, S., Vanderleyden, J., and Remans, R. (2007). Indole-3-acetic acid in microbial and microorganism-plant signaling. *FEMS Microbiol. Rev.* 31 (4), 425–448. doi: 10.1111/j.1574-6976.2007.00072.x

Swarup, K., Benková, E., Swarup, R., Casimiro, I., Péret, B., Yang, Y., et al. (2008). The auxin influx carrier LAX3 promotes lateral root emergence. *Nat. Cell Biol.* 10 (8), 946–954. doi: 10.1038/ncb1754

Tamás, L., Mistrík, I., Alemayehu, A., Zelinová, V., Bočová, B., and Huttová, J. (2015). Salicylic acid alleviates cadmium-induced stress responses through the inhibition of cd-induced auxin-mediated reactive oxygen species production in barley root tips. *J. Plant Physiol.* 173, 1–8. doi: 10.1016/j.jplph.2014.08.018

Tezuka, K., Miyadate, H., Katou, K., Kodama, I., Matsumoto, S., Kawamoto, T., et al. (2010). A single recessive gene controls cadmium translocation in the

cadmium hyperaccumulating rice cultivar cho-Ko-Koku. *Theor. Appl. Genet.* 120 (6), 1175–1182. doi: 10.1007/s00122-009-1244-6

Ulmasov, T., Hagen, G., and Guilfoyle, T. J. (1997). ARF1, a transcription factor that binds to auxin response elements. *Science* 276 (5320), 1865–1868. doi: 10.1126/science.276.5320.1865

Vázquez-Chimalhua, E., Barrera-Ortiz, S., Valencia-Cantero, E., López-Bucio, J., and Ruiz-Herrera, L. F. (2021). The bacterial volatile n, n-dimethyl-hexadecylamine promotes arabidopsis primary root elongation through cytokinin signaling and the AHK2 receptor. *Plant Signaling Behav.* 16 (4), 1879542. doi: 10.1080/15592324.2021.1879542

Wang, S., Bai, Y., Shen, C., Wu, Y., Zhang, S., Jiang, D., et al. (2010a). Auxin-related gene families in abiotic stress response in sorghum bicolor. *Funct. Integr. Genomics* 10 (4), 533–546. doi: 10.1007/s10142-010-0174-3

Wang, Y., Deng, D., Bian, Y., Lv, Y., and Xie, Q. (2010b). Genome-wide analysis of primary auxin-responsive Aux/IAA gene family in maize (Zea mays. l.). *Mol. Biol. Rep.* 37 (8), 3991–4001. doi: 10.1007/s11033-010-0058-6

Wang, S., and Fu, J. (2011). Insights into auxin signaling in plant–pathogen interactions. *Front. Plant Sci.* 2, 74. doi: 10.3389/fpls.2011.00074

Wang, S., Xu, Y., Li, Z., Zhang, S., Lim, J. M., Lee, K. O., et al. (2014). OsMOGS is required for n-glycan formation and auxin-mediated root development in rice (Oryza sativa l.). *Plant J.* 78 (4), 632–645. doi: 10.1111/tpj.12497

Won, C., Shen, X., Mashiguchi, K., Zheng, Z., Dai, X., Cheng, Y., et al. (2011). Conversion of tryptophan to indole-3-acetic acid by TRYPTOPHAN AMINOTRANSFERASES OF ARABIDOPSIS and YUCCAs in arabidopsis. *Proc. Natl. Acad. Sci.* 108 (45), 18518–18523. doi: 10.1073/pnas.1108436108

Xu, Z.-M., Li, Q.-S., Yang, P., Ye, H.-J., Chen, Z.-S., Guo, S.-H., et al. (2017). Impact of osmoregulation on the differences in cd accumulation between two contrasting edible amaranth cultivars grown on cd-polluted saline soils. *Environ. Pollut.* 224, 89–97. doi: 10.1016/j.envpol.2016.12.067

Xu, L., Wu, C., Oelmüller, R., and Zhang, W. (2018). Role of phytohormones in piriformospora indica-induced growth promotion and stress tolerance in plants: more questions than answers. *Front. Microbiol.* 9 (1646). doi: 10.3389/fmicb.2018.01646

Yoo, S.-D., Cho, Y.-H., and Sheen, J. (2007). Arabidopsis mesophyll protoplasts: A versatile cell system for transient gene expression analysis. *Nat. Protoc.* 2 (7), 1565–1572. doi: 10.1038/nprot.2007.199

Yu, C., Sun, C., Shen, C., Wang, S., Liu, F., Liu, Y., et al. (2015). The auxin transporter, os AUX 1, is involved in primary root and root hair elongation and in cd stress responses in rice (Oryza sativa l.). *Plant J.* 83 (5), 818–830. doi: 10.1111/tpj.12929

Yu, J., Yu, Z., Fan, G., Wang, G., and Liu, X. (2016). Isolation and characterization of indole acetic acid producing root endophytic bacteria and their potential for promoting crop growth. 18, 1381–1391.

Zhang, H., Kim, M.-S., Krishnamachari, V., Payton, P., Sun, Y., Grimson, M., et al. (2007). Rhizobacterial volatile emissions regulate auxin homeostasis and cell expansion in arabidopsis. *Planta* 226 (4), 839. doi: 10.1007/s00425-007-0530-2

Zhao, Y. (2010). Auxin biosynthesis and its role in plant development. *Annu. Rev. Plant Biol.* 61, 49. doi: 10.1146/annurev-arplant-042809-112308

Zhao, H., Ma, T., Wang, X., Deng, Y., Ma, H., Zhang, R., et al. (2015). OsAUX 1 controls lateral root initiation in rice (O ryza sativa l.). *Plant Cell Environ.* 38 (11), 2208–2222. doi: 10.1111/pce.12467

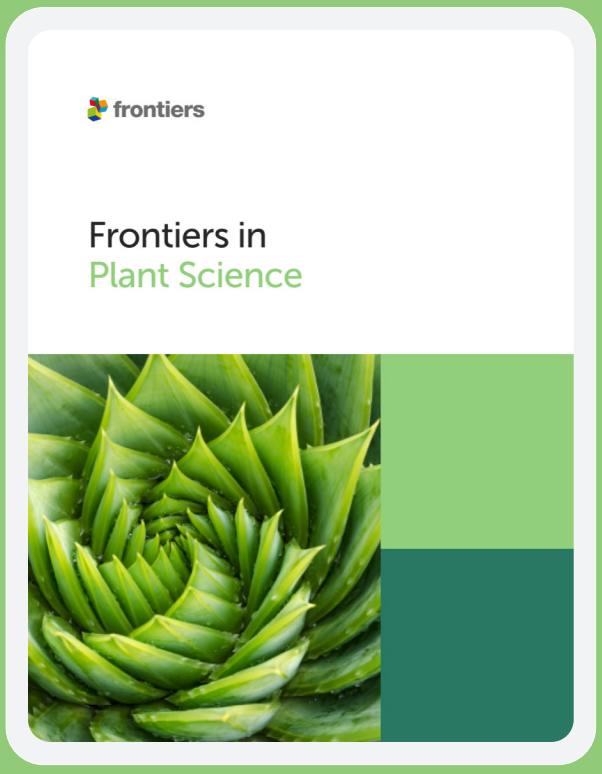
Frontiers in Plant Science

Cultivates the science of plant biology and its applications

The most cited plant science journal, which advances our understanding of plant biology for sustainable food security, functional ecosystems and human health.

Discover the latest Research Topics

See more →



Frontiers

Avenue du Tribunal-Fédéral 34
1005 Lausanne, Switzerland
frontiersin.org

Contact us

+41 (0)21 510 17 00
frontiersin.org/about/contact